The cover illustration depicts two lead nuclei (gray-colored nucleons) colliding head on at relativistic speed to create a quark−gluon plasma (QGP), illustrated by the liberation of red, green, and blue color-charged quarks at the point of interaction and the emission of photons depicted by yellow particles further away from the QGP. As described by Andreas Ipp and Peter Somkuti (*Physical Review Letters* **109**, 192301, 2012, http://journals.aps.org/prl/abstract/10.1103/PhysRevLett.109.192301), in the QGP the quarks and gluons are liberated and able to move freely, unlike their bound state within a nucleon, and the creation of the plasma is very short-lived. The plasma duration is only several yoctoseconds (10^{-24} s). Ipp and Somkuti (2012) describe how the photon emissions (ie, light pulses created by the QGP) can be measured instrumentally to produce the world's fastest stopwatch. (Illustration reproduced with permission, Technical University of Vienna © TU Wien.)

Radioactivity

Introduction and History, From the Quantum to Quarks

Second Edition

Michael F. L'Annunziata

ELSEVIER

AMSTERDAM • BOSTON • HEIDELBERG • LONDON • NEW YORK • OXFORD • PARIS
SAN DIEGO • SAN FRANCISCO • SINGAPORE • SYDNEY • TOKYO

Elsevier
Radarweg 29, PO Box 211, 1000 AE Amsterdam, Netherlands
The Boulevard, Langford Lane, Kidlington, Oxford OX5 1GB, UK
50 Hampshire Street, 5th Floor, Cambridge, MA 02139, USA

Copyright © 2016, 2007 Elsevier B.V. All rights reserved.

No part of this publication may be reproduced or transmitted in any form or by any means, electronic or mechanical, including photocopying, recording, or any information storage and retrieval system, without permission in writing from the publisher. Details on how to seek permission, further information about the Publisher's permissions policies and our arrangements with organizations such as the Copyright Clearance Center and the Copyright Licensing Agency, can be found at our website: www.elsevier.com/permissions.

This book and the individual contributions contained in it are protected under copyright by the Publisher (other than as may be noted herein).

Notices
Knowledge and best practice in this field are constantly changing. As new research and experience broaden our understanding, changes in research methods, professional practices, or medical treatment may become necessary.

Practitioners and researchers must always rely on their own experience and knowledge in evaluating and using any information, methods, compounds, or experiments described herein. In using such information or methods they should be mindful of their own safety and the safety of others, including parties for whom they have a professional responsibility.

To the fullest extent of the law, neither the Publisher nor the authors, contributors, or editors, assume any liability for any injury and/or damage to persons or property as a matter of products liability, negligence or otherwise, or from any use or operation of any methods, products, instructions, or ideas contained in the material herein.

British Library Cataloguing-in-Publication Data
A catalogue record for this book is available from the British Library

Library of Congress Cataloging-in-Publication Data
A catalog record for this book is available from the Library of Congress

ISBN: 978-0-444-63489-4

Library of Congress Control Number: 2015958159

For information on all Elsevier publications
visit our website at https://www.elsevier.com

Publisher: John Fedor
Acquisition Editor: Kathryn Morrissey
Editorial Project Manager: Jill Cetel
Production Project Manager: Mohanapriyan Rajendran
Designer: Greg Harris

Typeset by TNQ Books and Journals

To my wife Maria del Carmen (aka Reyna)
and son and daughter Michael and Carmen Elena.
In memory of our son Frank.

About the Author

Michael F. L'Annunziata earned his BSc degree in 1965 from St. Edward's University, and his MSc and PhD in 1967 and 1970 at the University of Arizona. His graduate thesis research in the 1960s dealt with the analysis of radionuclides and chemical remediation of the environment in the event of possible nuclear fallout. His main research interests are focused on the development of chemical and instrumental methods for the detection and measurement of radioactive nuclides and the utilization of radionuclides as tracers in biological research. L'Annunziata was formerly head of fellowships and training at the International Atomic Energy Agency (IAEA) in Vienna, Austria, and served as a representative for the IAEA in fact-finding, planning, and implementation assignments on peaceful applications of nuclear energy for development in over 50 countries from 1976 to 2007. He is the author and editor of several books, including *Radionuclide Tracers, Their Detection and Measurement*, published in 1987, and the *Handbook of Radioactivity Analysis*, now in its third edition, published in 2012. His more lengthy biography has been included in the annual editions of *Who's Who in the World* from 1987 to 2016.

Foreword

Our knowledge of the atom and the energy that it harnesses increases rapidly with each passing year. This book gives the reader an opportunity to walk through the ages and delve into the lives and works of numerous pioneers who have made discoveries contributing to our atomic knowledge, and the remarkable technical and scientific applications that have emerged to improve lives and well-being around the world.

In this second edition, I am pleased that the author has expanded extensively on the vital role that the atom and its energy play in many aspects of our daily life. It is interesting to note how important nuclear techniques are in both the diagnosis and the therapy of many forms of cancer, for example, but we also make use of bandages and gauzes to dress wounds and hypodermic needles to administer vaccines, all of which have been sterilized by ionizing radiation.

Furthermore, ensuring the quantity and quality of the world's food supply is a never-ending challenge, and it is being met with the aid of nuclear techniques to research and optimize crop nutrition and water use efficiency, plant breeding, animal health and production, and the use of radiation to control and eradicate insects pests that act as vectors of hugely harmful diseases for humans, livestock, and crops.

Nuclear applications are being used to monitor our water and marine resources, and contribute to the essential data needed as the world begins to tackle the issues caused by ocean acidification and climate change. And fascinating research into harnessing fusion, a potentially endless source of power, free of the radioactive waste associated with current nuclear fuels, is another of the most exciting developments that will unfold over the coming years.

All countries of the world benefit from nuclear science and its applications, and I note the crucial role of the International Atomic Energy Agency (IAEA), with over 160 member states, in coordinating research, training, and the implementation of nuclear techniques worldwide to help satisfy basic needs that are essential for well-being and development.

This second edition offers the reader an expanded and up-to-date account of the historical developments in nuclear science. The discoveries, which were made from as early as the late 19th century through to today, have enabled us to develop and refine the applications so essential to modern life.

I note that this very readable book presents the principles of nuclear science in an easily accessible format for the scientist, teacher, student, or ordinary reader. Nuclear science and its applications are here to stay, and this book provides a good review of how we have arrived where we are today.

Professor Aldo Malavasi, PhD
Deputy Director General
Department of Nuclear Sciences and Applications
International Atomic Energy Agency, Vienna, Austria

Preface to the First Edition

This book describes the origins and properties of the various types of radiation emitted by radioactive nuclides, as well as cosmic radiation, cosmic-ray showers, and Cherenkov radiation. It includes the principles of radionuclide decay, and a historical narrative of discoveries that revealed the properties of the atomic nucleus, atomic structure, and nuclear decay and its radiations. These discoveries revealed, as described in this book, a source of energy vital to our well-being and development. Before each chapter are accounts of the lives and works of early pioneers, from the discovery of radioactivity by Henri Becquerel in 1896, only a few months after the discovery of x-radiation by Wilhelm Röntgen in 1895, to around 1960 when many applications of nuclear energy of benefit to mankind were beginning to take hold in medicine, biology, food and agriculture, hydrology, industry, nuclear power, and other fields vital to our basic needs.

The book is divided into two parts: one providing biographical accounts of the lives and works of pioneers in this field, and the other part detailing the origins and properties of the various types of radiation and nuclear decay. The biographical accounts are found in the sections entitled Radioactivity Hall of Fame, which appear before each chapter of the book. The lives and works of the pioneers are not presented in purely chronological order; rather, before each chapter I include as far as possible the biographical accounts of those who contributed most to our knowledge of the material presented in the subsequent chapter.

The Introduction includes an overview of some of the many applications of radioactive sources that play an important role in our day-to-day lives. In this, it was my objective to highlight how we have become dependent in so many ways on a source of energy which has enriched our lives. Radioactive sources and the various types of radiation that they emit are invisible to us, and thus the benefits these energy sources bring to us each day through radiation technology usually do not cross our minds.

It is my hope that this book will serve as a teaching text for those who are or may become interested in physics and chemistry. It describes in detail how pioneers in these two fields joined forces to unravel the mysteries of natural and artificial radioactive sources, their invisible radiations, and the numerous ways that this energy source can be applied to improve our lives and well-being.

In the sections entitled *Radioactivity Hall of Fame*, I have included the lives and works of over 60 research pioneers, most of whom were awarded the Nobel Prize. The experiments they carried out and the reasoning they used both to devise their experiments and to arrive at their findings are provided in detail. Many of the trials and tribulations of their lives are also included. It is my hope that they will serve as examples to students in any field of endeavor. Specifically, I hope the student will not only extract from this book the romance of science, but also take note of the tremendous perseverance displayed by these pioneers. They encountered many difficulties and sometimes seemingly insurmountable obstacles in life and work, and without doubt fear of failure; nevertheless, these obstacles did not hinder them but only motivated them further. To illustrate my point I will use one example from many in the text of this book. It is taken from the biographical sketch of Ernest Lawrence (1901−1958), who conceived and built the cyclotron, a device found today in many hospitals for on-site production of artificial radioisotopes of short half-life needed in medical diagnosis and treatment. The text describes how one day in 1929 Ernest Lawrence read an article by Rolf Wideröe, a Norwegian physicist, discussing the acceleration of positive ions across an increasing voltage potential in a linear device. On that day in 1929, after reading Wideröe's paper, Lawrence invented the principle of the cyclotron. Conceiving the principle of a new concept is one matter, but making it happen may be altogether a seemingly impossible hurdle. At the Nobel Prize award ceremony held at the University of California, Berkeley on 29 February, 1940, Professor R. T. Birge stated:

> *The next morning Dr. Lawrence told his friends that he had found a method for obtaining particles of very high energy, without the use of any high voltage. The idea was surprisingly simple and in principle quite correct—everyone admitted that. Yet everyone said, in effect, "Don't forget that having an idea and making it work are two very different things"… In this connection I can quote with profit some remarks made by Dr. W. D. Coolidge, when he presented to Dr. Lawrence, in 1937, the Comstock Prize of*

the National Academy of Sciences… "Dr. Lawrence envisioned a radically different course—one which did not have those difficulties attendant upon the use of potential differences of millions of volts. At the start, however, it presented other difficulties and many uncertainties, and it is interesting to speculate on whether an older man, having had the same vision, would have ever attained its actual embodiment and successful conclusion. It called for boldness and faith and persistence to a degree rarely matched."

This statement is a lesson to us in all fields of work and whatever the pursuit. Many good ideas that conform with known laws of nature may come to us, but to turn these ideas or inventions into reality can be an insurmountable task to most. Often it is difficult to comprehend the almost endless hours of toil, frustration, and sometimes borderline despair that one encounters, and to have the needed stubborn determination to find solutions to make an idea become a reality, We can be certain that Lawrence and many others who have achieved greatness have faced these tremendous hurdles. It is my hope that, in relating these stories, the student will find inspiration and examples to follow in the pursuit not necessarily of greatness, but of achievement and satisfaction in whatever work or endeavor their lives may bring.

While writing I thought how best to portray the greatness of the achievements of the pioneers described in this book. I thought of doing what is common, namely providing copies of historic photographs, as we have seen in other books, such as Pierre and Marie Curie working together in their Paris laboratory or Lise Meitner and Otto Hahn working in Germany as a team in physics and chemistry. Instead, I thought it best to underscore the significance of their work by illustrating postage stamps issued in many countries commemorating their discoveries or the beneficial applications that their discoveries have brought to mankind. It took time and effort to obtain the needed commemorative stamps, but it was worth the effort. There is no better way to draw attention to the significance of the work accomplished by these pioneers than to see that many nations have issued postage stamps commemorating their achievements.

In the end I hope this book will serve not only to inspire the student with the historical romance of discovery, but also serve as a teaching text for many of the basic principles of radioactivity, its beneficial applications, nuclear decay, and radiation physics and chemistry.

I have omitted specific chapters on the detection and measurement of radiation and radionuclide analysis, as being beyond the scope of this book. This subject matter is covered in detail in other more lengthy books, including an earlier text, *Handbook of Radioactivity Analysis*, second edition, edited by the author and published by Elsevier Science, Amsterdam in 2003.

Mention of commercial products in this book does not imply recommendation or endorsement by the author. Other and more suitable products may be available. The names of products are included for convenience or information purposes only.

I want to thank Dr. Ramkumar Venkataraman for his encouragement and review of some of the text. However, I bear sole responsibility for any errors or omissions. The encouragement of Professor Emeritus Romard Barthel, PhD, CSC, and his stimulating and dynamic lectures in physics and mathematics at St. Edward's University during 1961−1962 will always be remembered with gratitude, appreciation, and esteem. My appreciation is extended to editorial staff of Elsevier, Amsterdam, including Dr. Andrew D. Gent, Dr. Egbert van Wezenbeek, and Joan Anuels, for their encouragement, recommendations, and patience during the writing of this book, and to Joan Anuels and Betsy Lightfoot for their constant attention to every detail of the book. I thank my wife Reyna for her steadfast support, understanding, and patience.

Michael F. L'Annunziata, PhD
Oceanside, CA
February 2007

Preface to the Second Edition

During the preparation of the first edition, published in 2007, I was only able to provide the early history of the development of the science concerning the atom, its nucleus, and nuclear decay up to around 1950. Nevertheless, the book was well received, as evidenced by its appearance in 2008 in the top 10 of the *Library Journal*'s best sellers list in physics. When Elsevier invited me to prepare an expanded second edition, I relished both the challenge and the opportunity. This gave me the chance to expand the book to the present, and describe the historical developments that have led to our current understanding of the science of the atom, its nucleus, and the nuclear decay that gives rise to radioactivity.

I have included in this new second edition a review of our current understanding of the building blocks of matter, the fundamental forces in nature, and the role of quarks and the force particles, ie, gluons, photons, and the $W^{\pm}$ and Z^{0} bosons, in nuclear stability and decay. This expansion of the book compelled me to augment its subtitle to include *From the Quantum to Quarks*, which more accurately reflects its comprehensive content.

Readers familiar with the first edition will notice that I have included more photographs of the pioneers and Nobel Laureates who have contributed in a large way to our current knowledge of nuclear science—I heeded the requests of readers to do so. Also, I have continued to include throughout the book copies of postage stamps that commemorate the pioneers and the important contributions they made to our current understanding of this fascinating science. The inclusion of commemorative postage stamps of the pioneers highlights the importance of their work and the recognition and celebrity status attributed to them for discoveries that have had an important impact on our daily lives.

I have expanded extensively the introductory chapter, entitled "Radioactivity and Our Well-Being." This was warranted by the numerous advances that have been made since the first edition, including in the application of radioactivity to medical diagnosis and treatment, biological and agricultural research, the study of our water and marine resources, radiation processing in industry, and the continued development of nuclear fusion as a very promising safe source of electric power relatively free of radioactive waste and with an inexhaustible source of fuel, to mention just a few beneficial applications.

Included in this expanded second edition is the dark history of this science, including the development of the atomic bomb based on nuclear fission chain reactions, the development of the yet worse and more devastating hydrogen bomb, based on both fission and fusion, and the nuclear arms race that followed. With this in mind, I have provided an overview of the historic developments that have taken place toward the nonproliferation of nuclear weapons, including the very early Russell−Einstein Manifesto, the work of the late nuclear physicist and Nobel Laureate for Peace Joseph Rotblat (1908−2005), the Pugwash Conferences on Science and World Affairs, and the International Atomic Energy Agency (IAEA) of the United Nations, among other pioneers and organizations, that have sought to promote the ultimate and vital goal of nuclear nonproliferation and disarmament.

Throughout the text there are numerous examples of calculations requiring mostly elementary algebra that demonstrate many of the principles described in this book, such as the equivalence of mass and energy ($E = mc^2$), and the energies liberated in nuclear reaction and decay. These calculations are included to aid the student in his or her understanding of the principles outlined in the book, as well as to demonstrate the sound basis upon which the principles are founded. Thus it is my hope that this updated and expanded edition will continue to serve as a suitable text for classrooms. It is my hope that the book will continue to inspire the reader, either student or layperson, with the romance of discovery, and to enhance appreciation of the advances that have been made in our understanding of the atom, its nucleus, and the numerous beneficial applications of nuclear decay (ie, radioactivity) that continue to improve our daily lives.

I want to thank my close friend and former IAEA colleague, Bogdan Lisovich, who has encouraged me in my scientific writing over the past four decades. His friendship and encouragement provide invaluable support to my endeavors in this

field, for which I remain forever grateful. Appreciation is extended to Beth Campbell, Katey Birtcher, and Kathryn Morrissey at Elsevier for their assistance in the planning of this book, and to Jill Cetel, who has led the editorial team at Elsevier and guided me through book production. I wish also to thank Mohanapriyan Rajendran, project manager of book production at Chennai Elsevier, and his staff for their fine work and patience during the preparation of this book. I bear sole responsibility for any errors or omissions. Again and as always, I remain immensely grateful to my wife Maria del Carmen (Reyna) for her steadfast support, understanding, and unflagging patience.

Michael F. L'Annunziata, PhD
Oceanside, CA
31 March, 2016

Acronyms, Abbreviations and Symbols

A	Mass number
AA	Antiproton accumulator
a	Years (anni)
Å	Angstrom (10^{-10} m = 0.1 nm)
Ab	Antibody
AD	Anno Domini
Ag	Antigen
AIP	American Institute of Physics
α	Alpha particle, internal conversion coefficient, fine structure constant
$\propto$	Proportional to
amu	Atomic mass unit
ANL	Argonne National Laboratory
$\sim$	Approximately
APS	Advanced Photon Source, Argonne, IL, USA
ARS	Agricultural Research Service, Washington, DC
atm.	Standard atmospheric pressure (760 mm Hg, 760 Torr)
B	Binding energy
B	Baryon quantum number
B^+, B^0	B meson
b	Bottom or beauty quark
$\overline{b}$	Antibottom quark
B/A	Binding energy per nucleon
barn	10^{-24} cm^2
BEH	Brout-Englert-Higgs mechanism
BEPC	Beijing Electron-Positron Collider, Beijing, China
BNCT	Boron neutron capture therapy
BP	Before present
Bq	Becquerel = 1 disintegration per second (1 dps)
BYU	Bringham Young University, Provo, Utah
β	Particle relative phase velocity, beta particle
$\beta\beta$	Double-beta decay
β^-	Negatron, negative beta particle
β^+	Positron, positive beta particle
β^-n	Beta-delayed neutron emission
β^+p	Beta-delayed proton emission
c	Speed of light in a vacuum (2.9979×10^8 m/s)
c	Charm quark
$\overline{c}$	Anticharm quark
°C	Degrees Celsius
C	Coulomb (2.997×10^9 esu)
CC	Charged current (interaction)
cal	Calorie (4.186 J)
CalTech	California Institute of Technology, Pasadena, CA

CAT	Computed axial tomography
CCD	Charge-coupled device
CEA	Commissariat à l'Energie Atomique, Paris
CERN	European Organization for Nuclear Research, Geneva
CFR	Center des Faibles Radioactivités, Gif-sur-Yvette, France
Ci	Curie (2.22×10^{12} dpm $= 3.7 \times 10^{10}$ dps $= 37$ GBq)
cm	Centimeter (10^{-2} m)
CMB	Cosmic microwave background
CMBR	Cosmic microwave background radiation
CN	Carbon−nitrogen (solar energy cycle)
CNRS	Center National de la Recherche Scientifique, France
COBE	Cosmic Background Explorer (satellite)
COSMOS	Cosmic-Ray Soil Moisture Observing System
CP	Charge parity
CPM, cpm	Counts per minute
CRF	Controlled thermonuclear fusion
CPY	Counts per year
3D-CRT	Three-dimensional conformal radiotherapy
CT	Computed tomography
3D-CT	Three-dimensional computed tomography
CTR	Controlled thermonuclear reactor
D	Deuterium
d	Days, deuteron, down quark
$\overline{\mathrm{d}}$	Antidown quark
D−D	Deuterium−deuterium fusion
Δ^{++}, Δ^{+}, Δ^{0}, Δ^{-}	Delta baryon
δ	Delta values, parts per thousand or ‰
DDR	German Democratic Republic
DEMO	Demonstration power plant
DIC	Dissolved inorganic carbon
DiMF	Decay in a magnetic field
DNA	Deoxyribonucleic acid
DPM, dpm	Disintegrations per minute
DPS, dps	Disintegrations per second
D−T	Deuterium−tritium (fusion or plasma)
e^{-}	Electron
e^{+}	Positron
$e^{\pm}$	Positron−negatron pair
ε	Electron capture
E	Energy, detection efficiency
E_e	Electron energy
E_γ	Gamma-ray energy
E_K	Kinetic energy
$E_{\max}$	Maximum energy
E_{th}	Threshold energy
E/A	Energy per nucleon
EBRT	External beam radiation therapy
EC	Electron capture
ECAS	Emergency Committee of Atomic Scientists
e/m	Charge-to-mass ratio
ENS	Ecole Normale Supérieure, Paris
erg	Energy unit (100.0×10^{-9} J $= 6.2415 \times 10^{11}$ eV)
EPR	Enhanced permeability and retention
ES	Electron scattering

EPA	Environmental Protection Agency, Washington, DC
ESRF	European Synchrotron Radiation Facility, Grenoble
esu	Electrostatic unit (3.335×10^{-10} C)
η	Eta meson
ETH	Eidgenössische Technische Hochschule, Zurich
EU	European Union
EUR	Euro
eV	Electron volt (1.602×10^{-19} J $= 1.602 \times 10^{-12}$ erg)
FAO	Food and Agriculture Organization, Rome
FIAN	Fizicheskii Institut Akademya Nauk, USSR
FLNR	Flerov Laboratory of Nuclear Reactions, Dubna
fm	Fermi or femtometer (10^{-15} m)
fp	Fission products
FPD	Flat panel detector
ft	Foot (0.3048 m)
G	Gauss (100.0×10^{-6} T)
g	Gram, gluon
γ	Gamma radiation, photon
GBq	Giga becquerels (10^9 dps)
GEM	Gas electron multiplier
GeV	Giga electron volts (10^9 eV)
GSI	Gesellschaft für Schwerionenforschung mbH, Darmstadt
Gy	Gray $= 1$ J/kg $= 6.24 \times 10^{12}$ MeV/kg
H	Magnetic field strength
H^0	Higgs boson
h	Hours
h	Planck constant (6.626×10^{-34} J s or 4.136×10^{-15} eV s), hours
$\hbar$	Planck constant, reduced ($h/2\pi = 1.054 \times 10^{-34}$ J s $= 6.582 \times 10^{-22}$ MeV s)
HABS	Harmful algal blooms
HDR	High dose rate
HTGR	High-temperature gas-cooled reactor
Hz	Hertz (s^{-1}), ie, one cycle per second
IAEA	International Atomic Energy Agency, Vienna
IBA	Ion-beam analysis
IC	Internal conversion
ICE	Initial cooling experiment
ICRP	International Commission on Radiation Protection, Ottawa, Ontario, Canada
ICRU	International Commission on Radiation Units and Measurements Bethesda, MD, USA
IEC	Inertial electrostatic confinement
IECF	Inertial electrostatic confinement fusion
IMRT	Intensity modulated radiation therapy
in.	inch (2.54 cm)
IP	Intersecting point
ISR	Intersecting storage rings
IT	Isomeric transition
ITER	International Thermonuclear Experimental Reactor, St. Paul-lez-Durance, France
J	Joule (0.2389 cal or 1×10^7 erg $= 6.2415 \times 10^{18}$ eV $= 1$ kg m^2/s^2)
J/Ψ	J/psi meson
JET	Joint European Torus, Abingdon, Oxfordshire, UK
JHA	Juvenile hormone analog
JINR	Joint Institute for Nuclear Research, Dubna
K	Degrees Kelvin
K	Kinetic energy
K^+, K^-, K^0	Positive, negative, and neutral kaon or K meson

kBq	Kilobecquerel (10^3 dps)
keV	Kiloelectron volts (10^3 eV)
kG	Kilogauss (10^3 G)
kg	Kilogram (10^3 g)
kGy	Kilogray (10^3 Gy)
km	Kilometer (10^3 m)
km.w.e	km-water equivalent
kV	Kilovolt (10^3 V)
kW•h	Kilowatt-hour
KWI	Kaiser Wilhelm Institute, Berlin
L, l	Liters
ℓ	Electron orbital quantum number
Λ^0	Lambda baryon
λ	Wavelength, decay constant
λ_{nr}	Nonrelativistic wavelength
λ_r	Relativistic wavelength
LANL	Los Alamos National Laboratory, Los Alamos, NM, USA
LEAR	Low-energy antiproton ring
LEP	Large Electron-Positron Collider, Geneva
LET	Linear energy transfer
LHC	Large Hadron Collider, Geneva
LINAC	Linear accelerator
LLNL	Lawrence Livermore National Laboratory, Livermore, CA, USA
m	Particle mass, metastable nuclear state
m_0	Particle rest mass
m_ℓ	Electron magnetic quantum number
m_r	Speed-dependent particle mass, relativistic mass
m_s	Electron spin quantum number
m	Meters, minutes
M	Nuclide or nucleon mass
MBq	Megabecquerels (10^6 dps)
MCi	Megacurie (10^6 Ci)
mCi	Millicurie (10^{-3} Ci) = 2.22×10^9 dpm = 3.7×10^7 dps = 37 MBq
MCP-PMT	Microchannel plate photomultiplier tube
MeV	Megaelectron volts (10^6 eV)
mg	Milligram (10^{-3} g)
MIT	Massachusetts Institute of Technology, Cambridge, MA, USA
mL	Milliliter (10^{-3} L)
mM	Millimolar (10^{-3} M)
mm	Millimeter (10^{-3} m)
mrad	Milliard (10^{-3} rad = 10 μGy), milliradian
mrem	Millirem (10^{-3} rem)
MRI	Magnetic resonance imaging
ms	Milliseconds (10^{-3} s)
mSv	Millisievert (10^{-3} Sv)
μ	Linear attenuation coefficient
μ_m	Mass attenuation coefficient
μ^+, μ^-	Positive muon, negative muon
μ	Micron (10^{-6} m)
μCi	Microcurie (10^{-6} Ci)
μGy	Microgray (10^{-6} Gy)
μL	Microliter (10^{-6} L)
μm	Micrometer (10^{-6} m)
μs	Microseconds (10^{-6} s)

MWPC	Multiwire proportional chamber
MW	Megawatt (10^6 W)
n	Neutron
$\overline{\text{n}}$	Antineutron
n	Index of refraction, electron principle quantum number
N	Neutron number
N_A	Avogadro's number (6.022×10^{23} atoms/mol)
NAA	Neutron activation analysis
NAS	National Academy of Sciences, Washington, DC, USA
NC	Neutral current (interaction)
NCD	Neutral current detector
nCi	Nanocurie (10^{-9} Ci)
NCT	Neutron capture therapy
NDFF	Nitrogen derived from fertilizer
NDFS	Nitrogen derived from soil
NDT	Nondestructive testing
NIST	National Institute of Standards and Technology, Gaithersburg, MD, USA
nm	Nanometer (10^{-9} m)
NMR	Nuclear magnetic resonance
n/p	Neutron/proton ratio
NRC	National Research Council, Washington, DC, USA
NRL	National Radiation Laboratory, Christchurch, New Zealand
ns	Nanoseconds (10^{-9} s)
ν	Neutrino, photon frequency, particle velocity
$\overline{\nu}$	Antineutrino
$0\nu\beta\beta$	Neutrinoless double-beta decay
$2\nu\beta\beta$	Two-neutrino double-beta decay
N/Z	Neutron/proton ratio
Ω^-	Omega minus baryon (hyperon)
OTPC	Optical time projection chamber
P	Parity quantum number
p	Particle momentum
p^+, p	Proton
$\overline{\text{p}}$	Antiproton
PDFF	Phosphorus derived from fertilizer
PDFS	Phosphorus derived from soil
PET	Positron emission tomography
PGA	Phosphoglyceric acid
PGNAA	Prompt gamma neutron activation analysis
π	3.141592
π^+, π^-, π^0	Positive, negative, and neutral pion or pi meson
PID	Particle identification
PIGE	Proton-induced gamma-ray analysis
PIXE	Proton-induced X-ray emission
PMT	Photomultiplier tube
pp	Pyriproxyfen
ppm	Parts per million
PS	Proton synchrotron
Q	Charge quantum number
Q	Q value, energy released by a reaction, decay energy
Q_α	Alpha decay energy
Q_β	Beta decay energy
$Q_{\beta\beta}$	Double-beta decay energy
Q_{EC}	Electron capture decay energy

QCD	Quantum chromodynamics
QD	Quadrupole
QED	Quantum electrodynamics
QGP	Quark−gluon plasma
QND	Quantum nondemolition
R	Roentgen $= 2.58 \times 10^{-4}$ C/kg of air, particle range
RaB	Radium B (^{214}Pb)
RaC	Radium C (^{214}Bi)
RaD	Radium D (^{210}Pb)
rad	Radiation absorbed dose (100 erg/g = 10 mGy), radian
RBA	Receptor binding assay
rem	Roentgen equivalent mammal (10 mSv)
RF	Radiofrequency
ρ	Density (g/cm^3), neutron absorption cross-section, particle path radius of curvature
ρ^+, ρ^-	Rho meson
RIA	Radioimmunoassay
RICH	Ring imaging Cherenkov (counter)
RIKEN	Japanese Natural Sciences Research Institute, Saitama, Japan
RHIC	Relativistic Heavy Ion Collider, Upton, NY, USA
RNA	Ribonucleic acid
s	Seconds, strange quark
$\bar{s}$	Antistrange quark
S	Strangeness quantum number
SAM	Substitute Alloys Materials Project
SANS	Small-angle neutron scattering
sec.	Seconds
SF	Spontaneous fission
SI	Système International d'Unités
Σ^+, Σ^0, Σ^-	Sigma hyperon (positive, neutral, and negative)
σ	Reaction cross-section, neutron absorption cross-section
SIT	Sterile insect technique
SLAC	Stanford Linear Accelerator Center, Menlo Park, CA, USA
SMNG	Soil moisture neutron gauge
SNO	Sudbury Neutrino Observatory, Sudbury, Ontario, Canada
SPA	Scintillation proximity assay
SPECT	Single photon emission computed tomography
SPS	Superproton synchrotron
sr	Steradian
SRM	Secondary Modern Reference
SSD	Surface shaded density
SSPT	Spot-scanning proton beam therapy
STP	Standard temperature and pressure
Sv	Sievert (1 Sv = 1 Gy = 100 rem = 1 J/kg)
T	Tritium, tesla (10^4 G)
T	Particle kinetic energy
t	Top quark
$\bar{t}$	Antitop quark
t	Time
$t_{½}$	Half-life
TA-GVHD	Transfusion-associated graft versus host disease
τ	Particle lifetime, tau lepton
TeV	Teraelectron volts (10^{12} eV)
TFTR	Tokamak Fusion Test Reactor
ThA	Thorium A (^{216}Po)

ThB	Thorium B (^{212}Pb)
ThC	Thorium C (^{212}Bi)
ThC″	Thorium C″ (^{208}Tl)
TNT	Trinitrotoluene (dynamite)
TOA	Top of the atmosphere
TOF	Time of flight
Tokamak	Russian *toroidal'naya kamera ee magnetnaya katushka*, meaning "torus-shaped magnetic chamber"
TOP	Time of propagation
TPC	Time projection chamber
TT	Transfer tunnel
u	Atomic mass unit (1/12 m of $^{12}C = 1.66054 \times 10^{-27}$ kg) or 931.494 MeV/c^2, up quark
$\overline{u}$	Antiup quark
u	Particle speed
u_{nr}	Nonrelativistic particle speed
u_r	Relativistic particle speed
UA1	Underground Area 1 (CERN experimental detector)
UA2	Underground Area 2 (CERN experimental detector)
UIC	Uranium Information Center
ULB	Université libre de Bruxelles
USDA	US Department of Agriculture
USSR	Union of Soviet Socialist Republics
UV	Ultraviolet
V	Volt
W	Watt (1 J/s)
$W^{\pm}$	W^+ or W^- boson
Ξ	Xi baryon (hyperon)
XRD	X-ray diffraction
XRF	X-ray fluorescence
y	Years
Z^0	Z^0 boson
Z	Atomic number or nuclear charge
Z/N	Proton/neutron ratio

Introduction

Radioactivity: Introduction and History, From the Quantum to Quarks, in an updated and much expanded second edition, provides an introduction to radioactivity and our knowledge of the building blocks of matter, the fundamental forces in nature, and the role of quarks and force particles, ie, gluons, photons, and the $W^{\pm}$ and Z^0 bosons, in nuclear decay. The book answers many questions for the student, teacher, and practitioner as to the origins, properties, detection, measurement, and everyday life applications of radioactivity in fields such as medicine, biological research, and industry. This new edition provides the reader with a much expanded historical account of the lives and major achievements of over a hundred famous pioneers and Nobel Laureates who have contributed to our knowledge of the science of the atom and its structure, nuclear stability, and decay, from the discovery of radioactivity in 1896 through to the present. Written at a level that most students and teachers can appreciate, it includes many calculations that they may use in class work. *Radioactivity: Introduction and History, From the Quantum to Quarks* also serves as a refresher for experienced practitioners who use nuclear science and radioactive sources in their fields of work.

- Provides entry-level overviews of every form of radioactivity, including natural and artificial sources and radiation of cosmic origin, as well as an introduction to the role of the building blocks of matter, the fundamental forces in nature, and the role of quarks and force particles, ie, gluons, photons, and the $W^{\pm}$ and Z^0 bosons, in nuclear stability and decay.
- Includes many solved problems to practical questions concerning nuclear decay, nuclear radiation, and its interaction with matter.
- Gives historical accounts of the major achievements of pioneers and Nobel Laureates, from 1895 to the present, who have contributed to our current knowledge of the atom, its nucleus, and nuclear decay.

Chapter 1

Radioactivity and Our Well-Being

At the IAEA [International Atomic Energy Agency], we work daily on every continent to put nuclear and radiation techniques in the service of humankind. In Vietnam, farmers plant rice with greater nutritional value that was developed with IAEA assistance. Throughout Latin America, nuclear technology is being used to map underground aquifers, so that water supplies can be managed sustainably. In Ghana, a new radiotherapy machine is offering cancer treatment to thousands of patients. In the South Pacific, Japanese scientists are using nuclear techniques to study climate change. In India, eight new nuclear plants are under construction, to provide clean electricity for a growing nation …These projects, and a thousand others, exemplify the IAEA ideal: Atoms for Peace.

From the Nobel Lecture of Mohamed ElBaradei (2005 Nobel Laureate for Peace) on December 10, 2005.

Radioactivity, also referred to as nuclear decay, is the process of spontaneous decay and transformation of unstable atomic nuclei accompanied by the emission of radiation (also referred to as nuclear radiation). This book focuses on nuclear structure, nuclear stability and decay, the properties of various types of nuclear radiation, and an historical account of the lives and discoveries of the pioneers in this field of science. In light of the fundamental nature of this subject matter, the writer felt the need to expound firstly on the peaceful applications of radioactivity and its properties, upon which we depend dearly. This chapter provides a brief sketch of only a very few examples of applications of radioactivity that improve and enrich our lives.

Nuclear radiation and sources of radioactivity, ie, radionuclides, have become a necessary part of our daily lives. The quantity and quality of our food, our health, our general well-being, and consequently our extended lifespan are due in large part to radioactive sources and their numerous applications in medicine, biology, agriculture, industry, and electric power generation. The significance of the role that radioactivity plays in improving our lives was commemorated with a postage stamp illustrated here issued by France in 1965. The stamp shows an artistic depiction of an atom together with drawings representing four fields where radioactivity and nuclear energy play a significant role in development, namely medicine, agriculture, industry, and nuclear power for electricity.

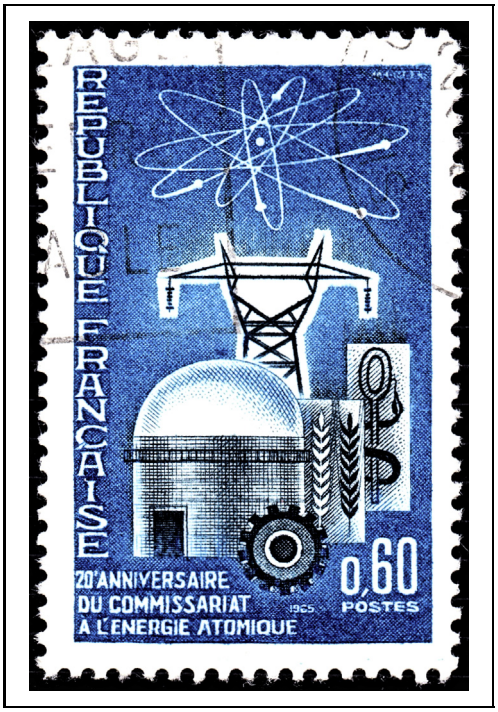

Radioactivity: Introduction and History, From the Quantum to Quarks. http://dx.doi.org/10.1016/B978-0-444-63489-4.00001-0
Copyright © 2016 Elsevier B.V. All rights reserved.

Our dependence on radioactivity began only a few years after its discovery by Henri Becquerel in 1896. Not long thereafter, at the beginning of the 20th century, Marie and Pierre Curie (Curie, 1905) spearheaded the use of radium for the treatment of cancer. We may consider their work to be the first peaceful application of nuclear energy and the birth of modern nuclear medicine, upon which we now depend for the diagnosis and treatment of cancer and many other illnesses. Not long afterward, Rutherford in 1919 demonstrated the first artificial production of the stable isotope oxygen-17 by bombarding the nucleus of nitrogen-14 with α particles. In the 1930s the example of Rutherford was followed by Frédéric Joliot and Irene Joliot-Curie, who in 1934 achieved the first artificial production of radioisotopes by bombarding various elements such as Be, B, and Mg with α particles from polonium. About the same time, in 1931 Ernest Lawrence built the first working cyclotron capable of accelerating protons, deuterons, or helium ions (α particles) to energies capable of penetrating atomic nuclei and thereby producing numerous stable and radioactive isotopes that would find many peaceful applications in improving the well-being of humanity the world over. By 1940 the cyclotron developed by Lawrence and his coworkers artificially produced as many as 223 radioactive isotopes, many of which proved to be of immediate and immense value in medicine and studies in the biological sciences. Small cyclotrons are used to this day on-site at hospitals to produce short-lived radioisotopes for the diagnosis and treatment of various cancers and other diseases. The invention of the cyclotron, and the many radioactive isotopes that were produced as a result, heralded the beginning of an era when peaceful applications of radioactive isotopes expanded worldwide and proved to be of great benefit to humanity.

Within this book the reader will find information on the origins and properties of the various types of nuclear radiation, plus an historical account of the lives and works of many early pioneers and Nobel Laureates who opened the doors to the application of radioactive sources in fields of science that have been of great benefit to humankind. The following sections describe a small number of the countless applications of radioactive isotopes and nuclear radiation in medicine, biological research, food and agriculture, water resource management, industry, environmental protection, and nuclear power. Comprehensive reviews on current trends and advances in peaceful applications of isotopes and nuclear radiation are found in the *Nuclear Technology Review* published annually by the International Atomic Energy Agency (IAEA), Vienna, as well as numerous books and training manuals published by the IAEA each year. Only a few examples of these peaceful applications, some of which are cited from the *Nuclear Technology Review* and other sources, are presented below.

1.1 HUMAN HEALTH

Among the many applications of nuclear radiation for human health, the technique of medical radiation imaging for cancer diagnosis and treatment is utilized worldwide; and research in its development and applications is making constant advances with each passing day. Imaging by means of radiation techniques is often the first step in clinical management and diagnostic radiology; and nuclear medicine studies play important roles in screening, staging, monitoring of treatment, and long-term surveillance of cancer patients. Numerous imaging techniques are available to doctors. The techniques that include X-radiation and nuclear radiation are X-ray radiography, X-ray computed tomography (CT), also referred to as computerized tomography, single photon emission computed tomography (SPECT), and positron emission tomography (PET). In conjunction with imaging techniques, which may be used to diagnose and monitor cancer and other illnesses, the physician has recourse to numerous nuclear methods of treating cancer, including radiation therapy, brachytherapy, proton beam and heavy ion therapy, boron neutron capture therapy (BNCT), and the application of radioactive nanoparticles to cancer diagnosis and therapy. These nuclear techniques are described briefly in the following paragraphs.

1.1.1 X-Ray Diagnostic Radiography

X-radiation, as described in this book, is not of nuclear origin, but rather originates from electron energy. It is nevertheless included here because X-rays are electromagnetic radiation of properties similar to γ-radiation, which is of nuclear origin. The potential of X-rays in medical diagnosis became immediately clear following their discovery by Wilhelm Röntgen in 1895. Most of us have had X-ray images taken of some part of our body, as physicians use them to diagnose broken limbs or very commonly to screen for afflictions such as pneumonia, tuberculosis, or breast cancer. The physician exposes the patient's body to a beam of X-radiation, which passes through the body and is partially absorbed or attenuated by parts of the body. Variation between bone and tissue densities will attenuate the X-rays to differing degrees, producing a photographic film or digital image of the X-radiation intensities passing through the body. Most X-rays currently taken are grayscale digital images.

Research is currently under way into the production of colored X-ray images, which can provide more contrast for the identification of infirmities not easily identified with the conventional grayscale images (Boone et al., 2014; Egan et al.,

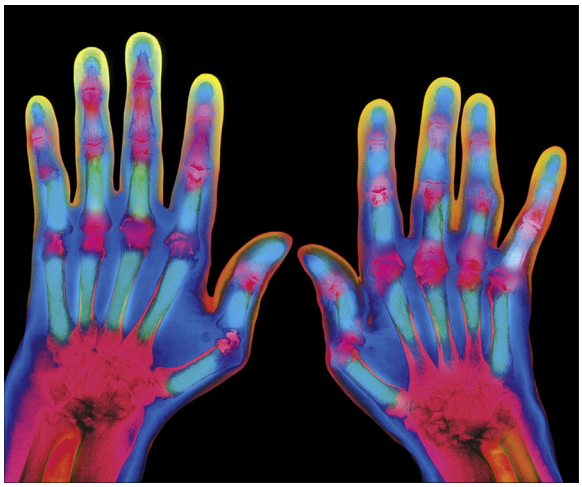

FIGURE 1.1 Colored X-ray of severe rheumatoid arthritis, with swelling and bone deformation shown in pink. *From Emery, P., Buch, M.H., May 5, 2012. Towards an optimum strategy in rheumatoid arthritis. Lancet 379, 1682–1683, with permission from Elsevier © 2012.*

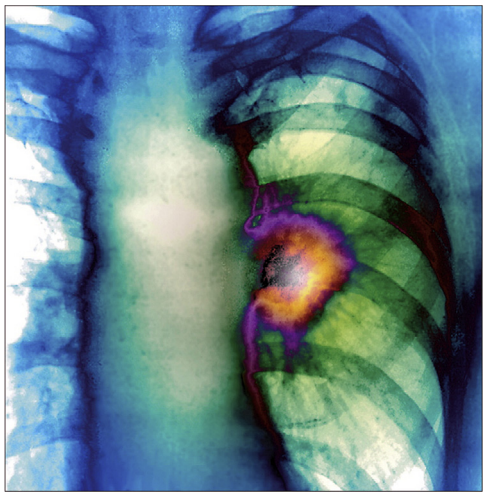

FIGURE 1.2 Colored X-ray of the left lung of a patient with lung cancer. *From Soo, R.A., et al., 2009. First-line systemic treatment of advanced stage non-small-cell lung cancer in Asia: consensus statement from the Asian Oncology Summit 2009. Lancet 10 (11), 1102–1110, reprinted with permission from Elsevier © 2009.*

2014). Pixelated energy-dispersive X-ray detectors capture X-rays of differing energies to acquire structural and chemical information provided by the different X-ray emissions. The differing wavelengths of the X-rays provide pseudo-color-coded discrimination, giving images of the different structural and chemical composition of objects. Research is under way to develop this technique for applications in medical diagnosis. Some examples of colored X-ray images are provided in Figs. 1.1 and 1.2.

1.1.2 X-Ray Computed Tomography

The advent of computer technology and more recent digital technology facilitated the development of X-ray CT, also referred to as computed axial tomography (CAT or CAT scan). X-ray CT can provide a three-dimensional image of the internal structure and organs of the human body from numerous X-ray images taken around the body in a precise axis of rotation. The important role of computed tomography in medical diagnosis was commemorated in a postage stamp issued by the United Kingdom illustrated here. The various densities of the structures and organs of the human body absorb the X-radiation to different degrees and thus, with computer data processing, produce an image of the organs and structures to give the physician information that might reveal abnormalities such as tumors.

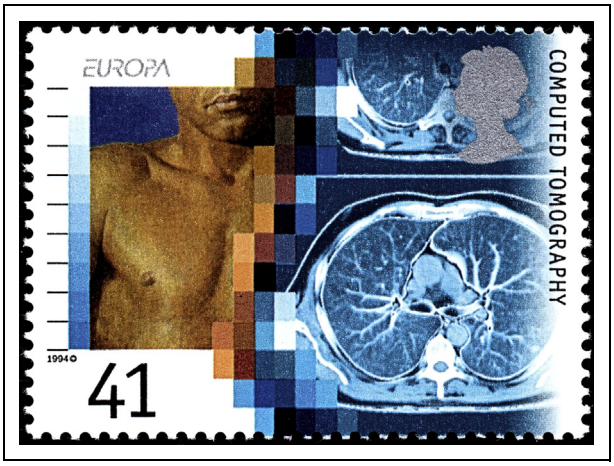

Helical CT scans, shown in the postage stamp, are obtained by rotating the X-ray source in a circular fashion 360 degrees around the patient. The technique is illustrated in Figs. 1.3 and 1.4. The patient lies flat on a table that moves at a designated speed through a circular array of X-ray detectors surrounding the patient. The X-ray source is rotated around the patient while irradiating the body with an X-ray beam in the shape of a cone that will encompass the body width of the patient. X-rays

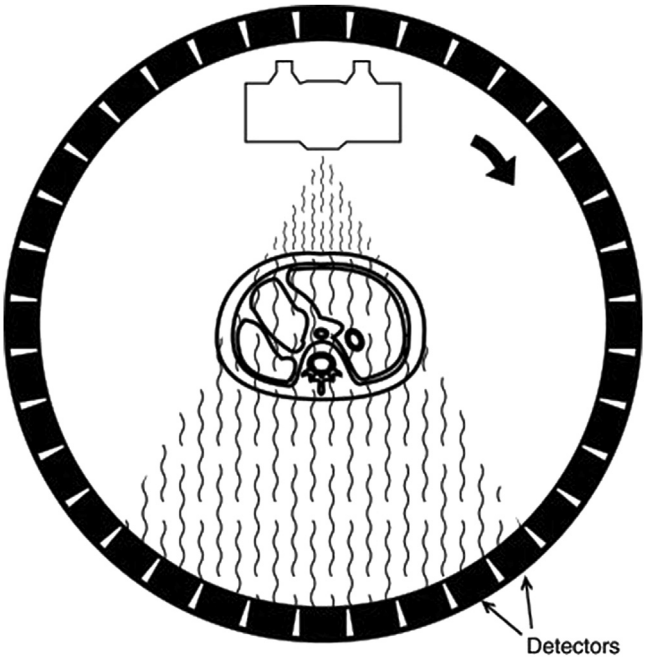

FIGURE 1.3 CT utilizes an array of detectors surrounding a patient (illustrated here as a cross-sectional image of the patient's body in the center of the figure), from which an image is constructed from the transmitted beam. *From McLean, I.D., Martensen, J., 2014. Specialized imaging. In: Marchiori, Dennis (Ed.), Clinical Imaging, third ed. Elsevier Science, Amsterdam, pp. 44–78, reprinted with permission from Elsevier © 2014.*

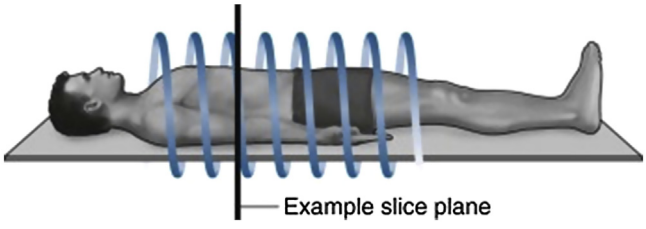

FIGURE 1.4 Typical scanning pathway for spiral CT. *From McLean, I.D., Martensen, J., 2014. Specialized imaging. In: Marchiori, Dennis (Ed.), Clinical Imaging, third ed. Elsevier Science, Amsterdam, pp. 44–78, reprinted with permission from Elsevier © 2014.*

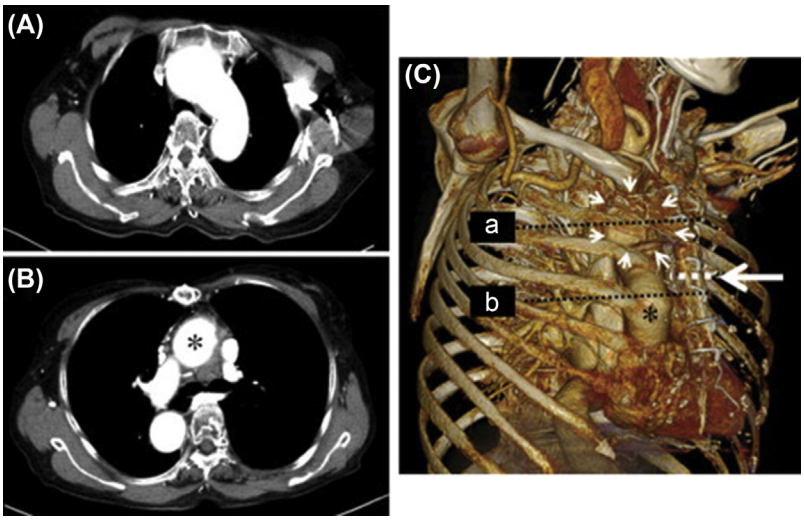

FIGURE 1.5 (A) Preoperative 2D-CT scan showing a dense aortic aneurysm adhering to the sternum (breastbone). (B) Preoperative 2D-CT scan showing the safe space between the ascending aorta (*) and the sternum. (C) Preoperative 3D-CT scan showing the relationships between the aorta, aneurysm, heart, and sternum. The *large white arrow* indicates the transection level of sternum, which is located below the aneurysm (*small white arrows*). The *a* and *b* symbols in (C) indicate the CT scan levels of image (A) and image (B), respectively. *From Kamohara et al. (2011), printed with permission from Elsevier © 2011.*

transmitted through the patient's body will be attenuated to different degrees by the different bone and tissue densities. The X-ray detectors receive the attenuated beam transmitted through the patient and transfer the attenuated beam intensities into electrical signals that are processed by a computer to generate a digital image. Data collected on the transmitted X-rays on completing a 360° scan can be processed by a computer to construct a cross-sectional image of a slice of the patient's body, as illustrated in Fig. 1.5A and B. Numerous scans of cross-sectional slices can be made by the physician along the body to obtain anatomical images that can provide diagnostic information on abnormalities such as tumors. Such helical CT scans can be obtained on entire anatomical sections of a patient in a matter of seconds.

Data from cross-sectional images collected from numerous spiral scans can be processed by a computer to construct a three-dimensional image, known as three-dimensional CT (3D-CT). The individual cross-sectional images of slices of the body are referred to as two-dimensional CT (2D-CT). Three-dimensional images can be useful to a physician in assessing complex bone fractures and other pathologies (McLean and Martensen, 2014). An example of a 3D-CT image of a patient taken to assist a physician prior to surgery is shown in Fig. 1.5C.

The 3D-CT scan of Fig. 1.5C is an excellent example of an image of the internal organs and chest bones of a patient. However, sometimes the physician is only interested in repairing bones, and prefers an image of the skeletal structure unmasked by body tissue. A surface shaded density (SSD) three-dimensional (3D) technology, which is computer formatting available with CT, allows 3D reconstructions of calcified tissue (bones) to be imaged without adjacent body tissue (Calloway et al., 2011). An example is shown in Fig. 1.6, which illustrates a 2D-CT scan (on the left) of a sectional slice of the chest of a patient. The scan gives the physician information on the location of a tumor in the rib cage (irregularly shaped object at the left of the grayscale image). The exact location of the tumor is not available from this

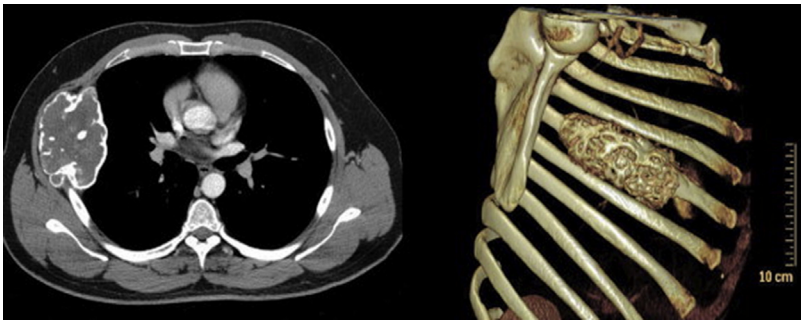

FIGURE 1.6 On the left is a 2D-CT image of a cross-sectional slice of the rib cage of a patient, illustrating a tumor on the very left of the image. On the right is an enhanced 3D-CT image providing the physician with the exact location of the tumor on the fifth rib. *From Rambalde et al. (2013), reprinted with permission from Elsevier © 2013 Elsevier España, S.L. and SEMNIM. All rights reserved.*

2D-CT image. But a 3D-CT scan with SSD (on the right) gives a clear image of the skeletal structure of the patient, with the exact location of the tumor on the fifth rib.

Since its development in the early 1970s, CT has become the standard for the evaluation of patients with malignancies because of its excellent definition of anatomical details. Allan M. Cormack and Godfrey N. Hounsfield shared the Nobel Prize in Physiology and Medicine in 1979 for the development of computer-assisted tomography.

Synchrotron radiation, as a highly collimated and intense beam of X-rays, can serve as an excellent radiation source for CT. The properties and applications of synchrotron radiation are discussed in the chapter entitled "Electromagnetic Radiation: Photons."

1.1.3 Single Photon Emission Computed Tomography

SPECT is a nuclear diagnostic imaging technique that requires the administration of a radioactive pharmaceutical to the patient. A radiopharmaceutical is a drug labeled with a relatively short-lived radioactive nuclide. The radionuclides used in SPECT are short-lived gamma-ray-emitting nuclides, such as gallium-67 ($t_{½} = 78.3$ h), technetium-99m ($t_{½} = 6.0$ h), indium-111 ($t_{½} = 2.8$ days), iodine-123 ($t_{½} = 13.0$ h), rhenium-186 ($t_{½} = 3.7$ days), and thallium-201 ($t_{½} = 74$ h). All of these nuclides decay with relatively short half-lives ($t_{½}$), with the emission of γ rays. The gamma radiation emitted from the body of the patient is required to produce an image, while the short half-life of the radioactivity source is required to minimize harm to the patient. When administered to the patient, the radiopharmaceutical will distribute itself throughout the body, sometimes settling at higher concentrations where an injury, tumor, or infection is located. The γ rays are emitted equally in all directions. The patient, lying flat on a bed, is scanned by a detector containing a radiation collimator (see Fig. 1.7) which permits only the γ rays emitted in the direction of the detector to be registered. An image is constructed by a computer from the gamma-ray emissions detected after rotating the detector with its collimator 360 degrees around the patient. This provides an image of the radiation intensities emitted from within the body of the patient. The various tissues and organs attenuate the emitted gamma-ray photons to varying degrees depending on the tissue densities and their absorption coefficients, and a computer can construct an image from the gamma-ray photon intensities and angles of emission.

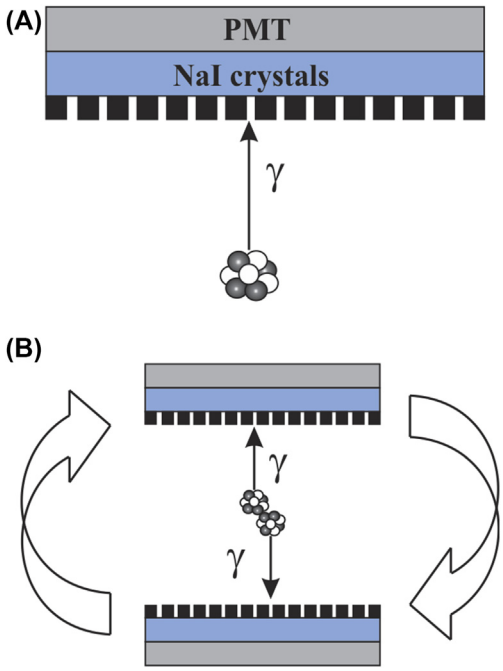

FIGURE 1.7 The mechanism of SPECT. (A) A gamma camera consisting of a lead collimator (represented by solid black objects separated with narrow openings), NaI crystal scintillators, and photomultiplier tubes (PMTs) receives the energy of a gamma-ray photon emitted from the body of a patient (not illustrated), who was previously administered a radiopharmaceutical. The gamma-ray photon, which passes the collimator and is incident at a 90 degrees angle to the gamma camera, is converted to an electrical signal processed by a computer (not illustrated). (B) The gamma camera is rotated 360 degrees around the body of the patient, receiving and processing, via a computer, numerous gamma-ray emissions at all angles from the radionuclides within the body of the patient. For simplicity only two radioactive atoms are illustrated here, among millions originating from the radiopharmaceutical; and only two radioactive atoms are illustrated with the gamma camera at two locations only (above and below the body of the patient). *Figure is from Velikyan (2014), printed with permission from Elsevier © 2014.*

The detector may be moved to image the front, rear, or side of a patient; or it may be rotated in a 360 degrees fashion around the patient. Only short-lived radionuclides are used so that the radioactivity administered to the patient will decay in a short term and not cause harm. In the chapter entitled "Radionuclide Decay, Radioactivity Units, and Radionuclide Mass" the author provides an example of a calculation illustrating the short duration that Tc-99m remains in the human body after it is administered to a patient. SPECT and PET, which is described subsequently in this chapter, are nuclear medicine functional imaging techniques which have the ability to detect cancerous involvement based on molecular and biochemical processes within the tumor tissue.

The important role of SPECT as a tool in cancer diagnosis was commemorated in a postage stamp issued by Germany in 1981, when SPECT was in its infant stage and low-resolution two-dimensional scans were the order of the day. The colors produced by the CT image, as illustrated on this stamp, provide the doctor with an indication of radiation intensities emitted by the radioactive source in the patient: diminishing radiation intensities are identified by the colors red > yellow > green > blue. (See Fig. 1.10 for an example of the color coding used in tomographic images, which provides a measure of radiation intensities in various parts of the organs of a patient.)

The modern fusion of data from the two scanning techniques of SPECT and CT is known as hybrid SPECT/CT. Hybrid imaging can provide improved imaging and information to the physician on the internal anatomy and organ function. The integration of imaging techniques gives the physician additional morphological information which can provide the exact location of lesions in the body. This can otherwise be difficult to determine, for example in the abdominal region (Velikyan, 2014). The early identification of abnormalities, including tumors, permits early treatment of disease and enhanced chances for recovery.

1.1.4 Positron Emission Tomography

PET is yet a more sophisticated form of tomographic imaging with a radioactive source, and can provide 3D images of body organs and a display of the dynamics of radioisotope-labeled compound metabolism in organs. A positron-emitting radionuclide, such as carbon-11 ($t_{½} = 20.4$ min), nitrogen-13 ($t_{½} = 9.96$ min), oxygen-15 ($t_{½} = 2.03$ min), fluorine-18 ($t_{½} = 109.7$ min), copper-64 ($t_{½} = 12.7$ h), gallium-66 ($t_{½} = 9.45$ h), gallium-68 ($t_{½} = 68.3$ min), bromine-76 ($t_{½} = 16.2$ h), and rubidium-82 ($t_{½} = 1.27$ min) among others, in the chemical form of a radiopharmaceutical is first administered to the body of a patient by intravenous injection. The patient is placed in a declining position within a chamber containing numerous radiation detectors that surround the body in a complete 360 degrees circle (see Fig. 1.8).

The positrons emitted by the radionuclide atoms in the patient become annihilated only a few millimeters from their originating atomic nuclei, resulting in the emission of annihilation radiation, namely two 0.511 MeV γ rays in opposite directions (180 degrees apart) for each positron annihilation, as illustrated in Fig. 1.9. The properties of positron radiation and annihilation are discussed in detail later in this book. The multiple radiation detectors, mounted in a circle, are

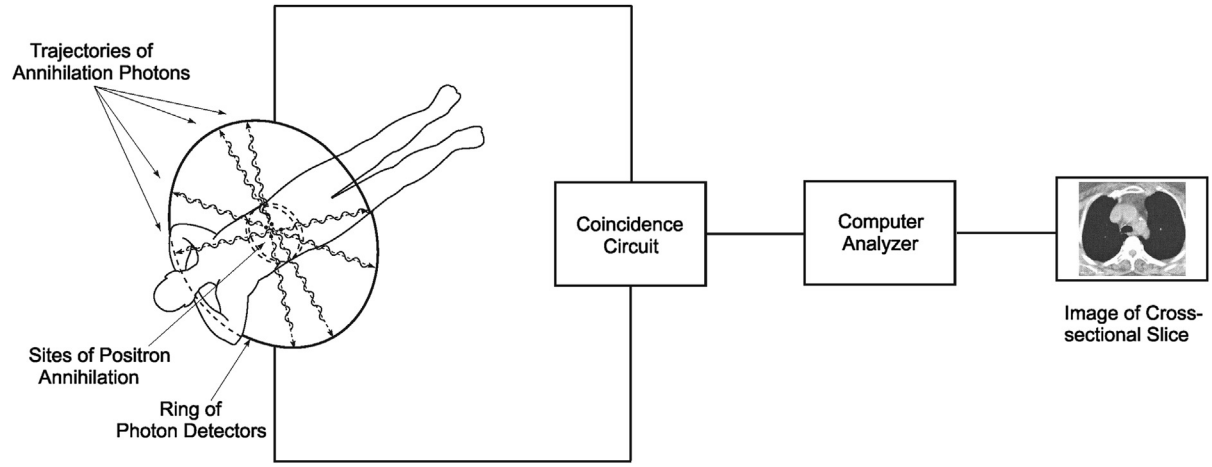

FIGURE 1.8 Positron-annihilation detection by a photon-detector ring in a PET instrument, illustrating the line segment (cross-sectional slice) in which the positron-emitting nuclides reside. Many thousands of positron annihilations are detected by the ring of photon detectors. The photons arriving from opposite detectors (180 degrees) in coincidence pass the coincidence circuit and are analyzed by the computer. From the data collected, an image of the relative intensities of the radioactive (positron-emitting) sites within the cross-sectional slice are plotted to provide an image of the structure and organs of the patient.

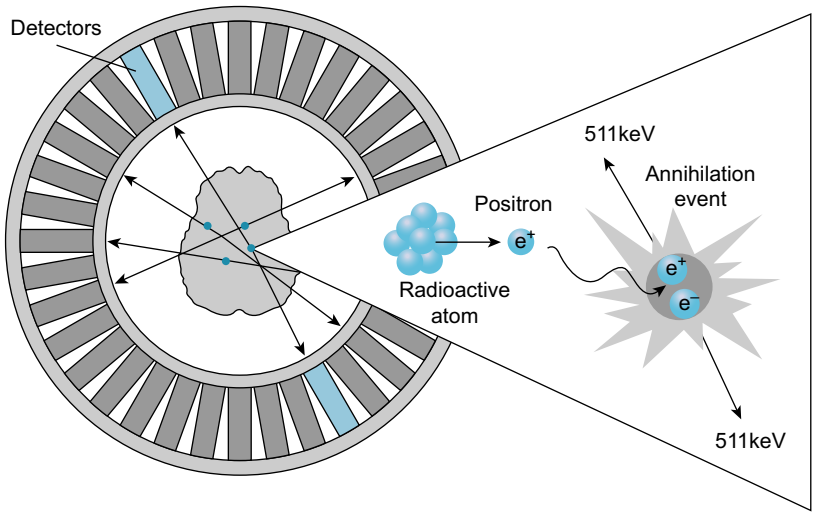

FIGURE 1.9 When a nucleus decays by positron emission, a proton in the nucleus converts into a neutron with the emission of a positron (e^+) and a neutrino. The positron and neutrino are ejected from the nucleus; the neutrino leaves without incident, while the positron quickly interacts with a nearby electron as an annihilation event. The positron−electron annihilation event creates two 511 keV gamma rays (photons) that are emitted in opposite directions from the patient placed in the center of the gantry. Within the gantry, photomultiplier−scintillator detectors record the locations of emitted gamma rays. This information is assessed by mathematical algorithms over many iterations (typically 107−108) and at many different angles around the patient to map an image detailing where the radioactive substance has accumulated. The intensity detected at any point in the patient directly relates to the concentration of the radiotracer in the tissue. *From McLean, I.D., Martensen, J., 2014. Specialized imaging. In: Marchiori, Dennis (Ed.), Clinical Imaging, third ed. Elsevier Science, Amsterdam, pp. 44−78, reprinted with permission from Elsevier © 2014.*

positioned around the body of the patient where the labeled organ or radionuclide localization is expected. Two of the many detectors surrounding the body become activated when two γ-ray photons, originating from one positron−electron annihilation, simultaneously reach detectors 180 degrees apart (see Figs. 1.8 and 1.9). The coincidence detection of annihilation photons accurately determines the line segments in which the radionuclides resided. Many thousands of line segments are analyzed by a computer to reconstruct the distribution of the decayed radionuclides, producing a tomographic image in a cross-sectional slice of the organ where the radiopharmaceutical has concentrated. Computer analysis of the line-segment origins of the annihilation radiations yields a tomographic density map or image of the various organs and anomalies (eg, tumors) in the narrow region (slice) of the patient's body.

McLean and Martensen (2014) note that PET offers the advantage that many of the positron-emitting radionuclides used are isotopes of elements that reside naturally in the body, including oxygen (O-15), nitrogen (N-13) carbon (C-11), and fluorine (F-18). They also note that the most widely used radioisotope for PET in the form of a labeled

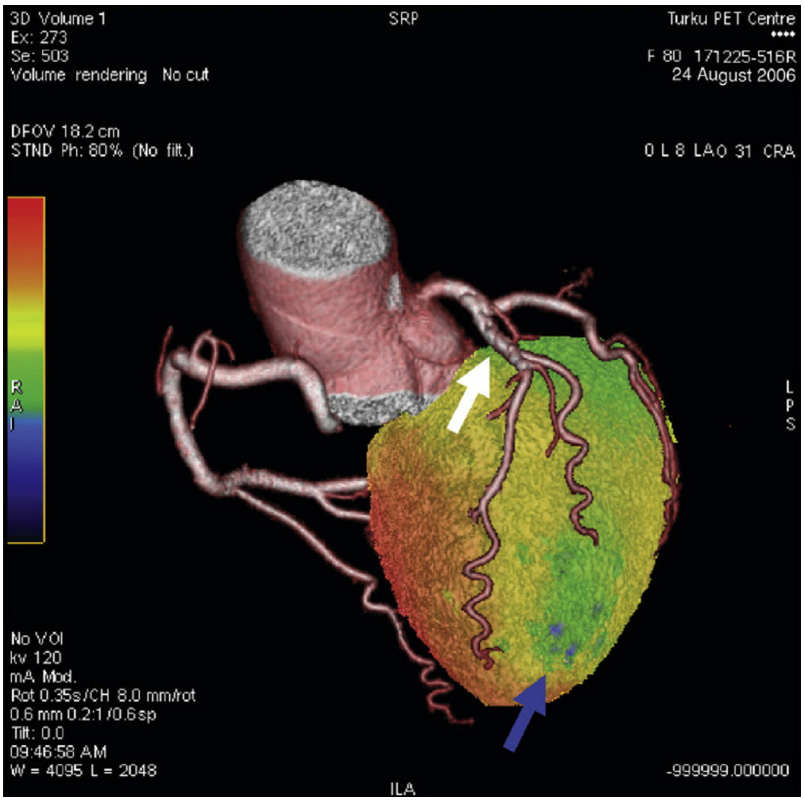

FIGURE 1.10 Hybrid imaging by PET/CT. Hybrid imaging of multidetector-row CT coronary angiography and PET perfusion during adenosine stress. A three-dimensionally rendered image of the anterior view of the heart by PET image and the coronary tree visualized by multidetector row CT are shown. On multidetector-row CT, obstructive plaques were detected in the proximal segment of the left anterior descending coronary artery and in the first diagonal branch (*white arrow*). However, in the myocardial region, supplied by the diagonal branch, myocardial perfusion was reduced (*blue arrow*), whereas in other regions preserved perfusion was detected. *From Schroeder, S., et al., 2008. Cardiac computed tomography: indications, applications, limitations, and training requirements: report of a writing group deployed by the Working Group Nuclear Cardiology and Cardiac CT of the European Society of Cardiology and the European Council of Nuclear Cardiology. Eur. Heart J. 29 (4), 531–556, reprinted with permission of Oxford University Press.*

radiopharmaceutical is 2-(fluorine18)-fluoro-2-deoxy-D-glucose (FDG), which is commonly used to evaluate brain function and malignancy. FDG is structurally very similar to glucose, a common naturally occurring carbohydrate with the substitution of the fluorine-18 radionuclide in the molecule. Also, it is important to point out that all of the positron-emitting radionuclides used for PET, listed in the first paragraph of this subsection, have short half-lives (of the order of minutes or hours). A short half-life is important, as it permits several scans to be taken of a patient in a matter of minutes while minimizing any harm to the patient due to nuclear radiation.

PET scans of a patient, with the accumulated data from numerous line segments at all angles, can be processed by a computer to construct 3D images. Often PET is fused with data from another imaging technique, such as CT, to yield hybrid PET/CT, which can provide the physician with improved visual diagnostics of anatomic and functional abnormalities. DiCarli and Murthy (2011) notes PET/CT and SPECT/CT can give the physician the opportunity to delineate cardiac and vascular anatomic abnormalities and their physiologic consequences in a single setting. An example is provided by the PET/CT image of the heart illustrated in Fig. 1.10.

PET is not a new concept. It was reviewed by the author almost 30 years ago (L'Annunziata, 1987); however, with the advances of computer science in the past two decades, PET imaging technology has advanced almost exponentially, and it is now a dominant topic of many medical imaging meetings and nuclear medicine publications. PET serves as a tool in the diagnosis of many cancers. The diagnosis and treatment of other conditions with PET, such as cardiovascular disease and brain degenerative diseases like Alzheimer's and depression, are under intensive research.

Other imaging techniques that do not involve radioactivity are available to the medical profession, such as magnetic resonance imaging, described later in this book. Often it is a combination of imaging techniques that provides the physician with a hybrid image yielding the information needed to arrive at the correct diagnosis.

1.1.5 Radiation Therapy

Radiation oncology, which is the branch of medicine that deals with the radiation imaging and treatment of cancerous tumors, is a field of science with a very long history. As described in this book, Marie and Pierre Curie recognized the potential of nuclear radiation for the treatment of cancer. After the death of her husband in 1906 and receiving a second Nobel Prize in 1911 for her discovery of radium and polonium, the isolation of radium, and the study of its properties, Marie Curie spearheaded the application of nuclear radiation from radium for the treatment of cancer. Since that time, countless patients suffering from many types of cancer, including brain, neck, lung, breast, cervical, rectal, and prostate cancer, have been treated and continue to be treated today with radiation therapy.

1.1.5.a External Beam Radiation Therapy

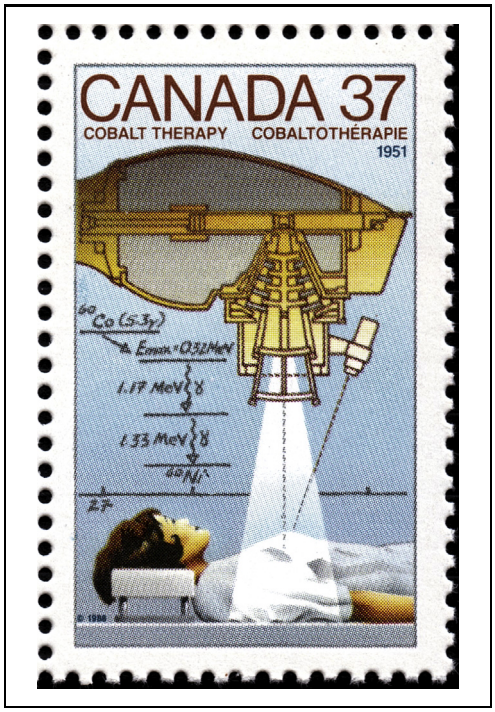

One common type of cancer treatment is external beam radiation therapy (EBRT), which involves directing a beam of γ-ray photons from an external radiation source or X-ray photons produced by a linear accelerator on to the cancer of a patient, or the use of external beams of electrons, protons, or neutrons produced by a linear accelerator (discussed later in this section). One common external source of gamma radiation for cancer therapy is cobalt-60, often referred to as cobalt therapy. The importance of cobalt therapy in the treatment of cancer was heralded by a postage stamp issued in Canada, which commemorated the world's first treatment of a cancer patient using cobalt-60 radiation on October 27, 1951 at the Ontario Institute of Radiotherapy, known today as the London Regional Cancer Center. On October 27, 2001 the Cancer Center celebrated 50 years of cobalt-60 radiotherapy (Battista and van Dyk, 2002). The stamp illustrates a cobalt therapy device, which contains a source of cobalt-60, situated above a patient. The device directs a narrow beam of gamma radiation on to the cancer cells of the patient to kill the malignant cells while causing minimal damage to the healthy cells. The stamp also illustrates the decay scheme of the cobalt-60 radiation source. Cobalt-60 decays, with a half-life of 5.3 years, to the element nickel-60 by the emission of a 0.32 MeV beta particle. The nickel-60 daughter nuclide is formed at an excited energy state, and loses this energy immediately with the emission of two gamma rays of energies 1.17 and 1.33 MeV, settling at a stable nuclear state. The origins and properties of gamma radiation are discussed later. It is the gamma radiation from the cobalt-60 decay that is directed on to the cancer by careful collimation of the beam, providing pinpoint irradiation of the cancer cells. More commonly today X-ray photons, which have similar properties to gamma-ray photons, are produced by a linear accelerator, and the beam of rays are directed on to the tumor with a dose of radiation sufficient to kill the tumor with minimal damage to surrounding healthy tissue.

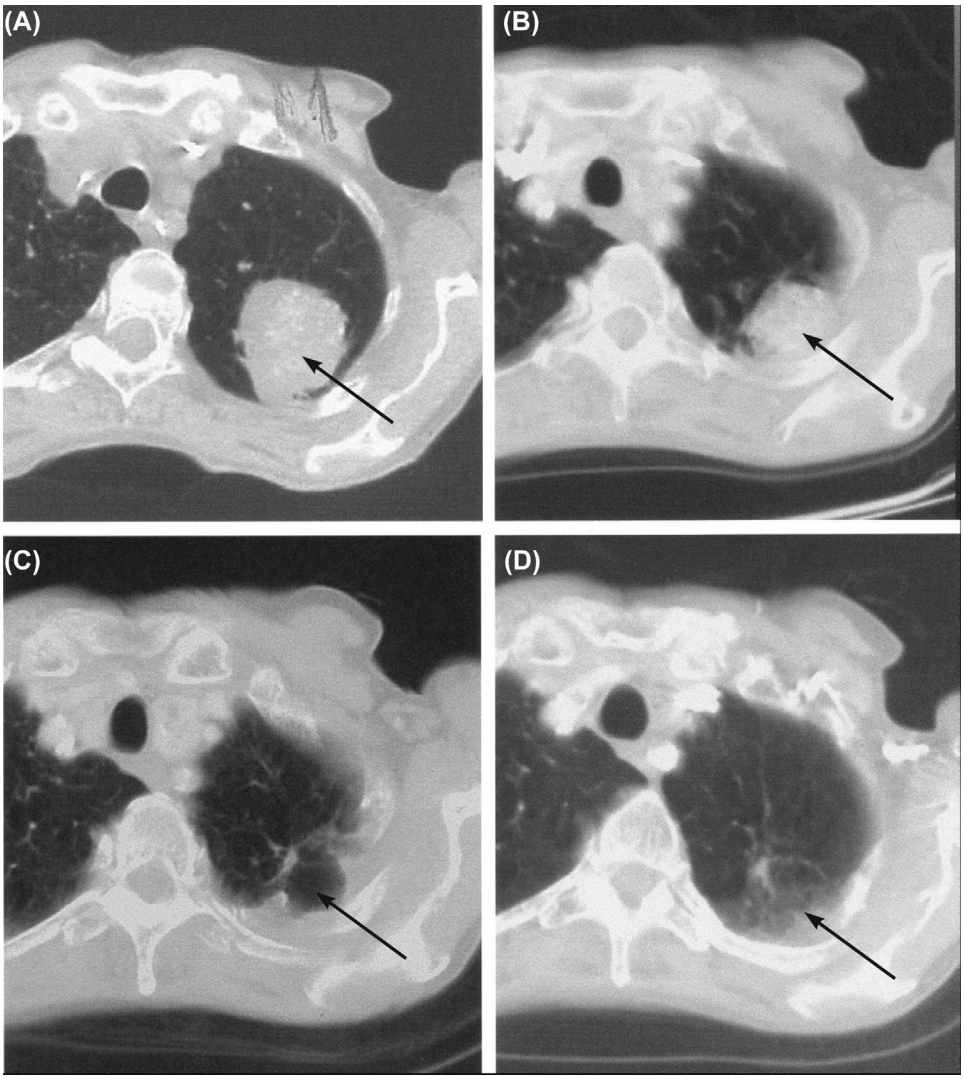

FIGURE 1.11 CT scans illustrating (A) bronchial carcinoma, indicated with *arrow*, before radiotherapy with a single dose (30 Gy) of irradiation; (B) partial remission after 10 months; (C) complete remission 21 months after irradiation, leaving a scarlike fibrosis; and (D) dense consolidation after 48 months. *From Fritz, P., et al., 2006. Stereotactic, single-dose irradiation of stage I non-small cell lung cancer and lung metastases. Radiat. Oncol. 1, 30, with permission © Fritz et al.; licensee BioMed Central Ltd.*

An excellent example of the benefits of radiation therapy in cancer treatment is provided by Fig. 1.11, which illustrates complete cancer remission in a patient 21 months after irradiation with a dose of 30 gray (Gy). The figure illustrates helical CT scans of the patient's lungs at four different time intervals, giving the physician information on the progress the patient is making following radiation therapy. The helical CT scans of Fig. 1.11 illustrate how the physician can see, in this case, images of complete cancer remission 21 months after radiation therapy; and the cancer tissue transformed into a dense benign consolidation 48 months after radiation therapy. The gray is a unit of absorbed dose—that is, the energy of radiation absorbed per unit mass of absorber. The absorber in this case is body tissue or tumor cells. The gray is defined specifically as the amount of energy in MeV absorbed per kilogram of absorber, or $1\ \text{Gy} = 6.24 \times 10^{12}$ MeV/kg. Radiation dose is discussed later in this book.

A modern application of gamma radiation therapy from cobalt-60 decay is radiosurgery using the Leksell Gamma Knife®, which was first developed by Swedish neurosurgeon Lars Leksell at the Karolinska Institute. The purpose of the Gamma Knife® is to treat tumors of the brain which are located deep within the brain, rendering conventional surgery impossible or extremely hazardous to the patient. The Gamma Knife® consists of an aluminum head frame or helmet that allows cobalt-60 gamma rays to be collimated at 200 positions surrounding the 3D coordinates of the helmet. The gamma rays originating from the cobalt-60 sources are directed by collimators to yield a fine pinpoint beam of gamma rays targeted

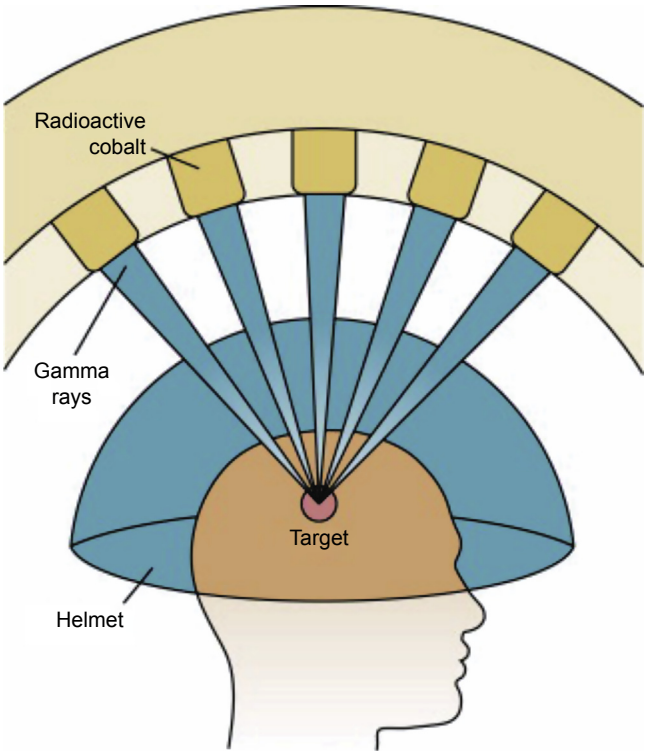

FIGURE 1.12 Schematic depiction of Leksell Gamma Knife® irradiation of an intracranial target (eg, cancer tumor). Sources in the primary collimator generate γ rays, which penetrate through holes in the secondary collimator helmet to converge with pinpoint accuracy on to a target from multiple directions. This convergence maximizes dose at the radiation isocenter, which is the point where the radiation beams intersect. Only five collimators are illustrated in the figure for simplicity; however, 200 of these collimators in the Leksell Gamma Knife® are uniformly distributed around the 3D coordinates of the helmet surrounding the skull. *Adapted from National Regulatory Commission file photo. From Loeffler, J., et al., 2012. Chapter 45 — Application of current radiation delivery systems and radiobiology. In: Ellenbogen, Richard, Abdulrauf, Saleem, Sekhar, Laligam (Eds.), Principles of Neurological Surgery, third ed. Saunder, New York, pp. 697–706, reprinted with permission from Elsevier © 2012.*

at a single area where the tumor is located, as illustrated in Fig. 1.12. The location of the tumor is determined by imaging techniques such as those previously described. Because the radiation beams are collimated on to the target tumor, the cancerous cells can be killed with minimal radiation damage to surrounding brain tissue. Thus surgery of the tumor is performed without opening the patient's skull. When the radiation treatment is performed at one sitting, the procedure is referred to as stereotactic radiosurgery; when it is performed over several treatment sessions, it is known as stereotactic radiotherapy. More detailed information on the Gamma Knife® can be obtained from reviews by Finger (2009) and Loeffler et al. (2012).

Advances in computer processing have enabled computer control of radiation therapy to optimize irradiation of cancerous tissue while avoiding harmful irradiation of neighboring healthy tissue. With this objective in mind, developments in computer-controlled radiation therapy have led to **3D conformal radiotherapy** (3D-CRT). As described in the IAEA *Nuclear Technology Review* (2011), 3D-CRT combines CT with 3D radiation treatment to shape the dose distribution of the radiation as closely as possible to the shape of the tumor by focusing the radiation beam in three dimensions. 3D-CRT determines the design and delivery of radiotherapy treatment based on a 3D image of the tumor collected by the computer, resulting in the delivery of radiation shaped to treat only the tumor target tissue. Thus healthy tissue is preserved, because the prescribed dose of radiation is delivered to the irregular shape of the tumor. Fig. 1.13 illustrates how a gantry containing the radiation source is rotated to administer radiation at various angles conforming to the irregular shape of the tumor.

A further development to 3D-CRT is **intensity modulated radiation therapy** (IMRT). In IMRT the prescribed dose is first specified by the physician, as in conventional radiation therapy. Then, on the basis of the irregular shape of the tumor as found in 3D-CRT, computer algorithms determine the optimum configuration of radiation beam directions and intensities to give the patient an optimized delivery of radiation dose to the tumor while minimizing radiation delivery to healthy tissue. An example of various radiation beam orientations determined by CT in conjunction with 3D-CRT and IMRT is provided in Fig. 1.14.

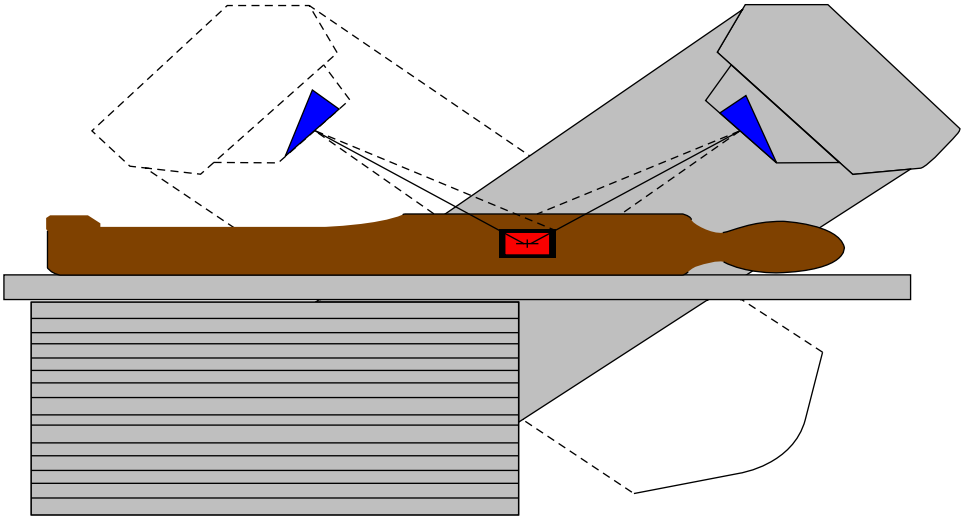

FIGURE 1.13 Block diagram of radiation beam orientations in 3D conformal radiotherapy. Two orientations are shown, with radiation beams (*solid and dashed lines*) leading from the gantry wedge (*blue triangle*) to the tumor or treatment volume (*red square*) in a supine patient (*brown*). The gantry is illustrated in white or gray according to orientation. *From Gearheart, D.M., et al., 2007. An improved approach to external beam radiation therapy for intra-abdominal cavity lesions for rural cancer centers. Med. Dosim. 32 (4), 271–277, reprinted with permission from Elsevier © 2007.*

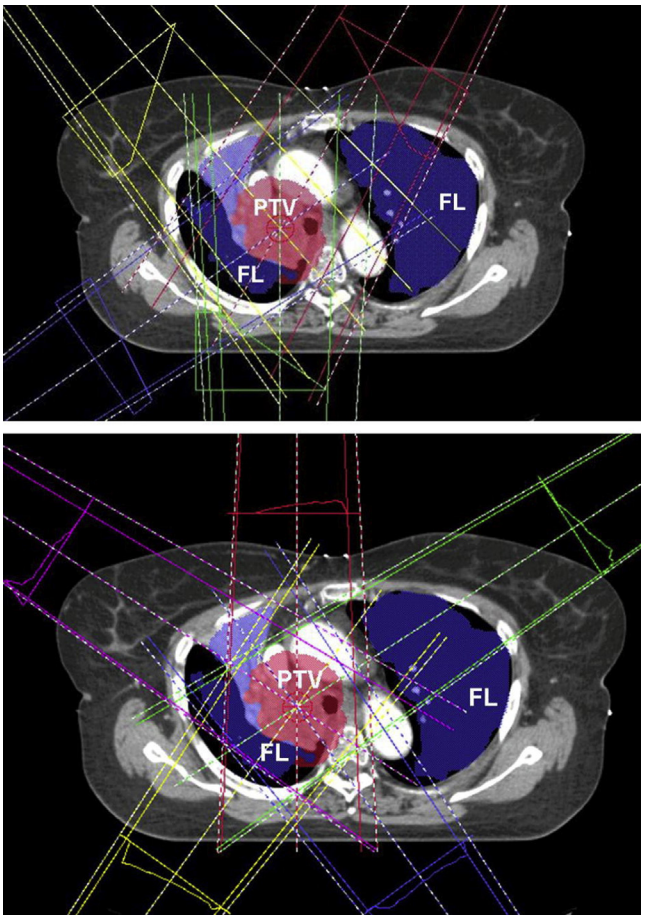

FIGURE 1.14 A CT/SPECT sectional image of a patient with lung cancer. The tumor is labeled PTV (planned treatment volume), and FL represents functional lung. The beam orientations (*colored lines*) of 3D-CRT (upper figure) and IMRT (lower figure) for radiotherapy aim at optimal irradiation of the PTV and maximal avoidance of functional lung. *From Lavrenkov, K., et al., 2007. A potential to reduce pulmonary toxicity: the use of perfusion SPECT with IMRT for functional lung avoidance in radiotherapy of non-small cell lung cancer. Radiother. Oncol. 83 (2), 156–162, reprinted with permission from Elsevier © 2007.*

Another development of 3D-CRT is **four-dimensional conformal radiotherapy** (4D-CRT), which takes into account the fourth dimension, namely time, in the delivery of radiation to a cancer tumor. As defined in the *Nuclear Technology Review* (2011), 4D-CRT is computer-driven respiratory-gated radiotherapy that enables the analysis of chest movement and triggers the treatment beam of radiation to be synchronized with the respiratory cycle. The computer determines the specific respiratory phase of inhalation and exhalation of the patient for irradiation treatment. This ensures that the radiation target (eg, tumor) will always receive an optimum radiation beam while excessive exposure of radiation to healthy tissue is avoided.

1.1.5.b Brachytherapy

Brachytherapy is radiation therapy that involves the deployment or placement of radioactive sources (called "seeds") in intimate contact with the cancerous tumor or the gland within which the tumor is located. The radioactive sources are small, each about the size of a grain of rice. A brachytherapy seed is illustrated in the center of Fig. 1.15. Their small size permits their insertion into or onto tumors, allowing the radiation emanating from the seeds to interact and kill neighboring tumor cells but causing minimal harm to healthy tissue further away from the tumor.

The word brachy is derived from Greek *brakhus*, meaning "short." Thus brachytherapy signifies radiation therapy provided over a short distance, as the radioactive seeds are inserted into or directly on the tumor so the radiation travels only the short distance to the cancer and a small amount of surrounding tissue. This is very much in contrast to EBRT, previously described, where the radiation source is external to the patient's body and generally must travel through healthy tissue before reaching the cancer target area within the body.

Some radioactive sources used for brachytherapy are iridium-192 (half-life = 74.17 days), iodine-125 (half-life = 60.25 days), and palladium-103 (half-life = 16.96 days). These radionuclides have relatively short half-lives, permitting brachytherapy seeds to be inserted into a cancerous tumor and never removed. The radioactivity in the seeds decays, emitting lethal radiation to cancer cells, until no detectable radiation remains in the seeds. This is often the practice with the treatment of prostate cancer: the seeds are never removed, but remain harmlessly in the prostate for the rest of the patient's life. Fig. 1.16 illustrates a prostate gland treated with brachytherapy seeds, with the radiation isodose being received by the cancerous gland while healthy neighboring tissues receive a diminished and less harmful dose of radiation.

Alternatively, high-dose-rate (HDR) radioactive sources have been developed whereby the physician inserts a very small plastic catheter into the prostate gland of the patient, and then gives the patient a series of HDR radiation treatments by inserting a radioactive source through the catheter. The catheter and radiation source are removed after a controlled dose has been administered, and no radioactive material is left in the tumor.

Radioactive sources of longer half-life are used in the brachytherapy of other cancers; but the radioactive source is removed from the tumor after the prescribed dose of radiation is administered to the cancer cells. Brachytherapy may be used to treat numerous types of cancer in addition to prostate cancer, including cervical, esophageal, breast, and skin cancers. For additional and more comprehensive information on brachytherapy and its applications in cancer treatment, the reader may peruse articles by Swallow and Kirby (2008), Vetter (2010), Souza et al. (2011), Unno et al. (2011), and Gambarini et al. (2014).

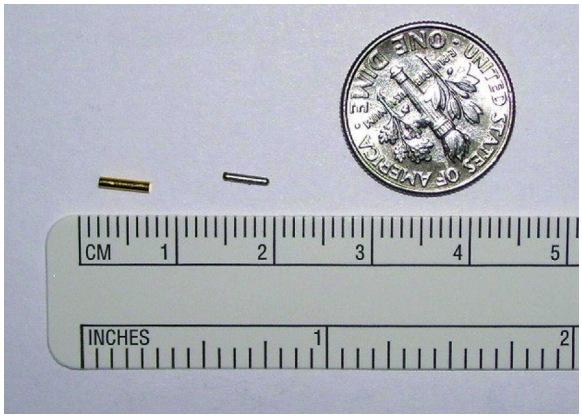

FIGURE 1.15 Illustrated are a gold fiducial marker on left, radioactive brachytherapy seed in the center, and a dime (small US coin worth 10 cents) on the right. The fiducial marker on the left is not radioactive, and not utilized in brachytherapy. *From Linden, R.A., et al., 2009. Technique of outpatient placement of intraprostatic fiducial markers before external beam radiotherapy. Urology 73 (4), 881–886, reprinted with permission from Elsevier © 2009.*

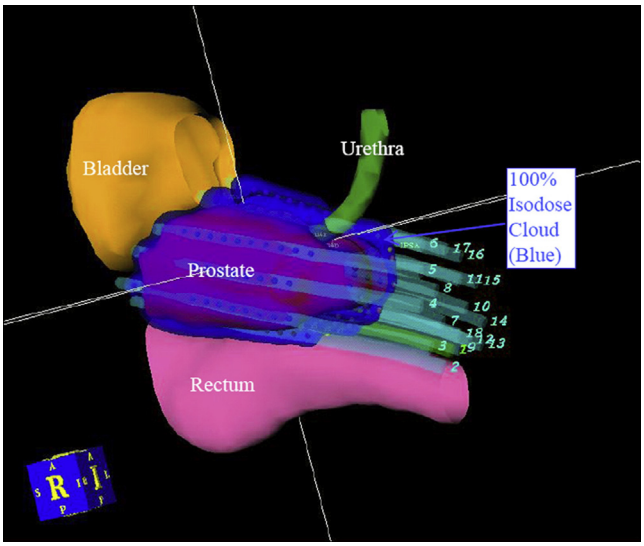

FIGURE 1.16 Computer-generated 3D reconstruction of prostate gland and neighboring organs. The prostate, colored red, is the target volume for irradiation by brachytherapy seeds containing radioactive ^{125}I or ^{103}Pd. Numerous seeds are illustrated within several injection canals inserted in the prostate. The 100% isodose distribution (colored blue) represents the zones that receive equal doses of radiation. Notice that the 100% isodose encompasses the entire cancerous prostate gland while infringing minimally into regions of neighboring healthy tissue. *Figure from Demanes, D.J., et al., 2011. High-dose-rate monotherapy: safe and effective brachytherapy for patients with localized prostate cancer. Int. J. Radiat. Oncol. Biol. Phys. 81 (5), 1286–1292, reprinted with permission from Elsevier © 2011.*

1.1.5.c Proton Beam and Heavy Ion Therapy

Advances have been made in EBRT whereby proton beams are produced by a particle accelerator in the hospital for the treatment of cancerous tumors. The protons undergo less scatter than X-ray and gamma-ray photons. An additional advantage of proton beam therapy over X-ray or gamma-ray photon therapy is that the proton beam, consisting of a charged particle of relatively high mass, will dissipate most of its energy via ionization when it reaches the end of its range of travel in human tissue. This is shown in Fig. 4.4 of the chapter entitled "Alpha Radiation," which illustrates that positively charged particles of relatively high mass (eg, proton or helium nucleus) dissipate their energy in matter via ionization, producing the greatest number of ion pairs as the particles slow down and reach the end of their path of travel. Thus if the energy of the proton beam is selected to enable the proton to travel through human tissue to a depth sufficient to reach a cancerous tumor, the proton beam will go no further and will dissipate most of its energy via ionization within the tumor, causing minimal damage to healthy tissue. The greater ionization at the tumor site produced by protons, in contrast to that produced by X-ray or gamma-ray photons, causes a greater degree of damage to cancer cells and makes it more difficult for the damaged cells to repair themselves and survive. Consequently, with protons, higher dose rates to diseased tissues are sometimes possible while inflicting minimal damage to healthy tissue. A modern dedicated proton beam therapy unit is illustrated in Fig. 1.17. This unit combines X-ray imaging with proton beam therapy. Because the tumor is not always static—depending on its location, it can sometimes move within the body of a patient as a result of respiration (inhalation and exhalation)—X-ray imaging can be used simultaneously with proton beam therapy, which is known as spot-scanning proton beam therapy. Due to the positive charge on the proton, a magnetic field can be used to deflect and direct the proton beam to scan or cover only the area or region of the tumor and thereby minimize damage to neighboring healthy tissue and organs.

Ions heavier than protons, such as carbon ions, can be accelerated to provide a heavy ion beam for the treatment of tumors. Carbon ions are much heavier than protons, and their high mass and charge create greater ionization than protons when the carbon ions reach the end of their path of travel. The degree of ionization is measured by the number of ion pairs produced in tissue per millimeter of path of travel, referred to as specific ionization. Like protons, the specific ionization of carbon ions is greatest when the ions slow down and reach the end of their travel, but carbon ions are about 12 times the mass of protons and thus produce at least a 12-fold greater specific ionization than protons within a tumor. If the carbon ions are accelerated with sufficient energy to reach the tumor, they will travel no further and deposit more ionization than protons within the tumor, giving more assurance of a kill to harmful cancer cells within the tumor. Carbon ions, like protons, deposit much less energy via ionization in healthy tissue than X-ray and gamma-ray photons as they enter the

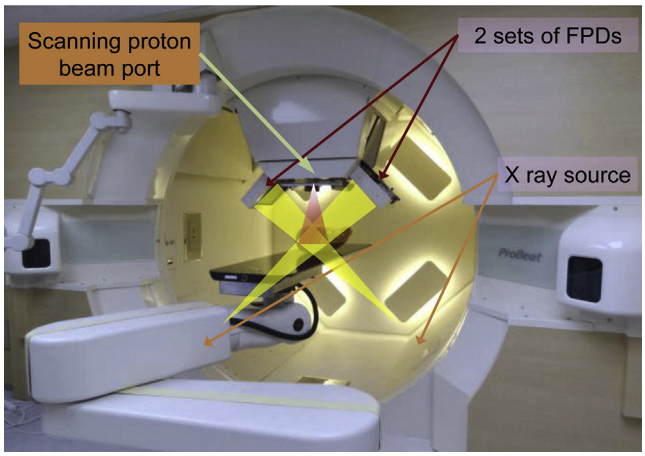

FIGURE 1.17 A spot-scanning proton beam therapy unit. The proton beam (brown) travels from the proton beam port toward the patient (not illustrated). The patient lies on the black table under the beam. X-ray sources can be used to image the tumor, particularly nonstatic tumors, so the proton beam can be scanned to encompass only the tumor. X-ray images are provided by flat panel detectors (FPDs), which are modern X-ray imaging detectors providing fast images with minimal X-ray dose to the patient. *Figure from Shimizu, S., et al., 2014. Preliminary analysis for integration of spot-scanning proton beam therapy and real-time imaging and gating. Phys. Med., in press, reprinted with permission from Elsevier © 2014.*

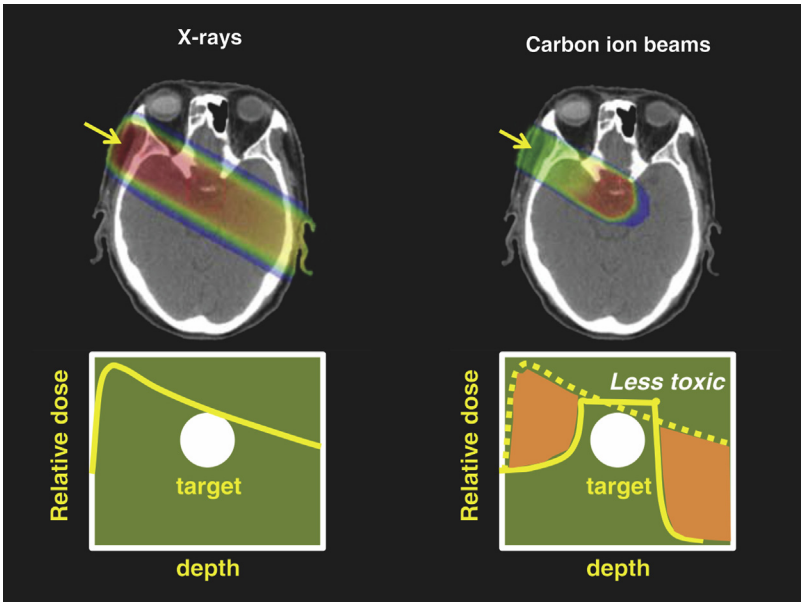

FIGURE 1.18 The difference of dose distribution by one beam port between X-ray photons and carbon ion beams. The intensity of radiation deposited in the tissue, illustrated in the sectional image of a patient's skull, is provided by the color scheme red > yellow > green > blue. In the case of X-ray photons, more radiation is deposited in healthy tissue before reaching the tumor; but in the case of a carbon ion beam, more radiation is deposited (*red color*) in the tumor than in healthy tissue. *Figure from Ohno, T., 2013. Particle radiotherapy with carbon ion beams. EPMA J. 4, 9, printed with permission © 2013 Ohno; licensee Biomed Central Ltd.*

body of the patient and travel to the tumor. X-ray and gamma-ray photons deposit more energy within healthy tissue as they travel on toward the tumor within the body of the patient. Thus the destructive effect of X-ray or gamma-ray photons on cancerous tumors is less specific than that provided by properly focused proton or carbon ion beams. The comparison between the effects of X-ray photons and carbon ion beams is illustrated very clearly in Fig. 1.18. Although Fig. 1.18 compares the effects of X-ray photons with carbon ion beams, it can be safely stated that gamma-ray photons produce similar effects to X-ray photons in human tissue; and proton ion beams act similarly, although to a lesser extent, to carbon ion beams in tissue.

The advantage of carbon ion beam therapy over X-ray photon therapy is illustrated in Fig. 1.18. On the left, an X-ray photon beam is directed toward a tumor in the center of the brain. The X-ray photon beam travels through the entire brain,

depositing a higher dose in healthy tissue upon entering the skull before reaching the tumor in the center of the brain. In the case of the carbon ion beam, the carbon ions, which travel only as far as the tumor, deposit their highest dose of radiation at the site of tumor and deposit minimal radiation in healthy tissue upon entering the skull and during travel to the tumor site. Gamma-ray photons interact in human tissue similarly to X-ray photons, and protons interact similarly to carbon ions; but a carbon ion beam can provide a more lethal dose to tumors than a proton beam, because of the much higher mass of carbon ions and the consequent higher specific ionization they produce.

The IAEA *Nuclear Technology Review* (2013a) reports rapid growth of proton beam and carbon ion beam therapy centers around the world. In particular, there are now 40 particle therapy centers worldwide, including six carbon ion beam centers; and at least 25 additional facilities are under development (Peeters et al., 2010).

1.1.5.d Boron Neutron Capture Therapy

Neutron capture therapy (NCT) involves the treatment of malignant tumors that cannot be treated effectively by other methods due to the particular invasive character of the tumor or its inoperable characteristics. The method encompasses two stages. A pharmaceutical or drug containing in its molecular structure an element with a high cross-section for the capture of thermal or slow neutrons, such as boron-10, is administered. The drug should ideally concentrate in the tumor cells—that is, it should have a specificity to settle after administration in tumor cells rather than healthy tissue. The patient and tumor are irradiated with epithermal neutrons, which have an energy in the range of 0.4–100 eV. While passing through tissue and before reaching the tumor, the epithermal neutrons lose energy via collisions, mainly with protons in the bodily tissue, and thus are slowed down to the thermal energy range of <0.4 eV. When the thermal neutrons reach the tumor cells, they are captured mainly by the boron-10 previously administered to the patient in a tumor-specific drug. The capture of thermal neutrons by the boron-10 isotopes distributed throughout the tumor cells results in the production of boron-11 isotopes, which in turn undergo fission into high-energy alpha particles (helium nuclei) and high-energy nuclei of lithium-7, as illustrated in Fig. 1.19. The range of travel of these ionizing particles is very short, ~5–9 μm, which is the size of a single cell. Both particles possess high energy, a positive charge, and relatively high mass, which gives them great power to deposit much energy via ionization (ie, high linear energy transfer) over a short distance (a few μm); this causes much ionization damage within the cancerous cell and delivers a lethal blow. When boron-10 is used in this way to kill malignant tumor cells selectively, the method is known as boron neutron capture therapy (BNCT).

BNCT has a potential advantage over other therapeutic methods previously described, because it is both biologically and physically specific: it is biologically specific when sufficient boron-loaded drug can be administered to concentrate in tumor cells, so it is biologically focused at the cellular level, as illustrated in Fig. 1.20; and it is physically specific because the neutron capture fission reaction will occur only with boron-10 isotopes and not with other isotopes of the elements C,

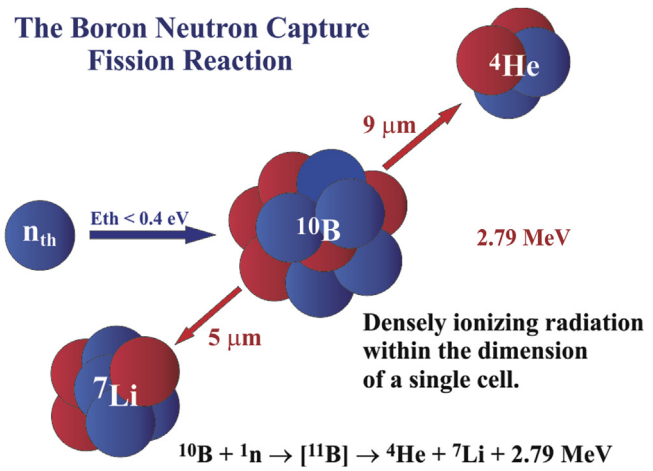

FIGURE 1.19 Schematic of the boron neutron capture fission reaction. BNCT is based on the neutron capture reaction $^{10}B(n,\alpha)^{7}Li$, where a ^{10}B atom captures a low-energy thermal neutron ($E_{th} < 0.4$ eV) and spontaneously decays to produce the linear recoiling particles ^{4}He (α particle) and ^{7}Li. In tissues these particles have short penetration ranges, approximately the width of a single cell (5 μm for ^{7}Li and 9 μm for ^{4}He). The average linear energy transfer is high (^{7}Li, 162 keV/μm; ^{4}He, 196 keV/μm), which results in densely ionizing radiation restricted to the track of each particle. *From Chandra, S., Lorey II, D.R., 2007. SIMS ion microscopy imaging of boronophenylalanine (BPA) and $^{13}C^{15}N$-labeled phenylalanine in human glioblastoma cells: relevance of subcellular scale observations to BPA-mediated boron neutron capture therapy of cancer. Int. J. Mass Spec. 260, 90–101, reprinted with permission from Elsevier © 2007.*

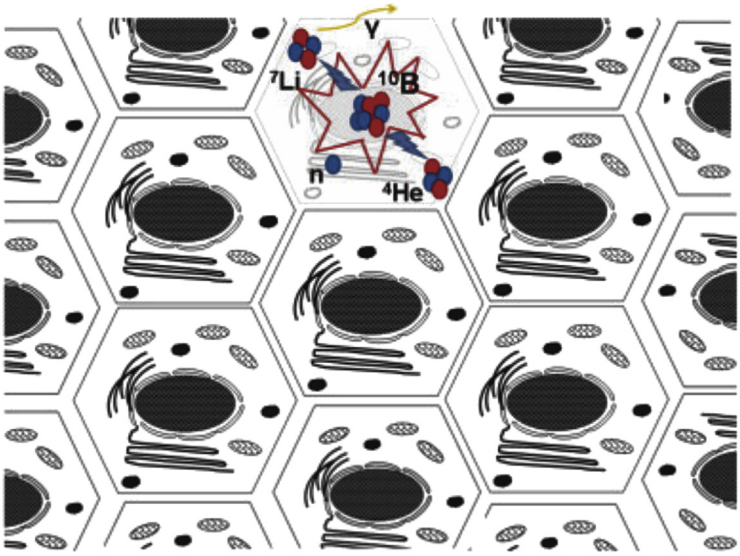

FIGURE 1.20 Therapeutic mechanism of BNCT. The boron-10 residing within a tumor cell captures a thermal neutron and undergoes fission, with the release of high-energy ^{4}He and ^{7}Li nuclei which deal a lethal blow of ionization within the cell. *Figure from Evangelisti, L., et al., 2013. Boron neutron capture therapy and ^{18}F-labelled borophenylalanine positron emission tomography: a critical and clinical overview of the literature. Appl. Radiat. Isot. 74, 91–101, reprinted with permission from Elsevier © 2013.*

H, O, N, or P common in human tissue. As noted by Professor Akira Matsumura of the Faculty of Medicine, University of Tsukuba, Japan and then president of the International Society for Neutron Capture Therapy, in his announcement of the 15th International Congress on Neutron Capture Therapy in September 2012:

> *Boron Neutron Capture Therapy is attracting increasing interest and demand as the "next-generation charged particle therapy" after proton and carbon ion therapy since it is the only radiation therapy that can focus on the cellular level.*
>
> http://square.umin.as.jp/ICNCT15/general/.

Much research and clinical trials are now ongoing around the world to establish BNCT "as an accepted and mainstream modality for several cancers" (Kreiner et al., 2011), including head and neck cancers. Research is under way to determine the most efficient boron-loaded drugs that will settle in sufficient concentration in tumor cells, and the most efficient means of delivery of epithermal neutrons via research reactors or accelerator-created neutrons in the hospital setting. This was highlighted in the announcement of the 16th International Congress on Neutron Capture Therapy, held in Helsinki, Finland in June 2014, which included the statement by Dr. Leena Kankaanranta, oncologist and president of the International Society of Neutron Capture Therapy, noting that key developments to be discussed are "the development of hospital-deployable accelerator-based neutron sources and next-generation boron targeting agents for BNCT, as well as highlights of the latest biological, biophysical and clinical research" (http://icnct16.org/welcome-message/).

Another isotope receiving attention in NCT is gadolinium-157, which has a thermal neutron capture cross-section much higher than that of boron-10; however, research into the application of gadolinium-157 in NCT is far behind developments made with boron-10. An excellent review of NCT is provided by Issa et al. (2013). The IAEA reports that 20 countries now have BNCT facilities, although the technique is still in clinical trial stages (http://www.naweb.iaea.org/napc/physics/research_reactors/database).

1.1.6 Radioactive Nanoparticles in Cancer Imaging and Therapy

Various methods to treat cancerous tumors have been discussed, including the use of X-ray and gamma-ray photons as well as proton and carbon ion irradiation. These irradiation techniques, while effective in treating cancer, cause harm to healthy tissue to varying degrees as chemotherapy, which is a well-known nonradiation method for treating cancer, also harms healthy tissue. A relatively new approach to the treatment of malignant tumors is to employ radioactive nanoparticles, which can target cancer cells specifically without harm to healthy tissue. This enters the realm of a recent and rapidly expanding field called nanomedicine.

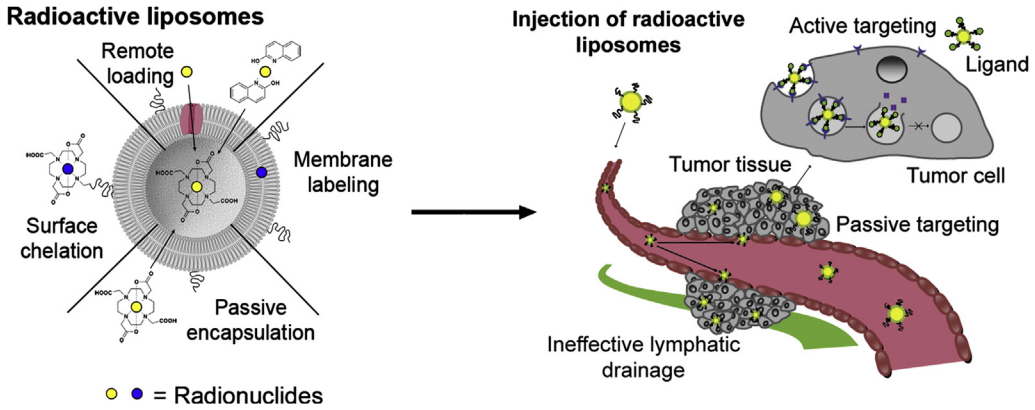

FIGURE 1.21 Left: A schematic diagram of a radioactive liposome nanoparticle illustrating remote loading, membrane labeling, passive encapsulation, and surface chelation methods for preparing radioactive liposomes. Radionuclides can be associated with the lipid membrane by hydrophobic interaction, through membrane conjugation, or surface chelation using chelator−lipid conjugates in preformed liposomes (blue radionuclides). Radionuclides can either be encapsulated inside liposomes during lipid hydration, or transported through the lipid membrane of preformed liposomes by ionophores or lipophilic chelators (yellow radionuclides). In the latter case, the radionuclides are trapped inside the aqueous lumen by a hydrophilic chelator with high affinity for the radionuclide. Right: Illustration of passive and active in vivo targeting of liposomes in tumor tissue. *From Petersen, A.L., et al., 2012. Liposome imaging agents in personalized medicine. Adv. Drug Deliv. Rev. 64, 1417−1435, reprinted with permission from Elsevier © 2012.*

Nanoparticles are by definition very small particles measured in nanometers (nm) in diameter. A certain class of nanoparticles is the liposome, composed of a spherical particle with a dual layer of lipids. Liposomes can be artificially prepared from biological membranes to vary in size from 50 to 300 nm, and used to carry drugs through the bloodstream to treat cancer. Such liposomes can be loaded with the radioactive isotopes (radionuclides) that are instrumental in SPECT and PET imaging of cancerous tumors, or used to deliver lethal blows of ionizing radiation within tumor cells with the purpose of killing the cancerous cells without harming cells of healthy tissue.

Various methods may be used to load radionuclides on to the liposomes, as illustrated and described in Fig. 1.21. Once loaded with a particular radioisotope, the radioactive liposomes are injected into the bloodstream of the patient. The liposomes circulate throughout the normal blood vessels; but when they encounter blood vessels associated with cancerous tissue, they passively escape from the blood vessels and enter the tumor cells. This is known as passive targeting, and is a consequence of the enhanced permeability and retention effect. Passive targeting of tumor cells by this effect is based on the fact that healthy blood vessels contain pores measuring 2−6 nm wide; whereas blood vessels associated with tumors contain pores that are much wider, from a few hundred to a few thousand nanometers (IAEA, 2013a). The much wider pores in tumor-associated blood vessels are due to the rapid growth of cancer cells relative to healthy tissue, and the need of cancerous tissue to develop blood vessels rapidly to sustain its requirement for oxygen and nutrients. Thus the nanoparticles loaded with radionuclides passively enter the wider pores of the leaky blood vessels associated with a cancerous tumor, and then reach and enter the tumor cells by active targeting, as illustrated in Fig. 1.21. Active targeting of tumor cells occurs after the nanoparticles passively escape from the blood vessels and reach the tumor. The presence of ligands grafted at their surface allows active targeting by binding to receptors overexpressed on tumor cells, resulting in enhanced accumulation and cell uptake through receptor-mediated endocytosis (Sanna et al., 2013). Endocytosis is a process by which cells absorb large molecules by engulfing them. The selective absorption of the radioisotope-loaded nanoparticles (eg, liposomes) in the tumor cells by the enhanced permeability and retention effect results in the localization of the radioisotope in the tumor while avoiding healthy tissue. The radioisotopes in the tumor cells can provide enhanced SPECT or PET imaging of cancers for improved treatment, or they can deliver lethal ionizing radiation to the cancerous cells.

The application of nanoparticles to the treatment of cancer is a rapidly growing field currently undergoing widespread research around the world. The IAEA *Nuclear Technology Review* (2013) noted that in one year alone as many as 240 nanosized products entered the pharmaceutical research pipeline; and nanoliposomes, which are hollow bubbles enclosed by two layers of lipids (see Fig. 1.21), have been the nanocarrier of choice for the delivery of therapeutic radionuclides contained in their internal cavity or bound to their surface. Numerous radionuclides are listed in the *Nuclear Technology Review* (2013) for application in liposome-based nanotargeted cancer radiopharmaceuticals; among these are ^{67}Cu (half-life = 62.0 h, β^-, E_{max} = 0.58 MeV), ^{90}Y (half-life = 64.1 h, β^-, E_{max} = 2.28 MeV), ^{131}I (half-life = 8.04 days, β^-, E_{max} = 0.61 MeV), ^{186}Rh (half-life = 3.72 days, β^-, E_{max} = 1.1 MeV), ^{188}Rh (half-life = 16.9 h, β^-, E_{max} = 2.1 MeV), and ^{225}Ac (half-life = 10.0 days, α, 5.8 MeV). Notice that the half-lives of the therapeutic radionuclides are relatively short, ranging from several hours to days; and they emit highly ionizing beta or alpha radiation. The relatively short half-lives give sufficient

time for the radiation to be emitted into the cancer cells over a relatively short period before decaying to undetectable levels, thereby minimizing harm to the patient. When nanoparticles are used for imaging rather than therapy, radionuclides that emit gamma radiation, such as ^{67}Ga, ^{111}In, ^{123}I and ^{99m}Tc, are used for SPECT; and radionuclides that emit positron radiation, such as ^{18}F, ^{64}Cu and ^{124}I, are used for PET imaging (Petersen et al., 2012).

The stable isotope boron-10 may also be loaded on to nanoparticles for targeting cancerous tissue. Once the ^{10}B is concentrated in the cells of the tumor, the patient can be irradiated with epithermal neutrons. As previously discussed in the section on BNCT, the epithermal neutrons are slowed down after passing through body tissue and captured by the ^{10}B nuclei to become ^{11}B nuclei, which undergo immediate fission to highly ionizing ^{4}He and ^{7}Li nuclei within the cancerous cells, dealing a lethal blow to them.

1.2 BIOLOGICAL RESEARCH

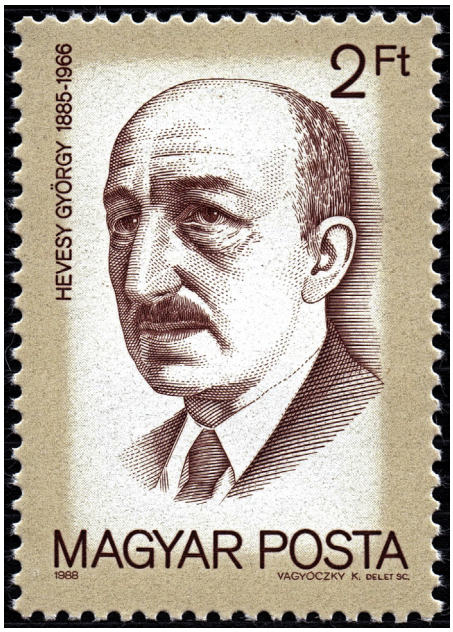

George de Hevesy (1885–1966)

The applications of radioactive isotopes in biological research began with George de Hevesy, who was awarded the Nobel Prize in Chemistry in 1943 for, in the words of the Nobel Committee, "his work on the use of isotopes as tracers in the study of chemical processes." In 1913 de Hevesy was among the first to discover that radioactive isotopes of an element could be used to trace the chemical processes of that element in inert and living systems. Because radioisotopes are chemically inseparable from the stable isotopes of a given element—that is, they possess the same electron shell—de Hevesy demonstrated that a radioactive isotope in trace amounts could be mixed with the stable isotope of the same element, and all the chemical or biological transformations of that element could be followed by detecting and measuring the radiation emitted by the radioactive tracer isotope. George de Hevesy's discovery of the application of isotopes as tracers started when he traveled to Manchester, England in 1910 to study under Ernest Rutherford. At Manchester, Rutherford had a large supply of radioactive lead containing radioactive isotopes known as radium D (RaD), which had been donated by the Austrian government. Rutherford gave George de Hevesy the assignment of separating the RaD from lead. The RaD was of little use as a radiation source, because the lead would absorb much of the radiation. Thus one day, as related by de Hevesy (1944), Rutherford addressed de Hevesy in the basement of the Institute of Physics at the University of Manchester where the radioactive lead was stored, saying "My boy, if you are worth your salt, you try to separate RaD from all that lead." George de Hevesy was an enthusiastic budding scientist and made numerous attempts, working for almost two years at the task of separating the RaD chemically from the lead. Having failed completely at this, and to make the best of a depressing situation, he decided that RaD could not be separated chemically from lead and thus could be used as a radioactive tracer to study the chemical pathways of stable (nonradioactive) lead. De Hevesy was correct in this conclusion, as it was later discovered that RaD is a radioactive isotope of lead, namely Pb-210, which cannot be separated chemically from the element lead.

De Hevesy went on to the Vienna Institute of Radium Research, as it had more radium at its disposal than any other institution. There he met with Frederic Paneth, who had also carried out abortive tests to separate RaD from lead.

George de Hevesy's first experiment with radioisotope tracers was carried out with Frederic Paneth in 1913 at the Vienna Institute. They were able to determine the solubility of highly insoluble lead compounds with the use of tracer amounts of radioactive lead (de Hevesy and Paneth, 1913a,b). George de Hevesy later demonstrated in numerous works how radioisotopes could be applied to determine the fate of inorganic and organic compounds in living systems, such as plants, animals, and the human organism. For example, if we want to determine the pathways of a carbon atom in an organic compound within a living system, such as a certain atom of an amino acid, protein, nucleic acid, carbohydrate, lipid, vitamin, etc. the atom in that chemical compound need only be labeled with a radioactive isotope of carbon, namely carbon-14. From the radiation emissions of the radioisotope tracer, the chemical pathways of the carbon atom can then be followed. Since the pioneering experiments of de Hevesy, countless biological pathways of carbon, hydrogen, phosphorus, sulfur, and other elements in plants, animals, and microorganisms have been elucidated with the use of radioisotope tracers—in this case, carbon-14, tritium (hydrogen-3), phosphorus-32, and sulfur-35, respectively. Where suitable radioactive isotopes are not available, such as is the case with nitrogen, the anabolic and catabolic reactions involving nitrogen in living systems are studied with the stable isotope nitrogen-15. Since the first demonstration in 1913 by George de Hevesy, who is the father of the isotope tracer technique, innumerable examples may be seen in the scientific literature, and the knowledge gained in these studies and applied to medicine, agricultural production, and the biological sciences in general has been invaluable. One can safely state that almost every biological cycle of carbon compounds that we know today, all vital for human health and nutrition, has been elucidated with the use of the aforementioned radioactive isotopes as well as many stable isotopes (eg, ^{2}H, ^{13}C, and ^{15}N). George de Hevesy also pioneered the use of stable isotopes as tracers in the biological and chemical sciences after deuterium, the heavy stable isotope of hydrogen, was discovered by Harold Urey in 1932. Biological cycles such as carbohydrate metabolism, the Krebs cycle, lipid metabolism, photosynthesis, biosynthesis and modes of action of nucleic acids and proteins, metabolic regulation, etc. have been studied with the aid of radioactive isotope tracers.

A classic example of the use of a radioactive tracer in the biological sciences can be taken from the work of Melvin Calvin, who together with coworkers used the radioactive isotope carbon-14 as a tracer for CO_2 to elucidate the initial biochemical pathways in plant photosynthesis. He was awarded the Nobel Prize in Chemistry in 1961 for, in the words of the Nobel Committee, "his research on the carbon dioxide assimilation in plants."

Melvin Calvin (1911–1997)

It was, of course, known then that plants needed carbon dioxide and light to grow; but knowledge was lacking of the biochemical mechanisms whereby plants capture CO_2 from the atmosphere and assimilate the carbon from this gaseous substance into the building blocks of plant matter and food upon which we depend. Melvin Calvin and coworkers

(Calvin, 1949, 1953; Calvin and Benson, 1948; Bassham et al., 1950; Calvin et al., 1950; Benson et al., 1952) carried out experiments by feeding carbon dioxide labeled with the radioactive tracer carbon-14 (ie, $^{14}CO_2$) to photosynthesizing plant chloroplasts over different time intervals. During short exposure periods ($\sim$1 s) the major fraction of the radioisotope label was encountered in the three-carbon (C_3) compound, phosphoglyceric acid (PGA, **3**) as shown below; this was concluded to be the first product of photosynthesis. PGA was found to be a product of the condensation of the $^{14}CO_2$ with ribulose 1,5-biphosphate (**1**) catalyzed by a carboxylase enzyme to produce the 2-carboxy-3-ketoribitol 1,5-biphosphate intermediate (**2**), which then undergoes hydrolysis to PGA (**3**). The asterisks in the illustrated reactions mark the positions of the carbon-14 radioisotope label.

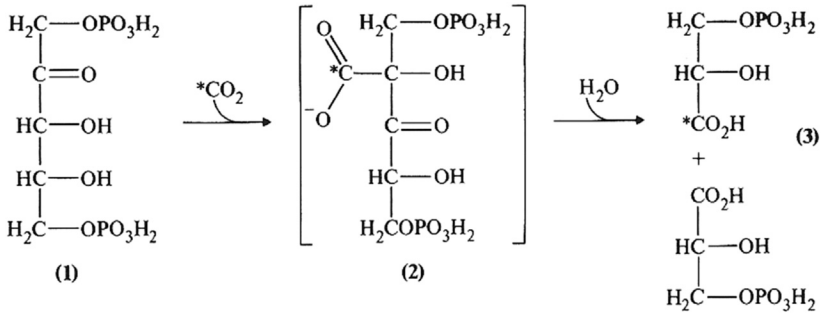

The first step of this Calvin–Benson–Bassham cycle, producing a C_3 compound as a first product of photosynthesis, was considered the general pathway for CO_2 fixation in all plants. However, subsequent work by Kortschak, Hartt, and coworkers (Kortschak et al., 1965; Kortschak and Hartt, 1966) with sugarcane showed that, for very short periods of photosynthesis with $^{14}CO_2$, the carbon-14 label was found mostly in the four-carbon compounds (C_4), aspartic (**4**) and malic (**6**) acids, with only a small portion of the isotope label residing in the three-carbon PGA (**3**). For example, when an attached sugarcane leaf was exposed to $^{14}CO_2$ for 2 s and killed with 80% alcohol, the radioactivity intensities of the ^{14}C label in malate, aspartate, PGA, and hexose monophosphates were 54%, 37%, 7%, and 2%, respectively. The pathways of carbon in this newly discovered cycle were elucidated by Hatch and Slack (1966) by counting the radioactivity (ie, measuring its intensity) in the specific carbon atoms of malate, aspartate, and PGA after isolation of the compounds from the plant and selective chemical degradation of their carbon atoms.

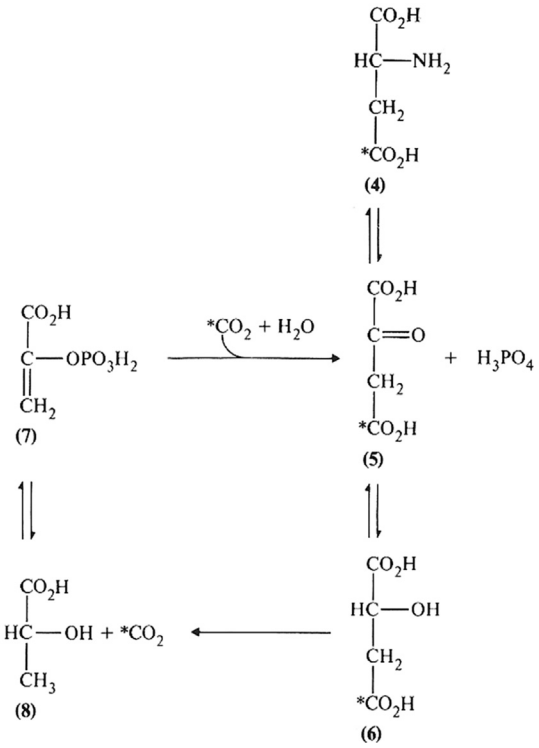

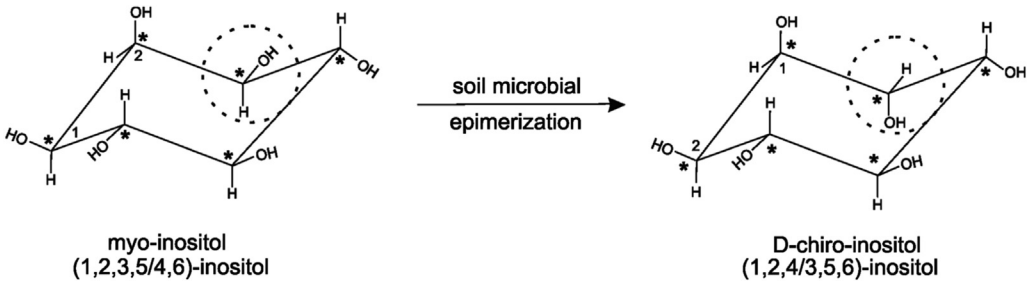

FIGURE 1.22 The microbial epimerization of uniformly label [^{14}C]myo-inositol to [^{14}C]chiro-inositol in soil. The asterisks represent the locations of the carbon-14 radioisotope labels and the dotted circles enclose the only carbon atom that differs in the structure of the two molecules. These reactions are important, because inositol phosphates can be a major source of soil organic phosphorus important to soil fertility and plant nutrition. *From L'Annunziata, M.F., et al., 1977. Microbial epimerization of myo-inositol to chiro-inositol in soil. Soil Sci. Soc. Am. J. 41, 733–736.*

This work on photosynthesis clearly distinguished two types of plants, namely C_3 and C_4 plants, and this knowledge plus measurements on the energy requirements for the various biochemical reactions involved were used to improve crop production around the globe as a function of climate variations, among other factors. For example, the C_4 plants like sugarcane and maize display higher net photosynthesis in regions of strong light intensity, such as in the tropical areas of Brazil where fuel produced from sugarcane and alcohol is a viable energy source. In temperate regions, where light intensities are lower, the C_3 plants have higher rates of net photosynthesis and a potential for high crop production.

Radioactive isotopes are sensitive tracers that are helpful in the elucidation of biochemical pathways. For the method to be conclusive it is necessary to start with a compound precursor labeled with a radioisotope, for example ^{14}C, ^{3}H, or ^{32}P. Biological transformations of the radioactive precursor molecule may lead to a number of product compounds; these would also be radioactive if the atom or atoms that are labeled in the precursor also reside in the product compounds. Thus if we start with an organic compound **A** labeled with ^{14}C, which undergoes transformation to product compounds **B** and **C**, etc. and if compounds **B** and **C** are also radioactive, we can conclude that the isotope-labeled carbon atom(s) in the product compounds originated from compound **A**. This is illustrated by the following reaction sequence:

$$[^{14}\text{C}]\text{-Molecule } \mathbf{A} \rightarrow [^{14}\text{C}]\text{-Molecule } \mathbf{B} \rightarrow [^{14}\text{C}]\text{-Molecule } \mathbf{C} \rightarrow \ldots$$

The tracer technique is useful in determining very complex sequences of biological reactions, such as the intricate carbon transformations that occur in plant photosynthesis described above. The method is complicated by the need to isolate each product compound and determine its molecular structure, in addition to measuring the radioactivity intensity emanating from the radioisotope label in each compound. Although the technique may be tedious, the radioisotope tracer method is vital in proving the origin of compounds that are very similar in structure. For example, the writer and coworkers (L'Annunziata et al., 1977; L'Annunziata and Gonzalez, 1977) used the radioisotope carbon-14 to demonstrate microbial transformations of inositol and inositol phosphates in soil. Fig. 1.22 shows a biochemical transformation of myo-inositol to D-chiro-inositol, demonstrated using carbon-14.

The two molecules illustrated in Fig. 1.22 are stereoisomers. The gross similarities of the two molecules, which share the same chemical formula and differ only in the spatial orientation of the proton and hydroxyl group at one carbon atom, make the biological origin of the product compound difficult to ascertain without the aid of a radioisotope label. The intensities of the radioactivity in the precursor and product compounds can also give a quantitative measure of the degree to which the metabolism occurs.

Radioisotopes as tracers in the biological sciences remain a vital tool for the elucidation of anabolic and catabolic reaction pathways. Examples in the scientific literature of the application of radioactive isotopes as tracers since the first demonstration by George de Hevesy in 1913 are numbered in the millions. For additional information on applications of radioactive tracers in the biosciences the reader may peruse books by Sarkadi-Priboczki (2013), L'Annunziata (2012a), Nasser (2009), Lappin and Temple (2006), Larijani et al. (2006), Volkman (2006), Wolfe and Chinkes (2004), Slater (2002), Cobelli and Gianna, D. F. (2001), Billington (1992), Wolfe (1992), and L'Annunziata (1984).

1.3 FOOD AND AGRICULTURE

Scientific research is vital to improving the quantity and quality of food needed to meet the growing demand of the world population. Radioactive and stable isotopes and nuclear radiation serve as useful tools in research aimed at increasing

world food production. In the foreword of a review book, *Isotopes and Radiation in Agricultural Sciences* (L'Annunziata and Legg, 1984a,b), Hans Blix, then IAEA director general, wrote:

> *Nuclear techniques in agricultural research have played a major role in increasing world food production to the level at which it is today. A few areas in which these techniques, largely based on the use of isotopes and radiation, have attained prominence are insect pest control, food preservation, plant nutrition, animal health and production, crop management and pesticide residue studies. Nuclear methods have contributed in no small way to our understanding of biological processes and, when translated into practice, have made a subsequent impact in various fields of agriculture… While there have been remarkable advances in the agricultural sciences in recent years, the need for increasing global food production is still critical and will become more so as time goes on. If further advances are to be made in this respect, our need for nuclear techniques will become even greater.*

The applications of nuclear techniques aimed at increasing agricultural production are numerous, and only a few examples are cited here.

1.3.1 Insect Pest Control

In the field of insect pest control, one of the greatest boons to improving agricultural production and human health, while at the same time improving the environment, has been the use of the sterile insect technique (SIT) to control or eradicate insect pests that cause damage to crops, livestock, and human health. SIT involves the mass rearing of an insect pest and the sterilization of the reared insects by means of high doses of gamma radiation from a sealed source of a radioisotope such as cobalt-60 or caesium-137. The use of X-rays to sterilize insects is currently under study as an alternative to gamma radiation (IAEA, 2012). Self-contained low-energy (a few 100 keV) X-ray irradiators offer the advantage that the source of X-rays is available only when the power is turned on, so much less shielding is required. Following irradiation, the sterile insects, particularly the males, are released into the wild by various techniques, such as aircraft drops of irradiated insect pupae. The sterile males generally mate many times with female insects they encounter in the wild, whereas the female insects mate only once. Thus if sufficient male insects of a particular species are reared, sterilized, and released into the wild in a healthy and competitive, albeit sterilized, state, the population of that species can be made to drop. When sufficient numbers of the insect species are reared, sterilized, and dispersed over large regions of land, the species can be eradicated from a region. Reinfestation could occur, but an SIT program can be maintained to keep the insect species out of a particular region, if not eradicate the species altogether. In addition to eradicating or controlling harmful insect pests, SIT offers the advantage of conserving the environment by avoiding the use of harmful insecticides and sparing from harm the very useful and beneficial insects, such as bees.

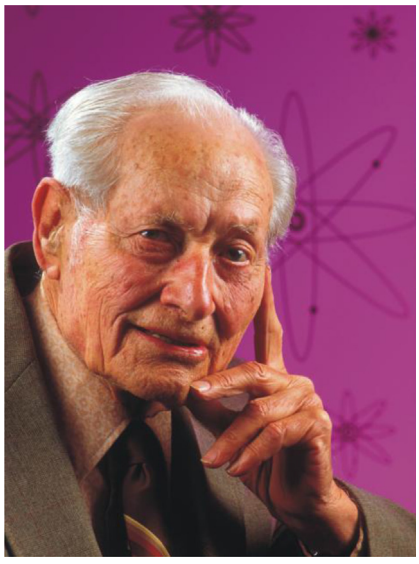

E. F. Knipling (1909–2000) from US National Academy of Sciences

Edward F. Knipling was the father of SIT. He first developed the sterile male theory of autocidal control of the screwworm fly in 1938 after joining the Agricultural Research Service of the US Department of Agriculture in Menard, Texas that year (USDA-ARS, 2006). The screwworm fly is a destructive pest of livestock, and was causing losses of several hundreds of millions of dollars annually in the USA (Kloft, 1984). The USDA-ARS also reports that Edward F. Knipling and coworkers R.C. Bushland, H.J. Muller, and E.D. Hopkins, among many others, began research on the radiation sterilization of the screwworm in 1950, followed by field tests on Sanibel Island, Florida in 1951−1953. They then successfully eradicated the screwworm from the island of Curaçao, off the coast of Venezuela, in 1954 using radiation-sterilized flies reared at a laboratory in Orlando, Florida. The sterile flies were shipped and released on Curaçao marking the first successful eradication of an insect pest by SIT. As reported in the *Nuclear Technology Review* (2004c), the screwworm pest was eradicated from all of North and Central America by use of SIT, and it is estimated that the eradication has provided annual benefits to the livestock industry in the region, through improved livestock productivity and health, that exceed the overall investment in the eradication campaign over 45 years.

Knipling (1955) was the first to publish the technique of insect control or eradication through the use of sexually sterile males. In this historic paper he demonstrated mathematically that insecticide applications become less efficient and SIT more efficient as the insect population is reduced. Edward Knipling subsequently published in 1957, 1959, and 1960 more earthshaking papers on SIT, with titles such as "Controlled Screwworm Eradication by Atomic Radiation," "Sterile-male Method of Population Control," and "Use of Insects for their Own Destruction." He had a very long and successful career in the continued development of his SIT technique as well as other methods of insect control, and published works as recently as in 1998, two years before his death. Knipling did not receive the Nobel Prize for his discovery of SIT, but certainly deserved such a prize, as SIT has proven to be a successful technique for the control and eradication of numerous harmful insect pests around the world. He was admitted to the US National Academy of Sciences, and was a recipient of the Presidential Medal for Merit, the FAO Medal and World Food Prize, and the Japan Prize, as well as numerous honorary doctoral degrees (Adkisson and Tumlinson, 2003). For additional information on his life and work, the reader may peruse an historical account by Waldemar Klassen (2003), a former coworker of Knipling and former colleague of the writer.

SIT has proven to be a useful method for the control of numerous insect pests in addition to the screwworm, including the Mediterranean fruit fly or "Medfly," olive fruit fly, onion fly, pink bollworm, codling moth, cactus moth, boll weevil, stable fly, horn fly, certain species of mosquito, and the tsetse fly. The control and eradication of the tsetse fly is vital to the development of certain countries of Africa where the insect acts as a vector of the "sleeping sickness" affecting the livestock and human population. The joint FAO/IAEA Division of the United Nations in Vienna, Austria oversees around the world SIT control and eradication programs against the Medfly, tsetse fly, and malaria mosquito. The use of SIT to control the malaria mosquito is a relatively new and vital challenge for the scientific community. The joint FAO/IAEA Division initiated a project in 2004 (*Nuclear Technology Review*, 2006) to assess the feasibility of using SIT for mosquito control. Research is now focused on the mosquito species *Anopheles arabiensis*, which is the second most important vector of malaria in Africa. The control or even eventual eradication of malaria in Africa would be one of the greatest achievements of the century for the betterment of humankind.

In addition to controlling mosquito populations in the fight against malaria, there is interest in applying SIT against mosquitoes that transmit virus diseases such as dengue and chikugunya fever. The IAEA *Nuclear Technology Review* (IAEA, 2007) reports that an experimental pilot plant has been established in Rimini, Italy to utilize SIT to control the mosquito *Aedes albopictus*, the vector of dengue. At this SIT plant, methods have been developed for the production of large numbers of male pupae for sterilization and release into the environment. Sterile male releases in the area of Rimini have resulted in significant reductions in the population density of the vector of this disease.

An innovative approach to SIT is "boosted SIT" to control mosquitoes, described by Bouyer and Lefrançois (2014), which entails the mass breeding of male mosquitoes, their sterilization by ionizing radiation followed by coating the sterilized males with pyriproxyfen (PP), a juvenile hormone analog. The sterile PP-coated males are released and dispersed in large numbers in the wild over large areas by helicopter. Mating of the sterilized PP-coated males with wild fertile female mosquitoes then follows. After unsuccessful mating with the sterile male, the female becomes permanently contaminated with the PP. Thus, when females lay their eggs in larval sites, the growth hormone prevents adult metamorphosis of all larvae including those that originate from fertile offspring. Even if the fertile and PP-contaminated female mates with a wild fertile male, there will be no offspring due to the PP contamination at the larval site. The addition of PP to the radiation-sterilized males adds a boost to SIT, because it wields a "double whammy" to this harmful insect pest by preventing the survival of all larvae, those from females that had mated with sterile males or fertile males. An illustration of the general procedure is provided in Fig. 1.23.

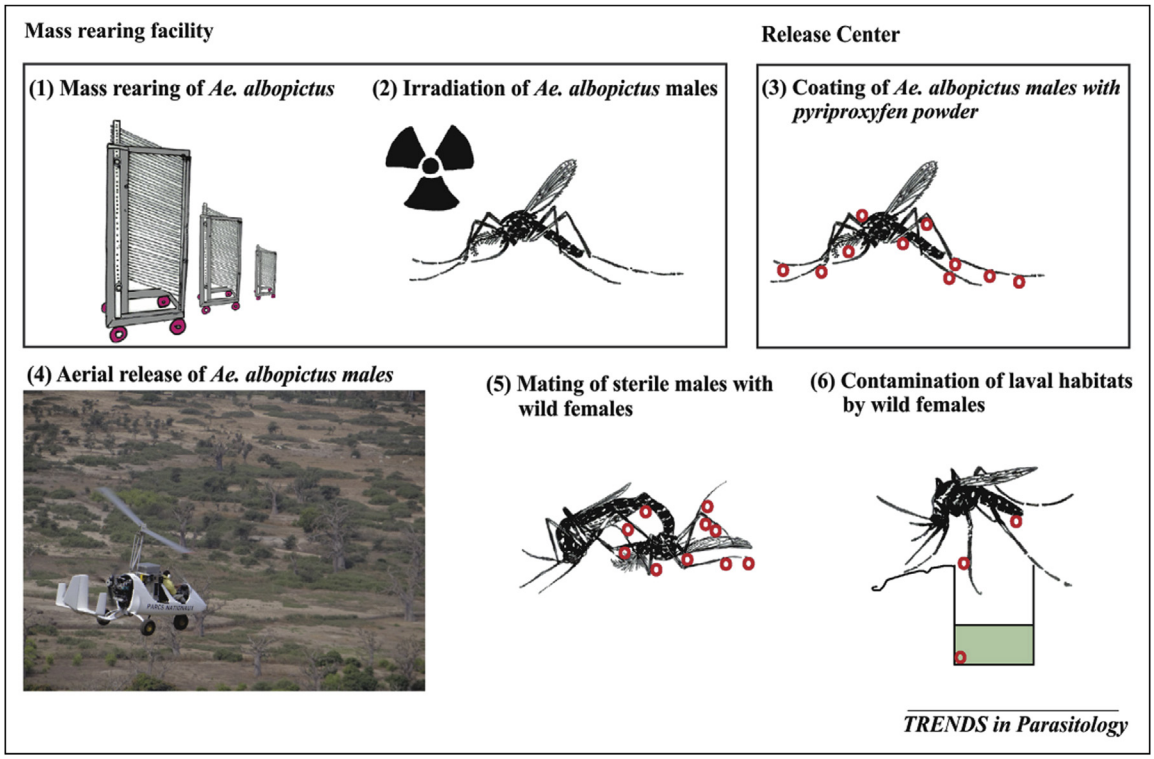

FIGURE 1.23 Presentation of the "boosted SIT" concept. Males of *Aedes albopictus* are coated with PP (*red circles*) and then released by air. They mate with wild females, which will in turn contaminate their larval habitats. To avoid contaminating the colony, males must be coated in a release center separated from the mass-rearing facility. The larval-tray rearing of *Ae. albopictus* illustrated in (1) represents the system presently used at the Insect Pest Control Laboratory, Joint FAO/IAEA Program of Nuclear Techniques in Food and Agriculture, Vienna, Austria (http://www-naweb.isaea.org/nafa/ipc/public/IPC-NL-82.pdf). The gyrocopter in (4) is the machine presently used to release *Glossina palpalis gambiensis* from Kalahari aerodrome, Saly, Senegal in the framework of a national tsetse elimination campaign (http://www.fao.org/news/story/pt/item/211898/icode/). It is equipped with a smart release machine, the most advanced release machine from the Mubarqui group, Cuidad Victoria, Mexico (ftp://ftp.fao.org/docrep/fao/010/a1195e/a1195e08.pdf). For large areas, this machine can be installed on board small planes. *From Bouyer and Lefrançois (2014), reprinted with permission from Elsevier © 2014.*

The boosted SIT concept, as illustrated in Fig. 1.23, involves (1) mass rearing of the mosquito using larval trays; (2) irradiation sterilization of males with gamma or X-radiation; (3) coating the sterile males with PP, a juvenile hormone analog, shown as red dots; (4) aerial release of the sterile and PP-coated males; (5) mating of the mass-reared sterile males with wild females, which includes contaminating the females with the juvenile hormone analog (red dots); and (6) females lay infertile eggs in communal larval habitats, contaminating the habitat and preventing the maturing of eggs originating from fertile wild mosquitoes.

For additional information on SIT the reader is invited to peruse books by Dyck et al. (2005), Vreysen et al. (2007), and Khaton and Shaik (2011).

1.3.2 Fertilizer and Water Use Efficiency

Another field of agriculture where radioactivity and nuclear techniques have played vital roles in development is research on the optimization of crop nutrition and water use efficiency. The efficient use of fertilizer to maximize crop production is measured with radioactive and stable isotope tracers, and the most cost-effective application of water for crop irrigation, upon which optimum fertilizer utilization depends, is measured with neutron radiation. As noted by Menzel and Smith (1984):

> *Increasing fertilizer costs and the necessity for minimizing environmental pollution have given added impetus to fertilizer disposition studies…tracer fertilizers [i.e., isotope-labeled fertilizers] provide the only definitive means for determining both the behavior and fate of applied nutrients. A basic assumption is that the isotopically labeled element behaves in an identical manner to the non-labeled element both physically and chemically, and a plant cannot distinguish between [isotope] labels.*

1.3.2.a Fertilizer Use Efficiency

In research studies on fertilizer use efficiency, radioactive isotopes are not applied in the open field; however, greenhouse experiments with radioactive isotopes of plant nutrients (eg, ^{32}P, ^{33}P, ^{35}S and ^{65}Zn) can provide scientists with the information needed to make recommendations to farmers to help achieve the optimum utilization of plant nutrient elements from soil and fertilizer. For example, a research scientist may use a fertilizer labeled with the radioisotope of phosphorus, ^{32}P, and apply it to the soil to measure percentage use of the fertilizer nutrient by plant crops. The radioactive fertilizer phosphorus has a specific activity, defined as the intensity of the radioactivity per unit weight of the element or

$$^{32}\text{P specific activity} = \frac{\text{DPM}}{\text{gP}} \quad [1.1]$$

where DPM is the radioactivity in units of disintegrations per minute, and gP represents the weight of the element phosphorus in grams. The weight of the phosphorus in the fertilizer is the sum of the weights of the radioactive isotope ^{32}P plus the natural stable isotope ^{31}P. However, the weight of the radioisotope tracers used in such studies is so small that the contribution of the radioisotope ^{32}P weight to the total weight of phosphorus can be neglected (see Eqs. 18.56 and 18.57 of the chapter entitled "Radionuclide Decay, Radioactivity Units, and Radionuclide Mass," which demonstrate that 1 mCi of ^{32}P comprises only 3.5 ng or 3.5×10^{-9} g). When the researcher adds the radioactive fertilizer to the soil, the plant absorbs phosphorus from two sources, namely the phosphorus derived from the fertilizer (PDFF) and the phosphorus derived from the soil (PDFS). The specific activity of the radioactive tracer ^{32}P in the plant is lower than that of the radioactive fertilizer, because of the absorption of stable ^{31}P from the soil by the plant. The reduction in ^{32}P specific activity is referred to as isotope dilution, and the degree of isotope dilution serves to measure the proportions of phosphorus in the plant that came from the fertilizer and from the soil from the following:

$$\%\text{PDFF} = \frac{^{32}\text{P specific activity in plant}}{^{32}\text{P specific activity in fertilizer}} \times 100 \quad [1.2]$$

where %PDFF is the percentage of phosphorus in the plant derived from the fertilizer. The remaining phosphorus in the plant is derived from the soil or

$$\%\text{PDFS} = 100\% - \%\text{PDFF} \quad [1.3]$$

Radioisotopes of phosphorus have relatively short half-lives (^{32}P, half-life = 14.3 days; ^{33}P, half-life = 25.3 days), which limits considerably the time available to carry out experiments with these isotopes as tracers. Long-term research on the dynamics of phosphorus in the soil is not possible with radioisotopes. Also, phosphorus has only one stable isotope, which eliminates any possibility of using stable isotopes of phosphorus as tracers. However, the IAEA *Nuclear Technology Review* (IAEA, 2011) reports that a new approach to studying the dynamics of phosphorus in cropping systems has been investigated whereby researchers measure stable isotopes of oxygen in inorganic and organic soil phosphorus compounds. Tamburini et al. (2010) developed a method for accurately measuring the stable isotope oxygen-18 (^{18}O) in different soil phosphorus fractions. As reported by the IAEA (2011) "Soils under different farm management practices (eg, fertilizer or manure applications) showed varying ^{18}O signatures in soil phosphorus indicating the potential of ^{18}O as an isotopic tracer for studying phosphorus cycling, tracing phosphorus sources and ultimately providing a better understanding of soil phosphorus dynamics in agro-ecosystems."

In the case of the element N, which is another major plant nutrient, there is no suitable radioactive isotope that could be used by researchers to assess fertilizer use efficiency. In this case, they use the stable isotope of nitrogen or ^{15}N as the tracer. In nature, the element nitrogen consists of a mixture of two isotopes, $^{14}N + {}^{15}N$, with abundances of 99.634% and 0.366%, respectively. There is consequently much more ^{14}N than ^{15}N in nature. However, researchers have been able to enrich the isotope ^{15}N in samples of natural nitrogen to produce nitrogen with a $^{15}N\%$ abundance greater than 0.366% so that this stable isotope may be used as a tracer in experiments such as fertilizer use efficiency studies. (See Radioactivity Hall of Fame, Part V for a biographical sketch of Gustav Hertz, who was the first to devise a method of isotope enrichment.) The amount of enrichment of ^{15}N in excess of its natural abundance is defined as

$$\%^{15}\text{N atomic excess} = \%^{15}\text{N in the sample} - 0.366\% \quad [1.4]$$

Thus, as in the previous example taken in research with fertilizers labeled with a radioactive isotope, researchers can use a fertilizer with a known $\%^{15}N$ atomic excess to measure the plant utilization of the nitrogen from the fertilizer according to the following

$$\%\text{NDFF} = \frac{\%^{15}\text{N atomic excess in plant}}{\%^{15}\text{N atomic excess in fertilizer}} \times 100 \quad [1.5]$$

where %NDFF is the percent nitrogen in the plant derived from the fertilizer. The $\%^{15}N$ atomic excess in the plant is always less that of the fertilizer because the plant roots also absorb nitrogen from the soil, which contains ^{14}N at its natural abundance. Thus the remaining nitrogen in the plant must be derived from the soil or

$$\%NDFS = 100\% - \%NDFF \quad [1.6]$$

1.3.2.b Soil Moisture Neutron Gauge

While scientists measure fertilizer use efficiency with the aid of isotope techniques, they also study the conditions that can optimize the plant nutrient use efficiency, such as the soil moisture. A source of fast neutron radiation is used by scientists to measure and monitor the water content of soils in the field.

The chapter entitled "Neutron Radiation" of this book gives much information on the sources and properties of neutron radiation. Neutrons are classified according to their energy: fast neutrons possess energies in the range of ~200 keV−10 MeV, while slow (thermal) neutrons are lower in energy, in the range of ~0.003−0.4 eV. As discussed in subsection 10.4 of the chapter entitled "Neutron Radiation," collisions of fast neutrons with nuclei can result in scattering of the neutrons, yielding recoil nuclei, whereby part of the kinetic energy of the neutrons is transferred to the nuclei with which they collide. A fast neutron loses more energy when colliding with a nucleus of similar mass, ie, the proton nucleus (^1H), similar to the collision of two billiard balls. One billiard ball can transfer almost all its energy to another billiard ball. Less energy is lost by collision of a fast neutron with a nucleus of higher mass, for example ^{28}Si, somewhat like the collision of a billiard ball with a bowling ball.

To measure soil moisture, the scientist makes use of a soil moisture neutron gauge (SMNG), which consists of a source of fast neutrons and a detector of slow neutrons within a compact cylinder that can be inserted into a narrow well in the soil. The scientist lowers the SMNG into the well, as shown in Fig. 1.24, and in so doing the fast neutrons that are emitted will collide with the various nuclei of the soil matter as well as with nuclei of soil water molecules. A sphere or cloud of slow (thermal) neutrons is created around the source of fast neutrons through numerous collisions of the fast neutrons with the nuclei of water molecules and nuclei of other elements in the soil, as illustrated in Fig. 1.24. Because water molecules are high in protons relative to soil mineral matter, the rate of attenuation of the fast neutrons to slow neutrons will be a function of the moisture content in the soil. The slow neutrons are counted with a gas ionization detector, which is located next to the source of fast neutrons. The rate of production of slow (thermal) neutrons is calibrated with soil moisture content. In this fashion, irrigation can be programmed when needed to maximize crop yields with the most efficient use of fertilizer while conserving water resources.

Numerous articles and books are available on nuclear techniques like the SMNG and other methods used to optimize crop nutrient and water use efficiency, including a review book edited by L'Annunziata and Legg (1984a), more recent books published as proceedings of international symposia (IAEA, 2000a, 2002, 2005e, 2008), and a review article by Susha Lekshmi et al. (2014).

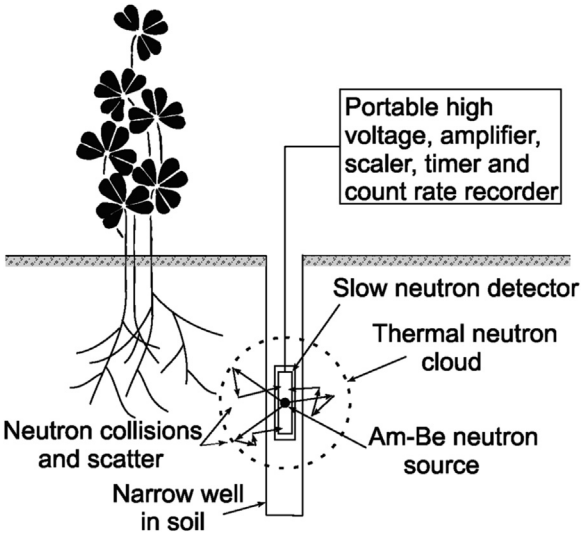

FIGURE 1.24 Schematic illustration of an SMNG. *Adapted from Nielsen, D.R., Cassel, D.K., 1984. Soil water management, pp. 35–65. In: L'Annunziata, M.F., Legg, J.O. (Eds.), Isotopes and Radiation in Agricultural Sciences. In: Soil-Plant-Water Relationships, vol. 1. Academic Press, London, p. 292, with permission from Elsevier © 1984.*

1.3.2.c Cosmic Ray Soil Moisture Observing System

The SMNG described above can measure soil moisture content only over small areas of a field, specifically the areas surrounding the narrow well where the SMNG is inserted manually into the soil. A relatively new development in the measurement of soil moisture and water resources that can cover vast areas of agricultural land without the need to insert probes into the soil involves the use of cosmic ray neutrons (Zreda et al., 2008). As described in the chapter entitled "Cosmic Radiation," particles of cosmic radiation (primary particles) collide at the top of the atmosphere with nuclei of atoms of our atmosphere, thereby smashing the atoms and creating a cascade of secondary nuclear collisions; this results in the production of numerous nucleons and subatomic particles, including numerous fast (high-energy) neutrons, as illustrated in Fig. 1.25. This cascade of nucleons and atomic particles is referred to as a cosmic ray shower. Many high-energy nucleons, including fast neutrons of the cosmic ray showers, enter the surface of the Earth and undergo numerous collisions with nuclei of soil minerals, organic matter, and soil moisture. As described in the chapter entitled "Neutron Radiation," fast neutrons lose more energy when they collide with a nucleon of similar mass, such as the proton. Thus collisions of fast neutrons with protons of soil moisture are the main process by which the fast (high-energy) neutrons lose their energy to become thermal (low-energy) neutrons. The thermalized neutrons diffuse into the air above the soil surface to reduce the number (ie, intensity) of fast neutrons, which are detected by a neutron detector mounted on the soil surface. The fast neutron intensity above the soil surface is inversely proportional to soil moisture (Zreda et al., 2008), which is the concept used to measure soil moisture by fast neutron detection.

The method shown in Fig. 1.25 has been established as a network of stationary neutron probes named the Cosmic Ray Soil Moisture Observing System (COSMOS), designed for long-term soil moisture monitoring (Zreda et al., 2012). As described by Dong et al. (2014), a stationary COSMOS probe (white box in center of the field in Fig. 1.25) contains two detectors, one sensitive to fast neutrons and the other to slow or thermal neutrons (Desilets et al., 2010; Zreda et al., 2012). The neutron detectors which constitute a COSMOS probe are mounted on a pole 1 m above the soil surface. The horizontal footprint of a COSMOS probe is reported to be a circle with a diameter of ~600 m at sea level (Desilets and Zreda, 2013), as illustrated in Fig. 1.25. This diameter of the circular footprint is only approximate, because it decreases with increasing atmospheric pressure and water vapor (Zreda et al., 2012; Desilets and Zreda, 2013; Rosolem et al., 2013), as collisions of fast neutrons with protons of water vapor in the atmosphere will attenuate or reduce the intensity of fast neutrons to some degree. The effective soil depth of measurement of a COSMOS probe varies according to soil moisture content from ~76 cm for a completely dry soil with no organic matter present

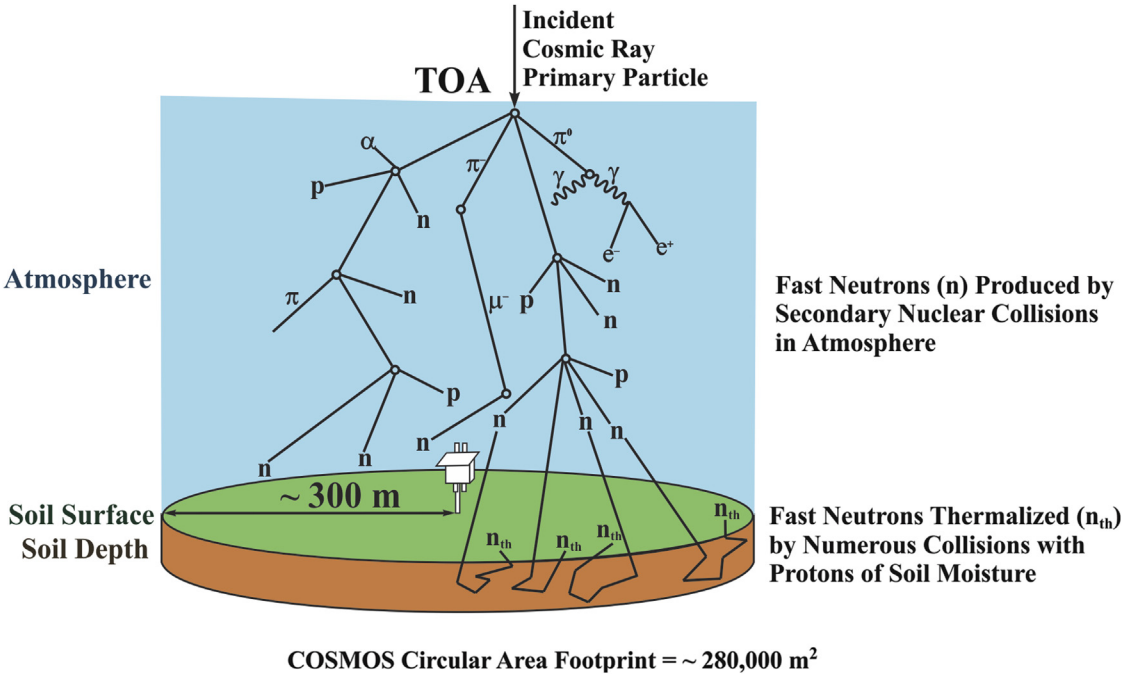

FIGURE 1.25 Principles of the Cosmic Ray Soil Moisture Observing System (COSMOS). Incident cosmic ray primary particles collide with nuclei at the top of the atmosphere (TOA) and create a cascade of secondary collisions, resulting in a shower of nucleon and subatomic particles, including fast (high-energy) neutrons. Nucleons and fast neutrons of the showers of cosmic radiation enter the soil to undergo further collisions therein. The fast neutrons (n) lose energy mainly through collisions with protons of soil moisture to become thermal (low-energy) neutrons (n_{th}), which diffuse from the soil back into the air above the soil surface. Neutron detectors are mounted on a pole 1 m above the soil surface located in the center of the field (white box), and measure a reduction in the intensity of fast neutrons above the soil surface proportional to the level of moisture in the soil. *Adapted from National Center for Atmospheric Research, Computational & Information Systems Laboratory Annual Report 2012, http://www.nar.ucar.edu/2012/lar/cisl/data-assimilation-research.html.*

(ie, no protons) to ~ 12 cm for a saturated soil (Zreda et al., 2008). The COSMOS probe effectively measures the water content of soils at the normal root depth of crops over a very large area. As noted in the *Nuclear Technology Review* (IAEA, 2012), the COSMOS probe is robust, can be easily installed in the field, and can measure soil moisture data over an area 1000 times as large as a conventional soil moisture neutron probe. Compared to all other methods, this new technique saves time and labor, and is most economic for measurements of soil moisture over large areas of irrigation. A review of the state of the art of large-scale soil moisture monitoring is provided by Ochsner et al. (2013).

1.3.2.d Isotopic Water Signatures

Water molecules contain atoms of hydrogen and oxygen (H_2O), which consist mostly of the stable isotopes ^{1}H with a natural abundance of 99.985% and ^{16}O with a natural abundance of 99.76%. Other naturally occurring stable isotopes of hydrogen and oxygen are deuterium or ^{2}H with a natural abundance of 0.015% and ^{17}O and ^{18}O with natural abundances of 0.04% and 0.20%, respectively. Van den Akker et al. (2011a,b) recently demonstrated that alterations in the isotopic content or signatures of water, namely the heavy isotopes of deuterium and ^{18}O, can be used to measure the loss of water from crop lands. This new approach is based on the principle that during evaporative or transpirative water loss, the lighter isotopes of water (^{1}H and ^{16}O) will volatilize or evaporate more readily than the heavier isotopes (^{2}H and ^{18}O), thereby leaving behind an enrichment of the heavier isotopes according to the degree of water loss by evaporation or transpiration. When water losses from the crop fields occur by evaporation or transpiration, there is a concentrating effect that can result in increased salinity and reduced water quality, which can be detrimental to plant growth. Van den Akker et al. (2011a,b) demonstrate that combining chloride analysis together with the isotopic analysis of ^{2}H and ^{18}O can be useful in suggesting which management strategies are most effective in improving water use efficiency and water quality.

1.3.3 Animal Health and Production

The IAEA *Nuclear Technology Review* (2004c, 2005b, 2006) outlines the scope of applications of nuclear techniques in scientific research around the world directed to the improvement of animal productivity and health. Among these applications is the traditional radioimmunoassay (RIA), which is an analytical method capable of measuring very low concentrations (femtomolar or 10^{-15} M) of hormones and other antigens in living systems (eg, blood or plasma) utilizing antigens labeled with a radioactive isotope. The RIA technique was discovered by Rosalyn Yalow (1921–2011) and Solomon Berson (1918–1972), and demonstrated to the scientific community in 1959. Rosalyn Yalow was awarded the Nobel Prize in Physiology and Medicine in 1977 for, in the words of the Nobel Committee, "the development of radioimmunoassay of peptide hormones." She is honored by a postage stamp issued by Sierra Leone. Yalow and Berson (1959) demonstrated that the binding of a radioisotope-labeled antigen, such as insulin, to a fixed concentration of antibody is a quantitative function of the amount of insulin present. This formed the basis for the quantitative analysis of insulin in human plasma. RIA was described by Yalow in her Nobel Lecture (Yalow, 1977) given on December 8, 1977:

Rosalyn Yalow (1921–2011)

Radioimmunoassay (RIA) is simple in principle…The concentration of the unknown unlabeled [non-radioactive] antigen is obtained by comparing its inhibitory effect on the binding of radioactively labeled antigen to specific antibody with the inhibitory effect of known standards.

The method is very sensitive. In his presentation speech for the Nobel Prize, Professor Rolf Luft stated:

Rosalyn Yalow's name is forever associated with her methodology of measuring the presence of hormones in the blood at concentrations as low as one thousand billionths of a gram per milliliter of blood.

Yalow and Berson's first report on the discovery of RIA was concerned with the analysis of insulin (Yalow and Berson, 1959). In the Mayo Clinic Proceedings, Kyle and Shampo (2002) noted the following concerning the discovery:

Yalow's report was initially rejected by a journal editor, who did not believe that insulin could produce antibodies. The radioimmunoassay technique proved to be so sensitive that a Swedish scientist likened its power to detecting half a lump of sugar in a lake 62 miles square and 30 feet deep.

The RIA technique involves the competing reactions illustrated in Fig. 1.26. The competing reactions result from mixing a known quantity of radioactive antigen (Ag*), referred to as a labeled antigen in Fig. 1.26, such as a hormone labeled with the radioisotope ^{125}I, with a known quantity of its antibody (Ab). This results in the formation of a specific amount of the radioactive antigen attached to the antibody as a radioactive antigen–antibody complex (Ag*Ab). It is important that the amount of antibody (Ab) added as a reagent is limited in quantity with respect to the amount of antigen (Ag) to be analyzed in the sample. If one then adds a small amount of sample (eg, blood or plasma) that contains the antigen (Ag) to be analyzed, this newly added antigen will also become attached to the antibodies (Ab), resulting in a competitive removal of a certain amount of the radioactive antigen (Ag*) from the Ag*Ab complex. The amount of radioactive antigen removed from its antibodies, measured by a radioactive detector, is a function of the amount of antigen present in the sample under analysis. Following the preparation of a calibration curve with known amounts of antigen standard, the amount of reduction in radioactivity of the Ag*Ab complex can be correlated to an exact amount of antigen in the sample.

The competitive reaction shown in Fig. 1.26 is illustrated in terms of the preparation of a standard calibration curve, shown underlying Fig. 1.27, used by Feher (2012) to describe the RIA technique in general principles of endocrinology. The same procedure is used for the measurement of various hormones and other types of antigens in studies of animal health and production. As illustrated in Fig. 1.27, the preparation of a calibration curve involves several steps. *Step 1*: a limited amount of antibodies (less than the amount of antigen to be added) is incubated in a series of tubes (~10–15 tubes, but only one tube is illustrated in the figure), a constant amount of radioactively labeled hormone (antigen, eg, ^{125}I-labeled antigen) is added to each tube, and various known amounts of unlabeled hormone standard are added to each tube. *Step 2*: the tubes are allowed to incubate, so the radioisotope-labeled hormone (Ag*) and the unlabeled hormone (Ag) compete for binding sites on the antibodies (Ab). Adding a greater amount of unlabeled hormone results in a reduced amount of radioisotope-labeled hormone bound to antibody. *Steps 3 and 4*: the hormone–antibody complex is precipitated and the supernatant containing free (unbound) hormone (both radioactive, Ag*, and unlabeled unbound hormone, Ag) is removed after centrifugation. *Step 5*: the bound radioactivity at the bottom of the tubes (Ag*Ab) is measured with a radiation counter. The series of 10–15 tubes to which were added increasing amounts of standard unlabeled hormone (antigen) will register diminishing radioactivity in the bound fraction of hormone–antibody complex at the bottom of each tube. A plot of radioactivity measured/radioactivity added (ie, bound radioactivity/total radioactivity), illustrated in Fig. 1.27 as bound ^{125}I/total ^{125}I, versus the amount of standard unlabeled hormone added to each tube provides a standard calibration curve against which samples containing unknown amounts of hormone can be determined. When a sample containing an unknown amount of hormone (eg, from blood or plasma) must be analyzed, the procedure described above and illustrated in Fig. 1.27 is followed, but only one tube is needed (or a few tubes for replicate analysis); and in Step 1 the sample containing the unknown amount of hormone is added in lieu of a standard. The ratio of bound radioactivity measured/total radioactivity added found in Step 5 is then used to obtain from the standard curve the amount of unlabeled hormone in the

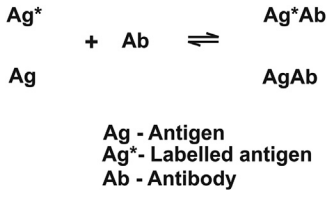

FIGURE 1.26 The principle of the RIA technique. *From Sharma et al. (2014), reprinted with permission from Elsevier © 2014.*

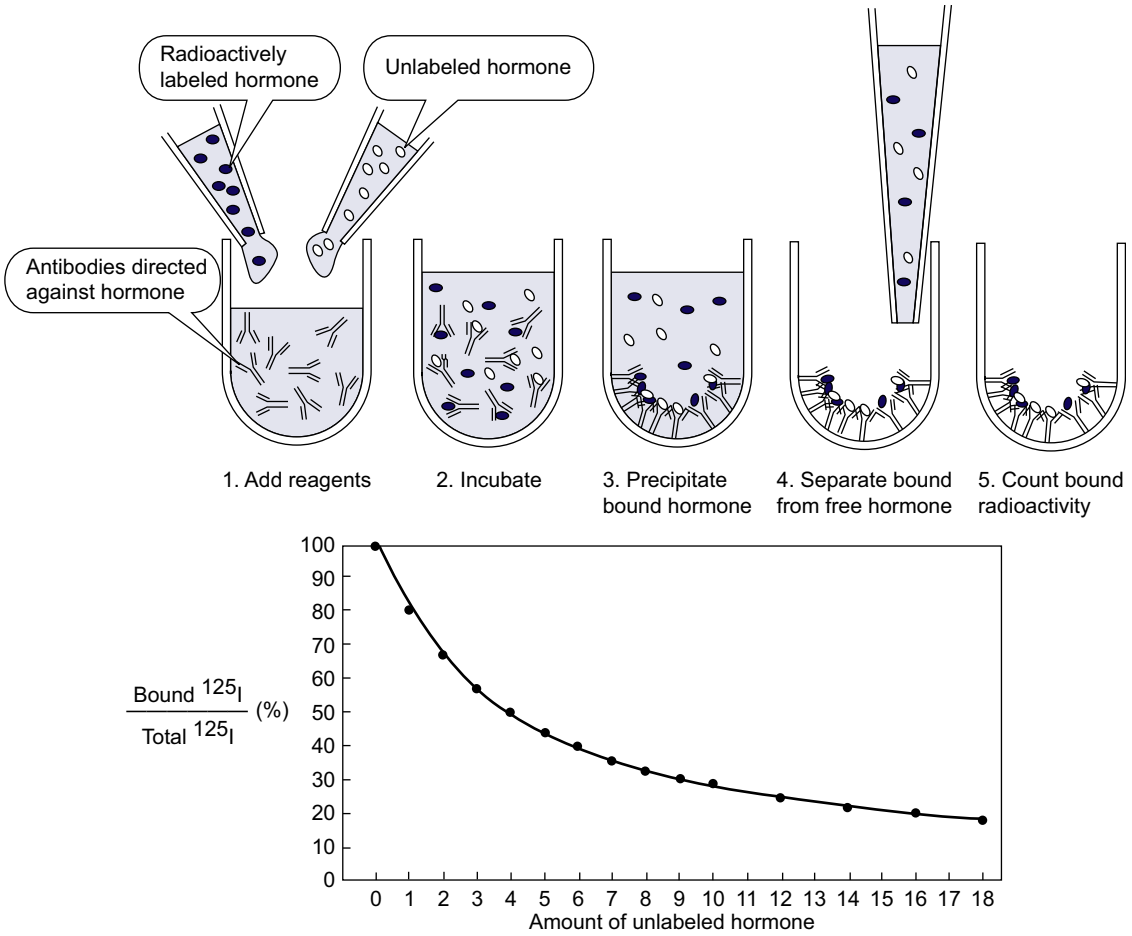

FIGURE 1.27 Basic principles of RIA. Antibodies against the hormone are incubated in a series of tubes containing a constant amount of radioactively labeled hormone and various amounts of standard unlabeled hormone, or samples containing unknown amounts of hormone. The labeled and unlabeled hormones compete for binding sites on the antibodies. When more unlabeled hormone is present, less radioactivity binds to the antibody. After equilibration, the antibody–hormone complex is precipitated and collected into a pellet by centrifugation. The free unlabeled and radioactive hormone is removed and the bound radioactivity is measured using a radiation counter. Plots of the percentage of radioactivity bound against unlabeled hormone concentration are highly nonlinear. The amount of hormone in the unknowns is determined by interpolation. *From Feher, J.J., 2012. Quantitative Human Physiology, An Introduction. Elsevier, p. 904, reprinted with permission from Elsevier © 2012.*

unknown sample. The method is very sensitive, and very weak solutions in the femtomolar (fmol) or nanomolar (nmol) concentrations of antigen can be measured.

The radioactivity of antigen–antibody complex is measured in modern scintillation analyzers. The techniques for measuring radioactivity in bound antigen–antibody complexes, including related scintillation proximity assays and receptor binding assays, are described in detail by the writer (L'Annunziata, 2012c).

The IAEA *Nuclear Technology Review* (2004c, 2006, 2008) points out that RIA, which employs radioisotopes in the measurement of a given molecule in a biological system, remains an important technology in the field of animal reproduction and breeding. Also, the *Nuclear Technology Review* (IAEA, 2013a) underscores that nuclear and nuclear-related techniques are used either as tracers (eg, isotopic labeling of nutritive components to trace their metabolic pathways) or as laboratory methods (eg, RIA and molecular-based genetic analysis) for measuring targeted parameters in studies of animal health and production. The radioisotope ^{125}I is commonly employed in RIA to determine the concentrations of hormones and metabolites in the blood or milk of farm animals. For example, RIA of the reproductive hormone progesterone is reported to be an indispensable tool that provides information needed by farmers for breeding management programs, and it can help monitor the utility of the artificial breeding services provided to farmers by government, cooperative, or private organizations. RIA is also reported to be a very simple and robust technique for the analysis of harmful residues (antigens) in food of animal origin, such as products resulting from the misuse of veterinary drugs. Numerous advances continue to be made in animal health and production and human health using RIA techniques, which is evidenced by the numerous scientific papers currently appearing in journals such as *General and Comparative Endocrinology*, *Animal Production Science*, *Domestic Animal Endocrinology*, *Journal of Immunological Methods*, *European Journal of Pharmacology*, *Clinical Biochemistry*, *and Analytical Biochemistry*, among others.

For additional information on the RIA technique the reader may peruse papers by Cole (2010), Feher (2012), and Sharma et al. (2014) and books by Chard (1995), Patrono et al. (2011), Heding (2012), and L'Annunziata (2012c).

The *Nuclear Technology Review* (IAEA, 2010, 2012) points to methodologies where radioactive tracers are applied to studies of animal health and production. Among these are molecular diagnostics, which increase the sensitivity of testing and detecting animal diseases, and technologies such as $^{35}S/^{32}P$ dual radioisotope phosphor-imaging gene sequencing and the incorporation of radioactive ^{32}P, ^{33}P, or ^{35}S into short DNA synthetic probes to permit the identification of genes that influence animal traits of interest and parentage. Such testing can help determine which animals carry superior forms of genes of interest to improve accuracy of selection and increase animal productivity. The *Nuclear Technology Review* (IAEA, 2010) highlights "isotope-based nucleic acid hybridization approaches used to detect genetic material in host tissues that will allow direct identification of infected animals as well as provide information of epidemiological importance in relation to the strain type or variant of the agent. These tests make use of suitable DNA probes labeled with radioactive ^{35}S or ^{32}P and their amplification in vitro by a nucleic acid polymerase chain reaction to increase the amount of the specific target." Upham and Englert (2003) and Barthe et al. (2012) provide detailed information on some of the analytical techniques used in this field.

Stable isotopes are also useful tools in studies to improve animal production and health. As highlighted in the *Nuclear Technology Review* (IAEA, 2007, 2008) and journal articles (Norman et al., 2009; Monahan et al., 2012; Stefański et al., 2013; Devincenzi et al., 2014), the stable isotopes of carbon and nitrogen, namely ^{13}C and ^{15}N, are used to label animal feed or specific compounds administered to the rumen of ruminant animals to measure nutrient uptake or study the metabolism of important feed components such as amino acids, protein, carbohydrates, and vitamins. Another stable isotope of hydrogen, namely deuterium (^{2}H), is used in the form of heavy water (D_2O) in isotope dilution analysis to measure animal lean body mass, fat content, body composition, total body water, and milk intake by calves (IAEA, 2008; Argo et al., 2012; Dugdale et al., 2011, 2012; Munn et al., 2012; Pichler et al., 2013).

Birds and wild animals can play a key role as vectors of animal disease. Migratory birds, for example, can play a role as carriers in the spread of avian flu from infected to uninfected areas. Stable isotope profiles of ^{13}C, ^{15}N, and ^{2}H are used to study animal movement, including the origin and breeding habits of migratory birds (Hobson, 2007, 2008; Mizota, 2009; Marra et al., 2010; Liedvogel et al., 2011), which may be used to assess risk of the spread of diseases such as avian influenza (IAEA, 2009; Bridge et al., 2014).

1.3.4 Plant Breeding

Plant breeding is the science of the manipulation of plant species through pollination, genetic engineering, and selection of progeny for the purpose of creating new and improved plant genotypes and phenotypes with desirable characteristics, such as disease or insect pest resistance, salt or draught tolerance, crop quality, increased yields, etc. Mutations induced in plants with the aid of gamma rays, X-rays, fast neutrons, and heavy ions or by means of chemical mutagens aid the plant breeder by increasing germplasm variability.

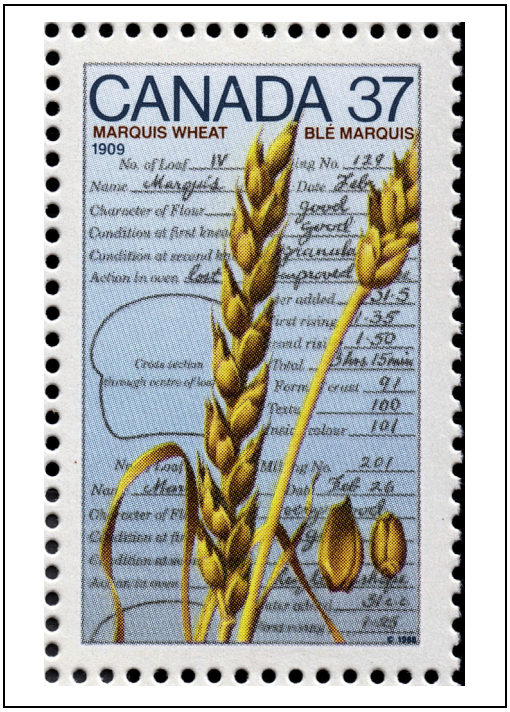

The significant role that plant breeding can have in the improvement of crop quality and yield was highlighted by a postage stamp issued in Canada in 1988. The stamp commemorates the national breeding program that generated the Marquis wheat in 1909. The new variety obtained through plant breeding provided better baking quality, higher yields, earlier maturity, and shorter straw then other wheat varieties (Morrison, 1960; Fedak, 2002).

Norman E. Borlaug (1914–2009)

The impact of plant breeding in alleviating starvation in the world by the creation of new crop varieties with improved quality and yields was recognized through the work of geneticist Norman Borlaug (1914−2009), who was awarded the Nobel Peace Prize in 1970 for his "green revolution," born from the impressive results he achieved in wheat improvement through plant breeding and the organized exploitation of the results of this improvement for agriculture, particularly in the developing world. Borlaug's work drew the attention of the world to the importance of plant breeding. Aase Lionaes (1970), chair of the Nobel Committee, underscored the significance of Norman Borlaug's work at the presentation of the Nobel Prize on December 19, 1970:

> *Dr. Borlaug went to the International Maize and Wheat Improvement Center in 1944…Ever since that day, twenty five years ago, when Dr. Borlaug started his work on the improvement of grain, and right up to the present, he has devoted all his energy to achieving the historical result which today is referred to as the "green revolution". This revolution will make it possible to improve the living conditions of hundreds of millions of people in that part of the globe which today might be called as the "non-affluent world."…*
>
> *The purpose of this research, Dr. Borlaug continues, was to endeavor to develop a variety of wheat with greater yields, with a great degree of resistance to diseases, and with qualities that rendered it suitable for use in connection with improved agronomic methods,…*
>
> *The most important event…was the development of the so-called "dwarf varieties". After years of research on the part of Dr. Borlaug and his collaborators to develop, by crossing and selection, the so-called Japanese breed of wheat, they evolved the new world-famous "dwarf variety". These are breeds of wheat which, unlike previously known long-bladed varieties, have short blades…The new dwarf varieties…provide an increase of yield per decare from the previous maximum of 450 kilos to as much as 800 kilos per decare. These varieties can be used in various parts of the world because they are not affected by varying lengths of daylight. They are better than all other kinds in both fertilized and non-fertilized soil, and with and without artificial irrigation. In addition they are highly resistant to the worst enemy of wheat, rust fungus or oromyces. Thanks to these high-yield breeds of wheat, Mexico was self-supporting in this grain in 1956, and in recent years this country has exported several hundred thousand tons annually…*
>
> *Once the seed corn had been introduced [into Pakistan] and had yielded superb results in the form of increased crops, the triumphal march of the green revolution was ushered in. Pakistan's present-day wheat production amounts to several million tons, and the country is self-supporting in wheat…*

The highest results [of wheat production] in the history of India was achieved in 1968 [after the introduction of Borlaug's new wheat] with a crop of seventeen million tons…After the successful results achieved in Mexico, India, and Pakistan, the new varieties of wheat were introduced into certain parts of Turkey, Afghanistan, [Islamic Republic of] Iran, Iraq, Tunisia, Morocco, and Lebanon…The new variety of wheat will be able to affect a total transformation of the economic picture in the developing countries.

The induction of mutation in plants by nuclear radiation has proven to be a useful tool for plant breeders in crop improvement. Mutation induction for increasing germplasm variability is carried out with gamma rays, X-rays, fast neutrons, heavy ion beams, and cosmic radiation, in addition to chemical mutagens. Among the methods used to induce mutations, the IAEA *Nuclear Technology Review* reports that "the majority (88%) of mutant varieties are developed through irradiation (eg, fast neutrons, X-rays, and more than 64% through gamma irradiation)." Chemical mutagens as a tool account for 10% of mutation induction in plants, and the remaining 2% are derived from other nuclear techniques (IAEA, 2009), which may include the radioisotope labeling of nucleic acids used as probes for genetic fingerprinting, mapping and marker-assisted selection, and mutagenesis for the analysis of gene function, as reported in the IAEA *Nuclear Technology Review* (IAEA, 2006).

One of the most recently developed techniques for the induction of mutations in plants is the use of accelerator-produced heavy ion beams consisting of nitrogen ions $\left({}^{14}N^{7+}\right)$ or carbon ions $\left({}^{12}C^{6+}\right)$, reported by numerous researchers including Zhou et al. (2006), Krasaechai et al. (2009), Wu et al. (2009), Phanchaisri et al. (2012), Murai et al. (2013), and Shi et al. (2014). Plant seeds are exposed to the heavy ion beams produced by laboratory cyclotrons; and the optimum radiation dose, which will produce maximum mutation without delivering damaging or lethal effects, is determined through experimentation. An example of the experimental method used to find the optimal radiation dose can be taken from the work of Murai et al. (2013), illustrated in Fig. 1.28.

In this example Murai et al. (2013) irradiated dry seeds, packed as a monolayer in a plastic bag, with a range of doses of 20, 30, 40, 50, or 60 Gy (gray) of $^{12}C^{6+}$ ions, which may impart a linear energy transfer (LET) to seeds at a rate of 30−50 keV/μm. The monolayer of seeds ensures a uniform dose of radiation to all seeds. The gray, abbreviated Gy, is a measure of absorbed dose in units of energy absorbed per mass of absorber, and is defined in detail in the chapter entitled "Cosmic Radiation." The term LET is the amount of energy deposited by ionizing radiation per length of travel of the radiation within an absorbing medium (eg, seeds). LET is discussed in detail in the chapter entitled "Beta Radiation and

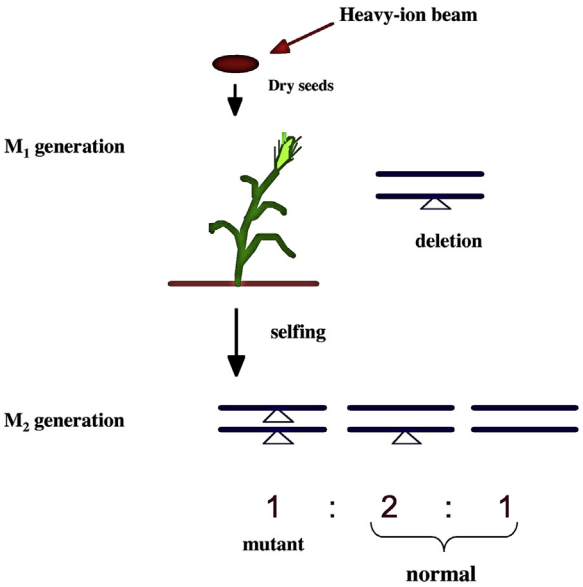

FIGURE 1.28 Screening strategy for identifying mutants induced by ion beam mutagenesis. Dry seeds are irradiated with ion beam and sown in the field. In the M_1 generation, an induced deletion is hemizygous: one allele is normal and the other has been deleted. M_2 seeds are obtained by selfing M_1 plants. Ten individual plants per M_2 line are examined in the following year. In the M_2 generation, mutant plants homozygous for the deletion are expected in the Mendelian ratio of 1 (mutant):3 (wild type). *From Murai, K., et al., 2013. A large-scale mutant panel in wheat developed using heavy-ion beam mutagenesis and its application to genetic research. Nucl. Instrum. Methods Phys. Res. Sect. B 314, 59−62, printed with permission from Elsevier © 2013.*

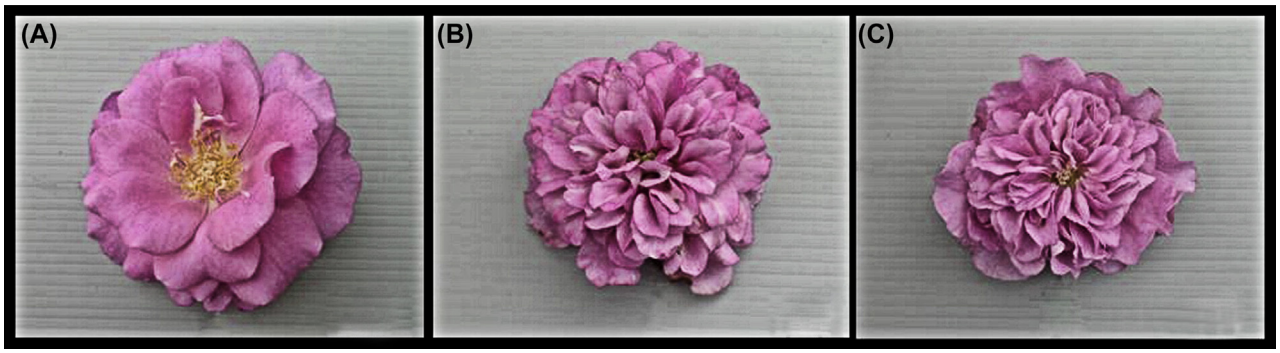

FIGURE 1.29 Mutants of rose variety Shocking Blue induced by ion beam. (A) Control. (B) Bombarded with a fluence of 1×10^{16} ions/cm^2 at 80 keV. (C) Bombarded with a fluence of 1×10^{16} ions/cm^2 at 100 keV. *From Krasaechai, A., et al., 2009. Low-energy ion beam modification of horticultural plants for induction of mutation. Surf. Coat. Technol. 203, 2525–2530, reprinted with permission from Elsevier © 2009.*

FIGURE 1.30 Inflorescence of Kentucky bluegrass. Right: Normal "Nassau." Left: PM2, a dwarf mutation of "Nassau" Kentucky bluegrass induced by exposing seeds to space radiation. *From Han, L., et al., 2011. A male- and female-sterile mutant of Kentucky bluegrass (*Poa pratensis *L.) induced by space radiation. Sci. Hortic. 131, 67–73, reprinted with permission from Elsevier © 2011.*

Beta Decay." As described by Murai et al. (2013) and illustrated in Fig. 1.28, the irradiated seeds, known as the M_1 generation, are sown in an experimental field. The germination rate of seeds in the M_1 generation is recorded according to the radiation dose administered. Following plant growth, the spikes of the M_1 plants are bagged and the seeds are harvested from each spike and sown in the field to produce the M_2 generation. The M_2 generation is screened for mutation by determining the frequency of albino plants as a function of radiation dose administered to the seeds. An example of mutation in a rose flower induced by two beam intensities of $^{14}N^{7+}$ ions is illustrated in Fig. 1.29. DNA fingerprinting is used to confirm mutations by comparing the DNA profiles of lines derived from control and irradiated seed (Krasaechai et al., 2009; Wu et al., 2009; Shi et al., 2014).

A relatively new approach to mutation plant breeding is the induction of mutation in outer space, whereby the genetic material in plant seeds is exposed to an altogether different environment to that on Earth. Plant seeds are launched into space on recoverable satellites, and in orbit they are exposed to the combined effects of a high vacuum, cosmic ray irradiation, very low gravity, and a weak magnetic field. Plant seeds which are not sent into space serve as controls. The control seeds are even reported to be taken to the launch pad along with the seeds that are sent into space, although not launched (Wu et al., 2010), which ensures that the control seeds are submitted to the same environment on Earth as the seeds sent into space. After seeds are launched into space and recovered on Earth, they are planted together with the control seeds. Mutation identification and seed selection follows for seed yielding improved varieties. An example of an improved variety of bluegrass following mutation in space is illustrated in Fig. 1.30.

The joint FAO/IAEA Division in Vienna, Austria carries out extensive coordinated research programs with member states utilizing nuclear and conventional techniques in mutation plant breeding. The induced mutations created by radiation and chemicals have led to major advances in plant breeding for crop improvement. The beneficial mutants have been selected and used by plant breeders for over 50 years. The *Nuclear Technology Review* (IAEA, 2010) reports that, to date, approximately 3100 officially registered mutant varieties of more than 170 different plant species worldwide are listed in the FAO/IAEA Mutant Variety and Genetic Stock Database (http://mvgs.iaea.org). Examples cited in the *Nuclear Technology Review* (IAEA, 2013a) are mutation breeding to develop new varieties that can provide greater yields and productivity in harsh and variable climates, such as hardy barley mutant varieties which survive and give improved yields under the harsh climate conditions at 5000 m above sea level in Peru. These new varieties have improved the prosperity and health of 7 million Andean people. Also cited are new salt-tolerant rice mutant varieties that can withstand and give improved yields in saline soils, expanding the arable land in Bangladesh.

The *Nuclear Technology Review* (IAEA, 2005b) reports that mutation induction coupled to selection remains the most "clean" and inexpensive way to create varieties by changing single characteristics without touching the general phenotype. Major successes are reported for mutagenesis-enhanced breeding in the USA (rice, barley, sunflower, grapefruit, peppermint), Pakistan (cotton), India (blackgram), Australia and Canada (linseed), Japan (pear), and China and Australia (rice). Mutant varieties of oil seeds and pulses are released for commercial cultivation. Other changes created through induced mutation with nuclear radiation and chemicals are disease and pest resistance and crop nutritional and processing quality. An increasing number of private enterprises is involved in research in mutation-induction breeding for ornamental flowers as well as industrial and food crops.

1.4 WATER RESOURCES

Water, like the air we breathe, is a valuable and vital resource. It is in great demand for domestic use, agricultural irrigation, and industrial productivity. Many people in many nations do not have adequate water supplies, and scientific research into maintaining and improving the supply and quality of our water is vital to human development and the conservation of the environment. The proper management of our water resources, including groundwater, is vital to meeting current and future water needs throughout the world. Nuclear techniques, namely the use of isotopes, help us manage our water resources. This is underscored in the *Nuclear Technology Review* (IAEA, 2011):

> *It is estimated that more than 97% of the Earth's available fresh water is located underground, yet this vital resource is often poorly understood and poorly managed. Stable and radioactive isotope techniques are cost-effective tools in hydrological investigations and assessments, and are critical in supporting effective water management. Isotopes are commonly employed to investigate:*
>
> - *Sources and mechanisms of groundwater recharge;*
> - *Groundwater age and dynamics;*
> - *Interconnections between aquifers;*
> - *Interaction between surface water and groundwater;*
> - *Groundwater salinization;*
> - *Groundwater pollution.*

By tracing changes in the isotopic composition of water resources, isotope hydrologists can obtain valuable data on hydrological dynamics that could otherwise be impossible or immensely difficult to obtain. Isotopes are used to measure the processes of the hydrologic cycle in catchments, illustrated in Fig. 1.31, including the groundwater origins, the dating and renewal rate of groundwater, sources of pollution or contaminant intrusions into groundwater, etc.

Many of the isotopes used by hydrologists to study the hydrolytic cycle are natural isotopes of the elements H, O, C, N, S, and the noble gases of the elements Ar, Ne, and Kr, among others. The isotopes of these elements serve as tracers with which hydrologists can measure water movement or cycling in the environment as a result of isotope exchange and movement in the hydrological cycle. The major elements and their isotopes used in studies of water resources and their role in the hydrological cycle are illustrated in Fig. 1.32.

Many chemical elements of the periodic table, including those noted in Fig. 1.32, are composed of more than one isotope. The specific isotopes of the chemical elements illustrated in Fig. 1.32, which serve as tracers in studies of our water resources, include the isotopes of hydrogen (^{1}H, ^{2}H, ^{3}H), oxygen (^{16}O, ^{18}O), carbon (^{12}C, ^{13}C and ^{14}C), nitrogen (^{14}N and ^{15}N), sulfur (^{32}S, ^{34}S), and the noble gases helium (^{3}He, ^{4}He), argon (^{39}Ar), and krypton (^{85}Kr). Among these isotopes, all are stable with the exception of ^{3}H, ^{14}C, ^{39}Ar, and ^{85}Kr, which are radioactive. The isotopes that make up a

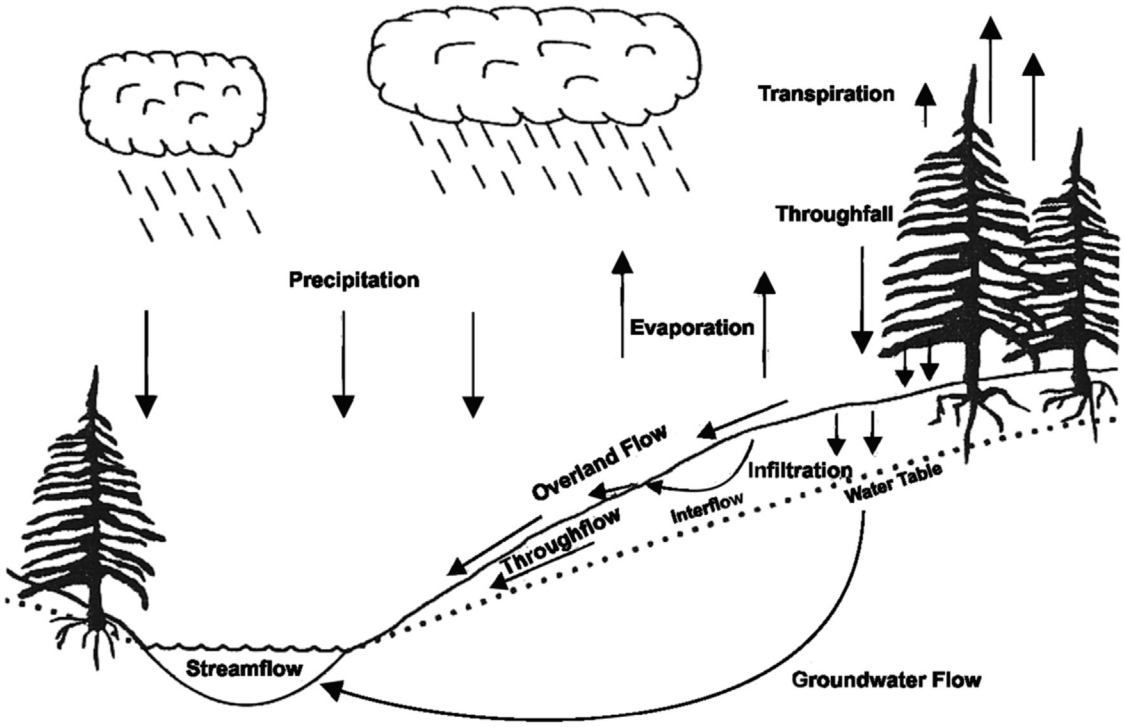

FIGURE 1.31 Catchment hydrologic processes composing a local hydrologic cycle. Each of these processes can be assessed by lithogenic and cosmogenic nuclides. *From Nimz, G.J., 1998. Lithogenic and cosmogenic tracers in catchment hydrology, pp. 247–289. In: Kendall, C., McDonnell, J.J. (Eds.), Isotope Tracers in Catchment Hydrology. Elsevier Science, Amsterdam, p. 839, reprinted with permission from Elsevier © 1998.*

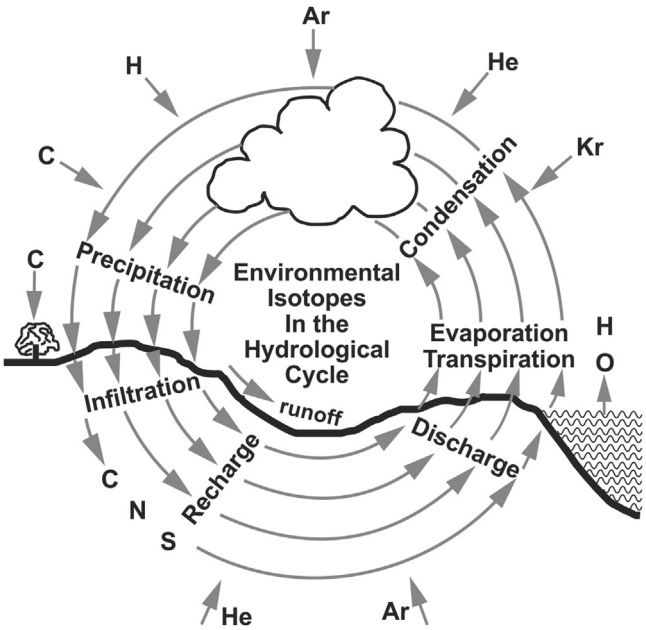

FIGURE 1.32 The hydrologic cycle and environmental isotopes. *From Trček, B., Zojer, H., 2010. Recharge of springs, pp. 88–127. In: Neven Kresic, Zoran Stevanovic (Eds.), Groundwater Hydrology of Springs. Elsevier, Amsterdam, p. 573, reprinted with permission from Elsevier © 2010.*

given chemical element on Earth have a certain natural abundance. For example, the natural abundances of the isotopes of some common elements, expressed as a percentage, are hydrogen (consisting of the isotopes ^{1}H, 99.9885%; ^{2}H, 0.0115%; ^{3}H, trace), carbon (^{12}C, 98.93%; ^{13}C, 1.07%; ^{14}C, trace), nitrogen (^{14}N, 99.636%; ^{15}N, 0.364%), and oxygen (^{16}O, 99.757%; ^{17}O, 0.038%; ^{18}O, 0.205%). If we take oxygen as an example, if we are able to collect a sample of 1 million atoms of the chemical element oxygen, we expect to find that the sample would contain on average 997,570 atoms of the

isotope ^{16}O, 380 atoms of ^{17}O, and 2050 atoms of ^{18}O. However, certain physical and chemical processes in nature, such as illustrated in Figs. 1.31 and 1.32 and including evaporation, condensation, precipitation, infiltration, recharge of groundwater, runoff, etc. can result in slight enrichments or depletions of the abundance of one isotope of a given element relative to another isotope of the same element.

Hydrologists analyze the relative amounts of two isotopes of a chemical element to observe slight deviations in their natural abundance that could identify a physical process that a given water resource has undergone. Because these naturally occurring deviations in isotope abundance are small, hydrologists express them in terms of parts per thousand (units ‰ or per mil) rather than as a percentage. As described by Kendall et al. (2014) and Trček and Zojer (2010), the stable isotopic compositions of substances, which will define deviations between two stable isotopes such as $^{18}O/^{16}O$, $^{13}C/^{12}C$, $^{15}N/^{14}N$, and $^{2}H/^{1}H$, are reported as delta (δ) values in parts per thousand or ‰, defined as

$$\delta\ (\text{in } ‰) = (R_{\text{sample}}/R_{\text{standard}} - 1) \times 1000 \qquad [1.7]$$

where R_{sample} is the ratio of the heavy isotope to light isotope of the element of interest in the sample, and R_{standard} is the ratio of heavy to light isotope of a corresponding international standard substance. A negative value of δ signifies a sample depleted in the heavy isotope relative to that of the standard, and a positive value of δ indicates that the sample is enriched in the heavy isotope relative to that of the standard. The value of delta in parts per thousand or per mil is expressed as that of the heavy isotope, such as $\delta^{18}O$, $\delta^{13}C$, $\delta^{15}N$, or $\delta^{2}H$. For example, the measurement of $\delta^{18}O$ of a substance is calculated according to Eq. [1.7] as

$$\delta^{18}O\ (\text{in } ‰) = \left(\frac{(^{18}O/^{16}O)_{\text{sample}}}{(^{18}O/^{16}O)_{\text{standard}}} - 1\right) \times 1000 \qquad [1.8]$$

Isotope ratios are often determined by mass spectrometry.

Hydrologists may take $\delta^{18}O$ measurements of water resources to see how these reveal the processes that water has undergone in the hydrologic cycle. For example, if we consider the physical process of evaporation of water molecules, we find that water molecules containing the lighter ^{16}O isotope (ie, $H_2{}^{16}O$) will evaporate more readily than molecules containing the heavier ^{18}O isotope (ie, $H_2{}^{18}O$), which results in a slight enrichment of the lighter ^{16}O isotope over the heavier ^{18}O isotope in water vapor. The reverse process of condensation yields the opposite result—that is, molecules of water containing the heavier isotope ^{18}O condense more readily than molecules containing the lighter ^{16}O isotope. Thus rain will contain a slight enrichment of the heavier ^{18}O isotope over the lighter ^{16}O. A similar isotope effect occurs with water molecules containing the lighter isotope of hydrogen (^{1}H) compared to molecules containing a heavier isotope of hydrogen (^{2}H). These isotope effects in water are monitored by hydrologists by measuring the $^{18}O/^{16}O$ and $^{2}H/^{1}H$ isotope ratios and calculating $\delta^{18}O$ and $\delta^{2}H$. Examples of $\delta^{18}O$ values for water vapor and rain are shown in Fig. 1.33, illustrating that the enrichment of the lighter isotope of oxygen (^{16}O) is greatest in water vapor due to the easier vaporization of water molecules containing the lighter isotope. In turn, rain droplets show a drop in negative $\delta^{18}O$ values due to the easier

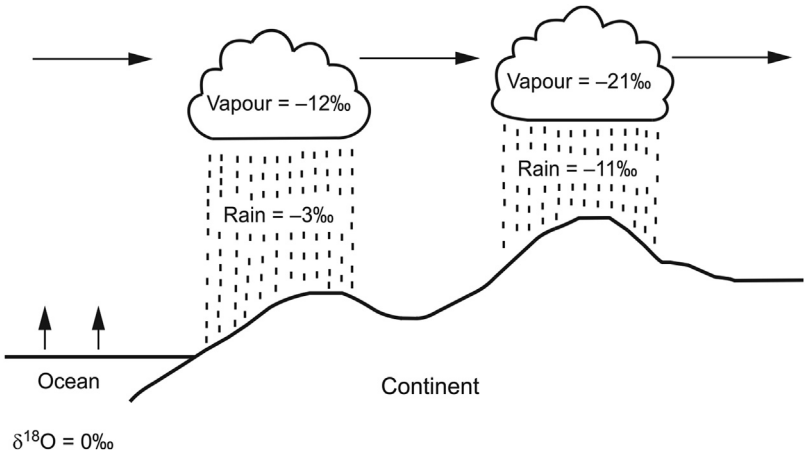

FIGURE 1.33 Origin of variations in the $\delta^{18}O$ of meteoric waters as moisture rains out of air masses moving across a continent. *From Kendall, C., et al., 2014. Environmental isotope applications in hydrologic studies. In: Heinrich Holland, Karl Turekianpp (Eds.), Treatise on Geochemistry, second ed. In: Surface and Groundwater, Weathering and Soils, vol. 7. Elsevier, Amsterdam, pp. 274–327, reprinted with permission from Elsevier © 2014.*

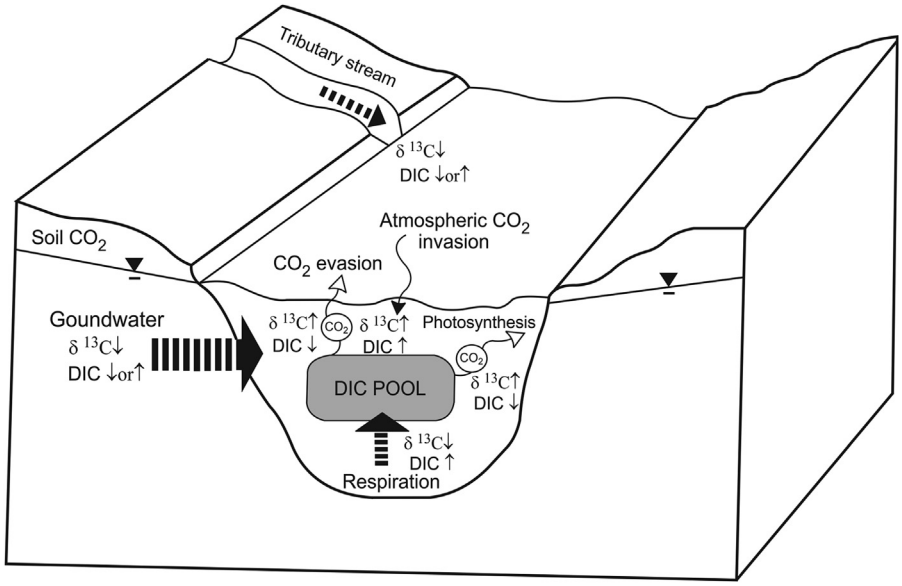

FIGURE 1.34 Schematic showing how various in-stream processes can affect the $\delta^{13}C$ of dissolved inorganic carbon (DIC). *From From Kendall, C., et al., 2014. Environmental isotope applications in hydrologic studies. In: Heinrich Holland, Karl Turekianpp (Eds.), Treatise on Geochemistry, second ed. In: Surface and Groundwater, Weathering and Soils, vol. 7. Elsevier, Amsterdam, pp. 274–327. Modified from Atekwana, E.A., Krishnamurthy, R.V., 1998. Seasonal variations of dissolved inorganic carbon and $\delta^{13}C$ of surface waters: application of a modified gas evolution technique. J. Hydrol. 205, 265–278, reprinted with permission from Elsevier © 2014.*

condensation of water molecules containing the heavier isotope (^{18}O). Also, as reported by Kendall et al. (2014), the $\delta^{18}O$ and $\delta^{2}H$ of rain precipitation are influenced by altitude and distance inland along different storm tracks, among other environmental conditions; and, as illustrated in Fig. 1.33, the rainout from clouds in successive rainstorms as clouds move across a continent will exhibit increasingly lower δ values.

Hydrologists can derive much information on the movement and mixing of water resources when the $\delta^{18}O$ or $\delta^{2}H$ values differ significantly between different bodies of water. For example, Trček and Zojer (2010) point out that the ^{18}O and ^{2}H composition of groundwater on average is equal generally to a weighted average of the precipitation ^{18}O and ^{2}H composition, whereas surface water is enriched more with the heavier isotopes than in precipitation, due to the evaporation process, which results in the easier evaporation of water molecules containing the lighter ^{16}O isotope.

Another illustrative example of isotope tracers in hydrologic studies involves measurement of the ratios of the stable isotopes of carbon, namely $^{13}C/^{12}C$, which yields values of $\delta^{13}C$ according to Eq. [1.7]. Kendall et al. (2014) underscore the utility of $\delta^{13}C$ measurements as indicators of reactions taking place within rivers along their courses of flow, as illustrated in Fig. 1.34. They point out that $\delta^{13}C$ signatures of dissolved inorganic carbon (DIC) in large rivers are the result of CO_2 exchange with the atmosphere, dissolution and precipitation of carbonate minerals, and photosynthesis and respiration within river bodies. As illustrated in Fig. 1.34, smaller tributaries exhibit lower $\delta^{13}C$ values of DIC, while further downstream in the main river, shifts in the $\delta^{13}C$ of DIC occur due to the photosynthetic assimilation of CO_2 and equilibrium with the atmosphere (Kendall et al., 2014).

Another isotopic technique involves the measurement of $^{36}Cl/Cl$, ie, the ratio of the isotope ^{36}Cl to the total chlorine in a sample, because the atmospheric input of ^{36}Cl to the chlorine content of water can be used as a groundwater tracer (Caffee et al., 1992; Nimz et al., 1993, 1997, and Nimz 1998). The atmospheric thermonuclear weapons tests during the 1950s and 1960s enriched the atmosphere with ^{36}Cl, which has a half-life of 3×10^5 years. Water older than 1950 (>50 years), which is water that has not mixed with water exposed to the atmosphere for over 50 years, is lower in ^{36}Cl radioactivity than younger water. Thus the $^{36}Cl/Cl$ ratios can be used to discriminate between older and younger water that may be recharged in a catchment. This isotope is particularly applicable to the dating of groundwaters that range between 500,000 and 1 million years of age (Trček and Zojer, 2010).

The $^{36}Cl/Cl$ ratios of rainwater and groundwater have been used to determine the amount of water lost from catchments as a result of evapotranspiration (Nimz, 1998; Paul et al., 1986; Magaritz et al., 1990). Rainwater increases in solute, including chloride ion, concentration as it enters the soil profile, due to a combination of evapotranspiration and Cl acquired from soil mineral leaching. The evapotranspiration process increases the chloride concentration but does not alter

the ^{36}Cl/Cl ratio, whereas the soil mineral contribution of chloride does alter the ratio. The ratio is reduced by the addition of Cl from soil minerals. Thus by accurate measurement of the ^{36}Cl isotope and total chloride content of precipitation and groundwater, research hydrologists can factor out the soil mineral contribution of chloride to the soil water and calculate the chloride contribution due to evapotranspiration.

The *Nuclear Technology* Review (IAEA, 2012) reported that new developments are being made in the utilization of isotopes of the noble gases to date groundwater over several age ranges. Specifically it is noted that the Argonne National Laboratory, USA and Heidelberg University, Germany have developed atom-trap trace analysis techniques which permit the dating of recently recharged groundwater (up to 100 years) with the radioactive isotope ^{85}Kr, which has a half-life of 10.70 years. Argon-39, with a half-life of 269 years, has been applied to the determination of groundwater recharge with an age of 2000 years. Krypton-81, a long-lived isotope with a half-life of 2.3×10^5 years, is used to determine the age of groundwater in deep aquifers that can reach up to 1 million years old (IAEA, 2012; *New York Times*, 2011).

Many other examples of isotope tracers may be cited, but this is beyond the scope of this chapter and only a few examples are provided here. Thorough reviews of the isotope tracer techniques used in studies of catchment hydrology are provided in books edited by Holland and Turekian (2014) and Kendall and McDonnell (1998). Comprehensive reviews by Bullen and Kendall (1998), Nimz (1998), and Trček and Zojer (2010) cite numerous isotopes as tools for measuring the dynamics of catchment hydrologic processes, such as variations in ^{87}Sr natural abundance, or δ^{87}Sr, which varies in waters depending on the water origin (eg, bedrock, soil leachate, rain, etc.) in the catchment. Precise measurements of variations in isotope natural abundances are made with a mass spectrometric analysis.

Nimz (1998) and Bullen and Kendall (1998) give a detailed account of many applications of lithogenic and cosmogenic stable and radioactive isotopes, including ^{3}H, ^{6}Li, ^{7}Li, ^{7}Be, ^{8}Be, ^{10}Be, ^{10}B, ^{11}B, ^{14}C, ^{22}Na, ^{24}Na, ^{39}Ar, ^{41}Ca, ^{129}I, ^{204}Pb, ^{206}Pb, ^{208}Pb, ^{234}U, and ^{238}U, among other isotopes, to the measurement of the catchment hydrologic processes. For additional reading on detailed accounts of the isotope techniques used to assess and improve our water resources see book chapters by Gonfiantini et al. (1998), Trček and Zojer (2010), and Kendall et al. (2014), and books by Bullen and Kendall (1998), the IAEA (2000b, 2004a), Gat (2005), Singh and Kumar (2005), Aggarwaal et al. (2012), Ferronsky and Polyakov (2012), and Holland and Turekian (2014).

1.5 MARINE RESOURCES

Radioactive and stable isotopes are vital tools used by the scientific community to study and preserve our marine resources. The IAEA *Nuclear Technology* Review highlights the current nuclear techniques, including the use of radioactive and stable isotopes to monitor the oceans, marine life, and the impact the oceans have on our overall environment and climate change (IAEA, 2007, 2008, 2009, 2010, 2011, 2012, 2013). A few of the major studies undertaken by marine scientists with the aid of radioactive and stable isotopes, which may serve as examples, are described here.

1.5.1 Climate Change and Marine Acidification

Global warming and climate change are currently major concerns, as global warming has an effect on our climate. Drought, flooding, and storms all affect agricultural production and our oceans. The increase of atmospheric CO_2 around the globe as a result of increased burning of fossil fuels and deforestation is at the root of global warming. The world's oceans play an important role in regulating global warming to some extent, as they absorb heat and additional CO_2 by way of physical and biological processes; however, this can have an impact on the marine environment, which in turn can affect our well-being. It is reported that the average temperature of the upper layers of the ocean has increased by 0.6°C in the past 100 years (IPCC, 2007; Bijma et al., 2013). The rate of temperature rise in the oceans should increase during this century, alongside a corresponding increase in atmospheric CO_2.

Adverse effects of climate change on the marine environment include the acidification of oceans and ocean warming, producing in turn deoxygenation, which is a reduction of the oxygen levels of the ocean environment. Bijma et al. (2013) note that the combined impact of warming, acidification, and deoxygenation is already having a dramatic effect on marine flora and fauna, with significant changes in the distribution of populations and a decline of sensitive species. They underscore that the interactive effects of this deadly trio (warming, acidification, and deoxygenation) reflect similar events in the Earth's past, which were often coupled with extinctions of major species groups. Global warming will increase stratification and impact primary production, as shown in Fig. 1.35, altering patterns of nutrient input in addition to acidification (Rost et al., 2008; Hönisch et al., 2012; Bijma et al., 2013).

The isotopes of carbon, namely ^{13}C/^{12}C, measured as δ^{13}C according to Eq. [1.7], serve as a signature of greenhouse gases (eg, CO_2) which can be tracked when absorbed by the oceans to facilitate measurement of the extent to

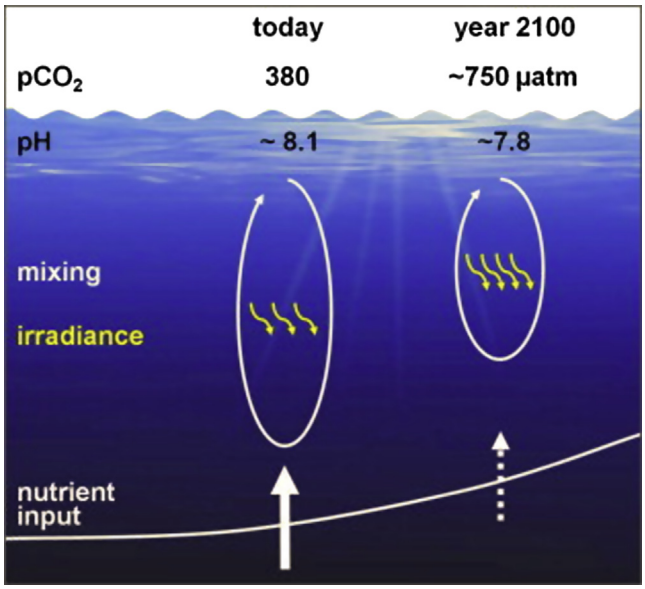

FIGURE 1.35 Main putative physico chemical changes in the oceanic ecosystem occurring in this century. Ocean acidification (reduction of pH) of the surface ocean is expected to intensify. Rising temperatures will impact surface ocean stratification, which in turn will affect the surface water light regime and nutrient input from deeper layers. Phytoplankton will be affected by these environmental changes in many ways, altering the complex balance of biogeochemical cycles and climate feedback mechanisms. *From Bijma, J., et al., 2013. Climate change and the oceans − what does the future hold? Mar. Pollut. Bull. 74, 495−505, reprinted with permission from Elsevier © 2013. Modified after Rost, B., et al., 2008. Sensitivity of phytoplankton to future changes in ocean carbonate chemistry: current knowledge, contradictions and research directions. Mar. Ecol. Prog. Ser. 373, 227−237.*

which the oceans acts as a sink for greenhouse gases (IAEA, 2013b). Menviel et al. (2012) point out that fractionation of ^{13}C (ie, isotope effects between ^{13}C and ^{12}C) occurs during marine photosynthesis and the air−sea gas exchange of CO_2; that is, during the formation of hydrogen carbonate $\left(HCO_3^-\right)$ when atmospheric CO_2 is trapped by the oceans.

A deleterious effect of global warming and the warming of our oceans is deoxygenation of marine waters. Isotope signatures provided by $^{18}O/^{16}O$, measured as $\delta^{18}O$, in the shells of marine microfossils high in carbonate and in long-lived corals have given scientists information on past sea temperatures (IAEA, 2013b). An interesting example, described by Basu (2003), is the measurement of $\delta^{18}O$ to study the temperature changes of ocean waters that may be correlated with prehistoric climatic changes. Due to the higher mass of ^{18}O, its rates of reaction are slower than those involving ^{16}O in biochemical processes (ie, isotope effect). Thus the $^{18}O/^{16}O$ ratio in organic matter of the oceans is lower than the $^{18}O/^{16}O$ ratio of the seawater. At elevated temperatures, the reaction rates of the ^{18}O in living organisms are faster and the $^{18}O/^{16}O$ ratios thus increase. Certain types of amebas, such as the Foraminifera, have lived in our oceans for millions of years. They form a siliceous shell around their bodies, and leave these behind as an ever-accumulating layer of lime and silica at the ocean bottom. Examination of the $^{18}O/^{16}O$ isotopic ratios of the remains of these ancient organisms can give information on the temperatures during prehistoric times when correlated with information provided by isotope dating (Bornemann et al., 2003; Mora, 2003; Mutterlose et al., 2005).

Radioactive and stable isotopes are used to study the acidification of our oceans. Isotopes of boron ($^{11}B/^{10}B$, measured as $\delta^{11}B$ according to Eq. [1.7]) in long-lived massive corals are used to determine past changes in ocean pH and how these changes differ from the current human-driven rise in atmospheric CO_2 and the consequent reduction in ocean pH (IAEA, 2008, 2013b; Rollion-Bard et al., 2011; Hönisch and Allen, 2013).

The effect of ocean acidification is studied with the radioactive isotope of calcium, namely ^{45}Ca, which helps researchers determine the effects of lowered pH on the development of commercially important fish and mollusks, and the rates of calcification in corals (IAEA, 2013). Corals serve as a breeding ground and habitat of fish, help defend against erosion, and provide an important income from the tourist industry (IAEA, 2008). Calcium-45 emits beta radiation with a half-life of 165 days, which is sufficiently long to carry out research over a period of several years. This radioisotope is also used to measure rates of calcification in sea butterflies and cockles from the Arctic, which are important food sources of whales, walruses, and seabirds (IAEA, 2009).

1.5.2 Ocean Water Transport and Circulation

Measurements of natural and anthropogenic radioactive isotopes in ocean waters are used to determine ocean circulation and mixing between shallow and deep currents. The anthropogenic radionuclides originate artificially from human activity, and can include ^{3}H, ^{14}C, ^{90}Sr, and ^{137}Cs, among others, that originated mostly from atmospheric nuclear weapons tests during the 1960s, dispersed around the globe in the atmosphere, and were subsequently deposited on the Earth's continents and oceans. Some radionuclides are both natural and anthropogenic. Carbon-14, for example, is produced naturally in our upper atmosphere when cosmic rays interact with nuclei of the atmosphere and produce neutrons. Some of the resulting neutrons are captured by nuclei of nitrogen atoms in the atmosphere to produce ^{14}C. Carbon-14 has a half-life of 5730 years. Thus the naturally produced ^{14}C can remain on Earth over several half-lives before it decays to undetectable levels, giving time for it to penetrate into the slow-mixing deep waters of the oceans. In contrast, the anthropogenic ^{14}C produced by atmospheric nuclear weapons testing in the 1960s has had sufficient time to penetrate only the surface waters of the oceans. By discriminating between natural and anthropogenic (bomb) radiocarbon, scientists are able to discern and measure both the surface and deep circulating currents of our oceans (IAEA, 2007; Kumamoto et al., 2011; Chikamoto et al., 2012; Poirier et al., 2012; Siegert, 2013). In addition, other anthropogenic radioactive isotopes, including ^{3}H, ^{137}Cs, ^{90}Sr, and isotopes of plutonium ($^{240}Pu/^{239}Pu$), are used to study ocean water circulation and mixing (Aoyama et al., 2013; Hirose et al., 2013; Lee et al., 2013; Povinec et al., 2013; Tsumune et al., 2013). A concise map of circulating deep and shallow currents in global oceans is illustrated in Fig. 1.36.

1.5.3 Harmful Algal Blooms in Marine Coastal Waters

Algal blooms are the result of a rapid production of numerous microscopic algal populations (phytoplankton species), and harmful algal blooms (HABs) are blooms producing toxins that can enter the human food chain. HABs are sometimes referred to as red tides, due to the red or brown color staining the ocean waters from the immense algal populations that develop. The toxins that HABs produce can cause potentially fatal ciguatera fish poisoning and paralytic and diarrheic shellfish poisoning, among other similar illnesses, following the ingestion of bivalve mollusks (eg, clams, mussels, oysters, and scallops) or reef fish that have accumulated the toxins produced by the algal blooms in the ocean waters. In addition to the potentially fatal outcome of toxins produced by HABs, there is the potential economic toll on countries that export shellfish, when restrictions on export are levied in the absence of proper screening and analysis for toxins and labeling of exports. An analytical technique called receptor binding assay (RBA), which makes use of a radioactive isotope as a tracer,

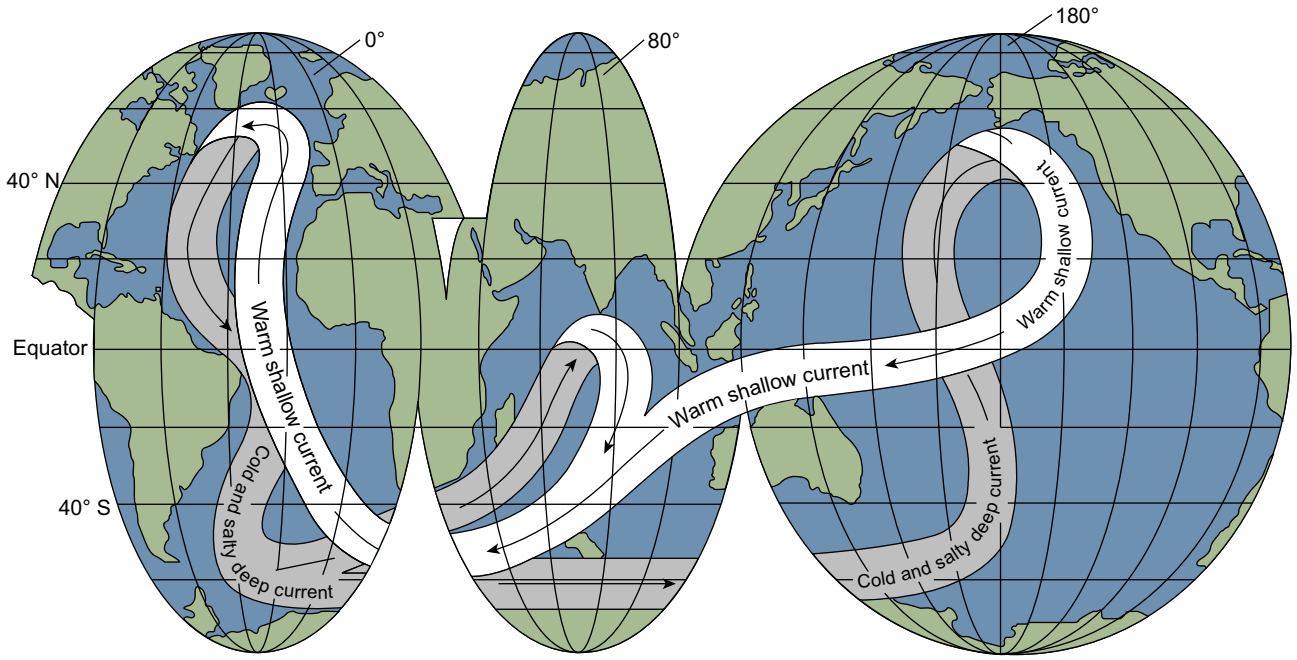

FIGURE 1.36 Schematic diagram of the global ocean circulation system illustrating cold and deep currents and warm and shallow currents. *From Siegert, M.J., 2013. Glacial landforms, ice sheets | growth and decay. In: Elias, Scott A. (Ed.-in-chief), Encyclopedia of Quaternary Science, second ed. Elsevier, Amsterdam, pp. 877–883, reprinted with permission from Elsevier © 2013.*

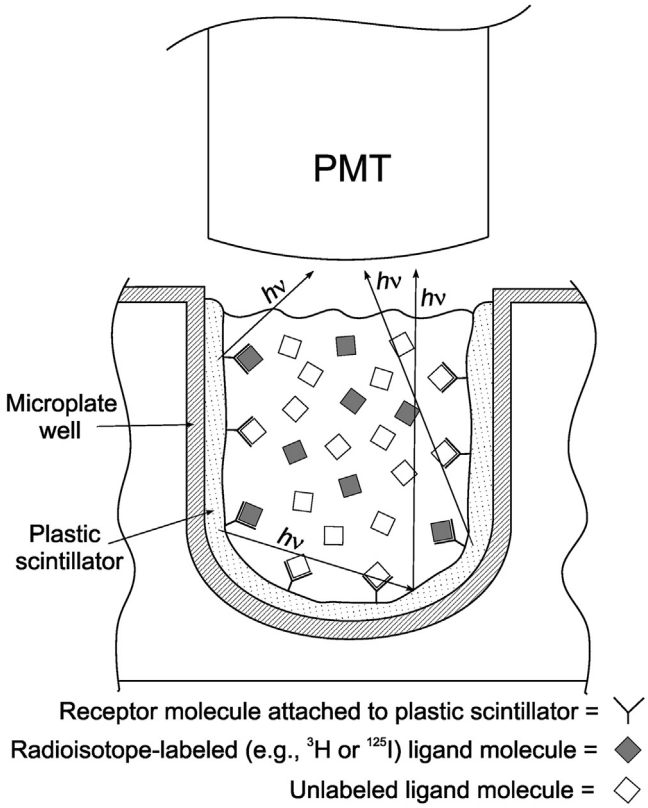

FIGURE 1.37 Artistic depiction of a magnified cross-section of a sample well in a microplate. The well is coated with plastic scintillator. On the surface of the scintillator a layer of receptor molecules is attached. When radioisotope-labeled antigen molecules bind to the receptor molecules, the binding brings the radioisotope into close proximity to the plastic scintillator. The energy of the short-range emissions from radioactive decay of the radioisotope-labeled ligand molecules will excite the scintillator when the radioactive ligand molecules are bound to receptor molecules on the surface of the scintillator-coated microplate wells. The radiation energy absorbed by the scintillator is emitted as photons ($h\nu$) of visible light, which travel through the solution and are detected by a photomultiplier tube (PMT).

is used to analyze toxins derived from harmful algal blooms. The IAEA (2011) reported that "the receptor binding assay (RBA) method, a nuclear technology based on the use of radiolabeled toxins, was identified at the annual meeting of AOAC International (The Scientific Association Dedicated to Analytical Excellence) in 2010 as one of the two developed alternative methods that have been successfully tested in prevalidation studies and will be important for the national regulatory authorities for shellfish export."

The RBA is a very sensitive analytical technique commonly used in biological sciences for the measurement of minute concentrations (femptomolar or 10^{-15} M to nanomolar or 10^{-9} M concentration) of antigen in solution. The technique uses a microplate of sample wells made of white light-reflecting plastic. The wells are coated with plastic scintillator and can contain small volumes (80−1500 μL) of solutions to be analyzed for antigens. Molecules of a suitable receptor are adhered to the surface of the plastic scintillator in an immobilized state, as illustrated in Fig. 1.37.

Once the receptor molecules are immobilized on the scintillator, a radioisotope-labeled ligand is added. The ligand will then bind with the receptor molecules and thereby come into close proximity with the scintillator. Generally a radioisotope that emits low-energy beta particles, such as ^{3}H ($E_{max} = 0.018$ MeV), or a radioisotope that emits Auger electrons, such as ^{125}I, is used as the isotope label. Low-energy beta particle emissions from ^{3}H decay only travel about 1.5 μm in water before coming to a stop, and Auger electrons only a little further. Ranges of travel of various types of nuclear radiation in different media are described in this book. The short range of travel of the decay emissions ensures that only those emissions resulting from the radioactive decay of radioisotope-labeled ligand molecules bound to the receptor molecules interact with the plastic scintillator, resulting in the emission of visible light. The radiation emissions of radioisotope-labeled ligand molecules not bound to receptor molecules in the microplate sample-well solution do not reach the scintillator. The photons of visible light emitted by the scintillator are detected by a PMT above the sample well (see Fig. 1.37). The PMT converts the light photons to an electric pulse, and the pulses are counted. If, however, we now add another competing ligand which is not labeled with radioisotope (eg, ligand molecules found in the extracts of shellfish or

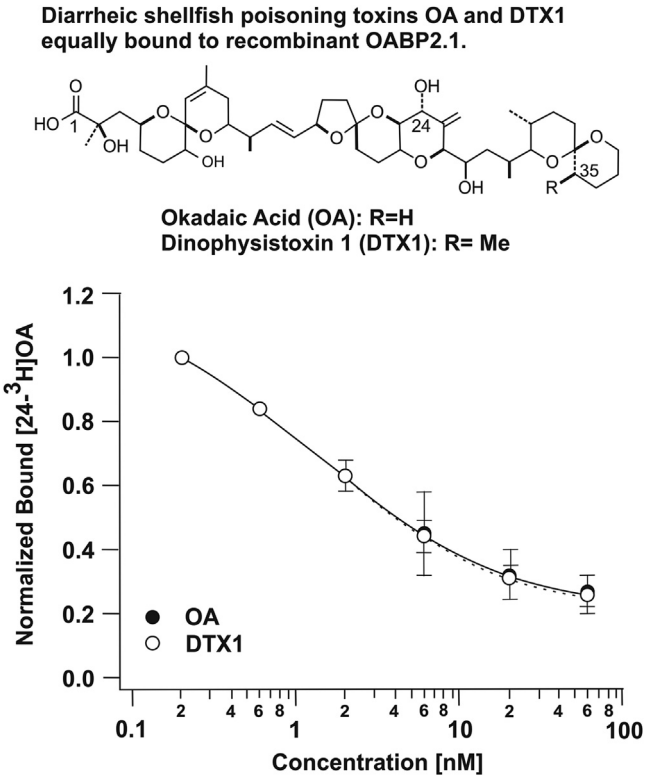

FIGURE 1.38 Replacement of [24-^{3}H]OA binding to recombinant OABP2.1 with various concentrations of OA (closed circles with straight line) or DTX1 (open circles with dotted line). The OABP2.1 is the receptor molecule or binding protein upon which the radioisotope-labeled and nonlabeled toxins (ie, OA and DXT1) will bind. *From Konoki, K., et al., 2010. Binding of diarrheic shellfish poisoning toxins to okadaic acid binding proteins purified from the sponge* Halichondria okadai. *Bioorg. Med. Chem. 18, 7607–7610, reprinted with permission from Elsevier © 2010.*

reef fish that may have ingested toxins from HABs), the added ligand will displace the radioisotope-labeled ligand on the receptor molecules according to the competitive affinity for the receptor and its concentration in the solution (see Fig. 1.37). The displacement of radioisotope-labeled ligand from the receptor molecules into the medium solution of the sample well and away from the scintillator results in a reduction in the radiation–scintillator interactions and in the number of photons emitted. The greater the concentration of unlabeled ligand in the solution (eg, shellfish extract), the greater the reduction in the emission rate of light photons from the scintillator. Thus, with the aid of a standard curve, the unknown concentration of ligand in solution can be determined by the rate of emission of light photons. An example of such a standard curve used for the analysis of toxins that produce shellfish poisoning is illustrated in Fig. 1.38. Notice in the standard curve that at the lowest concentration of toxin in a shellfish extract, the radioactivity of the ^{3}H-labeled ligand attached to the receptor molecule is at a maximum (normalized to 1.0); but as the concentration of unlabeled toxin extracted from the shellfish increases, the amount of radioactivity attached to the receptor molecules diminishes.

Reguera et al. (2013) report that RBA is a simple, sensitive (ppb range), and high-throughput method that can be used for early warning of neurotoxins, such as paralytic shellfish poisoning, ciguatera fish poisoning, and neurotoxic shellfish poisoning, in shellfish and fish. The RBA analysis described here is also known as scintillation proximity assay, because only receptor-bound radioisotope-labeled ligands in close proximity to the scintillator can be detected and counted. In many bioscience laboratories around the world RBAs are performed to analyze very minute concentrations of various types of antigens or ligand molecules. RBAs and scintillation proximity assays are described in detail in an earlier book by the writer (L'Annunziata, 2012c).

1.5.4 Other Isotope Applications in Marine Science

Numerous other isotope techniques are used to study the physical and chemical processes in our oceans, including the application of natural isotope ratios such as $^{87}Sr/^{86}Sr$, $^{206}Pb/^{207}Pb$, $^{143}Nd/^{144}Nd$, and $^{187}Os/^{186}Os$ to answer geologic questions of plate tectonics based on the isotopic composition of seawater and the mineral composition of the sea bedrock (National Academy of Sciences, 1992).

One way of dating ocean floors is the $^{40}Ar/^{39}Ar$ method, which is based on the decay of ^{40}K to ^{40}Ar (McDougall and Harrison, 1999; Koppers et al., 2000, 2003; Yamasaki et al., 2011; Salvany et al., 2012). The isotope ^{40}K decays with a half-life of 1.26×10^9 years, providing a means of dating well beyond the scope of ^{14}C dating.

There are many other applications of radioactive and stable isotopes in the study and preservation of our ocean waters. These are too numerous to describe in this introductory chapter. For further information, comprehensive treatments of the applications of these isotopes to marine studies can be found in books by Caroll and Lerche (2003), Povinec and Sanchez-Cabeza (2006), Schulz and Zabel (2006), and Volkman, 2006, a symposium series (IAEA, 2013b), and book chapters by Povinec et al. (2012) and Bradley (2015).

1.6 RADIATION TECHNOLOGY

Applications of radiation technology, including the industrial applications of nuclear radiation, are widespread throughout the world and vital to our well-being, and only a few examples are noted here. Among the many applications are the research reactor and cyclotron production of radioisotopes required for radiopharmaceuticals in medical diagnosis and treatment of cancer and other infirmities, described earlier; neutron radiation applied to the nondestructive testing of materials; X-ray diffraction, emission, and fluorescence analysis; sterilization of medical products with high levels of gamma radiation; and use of electron beams to process materials such as those needed in rubber vulcanization and wood curing.

1.6.1 Research Reactors and Accelerators

This book describes the discovery of neutrons by James Chadwick in 1932, the properties of neutron radiation, and the production of neutrons by various means, including controlled nuclear fission. Another source of neutron radiation described here is the charged particle accelerator, such as the cyclotron, first conceived by Ernest Lawrence in 1929 and put into operation in 1931. Research reactors and cyclotrons are major sources of neutrons utilized in the production of radioisotopes, and furthermore, the cyclotron can produce a wide range of radioactive isotopes depending on the particle accelerated (proton, deuteron, or helium nucleus) against different target materials.

Many of the radioactive isotopes produced by either research reactors or cyclotrons are vital to our well-being, as they are used at hospitals and clinics for medical diagnosis and treatment, such as the medical imaging and radiotherapy techniques described earlier. Among the radioactive isotopes required in medicine are ^{99m}Tc, used mostly in medical diagnosis, ^{67}Ga, ^{103}Pd, ^{125}I, ^{131}I, ^{192}Ir, and ^{201}Tl, used as seeds in the treatment of prostate cancer, other therapeutic agents containing ^{90}Y, ^{153}Sm, ^{186}Re, ^{165}Dy, and ^{177}Lu, positron-emitting radionuclides, ^{18}F, ^{11}C, ^{15}O, ^{13}N, ^{64}Cu, ^{66}Ga, ^{68}Ga, ^{76}Br, and ^{82}Rb, required for medical imaging of the human body to permit detailed visualization of the organs within the body and attached tumors, and ^{60}Co for radiation therapy, to mention just a few. Other radioactive isotopes are needed for important research in the biological and agricultural sciences, and some of the applications have been cited earlier. There are currently 266 research reactors operating in 70 countries of the world and approximately 650 cyclotrons operating worldwide. Small cyclotrons located at hospital facilities allow short-lived radioisotopes to be produced on site for the diagnosis and treatment of various diseases.

Research reactors also act as a source of neutron beams serving research and industrial needs for nondestructive testing and analysis of materials, including techniques such as neutron scattering and diffraction for atomic structure determinations, neutron radiography, and neutron activation analysis. These are described briefly in the following subsections.

1.6.2 Neutron Diffraction and Scattering

The importance of neutron beam technology for human development and well-being was recognized by the Nobel Committee when it awarded the Nobel Prize in Physics in 1994 to Bertram N. Brockhouse (1918–2003) and Clifford G. Shull (1915–2001) for, in the words of the Nobel Committee, "pioneering contributions to the development of neutron scattering techniques for studies of condensed matter," and particularly to Bertram Brockhouse "for the development of neutron spectroscopy" and to Clifford Shull "for the development of the neutron diffraction technique."

As a background to the modern applications of neutron diffraction and scattering, we can recall the work of Albert Einstein in 1905, described in this book, when he demonstrated that a photon of light or a light quantum possess a dual nature—that of a wave and that of a particle. For this work, Einstein was awarded the Nobel Prize in Physics in 1921. Also described in the book is the work of Louis de Broglie, who demonstrated in 1923 that particles with kinetic energy to

which we can assign a mass at rest, such as a proton, electron, or neutron, also has a dual nature, with the properties of a wave as well as the properties of a particle, such as light. Along these same lines of thought, this chapter describes the pioneering work of Max von Laue in 1912 when he discovered the diffraction of X-rays by crystalline substances, and that of Sir William Henry Bragg and Sir William Lawrence Bragg in 1914, a father-and-son team who determined the interatomic distances of atoms in a crystal by means of X-ray diffraction. These previous findings led to the work of Brockhouse and Shull, which is described in the words of Professor Carl Nordling of the Royal Swedish Academy of Sciences in his speech when presenting the Nobel Prize to them on December 8, 1994:

> *…they knew that neutrons possessed a dual nature that was characteristic of their tiny world: the ability to behave both as particles and as waves. In their latter guise, neutrons have been reflected against the atomic planes of a crystal in the same way x-rays previously had. This provided a hint that, someday, neutrons might become a tool for studying the microstructure of matter at the atomic level. The door was already ajar, but had not yet been opened wide…Shull took advantage of the fact that the wavelength of neutrons from a reactor may be roughly equal to the distance between the atoms in a solid body or a liquid. When the neutrons bounce against atomic nuclei, they do not lose energy, but their scattering is concentrated in directions that are determined by the structure in which the atoms are arranged. Shull revealed that neutrons could answer questions that the x-ray diffraction method had failed to answer, such as where the atoms of the light element hydrogen are located in an ice crystal.*

Neutrons of specific energy, when directed as a beam toward a crystalline substance, may exit from the substance without any loss of energy (elastic scattering), exit with some loss of energy (inelastic scattering), or exit at specific angles or directions (diffraction). As in X-ray diffraction, described in this book, a neutron beam from a research reactor may be directed toward a crystalline material. Most of the neutrons exit the crystal without loss of energy and are diffracted by the crystal. A neutron detector may be rotated around the crystal to determine the angles of diffraction to yield a diffraction pattern, from which the positions and distances of the atoms on the crystalline sample may be determined. As discovered by Shull, this is particularly sensitive in determining the positions of hydrogen atoms, which are similar in mass to the neutron and cannot be revealed by X-ray diffraction. This technique has proven to be of great value in the biological sciences, where the determination of the structure of proteins, viruses, and other macromolecules and their complexes with DNA and other nucleic acids is vital to our understanding of their modes of action in living systems. An illustrative example is taken from the work of Shu et al. (2000), illustrated in Fig. 1.39, which shows the locations of hydrogen atoms bound to a residue of myoglobin, the primary oxygen-carrying pigment of muscle tissue. This work demonstrated the enhanced structural information obtained when hydrogen is replaced by deuterium in the molecular structures. As noted in the *Nuclear Technology* Review (IAEA, 2006) "The similar scattering signal, using small angle neutron scattering (SANS) from deuterium, carbon, nitrogen and oxygen allows the full determination of the positions and dynamics of the atoms in biological structures. The non-destructive method using neutrons is an ideal complementary tool of investigation if combined with X-ray scattering and/or nuclear magnetic resonance (NMR) measurements." For an overview of neutron techniques in studies of structural biology, see a review paper by the father of neutron protein crystallography, Benno Schoenborn (2006).

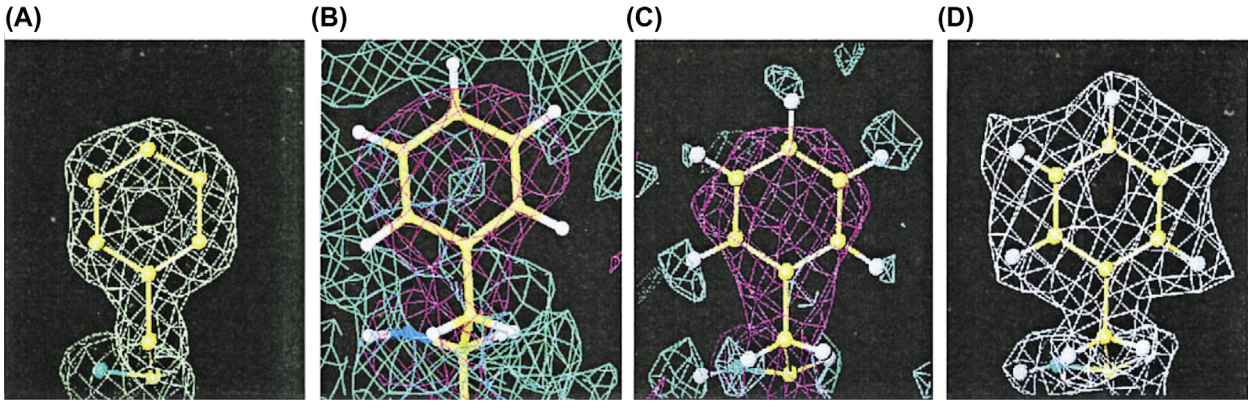

FIGURE 1.39 Fourier density maps of a unit of myoglobin from diffraction pattern data obtained using (A) X-rays where no hydrogen atoms are visible; (B) neutrons where no isotope labels were added; (C) a calculated structure equivalent to (B); (D) enhanced image taken with neutrons and a sample where the hydrogen atoms were replaced by deuterium. *From Shu, F., Ramakrishnan, V., Schoenborn, B.P., 2000. Enhanced visibility of hydrogen atoms by neutron crystallography on fully deuterated myoglobin. Proc. Natl. Acad. Sci. U.S.A. 97 (8), 3872–3877, reprinted with permission from National Academy of Science, USA © 2000.*

1.6.3 Neutron Radiography

Neutron radiography is an imaging technique similar to X-ray radiography. A neutron beam is directed toward an object and an image is formed on photographic film or a digital detector system sensitive to neutron radiation. The image produced may look like an X-ray image, but objects often invisible to X-ray radiography are visible in neutron radiography.

The many properties of neutrons are described in this book. Neutron properties which make them particularly suitable for radiography are their neutral charge and their ability to transfer significant amounts of their energy to nuclei of light elements by inelastic scattering. Because of the lack of charge on the neutron, a neutron beam from a research reactor or other source is able to penetrate matter easily, somewhat like X-rays are able to pass through materials of varying densities. However, unlike X-rays, neutrons are sensitive to light elements, such as hydrogen, lithium, boron, and carbon. As described in more detail in this book, elements of high atomic number will attenuate X-rays to the greatest extent, whereas neutrons are attenuated most by elements of low atomic number. As a consequence, the images that neutrons produce after passing through an object will be particularly revealing of substances containing light elements, which would be invisible with X-rays. Thus neutron radiography complements X-ray radiography. This is illustrated by comparison of the neutron and X-ray radiographs shown in Fig. 1.40.

Neutron radiography is often used in quality control, such as the inspection of components inside manufactured devices that would generally not be visible through X-ray radiography. Some applications of neutron radiography are inspections of manufactured components of many types, such as those engineered for the aircraft, aerospace, and automotive industries, to check for precision manufacture of turbine engine blades; corrosion; flaws in adhesive bindings; internal flaws; missing or misplaced O-rings or other components; and cracks, inclusions, and voids or other types of internal defects in materials. Neutron radiography is also applied in the biomedical and agricultural fields. Examples cited in the *Nuclear Technology* Review (IAEA, 2006) are the monitoring of boron distribution needed for BNCT in the treatment of cancer; the inspection of heart valves and materials used in dentistry; and water movement in plants, including the distribution and transport of neutron-capturing elements such as gadolinium, samarium, and cadmium in plant leaves. The neutron-capturing properties of the elements are described in the chapter entitled "Neutron Radiation."

Advances in neutron radiography applications are described in papers by Sinha et al. (2014), Tharwat et al. (2014), and Tremsin et al. (2014). For further reading, books by Domanus (2004), Harms and Wyman (2005), Downing and Arif (2008), Anderson et al. (2010), and von der Hardt and Röttger (2013) provide comprehensive treatments on neutron radiography.

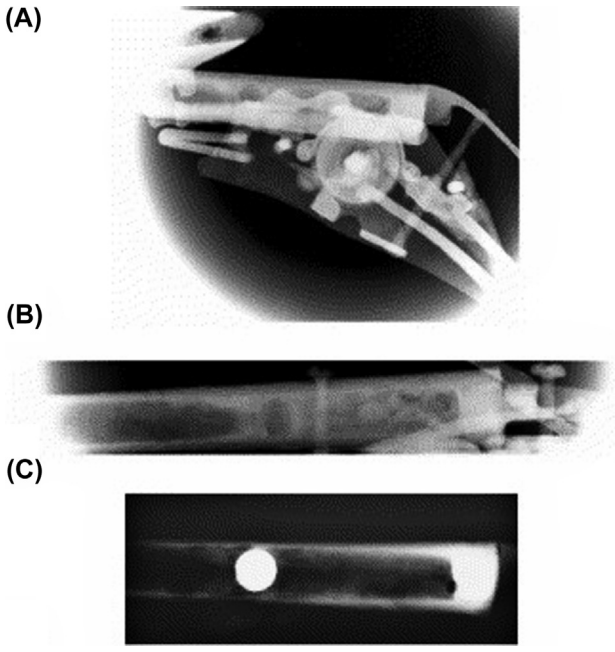

FIGURE 1.40 Neutron and X-ray radiographs of a 16th-century wheel-lock pistol discovered in a river in Slovenia. The wheel-lock mechanism and indications of the presence of gunpowder can be seen in the neutron radiographs of the pistol (A) and the barrel (B). The lead bullet cannot be directly observed in the neutron radiograph; its presence in the barrel is concealed by the detection of mud, corrosion products, and gunpowder clogged around the bullet. The position of the lead bullet is clearly revealed by the X-ray radiograph (C). *From Rant, J., et al., 2006. Neutron radiography examination of objects belonging to the cultural heritage. Appl. Radiat. Isot. 64, 7–12, reprinted with permission from Elsevier © 2006.*

1.6.4 Neutron Activation Analysis

Neutron activation analysis (NAA) is a method that utilizes a neutron beam to determine the concentrations of elements in a given substance. The technique involves irradiating the material to be analyzed with a neutron beam, which results in the capture of neutrons by various nuclei of the elements in the substance, yielding many radioactive isotopes. The energies and intensities of the gamma-ray emissions of the radioisotopes produced are then measured with a sensitive semiconductor detector, and the elements in the sample and their concentrations are determined by correlating the gamma-ray energy lines and their intensities with standards irradiated simultaneously with the unknown substance. Fig. 1.41 illustrates, as an example, the gamma-ray emissions resulting from the capture of a neutron by a stable isotope of bromine ($^{81}_{35}$Br), which are relevant in the NAA of bromine.

In the NAA process, a material containing bromine is irradiated with neutrons, starting the sequence of events illustrated in Fig. 1.41. A stable isotope of bromine ($^{81}_{35}$Br) captures a neutron, yielding a nucleus at an excited energy state ($^{82}_{35}$Br*) which immediately emits gamma rays (prompt γ rays) upon deexcitation to yield $^{82}_{35}$Br at a lower energy state. The $^{82}_{35}$Br is unstable and decays by beta particle emission (β^-) with a half-life of 35.3 h to $^{82}_{36}$Kr*, which is in an excited energy state, emitting gamma rays to yield the stable isotope $^{82}_{36}$Kr. The intensities of the decay gamma rays emitted by $^{82}_{36}$Kr*, which possess very specific energy lines, are measured by a suitable radiation counter. When the gamma-ray intensities of a sample containing an unknown amount of bromine are correlated with the gamma-ray intensities produced by standard samples of bromine irradiated together with the unknown, the amount of bromine in the unknown sample can be determined. NAA is an excellent method to analyze trace amounts of elements in the presence of many other elements, provided that the element of interest has a suitable neutron capture cross-section and yields suitable radiation emissions that can be measured in the presence of radiation emitted by isotopes originating from other elements in the sample. Holbert and Murray (2015) point out that it is possible with NAA to detect quantities as low as a millionth of a gram in 76 elements, a billionth of a gram in 53 elements, and a trillionth of a gram in 11 elements of the periodic table.

A variant of NAA is prompt gamma neutron activation analysis (PGNAA), which entails the measurement of the initial "prompt gamma-rays" that are emitted by an excited nucleus immediately after capturing a neutron instead of the measurement of gamma rays emitted by a nucleus resulting from subsequent nuclear decay. Fig. 1.41 illustrates the emission of gamma rays promptly after the capture of a neutron by a nucleus of an atom. PGNAA is fast, as it is based on the immediate gamma-ray emissions following neutron capture. Analysis in some cases can take only minutes to complete. PGNAA is nondestructive, as the production and detection of a radioactive daughter nuclide is not necessary. In general, PGNAA does not produce long-lived radioactive nuclides in the sample, permitting the analyzed sample to be used for other purposes. Thus PGNAA has found many uses for fast analysis of elements in the coal, mineral, and steel industries. For example, scrap metal needed for the steel industry is analyzed rapidly by moving the metal scrap on a conveyor belt while simultaneously bombarding the metal with neutrons from a californium-252 source. Neutron capture by impurities in the scrap metal produces prompt gamma rays that are then analyzed in minutes for their intensities and energy lines by a detector coupled to a computer (Madias, 2014).

NAA was first conceived by Nobel Laureate George de Hevesy while working with Hilde Levi (1909–2003) at the Niels Bohr Institute of Theoretical Physics in Copenhagen, and first published in 1936 (de Hevesy and Levi, 1936a,b).

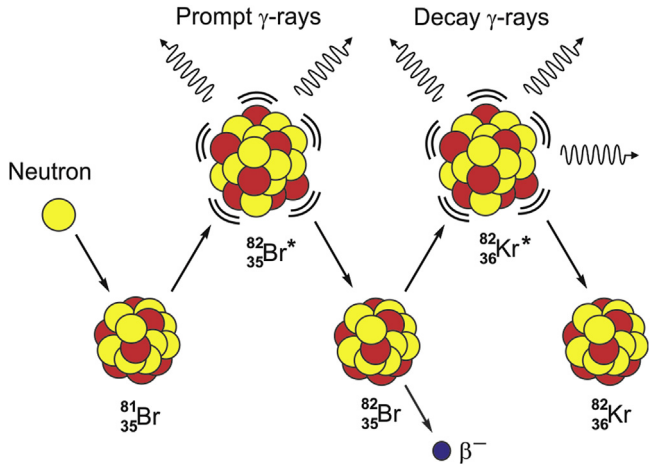

FIGURE 1.41 Neutron capture by stable bromine-81 and subsequent gamma-ray (γ-ray) emissions relevant in the NAA of the element bromine. *Figure from Kim et al. (2013b), reprinted with permission from Elsevier © 2013.*

Hilde Levi received her doctorate in physics and chemistry at the University of Berlin in 1934, during the early phase of Hitler's dictatorship. Because of her Jewish heritage, she left Germany and obtained assistance from the Danish branch of the International Federation of University Woman, which arranged her connections to Denmark and employment at the Niels Bohr Institute (Aaserud, 2003). There she became a collaborator in research with George de Hevesy during the time of his pioneering work on the application of isotope tracers in biological research. In a biography of George de Hevesy, Hilde Levi (1985) related her recollections of this historic discovery:

> *The most important discovery from this short period of research was the basic development of neutron activation analysis. As discussed in a previous chapter, the separation and purification of the different elements within the group of rare earths was exceedingly complex. Chemists in many countries were still laboring with this problem using the classical methods of analytical chemistry. Hevesy suggested that — as a means of identification — we make use of the characteristic decay period of each of these elements and of their relative intensities of activation after neutron bombardment. In this way, their presence could be determined in any unknown mixture. In the early phase of this work we observed that, with the neutron sources available, the strongest activity was induced in the rare earth element dysprosium. It was therefore easy to detect even a minute amount of dysprosium compound present as an impurity in the salt of any other rare earth element. This finding was published in 1936.*

Frame (1997) also relates an interesting story of de Hevesy's discovery of NAA, taken in part from de Hevesy's biography (Levi, 1985).

Hilde Levi (1909–2003)
With permission courtesy of
AIP Emilio Segre Visual Archives,
Gift of Jost Lemmerich

Because of its high level of sensitivity for the trace elements (<0.01%) and accuracy, NAA is widely used in many fields of study, including the biological sciences, agriculture, industry, and food and nutrition (Filby, 1995). It is also often used in forensic science, because of characteristic signatures displayed by the gamma spectra after neutron irradiation of samples (IAEA, 2006), as well as in trace element analysis for applications such as the verification of archeological artifacts and precious paintings. The reader will find thorough treatments of NAA in books by Keisch (2003), Baas (2004), Molnar (2004), Naeem (2012), and US EPA (2013).

1.6.5 X-Ray Diffraction, Emission, and Fluorescence Analysis

X-radiation is useful in various analytical techniques, including the structural analysis of inorganic and organic crystals by X-ray diffraction and the nondestructive analysis of the elemental content of materials by proton-induced X-ray emission (PIXE) or X-ray fluorescence (XRF) spectrometry. These analytical methods are described briefly here.

1.6.5.a X-Ray Diffraction/Crystallography

The Hall of Fame III in this book describes how Max von Laue (1879–1960) first recognized in 1912 that X-rays possess wavelengths of an order of magnitude similar to the distances between the lattices in crystalline substances. If the distance between the atoms of a crystalline substance was ~1Å or 10^{-10} m, von Laue concluded that X-rays of similar wavelength would be diffracted between the arrays of atoms that form spatial lattices in a crystal. He and his coworkers irradiated a copper sulfate crystal with X-rays and discovered that the X-rays were deflected at certain maxima, which were recorded on a photographic plate as spots at certain distances from a central spot created by the primary X-ray. Max van Laue provided evidence for the wave nature of X-radiation and the lattice theory of crystal structure. He also demonstrated that the wavelengths of X-rays could be determined by the dimensions of the crystal space lattice—that is, the interatomic distances within the crystal structure. Following von Laue's discovery of the wave nature of X-rays, the father-and-son team of William Henry Bragg (1862–1942) and William Lawrence Bragg (1890–1971) built an X-ray diffraction spectrometer and derived the mathematical formula which enabled the precise measurements of the interatomic distances within a crystal structure. As described by William Lawrence Bragg in his Nobel Lecture in 1915:

> *…a very strong reflection [of x-rays] appeared when a given crystal face was set at certain definite angles…These same lines [of reflection] could be recognized in the reflections from other faces, and the measurement of the angles at which they appeared proved a most powerful method of finding the arrangement of the atoms in the crystal.*

From such X-ray diffraction, W.H. and W.L. Bragg reported the crystalline structure of NaCl, demonstrating that the metal atom Na was situated in the crystal equally distant from the six Cl atoms nearest to it, and vice versa. Prior to this it had always been thought that the NaCl molecules were situated equally distant to each other in the crystal. By 1922 the pair had determined the atomic structures of several crystalline materials, including diamond, calcite, graphite, ice, and the organic crystalline structure of naphthalene. This original work by the Braggs gave birth to the field of X-ray crystallography—the study of the atomic structure of crystals by X-ray diffraction. With this technique Rosalind Franklin (1920–1958) determined the X-ray diffraction pattern of DNA, which was a critical step in the elucidation of the helical structure of DNA. X-ray crystallography has advanced to become a vital analytical technique for determining the atomic arrangements in many large and complex molecular structures that are of particular importance in the medical and biological sciences.

Modern crystallography, which makes use of X-ray diffraction in crystalline material, is reviewed eloquently by Garcia-Granda and Montejo-Bernardo (2013). A mathematical computation, known as Fourier analysis, is performed by computer on data collected from the angles and intensities of the diffracted X-rays. This analysis gives a 3D map of the electron densities within the crystal, known as an electron density map. Because the electrons occupy the outer shells of the atoms in the crystal, the positions of the atoms in the crystal are determined as well as the lengths of their chemical bonds. An electron density map of the organic compound benzimidazole obtained by high-resolution X-ray diffraction of a benzimidazole crystal is illustrated in Fig. 1.42. The map shows the electronic density structure of the molecule and the locations of each of the carbon, hydrogen, and nitrogen atoms within the molecule. The structural formula of benzimidazole is written alongside the electron density map for comparative purposes.

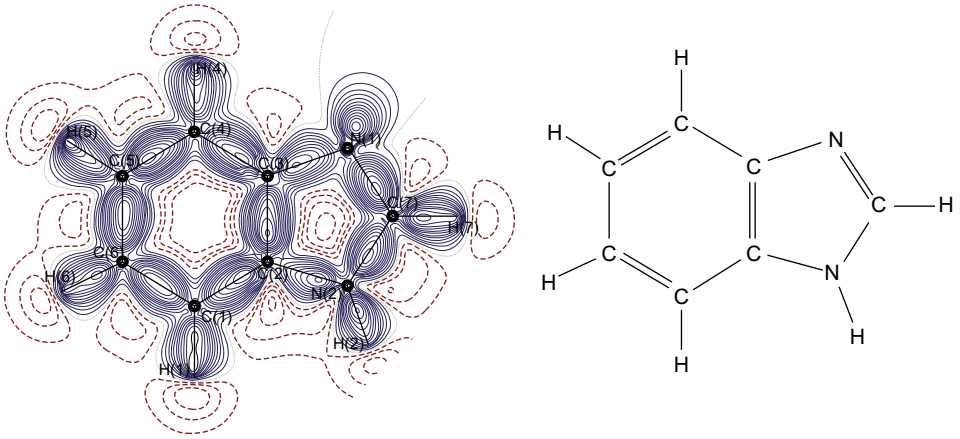

FIGURE 1.42 Left: Electron density map of benzimidizole determined by high-resolution X-ray diffraction. Right: Structure of the benzimidizole molecule. *Electron density map is from Stephen, A.D., et al., 2011. Exploring the bond topological and electrostatic properties of benzimidazole molecule via experimental and theoretical charge density study. J. Mol. Struct. 989, 122–130, reprinted with permission from Elsevier © 2011.*

X-ray crystallography to produce an electron density map of a molecule, and thus a picture of the atoms in a crystal, is analogous in certain respects to day-to-day photography with visible light. When we take a photograph with a camera, visible light reflects off the object being photographed. The dark or shaded areas of the object absorb more light then the other parts, and the reflected light is captured by the camera to produce an outline of the object constructed by the variations in absorption and reflection of light by that object. The wavelengths of visible light are too long to map or picture the inner structure of matter; however, X-rays have a wavelength equivalent to the distance between each atom ($\sim 10^{-10}$ m) of a molecule and thus can pass through the interspatial lattices of a crystal and be diffracted by it, from which the atomic structures are mapped.

Synchrotron radiation, which originates when charged particles are accelerated at relativistic speeds, is an excellent source of X-rays for application in X-ray crystallography. Papiz and Winter (2010) underscore the need to utilize X-radiation produced when charged particles are accelerated in synchrotron storage rings, which have the capacity to yield the most intense X-ray beams with the best optical properties by producing X-rays over a narrow spectral range.

X-ray crystallography is an invaluable tool in studies of medicine, biology, and the pharmaceutical sciences. The complex structure of very large molecules, such as proteins, enzymes, and nucleic acids, can be determined and the relative locations of each atom in the molecule accurately delineated. The significance of this field was recognized by the Nobel Committee in 1962 when it awarded the Nobel Prize to John Kendrew (1917–1997) and Max Perutz (1914–2002) for their determination of the structure of myoglobin by high-resolution X-ray crystallography. Also, Dorothy Hodgkin was awarded the Nobel Prize in 1964 in the words of the Nobel Committee "for her determination by x-ray techniques of the structures of important biochemical molecules [including penicillin and Vitamin B12]." Structural information obtained by X-ray crystallography is essential to the medical and biological sciences. For example, it is necessary to see the 3D structure of enzymes and their active sites to determine their function in catalyzing biochemical reactions. The structure of fumarase, a very complex enzyme that plays a key role in metabolic pathways, determined by X-ray crystallography is illustrated in Fig. 1.43. Fumarase is composed of four subunits comprising 510 amino acids with a molecular weight of 54,637 Da. In the medical sciences, our knowledge of the 3D chemical structures of pharmaceutical drugs and the target molecules upon which they interact, obtained by X-ray crystallography, are vital to the development of new and improved drugs.

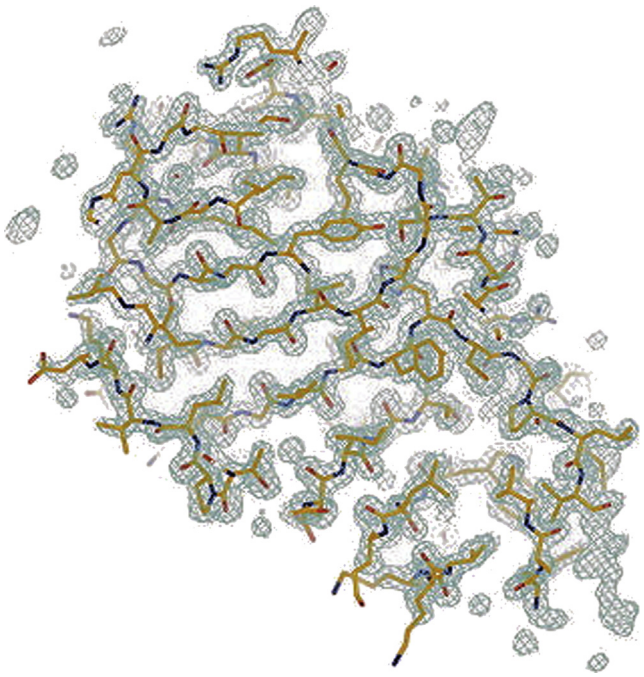

FIGURE 1.43 The crystal structure of fumarase from *Archaeoglobus fulgidus* at 1.66 Å resolution determined by X-ray crystallography. The peptide bonds linking amino acids are illustrated in blue, carbon atoms in yellow, and oxygen atoms in red. Structure determined by the Joint Center for Structural Genomics, to be published (PDB code: 2isb). *Figure from Papiz, M.Z., Winter, G., 2010. Biomolecular X-ray crystallography, structure determination methods. In: Lindon, John (Ed.-in-chief), Encyclopedia of Spectroscopy and Spectrometry. Elsevier, Amsterdam, pp. 185–193, reprinted with permission from Elsevier © 2010.*

1.6.5.b Proton-Induced X-Ray Emission (PIXE)

PIXE is a nondestructive analytical technique used to determine the elemental content of a substance from the X-ray emissions caused by the irradiation of the substance with protons. The technique involves the irradiation of a substance with protons accelerated at an energy of ~3 MeV. Accelerated protons collide with inner orbital electrons (K or L orbital) of the elements in the sample under analysis, resulting in a cascade of electrons falling from outer higher-energy orbitals to inner orbitals with a concomitant emission of X-radiation at energy lines characteristic of each element. A suitable detector of X-rays emitted by the sample, such as s silicon drift detector, is used to measure the intensities of the X-rays emitted at different energy lines, from which the elements in the substance under analysis can be identified and quantified (Verplancke et al., 2012). The elements are identified according to the X-ray energy lines that are characteristic of each element; and the X-ray intensities at specific energies are used to quantify each element in the sample under analysis. Pure element standards serve as reference material to calibrate the X-ray detector response to X-rays emitted by the sample at various energy lines. A typical spectrum resulting from the PIXE analysis of paint used by Antonello de Messina, one of the great Italian masters of the 15th century, in the famous painting "Ritratto Trivulzio" is illustrated in Fig. 1.44.

PIXE is an excellent method for elemental analysis when a nondestructive method is required for the measurement of elements of atomic number greater than 11 ($Z > 11$). The analysis of elements of low atomic number ($Z < 17$), including Li, B. F, Na, Mg, Al, and Si, can be carried out with proton-induced gamma-ray analysis (PIGE) resulting from nuclear reaction between accelerated protons and the nuclei of the light elements. The light elements have a lower coulomb barrier than the heavier elements, and thus protons accelerated at energies of only 2.0−3.5 MeV will interact with the nuclei of the light elements, with the concomitant emission of gamma radiation. Because proton energies used in PIGE are similar to those used in PIXE, both methods of analysis may be used simultaneously. The acronym PIXE may also refer to particle-induced X-ray emission, as other particles, such as the accelerated electrons, may be used in lieu of accelerated protons; however, accelerated electrons produce considerable bremsstrahlung radiation, which can interfere with the measurement of X-radiation emitted by the sample under analysis. PIXE is also known as a form of ion beam analysis, because a beam of charged particles is accelerated to collide with a sample to analyze its elemental composition from the resulting radiation emissions.

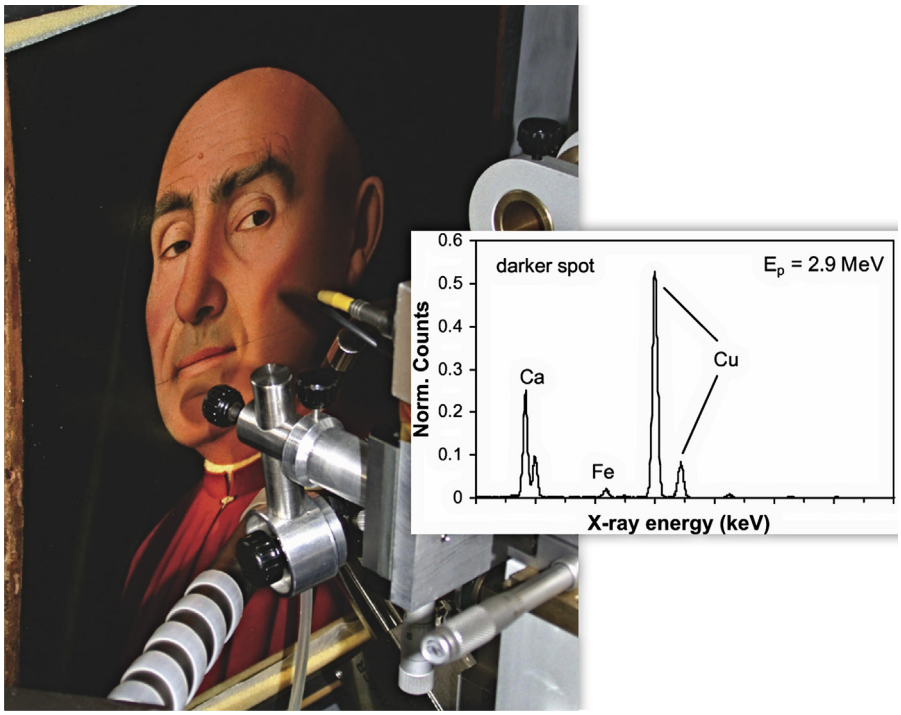

FIGURE 1.44 The "Ritratto Trivulzio" by Antonello de Messina at the scanning microbeam line at the Laboratorio di tecniche nucleari per i Beni Culturali of the Instituto Nazionale di Fisica Nucleare, Florence, Italy. The overlapping graph illustrates X-ray peak intensities for the elements Ca, Fe, and Cu in a spot of the dark headcloth in the painting. The paint used for the headcloth was identified as a Cu-based pigment, such as the blue pigment azurite. *Figures from Grassi, N., 2009. Differential and scanning-mode external PIXE for the analysis of the painting "Ritratto Trivulzio" by Antonello da Messina. Nucl. Instrum. Methods Phys. Res. Sect. B 267, 825−831, reprinted with permission from Elsevier © 2009.*

PIXE is useful in analyzing materials that should not be destroyed, such as analysis required in the measurement and characterization of prehistoric pigments and ancient artifacts, and the characterization of paints used by the masters of centuries past. Excellent examples of PIXE analysis in studies of cultural heritage and reviews on its applications are available from Grassi (2009), Sokaras et al. (2011), Jeynes et al. (2012), Kakuee et al. (2012), Beck (2014), Rizzutto et al. (2014), and Zucchiatti and Redondo-Cubero (2014).

1.6.5.c X-Ray Fluorescence

XRF analysis is a nondestructive method for the identification and quantitative determination of the elements in a sample, involving the irradiation of a substance with X-rays followed by measurement of the fluorescent X-radiation emitted by the sample. When X-rays are directed toward a substance, ionization of inner electron orbitals of the various atoms in the sample can occur, followed by a cascade of electrons falling from outer orbitals to lower-energy orbitals as a result of the void created by any electron emitted from an inner shell. Each element emits characteristic X-ray energy lines, which are measured to identify the elements in the substance. The intensities of the X-ray emissions at energy lines characteristic of each element in the sample are used to quantify the elemental composition of the sample. The method is referred to as fluorescence analysis, because the X-ray emissions are lower in energy than the X-radiation used; the X-ray emissions are secondary emissions resulting from excitation of atomic electron orbitals.

XRF is a commonly employed method of analysis in a wide range of sample types, such as soil, minerals, metal, ceramic, prehistoric artifacts, ancient paintings, glass, and a wide range of materials encountered in forensic investigations and studies of cultural heritage. The technique is not new, as the writer used XRF analysis in 1965 for the quantitative determination of strontium in soils; however, over the years many improvements have been made in the detection and measurement of the X-ray emissions (Verplancke et al., 2012). XRF can be used to measure almost every element in the periodic table, from lithium ($Z = 3$) up to nobelium ($Z = 102$). Relatively inexpensive XRF instrumentation is commercially available, which makes XRF a widely popular technique compared to other nondestructive analytical methods previously described.

An interesting example of XRF analysis in studies of cultural heritage is provided by the work of Kantarelou et al. (2011), who used XRF to analyze the elemental composition of ancient coins of Greece. A silver coin of Ptolemy I from Ancient Greece and the XRF analysis of its elemental composition are illustrated in Fig. 1.45. The X-ray emission spectra show peaks of emissions at energy lines corresponding to Ag, Fe, Cu, Au, and Pb from the surface of the coin irradiated with 40 kV X-rays. The peaks labeled Rh* are emissions from the rhodium anode of the X-ray tube used to irradiate the coin. Quantitative analysis of the coin obtained from the peak intensities correlated with standards yielded average values of 98.5% Ag, 0.5% Au, 0.3% Pb, 0.1% Cu, and trace amounts of Fe and other metals. Kantarelou et al. (2011) concluded that data on the elemental composition of various coins provided important information about possible sources of silver during the Ptolemaic period, and gradual coinage debasement after 270 BC for economic or technical reasons. The reader may also peruse a paper by de Viguerie et al. (2010) describing XRF analysis of the famous "Mona Lisa" by Leonardo da Vinci, which gave insight into his painting technique.

1.6.6 Radiation Processing

Radiation processing is the use of high doses of ionizing radiation to alter the biological, physical, or chemical properties of the irradiated substances. It is a field of science that is out of view and out of mind to the general public, but one to which we owe dearly for our well-being and comfort. The importance of radiation processing in our day-to-day lives was underscored by the IAEA (2004b):

Radiation Processing: The Invisible Performer

Unknown to the general public, and even to the scientific community, radiation technology has sneaked into our daily routine to enrich the quality of our life in many ways. Today, you may be using radiation processed materials in some form or the other, for example, the car you drive or the television set you watch may be equipped with radiation crosslinked wires or cables, the hot water pipe line bringing warmth to your homes might be made of radiation crosslinked plastic material, the long lasting alkaline battery you use in the camera or watch may use radiation cured membranes to enhance its lifetime, the safe hamburger you ate may have contained meat or spices pasteurized by radiation…or if you have been unfortunate to have stayed in the hospital, the sterile syringe or the catheter the doctor used might have been sterilized by radiation processing to make it absolutely safe. The examples are numerous. At present, the value of irradiated products produced exceeds several billion dollars and the industry is expanding at a fast rate all over the world…

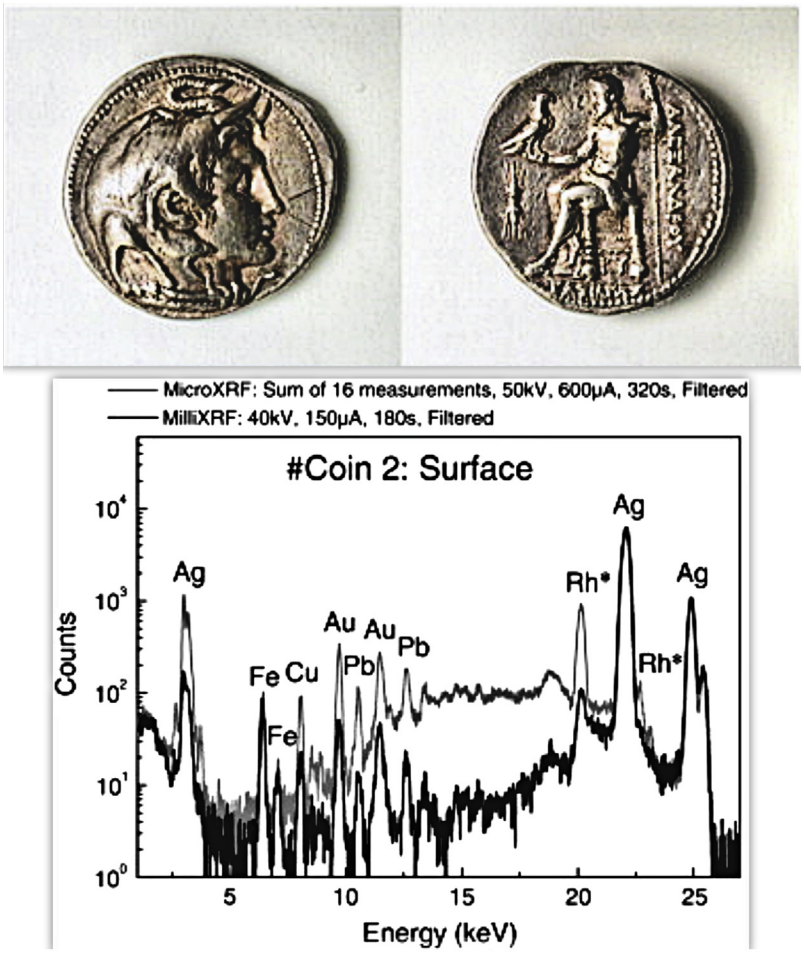

FIGURE 1.45 Top: Tetradrachm of the reign of Ptolemy I from the collection of "Ioannes Demetriou" (Numismatic Museum of Athens). Bottom: XRF spectrum of the coin surface. *From Kantarelou et al. (2011), reprinted with permission from Elsevier © 2011.*

Some of the industrial applications of radiation processing are described below.

1. **Sterilization of healthcare products**. Most healthcare products, such as bandages, syringes, gloves, surgical blades, sutures, catheters, pharmaceuticals, and many other items used during surgery or outpatient treatment, are sterilized with high doses of ionizing radiation. Even the standard bandages that we often apply at home to minor cuts and bruises are sterilized by high doses of radiation. The advantages are that the sterilization does not require heat or autoclave, and the items are sterilized after they are packed or sealed in wrappings impermeable to air or bacteria, which keeps them sterile until their time of use (Choppin et al., 2013a,b; Lambert and Martin, 2013; Soliman et al., 2013).
2. **Irradiation of blood to prevent transfusion-associated graft versus host disease**. This is a rare but lethal complication of transfusion generally associated with immunosuppressed patients. The problem is usually prevented by the irradiation of cellular blood components (red cells and platelets) with suitable doses of gamma radiation before transfusion (Williamson, 1998; Kaufman, 2010; Lerouge, 2010; Cheryl et al., 2012).
3. **Sterilization of tissue from human donors in transplant surgery to reduce infection rate** (Yang et al., 2013; Allaveisi et al., 2013).
4. **Preparation of sterile hydrogels**. Ionizing radiation is used both to prepare and to sterilize hydrogels, which have practical medical applications. Hydrogels are cross-linked polymeric chains created with slight heat and gamma irradiation of synthetic and natural monomers with natural polymers like agar. The hydrogels are molded according to need in foil impermeable to air or bacteria. Practical applications are contact lenses (silicone hydrogels, polyacrylamides), dressings for burns and other hard-to-heal wounds, disposable diapers, etc. (Gupta and Agarwal, 2011).

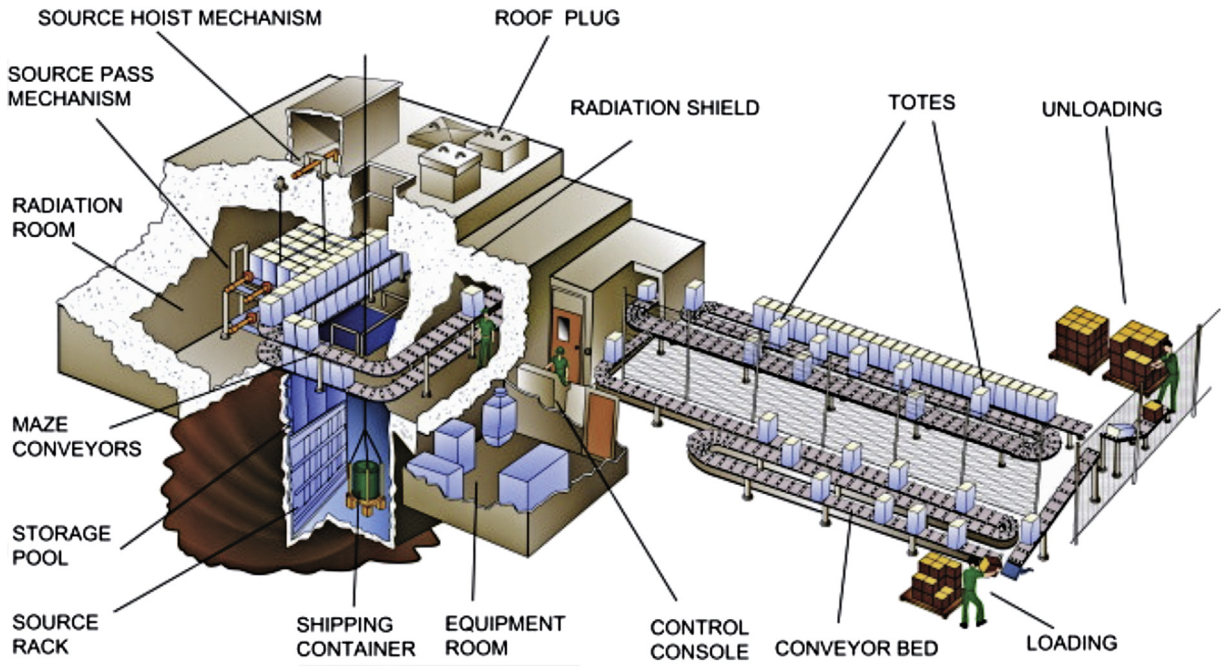

FIGURE 1.46 A high-volume ^{60}Co irradiation facility. *Courtesy of Nordion, Inc., Ottawa, ON, Canada.*

5. **Irradiation of food and agricultural products**. Various types of food and agricultural products may be treated with ionizing radiation for objectives including disinfestation of seed products, flours, fresh and dried fruit, spices etc. sprout inhibition, killing pathogenic bacteria in meat, poultry, and fish, increasing food shelf life, etc. The US Food and Drug Administration approved the irradiation of spinach as a measure to reduce outbreaks of bacterial infection (IAEA, 2010). Radiation treatment of food helps prevent spoilage by killing or attenuating pathogenic microorganisms and preventing the reproduction of insect pests that often accompany agricultural products. For example, irradiation can inhibit sprouting in potatoes, onions, and garlic; extend the shelf life of strawberries and other types of fruit by delaying mold growth and decay; delay spoilage of poultry, meat, and fish by killing pathogenic bacteria like *Salmonella*; and increase the shelf life of spices by killing microorganisms and insects. The *Nuclear Technology Review* (IAEA, 2013a) reports that gamma radiation is predominantly used for this purpose, although the use of electron beam and X-radiation for irradiation of food is increasing worldwide. For example, 95% of the 170 food irradiation facilities in China use gamma radiation; and in the European Union 26 irradiation facilities use gamma radiation and six use electron beams (IAEA, 2013a). A high-throughput gamma-irradiation facility is illustrated in Fig. 1.46.
6. **Synthesis of radiation-cured rubber free of carcinogenic compounds**. Ionizing radiation may be used in conventional rubber vulcanization for the manufacture of tires, disposable gloves, and other rubber products (El-Nemr, 2011; Scagliusi et al., 2012).
7. **Manufacture of radiation-induced heat-shrinkable plastics and curing of coatings and adhesives**. Ionizing radiation is used in the manufacture of plastics for the packing industry. This may include radiation cross-linking in the manufacture of wire insulations, plastic piping, and other materials to increase their resistance to heat, chemical attack, and/or mechanical damage, and radiation grafting of polymers to other materials (Drobny, 2012a,b,c). Radiation curing of coatings and adhesives is an attractive technology for the fabrication of high-performance composite materials (Martin et al., 2014).
8. **Manufacture of radiation-cured wood polymer composites**. Radiation curing of wood polymer composites, which are often used for flooring, gives resistance to insect attack, moisture, fire, and abrasion. Also, radiation curing of surface coatings of wood, plastics, and metals increases their potential for use in the industrial manufacture of a wide spectrum of goods and electronic appliances (Cleland and Stichelbaut, 2013).
9. **Irradiation of hospital waste to kill disease-causing bacteria and microorganisms**. Ionizing radiation can be used to convert hazardous hospital waste to conventional refuse.
10. **Gamma-ray and X-ray sterilization of insects released in the wild to control and eradicate insect pests by SIT**. The mass rearing of insects, their sterilization, and release of sterile males in the wild to control and eradicate insect pests is described in detail in Section 1.3.1 of this chapter.

11. **Use of electron-beam radiation to process polluting industrial emissions of NO_x and SO_2 and purify flue gas emitted into the atmosphere**. Electron-beam radiation converts the oxides of nitrogen and sulfur to a residue that can be used as fertilizer. Both nitrogen and sulfur are major nutrients required by crops for optimum growth. Their removal from industrial flue gas helps reduce acid rain while leaving a valuable by-product (Chmielewski et al., 2012; Calinescu et al., 2013; Gogulancea and Lavric, 2014).
12. **Irradiation of domestic sewage sludge with ^{60}Co gamma radiation or accelerator electron-beam radiation**. Irradiation of sewage sludge can have various advantages, including killing pathogenic microorganisms for safe release of the sludge into the environment (Benny et al., 2011; Jebri et al., 2013), the degradation of organic chemical contaminants that would cause an environmental risk (Bao et al., 2014), the promotion of sludge disintegration and solubilization in treatment waters (Chu et al., 2011; Kim et al., 2013b; Xie et al., 2014), and reduction of algal toxicity and the toxicity of antimicrobial compounds (Kim et al., 2013a).
13. **Use of gamma radiation or electron beams in preparing attenuated vaccines to combat disease**. Ionizing radiation is effective in attenuating viruses to create vaccines capable of providing immunization against disease. For example, the *Nuclear Technology Review* (IAEA, 2012) reports that radiation-attenuated virus-based vaccines have been successfully developed for a number of infectious diseases, including polio, yellow fever, measles, and smallpox. Promising advances have been made in the development of a gamma-radiation-attenuated vaccine for malaria (*New York Times*, 2011; *New England Journal of Medicine*, 2011), which would be the first vaccine for a human disease caused by a parasite. Research is currently under way to have an effective, safe, and deployable malaria vaccine before the year 2020.
14. **Radiation sterilization of contaminated mail**. After letters postmarked on October 9, 2001 contaminated with powdered anthrax (spores of *Bacillus anthracis*) were mailed to US senators and news media figures, the US Postal Service began irradiating mail with an electron beam from a linear accelerator (Courtesy, 2014; Desrosiers et al., 2005). Currently mail addressed to US federal government offices and congressional offices is irradiated with electron-beam technology to sterilize it (US EPA, 2014).
15. **Radiation processing of natural polymers**. Many polymers harvested as natural resources, including starch (polysaccharides from crops such as potato, cassava, and maize), chitin (an *N*-acetylglucosamine polymer from the exoskeletons of crabs, lobsters, and shrimp), keratin (polypeptides from animal horn, hair, and nails), alginate (anionic polysaccharide from algae cell wall), pectin (heteropolysaccharide from plant cell walls), and carrageenan (linear sulfated polysaccharides from seaweed), among others, are processed with gamma or electron-beam radiation. Irradiation of natural polymers facilitates degradation, grafting, and cross-linking to produce hydrogels, nanoparticles, controlled drug delivery systems, and other products useful in medicine, agriculture, and biotechnology (Ražem and Katušin-Ražem, 2008; Liu et al., 2009; Huang et al., 2009; Arvanitoyannis, 2010).

Gamma radiation from cobalt-60 sources is most commonly used for large-scale sterilization of healthcare products, food, and industrial materials. Accelerated electron beams are also used as a source of radiation. An electron beam can be converted to a source of penetrating X-radiation when the beam is directed toward a high−atomic number target such as tungsten. A typical industrial-scale cobalt-60 irradiation facility is illustrated in Fig. 1.46.

The products to be irradiated are placed in standard boxes, known as totes. The boxes are transported on a conveyer belt into the radiation room, where a cobalt-60 source of gamma radiation is hoisted up from its storage pool below ground to a position between the boxes. The boxes remain exposed to the gamma radiation for the period of time necessary to receive the calculated dose, measured in units of the gray (Gy), required to achieve the objectives of the radiation, according to the cobalt-60 gamma-ray activity measured in units of the curie (Ci) or becquerel (Bq). (Units of radiation activity and radiation dose are described in this book.) Typical dose requirements for radiation processing applications in units of kilogray (kGy) are reported by the IAEA (2005c) as follows: irradiation of blood for preventing transfusion-associated graft versus host disease (0.02−0.04 kGy); irradiation of potatoes, onions, and garlic to prevent sprouting (0.05−0.15 kGy); irradiation sterilization of insect pests (0.1−0.5 kGy); irradiation of strawberries and other fruits to extend shelf life (1−4 kGy); irradiation of fish, poultry, and meat to delay spoilage and kill pathogenic bacteria (1−7 kGy); irradiation of spices to extend shelf life by killing microorganisms and insects (1−30 kGy); irradiation sterilization of healthcare products (15−30 kGy); and irradiation of polymers for cross-linking and grafting (0.2−250 kGy). Electron-beam radiation sterilization of mail by the US EPA uses a dose of 56 kGy (US EPA, 2014).

Data provided by the *Nuclear Technology Review* (IAEA, 2004) shows that there are over 160 industrial gamma-ray irradiation facilities working worldwide on a service basis; and more than 20% of these are equipped with facilities in excess of 1 MCi of ^{60}Co. There are approximately 1200 electron-beam facilities applied to radiation processing worldwide.

As noted in the numerous examples cited in this chapter, radiation processing and radioisotope applications have a great impact on social and industrial development of nations worldwide. The benefits include the betterment of human health, comfort, and environmental protection. In addition, the economic impact of radiation processing and radioisotope applications is substantial. The output of a few industrial applications for the sterilization of medical supplies, the production of semiconductors for detection and measurement of radiation, and the production of radiation-cured radial tires in Japan and the United States amounted to US$39.3 and US$55.5 billion, respectively (IAEA, 2004c).

1.7 NUCLEAR POWER

There are three peaceful applications of nuclear power, namely nuclear fission for generation of electricity; desalination of seawater, which requires a large source of economically feasible energy, easily provided by nuclear power; and nuclear fusion, the source of power for the electricity of the future. These applications are treated below.

1.7.1 Nuclear Fission

This book describes the discovery of nuclear fission in early 1939 by Otto Hahn and Fritz Strassmann, with critical interpretation provided by Lise Meitner and Otto Frisch. This was followed by the calculations of Robert Anderson, Enrico Fermi, and Leo Szilard in July 1939 to give the approximate number of two neutrons produced per each neutron-induced fission of a uranium-235 nucleus; and in August the same year Walter Zinn and Leo Szilard made more precise calculations, arriving at the average number of approximately 2.3 neutrons. These historic findings, all within the period of one year, illustrated the possibility of a nuclear chain reaction, which could be controlled to release and harness immense amounts of energy for electric power through nuclear fission. The first successful demonstration of a controlled nuclear chain reaction on December 2, 1942 by Enrico Fermi and collaborators at the University of Chicago is described in this book. Two years later, in December 1944, Enrico Fermi and Leo Szilard jointly filed a highly classified patent as co-inventors of the atomic pile, describing how the self-sustained nuclear chain reaction had been achieved and could be used for nuclear power.

The invention of the nuclear reactor for the peaceful application of nuclear energy to provide electric power to cities was declared by some to be one of the most significant inventions of all time, comparable to those of the telegraph and telephone by Samuel Morse and Alexander Graham Bell. In 1944 the "New Piles Committee" was formed, with the participation of Enrico Fermi, Leo Szilard, and Nobel Laureates James Frank and Eugene Wigner among other physicists, chemists, and engineers, including Walter Zinn and Alvin Weinberg. The New Piles Committee meetings explored and recommended designs for peaceful electricity-producing nuclear reactors. Many new reactor concepts were presented, and would become the modern power reactors that supply the needed electricity for cities around the world.

Not until after the Second World War, on December 20, 1951, was electricity finally generated from a nuclear power reactor—the Experimental Breeder Reactor-I at the National Reactor Testing Station in Idaho, USA (IAEA, 2004). The breeder reactor, first conceived by Fermi and Szilard, is described in this book. Today, we have already celebrated 60 years of the comforts and benefits of nuclear power. Data from the *Nuclear Technology Review* (IAEA, 2013a, 2015) shows that at the end of 2014 there were 438 nuclear power plants in operation in 31 countries, supplying approximately 16% of the world's electricity. There were 70 new power reactors under construction in 2015 in nine countries, and it is foreseen that the use of nuclear power will grow worldwide to meet the expanding energy needs of this century. The critical role that nuclear power plays as a source of energy was commemorated in a postage stamp issued in Finland, which depicts a reactor core producing heat from nuclear fission, and a wave of electricity generated from that heat. Use of nuclear power worldwide is expected to grow, as forecast by an international meeting in Paris of 74 government representatives organized by the IAEA in March 2005 on the future role of nuclear power. The meeting concluded with the affirmation of the vast majority of participants that nuclear power would contribute to a great extent to helping the world meet its energy needs through the 21st century. The foreseen growth in nuclear power is due to several factors, including the growing demand for energy to sustain development around the world, the environmental constraints and the need to reduce global pollution from greenhouse gas emissions by reducing burning of fossil fuels, concerns over future energy supplies, and lower generating costs and improvements in nuclear power safety. The *Nuclear Technology Review* (IAEA, 2006, 2013, 2015) gives an overview of the current and future advances in fission, which include cost reductions, safety enhancements, and proliferation resistance. It concludes that if we are to meet even a fraction of the economic aspirations of the developing world, energy supplies must expand significantly; and that

demand for oil and natural gas will grow faster than supply. Concerning the future of nuclear power, the *Nuclear Technology Review* (IAEA, 2013a) notes: "When studying their energy choices, a significant number of countries are considering nuclear power as an option. The factors contributing to the continuing interest in nuclear power include the increasing global demand for energy, as well as concerns about climate change, volatile fossil fuel prices and security of energy supply." However, after the 21st century the world is expected to enjoy a much safer and more efficient source of electric power, namely fusion, which is discussed in Section 1.7.3.

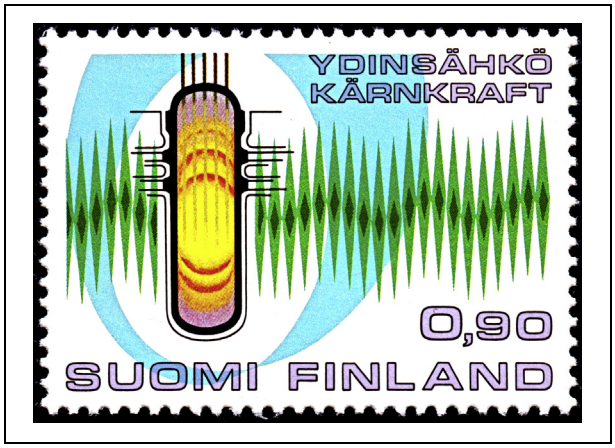

1.7.2 Desalination

Desalination refers to the removal of the excess salt or other minerals from water, such as seawater, to obtain fresh water suitable for irrigation or human consumption. The desalination process may include several steps, such as multistage flash distillation or reverse osmosis using semipermeable membranes. Details of the techniques involved are described in books, including IAEA (2001), El-Dessouky and Ettouney (2002), Lauer (2006), and Escobar and Schafer (2010). Desalination requires high inputs of energy from electric power tapped from conventional fossil-fuel-burning plants, nuclear power, or a combination of the two.

Current and future global needs for fresh water were underscored by the *Nuclear Technology Review* (IAEA, 2004c): "Of all the earth's water only 2.5% is freshwater and 70% of the freshwater is frozen in the icecaps of the Antarctica and Greenland, and most of the remaining freshwater is found in the form of soil moisture or deep within inaccessible aquifers, or arrives on earth in the form of monsoons or floods that are difficult to contain or exploit. This leaves very little, less than 0.08%, of the earth's fresh water available for human consumption. There are currently about 2.3 billion people living worldwide in water-stressed or water-scarce areas. By the year 2025 it is foreseen that the number of people suffering from water stress or scarcity will increase to 3.5 billion."

There were over 17,000 desalination plants in operation worldwide in 2014, according to the International Desalinization Association (http://idadesal.org/desalination-101/desalination-by-the-numbers/), and about 60% are located in the Middle East. To meet the growing needs for fresh water, the demand for the desalination of seawater is on the rise, and it is foreseen that the need for fresh water from the sea will increase unabated through the century as countries develop and increase in population, with concomitant needs for increased water supply for agricultural production and human consumption. The high energy inputs for desalination are provided largely by conventional fossil fuel power plants, although nuclear power is used in some countries, and the role of nuclear power in desalination is foreseen to increase for many of the same reasons presented for the predicted increase in nuclear power in general. An additional factor in the increased role of nuclear power in desalination was underscored in the *Nuclear Technology Review* (IAEA, 2004c), where it was noted that the high-temperature gas-cooled reactor (HTGR), which is one of the leading reactor concepts for future power needs, is particularly suited for desalination. The advantage of the HTGR for desalination is the virtually cost-free waste heat produced by the reactor in the desired temperature range of 100−120°C, which is needed for seawater desalination—of the total production costs of desalination, 30−50% is attributed to energy costs. There is thus a high potential of increased use of nuclear power, particularly the HTGR, since it has the advantage of offering increased thermal energy utilization, in addition to electricity, as a safe, clean, and economically competitive heat source (IAEA, 2005d).

1.7.3 Nuclear Fusion

1.7.3.a Principles

Nuclear fusion is the process whereby nuclei join together into one nucleus. Such an occurrence is not possible at normal temperatures, because the repulsive coulombic forces between the positive charges of atomic nuclei prevent them from mingling in the required close proximity for them to coalesce into one. However, at temperatures of about 100 million degrees Centigrade the nuclei of atoms become plasmas in which nuclei and electrons move freely, with high kinetic energy sufficient for the nuclei to overcome their repulsive forces and combine. Because of the high temperatures required, the process is also referred to as thermonuclear fusion. The theory, principles, and energies released in various fusion reactions are discussed in detail in the chapter entitled "Neutron Radiation" of this book.

The fusion of light elements, such as deuterium (^{2}H) and tritium (^{3}H), releases an energy per nucleon (MeV/u) or energy per unit of material considerably greater than can be achieved by nuclear fission. Thermonuclear fusion requires energy to reach high temperatures and maintain nuclear plasma, but once achieved, the energy output is greater than the input. An additional advantage of the nuclear fusion of deuterium and tritium is that no hazardous radioactive wastes are direct products of the reaction; the products are alpha particles and neutrons. The neutrons can produce some radioactive isotopes in the surrounding reactor shielding material, but most would be short-lived and there is no need to store radioactive waste in geological deposits for long periods, as is the custom with nuclear fission.

1.7.3.b Past and Future Developments

TOKAMAK, Russia

Fusion reactors are under development to achieve nuclear fusion as a practical energy source. The reactors are based on maintaining plasmas at high temperature through magnetic confinement in a tokamak. The word "tokamak" is derived from the Russian *toroidal kamera ee magnetnaya katushka*, meaning "torus-shaped magnetic chamber," which was initially designed in 1951 by Soviet physicists and Nobel Laureates Andrei Sakharov and Igor Tamm (UIC, 2005). The significance of the Russian tokamak was commemorated with a postage stamp issued in Russia in 1987. The upper portion of the stamp illustrates the deuterium–tritium (D-T) fusion reaction, and the lower portion shows the tokamak reactor with a section cut away to illustrate the vacuum chamber where the plasma is contained for D-T fusion. The various components of the tokamak are described in the next subsection. A momentous D-T plasma-burning experiment was performed with 0.2 g of tritium fuel with the Joint European Torus reactor in the UK in 1991; and a higher-power D-T experimental program with 20–30 g of tritium was continued on the tokamak fusion test reactor at Princeton in 1993. The European reactor achieved 16 MW of fusion power over approximately 1 s in 1997; and a long-duration plasma of 4.5 min was sustained with a

heating power of 3 MW in the Tore Supra device at Cadarache, France in 2002 (Magaud et al., 2004). The experimental advanced superconducting tokamak in China had a successful plasma test in 2006 (Wan et al., 2007; Xiao et al., 2008). This tokamak was an advanced design for toroidal and poloidal magnetic confinement of plasma; this design is currently under construction in Cadarache by the international ITER project described in the next paragraph. In addition, a plasma function with diagnostic tests was conducted on the Korea Superconducting Tokamak Advanced Research (KSTAR) fusion reactor in 2008 (Park et al., 2010).

Under the auspices of the IAEA, the international project ITER, meaning "the way" in Latin, to signify "the way to new energy," was created in 1988 with the purpose of designing and constructing a fully operational prototype fusion reactor. There are seven signatories of ITER (China, the European Union, India, Japan, the Russian Federation, the Republic of Korea, and the United States), all of which will provide the financial input and technical cooperation required for the construction and operation of the reactor. The design of the ITER Tokamak fusion reactor was approved by the signatory members in 2001; and the site where the reactor would be constructed was agreed in 2005 to be in southern France at Cadarache, near Aix-en-Provence. The fusion reactor now under construction will begin plasma experimentation in 2020, and the reactor is expected to be fully functional with D-T fusion by 2027. The prototype reactor is intended to demonstrate that fusion can produce relatively safe energy with a high net energy yield—that is, more energy output than energy put into the system. Fusion energy production via a large-scale commercial reactor with the capacity to generate electric power and produce its own tritium fuel will be the next step after ITER. This full-scale commercial fusion reactor is planned with the project DEMO, or demonstration power plant. DEMO is expected to begin operation around the year 2030, with connection to the electrical grid in 2040.

1.7.3.c Fusion Power Reactor

A schematic cutaway view of a fusion power reactor, based on magnetic confinement of the hot plasma, is illustrated in Fig. 1.47. Five major components of the reactor are identified by the encircled letters A—E. Firstly, D-T fuels are introduced into an inner vacuum chamber at A. This is a closed chamber with the shape of a torus. The D-T are heated in excess of 150 million °C and enter into the plasma state (B). Heating, which is required to take the D-T to the plasma state illustrated at (A) in Fig. 1.47, is accomplished by three means: ohmic heating, which is the result of the changing magnetic fields used to confine the plasma within the center of the vacuum chamber—these magnetic fields create a very intense electrical current through the plasma, causing the charged particles to travel and collide, creating a resistance and heat; neutral beam injection; and high-frequency electromagnetic waves. As described by ITER (http://www.iter.org/sci/plasmaheating), neutral beam

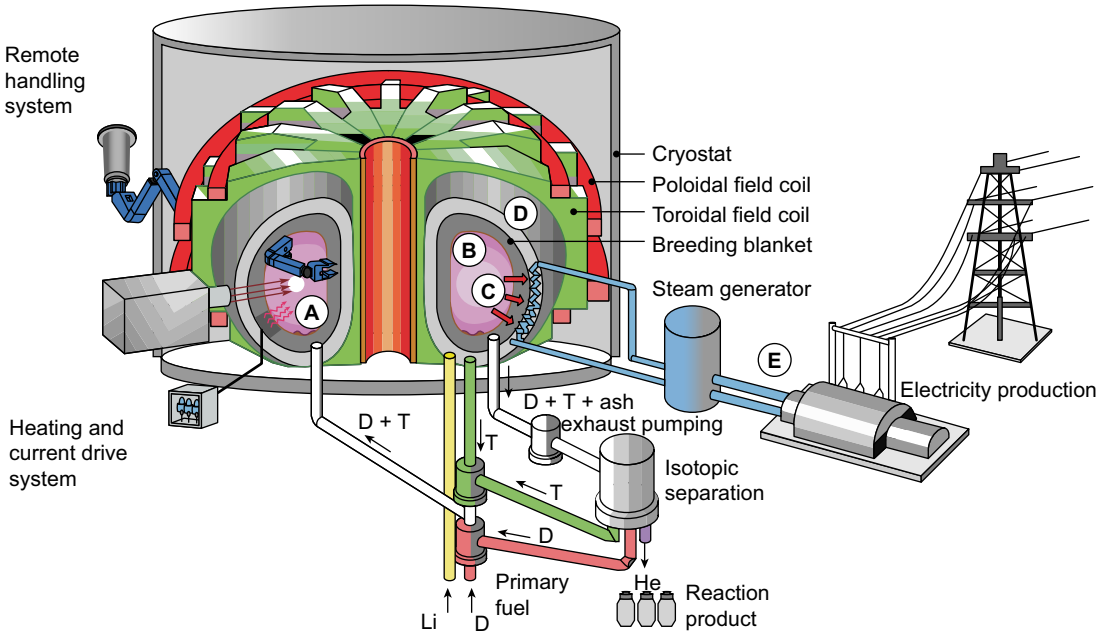

FIGURE 1.47 Schematic and cutaway view of a fusion reactor based on a magnetic confinement of plasma: (A) vacuum chamber, (B) plasma, (C) plasma radiation, (D) blanket, and (E) electricity production. *From Magaud, P., et al., 2004. Nuclear fusion reactors. In: Cleveland, Cutler J. (Ed.-in-chief), Encyclopedia of Energy. Elsevier, pp. 365—381, printed with permission from Elsevier © 2004.*

injection involves accelerating high-energy particles into the plasma. Deuterium particles are accelerated to the required energy level and subsequently stripped of their electrons with an "ion beam neutralizer." Upon entering the plasma at high velocity, the high-energy deuterium nuclei undergo collisions and thus transfer their energy to the plasma particles. This process brings the temperature of the plasma close to that required for D-T fusion. Irradiation with high-frequency electromagnetic radiation increases the temperature of the plasma to the desired ~150 million °C, which is more than sufficient for fusion to occur. The hot plasma is kept within the central region of the inner chamber by magnetic confinement using toroidal and poloidal field coils. The plasma produces energy with the fusion of D-T and the emission of 3.52 MeV helium nuclei and 14.06 MeV neutrons according to the fusion reaction

$$^{2}_{1}\mathrm{H} + ^{3}_{1}\mathrm{H} \rightarrow ^{4}_{2}\mathrm{He} + ^{1}_{0}\mathrm{n} + 17.58\ \mathrm{MeV} \qquad [1.9]$$

The high-energy 14.06 neutrons account for 80% of the energy liberated from this nuclear fusion. The high-energy neutrons possess no charge and thus can penetrate the magnetic confinement and deposit energy into the outer blanket of the chamber. The energy liberated is absorbed by this outer chamber blanket, illustrated at (C) in Fig. 1.47, and the heat is utilized to produce steam to operate a turbine and generate electricity at (E). The neutrons thus lose energy and are absorbed by lithium nuclei in a breeding blanket at (D). The breeding blanket contains a high concentration of lithium to produce tritium according to the reaction

$$^{1}_{0}\mathrm{n} + ^{6}_{3}\mathrm{Li} \rightarrow ^{3}_{1}\mathrm{H} + ^{4}_{2}\mathrm{He} + 4.78\ \mathrm{MeV} \qquad [1.10]$$

With the breeder blanket, the ITER fusion reactor will be equipped to produce more tritium fuel than it consumes to produce power. The tritium produced by the reactor can be introduced along with deuterium as fuel when required. Ash, consisting of helium ions and unconsumed D-T, is extracted from the inner chamber, as illustrated in Fig. 1.47, and separated to collect the helium; and the unconsumed D-T are reintroduced into the inner chamber. The cryostat, illustrated in Fig. 1.47, is the cooling system and physical enclosure surrounding the vacuum chamber, providing thermal insulation for the superconducting magnets required for plasma confinement.

1.7.3.d Plasma Magnetic Confinement

Magnetic confinement is required to keep the D-T nuclei from escaping, so that they may fuse and release energy. The toroidal field coils of the ITER reactor run perpendicular to the plasma of charged nuclei and electrons, as illustrated in Fig. 1.48, creating a high magnetic energy of 41 GJ and a maximum magnetic field strength of approximately 12 T (ITER,

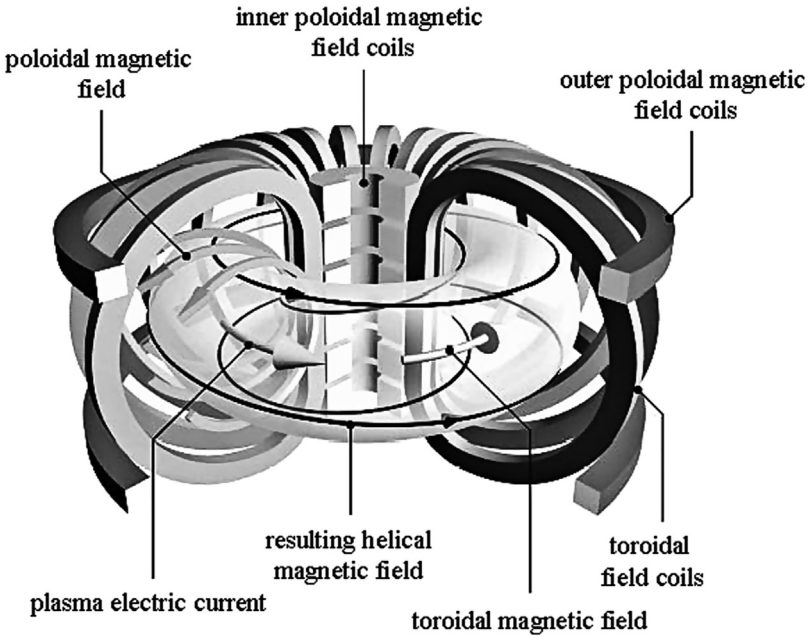

FIGURE 1.48 Tokamak magnetic configuration. *From Gaye, O., et al., 2013. Robust stabilization of the current profile in tokamak plasmas using sliding mode approach in infinite dimension. Control Eng. Pract. 21 (10), 1350–1358, reprinted with permission from Elsevier © 2013.*

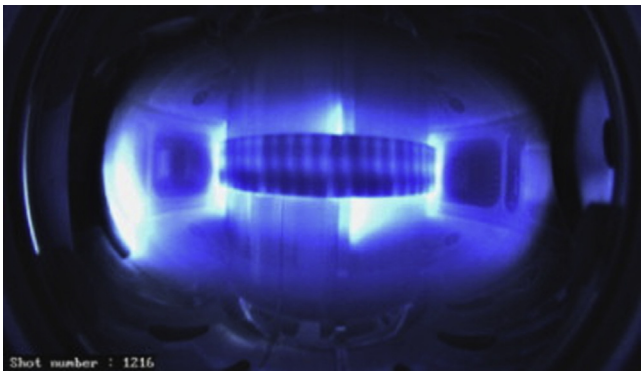

FIGURE 1.49 Image of the magnetically confined plasma in the KSTAR fusion reactor, taken with a remote visible TV with 210 Hz frame at shot 1216. *From Park, M., et al., 2010. Data acquisition system implemented with various platforms for KSTAR diagnostic systems. Fusion Eng. Des. 85, 350–355, reprinted with permission from Elsevier © 2010.*

http://www.iter.org/mach/magnets). As described by ITER, the poloidal field coil system consists of six horizontal coils outside the toroidal coils. The poloidal field magnets squeeze the plasma inward, away from the walls of the vacuum chamber housing the plasma. The poloidal field, which is created by the magnets and the charged particles traveling in the plasma, twists the magnetic field lines to maintain the shape and stability of the plasma. Thus the hot plasma is confined to travel within the torus-shaped inner chamber of the fusion reactor, away from the walls of the chamber. A plasma squeezed within the chamber with its toroidal and poloidal magnetic fields is illustrated in Fig. 1.48. The figure shows the directions of the toroidal and poloidal magnetic fields, which maintain the hot donut-shaped plasma within the inner chamber. The toroidal field lines run horizontally together with the plasma ions, whereas the poloidal field lines run vertically around the plasma, pinching it inward away from the chamber walls.

An image of the plasma within which D-T fuse at high temperature, taken with a remote visible TV, is provided in Fig. 1.49. The central high-temperature region of the plasma emits radiation of wavelengths invisible to our eyes; however, the image is that of the colder outer regions of the magnetically confined plasma. From the image one can visualize how the plasma is confined within the torus-shaped inner chamber of the fusion reactor.

1.7.3.e Size and Energy Output of the ITER Tokamak

The ITER reactor will be the most complicated device ever manufactured, with over 1 million parts and weighing over 23,000 tons. As described by ITER (https://www.iter.org/construction/assembly), the assembly will require 1.5 million person-hours over a period of four years. It will measure 30 m in diameter and approximately 30 m in height. The reactor will contain 10,000 tons of magnets, which will shape and confine the hot plasma inside the vacuum chamber assembly. The magnetic field generated will be over 200,000 times stronger than that of planet Earth (https://www.iter.org/mach). The inner surface of the vacuum chamber, within which the plasma will be contained, will be covered with 440 blanket modules measuring 1×1.5 m and weighing approximately 4 tons. These blanket modules will serve to shield the vacuum vessel of high-energy neutrons produced by the fusion reaction (https://www.iter.org/mach). Fig. 1.50 gives a cutaway view of the ITER Tokamak, showing a portion of the donut-shaped plasma within the vacuum chamber where the D-T fusion occurs during reactor operation.

The ITER Tokamak is designed to produce 500 MW of fusion power from 50 MW of input power to yield a Q value $\geq$10, which is a 10-fold net energy output. In other words, the ITER fusion reactor should produce 10 times the energy that it will consume.

1.7.3.f Advantages of Fusion

Fusion is the energy of the future; and we may state optimistically that it is the energy of the relatively near future. The fusion of D-T in a tokomak reactor has been demonstrated. As described, the ITER reactor will begin plasma experimentation in the year 2020; and the DEMO reactor, which will be the first full-scale fusion power plant, is planned to begin operation in 2030 with connection to the electric power grid in 2040. In the next three decades we should see a functioning full-scale fusion power plant producing relatively safe electricity and more power output than the energy consumed by the reactor. By the next century, we can expect and hope that fusion will be the energy of choice over the reactors that now produce considerable radioactive waste. Thus fusion reactors and solar and wind power constitute sources of electricity that produce neither greenhouse gases nor long-lived radioactive waste.

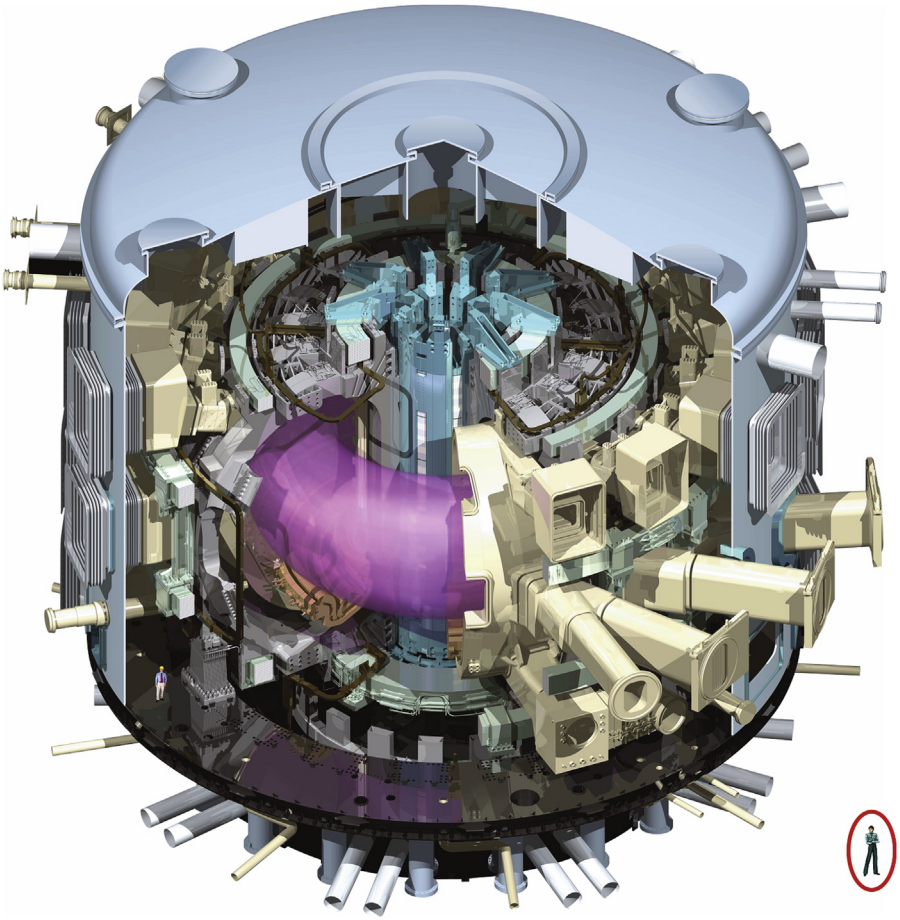

FIGURE 1.50 A cutaway view of the ITER Tokamak fusion reactor showing part of the donut-shaped plasma (colored purple) inside the vacuum vessel. In the lower right-hand corner is an image of a person standing next to the reactor, circled in red, which serves as a reference to the relative size of the reactor. *Courtesy of ITER, © ITER Organization, http://www.iter.org/.*

Current optimism over fusion reactors for electric power is based on overwhelming advantages that D-T fusion offers over current nuclear fission power reactors. These advantages are described briefly below.

1. **No danger of a runaway nuclear chain reaction**. Unlike nuclear fission, any misfortune such as a tsunami, earthquake, or simple negligence would not result in any out-of-control chain reaction that could spew radioactive contamination into the environment. Nuclear chain reactions are not involved in a fusion reactor. Any misfortune that could break the reactor would automatically and immediately shut the fusion reaction down, because the continuous heating and feeding of D-T into the plasma would be disrupted. As noted by Magaud et al. (2004), the slightest uncontrolled interference with the environment of a fusion reactor causes the rapid cooling and automatic shutdown of the fusion reaction.
2. **No long-lived radioactive waste**. Fusion reactors do not use or produce long-lived radioactive materials, and do not produce long-lived fission products. The fusion of D-T produces alpha particles and high-energy neutrons. The neutrons produce heat and more tritium fuel upon reaction with Li-6, and mostly short-lived radionuclides when neutrons are absorbed by nuclei of the materials with which the fusion reactor is constructed. These materials have a relatively short half-life and would not require the deep underground storage facilities for long-lived radioactive waste now necessary for current fission reactor waste. In point of fact, if we compare an equal amount of energy produced by a fusion reactor and a coal-burning plant, the burning of coal produces more long-term radioactive waste, as the ash from coal burning contains long-lived radioactive uranium and thorium (Magaud et al., 2004). Fig. 1.51 illustrates the relative amounts of long-lived radioactive waste that result from fission, coal, and fusion. Fission and coal burning leave significant radioactive waste beyond 500 years; whereas after only 50 years of fusion reactor shutdown there is no significant long-lived radioactive waste and no need for deep underground waste storage.

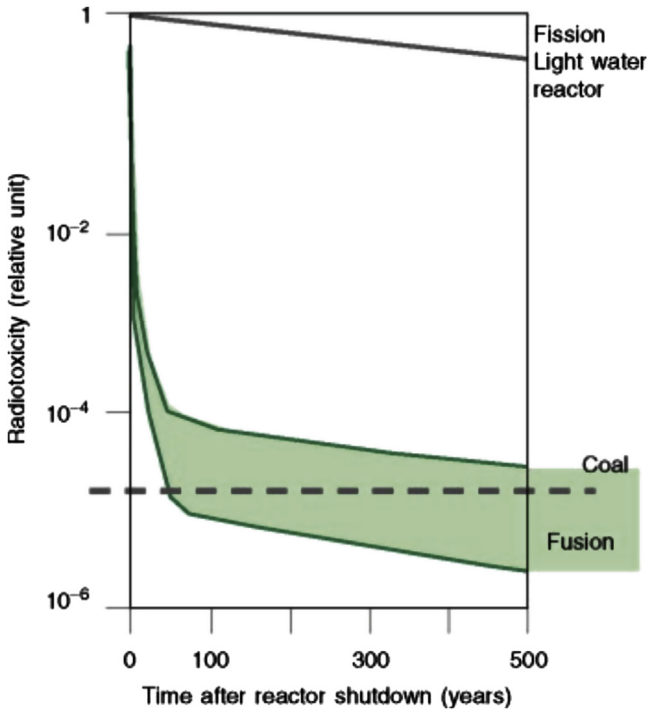

FIGURE 1.51 Radiotoxicity of fusion waste after reactor shutdown. The green shaded area shows the significant difference between coal and fusion with respect to long-term radioactive waste production. *Figure from Magaud, P., et al., 2004. Nuclear fusion reactors. In: Cleveland, Cutler J. (Ed.-in-chief), Encyclopedia of Energy. Elsevier, pp. 365–381, reprinted with permission from Elsevier © 2004.*

3. **No radioactive fuel is required**. The fuels required for fusion are deuterium and lithium, both of which are not radioactive. Although the fusion of D-T is the reaction liberating energy for power, the elements considered as fuel components for fusion are deuterium and lithium, as they are the elements required in relatively large quantities. Tritium is needed only in relatively small quantities for the startup of the fusion reaction. The tritium, which is radioactive but with a relatively short half-life, would be produced by the neutrons emitted during fusion and subsequently fed into the fusion chamber when needed. All the tritium needed for power would be produced by the fusion reactor.
4. **The only fuel elements required for fusion, deuterium and lithium, are abundantly available**. Deuterium is readily extracted from seawater, which contains inexhaustible amounts (33 g of deuterium/m^3 of seawater); and lithium would be used in the reactor to breed the required tritium for the fusion reactor. Magaud et al. (2004) note that <1 kg of deuterium and <10 kg of naturally occurring lithium would be required for a day's generation of 1000 MWe of power. Lithium deposits are massive, with global deposits totaling 31.1 million tons of Li (Kesler et al., 2012). In addition, the world's oceans contain 44.8 billion tons of recoverable lithium (Yaksic and Tilton, 2009).
5. **Extraction of fuel for fusion will have minimal effect on the environment**. Obtaining deuterium and lithium fuel for fusion from seawater will cause minimal effect on the environment; whereas the mining of uranium deposits for fission reactor fuel has a significant effect on the environment.
6. **The fusion reactor will yield more power than energy input**. The ITER prototype fusion reactor requires 50 MW of input power and is designed to produce 500 MW of output power. The reactor will have a Q value ≥ 10; that is, it is designed to produce 10 times the power it will consume. This will be the first reactor to produce net energy (https://www.iter.org/proj/itermission).
7. **No need to evacuate the population in the event of a severe accident**. The overall radioactivity at a fusion reactor would be minimal. The only radioactive isotope involved in the production of fusion energy is tritium; and because tritium is not a fuel component but produced in the lithium breeding blanket to be fed into the plasma as needed, the tritium inventory on site would be minimal. Also, as noted by Magaud et al. (2004), to minimize emission there would be "three confinement barriers: the vacuum vessel, the cryostat, and the reactor building itself…there is no accident sequence that could impugn reactor integrity. Even in the event of a severe accident, it would not be necessary to evacuate the population."
8. **Overall costs of fusion energy would be comparable to those of renewable resources**. Magaud et al. (2004) give an excellent review of the overall costs of fusion power relative to other sources, such as fossil fuel, fission, and renewable resources like solar and wind. A brief summary is provided here. The principal direct costs in the utilization of all energy sources are

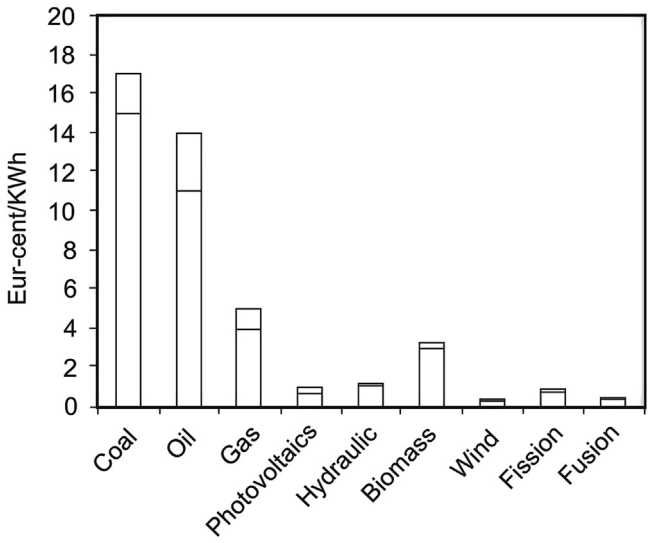

FIGURE 1.52 Comparison of externalities (external costs) of several energy sources in units of euro cents per kilowatt-hour. *From Magaud, P., et al., 2004. Nuclear fusion reactors. In: Cleveland, Cutler J. (Ed.-in-chief), Encyclopedia of Energy. Elsevier, pp. 365–381, reprinted with permission from Elsevier © 2004.*

investment, operation, maintenance, replacement of components, and fuel. Fuel costs of fusion account for less than 1% of the total kilowatt-hour costs; whereas in nuclear fission, fuel costs amount to ~35% of direct costs. Other costs, called externalities, are measured in terms of the cost of effects on our environment and health, and include fuel extraction, plant construction, operation, accident, dismantlement, and disposal of dismantled power sources. For example, the nuclear fuel cycle required for nuclear fission involves mining and nuclear enrichment, which have an effect on our environment. So do the mining and burning of coal. Fusion is predicted to have one of the lowest costs per kilowatt-hour of energy produced, similar to that of renewable resources such as wind and solar, as determined by the European Union (ExternE Studies, http://www.externe.info/externe_d7/) by evaluation of indirect or external costs and illustrated in Fig. 1.52.

1.8 SUMMARY

In summary, the peaceful applications of radioactive sources are numerous and encompass a wide spectrum of fields, from medicine, biology, agriculture, and the environment to industry, nondestructive analysis, and power production. Radioactive sources and nuclear energy applied to peaceful means have enriched our lives in so many ways. The significance of the many peaceful applications of nuclear energy was commemorated by a postage stamp from Canada portraying an atom superimposed over a microscope on one side and a nuclear reactor with electric grid on the other. In the not too distant future, fusion will be demonstrated to be a substitute for the nuclear reactor as a safer and more powerful source of electricity. Only a few examples of peaceful applications and how these touch our everyday lives are provided in this introduction, but the writer hopes that through these the reader will appreciate the significance of the material presented in the rest of the book, if he or she is not already well informed of this realm of science.

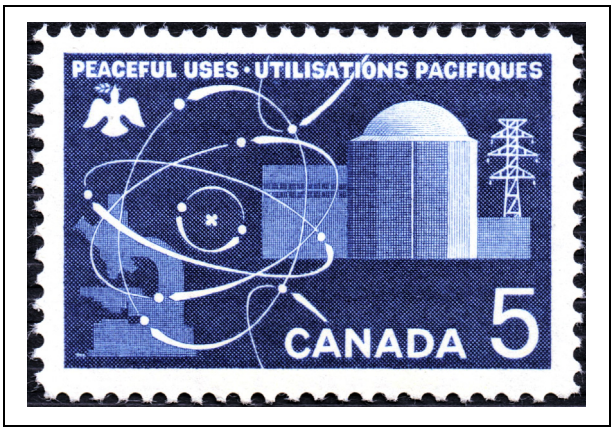

Chapter 2

Basic Concepts and Definitions

I call (them) "isotopes" or "isotopic elements", because they occupy the same place (from the Greek) in the Periodic Table. They are chemically identical, and save only as regards the relatively few physical properties which depends on atomic mass directly, physically identical also.

This is a quote from Nobel Laureate Frederick Soddy (1913a,b), who coined the word "isotopes" to refer to atoms that have the same atomic number (ie, the number of protons in the nucleus) but different mass number (ie, the number of protons plus neutrons in the nucleus). Soddy recognized that these are atoms of the same element in the periodic table, but of different mass.

Radioactivity is the emission of radiation originating from a nuclear reaction or the spontaneous decay of unstable atomic nuclei. The term "radioactive decay" refers to the process whereby unstable atomic nuclei decay with the loss of energy by the emission of elementary particles (eg, alpha particles, beta particles, neutrons, or gamma-ray photons) directly from the nucleus, or the emission of particles from electron shells of atoms (eg, Auger electrons and X-ray photons) within which the nucleus resides. The rate of decay or disintegration rate of a radionuclide (ie, a specific radioactive isotope of an element) is directly proportional to the mass of the radionuclide.

2.1 PROPERTIES OF ATOMIC CONSTITUENTS

The properties of the atomic constituents that are relevant to topics dealt with in this book are rest mass, charge, spin, magnetic moment, and stability. The atomic constituents in this section are limited to the proton, neutron, and electron (Table 2.1). The properties of particles that are found in the underlying structure of protons and neutrons, namely quarks and gluons, are discussed later in the book. Several units of rest mass are given in Table 2.1, as these are used throughout the book, including the expression of mass in terms of energy, the electron volt, or joule, the unit of energy established by the International System of Units. A brief description of the terms used for the properties of atomic constituents is as follows.

Rest mass: The rest mass, which is the mass of the particle at rest relative to an observer, is expressed in four units, namely kilograms (kg) or atomic mass units (u), and the energy equivalence of the rest mass ($E = m_0c^2$) in joules (J) or electron volts (eV). The atomic mass unit (u) is defined in terms of the stable carbon nuclide ^{12}C, which is assigned an

TABLE 2.1 Properties of Atomic Constituents

Property	Proton	Neutron	Electron
Rest mass	1.67262×10^{-27} kg	1.67492×10^{-27} kg	9.10938×10^{-31} kg
	1.50327×10^{-10} J	1.50534×10^{-10} J	8.18710×10^{-14} J
	938.271 MeV	939.565 MeV	0.510998 MeV
	1.007276466 u	1.008664915 u	0.0005485799 u
Charge	$+e$	Zero	$-e$
	$+1.602 \times 10^{-19}$ C		-1.602×10^{-19} C
Spin	½	½	½
Magnetic moment	1.410×10^{-26} J/T	-0.966×10^{-26} J/T	928.476×10^{-26} J/T
Stability	Stable	10.2 min half-life	Stable

Radioactivity: Introduction and History, From the Quantum to Quarks. http://dx.doi.org/10.1016/B978-0-444-63489-4.00002-2
Copyright © 2016 Elsevier B.V. All rights reserved.

atomic mass of exactly 12 u where 1 u = 1.660540×10^{-27} kg. The rest mass of the proton or neutron is approximately 1,840 times that of the electron.

Charge: The charge on the particle is expressed on the basis of the unit electron charge $+e$ or $-e$ or in units of the coulomb (C). The neutron is neutral or without charge. A **neutral atom** is one that possesses a number of external electrons equal to the number of protons in the nucleus. It may be expressed as ${}^{A}_{Z}\mathrm{X}$, where Z is the **nuclear charge** or **proton number**, ie, the number of protons in the nucleus A is the **mass number** of the nucleus or the sum of the number of protons and neutrons in the nucleus. The number of electrons that the atom possesses is assumed to equal that of Z when the atom is a neutral atom.

Spin: In 1920 Otto Stern and Walter Gerlach observed two spin states of the electron; that is, the electron possesses a magnetic dipole moment which may be quantized in either of two directions, namely with or against an external magnetic field, ie, spin-up or spin-down. The spin states are assigned the values $+\frac{1}{2}\hbar$ or $-\frac{1}{2}\hbar$ where $\hbar$ is Planck's constant reduced or $h/2\pi$. The spin states are abbreviated as $+\frac{1}{2}$ and $-\frac{1}{2}$. The proton, neutron, and electron possess half-integer spin states. Particles with half-integer spins belong to a class of particles called **fermions** (named after Enrico Fermi). Fermions obey the Pauli exclusion principle, which states that no two identical fermions can occupy the same quantum state (energy state) at any given time, as described further on in this book. The property of spin and the Pauli exclusion principle enable the assignment of protons and neutrons to specific quantum levels or shells within the nucleus, and electrons to specific orbitals away from the nucleus.

Magnetic moment: The magnetic moments of the proton and neutron are about a thousandfold smaller than that of the electron. Although the neutron is of neutral charge, it possesses a magnetic moment due to its underlying quark constituents that possess charge. The positive or negative signs designated to the magnetic moments indicate that the spin vectors and the magnetic moments are in opposite direction. The magnetic moments are important properties that establish the basis for magnetic resonance imaging and spectroscopy.

Stability: The neutron is unstable outside the confines of the nucleus. Once outside the nucleus, a neutron has a mean half-life of 10.2 min.

2.2 NUCLIDE NOMENCLATURE

The fact that the atom contains a massive center was discovered by Ernest Rutherford (1911) following experiments that revealed the backscattering of α particles by atoms of gold, as discussed in detail later in this book. The "nucleus" as a massive positively charged center of the atom was proposed by Rutherford (1913) and Niels Bohr (1913) in their classic papers on the structure of the atom. However, it was not until James Chadwick (1932a,b, 1935) discovered the neutron and determined its mass that the structure of an atomic nucleus could be explained to contain a definite number of protons and neutrons. Consequently the terms nuclide, radionuclide, and others related to the atomic nucleus could then be derived, and these are defined in the following paragraphs.

Nuclide: A nuclide is a species of an atom that is characterized by the number of protons (Z) and number of neutrons (N) in its nucleus, and in some cases by the energy state of the nucleus. A symbol for a nuclide can be written in the form ${}^{A}_{Z}\mathrm{X}_{N}$, where X is the symbol for the chemical element, Z is the atomic number or number of protons in the nucleus, A is the mass number or the number of protons plus neutrons in the nucleus, and N is the number of neutrons in the nucleus. Generally, when A and Z are noted with the nuclide symbol, the neutron number N is not written, as it is deduced (ie, $N = A - Z$). For example, the nuclide written as ${}^{90}_{38}\mathrm{Sr}$ represents an atom of the element strontium with a nucleus containing 38 protons and a mass number of 90; and, by difference, we may deduce that the nucleus contains 52 neutrons. The nuclide may also be written in a more abbreviated form as ${}^{90}\mathrm{Sr}$, since the atomic number of the element strontium is known and an invariable number for that element.

There are 266 stable nuclides and 83 unstable or radioactive nuclides that exist naturally on Earth. More than 3000 artificially produced radioactive nuclides are known. The radioactive nuclides are referred to as **radionuclides**. All the nuclides, both stable and radioactive, are organized in "the Chart of the Nuclides." The Chart provides a block containing the properties of each nuclide, which is plotted according to its Z versus N. Small parts of the Chart of the Nuclides are illustrated in Figs. 6.5 and 6.11 of the chapter entitled "Beta Radiation and Beta Decay" of this book. The entire Chart of the Nuclides and the nuclear data for each nuclide can be viewed online on the website of the National Nuclear Data Center (NNDC) of the Brookhaven National Laboratory (http://www.nndc.bnl.gov/nudat2/), or on that of the International Atomic Energy Agency (http://www-nds.iaea.org/relnsd/vcharthtml/VChartHTML.html). The term isotope, which is frequently and erroneously used for the term nuclide, is discussed and defined below.

Isotopes: Nobel Laureate Frederick Soddy coined the word "isotopes" (Soddy, 1913a,b) to refer to atoms that have the same atomic number (ie, the number of protons in the nucleus) but different mass number (ie, number of protons plus

neutrons in the nucleus). Soddy recognized that these are atoms of the same element in the periodic table but of different mass. In his words, Soddy (1913a) explained:

> *I call (them) "isotopes" or "isotopic elements", because they occupy the same place (from the Greek) in the periodic table. They are chemically identical, and save only as regards the relatively few physical properties which depend on atomic mass directly, physically identical also.*

Soddy went further by alluding to the fact that not only can we consider the radioactive atoms of different mass of specific elements as "isotopes," but that many, if not most, of the stable elements may actually consist of a mixture of isotopes. In his Nobel lecture, Soddy (1922) gave credit to the Swedish scientists Strömholm and Svedberg (1909a,b) by quoting them as follows:

> *Perhaps, one can see, as an indication in this direction, the fact that the Mendeleev scheme (Periodic Table of Elements) is only an approximate rule as concerns the atomic weight, but does not possess the exactitude of a natural law; this would not be surprising if the elements of the scheme were mixtures of several homogeneous elements of similar but not completely identical atomic weight.*

Isotopes are nuclides that have the same atomic number (Z), meaning the same number of protons; but they differ in their number of neutrons (N). Thus they differ in their mass number (A), which is the sum of the number of protons and neutrons in the nucleus. Because isotopes have the same atomic number, they are nuclides of the same chemical element. For example, five isotopes of the chemical element carbon are ${}^{10}_{6}\mathrm{C}$, ${}^{11}_{6}\mathrm{C}$, ${}^{12}_{6}\mathrm{C}$, ${}^{13}_{6}\mathrm{C}$, ${}^{14}_{6}\mathrm{C}$, where the subscript and superscript represent the atomic number Z and mass number A, respectively, and the number of neutrons in the nucleus N is calculated as $A-Z$. Among the five isotopes of carbon listed above, ${}^{10}_{6}\mathrm{C}$, ${}^{11}_{6}\mathrm{C}$ and ${}^{14}_{6}\mathrm{C}$ are radioactive, and thus referred to as **radioisotopes**. The other two isotopes of carbon listed above, namely ${}^{12}_{6}\mathrm{C}$ and ${}^{13}_{6}\mathrm{C}$, are stable. The natural isotopes that make up the element of carbon are ${}^{12}_{6}\mathrm{C}$, ${}^{13}_{6}\mathrm{C}$, and ${}^{14}_{6}\mathrm{C}$.

Isotope natural abundance: Of the elements found in nature, isotopes occur at a particular natural abundance. The term "natural abundance" refers to the relative abundance of an isotope that occurs naturally on Earth. For example, among the five isotopes of carbon listed above, ${}^{12}_{6}\mathrm{C}$ and ${}^{13}_{6}\mathrm{C}$ occur naturally at abundances of 98.90% and 1.10%. The isotope ${}^{14}_{6}\mathrm{C}$ is naturally occurring in only a small trace ($\sim 10^{-10}$% natural abundance), as it is formed continuously by the interaction of neutrons of the cosmic ray showers with nitrogen-14 in the upper atmosphere, as described by Eq. VIII.37 in Hall of Fame, Part VIII of this book. The isotope ${}^{14}\mathrm{C}$ is radioactive, and thus a radioisotope of carbon. The percentage natural abundances of the isotopes for each element should add up to 100%. Another example is the naturally occurring isotopes of potassium, namely ${}^{39}_{19}\mathrm{K}$, ${}^{40}_{19}\mathrm{K}$, and ${}^{41}_{19}\mathrm{K}$, which occur at natural abundances of 93.2581%, 0.0117%, and 6.7302%, respectively. The isotopes ${}^{39}\mathrm{K}$ and ${}^{41}\mathrm{K}$ are stable isotopes; however, the isotope ${}^{40}\mathrm{K}$ is a radioisotope that decays with a half-life of 1.26×10^{9} years. Since the naturally occurring isotopes are remnants of the nucleosynthesis of the Earth, which is 2.54×10^{9} years old (Dalrymple, 2001), the isotope ${}^{40}\mathrm{K}$ has had time to decay since the Earth's creation. When only one isotope of an element exists naturally on Earth, its natural abundance is expressed as 100%. Examples are ${}^{19}_{9}\mathrm{F}$, ${}^{27}_{13}\mathrm{Al}$, ${}^{31}_{15}\mathrm{P}$, ${}^{45}_{21}\mathrm{Sc}$, ${}^{55}_{25}\mathrm{Mn}$, ${}^{59}_{27}\mathrm{Co}$, ${}^{89}_{39}\mathrm{Y}$, ${}^{127}_{53}\mathrm{I}$, ${}^{133}_{55}\mathrm{Cs}$, ${}^{209}_{83}\mathrm{Bi}$, and ${}^{232}_{90}\mathrm{Th}$.

Further up the Chart of the Nuclides are found the last of the natural isotopes, namely isotopes of uranium. Three of the isotopes of uranium are found naturally on Earth, namely ${}^{234}_{92}\mathrm{U}$, ${}^{235}_{92}\mathrm{U}$, and ${}^{238}_{92}\mathrm{U}$, at abundances of 0.0055%, 0.720%, and 99.2745%, respectively. The isotope ${}^{238}\mathrm{U}$, which is the most abundant, has a half-life of 4.5×10^{9} years. It has not undergone even a half-life of decay since the formation of the Earth. However, the isotopes ${}^{234}\mathrm{U}$ and ${}^{235}\mathrm{U}$, with half-lives of 2.4×10^{5} years and 7.1×10^{8} years, respectively, have undergone considerable decay since the formation of the Earth. All nuclides of atomic number greater than that of uranium do not occur naturally and have been produced artificially by humans, as described further on in this book.

Isobars: Isobars are nuclides that possess the same mass number (A), but different atomic number (Z). For example, ${}^{56}_{28}\mathrm{Ni}$, ${}^{56}_{27}\mathrm{Co}$, ${}^{56}_{26}\mathrm{Fe}$, ${}^{56}_{25}\mathrm{Mn}$, and ${}^{56}_{24}\mathrm{Cr}$ are isobars. In mass spectrometry, where nuclides are separated and analyzed according to their mass, isobars can cause interference, and special techniques may be required to discriminate between nuclides of the same mass number (Kusnir et al., 2004; Litherland et al., 2007; Plaβ et al., 2008). In beta decay, discussed later in this chapter, the parent and daughter nuclides are always isobars.

Isomers: Nuclear isomers are different energy states of the same nucleus, with different half-lives and even different modes of decay. A well-known example is ${}^{99}_{43}\mathrm{Tc}$, which may have two isomeric states. The isomers of ${}^{99}\mathrm{Tc}$ are ${}^{99}_{43}\mathrm{Tc}$, which decays by negatron emission to ${}^{99}_{44}\mathrm{Ru}$ with a half-life of 2.14×10^{5} years, and ${}^{99m}_{43}\mathrm{Tc}$, which decays by gamma emission to ${}^{99}_{43}\mathrm{Tc}$ with a half-life of 6.00 h. Isomeric states of nuclides other than the ground state are represented with a superscript "m" following the mass number. The isomer ${}^{99m}\mathrm{Tc}$ is commonly used in the field of nuclear medicine as a diagnostic imaging

source injected into the human body, as described in the "Introduction: Part A, Radioactivity and Our Well Being". When more than two excited isomeric states of a nuclide exist, the nuclear isomers are labeled as m_1, m_2, etc., in order of increasing excitation energy. For example, the isomers of ^{152}Eu are identified as $^{152}_{63}$Eu of 13.2 years half-life, $^{152m_1}_{63}$Eu of 9.3 h half-life, and $^{152m_2}_{63}$Eu of 1.6 h half-life. There are over 950 isomeric states known to exist among the nuclides. They are not considered as individual nuclides, but rather as isomers of individual nuclides.

Isotones: Nuclides that have the same number of neutrons but different mass numbers are isotones. For example, $^{33}_{15}$P, $^{34}_{16}$S, $^{35}_{17}$Cl, $^{36}_{18}$Ar, and $^{37}_{19}$K are isotones; their nuclei all contain 18 neutrons. Isotones may be found in the Chart of the Nuclides, which plots the nuclides according to their Z versus N, as the column of nuclides having the same number N.

Nucleon: The word nucleon is used to signify either a proton or a neutron in the atomic nucleus. Thus the atomic nucleus consists of nucleons.

2.3 MASS AND ENERGY

The rest masses of the proton and neutron are of the order of 10^{-27} kg (see Table 2.1), and consequently the masses of the atomic nuclei are also very small. Due to the very small masses, most calculations involving atomic nuclei, such as nuclear decay energy, binding energy, and energies of nuclear reactions, make use of a more convenient scale of unit, namely the atomic mass unit (u).

The atomic mass unit is defined in terms of the stable carbon nuclide ^{12}C, which is assigned an atomic mass of exactly 12.000000 u. Thus the atomic mass unit is by definition exactly $1/12$ the rest mass of ^{12}C, or

$$1\ \text{u} = 1.66053873 \times 10^{-27}\ \text{kg}. \qquad [2.5]$$

The masses of all the nuclides in atomic mass units are available in reference tables, such as those listed in the *Handbook of Chemistry and Physics* (Haynes, 2013).

The International System of units for energy is the joule (J); but the electron volt (eV) remains a very popular unit for expressing energy in nuclear decay, nuclear reactions, nuclear binding, etc. The eV is, by definition, the amount of kinetic energy gained by an electron when accelerated through a potential difference of 1 V. The eV is equivalent to the following units:

$$1\ \text{eV} = 1.602176462 \times 10^{-19}\ \text{J} = 1.602176462 \times 10^{-12}\ \text{erg} \qquad [2.6]$$

The erg is a unit of energy in the centimeter-gram-second system of units, and less commonly used in nuclear energy calculations. From the above relation, the erg is equivalent to 10^{-7} J or 6.2415097×10^{11} eV.

Calculations concerning nuclear decay energy, nuclear reaction energy, nuclear binding energy, etc. generally require the conversion of mass to energy. A common factor used in such calculations is one that can convert atomic mass units (u) to units of the eV. The conversion factor is found using Einstein's equation to convert the mass of 1 u to energy or

$$E = m_0 c^2 \qquad [2.7]$$

where E is energy in joules, m_0 is the rest mass in kilograms, and c is the velocity of light in a vacuum or 2.99792458×10^8 m/s. If, by definition, the mass of 1 u = $1.66053873 \times 10^{-27}$ kg, the energy equivalent to 1 u is calculated as

$$E = \left(1.66053873 \times 10^{-27}\ \text{kg/u}\right)\left(2.99792458 \times 10^{8}\ \text{m/s}\right)^2 = 14.92417783 \times 10^{-11}\ \text{J/u} \qquad [2.8]$$

The energy in units of joules is then converted to units of eV, as 1 eV = $1.602176462 \times 10^{-19}$ J or

$$E = \frac{14.92417783 \times 10^{-11}\ \text{J/u}}{1.602176462 \times 10^{-19}\ \text{J/eV}} = 9.31494013 \times 10^{8}\ \text{eV/u} = 931.494013\ \text{MeV/u} \qquad [2.9]$$

Thus 1 u = 931.494013 MeV or 931.494013 MeV/c^2. The latter units of MeV/c^2 are used conveniently when converting atomic mass units to MeV energy in Einstein's equation according to the following

$$E = mc^2 = \left[(\text{atomic mass units})\left(931.494013\ \text{MeV}/c^2\right)\right]c^2 \qquad [2.10]$$

Eq. [2.10] is used to convert conveniently atomic mass units (u) to units of energy in MeV. Examples are given throughout this book in calculations of nuclear decay energy, nuclear reaction energy, and nuclear binding energy.

2.4 *Q* VALUE

The Q value of a nuclear reaction is a measure of the energy "released" or "absorbed" by the reaction. When the Q value is positive ($Q > 0$), energy is "released" by the reaction with a conversion of the rest mass of the reactants into kinetic energy of the products. When the Q value is negative in magnitude ($Q < 0$), an input of energy is needed for the reaction to proceed, as energy is consumed in the reaction. In other words, when Q is negative, kinetic energy must be added to one or more of the reactants (ie, bombarding particles) up to a threshold (ie, required) energy for the reaction to proceed. When the value of $Q = 0$, kinetic energy is neither consumed nor released. In this case no reaction occurs, with the exception of an elastic collision.

The Q value of a nuclear reaction is calculated by the mass difference of the nuclear reactants and nuclear products, or

$$Q = K_{\text{Products}} - K_{\text{Reactants}} = (m_R - m_P)c^2 \quad [2.11]$$

where K_{Products} is the kinetic energy of the reaction products, $K_{\text{Reactants}}$ is the kinetic energy of the reactants or incident particles involved in the reaction, and m_R and m_P are the rest masses of the reactants and products of the nuclear reaction.

If we know the Q value of a nuclear reaction and the kinetic energies of the reactants, we can calculate the kinetic energies of the products according to Eq. [2.11] or

$$K_{\text{Products}} = Q + K_{\text{Reactants}} \quad [2.12]$$

Examples of the application of Eqs. [2.11] and [2.12] to a nuclear reaction are provided in the following paragraphs.

As nuclear particles and nuclei of atoms are involved in nuclear reactions, we need to know the masses of the nuclei or nuclear particles to calculate a reaction Q value. In lieu of using rest masses of the atomic nuclei, it is common to use the atomic masses (u) available in reference tables, such as those of the *Handbook of Chemistry and Physics*. However, it is important to keep in mind that atomic masses include the masses of the atomic electrons. To eliminate error that might occur from the added masses of the atomic electrons, it is important to ensure that the number of electrons added to either side of the reaction is equal, so the difference of the electron masses of the reactants and products is zero when using Eq. [2.11]. Let us take an example and calculate the Q value of the first manmade nuclear reaction, whereby Earnest Rutherford in 1919 discovered the proton (described later in this book). The reaction is as follows:

$$^{4}_{2}\text{He} + {}^{14}_{7}\text{N} \rightarrow {}^{17}_{8}\text{O} + {}^{1}_{1}\text{H} \quad [2.13]$$

In this reaction the alpha particle interacts with an atom of ^{14}N to form an atom of ^{17}O, with the ejection of a proton from the nucleus. The atomic masses may be used to calculate the Q value of the reaction according to Eq. [2.11] as follows:

$$\begin{aligned} Q &= [(M_{^4\text{He}} + M_{^{14}\text{N}}) - (M_{^{17}\text{O}} + M_{^1\text{H}})]c^2 = [(4.00260325\ \text{u} + 14.00307401\ \text{u}) - (16.9991315\ \text{u} + 1.007825032\ \text{u})]c^2 \\ &= (-0.001279272\ \text{u})c^2 \end{aligned} \quad [2.14]$$

By using atomic masses, we have added nine electron masses to each side of the reaction, and their difference is zero from Eq. [2.14]. Converting atomic mass units to energy according to Eq. [2.10] gives the Q value in units of MeV energy or

$$Q\ \text{value} = E = mc^2 = \left[(-0.001279272)\left(931.494013\ \text{MeV}/c^2\right)\right]c^2 \quad [2.15]$$

$$Q\ \text{value} = -1.192\ \text{MeV}$$

Atomic masses are conveniently used in such calculations, in lieu of nuclear masses, provided an equal number of electrons are included on either side of the reactants or products, as in Eq. [2.14]. The negative energy value above demonstrates that the reaction is endoergic or endothermic—that is, the reaction requires a net energy input of 1.192 MeV. When the Q value is positive, the nuclear reaction is exoergic or exothermic, resulting in a net release of energy. There are small differences in the binding energies of the electrons when using atomic masses; however, the differences in the binding energies are negligible and ignored.

The Q value for nuclear reactions and nuclear decays can be obtained using the QCALC computer program via the internet on the NNDC website (http://www.nndc.bnl.gov/qcalc/). In the case of a nuclear reaction, all that is required is to input on the site the symbols for the reactants and that of a product. For example, we can take Eq. [2.13] and, on the NNDC

website, input the symbol for the **target** nucleus as 14N (without superscript for the mass numbers), the symbol for the **projectile** 4He, and the symbol for the **ejectile** 1H. The QCALC program can then in an instant calculate the Q value to be −1191.87 keV, which is equivalent to −1.192 MeV calculated above.

When the reaction has a negative Q value, as in the example above, energy must be added for the reaction to proceed. According to the calculation of Eq. [2.15], a minimum of 1.2 MeV of kinetic energy must be added to the bombarding particle for the reaction to proceed. In the reaction described by Eq. [2.13], Ernest Rutherford (1919) used alpha particles from radium C, which possess a kinetic energy of 7.7 MeV—well above the threshold energy for the reaction to proceed. The kinetic energy of the reaction products (K_{Products}) when 7.7 MeV alpha particles are bombarded on to ^{14}N nuclides at rest are calculated according to Eq. [2.12] as

$$K_{\text{Products}} = Q + K_{\text{Incident alpha-particle}} = -1.2\ \text{MeV} + 7.7\ \text{MeV} = 6.5\ \text{MeV} \quad [2.16]$$

The 6.5 MeV is shared between the product nuclides of Eq. [2.13], namely the ^{17}O and ^{1}H.

2.5 NATURALLY OCCURRING RADIONUCLIDES

If we take into account the age of the Earth, 4.5×10^9 years, and the characteristic property of radionuclide half-life decay, one of the following conditions would have to be met for a natural radioactive nuclide to occur on Earth: (1) the radionuclide is produced continuously on Earth or in its atmosphere by a natural phenomenon; (2) the radionuclide is very long-lived and has a half-life of the order of $\geq 10^9$ years; or (3) a short-lived radionuclide exists in equilibrium with a naturally occurring long-lived parent radionuclide. These categories of naturally occurring radionuclides are discussed below.

TABLE 2.2 Production Rates of Several Isotopes in the Earth's Atmosphere, Arranged in Order of Decreasing Half-lives[a]

Isotope	Half-life	Production Rate (Atoms/cm^{2}s)		Global Inventory
		Troposphere	Total Atmosphere	
^{3}He	Stable	6.7×10^{-2}	0.2	3.2×10^3 tons[b]
^{10}Be	1.5×10^6 y	1.5×10^{-2}	4.5×10^{-2}	260 tons
^{26}Al	7.1×10^5 y	3.8×10^{-5}	1.4×10^{-4}	1.1 tons
^{81}Kr[c]	2.3×10^5 y	5.2×10^{-7}	1.2×10^{-6}	8.5 kg
^{36}Cl	3.0×10^5 y	4×10^{-4}	1.1×10^{-3}	15 tons[d]
^{14}C	5730 y	1.1	2.5	75 tons
^{39}Ar[e]	268 y	4.5×10^{-3}	1.3×10^{-2}	52 kg
^{32}Si	~150 y	5.4×10^{-5}	1.6×10^{-4}	0.3 kg
^{3}H	12.3 y	8.4×10^{-2}	0.25	3.5 kg
^{22}Na	2.6 y	2.4×10^{-5}	8.6×10^{-5}	1.9 g
^{35}S	87 d	4.9×10^{-4}	1.4×10^{-3}	4.5 g
^{7}Be	53 d	2.7×10^{-2}	8.1×10^{-2}	3.2 g
^{37}Ar	35 d	2.8×10^{-4}	8.3×10^{-4}	1.1 g
^{33}P	25.3 d	2.2×10^{-4}	6.8×10^{-4}	0.6 g
^{32}P	14.3 d	2.7×10^{-4}	8.1×10^{-4}	0.4 g

d, days; *y*, years.
[a] *Based on Lal and Peters (1967).*
[b] *The inventory of this stable nuclide is based on its atmospheric inventory, which includes an appreciable contribution from crustal degassing of ^{3}He.*
[c] *Based on an atmospheric ^{81}Kr/Kr ratio of $(5.2 \pm 0.4) \times 10^{-13}$.*
[d] *Includes a rough estimate of ^{36}Cl produced by the capture of neutrons at the Earth's surface.*
[e] *Based on an atmospheric ^{39}Ar/Ar ratio of (0.107 ± 0.004) dpm/L Ar (STP).*
From Lal (2009), reprinted with permission from Elsevier Publishers.

2.5.1 Radionuclides of Cosmogenic Origin

A number of radionuclides are produced on a continuous basis by the interaction of cosmic ray particles with nuclei in the Earth's atmosphere. The cosmogenic isotopes are created by the interactions of high-energy primary and secondary particles of cosmic radiation with nuclei of gaseous molecules of the atmosphere (eg, N_2, O_2, Ar, etc.), resulting in the fragmentation of the target nuclei, or by the capture of thermal neutrons of cosmic radiation showers with target nuclei of the atmosphere (see the chapter: Cosmic Radiation for additional information on cosmic ray interactions in the Earth's atmosphere). As reported by Lal (2009), most of the cosmic ray energy (>98%) is dissipated in the Earth's atmosphere. Secondary particles of cosmic radiation produce nuclear reactions at a much-reduced rate, with the Earth's superficial reservoirs including the hydrosphere, cryosphere, and lithosphere. Cosmogenic radionuclides are therefore produced to the greatest extent in the Earth's atmosphere. Table 2.2 provides a list of cosmogenic nuclides, their half-lives, rate of production in the atmosphere, and the global mass of these naturally occurring nuclides. Short-lived radionuclides are not included. Once produced in the atmosphere, radionuclides such as ^{3}H, ^{7}Be, ^{10}Be, ^{26}Al, and ^{36}Cl, will find their way to the Earth's surface; whereas radionuclides in gaseous form, such as $^{14}CO_2$, ^{37}Ar, ^{39}Ar and ^{81}Kr, find their way into oceans and rivers via air exchange.

2.5.2 Long-Lived Radionuclides

Based on the age of the Earth (4.5×10^9 years), we can expect that all noncosmogenic radionuclides with a half-life $<10^8$ years that were formed during the formation of the Earth and are not in equilibrium with a parent nuclide in a naturally occurring decay chain will have decayed to an undetectable level. Table 2.3 lists the naturally occurring

TABLE 2.3 Long-Lived Naturally Occurring Radionuclides[a]

Nuclide	Half-life (years)	Isotope Abundance (%)	Decay Mode(s)	Decay Product(s)
$^{40}_{19}K$	1.26×10^9	0.0117	β^-, EC	$^{40}_{20}Ca$ (β^-), $^{40}_{18}Ar$ (EC)
$^{50}_{23}V$	1.4×10^{17}	0.250	β^-, EC	$^{50}_{24}Cr$ (β^-), $^{50}_{22}Ti$ (EC)
$^{87}_{37}Rb$	4.88×10^{10}	27.835	β^-	$^{87}_{38}Sr$
$^{113}_{48}Cd$	9×10^{15}	12.22	β^-	$^{113}_{49}In$
$^{115}_{49}In$	4.4×10^{14}	95.71	β^-	$^{115}_{50}Sn$
$^{123}_{52}Te$	1.3×10^{13}	0.908	EC	$^{123}_{51}Sb$
$^{138}_{57}La$	1.06×10^{11}	0.0902	β^-, EC	$^{138}_{58}Ce$ (β^-), $^{138}_{56}Ba$ (EC)
$^{142}_{58}Ce$	5×10^{16}[b]	11.08	α	$^{138}_{56}Ba$
$^{144}_{60}Nd$	2.1×10^{15}	23.80	α	$^{140}_{58}Ce$
$^{147}_{62}Sm$	1.06×10^{11}	15.0	α	$^{143}_{60}Nd$
$^{148}_{62}Sm$	7×10^{15}	11.3	α	$^{144}_{60}Nd$
$^{152}_{64}Gd$	1.1×10^{14}	0.20	α	$^{148}_{62}Sm$
$^{176}_{71}Lu$	3.8×10^{10}	2.59	β^-	$^{176}_{72}Hf$
$^{174}_{72}Hf$	2.0×10^{15}	0.162	α	$^{170}_{70}Yb$
$^{180}_{73}Ta$	$>1.2 \times 10^{15}$	0.012	β^-, EC	$^{180}_{74}W$ (β^-), $^{180}_{72}Hf$ (EC)
$^{187}_{75}Re$	4.4×10^{10}	62.60	β^-	$^{187}_{76}Os$
$^{186}_{76}Os$	2.0×10^{15}	1.58	α	$^{182}_{74}W$
$^{190}_{78}Pt$	6.5×10^{11}	0.01	α	$^{186}_{76}Os$
$^{232}_{90}Th$	1.4×10^{10}	100.0	α	$^{228}_{88}Ra$
$^{235}_{92}U$	7.04×10^8	0.720	α	$^{231}_{90}Th$
$^{238}_{92}U$	4.46×10^9	99.27	α	$^{234}_{90}Th$

[a] *Data from Lide (2010).*
[b] *Half-life from Macfarlane and Kohman (1961).*

long-lived radionuclides according to increasing atomic number (Z), together with their half-lives, relative isotope abundances, decay modes, and decay products. Two decay products are listed when there are two modes of decay. All the decay products are stable with the exception of the decay products of ^{148}Sm and ^{152}Gd, which decay to the very long-lived ^{144}Nd and ^{148}Sm, respectively, and ^{232}Th, ^{235}U, and ^{238}U, which are long-lived parent radionuclides of the thorium, uranium, and actinium decay chains described in the next subsection. Not listed in the table are 10 radionuclides that are exceptionally long-lived. These decay via a double-beta ($\beta\beta$) decay mode with half-lives ranging between 10^{18} and 10^{24} years. Double-beta decay is the rarest form of nuclear decay, discussed in the chapter entitled "Beta Radiation and Beta Decay."

2.5.3 Natural Radioactive Decay Chains

There are three naturally occurring decay chains, which begin with one of three long-lived parent nuclides. The three decay chains, namely the ^{232}Th or thorium decay chain (4n), the ^{238}U or uranium decay chain (4n + 2), and the ^{235}U decay chain, also referred to as the actinium decay chain (4n + 3), are illustrated in Figs. 2.1–2.3, respectively. The notations 4n, 4n + 2, and 4n + 3 refer to the mass number A for all nuclides in the respective decay chains, where n is a positive integer between 50 and 60. The notations are derived from the fact that the mass number (A) for all radionuclides in a given decay chain is a multiple of 4 because α decay results in a mass reduction of 4, whereas the mass number between parent and daughter does not change in β decay. Thus the mass numbers in the respective series agree with the relations $4n = A$, $4n + 2 = A$, and $4n + 3 = A$, where n is an integer between 50 and 60. There are radionuclides in the decay chains with very short half-lives (of the order of minutes and seconds). These short-lived nuclides have survived the billions of years since the formation of the Earth due to an equilibrium that develops between a long-lived parent and its shorter-lived daughters. Equilibrium between parent and daughter nuclides is discussed in detail in the chapter entitled "Radionuclide Decay, Radioactivity Units, and Radionuclide Mass". All radionuclides in the thorium, uranium, and actinium decay chains terminate with a stable isotope of lead, namely ^{208}Pb, ^{206}Pb, and ^{207}Pb, respectively.

2.6 ARTIFICIALLY PRODUCED RADIONUCLIDES

There are over 1300 artificially produced radionuclides. These are made by nuclear reactions, often facilitated by a nuclear reactor or particle accelerator. A brief historical account of the development of manmade radionuclides, including the synthetic elements, all of which are radioactive, is provided here.

Frédéric Joliot and Irène Joliot-Curie (daughter of Pierre and Marie Curie) were in 1934 the first to produce artificially a radioactive nuclide, ^{30}P. The nuclide emits positrons, which are electrons of positive charge and the antiparticle of the negative electron. Positrons were discovered in cosmic radiation only two years earlier by Carl D. Anderson (1932, 1933a).

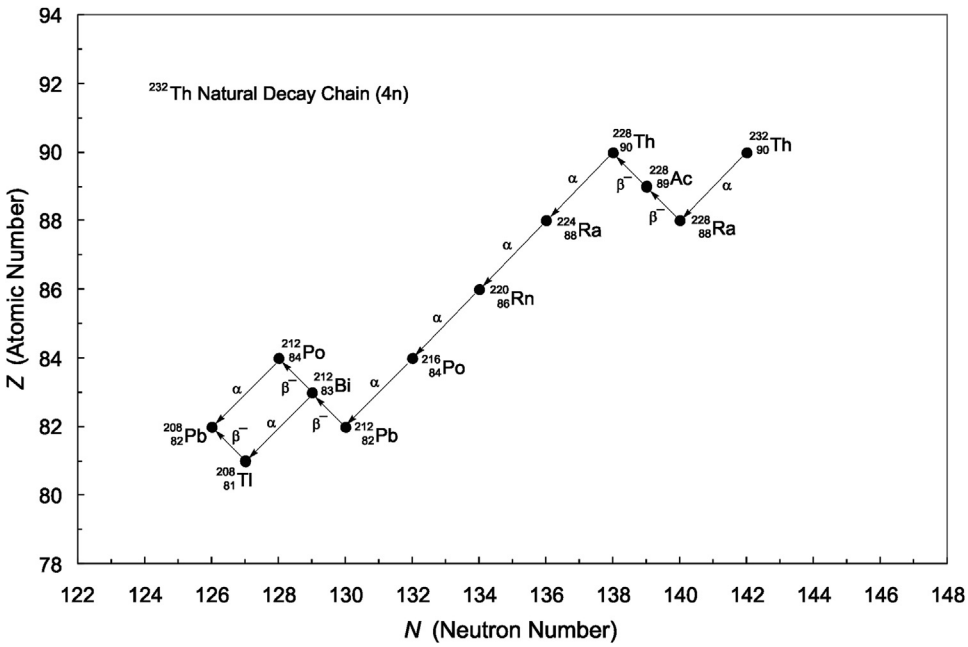

FIGURE 2.1 The ^{232}Th natural decay chain.

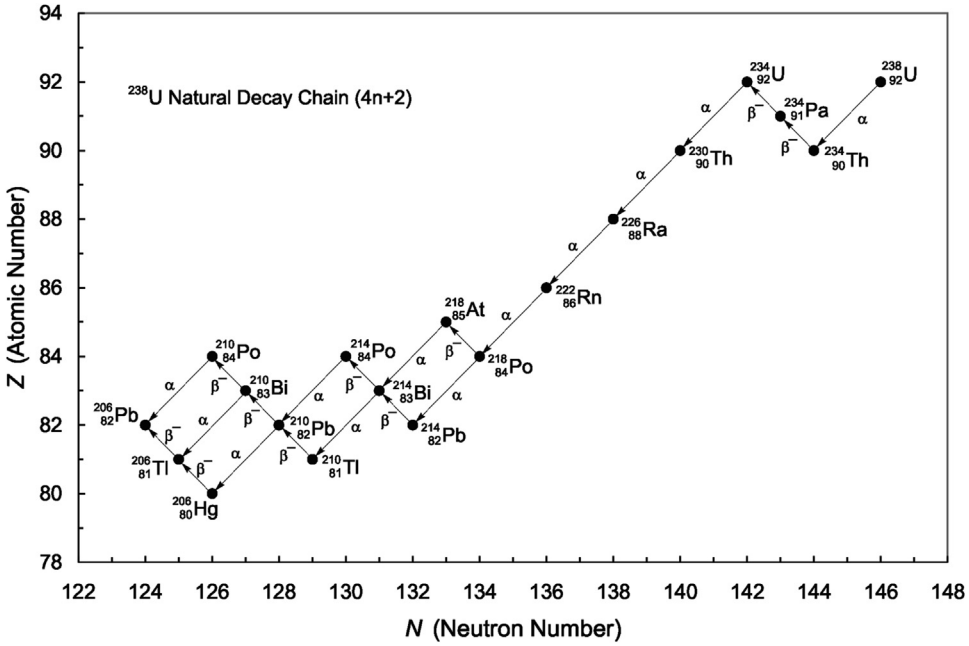

FIGURE 2.2 The ^{238}U natural decay chain.

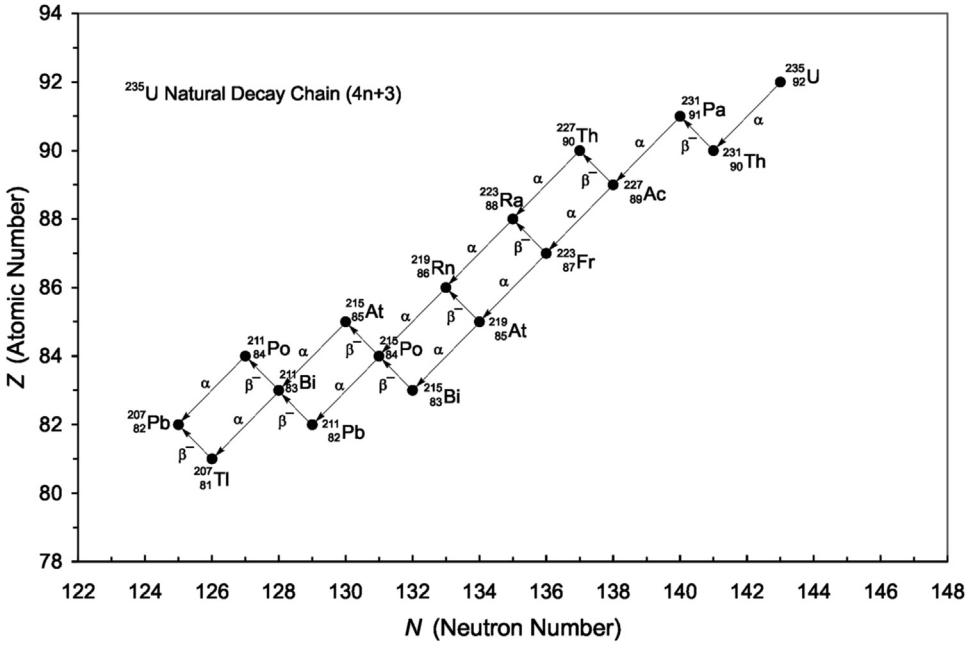

FIGURE 2.3 The ^{235}U natural decay chain, also referred to as the actinium decay chain.

The discovery by the Joliot-Curies of artificially produced radioisotopes came about when they began their search for positrons. They decided to irradiate various metals with alpha particles of different energies to see if the result would be the production of a predominance of neutrons or positrons. They irradiated aluminum foil with alpha particles from a polonium source. The energy of the alpha particles colliding with the aluminum could be controlled by placing the polonium at various distances from the aluminum. The irradiation of aluminum foil by the polonium alpha particles produced neutrons and positrons. When the polonium source was moved away from the aluminum to a distance beyond the reach of the alpha particles (the alpha particles from polonium-216 have an energy of 6.78 MeV and cannot travel beyond 5.3 cm in dry air, as calculated in the chapter entitled "Alpha Radiation"), the neutron emission from the alpha-irradiated aluminum would

cease; however, to their amazement, the Joliot-Curies discovered that the positron emission continued. They measured the positron emission with a Geiger counter and found that the number of positrons emitted diminished with time, with an average lifetime of less than 5 min. The interaction of the alpha particles with the aluminum foil produced a new radioactive isotope of short half-life, previously unknown to mankind.

The Joliot-Curies were able to demonstrate that the new isotope was chemically equivalent to elemental phosphorus, and it was radioactive phosphorus. By balancing the transformation of the nuclear reaction between alpha particles and aluminum-yielding neutrons, they could write the reaction

$$^{27}_{13}\mathrm{Al} + {}^{4}_{2}\mathrm{He} = {}^{30}_{15}\mathrm{P} + {}^{1}_{0}\mathrm{n} \qquad [2.17]$$

They used the equal sign rather than an arrow in this reaction to demonstrate that the sum of the mass numbers and atomic numbers on one side of the nuclear reaction should equal those on the other side, ie, $27 + 4 = 30 + 1$ for the mass numbers and $13 + 2 = 15 + 0$ for the atomic numbers. Expressing nuclear reactions was not the practice at that time, and the Joliot-Curies were among the first to introduce the method.

The Joliot-Curies demonstrated that the new radioactive isotope of phosphorus emitted positrons. The new radioisotope, phosphorus-30, decays to stable silicon-30 with positron emission and a short half-life of 2.5 min according to the following:

$$^{30}_{15}\mathrm{P} \rightarrow {}^{30}_{14}\mathrm{Si} + \beta^{+} \qquad [2.18]$$

Thus the Joliot-Curies not only produced a previously nonexistent radioisotope, but they were the first to produce positrons in the laboratory.

By irradiating other metals, such as boron and magnesium, with alpha particles the Joliot-Curies were able to produce radioactive nitrogen and radioactive silicon, according to the following reactions (Joliot-Curie and Joliot, 1934a,b,c):

$$^{10}_{5}\mathrm{B} + {}^{4}_{2}\mathrm{He} \rightarrow {}^{13}_{7}\mathrm{N} + {}^{1}_{0}\mathrm{n} \qquad [2.19]$$

$$^{24}_{12}\mathrm{Mg} + {}^{4}_{2}\mathrm{He} \rightarrow {}^{27}_{14}\mathrm{Si} + {}^{1}_{0}\mathrm{n} \qquad [2.20]$$

These radioisotopes of nitrogen and silicon decay by positron emission.

The Joliot-Curies were awarded the Nobel Prize in Chemistry the year following the report of these discoveries. The rapid award of the Nobel Prize underscored the impact this discovery had on the scientific community and the advancement of science. Their work firmly established a new branch of chemistry called "radiochemistry." As explained by Frédéric Joliot in his part of the Nobel lecture:

> *The succession of radioactive transformations provides numerous examples in which the quantities of radio-elements are extremely small and not capable of being weighed, yet nevertheless, by the methods of radiochemistry it has been possible to examine correctly their chemical properties, and identify some of them as being isotopes of elements… This special kind of chemistry in which one handles unweighable quantities, sometimes of the order of 10^{-16} g, is made possible thanks to the fact that one can determine and follow by measuring the radiation emitted, infinitesimal traces of radioactive matter dispersed in the midst of other matter.*

While this work established radiochemistry as a new branch of chemistry, the Joliot-Curies were the first to coin the terminology, to which we are now very accustomed, when referring to radioactive elements. In their Nobel lecture Frédéric Joliot stated:

> *We have proposed that these new radio-elements (isotopes, not found in nature, of known elements) be called radio-nitrogen (for radioactive isotopes of nitrogen), radio-phosphorus (for radioactive isotopes of phosphorus) …*

Only two years after the Joliot-Curies reported the synthesis of radionuclides by the alpha particle bombardment of nuclei, Enrico Fermi and his coworkers reported the synthesis of new radionuclides by neutron bombardment of nuclei. This work, which is discussed in more detail in Hall of Fame, Part II, yielded 63 previously unknown artificial radionuclides by the following three nuclear reactions:

$$(1)\quad {}^{A}_{Z}\mathrm{X} + {}^{1}_{0}\mathrm{n} \rightarrow {}^{A-3}_{Z-2}\mathrm{X} + {}^{4}_{2}\mathrm{He} \qquad [2.21]$$

$$(2)\quad {}^{A}_{Z}\mathrm{X} + {}^{1}_{0}\mathrm{n} \rightarrow {}^{A}_{Z-1}\mathrm{X} + {}^{1}_{1}\mathrm{H} \qquad [2.22]$$

$$(3)\quad {}^{A}_{Z}\mathrm{X} + {}^{1}_{0}\mathrm{n} \rightarrow {}^{A+1}_{Z}\mathrm{X} \qquad [2.23]$$

where ${}^{A}_{Z}\mathrm{X}$ is a symbol for any element X with atomic number Z and mass number A, and n is the symbol for the neutron. Fermi found the first and second reactions to occur chiefly among the light elements, and the third type of reaction was found to occur most often among the heavy elements. More than one of these reactions would sometimes occur when elements were bombarded with neutrons. In Fermi's words in his Nobel lecture:

> *In many cases the three processes are found at the same time in a single element. For instance, neutron bombardment of aluminum that has a single isotope ^{27}Al, gives rise to three radioactive products: ^{24}Na, with a half-life of 15 hours by process (1); ^{27}Mg, with a period (half-life) of 10 minutes by process (2); and ^{28}Al with a period (half-life) of 2 to 3 minutes by process (3).*

In addition to these three neutron reactions described by Fermi, he and his coworkers were able to observe the production of artificial radioactive isotopes by a fourth process:

> *The primary neutron does not remain bound in the nucleus, but knocks off instead, one of the nuclear neutrons out of the nucleus; the result is a new nucleus, that is isotopic with the original one and has an atomic weight less by one unit.*

This fourth neutron interaction, where the mass number is reduced by one (loss of a neutron) and the atomic number remains unaltered, can be written as follows:

$$(4)\quad {}^{A}_{Z}\mathrm{X} + {}^{1}_{0}\mathrm{n} \rightarrow {}^{A-1}_{Z}\mathrm{X} + 2{}^{1}_{0}\mathrm{n} \qquad [2.24]$$

Fermi knew that neutrons, because of their neutral charge, did not have to overcome the coulombic barrier to penetrate the nucleus of an atom. Furthermore, he discovered that by placing a water or paraffin barrier between a neutron source and its target nuclei, the energy of the neutrons could be reduced to that corresponding to thermal agitation, ie, the energy of the neutrons and their speed are reduced. At this reduced energy state, the slow neutrons could diffuse through target atoms and be captured by the target nuclei. Thus by using slow neutron bombardment, Fermi and his coworkers were able to produce more than 400 new radioisotopes of all known elements, with the exception of hydrogen and helium.

At the same time that Enrico Fermi was producing radionuclides by means of neutron bombardment of target nuclei, Ernest Lawrence was developing a cyclotron capable of accelerating protons, deuterons and helium nuclei to very high energies. This work, discussed in detail in Hall of Fame, Part VIII, yielded many new artificial radionuclides, as the high energy of the accelerated particles could easily penetrate the coulombic barrier of target nuclei.

The discovery of nuclear fission by Otto Hahn and Fritz Strassman with the collaboration of Lise Meitner in 1939 led to the discovery of the first nuclear reactor in 1942 by Enrico Fermi and coworkers. This work is discussed in more detail in Hall of Fame, Part II. Today, the nuclear reactor and the cyclotron are the main instruments for the artificial production of radionuclides. There are now more than 1300 artificially produced radionuclides. Many of these radionuclides are vital for

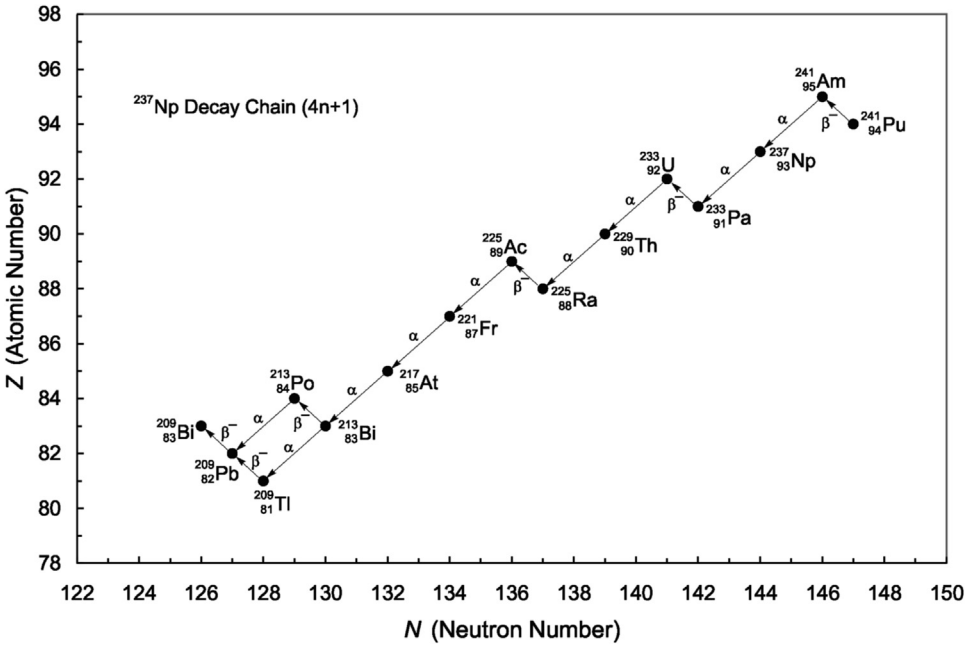

FIGURE 2.4 The neptunium decay chain.

medical diagnosis and treatment, the sterilization of medical implements and supplies, and applications in industry, and scientific research.

Elements with atomic number $Z > 92$, which are elements with atomic number higher than that of uranium, are artificially produced. They are all radioactive. By means of the cyclotron, Glenn T. Seaborg pioneered the synthesis of many artificial elements. This work is described in detail in Hall of Fame, Part VIII. There are no natural elements beyond $Z = 92$, because they all have half-lives too short to have survived since the formation of the Earth. Also, there is the $4n + 1$, illustrated in Fig. 2.4, which consists of mostly artificially produced radionuclides. It is called the neptunium decay chain after ^{237}Np, which is the longest-lived nuclide of the chain with a half-life of 2.1×10^6 years. There are currently over 20 artificially produced elements.

Chapter 3

Hall of Fame: Part I

Democritus (c.460–370 BC), Wilhelm C. Röntgen (1845–1923), Ivan Pavlovich Puluj (a.k.a. Johann Puluj, 1845–1918), Henri Becquerel (1852–1908), Pierre (1859–1906) and Marie Curie (1867–1934), Paul Villard (1860–1934), Ernest Rutherford (1871–1937), Johannes "Hans" Geiger (1882–1945), Hendrick A. Lorentz (1853–1928), James Clerk Maxwell (1831–1879), Pieter Zeeman (1865–1943), Jean B. Perrin (1870–1942), Joseph John Thomson (1856–1940), Hantaro Nagaoka (1865–1950), and Philipp Lenard (1862–1947)

Radium gives out three distinct types of radiation:

1) *The α rays, which are very absorbed by thin layers of matter, and which give rise to the greater portion of the ionization of the gas observed under the usual experimental conditions.*
2) *The β rays, which consist of negatively charged particles projected with high velocity, and which are similar in all respects to cathode rays produced in a vacuum tube.*
3) *The γ rays, which are non-deviable by a magnetic field, and which are of a very penetrating character.*

Quotation from Earnest Rutherford (1903), who assigned the terms alpha, beta, and gamma to the various types of radiation out of convenience and for lack of any other basis for naming the previously unfamiliar radiations.

DEMOCRITUS (C.460–C.370 BC)

Democritus was a Greek philosopher born in Abdera in the north of Greece. He was a student of Leucippus, who proposed the atomic theory of matter. There is little documentation on the philosophy of Leucippus; however, it was Democritus, who elaborated extensive works on his theories on the atomic structure of the physical world, of the universe, and the void of space. Although Democritus was a philosopher, he is included here among the list of great pioneers of physics and chemistry of the 19th and 20th centuries, because many of his teachings on the structure of matter were demonstrated finally by scientists over 2000 years after his death.

Democritus (c.460–c.370 B.C.)

Democritus taught the theory of atomism, which held to belief that indivisible and indestructible atoms are the basic components of all matter in the universe. Thus the word "atom" is derived from the Greek *atomos*, meaning indivisible. It was not until 20 centuries after Democritus that Rutherford, Bohr, Soddy, and others demonstrated the atom to be the smallest unit of an element consisting of a positively charged nucleus surrounded by electrons equal to the number of

Radioactivity: Introduction and History, From the Quantum to Quarks. http://dx.doi.org/10.1016/B978-0-444-63489-4.00003-4
Copyright © 2016 Elsevier B.V. All rights reserved.

protons in the nucleus. Although modern science has demonstrated that the atom can be broken down into its component protons, neutrons, and electrons, and the nucleons (protons and neutrons) further divided into their constituent quarks and gluons, atoms remain the basic components involved in chemical reactions with the exception of a limited removal, exchange, or transfer of electrons. The atom is also the basic unit of elements that are the source of nuclear energy. The postage stamp illustrated here was issued by Greece in 1961 to commemorate Democritus' teachings of atomism and the development of peaceful applications of atomic energy in the world.

Democritus was not alone in the teaching of atomism, but his writings on this philosophy were most extensive. He held that atoms were the tiniest of particles, too small to be perceived by the senses, of which all matter was composed, and that the atoms differed in size, shape, and mass. He also argued that atoms were in constant motion and could coalesce to form the larger bodies of matter that we can see, feel, and taste. The properties of matter that we can perceive with the senses, such as color, taste, and hardness, were the result of the interactions of atoms that constituted a given substance and the interactions of atoms with our body. For example, the taste of a substance would be the result of the interactions of atoms with the atoms of our tongue. Democritus also held to the belief of the existence of the "void" or empty space to which atoms or matter can move into. He argued that the lights of the Milky Way were the lights of distant stars, and that there existed other worlds, some with suns and moons, and others without. Likewise there would be other worlds with animal life, plants, and water, and others without.

Much of Democritus' philosophy of atomism was demonstrated by modern science to be true. In honor of Democritus, a major scientific research center in Greece is named the National Center of Scientific Research "Democritus" (NCSR Democritus). This national institution is dedicated to research on natural science and peaceful applications of atomic energy for development. It was formerly called the Nuclear Research Center "Democritus" from the time of its founding in 1959 until 1985.

For additional reading on one of the greatest philosopher-scientists from antiquity, see Taylor's book, *The Atomists* (1999).

WILHELM C. RÖNTGEN (1845–1923)

Wilhelm Conrad Röntgen was born in 1845 in Lennep, Prussia, which is now Remscheid, Germany. He was awarded the very first Nobel Prize in Physics in 1901. The award was granted for the extraordinary services he had rendered by the discovery of Röntgen rays, more commonly referred to as X-rays.

Wilhelm C. Röntgen (1845–1923)

He attempted to begin his higher education in the Netherlands at the University of Utrecht, but could not satisfy the requirements for admission. Instead he passed the entrance examinations for admission into the Swiss Federal Institute of Technology (Eidgenössische Technische Hochschule) in Zurich, Switzerland. Here he graduated with a PhD in physics in 1869, having studied under August Kundt, who was a renowned professor of outstanding students including Ivan Pavlovich Puluj (a.k.a. Johan Puluj) and Pyotr N. Lebedev. Professor August Kundt moved to the University of Strassburg; and Wilhelm Röntgen moved as well to the same university and there he became a lecturer in 1874. For a short period in 1875, he was professor at the Academy of Agriculture at Hohenheim, Württemberg before returning to the University of Strassburg in 1876 as professor of physics. Later in life, Röntgen occupied several chairs in physics, firstly at the University of Giessen in 1879, at the University of Würzburg in 1888, and, after his discovery of X-rays, at the University of Munich in 1900 (https://en.wikipedia.org).

Röntgen discovered the mysterious invisible rays on November 8, 1895 when he was studying cathode rays, ie, the current that would flow through a partially evacuated glass tube (cathode-ray tube, then referred to as a Crookes tube). With such a tube covered in black paper and in a dark room, he noticed that a paper plate covered with the chemical barium platinocyanide would become fluorescent (give off light) even at a distance of 2 m from the cathode ray tube. He was able to demonstrate that the invisible rays came from the collision of the cathode rays (electrons) with the glass surface of the

cathode-ray tube or from the collision of the cathode rays with other materials such as aluminum inserted into the glass of the tube. Further studies by Röntgen demonstrated that these rays could travel through various materials to varying extents, when these were placed in the path of the invisible rays, and the transmitted rays could be measured with photographic plates. He gave these mysterious rays the name X-rays, because of their unknown nature and "for the sake of brevity," as he stated in his original paper (Röntgen, 1895, 1896):

> *A piece of sheet aluminum, 15 mm thick, still allowed the X-rays (as I will call the rays, for the sake of brevity) to pass, but greatly reduce the fluorescence.*

Röntgen was a very modest man, as evidenced by the fact that after making such a revolutionary discovery he went into isolation for almost two months to thoroughly research these mysterious rays. It was not until December 28, 1895 did he make an official report entitled "Über eine neue Art von Strahlen" on his discovery to the Wurzburg Physical-Medical Society (Röntgen, 1895). His original report was translated shortly thereafter and published in the journal *Nature* on January 23, 1896 under the title "On a New Kind of Rays" (see Röntgen, 1896). In his original report, Röntgen (1895, 1896) demonstrated the properties of these newly discovered rays and demonstrated that the rays could be attenuated to different degrees according to the densities of the absorber. He showed that platinum, lead, zinc, and aluminum would be transparent to the X-rays to different magnitudes, and he experimentally determined the relative differences of these metals to X-ray transmission with the following data.

	Thickness (mm)	Relative thickness	Density
Platinum	0.018	1	21.5
Lead	0.050	3	11.3
Zinc	0.100	6	7.1
Aluminum	3.500	200	2.6

As a result of the transparency of various materials to X-rays, Röntgen reported the images of items enclosed within metal boxes and the images of the bones of the fingers of a human hand when the hand is placed on the surface of photographic film. The varying degrees of transmission of metal and human flesh were illustrated by the X-ray image of his wife's hand with a ring on the third finger. This was one of the very first X-ray images illustrated in Röntgen's original paper (1895, 1896) together with that of a compass card and needle enclosed in a metal case, illustrated in Fig. I.1. The

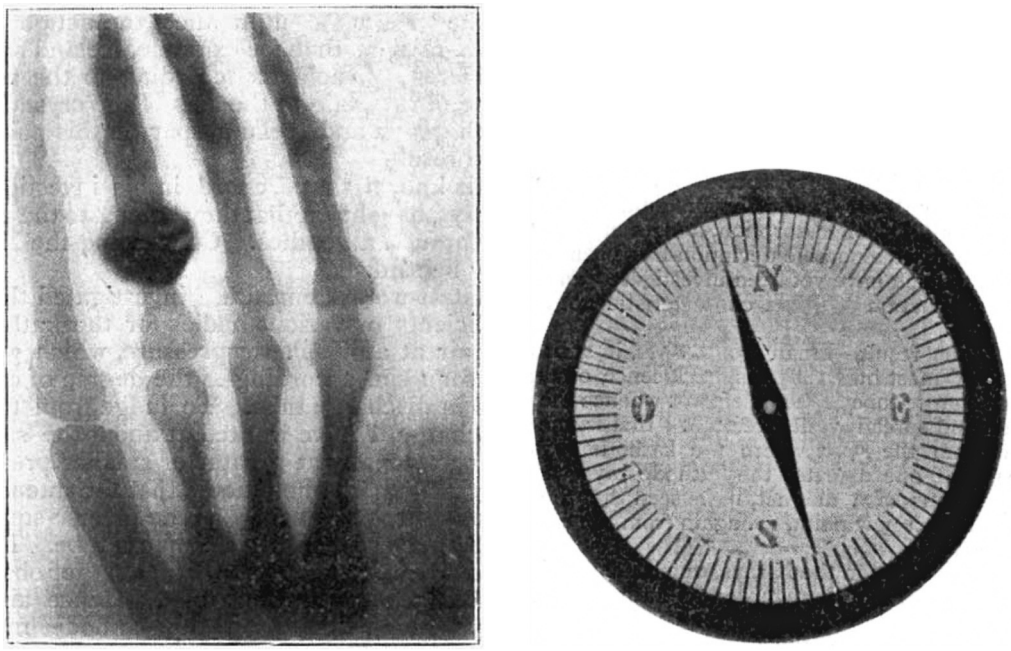

(A) (B)

FIGURE I.1 The very first X-ray images reported by Wilhelm Röentgen: (A) an image of his wife's left hand with ring on the third finger, and (B) a compass card and needle completely enclosed in a metal case. *From Roentgen, W.C., 1895. Über eine neue Art von Strahlen. Sitzungsberichte der Würzburger Physik-medic Gesellschaft 9, 132–141; Roentgen, W.C., 1896. On a new kind of rays. Nature 53 (1369), 274–276.*

postage stamp above, issued in 1995 to commemorate the 100th anniversary of Röntgen's discovery, also depicts the famous X-ray image of the left hand of Röentgen's wife, Anna Berta Ludwig (1872−1919).

Only days after Röntgen's report on December 28, 1895, the news proliferated through the world press, and an "X-ray mania" spread across the globe. One can only imagine the thoughts that went through the minds of the public and scientists alike when they saw for the first time the skeletal structure of a living human being or were able to "see through" a closed wood or metal container and observe its contents.

The image that X-rays produced on a photographic plate after traveling through a substance with varying transparencies to X-rays were referred to then as a "röntgenogram," and in 1896 the Wurzburg Physical Medical Society officially named these mysterious rays "Röntgen rays." Nowadays we call these images X-ray images. The medical ramifications of the early X-ray image of bones of the human hand became immediately clear, and Röntgen was awarded an honorary degree of Doctor of Medicine by the medical faculty of his own University of Würzburg. Numerous awards and honorary degrees were showered upon him, but he nevertheless remained a modest man, refusing to take out any patents on his work so that the scientific and medical community could advance without obstacle.

The early cathode-ray tubes used by Röntgen consisted of simple evacuated or partially evacuated glass tubes with a cathode (negative electrode) at one end of the tube and the anode (positive electrode) located off the side or at the other end of the tube. In these early tubes, with the application of a high voltage to the electrodes, electrons would escape from the cathode (cathode rays) and be accelerated toward the anode located off to the side of the tube. Many of the electrons upon acceleration would acquire sufficient energy to speed by the anode and hit the glass of the tube. Upon colliding with the glass, electron kinetic energy would be lost as x-radiation. These X-rays are also referred to as "Bremsstrahlung," meaning "braking radiation," since the accelerated electrons are forced to divert their path when they approach the nuclei of the glass atoms or target nuclei, causing the accelerated electrons to undergo a slowing-down or deceleration. The deceleration of the electrons results in the emission of the electron energy as x-radiation.

Not long after Röntgen's discovery, much work went into improving the efficiency of the production of X-rays by the development of X-rays tubes as modified cathode-rays tubes. Such a tube from the early 1900s is illustrated (Fig. I.2) in the postage stamp issued by the Czech Republic in 1995 to commemorate 100 years of Röntgen's discovery of X-rays. The stamp illustrates a typical X-ray tube of the time. The glass tube was partially evacuated to remove excess gas and

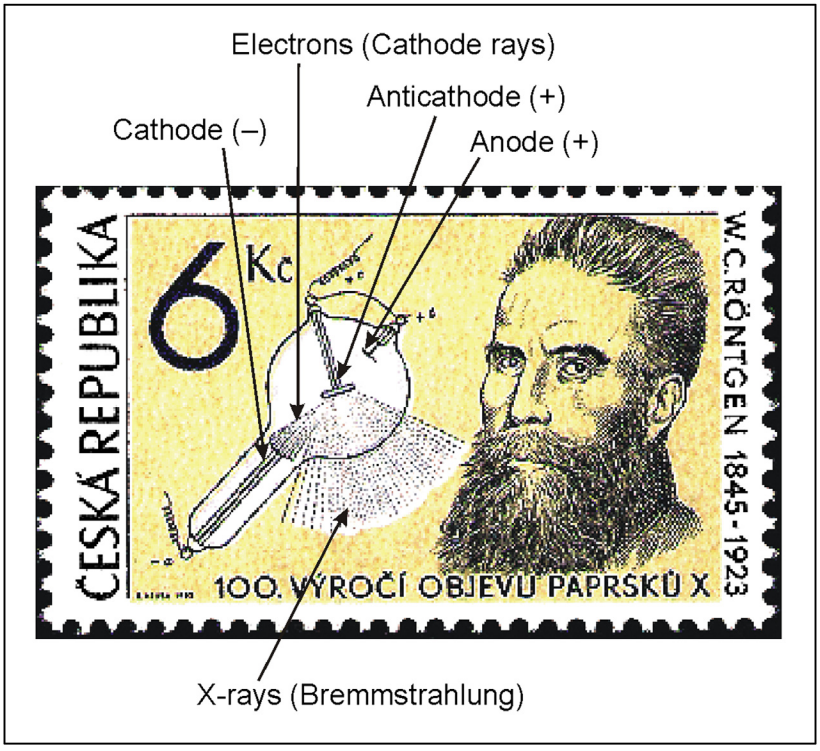

FIGURE I.2 The components of an early X-ray tube and bust of W.C. Röntgen on a postage stamp from the Czech Republic issued to commemorate the 100th anniversary of his discovery of X-rays.

maximize the efficiency of X-ray production. Upon application of a high-voltage potential to the electrodes, electrons escaping from the cathode would accelerate toward the positively charged anticathode. The anticathode was the name attributed to a target in the X-ray tube against which the electrons would collide to produce the x-radiation. The name anticathode is derived from the fact that the anode is oppositely charged from that of the cathode. The anticathode was made of a metal of high atomic number such as platinum or tungsten, as X-ray output efficiency was proportional to the target atomic number (see Eq. [6.91] of the chapter entitled "Beta Radiation and Beta Decay"). It was orientated at a 45 degree angle, as illustrated, to disperse the X-rays away from the electron beam out of the glass tube. The anode, located behind the anticathode, would accelerate the electrons from the cathode. The accelerating electrons would collide with the anticathode placed directly between the cathode and anode.

Röntgen's discovery and his numerous investigations on X-rays revolutionized the fields of medicine and physics. The vital fields of radiology and nuclear medicine, which many of us often take for granted today, were given birth on the day of this revolutionary discovery as commemorated by the postage stamp from Mexico in 1995. We should keep in mind that Röntgen was the first to discover artificial x-radiation, and it was only shortly after, in 1896, that Henri Becquerel discovered natural radioactivity.

IVAN PAVLOVICH PULUJ (A.K.A. JOHANN PULUJ 1845–1918)

Ivan Pavlovich Puluj, best known as Johann Puluj in Western Europe, was a pioneering Ukranian-born physicist and inventor in the late 19th and early 20th centuries. He contributed greatly to our understanding of the properties and origin of cathode rays, the properties of X-rays, and the interpretation of the origin of x-radiation. Puluj and others demonstrated the implementation of X-rays in the field of medical imaging practically from the day that x-radiation was first reported by Wilhelm Röntgen in December of 1895.

Ivan P. Puluj (1845–1918)

Ivan P. Puluj was born on February 2, 1845 in the Austro-Hungarian Empire, now Western Ukraine, in the small urban settlement of Hrymailiv in the Husiatyn Raion (district) of Ternopil Oblast. Biographical data are available from the Österreichisches Biographisches Lexicon 1815–1950 (Austrian Biographical Lexicon, Austrian Academy of Sciences, http://www.biographien.ac.at) and Wikipedia (https://de.wikipedia.org), from which some biographical data is taken. Information on the scientific works of Ivan Puluj was obtained from his scientific papers cited in this chapter.

Growing up in what is now Western Ukraine, he completed his secondary education at the Humanistischen Gymnasium Ternopil during 1857–65, where all instruction was carried out in the German language. Puluj then entered the University of Vienna, where he initially studied theology and philiosophy (1865–69). He continued his studies at the University of Vienna in physics, mathematics, and astronomy until 1972. His studies were funded with a Franz-Josef scholarship.

Another source of support was provided by tutoring within Viennese families. From 1872 to 1874, Puluj was assistant to Prof. Victor von Lang, whose research focused on internal friction and temperature of gases. From 1874 to 1875, Puluj was a lecturer in mathematics and physics at the Imperial and Royal Naval College in Fiume, which is now Rijeka, Croatia. He completed his doctorate degree at the University of Strasbourg on the internal friction of gases under Prof. August Kundt. Among the students of the scientific school of August Kundt was the famous Russian pioneer in the field of physics, Pyotr N. Lebedev, whose work is discussed in Hall of Fame, Part VII of this book. During his stay at the University of Strasbourg, Puluj met Wilhelm Röntgen, who was also a student of August Kundt at the University of Strasbourg. Both Puluj and Röntgen were of the same age; but little is known about whether they had any working or social relationship at the University of Strasbourg.

At the 1878 Paris Exhibition, Puluj was awarded a silver medal for the invention of a device used for the measurement of the mechanical equivalent of heat. From 1876 to 1883, Puluj was assistant professor and lecturer (Privatdozent) at the University of Vienna. After 1882, he focused his efforts on theoretical and practical electrical engineering. He was appointed professor of experimental and technical physics at the Czech Technical University in Prague (Prague Polytechnical University) in 1884 where he remained until 1916. In 1916, he was offered the position of Austrian Minister of Education, which he declined for reasons of health.

During the 1880s, Puluj did extensive theoretical and technical research using Crookes tubes, which were experimental electric discharge tubes invented by the English Physicist William Crookes (and others). Crookes tubes were partially evacuated glass tubes containing electrodes at generally opposite ends, and were instrumental to the discovery of X-rays by Wilhelm Röntgen in 1895 and electrons by J.J. Thomson in 1897. Puluj's extensive works involving the then-unknown emissions from the cathode of the Crookes tubes were precursors to the discoveries of X-rays by Röntgen and the electron by Thomson.

As early as 1883, Puluj presented experimental work that characterized the cathode rays, that is, the characterization of the emissions from the cathode of a Crookes tube or the emissions from the cathode of other tubes, known as electrical radiometers. In the case of electrical radiometers, the cathode rays were known to cause the rotation of a wheel with blades within the radiometer similar to the rotation of the blades of a fan. Puluj (1883) provided evidence that matter of some sort (electrons were yet to be discovered) was emitted with sufficient kinetic energy to cause the blades of the electrical radiometer to rotate in certain directions. He referred to the emissions from the cathode as radiant electrode matter, which he described in a book published in 1883 entitled *Strahlender Elektroden-Materie und der sogenannte vierte Aggregatzustand* (Puluj, 1883, p. 37), when he was a lecturer of physics (Privatdocent für Physik) at the University of Vienna. In a translation of this work published six years later by the Physical Society of London (Puluj, 1889), the title was written *Radiant Electrode Matter and the So-Called Fourth State of Matter*. In this important work, Puluj demonstrated that particle emissions emanated from the negative electrode—and not from the positive electrode. For the purpose of this demonstration, he constructed an electrical radiometer with the electrodes offset from the center, as illustrated in Fig. I.3. This allowed the "radiant electrode matter" to become focused onto the blades of a rotating wheel in the center of the radiometer. The experiment, as described in his words, first published in German (Puluj, 1883) and later in English (Puluj, 1889) is as follows (with the writer's comments in brackets):

> *The sketch fig. 32 [See Fig. I.3 of this book] represents an electrical radiometer which I have constructed. A small wheel of unblackened mica is suspended on a needle-point by means of a small glass cap, and two flat electrodes are fused eccentrically into the glass vessel. To obtain a stronger action the electrodes were bent cylindrically, so that their focal line fell on about the middle of a wing when the latter was between the two electrodes.*
>
> *Fig. 33b [See Fig. I.3 of this book] represents the section of the apparatus: the small wheel revolves in the direction of the motion of radiant electrode matter, from the negative towards the positive pole. [In this report, Puluj cited the work of another researcher who concluded erroneously that the material particles were emitted from the positive electrode. Puluj thus wanted to provide strong evidence that the matter particles were emitted from the negative electrode and not from the positive.]*
>
> *It was of great interest to me to determine whether this rotation in the direction of the emission of the particles from the positive electrode also took place at a pressure at which the radiant electrode matter appears. I made the experiment with a radiometer represented in fig. 34 [See Fig. I.3 of this book], which is furnished with two wire electrodes. At a pressure of 0.03 mm. the little wheel revolved in a direction opposite to that in which it would have rotated with flat electrodes.*

Puluj (1883, 1889) continued the experiment described above to demonstrate that the "electrode matter" was emitted from the negative electrode and not from the positive electrode. The description of the experiment in his written words is the following (See Fig. I.4 to follow Puluj's description):

> *The question now arises: Are the particles emitted from the positive or negative electrode, and how is that inversion of the direction of rotation to be explained?*

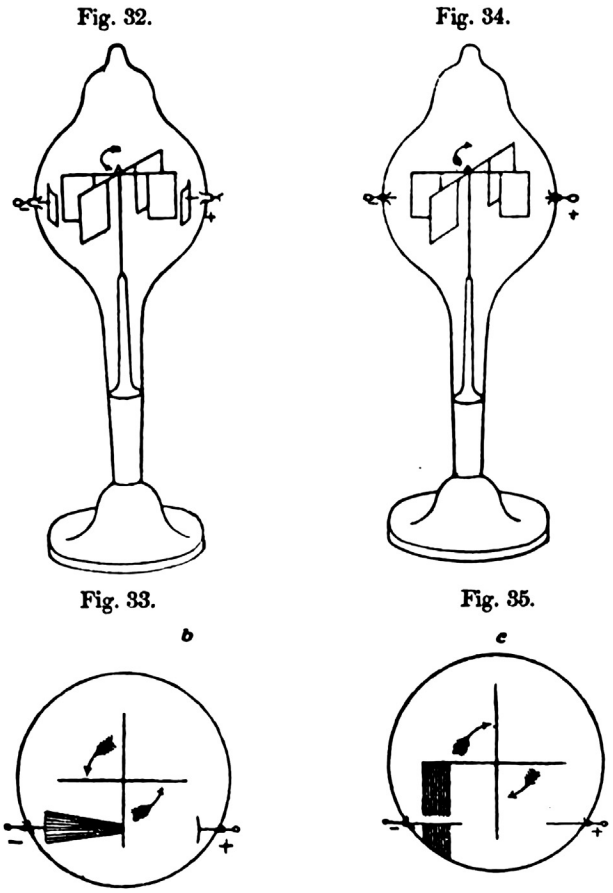

FIGURE I.3 Electrical radiometers constructed by Puluj (1883, 1889) with rotating wheel in the center and electrodes offset from the center of the glass bulb (Side views of two distinct radiometers are provided above by Puluj's Figs. 32 and 34.). Views from above the radiometers are provided by Puluj in diagrams b and c below each radiometer. The radiometer of Fig. 33b above contains wide electrodes, which are concaved slightly to focus the "electrode matter" or rays onto the blades of the central wheel, causing the wheel to move in a counter-clockwise direction. The rays are illustrated as numerous lines emitted from the negative electrode. On the other hand, the electrodes of Puluj's radiometer illustrated in Fig. 35c above are long wires, which Puluj used to demonstrate that the "electrode matter" was emitted perpendicular to the negative electrode (cathode), causing the blades to move in the opposite clockwise direction. *From Puluj, J., 1883. Strahlende Elektroden-Materie und der sogenannte vierte Aggregatzustand. Druck und Verlag von Carl Gerold's Sohn, Vienna, p. 86; Puluj, J., 1889. Radiant Electrode Matter and the So-Called Fourth State. Physical Memoirs Selected and Translated from Foreign Sources. Physical Society of London, vol. 1, Part 2, Taylor and Francis, London, pp. 233–331.*

> *This question is solved by the following very simple experiment.*
>
> *If an induction-current be passed through a cylindrical glass vessel into which a long wire reaches almost to the middle, on using this as a negative electrode the vessel shows a phosphorescent equatorial zone (fig. 36), which luminous phenomenon assumes an oblique position, as regards the electrodes, as soon as a horseshoe magnet is placed about the glass vessel in the manner represented in fig. 37 and fig. 38.*
>
> *The luminous equatorial zone can only be formed by the particles of the electrode being emitted perpendicularly to the axis of the wire in all directions. That, too, the last section of the wire emits particles perpendicular to the surface is self-evident, only their number is very small in proportion with those thrown off sideways.*
>
> *It is now easy to understand why, with the same direction of current, the small wheel in the radiometer with wire electrodes turns in the opposite direction to that with plate electrodes. It is at once evident from the sketch, fig. 35, that the lateral emission of the wire must turn the wheel in the opposite direction.*

Puluj wrote all of his scientific works as J. Puluj (Johann Puluj), which was the name by which Ivan P. Puluj was known throughout Europe. Johann Puluj's conclusions concerning "electrode matter" (ie, electrode particles) originating from the negatively charged electrode (cathode) in the electrical radiometer described above were major contributions that would be vital to the future discovery of the electron and its properties by J.J. Thomson in 1897. The acceptance of Johann Puluj's conclusions concerning the negatively charged electrode particles emitted by the cathode was reported in 1880 in the journal *Science* (Glaser, 1880) in a critic of one of the works of William Crookes. The following relevant excerpts from

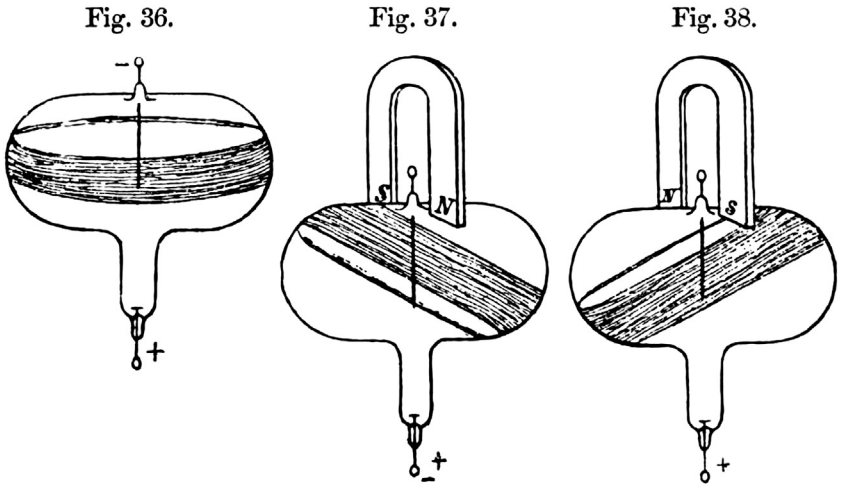

FIGURE I.4 Puluj's demonstration of an induction current, which is passed through a cylindrical glass vessel with a long negative electrode that reaches from the top to the middle of the vessel. In Fig. 36, the lines illustrate a phosphorescent equatorial zone running perpendicular to the electrode. A horseshoe magnet with its poles oriented in two different directions in Figs. 37 and 38 demonstrates two different oblique orientations of the luminous phenomenon. *From Puluj, J., 1883. Strahlende Elektroden-Materie und der sogenannte vierte Aggregatzustand. Druck und Verlag von Carl Gerold's Sohn, Vienna, p. 86; Puluj, J., 1889. Radiant Electrode Matter and the So-Called Fourth State. Physical Memoirs Selected and Translated from Foreign Sources. Physical Society of London, vol. 1, Part 2, Taylor and Francis, London, pp. 233–331.*

the 1880 article in the journal *Science* underscore the contributions of Puluj to what would become our knowledge of some properties of the electron demonstrated 17 years later by J.J. Thomson in his experimental verification and discovery of the electron in 1897. (The writer's comments are in brackets.)

> *It may interest the readers of "SCIENCE" to know the opinion held in Germany respecting those phenomena which led Mr. W. Crookes to believe he had discovered a fourth state of matter. For this purpose we have translated and abridged an article by Dr. J. Puluj, the well-known scientist of Vienna, published in the "Chemiker Zeitung"…*
>
> *Dr. Puluj's experiments go to show that Mr. Crookes' so-called radiant matter "consists of negative electric particles," which are torn off from the negative electrode and hurled away with immense rapidity. These electrode particles form a very beautiful metallic mirror on the glass walls… Because the electrode particles are negative electric, they represent a positive electric current, which moves in an opposite direction from the former. The electrode particles in motion are, therefore, real elements of an electric current,…*
>
> *The Vienna scientist (J. Puluj) draws from his observations the conclusion that the forces by which the electrode particles are torn off are not interior but exterior forces. [These were determined by J.J. Thomson 17 years later to be electrons, which are the exterior components of the atom.] When the electric current passes through the electrode, there is, according to his opinion, really a stream of extremely fine matter (ether) flowing,…. [The extremely fine matter was determined to be electrons, which would not be discovered until 1897 by J.J. Thomson. Also, at the time of this article in the journal* Science *(1880), the general thought was that a vacuum contained an 'ether'.]*

Johann Puluj became very well known for his phosphorescent lamp, known as Puluj's lamp, which is illustrated in Fig. I.5. Puluj's lamp, first designed by Puluj in 1881, would become an X-ray tube after the discovery of X-rays was announced by Wilhelm Röntgen in December of 1895. Puluj (1883, 1889) described the phosphorescent lamp in his book on *Radiant Electrode Matter*. A description of the lamp in Puluj's own words (Puluj 1883, 1889), with the writer's comments in brackets, is the following:

> *It [phosphorescent lamp] consists of a simple glass tube having in the centre an obliquely placed elliptical plate of mica covered with sulphide of calcium. Below the mica plate [above the mica plate in Fig. I.5] is a disc of aluminum of the same diameter as the section of the tube which serves as the cathode. Above the mica plate [below the mica plate in Fig. I.5] is the much smaller anode.*
>
> *The light of the phosphorescent lamp is sufficiently brilliant to light a room, and it is possible to read even at some distance from it.*
>
> *The light intermits as often in a second as the primary current is broken; on account of the longer duration of the impression of light, however, the lamp appears continuously luminous, and the intermittent character of the light is only recognized by observing bodies in motion, which then appear multifold. [Puluj (1883, 1889) continues in his book to describe numerous experiments that can carried out with this intermittent character of the light.]*

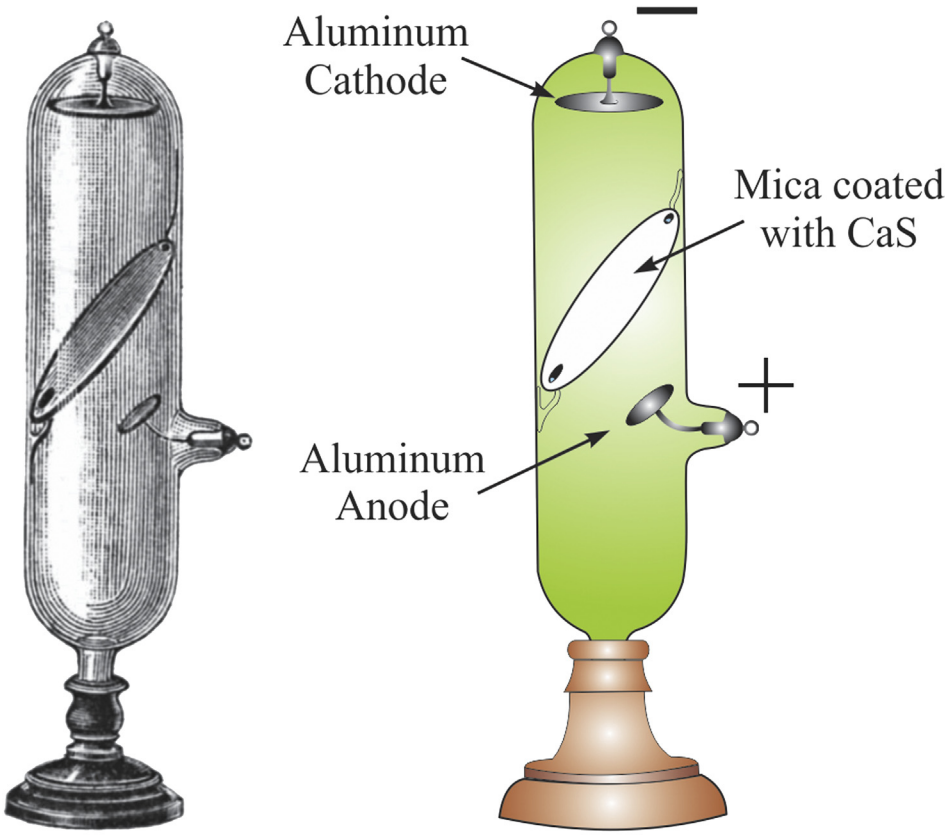

FIGURE I.5 Puluj's phosphorescent lamp on a wooden stand. (A). A contemporary drawing (c.1895). *(Courtesy of the Museum of Experimental Physics, University of Innsbruck http://physik.uibk.ac.at/museum/de/details/tubes/puluj.html.).* (B). A drawing adapted by the writer to illustrate more clearly the electrodes and the CaS-coated mica plate with a greenish internal color to represent the fluorescent color emitted by the lamp.

The light emitted from Puluj's lamp was due to fluorescence created by the interactions of what Puluj referred to as electrode matter, now known to be electrons, with the calcium sulfide on the mica plate, which would emit a green light when the CaS was deposited onto the mica plate. Puluj's tube was mass produced in the early 1880s by Stoehrer, of Leipzig, Germany and shipped to buyers worldwide. Thus, the Puluj phosphorescent lamps were already available in some American laboratories and particularly at the Physical Laboratory of Dartmouth College in Hanover, New Hampshire, USA in January of 1896 when the first news of Röntgen's discovery of X-rays reached North America by cable (Frost, 1896, 1930). Only eight weeks after the news of Röntgen's discovery of X-rays reached the USA, Puluj's fluorescent lamp, among other Crookes tubes, were tested as X-ray tubes by Edwin Brandt Frost and Prof. C.F. Emerson at the Physical Laboratory of Dartmouth College. It was in this laboratory where the very first application of X-rays to medical imaging in the USA was reported (Frost, 1896). In the journal *Science*, dated March 17, 1896, Edwin B. Frost (Frost, 1896) wrote the following:

> *Photographs [x-ray images] have been obtained with several of the Crookes tubes in the cabinet of the Dartmouth Laboratory, but the one referred to in a previous communication is by far the most efficient, and it has been used in nearly all the experiments now to be described. This tube was made by Stoehrer, of Leipzig, being No. 1147 of his catalogue, where it is designated as Puluj's neue Phosphorescenz-Lampe. It contains a mica diaphragm coated with some phosphorescent substance, and gives quite a brilliant green light when in action (although this brilliancy is doubtless immaterial to the production of the X-rays). As to the source of the X-rays developed by this tube it may be stated that a variety of experiments have shown that they originate in the diaphragm itself where exposed to the cathode rays, and not to any appreciable degree in the glass around the diaphragm.*

Thirty-four years later, Edwin B. Frost (Frost, 1930) provided a historical account of the days of the very first X-ray images taken with Puluj's tube (ie, phosphorescent lamp) in the United States on February 1, 1896. An excerpt of this account, which appeared in the Dartmouth Alumni Magazine, from Frost (1930) is the following:

> *No one could ever forget the interest felt in watching the development of these first plates on that Saturday evening, either January 24 or February 1, 1896, probably the latter. It did not take long to find where the rays were most active around the tubes, and the Puluj tube proved to be the most efficient. I suspect, in fact, that it was one of the best tubes in America for the next few weeks. It was handled carefully and was not burned out, as were many of the tubes used in other laboratories.*

Johann Puluj was also among the first to demonstrate the application of X-rays to medical imaging. Four months after the first X-ray images were reported by Wilhelm Röntgen in 1895, Johann Puluj provided an image of an entire seven-month-old human fetus, which was stillborn. The image can be found in the journal *The Photogram*, April 1896, Vol III (No. 28), pp. 106–107. An excerpt from *The Photogram*, with the writer's notes in brackets, is the following:

> *Professor Puluj, of the Imperial Technical High School, at Prague, sent an important paper to the Imperial Academy of Sciences at Vienna upon "The formation of Röntgen rays and their photographic action"…Fifteen years ago [1881], he designed a tube which, besides the ordinary electrodes, contained a mica screen coated with calcium sulfide [see Fig. I.5] from which proceeds not only the visible phosphorescent rays but the new X-rays with such intensity that very distinct images of small objects can be obtained in two seconds. This tube was described in the* Berichte der K. Akad. d Wissen., Wien*, 1881 and in the* Physical Memoirs of Physical Society, London, 1889, vol. 1, part 2, p. 204…*Our illustration is a reproduction of a seven months human fetus, kindly supplied by Professor Dr. Puluj, and is the first complete human skeleton ever radiographed…*

Puluj's fluorescent lamp, which was designed by Puluj in 1881, as well as many Crookes tubes used by Puluj and others, were producing fluorescence that was easily visible and recognized by all; however, these tubes also produced invisible rays (ie, X-rays), which they did not recognize until Wilhelm Röntgen announced his discovery in December of 1895. The discovery of the invisible X-rays and the utility of these rays to produce images of the skeletal structure of the human hand or an image of an item enclosed in a wooden or metal container were first demonstrated by Röntgen. This fact was acknowledged by Johann Puluj in a short note received by the editors of the *Proceedings of the Physical Society of London* on March 13, 1896 (Puluj, 1896). In this short note, Puluj referred to the newly discovered invisible rays as Röntgen rays, and the images that the X-rays would produce as Röntgen photographs. An excerpt of Puluj's comments in this note is the following:

> *Herr Puluj [the writer] sent for exhibition some Röntgen photographs taken by means of a form of Crookes tube which he had described in a memoir published in 1889. With this tube he has succeeded in obtaining impressions with exposures of only two seconds… Each portion of the glass or screen bombarded by the cathode stream becomes the starting-point of ether waves, which, according to their oscillation period and oscillation character, are either visible rays (phosphorescence) or invisible Röntgen rays.*

In the above acknowledgment by Puluj that Röntgen was both the discoverer of X-rays (ie, Röntgen rays) and X-ray imaging (ie, Röntgen photographs), he provided one of the first explanations of the origin of the X-rays. In this note, Puluj refers to the oscillation period and character of these invisible rays originating as ether waves. The reader will recall that all physicists, at the time, considered a vacuum to contain an "ether." The Crookes tube referred to by Puluj above is the Puluj fluorescent lamp described previously and illustrated in Fig. I.5.

An excellent review of Puluj's work and contributions to the science of the newly discovered X-rays was provided by Savchuk (2006) with numerous literature references to support his conclusions. In this review, Savchuk (2006) listed four contributions made by Puluj with detailed historical evidence for each. The reader may peruse this paper for additional information. The contributions are only briefly listed here as follows:

1. The discovery of the ionizing properties of X-rays is attributed to Puluj.
2. Puluj was the first to investigate the spatial distribution of X-rays and that X-rays are emitted by the anticathode mainly at an angle perpendicular to it.
3. Puluj's tube designed in 1881 (see Fig. I.5) had the main features of a modern X-ray tube. It was Puluj's tube (Puluj's fluorescent lamp) that was used to produce the first X-ray images in America at Dartmouth College in 1896.
4. Puluj was the first to provide a correct explanation of the mechanism for the production of x-radiation.

Johann Puluj (a.k.a. Ivan Pavlovich Puluj) was one of the foremost pioneers in the field of physics during the 1880s and 1890s. He was born Ukrainian and remained a patriot of Ukraine. He assisted politically persecuted Ukrainians seek asylum in Prague during World War I; and he campaigned for the establishment of a Ukrainian university in Lvov

(Mayba et al., 1997). While occupying the position of professor of experimental and technical physics at the Czech Technical University in Prague (Prague Polytechnical University), Puluj wrote a book entitled *Ukrainia und ihre internationale politische Beudeutung*, which is translated to "Ukraine and its international political importance," published in Vienna in 1915. The following year he was offered the political position of Austrian Minister of Education, which he had to decline for reasons of health. Johann Puluj died in Prague on January 31, 1918, where he is buried. The Ukraine National Technical University in Ternopil (TNTU) is named after Ivan Puluj.

HENRI BECQUEREL (1852–1908)

Antoine Henri Becquerel was born in Paris, France in 1852. He was awarded the Noble Prize in Physics in 1903 for, in the words of the Nobel Committee, "the extraordinary services he has rendered by his discovery of spontaneous radioactivity."

Becquerel (1852–1908)

In the beginning of 1896, on the very day that news reached Paris of the discovery of X-rays, Henri Becquerel thought of carrying out research to see whether or not natural phosphorescent materials emitted similar rays. He was then professor of the École Polytechnic, where he went to work on some uranium salts that he had inherited from his father, who had previously studied phosphorescence as professor of applied physics at the Polytechnic. Henri Becquerel placed samples of uranium sulfate onto photographic plates, which were enclosed in black paper or an aluminum sheet to protect the plates from exposure to light. After developing the photographic plates, he discovered that the uranium salt emitted rays that could pass through the black paper and even a metal sheet or thin glass positioned between the uranium salts and the photographic plates. Becquerel reported his findings to the French Academy of Sciences in February and March of 1896 (Becquerel, 1896a,b), and summarized his discovery in 1901 in the journal *Nature* as follows:

> *At the commencement of the year 1896, in carrying out some experiments with the salts of uranium, the exceptional optical properties of which I had been studying for some time, I observed that these salts emitted an invisible radiation, which traversed metals and bodies opaque to light as well as glass and other transparent substances. This radiation impressed a photographic plate and discharged from a distance electrified bodies — properties giving two methods of studying the new rays.*

At first he thought the rays were a result of phosphorescence, that is, excitation of the crystals by sunlight forcing the crystals to give off their own rays. However, Henri Becquerel carried out further tests demonstrating that the rays emanating from the uranium salts were independent of any external source of excitation including light, electricity, or heat, and the intensity of the rays did not diminish appreciably with time. "We were thus faced with a spontaneous phenomenon of a new order," which were his words during his Nobel lecture given on December 11, 1903.

Becquerel provided evidence that all uranium salts emitted the same radiation, and that this was a property of the uranium atom particularly, since uranium metal gave off much more intense radiation than the salts of that element. He was also able to demonstrate that the radiation was different from the X-rays discovered by Röntgen. The new radiation produced ionization and the intensity of the radioactivity could be measured by this ionization, as in his words, "the uranium discharged electrically-charged materials located some distance away." Even to this day, some pocket dosimeters used by radiation workers measure the radiation dose according to the degree of electrical discharge caused by ionizing radiation impinging onto an electrically charged chamber that can fit into a shirt pocket. Not only did these rays produce ionization, but he was able to demonstrate that a large portion of these rays could be deflected by a magnetic field and were charged particles of property similar to cathode rays. In the journal *Nature*, Becquerel (1901) described his findings as follows, with the writer's comments in brackets:

> *…in an electric field the radiation of radium undergoes a parabolic inflection in the contrary sense to the [magnetic] field, as would be the case with a flux of negatively charged particles. The comparison of electrostatic and magnetic deviations allows of the determination, like that of Prof. J.J. Thomson for the cathode rays, of the velocity of the particles. For the particular radiations defined by* $H\rho = 1600$ *[product of magnetic field strength and radius of curvature of the electron, which is proportional to the electron energy; see Eq. VI.24 in Radioactivity Hall of Fame VI], the velocity has been found equal to* 1.6×10^{10} *– about one half of that of light.*

In recognition of his discovery of radioactivity, Henri Becquerel shared the Nobel Prize in Physics in 1903 with Pierre and Marie Curie, who were awarded the prize for their extensive research into this newly discovered radioactivity.

PIERRE CURIE (1859–1906) AND MARIE CURIE (1867–1934)

Pierre Curie and Marie Curie shared the Nobel Prize in Physics in 1903 with Henri Becquerel. The Curies were awarded the prize in recognition of "their joint researches on the radiation phenomena discovered by Professor Henri Becquerel."

Pierre Curie was born in Paris in 1859. He received the doctor of science degree in 1895 and was then appointed professor in the school of physics. His wife, Marie Curie, was born Maria Sklodowska in Warsaw, Poland in 1867. Maria left Poland in 1891 after years of hard work and saving to finance her own education as well as providing for the education of her sister. When she saved what she thought would be enough for her education, she traveled to Paris to continue her studies of physics and mathematical sciences at the Université Paris "La Sorbonne." It was

Pierre (1859–1906)

Marie (1867–1934)

impossible for her to continue her education to get a university degree under the czarist control of Poland at that time. In France she changed her name from Maria to the more locally customary name of Marie. Although Marie had barely the resources to survive, living in the most modest dwelling with barely enough to eat, she studied hard and was the top of her class receiving licentiateships in physics and the mathematical sciences. She was sometimes so engrossed in her studies that she would forget to eat, and it was reported that she once fainted in class for lack of nourishment.

While Marie was studying in 1894, she and Pierre met. Pierre was professor of the Municipal School of Industrial Physics and Chemistry and already a well-known scientist in the field of crystal chemistry and physics. They fell in love and married in 1895. She encouraged Pierre to complete his doctorate degree that year, and he provided Marie with his laboratory as well as encouragement to pursue her research interests.

Two recent discoveries in physics sparked Madame Curie's interest. The first was the discovery of X-rays by Röntgen in 1895, and the other was the discovery the following year by Becquerel of spontaneous radiation emitted by uranium. She decided to study the mysterious rays emitted by uranium and to apply this work for a doctorate degree. The fact that no woman yet in the world had earned a doctorate degree did not thwart her efforts. Obstacles in life only seemed to motivate Madame Curie. She discovered in 1898 that not only uranium gave off the mysterious rays discovered by Becquerel, but thorium did as well; this was independently discovered by Gerhard Schmidt in Germany the same year.

Madame and Pierre Curie observed that the intensity of the spontaneous rays emitted by uranium or thorium increased as the amount of uranium or thorium increased. They concluded that these rays were a property of the atoms or uranium and thorium; thus they decided to coin these substances as "radioactive." The emanation of such spontaneous rays from atoms would now be referred to as "radioactivity."

Madame Marie Curie pursued her studies with all materials that contained uranium and thorium and discovered that the uranium ore pitchblende exhibited more radioactivity than could be attributed to its content of uranium or thorium. On this basis she made the assumption that there were one or more radioactive elements in pitchblende other than uranium and thorium. Through tedious chemical separations and analyses, Madam and Pierre Curie worked as a team and found that another radioactive element with chemical properties similar to bismuth was present in pitchblende. She named this new element "polonium" in honor of her native country. They found yet a second new radioactive element in the pitchblende ore with chemical properties close to that of barium, and they named that new element "radium" from the Latin word *radius*, meaning "ray." The new elements were encountered only as traces in pitchblende; and the Curies had to tediously process and fractionate over a ton of pitchblende ore to extract only minute quantities of the new elements. They spent their life savings to procure the pitchblende, and in the words of Madame Curie "it took several years to show unequivocally that pitchblende contains at least one highly-radioactive material which is a new element in a sense that chemistry attaches to the term."

The procedures devised by Pierre and Marie Curie for the extraction of these new radioactive elements were very exhausting physically, and the radiation doses they received from this tedious work and handling of this material surely affected their health. They both suffered from ill health due possibly to a combination of excessive work and radiation sickness. Due in part to ill health, Pierre delivered the Nobel Laureate address on June 6, 1905, two years after they were awarded the coveted prize. In 1903, the year Pierre and Marie Curie were awarded the Nobel Prize in Physics, Marie also became the first woman to receive a doctorate degree in France. Pierre was promoted to professor at La Sorbonne.

The effects of excessive doses of radiation to one's health were then unknown, although Pierre demonstrated that high doses of radiation could damage human tissue. In the Nobel address (Curie, 1905), he stated:

> *Radium rays have been used in the treatment of certain diseases (lupus, cancer, etc.). In certain cases their action may become dangerous. If one leaves a small glass ampoule with several centigrams of a radium salt in one's pocket for a few hours, one will feel absolutely nothing. But 15 days afterwards a 'redness' will appear on the epidermis, and then a sore which will be very difficult to heal. A more prolonged action could lead to death. Radium must be transported in a box of lead.*

Over 100 years ago at the Nobel lecture, Pierre Curie had the wisdom to comprehend, like a double-edged sword, the potential benefits and dangers that radioactivity presented. He noted the immediate benefits found in using radiation from radium to treat cancer, while on the other hand he stated:

> *It can even be thought that radium could become very dangerous in criminal hands, and here the question can be raised whether mankind benefits from knowing the secrets of Nature, whether it is ready to profit from it or whether this knowledge will not be harmful for it. I am one to believe with [Alfred] Nobel that mankind will derive more good than harm from the new discoveries.*

So far to this day mankind has not betrayed Pierre's belief.

Approximately 10 months after presenting the Nobel address, Pierre met with a tragic accident and died instantly after being struck by a horse-drawn carriage while crossing a street in Paris. Marie suffered from his demise, as they were deeply in love. Like most determined and driven individuals, this tragedy forced her deeper into her work. She was awarded the Nobel Prize in Chemistry in 1911. Marie Curie then became not only the first woman to receive a Nobel Prize, but also the only person to ever receive a second Nobel Prize in two distinct sciences. The prize was awarded "in recognition of her services to the advancement of chemistry by the discovery of the elements radium and polonium, by the isolation of radium and the study of the nature and compounds of this remarkable element."

The French Academy of Sciences rejected Marie's bid for admission into the Academy. No woman had yet been admitted into the Academy and she was not of French descent. Nevertheless, following the death of Pierre she took over his classes, and was appointed professor to become the first woman ever to teach at La Sorbonne. Much of her work later in life was devoted to finding medical applications of radioactivity including radium therapy for the treatment of illnesses such as cancer, and the medical applications of X-rays. She played a vital role in the establishment of the Radium Institute in Paris (Institut du Radium) in 1909, which was established by the University of Paris and the Institut Pasteur. Marie Curie directed the Radium Institute, which carried out research on radiation chemistry and physics, while Dr. Claudius Regaud was director of the Pasteur Institute, which researched the biological effects and medical applications of radioactivity. Marie Curie and Dr. Claudius Regaud joined forces and created the Curie Foundation in 1920 with the objective of supporting the Radium Institute for the applications of radioactivity in medicine. The Curie Foundation established its first hospital in 1922, which spearheaded innovative applications of radiation therapy in cancer treatment. The Radium Institute and Curie Foundation united in 1970 to form the Curie Institute, which is today a leading research center of the world in medical biology, with a hospital specialized in cancer treatment including radiation oncology (https://en.wikipedia.org/wiki/Curie_Institute_(Paris)). Many of the techniques used today throughout the world for the diagnosis and treatment of cancer utilize nuclear radiation for imaging and therapy, as described in detail in the introductory chapter of this book, thanks to the pioneering work of Marie Curie with the collaboration of Dr. Claudius Regaud. The postage stamp illustrated here commemorates the Curies' discovery of radium and Marie Curie's efforts to apply this radioactive source in the international fight against cancer.

Marie Curie suffered hardship and many obstacles in her life, and these obstacles only seemed to motivate her further. Also her modesty was unsurpassed. It is reported that she wore the same black dress to receive both Nobel Prizes in 1903 and 1911. Her life, determination, and perseverance to overcome all obstacles should serve as an example for us all. Many very informative books have been written about Marie Curie, including those by Noami Pasachoff (1996), Susan Quinn (1996), Barbara Goldsmith (2004), and a biography by her daughter Eve Curie (1938).

Marie Curie died of leukemia on July 4, 1934, a disease she likely acquired from excessive exposure to the radioactive materials she studied. Albert Einstein eulogized on her death, stating "Marie Curie is of all celebrated beings, the only one whom fame had not corrupted." Her determined work, personal sacrifice, and devoted efforts to help mankind through

medical applications of radioactivity had revolutionized the sciences of physics, chemistry, and medicine. In a book, Richard Rhodes (1986) eloquently characterized her passing by writing the following, with the author's comment in brackets:

> *As if to mark in some distant inhuman ledger the end of one age and the beginning of another, Marie Sklodowska Curie, born in Warsaw, Poland, on November 7, 1867 died that day of Szilard's filing, July 4, 1934. [The date July 4, 1934 was the day of Leo Szilard's filing of a patent, No. 630,726 in the UK, on the principles of making the atomic bomb (See the short biography of Leo Szilard in Hall of Fame, Part IV).]*

In 1995, President François Mitterrand of France transferred the ashes of Marie Curie and those of her husband Pierre to rest under the famous dome of the Panthéon in Paris alongside the remains of France's greatest dignitaries. The inscription on the Panthéon's ornamental front used to read "To the fatherland's great men, in gratitude." This could be interpreted literally until the remains of Marie Curie were laid to rest among these great men. President Mitterrand conferred the added value of "beings" to the term "men" to set things right and enable the country and world to honor a nonnational among other great French personalities, who had contributed greatly to French prestige. It is said that nobody has sacrificed and contributed so much to scientific research and humankind as Marie Curie.

PAUL VILLARD (1860–1934)

Paul Ulrich Villard discovered gamma radiation in the year 1900. He received very little recognition for his discovery. His work remained largely forgotten by the scientific community until the 100th anniversary of his discovery, when Gerward (1999) and Gerward and Rassat (2000) published thorough historical accounts of Villard's life and work. Most of the biographical data presented here was obtained from their reports.

Paul Villard (1860–1934)

© Académie des Sciences de l'Institut de France, with permission.

Paul Villard was born in a village near Lyon, France on September 28, 1860. He entered the École Normale Supérieure in Paris in 1881, and upon graduation he taught at various lycées and finally at the Lycée of Montpellier. Villard had a strong interest in scientific research. He thus established a scientific liaison with staff of the local university, which provided him with a small research laboratory. He enjoyed scientific research and preferred to be in Paris, which was then the heart of research in the physical and chemical sciences. Having sufficient financial resources to cover his needs, Villard was free to move to Paris, where he enjoyed the hospitality of the Chemistry Department of the École Normale at rue

d'Ulm. He was provided a small laboratory at the École Normale for his personal scientific research, where he remained for his entire scientific career until late in life, when he would retire outside of Paris.

His early scientific work during 1888–96 was devoted to the synthesis and chemistry of gaseous hydrates (1894a,b). Villard (1896) is recognized as the discoverer of the noble gas hydrates including the hydrate of argon. The element was discovered in 1894 by Nobel Laureates Lord Rayleigh (John William Strutt) and Sir William Ramsey. The gas hydrates are solid compounds of crystalline structure in a water matrix produced under high pressure and low temperature. Villard's pioneering work in this field is cited often in the scientific literature on gaseous hydrates.

The very year that Villard (1896) reported his discovery of argon hydrate, Henri Becquerel made his discovery of radioactivity. The year prior to Henri Becquerel's discovery of radioactivity, Wilhelm Röntgen discovered x-radiation, and Marie Curie discovered in 1898 that uranium and thorium also emitted radioactivity. Before the end of 1898, Pierre and Marie Curie had discovered new radioactive elements, which they named polonium and radium. Research in the field of radioactivity became the new frontier, and Villard would take part in the exploration.

In the field of radiation, Villard began his research using a Crookes tube to study the effect of magnetic fields on cathode rays and chemical effects of X-rays during 1897–99. He discovered that X-rays would produce both physical and chemical changes in substances (Villard, 1899, 1900a). Villard next obtained samples of radium from the Curies, and at first attempted to study the rays emitted by radium that could be deflected by a magnetic field, referred to as deviable rays, because he considered these rays to be similar to the deviable cathode rays. Although unknown at the time, the deviable rays emitted by radioactive atoms were beta particles identical in property to electrons that constituted cathode rays. In his attempt to measure the "refraction" of the deviable rays emitted by radium, Villard (1900b) discovered a yet-unknown nondeviable highly penetrating radiation, which was to be named years later by Rutherford (1903) as gamma radiation. Villard's discovery of gamma radiation was reported to the French Academy of Sciences (Villard, 1900b,c) and at the meetings of the French Society of Physics (1900d). The experimental procedures used by Villard are related in detail by Gerward (1999), and only his final and conclusive experiment reported to the French Society of Physics in 1900 is described below. Villard did not provide any diagrams of his experimental arrangements, which led to the discovery of gamma rays; however, the writer sketched Fig. I.6 to facilitate the description of an experiment reported by Villard.

Villard placed a sample of barium chloride containing radium within a lead shield that contained an opening, which essentially provided a collimated beam of the radiation from the radium source, as illustrated in Fig. I.6. To the radiation beam he exposed two photographic plates wrapped in black light-tight protective paper. Between the two plates was sandwiched a 0.3-mm thick lead barrier. A magnetic field was applied to the collimated beam to deflect the deviable rays. Alpha particles emitted by the radium are ignored, because these are absorbed by the protective paper wrapping of the photographic plates. The magnetic field caused a deviation of the beta particles, whereas a very penetrating radiation remained unaffected or undeviable by the magnetic field, as evidenced from the images produced by the radium emanations on the developed photographic emulsions. The developed photographic emulsion A, which was the first to

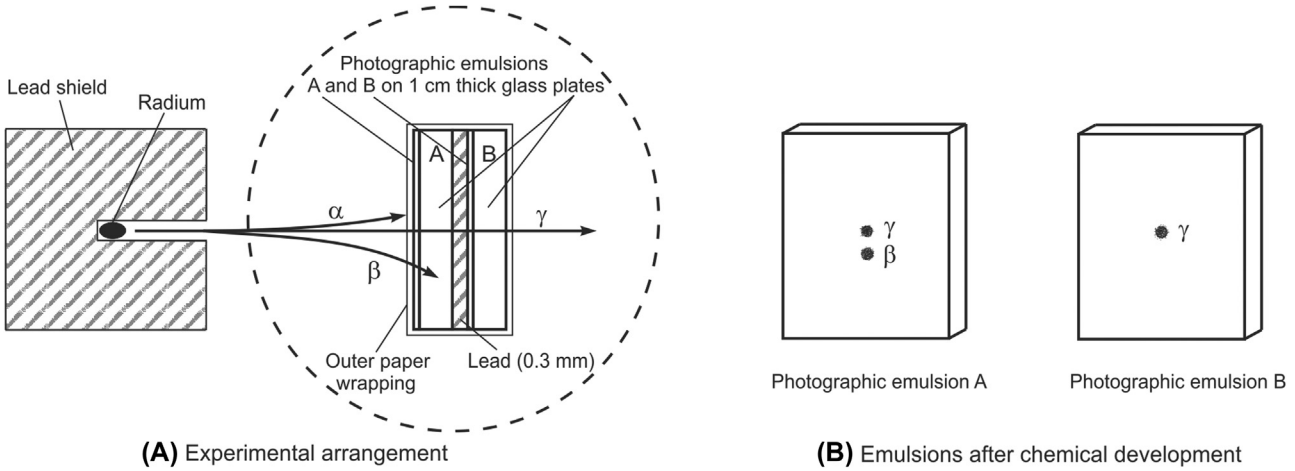

FIGURE I.6 Paul Villard's (A) experimental arrangement and (B) experimental results that lead to his discovery of gamma rays in 1900. Photographic plates A and B consisting of emulsion set on 1-cm thick glass supports were separated from each other by a 3-mm thick lead barrier and wrapped in an envelope of light-tight paper. The *dashed circle* represents the pole of a magnet from which the lines of force are directed into the plane of the page perpendicular to the path of radiation emitted by the radium source.

receive the nuclear radiations from the radium, showed two spots produced by two types of radiation, one deviable (marked β) and the other undeviable (marked γ) in the magnetic field. The second photographic emulsion B, which was placed behind a 0.3-mm thick lead barrier, yielded only one spot produced by a highly penetrating radiation unaffected by the magnetic field. The intensity of the spot on emulsion B was the same as that on emulsion A, indicating that its intensity remained unaffected to any observable extent by the lead barrier. The spot was also more clearly discernable, because it was not clouded by the deviable beta particles. Villard concluded that his experimental evidence demonstrated a radiation of property similar to X-rays, but with a greater penetrating power than x-radiation. In the journal *Nature*, Becquerel (1901) acknowledged Villard's discovery of gamma rays, which had not yet been named as such, with the following statement:

> *…there exists two kinds of radiations, one not capable of deviation [in a magnetic field] and of which the nature is still unknown, the other capable of deviation, which later experiments have identified with the cathode rays [later identified as beta-particles]… I might add that recently Mr. Villard has proved the existence in the radium radiation of very penetrating rays, which are not capable of deviation.*

Villard did not venture to name this newly discovered highly penetrating radiation. He was a modest person, possibly uninterested in fame or in the highly competitive pursuits of his fellow scientists in this new frontier. Gerward (1999) researched the scientific literature and found that it was Rutherford (1903), who was first to name the highly penetrating radiation discovered by Villard, as gamma rays. A few years prior to Villard's discovery, Rutherford (1899) had already named two types of nuclear radiation as "alpha" and "beta," which he characterized on the basis of their relative penetrative power in matter, that is, alpha radiation would be more easily absorbed by matter than beta radiation. In harmony with this nomenclature, Rutherford (1903) assigned the term gamma rays to the yet more penetrating radiation. In the *Philosophical Magazine*, Rutherford (1903) named and characterized the three types of nuclear radiation on the basis of their penetration power in matter as follows:

> *Radium gives out three distinct types of radiation:*
>
> *(1) The α rays, which are very easily absorbed by thin layers of matter, and which give rise to the greater portion of the ionization of the gas observed under the usual experimental conditions.*
> *(2) The β rays, which consist of negatively charged particles projected with high velocity, and which are similar in all respects to cathode rays produced in a vacuum-tube.*
> *(3) The γ rays, which are non-deviable by a magnetic field, and which are of a very penetrating character.*
>
> *These rays differ very widely in their power of penetrating matter. The following approximate numbers, which show the thickness of aluminum traversed before the intensity is reduced to one-half, illustrate this difference:*

Radiation	Thickness of Aluminum (cm)
α rays	0.0005
β rays	0.05
γ rays	8

As noted by Rutherford in the above quotation, ionization in a gas was one of the principal properties of nuclear radiation, which helped distinguish the radiation type. It was well understood at the time that the three rays possessed different powers of ionization in matter. The number of ion pairs formed in a gas by α-, β-, and γ-rays of given energy per path length of travel would differ according to the relationship α-rays > β-rays > γ-rays. Consequently, the property of ionization power of a given radiation was used to also measure the intensity of that radiation.

Villard discontinued his research on nuclear radiation and went on to research cathode rays and X-rays. He introduced the concept of the ionization of air by X-rays to help radiologists measure the intensity of X-rays that would be administered to patients (Villard, 1908). Prior to instrumental methods of measuring X-ray intensity, radiologists would practice the long-term harmful technique of using the X-ray image of their hand to measure adequate X-ray exposure times for patients. Van Loon and van Tiggelen (2004) provide a historical account of Villard's contribution to radiation dosimetry in the monitoring of medical exposure. Villard (1908) introduced the Villard unit as a measure of radiation intensity, which was defined as "the quantity of radiation which liberates by ionization one esu of electricity per cm^3 of air under normal conditions of temperature and pressure." Van Loon and van Tiggelen (2004) report that the Villard unit was adopted 10 years later as the "e" unit by Krönig and Friedrich (1918), and modified by H. Behnken (1927) to become the "R" unit (ie, Röntgen Unit) or "German unit of x-radiation."

In 1908 Villard was appointed a member of the French Academy of Sciences. He retired outside of Paris and died in Bayonne, France on January 13, 1934.

ERNEST RUTHERFORD (1871–1937)

Earnest Rutherford was born on August 10, 1871 in Nelson, New Zealand. He was awarded the Nobel Prize in Chemistry in 1908 "for his investigations into the disintegration of the elements, and the chemistry of radioactive substances." He was still a young man of 37 years at the time of this award, and most of his major achievements and contributions to the science of radioactivity and the field of nuclear physics were made by Rutherford after receiving the Nobel Prize.

Ernest Rutherford (1871–1937)

Rutherford grew up as a farm boy in New Zealand, raised by parents who had emigrated from Britain with modest means but who had instilled in their children the power of knowledge and the importance of completing all their schoolwork to the best of their abilities. Ernest excelled in science and mathematics, and could only achieve a higher education through financial aid with scholarships. He won a scholarship to Nelson College, where he learned elementary science and mathematics and excelled to win another scholarship to continue his education at Canterbury College, which is now the University of Canterbury in New Zealand. Although Rutherford worked hard and had an inquisitive mind, he credited his teacher, Prof. Alexander Bickerton at Canterbury, who displayed such an enthusiasm for science, it gave him the stimulus to pursue scientific research on his own. At Canterbury Rutherford won another scholarship as a research student at the Cavendish Laboratory, University of Cambridge under J.J. Thomson, who would later in life also win the Nobel Prize in Physics. At Cambridge, Rutherford stood out as a great experimenter and thinker, who could make major discoveries concerning radioactivity and atomic structure without expensive equipment and only limited resources.

Rutherford was captivated with the recent discoveries of X-rays by Röntgen and the subsequent discovery by Becquerel of the mysterious natural radiations from uranium. Because Becquerel showed that the radiations from uranium could, as well as X-rays, discharge an electrified body (ie, cause ionization), he decided to examine the effect of placing successive layers of aluminum foil over uranium oxide on the efficiency of the emanations to cause the electrical discharge. From this experiment he made his first discovery concerning radioactivity, stating at his Nobel address:

> *"…[I] was led to the conclusion that two types of radiation of very different penetrating power were present – one that is very readily absorbed, which will be termed for convenience the α-radiation, and the other of a more penetrative character, which will be termed the β-radiation, … and when a still more penetrating type of radiation from radium was discovered by Villard, the term γ-rays was applied to them.*

These terms devised by Rutherford soon took acceptance and came into common use by the scientific community as the convenient nomenclature, which remains today, for identifying these three types of radiation.

In addition to the different penetrating powers of α-, β-, and γ-radiation, other properties were used to identify these mysterious radiations, such as the differing deflections that the three radiations undergo in electric or magnetic fields. Alpha radiation was known to possess a positive charge, because it would be deflected toward the negative electrode in an electric field potential, while beta particles were known to be negatively charged due to their deflection in the opposite direction toward the anode or positive electrode. Gamma radiation would not undergo any deflection whatsoever, as illustrated in Fig. I.7. Likewise, the alpha and beta radiations, when traveling in a path perpendicular to the lines of force of

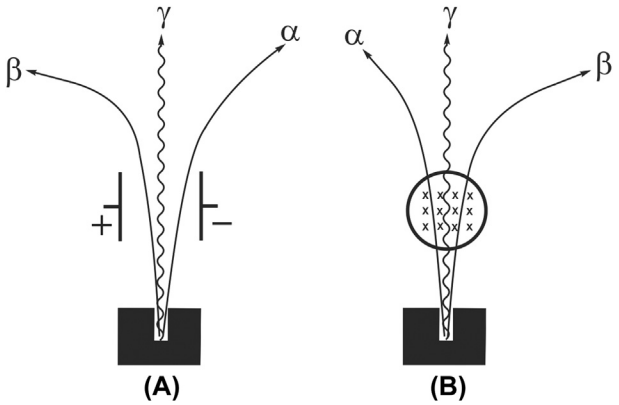

FIGURE I.7 Paths of travel of collimated beams of alpha, beta, and gamma radiation in (A) electric and (B) magnetic fields. Beam collimation is provided by placing the radiation source in a hole drilled within shielded containers (eg, lead) of which cross-sections are illustrated. The electric field in (A) is illustrated by positive and negatively charged electrodes separated by a space through which the radiations pass; and the magnetic field in (B) is illustrated by the circle to depict the pole of a magnet through which the lines of force of magnetic flux (marked by the symbol x) are directed into the plane of the page (z-axis) perpendicular to the radiation paths in the xy-axis.

a magnetic field, will be deflected in opposite directions, which is a characteristic of charged particles. Radiation that carries no electric charge would continue along a straight undeviating path in either electric or magnetic fields.

After 3 years at the Cavendish laboratory, Rutherford moved in 1898 to McGill University in Montreal at the age of 27 to take on the position of professor of physics. It is at McGill University where he began to make his major discoveries in the field of nuclear physics. The first of these was the discovery that radioactive atoms that emit α-particles or β-particles disintegrate into atoms of lighter weight, in other words, atoms of an element such as radium that emit α-particles undergo transformations to atoms of a lighter and consequently different element. Rutherford and coworkers were able to demonstrate that the alpha particle was an atom of helium (later to be determined to be a nucleus of helium), and that helium gas would accumulate or be entrapped in minerals that contained radium. Furthermore, he demonstrated that the lighter atom produced as a product of the decay of radium would likewise be radioactive, and in turn, decay to another even lighter atom, and so on until the final product atom was stable. It was for this work that Rutherford received the Nobel Prize in Chemistry. Although a great honor for such a young scientist, it was ironic for Rutherford to go through life as a Nobel Laureate of Chemistry. He was a physicist and considered physics as the most important science of all. At the Nobel Prize presentation address on December 10, 1908, Prof. K.B. Hasselberg, President of the Royal Academy of Sciences, explained:

> *Though Rutherford's work has been carried out by a physicist and with the aid of physical methods, its importance for chemical investigation is so far-reaching and self-evident, that the Royal Academy of Sciences has not hesitated to award to its progenitor the Nobel Prize designed for original work in the domain of chemistry.*

Rutherford's work in conjunction with numerous collaborators including Frederick Soddy, led to the conclusion that one chemical element can transform into other elements, which was previously only a centuries-old belief of alchemists, who tried to change lead into gold. Prof. Hasselberg in his speech of award presentation, had foresight when he added further:

> *[Rutherford's] disintegration theory [of atoms] and the experimental results upon which it is based, are synonymous with a new department of chemistry.*

We can thus give credit to Rutherford for giving birth to the field of radiochemistry.

Rutherford's best work was yet to come after the Nobel Prize. In 1907 he moved to England to fill the position of professor of physics at Manchester University. It was at Manchester where Rutherford had a list of research topics to explore, and one of these was the deflection that alpha particles would undergo when passing through thin foils (approx. 5×10^{-5} cm thick) of materials such as mica, aluminum, gold, etc. He knew that the alpha particles, as they travel at high speed, would traverse the foils as if the foil material was not even in the alpha-particle path, and that the flux of alpha-particle radiation would undergo only a very slight dispersion upon exiting the foils. This was understandable to him as strong electrical charges, expected to occur in atoms, could cause the slight deflection of the positively charged alpha particles.

The story goes that he was approached by his research assistant at Manchester, Dr. Wilhelm "Hans" Geiger (best known as the person who developed the Geiger counter, still used today for the monitoring of radioactivity). Geiger had asked Rutherford "What do you suggest we give the new student Ernest Marsden to do?" Rutherford proposed that they try to see if any alpha particles would bounce back, that is, not traverse the foil but be deflected by over 90 degrees back toward the direction from which the particle had originated. Rutherford did not expect to see any such deflection, but it had to be investigated. They could observe the alpha-particle path of travel and see and count the deflections by means of a zinc sulfide screen that would produce a microscopic fluorescence (flash of light scintillation) in the dark when each individual alpha particle hit the screen. They used radium as the source of the alpha-particle beam to bombard a thin foil of gold. Geiger later informed Rutherford that they could see the occasional deflection by greater than 90 degrees of one alpha particle for every 8000 particles traversing the gold foil. (See the following biographical sketch of Wilhelm "Hans" Geiger for a detailed description of this experiment.) The commemorative postage stamp above illustrates this phenomenon. The stamp illustrates a central nucleus surrounded by five electrons and the path (arrows) of three alpha particles. One of the alpha particles is illustrated hitting the nucleus of an atom of gold and bouncing back. In a presentation given by Rutherford years later, he described his reaction to this discovery by stating:

> *It was quite the most incredible event that ever happened to me in my life. It was as incredible as if you fired a 15-inch shell at a piece of tissue paper and it came back and hit you.*

Rutherford grasped this discovery to conclude that there had to be a massive core or nucleus in the atoms of materials that would cause colliding alpha particles to bounce back. By using high-energy (7.7-MeV) alpha particles, that would travel at highest speeds, Rutherford was able to calculate the distance of closest approach and consequently the radius of the atomic nucleus to be approx. 5×10^{-15} m (see chapter: Alpha Radiation).

In addition to the alpha-particle scattering experiment described above, which was carried out with the assistance of Hans Geiger, Ernest Rutherford undertook numerous ground-breaking experiments with Geiger. Some of these are described in the following biographical sketch on Wilhelm "Hans" Geiger. One very important experiment, which he undertook with Geiger (Rutherford and Geiger, 1908a), confirmed the charge and nature of the alpha particle. Rutherford had determined in previous years that the alpha particle was positively charged (Rutherford 1905a,b); however, a few years later Rutherford and Geiger (1908a) described their detailed measurement of the double charge on the alpha particle and their determination that the alpha particle was equivalent to a nucleus of the helium atom.

Rutherford and Geiger's precise determination of the charge on the alpha particle made use of the apparatus illustrated in Fig. I.8. As described by Rutherford and Geiger (1908a), the apparatus consisted of a 4-cm diameter cylindrical glass tube HH closed at both ends with ground glass stoppers D and E. The radioactive source is located at R, which is attached to the lower stopper E. The radiation travels into the testing chamber, which is attached to the upper stopper D via an ebonite tube F. The testing chamber contains two parallel plates, A and B, situated approximately 2 mm apart. Plate B was made of brass with a circular opening, 1.92 cm in diameter, covered with a thin sheet of aluminum. Likewise, the upper chamber AC consists of a shallow brass plate with an opening of 2.5 cm, which is also covered with a thin sheet of aluminum foil. The aluminum foil exhibited only a minimal stopping power for alpha particles equivalent to $\sim$5 mm of air. Plate B was connected via a side glass tube to a battery, while the other pole was earthed. The chamber AC, insulated from plate B, was connected to an electrometer. The entire apparatus was situated between the poles NS of an electromagnet, which is illustrated with dashed lines in Fig. I.8.

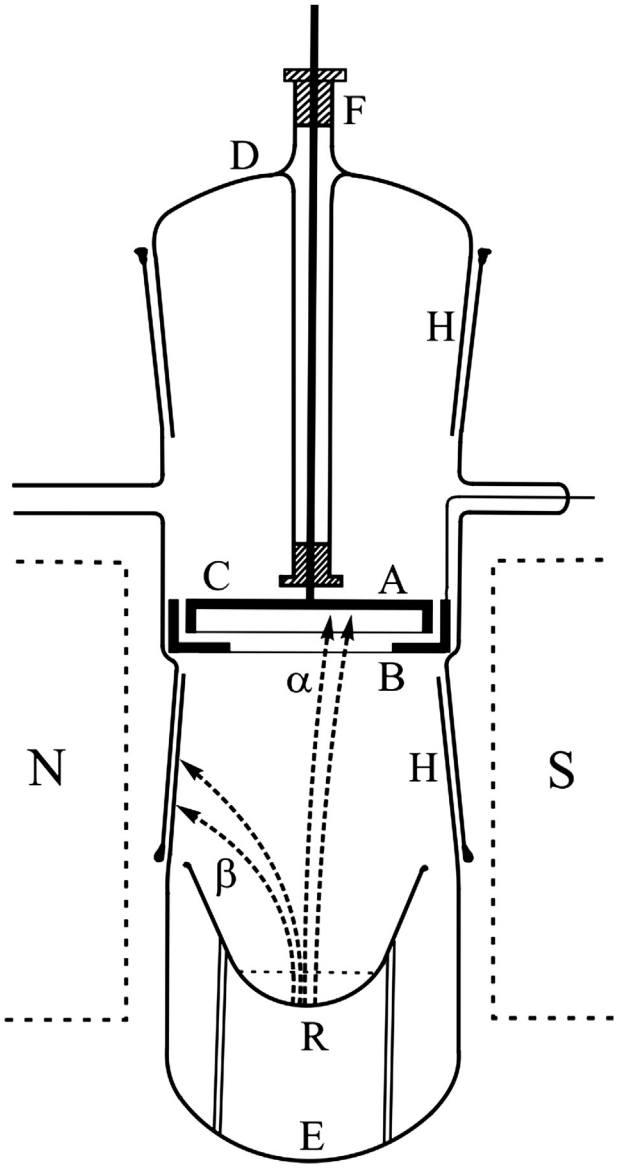

FIGURE I.8 Apparatus used for the measurement of the charge on the alpha particle. The illustrated paths of deflections of alpha and beta particles was added by the author. *From Rutherford and Geiger (1908a).*

The magnetic field was required to deflect beta particles, that are emitted from the radioactive source, away from the detector plates AC and B.

A vacuum pump was attached to the arm at the left of the figure to remove air from the chamber, as best as possible, in order to minimize any ionization of air molecules by alpha particles. Ionization within the chamber could produce variation in the measurement of positive charge of the alpha particles by the upper collection plate. The source of radium used by Rutherford and Geiger, emits both alpha and beta particles. The magnetic field would deflect all beta particles away to one side of the glass tube, as illustrated in Fig. I.8, so that beta particles do not deposit any charge on the collecting plate AC and interfere with the charge collected from alpha particles.

With the apparatus under a strong magnetic field, the upper plate AC receives a positive charge. The positive charge received by the upper plate was measured under two conditions, namely with the lower plate B connected to a positive potential (+V) or negative potential (−V). Rutherford and Geiger (1908a) made calculations based on the basis of current collected i_1, when plate B was connected to a positive potential, and i_2, the current collected when plate B was connected to a negative potential. The magnitude of i_2 was always smaller than i_1; and their magnitudes depended on the level of vacuum inside the vessel. The chamber was not under a perfect vacuum; and Rutherford and Geiger (1908a) thus named

the current collected when the alpha particle traveled through the gas of the chamber as i_0. Thus, they defined the current observed when the voltages on plate B were positive as:

$$i_1 = i_0 + nE \quad [I.1]$$

where n is the number of alpha particles passing into the upper plate AC per second and E is the charge on each alpha particle; and when the voltage on plate B is reversed, the ionization current caused by the alpha particles was reversed, although equal in magnitude, and:

$$i_2 = nE - i_0 \quad [I.2]$$

Adding Eqs. [I.1] and [I.2] gives:

$$i_1 + i_2 = 2nE \quad [I.3]$$

or:

$$nE = 1/2(i_1 + i_2) \quad [I.4]$$

The number n of α-particles reaching the upper collection plate AC of Fig. I.8 was defined as:

$$n = KQN \quad [I.5]$$

where K is the fraction of the total number of α-particles emitted by the radioactive source reaching the upper collection plate AC, Q is the quantity of pure radium in grams, and N is the number of α-particles emitted per second per gram of pure radium. Thus, the number of α-particles emitted per second by the radioactive source in the apparatus is $R = QN$. The values of K and Q are measured, and the value of N is determined from measurements of count rate. The value of K, that is the fraction of α-particles striking the upper plate AC, was calculated easily to be $K = 0.0172$ on the basis of the geometry of the apparatus and under the assumption that all of the α-particles are emitted equally from the source in all directions. The value of N, ie, the number of α-particles emitted per second per gram of radium, was determined to be 3.4×10^{10}. (Rutherford's calculation of Q was amazingly close to the true value, which is known currently to be 3.65×10^{10} α-particles per second per gram of radium.) Thus, Rutherford and Geiger (1908a) measured the charge on each α-particle with the apparatus illustrated in Fig. I.8 using the equation:

$$E = (i_1 + i_2)/2KQN \quad [I.6]$$

Following the collection of numerous values of i_1 and i_2, Rutherford and Geiger calculated a mean value of E for a single α-particle in electrostatic units (e.s.u.) to be $E = 9.4 \times 10^{-10}$ e.s.u., and from additional experiments not described here for brevity they obtained the value of $E = 9.1 \times 10^{-10}$ e.s.u. An average of the two values was taken as the charge on the α-particle, E_α, or:

$$E_\alpha = 9.3 \times 10^{-10} \text{ e.s.u.} \quad [I.7]$$

Rutherford and Geiger noted that the charge on the electron, E_e, from early work of Millikin and Begeman (1908), was:

$$E_e = 4.1 \times 10^{-10} \text{ e.s.u.} \quad [I.8]$$

which is approximately one-half that of the α-particle. Thus, Rutherford and Geiger found the α-particle charge to be twice that of the electron but of opposite sign. On the basis of their calculation of the charge on the α-particle to be $E = 9.4 \times 10^{-10}$ e.s.u., Rutherford reported that the charge on the electron E_e should be one-half of their determined charge on the α-particle or $E_e = 4.65 \times 10^{-10}$ e.s.u., that is:

$$\frac{E_\alpha}{E_e} = \frac{2e}{e} = \frac{9.3 \times 10^{-10} \text{ e.s.u.}}{4.65 \times 10^{-10} \text{ e.s.u.}} \quad [I.9]$$

After determining the charge on the α-particle to be $+2e$, Rutherford and Geiger (1908a) went further to make measurements of the deflection of the α-particle relative to that of the proton in a magnetic field by measurements of the charge/mass or e/m ratio for each particle. They concluded that the α-particle had a mass that was four times that of the proton and equivalent to the mass of the helium nucleus. Also, it was concluded that the loss of an α-particle from an atom would create another different atom with the reduction in mass number of 4. They worded their finding as follows:

*Taking into account probable experimental errors in the estimates of the e/m for the α-particle, we may conclude that an α-particle is a helium atom [*i.e., *helium nucleus], or, to be more precise, the α-particle, after it has lost its positive charge is a*

*helium atom…There is direct evidence in the case of radium that each of the α-ray changes is accompanied by the expulsion of one α-particle from each atom. Consequently, since the atomic weight [*i.e.*, mass number] of radium is 226, the atomic weight of the emanation is 222, and of radium A is 218.*

What Rutherford and Geiger were reporting was eventually reconfirmed by others that radium-226 decays with the successive emission of an α-particle according to the following:

$$^{226}_{88}\text{Ra} \xrightarrow{\alpha} {}^{222}_{86}\text{Rn} \xrightarrow{\alpha} {}^{218}_{84}\text{Po} \ldots \qquad \text{[I.10]}$$

From here on, Rutherford was able to begin to formulate the structure of atoms with a central massive nucleus, the structure that holds today. Rutherford's findings were the initial step that provided the foundation upon which other physicists, including Niels Bohr, Werner Heisenberg, and others, were able to elaborate the structure of the atom as we know it today.

In a letter to the editor of the journal *Nature*, concerning the structure of the atom, published on December 11, 1913, Rutherford postulated correctly the atomic nucleus as the origin of α- and β radiation. In his letter he stated the following:

There appears to me no doubt that the α-particle does arise from the nucleus, and I have thought for some time that the evidence points to the conclusion that the β particle has a similar origin. This point has been discussed in some detail in a recent paper by Bohr (Phil. Mag., September 1913). The strongest evidence in support of this view is, to my mind, (1) that the β ray, like the α ray transformations, are independent of physical and chemical conditions, and (2) that the energy emitted in the form of β and γ rays by the transformation of an atom of radium C is much greater than could be expected to be stored up in the external electronic system.

Rutherford's next great discovery came in 1919, when he reported the first evidence of a manmade nuclear reaction, that is, the splitting of the atom. This he was able to demonstrate when a high-speed alpha particle would strike the nucleus of an atom and rearrange it into two different atoms. Rutherford observed that when alpha particles would strike air, he could detect scintillation on a zinc sulfide screen produced at a distance well beyond the distance of alpha-particle range of travel corresponding to the range of travel of hydrogen atoms (protons). He demonstrated that the production of high-speed hydrogen atoms by collision of alpha particles with air arose from the collision of the alpha particles with nitrogen atoms only, because the effect would not occur with other constituents of air such as oxygen or carbon dioxide. Furthermore, when pure nitrogen was the target, the scintillations produced by the product hydrogen nuclei (protons) were greater then when air was bombarded with alpha particles (air contains only 79% nitrogen). Rutherford was also able to show that the number of swift atoms of oxygen produced by the alpha-particle collisions was about the same as the corresponding number of hydrogen nuclei (protons). This first manmade nuclear reaction is illustrated in the commemorative stamp from New Zealand shown here. The stamp illustrates the historic nuclear reaction where an atom of nitrogen-14, the most common isotope of nitrogen, denoted as $^{14}_{7}\text{N}$, because its nucleus contains seven protons and seven neutrons, interacts with the colliding alpha particle or helium nucleus ($^{4}_{2}\text{He}$). In the collision, a proton ($^{1}_{1}\text{H}$) is ejected and two protons and two neutrons from the alpha particle can coalesce with the remaining nucleons of the original nitrogen to yield a nucleus having eight protons and nine neutrons, namely, the isotope oxygen-17 denoted above as $^{17}_{8}\text{O}$. This was the very first artificial transformation of one element into another, which was the age-old dream of alchemists.

Nobel Laureate Cecil Powell (1903–69) in his autobiography published in 1987, related that he was only 19 years of age when he arrived at the Cavendish Laboratory as a research student to C.T.R. Wilson, and at this time he recalls Rutherford researching alpha-particle induced transmutations. Powell related his following recollections:

> *When I arrived in 1922, Rutherford had already, in 1919, demonstrated the artificial disintegration of the light elements by bombarding them with fast alpha-particles from radioactive sources. We used to see him disappearing from time to time into a partitioned corner in his laboratory, with his assistant [George] Crowe, to count the scintillations which recorded the ejected protons. This involved long periods of darkness viewing a zinc sulfide screen under a low-powered microscope, and they used to emerge after an hour or so, blinking in the sudden light, like miners coming out of the pit.*

As a result of the above manmade nuclear reaction where protons were emitted as a product, Rutherford has been given the honor of discovering the third elementary particle in matter, the proton. To put this discovery in perspective, the first elementary particle to be discovered was the electron from the work of J.J. Thomson in 1897 (see biographical sketch further on in this chapter), and the second elementary particle to be discovered was the photon from the work of Albert Einstein in 1905 (see Radioactivity Hall of Fame, Part III).

Rutherford contributed much more to the study of radioactivity and nuclear physics, including the fact that all radioactive atoms have differing rates of decay, including the concepts of half-life and decay constant that are invariable properties of each radioactive nucleus or radionuclide of given atomic number (proton number) and mass number (number of protons + neutrons in the nucleus (see chapter: Radionuclide Decay, Radioactivity Units, and Radionuclide Mass)).

Another contribution among many others made by Rutherford deserves mention. This is the development, together with Hans Geiger, of the first electronic means of detecting and counting individual alpha-particle emissions from radioactive atoms. (See the next biographical sketch on Johannes "Hans" Geiger for a detailed description of this electronic counter of alpha particles.) The alpha-particle emissions were allowed to travel through a small opening or window into a vessel containing air or other gas exposed to an electric potential. The vessel is referred to today as an ionization chamber. Upon entering the vessel, the alpha particle, which carries a double positive charge, would cause ionization of the gas, and the ions produced by the alpha particle would accelerate toward electrodes of the chamber, thereby magnifying the ionization within the gas. The positive and negative ions produced by the alpha particle would be collected by their opposing electrodes and thereby produce a pulse that would cause a deflection of the electrometer needle. This instrument was the precursor of more modern Geiger counters, but it served its purpose, as Rutherford and Geiger were able to count each alpha-particle emission from a radium sample and calculate its specific activity. In the words of Rutherford in his Nobel lecture:

> *In this way it was shown that 3.4×10^{10} alpha-particles are expelled per second from one gram of radium.*

This was very close to the real value of 3.7×10^{10}, which is the unit used today to define the unit of radioactivity known as the Curie (Ci), where $1\text{Ci} = 3.7 \times 10^{10}$ disintegrations per second (see chapter: Radionuclide Decay, Radioactivity Units, and Radionuclide Mass). For the entire text of Rutherford's Nobel lecture as well as those of other Nobel Laureates in chemistry and physics, the reader may consult the website of the Nobel Foundation (http://nobelprize.org) as well a book edited by Elsevier entitled *Nobel Lectures, 1901–1970*.

At Manchester, many famous nuclear physicists and future Nobel Laureates worked and collaborated with Rutherford including Frederick Soddy, Henry G.J. Moseley, George de Hevesy, and Niels Bohr. At Rutherford's

laboratory in Montreal, Otto Hahn, who later discovered nuclear fission with the collaboration of Fritz Strassmann and Lise Meitner, also worked with Rutherford. At the Cavendish laboratory, other future Nobel Laureates of physics collaborated with Rutherford including James Chadwick, Patrick Blackett, John Cockroft, Ernest Walton, George P. Thomson, Edward V. Appleton, Cecil Powell, and Francis W. Aston, among others. The commemorative stamp from Canada illustrated above celebrated the centennial of Rutherford's birth. The stamp illustrates a reprint of Ray Webber's art work as described by the Canada Post Office as a burst of light symbolizing, "the great energy that the harnessing of the atom has given to us and which, unseen, affects so much of all our lives." It is said that Ernest Rutherford was the greatest experimental physicist of the 20th century, while Albert Einstein was the greatest theoretical physicist of the century.

For further reading on the life and accomplishments of Rutherford, the reader may peruse books by Boltz (1970), Heilbron (2003), and Pasachoff (2005).

JOHANNES "HANS" GEIGER (1882–1945)

Johannes "Hans" Geiger was born Johannes Wilhelm Geiger on September 30, 1882 in Neustadt an der Weinstrasse, which was at the time named Neustadt an der Haardt, Germany. He is best known as Hans Geiger, where Hans is a common short for Johannes. His father was professor of languages at the University of Erlangen. where the young Hans studied mathematics and physics and was awarded the doctorate degree in 1906.

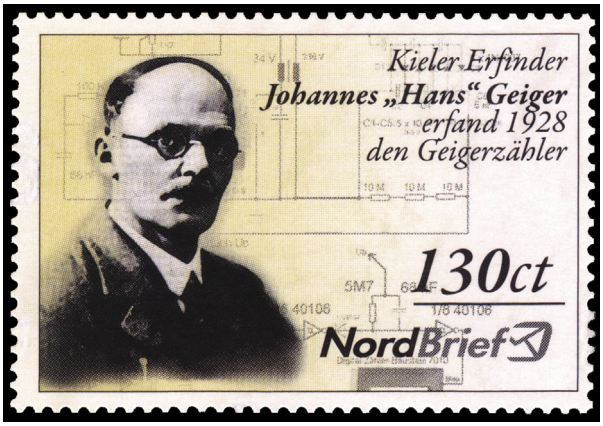

Johannes "Hans" Geiger (1882–1945)

After receiving the doctorate degree, Hans Geiger was appointed to the Physics Institute of the University of Manchester. Shortly thereafter in 1907, Ernest Rutherford, who would become known as the most renowned experimental physicist of the 20th century, became Director of the Physics Institute. Ernest Rutherford recognized Geiger's knowledge and ability in experimental physics and took him under his wing to perform experiments that would greatly improve our knowledge of radioactivity and the structure of the atom.

One of the most significant of Geiger's contributions to physics was made shortly after the arrival of Rutherford as Director of the Institute of Physics. At that time, a student by the name of Ernest Marsden was arriving at the institute, and they needed to give him something to do. Rutherford was interested in knowing what would happen when alpha particles interacted with very thin metal foils (5×10^{-5} cm thick). It was expected that the alpha particles would travel through the foils without much interference; however, it was necessary to know if any alpha particles would be deflected by the foil back toward the direction from which they originated. Thus, Rutherford directed Hans Geiger to investigate this together with Ernest Marsden.

An experimental arrangement used by Geiger and Marsden (1909) to determine if alpha particles would be deflected by thin metal foils is illustrated in Fig. I.9. A source of radium with an activity equivalent to the emission of $\sim 3.4 \times 10^{10}$ alpha particles per second was placed on a planchet A resting on a lead plate P. Many of the alpha particles emitted from the sample on A will strike the metal foil (reflector R) at a 90 degree angle and pass directly through it. A very small number, 1 in 8000 alpha particles, emitted from A would be deflected from the metal foil R back into a scintillation screen S. The scintillation screen was made of zinc sulfide, which would emit a flash of light after absorbing energy from an alpha particle. The light flashes on the screen S could be observed in a dark room with a microscopic lens M and manually

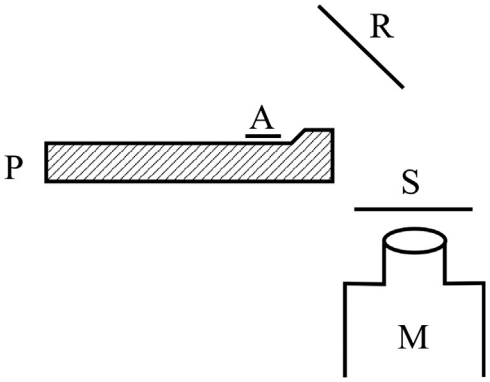

FIGURE I.9 Experimental arrangement reported by Geiger and Marsden to count the number of alpha particles deflected by thin metal foils at large angles back in the direction from which they originated. The components are defined as follows: P is a lead (Pb) barrier supporting the alpha-particle emitting sample A placed on a planchet, R is a metal foil that is bombarded with alpha particles among which 1 in 8000 on average are deflected into a scintillation screen S, from which are counted flashes of light with a microscope lens M in a darkroom. *From Geiger, H., Marsden, E., 1909. On a diffuse reflection of the α-particles. Proc. Royal Soc. A 82, 495–500.*

counted. The observer had to dark-adapt his or her eyes for approximately 30 min prior to counting and limit the counting period to 1 min before rotating with another person to avoid miscounting. Rutherford used the backscattering of alpha particles by thin metal foils to demonstrate that the alpha particles, for the most part, would travel through atoms, which contained mostly empty space; and occasionally an alpha particle (1 in 8000 on average) would collide with a relatively small (on an atomic scale) nucleus of the atom. In their paper, Geiger and Marsden (1909) noted:

> *A small fraction of the α-particles falling upon a metal plate have their directions changed to such an extent that they emerge again at the side of incidence…If the high velocity and mass of the α-particle is taken into account, it seems surprising that some of the α-particles, as the experiment shows, can be turned within a layer of 6×10^{-5} cm of gold through an angle of 90°, and even more…Three different determinations showed that of the incident α-particles about 1 in 8000 was reflected, under the described conditions.*

Geiger and Marsden's experimental setup aided Rutherford in his discovery of the atomic nucleus. With the use of high-energy alpha particles, which would collide with a nucleus at its closest possible approach, Rutherford extended these experiments further to calculate the radius of the nucleus to be $\sim 5 \times 10^{-15}$ m. (See the biographical sketch on Rutherford in this section of the Hall of Fame.)

Counting the flashes of light from alpha-particle interactions with scintillation screen in the dark as described above was prone to error, particularly when counting periods exceeded 1 min. One had to remain focused and the count rates kept low to reduce miscounting. Women, for some reason, were found to be the most efficient in providing the most accurate count rates. At the time, this was the only means of counting emissions from radioactive sources; and the accuracy of this method was unknown, because there was no other method to which the results (ie, count rates obtained) could be compared. As noted by Rutherford and Geiger (1908b):

> *With the aid of a microscope, it is not very difficult to count the number of scintillations appearing per second on a screen of known area [of phosphorescent zinc sulfide] when exposed to a source of α-rays. The doubt, however, at once arises whether every α-particle produced a scintillation,…No confidence can be placed in such a method of counting the total number of α-particles (except as a minimum estimate) until it can be shown that the number so obtained is in agreement with that determined by some other independent method which does not involve such obvious uncertainties.*

To facilitate and improve the accuracy of radiation counting, Rutherford and Geiger (1908b) constructed an electrical means of counting α-particle emissions from radioactive sources. Their approach was to construct a chamber containing a neutral gas with an internal anode wire with the chamber wall acting as the cathode. With a strong electric field across the anode and cathode, alpha particles would produce ions within the gas and thereby produce a voltage pulse to be measured with an electrometer. As reported by Rutherford and Geiger (1908b):

> *We had recourse to a method of automatically magnifying the electrical effect due to a single α-particle. For this purpose we employed the principle of production of fresh ions by collision. In a series of papers Townsend (1901-3a,b) has worked out the conditions under which ions can be produced by collisions with the neutral gas molecules in a strong electric field.*

In the above statement, they refer to the pioneering work of John Sealy Townsend (1868−1957), who discovered the Townsend Discharge, which is a gas ionization mechanism whereby free electrons produced by the ionization of a gas are accelerated by an electric field; and the acceleration of the electrons through ion impact with gas molecules creates a multiplication of electrons referred to as avalanche multiplication, resulting in the conduction of electricity in the gas. When the gas multiplication ceases, the conduction of electricity also ceases.

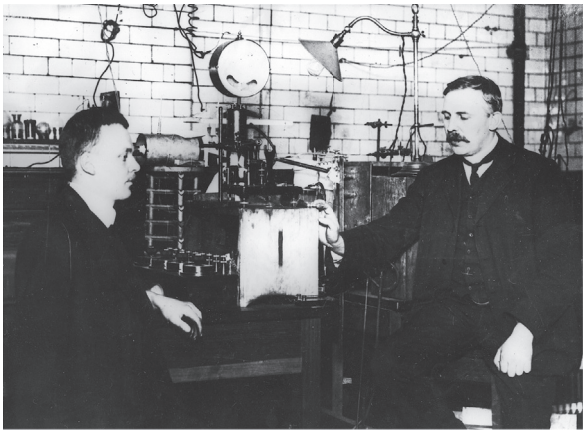

Hans Geiger (profile) left and Ernest Rutherford, right (cerca 1908) in the Schuster Laboratory, University of Manchester. The electronic counter of alpha-particles with its detector vessel and the electrometer needle gauge appear to be situated between Geiger and Rutherford. Courtesy Emilio Segrè Visual Archives, Physics Today Collection.

The very first electronic detector of alpha particles constructed by Rutherford and Geiger (1908) is illustrated in Fig. I.10. A radioactive source emitting alpha particles was adhered to a support plate R, illustrated in Fig. I.10. The detector vessel was filled with an inert gas, such as CO_2. With the stopcock B closed, no alpha particles enter the chamber of the detector vessel D; and when a sufficient potential difference is applied to the central wire, acting as the anode, and detector vessel wall, acting as the cathode, the needle of the electrometer will display a minimal response due to ionization in the chamber from background radiation and electronic noise. Upon the opening of stopcock B, alpha particles from the radioactive source on plate R pass through the stopcock opening and enter the detector vessel. The alpha particles create ionization in the gas, whereby the positively charged gas molecules travel toward the wall of the detector vessel, acting as the cathode; and the electrons ejected from the gas molecules are accelerated toward the central anode wire, producing an ever increasing number of ion pairs. This creates an avalanche of ion pairs, resulting in a corresponding response by the electrometer. The potential difference applied across the anode and cathode of the detector vessel D was sufficient only to produce ionization by alpha particles. This was demonstrated by Rutherford and Geiger by placing a sheet of mica at the

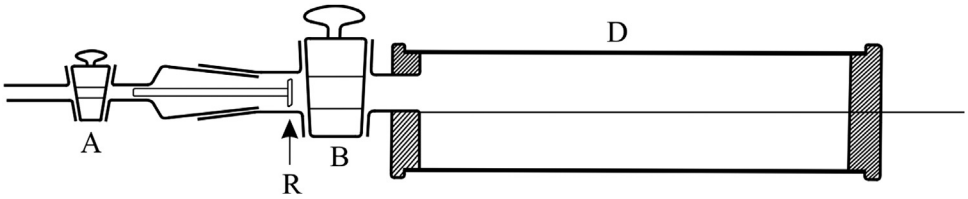

FIGURE I.10 The first electronic apparatus constructed to count alpha-particle emissions from radioactive sources. The stopcock A was used to enable the extraction and addition of counting gas to the detector vessel D, consisting of a brass cylinder 25 cm in length and 1.7 cm in internal diameter. The radioactive sample emitting alpha particles is adhered onto a plate R of 1 cm diameter, which is located about 5 cm from the opening of the detector vessel. The stopcock B permits the closing and opening of the detector vessel to the alpha-particle emissions from plate R. The detector vessel contains a central insulated wire of 0.45 mm diameter, which serves as the anode connected to an electrometer, while the outer wall of the vessel D is connected the negative terminal of a battery, acting as the cathode. The central-wire anode and outer-wall cathode of the detector vessel D are insulated with ebonite corks at either end of the vessel. *From Rutherford, E., Geiger, H., 1908b. An electrical method of counting the number of α-particles from radioactive substances. Proc. Royal Soc. A 81, 141−161.*

opening of the detector vessel. The sheet of mica, which was of a thickness capable of absorbing all alpha particles but not beta particles, would prevent any response from the electrometer, demonstrating that beta particles were undetectable by this instrument. Rutherford and Geiger (1908b) described this as follows:

Under ordinary conditions, the effect due to β-particles is very small compared to that due to an α-particle, and is not detectable.

Hans Geiger discovered years later that the potential difference applied across the electrodes (∼700 V) was very low, preventing the efficient detection of beta particles. In a historical review, Trenn (1986) notes that Rutherford and Geiger had constructed the first proportional counter, because they reported that the magnitude of the output pulse varied with the incident alpha-particle energy.

While at the Physics Institute of the University of Manchester, Hans Geiger collaborated with the British physicist, John Mitchell Nutall, and together they developed a method of measuring the ranges of alpha particles of various energies in air (Geiger and Nuttall, 2011). To measure the ranges of alpha particles in air they constructed an apparatus illustrated in Fig. I.11. It consisted of a glass bulb 7.95 cm in diameter; and the inside wall of the glass bulb was silvered and connected to a 700-V battery. The radioactive source of alpha particles was placed as a thin film in the center of the bulb on a small metal disk B connected to an electrometer by means of a wire H. A brass tube, labeled KK, surrounded the wire H, and it was insulated from the wire with ebonite plugs. The tube KK provided electrostatic protection preventing any electrical leak from the glass bulb to the wire. The apparatus is air-tight via a ground-glass joint E, which is sealed with the

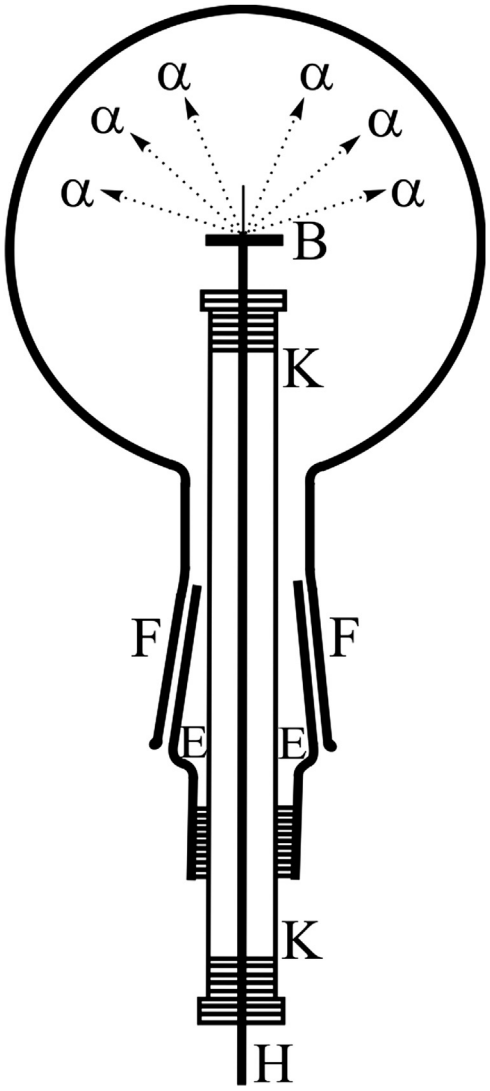

FIGURE I.11 Geiger–Nuttall apparatus for the measurement of the ranges of alpha particles of various energies in air. The *dashed arrows*, which illustrate possible alpha particle trajectories, were inserted by the author. *From Geiger, H., Nuttall, J.M., 1911. LVII. The ranges of the α particles from various radioactive substances and a relation between range and period of transformation. Phil. Mag. Series 6, 22 (130), 613–621.*

corresponding joint F. The length of the wire was carefully adjusted by Geiger and Nuttall so that the radioactive source of alpha particles on plate B was exactly in the center of the bulb. Hans Geiger and John Nuttall plotted linear relationships between ionization (measured with the electrometer) versus air pressure (centimeters of Hg) in the glass bulb. They found that as the air pressure was increased so did the ionization increase linearly; and when the pressure reached a certain magnitude, the ionization caused by the alpha particle no longer increased. The cessation in the increase of ionization was due to the fact that the alpha particle had reached the end of its range and thereby ceased to produce more ion pairs in the air. The air pressure at which the increase in ionization ceased was referred to as the critical pressure. Geiger and Nuttall (1911) explained the process as follows (with the author's comments in brackets):

> *From the critical pressure [the pressure at which ionization no longer increases] and the radius of the bulb [7.95 cm], the range of the α-particles can easily be deduced.*

Measuring the ranges of alpha particles of various energies in centimeters of air emitted by different radioactive sources was only the beginning. Geiger and Nuttall (1911) went further by finding a relationship between alpha-particle energy and half-life decay of radionuclides. By correlating half-life measurements with the range of alpha particles emitted by several radionuclides, Geiger and Nuttall (1911) determined the best-fit linear relationship between the two variables and reported the following equation, which is known as the Geiger–Nuttall Law:

$$\log\lambda = a \log R + b \qquad \text{[I.11]}$$

where λ is the radionuclide decay constant, R is the alpha-particle range (cm), and a and b are constants that provided the best fit to the experimental data. Since $\lambda = 0.693/t_{1/2}$, where $t_{1/2}$ is the half-life (see Eq. [18.11] in the chapter entitled "Radionuclide Decay, Radioactivity Units, and Radionuclide Mass"), it is clear from Eq. (I.11) that for smaller values of $t_{1/2}$ (ie, shorter half-lives) there are correspondingly increasing magnitudes of the alpha-particle range (R). The range of travel of the alpha particle is proportional to its energy. Thus, the shorter the half-life of the radionuclide, the greater will be its decay energy, that is, the greater will be the energy of the alpha-particle. A detailed treatment of the Geiger–Nuttall Law and how this law is used to interpret nuclear stability is provided in the chapter entitled "Alpha Radiation."

As a leading authority on radioactivity and its measurement, Hans Geiger left England in 1912 to take up a position with the Physikalisch Technische Reichsanstalt in Berlin, which is the national metrology institute. The institute is now the Physikalisch Technische Bundesanstalt (PTB) with headquarters in Braunschweig, Germany. At the institute in Berlin, Geiger set up a radioactivity metrology laboratory and obtained his *Habilitation*. The Habilitation is the highest academic degree that one can achieve in many countries of Europe, and it is a requisite for any teaching position at the university level.

While at the PTB in Braunschweig, Geiger wanted to develop an electronic counter capable of detecting and counting all types of ionizing radiation including alpha, beta, and gamma radiation. As discussed earlier, Geiger had collaborated years previously with Rutherford; and they reported in 1908 that their electronic instrument could detect only alpha particles for the most part. The low voltage potential applied across the electrodes of their ionization detector was sufficient mostly for the collection of pulse events due to ion pairs produced by alpha particles. At the PTB in Berlin, Geiger continued his research into the electronic ionization counter. He discovered (Geiger, 1913) that a central wire in the shape of a needle improved the sensitivity of the ionization detector for alpha, beta, and gamma radiation, which was called the point counter or *Spitzenzähler* (Trenn, 1986). A simple diagram of the point counter developed by Hans Geiger in 1913 is illustrated in Fig. I.12. On the left of the detector is illustrated an opening or window, which could be sealed with very thin mica possessing only a minimal stopping power for alpha particles equivalent to 5 mm of air. This window permits the entrance of alpha particles into the detector chamber. This instrument was an improvement over that of the earlier detector,

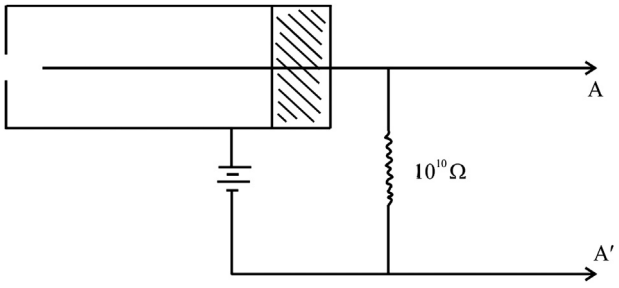

FIGURE I.12 The point counter or *Spitzenzähler* developed by Hans Geiger in 1913 for the detection of alpha, beta, and gamma radiation. A and A′ lead to an amplifier and register of output pulses. *From Trenn, T.J., 1986. The Geiger-Müller counter of 1928. Ann. Sci. 43 (2), 111–135. Reprinted by permission of the publisher, Taylor & Francis, Ltd., http://www.tandf.co.uk/journals.*

which he developed in 1908, illustrated earlier in Fig. I.10; however, the development of the electronic counter as a very sensitive and reliable instrument for the measurement of ionizing radiation still required more research. The central needle of the detector is illustrated as the cathode and outer wall as anode at a low potential (~1200 V); however, future development of the counter by Geiger would result in a reversing of the polarity with the central wire needle as the anode and the application of a higher potential across the electrodes.

When World War I broke out in 1914, Hans Geiger had to take a respite from science, and he served as an artillery officer for the German army. The American Physical Society (2012) reports that the war took a toll on Geiger, as he developed severe painful rheumatism due to the harsh conditions in the trenches of that war, which plagued him for the rest of his life.

In 1925, Geiger moved to Kiel, Germany with an appointment to the Chair in Experimental Physics at the University of Kiel (Korff, 2013). At the University of Kiel, Hans Geiger continued research on the measurement of radioactivity; and it is here where he would develop the Geiger–Müller counter with the collaboration of Walter Müller (1905–79), who was a young postdoctoral research assistant at the University of Kiel. Trenn (1986) relates in a comprehensive historical review that in 1927 Walter Müller was assigned the task of investigating the workings of the point counter. He tested many properties of the radiation counter, including varying the polarity of the needle point and wall of the detector, internal gas pressure, condition of the needle point, and humidity and voltage applied, among other factors. Müller found improved performance with a pressure of 2.1 mm and a positive voltage of 1200 V on the central wire anode (Trenn, 1986). Geiger and Müller made many tests with external sources of alpha, beta, and gamma emitters from 1927 to 1928 to demonstrate that the detector responded to radioactive sources according to their activities and distance between the detector and source. Lead shielding of the detector was used to demonstrate that radiation counts in the absence of radioactive sources were due to external (eg, cosmic radiation). Trenn (1986) reports the story that Müller measured a radiation-counting plateau of the detector in the range of 1310 and 1340 V of a detector, which was specifically selected to give to Ernest Rutherford for his personal research on the atom and radioactivity. A counting plateau, as determined by Müller in 1928, is to this day very familiar to all researchers who use Geiger–Müller radioactivity counters. Each Geiger–Müller detector will display a region of voltage applied to the anode with relatively little or negligible change in counts. There is thus a flat region or plateau, which is obtained when the counts registered by the detector are plotted against the voltage applied. The optimum operation voltage is selected in the middle of this region or plateau.

Trenn (1986) provides the following excerpt of a letter on the matter, which Geiger sent to Rutherford on August 17, 1928 following their successful research (reprinted by permission of the publisher, Taylor & Francis, Ltd. © 1986, http://www.tandf.co.uk/journals):

> *I am sending you one of the new counting tubes… There is not the slightest difficulty to get it going. The data of the tube are given on the paper annexed. The tube N'22 is rather a small one, but larger tubes need a great amount of lead or iron to protect them against stray radiation. Dr. Müller, who works with me, has got sufficient experience now so that we can send you some more tubes and of any dimensions if they are of use to you.*

Hans Geiger and Walter Müller published their findings (Geiger and Müller, 1928a,b, 1929a,b), and today their detector is of widespread use throughout the world to count alpha, beta, and gamma emission from radioactive sources. When the efficiencies of detection are determined for a particular detector with radioactive standards, the exact disintegration rates of sources of radioactivity can be calculated. Modern Geiger–Müller counters are very similar to the one developed by Hans Geiger and Walter Müller in 1928 and 1929. These Geiger–Müller counters have improved front-end windows on the detector often made of thin synthetic Mylar to permit alpha-particles, weak beta particles, as well as the penetrating gamma radiation to enter the detector chamber; improved noble gas mixtures within the detector; and improved electronics for counting individual radiation particles and background radiation discrimination.

The well-known and popular instrument today is referred to as a Geiger–Müller counter or abbreviated as the GM counter in honor of Hans Geiger and Walter Müller. The postage stamp of Hans Geiger with electronic circuitry in the background, illustrated previously, honors Hans Geiger, who took the lead in this work. A portable version of this instrument is called the Geiger counter, which is often used today as a handheld instrument to survey for radioactivity.

After completing his research on what is now referred to as the Geiger–Müller counter, Hans Geiger took up positions at the University of Tübingen from 1929 to 1936 and finally was appointed to the Physics Chair at the Technische Hochschule in Berlin from 1936 to 1945.

The American Physical Society (APS, 2012) reports that Geiger was a member of the Uranium Club (Uranproject or Uranverein), which was the clandestine German effort to develop and produce a nuclear weapon, which splintered in 1942 after it was decided that nuclear fission would not be instrumental in ending the war. The APS (2012) also notes that Geiger denounced the politicization of the universities when the National Socialist Party came into power and signed a petition with 74 other colleagues urging the new government not to interfere with their work. Geiger lived to see the Nazi regime fall from power; however, he died shortly thereafter in Potsdam on September 25, 1945.

HENDRICK A. LORENTZ (1853–1928)

Hendrik Antoon Lorentz was born on July 18, 1853 at Arnhem, the Netherlands. He shared the Nobel Prize in Physics 1902 with Pieter Zeeman also of The Netherlands "in recognition of the extraordinary service they rendered by their researches into the influence of magnetism upon radiation phenomena."

Lorentz (1853–1928)

Lorentz entered the University of Leyden in 1870, and as a gifted student, obtained his BSc degree in mathematics and physics in only one year. He was awarded a doctorate degree at Leyden in 1875 for his work on the reflection and refraction of light. Three years later, Lorentz was appointed Chair of Theoretical Physics at Leyden. In 1912 he became Director of the Teyler Institute in Haarlem and Secretary of the Dutch Society of Sciences. Nevertheless, remaining faithful to his alma mater, he never relinquished his position as professor at Leyden, where he was well-known for weekly lectures, which he continued from 1912 for the remainder of his life.

For the entire of his scientific career Lorentz did much to develop and extend the theory of James Clerk Maxwell (1831–79), which expounded electric current oscillations would create alternating electric and magnetic fields, and radiated electromagnetic waves would have the same physical properties of light. His early studies on electromagnetic radiation were focused on defining empirical formulas for the varying velocities of light in differing liquid, solid, and gaseous substances, and hence the index of refraction, as a function of the density and chemical composition of the media. This work has relevance to our understanding of the threshold energies for the production of Cherenkov radiation by charged particles in media of differing refractive index (see the chapter: "Cherenkov Radiation").

Lorentz is best known for his later work, which resulted in the derivation of mathematical formulas that defined the phenomena known today as the Lorentz transformations. These calculations were based on his finding that electromagnetic forces between charges are subject to slight alterations due to their motion, resulting in minute contractions in the sizes of the moving bodies. The Lorentz transformations are formulas that relate the space and time coordinates of two inertial observers moving at relative speeds up to but less than the speed of light (2.99×10^8 m/s); and these transformations permit the calculations for the solutions of the resulting changes in size, mass, and time for the moving objects. In his Nobel lecture, Lorentz provided the following explanation for these transformations:

> *Consider for example the case in which water is flowing along a tube and a beam of light is propagated within this water in the direction of flow. If everything that is involved in the light vibrations is subject to the flowing movement, then the propagation of light in the flowing water to the rate of flow of the water will in relation to the latter behave in exactly the same way as in still water. The velocity of propagation relative to the wall of the tube can be found by adding the velocity of propagation in the water to the rate of*

flow of the water, just as, if a ball is rolling along the deck of a ship in the direction in which it is traveling, the ball moves relative to an observer on the shore as the sum of the two speeds − the speed of the ship and the speed at which the ball is rolling.

(Nobel Lectures, Physics, 1901−1921) and from "Hendrik A. Lorentz—Nobel Lecture: The Theory of Electrons and the Propagation of Light." Nobelprize.org. Nobel Media AB 2014. Web: August 26, 2015, http://www.nobelprize.org/nobel_prizes/physics/laureates/1902/lorentz-lecture.html.)

Lorentz's concepts and his mathematical transformations were the precursor to Einstein's theory of relativity. In the biographical sketch of Albert Einstein, provided in Hall of Fame III, a discussion of Einstein's relativity is included together with Einstein's application of the Lorentz transformations in relativistic calculations. A derivation of the Lorentz transformations is found in Appendix C. In Einstein's writings on relativity (Einstein, 1916a,b), he provided examples of how measurements made from one frame of reference on another frame of reference will yield different measurements of time and length dependent on the frame of reference from which the measurements are taken and the velocity v at which an object is traveling relative to an observer.

In the biographical sketch of Hendrik A. Lorentz provided by the Nobel Foundation in a link to the Nobel Prize in Physics awarded to Lorentz, the following is stated:

The so-called Lorentz transformation (Lorentz, 1904) was based on the fact that electromagnetic forces between charges are subject to light alterations due to their motion, resulting in a minute contraction in the size of moving bodies. It … paved the way for Einstein's special theory of relativity.

Hendrik A. Lorentz married Aletta Catharina Kaiser in 1881. She was the daughter of K.W. Kaiser, a professor of the Academy of Fine Arts, director of the world-known Rijksmuseum (National Gallery) of The Netherlands, and designer of the first postage stamps of The Netherlands. Hendrick Lorentz died in Haarlem, The Netherlands, on February 4, 1928.

JAMES CLERK MAXWELL (1831−1879)

James Clerk Maxwell was born on June 13, 1831 in Edinburgh, Scotland. He is considered one of the greatest scientists of all times, who made contributions of significance similar to those of Isaac Newton and Albert Einstein.

James Clerk Maxwell, 1855, at 24 years of age (Trinity College Library, Cambridge University. Courtesy AIP Emilio Segrè Visual Archives.

Maxwell entered The Edinburgh Academy at 10 years of age and presented his first paper in mathematics to the Edinburgh Royal Society at 14 years of age. The work was presented by Prof. James Forbes of Edinburgh University, because Maxwell was considered to be too young of age to be allowed to present the work himself. He continued his higher

education at the University of Edinburgh at the age of 16, and three years later continued studies at Trinity College, University of Cambridge. At 24 years of age, Maxwell was appointed professor of physics at Marischal College, University of Aberdeen. Three years later, he was appointed professor at Kings College, London.

At Marischal College, Maxwell was at least 15 years younger than any of the faculty. It is here where Maxwell focused his efforts on the composition of Saturn's rings, because it was a problem selected by St. John's College at the University of Cambridge. The person presenting the best explanation would be awarded the Adams Prize together with a monetary award. Maxwell mathematically demonstrated (Maxwell, 1859, 1862a) that the rings surrounding the planet could not be either solid or liquid. He explained that they had to be composed of many small pieces of rock that orbited Saturn. It was not until the photos from space exploration with Voyager flybys in 1980 and 1981 that it was confirmed that the rings do indeed consist of relatively small rocks or minerals orbiting the planet.

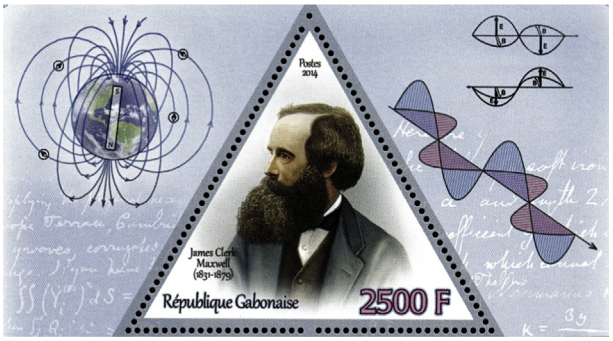

James Clerk Maxwell (1831–1879)

Maxwell's greatest contribution was the unification of electricity and magnetism. His findings in the 19th century had the greatest impact on modern physics of the 20th century. In his treatise "On the Physical Lines of Force," published in four parts (Maxwell, 1861a,b, 1862b,c), Maxwell calculated that electromagnetic radiation travels together at the speed of light; and he clarified the inseparability of electricity and magnetism when he stated in these publications:

> *…we can scarcely avoid the interference that light consists in the transverse undulations of the same medium, which is the cause of electric and magnetic phenomena.*
>
> James Clerk Maxwell Foundation, http://www.clerkmaxwellfoundation.org/.

With the above and subsequent publications, James Clerk Maxwell (1865, 1873) made his major contributions to modern radiation physics by explaining mathematically that light consisted of waves of oscillating electric and magnetic fields. The triangular postage stamp issued in Gabon illustrated here commemorates the findings of Maxwell. On the left of the stamp's attached sheet is illustrated magnetic fields of the earth created by the motion of molten iron alloys in the earth's core as the earth rotates about its axis, creating a magnetic dipole. On the right is illustrated a photon traveling in the direction of the arrow with perpendicular oscillating electric and magnetic fields.

Even heat, which can manifest itself in the form of visible light, is an electromagnetic phenomenon as explained by Maxwell (1865) in his "Dynamical Theory of the Electromagnetic Field" (with author's words in brackets) as follows:

> *This velocity [of electromagnetic disturbance] is so nearly that of light, that it seems we have a strong reason to conclude that light itself (including radiant heat and other radiations, if any) is an electromagnetic disturbance in the form of waves propagated through the electromagnetic field…*

In his words noted above, Maxwell includes "other radiations, if any," as radio waves, ultra violet radiation, X-rays, and gamma radiation had not yet been discovered. However, Maxwell includes all radiations into the category of electromagnetic phenomena.

Radiation, as described by Maxwell, can be depicted as illustrated in Fig. I.13, with transverse undulations of electric and magnetic fields. As the electromagnetic radiation (ie, photon) propagates in the direction y as illustrated in Fig. I.13, the electric and magnetic fields oscillate in opposite directions. For example, as the photon propagates starting at the origin O, the electric fields (blue) and magnetic fields (red) coincide perpendicular to each other and flip in opposite directions. In the completion of one wavelength of travel (λ), the fields will simultaneously return to their original direction. The simultaneous oscillation of electric and magnetic fields continues as the photon travels on. The number of wavelengths or oscillations that occur in 1 s is the radiation frequency known as the Hertz (Hz) and it has units of inverse seconds (s^{-1}).

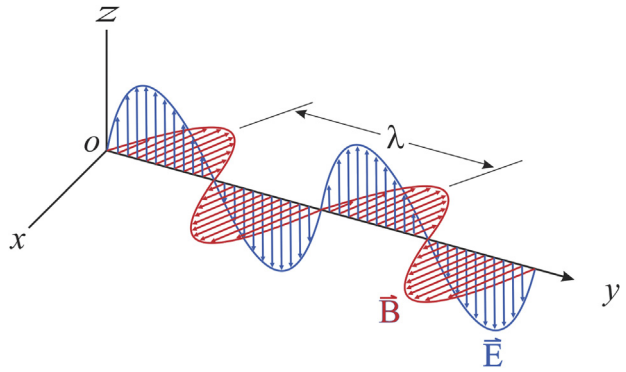

FIGURE I.13 An electromagnetic radiation wave, which is also a photon particle or packet of energy, is illustrated traveling in the direction of the y axis. It consists of oscillating electric $(\vec{E})$ and magnetic fields $(\vec{B})$ perpendicular to each other.

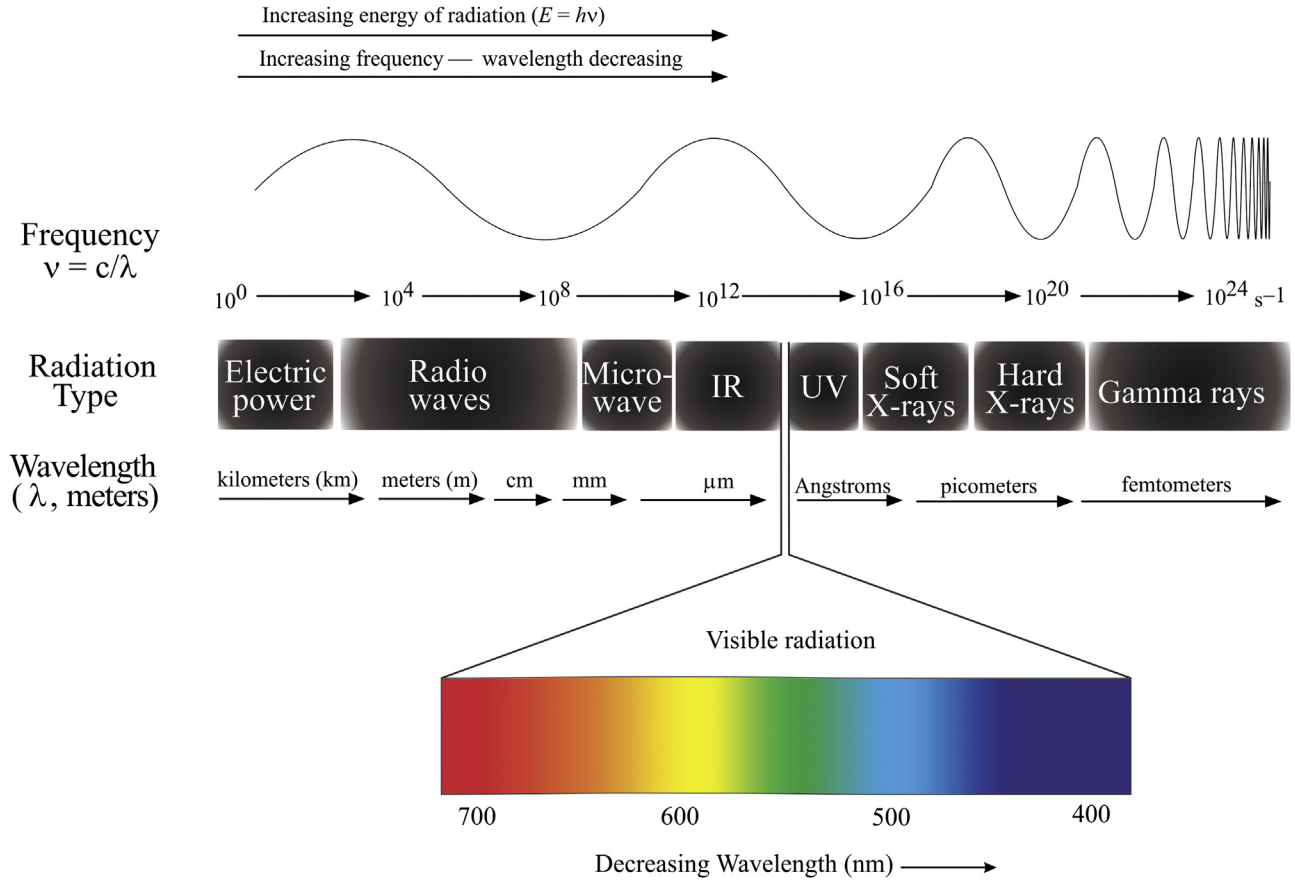

FIGURE I.14 The electromagnetic radiation spectrum is illustrated above by classifying the types of radiation as a function (from left to right) of decreasing wavelength (λ) and increasing frequency (ν). As the wavelength of the radiation decreases, its frequency (ν) and its energy ($E = h\nu$) increase, where h is Planck's constant ($h = 6.626 \times 10^{-34}$ J s). There are no sharp lines of demarcation between the radiation types, as their wavelengths and frequencies can overlap between neighboring radiation types. Thus, the wavelengths and frequencies given above are only approximate. The uppermost wave in the figure is provided as an abstract illustration of how radiation frequency increases with decreasing wavelength. Radiation, visible to the human eye, is found in a very narrow region between the infrared (IR) and ultra violet radiation (UV) bands with wavelengths in the region of 380–740 nanometers (nm) yielding the colors of violet, blue, green, yellow, orange, and red.

Radio waves, X-rays, and gamma rays had not been discovered during the lifetime of Maxwell. In 1888, Heinrich Hertz discovered radio waves. Heinrich Hertz (1857–94) was a German physicist, who demonstrated Maxwell's electromagnetic wave theory with the discovery of radio waves when he was professor at the University of Karlsruhe (Hertz, 1887a,b, 1888a,b). Electromagnetic radiation of shorter wavelength including X-rays and gamma rays would come a decade later after the discoveries of Wilhelm Röntgen in 1895, Henri Becquerel in 1896, and Paul Villard in the year 1900. Thus a wide spectrum of radiation—from the long-wavelength radio waves to increasingly shorter wavelengths including the microwave, infra-red, visible light, ultra-violet, X-rays, and gamma rays—constitutes electromagnetic radiation. The radiation spectrum, as illustrated in Fig. I.14, reads from left to right with decreasing wavelength, increasing frequency, and increasing energy.

Maxwell's theory of electromagnetic radiation is considered to be his greatest contribution to modern physics. Nevertheless, he made many contributions including (1) defining white light as a mixture of red, yellow, green, and blue; and (2) the production of the first color photograph using filters and superimposing projections of photos through filters. In the photo of Maxwell provided in the preceding pages, he is holding a color wheel, which he used to demonstrate the constitution of white light.

PIETER ZEEMAN (1865–1943)

Pieter Zeeman was born on May 25, 1865 at Zonnemaire a village on the Isle of Schouwen, the Netherlands. He shared the Nobel Prize in Physics 1902 with Hendrick Lorentz "in recognition of the extraordinary service they rendered by their researches into the influence of magnetism upon radiation phenomena."

Zeeman (1865–1943)

Zeeman studied at Leyden University from 1885 to 1893, the year he was awarded the doctoral degree. At Leyden he was a pupil of two Nobel Laureates, Heike Kamerlingh Onnes (Physics 1913) and Hendrick Lorentz, with whom he shared the Nobel Prize in 1902. In 1896, Pieter Zeeman discovered that a magnetic field would alter the frequency of light emitted by a glowing gas, called the Zeeman effect. The magnetic field would alter the spectral line corresponding to the frequency of the light into a triplet or even a more complex multiplet of lines. This discovery was significant, because it was the very first to link the properties of light with electricity and magnetism. Zeeman explained the origin of the light and how the magnetic field would have an effect on its line of emission based on the theory of Lorentz. In his Nobel lecture he stated: "This theory assumes that all bodies contain small electrically charged mass particles, 'electrons,' and that all electrical and optical processes are based on the position and motion of the 'electrons'…as soon as the electron is exposed to the effect of a magnetic field, its motion changes." Zeeman reported his work in the *Proceedings of the Physical Society of Berlin* in 1896, and this was published in the English language in the journal *Nature* on February 11, 1897. At the time of Zeeman's discovery, not much was known of electrons or of their position in atoms, before it could be explained fully that light emissions originated from electron orbital transitions in atoms, and that electrons had an intrinsic spin and their own magnetic field the alignment of which could be controlled by external magnetic fields. It was only the year after Zeeman's discovery that J.J. Thomson published his paper in 1897, where he reported the unequivocal discovery of the electron, the first atomic particle to be discovered, and reported its properties including charge and mass.

JEAN B. PERRIN (1870–1942)

Jean Baptiste Perrin was born in Lille, France on September 30, 1970. He was awarded the Nobel Prize in Physics 1926. In the words of Prof. C.W. Orseen, member of the Nobel Committee for Physics of the Royal Swedish Academy of Sciences, at the Nobel Prize award ceremony on December 10, 1926 "The object of the researches of professor Jean Perrin, which have gained for him the Nobel Prize in Physics for 1926, was to put a definite end to the long struggle regarding the existence of molecules." Prof. Jean Perrin demonstrated experimentally what Albert Einstein had theorized concerning Brownian movement, namely, that the constant displacement of microscopic particles in a liquid observed under the lens of a microscope are the result of collisions or shocks due to the constant movement of molecules in the liquid.

Jean B. Perrin (1870–1942)

Jean Perrin was educated at the École Normal Supérieure in France where he became an assistant in physics from 1894 to 1897. This is the time that Jean Perrin undertook research on cathode rays, which would set the stage for J.J. Thomson's discovery of the electron in 1897. Jean Perrin received the doctor of science degree in 1897 at the Sorbonne, University of Paris with his doctoral dissertation on cathode and Röntgen rays. He remained professor at the Sorbonne until 1940, when the Germans invaded France.

Perrin's early work on cathode rays, presented to the Paris Academy of Sciences on December 30, 1895 (Perrin, 1895) with a translation in English appearing in the journal *Nature* in 1896 (Perrin, 1896), proved to be an important contribution that set the stage for J.J. Thomson's discovery of the electron (see the biographical sketch on J.J. Thomson in this section). In the late 19th century, cathode rays were mysterious rays produced in partially evacuated glass tubes with positive and negative electrodes embedded on opposite ends to which a high voltage was applied across the electrodes. These glass tubes were commonly referred to as Crookes tubes, which were named after the English physicist William Crookes (1832–1919), a pioneer of vacuum tubes (Crookes, 1878). The tubes were observed to emit a mysterious glow or light originating from the cathode on to the opposite end of the tube of which the origin was uncertain. In his presentation to the Paris Academy of Sciences on December 30, 1895, Perrin noted that there were two schools of thought over the origin of the cathode rays. Some physicists, including G. Hertz and P. Lenard, thought that the production of cathode rays was a phenomenon similar to light due to vibrations in the "ether." (At that time, it was believed that absolute space required a medium to propagate; and this medium was referred to as the "ether." It is now known that there is no "ether" of this type, and that light will propagate in a vacuum.) The second school of thought, held by physicists including J. Puluj, W. Crookes, and J.J. Thomson, considered the cathode rays were formed by negatively charged matter traveling at high velocity. Jean Perrin (1895) demonstrated that the cathode rays are indeed negatively charged matter, which traveled with high velocity across the tube.

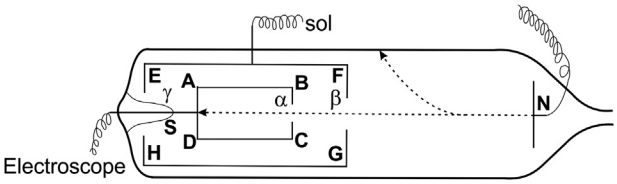

FIGURE I.15 Glass tube utilized by Jean Perrin to characterize cathode rays. The *dashed lines with arrows* are not in the original paper of Perrin. These were inserted by the writer. *From Perrin, J., December 30, 1895. New Experiments on the Kathode Rays. Paris Academy of Sciences.*

An experimentally modified Crookes tube, utilized by Perrin, is illustrated in Fig. I.15. A metal cylinder, referred to as a Faraday cylinder and labeled A, B, C, and D, within an evacuated glass tube served as an electrode connected by wire at S to an electroscope, which would measure the magnitude of electric charge collected. The Faraday tube had an opening at α; and this tube was surrounded by an outer cylinder labeled E, F, G, and H with openings at β and γ. This outer cylinder was permanently connected to the earth (sol) to protect the Faraday cylinder from external electrical influence. The cathode or negative electrode was a metal plate located at the opposite end of the tube at N and fixed at a distance of 10 cm from an outer cylinder E, F, G, and H. The anode or positive electrode as noted by Perrin (1895, 1896) was formed by the protecting cylinder E, F, G, and H through which "a pencil of cathode rays could pass into the Faraday cylinder." In the absence of an external magnetic field, the cathode rays would travel from electrode N through the opening of cylinder E, F, G, and H at β and into the Faraday cylinder at α, which is illustrated by the straight dashed lined with arrow.

Perrin (1895, 1896) reported that the Faraday cylinder would become charged with negative electricity when the cathode rays entered through the opening at α (*straight dashed line with arrow*). However, when the entire vacuum tube was placed between the poles of an electromagnet, the Faraday cylinder would not become charged. This was due to the magnetic field deflecting the cathode rays away from the Faraday cylinder, illustrated by the curved dashed line with arrow directed toward the glass wall of the vacuum tube. Perrin concluded that the cathode rays consisted of negative electricity, because the Faraday cylinder would become negatively charged only when the cathode rays entered the cylinder. The deflection of the cathode rays with the magnetic field offered evidence that the cathode rays consisted of charged matter rather than light phenomenon. He noted the following:

> *By means of a magnet this action [collection of negative charge by the Faraday cylinder] could be entirely suppressed. These results as a whole do not appear capable of being easily reconciled with the theory which regards the kathode rays as an ultra-violet light. On the other hand, they agree well with the theory which regards them as a material radiation, and which, as it appears to me, might be thus enunciated. (At the time, cathode was spelt 'kathode'.)*

This work of Jean Perrin set the stage for Nobel Laureate J.J. Thomson's work reported in 1898 that the cathode rays consisted of particles of negative charge, namely electrons, possessing a specific charge-to-mass (*e*/*m*) ratio. (See the biographical sketch of J.J. Thomson in this section.)

The work for which Jean Perrin is most remembered is his work with aqueous emulsions of gamboge particles, which are emulsions of particles isolated from vegetable sap. Perrin was able to isolate microscopic gamboge particles of uniform size in aqueous solutions; and with these, take measurements of the Brownian movements of these particles through the microscope lens. Brownian movement, which is the continuous tortuous paths and movements taken by microscopic particles suspended in liquids, was interpreted theoretically and mathematically by Einstein in 1905 as the result of the effects of atoms and molecules of the solvent, which are in constant movement or agitation. By preparing spherical emulsions of constant and measureable radius, Perrin was able to confirm Einstein's formulas for particle displacement (translational movement) and rotation, as the particle in the emulsion will rotate about its axis when it is displaced in the solution by collision with a molecule or atom of the solvent. In his Nobel lecture, Perrin explained:

> *In several series of measurements I varied, with the aid of several collaborators, the size of the grains [grains of emulsion] in the ratio of 1 to 70,000) as well as the nature of the liquid (water, solutions of sugar or urea, glycerol) and its viscosity (in the ratio of 1 to 125). They gave values between 55×10^{22} and 72×10^{22}, with differences which could be explained by experimental errors. This agreement is such that it is impossible to doubt the correctness of the kinetic theory of the translational Brownian movement…Einstein's theory does not introduce simplifying approximations and, like the measurement of height distribution, lends itself to a precise determination of Avogadro's number.*

The methodology behind Perrin's calculation of Avogadro's number from measurements of the displacement of microscopic particles as a result of Brownian motion can be obtained from his original and very extensive paper (Perrin, 1909); books, which are multiple publications of a translation by Frederick Soddy of Perrin's original papers (Perrin, 1910, 2010, 2014); and a repeat of Perrin's measurements using modern instrumentation (Newburgh et al., 2006). Avogadro's number is known today to be a constant having the value of 6.022×10^{23} atoms or molecules per mole of substance. A mole of substance is the weight of that substance in grams equivalent to its atomic or molecular weight. For example, a mole of pure hydrogen atoms weighs 1.0 g, and a mole of hydrogen molecules (H_2) weighs 2.0 g. The constant number of 6.022×10^{23} atoms or molecules per mole of substance is called Avogadro's number in honor of the Italian physicist Amadeo Avogadro (1776–1856), who made significant contributions to molecular theory including the relationship of the mass of a given volume of gas and its molecular weight.

Jean Perrin was the creator of the renowned Center Nacional de la Recherche Scientifique (CNRS) with headquarters in Paris. This institute was founded to provide careers in scientific research outside of the universities. This national research center now encompasses several research institutes in the fields of physics, chemistry, biological science, engineering, ecology, and environmental science; the humanities and social sciences; and the information and technological sciences. Jean Perrin fled to the United States in 1940 when France was occupied by the German army. He died in the United States on April 17, 1942. After the war, his remains were returned to France in 1948 on the French battleship Jeanne d'Arc. His remains were buried together with the remains of many distinguished French citizens and national heroes in the Panthéon in Paris.

JOSEPH JOHN THOMSON (1856–1940)

J.J. Thomson was born on December 18, 1856 in Cheetham Hill, a suburb of Manchester, England. He was awarded the Nobel Prize in Physics 1906, as stated by the Nobel Committee "in recognition of the great merits of his theoretical investigations on the conductivity of electricity by gases."

J.J. Thomson (1856–1940)

Thomson became a Fellow of Trinity College, Cambridge in 1880 and remained a member of the college for the remainder of his life. He was Cavendish Professor of Experimental Physics at Cambridge from 1884 to 1918. During Thomson's tenure at the Cavendish Laboratory at Trinity College, Rutherford received a scholarship in 1894 as a research student at the Cavendish Laboratory. Rutherford was only 23 years of age then, and Thomson recognized Rutherford as a budding scientist. Rutherford worked with Thomson for a few years up to about 1897 on the behavior of ions in gases produced by X-rays, on the mobility of ions in electric fields, and on the production of ions from metals exposed to light (photoelectric effect).

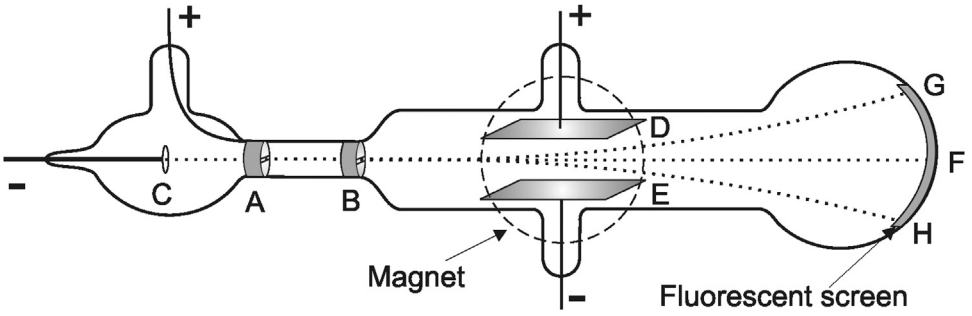

FIGURE I.16 Thompson's cathode-ray tube. The cathode rays are emitted from the negatively charged plate C, accelerated and collimated by positively charged anodes A and B. An electric field potential is applied to the cathode rays by plates D and E and the magnetic field is applied by an external magnet illustrated by the circle.

Thomson's greatest contribution to physics was the discovery of the electron and its properties, the first atomic particle to be discovered. To identify and study the electron, Thomson used a cathode-ray tube illustrated in Fig. I.16, which is drawn as it appeared in Thomson's original paper (Thomson, 1897), with the exception that the lines illustrating possible paths of travel of the electrons were added by the writer to the original sketch. The apparatus was used to study the cathode rays, which were then only unknown rays emitted from the cathode C. The rays were accelerated by positively charged anodes A and B with slits to collimate the beam. The beam of rays would travel across the length of the tube to the far right, which was coated with a fluorescent screen. The fluorescent screen would allow a visual measurement of the location of the beam that hit the glass wall at the far-right hand of the tube. Upon striking the fluorescent screen, the beam would produce a pinpoint green-colored phosphorescence similar to the phosphorescence we would see on old computer screens. At the time of Thomson's work there was controversy as to the nature of these rays. As explained by Thomson in his Nobel lecture, "some thought the rays were negatively-charged electrified bodies shot off from the cathode with high velocity; the other view was that the rays were some kind of ethereal vibration or waves." Thomson demonstrated that the rays consisted of negatively charged particles by using both electric and magnetic fields to deflect the cathode rays. When a positive potential was applied to electrode D with respect to electrode E, the cathode ray would deflect upwards as illustrated and travel onwards to a position G, with the degree of deflection depending on the potential applied to the electrode D. Likewise, when the electric field applied to D and E was shut off, and a magnetic field applied perpendicular to the rays, the rays could be seen to be deflected in the opposite direction to a position H on the phosphorescent screen, the degree of deflection again dependent on the strength of the magnetic field. Earlier experimenters could not observe the cathode-ray deflections due to electrical or magnetic fields, because the experiments were carried out with a gas present inside the tube; and as noted by Thomson "the gas will become a conductor of electricity and the rays will be surrounded by a conductor, which will screen them (the electrons) from the effect of electric force."

Thomson applied both the electric and magnetic fields simultaneously to determine the velocity of the particles, which he called "negative corpuscles." Firstly, when the magnetic field was applied, he defined the force acting upon the particles traveling perpendicular to the lines of magnetic force as Hev, where H is the magnetic force, e is the charge on the particle, and v is its velocity. Likewise, he defined the electric force acting upon the particle as Xe, where X was the electric force. Thomson would then adjust the magnetic field to exactly balance the force due to the electric field so that the beam would not undergo any deflection and travel straight onto point F in Fig. I.16. In such as case:

$$Hev = Xe \tag{I.12}$$

and:

$$v = \frac{X}{H} \tag{I.13}$$

Since the electric and magnetic fields of force, X and H respectively, were applied, these could be easily measured. Thomson, thereby calculated the velocity of the particles at 9.7×10^7 m per second or one-third the speed of light. In Thomson's words:

their velocity is much greater than the velocity of any other moving body with which we are acquainted.

Thomson went further now to determine the charge-to-mass ratio (e/m) of this new negative particle. The degree (angle) of deflection of the beam, due to either electric or magnetic force fields, is a function of the charge, mass, and velocity of

the particle. From the angle of deflection, Thomson calculated the ratio *e/m* to be 1.7×10^{11} C/kg. This was very close to the currently accepted value of 1.758820×10^{11} C/kg. The new particle was also the smallest particle to be known at that time, as in Thomson's own words:

> *for the corpuscle in the cathode rays the value* e/m *is 1,700 times the value of the corresponding quantity for the charged hydrogen atom.*

Thomson noted that this new negatively charged particle not only occurred in the cathode rays, but it was widely distributed. As Thomson stated (with the writer's comments in brackets):

> *"They are given off by metals when raised to a red heat; indeed any substance when heated gives off corpuscles to some extent." "The corpuscles [electrons] are also given off by alkali metals, when these are exposed to light. [This phenomenon was later on studied by others as the photoelectric effect.]…" "They are being continuously given out in large quantities and with very great velocities by radioactive substances."*

It was not known during Thomson's work; but it was discovered years later, that beta particles from radioactive sources and electrons only differed in their origins. Beta particles originate from the decaying nuclei of unstable or radioactive atoms, and electrons originate from the outer regions or orbitals of atoms.

The term "electron" was coined by George Johnstone Stoney, professor of Queen's College (now University College), Galway, Ireland in a paper in *The Scientific Transactions of the Royal Society*, Dublin in 1891.

HANTARO NAGAOKA (1865–1950)

Hantaro Nagaoka was born in Nagasaki, Japan on August 15, 1865. As noted by Nobel Laureate Hedeki Yukawa (1951), who wrote Nagaoka's obituary in the journal *Nature*, Prof. Hantaro Nagaoka was born in a time of turmoil when Japan was beginning to break its two centuries of isolation from the rest of the world and reopen its trade and diplomatic relations with countries of Europe and North America. He is most famous for his prediction of the atomic nucleus in 1904 with his electron-orbital theory of the atom, which would be the precursor to the atomic model proposed by Ernest Rutherford and Niels Bohr.

Hantaro Nagaoka (1865–1950)

In 1887, Hantaro Nagaoka graduated from Tokyo Imperial University, which is now the University of Tokyo. After receiving his doctorate degree in 1893, Nagaoka traveled to Europe to study at the Universities of Berlin, Munich, and Vienna. He participated in The Inaugural International Congress of Physics in Paris 1900, which was a meeting at which Pierre and Marie Curie presented their work on radioactivity. Radioactivity had been discovered in 1895 by Henri Becquerel in France, only five years prior to this meeting. Certainly Nagaoka's studies in Europe and the surging interest in radioactivity and the atom in Europe sparked his interest in this field of physics.

Around the time of Nagaoka's studies in Europe, J.J. Thomson discovered the electron, which was described previously in this chapter. Later in 1904, after Nagaoka's return to Japan, Thomson (1904) proposed the structure of the atom, which is now called the "plum pudding model" or the "blueberry muffin model." This model for the atom, as Thomson (1904) proposed, would consist of negatively charged electrons, which he named corpuscles, distributed within a sphere of uniform positive charge. As Thomson (1904) noted in his paper on the structure of the atom, "we suppose that the atom consists of a number of corpuscles moving about in a sphere of uniform positive electrification." This sphere of uniform positive charge would be similar to that of a pudding or soup within which the corpuscles (ie, electrons) would move about or be distributed. Some prefer to call this the blueberry muffin model, as the electrons would be distributed like blueberries or raisins about the muffin-like medium of positive charge.

Contrary to Thomson's model of the atom, Hantaro Nagaoka proposed in the journal *Nature* (Nagaoka, 1904a) from the Physics Laboratory of Tokyo University, that the atom would consist of a central positive charge surrounded by negative electrons orbiting about the central positive charge. In the journal *Nature*, Nagaoka (1904a) described the atom as follows:

> *The system consists of a large number of particles of equal mass arranged in a circle of equal angular intervals, and repelling each other with forces inversely proportional to the square of distance between the particles; at the centre of the circle is placed a large particle attracting the other particles forming the ring according to the same law of force…Evidently the system here considered will be approximately realized if we place negative electrons in the ring and a positive charge at the centre.*

Likewise, in the *Philosophical Magazine*, Nagaoka (1904b) proposed the same structure of the atom, which included electrons orbiting a central positive charge, on the basis of experimental findings of the regularity of spectral lines characteristic of atoms. In the *Philosophical Magazine*, Nagaoka (1904b) wrote the following (with the writer's comments in brackets):

> *…to find a system whose modes of vibration are brought into complete harmony with the regularity observed in spectral lines…I propose to discuss a system whose small oscillations accord qualitatively with the regularity observed in the spectra of different elements and by which the influence of the magnetic field on band- and line-spectra is easily applicable…The system, which I am going to discuss consists of a large number of particles [*i.e.*, electrons] arranged in a circle of equal angular intervals and repelling each other with forces inversely proportional to the square of the distance; at the centre of the circle, place a particle of large mass [*i.e.*, nucleus] attracting the other particles to the same law of force.*

Nagaoka did not use the word "nucleus" for his "positive charge at the center" and "particle of large mass" at the center of the atom, because it would not be until seven years later that Rutherford (1911) would discover Nagaoka's positive charge at the center of large mass. In 1911, Rutherford's experiment in α-particle scattering with gold foil would lead to his discovery of the positively charged nucleus of large mass. In his paper on α-particle scattering and the structure of the atom, Rutherford (1911) gives credit to Nagaoka for postulating the central positive nucleus of the atom by the following:

> *It is of interest to note that Nagaoka (1904) has mathematically considered the properties of the Saturnian atom, which he supposed to consist of a central attracting mass surrounded by rings of rotating electrons. He showed that such a system was stable if the attracting force was large. From the point of view considered in his paper, the change of a large deflection [of α-particles] would practically be unaltered…*

The structure of the atom, as proposed by Hantaro Nagaoka, is illustrated in the postage stamp shown in this section commemorating his theory. Nagaoka's atom would serve as the precursor to the atomic models later formulated by Rutherford (1911, 1913) and Bohr (1913, 1921a,b, 1922) and the current models of the atom with a central nucleus.

Together with coworkers at the Institute of Physical and Chemical Research in Tokyo, Nagaoka et al. (1924) reported the spectral lines of isotopes of mercury; and as a consequence, they predicted the possibility of converting mercury into gold in view of the fact that mercury has one additional proton in the nucleus compared to gold, The atomic numbers of mercury and gold are 80 and 79, respectively. Nagaoka et al. (1924) reported the following in the journal *Nature*:

> *It should be pointed out that, if the…assumption as to the mercury nucleus is valid, we can perhaps realize the dream of alchemists, by striking out a H-proton from the nucleus by α-rays, or by some other powerful methods of disruption.*

Reprinted by permission from Macmillan Publishers Ltd. © 1924. http://www.nature.com/nature/index.html.

The transmutation of mercury into microscopic particles of gold was demonstrated shortly thereafter by Nagaoka (1925a,b,c). He and coworkers applied an intense electric field to mercury atoms using a short spark gap with a conduction coil to produce a potential difference of 15×10^4 V/cm maintained for 4 h. The product tested positively for gold with a Purple of Cassius test, which is a chemical test for gold involving the formation of a purple pigment when gold salts react with tin(II) chloride. Gold particles were observed under microscopic examination with 150× magnification.

Miethe (1924) in Germany also reported traces of gold produced with a high potential produced by mercury vapor lamps. Nagaoka (1925a,b) postulated that, in the process, the mercury atom loses a proton to undergo transmutation to an atom of gold. However, Frederick Soddy (1924) and Russell (1925) noted that a transmutation could have taken place by the capture of an electron by a proton in the nucleus. In any case, it was apparent to all that this would not be an economical means of producing gold.

From his research on the transmutation of mercury into gold, Hantaro Nagaoka was a pioneer in demonstrating the potential of transmutation. As described further on in this book Enrico Fermi was awarded the Nobel Prize in 1938 for his demonstrations of the existence of many new radioactive elements produced by neutron capture. Currently Nagaoka's objective of converting mercury to gold can be carried out, although not economically, with a nuclear reactor. Stable atoms of mercury (^{196}Hg), which occur in nature at a 0.15% natural abundance, can be irradiated with slow neutrons from a nuclear reactor to produce an unstable isotope of mercury (^{197}Hg). The atoms of ^{197}Hg decay by electron capture with a 64.1-h half-life to form stable atoms of gold (^{197}Au). The reactions are illustrated as follows:

$$^{196}_{80}\mathrm{Hg} + {}^{1}_{0}\mathrm{n} \xrightarrow{\text{neutron capture}} {}^{197}_{80}\mathrm{Hg} \xrightarrow[t_{1/2} = 64.1\ \mathrm{h}]{\text{E.C.}} {}^{197}_{79}\mathrm{Au} \qquad \text{[I.14]}$$

Hantaro Nagaoka produced many scientific papers including studies related to atomic spectra of the elements and their isotopes (Nagaoka, 1904a,b,c, 1908a, 1924; Nagaoka and Sugiura, 1923a,b, 1924), the kinetic theory of gases (Nagaoka, 1903), the Zeeman effect (Nagaoka, 1908b, 1909, 1910; Nagaoka and Takamine, 1913), and geophysics including the study of earthquakes (Nagaoka, 1907, 1932). He was professor of Tokyo Imperial University from 1896 to 1926. Nagaoka then undertook research at the Institute of Physical and Chemical Research in Tokyo; and he became the first president of Osaka Imperial University in 1931, which is now known as Osaka University. Nagaoka received many honors in Japan and abroad including an honorary doctorate degree from the University of Cambridge in 1925. As noted by Yukawa (1951), Prof. Hantaro Nagaoka had inspired and motivated many young budding scientists in Japan at a time when Japan strove eagerly to catch up with Western science and technology. Hantaro Nagaoga was actively engaged in scientific research right up to the date of his passing on December 10, 1950.

PHILIPP LENARD (1862–1947)

Philipp von Lenard was born on June 7, 1862 in Pozsony, a part of the Austro-Hungarian Empire, which is now Bratislava, Slovakia. He received the Nobel Prize in Physics 1905 "for his work on cathode rays."

Philipp Lenard (1862–1947)

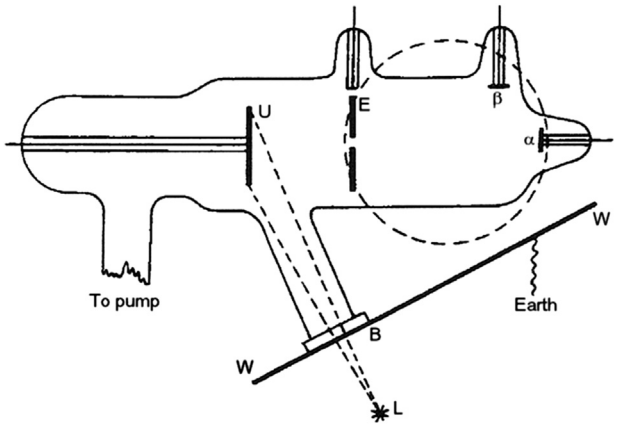

FIGURE I.17 Cathode ray tube used by Philipp Lenard to produce photoelectrons and demonstrate that the photoelectron kinetic energy (velocity) was independent of the light intensity, but dependent only on the wavelength of the light producing the photoelectrons.

Lenard completed his PhD degree in physics in 1886 at the University of Heidelberg. He subsequently worked as a privatdozent and assistant to Heinrich Hertz at the University of Bonn from 1892 to 1894, and after a few short stints as professor in other universities, he was appointed professor ordinarius at the University of Kiel in 1898. In 1892 at Bonn, Hertz had discovered that when aluminum foil was placed in the path of the cathode rays, within the cathode ray tube, the rays would pass through the foil and cause uranium glass to glow (Hertz, 1892). A cathode-ray tube of the type used by Hertz is illustrated in the previous biographical sketch on J.J. Thomson. Lenard took it upon himself to test aluminum foil as a substance that could be used as a possible window through which the cathode rays might be directed out of the tube. After several experiments in 1894, he was successful in finding a proper thickness of aluminum foil that could be used to close an opening in the cathode-ray tube to assure the maintenance of a vacuum inside the tube (the cathode rays, ie, electrons traveled best under maximum vacuum) while permitting the cathode rays to travel through the thin aluminum layer (Lenard, 1894). The aluminum-sealed opening became known as the "Lenard window." The window, for the first time, allowed cathode rays to exit the tube and come out into the "open air," although the rays could not travel very far in air (approx. 8 cm). Previously these rays (ie, electrons) were limited to the confines of the cathode ray tube; the electrons generated were now able to be studied "out in the open."

Lenard extended another finding of Hertz. In 1887, Heinrich Hertz was the first to observe that metal plates would give off negative electricity (electrons) when exposed to ultraviolet light (Hertz, 1887b). This phenomenon is known as the photoelectric effect (see the chapter: "Electromagnetic Radiation: Photons"). To study the photoelectric effect further, Lenard constructed a special cathode-ray tube, illustrated in Fig. I.17. The tube was equipped with a quartz window B through which ultraviolet light could pass. The UV light originating from position L would pass through the quartz window and strike a metal plate U within the evacuated tube. The impact of the UV photons onto the metal would force electrons to be ejected from the metal surface. These electrons, referred to as photoelectrons, would then travel in the tube straight on toward the collector plate labeled α. The path of the photoelectrons could be deflected upwards toward the collector labeled β when the poles of a magnet, depicted by a dashed circle in the diagram, were placed perpendicular to the path of the electrons. The tube and external magnet (not visible) provided evidence that the particles emitted from the metal plate U were indeed electrons from data collected including angle of deflection, particle velocity, and magnetic field strength, from which the charge-to-mass (e/m) ratio could be calculated (see bio-sketch on J.J. Thomson.). The ion collectors α and β were connected to electrometers that would provide data on the photoelectron intensity via the photoelectric current produced at the collectors (Lenard, 1899).

Lenard was able to measure the photoelectron intensity from the photoelectric current, and the speed or kinetic energy of the photoelectrons as a function of the intensity and frequency of the light hitting the metal target (Lenard, 1902). He concluded that the electron velocity (kinetic energy) was independent of the light intensity, but that the velocity would vary only according to the wavelength of the light, and that highest velocities were attained for shorter wavelengths of light. Lenard provided excellent experimental data on the photoelectric effect, but erred in his interpretation of the facts, which is reflected in his misinterpretation stated as follows in his Nobel lecture: "I have found that the velocity [of the electrons] is independent of the ultraviolet light intensity, and thus concluded that the energy of escape [of the electrons from the metal surface] does not come from the light at all…." It was only a few years later in 1905 when Albert Einstein fully explained the photoelectric effect after grasping Max Planck's calculations and showing that light not only traveled as waves but also

as packets of energy or particles, which he named "energy quanta," and that the energy of the photoelectron did indeed come from the light and depended on the energy or wavelength of the photon. Einstein was awarded the Nobel Prize in Physics 1921 for his discovery of the new law of the photoelectric effect. (See Albert Einstein in Radioactivity Hall of Fame, Part III for a more thorough treatment of the photoelectric effect and Einstein's explanation of it.)

The following interpretation of Lenard is provided in *Nobel Lectures, Physics 1901−1921*, Elsevier, Amsterdam (with the writer's comment in brackets):

> *…Lenard never forgave Einstein for discovering and attaching his own name to this law [The law of the photoelectric effect]… Lenard was an experimentalist of genius, but more doubtful as a theorist. Some of his discoveries were great ones and others were very important, but he claimed for them more than their true value. Although he was given many honours…he believed that he was disregarded and this probably explains why he attacked other physicists in many countries. He became a convinced member of Hitler's National Socialist Party and maintained unreserved adherence to it. The party responded by making him the Chief of Aryan or German Physics.*

Philipp von Lenard died on May 20, 1947 in Messelhausen, Germany. For additional information on the life and work of Philipp von Lenard, the reader may peruse a detailed biography provided by the Nobel Foundation (Nobelprize.org. Nobel Media AB 2014. Web: August 26, 2015, http://www.nobelprize.org/nobel_prizes/physics/laureates/1905/lenard-bio.html).

Chapter 4

Alpha Radiation

It was quite the most incredible event that ever happened to me in my life. It was as incredible as if you fired a 15-inch shell at a piece of tissue paper and it came back and hit you.

Earnest Rutherford at a Bakerian Lecture: "Nuclear Constitution of Atoms" (1920), where he described his observation of the back-scattering of alpha particles and his discovery of the atomic nucleus.

4.1 INTRODUCTION

Alpha decay is the nuclear decay process whereby the parent nucleus emits an alpha particle. The alpha particle, structurally equivalent to the nucleus of a helium atom and denoted by the Greek letter α, consists of two protons and two neutrons. Alpha particles are emitted as decay products of many radionuclides that possess a large nucleus, predominantly of atomic number greater than 81. For example, the radionuclide americium-241 decays by alpha-particle emission to yield the daughter nuclide ^{237}Np according to the following equation:

$$^{241}_{95}\mathrm{Am} \rightarrow {}^{237}_{93}\mathrm{Np} + {}^{4}_{2}\mathrm{He} + 5.638\ \mathrm{MeV} \qquad [4.1]$$

The loss of two protons and two neutrons from the americium nucleus results in a mass reduction of four and a charge reduction of two on the nucleus. In nuclear equations such as the preceding one, the subscript denotes the charge on the nucleus (ie, the number of protons or atomic number, also referred to as the Z number) and the superscript denotes the mass number (ie, the number of protons plus neutrons, also referred to as the A number). The 5.638 MeV of Eq. [4.1] is the decay energy, which is described subsequently.

4.2 DECAY ENERGY

The energy liberated during nuclear decay is referred to as decay energy. Many reference books report the precise decay energies of radioisotopes. The energy released in alpha decay will be reviewed in this section and the decay of ^{241}Am will be taken as an example. The value reported by the National Nuclear Data Center of the Brookhaven National Laboratory (http://www.nndc.bnl.gov/qcalc) for the decay energy of ^{241}Am, illustrated in Eq. [4.1], is 5.638 mega-electron volts (MeV).

The alpha decay equation may be described in general terms as follows:

$$^{A}_{Z}P \rightarrow {}^{A-4}_{Z-2}D + {}^{4}_{2}\mathrm{He} + K_T \qquad [4.2]$$

where $^{A}_{Z}P$ is the parent nucleus of atomic number Z and mass number A, $^{A-4}_{Z-2}D$ is the daughter nucleus of atomic number $Z-2$ and mass number $A-4$, $^{4}_{2}$He is the alpha particle equivalent to a helium nucleus, and K_T is the total kinetic energy released in the alpha-decay. The total kinetic energy released, also referred to as the decay energy (Q_α), is shared between the alpha particle, recoil daughter nucleus, and gamma-radiation, or:

$$Q_\alpha = K_T = E_\alpha + E_{\mathrm{recoil}} + E_\gamma \qquad [4.3]$$

where E_α is the kinetic energy of the alpha-particle, E_{recoil} is the kinetic energy of the recoil daughter nucleus, and E_γ is the energy lost as gamma radiation from the daughter nucleus, when the daughter nucleus is left at an excited energy state and decays to its ground state. We will use the symbol E for kinetic energy, rather than K, when referring to the kinetic energy of the radiation and recoil nuclei, as it is the symbol most commonly used, and the kinetic energy is inferred. The decay

Radioactivity: Introduction and History, From the Quantum to Quarks. http://dx.doi.org/10.1016/B978-0-444-63489-4.00004-6
Copyright © 2016 Elsevier B.V. All rights reserved.

energy is represented by Q as the "Q value." The decay energy of 5.638 MeV of Eq. [4.1] above may be written as Q_α for alpha-decay energy, which may be composed of the energies of the alpha particle, recoil daughter nucleus, and gamma radiation described in Eq. [4.3]. Energy and mass are conserved in the decay process; that is, the energy liberated in radioactive decay is equivalent to the loss of mass by the parent radionuclide (eg, ^{241}Am) or, in other words, the difference in masses between the parent radionuclide and the product nuclide and particle.

We can calculate the energy liberated in the decay of ^{241}Am, as well as for any radionuclide decay, by accounting for the mass loss in the decay equation. Using Einstein's equation for equivalence of mass and energy:

$$E = mc^2 \quad [4.4]$$

we can write the general equation for the energy equivalence to mass loss as:

$$Q = (\text{mass of parent nuclide} - \text{mass of decay products})c^2 \quad [4.5]$$

For the decay of ^{241}Am described in Eq. [4.1] above, we can write Eq. [4.5] as:

$$Q_\alpha = \left(M_{241_{\text{Am}}} - M_{237_{\text{Np}}} - M_\alpha\right)c^2 \quad [4.6]$$

where Q_α is the disintegration or alpha decay energy, $M_{241_{\text{Am}}}, M_{237_{\text{Np}}}$ and M_α are the masses of ^{241}Am, ^{237}Np, and the alpha-particle, and c is the speed of light in a vacuum. We may use atomic mass units (u) for the calculation, because the electron masses included with atomic mass units may be ignored. The number of electrons on both sides of the decay Eqs. [4.1] and [4.2] are equal, and we can ignore the negligible differences in the binding energies of the electrons. When the nuclide masses are expressed in the more convenient atomic mass units (u), the energy liberated in decay equations can be calculated in units of megaelectron volts according to the equation:

$$Q_\alpha = \left(M_{241_{\text{Am}}} - M_{237_{\text{Np}}} - M_\alpha\right)(931.494\ \text{MeV/u}) \quad [4.7]$$

The precise atomic mass units obtained from reference tables (Holden, 1997a) can be inserted into Eq. [4.7] to obtain:

$$Q_\alpha = (241.056822\ \text{u} - 237.048166\ \text{u} - 4.00260325\ \text{u})(931.494\ \text{MeV/u}) = (0.00605275\ \text{u})(931.494\ \text{MeV/u})$$
$$= 5.638\ \text{MeV}$$

The energy liberated is shared between the daughter nucleus and the α-particle. If the parent nuclide (eg, ^{241}Am) is at rest when it decays, most of the decay energy will appear as kinetic energy of the liberated less-massive α-particle and only a small fraction of the kinetic energy remaining with the recoiling massive daughter nuclide (eg, ^{237}Np). The kinetic energy of the recoiling daughter nuclide is comparable to that of a recoiling canon after a shell is fired; the shell being analogous to that of the α-particle shooting out of the nucleus, as illustrated in Fig. 4.1.

Fig. 4.2 illustrates the transitions involved in the decay of ^{241}Am. The interpretation of this figure is given in the following paragraph. There are five major α-particle transitions in the decay of ^{241}Am, each involving an α-particle emission at different energies and relative intensities. These are illustrated in Fig. 4.2. The decay energy of 5.638 MeV for ^{241}Am calculated above and reported in the literature is higher than any of the α-particle energies provided in Fig. 4.2. This is because there remains also the recoil energy of the daughter nucleus and any gamma-ray energy that may be emitted by the daughter, when its nucleus remains at an excited state. The emission of gamma radiation often accompanies radionuclide decay processes that occur by alpha-particle emission. Gamma radiation is described in the chapter entitled "Electromagnetic Radiation: Photons." The recoil energy, E_{recoil}, of the daughter nucleus can be calculated by the equation:

$$E_{\text{recoil}} = (M_\alpha / M_{\text{recoil}})E_\alpha, \quad [4.8]$$

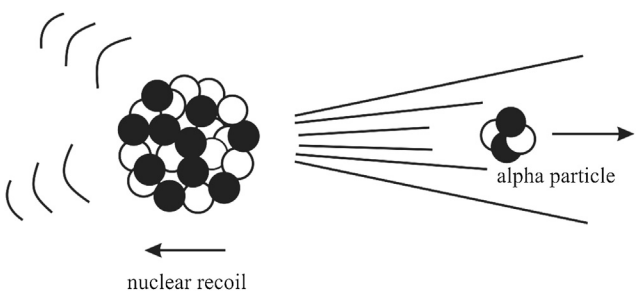

FIGURE 4.1 The alpha particle shoots out of a nucleus. In the decay of nuclides by alpha-particle emission, the alpha particle will shoot out of the nucleus, and the daughter nucleus will recoil similar to that of a canon that recoils upon firing a shell from its barrel.

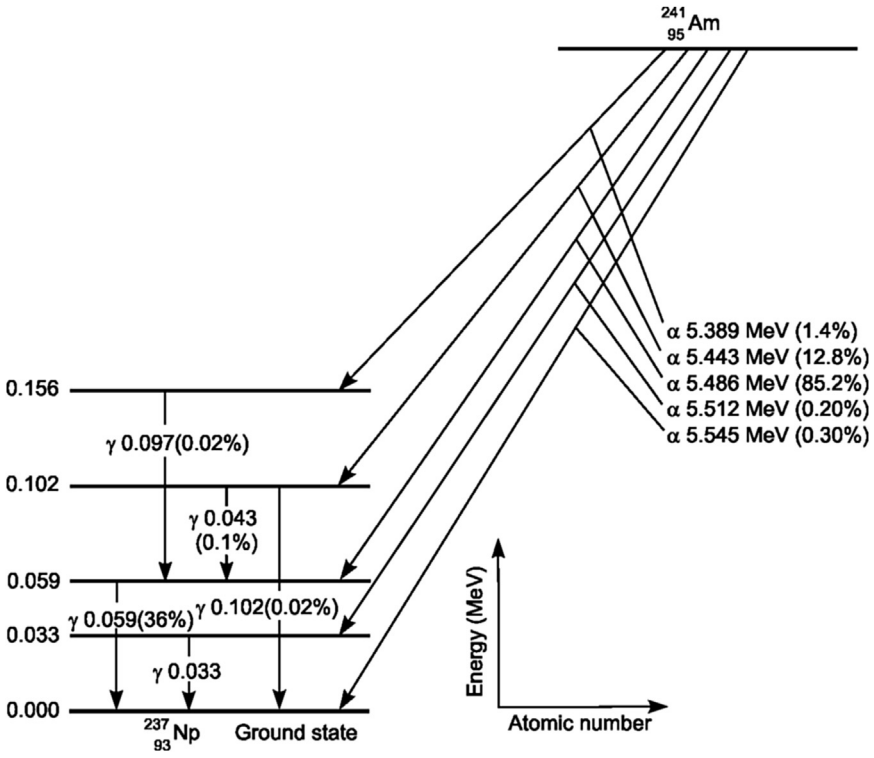

FIGURE 4.2 Decay scheme of ^{241}Am. The relative intensities of alpha-particle and gamma-ray emissions are expressed in percent beside the radiation energy values in MeV.

which is derived in the chapter entitled "The Atomic Nucleus", where M_α is the mass of the alpha particle as defined in Eq. [4.7], M_{recoil} is the mass of the recoil nucleus, and E_α is the α-particle energy. For example, the recoil energy of the ^{237}Np daughter nucleus for the transition of the 5.545-MeV alpha particle (Fig. 4.2) can be calculated according to Eq. [4.8] as:

$$E_{\text{recoil}} = (4.00260325\ \text{u}/237.048166\ \text{u})5.545\ \text{MeV} = (0.0168851897)(5.545\ \text{MeV}) = 0.0936\ \text{MeV}$$

The transition energy, E_{trans}, for the above α-particle emission is the sum of the α-particle and recoil nuclear energies or:

$$E_{\text{trans}} = E_\alpha + E_{\text{recoil}} = 5.545\ \text{MeV} + 0.0936\ \text{MeV} = 5.638\ \text{MeV} \quad [4.9]$$

In the above case, the transition energy turns out to be equal to the reported and calculated decay energy, because as illustrated in Fig. 4.2, the ^{241}Am radionuclides decay directly to the ground state whenever 5.545 MeV α-particles are emitted. This is not the case when α-particles of other energies are emitted from ^{241}Am. If we take, for example, the 5.486 MeV α-particle transition of Fig. 4.2, the decay energy, E_{decay}, would be the sum of the transition energy plus gamma-ray energy, E_γ, emitted from the daughter nucleus, or:

$$\begin{aligned} E_{\text{decay}} &= E_{\text{trans}} + E_\gamma = E_\alpha + E_{\text{recoil}} + E_\gamma = E_\alpha + (M_\alpha/M_{\text{recoil}})E_\alpha + E_\gamma \\ &= 5.486\ \text{MeV} + (4.00260325\ \text{u}/237.048166\ \text{u})(5.486\ \text{MeV}) + 0.059\ \text{MeV} \\ &= 5.486\ \text{MeV} + 0.0926\ \text{MeV} + 0.059\ \text{MeV} = 5.638\ \text{MeV} \end{aligned} \quad [4.10]$$

The gamma-ray energy emitted from the daughter nucleus for the 5.486 MeV α-particle transition in ^{241}Am decay is found in Fig. 4.2. Gamma-ray energy values of other radionuclides are available from reference tables (Browne et al., 1986; Firestone et al., 1996; L'Annunziata, 2012f; Lederer and Shirley, 1978).

As described in the previous paragraphs, alpha particles are emitted with a certain quantum of energy as the parent nuclide decays to a lower energy state. The energy emitted from radionuclides as nuclear radiation can be described by a decay scheme such as that given in Fig. 4.2. Decay schemes are written such that the energy levels of the nuclides are plateaus along the ordinate, and these energy plateaus are distributed along the abscissa according to atomic number. The alpha particles, as the example shows (Fig. 4.2), are emitted with certain magnitudes of kinetic energy, which is most often

expressed in units of kiloelectron volts (keV) or megaelectron volts (MeV). The energies of alpha particles from most nuclear decay reactions fall within the range 4−10.5 MeV.

Alpha particles are emitted from unstable nuclei with discrete quanta of energy, often leaving the daughter nuclide at an excited energy state. In such cases, when the daughter nuclide occurs at an elevated energy state, it may reach the ground state via the emission of energy in the form of electromagnetic gamma radiation, as illustrated in Fig. 4.2.

The nuclei of daughter atoms of alpha particle-emitting nuclides are often unstable themselves and may decay by further alpha- or beta-particle emission. Thus, alpha particle-emitting nuclides may consist of a mixture of radionuclides, all part of a decay chain, as illustrated in Figs. 2.2−2.5 described previously in chapter "Basic Concepts and Definitions" of this book. Additional reading on radionuclide alpha decay is available from Das and Ferbel (1994).

4.3 ALPHA DECAY-ENERGY AND HALF-LIFE RELATIONSHIP

Alpha particles are emitted by radionuclides with distinct energies that range between 4 and 10 MeV; and half-lives of alpha-particle emitting nuclides will vary over a wide range of time from 10^{10} years to microseconds. Radionuclides emitting alpha particles of low energy decay with long half-lives, whereas those emitting alpha particles of high energy have short half-lives.

A relationship between alpha decay energy and the half-life of the nuclide was recognized very early in the history of the study of radionuclide decay. German physicist Hans (Johannes Wilhelm) Geiger, best known for the Geiger-Müller counter, and British physicist John Mitchell Nuttall (Geiger and Nuttall, 1911), were the first to measure a relationship between alpha-particle energy and half-life decay of even-Z even-A radionuclides—that is, radionuclides that had an even number of protons and even mass number. By correlating half-life measurements with the range of alpha particles emitted by several radionuclides, Geiger and Nuttall (1911) determined the best-fit linear relationship between the two variables and reported the following equation, which is known as the Geiger−Nuttall Law:

$$\log\lambda = a \log R + b \qquad [4.11]$$

where λ is the radionuclide decay constant, R is the alpha-particle range (cm), and a and b are constants that provided the best fit to the experimental data. Since $\lambda = 0.693/t_{1/2}$, where $t_{1/2}$ is the half-life (see the chapter entitled: "Radionuclide Decay, Radioactivity Units, and Radionuclide Mass"), it is clear from Eq. [4.11] that for shorter values of half-life ($t_{1/2}$) there are correspondingly increasing magnitudes of the alpha-particle range (R). The range of travel of the alpha particle is proportional to its energy. Consequently, the Geiger−Nuttall Law provided a correlation between radionuclide decay half-life and alpha decay energy. Other variations of the best-fit equation were reported subsequently to the work of Geiger and Nuttall, which provided best-fit empirical equations for specific radionuclide decay series (Beckerly, 1945), but the correlation of half-life decay and decay energy remained the same.

Alpha-decay energy and half-life of heavy elements of even Z even A were studied by Perlman and Ypsilantis (1950a,b) on the basis of the shell structure of nuclei. They found a direct and exponential relationship between half-life and alpha-decay energy for many even Z even A radioisotopes of the heavy elements, which is illustrated in Fig. 4.3.

Radionuclides that are not even Z and even A (ie, even Z odd N, odd Z even N, or odd Z odd N) also obey the general rule whereby nuclides with low alpha-decay energy exhibit long half-lives, and nuclides with high alpha-decay energy exhibit short half-lives. However, these nuclides exhibit longer half-lives than even−even nuclides, because these nuclides must first transition to an excited state prior to the formation of the alpha particle, which is an even−even nucleus of two protons and two neutrons. The alpha particle must be assembled within the nucleus from proton and neutron nuclear shells; and the transition to the excited nuclear state will prolong the nuclear decay to yet longer half-lives (Perlman et al., 1950; Evans, 1972; Loveland, 2004).

The shorter half-lives exhibited by radionuclides with high alpha-decay energies compared to the longer half-lives of nuclides with lower decay energies is explained on the basis of the nuclear potential barrier that the alpha particle must overcome to penetrate or escape from the nucleus. By bombarding a thin foil of uranium with 8.75-MeV alpha particles, Ernest Rutherford (1927) demonstrated that the high-energy alpha particles were scattered by the uranium nuclei at a distance of 30×10^{-13} cm from the center of the nucleus, as illustrated in Fig. 4.4. A Coulomb potential barrier, which is inversely proportional to the distance from the center of the nucleus, repels incoming alpha particles as well as inhibits their escape from the nucleus. Question therefore arose as to how alpha particles, which are emitted from decaying nuclei with energies as low as 4 MeV, escape from the nucleus. George Gamow (1928) and Gurney and Condon (1928) independently used Schrödinger's wave mechanics to demonstrate that, within the nucleus, the alpha particle as a wave need not pass over the Coulomb barrier, but that the alpha-particle wave could tunnel its way through the potential barrier and escape from the nucleus. The probability of the alpha-particle escape will be a function of the energy of the alpha particle and the amount of

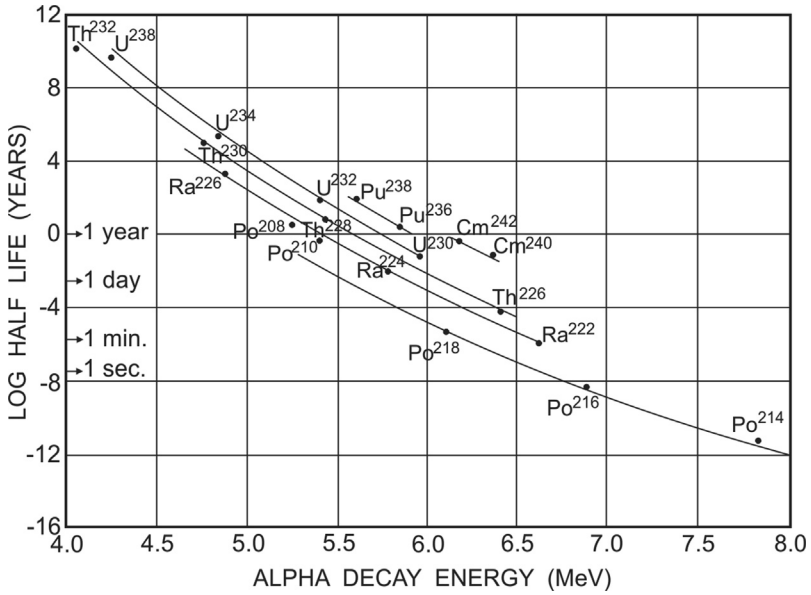

FIGURE 4.3 Observed values of half-life and total alpha-decay energy for each nuclide. The mass number of the radioactive parent nuclide is given at each point. The curves represent the theoretical values for radioactive parents having the same atomic number (isotopes). The range in half-life for the radionuclides, in the curves provided, are 1.6×10^{-4} s for ^{214}Po to 1.4×10^{10} y for ^{232}Th. *(From Perlman, I., and Ypsilantis, T.J., 1950a. Consistency of nuclear radii of even-even nuclei from alpha-decay theory. United States Atomic Energy Commission Report UCRL-613, February 27, 1950, 15.)*. The reader will note from the figure that, at the time of this report, the mass numbers were written as superscripts to the right of the element symbol. Currently mass numbers are written as superscripts to the left of the element symbol.

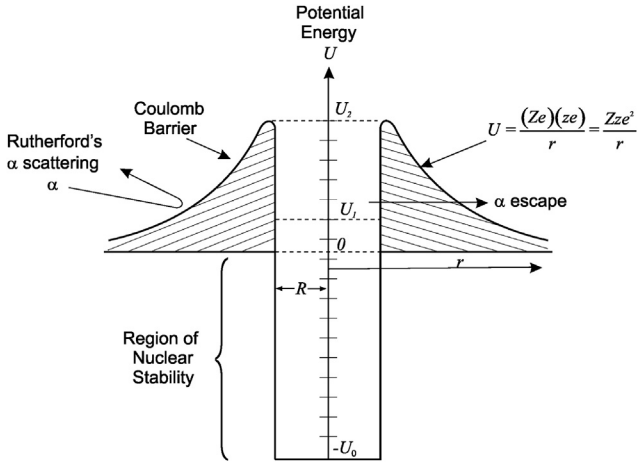

FIGURE 4.4 Nuclear potential barrier and potential energy well based on schematics of Gamow (1930) and Evans (1955). The nuclear radius is from 0 to R; and the distance from the center of the nucleus is r. The potential energy of the bound nucleus within the well is considered constant from $-U_0$ to 0. The Coulomb potential barrier U is inversely proportional to the distance from the center of the nucleus according to $U = (Ze)(ze)/r$ or Zze^2/r, where Z is the atomic number or charge on the nucleus and z is the proton number of the alpha particle ($z = 2$). Excess energy of the unstable nucleus, required for alpha-particle emission, is represented by the energy level U_1 along the potential energy scale; and the height of the potential barrier occurs at U_2 where $r = R$. For a perspective on the nuclear dimensions, data from Evans (1955) for the uranium nucleus ($Z = 92$) are the following: $R \approx 9.3 \times 10^{-13}$ cm, $U_1 \approx 4$ MeV, and $U_2 \approx 28$ MeV.

potential barrier that the alpha particle must overcome. Alpha-decay energies, among all of the alpha-decaying radionuclides, vary between approximately 4 and 10 MeV. A high alpha-decay energy yields alpha particles with a reduced Coulomb barrier to overcome, which augments the probability for alpha-particle escape resulting in a shorter half-life. The opposite would be the case for a low alpha-decay energy, which would yield alpha particles with a greater Coulomb barrier or reduced penetrability and thus lower probability of escape, resulting in a longer decay time or half-life.

4.4 ALPHA PARTICLE INTERACTIONS WITH MATTER

Now consider what happens to an alpha particle that dissipates its kinetic energy by interaction with matter. Alpha particles possess a double positive charge due to the two protons present. This permits ionization to occur within a given substance (solid, liquid, or gas) by the formation of ion pairs due to coulombic attraction between a traversing alpha particle and atomic electrons of the atoms within the material the alpha particle travels. The two neutrons of the alpha particle give it additional mass, which further facilitates ionization by coulombic interaction or even direct collision of the alpha particle with atomic electrons. The much greater mass of the alpha particle, 4 atomic mass units (u), in comparison with the electron (5×10^{-4} u) facilitates the ejection of atomic electrons of atoms through which it passes, either by direct collision with the electron or by passing close enough to it to cause its ejection by coulombic attraction. The ion pairs formed consist of the positively charged atoms and the negatively charged ejected electrons. The alpha particle continues along its path suffering, for the most part, negligible deflection by these collisions or coulombic interactions because of the large difference in mass between the alpha particle and the electron. Thus an alpha particle travels through matter producing thousands of ion pairs (see the following calculation) in such a fashion until its kinetic energy has been completely dissipated within the substance it traverses.

In air, an alpha particle dissipates an average of 35 eV (electron volts) of energy per ion pair formed. Before it stops, having lost its energy, an alpha particle produces many ion pairs. For example, as a rough estimate, a 5-MeV alpha particle will produce 1.4×10^5 ion pairs in air before coming to a stop:

$$\frac{5 \times 10^6 \text{ eV}}{35 \text{ eV/ion pair}} = 1.4 \times 10^5 \text{ ion pairs in air} \qquad [4.12]$$

The thousands of interactions between a traveling alpha particle and atomic electrons can be abstractly compared with a traveling bowling ball colliding with stationary ping-pong balls. Because of the large mass difference of the two, it will take thousands of ping-pong balls to stop a bowling ball. The additional stopping force of electrons is the binding energy of the atomic electrons.

The amount of energy required to produce ion pairs is a function of the absorbing medium. For example, argon gas absorbs approximately 25 eV per ion pair formed, and a semiconductor material requires only 2−3 eV to produce an ion pair. Ionization is one of the principal phenomena utilized to detect and measure radionuclides. The energy threshold for ion pair formation in semiconductor materials is approximately 10 times lower than in gases, which gives semiconductor materials an important advantage as radiation detectors when energy resolution in radioactivity analysis is an important factor.

In addition to ionization, another principle mechanism by which alpha particles and charged particles, in general, may impart their energy in matter is via electron excitation. This occurs when the alpha particle fails to impart sufficient energy to an atomic electron to cause it to be ejected from the atom. Rather, the atoms or molecules of a given material may absorb a portion of the alpha-particle energy and become elevated to a higher energy state. Depending on the absorbing material, the excited atoms or molecules of the material may immediately fall back to a lower energy state or ground state by dissipating the absorbed energy as photons of visible light. This process, referred to as fluorescence, was first observed by Sir William Crookes in London in 1903 (Crookes, 1903a,b) and soon confirmed by Julius Elster and Hans Geitel the same year in Wolfenbüttel, Germany (Julius Elster and Hans Geitel, 1903). They observed fluorescence when alpha particles emitted from radium bombarded a zinc sulfide screen. In darkness, individual flashes of light were observed and counted on the screen with a magnifying glass with the screen positioned a few millimeters from the radium source. The phenomenon of fluorescence is very significant and utilized in the detection and measurement of radionuclides. Thus, as described in the previous paragraphs, alpha particles as well as other types of charged particles dissipate their energy in matter mainly by two mechanisms: ionization and electron excitation.

Because the atomic "radius" is so very much larger ($\approx 10^{-10}$ m) than the "radius" of the nucleus ($\approx 10^{-14}$ m), the interactions of alpha particles with matter via direct collision with an atomic nucleus are few and far between. In this case, though, the large mass of the nucleus causes deflection or ricocheting of the alpha particle via coulombic repulsion without generating any change within the atom. Such deflection was discovered in the early part of this century by Ernest Rutherford and his assistants Hans Geiger and Ernest Marsden (Rutherford, 1906; Geiger, 1908; Geiger and Marsden, 1909), who bombarded very thin gold foil (only 4×10^{-5} cm thick) with alpha particles and observed the occasional deflection of an alpha particle (about 1 in 8000) by more than 90 degrees, even directly backwards toward the alpha-particle source. Lord Rutherford took advantage of this discovery to provide evidence that the greater mass of an atom existed in a minute nucleus. In his own words at a seminar, Rutherford expressed his reaction to the observed

alpha-particle back-scattering with the following statement, related by N. Feather (1940) in a biographical essay a few years following his death:

> *It was quite the most incredible event that ever happened to me in my life. It was almost as incredible as if you fired a 15-inch shell at a piece of tissue paper and it came back and hit you. On consideration, I realized that the scattering backwards must be the result of a single collision, and when I made calculations I saw that it was impossible to get anything of that order of magnitude unless you took a system in which the greater part of the mass of the atom was concentrated in a minute nucleus.*

The discovery of the deflection of alpha particles by matter in the direction backward from which they came was, in the opinion of Rutherford, an opportunity to explore the structure of the atom. As he reported (Rutherford, 1911):

> *It seems reasonable to suppose that the [α-particle] deflection of a large angle is due to a single atomic encounter…it should be possible from a close study of the nature of the deflection to form some idea of the constitution of the atom to produce the effects observed.*

There was at that time little concrete evidence on the structure of the atom. To explain and predict the deflections, Rutherford considered the atom as containing a large positive charge at its center surrounded by the distribution of negative electricity (electrons). By considering that the velocity of a massive positively charged particle (α-particle) would not be changed appreciably by its passage through the atom, Rutherford (1911) derived the path that the α-particle would take as it approached close to the center of an atom. He stated the following (with the writer's comments in brackets):

> *The path of the α-particle under the influence of a repulsive force [coming from the nucleus] varying inversely as the square of the distance will be a hyperbola with the center of the atom S as the external focus. [The original figure of the hyperbola, taken from Rutherford's paper of 1911, is illustrated here on a stamp, that was issued in 1971 commemorating 100 years since Rutherford's birth]. Suppose the particle to enter the atom in the direction PO [O is the position of the circle in the hyperbola illustrated on the commemorative postage stamp], and that the direction of motion on escaping the atom is OP′. OP and OP′ make equal angles with the line SA, where A is the aspe [foci] of the hyperbola. p = SN = perpendicular distance from the [atom] center on direction of initial motion of the α-particle.*

By assigning two velocity variables to the α-particle entering the atom to position A and departing or backscattering from position A, and considering angular momentum and conservation of energy, Rutherford derived the equation $b = 2p \cot \theta$ for the calculation of the factor b, which would be the distance of closest approach of the α-particle to the atom center. Initial estimates from his paper of 1911 gave the value of b for an α-particle of velocity 2.09×10^9 cm/s to be 3.4×10^{-12} cm.

Rutherford went even further to make use of this interaction to determine the nuclear radius of aluminum. By selecting a metal foil of low Z (aluminum, $Z = 13$) and thus low Coulomb barrier to alpha penetration, and applying alpha particles of high energy (7.7 MeV), whereby defined alpha-particle scattering at an acute angle due to Coulombic repulsion would begin to fail, Rutherford (1919, 1920a,b) was able to demonstrate that the distance of closest approach of these alpha particles to the atom center according to Coulomb's law was equivalent to the nuclear radius of aluminum, $\sim 5 \times 10^{-15}$ m.

Scattering of alpha particles at angles of less than 90 degree may occur by coulombic repulsion between a nucleus and a particle that passes in close proximity to the nucleus. These deflected particles continue traveling until sufficient energy is lost via the formation of ion pairs. The formation of ion pairs remains, therefore, the principal interaction between alpha particles and matter.

4.5 ALPHA PARTICLE RANGES

The high mass and charge of the alpha particle, relative to other forms of nuclear radiation, give it greater ionization power but a poorer ability to penetrate matter. In air, alpha particles may travel only a few centimeters. This short range of travel varies depending on the initial energy of the particle. For example, a 5.5-MeV alpha particle, such as that emitted by the radionuclide ^{241}Am previously described, has a range of approximately 4 cm in dry air at standard temperature and pressure, as estimated by empirical formulas, such as Eqs. [4.13] and [4.14] provided below:

$$R_{\text{air}} = (0.005E + 0.285)E^{3/2} \quad [4.13]$$

where R is the average linear range in cm of the alpha particle in air and E is the energy of the particle in MeV. The empirical formula is applied for alpha particles in the energy range of 4−15 MeV. According to calculations of Fenyves and Haiman (1969), the ranges of alpha particles with energies between 4 and 7 MeV can be estimated by using a simplified version of Eq. [4.13] as follows:

$$R_{\text{air}} = 0.3\,E^{3/2} \quad [4.14]$$

Ranges of alpha particles in air over a more wide range of alpha-particle energy can be obtained from Fig. A.1 of Appendix A. For example, taking the value of 5.5 MeV for the energy of the alpha particle, we obtain the range in units of mass thickness from Fig. A.1 of Appendix A to be 0.005 g/cm^2 of dry air. If the density (σ) of dry air is known to be 0.001226 g/cm^3, we can calculate the linear range of the 5.5 MeV alpha particle in terms of distance of travel in dry air by dividing the range in mass thickness by the density of dry air, or:

$$\text{Range of 5.5 MeV } \alpha \text{ in dry air} = \frac{0.005 \text{ g/cm}^2}{0.001226 \text{ g/cm}^3} = 4.07 \text{ cm}$$

A thorough treatment of range calculations for charged particles is available from Fenyves and Haiman (1969). The approximate 4-cm range of 5.5-MeV alpha particles in air is illustrated in Fig. 4.5. There is no abrupt drop in the number of alpha particles detected at the calculated range of 4 cm owing to statistical variations in the number of collisions that the particles may have with air molecules and to variations in the amount of energy loss by the particles for each ion pair formed. After being halted, an alpha particle acquires two free electrons through coulombic attraction and is converted to helium gas.

In materials other than air, such as liquids and solids, the range of alpha particles is obviously much shorter owing to the higher densities of the medium, which enhance the number of collisions a particle may undergo per path length of travel. The range of alpha particles in liquids and solids may be approximated by comparison with ranges in air according to the formula:

$$R_{\text{cm}} = 0.00032\left(A^{1/2}/\rho\right)R_{\text{air}} \quad [4.15]$$

described in a previous text (L'Annunziata, 1987), where R_{cm} is the average range in cm of the alpha particle in an absorber other than air, A is the atomic weight of the absorber, ρ is the absorber density in g/cm^3, and R_{air} is the calculated average

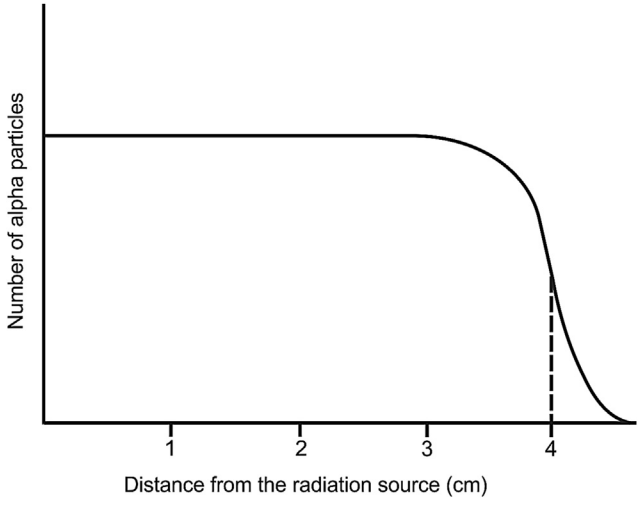

FIGURE 4.5 Range of 5.5-MeV alpha particles in air.

linear range of the alpha particle in air (from Eqs. [4.13] and [4.14]). For example, the linear range of the 5.5-MeV alpha particles emitted by ^{241}Am in aluminum ($A = 26.98$ and $\rho = 2.7$ g/cm^3) according to Eq. [4.15] is calculated as:

$$R_{cm} = 0.00032\left(\sqrt{26.98}\Big/2.7\right)(4.0\text{ cm}) = 2.4 \times 10^{-3}\text{ cm} = 24\ \mu\text{m}$$

The linear ranges of alpha particles in liquids and solid materials are too short to measure with conventional laboratory instrumentation. The alternative is to express range in units of weight of absorber material per unit area, such as mg/cm^2, which is a measure of milligrams of absorber per square centimeter in the absorption path, or in other words, a measure of absorber thickness. If we multiply the linear range of the alpha particle measured in cm of absorber material by the density of the absorber in units of mg/cm^3, the range of the alpha particle in an absorber will be expressed in terms of the weight of absorber per unit area (mg/cm^2) as described by Eq. [4.16], as follows:

$$R_{mg/cm^2} = (R_{cm})(\rho) \qquad [4.16]$$

where R_{mg/cm^2} is the range of alpha particles of a given energy in units of mg/cm^2, also referred to as mass thickness units or material surface density; R_{cm} is the linear range of the alpha particles; and ρ is the absorber density. For example, the linear range of the 5.5-MeV alpha particles in aluminum ($\rho = 2.7$ g/cm^3), calculated above with Eq. [4.15], is converted to range in mass thickness units according to Eq. [4.16] as follows:

$$R_{mg/cm^2} = \left(2.4 \times 10^{-3}\text{ cm}\right)\left(2700\text{ mg}/\text{cm}^3\right) = 6.4\text{ mg}/\text{cm}^2$$

Therefore, the mass thickness of 6.4 mg/cm^2 of aluminum absorber is sufficient to absorb alpha particles of 5.5 MeV energy.

Ranges of alpha particles as well as other charged particles such as protons and deuterons of a given energy in absorber elements of atomic number $Z > 10$ in units of absorber mass thickness can be calculated directly by comparison to the calculated range of the same charged particles of the same energy in air according to the following formula described by Friedlander et al. (1964):

$$\frac{R_Z}{R_{air}} = 0.90 + 0.0275Z + (0.06 - 0.0086Z)\log\frac{E}{M} \qquad [4.17]$$

where R_Z is the range of the charged particle in mass thickness units, mg/cm^2, R_{air} is the range of the charged particle in air in the same mass thickness units, Z is the atomic number of the absorber element, E is the particle energy in MeV, and M is the mass number of the particle (ie, one for protons, two for deuterons, and four for alpha particles). The following example will illustrate the use of the above empirical formula (Eq. [4.17]) to calculate the range R_Z of 5.5 MeV alpha particles ($M = 4$) in aluminum ($Z = 13$). In this example, Eq. [4.17] requires the value of R_{air} for 5.5-MeV alpha particles, which is determined according to Eq. [4.16] as the product of the 5.5-MeV alpha-particle linear range in air (previously calculated) and the density of air at STP ($\rho = 1.226$ mg/cm^3), that is, $R_{air} = (4.0\text{ cm})(1.226\text{ mg/cm}^3) = 4.90$ mg/cm^2. The range of the 5.5-MeV alpha particles in aluminum in mass thickness units (mg/cm^2) is then calculated according to the empirical formula of Eq. [4.17] as:

$$\begin{aligned}
R_z &= \left(0.90 + 0.0275(13) + (0.06 - 0.0086(13))\log\frac{5.5}{4}\right)(R_{air}) \\
&= (0.90 + 0.3575 + (0.06 - 0.1118)\log 1.375)(4.90\text{ mg/cm}^2) \\
&= (1.2575 + (-0.0518)\log 1.375)(4.90\text{ mg/cm}^2) \\
&= (1.2575 - 0.0518\log 1.375)(4.90\text{ mg/cm}^2) \\
&= (1.2575 - 0.007164)(4.90\text{ mg/cm}^2) \\
&= 1.2503(4.90\text{ mg/cm}^2) \\
&= 6.1\text{ mg/cm}^2
\end{aligned}$$

The formula provided by Eq. [4.17] is applicable to charged particles over a wide range of energies (approximately over the range 0.1−1000 MeV) and for absorber elements of $Z > 10$. For lighter absorber elements, the term $0.90 + 0.0275Z$ is replaced by the value 1.00 with the exception of hydrogen and helium, where the value of 0.30 and 0.82 are used, respectively (Friedlander et al., 1964).

Where alpha particles alone are concerned, the range in mass-thickness units can be calculated according to Eq. [4.18] described by Ehman and Vance (1991), as follows:

$$R_{\text{mg/cm}^2} = 0.173E^{3/2}A^{1/3} \quad [4.18]$$

where E is the energy of the alpha particle in MeV and A is the atomic weight of the absorber. If we continue to use the 5.5-MeV alpha particles emitted from ^{241}Am as an example, we can calculate their range in mass thickness units in aluminum according to Eq. [4.18] as follows:

$$R_{\text{mg/cm}^2} = 0.173(5.5)^{3/2}(27)^{1/3} = 6.6\ \text{mg/cm}^2.$$

Ranges reported in mass-thickness units (mg/cm^2) of absorber can be converted to linear range (cm) in that same absorber material from the absorber density (ρ) from the relationship described in Eq. [4.16] or:

$$R_{\text{cm}} = \frac{R_{\text{mg/cm}^2}}{\rho} \quad [4.19]$$

For example, the linear range of the 5.5-MeV alpha particles in aluminum ($\rho = 2.7$ g/cm^3) is calculated as:

$$R_{\text{cm}} = \frac{6.6\ \text{mg/cm}^2}{2700\ \text{mg/cm}^3} = 0.0024\ \text{cm} = 24\ \mu\text{m}.$$

When the absorber material is not a pure element, but a molecular compound (eg, water, paper, polyethylene, etc.) or mixture of elements, such as an alloy, the ranges of alpha particles in the absorber are calculated according to Eq. [4.20] on the basis of the atomic weights of the elements and their percent composition in the absorber material, or in other words, the weight fraction of each element in the complex material. Thus the range in mass-thickness units for alpha particles in absorbers consisting of compounds or mixtures of elements is calculated according to the equation:

$$\frac{1}{R_{\text{mg/cm}^2}} = \frac{w_1}{R_1} + \frac{w_2}{R_2} + \frac{w_3}{R_3} + \cdots \frac{w_n}{R_n}. \quad [4.20]$$

where $R_{\text{mg/cm}^2}$ is the range of the alpha-particles in mass-thickness of the complex absorber material, w_1, w_2, w_3 … w_n are the weight fractions of each element in the absorber, and R_1, R_2, R_3 … R_n are the ranges in mg/cm^2 of the alpha particle of defined energy in each element of the absorber. For example, the range of 5.5-MeV alpha particles in Mylar (polyethylene terephthalate) in units of mass thickness is calculated as follows:

$$\frac{1}{R_{\text{mg/cm}^2}} = \frac{w_C}{R_C} + \frac{w_H}{R_H} + \frac{w_O}{R_O}$$

where w_C, w_H, and w_O are the weight fractions of carbon, hydrogen, and oxygen, respectively, in Mylar; and R_C, R_H, and R_O are the mass-thickness ranges of the alpha particles in pure carbon, hydrogen, and oxygen, respectively. The ranges of 5.5-MeV alpha particles in carbon, hydrogen, and oxygen are calculated according to Eq. [4.18] as:

$$R_C = 0.173(5.5)^{3/2}(12)^{1/3} = 5.10\ \text{mg/cm}^2$$

$$R_H = 0.173(5.5)^{3/2}(1)^{1/3} = 2.23\ \text{mg/cm}^2$$

$$R_O = 0.173(5.5)^{3/2}(16)^{1/3} = 5.62\ \text{mg/cm}^2$$

The weight fractions of the carbon, hydrogen, and oxygen in Mylar [$-(C_{10}H_8O_4)_n-$] are calculated as:

$$w_C = (12 \times 10)/192 = 0.625$$

$$w_H = (1 \times 8)/192 = 0.042$$

$$w_O = (16 \times 4)/192 = 0.333$$

The calculated ranges of the 5.5-MeV alpha particles in each element and the values of the weight fractions of each element in Mylar can now be used to calculate the alpha-particle range in Mylar in mass-thickness units according to Eq. [4.20] as:

$$\frac{1}{R_{\text{Mylar}}} = \frac{0.625}{5.10} + \frac{0.042}{2.23} + \frac{0.333}{5.62} = 0.200$$

$$R_{\text{Mylar}} = 1/0.200 = 5.0\ \text{mg/cm}^2$$

The linear range of these alpha particles in Mylar are obtained from range in mass-thickness units and the density of Mylar ($\rho = 1.38\ \text{g/cm}^3$) as:

$$R_{\text{cm}} = \frac{5.0\ \text{mg/cm}^2}{1380\ \text{mg/cm}^3} = 0.0036\ \text{cm} = 36\ \mu\text{m}.$$

To provide illustrative examples, the values of the ranges of 5.5-MeV alpha particles in units of mass-thickness of various absorber materials are provided in Table 4.1. These values represent the milligrams of absorber per square centimeter in the alpha-particle absorption path. It can be difficult to envisage alpha-particle distance of travel from the values of range when expressed in units of mass thickness. However, it is intuitively obvious that, the greater the charge on the nucleus of the absorber (ie, absorber atomic number, Z), the greater the atomic weight of the absorber (A), and the greater the absorber density (ρ), the shorter will be the path length of travel of the alpha particle through the absorber. This is more evident from the calculated values of linear range of 5.5-MeV alpha particles in various gaseous, liquid, and solid absorbers provided in Table 4.2. From the linear ranges we can see that 5.5-MeV alpha particles could not pass through fine commercial aluminum or copper foils 0.0025 cm thick. Although commercial paper varies in thickness and density, the linear range in paper calculated in Table 4.2 illustrates that 5.5-MeV alpha particles would not pass through 0.0034-cm thick paper, which has an average density value of 1.45 g/cm^3. Also, the alpha particles of the same energy would not pass through a layer of Mylar only 0.0036 cm thick. Mylar is a polymer sometimes used as a window for gas ionization detectors. From our previous calculations in this chapter we can see that a Mylar window of mass thickness 5 mg/cm^2 would not allow 5.5-MeV alpha particles to pass into the gas ionization chamber. A sample emitting such alpha particles would have to be placed directly into the chamber in a windowless fashion to be detected and counted.

From the above treatment it is clear that the range of alpha-particle travel depends on several variables including (1) the energy of the alpha particle, (2) the atomic number and atomic weight of the absorber, and (3) the density of the absorber. The higher the alpha-particle energy, the greater will be its penetration power into or through a given substance as more coulombic interactions of the alpha particle with the electrons of the absorber will be required to dissipate its energy before coming to rest. Also, if we consider alpha particles of given energy, the alpha-particle ranges will be shorter in absorbers of higher atomic number or atomic weight, as the absorber atoms will contain a higher number of atomic electrons. An increase in the number of atomic electrons in an absorber material would increase consequently the number of coulombic interactions of the alpha particle per path length of travel.

TABLE 4.1 Ranges of 5.5-MeV Alpha Particles in Various Absorbers in Units of Surface Density or Mass Thickness

Water[a] (mg/cm^2)	Paper[a,b] (mg/cm^2)	Aluminum[c] (mg/cm^2)	Copper[c] (mg/cm^2)	Gold[c] (mg/cm^2)
4.8	4.9	6.6	8.9	12.9

[a]*Calculated with empirical formula provided by Eq. [4.20] on the basis of the weight fraction of each element in the absorber.*
[b]*Cellulose $(C_6H_{10}O_5)_n$ calculated on the basis of the weight fraction of each element in the monomer.*
[c]*Calculated with empirical formula provided by Eq. [4.18].*

TABLE 4.2 Linear Ranges of 5.5-MeV Alpha Particles in Various Absorbers in Units of cm and μm or 10^{-6} m

Air[a]	Water[b]	Mylar[b,c]	Paper[b,d]	Aluminum[b]	Copper[b]	Gold[b]
4 cm	0.0048 cm	0.0036 cm	0.0034 cm	0.0024 cm	0.001 cm	0.00075
40,000 μm	48 μm	36 μm	34 μm	24 μm	10 μm	7.5 μm

[a]*Calculated with empirical formula provided by Eqs. [4.13] and [4.14].*
[b]*Calculated by dividing the range in mass thickness by the absorber density according to Eq. [4.19].*
[c]*Polyethylene terephthalate, $\rho = 1.38\ \text{g/cm}^3$.*
[d]*Cellulose $(C_6H_{10}O_5)_n$, $\rho = 1.45\ \text{g/cm}^3$.*

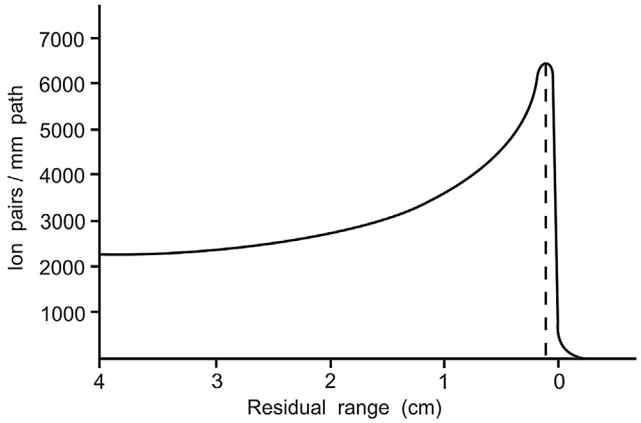

FIGURE 4.6 Specific ionization of an alpha particle in air along its range of travel. A 5.5-MeV alpha particle will travel only 4.0 cm in dry air before coming to a stop (residual range = 0 in the above graph). The maximum ionization (ion pairs/mm path traveled) produced by the alpha-particle occurs only 2–3 mm (dashed line) before the particle reaches the end of its range.

As the alpha particle travels through air and undergoes energy loss via numerous collisions, the velocity of the particle obviously diminishes. At reduced velocity and consequently reduced momentum, an alpha particle is more affected by coulombic attraction within the vicinity of a given atom. Progressive reduction in the velocity of travel of the alpha particle therefore results in an increase in the number of ion pairs produced per millimeter of path length of travel. The increase in ionization per path length of travel of an alpha particle is illustrated in Fig. 4.6. The highest specific ionization (number of ion pairs formed per millimeter of path) occurs shortly before termination of the alpha particle's travel, some 2 or 3 mm before the end of its range.

Chapter 5

Hall of Fame: Part II

Frederick Soddy (1877−1956), C.T.R. Wilson (1869−1959), Frédéric Joliet (1900−1958) and Irène Joliet-Curie (1897−1956), Enrico Fermi (1901−1954), Wolfgang Pauli (1900−1958), Frederick Reines (1918−1998) and Clyde Cowan, Jr. (1919−1974), and Otto Stern (1888−1969)

Everything comes to him, who knows how to wait.

Wolfgang Pauli in a cable reply dated June 15, 1956 after Frederick Reines and Clyde Cowen informed Pauli that they had discovered the neutrino, which Pauli had postulated 26 years earlier.

FREDERICK SODDY (1877−1956)

Frederick Soddy was born in Eastbourne, Sussex, England on September 2, 1877. He was awarded the Nobel Prize in Chemistry in 1922, in the words of the Nobel Committee, "for his contributions to our knowledge of the chemistry of radioactive substances, and his investigations into the origin and nature of isotopes."

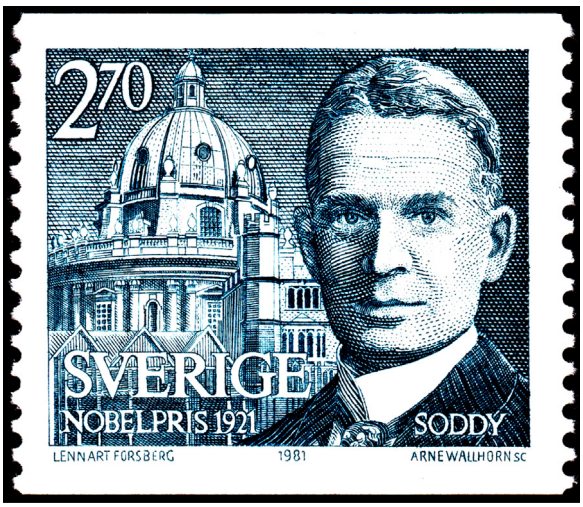

Frederick Soddy (1877-1956)

Soddy studied at Eastbourne College and the University College of Wales, Aberystwyth and, after obtaining a scholarship. At Merton College, Oxford, he graduated with highest honors in chemistry in 1898. After a couple of years of research at Oxford, Frederick Soddy joined the Chemistry Department at McGill University, Montreal, Canada where he worked with Rutherford during the period of 1900 to 1902. It is with Rutherford at McGill University where Soddy began to do pioneering work in the field of radioactivity. Rutherford (1900) was the first to define the concept of radioactive decay in terms of half-life, that is, the time it takes for a radioactive sample to lose one-half of its original radioactivity. In 1900 Rutherford had also determined the equations that define the rates of decay of radioactive atoms (see the chapter: "Radionuclide Decay,

Radioactivity: Introduction and History, From the Quantum to Quarks. http://dx.doi.org/10.1016/B978-0-444-63489-4.00005-8
Copyright © 2016 Elsevier B.V. All rights reserved.

Radioactivity Units, and Radionuclide Mass" and Eq. [II.1], below). Subsequently Rutherford and Soddy (1902) reported the rates of transformation of one radioactive element (parent nuclide) into another element (daughter nuclide). They demonstrated that the rate of decay of the parent nuclide would govern the rate of formation of the daughter nuclide. The terminology "parent" and "daughter" nuclides were not used by them in this initial report, because such nomenclature had not yet been adopted at this early stage of development. They defined the exponential decay equation for radioactive nuclides in accord with Rutherford's initial mathematical findings (Rutherford, 1900), which are now used universally in this field of science, namely:

$$I/I_0 = e^{-\lambda t} \qquad \text{[II.1]}$$

where I is the intensity of the radioactivity after a given time t measured in seconds, minutes, days, or years, I_0 is the initial intensity of radioactivity or the intensity at the time observations are initiated, λ is the decay constant with units of reciprocal time, and e is the base to the natural logarithm (see Eq. [18.6] and the chapter: "Radionuclide Decay, Radioactivity Units, and Radionuclide Mass" for a more detailed treatment of radionuclide decay). They also defined another equation, now widely used, that defines the rate of production of daughter element (nuclide) from the parent as:

$$I/I_{\max} = 1 - e^{-\lambda t} \qquad \text{[II.2]}$$

where I is the intensity of radioactivity of the daughter after a given period of time t, and $I_{\max}$ is the intensity of the radioactivity of the daughter nuclide when its maximum value is reached. See Eq. [18.33] in the chapter "Radionuclide Decay, Radioactivity Units, and Radionuclide Mass" for the practical applications of this equation. The important conclusions made by Rutherford and Soddy from their work were concerned with the nature of radioactivity. They stated in their paper:

> *This property (radioactivity) is the function of the atom and not of the molecule. Uranium and thorium possess the property (radioactivity) in whatever molecular condition they occur…The intensity of the radiation appears to depend only on the quantity of active element present.*

After completing the above work with Rutherford, Soddy moved to the University College, London where he worked with Sir William Ramsay. In their joint work, Ramsay and Soddy (1903) demonstrated that the alpha particles that constitute the radioactive emanations from radium turned into helium gas. They trapped the emanations from 50 mg of radium bromide in a glass tube and studied the contents by spectroscopic means. At first they could not recognize the spectrum as that of any known element, but after a few days the contents of the tube produced spectroscopic lines characteristic of helium. This was an important discovery, because it provided evidence that alpha particles consisted of helium nuclei. It is now known that alpha particles, when they lose their energy traveling through matter, come to a stop and acquire two free electrons and form helium gas. The following year (1904), Sir William Ramsay was awarded the Nobel Prize in Chemistry for his discovery of the inert gases, such as helium, and their location in the periodic table.

After two short stints of work under the influence of the two Nobel Laureates Ernest Rutherford and William Ramsay, Frederick Soddy went on at the young age of 27 to the University of Glasgow, where he became lecturer in physical chemistry and radioactivity. He remained at Glasgow University from 1904 to 1914, during which time he would conduct yet more pioneering work on radioactivity. While at Glasgow, Soddy carried out studies that established the "Displacement Law" or "Periodic Law" of radioactive elements (radionuclides). In the journal *Nature* (Soddy, 1913a), he stated the law clearly in the following words:

> *The successive expulsion of one α and two β particles in three radioactive changes in any order brings the inter-atomic charge of the element back to its initial value, and the element back to its original place in the (Periodic) table, though its atomic mass is reduced by four units.*

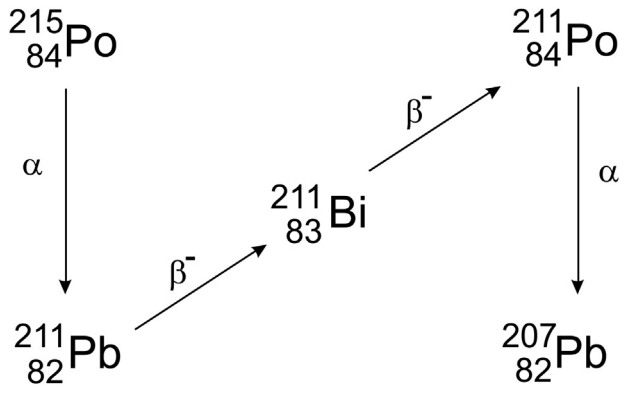

FIGURE II.1 Soddy's displacement or Periodic Law, as illustrated with polonium and lead isotopes, a part of the ^{235}U natural decay chain.

An example of Soddy's displacement law can be taken from a part of Fig. 2.3 of the ^{235}U natural decay chain from chapter "Basic Concepts and Definitions,", which is illustrated here in Fig. II.1.

As illustrated in Fig. II.1, Soddy demonstrated that the emission of an α-particle would produce an element that is two atomic numbers lower, while the emission of a β-particle would displace an atom one atomic number higher. In Fig. II.1, we see that the radioactive atom of polonium-215 emits an α-particle to become an atom of lead-211, which in turn decays by the emission of a β-particle to become radioactive bismuth-211. The bismuth atom also decays by the emission of a β-particle to become polonium, the same element of atomic number 84 from which it had originated, but with a mass of four units less. The emission of an α-particle from the polonium-211 brings the atom back to the element lead with four mass units less than the atom of lead-211. The parent and product atoms of atomic number 84 are of the same element polonium, but of different mass. The two distinct atoms of polonium (ie, ^{215}Po and ^{211}Po and of lead (ie, ^{211}Pb and ^{207}Pb)) illustrated in Fig. II.1 are today known as "isotopes" (ie, isotopes of polonium and isotopes of lead), because Soddy (1913a,b) coined the term "isotopes" to refer to such atoms that have the same atomic number (ie, the number of protons in the nucleus) but a different mass number (ie, number of protons plus neutrons in the nucleus). Soddy recognized that these are atoms of the same element in the periodic table but of different mass. In his words, Soddy (1913a) explained:

> *I call (them) "isotopes" or "isotopic elements," because they occupy the same place (from the Greek) in the periodic table. They are chemically identical, and save only as regards the relatively few physical properties which depend on atomic mass directly, physically identical also.*

Soddy went further by alluding to the fact that not only can we consider the radioactive atoms as "isotopes" of known elements, but that many, if not most, of the stable elements may actually consist of a mixture of isotopes. In his Nobel Lecture, Soddy (1922) gave credit to the Swedish scientists Strömholm and Svedberg (1909a,b) by quoting them as follows:

> *Perhaps, one can see, as an indication in this direction, the fact that the Mendeleev scheme (Periodic Table of Elements) is only an approximate rule as concerns the atomic weight, but does not possess the exactitude of a natural law; this would not be surprising if the elements of the scheme were mixtures of several homogeneous elements of similar but not completely identical atomic weight.*

In a subsequent paper (Soddy, 1913c) and in his Nobel Lecture (1922), Soddy mapped out his Periodic Law, which shed much light on the identification of isotopes. Fig. II.2 is the original Fig. 2, taken from Soddy's Nobel lecture (1922), which illustrates his charting of the radioactive elements and the Periodic Law.

This work advanced knowledge considerably about the identities of radioactive atoms and where these resided in the periodic table of elements. The radioactive atoms were then identified, just as they are to this day, by their decay rate (ie, half-life), energies and types of radiation they emitted, or from their parent atoms. But in the early part of the 20th century, the radioactive atoms were named after the parent atom, for one of two reasons: it was thought that the daughter atom was of the same element as the parent or it was simply not known what element the daughter atom was. For example, as illustrated in Soddy's figure above, the radioactive atoms previously referred to as thorium A, thorium B, and thorium C originated from thorium, but were not thorium at all. Rather, the three radioactive atoms were isotopes of the elements polonium, lead, and bismuth, respectively. Soddy's work was the precursor to the chart of the nuclides, which is the current chart of all known isotopes of the atomic elements.

In 1914 at the age of 37, Soddy was appointed to the position of professor of chemistry and chair at the University of Aberdeen, where he remained until 1919 to take on a position of professor of chemistry at Oxford University. He remained at Oxford until 1936, retiring after the death of his wife.

It is interesting to note that Soddy's greatest contribution to science, the work for which he won the Nobel Prize, was confined to the short period from 1902 to 1914. After that period he diverted his attention from radioactivity to other interests, which were summarized succinctly in *Nobel Prize Lectures in Chemistry, Vol. 1, 1901–1921* (1967) as follows: After his period at Glasgow (1914) he did no further work in radioactivity and allowed the later developments to pass him by. His interest was diverted to economic, social and political theories which gained no general acceptance, and to unusual mathematical and mechanical problems.

C.T.R. WILSON (1869–1959)

Charles Thomson Rees Wilson was born in Glencorse Parish near Edinburgh, Scotland on February 14, 1869. He received the Nobel Prize in Physics in 1927 "for his method of making the paths of electrically charged particles visible by condensation of vapor."

Wilson initially studied biology at the University of Manchester with intentions of earning a degree in medicine. He won a scholarship to Cambridge in 1888, where his interests changed from medicine to physics and chemistry, and graduated in 1892.

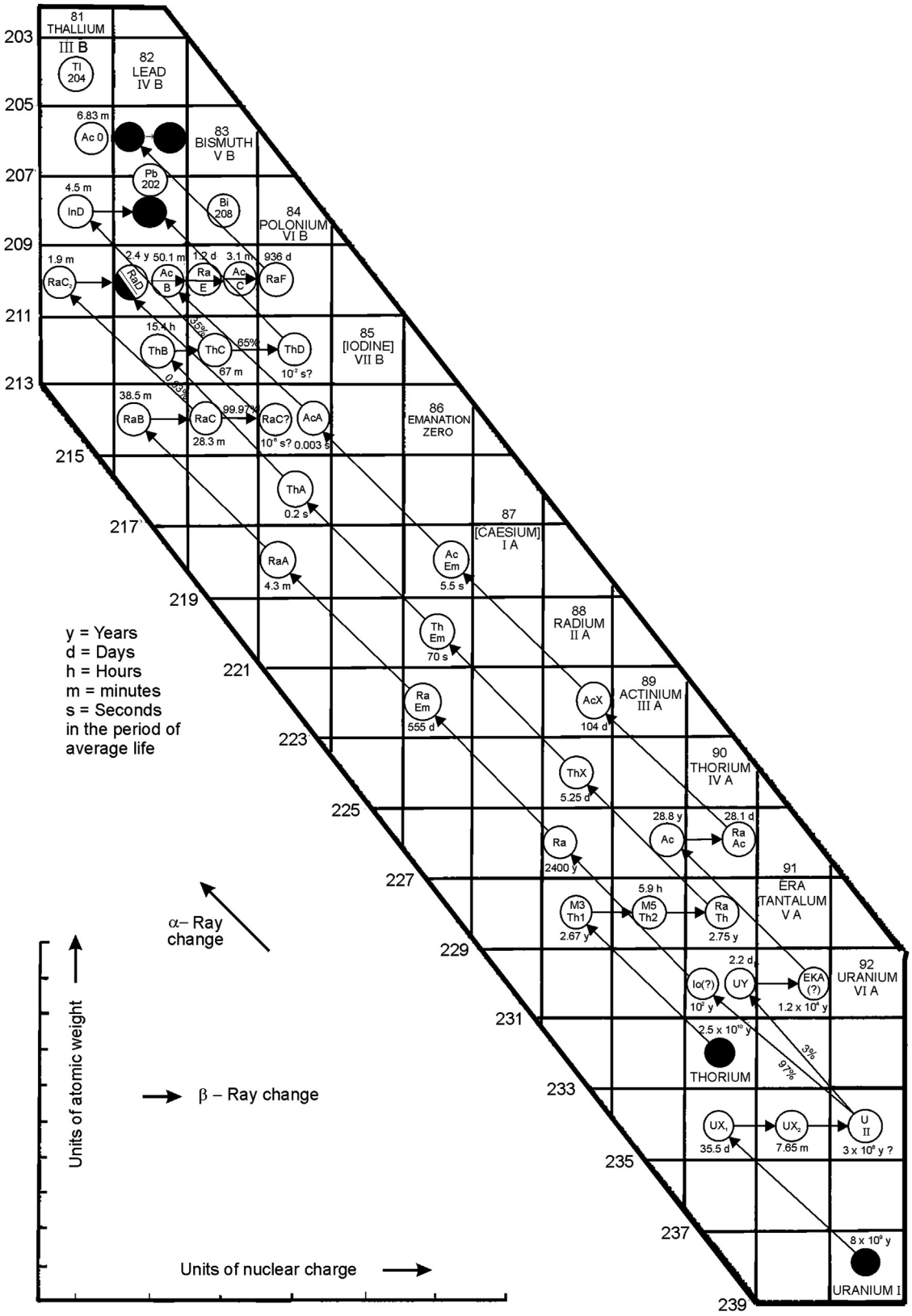

FIGURE II.2 Radio-elements and Periodic Law. All elements in the same vertical column are isotopes…are chemically non-separable. *Soddy, F., 1922. The origins of the conceptions of isotopes. Nobel Lecture, December 12, 1922. In: Nobel Lectures, Chemistry 1901–1921 (1966), Elsevier Publishing Co., Amsterdam, with permission from The Nobel Foundation © 1922.*

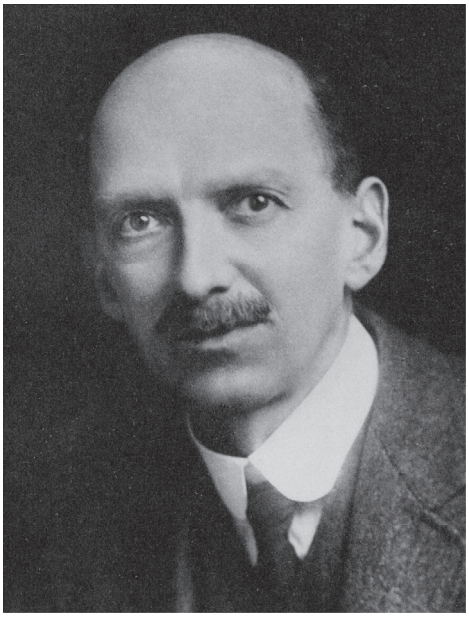

C.T.R. Wilson (1869-1959)
Photograph by A.B. Lagrelius and Westphal, Stockholm, with permission, courtesy AIP Emilio Segre Visual Archives, Weber Collection.

In his Nobel lecture, Wilson explained how he became interested in cloud and mist formation and eventually discovered a method of making visible the paths of travel of subatomic particles. During September of 1894, he spent a few weeks at an observatory located on the summit of Ben Nevis, the highest of the Scottish Hills. The beautiful optical phenomena that the sun produced when its rays passed through the clouds surrounding the hilltop and the shadows cast on the mist and cloud glories excited his interest in the possibility of reproducing this effect in the laboratory. In early 1895, Wilson first tried to make clouds in the laboratory by expanding moist air. It was known then that dust particles in the air served as nuclei for the formation of clouds, and during his experimentation he discovered that even if all dust particles were removed, whereby no cloud formation should occur, he could still achieve a cloud formation if the air expansion and supersaturation would exceed a certain limit. His studies indicated that a cloud would form in dust-free air that had an expansion ratio of $v_2/v_1 = 1.25$, where v_2 and v_1 are the expanded and initial volumes of air, respectively, resulting in an approximately fourfold supersaturation of air moisture. He also observed that an even more rapid critical dust-free air expansion yielded an approximately eightfold supersaturation of the water vapor, and expansions exceeding this limit produced dense cloud formation. It was clear to Wilson at this point in his work that a critical supersaturation of water vapor could be reached where cloud formation would occur with nothing more than the gas molecules of air.

The news of Röntgen's discovery of X-rays reached Scotland in a short time during late 1895, and by early 1896 J.J. Thomson was already studying the ionization (conductivity) of air by the newly discovered X-rays. That very year Wilson got hold of one of the X-ray tubes manufactured in Thompsons lab to see what effect these rays would have on his new synthetic clouds. When exposing the expanding moist air to the X-rays, Wilson discovered that a dense long-lasting fog would be produced when the expansion ratio exceeded 1.25. The X-rays were apparently producing condensation nuclei in the supersaturated air to enable the formation of the long-lasting fog or mist. During the following two years, Wilson studied the effects of several forms of radiation on the cloud formations, including the effects of X-rays, the newly discovered Becquerel rays from uranium, and ultraviolet light.

During the first decade of the 20th century, the corpuscular nature of radioactivity, such as alpha and beta particles and the ionization that these particles produced in air, was known (see Rutherford in Hall of Fame, Part I). Sometime around 1910, Wilson decided to build his cloud chamber with the idea of possibly visualizing and even photographing the tracks or paths of travel of the various radiations by the ionization and consequent condensation or miniature clouds these might form. The expansion chamber or cloud chamber designed by Wilson in 1911 for these studies is illustrated in Fig. II.3.

The diameter of the cylindrical cloud chamber (A) is 16.5 cm and the expansion depth (height) is 3.4 cm. The chamber contains a hollow piston or "plunger" (M) that moves up or down within a fixed outer cylinder according to the pressure

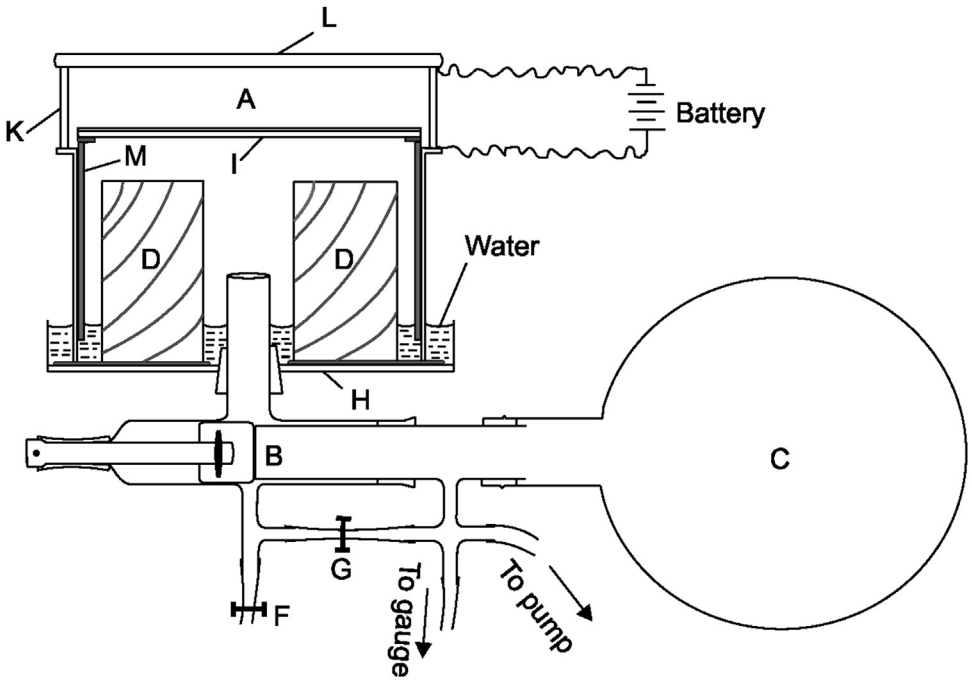

FIGURE II.3 Wilson Cloud Chamber (1912). The charged-particle tracks were produced in the expansion space above the piston, and these were observed and photographed with proper illumination as described in the text. An electric field potential was applied to the cloud chamber expansion space to remove any ions that may be present in the water vapor prior to the entry of ionizing charged particles under observation. The original Wilson cloud chamber is on exhibit at the Cavendish Laboratory Museum, University of Cambridge. *See Wilson, C.T.R., 1911. On the method of making visible the paths of ionizing pasrticles through a gas. Proc. R. Soc. London A85, 285–288, Wilson, C.T.R., 1912. On the expansion apparatus for making visible the tracks of ionizing particles in gases and some results obtained by its use. Proc. R. Soc. London A87, 277–291, and Wilson, C.T.R., 1923. Investigations on X-rays and β-rays by the cloud method. I. X-rays. Proc. R. Soc. London A104, 1–24 for details.*

differential within and outside of the piston. The chamber is sealed with a pool of water within which the piston is able to move. A vacuum is applied to the round glass chamber (C) with a suitable pump, and rapid expansion of the air within the chamber (region A) is achieved by opening the valve (B) to the vacuum chamber (C). The vacuum will suck air out of the hollow piston, forcing it to move in the downward direction, thereby rapidly expanding the moist air in the cloud chamber (A), which is the expansion space above the piston. The floor (I) of the cloud chamber drops suddenly when valve (B) is opened to the evacuated chamber (C) until it is brought to a sudden stop when the plunger hits the rubber-covered base (H). The expansion of the chamber would yield the supersaturation of moisture required for particle track formation while simultaneously triggering the flash of a camera. Pinch-cocks (F) and (G) on rubber tubing connections allowed for opening communication with the atmosphere to control the air in the cloud chamber and adjustment of the plunger (piston) providing the desired volume to the chamber (~750 mL). A hollow cylinder of wood (D) is enclosed inside the inner piston, which reduces the volume of air passing through the connecting tubes at each expansion. The top (L), walls (K), and floor (I) of the cloud chamber were made of glass. To permit visualization and photography of the charged-particle tracks in the cloud chamber, a dark background was provided by painting the base of the expansion chamber black and coating the walls with gelatin. Wilson found that an expansion ratio of at least 1.25, yielding a fourfold supersaturation of water vapor, was sufficient for negative particles such as Compton electrons produced by X-rays to condense water along the electron tracks in ionized air. However, for positively charged particles, such as alpha particles, the expansion ratio had to exceed 1.31, corresponding to an approximately sixfold supersaturation of water vapor to yield the condensation of the water vapor along the particle tracks. The water vapor would condense along the charged-particle path of travel as illustrated in Fig. II.4.

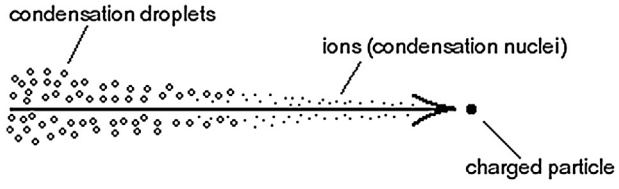

FIGURE II.4 The formation of condensation droplets onto ions formed along the path of travel of a charged particle in a Wilson Cloud Chamber.

The ions produced by the charged particle as it traveled through the air of the chamber would act as seeds or condensation nuclei on which very minute droplets the size of large molecules would form. To achieve the proper conditions so that the charge-particle tracks could be observed and photographed, the following conditions had to be met, in the words of C.T.R. Wilson in his Nobel lecture:

> *The expansion must be effected without stirring up the gas (air); this condition is secured by using a wide, shallow cloud chamber of which the floor can be made to drop suddenly and so produce the desired increase in volume. The cloud chamber must be freed not only from "dust" particles, but from ions other than those produced by the ionizing particles under observation.*

It was not only desirable to observe the particle tracks, but also photograph these for subsequent detailed study. With this in mind, Wilson further explained:

> *For the purpose of obtaining sharp pictures of the tracks, the order of operations has to be firstly, the production of the necessary super-saturation by sudden expansion of the gas; secondly, the passage of the ionizing particles through the super-saturated gas (air); and finally, the illumination of the cloud condensed on the ions along the track.*

The commemorative postage stamp pictured here illustrates numerous straight tracks produced in Wilson's Cloud Chamber by alpha particles emitted in all directions from a radium source. Other interesting particle-track photographs taken by Wilson with his cloud chamber and described in his Nobel lecture on December 12, 1927 are illustrated in Figs. II.5–II.8. The track in Fig. II.5 is that of an alpha particle. Alpha particle tracks are generally straight and wider than those produced by beta particles or electrons. This is because alpha particles produce a higher specific ionization (ion pairs

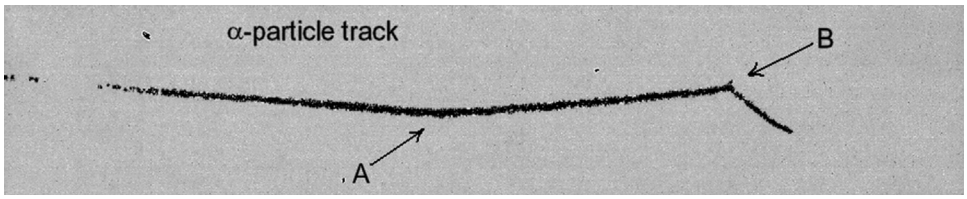

FIGURE II.5 A track produced by an alpha particle. The bend (A) and deflection (B) in the track were interpreted by Wilson as a close encounter of the alpha particle with an atomic nucleus and a collision with a nucleus, respectively. *From Wilson, C.T.R., 1927. On the cloud method of making visible ions and the tracks of ionizing particles. Nobel Lecture, December 12, 1927. In: Nobel Lectures, Physics 1922–1941, Elsevier Science Publishers, Amsterdam, with permission © The Nobel Foundation 1927.*

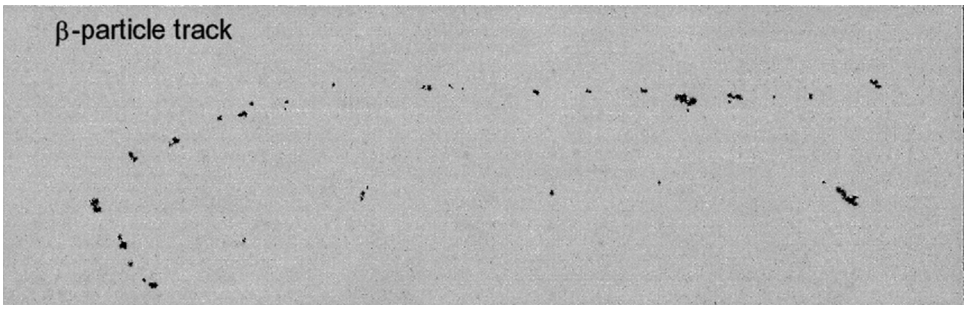

FIGURE II.6 A track of a beta particle. Beta particles and electrons yielded thinner tracks than alpha particles. The tracks would be straight for high-energy electrons, but low-energy electrons would have more tortuous paths, as illustrated. *From Wilson, C.T.R., 1927. On the cloud method of making visible ions and the tracks of ionizing particles. Nobel Lecture, December 12, 1927. In: Nobel Lectures, Physics 1922–1941, Elsevier Science Publishers, Amsterdam, with permission © The Nobel Foundation 1927.*

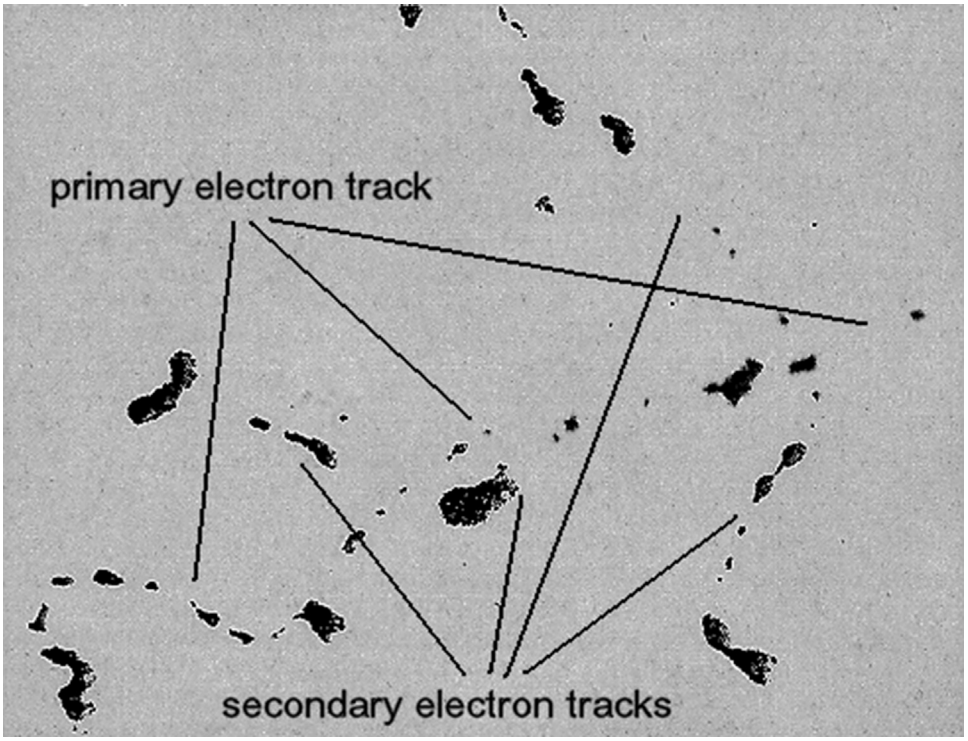

FIGURE II.7 A track produced by a primary electron and four branching tracks produced by secondary electrons. *From Wilson, C.T.R., 1927. On the cloud method of making visible ions and the tracks of ionizing particles. Nobel Lecture, December 12, 1927. In: Nobel Lectures, Physics 1922–1941, Elsevier Science Publishers, Amsterdam, with permission © The Nobel Foundation 1927.*

per mm of path traveled) and they have a much higher mass than the electron. The usual straight path of an alpha particle may bend when it comes into close proximity to an atomic nucleus, such as point A in Fig. II.5; or the alpha particle may deflect sharply if it collides with a nucleus, as illustrated by point B in Fig. II.5. Wilson illustrated in Fig. II.6 how the beta particle of much lower mass than the alpha particle produces tracks that are thinner than those produced by alpha particles, and they will also bend or undergo numerous deflections by collisions with atomic electrons. The collisions of electrons with other electrons is illustrated in Wilson's photograph in Fig. II.7. This photograph shows a long, winding track of a primary electron and four branches of tracks made by secondary electrons. The secondary electrons are the result of collisions of the primary electron with atomic electrons in the cloud chamber. One can also see that the electron tracks become much wider at the very end of each track. This is a

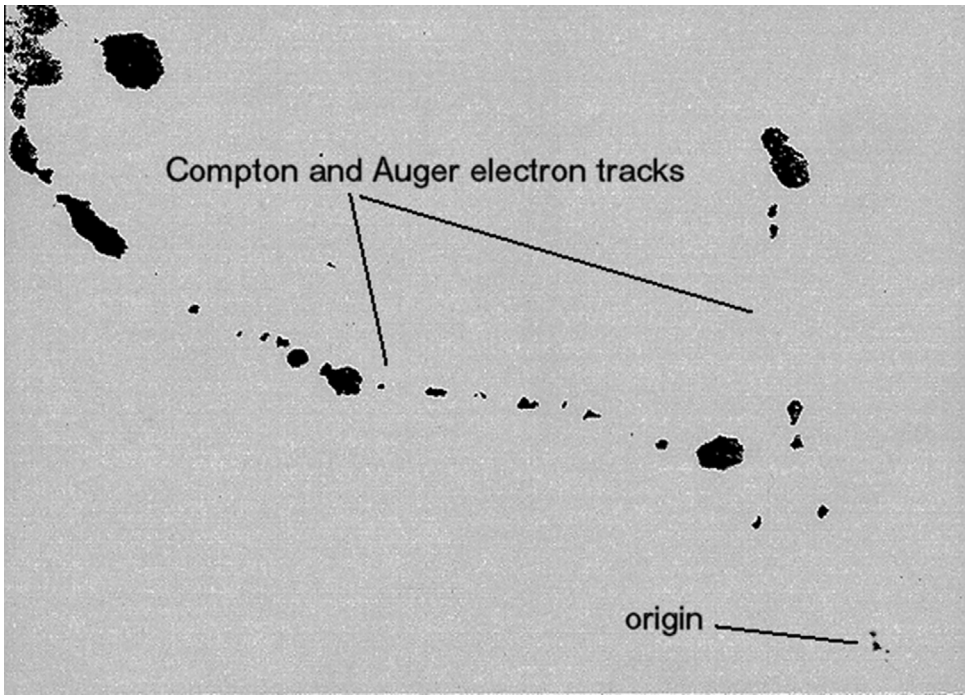

FIGURE II.8 Two branching tracks produced by Compton and Auger electrons originating from the same atom. *From Wilson, C.T.R., 1927. On the cloud method of making visible ions and the tracks of ionizing particles. Nobel Lecture, December 12, 1927. In: Nobel Lectures, Physics 1922–1941, Elsevier Science Publishers, Amsterdam, with permission © The Nobel Foundation 1927.*

common trait in Wilson's cloud chamber track images. He explains that as the electron loses energy its path becomes more tortuous, and as it slows down will accumulate more condensation. The tracks of high-energy electrons and beta particles generally yielded straight thin tracks. The two tracks illustrated in Fig. II.8 are interpreted by Wilson as one produced by a Compton electron possibly ejected from a K shell of an atom when irradiating the cloud chamber with X-rays, and the other track arising from the same atom would be that of an Auger electron ejected from an outer shell of the atom after absorbing the energy released from orbital electron transitions following the ejection of a Compton electron.

The significance of Wilson's work in the development and application of the cloud chamber cannot be underestimated. For the first time he made it possible to observe the interactions of charged particles with matter by photographing their tracks before and after collision with atomic particles. At the time of his work he was able to put into clear view in black-and white photographs many interactions of atomic particles, such as the existence of Compton scatter electrons, Rutherford's alpha-particle interactions with atomic nuclei, the production of secondary electrons from primary (fast) electron collisions, and the existence of delta rays, which are very fast high-energy electrons produced by head-on collision of heavy particles with electrons, among other interactions.

FRÉDÉRIC JOLIET (1900–1958) AND IRÈNE JOLIET-CURIE (1897–1956)

Frédéric Joliet and Irène Joliet-Curie shared the Nobel Prize in Chemistry in 1935 "in recognition of their synthesis of new radioactive elements."

Jean Frédéric Joliet was born in Paris on March 19, 1900. He studied at the Ecole de Physique et Chemie, Paris, and in 1925 became a laboratory assistant to Marie Curie at the Radium Institute in Paris. Then Irène Curie, a daughter of Marie and Pierre Curie, was given the task of teaching Frederick the laboratory methods used when working with radioactive materials. Frédéric and Irène married in 1926. Frédéric completed his doctorate degree in 1930 with a thesis on the electrochemistry of the radioactive elements, and became lecturer of the faculty of Science in 1935. Frédéric Joliet and Irène Joliet-Curie had two children and, like Pierre and Marie Curie, devoted their lives to their work as a team in laboratory research on radioactivity and to the education of their children.

Frédéric and Irène Joliet-Curie

Irène Curie was born in Paris on September 12, 1897. She was the eldest of two daughters born to Pierre and Marie Curie. The year that she met Frédéric, Irène received her doctorate degree in 1925 with a thesis on polonium alpha radiation, the element discovered by her mother.

Their work yielded crucial evidence that led to the discovery of the neutron, but the discovery of this elementary particle eluded their grasp. In early 1932 the Joliet-Curies reported that the highly penetrating radiation emitted when the alpha-particle emitter polonium was in contact with beryllium could knock out high-energy protons from paraffin and other hydrogenous materials and that the radiation responsible for this was gamma rays (Joliot-Curie and Joliot, 1932). At the Cavendish Laboratory, James Chadwick recognized the findings of the Joliot-Curies to be startling and very significant, but the radiation capable of knocking out protons could not be gamma rays, but another source of unknown radiation consisting of a particle with a mass or energy equivalent to the mass of the proton. Chadwick then set about in a matter of weeks to discover this new particle as the neutron (see Hall of Fame, Part IV).

Although they missed the opportunity to discover the neutron, the Joliot-Curies were the first to synthesize new radioactive elements (isotopes), for which they were awarded the Nobel Prize. By the time the Joliot-Curies began their work together it was well understood, following the discoveries of Rutherford and Soddy, that one element would transform itself into another element by radioactive decay. In their jointly prepared Nobel lecture presented on December 12, 1935 (they split their lecture so that Irène Joliot-Curie would present the first half of the lecture followed by Frédéric Joliot, who gave the remaining part), the Joliot-Curies explained that, when writing these transformations "the atomic weight is placed above and to the left of the chemical symbol, and the atomic number to the left and below." The following transformation of radium into the radioactive radon gas served as an example:

$$^{226}_{88}\mathrm{Ra} \rightarrow {}^{222}_{86}\mathrm{Rn} + {}^{4}_{2}\mathrm{He}\ (\text{alpha particle}) \qquad \text{[II.3]}$$

We should keep in mind that the neutron was discovered only in 1932, and the term "mass number" (representing the sum of protons and neutrons in the nucleus) did not yet exist. Hence, the Joliot-Curies referred to the superscript mass number as the atomic weight.

Much had occurred in 1932, first the discovery of the neutron by James Chadwick, which the Joliot-Curies missed. This was followed by the discovery of the positron (positively charged electron) in cosmic ray showers by Carl Anderson from Caltech later that year. The Joliot-Curies now searched for the positron, which they thought they had also missed. They not only found the missed positron (the first artificially produced positron), but they also made a new discovery, the first artificially produced radioactive isotopes.

The discovery of the Joliot-Curies of artificially produced radioisotopes came about when they began their search for their missed positrons. They decided to irradiate various metals with alpha particles of different energies to see if the result would be the production of a predominance of neutrons or positrons. It was already known that neutrons would result from the irradiation of beryllium metal with alpha particles according to the following transformation:

$$^{9}_{4}\mathrm{Be} + {}^{4}_{2}\mathrm{He} \rightarrow {}^{12}_{6}\mathrm{C} + {}^{1}_{0}\mathrm{n} \qquad \text{[II.4]}$$

They irradiated aluminum foil with alpha particles from a polonium source. The energy of the alpha particles colliding with the aluminum could be controlled by placing the polonium at various distances from the aluminum. The irradiation of aluminum foil by the polonium alpha particles produced neutrons and positrons. When the polonium source was moved

away from the aluminum to a distance beyond the reach of the alpha particles (the alpha particles from polonium-216 have an energy of 6.78 MeV, and these cannot travel beyond 5.3 cm in dry air as calculated according to Eq. [3.14] of the chapter entitled "Alpha Radiation"), the neutron emission from the alpha-irradiated aluminum would cease; however, to their amazement, the Joliot-Curies discovered that the positron emission would continue. They measured the positron emission with a Geiger counter and found that the number of positrons emitted would diminish with time with an average lifetime of less than 5 min. The interaction of the alpha particles with the aluminum foil produced a new radioactive isotope, yet unknown to mankind.

The Joliot-Curies were able to demonstrate that the new isotope was radioactive phosphorus using the following tests and reasoning:

1. By balancing the transformation of the nuclear reaction between alpha particles and aluminum yielding neutrons, they could write the reaction:

$$^{27}_{13}\mathrm{Al} + ^{4}_{2}\mathrm{He} = ^{30}_{15}\mathrm{P} + ^{1}_{0}\mathrm{n} \qquad \text{[II.5]}$$

   The Joliot-Curies used the equals sign rather than an arrow for the above reaction to demonstrate that the sum of the mass numbers and atomic numbers on one side of the equation should equal those on the other side, ie, $27 + 4 = 30 + 1$ for the mass numbers and $13 + 2 = 15 + 0$ for the atomic numbers. Expressing nuclear reactions was not a practice at that time. The Joliot-Curies were one of the first to introduce the practice.
2. The Joliot-Curies took a piece of aluminum foil that had been irradiated with alpha particles and placed it into a test tube containing hydrochloric acid. The aluminum would react to produce hydrogen gas as expected according to the reaction:

$$2\ \mathrm{Al} + 6\ \mathrm{HCl} \rightarrow 2\ \mathrm{AlCl_3} + 3\ \mathrm{H_2}\uparrow \qquad \text{[II.6]}$$

   They collected the hydrogen gas in an inverted test tube, as illustrated in Fig. II.9. The new radioactive substance emitting positrons was carried over with the hydrogen gas into the test tube as illustrated in the figure.
3. Finally by taking another piece of aluminum foil, which had previously been irradiated with alpha particles, and dissolving this metal in a mixture of acid and chemical oxidant to which was added a small quantity of sodium phosphate and a zirconium salt, the Joliot-Curies found that the zirconium phosphate formed and its precipitates carried with it the new radioactive substance.

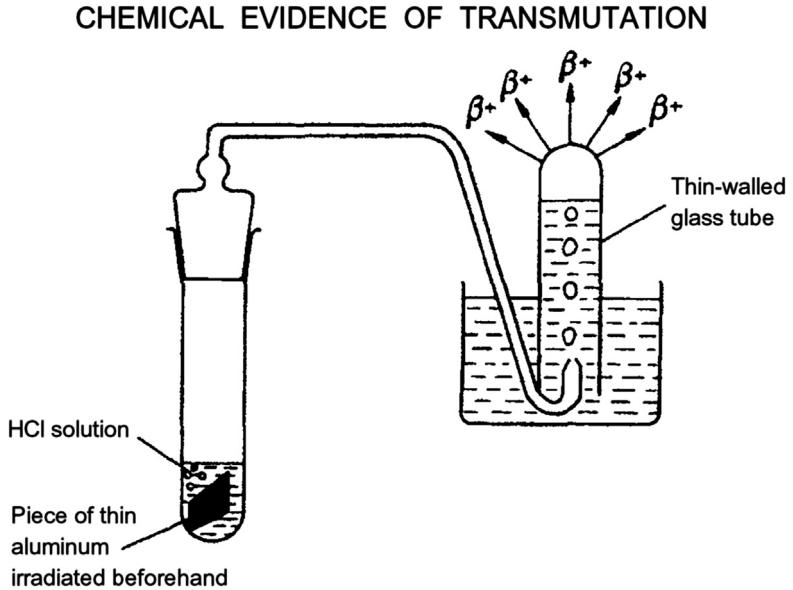

FIGURE II.9 Acid treatment of aluminum foil irradiated with alpha particles. *From Joliot, F., Joliot-Curie, I. 1935. Chemical evidence of the transmutation of elements. Nobel Lecture on December 12, 1935. In: Nobel Foundation Staff (Eds.), Nobel Prize Lectures in Chemistry, 1901–1970 (1967), vol. 1, 1901–1921, vol. 2, 1922–1941, vol. 3, 1942–1962. Elsevier Science, Amsterdam, with permission © The Nobel Foundation 1935.*

From the above tests, the Joliot-Curies could conclude that the new radioactive isotope was that of phosphorus, which emits positrons. The new radioisotope, phosphorus-30, decays to stable silicon-30 with positron emission and a short half-life of 2.5 min according to the following:

$$^{30}_{15}\mathrm{P} \rightarrow {}^{30}_{14}\mathrm{Si} + \beta^{+} \qquad \text{[II.7]}$$

Thus, the Joliot-Curies not only produced a previously nonexistent radioisotope, but they were the first to produce positrons in the laboratory.

By irradiating other metals, such as boron and magnesium, with alpha particles, the Joliot-Curies were able to produce radioactive nitrogen and radioactive silicon according to the following reactions (Joliot-Curie and Joliot, 1934a,b,c):

$$^{10}_{5}\mathrm{B} + {}^{4}_{2}\mathrm{He} \rightarrow {}^{13}_{7}\mathrm{N} + {}^{1}_{0}\mathrm{n} \qquad \text{[II.8]}$$

$$^{24}_{12}\mathrm{Mg} + {}^{4}_{2}\mathrm{He} \rightarrow {}^{27}_{14}\mathrm{Si} + {}^{1}_{0}\mathrm{n} \qquad \text{[II.9]}$$

The radioisotopes of nitrogen and silicon above decay by positron emission.

The Joliot-Curies were awarded the Nobel Prize in Chemistry the very year following the report of these discoveries. The rapid award of the Nobel Prize underscored the impact that this discovery had on the scientific community and the advancement of science. Their work established firmly a new branch of chemistry called "radiochemistry." As explained by Frédéric Joliot in his part of the Nobel lecture:

> *The succession of radioactive transformations provides numerous examples in which the quantities of radio-elements are extremely small and not capable of being weighed, yet nevertheless, by the methods of radiochemistry it has been possible to examine correctly their chemical properties, and identify some of them as being isotopes of elements…This special kind of chemistry in which one handles unweighable quantities, sometimes of the order of 10^{-16} g, is made possible thanks to the fact that one can determine and follow by measuring the radiation emitted, infinitesimal traces of radioactive matter dispersed in the midst of other matter.*

While this work established firmly "radiochemistry" as a new branch of chemistry, the Joliot-Curies were the first to coin the terminology, which we are very accustomed to, when referring to radioactive elements. In their Nobel lecture, Frédéric Joliot stated:

> *We have proposed that these new radio-elements (isotopes, not found in nature, of known elements) be called radio-nitrogen (for radioactive isotopes of nitrogen), radio-phosphorus (for radioactive isotopes of phosphorus)….*

At the time of this great discovery, Irene's mother, Marie Curie, was ailing from leukemia after many years of extensive overexposure to radiation and would not live to the see her daughter and son-in-law receive the Nobel Prize. This would be the second Nobel Prize to be granted a woman and the daughter whom she and her late husband Pierre had helped form into a pioneering scientist. Nevertheless, the Joliot-Curies related the satisfaction that the ailing Marie Curie got from knowing of this great discovery. This was conveyed in Frédéric's words taken from a historical account by Rhodes (1986):

> *Marie Curie saw our research work and I will never forget the expression of intense joy which came over her when Irène and I showed her the first artificially radioactive element in a little glass tube. I can still see her taking in her fingers (which were already burnt with radium) this little tube containing the radioactive compound…To verify what we had told her she held it near a Geiger-Müller counter and she could hear the rate meter giving off a great many "clicks". This was doubtless the last great satisfaction of her life.*

When reporting their discovery, the Joliot-Curies suggested that possibly more artificial radioisotopes might be produced by collisions of other particles with atomic nuclei, particles such as protons, neutrons, deuterons, etc. It didn't take long for this to happen. Many researchers all over the world started to make radioisotopes. In just two years' time since the discovery of the first artificial transmutation, Frédéric Joliot related in his Nobel lecture (Nobel Lectures, Chemistry, 1922−1941):

> *In England and the United States, where physicists have at their disposal equipment of very high voltages, several new elements were prepared using protons and deuterons as projectiles. In Italy first, and then in other countries, research workers, in particular, Fermi and his co-workers, used neutrons, projectiles which are outstandingly suitable to cause transmutations…among which were radio-phosphorus (^{32}P), and more than fifty new radio-elements…It was indeed a great source of satisfaction for our lamented teacher Marie Curie to have witnessed this lengthening of the list of radioelements, which she had had the glory, in company with Pierre Curie, of beginning.*

After receiving the Nobel Prize, Irène Joliot-Curie together with Paul Savitch continued research into the formation of radioelements, this time by irradiation of uranium and thorium with neutrons. They came close to discovering the phenomena of nuclear fission (Joliot-Curie and Savitch, 1938a,b, 1939); but the discovery of fission was reported by Otto Hahn and Fritz Strassmann (1939b) and explained by Lise Meitner and Otto Frisch (1939). Their contributions to advances in nuclear fission and its eventual application to nuclear power for electricity were commemorated in the above postage stamp from France illustrated at the beginning of this biographical sketch. The postage stamp illustrates, in the foreground superimposed with the busts of the Joliot-Curies, an artistic depiction of a nucleus, followed by the liquid-drop effect after it absorbs a neutron, and its fission into two smaller nuclides. The chain reaction of subsequent fission reactions caused by the emission of more than one neutron on the average per fission is illustrated in the left-hand portion of the stamp.

The synthesis of new manmade radioisotopes by the Joliot-Curies had a tremendous impact on advances in the biological and medical sciences. Following their discoveries, scientists in many parts of the world began to artificially make many more new radioactive isotopes that could be used as tracers in research. Most of the biological transformations, including catabolic and anabolic transformations in living systems that we understand today, are due to research using artificially made radioisotopes such as ^{3}H, ^{14}C, ^{32}P, ^{35}S, etc. Medical applications of manmade radioisotopes that have resulted include techniques such as radiotherapy with radioactive sources, computed tomography, positron emission tomography, and the use of radiopharmaceuticals for the diagnosis and treatment of cancer. The stamp illustrated here from Mauritania commemorates the significance of the Joliot-Curie discovery of manmade radioisotopes, as countless lives have been saved by the applications of radiopharmaceuticals in the treatment of cancer. The stamp from Mauritania illustrates a pharmaceutical containing a short-lived radioisotope which, when administered to a cancer patient, will travel and concentrate directly at the location of a particular tumor and provide data for the imaging, diagnosis, and treatment of cancer before the radioactivity dissipates to a level harmless to the patient.

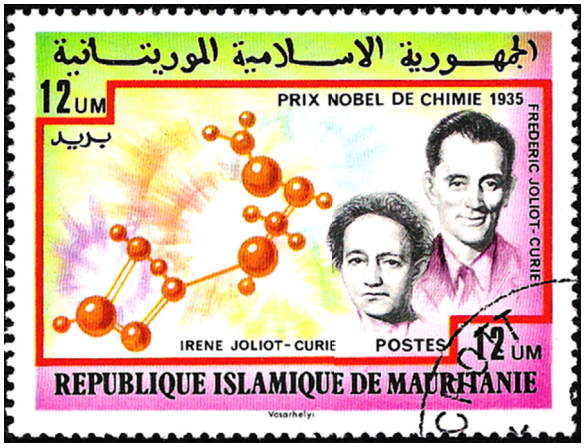

Frédéric and Irène Joliet-Curie

Frédéric Joliot was admitted to the French Academy of Science; however, Irène Joliot-Curie was not admitted. Like her mother, women were not yet granted that privilege. She was, however, appointed to Undersecretary of State for Scientific Research, and her husband to the first High Commissioner for Atomic Energy in France. They both passed away before reaching the age of 60. Two years before Frédéric's demise, Irène died in 1956 of leukemia, a disease she may have contracted like her mother from overexposure to radioactivity from childhood to her pioneering years of research.

ENRICO FERMI (1901–1954)

Enrico Fermi was born in Rome, Italy on September 29, 1901. He received the Nobel Prize in Physics in 1938 "for his demonstrations of the existence of new radioactive elements [radioisotopes] produced by neutron radiation, and for his related discovery of nuclear reactions brought about by slow neutrons."

Fermi had a natural aptitude for physics and mathematics. According to historical accounts by Rhodes (1986, 1999), Enrico Fermi discovered physics at the age of 14 after he encountered two old volumes on elementary physics in the book stacks of Rome's Campo dei Fiori. He read these books thoroughly with such intense interest, sometimes correcting the mathematics, that he had not even noticed that the books were written in Latin. He earned his doctorate degree in physics at the University of Pisa at 21 years of age. After short fellowships in Göttingen and Leyden, Fermi became lecturer in

physics at the University of Florence from 1924 to 1926. In 1927 he was elected professor of theoretical physics at the University of Rome, the youngest scientist to be elected professor since Galileo. Fermi retained this post until he was awarded the Nobel Prize in 1938; an opportunity he took to escape from Mussolini's fascist regime and emigrate with his family to the United States.

Enrico Fermi (1901-1954)

Enrico Fermi is well known for his elaboration in 1934 of the beta-decay process of radioisotopes, often referred to as "Fermi beta decay." The mystery was how beta particles, which are equivalent to electrons, could originate and be expelled from an atomic nucleus. Fermi proposed that within the nucleus of a radioactive atom, the neutron may decay to a proton and vice versa, a proton into a neutron. He proposed the existence of a weak interaction as a new force within the nucleus, which permits a neutron to decay into a proton and a negatively charged electron ($n \rightarrow p^+ + e^-$), or vice versa, a proton could decay into a neutron and a positively charged electron ($p^+ \rightarrow n + e^+$). The weak interaction would allow a nucleon (proton or neutron) to transform itself into the other to achieve nuclear stability. This force would be weaker than the strong nuclear force or strong interaction that binds the nucleons together in the nucleus. The weak interaction proposed by Fermi has advanced into a unified electroweak theory (Nobel Prize in Physics, 1979, awarded to Sheldon L. Glashow, Abdus Salam, and Steven Weinberg "for their contributions to the theory of unified weak and electromagnetic interaction between elementary particles"), as it has subsequently been discovered that the weak interactions and electromagnetic interactions are of similar strengths at short distances typical of nucleons (10^{-18} m). These two forces can this be combined into what is called the electroweak force.

The beta-decay theory of Fermi explains the origins for either a negative beta particle or positive beta particle from a decaying nucleus. However, an additional mystery to beta-particle radiation was the broad range of energies that a beta particle could possess, from near zero to a maximum energy, when it is emitted from a radioactive atom. When an unstable nucleus emits radiation, it decays from a higher energy state to a nucleus with a lower energy state, and the energy difference in these two states should exactly correspond to the sum of the energies of the radiations emitted by the decaying nucleus. This could easily be observed when alpha particles or gamma radiation were emitted from nuclides with discrete energies that corresponded to the energy transitions of the parent and daughter nuclides. The emission of a beta particle from a nucleus that could possess any energy between zero and a maximum value would appear to contradict the laws of conservation of energy, except that Wolfgang Pauli had proposed in 1930 the existence of a neutral particle of near-zero rest mass that would share the decay energy with the beta particle. Pauli called this particle the "neutron," as this was prior to the time when the neutron was discovered (Chadwick, 1932a,b) and prior to Fermi's beta-decay theory (1934). Fermi coined Pauli's neutral particle as the "neutrino," from the Italian meaning "little neutral one." The Fermi beta-decay including the accompanying neutrino (ν) can be written as follows:

$$n \rightarrow p^+ + \beta^- + \overline{\nu} \qquad \text{[II.10]}$$

$$p^+ \rightarrow n + \beta^+ + \nu \qquad \text{[II.11]}$$

When the neutron transforms itself into a proton in a decaying nucleus, a negative beta particle (negatron) would be ejected from the nucleus together with an antineutrino. The opposite would occur when a proton transforms itself into a neutron in a decaying nucleus, that is, a positive beta particle (positron) would be ejected from the decaying nucleus together with a neutrino. As the two transformations involve the inverse or opposite of the other, the beta particle and neutrino emitted in one of the decay processes are the antiparticles of the beta and neutrino radiations emitted in the other decay process. Also, a decay process that involves the emission of a negative beta particle would result in a daughter nucleus with one unit higher in atomic number (an additional proton in the nucleus), whereas nuclear decay with the emission of a positive beta particle would produce a daughter nucleus one unit lower in atomic number (one less proton in the nucleus). Examples of the nuclear transitions that occur in negative beta decay and positive beta decay are illustrated in Figs. II.10 and II.11.

Example: decay of carbon-14:

$$^{14}_{6}\mathrm{C} \rightarrow {}^{14}_{7}\mathrm{N} + \beta^{-} + \overline{\nu} + 0.156\ \mathrm{MeV} \qquad \text{[II.12]}$$

Example: decay of nitrogen-13:

$$^{13}_{7}\mathrm{N} \rightarrow {}^{13}_{6}\mathrm{C} + \beta^{+} + \nu + 1.190\ \mathrm{MeV} \qquad \text{[II.13]}$$

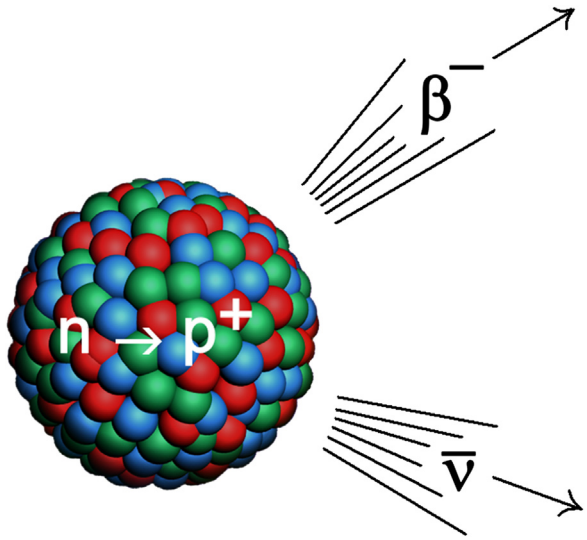

FIGURE II.10 Negative beta decay. A neutron transforms itself into a proton in the nucleus with the production and emission of a negative beta particle (negatron) and antineutrino from the nucleus. The energy of decay is carried off by the negatron and antineutrino.

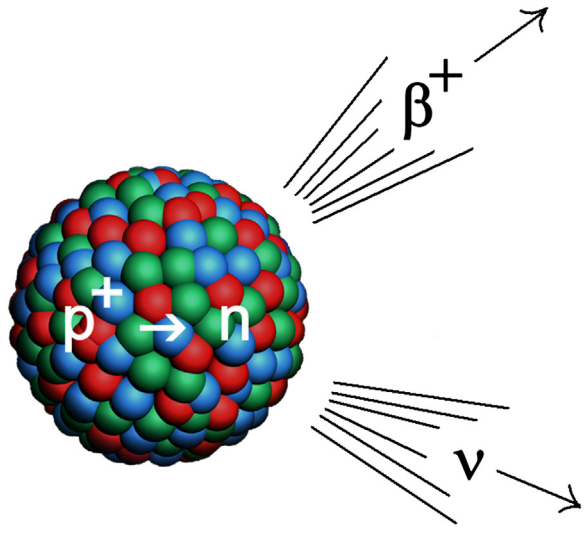

FIGURE II.11 Positive beta particle decay. A proton transforms itself into a neutron in the nucleus with the production and emission of a positive beta particle (positron) and neutrino. The energy of decay is carried off by the positron and neutrino.

Fermi's original manuscript on the transformations of nucleons within the nucleus was rejected by the editors of the journal *Nature* because of its theoretical nature, and therefore his first reports on the beta-decay theory were published in the Italian and German languages (Fermi, 1934a,b). Evidence for these transformations was provided years later by Snell and Miller (1948), who demonstrated that the neutron, when outside the confines of a stable nucleus, would decay to a proton and an electron with a lifetime of 15 min (see the chapter: "Neutron Radiation") according to the scheme:

$$n \rightarrow p^{+} + e^{-} + \overline{\nu} + 0.782\ \text{MeV} \qquad \text{[II.14]}$$

Although Fermi is well remembered for his beta-decay theory, the Nobel Prize was awarded him in 1938 for his contribution to the application of neutron radiation to the production of many new radioactive isotopes and to his discovery that certain nuclear reactions are brought about by slow neutrons. In his Nobel lecture (December 12, 1938), Fermi acknowledged that Rutherford was the first to start the technique of nuclear bombardments using high-energy alpha particles to enable the transmutation of one element into another in 1919 (see Rutherford, Hall of Fame, Part I). Fermi further noted that immediately after the discoveries of the artificial production of radioactive elements (radioisotopes) by the Joliot-Curies in 1934 by alpha−particle-induced nuclear reactions, he thought that alpha particles might not be the only type of bombarding projectiles that could produce artificial radioactivity, particularly for atoms with an atomic number greater than 20, and began then to investigate the effects of bombarding various elements with neutrons.

Fermi observed that neutrons having no electric charge should be able to reach the nuclei of all atoms without having to overcome the Coulombic barrier of the surrounding negatively charged atomic electrons or positively charged nucleus. He knew that the neutron would not be hindered by the atomic electrons, and that the probability of nuclear collisions by neutrons would be higher than that achievable with charged projectiles such as alpha particles or protons. As a source of neutrons he used a small glass bulb of beryllium powder together with 800 mCi of radon, which provided a source of neutrons with an emission rate of 2×10^{7} neutrons per second. The alpha particles from the radon interact with the beryllium nucleus to produce neutrons (see Eq. [10.19] of the chapter entitled "Neutron Radiation"). The initial results obtained by Fermi in early 1934 (Fermi, 1934c,d; Fermi et al., 1934) and his coworkers from 1934 to 1940, including H. Anderson, E. Amaldi, O. D'Agostino, F. Rasetti, E. Segré, and L. Szilard (Amaldi and Fermi, 1935, 1936a,b; Amaldi et al., 1937; Anderson et al., 1939a,b; Fermi and Amaldi, 1936, 1938; Fermi, 1940a,b; Fermi et al., 1934, 1938) yielded 63 artificial radioisotopes produced by the following three types of nuclear reactions using Fermi's original notation:

$$(1) \quad {}^{M}_{Z}A + {}^{1}_{0}n \rightarrow {}^{M-3}_{Z-2}A + {}^{4}_{2}He \qquad \text{[II.15]}$$

$$(2) \quad {}^{M}_{Z}A + {}^{1}_{0}n \rightarrow {}^{M}_{Z-1}A + {}^{1}_{1}H \qquad \text{[II.16]}$$

$$(3) \quad {}^{M}_{Z}A + {}^{1}_{0}n \rightarrow {}^{M+1}_{Z}A \qquad \text{[II.17]}$$

where ${}^{M}_{Z}A$ is a symbol for any element A with atomic number Z and mass number M, and n is the symbol for the neutron. Fermi found reactions (1) and (2) to occur chiefly among the light elements (there were 92 known elements at the time), and the reaction of type (3) were found to occur most often among the heavy elements. More than one of the above reactions would sometimes occur when elements were bombarded with neutrons. In Fermi's words at his Nobel lecture:

> *In many cases the three processes are found at the same time in a single element. For instance, neutron bombardment of aluminum that has a single isotope ^{27}Al, gives rise to three radioactive products: ^{24}Na, with a half-life of 15 hours by process (1); ^{27}Mg, with a period [half-life] of 10 minutes by process (2); and ^{28}Al with a period [half-life] of 2−3 minutes by process (3).*

In addition to the three neutron reactions described above by Fermi, he and his coworkers were also able to observe the production of artificial radioactive isotopes by a fourth process:

> *The primary neutron does not remain bound in the nucleus, but knocks off instead, one of the nuclear neutrons out of the nucleus; the result is a new nucleus, that is isotopic with the original one and has an atomic weight less by one unit.*

This fourth neutron interaction, where the mass number is reduced by one (loss of a neutron) and the atomic number remains unaltered, can be written as follows:

$$(4) \quad {}^{M}_{Z}A + {}^{1}_{0}n \rightarrow {}^{M-1}_{Z}A + {}^{1}_{0}n \qquad \text{[II.18]}$$

Only about 6 months after their first experiment with neutron bombardment, Fermi made a great discovery. He found that the neutron irradiation of elements became more effective in producing new radioisotopes when the neutrons were made to slow down, by allowing the neutron beam to pass through a given barrier of water or paraffin. By so doing, the fast

neutrons are slowed down to become thermal neutrons, or in other words, neutrons corresponding to thermal agitation. In his Nobel lecture, Fermi explained the properties of thermal neutrons:

> *After their energy is reduced to a value corresponding to thermal agitation, the neutrons go on diffusing without further change of their average energy. All of the processes of capture of slow neutrons by any nucleus are generally accompanied by the emission of gamma rays: Immediately after the capture of the neutron, the nucleus remains in a state of high excitation and emits one or more gamma-quanta, before reaching the ground state.*

The idea of slowing down neutrons to improve the efficiency of neutron capture was contrary to what one would believe at that time, because previously only charged particles were used to bombard atomic nuclei and the higher the speed of the charged particle, the greater the probability of penetrating the Coulombic barrier of the atoms to yield a reaction. Because neutrons have no difficulty diffusing into close proximity of atomic nuclei, Fermi and his coworkers were able to produce more than 400 new radioisotopes using slow neutron bombardment of all known elements with the exception of hydrogen and helium.

Fermi also discovered a neutron capture anomaly whereby the strongest capture of a neutron by a nucleus could occur at a precise speed, referred to as a resonance effect. He noted that "elevated neutron absorption by nuclei at precise neutron speeds was explained by Bohr, Breit, and Wigner as due to resonance with a virtual energy level of the compound nucleus (ie, the nucleus composed of the bombarded nucleus and the neutron)." Resonance effects are illustrated in Fig. 10.12 of the chapter entitled "Neutron Radiation."

Upon receiving the Nobel Prize in 1938, Enrico Fermi immigrated with his family to the United States, and he was appointed professor of physics at Columbia University in 1939, a post which he held until 1942. His work up to 1938 on neutron reactions was the final precursor needed for the discovery of nuclear fission by Otto Hahn and Fritz Strassmann in 1939 and Fermi's next great achievement, the construction of the first nuclear reactor.

Enrico Fermi collaborated with Leo Szilard in the construction of the first nuclear reactor. Leo Szilard was a renowned theoretical physicist and lifelong friend of Albert Einstein (see Hall of Fame, Part IV). Fermi's great knowledge of neutron physics, and Szilard's determination to beat Germany at the production of the atomic bomb was an excellent combination for the successful working reactor. In the words of Richard Rhodes (1999):

> *In 1939, still official enemy aliens, Fermi and Szilard co-invented the nuclear reactor at Columbia University, sketching out a three-dimensional lattice of uranium slugs dropped into holes in black, greasy blocks of graphite moderator, with sliding neutron-absorbing cadmium control rods to regulate the chain reaction.*

As soon as it became known that neutron-induced fission of uranium-235 would yield more than one neutron per fission (2.4 neutrons on the average for ^{235}U fission, and a high amount of energy, $\sim$194 MeV) Fermi, Szilard, and others knew that a fission chain reaction would be possible, which would release large amounts of energy. The reactor they built was given the name of an "atomic pile," coined by Fermi, because their unique apparatus had the appearance of a pile of uranium fuel, graphite moderator, and cadmium control elements. Fermi knew from his previous work with neutrons that cadmium has a very high efficiency for absorbing slow (thermal) neutrons and should serve to control the chain reaction, since fission in ^{235}U is optimal at thermal incident neutron energies. They assembled the pile in such a way that neutrons would be produced with the correct energy needed to create fission in the uranium, whereby the splitting of uranium nuclei would create additional neutrons and keep the chain reaction going to produce energy with the application of cadmium rods to control the reaction. The reactor "pile" was assembled by Fermi and his team on a squash court under the stands of the University of Chicago's Stagg (football) Field in late 1942. On December 2, 1942, under the direction of Enrico Fermi, the reactor went critical, that is, the chain reaction was sustained with the production of a neutron for every neutron absorbed by the uranium nucleus. Fermi allowed the reactor to continue as a carefully controlled chain reaction for 4.5 min at one-half watt of power. A plaque at the site of the first "atomic pile" commemorates this historic event with the words "On December 2, 1942, man achieved here the first self-sustaining chain reaction and thereby initiated the controlled release of nuclear energy." Two years later, Fermi and Szilard filed for a joint patent on the detailed construction and operation of a nuclear reactor, which was maintained secret and the patent finally released in 1955 (see the biographical sketch on Leo Szilard in Hall of Fame, Part IV). Four years after the successful construction of the reactor "pile" and the sustained nuclear chain reaction at the University of Chicago, alumni of the Metallurgical Laboratory (Met Lab), which was part of the Manhattan Project to develop the atomic bomb, reunited with Enrico Fermi on December 2, 1946. Their group photo is provided in Fig. II.12.

The first nuclear reactor was a giant step for mankind, as it has had since Fermi's "atomic pile" and continues to have a vital role in development for peaceful applications, including (1) the production of isotopes for medical, biological, and other vital sciences; (2) the production of heat that can drive steam turbines and generate enormous amounts of electricity;

FIGURE II.12 Alumni of the Metallurgical Laboratory (Met Lab) pose on the steps of Eckhart Hall on the campus of the University of Chicago on December 2, 1946 (the fourth anniversary of Chicago Pile 1 first going critical). Front row, left to right: Enrico Fermi, Walter Zinn, Albert Wattenberg, and Herbert Anderson. Middle row, left to right: Harold Agnew, William Sturm, Harold Lichtenberger, Leona W. Marshall, and Leo Szilard. Back row, left to right: Norman Hilberry, Samuel Allison, Thomas Brill, Robert Nobles, Warren Nyer, and Marvin Wilkening. *Digital Photo Archive, Department of Energy, courtesy AIP Emilio Segre Visual Archives.*

and (3) the production of neutrons for research. A fourth ominous application of the nuclear reactor is, of course, for the production of plutonium (see the chapter: "Neutron Radiation") for nuclear weapons. The peaceful applications of nuclear power have an enormous impact on our daily lives. This is underscored in chapter "Radioactivity and Our Well Being" of this book and in an article by ElBaradei (2004), where he notes:

> *At the end of last year there were 440 nuclear power units operating worldwide. Together, they supply about 16% of the world's electricity. That percentage has remained relatively steady for almost 20 years—meaning that nuclear electricity generation has grown at essentially the same rate as total electricity use worldwide.*

After overseeing the assembly and operation of the first self-sustaining nuclear chain reaction, Fermi joined a group of eminent physicists and chemists in the Manhattan Project at Los Alamos, New Mexico, which was established in mid-1943 under the direction of J. Robert Openheimer, as part of America's efforts during the Second World War. Fermi played a vital role in this project. In an address marking the centennial celebration of the birth of Enrico Fermi on November 27, 2001, Dr. John H. Marburger III, the Science Advisor to the President of the United States, noted that in the preparations for testing the bomb, Fermi's help was invaluable, and quoted Emilio Segré (Fermi's lifelong friend and collaborator, and a Nobel Laureate in Physics in 1959), as follows:

> *This was one of those occasions when Fermi's dominion over all physics, one of his most startling characteristics, came into its own. The problems involved in the Trinity test ranged from hydrodynamics to nuclear physics, from optics to thermodynamics, from geophysics to nuclear chemistry. Often they were closely interrelated, and to solve one it was necessary to understand all the others. Even though the purpose was grim and terrifying, it was one of the greatest physics experiments of all time. Fermi completely immersed himself in the task. At the time of the test he was one of the very few persons (or perhaps the only one) who understood all the technical ramifications of the activities at Alamogordo.*

Enrico Fermi became an American citizen in 1944 and held the position of professor at the University of Chicago's Institute for Nuclear Studies from 1946 until his untimely death in 1954 from stomach cancer. During his last years at the

University of Chicago, he concentrated his efforts on high-energy physics and the origins of cosmic radiation, which still remains the source of high-speed particles with energies not yet achieved by any manmade accelerator.

WOLFGANG PAULI (1900–1958)

Wolfgang Pauli was born in Vienna on April 25, 1900. He received the Nobel Prize in Physics in 1945 for "his discovery of the Exclusion Principle also called the Pauli Principle." Also Pauli made a major contribution to the understanding of beta-particle emissions from radioactive atoms by proposing the existence of the neutrino, a particle of zero charge and near zero rest mass that is emitted from the nucleus during beta decay.

Wolfgang Pauli graduated in 1918 from the Döblinger Gymnasium in Vienna after comprehensive studies in the fields of physics and mathematics. Pauli was a gifted and ambitious student, often preferring to study Einstein's works on relativity during his classes at the Döblinger Gymnasium, which he sometimes considered boring. Having graduated with distinction, Pauli became a pupil of Arnold Sommerfeld at the Ludwig-Maximilian University of Munich, where he received his doctorate degree in 1921. During his budding years as a student at the University of Munich, Pauli wrote a most comprehensive and knowledgeable book on Einstein's theory of relativity, which illustrated in Einstein's words Pauli's "sureness of mathematical deduction and profound insight." Einstein recognized the genius in Pauli and considered Pauli his intellectual successor, and it was Einstein who, later in life, would nominate Pauli for the Nobel Prize. Pauli continued to study with great physicists of the time, including a year with Max Born at the University of Göttingen followed by a year with Niels Bohr at the University of Copenhagen. After a few years as lecturer at the University of Hamburg (1923–1928), Pauli was appointed professor of theoretical physics at the Swiss Federal Institute of Technology in Zurich (Eidgenössische Technische Hochschule, or ETH, Zurich). The German annexation of Austria in 1938 placed a threatening cloud over Pauli. He was partly of Jewish decent, and the possibility of German occupation of Switzerland forced him to flee. He was invited to the United States in 1939 by Albert Einstein as visiting professor of the Institute of Advanced Studies at Princeton University, and elected as chair of theoretical physics at Princeton in 1940.

Wolfgang Pauli (1900-1958)

Wolfgang Puali was awarded the Nobel Prize in Physics in 1946 for his discovery of the Exclusion Principle proposed in 1925, which states that no two electrons in an atom could possess the same quantum numbers, that is, no two electrons in an atom could exist at the same quantum or energy state. In his Nobel lecture (December 13, 1946), Pauli explained that he began to formulate his thoughts on the Exclusion Principle after listening to a series of lectures given by Niels Bohr in 1922 at the University of Göttingen, where he explained:

> *…the spherically symmetric atomic model, the formation of the intermediate shells of the atom and the general properties of the rare earths. The question, as to why all electrons for an atom in its ground state were not bound in the innermost shell, had been emphasized by Bohr as a fundamental problem….*

Pauli's Exclusion Principle solved the problem by providing "a general explanation for the closing of every electron shell [of an atom]" (Nobel Lectures, Physics, 1942−1962). The Pauli Exclusion Principle can be visualized by first considering the definition of the four quantum numbers. Three quantum numbers originate from the space geometry of the electron, while the fourth arises from the electron spin, and these are defined as follows:

1. **Principal quantum number**, assigned values of $n = 1, 2, 3\ldots$, correspond to the principal energy level of the electron. For example, $n = 1$ for a K electron (an electron in the innermost K shell or lowest energy level), $n = 2$ for an L electron, $n = 3$ for an M electron, $n = 4$ for an N electron, etc.
2. **Orbital quantum number**, assigned values of $\ell = 0, 1, 2, 3\ldots n - 1$, correspond to values of the angular momentum of the electron.
3. **Magnetic quantum number**, assigned values of whole numbers from $m_\ell = -\ell$ to $+\ell$, correspond to the possible properties of an electron in a magnetic field. For example, when $\ell = 2$, m_ℓ can have values of -2, -1, 0, $+1$, and $+2$.
4. **Spin quantum number**, $m_s = +½$ or $-½$, corresponds to the two possible spin vectors or orientations of an electron in a magnetic field with spin vectors classified as spin up (+ or ↑) and spin down (− or ↓).

An example can be taken by arbitrarily selecting an element and applying the rules of the Pauli Exclusion Principle to demonstrate how the principle can explain the intermediate and main electron energy levels of an atom. For example, zinc has an atomic number of 30 (ie, 30 protons), and its 30 orbital electrons may possess the quantum numbers listed in Table II.1.

According to the Pauli Exclusion Principle, the maximum number of electrons allowable in the sublevels of the energy levels K, L, M, N, and O are illustrated below with increasing energy and distance from the nucleus. The letters s, p, d, *or* f are used to identify the number of electrons encountered in a sublevel (see Fig. II.13). The nomenclature used to specify the electron configurations of the elements depicts both the numbers of electrons in the main and sublevels, such as the following using the above case of zinc as an example: the electron configuration of zinc would be described as $1s^2$, $2s^2$, $2p^6$, $3s^2$, $3p^6$, $3d^{10}$, $4s^2$, which would read as $2s$ electrons in the first main level, $2s$ electrons in the second main level, $6p$ electrons in the second mail level, $2s$ electrons in the third main level, etc. To shorten the notations in the nomenclature, it is possible to add a configuration to the known configuration of another element such as one of the inert gases, such as He, Ne, Ar, or Kr. For example, the electron configuration for zinc may be simplified to Ar-$3d^{10}$, $4s^2$, because the configuration of the 18 electrons of argon is $1s^2$, $2s^2$, $2p^6$, $3s^2$, $3p^6$. There are some irregularities in the electron configurations of the elements, and the exact configurations are found in reference tables such as those provided by Weise and Martin (1989), Lide (1997, 2010). However, the Pauli Exclusion Principle is precise in that it excludes, without exception, the number of electrons from exceeding 2, 6, 10, and 14 in the s, p, d, and f sublevels; or 2, 8, 18, 32, and 32, in the K, L, M, N, and O main levels, respectively.

The Pauli Exclusion Principle applies to all fermions (odd half-integer spin particles, i.e., half an odd integer) in a given atom, which includes protons and neutrons in addition to the electrons. The principle solved the electronic structure of the atom, which was clearly emphasized in the following excerpt from an obituary that appeared in *The Times* of London on the eve of Pauli's death on December 15, 1958:

> *The quantum theory of the atoms accounts in some detail for many of the properties of the 100 or so chemical elements, and in this feat of generalization, Pauli's Exclusion Principle played a necessary part. Although the theory of the nucleus of the atom is in a less satisfactory state than that of the electronic or outer structure of the atom, it appears that in the nucleus too, Pauli's Exclusion Principle operates.*

It might be said that Wolfgang Pauli is equally famous for his bold hypothesis in 1930 for the existence of the neutrino as for his monumental Exclusion Principle for which he received the Nobel Prize. In 1930, physicists were perplexed over the fact that beta particles were emitted from radioactive atoms with a broad range of energies. That is, the energy of the beta particle could not be predicted on the basis of the radionuclide decay energy. The emissions of alpha particles and gamma rays from the nuclei of atoms could be easily explained. The energy of an alpha particle emitted from a given radionuclide always possessed a discrete energy, which represented the decay energy of the radionuclide less the recoil energy of the nucleus. Likewise gamma rays were of discrete energies representing the energy lost by the nucleus as it decayed from an excited to a more stable state. Beta-particle emission presented a totally different and perplexing picture. The energy of a beta particle could not be predicted on the basis of the decay energy of the radionuclide. For example, a radionuclide that decays by beta-particle emission, such as ^{32}P, has a decay energy of 1.7106 MeV, which is the energy lost by the radioactive ^{32}P when it decays by beta-particle emission to the stable nuclide ^{32}S. However, a beta particle emitted in the nuclear decay of ^{32}P would have an energy ranging from close to zero to a maximum energy close to the decay energy of the nucleus (see Fig. 6.1 of the chapter: "Beta Radiation and Beta Decay"). The law of energy conservation required that the energy of the radiation emitted from the radioactive atom should equal its decay energy.

TABLE II.1 Possible Quantum Numbers for Electrons in Atomic Orbitals for Zinc (Atomic Number 30) Starting with the Lowest *K* Energy Level

Main Quantum Level[a]	Quantum Number				Electrons in Sublevels or Subshells[f]	Orbital Type[g]	Electrons in Main Levels[h]
	Principal[b] n	Orbital[c] ℓ	Magnetic[d] m_ℓ	Spin[e] m_s			
K	$n = 1$	$\ell = 0$	$m_\ell = 0$	$m_s = +$ $m_s = -$	2	*s*	2
L	$n = 2$	$\ell = 0$	$m_\ell = 0$	$m_s = +$ $m_s = -$	2	*s*	
		$\ell = 1$	$m_\ell = -1$	$m_s = +$ $m_s = -$			
			$m_\ell = 0$	$m_s = +$ $m_s = -$			
			$m_\ell = +1$	$m_s = +$ $m_s = -$	6	*p*	8
M	$n = 3$	$\ell = 0$	$m_\ell = 0$	$m_s = +$ $m_s = -$	2	*s*	
		$\ell = 1$	$m_\ell = -1$	$m_s = +$ $m_s = -$			
			$m_\ell = 0$	$m_s = +$ $m_s = -$			
			$m_\ell = +1$	$m_s = +$ $m_s = -$	6	*p*	
		$\ell = 2$	$m_\ell = -2$	$m_s = +$ $m_s = -$			
			$m_\ell = -1$	$m_s = +$ $m_s = -$			
			$m_\ell = 0$	$m_s = +$ $m_s = -$			
			$m_\ell = +1$	$m_s = +$ $m_s = -$			
			$m_\ell = +2$	$m_s = +$ $m_s = -$	10	*d*	18
N	$n = 4$	$\ell = 0$	$m_\ell = 0$	$m_s = +$ $m_s = -$	2	*s*	2

[a] *The electron energy level* K *is the closest to the nucleus and contains no sublevel. Other levels, namely,* L, M, N, O, *etc., are of increasing energy and distance from the nucleus, and these contain sublevels.*
[b] *The principal quantum number are assigned values of* n = *1, 2, 3….*
[c] *The orbital quantum number is assigned values according to* $\ell = 0, 1, 2, 3 \ldots n - 1$.
[d] *The magnetic quantum number is assigned values in the range of* $m_\ell = -\ell$ *to* ℓ.
[e] *The spin quantum number can have only two possibilities,* +½ *or* −½. *The* + *or* − *signs are used to denote the possible spin orientations.*
[f] *The maximum number of electrons in the sublevel is* $2(2\ell + 1)$. *When a subshell is filled, any additional electrons that an atom would possess, must go into the next and higher-energy sublevel.*
[g] *The term "orbital" does not refer to fixed orbits or circular paths about the nucleus. Following the work of Schrödinger and others, a certain electron cannot be located at any fixed distance from the nucleus. The term "orbital" thus refers to a region in space about the nucleus where an electron has the highest probability of being found.*
[h] *The number of electrons in the main levels is the sum of the electrons in the sublevels.*

Some leading scientists, including Niels Bohr, postulated that possibly the laws of conservation of energy might have some restricted validity in certain circumstances, such as in beta decay. Pauli, however, concluded that there can never be any alternatives or limitations to the fundamental law of energy conservation. Therefore, in a bold move, he postulated the neutrino as a small neutral particle of zero charge and near zero mass that was simultaneously emitted from the nucleus together with the beta particle. The neutrino and beta particle would share the decay energy of the nucleus. While Pauli was

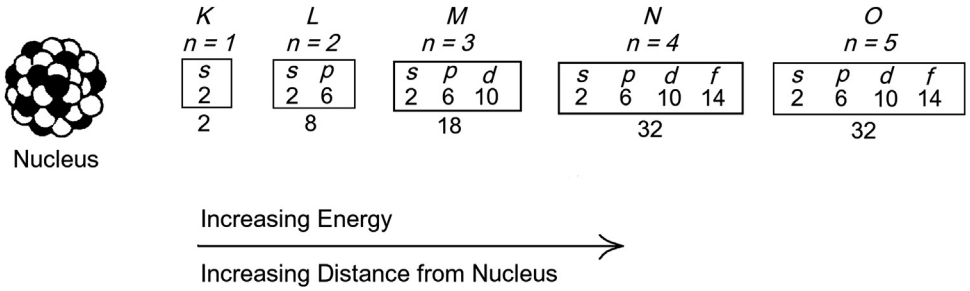

FIGURE II.13 Maximum number of electrons in the main levels (*K*, *L*, *M*, *N*, and *O*) and sublevels (*s*, *p*, *d*, and *f*) of electron energies of neutral atoms in the ground (unexcited) state.

convinced of his hypothesis, it would have been too bold to publish. He therefore, put his hypothesis in a letter addressed to the participants of a conference on radioactivity at Tübingen, Germany on December 4, 1930. The letter was addressed to all present "Liebe Radioactive Damen und Herren," and is translated as follows:

Open Letter to the Radioactivity Group
at the Regional Meeting at Tübingen

Zurich , 4 Dec. 1930
Gloriastrasse

From
Physics Institute of the Federal Institute of Technology (ETH)
Zurich

Dear Radioactive Ladies[1] and Gentleman,

I beg you to most favorably listen to the carrier of this letter. He will tell you that, in view of the wrong statistics of the N and the Li[6] nuclei and of the continuous beta spectrum, I have hit upon a desperate remedy to save the exchange theorem of statistics and the law of conservation of energy. This is the possibility that electrically neutral particles exist which I will call neutrons[2], which exist in nuclei, which have a spin ½ and obey the exclusion principle, and which differ from the photons also in that they do not move with the velocity of light. The mass of the neutrons [i.e., neutrinos][3] should be of the same order as those of the electrons and should in no case exceed 0.01 proton masses. The continuous beta spectrum would then be understandable if one assumes that during beta decay with each electron a neutron [i.e., neutrino][3] is emitted in such a way that the sum of the energies of neutron [i.e., neutrino][3] and electron [i.e., beta-particle][4] is constant.

I admit that my remedy may seem incredible, because one should have seen these neutrons [i.e., neutrinos][3] long ago, if they really exist.[5] But only he who dares can win and the difficult situation caused by the continuous beta spectrum is illuminated by a remark of my honored predecessor, Mr. Debye, who told me recently in Brussels: Oh, it is best not to think at all, just as with the new taxes. Henceforth every possible solution must be discussed. So, dear radioactive people, because I am indispensable here due to a ball[6] which will take place in Zurich during the night from December 6 to 7. With my best regards to you and also to Mr. Back.

Your humble servant,
W. Pauli

1. A lady at this meeting was Lise Meitner, a key figure later in the discovery of nuclear fission.
2. Pauli called this particle the neutron in this letter; however, Enrico Fermi, changed the name of this neutral particle of near-zero mass to the "neutrino" from the Italian meaning "little neutral one". The neutron, a particle of relatively high mass and neutral charge in the nucleus was discovered by Chadwick in 1932.
3. The actual name of neutrino, while not included in Pauli's letter, is included here for clarification with the reader as to the real particle referred to by Pauli.
4. Pauli used the word electron in his letter while referring to the beta particle, because the beta particle is an electron originating from the decay of the nucleus of the atom.
5. Pauli was being too courteous or playing up to his audience. It would really have been difficult or impossible to detect these particles during the time of Pauli's letter or earlier, because of the particle's neutral charge and near-zero rest mass. So difficult were the neutrinos to detect that it was not until over 25 years later (June 1956) did technology permit Frederick Reines and Clyde Cowan, Jr. to finally achieve the detection of the neutrino.
6. The writer believes that Pauli's reference to the ball in this letter was simply an excuse not to attend the conference; and that he preferred his letter be read to all that were present. In this way, he would not have to listen to any ridiculous objections to his proposal for the existence of the neutrino.

Pauli's hypothesis was taken by Enrico Fermi to elaborate the beta-decay process in 1934, when Fermi also adopted the name "neutrino" for this particle, since another particle of neutral charge and mass similar to the proton was discovered by Chadwick in 1932 and named the neutron. The beta-decay process and examples of how the beta particle and neutrino

share the nuclide decay energy is described in detail in this section in the biographical sketch of Enrico Fermi and in the chapter entitled "Beta Radiation and Beta Decay."

FREDERICK REINES (1918–1998) AND CLYDE L. COWAN, JR. (1919–1974)

Frederick Reines was awarded the Nobel Prize in Physics in 1995 "for the detection of the neutrino"; and it is said that Clyde Cowan would have shared that Nobel Prize for his collaboration with Frederick Reines, if the Nobel Prize were awarded posthumously. It was Wolfgang Pauli, who in 1930 first postulated the neutrino in a desperate attempt to explain the wide spectrum of beta-particle energies emitted from radioactive atoms and the need to postulate a neutral elusive particle of near-zero rest mass to conform to the laws of conservation of energy in radionuclide decay (see Wolfgang Pauli in this section). Not until 1956, some 26 years later, was the neutrino demonstrated to exist after the extraordinary scientific collaboration and determination of Frederick Reines and Clyde Cowan, Jr.

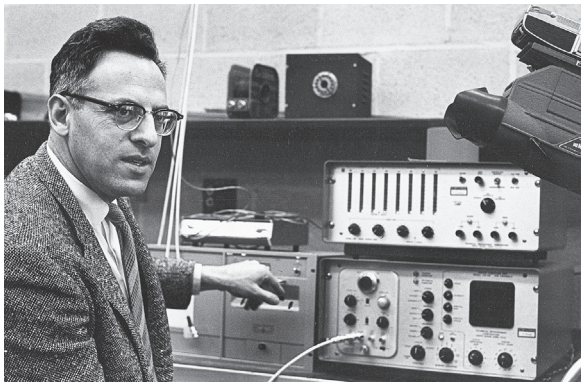

Frederick Reines (1918-1998)
With permission. Courtesy of AIP Emilio Segre Visual Archives.

Frederick Reines was born in Paterson, New Jersey on March 16, 1918 of Russian immigrant parents. During his first two years of high school, he was more interested in literature and did not excel in his science studies. However, during his junior and senior years, his science teacher at Union Hill High School, in Union City, New Jersey took an interest in young Frederick, and encouraged him to pursue science. By the time he graduated from high school, Frederick Reines was determined to be a pioneering physicist. Upon graduation, his ambition as noted in the high school yearbook was "to be a physicist extraordinaire." This is another example, as in the life of Ernest Rutherford (see Rutherford, in the chapter: "Alpha Radiation"), of how one teacher can have a pivotal influence on the life achievements of a student. Frederick Reines was also a gifted singer, and he was encouraged by others to pursue a career as a professional singer. So good was his talent that he was awarded cost-free coaching at the Metropolitan Opera. Nevertheless, he decided against a singing career. Frederick Reines' determination to become a "physicist extraordinaire" was set in stone.

After high school, Frederick Reines gained admission to the renowned Massachusetts Institute of Technology (MIT) and had promise of a scholarship. However, he selected the Stevens Institute of Technology because of the enthusiasm for Stevens displayed by an admissions officer in a chance encounter. At Stevens he received his undergraduate degree in Engineering in 1939 and a Master of Science degree in mathematical physics in 1941. While working on his PhD dissertation on "The Liquid Drop Model for Nuclear Fission," Frederick Reines was recruited in 1944 to work under Richard Feynman on the Manhattan Project at the Los Alamos National Laboratory. He found the Los Alamos to be the most stimulating environment for scientific advancement. In his own words, Frederick Reines noted that "During my participation in the Manhattan Project and subsequent research at Los Alamos, encompassing a period of 15 years, I worked in the company of perhaps the greatest collection of scientific talent the world has ever known" (Barany, 1999). It was at Los Alamos that Frederick Reines began a fruitful collaboration with Clyde Cowan that led to the detection of the neutrino.

Clyde L. Cowan, Jr. was born in Detroit, Michigan on December 6, 1919. He received a Bachelor of Science degree in 1940 at the Missouri School of Mines and Metallurgy, which is now part of the University of Missouri. He was awarded his Master of Science and PhD degrees in physics at Washington University, St. Louis in 1947 and 1949, respectively. During World War II, Cowan joined the U.S. Army and was a second lieutenant with the 51st Troop Carrier Wing. During

the war he was stationed in England and was assigned to work on the newly developed radar. He was awarded the Bronze Star for his significant contributions to the improvement of radar. In 1949, Cowan joined the scientific team at the Los Alamos National Laboratory, and in 1951 he became group leader of the Nuclear Weapons Test Division at Los Alamos.

Clyde Cowan, Jr. (1919-1974)
With permission, courtesy of the Smithsonian Institution Archives, Image # SIA Acc. 90-105 [SIA2008-0297], http://siarchives.si.edu/.

Frederick Reines and Clyde Cowan began their historic collaboration in 1951 at Los Alamos to detect the neutrino. Reines primarily wanted to do something big, deserving of a "physicist extraordinaire," and personally decided to accomplish the detection of the neutrino postulated by Pauli in 1930. He first consulted with Enrico Fermi in 1951 at Los Alamos about the idea. Reines decided that a nuclear weapon test would serve as the best source of neutrinos, because of the immense number of fissions that would occur and the concomitant numerous beta-particle emissions from fission products that would result. He decided that he would also need a very large detector, because of the elusive nature of the neutrino. Enrico Fermi agreed with Reines that a weapon test would be the best source of neutrinos, but that the design of a detector large enough and capable of detecting a neutrino interaction would be a tremendous hurdle. Later that year Reines proposed the idea to Clyde Cowan, who was a good experimentalist with a sense of daring, and they set out to solve this challenging problem even without having in mind the design of a detector.

During their initial assessment of the problem of the detection of the neutrino, Frederick Reines and Clyde Cowan first had to consider the following questions: (1) What features of the neutrino interaction would they use for signals? (2) How large a detector would be needed? (3) How many counts would they expect to obtain from neutrino interactions? To select a possible neutrino interaction that could provide a signal to a detector, they considered two processes of reverse beta decay that would be possible according to the Pauli-Fermi beta-decay theory. The two possible reverse beta-decay processes are the following:

$$(1) \quad \overline{\nu} + p^+ \rightarrow n + \beta^+ \ \text{ ie, } \ \overline{\nu} + {}^{A}_{Z}X \rightarrow {}^{A}_{Z-1}Y + \beta^+ \qquad \text{[II.19]}$$

where an antineutrino would interact with a proton to yield a neutron plus a positron (positive electron), that is, the anti-neutrino would cause a nuclide X of charge Z and mass number A to convert to a nuclide Y of charge $Z - 1$ with the emission of a positron; or:

$$(2) \quad \nu + n \rightarrow p^+ + \beta^- \ \text{ ie, } \ \nu + {}^{A}_{Z}X \rightarrow {}^{A}_{Z+1}Y + \beta^- \qquad \text{(II.20)}$$

where a neutrino would interact with a neutron of a nucleus to yield a proton and a negatron (negative electron). They selected the first possible neutrino interaction (Eq. [II.19]), because the positron produced by the first process could provide a signal from positron annihilation (ie, the emission of two gamma rays of 0.51 MeV in opposite directions). Liquid scintillation

detection, which uses organic fluor solutions, had been newly discovered by Kallman (1950) and Reynolds et al. (1950), and Reines and Cowan decided that a detector composed of liquid scintillation fluor surrounded by numerous photomultiplier tubes to convert light emissions into electrical pulse signals would serve their purpose. The largest detector ever manufactured at that time was only $\sim 1\ m^3$ in volume, which was thousands of orders of magnitude smaller than what would be needed to detect a neutrino interaction. A liquid detector provided the versatility of manufacturing a detector to almost any size and geometry.

Because of the neutral charge and near zero mass of the neutrino, they knew a very large detector would be required. Their initial estimations based on a neutrino of a few MeV in energy yielded a cross-section of $\sim 10^{-44}\ cm^2$, which represents a miniscule interaction probability proportional to a mean free path of ~ 1000 light years of liquid hydrogen. Such estimates made the idea of detecting a neutrino seem almost impossible, and the comments from some pioneering physicists were not encouraging. In his Nobel Laureate address, Frederick Reines noted that Wolfgang Pauli remarked during a visit to Caltech, "I have done a terrible thing. I have postulated a particle that cannot be detected." Also Hans Bethe and Rudolf Peierls (1934) wrote in the journal *Nature* "there is no practically possible way of observing the neutrino." In 1954, during Reines' search for the neutrino, he confronted Bethe concerning his pronouncement in the journal *Nature*, and Bethe replied in good humor, "Well, you shouldn't believe everything you read in the papers." A major obstacle that Reines and Cowan had to overcome was the general belief that the neutrino was undetectable. Also, there was no evidence of any kind that the neutrino existed. Nevertheless, the existence of the neutrino was generally accepted by the scientific community. The elusive and then theoretical particle provided the only explanation for the wide spectrum of energies encountered in beta decay.

Knowing the difficult task at hand, Reines and Cowan nevertheless forged ahead in their quest. They discarded their plans to use a nuclear weapons test as a source of neutrinos, and decided to make an initial test at one of the nuclear reactors of the Hanford Engineering Works in Hanford, Washington, which would serve as a suitable source of neutrinos, and where the detector could be adequately shielded to reduce gamma and neutron background radiation. They constructed a 300-L liquid scintillator surrounded by 90 photomultiplier tubes each 5 cm in diameter. The positron produced by the neutrino interaction (Eq. [II.19]) would excite the liquid scintillator, resulting in a flash of light that would be detected as a signal by the photomultiplier tubes. The neutron produced by the neutrino interaction with a water proton would produce a delayed gamma pulse as a result of neutron capture. To reduce backgrounds even further, they decided to count only the delayed coincidence between the positron and neutron capture pulse. After months of testing at the Hanford reactor (see Fig. II.14), results were inconclusive because of high backgrounds from reactor-independent signals arising from cosmic radiation.

In spite of the difficulties encountered, they continued to forge ahead with the design of a larger detector that would be yet more discriminating in its rejection of background, because of the very specific signals that would be used as the antineutrino signature. The newly designed detector would be taken to a new 700-MW nuclear reactor at the Savannah River Plant in Aiken, South Carolina. The modified detection scheme is illustrated in Fig. II.15, and a sketch of the new detector is provided in Fig. II.16. The target chamber would consist of 200 L of water containing 40 kg of dissolved $CdCl_2$ sandwiched between two tanks of 1400 L of liquid scintillator solution. Each end of the scintillator tanks was viewed by 55 photomultiplier tubes. The water would provide target protons for antineutrinos. As illustrated in Fig. II.15, the interaction of an antineutrino with a water proton would create a neutron (n) and a positron (β^+). The positron would be annihilated when coming to rest and in contact with an electron, and the resulting annihilation radiation (two 0.51-MeV gamma rays emitted in opposite directions) would be detected in coincidence by the two liquid scintillation detectors above and below the water tank. The neutron produced by the antineutrino interaction would slow down quickly ($\sim 10\ \mu s$) in the water and be captured by a cadmium nucleus in the water target chamber. The characteristic multiple gamma rays following the neutron capture would be detected in coincidence by the liquid scintillation detectors. The antineutrino signature would therefore consist of a delayed coincidence between the prompt pulses produced by the β^+ annihilation and the pulses produced microseconds later by the neutron capture in cadmium.

With the unique signature for the antineutrino provided by the detector design devised by Reines and Cowan, the high neutron flux produced by the Savannah River reactor ($1.2 \times 10^{13}/cm^2\ s$), and reduced cosmic ray backgrounds from massive shielding 11 m from the reactor and 12 m underground were essential to the success of their experiment. Nevertheless, a detector running time of 100 days over a period of about one year was required to provide sufficient conclusive signals from the antineutrino signature. Frederick Reines and Clyde Cowan, Jr. and their coworkers provided conclusive evidence for the antineutrino signature signals by demonstrating, among other evidence, the following: (1) the first signal pulse of the delayed coincidence pair (two gamma rays) was demonstrated to be due to the positron annihilation by varying the thickness of a lead sheet interposed between the water target and one of the liquid scintillators, thereby reducing the positron detection efficiency in one of the detector triads and not in the others; (2) the second signal pulse was shown to be due to a neutron by varying the cadmium concentration in the target water. Removal of the

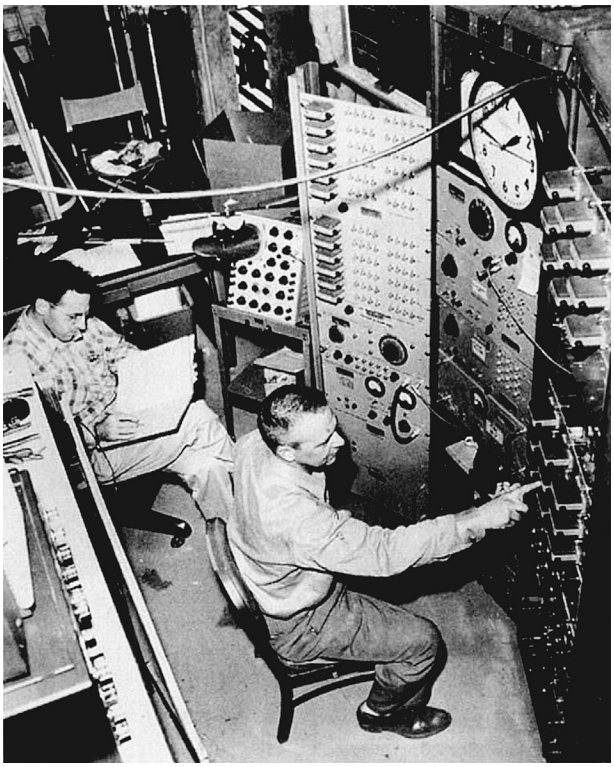

FIGURE II.14 Frederick Reines (left) and Clyde Cowan, Jr. (right) with some of the equipment used at the Hanford experiment. *From Reines, F., 1995. The neutrino: from poltergeist to particle. Nobel Lecture, December 8, 1995. In: Barany, A. (Ed.), The Nobel Prizes 1999 Les Prix Nobel: Nobel Prizes, Presentations, Biographies, and Lectures, Almquiest & Wiksell International, Stockholm. Nobel Lecture, with permission © The Nobel Foundation 1995.*

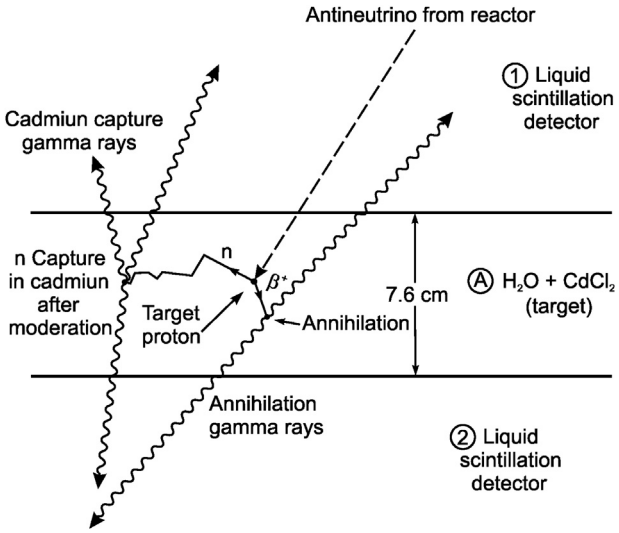

FIGURE II.15 Detection scheme used by Reines and Cowan for the antineutrino signature signal. An antineutrino is illustrated entering the tank of aqueous $CdCl_2$ solution and striking a target proton. The proton converts to a neutron and positron. The positron annihilates on an electron with the emission of two 0.511-MeV gamma rays in opposite directions detected by the liquid scintillator in tanks above and below the water target tank. The neutron produced by the antineutrino interaction slows down in the water and is captured by a cadmium nucleus and the resulting gamma rays are detected by the liquid scintillator in the adjacent tanks approximately 10 μs after the positron annihilation. *From Reines, F., 1995. The neutrino: from poltergeist to particle. Nobel Lecture, December 8, 1995. In: Barany, A. (Ed.), The Nobel Prizes 1999 Les Prix Nobel: Nobel Prizes, Presentations, Biographies, and Lectures, Almquiest & Wiksell International, Stockholm. Nobel Lecture, with permission © The Nobel Foundation 1995.*

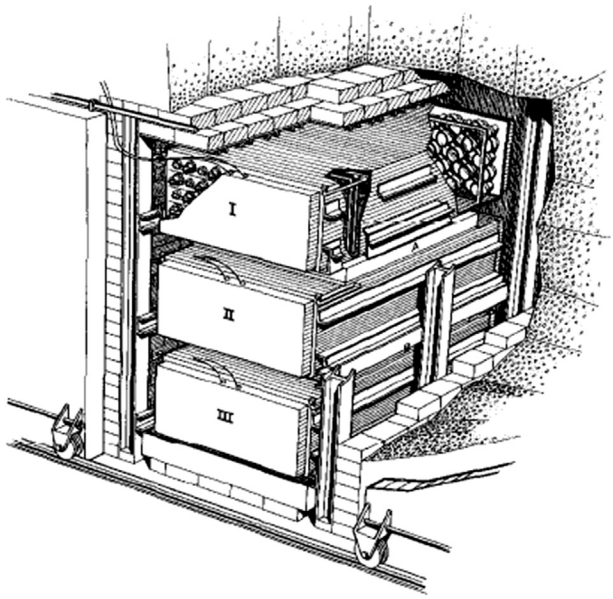

FIGURE II.16 A sketch of the equipment used by Reines and Cowan for the detection of the antineutrino. Tanks marked I, II, and III contained 1400 L of liquid scintillator solution and are viewed on each end with 55 photomultiplier tubes. Thinner tanks marked A and B were filled with 200 L of water, providing target protons for the antineutrinos, and 40 kg of $CdCl_2$ was dissolved in each water target solution to provide Cd nuclei that would capture the product neutrons. *From Reines, F., 1995. The neutrino: from poltergeist to particle. Nobel Lecture, December 8, 1995. In: Barany, A. (Ed.), The Nobel Prizes 1999 Les Prix Nobel: Nobel Prizes, Presentations, Biographies, and Lectures, Almquiest & Wiksell International, Stockholm. Nobel Lecture with permission © The Nobel Foundation 1995.*

cadmium, as expected for antineutrinos, totally removed the correlated count rate; and (3) the time interval spectrum between the first and second pulse signals agreed with that expected for annihilation and neutron-capture gamma rays. For additional reading on the history of this magnificent feat, see papers by Cowan and Reines (Cowan, 1964; Cowan et al., 1953, 1956; Reines, 1979, 1982; Reines and Cowan, 1953; Reines et al., 1960) and a review of this work in *Los Alamos Science* (1997).

After the discovery of the neutrino, Reines and Cowan sent a telegram on June 14, 1956 to Wolfgang Pauli at Zurich University to inform him of their successful detection of the neutrino. It was Pauli, who as a young man in 1930, had postulated the existence of the neutrino as a desperate measure to explain the broad spectrum of beta-particle energies emitted from decaying nuclides. The telegram is illustrated in Fig. II.17 and reads as follows: "We are happy to inform you that we have definitely detected neutrinos from fission fragments by observing inverse beta decay of protons. Observed cross section agrees well with expected six times ten to minus forty four square centimeters."

It is reported that Pauli and friends celebrated in Zurich that evening, and Pauli had sent immediately a reply letter (ie, night letter or cable) illustrated in Fig. II.18 to Reines and Cowan, which reads as follows: "Thanks for message. Everything comes to him who knows how to wait."

Pauli died exactly 18 months later, on December 15, 1958 in Zurich. He waited 26 years for the neutrino to be detected, and many of the most renowned physicists of the time did not believe that the neutrino could ever be detected and would remain a postulated particle. One can only imagine the immense satisfaction that Pauli could cherish during the remaining months of his life and the immeasurable sense of accomplishment felt by Frederick Reines and Clyde Cowan, Jr. after completing this colossal achievement.

A very practical outcome of the work of Reines and Cowan was the development of large radioactivity detectors. Among these is the whole-body counter, which is now a very practical means of measuring low levels of natural radiation or internal contamination in the human body. A person can step into a chamber or be lying down on a bed with surrounding detectors capable of measuring body radioactivity. One of the first whole-body counters was demonstrated to the public in 1958 at the Atoms for Peace Conference in Geneva.

Frederick Reines went on to head a research group at the University of California, Irvine (UCI) and became Dean of the School of Physical Sciences until 1974. He continued at UCI as professor of physics and became professor emeritus there in 1988. He was awarded the Bruno Rossi Prize in 1989 for the joint observations of his group at UCI and the Kamiokande Experiment in Japan of neutrinos from supernova 1987A. His research group at UCI had large detectors that they used to

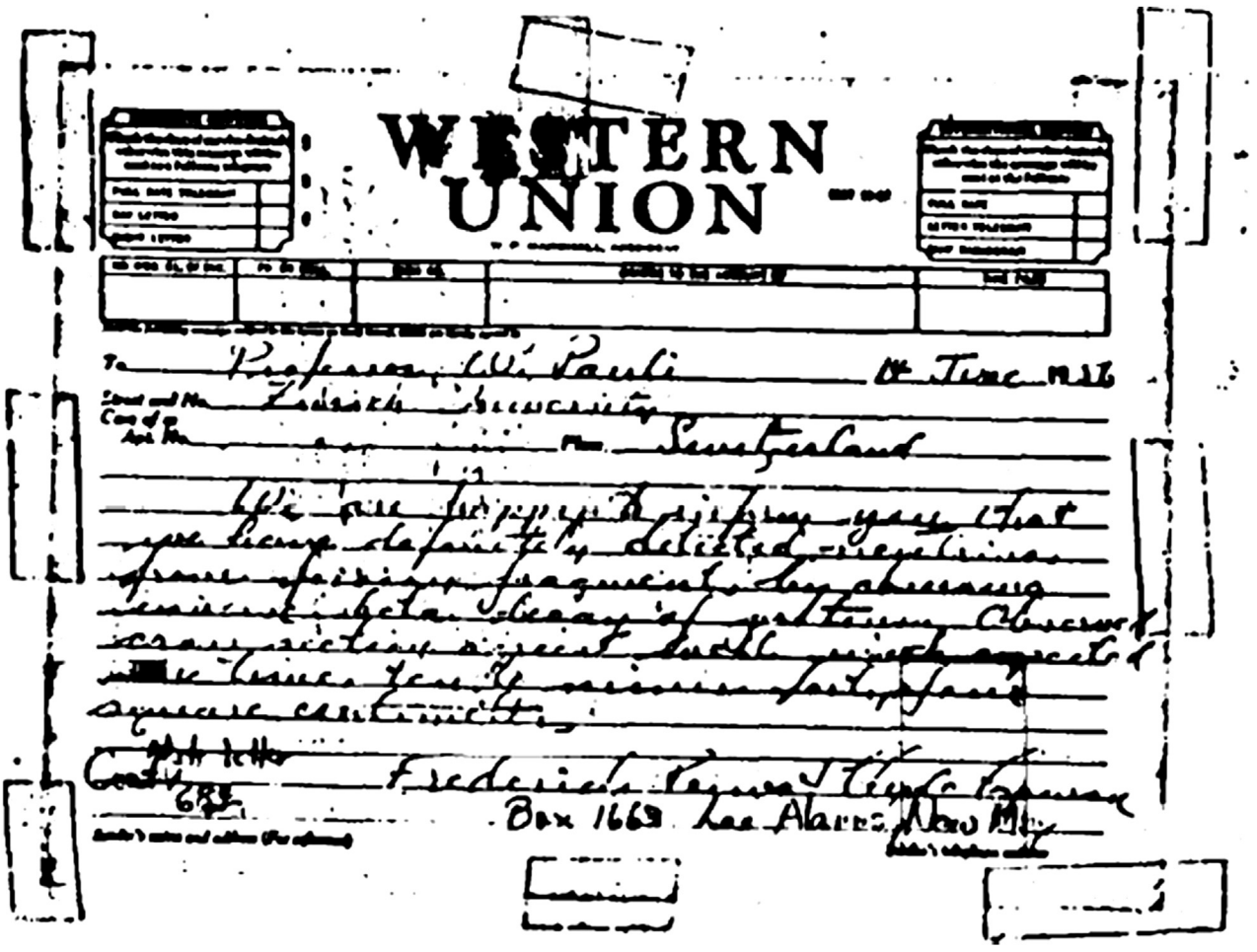

FIGURE II.17 Telegram dated 14 June 1956 from Reines and Cowan to Wolfgang Pauli informing him of their discovery of the neutrino. *From Reines, F., 1995. The neutrino: from poltergeist to particle. Nobel Lecture, December 8, 1995. In: Barany, A. (Ed.), The Nobel Prizes 1999 Les Prix Nobel: Nobel Prizes, Presentations, Biographies, and Lectures, Almquiest & Wiksell International, Stockholm. Nobel Lecture, with permission © The Nobel Foundation 1995.*

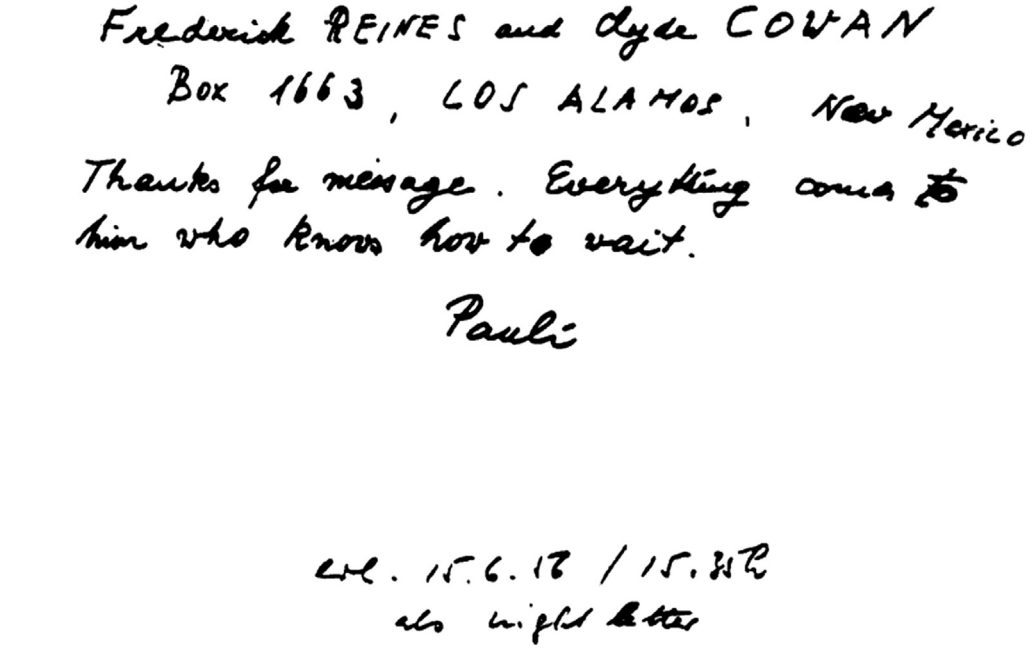

FIGURE II.18 Reply letter (ie, night letter or cable) dated June 15, 1956 to Reines and Cowan from Wolfgang Pauli thanking them for informing him of the discovery of the elusive neutrino that he had postulated 26 years earlier. *From Reines, F., 1995. The neutrino: from poltergeist to particle. Nobel Lecture, December 8, 1995. In: Barany, A. (Ed.), The Nobel Prizes 1999 Les Prix Nobel: Nobel Prizes, Presentations, Biographies, and Lectures, Almquiest & Wiksell International, Stockholm. Nobel Lecture, with permission © The Nobel Foundation 1995.*

detect neutrinos originating from stellar collapse, and these detectors were adorned with signs identifying each as "Supernova Early Warning System." He died on August 26, 1998.

After the discovery of the neutrino, Clyde Cowan, Jr. was awarded a Guggenheim Fellowship for studies on the physics of neutrinos and neutrino interactions. He went on to become professor of physics at the Catholic University of America in 1958 and an inspiration to many of his students until his early death in 1974.

OTTO STERN (1888–1969)

Otto Stern was born into a prosperous Jewish family of merchants on February 17, 1888 in Sorau, Upper Silesia, Germany, which is now Żary, Poland. His family moved to Breslau (now Wroclaw, Poland) in 1892. In Breslau, Otto Stern attended Johannes Gymnasium from 1897 to 1906. He graduated with a PhD degree in the field of physical chemistry from the University of Breslau in 1912.

Otto Stern (1888-1969)

Stern was interested in getting to know Albert Einstein and possibly study under him. He enjoyed financial independence, so he had the liberty and sense of adventure to go where Einstein would happen to be. Stern's professor contacted Fritz Haber, who knew Einstein; and Einstein was willing to accept him (Segré, 1973). Thus he joined Einstein at the University of Prague in 1912 and subsequently at the University of Zurich. In Zurich, he became Privatdocent of physical chemistry at the Eidgenössische Technische Hochschule in 1913. Informal discussion with Albert Einstein and other renowned physicists in Zurich provided Otto Stern with a good foundation in quantum theory, before Niels Bohr published his quantum theory of the hydrogen atom (See Bohr in Hall of Fame, Part V).

In 1914, Stern took on a position as Privatdocent of theoretical physics at the University of Frankfurt am Main, where he remained until 1921, except during a period of military service; and during 1921–1922 he became associate professor of theoretical physics at the University of Rostock.

It was at the University of Frankfurt where he collaborated with Walther Gerlach (1889–1979) in the study of the effects of inhomogeneous magnetic fields on "molecular rays" or "molecular beams." Otto Stern established himself as a leading expert in the experimental preparation of what was referred to as molecular rays or molecular beams. As noted by Emilio Segré (1973) in a biographical memoir, up to 1934 all of the important research involving molecular beams was carried out in Stern's laboratory; and all other molecular beam laboratories were established by persons who learned under Stern or by pupils of his pupils. Molecular beams, first discovered by the French physicist Louis Dunoyer (1911), consisted of heating an atomic or molecular substance in an oven having a very small opening through which the atomic vapor would escape and travel in a vacuum as a thin straight beam. The atoms would travel along a straight path, because in a vacuum

the atoms possessing kinetic energy would not encounter any atoms with which they could collide, and thereby travel along a straight path without scatter. Otto Stern perfected the technique with improved methods of creating and maintaining such beams under vacuum (Stern 1920, 1921).

In 1923, Otto Stern was appointed professor of physical chemistry and laboratory director at the University of Hamburg (Nobel Lectures, Physics 1942–1962). Otto Stern's work in Hamburg ended in 1933 by his resignation, because of the Nazis; and his pretext was the dismissal of his former student and collaborator, Immanuel Estermann (1900–1973), and an order to remove Einstein's portrait from his office (Segré, 1973). In a biographical memoir, Emilio Segré (1973) notes that Stern emigrated to accept a research professorship at the Carnegie Institute of Technology in Pittsburg, Pennsylvania where he set up a molecular beam laboratory together with Immanuel Estermann. Stern became a naturalized American citizen in 1939 and assisted in the war effort during World War II as a consultant to the War Department. After the war, Stern retired from the Carnegie Institute and moved to Berkeley, California. The Carnegie Institute of Technology became the Carnegie Mellon University in 1967. Otto Stern died in Berkeley from a heart attack on August 17, 1969.

Otto Stern received the Nobel Prize in Physics in 1943, in the words of the Nobel Committee, "for his contribution to the development of the molecular ray method and his discovery of the magnetic moment of the proton." The outcome of this work with molecular beams was unexpected; and the outcome demonstrated the magnetic properties of the electron and proton and the two possible spin quantum states of these particles. In the Nobel award ceremony speech on December 10, 1944, Professor E. Hulthén, Member of the Nobel Committee for Physics, described the experimental setup and discovery as follows (with the writer's notes in brackets):

> *There is a certain relation between electric and magnetic phenomena in that the magnetic field can generally be ascribed to the presence of electric currents…However, certain difficulties arose when it came to accounting in detail for the influence of the magnetic field on the movement of electrons…in the interior of the atom…The experiment [Gerlach and Stern 1922a,b] was carried out in Frankfurt in 1920 by Otto Stern and Walter [Walther] Gerlach, and was arranged as follows: In a small electrically heated furnace, was bored a tiny hole, through which the vapor [of silver atoms] flowed into a high vacuum so as to form thereby an extremely thin beam of vapor. The molecules in this so-called atomic or molecular beam all fly forwards in the same direction without any appreciable collisions with one another, and they were registered by means of a detector [a photographic plate]…On its way between the furnace and the detector the beam is affected by a non-homogeneous magnetic field, so that the atoms—if they really are magnetic—become unlinked in one direction or another, according to the position which their magnetic axles may assume in relation to the field. The classical conception was that the thin and clear-cut beam would consequently expand into a diffuse beam, but in actual fact the opposite proved to be the case. The two experimenters found that the beam divided up into a number [split into two beams] of relatively still sharply defined beams, each corresponding to one of the just mentioned discrete positional directions of the atoms in relation to the field. This confirmed the space-quantization hypothesis [see Fig. II.19]. Moreover, the experiment rendered it possible to estimate the magnetic factors [magnetic moment] of the electron, which proved to be in close accord with the universal magnetic unit, the so-called "Bohr's magneton"…[1 Bohr magneton = 9.274×10^{-24} J/Tesla].*
>
> *It had already been realized when studying the fine structure of the spectral lines that the actual nucleus of the atom, like the electron, possesses a rotation of its own, a so-called "spin"…The immense interest attaching in this connection to a determination of the magnetic factors of the hydrogen nucleus, the so-called proton, was due to the fact that the proton, together with the recently discovered neutron, forms the basic constituent of all the elements of matter; and…as far as the proton is concerned, its magnetic factor would be as many times smaller than the electron's as its mass is greater than the electron's, implying that the magnetic factor of the proton must be, in round figures, 1850 times smaller than the electron's. Naturally then, it aroused great interest when, in 1933, Stern and his colleagues [Frisch and Stern, 1933, Estermann and Stern, 1933, and Estermann et al., 1933] made this determination according to the molecular beam method, it being found that the proton factor was about 2½ times greater than had theoretically been anticipated. [This was in close agreement with the current values of the magnetic moments of the proton and electron, which are 1.410×10^{-26} J/T and 928.4×10^{-26} J/T, respectively].*

The Stern–Gerlach experiment described above utilized a beam of silver atoms heated in an oven to the vapor state. Silver atoms have an atomic number of 47 ($Z = 47$); and of its orbital electrons, 46 are found in filled atomic orbitals and the last electron (47th) remains alone in an outer orbital unshared with any other electron. Thus, a beam of silver atoms having this one electron in an outer orbital would act in a magnetic field similar to a hydrogen atom with a single electron, and its beam can produce an image readily with a photographic emulsion, which contains silver halide.

In the Nobel Award Ceremony Speech cited above, Professor E. Hulthén of the Nobel Committee made reference to "the electron, possesses a rotation of its own, a so-called *spin*." The concept of electron spin did not originate with Stern and Gerlach, who carried out their experiment in 1920; although their experiment demonstrating the splitting of the atomic beam of silver atoms provided evidence for the spin and magnetic moments of the electron. In 1925, George Uhlenbeck

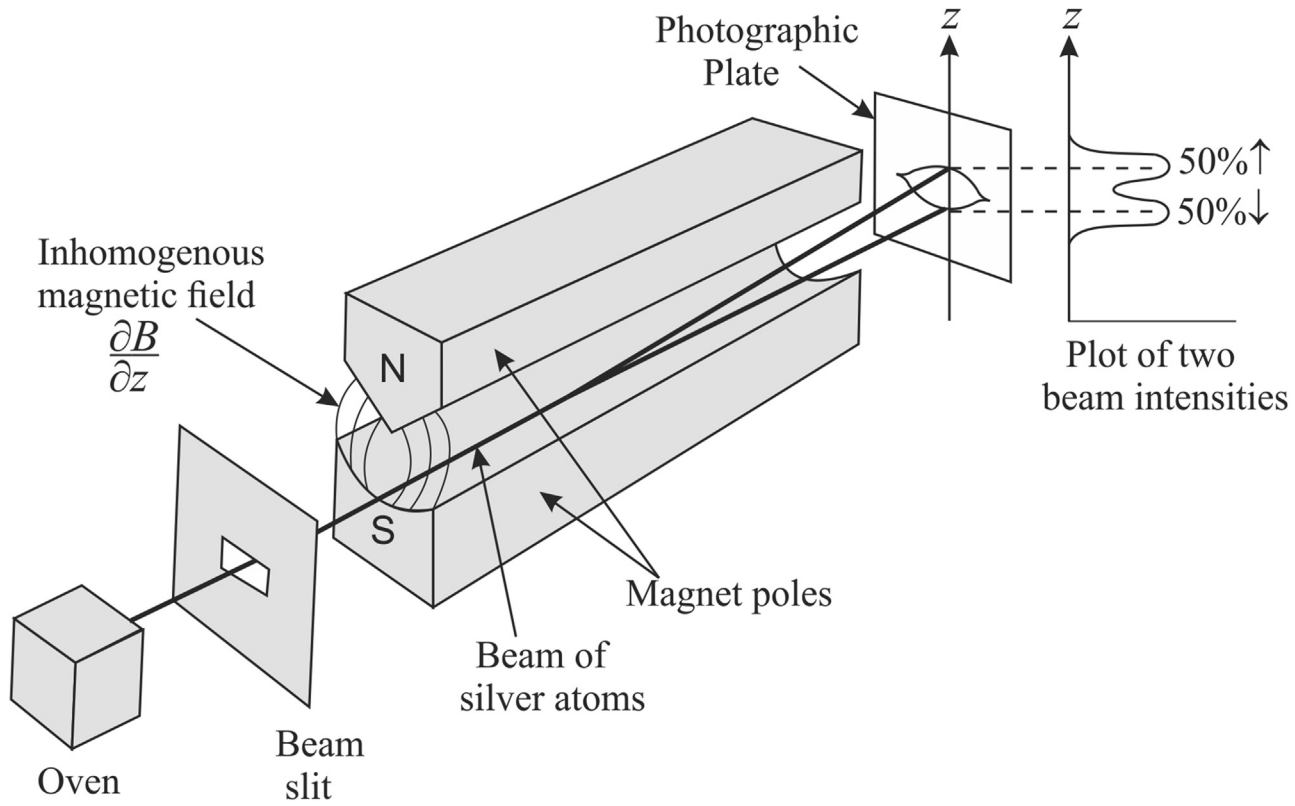

FIGURE II.19 Basic components of the Stern–Gerlach experiment. Under vacuum, a beam of silver atoms generated at the oven passes through a collimating slit and on through an inhomogeneous magnetic field, which splits the single beam into two separate beams of equal intensity. A photographic plate would register the beam intensities. One-half of the beam would move in the upward direction and the other half in the downward direction. The illustration is based on a description depicted on the commemorative plaque at the entrance of the Physikalischer Verein building, which housed the Physics Institute of Frankfurt University from 1914 to 2005.

(1900–1988) and Samuel Goudsmit (1902–1978) at the Instituut voor Theoretische Natuurkunde at Leiden in The Netherlands (now known as the Instituut Lorentz of Leiden University), first proposed the property of spin to the electron. Their paper (Uhlenbeck and Goudsmit, 1925) was published in the journal *Die Naturwissenschaften* in the German language. In a historical account celebrating 50 years of spin, Uhlenbeck (1976) recalled their idea proposed in the paper submitted on October 17, 1925, that each atomic electron rotates with an angular momentum of ½$\hbar$ carrying with it a magnetic moment equal to one Bohr magneton, which is defined as $e\hbar/2m_e$, where e is the electron charge, $\hbar$ is Plank's constant reduced or $h/2\pi$, and m_e is the electron mass. A few months later, Uhlenbeck and Goudsmit (1926) published their hypothesis of the electron spin quantum number in the journal *Nature*.

The electron spin was originally interpreted as a particle rotating on its axis such as a spinning top rotates on it axis. However, in quantum physics the electron is an elementary particle and classified as a point source, which would not have dimensions. Also, the spin of larger particles, such as the proton, is often metaphorically described in terms of a particle spinning on its axis like a spinning top. However, this classical physics explanation is discarded in quantum physics. The term "spin" in quantum physics refers to a quantum number, which for the electron, proton, and neutron can possess two values, referred to as "spin up" (↑) or "spin down" (↓) with values of $+\frac{1}{2}\hbar$ or $-\frac{1}{2}\hbar$, respectively, where $\hbar$ is Planck's reduced constant or $h/2\pi$. The spin quantum number of the electron is one of several quantum numbers that characterize the electron, such as principal quantum number (n), and the orbital (ℓ) and magnetic (m_ℓ) quantum numbers characterize the atomic electron and its relative positon in the atom. All subatomic particles possess quantum numbers including charge and spin, which together with the particle mass, characterize each particle.

The spin quantum numbers of subatomic particles are often explained on the basis of the spins of their underlying quark structure, as provided in the following examples:

1. The "spin ½ baryons" are baryons of half-integer spin such as the proton (p) and neutron (n). These particles contain three quarks each with spin $+\frac{1}{2}\hbar$, $+\frac{1}{2}\hbar$, and $-\frac{1}{2}\hbar$, which are summed to give a total spin of ½$\hbar$.

2. The "spin 3/2 baryons" or "triple-spin baryons" are baryons with their underlying quarks aligned each with spin $+½\hbar$, $+½\hbar$, and $+½\hbar$, which sum to give a total spin of $3/2\hbar$. Baryons of this type include the delta (Δ) and omega (Ω) particles.
3. The "spin 0 mesons" or "zero-spin mesons" contain two quarks with nonaligned spins of $+½\hbar$ and $-½\hbar$, which sum to a spin of zero. Mesons of this type include the pion (π), kaon (K), and eta (η) particles.
4. The "spin 1 mesons" or "double-spin mesons" contain two quarks with aligned spins of $+½\hbar$ and $+½\hbar$, which sum to give a total spin of 1.

The above explanation is commonly used in describing the origin of the total spin of a particle. This explanation, although convenient, may need to be modified in the future, as described by Moskowitz (2014) in *Scientific American.* Moskowitz (2014) describes the current work of researchers at the Relativistic Heavy-Ion Collider (RHIC) at Brookhaven National Laboratory in Upton, N.Y. Gluons are bosons, like the photon, which have a spin of 1. Gluons constitute a strong nuclear force that bind the quarks together in the proton; and the gluons constitute over 99% of the mass of the proton. As reported by Moskowitz (2014), research at the RHIC indicates that the quarks may contribute only up to 25% of the proton's spin. The remaining contribution to the spin of the proton may be derived from its constituent gluons. Research work is currently underway to solve what is referred to as the "proton spin crisis" (Moskowitz, 2014).

For a very comprehensive account of the life and work of Otto Stern, the reader may peruse a paper by Toennies et al. (2011) and a biographical memoir by Emilio Segré (1973).

Chapter 6

Beta Radiation and Beta Decay

However, even if the radiation formula should prove itself to be absolutely accurate, it would still only have, within the significance of a happily chosen interpolation formula, a strictly limited value. For this reason, I buried myself, from then on, that is, from the day of its establishment, with the task of elucidating a true physical character for the formula… after some weeks of the most strenuous work of my life, light came into the darkness, and a new undreamed of perspective opened up for me.

This quote from Max Planck on 2 June 1920 describes his general formula for black-body radiation that fitted both low and high radiation frequencies and included a constant $h = 6.626 \times 10^{-34}$ J s, named Planck's constant in his honor. In this statement he refers to his discovery of the quantum theory and the role of Planck's constant h in the new field of quantum physics, which he was about to open (Planck's quantum theory is discussed in detail in Hall of Fame, Part III).

6.1 INTRODUCTION

Beta particles, which constitute beta radiation, have the same mass and charge as electrons. A beta particle differs from the electron in its origin. The beta particle, which may be either negatively charged (negatron) or positively charged (positron), is created during the decay of the nucleus of an atom. A beta particle is emitted from the nucleus of an atom during radioactive decay. The electron, however, occupies regions outside the nucleus of an atom. The beta particle, like the electron, has a very small mass compared to the proton or neutron. Its mass is 1/1836 that of the proton mass and 1/1838 that of the neutron mass. The beta particle has an origin in addition to that of the nucleus. The beta particle may be produced in pairs, one positive and the other negative in charge, by the conversion of gamma radiation energy into the mass of two beta particles in the vicinity of a nucleus. This phenomenon is referred to as pair production. The origins, properties, and interaction of beta particles with matter are discussed in this chapter.

A nuclear decay process, referred to as beta decay, results in some circumstances in the emission of beta radiation. Beta decay may be defined as any nuclear decay process whereby the mass number (A) of the nucleus remains the same and the atomic number (Z) changes. There are three main types of beta decay.

1. Negatron (β^-) emission, which involves the emission of a negative beta particle or negative electron from the nucleus.
2. Positron (β^+) emission, whereby a positive beta particle or positively charged electron is emitted from the nucleus.
3. Electron capture (EC), which does not result in the emission of any beta particle.

Each of these beta decay processes will be treated in detail in the following sections.

6.2 NEGATRON (β^-) EMISSION

Negatron emission can be described by the general equation

$$ {}^{A}_{Z}P \rightarrow {}_{Z+1}{}^{A}D + \beta^- + \overline{\nu} + K_T \qquad [6.1] $$

where ${}^{A}_{Z}P$ is the parent nuclide of atomic number Z and mass number A, ${}_{Z+1}{}^{A}D$ is the daughter nuclide of atomic number $Z + 1$ and the same mass number as the parent, β^- is the negatron or negative beta particle, $\overline{\nu}$ is the antineutrino, and K_T is the total kinetic energy released in the beta decay process. The total kinetic energy released, also referred to as the decay energy (Q_β), is shared between the negatron, antineutrino, recoil daughter nucleus, and any gamma radiation that may be emitted by the daughter nucleus. Gamma-ray emission can occur when the daughter nuclide is left in an excited energy state and decays to a lower energy state or ground (stable) state, with the emission of energy as gamma-ray photons.

Radioactivity: Introduction and History, From the Quantum to Quarks. http://dx.doi.org/10.1016/B978-0-444-63489-4.00006-X
Copyright © 2016 Elsevier B.V. All rights reserved.

Gamma-ray emission does not occur in all cases of negatron emission. There are some nuclides, described later in this section, that decay with the emission of negatrons directly to the stable ground state without the emission of gamma radiation. The decay energy, Q_{β^-}, may be defined as

$$Q_{\beta^-} = K_T = E_{\beta^-} + E_{\overline{\nu}} + E_{\gamma} + E_{\text{recoil}} \quad [6.2]$$

where E_{β^-} is the kinetic energy of the negatron, $E_{\overline{\nu}}$ is the kinetic energy of the antineutrino, E_{γ} is the gamma-ray energy, which is emitted when the daughter nucleus is at an elevated energy state and drops to a more stable or ground state, and E_{recoil} is the kinetic energy of the recoil daughter nucleus. The recoil energy can be ignored in most calculations of beta decay energy, because it may be only a few electron volts (eV), compared to the fractional or multiple magnitudes of million electron volts (MeV) energy possessed by the beta particle, antineutrino, and gamma radiation (see the Section 20.11 in the chapter: "The Atomic Nucleus"). We should keep in mind that there is a maximum energy shared by the beta particle and antineutrino $\left(E_{\beta^-} + E_{\overline{\nu}}\right)$, which is often referred to as the $E_{\max}$ of the beta particle.

6.2.1 Basic Principles

A negatron or negative beta particle (β^-) is an electron emitted from the nucleus of a decaying radionuclide that possesses an excess of neutrons or, in other words, a neutron/proton (n/p) imbalance. The nuclear instability caused by the n/p imbalance results in the conversion of a neutron to a proton within the nucleus. The balance of charge is conserved by the simultaneous formation of an electron (negatron) according to the equation

$$\text{n} \rightarrow \text{p}^+ + \beta^- + \overline{\nu}. \quad [6.3]$$

A neutrino (ν), which is a particle of zero charge, accompanies beta particle emission. The neutrino can be identified further as two types with opposite spin, namely the antineutrino ($\overline{\nu}$), which accompanies negative beta particle (negatron) emission, and the neutrino (ν), which accompanies positive beta particle (positron) emission. Because the neutrino and antineutrino have similar properties, with the exception of spin, it is common to use the word "neutrino" to simplify references to both particles. The explanation for the neutrino and its properties, also emitted from the decaying nucleus, is given later in this section. The electron formed as a product of nuclear decay cannot exist within the nucleus; and it is thus ejected as a negatron or negative beta particle, β^-, with an energy equivalent to the mass difference between the parent and daughter atoms, less than the energy of the antineutrino or neutrino in the case of positron emission, and any gamma-ray energy that may be emitted by the daughter nucleus if the nucleus is left in an excited energy state, and recoil energy of the daughter nucleus, as described by Eq. [6.2]. Tritium (^{3}H), for example, decays with β^- emission according to the following:

$$^{3}_{1}\text{H} \rightarrow {}^{3}_{2}\text{He} + \beta^- + \overline{\nu} + 0.0186\ \text{MeV} \quad [6.4]$$

The ^{3}H nucleus decays directly to the ground state of ^{3}He, thus there is no gamma-ray energy emission in this case. The value of 0.0186 MeV (megaelectron volts) is the maximum energy the beta particle may possess. The unstable tritium nucleus contains two neutrons and one proton. The transformation of a neutron to a proton within the tritium nucleus results in a charge transfer on the nucleus from +1 to +2 without any change in the mass number. Although there is no change in the mass number, the mass of the stable helium isotope produced is slightly less than that of its parent tritium atom. Eqs. [6.5]–[6.10] illustrate other examples of β^- decay, which decay to stable daughter nuclides whereby no gamma-ray emission occurs.

$$^{14}_{6}\text{C} \rightarrow {}^{14}_{7}\text{N} + \beta^- + \overline{\nu} + 0.156\ \text{MeV} \quad [6.5]$$

$$^{32}_{15}\text{P} \rightarrow {}^{32}_{16}\text{S} + \beta^- + \overline{\nu} + 1.710\ \text{MeV} \quad [6.6]$$

$$^{35}_{16}\text{S} \rightarrow {}^{35}_{17}\text{Cl} + \beta^- + \overline{\nu} + 0.167\ \text{MeV} \quad [6.7]$$

$$^{36}_{17}\text{Cl} \rightarrow {}^{36}_{18}\text{Ar} + \beta^- + \overline{\nu} + 0.714\ \text{MeV} \quad [6.8]$$

$$^{45}_{20}\text{Ca} \rightarrow {}^{45}_{21}\text{Sc} + \beta^- + \overline{\nu} + 0.258\ \text{MeV} \quad [6.9]$$

$$^{89}_{38}\text{Sr} \rightarrow {}^{89}_{39}\text{Y} + \beta^- + \overline{\nu} + 1.490\ \text{MeV} \quad [6.10]$$

The energies of beta particle decay processes are usually reported as the maximum energy, $E_{\max}$, that the emitted beta particle or antineutrino may possess. The maximum energy is reported because beta particles are emitted from

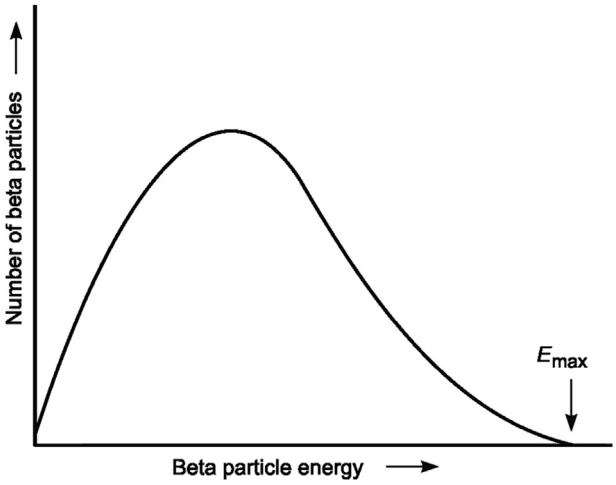

FIGURE 6.1 General beta particle energy spectrum.

radionuclides with a broad spectrum of energies. A typical spectrum is illustrated in Fig. 6.1. The shape of the beta particle energy spectra will vary among the beta-emitting radionuclides, but all beta-emitting radionuclides will display a wide spectrum of energies between zero and E_{max}. Unlike alpha particles, which have a discrete energy, beta particles are emitted with a wide spectrum of energies ranging from zero to E_{max}.

The majority of beta particles emitted have energies of approximately $1/3E_{max}$. Only a very small portion of the beta particles is emitted with the maximum possible energy from any radionuclide sample. In 1930 Wolfgang Pauli was the first to postulate why beta particles were not emitted with fixed quanta of energy, quite the contrary to what is observed in alpha particle emission. He proposed the existence of an elusive neutral particle of near-zero rest mass, the neutrino, in a letter to participants at a regional meeting on radioactivity in Tübingen, Germany. The neutrino was considered elusive, because if it existed its zero charge and near-zero rest mass would make it undetectable by conventional means, allowing a neutrino to penetrate matter easily and even pass through the entire Earth without causing a single interaction. The neutrino is emitted simultaneously with the beta particle from the decaying nucleus and shares the energy of decay with the beta particle. For example, if a beta particle was emitted from tritium (decay energy = 0.0186 MeV) with an energy of 0.0086 MeV, the accompanying neutrino would possess the remaining energy of 0.01 MeV—that is, the decay energy less than the beta particle energy (0.0186 − 0.0086 MeV). Consequently, if we observe any number of beta particles emitted from a tritium sample or other beta-emitting nuclide sample (eg, ^{14}C, ^{32}P, ^{90}Sr), they would possess different energies and display an energy spectrum from zero to E_{max}, as illustrated in Fig. 6.1.

6.2.2 Inverse Beta Decay

With Pauli's postulation of the neutral particle, Enrico Fermi elaborated the beta decay theory in 1934 and took the word neutrino from the Italian language, meaning "little neutral one." The particle remained elusive until the observation of the neutrino was demonstrated by Frederick Reines and Clyde Cowan, Jr in 1956 (see Hall of Fame, Part II for a detailed description of Reines and Cowan's detection of the neutrino). They confirmed the existence of the neutrino by demonstrating inverse beta decay where an antineutrino interacts with a proton to yield a neutron and a positron

$$\overline{\nu} + p^+ \rightarrow n + e^+ \qquad [6.11]$$

In the same year, Lee and Yang (1956) proposed that neutrinos and antineutrinos possessed left-handed and right-handed spins, respectively. Inverse beta decay remains an important nuclear process utilized in the measurement of solar neutrinos today (Gratta and Wang, 1999; Zuber, 2003; Ianni et al., 2005; Fukuda et al., 2010).

An inverse beta decay, first proposed by Raghaven (1976), which involves the interaction of a neutrino with the neutron of ^{115}In is the following:

$$\nu + {}^{115}_{49}In \rightarrow {}^{115}_{50}Sn^* + e^- \qquad [6.12]$$

which can be written in general terms illustrating only the nucleons as

$$\nu + \mathrm{n} \rightarrow \mathrm{p}^{+} + e^{-} \qquad [6.13]$$

The superscript asterisk in Eq. [6.12] represents an excited state of ^{115}Sn, which decays into the ground state with a lifetime of 4.76 μs and emits two gamma-ray photons of 116 and 497 keV. This provides a triple coincidence signal, namely the emitted electron together with the two gamma-ray photons, which can be detected among huge backgrounds (Fukuda et al., 2010). Also, the neutrino energy may be calculated from the energy of the prompt electron according to the equation

$$E_{e^-} = E_{\nu} - (E_f - E_i) \qquad [6.14]$$

where E_{e^-} is the energy of the electron produced, E_{ν} is the neutrino energy, and E_f and E_i are the final and initial energies of the nuclear state involved in the transition (Zuber, 2003). In the case of neutrino interactions with ^{115}In, Eq. [6.14] may be written, according to Fukuda et al. (2010), as

$$E_{e^-} = E_{\nu} - 118 \text{ keV} \qquad [6.15]$$

Thus, neutrino spectroscopy is possible.

In general, the detection principle of solar neutrinos involving the inverse beta decay reaction of Eq. [6.13], as described by Zuber (2003), may involve one of the following two reactions:

$$\nu + {}^{A}_{Z}\mathrm{A} \rightarrow {}_{Z+1}{}^{A}\mathrm{B}_{\mathrm{g.s.}} + e^{-} \rightarrow {}_{Z+2}{}^{A}\mathrm{C} + e^{-} + \overline{\nu} \quad (e - e \text{ tag}) \qquad [6.16]$$

or

$$\nu + {}^{A}_{Z}\mathrm{X} \rightarrow {}_{Z+1}{}^{A}\mathrm{Y}^{*} + e^{-} \rightarrow {}_{Z+1}{}^{A}\mathrm{Y}_{\mathrm{g.s.}} + \gamma \quad (e - \gamma \text{ tag}) \qquad [6.17]$$

The reaction described in Eq. [6.16] involves the interaction of a neutrino with a neutron of nuclide ${}^{A}_{Z}\mathrm{A}$ of atomic number Z and mass number A producing a nuclide ${}_{Z+1}{}^{A}\mathrm{B}_{\mathrm{g.s.}}$ at its ground state and a beta particle (e^{-}). The nuclide ${}_{Z+1}{}^{A}\mathrm{B}_{\mathrm{g.s.}}$ undergoes beta decay to nuclide ${}_{Z+2}{}^{A}\mathrm{C}$ with the emission of a beta particle (e^{-}) and antineutrino ($\overline{\nu}$). This reaction has an $e - e$ tag whereby a coincidence signal between the two electron emissions provides the signature for the neutrino detection. The reaction described by Eq. [6.17] depicts a neutrino interacting with a neutron of nuclide ${}^{A}_{Z}\mathrm{X}$ producing nuclide ${}_{Z+1}{}^{A}\mathrm{Y}^{*}$ at an excited energy state, indicated by the superscript asterisk, plus an electron or beta particle (e^{-}). The nuclide ${}_{Z+1}{}^{A}\mathrm{Y}^{*}$ then undergoes deexcitation to its ground state ${}_{Z+1}{}^{A}\mathrm{Y}_{\mathrm{g.s.}}$ with the emission of a gamma-ray photon. This reaction has an $e - \gamma$ tag whereby a coincidence signal between the electron and one or more gamma-ray photon emissions provides the signature for the neutrino detection. The neutrino energies are determined by Eq. [6.14]. Zuber (2003) provides a review of these two approaches to neutrino detection and spectroscopy. The interaction of a neutrino with ^{115}In previously discussed (Eq. [6.12]), utilized by Fukuda et al. (2010), is an example of the generic reaction yielding an $e - \gamma$ tag depicted by Eq. [6.17], which is specifically

$$\nu + {}^{115}_{49}\mathrm{In} \rightarrow {}^{115}_{50}\mathrm{Sn}^{*} + e^{-} \rightarrow {}^{115}_{50}\mathrm{Sn} + \gamma(116 \text{ keV}) + \gamma(497 \text{ keV}) \qquad [6.18]$$

An example of the generic reaction depicted in Eq. [6.16] is the following:

$$\nu + {}^{13}_{6}\mathrm{C} \rightarrow {}^{13}_{7}\mathrm{N}_{\mathrm{g.s.}} + e^{-} \rightarrow {}^{13}_{6}\mathrm{C} + e^{+} \qquad [6.19]$$

This reaction was utilized by Ianni et al. (2005) for the detection of neutrinos. The reaction provides an $e - e$ tag, as the beta particle (e^{-}) produced in the reverse beta decay yields one signal while the positron (e^{+}) produced in the subsequent decay of ^{13}N provides a time and space coincidence signal and signature for the neutrino detection.

6.2.3 Neutrino Mass

From its inception by Pauli in 1930 up to recent years, the neutrino or antineutrino had been thought to have no rest mass or a near-zero rest mass. But on June 5, 1998 the Super-Kamiokande Collaboration, including scientists from 23 institutions in Japan and the United States, announced at the Neutrino 98 International Physics Conference in Takayama, Japan, that neutrinos possessed a definite mass (Gibbs, 1998; Kesterbaum, 1998; Kearns et al., 1999; Nakahata, 2000). The mass was not reported, but evidence was provided that the neutrino did possess mass although it was considered to be "very small," at least 0.07 eV, which would be less than a millionth of the electron mass. Evidence for the neutrino mass was provided by demonstrating that neutrinos can "oscillate" from one type or flavor into another (ie, electron-, muon-, and tau-neutrinos) as

they travel through space and matter. Oscillation is the changing of neutrino types back and forth from one type or flavor to another; and this could occur only if the neutrino possessed mass. The Nobel Prize in Physics in 2015 was awarded to two key scientists of two large research groups, namely Takaaki Kajita, affiliated with the Super-Kamiokande detector in Japan, and Arthur B. McDonald, affiliated with the Sudbury Neutrino Observatory in Canada, for the discovery of neutrino oscillations as evidence that neutrinos have mass. At the time of the Nobel award, Kajita was director of the Institute for Cosmic Ray Research and professor at the University of Tokyo, Kashiwa, Japan; and McDonald was professor emeritus at Queen's University, Kingston, Canada.

At the Neutrino 2000 Conference held in Sudbury, Canada on 16–21 June 2000, groups from the University of Mainz, Germany (Bonn et al., 2001) and the Institute for Nuclear Research, Moscow (Lobashev et al., 2000) reported the mass of the neutrino to be between 2.2 and 2.5 eV/c^2, respectively, at 95% confidence levels. It is common to express subatomic particle mass in units of energy based on equivalence of mass and energy ($E = mc^2$), so the particle mass m is measured in units of E/c^2 or eV/c^2. Neutrino mass experiments are reviewed by Kraus et al. (2005), Otten and Weinheimer (2008), Beck (2010), and Kristiansen et al. (2010). Beck (2010) underscores that the results from previous research reported by the Triosk (Russia) and Mainz (Germany) neutrino mass experiments (see Lobashev et al., 1999a,b,c, 2000; Kraus et al., 2005) have set the best upper limits of 2.3 eV/c^2 with a 95% confidence limit on the neutrino mass. Beck (2010) also reports that the KATRIN (KArlsruhe TRItiun Neutrino) experiment is under preparation to search for the mass of the electron neutrino with a sensitivity of 0.2 eV/c^2. With this objective, the KATRIN experiment will perform a precision measurement of the endpoint region of the β decay spectrum of tritium, the shape of which depends highly on the neutrino mass. A windowless gaseous tritium source is used in a transport system that guides the beta particles of tritium without energy loss to PIN diode detectors, described by Wüstling et al. (2006). A pre-spectrometer rejects all beta particles with energy <200 eV below the β spectrum endpoint, and the beta particle energies can be measured with a resolution of 0.93 eV. The collection of data to obtain the neutrino mass started in 2012 and will continue for 5 years.

To put the mass of the neutrino in perspective, we can take the current experimental value of the upper limit to the neutrino rest mass, $m_\nu = 2.3$ eV/c^2, and convert this to kilograms as follows.

By definition $1\text{ eV} = 1.60 \times 10^{-19}$ J and, from the equation $E = mc^2$, we can calculate the neutrino rest mass in kilograms as

$$\begin{aligned} m_\nu &= E/c^2 \\ &= (2.3\text{ eV})\left(1.6 \times 10^{-19}\text{ J/eV}\right)\Big/\left(3.0 \times 10^{8}\text{ m/s}\right)^2 \\ &= 4.1 \times 10^{-36}\text{ kg} \end{aligned} \qquad [6.20]$$

If we compare the rest mass of the neutrino, m_ν, to that of the miniscule electron, m_e, we see that the neutrino rest mass is approximately 4 millionths that of the electron, or

$$m_\nu/m_e = 4.1 \times 10^{-36}\text{ kg}/9.1 \times 10^{-31} = 4.5 \times 10^{-6}$$

6.2.4 Negatron Decay Energy

The general reaction for negatron emission was described by Eq. [6.1]. It is provided here again for a treatment on negatron decay energy calculations:

$$^{A}_{Z}P \rightarrow {}^{A}_{Z+1}D + \beta^- + \overline{\nu} + K_T \qquad [6.21]$$

where $^{A}_{Z}P$ is the parent nuclide of atomic number Z and mass number A, $^{A}_{Z+1}D$ is the daughter nuclide of atomic number $Z + 1$ and the same mass number as the parent, β^- is the negatron or negative beta particle, $\overline{\nu}$ is the antineutrino, and K_T is the total kinetic energy released in the beta decay process.

In terms of nuclear masses, we may write Eq. [6.21] as

$$_{Z}M_P = {}_{Z+1}M_D + m_e + K_T \qquad [6.22]$$

where $_{Z}M_P$ and $_{Z+1}M_D$ are the masses of the parent and daughter nuclei of atomic numbers Z and $Z + 1$, respectively, and m_e is the mass of the beta particle (ie, one electron mass). We may use atomic mass units (u) to calculate the mass difference of the parent and daughter nuclei by adding firstly Z atomic electron masses to each side of Eq. [6.22] to give

$$_{Z}M_P + Zm_e = {}_{Z+1}M_D + (Z+1)m_e + K_T \qquad [6.23]$$

The mass difference of the parent and daughter nuclei is equivalent to the decay energy $\left(Q_{\beta^-}\right)$. We can now calculate the decay energy Q_{β^-} by the difference of the parent and daughter nuclide atomic masses, after adding Z atomic electrons to each side of the equation and ignoring the small difference in the binding energies of the electrons in the two nuclides, as

$$Q_{\beta^-} = ({}_{Z}M_P - {}_{Z+1}M_D)c^2 = K_T = E_{\beta^-} + E_{\overline{\nu}} + E_\gamma + E_{\text{recoil}} \quad [6.24]$$

where c is the velocity of light in a vacuum and the product Mc^2 yields the energy equivalence of the mass, E_{β^-} is the kinetic energy of the negatron, $E_{\overline{\nu}}$ is the kinetic energy of the antineutrino, E_γ is the gamma-ray energy, which only appears with the decay of a daughter nucleus when left at an excited energy state, and E_{recoil} is the kinetic energy of the daughter recoil nucleus. As previously described, the recoil energy, E_{recoil}, is generally relatively very small (a few eVs) and will be ignored here. Also, if there is no gamma radiation emitted by the daughter nucleus, we can exclude the term E_γ. The remaining decay energy $\left(E_{\beta^-} + E_{\overline{\nu}}\right)$ is shared as kinetic energy between the beta particle and antineutrino, most often referred to as the $E_{\max}$.

A simple example is that of the radionuclide ^{14}C, which decays by negatron emission without the emission of gamma radiation to the stable daughter nuclide ^{14}N according to the following:

$${}^{14}_{6}\text{C} \rightarrow {}^{14}_{7}\text{N} + \beta^- + \overline{\nu}\ (E_{\max} = 0.156\ \text{MeV}) \quad [6.25]$$

The decay scheme is illustrated in Fig. 6.2.

The decay energy of ^{14}C can be calculated according to Eq. [6.24] using atomic mass units (u) of the parent and daughter atoms as follows:

$$\begin{aligned} Q_{\beta^-} &= (M_{14_C} - M_{14_N})c^2 \\ &= (14.00324199\ \text{u} - 14.00307401\ \text{u})(931.494\ \text{MeV/u}) \\ &= 0.156\ \text{MeV} \end{aligned} \quad [6.26]$$

where 931.494 is the energy equivalence of 1 atomic mass unit, as derived previously in chapter "Basic Concepts and Definitions." The energy of 0.156 MeV, calculated above, is shared between the beta particle and antineutrino. Thus the maximum energy that the beta particle or antineutrino may possess is 0.156 MeV. The online computer calculation (www.nndc.bnl.gov/qcalc) agrees with the above beta decay energy to be 156 keV or 0.156 MeV.

We may now look at a more complex example of ^{137}Cs decay, where negatron β^- emission occurs with more than one energy maxima, or via what is referred to as a branching decay mode, and which decays with the emission of gamma radiation from the nucleus of the daughter nuclide ^{137}Ba. The decay equation is:

$${}^{137}_{55}\text{Cs} \rightarrow {}^{137}_{56}\text{Ba} + \beta^- + \overline{\nu} + \gamma \quad [6.27]$$

The decay scheme of ^{137}Cs to stable ^{137}Ba is illustrated in Fig. 6.3.

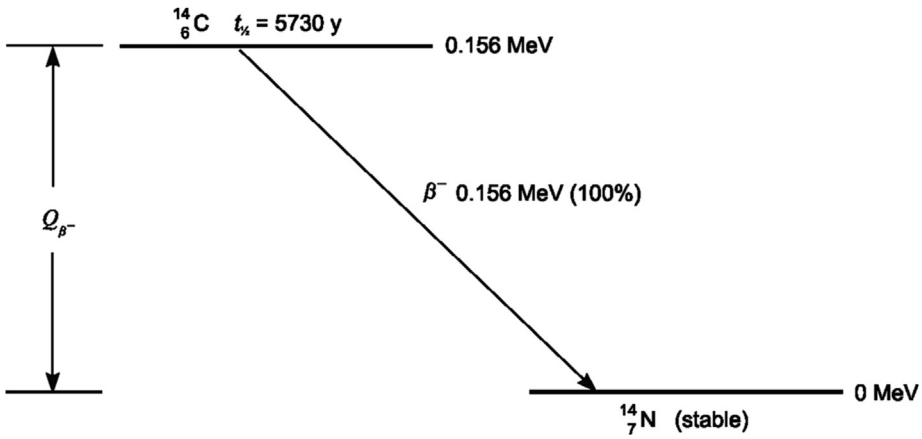

FIGURE 6.2 Negatron beta decay scheme of ^{14}C. The radionuclide ^{14}C decays to stable ^{14}N by negatron emission. Nuclear decay occurs entirely (100%) by emission of a negatron (β^-) and antineutrino ($\overline{\nu}$) with an energy maximum of 0.156 MeV, which is shared by the negatron and antineutrino.

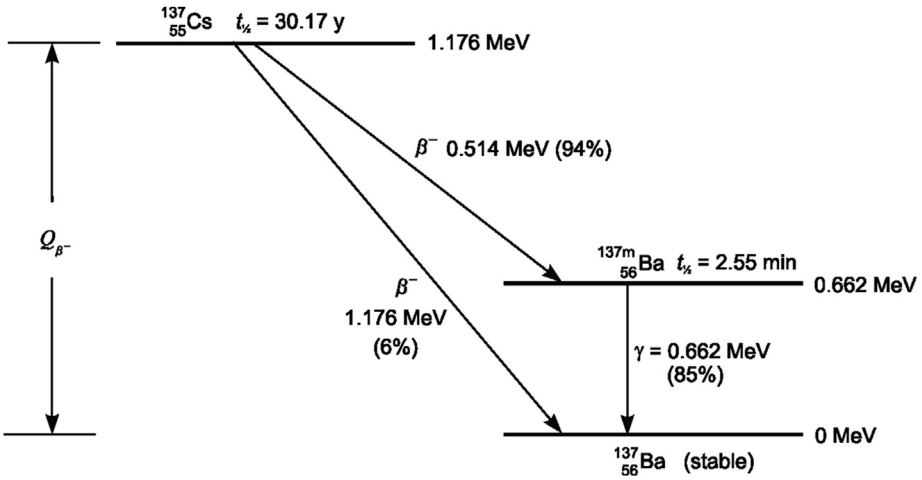

FIGURE 6.3 Negatron beta decay scheme of ^{137}Cs. The radionuclide ^{137}Cs decays to stable ^{137}Ba via two branching negatron emissions with energy maxima of 1.176 MeV at a relative intensity of 6% and 0.514 MeV at an intensity of 94%. Negatrons with energy maxima of 0.514 MeV produce a metastable ^{137m}Ba daughter, which decays to stable ^{137}Ba with the emission of a gamma-ray photon of 0.662 MeV at an 85% intensity.

The decay energy of ^{137}Cs is calculated as follows:

$$\begin{aligned} Q_{\beta^-} &= (M_{137_{Ca}} - M_{137_{Ba}})c^2 = E_{\beta^-} + E_{\overline{\nu}} + E_{\gamma} + E_{\text{recoil}} \\ &= (136.907085\ \text{u} - 136.905822\ \text{u})(931.494\ \text{MeV/u}) \\ &= 1.176\ \text{MeV} \end{aligned} \qquad [6.28]$$

The calculated 1.176 MeV decay energy is the energy liberated from ^{137}Cs decay to the ground state of stable ^{137}Ba. One branch of this decay occurs at 94% intensity (abundance) via the emission of a negatron and antineutrino with an E_{max} of 0.514 MeV, followed by the emission of gamma radiation of 0.662 MeV from the daughter nuclide ^{137m}Ba, which is metastable, decaying to the stable ^{137}Ba (see Fig. 6.3). The remaining 6% of the negatron emissions (ie, 100−94%) arise from the decay of ^{137}Cs directly to the ground state of stable ^{137}Ba, with the entire 1.176 MeV of decay energy shared by the negatron (β^-) and antineutrino ($\overline{\nu}$). The "QCalc" online (www.nndc.bnl/gov/qcalc) computer-calculated decay energy is found to be 1176 keV or 1.176 MeV.

More complex negative beta decay schemes occur, such as that of the radionuclide ^{131}I to stable ^{131}Xe, illustrated in Fig. 6.4.

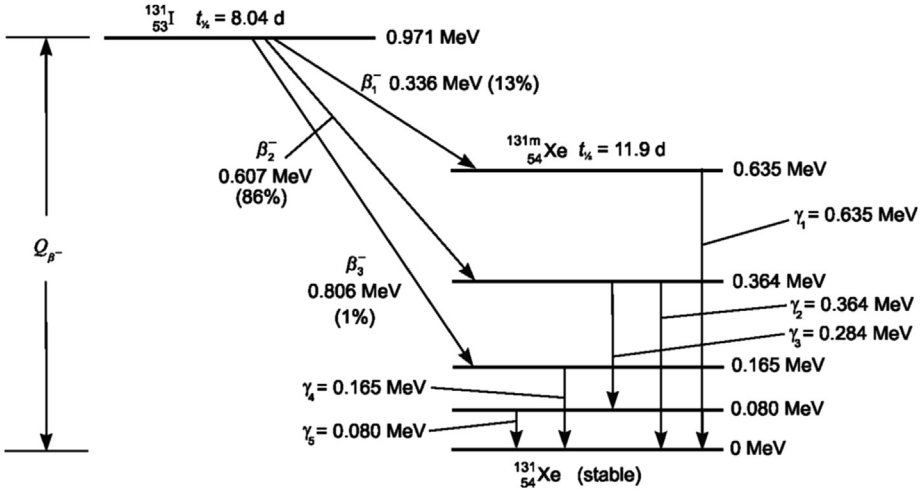

FIGURE 6.4 Negatron decay scheme of ^{131}I. The radionuclide ^{131}I decays to stable ^{131}Xe via three branching negatron emissions with energy maxima at 0.336, 0.607, and 0.806 MeV, producing metastable ^{131m}Xe at three energy levels and yielding several gamma-ray lines of emissions, namely $\gamma_1 = 0.635$ MeV, $\gamma_2 = 0.364$ MeV, $\gamma_3 = 0.284$ MeV, $\gamma_4 = 0.165$ MeV, and $\gamma_5 = 0.080$ MeV.

The decay energy of ^{131}I to stable ^{131}Xe is calculated as

$$\begin{aligned} Q_{\beta^-} &= (M_{131_I} - M_{131_{Xe}})c^2 = E_{\beta^-} + E_{\bar{\nu}} + E_\gamma + E_{\text{recoil}} \\ &= (130.906125\ \text{u} - 130.905083\ \text{u})(931.494\ \text{MeV/u}) \\ &= 0.971\ \text{MeV} \end{aligned} \quad [6.29]$$

The online computer-calculated decay energy (www.nndc.bnl/gov/qcalc) is determined to be 970.8 keV or 0.971 MeV, as calculated above.

In summary, if we ignore the relatively very small nuclear recoil energy, we find that the β^- energy maxima and the gamma-ray emission energies for the three beta decay branches of ^{131}I decay, illustrated in Fig. 6.4, yield the total decay energy of 0.971 MeV, as follows:

β^- Branch 1 of 13% Intensity: $E_{\beta_1^-} + E_{\bar{\nu}} + \gamma_1 = E_{\max}$ of 0.336 MeV + γ_1 of 0.635 MeV = 0.971 MeV

β^- Branch 2 of 86% Intensity: $E_{\beta_2^-} + E_{\bar{\nu}} + \gamma_2 = E_{\max}$ of 0.607 MeV + γ_2 of 0.364 MeV = 0.971 MeV

β^- Branch 3 of 1% Intensity: $E_{\beta_3^-} + E_{\bar{\nu}} + \gamma_4 = E_{\max}$ of 0.806 MeV + γ_3 of 0.165 MeV = 0.971 MeV

6.3 POSITRON (β^+) EMISSION

Positron emission can be described by the general equation

$$^A_Z P \rightarrow {}^A_{Z-1} D + \beta^+ + \nu + K_T \quad [6.30]$$

where $^A_Z P$ is the parent nuclide of atomic number Z and mass number A, $^A_{Z-1} D$ is the daughter nuclide of atomic number $Z - 1$ and the same mass number as the parent, β^+ is the positron or positive beta particle, ν is the neutrino, and K_T is the total kinetic energy released in the beta decay process.

6.3.1 Basic Principles

In contrast to negatron emission from nuclei having n/p ratios too large for stability, positrons, which consist of positively charged electrons (positive beta particles), are emitted from nuclei having n/p ratios too small for stability—that is, those which have an excess of protons.

To attain nuclear stability, the n/p ratio is increased. This is realized by a transformation of a proton to a neutron within the nucleus. The previously discussed change of a neutron to a proton in a negatron-emitting nuclide (Eq. [6.3]) may now be considered in reverse for the emission of positrons. Eq. [6.31] describes such a transformation

$$\text{p}^+ \rightarrow \text{n} + \beta^+ + \nu \quad [6.31]$$

The decay of the radionuclide ^{11}C may be cited as an example of a nuclide that decays by positron emission:

$$^{11}_6\text{C} \rightarrow {}^{11}_5\text{B} + \beta^+ + \nu \quad [6.32]$$

Note that the mass number does not change, but the charge on the nucleus (Z number) decreases by 1. As in negatron emission, a neutrino, ν, is emitted simultaneously with the positron (beta particle), and shares the decay energy with the positron. Thus positrons, like negatrons emitted from a given radionuclide sample, may possess a broad spectrum of energies from near zero to $E_{\max}$, as illustrated in Fig. 6.1.

Decay by positron emission can occur only when the decay energy is significantly above 1.02 MeV. This is because two electrons of opposite charge are produced (β^+, β^-) within the nucleus, and the energy equivalence of the electron mass is 0.51 MeV (see Section 8.8.4 in the chapter: "Electromagnetic Radiation: Photons"). The positive electron, β^+, is ejected from the nucleus and the negative electron, β^-, combines with a proton to form a neutron:

$$\beta^- + \text{p}^+ \rightarrow \text{n} \quad [6.33]$$

From the Chart of the Nuclides, it is possible to cite specific examples of the n/p imbalance in relation to negatron and positron emission. Fig. 6.5 illustrates a segment of the Chart of the Nuclides and the relative positions of the stable nuclides (shaded areas) and their neighboring radionuclides. The nuclides are positioned as a function of the number of protons, Z, and the number of neutrons, N, in their respective nuclei. Dashed arrows are placed through the blocks that segregate

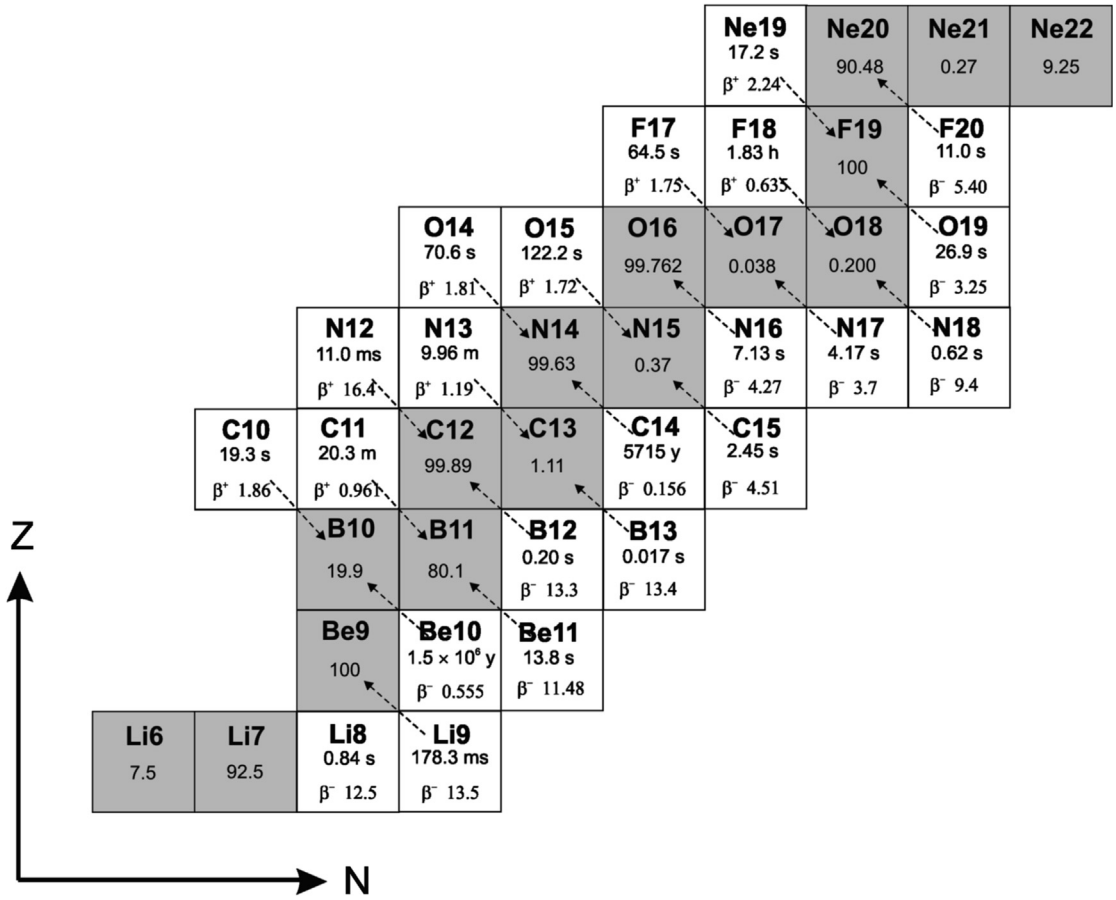

FIGURE 6.5 A segment of the Chart of the Nuclides showing the relative positions of some stable (*shaded*) and unstable nuclides. The ordinate Z and absicca N represent the number of protons (atomic number) and the number of neutrons (neutron number) within the nucleus, respectively. The mass number (number of protons + neutrons) in the nucleus of an isotope is provided alongside the abbreviation of the element. For example, the isotope ^{14}C (carbon-14) is written in the chart as C14. Radionuclides that undergo positron emission (β^+) are illustrated with *arrows* pointing downward to stable nuclide products of a lower atomic number; and radionuclides undergoing negatron (β^-) emission are illustrated with arrows pointing upward to stable nuclide products of a higher atomic number. The maximum beta particle energy in units of MeV is provided alongside the positron or negatron symbol. Numbers in shaded areas are the percentage of natural abundances of the stable isotopes, which for each element should add up to 100%. For example, the element lithium (Li) exists in nature as a combination of two stable isotopes, namely ^6Li and ^7Li, with abundances of 7.5% and 92.5%, respectively. When only one stable isotope of an element exists, its natural abundance will be expressed as 100%, such as is the case for ^9Be and ^{19}F illustrated above. The half-lives of the unstable nuclides are given in units of seconds (s), milliseconds (ms), minutes (m), hours (h), and years (y).

radionuclides interrelated with common daughter nuclides resulting from β^- or β^+ decay processes. For example, the stable nuclide ^{12}C of atomic number 6 has a nucleus with an n/p ratio of 6/6. However, the nuclide ^{12}N of atomic number 7 has an unstable n/p ratio of 5/7, an excess of protons. Thus this radionuclide ^{12}N decays to ^{12}C via positron emission according to the equation

$$^{12}_{7}\mathrm{N} \rightarrow {}^{12}_{6}\mathrm{C} + \beta^+ + \nu \qquad [6.34]$$

as indicated by a dashed arrow in Fig. 6.5.

The nuclide ^{12}B of atomic number 5 has the unstable n/p ratio of 7/5, an excess of neutrons. This nuclide thus decays to ^{12}C by negatron emission according to the equation

$$^{12}_{5}\mathrm{B} \rightarrow {}^{12}_{6}\mathrm{C} + \beta^- + \overline{\nu} \qquad [6.35]$$

Similar reasoning may be used to explain positron and negatron decay of the unstable nuclides shown in Fig. 6.5 to the stable products ^{13}C, ^{14}N, and ^{15}N, etc. The interrelationship between β^- and β^+ decay leading to the formation of stable nuclides is to be found throughout the Chart of the Nuclides. Nuclear stability with n/p ratios close to unity only exists with nuclides of low atomic number ($Z \leq 20$), as discussed in the chapter entitled "The Atomic Nucleus" and in the following section of this chapter.

6.3.2 *N*/*Z* Ratios and Beta Decay

Negatron and positron emission were discussed previously as processes whereby unstable nuclei may achieve stability via neutron or proton transformations in negatron and positron beta decay processes, respectively. These processes in the nucleus of the radionuclide result in a change in the n/p or *N*/*Z* ratio of the nucleus.

If we look throughout the Chart of the Nuclides, we notice that the stable nuclides of low atomic number will have an *N*/*Z* ratio of approximately 1. However, as the atomic number increases ($Z > 20$), the *N*/*Z* ratio of the stable nuclides increases gradually and reaches as high as approximately 1.5 (eg, $^{209}_{83}$Bi, $Z = 83$, $N/Z = 1.518$). This is illustrated in Fig. 20.7 in the chapter entitled "The Atomic Nucleus." There are no stable nuclides of an atomic number greater than 83.

The nature of nuclear forces and the relationship of *N*/*Z* ratio to nuclear stability are discussed in detail in the chapter entitled "The Atomic Nucleus," and by Serway et al. (2005) and Sundaresan (2001). In brief, the importance of *N*/*Z* ratio to nuclear stability is explained by the fact that there exists a short-range attractive nuclear force, which extends to a distance of $\approx$2 fm (2 fermi or 2×10^{-15} m). This attractive force has charge independence, and is a consequence of the relative spins of the protons and neutrons and their relative positions in the nucleus. These binding exchange forces therefore exist, regardless of charge on the particles, between two protons, two neutrons, and a proton and neutron. While the attractive nuclear forces will tend to hold the nucleus together, at the same time there are repelling coulombic forces between the positively charged protons that act to force them apart. For nuclides of low *Z*, the attractive nuclear forces exceed the repelling coulombic forces when $N \approx Z$. However, increasing the number of protons (eg, $Z > 20$) further increases the strength of the repelling coulombic forces over a larger nucleus, which will tend to force the nucleus apart. Therefore additional neutrons, $N > Z$, provide additional attractive nuclear forces needed to overcome the repelling forces of the larger proton population. As the atomic number increases further, $Z > 83$, all nuclides are unstable. Even though *N*/*Z* ratios reach 1.5, nuclear stability is not achieved when the number of protons in the nucleus exceeds 83.

6.3.3 Positron Decay Energy

The general reaction for positron emission was described by Eq. [6.30]. It is provided here again for a treatment on positron decay energy:

$$ {}^{A}_{Z}P \rightarrow {}^{A}_{Z-1}D + \beta^{+} + \nu + K_T \qquad [6.36] $$

where ${}^{A}_{Z}P$ is the parent nuclide of atomic number Z and mass number A, ${}^{A}_{Z-1}D$ is the daughter nuclide of atomic number $Z - 1$ and the same mass number as the parent, β^{+} is the positron or positive beta particle, ν is the neutrino, and K_T is the total kinetic energy released in the beta decay process.

In terms of nuclear masses, Eq. [6.36] may be written as

$$ {}_{Z}M_P = {}_{Z-1}M_D + m_e + K_T \qquad [6.37] $$

where ${}_{Z}M_P$ and ${}_{Z-1}M_D$ are the masses of the parent and daughter nuclei of atomic number Z and $Z - 1$, respectively, and m_e is the mass of the positron (ie, one electron mass). Atomic mass units (u) may be used to calculate conveniently the mass difference of the parent and daughter, if we add Z atomic electron masses to each side of Eq. [6.37] and ignore the negligible difference in electron binding energies of the parent and daughter atoms. Adding Z atomic electrons to each side of Eq. [6.37] gives

$$ {}_{Z}M_P + Zm_e = {}_{Z-1}M_D + (Z+1)m_e + K_T \qquad [6.38] $$

and

$$ {}_{Z}M_P = {}_{Z-1}M_D + 2m_e + K_T \qquad [6.39] $$

The mass difference of the parent and daughter nuclei is equivalent to the decay energy, Q_{β^+}. The decay energy, Q_{β^+}, may be calculated now using atomic mass units and taking the product of mass and c^2 to determine the energy equivalence of mass using Eq. [6.39] to give

$$ Q_{\beta^+} = ({}_{Z}M_P - {}_{Z-1}M_D)c^2 = 2m_e c^2 + K_T \qquad [6.40] $$

or

$$ Q_{\beta^+} = ({}_{Z}M_P - {}_{Z-1}M_D)c^2 = 2m_e + E_{\beta^+} + E_{\nu} + E_{\gamma} + E_{\text{recoil}} \qquad [6.41] $$

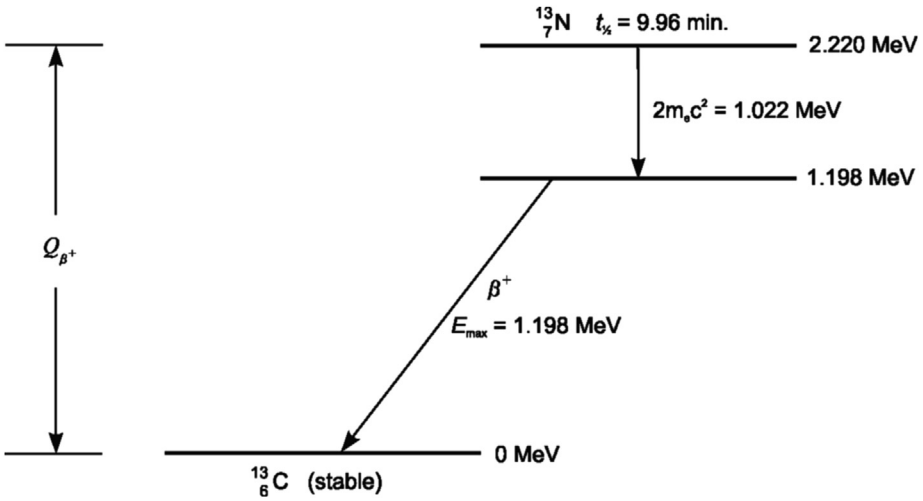

FIGURE 6.6 Beta decay of ^{13}N to stable ^{13}C by positron (β^+) emission. The scheme illustrates the energy equivalence (1.022 MeV) of two electron masses (e^+e^-) required for positron emission. The remaining 1.198 MeV energy is shared by the β^+ and ν.

where ${}_ZM_P - {}_{Z-1}M_D$ is the mass difference of the parent and daughter nuclides, c is the speed of light in a vacuum, and $2m_ec^2$ is the energy equivalence of two electron masses or 1.022 MeV, which is the energy required for the creation of the e^+e^- pair in the positron decay process described in Section 6.3.1. The terms $E_{\beta^+} + E_\nu$ are the shared positron and neutrino kinetic energies, which combined are often referred to as the $E_{\max}$ of the beta decay. The term E_γ is gamma-ray energy that may be emitted by the daughter nucleus, and E_{recoil} is the nuclear recoil energy, which is relatively small (measured in eV) and can be ignored as negligible when calculating the overall decay energy (measured in MeV).

We may take an example of a simple case of positron emission in the decay of ^{13}N where there is no gamma radiation from the daughter nucleus—that is, the ^{13}N nucleus decays directly to ^{13}C at its stable ground state with the emission of a positron and neutrino with maximum energy 1.198 MeV. The scheme for the decay of ^{13}N is illustrated in Fig. 6.6.

The $E_{\max}$ is the combined energy of the positron and neutrino $\left(E_{\beta^+} + E_\nu\right)$—that is, the energy shared by the positron and neutrino. In other words, the $E_{\max}$ is the maximum energy of the positron when the neutrino is at its minimum energy, or vice versa.

The decay energy, Q_{β^+}, for ^{13}N decay is calculated as

$$\begin{aligned} Q_{\beta^+} &= (M_{13_N} - M_{13_C})c^2 \\ &= (13.0057386\ \text{u} - 13.0033548\ \text{u})(931.494\ \text{MeV/u}) \\ &= 2.2204\ \text{MeV} \end{aligned} \quad [6.42]$$

which is the magnitude of the decay energy for ^{13}N listed in standard reference tables (eg, Table of the Isotopes in Lide, 2010). The maximum energy of the β^+ or neutrino in this case may be calculated easily according to Eq. [6.41] by ignoring the nuclear recoil energy (E_{recoil}), because of its small value, and ignoring the gamma-ray energy (E_γ), because in this example no gamma-ray energy arises from the daughter nucleus following beta decay. Thus the maximum energy of the β^+ or neutrino is

$$\begin{aligned} E_{\max} &= E_{\beta^+} + E_\nu = Q_{\beta^+} - 2m_ec^2 \\ &= 2.220\ \text{MeV} - 1.022\ \text{MeV} \\ &= 1.198\ \text{MeV} \end{aligned} \quad [6.43]$$

The above value of 1198 keV or 1.198 MeV can be calculated online via the National Nuclear Data Center website (www.nndc.bnl.gov/qcalc).

A more complex example is that of the decay of ^{22}Na, which decays by positron (β^+) emission and EC decay with the emission of gamma radiation according to the decay (Eqs. [6.44] and [6.45]) and the decay scheme illustrated in Fig. 6.7.

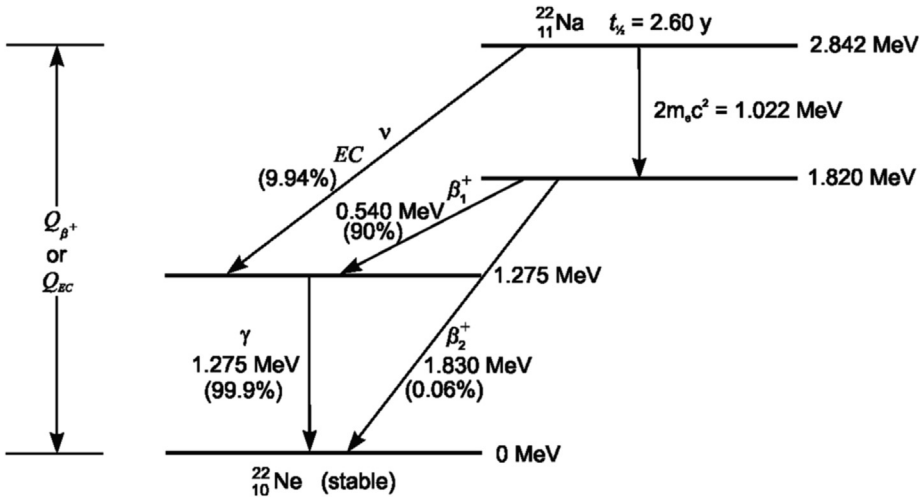

FIGURE 6.7 Beta decay scheme of ^{22}Na by competing positron (β^+) and EC decay. Positron emission occurs in 90.06% of the nuclear decays and EC on the remaining 9.94%. Decay by EC involves the emission of a monoenergetic neutrino of 1.567 MeV (ie, $E_\nu = 2.842 - 1.275$ MeV) to metastable ^{22}Ne. Positron emission occurs with the consumption of the energy equivalence of two electron masses (ie, $2m_ec^2$), followed by two branching positron emissions with intensities of 90% and 0.06%.

Positron emission (90.06%):

$$\begin{aligned} &^{22}_{11}\mathrm{Na} \rightarrow {}^{22}_{10}\mathrm{Ne} + \beta^+ + \nu + \gamma(90.0\%) \text{ and} \\ &^{22}_{11}\mathrm{Na} \rightarrow {}^{22}_{10}\mathrm{Ne} + \beta^+ + \nu(0.06\%) \end{aligned} \quad [6.44]$$

Electron capture (9.94%):

$$^{22}_{11}\mathrm{Na} \rightarrow {}^{22}_{10}\mathrm{Ne} + \nu + \gamma(9.94\%) \quad [6.45]$$

As illustrated in Fig. 6.7, the radionuclide ^{22}Na may decay by EC in addition to positron emission. EC is a decay mode that competes with positron emission, as discussed in the following section. In this case, 90.06% of the ^{22}Na radionuclides decay via positron emission and the remaining 9.94% decay via EC. When the decay energy, Q_{β^+}, is well above 1.022 MeV (the minimum energy required for e^+e^- pair production), positron emission will predominate over EC decay.

The decay energy for ^{22}Na may be calculated according to Eq. [6.40] as

$$\begin{aligned} Q_{\beta^+} &= (M_{^{22}\mathrm{Na}} - M_{^{22}\mathrm{Ne}})c^2 \\ &= (21.994437\ \mathrm{u} - 21.9913855\ \mathrm{u})(931.494\ \mathrm{MeV/u}) \\ &= 2.842\ \mathrm{MeV} \end{aligned} \quad [6.46]$$

which is in agreement with the magnitude of the decay energy for ^{22}Na listed in standard reference tables (eg, Table of the Isotopes in Lide, 2010). The calculated decay energy corresponds to the theoretical value described by Eq. [6.41], which is

$$Q_{\beta^+} = 2m_ec^2 + E_{\beta^+} + E_\nu + E_\gamma + E_{\mathrm{recoil}} \quad [6.47]$$

where $E_{\beta^+} + E_\nu = \beta^+_{\mathrm{max}}$ and, if we ignore the relatively very small value of E_{recoil}, we calculate

$$\begin{aligned} Q_{\beta_1^+} &= 2m_ec^2 + \beta^+_{\mathrm{max}} + E_r \\ &= 1.022\ \mathrm{MeV} + 0.540\ \mathrm{MeV} + 1.275\ \mathrm{MeV} \\ &= 2.84\ \mathrm{MeV} \end{aligned} \quad [6.48]$$

which is in accord the β_1^+ transition illustrated in Fig. 6.7, and

$$\begin{aligned} Q_{\beta_2^+} &= 2m_ec^2 + \beta^+_{\mathrm{max}} \\ &= 1.022\ \mathrm{MeV} + 1.830\ \mathrm{MeV} \\ &= 2.85\ \mathrm{MeV} \end{aligned} \quad [6.49]$$

which is in agreement with the β_2^+ transition illustrated in Fig. 6.7 whereby ^{22}Na decays directly to the stable ground state of ^{22}Ne without gamma emission in 0.06% of the nuclear decays.

6.4 ELECTRON CAPTURE

The EC decay process is described by the following general equation:

$$ {}^{A}_{Z}P + e \xrightarrow{\text{EC}} {}^{A}_{Z-1}D + \nu + K_T \qquad [6.50] $$

where ${}^{A}_{Z}P$ is the parent nuclide of atomic number Z and mass number A, e is an orbital electron captured by the nucleus of the parent nuclide, ${}^{A}_{Z-1}D$ is the daughter nuclide of atomic number $Z-1$ and the same mass number as the parent, ν is the neutrino, and K_T is the total kinetic energy released in the beta decay process.

6.4.1 Basic Principles

EC is another form of beta decay. The change in atomic number is the same as occurs with positron (β^+) emission. EC competes with positron emission, and most radionuclides that decay by positron emission also decay by EC to the same daughter nuclide.

Another mechanism, in addition to positron emission, by which an unstable nucleus can increase its n/p ratio is via the capture by the nucleus of a proximate atomic electron (eg, K- or L-shell electron). The absorbed electron combines with a proton to yield a neutron within the nucleus as follows:

$$ e^- + \text{p}^+ \rightarrow \text{n} + \nu + \text{inner bremsstrahlung} + \text{X-rays} + \text{Auger electrons} + \gamma \qquad [6.51] $$

The decay process is known as EC, sometimes referred to as K capture because most of the electrons are captured from the K shell, which is closest to the nucleus. A neutrino, ν, is emitted, accompanied by the emission of internal bremsstrahlung, which is a continuous spectrum of electromagnetic radiation that originates from the atomic electron as it undergoes acceleration toward the nucleus. Unlike the beta decay process, which results in the emission of a neutrino from the nucleus with a broad spectrum of energies, the neutrino emitted from the EC decay process does not share the transition energy with another particle, and therefore it is emitted with a single quantum of energy equal to the transition energy less the atomic electron binding energy. The capture of an atomic electron by the nucleus leaves a vacancy in an electron shell, and this is usually filled by an electron from an outer shell, resulting in the production of X-radiation (see also the chapter: "Electromagnetic Radiation: Photons"). The electron that fills the vacancy leaves yet another vacancy at a more distant shell. A cascade of electron vacancies and subsequent filling of vacancies from outer electron shells occurs, with the production of X-rays characteristic of the daughter atom. The X-rays will either travel out of the atom or the energy emitted by the electron transition will be transferred to an outer orbital electron, causing the electron to be ejected as an Auger electron. Gamma radiation is illustrated in the above Eq. [6.51], because it is emitted only when the daughter nuclide is left at an unstable elevated energy state (see Figs. 6.7–6.9).

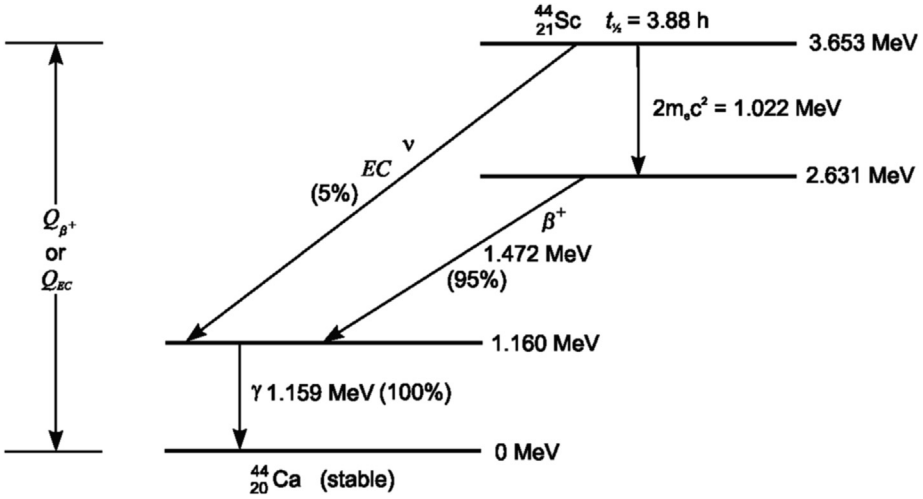

FIGURE 6.8 Beta decay scheme of ^{44}Sc by competing EC decay and positron (β^+) emission. The high decay energy of 3.653 MeV favors β^+ emission, as it is well above the minimum 1.022 MeV or $2m_ec^2$ required for positron emission. EC decay occurs in only 5% of the nuclear decays and β^+ emission in the remaining 95%. Both EC and β^+ decay yield metastable ^{44m}Ca, which decays to stable ^{44}Ca with gamma-ray emission of 1.159 MeV.

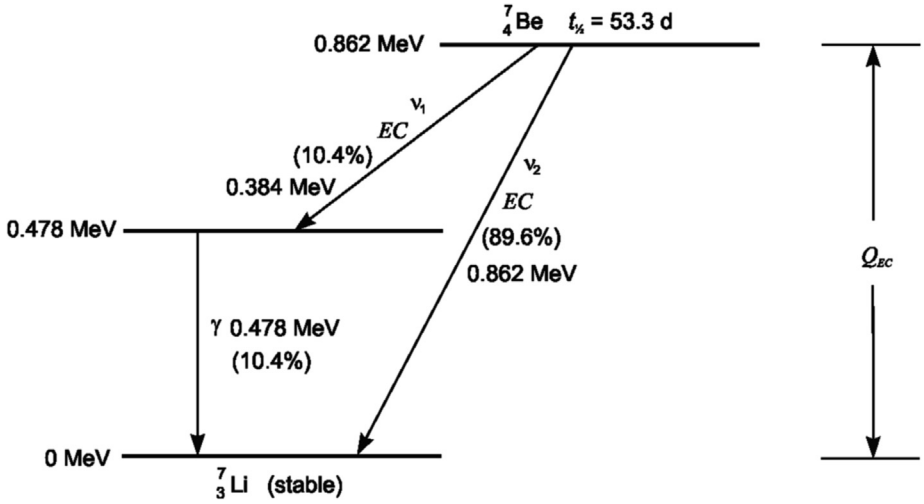

FIGURE 6.9 Decay scheme of ^{7}Be. The decay occurs exclusively by branching electron capture. In 10.4% of the transitions, ^{7}Be emits a monoenergetic neutrino of 0.384 MeV (ie, 0.862 − 0.478 MeV) followed by the emission of a 0.478 MeV gamma-ray photon. The remaining EC decay events occur with the emission of a monoenergetic neutrino of 0.862 MeV directly to the ground state of stable ^{7}Li in 89.6% of the decay transitions.

The EC decay process may compete with β^+ emission; that is, some radionuclides may decay by either EC or β^+-emission. As discussed previously, positron emission requires a transition energy of at least 1.022 MeV, the minimum energy required for pair production in the nucleus (ie, two electron rest mass energies or 2×0.511 MeV). Positron emission will therefore not compete with EC for decay transitions less than 1.022 MeV. In general, positron emission will predominate when the transition energy is high (well above 1.022 MeV) and for nuclides of low atomic number, while the EC decay process will predominate for low transition energies and nuclides of higher atomic number. The decay transitions of ^{22}Na and ^{65}Zn serve as examples. In the case of ^{22}Na, decay by β^+ emission predominates (90%) as compared with decay via EC (10%)

$$^{22}_{11}\text{Na} \rightarrow {}^{22}_{10}\text{Ne} + \beta^+ + \nu + \gamma \ (90\%) \qquad [6.52]$$

and

$$^{22}_{11}\text{Na} \xrightarrow{\text{EC}} {}^{22}_{10}\text{Ne} + \nu + \gamma \ (10\%) \qquad [6.53]$$

The transition energy of ^{22}Na is 2.842 MeV (Holden, 1997a), well above the 1.022 MeV minimum required for positron emission. Thus positron emission predominates. On the other hand, taking the following example of the nuclide ^{65}Zn, we see that EC predominates over β^+ emission:

$$^{65}_{30}\text{Zn} \rightarrow {}^{65}_{29}\text{Cu} + \beta^+ + \nu + \gamma \ (1.5\%) \qquad [6.54]$$

and

$$^{65}_{30}\text{Zn} \xrightarrow{\text{EC}} {}^{65}_{29}\text{Cu} + \nu + \gamma \ (98.5\%) \qquad [6.55]$$

In the case of ^{65}Zn, the transition energy is only 1.35 MeV (Holden, 1997a), which is not much above the minimum energy of 1.02 MeV required for positron emission. Consequently, EC decay predominates.

6.4.2 EC Decay Energy

The general decay equation for EC was described by Eq. [6.50]. It is provided here again for a treatment on EC decay calculations:

$$^{A}_{Z}P + e \xrightarrow{\text{EC}} {}^{A}_{Z-1}D + \nu + K_T \qquad [6.56]$$

where $^{A}_{Z}P$ is the parent nuclide of atomic number Z and mass number A, e is an orbital electron captured by the nucleus of the parent nuclide, $^{A}_{Z-1}D$ is the daughter nuclide of atomic number $Z - 1$ and the same mass number as the parent, ν is the neutrino, and K_T is the total kinetic energy released in the beta decay process.

In mass and energy terms, Eq. [6.56] can be written as

$$ {}_{Z}M_{P} + m_{e} = {}_{Z-1}M_{D} + K_{T} \quad [6.57] $$

where ${}_{Z}M_{P}$ is the mass of the parent nuclide of atomic number Z, m_e is the mass of the atomic electron captured by the nucleus, and ${}_{Z-1}M_{D}$ is the mass of the daughter nucleus of atomic number $Z-1$. We may use atomic mass units (u) to calculate conveniently the mass difference of the parent and daughter nuclei and arrive at the decay energy by firstly adding $Z-1$ atomic electrons to each side of Eq. [6.57], which yields

$$ {}_{Z}M_{P} = {}_{Z-1}M_{D} + K_{T} \quad [6.58] $$

The mass difference of the parent and daughter nuclei is equivalent to the decay energy (Q_{EC}). We can now calculate the decay energy Q_{EC} by the difference of the parent and daughter nuclide atomic masses, ignoring the small difference in the binding energies of the electrons in the two nuclides, as

$$ Q_{\mathrm{EC}} = \left({}_{Z}M_{P} - {}_{Z-1}M_{D}\right)c^{2} = K_{T} = E_{\nu} + E_{\gamma} + E_{\mathrm{recoil}} \quad [6.59] $$

where c is the velocity of light in a vacuum and the product Mc^2 yields the energy equivalence of the mass, E_ν is the kinetic energy of the neutrino, E_γ is the gamma-ray photon energy, which only appears with the decay of the daughter nucleus when it is left at a metastable or excited energy state, and E_{recoil} is the kinetic energy of the daughter recoil nucleus. As in the previously described beta decay processes, we will ignore the relatively very small recoil energy when calculating the overall decay energy.

As an example, let us look at the decay scheme of ^{44}Sc, which decays by EC and positron emission. The decay equations are

$$ {}^{44}_{21}\mathrm{Sc} \xrightarrow{\mathrm{EC}} {}^{44}_{20}\mathrm{Ca} + \nu + \gamma\ (5\%) \quad [6.60] $$

and

$$ {}^{44}_{21}\mathrm{Sc} \rightarrow {}^{44}_{20}\mathrm{Ca} + \beta^{+} + \nu + \gamma\ (95\%) \quad [6.61] $$

The decay scheme is illustrated in Fig. 6.8.

The scheme in Fig. 6.8 illustrates that 5% of the ^{44}Sc nuclides decay by EC, and the remaining 95% decay with positron emission with a positron E_{max} of 1.472 MeV. The ^{44}Ca product nuclides then decay to a stable ground state with the emission of gamma radiation of 1.159 MeV energy.

The decay energy for either mode of decay (EC or β^+ emission) is calculated according to Eqs. [6.59] and [6.46], respectively, as follows.

For EC

$$ \begin{aligned} Q_{\mathrm{EC}} &= \left({}_{Z}M_{P} - {}_{Z-1}M_{D}\right)c^{2} = E_{\nu} + E_{\gamma} + E_{\mathrm{recoil}} \\ &= \left(M_{44_{\mathrm{Sc}}} - M_{44_{\mathrm{Ca}}}\right)c^{2} \\ &= (43.959403\ \mathrm{u} - 43.955481\ \mathrm{u})(931.494\ \mathrm{MeV/u}) \\ &= 3.653\ \mathrm{MeV} \end{aligned} \quad [6.62] $$

which is in agreement with the decay energy provided in standard reference tables (eg, Holden, 1997a). As we know that the gamma-ray energy $E_\gamma = 1.159$ MeV (see Fig. 6.8) and if we disregard the very small magnitude of the recoil energy, we can calculate the neutrino energy in this case as

$$ E_{\nu} = Q_{\mathrm{EC}} - E_{\gamma} = 3.653\ \mathrm{MeV} - 1.159\ \mathrm{MeV} = 2.494\ \mathrm{MeV} \quad [6.63] $$

The neutrino energies are monoenergetic in the case of the EC decay mode.

For positron emission

$$ \begin{aligned} Q_{\beta^{+}} &= \left({}_{Z}M_{P} - {}_{Z-1}M_{D}\right)c^{2} = 2m_{e}c^{2} + E_{\beta^{+}} + E_{\nu} + E_{\gamma} + E_{\mathrm{recoil}} \\ &= \left(M_{44_{\mathrm{Sc}}} - M_{44_{\mathrm{Ca}}}\right)c^{2} = 3.653\ \mathrm{MeV}\ (\text{as calculated in Eq. [6.62]}) \end{aligned} \quad [6.64] $$

If we again ignore the very small recoil energy of the daughter nucleus and combine the positron and neutrino energies as $E_{\mathrm{max}} = E_{\beta^+} + E_\nu$, we can arrive at the decay energy taking the values from Fig. 6.8 as

$$\begin{aligned} Q_{\beta^+} &= 2m_e c^2 + E_{\max} + E_\gamma \\ &= 1.022\ \text{MeV} + 1.472\ \text{MeV} + 1.159\ \text{MeV} \\ &= 3.653\ \text{MeV} \end{aligned} \quad [6.65]$$

The decay energy of 3.653 MeV is well above the minimum energy for e^+e^- pair production ($2m_ec^2$ or 1.022 MeV) required for positron emission. Thus the EC decay does not compete well against positron emission in the case of ^{44}Sc, which decays via positron emission in 95% of the disintegrations and by EC decay in the remaining 5%.

Let us take another example, which is that of ^{7}Be decaying exclusively by EC according to the following equation:

$$^7_4\text{Be} \xrightarrow{\text{EC}} {}^7_3\text{Li} + \nu + \gamma \quad [6.66]$$

The decay energy is calculated as

$$\begin{aligned} Q_{\text{EC}} &= (M_{^7\text{Be}} - M_{^7\text{Li}})c^2 \\ &= (7.016929\ \text{u} - 7.016004\ \text{u})(931.494\ \text{MeV/u}) \\ &= 0.862\ \text{MeV} \end{aligned} \quad [6.67]$$

which is in agreement with the magnitude of the decay energy reported in standard reference tables (eg, Holden, 1997a). The decay energy is not sufficient to satisfy the minimum energy requirement of 1.022 MeV for positron emission in this case. Thus there is no competition here between EC and β^+ decay modes, and the ^{7}Be nuclides decay exclusively by EC according to the decay scheme illustrated in Fig. 6.9.

The daughter nuclide, ^{7}Li, emits a gamma ray of 0.478 MeV in 10.4% of the transitions. The neutrino energy from the EC decay of ^{7}Be in these transitions is derived from the difference of the decay energy and gamma-ray energy, while ignoring the relatively very small recoil energy according to Eq. [6.63], or

$$\begin{aligned} E_\nu &= Q_{\text{EC}} - E_\gamma \\ &= 0.862\ \text{MeV} - 0.478\ \text{MeV} \\ &= 0.384\ \text{MeV} \end{aligned} \quad [6.68]$$

The remaining 89.6% of the transitions are due to a neutrino emission of 0.862 MeV directly to the stable ground state of the daughter nuclide without any gamma-ray emission. Neutrinos emitted in the EC decay process are monoenergetic. They do not possess any broad spectrum of energies, contrary to the neutrinos emitted during β^+ or β^- emission, because the neutrinos emitted from the nucleus in EC decay do not share the decay energy with any other particle.

There is nuclear recoil of the daughter nucleus during EC decay resulting from the emission of the neutrino. We should keep in mind that it is the daughter nucleus that undergoes recoil, because when a neutrino is emitted from the parent nucleus, the parent becomes the daughter. The nuclear recoils in EC decay have been measured by researchers, confirming the monoenergetic character of the emitted neutrino. The calculation of nuclear recoil energies is discussed in detail in the chapter entitled "The Atomic Nucleus."

The ^{7}Li ion will recoil at two energy maxima corresponding to the neutrino emissions of 0.862 and 0.384 MeV calculated above. The maximum recoil energy corresponding to the neutrino emission of 0.862 MeV is calculated, according to Eqs. [20.97] and [20.114] of the chapter entitled "The Atomic Nucleus," to be 56.84 eV. This agrees with the experimental measurement of the ^{7}Li recoil energy reported by 2002 Nobel Laureate Raymond Davis, Jr (1952) to be 56 ± 1 eV. The recoil energy in this case is relatively high (>10 eV), because of the relatively low mass of the ^{7}Li nucleus. Nevertheless, the recoil energy here may be ignored as negligible when calculating the decay energy, which has units of MeV.

6.4.3 Chemical and Pressure Effects on EC Decay Rates

In general, the chemical and physical environments of radionuclides do not control nuclear decay processes. However, because the EC decay process involves the capture of an orbital electron by the nucleus, atomic or molecular binding effects, which vary with chemical structure, can influence the EC decay process. Also, external pressure that may alter electron densities in the vicinity of the nucleus could also have an altering effect on the EC decay rate.

Emilio Segré (1947) at the Berkeley Radiation Laboratory of the University of California in the USA and Raymond Daudel (1947) at the Curie Laboratories of the Radium Institute in Paris, France were the first to suggest independently that the rate of disintegration of nuclei decaying by EC or internal conversion would be subject to extranuclear environments. Numerous works were published from 1948 to the 1970s confirming the effect of the chemical environment on the decay rate of ^{7}Be, and these are reviewed by Huh (1999). The effect of pressure on the decay constant of ^{99}Tc was first confirmed by Bainbridge (1952), and the mathematical expression for the shift in the binding energy of the atomic electron under pressure, which would affect EC decay rates, was derived by Mukoyama and Shimizu (1974).

During the last two decades or so, much attention has been given to experimentation related to chemical and pressure effects on radionuclide EC decay rates, due to the technological advances in detector instrumentation with improved detection efficiencies and energy resolution of semiconductor detectors that can now yield more precise decay rate measurements. Utilizing a 100% efficiency high-purity germanium detector, Huh (1999) was able to determine the decay constant of ^{7}Be in three chemical environments, namely $Be^{2+}(OH_2)_4$, $Be(OH)_2$, and BeO, with a precision of 0.01%, resulting in a ~1.5% difference in the decay rates of ^{7}Be in $Be(OH)_2$ and BeO. Also, Ray et al. (1999) found the decay rate of ^{7}Be implanted in Au was $0.72 \pm 0.07\%$ lower than ^{7}Be implanted in Al_2O_3. The variation in decay rates of the ^{7}Be was considered to be a result of the change in the electron density around the nucleus of ^{7}Be due to its association with different anions, and the atomic electron affinity and geometry of the lattice within which the ^{7}Be was implanted. EC occurs mostly with electrons in closest proximity to the nucleus, such as electrons from the *K* shell; and any chemical bond or environment that would force atomic electrons closer to the nucleus or reduce the electron binding energy would increase the EC decay rate.

The combination of chemical environment and pressure can affect EC decay rates. Liu and Huh (2000) found a steady increase in the decay constant of ^{7}Be in $Be(OH)_2$ as a function of pressure over the range of 1 atm−441 kbar. The decay constant increased by 1% at 441 kbar compared to the decay constant at 1 atm, which corresponded to a change in half-life from 53.414 ± 0.003 days at 1 atm to 52.884 ± 0.022 days at 441 kbar pressure. These results were consistent with calculations made by Tossell (2002) on the effects of Be−O bond compression in $Be(OH)_4^{2-}$ on the energy and the electron density at the nucleus of ^{7}Be, which indicates that several 100 kbar pressure could increase the electron density by 1% or more. This would expectedly facilitate the capture of an orbital electron by the nucleus and increase the decay rate. Lee and Steinle-Neumann (2008) demonstrated a 0.1−0.2% increase in the decay constant of ^{7}Be as a metal, chloride, or oxide under a pressure of 25 GPa. The radionuclides ^{22}Na and ^{40}K in metallic form showed an increase of 0.06% and 0.025% in their decay constants, respectively, at 25 GPa pressure. Ray et al. (2009) also observed an increase in the orbital EC rates of ^{109}In and ^{110}Sn by $1.00 \pm 0.17\%$ and $0.48 \pm 0.25\%$, respectively, when implanted in the smaller Au lattice compared to implantation in a larger Pb lattice. They interpret the increased decay rates as being due to an increase in the eigenstate energies of an atom under spatial confinement. This effect would increase the electron density of the orbital electrons at the nucleus, and thus increase the decay rate of an electron capturing radioactive nucleus.

While the fluctuations in the observed EC decay rates may appear small, Zito and Schiferl (1987) indicate that the effects may be significant in terms of stellar energetics. They note that pressure-dependent decay may be an important source of heat generation in Jovian planets where central pressures may reach megabars. They give the example of Jupiter's rock−ice core, which contains as much potassium as Earth's continental crust, and that ^{40}K decay accounts for about 11.5% of the total excess energy output of Jupiter. This energy divided into two parts gives 9.3% due to normal (zero-pressure) beta and EC decay, and the remaining 2.2% would be due to pressure effects alone on the EC decay rate. Also, they surmise that pressure effects on the EC decay rate of ^{90m}Nb could account for 14% of the total energy output of Jupiter's core. The high pressures in Saturn, Uranus, and Neptune could have a role in pressure-accelerated EC decay as an important heat source in these planets. Zito and Schiferl (1987) also provide convincing arguments in support of the role of ^{50}V, ^{123}Te, ^{138}La, ^{40}K, ^{26}Al, and ^{36}Cl, which undergo EC decay, in stellar energetics. They note that peculiar A stars are enriched in La isotopes by a factor of 600 over normal stars, and other stars breed significant amounts of ^{26}Al and ^{36}Cl. They point out that sudden pressure changes in the interior of these stars could result in EC outbursts.

6.5 BRANCHING β^-, β^+, AND EC DECAY

It is a common practice to characterize radionuclide beta decay according to negatron (β^-) emission, positron (β^+) emission, and/or EC. However, there are also several radionuclides of odd atomic number *Z* and even mass number *A* that decay via all beta decay modes, namely β^-, β^+, and EC decay, to varying degrees, yielding two daughter nuclides that differ by two units of atomic number. Their decay may be described by the branching pathways illustrated in Fig. 6.10, where the parent nuclide ${}^{A}_{Z}P$ decays in two directions, namely by β^- emission to a daughter nuclide ${}^{A}_{Z+1}D$ of atomic number

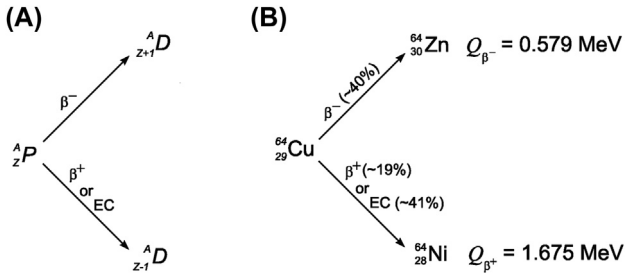

FIGURE 6.10 Branching β^-, β^+, and EC decay illustrated by (A) the general decay reaction of a parent nuclide ${}^{A}_{Z}P$ to daughter nuclides ${}^{A}_{Z+1}D$ and ${}^{A}_{Z-1}D$, and (B) the decay of ${}^{64}_{29}$Cu to the daughter nuclide ${}^{64}_{30}$Zn by negatron (β^-) emission and to the daughter nuclide ${}^{64}_{28}$Ni by positron (β^+) emission or EC decay. The intensities of the three modes of decay—that is, their branching ratios—are ~40% for negatron emission, ~19% for positron emission, and ~41% for EC decay.

$Z+1$, by β^+ emission, and by EC decay to a daughter nuclide ${}^{A}_{Z-1}D$ of atomic number $Z-1$. This decay phenomenon is also referred to as "dual beta decay"; however, it should not be confused with "double beta decay," which is an altogether different and more elusive decay process described in a subsequent section of this chapter.

Radionuclides that decay by means of this branching β^-, β^+, and EC decay are listed in Table 6.1, together with the relative intensity (%) to which these three beta decay modes occur, and the decay energies of each mode and their daughter nuclides. These radionuclides can be found in the Chart of the Nuclides, together with their neighboring isobars that are stable. A segment of the Chart of the Nuclides illustrating the positions of ^{36}Cl and ^{40}K, which decay by the three β^-, β^+, and EC modes, and their neighboring stable daughter isobars is provided in Fig. 6.11.

The decay schemes of ^{36}Cl and ^{40}K exhibit very low relative occurrences of their β^+ decay modes, namely 0.002% and 0.3%, respectively, which may be due to their relatively low decay energies of $\left(Q_{\mathrm{EC},\beta^+}\right)$ of 1.142 and 1.505 MeV, respectively (see Table 6.1). Positron decay will compete and predominate over the EC decay mode when the decay energy is well above 1.022 MeV, which is the energy required for the production of an e^+e^- pair needed for the positron decay mode. Two nuclides listed in Table 6.1, namely ^{64}Cu and ^{74}As, have higher decay energies $\left(Q_{\mathrm{EC},\beta^+}\right)$ of 1.675 and 2.562 MeV, respectively, yielding more significant intensities of 19% and 31%, respectively, for their β^+ decay modes, as listed in Table 6.1.

There are an additional 25 radionuclides that decay by branching negatron (β^-) and EC decay modes, whereas positron (β^+) emission does not occur. These radionuclides decay according to the general scheme provided in Fig. 6.10, with the exception that the positron (β^+) decay mode does not occur. The properties of these radionuclides, their decay modes, and product nuclides are included in the tables of radioacive isotopes found in reference books, including Lide (2010), L'Annunziata (2012f), and the database of the Brookhaven National Laboratory, NuDat 2.6 (2012, www.nnde.bnl.gov/nudat2). They can be easily identified by the fact that both β^- and EC decay modes are listed, and there are two product nuclides rather than the customary one nuclide product. Although positron emission does not occur in these cases, the parent nuclide of atomic number Z decays to two daughter nuclides of atomic numbers $Z+1$ and $Z-1$. These nuclides, which do not decay by positron emission, have mostly low decay energies ($Q_{\mathrm{EC}} < 1.0$ MeV). The decay energies are below the minimum decay energy, equivalent to two electron masses (1.022 MeV), for the production of an e^+e^- pair required in the positron decay mode.

6.6 DOUBLE-BETA ($\beta\beta$) DECAY

Double-beta decay is the rarest of all radioactive decay processes ever observed. It may be described by the following general equation:

$$ {}^{A}_{Z}P \rightarrow {}^{A}_{Z+2}D + 2\beta^- + 2\overline{\nu} \qquad [6.69] $$

The parent nucleus transforms to a daughter nucleus of the same mass number A, but with an increase in atomic number Z by two. In accordance with the beta decay scheme, within the nucleus of the parent nuclide two neutrons decay to two protons with the simultaneous emission of two beta particles and two antineutrinos, or

$$ 2\mathrm{n} \rightarrow 2\mathrm{p}^+ + 2\beta^- + 2\overline{\nu} \qquad [6.70] $$

TABLE 6.1 Radionuclides that Decay via Branching β^-, β^+, and EC

Radionuclide	Decay Modes (%)	Decay Energies (MeV)	Product Nuclides
$^{36}_{17}$Cl	β^- (98%)	Q_{β^-}, 0.708	$^{36}_{18}$Ar (β^-)
	β^+ (0.002%)	$Q_{\beta^+,EC}$, 1.421	$^{36}_{16}$S (β^+, EC)
	EC (1.9%)		
$^{40}_{19}$K	β^- (89%)	Q_{β^-}, 1.311	$^{40}_{20}$Ca (β^-)
	β^+ (0.3%)	$Q_{\beta^+,EC}$, 1.505	$^{40}_{18}$Ar (β^+, EC)
	EC (10.7%)		
$^{64}_{29}$Cu	β^- (40%)	Q_{β^-}, 0.579	$^{64}_{30}$Zn (β^-)
	β^+ (19%)	$Q_{\beta^+,EC}$, 1.675	$^{64}_{28}$Ni (β^+, EC)
	EC (41%)		
$^{74}_{33}$As	β^- (32%)	Q_{β^-}, 1.353	$^{74}_{34}$Se (β^-)
	β^+ (31%)	$Q_{\beta^+,EC}$, 2.562	$^{74}_{32}$Ge (β^+, EC)
	EC (37%)		
$^{80}_{35}$Br	β^- (92%)	Q_{β^-}, 2.004	$^{80}_{36}$Kr (β^-)
	β^+ (2.6%)	$Q_{\beta^+,EC}$, 1.871	$^{80}_{34}$Se (β^+, EC)
	EC (5.7%)		
$^{84}_{37}$Rb	β^- (3%)	Q_{β^-}, 0.894	$^{84}_{38}$Sr(β^-)
	β^+ (22%)	$Q_{\beta^+,EC}$, 2.681	$^{84}_{36}$Kr(β^+, EC)
	EC (75%)		
$^{102}_{45}$Rh	β^- (22%)	Q_{β^-}, 1.150	$^{102}_{46}$Pd(β^-)
	β^+ (14%)	$Q_{\beta^+,EC}$, 2.323	$^{102}_{44}$Ru (β^+, EC)
	EC (64%)		
$^{108}_{47}$Ag	β^- (97%)	Q_{β^-}, 1.650	$^{108}_{48}$Cd (β^-)
	β^+ (0.2%)	$Q_{\beta^+,EC}$, 1.922	$^{108}_{46}$Pd (β^+, EC)
	EC (2.8%)		
$^{126}_{53}$I	β^- (47.3%)	Q_{β^-}, 1.258	$^{126}_{54}$Xe (β^-)
	β^+ (1%)	$Q_{\beta^+,EC}$, 2.155	$^{126}_{52}$Te (β^+, EC)
	EC (51.7%)		
$^{130}_{55}$Cs	β^- (1.6%)	Q_{β^-}, 0.370	$^{130}_{56}$Ba (β^-)
	β^+ (43.6%)	$Q_{\beta^+,EC}$, 2.979	$^{130}_{54}$Xe (β^+, EC)
	EC (54.8%)		

Data from Lide, D.R., 2010. CRC Handbook of Chemistry and Physics, 81st ed. CRC Press, Boca Raton, pp. 10–220, Firestone, R.B., et al., 1996. Table of Isotopes, 8th ed., vols. I and II, John Wiley & Sons, New York, and National Data Center, Brookhaven National Laboratory, www.nndc.bnl.gov/nudat2/.

6.6.1 Discovery and Current Research

Double-beta decay was first predicted by Nobel Laureate Maria Goeppert-Mayer (1935) at Johns Hopkins University, who calculated a predicted half-life of over 10^{17} years. Not until 1987 did Steven R. Elliott, Alan A. Hahn, and Michael K. Moe at the University of California, Irvine report the first observation of double-beta decay in a sample of ^{82}Se, enriched from

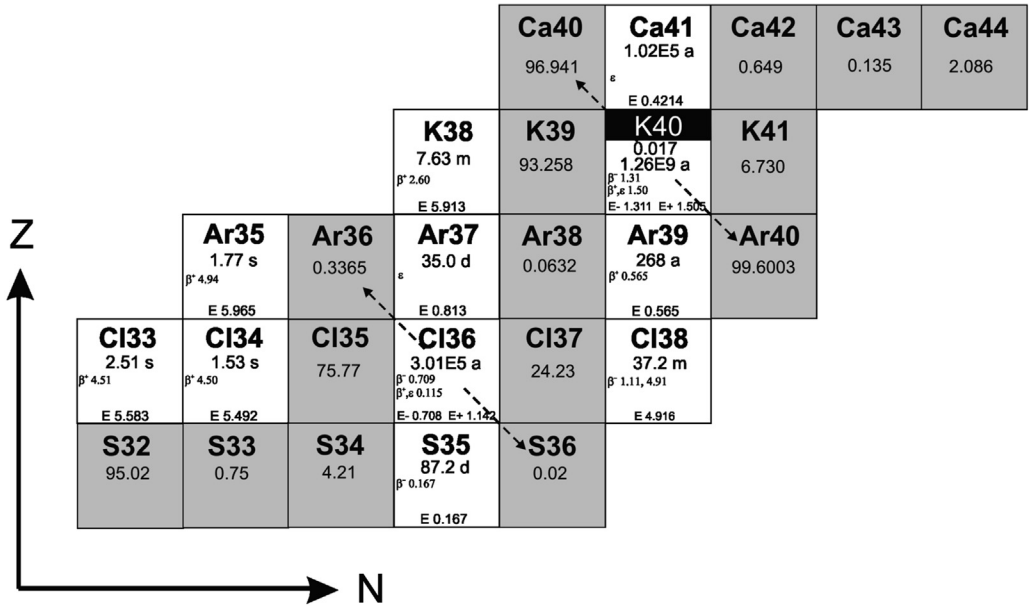

FIGURE 6.11 A segment of the Chart of the Nuclides illustrating the location of $^{36}_{17}$Cl and $^{40}_{19}$K, which decay to neighboring stable isobars (indicated by *arrows*) via negatron (β^-) emission with increasing Z, and via positron (β^+) emission and EC with decreasing Z. The stable and naturally occurring nuclides are shaded blocks, and the percentage of natural abundance of the isotope is included in the center of the shaded block. ^{40}K is a naturally occurring but radioactive isotope of potassium, and is thus displayed differently with a black bar over the symbol of the element and the mass number of the isotope. Units of half-life are abbreviated as "s," "m," "d," or "a" for seconds, minutes, days, or anni (years). Beta decay modes are abbreviated as β^-, β^+, and ε for negatron, positron, and EC, respectively, with decay energies in MeV. The decay energy of a radionuclide is in MeV at the bottom of each block alongside the letter E. Two decay energies are given for the radionuclides ^{36}Cl and ^{40}K, because of their branching beta decay modes. The value after the negative sign (E−) is the decay energy for the negatron decay mode, and the value with a positive sign (E+) is the decay energy for the positron and EC decay modes.

its natural abundance of 8.7% to an isotope abundance of 97% to provide more source material for the double-beta decay as well as reduce contamination in the sample from other sources (Elliott et al., 1986, 1987; Moe, 1986; Moe and Rosen, 1989).

The rarity of this decay process is manifested by the very long half-lives (from 10^{18} to 10^{24} years) of the nuclides that decay by this process. Because of the rarity of double-beta decay, its observation in the laboratory is extremely difficult, requiring highly enriched radionuclide sources and sophisticated coincidence (double-beta) counting instrumentation capable of extreme suppression or vetoing of background radiation (Elliott et al., 2006; Gómez et al., 2007; Campbell et al., 2008; Gehman et al., 2010; McGrath et al., 2010). Thus double-beta decay is not measured routinely, and is not relevant to the general measurement of radioactivity. Nevertheless, double-beta decay is discussed briefly here, because our knowledge of its existence helps us understand more fully the beta decay process.

6.6.2 $\beta\beta$ Decay Energy

The double-beta decay of ^{82}Se, as observed by Elliott et al. (1987), can be written as follows:

$$^{82}_{34}\mathrm{Se} \xrightarrow{t_{1/2}=9.2\times10^{19}\ \text{years}} {}^{82}_{36}\mathrm{Kr} + 2\beta^- + 2\overline{\nu} \qquad [6.71]$$

This decay equation would only be possible if the daughter nucleus, ^{82}Kr, is lighter than the nucleus of its parent ^{82}Se. As explained by Moe and Rosen (1989), the mass of the daughter nucleus is diminished by the mass equivalent to its binding energy, the energy needed to pull the nucleus apart. Thus a more tightly bound nucleus is lighter than a more loosely bound nucleus containing the same number of nucleons. The number of nucleons or mass number (82) in the above equation remains the same; but the nucleus of ^{82}Kr is lighter than its parent ^{82}Se, and the difference in mass of the two nuclei would yield the mass equivalent to the decay energy, $Q_{\beta\beta}$. In mass terms Eq. [6.71] may be written as

$$_{Z}M_{P} = {}_{Z+2}M_{D} + 2m_{e} \qquad [6.72]$$

where ${}_{Z}M_{P}$ and ${}_{Z+2}M_{D}$ are the masses of the parent and daughter nuclei of atomic numbers Z and $Z+2$, respectively, and $2m_e$ is the mass of two beta particles (ie, two electron masses). We may use atomic mass units (u) to calculate the mass difference of the parent and daughter nuclei by firstly adding Z atomic electron masses to each side of Eq. [6.72] to give

$$ {}_{Z}M_{P} + Zm_e = {}_{Z+2}M_{D} + (Z+2)m_e \qquad [6.73] $$

The decay energy, $Q_{\beta\beta}$, may then be calculated by the difference in parent and daughter nuclide atomic mass units, ignoring the small difference in the binding energies of the electrons in the two nuclides, or

$$ \begin{aligned} Q_{\beta\beta} &= (M_{82_{Se}} - M_{82_{Kr}})c^2 \\ &= (81.916700\ \text{u} - 81.913485\ \text{u})(931.494\ \text{MeV/u}) \\ &= 2.99475\ \text{MeV} \end{aligned} \qquad [6.74] $$

The above calculated value is in agreement with the decay energy reported by the National Nuclear Data Center of the Brookhaven National Laboratory, which is is 2.995 MeV (NNDC, 2010a, www.nndc.bnl.gov/qcalc/). Fig. 6.12 illustrates the decay scheme of ^{82}Se of higher mass to ^{82}Kr of lower mass, and the mass difference of the two is equivalent to the decay energy, $Q_{\beta\beta}$. The decay energy is shared as energy of four particles, namely two beta particles and two antineutrinos. Single-beta decay of ^{82}Se to ^{82}Br, a nuclide of higher mass, is energetically forbidden, as depicted in Fig. 6.12.

The National Nuclear Data Center currently lists 10 nuclides that are known to undergo double-beta decay: ${}^{48}_{20}$Ca, ${}^{76}_{32}$Ge, ${}^{82}_{34}$Se, ${}^{96}_{40}$Zr, ${}^{100}_{42}$Mo, ${}^{116}_{48}$Cd, ${}^{128}_{52}$Te, ${}^{130}_{52}$Te, ${}^{150}_{60}$Nd, and ${}^{238}_{92}$U. These nuclides have an even number of protons and an even number of neutrons. They exhibit a significant stability to beta decay, with half-lives that vary over the range of 10^{19}–10^{24} years. The stability of these nuclei, as described by Moe and Rosen (1989), may be due to their "even–even" characteristic—that is, their nuclei consist of an even number of protons and neutrons versus a neighboring "odd–odd" nucleus in the Chart of the Nuclides with the same number of nucleons consisting of an odd number of protons and neutrons. The strong nuclear force that holds the nucleus together binds pairs of like particles more tightly than unlike particles. Thus a nucleus with an even number of protons and even number of neutrons can pair and be bound more tightly than a nucleus with the same mass number but with an odd number of protons and odd number of neutrons. For example, the nucleus of ${}^{82}_{34}$Se contains 34 protons and 48 neutrons, whereas its neighboring isobar, ${}^{82}_{35}$Br, contains the odd numbers of 35 protons and 47 neutrons. The mass of the ^{82}Br nucleus is slightly higher than that of ^{82}Se, as illustrated in Fig. 6.12. The diminished mass of the ^{82}Se is due to its higher binding energy. Thus the ^{82}Se is a more tightly bound nucleus than the ^{82}Br, and the transition by beta decay from ^{82}Se to ^{82}Br is forbidden energetically, as illustrated in Fig. 6.12.

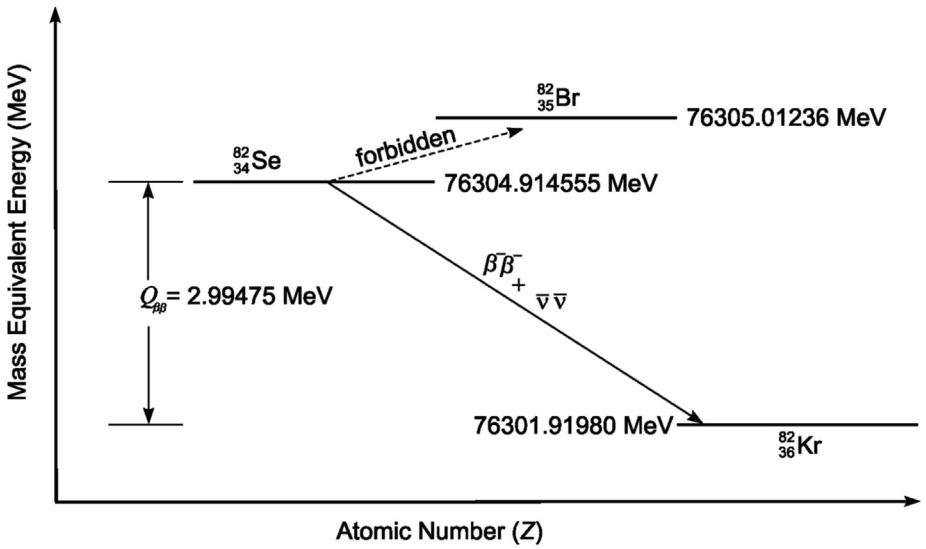

FIGURE 6.12 Double-beta decay of ${}^{82}_{34}$Se to ${}^{82}_{36}$Kr. The decay energy, $Q_{\beta\beta}$, of 2.99475 MeV (equivalent to the mass difference between the ^{82}Se and ^{82}Kr) is shared by the two beta particles and two antineutrinos created in the process from the two neutrons of the parent nucleus ${}^{82}_{34}$Se. Transition via beta decay of ^{82}Se to ^{82}Br is forbidden energetically, as the mass of ^{82}Br is greater than that of ^{82}Se. The double-beta decay occurs with the simultaneous emission of two beta particles and two antineutrinos.

As discussed in previous sections, beta decay is not confined to negatron emission. There are also positron and EC decay processes, which are other forms of beta decay. Thus there may theoretically be double-beta ($\beta^+\beta^+$) and double-capture (ECEC) decay processes, and research is under way to observe these alternatives (Barabash et al., 2007, 2008; Kolhinen et al., 2010). In a single positron emission a minimum decay energy of 1.022 MeV was discussed previously (Section 6.3.3). Double $\beta^+\beta^+$ would then require a minimum of 2.044 MeV decay energy.

6.6.3 Neutrinoless $\beta\beta$ Decay

There is much research currently under way on double-beta decay, particularly with respect to the search for neutrinoless double-beta decay by many research groups in the world—just a few of the research papers are Eliott and Vogel (2002), Kazkaz and Majorana Collaboration (2005), Fiorini (2007, 2008), Rahaman et al. (2008), Daraktchieva and NEMO Collaboration (2009), Dracos (2009), Avignone III (2010), Freitas et al. (2010), Majorovits (2010), and Šimkovic (2010). In accordance with the standard model, which explains the continuous spectrum of beta energies emitted from decaying nuclei, the neutrino always accompanies beta emission—that is, specifically the antineutrino accompanies negatron (β^-) emission and the neutrino accompanies positron (β^+) emission; and accordingly two antineutrinos would accompany double $\beta^-\beta^-$ decay and two neutrinos would accompany $\beta^+\beta^+$ emission. However, beyond this standard model there is the possibility that the neutrino could be its own antiparticle, referred to as a Majorana neutrino in honor of the exceptionally gifted Italian mathematician and theoretical physicist Ettore Majorana (1906−1938, his presumed year of death), who first postulated the possibility. According to this theory, if the neutrino possesses a mass (now estimated to have a mass upper limit of 2.3 eV/c^2) and is its own antiparticle, a neutrino emitted in one beta decay could be reabsorbed in the second beta decay, resulting in a double-beta decay in which no neutrinos are emitted, ie, a neutrinoless double-beta decay, often abbreviated as $0\nu\beta\beta$. The search for the neutrinoless double-beta decay is important because it would reaffirm the mass of the neutrino, as only a particle with a definite rest mass can oscillate from one form into another.

Ettore Majorana (1906-1938?)
Ettore Majorana was an exceptionally gifted theoretical physicist and mathematician, who was a member of Enrico Fermi's 'Via Panisperna boys' (Ragazzi di via Panisperna), which was the name Fermi's young research group acquired from the name of the street where their laboratory was located in Rome. Majorana mysteriously disappeared at 32 years of age. The reader will find a biography by Holstein (2009) to be an excellent review of the short and fascinating life of Ettore Majorana

Diagrams of the double-beta decay processes that would occur in a decaying nucleus for the two neutrino double-beta decay ($2\nu\beta\beta$) and the yet to be observed neutrinoless double-beta decay ($0\nu\beta\beta$) are illustrated in Fig. 6.13. In both cases, two neutrons (n) transform into two protons (p) in the nucleus when two down quarks (d) in the two neutrons change into

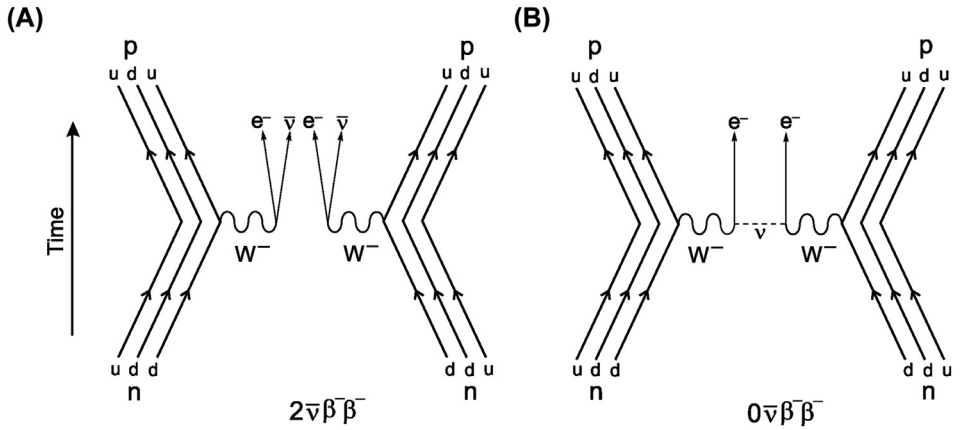

FIGURE 6.13 Feynman diagrams illustrating double-beta decay via (A) two-antineutrino double-beta decay $\left(2\bar{\nu}\beta^{-}\beta^{-}\right)$, and (B) neutrinoless double-beta decay $(0\nu\beta^{-}\beta^{-})$.

two up quarks (u) with the emission of two W^{-} bosons. The $W^{\pm}$ bosons were discovered at the super proton synchrotron proton-antiproton collider at CERN (the European Organization for Nuclear Research) in 1983 by the UA1 and UA2 collaborators (Arnison et al., 1983a,b; Banner et al., 1983; Bagnaia et al., 1983). These particles are the carriers of the weak interactions between elementary particles and are responsible for the weak decays of the particles (Sundaresan, 2001). As illustrated in Fig. 6.13, the two W^{-} bosons transform into two high-energy electrons (beta particles) and two anti-neutrinos. In the case of neutrinoless double-beta decay (yet to be observed), the Majorana neutrino emitted in one stage of the decay is reabsorbed in the second stage and two high-energy electrons are emitted without neutrinos.

In the $2\nu\beta\beta$ process the two beta particles that are emitted simultaneously share the total decay energy, $Q_{\beta\beta}$, with the two neutrinos. Thus the decay energy is shared between four particles, namely the two neutrinos and two beta particles. In the $0\nu\beta\beta$ process the two beta particles emitted share the entire decay energy, as there are no neutrinos emitted with which to share the decay energy. The beta particle energy spectra for $2\nu\beta\beta$ and $0\nu\beta\beta$ decay are illustrated in Fig. 6.14. The two beta particle spectra are very distinct. In the $2\nu\beta\beta$ decay process the numbers of beta particles (N) vary over a wide range of energy plotted as the sum of the two beta particle energies divided by the decay energy, ie, $\sum\left(E_{\beta_1}+E_{\beta_2}\right)/Q_{\beta\beta}$. The beta particle energy spectrum for the $2\nu\beta\beta$ decay encompasses the continuous energy range with a spectral shape similar to that of the single beta particle emission, because they share the decay energy with neutrinos. Notice in Fig. 6.14 that the endpoint of the continuous beta particle spectrum of the $2\nu\beta\beta$ decay does not reach the value of 1.0. This is due to the fact that the two beta particles emitted in the $2\nu\beta\beta$ decay process must share decay energy with two neutrinos, and thus

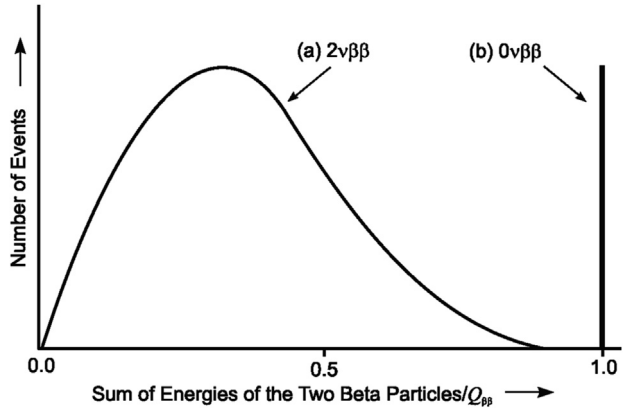

FIGURE 6.14 Beta particle energy spectra for (a) two-neutrino double-beta decay ($2\nu\beta\beta$), and (b) neutrinoless double-beta decay ($0\nu\beta\beta$). In the $2\nu\beta\beta$ decay process the sum of the two beta particle energies divided by the decay energy, $\sum\left(E_{\beta_1}+E_{\beta_2}\right)/Q_{\beta\beta}$, displays a continuous spectrum and the maximum will never reach 1.0; whereas the spectrum for $0\nu\beta\beta$ displays a single line at $\sum\left(E_{\beta_1}+E_{\beta_2}\right)/Q_{\beta\beta}=1$.

the sum of the two beta particle energies can never equal the decay energy, $Q_{\beta\beta}$. However, the beta particle energy spectrum for the $0\nu\beta\beta$ decay, where neutrinos are not emitted and thus do not escape with any of the decay energy, displays a single energy line for the sum of the two beta particle energies, and this line occurs at $\sum\left(E_{\beta_1} + E_{\beta_2}\right)/Q_{\beta\beta} = 1$. Currently research is under way in the search for the sum of the two beta particles to equal the decay energy, $Q_{\beta\beta}$, or where $\sum\left(E_{\beta_1} + E_{\beta_2}\right)/Q_{\beta\beta} = 1$, which would confirm $0\nu\beta\beta$ decay.

6.7 BETA PARTICLE INTERACTIONS WITH MATTER

Owing to the very low mass of the β^- electron compared with the alpha particle, it travels at a much higher velocity than an alpha particle of equivalent energy. Because of its greater velocity, lower mass, and lower charge, the specific ionization produced in air by the traveling beta particle is much lower (by a factor of 1000) than that of an alpha particle of equivalent energy.

Like the alpha particle, the beta particle interacts with matter via ionization and electron orbital excitation as it dissipates its kinetic energy. A third mechanism of interaction with matter, which distinguishes the beta particle, is radiative energy dissipation via bremsstrahlung production (see the chapter: "Electromagnetic Radiation: Photons"). Thus, as described by Turner (1995), the stopping power for beta particles (β^- or β^+) is the sum of the collisional and radiative contributions or

$$\left(-\frac{dE}{dx}\right)^{\pm}_{\text{tot}} = \left(-\frac{dE}{dx}\right)^{\pm}_{\text{col}} + \left(-\frac{dE}{dx}\right)^{\pm}_{\text{rad}} \qquad [6.75]$$

where the superscript $\pm$ refers to positively or negatively charged electrons. The radiative contribution—that is, the absorption of beta particle energy with the concomitant emission of bremsstrahlung radiation—is significant with high-energy beta particles (eg, ^{32}P or ^{90}Y beta particle emissions) in absorbers of high atomic number (eg, Pb-glass). Bremsstrahlung radiation is discussed in the chapter entitled "Electromagnetic Radiation: Photons."

Collision interactions of beta particles are somewhat different than those that occur with alpha particles. A beta particle may collide with an orbital electron or come into close proximity to it and cause the electron to be ejected, resulting in the formation of an ion pair. Considerable scattering of beta particles occurs in such collisions, because the mass of the beta particle is equivalent to that of an atomic electron. This is in direct contrast to the alpha particle, which for the most part retains a relatively undeviating path while passing through matter and interacting with atomic electrons. The mass equivalence of beta particles and electrons is an important factor that gives bombarding beta particles the power to impart a major portion of their kinetic energy to atomic electrons in a single collision. The atomic electrons ejected upon beta particle collisions themselves cause ionization in a similar fashion. This is referred to as secondary ionization, and the ionization caused by the first beta particle-electron collisions is classified as primary ionization. Because the major portion of beta particle energy may be imparted to an atomic electron upon collision, secondary ionization may account for as much as 80% of the total ionization produced in a given material bombarded by beta particles.

The probability of beta particle interactions with atomic electrons increases with the density of the absorbing material. Beta particle absorption is consequently proportional to the density and thickness of an absorber. Figs. A.2–A.3 of Appendix A provide graphs where the range in units of g/cm^2 in substances of low atomic number can be estimated for beta particles of energies from 0.01 to 10 MeV. The range of beta particles expressed in terms of surface density or mass thickness (g/cm^2) of absorber can be converted to absorber thickness (cm) when the absorber density (g/cm^3) is known. Several empirical formulas exist for calculating beta particle ranges, solved on the basis of the $E_{\max}$ of the beta particle. The formulas reported by Glendenin (1948) are

$$R = 0.542E - 0.133 \quad \text{for} \quad E > 0.8\ \text{MeV} \qquad [6.76]$$

and

$$R = 0.407E^{1.38} \quad \text{for} \quad 0.15\ \text{MeV} < E < 0.8\ \text{MeV} \qquad [6.77]$$

where R is the beta particle range in g/cm^2 and E is the energy of the beta particle (ie, $E_{\max}$) in MeV. Also, the empirical formula of Flammersfield (1946) described by Paul and Steinwedel (1955) can be used:

$$R = 0.11\left(\sqrt{1 + 22.4E^2} - 1\right) \quad \text{for} \quad 0 < E < 3\ \text{MeV} \qquad [6.78]$$

This formula provides calculated ranges in units of g/cm^2 in close agreement to those obtained from Eqs. [6.76] and [6.77] or those found in Figs. A.2–A.4 in Appendix A. This empirical formula and the graphs in the appendix are suitable for low atomic number absorbers, such as aluminum ($Z = 13$). Semiempirical equations developed by Tabata et al. (1972) and described in detail by Tsoulfanidis (1995) yield beta particle or electron ranges in absorber elements and compounds of a wide range of atomic numbers. For negatrons or electrons exceeding 2.5 MeV up to 10 MeV, the empirical formula from Katz and Penfold (1952) and the US. Public Health Service (1970), may be used:

$$R = 0.530E - 0.106 \quad \text{for} \quad 2.5\ \text{MeV} < E < 10\ \text{MeV} \qquad [6.79]$$

where R is the negatron or electron range in g/cm^2. Eq. [6.79] is derived from the experimentally determined energy–range correlation provided in Fig. A.4 of Appendix A.

According to Eq. [6.76], a 1.0-MeV negatron has a calculated range of 0.409 g/cm^2. This value may be divided by the density, ρ, of the absorber material to provide the range in centimeters of absorber thickness. Thus it can be estimated that a 1.0 MeV negatron travels approximately 334 cm in dry air ($\rho = 0.001226$ g/cm^3 at standard temperature and pressure (STP)), 0.40 cm in water ($\rho = 1.00$ g/cm^3), and 0.15 cm in aluminum ($\rho = 2.7$ g/cm^3). The effect of absorber density on beta particle range is obvious from the foregoing examples, which demonstrate that 1 cm of dry air has about the same stopping power as 0.004 mm of aluminum.

The range of beta particles in matter is considerably greater than that of alpha particles of the same energy. Again, this is due to the lower mass, lower charge, and higher velocity of travel of the beta particle in comparison with an alpha particle of equivalent energy. The significance of this difference may be appreciated by reference to Table 6.2, in which the alpha particle, beta particle, and/or electron ranges in air as a function of particle energy are compared.

To put the data of Table 6.2 into historical perspective, it is interesting to recall the origin of the names "alpha and beta radiation." Before alpha and beta particles were characterized fully, Ernest Rutherford (1899) carried out experiments demonstrating that two types of radiation existed: one radiation that was most easily absorbed by matter, and another that possessed a greater penetrating power. Out of convenience, he named these radiations as "alpha" and "beta." Not much

TABLE 6.2 Ranges of Alpha and Beta Particles (or Electrons) of Various Energies in Air

	Range (mg/cm^2 Air)		Range (cm Air)[c]	
Energy (MeV)	Alpha Particle[a]	Beta Particle[b]	Alpha Particle	Beta Particle
0.1	0.17	16	0.1	13
0.5	0.42	200	0.3	163
1.0	0.67	490	0.5	400
1.5	0.95	790	0.7	644
2.0	1.3	1010	1.1	824
2.5	1.7	1400	1.4	1142
3.0	2.1	1700	1.7	1386
4.0	3.1	2200	2.5	1794
5.0	4.4	2700	3.6	2202
6.0	5.8	3200	4.7	2610
7.0	7.3	3700	5.9	3010
8.0	9.0	4200	7.3	3425

[a] *From the range–energy relationship provided in Fig. A.1 of Appendix A. More accurate values can be obtained from data provided by the National Institute of Standards and Technology (NIST) Database ASTAR (2010) for CSDA (continuous slowing down approximation) ranges: www.nist.gov/pml/data/star/index.cfm.*

[b] *From the range–energy relationship provided in Fig. A.2 of Appendix A. More accurate values can be obtained from data provided by the NIST Database ASTAR (2010) for CSDA ranges: www.nist.gov/pml/data/star/index.cfm.*

[c] *Calculated from the range in mass thickness units (mg/cm^2) and the density of dry air at STP, $\rho_{air} = 1.226$ mg/cm^3, according to Eq. [4.19] in chapter "Alpha Radiation."*

later Paul Villard (1900b,c) in France discovered a yet more penetrating radiation. In harmony with the nomenclature assigned to the "alpha" and "beta" radiation, Rutherford (1903) coined the term "gamma rays" to the yet more penetrating radiation. In the *Philosophical Magazine* Rutherford (1903) named and characterized the three types of nuclear radiation on the basis of their penetration power in matter as follows:

Radium gives out three distinct types of radiation:

(1) The α rays, which are very easily absorbed by thin layers of matter, and which give rise to the greater portion of the ionization of the gas observed under the usual experimental conditions.
(2) The β rays, which consist of negatively charged particles projected with high velocity, and which are similar in all respects to cathode rays produced in a vacuum tube.
(3) The γ rays, which are non-deviable by a magnetic field, and which are of a very penetrating character.
These rays differ very widely in their power of penetrating matter. The following approximate numbers, which show the thickness of aluminum traversed before the intensity is reduced to one-half, illustrate this difference:

Radiation	*Thickness of Aluminum (cm)*
α rays	*.0005*
β rays	*.05*
γ rays	*8*

It is important to emphasize that although all beta particles can be completely absorbed by matter, the shields we select can be of great consequence. Hazardous bremsstrahlung radiation can be significant when high-energy beta particles interact with shields of high atomic number. The phenomenon of bremsstrahlung production is discussed further in the chapter entitled "Electromagnetic Radiation: Photons."

Positrons dissipate their energy in matter via the same mechanisms as previously described for negatrons, which is understandable, as both are electrons. The scattering of positrons by atomic nuclei (ie, elastic scattering) is less than that for negatrons of the same energy when traveling through matter of a given atomic number Z, as demonstrated by Fowler and Oppenheimer (1938), Lipkin and White (1950), and Feshbach (1952). The mass attenuation coefficients of positrons in the energy range of $0.3\ \text{MeV} < E_{\max} < 3.6\ \text{MeV}$ are always slightly lower than that of negatrons of the same energy when traveling through matter of the same atomic number, as demonstrated by Singh and Batra (1987). Calculated and observed mass attenuation coefficients for positrons and negatrons over the energy range of 0.3−3.6 MeV in absorber materials of atomic number 10−90 are provided by Singh and Batra (1987). The role of mass attenuation coefficients in the absorption and transmission of negatrons and positrons in various materials is discussed in more detail in the next section on beta particle absorption and transmission. Section 6.9 provides more information for calculating the ionization-excitation stopping powers for negatrons and positrons due to collision interactions with absorbers, and the differences between negatron and positron stopping powers are demonstrated to not exceed 10%. However, positrons are unique, in that these particles produce annihilation gamma radiation in matter, discussed in the chapter entitled "Electromagnetic Radiation: Photons."

6.8 BETA PARTICLE ABSORPTION AND TRANSMISSION

Early research work on measuring the range of beta particles involved placing absorbers of increasing thickness between the radioactive source and the detector. The detector would measure the beta particles transmitted through the absorber. Increasing the absorber thickness would increasingly diminish the number of beta particles transmitted on to the detector. The transmission of beta particles was then plotted against absorber thickness, as illustrated in Fig. 6.15, in an attempt to determine the thickness of absorber required to stop all the beta particles. Unfortunately, the plots could not be used directly to determine accurately beta particle ranges; rather they had to be compared to an absorption curve of a beta emitter of known range by what became known as Feather analysis (Feather, 1938; Glendenin, 1948). An auspicious outcome of this work was the observation that the plots of beta particle absorption had more or less an exponential character. When

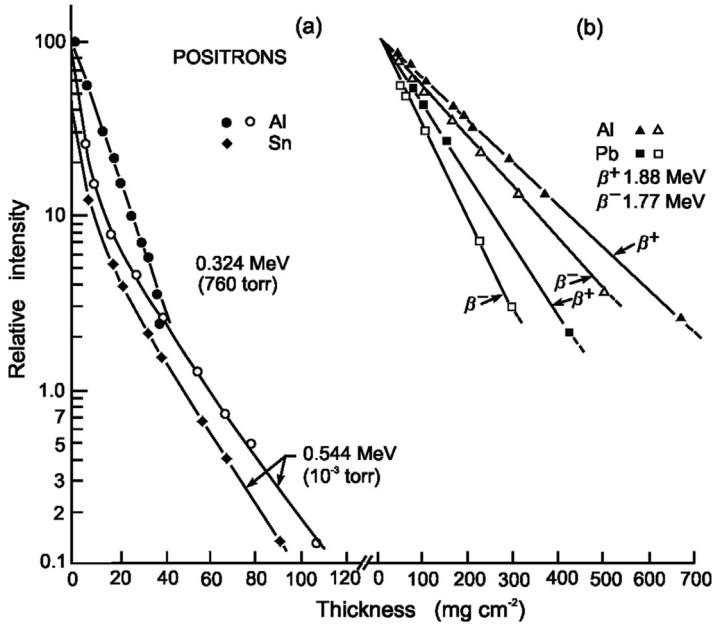

FIGURE 6.15 The relative measured transmission ($I/I_0 \times 100$ of Eq. [6.80]) of positrons of 0.324, 0.544 (two curves in part (a)), 1.77, and 1.88 MeV (two curves in part (b)) in Al, Sn, and Pb and negatrons of 1.77 and 1.88 MeV in Al and Pb (two curves in part (b)). The semilogarithmic plot is linear over a specific range of absorber thickness. For the set of *curves* in (b), the scale along the *x*-axis is different. *From Singh, B., Batra, R.K., 1987. A method for calculating mass attenuation coefficients of beta particles. Appl. Radiat. Isot. 38 (12), 1027–1031, reprinted with permission from Elsevier © 1987.*

plotted logarithmically against absorber thickness, the beta particle absorption and/or transmission through the absorber was linear or near linear, as illustrated in Fig. 6.15. This was a fortuitous outcome of the continuous energy spectrum of beta particles emitted from any given source. These findings are quite a contrast to the absorption curve of alpha particles discussed previously (Fig. 4.6 of the chapter: "Alpha Radiation"), where the alpha particle intensity remains constant and then comes to an almost abrupt stop.

The curves illustrated in Fig. 6.15 are characteristic of beta particles. The linear segment of the semilogarithmic plot of activity transmitted versus absorber thickness levels off horizontally (not illustrated in Fig. 6.15) due to a background of bremsstrahlung radiation (see the chapter: "Electromagnetic Radiation: Photons" for a discussion on bremsstrahlung radiation). Negatrons and positrons both display a linear semilogarithmic plot, with the exception that in the case of positrons the plot has an added background due to annihilation radiation (Glendenin, 1948). Because beta particles have a definite range in matter, beta particle transmission is not purely logarithmic, as we shall see is the case for gamma radiation (see the chapter: "Electromagnetic Radiation: Photons"). The curves may not display a purely exponential character and the plots may have a degree of concavity to them depending on the distance of the source and detector to the absorber and on the shape of the beta particle continuous energy spectrum. The greater the atomic number of the beta particle emitter, and the more the beta spectrum is displaced toward the lower energies, the more nearly exponential (linear) will be the absorption curve (Glendenin, 1948). It is common to express the amount of absorber in mass thickness units—that is, mass per unit area (eg, g/cm^2), which is the product of absorber thickness and density—as it is easier to measure accurately very thin absorbers simply from their weight.

Based on the exponential character of beta particle absorption, we can describe the transmission of beta particles through the absorber as

$$I = I_0 e^{-\mu x} \qquad [6.80]$$

where I is intensity of the beta particles (DPM) transmitted through the absorber and DPM signifies disintegrations per minute or beta particles detected per minute time, I_0 is the initial intensity of beta particles (DPM) incident on the absorber, μ is the linear absorption coefficient in units of cm^{-1}, and x is the absorber thickness in cm. If we express absorber thickness in mass thickness units (eg, mg/cm^2 or g/cm^2), we can rewrite Eq. [6.80] as

$$I = I_0 e^{-(\mu/\rho)(\rho x)} \qquad [6.81]$$

or

$$\frac{I}{I_0} = e^{-(\mu/\rho)(\rho x)} \qquad [6.82]$$

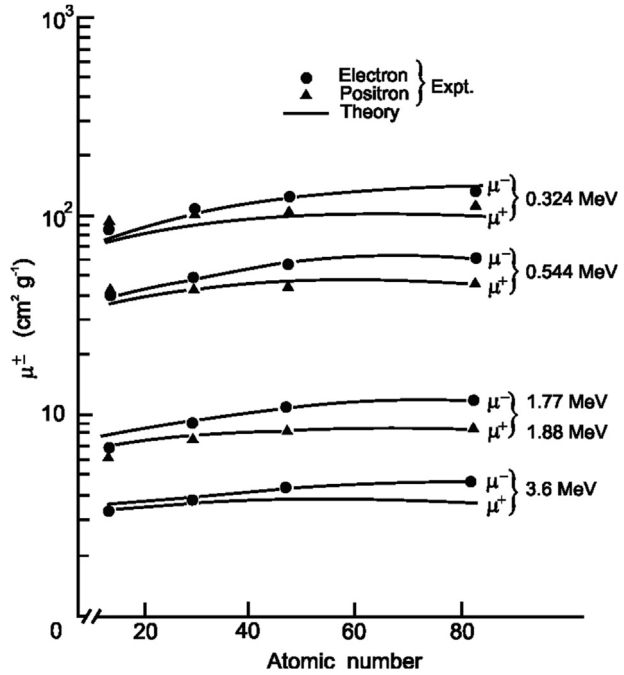

FIGURE 6.16 Mass attenuation coefficient μ (or μ/ρ of Eq. [6.83]) versus atomic number Z for positrons and negatrons (electrons) at different energies. *From Singh, B., Batra, R.K., 1987. A method for calculating mass attenuation coefficients of beta particles. Appl. Radiat. Isot. 38 (12), 1027–1031, reprinted with permission from Elsevier © 1987.*

and

$$\ln \frac{I}{I_0} = -(\mu/\rho)(\rho x) \qquad [6.83]$$

where μ/ρ is the mass absorption coefficient (also referred to as mass attenuation coefficient) in units of cm^2/g (that is, the linear absorption coefficient divided by the absorber density) and ρx is the absorber thickness in mass thickness units g/cm^2 (that is, the product of the absorber density and absorber thickness). Mass attenuation coefficients for positrons are calculated by Singh and Batra (1987) over the energy range of 0.1–5.0 MeV in various absorbers of atomic number ranging from Al ($Z = 13$) to Pb ($Z = 82$). The mass attenuation coefficients of negatrons are higher than those of positrons over the energy range of 0.3–3.6 MeV, as illustrated in Fig. 6.16.

Eq. [6.83] can be used to determine experimentally the unknown thickness of absorber materials. A standard curve is plotted with the ratio I/I_0 on a logarithmic scale versus mass thickness (ρx) of the absorber on a linear scale, as illustrated in Fig. 6.15. A value for I in DPM units is determined with a detector by measuring the beta particle intensity transmitted through a given absorber thickness. This is repeated with absorbers of different thickness. The magnitude of the incident beta particle intensity, I_0, is a constant value and determined with the detector in the absence of absorber. The linear portion of the plot has a negative slope, such as that illustrated in Fig. 6.15, and from least squares analysis the mass attenuation coefficient μ/ρ is determined (Singh and Batra, 1987; Yi et al., 1999). Consequently, the thickness of an unknown similar material can be determined from the measured intensity, I, of the transmitted beta particle radiation after placing the material between the beta particle source and the detector without altering the counting geometry. The sample thickness is calculated or determined directly from the aforementioned curve (Tumul'kan, 1991; Clapp et al., 1995). A diagram of an arrangement used in a beta thickness gauge for industrial testing of uniformity or defects in sheets or films of material is illustrated in Fig. 6.17.

Beta particle transmission has many practical applications today in industrial manufacturing. Beta particle sources and detectors are placed on the production line to test for thickness, uniformity, and defects in the manufacture of paper, metal, and plastic films (Yoshiyuki and Hiroshi, 1999; Gardner et al., 2004), online inspection of sewn seams or fabric density in the textile industry (Ogando, 1993; Clapp et al., 1995; Mapleston, 1997; Titus et al., 1997; Kim et al., 2009a), and in agronomic research to measure leaf water content (Mederski, 1961; Mederski and Alles, 1968; Nakayama and Ehrler, 1964; Jones, 1973; Obregewitsch et al., 1975; Barthakur, 1983) or the biomass of a prairie (Knapp et al., 1985). These are

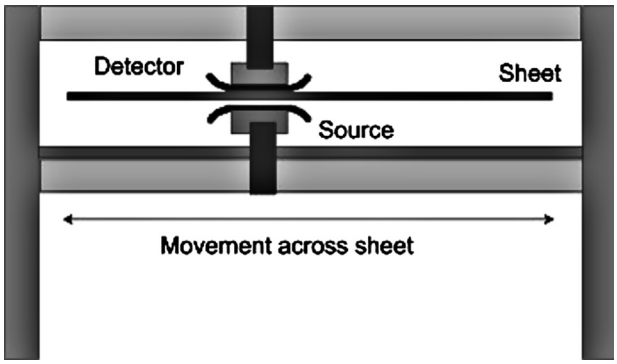

FIGURE 6.17 A beta thickness gauge. The beta radiation source and detector are mounted on a frame and constantly traverse a sheet to measure the mass thickness, ie, weight per unit area. The thickness is then obtained from the known density of the material. *From Wagner Jr., J.R., et al., 2014. Extrusion, 2nd ed. Elsevier, Amsterdam, pp. 620, reprinted with permission from Elsevier © 2014.*

commonly referred to as beta transmission thickness gauges. The beta particle sources used depend on the absorber thickness to be measured and the E_{max} of the beta particles. Sources commonly used are ^{14}C ($E_{max} = 0.156$ MeV), ^{147}Pm ($E_{max} = 0.224$ MeV), ^{85}Kr ($E_{max} = 0.672$ MeV), ^{204}Tl ($E_{max} = 0.763$ MeV), and ^{90}Sr (^{90}Y) in secular equilibrium (E_{max} of ^{90}Sr and $^{90}Y = 0.546$ and 2.280 MeV, respectively). A source of low beta particle E_{max} (eg, ^{14}C or ^{147}Pr) is used to measure the finest thickness of material (Jaklevic et al., 1983; Balasubramanian, 1997, 1998), and the sources are changed according to beta particle energy and material density and thickness to be tested. Practical references for radioisotope thickness gauge measurements are provided by Johansen and Jackson (2004) and Wagner et al. (2014).

6.9 STOPPING POWER AND LINEAR ENERGY TRANSFER

Throughout this book information is provided on the mechanisms of interaction of radiation with matter. In summary, we can state that the principle mechanisms of interaction of charged particles (eg, alpha particles, protons, deuterons, and electrons or beta particles) with matter, which result in significant charged-particle energy loss, are ionization via coulombic interactions of the charged particles with atomic electrons of the absorbing medium; electron orbital excitation of the medium, which occurs when the energy transfer through coulombic interaction is not sufficient actually to eject an electron from an atom; and the radial emission of energy as bremsstrahlung when a charged particle (eg, electron or beta particle) decelerates as it approaches an atomic nucleus. Release of particle energy by bremsstrahlung radiation becomes increasingly significant as the beta particle energy and absorber atomic number increase. On the other hand, electromagnetic radiation (ie, the photon) dissipates its energy in matter via three possible mechanisms, namely the photoelectric effect, Compton scattering, and pair production (see the chapter: "Electromagnetic Radiation: Photons"). The photoelectric effect and Compton scattering generate ion pairs directly within the absorbing medium, whereas pair production results in the creation of charged particles (positrons and negatrons) that will subsequently dissipate their energy via ionization, electron excitation, and, in the case of positrons, annihilation. Also, as described in the chapter entitled "Neutron Radiation," energetic neutrons will dissipate their energy in matter through elastic collisions with atomic nuclei of the absorbing medium. When hydrogen is present in the absorbing material, the bulk of the fast neutron energy is passed on to the hydrogen nuclei. In turn, the kinetic energy of these protons is absorbed in the medium via ionization and excitation processes. Low- and high-energy neutrons are absorbed principally via inelastic neutron reactions, which can result in the production of charged particles and gamma radiation.

The radiation properties (eg, charge, mass, and energy) and mechanisms of interaction previously described govern the rate of dissipation of energy, and consequently the range of travel of the nuclear radiation in an absorber. This brings in the concepts of stopping power and linear energy transfer (LET), which are described subsequently.

6.9.1 Stopping Power

Stopping power is defined by the International Commission on Radiation Units and Measurements (ICRU; Taylor et al., 1970) as the average energy dissipated by ionizing radiation in a medium per unit path length of travel of the radiation in the medium. It is, of course, impossible to predict how a given charged particle will interact with any given atom of the absorber medium. Also, when we consider that the coulombic forces of charged particles will interact simultaneously with

many atoms as they travel through the absorbed medium, we can only predict an average effect of energy loss per particle distance of travel. Taking into account the charge, mass, and speed (energy) of the particle and the density and atomic number of the absorbing medium, Hans Bethe (1933) and Bethe and Ashkin (1953) derived the formula for calculating the stopping power resulting from coulombic interactions of heavy charged particles (eg, alpha particles, protons, and deuterons) traveling through absorber media. Rohrlich and Carlson (1954) have refined the calculations to include energy losses via bremsstrahlung radiation, significant when high-energy electrons and beta particles interact with absorbers of high atomic number. Also, refinements to the stopping power formulae in the low-energy ranges of heavy particles have been made by several researchers, including Bohr and Lindhard (1954), Lindhard and Scharff (1960, 1961), Northcliffe (1963), and Mozumder et al. (1968). Derivations of stopping power formulas can be obtained from texts by Friedlander et al. (1964), Roy and Reed (1968), Segré (1968), and Evans (1972). The formulas for the stopping power of charged particles due to coulombic interactions (ie, ionization and electron orbital excitation) are most clearly defined by Tsoulfanidis (1995) as the following.

1. For heavy charged particles (eg, protons, deuterons, and alpha particles),

$$\frac{dE}{dx} = 4\pi r_0^2 z^2 \frac{mc^2}{\beta^2} NZ\left[\ln\left(\frac{2mc^2}{I}\beta^2\gamma^2\right) - \beta^2\right] \qquad [6.84]$$

2. For electrons or negatrons (negative beta particles),

$$\frac{dE}{dx} = 4\pi r_0^2 \frac{mc^2}{\beta^2} NZ\left\{\ln\left(\frac{\beta\gamma\sqrt{\gamma-1}}{I}mc^2\right) + \frac{1}{2\gamma^2}\left[\frac{(\gamma-1)^2}{8} + 1 - \left(\gamma^2 + 2\gamma - 1\right)\ln 2\right]\right\} \qquad [6.85]$$

3. For positrons (positive beta particles),

$$\frac{dE}{dx} = 4\pi r_0^2 \frac{mc^2}{\beta^2} NZ\left\{\ln\left(\frac{\beta\gamma\sqrt{\gamma-1}}{I}mc^2\right) - \frac{\beta^2}{24}\left[23 + \frac{14}{\gamma+1} + \frac{10}{(\gamma+1)^2} + \frac{4}{(\gamma+1)^3}\right] + \frac{\ln 2}{2}\right\} \qquad [6.86]$$

where $\frac{dE}{dx}$ is the particle stopping power in units of MeV/m, r_0 is the classical electron radius $= 2.818 \times 10^{-15}$ m, z is the charge on the particle ($z = 1$ for p, d, β^-, β^+ and $z = 2$ for α), mc^2 is the rest energy of the electron $= 0.511$ MeV (see Eq. [8.42] of the chapter: "Electromagnetic Radiation: Photons"), N is the number of atoms per m^3 in the absorber material through which the charged particle travels ($N = \rho(N_A/A)$ where ρ is the absorber density in units of g/cm^3, N_A is Avogadro's number $= 6.022 \times 10^{23}$ atoms per mol, A and Z are the atomic weight and atomic number, respectively, of the absorber, $\gamma = (T + mc^2)/mc^2 = 1\Big/\sqrt{1-\beta^2}$ where T is the particle kinetic energy in MeV and m is the particle rest mass, (eg, proton $= 938.2$ MeV/c^2, deuteron $= 1875.6$ MeV/c^2, alpha particle $= 3727.3$ MeV/c^2, and negatron or positron $= 0.511$ MeV/c^2), β is the relative phase velocity of the particle $= v/c$, ie, the velocity of the particle in the medium divided by the speed of light in a vacuum $= \sqrt{1-(1/\gamma^2)}$ (see also the chapter: "Cherenkov Radiation" for a treatment on β), and I is the mean excitation potential of the absorber in units of eV approximated by the equation

$$I = \left(9.76 + 58.8Z^{-1.19}\right)Z, \quad \text{when } Z > 12 \qquad [6.87]$$

where pure elements are involved, as described by Tsoulfanidis (1995). However, when a compound or mixture of elements is concerned, a mean excitation energy, $\langle I\rangle$, must be calculated according to Bethe theory, as follows

$$\langle I\rangle = \exp\left\{\left[\sum_j w_j(Z_j/A_j)\ln I_j\right]\Big/\sum_j w_j Z_j/A_j\right\} \qquad [6.88]$$

where w_j, Z_j, A_j, and I_j are the weight fraction, atomic number, atomic weight, and mean excitation energy, respectively, of the jth element (Seltzer and Berger, 1982a). See Anderson et al. (1969), Snow et al. (1973), Janni (1982), Seltzer and Berger (1982a,b, 1984), Berger and Seltzer (1982), and Tsoulfanidis (1995) for experimentally determined values of I for various elements and thorough treatments of stopping power calculations. Values of mean excitation potentials, I, for 100 elements and many inorganic and organic compounds are provided by Seltzer and Berger (1982a, 1984).

An example of the application of one of the above equations would be the following calculation of the stopping power for a 2.280 MeV beta particle (E_{max}) emitted from ^{90}Y traveling through an aluminum absorber. Of course, the beta particles emitted from ^{90}Y encompass a wide spectrum of energies between zero and a maximum value or E_{max}. It is the E_{max} that will be used in this example. The solution is as follows.

Firstly, the calculation of relevant variables is

$$\gamma = \frac{2.280\ \text{MeV} + 0.511\ \text{MeV}}{0.511\ \text{MeV}} = 5.462$$

$$\beta = \sqrt{1 - \frac{1}{\gamma^2}} = 0.9831 \ \text{ and } \ \beta^2 = 0.9665$$

The atomic weight A for aluminum is 27, atomic number Z is 13, and its density ρ is 2.70 g/cm^3. The mean excitation potential, I, for aluminum is 166 eV, is obtained from Seltzer and Berger (1982a). From Eq. [6.85] the stopping power for the 2.280 MeV beta particle traveling through aluminum is calculated as

$$\frac{dE}{dx} = 4(3.14)\left(2.818 \times 10^{-15}\ \text{m}\right)^2 \left(\frac{0.511\ \text{MeV}}{0.9665}\right)\left(2.70\ \text{g/cm}^3\right)\left(\frac{6.022\ \times\ 10^{23}\ \text{atoms/mol}}{27\ \text{g/mol}}\right)\left(\frac{10^6\ \text{cm}^3}{\text{m}^3}\right)$$

$$\times\ (13)\left\{\begin{array}{l} \ln\left(\dfrac{(0.9831)(5.562)\sqrt{4.462}}{166\ \text{eV}}(0.511\ \text{MeV})(10^6\ \text{eV/MeV})\right) \\ + \dfrac{1}{2(5.462)^2}\left[\dfrac{(4.462)^2}{8} + 1 - (5.462^2 + 2{\cdot}5.462 - 1)\right]\ln 2 \end{array}\right\} = 431.4\ \text{MeV/m}$$

The term (10^6 cm^3/m^3) is included in the above equation to maintain consistency of units, thus converting the units of density expressed in g/cm^3 to units of g/m^3. In SI units the stopping power can be expressed in units of J/m or

$$(431.4\ \text{MeV/m})\left(1.602 \times 10^{-13}\ \text{J/MeV}\right) = 6.91 \times 10^{-11}\ \text{J/m}$$

The stopping power is often expressed in units of MeV cm^2/g or J m^2/kg, which provides values for stopping power without defining the density of the absorber medium (Taylor et al., 1970; Tsoulfanidis, 1995). In these units the above calculation can also be expressed as

$$\frac{1}{\rho}\left(\frac{dE}{dx}\right) = \frac{4.314\ \text{MeV/cm}}{2.70\ \text{g/cm}^3} = 1.60\ \text{MeV cm}^2/\text{g} \qquad [6.89]$$

Eq. [6.85] used above to calculate the stopping power for the 2.280 MeV beta particle from ^{90}Y in aluminum accounts only for energy of the beta particle lost via collision interactions resulting in ionization and electron orbital excitations. The equation does not account for radial energy loss via the production of bremsstrahlung radiation, which can be very significant with beta particles of high energy and absorber materials of high atomic number. Thus a complete calculation of the stopping power must include the radial energy loss via bremsstrahlung as described by Eq. [6.75], which is,

$$\left(\frac{dE}{dx}\right)_{\text{total}} = \left(\frac{dE}{dx}\right)_{\text{ion.}} + \left(\frac{dE}{dx}\right)_{\text{rad.}} \qquad [6.90]$$

where $(dE/dx)_{total}$ is the rate of total beta particle or electron energy loss in an absorber, $(dE/dx)_{ion.}$ is the rate of energy loss due to ionization, and $(dE/dx)_{rad.}$ is the rate of energy loss due to bremsstrahlung radiation production. We must keep in mind that each stopping power calculation, such as the above example, provides values for only one beta particle or electron energy. However, beta particles are emitted with a broad spectrum of energies from zero to E_{max}, the majority of which may posses an average energy, E_{av}, of approximately one-third of E_{max}.

The ratio of beta particle energy loss via bremsstrahlung emission to energy loss via collision interactions causing ionization and excitation is described by the relation

$$\frac{E_{\text{Brems.}}}{E_{\text{ioniz.}}} = \frac{EZ}{750} \qquad [6.91]$$

where E is the beta particle energy in MeV and Z is the atomic number of the absorber material (Friedlaner et al., 1964; Evans, 1972; Tsoulfanidis, 1995). From Eqs. [6.90] and [6.91] we can write

$$\left(\frac{dE}{dx}\right)_{\text{rad.}} = \frac{ZE}{750}\left(\frac{dE}{dx}\right)_{\text{ion.}} = \frac{(13)(2.280)}{750}(4.314\ \text{MeV/cm}) = 0.170\ \text{MeV/cm} \qquad [6.92]$$

The total stopping power of the 2.280 MeV beta particle in aluminum according to Eqs. [6.90] and [6.92] is thus

$$\left(\frac{dE}{dx}\right)_{\text{total}} = \left(\frac{dE}{dx}\right)_{\text{ion.}} + \frac{EZ}{750}\left(\frac{dE}{dx}\right)_{\text{ion.}} = 4.314\ \text{MeV/cm} + 0.170\ \text{MeV/cm} = 4.48\ \text{MeV/cm} \qquad [6.93]$$

Beta particle loss via bremsstrahlung radiation of the 2.280 MeV beta particles from ^{90}Y is low in aluminum, namely 0.170/4.48 or 3.79% of the total energy loss. However, bremsstrahlung production will increase as the absorber atomic number (Z) and beta particle or electron energy increase. Bremmstrahlung is highly penetrating electromagnetic radiation, and thus low atomic number absorbers such as aluminum or plastic (high in carbon and hydrogen) of adequate thickness may be evaluated as shields against beta particles and electron radiation. Shielding material of high atomic number elements, such as lead, will yield higher levels of bremsstrahlung radiation. The effect of atomic number (Z) and beta particle or electron energy (E) on the ratio of energy loss via bremstrahlung production to ionization energy is illustrated in Fig. 6.18.

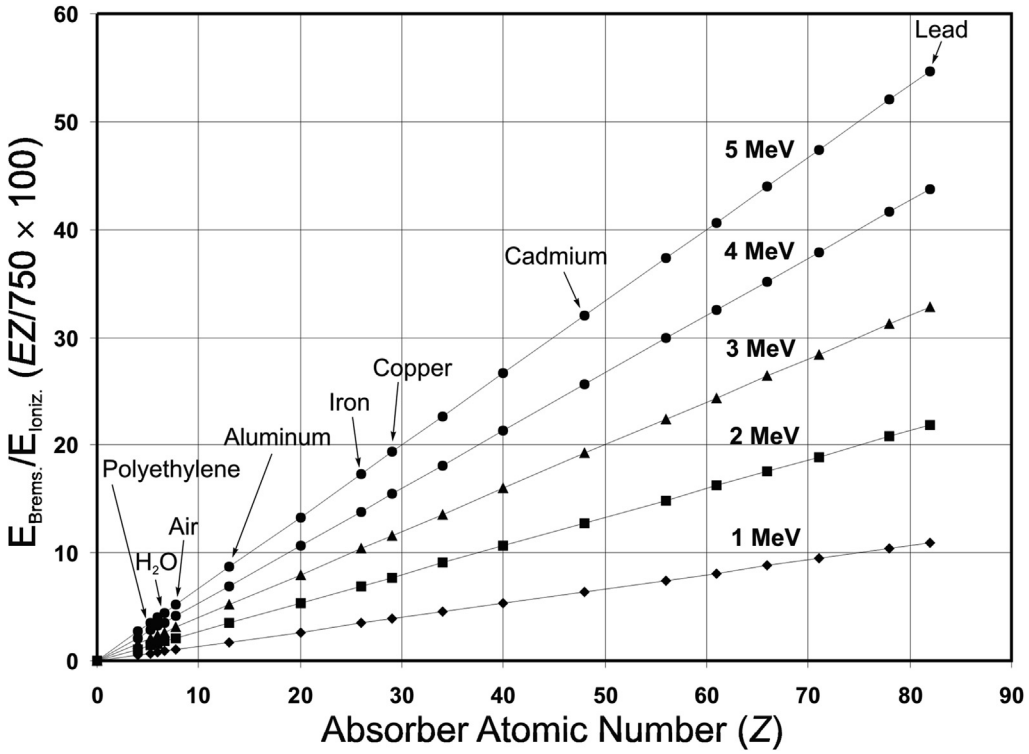

FIGURE 6.18 Ratio of energy loss via bremsstrahlung production to ionization expressed as a percentage ($EZ/750 \times 100$) for beta particles or electrons of energies (E) ranging from 1 to 5 MeV as a function of absorber atomic number (Z). Some common absorbers are identified above data points corresponding to their atomic number (Z) or effective atomic number (Z_{ef}) for observers that are compounds.

The effective atomic numbers of compounds such as polyethylene $(-C_2-H_4)_n$, ($Z_{ef} = 5.28$), water ($Z_{ef} = 6.60$), and air ($Z_{ef} = 7.3$) provided in Fig. 6.18 are a function of the weight fraction of each element in the compound, calculated according to the equation

$$Z_{ef} = \frac{\sum_{i=1}^{L} w_i (Z_i^2/A_i)}{\sum_{i=1}^{L} w_i (Z_i/A_i)} \quad [6.94]$$

where L is the number of elements in the compound, w_i is the weight or mass fraction of element i, Z_i is the atomic number of element i, and A_i is the atomic weight of element i (Tsoulfanidis, 1995; Andreo et al., 2005). As illustrated in Fig. 6.18, absorbers of low atomic number as protective shields will yield less harmful highly penetrating bremsstrahlung radiation, particularly when absorbers of high-energy (MeV) beta particles or electrons are needed.

6.9.2 Linear Energy Transfer

The ICRU (Taylor et al., 1970) defines LET (L) of charged particles in a medium as

$$L = \frac{dE_L}{dl} \quad [6.95]$$

where dE_L is the average energy locally imparted to the medium by a charged particle of specified energy in traversing a distance dl. The term "locally imparted" refers either to a maximum distance from the particle track or to a maximum value of discrete energy loss by the particle beyond which losses are no longer considered as local. LET is generally measured in units of keV/μm. The ICRU recommends, when a restricted form of LET is desired, that the energy cut-off form of LET be applied because this can be evaluated using restricted stopping power formulae (Taylor et al., 1970). The energy-restricted form of LET or L_Δ is therefore defined as that part of the total energy loss of a charged particle which is due to energy transfers up to a specified energy cut-off value

$$L_\Delta = \left(\frac{dE}{dl}\right)_\Delta \quad [6.96]$$

where the cut-off energy (Δ) in eV units must be defined or stated. If no cut-off energy is applied, then the subscript ∞ is used in place of Δ, where L_∞ would signify the value of LET which includes all energy losses and would therefore be equal to the total mass stopping power.

Fig. 6.19 illustrates charged particle interactions within an absorber involved in the measurement of LET. The possible types of energy loss, ΔE, of a charged particle of specified energy E traversing an absorber over a track length Δl is illustrated, where O represents a particle traversing the absorber without any energy loss, U is the energy transferred to a localized interaction site, q is the energy transferred to a short-range secondary particle when $q \leq \Delta$, Δ is a selected cut-off energy level (eg, 100 eV), Q' is the energy transferred to a long-range secondary particle (eg, formation of delta rays) for which $Q' > \Delta$, γ is the energy transferred to photons (eg, excitation fluorescence, Cherenkov photons, etc.), r is a selected

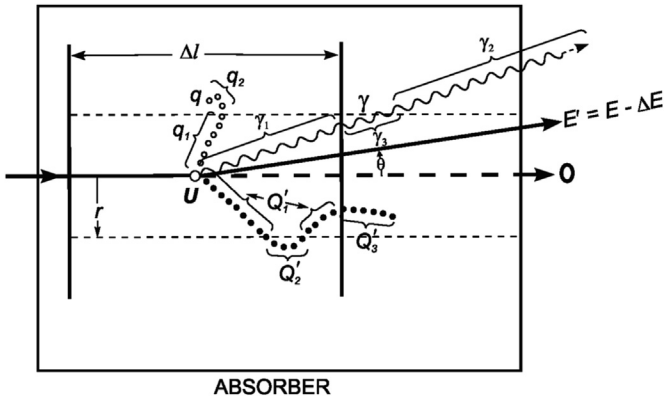

FIGURE 6.19 Diagram of the passage of particle of energy E through a thickness Δl of material, illustrating the several types of energy loss that may occur. *From Taylor, L.S., et al., 1970. Linear Energy Transfer. ICRU Report 16. International Commission on Radiation Units and Measurements, Washington, DC, reprinted with permission from ICRU © 1970.*

TABLE 6.3 Track Average Values of LET (L_Δ) in Water Irradiated With Various Radiations

Radiation	Cut-off Energy, Δ (eV)	L_Δ (keV/μm)
^{60}Co gamma rays	Unrestricted	0.239
	10,000	0.232
	1000	0.230
	100	0.229
22 MeV X-rays	100	0.19
2 MeV electrons (whole track)	100	0.20
200 kV X-rays	100	1.7
^{3}H beta particles	100	4.7
50 kV X-rays	100	6.3
5.3 MeV alpha particles (whole track)	100	43

Taylor, L.S., et al., 1970. Linear Energy Transfer. ICRU Report 16. International Commission on Radiation Units and Measurements, Washington, DC, reprinted with permission from ICRU © 1970.

cut-off distance from the particle's initial trajectory or path of travel, and θ is the angle of particle scatter. The interactions q, Q, and γ are subdivided in Fig. 6.19 when these fall into different compartments of the absorber medium. See Taylor et al. (1970) for methods used for the precise calculations of LET. Some examples of LET in water for various radiation types are given in Table 6.3. The table clearly illustrates that radiation of a given energy with shorter range in a medium will yield higher values of LET than radiations of the same energy with longer ranges in the same medium. This may be intuitively obvious, because the shorter the range of the radiation the greater is the energy dissipated per unit path length of travel. We can take this further and generalize that the following radiation types will yield LET values of decreasing orders of magnitude (the heavier charged particles are considered here to be of the same energy for purposes of comparison) according to the sequence:

Decreasing LET:

↓
Fission Products
Alpha Particles
Deuterons
Protons
Low-energy x Rays and Beta Particles
High-energy x Rays and Beta Particles
Gamma Radiation and High-energy Beta Particles

[6.97]

Although electromagnetic X- and gamma radiations are not charged particles, these radiations do have the characteristics of particles (photons) that produce ionization in matter. They are therefore included in the above sequence and among the radiations listed in Table 6.3.

The term "delta rays" is used to identify energetic electrons that produce secondary ionization. When a charged particle, such as an alpha particle, travels through matter, ionization occurs principally through coulombic attraction of orbital electrons to the positive charge on the alpha particle, with the ejection of electrons of such low energy that these electrons do not produce further ionization. However, direct head-on collisions of the primary ionizing particle with an electron do occur occasionally, whereby a large amount of energy is transferred to the electron. The energetic electron will then travel on in the absorbing matter to produce secondary ionization. These energetic electrons are referred to as delta rays. Delta rays form ionization tracks away from the track produced by the primary ionizing particle. The occurrence and effects of delta rays in radiation absorption are applied to studies of radiation dosimetry (Casnati et al., 1998; Cucinotta et al., 1998).

TABLE 6.4 Range and Estimated LET Values for Various Charged Particle Radiations in Water in Order of Decreasing Mass[a]

Nuclide	Radiation Energy (MeV)	Range in Water (mm)	Average LET in Water (keV/μm)
Thorium-232	α, 4.0	0.029[b]	138
Americium-241	α, 5.5	0.048[b]	114
Thorium-227	α, 6.0	0.055[b]	109
Polonium-211	α, 7.4	0.075[b]	98
……..	d, 4.0	0.219[c]	18.3
……..	d, 5.5	0.377[c]	14.6
……..	d, 6.0	0.440[c]	13.6
……..	d, 7.4	0.611[c]	12.1
……..	p, 4.0	0.355[d]	11.3
……..	p, 5.5	0.613[e]	9.0
……..	p, 6.0	0.699[f]	8.6
……..	p, 7.4	1.009[g]	7.3
Tritium	β^-, 0.0186 (E_{max})	0.00575[h]	3.2[h]
Carbon-14	β^-, 0.156 (E_{max})	0.280[h]	0.56[h]
Phosphorus-32	β^-, 1.710 (E_{max})	7.92[h]	0.22[h]
Yttrium-90	β^-, 2.280 (E_{max})	10.99[h]	0.21[h]

[a]*The deuteron (d) and proton (p) energies were arbitrarily selected to correspond to the alpha particle (α) energies to facilitate the comparison of the effects of particle mass and charge on range and LET.*
[b]*Calculated according to Eqs. [4.19] and [4.20] of chapter "Alpha Radiation."*
[c]*The deuteron range is calculated from the equation* $R_{Z,M,E} = M/Z^2 R_{p,E/M}$. *The equation provides the range of a particle of charge Z, mass M, and energy E, where* $R_{p,E/M}$ *is the range in the same absorber of a proton of energy E/M (Friedlander et al., 1964).*
[d]*Calculated according to Eqs. [4.17], [4.19], and [4.20] of chapter "Alpha Radiation."* $R_{air} = 28.5$ *mg/cm*^{2} *(Friedlander et al., 1964).*
[e]*Calculated according to Eqs. [4.17], [4.19], and [4.20] of chapter "Alpha Radiation."* $R_{air} = 49.5$ *mg/cm*^{2} *(Friedlander et al., 1964).*
[f]*Calculated according to Eqs. [4.17], [4.19], and [4.20] of chapter "Alpha Radiation."* $R_{air} = 56.5$ *mg/cm*^{2} *(Friedlander et al., 1964).*
[g]*Calculated according to Eqs. [4.17], [4.19], and [4.20] of chapter "Alpha Radiation."* $R_{air} = 82.0$ *mg/cm*^{2} *(Friedlander et al., 1964).*
[h]*Calculations are based on the maximum energy* (E_{max}) *of the beta particles. When the lower value of average beta particle energy* (E_{av}) *is used, the calculated value of range is shorter and LET higher. The range was calculated according to the empirical formula* $R = 0.412E^{1.27-0.0954\ln E}$ *available from the curve provided in Fig. A.4, Appendix A.*

When we compare particles of similar energy, we can state that the ranges of particles of greater mass and charge will obviously be shorter and the magnitude of their LET values will be consequently higher in any given medium. The relationship between mass, charge, energy, and range of particles and their corresponding LET values can be appreciated from Table 6.4. The LET values in Table 6.4 are estimated by dividing the radiation energy by its range or path length in the medium. Such a calculation provides only an estimate of the LET, because the energy dissipated by the radiation will vary along its path of travel, particularly in the case of charged particles. More energy is released when the particle slows down before it comes to a stop, as illustrated in Fig. 4.6 of the chapter entitled "Alpha Radiation," when energy liberated in ion pair formation is the highest. Nevertheless, the LET values provided in Table 6.4 give good orders of magnitude for comparative purposes.

The concept of LET and the calculated values of LET for different radiation types and energies can help us interpret and sometimes even predict the effects of ionizing radiation on matter. For example, we can predict that heavy charged particles, such as alpha radiation, will dissipate their energy at shorter distances within a given absorber body than the more penetrating beta or gamma radiations. Also, low-energy X-radiation can produce a similar effect as certain beta radiations. The order of magnitude of the LET will help us predict the penetration power and degree of energy dissipation in an absorber body, which is critical information in studies of radiation chemistry, radiation therapy, and dosimetry, among others. For additional information the reader is referred to works by Ehman and Vance (1991), Farhataziz and Rodgers (1987), and Spinks and Woods (1990).

Chapter 7

Hall of Fame: Part III

Max Planck (1858–1947), Louis de Broglie (1892–1987), Albert Einstein (1879–1955), Arthur H. Compton (1892–1962), Wu Youxun (1897–1977), Yoshio Nishina (1890–1951), Max von Laue (1879–1960), Sir William Henry Bragg (1862–1942) and Sir William Lawrence Bragg (1890–1971), Rosalind Franklin (1920–1958), Henry G.J. Moseley (1887–1915), Charles Glover Barkla (1877–1944), Manne Siegbahn (1886–1978), Robert A. Millikan (1868–1953) and Harvey Fletcher (1884–1981), and Homi J. Bhabha (1909–1966).

Thus to describe the properties of matter as well as those of light, waves and corpuscles have to be referred to at one and the same time. The electron can no longer be conceived as a single, small granule of electricity: it must be associated with a wave and this wave is no myth; its wavelengths can be measured and its interferences predicted…And it is on this concept of the duality of waves and corpuscles in Nature, expressed in a more or less abstract form, that the whole recent development of theoretical physics has been founded and that all future developments of this science will apparently have to be founded.

Prince Louis Victor de Broglie in his Nobel lecture on December 12, 1929.

MAX PLANCK (1858–1947)

Max Karl Ernst Ludwig Planck was born in Kiel, Germany on April 23, 1858. He was awarded the Nobel Prize in Physics in 1918 "in recognition of the services he rendered to the advancement of physics by his discovery of energy quanta."

Max Planck (1858-1947)

Max Planck entered the University of Munich in 1874 to study physics and mathematics and transferred to the University of Berlin in 1877 to broaden his studies. In Berlin he was able to attend lectures by the prominent physicists Hermann von Helmholtz and Gustav Kirchhoff. At the age of 21, he received the doctor of philosophy degree in physics after defending his dissertation in Munich "On the Second Law of the Mechanical Theory of Heat." He submitted his Habilitation thesis the following year to become a university teacher, and began to serve at the university as a lecturer without salary. The lack of

Radioactivity: Introduction and History, From the Quantum to Quarks. http://dx.doi.org/10.1016/B978-0-444-63489-4.00007-1
Copyright © 2016 Elsevier B.V. All rights reserved.

remunerative compensation for his university lectures forced him to live with his parents in Munich, which he considered to be an unfavorable burden on them. He felt the need to demonstrate to the scientific community his worth as a physicist in order to gain a professorship. For the next five years (1880−1885), Max Planck established himself as a private lecturer or Privatdozent in physics at the University of Munich until he was able to get an appointment to the position of associate professor of theoretical physics at the University of Kiel in 1885, where he remained until 1889. His appointment at the University of Kiel at the age of 27 provided him with the financial resources necessary to marry Marie Merck (1861−1909) on March 31, 1887. After the death of Gustav Kirchhoff in 1887, Max Planck was able to succeed him as Chair of Theoretical Physics at the University of Berlin in 1888, starting as associate professor and director of the Institute of Theoretical Physics, and then advancing to full professorship in 1892. He remained at the University of Berlin until his retirement in 1926.

Upon his arrival in Berlin, Max Planck joined the German Physical Society and remained a very active and devoted member for three decades, serving in various years on the Society's board as treasurer, committee member, and chairman. The year 1929 marked the 50th anniversary of his doctoral degree, and the German Physical Society established on that occasion the Max Planck Medal. Albert Einstein was a recipient of the medal in 1929. The medal is bestowed annually by the German Physical Society, and it remains the reward of highest honor granted by the Society.

Max Planck's main contributions originated from his work on thermal radiation, the results of which opened the field of quantum physics and provided the groundwork for subsequent discoveries on the properties of light waves and other classes of electromagnetic radiation including X-rays and gamma rays. Several key discoveries on the properties of radiation were made prior to Planck's, and a brief description of this earlier work is provided here. Very early observations on the properties of thermal radiation were documented in 1792 by Thomas Wedgewood, the famous British manufacturer of Wedgewood porcelain. Wedgewood observed that all objects in his ovens, where he prepared fine china, would glow the same red color when they reached a certain temperature, regardless of their size, shape, or composition. It was not until 1859 that Gustav Kirchhoff demonstrated that, with any object in thermal equilibrium with radiation, the emitted energy is proportional to the energy absorbed by the object. An example of such a case would be the heated walls of a kiln with its door closed and at a constant temperature. The radiation within the walls of the kiln would be in thermal equilibrium when the radiation energy within the kiln is absorbed, exchanged, and reemitted many times over until the entire walls of the cavity of the kiln are in thermal equilibrium. The radiation in thermal equilibrium within the walls of a kiln is similar to the radiation emitted by a black body, which is an object that absorbs radiation of all wavelengths or frequencies and therefore would appear black. A black body emits the energy it absorbs in accord with Kirchhoff's observations; and the energy emitted is a function of the temperature of the black body and frequency of the emitted light, and independent of the size, shape, and chemical nature of the black body. Wilhelm Wien, in 1893, mathematically defined the spectral density of a black-body cavity, that is, the energy per unit volume per unit frequency within a black-body cavity, as a function of black-body temperature. The equation derived by Wien became known as Wien's exponential law, because the energy density was an exponential function of the radiation frequency and black-body temperature. Radiation spectroscopists at the time determined experimentally that Wien's law fit well for the short wavelengths of radiation (0−4 μm) over a wide range of temperatures (400−1600K), but that the law failed for longer radiation wavelengths (Serway et al., 2005).

Over a period of 6 years, Planck labored to find a general formula that would describe the energy density of black-body radiation that would fit for both low and high radiation frequencies. In October of 1900, Planck found such a formula, which included a constant $h = 6.626 \times 10^{-34}$ J s, which is called Planck's constant in his honor. The postage stamp illustrated here was issued by the German Democratic Republic in honor of Max Planck and his discovery of the Planck constant h. While this was a great achievement, it did not satisfy Plank's efforts to find more meaning for his formula. In his Nobel lecture he expressed his struggles toward this goal as follows:

> *However, even if the radiation formula should prove itself to be absolutely accurate, it would still only have, within the significance of a happily chosen interpolation formula, a strictly limited value. For this reason, I buried myself, from then on, that is, from the day of its establishment, with the task of elucidating a true physical character for the formula,…after some weeks of the most strenuous work of my life, light came into the darkness, and a new undreamed of perspective opened up for me.*

Max Planck was referring to his discovery of quantum theory, which we have yet to describe, and the role of Plank's constant h in the new field of quantum physics that he was about to open. In the course of his efforts, Max Planck correlated black-body radiation to radiation produced by many oscillators, which he called resonators, within the cavity surrounded by a sphere of reflecting walls from which he developed quantum theory. In his Nobel lecture of June 2, 1920 he described his thoughts at the time as follows:

> *Heinrich Hertz's linear oscillator, whose laws of emission, for a given frequency, …seemed to me to be a particularly suitable device for this purpose. If a number of such Hertzian oscillators are set up within a cavity surrounded by a sphere of reflecting walls, then by analogy with audio oscillators and vibrating resonators, energy will be exchanged between them by the output and absorption of electromagnetic waves, and finally stationary radiation corresponding to Kirchhoff's Law, the so-called black-body radiation, should be set up within the cavity.*

Planck expected that the vibrating resonators would emit radiation within the reflecting walls of a cavity over a continuous spectrum of wavelengths with frequencies corresponding to the varying frequencies of the vibrating resonators. However, to fit experimental observations, Planck had to envisage that the vibrating resonator could not possess energies corresponding to all frequencies, but that the energy levels would correspond to discrete multiples of $h\nu$ (Serway et al., 2005), or:

$$E_{\text{resonator}} = nh\nu \qquad \text{[III.1]}$$

where $n = 1, 2, 3\ldots$ and ν is the resonator frequency. Therefore, as illustrated in Fig. III.1, the radiation emitted by the resonator could only occur as "packets" of energy when the energy of the resonator would drop from a high energy level to a lower one, or:

$$\Delta E = h\nu \qquad \text{[III.2]}$$

It was found that radiation is emitted at discrete energies corresponding to differences in energy states of a body, and the energies of emitted radiations would be found as the product of Planck's constant, h, having units of energy $\times$ time and the radiation frequency, ν. Planck named the discrete radiation energy "the quantum" from the Latin *quantus* meaning "how great." Eq. [III.2] is referred to as the Planck–Einstein equation, as Einstein in 1905 was able to demonstrate that

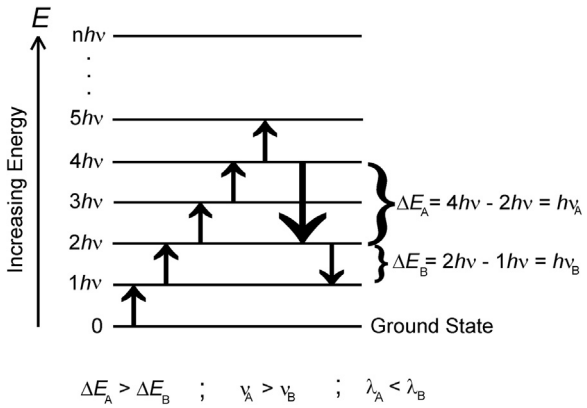

FIGURE III.1 Planck's quantum theory. The energy levels of a vibrating resonator or black body would not correspond to energies of all frequencies ν, but the energy levels would correspond to multiples of $h\nu$. The energy emitted by the resonator or body could only occur as "packets" of energy when the energy of the body would drop from a higher energy level to a lower one, or $\Delta E = h\nu$. The arrows pointed upward correspond to increasing energy levels, and the two arrows pointed downward illustrate two distinct emissions of energy and radiation frequencies.

light not only traveled as waves of electromagnetic radiation but also as discrete packets of energy, which he named "energy quanta" or photons.

To commemorate the significance of quantum theory, the postage stamp illustrated here was issued in Germany in 1994. It pictures a black-body cavity or kiln in which an opening is created and from which radiation is emitted. The energy of that radiation is illustrated as equivalent to Planck's constant h times the radiation frequency.

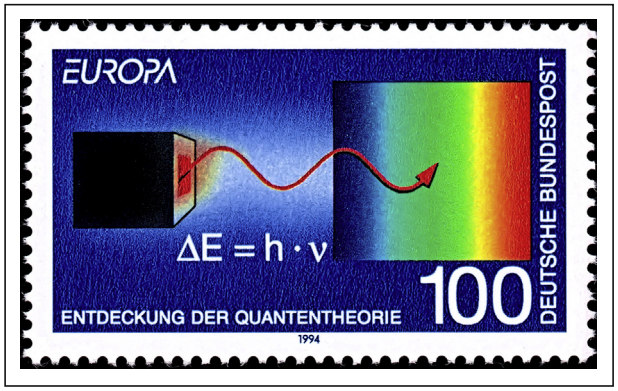

Max Planck's discovery of the quantum was one of the greatest contributions to science of the 20th century. It led to Einstein's interpretation of the photoelectric effect and his discovery of the photon; and it opened the door to our understanding of the properties of radiation and its interaction with matter. Planck's equation for the energy quantum, namely, $E = h\nu$, is used universally in science and in many parts of this book. Planck's discovery was again commemorated in 2008 by the postage stamp with his picture illustrated here.

After the death of his wife Marie in 1909, Planck married her cousin Marga von Hösslin. He remained in Germany throughout the Second World War and had to cope with the power and intervention of the National Socialists in Germany. He was President of the Kaiser Wilhelm Society, and thus headed the primary research institution in Germany from 1930 to 1938. His leadership was notable in hindering the Nazis from engulfing the Society, and in maintaining high scientific standards, but he was unable to prevent the Nazis from overrunning the Society (Max-Planck Society). During the last few years of his life, he suffered great hardship and loss. In 1944, his home in the Berlin suburb of Grunewald was totally destroyed together with most of his possessions and scientific papers after an Allied air bombing raid. That same year on July 20th his son Erwin, who was also his close friend and trusted advisor, was arrested for participating in an assassination attempt on Hitler's life. After the war in 1945, American colleagues escorted the world-famous physicist to Göttingen, where he spent the remaining years of his life until his death in October, 1947. His wife Marga wrote Lise Meitner on June 16, 1947: "But I can assure you of one thing: without the help of our friends abroad, my husband would very certainly not have survived the winter" (Max-Planck Society).

LOUIS DE BROGLIE (1892–1987)

Prince Louis-Victor de Broglie was born at Dieppe (Seine Inférieure) on August 15, 1892. He was awarded the Nobel Prize in Physics in 1929 "for his discovery of the wave nature of electrons."

de Broglie (1892-1987)

After completing his secondary school education at the Lycée Janson de Sailly in 1909, Louis de Broglie decided to pursue studies in literature and history, and was awarded a degree in history at the Sorbonne in 1910, contemplating a career in the diplomatic service; but he also had an interest in science. When given a research topic in history, he gave serious thought to his goals in life and his interest in science prevailed. He decided to pursue studies in physics and mathematics and obtain a degree in theoretical physics. In 1913 he was awarded his License de Sciences at the Sorbonne. De Broglie was then conscripted into military service for the duration of the war of 1914 to 1918, and was stationed at the Eifel Tower in the wireless section of the army. After the war, de Broglie pursued studies in theoretical physics, taking an interest in the X-ray research work of his elder brother Maurice de Broglie, which strengthened his interest in science while working for his doctorate degree in theoretical physics in the early 1920s. During his Nobel lecture on December 12, 1929, de Broglie elucidated his thoughts on physics at the time of his graduate studies for the doctorate degree as follows:

> *I was attracted to theoretical physics by the mystery enshrouding the structure of matter and the structure of radiations, a mystery which deepened as the strange quantum concept introduced by Planck in 1900 in his research on black-body radiation continued to encroach on the whole domain of physics.*

While pursuing his university studies in theoretical physics, de Broglie focused his interest in problems related to quanta. The year prior to presenting his dissertation, de Broglie (1923a,b,c) presented his thoughts on the dual nature of matter and light, that is, matter could be interpreted as having the properties of light with wavelength and frequency, or the properties of a particle with mass. For example, de Broglie (1923a) referred to the wavelength and associated frequency of particulate matter as follows:

> *An observer bound to the portion of matter will associate with it a frequency determined by its internal energy, namely by its "mass at rest". An observer for whom a portion of matter is in steady motion with velocity* βc*, will see this frequency lower in consequence of the Lorentz-Einstein time transformation.*

The term β in de Broglie's statement refers to the relative phase velocity of a particle of matter, that is, the velocity of the particle in a medium (eg, air) divided by the velocity of light in a vacuum, ie, $c = 2.99 \times 10^{10}$ cm/s. (See the following biographical sketch on Albert Einstein for an example of a time transformation calculation based on an observer on earth detecting the arrival of a cosmic particle.) De Broglie (1923a), in turn, referred to light as having the properties of particles with mass, when he wrote the following:

> *A radiation of frequency* ν *has to be considered as divided into atoms of light of very small internal mass (*$\sim 10^{-50}$ *gm) which move with a velocity very nearly equal to* c *given by* $m_0c^2 \Big/ \sqrt{1-\beta^2} = h\nu$.

In 1924 at Paris University, he delivered his doctoral dissertation on *Recherches sur la Théorie des Quanta* (Research on the Quantum Theory). What is very astonishing is that de Broglie received the Nobel Prize mainly for the work he did in his doctoral dissertation presented to the Faculty of Sciences only five years prior to his receiving the Nobel Prize in Physics. His dissertation expounded on the dual particle and wave nature of the electron and other matter. His ideas, based on previous work of Planck and Einstein, were first received with astonishment, but subsequently accepted universally following demonstrations by experimental work on electron diffraction by crystals carried out by Davisson and Gerner at Bell Laboratories, New York in 1927, and by others.

The significance of de Broglie's findings was explained by Prof. C.W. Oseen, Chairman of the Nobel Committee for Physics of the Royal Swedish Academy of Sciences, on December 10, 1929 as follows:

> *Louis de Broglie had the boldness to maintain that not all properties of matter can be explained by the theory that it consists of corpuscles…there are others, according to him, which can be explained only by assuming that matter is, by its nature, a wave motion. At the time when no single known fact supported this theory, Louis de Broglie asserted that a stream of electrons, which passed through a very small hole in an opaque screen, must exhibit the same phenomena as a light ray under the same conditions. It was not quite in this way that Louis de Broglie's experimental investigation concerning his theory took place. Instead, the phenomena arising when beams of electrons are reflected by crystalline surfaces, or when they penetrate thin sheets, etc. were turned to account. The experimental results obtained by these various methods have fully substantiated Louis de Broglie's theory. It is thus a fact that matter has properties, which can be interpreted only by assuming that matter is of a wave nature.*

Prof. Orseen concluded his remarks on the work of de Broglie with the following statement, which underscored the impact of de Broglie's findings:

> *Hence there are not two worlds, one of light and waves, one of matter and corpuscles. There is only a single universe. Some of its properties can be accounted for by the wave theory, others by the corpuscular theory.*

Louis de Broglie expounded on his approach to the findings of his theoretical work as follows:

> *I thus arrived at the following overall concept which guided my studies: for both matter and radiations, light in particular, it is necessary to introduce the corpuscle concept and the wave concept at the same time. In other words, the existence of corpuscles accompanied by waves has to be assumed in all cases…it must be possible to establish a certain parallelism between the motion of a corpuscle and the propagation of the associated wave.*

He derived the fundamental relation of his theory as the wavelength of the electron or other particle in motion as:

$$\lambda = \frac{h}{p} \qquad \text{[III.3]}$$

where λ is the wavelength of the particle, that is, the distance between two consecutive peaks of the particle wave, h is Planck's constant (6.626×10^{-34} J s), and p is the particle momentum. De Broglie noted that for electrons that are not extremely fast (not relativistic), the electron momentum could be expressed as:

$$p = m_0 v \qquad \text{[III.4]}$$

where m_0 is the rest mass of the electron and v its velocity. The wavelength of the electron could then be calculated as:

$$\lambda = \frac{h}{m_0 v} \qquad \text{[III.5]}$$

This Eq. [III.5] is the basic formula for calculating the de Broglie wavelength of a particle. The discovery of de Broglie, described in his doctoral dissertation of 1924, is commemorated in the postage stamp illustrated here that was issued in France in 1994.

Louis de Broglie calculated the wavelength of an electron that is accelerated through a specific voltage potential after deriving the following:

For the nonrelativistic case, the energy of the electron can be expressed as:

$$eV = \frac{1}{2}m_0v^2 \qquad \text{[III.6]}$$

and since $p = m_0v$, we can write:

$$\frac{p^2}{2m_0} = \frac{m_0^2v^2}{2m_0} = \frac{1}{2}m_0v^2 = eV \qquad \text{[III.7]}$$

Thus:

$$p = \sqrt{2m_0eV} \qquad \text{[III.8]}$$

and:

$$\lambda = \frac{h}{p} = \frac{h}{\sqrt{2m_0eV}} \qquad \text{[III.9]}$$

He demonstrated that the wavelength of the electron that had been accelerated some tens of volts would have a dimension of the order of the angstrom unit. For example, an electron that is accelerated across a potential of 100 V would have a wavelength calculated according to Eq. [III.9] as:

$$\lambda = \frac{h}{\sqrt{2m_0eV}} = \frac{6.626 \times 10^{-34}\ \text{J s}}{\sqrt{2(9.11 \times 10^{-31}\ \text{kg})(1.6 \times 10^{-19}\ \text{C})(100\ \text{V})}} = 1.2 \times 10^{-10}\ \text{m} = 1.2\ \text{Å}$$

De Broglie concluded that with a wavelength of the order of magnitude of the angstrom unit, it would be expected that crystals, which have similar atomic dimensions, could cause the diffraction of these electron waves similar to the diffraction of X-rays in crystals. In his Nobel lecture he noted the following:

> *A natural crystal such as rock salt, for example, contains nodes composed of the atoms of the substances making up the crystal and which are regularly spaced at distances of the order of an Angström. These nodes act as diffusion centers for the waves, and if the crystal is impinged upon by a wave, the wavelength of which is also of the order of an Angström, the waves diffracted by the various nodes are in phase agreement in certain well-defined directions and in these directions the total diffracted intensity is a pronounced maximum. The arrangement of these diffraction maxima is given by the nowadays well-known mathematical theory developed by von Laue and Bragg, which defines the position of the maxima as a function of the spacing of the nodes in the crystal and of the wavelength of the incident wave…However, if the electron is assumed to be associated with a wave and the density of an electron cloud is measured by the intensity of the associated wave, than a phenomenon analogous to the Laue phenomenon ought to be expected for electrons. The electron wave will actually be diffracted intensely in the directions which can be calculated by means of the Laue-Bragg theory from the wavelength* $\lambda = \text{h/mv}$*, which corresponds to the known velocity* v *of the electrons impinging on the crystals.*

Proof of Louis de Broglie's theory of the wave nature of the electron was provided by Davisson and Germer at the Bell Laboratories, New York in 1927 when they demonstrated that the phenomenon of electron diffraction by crystals was possible, and that the diffraction obeys exactly and quantitatively the laws of wave mechanics. Davisson and Germer shared the honor of being the first to observe the phenomenon of electron diffraction by a method analogous to that of von Laue for X-rays.

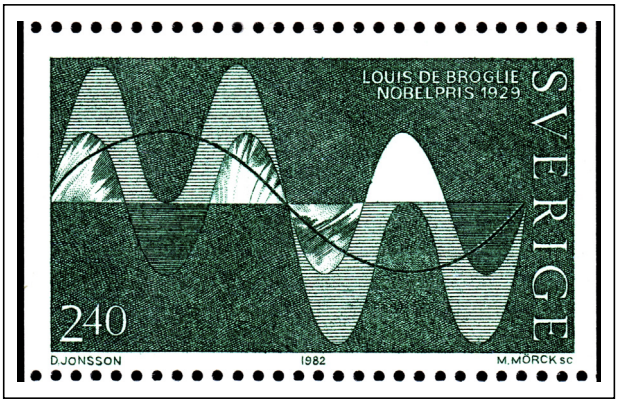

The postage stamp illustrated here was issued in Sweden in 1982 to commemorate de Broglie's discovery of the wave nature of matter. The impact of de Broglie's findings on modern physics was underscored when he concluded his Nobel lecture with the following:

> *Thus to describe the properties of matter as well as those of light, waves and corpuscles have to be referred to at one and the same time. The electron can no longer be conceived as a single, small granule of electricity; it must be associated with a wave and this wave is no myth; its wavelength can be measured and its interferences predicted…And it is on this concept of the duality of waves and corpuscles in Nature, expressed in a more or less abstract form, that the whole recent development of theoretical physics has been founded and that all future development of this science will apparently have to be founded.*

After presenting his doctoral dissertation in 1924, de Broglie completed two years of compensation-free lectures at the Sorbonne, after which he was appointed to the faculty of the Institut Henri Poincaré in Paris, which was newly established for the purpose of teaching and development of mathematical and theoretical physics. In 1932 he was appointed to the Chair of Theoretical Physics at the Faculty of Sciences at the University of Paris only eight years after receiving his doctorate at the same university. From 1930 to 1952, de Broglie continued studies on wave mechanics, Dirac's electron theory, the new theory of light photons, etc., during which time he was the author of 25 books. Many of these books were based on his courses; and students traveled from many parts of the world and within France to work with him. Many doctorate dissertations were prepared by students under his guidance.

Louis de Broglie received many awards including the first Kalinga Prize awarded by UNESCO for his efforts in explaining modern physics to the layperson. He was an elected member of the French Academy of Sciences and its Permanent Secretary for the mathematical sciences since 1942. Louis de Broglie died on March 19, 1987.

ALBERT EINSTEIN (1879–1955)

Albert Einstein was born at Ulm in Württemberg, Germany, on March 14, 1879. He was awarded the Nobel Prize in Physics in 1921 "for his services to theoretical physics and especially for his discovery of the law of the photoelectric effect." Einstein was the greatest theoretical physicist of the 20th century. He is known for making many contributions to science and mankind including his interpretation of quantum physics and the photoelectric effect, for which he received the Nobel Prize; his theory of relativity including the demonstration of the equivalence of mass and energy; his correspondence with President Franklin Delano Roosevelt warning of the potential of Germany to build a neutron fission bomb; his pacifism; and his philosophy. This biographical sketch will, in addition to providing information on his life and the impact it has made on our lives, underscore mostly Einstein's scientific contributions to the field of our understanding of the properties of radioactivity.

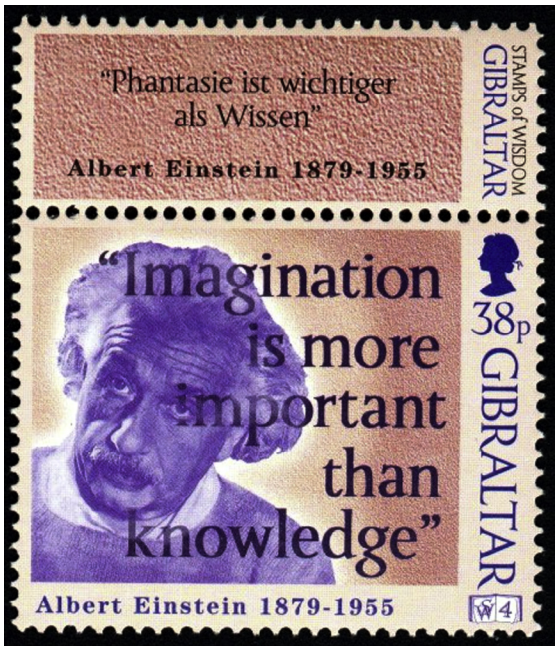

Albert Einstein (1879-1955)

Early Years

When Einstein was six weeks of age his family moved to Munich, where he began his elementary education at Luitpold Gymnasium. His family moved to Italy in 1894, but Einstein remained in Munich. In 1895 he tried to gain admission to the Eidgenössische Technische Hochschule (ETH) or Swiss Federal Polytechnic School in Zurich, but failed the entrance exam. In 1896 he renounced his German citizenship and remained stateless until being granted Swiss citizenship in 1901. Also in 1896, Einstein gained admission to the ETH and graduated in 1900 with a diploma as a teacher in mathematics and physics. After graduation he was unsuccessful in getting a job as a teacher in any university, and at the time gave up his ambitions to do so. Instead Einstein had to take temporary teaching employment in high schools in Winterthur and Schaffhausen during 1901. With the help of Marcel Grossman, a friend and classmate at the ETH, Einstein was appointed in 1902 as a clerk at the Swiss Patent Office in Bern, where he worked until 1909.

Discovery of the Photon Particle

During the time of his employment at the Patent Office and during his spare time Einstein produced a great amount of his most remarkable work, without any close association with other scientific colleagues or scientific literature. At the age of 26, he wrote three historic papers in his spare time and submitted these to the prestigious journal *Annalen der Physik* requesting publication "provided there was room" in the journal. All papers were published in the same journal issue in 1905. The first paper was Einstein's interpretation of Max Planck's quantum theory of radiation. He applied Planck's quantum theory to the interpretation of the photoelectric effect and explained the dual nature of light, that is, light may behave as a particle (ie, photon) or as a wave. The phenomenon of the photoelectric effect was already well known. It was for Einstein's interpretation of the photoelectric effect that he was awarded the Nobel Prize in Physics in 1921.

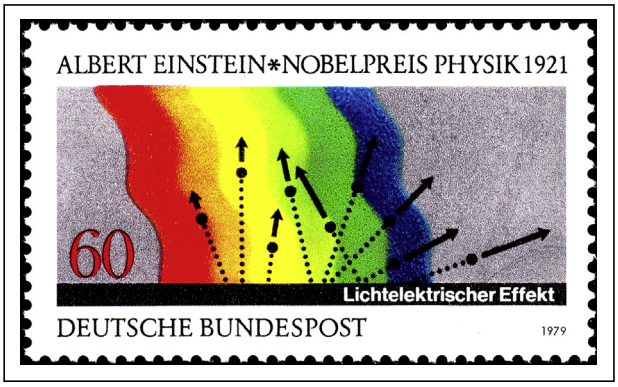

The photoelectric effect is the process whereby the energy from electromagnetic radiation, such as visible light or gamma radiation, hits an atomic electron, whereby the energy of the radiation is transferred in its entirety to the electron, causing the electron to be ejected from the atom. An artist's depiction of the photoelectric effect is illustrated in the postage stamp from Germany issued in 1979. The stamp illustrates visible light of various wavelengths (colors) striking the surface of a substance (eg, metal plate), causing the ejection of electrons from the surface of the plate.

Credit for the discovery of the photoelectric effect has been given to Heinrich Hertz, who in 1887 found that an electrical spark passing between two spheres would occur more readily if its path were illuminated with the light from another electrical discharge. A more thorough study by the German physicist Wilhelm Hallwachs in 1888 demonstrated that under certain conditions a negatively charged body, eg, a metal plate, illuminated with light of a particular color, loses its negative charge and ultimately assumes a positive charge (Arrhenius, 1922). Philipp Lenard (1902) demonstrated that the photoelectron velocity (ie, its kinetic energy) was independent of the light intensity, but that the electron velocity would vary only according to the wavelength of the light, and the highest velocities were attained when shorter wavelengths of light would hit a metal electrode (see Philipp Lenard, Hall of Fame, Part I). Increasing the light intensity would increase the number of photoelectrons, but not their energies.

Einstein was able to demonstrate in his first paper submitted to *Annalen der Physik* (Einstein, 1905a) that when a quantum of light hits a substance such as a metal plate, it can at most yield all of its energy to an electron. A part of the energy of the light quantum is consumed in knocking the electron out of its atom and the remaining energy will stay with the electron as kinetic energy of the electron. Einstein was awarded the Nobel Prize for his findings described in his first publication of 1905, and Prof. S Arrhenius, Chairman of the Nobel Committee for Physics, announced that the Nobel Committee named these findings as Einstein's Law of the Photoelectric Effect. The law states that the light quantum must have sufficient energy for the electron to become detached or released from its structure (electron binding energy) and provide the remaining energy to the electron as kinetic energy.

Only light having a frequency greater than a certain limit [greater than the electron binding energy] is capable of inducing a photoelectric effect, however high the intensity of the irradiating light. If this limit is exceeded, the effect is proportional to the light intensity at a constant frequency.

Arrhenius (1922).

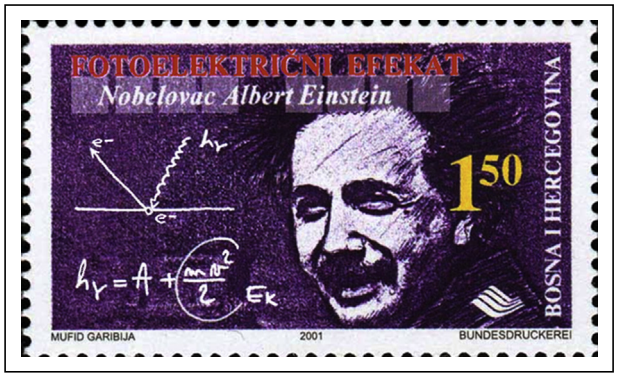

This effect can occur in any substance gas, liquid, or solid, provided the frequency of the light quantum is of sufficient energy to liberate an electron from its atom and thereby cause ionization. A postage stamp from Bosnia and Hertzegovina issued in 2001 commemorates Einstein's findings. The stamp illustrates a quantum of light ($h\nu$) striking a substance, such as a metal plate, and an electron is ejected. The stamp provides the equation describing the photoelectric effect, where:

$$h\nu = A + \frac{mv^2}{2} \qquad \text{[III.10]}$$

The equation states that the light quantum ($h\nu$) is proportional to the electron-binding energy (A) plus the kinetic energy of the electron ($E_K = \frac{1}{2}mv^2$). In the chapter entitled "Electromagnetic Radiation: Photons" the equation is described in reverse, that is, the kinetic energy of the photoelectron is proportional to the light quantum less the electron-binding energy (see Eq. [8.31] of the chapter "Electromagnetic Radiation: Photons"). In summary, Einstein grasped the calculations of Planck to explain that light not only traveled as waves but also as particles of energy (energy quanta). Today we refer to these energy quanta as photons, which are classified by particle physicists as one of the elementary particles of nature. The photoelectric effect is also one of the key interactions now used in gamma-ray spectrometry to identify radioactive sources when the energy imparted to an electron of a radiation detector is proportional to the energy of the gamma-ray photon. For his interpretation of the energy quanta of photons, Einstein is credited with the discovery of the photon as a particle.

The significance of Einstein's Law of the Photoelectric Effect was emphasized by the Chairman of the Nobel Committee (Gullstrand, 1925) when he stated:

A logical consequence of Planck's theory is that a transition from one [energy] state to another can only take place in such a way that an integral number of energy quanta is emitted or absorbed. An exchange of energy between matter and radiation, therefore — that is to say an emission or absorption of radiation — can be effected only by the transmission of an integral number of energy quanta. It was not Planck, however, but Einstein, that drew this conclusion, which involves the law of the photoelectric effect — a law that now, especially thanks to Millikan's work, has been verified in a brilliant manner. It is through Einstein's law that the Planck's constant and the whole quanta theory have attained their greatest importance.

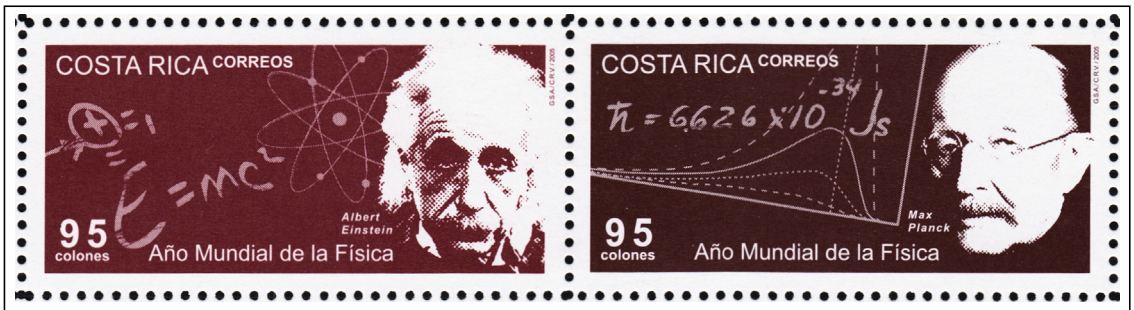

Einstein and Planck, World Year of Physics 2005

The above statement underscores the very close link between Max Planck's quantum theory and Albert Einstein's interpretation of the photon as a particle possessing an integral number of energy quanta. Thus, the work of Einstein was celebrated together with that of Planck in the postage stamps issued by Costa Rica illustrated here.

Einstein's quantum theory of the photon as an elementary particle was not universally accepted at the time that Einstein provided his explanation of the photoelectric effect in 1905. In particular, Robert A. Millikan (1968−1953), Nobel Laureate of Physics in 1923, was among those in disbelief. Millikan (1914, 1916a,b, 1921) devoted 10 years of effort into research on the photoelectric effect to disprove Einstein's interpretation of Planck's quantum theory to describe the photon as an elementary particle in an explanation of the photoelectric effect. All of Millikan's extensive research into the photoelectric effect only provided more evidence in support of Einstein's theory of the light quantum or photon. In view of Millikan's extensive research on the photoelectric effect, the Nobel Committee awarded the Nobel Prize in Physics in 1921 to Albert Einstein. The reader will find more information on this matter in the biographical sketch of Robert A. Millikan provided further on in the chapter.

Discovery of Molecular Dimensions in Brownian Motion

Another paper written by Einstein, when he was a patent clerk, explained Brownian motion (Einstein, 1905d), which was first observed by botanist Robert Brown in 1828. Most students of biology have witnessed Brownian motion when they observed in the lens of an optical microscope the erratic and jittery movement of microscopic substances in a liquid, such as pollen grains suspended in water on a microscope slide. Einstein provided calculations that could account for Brownian motion as that due to random collisions of molecules with the microscopic particle in the fluid, and his calculations provided an accurate measurement of the dimensions of the still-hypothetical molecules. His findings provided the first evidence for the existence of atom-sized molecules in matter and that the kinetic-energy theory could explain how heat would have an effect on the motion of atoms and molecules. From this paper Einstein wrote a thesis titled *Eine neue Bestimmung der Molekuldimensionen* (A New Determination of Molecular Dimensions), which earned him a doctorate degree from the University of Zurich in 1905. He dedicated the thesis to Marcel Grossman, his friend and former classmate at the ETH.

Relativity

The third of Einstein's papers submitted to *Annalen der Physik* in 1905 (Einstein, 1905b) proposed his theory of special relativity. Einstein's *Principle of Relativity* is based on two postulates: (1) that in making observations or measurements in physics, there should be no preferred inertial (nonaccelerating) frame; in other words, for all inertial observers, the laws of physics are the same; and (2) the speed of light in a vacuum is a constant ($c = 2.99 \times 10^8$ m/s) for all inertial observers, regardless of the velocity of travel of the source. Einstein developed his principle of relativity into what would be referred to later as the special theory of relativity that would provide an analysis of space and time. The special theory of relativity can be used to explain changes of length, time, and mass when an observer in one inertial frame makes measurements of length, time, and mass of another body or clock in another inertial frame. A person in one inertial frame of reference can make measurements of length, time, and mass on another inertial frame, and vice versa. Space, time, mass, and speed are all relative depending on which inertial frame of reference is used. In his Nobel lecture on the theory of relativity delivered to the Nordic Assembly of Naturalists at Gothenburg on July 11, 1923 (http://www.nobelprize.org), Einstein underscored the two principles upon which the special theory of relativity is based (Einstein, 1923) as follows:

> *The special theory of relativity is an adaption of physical principles to Maxwell-Lorentz electrodynamics. From earlier physics it takes the assumption that Euclidian geometry is valid for the laws governing the position of rigid bodies, the inertial frame and the law of inertia. The postulate of the equivalence of inertial frames for the formulation of the laws of Nature is assumed to be valid for the whole of physics (special relativity principle). From Maxwell-Lorentz electrodynamics it takes the postulate of invariance of the velocity of light in a vacuum (light principle).*

Relativistic Length Contraction and Time Dilation

In Einstein's treatise on relativity (Einstein, 1916a), he explained that when making measurements of events from frames of reference that are in uniform motion, we must define the events by four coordinates, namely the space coordinates x, y, and z as well as the time coordinate t. Thus any event, wherever it takes place, would be fixed in space by the perpendicular space coordinates x, y, and z and a fixed time t (see Fig. III.2). The same event, relative to another frame of reference, is also fixed in space and time according to the space-time coordinates x', y', z', t'. In his treatise on relativity, Einstein (1916a) explained that the world we live in should be considered as a four-dimensional space-time continuum.

Einstein (1916a) demonstrated that events measured from one frame of reference (eg, O, where the events are measured by an observer at O) on another frame of reference (eg, O', where the same events are measured by an observer at O'),

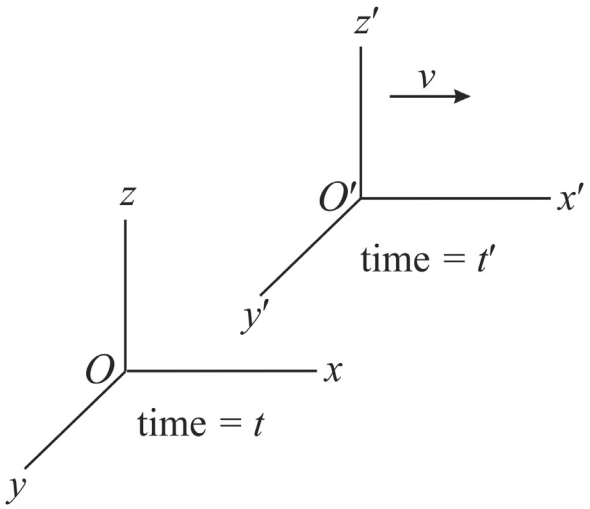

FIGURE III.2 Two frames of reference in space and time. An event in space and time in reference frame O' is defined by space–time coordinates x', y', z' and time t', traveling at a velocity v relative to reference frame O, defined by coordinates x, y, z, and t.

which is traveling at a velocity v relative to the observer at O, will yield different measurements of time (eg, time dilation) and length (eg, length contraction), which is dependent on the frame of reference from which the measurements are taken and the velocity (v). The differences in measurement of time and length taken from the two frames of reference will be greater as the velocity v approaches the unattainable speed of light c (ie, speed of light in a vacuum $= 2.9979 \times 10^8$ m/s).

The problem of relativity was presented by Einstein (1916a) with a question, which may be worded as follows: What are the values of x', y', z', and t' of an event with respect to frame O', when we know the values of x, y, z, and t, of the same event with respect to reference frame O. He explained that the solution to the problem must satisfy a law of the transmission of light in a vacuum, abbreviated by the symbol c, as a constant. Einstein indicated that for the coordinate systems illustrated in Fig. III.2, the problem is solved by the following Lorentz transformations, named after Nobel laureate Hendrik A. Lorentz (see the biographical sketch of H.A. Lorentz in Hall of Fame, Part I and a derivation of the Lorentz transformations in Appendix C of this book):

$$\text{length:} \quad x' = \frac{x - vt}{\sqrt{1 - (v^2/c^2)}}, \quad y' = y \quad \text{and} \quad z' = z \qquad \text{[III.11]}$$

$$\text{time:} \quad t' = \frac{t - \frac{v}{c^2}x}{\sqrt{1 - (v^2/c^2)}} \qquad \text{[III.12]}$$

Length Contraction in Relativity

Fig. III.3 illustrates an observer (with waving hands) in reference frame O', who takes a measurement in his or her own frame of reference; and measures the length of an object at time t' along the x-axis to extend from x'_a to x'_b. Since the object is measured by O' in his or her own frame of reference, the object is at rest with respect to the observer O'. At the same time, another observer in reference frame O takes a measurement of the same object in the reference frame O' to extend from x_a to x_b. Reference frame O' is traveling at a velocity v with respect to reference frame O. The measurement made by the observer in reference frame O will be smaller than that made by the observer in reference frame O' according to the Lorentz transformation defined in Eq. [III.11] above.

Let us look at Eq. [III.11] of the Lorentz transformation with respect to the specific example provided in the previous paragraph. The Lorentz transformation that defines changes in length along the x-axis (Eq. [III.11]) is the following:

$$x' = \frac{x - vt}{\sqrt{1 - (v^2/c^2)}} \qquad \text{[III.13]}$$

where x' is a coordinate along the x-axis measured at time t' in reference frame O' as measured by an observer in the same reference frame, which is traveling at the velocity v with respect to another reference frame O. The variable x is the

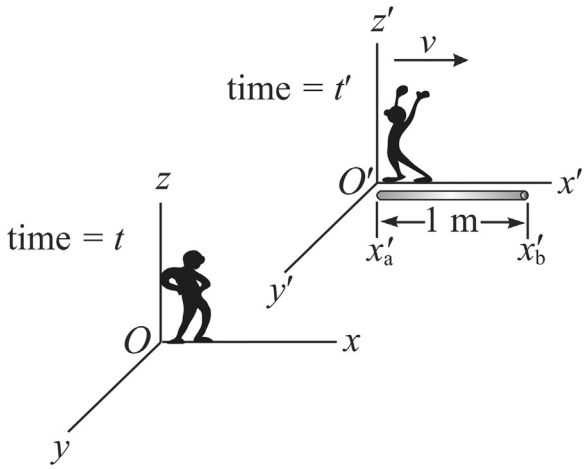

FIGURE III.3 Two frames of reference in space and time. An event in space and time in reference frame O' is defined by space–time coordinates x', y', z' and time t', traveling at a velocity v relative to reference frame O, defined by coordinates x, y, z, and t. An observer at O (with hands on hips) may take measurements of length and time on the frame of reference at O' (where there is an observer with hands waving) and measure length to be contracted (ie, shorter) and time dilated (ie, longer interval of time) than the length and time measured by the observer at O'. The observer at O', who makes measurements of an event from his or her own reference frame, would experience different measurements, because the measurements would be made of an event that would be at rest with respect to the observer. A rod is illustrated in the reference frame O', which would measure 1 m by the observer at O', because the rod would be at rest with respect to the observer at O'. However, the rod measured by the observer in the reference frame O would measure the rod to be contracted or shorter than 1 m in length; and the amount of contraction would be a function of the velocity v at which the reference frame O' is traveling with respect to reference frame O.

coordinate along the x-axis measured by an observer in reference frame O at time t; and c is the invariable speed of light in a vacuum. With respect to the example given in the previous paragraph, we can express the two measurements taken by the two observers in the two reference frames with the Lorentz transformation Eq. [III.11] as follows:

$$x_b' - x_a' = \frac{(x_b - x_a) - v(t' - t)}{\sqrt{1 - (v^2/c^2)}} \qquad \text{[III.14]}$$

where $x_b' - x_a'$ are the measurements along the x-axis (length of an object) in reference frame O' taken by an observer in the same reference frame where the object would be at rest with respect to the observer, which we can now call L_r; and $x_b - x_a$ are the measurements of the same object made by an observer in reference frame O, which we may call L. If the measurements are made by the two observers in the two reference frames at the same time, $t' = t$ and $t' - t = 0$, and Eq. [III.14] becomes:

$$L_r = \frac{L}{\sqrt{1 - (v^2/c^2)}} \qquad \text{[III.15]}$$

where L_r is the length of the object that is at rest with respect to the observer (at O') traveling at the velocity v with respect to an observer O in another reference frame, and L is the length of the object in reference frame O' measured by an observer in reference frame O. Eq. [III.15] may be written as:

$$L = L_r\sqrt{1 - (v^2/c^2)} \qquad \text{[III.16]}$$

The above Eq. [III.16] states that an observer in a reference frame, who measures an object (L) in another reference frame that is traveling at a velocity v with respect to the observer, will be contracted (ie, smaller) with respect to the measurement L_r taken by another observer, who makes the measurement in the reference frame where the object is at rest with respect to that observer. Thus, L is always smaller than L_r (ie, $L < L_r$) by the factor $\sqrt{1 - (v^2/c^2)}$; and the degree of contraction is dependent on the velocity v. As the velocity v increases and approaches the unattainable speed of light c, the value of L decreases, that is, contraction increases.

Einstein (1916a) provided examples of how measurements from one frame of reference on another frame of reference will yield different measurements of time and length dependent on the frame of reference from which the measurements are taken and the velocity v at which one frame of reference is traveling with respect to the other. As an example, he chose a meter-rod situated in Fig. III.3 in the coordinate system (reference frame) O' at $x' = 0$ at one end and $x' = 1$ m at the other

end of the rod. He then proceeded to calculate the length of the meter-rod relative to the system O at a particular time t. Using Eq. [III.13] of the Lorentz transformation reduced to Eq. [III.16], Einstein shows that at time $t = 0$, the value of $x = 0$ for the beginning of the rod, that is:

$$x = 0\left(\sqrt{1 - (v^2/c^2)}\right) \qquad \text{[III.17]}$$

and the end of the rod, would measure:

$$x = 1\ \text{m}\left(\sqrt{1 - (v^2/c^2)}\right) \qquad \text{[III.18]}$$

Thus when the meter-rod is traveling at the speed v relative to O, the meter-rod is shorter as judged from O according to the factor $\sqrt{1 - (v^2/c^2)}$; and the faster that the rod is traveling relative to O, the shorter will be the rod as measured from O. The degree of rod contraction is a function of the velocity v, and it is significant at relativistic speeds, that is, when v approaches c, the unattainable speed of light.

Time Dilation in Relativity

Another example proposed by Einstein (1916a) in his treatise on relativity included a clock, which is permanently situated at the origin ($x = 0$) of the frame of reference O, which travels at the velocity v relative to the reference frame O' (see Fig. III.4). He then assigned two successive ticks of the clock as $t = 0$ for the first tick and $t = 1$ s for the following tick. Using the Lorentz transformation provided by Eq. [III.12], Einstein (1916a) calculated the time for the two ticks measured from the frame of reference O' to be $t = 0$ for the start and $t = 1/\sqrt{1 - (v^2/c^2)}$ for the following tick of the clock. Thus, from the reference frame of O', Einstein demonstrated that the time between two ticks of the clock is not 1 s, but rather the dilated time of $t = 1/\sqrt{1 - (v^2/c^2)}$ seconds. Thus, when measured from the frame of reference O', the time is enlarged; and the greater the velocity v, the longer the time will be measured to run when judged from O'. As explained by Einstein (1916a), the value of v can never reach c, which remains an unattainable limiting velocity.

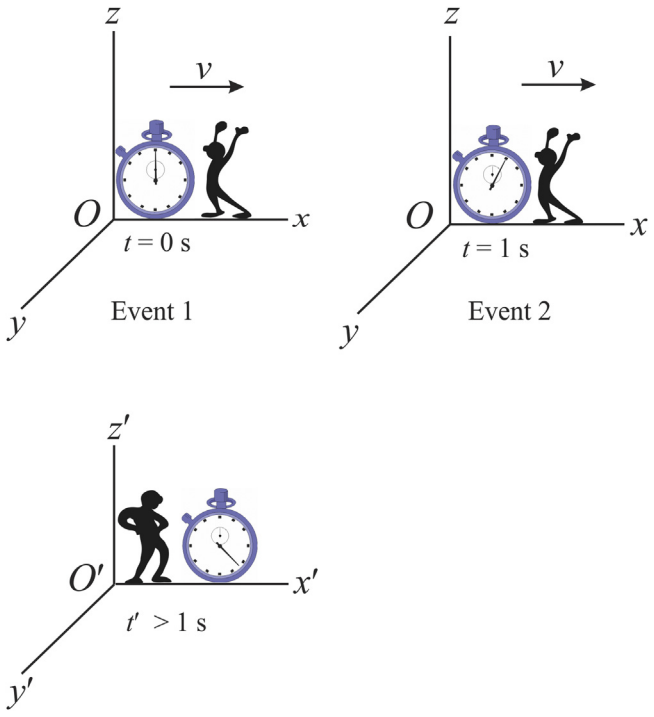

FIGURE III.4 An observer in reference frame O measures two events with a clock situated at the origin. In reference frame O, the clock remains at the origin, that is, it does not move with respect to the observer in that reference frame. The reference frame O travels at a velocity v with respect to the frame of reference O'. However, the clock in reference frame O is at rest with respect to the observer in that reference frame, who measures the time interval between the two events to be 1 s. An observer in the frame of reference O' sees the two events as occurring in two locations and measures the time interval between these events to be $t' > 1$ second.

In the above example, Einstein (1916a) used the Lorentz transformation provided in Eq. [III.12], namely:

$$t' = \frac{t - \frac{v}{c^2}x}{\sqrt{1 - (v^2/c^2)}} \qquad \text{[III.19]}$$

and:

$$\Delta t' = \frac{(t_2 - t_1) - \frac{v}{c^2}(x_2 - x_1)}{\sqrt{1 - (v^2/c^2)}} \qquad \text{[III.20]}$$

where x_2 and x_1 are the positions of the clock at the origin of reference frame O. The clocks remain at rest with respect to the observer in frame O; and thus, $x_2 - x_1 = 0$. Eq. [III.20] is then written as:

$$\Delta t' = \frac{\Delta t_r}{\sqrt{1 - (v^2/c^2)}} \qquad \text{[III.21]}$$

where $\Delta t_r = t_2 - t_1$, that is, the time interval measured by the observer in reference frame O where the clocks are at rest with respect to the observer. Thus, the time interval measured by the observer at O' is the time interval:

$$\Delta t' = \frac{1\text{ s}}{\sqrt{1 - (v^2/c^2)}}, \qquad \text{[III.22]}$$

which is a dilated or longer time interval than 1 s, that is $\Delta t' > \Delta t_r$. The length of the time interval is greater than 1 s by the factor $1/\sqrt{1 - (v^2/c^2)}$; and this dilated time will be greater as the velocity v increases and approaches c, the unattainable velocity of light in a vacuum.

The above results would be the same if we were to consider the reference frames O and O' in reverse, that is, if the reference frame O' would be moving with the velocity v with respect to O, the observer at O would measure the same results with the following Lorentz transformation with the expression Δt rather than $\Delta t'$:

$$\Delta t = \frac{\Delta t_r}{\sqrt{1 - (v^2/c^2)}} \qquad \text{[III.23]}$$

Real examples of relativistic calculations of time dilation and length contraction with respect to the measurement of muons in the showers of cosmic radiation are provided in the following section.

Evidence for Relativity Provided by Muons in the Showers of Cosmic Radiation

Muons are produced high in the atmosphere at an altitude of $\sim$15 km, where high-energy cosmic ray nucleons encounter and undergo collision with nuclei of the atmospheric gases. The muons produced high in the atmosphere are components of the showers of cosmic radiation; and these muons travel toward the earth reaching the ground (sea level) with a mean energy of $\approx$4 GeV at speeds close to the speed of light ($>0.99c$).

One might ask at this point the following question: If muons of the cosmic radiation showers are produced high in the earth's atmosphere (at altitudes of $\sim$15,000 m or higher), travel at speeds close to the speed of light, and have an average lifetime of only 2.2×10^{-6} s, how could such muons be detected to reach the earth's surface? The question is an obvious one, as it would appear with classical mathematics that, with such a short lifetime, muons would never be expected to reach the earth. Let's say, for example, that a muon is produced at the altitude of 15,000 m and it travels at the speed v of $0.9993c$, which would correspond to a speed in units of m/s as:

$$0.9993c = (0.9993)\left(2.9979 \times 10^8\ \text{m/s}\right) = 2.9958 \times 10^8\ \text{m/s}. \qquad \text{[III.24]}$$

The classical calculation of its average distance d of travel during its lifetime would be:

$$d = (v)(t) = \left(2.9958 \times 10^8\ \text{m/s}\right)\left(2.2 \times 10^{-6}\ \text{s}\right) = 659.1\ \text{m} \qquad \text{[III.25]}$$

Thus, the muon would be expected to decay, according to classical transformations, after traveling only 659 m on the average and, therefore, never be detected an earth. However, for such a muon viewed by an observer on earth,

he or she would view the two events A, the creation of the muon and B, the decay of the muon, to occur in two locations in space–time coordinates. Einstein's theory of relativity utilizing the Lorentz time transformations demonstrate that the two events, A and B, separated by the time interval Δt, will be dilated to the time interval Δt_{earth}, when viewed by an observer on earth. The time dilation, as described by Einstein (1916a), is calculated according to the following:

$$\Delta t_{\text{earth}} = \frac{\Delta t_r}{\sqrt{1-(v^2/c^2)}} \qquad \text{[III.26]}$$

where v is the velocity of the particle and c is the invariable speed of light in a vacuum. For the muon traveling at $0.9993c$, we can calculate Δt_{earth} or the observed dilated lifetime of the muon as follows:

$$\Delta t_{\text{earth}} = \frac{\Delta t_r}{\sqrt{1-(v^2/c^2)}} = \frac{2.2\times10^{-6}\ \text{s}}{\sqrt{1-(0.9993)^2}} = \frac{2.2\times10^{-6}\ \text{s}}{0.0374} = 58.8\times10^{-6}\ \text{s} \qquad \text{[III.27]}$$

According to the dilated time of 58.8×10^{-6} s, the observer on earth will determine that the muon would travel, before it decays, a distance of:

$$d = (v)(\Delta t_{\text{earth}}) = \left(2.9958\times10^{8}\ \text{m/s}\right)\left(58.8\times10^{-6}\ \text{s}\right) = 17,615\ \text{m}, \qquad \text{[III.28]}$$

which is well beyond the distance of 15,000 m elevation when it was created, permitting its detection on earth. The distance is only an average figure, because the muon lifetime of 2.2×10^{-6} s is an average lifetime. For thorough treatments of relativistic space–time measurements and the applications of Lorentz transformations to these measurements, see books by Einstein (1916a), Wolfson (2003), Gautreau and Savin (1999), and Serway et al. (2005).

The example provided here is a realistic one, and the relativistic time dilation has been demonstrated by Bailey et al. (1977, 1979) based on the historical tests of Rossi and Hall (1941). The historical work of Rossi and Hall entailed the measurement of the muon flux on Mt. Washington in New Hampshire at the altitude of 1900 m and at the mountain base, as illustrated in Fig. III.5. They found that the muon flux at both altitudes did not differ greatly, but only by the ratio of 1.4, that is, the muon flux was 1.4 times as high at the altitude of 1900 m compared to the ground level. Calculations based on a muon half-life of 1.5×10^{-6} s (ie, average lifetime of 1.5×10^{-6} s/ln 2 = 2.2×10^{-6} s), the muon flux ratio for the two altitudes, should have been approximately 22 even when attributing the highest unrealistic speed of light to the muons. The

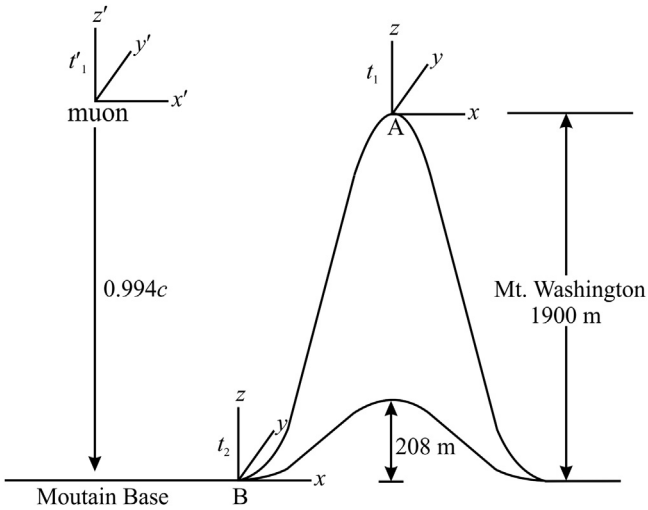

FIGURE III.5 Observers at the peak of Mt. Washington measure the intensity of muons in the atmosphere at (A) the altitude of 1900 m (mountain peak) and at (B) the base of the mountain. To the left in the figure, a path of travel taken by a muon is illustrated. Only one muon path of travel is illustrated for simplicity, although numerous muons are produced in the showers of cosmic radiation. The muon is illustrated traveling toward the earth at the relativistic speed of $0.994c$. Relativistic calculations show that the mountain height would be squeezed or contracted in space to only 208 m when measured from the reference frame of the muon.

actual low ratio of 1.4 could only be explained by applying the time dilation calculations for muons traveling at the speed of $0.994c$, which are the following:

$$\Delta t_{\text{earth}} = \frac{\Delta t}{\sqrt{1-(v^2/c^2)}} = \frac{2.2\times10^{-6}\ \text{s}}{\sqrt{1-(0.994)^2}} = \frac{2.2\times10^{-6}\ \text{s}}{0.1094} = 20.1\times10^{-6}\ \text{s} \quad \text{[III.29]}$$

The dilated muon lifetime of 20.1×10^{-6} s measured by observers in the space–time reference frame of earth demonstrates that the muons measured at the 1900 m mountain peak altitude and at the base of the mountain, have a measured lifetime long enough to travel ~6000 m well beyond the base of the mountain, calculated as follows:

$$d = (v)(\Delta t_{\text{earth}}) = (0.994c)(\Delta t_{\text{earth}}) = (.994)\left(2.9979\times10^{8}\ \text{m/s}\right)\left(20.1\times10^{-6}\ \text{s}\right) = 5989\ \text{m} \quad \text{[III.30]}$$

The above calculation demonstrated the time dilation for the decay of the muon when observing the muon travel from the reference frames of observes on earth (Fig. III.5), which explains why the muon of short lifetime (2.2×10^{-6} s) created high in the atmosphere can be observed (ie, detected) at sea level. However, there is yet another aspect of relativity providing evidence for the observation of muons at sea level. As noted by Einstein, when traveling at relativistic speeds (ie, speeds approaching the speed of light), measurements made in the space–time reference frame where they occur in different places will yield a contraction of objects compared to their sizes when measured in a reference frame where they occur at the same place. For example, an observer on the mountain would measure its altitude to be 1900 m; however, if an observer could travel with the muon at $0.994c$, he or she would take two separate measurements, namely, one of the peak and one of the base of the mountain (two events) and find the height of the mountain to be contracted by the factor $\sqrt{1-(v^2/c^2)}$ previously described by Einstein (1916a) and discussed earlier in this section. The measured height of the mountain (x), from the reference frame of the muon, would be squeezed or contracted in space according to the following:

$$x = (1900\ \text{m})\left(\sqrt{1-(v^2/c^2)}\right) = (1900\ \text{m})\left(\sqrt{1-(0.994)^2}\right) = 208\ \text{m} \quad \text{[III.31]}$$

Thus the muon in the atmosphere traveling at $0.994c$ at the height of the mountain peak encounters a mountain squeezed in space to only 208 m from the mountain peak to its base (Fig. III.5), which is more than enough distance for it to reach earth. One might question these calculations by asking "What is the true height of the mountain, 1900 or 208 m?" Both calculations are correct relative to the inertial frame of reference in which the measurements are taken; the height of the mountain will depend on the reference frame (space–time coordinates) of an observer who makes the measurement, namely, an observer located at the mountain, who measures the height to be 1900 m or an observer traveling close to the speed of light ($0.994c$) in the reference frame of the muon, who measures the height (208 m from peak to base) of the mountain while traveling past the mountain at this relativistic speed.

Evidence for Relativity From Particle Accelerator Experiments

Experiments at CERN by Bailey et al. (1977, 1979) involved accelerating muons in a storage ring to speeds of up to $0.9994c$. These experiments provided evidence for Einstein's theory of relativity by demonstrating the measured dilated lifetime of the muons that travel at relativistic speeds. The rates of decay of the accelerated muons were measured by detecting their electron decay-product emissions. The accelerated muons were found to have a lifetime of 29.3 times longer than a muon at rest (ie, at rest in the reference frame of the observer). This agrees perfectly with the following dilated lifetime of the muon calculated according to the following:

$$\Delta t = \frac{\Delta t_0}{\sqrt{1-(v^2/c^2)}} \quad \text{[III.32]}$$

where Δt_0 is the lifetime of the muon at rest, v the speed of the muon, and c the speed of light. The dilated lifetime of the muon at $0.9994c$ is calculated to be:

$$\Delta t = \frac{2.2\times10^{-6}\ \text{s}}{\sqrt{1-(0.9994)^2}} = 63.52\times10^{-6}\ \text{s} \quad \text{[III.33]}$$

The increase in the observed lifetime of the accelerated muons over the muons at rest (ie, at rest in the reference frame of the observer) is:

$$\frac{\Delta t}{\Delta t_0} = \frac{63.52 \times 10^{-6}\ \text{s}}{2.2 \times 10^{-6}\ \text{s}} = 28.9 \qquad \text{[III.34]}$$

Equivalence of Mass and Energy ($E = mc^2$)

As a consequence of his special theory of relativity, Einstein (1905c) concluded that energy was equivalent to mass, that is, if a body emitted energy, the mass of the body would decrease proportionally to the amount of energy lost. In his explanation of the fundamental ideas and problems of the theory of relativity, he stated (Einstein, 1923) the following:

The special relativity theory…united the momentum and energy principle, and demonstrated the like nature of mass and energy.

He expressed this relationship of mass and energy with the equation:

$$E = mc^2 \qquad \text{[III.35]}$$

where E is energy, m is mass, and c the velocity of light in a vacuum. Einstein's equation of equivalence of mass and energy has been demonstrated many times over, and it is an equation of standard use in the study of radioactivity and nuclear decay processes. For example, it is known that a quantum of gamma radiation must possess a minimum of 1.02 MeV

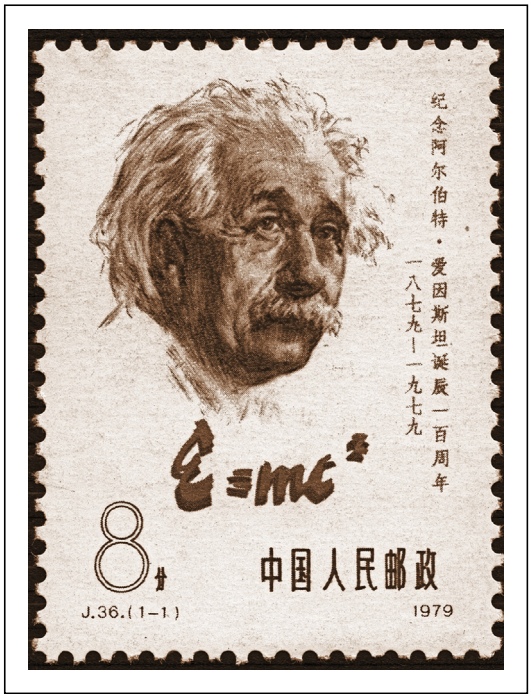

of energy for it to be converted to two electrons (positron and negatron pair) when the gamma-ray photon interacts with the coulombic field of a nucleus. This phenomenon is referred to as pair production, because the mass of two electrons is created from the energy of the gamma-ray photon. Using Einstein's Eq. [III.35], the equivalent energy of one electron can be calculated from the electron mass of 9.109×10^{-31} kg as:

$$E = mc^2 = \left(9.109 \times 10^{-31}\ \text{kg}\right)\left(2.997 \times 10^{8}\ \text{m/s}\right)^2 = 8.182 \times 10^{-14}\ \text{J} \qquad \text{[III.36]}$$

The joule (J) as a unit of energy can be converted mathematically to other units of energy. The amount of energy in joules calculated above, as equivalent to one electron mass, can be converted to another unit of energy, the electron-volt, as follows:

$$8.182 \times 10^{-14}\ \text{J}/1.602 \times 10^{-19}\ \text{J/eV} = 0.511\ \text{MeV} \qquad \text{[III.37]}$$

Therefore, the mass of one electron is equivalent to 0.511 MeV, and the mass of two electrons would be twice that amount or 1.02 MeV, which is exactly the amount of energy that a gamma ray must possess when its energy is converted to the mass of two electrons in the process of pair production (see "Pair Production" in the chapter entitled "Electromagnetic

Radiation: Photons"). Likewise we can consider this calculation in the reverse. The mass of the positively charged electron (positron) will be converted to energy as gamma radiation when it losses kinetic energy, slows down, and encounters a negatively charged electron, its antiparticle. In such an encounter, both electrons become annihilated and the masses of the two electrons are converted to energy in the form of two gamma-ray photons of 0.511 MeV energy that are emitted in opposite directions from their site of encounter (see "Annihilation Radiation" in the chapter entitled "Electromagnetic Radiation: Photons"). Einstein's equation of equivalence of mass and energy is used often to calculate the energy lost by nuclides that undergo radioactive decay transitions from the differences in mass of parent and daughter nuclides. See the example calculations for ^{241}Am decay given in the chapter entitled "Alpha Radiation." The stamp illustrated here, issued in China in 1979, is one example of many issued from many countries that commemorate Einstein's work and his equation of the equivalence of mass and energy.

Energy and Mass in Relativity

In Einstein's treatise on relativity (1916a), he wrote on the relationship of energy and mass. He explained that, in the theory of relativity, the kinetic energy of a body of mass m is not given by the conventional expression:

$$E = 1/2mv^2, \qquad \text{[III.38]}$$

but rather by the expression:

$$E = \frac{mc^2}{\sqrt{1-(v^2/c^2)}} \qquad \text{[III.39]}$$

where the energy E approaches infinity, as the velocity v of the body approaches the speed of light c. Thus, the velocity v always remains below the unattainable speed of light c.

Einstein (1916a) elucidated that if a body, which he referred to as a material point (eg, nuclear particle), takes up energy, its energy will increase by an amount:

$$E_0 = mc^2 \qquad \text{[III.40]}$$

The increase in energy also represents an increase in mass. Thus, Einstein (1916a) wrote the increase in energy of the particle E_0 into Eq. [III.40] to give:

$$E = \frac{mc^2 + E_0}{\sqrt{1-(v^2/c^2)}} \qquad \text{[III.41]}$$

or:

$$E = \frac{(m + E_0/c^2)c^2}{\sqrt{1-(v^2/c^2)}}, \qquad \text{[III.42]}$$

which expresses that the body, to which energy is added, has the energy of a body of mass $(m + E_0/c^2)$ moving at a velocity v.

Eq. [III.42] may be written as:

$$mc^2 = \frac{m_0c^2}{\sqrt{1-(v^2/c^2)}} \quad \text{where} \quad m_0 = m + E_0/c^2 \qquad \text{[III.43]}$$

and:

$$m = \frac{m_0}{\sqrt{1-(v^2/c^2)}} \qquad \text{[III.44]}$$

where m is the relativistic mass of the body, sometimes written as m_r; and m_0 is the rest mass of the body, or in other words the mass of the body as measured in the coordinates of the observer, which would be at rest with respect to the observer, because the body and the observer in the same coordinates are traveling at the same velocity.

The expression of Eq. [III.39] is used in the chapter entitled "Neutron Radiation" to define the energy of particles that travel at speeds approaching the speed of light (ie, relativistic speeds). The equation is expressed in the chapter entitled "Neutron Radiation" as:

$$E = \gamma mc^2 \quad \text{where} \quad \gamma = \frac{1}{\sqrt{1-(u^2/c^2)}} \quad \text{and} \quad u = v \qquad \text{[III.45]}$$

The symbol u is often used in place of v when particle speeds are relativistic. Einstein (1916a) explained in Eq. [III.45] that as the energy of a body (eg, nuclear particle) is increased, so is its mass increased. He expounded on this by clarifying that the law of conservation of energy must hold not only for one coordinate system O, but also for all coordinate systems, such as O', that are in uniform motion relative to O (see Fig. III.2). Einstein (1916a) elaborated that when the energy of a body is increased by an amount E_0, its mass increases by the amount E_0/c^2. He stated that the inertial mass of a body is a variable; namely, the inertial mass of the body will vary according to the change in energy of the body. In turn, the inertial mass of a body is also a measure of its energy.

Relativistic Mass Calculations

In Eq. [III.44], Einstein described that the rest mass of a body, m_0, which is the mass of a body when measured in the reference frame of an observer, would be measured to possess a higher mass, m, when the body is observed traveling at a velocity, v, relative to an observer; and the value of m is referred to the relativistic mass.

The relativistic speed of a 100-GeV cosmic ray proton is calculated in the chapter entitled "Cosmic Radiation" from its kinetic energy (Eqs. [14.1]–[14.5]) to be $0.999956c$. As noted in Einstein's Eq. [III.44], we may calculate the relativistic mass, m, of the proton from its known rest mass (1.67262×10^{-27} kg) and its velocity, to be:

$$m = \frac{m_0}{\sqrt{1-(v^2/c^2)}} \qquad \text{[III.46]}$$

$$m = \frac{1.67262 \times 10^{-27}\ \text{kg}}{\sqrt{1-\left((0.999956c)^2/c^2\right)}}$$

$$m = \frac{1.67262 \times 10^{-27}\ \text{kg}}{\sqrt{1-(0.999956)^2}} = 178.3038 \times 10^{-27}\ \text{kg}$$

The ratio of the relativistic mass to the rest mass (m/m_0) of the proton traveling at $0.999956c$ is:

$$m/m_0 = 178.3038 \times 10^{-27}\ \text{kg}/1.67262 \times 10^{-27}\ \text{kg} = 106.6 \qquad \text{[III.47]}$$

The measured mass of the high-energy proton traveling at $0.999956c$ relative to an observer is calculated to be over 100-fold greater than its mass when measured in the reference frame of an observer or its mass at rest.

Einstein's relativity calculations can be applied to photons of light, which are also particulate in nature. We know from Einstein's interpretation of the photoelectric effect, for which he was awarded the Nobel Prize, that the energy of a photoelectron is directly proportional to the energy of the photon, which had collided with the electron to cause its emission from an atom (see the chapter: "Electromagnetic Radiation: Photons"). The greater the energy of the photon, that is, the shorter its wavelength, the greater will be the energy of the photoelectron. Einstein demonstrated that the energy of the photoelectron depended on the energy of the photon that collided with the atomic electron, or the product of Planck's constant times the photon frequency according to the formula:

$$E_{\text{photon}} = mc^2 = h\nu = \frac{hc}{\lambda} \qquad \text{[III.48]}$$

and from the above equations, the effective mass of the photon can be written as:

$$m = \frac{h}{\lambda c} \qquad \text{[III.49]}$$

where m is the photon mass, c is the speed of light in a vacuum (2.9979×10^8 m/s), h is Planck's constant (6.626×10^{-34} J s), ν is the photon frequency in units of s^{-1}, and λ is the photon wavelength in meters. From Eq. [III.49], the effective mass of the photon as a function of its wavelength can be calculated. For example, the effective mass of a photon of 450 nm wavelength, which is in the visible blue wavelength of light, is calculated as:

$$m = \frac{6.626 \times 10^{-34}\ \text{J s}}{(4.50 \times 10^{-7}\ \text{m})(2.9979 \times 10^8\ \text{m/s})} = 4.91 \times 10^{-36}\ \text{kg}$$

The above units of J s^2/m^2 convert to kilograms or kg as follows:

$$\frac{\text{J s}^2}{\text{m}^2} = \frac{\text{N m s}^2}{\text{m}^2} = \frac{\text{N s}^2}{\text{m}} = \frac{\text{m kg/s}^2\ \text{s}^2}{\text{m}} = \text{kg}$$

where N is the Newton, a unit of force, which is equivalent to m kg/s^2. As seen from Eq. [III.49], the energy and consequently the mass of the photon are wavelength dependent.

The velocity of a photon, outside of a vacuum (ie, in a transparent medium such as air, water, glass, etc.), is wavelength dependent; and it will travel at the velocity of v relative to c, although the differences between v and c are very small. Einstein's equation for the relativistic mass of a particle (Eq. [III.46]) is used by joint authors Grado-Caffaro and Grado-Caffaro (2010, 2014) to arrive at an equation for the relativistic mass of a photon as a function of its wavelength. They conclude that the rest mass of the photon is nonzero, but that this mass is very small, that is, the velocity of the photon as a function of its wavelength, that is $v(\lambda)$, is extremely near c.

Interaction of Gravitational Mass and Photons

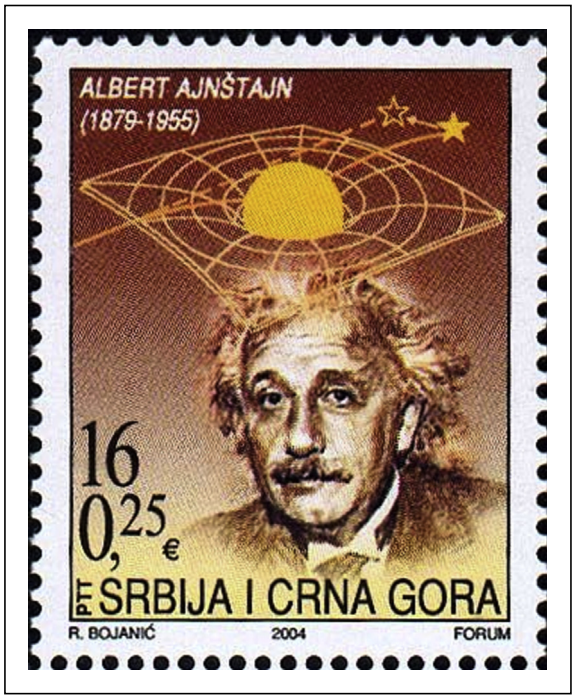

Einstein extended his special theory of relativity to phenomena involving acceleration into his general theory of relativity, which he wrote in 1915 (Einstein, 1916b). He proposed that as mass was equivalent to energy, as described above, the same principle of equivalence would require that gravitational mass would interact with the mass of photons of visible light (electromagnetic radiation). From this reasoning, Einstein predicted the deflection of the light from stars as the light would pass near a massive body such as the sun (Einstein, 1911). The gravitational pull of the sun would attract and bend the light from a distant star as that light passed near the body of the sun. Einstein concluded that this deflection of light toward the body of the sun could be observed from earth when the light of the sun would be blocked by a total eclipse. In 1913, prior to the total eclipse of May, 1919, Einstein diagrammed a sketch illustrating how the gravity of the sun would deflect light near the sun making stars to appear to observers on earth that they have shifted their position in space. Einstein's prediction was found to be true when British astronomers in May of 1919 took photographs of the total eclipse of the sun. The British astronomer Arthur Eddington demonstrated Einstein's prediction to be true. He spotted a star that should have been hidden behind the sun. Photographs of the total eclipse illustrated how the positions of some stars deviated from their positions when the stars were photographed on other occasions with the sun in a different location in the sky. This finding made Einstein an instant celebrity. The London Times on November 7, 1919 ran the headline "Revolution in Science, New Theory of the Universe, Newtonian Ideas Overthrown." The demonstration of Einstein's theory is commemorated in the stamp issued by Serbia in 2004. The stamp illustrates how the bending of the light near the sun gave the appearance that the distant star was located to the side rather than directly behind the sun. Eddington commented that it was the greatest moment of his life when he measured the image of a star and found that the sun's gravity warped the space through which the light had traveled.

The effect was reconfirmed in photographs taken during the solar eclipse of 1922. As noted by the American Institute of Physics:

> *The eclipse experiments, like most important new science, were done at the very limit of available techniques. It was not until the 1960s, with vastly improved methods, that the gravitational bending of light could be demonstrated beyond reasonable doubt. Until then one could almost say that the logic and beauty of Einstein's theory did as much to confirm the observations as the observations did to confirm his theory.*

Eddingtons findings during the solar eclipse of 1919 confirming Einstein's predictions were commemorated with the postage stamp issued in 2009 by São Tomé and Príncipe illustrated here.

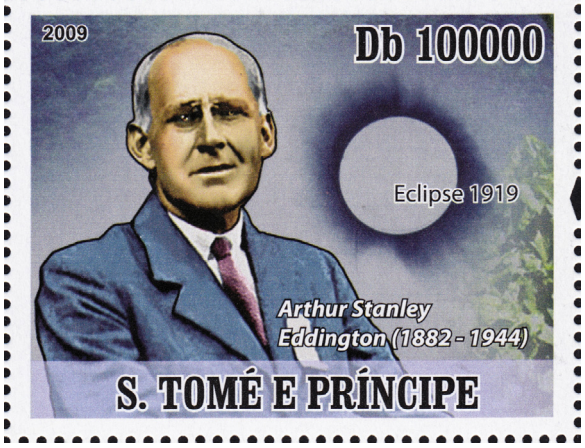

Arthur S. Eddington (1882-1994)

In addition to the deflection of light by the sun's gravity described above, Einstein made several predictions from general relativity theory including the perihelic orbit of the planet Mercury (Einstein, 1915). In his Nobel lecture presented on July 11, 1923 (see clarification below for the lateness and subject matter of the lecture), Einstein underscored some of the predictions of his theory when he stated:

> *The considerations mentioned led to the theory of gravity which yields the Newtonian theory as a first approximation and furthermore it yields the motion of the perihelion of Mercury, the deflection of light by the sun, and the red shift of spectral lines [due to an expanding universe]…*
>
> Einstein (1923).

Professorships in Switzerland, Czech Republic, Germany, and USA

Einstein's publications in *Annalen der Physik* in 1905 (Einstein, 1905a–c), while a clerk in the Swiss Patent Office, put him in great demand by universities and research institutes, which previously knew nothing of him. In 1908 he became Privatdozent in Bern and in 1909 became Professor Extraordinary at the University of Zurich. In 1911 he was appointed Professor of Theoretical Physics at the Karl-Ferdinand University in Prague; and returned to Zurich in 1912 to take up a chair at the Eidgenössische Techische Hochschule (ETH), the prestigious polytechnic school of Switzerland, which had rejected his admission as a student in 1895. In 1914, Einstein was appointed director of the Kaiser Wilhelm Institute of Physics in Berlin and professor of the University of Berlin. At the outbreak of World War I in 1914, Einstein's pacifist sympathies were brought into public view. Ninety-three leading German intellectuals, including physicists such as Max Planck, signed a manifesto defending Germany's war conduct. Einstein and three others signed an antiwar countermanifesto (American Institute of Physics). He became a citizen of Germany in 1914 and remained in Berlin until 1933, when he renounced his citizenship during the rise of fascism and emigrated to the United States to take on a position of professor of theoretical physics at Princeton. He earned American citizenship in 1940 and retired from his post at Princeton in 1945.

Some wonder why Einstein was awarded the Nobel Prize in Physics in 1921 mostly for his contributions to the understanding of the photoelectric effect and not for his extensive works on relativity for which he is best known. Einstein's theories of relativity remained controversial among the less flexibly minded physicists of the Nobel Committee at the time of

the awarding of the Nobel Prize. He therefore was awarded the prize not for his contributions to relativity, but for a paper he wrote on the photoelectric effect in 1905. A possible indication of the hard feelings at the time may be manifested by the fact that Einstein did not present himself to receive the Nobel Prize, as he was on a voyage to Japan, and moreover, he presented his Nobel lecture not on the subject matter for which he was awarded the Nobel Prize but rather on the *Fundamental Ideas and Problems of the Theory of Relativity*. In addition, he did not deliver his Nobel lecture in Sweden, but to the Nordic Assembly of Naturalists at Gothenburg on July 11, 1923 (Einstein, 1923). Einstein had been nominated many times over for the Nobel Prize, and according to a report by Schultz (2005), he was nominated 11 different years before finally getting the prize. As reported by Schultz (2005), one Nobel Committee member wrote "Einstein must never receive a Nobel Prize even if the entire world demands it." And, when finally awarded the prize for his interpretation of the photoelectric effect attributing to light the dual properties of wave and particle (photon), the Nobel Committee directed Einstein not to mention relativity in his acceptance lecture. Well, Einstein ignored the request of the Committee and only discussed relativity.

Einstein's Letter to President Franklin D. Roosevelt

During the Second World War, nuclear physicists approached Einstein for help in drawing the attention of the American Government to the threat of German research on nuclear fission and the possibility that Germany would develop a nuclear weapon. Although he was a pacifist against war of any kind, Einstein agreed to help urge the American Government to pursue research into the making of a nuclear weapon in light of Hitler's aggression and fear of what could happen if Hitler were to acquire nuclear weapons. With the assistance of his longtime friend and colleague, Leo Szilard, Einstein signed a letter drafted by Szilard and addressed to Franklin Delano Roosevelt, President of the United States, on August 2, 1939. The original letter can be found in the archives of the Franklin D. Roosevelt Library, Hyde Park, New York, and may be accessed via the U.S. Government archives via http://research.archives.gov/description/593374. A portion of the letter is provided in the biographical sketch of Leo Szilard in Hall of Fame, Part IV of this book. In brief, the letter underscores the work of Enrico Fermi and Leo Szilard, which indicates that uranium can be converted into an important source of energy; and that "watchfulness" and "quick action" on the part of the presidential administration may be needed due to the following: (1) a nuclear chain reaction may be possible with uranium in which "vast amounts of power" and large quantities of radioactive elements could be generated; (2) this could lead to the construction of very powerful bombs; and (3) Germany has halted the "sale of uranium from Czechoslovakian mines, which they have taken over"; and some of the American work on uranium "is now being repeated at the Kaiser-Wilhelm-Institut in Berlin."

With the assistance of Alexander Sachs, Special Counsel to the Director of Strategic Services, the letter was hand-carried to President Roosevelt on October 11, 1939. This letter was instrumental in the eventual establishment, with the approval of FDR, in 1941 of the American project for the development of the atomic bomb.

Einstein explained his position in urging the American President to pursue the creation of an atomic bomb when he stated the following (American Institute of Physics, http://www.aip.org/history/einstein/ae44.htm http://www.aip.org/):

> *Because of the danger that Hitler might be the first to have the bomb, I signed a letter to the President, which had been drafted by [Leo] Szilard. Had I known that the fear was not justified, I would not have participated in opening this Pandora's box, nor would Szilard. For my distrust of governments was not limited to Germany.*

Einstein the Pacifist

Aside from his letter to President Roosevelt, Einstein contributed in no other way to the creation of the atomic bomb. Einstein was a true pacifist.

In 1946, the year after the atomic bombs were dropped on Hiroshima and Nagasaki, Albert Einstein and Leo Szilard established the Emergency Committee of Atomic Scientists (ECAS). Founding members of the ECAS included Albert Einstein as Chairman, Harold C. Urey as Vice Chairman, and Hans Bethe, Leo Szilard, Linus Pauling, Victor F. Weisskopf, Thorfin R. Hogness, Edward U. Condon, Philip M. Morse, and Selig Hecht (see Fig. III.6). The ECAS had the objectives of calling the attention of the public to the dangers of nuclear weapons and to promote the peaceful applications of atomic energy. The committee was established after Leo Szilard's "Petition to the President of the United States," signed by 70 members of the Manhattan Project urging against the use of the atomic bomb against Japan. The Emergency Committee solicited private contributions in support of groups interested in the field of atomic information and education as well as the National Committee for Atomic Information. The ECAS remained active from 1946 to 1952. The official papers, records, correspondence, memoranda, and minutes of meetings are available at the Special Collections Research Center of the University of Chicago.

FIGURE III.6 Meeting of the Emergency Committee of Atomic Scientists at the Institute for Advanced Study, Princeton on November 1946. Left to right standing: Victor Weisskopf, Leo Szilard, Hans Bethe, Thorfin R. Hogness, and Philip M. Morse; left to right sitting: Harold C. Urey, Albert Einstein, and Selig Hecht. *Courtesy of the AIP Emilio Segre Visual Archives, Gift of Joseph P. Baratta.*

One week before his death, Albert Einstein signed his last letter to Bertrand Russell, whereby he agreed that his name be included in a manifesto urging all nations to abolish nuclear weapons. This letter is known as the Russell–Einstein Manifesto. The manifesto is included in its entirety in Hall of Fame, Part IV for the benefit of the reader. It is an important letter calling for the abolition of nuclear weapons for the sake of mankind; and it was the first big step taken in the cause for nuclear nonproliferation.

Einstein was also a philosopher with a strong kinship to mankind, which is evidenced by his writings, particularly his essay "The World as I See It" published in *Living Philosophies* (Einstein, 1931) and in a book edited by Seelig (1954).

For a long period of his life starting before 1920 up to his death in 1955, Einstein struggled without success to define a unified field theory that would unite electromagnetism and gravity and space and time. Einstein died on April 18, 1955 in Princeton, New Jersey.

ARTHUR H. COMPTON (1892–1962)

Arthur Holly Compton was born in Wooster, Ohio on September 10, 1892. He was awarded the Nobel Prize in Physics in 1927 "for his discovery of the phenomenon named after him–the Compton Effect."

Arthur Compton graduated in 1913 from the College of Wooster with a Bachelor of Science degree. He then went to Princeton University, where he received his MA degree in 1914 and his PhD in physics in 1916. His doctoral dissertation was on the angular distribution of X-rays reflected by crystals. Compton then took on a year as physics instructor at the University of Minnesota before taking on a position as a research engineer for the Westinghouse Company until 1919. He left industrial engineering to do research of his choosing when he received a research fellowship from the National Research Council, which enabled him to continue research with X-ray and gamma-ray scattering at the Cavendish Laboratory, Cambridge University, where he carried out his first tests on wavelength variations of X- and gamma rays as a function of scattering angle. After a year at Cambridge, he became Professor and Head of the Department of Physics at Washington University, St. Louis in 1920 and subsequently succeeded Robert A. Millikan as Professor of Physics at the University of Chicago in 1923, a post he occupied until the end of the Second World War in 1945 (*Nobel Lectures, Physics 1922–1941*).

A. H. Compton (1892-1962)

Arthur Compton is best known for his work on the scattering of X-rays and gamma rays when he discovered the increase in wavelength of an X-ray or gamma ray after the incident radiation was scattered by an electron in matter, demonstrating that the scattered radiation had lost energy to an atomic electron (Compton, 1923a) known as the Compton Effect. It was for this work that Compton received the Nobel Prize in Physics in 1927. He studied the x-radiation scattered by low-atomic-weight materials. By irradiating substances with homogeneous or monochromatic X-rays, that is, X-rays of a specific wavelength, he found that the rays would be divided into two lines or wavelengths; one line would be of one and the same wavelength as the incident radiation, and the other would be the scattered rays of a longer wavelength. The change in wavelength would be independent of the irradiated material, but dependent on the angle between the incident and scattered rays.

Compton explained this phenomenon on the basis of the quantum theory of light. In his account for the quantum theory of the scattering of X-rays and gamma rays by light elements, Compton (1923a) stated:

> *The hypothesis is suggested that when an x-ray quantum is scattered it spends all of its energy and momentum upon some particular electron. This electron, in turn, scatters the ray in some definite direction. The change in momentum of the x-ray quantum, due to the change in its direction of propagation, results in a recoil of the scattering electron. The energy in the scattered quantum is thus less than the energy of the primary quantum by the kinetic energy of recoil of the scattering electron.*

Compton elucidated that, of the total energy of the primary beam incident on a material, a fraction of the energy reappears as scattered radiation, while the remainder is absorbed and transformed into kinetic energy of recoil of the scattering electrons. The Compton Effect is illustrated in Fig. III.7. The scattered quantum is of longer wavelength (λ') and thus lower in energy than the incident quantum of shorter wavelength (λ). The change in wavelength can be calculated as a function of the angle of deflection of the scattered ray as derived by Compton according to the equation:

$$\lambda' - \lambda = \frac{h}{mc}(1 - \cos\phi) \qquad \text{[III.50]}$$

where h is Planck's constant, m is the mass of the scattering electron, c the velocity of light in a vacuum, and ϕ is the angle between the incident and scattered ray. The expression h/mc has the value of 0.024 Å. The difference in energy of the two wavelengths is manifested as the kinetic energy of the recoil electron less the electron-binding energy. As the electron-binding energy is relatively small, it can be ignored. Compton (1923) thus described the energy of the scattered quantum ($h\nu_\phi$) as being equal to that of the incident quantum ($h\nu_0$) less the kinetic energy of recoil of the scattering electron, or:

$$h\nu_\phi = h\nu_0 - mc^2\left(\frac{1}{\sqrt{1-\beta^2}} - 1\right) \qquad \text{[III.51]}$$

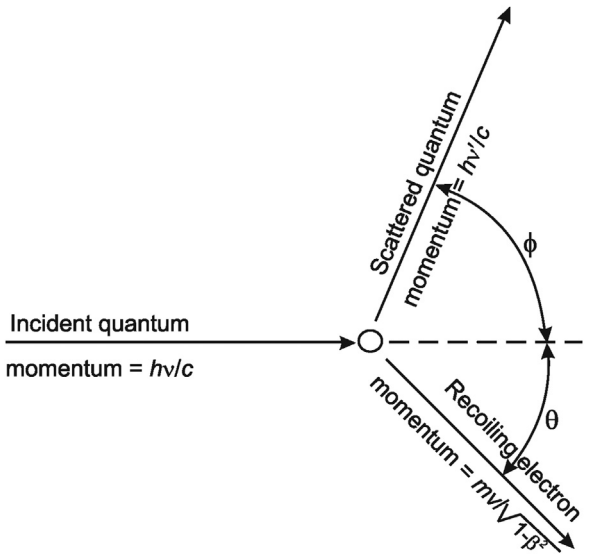

FIGURE III.7 The Compton Effect. An incident X-ray or gamma-ray photon is deflected through an angle ϕ by an electron, which in turn recoils at an angle θ, taking part of the energy of the photon. The symbol β represents the relative phase velocity of the recoil electron, that is, the ratio of the velocity of the electron to the velocity of light. *Adapted from Compton, A.H., 1927. X-rays as a branch of optics. Nobel Lecture, December 12, 1927. In: Nobel Lectures, Physics, 1922–1941. (1965). Elsevier Publishing, Amsterdam, with permission of The Nobel Foundation © 1927.*

where β is the relative phase velocity of the electron or the ratio of the velocity of recoil of the electron to the velocity of light.

When Compton (1923a,b) first presented his theory, the scientific community reacted with both amazement and some opposition. However, Compton and others, including Wu Youxun (Woo, 1925), a collaborator of Compton at the University of Chicago, were able to provide evidence by several methods, including (1) exact spectrometric analysis of the incident and scattered X-ray or gamma-ray lines; (2) visualization of the directions of the scattered photon and recoil electron tracks by means of the Wilson cloud chamber (Compton, 1927); and (3) coincident detection methods developed by Bothe and Geiger (1924) and Compton and Simon (1925a,b), by which it could be established that the scattered X-ray photon and recoil electron appear at the same instant.

In his Nobel lecture, Compton (1927) explained that an examination of the spectrum of the scattered (secondary) X-rays and incident (primary) X-rays showed that the primary beam would be split into two parts, as illustrated in Fig. III.8, one of the same wavelength and the other of an increased wavelength. When different primary wavelengths are used, the same difference in wavelength between the two components is encountered, but the relative intensities of the two components change. For the longer wavelengths of incident radiation, the unmodified ray has the greatest intensity, whereas for shorter wavelengths of incident radiation, the scattered (modified) ray is predominant; and when very hard gamma rays are used (very short wavelengths) as incident rays, all of the rays end up as scattered (modified) radiation.

Very conclusive evidence for the Compton Effect was provided by visualization of the directions of emission of the scattered photon and recoil electron by means of the Wilson expansion cloud chamber. The experimental setup used by Compton and coworkers is illustrated in Fig. III.9. A photograph taken by Compton in the Wilson cloud chamber showing the electron recoil track and associated secondary β-track produced by the scattered X-ray photon is given in Fig. III.10. In his Nobel lecture on December 12, 1927, Compton explained his method as follows (with the writer's comments in brackets):

> *A narrow beam of x-rays enters a Wilson expansion cloud chamber. Here it produces a recoil electron. If the photon theory [Compton Effect] is correct, associated with this recoil electron, a photon is scattered in the direction ϕ. If it should happen to eject a β-ray, the origin of the β-ray tells the direction in which the photon was scattered. [The term β-ray was adopted by Compton for convenience and it refers to a photoelectron produced by the scattered x-ray photon]. A measurement of the angle θ at which the recoil electron is ejected and the angle ϕ of the origin of the secondary β-particle, shows close agreement with the photon formula. This experiment is of special significance, since it shows that, for each recoil electron there is a scattered photon, and that the energy and momentum of the system photon plus electron are conserved in the scattering process.*

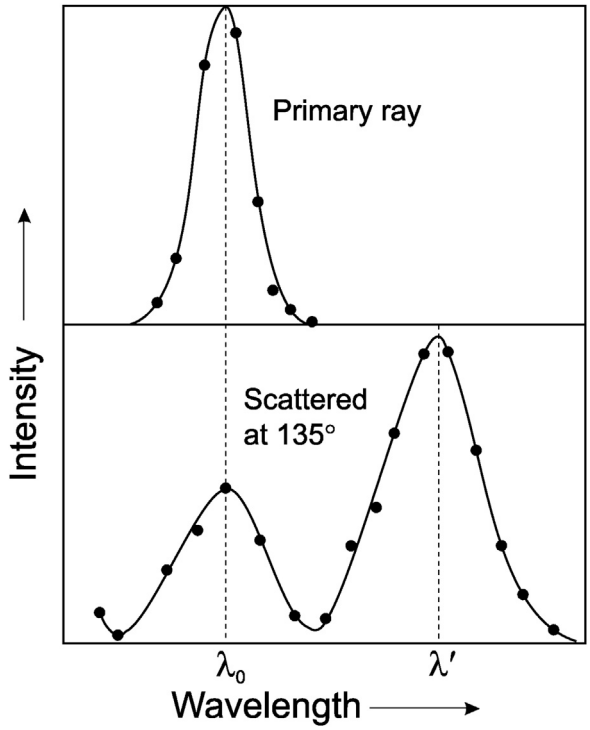

FIGURE III.8 A typical spectrum of scattered X-rays, showing the splitting of the primary (incident) ray (λ_0) into a modified (scattered, λ') and unmodified ray. *Adapted from Compton, A.H., 1927. X-rays as a branch of optics. Nobel Lecture, December 12, 1927. In: Nobel Lectures, Physics, 1922–1941. (1965). Elsevier Publishing, Amsterdam, with permission of The Nobel Foundation © 1927.*

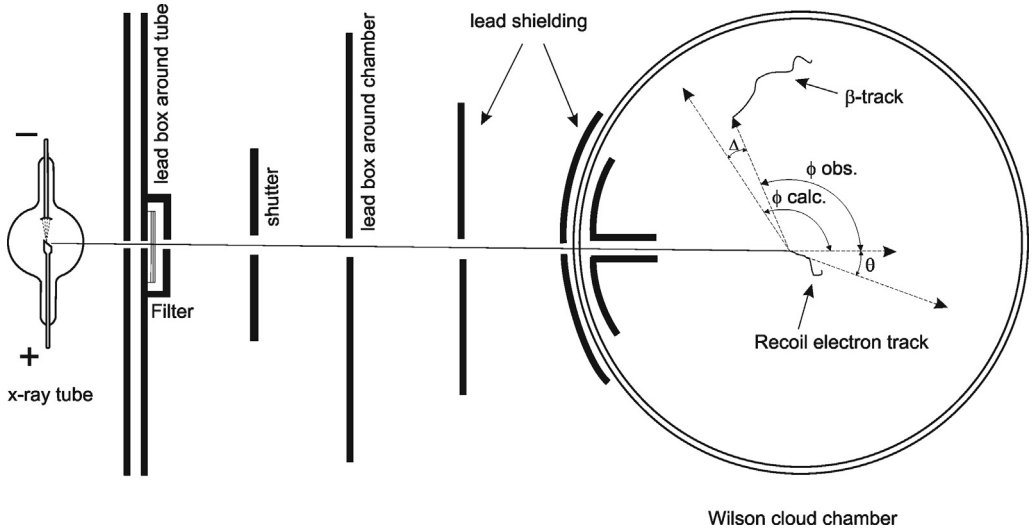

FIGURE III.9 A schematic illustration of the experimental setup used by Compton to observe and measure the recoil electron and X-ray scatter angles relative to the incident X-ray photon. The circular cloud chamber measured 18 cm in diameter and 4 cm deep. It is traversed by a carefully shielded narrow beam of homogeneous (monochromatic) X-rays. A photograph is taken of the electron recoil track as well as the track of a photoelectron [now referred to as a Compton electron] produced by the scattered X-ray (identified by Compton from the β-track). A line is manually drawn on the photograph from the beginning of the electron recoil track to the beginning of the β-track, which provides the direction of the X-ray after scattering. An electron recoiling at an angle θ is associated with an X-ray photon scattered simultaneously through an angle ϕ. The angle Δ represents the difference between the observed and calculated angles ϕ of Compton photon scatter *Adapted from Compton, A.H., 1927. X-rays as a branch of optics. Nobel Lecture, December 12, 1927. In: Nobel Lectures, Physics, 1922–1941. (1965). Elsevier Publishing, Amsterdam, with permission of The Nobel Foundation © 1927.*

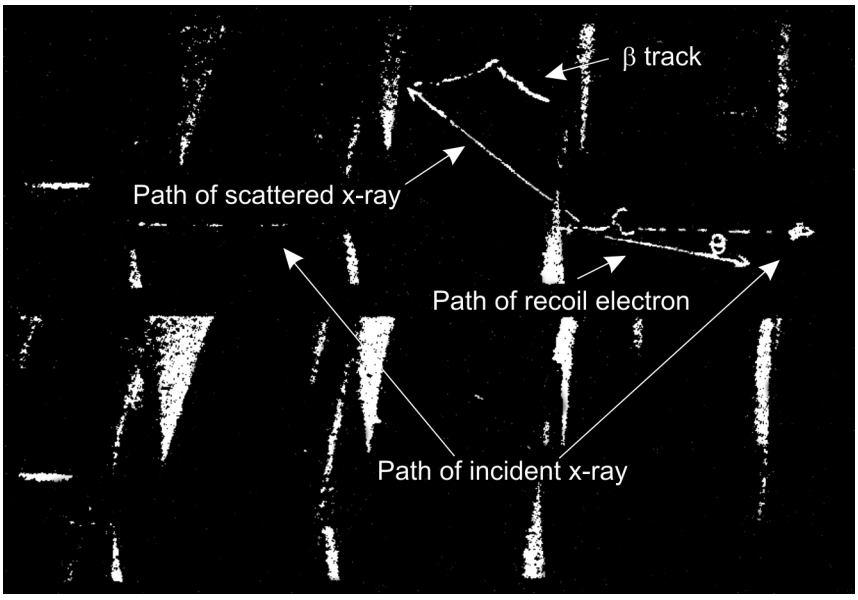

FIGURE III.10 Photograph taken in the Wilson cloud chamber showing an electron recoil track and the β-track produced by the scattered X-ray photon. The direction of travel of the scattered photon is found by drawing a line on the photograph from the beginning of the electron recoil track to the beginning of the β-track. The photograph was modified with lettering. *From Compton, A.H., 1927. X-rays as a branch of optics. Nobel Lecture, December 12, 1927. In: Nobel Lectures, Physics, 1922–1941. (1965). Elsevier Publishing, Amsterdam, with permission of The Nobel Foundation © 1927.*

It was Prof. Manne Siegbahn, Nobel Laureate in Physics in 1924 and member of the Nobel Committee in Physics, who gave the presentation speech during the awarding of the Nobel Prize to Arthur Compton on December 10, 1927. Manne Siegbahn summarized the Compton Effect and its significance as follows:

> *Compton deduced a new kind of corpuscular theory [It reconfirmed Einstein's theory of the photon as an elementary particle.], with which all experimental results showed perfect agreement within the limits of experimental error. According to this theory, a quantum of radiation is re-emitted in a definite direction by a single electron, which in so doing must recoil in a direction forming an acute angle with that of the incident radiation. In its mathematical dress this theory leads to an augmentation of the wavelength of the incident radiation and implies a velocity of the recoil electron that varies between zero and about 80% of the velocity of light, when the angle between the incident and the scattered radiation varies between zero and 180°. This theory predicts recoil electrons with a velocity generally much smaller than that of the electrons which correspond to [Einstein's] photoelectric effect…Finally, the fact deserves to be emphasized that the Compton effect has proved to be of decisive influence upon the absorption of short-wave electromagnetic – especially radioactive – radiation…*

From 1930 to 1940, Compton became a leading research physicist on cosmic radiation (Compton, 1932, 1933). Leading a worldwide study of the geographic variations of cosmic ray intensities, he confirmed the findings of J. Clay from Amsterdam, who observed geographic variations in the intensity of cosmic radiation and a consistent lower intensity near the equator as a result of a Dutch cosmic ray expedition in 1933 (Clay, 1934). Compton confirmed these findings from data on the cosmic ray intensities obtained by eight different expeditions at 69 stations distributed at representative points over the earth's surface (Compton, 1933).

While at the University of Chicago during World War II, Compton collaborated with Enrico Fermi, Leo Szilard, Eugene P. Wigner, and others on the first uranium fission reactor (see Enrico Fermi in Hall of Fame, Part II) and subsequently in the establishment of the large plutonium-producing reactors in Hanford, Washington (*Nobel Lectures, Physics 1922–1941*).

Arthur Compton died on March 15, 1962 in Berkeley, California.

WU YOUXUN (1897–1977)

Wu Youxun was born in Gao'an Jiangxi, China in 1897. He graduated with a major in physics from the Nanking Higher Normal School located in Nanjing, Jiangsu, China. The school is one of the oldest (founded about 258 AD) and most prestigious institutions of learning in China, and is now named Nanjing University.

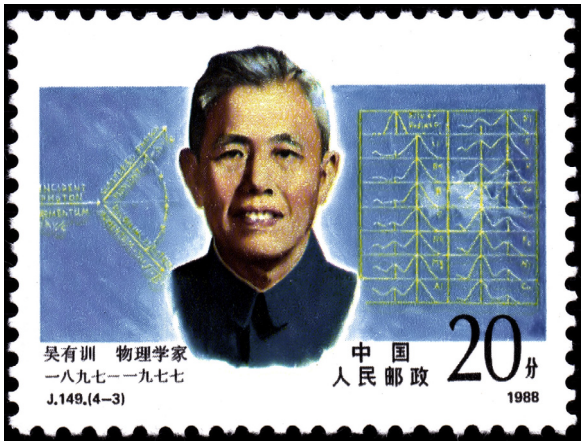

Wu Youxun (1897-1977)

With a fellowship from the Government of China, Wu Youxun received a doctorate in physics from the University of Chicago. He completed his doctorate degree with a dissertation in 1925 entitled "The Compton Effect" (Woo, 1925a), which was a result of close collaboration with Arthur H. Compton, who was awarded the 1927 Nobel Prize in Physics for the discovery of the Compton Effect. The scientific papers of Wu Youxun are authored under the name Woo, Yui Hsun according to the phonetic spelling of Wu Youxun; and his name is abbreviated in some publications as Y.H. Woo.

Wu Youxun carried out extensive and thorough studies on the Compton Effect, including the distribution of energy between incident and scattered rays (Woo, 1926), the intensity of scattered rays by recoiling electrons (Woo, 1925a,b), the effect of temperature on Compton scattering (Woo, 1931a), and Compton scattering in various materials including calcite crystal (Woo, 1924), lithium, boron, carbon, water, sodium (Compton and Woo, 1924), rock salt, magnesium, aluminum, silicon, sulfur (Woo, 1925b,c), and gases (Woo, 1930a,b, 1931a,b,c, 1932). The postage stamp of Wu Youxun illustrates, on the left, the deflection of an incident X-ray or gamma-ray photon and the recoiling electron at specific angles with respect to the incident photon (see Fig. III.7 in the biographical sketch of Arthur Compton for a clearer picture), and on the right, peak intensities for incident photons of wavelength λ and deflected photons of wavelength λ' (see Fig. III.8 in the biographical sketch of Arthur Compton for a general example). Wu Youxin demonstrated thoroughly the Compton Effect by irradiation matter with X-ray photons of given energy (ie, specific wavelength), and plotting the intensities of the incident photon wavelength λ and deflected photon wavelength λ' whereby:

$$\lambda' - \lambda = \frac{h}{mc}(1 - \cos\phi) = 0.024(1 - \cos\phi) \text{ Å units} \qquad \text{[III.52]}$$

where λ and λ' are the incident and deflected photon wavelengths, respectively, h is Planck's constant, m is the electron mass, c is the speed of light in a vacuum, ϕ is the angle of deflection of the scattered photon relative to the path of the incident photon, and 0.024 Å is the value of the term h/mc in Å units. As cited above, Wu Youxun published numerous papers in the *Proceedings of the National Academy of Sciences*, *Physical Review*, and *Nature* describing and demonstrating the Compton Effect as a result of his close collaboration with Compton; so close that many called this phenomenon the "Compton−Wu Effect."

After completing his doctorate degree at the University of Chicago, Wu Youxun returned to China in 1926, where he became a faculty member of Jiangxi University. By 1928 Wu Youxun became professor of physics at the National Southeastern University, and professor of Tsing Hua University and of Beijing University. From 1937 to 1945, Wu Youxun was dean of the College of Science of the National Southwestern Associated University in Kunming; and in 1946 he was professor of the National Jiatong University. In 1950 Wu Youxun became director of the Institute of Physics, of the Chinese Academy of Sciences (CAS). He held the position of Vice President of the CAS from 1950 for the remainder of his life; and he was appointed Vice Chairman of the China Association for Science and Technology from 1958 to the time of his death in 1977 (Bartke, 1997).

Wu Youxun was the teacher and motivator of many prominent physicists in China; and he was very instrumental in the establishment and strengthening of the field of modern physics in China. Wang (2007) noted that Wu Youxun was the teacher of many of the first-generation Chinese physicists, including the physicists who would become leaders of the bomb projects. In honor of the contributions of Wu Youxun, the China Physical Society (CPS) awards each year the Wu Youxun Prize to a physicist in the field of nuclear physics.

YOSHIO NISHINA (1890–1951)

Formation into Japan's Pioneer of Modern Physics

Yoshio Nishina was born on December 6, 1890 in the village of Satosho near the city of Okayama, Japan. He attended the elite sixth national high school in Okayama. This school was prestigious and equivalent to a junior college, as most graduates were qualified to continue their education in an imperial university. Nishina graduated from the Tokyo Imperial University with honors in the field of electrical engineering. He was not deeply interested in pursuing a career in electrical engineering, and became more interested in electrochemistry. With a new interest in chemistry, Nishina accepted an invitation from Prof. Kujirai to join a newly established institute for physics and chemistry at RIKEN (Kubo, 2008). RIKEN remains a major institution for scientific research in Japan, staffed by about 3000 scientists and campuses throughout Japan The acronym RIKEN comes from the Japanese "Rikagaku Kenkyūsho," which stands for the Institute of Physical and Chemical Research.

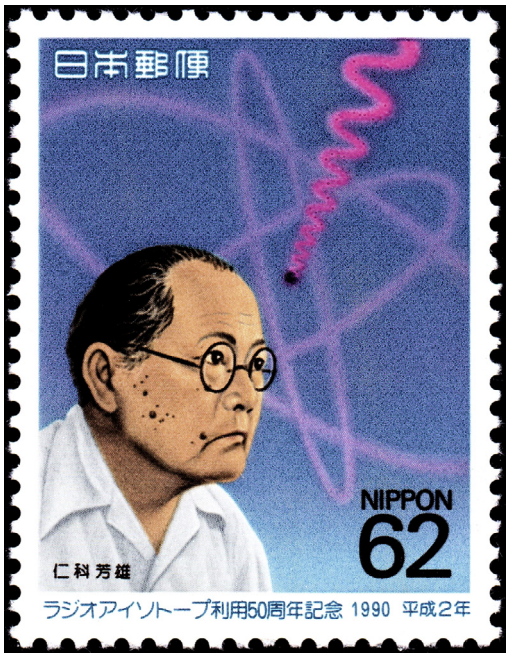

Yoshio Nishina (1890-1951)

As a research fellow at RIKEN, Yoshio Nishina became a graduate student in the school of physics at the Tokyo Imperial College, where he studied physics under the guidance of Prof. Hantaro Nagaoka, who was the most esteemed scientist in the field of nuclear physics in Japan at that time, and also an esteemed research scientist at RIKEN. Prof. Nagaoka was well known worldwide from his publications in nuclear physics; and Rutherford (1911) gave Nagaoka credit for postulating in 1904 the central positive nucleus of the atom. (See the biographical sketch on Prof. Hantaro Nagaoka in Hall of Fame, Part I.) Under the umbrella of Prof. Nagaoka, it is of little surprise that, after three years of study, Yoshio Nishina was selected to study physics in the laboratory of Lord Rutherford in Europe.

In 1921, Nishina went to study at the Cavendish Laboratory under the direction of Ernest Rutherford followed by studies at the University of Göttingen and with Niels Bohr in Copenhagen. During his studies and research in Europe from 1921 to 1927, Nishina wrote several scientific papers on X-ray absorption spectroscopy in collaboration with others (Coster et al., 1923; Nishina, 1925; Nishina and Ray, 1926; Aoyama et al., 1927). In collaboration with Oskar Klein in Copenhagen, Yoshio Nishina derived the Klein–Nishina formula that defines the differential cross-section of photons scattered from a single free electron (Klein and Nishina, 1928, 1929). It may be of interest to the reader to note here that the name Coster cited in the previous phrase among the authors with whom Nishina had collaborated is the Dutch physicist Dirk Coster (1889–1950), who assisted and accompanied Lise Meiter in her escape from Nazi Germany to Sweden by way of the Netherlands on July 17, 1938 (see the biographical sketch on Lise Meitner in Hall of Fame, Part IV). As related by Ryogo Kubo (1990), Yoshio Nishina traveled to Hamburg in 1928 to study under Nobel Laureate Wolfgana Pauli, who would be awarded the Nobel Prize in Physics in 1945, and to collaborate with Isador Isaac Rabi (Nishina and Rabi, 1928), who would become Nobel Laureate in Physics in 1944.

Pioneer of Modern Physics

Upon his return to Japan from Europe via the United States, Yoshio Nishina returned to work at RIKEN in the laboratory of his mentor, Prof. Hantaro Nagaoka. As related by Prof. Ryogo Kubo (1990, 2008), former President of the Nishina Memorial Foundation, in an address presented at the Nishina Centennial Symposium on December 5, 1990, Yoshio Nishina was successful in inviting Werner Heisenberg and Paul A.M. Dirac to Japan in 1929. Nishina helped the young generation of physicists in Japan understand the lectures of Heisenberg and Dirac; and at the same time became popular in the academic community as a leading authority in Japan in the field of quantum mechanics. He was invited to lecture at Kyoto and Hokkaido, during which time he met two budding physicists and future Nobel Laureates, Hideki Yukawa and Sin-itiro Tomonaga, who regarded Nishina as their teacher and who would eventually succeed Nishina in helping Japan become a leading country in modern physics.

By the year 1931, Yoshio Nishina was provided his own laboratory at RIKEN, where he would establish one of the largest research groups in the world with over 100 scientific staff with research focused on mainly quantum mechanics, nuclear physics, cosmic ray research, and research with cyclotron-generated high-energy proton beams. It was Yoshio Nishina's intention to steer Japan into becoming a leading scientific country comparable to the United States and countries of Europe (Kubo, 1990, 2008).

Yoshio Nishina and his collaborators at RIKEN undertook much research on cosmic radiation, at various altitudes in the atmosphere to the top of Mt. Fuji and deep underground at a depth equivalent to 1400 m of water (Nishina et al., 1937, 1939a, 1940a,b, 1941a). They detected a new particle in cosmic radiation, with a mass of $180 \pm 20\ m_e$ (where m_e is the mass of the electron), with the use of cloud chambers (Nishina et al., 1937, 1939a). It was thought at the time that this was the meson postulated by Nobel Laureate Hideki Yukawa; however, it turned out to be the muon, which was also discovered by Neddermeyer and Anderson (1938).

In 1937, Nishina completed the construction of a 27-in. cyclotron. After products of neutron bombardment of uranium were discovered by Otto Hahn and Fritz Strassman, which were identified as products of nuclear fission by Lise Meitner and Otto Frisch in 1939, the field of nuclear fission attracted much interest among theoretical physicists. Once it was finally determined that more than two neutrons were emitted on the average in the neutron-induced fission of uranium-235 (Zinn and Szilard, 1939), it could be said that "the cat was out of the bag" and nuclear physicists throughout the world could became aware of the potential for a nuclear chain reaction that could liberate large quantities of energy. The cyclotron could serve as an excellent neutron source; and Yoshio Nishina joined the scientific community worldwide in research in nuclear fission (Nishina et al., 1939b, 1940c,d, 1941b, 1942).

With the cooperation and friendship with Earnest Lawrence at Berkeley, Yoshio Nishina was able to procure a very large electromagnet from the same American company that had provided the electromagnet to Lawrence for the construction of his large cyclotron at Berkeley (see the biographical sketch on Ernest Lawrence in Hall of Fame, Part VIII). By 1944, Nishina had completed the construction of a 60-in cyclotron at RIKEN (Kimura, 1951). Thus, with the leadership of Nishina, Japan had become the second country in the world to possess such a large cyclotron for research in nuclear physics.

Work on Atomic Bomb Project

In his address at the Nishina Centennial Symposium, Tokyo, Ryogo Kubo, a prominent Japanese mathematical physicist, Boltzman medalist, and formerly affiliated with the University of Tokyo and Kyoto University, on December 5, 1990 (Kubo, 1990, 2008) acknowledged Nishina's involvement in Japan's effort to develop a nuclear bomb; however, Kubo intimated that Nishina had no choice but to engage in the nuclear bomb project during the Second World War; and that Nishina and others concluded that a nuclear bomb could not be developed within the time span required by the military. In his address he noted:

> *In 1937, Niels Bohr visited Japan with his family in response to Nishina's longstanding invitation, and gave great encouragement to Japanese scientists. It was almost the last days of the happy time, because Japan was becoming internationally isolated by her militaristic policies, finally rushing into the reckless war. During the wartime, Nishina's group had to engage in the project to develop the nuclear bomb. The scale of the project was nothing compared to the Manhattan project and the researchers concluded that it was impossible to produce a nuclear bomb within fifty years. Japan was already losing the war then, and finally there came the disasters of Hiroshima and Nagasaki.*

In 1978, the News and Comment Section of the journal *Science*, in an article entitled "Nuclear Weapons History: Japan's Wartime Projects Revealed" (Shapley, 1978), relates information on the involvement of Yoshio Nishina and other

nuclear physicists in Japan's atom bomb project from the diary of Masa Takeuchi, a worker at Nishina's laboratory who was assigned to the thermal diffusion project, and a memoir of Bunsabe Arakatsu, a physicist from Kyoto. It was noted in this article that the Japanese scientists were ordered to do whatever they could to develop a bomb. Takeuchi's diary noted that he and other scientists at RIKEN, all under Yoshio Nishina, did the work they were ordered to do but were unenthusiastic.

In 1995, the News section of the journal *Nature*, entitled "Physicists Reveal Glimpses of Japan's Atomic Bomb Effort" (Swimbanks, 1995) reported about a press conference in Tokyo where Tatsusaburo Suzuki, 83 years of age at the time of the press conference, was sent by the military in 1944 to work on the bomb project at RIKEN. He reported that Japan had the necessary expertise to build the bomb, but lacked the required resources. In this article of the journal *Nature*, it was reported that a leading Japanese physicist, then a student at Osaka University during the war, reported that there were three institutes in Japan working on the "uranium bomb." One group was headed by Hoshio Nishina at RIKEN, a second group was led by Seishi Kikuchi at Osaka University, and a third group was at Kyoto University.

Kenji Ito (2002) of the University of Tokyo provides a thorough study and analysis of Yoshio Nishina's wartime discourse. He noted that, during the war, Nishina was Japan's supreme authority on atomic physics and thus he led one of the principal wartime "nuclear power projects." Ito preferred to refer to the atomic bomb project as a nuclear power project, as in his words:

> *Like the Germans, the Japanese did not get far enough to have to decide whether to build a bomb or a reactor; therefore, "nuclear power project" is more appropriate than "atomic bomb project."*

El Naschie (2000) discusses Yoshio Nishina's estimate of the critical mass for fast neutron fission within the context of Japan's early nuclear research before and during World War II. He analyzes Japan's advanced intellectual capacity and development in nuclear physics comparable to that of the United States and Germany. He emphasized Japan's transition from intelligence to wisdom in banning the development of nuclear weapons altogether, which should serve as an example to all nations:

> *Prof. Nishina…was by any standards an incredible scientist and an outstanding engineer and physicist of the highest calibre. Nishina was never honoured by a Nobel Prize, however he has achieved far more than that by establishing the Japanese Modern School of Physics which in turn produced Nobel Laureates such as his student H. Yukawa…the basic idea which we are never tired of repeating in the hope that it can bring home the message namely that all powers participating in World War II could have produced nuclear weapons…Nishina understood the design of cyclotrons and made better guesses at the critical mass than the comparable one made in the USA at the very early stages of a bomb project…From all the nations which participated in the last great war, Japan seems to be the only one who has consistently shrugged from war and from developing nuclear capabilities for military purposes. If this is correct then they seem to have achieved a rare transformation from intelligence to wisdom, a process which one could recommend to every nation without the slightest hesitation.*
>
> From El Naschie, Reprinted with permission from Elsevier © 2000.

Heartbreaking Loss and Recovery

In April of 1945, an aerial bombing destroyed Yoshio Nishina's small 27-inch cyclotron and much of the facilities at RIKEN. Nishina's large 60-inch cyclotron escaped damage. Then came the dreadful atomic bombings of Hiroshima on August 6 and Nagasaki on August 9, 1945. The destruction caused by the bomb dropped on Hiroshima is described by the following quotation of Prof. Robert J. Lifton, quoted in a paper by El Naschie (2000):

> *I climbed Hikiyama Hill and looked down…I was shocked by the sight. What I felt then and still feel now just can't explain with words…Hiroshima didn't exist – that was mainly what I saw – Hiroshima just didn't exist.*
>
> Prof. Robert J. Lifton.

As Nishina was the leading figure in nuclear physics, he was sent to assess the cause of the destruction. Nishina knew immediately that the bombs were atomic; and Nishina's report to the Japanese Government is noted by Kubo (1990, 2008) to have been a decisive factor in Japans radio broadcast of surrender on August 15, 1945.

Later more tragedy befell Nishina, as reported by Kubo (1990, 2008) and Kim (2006), when the American occupation forces arrived at RIKEN unexpectedly only a few months after the surrender, to disarm Nishina's large 60-inch cyclotron. Nishina pleaded with the soldiers, as this represented a great part of his life's work and was an important tool for Japan's recovery. Nevertheless, the forces dismantled the cyclotron and dropped its components into the deep waters of Tokyo Bay to never be recovered. American scientists expressed their criticism over the destruction of the cyclotron, and the American Secretary of War later acknowledged this destruction as an error on the part of the U.S. War Department.

Yoshio Nishina and I.I. Rabi (1948) in Tokyo Nishina Memorial Foundation, courtesy AIP Emilio Segre Visual Archives

Further hardship ensued a year later, in 1946, when RIKEN, which was the heart of physics research in Japan, was ordered by the occupation forces to dissolve. Now Yoshio Nishina was left with nothing but to start from scratch to build up again a research institute and staff to reconstruct Japan's scientific infrastructure. He then had to give up science per se and become an administrator to establish a research institution and find funds to pay staff. In the address of Prof. Ryogo Kubo (1990), Yoshio Nishina established a new company by the name of RIKEN Co., and through this company managed the industrial production of penicillin. This provided financial support for the research activities of staff; and Nishina then became president of RIKEN as a company. Nishina saved RIKEN, which is now a major research institution with 3000 staff on seven campuses across the country devoted to research in the chemical, physical, and biological sciences. With the help of Nishina, RIKEN is at the forefront of science; and two RIKEN scientists have won the Nobel Prize in Physics, Hideki Yukawa in 1949 and Sin-Itiro Tomonaga in 1965, both of whom regarded Yoshio Nishina as their teacher. The strenuous work of recovery from such loss after the war led to declining health, and Yoshio Nishina died at the young age of 60 years on January 10, 1951.

MAX VON LAUE (1879–1960)

Max von Laue was born in Pfaffendorf (near Koblenz), Germany on October 9, 1879. He was awarded the Nobel Prize in Physics in 1914 "for his discovery of the diffraction of X-rays by crystals."

von Laue (1879-1960)

Von Laue remained keenly interested in physics since he was a young man, and as he noted in his Nobel lecture "that goes back to the days in which I was privileged to receive first-class instruction at the famous old Protestant Gymnasium in Strassburg, Alsatia—my particular attention was drawn to the field of optics, and within that field the wave theory of light" (von Laue, 1915). After a year in military service in 1898, he went to the University of Strassburg to study physics, chemistry, and mathematics. Soon he moved on to study for short periods at the University of Göttingen and a semester at the University of Munich, until in 1902 he went to the University of Berlin to work under Max Planck. Von Laue recalled that:

> *the lectures, which I heard during my student days from Profs. W. Voigt, Max Planck, and O. Lummer provided me at that time…with thorough experimental and theoretical knowledge; and as I had been finally able to cultivate what one could almost term a special feeling or intuition for wave processes.*
>
> von Laue (1915).

Max von Laue received his doctorate from the University of Berlin in 1903, after which he returned for two years to the University of Göttingen, until receiving a post as assistant to Max Planck in 1905 at the Institute for Theoretical Physics at Berlin, where he continued research on radiation fields and light waves.

In 1909, Max von Laue became Privatdozent at the University of Munich lecturing on optics, thermodynamics, and relativity theory. It was upon his arrival at Munich that von Laue began to concentrate his thoughts on the true nature of X-rays. It was not that long since Röntgen discovered X-rays in 1895, and there was much debate in the scientific community about the true nature of X-rays. The debate surrounded the question of whether X-rays had the properties of light waves or were the rays of particulate nature. Since the discovery of X-rays, Röntgen and others made efforts to observe the diffraction or interference of the rays that could provide evidence as to whether the X-rays represented a wave phenomenon or the emission of small particles. Some argued that, according to Maxwell–Lorentz electrodynamics, electromagnetic waves must be produced whenever electricity carriers alter their velocity, which is precisely what occurs in the creation of X-rays. Others experts maintained at the time that X-rays were corpuscular in nature, because X-rays would, upon striking a substance, excite the creation of secondary X-rays and at the same time they would free electrons from the substance. The velocities of the electrons emitted were not dependent on temperature of the substance bombarded or on the intensity of the x-radiation, but rather on the energy of the x-radiation. The velocities of the electrons knocked out of the bombarded substance would increase with radiation hardness or energy. From the quantum theory of Planck and Einstein's then-recent revelations on the photoelectric effect, Max von Laue and others could see that the X-rays had properties similar to light rays in the photo-electric effect. Nevertheless, there was the need to demonstrate the true nature of X-rays. On the assumption that X-rays were of wave nature, Wilhelm Wien and Arnold Sommerfeld used Planck's new quantum theory to arrive at an estimate of the X-ray wavelengths to lie between 10^{-10} and 10^{-9} cm, which would give them a wavelength shorter than visible light.

In 1912, von Laue became Professor of Physics at the University of Zurich, and in February of that year he was approached by P.P. Ewald about a research problem concerning crystal optics. Von Laue related (von Laue, 1915):

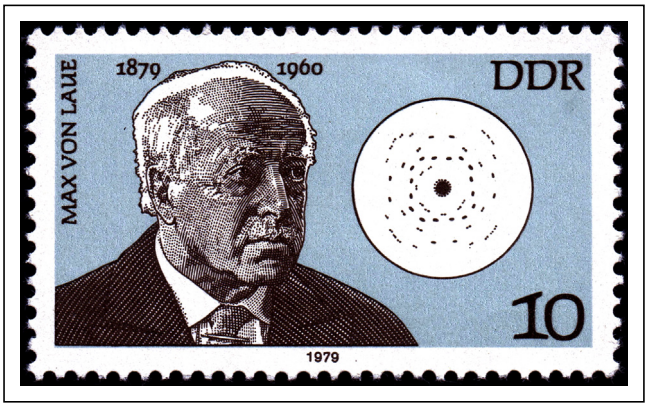

During the conversation I was suddenly struck by the obvious question of the behavior of waves which are short by comparison with the lattice constants of the [crystal] space lattice. And it was at that point that my intuition for optics suddenly gave me the answer:…The fact that the lattice constant in crystals is of an order of 10^{-8} cm was sufficiently known from the analogy with other interatomic distances in solid and liquid substances, and…the order of X-ray wavelengths was estimated by Wien and Sommerfeld to be 10^{-9} cm. Thus the ratio of wavelengths and lattice constants was extremely favorable if X-rays were to be transmitted through a crystal.

Shortly thereafter, at the University of Munich, Max von Laue and his associates W. Friedrich and P. Knipping carried out an experiment whereby they irradiated a crystal of copper sulfate with X-rays. A photographic plate was placed behind the crystal. Right from the outset they observed on the photographic plate a considerable number of deflected X-rays together with an image of the primary ray. The deflection maxima left images on the photographic plate as spots at defined distances from a larger center spot produced by the primary X-ray (Friedrich et al., 1912; von Laue, 1912). The deflected maxima represented the crystal lattice spectra as von Laue anticipated. One of the original crystal X-ray diffraction images taken by von Laue and his coworkers is illustrated as spots on a circular photographic plate in the postage stamp from the former German Democratic Republic (DDR) issued in 1979. A more intricate crystal diffraction image, such as those produced by more complex crystalline substances, is illustrated in another stamp from the Federal Republic of Germany, also issued in 1979, commemorating 100 years since the birth of Max von Laue.

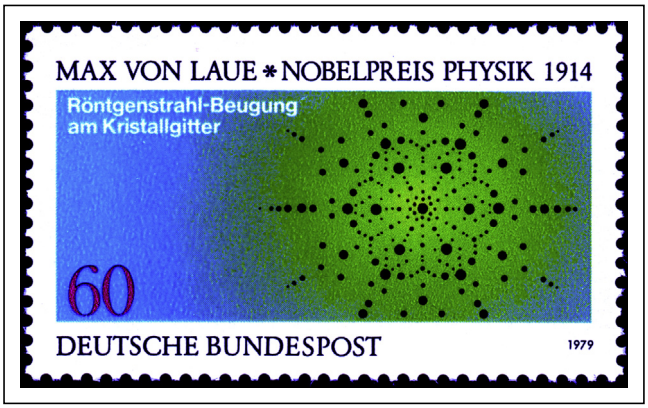

Max von Laue was able to demonstrate that the spots on the photographic plates represented X-ray diffraction maxima produced by crystal lattice points of interference, corresponding with three integral numbers that originated from three space-lattice periodicities, the ratios of which determine the position of each point of interference (von Laue, 1915). This discovery provided evidence for the wave nature of X-rays and also the lattice theory of crystals. The wavelengths of the X-rays could then be determined by the dimensions of the crystal space lattice. However, for this to be done, it would be necessary to know the exact molecular structure of the crystals. Such work was soon to follow with the discoveries of William Henry Bragg and his son William Lawrence Bragg. The significance of Max von Laue's discovery was underscored by Prof. G. Granqvist, Chair of the Nobel Committee for Physics, when he stated

As a result of von Laue's discovery of the diffraction of x-rays in crystals proof was thus established that these light waves are of very small wavelengths. However, this discovery also resulted in the most important discoveries in the field of crystallography. It is now possible to determine the position of atoms in crystals.

Granqvist (1915).

In 1914, von Laue moved to Frankfurt on Main as professor of Theoretical Physics at the Goethe University; and in 1916 worked at the University of Würzburg on wireless communication for the war effort. In 1917 he worked under Albert Einstein as Second Director of the Institute for Physics at Berlin-Dahlem. From 1919 to 1943, von Laue was professor of physics at the University of Berlin. During this period von Laue made significant contributions to the understanding of superconductivity.

During the reign of Hitler and the National Socialist Power in Germany, Max von Laue defended scientific views, such as Einstein's theory of relativity, that were not approved by the party or by party loyalists such as Philipp Lenard. Von Laue was the only member of the Berlin Academy to protest a statement by the President of the Academy, who claimed that the resignation of Albert Einstein from the Academy was no loss (*Nobel Lectures, Physics 1901–1921*). He welcomed the arrival of the French troops; and he was taken by an Anglo-American mission to England with other German scientists until 1946, when he returned to Göttingen as Acting Director of the Max Planck Institute and professor of the University. In 1951, von Laue was appointed Director of the Fritz Haber Institute for Physical Chemistry in Berlin-Dahlem, where he continued work on X-ray optics. He retired in 1958, and on April 24, 1960 succumbed to injuries suffered in an auto accident while driving alone to his laboratory on the Berlin autobahn at the age of 80.

SIR WILLIAM HENRY BRAGG (1862–1942) AND SIR WILLIAM LAWRENCE BRAGG (1890–1971)

Sir William Henry Bragg shared the Nobel Prize in Physics in 1915 with his son, Sir William Lawrence Bragg, "for their services in the analysis of crystal structure by means of X-rays."

Sir William Henry Bragg was born in Westward, Cumberland, England on July 2, 1862. He was educated at Market Harborough Grammar School and King William's College, Isle of Man. William Henry was elected a scholar of mathematics at Trinity College, Cambridge in 1882, where he studied for two years, achieving high honors in the final mathematics examinations. He then studied physics at the Cavendish Laboratory during part of 1885, being elected that year as Professor of Physics and Mathematics at the University of Adelaide, South Australia. He returned to England in 1909 to become Cavendish Professor of Physics at the University of Leeds, where he remained until 1915. During his tenure at Leeds, William Henry focused his work on the study of X-rays, which he at first thought were elementary particles until the work of Max von Laue of 1912 demonstrated that X-rays had wavelengths of the order of magnitude equivalent to the distances of crystal lattices (10^{-8} cm) and thus the crystal lattices could serve as molecular X-ray diffraction gratings. At Leeds, Willam Henry designed the Bragg X-ray spectrometer and began work with his son William Lawrence on studies of X-ray diffraction by crystalline materials. Their joint studies provided information as soon as 1914 on the interatomic distances and structure of crystals as well as X-ray wavelengths, whereby father and son were awarded jointly the Nobel Prize in Physics in 1915. From 1915 to 1925, William Henry was Quain Professor of Physics at University College, London. In 1923 William Henry became Head of the Royal Institution, where he remained in service until his death in 1942.

W. H. (1862-1942) and W. L. Bragg (1890-1971)

Sir William Lawrence Bragg was born in Adelaide, South Australia on March 31, 1890 the son of Sir William Henry Bragg. He attended St. Peter's College at Adelaide and thereafter studied mathematics at Adelaide University, graduating with honors in 1908. When his father returned to England in 1909 with his son, William Lawrence entered Trinity College, Cambridge and graduated with honors in Natural Science in 1912. William Lawrence started work on X-ray diffraction in 1912 and published his first paper on the diffraction of short electromagnetic waves in the Proceedings of the Cambridge Philosophical Society (Bragg, 1913). This was followed by another paper on the analysis of crystals by the X-ray spectrometer the following year (Bragg, 1914a). In 1912, William Lawrence started a collaboration in the field of X-ray diffraction and crystal structure with his father, who then developed the very first X-ray diffraction spectrometer.

The combined efforts of father and son from 1912 to 1914 earned them the joint Nobel Prize in 1915. William Lawrence, who delivered the Nobel lecture in 1915, is still the youngest person (25 years) to receive the Nobel Prize. Prior to winning the Nobel Prize, young William Lawrence wrote a thorough text that gave birth to X-ray diffraction as a standard method for the determination of crystalline structures (Bragg, 1914b). From 1915 to 1919, William Lawrence served as Technical Advisor on Sound Ranging for the General Headquarters, British Troops in France. From 1919 to 1937 he held the post of Langworthy Professor of Physics, University of Manchester (*Nobel Lectures, Physics 1901–1922*). From 1937 to 1938 he was Director of the National Physical Laboratory, but despised pure administration. He served also in World War II, and after the war succeeded Rutherford as Cavendish Professor of Experimental Physics at Cambridge. In 1948, William Lawrence became interested in the structure of protein and nucleic acids. He did not play any direct part in the X-ray diffraction study and 1953 discovery of the helical structure of DNA derived from the work of Rosalind Franklin, James Watson, Francis Crick, and Maurice Wilkins; however, the X-ray diffraction technique developed by William Lawrence Bragg was a vital tool in the discovery of the nucleic acid structure. James Watson admitted that the X-ray method developed by Bragg 40 years before was at the heart of this profound insight into the nature of life itself (University of Cambridge, Cavendish Laboratory). In 1953, William Lawrence became resident professor of the Royal Institution, London and remained in that position until his retirement in 1966. He passed away in Waldringfield on July 1, 1971.

When awarded the Nobel Prize, William Lawrence was only 25 years of age, the youngest person ever to receive the Nobel Prize. The fact that the joint research and Nobel Prize was the result of collaboration between father and son led many to believe that the father had initiated the research, a fact that upset the son (University of Cambridge, Cavendish Laboratory). The credit for this joint work was clarified by Prof. G. Granqvist, Chairman of the Nobel Committee, in the Nobel presentation speech (Granqvist, 1915), when he stated:

> *The problem of calculating the crystal structures was a discovery of epoch-making significance when W.L. Bragg [the son] found out that the phenomenon could be treated mathematically as a reflection by the successive parallel planes [i.e., the atomic planes of a crystal] that may be placed so as to pass through the lattice points, and that in this way the ratio between the wavelengths and the distances of the said planes from each other can be calculated by a simple formula from the angle of reflection…The instrument requisite for the said purpose, the so-called x-ray spectrometer, was constructed by Prof. W.H. Bragg, W.L. Bragg's father, and it has been with the aid of that instrument that father and son have carried out, in part conjointly, in part each on his own account, a series of extremely important investigations respecting the structure of crystals.*

Giving much deliberation on the work of Max von Laue (see von Laue in this section), who demonstrated the wave nature of X-rays and that the diffracted wave pattern was a function of the symmetry of the underlying crystal structure, W.L. Bragg considered the diffraction effects as a reflection of the X-rays by the planes of the crystal structure. In his Nobel lecture given at the Royal Swedish Academy of Sciences in Stockholm on September 6, 1922, W.L. Bragg stated how he approached the mathematical solution to the application of X-ray diffraction to the determination of crystal structure (Bragg, 1922). In the lecture he stated:

> *The points of a space lattice may be arranged in series of [atomic] planes, parallel and equidistant from each other. As a pulse passes over each diffracting point, it scatters a wave, and if the number of points are arranged on a plane the diffracted wavelets will combine together to form a reflected wave front, according to the well-known Huygens construction. The pulses reflected by successive [atomic] planes build up a wave train given by the formula:*

$$n\lambda = 2d \sin \theta \qquad \text{[III.53]}$$

> *In this impression,* n *in an integer,* λ *is the wavelength of the x-rays,* d *the spacing of the [atomic] planes, and* θ *the glancing angle at which the x-rays are reflected.*

Eq. [III.53] has become to be known as Bragg's Law, and the diffraction of X-rays according to Bragg's Law is illustrated in Fig. III.11. The figure illustrates two atomic planes in a crystal separated by the distance d. The diffracted rays are those reflected at an angle θ to the atomic planes, and such reflection requires a coherence of rays that are in-phase yielding a reinforced beam, which can be detected by the spectrometer at a given angle θ by an ionization detector or with photographic film in a circular Bragg camera. The reflection of the rays in-phase as a coherent beam requires incident X-ray wavelengths that are integer multiples along the X-ray path of travel between the two atomic planes. Only those X-rays with wavelengths of 1λ, 2λ, 3λ…over the path length of travel ($2d \sin\theta$) between each successive crystal atomic plane will produce coherent reflected X-ray beams. By measurement of the angle of reflection θ of an incident monochromatic X-ray of known wavelength, the spacing d between each atomic plane can be measured.

In addition to the measurements of the d spacing of the atomic planes, W.H. and W.L. Bragg extended their diffraction experiments of various crystalline materials to determine their structure or atomic arrangements. As explained by William Lawrence in the Nobel lecture:

> *In examining the effect for varying angles of incidence my father discovered that a very strong reflection appeared when a given crystal face was set at certain definite angles. Since the relationship [diffraction] must hold between glancing angle and wavelength, this constituted the first evidence of the existence of characteristic [x-ray] lines in the radiation given off by the anticathode [of the x-ray tube]. These same lines could be recognized in the reflections from other faces, and the measurement of the angles at which they appeared proved a most powerful method of finding the arrangement of the atoms in the crystal.*

The method used by the father and son team to analyze crystal structure by X-rays, as described in the Nobel Lecture, was firstly to find the dimensions of a unit cell of the crystal space lattice, which has for its sides the basic atomic structure. To achieve this they would measure the angle θ by which a monochromatic beam of X-rays would be reflected by various faces of the crystal (see a diagram of their X-ray spectrometer in Fig. III.12). A small crystal would

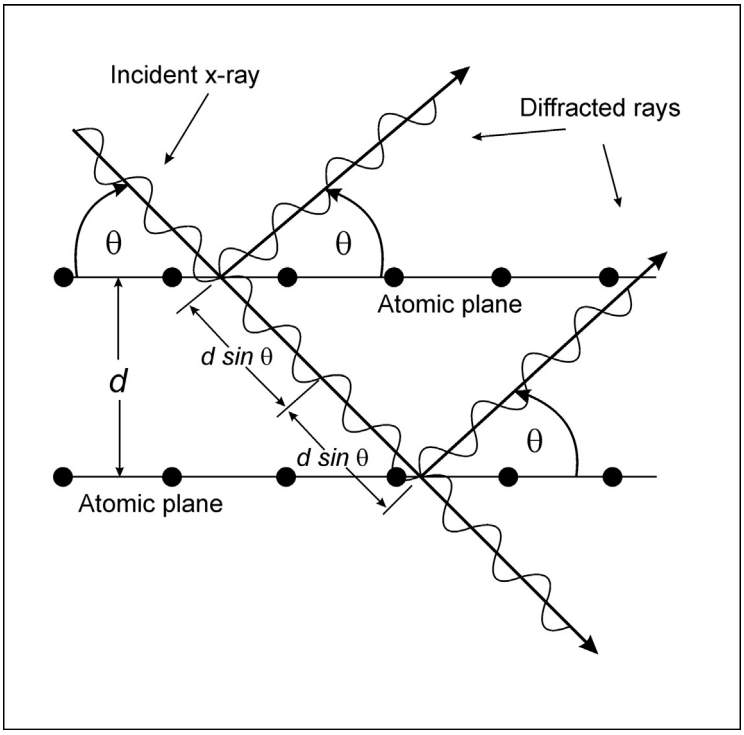

FIGURE III.11 The diffraction of X-rays by the atomic planes of a crystal. The rays are diffracted according to Bragg's Law, $n\lambda = 2d \sin\theta$, where λ is the X-ray wavelength, d is the spacing of the atomic planes, and θ is the glancing angle at which the X-rays are reflected.

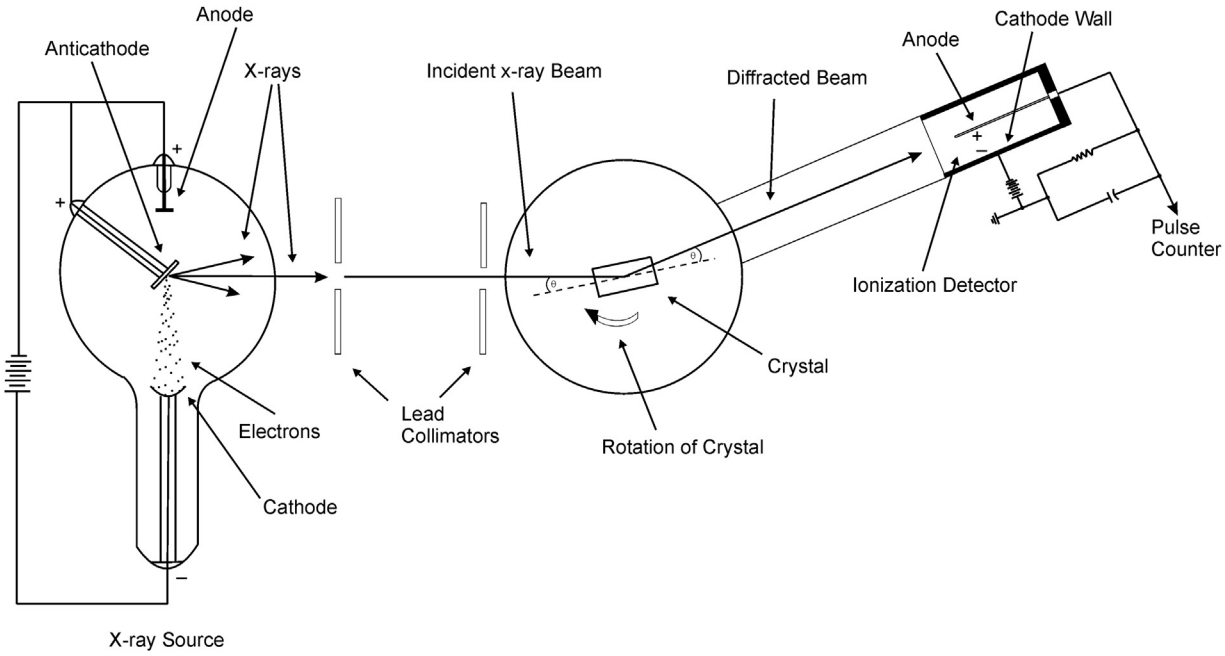

FIGURE III.12 Bragg's X-ray spectrometer.

be set at the center of the instrument as illustrated, adjusted so that a zone of the crystal is parallel to the axis, and then the crystal is rotated to permit the reflections of various faces to be measured by the ionization detector in turn. The *d* spacing of the atomic planes parallel to any crystal face under examination could then be calculated according to Eq. [III.53]. The dimensions of a unit cell are then found by the measurement of *d* for several crystal faces. When the dimension of the unit cell is known, the number of atoms in the unit cell is calculated from the crystal density and mass of each atom. The second step in the structural analysis is to determine how the atoms are grouped to form the unit cell. The structure or the manner in which the atoms are grouped in the unit cell will influence the strengths of the various X-ray reflections. This is so, because the X-rays are diffracted by the electrons grouped about the nucleus of each atom. In some directions of the X-ray beam the atoms give a strong scattered beam, whereas in other directions the effects of the electron densities annul each other by interference. The exact arrangement of the atoms indicated by the electron density distributions are deduced by comparing the strengths of the X-ray reflections from different faces and in different orders. When placed in the spectrometer, the crystal was set at the center of the instrument and adjusted so that a zone of the crystal was parallel to the axis; and then the crystal would be rotated round so that the reflections of various faces would be observed in turn. The X-ray spectrometer measures the angles between planes of the crystal structure, and the spacings of the planes.

W.H. and W.L. Bragg analyzed several crystal types, reporting their atomic arrangements and the spacing between the atoms. One of these was the cubic crystalline lattice of sodium chloride (rock salt), whereby they reported for the first time that the arrangement of atoms in sodium chloride were alternate Na and Cl atoms and not associated in the crystal as molecular NaCl. In other words, a Na atom was surrounded by six Cl atoms, and vice versa. The atomic arrangement of the sodium chloride crystal is illustrated in the postage stamp issued by the United Kingdom, which commemorates the achievement of W.H. and W.L. Bragg. The stamp illustrates a unit cell of sodium chloride crystal, where the central atom (ie, sodium ion, blue ball) is surrounded by six atoms of the other ion (ie, chloride, green ball). As stated by William Lawrence Bragg in his Nobel lecture:

> *For the first time the exact arrangement of the atoms in solids has become known, we can see how far the atoms are apart and how far they are grouped…One type of chemical binding has already been confirmed. In a structure of sodium chloride the atoms of sodium and chlorine are not associated into chemical molecules, but are arranged alternately equidistant from several neighbors.*

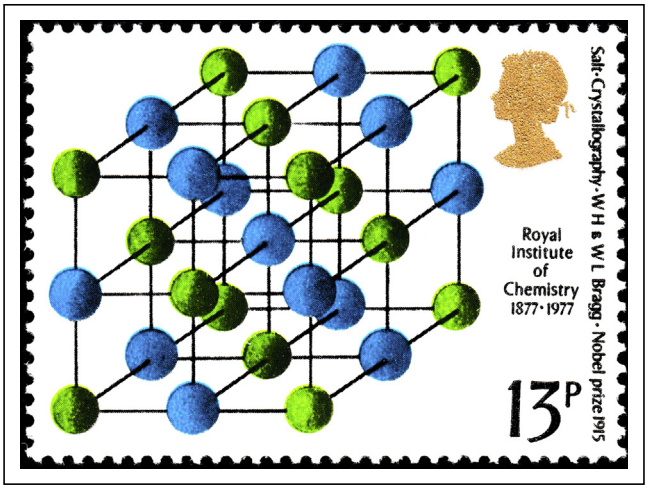

Prior to their discovery of the atomic arrangements of the crystalline structure of NaCl in 1914, it was always imagined that crystalline materials such as NaCl, KCl, KI, KBr, etc. were molecular associations, not associations of the separate ions or atoms in the crystal. The importance of this discovery was underscored by Prof. G. Granqvist (1915), Chairman of the Nobel Committee, when he stated at the Nobel presentation speech:

> *From these investigations it follows that a metal atom in the crystals of the alkaloid salts is situated at one and the same distance from the six haloid atoms nearest to it, and vice versa – a relationship that was found to prevail,* mutatis mutandis*, in all the crystals examined. That means the exceedingly important discovery, both for molecular physics and chemistry, is that the crystals consist of atomic lattices and not, as has been always imagined, of molecular ones.*

The above statement of Prof. Granqvist can give some insight into the impact of the findings, as when this discovery was first reported (Bragg, 1914a,b) some members of the scientific community were initially in disbelief. I personally had the good fortune to meet Sir William Lawrence Bragg around 1968 during my graduate student days. I recall him relating that he had saved correspondence, received soon after his publications of the discovery in 1914, from some of the scientific community stating that he must be out of his mind.

By the time of the Nobel lecture given by William Lawrence Bragg on September 6, 1922, 7 years after the Nobel Prize was awarded to Sir Lawrence and his father, they had determined the atomic structures of several crystalline materials including diamond, magnetite, calcite, graphite, ice, and the organic crystalline structure of naphthalene, among others.

In conclusion, the discovery of X-ray diffraction by crystalline compounds was the beginning of a new era. It would provide us with a new tool that could afford images of the small atomic world, the dimensions of which the light microscope could not provide. W.L. Bragg clearly pointed this out when he stated in the Nobel Lecture:

> *The examination of crystal structure, with the aid of x-rays has given us for the first time an insight into the actual arrangement of the atoms in solid bodies. The study of structure by means of a microscope is limited by the coarseness of the light which illuminates the object, for we can never hope to see details smaller than the wavelength of the light. By using x-rays with their very short wavelengths, this limit of minuteness has at one step been decreased ten thousand times, for the wavelength of the x-rays is of a smaller order than the dimensions of the atomic structure. We are actually looking into the interior of the molecule and the atom with this fine-grained form of light.*

From the original work of W.H. and W.L. Bragg, the field of X-ray crystallography, that is, the study of crystal structures by X-ray diffraction, was given birth and remains a vital analytical technique today. With the aid of modern computers, the diffraction images, that is the images of the X-rays diffracted off the electrons in a crystal structure, are recorded and processed by computer. From this data, the electron density maps of the molecular structure in a crystalline material are constructed with the aid of computer processing, and thereby the arrangement of the atoms of a molecular

structure can be determined. The molecular structures of innumerable inorganic, organic, and biological compounds have been determined by X-ray diffraction.

ROSALIND FRANKLIN (1920–1958)

A biographical sketch of Rosalind Franklin is warranted here, because her work, which entailed mostly the utilization of X-ray diffraction, contributed significantly to one of the greatest discoveries of the 20th century. The X-ray diffraction data obtained by Rosalind Franklin (1920–1958), was a critical component in the elucidation of the double helical structure of DNA, which was crucial to the unraveling of the code of life.

The following is an excerpt of biographical information from Profiles in Science, Rosalind Franklin Papers, reproduced with permission of the National Library of Medicine (NLM), National Institutes of Health (NIH) with comments of the author in brackets, http://profiles.nlm.nih.gov/ps/retrieve/Narrative/KR/p-nid/183:

> *Science and everyday life cannot and should not be separated. Science, for me, gives a partial explanation of life. In so far as it goes, it is based on fact, experience, and experiment. …In my view, all that is necessary for faith is the belief that by doing our best we shall come nearer to success and that success in our aims (the improvement of the lot of mankind, present and future) is worth attaining.*
>
> Rosalind Franklin in a letter to Ellis Franklin [her father], c. summer 1940.

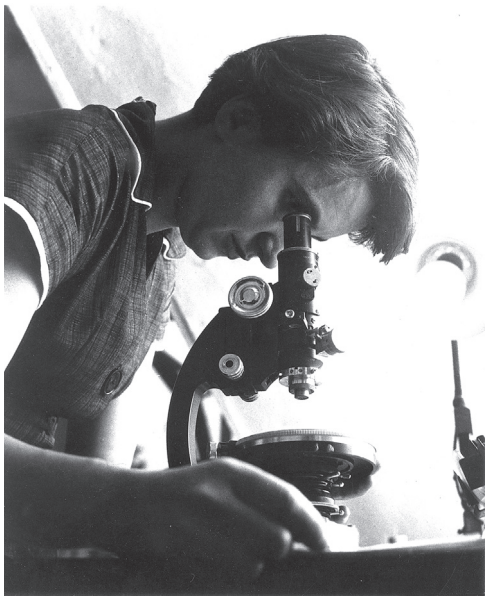

Rosalind Franklin (1954)
Printed with permission © Henry Grant Collection/Museum of London

Rosalind Elsie Franklin, the brilliant chemist whose X-ray diffraction studies provided crucial clues to the structure of DNA and quantitatively confirmed the Watson–Crick DNA model, was born in London on July 25, 1920. Rosalind attended St. Paul's School for Girls, which emphasized preparing its graduates for careers, not just for marriage. She had demonstrated an early aptitude for math and science, and an easy facility for other languages (she would eventually speak excellent French, good Italian, and passable German).

"All her life," Franklin's mother later noted, "Rosalind knew exactly where she was going, and at 16, she took science for her subject." Rather than stay an extra year for more college preparation, she left St. Paul's in 1938 to enter Newnham College, one of two women's colleges at Cambridge University. At Cambridge, Franklin majored in physical chemistry. Cambridge also took in a number of war refugees, including the French scientist Adrienne Weill, who arrived at Newnham in 1940, and became Franklin's mentor and friend.

Franklin received her BA in 1941, and was awarded a scholarship for a further year of research, and a research grant from the Department of Scientific and Industrial Research. She spent that year in the laboratory of R.G.W. Norrish, a noted pioneer in photochemistry. In 1942, with the war still on, she had to decide whether to be drafted for more traditional war work or pursue a PhD-oriented research job in a field relevant to wartime needs. She chose the latter, and began work with the recently organized British Coal Utilisation Research Association (BCURA) that summer. For the next 4 years, Franklin worked to elucidate the microstructures of various coals and carbons, and explain why some were more permeable to water, gases, or solvents and how heating and carbonization affected permeability. In this original work, she found that the pores in coal have fine constrictions at the molecular level, which increase with heating, and vary according to the carbon content of the coal. These act as "molecular sieves," successively blocking penetration of substances according to molecular size. Franklin was the first to identify and measure these microstructures, and this fundamental work made it possible to classify coals and predict their performance to a high degree of accuracy. Her work at BCURA yielded a doctoral thesis—she received her PhD from Cambridge in 1945—and five scientific papers.

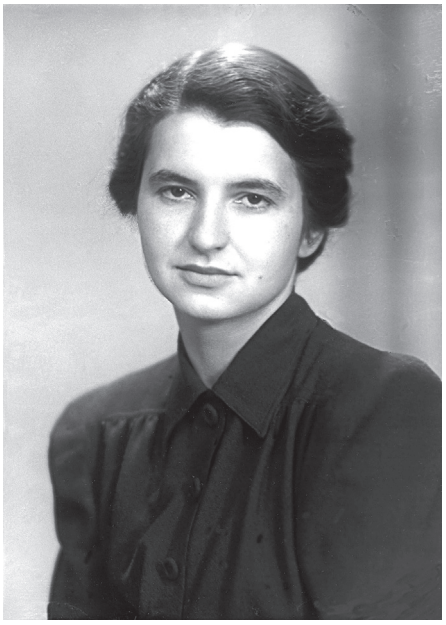

Rosalind Elise Franklin (11 June 1946) by Elliott & Fry © National Portrait Gallery, London with permission

After the war, Franklin began searching for different work. Adrienne Weill, who had returned to France, helped her get a position in Jacques Mering's lab at the Laboratoire Central des Services Chimique de l'Etat in Paris. At the "labo" she learned how to analyze carbons using X-ray crystallography (also called X-ray diffraction analysis), becoming very proficient with the technique. Her work detailing the structures of graphitizing and nongraphitizing carbons helped form the basis for the development of carbon fibers and new heat-resistant materials, and earned her an international reputation among coal chemists. She also enjoyed the collegial professional culture of the Laboratoire Central, and formed many lifelong friendships there.

Though very happy in France, Franklin began seeking a position in England in 1949. Her friend Charles Coulson, a theoretical chemist, suggested she look into doing X-ray diffraction studies of large biological molecules. In 1950 she was awarded a 3-year Turner and Newall Fellowship to work in John T. Randall's Biophysics Unit at King's College, London. Randall had originally planned to have Franklin build up a crystallography section and work on analyzing proteins. At the suggestion of the assistant lab chief, Maurice Wilkins, however, Randall asked Franklin to investigate DNA instead. Wilkins had just begun doing X-ray diffraction work on some unusually good DNA samples. He expected that he and Franklin would work together, but Randall's communication to Franklin did not convey this; it said that only she and graduate student Raymond Gosling would do the DNA work. Her subsequent relations with Wilkins suffered from this misunderstanding (and perhaps from Franklin's unhappiness with the less collegial culture at King's). Within 6 months of her arrival at King's in early 1951, they were having very little to do with each other. Working with Gosling, Franklin took increasingly clear X-ray diffraction photos of DNA, and quickly discovered that there were two forms—wet and

dry—which produced very different pictures. The wet form, she realized, was probably helical in structure, with the phosphates on the outside of the ribose chains. Her mathematical analyses of the dry form diffractions, however, did not indicate a helical structure, and she spent over a year trying to resolve the differences. By early 1953 she had concluded that both forms had two helices (see Fig. III.13 for the two forms of DNA).

Meanwhile, at the Cavendish Laboratory at Cambridge, Francis Crick and James Watson were working on a theoretical model of DNA. Though not in close communication with Franklin, in January 1953 they gleaned crucial insights about DNA's structure from one of her X-ray diffraction photos (see Fig. III.14) shown to them by Wilkins, and from a summary of her unpublished research submitted to the Medical Research Council. Watson and Crick never told Franklin that they

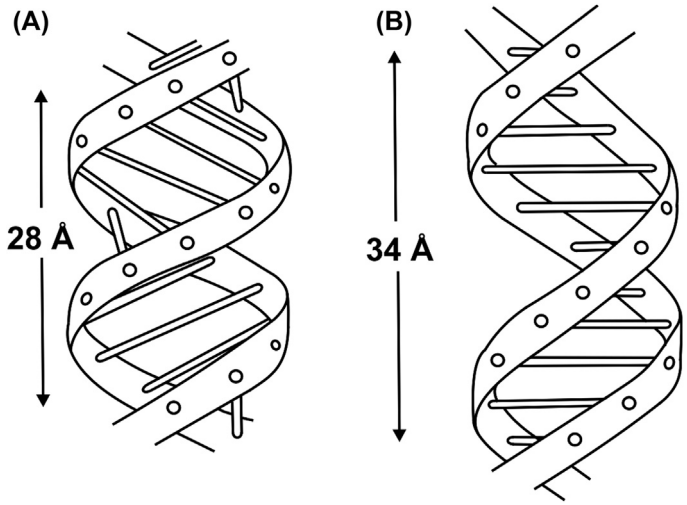

FIGURE III.13 Diagram illustrating the principal differences between the A (dry, on the left) and B (wet, on the right) forms of DNA. The ribbons symbolize the phosphate–sugar chains, and the rods the pairs of hydrogen-bonded bases holding the chains together. In the A structure, in which the molecules are tightly packed in a crystal, each chain contains 11 nucleotides in the axial repeat distance of 28 Å. In the B structure, in which the molecules are essentially free, there are 10 nucleotides in the axial repeat of 34 Å. The molecule is 30% shorter in the A than the B form. *From Klug, A., 1968. Rosalind Franklin and the discovery of the structure of DNA. Nature 219 (5156), 808–810, 843–44, reprinted by permission from Macmillan Publishers Ltd © 1968.*

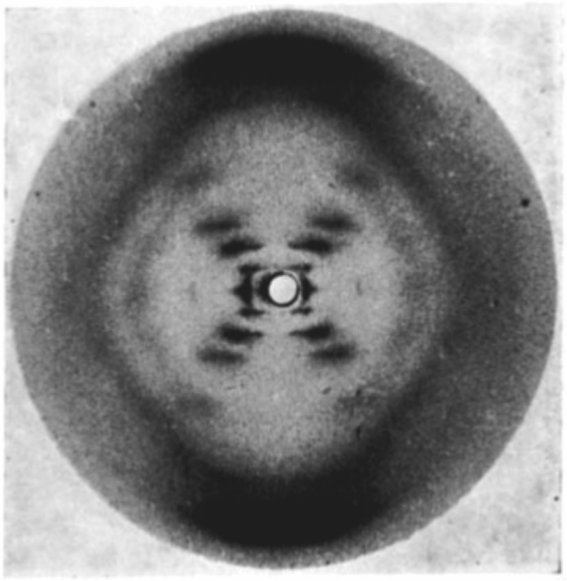

FIGURE III.14 X-ray diffraction pattern obtained by Rosalind Franklin and her student Raymond Gosling crucial to the structural determination of DNA. *From Franklin, R.E., Gosling, R.G., 1953c. Molecular configuration in sodium thymonucleate. Nature 171 (4356), 740–741, reprinted by permission from Macmillan Publishers Ltd © 1953c.*

had seen her materials, and they did not directly acknowledge their debt to her work when they published their classic announcement in the journal *Nature* that April (Watson and Crick, 1953). Crick later admitted that Franklin was two steps away from realizing the correct structure in the spring of 1953.

By that time, Franklin had arranged to transfer her fellowship to J.D. Bernal's crystallography laboratory at Birkbeck College, where she turned her attention to the structure of plant viruses, particularly tobacco mosaic virus (TMV). Working with a team that included future Nobelist Aaron Klug, Franklin made meticulous X-ray diffraction photos of the viruses. Her analyses of the diffraction patterns revealed, among other things, that TMV's genetic material (RNA) was embedded in the inner wall of its protective protein shell. This work involved collaboration with many other virus researchers, particularly in the United States. Her expertise in virus structures was recognized by the Royal Institution in 1956, when its director honored her with a request to construct large-scale models of rod-shaped and spherical viruses for the 1958 Brussels World's Fair Science Exhibition.

In the fall of 1956, Franklin was diagnosed with ovarian cancer. For the next 18 months she underwent surgeries and other treatments; she had several periods of remission, during which she continued working in her lab and seeking funding for her research team. She died in London on April 16, 1958.

Throughout her 16-year career, Franklin published steadily: 19 articles on coals and carbons, five on DNA (Franklin and Gosling, 1953a,b,c,d, 1955), and 21 on viruses. During her last few years, she received increasing numbers of invitations to speak at conferences all over the world, and it is likely that her virus work would have earned awards and other professional recognition, had she lived to continue it.

Franklin's scientific achievements, both in coal chemistry and virus structure research, were considerable. Her peers in those fields acknowledged this during her life and after her death. But it is her role in the discovery of DNA structure that has garnered the most public attention. Crick, Watson, and Wilkins shared the 1962 Nobel Prize for Physiology or Medicine for their work on the structure of DNA. None gave Franklin credit for her contributions at that time. Franklin's work on DNA may have remained a quiet footnote in that story had Watson not caricatured her in his 1968 memoir, The Double Helix. There he presented Franklin as "Rosy," a bad-tempered, arrogant bluestocking who jealously guarded her data from colleagues, even though she was not competent to interpret it. His book proved very popular, even though many of those featured in the story—including Crick, Wilkins, and Linus Pauling—protested Watson's treatment of Franklin, as did many reviewers. In 1975, Franklin's friend Anne Sayre published a biography in angry rebuttal to Watson's account, and Franklin's role in the discovery became better known. Numerous articles and several documentaries have attempted to highlight her part in "the race for the double helix," often casting her as a feminist martyr, cheated of a Nobel Prize both by misogynist colleagues and by her early death. However, as her second biographer, Brenda Maddox, has noted, this too is caricature, and unfairly obscures both a brilliant scientific career and Franklin herself. (From Profiles in Science, Rosalind Franklin Papers reproduced with permission of the National Library of Medicine (NLM), National Institutes of Health (NIH) with comments of the author in brackets, http://profiles.nlm.nih.gov/ps/retrieve/Narrative/KR/p-nid/183.)

Three papers were published back-to-back in the same volume of the journal *Nature*. The first was that by Watson and Crick (1953), the second by Wilkins et al. (1953), and the third paper by Franklin and Gosling (1953c). The paper by Watson and Crick provided a figure of the helical structure of DNA with its double helical chain of sugar phosphates and interlocking bases holding the chains together. Published alongside the paper by Watson and Crick (1953) were papers by Wilkins et al. (1953) and Franklin and Gosling (1953c), which provided X-ray diffraction patterns and analysis that supported the Watson and Crick model. The A and B forms of the DNA double helix were described by Franklin and Gosling (1953c) by means of complex mathematical analysis of the X-ray diffraction image illustrated in Fig. III.14. Franklin and Gosling (1953c) noted the following:

> *Structure B is derived from the crystalline structure A when the sodium thymonucleate fibers take up quantities of water in excess of about 40 per cent of their weight. The change is accompanied by an increase of about 30 per cent in the length of the fiber, and by a substantial rearrangement of the molecule…In the present case [Form B], the fiber axis period is 34 Å and the very strong reflection at 3.4 Å lies on the tenth layer line…This suggests strongly that there are exactly 10 residues per turn of the helix. If this is so…the radius [r] of the helix can be obtained. In the present instance, measurements…all lead to values of* r *of about 10 Å. Since this linear array of maxima is one of the strongest features of the x-ray diagram, we must conclude that a crystallographically important part of the molecule lies on a helix of this diameter. If ten phosphorus atoms lie on one turn of a helix of radius 10 Å, the distance between neighboring atoms in a molecule is 7.1 Å. This corresponds to the P···P distance in a fully extended molecule, and therefore provides a further indication that the phosphates lie on the outside of the structural unit.*
>
> From Franklin and Gosling (1953c), reprinted by permission from Macmillan Publishers Ltd © 1953.

The history behind the three back-to-back papers by Watson and Crick (1953), Wilkins et al. (1953), and Franklin and Gosling (1953c) appeared in an editorial entitled "Due Credit" in the journal *Nature* (Editorial, 2013). The editorial included comments on an interview with Raymond Gosling, who was the PhD student of Rosalind Franklin and coauthor of her papers on the X-ray diffraction determination of the structure of DNA. Gosling was 86 years of age at the time of the interview, and his comments and an excerpt of the editorial follow:

> *In the interview, a humble Gosling fondly recalls Franklin's response to Crick and Watson's model of the double helix was gracious and sanguine: "She didn't use the word 'scooped.' What she actually said was, 'We all stand on each other's shoulders.'"*
>
> *All three papers appeared with no peer review – unthinkable now. The head of the King's College biophysics unit, John Randall, belonged to the same London gentleman's club – the Athenaeun – as Lionel ('Jack') Brimble, co-editor of* Nature. *Randall convinced Brimble to publish Wilkin's paper alongside Watson and Crick's; Franklin's paper was added only after she petitioned for its inclusion.*
>
> *This cavalier approach to submissions extended to the awarding of credit. Watson and Crick's paper features only a glancing concession to being "stimulated by a knowledge of the general nature of [Wilkins and Franklin's] unpublished experimental results and ideas."*

Reprinted by permission from Macmillan Publishers Ltd © 2013.

A commentary published in the journal *Nature* (Fuller, 2003) underscores the significance of the scientific information concerning Franklin's X-ray diffraction work passed on to Watson without Franklin's consent and the possible consequences of this work, had Franklin not suffered an early demise. An excerpt of the commentary is included here, with the author's comment in brackets, as follows:

> *The proposed double-helical model for DNA is commonly described as the most significant discovery of the second half of the twentieth century… Franklin has loyal, influential and persistent champions, and in particular has had her reputation boosted, mainly at Wilkins' expense. Some have gone so far as to ask whether, if Franklin, who died at the age of 37 in 1958, had lived, she would have shared the Nobel Prize for the discovery of the structure of DNA. As the prize is never shared by more than three people, the implication is that Wilkins would have been excluded…In the much improved B-type pattern [x-ray diffraction pattern, see Fig. III.13] obtained by Franklin and Gosling in May 1952, the helical features are very clear. It was this pattern that Gosling passed to Wilkins without any caveat regarding its use. Wilkins, perhaps naively, but totally in character with his strong commitment to sharing scientific information, showed it to Watson on his crucial visit to King's at the end of January 1953. Watson immediately recognized this as the clearest evidence yet for a helical structure.*

From Fuller (2003), reprinted by permission from Macmillan Publishers Ltd © 2003.

In an article in the journal *Nature*, Aaron Klug (1986), Nobel Laureate and scientific colleague of Rosalind Franklin, provided a detailed account of Franklin's work in the period before the presentation of the DNA structural model by Watson and Crick. In the words of Klug:

> *in order to place the helical question [of the structure] in context, and to summarize the contributions she made to the proof of the structure…The importance of Franklin's work has been lost sight of, partly because of her untimely death*

From Klug (1986), reprinted by permission from Macmillan Publishers Ltd © 1986.

One of the most revealing pieces of evidence of the importance of Rosalind Franklin's contribution to the structure of DNA was provided in a letter dated December 31, 1961 written by Crick the year before he, Watson, and Wilkins received the Nobel Prize for their work on the structure of DNA. The content of Crick's letter was reported in the journal *Nature* (Zallen, 2003). An excerpt of the report is the following:

> *Some years ago while working in the archives of the Pasteur Institute in Paris, I came across a document that may be of interest in relation to the appropriateness of the inclusion of Wilkins as a recipient of the 1962 Nobel prize for this work. The document is a letter dated 31 December 1961, and an accompanying overview of the DNA work from Crick to his friend Jacques Monod…Crick writes about Wilkins as follows: 'On the matter of Maurice Wilkins. I think his contribution was two-fold. He initiated the careful x-ray work on DNA, and since 1953 he has done numerous extensive, accurate and painstaking studies on*

it…However, the data which really helped us to obtain the structure was mainly obtained by Rosalind Franklin, who died a few years ago.

From Zallen (2003), reprinted by permission from Macmillan Publishers Ltd © 2003.

The importance of Rosalind Franklin's contribution to the discovery of the structure of DNA with X-ray crystallography was underscored in a publication of the American Institute of Physics (Elkin, 2003). An excerpt is the following:

Watson and Crick could not have proposed their celebrated structure for DNA as early in 1953 as they did without access to experimental results [including x-ray crystallography data] obtained by King's College scientist Rosalind Franklin. Franklin had died of cancer in 1958 at age 37, and so was ineligible to share the honor [Nobel Prize in Physiology and Medicine 1962]. Her conspicuous absence from the awards ceremony—the dramatic culmination of the struggle to determine the structure of DNA—probably contributed to the neglect, for several decades, of Franklin's role in the DNA story.

Reproduced with permission from Elkin (2003), © 2003 American Institute of Physics.

Rosalind Franklin has been given numerous posthumous recognitions. Only a few will be mentioned here, including (1) the naming of the Rosalind Franklin Molecular Biology Laboratory at the Birkbeck University of London, School of Science; (2) the Rosalind Franklin Award bestowed annually by the Royal Society for outstanding contributions to any area of science, technology, engineering, or mathematics; (3) the naming of the Rosalind Franklin University of Medicine and Science, Chicago, Illinois, USA; (4) the placing of Rosalind Franklin's portrait alongside those of the 1962 Nobel Laureates Watson, Crick, and Wilkins at the National Portrait Gallery in London; and (5) the establishment of the Rosalind E. Franklin Award bestowed annually by the American National Cancer Institute to honor the commitment of women in cancer research.

Other historic but less dramatic examples of the vital role of X-ray diffraction to scientific development was the determination of the crystal structure of myoglobin, a protein of 153 amino acids, which is the primary oxygen-carrying pigment of muscle tissue. In 1957 John Kendrew (1917–1997) and Max Perutz (1914–2002) determined the structure of myoglobin by high-resolution X-ray crystallography and were awarded the Nobel Prize in Chemistry in 1962. Two years later, Dorothy Hodgkin (1910–1994) was awarded the Nobel Prize in Chemistry in 1964 "for her determination by X-ray techniques of the structures of important biochemical substances [including penicillin and Vitamin B12]."

HENRY G.J. MOSELEY (1887–1915)

Henry Gwyn Jeffreys Moseley was born in Weymouth, England on November 23, 1887. He did not receive the Nobel Prize, because of his untimely death at the age of 27. His contributions to atomic physics and X-ray spectrometry of the elements were of great importance; and it was stated by the Chairman of the Nobel Committee (Gullstrand, 1925), that Moseley would have been awarded the Nobel Prize, if he had survived.

In 1906, Moseley entered Trinity College of the University of Oxford, and graduated in 1910 with a second degree in Physics. Upon graduation he went to Manchester University to work under Ernest Rutherford. At Manchester, he was given a full-time teaching position, but he had ambitions to become a research physicist. After a year of teaching, Moseley was relieved of his duties and allowed to do scientific research. It was in 1911 that W.H. and W.L. Bragg at the University of Leeds were carrying out research in X-ray diffraction, which caught his interest. By the time Moseley started his work, it was known that the diffraction of X-rays by a crystal made it possible to accurately determine the frequencies and wavelengths of x-radiation. In addition, it had been demonstrated that an element would emit its characteristic x-radiation, if excited by a beam of sufficiently fast cathode rays. Moseley devised an apparatus whereby he could bombard individually all of the known and available elements with cathode rays and measure the wavelengths of the X-rays emitted by each element (Moseley, 1913, 1914). To measure the wavelengths (λ), Moseley directed the X-rays at a crystal of potassium ferrocyanide and measured the angle of diffraction (θ) according to Bragg's Law:

$$n\lambda = 2d \sin\theta \qquad \text{[III.53]}$$

Henry Moseley in the Balliol-Trinity Laboratory surrounded by shelves of laboratory equipment, Oxford, England, circa 1910 University of Oxford, Museum of the History of Science, courtesy AIP Emilio Segre Visual Archives, Physics Today Collection

where d is the spacing of the interatomic planes of the crystal ($d = 8.454 \times 10^{-8}$ cm). He determined the order of the diffraction ($n = 1$, 2, or 3…) by imaging the diffracted light on photographic film. Diffraction of the first order ($n = 1$) was more intense than that of the second and third orders. In his first report, Moseley (1913) measured the X-ray emission spectra of 21 elements of increasing numbers of the periodic table of the elements from aluminum to silver and determined the wavelengths of the α and lower-intensity β lines that belong to Barkla's K series. Charles Glover Barkla (1877−1944) identified the x-radiation resulting from atomic electron transitions to the K shell as K X-rays, and X-rays emitted as a result of atomic electron transitions to the L shell as L X-rays. In a subsequent paper, Moseley (1914) measured the wavelengths of the L series of X-ray emissions of 24 elements of increasing numbers of the periodic table of the elements from zirconium to gold. Of the L-series, he measured the wavelengths of α, β, γ, and δ lines of decreasing wavelengths and decreasing intensities. Moseley then plotted the square root of the radiation frequencies or the logarithm of the radiation wavelengths against a characteristic integer (N) assigned to each element. Starting with aluminum, being the 13th element in the periodic table, he assigned aluminum the number N = 13. The next element, silicon, was assigned the next highest integer, N = 14; phosphorus, N = 15; etc. A copy of his plots is illustrated in Fig. III.15. The plots showed an incredibly straight-line relationship between the assigned integer N and the x-radiation frequencies for each element. From this relationship, he concluded the following (Moseley, 1914), with the writer's comments in brackets:

> *Now if either the elements were not characterized by these integers or any mistake had been made in the order chosen, or in the number of places left for unknown elements [places for three unknown elements in the periodic table were found, see Fig. III.15], these irregularities would at once disappear. We can therefore conclude from the evidence of the x-ray spectra alone, without using any theory of atomic structure, that these integers are really characteristic of the elements. Further, as it is improbable that two different stable elements should have the same integer, three, and only three, more elements are likely to exist between Al and Au. As the x-ray spectra of these elements can be confidently predicted, they should not be difficult to find…Now Rutherford has proved that the most important constituent of an atom is its central positively charged nucleus, and van der Broek has put forward the view that the charge carried by this nucleus is in all cases an integral multiple of the charge on the hydrogen nucleus. There is ever reason to suppose that the integer which controls the x-ray spectrum is the same number of electrical units in the nucleus…*

From Moseley's discovery as stated above, it was clear that his number N could be identified with the atomic number Z, which is the number of protons in the nucleus. The atomic number, therefore, was a meaningful number with respect to atomic structure, and not just an arbitrary number assigned to an element in the periodic table of elements. Also, this number was related to the electron distributions about the atom according to Bohr Theory. Another outcome of this work was Moseley's confident identification of three gaps or missing elements in the periodic table, namely elements of atomic

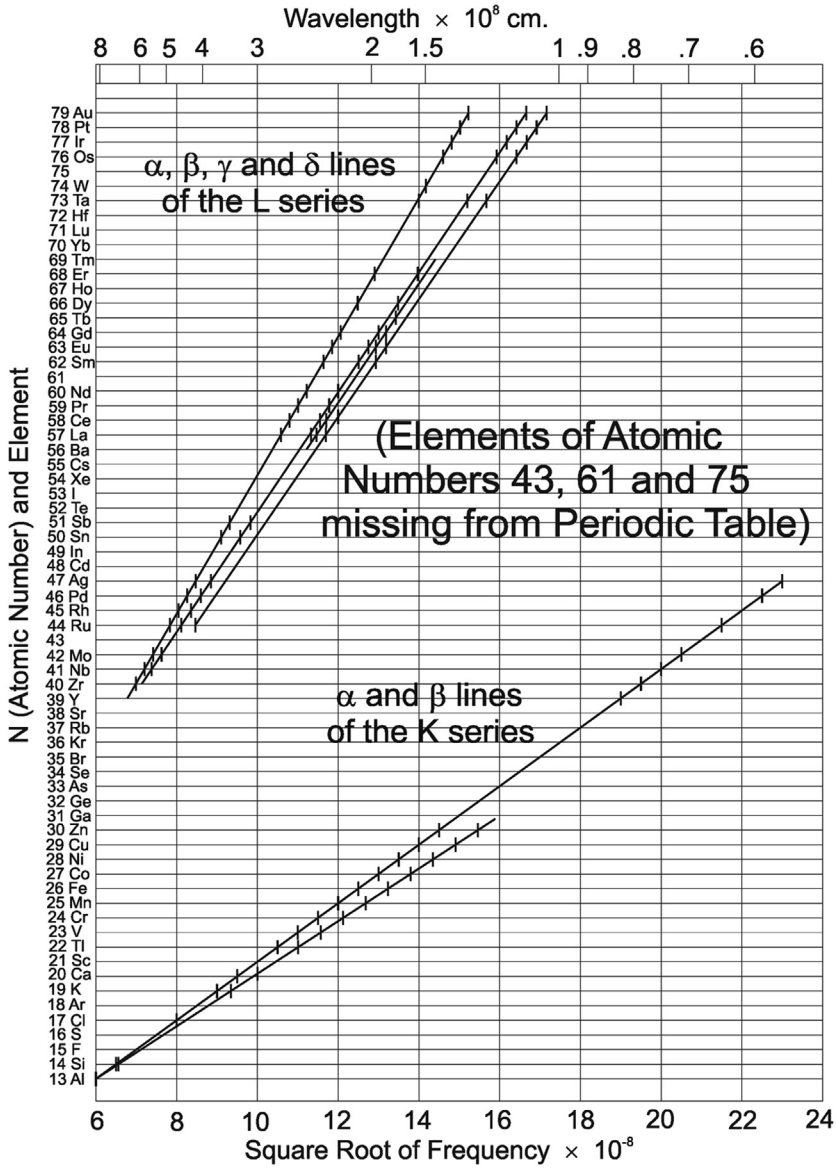

FIGURE III.15 Artist's portrayal of Moseley's original 1914 graph of the frequencies and wavelengths of X-rays emitted by all of the then-known elements plotted against each element and an integer N assigned to each element from Aluminum (Al, assigned N = 13) to Gold (Au, assigned N = 79). Three missing and yet-unknown elements are listed with blank spaces adjacent to integers N = 43, 61, and 75. The two lines of the lower curves (elements N = 13−47) are X-rays resulting from α and β lines of the *K* series of electron transitions; and the four lines of the upper curves (elements N = 40−79) are X-rays resulting from α, β, γ, and δ lines of the L series of electron transitions. *From Moseley, H.G.J., 1914. The high frequency spectra of the elements. Phil. Mag. 27 (2), 703−713. The original Moseley graph, drawn by his own hand, may be seen in the Moseley Room of the Cavendish Laboratory, University of Oxford.*

numbers 43, 61, and 75. Moseley could predict that there were three elements missing from the periodic table and yet to be discovered. Two of these elements were technetium ($Z = 43$) and promethium ($Z = 61$), both of which are radioactive and made artificially. Technetium was the very first element to be made artificially and discovered in Italy by Carlo Perrier and Emilio Segre (Perrier and Segre, 1937). Promethium was identified as a product of uranium fission in 1945. The third element predicted by Moseley ($Z = 75$) was the stable natural element rhenium, which was discovered eventually in 1925 in platinum ores. Another outcome from Moseley's work was the potential of identifying or analyzing any element in the periodic table from its X-ray emissions.

The same month of Moseley's first publication of 1913 relating X-ray emission frequencies to the atomic number of the element, Rutherford wrote a letter to the editor of the journal *Nature* on December 11, 1913 (Rutherford, 1913), which

underscored the importance of Moseley's findings as related to the structure and properties of the atom. In his letter Rutherford stated the following:

> *The original suggestion of van der Broek that the charge of the nucleus is equal to the atomic number and not to half the atomic weight seems to me very promising. This idea has already been used by Bohr in his theory of the constitution of atoms. The strongest and most convincing evidence in support of this hypothesis will be found in a paper by Moseley in* The Philosophical Magazine *of this month. He there shows that the frequency of the X radiations from a number of elements can be simply explained if the number of unit charges on the nucleus is equal to the atomic number. It would appear that the charge on the nucleus is the fundamental constant which determines the physical and chemical properties of the atom,…*

In his above letter, Rutherford came close to predicting the proton as the source of the positive charge on the nucleus. It would be only 6 years later that Rutherford would discover the proton. (See Rutherford in Hall of Fame, Part I.)

In 1914, Henry Moseley had planned to return to Oxford to continue his research, but the First World War broke out, and he volunteered for active service against the advice of family and of the Army itself (Clarendon Laboratory Archive, Oxford Physics). He served under the Royal Engineers and was killed on the Gallipoli Peninsula on August 10, 1915 at the age of 27 years. It is said that World War I was an unjustified war solely on the basis of the loss of Henry Moseley. As evidenced from his work as a budding scientist, we can only imagine the additional contributions and advancements to science that he could have made, had he lived. He had accomplished more in about 3 years of research than most could accomplish in a lifetime, and his findings were worthy of the Nobel Prize. The significance of Moseley's work was underscored by the Chairman of the Nobel Committee on December 10, 1925 (Gullstrand, 1925) when he stated:

> *He [Moseley] discovered the simple mathematical law by means of which the frequencies determined by the position of the lines — and consequently the corresponding wavelengths — can be obtained by what is known as the atomic number, i.e. the number of the element in a series in which all the elements are arranged with a generally increasing atomic weight. As the atomic number has proved to distinguish the elements better than the atomic weight, it has now attained the very greatest importance for atomic physics of the present day. Moseley fell at the Dardanelles before he could be awarded the prize, but his researches had directed attention to the merits of Barkla, who consequently in 1918 was proposed for the Nobel Prize, which was awarded to him without delay.*

The Museum of the History of Science in Oxford has some of Moseley's original experimental apparatus. The original graph, artistically approximated by Fig. III.15, published by Moseley in the *Philosophical Magazine* in 1914, is in the Moseley Room of the Clarendon Laboratory.

CHARLES GLOVER BARKLA (1877–1944)

Charles Glover Barkla was born in Widness, Lancashire, England on June 7, 1877. He was awarded the Nobel Prize in Physics in 1917 "for his discovery of the characteristic Röntgen radiation of the elements."

Charles Glover Barkla (1877-1944)

Charles Barkla was educated at the Liverpool Institute and he received his university degree in physics in 1898 with first-class honors at the University College Liverpool followed by a master's degree the following year. In 1899 he received a scholarship, which enabled him to work in the Cavendish laboratory with J.J. Thomson at Trinity College, Cambridge. In

1900 Barkla moved to King's College, and in 1902 he returned to the University College Liverpool. He was promoted at the University in Liverpool from 1905 to 1909 from demonstrator to assistant lecturer in physics, and special lecturer in advanced electricity. In 1909 he became Wheatstone Professor of Physics at the University of London. In 1913, Barkla was awarded the Chair in Natural Philosophy at the University of Edinburgh, which he occupied for the remainder of his life.

Barkla devoted most of his scientific career to the study of X-rays. Among his many contributions is the finding that when X-rays (eg, from an X-ray tube) traverse matter of any kind, the matter becomes a source of x-radiation similar to the primary radiation used to bombard the matter. He found that this secondary radiation, also referred to as scattered x-radiation, displayed a definite degree of polarization with respect to the primary X-rays originating from an X-ray tube. He thus demonstrated that X-rays consist of oscillating waves in different directions and these could be separated or polarized. Thus X-rays had properties similar to light.

His most significant contribution was the discovery that each element has its own line spectrum in the X-ray region. That is, when any substance is irradiated by X-rays, it emits x-radiation characteristic of the elements in the substance. He found that, upon bombardment by an X-ray beam, the line spectra or X-ray energies emitted by any element are characteristic of that element irrespective of the chemical composition of the substance within which the element may be found. This formed the basis for the analytical technique known as X-ray fluorescence. In his Nobel lecture presented on June 3, 1920, Barkla explained his findings as follows:

> *Each element when traversed by x-rays emits x-radiations characteristic of the element; each characteristic radiation is unaffected by changes in the physical condition or state of chemical combination of the radiating element, and its quality is independent of that of the exciting primary radiation. But only primary radiations of shorter wavelength are able to excite the characteristic x-radiations…all of the radiations hitherto definitely observed have fallen into three series, the K-, L-, and M-series [the M-series was discovered by Siegbahn and his collaborators].*

The K-, L- and M-series referred to by Barkla are X-ray lines emitted by atoms of elements as a result of atomic electron energy transitions from outer to inner shells. Electron transitions to the K shell belong to the K-series, transitions to the L shell belong to the L-series, etc. Barkla's findings provided important information regarding the concept of the atomic structure, as they provided evidence for electron energy levels. Prof. G. Granqvist, Chairman of the Nobel Committee, noted in his presentation speech:

> *Barkla's discovery, that two domains of differing hardness are to be differentiated in the characteristic radiation, is of fundamental importance as regards the modern conception of the structure of atoms. Barkla has named the two domains the K-series and the L-series respectively. Thus every chemical element, when irradiated by x-rays, emits two rays of different penetrability, that is to say, every element can by fluorescence emit an x-ray spectrum of two lines or line-groups, the so-called K-series and L-series. Of these the K-series have the greater penetrability.*

In addition to grasping the X-ray fluorescence data to provide information concerning energy levels of electrons, Barkla went further to obtain experimental data on X-ray absorption to obtain information on the number of electrons per atom. First he determined that the secondary radiation resulting from X-ray bombardment of matter consisted of two types, namely, electrons and X-rays of the K- and L-series. X-rays of the primary radiation were colliding with atomic electrons and liberating them from the atom by mechanisms such as the photoelectric effect. This caused electron vacancies in the atoms, which would be filled by electrons from outer shells to yield the secondary K- and L-series X-rays. He then utilized the following equation derived by J.J. Thomson, which describes the fraction (f) of a primary X-ray beam lost by scattering per centimeter of substance traversed to determine the number of electrons per atom of element bombarded by X-rays:

$$f = \frac{8\pi}{3} N \frac{e^4}{m^2} \mu^2 \qquad \text{[III.54]}$$

where N is the number per cubic centimeter of particles of charge e and mass m. With precise measurements of N, e/m, and e, the calculated values for the number of electrons per atom were as noted in his Nobel lecture:

> *one electron per atom of hydrogen, 6 per atom of carbon, 7 per atom of nitrogen, 8 for oxygen, 15 or 16 for sulfur, and so on. As these conclusions regarding the number of electrons (outer electrons) within the atom have been confirmed by the researches of Rutherford, Bohr and Moseley, it is perfectly legitimate to use the agreement as evidence in support of the theory of radiation upon which it was based*
>
> Nobel Lectures, Physics 1901–1921.

Barkla died at Braidwood, Edinburgh on October 23, 1944 the year after the death of his youngest son Flight Lieutenant Michael Barkla, also a brilliant scholar, who was killed in action in World War II.

MANNE SIEGBAHN (1886–1978)

Karl Manne Georg Siegbahn was born in Örebro, Sweden on December 3, 1886. He was awarded the Nobel Prize in Physics in 1924 "for his discoveries and research in the field of X-ray spectroscopy."

Siegbahn (1886-1978)

Manne Siegbahn received his doctorate in physics at the University of Lund in 1911. During his years as a graduate student he served as assistant to Johannes (Janne) Robert Rydberg in the Physics Institute of Lund University. After receiving his doctorate degree, he was appointed lecturer and in 1915 deputy professor of physics. Following the death of Rydberg in 1919, Manne Siegbahn was appointed full professor at Lund in 1920. He became professor of physics at Uppsala University in 1923 and research professor of experimental physics at the Royal Swedish Academy of Sciences in 1937. From 1937 to 1964 he served as Director of the Nobel Institute of Physics in Stockholm.

Siegbahn's major discoveries were obtained from research in the field of X-ray spectroscopy during the years 1912 to 1937. Research on x-radiation at this time, in addition to applications in medicine, were focused in two directions, namely, (1) the use of X-rays to research the structures of crystalline lattices as pioneered by Sir William and Sir Lawrence Bragg; and (2) spectral investigation of the x-radiation itself pioneered by Manne Siegbahn, which would provide much information on the electronic structure of the atom. He firstly made many improvements that would facilitate the study of the X-ray spectral lines including the design of improved vacuum pumps and X-ray tubes that yielded more intense x-radiation together with the construction of improved crystal and linear gratings, which provided increased accuracy of measuring X-ray spectral frequencies or wavelengths. Siegbahn thus brought X-ray spectroscopy to a new level, which would provide new information on the electron within the structure of the atom, and the characteristic X-ray emissions of the elements. The contributions of Siegbahn were highlighted in the Nobel presentation speech of Prof. A. Gullstrand, Chairman of the Nobel Committee for Physics on December 10, 1925 (Gullstrand, 1925) when he stated:

> *It had already become clear that the x-radiation must arise in the inner parts of the atoms, and that consequently exact spectroscopic investigations form the only means for an experimental research of those parts. Clearly perceiving this fact, Siegbahn has in the course of ten years' assiduous and systematic labor devised a series of improvements and new designs dealing with almost every detail of the various apparatus and so constantly increased the exactitude of his measurements…The high level to which he has brought x-ray spectroscopy can perhaps be best defined by the statement that the exactitude with which wavelengths can now be measured by his methods is a thousand times greater than that attained by Moseley. It was only to be expected that these more accurate means would in his hands be used for a series of new discoveries. Thus to begin with, he has found a large number of new lines in the K- and L-series. Moreover he has made the experimental discovery of a new characteristic x-radiation, the M-series; and another such radiation, the N-series…*

Moseley had originally identified two K-lines and four L-lines (see Moseley in this Part III of the Hall of Fame). Manne Siegbahn, 10 years later, identified many new lines of X-ray frequencies or energy quanta within the different series for the known 92 elements. He subjected 42 elements to a fresh investigation of the K-series and identified four lines of the K-series for 27 elements and even eight fainter lines for the lighter elements. Of the L-series, he identified 28 lines for some 50 elements. A new M-series was discovered by Siegbahn for 16 elements and another new N-series was measured for three of the heaviest elements, which included five lines belonging to uranium and thorium.

Manne Siegbahn's work provided much insight into the role of the electron in the structure of the atom. The wavelengths or frequencies of the various lines reflected the energy quanta emitted by the X-rays and consequently the energy states of the electrons in the K-, L-, M-, and N-orbitals of the elements. The impact of the findings of Siegbahn on our knowledge of the electron configurations in the atom was emphasized in the Nobel Prize presentation Speech (Gullstrand, 1925) with the statement:

In an element that can emit both K-and L-rays, the former radiation has much shorter wavelengths and consequently greater frequencies than the latter. As the energy quanta are proportional to the frequencies, therefore, the K radiation involves a larger change in the energy of the atom than the L radiation; and in the atomic theory this is as much as to say that an orbit into which an electron falls on emission of a K-line must lie nearer the nucleus than an orbit to which an electron falls on emission of an L-line. In this way it was inferred that there is a K-level nearest the nucleus, outside that an L-level, and after that an M-level and an N-level, all these four being experimentally determined [by Manne Siegbahn].

In his Nobel lecture, Manne Siegbahn explained the various lines of X-ray emission by the elements as electron rearrangements within the atom. He stated:

Let us assume that at a given moment a certain atom is in such state that its total energy has the value E_t. *At that moment a rearrangement occurs within the atom which has the effect of reducing the total energy to* E_0. *In the course of the process of rearrangement the quantity of energy liberated is therefore:*

$$h\nu = E_t - E_0 \qquad \text{[III.55]}$$

According to the Einstein–Bohr formula there is thus a relationship between the frequency ν_1 *for the wave and the energy liberated from the atom:*

$$\nu_1 = \frac{E_1 - E_0}{h} \qquad \text{[III.56]}$$

where h *is Planck's constant. We can therefore imagine that the energy of the atom during [another] rearrangement of this nature, is then changed from* E_2 *to* E_0 *during which a wave frequency* ν_2 *is emitted. Thereby:*

$$\nu_2 = \frac{E_2 - E_0}{h} \qquad \text{[III.57]}$$

The series can be continued further:

$$\nu_3 = \frac{E_3 - E_0}{h}, \text{ and so on.} \qquad \text{[III.58]}$$

By measuring the wavelengths it is possible experimentally to determine a series of ν*-values:* ν_1, ν_2, ν_3,*…It would, however, require a special and not always simple analysis of the wavelengths available in order to select and bring together those frequency values which belong to one and the same series.*

Manne Siegbahn measured X-ray spectra lines for the K-, L-, M-, N-series for the 92 elements and, even for the heaviest elements, the O-, and P-series (X-ray lines from electron transitions to the O- and P-orbitals). He confirmed that X-ray emissions from atoms are the result of electron transitions in atomic orbitals. In his Nobel lecture he explained the mechanism of X-ray emission by the elements and the relevance of these findings to our understanding of the atom as follows:

For the x-ray spectra, too, we must assume that light emission takes place when an electron, but in this instance one belonging to the inner electron system of the atom, moves from one quantum orbit to another while the state of all the remaining electrons is not altered to any significant extent…x-ray spectroscopy measurements provide us with a quantitative and thorough knowledge of the energy content and energy relationships within each particular atom. Any further work on the structure of the atom must rest upon this firm, empirical foundation.

Later in life, as Director of the Nobel Institute of Physics in Stockholm (1937–1962), Manne Siegbahn oversaw much scientific research toward problems in nuclear physics, and he lectured extensively in the most prestigious scientific research institutes of Europe, the United States, and Canada. His son Kai Siegbahn (born 1918) followed in his footsteps by occupying the Chair of the Physics Department of Uppsala University (since 1954), and by winning the Nobel Prize in Physics 1981.

Manne Siegbahn died in Stockholm, Sweden on September 26, 1978.

ROBERT A. MILLIKAN (1868–1953) AND HARVEY FLETCHER (1884–1981)

The biographical sketches of Robert Millikan and Harvey Fletcher are included jointly here, because a major contribution to the field of atomic physics, namely, the determination of the charge on the electron, was carried out with the joint efforts of Millikan and his graduate student Fletcher. A review of the memoirs of Millikan and Fletcher is provided by Perry (2007), who concludes from the differences in the autobiographical accounts that it is uncertain who deserves most credit for the determination of the charge on the electron, Millikan or Fletcher. In other words, both deserve credit for this important finding.

Robert Andrews Millikan was born in Morrison, Illinois, USA on March 22, 1868. He was awarded the Nobel Prize in Physics in 1923 "for his work on the elementary charge of electricity and on the photoelectric effect."

Milliken (1868-1953)

Millikan was a descendant of New England settlers, who had come to America before 1750 and who were pioneer settlers in the Middle West. He was brought up in a rural environment, attending Maquoketa High School in Iowa. In 1891 he graduated from Oberlin College in Ohio with major studies in Greek and Mathematics. At Oberlin he taught himself physics, as he was disappointed with the content or scope of the short physics course that the college offered at the time. After graduation, Millikan accepted a teaching post in physics for 2 years mostly for the need of money, and during this time he developed an interest in physics, which would become his lifelong passion. Millikan continued his education at Columbia University, and was appointed a fellow in physics after receiving a master's degree at the university. He was awarded the PhD degree in physics at Columbia in 1895. The following year Millikan studied at the Universities of Berlin and Göttingen, as it was popular and thought advisable then for Americans to study advanced physics in Germany. Upon the invitation of A.A. Michelson, he returned to take on a position as a teaching and research assistant at the University of Chicago in 1896. He taught class with a passion becoming an eminent educator and author of several textbooks on physics for both high school and college students. As noted by the American Institute of Physics, Millikan only became an associate professor at the age of 38 when, on average, an American physicist with published research would become professor at the age of 32. He later recalled:

> *Although I had for ten years spent on research every hour I could spare from my other pressing duties, by 1906 I knew that I had not yet published results of outstanding importance, and certainly had not attained a position of much distinction as a research physicist.*

Millikan thus decided to curtail his writing of textbooks and make one great effort to make his mark in physics by accurately measuring the charge carried by an electron, which he and Harvey Fletcher successfully accomplished by 1910 (Millikan, 1911); and Milliken improved the measurements with greater precision 2 years later (Millikan, 1913), demonstrating once and for all the elementary particulate nature of the electron and electricity. He was awarded full

professorship at the University of Chicago shortly after his first publication on the elementary electrical charge. He subsequently went to work earnestly to disprove Einstein's concept of the photon as an elementary particle in the photoelectric effect, and after 10 years of effort by 1921 (Millikan, 1914, 1916a,b, 1921) all of his research in this direction proved to be a great contribution to physics, because it gave more credence to Einstein's light quantum or photon. Millikan was thus awarded the Nobel Prize in Physics in 1923 for his dual contribution on his measurement of the elementary charge of electricity and the photoelectric effect.

The significance of Millikan's work on the charge of the electron was highlighted by Prof. A. Gullstrand, Chairman of the Nobel Committee (Gullstrand, 1923), when he stated:

> *Millikan's aim was to prove that electricity really has the atomic structure, which, on the base of theoretical evidence, it was supposed to have. To prove this it was necessary to ascertain, not only that electricity, from whatever source it may come, always appears as a unit of charge or as an exact multiple of units, but also that the unit is not a statistical mean, as, for instance, has of late been shown to be the case with atomic weights. In other words it was necessary to measure the charge of a single ion with such a degree of accuracy as would enable him to ascertain that this charge is always the same, and it was necessary to furnish the same proofs in the case of free electrons. By a brilliant method of investigation and by extraordinary exact experimental technique Millikan reached his goal.*

To prove the nature and charge of the electron, Millikan and Fletcher devised their famous oil-drop experiment. They devised the apparatus, illustrated in Fig. III.16, which contains two horizontal metal plates separated by a short distance and joined only by an electric field of about 6000 V/cm. The air between the plates was ionized by means of X-rays or suitable radioactive source.

The positively charged upper plate contained a pinhole in its very center, over which an atomizer was arranged to spray minute oil droplets with a radius of approximately 1/1000 of a millimeter. Eventually one of the oil droplets would fall through the pinhole and enter the region between the plates. The space between the plates was illuminated so that Millikan and Fletcher could observe the oil droplet with a telescope. The oil drop would appear in the telescope as a bright star with a dark background. The eyepiece of the telescope contained cross-hairs so that Millikan and Fletcher could measure the time that the droplet needed to pass between each cross-hair and thereby measure the velocity of fall of the oil drop, which would be only a fraction of a millimeter per second. The oil droplet would be charged with electricity from the friction produced during the droplet formation by the atomizer. When the drop would fall and approach the lower plate, Millikan and Fletcher would switch on the electric field so that the drop would rise through the attractive forces of the positively charged upper plate. The velocity of rise of the droplet was measured with the telescope. After its rise, the charge to the plates would be turned off, and the oil drop would begin to fall again. The fall and rise of the drop could be repeated many times during a period of several hours by simply connecting or short-circuiting the charge to the metal plates, and each time Millikan and Fletcher could repeat the measurements of the velocity of fall or velocity of rise by use of a stopwatch or chronometer. The velocity of fall of the oil droplet was always constant, but its velocity of rise would vary and increase

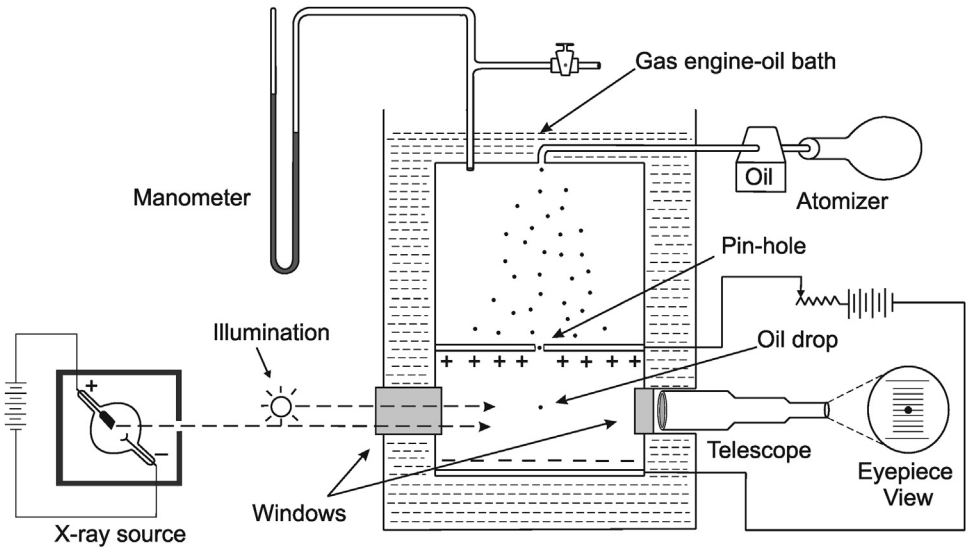

FIGURE III.16 Schematic of the Millikan–Fletcher oil-drop apparatus.

according to the amount of charge that the droplet had acquired from the ionized air between the plates. X-rays directed into the space between the plates would produce ionized air, and the oil droplet would rise at a velocity that would increase proportionally to the charge it had acquired. The droplet would increase in velocity upwards by a certain value or an exact multiple of that value. Thus, Millikan and Fletcher could demonstrate that the oil droplet had acquired one or more units of electrical charge, each charge of exact equal strength. They were thus able to measure the charge of a single ion with a precision of 1 in a 1000. Some experimental data presented by Millikan in his Nobel lecture on May 23, 1924, provided in Table III.1, illustrate how exact were the measurements of the multiples of velocity of rise.

With reference to the data provided in Table III.1, Millikan commented:

> *…speeds exactly two times, three times, four times, five times, etc. (always within the limits of observational error − still less than a percent) could be communicated to the droplet, but never any fraction of these speeds. He who has seen that experiment, and hundreds of investigators have observed it, has literally seen the electron. For he has measured (in terms of speed) the smallest of the electrical forces, which a given electrical field ever exerts …by its aid [the experiment] he can count the number of electrons in a given small electrical charge with exactly as much certainty as he can attain in counting his fingers and his toes…but the electron itself, which man has measured, as in the case shown in the table, is neither an uncertainty nor an hypothesis. It is a new experimental fact that this generation in which we live has for the first time seen, but which anyone who wills may henceforth see.*

Millikan and Fletcher applied Stokes' law and the oil-drop velocity of free-fall under gravity and oil-drop velocity of rise in an electric field to calculate the exact charge on the electron in terms of electrostatic units, which can be converted to coulombs, which is the SI unit for electric charge. Stokes' law, which was discovered by George Stokes (1819−1903), predicts the drag or frictional force D that is exerted on a spherical ball moving through a viscous medium. It is defined by the equation:

$$D = 6\pi a\eta v \qquad \text{[III.59]}$$

where the variable a is the radius of the sphere or droplet, η is the viscosity of the medium, and v is the velocity of the ball or droplet. Millikan and Fletcher had to apply a correction factor to the equation, because of the very small radius of the oil droplets they created and the fact that the droplet would fall or rise is an almost frictionless evacuated chamber. They then defined the forces acting on the oil droplet during its free-fall when the electric field was turned off and during its rise when the electric field was turned on. These forces are illustrated in Fig. III.17, where b according to Stokes' law is the drag force

TABLE III.1 Velocities of Rise (Electric Field On) and Fall (Electric Field Off) of Oil Droplets

Time of Fall 1.303 cm Under Gravity (s)	Time of Rise 1.303 cm in Field (s)	Mean Times of Rise in Field (s)	Divisors for Speeds Due to Field	The Electron in Terms of Speed
120.8	26.2			
121.0	11.9			
121.2	16.5	67.73	1	3.007
120.1	16.3	26.40	2	3.009
120.2	26.4	16.50	3	2.993
119.8	67.4	11.90	4	3.008
120.1	26.6			
–	16.6			
120.2	16.6	Mean time of fall under gravity = 120.35		
–	16.4			
120.2	68.0			
119.9	67.8			
–	26.4			

From Millikan, R.A., 1924. The electron and the light-quant from the experimental point of view. Nobel Lecture, May 23, 1924. In: Nobel Lectures, Physics 1922−1941. (1965). Elsevier Publishing, Amsterdam, with permission from the Nobel Foundation © 1924.

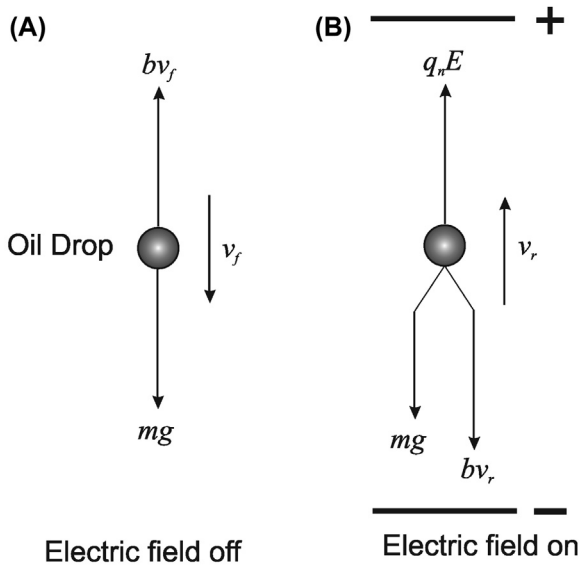

FIGURE III.17 Forces defining (A) the velocity of free-fall, v_f, of the oil drop in the absence of an electric field, and (B) the velocity if rise, v_r, of the oil drop in the presence of an electric field.

proportional to the velocity of the droplet, m is the droplet mass, g is the acceleration due to gravity, q_n is the charge on the droplet, and E is the electric field strength.

When the electric field of Millikan and Fletcher's apparatus is turned off, the oil drop will fall with the velocity v_f, under the force of gravity mg, against the drag force defined by Stokes' law, $D = bv_f$, and when the electric field is turned on, the oil droplet would rise with the velocity v_r, proportional to the electric charge on the droplet, q_n and the electric field strength E, and against the gravitational and drag forces. Millikan and Fletcher derived the equation for calculating the charge on the electron by defining the velocities of fall and rise of the droplet in the absence and presence of an electric field according to the following:

(A) With the electric field off, the oil drop is static when:

$$bv_f = mg \qquad \text{[III.60]}$$

and the drop will fall with a velocity:

$$v_f = \frac{mg}{b} \qquad \text{[III.61]}$$

(B) With the electric field on, the oil drop remains static when:

$$q_nE = mg + bv_r \qquad \text{[III.62]}$$

and the drop rises with the velocity:

$$v_r = \frac{(q_nE - mg)}{b} \qquad \text{[III.63]}$$

Millikan and Fletcher solved Eqs. [III.61] and [III.63] to provide the working equations defining the charge on the electron as:

$$q_n = \frac{mg}{Ev_f}(v_f + v_r) \qquad \text{[III.64]}$$

or:

$$q_n = \frac{mgt_f}{E}\left(\frac{1}{t_f} + \frac{1}{t_r}\right) \qquad \text{[III.65]}$$

where q_n is the unit charge on the electron, and t_f and t_r are the respective times required for the oil drop to fall under gravity and to rise under the electric field E. If the electron acquires more than one unit of charge in the ionized air of Millikan and Fletcher's apparatus, the oil drop would rise at a higher velocity while its rate of fall in the absence of the electric field always remained constant. Therefore, Millikan and Fletcher defined the equation for the charge on the electron that rose at the faster rate, due to additional units of charges acquired, as:

$$q_{n+n'} = \frac{mgt_f}{E}\left(\frac{1}{t_f}+\frac{1}{t'_r}\right) \qquad \text{[III.66]}$$

Eq. [III.66] would yield various values for the charge on the electron that would be successive multiples of the unit charge on the electron, as defined by Eq. [III.65]. This was explained by Millikan in his classic paper in *The Physical Review* (Millikan, 1913) as follows:

> *Now Eqs. (11) and (12) (Eqs. [III.65] and [III.66]) show, since* $\mathrm{mgt_f/E}$ *remains constant, that, as the drop changes charge, the successive values of its charge are proportional to the successive values assumed by the quantity* $(1/t_f + 1/t_r)$ *and the elementary charge itself is obviously this same constant factor* $\mathrm{mgt_f/E}$ *multiplied by the* greatest common divisor *of all these successive values.*

From the experimental data measured from 23 oil drops, Millikan calculated the electron charge, q, which he represented with the symbol e as follows:

$$e = 4.774 \pm 0.009 \times 10^{-10} \text{ electrostatic units},$$

which is expressed currently in the SI unit of coulombs (C) as:

$$e = 1.602 \times 10^{-19} \text{ C}$$

As Millikan was able to provide a most precise measurement of the electron charge, he was also able to report (Millikan, 1913) new and more precise calculated values of several other physical constants including the Avogadro constant (N_A), which he recalculated from the Faraday constant ($F = N_A e$) and Planck's constant (h).

Millikan could not accept at first Einstein's interpretation of the photoelectric effect, that is, Einstein's concept of the photon as an elementary particle or "quantum of light" that could collide, as a particle. The photoelectric effect was a proven phenomenon (see Lenard in Radioactivity Hall of Fame, Part I) whereby a photon of light collides with an atomic electron in a substance, such as a metal surface to cause the electron to be emitted as a free electron with the same energy as the photon (less the small binding energy of the electron in the atom from which it came); however, for over a decade Millikan could not come to terms with Einstein's concept of the corpuscular nature of light. He thus devoted about 10 years of research to disprove Einstein's concept. In his Nobel lecture, Millikan commented:

> *This…semicorpuscular conception of localized radiant energy was taken up in 1905 by Einstein who, by combining it with the facts of quanta discovered by Planck through his analysis of black-body radiation, obtained an equation which should govern, from his viewpoint, the interchange of energy between waves and electrons, viz.* $\frac{1}{2}\mathrm{mv}^2 = \mathrm{h}\nu - \mathrm{A}$ *(Einstein equation), the first term representing the energy with which the electron escapes, the second term Planck's energy quantum for the particular light employed, and the last the work necessary to get the electron out of the metal. After 10 years of testing and changing and learning and sometimes blundering, all efforts being directed from the first toward the accurate experimental measurement of the energies of emission of photoelectrons, now as a function of temperature, now of wavelength, now of material, this work resulted, contrary to my own expectation, in the first direct experimental proof in 1914 of the exact validity, within narrow limits of experimental error, of the Einstein equation, and the first direct photoelectric determination of Planck's* h*…In view of all these methods and experiments the general validity of Einstein's equation is, I think, now universally conceded, and to that extent the reality of Einstein's light-quanta may be considered as experimentally established. But the conception of localized light-quanta out of which Einstein got his equation must still be regarded as far from being established.*

From the last sentence of Millikan's statement taken from his Nobel lecture given on May 23, 1924, he still could not accept Einstein's concept of the photon, even after proving many times over the validity of Einstein's equation and Planck's constant. However, in his autobiography published in 1950, Millikan admitted to eventually yielding to universal thinking and accepted Einstein's conception of the photon, as a chapter in his autobiography (Millikan, 1950) is titled "The Experimental Proof of the Existence of the Photon—Einstein's Photoelectric Equation."

Because of the extensive experimental research that Millikan put into the photoelectric effect, the Nobel Committee decided to award the Nobel Prize in Physics in 1921 to Albert Einstein in the words of the Nobel Committee "especially for his discovery of the law of the photoelectric effect." The Nobel Committee acknowledged that

Millikan's extensive experimental research on the photoelectric effect convinced them to award the prize to Einstein. This was clearly admitted when Prof. A. Gulstrand, Chairman of the Nobel Committee, stated in the Nobel presentation speech of 1923:

> *In justifying the reward of Millikan the Academy has not omitted to refer also to his investigations of the photoelectric effect. Without going into details I will only state that, if these researches of Millikan had given a different result, the law of Einstein would have been without value, and the theory of Bohr without support. After Millikan's results both (Einstein and Bohr) were awarded a Nobel Prize for Physics last year.*

Millikan remained professor at the University of Chicago until 1921. In 1921 he was appointed Director of the Norman Bridge Laboratory of Physics at the California Institute of Technology (Caltech), Pasadena and made Chairman of the Executive Council of the Institute, a post he held until his retirement in 1946 (*Nobel Lectures, Physics 1922–1941*, 1965). It was George Ellery Hale (1868–1938), the famed astronomer and astrophysicist of the time, who lured Millikan to join him at the new California Institute of Technology. Under Millikan's guidance, Caltech soon became one of the top American centers of research. At Caltech, Millikan pioneered research on the phenomena that he named "cosmic rays." He designed many small electroscopes and Geiger–Müller detectors of cosmic radiation that could be taken on aircraft and high-altitude balloons, and contributed much to our knowledge of the latitude effect of cosmic radiation at high altitudes (Millikan and Bowen, 1926; Millikan and Cameron, 1928; Millikan and Neher, 1935; Bowen et al., 1934, 1936, 1937; see also chapter: Cosmic Radiation). He stubbornly insisted that cosmic rays consisted in whole or in large part of electromagnetic radiation (American Institute of Physics), contrary to the belief of others, such as Arthur Compton, who considered cosmic rays to consist mostly of charged particles. Even to this day some tables of electromagnetic radiation wavelengths and frequencies still equate cosmic rays with gamma rays. See the chapter entitled "Cosmic Radiation" for information on cosmic rays.

Millikan died on December 19, 1953 in San Marino, California. During the early 1980s his reputation was tarnished with accusations of having swindled his graduate student, Harvey Fletcher (1884–1981) out of credit for the oil-drop experiment (Kirkham, 1982; Schroeder, 1982; Halevi, 1982; Brower, 1985). Harvey Fletcher wrote a manuscript autobiography that included an account of his work in the famous oil-drop experiment for which his thesis advisor, Robert A. Millikan, won, in part, the Nobel Prize in 1923. Fletcher wrote the manuscript with instructions that it be published only posthumously, so there would be no doubt that Fletcher had no personal interest motivating its publication. Harvey Fletcher's account of his work with Millikan on the oil-drop experiment was published in *Physics Today* in June, 1982 (Fletcher, 1982).

In his memoir on the oil drop experiment, Fletcher (1982) accounts that after Millikan assigned him the thesis work of finding a liquid substance other than water to be used for the determination of the charge of the electron (e), Fletcher went immediately to design a crude oil-drop apparatus. In his autobiography Fletcher relates the following (with the author's comments in brackets):

> *I went immediately to find Millikan [after Fletcher had set up the initial crude oil-drop apparatus], but could not find him so I spent the rest of the day playing with these oil droplets and got a fairly reasonable value of* e *before the day ended. The next day I found him. He was very much surprised to learn that I had a setup that was working. He came down to the laboratory and looked through the telescope and saw the same beautiful sight of the starlets jumping around that I had already seen and have described above. He was very much excited, especially after turning on the field. After watching for some time he was sure we could get an accurate value of* e *by this method. He stopped working with Begeman [another graduate student with whom Millikan was working on the possibility of utilizing water droplets and an expansion cloud chamber to determine* e*] and started to work with me. We were together nearly every afternoon for the next two years…My name ran right along with Professor Millikan's in the newspapers…This was all great publicity, but I began to wonder if this work was to be my thesis as Millikan had promised at that first conference in December 1909. However, during the spring of 1910 we started together writing a paper to be published about this new research. I wrote more of it than he did, particularly about the modification of Stokes' law and the arrangements of the data…All the time I thought we were to be joint authors…Phyllis [Fletcher's daughter] was born 21 May 1910, and as you will see, that is about the time, we finished this first paper [on the electron charge and the correction of Stokes' Law]. When she was about one month old, I was babysitting with her as Lorena [Fletcher's wife] had gone out somewhere with some of her friends. Answering a knock, I went to the door and was surprised to see Millikan. I wondered why he had come to our humble apartment. I soon found it was to decide who was to be the author of the paper [on the charge of the electron and the correction to Stokes' Law]. There were four other papers in the formative stage that were coming out of these oil-drop experiments and I had expected*

they would all be joint papers. He said that if I used a published paper for my doctor's thesis that I must be its sole author. The five papers on which we did the experimental work together were:

- *"The Isolation of an Ion: A Precision Measurement of Its Charge, and the Correction of Stokes' Law."* Science*, September 30, 1910—Millikan.*
- *"Causes of Apparent Discrepancies and Recent Work on the Elementary Electrical Charge."* Phys. Z.*, January 1911—Millikan and Fletcher.*
- *"Some Contributions to the Theory of Brownian Movements, with Experimental Applications."* Phys. Z.*, January 1911—Fletcher.*
- *"The Question of Valency in Gaseous Ionization."* Phil. Mag. *June 1911—Millikan and Fletcher.*
- *"A Verification of the Theory of Brownian Movements and a Direct Determination of the Value of* Ne *for Gaseous Ionization."* Phys. Rev.*, August 1911, and* Le Radium*, 1 July 1911—Fletcher.*

It was obvious that he wanted to be the sole author on the first paper [the paper providing a measurement of the charge on the electron and the modifications of Stokes' law]. I did not like this, but I could see no other way out so I agreed to use the fifth paper listed above as my thesis [a paper on the verification of the theory of Brownian movement and a direct determination of the value of Ne *for gaseous ionization published in 1911 a year after the first paper authored solely by Millikan]…People have frequently asked me if I had bad feelings toward Millikan for not letting me be a joint author with him on this first paper, which really led to his getting the Nobel Prize. My answer has always been no. It is obvious that I was disappointed as I had done considerable work on it, and had expected to be a joint author. But Millikan was very good to me while I was at Chicago. It was through his influence that I got into the graduate school. He also found remunerative jobs for me to defray all my personal and school expenses for the last two years. Above this was the friendship created by working intimately together for more than two years. This lasted throughout our lifetime. When he wrote his memoirs shortly before he died he had probably forgotten some of these early experiences.*

From Fletcher (1982); reprinted with permission from AIP Publishing LLC © 1982.

Following the above account by Fletcher, letters to the editor of *Physics Today* and the *Journal of Chemical Education* proposed that the well-known Millikan oil drop experiment be called the "Millikan–Fletcher oil drop experiment" (Kirkham, 1982; Schroeder, 1982; Halevi, 1982; Brower, 1985). For example, Halevi (1982) wrote:

*I was impressed by the ring of truth in Harvey Fletcher's posthumous description of the Millikan-*Fletcher *oil drop experiment. By excluding Fletcher from coauthorship in the 1910* Science *paper, Millikan stretched scientific ethics beyond its breaking point. ("A PhD for you, a Nobel for me, is that okay for you, Mr. Fletcher?"). I hope that Nobel Prize committee members and historians of science will take notice.*

Reprinted with permission © 1982 AIP Publishing LLC.

Another example is taken from Brower (1985), who wrote:

Fletcher did not want this account published until after his death, so that no personal interest could be attributed to its publication. It seems clear that the actual oil drop apparatus was in fact designed by Fletcher and the work with the oil drops was to have been Fletcher's doctoral thesis. However, when the success of the experiment became apparent along with much attendant publicity, Millikan struck a "deal" with Fletcher. Since Millikan had helped Fletcher's entrance into graduate school and had aided him in other ways, Fletcher agreed to Millikan's sole authorship of the first (Millikan, 1910) of a series of five papers on the subject…Fletcher states he wrote a goodly portion of the first paper, particularly about the Stokes Law modification and the organization of data. I am inclined to agree with other letters to Physics Today *that the experiment be referred to as the Millikan-Fletcher oil drop experiment.*

Reprinted with permission © 1985 American Chemical Society.

A defense of Millikan was given by Goodstein (2001) in a speech addressed to Sigma Xi, The Scientific Research Society. A quotation from the defense is the following:

No doubt Millikan understood that the measurement of e *would establish his reputation, and he wanted full credit. Fletcher understood this too, and he was somewhat disappointed, but Millikan had been his protector and champion throughout his graduate career, so he had little choice but to accept. This coercion is the source of the assertion that Millikan mistreated his*

graduate students. And in this case he probably did. Still the two men remained [sic] good friends throughout their lives, and Fletcher saw to it that his account of this unflattering episode was not published until after Millikan's death (and after his own).

Reprinted by permission of *American Scientist*, magazine of Sigma Xi, The Scientific Research Society.

A more recent editorial, which included remarks on the oil drop experiment entitled "Plagiarism: Words and Ideas" by Resnik (2012), appeared in the journal *Accountability in Research*. The observations in this editorial were the following:

The history of science unfortunately contains numerous examples of teachers taking ideas from students without giving them appropriate credit (Shamoo and Resnik, 2009). Robert Millikan won the Nobel Prize in Physics in 1923 for determining the charge of an electron. Millikan's results were based on a paper he published in the journal Science *in 1910 reporting experiments involving the suspension of electrically charged oil drops in magnetic fields. Harvey Fletcher was a graduate student who was working with Millikan at the University of Chicago. Fletcher made numerous suggestions that were crucial for executing the oil drop experiment, including the idea that oil drops should be used instead of water, because water evaporates too quickly to obtain accurate measurements. Fletcher was not listed as an author on Millikan's famous paper, although he was listed as an author on other papers with Millikan. In recalling their relationship, Fletcher said that he was disappointed that he was not named as an author on the paper that led to the Nobel Prize, but he bore no bad feelings toward Millikan because Millikan helped him advance his scientific career (Fletcher, 1982).*

From Resnik (2012), http://www.tandfonline.com/doi/full/10.1080/08989621.2012.718677#.U-PDu8J0yUm, Reprinted with permission © 2012 Taylor and Francis Group LCC.

During the First World War, Robert Millikan became Vice Chairman of the National Research Council, where he assisted in the development of antisubmarine devices. He remained professor at the University of Chicago until 1920; and he was eventually recruited in 1921 to join the California Institute of Technology (Caltech). When he joined Caltech, Millikan was one of the most influential and admired physicists in the country; and he was appointed as Director of the Norman Bridge Laboratory of Physics and Chairman of the Executive Council of the Institute. At Caltech, Millikan raised the institute to become one of the leading institutes of teaching and research in physics. Although Millikan was one of the most admired and respected physicists in the country, some at Caltech were not as respectful toward Millikan, as depicted in the photograph shown in Fig. III.18, which appeared in Goodstein's book "Millikan's School," published in 1991. The photograph was that of a construction site at Caltech, where someone had inscribed as graffiti "JESUS SAVES"; and another added below "BUT MILLIKAN GETS CREDIT." Robert Millikan received approximately 25 honorary doctorate degrees and numerous medals in addition to that of the Nobel Prize. He died on December 19, 1953 in San Marino, California.

Relating to the value of the charge on the electron as determined by the oil drop experiment, Nobel Laureate Richard Feynman (1918−1988) provided words of advice to the student body at the California Institute of Technology in a commencement address in 1974. His speech was entitled "Cargo Cult Science: Some Remarks on Science, Pseudoscience, and Learning How to Not Fool Yourself." A relevant excerpt of his remarks is quoted as follows, with the author's comments in brackets:

We have learned a lot from experience about how to handle some of the ways we fool ourselves. One example: Millikan measured the charge on an electron by an experiment with falling oil drops and got an answer which we know now not to be quite right. It's a little bit off, because he had the incorrect value for the viscosity of air. It's interesting to look at the history of measurements of the charge of the electron, after Millikan. If you plot them as a function of time, you find that one is a little bigger than Millikan's, and the next one's a little bigger than that, and the next one's a little bigger than that, until finally they settle down to a number which is higher.

Why didn't they discover that the new number was higher right away? It's a thing that scientists are ashamed of—this history—because it's apparent that people do things like this: When they got a number that was too high above Millikan's, they thought something must be wrong—and they would look for and find a reason why something might be wrong. When they got a number closer to Millikan's value they didn't look so hard. And so they eliminated the numbers that were too far off, and did other things like that. We've learned those tricks nowadays, and now we don't have that kind of disease…The first principle is that you must not fool yourself—and you are the easiest person to fool…After you've not fooled yourself, it's easy not to fool other scientists." [In his address Richard Feynman refers only to Millikan as discover of the charge on the electron, because it was not known until 1982 that Harvey Fletcher played a major role in this discovery.]

Harvey Fletcher was born in Provo, Utah, USA on September 11, 1884. Fletcher entered the Brigham Young Academy in 1901, which was then the only school in the Utah Valley where a student could get an education beyond the eighth grade including a college degree. Brigham Young Academy would become Brigham Young University (BYU) in 1903. There

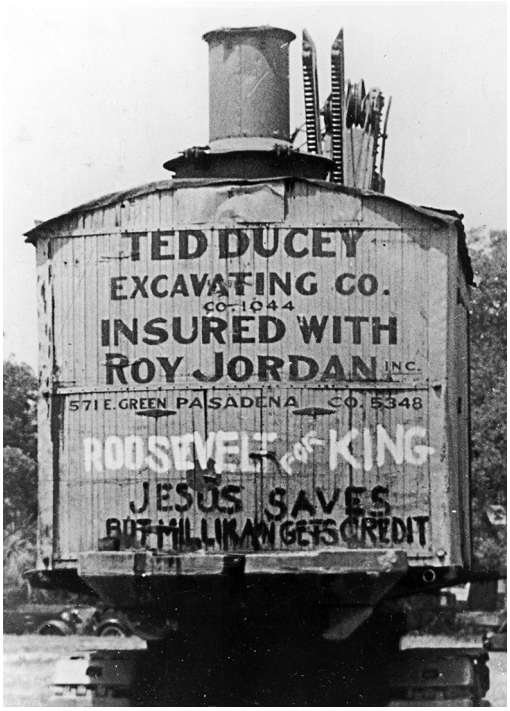

FIGURE III.18 Graffiti at the construction site of Caltech's Kerckhoff Laboratories in 1937 where the words "JESUS SAVES" was inscribed by one person; and another added below "BUT MILLIKAN GETS CREDIT." *Courtesy of the Archives, California Institute of Technology.*

Fletcher failed his first course in physics; and on reflection that he didn't take the course seriously, repeated it to achieve the highest grade in the class. Later in life as an accomplished and esteemed university professor of physics, he would often relate, to the delight of his students, the fact that he had failed his first physics course. Harvey Fletcher graduated from BYU in 1907; and he taught physics and mathematics there for a year before deciding to pursue a doctorate degree in physics.

Harvey Fletcher (1884-1981)
Courtesy AIP Emilio Segrè Visual Archives

After marriage in 1908, Harvey Fletcher moved to Chicago with his wife Lorena to pursue a PhD degree in physics at the University of Chicago without having an acceptance letter from the university. The office of admissions at the prestigious University of Chicago did not accept his education as accredited from the newly formed Brigham Young University, and required that Fletcher complete successfully a 4-year undergraduate study at the university before entering graduate school. Harvey Fletcher discussed his predicament with Robert A. Millikan, who was then assistant professor of physics, and Millikan kindly offered to help Fletcher by suggesting that if he could successfully complete the first year of graduate course work in physics, Millikan would try to get him accepted into the doctoral program. Harvey Fletcher thus entered in the doctoral program in physics; and 4 years later, he would graduate top of the class to become the first summa cum laude in physics at the University of Chicago.

The pioneering work of Harvey Fletcher together with Robert Millikan in the determination of the charge on the electron is described above. He did not receive the Nobel Prize for this work, because he was not included as coauthor of the publication of this work with Millikan. Fletcher thus led a more unpretentious life although one of great achievement in education and research. Upon graduation from the University of Chicago in 1911, Harvey Fletcher was appointed Chairman of the Department of Physics at BYU, where he had the opportunity to teach and develop the department, which put out many distinguished students including Vern O. Knudson, who became Chancellor of the University of California at Los Angeles. In 1916 he finally accepted an open invitation to join the research and development department of the Western Electric Company in New York City, an opportunity that had been available to him since his graduation from BYU. This was the department where most of the research of the American Telephone and Telegraph Company was conducted. He was elected a fellow of the American Physical Society in 1920 and in 1921 a member of the American Association for the Advancement of Science (AAAS). In 1928, Fletcher was appointed director of acoustical research; and in 1933, he became director of all physical research in the Bell Telephone Laboratories. In this capacity, Fletcher was responsible for the successful development of the Western Electric hearing aids, which were among the first in the nation and a tremendous aid to those hard of hearing throughout the world. In 1929, he was elected President of the American Federation of Organizations of the Hard of Hearing and President of the Acoustical Society of America.

The Bell Laboratory Systems under Harvey Fletcher manufactured the first artificial larynx, which provided the handicapped with the ability to speak, which seemed miraculous to those in need and provided some notoriety to Fletcher. Under his direction at Bell Laboratories, scientists and their assistants were able to produce the very first stereophonic sound transmission in 1933 and stereophonic recording in 1939. Fletcher's responsibilities at Bell Laboratories as director of physical research included the supervision of the work of prominent scientists including Nobel Laureates William A. Shockley, Walter H. Brattain, and John Bardeen, credited with the development of the transistor and pioneering work on semiconductors; Dean Wooldridge, who was instrumental in the development of the magnetic tape; and Nobel Laureate Charles Townes, among other prominent physicists. Harvey Fletcher was elected a member of the National Academy of Sciences in 1935. During the United States involvement in World War II from 1941 to 1945, Fletcher supervised research in the Office of Scientific Research and Development, which was an agency of the United States federal government created to coordinate scientific research for military purposes during World War II. As a renowned scientist in the acoustical field, he supervised the secret research in several prestigious institutions in the war effort. For his work in this group effort, Fletcher received several citations including one awarded by President Truman. Harvey Fletcher was the author of 40 papers and two books on speech and hearing. Upon his retirement from Bell Laboratories in 1949, Harvey Fletcher accepted a position as professor of electrical engineering at Columbia University; and in 1952 he moved back to his old school, the Brigham Young University, as director of research. In 1953 he was appointed as Chairman of the Department of Engineering Science at BYU, and oversaw its transformation into the College of Physical and Engineering Sciences. Harvey Fletcher was awarded honorary degrees from several universities; and he actively carried our scientific research at BYU from 1960 to his death in 1981 at the age of 96. (Biographical information is from Gardner, 1981, and Fletcher, 1992.)

HOMI J. BHABHA (1909–1966)

Homi Jehangir Bhabha was born on October 30, 1909 in a prominent industrial Parsi family in Bombay (now Mumbai), India. Homi Bhabha is well known for his contributions to nuclear physics, in particular calculations of electron-positron scattering, which is called "Bhabha scattering" in his honor, and his contributions to the origin and mechanisms of the production of cosmic ray showers. He was crucial to the establishment of prominent institutions of research and development of nuclear energy in India; and he is thus regarded as the "father of the Indian nuclear energy program." The leading institution of nuclear research, named in honor of Homi J. Bhabha, is the Bhabha Atomic Research Centre (BARC) located in Trombay, Mumbai, India. The postage stamp illustrated here commemorates the life and

contributions of Homi Bhabha to nuclear energy development with the likeness of Bhabha overlooking a nuclear research institute and reactor.

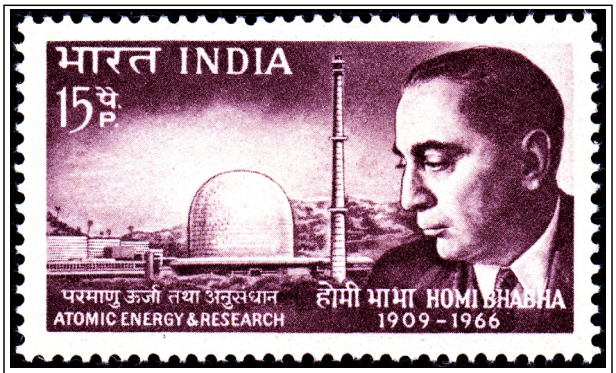

Homi J. Bhabha (1909-1966)

At the age of 15, Bhabha entered the Elphinstone College in Bombay and subsequently the Royal Institute of Science, also in Bombay. Three years later he entered the Gonville and Caius College in Cambridge, which is one of the oldest and largest colleges of the University of Cambridge. Bhabha's father and his uncle, Sir Dorab J. Tata, had high hopes that Bhabha would graduate as an engineer to ultimately join the Tata Iron and Steel Company; however, at Cambridge, Bhabha developed a passion for theoretical physics. Bhabha wrote his father in 1928 to explain his passion for a field of work in physics and to ask for permission to pursue studies in this field. An excerpt of this letter, taken from Vigyan Prasar, which is an autonomous organization promoting the understanding and appreciation of scientific principles under the Department of Science and Technology of the Government of India, is the following:

> *I seriously say to you that business or job as an engineer is not the thing for me. It is totally foreign to my nature and radically opposed to my temperament and opinions. Physics is my line. I know I shall do great things here. For, each man can do best and excel in only that thing of which he is passionately fond, in which he believes, as I do, that he has the ability to do it, that he is in fact born and destined to do it…I am burning with a desire to do physics. I will and must do it sometime. It is my only ambition. I have no desire to be a "successful" man or the head of a big firm. There are intelligent people who like that and let them do it…It is no use saying to Beethoven "You must be a scientist for it is great thing" when he did not care two hoots for science; or to Socrates "Be an engineer; it is work of intelligent man." It is not in the nature of things. I therefore earnestly implore you to let me do physics.*
>
> From: http://www.vigyanprasar.gov.in/scientists/bhabha/BHABHANEW.HTM.

From Bhabha's letter, it is clear he had no doubt that to be successful and achieve greatness, one must have a passion in their life's work regardless of the field or endeavor. Bhabha's father conceded to his son's wishes under the condition that he pass the Mechanical Tripos at Cambridge, which he successfully passed with honors in 1930. This provided Bhabha the opportunity to subsequently study and pass the Mathematics Tripos at Cambridge in 1932, also with honors, and with an award of a traveling scholarship in mathematics. At Cambridge, Bhabha studied under Nobel laureates Paul A.M. Dirac and Erwin Schroedinger, He was awarded a doctorate degree in nuclear physics at Cambridge after the publication of a paper on cosmic radiation (Bhabha, 1933) where he calculated the cross-sections for the various processes occurring in the atmosphere resulting in the showers of cosmic radiation. In this paper Bhabha thanked Prof. Paul A.M. Dirac, Lucasian Professor of Mathematics at Cambridge, for his interest and review of this paper. As a result of this paper, Bhabha was awarded an Isaac Newton scholarship, whereby he continued studies at Cambridge and in Copenhagen under Niels Bohr. In 1935, Bhabha completed his doctoral studies in theoretical physics under the supervision of Ralph H. Fowler, who held the Chair of Theoretical Physics at the Cavendish Laboratory. Shortly thereafter, Bhabha (1936) published on the cross-section for electron-positron scattering, which is referred to worldwide as "Bhabha scattering." The process of Bhabha scattering, first calculated by Bhabha, involves an elastic scattering process $e^+e^- \rightarrow e^+e^-$ whereby positrons and electrons are scattered by the exchange of a virtual photon between them, as illustrated in Fig. III.19, as explained by quantum electrodynamics. Fig. III.19 is that of a Feynman diagram depicting a positron (e^+) and electron (e^-) approaching each other; and the emission and absorption of a photon (γ) causes the scattering of the positron and electron in opposing directions.

Bhabha scattering is commonly used in high-energy physics. All large electron-positron (LEP) experiments that involve the collisions of high-energy electrons and positrons, use luminosity detectors. A luminosity detector provides a measure of

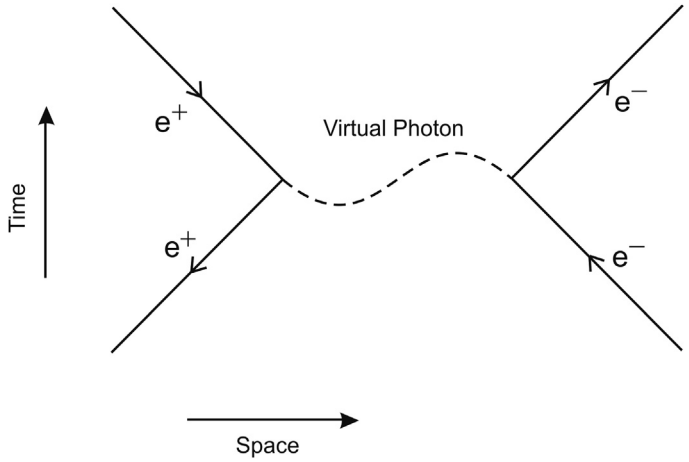

FIGURE III.19 Feynman diagram for Bhabha scattering.

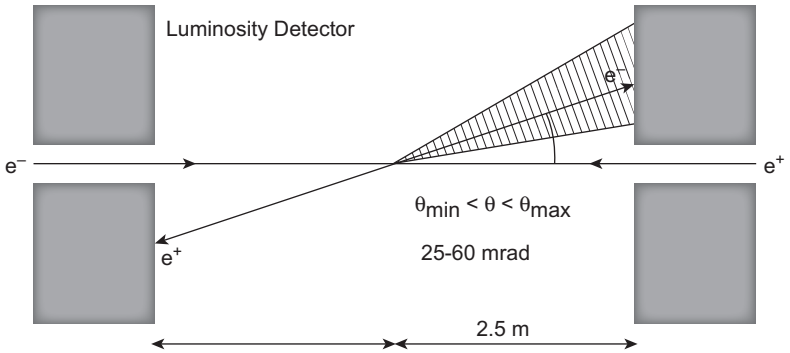

FIGURE III.20 Luminosity measurement at an e^+e^- collider. Electron and positron beams collide at the center of the figure, resulting in Bhabha scattering ($e^+e^- \rightarrow e^+e^-$); and the positrons and electrons scattered at angle θ are detected at opposite directions from the point of interaction. The detectors of Bhabha-scattered positrons and negatrons are represented by shaded blocks. The distance of the luminosity detectors to the interaction point is about 2.5 cm. *From Grönewald (1999); reprinted with permission from Elsevier © 1999.*

the beam interaction rate, which is a function of the beam geometry, density, and energy. Luminosity detectors provide a count rate of scattered electrons and positrons (dR/dt); and the luminosity (L) is calculated with theoretically calculated Bhabha scattering cross-sections (q). As described by Potter (1994), the luminosity is the most important parameter after the beam energy at a colliding beam facility; and it is defined as the interaction rate per unit cross-section, ie, $L = (dR/dt)/q$. A diagram of a luminosity detector used to monitor Bhabha scattering at an intersection point in an e^+e^- collider is illustrated in Fig. III.20.

Bhabha's work at the Gonville and Caius College at Cambridge focused on explaining the origins of the cosmic radiation showers (Bhabha, 1937, 1938a,b). Together with W. Heitler of the University of Bristol (Bhabha and Heitler, 1937), Bhabha published the explanation for the production of a cascade of gamma radiation and elementary particles and calculations of the nuclear processes that occur including electron-positron pair production when the primary cosmic rays interact with nuclei of the atmosphere to produce cosmic ray showers.

High-energy particles in the cosmic ray showers travel at speeds close that of light (ie, relativistic speeds). Thus, Bhabha (1938b) was the first to predict that cosmic ray particles traveling at such high speed would exhibit time dilation according to Einstein's theory of relativity, whereby the decay times of the particles as measured on earth would be longer than those measured in the same time-frame at the cosmic ray particle. In the journal *Nature*, Bhabha (1938b) predicted time dilation in the decay of high-energy cosmic ray particles as follows (with the author's comments in brackets):

> *A positive U-particle [now known to be a muon with the decay mode* $\mu^+ \rightarrow e^+ + \nu$*] at rest may disintegrate spontaneously into a positive electron and a neutrino. This disintegration being spontaneous, the U-particle may be described as a 'clock,' and hence it follows merely from considerations of relativity that the time of disintegration is longer when the particle is in motion. We believe*

that this may have to do with the fact observed by Blackett and others that below 2×10^8 e.v. [200 MeV] most cosmic ray particles are electrons, above this energy heavy electrons. [What was then referred to as heavy electrons are now known as muons, which have a mass of ~200 times that of electrons.]

Reprinted by permission from Macmillan Publishers Ltd. © 1938.

In his prediction cited above, Bhabha indicates that with sufficient energy a particle will travel at relativistic speeds, and thus its decay time would be dilated to such an extent that an observer would be able to detect the cosmic ray particle on earth at sea level. Bhabha's prediction was demonstrated by Bailey et al. (1979) based on tests of Rossi and Hall (1941). The muon has an average lifetime of 2.2×10^{-6} s; and in that lifetime, most muons would be expected to decay before reaching earth. However, a muon traveling at a speed close to that of light (eg, $0.994c$) would have a calculated dilated lifetime of 20.1×10^{-6} s when measured by an observer in the space–time reference frame of earth. The lifetime measured in the time-frame of an observer on earth is almost 10 times as long as that which is measured in the time-frame of the muon. The dilated lifetime of the muon measured on earth is long enough for the muon to travel at a distance of ~6000 m in the earth's atmosphere and be detected on earth. (Calculations of this time dilation are provided in this Hall of Fame, Part III in the biographical sketch of Albert Einstein under the heading "Evidence for Relativity Provided by Muons in the Showers of Cosmic Radiation.") In 1935, Hideki Yukawa predicted a particle that would account for the strong interactions that could hold protons and neutrons together in the atomic nucleus. This particle was discovered in cosmic radiation and called the "mesotron." In a note in the journal *Nature*, Homi Bhabha (1939) proposed the name "meson" for this new particle, which is the name finally adopted. The particle postulated by Yukawa is called the π meson; and all mesons are now known as composite particles containing two quarks.

Excellent biographical memoirs of Homi J. Bhabha are written by Penney (1967), published by The Royal Society, and by Mahatni (2014), which is available from the website of Vigyan Prasar, an autonomous organization under the Department of Science and Technology of the Government of India, from which some of the biographical information presented here was obtained. In 1940, Bhabha joined the Indian Institute of Science at Bangalore, which was headed by Nobel Laureate Chandrasekhara Venkata Raman (1888–1970). Bhabha was assigned the post of Readership in Theoretical Physics and was promoted to a professorship there in 1944. At this institute, Bhabha established a group of young scientists to carry out research on cosmic radiation. In 1944 Bhabha began his efforts to form a high-caliber research institute in India by writing a letter to Sir Sorab Saklavata, Chairman of the Sir Dorab Data Trust. His letter read in part as follows:

There is at the moment in India no big school of research in the fundamental problems of physics, both theoretical and experimental. There are, however, scattered all over India competent workers who are not doing as good work as they would do if brought together in one place under proper direction. It is absolutely in the interest of India to have a vigorous school of research in fundamental physics, for such a school forms the spearhead of research not only in less advanced branches of physics but also in problems of immediate practical application in industry…Moreover, when nuclear energy has been successfully applied for power production in say a couple of decades from now, India will not have to look abroad for its experts but will find them ready at hand. I do not think that anyone acquainted with scientific development in other countries would deny the need in India for such a school as I propose.

From Penney (1967); reprinted with permission from The Royal Society © 1967.

Bhabha's proposal was accepted and the trustees of the Sir Dorab Data Trust agreed to provide financial backing with the Government of India as a joint founder of the new Tata Institute of Fundamental Research, which was inaugurated in 1945 in a house in Mumbai, which was then the city of Bombay, India. It was later in 1948 moved into old buildings of the Royal Bombay Yacht Club. The foundation stone of the institute was laid in 1954 by Pt. Jawaharial Nehru, who was the first Prime Minister of India and a central figure in Indian politics for much of the 20th century. Nehru also inaugurated in 1962 the opening of the then-new and current institute in Mumbai. Bhabha had published many papers in theoretical nuclear physics prior to 1955; however, his efforts later were focused in directing research at the institute and nuclear power development in the country.

Bhabha was appointed chairman of a commission in the Ministry of Natural Resources and Scientific Research, which would oversee the responsibilities of the central government in its activities set forth by a newly established Atomic Energy Act in 1948. This Act provided the government of India with the power to oversee all development of nuclear power in India. While the Tata Institute would develop to become a leading research institute in the world, another institute was needed to satisfy the development of atomic energy and, under Homi J. Bhabha, the commission agreed to build a new Atomic Energy Establishment in 1948 at Trombay, Mumbai, India. The Atomic Energy Establishment began to function in

1954 for the development of the atomic energy program in India. This put India on the road to becoming an independent country in the field of physics capable of research and development of new designs for modern nuclear power needed to satisfy the needs of the country for electric power and industrial development.

As noted in the biographical memoir by Mahatni (2014), during the course of his scientific career, Bhabha was elected a Fellow of the Royal Society in 1941. He was awarded the Adams Prize in 1943 by Cambridge University for his work on cosmic rays, and the Hopkins Prize in 1948 by the Cambridge Philosophical Society. Bhabha was elected in 1963 to the U.S. National Academy of Sciences and as a Foreign Associate and Honorary Life Member of the New York Academy of Sciences. Bhabha received numerous other awards and honorary doctoral degrees for his leadership in research.

From left to right Homi J. Bhabha, M. G. K. Menon and Emilio Segrè at the Tata Institute of Fundamental Research in Bombay (now Mumbai), India
Courtesy of AIP Emilio Segrè Visual Archives, Segrè Collection

Homi J. Bhabha played an active role in advisory committees of the International Atomic Energy Agency (IAEA) in Vienna. Bhabha was killed in a tragic air accident when his plane crashed near the peak of Mont Blanc on January 24, 1966 while traveling to attend a meeting of the Scientific Advisory Committee (SAC) of the IAEA in Vienna. After Bhabha's passing, Prof. M.G.K. Menon succeeded Bhabha as Director of the Tata Institute of Fundamental Research up to the year 1974; and Prof. Menon has played a leading role in scientific research and development in India for over four decades. After Homi J. Bhabha's death, the main center of nuclear research and development in India was the Atomic Energy Establishment at Trombay; and on January 12, 1967, in a ceremony attended by numerous international scientific dignitaries, Mrs. Indira Ghandi, Prime Minister of India, renamed the Atomic Energy Establishment at Trombay the Bhabha Atomic Research Centre, also known as BARC.

Chapter 8

Electromagnetic Radiation: Photons

A logical consequence of Planck's theory is that a transition from one [energy] state to another can only take place in such a way that an integral number of energy quanta is emitted or absorbed. An exchange of energy between matter and radiation, therefore—that is to say an emission or absorption of radiation—can be affected only by the transmission of an integral number of energy quanta. It was not Planck, however, but Einstein, that drew this conclusion, which involves the law of the photoelectric effect … It is through Einstein's law that the Planck's constant and the whole quanta theory has attained their greatest importance.

Statement made by the Chairperson (Prof. A. Gullstrand) of the Nobel Committee on September 25, 1925 upon awarding the Nobel Prize for Physics. This statement attributes to Albert Einstein the discovery of the photon as a particle with energy quanta ($E = h\nu$) following Einstein's interpretation of the photoelectric effect. It is because of Albert Einstein's interpretation of the photoelectric effect and Max Planck's discovery of the quantum theory that the equation $E = h\nu$ is referred to as the Planck–Einstein relation.

8.1 INTRODUCTION

In the latter part of the 19th century, Heinrich Hertz (1887a,b) carried out a series of experiments demonstrating that an oscillating electric current sends out electromagnetic waves similar to light waves, but of different wavelength. Hertz proved, thereby, the earlier theory of James Clerk Maxwell (1831–1879), that electric current oscillations would create alternating electric and magnetic fields, and radiated electromagnetic waves would have the same physical properties of light (see Fig. I.13 in Hall of Fame, Part I). A subsequent discovery by Nobel Laureate Pieter Zeeman (1897) further linked the properties of light with electricity and magnetism when he discovered that a magnetic field would alter the frequency of light emitted by a glowing gas, which we now refer to as the Zeeman effect. The magnetic field would alter the spectral line corresponding to the frequency of the light into a triplet or even a more complex multiplet of lines. This discovery was significant, because it was the very first to link the properties of light with electricity and magnetism.

8.2 DUAL NATURE: WAVE AND PARTICLE

Not long after the discoveries of Hertz and Zeeman came the work of Max Planck, who in 1900 proposed a formula to explain that the vibrating particles in the heated walls of a kiln could radiate light only at certain energies. These energies would be defined by the product of a constant having the units of energy × time and the radiation frequency. The constant that he calculated became known as the universal Planck constant, $h = 6.626 \times 10^{-34}$ J s. Therefore, radiation would be emitted at discrete energies, which were multiples of Planck's constant and the radiation frequency, ν. Planck named the discrete radiation energy as the "quantum" from the Latin *quantus*, meaning "how great."

In 1905 Einstein grasped the calculations of Planck to explain and provide evidence that light not only traveled as waves but also existed as discrete packets of energy or particles, which he named "energy quanta." Today we refer to these energy quanta as photons. Einstein demonstrated the existence of the photon in his explanation of the photoelectric effect (see Section 8.8.2 of this chapter). He demonstrated that the energy of an electron (photoelectron) ejected from its atomic orbital after being struck by light was not dependent on the light intensity, but rather on the wavelength or frequency of the light. In other words, increasing the light intensity would increase the number of photoelectrons, but not their energy; whereas altering the frequency, and thus the energy, of the light would alter the energy of the photoelectron. In summary,

Radioactivity: Introduction and History, From the Quantum to Quarks. http://dx.doi.org/10.1016/B978-0-444-63489-4.00008-3
Copyright © 2016 Elsevier B.V. All rights reserved.

Einstein demonstrated that the energy of the photoelectron depended on the energy of the photon that collided with the electron, or the product of Planck's constant times the light frequency according to the formula:

$$E = h\nu = \frac{hc}{\lambda} \quad [8.1]$$

Eq. [8.1] is referred to as the Planck−Einstein relation (Woan, 2000). From this observation, Einstein is credited with discovering the photon as an elementary particle. Also, we may notice from Eq. [8.1] that the product of the photon frequency, ν, and wavelength, λ, always yields the velocity, c, the speed of light. The photon always travels at the constant speed in a vacuum, $c = 2.9979 \times 10^8$ m/s; it cannot travel at a speed less than c in a vacuum.

From our previous treatment, we see that the photon behaves as a particle, which could knock out an electron from its atomic orbital provided it possessed sufficient energy to do so, that is, an energy in excess of the electron binding energy. Therefore, the photon can be considered also as another elementary particle. In his explanation of the photoelectric effect, Einstein was the first to demonstrate the particulate nature of light, and it is for this work he won the Nobel Prize. Since these findings of Einstein, electromagnetic radiation is known to have a dual nature as energy that travels as a wave and particle.

Electromagnetic radiation may be classified according to its wavelength or origin. For example, we will see in this section of the chapter that gamma rays and X-rays are similar, but have different origins. Gamma rays arise from the nucleus of an atom while X-rays come from extranuclear electrons. The classification of electromagnetic radiation according to wavelength and frequency is illustrated in Fig. I.14 in Hall of Fame, Part I.

Since electromagnetic radiation or photons have properties of particles, they should also possess momentum. We calculate momentum as the product of mass and velocity. For relativistic conditions, the mass of a particle is a function of its speed according to Eq. [III.44] of Hall of Fame, Part III and Eq. [10.6] of the chapter entitled "Neutron Radiation," or:

$$m = \frac{m_0}{\sqrt{1 - (u^2/c^2)}} \quad [8.2]$$

where m and m_0 are the particle relativistic and rest masses, u is the particle speed, and c is the speed of light. Grateau and Savin (1999) transform Eq. [8.2] by squaring both sides and then multiplying each side by c^4 $[1 - (u^2/c^2)]$ to yield the equation:

$$m^2c^4 - m^2u^2c^2 = m_0^2c^4 \quad [8.3]$$

Using $E = mc^2$ and $E_0 = m_0c^2$ to define the relativistic and rest energies and $p = mu$ to define the particle momentum together with the fact that the rest energy of the photon is zero, ie, $m_0 = 0$, Eq. [8.3] becomes:

$$E^2 - p^2c^2 = \left(m_0c^2\right)^2 \quad [8.4]$$

$$E^2 - p^2c^2 = 0 \quad [8.5]$$

and:

$$p = \frac{E}{c} \quad [8.6]$$

From Eqs. [8.1], [8.5], and [8.6] we can further describe the photon momentum as:

$$p = \frac{E}{c} = \frac{h\nu}{c} = \frac{h}{\lambda} \quad [8.7]$$

To illustrate the use of the above equations defining the relationships of photon properties, let us calculate the wavelength, frequency, and momentum of a 2-MeV gamma-ray photon. From Eq. [8.1] we can write the equation for calculating the wavelength as:

$$\lambda = \frac{hc}{E} \quad [8.8]$$

Planck's constant, h, can be converted from units of J s to eV s as:

$$h = \frac{6.626 \times 10^{-34}\ \text{J s}}{1.602 \times 10^{-19}\ \text{J/eV}} = 4.136 \times 10^{-15}\ \text{eV s} \quad [8.9]$$

and hc is calculated as:

$$\begin{aligned} hc &= \left(4.136 \times 10^{-15}\ \text{eV s}\right)\left(2.9979 \times 10^{8}\ \text{m/s}\right) \\ &= 12.399 \times 10^{-7}\ \text{eV m} \\ &= 12.4\ \text{keV Å} \end{aligned} \quad [8.10]$$

The wavelength of the 2.0-MeV gamma ray according to Eq. [8.8] becomes:

$$\lambda = \frac{12.4\ \text{keV Å}}{2 \times 10^{3}\ \text{keV}} = 0.0062\ \text{Å}$$

The frequency is calculated according to Eq. [8.1] as:

$$\nu = \frac{c}{\lambda} = \frac{2.9979 \times 10^{8}\ \text{m/s}}{0.0062 \times 10^{-10}\ \text{m}} = 484 \times 10^{18}\ \text{s}^{-1}$$

$$= 4.84 \times 10^{20}\ \text{Hz}$$

The momentum is expressed according to Eq. [8.6] as:

$$p = \frac{E}{c} = 2.0\ \text{MeV}/c$$

Notice that relativistic calculations of momentum have units of MeV/c, while conventional units of momentum are derived from mass times velocity or kg m/s. Units of MeV/c can be converted to the conventional units with the conversion factor 1 MeV/$c = 0.534 \times 10^{-21}$ kg m/s (Gautreau and Savin, 1999).

8.3 GAMMA RADIATION

Radionuclide decay processes often leave the product nuclide in an excited energy state. The product nuclide in such an excited state either falls directly to the ground state or descends in steps to lower energy states through the dissipation of energy as gamma radiation.

A nuclide in an excited energy state is referred to as a nuclear isomer, and the transition (or decay) from a higher to a lower energy state is referred to as isomeric transition. Gamma rays are emitted in discrete energies corresponding to the energy state transitions a nuclide may undergo when in an excited state. The energy, E_γ, of a gamma ray may be described as the difference in energy states of the nuclear isomers:

$$E_\gamma = h\nu = E_1 - E_2 \quad [8.11]$$

where $h\nu$ is the energy of the electromagnetic radiation described previously in Section 8.2, and E_1 and E_2 represent the energy levels of the nuclear isomers.

Let us consider the decay schemes of some radionuclides to illustrate the process in more detail.

Fig. 8.1 shows the decay scheme of $^{86}_{37}$Rb with a half-life of 18.8 days. This nuclide decays by β^- emission with an increase in atomic number to $^{86}_{38}$Sr. Eighty-eight percent of the beta particles emitted have a maximum energy of 1.77 MeV; the remaining 11% have a maximum energy of 0.70 MeV. The percentages cited and illustrated in the figure are referred to as transition probabilities or intensities. Obviously, a greater quantum of energy is released by the 1.77-MeV beta-decay process. As a consequence, the ^{86}Sr product nuclides that result from β^- emission of 0.70 MeV (11%) are at a higher energy state than those that result from β^- emission of 1.77 MeV. The energy difference of the two ^{86}Sr product nuclide isomers, $E_1 - E_2$, is equivalent to the difference of the two β^- energies, 1.77 − 0.70 MeV = 1.07 MeV. Consequently, the ^{86}Sr nuclide isomers, which are products of the 0.70-MeV beta-decay process, can emit the remaining energy as 1.07-MeV gamma-ray photons.

As illustrated in Fig. 8.1, 11% of the parent ^{86}Rb nuclides decay to an ^{86}Sr nuclear isomer at an elevated energy state. Not all of these isomers decay immediately to the ground state. Only 8.8% of the ^{86}Rb → ^{86}Sr disintegrations result in the emission of a gamma-ray photon of 1.07 MeV. For example, a 37-kBq sample of ^{86}Rb by definition would emit 2.22×10^6 beta particles in 1 min (37,000 dps × 60 s/min). However, only $(2.22 \times 10^6)\ (0.088) = 1.95 \times 10^5$ gamma-ray photons of 1.07 MeV can be expected to be emitted in 1 min from this sample.

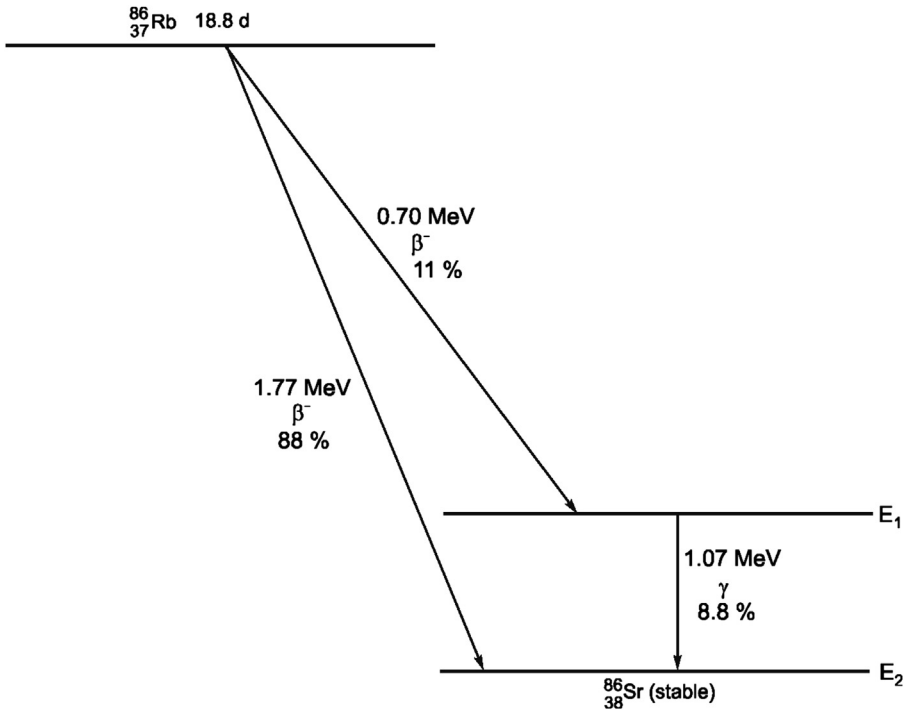

FIGURE 8.1 Decay scheme of $^{86}_{37}$Rb.

Fig. 8.2 shows the somewhat more complicated decay scheme of $^{144}_{58}$Ce, which has a half-life of 284.5 days. This nuclide decays by β^- emission with an increase in atomic number to $^{144}_{59}$Pr. In this case, three distinct β-decay processes produce three nuclear isomers of the daughter ^{144}Pr. Seventy-five percent of the beta particles emitted have a maximum energy of 0.31 MeV, 20% have a maximum energy of 0.18 MeV, and the remaining 5% have a maximum energy of

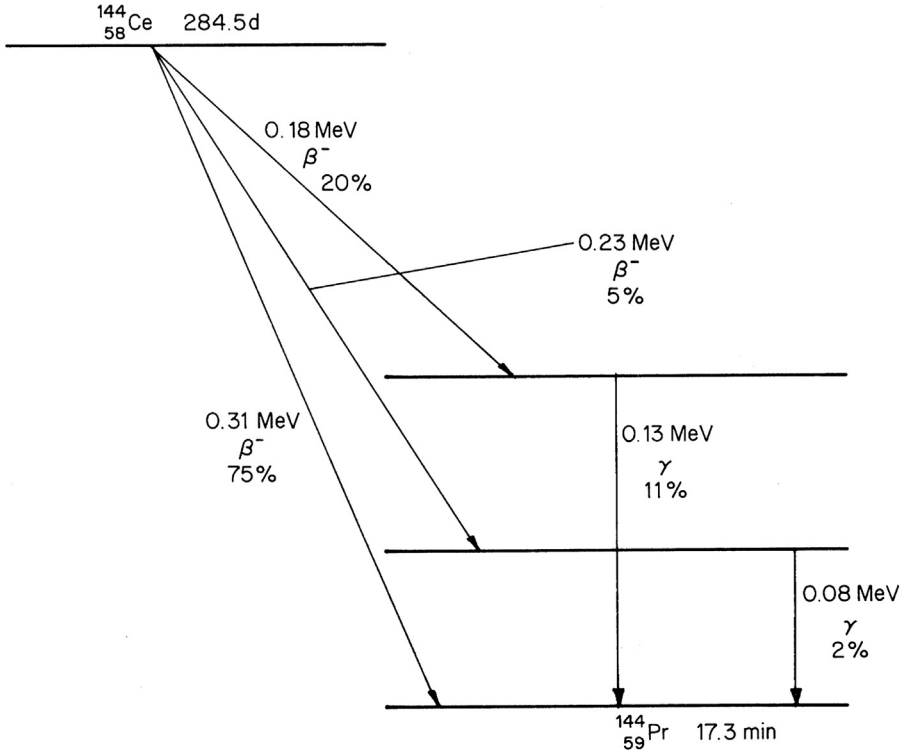

FIGURE 8.2 Decay scheme of $^{144}_{58}$Ce.

0.23 MeV. Obviously, a greater amount of energy is released by the 0.31 MeV β-decay process. As a consequence, ^{144}Pr nuclides that result from β^- emission of 0.23 MeV can decay to the ground state with the emission of gamma-ray photons with an energy equivalent to 0.08 MeV, that is, 0.31 − 0.23 MeV. Likewise, ^{144}Pr isomers at an even higher energy state are products of the 0.18-MeV β-decay process. These can decay to the ground state with the emission of gamma-ray photons of energy 0.13 MeV, that is, 0.31 − 0.18 MeV. Not all of the product isomers decay with the immediate emission of gamma radiation, and the abundance of these transitions is given in Fig. 8.2.

It is also possible that essentially all of the product nuclides of a decay reaction will be at an excited or elevated energy state and subsequently fall to a lower energy state by the emission of gamma radiation.

The decay scheme of the nuclide $^{22}_{11}$Na with a 2.6-year half-life serves as an example (see Fig. 8.3). The $^{22}_{11}$Na nuclides decay by both electron capture (EC) and β^+ emission, at relative proportions of 10% and 90%, respectively, to yield immediate $^{22}_{10}$Ne product nuclides in an elevated energy state. Only a trace of the ^{22}Na nuclides (0.06%) decay directly to the ground state. All of the $^{22}_{10}$Ne isomers in the excited energy state decay immediately with the emission of gamma-ray photons of 1.28 MeV energy, which is equivalent to the difference of the energy levels of the two $^{22}_{10}$Ne isomers and also equivalent to the difference in energies released by the two β^+-decay processes (1.82 − 0.54 MeV).

Isomeric transition, as described earlier, is a decay process in which γ emission is the sole process of eliminating energy from an excited nucleus. This mode of decay is referred to as isomeric transition because neither the mass number, *A*, nor the atomic number, *Z*, of a nuclide (^A_ZX) changes in the decay process, and the nuclides are considered to be in isomeric energy states.

In the previous examples (Figs. 8.1−8.3), the isomeric energy state transitions are short-lived; that is, they occur virtually immediately after the other decay processes (eg, β^-, β^+, and EC); and the half-life of the parent nuclide is dependent on these initial processes. If, however, the isomeric transitions are long-lived, the nuclide is considered to be in a metastable state. These nuclides are denoted by a superscript *m* beside the mass number of the nuclide. The radionuclide $^{119m}_{50}$Sn with a 250-day half-life is an example. Its decay scheme, shown in Fig. 8.4, illustrates the emission of two γ photons of 0.065 and 0.024 MeV energy falling from the 0.089-MeV excited state to the ground (stable) state.

Gamma radiation is not produced in all radionuclide decay processes. Instead, some radionuclides decay to a product nuclide at an unexcited ground state. An example is the commonly used radionuclide ^{32}P, which decays by beta-particle emission to the ground state as depicted in Fig. 8.5.

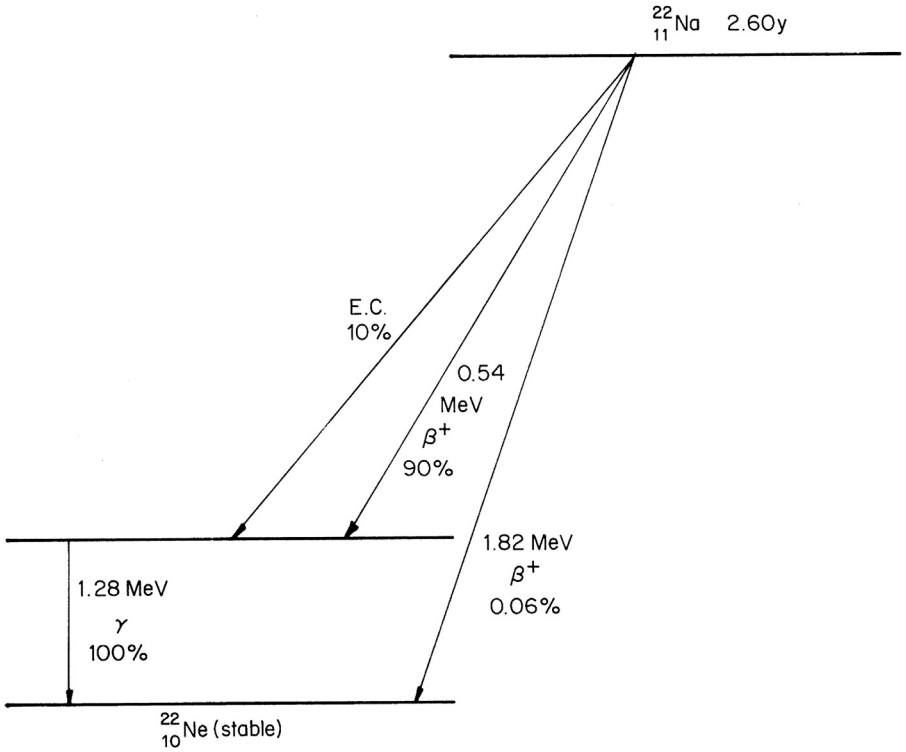

FIGURE 8.3 Decay scheme of $^{22}_{11}$Na.

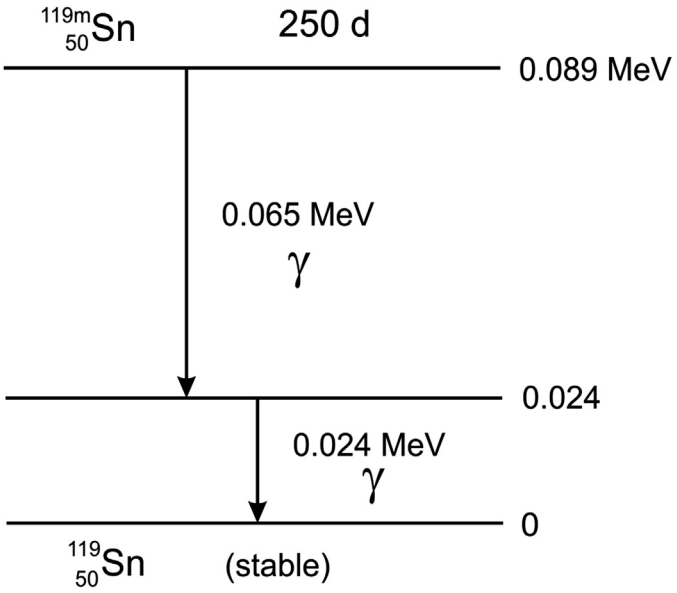

FIGURE 8.4 Decay scheme of $^{119m}_{50}$Sn.

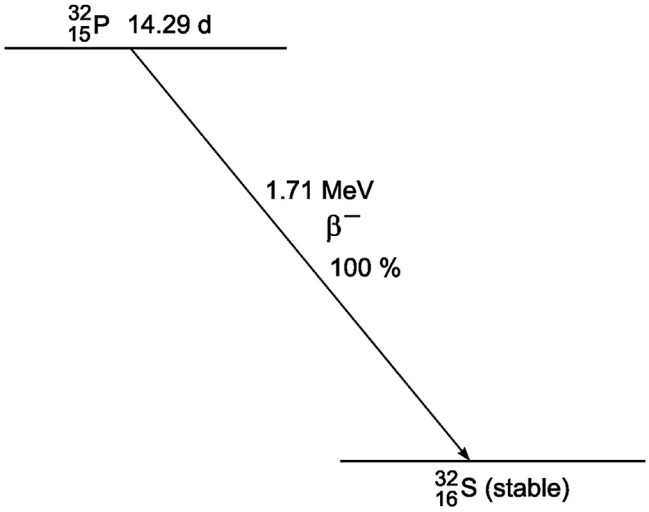

FIGURE 8.5 Decay scheme of $^{32}_{15}$P.

8.4 ANNIHILATION RADIATION

The negatron or negative beta particle, produced by β decay or by pair production (see Section 8.8.4 of this chapter), will travel through matter until it has completely dissipated its kinetic energy via ionization, electron excitation, or bremsstrahlung. The negatron then at rest acts as an atomic or free electron in matter.

A positron or positive beta particle, however, may be considered an "antiparticle" of an electron and consequently, in the electron environment of atoms, has a definite instability. A given positron emitted by pair production or by β^+ decay will also dissipate its kinetic energy in matter via interactions described previously for the case of the negatron. However, as the positron loses its kinetic energy and comes to a near stop, it comes into contact with an electron (Fig. 8.6) with nearly simultaneous annihilation of the positron and the electron masses and their conversion into energy. The annihilation involves the formation of positronium, which is a short-lived association of the positron and electron. Its lifetime is only approximately 10^{-10} or 10^{-7} s, depending on whether the spin states of the associated particles are parallel (*ortho*-positronium) or opposed (*para*-positronium). The *para*-positronium is the shorter-lived spin state. The energy released in

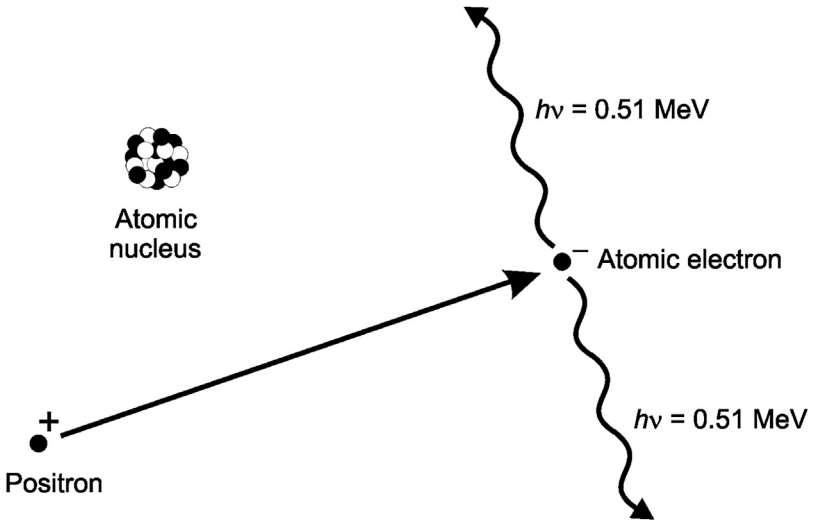

FIGURE 8.6 Annihilation. The interaction between a positron and an electron, and the conversion of their masses into two photons of 0.511-MeV energy.

this annihilation appears as two photons emitted in opposite directions. This transformation of mass into energy, considered as the reverse of pair production, is described as:

$$e^+ + e^- = 2h\nu = 2E_\gamma \qquad [8.12]$$

where a positron, e^+, and electron, e^-, combine to form two gamma-ray photons of energy E_γ. To maintain the equivalence of mass and energy (see Eq. [8.42]), the equivalent of two electron rest masses (0.511 MeV) must appear as photon energies (see Section 8.8.4 of this chapter). In agreement with Eqs. [8.12] and [8.42], the annihilation results in the emission of two 0.511-MeV photons in opposite directions.

8.5 CHERENKOV RADIATION

Charged particles, when they possess sufficient energy, may travel through a transparent medium at a speed greater than the speed of light in that medium. This occurrence causes the emission of photons of light known as Cherenkov radiation. These photons extend over a spectrum of wavelengths from the ultraviolet into the visible portion of the electromagnetic radiation spectrum.

The photon emission is a result of a coherent disturbance of adjacent molecules in matter caused by the traveling charged particle, which must possess a certain threshold energy. This phenomenon has practical applications in the measurement and detection of radionuclides that emit relatively high-energy beta particles (L'Annunziata, 2012e). The theory and applications of Cherenkov radiation are discussed in detail in the chapter entitled "Cherenkov Radiation".

8.6 X-RADIATION

X-radiation is electromagnetic radiation similar to gamma (γ) radiation. Both X-rays and γ-rays are identical in their properties. Both X-rays and γ-rays are photons that possess a quantum of energy defined by Eq. [8.1], namely, $E = h\nu$, which is the product of Planck's constant and the frequency of the radiation. X-rays and γ-rays differ only in their origin. X-rays originate from electron energy transitions, whereas γ-rays originate from the nucleus of an atom, as described in the previous paragraphs, when a nucleus at an elevated energy state decays to a lower, more stable energy state. There are two types of X-rays, which are the following:

1. Electromagnetic radiation characterized by discrete spectral lines of energy resulting from electron transitions in shells of the atoms (eg, *K*, *L*, *M*,… shells) from which they originate. These are X-ray emissions produced when an electron from a given shell is ejected from an atom and an electron from outer shell fills the vacancy left by the ejected electron. This is followed generally by a cascade of electron transitions from outer electron shells, since the filling of one electron vacancy by the transition of an electron from an outer to inner shell will leave another electron vacancy in the outer shell. For example, an electron vacancy in the *K*-shell created by the capture of an electron by the nucleus

(eg, EC or *K*-capture decay) is filled by an electron in the next outer *L*-shell, creating an electron vacancy in that shell, which is followed by the filling of that electron vacancy by an electron in the next outer *M*-shell, etc. The spectra of these discrete energy lines of electromagnetic radiation are characteristic of the atoms from which they originate.

2. Electromagnetic radiation characterized as a broad smear of continuous energies referred to as **bremsstrahlung**, which is produced by electrons or other charged particles, such as protons and alpha-particles, as they are accelerated towards an atomic nucleus and are deflected by the Coulomb field of the nucleus. This was the type of X-ray discovered by Wilhelm Röntgen in 1895, who was the first to discover X-rays. Röntgen discovered the mysterious invisible rays on November 8, 1895 when he was studying cathode rays, ie, the current that would flow through a partially evacuated glass tube (cathode-ray tube then referred to as a Crooke's tube). With such a tube covered in black paper and in a dark room, he noticed that a paper plate covered with the chemical barium platinocyanide would become fluorescent (give off light) even at a distance of 2 m from the cathode ray tube. He was able to demonstrate that the invisible rays came from the collision of the cathode rays (electrons) with the glass surface of the cathode-ray tube or from the collision of the cathode rays with other materials such as aluminum inserted into the glass of the tube. Further studies by Röntgen demonstrated that these rays could travel through various materials to varying extents, when these were placed in the path of the invisible rays, and the transmitted rays could be measured with photographic plates. He gave these mysterious rays the name X-rays, because of their unknown nature and "for the sake of brevity," as he stated in his original papers (Roentgen, 1895, 1896).

8.6.1 X-Rays Characterized by Discrete Spectral Lines

In the chapter entitled "Beta Radiation and Beta Decay," the electron capture (EC) or *K* capture decay process is discussed, whereby an electron from one of the atomic shells (generally the innermost *K* shell) is absorbed by the nucleus, where it combines with a proton to form a neutron. No particle emission results from this decay process. However, the vacancy left by the electron from the *K* shell is filled by an electron from an outer shell (generally the adjacent *L* shell). Transitions produced in electron shell energy levels result in the emission of energy as x-radiation. This radiation consists of photons of electromagnetic radiation similar to gamma radiation. X-radiation and gamma radiation differ only in their origin. X-rays arise from atomic electron energy transitions and gamma rays from transitions between nuclei of different energy states. The production of x-radiation from atomic electron transitions is illustrated in Fig. 8.7.

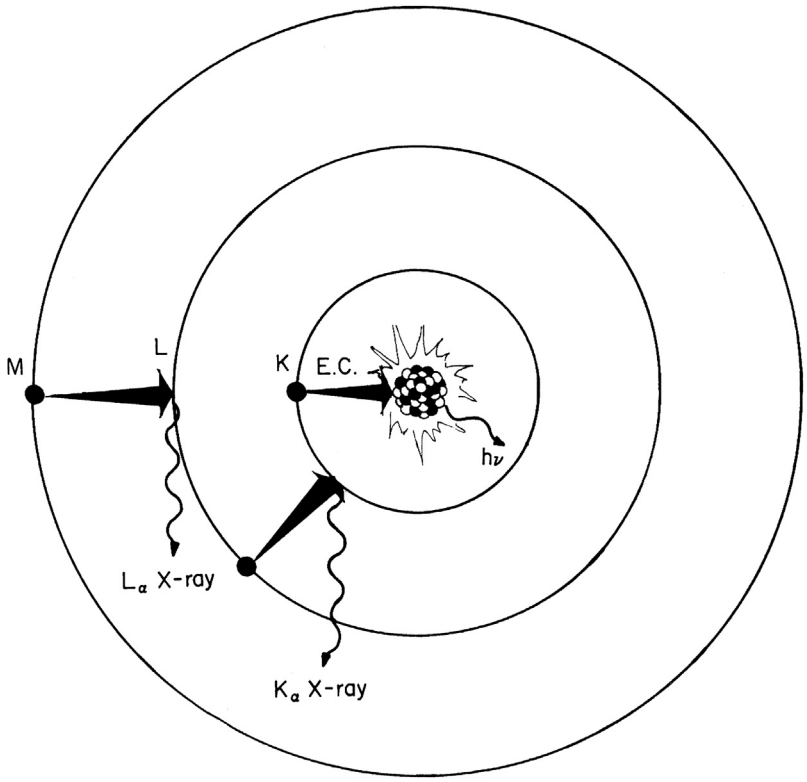

FIGURE 8.7 Electron capture (EC) decay and the accompanying gamma ($h\nu$) and x-radiation.

When an electron transition occurs from the outer L shell to an inner K shell, the energy emitted is equivalent to the difference between the K and L electron binding energies. The electron transitions that ensue in the filling of vacancies result in energy lost by the atom as x-radiation, which is equivalent to the difference of the electron binding energies of the outer, E_{outer}, and its new inner state, E_{inner}, as described by:

$$h\nu = E_{\text{outer}} - E_{\text{inner}} \quad [8.13]$$

The radiation emitted consists of a discrete line of energy characteristic of the electron shell, and consequently of the atom from which it arises.

The production of X-rays in radionuclide decay is, however, more complex. The filling of one electron vacancy in an inner shell is followed by a series of electron transitions in an overall adjustment of electrons in outer shells. This gives rise to further X-rays with lines characteristic of outer shells. Such electron transitions, each resulting in the emission of discrete lines of characteristic X-rays, are illustrated in Fig. 8.8. The transitions are identified by a letter corresponding to the shell (K, L, M, etc.) with vacancy giving rise to the X-ray photon and a subscript (α, β, γ, etc.) to identify, from among a series of outer electron shells of the atom, the shell from which the electron vacancy is filled. For example, an X-ray arising from an electron transition from the L to the K shell is denoted as K_α, and that arising from a transition from the M to the K shell as K_β. Transitions involving the filling of electron vacancies in the L shell from outer M, N, and O shells are denoted by L_α, L_β, and L_γ.

Because x-radiation is characteristic of the atom from which it arises, it is customary to identify the element along with the X-ray photon (eg, Cr K X-rays, Hg L X-rays, etc.). In these examples, the fine structure of the X-ray emissions is not given and the lines are grouped together as K and L X-rays.

The complexity of X-ray lines emitted and their abundances of emission are compounded by the existence of other mechanisms of X-ray production in unstable atoms. One of these mechanisms is the production of Auger electrons. An X-ray emitted from an atom may produce an Auger electron via an internal photoelectric effect (see chapter: Atomic Electron Radiation), which results in the emission of an atomic electron from a shell farther away from the nucleus. The vacancy left by the Auger electron gives rise to additional X-rays characteristic of outer shells following the electron readjustments that ensue. Auger electrons can be emitted from a variety of electron shells, followed by an equal variety of characteristic X-rays from subsequent electron adjustments in outer shells.

Any process that would cause the ejection of an atomic electron of an inner shell can result in the production of x-radiation. Other processes not yet mentioned in this section that involve the ejection of atomic electrons are the emission of internal-conversion electrons (see the chapter: "Atomic Electron Radiation") and radiation-induced ionization.

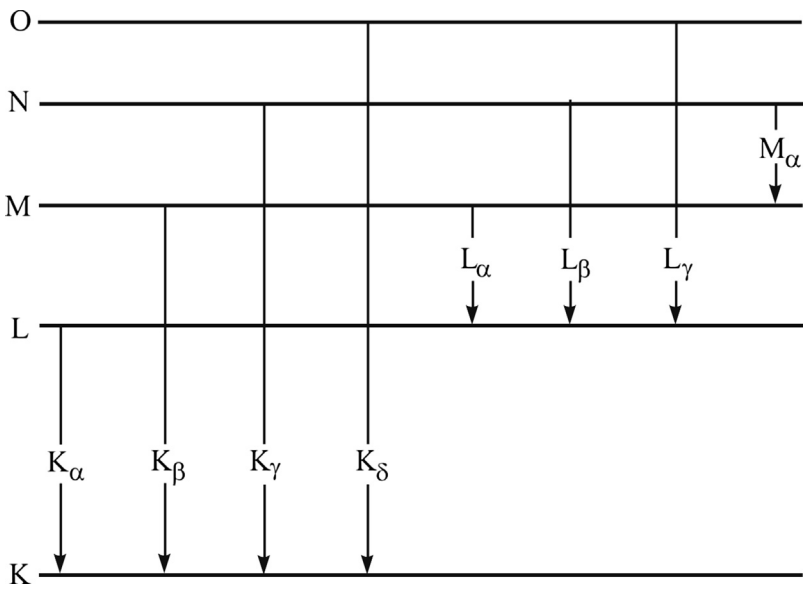

FIGURE 8.8 Atomic electron energy levels or shells (K, L, M, etc.) and lines of transition corresponding to characteristic X-rays (K_α, K_β, K_γ, etc.).

8.6.2 Bremsstrahlung

Bremsstrahlung is a type of x-radiation that is characterized by a broad smear of continuous energies of electromagnetic radiation anywhere in the range between zero and an energy maximum. In general, any charged particle that undergoes acceleration will emit electromagnetic radiation; thus an accelerating charged particle will emit bremsstrahlung when it is made to decelerate upon being deflected from its path of travel by collision or near encounter with an atomic nucleus. Charged particles undergoing acceleration, such as beta particles, electrons, protons, deuterons, and alpha particles, can emit bremsstrahlung as these particles decelerate in a series of collisions with atomic nuclei. This mechanism is illustrated in Fig. 8.9, where a beta particle traveling through matter approaches a nucleus and is deflected by it. This deflection causes a deceleration of the beta particle and consequently a reduction in its kinetic energy with the emission of energy as a photon of bremsstrahlung, which is taken from the German language meaning "braking radiation." The phenomenon is described by:

$$h\nu = E_i - E_f \qquad [8.14]$$

where $h\nu$ is the energy of the photon of bremsstrahlung, E_i is the initial kinetic energy of the beta particle prior to collision or deflection, producing a final kinetic energy E_f of the electron.

As described by Evans (1972) the acceleration produced by a nucleus of charge Ze on a particle of charge ze and mass M is proportional to Zze^2/M, where Z is the atomic number of the nucleus, e is the elementary charge $= 4.803 \times 10^{-10}$ esu, and z is the particle atomic number or 1 for electrons and protons, 2 for alpha particles. Thus, the bremsstrahlung intensity, which is proportional to the square of the product of the amplitude and the charge ze, will vary according to $Z^2z^4e^6/M^2$ (Evans, 1972). From this relation, it is seen that the production of bremmstrahlung per atom of absorber is proportional to the square of the atomic number of the absorber material, and that the total bremsstrahlung is inversely proportional to the square of the mass M of the accelerating charged particle. It is intuitively obvious, and it has been demonstrated through experiment, that an absorber material of higher atomic number will yield a greater production of bremsstrahlung per atom, because the size of the nucleus as well as its charge increases with atomic number and thus the probabilities of interaction of the accelerating charged particle with a nucleus will be a function of the magnitude of the charge on the nucleus as well

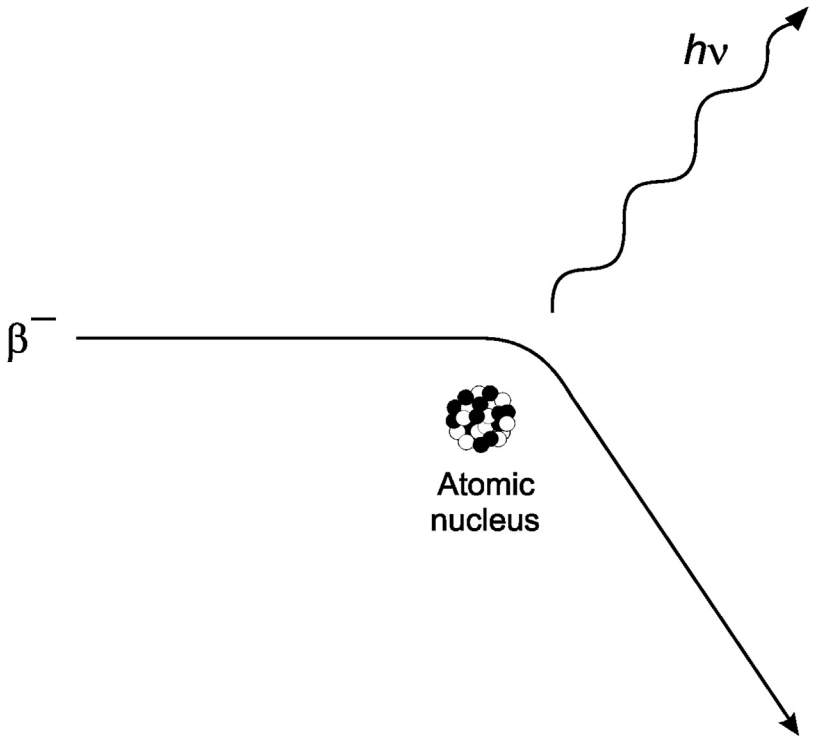

FIGURE 8.9 Bremsstrahlung production. A beta particle is deflected by an atomic nucleus and loses kinetic energy with the emission of a photon of x-radiation.

as the nuclear size. For example, a charged particle (eg, electron or beta particle) of given energy will yield more bremsstrahlung upon interaction with absorber material consisting of pure Pb than one of Cu or C (eg, graphite), that is, bremsstrahlung in Pb ($Z = 82$) > Cu ($Z = 29$) > C ($Z = 6$). The inverse proportionality of bremsstrahlung to the square of the mass M of the charged particle, yields as an outcome that bremsstrahlung production by electrons ($M = 0.0005485$ u) is the most significant among all other charged particles, which are of much higher mass, eg, the muon ($M = 0.1134$ u), proton ($M = 1.007$ u), deuteron ($M = 2.014$ u), or the alpha particle ($M = 4.001$ u). For example, the muon, which has a mass equivalent to 206.7 times that of the electron, would yield less bremsstrahlung than an electron of equal energy in the same absorber medium by a factor of more than 42,000, ie, $M_\mu^2/M_e^2 = 0.1134^2/0.0005485^2 = 42{,}700$. A proton of the same energy and in the same absorber material would yield still less bremsstrahlung than that of the electron by a factor of $M_p^2/M_e^2 = 1.007^2/0.0005485^2 = 3.37 \times 10^6$. Nevertheless, bremsstrahlung from accelerated charged particles, such as accelerated protons, is significant (Huisman et al., 2000; Volkerts et al., 2001; Mahjour-Shafiei et al., 2006; Cohen et al., 2008; Johansson and Wilkin, 2009).

The tremendous difference between the magnitudes of bremsstrahlung production by protons and electrons of the same energy in a given absorber material described in the previous paragraph (ie, $M_p^2/M_e^2 = 1.007^2/0.0005485^2 = 3.37 \times 10^6$) was utilized by Olzem et al. (2007) to measure cosmic-ray positron radiation through bremsstrahlung conversion. A major difficulty in the measurement of cosmic-ray positrons in the energy range of 50 GeV is the high background of cosmic-ray protons, which exceed the number of positrons by a factor of 10^4 (Aguilar et al., 2002; Beatty et al., 2004). The researchers (Olzem et al., 2007) took advantage of the fact that proton bremsstrahlung is suppressed by a factor of more than 3.37×10^6 with respect to the electron (ie, positrons). By detecting the bremsstrahlung produced by the high-energy (1−50 GeV) cosmic-ray positrons, the proton background in this same energy range is suppressed by a factor of more than 3×10^6. Bremsstrahlung by cosmic-ray pions is also significantly suppressed compared to electron bremsstrahlung by a factor of $M_\pi^2/M_e^2 = 0.1485u^2/0.0005485\,u^2 = 7.3 \times 10^4$. A diagram illustrating the process of cosmic-ray positron bremsstrahlung conversion is given in Fig. 8.10.

As illustrated in Fig. 8.10, a primary cosmic-ray positron enters into the detector material from above, producing a bremsstrahlung photon. The bremsstrahlung photon then converts into a positron−electron pair. Three particles are observed in the tracking detector, namely, the positron and negatron each of 0.511-MeV energy created in the pair production, which are highly deflected in a magnetic field, and the incident high-energy positron, which is only slightly deflected in the magnetic field. Olzem et al. (2007) report that additional background rejection of cosmic-ray mesons and protons is provided by the photon emission angles, which are essentially zero for high-energy positrons and significantly larger than zero for mesons and protons due to their higher mass.

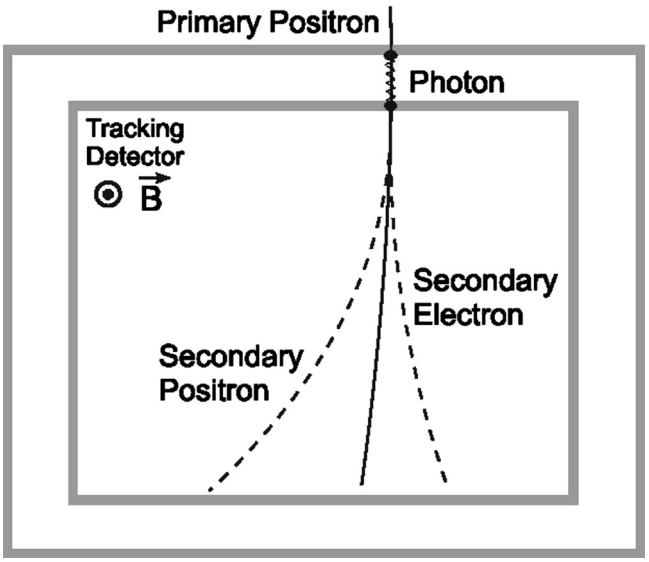

FIGURE 8.10 Signature of pair production by a bremsstrahlung photon. *From Olzem, J., et al., 2007. Cosmic-ray positron identification through bremsstrahlung conversion. Nucl. Phys. B (Proc. Suppl.) 173, 51−55. Reprinted with permission of Elsevier © 2007.*

8.6.2.1 Bremsstrahlung in Beta-Particle Absorbers

When beta particles from a particular radionuclide source strike an absorber material, a wide spectrum of bremsstrahlung photon wavelengths (or energies) will be produced. The bremsstrahlung photon energies will range from zero to a maximum photon energy, $h\nu_{max}$. The broad spectrum of bremsstrahlung is due to the broad possibilities of different interactions, ie, deflections or collisions, that the beta particles can have with atomic nuclei of the absorber and the broad spectrum of beta-particle energies emitted from any given radionuclide. In a given spectrum of bremsstrahlung, the shortest wavelength, λ_{min}, is observed when a beta particle or electron undergoes a direct collision with the nucleus of an atom and loses all of its kinetic energy, $h\nu_{max}$, as bremsstrahlung or x-radiation according to the relation:

$$h\nu_{max} = \frac{hc}{\lambda_{min}}, \qquad [8.15]$$

which follows the energy-wavelength Planck–Einstein relation previously described by Eq. [8.1].

Let us consider an example of a 1710-keV beta particle from ^{32}P ($E_{max} = 1.71$ MeV) striking a nucleus. If the beta particle loses all of its energy in the collision, the wavelength of the bremsstrahlung emitted from this interaction according to Eq. [8.15] would be:

$$\lambda = \frac{hc}{h\nu_{max}} = \frac{12.4 \text{ keV Å}}{1710 \text{ keV}} = 0.00725 \text{ Å}$$

See Eq. [8.10] for the conversion of the constant hc to convenient units of eV m or eV Å. Bremsstrahlung production by high-energy beta particles in absorber material of high atomic number is significant (see Section 6.9.1 of the chapter: "Beta Radiation and Beta Decay"). Consequently to reduce the production of bremsstrahlung in radiation shielding against the harmful effects of high-energy beta particles, an absorber of low atomic number (eg, plastic) may be preferred over one of high atomic number (eg, Pb-glass).

Ionization and electron excitation were previously described as predominant mechanisms by which a traveling beta particle may lose its kinetic energy in matter (see the chapter: "Beta Radiation and Beta Decay"). However, the production of bremsstrahlung may also be another significant mechanism for the dissipation of beta-particle energy, particularly as the beta-particle energy and the atomic number of the absorber increase (Kudo, 1995). A more thorough treatment is found in Section 6.9 of the Chapter entitled "Beta Radiation and Beta Decay," which includes examples of calculations involved to determine the degree of bremsstrahlung production as a function of beta-particle energy and absorber atomic number. In general terms, we can state that for a high-energy beta particle such as the beta particle of highest energy emitted from ^{32}P ($E_{max} = 1.71$ MeV) in a high–atomic-number absorber such as lead (Pb = 82), bremsstrahlung production is significant. In a substance of low atomic number such as aluminum (Al = 13), bremsstrahlung production by a 1.7-MeV beta particle is reduced more than sixfold as compared to lead (see Fig. 6.18 of the chapter: "Beta Radiation and Beta Decay").

In view of the wide spectrum of beta-particle energies emitted from radionuclides and the wide variations of degree of beta-particle interactions with atomic particles, the production of a broad spectrum, or smear, of photon energies of bremsstrahlung is characteristic. This contrasts with x-radiation, which is emitted as a result of atomic electron rearrangement processes, resulting in the emission of discrete lines of photon energy.

8.6.2.2 Artificially Produced Bremsstrahlung

An apparatus used to artificially produce X-rays, such as those employed in medical diagnosis or X-ray diffraction, functions on a similar principle as bremsstrahlung described previously. The X-ray apparatus consists of an evacuated tube containing a cathode filament and a metal anode target such as tungsten ($A = 74$). A voltage potential is applied to the tube so that electrons emitted from the cathode accelerate towards the anode. Upon colliding with the tungsten anode, the accelerated electrons lose energy as bremsstrahlung x-radiation. For example, an electron accelerated in an X-ray tube to an energy of 40 keV, which loses all of its energy upon impact with a tungsten nucleus, would produce a single X-ray photon of wavelength calculated as:

$$\lambda = \frac{hc}{h\nu} = \frac{12.4 \text{ keV Å}}{40 \text{ keV}} = 0.31 \text{ Å} = 0.031 \text{ nm} \qquad [8.16]$$

A broad spectrum of bremsstrahlung is produced due to the various degrees of deflection or collision of the accelerated electrons with the target nuclei.

Electron accelerators are a good source of bremsstrahlung currently employed in food irradiation for the preservation and extension of the shelf-life of food (Miller, 2003, 2005; Mehta et al., 2003; Auslender et al., 2004; Farkas, 2004, 2006; Farkas and Mohácsi-Farkas, 2010). Food irradiation is the process where food is exposed to ionizing energy, utilizing gamma photons emitted by ^{60}Co (or less frequently by ^{137}Cs), machine-generated X-rays (bremsstrahlung) of up to 5 MeV, or accelerated electrons of up to 10 MeV kinetic energy (Farkas, 2004). The use of accelerator sources is gradually replacing the use of radioisotope sources for the irradiation of food, mainly because the generation of the radiation can be controlled by a simple on-off switch (Cleland et al., 1991; Miller, 2003). The accelerators may be used to irradiate food directly with the electron beam or indirectly with the bremsstrahlung radiation produced after the electron beam strikes a converter material. To avoid the possibility of measurable food activation via photonuclear reactions, the kinetic energy of the electron beam is limited by regulation to 10 MeV, and the kinetic energy regulation for bremsstrahlung irradiation of foods is limited to 5 MeV.

Bremsstrahlung, electron beams, and gamma radiation have numerous industrial applications, which include, in addition to food preservation, the sterilization of health care products, the irradiation of blood to prevent transfusion-associated graft versus host disease, the sterilization of tissue for transplant surgery, the synthesis of radiation-cured rubber, and the manufacture of radiation-cured wood polymer composites, etc. These applications are reviewed in chapter "Radioactivity and Our Well Being" of this book.

8.6.2.3 Inner or Internal Bremsstrahlung

Bremsstrahlung of very low intensity, referred to as inner or internal bremsstrahlung, also occurs during the transformation of the nucleus in electron capture decay processes and beta particle emission. The bremsstrahlung is a continuous spectrum of X-ray photons that originates within the transforming atoms and can be attributed to the sudden change of nuclear charge when the beta particle is emitted or when an orbital electron is captured (Evans, 1972). Internal bremsstrahlung is explained by Cengiz and Almaz (2004) to occur during the emission of a β^- particle from the nucleus, as the β^- particle undergoes an acceleration at its birth and emits bremsstrahlung in the field of the emitting nucleus. The magnitude of inner bremsstrahlung was calculated to be approximately 1/137 quantum of internal bremsstrahlung per beta particle emitted from the nucleus (Knipp and Uhlenbeck, 1936; Evans, 1972). Internal bremsstrahlung spectra for several nuclides that emit β^- particles were calculated by Cengiz and Almaz (2004). This radiation was named inner or internal bremsstrahlung, because it originates from the nucleus, the internal part of the atom, in contrast to external bremsstrahlung that occurs when an external beta particle approaches an atom external to it from another source and is deflected by the nucleus of that atom.

In the electron capture decay process, the quantum of energy not carried away by the neutrino is emitted as internal bremsstrahlung. Thus, in electron capture decay, internal bremsstrahlung may possess energies between zero and the maximum, or transition energy of a radionuclide. When gamma radiation is also emitted, the internal bremsstrahlung may be masked by the more intense gamma rays and go undetected. However, in the absence of gamma radiation, the upper limit of the internal bremsstrahlung can be used to determine the transition energy of a nuclide in electron capture decay. Some examples of radionuclides that decay by electron capture without the emission of gamma radiation are as follows:

$$^{55}_{26}\mathrm{Fe} \rightarrow {}^{55}_{25}\mathrm{Mn} + \nu + h\nu \quad (0.23\ \mathrm{MeV}) \qquad [8.17]$$

$$^{37}_{18}\mathrm{Ar} \rightarrow {}^{37}_{17}\mathrm{Cl} + \nu + h\nu \quad (0.81\ \mathrm{MeV}) \qquad [8.18]$$

and:

$$^{49}_{23}\mathrm{V} \rightarrow {}^{49}_{22}\mathrm{Ti} + \nu + h\nu \quad (0.60\ \mathrm{MeV}) \qquad [8.19]$$

where $h\nu$ is the internal bremsstrahlung, the upper energy limits of which are expressed in MeV.

8.6.2.4 Nuclear Bremsstrahlung (Nuclear Startstrahlung)

Nuclear bremsstrahlung was identified in proton−neutron capture and proton−deuteron fusion reactions by Nie Luo, Magdi Ragheb, and George Miley at the University of Illinois (Luo et al., 2010). This class of bremsstrahlung refers to electromagnetic radiation of low energy (ie, soft X-rays of a few hundred eV to a few keV) emitted by a proton or deuteron, or both as these undergo acceleration during the fusion of a proton with a neutron or the fusion of a proton with a deuteron. Luo et al. (2010) loosely assigned the name of nuclear bremsstrahlung to this phenomenon and have ventured to also call it nuclear startstrahlung, from the German meaning "take-off radiation," depicting the acceleration of these nuclear particles as the origin of the soft X-rays. The identification of this class of bremsstrahlung opens the door to new plasma diagnostics

such as in the identification of the parasitic D−D fusion reaction in future thermonuclear reactors based on D−T fusion. The D−D fusion reaction produces protons according to:

$$d + d \rightarrow {}^{3}\mathrm{H} + p \quad Q = 4.04\ \mathrm{MeV} \qquad [8.20]$$

The D−T thermonuclear reaction is an excellent source of neutrons, as described in the chapter entitled "Neutron Radiation." The protons and neutrons generated can, in turn, participate in the thermonuclear process via other reactions including the fusion of a proton with a neutron according to:

$$p + n \rightarrow {}^{2}\mathrm{H} + \gamma + \text{x-rays} \quad Q = 2.23\ \mathrm{MeV} \qquad [8.21]$$

and the fusion of a proton with unreacted deuterium fuel according to the reaction:

$$p + d \rightarrow {}^{3}\mathrm{He} + \gamma + \text{x-rays} \quad Q = 5.49\ \mathrm{MeV} \qquad [8.22]$$

both of which give rise to the nuclear bremsstrahlung, which are included in the above two reactions.

The process of nuclear bremsstrahlung, in the simplest case of $p-n$ capture, is illustrated in Fig. 8.11. As described by Luo et al. (2010), the proton and neutron are attracted to each other by the strong nuclear force, and this attraction causes

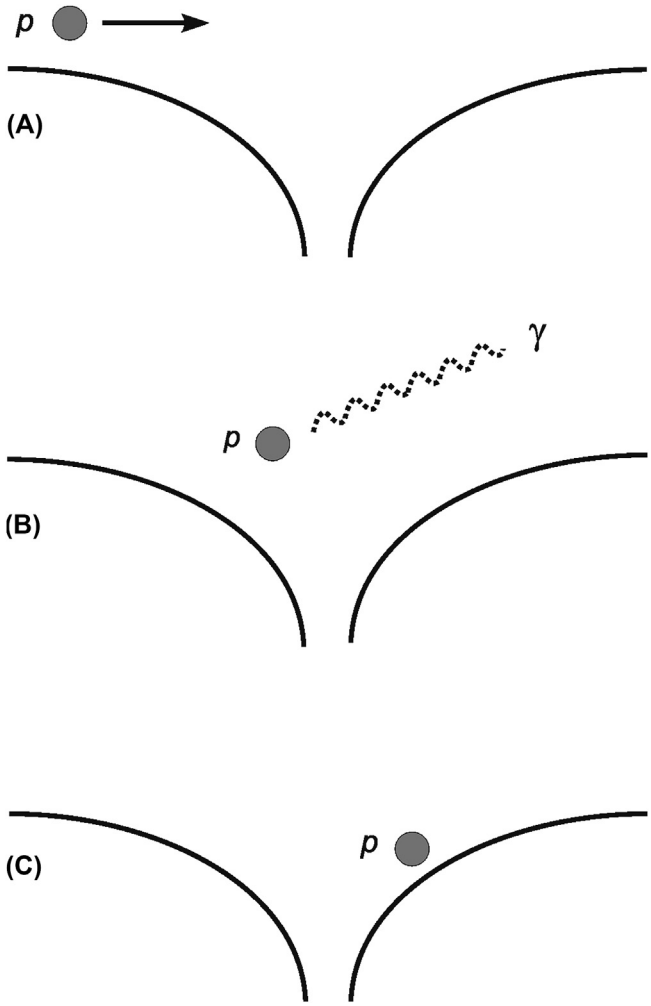

FIGURE 8.11 The nuclear bremsstrahlung process that releases soft X-rays in the proton−neutron capture and proton−deuteron fusion. The solid curves represent the attractive nuclear potential of a neutron (or deuteron) felt by a proton. The length dimension shown is ~10 fermi. (A) The proton, having an initial positive kinetic energy of several keV, is moving towards the neutron (or deuteron) due to nuclear attraction. (B) The proton accelerates in the process, and therefore starts radiating electromagnetic waves, ie, photons. (C) The proton, having lost all of its initial kinetic energy and maybe more, now has a total energy of negative value, ie, it is now a bound state around the neutron (or deuteron). Afterward it may emit a gamma of 2.23 MeV for proton−neutron fusion (or 5.49 MeV for proton−deuteron fusion) and then combine with the neutron (or deuteron) to finally form ^{2}H (or ^{3}He). The acceleration of the neutron is radiation-free, because the neutron is without charge. In p−d fusion, the accelerating deuteron also radiates, but this is not illustrated in the figure for clarity. *From Luo et al. (2010) with permission of Elsevier © 2010.*

both particles to accelerate toward each other. Due to the charge on the accelerating proton, electromagnetic radiation is generated of the bremsstrahlung type. Luo et al. (2010) refer to this as a nuclear bremsstrahlung or nuclear startstrahlung, to accentuate its origin in acceleration due to the strong nuclear force.

The fusion of the proton with deuterium yields the nuclear bremsstrahlung similar to the case of the proton and neutron fusion. However, Luo et al. (2010) explain that the Coulomb repulsion of proton and deuterium add a degree of complication to the process. They explain that the Coulomb barrier is overcome by quantum mechanical tunneling; and the strong nuclear force still causes both particles to accelerate toward each other, although the particles accelerate at different rates because of their mass difference. As both the proton and deuteron are charged they radiate quanta of electromagnetic radiation. Because the two charged particles are accelerating towards each other, they travel in opposite directions, and the radiation they emit will tend to cancel each other; however, the cancellation is not complete, because the two particles accelerate at different rates due to their mass difference.

8.6.3 X-Rays From Beta-Particle Emissions

All beta-emitting radionuclides, even those radionuclides classified as pure beta-emitters that are not the source of any gamma radiation, including ^{3}H, ^{14}C, ^{32}P, ^{35}S, ^{45}Ca, ^{63}Ni, ^{89}Sr, ^{90}Y, and ^{123}Sn, among others, will produce X-ray photons. For example, the measurement of bremsstrahlung from the beta particles of ^{3}H has been demonstrated as a method for the monitoring of the fuel-processing system in the development of thermonuclear fusion reactors (Shu et al., 2004, 2006). This section will describe X-ray production by beta particles in thick-target materials. Thick-target materials include any absorber within which a beta particle will come to a complete stop. When beta particles are emitted from decaying nuclei and escape the atom from which they originated, and are absorbed by materials before coming to a stop, X-ray photons are created by several distinct physical phenomena, which are enumerated as follows:

1. **External bremsstralung**, which is a continuous spectrum of X-rays produced when the accelerating beta particle traverses atoms of absorber material and is deflected by the Coulomb field of atomic nuclei, causing the beta particle to decelerate and emit electromagnetic radiation. This is the major source of X-ray energy that a beta particle will radiate. As discussed previously, the energy of the electromagnetic radiation emitted ($E = h\nu$) is proportional to the initial energy of the beta particle and the atomic number (Z) of the absorber. Thus, the bremsstrahlung energy loss (I) in MeV is written as:

$$I \simeq kZE^2 \qquad [8.23]$$

or:

$$I/E \simeq kZE \qquad [8.24]$$

where I/E is the fraction of incident beta-particle energy lost as bremsstrahlung and $k = 0.0007\ \text{MeV}^{-1}$ is a normalization constant (Evans, 1972; Faw and Shultis, 2004). Table 8.1 illustrates the effect of atomic number Z on the conversion of beta-particle energy to bremsstrahlung in a thick target according to the approximation given by Eq. [8.23]. The estimates of energy conversion for a 1-MeV electron in aluminum and a 2-MeV electron in lead listed in Table 8.1 agree with estimates quoted by Choppin et al. (2002) and Faw and Schultis (2004), respectively. Molybdenum (Mo) and tungsten (W), listed in Table 8.1, are relatively high-Z materials with heat stability used as target materials for the production of bremsstrahlung X-rays in commercial medical diagnostic X-ray tubes (Mavunda et al., 2004).
2. **Internal bremsstrahlung**, which occurs during the emission of the beta particle from the nucleus, as the beta particle accelerates at its birth and emits a continuous spectrum of X-rays in the field of the emitting nucleus (Cengiz and Almaz, 2004). This mechanism of bremsstrahlung production is in direct contrast to that of outer bremsstrahlung, whereby the beta particle approaches a nucleus from outside the atom, as described in the previous section.
3. **X-rays corresponding to line spectra characteristic of the absorber material**, which are produced when the beta particle traverses the absorber and produces ionization in inner electron shells (K, L, M,… shells). The electron vacancies in the inner shells are filled by electrons from outer shells with the concomitant emission of X-rays. These X-rays consist of discrete lines of energy characteristic of X-ray lines of the absorber material.
4. **X-rays corresponding to line spectra characteristic of the emitting atom**, which are produced when the beta particle produces ionization as it accelerates out of the atom from which it was created. Ionization of internal electron shells (K, L, M,… shells) of the emitting atom leaves electron vacancies, which are filled by electrons from outer shells, producing X-rays of discrete energy lines characteristic of the emitting atom. The probability of this internal ionization followed by X-ray emission by the β-emitting atom is of the order of 10^{-4} (Levinger, 1953; Boehm and Wu, 1954; Evans, 1972).

TABLE 8.1 Approximate Incident Beta-Particle Energy Loss (*I*/*E*) as Bremsstrahlung in Various Thick Targets[a]

	Fraction of Incident Beta-Particle Energy Loss (*I*/*E*)					
Incident Energy (*E*)	H_2O ($Z = 6.6$)[b]	Al ($Z = 13$)	Cu ($Z = 29$)	Mo ($Z = 42$)	W ($Z = 74$)	Pb ($Z = 82$)
0.1 MeV	0.05%	0.09%	0.2%	0.3%	0.5%	0.6%
0.2	0.09	0.2	0.5	0.6	1.0	1.1
0.5	0.2	0.5	1.0	1.5	2.6	2.9
1.0	0.5	0.9	2.0	2.9	5.2	5.7
1.5	0.7	1.4	3.0	4.4	7.8	8.6
2.0	0.9	1.8	4.1	5.9	10.4	11.5
2.5	1.1	2.3	5.1	7.4	13.0	14.4

[a]*Calculated according to* $I/E \approx (0.0007\ MeV^{-1})\ ZE$, *where* I *is the total bremsstrahlung energy (MeV),* E *is the incident electron or beta-particle energy (MeV), and* Z *is the atomic number of the thick-target absorber.*
[b]*For* H_2O, *a compound absorber, the effective or modified atomic number is used as calculated by Markowicz and VanGrikin (1984) and Manjunatha and Rudraswamy (2009, 2010), namely,* $Z_{mod} = \sum_i^l (W_i Z_i^2/A_i)/\sum_i^l (W_i Z_i/A_i)$ *where* W_i, Z_i, *and* A_i *are the weight fraction, atomic number, and mass number, respectively, of the* ith *element.*

8.7 SYNCHROTRON RADIATION

Synchrotron radiation is electromagnetic radiation emitted by charged particles of low mass (eg, negatrons or positrons) traveling at relativistic speeds (ie, close to the speed of light) as the particles are made to undergo radial acceleration when deflected in a magnetic field. The radiation emitted covers a broad spectrum from the long microwaves to the shorter wavelengths of hard X-rays. Synchrotron radiation is produced both naturally and artificially.

8.7.1 Synchrotron Radiation From Natural Sources

A natural source of synchrotron radiation is observed in certain light emissions from astronomic bodies. An example is provided by the light emitted from the Crab Nebula, which is the remnant of a supernova explosion of a massive star. An excellent image of the Crab Nebula obtained by the Spitzer Space Telescope is given in Fig. 8.12, which shows the bluish-white light originating from synchrotron radiation caused by clouds of relativistic electrons deflected radially by the magnetic field of a rotating neutron star.

8.7.2 Discovery of Synchrotron Radiation

The first artificial production of synchrotron radiation was reported in 1947 by Frank Elder, Anatole Gurewitsch, Robert Langmuir, and Herb Pollock in a letter entitled "Radiation from Electrons in a Synchrotron" in the journal *Physical Review* (Elder et al., 1947). They followed their initial observations with a paper on the properties of the radiation and its origin the following year entitled "Radiation from Electrons Accelerated in a Synchrotron" (Elder et al., 1948). In this work, they concluded that the radiation emissions were due to "high-energy electrons subjected to large radial accelerations." The radiation was named synchrotron radiation, as it was discovered to occur when electrons are accelerated to relativistic speeds in a synchrotron where the electron path is diverted radially with a magnetic field. The phenomenon is illustrated in Fig. 8.13, which shows electrons traveling near the speed of light in a storage ring, which is a ring-shaped chamber where electrons, traveling at near light speed originating from a booster synchrotron, are stored for research. The synchrotron radiation is emitted when the path of travel of the electron is forced to bend in a magnetic field.

The discovery of synchrotron radiation followed the construction of the synchrotron and the testing of the synchrotron principle. It was foreseen in the early 1940s that, as a charged particle is accelerated to relativistic speeds (ie, speeds approaching the speed of light), the relativistic mass of the particle would increase to the point that it would not be possible to maintain that particle in a constant orbit. Thus, current thought prevailed that there would be a limit to the speed to which the charged particle could be kept in a constant orbit. Wilson (1996) and Wei (2003) provide good historical accounts that led to the discovery of the synchrotron. In 1943, Sir Marcus Oliphant (1901–2000), an Australian physicist, was working

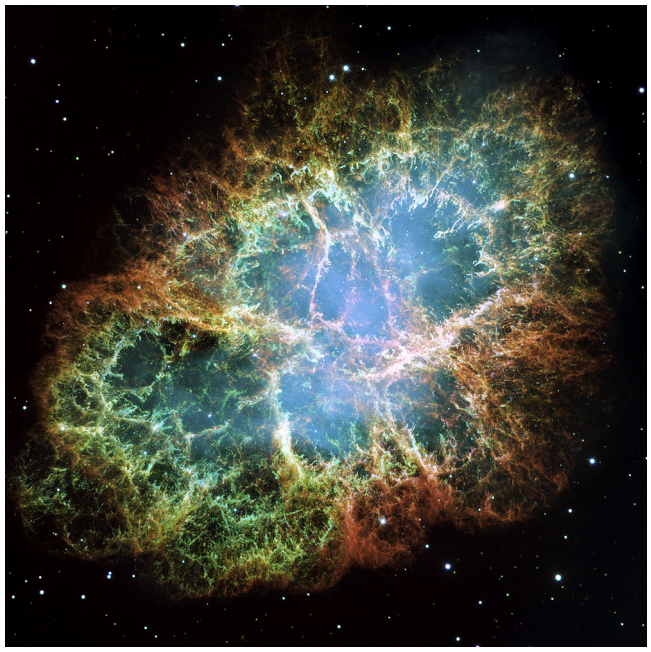

FIGURE 8.12 Image of the Crab Nebula photographed by the NASA Hubble Space Telescope's Wide Field and Planetary Camera released to the public on December 1, 2005. The bluish-white regions originate from synchrotron radiation produced by clouds of high-energy electrons traveling radially at relativistic speeds under the influence of a magnetic field of a rapidly rotating neutron star. The Crab Nebula is located in the Constellation Taurus, about 6500 light years from earth, and the image along the bottom measures 12 light years. *Courtesy of NASA, ESA, J. Hester, and A. Loll (Arizona State University).*

with Earnest Lawrence at the Oak Ridge National Laboratory on the Manhattan Project. As related by Wilson (1996), Marcus Oliphant, while at Oak Ridge, was planning to return to his professorship post at the University of Birmingham; and in September of 1943, he wrote a memorandum to the Department of Scientific and Industrial Research (DSIR) in the UK (Oliphant, 1943) in which he proposed a new method of acceleration as follows:

> *Particles should be constrained to move in a circle of constant radius thus enabling the use of an annular ring of magnetic field…which would be varied in such a way that the radius of curvature remains constant as the particles gain energy through successive accelerations by an alternating electric field applied between coaxial hollow electrodes.*

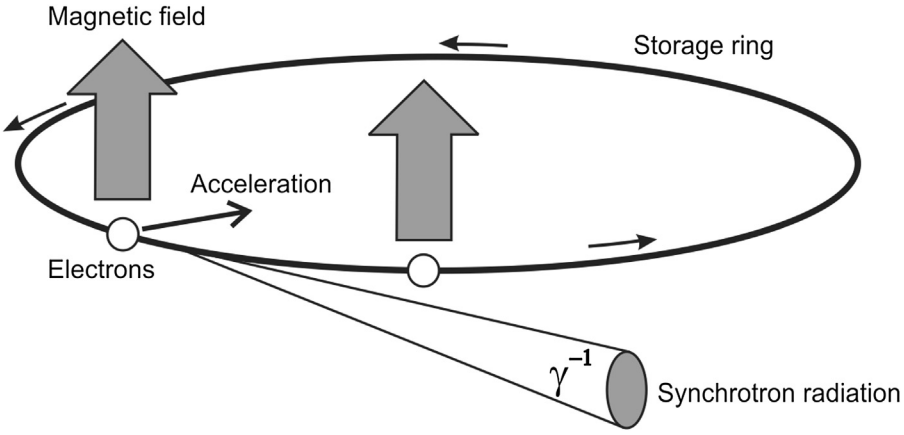

FIGURE 8.13 Synchrotron radiation caused by a bending magnet, when electrons traveling at relativistic speeds are caused to travel radially in a storage ring linked to a booster cyclotron. The high-energy electrons produce synchrotron radiation every time they are deflected by a magnetic field. The synchrotron radiation is concentrated into a cone with an angle on the order of γ^{-1}. *From Yagi, N., 2014. Synchrotron radiation, pp. 17–33, In Comprehensive Biomedical Physics. In: Brahme, A. (Ed.-in-Chief), Radiation Sources and Detectors, vol 8. Elsevier, Amsterdam, pp. 418; reprinted with permission from Elsevier © 2014.*

Oliphant is thus considered as the originator of the synchrotron concept (Wilson, 1996; Wei, 2003). However, shortly thereafter the Russian Physicist Vladimir I. Veksler (1907−1966) and Edwin M. McMillan (1907−1991) at the University of California, Berkeley independently proposed the concept of phase stability upon which the operation of the synchrotron is based (Veksler, 1944, 1945; McMillan, 1945). As defined by Wei (2003), synchrotrons are circular accelerators in which charged particles are accelerated with electric fields and constrained to move in fixed orbits by magnets whose fields vary in time such that the radius of curvature of the particle beam remains constant as the particles gain energy. Increasing energy and acceleration are attributed to the particles, as described in Oliphant's memo, by alternating electric fields, which are produced by resonating radiofrequency (rf) cavities.

At the General Electric Company in Schenectady, New York, Frank Elder, Anatole Gurewitsch, Robert Langmuir, and Herb Pollock and their staff constructed a 70-MeV synchrotron to test the synchrotron principle of phase stability (Elder et al., 1947, 1948). During a test run of the newly constructed synchrotron, synchrotron radiation was discovered. As related in a published memoir on "The Discovery of Synchrotron Radiation," Pollock (1983) recorded in his laboratory notebook the following account on April 24, 1947 (reproduced with permission © 1983 American Association of Physics Teachers):

> *Frank Elder worked on the design of the power circuit and the laminated magnet, which was assembled by machinist Floyd Haber. Anatole Gurewitsch focused on the 163-Mc rf cavity resonator design…Robert Langmuir and Pollock put the various components together and on 24 October 1946 we were able to tell Edwin McMillan in Berkeley that we had a synchrotron beam and that no problem had been encountered…for synchrotron acceleration to 70 MeV…On that day in April [24 April 1947] Langmuir and Pollock were running the machine and as usual were trying to push the electron gun and its associated pulse transformer to the limit. Some intermittent sparking had occurred, and Haber was asked to observe with a mirror around the protective concrete wall which separated the machine from the control room…When Haber looked around the corner of the wall he noticed a very bright spot of light…At first we thought it might be due to Cerenkov radiation, but it soon became clear that we were seeing Iwanenko and Pomeranchuk radiation …We observed the bright spot with mirrors, looking tangent to the orbit at two or three points in the room…The beam appeared stable and of small cross section (perhaps 1 mm square).*

The Iwanenko and Pomeranchuk radiation, referred to in Pollock's notes, is the prediction made in 1944 by the Russian physicists Dimitri Iwanenko (1904−1994) and Isaak Pomeranchuk (1913−1966) in their joint papers (see Iwanenko and Pomeranchuk, 1944a,b) of the emission of radiation by electrons traveling at relativistic speeds in a magnetic field. Iwanenko and Pomeranchuk (1944a,b) thought that this radiation emission might be a limiting factor in achieving maximal electron energies in the development of electron accelerators. However, the radiation emission (ie, synchrotron radiation) is named after the instrument within which it was first observed and which today remains the principle source of this radiation for experimental research. A very thorough review of the history of synchrotron radiation, including the theory on radiation from accelerated electrons from as early as 1912, is provided by Blewett (1988).

8.7.3 Synchrotron Radiation and Accelerated Electron Properties

Synchrotron radiation is currently the brightest source of X-rays available for numerous practical research applications, which will be discussed further on in this section. Suortti (2003) and Owens (2012) report that the synchrotron light emissions are very intense; and the brilliance is measured in the number of photons per second per mm^2 per $mrad^2$. Modern synchrotrons yield a brilliance of up to 10^{20} photons/s/mm^2/$mrad^2$ (Owens, 2012). The X-ray beam of synchrotron radiation is generally very highly collimated with an angular spread of only 1 mrad (Teresawa and Kihara, 1996). As illustrated previously in Fig. 8.13, the angular spread of the synchrotron radiation cone is:

$$\gamma^{-1} = \sqrt{1-\beta^2} \text{ where } \beta = v/c \text{ and } \gamma = \frac{1}{\sqrt{1-(v^2/c^2)}} \quad [8.25]$$

The variable β is the relative phase velocity of the electron, that is, the ratio of the velocity of the electron (v) to the speed of light in a vacuum (c), and γ is the Lorentz transformation factor described previously for relativistic calculations of mass, length, and time. According to Eq. [10.3] of the chapter entitled "Neutron Radiation" and Eq. [III.45] in Hall of Fame, Part III, the total energy (E) of a particle is the sum of its kinetic (K) and rest energies (mc^2) or:

$$E = K + mc^2 = \gamma mc^2 \quad [8.26]$$

According to Eq. [8.26], the synchrotron cone angle γ^{-1} can be expressed as:

$$\frac{1}{\gamma} = \frac{mc^2}{E} \quad [8.27]$$

where the rest energy (mc^2) for the electron is 0.511 MeV. Thus, as the electron energy E increases, the synchrotron cone angle decreases. Teresawa and Kihara (1996) report $1/\gamma = 0.064$ mrad for $E = 8.0$ GeV electron, which is calculated according to Eq. [8.27] as:

$$\frac{1}{\gamma} = \frac{mc^2}{E} = \frac{0.511 \text{ MeV}}{8 \times 10^3 \text{ MeV}} = 0.0000638 \text{ rad} = 0.0638 \text{ mrad} \quad [8.28]$$

which represents only a 0.64-mm spread of the synchrotron radiation at a distance of 10 m from the source, or a 6.4-mm spread at a distance of 100 m. Synchrotron radiation is thus a very highly collimated beam. The radiation is highly polarized and emitted as pulsed light with short durations of 1 ns or less (Owens, 2012).

Teresawa and Kihara (1996) provide an example of electrons accelerated in a synchrotron to an energy of 1.0 GeV. They report the phase velocity $\beta = 0.999999868$, that is, the velocity (v) of the electron would be $0.999999868c$ and $\gamma = 1957$, that is, the electron traveling at the relativistic speed, close to that of light, would possess a mass 1957 times that of that of its rest mass. This is found according to Eq. [8.27] or:

$$E = \gamma mc^2 \text{ and } \gamma = \frac{E}{mc^2} = \frac{1 \text{ GeV}}{0.511 \text{ MeV}} = \frac{1 \times 10^3 \text{ MeV}}{0.511 \text{ MeV}} = 1956.95 \quad [8.29]$$

Also from the value of γ, the velocity of the electron (v) relative to the speed of light in a vacuum (c) can be calculated with the expression for the Lorentz transformation factor as:

$$\gamma = \frac{1}{\sqrt{1 - (v/c)^2}} \quad [8.30]$$

Substituting the value of 1957 for γ and calculating the velocity (v) of the electron according to Eq. [8.30] gives:

$$1957 = \frac{1}{\sqrt{1 - (v/c)^2}}$$

$$1 - (v/c)^2 = \left(\frac{1}{1957}\right)^2$$

$$(v/c)^2 = 0.9999997389$$

$$v/c = \sqrt{0.9999997389}$$

$$v = 0.999999869c$$

Thus, the 1 GeV electron in the synchrotron is measured to have a relativistic mass of 1957 times that of its rest mass and travels at a velocity of 0.999999869 times the velocity of light in a vacuum.

The Advanced Photon Source at Argonne National Laboratory is a synchrotron radiation source, which can achieve an electron energy output of 7.0 GeV. The calculated mass of an electron of 7.0 GeV energy in the synchrotron according to Eq. [8.29] would possess a sevenfold increase in mass over the previously calculated 1.0 GeV electron, that is, a mass of 13,698.6 times its rest mass. However, the velocity of the 7.0 GeV electron is calculated as above in Eq. [8.30] to be $0.9999999974c$, which is essentially the same as the 1.0 GeV electron, close to that of the unattainable speed of light in a vacuum.

8.7.4 Synchrotron Radiation Production and Applications

Synchrotron radiation sources generally consist of the following basic elements: (1) an electron gun and linear accelerator (LINAC), (2) a booster synchrotron, (3) a storage ring, (4) synchrotron radiation beam-lines, and (5) experimental work stations at each synchrotron radiation beam-line. An illustration of a modern synchrotron light source with an identification of its basic elements is given in Fig. 8.14. The electron gun provides the initial source of electrons, which are emitted by thermionic emission from a heated cathode, which consists of a heated block of negatively charged metal. A linear accelerator or linac, which is labeled as the injector in Fig. 8.14, will accelerate the electrons to an energy sufficient for the

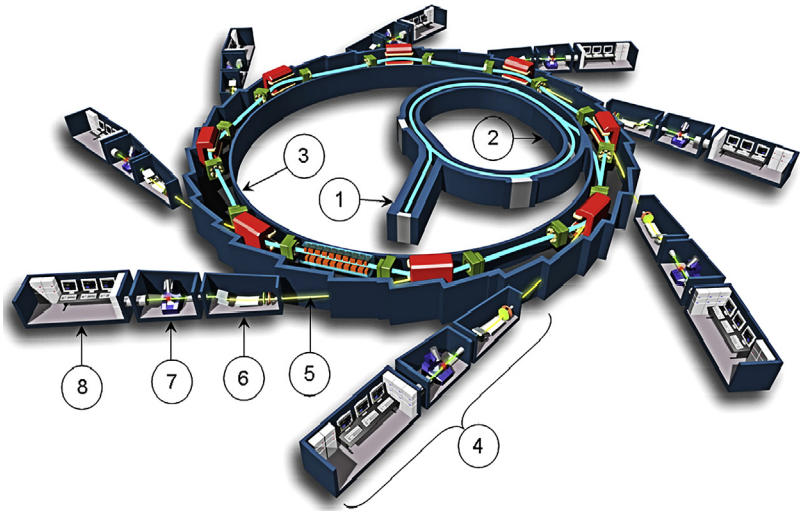

FIGURE 8.14 Essential elements of the third-generation 2.75-GeV Soleil Light Source at Saint-Aubin, France (http://www.synchrotron-soleil.fr/; printed with permission © Synchrotron SOLEIL—EPSIM/J.F. SANTARELLI). Its major components are (1) the injector, (2) booster ring, (3) storage ring, (4) experimental station consisting of (5) a beam-line, (6) optics and monochromator hutch, (7) experimental hutch, and (8) control room. Generally the experimental stations are custom designed for specific applications. *From Owens, A., 2012. Synchrotron light sources and radiation detection metrology. Nucl. Instrum. Methods Phys. Res., Sect. A 695, 1—12.*

electrons to be injected into a booster synchrotron ring. The energy output of the LINAC of the Advanced Photon Source (Synchrotron) of the Argonne National Laboratory will accelerate the electrons to 375 MeV (0.375 GeV). These electrons travel at a speed of 0.9999990715c or 99.99990715% of the speed of light calculated according to Eqs. [8.29] and [8.30] described previously. The high-energy electrons are then fed into a booster synchrotron ring to accelerate the electrons further with radio frequency energy sources. Electron energies achieved at the booster synchrotron will vary from 2 to 8 GeV at different synchrotron facilities around the world (Clarke, 2005). The booster synchrotron at the Advanced Photon Source (Synchrotron) of the Argonne National Laboratory produces an electron energy output of 7.0 GeV with an electron velocity of 0.9999999974c or 99.99999974% of the velocity of light. The high-energy electrons produced by the booster synchrotron are then fed into a storage ring where the electrons will travel at relativistic speed in a circular path controlled by bending magnets, which also serve as the source of synchrotron radiation needed for practical research with X-rays in numerous fields of science. The synchrotron radiation beam-lines, illustrated in Fig. 8.14, lead into individual experimental stations where individualized experimentation with the synchrotron radiation, generally the x-radiation, is carried out. The circulating electrons will lose energy with the emission of synchrotron radiation; and the lost energy is replenished with surges of energy from radio frequency cavities as the electrons circulate in the ring. Eventually electrons are lost by interactions with molecules of gas that reside in the imperfect vacuum chamber within which the electron beam travels; however, beams can last in storage rings for many hours (eg, over 60 h). Electron beams in storage rings are regularly replenished with the booster synchrotron to maintain the production of synchrotron radiation according to the needs of the research community.

The storage ring is not a perfect circle; rather it is considered as a polygon, as it will contain straight sections allowing for the insertion devices, referred to as wigglers and undulators, as illustrated in the simplified diagram of Fig. 8.15. The wigglers and undulators consist of varying poles of numerous magnets (see Fig. 8.16) to provide tightly curved transverse displacements of the particle beam (Clarke, 2005). The wigglers use the poles of the various magnets to deflect the electron beam back and forth or from side to side, such as to "wiggle" the electron beam, and at each wiggle, synchrotron radiation is emitted as a wide horizontal fan of X-rays capable of feeding more than one work station with X-rays where each work station can take a portion of slice of the fan for research (Mitchell et al., 1999). An undulator, as described by Mitchell et al. (1999), operates in a similar fashion as the wiggler, but with a shorter period between each magnetic pole maintaining the deflected beam within the original beam envelope. The photons emitted at each pole result in partially coherent X-rays concentrated in a more narrow beam with enhanced brilliance. With N bending magnets, the brilliance is enhanced in indulators by a factor of N^2 emitted over a narrow bandwidth (Owens, 2012), whereas with wigglers, the brilliance is enhanced only by a factor of N bending magnets.

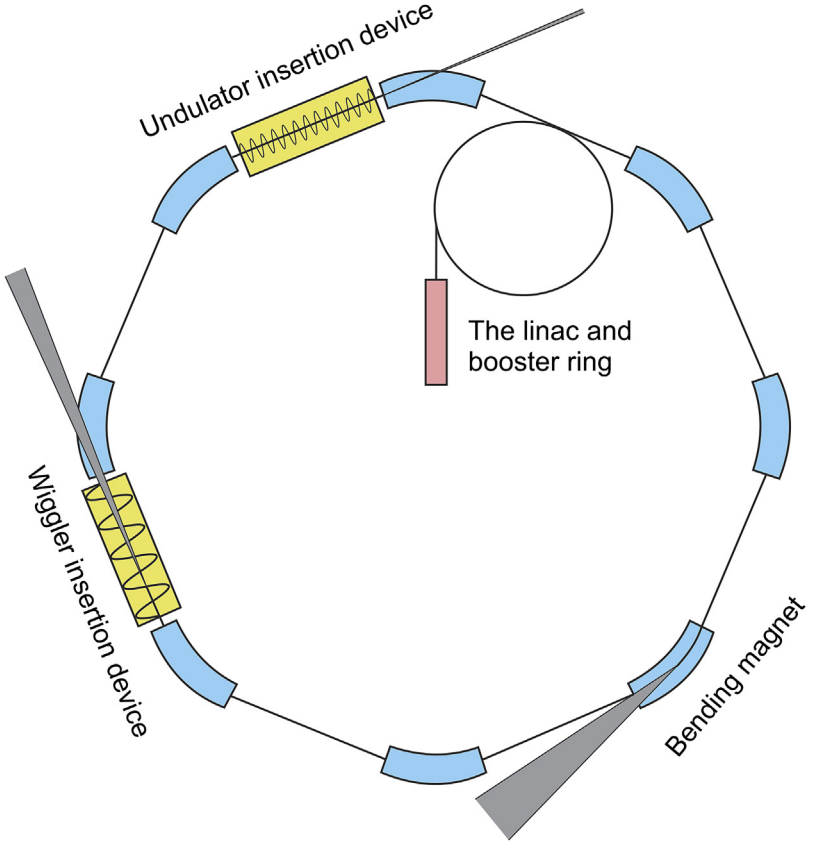

FIGURE 8.15 Schematic of a synchrotron radiation source showing the linac, inner synchrotron booster ring, outer storage ring, and the magnetic devices that produce synchrotron X-ray radiation. In the storage ring are illustrated bending magnets and wiggler and undulator insertion devices with synchrotron radiation emitting from each device. The properties of the source and resulting X-ray beam are described by a flux (photons/second/unit energy bandwidth), a brilliance (photons/second/mm^2/mrad^2/unit energy bandwidth), and a divergence (mrad). *From Mitchell, E., et al., 1999. Demystifying the synchrotron trip: a first time user's guide. Structure 7 (5), R111–R121; reprinted with permission from Elsevier © 1999.*

Many insertion devices are installed generally within the storage ring, which provides numerous synchrotron radiation beam-lines for research and practical applications. Synchrotron radiation facilities can have large storage rings with a circumference exceeding a kilometer and with well over 40 beam-lines and their associated workstations. Some storage rings of this magnitude include the European Synchrotron Radiation Facility (ESRF) in Grenoble, France, the Advanced Photon Source (APS) at Argonne, IL, USA, and the 8-GeV Super Photon Ring (Spring-8) at Nishi Harima, Japan. An example of the magnitude of such facilities is provided by an aerial photograph of the APS and an illustration of its associated work stations in Figs. 8.17 and 8.18, respectively.

There are over 70 synchrotrons worldwide; and many of these are wholly or partially dedicated to the generation of synchrotron radiation for research (Sorensen et al., 2006). The IAEA maintains a database of synchrotron radiation facilities worldwide with links to the individual websites of these synchrotron radiation sources (http://www.iaea.org/). Synchrotron radiation facilities generally provide the opportunity for research groups to reserve a workstation coupled to a beam-line for independent research.

Many applications of synchrotron radiation are available in almost every field of science including the biological and life sciences, geology and soil science, physics, chemistry, and materials science. Examples of synchrotron radiation applications in the scientific journal literature number in the thousands; only a few examples will be cited here. Among these applications are the structural determinations of macromolecules by X-ray diffraction (Wasserman et al., 2012; Garino et al., 2014; Gutiérrez-Fernández et al., 2014); imaging by means of X-ray computed tomography (Meneses et al., 2012; Almeida et al., 2014; Basnayaka et al., 2014); X-ray spectroscopy (Sayen and Guillon, 2014; Sutton and Newville, 2014; Young, 2014); infrared spectroscopy (McKellar, 2010; Miura et al., 2010; Marcelli et al., 2012); X-ray fluorescence

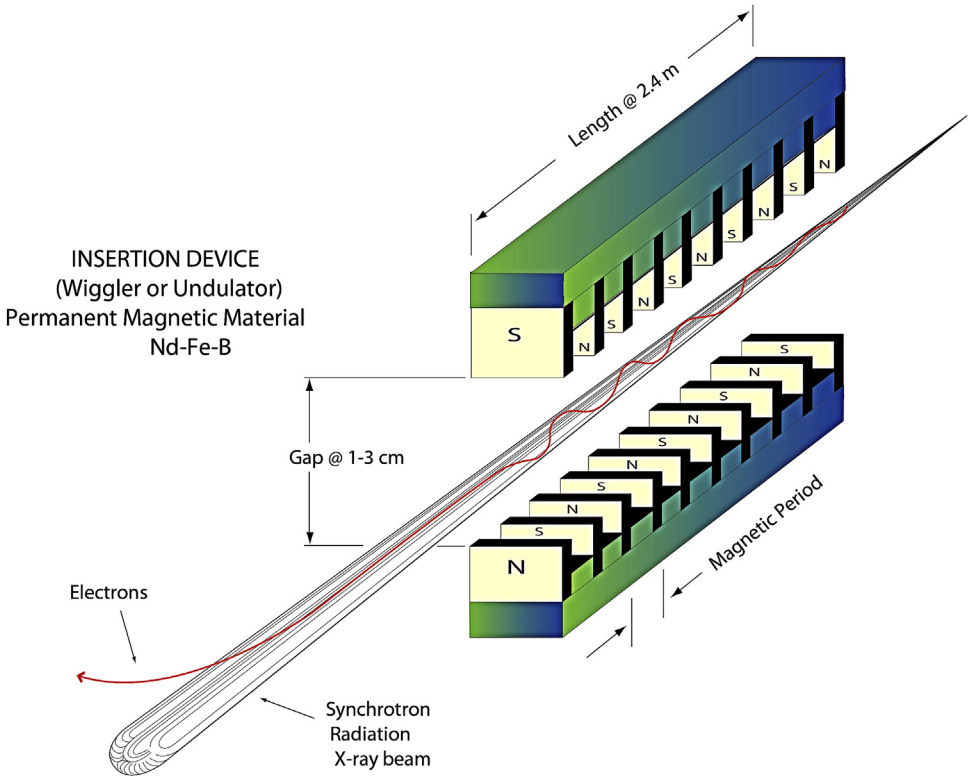

FIGURE 8.16 Basic structure and mechanism of a wiggler or undulator insertion device. *Courtesy of Advanced Photon Source, Argonne National Laboratory, Argonne, IL, USA (http://www.aps.anl.gov/).*

analysis (Lis et al., 2014; Baldassini et al., 2015); and nanotechnology (Wu and Becker, 2011; Zhu et al., 2014), among other fields where an X-ray or infrared or other suitable bandwidth of radiation source of high collimation and brilliance can be applied. For a general review of the many applications of synchrotron radiation, the reader may peruse reviews by Abela et al. (2010) and Martins and Silva (2014).

FIGURE 8.17 Aerial photograph of the Advanced Photon Source of the Argonne National Laboratory, Argonne, IL, USA, which houses a 1.1-km storage ring for the production and application of synchrotron radiation. *Courtesy of Advanced Photon Source, Argonne National Laboratory, Argonne, IL, USA (http://www.aps.anl.gov/).*

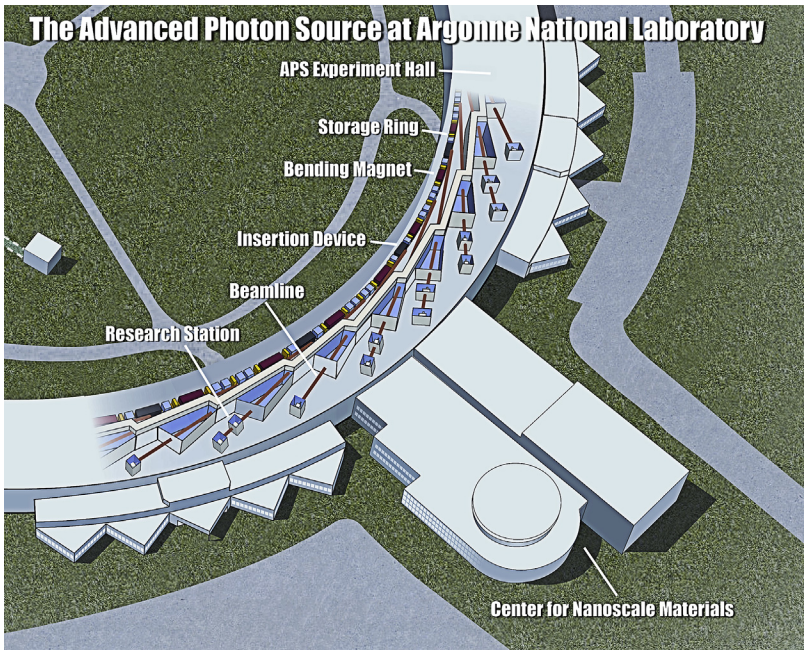

FIGURE 8.18 An artistic view of the layout within the experimental hall of the Advanced Photon Source storage ring illustrating the various workstations linked to synchrotron radiation beam-lines and components of the storage ring. *Courtesy of Advanced Photon Source, Argonne National Laboratory, Argonne, IL, USA (http://www.aps.anl.gov/).*

8.8 INTERACTION OF ELECTROMAGNETIC RADIATION WITH MATTER

8.8.1 Introduction

The lack of charge or rest mass of electromagnetic radiation, such as gamma and x-radiation, hinders their interaction with, and dissipation of their energy in matter. Consequently, gamma radiation and X-rays have greater penetration power and longer ranges in matter than the massive and charged alpha and beta particles of the same energy. Nevertheless, gamma and x-radiation are absorbed by matter, and the principal mechanisms by which this type of radiation interacts with matter are discussed in this section.

8.8.2 Photoelectric Effect

The energy of a photon may be completely absorbed by an atom. Under such circumstances, the entire photon energy is transferred to an electron of the atom and the electron is ejected, resulting in the formation of an ion pair. Consequently, the energy of the emitted electron is equal to the energy of the impinging photon less the binding energy of the electron. This is described by the photoelectric equation of Einstein:

$$E_e = h\nu - \phi \qquad [8.31]$$

where E_e is the energy of the ejected electron, $h\nu$ is the energy of the incident photon, and ϕ is the binding energy of the electron or the energy required to remove the electron from the atom. The ejected electron is identical in properties to a beta particle and produces ionization (secondary ionization in this case) as it travels through matter as previously described for beta particles.

The photoelectric effect occurs in the inner electron shells, predominately in the *K*-electron shell, of the atom as explained in the penultimate paragraph of this chapter. When an electron from an inner atomic *K* or *L* shell is ejected, electrons from outer shells fall to inner electron shells to fill the resulting gap. These transitions in electron energy states require a release of energy by the atomic electrons, which appears as soft (low-energy) X-rays. X-radiation is identical in properties to gamma radiation. The essential difference lies in the origin of the two radiations. As previously described, gamma radiation originates from energy state transformations of the nucleus of an atom, whereas x-radiation originates from energy state transformations of atomic electrons.

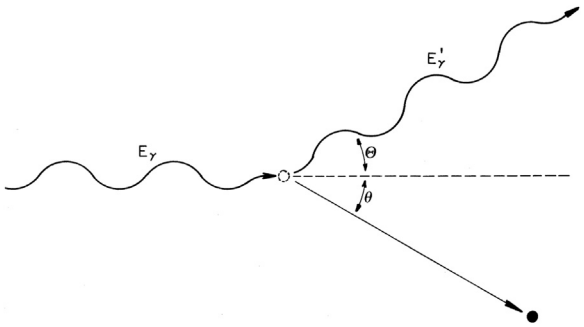

FIGURE 8.19 The Compton effect. An incident photon collides with an atomic electron and imparts energy to it, the photon and electron being deflected at angles Θ and θ, respectively, to the trajectory of the incident photon.

8.8.3 Compton Effect

There is a second mechanism by which a photon (eg, X-ray or gamma ray) transfers its energy to an atomic orbital electron. In this interaction, illustrated in Fig. 8.19, the photon, E_γ, imparts only a fraction of its energy to the electron and in so doing is deflected with energy E'_γ at an angle Θ, while the bombarded electron is ejected at an angle θ to the trajectory of the primary photon. This interaction is known as the Compton effect and also as Compton scattering. The result of this interaction is the formation of an ion pair, as in the case of the photoelectric effect. However, the deflected photon continues traveling through matter until it dissipates its entire kinetic energy by interacting with other electrons in a similar fashion or via other mechanisms of interaction with matter discussed in this section. The ejected electron, being identical in properties to a beta particle, loses its energy through the ionization it causes according to mechanisms previously described.

Our understanding of the Compton effect comes from the original work of Arthur H. Compton (1923a,b), who discovered that X-ray photons scattered by thin foils underwent a wavelength shift. The shift in wavelength of the scattered photon with respect to that of the incident photon was a function of the angle of scatter, Θ. To interpret this effect, Compton treated x radiation as photon particles or quanta according to the Einstein–Plank relation $E = h\nu$ (see Eq. [8.1]) and the scattering to occur as photon–electron collisions somewhat like billiard-ball collisions as illustrated in Fig. 8.19. Compton derived the equation, which describes the wavelength shift between the incident and scattered photons and angle of scatter, as:

$$\lambda' - \lambda = \frac{h}{m_0 c}(1 - \cos\Theta) \qquad [8.32]$$

where λ' and λ are the wavelengths of the deflected and incident photons, h is Planck's constant, m_0 is the rest mass of the electron, c is the speed of light, and Θ is the angle of scatter of the photon relative to the photon trajectory.

The Compton-scatter photon will always be of longer wavelength (lower energy) than the incident photon, because of energy lost in the collision with the electron. For example, let us calculate the wavelength shift and energy loss by an incident photon of wavelength 0.300 nm that collides with an electron, and where the photon is scattered at an angle of 70 degrees. The wavelength of the scattered photon is calculated according to Eq. [8.32] as:

$$\begin{aligned}\lambda' &= \lambda + \frac{h}{m_0 c}(1 - \cos\Theta)\\ &= 3.0 \times 10^{-10}\ \text{m} + \frac{6.626 \times 10^{-34}\ \text{J s}}{(9.109 \times 10^{-31}\ \text{kg})(2.997 \times 10^{8}\ \text{m/s})}(1 - \cos 70^\circ)\\ &= 3.0 \times 10^{-10}\ \text{m} + 2.43 \times 10^{-12}\ \text{m}\,(1 - 0.342)\\ &= 0.3016\ \text{nm}\end{aligned}$$

The energy lost by the incident photon according to the Einstein–Planck relation (Eq. [8.1]) is given by:

$$\begin{aligned}\Delta E &= E_\gamma - E'_\gamma \\ &= \frac{hc}{\lambda} - \frac{hc}{\lambda'} \\ &= \frac{12.4\ \text{keV Å}}{3.00\ \text{Å}} - \frac{12.4\ \text{keV Å}}{3.016\ \text{Å}} \\ &= 4.133\ \text{keV} - 4.111\ \text{keV} = 0.022\ \text{keV}\end{aligned}$$

and the fraction of photon energy lost becomes:

$$\frac{\Delta E}{E} = \frac{0.022\ \text{keV}}{4.133\ \text{keV}} = 0.0053 = 0.53\%$$

We can calculate directly the energy of the Compton scatter photon, λ', if we know the incident X-ray or gamma-ray photon energy and angle of scatter of the photon according to the equation:

$$E'_\gamma = \frac{E_\gamma}{1 + (E_\gamma/mc^2)(1 - \cos\Theta)} \qquad [8.33]$$

where E'_γ is the energy of the Compton scatter photon, E_γ is the incident photon energy, mc^2 is the rest energy of the electron (511 keV or 0.511 MeV, see Section 8.8.4), and Θ is the Compton photon angle of scatter (Tait, 1980). If we take the data from the previous example, where the incident photon energy was 4.133 keV and the angle of scatter was 70 degrees, we can calculate the energy of the Compton photon according to Eq. [8.33] to be:

$$E'_\gamma = \frac{4.133\ \text{keV}}{1 + (4.133\ \text{keV}/511\ \text{keV})(1 - \cos 70^\circ)} = 4.111\ \text{keV}$$

The result is in agreement with the calculations above using Eq. [8.32] derived by Compton.

8.8.4 Pair Production

The interactions of gamma radiation with matter, considered earlier, involve the transfer of γ energy, in whole or in part, to atomic electrons of the irradiated material. Pair production, as another mechanism of γ-energy dissipation in matter, results in the creation of matter (ie, electrons) from the γ energy. The particles produced are a negatron and a positron from an individual gamma-ray photon that interacts with the coulombic field of a nucleus (see Fig. 8.20). Consequently, this phenomenon involves the creation of mass from energy. Carl D. Anderson at the California Institute of Technology (Caltech) received the 1936 Nobel Prize in physics for his discovery of the positron, the first experimental evidence of

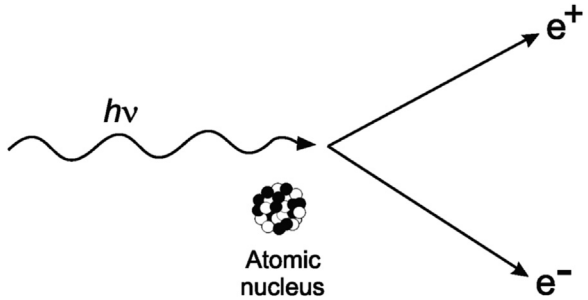

FIGURE 8.20 Pair production. The conversion of a gamma-ray photon into a negatron and positron pair.

antimatter. He and his graduate student Seth Neddermeyer also reported in their findings (Anderson and Neddermeyer, 1933) the first observation of pair production, which they described as follows:

> *One of the most striking phenomena, which have been observed in this experiment is the occasional simultaneous appearance of paired tracks consisting of one positive particle and one negative with a common point of origin…The process, which gives rise to the positrons is at present not known, but so far as these data go they are in accord with the view expressed by Blackett and Occhialini (1933) that the two particles may be formed by a process in which the energy of approximately 1 MeV required for the formation of a positive and negative electron is supplied by the impinging radiation.*

It was Nobel Laureate Patrick Blackett and his coworker G.P.S. Occhialini (1933) who recognized that the two particles, positron and negatron, are formed by the process known as pair production, whereby the energy of 1.02 MeV required for the production of the two particles is provided by the gamma radiation. In his Nobel Lecture, Anderson (1936) explained the pair-production phenomena as follows:

> *…that the appearance of pairs of positive and negative electrons could be understood in terms of this theory [Dirac's theory] as the "creation" of a positive-negative electron pair in the neighborhood of an atomic nucleus. The energy corresponding to the proper mass of both of the particles, as well as to their kinetic energies is supplied, according to this view, by the incident radiation. Since the energy corresponding to the proper mass of a pair of electrons is approximately 1 MeV, one should expect gamma rays of energy greater than this amount to produce positrons in their passage through matter, and further that the sum of the kinetic energies of the positive and negative electrons should be equal to the energy of the radiation producing them diminished by approximately 1 MeV.*

In the above statement, Anderson described the process of pair production, first theorized by Dirac (1928a,b), observed through cloud-chamber track photographs by Anderson and Neddermeyer (1933), and interpreted by Blackett and Occhialini (1933). The gamma-ray photon energy required for pair production is, as noted above by Anderson, equivalent to the sum of the masses of the electron and positron described by the equation:

$$E_{\text{pair}} = m_{e^-}c^2 + m_{e^+}c^2 = 2mc^2 = 2(0.511\ \text{MeV}) = 1.022\ \text{MeV} \qquad [8.34]$$

The gamma-ray photon energy in excess of 1.022 MeV appears as the kinetic energy of the electron and positron created, and the overall pair-production phenomena can be expressed as:

$$h\nu = 2mc^2 + E_{e^-} + E_{e^+} \qquad [8.35]$$

where $h\nu$ is the gamma-ray photon energy, $2mc^2$ is the energy equivalence of the mass of two electrons, and E_{e^-} and E_{e^+} are the kinetic energies of the electron and positron, respectively. In pair production, gamma-ray energy in excess of 1.02 MeV appears as kinetic energy of the negatron and positron produced. By the time of his Nobel Lecture in 1936, three sources of positrons were known, and Anderson took the opportunity of his lecture to describe these, which are the following: (1) cosmic ray showers of electron–positron pairs via pair production from cosmic gamma radiation, (2) pair production via the absorption of gamma radiation in excess of 1 MeV from radionuclide sources, and (3) positron emission via beta decay from radioactive elements, such as ^{30}P, ^{13}N, and ^{27}Si, artificially produced by Joliot-Curie and Joliot (1934a,b,c), which decay by positron emission.

The creation of an electron requires a certain quantum of energy of a gamma-ray photon, which may be calculated according to Einstein's equation for the equivalence of mass and energy:

$$E = m_e c^2 \qquad [8.36]$$

where E is energy, m_e is the electron rest mass, and c is the speed of light in a vacuum. Thus, the rest energy of the electron (negatron or positron) is calculated as:

$$E = \left(9.109 \times 10^{-31}\ \text{kg}\right)\left(2.997 \times 10^{8}\ \text{m/s}\right)^2 = 8.182 \times 10^{-14}\ \text{J}$$

Since by definition, $1\ \text{eV} = 1.602 \times 10^{-19}$ J, the electron rest energy in joules is converted to electron volts as:

$$8.182 \times 10^{-14}\ \text{J} / 1.602 \times 10^{-19}\ \text{J/eV} = 5.11 \times 10^{5}\ \text{eV} = 0.511\ \text{MeV}$$

Thus, the creation of an electron (negatron) requires a minimum energy of 0.511 MeV. However, a gamma ray of 0.511 MeV energy cannot alone create a negatron, as there must also be the simultaneous creation of its antiparticle, the positron of equal mass and opposite charge. The minimum gamma ray photon energy required for the creation of the negatron–positron pair is, as described by Eq. [8.34] above, 2(0.511) or 1.022 MeV. Thus, the absorption by matter of gamma radiation greater than 1.02 MeV may result in pair production. The probability of pair production increases in proportion to the magnitude of gamma-ray photon energy above 1.02 MeV, and pair

TABLE 8.2 Examples of Nuclides That Exhibit Internal Pair Production, Their Gamma Radiations, and Relative Intensities of the Positron–Negatron Pairs

	Gamma Radiations		
Nuclide	Energy (MeV)	Abundance (%)	Pair/Gamma Ratio[a] ($e^{\pm}/\gamma$)
^{24}Na	1.369	100	6×10^{-5}
	2.754	100	7×10^{-4}
^{56}Mn	1.81	29	5.6×10^{-4}
	2.11	15	4.6×10^{-4}
^{59}Fe	1.099	57	1.4×10^{-4}
	1.292	43	1.1×10^{-4}
^{60}Co	1.17	100	3.7×10^{-5}
	1.33	100	Combined[a]
^{142}Pr	1.576	4	1.1×10^{-4}
^{144}Pr	1.489	0.3	1.9×10^{-4}
	2.186	0.7	6.7×10^{-4}
^{154}Eu	1.274	37	8.0×10^{-5}

[a]*The value of* $(e^{\pm}/\gamma)$ *of* 3.7×10^{-5} *for* ^{60}*Co represents the pair/gamma ratio for both gamma emissions combined.*

production is the predominant mechanism of absorption of photons of energies of 5 MeV and above (see Figs. 8.23 and 8.24).

As discussed previously in Section 8.4, a positron will produce annihilation radiation when it comes to rest in the proximity of a negative electron, ie, its antiparticle, resulting in the simultaneous conversion of two electron masses into two gamma-ray photons of 0.511 MeV energy.

Pair production does not occur only in the vicinity of atomic nuclei bombarded by gamma radiation. It may also originate from nuclei that emit gamma radiation with transition energies greater than 1.02 MeV. This is referred to as internal pair production, and the mechanism competes to a small extent with the emission of gamma radiation. The degree to which this competition occurs is measured by the ratio of intensities of positron–negatron pairs to gamma radiation or $(e^{\pm}/\gamma)$. Some examples of nuclides that emit such positron–negatron pairs and the intensities of these pairs relative to gamma radiation are given in Table 8.2.

A practical application of internal pair production to the nondestructive activity analysis of ^{90}Y and ^{90}Sr was reported by Selwyn et al. (2007). The nuclide ^{90}Y decays by negatron emission with a Q value of 2280.1 keV, as illustrated in Fig. 8.21. The activity of ^{90}Y is determined traditionally by liquid scintillation or Cherenkov counting of the high-energy

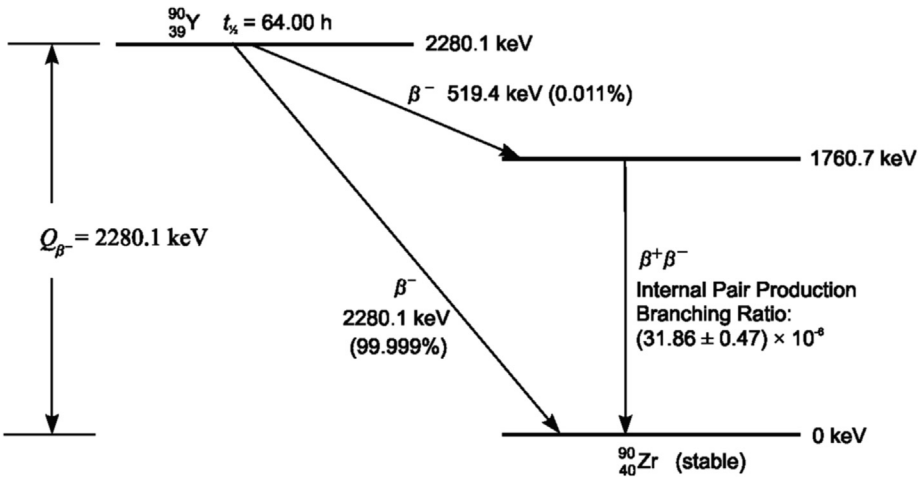

FIGURE 8.21 Decay scheme of ^{90}Y.

negatron emissions, which have an E_{max} of 2280.1 keV, as this beta transition occurs at an intensity of 99.999% to the ground state of stable ^{90}Zr (L'Annunziata and Passo, 2012; L'Annunziata, 2012c). There is a very small branching beta transition with an E_{max} of 519.4 keV, which occurs at an intensity of 0.011%, to metastable ^{90}Zr at the energy level of 1760.7 keV (see Fig. 8.21). This is well above the 1022 keV required for internal pair production, that can occur in the transition from 1760.7 keV to the ground state of ^{90}Zr. Selwyn et al. (2007) measured the internal pair production branching ratio for this transition to be $(31.86 \pm 0.47) \times 10^{-6}$ by measuring the count rate of the 511 keV peak with a high-purity germanium detector (HPGe) produced by the positron (β^+) annihilation that follows pair production. The high-energy beta emissions of ^{90}Y produce Bremstrahlung background radiation, which had to be subtracted from the overall count rate to get an accurate measurement of the net count rate at the 511-keV peak. With the known branching ratio for the internal pair production, and measurement of the net count rate and detection efficiency of the 511 keV positron (β^+) annihilation photons, the ^{90}Y activity of unknown samples can be determined. The activity of ^{90}Sr can be calculated from the measured activity of ^{90}Y, as their activities are equal when in secular equilibrium (L'Annunziata, 1971; see also the chapter: "Radionuclide Decay, Radioactivity Units, and Radionuclide Mass").

8.8.5 Combined Photon Interactions

Because of its zero rest mass and zero charge, gamma radiation has an extremely high penetration power in matter in comparison with alpha and beta particles.

Materials of high density and atomic number (such as lead) are used most often as absorbers to reduce x- or gamma radiation intensity. Radiation intensity, I, is defined here as the number of photons of a radiation beam that traverse a given area per second, the units of which can be photons $cm^{-2}\ s^{-1}$. Suppose a given absorber material of thickness x attenuates or reduces the intensity of incident gamma radiation by one-half. Placing a similar barrier of the same thickness along the path of the transmitted gamma radiation would reduce the intensity again by one-half. With three barriers each of thickness x and an initial gamma-ray intensity I_0, there is a progressive drop in the transmitted gamma-ray intensities: $I_1 = \frac{1}{2}I_0$, $I_2 = \frac{1}{2}I_1$, $I_3 = \frac{1}{2}I_2$, and $I_n = \frac{1}{2}I_{n-1}$. Obviously, incident x- or gamma radiation may be reduced from I_0 to I_3 by using a $3x$ thickness of the same material as an absorber. Consequently, the intensity of the transmitted electromagnetic radiation is proportional to the thickness of the absorber material and to the initial intensity of the radiation. An increasing absorber thickness increases the probability of photon removal, because there is a corresponding increase of absorber atoms that may attenuate the incident photons via the photoelectric effect, the Compton effect, and pair production mechanisms.

If gamma-ray attenuation with respect to absorber thickness is considered, the change in gamma-ray intensity, ΔI, with respect to the absorber thickness, Δx, is proportional to the initial gamma-ray photon intensity, I. This may be written as:

$$\Delta I/\Delta x = -\mu I \qquad [8.37]$$

where μ is the proportionality constant, referred to as the linear attenuation coefficient or linear absorption coefficient. Its value is dependent on the atomic composition and density of the absorber material. The change in intensity over an infinitely thin section of a given absorber material may be expressed as:

$$dI/dx = -\mu\, I \qquad [8.38]$$

or:

$$dI/I = -\mu\, dx \qquad [8.39]$$

Integrating Eq. [8.39] over the limits defined by the initial intensity, I_0, to the transmitted intensity, I, and over the limits of absorber thickness from zero to a finite value x, such as:

$$\int_{I_0}^{I} dI/I = -\mu \int_{0}^{x} dx \qquad [8.40]$$

gives:

$$\ln I - \ln I_0 = -\mu x \qquad [8.41]$$

or:

$$\ln(I_0/I) = \mu x \qquad [8.42]$$

Eq. [8.42] may be written in exponential form as:

$$I = I_0 e^{-\mu x} \quad [8.43]$$

which is somewhat similar to the exponential attenuation of neutrons discussed in the chapter entitled "Neutron Radiation."

Because gamma ray absorption is exponential, the term half-value thickness, $x_{1/2}$, is used to define the attenuation of gamma radiation by matter. Half-value thickness is the thickness of a given material of defined density that can reduce the intensity of incident gamma radiation by one-half. The half-value thickness may also be defined according to Eq. [8.42], in which the initial gamma ray intensity, I_0, is given an arbitrary value of 1 and the transmitted intensity must, by definition, have a value of 1/2, or:

$$\ln 1/0.5 = \mu x_{1/2} \quad [8.44]$$

or:

$$\ln 2 = \mu x_{1/2} \quad [8.45]$$

and:

$$x_{1/2} = 0.693/\mu \quad [8.46]$$

From the linear attenuation coefficient, μ, of a given material and gamma-ray photon energy, it is possible to calculate the half-value thickness, $x_{1/2}$. The linear attenuation coefficient has units of cm^{-1}, so that a calculated half-value thickness is provided in units of material thickness (cm). Linear attenuation coefficients for some materials as a function of photon energy are provided in Table 8.3. The table refers to these as total linear attenuation coefficients, because they constitute the sum of coefficients due to Compton, photoelectric, and pair-production interactions. Celiktas (2011) reports on the development of the experimental methods that may be used to determine gamma-ray linear attenuation coefficients. Calculated half-value thicknesses of various absorber materials as a function of gamma-ray energy are illustrated in Fig. 8.22 to illustrate some examples of the varying amounts of absorber material required to attenuate gamma-ray photons. The linear attenuation coefficient is a constant for a given absorber material and gamma-ray photon energy and has units of reciprocal length such as cm^{-1}. It is, however, dependent on the state of the absorber or the number of atoms per unit volume of absorber. A more popular coefficient is the mass attenuation coefficient, μ_m, which is independent of the physical state of the absorber material and is defined as:

$$\mu_m = \mu/\rho \quad [8.47]$$

TABLE 8.3 Total Linear Attenuation Coefficients (cm^{-1}) for Gamma-Ray Photons in Various Materials[a]

Photon Energy (MeV)	Water	Aluminum	Iron	Lead
0.1	0.167	0.435	2.704	59.99
0.2	0.136	0.324	1.085	10.16
0.4	0.106	0.2489	0.7223	2.359
0.8	0.0786	0.1844	0.5219	0.9480
1.0	0.0706	0.1658	0.4677	0.7757
1.5	0.0575	0.1350	0.3812	0.5806
2.0	0.0493	0.1166	0.3333	0.5182
4.0	0.0339	0.0837	0.2594	0.4763
8.0	0.0240	0.0651	0.2319	0.5205
10.0	0.0219	0.0618	0.2311	0.5545

[a]*Data from Argonne National Laboratory, ANL-5800 (1963), Hubbell (1969), and Berger et al. (2010).*

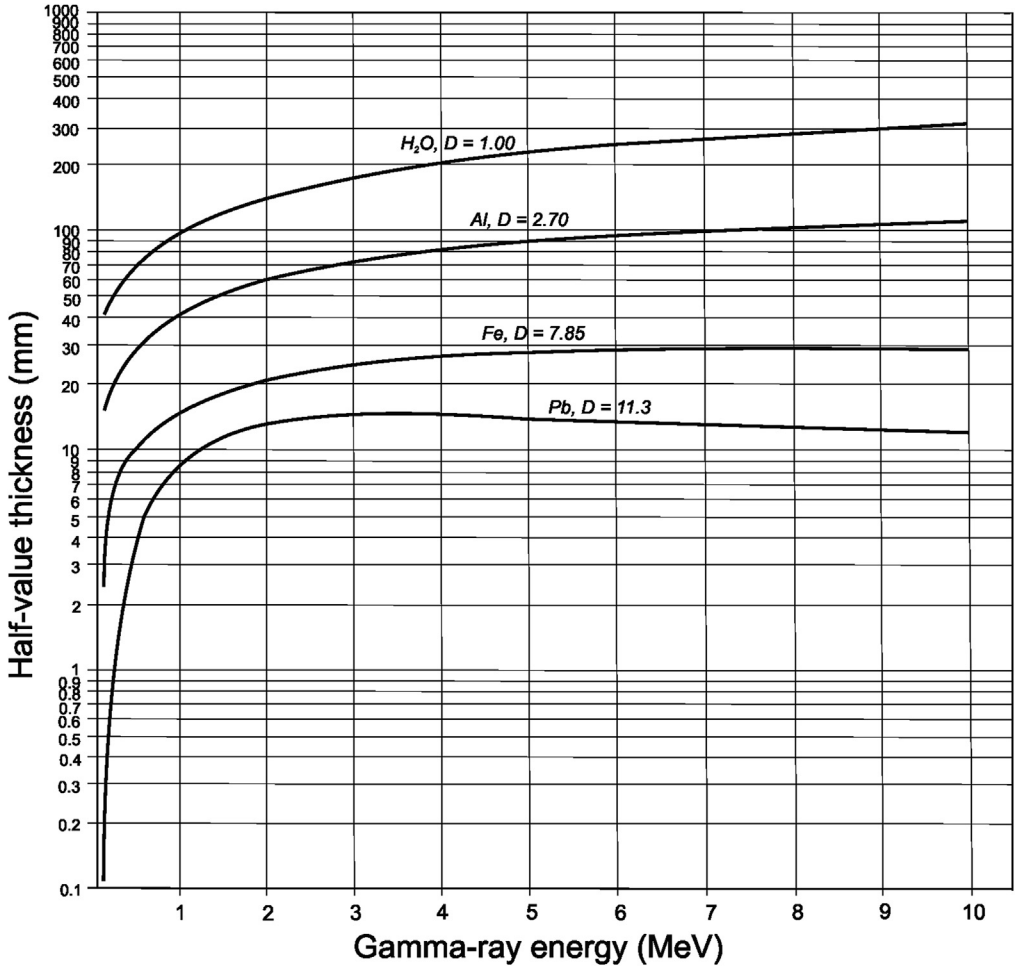

FIGURE 8.22 Half-value thicknesses of various materials as a function of gamma-ray energy. *D* is the density of each material. *From L'Annunziata, M.F., 1987. Radionuclide Tracers, Their Detection and Measurement. Academic Press, London, pp. 505, reprinted with permission from Elsevier © 1987 Academic Press.*

where ρ is the density of the absorber in units of g/cm^3, and μ_m has units of cm^2/g. Some examples of mass attenuation coefficients according to X- and gamma-ray photon energy are provided in Table 8.4. Using the mass attenuation coefficient, Eq. [8.43] transforms to:

$$I = I_0 e^{-\mu_m \rho x} \quad [8.48]$$

and the half-value thickness is calculated according to Eq. [8.46] as:

$$x_{1/2} = 0.693/\mu_m \rho \quad [8.49]$$

Mass attenuation coefficients for X- or gamma-ray photons over a wide range of energies from 1 keV to 1000 MeV in 100 elements are available from Berger and Hubbell (1997). In addition, mass attenuation coefficients for any element, chemical compound, mixtures of elements, or mixtures of compounds over the X-ray or gamma-ray photon energy range of 1 keV to 10^5 MeV are available from a database, which can be found at the following National Institute of Standards and Technology (NIST) website: http://physics.nist.gov/PhysRefData/Xcom/html/xcom1.html. A sample of mass attenuation coefficients over the range of 5 keV to 10 MeV in a few materials is given in Table 8.4. The following calculation illustrates the use of the data from Tables 8.3 and 8.4 to calculate half-value thickness and radiation attenuation:

Let us calculate the half-value thickness of lead ($\rho = 11.3$ g/cm^3) for 2.0-MeV gamma radiation, and further calculate what reduction in radiation intensity would result if we positioned four times the half-value thickness of lead in the path of the radiation beam. First, the linear attenuation coefficient, μ, or mass attenuation coefficient, μ_m, for 1.0-MeV

TABLE 8.4 Total Mass Attenuation Coefficients (cm^2/g) for X- or Gamma-Ray Photons in Various Materials[a]

Photon Energy (MeV)	Air	Water	Aluminum	Iron	Lead
0.005	38.3	42.0	193	140	730
0.01	4.6	5.1	26.2	171	131
0.05	0.187	0.208	0.368	1.96	8.04
0.1	0.151	0.167	0.170	0.372	5.55
0.2	0.123	0.136	0.122	0.146	0.999
0.4	0.0953	0.106	0.0922	0.0919	0.208
0.8	0.0706	0.0786	0.0683	0.0664	0.0836
1.0	0.0655	0.0706	0.0614	0.0595	0.0684
1.5	0.0517	0.0575	0.0500	0.0485	0.0512
2.0	0.0445	0.0493	0.0432	0.0424	0.0457
4.0	0.0307	0.0339	0.0310	0.0330	0.0420
8.0	0.0220	0.0240	0.0241	0.0295	0.0459
10.0	0.0202	0.0219	0.0229	0.0294	0.0489

[a]*Data from Argonne National Laboratory, ANL-5800 (1963), Hubbell (1969), Berger and Hubbell (1997), and Berger et al. (2010), available at National Institute of Standards and Technology (NIST): http://physics.nist.gov/cgi-bin/Xcom/xcom3_1.*

photons in lead are obtained from either Table 8.3 or 8.4, and the half-value thickness of lead for 2.0 MeV photons is calculated as:

$$x_{1/2} = \frac{0.693}{\mu} \text{ or } \frac{0.693}{\mu_m \rho} \quad [8.50]$$

or:

$$x_{1/2} = \frac{0.693}{0.5182\ \text{cm}^{-1}} \text{ or } \frac{0.693}{(0.0457\ \text{cm}^2/\text{g})(11.3\ \text{g/cm}^3)}$$

$$x_{1/2} = 1.34\ \text{cm}$$

Thus, a barrier of 1.34-cm thickness of lead is sufficient to reduce the radiation intensity of 2.0-MeV photons by 1/2 or 50%. According to Eq. [8.43], the relation between the initial radiation intensity, I_0, and the transmitted intensity, I, is:

$$\frac{I}{I_0} = e^{-\mu x} \quad [8.51]$$

and for $x = 1.34$, if the initial radiation intensity is given an arbitrary value of 2, the transmitted intensity would be 50% of the initial intensity or equal to 1. We then can write:

$$\frac{I}{I_0} = \frac{1}{2} = e^{-1.34\mu} \quad [8.52]$$

If we employ four times the half-value thickness of lead or $4 \times 1.34\ \text{cm} = 5.36\ \text{cm}$, we can calculate that the transmitted radiation would be reduced to the following:

$$\frac{I}{I_0} = \left(e^{-1.34\mu}\right)^4 = \left(\frac{1}{2}\right)^4$$

or:

$$e^{-5.36\mu} = \frac{1}{16} = 0.0625 = 6.25\%\ \text{transmitted}$$

The remaining 15/16 or 93.75% of the initial radiation is attenuated by the 5.36-cm lead barrier.

In general, we need not know the half-value thickness of the material or shield, but simply obtain the linear or mass attenuation coefficient for a given energy of x- or gamma radiation from reference tables and use Eqs. [8.43] or [8.48] to calculate the magnitude of radiation attenuation for any thickness of the absorber material. For example, if we used only 2.5 cm of lead barrier, the attenuation of 2.0-MeV gamma rays could be calculated as:

$$\frac{I}{I_0} = e^{-\mu x} = e^{-\mu_m \rho x} \quad [8.53]$$

and:

$$\frac{I}{I_0} = e^{-\left(0.5182\ \text{cm}^{-1}\right)(2.5\ \text{cm})} = e^{-\left(0.0457\ \text{cm}^2/\text{g}\right)\left(11.3\ \text{g}/\text{cm}^3\right)(2.5\ \text{cm})}$$

$$= e^{-1.29} = 0.275 = 27.5\%\ \text{transmitted}$$

Thus, the 2.0-MeV radiation transmitted through a shield of 2.5 cm of lead would be 27.5% of the initial radiation intensity. The remaining 72.5% of the initial gamma radiation is attenuated by the 2.5-cm lead barrier.

As previously discussed, the absorption of gamma radiation is a process that principally involves three mechanisms of attenuation: the Compton effect, the photoelectric effect, and pair production. The attenuation coefficients just discussed above are also referred to as total attenuation coefficients, because they consist of the sum of three independent coefficients or:

$$\mu = \mu_c + \mu_e + \mu_p \quad [8.54]$$

where μ_c, μ_e, and μ_p are attenuation coefficients for Compton, photoelectric, and pair-production processes. The attenuation coefficients are proportional to the probabilities of occurrence of these radiation attenuation processes and can be used as a measure of the relative roles these processes play in the absorption of gamma-ray photons.

Accordingly, the total and partial mass attenuation coefficients can be written as:

$$\mu_m = \mu/\rho = \mu_c/\rho + \mu_e/\rho + \mu_p/\rho \quad [8.55]$$

Figs. 8.23 and 8.24 provide a graphic representation of the relative frequency of occurrence of the Compton, photoelectric, and pair production processes in aluminum and sodium iodide absorbers as a function of photon energy. From these curves, it is seen that the photoelectric effect plays a predominant role in total gamma-ray attenuation at lower gamma-ray energies and with absorber materials of higher atomic number. We can also note from these figures that pair production becomes significant at photon energies above 1 MeV, as the threshold energy for pair production is 1.022 MeV. Data on the total and partial mass attenuation coefficients as a function of photon energy for any element, chemical compound, mixture of elements, or mixture of compounds over the photon energy range of 1 keV to 10^5 MeV is available from the following website of the National Institute of Standards and Technology: http://physics.nist.gov/PhysRefData/Xcom/html/xcom1.html.

In some absorber materials of relatively high density, absorption edges can be measured for low photon energies, such as the *K* edge illustrated in Fig. 8.24. The absorption edge is a discontinuity in the attenuation coefficient curve for the photoelectric effect that is caused when photon energies are less than the binding energies of electrons of a certain shell (eg, *K* shell), which reduces the number of electrons that may be ejected by the photoelectric effect. When photons possess the threshold binding energy of electrons of that shell, there is a sudden surge in attenuation owing to the ejection of electrons from that shell via photoelectric interactions.

The photoelectric effect will occur primarily in the *K*-electron shell. At such photon energies (>*K*-shell binding energy), the probability of the photoelectric effect occurring in the *L*-shell is only about 20% and even less probable for outer shells (Friedlander et al., 1964). Such a phenomenon may appear strange, considering that the binding energies of the electrons are lower in shells further away from the nucleus. If one considers only the binding energies of the electrons, it would appear, although incorrectly, that for photon energies in excess of the *K*-shell binding energy, electrons further away from the nucleus (eg, *L*-, *M*-, *N*-shells) would be ejected as photoelectrons more easily. This is not the case, because energy and momentum must be conserved in the process; and the atom, because of its much higher mass, will carry off the excess momentum while taking away negligible energy in the process. The entire photon energy is transferred to the photoelectron less its binding energy. Consequently, the photoelectric effect cannot occur with a free electron, because there is no atom to carry off excess momentum, as demonstrated by Gautreau and Savin (1999). In the same sense, when the photon energy is

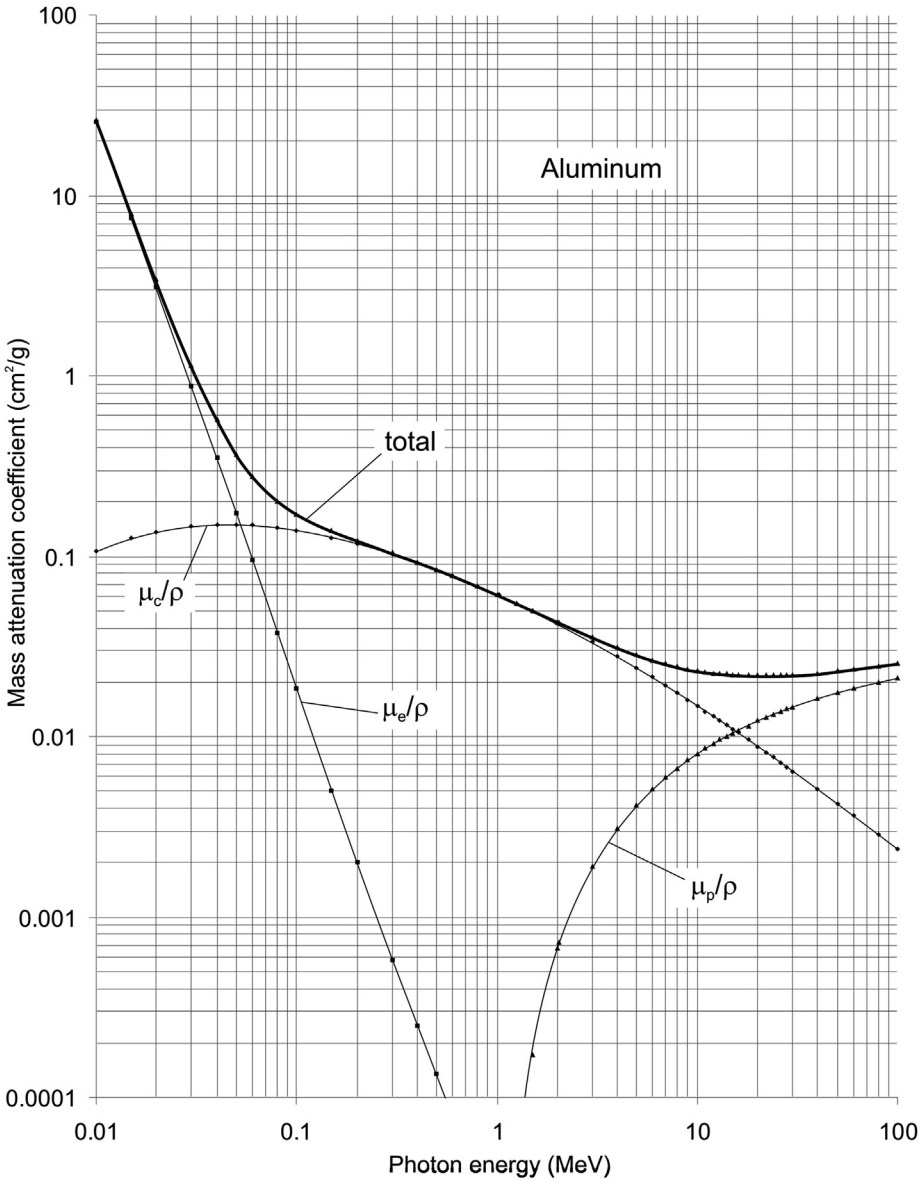

FIGURE 8.23 Mass attenuation coefficients for photons in aluminum. The total attenuation is given by the solid line, which is the sum of the partial attenuations due to the Compton effect, μ_c/ρ; the photoelectric effect, μ_e/ρ; and pair production, μ_p/ρ. *Drawn from data of Hubbell et al. available from the website of the National Institute of Standards and Technology: http://physics.nist.gov/PhysRefDate/Xcom/html/xcom1.html.*

much greater than the electron binding energy, the electrons, such as those in the outer shells with very low binding energies, act more like free electrons. These electrons contribute less to photon attenuation by the photoelectric effect. As explained by Lilley (2001), the conservation of energy and momentum is the reason why the most tightly bound electrons contribute most to photoelectric absorption for $E_\gamma > B_K$, where E_γ is the photon energy and B_K is the K-shell electron binding energy, and also why there is a marked dependence of photon attenuation on photon energy and absorber atomic number. The photon absorption in NaI, illustrated in Fig. 8.24, shows a K edge at $\sim$0.033 MeV or 33 keV. This corresponds to the electron binding energy in the K shell of iodine, which from reference tables (Lide, 2010) is reported to be 33,169 eV or 33.1 keV. Photon attenuation by the photoelectric effect for photon energies in excess of 33 keV occur predominantly with the K-shell electrons. There is no K edge observed for sodium in Fig. 8.24 for the NaI absorber, because the binding energy of the K-shell of sodium is only 1070 eV or 1.07 keV, a factor of 10 lower than the photon energy scale provided in the figure. At much lower photon energies, corresponding to L- and M-shell electron binding energies, characteristic L and M edges can be observed. The binding energies of electrons in the various atomic electron shells of the elements are listed in reference tables, such as those provided by Lide (2010).

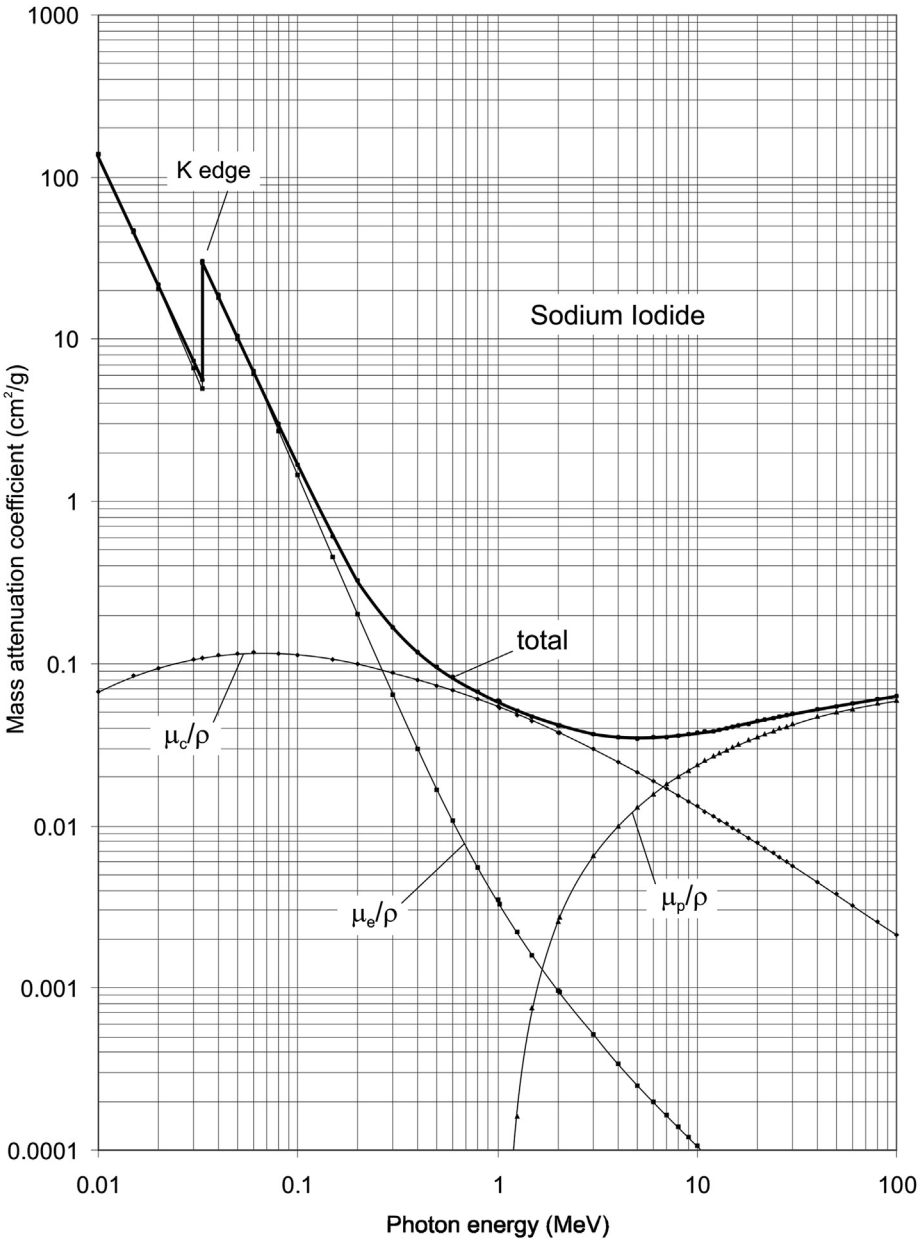

FIGURE 8.24 Mass attenuation coefficients for photons in sodium iodide. The total attenuation is given by the solid line, which is the sum of the partial attenuations due to the Compton effect, μ_c/ρ; the photoelectric effect, μ_e/ρ; and pair production, μ_p/ρ. *Drawn from data of Hubbell et al. available from the website of the National Institute of Standards and Technology: http://physics.nist.gov/PhysRefDate/Xcom/html/xcom1.html.*

As illustrated in Figs. 8.23 and 8.24, the pair production process does not occur at gamma-ray energies below the threshold value of 1.02 MeV, as expected, in accord with the combined positron and negatron rest energies (ie, 2×0.511 MeV) required for pair production. A thorough treatment of the attenuation and absorption of gamma radiation in matter is available from Hubbell (1969), Krane (1988), Lilley (2001), Serway et al. (2005), and Turner (1995).

Chapter 9

Hall of Fame: Part IV

James Chadwick (1891−1974), Lise Meitner (1878−1968) and Otto Hahn (1879−1968), Leo Szilard (1898−1964), Joseph Rotblat (1908−2005), Edward Teller (1908−2003)

In the tragic situation which confronts humanity we feel that scientists should assemble in conference to appraise the perils that have arisen as a result of the development of weapons of mass destruction…We are speaking on this occasion, not as members of this or that nation, continent, or creed, but as human beings, members of the species Man, whose continued existence is in doubt…We have to learn to think in a new way. We have to learn to ask ourselves, not what steps can be taken to give military victory to whatever group we prefer, for there are no longer such steps; the question we have to ask ourselves is: what steps can be taken to prevent a military contest of which the issue must be disastrous to all parties…

Excerpt from the Russell−Einstein Manifesto proclaimed on July 9, 1955 and signed by Bertrand Russell, Albert Einstein, Joseph Rotblat, and eight other Nobel Laureates and dignitaries. The Russell−Einstein Manifesto was the precursor to the Pugwash Conferences on Science and World Affairs founded by Joseph Rotblat. The Nobel Committee awarded the Nobel Peace Prize for 1995 in two equal parts to the Pugwash Conferences on Science and World Affairs and to Joseph Rotblat in the words of the Nobel Committee "for their efforts to diminish the part played by nuclear arms in international politics and, in the longer run, to eliminate such arms."

JAMES CHADWICK (1891−1974)

James Chadwick was born in Cheshire, England on October 20, 1891. He was awarded the Nobel Prize in Physics in 1935 "for the discovery of the neutron."

James Chadwick (1891–1974)

Radioactivity: Introduction and History, From the Quantum to Quarks. http://dx.doi.org/10.1016/B978-0-444-63489-4.00009-5
Copyright © 2016 Elsevier B.V. All rights reserved.

After attending Manchester High School, Chadwick entered Manchester University in 1908 and graduated from the Honours School of Physics in 1911. He then went to study under Ernest Rutherford at the Physics Laboratory in Manchester on research studies related to radioactivity, and graduated with a master of science degree in 1913. A stint with Rutherford was the springboard for the successful careers of many famous physicists and future Nobel Laureates interested in pursuing studies on radioactivity and the structure of the atom. After receiving the MSc degree in 1913, Chadwick was awarded a scholarship to study under Prof. Hans Geiger, also a former student of Rutherford, at the Physikalisch Technische Reichsanstalt in Charlottenburg, Berlin. During the war, Chadwick was interred in the Zivilgefangenenlager (civilian prisoners camp) in Ruhleben until 1919. He then returned to England to work again under Ernest Rutherford, who was then at the Cavendish Laboratory, Cambridge, and to continue his studies in physics at the Gonville and Caius College in Cambridge. At this time Rutherford had already accomplished the very first artificial nuclear transmutation by splitting atoms of nitrogen with alpha particles, yielding oxygen atoms and protons (see Rutherford, Hall of Fame, Part I). Chadwick worked with Rutherford on studies related to the structure of the nucleus and on the successful nuclear transmutation of other elements (*Nobel Lectures, Physics 1922–1941*).

While at the Cavendish Laboratory in 1932, James Chadwick made a discovery for which he received the Nobel Prize. He demonstrated the existence of the neutron, accurately determined its mass, and thereby explained the structure of the atomic nucleus. The existence of the neutron was first suggested by Rutherford in his Bakerian Lecture delivered on June 3, 1920 (Rutherford, 1920a,b), but because of the particle's neutral charge, its detection was difficult and the particle remained elusive until Chadwick's discovery in 1932.

Two years prior to Chadwick's discovery of the neutron it had been shown by Bothe and Becker (1930) that some light elements, particularly beryllium, when bombarded by alpha particles from polonium, would emit an unknown, very penetrating radiation resembling gamma radiation. At the time, the unknown radiation originating from the interaction of alpha particles with light elements, such as boron and beryllium, was referred to as "beryllium radiation," because the radiation was more intense with beryllium. Subsequently Irène Joliot-Curie (1931) and Webster (1932) demonstrated that the "beryllium radiation" had a penetration power much greater than any gamma radiation known to exist. The radiation was reported to be able to pass through a brass plate several centimeters thick, without any noteworthy loss of velocity, or through several kilometers of air, before losing its energy of motion. Also, Irène Joliot-Curie and Frédéric Joliot (1932) made a key observation that the unknown radiation from beryllium and from boron would eject protons when interacting with materials containing hydrogen such as paraffin. They showed that the protons were ejected with a high velocity of approximately 3×10^9 cm/s and estimated the quantum energy of the presumed gamma radiation to be extremely high, about 50 MeV. They had thought that the protons were ejected by the energy quanta of the mysterious radiation by a process similar to the Compton Effect. The Joliot-Curies came very close to discovering the neutron, but it eluded them. They unfortunately were fixated on their conviction that the radiation coming from beryllium was gamma radiation. The discovery of the neutron was almost at their grasp, but they failed to consider that the radiation could be a particle of relatively high mass and neutral charge. Chadwick shortly thereafter, after a series of experiments including repeating the paraffin experiment of the Joliot-Curies, identified the mysterious radiation as neutron radiation and not a quantum of gamma radiation.

On the basis of the findings described above and by a combination of intuition, logical thought, and experiment, James Chadwick (1932a,b) was able to prove that the "beryllium radiation" was not gamma radiation but the elusive neutron. To demonstrate the existence of the neutron and its properties, Chadwick made several systematic observations and experiments including (1) disproving on the basis of conservation of energy that the high energy emitted by the "beryllium radiation" was a quantum of gamma radiation; (2) demonstrating the particulate nature of the neutral radiation by observing recoil atoms of light elements including lithium, beryllium, boron, carbon, and nitrogen; (3) measuring the approximate mass of the neutral particle on the basis of recoil atom velocities; and (4) deducing the precise mass of the neutron from the mass–energy relations of the nuclei involved in the emission of the neutron.

Chadwick's first consideration that led to his discovery of the neutron was the improbability that a nuclear reaction involving an alpha particle with kinetic energy of only 5 MeV interacting with a beryllium nucleus could yield a high-energy gamma quantum of 50 MeV. In line with the laws of conservation of energy and momentum, Chadwick was convinced that there was another explanation for the identity of this highly penetrating radiation. He then proceeded to study the interaction of the "beryllium radiation" with protons from paraffin as well as atoms of other light elements. Such interactions via collisions of the unknown "beryllium radiation" would produce recoil atoms not only with hydrogen of paraffin (producing free protons), but also recoil atoms of the light elements. Fig. IV.1 illustrates the basic experimental setup Chadwick used to observe the recoil atoms produced by the mysterious "beryllium radiation."

As illustrated in Fig. IV.1, Chadwick produced proton recoil atoms by placing a paraffin barrier in the path of the "beryllium radiation." He could then measure the ranges and hence velocities of the protons by counting the protons that reached the ionization counter after interposing aluminum foil of different thicknesses between the wax and the counter. He measured the maximum range of the protons to be equivalent to 22 cm of air, corresponding to a velocity of about 3.3×10^9 cm per second (Chadwick, 1932a,b). He concluded that such a velocity could arise from a collision of a particle

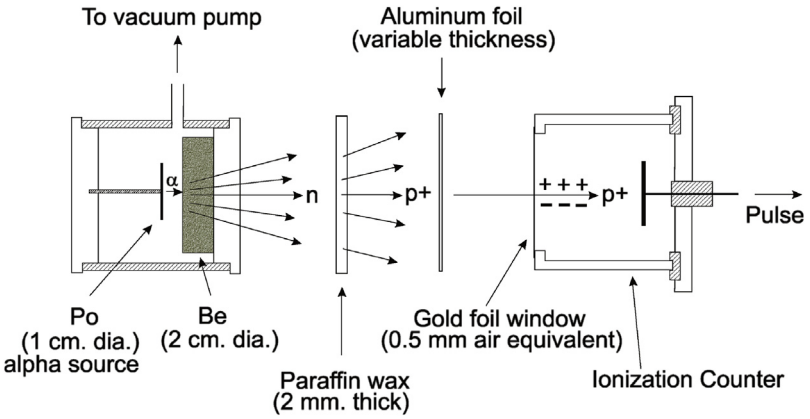

FIGURE IV.1 Schematic illustration of Chadwick's experimental setup of 1932 used in the discovery of the neutron and its properties. The aluminum foil of various thicknesses was used to determine the ranges of the recoil protons ejected from the paraffin. Also, Chadwick removed the paraffin layer and aluminum foil and inserted a brass plate coated with one of the following light elements—Li, Be, B, C, and N—very close to the ionization counter to measure the recoil atoms of the elements from direct neutron collisions. In another variation of the setup, Chadwick removed all paraffin and metal foils or plates between the neutron source and ionization counter and filled the ionization counter with hydrogen, helium, nitrogen, oxygen, or argon gas to observe the number of recoil atoms produced by neutron collisions with atoms of the different gases (see Chadwick, 1932b).

of similar mass as the proton, that is, the neutron, because a head-on collision between particles of equal mass could entail the transfer of practically all of the energy of one particle to the other, such as the head-on collision of one billiard ball with another. Chadwick arrived at the following "neutron hypothesis" prior to presenting still more evidence in support of his hypothesis (Chadwick, 1932b):

> *It is evident that we must either relinquish the application of conservation of energy and momentum in these collisions or adopt another hypothesis about the nature of the radiation. If we suppose that the radiation is not a quantum radiation, but consists of particles of mass very nearly equal to that of the proton, all the difficulties connected with the collisions disappear, both with regard to their frequency and to the energy transfer to different masses. In order to explain the great penetrating power of the radiation we must further assume that the particle has no net charge…The experiments showed that the maximum velocity of the protons ejected from paraffin wax was about 3.3 × 10^9 cm per second. This is therefore the maximum velocity of the neutrons emitted from beryllium bombarded by α-particles of polonium.*

Chadwick made additional measurements of recoil atoms of other light elements, including lithium, beryllium, boron, carbon, and nitrogen, which provided additional evidence that the "beryllium radiation" was a nuclear particle of mass similar to that of the proton. In one of these studies, he removed the paraffin layer and aluminum foil barriers to the neutron source (see Fig. IV.1) and inserted a brass plate coated with one of the following light elements—Li, Be, B, C, and N—very close to the ionization counter to measure the recoil atoms of the elements from direct neutron collisions. The recoil atoms would be liberated from the elemental coating on the brass plate and would, in turn, produce ionization and a consequent pulse count for each ion entering into the counter. The brass plate coated with any one of the light elements had to be placed very close to the ionization counter, because the recoil atoms of these elements could only travel a few millimeters in air. The counter was equipped with a very thin gold foil window equivalent to an absorbing power of only 0.5 mm of air. In each case, Chadwick found that the number of counts registered would increase when one of the light elements was bombarded with the neutron radiation. The magnitude of the pulses, measured by oscillograph deflections, produced by the light-element recoil atoms was larger than those produced by proton recoil atoms. Chadwick concluded that this was due to the greater atomic size and consequent greater ionization power that the light-element recoil atoms would have over the relatively smaller proton recoil atoms. The fact that the "beryllium radiation" could produce recoil atoms from collisions with such elements considerably larger than hydrogen provided Chadwick with additional conclusive evidence that the "beryllium radiation" was the particulate neutron radiation and not quanta of gamma radiation. He made this clear in the simple statement:

> *In general, the experiment results show that if the recoil atoms are to be explained by collision with a quantum, we must assume a larger and larger energy for the quantum [e.g. 90 MeV for nitrogen recoil] as the mass of the struck atom increases.*
>
> (Chadwick, 1932b).

Chadwick proceeded to measure the mass of the neutron as conclusive proof that the neutron was indeed a fundamental nuclear particle. He used three approaches to this problem. The first approach was to get an approximate mass of the neutron by measuring and comparing the relative velocities and masses of the recoil nitrogen and proton atoms. With the

assistance of Norman Feather (see Feather, 1932), Chadwick measured the ranges of the nitrogen and proton recoil atoms by photographing these from tracks of the recoil atoms produced in a Wilson cloud chamber (see C.T.R. Wilson in Hall of Fame, Part II). Chadwick calculated the maximum velocity that could be attributed to a hydrogen atom (proton recoil) from collision with a neutron as:

$$U_H = \frac{2M}{M+1}V \qquad \text{[IV.1]}$$

where U_H is the hydrogen atom (proton recoil) velocity and M and V are the mass and velocity of the neutron, respectively. Likewise, the maximum velocity, U_N, that could be given to a nitrogen atom (nitrogen recoil) upon collision with a neutron was calculated by Chadwick as:

$$U_N = \frac{2M}{M+14}V \qquad \text{[IV.2]}$$

Then the ratio of the two velocities of the recoil atoms could be written as:

$$\frac{M+14}{M+1} = \frac{U_H}{U_N} \qquad \text{[IV.3]}$$

The maximum range of the nitrogen recoil atom was measured at 3.5 mm in air, which corresponded to a velocity, U_N, of 4.7×10^8 cm/s. The previously deduced maximum velocity for the proton (hydrogen recoil) atom, U_H, was taken by Chadwick as 3.3×10^9 cm/s. Therefore, Chadwick (1932a,b) estimated the mass, M, of the neutron as:

$$\left(\frac{M+14}{M+1}\right) = \frac{U_H}{U_N} = \frac{3.3 \times 10^9}{4.7 \times 10^8}$$

$$M = 1.15$$

which was very close to the mass of the proton.

Because the ranges and velocities of the recoil atoms could not be so accurately determined, the above calculation of the neutron mass was only an approximation. Chadwick went further to a second approach to getting a more accurate measurement of the neutron mass. For this, he turned to consider the energy relations in one of the disintegration processes in which a neutron is liberated from an atomic nucleus and where the masses of the atomic nuclei concerned in the process were already accurately known. He took the process where boron (^{11}B) would liberate neutrons when bombarded with alpha particles (^{4}He) from polonium, that is:

$$^{11}_{5}\mathrm{B} + ^{4}_{2}\mathrm{He} \rightarrow ^{14}_{7}\mathrm{N} + ^{1}_{0}\mathrm{n} \qquad \text{[IV.4]}$$

From the calculated maximum velocities of the particles concerned, namely the alpha particle from polonium, the recoil atom of nitrogen, and the neutron, Chadwick could calculate the kinetic energy (K.E.) of each particle concerned, and considering that energy and momentum were conserved in the collisions, he wrote the following energy equation:

$$\text{mass of } ^{11}\mathrm{B} + \text{mass of } ^{4}\mathrm{He} + \text{K.E. of } ^{4}\mathrm{He} = \text{mass of } ^{14}\mathrm{N} + \text{mass of } ^{1}\mathrm{n} + \text{K.E. of } ^{14}\mathrm{N} + \text{K.E. of } ^{1}\mathrm{n} \qquad \text{[IV.5]}$$

or:

$$11.00825\ \mathrm{u} + 4.00106\ \mathrm{u} + 0.00565\ \mathrm{u} = 14.0042\ \mathrm{u} + \text{mass of } ^{1}\mathrm{n} + 0.00061\ \mathrm{u} + 0.0035\ \mathrm{u} \qquad \text{[IV.6]}$$

and:

$$\text{mass of } ^{1}\mathrm{n} = 1.0066\ \mathrm{u} \qquad \text{[IV.7]}$$

Chadwick estimated an error of ± 0.003 and the mass of the neutron to be somewhere between 1.005 and 1.008 u. This was very close to the actual value of 1.00866 u taken from tables of physical constants (Lide, 1997) and the neutron/proton mass ratio from current tables is 1.001378. In his calculations, Chadwick converted the kinetic energy of the particles from units of MeV to atomic mass units (u) according to Einstein's equation of equivalence of energy and mass and the calculated conversion unit of 931.494 MeV/u (see the chapter: "Alpha Radiation"). For example, the kinetic energy of the alpha particle (K.E. of ^{4}He) from polonium in Eq. [IV.5] has an average energy of 5.26 MeV. Its energy was converted to atomic mass units (u) in Eq. [IV.6] as follows:

$$\frac{5.26\ \mathrm{MeV}}{931.494\ \mathrm{MeV/u}} = 0.00565\ \mathrm{u} \qquad \text{[IV.8]}$$

A third and most accurate approach to the problem of the mass of the neutron was taken by Chadwick and Goldhaber (1934). The method they designed involved the disintegration of a nucleus into its component nucleons by means of gamma-ray bombardment. They selected a radioactive source that emitted gamma rays of sufficient energy to break apart a

deuterium nucleus into its component proton and neutron. The necessary condition for this was that the gamma-ray energy of the source should be greater than the binding energy of the proton and neutron, that is, an energy greater than that which holds the proton and neutron together forming the deuterium nucleus. In the words of Chadwick and Goldhaber (1934):

> *Heavy hydrogen was chosen as the element first to be examined, because the diplon has a small mass defect and also because it is the simplest of all nuclear systems and its properties are as important in nuclear theory as the hydrogen atom is in atomic theory. The disintegration to be expected is:*

$$^{2}_{1}\mathrm{H} + h\nu \rightarrow {}^{1}_{1}\mathrm{H} + {}^{1}_{0}\mathrm{n} \qquad \text{[IV.9]}$$

> *Since the momentum of the quantum is small and the masses of the proton and neutron are nearly the same, the available energy,* $\mathrm{h}\nu - \mathrm{W}$*, where* W *is the binding energy of the particles, will be divided nearly equally between the proton and the neutron.*

The term "diplon" used by Chadwick and Goldhaber refers to the nucleus of the recently discovered deuterium (heavy hydrogen nucleus) consisting of only one proton and one neutron. By "mass defect" of the nucleus, Chadwick and Goldhaber refer to the fact that the mass of the nucleus is always less than the combined masses of the separate nucleons. This difference in mass of the deuterium nucleus and the combined masses of the proton and neutron would be the binding energy of the deuterium nucleus. According to Einstein's equation of equivalence of mass and energy ($E = mc^2$), we can equate this difference in mass to the energy required to bind the proton and neutron together in the nucleus of deuterium, that is, the "binding energy." This binding energy is also the energy released when the deuterium nucleus is created by nuclear fusion, and it is the amount of energy needed to break apart the deuterium nucleus into its component proton and neutron. They therefore selected the isotope of Thorium C″, which is known today as ^{208}Tl. This isotope of thallium decays by beta particle emission with maximum energies of 1.8 MeV followed by the emission of a gamma ray of 2.62-MeV energy. Chadwick and Goldhaber estimated that the gamma ray from Thorium C″, if imparted to a nucleus of deuterium, would be more than sufficient to break it apart into its constituent proton and neutron. The result was exactly as they had hoped. An artist's depiction of the experimental arrangement they used is illustrated in Fig. IV.2.

Gamma rays from the Thorium C″ were sufficient to produce pulse events in the ionization chamber due to the proton produced by the splitting of the deuterium nucleus. From the magnitude of the pulse events, the energy of the proton could be determined to be 0.25 MeV. Since the proton and neutron have masses of similar magnitude, Chadwick and Goldhaber deduced that they would be ejected from the nuclear disintegration with equal energies, that is, 0.25 MeV each. They provided further evidence that the 2.62-MeV gamma ray from the Thorium C″ was indeed causing the splitting of the deuterium nucleus by replacing the Thorium C″ source with radium C, ie, ^{212}Bi. The 1.6-MeV gamma rays from radium C would produce no pulse events over background, as this gamma radiation was not of sufficient energy to exceed the binding energy to break apart the deuterium nucleus.

From the results obtained and from the then-known atomic masses of deuterium (2.0136 u) and proton (ie, hydrogen atom = 1.0078 u), and by use of Einstein's equation of mass and energy equivalence ($E = mc^2$), Chadwick and Goldhaber could calculate the mass of the neutron. The following reaction of their photon-induced splitting of deuterium can be written:

$$^{2}_{1}\mathrm{H} + h\nu \rightarrow {}^{1}_{1}\mathrm{H} + \text{proton energy} + {}^{1}_{0}\mathrm{n} + \text{neutron energy} \qquad \text{[IV.10]}$$

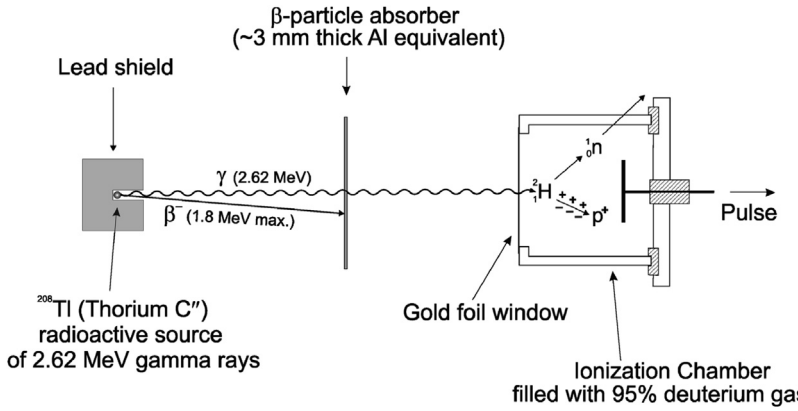

FIGURE IV.2 Artist's depiction of Chadwick and Goldhaber's experimental arrangement for the determination of the mass of the neutron. Gamma radiation of 2.62 MeV from a source of Thorium C″ was directed toward an ionization chamber filled with 95% pure deuterium gas. An absorber equivalent to 3 mm of aluminum would be required to prevent the beta particles from entering the chamber. Upon impact with a deuterium nucleus in the ionization chamber, the 2.62-MeV gamma ray would break the nucleus into its constituent neutron and proton. The neutron would escape from the chamber without effect, and the proton would be fully stopped producing ion pairs during its travel in the deuterium gas. The magnitude of the pulse produced by the proton could be calibrated to measure electron volts of energy absorbed by the ionization chamber.

Because the mass of deuterium includes the mass of an electron, we must use atomic mass units. Eq. [IV.10] in units of mass or energy can be written as:

$$2.0136\ \text{u} + 2.62\ \text{MeV} \rightarrow 1.0078\ \text{u} + 0.25\ \text{MeV} + {}^{1}_{0}\text{n} + 0.25\ \text{MeV} \qquad \text{[IV.11]}$$

The gamma-ray energy of 2.62 MeV and the proton and neutron energies of 0.25 MeV can be converted to atomic mass units with Einstein's equation. His equation may be used to determine the factor for converting energy in eV to atomic mass units (u) as follows:

$$E = mc^2 \qquad \text{[IV.12]}$$

where m is mass in kilograms and c is the constant velocity of light in a vacuum (2.9979×10^8 m per second. If by definition, the mass of 1 u = 1.6605×10^{-27} kg, the energy equivalent of 1 atomic mass unit could be calculated as:

$$\begin{aligned} E &= (1.6605 \times 10^{-27}\ \text{kg})(2.9979 \times 10^{8}\ \text{m/s})^2 \\ &= 14.924 \times 10^{-11}\ \text{J} \end{aligned} \qquad \text{[IV.13]}$$

The calculated energy in units of joules (J) is then converted to units of electron volts according to the conversion factor 1 eV = 1.602×10^{-19} J, or:

$$\begin{aligned} E &= 14.924 \times 10^{-11}\ \text{J}/1.602 \times 10^{-19}\ \text{J/eV} \\ &= 9.315 \times 10^{8}\ \text{eV} = 931.5\ \text{MeV} \end{aligned} \qquad \text{[IV.14]}$$

Thus 1 u = 931.5 MeV is established as a factor for converting energy into mass and vice versa. With this conversion factor, the energies in MeV of the gamma-ray photon and of the proton and neutron of Eq. [IV.11] can be converted to atomic mass units, providing all of the values in mass units as follows:

$$2.0136\ \text{u} + \left(\frac{2.62\ \text{MeV}}{931.5\ \text{MeV/u}}\right) \rightarrow 1.0078\ \text{u} + \left(\frac{0.25\ \text{MeV}}{931.5\ \text{MeV/u}}\right) + {}^{1}_{0}\text{n} + \left(\frac{0.25\ \text{MeV}}{931.5\ \text{MeV/u}}\right) \qquad \text{[IV.15]}$$

or:

$$2.0136\ \text{u} + 0.0028\ \text{u} \rightarrow 1.0078\ \text{u} + 0.00027\ \text{u} + {}^{1}_{0}\text{n} + 0.00027\ \text{u} \qquad \text{[IV.16]}$$

And the mass of the neutron would be calculated as:

$$\begin{aligned} {}^{1}_{0}\text{n} &= 2.0136\ \text{u} + 0.0028\ \text{u} - 1.0078\ \text{u} - 0.00027\ \text{u} - 0.00027\ \text{u} \\ &= 1.0081\ \text{u} \end{aligned} \qquad \text{[IV.17]}$$

With an estimate of errors, Chadwick and Goldhaber (1934) reported the mass of the neutron as 1.0081 u ± 0.0005. This was yet the closest to the current value for the mass of the neutron of 1.00866 u taken from tables of physical constants (Lide, 1997). They then were able to report the binding energy of the deuterium nucleus as 2.1 MeV by taking the difference of the mass of deuterium and that of the sum of its proton and neutron masses, or:

$$\begin{aligned} \text{Binding Energy of } {}^{2}_{1}\text{H} &= (\text{Mass of } {}^{1}_{1}\text{H} + \text{Mass of } {}^{1}_{0}\text{n}) - \text{Mass of } {}^{2}_{1}\text{H} \\ &= (1.0078\ \text{u} + 1.0081\ \text{u}) - 2.0136\ \text{u} \\ &= 0.0023\ \text{u} \end{aligned} \qquad \text{[IV.18]}$$

Converting the 0.0023 u into units of MeV yields:

$$\text{Binding Energy of } {}^{2}_{1}\text{H} = (0.0023\ \text{u})(931.5\ \text{MeV/u}) = 2.1\ \text{MeV} \qquad \text{[IV.19]}$$

Chadwick's discovery of the neutron, its mass, and its charge provided science finally with what was missing to formulate the basic structure of the nucleus and the atom. The importance of this milestone was emphasized by Prof. H. Pleijel, Chairman of the Nobel Committee for Physics on December 10, 1935, when he stated:

> *The existence of the neutron having thus been proved…The nucleus of atoms is nowadays considered to be composed of a number of protons and neutrons…about the nucleus there circle in the atom electrons…Isotopes are formed by surplus or lack of the number of neutrons in the solid atom…The existence of the neutron having been fully established, scientists have come to a new conception of the structure of atoms which agrees better with the distributions of energy within the nuclei of atoms. It has proved obvious that the neutron forms one of the building stones of atoms and molecules and thus also of the material universe.*

In 1935 Chadwick left Cambridge to occupy the Lyon Jones Chair of Physics at the University of Liverpool. From 1943 to 1946, he worked in the United States as head of the British team on the Manhattan Project for the development of the atomic bomb. Afterward he returned to England, and in 1948 retired from his post at the University of Liverpool to become Master of Gonville and Caius College at Cambridge until his retirement in 1959. Chadwick served as a part-time member of the United Kingdom Atomic Energy Authority from 1957 to 1962 (*Nobel Lectures, Physics 1922–1941*). James Chadwick died on July 24, 1974.

LISE MEITNER (1878–1968) AND OTTO HAHN (1879–1968)

The biographical sketches of Lise Meitner and Otto Hahn are included jointly here because they worked closely together and collaborated professionally for over 30 years. Many of their major contributions to science, including the discovery of nuclear fission, for which they deserve equal credit, were the result of their mutual collaboration. Austria has honored Lise Meitner with a postage stamp illustrated here, which was issued to commemorate the ten-year anniversary of her death.

Lise Meitner (1878–1968)

Lise Meitner was born in Vienna, Austria on November 7, 1878 to Jewish parents. Her father was a successful Jewish lawyer. Although of Jewish heritage, Lise Meitner did not practice the Jewish faith. When she and her two sisters were young adults, Lise converted to Protestantism and her sisters to Catholicism, but she was not outwardly religious.

When Lise Meitner was a young girl her parents provided her with private tutoring, as a good formal education for women at that time was difficult. She was gifted in the subjects of physics and mathematics. In a biography by Ruth Lewin Sime (1996), *Lise Meitner: A Life in Physics*, we can appreciate the adverse social and cultural conditions she had to surmount. She passed the entrance exam to the University of Vienna in 1901 after the restrictions on female students were lifted. At the prestigious University of Vienna, she majored in physics and studied under Ludwig Boltzmann. Science, at that time, was the domain of men. Consequently her performance had to be outstanding to overcome bias of some unsympathetic professors and students. She could often find herself as the only woman in a class of over 100 men. Lise Meitner graduated with a doctorate degree in physics from the University of Vienna in 1905. She wanted to continue her studies in theoretical physics at the University of Vienna, but to her great distress, Boltzmann had taken his life in 1906 during one of his attacks of depression (Frisch, 1978).

Lise Meitner's doctoral dissertation was titled "Wärmeleitung in inhomogenen Körpern" (Heat Conduction in Inhomogeneous Solids). After graduation she worked at the Institute for Theoretical Physics in Vienna and wrote her first paper on radioactivity in 1907 "Über die Absorption von α- und β-Strahlen" (Concerning the Absorption of α- and β-rays). Meitner was able to demonstrate that α-particles do not travel in straight lines, but that in passing through matter, they undergo slight irregular deflections (Frisch, 1978). Ernest Rutherford later discovered the backscattering of α-particles and the existence of the atomic nucleus in 1911. There were then few opportunities in Vienna for women in physics, so with financial assistance from her parents, she moved to Berlin to pursue studies and research on nuclear physics. In Germany she would meet with the great physicists Max Planck and Albert Einstein and began to study and work under Max Planck, the leading theoretical physicist at the time. Planck let her attend lectures and assist in evaluating the essays of students and

to organize seminars. Planck was puzzled by her quest for knowledge and need to carry out research in theoretical physics, possibly because she was a woman, and asked, "You have the doctorate, what more do you want?" (Frisch, 1978). Eventually Lise Meitner would team up with a young chemist Otto Hahn at the Kaiser Wilhelm Institute (KWI), with whom she would carry on a very successful research collaboration in the field of radioactivity for over 30 years, most of her career. At the start of their collaboration, Otto Hahn had suggested that the young woman physicist help him install and operate the new physical instruments used to measure radioactive sources. As related by Otto Frisch (1978), the suggestion of Hahn alarmed his boss, Emil Fischer, who did not want women in his laboratory for fear, it was said, that "their fuzzy hair might catch fire from a Bunsen burner." Frisch (1978) relates that women's education was regularized in 2 years' time and the ban lifted. In the meantime, Hahn and Meitner were given an old carpentry shop to set up their equipment.

Otto Hahn was born on March 8, 1879 in Frankfurt on Main, Germany. He studied chemistry at universities in Marburg and Munich and graduated with his doctorate degree in organic chemistry at Marburg in 1901. After receiving the doctorate degree, he remained in Marburg as an assistant at the Chemical Institute for 2 years before transferring to the University College, London to work under Sir William Ramsay (Nobel Laureate in Chemistry 1904), where he started his research work on radioactivity. From the autumn of 1905 to the summer of the following year, Hahn worked with Ernest Rutherford at the Physical Institute of McGill University in Montreal, Canada. Here he carried out research with Rutherford on alpha radiation from thorium and actinium. Otto Hahn returned to Germany in 1906 and moved to Berlin as university lecturer at the Chemical Institute of the university, and also Head of the Radiochemistry Department of the Kaiser Wilhelm Institute. At the end of 1907, Otto Hahn began his long and fruitful collaboration with Lise Meitner after her arrival from Vienna. Their collaboration would last over 30 years until July 1938. Hahn helped Meitner, as it was not easy for a woman to work at the institute and they had a mutual interest in research into the field of radioactivity. They also made a perfect team; he as the chemist with the knowledge and ability to separate and isolate the many radioactive elements they would encounter, and she as the physicist with the theoretical knowledge needed to interpret the physical properties of radiation and its interaction with matter. Their collaboration was interrupted from 1914 to 1918 when Hahn was recruited into the war effort, where he applied his scientific knowledge as a chemical-warfare specialist. Lise Meitner was also recruited into the war effort, but used her expertise in X-ray physics to save lives of injured soldiers as an X-ray nurse. They continued their research collaboration at the Kaiser Wilhelm Institute (KWI) in 1918.

Otto Hahn (1879–1968)

When Lise Meitner arrived at the KWI in Berlin in 1907, she was a woman in a man's world, and was not immediately welcomed except by a few who knew her talents. The previously noted biography of Lise Meitner by Ruth Lewin Sime (1996), a more recent biography by Patricia Rife (1999), *Lise Meitner and the Dawn of the Nuclear Age*, and a critique on the book by Goldstein (2001), as well as an article on Lise Meitner's life by Bartusiak (1996), provide much insight into the obstacles that she as a woman and accomplished physicist at that time encountered, and the perseverance, hard work, and lifelong battle for the ultimate truth in nuclear physics, which enabled her to overcome most obstacles. Some of their impressions are summarized herein. It was an uphill battle for her to gain recognition, as she was the first among women in both

Austria and Germany to be allowed into the institutions of higher learning and research. When she started to work at the KWI in 1907, Lise Meitner was compelled to set up her lab in a converted carpentry shop in the building basement as it was unimaginable to some in management to have a woman work in a laboratory that belonged to men. However, her knowledge and perceptive abilities in nuclear physics quickly established her as an outstanding scientist at the KWI. Lise Meitner and Otto Hahn collaborated as equal partners and Hahn always insisted that she be provided with due credit and be included as coauthor on all of their collaborative research at least during the years she remained at the KWI. For many years Lise Meitner worked with Otto Hahn without salary, as women had no official status at the institute. She received financial assistance from her parents and a meager stipend from her friend, Max Planck, while working at the institute. Eventually by the year 1916, she received a salary comparable to that of Otto Hahn even though she had already for several years carried out equal responsibilities as Hahn. In 1918 she became Head of the Radiophysics Department at the KWI.

During the early stages of their collaboration one of the only precise instruments available to them for measuring radioactive sources was the gold leaf electroscope. With the aid of a stopwatch, they could measure an ionization current by the rate of movement of the gold leaf of the electroscope across a reference scale (see Fig. VI.1 and a treatment on the electroscope in Hall of Fame, Part VI). In a biographical sketch, Otto Frisch (1978) relates a story about Lise Meitner using the gold leaf electroscope at the time a mailman entered the room. His story goes as follows:

> *It [gold-leaf electroscope] was surprisingly sensitive. On one occasion Lise Meitner peering through the eyepiece, greatly startled the postman who had just entered the room by telling him that he had a letter from Manchester in his bag! Rutherford occasionally sent her some radon in a small glass tube, just wrapped in cardboard; unthinkable under today's safety rules, which would demand a leaden box with inch-thick walls. Hahn and Meitner, to work fast and unencumbered by gloves, often risked and got small burns on their fingers, sometimes slow to heal; but neither of them suffered serious injury.*

As in the case of Marie Curie, Lise Meitner volunteered her expertise in the new X-ray technology as an X-ray nurse (Röntgenschwester) during the war. She worked to exhaustion to help in the diagnosis of many severely injured soldiers for the Austrian army in a military hospital on the East Front. By 1922 Lise Meitner became the first woman to be appointed as extraordinary professor of experimental nuclear physics at the University of Berlin. This was a more prestigious position that would draw more attention both nationally and internationally than that of a researcher at the KWI. During these times such accomplishments for a woman were remarkable. For example, when the name of Prof. Meitner had become well known, a book publisher inquired about getting the collaboration of Prof. Meitner in the production of an encyclopedia. After finding out that Prof. Meitner's first name was Lise, he would have nothing to do with a lady as author of any chapter. Lise Meitner remained in Berlin as long as possible, but she had to flee for her life to Sweden in 1938. The German *Anschluss* or annexation of Hitler's regime with Austria made Lise Meitner a German citizen and thereby subject to all of the anti-Semitic laws of the Nazi state. Her long career in Berlin and collaboration with Otto Hahn resulted in several historic discoveries. She was eventually honored by Germany with the postage stamp issued from 1986 to 1991. The stamp, shown here, illustrates how she appeared as a young girl, when she embarked on a career of discovery in nuclear physics.

One of the first major outcomes of her collaboration with Otto Hahn at the KWI was the discovery of element 91, protactinium. The element is radioactive, as all natural elements of atomic number greater than 83 are radioactive. They identified the element as a radioactive isotope and the parent substance of actinium (Hahn and Meitner, 1918). They named it "protoactinium" from the Greek "prōtos," meaning first, because it held the first place after uranium in the uranium-actinium decay series, better known today as the uranium-235 decay series, illustrated in Fig. IV.3. The name of the element was shortened in 1949 to protactinium, and the isotope (^{231}Pa) in the decay series identified by Hahn and Meitner is highlighted in Fig. IV.3. Soddy and Cranston (1918) also independently identified the isotope as the parent of actinium. The two papers reporting the discovery were published almost simultaneously in two different journals, and consequently both parties shared the credit for the discovery. Another isotope of protactinium (^{234m}Pa) of very short half-life (1.18 min) was discovered earlier by Kasimir Fajans and Otto H. Göring of Karlsruhe in 1913. They called the isotope "brevium," meaning brief (Fajans and Göring, 1913). Hahn and Meitner discovered the more stable isotope (^{231}Pa) of the element, which has a half-life of 3.3×10^4 years.

Lise Meitner (1923) discovered Auger (pronounced OH-ZHAY) electrons. The French physicist Pierre Victor Auger (1899−1993) also independently discovered Auger electrons and carried out studies on the electron emissions from atoms (Auger, 1923, 1925a,b). Although both Lise Meitner and Pierre Auger independently discovered the atomic electron emissions about the same time, only Auger's name has been attached to this phenomenon. Auger electrons are atomic electrons that are emitted from atoms after acquiring energy from an atomic electron transition within the atom. For a detailed discussion of Auger electrons and their origins, see the biographical sketch on Pierre Victor Auger in Hall of Fame, Part V.

By 1937, Lise Meitner and Otto Hahn, together with a German chemist Fritz Strassmann at the KWI, had identified about 10 previously unknown radioactive isotopes of the elements in the uranium decay series. They, as well as others,

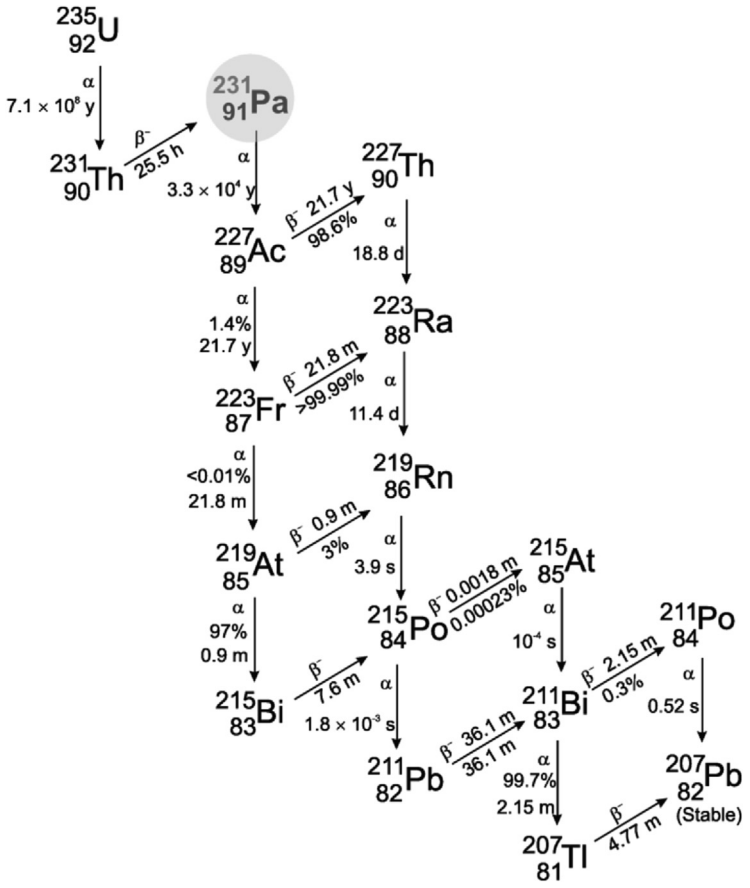

FIGURE IV.3 The uranium-235 decay series. The protactinium-231 discovered by Hahn and Meitner is highlighted with a *gray circle*. They named the element "protoactinium" from the Greek "prōtos," meaning first and the parent of actinium-227. In the figure we can see that it is the first element after uranium in the decay series according to atomic number. Uranium has the atomic number 92, and protactinium has the next lower atomic number of 91. The decay modes are identified as α or β^- and percentages included for branching decay. The abbreviations s, m, h, d, and y represent the half-lives of the radioisotopes in seconds, minutes, hours, days, or years.

including Enrico Fermi's group in Rome and Irene Joliot-Curie and Paul Savitch in Paris, were researching the transmutation of uranium under the effect of neutron bombardment. This work would in short time lead to Lise Meitner's greatest discovery. Lise Meitner was very productive at the KWI in Germany, well known internationally by 1937, and happy with her work. Albert Einstein had once said "She is our German Marie Curie." The most significant scientific contribution made by Lise Meitner was her collaboration with Otto Hahn in the discovery and interpretation of nuclear fission. This discovery was not made until February of 1939 after her escape from Nazi Germany in July of 1938.

Although a Protestant, Lise Meitner was of Jewish decent, and after the annexation of Austria by Germany in 1938, she became a German citizen and subject to all of the anti-Semitic laws or decrees of Hitler's Nazi regime. With her job and life in peril, Lise Meitner escaped to Sweden on July 17, 1938 by way of The Netherlands in the company of Dirk Coster (1889−1950), the Dutch physicist, who together with George de Hevesy in Copenhagen discovered the element hafnium (Hf) taken from the word *Hafnia*, Latin for Copenhagen. Lise Meitner's escape from Germany was a dangerous one, and the details of her preparation and escape can be found in a detailed account by Rhodes (1986).

During Lise Meitner's escape to Sweden, Otto Hahn and Fritz Strassmann continued their research on the transmutations that occur upon the neutron bombardment of uranium. Similar work by Joliot-Curie and Savitch in Paris also continued. In Sweden, Lise Meitner had been provided a position in Manne Siegbahn's Institute of Physics in Stockholm. Here she was provided with a place to work, but with insufficient equipment, staff, or funds to carry out significant work. Nevertheless, by correspondence Otto Hahn kept Lise Meitner informed of the details of their work in Germany on the transmutations resulting from the neutron bombardment of uranium, and he asked Lise Meitner for guidance and input into the interpretation of their findings. By December 1938, Hahn and Strassmann had confirmed through fractionation and recrystallization of the numerous transmutation products with barium carrier that radioactive barium (atomic number 56) was one of the products of neutron bombardment of uranium (atomic number 92). Such a result was inconceivable to him, as he or anyone else could not then imagine how uranium with its large nucleus containing 92 protons, could yield such a small atomic nucleus as barium with only 56 protons. As related in detailed accounts by Rhodes (1986) and Sime (1996), Hahn wrote Meitner on December 19, 1938 requesting advice as follows:

> *Perhaps you can suggest some fantastic explanation…We understand that it* can't *break up into barium….So try to think of some other possibility. Barium isotopes with much higher atomic weights than 137? If you can think of anything that might be publishable, then the three of us would be together in this work after all. We don't believe this is foolishness or that contaminations are playing tricks on us.*

Lise Meitner wrote Hahn back the same week of his letter accepting the fact that barium was a product of slow-neutron bombardment of uranium and informing him that, although it is difficult to believe, anything is possible. As related by Richard Rhodes (1996), Hahn and Strassmann on December 23rd had reconfirmed that the barium isotope was the product, because it would decay to the element lanthanum only one atomic number higher. Hahn was anxious to find an understanding as to what type of phenomenon was occurring, and he was fearful that others, such as Joliot-Curie and Savitch, might soon make the same discovery—a race was on and the matter was urgent. As related by Rhodes (1986) and Sime (1996), Hahn wrote Lise Meitner again in late December desperate for an explanation of the results:

> *We cannot hush up the results, even though they may be absurd in physical terms. You can see that you will be performing a good deed if you find an explanation. When we finish tomorrow or the day after I will send you a copy of the manuscript.*

Hahn's letter to Stockholm did not immediately reach Meitner's hands, as she was away from Stockholm meeting with her nephew, physicist Otto Frisch, in the village of Kungälv, Sweden. He had arrived from Copenhagen. While hiking in Kungälv on December 19th, Lise Meitner discussed with Otto Frisch the problem of barium—that is, how could barium of such low atomic number (56), be a product of neutron bombardment of uranium of high atomic number (92). As related by Frisch (1978), they thought of Bohr's theory that the nucleus of an atom was like that of a liquid drop. It then occurred to Lise Meitner that the large uranium nucleus made unstable by its high electric charge might burst and divide itself into two smaller nuclei when shaken up by a neutron, such as a living cell becomes two smaller cells by fission. In the outdoors of that winter day, Lise Meitner sketched the form of a liquid drop to simulate the uranium nucleus, which after capturing a neutron, could become so unstable as to elongate into a dumbbell shape with opposing positive forces of the nuclear protons and break apart into two smaller nuclei. Meitner and Frish then and there on that winter hike made calculations of the immense energy that would be liberated upon splitting the uranium nucleus—approximately 200 MeV. Nuclear fission had been discovered by Meitner and Frisch while hiking in December of 1938. They coined the word "fission" by borrowing the word from biology, a term used to describe splitting bacteria cells (Michaudon, 2000). Rhodes (1986) relates, in his detailed historical account, within a few days of her discovery of fission, Meitner wrote Hahn the following on January 1, 1939:

> *We have read your work very thoroughly and consider it* perhaps *possible energetically after all that such a heavy nucleus bursts.*

On January 3rd, after reviewing Hahn's paper (Hahn and Strassmann, 1939a) proving barium to be a product of neutron bombardment of uranium, she wrote Hahn explaining to him that what was occurring in the production of barium from uranium was definitely a splitting of the nucleus, but she did not go further with providing him with any further information concerning a theory on how the nucleus of uranium could split. She wrote the following:

> *I am fairly* certain *now that you really have a splitting towards barium and I consider it a wonderful result for which I congratulate you and Strassmann very warmly.*

Now that Hahn and Strassmann (1939a) would publish their experimental results proving that barium was a product of neutron bombardment of uranium (their paper was published in January 1939), Meitner and Frisch intended to publish the interpretation of these results. In an article published in the journal *Nature* on February 11, 1939 entitled "Disintegration of Uranium by Neutrons: A New Type of Nuclear Reaction," Meitner and Frisch were the first to describe and name the phenomenon of nuclear fission. An excerpt from Meitner and Frisch (1939) describing fission for the first time is the following (reprinted by permission from MacMillan Publishers, Ltd., http://dx.doi.org/10.1038/143239a0):

> *…Hahn and Strassmann (1939a) were forced to conclude that isotopes of barium (Z = 56) are formed as a consequence of the bombardment of uranium (Z = 92) with neutrons…In the basis, however of present ideas about the behaviour of heavy nuclei (Bohr, 1936), an entirely different and essentially classical picture of these new disintegration processes suggests itself. On account of their close packing and strong energy exchange, the particles of a heavy nucleus would be expected to move in a collective way which has some resemblance to the movement of a liquid drop. If the movement is made sufficiently violent by adding energy, such a drop may divide itself into two smaller drops…It seems therefore possible that the uranium nucleus has only small stability of form, and may, after neutron capture, divide itself into two nuclei of roughly equal size (the precise ratio of sizes depending on final structural features and perhaps partly on chance). These two nuclei will repel each other and should gain a total kinetic energy of approximately 200 MeV, as calculated from nuclear radius and charge. This amount of energy may actually be expected to be available from the difference in packing fraction between uranium and the elements in the middle of the periodic system. The whole fission process can be described in an essentially classical way…*

An illustration of neutron capture of uranium, as it is currently known today, is provided in Fig. IV.4. The figure also illustrates uranium fission with the unstable ^{236}U nucleus oscillating like a liquid drop, as first described by Meitner and Frisch in 1939.

Meitner and Frisch (February 11, 1939) went even further to explain in their historic paper reporting nuclear fission for the first time that, if one of the fission products (eg, X of Fig. IV.4) was barium ($Z = 56$), then the other fission product (eg, Y of Fig. IV.4) must be krypton ($Z = 36$), as the atomic number of the two fission products must equal 92, the atomic number of the parent element uranium. In their paper, Meitner and Frisch (1939) stated:

> *After division, the high neutron/proton ratio of uranium will tend to readjust itself by beta decay to the lower value suitable for lighter elements. Probably each part will give rise to a chain of disintegrations. If one of the parts is an isotope of barium (Meitner, Strassmann, and Hahn, 1938), the other will be krypton (Z = 92 − 56),…*

In the above statement, Meitner and Frisch gave one specific example of two fission fragments of uranium-236; however, they noted that numerous different fission fragments are possible. The example provided in the above quotation can be written as follows:

$$^{235}_{92}\mathrm{U} + {}^{1}_{0}\mathrm{n} \rightarrow {}^{236}_{92}\mathrm{U} \xrightarrow{\text{fission}} {}_{56}\mathrm{Ba} + {}_{36}\mathrm{Kr} + \mathrm{x}\,{}^{1}_{0}\mathrm{n} \qquad \text{[IV.20]}$$

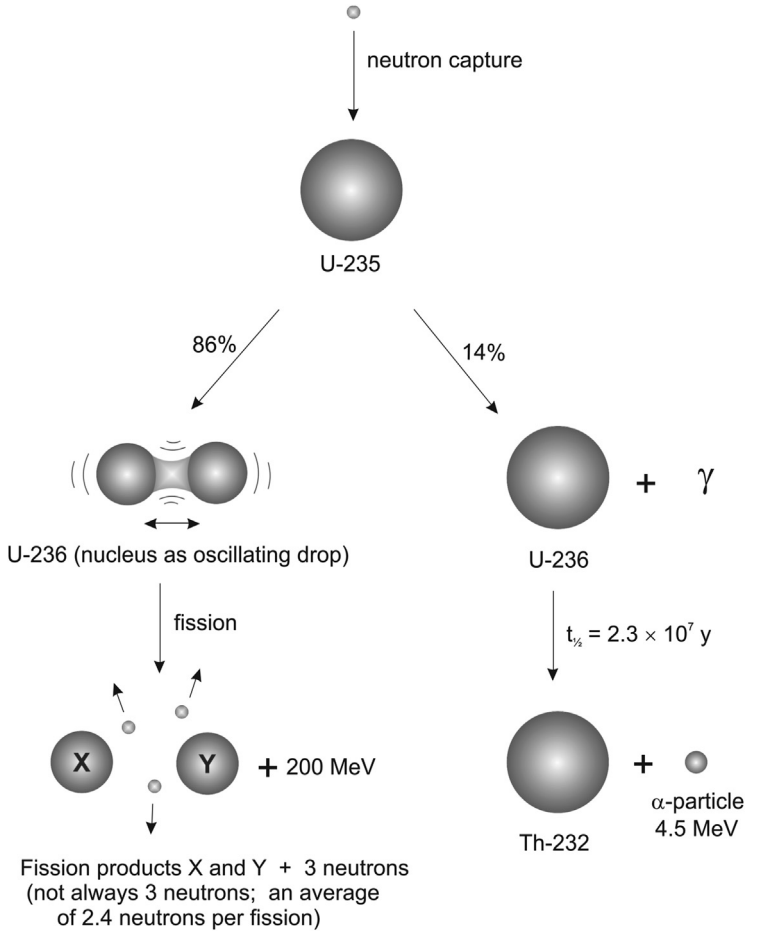

FIGURE IV.4 Uranium-235 neutron capture. The capture of a slow neutron by uranium-235 yields the nuclide uranium-236. A small number of the neutrons captured (14%) yield a U-236 nucleus that decays with a long half-life ($t_{½}$) to thorium-232 with the emission of an α-particle and 4.5 MeV energy. A larger number of the neutrons captured by U-235 (86%) yield a U-236 nucleus which is highly unstable, capable of oscillating like a liquid drop and breaking into two smaller nuclides, X and Y, of different masses and of atomic numbers that add up to 92 (the atomic number of the parent uranium) plus the emission of an average of 2.4 neutrons and a lot of energy (approximately 200 MeV). The emission of three neutrons is illustrated above.

The x in the last term of Eq. [IV.20] represents an indeterminate number of neutrons. The number of neutrons emitted from uranium-236 fission will vary, and the average number is 2.4. The fission reaction first explained by Meitner and Frisch was commemorated by a postage stamp shown here issued by the German Democratic Republic (DDR) in 1979. The stamp pictures only Otto Hahn together with the historic fission reaction. Lise Meitner had not been given equal credit for the work leading to the discovery or for her part in the discovery of fission. Due recognition would not come until the award of the Fermi Prize to Meitner, Hahn, and Strassmann in 1966 for the discovery of nuclear fission only a couple of years prior to the deaths of Hahn and Meitner in 1968.

Meitner and Frisch also tried to explain the relative stability of some of the uranium isotopes, that is, why they don't all undergo fission (eg, U-236, with a long half-life illustrated in Fig. IV.4). In their paper announcing fission, they provided the following explanation:

> *The formation of this body [uranium nucleus] is a typical resonance process [Bethe and Placzec, 1937], the compound state must have a life-time of a million times longer than the time it would take the nucleus to divide itself. Perhaps this state corresponds to some highly symmetrical type of nuclear matter, which does not favor fission of the nucleus.*

In this paper Meitner and Frisch (1939) also described fission of thorium for the first time. An excerpt of that statement is the following:

> *By bombarding thorium with neutrons, activities are which have been ascribed to radium and actinium isotopes (Meitner, Strassmann, and Hahn, 1938). Some of these periods [half-lives] are approximately equal to periods of barium and lanthanum isotopes resulting from the bombardment of uranium. We should therefore like to suggest that these periods [half-lives] are due to a fission of thorium, which is like that of uranium and results partly in the same products.*

Hahn and Strassmann (1939b) published their paper providing the analytical chemistry proof of uranium fission as well as the fission of thorium on February 10, 1939, one month after the publication of Meitner and Frisch's paper describing nuclear fission. They also identified the fission fragments of radioactive strontium ($Z = 38$) and yttrium ($Z = 39$) for the first time. Although Hahn and Strassmann did not include Lise Meitner as coauthor of the paper, they did acknowledge her contribution to the work at the end of the paper as follows:

In a rather short time it has been possible to identify numerous new reaction products described above — with considerable certainty, we believe — only because of the previous experience we had gathered, in association with L. Meitner, from the systematic study of uranium and thorium reaction products.

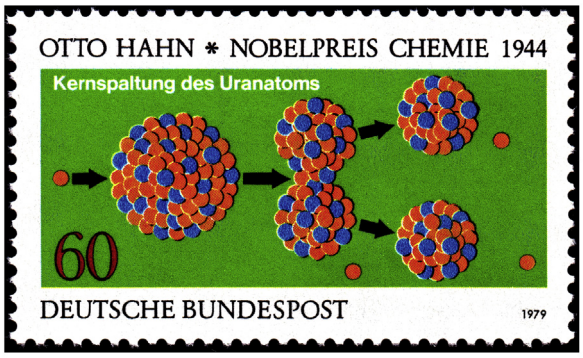

Nuclear Fission

The postage stamp shown here was issued in Germany in 1979. It illustrates the fission of a uranium nucleus as initially proposed by Meitner and Frisch in 1939. The stamp illustrates from left to right a neutron being captured by a uranium nucleus, which forms an unstable "liquid-drop" or dumbbell shape and then undergoes fission to two separate and smaller atomic nuclei (fission products) and three neutrons. The stamp does not cite Lise Meitner for her role in the discovery of nuclear fission, but only Otto Hahn, who received the Nobel Prize in Chemistry in 1944 for the discovery of nuclear fission. This was an apparent oversight on the part of the Nobel Committee and particularly an omission on the part of Otto Hahn for not giving her sufficient credit to share the Nobel Prize. The truth about this unfortunate discrimination has come to public light with the detailed biographies of Lise Meitner written by Sime (1996) and Rife (1999). The questions about the unfairness which Lise Meitner was dealt concerning the credit due her were highlighted by Goldstein (2001), and a relevant excerpt of his comments is the following (reprinted with permission © 2001 Peace History Society and Consortium on Peace History Research, Education and Development, John Wiley & Sons, Inc. All Rights Reserved):

The history of fission's discovery raises many questions. Why was Meitner not included as co-author on Hahn and Strassmann's paper? Rife (1999) doesn't consider this point, but the fact that Meitner had been an active partner in this particular research until her escape in July reasonably should have led to her inclusion on the paper. Sime's book (1996) speculated that it might have been dangerous for Hahn to include this recently escaped non-Aryan as a co-author. Most of the scientists involved in this line of research knew that Meitner had been an equal partner in the work anyway. Unfortunately, though, after the war Hahn continued to downplay Meitner's role in the research, as Rife (1999) shows. During the war "he refused to take a stand on the politics in and out of his Institute: the Third Reich was blinding Hahn and he began to discount Meitner's insights and contributions he had frantically sought out *months earlier. We witness here appeasement, professional cowardice, and worse (Rife, 1999, p. 213). Perhaps Hahn's initial lapse is understandable, given that the editor or some other authorities may have rejected the groundbreaking paper for political reasons, although Hahn knew the editor personally. More likely he would have had to stand up to the Nazi dictatorship of the Institute and the official scientific establishment, thereby jeopardizing his position. And when he finally received recognition for the paper and the acclaim from his German colleagues that followed, he was not about to share credit with Meitner. There is no question that his behavior was scurrilous. He must have constructed a tortuous self-justification to assuage his guilt for deserting his decades-long collaborator and friend. He never adequately acknowledged her essential role in the discovery, even long after he was awarded the Nobel Prize and was a leading figure in post-war German science.*

Lise Meitner and Otto Hahn

The Nobel Committee overlooked Lise Meitner when they awarded the Nobel Prize in Chemistry in 1945 to only Otto Hahn even though she had collaborated with Otto Hahn for three decades right up to July 1938, when she escaped from Nazi Germany, and the work that led to the discovery of fission was concluded only a few months later. The absence of Lise Meitner's name as coauthor to Hahn and Strassmann's paper of February 1939 may have contributed to this mistake of the Nobel Committee, although never acknowledged by the Royal Swedish Academy of Sciences. Niels Bohr tried to assure priority credit to Lise Meitner for her interpretation of fission, but this was not sufficient to prevent the 1944 Nobel Prize in Chemistry from being awarded exclusively to Otto Hahn (Goldstein, 2001), which was announced after the war on November 15, 1945. This mistake certainly had been gnawing at the consciences of the scientific community for at least two decades since the awarding of the Nobel Prize to only Otto Hahn. Some rectification of the error was made with the award of the United States Fermi Prize in 1966 to Hahn, Meitner, and Strassmann. The Enrico Fermi Award was established in 1954. It is the most prestigious science and technology award given by the U.S. Government. It recognizes scientists of international stature for their lifetimes of exceptional achievement in the development, use, or production of energy. The Fermi Award in 1966 was bestowed equally to Lise Meitner, Otto Hahn, and Fritz Strassmann "for contributions to nuclear chemistry and extensive experimental studies contributing to the discovery of fission." A yet greater honor was bestowed posthumously to Lise Meitner when element 109 was named Meitnerium in 1997 in honor of Lise Meitner, the Austrian physicist who first interpreted the phenomenon of nuclear fission. Finally, following the detailed historical accounts of Lise Meiner's life and work by Sime (1996), Rife (1999), and others, the general public has come to realize the mistake, and consequently the very first postage stamp that honors both Lise Meitner and Otto Hahn for the discovery of fission was issued by St. Vincent and The Grenadines in the year 2000. The stamp shown here is that of a famous photo taken of Lise Meitner and Otto Hahn in 1913 in their laboratory at the Kaiser Wilhelm Institute in Berlin-Dahlem many years prior to her escape from Germany in 1938. The fitting statement of the stamp reads "1938: The discovery of Fission."

Albert Einstein called her "Our Madame Curie" (Frisch, 1978). The life of Lise Meitner, like that of Marie Curie, should serve as an example for all on how hard work and dedication can overcome many obstacles no matter how insurmountable they may appear. Goldstein (2001) put it very clearly when he wrote:

> *Though she was never given the same level of recognition and reward as her collaborator Hahn, Lise Meitner's single-minded dedication to physics while faced with a myriad of obstacles is proof of an extraordinary person. And with such extraordinary people we want to know how they came to be.*

Her life was difficult, as she apparently encountered obstacles at almost every turn; nevertheless, Lise Meitner had a life full of satisfaction and fulfillment. We can be certain of this from the following quotation of Lise Meitner, 5 years before her death, from a biography by Rosner and Strohmaier (2003) and a review article in the CERN Courier (2004):

I believe that all young people think about how they would like their lives to develop. When I did so, I always arrived at the conclusion that life need not be easy; what is important is that it not be empty. And this wish I have been granted.

Lise Meitner retired in 1960 in Cambridge, England. She continued to lecture and visit friends up to 1964, when she suffered a heart attack after a strenuous trip to the United States. She recovered from the heart attack, and the following year was awarded the Enrico Fermi Prize with Otto Hahn and Fritz Strassmann for contributions to nuclear chemistry and the discovery of nuclear fission. Glenn T. Seaborg, then Chairman of the U.S. Atomic Energy Commission, went to Cambridge to present her share of the award (Frisch, 1978). Lise Meitner died on October 27, 1968. Otto Hahn, after receiving the Nobel Prize in 1945, continued his research on the identification and separation of many radioactive isotopes that arise through fission. He died a few months before Lise Meitner on July 28, 1968 (Nobel Lectures in Chemistry, 1901−1970).

LEO SZILARD (1898−1964)

Leo Szilard (1898–1964)

Leo Szilard was born Leo Spitz on February 11, 1898 to an affluent Jewish family in Budapest, Austro-Hungary. The family name was changed to Szilard in 1900. He was one of the world's greatest thinkers among the physicists of the 20th century. His mind was never idle, always conceiving new scientific theories and inventions. He is recognized mostly for his pioneering thought and contributions to nuclear physics, his numerous patents of instruments that have revolutionized 20th-century nuclear physics, his patent for the atomic bomb and his spearheading of the formation of a program for its development, the design and patent for the first nuclear reactor (joint patent with Enrico Fermi), and his efforts to prevent the nuclear arms race after the Second World War. Szilard did not win the Nobel Prize for any of his achievements; however, two of his patents, which were for the design and operation of the cyclotron and electron microscope, would be developed subsequently by Ernest Lawrence and Ernst Ruska, respectively, providing them with the instrumentation to make discoveries and merit the Nobel Prize. Other inventions, patents, and scientific discoveries of Leo Szilard, which are described subsequently, established his legacy forever among the greatest physicists of the century.

Leo Szilard graduated from the University of Budapest in 1916 winning the Eötvös Prize, the Hungarian National Prize in mathematics (Rhodes, 1986). His main interest was physics, but at that time in Hungary there were no professional opportunities in physics. Thus, he decided to begin his higher education in engineering at the Budapest Technical

University. However, his studies in Hungary were cut short as he was drafted into the Austro-Hungarian Army in 1917 and honorably discharged in 1918 while on leave after recovering from influenza. He was fortunate to escape death, as most of his fellow troops were killed. It was a war that stole so many potentially productive young souls from either side of the trenches, including the budding physicist Henry G.J. Moseley (see Hall of Fame, Part III).

In 1919 Szilard left his homeland both to escape the anti-Semitic regime there and to pursue studies in Berlin, which was one of the leading centers of the world for scientific learning and research. He enrolled in the Technische Hochschule (Institute of Technology) in Berlin-Charlottenburg as an engineering student in 1920, but only shortly thereafter, the following year, he would begin a career in physics, transferring to the University of Berlin where some of the greatest physicists of the time were located including Nobel Laureates Albert Einstein, Max Planck, and Max von Laue.

It was at the University of Berlin where Leo Szilard at the age of 23 would demonstrate his amazing intellect by completing his doctoral thesis or dissertation in physics in 1922 only one year after enrolling in the university. A detailed account of Szilard's early accomplishment as a university student is given by Rhodes (1986); only a brief summary will be given here. The award of a university doctoral degree in the sciences at the University of Berlin required the satisfactory completion of four years of course work and a dissertation describing a truly original work. The dissertation could describe either a noteworthy discovery or research results that would contribute significant knowledge to a particular field of science. The topic of the dissertation could be of the student's choice or one selected by his or her supervisor. Following approval of the dissertation by a committee of professors, the final requirement is the completion of a rigorous oral examination. These requirements for a doctoral degree in the sciences still exist today in the major universities of the world. Max von Laue would accept only outstanding students to supervise in their doctoral work, and Leo Szilard was one of those. Szilard went to von Laue during his first year as a student to request a topic for his dissertation. Von Laue gave Szilard a very perplexing problem on relativity, possibly to put Leo Szilard in a humble position or just to challenge him and observe his reaction.

For 6 months Szilard worked on the thesis problem that von Laue had given him and was convinced that it could not be solved. He then abandoned the thesis topic and just put his mind to thought for 3 weeks to whatever idea would come to mind. A topic on thermodynamics came to him, and from time-to-time he would put to paper whatever ideas materialized in his mind. Over a period of only 3 weeks he was convinced that he had a manuscript that was truly original. Szilard was afraid to take the manuscript to Max von Laue, because it was not the topic given him to work on. Instead, he cornered Einstein after a seminar and asked him if he would look at what he was working on. Einstein asked him specifically what he was doing. When Szilard told Einstein the topic, Einstein replied that it could not be done. However, after Szilard gave Einstein a 5- to 10-minute detailed explanation of what he had done, Einstein understood. This boosted Szilard's confidence to take his manuscript to von Laue as his completed dissertation. The manuscript was entitled "Uber die thermodynamischen Schwankungserscheinungen" (About the Thermodynamic Fluctuation Phenomena). In this work, Szilard mathematically demonstrated that the Second law of Thermodynamics covers not only the mean values, as was up to then believed, but also determines the general form of the law that governs the fluctuating values. The dissertation presented ideas that would be the foundation of modern information theory (USCD, 2005 MSS 0032). The following morning, Max von Laue called Leo Szilard to inform him that his thesis was accepted for his doctorate degree, which he earned "cum laude" in 1922. Leo Szilard would then begin a lifelong friendship and collaboration with Albert Einstein. Subsequently Leo Szilard published additional works on the topic of his thesis in the journal *Zeitschrift für Physik* (Szilard, 1925, 1929).

Szilard did his postdoctoral work on X-ray diffraction in crystals at the Kaiser Wilhelm Institute in Berlin-Dahlem until 1925, when his paper on thermodynamics (Szilard, 1925) was accepted for his *Habilitationsschrift*. He was thereafter appointed as a private lecturer (*Privatdozent*) in 1927 at the University of Berlin. While remaining in Berlin from 1925 to 1933, Szilard applied for numerous German patents, some of these with Albert Einstein. Some of the most prominent German patents and patent applications submitted by Szilard are described by Telegdi (2000) with diagrams. Among these are the patent applications for particle accelerators in great detail including the linac or linear accelerator, cyclotron, and betatron, which Szilard submitted January 17, 1929. Ernest Lawrence, who won the Nobel Prize in Physics in 1939 "for the invention and development of the cyclotron and for the results obtained with it," did not get the idea for the cyclotron until the summer of 1929, when he came across a publication of the Norwegian engineer Rolf Wideröe (1928) concerning his idea for the linac or linear accelerator; although the linear accelerator was first reported by the Swedish scientist Gustaf Ising (1924). The year following Wilderöe's paper, Ernest Lawrence (1930) published the cyclotron principle in the journal *Science*. It is recognized clearly that Leo Szilard was the first to conceive of the principle of the cyclotron for accelerating charged nuclear particles, which was very instrumental in producing many artificial radioactive elements. However, the Nobel Prize would go to Ernest Lawrence, who developed the cyclotron and demonstrated its utility.

Gene Dannen (1997, 1998, 2001) has thoroughly reviewed the life and work including the many patents of Leo Szilard. Dannen (1998) provides the following comments of Dennis Gabor, one of Szilard's close associates in Berlin:

Dennis Gabor (1900–1979)

Dennis Gabor, who won the 1971 Nobel Prize for the invention of holography, was one of Szilard's best friends in Berlin. "He used to discuss all his inventions with me," Gabor later recalled. "I was so full of admiration that I felt stupid in his presence. Of all the many men I have met in my life, he was, by far, the most brilliant." Gabor also said of Szilard. "Had he pushed through to success all his inventions, we would now talk of him as the Edison of the 20th century."

Gene Dannen (1998) also relates the following circumstances around Leo Szilard's patent on the electron microscope and his urging that Dennis Gabor build it:

It is not as well known that Szilard also foresaw, and filed for patent on, the electron microscope. Dennis Gabor later recalled how, in 1928 at the Café Wien in Berlin, Szilard tried to convince him to build such a microscope. Gabor told Szilard that such a device would be useless. Gabor told Szilard, and I quote, "one cannot put living matter into a vacuum and everything will burn away to a cinder under the electron beam." Gabor later regretted that he had not taken Szilard's advice. It was only a few years later that work on developing electron microscopes began at several different laboratories. Szilard filed for patent on the electron microscope on July 4, 1931.

Historians have pondered over the question of why Szilard did not pursue his patent applications onto the development and application of the instruments he conceived. Gene Dannen (1998) has carefully studied this question and points out the following:

Why, in fact, were so many of Szilard's inventions not developed further? It is often said that Szilard was psychologically incapable of pursuing his ideas to completion. I would like to disagree with that answer. It is certainly true that Szilard was willing to drop one idea when a more important idea came along. And he was a person with so many important ideas. But when you are so far ahead of your time as Szilard often was, the obstacles of the acceptance of your ideas can be almost insurmountable. In the case of each of Szilard's inventions, there were specific reasons why they were not developed. Above all other reasons loomed the largest: the lack of a peaceful world in which to pursue them.

Reprinted with permission, Eötvös Physical Society © 1988, Budapest.

Leo Szilard could not pursue the development of most of his patents, because he became overwhelmed with Hitler's rise to power and the need to escape his anti-Semitic regime. However, we will see further on in this biosketch that Leo

Szilard did pursue the development of his patent for the atomic bomb. He would pursue this out of fear for Hitler's regime, to beat German scientists in the development of the bomb, and with the hope of keeping the bomb in the hands of the free world.

A number of patents were filed by Leo Szilard together with Albert Einstein in the development of refrigerators without moving parts. This work was outside the scope of nuclear physics, as it involved thermodynamics. They developed the first cooling system that involved liquid sodium metal as the refrigerant whereby the metal was pumped by a variable magnetic field. The Szilard–Einstein pump was developed into a prototype refrigerator by the German Electric Company (A.E.G.), for which Einstein and Szilard were paid handsomely for their patent. The subsequent discovery of Freon as a cheap refrigerant changed the direction of commercial production away from the Einstein–Szilard refrigerator. Dannen (1997) gives an excellent review of the history of the Einstein–Szilard refrigerators. He points out that had Freon not been implemented as a coolant, the Einstein–Szilard refrigerator might have been a common household appliance today and the problem of Freon diminishing the ozone layer less of a concern. Also Dannen (1997) points out that the Einstein–Szilard pump did find use eventually in the cooling of the nuclear breeder reactor.

After Hitler became Chancellor of Germany in January 1933, it would soon become unsafe for Leo Szilard to remain in the country. He escaped by train from Berlin to Vienna in April one day before it would have become impossible or very difficult for him to leave the country. Richard Rhodes (1986) writes that on the weekend of April first, Julius Streicher directed a national boycott of Jewish businesses, and Jews were beaten in the streets. Rhodes then quotes Szilard concerning his escape as follows:

> *I took a train from Berlin to Vienna on a certain date, close to the first of April, 1933. The train was empty. The same train the next day was overcrowded, was stopped at the frontier, the people had to get out, and everybody was interrogated by the Nazis. This just goes to show that if you want to succeed in this world you don't have to be much cleverer than other people, you just have to be one day earlier.*

Leo Szilard tried for months to help other Jewish scholars who were evicted from their professional posts in Germany to emigrate and find jobs in other countries of the world. Later, in 1933, Szilard moved to London. On September 12, 1933 Szilard read a news report in *The Times* where Rutherford was interviewed. The reporter had asked Rutherford what were his thoughts concerning nuclear transmutations and nuclear energy. Rutherford replied that charged particles, such as the proton, could eventually be accelerated with sufficient high voltage to eventually transform all of the elements. He added that the energy released would be too small to produce energy on a large scale for power and anyone who looked for transmutation as a source of power was talking "moonshine". Szilard agreed with Rutherford's comments concerning accelerated protons, that these would not be a useful source of energy. He knew that the proton had to overcome the Coulombic barrier of its repelling positive charge with that of the atomic nucleus. However, he thought that the neutron, because of its neutral charge, should be able to penetrate the Coulombic barrier of the electron shells of an atom and collide with the nucleus without any external force and cause a reaction or transmutation of the nucleus. Szilard's mind was restless. While standing at a street corner in London in the following month of October and during the time that it took a traffic light to change, the idea of the possibility of a neutron-induced nuclear chain reaction hit him. Szilard knew that in chemistry there existed chain reactions where one reaction could yield two products that could further interact with other reactants to produce four products, and these could react to produce eight products, etc. resulting in an exponential increase in reactions. The chain reactions could be very numerous and limited only by the quantity of reactants available. He thought that if a chain reaction with neutrons would occur, that is, if a neutron would be able to interact with an atomic nucleus to produce more than one neutron and the additional neutrons created would interact with other atomic nuclei to produce yet more neutrons in a chain reaction, a tremendous amount of energy could be liberated. Szilard could foresee that the initial neutron reaction and the resultant multiplication of neutrons should occur in a very short period of time, in microseconds, as nuclear reactions would be fast, producing an explosion of unforeseeable magnitude. Leo Szilard was the first to conceive the possibility of obtaining large amounts of energy and even an explosion from nuclear transmutations.

Having formulated further his initial idea of the potential energy that could be released from neutron-induced chain reactions, Leo Szilard filed for a patent on June 28, 1934, which contained the basic concepts of a nuclear chain reaction, nuclear power (ie, the production of steam by a nuclear power plant as an energy source), the concept of "critical mass," that is, the minimum mass of a material required for a sustained nuclear chain reaction, and the possibility of an "explosion" that could result from this chain reaction. He was awarded British Patent no. 630,726 entitled "Improvements in or Relating to the Transformation of Chemical Elements." He applied for this patent 5 years before the splitting of atoms with the emission of neutrons, which is the source of nuclear chain reactions, was discovered by Hahn and Strassman in 1939 and interpreted by Lise Meitner and Otto Frisch (1939). A clipping from the first page of Leo Szilard's patent registered with the British Patent Office in 1934 is illustrated in Fig. IV.5. The patent, no. GB 630,726, includes 8 pages of text and 11 detailed

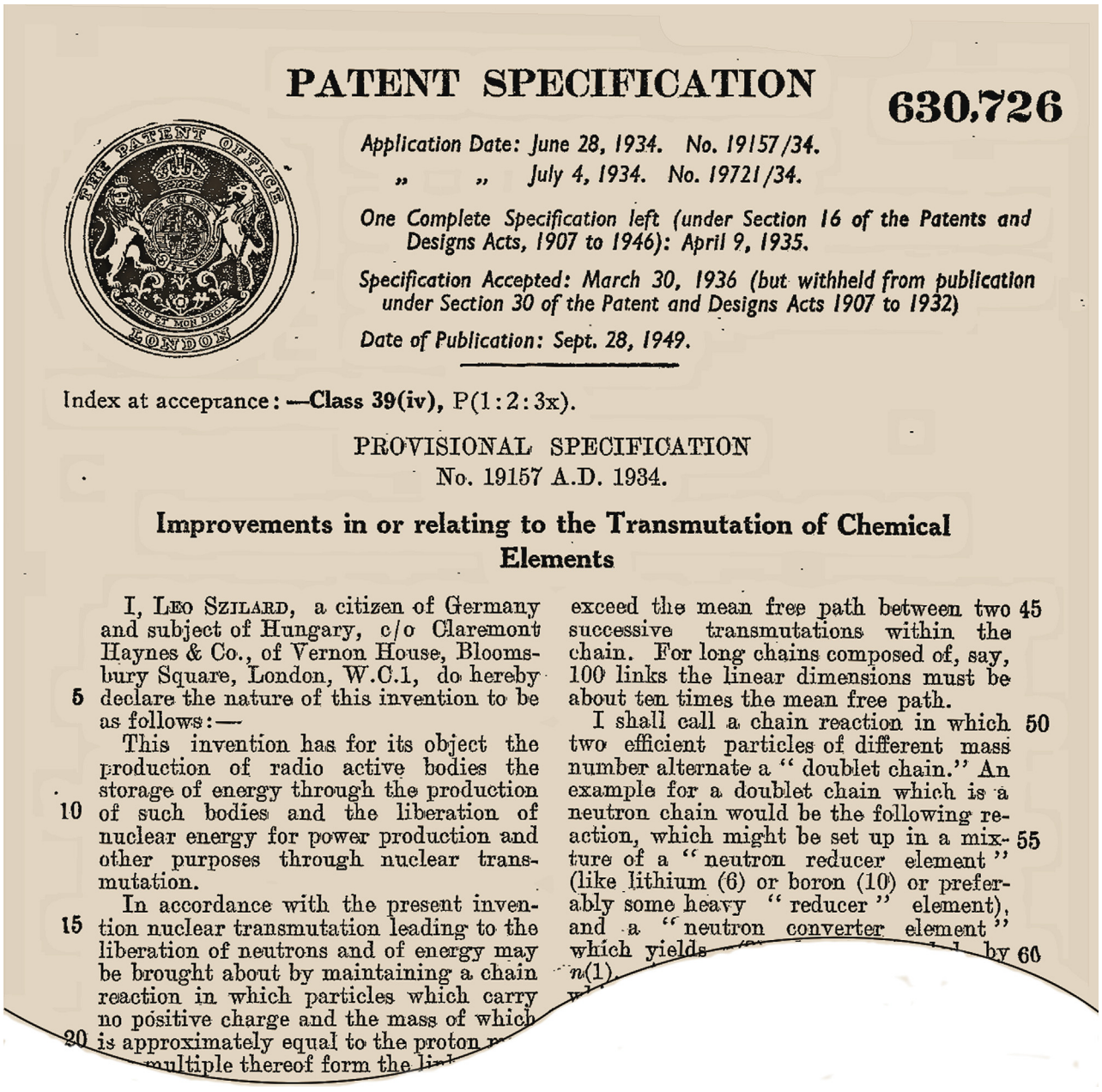

PATENT SPECIFICATION

630,726

Application Date: June 28, 1934. No. 19157/34.
„ „ July 4, 1934. No. 19721/34.

One Complete Specification left (under Section 16 of the Patents and Designs Acts, 1907 to 1946): April 9, 1935.

Specification Accepted: March 30, 1936 (but withheld from publication under Section 30 of the Patent and Designs Acts 1907 to 1932)

Date of Publication: Sept. 28, 1949.

Index at acceptance: —**Class 39(iv)**, P(1:2:3x).

PROVISIONAL SPECIFICATION
No. 19157 A.D. 1934.

Improvements in or relating to the Transmutation of Chemical Elements

I, LEO SZILARD, a citizen of Germany and subject of Hungary, c/o Claremont Haynes & Co., of Vernon House, Bloomsbury Square, London, W.C.1, do hereby declare the nature of this invention to be as follows:—

This invention has for its object the production of radio active bodies the storage of energy through the production of such bodies and the liberation of nuclear energy for power production and other purposes through nuclear transmutation.

In accordance with the present invention nuclear transmutation leading to the liberation of neutrons and of energy may be brought about by maintaining a chain reaction in which particles which carry no positive charge and the mass of which is approximately equal to the proton [illegible] multiple thereof form the link[illegible] exceed the mean free path between two successive transmutations within the chain. For long chains composed of, say, 100 links the linear dimensions must be about ten times the mean free path.

I shall call a chain reaction in which two efficient particles of different mass number alternate a "doublet chain." An example for a doublet chain which is a neutron chain would be the following reaction, which might be set up in a mixture of a "neutron reducer element" (like lithium (6) or boron (10) or preferably some heavy "reducer" element), and a "neutron converter element" which yields [illegible] by $n(1)$ [illegible]

FIGURE IV.5 A clipping from the first page of Leo Szilard's British Patent no. 630,726 (application date 1934) for neutron-induced nuclear chain reactions, nuclear power from the energy of nuclear chain reactions, and the possibility of an explosion from nuclear chain reactions.

drawings of a nuclear reactor for power. This patent was applied by Leo Szilard 9 years before the first nuclear reactor was demonstrated by Enrico Fermi, Leo Szilard, and others at the University of Chicago in 1942. In lines 7 to 19 of Fig. IV.5, Szilard introduces the objective of his patent to produce energy for power production by means of chain reactions of nuclear transmutations initiated by neutrons. Also in lines 55 to 58, Szilard was the first to mention the need to have a neutron moderator to control the chain reaction. He refers here to the neutron moderator as a "neutron reducer element," as the term moderation of a nuclear chain reaction and the term "neutron moderator" did not come into use until several years later.

The application of nuclear chain reactions to the production of steam for power plant energy production is noted in lines 50 to 59 and 105 to 113 of the patent clipping illustrated in Fig. IV.6. Here Leo Szilard described how energy is liberated from the yet-undiscovered neutron-induced nuclear chain reactions, the transfer of this heat to a liquid in pipes composing a cooling system, and the piping of this hot liquid to a boiler for the production of steam in a power plant.

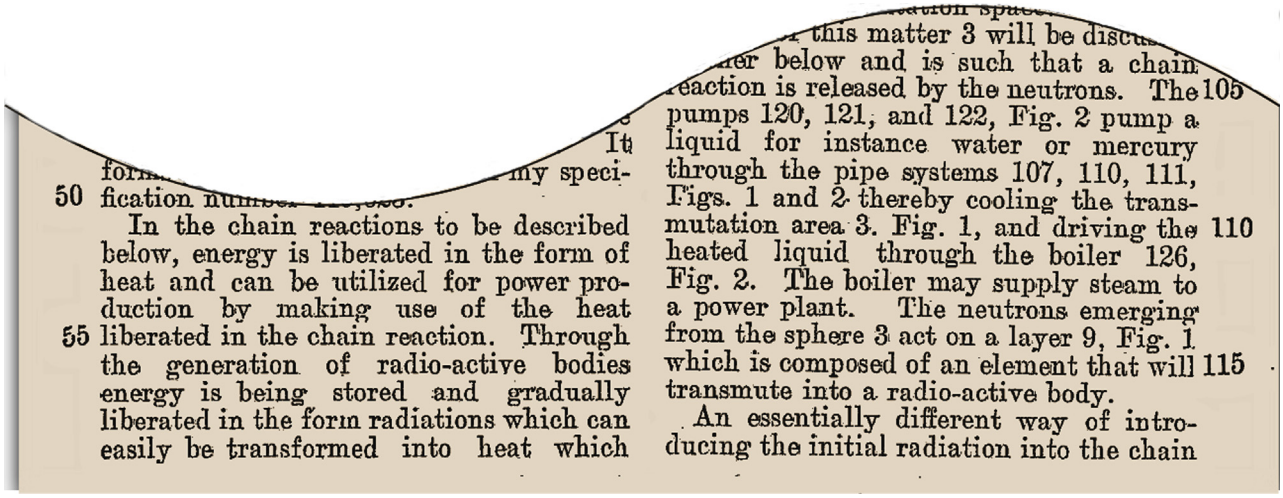

this matter 3 will be discu
er below and is such that a chain
eaction is released by the neutrons. The
pumps 120, 121, and 122, Fig. 2 pump a
liquid for instance water or mercury
through the pipe systems 107, 110, 111,
Figs. 1 and 2 thereby cooling the trans-
mutation area 3. Fig. 1, and driving the
heated liquid through the boiler 126,
Fig. 2. The boiler may supply steam to
a power plant. The neutrons emerging
from the sphere 3 act on a layer 9, Fig. 1
which is composed of an element that will
transmute into a radio-active body.
An essentially different way of intro-
ducing the initial radiation into the chain

It
my speci-
fication

In the chain reactions to be described below, energy is liberated in the form of heat and can be utilized for power production by making use of the heat liberated in the chain reaction. Through the generation of radio-active bodies energy is being stored and gradually liberated in the form radiations which can easily be transformed into heat which

FIGURE IV.6 A portion of a page of Leo Szilard's British Patent no. 630,726, first applied for in June 1934, which describes the engineering of a nuclear reactor for harnessing the heat of the chain reaction with a boiler to supply steam to a power plant. (See lines 55 to 59 and 110 to 113.)

The possibility of a nuclear explosion (ie, atomic bomb) was foreseen by Leo Szilard in his patent application of 1934, where he noted that an explosion would occur if a mass of fissionable material were accumulated larger than a critical value. In Fig. IV.7 lines 74 to 76, Leo Szilard noted: "If the thickness is larger than the critical value l_o, I can produce an explosion."

Szilard could foresee, long before nuclear fission was discovered and long before the term "critical mass" was coined, that exceeding the critical mass of fissionable material would produce an uncontrollable nuclear chain reaction and

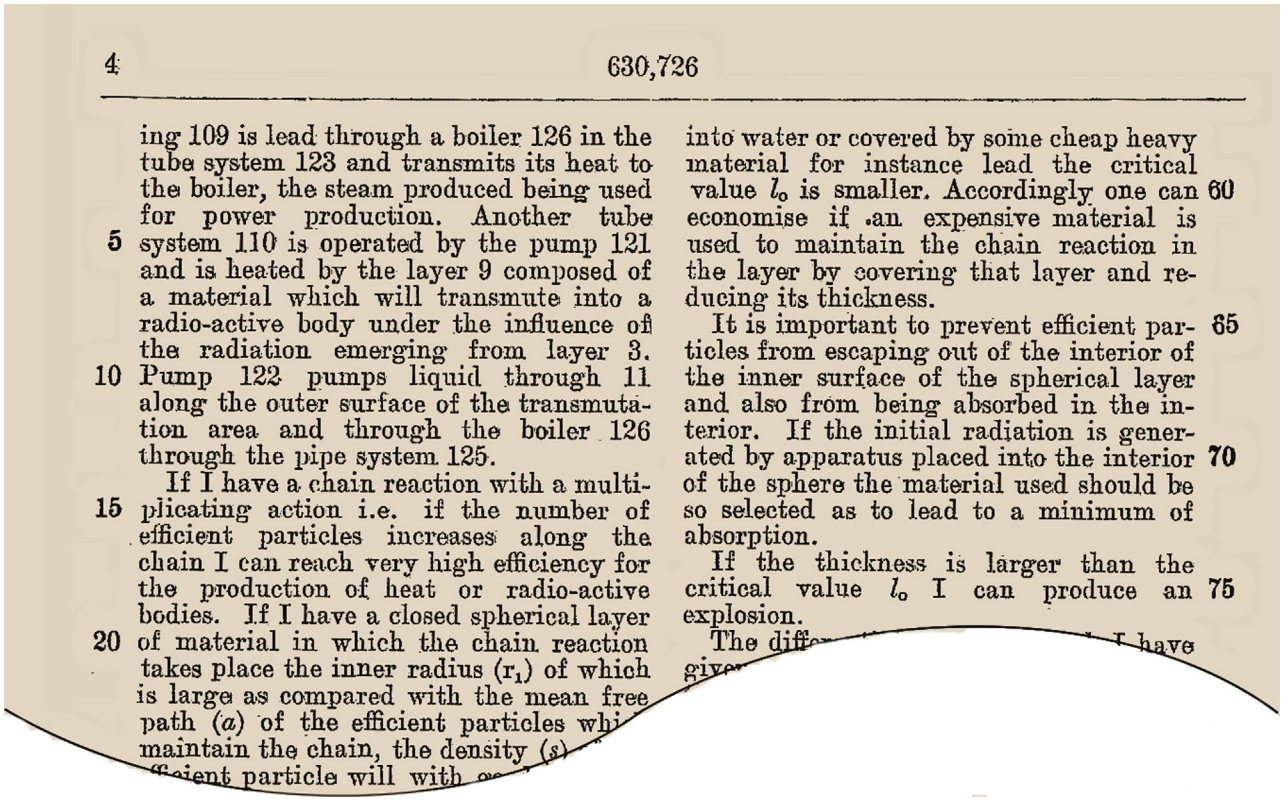

4 630,726

ing 109 is lead through a boiler 126 in the tube system 123 and transmits its heat to the boiler, the steam produced being used for power production. Another tube system 110 is operated by the pump 121 and is heated by the layer 9 composed of a material which will transmute into a radio-active body under the influence of the radiation emerging from layer 3. Pump 122 pumps liquid through 11 along the outer surface of the transmutation area and through the boiler 126 through the pipe system 125.

If I have a chain reaction with a multiplicating action i.e. if the number of efficient particles increases along the chain I can reach very high efficiency for the production of heat or radio-active bodies. If I have a closed spherical layer of material in which the chain reaction takes place the inner radius (r_1) of which is large as compared with the mean free path (a) of the efficient particles whi
maintain the chain, the density (s)
efficient particle will with

into water or covered by some cheap heavy material for instance lead the critical value l_o is smaller. Accordingly one can economise if an expensive material is used to maintain the chain reaction in the layer by covering that layer and reducing its thickness.

It is important to prevent efficient particles from escaping out of the interior of the inner surface of the spherical layer and also from being absorbed in the interior. If the initial radiation is generated by apparatus placed into the interior of the sphere the material used should be so selected as to lead to a minimum of absorption.

If the thickness is larger than the critical value l_o I can produce an explosion.

The diff
give
I have

FIGURE IV.7 The production of steam from the heat of nuclear chain reactions for energy (lines 1–21). Also, for the first time, the origins of the term "critical mass" required for the production of an atomic bomb is provided by Leo Szilard in lines 74 to 76, where he affirms "If the thickness is larger than the critical value l_o I can produce an explosion."

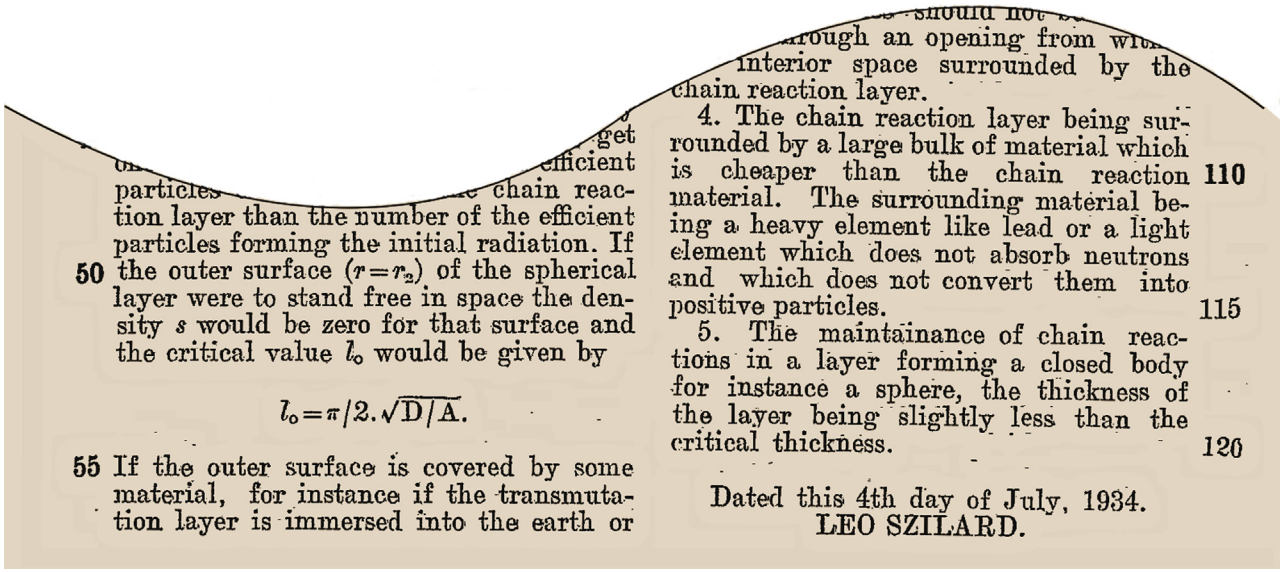

...should not ...
...rough an opening from wi...
interior space surrounded by the chain reaction layer.

4. The chain reaction layer being surrounded by a large bulk of material which is cheaper than the chain reaction material. The surrounding material being a heavy element like lead or a light element which does not absorb neutrons and which does not convert them into positive particles.

5. The maintainance of chain reactions in a layer forming a closed body for instance a sphere, the thickness of the layer being slightly less than the critical thickness.

Dated this 4th day of July, 1934.
LEO SZILARD.

...get
...efficient
particles ... chain reaction layer than the number of the efficient particles forming the initial radiation. If the outer surface ($r=r_2$) of the spherical layer were to stand free in space the density s would be zero for that surface and the critical value l_o would be given by

$$l_o=\pi/2.\sqrt{D/A}.$$

If the outer surface is covered by some material, for instance if the transmutation layer is immersed into the earth or

FIGURE IV.8 A portion of the last page from Leo Szilard's British Patent no. 630,726, first applied for in June 1934, which describes the need to keep the nuclear material required for the chain reaction below the critical mass, ie, "critical thickness," in order to avert any possibility of an explosion that would occur with an atomic bomb. See Lines 116 to 120, where Szilard clarifies: "The maintenance of chain reactions in a layer forming a closed body for instance a sphere, the thickness of the layer being slightly less than the critical thickness."

explosion. The term "critical mass" is the current term used to define the mass of fissionable material required to maintain a self-sustaining chain reaction at a constant rate. When the critical mass is exceeded, the atomic bomb is detonated. Szilard underscored the importance of keeping the chain-reacting material (referred to today as fissionable material) below its critical mass for reasons of safety. He noted this in statement no. 5 (lines 116−130) at the end of his 1934 patent application illustrated in Fig. IV.8. Also, in lines 108 to 115 of Fig. IV.8, Szilard emphasizes the use of materials that would minimize neutron loss.

Nuclear fission was not discovered until 1939. Consequently, the fissile materials required to produce neutron-induced nuclear chain reactions had not yet been discovered and there is no record that any such nuclear chain reactions had ever been discussed prior to Szilard's patent. The concepts of nuclear chain reactions, nuclear power from these chain reactions, or the possibility of an explosion (ie, a bomb) from these chain reactions didn't exist at the time of Szilard's patent. Szilard was clearly ahead of his time. The concept and mechanics of operation of a nuclear power plant based on the energy released from neutron-induced nuclear chain reactions is described in Szilard's Patent of 1934, which is 5 years before nuclear fission was discovered and eight years before Enrico Fermi, Leo Szilard' and others would demonstrate the first sustainable nuclear chain reaction in uranium at the University of Chicago in 1942.

Szilard was a pacifist and idealist, and the objective of his patent was not personal gain but for control over the harmful use of nuclear weapons. After a year's time he convinced the British Government to accept the patent in order to keep the concepts of the patent secret and inaccessible to the world. Later in life (July 16, 1939), Leo Szilard convinced Einstein to sign a letter to the President of the United States, which was the spark that eventually created the Manhattan Project, the secret American project for the production of the atomic bomb, out of fear that Germany could become the first to develop the weapon. Leo Szilard worked on the Manhattan Project. Rhodes (1986) and Loeber (2002) point out that Szilard tried to use his patent as a means to gain control of the decision-making process for the atomic bomb. He felt that the control of the bomb and its use should be in the hands of the wisest scientists and not in the hands of government officials. Rhodes (1986) noted that the U.S. Government rejected Szilard's claim to the atomic bomb on simple legalistic grounds, because he did not disclose the existence of his patent before joining the Manhattan Project.

When Szilard first conceived of neutron-induced chain reactions in 1933, he did not know what element or isotope would undergo such reactions. His patent had made a slight mention of uranium and thorium, but his thoughts were mistakenly on beryllium. He therefore, started a search for the chain-reacting element. With this in mind, Szilard began a collaboration of nuclear research with T.H. Chalmers at St. Bartholomew's Hospital. This research did not lead to the discovery of the neutron-induced chain reaction, but lead to other important discoveries including (1) the discovery of a

photoneutron (γ,n) source, that is, the induction of neutron emission by gamma or X-radiation; and (2) the Szilard–Chalmers effect, which is the rupture of a chemical bond between an atom and a molecule of which the atom is a constituent, as a result of a nuclear reaction or radioactive decay of that atom. The Szilard–Chalmers effect led to the Szilard–Chalmers process or reaction, which has enabled the isolation of high-specific activities of radionuclides. The two discoveries and their applications will be discussed briefly in subsequent paragraphs.

In his search for neutron emission that might initiate a neutron-induced chain reaction, Leo Szilard and T.H. Chalmers irradiated beryllium with radium gamma rays. They discovered a radiation from the beryllium that would induce radioactivity in iodine and concluded that neutrons were emitted from the beryllium by the gamma rays (Szilard and Chalmers, 1934a,b, 1935). Their report was the first where neutron emission was initiated by gamma radiation, and the reaction that they observed can be abbreviated as:

$$^{9}\mathrm{Be}(\gamma, \mathrm{n})^{8}\mathrm{Be} \qquad \text{[IV.21]}$$

which reads as follows:

^{9}Be target nuclide(gamma-ray projectile, neutron emitted)^{8}Be product nucleus.

This discovery was significant, because today photoneutron (γ,n) sources are useful portable sources of neutrons. A very common neutron source of this nature used today is the mixture of ^{124}Sb + Be, where the gamma rays from ^{124}Sb yield neutrons via a photonuclear reaction (see Section 10.3 of the chapter: "Neutron Radiation").

Szilard and Chalmers (1934b) used iodine as the indicator for neutrons, because the neutrons would induce radioactivity in iodine by creating radioiodine via neutron capture. A subsequent work was reported shortly thereafter by Brasch and coworkers together with Szilard and Chalmers and with the assistance of Lise Meitner in Berlin (Brasch et al., 1934), whereby the neutron emission from beryllium was induced by X-ray photons and neutron capture by bromine and the isolation of the product nuclide, radiobromine, was used as the neutron indicator.

An important outcome of this work was the discovery of the Szilard–Chalmers process whereby radionuclides may be easily separated and isolated from their parent atoms and consequently high specific activities of radionuclides may be obtained which otherwise would be difficult when both the target and product atoms are isotopes. For example, Szilard and Chalmers (1934a,b) surrounded 150 mg of radium (gamma-ray source) with 25 g of beryllium in a sealed container of 1-mm thick platinum. The Ra-Be neutron source was immersed in 100 mL of ethyl iodide. The neutrons produced radioactive iodine-128 from stable iodine-127 by neutron capture. The ^{128}I would precipitate as radioactive silver iodide ($Ag^{128}I$) after the addition of water containing silver ions (Ag^{+}). However, a control experiment without the neutron source produced no radioactivity over background in the silver iodide precipitate. This experiment indicated that the chemical bond between the carbon atom of the ethyl group and the ^{128}I was broken after ^{127}I neutron capture due to nuclear recoil following γ emission. They could conclude that the C–I chemical bond was broken following neutron capture, because free unbound ionic $^{128}I^{-}$ would precipitate with the Ag^{+} to produce radioactive $Ag^{128}I$ precipitate in the aqueous phase, according to the sequence illustrated in Fig. IV.9.

The energy of bonding between the carbon and iodine atoms is about 2 eV, which is higher than the neutron recoil energy. Consequently, the rupture of this bond is due to the gamma recoil when the ^{128}I undergoes gamma emission upon deexcitation after neutron capture. Some atoms of ^{128}I could recombine with the free ethyl group and even exchange with some stable atoms of ^{127}I, but if these processes are slow, and if these processes are further reduced by the addition of water or even alcohol to dilute the organic phase, the precipitate of radioactive inorganic iodide proceeds, yielding a highly enriched radioactive ^{128}I with minimal ^{127}I.

The Szilard–Chalmers process remains to this day a very practical application to the isolation of high specific activity radioactive sources from the medium in which the radionuclide sources were synthesized. A few examples taken from the literature are editorial reviews by Eckelman et al. (2008) and Köster et al. (2012); the isolation of high specific activity radioisotopes after cyclotron production (Bonardi et al., 2004; Birattari et al., 2001); and in order of increasing atomic number, the optimized production of ^{18}F (Alfassi et al., 1986); the production of high specific activity ^{51}Cr (Harbottle, 1954; Green and Maddock, 1949; Vimalnath et al., 2014); high specific activity ^{56}Mn (Zahn, 1967a,b); the preparation of high specific activity ^{64}Cu (Van Elteren et al., 1999; Gielow, 1990; Barnes et al., 1986; Hetherington et al., 1986; Sekine et al., 1986); and the production of high specific activity ^{99}Mo and ^{90}Y (Tomar et al., 2010); high specific activity radioisotopes of tin (Spano and Kahn, 1952); the preparation of high specific activity ^{117m}Sn for medical applications (Mausner et al., 1992); high specific activity radiohafnium complexes (Abbe and Marques-Netto, 1975; Marques-Netto and Abbe, 1975); the production of high specific activity ^{166}Ho (Zeisler and Weber, 1998); high specific activity ^{186}Re (Jia and Ehrhardt, 1997); and the concentration of high specific activities of the radioisotopes of group IV and V elements (Murin and Nefedov, 1955).

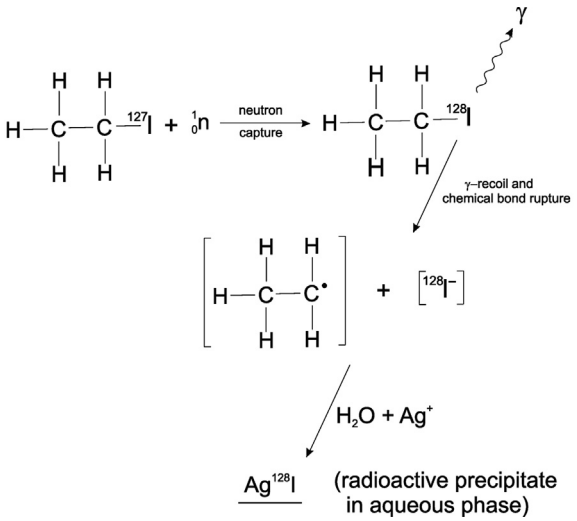

FIGURE IV.9 Szilard–Chalmers process. High specific activity ^{128}I is separated from the stable ^{127}I as a result of the Szilard–Chalmers effect. The capture of a neutron by the stable isotope ^{127}I in the ethyl iodide molecule creates radioactive ^{128}I. The neutron capture process leaves the ^{128}I nucleus in an excited state, which emits a gamma ray upon deexcitation. The gamma recoil causes a rupture of the chemical bond between the carbon atom of the ethyl group and the ^{128}I, thereby liberating the ^{128}I as an anion. The addition of water containing silver cations (Ag^+) to the organic solution enables the ionic $^{128}I^-$ to enter the aqueous phase and separate out as precipitated $Ag^{128}I$. The radioactivity of ^{128}I is detected by its beta particle emissions, and it decays with a half-life of 25 min.

On September 30, 1938 Germany, Italy, France, and Britain signed the Munich Pact, whereby Premier Édouard Daladier of France and prime Minister Neville Chamberlain of Britain, to avoid confrontation with German Chancellor Adolf Hitler, agreed to his demands that Germany occupy the Sudetenland, a region of Czechoslovakia bordered by Germany. Italy was represented at the Munich Pact by Benito Mussolini, who colluded with Hitler and had anti-Semitic laws enforced. At the time of the Munich Pact, Leo Szilard was a visiting professor in the United States. He had foresight to see the impending threat of Germany and moved to New York, where he carried on a collaboration from Columbia University with Walter Zinn. The foresight that Szilard displayed in escaping from Berlin and the Nazis in 1933 would again prove to be vital. It would be in the United States where Leo Szilard could safely carry out his efforts to beat Germany or any other aggressive nation in the development of an atomic bomb. On September 1, 1939, less than a year after the signing of the Munich Pact, Hitler invaded Poland; and France and England declared war on Germany, marking the beginning of World War II.

After the first explanation of neutron-induced fission by Lise Meitner and Otto Frisch on February 11, 1939, following the work of Otto Hahn and Fritz Strassman (1939a,b), it became clear to Leo Szilard that uranium would be the element that could sustain the nuclear chain reaction that he had patented over 5 years prior to the discovery of neutron-induced fission. In July of the same year, Herbert Anderson, Enrico Fermi, and Leo Szilard determined that there are about two neutrons produced for every neutron consumed in the fission of uranium-235 (Anderson et al., 1939a,b). Leo Szilard finally found the isotope that could sustain a neutron-induced chain reaction that could yield immense amounts of energy and even the atomic bomb that he had patented 6 years prior to this discovery. Szilard knew that the neutron yield had to be greater than one neutron produced per neutron consumed to maintain the chain reaction, and that the production of two neutrons for each neutron consumed left no doubt in his mind that the self-sustaining chain reaction was in his grasp. In the following month (August 14th), Walter Zinn at City College, New York together with Leo Szilard from Columbia University, New York reported a more precise number of 2.3 neutrons, on the average, produced for each thermal neutron absorbed in uranium (Zinn and Szilard, 1939). This is very close to the current more precise average number of 2.5 neutrons produced per thermal neutron absorbed in uranium-235. They also determined the general energy spectrum of the neutrons emitted in fission. The neutrons were classified as fast neutrons with an upper energy limit of about 3.5 MeV; however, Szilard knew that the fast neutrons could easily be thermalized (slowed down) with a low atomic number element or moderator such as graphite to sustain the chain reaction. From this work it was clear to Szilard that there was little doubt that the conditions needed for the self-sustaining neutron-induced chain reaction in uranium-235 could be made, and its demonstration would soon be a reality.

In Szilard's mind, time was of the essence. Szilard urged his lifelong friend Albert Einstein, then a theoretical physicist at Princeton, to send a letter to the President of the United States, Franklin Delano Roosevelt, to inform him of the threat of

Germany's nuclear research program and the danger that Germany could develop a nuclear weapon, urging the president to initiate a program for the weapon development. Leo Szilard knew that no scientist in the world could approach the President of the United States with what would appear to be an unbelievable, if not crazy, idea of harnessing the energy of the atom to produce atomic weapons that would tip the balance in the war against Germany. Szilard was determined to get a letter to President Roosevelt; and he knew that only Albert Einstein, who was the most celebrated scientist in the world and who had been invited previously to the White House for dinner as a celebrity, could capture the attention of the President. On July 16, 1939 Eugene Wigner, a fellow Hungarian and theoretical physicist, drove Leo Szilard to Albert Einstein's Peconic, Long Island summer residence (Leo Szilard did not drive a car) to convince Einstein of the danger that Germany had discovered nuclear fission, and that they would know how to develop the weapon and thereby win the war; and Szilard feared the worst. Leo Szilard thus convinced Einstein to sign a letter to the President with the intention of beating Germany to the development of this terrible weapon. Einstein was a pacifist; but he was convinced by Leo Szilard that there was no other choice but to beat Germany in the development of the bomb. As noted in a comprehensive book by Lanouette (2013), Albert Einstein would state later that he "really acted only as a mailbox" for Szilard, as his notoriety in his famous equation $E = mc^2$ and his letter to President Roosevelt are credited with the initiation of the American Manhattan Project to develop nuclear weapons. The development of the atomic bomb would not have been possible without Leo Szilard's determination to convince his friend, Albert Einstein, to sign a letter to President Roosevelt.

The famous letter, drafted by Szilard and signed by Einstein, was dated August 2, 1939. Leo Szilard hand-carried his drafted letter to Albert Einstein for signing. A fellow Hungarian and famous theoretical physicist, Edward Teller, would sometimes relate how he entered history by acting as a chauffeur for Szilard in this case. This is related in Edward Teller's Biographical Memoir by Dyson (2007) published by the National Academy of Sciences as follows:

> *Szilard, who could not drive a car, came to see Teller and asked him for a ride. Szilard had written a letter to President Roosevelt informing him of the discovery of fission and the possibility of nuclear bombs. The letter asked the President to set up a channel of communication between the government and the physicists working on nuclear chain reactions in America…Teller was needed as a chauffeur to bring Szilard and the letter to Einstein's summer home on Long Island. Einstein signed the letter and Szilard successfully delivered it to Roosevelt.*

Einstein's letter was hand carried to President Roosevelt on October 11, 1939 by Alexander Sachs, who was Special Counsel to the Director of Strategic Services during the war, and who could gain access to President Roosevelt, although with some difficulty, as described in detail by Lanouette (2013). A portion of Einstein's letter is provided in Fig. IV.10. President Roosevelt responded with a memorandum to Army Major General Edwin M. Watson that he prepare a reply letter to Albert Einstein; and Roosevelt requested the initiation of a study on the matter. Edwin M. Watson was the military advisor and Appointments Secretary to President Roosevelt. A copy of Roosevelt's memorandum to Watson, concerning Einstein's letter, is provided in Fig. IV.11; and the White House copy of the reply letter to Einstein is illustrated in Fig. IV.12.

An outstanding historical account by Gillon (2006), and a video presentation by the History Channel (Goodman et al. 2006) entitled "Einstein's Letter: July 16, 1939" in "10 Days that Unexpectedly Changed America", provides insight into the background of Einstein's letter and how Leo Szilard was able to get Einstein to sign that letter. The date of July 16, 1939 is noted as a day that unexpectedly changed America and not August 2, 1939, which is the date of Einstein's letter, because July 16, 1939 was the date that Leo Szilard, in the company of Eugene Wigner, visited Einstein (Wigner drove Szilard to Einstein's residence, because Szilard did not drive a car) to describe the immense energy that could be released from the newly discovered nuclear fission in uranium and to obtain Einstein's agreement in sending a letter to the President on the matter.

The historical significance of Einstein's first letter to President Roosevelt dated August 2, 1939 and drafted by Leo Szilard was highlighted in a 1946 *March of Time* newsreel where Albert Einstein and Leo Szilard reenacted the drafting and the signing of the letter of Albert Einstein to President Roosevelt on August 2, 1939. A still from that newsreel is provided in Fig. IV.13. An excerpt of the same film was rebroadcast in a historical account by Goodman et al. (2006) in the History Channel, A&E Television Networks Production "10 Days that Unexpectedly Changed America."

The secret American project to develop atomic weapons, which became known as the Manhattan Project (derived from its official name of the Manhattan Engineering District), was authorized by President Franklin D. Roosevelt on October 9, 1941. While working on this project, Rudolf Peierls (1907−1995) made initial calculations on the number of neutron chain reactions or neutron generations that would occur if a critical mass of uranium-235 could be confined in a small sphere about the size of a golf ball. See Fig. IV.14 for an illustration of the first four generations of a nuclear chain reaction. Rhodes (1986) relates that Peierls based his calculations on the assumption that the time between each neutron generation would be short, only a few microseconds. In reality, the neutron chain reactions are faster. The time it takes for one neutron to travel from one nucleus and hit another nucleus is about 10 ns (10^{-9} s). If the velocity of the approximately 2-MeV fission neutrons reach about 20 million meters per second (see Fig. 10.1 of the chapter: "Neutron Radiation") Peierls

Albert Einstein
Old Grove Rd.
Nassau Point
Peconic, Long Island

August 2nd, 1939

F. D. Roosevelt
President of the United States
White House
Washington, D. C.

Sir:

Some recent work by E. Fermi and L. Szilard, which has been communicated to me in manuscript, leads me to expect that the element uranium may be turned into a new and important source of energy in the immediate future. Certain aspects of the situation which has arisen seem to call for watchfulness and, if necessary, quick action of the part of the Administration. I believe therefore that it is my duty to bring to your attention the following facts and recommendations.

In the course of the last four months it has been made possible – through the work of Joliot of France as well as Fermi and Szilard in America – that it may become possible to set up a nuclear chain reaction in a large mass of uranium, by which vast amounts of power…would be generated…Now it appears almost certain that this could be achieved in the immediate future.

This new phenomenon would also lead to the construction of bombs, and it is conceivable…that extremely powerful bombs of a new type may thus be constructed…A single bomb of this type…might very well destroy the whole port together with some of the surrounding territory…

In view of this situation you may think it desirable to have some permanent contact maintained between the Administration and the group of physicists working on chain reactions in America…His task might comprise the following:

a) to approach Government departments, keep them informed of the further development, and put forward recommendations for Government action…

b) to speed up the experimental work, which is at present being carried on within the limits of the budgets of University laboratories, by providing funds…and perhaps also by obtaining the co-operation of industrial laboratories which have the necessary equipment.

I understand that Germany has actually stopped the sale of uranium from the Czechoslovakian mines which she has taken over. That she should have taken such early action might perhaps be understood on the ground that the son of the German Under Secretary of State, von Weizsäcker, is attached to the Kaiser-Wilhelm-Institut in Berlin where some of the American work on uranium is now being repeated.

Yours very truly,

(Albert Einstein)

FIGURE IV.10 Letter drafted by Leo Szilard and signed by Albert Einstein addressed to the President of the United States, Franklin D. Roosevelt. It is this letter that convinced President Roosevelt to initiate the American project to build atomic weapons. The entire two-page original letter, signed by Albert Einstein, is in the United States National Archives and available via http://research.archives.gov/description/593374. *Printed courtesy of The Albert Einstein Archives, The Hebrew University of Jerusalem.*

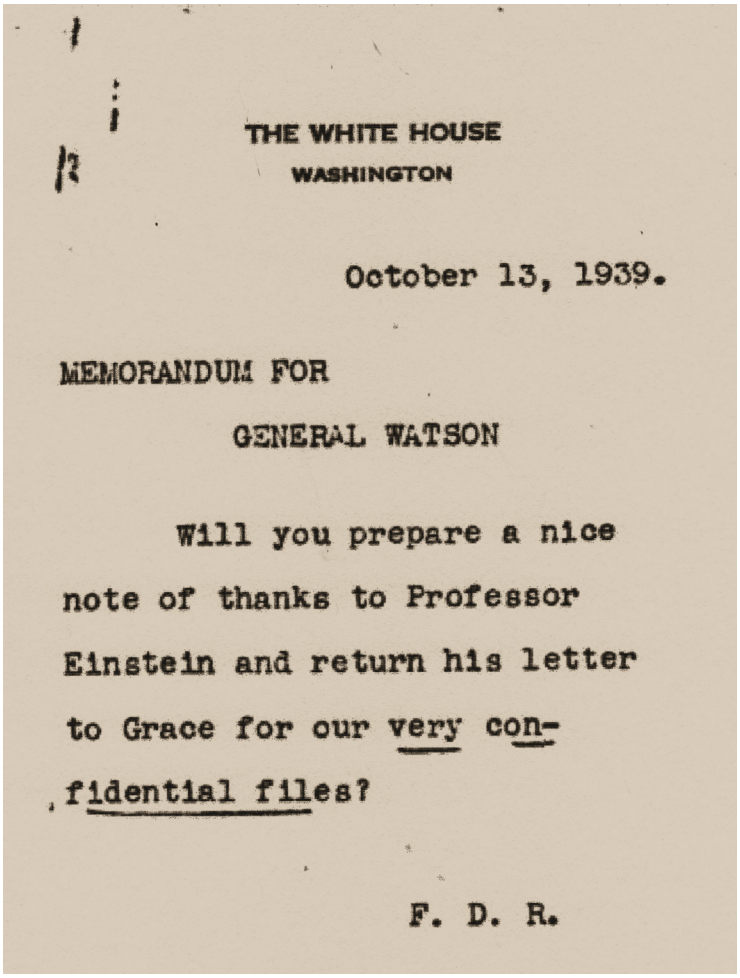

THE WHITE HOUSE
WASHINGTON

October 13, 1939.

MEMORANDUM FOR
GENERAL WATSON

Will you prepare a nice note of thanks to Professor Einstein and return his letter to Grace for our very confidential files?

F. D. R.

FIGURE IV.11 Memorandum from President Franklin D. Roosevelt to Major General Edwin M. Watson dated October 13, 1939 requesting a reply letter to Albert Einstein. *From FDR Presidential Library, http://docs.fdrlibrary.marist.edu/PSF/Box5/a64c01.jpg.*

estimated that only about 80 neutron generations would be achieved in the nuclear chain reaction before the explosion produced an expansion and dispersion of the U-235, thereby terminating the chain reaction.

We can make a simple calculation of the energy released by 80 neutron generations of the chain reaction based simply on the reaction as propagated by two neutrons per fission with the release of 200-MeV energy per fission (Table IV.1). The energy released after each generation (n) is exponential (2^n), as illustrated in Table IV.1 and Fig. IV.14, and the chain reaction culminates in an estimated energy release of 1.26×10^{26} MeV on the 80th neutron generation alone. The estimated energy of 1.21×10^{26} MeV provided in Table IV.1 is equivalent to approximately 4.6×10^{12} calories of heat calculated by converting MeV energy units to joules (J), which is a unit of power, ie, 1 J = 1 W s (watt second), and then to calories (cal), a unit of heat, as follows:

By definition:

$$1\ \text{MeV} = 1.60 \times 10^{-13}\ \text{J} \qquad \text{[IV.22]}$$

and:

$$1\ \text{J} = 0.239\ \text{cal}$$

Then, the energy released from the 80th neutron generation in joules and calories may be calculated as:

$$\begin{aligned} (1.21 \times 10^{26}\ \text{MeV})(1.60 \times 10^{-13}\ \text{J/MeV}) &= 1.94 \times 10^{13}\ \text{J} \\ (1.94 \times 10^{13}\ \text{J})(0.239\ \text{cal/J}) &= 4.63 \times 10^{12}\ \text{cal} \end{aligned} \qquad \text{[IV.23]}$$

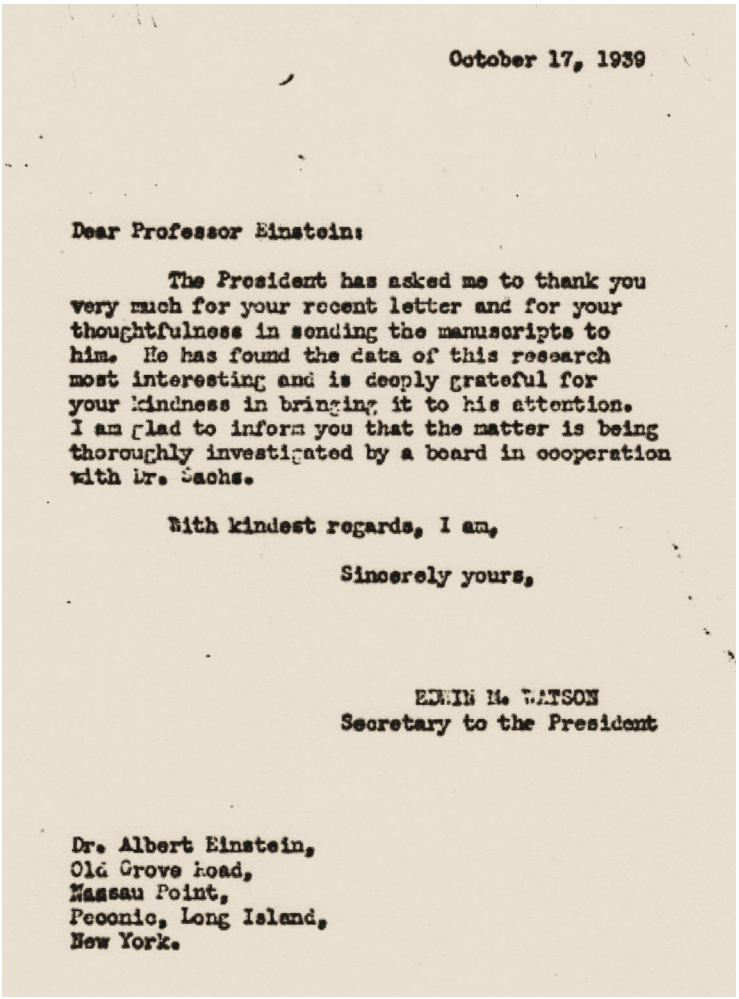

October 17, 1939

Dear Professor Einstein:

The President has asked me to thank you very much for your recent letter and for your thoughtfulness in sending the manuscripts to him. He has found the data of this research most interesting and is deeply grateful for your kindness in bringing it to his attention. I am glad to inform you that the matter is being thoroughly investigated by a board in cooperation with Dr. Sachs.

With kindest regards, I am,

Sincerely yours,

EDWIN M. WATSON
Secretary to the President

Dr. Albert Einstein,
Old Grove Road,
Nassau Point,
Peconic, Long Island,
New York.

FIGURE IV.12 White House reply letter from Major General Edwin M. Watson, Secretary to the President, to Albert Einstein dated October 17, 1939. *From FDR Presidential Library, http://docs.fdrlibrary.marist.edu/PSF/Box5/a64d01.jpg.*

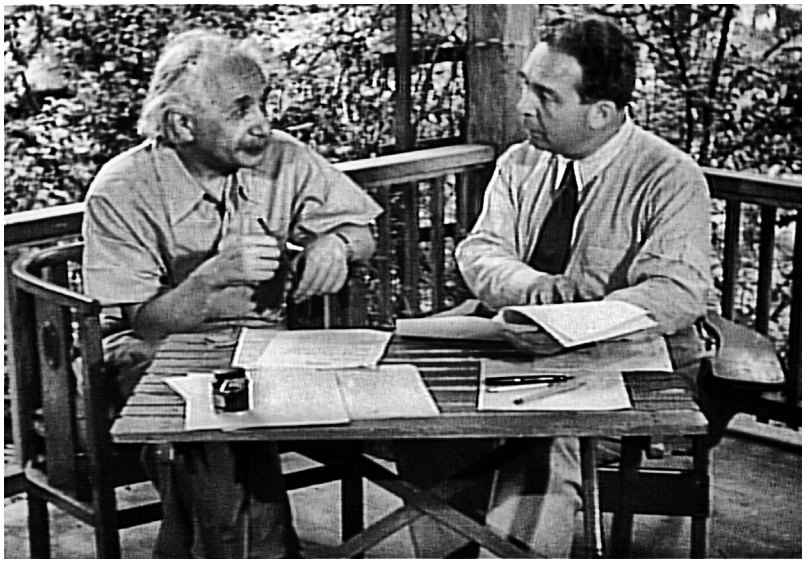

FIGURE IV.13 A still from a 1946 *March of Time* news film of Albert Einstein (left) and Leo Szilard on the porch of Einstein's home in Peconic, Long Island reenacting the August 1939 drafting and signing of a letter by Albert Einstein to President Franklin D. Roosevelt alerting to the potential of a German development of the atomic bomb, which sparked the initiation of the secret American Manhattan Project to develop nuclear weapons. *Courtesy of CriticalPast, with clearance from the Albert Einstein Archives, The Hebrew University of Jerusalem.*

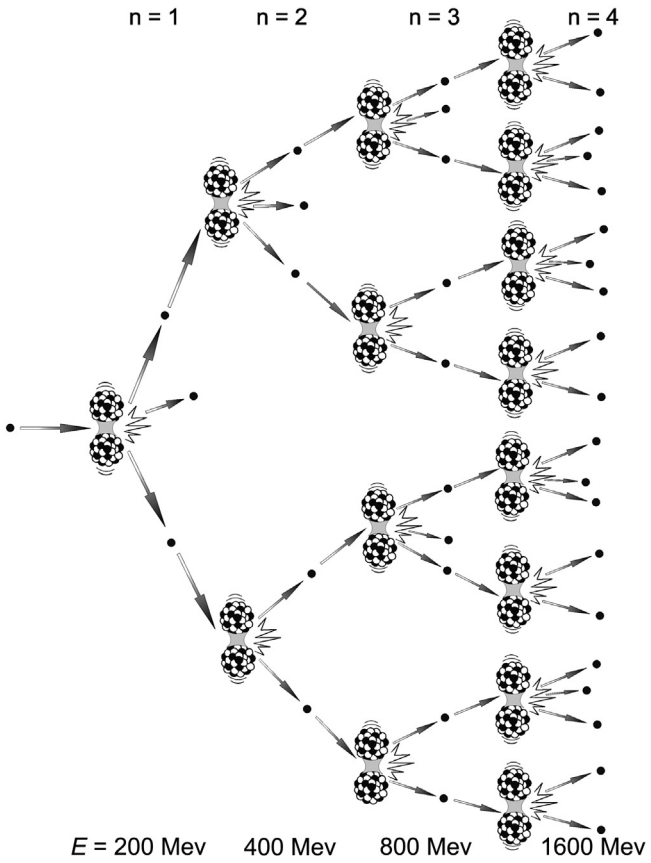

FIGURE IV.14 Neutron-induced nuclear chain reaction with uranium-235. On the far left of the figure is illustrated a neutron interacting with a U-235 nucleus, which becomes an unstable nucleus of U-236 oscillating as a liquid droplet. The U-236 nucleus is illustrated as bursting apart into two smaller nuclides (fission) with the emission of three neutrons. Two of the neutrons interact with two other nuclei of U-235 to cause nuclear fission of each with the concomitant emission of two or three neutrons from each nucleus. These neutrons then interact with four U-235 nuclei, which in turn produce yet more neutrons, etc. that propagate the exponential chain reaction. The chain reaction continues to produce increasing amounts of energy after each neutron generation (n). Only four neutron generations are illustrated, with the energy (E) emitted from each generation increasing exponentially according to 2^n or 200, 400, 800, 1600, 3200…n. The actual number of neutrons emitted per nuclear fission will vary, with the average being 2.4.

TABLE IV.1 Minimum Energy Yield From Various Generations of ^{235}U Fission Chain Reactions[a]

Fission Generation (n)	Minimum Energy Yield (MeV)		
1	200	or	2.00×10^2
5	3200	or	3.20×10^3
10	102,400	or	1.02×10^5
20	104,857,600	or	1.05×10^8
30	107,300,000,000	or	1.07×10^{11}
40	109,900,000,000,000	or	1.10×10^{14}
50	112,500,000,000,000,000	or	1.12×10^{17}
60	115,200,000,000,000,000,000	or	1.15×10^{20}
70	118,000,000,000,000,000,000,000	or	1.18×10^{23}
80	120,800,000,000,000,000,000,000,000	or	1.21×10^{26}

[a]*Energy yield is estimated on the basis of only two neutrons per fission and an energy emission of 200 MeV per fission, or* $\sum_{n=1}^{x}(2^n)(100)$, *where* n *is the neutron generation and the energy emitted after each generation undergoes an exponential multiplication* (2^n) *or 200, 400, 800, 1600, 3200…*n.

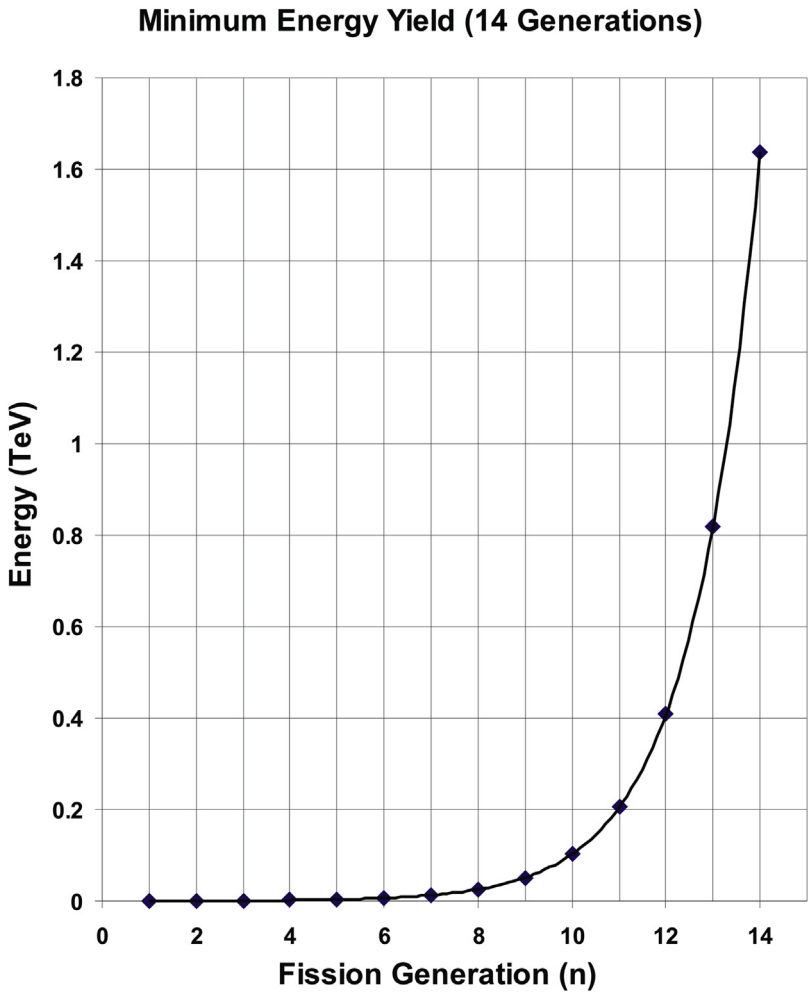

FIGURE IV.15 Estimated energy (TeV or 10^{12} eV) released from a neutron-induced fission chain reaction with uranium-235. The graph illustrates the energy released only up to the 14th generation of the chain reaction; however, the exponential increase in energy after each generation can be visualized.

If, by definition, 1 cal would be sufficient heat to raise the temperature of 1 g of water by 1°C, the 4 million−million calories of heat produced in the 80th neutron generation of the U-235 fission chain reaction would yield a staggering temperature hotter than the center of the sun (~15,000,000°C) and, if each reaction in the chain occurs in a period of time shorter than one-millionth of a second (eg, 10 ns), the timespan for the explosion to occur could be calculated to be less than 1 μs as follows:

$$(10\ \text{ns/neutron generation})(80\ \text{generations}) = 800\ \text{ns} = 0.8\ \mu\text{s} \qquad \text{[IV.24]}$$

the pressures from the explosion would be staggering. The exponential energy release after only 14 neutron generations is illustrated in Fig. IV.15.

Subsequent to the discovery of nuclear fission by Hahn and Strassman in 1939 and the more precise determination of the average number of 2.5 neutrons emitted in the thermal neutron induced fission of ^{235}U by Walter Zinn and Leo Szilard in 1939, Szilard feverishly collaborated with Enrico Fermi and others to demonstrate the first self-sustaining nuclear chain reaction with the construction of a nuclear reactor. As a prerequisite to the construction of an atomic bomb, the nuclear chain reaction had first to be demonstrated in a controlled fashion with the construction of a nuclear reactor.

During the planning of the first nuclear reactor, an important question was the selection of the proper moderator, which would be used to reduce the speed or energy of fast neutrons emitted in fission to the thermal energy state, as neutron capture by ^{235}U is optimal at thermal neutron energies. Examples of this collaboration can be found in personal letters

between Enrico Fermi and Leo Szilard now preserved in the Mandeville Special Collections Library of the University of California, San Diego. The following excerpt of a letter by Leo Szilard to Enrico Fermi in 1939 serves as an example:

Hotel King's Crown
420 West 116th Street
New York City

July 3rd, 1939

Dear Fermi,

This is to keep you informed of the trend of my ideas concerning chain reactions. It seems to me now that there is a good chance that carbon might be an excellent element to use in place of hydrogen…The capture cross-section of carbon is not known: the only experimental evidence available asserts an upper limit of 0.01 times 10^{-24} cm^2. If the cross-section were 0.01, carbon would be better than hydrogen, but the cross-section is perhaps much smaller, and it might be for instance 0.001. If it were so, carbon not only could be used in place of hydrogen, but would have great advantages…The concentration of uranium oxide in carbon could be kept very low, so that one could have about 2 gm. of carbon per cc. This compares favorably with ½ gram of water per cc at the most and means that the mean square of the displacement of a neutron for slowing down to thermal velocities would be only 1.5 times as large in the carbon-uranium oxide mixture. If capture by carbon can be neglected, the concentration of uranium oxide is determined by the consideration that the average displacement of a thermal neutron for capture by uranium in the mixture must not become too large. With this as a limiting factor about 1/10 of the weight of the mixture would have to be uranium, and that means that one would need only a few tons of uranium oxide if our present data about uranium are correct.

I personally would be in favor of trying a large-scale experiment with carbon—uranium oxide mixture if we can get hold of the material.

I intend to plunge in the meantime into an experiment designed for measuring small capture cross-sections for thermal neutrons…

If carbon should fail, our next best guess might be heavy water, and I have therefore taken steps to find out if it is physically possible to obtain a few tons of heavy water…

Yours,

(Leo Szilard)

Leo Szilard followed this up with another letter in only 2 days to Enrico Fermi on the same subject. An excerpt of that letter, which is available in the Mandeville Special Collections Library of the University of California, San Diego, is the following:

Hotel King's Crown
420 West 116th Street
New your City

July 5th, 1939

Dear Fermi,

…It seems that it will be possible to get sufficiently pure carbon at a reasonable price. Carbon would also have an advantage over hydrogen insofar as there is no change in the scattering cross-section in the transition from the resonance region to the thermal region. Consequently, if layers of uranium oxide of finite thickness are used, the diffusion of the thermal neutrons produced in the carbon to the uranium layer is not adversely affected as in the case of hydrogen by such a change. Whether this point is of any importance depends of course on the absolute value of the carbon cross-section…

With kind regards to all,

Yours,

(Leo Szilard)

Enrico Fermi replied quickly to Szilard's letters with confirmation that he was also thinking of carbon as the best moderator for their experiment aimed at demonstrating the first self-sustaining nuclear chain reaction. He agrees also with Leo Szilard concerning the possibility of using heavy water as the moderator. An excerpt of Fermi's letter to Szilard, which is available in the Mandeville Special Collections Library of the University of California, San Diego, is the following:

UNIVERSITY OF MICHIGAN
ANN ARBOR

DEPARTMENT OF PHYSICS

July 9, 1939

Dear Szilard,

Thank you for your letter. I was also considering the possibility of using carbon for slowing down the neutrons; in the obviously optimistic hypothesis that carbon should have no absorption at all for neutrons, and assuming for the resonance absorption band of uranium the usual data (which also I rather suspect to be optimistic) one finds from an elementary calculation that the ratio of the concentrations (ratio of the number of atoms) of uranium and carbon should be about one thousandth in order to avoid too much resonance absorption. According to my estimates a possible recipe might be 39000 Kg of carbon mixed with 600 Kg of uranium. If it were really so the amounts of materials would certainly not be too large…

I had discarded heavy water as too expensive; but if you can easily get several tons of it, it might work very nicely.

The cyclotron here will start working again next week and I hope to be able to get reliable information on the so-called resonance absorption of uranium. I shall inform you of the results.

Yours sincerely,

(Enrico Fermi)

P.S. I have received your second letter. If heavy water is too expensive, as I believe, it would be important to find some way of knowing something of the carbon absorption. It seems to me that the use of very thick layers of C might do the trick.

As discussed in the letters between Szilard and Fermi, carbon in the form of graphite blocks was selected as the moderator for the nuclear reactor. In 1939, Leo Szilard and Enrico Fermi coinvented the nuclear reactor at Columbia University by jointly sketching out a three-dimensional lattice of uranium slugs dropped into holes in black, greasy blocks of graphite moderator, with sliding neutron-absorbing cadmium control rods to regulate the chain reaction. The reactor with its heap of graphite blocks was referred to by Enrico Fermi as an "atomic pile." The first demonstration of the nuclear chain reaction in uranium was carried out by Enrico Fermi with the collaboration of Leo Szilard and others at the University of Chicago on December 2, 1942 (see Enrico Fermi in Hall of Fame, Part II). In December 1944, Enrico Fermi and Leo Szilard jointly filed for a highly classified patent as coinventors of the atomic pile, describing how the self-sustained nuclear chain reaction had been achieved. The patent (no. 2,708,656) remained classified for over 10 years; and it was not issued until May 18, 1955. They called it a "neutronic reactor," and they were listed as coinventors of the reactor. A clipping of the first page of their patent submitted to the United States Patent Office on December 19, 1944, is illustrated in Fig. IV.16.

The patent listing E. Fermi and L. Szilard as coinventors was highly detailed with 27 drawings and schematics; and 30 pages of text describing the construction and operation of the nuclear reactor. The patent provided detailed information, calculations, and drawings on (1) the chain fission reaction initiated by thermal neutrons, (2) neutron loss by absorption in uranium, absorption in the moderator, absorption by impurities in the system, and exterior neutron loss, (3) calculations for the measurement of neutron loss, (4) a reactor with a solid neutron moderator (eg, graphite), (5) a reactor having a liquid neutron moderator (eg, heavy water or D_2O), (6) reactors with other moderators, (7) the reduction and loss of neutrons due to resonance capture and impurities in the materials, (8) the effect of the cooling system on the neutron reactor, (9) an illustrative gas-cooled neutron reactor, (10) an illustrative liquid-cooled neutron reactor, (11) the

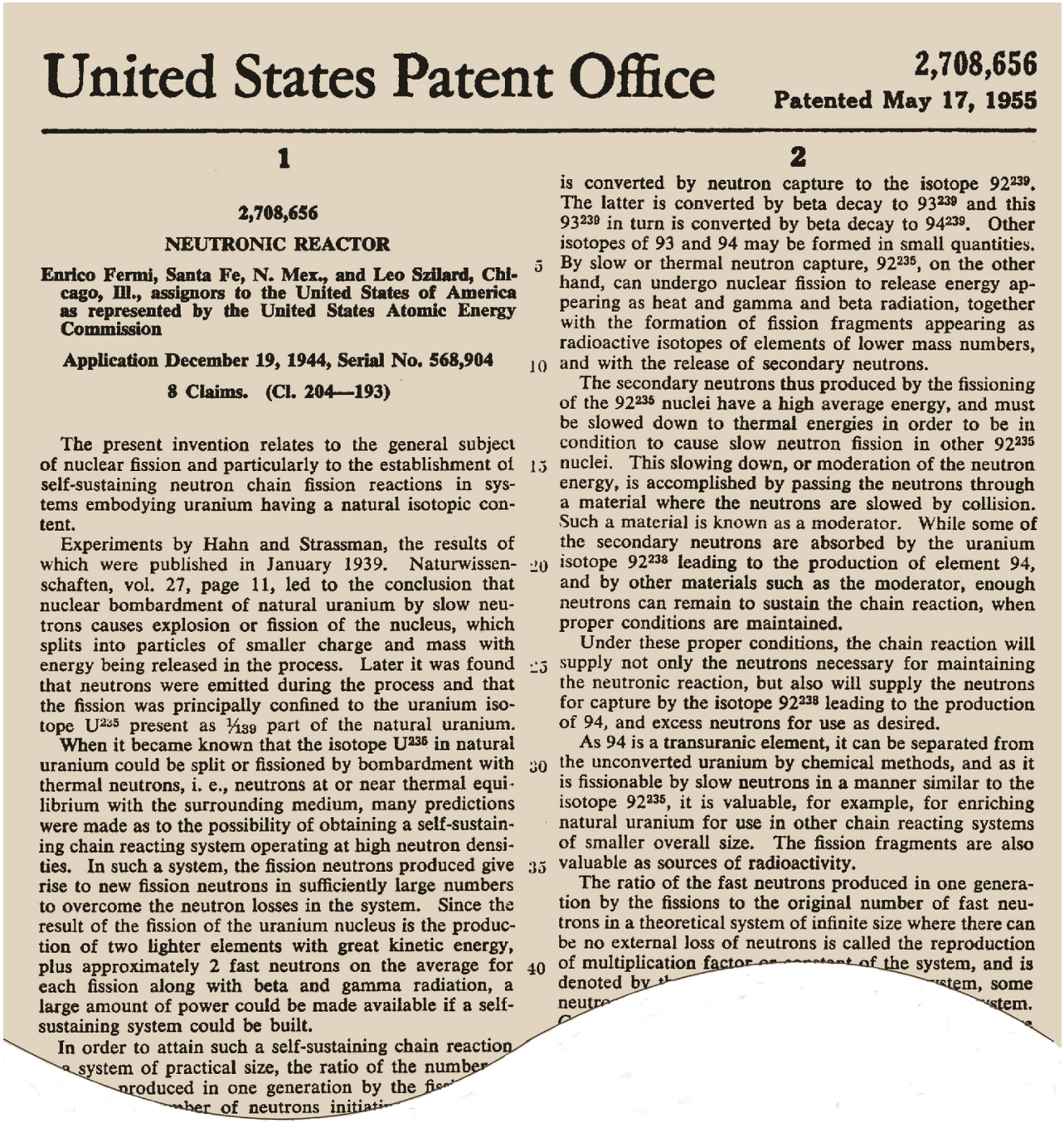

United States Patent Office

2,708,656

Patented May 17, 1955

1

2,708,656

NEUTRONIC REACTOR

Enrico Fermi, Santa Fe, N. Mex., and Leo Szilard, Chicago, Ill., assignors to the United States of America as represented by the United States Atomic Energy Commission

Application December 19, 1944, Serial No. 568,904

8 Claims. (Cl. 204—193)

The present invention relates to the general subject of nuclear fission and particularly to the establishment of self-sustaining neutron chain fission reactions in systems embodying uranium having a natural isotopic content.

Experiments by Hahn and Strassman, the results of which were published in January 1939. Naturwissenschaften, vol. 27, page 11, led to the conclusion that nuclear bombardment of natural uranium by slow neutrons causes explosion or fission of the nucleus, which splits into particles of smaller charge and mass with energy being released in the process. Later it was found that neutrons were emitted during the process and that the fission was principally confined to the uranium isotope U^{235} present as $1/139$ part of the natural uranium.

When it became known that the isotope U^{235} in natural uranium could be split or fissioned by bombardment with thermal neutrons, i. e., neutrons at or near thermal equilibrium with the surrounding medium, many predictions were made as to the possibility of obtaining a self-sustaining chain reacting system operating at high neutron densities. In such a system, the fission neutrons produced give rise to new fission neutrons in sufficiently large numbers to overcome the neutron losses in the system. Since the result of the fission of the uranium nucleus is the production of two lighter elements with great kinetic energy, plus approximately 2 fast neutrons on the average for each fission along with beta and gamma radiation, a large amount of power could be made available if a self-sustaining system could be built.

In order to attain such a self-sustaining chain reaction [illegible] system of practical size, the ratio of the number [illegible] produced in one generation by the fi[illegible] number of neutrons initiati[illegible]

2

is converted by neutron capture to the isotope 92^{239}. The latter is converted by beta decay to 93^{239} and this 93^{239} in turn is converted by beta decay to 94^{239}. Other isotopes of 93 and 94 may be formed in small quantities. By slow or thermal neutron capture, 92^{235}, on the other hand, can undergo nuclear fission to release energy appearing as heat and gamma and beta radiation, together with the formation of fission fragments appearing as radioactive isotopes of elements of lower mass numbers, and with the release of secondary neutrons.

The secondary neutrons thus produced by the fissioning of the 92^{235} nuclei have a high average energy, and must be slowed down to thermal energies in order to be in condition to cause slow neutron fission in other 92^{235} nuclei. This slowing down, or moderation of the neutron energy, is accomplished by passing the neutrons through a material where the neutrons are slowed by collision. Such a material is known as a moderator. While some of the secondary neutrons are absorbed by the uranium isotope 92^{238} leading to the production of element 94, and by other materials such as the moderator, enough neutrons can remain to sustain the chain reaction, when proper conditions are maintained.

Under these proper conditions, the chain reaction will supply not only the neutrons necessary for maintaining the neutronic reaction, but also will supply the neutrons for capture by the isotope 92^{238} leading to the production of 94, and excess neutrons for use as desired.

As 94 is a transuranic element, it can be separated from the unconverted uranium by chemical methods, and as it is fissionable by slow neutrons in a manner similar to the isotope 92^{235}, it is valuable, for example, for enriching natural uranium for use in other chain reacting systems of smaller overall size. The fission fragments are also valuable as sources of radioactivity.

The ratio of the fast neutrons produced in one generation by the fissions to the original number of fast neutrons in a theoretical system of infinite size where there can be no external loss of neutrons is called the reproduction of multiplication factor [illegible] of the system, and is denoted by [illegible] stem, some neutr[illegible] stem.

FIGURE IV.16 A portion of the first page of the Fermi–Szilard patent for the nuclear reactor, which they called the neutronic reactor.

use of different lattices in the reactor, (12) critical and operating sizes of the reactor, (13) control of the chain reaction by variation of the neutron losses, and (14) applications of neutron reactors.

The neutronic reactor patent application submitted by Enrico Fermi and Leo Szilard in 1944 would serve as a precursor for future development of nuclear reactors for research and electric power production. One of their drawings of a heavy water (D_2O) reactor, taken from their patent as an example, is illustrated in Fig. IV.17. Several other reactor designs are described in their original patent.

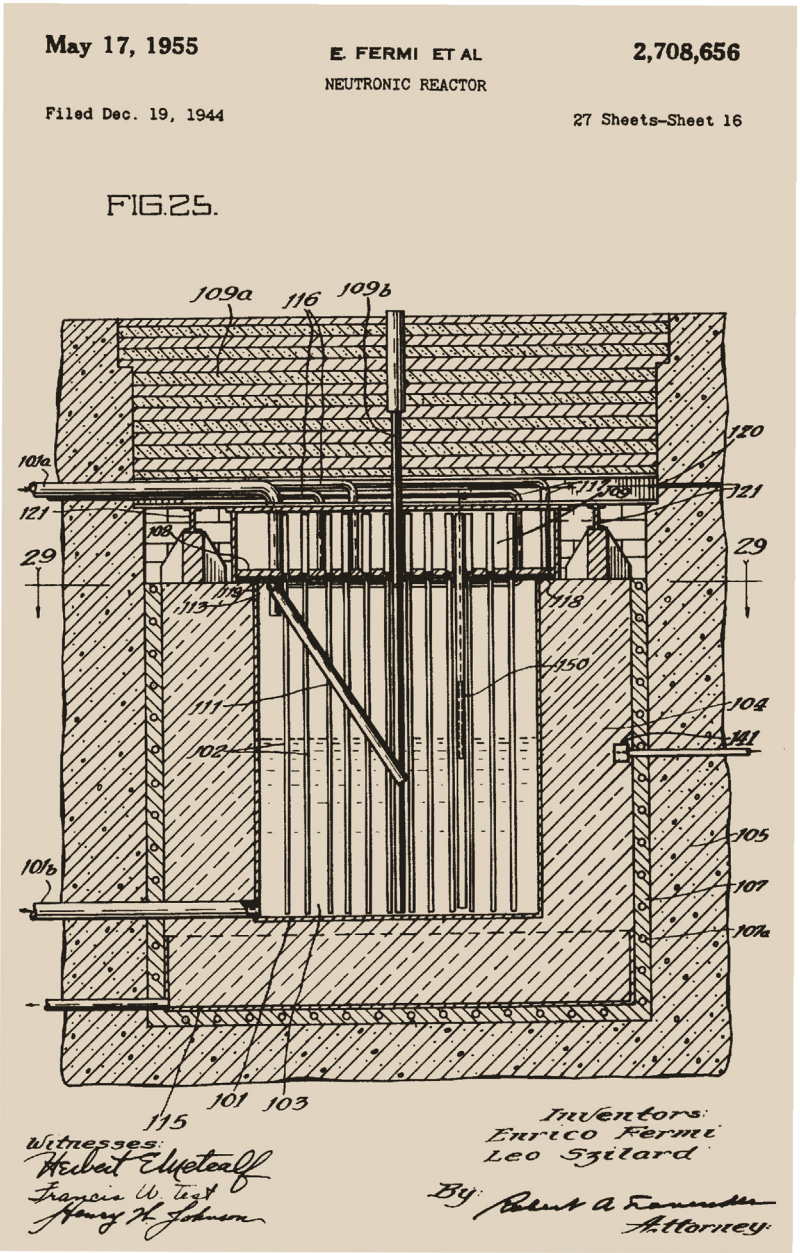

FIGURE IV.17 A vertical cross-section view of a "neutronic reactor" employing deuterium oxide (heavy water) as the moderator (from the joint patent no. 2,708,656 filed by Enrico Fermi and Leo Szilard on December 19, 1944 with the United States Patent Office). On the lower right-hand corner of the figure can be seen the names of Enrico Fermi and Leo Szilard as joint inventors of the nuclear reactor. The components of the reactor were identified according to the following numbering: **101**, reactor tank of cylinder shape; **101a** and **101b**, inlet and outlet pipes for the introduction and extraction of heavy water from the tank; **102**, uranium fuel rods 2.8 cm in diameter where the uranium metal is sheathed in 0.1-cm aluminum to prevent contamination of the D_2O moderator by fission products and prevention of corrosion of the uranium by the heavy water. The fuel rods extend in the heavy water to approximately 0.6 cm from the tank bottom; **103**, heavy water; **104**, graphite neutron reflector; **105**, concrete shield; **107**, metal shield; **107a**, metal tubing for reactor cooling through which light water is circulated; **108**, cover plate of stainless steel serving as a thermal shield and as a support for fuel rods and control and safety rods; **109**, space into which the upper ends of the uranium fuel rods and piping can be extended; **109a**, shield having alternate layers of iron and Masonite (compressed wood fiber) to shield penetrating radiation from the top of the tank; **109b**, tube or well of suitable diameter (eg, 10 cm) extending through the shields into the center of the tank to permit the bombardment of substances by high intensity neutron radiation for the production of radioactive isotopes or other purposes; **111**, hollow tube for the insertion or withdraw of control rods 10 cm in diameter containing a 0.2-cm layer of cadmium sandwiched between aluminum walls; **115**, pan of stainless steel for the collection of any expensive heavy water that may leak from the tank and drained from a collecting tube; **116**, pipes through which helium is introduced into the top of the reactor tank above the heavy water level; **117**, pipes for the circulation of helium above the heavy water; **118**, cadmium sheet to minimize the escape of slow neutrons; **119**, aluminum sheet to prevent electrolytic action between dissimilar metals in the tank interior; **120** and **121**, two pairs of crossed I beams; **141**, ionization chamber to monitor and control the neutron density and reactor power; **150**, shim rod or control rod to compensate for the xenon effect. The xenon effect is a poisoning or inhibition of the neutron-induced fission chain reaction caused by the production of the fission product ^{135}Xe, which is a short-lived (9.1 h half-life) radioisotope with a very high neutron absorption cross-section of 2.6×10^6 b. Buildup of ^{135}Xe in the reactor can significantly affect the operation of a reactor, because of its high capacity to absorb neutrons required to maintain the fission chain reaction.

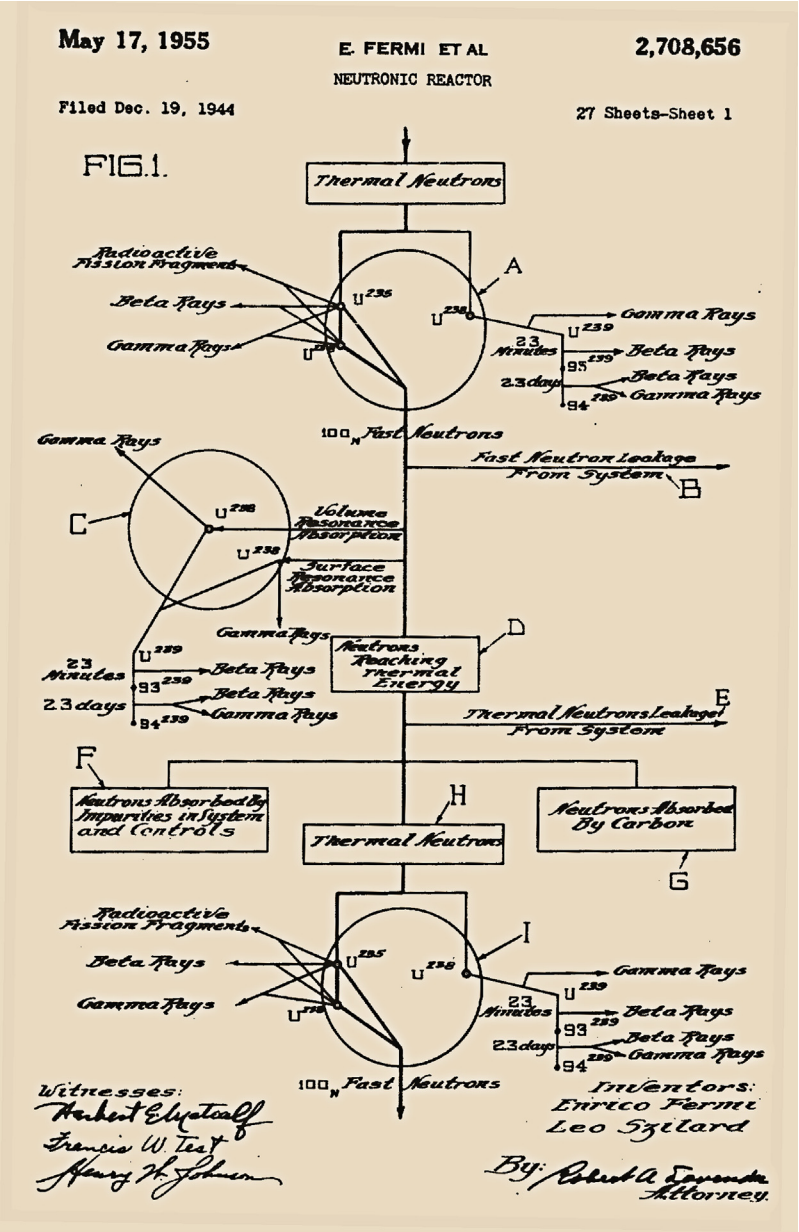

FIGURE IV.18 The chain fission reaction initiated by thermal neutrons in a uranium-fueled reactor depicted by Enrico Fermi and Leo Szilard in their patent filed on December 19, 1944. The names of the coinventors Enrico Fermi and Leo Szilard are found in the lower right-hand corner of the diagram. The sequence of events, as described by the inventors, in the thermal neutron–induced chain reaction is identified in the diagram as follows. (A) A uranium body (found in the nuclear fuel rods) from which fast neutrons are liberated as a result of the fission process. (B) A fast neutron loss due to leakage out of the reactor system. (C) A uranium body in which resonance absorption of neutrons by $^{238}_{92}$U takes place, at resonance energies above thermal energy, leading to the formation of element of atonic number 94, specifically plutonium, ie, $^{239}_{94}$Pu. (D) Neutron reaching thermal energy. (E) Thermal neutron loss by diffusion out of the system. (F) Thermal neutron loss by diffusion due to capture by impurities in the uranium, graphite, and controls. (G) Additional thermal neutron loss due to capture by graphite as the thermal neutrons diffuse through the graphite before entering uranium. (H) Thermal neutrons entering the uranium body. (I) A uranium body in which part of the thermal neutrons entering the body are absorbed by $^{238}_{92}$U leading to the formation of $^{239}_{94}$Pu. The remaining thermal neutrons in the uranium body are absorbed by $^{235}_{92}$U, producing new fissions and the emission of fast neutrons (see bottom of the figure). Additional fast neutrons are produced by fission of $^{238}_{92}$U.

The sequence of events that occur in the nuclear reactor during the thermal neutron–induced chain reaction in the uranium bodies of the nuclear fuel rods and in the surrounding moderator (eg, water, heavy water, or graphite) are illustrated in Fig. IV.18. Typical reactor moderators are water (H_2O), heavy water (D_2O), or graphite (an allotrope of carbon). The reactor moderator reduces the energy of fission neutrons via elastic collisions between the neutrons and

moderator atoms, thereby reducing the neutron energies from the fast to thermal energy state. The fission of ^{235}U in reactor fuel occurs optimally with thermal neutrons; however, fission results in the emission of fast neutrons. Thus the moderator in the nuclear reactor plays an important role in maintaining a chain reaction in the nuclear reactor by converting the fast neutrons from nuclear fission to thermal neutrons, facilitating the continued production of new fission reactions. Enrico Fermi and Leo Szilard, in their patent application of December 19, 1944, described in great detail the fission chain reaction process in their nuclear reactor. An excerpt of their description of the fission chain reaction process is the following:

We will consider the condition obtaining where thermal neutrons enter uranium body A (see top of Fig. IV.18). Some of these thermal neutrons will cause fission in the ^{235}U content of the uranium body to produce fast neutrons, the yield being at an average rate of about 2 neutrons per fission. As a result of this fission, fission fragments are released together with beta and gamma rays, thereby producing energy which, in the system, is manifested mostly by the heating of the uranium bodies with only a slight release of heat in the graphite. The actual average yield of fast neutrons by fission of ^{235}U is slightly higher, eg, by a few percent, than an average of 2 mentioned above. Some of the fast neutrons released in the fission ^{235}U by the thermal neutrons of this example almost immediately produce fast fission of ^{238}U in the same uranium body, with the production of additional fast neutrons.

*The fast neutrons leaving the uranium body, for example 100*n *neutrons (see Fig. IV.18), enter the mass of moderator, travel there through, and through the uranium bodies over paths long in comparison with the spacing of the uranium bodies, to undergo successive collisions that slow them down. A substantial portion of the fast neutrons are thus destined to be reduced, by about 100 elastic collisions apiece in the case of graphite (moderator) and mostly in the moderator, to thermal energy. Furthermore, during the extremely irregular path of the neutrons while they are being slowed down by elastic collisions, some of the neutrons will reach a uranium resonance absorption energy as they are about to enter a uranium body, such as C (see Fig. IV.18), and are absorbed immediately on or close to the surface of the uranium body; element 94 (ie, atomic number 94 or plutonium) is produced by the resonance absorption according to the following process:*

$$^{238}_{92}\mathrm{U} + \mathrm{n} \rightarrow {}^{239}_{92}\mathrm{U} + \gamma$$

$$^{239}_{92}\mathrm{U} \xrightarrow{23\ \mathrm{min}} {}^{239}_{93}\mathrm{Np} + \beta^- + \gamma$$

$$^{239}_{93}\mathrm{Np} \xrightarrow{2.3\ \mathrm{day}} {}^{239}_{94}\mathrm{Pu} + \beta^- + \gamma$$

A small amount of $^{240}_{94}Pu$ may also be found, formed by addition of a neutron to $^{239}_{94}Pu$. Capture of thermal neutrons by ^{238}U, as indicated in bodies A and C of Fig. IV.18, also results in production of element 94 by the same process.

The predominant isotope produced, $^{239}_{94}Pu$, is a long lived radioactive product with a half-life of about 20,000 years.

A large percentage of the original fast neutrons escape resonance capture and fast neutron leakage and are reduced to thermal energy within the system; thermal neutrons diffuse through the moderator in condition to produce fission if they promptly enter ^{235}U or element 94 without being captured by any other material.

The fission reaction is as follows:

$$^{235}_{92}\mathrm{U} + \text{neutron} = A + B + n\ \text{neutrons (average)}$$

A = *"light fission fragment, eg, Br, Kr, Rb, Sr, Y, Zr, Cd, Mo, Tc, Ru, Rh. Atomic mass, 83–99, inclusive, Atomic number, 35–45, inclusive.*

B = *"heavy" fission fragment, eg, Sb, Te, I, Xe, Cs, Ba, La, Ce, Pr, Nd. Atomic mass, 127–141 inclusive. Atomic number, 51–60 inclusive.*

*In any particular system, impurities will be present in both the moderator and the uranium. Thus, for example (see F of Fig. IV.18), if impurities necessarily present in the materials do not consume too many neutrons, some excess neutrons are available to be captured by "impurities" intentionally introduced for control purposes; ie, by a control rod, a small number of the neutrons are absorbed by the moderator (see G of Fig. IV.18), leaving sufficient thermal neutrons to enter a uranium body to produce new fast neutrons by fission (see H of Fig. IV.18), to repeat the cycle. In the uranium-graphite system about 72*n *thermal neutrons enter the uranium body to produce 100*n *new fast neutrons, ie, a survival of about 72% of the original 100*n *fast neutrons during the slowing process.*

The four neutron losses from the chain reaction referred to above are represented in Fig. IV.18, where the resonance absorption at C and the friction of thermal neutrons absorbed by ^{238}U at I represent the uranium absorption losses. Losses due to impurities are represented at F, those due to absorption in the moderator at G, and the leakage losses due to the finite size of the system at B and E.

The invention of the nuclear reactor for the peaceful application of nuclear energy capable of providing electric power to cities, as patented by Fermi and Szilard, was declared by some to be one of the most significant inventions of all time, comparable to those of communication, the telegraph and telephone, by Samuel Morse and Alexander Graham Bell. In 1944 around the time of writing the patent for the nuclear power reactor, Leo Szilard and Enrico Fermi participated in the "New Piles Committee" meetings together with Nobel Laureates James Frank and Eugene Wigner among other physicists, chemists, and engineers including Walter Zinn and Alvin Weinberg. The Committee meetings were held at the University of Chicago Metallurgical Laboratory to explore and recommend new designs for peaceful electric power-producing nuclear reactors. Many new reactor concepts were presented that would become the modern power reactors that supply the needed electricity for our cities today. The history and minutes of the New Piles Committee meeting are reviewed by Lawson and Krause (2004). Among the new reactor concepts and designs was that of the sodium-cooled "breeder reactor" proposed by Szilard and Fermi. The term "breeder reactor" was first proposed by Leo Szilard, as it refers to the type of reactor that produces more nuclear fuel or fissile material than it consumes. Although ^{235}U is the only naturally occurring fissile radionuclide, it stood to reason that if an excess of neutrons were produced in a thermal reactor (an average of 2.5 neutrons per ^{235}U fission) it would be possible to produce fissile ^{239}Pu or ^{233}U fuel (see Eqs. [10.36]–[10.41] of the chapter: "Neutron Radiation") in a reactor in excess of the fuel actually consumed in the reactor. This concept formed the basis for the new generation of "breeder" reactors.

The successful demonstration of a self-sustaining nuclear chain reaction in 1942 paved the way to the establishment of the Manhattan Project, which was a major undertaking culminating in the successful construction and eventual testing of the first nuclear weapon on July 16, 1945, and the utilization of the weapon against two of Japan's populous cities in early August of the same year. The Manhattan Project developed two nuclear weapon designs. The two designs are illustrated in Fig. IV.19. One design was a gun assembly, which employed a bullet of a subcritical mass of

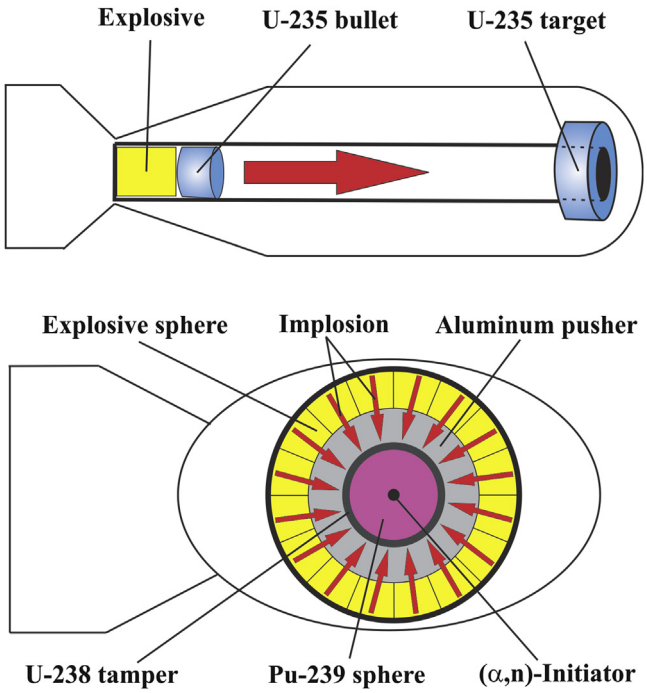

FIGURE IV.19 Two atomic bomb designs developed by the Manhattan Project. The upper device was the gun assembly whereby a bullet consisting of a subcritical mass of enriched uranium-235 is fired into a hollow target of uranium-235 to achieve a supercritical mass. The lower device was an implosion assembly whereby a sphere of conventional explosive is designed to focus the forces of the explosion inward to compress a sphere of enriched plutonium-239 into a supercritical mass.

enriched uranium-235 that was fired with conventional explosive down a gun barrel into a target of another subcritical mass of enriched fissile uranium-235. A bomb of this design, named "Little Boy," was dropped on Hiroshima on August 6, 1945. The device went supercritical, that is, in excess of its critical mass, when the bullet reached its target, creating a blast equivalent to 16 kilotons of TNT with intense nuclear radiation causing the immediate death of 80,000 persons and the total devastation of the city; and after a year, the casualties from radiation and injuries reached up to 160,000 of the inhabitants. The "Little Boy" bomb used 80% enriched uranium-235 with the bullet weighing approximately 39 kg and the target approximately 26 kg. The amount of uranium needed to achieve a critical mass of U-235 will depend on the percentage enrichment of U-235; and this data is available from Murray and Holbert (2015).

The second type of nuclear weapon, developed by the Manhattan Project, was designed to utilize an implosion creating an inward pressure to compress a sphere of highly enriched fissile plutonium-239 to more than twice its density to a supercritical mass. The implosion concept was determined to be more efficient with respect to the explosive yield per mass of fissile material. An implosion would produce an immediate compression of all of the fissile material in the bomb, which would react more efficiently than the gun assembly. The implosion design is illustrated in Fig. IV.19. Conventional explosive was designed to focus the force to implode from the detonated explosive inward. An aluminum sphere, referred to as a "pusher," further strengthened the implosion wave toward the inner sphere of uranium tamper and fissile plutonium-239. A sphere of uranium-238 was used as a tamper, which helped reflect neutrons back into the core of the fissile plutonium-239 and helped keep the core intact during the implosion. A source of neutrons, such as a combination of polonium and beryllium, served as a neutron initiator of the chain reaction and was located at the very center. (The alpha particles emitted by polonium react with stable beryllium to produce neutrons according to Eq. [10.19] of the chapter entitled "Neutron Radiation.") The implosion device, named "Fat Man" because if its round shape, was dropped on Nagasaki, Japan on August 9, 1945. It required less fissile material than the gun assembly, producing more explosive power. The bomb dropped on Nagasaki utilized 6.2 kg of highly enriched plutonium-239, producing an explosive force equivalent to 21 kilotons of TNT, and killing up to 80,000 people. In both bombings half of the people killed perished on the first day of the bombing; the remaining deaths in the subsequent months were the results of burns, radiation sickness, and injuries.

Before the bombs were dropped on Japan, numerous scientists who worked on the Manhattan Project, including Leo Szilard, tried to lobby against its use. In light of the official surrender of Germany to the allied forces in May of 1945, Leo Szilard began opposition to the use of the bomb on moral grounds. Szilard's efforts, first in patenting the possibility of an atomic bomb from a nuclear chain reaction and then promoting its development, were driven by the threat that Germany under the rule of Hitler could be first to develop the bomb. Now that the threat of Germany was a matter of the past and a peace treaty, other than an unconditional surrender of Japan appeared possible, he saw no justification to use the bomb against Japan. It was, however, believed by many that countless lives would have been lost on both sides over a prolonged war with Japan, if the bomb had not been used. Over a decade prior to the German surrender, Szilard had patented his original idea for the bomb in 1934 in order to maintain control over the eventual discovery of the nuclear chain reaction and then conferred his patent to the British War Office in 1935 to keep the patent a secret and out of the hands of those who might use the information for malicious objectives. It may appear ironic that Leo Szilard was a pacifist. We may say that Leo Szilard was the founder of nuclear arms control or what we now call nuclear nonproliferation (NNP). This is evidenced by his tireless efforts to reach the American President and prevent the deployment of the atomic bomb against Japan.

In March of 1945, Leo Szilard prepared a memorandum to President Roosevelt entitled "Enclosure to Mr. Albert Einstein's Letter of March 25, 1945 to the President of the United States." Szilard prepared the memorandum to avert the use of the bomb against Japan. In the memorandum, he warned that the use of the bomb would start an atomic arms race with Russia, and he raised the question on whether avoiding such an arms race might not be more important than the short-term goal of knocking Japan out of the war. Again, as in August of 1939, Leo Szilard realized that he could not personally get the memorandum to the President, so he asked Albert Einstein to sign a letter of introduction, a photocopy of which is illustrated in Fig. IV.20.

The letter of introduction signed by Albert Einstein together with Leo Szilard's memorandum is available in the Mandeville Special Collections Library of the University of California, San Diego. The letter signed by Einstein is interesting, because it purposely does not mention any specifics about Szilard's memorandum, because both Einstein and Szilard knew that the Government would not want scientists meddling in their affairs when it comes to policy-making. However, to give Szilard the opportunity to present his opinion to the Cabinet, Einstein's letter clearly points out that Einstein previously presented Szilard's views in a letter of August 2, 1939 concerning a neutron chain reaction in uranium; and, on the basis of that letter, the Government started the secret work in this field. Thus, Einstein points out, the

112 Mercer Street
Princeton, New Jersey
March 25, 1945

The Honorable Franklin Delano Roosevelt
The President of the United States
The White House
Washington, D. C.

Sir:

I am writing you to introduce Dr. L. Szilard who proposes to submit to you certain considerations and recommendations. Unusual circumstances which I shall describe further below induce me to take this action in spite of the fact that I do not know the substance of the considerations and recommendations which Dr. Szilard proposes to submit to you.

In the summer of 1939 Dr. Szilard put before me his views concerning the potential importance of uranium for national defense. He was greatly disturbed by the potentialities involved and anxious that the United States Government be advised of them as soon as possible. Dr. Szilard, who is one of the discoverers of the neutron emission of uranium on which all present work on uranium is based, described to me a specific system which he devised and which he thought would make it possible to set up a chain reaction in unseparated uranium in the immediate future. Having known him for over twenty years both from his scientific work and personally, I have much confidence in his judgment and it was on the basis of his judgment as well as my own that I took the liberty to approach you in connection with this subject. You responded to my letter dated August 2, 1939 by the appointment of a committee under the chairmanship of Dr. Briggs and thus started the Government's activity in this field.

The terms of secrecy under which Dr. Szilard is working at present do not permit him to give me information about his work; however, I understand that he now is greatly concerned about the lack of adequate contact between scientists who are doing this work and those members of your Cabinet who are responsible for formulating policy. In the circumstances I consider it my duty to give Dr. Szilard this introduction and I wish to express the hope that you will be able to give his presentation of the case your personal attention.

B F

Very truly yours,

A. Einstein

FIGURE IV.20 Photocopy of letter signed by Albert Einstein with the intention of encouraging President Franklin Delano Roosevelt to read Leo Szilard's memorandum with arguments in opposition to the use of the atomic bomb against Japan. *From the Harry S. Truman Presidential Library and Museum (http://www.trumanlibrary.org/); and with courtesy of The Albert Einstein Archives, Hebrew University of Jerusalem.) A carbon copy of the typed letter, also signed by Albert Einstein, is available from the Leo Szilard Papers, Mandeville Special Collections, University of California, San Diego Library.*

Government should listen to Szilard again. Also, Einstein's statement in his letter "Dr. Szilard, who is one of the discoverers of the neutron emission of uranium," should not be considered as a stretch or exaggeration, because Leo Szilard with Walter Zinn (Zinn and Szilard, 1939) jointly determined the more precise average number of neutrons emitted in fission following the capture of a thermal neutron by uranium-235.

Szilard's efforts to get to the President were related by him in an interview with a news reporter (U.S. News and World Report, 1960). Szilard suspected that his memorandum (even with Einstein's introductory letter) would not reach the President if it went through official channels. He consulted first with Nobel Laureate Arthur H. Compton (Compton Effect), who was in charge of the secret work of the University of Chicago Metallurgical Laboratory (Met Lab) in the Manhattan Project, and Arthur Compton agreed with Szilard and wished him success in getting the letter to the President. Szilard therefore requested and obtained an appointment to see the First Lady, Mrs. Eleanor Roosevelt, so that his letter could be handed over to the President in a sealed envelope. However, President Roosevelt died on April 12, 1945. Now Szilard was back to square one and had to find a way to get his letter/memorandum to President Harry S. Truman. Szilard and Walter Bartky, Associate Director of the Met Lab, met with Truman's Appointments Secretary, who agreed that the matter was serious and suggested that they meet with Secretary of State, Jimmy Byrnes. They agreed to meet with Byrnes and asked permission that Nobel Laureate Harold C. Urey accompany them to the meeting. Harold Urey was awarded the Nobel Prize in Chemistry in 1933 for his discovery of deuterium, an isotope of hydrogen also referred to as "heavy hydrogen." He had expertise in isotope separation and was part of the team that worked on the separation and enrichment of U-235 in the Manhattan Project. Urey's presence would add authority and prestige to the meeting. The three—Szilard, Bartky, and Urey—took the overnight train to Spartanburg, South Carolina to meet with Byrnes. Szilard related that after having read the memorandum, Byrnes commented that General Leslie Groves, who had headed the Manhattan Project and the development of the atomic bomb, informed him that Russia had no uranium and thus would not be able to participate in any atomic arms race, and that Byrnes was concerned over the Russian acquisition of Poland, Romania, and Hungary and he thought that the possession of the bomb by America would render the Russians manageable in Europe. When Leo Szilard returned to Chicago after the meeting, he learned that Byrnes had been appointed Secretary of State and consequently concluded that his arguments would be receiving no consideration. Consequently Szilard next considered addressing his concerns to the Secretary of War, Henry L. Stimson.

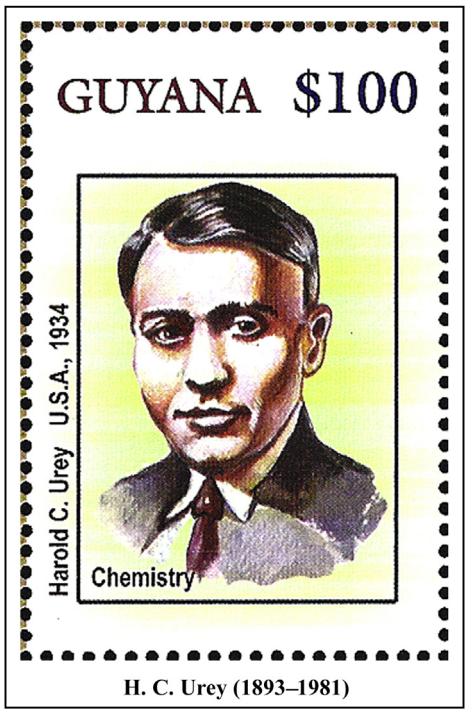

H. C. Urey (1893–1981)

On June 11, 1945 Leo Szilard coauthored The Franck Report, which was entitled "Report on Political and Social Problems" Manhattan Project, Metallurgical Laboratory, University of Chicago, addressed to Secretary Stimson, Secretary of War. The Report was prepared by a Committee consisting of Nobel Laureate James Franck (Chairman), Donald J. Hughes, J.J. Nickson, Eugene Rabinowitch, Nobel Laureate Glenn T. Seaborg, J.C. Stearns, and Leo Szilard. The eight-page report in summary urged that "the use of nuclear bombs in this war be considered as a problem of long-range national policy rather than military expediency, and that this policy be directed primarily to the achievement of an agreement permitting an effective international control of the means of nuclear warfare." As to the outcome of the Frank Report, Szilard commented "This report was addressed to Secretary Stimson, but none of those who participated in the writing of the report, including Prof. James Franck, had an opportunity to see Mr. Stimson."

On July 4, 1945, Leo Szilard drafted a Petition to the President of the United States opposing the use of the bomb, and by July 17, 1945, weeks before the bomb was dropped on Hiroshima on August 6, 1945, he got altogether 70 signatures on his petition including that of Nobel Laureate Eugene Wigner and other members of the Metallurgical Laboratory (Met Lab), the secret laboratory at the University of Chicago developed for the production of the atomic bomb. Szilard sent copies of his petition on July 4, 1945 to the laboratories at Oak Ridge and Los Alamos, where the secret work on the development of the atomic bomb was also carried out, and appealed that the scientists take a moral stand on the issue. Excerpts of his cover letter to obtain signatures on his petition are the following:

> *Enclosed is the text of a petition which will be submitted to the President of the United States. As you will see, this petition is based on purely moral considerations…On the basis of expediency, many arguments could be put forward both for and against our use of atomic bombs against Japan…However small the chance might be that our petition may influence the course of events, I personally feel that it would be a matter of importance if a large number of scientists who have worked in this field went clearly and unmistakably on record as to their opposition on moral grounds to the use of these bombs in the present phase of the war…The fact that the people of the United States are unaware of the choice which faces us increases our responsibility in this matter since those who have worked on "atomic power" represent a sample of the population and they alone are in a position to form an opinion and declare their stand.*

A photocopy of the "Petition to the President of the United States," signed by Leo Szilard, Eugene Wigner, and other scientists of the Manhattan Project (not all signatures visible), is provided in Fig. IV.21.

It is unknown whether the petition ever got to the President, although it is now available in the archives of the Harry S. Truman Presidential Library and Museum labeled SECRET and subsequently DECLASSIFIED (Fig. IV.21). Leo Szilard commented the following in an interview on August 15, 1960 with the *U.S. News and World Report*:

> *Some of those who signed insisted that the petition be transmitted to the President through official channels. To this I reluctantly agreed. I was, at this point, mainly concerned that the members of the project had an opportunity to go on record on this issue, and I didn't think that the petition would be likely to have an effect on the course of events. The petition was sent to the President through official channels, and I should not be too surprised if it were discovered one of these days that it hadn't ever reached him.*

After the war Leo Szilard abandoned physics and entered into research in the biosciences. Maurice Fox (1998) recounts his recollections of the time when Leo Szilard, after a meeting of atomic scientists in Chicago, invited Aaron Novick, a physical organic chemist, to join him on "an adventure in biology." Both scientist joined forces by first taking a phage course at Cold Spring Harbor, New York and a microbiology course at the Hopkins Marine Station of Stanford University at Pacific Grove, California. They invented the chemostat, a device for growing bacteria in continuous culture (Novick and Szilard, 1950). With the chemostat they were able to measure bacterial mutation rates (Novick and Szilard, 1951, 1952). Szilard could never rest, first with inventions and joint patents with Albert Einstein on refrigerators, and patents in nuclear physics, and later, in the field of biological sciences and tireless efforts to promote peace and nuclear arms control.

In his efforts to promote nuclear arms control and world peace, Szilard participated in the first three Pugwash Conferences on Science and World Affairs from 1957 to 1959. The objective of the Pugwash Conferences is to bring together, from around the world, influential scholars and public figures concerned with reducing the danger of armed conflict and seeking cooperative solutions to global problems. The name "Pugwash Conference" originated from the very first meeting, which took place in Pugwash, Nova Scotia in 1957. The Conferences from the very start have derived their inspiration from the *Russell–Einstein Manifesto* issued in London on July 9, 1955 by Nobel Laureates Bertrand Russell and Albert Einstein and signed by 10 other Nobel Laureates and eminent scientists. (See the following biographical sketch on Joseph Rotblat for further information on the Russell–Einstein Manifesto and the Pugwash Conferences.)

Again, by participating in the first three Pugwash Conferences, Leo Szilard was among the first who stood out among most of his colleagues in working toward a solution to the most difficult and vital challenge facing mankind, nuclear disarmament and world peace. The tireless efforts of Leo Szilard toward nuclear disarmament and world peace were summarized by Crow (2004) in his Addendum to "Szilard, A Personal Remembrance" by Werner Maas (2004) as follows:

> *After the war, he began devoting his creative imagination, his boundless energy, and his dogged persistence to social causes, especially attempts to assure that nuclear bombs would not be used. He concocted various schemes, scientific and political, to this end. He was instrumental in putting the development of nuclear energy into civilian rather than military hands at the Pugwash Conferences, in founding the* Bulletin of Atomic Scientists*, and, later, the Council for a Livable World.*

In 1959, Szilard was diagnosed with cancer of the bladder. He rejected the advice of his medical doctors, which included the conventional surgery and in situ use of a tubercular vaccine to stimulate the immune system (Allen, 2001). Rather, he designed his own radiation therapy (Crow, 2004). Szilard consulted with Jonas Salk, famous for developing the

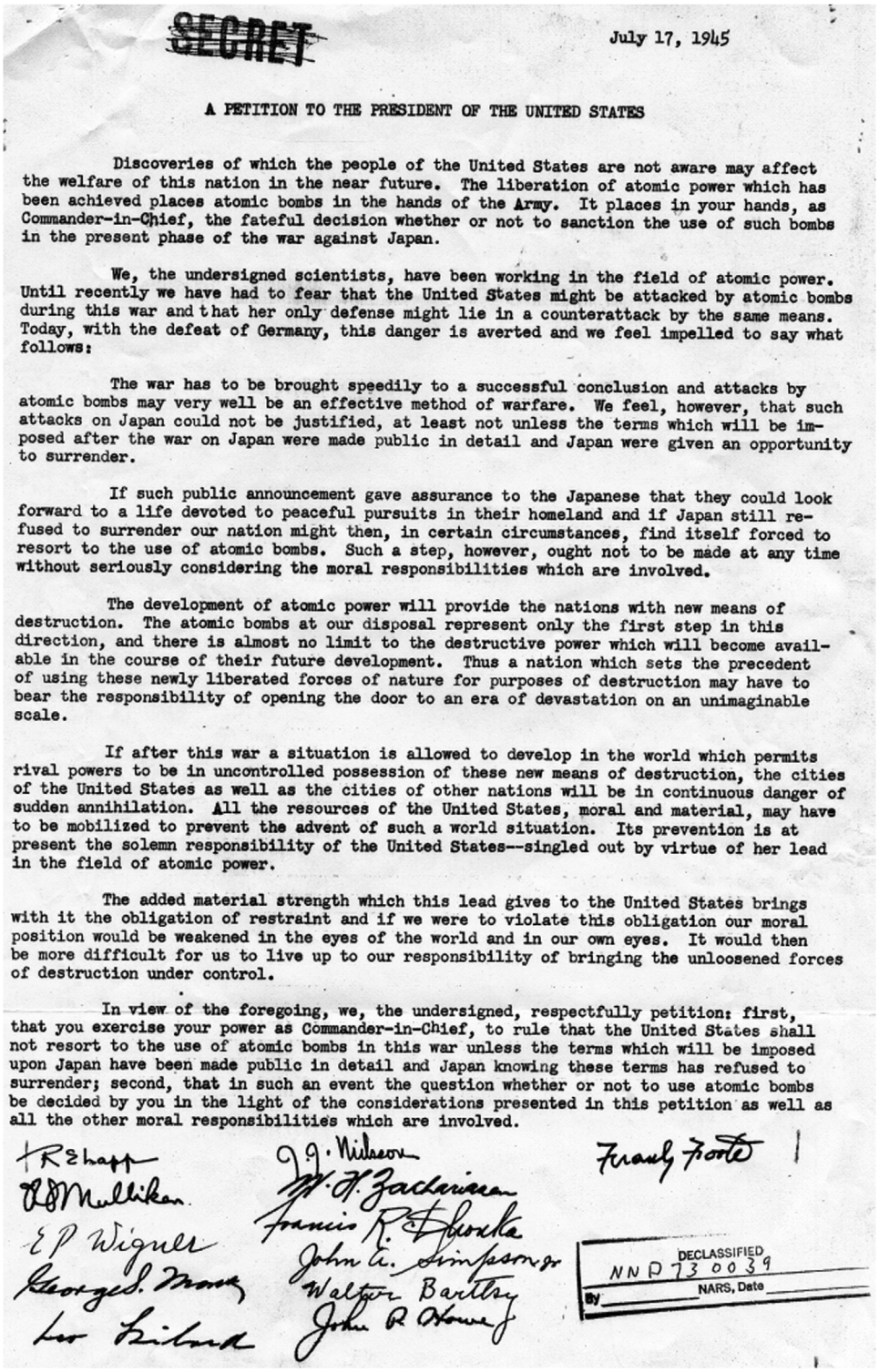

SECRET

July 17, 1945

A PETITION TO THE PRESIDENT OF THE UNITED STATES

Discoveries of which the people of the United States are not aware may affect the welfare of this nation in the near future. The liberation of atomic power which has been achieved places atomic bombs in the hands of the Army. It places in your hands, as Commander-in-Chief, the fateful decision whether or not to sanction the use of such bombs in the present phase of the war against Japan.

We, the undersigned scientists, have been working in the field of atomic power. Until recently we have had to fear that the United States might be attacked by atomic bombs during this war and that her only defense might lie in a counterattack by the same means. Today, with the defeat of Germany, this danger is averted and we feel impelled to say what follows:

The war has to be brought speedily to a successful conclusion and attacks by atomic bombs may very well be an effective method of warfare. We feel, however, that such attacks on Japan could not be justified, at least not unless the terms which will be imposed after the war on Japan were made public in detail and Japan were given an opportunity to surrender.

If such public announcement gave assurance to the Japanese that they could look forward to a life devoted to peaceful pursuits in their homeland and if Japan still refused to surrender our nation might then, in certain circumstances, find itself forced to resort to the use of atomic bombs. Such a step, however, ought not to be made at any time without seriously considering the moral responsibilities which are involved.

The development of atomic power will provide the nations with new means of destruction. The atomic bombs at our disposal represent only the first step in this direction, and there is almost no limit to the destructive power which will become available in the course of their future development. Thus a nation which sets the precedent of using these newly liberated forces of nature for purposes of destruction may have to bear the responsibility of opening the door to an era of devastation on an unimaginable scale.

If after this war a situation is allowed to develop in the world which permits rival powers to be in uncontrolled possession of these new means of destruction, the cities of the United States as well as the cities of other nations will be in continuous danger of sudden annihilation. All the resources of the United States, moral and material, may have to be mobilized to prevent the advent of such a world situation. Its prevention is at present the solemn responsibility of the United States--singled out by virtue of her lead in the field of atomic power.

The added material strength which this lead gives to the United States brings with it the obligation of restraint and if we were to violate this obligation our moral position would be weakened in the eyes of the world and in our own eyes. It would then be more difficult for us to live up to our responsibility of bringing the unloosened forces of destruction under control.

In view of the foregoing, we, the undersigned, respectfully petition: first, that you exercise your power as Commander-in-Chief, to rule that the United States shall not resort to the use of atomic bombs in this war unless the terms which will be imposed upon Japan have been made public in detail and Japan knowing these terms has refused to surrender; second, that in such an event the question whether or not to use atomic bombs be decided by you in the light of the considerations presented in this petition as well as all the other moral responsibilities which are involved.

J. R. Stark
R. S. Mulliken
E. P. Wigner
Leo Szilard
J. J. Nickson
W. H. Zachariasen
Francis R. Shonka
John A. Simpson Jr.
Walter Bartky
John R. Howe
Frank Foote

DECLASSIFIED
NND 730039
By _____ NARS, Date _____

FIGURE IV.21 Petition to the President of the United States drafted by Leo Szilard and signed by 70 members of the Manhattan Project weeks before the atomic bomb was dropped on Hiroshima, Japan. *From the Harry S. Truman Presidential Library and Museum, http://www.trumanlibrary.org/.*

polio vaccine, and he had seeds of radioactive silver implanted into his tumor. Again, Szilard was ahead of his time by designing at that time what was a nonconventional method of nuclear medicine to treat cancer. Sealed sources of Radium-226 had been used to treat external surface lesions caused by lupus since the early work of Marie and Pierre Curie (see Hall of Fame, Part I); however, the use of radioactive sources surgically implanted into tumors in body organs was yet to become recognized as an effective method to treat cancer until the 1980s, and by the year 2000, approximately 10% of the 120,000 patients treated each year for prostate cancer would be treated with radioactive seeds. The number of patients treated with radioactive seeds is predicted to increase in the future (Blasko et al., 1998; Coursey and Nath, 2000). The use of radioactive seeds for the treatment of cancer is today a highly developed method (see the chapter entitled "Radioactivity and Our Well-Being").

Leo Szilard's cancer was either cured or abated into remission until his death from a heart attack on May 30, 1964 in La Jolla, California, the very year he was appointed a Resident Fellow of the Salk Institute in La Jolla. A biography included with "The Register of Leo Szilard Papers 1898–1998" at the Mandeville Special Collections Library of the University of California, San Diego (UCSD, 2005) summarizes his life as follows:

> *Szilard lived a peripatetic life. After leaving Budapest in 1919 he had no true permanent residence. He stayed mostly in hotels, and his associations with various universities were usually tenuous. Because he had no long-term institutional affiliations, Szilard had difficulty in marshalling the material forces – such as clerical and laboratory staff – needed to follow through on many of his important ideas. Szilard was essentially a thinker, and he preferred to leave for others the tasks involved in implementing his ideas.*

For additional information on the life and works of Leo Szilard, the reader is invited to peruse a very comprehensive biography entitled "Genius in The Shadows, A Biography of Leo Szilard, the Man Behind the Bomb" by William Lanouette with Bela Szilard (brother of Leo Szilard) and with a Forward by Jonas Salk published in 2013 by Skyhorse Publishing.

JOSEPH ROTBLAT (1908–2005)

Joseph Rotblat was born in 1908 into a Jewish family in Warsaw, Poland. He shared the Nobel Peace Prize in 2005, which was awarded in two equal parts to "Joseph Rotblat and to the Pugwash Conferences on Science and World Affairs, for their efforts to diminish the part played by nuclear arms in international politics and, in the longer run, to eliminate such arms."

During his boyhood, Joseph Rotblat enjoyed prosperity, as his family bred horses and owned a horse-drawn carriage business. At the outbreak of the First World War, horses were seized for war, his family business was lost, and they entered into poverty. Joseph became an electrician as a source of income; but he was interested in physics, which he studied in the evenings. He entered into the Free University of Poland and earned an MA degree in 1932 and later a doctor of physics degree at the University of Warsaw in 1938. While earning his doctoral degree in physics, Joseph Rotblat carried out research as a Fellow in the Radiation Laboratory of the Polish Scientific Society, which was closely linked with the Free University of Poland, and was appointed Assistant Director of the Atomic Physics Institute of the Free University of Poland in 1937.

Joseph Rotblat (1908–2005)

As described in a biography by Underwood (2008), Joseph Rotblat held his professor and counselor Ludwick Wertenstein in high esteem. Ludwig Werteinstein had studied with Nobel Laureates Marie Curie in Paris and James Chadwick in Cambridge, who won the Nobel Prize in physics for the discovery of the neutron in 1935 (see the biosketch on James Chadwick in this Hall of Fame, Part IV). Rotblat admired Werteinstein's humanitarian approach to science, whereby a scientist had the responsibility to carry out scientific research for the betterment of humanity. Rotblat carried on this philosophy throughout his life and eventually would propose, later in life, that all scientist take a "Hippocratic Oath" to do no harm, similar to that taken by all medical doctors when they enter into their profession. Joseph Rotblat would eventually reject the neutral approach often taken by scientists who felt not responsible for the discoveries that they make regardless of the great harm that could arise from such discoveries. Research into the development of the atomic bomb, and chemical and biological means of mass destruction, serve as examples.

While studying at the Free University of Poland, Rotblat met a Polish literary student, Tola Gryn, who he married in 1937. In 1939, when Joseph Rotblat was in Warsaw, nuclear fission was discovered in Germany by Otto Hahn and Fritz Strassmann (1939a,b); and this was interpreted by Lise Meitner and Otto Frish (1939) as the splitting of a nucleus of U-236 following the capture of a neutron by U-235 with the release of a large amount of energy ($\sim$200 MeV) per fission. In May of 1939, Rotblat published a letter to the Editor of the journal *Nature* (Rotblat, 1939) that there would be more neutrons produced in a single fission than the one neutron captured by a U-235 nucleus. Very shortly thereafter, in a matter of weeks in America, Herbert Anderson et al. (1939b) determined that there were about two neutrons produced per neutron consumed in the fission reaction. Again, in a matter of weeks Walter Zinn and Leo Szilard published in the July–December issue of the journal *Physical Review* (Zinn and Szilard, 1939) a more precise average number of 2.3 neutrons produced for each neutron consumed or captured in the fission reaction. After Zinn and Szilard's paper in late 1939, the "cat was out of the bag" with the publication of the number of neutrons produced being significantly greater than the number captured by U-235. With this information in the international journals, physicists in many countries, including Germany and Japan (see the biosketch on Yoshio Nishina in Hall of Fame, Part II) could surmise the possibility of a chain reaction and even an explosion if a critical mass of U-235 could be compiled. Underwood (2008) reports that in early 1939 in Poland, the possibility of a bomb from U-235 fission had occurred to Joseph Rotblat; and that he calculated the chain reactions leading to the explosion could occur in less than a microsecond. (See the previous calculations of Eqs. [IV.22]–[IV.24] in the biosketch on Leo Szilard in this chapter.)

In 1939, Joseph Rotblat accepted a fellowship to work under Nobel Laureate James Chadwick at the University of Liverpool in the United Kingdom. James Chadwick had discovered the neutron in 1932 and determined its mass, for which he was awarded the 1935 Nobel Prize in Physics. This was a great opportunity for Joseph Rotblat, particularly because Chadwick occupied the Lyon Jones Chair of Physics at the University of Liverpool, where he wanted to build a cyclotron; and Joseph Rotblat could assist Chadwick and carry out research with the cyclotron. It was Rotblat's hope to later return to Warsaw to construct a cyclotron, which would be useful for the production of radioisotopes useful in medicine and the study of nuclear physics. The stipend provided by the fellowship was insufficient to support both Rotblat and his wife, so he left his wife behind in Warsaw until his stipend was increased later that year. Upon his return to Warsaw to take Tola to join him in Liverpool, she became too ill from appendicitis to travel. Again Joseph Rotblat had to return to Liverpool without her, with plans that his wife would soon follow him to Liverpool. The next day, Hitler invaded Poland; and Rotblat was never to see his wife again (Holdren, 2005). It is reported that he tried desperately to get his wife out of Poland into a neighboring country, but the borders were closed. It is thought that she perished in a concentration camp. This affected Joseph Rotblat; and he never remarried for lack of evidence of her eventual fate.

In 1943, Joseph Rotblat accompanied James Chadwick to join the Manhattan Project at the Los Alamos National Laboratory. Biographers of Joseph Rotblat clearly note that the development of an atomic bomb was against his moral judgment. However, Rotblat feared that the Germans would develop the atomic bomb first; and the Allies must be able to threaten Germany with retaliation against the use of such a weapon (Milne and Hinde, 2005). Only American and British citizens could work on the secret Manhattan Project, but Rotblat refused to give up his Polish nationality with the hope of someday returning to work in his country. General Leslie R. Grooves, who was in charge of the Manhattan Project, waived the restriction, which allowed Rotblat to work with Chadwick at the secret research facilities in New Mexico. By 1944 it became known that the German research on the bomb development had made little progress, and that the war with Germany would soon be won. Joseph Rotblat then resigned from the Manhattan Project on grounds of conscience and returned to Liverpool (Milne and Hinde, 2005). He was the only participant of the Manhattan Project to have resigned on moral grounds (Butcher, 2005) (See Fig. IV.22, which is a photo of Joseph Rotblat taken around the time of the Manhattan Project.).

After the bombings of Hiroshima and Nagasaki in 1945, which horrified Rotblat, he dedicated the remainder of his life to educating the public about atomic energy and championed nuclear disarmament and campaigned against weapons of

FIGURE IV.22 Joseph Rotblat at a young age, which was about the time when he resigned from the Manhattan Project. *Courtesy of the Pugwash Conferences on Science and World Affairs, http://pugwash.org/.*

mass destruction and potential annihilation. After the end of the Second World War, Rotblat became one of the founders of the Atomic Scientists Association (ASA), which was the British counterpart of the Federation of American Scientists (Holdren, 2005). The ASA was a nonpartisan group of prominent scientists, who educated the British public on the applications of nuclear energy and the dangers of nuclear weapons.

From 1946 to 1950 Joseph Rotblat served as chairman of the Cyclotron Panel of the UK Nuclear Physics Committee, which planned and supervised the building of cyclotrons for Harwell and Liverpool. Cyclotrons were and remain a very useful instrument for the production of radioisotopes that can be applied to medicine and practical biological research. Joseph Rotblat used his knowledge of nuclear physics for peaceful applications in medicine. Underwood (2008) provides an excellent summary of Rotblat's work in this field, which included the pioneering work on the use of the radioisotope ^{131}I for the treatment of thyroid disorders (Ansell and Rotblat, 1948), general applications of radioisotopes in medicine (Rotblat, 1949), the applications of a linear accelerator for the treatment of cancer (Rotblat, 1955a), and the effect of radiation dose on the life span and death of mice (Lindop and Rotblat, 1961, 1965). In 1949, Rotblat was appointed professor of physics to St. Barthomew's Hospital Medical College, which is a post he held until 1976 (Underwood, 2008).

On November 1, 1952, the United States tested its first thermonuclear bomb (ie, hydrogen bomb), which was a combined fission−fusion device, many times more powerful than the bomb dropped on Hiroshima on August 6, 1945. The Soviet Union carried out its first test of the hydrogen bomb only months later on August 12, 1953. The race was on to produce more and more powerful and horrendous bombs. Butcher (2005) relates that Joseph Rotblat knew about the secret American hydrogen bomb project from the time he was at Los Alamos, where he befriended the Polish scientist, Stanislaw Ulam, who worked with Edward Teller at Los Alamos. Edward Teller is often referred to as the father of the H-bomb (see the following biographical sketch on Edward Teller, who was at the opposite end of the spectrum with respect to weapons of mass destruction). As Butcher (2005) noted, as soon as Rotblat had learned about the bombing of Hiroshima, he became gravely concerned about the possibility of a more terrible hydrogen bomb and said:

> *I knew a little bit more than other people about what was going on. So I knew that it would begin an arms race and that the hydrogen bomb would come in. And then…for the first time I became worried about the whole future of mankind. Because…once you are going to develop these huge weapons, where are you going to stop? And this was my reaction on the 6th of August [1945].*

On March 1, 1954, the United States tested its first hydrogen bomb that contained dry fuel (see the following biosketch on Edward Teller) under the code name Castle Bravo at Bikini Atoll, Marshall Islands. It was the most powerful weapon yet, with a yield of 15 megatons of TNT, which was about 1000 times the strength of the bomb dropped on Japan in Hiroshima. The bomb became very notorious, because it released the highest level of radioactive contamination of any bomb tested. The radioactive fallout from what was supposed to be a secret test created an international incident and reaction to nuclear testing around the world. Butcher (2005) and Underwood (2008) describes Rotblat's reaction to this test after it became known that radioactive fallout from the test drifted in the atmosphere and contaminated the Japanese fishing

vessel *Daigo Fukuryū Maru* or Lucky Dragon and its crew of 23, which was 85 miles east of the Bikini Atoll. The radioactive fallout killed one fisherman on board and severely sickened others on board the vessel with radiation poisoning. Rotblat's immediate reaction was that the device tested had to be a fission−fusion or hydrogen bomb. While attending a conference on radiobiology in Belgium, Rotblat met Prof. Yasushi Nishiwaki, a Japanese scientist, who provided data on the radioactivity from the *Lucky Dragon*. Rotblat was convinced from the radioactive fission products that the bomb was a fission−fusion−fission device that released 1000 times more radioactivity than the fission bomb dropped on Hiroshima. Rotblat published his findings in the March 1955 issue of the *ASA Newsletter* and in the May issue of the *Bulletin of the Atomic Scientists* in the United States (Rotblat, 1955b). In the article Butcher (2005) cites the following statement of Joseph Rotblat:

> *It seems more than likely that should there be a full-scale atomic war—in which bigger and better [more powerful] hydrogen bombs now manufactured were used—it would have disastrous results for the whole world, partisans and neutrals alike, from the genetic point of view, quite apart from the immediate effects. But even without a war there is a probable risk of running into genetic trouble, if the tests of these weapons continue at the present rate.*

Rotblat's revelations created a political uproar, and internationally the public and scientists alike not involved with these secret nuclear tests wanted to know more on how these atmospheric tests would affect their health as well as the outcome of war with such weapons of mass destruction.

Joseph Rotblat had become an authority on the biological effects of radiation in both the scientific and public arenas from his research work in medical physics after abandoning the Manhattan project and from his public revelations on the hydrogen bomb, also known as the "Super" bomb, after the radioactive fallout that struck the Lucky Dragon. He appeared on a British Broadcasting Corporation (BBC) television program "Panorama" explaining the new hydrogen bomb to the public. It was then, on this television program, that Rotblat met Nobel Laureate Bertrand Russell, who had become very agitated over the increasing development and testing of nuclear weapons and the dangers of a thermonuclear war, and the worldwide catastrophic consequences of such a war. Bertrand Russell was a famous British philosopher, historian, mathematician, logician, social critic, and political activist, who was awarded the Nobel Prize in Literature in 1950 in the words of the Nobel Committee "in recognition of his varied and significant writings in which he champions humanitarian ideals and freedom of thought." Russell was very impressed by Joseph Rotblat's knowledge of nuclear physics and his stance against the threat of nuclear weapons; and he would afterward visit and call on Rotblat for information.

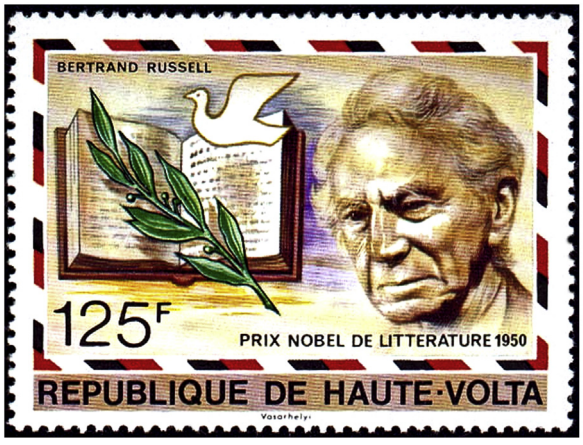

Bertrand Russell (1872–1970)

Bertrand Russell wanted to unite a number of renowned scientists from around the world to issue a joint statement alerting the world to the dangers of nuclear weapons. In a comprehensive historical account, Butcher (2005) noted that Russell felt the urge to "find some way of making the world understand the dangers into which it was running blindly, head on," which are words from Russell's autobiography (Russell, 1956). Because Albert Einstein was the most eminent scientist at the time, Bertrand Russell corresponded with Einstein on the wording of a declaration to the world of the dangers of nuclear weapons and the need to convene an international conference to discuss this danger and how to avert the use of nuclear weapons. Einstein provided his agreement to the basic text of the declaration in a final letter to Bertrand Russell dated April 11, 1955, only days before his death on April 18th (Butcher, 2005). It was the last message that Albert Einstein would relate to the public and together with Bertrand Russell in what would become known as the Russell−Einstein

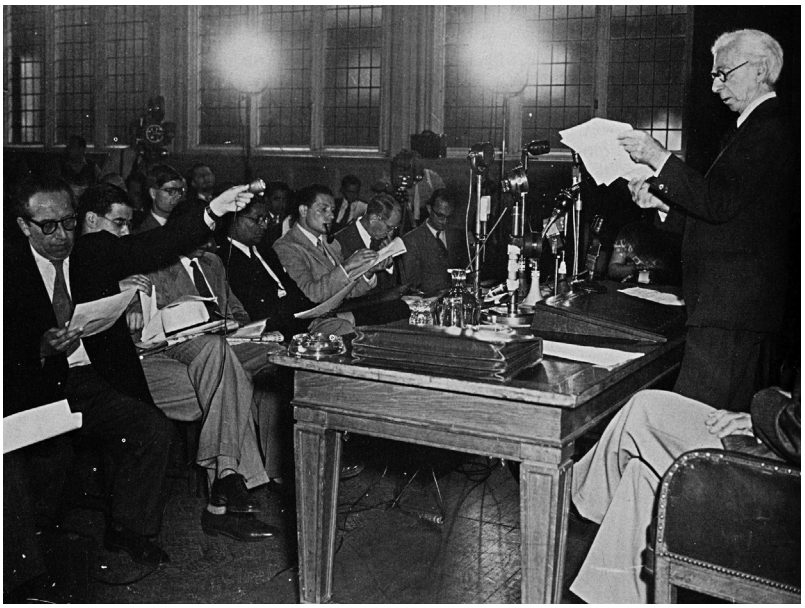

FIGURE IV.23 Bertrand Russell reading the proclamation of the Russell–Einstein Manifesto at a press conference in Caxton Hall, London on July 9, 1955. *From Butcher, S.I., 2005. The origins of the Russell-Einstein Manifesto. In: Jeffrey Boutwell (Ed.), Pugwash History Series, Number One, Pugwash Conferences on Science and World Affairs, pp. 1–35, with permission and the courtesy of the Pugwash Conferences on Science and World Affairs.*

Manifesto, which would plead with governments and the public not to let our civilization be destroyed by weapons of mass destruction. Bertrand Russell then obtained the signatures or agreements of other Nobel Laureates and eminent scientists, including the signature of Joseph Rotblat, to this manifesto.

To call the world's attention to the manifesto in a time of Government secrecy, Bertrand Russell needed to convene an international press conference. He invited Joseph Rotblat to chair the press conference, whereby Rotblat could answer authoritatively any technical questions that the press would have about thermonuclear weapons. Before a large audience of representatives of the press, radio, and television from around the world, Bertrand Russell proclaimed the manifesto with Joseph Rotblat chairing the press conference. A photo of the proclamation to the press is provided in Fig. IV.23.

The Manifesto reads as follows:

THE RUSSELL–EINSTEIN MANIFESTO, LONDON, JULY 9, 1955

In the tragic situation which confronts humanity, we feel that scientists should assemble in conference to appraise the perils that have arisen as a result of the development of weapons of mass destruction, and to discuss a resolution in the spirit of the appended draft.

We are speaking on this occasion, not as members of this or that nation, continent, or creed, but as human beings, members of the species Man, whose continued existence is in doubt. The world is full of conflicts; and, overshadowing all minor conflicts, the titanic struggle between Communism and anti-Communism.

Almost everybody who is politically conscious has strong feelings about one or more of these issues; but we want you, if you can, to set aside such feelings and consider yourselves only as members of a biological species which has had a remarkable history, and whose disappearance none of us can desire.

We shall try to say no single word which should appeal to one group rather than to another. All, equally are in peril, and, if the peril is understood, there is hope that they may collectively avert it.

We have to learn to think in a new way. We have to learn to ask ourselves, not what steps can be taken to give military victory to whatever group we prefer, for there no longer are such steps; the question we have to ask ourselves is: what steps can be taken to prevent a military contest of which the issue must be disastrous to all parties?

The general public, and even many men in positions of authority, have not realized what would be involved in a war with nuclear bombs. The general public still thinks in terms of the obliteration of cities. It is understood that the new bombs are more powerful than the old, and that, while one A-bomb could obliterate Hiroshima, one H-bomb could obliterate the largest cities, such as London, New York, and Moscow.

No doubt in an H-bomb war great cities could be obliterated. But this is one of the minor disasters that would have to be faced. If everybody in London, New York, and Moscow were exterminated, the world might, in the course of a few centuries, recover from the blow. But we now know, especially since the bikini test, that nuclear bombs can gradually spread destruction over a very much wider area than had been supposed.

It is stated on very good authority that a bomb can now be manufactured which will be 2,500 times as powerful as that which destroyed Hiroshima. Such a bomb, if exploded near the ground or under water, sends radioactive particles into the upper air. They sink gradually and reach the surface of the earth in the form of a deadly dust or rain. It was this dust which infected the Japanese fishermen and their catch of fish. No one knows how widely such lethal radioactive particles might be diffused, but the best authorities are unanimous in saying that a war with H-bombs might possibly put an end to the human race. It is feared that if many H-bombs are used there will be universal death, sudden only for a minority but for the majority a slow torture of disease and disintegration.

Many warnings have been uttered by eminent men of science and by authorities in military strategy. None of them will say that the worst results are certain. What they do say is that these results are possible, and no one can be sure that they will not be realized. We have not yet found that the views of experts on this question depend in any degree upon their politics or prejudices. They depend only, so far as our researches have revealed, upon the extent of the particular expert's knowledge. We have found that the men who know most are the most gloomy.

Here, then, is the problem which we present to you, stark and dreadful and inescapable: Shall we put an end to the human race; or shall mankind renounce war? People will not face this alternative because it is so difficult to abolish war.

The abolition of war will demand distasteful limitations of national sovereignty. But what perhaps impedes understanding of the situation more than anything else is that the term "mankind" feels vague and abstract. People scarcely realize in imagination that the danger is to themselves and their children and their grandchildren, and not only to a dimly apprehended humanity. They can scarcely bring themselves to grasp that they, individually and those whom they love are in imminent danger of perishing agonizingly. And so they hope that perhaps war may be allowed to continue provided modern weapons are prohibited.

This hope is illusory. Whatever arguments not to use H-bombs had been reached in time of peace, they would no longer be considered binding in time of war, and both sides would set to work to manufacture H-bombs as soon as war broke out, for, if one side manufactured the bombs and the other did not, the side that manufactured them would inevitably be victorious.

Although an agreement to renounce nuclear weapons as part of a general reduction of armaments would not afford an ultimate solution, it would serve certain important purposes. First, any agreement between East and West is to the good in so far as it tends to diminish tension. Second, the abolition of thermonuclear weapons, if each side believed that the other had carried it out sincerely, would lessen the fear of a sudden attack in the style of Pearl Harbor, which at present keeps both sides in a state of nervous apprehension. We should, therefore, welcome such an agreement though only as a first step.

Most of us are not neutral in feeling, but, as human beings, we have to remember that, if the issues between East and West are to be decided in any manner that can give any possible satisfaction to anybody, whether Communist or anti-Communist, whether Asian or European or American, whether White or Black, than these issues must not be decided by war. We should wish this to be understood, both in the East and in the West.

There lies before us, if we choose, continual progress in happiness, knowledge and wisdom. Shall we instead, choose death, because we cannot forget our quarrels? We appeal as human beings to human beings: Remember your humanity, and forget the rest. If you can do so, the way lies open to a new Paradise; if we cannot, there lies before you the risk of universal death.

Resolution

WE invite this Congress, and through it the scientists of the world and the general public, to subscribe to the following resolution:

> *In view of the fact that in any future world war nuclear weapons will certainly be employed, and that such weapons threaten the continued existence of mankind, we urge the governments of the world to realize, and to acknowledge publicly, that their purpose cannot be furthered by a world war, and we urge them, consequently, to find peaceful means for the settlement of all matters of dispute between them.*

Signed

Max Born, Percy W. Bridgman, Albert Einstein, Leopold Infeld, Frederic Joliot-Curie, Herman J. Muller, Linus Pauling, Cecil F. Powell, Joseph Rotblat, Bertrand Russell, Hideki Yukawa

Albert Einstein's signature and that of Bertrand Russell were key to its impact on the public and world governments. This was clearly emphasized by Butcher (2005), who noted

> *…Russell and Einstein were key figures in the success of the Manifesto. Together, they represented such intellectual and moral authority that it is doubtful that the Manifesto would have had nearly the same impact without their involvement…They both had long experience in the efforts to raise awareness about nuclear weapons. Albert Einstein's role in this respect was particularly poignant, given the fact that a letter from him to Franklin Delano Roosevelt (and drafted by Leo Szilard, another early Pugwash participant) was pivotal in the establishment of the U.S. Manhattan Project, the top-secret nuclear weapons program (Einstein, however, did not work on the Manhattan Project).*

At the 45th Pugwash Conference on Science and World Affairs held in Hiroshima, Japan on July 23 to 29, 1995, Joseph Rotblat commented on Albert Einstein's final letter of agreement to the text of the Manifesto days before Einstein's passing as follows:

> *…this gives the Manifesto extra poignancy: the last message from the man who was the symbol of the great heights the human intellect can reach, imploring us not to let all this be destroyed by human folly.*

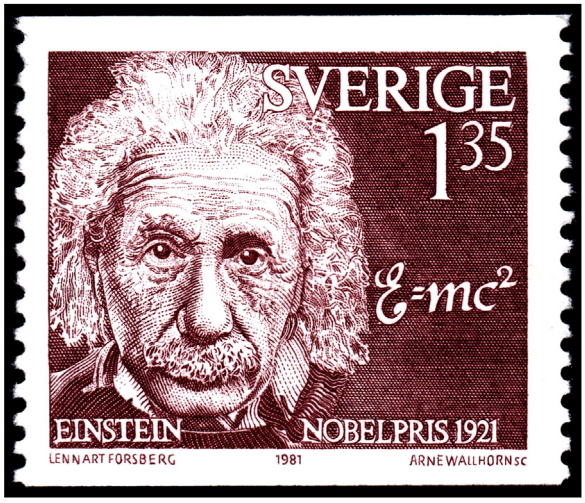

Albert Einstein (1879–1955)

The first paragraph of the Russell–Einstein Manifesto called for "scientists [to] assemble in conference to appraise the perils that have arisen as a result of the development of weapons of mass destruction, and to discuss a resolution." The Manifesto was the precursor to a first international conference in 1957 on how to avoid thermonuclear destruction, which was held in Pugwash on the northern coast of Nova Scotia, thanks to the generous sponsorship of philanthropist Cyrus Eaton (1883–1979), who wanted the scientists to use the peaceful settings of his birthplace for this important meeting. The first meeting was small, with the participation of 22 eminent scientists (seven from the United States, three each from the Soviet Union and Japan, two each from the United Kingdom and Canada, and one each from Australia, Austria, China, France, and Poland). Since the first meeting at Pugwash, in 1957, the Pugwash Conference on Science and World Affairs has evolved to include a continuing series of large international conferences held at many locations throughout the world with attendance numbering in the hundreds. The 60th Pugwash Conference on Science and World Affairs, entitled "Dialogue, Disarmament, and Regional and Global Security," took place in Istanbul, Turkey on November 1 to 5, 2013. It brought together approximately 200 leading current and former policy-makers, scientists, and other international opinion shapers from around the world to explore creative solutions to some of the world's most challenging problems (http://pugwash.org/). Over 300 Pugwash Conferences, Symposia, and Workshops have been held all over the globe. Joseph Rotblat was a driving force in

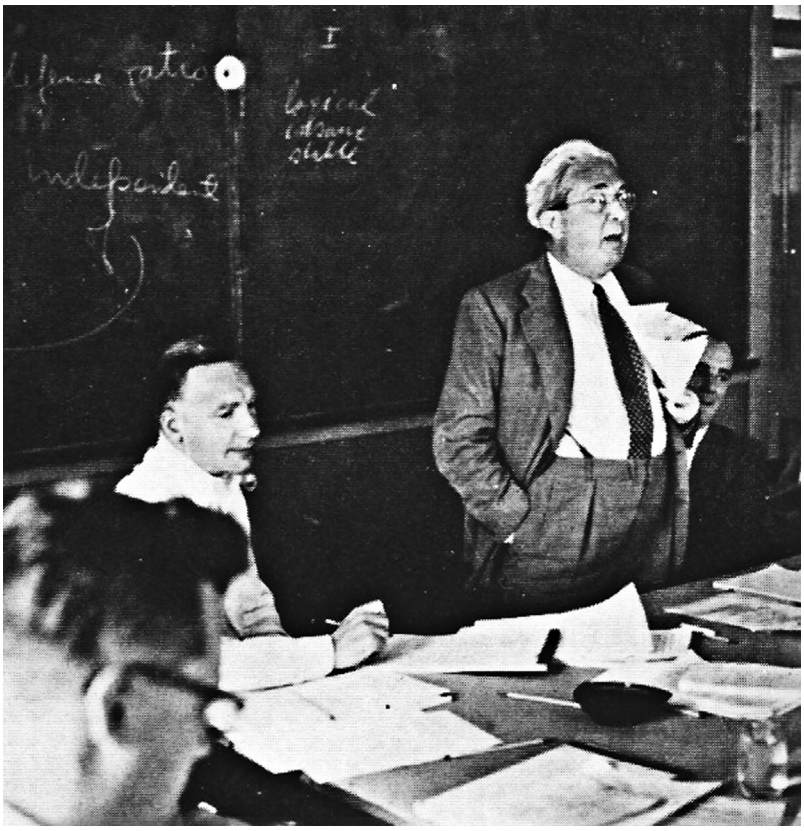

FIGURE IV.24 Joseph Rotblat (at left seated with back to blackboard) and Leo Szilard (standing) at the First Pugwash Conference on Science and World Affairs at Pugwash, Nova Scotia in 1957. *Courtesy of the Pugwash Conferences on Science and World Affairs, http://pugwash.org/.*

the Pugwash Organization since its inception, becoming Secretary General from 1957 to 1973, Chairman of the British Pugwash Group from 1978 to 1988, President from 1988 to 1997, and Emeritus President from 1997 to his death.

Leo Szilard, the nuclear physicist who drafted the letter signed by Einstein to Roosevelt that initiated the Manhattan Project, but later tried to prevent the use of the atomic bomb against Japan, had the foresight to know the important role that the Pugwash Conferences would play in saving the world from nuclear war and annihilation of the human race. A photograph of Joseph Rotblat and Leo Szilard at the first Pugwash Conference is provided in Fig. IV.24.

The participants of the Pugwash Conferences include distinguished scientists and eminent scholars, who are not representatives of governments. This provides them with the liberty of flexible and frank discussions not normally possible in official meetings between governments. Because of the eminent stature of many of the participants as advisors to governments, some of whom become holders of government positions, the important insights reached by the Pugwash Conferences rapidly penetrate into the appropriate levels of the policy-making branches of governments. As noted by the Nobel Foundation, the Pugwash movement during the cold war served as a channel of communication between the communist Eastern block and the Western democracies whereby participants played important roles behind the scenes in the realization of the nuclear test ban and nonproliferation treaties (http://www.nobelprize.org). Also, Milne and Hinde (2005) underscore that Pugwash has been one of the foremost advocates of détente and disarmament in the nuclear age. In addition, Pugwash provided the first links between Henry Kissinger and peace emissaries during the Vietnam war, and served as an informal channel of communication for officials and public figures in Arab-Israeli, Korean, and Kasmiri conflicts (Milne and Hinde, 2005).

As if to underscore the important efforts that the Pugwash Conferences have made and the vital need for the Conferences to continue, the Nobel Committee awarded the Nobel Peace Prize for 1995 in two equal parts to **Joseph Rotblat** (1908−2005) and to the **Pugwash Conferences on Science and World Affairs**. The rationale for the award was highlighted by the Nobel Committee in the following statement:

> *The Pugwash Conferences are based on the recognition of the responsibility of scientists for their inventions. They have underlined the catastrophic consequences of the use of the new weapons. They have brought together scientists and decision-makers to collaborate across political divides on constructive proposals for reducing the nuclear threat. The Pugwash*

Conferences are founded in the desire to see all nuclear arms destroyed and, ultimately, in a vision of other solutions to international disputes than war. The Pugwash Conference in Hiroshima in July this year declared that we have the opportunity today of approaching these goals. It is the Committee's hope that the award of the Nobel Peace Prize for 1995 to Rotblat and to Pugwash will encourage world leaders to intensify their efforts to rid the world of nuclear weapons.

In the closing of this brief biographical sketch, it is important to quote a small excerpt from Joseph Rotblat's Nobel address, which is the following:

I have to bring to your notice a terrifying reality: with the development of nuclear weapons man has acquired, for the first time in history, the technical means to destroy the whole of civilization in a single act. Indeed the whole human species is endangered, by nuclear weapons or by other means of wholesale destruction which further advances in science are likely to produce.

I have argued that we must eliminate nuclear weapons. While this would remove the immediate threat, it will not provide permanent security. Nuclear weapons cannot be disinvented. The knowledge of how to make them cannot be erased. Even in a nuclear-weapon-free world, should any of the great powers become involved in a military confrontation, they would be tempted to rebuild their nuclear arsenals. That would still be a better situation than the one we have now, because the rebuilding would take a considerable time, and in that time the dispute might be settled. A nuclear-weapon-free world would be safer than the present one. But the danger of the ultimate catastrophe would still be there.

The only way to prevent it is to abolish war altogether. War must cease to be an admissible social institution. We must learn to resolve our disputes by means other than military confrontation….

What we are advocating in Pugwash, a war-free world, will be seen by many as a Utopian dream. It is not Utopian. There already exist in the world large regions, for example, the European Union, within which war is inconceivable. What is needed is to extend these to cover the world's major powers.

http://www.nobelprize.org.

A little more than 3 months prior to his death at the age of 96, Joseph Rotblat wrote an editorial in the May 17, 2005 issue of *The New York Times* entitled "The 50-Year Shadow." An excerpt of his editorial is the following:

Fifty years ago, I joined Albert Einstein, Bertrand Russell and eight others in signing a manifesto warning of the dire consequences of nuclear war. This statement, the Russell-Einstein Manifesto, was Einstein's final public act. He died shortly after signing it. Now in my 97th year, I am the only remaining signatory. Because of this, I feel it is my duty to carry Einstein's message forward, into this 60th year since the destruction of Hiroshima and Nagasaki, which evoked almost universal opposition to any further use of nuclear weapons…Now two generations later, as the representatives of nearly 190 nations meet in New York to discuss how to advance the Nuclear Nonproliferation Treaty, we face the same perils and new ones as well. Today we confront the possibilities of nuclear terrorism and the development of yet more nuclear warheads…The two former superpowers still hold enormous nuclear arsenals. Other nations are increasingly likely to acquire nuclear arsenals on the excuse that they are needed for their security. The result could be a new arms race. Fifty years ago we wrote We have to learn to think in a new way. We have to learn to ask ourselves, not what steps can be taken to give military victory to whatever group we prefer, for there are no longer such steps; the question we have to ask ourselves is: what steps can be taken to prevent a military contest of which the issue must be disastrous to all parties?

That question is as relevant today as it was in 1955. So is the manifesto's admonition. "Remember your humanity, and forget the rest."

Joseph Rotblat received the Bertrand Russell Society Award in 1983 and the Albert Einstein Peace Prize in 1992. In the United Kingdom, Rotblat was appointed a Commander of the British Empire in 1965, and he was knighted by Queen Elizabeth in 1998. He died in London at the age of 96 on August 31, 2005.

For additional information the reader may want to peruse biographies by Andrew Brown (2012), Martin Underwood (2009), and Braun et al. (2007), and books on the quest for peace and the Pugwash Conferences by Rotblat (1962), Butcher (2005), and Rotblat and Ikeda (2006).

EDWARD TELLER (1908–2003)

Edward Teller was born in Budapest, Hungary on January 15, 1908 in an affluent and educated Jewish family. He was given the name of Ede Teller, which was anglicized to Edward Teller. The title of "father of the hydrogen bomb" was most often attributed to him, which he did not particularly like; he preferred to be known for his contributions to science and

education. To those who referred to him as the "father of the H-bomb," he would reply that the thermonuclear bomb was the work of many and that he was the father of two children.

At the time of his birth, Hungary was part of the Austro-Hungarian Empire; and the German language and culture played an important part of his life. His father was fluent in Hungarian and spoke German poorly; whereas, his mother spoke fluent German and poor Hungarian. World War I broke out in 1914 when Edward Teller was 6 years of age; and by the time he was 10 years of age, the end of the war brought independence to Hungary, which became subjected to turmoil under short-lived communist and fascist governments. Teller was fortunate to leave Hungary at the young age of 18 in 1926 to study in Germany; and he eventually escaped fascism in Germany to end up in America. Many of his friends, who did not escape, suffered tragic fates. This instilled in Edward Teller a deep abhorrence to both communism and fascism. These are the reasons why, when finally in America, Teller "saw it as his inescapable duty to keep America armed with the most effective weapons, with bombs for deterring attack, and with missiles for active defense" (Dyson, 2007).

Edward Teller (1908–2003)
On the left is illustrated the fusion of a deuterium nucleus with a tritium nucleus moving with arrows downward toward the center (white explosion) with the emissions (arrows outward) of a neutron and an alpha particle

As a young student in Budapest, Edward Teller excelled in mathematics with the highest grades. His father was worried that he could not make a good living in mathematics and pushed his son to study chemistry. To satisfy his father, he left Budapest to study chemical engineering in Karlsruhe, where he became very interested in physics, particularly the new quantum mechanics, which involved a lot of mathematics. He thus transferred to the University of Munich to study physics. While a student in Munich and traveling in a trolley car on his way to meet with friends, he missed his stop and jumped from the car. He slipped and half of his foot was severed. Dyson (2007) notes in his memoirs that Teller's mother was deeply saddened by the accident; however, Teller considered the accident only a nuisance, which did not affect what is important in life; and he thought that what doesn't kill you, only makes you stronger. The doctor had repaired what was left of his foot and with a prosthesis. Teller could go through life walking on the heel of his foot. The accident gave Edward Teller an excuse to transfer to the University of Leipzig to study quantum physics under Werner Heisenberg. At this time Teller was only 19 years of age; and Werner Heisenberg had published his famous uncertainty principle the year before in 1927 at the age of 26. Under Werner Heisenberg, Teller completed his PhD dissertation on the quantum states of the hydrogen molecule (Teller, 1930), which was followed a year later with work on diamagnetism in solids (Teller, 1931). With Gerhard Herzberg, who would eventually be awarded a Nobel Prize in 1977, Teller published a paper on the application of quantum mechanics to an explanation of the spectra of polyatomic molecules (Herzberg and Teller, 1933). In Germany he cultivated friendships and collaborated with other great physicists including Lev Landau, George Placzek, and James Franck.

Hitler came to power in Germany in 1933, which was when Teller became aware that there was no future for him in Germany. With the aid of other physicists, Teller was able to leave Germany to take up a position at Copenhagen, Denmark at the Institute of Theoretical Physics, which was headed by Niels Bohr. There he befriended George Gamow, a Russian physicist. After a year in Copenhagen, Gamow went to George Washington University in Washington, D.C. and Teller

married his childhood friend from Budapest, Augusta Harkanya nicknamed "Mici," with whom he shared over 60 years of matrimony. Teller and Mici moved together to London. After a short stint of less than a year at the University of London, Teller accepted an invitation from George Gamow to join him at George Washington University. He entered America in 1936; and became a naturalized citizen of the United States in 1941.

While at George Washington University, Edward Teller enjoyed the friendship and collaboration of theoretical nuclear physicists. With George Gamow, they established the Gamow–Teller Theory of weak interactions (Gamow and Teller, 1936, 1937); and with Herman Jahn a theory of polyatomic molecules with electrons in degenerate states (1937). These were happy days of freedom of research in theoretical physics for Edward Teller; but soon came the announcement of the discovery of nuclear fission in Germany by Otto Hahn and Fritz Strassmann in 1939. The work of Walter Zinn and Leo Szilard in the determination of 2.3 neutrons emitted per fission the same year confirmed the possibility of a nuclear chain reaction and a bomb that could be constructed from such a chain reaction. Thus, in June of 1939, Edward Teller moved from Washington to Columbia University to collaborate with Enrico Fermi and Leo Szilard in the construction of the first nuclear reactor (Dyson, 2007). With the demonstration of the first self-sustained nuclear reaction by Enrico Fermi and collaborators with the nuclear reactor at the University of Chicago on December 2, 1942, it was certain that an atomic bomb could be constructed. As noted in the National Academy of Sciences Biographical Memoirs (Dyson, 2007), Edward Teller worked on nuclear energy from 1939 and the construction of the first nuclear weapon from 1939 to 1945; 2 years at Columbia University helping Fermi design the first nuclear reactor, 2 years at the Metallurgical Laboratory in Chicago (part of the Manhattan Project) helping to design the plutonium production reactors at Hanford, and 2 years at the Los Alamos National Laboratory working on the design of nuclear bombs.

At the Los Alamos National Laboratory, Edward Teller wanted to pursue the design of a hydrogen bomb, which would be based on harnessing the energy of nuclear fusion of the light elements hydrogen and tritium into a more powerful bomb, than that based on fission. This type of bomb was referred to as the "Super." Teller had made some initial designs of the "Super" with Stanislaw Ulam, who was a Polish-American mathematician assigned by Hans Bethe, Director of the Theoretical Physics Division at Los Alamos, to work with Teller. The director of the bomb effort at Los Alamos, J. Robert Oppenheimer, rejected Teller and Ulam's more complicated approach to the development of the hydrogen bomb and insisted that the team at Los Alamos concentrate their efforts on a less complex bomb based on nuclear fission. However, during his two years at Los Alamos, Teller devoted about one-third of his time to the design of a hydrogen "Super" bomb (Dyson, 2007).

In 1946 Teller left Los Alamos and returned as professor to the University of Chicago. Here he enjoyed the academic life again and became close associates with Enrico Fermi and Maria Goeppert-Mayer. However, the nagging question on the possibility of developing a nuclear weapon based on fusion remained with Teller; and he returned to Los Alamos to persuade, without success, his former superiors at Los Alamos to pursue fusion as the means to the development of a thermonuclear weapon much more powerful than the fission bombs dropped on Japan in 1945 (IEEE Global History Network, 2014, http://www.ieeeghn.org). However, the Soviet Union detonated its first atomic bomb on August 29, 1949; and the American Government, surprised that the Russians had developed a bomb so quickly, began to become concerned for their safety. To assure weapon superiority, President Harry S. Truman announced on January 31, 1950 that he had directed the Atomic Energy Commission "to continue with its work on all forms of atomic energy weapons, including the so-called hydrogen or super-bomb" (History Today 17 September 2014, http://www.historytoday.com). Edward Teller and Stanislaw Ulam had carried out significant studies on a potential hydrogen bomb design. On March 9, 1951, Teller and Ulam prepared a jointly signed report titled "On Heterocatalytic Detonations I. Hydrodynamic Lenses and Radiation Mirrors," Report # LAMS-1225. Here they described how X-rays from a primary fission bomb could be made to provide sufficient heat and pressure with the reflection of X-rays off the bomb casing to compress and enable a secondary nuclear fusion bomb. The basic design of current thermonuclear weapons (ie, hydrogen bombs) is now referred to as the Teller–Ulam assembly.

The Teller–Ulam assembly is illustrated in Fig. IV.25. It functions in two stages, consisting of primary and secondary implosions. The primary stage involves an implosion fission bomb; and the secondary stage entails the detonation of the fusion/hydrogen bomb. In the primary stage, high explosive spherical lenses are detonated and the force of the explosion is focused inward (red arrows in spherical primary of Fig. IV.25) toward a spherical aluminum pusher and uranium-238 tamper, both of which strengthen the force of the implosion to compress a sphere of fissile plutonium-239 to its supercritical state, resulting in the explosion of this fission bomb. A sphere of deuterium (^{2}H) and tritium (^{3}H) are present in the very center of the primary fission implosion device to produce a limited amount of nuclear fusion, which will produce some fast neutrons to enhance the efficiency of nuclear fission reactions in the uranium-238 tamper. The energy released from the primary fission is transferred to ignite the secondary fusion stage. The X-rays emitted in the primary fission bomb

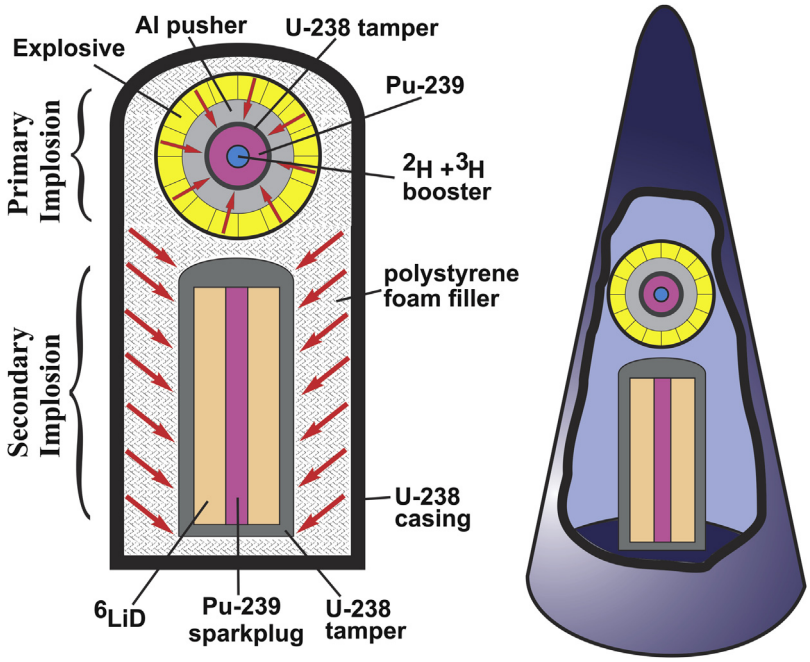

FIGURE IV.25 Left: Cross-sectional view of the Teller–Ulam assembly of a thermonuclear or hydrogen bomb. Right: A cut-out view of the contents of a thermonuclear-armed missile nose cone with a cross-sectional view of a miniaturized Teller–Ulam assembly.

irradiate the polystyrene foam filler and the X-rays reflect off the uranium-238 outer casing and direct inward (see red arrows in Fig. IV.25). The polystyrene foam burns to create a hot plasma and the reflecting X-rays create a force that compresses the lithium-6 deuteride (^{6}LiD) fusion fuel and plutonium-239 sparkplug. Upon compression, the plutonium-239 sparkplug reaches a supercritical mass and the resultant nuclear explosion creates sufficient heat for a thermonuclear explosion from the fusion of tritium and deuterium. The neutrons produced from the fission of Pu-239 convert the ^{6}Li to tritium according to the following reaction:

$$^{6}_{3}\mathrm{Li} + ^{1}_{0}\mathrm{n} \rightarrow ^{3}_{1}\mathrm{H} + ^{4}_{2}\mathrm{He} + 4.8\ \mathrm{MeV} \qquad [\mathrm{IV}.25]$$

The newly formed tritium produced from the above reaction fuses with the deuterium from the LiD to produce additionally more neutrons and a lot of energy according to the reaction:

$$^{3}_{1}\mathrm{H} + ^{2}_{1}\mathrm{H} \rightarrow ^{4}_{2}\mathrm{He} + ^{1}_{0}\mathrm{n} + 17.58\ \mathrm{MeV} \qquad [\mathrm{IV}.26]$$

This fusion reaction is depicted in the postage stamp of Edward Teller pictured earlier in this biographical sketch. The fast neutrons produced in the above fusion reaction will irradiate the uranium-238 tamper as well as the uranium-238 bomb casing, producing more energy as well as radioactive fission products, some of which are very hazardous to human health when detonated in the atmosphere, producing nuclear fallout.

The thermonuclear weapon, as described above, constitutes a fission-fusion-fission weapon. Joseph Rotblat alerted the public to the danger of this type of weapon after the American test under the code name of Castle Bravo at Bikini Atoll, Marshall Islands on March 1, 1954. This test deposited in the atmosphere significant radioactive fallout that had drifted and contaminated a Japanese fishing vessel, killing one sailor and sickening several others. The fishing vessel was 85 miles from the test site (see the pervious biographical sketch on Joseph Rotblat).

The neutron bomb, first conceived and developed by Samuel T. Cohen (1921–2010) in 1958 at the Lawrence Livermore National Laboratory, is a variant of the fission–fusion hydrogen bomb similar to that described above with the exception that fissionable uranium-238 is not used in the outer bomb casing. The bomb casing would be made of a nonfissionable material and kept as thin as possible. Also, U-238 as a tamper may be eliminated altogether. The purpose of removing U-238 in the neutron bomb is to increase the output of the fast neutrons from fusion, which otherwise would be consumed in the fission of U-238. The neutron bomb has less destructive power, measured in

kilotons equivalent of TNT rather than megatons; however, it can produce a high yield of lethal high-energy (14-MeV) neutrons arising from the fusion of deuterium and tritium. One objective of this bomb design was to kill personnel in advancing army tank divisions, as the intense source of lethal high-energy neutrons from this bomb would penetrate tank armor.

The testing of the Teller–Ulam hydrogen bomb mechanism was first carried out with liquid deuterium fuel. This took place at Eniwetok in the Marshall Islands on November 1, 1952. It was not a weapon that could be used in warfare, as it was a very large structure nicknamed "Mike" and intended only to test the feasibility of the Teller–Ulam mechanism of a primary nuclear fission explosion that would spark a secondary higher-energy yield from nuclear fusion of hydrogen nuclei. The bomb detonated with a yield equivalent to 10.4 megatons of TNT on the one-mile island of Elugelab. The island totally disappeared after the explosion. Less than a year later, on August 12, 1953, the Soviet Union tested its first hydrogen bomb, which was a "layer cake" design of alternating layers of uranium fission and hydrogen fusion fuel, developed by Andrei Sakharov. The Soviet bomb detonated with the much smaller yield of 400 kilotons; however, it was a hydrogen bomb that could be delivered by air.

With the testing of hydrogen bombs by the United States and Soviet Union, nuclear weapons testing now entered a new era of an arms race. After the successful testing of the Teller–Ulam mechanism on November 1, 1952, the United States detonated, on March 1, 1954 at Bikini Atoll, Marshall Islands, its first dry fuel hydrogen bomb of the Teller–Ulam assembly similar to that illustrated previously in Fig. IV.25. This test had the code name of Castle Bravo and yielded an explosion equivalent to 15 megatons of TNT, which was 1000 times the strength of the bomb dropped on Hiroshima, Japan in 1945. By 1961, the Soviet Union had tested a hydrogen bomb (October 30, 1961) which yielded an explosive force equivalent to approximately 60 million tons of TNT, which would be equivalent to 4000 times the strength of the bomb dropped on Hiroshima. At the height of the nuclear arms race in 1985, there were 68,000 active nuclear weapons in world stockpiles, which could destroy human life on earth many times over. Kristensen and Norris (2014) report, that as of mid-2014 there were approximately 16,300 nuclear warheads located at 98 sites in 14 countries. The countries include the United States, Russian Federation, United Kingdom, France, China, India, Pakistan, North Korea, Israel, and some European NATO countries.

To Edward Teller, the development of the hydrogen bomb was the best response to the Soviet threat (https://str.llnl.gov/str/Hacker.html); and to him it appeared that not enough effort in this direction was carried out at the Los Alamos National Laboratory. He lobbied the Atomic Energy Commission for a competing nuclear weapons laboratory, which opened its doors in 1952 as the Lawrence Livermore National Laboratory (LLNL) and a branch of the University of California Radiation Laboratory. The LLNL would become, like Los Alamos had become during the Manhattan Project, a first-order nuclear weapons design laboratory for the United States. The laboratory is officially named the Ernest Orlando Lawrence Berkeley National Laboratory, after Nobel Laureate Ernest O. Lawrence. Edward Teller served in positions as consultant, associate director, and director of the LLNL. On his 90th birthday celebration in 1998, Edward Teller delivered a speech to the staff of the LLNL titled "More Science in Livermore." A commentary by Bruce Tarter (1998), Director of the LLNL, quoted Edward Teller as stating "The Laboratory is the one thing in my life I am completely happy about." Tarter (1998) added that Edward Teller described briefly three specific contributions of the Laboratory that had really major importance, which were the following:

1. The first contribution was the introduction of very large computers into the scientific enterprise and leadership in this area.
2. The development of nuclear weapons that could be carried by submarines—a very difficult technical achievement, and one that changed the calculus of the Cold War, because it effectively negated the advantage of a first strike (by either side).
3. The work on strategic defense, which he and many others believed led to the collapse of the Soviet Union and the end to the Cold War.

The strategic defense here refers to the Strategic Defense Initiative (SDI), also known as "Star Wars," which was a program announced by President Ronald Reagan in March 1983 to use ground-based and space-based systems to protect the United States from ballistic missile attack. The administration of President Bill Clinton in 1993 renamed the initiative as the Ballistic Missile Defense Organization, and its scope was shifted from a global to the development of a more regional defense system.

On Edward Teller's 90th birthday, President William Jefferson "Bill" Clinton sent him a letter of congratulation and appreciation of his long service to his country. The entire letter can be found in the July/August 1998 issue of Science and

Technology Review, published by the Lawrence Livermore National Laboratory (https://str.llnl.gov/str/pdfs/07_98.pdf). An excerpt of that letter is the following:

THE WHITE HOUSE
WASHINGTON

January 14, 1998

Dr. Edward Teller
411 Gerona Road
Stanford, California 94305

Dear Dr. Teller:

…you can reflect with pride on a life and career dedicated to science, public service, and education. From your pathbreaking work on the Manhattan Project to your pivotal role in the creation of the Lawrence Livermore National Laboratory, you have brought together many disciplines and some of the world's finest scientific minds to confront and overcome the great challenges facing our nation in this century…

On behalf of our fellow Americans, I thank you for your extraordinary contributions to the security and success of our nation…

Sincerely,

(Bill Clinton)

As noted in the letter from President Clinton, Edward Teller served his government well. The development of thermonuclear weapons and the race to develop larger numbers and more sophisticated hydrogen bombs seemed to prevent a direct conflict between the Western bloc (United States and its NATO allies) and that of the East (USSR and the Warsaw Pact) during the Cold War (1946–1991) and after. At the peak of the race on thermonuclear weapons development in 1986, the world's stockpile of nuclear weapons amounted to approximately 60,000 (http://www.nrdc.org/), enough to destroy the human race many times over. Current military stockpiles contain a total of approximately 16,000 nuclear warheads reported by the Federation of American Scientists (http://fas.org/issues/nuclear-weapons/status-world-nuclear-forces/). Even with massive stockpiles of nuclear weapons intended to serve as a deterrent to war, the world came very close to a direct nuclear conflict between the Western and Eastern blocs during the Cuban Missile Crisis in 1962. The possession of nuclear weapons provides a false sense of security, with countries living under the fear that a military conflict involving nuclear weapons, intended as a deterrent, could break out, which would be disastrous to all. Is this peace? With this in mind, the Ig Nobel Prize for Peace in 1991 was awarded to Edward Teller with the following award statement: "father of the hydrogen bomb and first champion of the Star Wars weapons system, for his lifelong efforts to change the meaning of peace as we know it" (http://www.improbable.com/ig/winners/). The Ig Nobel Prizes honor achievements that "first make people laugh, and then make them think" (*Nature News* online: http://www.nature.com/news/2005). The Ig Nobel Prize is sometimes a veiled criticism; and the name of the prize is a play on the words "ignoble" and "Nobel Prize." Recipients, who attend the ceremony, generally receive their award from the hands of a genuine Nobel Laureate. The awards are presented each year in a gala ceremony at Harvard University's Sanders Theatre in various fields such as biology, chemistry, economics, education, literature, medicine, and peace; and the awards ceremony is broadcast live on major news and science sites including the following: http://www.improbable.com/ig/.

In a comprehensive review of Edward Teller's life and work, Hacker et al. (1998) note that the Lawrence Livermore National Laboratory was the result of vigorous efforts by Teller. He believed that a friendly competitor of the Los Alamos National Laboratory was required to accelerate the development of thermonuclear weapons and stimulate scientific discoveries. He was assisted by Earnest Lawrence. In addition to the development of thermonuclear weapons, Edward Teller was a leading advocate of safeguards for the operation of nuclear reactors for peaceful applications in research and power. He lead the study that culminated in the design of an inherently safe reactor, namely, the TRIGA (Test, Research, Isotopes–General Atomics), which became very popular around the world for peaceful applications in research and the preparation of isotopes, some of which are applicable to medicine and biological research.

Hacker et al. (1998) relate the political events of Edward Teller's youth and how these affected his scientific career. They note that in his youth, Teller experienced repression by the communists after Bela Kun seized power in Hungary and

later he and his family were persecuted by Nazis. After 1938, for fear of the Nazis, Edward Teller could not visit family and friends in Hungary. He never saw his father again; and he was not able to see his mother and older sister Emmi again until 1959. Also, his wife Mici lost her brother to the Nazis; and Emmi's husband suffered a similar fate. As noted by Hacker et al. (1998) "His own inclination was to pursue pure science; war turned him into an applied scientist who used his expertise to develop weapons in the service of the United States. His work on the hydrogen bomb was an important accomplishment, especially when the U.S. Government found out that the Soviets were developing their own H-bomb. That work also made possible an invulnerable submarine-based nuclear deterrent."

Left to Right: Glenn Seaborg, Edward Teller, President John F. Kennedy and Teller's wife 'Mici' in front of the White House during the Enrico Fermi Award Ceremony for Teller in 1962 (Digital Photo Archive, Department of Energy (DOE), courtesy of AIP Emilio Segre Visual Archives)

Edward Teller enjoyed teaching and was an outstanding lecturer. His career in teaching is outlined in detain by Hacker et al. (1998). In 1960, Teller proposed and helped establish a department of Applied Science as part of the University of California; and the first class of graduate students entered this program in the College of Engineering at the University of California, Davis with Edward Teller as its first chairman. From 1979 to the time of his death, Edward Teller was a Senior Fellow at the Hoover Institute for the Study of War, Revolution and Peace at Stanford University in Palo Alto, California. At the age of 82, he taught weekly classes in physics to Livermore-area high school students and their teachers and parents to stimulate their interest in science.

Numerous awards and honorary degrees have been bestowed on Edward Teller. Among the awards are the Enrico Fermi Award in 1962, the National Medal of Science for 1982, the Presidential Citizens Medal in 1989, and the Science Peace Prize in 1990 awarded by the Ettore Majorana Centre for Scientific Culture in Erice, Sicily. Edward Teller died at his home on the Stanford University campus in Palo Alto, California on September 9, 2003 at the age of 95.

Chapter 10

Neutron Radiation

In England and the United States where physicists have at their disposal equipment of very high voltages, several new elements were prepared using protons and deuterons as projectiles. In Italy first, and then in other countries, research workers, in particular, [Enrico] Fermi and his co-workers, used neutrons, projectiles which are outstandingly suitable to cause transmutations…among which were radio-phosphorus (^{32}P), and more than fifty new radio-elements…It was indeed a great source of satisfaction for our lamented teacher Marie Curie to have witnessed this lengthening of the list of radio-elements, which she had the glory, in company with Pierre Curie, of beginning.

Frédéric Joliet in his Nobel Lecture on December 12, 1935, who together with Irène Joliet-Curie was awarded the Nobel Prize in Chemistry for their synthesis of new radioactive elements.

10.1 INTRODUCTION

The neutron is a neutral particle, which is stable only in the confines of the nucleus of the atom. Outside the nucleus, the neutron decays with a mean lifetime of about 15 min. Its mass, like that of the proton, is equivalent to 1 u (atomic mass unit). Unlike the particulate alpha and beta nuclear radiation previously discussed, neutron radiation is not emitted in any significant quantities from radionuclides that undergo the traditional nuclear decay processes with the exception of a few radionuclides such as ^{252}Cf and ^{248}Cm, which decay to a significant extent by spontaneous fission. Significant quantities of neutron radiation occur when neutrons are ejected from the nuclei of atoms following reactions between the nuclei and particulate radiation. Due to the lack of charge, the neutron cannot directly produce any ionization in matter, again unlike alpha and beta radiation. The various sources, properties, and mechanisms of interaction of neutrons with matter are described subsequently.

10.2 NEUTRON CLASSIFICATION

Neutrons are generally classified according to their kinetic energies. There is no sharp division or energy line of demarcation between the various classes of neutrons; however, the following is an approximate categorization according to neutron energy:

- Cold neutrons: <0.003 eV
- Slow (thermal) neutrons: 0.003−0.4 eV
- Slow (epithermal) neutrons: 0.4−100 eV
- Intermediate neutrons: 100 eV−200 keV
- Fast neutrons: 200 keV−10 MeV
- High energy (relativistic) neutrons: >10 MeV

The energies of neutrons are also expressed in terms of velocity (meters per second) as depicted in the terminology used to classify neutrons. A neutron of specific energy and velocity is also described in terms of wavelength, because particles in motion also have wave properties. It is the wavelength of the neutron that becomes important in studies of neutron diffraction. The values of energy, velocity, and wavelength of the neutron, as with all particles in motion, are interrelated. The velocity of neutrons increases according to the square root of the energy, and the wavelength of the neutron is inversely proportional to its velocity. Knowing only one of the properties—the energy, velocity, or

Radioactivity: Introduction and History, From the Quantum to Quarks. http://dx.doi.org/10.1016/B978-0-444-63489-4.00010-1
Copyright © 2016 Elsevier B.V. All rights reserved.

wavelength—of a neutron, we can calculate the other two. We can relate the neutron energy and velocity using the kinetic energy equation:

$$E = \frac{1}{2}mv^2 \quad \text{or} \quad v = \sqrt{2E/m} \tag{10.1}$$

where E is the particle energy in joules (1 eV $= 1.6 \times 10^{-19}$ J), m is the mass of the neutron (1.67×10^{-27} kg), and v is the particle velocity in meters per second. The wavelength is obtained from the particle mass and velocity according to:

$$\lambda = \frac{h}{p} = \frac{h}{mv} \tag{10.2}$$

where λ is the particle wavelength in meters, h is Planck's constant (6.63×10^{-34} J s), p is the particle momentum, and m and v are the particle mass and velocity as previously defined. The correlation between neutron energy, velocity, and wavelength is provided in Fig. 10.1, which is constructed from the classical Eqs. [10.1] and [10.2] relating particle mass, energy, velocity, and wavelength. However, calculations involving high-energy particles that approach the speed of light will contain a certain degree of error unless relativistic calculations are used, as the mass of the particle will increase according to the particle speed. In chapter "Electromagnetic Radiation: Photons" we used the Einstein equation of equivalence of energy and mass, $E = mc^2$, to convert the rest mass of the positron or negatron to its rest energy (0.51 MeV). When gauging particles in motion, the *total energy* (E) of the particle is the sum of its kinetic (K) and rest energies (mc^2), or:

$$E = K + mc^2 = \gamma mc^2 \tag{10.3}$$

Thus the kinetic energy of the particle would be the difference between the *total energy* of the particle and its rest energy, or:

$$K = \gamma mc^2 - mc^2 \tag{10.4}$$

where:

$$\gamma = \frac{1}{\sqrt{1 - (u^2/c^2)}}, \tag{10.5}$$

u is the particle speed, and $u < c$. If we call the particle rest mass m_0, then the relativistic mass, m_r, which is the speed-dependent mass of the particle, is calculated as:

$$m_r = \frac{m_0}{\sqrt{1 - (u^2/c^2)}} \tag{10.6}$$

And from Eq. [10.4], the kinetic energy of the particle can be written as:

$$K = \frac{m_0}{\sqrt{1 - (u^2/c^2)}}c^2 - m_0c^2 \tag{10.7}$$

Eq. [10.7] can be transformed to read:

$$K + m_0c^2 = \frac{m_0c^2}{\sqrt{1 - (u^2/c^2)}} \tag{10.8}$$

and:

$$\frac{K + m_0c^2}{m_0c^2} = \frac{1}{\sqrt{1 - (u^2/c^2)}} \tag{10.9}$$

and:

$$\left(\frac{K}{m_0c^2} + 1\right)^2 = \frac{1}{1 - (u^2/c^2)} \tag{10.10}$$

which can be transformed to read:

$$\frac{u^2}{c^2} = 1 - \frac{1}{(K/m_0c^2 + 1)^2} \tag{10.11}$$

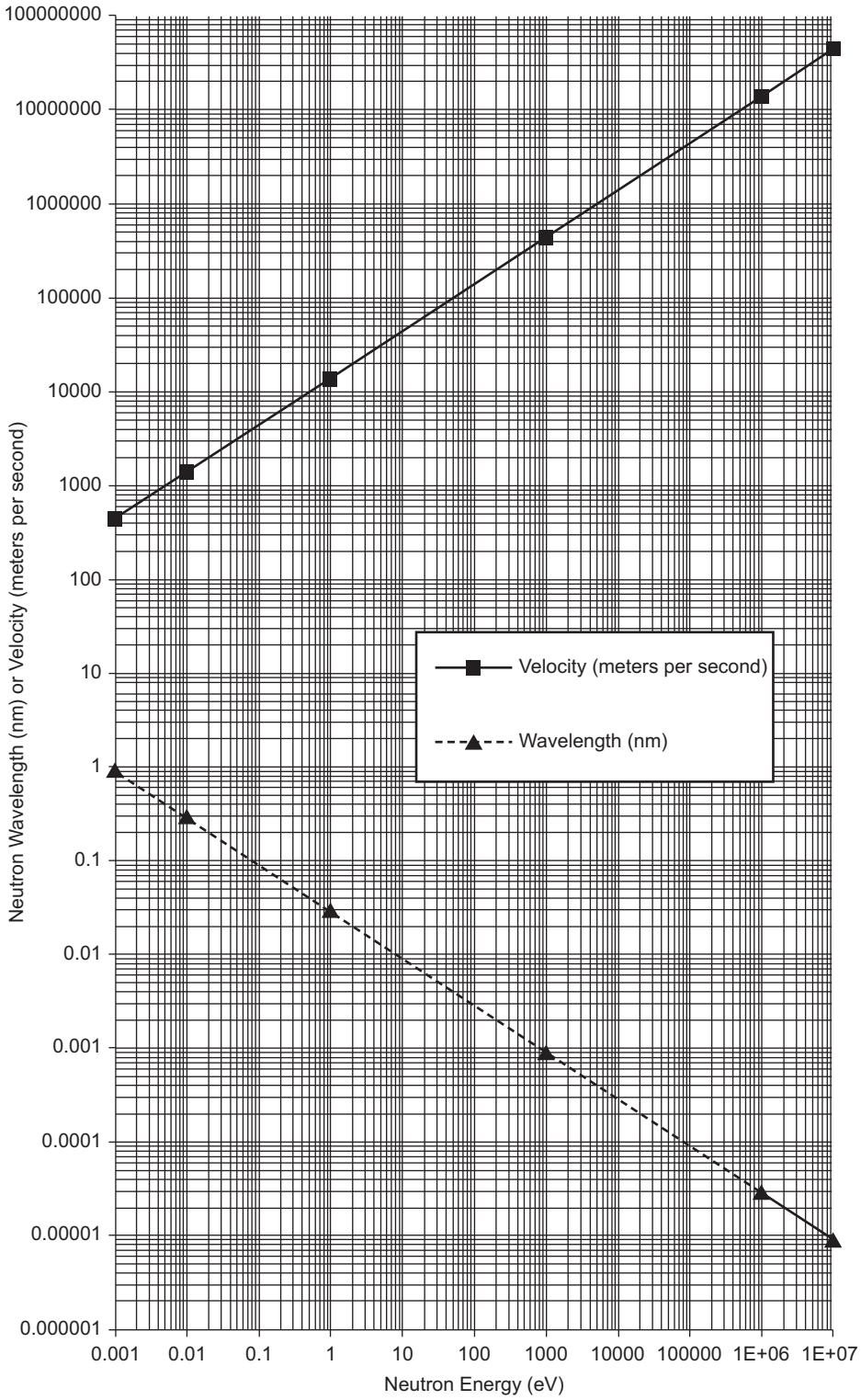

FIGURE 10.1 Correlation between neutron energy in electron volts (eV), velocity (m/s), and wavelength (nm). From the energy of the neutron in eV on the abscissa, a line is drawn vertically to cross the wavelength and velocity curves. The values of neutron wavelength and velocity are obtained directly from the ordinate. For example, to determine the wavelength and velocity of 0.025 eV thermal neutrons, the value of 0.025 eV is found on the abscissa. A line is then drawn vertically from the point of 0.025 eV to cross the values of 0.18 nm wavelength and 2200 m/s velocity.

and from Eq. [10.11] the relativistic speed of the particle can be defined as:

$$u_r = c\sqrt{1-\left(\frac{K}{m_0c^2}+1\right)^{-2}} \qquad [10.12]$$

where K is the kinetic energy, and the particle speed u is always less than c (Serway et al., 2005). The nonrelativistic speed is that described by Eq. [10.1], or $u_{nr} = \sqrt{2E/m_0}$.

To confirm the validity of the use of nonrelativistic calculations of particle speed for the construction of Fig. 10.1, let us use Eqs. [10.1] and [10.12] to compare the differences between the nonrelativistic and relativistic speeds of a neutron of 10 MeV kinetic energy. This energy was selected because it is the highest neutron energy included in Fig. 10.1, and differences between nonrelativistic and relativistic calculations increase with particle energy. The difference between the two calculated speeds is defined by the ratio of the two, or:

$$\frac{u_{nr}}{u_r} = \frac{\sqrt{2E/m_0}}{c\sqrt{1-(K/m_0c^2+1)^{-2}}} \qquad [10.13]$$

The rest energy of the neutron, mc^2, is first calculated as:

$$mc^2 = \left(1.6749\times10^{-27}\ \text{kg}\right)\left(2.9979\times10^{8}\text{m/s}\right)^2 = 1.505\times10^{-10}\ \text{J}$$

and:

$$\frac{1.505\times10^{-10}\ \text{J}}{1.602\times10^{-19}\ \text{J/eV}} = 939.5\ \text{MeV}$$

since by definition, $1\ \text{eV} = 1.602\times10^{-19}$ J. From Eq. [10.13], the ratio of the nonrelativistic and relativistic speeds is calculated as:

$$\frac{u_{nr}}{u_r} = \frac{\sqrt{2(10\ \text{MeV})(1.602\times10^{-13}\ \text{J/MeV})/1.6749\times10^{-27}\ \text{kg}}}{c\sqrt{1-((10\ \text{MeV}/939.5\ \text{MeV})+1)^{-2}}}$$

$$= \frac{4.3737\times10^{7}\ \text{m/s}}{0.1447751c} = \frac{4.3737\times10^{7}\ \text{m/s}}{(0.1447751)(2.9979\times10^{8}\ \text{m/s})}$$

$$= \frac{4.3737\times10^{7}\ \text{m/s}}{4.340\times10^{7}\ \text{m/s}} = 1.0078 = 0.78\%\ \text{error.}$$

The error between the nonrelativistic and relativistic calculations is small at this high neutron energy. However, if we consider higher neutron energies in excess of 10 MeV, the error of making nonrelativistic calculations increases.

As we observed above in the case of particle speed, we will also see that particle wavelength will also differ for nonrelativistic and relativistic calculations. In 1923, Louis Victor de Broglie first postulated that all particles or matter in motion should have wave characteristics, just as photons display both a wave and particle character. We therefore attribute the wavelength of particles in motion as de Broglie wavelengths. Let us then compare calculated nonrelativistic and relativistic wavelengths. From Eq. [10.2], we can describe the nonrelativistic wavelength, λ_{nr}, as:

$$\lambda_{nr} = \frac{h}{p} = \frac{hc}{pc} = \frac{hc}{cmv} = \frac{hc}{cm\sqrt{2E/m}} = \frac{hc}{\sqrt{2mc^2E}} \qquad [10.14]$$

where $p = mv = m\sqrt{2E/m}$. For relativistic calculations, the value of pc is calculated according to the following equation derived by Halpern (1988):

$$pc = \left[2m_0c^2K\left(1+\frac{K}{2m_0c^2}\right)\right]^{1/2} \qquad [10.15]$$

and the calculation for the relativistic de Broglie wavelength, λ_r, then becomes:

$$\lambda_r = \frac{hc}{pc} = \frac{hc}{[2m_0c^2K(1+(K/2m_0c^2))]^{1/2}} \quad [10.16]$$

We can then compare the difference between the nonrelativistic and relativistic wavelengths for the 10 MeV neutron as follows:

$$\frac{\lambda_{nr}}{\lambda_r} = \frac{hc/\sqrt{2m_0c^2E}}{hc/\left[2m_0c^2K\left(1+\left(K/2m_0c^2\right)\right)\right]^{1/2}}$$

$$= \frac{\left\{\begin{array}{l}[(6.626\times10^{-34}\ \text{J s})(2.9979\times10^{8}\ \text{m/s})/\\ 1.602\times10^{-13}\ \text{J/MeV}]/\sqrt{2(939.5\ \text{MeV})(10\ \text{MeV})}\end{array}\right\}}{\left\{\begin{array}{l}[(6.626\times10^{-34}\ \text{J s})(2.9979\times10^{8}\ \text{m/s})/1.602\times10^{-13}\ \text{J/MeV}]/\\ \sqrt{2(939.5\ \text{MeV})(10\ \text{MeV})[1+(10\ \text{MeV}/2(939.5\ \text{MeV}))]}\end{array}\right\}} \quad [10.17]$$

$$= \frac{12.3995\times10^{-4}\ \text{MeV nm}/\sqrt{18,790\ \text{MeV}^2}}{12.3995\times10^{-4}\ \text{MeV nm}/\sqrt{18,890\ \text{MeV}^2}}$$

$$= \frac{9.0456\times10^{-6}\ \text{nm}}{9.0217\times10^{-6}\ \text{nm}} = 1.0026 = 0.26\%\ \text{error}$$

From the above comparison of nonrelativistic and relativistic calculations of neutron wavelength and velocity, we see that the data provided in Fig. 10.1 based on nonrelativistic calculations are valid with less than 1% error for the highest- energy neutron included in that figure. However, if we consider higher energies beyond 10 MeV, where we classify the neutron as relativistic, the errors in making nonrelativistic calculations will increase with neutron energy. It will be clearly obvious to the reader that factors in Eq. [10.17] can be canceled out readily and the equation simplified to the following, which provides a quick evaluation of the effect of particle energy on the error in a nonrelativistic calculation of the de Broglie wavelength:

$$\frac{\lambda_{nr}}{\lambda_r} = \sqrt{1+\frac{K}{2m_0c^2}} \quad [10.18]$$

where K is the particle kinetic energy in MeV and m_0c^2 is the rest energy of the particle (eg, 939.5 MeV for the neutron and 0.511 MeV for the beta particle or electron). For example, a nonrelativistc calculation of the wavelength of a 50-MeV neutron would have the following error:

$$\frac{\lambda_{nr}}{\lambda_r} = \sqrt{1+\frac{50\ \text{Mev}}{2(939.5\ \text{Mev})}} = 1.0132 = 1.32\%\ \text{error.}$$

Note that the above-computed errors in nonrelativistic calculations of the de Broglie wavelength increased from 0.26% for a 10-MeV neutron to 1.32% for a 50-MeV neutron, and the error will increase with particle energy. Errors in nonrelativistic calculations are yet greater for particles of smaller mass (eg, beta particles) of a given energy compared to neutrons of the same energy. This is due obviously to the fact that particles of lower mass and a given energy will travel at higher speeds than particles of the same energy but higher mass. This is illustrated in Fig. 10.2, where the particle speed, u, is a function of the particle kinetic energy, K, and its mass or rest energy, m_0c^2. The particle energy in Fig. 10.2 is expressed as K/m_0c^2 to permit the reader to apply the curves for nonrelativistic and relativistic calculations to particles of different mass. For example, from the abscissa of Fig. 10.2, the values of K/m_0c^2 for a 2-MeV beta particle is 2 MeV/0.51 MeV = 3.9, and that for a 2-MeV neutron is 2 MeV/939.5 MeV = 0.0021. From Fig. 10.2 we see that the nonrelativistic calculation of the speed of a 2-MeV beta particle would be erroneously extreme (well beyond the speed of light), while there would be only a small error in the nonrelativistic calculation of the speed of the massive neutron of the same energy.

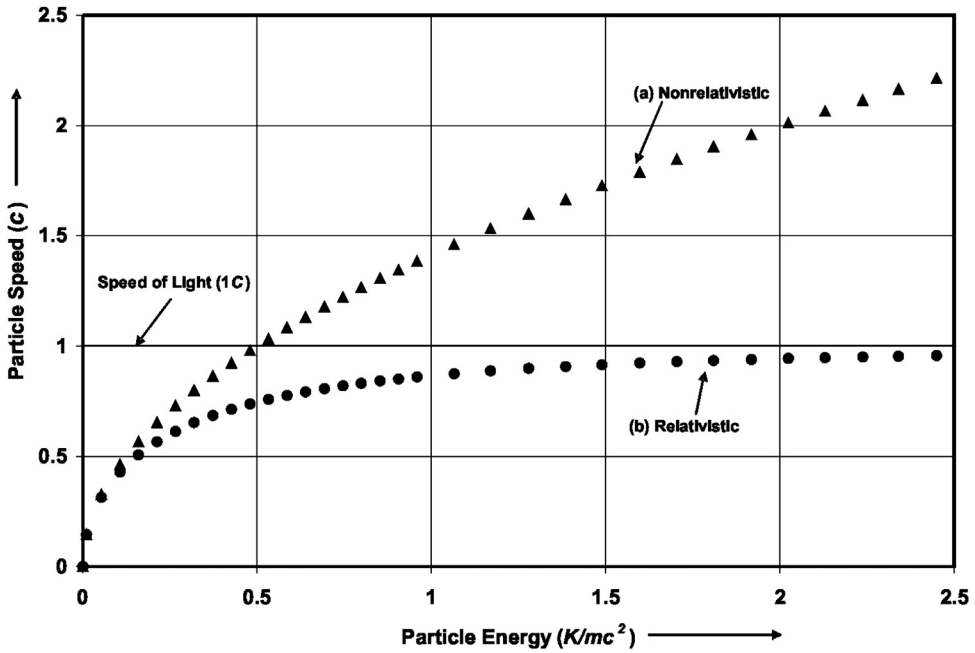

FIGURE 10.2 A graph comparing particle speeds derived from (a) nonrelativistic and (b) relativistic interpretations of the particle kinetic energy. The speeds in units of the speed of light ($1c = 2.9979 \times 10^8$ m/s) are plotted versus particle energy expressed as a ratio of its kinetic energy (K) over its rest energy (mc^2). In the nonrelativistic case, the particle kinetic energy is defined as $K = \frac{1}{2}mv^2$ and its speed is calculated according to $v = \sqrt{2K/m}$, whereas in the relativistic case, the particle kinetic energy is the difference between the total energy of the particle and its rest energy ($K = \gamma mc^2 - mc^2$) where $\gamma = 1\Big/\sqrt{1-(u^2/c^2)}$ and its speed $u = c\sqrt{1-((K/mc^2)+1)^{-2}}$ is always less than c.

10.3 NEUTRON SOURCES

Neutron sources are vital to our development and well-being. They serve to produce the energy we need and many of the radionuclides required for medical diagnosis and treatment of many forms of cancer, as well as numerous applications in industry including nondestructive testing and analysis. A review of current practical applications of neutrons and nuclear radiation is provided in the introduction of this book. There are several sources of neutrons, including (1) alpha–particle-induced (α,n) nuclear reactions (2) radionuclides that decay by spontaneous fission, (3) neutron-induced fission, (4) photoneutron (γ,n) sources, (5) charged-particle accelerator sources, and (6) nuclear fusion. A list of these sources is provided in Table 10.1, and a more detailed description of the sources of neutrons will be provided subsequently.

TABLE 10.1 Processes for Production of Neutrons and Short Description of Corresponding Spectral Fluence[a]

Process	Example	Neutron Fluence Energy Distribution
Spontaneous fission	$^{252}\mathrm{Cf} \rightarrow \mathrm{n} + \mathrm{FP}$	Maxwellian, $E_{mean} \sim 2$ MeV
Neutron-induced fission	$^{235}\mathrm{U(n,f)}$	
Radioisotope (α,n) sources	$\alpha + {}^{9}\mathrm{Be} \rightarrow {}^{12}\mathrm{C} + \mathrm{n}$	Mono[b] or polyenergetic
Photon reaction	$^{A}\mathrm{X}(\gamma,\mathrm{n})^{A-1}\mathrm{X}$	Mono[b] or polyenergetic neutrons (short half-life of γ-ray emitters)
	$\gamma + {}^{9}\mathrm{Be} \rightarrow {}^{8}\mathrm{Be} + \mathrm{n}$	
Charged particle direct reaction	$^{2}\mathrm{H(d,n)}^{3}\mathrm{He}$	Monoenergetic[b] neutrons
Charged particle breakup reaction	$^{2}\mathrm{H(d,np)}^{2}\mathrm{H}$	Broad energy distribution $E_{mean} \sim 0.5\ E_d$
Spallation reaction	$^{238}\mathrm{U(p,20n)}$	Broad energy distribution E_n max $\sim E_p$

[a] *From Lacoste (2010); reprinted with permission of Elsevier © 2010.*
[b] *Definition of monoenergetic neutron source from ICRU Report 63 (2000): "A neutron source can be consider "monoenergetic" if the energy spectrum consists of a single peak, which has an energy spread which is much less than the energy of the peak. The ideal source has a small energy spread and negligible neutron intensity at lower and higher energies."*

10.3.1 Alpha–Particle-Induced Nuclear Reactions

It is interesting to note that the method used by Chadwick to produce neutrons by alpha–particle-induced reaction, described in Hall of Fame, Part IV, remains an important method of producing a neutron source, particularly when a relatively small or easily transportable neutron source is required. The source may be prepared by compressing an alpha–particle-emitting radioisotope substance with beryllium metal. The nuclear reaction, which occurs between the alpha particle and the beryllium nucleus, terminates with the emission of a neutron and the production of stable carbon as follows:

$$^{9}_{4}\mathrm{Be} + {}^{4}_{2}\mathrm{He} \rightarrow {}^{12}_{6}\mathrm{C} + {}^{1}_{0}\mathrm{n} + 5.701\ \mathrm{Mev} \qquad [10.19]$$

where 5.701 MeV is the energy released in the reaction. The kinetic energy released in the reaction is determined by calculating the Q value of the reaction according to the following:

$$Q = (m_{\mathrm{reactants}})c^2 - (m_{\mathrm{products}})c^2 \qquad [10.20]$$

which for the above reaction is written as:

$$\begin{aligned} Q &= (M_{^{9}\mathrm{Be}} + M_{^{4}\mathrm{He}})c^2 - (M_{^{12}\mathrm{C}} + M_{^{1}\mathrm{n}})c^2 \\ &= [(9.012182\ \mathrm{u} + 4.00260325\ \mathrm{u})931.494\ \mathrm{MeV/u} - (12.000000\ \mathrm{u} + 1.00866492\ \mathrm{u})931.494\ \mathrm{MeV/u}] \\ &= 5.701\ \mathrm{MeV} \end{aligned} \qquad [10.21]$$

The calculated value agrees with the Q-value Calculator (QCalc) of the National Nuclear Data Center, Brookhaven National Laboratory (NNDC, 2016a: http://www.nndc.bnl.gov/qcalc/). The neutrons emitted from the reaction will have an average energy of ~5.5 MeV, as the kinetic energy released in the reaction is shared between the neutron and ^{12}C nucleus, and the neutron may possess varying energies and velocities as a consequence of the various directions of emission of neutrons from the nucleus.

Several alpha particle sources are used to produce neutrons via the preceding (α,n) reaction. Among these are the alpha emitters ^{241}Am, ^{242}Cm, ^{210}Po, ^{239}Pu, and ^{226}Ra. The alpha radiation source selected may depend on its half-life as well as its gamma-ray emissions. As noted previously in chapter "Alpha Radiation", gamma radiation often accompanies alpha decay. The use of an alpha source, which also emits abundant gamma radiation, requires additional protection for the user against penetrating gamma rays. For example, Am-Be sources are preferred over the Ra-Be sources of neutrons used in soil moisture probes (Nielsen and Cassel, 1984; O'Leary and Incerti, 1993), because the latter have a higher output of gamma radiation and require more shielding for operator protection.

The energies of the neutrons emitted from these sources will vary over the broad spectrum of 0–10 MeV. The neutrons produced by these sources vary in energy as a consequence of several factors, including the sharing of the liberated energy between the neutron and ^{12}C nucleus, the varying directions of emission of neutrons from the nucleus with consequent varying energies and velocities, and the variations in kinetic energies of the bombarding alpha particles.

The neutron activities available from these sources increase up to a maximum as a function of the amounts of alpha emitter and beryllium target material used. For example, as explained by Bacon (1969), the Ra-Be source, prepared by mixing and compressing radium bromide with beryllium powder, increases steadily in neutron activity (neutrons per second) for each gram of radium used as the amount of beryllium is increased to about 10 g; but no significant increase in neutron output is achieved if more beryllium is used. The maximum neutron output achieved is approximately 2×10^7 neutrons per second per gram of radium. Because alpha decay from any alpha–particle-emitting source occurs by means of random events, the production of neutrons by (α,n) reactions is also a random event. Therefore, these reactions can be referred to as "not time correlated." This is contrary to the case of neutron sources provided through fission, discussed subsequently.

Beryllium is not the exclusive element that may be used for the alpha–particle-induced neutron source. Other low Z elements may be packed with an alpha emitter (eg, boron or carbon), but their neutron yields is about six times lower than Be (Lacoste, 2010). For example, Skidmore et al. (2009) tested oxygen enriched with ^{18}O packed with ^{241}Am as a possible neutron energy source for planetary research. The neutron flux and energy yield from this source is compared to conventional sources of alpha emitters with Be as well as the ^{252}Cf spontaneous fission neutron source in Table 10.2.

Switchable neutron generators, that is, generators that may be turned on or off, of the (α,n) type are possible when the alpha emitter and target are not packed intimately. The alpha emitter need not be packed intimately with the target material,

TABLE 10.2 The Total Flux Emitted by the Neutron Sources per Second Integrated Over Energy

Neutron Source	Integrated Flux ($s^{-1}\,g^{-1}$)	Approximate Source Mass Required for 100-W Thermal Power Generation (g)
^{252}Cf	2.3×10^{12}	0.05
Am–Be	1.4×10^{6}	2000
Enriched AmO_2	3.7×10^{5}	2000
Pu–Be	7.2×10^{6}	2000

From Skidmore, M.S., et al., 2009. Neutron sources for in-situ planetary science applications. Nucl. Instrum. Methods Phys. Res. Sect. A 608, 403–409. Reprinted with permission of Elsevier © 2009.

but both must be close enough to allow the alpha particles to be absorbed by the target. Hertz et al. (2003) studied many combinations of alpha-emitter and target materials for switchable neutron sources, and they found the $^{9}Be(\alpha,n)$ generator with an ^{241}Am alpha-emitting source the most suitable as a switchable neutron source. In the "off" position, a mechanical device is used to prevent the alpha particles from reaching the Be target. These switchable neutron sources are classified as micromachines, because they can be constructed to have the dimensions of the same order of magnitude as the alpha-particle range.

10.3.2 Spontaneous Fission

About 100 radionuclides are known to decay by spontaneous fission (SF) with the emission of neutrons (Karelin et al., 1997) as an alternative to another decay mode, such as alpha decay. Spontaneous fission involves the spontaneous non-induced splitting of the nucleus into two nuclides or fission fragments and the simultaneous emission of more than one neutron on the average. This phenomenon occurs with radionuclides of high mass number, $A \geq 230$. The radionuclide ^{252}Cf is a good example of a commercially available spontaneous fission neutron source. It decays with a half-life of 2.65 years primarily by alpha emission (96.91% probability); the remainder of the ^{252}Cf decay processes occurs by spontaneous fission with a probability of 3.09% (Martin et al., 2000). Decay of ^{252}Cf by spontaneous fission produces an average number of 3.7 neutrons per fission. Because the sizes of the two fragments resulting from fission are not predictable, average sizes of the two fragments are determined. Consequently, the numbers of neutrons emitted from individual fissions are not the same; and an average number of neutrons produced per fission is determined. The fission rate of ^{252}Cf is 6.2×10^{5} SF/s/μg (Isotope Products Laboratories, 1995). The neutron emission from ^{252}Cf in units of neutrons per second per unit mass is reported to be 2.314×10^{6} neutrons/s/μg, with a specific activity of 0.536 mCi/μg (Martin et al., 2000; Skidmore et al., 2009). Thus, 1 mg of ^{242}Cf would emit 2.314×10^{9} neutrons per second. If we know the radionuclide specific activity and the % probability of decay by spontaneous fission, we can calculate the fission rate. For example, taking the specific activity and % probability of spontaneous fission reported above for ^{252}Cf, we can calculate the fission rate as the product of decay rate and probability of SF per decay, or:

$$(0.536\ \text{mCi}/\mu\text{g})\left(3.7 \times 10^{7}\ \text{dps}/\text{mCi}\right)(0.0309) = 6.13 \times 10^{5}\ \text{SF}/\text{s}/\mu\text{g} \qquad [10.22]$$

which is in close agreement with the value cited above. See chapter "Radionuclide Decay, Radioactivity Units, and Radionuclide Mass" for a discussion of radioactivity units and calculations.

The variations in fission fragment sizes and number of neutrons emitted per fission provide variable neutron energies over the range 0–5.5 MeV with an average neutron energy from ^{252}Cf of approximately 2.3 MeV. Small sources of ^{252}Cf are commercially available for a wide range of applications such as prompt-gamma neutron activation analysis of coal, cement, minerals, interplanetary analysis, petroleum contamination analysis in soil, detection of explosives and land mines, neutron radiography, and cancer therapy (Mercer et al., 2007; Skidmore et al., 2009). There is an increasing interest in the use of ^{252}Cf neutron sources in radiation therapy, or specifically neutron brachytherapy treatment of various types of cancer (Melhus and Rivard, 2006; Wang et al., 2008; and Ghassoun et al., 2010). Small commercial sources are described by Martin et al. (1997, 2000) among which are included 50-mg sources of ^{252}Cf providing a neutron intensity $>10^{11}$/s and measuring only 5 cm in length × 1 cm in diameter. They report also larger sources of mass >100 mg of ^{252}Cf that approach reactor capabilities for neutrons.

Another standard nuclide source of neutrons is ^{248}Cm, which provides a spontaneous fission intensity of only 4.12×10^4/s/mg and decays with a half-life of 3.6×10^5 years (Radchenko et al., 2000). The lower neutron flux intensity of this source limits its application, although it has the advantage of a very long half-life, providing invariability of sample intensity with time.

Some radionuclides of interest in nuclear energy and safeguards also decay by spontaneous fission. The isotopes of plutonium of even mass number, namely ^{238}Pu, ^{240}Pu, and ^{242}Pu, decay principally by alpha-particle emission but can also undergo spontaneous fission to a lesser extent at rates of 1100, 471, and 800 SF/s/g, respectively. The average number of neutrons emitted per fission is between 2.16 and 2.26 of broad energy spectrum (Canberra Nuclear, 1996). Because the neutrons produced with each fission occurrence are emitted simultaneously, we can refer to these emissions as "time correlated." Other isotopes of uranium and plutonium also undergo spontaneous fission, but at a much lower rate.

10.3.3 Neutron-Induced Fission

When the naturally occurring isotope of uranium, ^{235}U, is exposed to slow neutrons, it can absorb the neutron to form the unstable nuclide ^{236}U. The newly formed nucleus may decay by alpha-particle and gamma-ray emission with the long half-life of 2.4×10^7 years. This occurs in approximately 14% of the cases when ^{235}U absorbs a slow neutron. However, in the remaining 86% of the cases, the absorption of a slow neutron by ^{235}U results in the production of the unstable ^{236}U nuclide, which takes on the characteristics of an unstable oscillating droplet (see Fig. IV.4 of Hall of Fame, Part IV). This oscillating nuclear droplet with the opposing forces of two positively charged nuclides splits into two fragments, not necessarily of equal size, with the liberation of an average energy of 193.6 MeV. The general ^{235}U fission reaction may be written as:

$$^{235}_{92}\mathrm{U} + {}^{1}_{0}\mathrm{n} \rightarrow [^{236}_{92}\mathrm{U}] \rightarrow fp + \nu\,{}^{1}_{0}\mathrm{n} + E \qquad [10.23]$$

which represents the capture of one thermal neutron $^{1}_{0}$n by a nucleus of $^{236}_{92}$U to yield the release of fission products *fp* of varying masses plus an average yield of $\nu = 2.42$ neutrons and an overall *average* release of energy $E = 193.6$ MeV (Koch, 1995). The intermediate nuclide ^{236}U is shown in brackets in the above reaction. Most of this energy (over 160 MeV) appears in the form of kinetic energy of the two fission fragments. The remaining energy is shared among the neutrons emitted, with prompt gamma radiation accompanying fission and also beta particles and gamma radiation from decaying fission fragments and neutrinos accompanying beta decay. When a sample of ^{235}U is bombarded with slow neutrons, the fission fragments produced are rarely of equal mass. The ^{236}U intermediate nuclide breaks into fragments in as many as 30 different possible ways, producing, therefore, 60 different nuclide fission fragments. In a review, Koch (1995) provides a list of the fission fragments and their relative abundances as produced in a typical pressurized water reactor (PWR). The most common fission fragments have a mass difference in the ratio 3:2 (Bacon, 1969). Neutrons emitted from this fission process vary in energy over the range 0−10 MeV with an average neutron energy of 2 MeV, which are classified as fast neutrons.

Let us take one of many possible examples of ^{236}U fission to calculate the magnitude of energy liberated. One example of many possible fission reactions, that may be written conserving mass and charge of the ^{236}U nucleus with the emission of three neutrons, is the following:

$$^{235}_{92}\mathrm{U} + {}^{1}_{0}\mathrm{n} \rightarrow [^{236}_{92}\mathrm{U}] \rightarrow {}^{90}_{38}\mathrm{Sr} + {}^{143}_{54}\mathrm{Xe} + 3\,{}^{1}_{0}\mathrm{n} \qquad [10.24]$$

The energy liberated in the above fission reaction can be determined from its Q value, which is calculated according to Eq. [2.11], described in chapter "Basic Concepts and Definitions," as follows:

$$Q = (M_{\text{reactants}})c^2 - (M_{\text{products}})c^2 \qquad [10.25]$$

where $M_{\text{reactants}}$ and M_{products} are the combined masses of the nuclear reactants and products, respectively, and c is the velocity of light in a vacuum. For the fission reaction in Eq. [10.24], we can calculate its Q value as:

$$\begin{aligned} Q &= (M_{^{235}\mathrm{U}} + M_{^{1}\mathrm{n}})c^2 - (M_{^{90}\mathrm{Sr}} + M_{^{143}\mathrm{Xe}} + 3M_{^{1}\mathrm{n}})c^2 \\ &= [(235.043922\ \mathrm{u} + 1.00866492\ \mathrm{u}) - (89.907738\ \mathrm{u} + 142.9352\ \mathrm{u}) + 3(1.00866492\ \mathrm{u})] \times 931.494013\ \mathrm{MeV/u} \\ &= 171.1\ \mathrm{MeV}, \end{aligned} \qquad [10.26]$$

where 1 u = 931.494013 MeV or 931.494013 MeV/c^2.

The above-calculated Q value of 171.1 MeV is in agreement with the computer-calculated Q value determined with QCalc provided by the National Nuclear Data Center, Brookhaven National Laboratory (NNDC, 2016a): http://www.nndc.bnl.gov/qcalc/. As noted previously, most of the energy released appears as kinetic energy of the fission fragments ($\sim$165 MeV). The neutrons carry off about 2 MeV each on average. Additional energy is released from fission via gamma radiation and beta decay of the fission products and the neutrino radiation that accompanies beta decay. The total energy realized by the neutron-induced fission of ^{235}U, in the example given by Eq. [10.24], to the ultimate decay of the fission products ^{90}Sr and ^{143}Xe to their stable ground states is calculated by determining firstly the decay schemes of the two fission products as follows.

10.3.3.1 Decay of ^{90}Sr

$$\begin{array}{l} {}^{90}_{38}\mathrm{Sr} \rightarrow {}^{90}_{39}\mathrm{Y} + \beta^- + \bar{\nu} \\ \qquad\qquad \searrow \\ \qquad\qquad {}^{90}_{40}\mathrm{Zr}\ (\text{stable}) + \beta^- + \bar{\nu} \end{array} \qquad [10.27]$$

10.3.3.2 Decay of ^{143}Xe

$$\begin{array}{l} {}^{143}_{54}\mathrm{Xe} \rightarrow {}^{143}_{55}\mathrm{Cs} + \beta^- + \bar{\nu} + \gamma \\ \qquad\qquad \searrow \\ \qquad\qquad {}^{143}_{56}\mathrm{Ba} + \beta^- + \bar{\nu} + \gamma \\ \qquad\qquad\qquad \searrow \\ \qquad\qquad\qquad {}^{143}_{57}\mathrm{La} + \beta^- + \bar{\nu} \\ \qquad\qquad\qquad\qquad \searrow \\ \qquad\qquad\qquad\qquad {}^{143}_{58}\mathrm{Ce} + \beta^- + \bar{\nu} + \gamma \\ \qquad\qquad\qquad\qquad\qquad \searrow \\ \qquad\qquad\qquad\qquad\qquad {}^{143}_{59}\mathrm{Pr} + \beta^- + \bar{\nu} + \gamma \\ \qquad\qquad\qquad\qquad\qquad\qquad \searrow \\ \qquad\qquad\qquad\qquad\qquad\qquad {}^{143}_{60}\mathrm{Nd}\ (\text{stable}) + \beta^- + \bar{\nu} + \gamma \end{array} \qquad [10.28]$$

Thus, the final reaction to the stable nuclides can be written as:

$$^{235}_{92}\mathrm{U} + {}^{1}_{0}\mathrm{n} \rightarrow [{}^{236}_{92}\mathrm{U}] \rightarrow {}^{90}_{40}\mathrm{Zr} + {}^{143}_{60}\mathrm{Nd} + 3{}^{1}_{0}\mathrm{n} + 8\beta^- + 8\bar{\nu} + \gamma \qquad [10.29]$$

If we use atomic mass units to calculate the Q value of the above reaction, the eight additional atomic electrons of the $^{90}_{40}$Zr + $^{143}_{60}$Nd (100 atomic electrons) over the $^{235}_{92}$U (92 atomic electrons) force the eight electrons represented by the eight beta particles ($8\beta^-$) to drop out of the equation. Thus, we can calculate the Q value as:

$$\begin{aligned} Q &= (M_{^{235}\mathrm{U}} + M_{^{1}\mathrm{n}})c^2 - (M_{^{90}\mathrm{Zr}} + M_{^{143}\mathrm{Nd}} + 3M_{^{1}\mathrm{n}})c^2 \\ &= [(235.043922\ \mathrm{u} + 1.00866492\ \mathrm{u}) - (89.904702\ \mathrm{u} + 142.909810\ \mathrm{u}) + 3 \times 1.00866492\ \mathrm{u}] \times 931.494013\ \mathrm{MeV/u} \\ &= 197.55\ \mathrm{MeV} \end{aligned} \qquad [10.30]$$

The calculated Q value of 197.55 MeV represents the total energy released in the example of the neutron-induced fission of ^{235}U to the unstable ^{90}Sr and ^{143}Xe fission products, followed by the decay of these fission products, to the stable ^{90}Zr and ^{143}Nd nuclides. This calculated value is close to the estimated value of $\sim$202 MeV using average binding energies of the parent and daughter nuclides found in chapter "The Atomic Nucleus."

Let us take another example of many possible fission possibilities of the neutron-induced fission of ^{235}U. This example is one where the two fission products are of the same mass number, which is the following:

$$^{235}_{92}\mathrm{U} + {}^{1}_{0}\mathrm{n} \rightarrow [{}^{236}_{92}\mathrm{U}] \rightarrow 2\,{}^{117}_{46}\mathrm{Pd} + 2\,{}^{1}_{0}\mathrm{n} \qquad [10.31]$$

The fission products in this case are two nuclides of ^{117}Pd and two neutrons. The energy released by the neutron-induced fission is calculated as:

$$\begin{aligned} Q &= (M_{^{235}\mathrm{U}} + M_{^{1}\mathrm{n}})c^2 - (2M_{^{117}\mathrm{Pd}} + 2M_{^{1}\mathrm{n}})c^2 \\ &= [(235.043922\ \mathrm{u} + 1.00866492\ \mathrm{u}) - (2 \times 116.9178\ \mathrm{u} + 2 \times 1.00866492\ \mathrm{u})] \times 931.494013\ \mathrm{MeV/u} \\ &= 185.9\ \mathrm{MeV}, \end{aligned} \qquad [10.32]$$

which agrees with the value calculated by the National Nuclear Data Center's QCalc, Brookhaven National Laboratory (NNDC, 2016a): http://www.nndc.bnl.gov/qcalc/. The total energy yield, that includes the decay of the radioactive ^{117}Pd, can be calculated after firstly determining the decay scheme of two nuclides of ^{117}Pd to final stable daughter nuclides. The decay scheme is the following:

$$\begin{aligned} 2\,{}^{117}_{46}\mathrm{Pd} &\rightarrow 2\,{}^{117}_{47}\mathrm{Ag} + 2\beta^- + 2\bar{\nu} + \gamma \\ &\searrow \\ &\quad 2\,{}^{117}_{48}\mathrm{Cd} + 2\beta^- + 2\bar{\nu} + \gamma \\ &\quad\ \searrow \\ &\quad\ 2\,{}^{117}_{49}\mathrm{In} + 2\beta^- + 2\bar{\nu} + \gamma \\ &\quad\quad\ \searrow \\ &\quad\quad 2\,{}^{117}_{50}\mathrm{Sn}\ (\mathrm{stable}) + 2\beta^- + 2\bar{\nu} + \gamma \end{aligned} \qquad [10.33]$$

From the above reaction schemes, the total reaction of the neutron-induced fission of ^{235}U to two nuclides of ^{117}Sn can be written as follows:

$$^{235}_{92}\mathrm{U} + {}^{1}_{0}\mathrm{n} \rightarrow [{}^{236}_{92}\mathrm{U}] \rightarrow 2\,{}^{117}_{50}\mathrm{Sn} + 2\,{}^{1}_{0}\mathrm{n} + 8\beta^- + 8\bar{\nu} + \gamma \qquad [10.34]$$

The total energy released from this example of neutron-induced fission of ^{235}U is calculated as:

$$\begin{aligned} Q &= (M_{^{235}\mathrm{U}} + M_{^{1}\mathrm{n}})c^2 - (2M_{^{117}\mathrm{Sn}} + 2M_{^{1}\mathrm{n}})c^2 \\ &= [(235.043922\ \mathrm{u} + 1.00866492\ \mathrm{u}) - (2 \times 116.902955\ \mathrm{u} + 2 \times 1.00866492\ \mathrm{u})] \times 931.494013\ \mathrm{MeV/u} \\ &= 213.6\ \mathrm{Mev} \end{aligned} \qquad [10.35]$$

Thus, from the two examples of possible fission reactions taken above (Eqs. [10.29] and [10.34]), which include the decay of the fission products to stable nuclides, we calculated the energy released by the two fission processes as 197.5 MeV (Eq. [10.30]) and 213.6 MeV (Eq. [10.35]). We can see that approximately 200 MeV is the amount of energy released from the two examples taken of the neutron-induced fission of ^{235}U. The magnitude of the energy released from neutron-induced fission of ^{235}U would be an average figure, because the actual amount of energy released would depend on the fission reaction, and there are many possible ways that the ^{236}U could break into two nuclides. Some of the energy arises from fission product radioactivity including gamma-ray emission as fission product nuclides decay to lower energy states, beta-particle emission from fission product decay, and the emission of neutrinos that accompany beta decay. The energy released can be itemized into the various energy categories listed in Table 10.3, which are tallied to provide an approximate average figure for the energy released in neutron-induced fission of ^{235}U.

Because more than one neutron is released per fission, a self-sustaining chain reaction is possible with the liberation of considerable energy, forming the basis for the nuclear reactor as a principal source of neutrons and energy. In the case of ^{235}U, slow neutrons are required for neutron capture and fission to occur. The nuclear reactor, therefore, will be equipped with a moderator such as heavy water (D_2O) or graphite, which can reduce the energies of the fast neutrons via elastic scattering of the neutrons with atoms of low atomic weight. The protons of water also serve as a good moderator of fast

TABLE 10.3 Approximate Energy Released From Neutron-Induced ^{235}U Fission

Type	Energy Released (MeV)
Prompt energy	
Fission product kinetic energy	165
Neutrons (2.5 n/fission on average, ~2 MeV/n on average)	5
Gamma-ray emissions	7
Energy from fission-product decay	
Gamma-ray emissions	7
Beta radiation	6
Neutrinos	10
Total	200 MeV

neutrons, provided the neutrons lost via the capture process $^{1}H(n,\gamma)^{2}H$ can be compensated by the use of a suitable enrichment of the ^{235}U in the nuclear reactor fuel (Bryne, 1994).

The previously described fission of ^{235}U represents the one and only fission of a naturally occurring radionuclide that can be induced by slow neutrons. The radionuclides ^{239}Pu and ^{233}U also undergo slow neutron-induced fission; however, these nuclides are manmade via the neutron irradiation and neutron capture of ^{238}U and ^{232}Th, as illustrated in the following equations (Murray, 2009). The preparation of ^{239}Pu occurs by means of neutron capture by ^{238}U followed by beta decay as follows:

$$^{238}_{92}U + {}^{1}_{0}n \rightarrow {}^{239}_{92}U + \gamma \quad [10.36]$$

$$^{239}_{92}U \xrightarrow{t_{1/2}=23.5\,\text{min}} {}^{239}_{93}Np + \beta^{-} \quad [10.37]$$

$$^{239}_{93}Np \xrightarrow{t_{1/2}=2.35\,\text{days}} {}^{239}_{94}Pu + \beta^{-} \quad [10.38]$$

The preparation of ^{233}U is carried out via neutron capture of ^{232}Th followed by beta decay according to the following:

$$^{232}_{90}Th + {}^{1}_{0}n \rightarrow {}^{233}_{90}Th + \gamma \quad [10.39]$$

$$^{233}_{90}Th \xrightarrow{t_{1/2}=22.4\,\text{min}} {}^{233}_{91}Pa + \beta^{-} \quad [10.40]$$

$$^{233}_{91}Pa \xrightarrow{t_{1/2}=27.0\,\text{days}} {}^{233}_{92}U + \beta^{-} \quad [10.41]$$

Nuclides that undergo slow neutron-induced fission are referred to as fissile materials. Although ^{235}U is the only naturally occurring fissile radionuclide, it stands to reason that, if an excess of neutrons is produced in a thermal reactor, it would be possible to produce fissile ^{239}Pu or ^{233}U fuel in a reactor in excess of the fuel actually consumed in the reactor. This is referred to as "breeding" fissile material, and it forms the basis for the new generation of breeder reactors (Murray, 2009).

Other heavy isotopes, such as ^{232}Th, ^{238}U, and ^{237}Np, undergo fission but require bombardment by fast neutrons of at least 1 MeV energy to provide sufficient energy to the nucleus for fission to occur. These radionuclides are referred to as fissionable isotopes.

10.3.4 Photoneutron (γ,n) Sources

Many nuclides emit neutrons upon irradiation with gamma or x-radiation; however, most elements require high-energy electromagnetic radiation in the range 10−19 MeV. The gamma or X-ray energy threshold for the production of neutrons varies with target element. Deuterium and beryllium metal are two exceptions, as they can yield appreciable levels of neutron radiation when bombarded by gamma radiation in the energy range of only 1.7−2.7 MeV. The target material of D_2O or beryllium metal is used to enclose a β^{-}-emitting radionuclide, which also emits gamma rays. The gamma radiation

bombards the targets deuterium and beryllium to produce neutrons according to the photonuclear reactions $^{2}H(\gamma,n)^{1}H$ and $^{9}Be(\gamma,n)^{8}Be$, respectively. The photoneutron source $^{124}Sb + Be$ serves as a good example of a relatively high-yielding combination of gamma emitter with beryllium target. The ^{124}Sb gamma radiation of relevance in photoneutron production is emitted with an energy of 1.69 MeV at 50% abundance (ie, one-half of the ^{124}Sb radionuclides emit the 1.69-MeV gamma radiation following beta decay). A yield of 5.1 neutrons per 106 beta disintegrations per gram of target material has been reported (Byrne, 1994). The half-life ($t_{1/2}$) of ^{124}Sb is only 60.2 days, which limits the lifetime of the photoneutron generator; nevertheless, this isotope of antimony is easily prepared in the nuclear reactor by neutron irradiation of natural stable ^{123}Sb. An excellent example is that reported by Fantidis et al. (2009), whereby a SbBe neutron source was demonstrated to be very useful as a transportable neutron source applicable to a neutron radiography system. The particular advantage of such a neutron source is the ability to effectively have an on/off switching capability, because the production of neutrons can be stopped by simply removing the beryllium target from the antimony gamma-ray source. A unique application of the $^{9}Be(\gamma,n)^{8}Be$ reaction is reported by Moussavi-Zarandi (2008), who used the gamma emissions from a ^{124}Sb source to survey for the Be content of minerals in the exploration of potential beryllium mines. The neutrons emitted from the Be nucleus via the (γ,n) reaction are detected by a BF_3 neutron counter, providing a survey meter for Be exploration.

An alternative to a gamma source for the (γ,n) reaction is the use of electrostatic and linear accelerators (LINACs). Commercially available linear accelerators are capable of accelerating electrons against a high Z element, such as tungsten, to produce bremsstrahlung radiation. The bremsstrahlung photons interact with a converter material such as Be or BeD_2, which converts the photon beam to a neutron beam via the reactions $^{9}Be(\gamma,n)^{8}Be$ and $^{2}H(\gamma,n)^{1}H$. The symbol γ is used here to denote the nuclear reaction projectile although bremsstrahlung photons (X-rays), rather than gamma-rays, are the projectiles. This is done out of convenience, as bremsstrahlung and gamma-rays are photons which differ only in their origins. The target and converter materials are arranged with respect to the electron beam in a fashion such as that illustrated in Fig. 10.3. Alternatively, the electron beam may be directed to impinge immediately onto a Be or BeD_2 target material, whereby the bremsstrahlung photons that are produced interact directly with the Be or BeD_2 target to yield neutrons (Auditore, 2005).

In such an arrangement as illustrated in Fig. 10.3, neutrons are produced by means of the electron accelerator. The process, as described by Eshwarappa et al. (2007), entails the acceleration of electrons to impinge on a high Z target (eg, tungsten, W), which generates a cascade shower of bremsstrahlung photons with an energy spectrum having an end-point equal to the electron beam energy. The photons produced in this fashion travel through a suitable photoneutron target (eg, Be or BeD_2), producing excited compound nuclei of energy equal to the sum of the binding energy of the last neutron and the energy of the bremsstrahlung X-rays. When the excitation energy is larger than the binding energy of the last neutron in the compound nucleus, a neutron is emitted. Any excess energy is shared as kinetic energy of the neutron and the residual nucleus (Eshwarappa et al., 2007). Essentially the energy conversion follows the path of $e-\gamma-n$, that is, the accelerated electron energy is converted to bremsstrahlung photons, which subsequently yields neutrons.

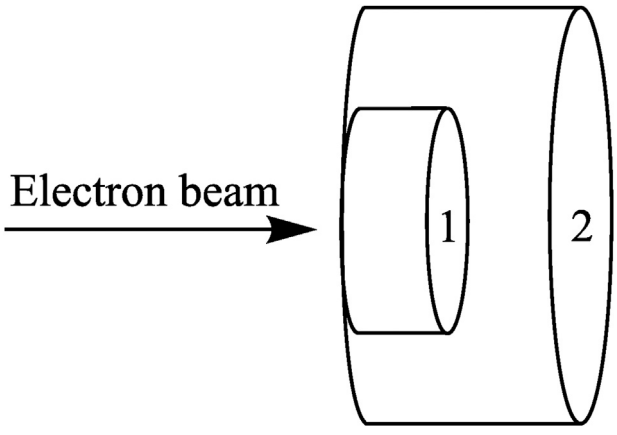

FIGURE 10.3 A photoneutron assembly consisting of (1) a disc of tungsten (W) target embedded within (2) a photoneutron converter consisting of Be or BeD_2. Typical dimensions are 2 × 8 cm (thickness × radius W target) and 10 × 12 cm or 60 × 60 cm Be or BeD_2 target. *From Rahmani, F., Shahriari, M., 2010. Hybrid photoneutron source optimization for electron accelerator-based BNCT. Nucl. Instrum. Methods Phys. Res. Sect. A 618, 48–53. Reprinted with permission from Elsevier © 2010.*

LINACs producing high-energy (15−25 MeV) photon beams are becoming widespread (Bevilacqua et al., 2007). Low-energy LINACs (<10 MeV) are found useful for neutron radiography and radiation boron-neutron capture therapy (BNCT) in radiation oncology. A 5-MeV electron LINAC with Be and BeD_2 targets can lead to thermal neutron beams of 8.48×10^7 n/cm^2/s/mA and 1.23×10^8 n/cm^2/s/mA, respectively (Auditore, 2005).

The use of LINACs for e−γ−n conversions as neutron sources in cancer therapy using BNCT is under development (Bevilacqua et al., 2007; Mameli et al., 2008; Martínez et al., 2010; Rahmani and Shahriari, 2010). BNCT entails the use of thermal neutrons to kill individual cancer cells (eg, brain tumors) with minimal damage to cancer-free cells. The principle and technique of BNCT is firstly the administration of a ^{10}B-loaded pharmaceutical to a cancer patient followed by the irradiation of the tumor with thermal neutrons, produced as previously described with the LINAC e−γ−n conversion. The ^{10}B-loaded pharmaceutical concentrates in the cancer cells, and the neutrons react with the ^{10}B to yield ^{7}Li and alpha-particles within the cancer cell according to ^{10}B(n,α)^{7}Li, that is:

$$ {}^{1}_{0}\mathrm{n} + {}^{10}_{5}\mathrm{B\text{-pharmaceutical}} \rightarrow {}^{7}_{3}\mathrm{Li} + {}^{4}_{2}\mathrm{He} \quad Q = 2.79\ \mathrm{MeV} \qquad [10.42] $$

The ^{7}Li and alpha particles share the kinetic energy liberated in the reaction. Their high mass attributes a high linear energy transfer (LET), high relative biological effectiveness (RBE), and short range of travel of 4.1 and 7.7 μm for the ^{7}Li and alpha particles, respectively (Eskandari and Kashian, 2009; Tanaka et al., 2009a; Rahmani and Shahriari, 2010). The total range of 11.8 μm is equivalent to the dimensions of a cell in the human body, thus providing BNCT with the advantage of cell selectivity over other methods of radiotherapy.

Accelerated electron-generated neutrons via the (γ,n) reactions have been reported to yield in a uranium target as many as 10^{-2} neutrons per accelerated electron at an electron energy of 30 MeV with a total yield of 2×10^{13} neutrons per second (Bryne, 1994). The accelerator is a good neutron source for the potential generation of nuclear fuels. Some other applications of photoneutrons produced by X-rays from electron accelerators are the detection of explosives by the measurement of photoneutron-induced gamma rays (Yang et al., 2007), photoneutron assay of highly enriched uranium via neutron-induced fission (Lakosi and Nguyen, 2008), and the elemental analysis of short-lived activation products (Patil et al., 2010a,b).

10.3.5 Accelerator Sources

The accelerator utilizes electric and magnetic fields to accelerate beams of charged particles such as protons, electrons, and deuterons into target materials. Nuclear reactions are made possible when the charged particles have sufficient kinetic energy to react with target nuclei. Some of the reactions between the accelerated charged particles and target material can be used to generate neutrons.

When electrons are accelerated, they gain kinetic energy as a function of the particle velocity. This kinetic energy is lost as bremsstrahlung electromagnetic radiation when the accelerated electrons strike the target material. Bremsstrahlung radiation is described in chapter "Electromagnetic Radiation: Photons." It is the Bremsstrahlung photons that interact with nuclei to produce neutrons according to the mechanisms described in the previous section under photoneutron (γ,n) sources.

Accelerated deuterons can be used to produce high neutron yields when deuterium and tritium are used as target materials according to the reactions ^{2}H(d,n)^{3}He and ^{3}H(d,n)^{4}He, respectively. In the deuterium energy range of 100−400 keV, it is possible to obtain neutron yields of the order of 10^{11} neutrons per second from these (d,n) reactions with relatively small electrostatic laboratory accelerators (Bryne, 1994; Kim et al., 2008; Eskandari and Kashian, 2009; and Park et al., 2009). The ^{2}H(d,n)^{3}He and ^{3}H(d,n)^{4}He reactions are referred to as the D−D and D−T neutron sources. When low-energy deuterons are used as projectiles, the D−D and D−T reactions yield 2.4 and 14.1 MeV fast monoenergetic neutrons, respectively (Eskandari and Kashian, 2009; Tracz et al., 2009; Sharma et al., 2010). The Q values for the D−D and D−T reactions are 3.27 and 17.58 MeV, respectively, which explains the energy of the neutrons liberated in these reactions. The remaining energy not carried away by the neutrons remains with the residual ^{3}He and ^{4}He nuclei of the D−D and D−T reactions. The two (d,n) reactions are the same as the fusion reactions discussed in the subsequent section of this chapter. The low energies of the deuteron projectiles required for the D−D and D−T reactions are advantageous when small accelerators are used in facilities that utilize neutrons for radiation therapy such as BNCT described in the previous sections of this chapter. Neutrons of higher energy (14−30 MeV) may be obtained from the D−T reactions by increasing the deuteron projectile energy, as the neutron energy is a function of the deuteron energy (Eskandari and Kashian, 2009). By means of a low-energy (350 keV) deuteron beam and a tritium target of 0.37 TBq of ^{3}H, Ochiai et al. (2007) report the D−T reaction yielding a neutron fluence of 1.5×10^{11} n/s, which was determined by counting the 3.5-MeV alpha-particles. The neutron flux from this generator could be increased 10-fold by increasing the thickness of the ^{3}H target (Csikai, 1987; Eskandari and Kashian, 2009).

By accelerating deuterons and protons to energies between 1.8 and 4 MeV, neutron generation using beryllium and lithium targets via the following reactions is routine: ^{9}Be(d,n)^{10}B, ^{7}Li(p,n)^{7}Be, and ^{9}Be(p,n)^{9}B (Bayanov et al., 2009a,b, 2010; Eskandari and Kashian, 2009; Feinberg et al., 2009; Iwashita et al., 2011). A higher-energy 30-MeV proton beam against a beryllium target was used by Tanaka et al. (2009b); and the fast neutrons were moderated for boron-neutron capture therapy.

The acceleration of protons in the energy range of ~0.5–5 GeV against targets of high atomic number will result in nuclear spallation with the emission of typically 20–30 high-energy neutrons per incoming proton, depending on the energy of the proton beam and the nature of the target material (Samec et al., 2009; Krása et al., 2010). Even higher yields of 40–50 neutrons emitted per proton projectile are possible at the very high proton energies of 4 and 5 GeV (Krása et al., 2010). Nuclear spallation is the process that occurs when a nucleus of high atomic number emits a large number of neutrons following impact by a high-energy projectile. Such reactions are abbreviated often with the notation (p,*x*n) which signifies a proton projectile with the emission of x number of neutrons (see Table 10.1). Such high-power neutron sources can yield a neutron flux of up to 10^{14} n/cm^2/s at the surface of the source. Some typical targets of high mass number, which have favorable spallation-neutron production characteristics, are Hg, W, ^{238}U, Pb, and Th (Aydin et al., 2008). Practical implications of neutron sources for the generation of nuclear fuels were noted previously in Section 10.3.3. Murray (2009) pointed out that a yield of as many as 50 neutrons per single charged-particle projectile could be used to produce new nuclear fuels via neutron capture by ^{238}U and ^{232}Th according to Eqs. [10.36]–[10.41] described previously.

When protons are accelerated at lower energies of 20–60 MeV against targets of intermediate mass number (eg, Cr and Cu), the spallation-neutron production characteristics are less favorable, that is, the yield of number of neutrons emitted per proton projectile is lower. Aydin et al. (2008) measured the spallation reaction cross-sections for protons in the energy range of up to 100 MeV against target nuclei consisting of isotopes of Cr and Cu. The neutrons emitted per proton projectile ranged from (p,n) at the low 20–30 MeV proton energies to (p,4n) at the higher 50–60 MeV proton energies. Thus, a cyclotron capable of accelerating protons to 20–60 MeV was found suitable for the production of neutrons from these target materials.

10.3.6 Nuclear Fusion

Nuclear fusion is the process whereby nuclei join together into one nucleus. The fusion of two atomic nuclei into one nucleus is not possible under standard temperature and pressure. This is because the repulsing coulombic forces between the positive charges of atomic nuclei prevent them from coming into the required close proximity of 10^{-15} m before they can coalesce into one. However, as described by Kudo (1995) and the Uranium Information Center (UIC, 2005) in reviews on nuclear fusion, if temperatures are raised to 100 million degrees, atomic electrons and nuclei can become plasmas in which the nuclei and electrons move independently at a speed of 1000 km/s, thereby giving the nuclei sufficient kinetic energy to overcome their repulsing forces and combine. The process is also referred to as thermonuclear fusion. Nuclear fusion reactors or controlled thermonuclear reactors (CTRs) are under development to achieve nuclear fusion as a practical energy source. The reactors are based on maintaining plasmas through magnetic and inertial confinement as described in chapter "Radioactivity and Our Well Being" of this book. Some fusion reactions produce neutrons.

The energy liberated during nuclear fusion is derived from the fact that the mass of any nucleus is less than the sum of its component protons and neutrons. This is because protons and neutrons in a nucleus are bound together by strong attractive nuclear forces described in chapter "The Atomic Nucleus." As explained by Serway et al. (2005), this energy is referred to as the binding energy (B), that is, the energy of work required to pull a bound system apart, leaving its component parts free of attractive forces, described by the equation:

$$Mc^2 + B = \sum_{i=1}^{n} m_i c^2 \qquad [10.43]$$

where M is mass of the bound nucleus, the m_i's are the free component particle masses (eg, protons and neutrons), and n is the number of component particles of the nucleus. From Eq. [10.43] we can see that if it is possible to overcome the repulsive forces of protons in nuclei and fuse these into a new nucleus or element of lower mass, energy will be liberated.

Nuclear fusion reactions of two types emit neutrons, and these are of prime interest in manmade controlled thermonuclear reactors. The first type is fusion between deuterium and tritium nuclei according to:

$$^{2}_{1}\mathrm{H} + {}^{3}_{1}\mathrm{H} \rightarrow {}^{4}_{2}\mathrm{He} + {}^{1}_{0}\mathrm{n} + 17.58\ \mathrm{MeV} \qquad [10.44]$$

We can confirm the energy released in the above reaction, (Eq. [10.44]), by using Einstein's equation for the equivalence of mass and energy. We can write firstly the atomic mass units for each component of the reaction and then calculate the energy equivalence in atomic mass units as follows:

$$^{2}_{1}\mathrm{H} + {}^{3}_{1}\mathrm{H} \rightarrow {}^{4}_{2}\mathrm{He} + {}^{1}_{0}\mathrm{n} + E \quad [10.45]$$

$$3.01604927\ \mathrm{u} + 2.014101778\ \mathrm{u} \rightarrow 4.00260324\ \mathrm{u} + 1.008664904\ \mathrm{u} + E \quad [10.46]$$

$$\begin{aligned} E &= (3.01604927\ \mathrm{u} + 2.014101778\ \mathrm{u})c^2 - (4.00260324\ \mathrm{u} + 1.008664904\ \mathrm{u})c^2 \\ &= (0.018882904\ \mathrm{u})c^2 \end{aligned} \quad [10.47]$$

Converting atomic mass units u into energy, where $1\ \mathrm{u} = 931.494\ \mathrm{MeV}/c^2$, yields:

$$\begin{aligned} E &= mc^2 \\ &= \left[(0.018882904\ \mathrm{u})\left(931.494\ \mathrm{Mev}/c^2\right)\right]c^2 \\ &= 17.58\ \mathrm{MeV} \end{aligned}$$

The fusion of deuterium and tritium is illustrated in Fig. 10.4.

Two other fusion reactions between two deuterium nuclei may proceed according to either of the following equations, which have approximately equal probabilities of occurring (Kudo, 1995):

$$^{2}_{1}\mathrm{H} + {}^{2}_{1}\mathrm{H} \rightarrow {}^{3}_{2}\mathrm{He} + {}^{1}_{0}\mathrm{n} + 3.27\ \mathrm{MeV} \quad [10.48]$$

and:

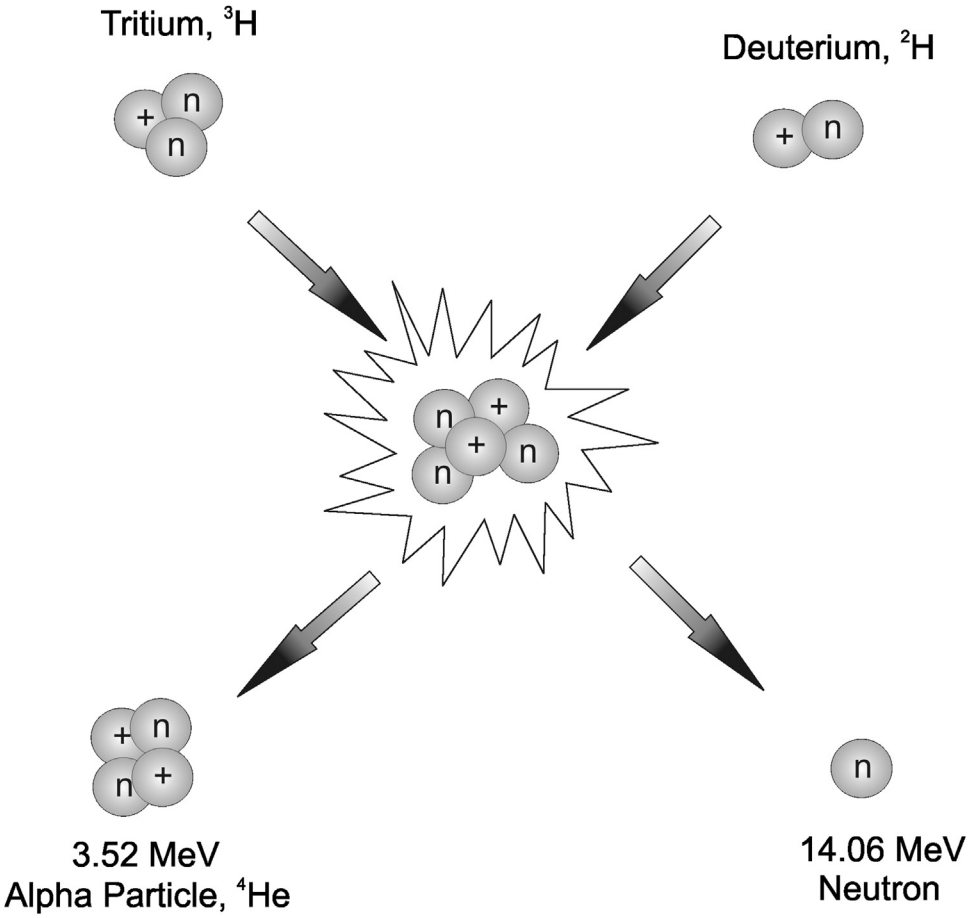

FIGURE 10.4 Fusion of deuterium and tritium. Under high temperature with magnetic field or inertial confinement, deuterium (^{2}H) and tritium (^{3}H) become plasmas whereby their electrons and nuclear protons (+), and neutrons (n) have sufficient kinetic energy to move about and interact free of their repulsive coulombic barriers. The nucleons coalesce forming a larger nucleus (center of figure), an alpha particle (^{4}He), and an excess neutron (n) with the emission of energy as kinetic energy of the alpha particle and neutron.

$$^{2}_{1}\mathrm{H} + {}^{2}_{1}\mathrm{H} \rightarrow {}^{3}_{1}\mathrm{H} + {}^{1}_{1}\mathrm{H} + 4.04\ \mathrm{MeV} \quad [10.49]$$

Another possible reaction in deuterium fusion is the formation of an alpha particle with the emission of gamma radiation as described by the following:

$$^{2}_{1}\mathrm{H} + {}^{2}_{1}\mathrm{H} \rightarrow {}^{4}_{2}\mathrm{He} + \gamma + 23.9\ \mathrm{MeV} \quad [10.50]$$

Although more energy is released in the above reaction, it has a low reaction cross-section, ie, low probability of occurrence, and most of the energy would be carried off by the gamma radiation (Lilley, 2001). The highly penetrating gamma rays would make it extremely difficult to sufficiently trap the energy for heat and electric power generation.

The fusion reaction between deuterium and tritium or D-T reaction (Eq. [10.44]) gives rise to a 14.06-MeV neutron and a 3.52-MeV alpha particle. This is the fusion reaction that is under research currently as a future source of energy that should someday replace nuclear fission power reactors as a safer source of electric power. The current advances in this direction are reviewed in chapter "Radioactivity and Our Well Being" of this book.

10.3.7 Inertial Electrostatic Confinement Fusion (IECF)

Under development are compact neutron sources, which utilize either D−D or D−T fusion reactions as well as D−^{3}He fusion. One instrument described by Miley and Sved (1997) is the inertial electrostatic confinement fusion (IECF) device, which accelerates deuteron ions producing fusion reactions as the ions react with a pure deuterium or deuterium−tritium plasma target. The device is compact, measuring 12 cm in diameter and 1 m in length, and provides a neutron flux of 10^{6}–10^{7} 2.5-MeV D−D n/s or 10^{8}–10^{9} 14-MeV D−T n/s. As described by Noborio et al. (2006), IECF involves a basically simple device, which can cause the fusion reaction, and it is expected to be used as a compact neutron-beam generator. The basic IECF device is illustrated in Fig. 10.5. The device consists of a spherical grounded anode and a grid cathode. Ions are generated by glow discharge in low-pressure deuterium gas ($< \sim 2$ Pa), and the ions are accelerated toward the center region by a high electric field. Within the center cathode, concentrated energetic ions collide with each other or with background neutral gases, resulting in the fusion reaction.

As described by Tomiyasu et al. (2010), ions are accelerated to fusion-relevant energies by the electric field between concentric electrodes and circulate inside the outer anode through the inner gridded cathode. The inner cathode consists of a spherical wire grid, which is highly transparent to ions. The objective, as described by Khachan and Samarian (2007), is to create a deep potential well in order to trap ions and confine them for a long enough time, for which reason the concept was called inertial electrostatic confinement (IEC). The first effective device of this type was reported by Hirsch (1967), who obtained a neutron output of $\sim 10^{8}$ D−D n/s and 10^{10} D−T n/s from a grided IECF device driven by six ion guns. In addition to the D−D and D−T fusion reactions as neutron sources described by Eqs. [10.51] and [10.52], the IECF device

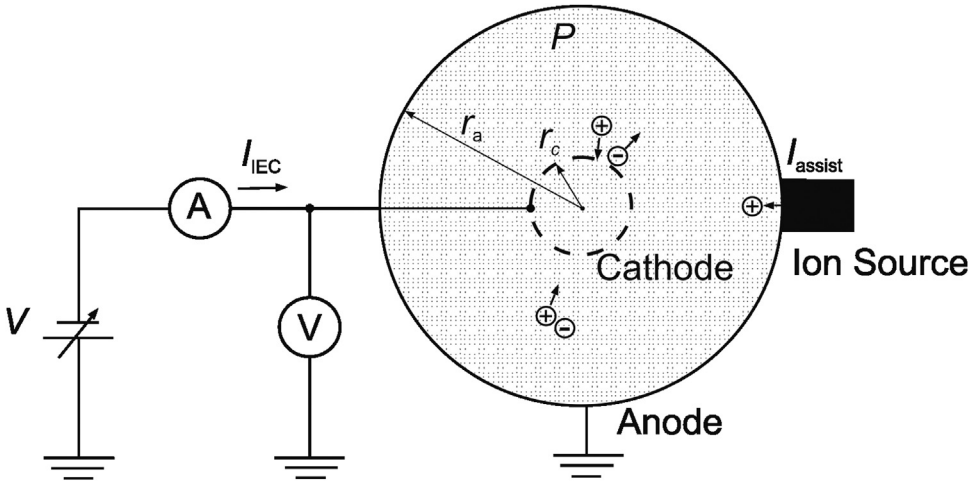

FIGURE 10.5 A schematic diagram of an IECF device and its geometrical and electrical parameters, namely, r_a = anode radius (17.10 cm), r_c = cathode radius (3 cm), P = gas pressure (0.07−0.2 Pa), V = discharge voltage (60−120 kV), I_{IEC} = discharge current (2 mA−4 A), and I_{assist} = injected ion current (2−200 mA). *From Noborio, K., et al., 2006. Confinement of ions in an inertial electrostatic confinement fusion (IECF) device and its influence on neutron production rate. Fusion Eng. Design 81, 1701−1705. Reprinted with permission of Elsevier @ 2006.*

is also a portable proton source yielding 10^8 protons/s utilizing the D−^{3}He fusion reaction (Eq. [10.53]) as described by Ashley et al. (2000) and Masuda et al. (2006). In summary, the fusion reactions that may yield neutrons and/or protons are the following:

$$\text{D}-\text{D fusion: } \begin{cases} {}^2_1\text{H} + {}^2_1\text{H} \rightarrow {}^3_2\text{He}(0.82\ \text{MeV}) + {}^1_0\text{n}(2.45\ \text{MeV})\ 50\% \quad Q = 3.27\ \text{MeV} \\ {}^2_1\text{H} + {}^2_1\text{H} \rightarrow {}^3_1\text{H}(1.01\ \text{MeV}) + {}^1_1\text{H}(3.03\ \text{MeV})\ 50\% \quad Q = 4.04\ \text{MeV} \end{cases} \quad [10.51]$$

$$\text{D}-\text{T fusion: } {}^2_1\text{H} + {}^3_1\text{H} \rightarrow {}^4_2\text{He}(3.52\ \text{MeV}) + {}^1_0\text{n}(14.06\ \text{MeV}) \quad Q = 17.58\ \text{MeV} \quad [10.52]$$

$$\text{D}-{}^3\text{He fusion: } {}^2_1\text{H} + {}^3_2\text{He} \rightarrow {}^4_2\text{He}(3.7\ \text{MeV}) + {}^1_1\text{H}(14.7\ \text{MeV}) \quad Q = 18.4\ \text{MeV} \quad [10.53]$$

The D−D fusion, as illustrated in Eq. [10.51], may occur via two possible reactions that have equal probabilities of occurrence, yielding either 2.45-MeV neutrons or 3.03-MeV protons. The D−T and D−^{3}He fusion reactions yield high-energy (14 MeV) neutrons or protons, respectively, according to Eqs. [10.52] and [10.53].

Although the concept of inertial electrostatic confinement fusion had an early beginning, only in the last several years has intense research been devoted to making this a compact portable neutron and proton source. In a review by Tomiyasu et al. (2010), two approaches have been taken to improve the IECF reaction rates, namely, (1) to increase the ion density by increasing the input current (Yamauchi et al., 2006; Ohnishi et al., 2007; Radel et al., 2007), and (2) to increase the ion energy by reducing the background gas pressure, which reduces the energy loss due to collisions with background neutral ions (Higashi et al., 2003; Piefer et al., 2005; Miley et al., 2005; and Takamatsu et al., 2006). Tomiyasu et al. (2010) proposed a magnetic-assisted electrostatic confinement whereby the ion motion can be controlled, as illustrated in Fig. 10.6. With the application of an appropriate magnetic field, the ions are forced to an azimuthal direction by Lorentz force as they are accelerated toward the center of the electric field.

In addition to efforts to increase the reaction rates achieved with the IECF device, research is conducted toward the practical applications of the device as a portable neutron source in light of its simple configuration and compact size. Applications of such a portable neutron and proton source include the detection and measurement of highly enriched uranium (Radel et al., 2007), the detection of explosives including land mine detection (Yoshikawa et al., 2007a,b; Takahashi et al., 2010), and isotope production (Cipiti and Kulcinski, 2005). Because of the simplicity and compact size of the IECF device, Yoshikawa et al. (2007a) list numerous applications subject to the expected improvements in reactions rates achieved by this neutron/proton source. These applications are listed in Fig. 10.7.

Another similar device is described by Tsybin (1997), which utilizes laser irradiation to create a plasma in an ion source. Compact neutron sources of these types can become competitive with other neutron sources previously described,

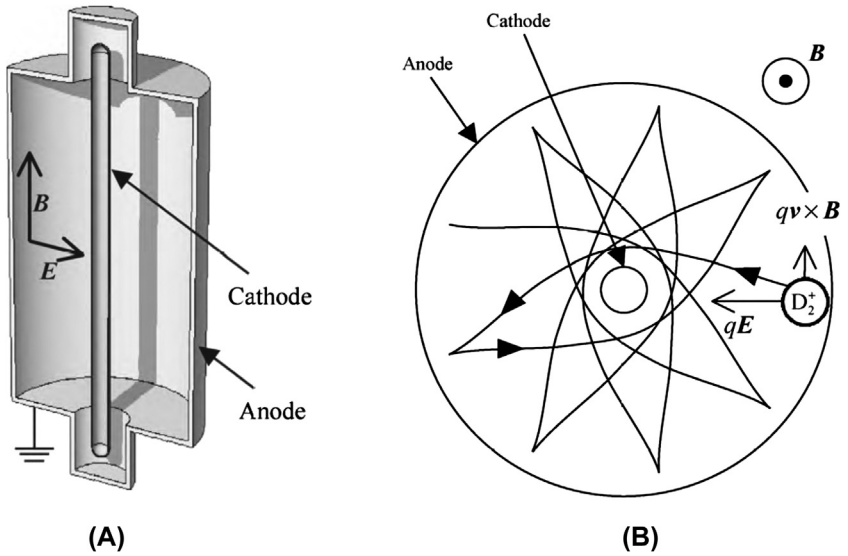

FIGURE 10.6 Schematic of (a) magnetic-assisted electrostatic confinement device, and (b) the motion of a deuterium molecular ion under the influence of the applied axial magnetic field. *From Tomiyasu, K., et al., 2010. Particle-in-cell simulation of magnetic-assisted electrostatic confinement device. Fusion Eng. Design 85 (5), 728–733. Reprinted with permission of Elsevier © 2010.*

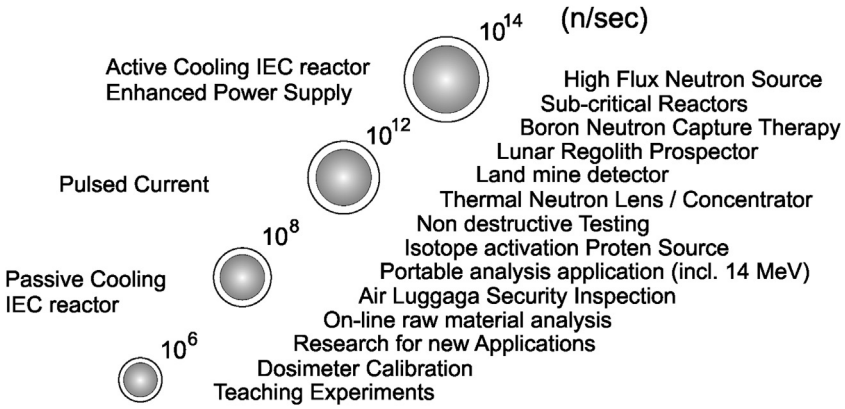

FIGURE 10.7 Applications of inertial electrostatic confinement fusion (IECF) devices. *From Yoshikawa, K., et al., 2007a. Research and development of a compact discharge-driven D–D fusion neutron source for explosive detection. Nucl. Instrum. Methods Phys. Res. Sect. B 261, 299–302. Reprinted with permission from Elsevier © 2007.*

such as ^{252}Cf and accelerator solid-target sources, because of advantages including (1) on-off capability, (2) longer lifetime without diminished neutron flux strength, and (3) minimum handling of radioactivity.

10.4 INTERACTIONS OF NEUTRONS WITH MATTER

If a neutron possesses kinetic energy, it will travel through matter much more easily than other nuclear particles of similar energy, such as alpha particles, negatrons, positrons, protons, or electrons. In great contrast to other nuclear particles, which carry charge, the neutron, because it lacks charge, can pass through the otherwise impenetrable coulombic barrier of the atomic electrons and actually collide with nuclei of atoms and be scattered in the process or be captured by the nucleus of an atom. Collision of neutrons with nuclei can result in scattering of the neutrons and recoil nuclei with conservation of momentum (elastic scattering) or loss of kinetic energy of the neutron as gamma radiation (inelastic scattering). The capture of a neutron by a nucleus of an atom may result in the emission of other nuclear particles from the nucleus (nonelastic reactions) or the fragmentation of the nucleus into two (nuclear fission). A brief treatment of the various types of neutron interactions, which are based on their scattering or capture by atomic nuclei, is provided next.

10.4.1 Elastic Scattering

The elastic scattering of a neutron by collision with an atomic nucleus is similar to that of billiard-ball collisions. A portion of the kinetic energy of one particle is transferred to the other without loss of kinetic energy in the process. In other words, part of the kinetic energy of the neutron can be transferred to a nucleus via collision with the nucleus, and the sum of the kinetic energies of the scattered neutron and recoil nucleus will be equal to the original kinetic energy of the colliding neutron. This process of interaction of neutrons with matter results only in scattering of the neutron and recoil nucleus. It does not leave the recoil nucleus in an excited energy state. Elastic scattering is a common mechanism by which fast neutrons lose their energy when they interact with atomic nuclei of low atomic number, such as hydrogen (^{1}H) in light water or paraffin, deuterium (^{2}H) in heavy water, and ^{12}C in graphite, which may be encountered in nuclear reactor moderators. It is easy to conceptualize what would occur when particles of equal or similar mass collide; the event would result in energy transfer and scattering without any other secondary effects, similar to what occurs in billiard-ball collisions.

Neutron scattering is the principal mechanism for the slowing of fast neutrons, particularly in media with low atomic number. Let us consider what occurs when a neutron collides with a nucleus and undergoes elastic scattering. Fig. 10.8 illustrates the direction of travel of an incident neutron with given kinetic energy (dashed line). The neutron collides with the nucleus. The nucleus is illustrated as undergoing recoil at an angle β, while the neutron is scattered at an angle α to the direction of travel of the incident neutron. The kinetic energy (E_k) lost by the neutron in this collision is defined by the equation:

$$E_k = \frac{4Mm_n}{(M+m_n)^2}\cos^2\beta \qquad [10.54]$$

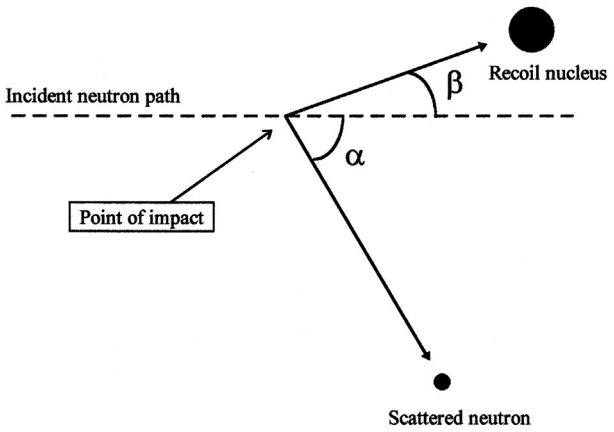

FIGURE 10.8 Elastic scattering of a neutron by collision of the neutron with an atomic nucleus. The neutron is scattered at an angle α and the nucleus recoils at an angle β to the direction of travel of the incident neutron.

where M is the mass of the nucleus, m_n is the mass of the neutron, and β is the recoil angle of the nucleus. A derivation of Eq. [10.54] is provided by Bacon (1969). Let us look at two extreme examples of elastic collisions between a neutron and a nucleus. In the first example, it is intuitively obvious from Eq. [10.54] that for a recoil angle $\beta = 90°$, $\cos^2\beta = 0$ and consequently $E_k = 0$. Under such a circumstance, the neutron is not deflected by the nucleus and there is no energy transfer to the nucleus. The neutron continues along its path without deflection until it encounters another nucleus. For the second case, however, let us consider the other extreme in which the recoil angle, $\beta = 0°$, where we have a head-on collision of the neutron with the nucleus of an atom. In this case, the maximum possible energy of the neutron is imparted to the nucleus, where $\cos^2\beta = 1$. For example, Table 10.4 provides the maximum fraction of the kinetic energy, calculated according to Eq. [10.54], that a neutron can lose upon collision with various atomic nuclei. As illustrated in Table 10.4, the neutron can transfer more energy to the nuclei of atoms, which have a low mass; and the highest fraction of its energy can be transferred to the nucleus of the proton, which is almost equal in mass to the neutron. Nuclides of low mass number are, therefore, good moderators capable of slowing down fast neutrons. The substances often used as neutron moderators are light water (H_2O), heavy water (D_2O), paraffin (C_nH_{2n+2}), and graphite (C).

10.4.2 Inelastic Scattering

We may picture a fast neutron colliding with a nucleus. The neutron is scattered in another direction as described in the previous paragraph; however, part of the neutron's kinetic energy is lost to the recoil nucleus, leaving it in an excited metastable state. Inelastic scattering can occur when fast neutrons collide with nuclei of large atomic number. The recoil

TABLE 10.4 Maximum Fraction of Kinetic Energy (E_k) a Neutron Can Lose Upon Collision With the Nucleus of Various Atoms, Listed in Increasing Mass in Atomic Mass Units (u)

Nuclide	Nuclide Mass, M	Neutron Mass, m_n	$E_k = (4Mm_n/(M+m_n)^2)\cos^2\beta$
^{1}H	1.007825	1.008665	4.065566/4.066232 = 0.999 or 100%
^{2}H	2.014102	1.008665	8.126217/9.137120 = 0.89 or 89%
^{9}Be	9.012182	1.008665	36.36109/100.41737 = 0.362 or 36.2%
^{12}C	12.000000	1.008665	48.41592/169.22536 = 0.286 or 28.6%
^{16}O	15.994915	1.008665	64.53404/289.12173 = 0.223 or 22.3%
^{28}Si	27.976927	1.008665	112.87570/840.16454 = 0.134 or 13.4%
^{55}Mn	54.938047	1.008665	221.65633/3130.0329 = 0.071 or 7.1%
^{197}Au	196.96654	1.008665	787.86616/39194.175 = 0.020 or 2.0%

nucleus may lose this energy immediately as gamma radiation or remain for a period of time in the excited metastable state. Inelastic scattering occurs mainly with fast neutron collisions with nuclei of large atomic number.

Neutron scattering is a common mechanism by which fast and intermediate neutrons are slowed down to the thermal neutron energy levels. Thermal neutrons have an energy level at which they are in thermal equilibrium with the surrounding atoms at room temperature. There is an energy range for thermal neutrons, as described earlier in this chapter; however, the properties of thermal neutrons are often cited at an energy calculated to be the most probable thermal neutron energy of 0.0253 eV at 20.43 °C corresponding to a velocity of 2200 m/s (Gibson and Piesch, 1985; Holden, 1997b). Fig. 10.1 may be used to find the velocity of the neutron at energy levels over the range 0.001 eV−10 MeV. For example, if we select the position 0.025 eV on the *X* axis and follow up the graph with a straight line to the upper curve, we find the value 2200 m/s. At the thermal energy state, the mechanisms of interaction of neutrons with matter change drastically, as discussed in the following section.

10.4.3 Neutron Capture

Because of the neutral charge on the neutron, it is relatively easy for slow neutrons, regardless of their low kinetic energy, to diffuse into the atom and "find themselves" in the vicinity of the nucleus without having to hurdle the coulombic forces of the atom. Once in close proximity to nuclei, it is easy for slow neutrons to enter into and be captured by nuclei to cause nuclear reactions. The capture of thermal neutrons, therefore, is possible with most radionuclides, and neutron capture is the main reaction of slow neutrons with matter. The power of a nucleus to capture a neutron depends on the type of nucleus as well as the neutron energy. The neutron absorption cross-section, σ, with units of 10^{-24} cm^2 or "barns," is used to measure the power of nuclides to absorb neutrons. A more detailed treatment of reaction cross-section and its units and application is provided in chapter "The Atomic Nucleus." Because the capture of thermal neutrons is possible with most radionuclides, references will cite the neutron cross-sections of the nuclides for comparative purposes at the thermal neutron energy of 0.0253 eV equivalent to a neutron velocity of 2200 m/s. This is also the energy of the neutron, which is in thermal equilibrium with the surrounding atoms at room temperature. For comparative purposes, therefore, Table 10.5 lists the thermal neutron cross-sections for neutron capture reactions in barns (10^{-24} cm^2) for several nuclides. The nuclides selected for Table 10.5 show a broad range of power for thermal neutron capture. Some of the nuclides listed have practical applications, which are referred to in various sections of this book.

The capture of a slow neutron by a nucleus results in a compound nucleus, which finds itself in an excited energy state corresponding to an energy slightly higher than the binding energy of the neutron in the new compound nucleus. This energy of excitation is generally emitted as gamma radiation. Neutron capture reactions of this type are denoted as (n,γ) reactions. Two practical examples of (n,γ) neutron capture reactions were provided earlier in this chapter in the neutron irradiation of ^{238}U and ^{232}Th for the preparation of fissile ^{239}Pu and ^{233}U (Eqs. [10.36] and [10.39]), respectively. Another interesting example of a (n,γ) reaction is the neutron capture by ^{235}U according to the following:

$$^{235}_{92}\mathrm{U} + {}^{1}_{0}\mathrm{n} \rightarrow {}^{236}_{92}\mathrm{U} + \gamma \qquad [10.55]$$

This neutron capture reaction is interesting, because the ^{236}U product nuclide decays by alpha emission with a very long half-life (2.4×10^7 y) in ~14% of the cases and decays by nuclear fission with emission of neutrons in the remaining 86% of the cases.

10.4.4 Nonelastic Reactions

Neutron capture can occur in nuclei resulting in nuclear reactions that entail the emission of nuclear particles such as protons (n,p), deuterons (n,d), alpha particles (n,α), and even neutrons (n,2n). These reactions may not occur in any specific energy range but may be prevalent at specific resonances, which are energy states of the excited compound nuclei that are specific to relatively narrow energies of the incident neutron. The effect of resonance in neutron capture by nuclei is discussed in more detail subsequently in this chapter. The (n,2n) reactions occur at very high incident neutron energies, >10 MeV (Gibson and Piesch, 1985). The (n,p) and (n,α) reactions can occur in the slow neutron capture and reaction with nuclides of low atomic number (low *Z*), where the coulombic forces of the electron shells are limited and present less a hurdle for the escape of charged particles from the confines of the atom. Some practical examples of these reactions are the (n,p) reaction used in the synthesis of ^{14}C by slow (thermal) neutron capture by ^{14}N:

$$^{14}_{7}\mathrm{N} + {}^{1}_{0}\mathrm{n} \rightarrow {}^{14}_{6}\mathrm{C} + {}^{1}_{1}\mathrm{H} \qquad [10.56]$$

TABLE 10.5 Cross-Sections σ in Barns for Thermal Neutron Capture Reactions of Selected Nuclides in Order of Increasing Magnitude

Nuclide	σ (Barns)
$^{3}_{1}H$	<0.000006
$^{16}_{8}O$	0.00019
$^{2}_{1}H$	0.00052
$^{12}_{6}C$	0.0035
$^{1}_{1}H$	0.332
$^{14}_{7}N$	1.8
$^{238}_{92}U$	2.7
$^{232}_{90}Th$	7.4
$^{55}_{25}Mn$	13.3
$^{233}_{92}U$	530
$^{235}_{92}U$	586
$^{239}_{94}Pu$	752
$^{6}_{3}Li$	940
$^{10}_{5}B$	3840
$^{3}_{2}He$	5330
$^{7}_{4}Be$	39,000
$^{155}_{64}Gd$	61,000
$^{157}_{64}Gd$	254,000

Data from Holden, N.E., 1997b. Neutron scattering and absorption properties. In: Lide, D.R., (Ed.), CRC Handbook of Chemistry and Physics, 77th ed. CRC Press, Boca Raton, FL, pp. 11-144–11-158 and Lide, D.R., 2010. CRC Handbook of Chemistry and Physics, 81st ed. CRC Press, Boca Raton, p. 10–220.

and the (n,p) and (n,α) reactions used to detect neutrons by the interaction of slow neutrons with ^{3}He and ^{10}B, respectively, according to Eqs. [10.57] and [10.58]:

$$^{3}_{2}He + ^{1}_{0}n \rightarrow ^{1}_{1}H + ^{3}_{1}H + 0.76\ MeV \quad [10.57]$$

$$^{10}_{5}B + ^{1}_{0}n \rightarrow ^{7}_{3}Li + ^{4}_{2}He + 2.8\ MeV \quad [10.58]$$

Either of these reactions is used to detect neutrons by using gas proportional detectors containing helium-3 gas or a gaseous form of boron (eg, boron trifluoride). Slow neutrons that penetrate these detectors produce either radioactive tritium (Eq. [10.57]) or alpha particles (Eq. [10.58]), which produce ionization in the gas. The ionization events or ion pairs formed can be collected and counted to determine a neutron count rate.

10.4.5 Nuclear Fission

The reaction of neutron-induced fission occurs when a neutron interacts with a fissile or fissionable nucleus and the nucleus becomes unstable, taking on the characteristics of an oscillating liquid droplet, which then fragments into two nuclides (fission fragments). At the same time, there is the release of neutrons (2.4 neutrons on the average for neutron-induced ^{235}U fission) and a relatively high amount of energy ($\sim$194 MeV for neutron-induced ^{235}U fission). Neutron-induced fission of natural ^{235}U and man-made ^{233}U and ^{239}Pu is optimal at thermal incident neutron energies; whereas neutron-induced

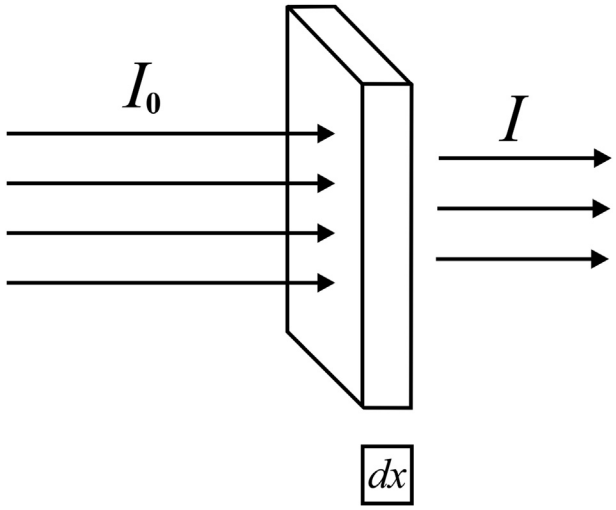

FIGURE 10.9 Attenuation of a neutron beam of intensity I_0 by an absorber material of unit area (cm^2) and thickness dx.

fission in ^{232}Th, ^{238}U, and ^{237}Np requires neutron energies of at least 1 MeV. A more detailed treatment of nuclear fission was provided previously in this chapter.

10.5 NEUTRON ATTENUATION AND CROSS-SECTIONS

As we have seen in our previous treatment of the neutron, there are several possible interactions of neutrons with nuclei. Among these are elastic scattering, inelastic scattering, neutron capture, nonelastic reactions, and neutron-induced nuclear fission. As we have seen in several examples, probabilities exist for any of these interactions to occur depending on the energy of the incident neutron and the type of nuclide with which the neutron interacts. We can define this probability of interaction by the term cross-section, which is a measure of the capturing power of a particular material for neutrons of a particular energy.

The range of neutrons in matter is a function of the neutron energy and the cross-section or capturing power of the matter or medium through which the neutrons travel. To define cross-section, let us consider an incident beam of neutrons of given intensity (I_0) or number (eg, neutrons/s), which impinges on a material of unit area (eg, cm^2) and thickness dx, as illustrated in Fig. 10.9.

The intensity (I) of the neutron beam traveling beyond the thickness dx will be reduced from the incident beam intensity according to the number of nuclei (n) per unit volume in the material and the "area of obstruction" (eg, cm^2) that the nuclei present to the oncoming beam. This area of obstruction is referred to as the cross-section of the material. On the basis of the description previously given, we can write the equation:

$$dI/dx = -n\sigma I \qquad [10.59]$$

which defines the change in beam intensity (dI) with respect to absorber thickness (dx) as proportional to the beam intensity (I) times a proportionality factor, which we may call the absorption coefficient or "obstruction coefficient" that the nuclei pose to the oncoming beam. The coefficient is a function of the number of nuclei (n) in the path of the neutron beam and the stopping power of the nuclei to interact with the neutron beam or, in other words, the neutron cross-section (σ) of the material through which the neutron beam travels. Eq. [10.59] may be written as:

$$dI/I = -n\sigma dx \qquad [10.60]$$

Eq. [10.60] is very similar to Eq. [8.45] of chapter "Electromagnetic Radiation: Photons" defining the attenuation of gamma radiation in matter, with the exception that the absorption coefficients and attenuation coefficients involved for neutron and gamma radiation, respectively, are very different. The negative sign of Eqs. [10.59] and [10.60] denotes the diminishing intensity of the neutron beam as a function of absorption coefficient and absorber thickness. The absorption coefficient $n\sigma$ is the combined effect of the number of nuclei (n) in the neutron beam path that might impede the continued

travel of neutrons and the power of the nuclei to react with the neutrons. Eq. [10.60] can be integrated over the limits of beam intensity from I_0 to I and absorber thickness from 0 to x as follows:

$$\int_{I_0}^{I} dI/I = -n\sigma \int_{0}^{x} dx \qquad [10.61]$$

to give the equation:

$$\ln I_0/I = n\sigma x \qquad [10.62]$$

or:

$$I = I_0 e^{-n\sigma x} \qquad [10.63]$$

which is the most simplified expression for the calculated beam intensity (I) that passes through an absorber of thickness (x) when the absorber material consists of only one pure nuclide and only one type of reaction between the neutron beam and nuclei is possible. If, however, different nuclides are found in the absorber material whereby various reactions between the neutron beam and the various different nuclei of the absorber material are possible, we must utilize the sum of the neutron cross-sections for all reactions that could take place.

We can use Eq. [10.62] to calculate the half-value thickness ($x_{1/2}$) or the thickness of absorber material needed to reduce the incident neutron beam intensity by one-half. If we give the initial beam intensity (I_0) a value of 1 and the transmitted intensity (I) a value of 1/2, we can write:

$$\ln 1/0.5 = n\sigma x_{1/2} \qquad [10.64]$$

and:

$$\ln 2 = n\sigma x_{1/2} \qquad [10.65]$$

or:

$$0.693 = n\sigma x_{1/2} \qquad [10.66]$$

The half-value thickness for neutron beam attenuation may be written:

$$x_{1/2} = 0.693/n\sigma \qquad [10.67]$$

where n is the number of nuclei per unit volume (cm^{-3}) and σ the neutron cross-section in cm^2. The neutron cross-section σ can be defined as the area in cm^2 for which the number of nuclei–neutron reactions taking place is equal to the product of the number of incident neutrons that would pass through the area and the number of target nuclei. The cross-section is defined in units of 10^{-24} cm^2 on the basis of the radius of atomic nuclei being about 10^{-12} cm. It provides a measure of the chances for the nuclei of a material being hit by a neutron of a certain energy. The unit of 10^{-24} cm^2 for nuclear cross-sections is called the barn. Tables in reference sources of nuclear data provide the neutron cross-sections in units of barns for various nuclides and nuclide energies. An example is the reference directory produced by McLane et al. (1988), which provides neutron cross-section values in barns and neutron cross-section curves for most nuclides over the neutron energy range 0.01 eV–200 MeV.

Let us take an example of 10-eV neutrons incident on a water barrier (ie, neutrons traveling in water). We may use Eq. [10.67] to estimate the half-value thickness, if we ignore the less significant interactions with oxygen atoms. This is because the neutron cross-section for hydrogen at 10 eV is about 20 b (Fig. 10.10) and that of oxygen is only 3.7 b (McLane et al., 1988), and there are twice as many hydrogen atoms as oxygen atoms per given volume of water. The half-value thickness may be calculated as follows. The value of n for the number of hydrogen nuclei per cm^3 of water may be calculated on the basis of Avogadro's number of molecules per mole. If 1 mol of water is equivalent to 18.0 g and the density of water is 1.0 g/cm^3, we can calculate the number of hydrogen nuclei per cm^3 as:

$$6.22 \times 10^{23} \text{ molecules } H_2O/18 \text{ cm}^3 = 3.45 \times 10^{22} \text{ molecules } H_2O/\text{cm}^3$$

$$n = \left(3.45 \times 10^{22} \text{ molecules } H_2O/\text{cm}^3\right)(2 \text{ hydrogen nuclei or } 2\,{}^{1}_{1}H/\text{molecule})$$

$$= 6.90 \times 10^{22}\,{}^{1}_{1}H \text{ nuclei}/\text{cm}^3.$$

By definition, 20 b is equal to 20×10^{-24} cm^2; and the half-value thickness may then be calculated as:

$$x_{1/2} = \frac{0.693}{(6.90 \times 10^{22}\ \text{cm}^{-3})(20 \times 10^{-24}\ \text{cm}^2)}$$

$$= \frac{0.693}{1.38\ \text{cm}^{-1}}$$

$$= 0.502\ \text{cm}$$

If we make the calculation for 1-keV (ie, 1000 eV) neutrons traversing water and use the value 4.1 b for the neutron cross-section of hydrogen nuclei at this neutron energy (Fig. 10.10 and McLane et al., 1988), we calculate a half-value thickness of:

$$x_{1/2} = \frac{0.693}{(6.90 \times 10^{22}\ \text{cm}^{-3})(4.1 \times 10^{-24}\ \text{cm}^2)}$$

$$= \frac{0.693}{0.283\ \text{cm}^{-1}}$$

$$= 2.45\ \text{cm}$$

As the examples illustrate in the case of the proton, the neutron cross-section (or barns) decreases as the energy or velocity of the neutron increases. That is, the neutron reactions with nuclei obey the general rule of having some proportionality to $1/v$, where v is the velocity of the neutron. This inverse proportionality of cross-section and neutron velocity is particularly pronounced in certain regions of energy as illustrated in the total neutron cross-section curves for protons and elemental boron in Figs. 10.10 and 10.11, respectively. However, this is not always the case with many nuclides at certain neutron energies where there exists a resonance between the neutron energy and the nucleus. At some specific or very narrow neutron energy ranges, certain nuclei have a high capacity for interaction with neutrons. The elevated neutron cross-sections at specific neutron energies appear as sharp peaks in plots of neutron cross-section versus energy, such as the

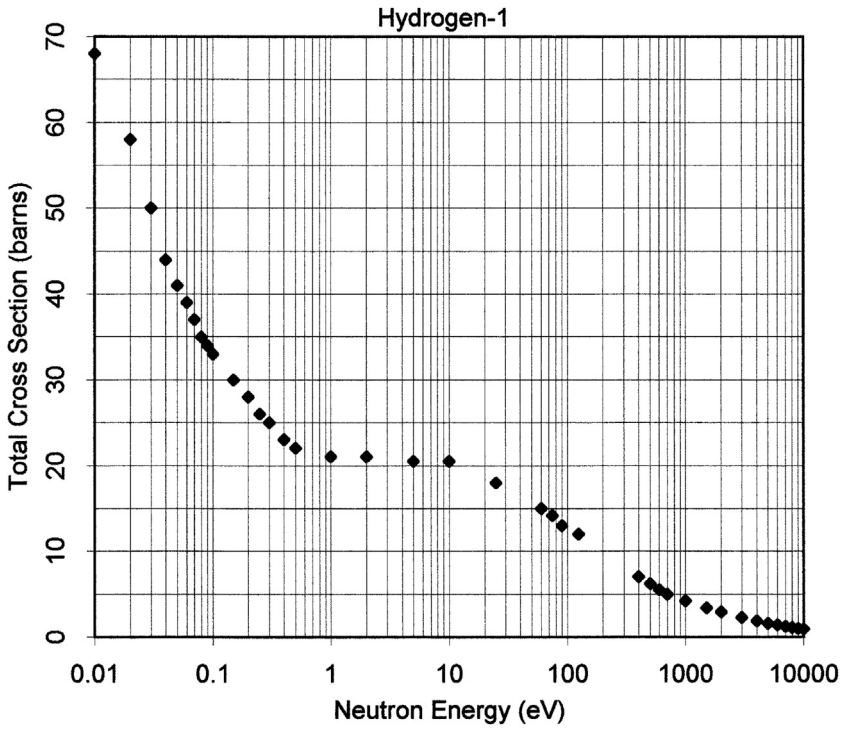

FIGURE 10.10 Total cross section curve for hydrogen-1 over the neutron energy range 0.01 eV−10 keV.

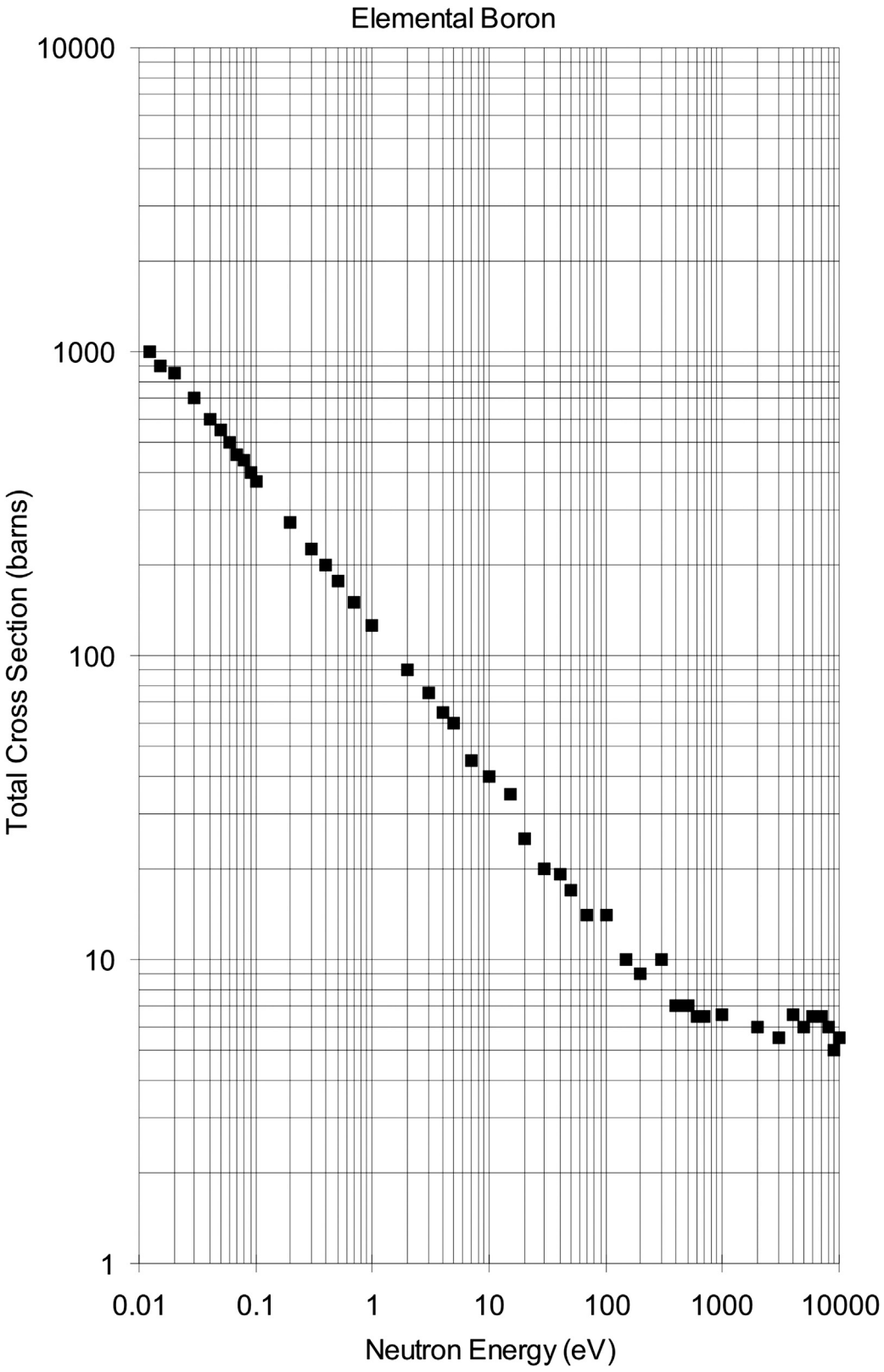

FIGURE 10.11 Total cross-section curve for elemental boron over the neutron energy range 0.01 eV−10 keV.

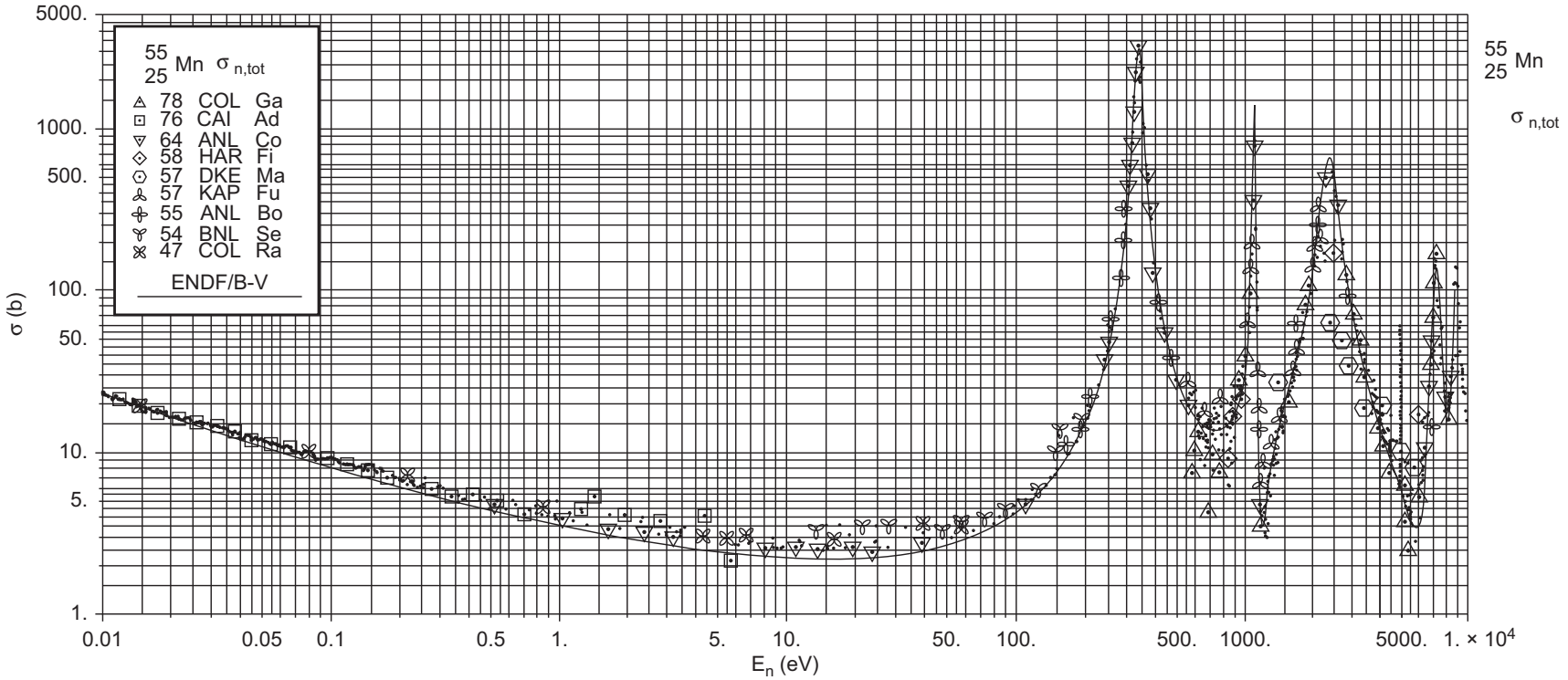

FIGURE 10.12 Total cross-section curve for manganese-55 over the neutron energy range of 0.01 eV−10 keV. The columns in the upper left-hand section of the graph provide the number of data points and an abbreviation of the laboratory that provided the data. *From McLane, V., et al., 1988. Neutron Cross Sections, vol. 2, Neutron Cross Section Curves for Z = 1 − 100. Academic Press, San Diego. Reprinted with permission from Elsevier © 1988.*

cross-section curve illustrated in Fig. 10.12 for ^{55}Mn. These peaks are called resonances and often occur with (n,γ) reactions. The high cross-sections occur when the energy of the incident neutron corresponds exactly to the quantum state of the excited compound nucleus, which is the newly formed nucleus consisting of a compound between the incident neutron and the nucleus. Most nuclides display both the $1/v$ dependence on neutron cross-section and the resonance effects over the entire possible neutron energy spectrum. We should keep in mind that neutron cross-sections can be specific and differ in value for certain reactions, such as proton (σ_p)- and alpha particle (σ_α)-producing reactions, fission reactions (σ_f), or neutron capture cross-sections (σ_c). The total neutron cross-section (σ_{tot}) would be the cross-section representing the sum of all possible neutron reactions at that specific neutron energy. For example, the thermal neutron cross-section for ^{235}U, which is the neutron cross-section at 0.0253 eV neutron energy corresponding to a neutron velocity of 2200 m/s at room temperature, can be given as $\sigma_c = 95$ b for the neutron capture cross-section, $\sigma_f = 586$ b for the fission cross-section, and $\sigma_\alpha = 0.0001$ b for the neutron cross-section for the alpha particle-producing reaction. These neutron cross-section values indicate that neutron fission would predominate at the thermal neutron energy of 0.0253 eV, although some neutron capture would also occur. The total neutron cross-section, σ_{tot}, would be the total of the three possible reactions or $\sigma_{tot} = 95\text{ b} + 586\text{ b} + 0.0001\text{ b} = 681$ b. In our treatment of slow neutron capture by ^{235}U in Section 10.4.3, illustrated by Eq. [10.55], we noted that about 14% of the slow neutron captures by ^{235}U nuclei result in the formation of a long-lived ^{236}U and gamma radiation; and the remaining 86% of the slow neutron captures result in nuclear fission. This is exactly what is predicted by the thermal neutron cross-section values just provided; that is, for ^{235}U:

$$\sigma_c/\sigma_{tot} = 95\text{ b}/681\text{ b} = 14\%\text{ neutron capture}$$

and:

$$\sigma_f/\sigma_{tot} = 586\text{ b}/681\text{ b} = 86\%\text{ fission}$$

10.6 NEUTRON DECAY

We have seen that fast neutrons may lose their energy through elastic and inelastic collisions with other nuclei, and if these neutrons do not undergo other reactions with nuclei, they may lose sufficient energy to reach thermal equilibrium with surrounding atoms and possibly be captured by atomic nuclei. The question remains of what would happen to a free neutron that is not captured by any atomic nucleus.

In chapter "Beta Radiation and Beta Decay" we discussed the transformation of the neutron within nuclei of radioactive atoms, which have a neutron/proton ratio too high for stability. In these unstable nuclides, the neutron breaks up into a proton, negatron (negative electron), and antineutrino (see Eq. [6.3] of chapter "Beta Radiation and Beta Decay"). If the neutron can transform itself in unstable nuclei, it stands to reason that the neutron might be unstable outside the protective boundaries of the stable nucleus. This is just the case, which A.H. Snell and L.C. Miller demonstrated in 1948. This work was followed with further studies by Robson (1950a,b) and Snell et al. (1950), which demonstrated neutrons in free flight in a vacuum would indeed decay with a lifetime in the range of 9–25 min with a release of 0.782 MeV of energy. Later, more accurate measurements of neutron decay by numerous researchers including Abele (2000), Arzumanov et al. (2000a,b), Pichlmaier et al. (2000), Snow et al. (2000), Coakley (2001), Nico et al. (2005), and Serebrov et al. (2005), among others, yielded the neutron lifetime declared by the Particle Physics Group to be 886.7 ± 1.9 s (Caso et al., 2005), which is close to 15 min. Much research has been carried out over the past several years to obtain the most accurate measurement of the neutron lifetime (Coakley, 2007; Wilkinson, 2007; Arzumanov et al., 2009; Dewey et al., 2009; Ezhov et al., 2009; Leung and Zimmer, 2009; Materne et al., 2009; Müller et al., 2009; O'Shaughnessy et al., 2009; Walstrom et al., 2009), which is an important physical parameter. The most accurate measurement of the neutron lifetime will help answer questions in particle physics and astrophysics. In particle physics, the neutron lifetime will help us address the weak interaction parameters within baryons (Walstrom et al., 2009), such as the transformation of a d quark into a u quark described in chapter "The Atomic Nucleus." In astrophysics, the neutron lifetime is a key process in establishing the model for the Big-Bang primordial nucleosynthesis whereby there was an equilibrium of neutrons and protons a few minutes after the Big Bang, described by Paul (2009). A treatment of the Big-Bang primordial nucleosynthesis is provided in chapter "Cosmic Radiation."

Various methods are used to measure the neutron lifetime including the trapping and magnetic storage of neutrons followed by the counting of decay products. Paul (2009) provides a very thorough review of the methods used worldwide to determine most accurately the lifetime of the neutron. The present world average of the neutron lifetime of $\tau_n = 885.7 \pm 0.8$ s was reported by the Particle Data Group (Amsler et al., 2008); however, research to achieve the

measurement of the lifetime of the neutron to a precision of ±0.1 s is currently under intensive research. The decay of elementary particles is characterized in terms of lifetime. The lifetime, usually symbolized as τ, is related to the term half-life, $t_{1/2}$, the mean time it takes for one-half of the particles to decay (Sundaresan, 2001) according to the relationship:

$$t_{1/2} = (\ln 2)\tau = 0.693\tau \quad [10.68]$$

The free neutron decays according to the scheme:

$$n \rightarrow p^+ + e^- + \overline{\nu} + 0.7823 \text{ MeV} \quad [10.69]$$

The 0.7823 MeV of energy released in the neutron decay corresponds to the difference in mass of the neutron and the sum of the masses of the products of the neutron decay, the proton plus the electron, or:

$$\begin{aligned} Q &= [m_n - (m_p + m_e)]c^2 \\ &= [1.008664915 \text{ u} - (1.007276466 \text{ u} + 0.0005485799 \text{ u})]\left(931.494013 \text{ MeV}/c^2\right)c^2 \\ &= 0.7823 \text{ MeV} \end{aligned} \quad [10.70]$$

which agrees with the value of $Q = 0.782347$ MeV provided by the National Nuclear Data Center's QCalc computer calculation of the Brookhaven National Laboratory (NNDC, 2016a): http://www.nndc.bnl.gov/qcalc/.

The neutron, therefore, outside the protective confines of the stable nucleus, has a very short lifetime.

Chapter 11

Hall of Fame: Part V

Niels Bohr (1885–1962), Gustav Hertz (1887–1975) and James Franck (1882–1964), Werner Heisenberg (1901–1976), Erwin Schrödinger (1887–1961), Max Born (1882–1970), and Paul Dirac (1902–1984), Clinton Davisson (1881–1958) and George Paget Thomson (1892–1975), and Pierre Victor Auger (1899–1993)

Joseph Thomson, the father, won the Nobel Prize in Physics in 1906 for his discovery that the electron is a particle; and George Thomson, the son, won the Nobel Prize in Physics in 1937 for his demonstration that the electron is not a particle, but a wave.

The above was a common joke among physicists after the Nobel Prize was awarded to George Thomson in 1937. This statement was only in jest, because all physicists then knew that George Thomson really demonstrated the de Broglie electron matter-wave, that is, he demonstrated the dual nature of the electron, that of a particle and a wave.

NIELS BOHR (1885–1962)

Niels Bohr was awarded the Nobel Prize in Physics 1922 "for his services in the investigation of the structure of atoms and the radiation emanating from them." He was born in Copenhagen, Denmark on October 7, 1885. His father was Professor of Physiology at Copenhagen University, and his mother also was from a family distinguished in education.

Bohr earned a master's degree in physics in 1909 and the doctorate degree in 1911 at Copenhagen University. His doctoral dissertation was a theoretical explanation of the properties of metals based on the electron theory. In 1911, Niels Bohr had a short stint at the Cavendish Laboratory, where he was able to witness the experimental work of J.J. Thomson on the properties of the electron. Subsequently in 1912 he worked in the laboratory of Ernest Rutherford in Manchester, where Rutherford was making discoveries on the properties of the atomic nucleus. These experiences with J.J. Thomson and Rutherford helped Bohr formulate his own ideas on the structure of the atom.

During the time of his doctoral work and following the stint in Rutherford's laboratory, Niels Bohr was confronted with Max Planck's quantum theory of radiation and Rutherford's experimental work on the atomic nucleus. By combining the concepts of Planck's quantum theory and Rutherford's atomic structure, Niels Bohr was able to formulate a quantum theory of atomic structure (Bohr, 1913, 1914), which remains to this day suitable in explaining the chemical and spectroscopic properties of the elements.

Bohr's starting point was Rutherford's theory of the atom based on Rutherford's experiments in alpha-particle scattering (see Hall of Fame, Part I). The Rutherford atom consisted of a positively charged nucleus with electrons revolving in orbits about the nucleus, the number of which were sufficient to neutralize the positive charge on the nucleus (ie, the number of electrons in each atom equaled the number of protons in the nucleus, or its atomic number). Also, the dimensions of the nucleus were very small in comparison to the size of the atom defined by the electron orbits, and almost all of the mass of the atom was concentrated in the nucleus. By taking Rutherford's atom, Max Planck's quantum theory of energy, and the simplest of all atoms, hydrogen, Niels Bohr was able to launch his quantum theory of atomic structure, referred to as the Bohr atom. With his quantum theory of atomic structure, Bohr was able to explain the spectra of radiation emitted by atomic electrons and the chemical properties of the elements based on electron groupings in quantum orbits.

Radioactivity: Introduction and History, From the Quantum to Quarks. http://dx.doi.org/10.1016/B978-0-444-63489-4.00011-3
Copyright © 2016 Elsevier B.V. All rights reserved.

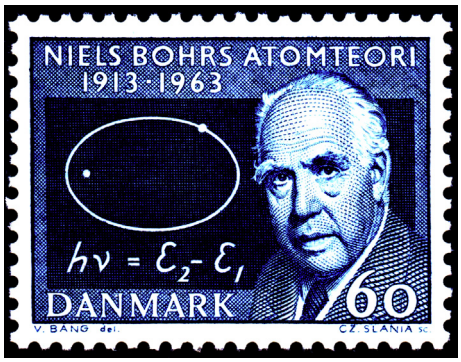

Niels Bohr (1885–1962)

Bohr (1913, 1914, 1921a,b) proposed that electrons exist in orbits about the nucleus at discrete distances and each orbit represented specific quantized energies. The energy of an electron would be proportional to its orbit, that is, the larger the orbit or the greater its radius, the higher would be the electron energy. Thus, when an atom absorbs energy from an external form of excitation, an atomic electron would jump from one orbit to another farther away from the atomic nucleus. Energy absorbed by the atom could be emitted from the atom as radiation when an electron falls from an outer to an inner orbit, as described by the equation:

$$h\nu = E_i - E_f \quad \text{or} \quad h\nu = E_u - E_l \qquad \text{[V.1]}$$

where h is Planck's constant, ν is the frequency of the emitted radiation, E_i and E_f are the initial and final electron energies, respectively, and E_u is the upper (higher) electron energy and E_l is the lower electron energy. Eq. [V.1] and the simplest of all atoms, the atom of hydrogen with its single orbital electron, are illustrated in the commemorative postage stamp from Denmark shown here. Bohr explained that energy can be absorbed or emitted by an atom only as a single quantum of energy or light photon ($h\nu$) equal to the energy differences of specific orbitals. He demonstrated that electrons could not possess any orbit, but only specific orbits, which he called "stationary states," and the orbits were defined by a quantum multiple of the angular momentum of the electron around the nucleus. Bohr (1913) stated:

> *If we assume that the orbit of the electron in the stationary states is circular, the results of the calculations can be expressed by the simple condition: that the angular momentum of the electron round the nucleus in a stationary state of the system is equal to an entire multiple of a universal value, independent of the charge on the nucleus…The great number of different stationary states we do not observe except by investigation of the emission and absorption of radiation.*

Bohr demonstrated that the angular momentum (L) of the electron in the various possible orbits was defined by the relation:

$$L = n(h/2\pi) \qquad \text{[V.2]}$$

where $n = 1, 2, 3,\ldots$ and h is Planck's constant. Thus, Bohr concluded that the angular momentum of the electron is quantized according to a quantum number n, and that the transition of an electron from one orbit (stationary state) to another as a result of the absorption or emission of energy by an atom could only occur in specific or quantized magnitudes.

With his quantum theory of atomic structure, Bohr derived and explained fully the Rydberg formula, which was a formula devised by the Swedish physicist Janne Rydberg (1854−1919) to calculate and predict the wavelengths of light photons emitted by hydrogen and later applied to the other elements of the periodic table to include, in addition to visible light, other types of electromagnetic radiation emitted by atoms. The Rydberg formula for hydrogen is the following:

$$\frac{1}{\lambda} = R_H\left(\frac{1}{n_l^2} - \frac{1}{n_u^2}\right) \qquad \text{[V.3]}$$

where λ is the radiation wavelength emitted by the hydrogen atom, R_H is the Rydberg constant for hydrogen ($R_H = 1.0967758 \times 10^{-3}$ Å^{-1}), and n_l and n_u are the lower and upper (higher) integers such that:

1. When $n_l = 1$ and $n_u = 2, 3, 4,\ldots \infty$, the Lyman series of wavelengths in the ultraviolet region are calculated.
2. When $n_l = 2$ and $n_u = 3, 4, 5,\ldots \infty$, the Balmer series of wavelengths in the visible region are calculated.
3. When $n_l = 3$ and $n_u = 4, 5, 6,\ldots \infty$, the Paschen series of wavelengths in the infrared region are calculated.
4. When $n_l = 4$ and $n_u = 5, 6, 7,\ldots \infty$, the Brackett series of wavelengths in the far infrared region are calculated.

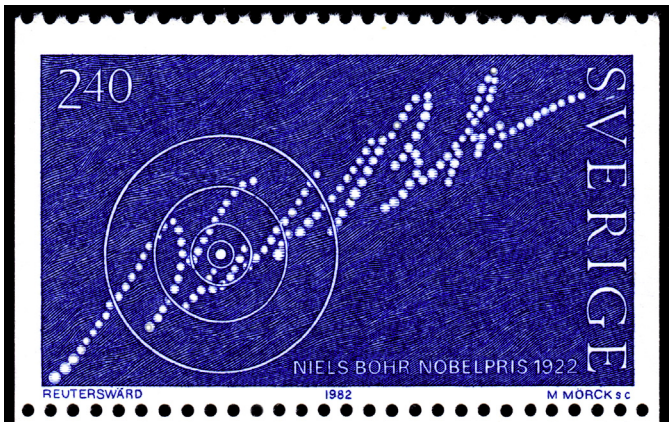

Bohr Atom and Signature of Niels Bohr

Although the Rydberg formula was well used by spectroscopists to calculate the lines of atomic absorption or emission, the formula was not fully understood until Niels Bohr derived the Rydberg constant and explained the origin of the specific lines of radiation emission or absorption on the basis of his quantum theory of atomic structure. Illustrated in the commemorative postage stamp from Sweden is a picture of the Bohr atom with the central nucleus and four of possibly more electron quantum orbitals. The Bohr atom is illustrated more clearly in Fig. V.1 taken from his Nobel lecture (Bohr, 1922). Using this simplified figure of the atom, Bohr explained the quantized transition that an electron can make in jumping from an inner to outer orbital, resulting in energy absorption or the transitions from an outer to an inner electron orbit, resulting in the emission of energy as quanta of radiation photons manifested by precise lines of electromagnetic radiation. In his own words, Bohr explained the radiation emission of hydrogen as follows:

> *We arrive at a manifold of stationary states for which the major axis of the electron orbit takes on a series of discrete values proportional to the square of the whole numbers. [The whole numbers that Bohr refers to here are* n_l^2 *and* n_u^2 *of the Rydberg formula.] The accompanying figure shows the relation diagrammatically. For the sake of simplicity the electron orbits in the stationary states are represented by circles, although in reality the theory places no restriction on the eccentricity of the orbit…The arrows represent the transition processes that correspond to the red and green hydrogen lines,* H_α *and* H_β*, the frequency of which is given by means of the Balmer formula (series) when we put* $n_l = 2$ *and* $n_u = 3$ *and 4, respectively. The transition processes are also represented which correspond to the first three lines of the series of ultraviolet lines found by Lyman in 1914, of which the frequencies are given by the formula when* n_l *is put equal to 1, as well as to the first line of the infrared series discovered some years previously by Paschen, which are given by the formula if* n_l *is put equal to 3. This explanation of the origin of the hydrogen spectrum leads us quite naturally to interpret this spectrum as the manifestation of a process whereby the electron is bound to the nucleus…the state of the atom can only be changed by the addition of energy whereby the electron is transferred to an orbit of larger dimensions corresponding to an earlier stage of the binding process.*

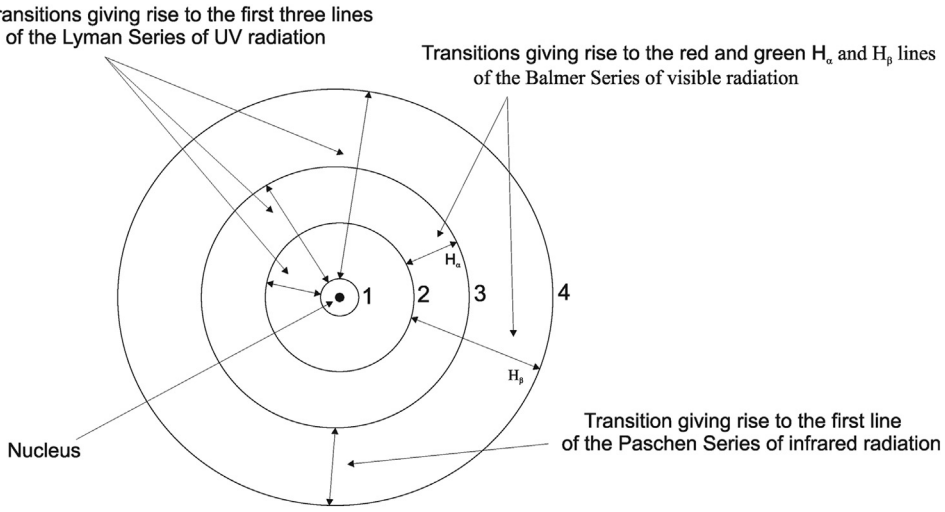

FIGURE V.1 Bohr's atomic representation of the hydrogen atom with quantized electron transitions according to the quantum numbers 1, 2, 3, and 4 giving rise to specific radiation emissions lines in the Lyman, Balmer, or Paschen series.

Using the Rydberg formula and Bohr's quantum theory of atomic structure, one can calculate the wavelengths (lines) of radiation emission for hydrogen and the other elements and the energy levels of the quantized electron orbits. For example, the electron transition from $n_u = 2$ to $n_l = 1$ will yield a photon in the first line of the Lyman series with a wavelength calculated according to Eq. [V.3] as:

$$\begin{aligned}\frac{1}{\lambda} &= R_H\left(\frac{1}{1^2}-\frac{1}{2^2}\right)\\ &= 1.0967758\times10^{-3}\ \text{Å}^{-1}\left(1-\frac{1}{4}\right)\\ &= 1.0967758\times10^{-3}\ \text{Å}^{-1}(0.75)\\ &= 8.2258185\times10^{-4}\ \text{Å}^{-1}\\ \lambda &= 1215\ \text{Å}\end{aligned} \qquad [V.4]$$

Similar calculations for radiation emissions as a result of electron transitions from $n_u = 3$ to $n_l = 1$ and $n_u = 4$ to $n_l = 1$, illustrated in Fig. V.1, yield according to Eq. [V.3] radiation emissions of 1025 and 972 Å, respectively. Radiation emission for transitions from orbitals farther out (eg, $n_u = 4, 5, 6, \ldots \infty$ to the innermost orbital $n_l = 1$) may be calculated in a similar fashion to yield other wavelengths of the Lyman series. If we consider the transition of $n_u = \infty$ to $n_l = 1$, we can calculate the energy level of the lowest or the innermost orbital as:

$$\begin{aligned}E_n &= -hcR_H\left(\frac{1}{n_l^2}-\frac{1}{\infty}\right)\\ &= -(4.136\times10^{-15}\ \text{eV s})(2.9979\times10^{8}\ \text{m/s})\left(1.0967758\times10^{-3}\ \text{Å}^{-1}\right)\left(\frac{1}{n^2}\right)\\ &= -(12.399\times10^{-7}\ \text{eV m})\left(1.0967758\times10^{-3}\ \text{Å}^{-1}\right)\left(\frac{1}{n^2}\right)\\ &= -\left(12.399\ \text{keV Å}\right)\left(1.0967758\times10^{-3}\ \text{Å}^{-1}\right)\left(\frac{1}{n^2}\right)\\ &= -\frac{0.01359\ \text{keV}}{n^2}\\ &= -\frac{13.59\ \text{eV}}{n^2}\end{aligned} \qquad [V.5]$$

Thus the energy of the electron in its lowest orbital closest to the nucleus (quantum number $n = 1$) is -13.59 eV. This energy corresponds exactly to the ionization energy of hydrogen, that is, the energy required to remove completely the electron from the hydrogen atom, namely, move it to an infinite distance from the nucleus, to form the hydrogen ion, H^+. The negative sign is used for the energy level, because the electron is in a bound state whereby the energy is not free. Higher energy levels of the hydrogen atom would be -3.40 eV for $n = 2$, -1.51 eV for $n = 3$, -0.85 eV for $n = 4$, -0.54 eV for $n = 5$, -0.38 eV for $n = 6$, and -0.28 eV for $n = 7$, etc. Energy levels of the Bohr atomic structure for hydrogen are illustrated in Fig. V.2.

A summary of Bohr's revolutionary quantum theory of atomic structure and the significance of Bohr's hypothesis were highlighted in a Nobel presentation speech given by Prof. C.W. Orseen, member of the Nobel Committee for Physics of the Royal Swedish Academy of Sciences on December 10, 1926. In Prof. Orseen's words:

> *It was only through a radical break with classical physics that Bohr was able to resolve the spectroscopic puzzles in 1913. Bohr's basic hypothesis can be formulated as follows: Each atom can exist in an unlimited number of different states. Each of these stationary states is characterized by a given energy level. The difference between two such energy levels, divided by Planck's*

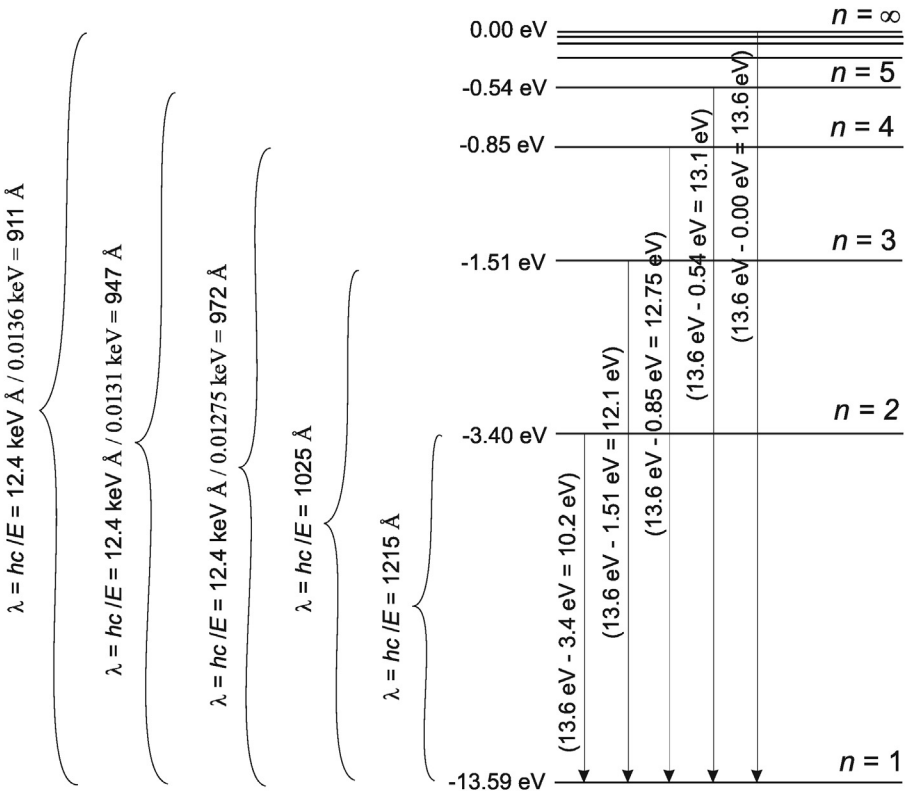

FIGURE V.2 Energy levels and energy transitions of Bohr's quantized atomic structure for hydrogen that yield the Lyman series (ultraviolet) of radiation emissions. The energy levels of hydrogen are represented as a plateau and the electron transitions from the outer higher-energy orbits to the lower are depicted as arrows pointing downwards. Some energies liberated as radiation quanta in units of electron volts and radiation wavelength in angstroms are provided.

constant h*, is the oscillation frequency of a spectral line that can be emitted by the atom [see Eq. [V.6]]…The extraordinary good agreement with experience obtained in this way, explains why after 1913 almost a whole generation of theoretical and experimental physicists devoted itself to atomic physics and its application in spectroscopy.*

$$\nu = \frac{E_2 - E_1}{h} \qquad [V.6]$$

The use of electron orbits about a central atomic nucleus as depicted by Bohr (ie, the Bohr atom) is not considered an accurate depiction of the atom; however, it remains to this day a very didactic method of illustrating the atom and of explaining radiation emission and absorption of electron origin and the chemical properties of the elements. Because electrons have properties of both particles and waves, that is, a dual nature as described by de Broglie (see Hall of Fame, Part III), Erwin Schrödinger took the dual nature of the electron to describe the electron and its properties with wave equations. Thus we may also picture atomic electrons as possessing energy levels, such as illustrated on Fig. V.2, rather than occupying definite orbits.

On the basis of his quantum theory of atomic structure, Bohr went further to explain the properties of the elements. In his paper on atomic structure (1921a), Bohr explained how the inert gases were different from the other elements because the atomic orbitals were completely filled, providing the atoms with "inherent stability," as it would be difficult (ie, require excessive energy) to remove any of the electrons from such atoms to form ions. He depicted the electron configurations of the inert gases as illustrated in Fig. V.3.

We can compare Bohr's early depiction of the above electron configurations and notice their close similarity to the current configurations taken from a modern *Handbook of Chemistry and Physics* (Lide, 1997) provided in Table V.1. The letters K, L, M,… are the principal electron energy levels with increasing energy and distance from the nucleus; *s*, *p*, *d*, and *f* are quantum energy sublevels also with increasing energy and distance from the nucleus; and $n = 1, 2, 3,\ldots$ are the principal quantum numbers. (See Wolfgang Pauli in Hall of Fame, Part II.)

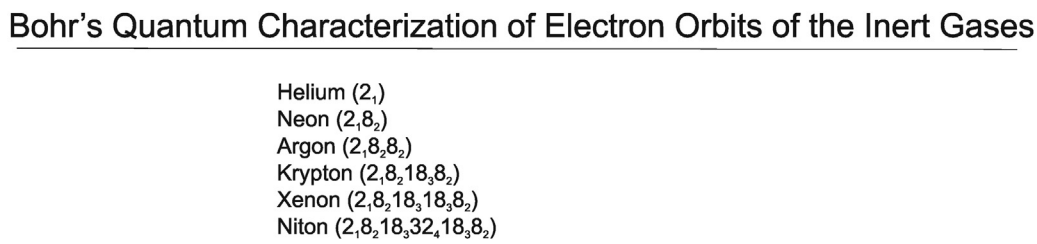

FIGURE V.3 Bohr's depiction of the quantum orbits of electrons of the inert gases (Bohr, 1921a). Niton, listed above, is now known as radon, with atomic number 86. In Bohr's words: "The large numbers denote the number of electrons in groups (shells) starting with the innermost group, and the small numbers (subscripts) denote the total number of quanta characterizing the electron orbits within each group (shell)."

TABLE V.1 Electron Configurations of Neutral Atoms in the Ground State

Atomic No.	Element	K ($n = 1$)	L ($n = 2$)		M ($n = 3$)			N ($n = 4$)				O ($n = 5$)				P ($n = 6$)		
		s	*s*	*p*	*s*	*p*	*d*	*s*	*p*	*d*	*f*	*s*	*p*	*d*	*f*	*s*	*p*	*d*
2	He	2																
10	Ne	2	2	6														
18	Ar	2	2	6	2	6												
36	Kr	2	2	6	2	6	10	2	6									
54	Xe	2	2	6	2	6	10	2	6	10		2	6					
86	Ra	2	2	6	2	6	10	2	6	10	14	2	6	10		2	6	

From Lide, D.R., 1997. CRC Handbook of Chemistry and Physics, 77th ed. CRC Press, Boca Raton.

During the time of his historic work on the structure of the atom (1913–1914), Niels Bohr was lecturer in physics at Copenhagen University. He subsequently held a similar position at Victoria University in Manchester from 1914 to 1916. Bohr returned to his home country in 1916 when he was appointed Professor of Theoretical Physics at Copenhagen University, and in 1920 he became Head of the Institute of Theoretical Physics, which was established for him.

After receiving the Nobel Prize in 1922, Niels Bohr diverted his attention from atomic electrons to the atomic nucleus and the disintegration and transmutation of radioactive atoms. Bohr was the first to conceive of a heavy atomic nucleus (ie, a nucleus of high atomic number) to display the properties of a liquid drop (Bohr, 1936); and it was Bohr's ideas on the properties of the atomic nucleus that helped Lise Meitner and Otto Frisch (1939) arrive at an explanation of nuclear fission through their interpretation of the work of Otto Hahn and Fritz Strassmann (1939a), who demonstrated the splitting of the uranium-235 nucleus after neutron capture (see Lise Meitner and Otto Hahn in Hall of Fame, Part IV). In his work on the disintegration of heavy nuclei, Bohr (1939) summarized these concepts as follows:

> *…any nuclear reaction initiated by collisions or radiation involves as an intermediate stage the formation of a compound nucleus in which the excitation energy is distributed among the various degrees of freedom in a way resembling the thermal agitation of a solid or liquid body…Since the effective cross-sections for the fission phenomena seem to be about the same order of magnitude as the cross-sections for ordinary nuclear reactions, we may therefore conclude that for the heaviest nuclei the deformation energy sufficient for the fission is of the same order of magnitude as the energy necessary for the escape of a single nuclear particle…These circumstances find their straightforward explanation in the fact, stressed by Meitner and Frisch, that the mutual repulsion between the electric charges in a nucleus will for highly charged nuclei counteract to a large extent the effect of the short-range forces between the nuclear particles in opposing a deformation of the nucleus.*

During the Nazi occupation of Denmark in the autumn of 1943, Bohr escaped to Sweden and was invited to England by the British Government. Bohr was then taken into confidence and informed of the secret Manhattan Project for the development of the atomic bomb, which was already at an advanced stage. During the last two years of the war, he spent time in England and America. Niels Bohr and his son, Aage Bohr, who would later become a Nobel Laureate in physics in 1975, joined the secret Manhattan Project at the Los Alamos National Laboratories. Bohr was not vital to the development of the atomic bomb, but he was an admired personality and served as a father-figure to other scientists in the project. Rhodes (1986) provides much insight into the role of Niels Bohr in the Manhattan Project, and provides the following

quote from Victor Weisskopf, Austrian émigré theoretician, who worked on the project at Los Alamos, which summarizes Bohr's role in the project:

In Los Alamos we were working on something which is perhaps the most questionable, the most problematic thing a scientist can be faced with. At that time physics, our beloved science, was pushed into the most cruel part of reality and we had to live it through. We were, most of us at least, young and somewhat inexperienced in human affairs, I would say. But suddenly in the midst of it, Bohr appeared in Los Alamos. It was the first time we became aware of the sense in all these terrible things, because Bohr right away participated not only in the work, but in our discussions. Every great and deep difficulty bears in itself its own solution….This we learned from him.

J. Robert Oppenheimer, theoretician and Director of the Manhattan Project at Los Alamos, noted that Bohr was not needed either for technical or theoretical aspects of the projects, but rather his persona had a tremendous positive effect on the project staff. Rhodes (1986), in his book, provided insight into the effect of Bohr's presence by quoting Oppenheimer in a postwar lecture as follows:

Bohr at Los Alamos was marvelous. He took a very lively technical interest…But his real function, I think for almost all of us, was not the technical one… In the unedited version of the lecture*: (Bohr) made the enterprise which looked so macabre seem hopeful.* In the edited version*: He made the enterprise seem hopeful, when many were not free of misgiving…Bohr spoke with contempt of Hitler, who with a few hundred tanks and planes had tried to enslave Europe for a millennium. He said nothing like that would ever happen again; and his own high hope that the outcome would be good….*

Niels Bohr was a pacifist, and he knew that he was not needed to produce the atomic bomb. He saw his own participation in the Manhattan Project as necessary so that he could bear witness and provide first-hand warning to President Franklin Roosevelt before the bomb was developed and tested and eventually to the world through the United Nations. Bohr feared that Germany, where nuclear fission was discovered in 1939, would eventually develop the atomic bomb, and the United States and England had to beat Germany to the race; however, Bohr had the foresight of the grave menace that nuclear weapons would present to the world and to the survival of the human race. In the beginning of 1944, Bohr had the opportunity to bring his views to the attention of the American and British governments, and in a memorandum dated July 3, 1944, Bohr wrote President Roosevelt on his concerns over the project for nuclear weapon development, the threat that nuclear weapons would present to the human race, and following the development of the weapon, the immediate need for an international nuclear nonproliferation regime to prevent a nuclear weapons race possibly under the auspices of the United Nations. In August 1944, Niels Bohr was granted a long meeting with the President. The following are some excerpts of Bohr's memorandum to President Roosevelt:

…The fact of immediate preponderance is, however, that a weapon of unparalleled power is being created which will completely change all future conditions of warfare. Quite apart from the question of how soon the weapon will be ready for use and what role it may play in the present war, the situation raises a number of problems which call for most urgent attention. Unless, indeed, some agreement about the control of the use of the new active materials can be obtained in due time, any temporary advantage, however great, may be outweighed by a perpetual menace to human security…especially the terrifying prospect of a future competition between nations about a weapon of such formidable character can only be avoided through a universal agreement in true confidence…The prevention of a competition prepared in secrecy will therefore demand such concessions regarding exchange of information and openness about industrial efforts including military preparations as would hardly be conceivable unless at the same time all partners were assured of a compensating guarantee of common security against dangers of unprecedented acuteness…Without impeding the importance of the project (Manhattan Project) for immediate military objectives, an initiative, aiming at forestalling a fateful competition about the formidable weapon, should serve to uproot any cause of distrust between the powers on whose harmonious collaboration the fate of coming generations will depend. Indeed, it would appear that only when the question is taken up among the United Nations of what concessions the various powers are prepared to make as their contribution to an adequate control arrangement, it will be possible for any one of the partners to assure themselves of the sincerity of the intentions of the others.

Bohr's fears of an eventual nuclear arms race with the development of weapons of unimaginable destructive power, and the need for the government to pursue a program for nuclear nonproliferation, were elaborated further in a subsequent memorandum to the President dated March 25, 1945 before the weapon was first tested on July 16, 1945. Bohr's memorandum contained the following relevant passages:

Above all, it should be appreciated that we are faced only with the beginning of a development and that, probably within the very near future, means will be found to simplify the methods of production of the active substances and intensify their effects to an extent which may permit any nation possessing great industrial resources to command powers of destruction surpassing all previous imagination.

Humanity will, therefore, be confronted with dangers of unprecedented character unless, in due time, measures can be taken to forestall a disastrous competition in such formidable armaments and to establish an international control of the manufacture and use of the powerful materials.

Any arrangement which can offer safety against secret preparations for the mastery of the new means of destruction would, as stressed in the memorandum, demand extraordinary measures. In fact, not only would universal access to full information about scientific discoveries be necessary, but every major technical enterprise, industrial as well as military, would have to be open to military control.

In this connection it is sufficient that the special character of the efforts which, irrespective of technical refinements, are required for the production of the active materials, and the peculiar conditions which govern their use as dangerous explosives, will greatly facilitate such control and should ensure its efficiency, provided only that the right of supervision is guaranteed.

Detailed proposals for the establishment of an effective control would have to be worked out with the assistance of scientists and technologists appointed by the governments concerned, and a standing expert committee, related to an international security organization, might be charged with keeping account of new scientific and technical developments and with recommending appropriate adjustments of the control measures.

On recommendations from the technical committee the organization would be able to judge the conditions under which industrial exploitation of atomic energy sources could be permitted with adequate safeguards to prevent any assembly of active material in an explosive state.

In an Open Letter to the United Nations dated June 9, 1950 (Bohr, 1950), Niels Bohr provided the above relevant contents of his memoranda to President Roosevelt and implored the United Nations in cooperation with its Member States to take the lead in working toward and achieving nuclear nonproliferation and to advance the peaceful applications of nuclear energy. The following are additional relevant excerpts of his Open Letter to the United Nations:

I address myself to the organization, founded for the purpose to further co-operation between nations on all problems of common concern, with some considerations regarding the adjustment of international relations required by modern development of science and technology… Everyone associated with the atomic energy project [nuclear weapons Manhattan Project] was, of course, conscious of the serious problems which would confront humanity once the enterprise was accomplished [ie, weapon developed]. Quite apart from the role atomic weapons might come to play in the war, it was clear that permanent grave dangers to world security would ensue unless measures to prevent abuse of the new formidable means of destruction could be universally agreed upon and carried out…Worldwide political developments have increased the tension between nations and at the same time the perspectives that great countries may compete about the possession of means of annihilating populations of large areas and even making parts of the earth temporarily uninhabitable have caused widespread confusion and alarm…The situation calls for the most unprejudiced attitude towards all questions of international relations. Indeed, proper appreciation of the duties and responsibilities implied in world citizenship is in our time more necessary than ever before…real co-operation between nations on problems of common concern presupposes free access to all information of importance for their relations. Any argument for upholding barriers for information and intercourse, based on concern for national ideals or interests, must be weighed against the beneficial effects of common enlightenment and the relieved tension resulting from openness…The development of technology has now reached a stage where the facilities for communication have provided the means for making all mankind a co-operating unit, and where at the same time fatal consequences to civilization may ensue unless international divergences are considered as issues to be settled by consultation based on free access to all relevant information…I turn to the United Nations with these considerations in the hope that they may contribute to the search for a realistic approach to the grave and urgent problems confronting humanity….

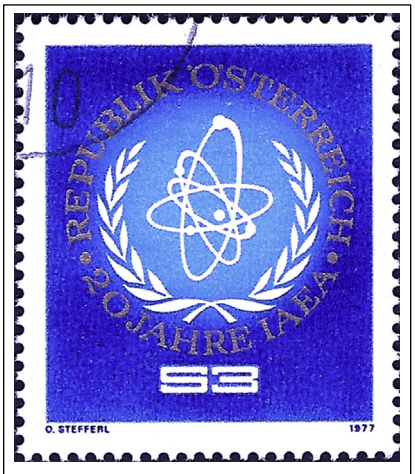

IAEA Emblem

Niels Bohr, in the above statements of his memoranda to President Roosevelt and in his Open Letter to the United Nations, displayed tremendous foresight in predicting the need for nuclear arms nonproliferation and the role of the United

Nations in this effort. What he wrote more than half a century ago in essence foretold the need for the current nuclear nonproliferation program that the IAEA of the United Nations actively pursues. Through his writings outlined above, Niels Bohr in 1950 gave birth to the IAEA's program of nuclear nonproliferation. In recognition of the efforts taken in the direction of nuclear nonproliferation, the IAEA and its Director General, Mohamed ElBaradei, were awarded the Nobel Peace Prize in 2005. The IAEA was founded in 1957. Its emblem is illustrated on the postage stamp issued in Austria in 1977 commemorating its 20th anniversary. The Headquarters of the IAEA are located in the Vienna International Center on the banks of the Danube River in Vienna, Austria, which is pictured in the commemorative stamp issued in Hungary in 1980.

IAEA and UN Headquarters, Vienna

The Nobel Prize was granted on October 7, 2005 with the following statement:

The Norwegian Nobel Committee has decided that the Nobel Peace Prize for 2005 is to be shared, in two equal parts, between the International Atomic Energy Agency (IAEA) and its Director General, Mohamed ElBaradei, for their efforts to prevent nuclear energy from being used for military purposes and to ensure that nuclear energy for peaceful purposes is used in the safest possible way.

At the time when the threat of nuclear arms is again increasing, the Norwegian Nobel Committee wishes to underline that this threat must be met through the broadest possible international cooperation. This principle finds its clearest expression today in the work of the IAEA and its Director General. In the nuclear non-proliferation regime, it is the IAEA which controls that nuclear energy is not misused for military purposes, and the Director General has stood out as an unafraid advocate of new measures to strengthen that regime. At a time when disarmament efforts appear deadlocked, when there is a danger that nuclear arms will spread both to states and to terrorist groups, and when nuclear power again appears to be playing an increasingly significant role, IAEA's work is of incalculable importance.

In his will, Alfred Nobel wrote that the Peace Prize should, among other criteria, be awarded to whoever has done most for the "abolition or reduction of standing armies." In its application of this criterion in recent decades, the Norwegian Nobel Committee has concentrated on the struggle to diminish the significance of nuclear arms in international politics, with a view to their abolition. That the world has achieved little in this respect makes active opposition to nuclear arms all the more important today.

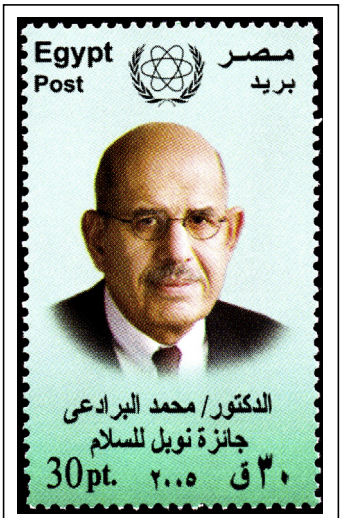

Mohamed ElBaradei (1942–)

Niels Bohr retained his post of Head of the Institute for Theoretical Physics at Copenhagen University, created for him in 1920, until his death in Copenhagen in 1962.

GUSTAV HERTZ (1887–1975) AND JAMES FRANCK (1882–1964)

Gustav Hertz and James Franck shared the Nobel Prize in Physics 1925 "for their discovery of the laws governing the impact of the electron upon an atom." Hertz and Franck were awarded the Nobel Prize for their work in providing experimental proof of Bohr's quantum theory of atomic structure. Prof. Orseen (1926), member of the Nobel Committee, in his presentation speech on the occasion of the Nobel Prize to Hertz and Franck, noted the following:

> *…When all that had been gained in the field of atomic physics seemed to be at stake, there is nobody who would have thought it advisable to proceed from the assumption that the atom can exist in different states, each of which is characterized by a given energy level, and that these energy levels govern the spectral lines emitted by the atoms in the way described [by Bohr's theory]. The fact that Bohr's hypotheses in 1913 have succeeded in establishing this, is because they are no longer mere hypotheses but experimentally proven facts. The methods of verifying these hypotheses are the work of James Franck and Gustav Hertz, for which they have been awarded the Physics Nobel Prize for 1925.*

Gustav Ludwig Hertz was born in Hamburg, Germany on July 22, 1887. He started his university studies at the University of Göttingen in 1906 and subsequently continued his studies at the Universities of Munich and Berlin. After graduating in 1911, Hertz was appointed as a Research Assistant at the University of Berlin. James Frank was a professor at the University of Berlin at the time, and the two started a collaboration on the interaction of electrons with gas atoms. This work led to their findings that gave experimental proof of Bohr's quantum theory of atomic structure and a joint sharing of the Nobel Prize in physics in 1925, which is described further on in this section. Hertz's research career was interrupted by his conscription into World War I; and he was wounded in action in 1915. He returned to the University of Berlin in 1917 as Privatdozent, and in 1920 entered into the private sector of research with the Philips Incandescent Lamp Factory at Eindhoven, where he continued experimental work on electron impact with gas atoms. In 1925, Hertz became Resident Professor of the University of Halle, and the following year he became Director of the Physics Institute of the university. At the end of 1927, he returned to Berlin and was given an appointment with the duties of creating a new physics institute at the Technische Hochschule (Technological University at Charlottenburg), where he managed to build an institute that paralleled its counterpart at the University of Berlin.

At his new Technische Hochschule in Berlin, Gustav Hertz did pioneering work on the separation of isotopes by means of a gaseous diffusion cascade. By 1932 he demonstrated the feasibility of isotope separation or isotope enrichment by gaseous diffusion (Hertz, 1933). He successfully separated the isotope neon-20 from neon-22 as well as deuterium (hydrogen-2), referred to as heavy hydrogen, from its most abundant isotope, which we refer to as normal hydrogen (hydrogen-1). The gaseous diffusion method is based on the principle that, in thermal equilibrium, two isotopes of the same energy will travel or diffuse with different velocities. The lighter isotopes, or the gaseous molecules within which the isotopes are bound, will travel with a higher velocity and therefore travel more rapidly through a porous membrane than the heavier isotopes. The difference in the rates of diffusion is proportional to the square root of the mass ratios or molecular weights of the light isotope over the heavier isotope, as described in Eq. [V.7] (Wooldridge, 1936; Wooldridge and Smythe, 1936):

$$\mu = \sqrt{\frac{M_L}{M_H}} \qquad [V.7]$$

where μ is the velocity of diffusion and M_L and M_H are the molecular weights of the gaseous molecules that contain the light and heavier isotopes, respectively. The apparatus used for isotope enrichment, as described by Wooldridge (1936), consisted of a length of clay tubing through which the gas containing the isotopes could be led. A region outside the tubing is kept evacuated so that part of the gas will diffuse through the porous walls of the clay tubing as the gas travels along the length of the tubing. As the gas containing the two isotopes travels through the tubing, the gas of lower molecular weight diffuses faster through the porous membrane of the clay tubing. Thus the gas that travels the entire length of the tubing without passing through the porous walls will be richer in the heavier isotope than the gas that was originally led into the tubing. When only two isotopes are involved in the process, the ratio of the number of heavy to light isotopes is increased by the factor E, the enrichment factor, given by Eq. [V.8]:

$$E = \sqrt[1-\mu]{\frac{\text{Volume of gas led into tubing}}{\text{Volume led out of tubing without diffusion}}} \qquad [V.8]$$

The method devised by Hertz was both simple and ingenious, whereby he was able to affect isotope enrichment by leading the gas containing the isotopes automatically through many successive diffusions in a closed system referred to as a diffusion cascade. Hertz led the gas through the successive diffusions by affecting the diffusion process in a chain of numerous chambers. Each chamber would consist of the porous clay tubing surrounded by its own evacuated glass jacket. The gas that diffuses through the porous walls was not discarded, but led back into the system at a point in the apparatus where the gas was introduced. The lighter constituent that had diffused through the wall of the tubing in the nth separation chamber (or *n*th stage) was sent back to the $(n-1)$th separation chamber. The light constituent of the $(n-1)$th chamber is sent back to the $(n-2)$th chamber, etc. This results in a net transfer of light molecules toward one end of the system (cascade) and the heavier molecules toward the other end. A simple illustration of Hertz's gaseous diffusion cascade is illustrated in the commemorative postage stamp issued by the German Democratic Republic (DDR).

Gustav Hertz (1887–1975) and his diffusion cascade apparatus

Gaseous diffusion was one of the methods used at the Oak Ridge National Laboratories in the Manhattan Project to enrich fissile uranium-235 for the production of the first atomic bomb. Natural uranium contains approximately 0.7% ^{235}U, and to enrich this isotope from ^{238}U required the use of a gaseous compound of uranium, namely uranium hexafluoride (UF_6). The production of 99% ^{235}U from natural uranium required approximately 4000 enrichment stages. The enrichment of isotopes for medical applications and biological research is currently in great demand. The enrichment of carbon-13 and nitrogen-15 to percent abundances greater than 99% is a common commercial practice together with the labeling of numerous organic and inorganic compounds with the enriched isotope ^{13}C or ^{15}N for metabolic studies in the biological sciences, which have resulted in many discoveries in medical, biological, and agricultural research (L'Annunziata, 1984).

In, 1934 Hertz could not continue as director of the research institute that he had founded at the Technische Hochschule in Berlin because of the anti-Semitic laws of the German Nazi regime, as his grandfather was of Jewish decent. He left the Technische Hochschule and took on a position in setting up a new research laboratory at Siemens in 1935. About 4 weeks prior to the testing of the first atomic bomb by the Americans in 1945, Hertz was flown to Moscow, and after World War II Hertz helped establish a research institute at Sukhumi on the Black Sea coast of the USSR, which had the principal task of developing the methodology for the separation of uranium isotopes, ie, the enrichment of uranium-235, in large quantities. Although there is no evidence of Hertz being involved directly in the Russian nuclear bomb program, he was a Nobel Laureate and respected scientist who could command the loyalty and following of other prominent scientists in the Russian research effort. In 1954 he took on a position as professor at the University of Leipzig and became professor emeritus of the university in 1961. He died in Berlin on October 30, 1975, where he returned after retiring from the University of Leipzig.

James Franck was born on August 26, 1882 in Hamburg, Germany. He started his university studies in the field of chemistry at the University of Heidelberg, and transferred to the field of physics at the University of Berlin, where he received the PhD degree in 1906. After a short stint as research assistant at Frankfurt-am-Main, James Franck returned to the University of Berlin as research assistant. In 1911 he became lecturer at the University of Berlin, where he remained until 1918, rising to the position of associate professor of physics. It was at the University of Berlin from 1912 to 1914 that Franck and Hertz collaborated in research that provided proof of Niels Bohr's quantum theory of atomic structure and for which both were awarded the Nobel Prize in physics. Their joint work is described further on in this section. During his stint at the University of Berlin, he took time to serve in World War I and was awarded the Iron Cross.

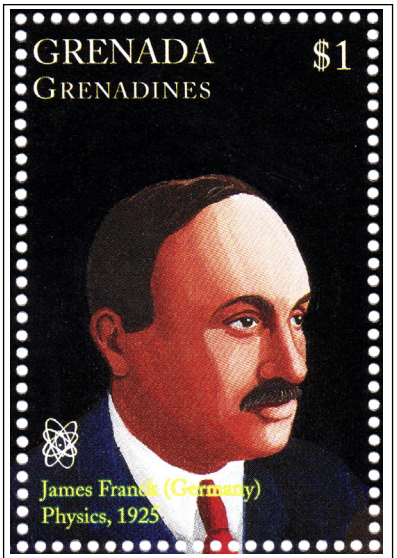

James Franck (1882–1964)

After the war, Franck was appointed Head of the Physics Division of the Kaiser Wilhelm Institute for Physical Chemistry at Berlin-Dahlem. In 1920, he was appointed Professor of Experimental Physics at the University of Göttingen. When the Nazi regime ruled Germany, James Franck showed his true character by resigning his post in protest of the Nazi anti-Semitic policies. As explained by Franck's former student and research collaborator (Rosenberg, 2004):

> *His resignation from his professorship as a public protest against emerging Nazism became a cause celebre in Germany. Although his World War I army service would have spared him from dismissal from his post under the new anti-Semitic laws, although only for the short term as we now know, he refused to accept his orders to dismiss many of his faculty, staff, and students under the new edicts dealing with racial and 'politically correct' classifications. Instead, he worked tirelessly as a private citizen from his home in Göttingen to locate scientific employment opportunities throughout the Western world for dozens of his colleagues.*

Franck left Germany altogether for Copenhagen, Denmark in 1933 as an academic refugee and took up a position of guest professor for a year in Niels Bohr's laboratory. In 1935 he was appointed professor at Johns Hopkins University, where he remained until 1938 when he became professor of physical chemistry at the University of Chicago.

During World War II, Franck served as Director of the Chemistry Division of the Metallurgical Laboratory, which was the center established for the secret Manhattan Project for the development of the atomic bomb. Franck and many other scientists of the Manhattan Project worked to develop the horrific bomb for one very specific reason, that being the threat of Nazi Germany where nuclear fission was discovered in 1939. Germany led by Hitler represented an evil that could not be tolerated. It had the technological skill needed to develop such a weapon and lacked the moral constraints against its use. But after Germany surrendered, many scientists were confronted with the moral implications of using the bomb and an international nuclear arms race that the use of the bomb could create. They knew that such an arms race would create the potential for a future nuclear war that would cause great worldwide destruction and the possibility of the eventual annihilation of the human race. With this in mind, James Franck chaired a Committee on the Political and Social Problems, University of Chicago Manhattan Project "Metallurgical Laboratory." The Committee, which included James Franck as chairman, Glenn T. Seaborg, and Leo Szilard, who was the first to conceive of the atomic bomb, among other scientists of the Manhattan Project, drafted "The Franck Report" on June 11, 1945, approximately five weeks before the first atomic bomb was tested at Los Alamos, New Mexico. The Franck Report, addressed to the U.S. Government, was by force a secret document asking it to refrain from using the bomb against Japan and instead recommended that the government detonate the weapon of mass destruction in an uninhabited desert area to be witnessed by an international team from the United Nations, which would put the United States and the world on a better footing toward the establishment of an international effort and program of safeguards toward nuclear nonproliferation. James Franck personally delivered the Franck Report to the United States Secretary of War, Henry Stimson, on June 11, 1945 (Rabinowitch, 1964; Rosenberg, 2004). The following excerpts of the Franck Report, which unfortunately have so far accurately predicted the current state of affairs concerning nuclear proliferation and the threat of nuclear annihilation, are very relevant in reminding the world of the threat of nuclear weapons and the need for a strong United Nations IAEA Program of Nuclear Nonproliferation (NNP).

THE FRANCK REPORT, JUNE 11, 1945, JAMES FRANCK (CHAIRMAN)

I. Preamble

The only reason to treat nuclear power differently from all other developments in the field of physics is its staggering possibilities as a means of political pressure in peace and sudden destruction in war…The scientists on this project do not presume to speak authoritatively on problems of national and international policy. However, we found ourselves, by the force of events, the last 5 years in the position of a small group of citizens cognizant of a grave danger for the safety of this country as well as for the future of all the other nations, of which the rest of mankind is unaware…The success we have achieved in the development of nuclear power is fraught with infinitely greater dangers than were all of the inventions in the past. All of us, familiar with the present state of nucleonics, live with the vision before our eyes of sudden destruction visited on our own country, of Pearl Harbor disaster, repeated in thousandfold magnification, in every one of our major cities…Protection can only come from the political organization of the world. Among all arguments calling for an efficient international organization for peace, the existence of nuclear weapons is the most compelling one. In the absence of an international authority which would make all resort to force in international conflicts impossible, nations could still be diverted from a path which must lead to total mutual destruction, by a specific international agreement barring a nuclear arms race.

II. Prospectives of Armaments Race

We cannot hope to avoid a nuclear armament race, either by keeping secret from the competing nations the basic scientific facts of nuclear power, or by cornering the raw materials required for such a race…All that these advantages can give us is the accumulation of a larger number of bigger and better atomic bombs…Such a quantitative advantage in reserves of bottled destructive power will not make us safe from sudden attack…If no efficient international agreement is achieved, the race of nuclear armaments will be on in earnest not later than the morning after our first demonstration of the existence of nuclear weapons. After this, it might take other nations 3 to 4 years to overcome our present head start….

III. Prospectives of Agreement

The prospect of nuclear warfare and the type of measures which have to be taken to protect a country from total destruction by nuclear bombing, must be abhorrent to other nations as to the United States. England, France, and the smaller nations of the European continent, with their congeries of people and industries, are in an entirely hopeless situation in the face of such a threat…There is no doubt that Russia too, will shudder at the possibility of a sudden disintegration of Moscow and Leningrad, almost miraculously preserved in the present war…Therefore, only lack of mutual **trust**, and not lack of **desire** for agreement, can stand in the path of an efficient agreement for the prevention of nuclear warfare. From this point of view, the way in which nuclear weapons, now secretly developed in this country, will be revealed to the world appears of great, perhaps fateful importance…Certain and perhaps important tactical results undoubtedly can be achieved (by the use of the atomic bomb on Japan), but we nevertheless think that the question of the use of the very first available atomic bombs in the Japanese war should be weighed very carefully, not only by military authority, but by the highest political leadership of this country. If we consider international agreement on total prevention of nuclear warfare as the paramount objective, and believe that it can be achieved, this kind of introduction of atomic weapons to the world may easily destroy all our chances of success. Russia, and even allied countries which bear less mistrust of our ways and intentions, as well as neutral countries, will be deeply shocked. It will be very difficult to persuade the world that a nation which was capable of secretly preparing and suddenly releasing a weapon, as indiscriminate as the rocket bomb and a 1000 times more destructive, is to be trusted in its proclaimed desire of having such weapons abolished by international agreement…It is not at all certain that the American public opinion, if it could be enlightened as to the effect of atomic explosives, would support the first introduction by our own country of such an indiscriminate method of wholesale destruction of civilian life. Thus from the "optimistic" point of view—looking forward to an international agreement on prevention of nuclear warfare—the military advantages and the saving of American lives, achieved by the sudden use of atomic bombs against Japan, may be outweighed by the ensuing loss of confidence and wave of horror and repulsion, sweeping over the rest of the world, and perhaps dividing the public opinion at home. **From this point of view a demonstration of the new weapon may best be made before the eyes of representatives of all United Nations, on the desert or barren land**. The best possible atmosphere for the achievement of an international agreement could be achieved if America would be able to say to the world, "You see what weapon we

had but did not use. We are ready to renounce its use in the future and to join other nations in working out adequate supervision of the use of this nuclear weapon."…One may point out that the scientists themselves have initiated the development of this "secret weapon" and it is therefore strange that they should be reluctant to try it out on the enemy as soon as it is available. The answer to this question was given above—the compelling reason for creating this weapon with such speed was our fear that Germany had the technical skill necessary to develop such a weapon without any moral constraints regarding its use….

IV. Methods of International Control

We now consider the question of how an effective international control of nuclear armaments can be achieved…Given mutual trust and willingness on all sides to give up a certain part of their sovereign rights, by admitting international control of certain phases of national economy, the control could be exercised…One thing is clear, any international agreement on prevention of nuclear armaments must be backed by actual and efficient controls. No paper agreement can be sufficient since neither this or any other nation can stake its whole existence on trust into other nations' signatures. Every attempt to impede the international control agencies must be considered equivalent to denunciation of the agreement. It hardly needs stressing that we as scientists believe that any systems of controls envisaged should leave as much freedom for the peace(ful) development of nucleonics as is consistent with the safety of the world.

In 1947, James Franck was named professor emeritus at the University of Chicago. He continued research work at the University of Chicago as Head of the Photosynthesis Research Group until 1956. He carried out a lot of pioneering work and theories on photosynthesis that cover a span of almost 30 years. His first paper on photosynthesis was published when he was at Johns Hopkins University (Franck, 1935), and his last with Rosenberg at the University of Chicago (Franck and Rosenberg, 1964). Franck's works in photosynthesis are reviewed by Rosenberg (2004) together with an excellent sketch of his life. Franck wrote on the fate of his theories on photosynthesis in one of his papers (Franck and Herzfeld, 1941) as follows:

> *The change in the situation (new methods of observation and new results) is indeed so far-reaching that practically all theories published hitherto are now obsolete…These theories have served the purpose for which they were developed; they have clarified the situation, they have stimulated new experiments, and most of them contained parts which have been used in each subsequent attempt… A theory… by its very nature can contain only a partial truth.*

Franck died in Germany when visiting Göttingen on May 21, 1964. In a short tribute to James Franck and his life, Rosenberg (2004) relates a story passed on to him by Franck as follows:

> *Another of his anecdotes expressed his pride in sharing the Nobel Prize with Bohr and Planck, because for safekeeping Bohr had dissolved all three of their gold Nobel medals in* agua regia *and stored them as a solution in an unmarked bottle in his Copenhagen laboratory during World War II, to be reprecipitated and cast into three new medals after the war.*

THE FRANCK–HERTZ EXPERIMENT

While at the University of Berlin from 1912 to 1914, James Franck and Gustav Hertz collaborated in research on the impact of electrons on atoms and the energy loss by electrons upon collision with atoms. In their collaborative work, Franck and Hertz (1914a,b) measured the kinetic energies of electrons before and after collisions with atoms, and demonstrated that an electron could lose its kinetic energy upon collision with an atom only when a certain quantum of energy is transferred to the atom. If the electron possessed kinetic energy less than that quantum, no kinetic energy of the electron would be transferred upon collision with an atom. An electron of kinetic energy greater than a given quantum, could transfer the quantum of energy to an atom upon collision with the atom and then continue traveling with any kinetic energy in excess of the transferred energy quantum. The atom with which the electron had collided would increase in energy from E_1 to E_2, corresponding to an absorption of that quantum of energy. Only energy corresponding to fixed quanta could be absorbed by the atom upon collision with electrons. Franck and Hertz were awarded the Nobel Prize in physics in 1925 for this work, because it demonstrated Bohr's quantum theory of atomic structure, that is, the atom can exist in only specific quantum energy states whereby the atomic electrons can only absorb and emit energy in discrete quanta. The quantum of energy emitted by the atom would correspond to the quantum of energy absorbed as defined by spectral lines or radiation frequencies, as defined by Eq. [V.6], ie, $\nu = (E_2 - E_1)/h$.

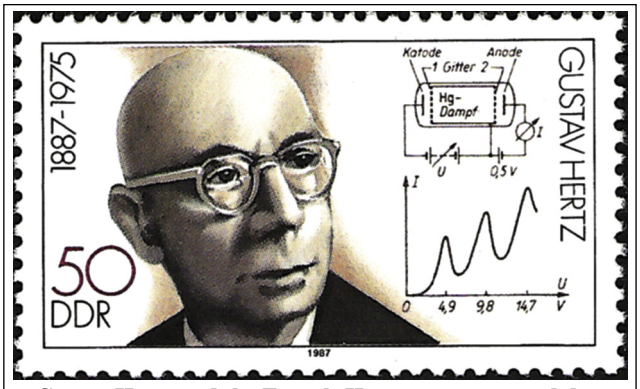

Gustav Hertz and the Franck-Hertz apparatus and data for Mercury

The experimental arrangement used by Franck and Hertz is illustrated in the postage stamp issued by the German Democratic Republic (DDR) in 1987 and in Fig. V.4. Their apparatus (Franck and Hertz, 1914a,b; Franck, 1926) consisted of an air-tight glass chamber containing mercury vapor. Within the chamber is located a tungsten wire heated to a bright-red glow by an electric current as a cathode or source of electrons. A few centimeters away from the electron source (G of Fig. V.4) is a positively charged wire-screen electrode (N) using the original notation of Franck (1926). The electrons emitted from the cathode will accelerate toward the positive wire screen. The kinetic energy that the electrons gained in the acceleration between G and N without collision with any atoms (ie, in the absence of any gas in the apparatus) is governed by the voltage potential applied according to the relationship:

$$E_e = \frac{1}{2}mv^2 = eV \qquad [V.9]$$

where $\frac{1}{2}mv^2$ is the kinetic energy of each electron traveling to the anode, e is the elementary electrical charge, and V is the applied potential difference between G and N. The energy of the electron can therefore be measured in units of electron

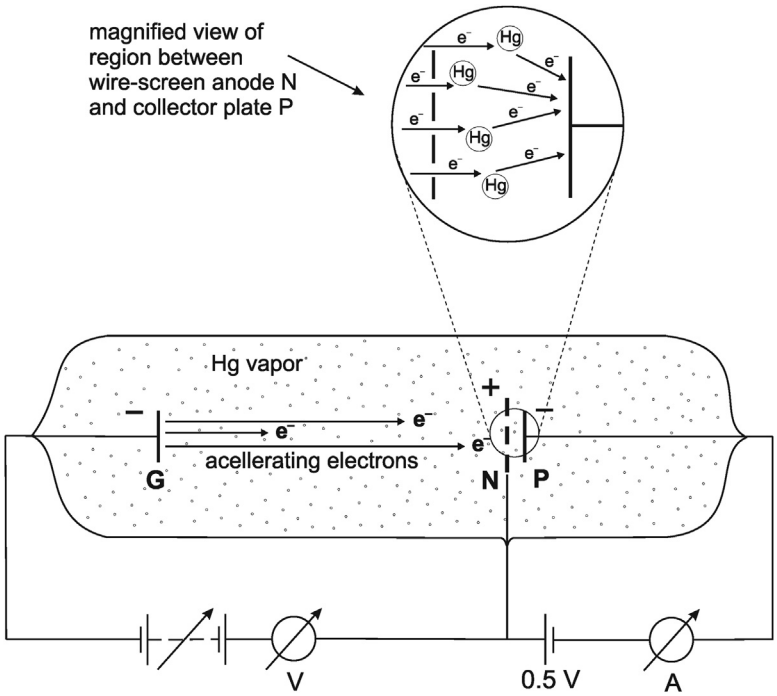

FIGURE V.4 The Franck–Hertz apparatus with mercury vapor. Electrons accelerated across the potential difference between electrodes G and N with energy greater than 0.5 V were collected at plate P. The electric current (amperes) collected at P was plotted against the accelerating voltage across G and N. The current collected at P would increase as the accelerating voltage was increased until the energy stage of 4.9 eV was reached, which would result in a sudden drop in current collected at P. This would repeat itself at additional increments of 4.9 eV as the accelerating voltage was further increased resulting in current drops at 9.8 and 14.7 V, etc. The current drops in increment of 4.9 eV illustrated that electron energy was transferred upon impact with Hg atoms between plates N and P (see magnified portion of illustration) in quantum increments of 4.9 eV only.

volts (eV) according to the accelerating voltage applied. Some of the accelerated electrons are caught by the screen with a specific energy of *x* eV, the value of which is subject to the voltage potential applied. Some of the electrons fly through the mesh and reach the electrode P to produce a negative current that flows to earth through a galvanometer, provided there is no field difference applied between N and P that would send the electrons back to N. With the apparatus described, Franck and Hertz introduced an electric field between N and P to determine the energy distribution of the electrons passing through the screen. We can call the electrode P a "collector plate," because it is the electrode that will collect the accelerated electrons passing through the wire-mesh anode N. Frank explains the function of the collector plate as follows:

> *By introducing an electric field between N and P the energy distribution of those electrons passing through the screen can be determined. If, for example, we take only 4-volt beams, which pass perpendicularly through the screen, than the electric current measured at the galvanometer as a function of a decelerating potential difference applied between N and P, must be constant, until P becomes 4 volts more negative than N. At this point the current must become suddenly zero since henceforth all electrons will be repelled from P that they return to N.*

Franck and Hertz introduced an inert gas, such as mercury vapor, into the chamber at a pressure that would ensure that the electrons accelerated through G and N would make many collisions with atoms of the gas when passing through the space between N and P. They then plotted the energy distribution of the electrons arriving at the collector plate P as a function of the accelerating voltage applied between G and N to determine whether the electrons had lost energy by impact or collision with the atoms of mercury. Franck and Hertz plotted the current collected at electrode P against the accelerating voltage applied across G and N. In this experiment they measured at the collector plate P all electrons with energy greater than the energy of 0.5-V beams. The plot is illustrated in the postage stamp issued by the German Democratic Republic, where the current collected (*I*) is plotted against the accelerating voltage (*V*) and the graph illustrated in Fig. V.5. The graph illustrates that the electron current at P increases with increasing acceleration until the critical energy stage is reached (4.9 eV), when the current

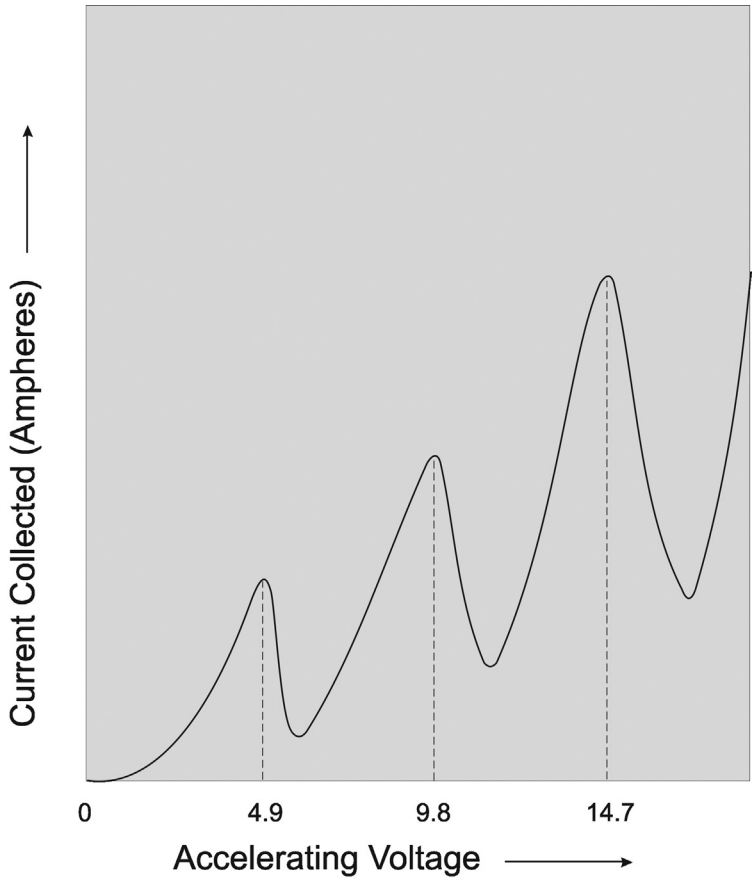

FIGURE V.5 The Franck–Hertz experiment with mercury vapor. Atoms of Hg absorb increments of 4.9-eV energy upon impact with accelerated electrons. *Modified from Franck, J., 1926. Transformations of kinetic energy of free electrons into excited energy of atoms by impacts. Nobel Lecture, December 11, 1926. In: Nobel Lectures, Physics 1922–1941, Elsevier Publishing Co., Amsterdam and commemorative postage stamp from the former DDR issued in 1987.*

collected falls suddenly. Further increasing the accelerating voltage causes the process to repeat itself, that is, the number of electrons with velocity greater than 0.5 V again increases until the critical value of the accelerating voltage reaches 9.8, a multiple of 4.9, and the current at the collector plate P again falls. The process repeats every time the accelerating voltage overreaches a multiple of the critical voltage of 4.9, that is, 9.8, 14.7 V, etc. as illustrated in the postage stamp and Fig. V.5.

The drop in the electron current collected at P at multiples of 4.9 V demonstrated that energy was removed from the accelerating electrons upon collision with mercury atoms and transferred to the atoms of mercury only in the quantized energy levels of 4.9 eV. This energy quantum corresponded to the 2.537-Å (254-nm) ultraviolet line in the emission spectrum of mercury, providing evidence to Bohr's theory that an atom can accept only discrete quantities of energy and can subsequently emit the energy only in discrete quantities. Frank (1926) interpreted the results according to Bohr's quantum theory of atomic structure as follows:

> *According to Bohr an atom can absorb as internal energy only discrete quantities of energy, namely those quantities which transfer the atom from one stationary state to another stationary state. If following on energy supply an exited energy state results from a transfer to a stationary state of higher energy, then the energy so taken up will be radiated in quanta fashion according to the* hν *relationship. The frequency of the absorption line having the longest wavelength…multiplied by Planck's constant, gives the energy required to reach the first state of excitation. These basic concepts agree in very particular with our results. The elastic collisions of low electron velocities show that for these impacts no energy is taken up as inner energy, and the first critical energy step results in just the amount of energy required for the excitation of the longest wave absorption line of Hg. Subsequently it appeared to me to be completely incomprehensible that we had failed to recognize the fundamental significance of Bohr's theory…I should like to mention that it later proved successful…to demonstrate also, from the current voltage curves, the stepwise excitation of a great number of quantum transitions, lying before the first excitation level and ionization.*

The experimental proof of the quantum atomic absorption and emission of energy provided by James Franck and Gustav Hertz set the stage for future scientific research in spectroscopy, an important phenomenon in chemistry and physics. In the words of Orseen (1926): "The extraordinary good agreement with experience obtained in this way (Frank–Hertz experiment) explains why after 1913 almost a whole generation of theoretical and experimental physicists devoted itself to atomic physics and its application in spectroscopy."

WERNER HEISENBERG (1901–1976), ERWIN SCHRÖDINGER (1887–1961), MAX BORN (1882–1970), AND PAUL A.M. DIRAC (1902–1984)

Werner Heisenberg, Erwin Schrödinger, and Paul Dirac were awarded the Nobel Prize in physics in 1932 and 1933 for their work on the "new atomic physics." The awards were presented in one ceremony on December 13, 1933. As expressed by Prof. H. Pleijel (1933) in his Nobel presentation speech "This year's Nobel Prizes for Physics are dedicated to the new atomic physics…awarded to those men, Heisenberg, Schrödinger, and Dirac, who have created and developed the basic ideas of modern atomic physics." In his Nobel presentation speech, Pleijel (1933) clearly outlined the historical developments that led to the creation and development of the "new physics," namely quantum and wave mechanics. Not included by the Nobel Committee at this time was the vital contribution of Max Born, his statistical interpretation of quantum mechanics from 1926 to 1927, for which the Nobel Prize eluded him until 1954. The historical development described in more detail earlier in this book, began with Max Planck, who in 1900 described light as a packet or quantum of energy, ie, a function of the wavelength or frequency, and Planck's constant, $E = h\nu$. Then Einstein, through his explanation of the photoelectric effect in 1905, demonstrated the particulate nature of the light photon. Planck demonstrated that light could only be absorbed and emitted by matter in discrete quantities of energy, the light quantum, and this energy divided by the frequency of the radiation would always yield the universal Planck's constant, h. Then Louis de Broglie in 1923 presented his ideas on the dual nature of matter and light or the particle-wave duality, that is, a particle in motion could be interpreted as having the properties of a particle with mass and as having the properties of light with a wavelength and frequency. De Broglie derived the wavelength of the particle as a function of Planck's constant, or $\lambda = h/p$, where p is the particle momentum. The dual nature of matter and light presented by Einstein and de Broglie was first received with astonishment, but accepted universally after Davisson and Germer demonstrated experimentally in 1927 the diffraction of electrons by crystals. Thus atomic particles had to be looked upon not only as having the properties of matter but also the properties of light, as explained by Pleijel (1933):

> *De Broglie's theory of matter-waves subsequently received experimental confirmation. If a relatively slowly traveling electron meets a crystal surface, diffraction and reflection phenomena appear in the same way as if an incident beam of waves were concerned. As a result of this theory one is forced to the conclusion to conceive of matter as not being durable, or that it can have*

definite extension of space. The waves, which form the matter, travel, in fact, with different velocity and must, therefore, sooner or later separate. Matter changes form and extent in space. The picture which has been created, of matter being composed of unchangeable particles, must be modified.

One of the phenomena that needed more clarification was Bohr's theory on the structure of the atom (Bohr 1913, 1914), which he constructed by taking the heavy positively charged nucleus as the center of the atom around which orbited the atomic electrons in fixed circular paths or stationary states. For the hydrogen atom, Bohr demonstrated that the atom could absorb energy only in fixed quanta, resulting in electron orbital transitions from inner to outer orbitals further away from the nucleus, and that the atom would emit this energy as a photon with a frequency that would be equivalent to the change in energy experienced by the electrons divided by Planck's constant or $\nu = (E_2 - E_1)/h$, where E_2 is the electron energy in an outer orbital after the atom had absorbed energy and E_1 is the initial electron energy in an inner orbital prior to the absorption of energy by the atom. This theory worked well for hydrogen (see Bohr in this section), but full agreement of this theory with atomic spectra did not hold for more complex atoms and molecules, which sparked the creation of the "new physics," as explained by Pleijel (1933):

The frequencies which Bohr thus obtained held good for a hydrogen atom which has only one electron, but when his method was applied to more complicated atoms and to certain optical phenomena, theory and practice did not agree. The fact that Bohr's hypothesis met the case for the hydrogen atom, however, suggests that Planck's constant was, in one way or another, a determining factor for the light-vibrations of the atoms. On the other hand, one had the feeling that it could not be right to apply the laws of classical mechanics to the rapid movements in the atom. Efforts made from various sides to develop and improve Bohr's theory proved also in vain. New ideas were required to solve the problem of oscillations of atoms and molecules. This solution started in 1925 upon the works of Heisenberg, Schrödinger, and Dirac in which different starting-points and methods were obtained.

The biographies and contributions of Heisenberg, Schrödinger, and Dirac are outlined subsequently.

Werner Heisenberg (1901−1976) was born in Würzburg, Germany on December 5, 1901. In 1920 he entered the University of Munich, where he pursued studies in theoretical physics, obtaining his PhD at the university in 1923. He then joined Max Born in studies of theoretical physics at the University of Göttingen. In 1926 he was appointed lecturer in theoretical physics under Niels Bohr at the University of Copenhagen, where he developed the first version of quantum mechanics, a mathematical matrix method of calculating the behavior of electrons and subatomic particles. As noted in his autobiography written at the time of his Nobel award (Heisenberg, 1933b), his new theory was based on what could be observed, for example, the radiation emitted by an atom. The paths of such radiation had clearly been visualized and photographed ingeniously by C.T.R. Wilson with his cloud chambers (see Hall of Fame, Part II). Heisenberg noted that we cannot always assign to an electron a position in space at a given time, nor follow it in its orbit, so therefore, we cannot assume that the planetary orbits postulated by Niels Bohr actually exist. He represented the electron's position and velocity not by ordinary numbers but by abstract mathematical matrices, formulating his new theory on the basis of matrix equations (Heisenberg, 1926a,b,c, 1929; Bohr et al., 1926).

Werner Heisenberg (1901–1976)

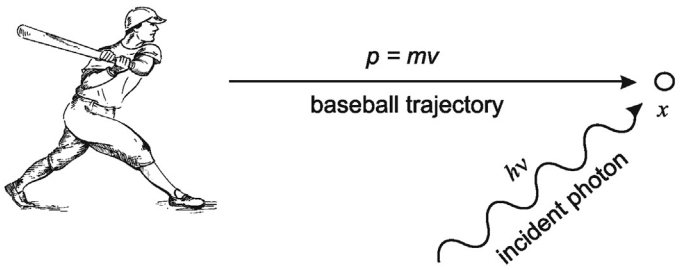

(A) light photon has negligible effect on baseball position (x)

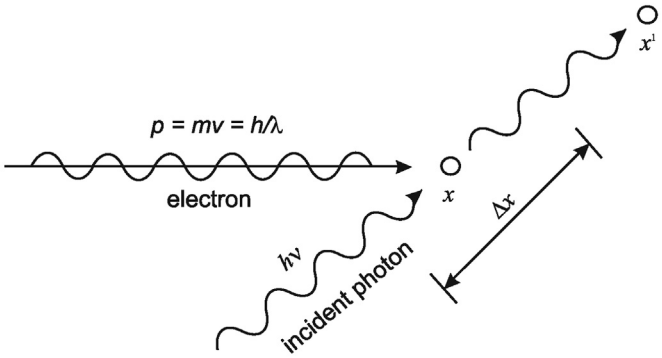

(B) light photon deflects electron matter-wave from position x to x'

FIGURE V.6 Artists' depiction of Heisenberg's explanation of the Uncertainty Principle. The momentum (p) and position (x) of a body of relatively large mass, such as a baseball illustrated in (A) above, will not be affected to any significant degree by the energy of the incident light photon (Heisenberg used the planets orbiting the sun instead of a baseball in his description; see Heisenberg's explanation taken from his Nobel lecture in this section); however, the momentum and position of a subatomic particle, such as the electron in (B), can be affected by a light photon. The uncertainty in the position (x) of the electron is depicted by (Δx). Thus both the location of the electron and its momentum cannot be measured with accuracy at any given time and remain uncertain.

In 1927 Heisenberg discovered and published his Uncertainty Principle, which is a basic concept of quantum theory. Before defining the Uncertainty Principle it is best to compare the concepts of classical physics with respect to velocity, mass, and position of large bodies of matter as compared to the same properties for the relatively small atomic particles. For example, with classical physics we can observe a baseball as it flies through the air after being hit by a batter and as light reflects off the ball. We can accurately determine the position (x) of the ball at a given time and its momentum (p) according to its mass (m) and velocity (v), where $p = mv$. However, at the small atomic level, when a photon of light hits an atomic particle, it can affect the momentum of the particle due to its low mass, as illustrated in Fig. V.6. Einstein explained that, in the photoelectric effect, a light photon is capable of imparting energy to an electron, providing it with momentum. Therefore, at the small atomic level, we cannot accurately measure both the momentum (p) and location (x) of the electron, as the particle will have wave properties as well as those of mass.

Heisenberg (1933a) explained the concept of the Uncertainty Principle in his Nobel lecture as follows:

> *This difference between classical and atomic physics is understandable, of course, since for heavy bodies such as the planets moving around the sun the pressure of the sunlight which is reflected at their surface and which is necessary for them to be observed is negligible; for the smallest building units of matter, however, owing to their low mass, every observation has a decisive effect on their physical behaviour. The perturbation of the system to be observed caused by the observation is also an important factor in determining the limits within which a visual description of atomic phenomena is possible. If there were experiments which permitted accurate measurement of all the characteristics of an atomic system necessary to calculate classical motion, and which, for example, supplied accurate values for the location and velocity of each electron in the system at a particular time, the result of these experiments could not be utilized at all in the formalism, but rather it would directly contradict the formalism. Again, therefore, it is clearly that fundamentally unverifiable part of the perturbation of the system caused by the measurement itself which hampers accurate ascertainment of the classical characteristics and thus permits quantum mechanics to*

be applied. Closer examination of the formalism shows that between the accuracy with which the location of a particle can be ascertained and the accuracy with which its momentum can simultaneously be known, there is a relation according to which the product of the probable errors in the measurement of the location and momentum is invariably at least as large as Planck's constant divided by 4π. In a very general form, therefore, we should have:

$$\Delta p \Delta q \geq \frac{h}{4\pi} \qquad [V.10]$$

where p *and* q *are canonically conjugated variables.*

The variable p represents the particle momentum and q its location. The postage stamp illustrated here commemorates Heisenberg's Uncertainty Principle and his original approximation that the product of the uncertainties of p and q are equivalent to the order of magnitude of Planck's constant h. The more common mathematical term for location is x. Thus Heisenberg's Uncertainty Principle is most often expressed as:

$$\Delta p \Delta x \geq \frac{h}{4\pi} \geq \frac{\hbar}{2} \qquad [V.11]$$

where Δp and Δx are the uncertainties of the particle momentum and location, h is Planck's constant ($h = 6.626 \times 10^{-34}$ J s), and $\hbar$ is equal to $h/2\pi$ or $\hbar = 1.054 \times 10^{-34}$ J s. Heisenberg's Uncertainty Principle simply states that it is not possible to accurately measure both the atomic particle (eg, electron) velocity or momentum and its location. Heisenberg's derivation from quantum mechanics showed that it is not possible to determine, in any given instant in time, both the velocity and the position of an atomic particle. It was demonstrated that the more accurately one tries to determine the velocity of the particle, the more uncertain becomes the determination of its position, and vice versa.

Let us take, for example, a hypothetical case where we can measure the velocity of an electron to be 2×10^8 m/s with an accuracy (eg, standard deviation) of 0.5%, and we want to know the uncertainty expected in the determination of the position (Δx) of that electron. According to Eq. [V.11], we can calculate the uncertainty as follows:

$$\Delta x \geq \frac{\hbar}{2\Delta p} \geq \frac{1.054 \times 10^{-34} \text{ J s}}{2(0.005)(m_e)(v)} \qquad [V.12]$$

where m_e and v are the electron mass and velocity, respectively. The relativistic mass (m_r) of the electron must be used, which is calculated according to Eq. [10.6] of the chapter entitled "Neutron Radiation," so that:

$$m_e = m_r = \frac{m_0}{\sqrt{1 - (v^2/c^2)}} \qquad [V.13]$$

where m_0 is the particle rest mass, v is the particle velocity, and c is the speed of light in a vacuum. The relativistic mass of the electron becomes:

$$m_r = \frac{9.109 \times 10^{-31} \text{ kg}}{\sqrt{1 - \left[\left(2 \times 10^8 \text{ m/s}\right)^2 / 2.99 \times 10^8 \text{ m/s}\right)^2\right]}}$$

$$= 12.25 \times 10^{-31} \text{ kg}$$

and:

$$\Delta x \geq \frac{1.054 \times 10^{-34} \text{ J s}}{2(0.005)(12.25 \times 10^{-31} \text{ kg})(2 \times 10^8 \text{ m/s})} \geq 0.43 \times 10^{-10} \text{ m} = 0.43 \text{ Å}$$

If the measurement of the electron velocity were made with a greater accuracy of 0.1%, the expected uncertainty of the electron position would increase to:

$$\Delta x \geq \frac{1.054 \times 10^{-34} \text{ J s}}{2(0.001)(12.25 \times 10^{-31} \text{ kg})(2 \times 10^8 \text{ m/s})} \geq 2.15 \times 10^{-10} \text{ m} = 2.15 \text{ Å}$$

Thus, increasing the accuracy of the measurement of one of the variables, the electron momentum, results in an increase in the uncertainty of the measurement of the other variable, the electron position.

Let us take another example that can illustrate the use of Heisenberg's Uncertainty Principle to calculate the uncertainty in the measurement of the momentum of an electron in the confines of an atomic nucleus (radius = 0.5×10^{-14} m) and

consequently the improbability of finding an electron in the nucleus. If we multiply Heisenberg's Eq. [V.11] by the speed of light (c) in both the numerator and denominator, we will obtain units of momentum in MeV/c, which are the conventional units for relativistic momentum, as described in the chapter entitled "Electromagnetic Radiation: Photons." Thus, Eq. [V.11] becomes:

$$\Delta p \geq \frac{hc}{4\pi\Delta xc} \tag{V.14}$$

Since $hc = 12.4$ keV Å (see Eq. [8.10] of the chapter: "Electromagnetic Radiation: Photons"), we can calculate the uncertainty in the measurement of the electron momentum in the atomic nucleus as:

$$\begin{aligned}\Delta p &\geq \frac{12.4 \text{ keV Å}}{4(3.14)\left(5 \times 10^{-5} \text{ Å}\right)c} \\ &\geq \frac{12.4 \text{ keV Å}}{6.28 \times 10^{-4} \text{ Å}c} \\ &\geq 1.97 \times 10^{4} \text{ keV}/c \\ &\geq 19.7 \text{ MeV}/c\end{aligned}$$

Converting the electron momentum to energy, including the rest-energy of the electron (m_0c^2), according to Eq. [8.4] of the chapter entitled "Electromagnetic Radiation: Photons" gives:

$$\begin{aligned}E^2 &= p^2c^2 + m_0c^2 \\ &= (19.7 \text{ MeV}/c)^2c^2 + \left(9.109 \times 10^{-31} \text{ kg}\right)\left(2.99 \times 10^{8} \text{ m/s}\right)^2 \\ &= (19.7 \text{ MeV}/c)^2c^2 + \left(8.143 \times 10^{-14} \text{ J}\right) \\ &= (19.7 \text{ MeV}/c)^2c^2 + \left(8.143 \times 10^{-14} \text{ J}/1.602 \times 10^{-19} \text{ J/eV}\right) \\ &= 388.1 \text{ MeV} + \left(0.51 \times 10^{6} \text{ eV}\right) \\ &= 388.1 \text{ MeV} + 0.51 \text{ MeV} \\ &= 388.6 \text{ MeV} \\ E &= 19.7 \text{ MeV}\end{aligned} \tag{V.15}$$

The energy of the electron would be of magnitude as great as its measured uncertainty of the momentum, that is:

$$E \geq 19.7 \text{ MeV}$$

No electron has ever been detected from isotope decay with an energy as high as 19.7 MeV. The highest beta-particle energy is 4.9 MeV from the decay of the radioactive isotope ^{38}Cl. While an electron (ie, beta-particle) is produced in nuclear beta-decay, the Heisenberg Uncertainty Principle demonstrates that the electron from beta-decay could not exist in the nucleus, but that the electron is only a product of the nuclear decay.

Heisenberg demonstrated that the uncertainties are not due to any experimental or instrumental error in measurement that may be made on the atomic particle, but rather they are due to the inherent quantum structure of atomic particles, that is, their wave-particle duality. Heisenberg's Uncertainty Principle in terms of energy and time variables is expressed as:

$$\Delta E\Delta t \geq \frac{h}{4\pi} \geq \frac{\hbar}{2} \tag{V.16}$$

which states that the precision with which we measure the energy of an atomic particle (ΔE) is limited by the time available (Δt) to measure the particle energy. The energy of the particle can be measured with perfect precision only if an infinite amount of time is used to measure the energy, ie, when $\Delta t = \infty$.

Heisenberg argued from quantum mechanics that the picture of the atom with fixed electron orbitals was not free of ambiguity, that is, we cannot definitely state that such particulate electron orbitals actually exist, because of the wave concept

of the electron. However, in his Nobel lecture, Heisenberg (1933a) clarified that the particulate and wave concepts of the atom remain useful for our visual interpretation of atomic structure and spectral emissions when he stated the following:

> *A visual description for the atomic events is possible only within certain limits of accuracy — but within these limits the laws of classical physics also still apply. Owing to these limits of accuracy as defined by the uncertainty relations, moreover, a visual picture of the atom free from ambiguity has not been determined. On the contrary the corpuscular and the wave concepts are equally serviceable as a basis for visual interpretation.*

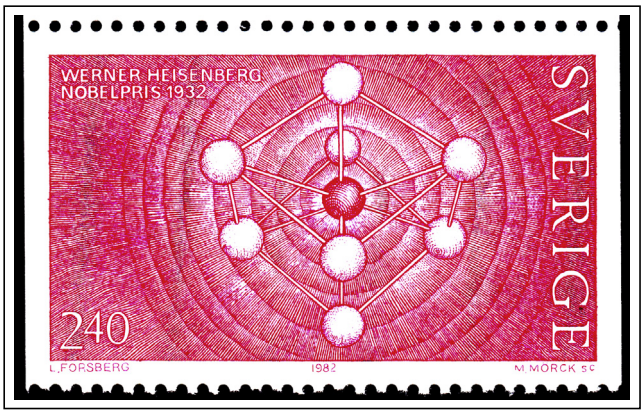

Niels Bohr (1928) presented his complementarity argument that the clearest analysis that can be derived from quantum mechanics must include both the corpuscular and wave nature of atomic particles, that is, both the particulate and wave nature of the electron are needed to complement each other in providing a complete description of the atomic particle. The duality of the wave-particle nature of matter was commemorated in the postage stamp illustrated here issued in Sweden in 1982, which provides an artistic abstract depiction of atoms as corpuscular matter forming a molecule and waves in the background. Heisenberg acknowledged Bohr's concept of complementarity in his Nobel lecture, when he stated:

> *For the clearest analysis of the conceptual principles of quantum mechanics we are indebted to Bohr who, in particular, applied the concept of complementarity to interpret the validity of the quantum mechanical laws. The uncertainty relations alone afford an instance of how in quantum mechanics the exact knowledge of one variable can exclude the exact knowledge of the other. This complementary relationship between different aspects of one and the same physical process is indeed characteristic for the whole structure of quantum mechanics.*

In 1927 Heisenberg was appointed Chair of Theoretical Physics at the University of Leipzig. He remained in Germany during World War II. In 1941 he was appointed Professor of Physics at the University of Berlin and Director of the Kaiser Wilhelm Institute for Physics. Heisenberg was involved in Germany's effort to develop the atomic bomb and nuclear energy for power, together with other notable German scientists; however, the German effort on the bomb development was eventually scuttled in 1942 due to the fact that three to four years would be needed to develop the weapon among other reasons, and Heisenberg (1946) wrote that German physicists "were spared the decision as to whether or not they should aim at producing atomic bombs" (Rhodes, 1986). A great historical debate started with the publication of "Brighter than a Thousand Suns" by Austrian writer and journalist Robert Jungk (1956), first published in German in 1956. After reading Jungk's book in 1956, Heisenberg sent him a letter concerning his role and that of German scientists in the atom bomb project. Jungk then published an excerpt of Heisenberg's letter, out of context, in the Danish edition of the book (Jungk, 1957). The excerpt of Heisenberg's letter in the Danish edition made it appear that Heisenberg was claiming to have purposely derailed the German bomb project. Heisenberg wrote in his letter to Jungk:

> *…we were convinced that the manufacture of atomic bombs was possible only with enormous technical resources. We knew that one could produce atom bombs but overestimated the necessary technical expenditure at the time. This situation seemed to us to be a favorable one, as it enabled the physicists to influence further developments. If it were impossible to produce atomic bombs this problem would not have arisen, but if they were easily produced the physicists would have been unable to prevent their manufacture. This situation gave the physicists at that time decisive influence on further developments, since they could argue with the government that atomic bombs would probably not be available during the course of the war…Under these circumstances we thought a talk with Bohr (Autumn of 1941) would be of value…Being aware that Bohr was under the surveillance of the German political authorities and that his assertions about me would probably be reported to Germany, I tried to conduct this talk in such a way as to preclude my life into immediate danger. This talk probably started with my question as to whether or not it was right for*

physicists to devote themselves in wartime to the uranium problem – as there was the possibility that progress in this sphere could lead to grave consequences in the technique of the war…He replied as far as I can remember with a counter-question, "Do you really think that uranium fission could be utilized for the construction of weapons?" I may have replied: "I know that this is in principle possible, but it would require a terrific effort, which, one can only hope, cannot be realized in this war." Bohr was shocked by my reply, obviously assuming that I had intended to convey to him that Germany had made great progress in the direction of manufacturing atomic weapons….

Nobel Laureate Hans Bethe (2000) provided evidence that Heisenberg did not work toward or try to build a bomb. Some of the evidence is presented by Bethe as follows:

The best evidence we have suggests that Heisenberg had no interest in building an atomic bomb. In mid-1942, Albert Speer, the weapons minister, asked Heisenberg whether he could produce a weapon in nine months. With a clear conscience he could answer "No."…If he wasn't trying to build a bomb, then why did Heisenberg work on the uranium project? He told me, in 1948, that he wanted to save the lives of a few young German physicists for the post-war period. I believe that this was indeed an important argument for him. An in judging his behavior during the war, we must remember that he was under enormous pressure, pressure virtually unimaginable for Americans or Englishmen. So Heisenberg didn't try to build a bomb, and apparently had no intention of doing so. Why then the visit to Bohr in 1941? What was he trying to communicate?...Perhaps he was trying to get Bohr to be a messenger of conscience, and wanted Bohr to persuade the allied scientists also to refrain from working on a bomb.

Heisenberg and other German scientists were taken prisoner by Allied troops after the war and sent to England. In 1946 he returned to Germany and reorganized the Institute for Physics at Göttingen, which was renamed the Max Planck Institute for Physics in 1948. While remaining Director of the Max Planck Institute, Heisenberg delivered extensive lectures in Cambridge in 1948, headed the German Delegation to the European Council for Nuclear Research, contemplating the founding of CERN, the European Organization for Nuclear Research, in Geneva, and he delivered the Gifford Lectures on "Physics and Philosophy" at the University of St. Andrews, Scotland in the winter of 1955–1956. From 1957 onwards Heisenberg was interested in plasma physics and a close collaborator of the International Institute of Atomic Physics in Geneva and participated for several years as chairman of the Scientific Policy Committee of the Institute. He was appointed the first President of the Alexander von Humboldt Foundation until his resignation in October 1975 shortly before his death from cancer at his home in Munich on February 1, 1976.

Erwin Schrödinger (1887–1961) was born in Vienna, Austria on August 12, 1887. He entered the Akademisches Gymnasium in Vienna at the age of 11 in 1898, where he was a gifted student of mathematics and physics. After graduation from the gymnasium in 1906, he entered the University of Vienna, where Fritz Hazenöhrl, the successor to Ludwig Boltzmann, and his lectures in theoretical physics had the greatest influence on him. Schrödinger received the doctorate degree in 1910 and completed his habilitation in 1914. With the outbreak of World War I he was ordered to serve as artillery officer at the Italian front. While carrying out active military service he published several papers in theoretical physics (Schrödinger, 1915a,b, 1917a,b) and received commendation for outstanding military service. After the war he continued his work in Vienna, where he was appointed associate professor at the university, where he worked on radioactivity, demonstrating the statistical nature of radioactive decay (Schrödinger, 1921). From 1920 to 1921, in a period of about 18 months, he held three positions: as professor at the University of Stuttgart and University of Breslau, and then Chair of Physics at the University of Zurich.

Erwin Schrödinger (1887–1961)

It was in Zurich where Schrödinger carried out his most fruitful work from 1921 to 1926. Here Schrödinger studied atomic structure and quantum statistics, and the turning point in his career was his reading of Louis de Broglie's papers on the dual nature of matter and light (de Broglie, 1923a,b,c,d). In 1926, Schrödinger published a series of papers revealing his revolutionary wave equation and the new physics of wave mechanics (Schrödinger, 1926a,b,c,d,e,f,g, 1927). Schrödinger was not happy with Bohr's quantum theory of atomic structure, as it held only for hydrogen and not the more complex atoms. Also, Heisenberg's Uncertainty Principle demonstrated that both the location and momentum of an electron could not be measured accurately, and thus, he considered Bohr's fixed electron orbits about the nucleus as an inadequate representation of the atom. Grasping the theory of matter—wave properties of the electron, Schrödinger created wave mechanics, In Schrödinger's wave mechanics he explained the movements of an atomic electron as a wave and calculated the coordinates of the electron according to a wave function (ψ) given by his equation:

$$-\frac{\hbar^2}{2m}\left\{\frac{d^2\psi}{dx^2}+\frac{d^2\psi}{dy^2}+\frac{d^2\psi}{dz^2}\right\}+U(r)\psi = i\hbar\frac{d\psi}{dt} \qquad [V.17]$$

described in detail by Levine (1999), McQuarrie (1983), Serway et al. (2005), and many others, where $\hbar$ is Planck's constant $h/2\pi$, m is the particle mass, ψ is the wave function, U is the potential energy as a function of the space coordinates $U(r) = U(x,y,z)$, and $i = \sqrt{-1}$. The solution of the Schrödinger equation provides a relation of the wave function ψ to the position or three-dimensional coordinates (x,y,z) of an electron in space, whereby ψ^2 will give the probability of finding and electron within given coordinates of the atom.

Schrödinger's Cat and the Superposition of States of Matter. Erwin Schrödinger (1935) devised a thought experiment as an aid to the interpretation and understanding of the superposition of different quantum states of matter. His thought experiment was only an imaginary one to relay a message and not an experiment that would ever be carried out. The imaginary experiment is illustrated in Fig. V.7; and the description of the experiment in Schrödinger's words, as translated by Trimmer (1980), is the following:

> *One can even set up quite ridiculous cases. A cat is penned up in a steel chamber, along with the following diabolical device (which must be secured against direct interference by the cat): in a Geiger counter there is a tiny bit of radioactive substance, so small, that* perhaps *in the course of one hour one of the atoms decays, but also with equal probability, perhaps none; if it happens,*

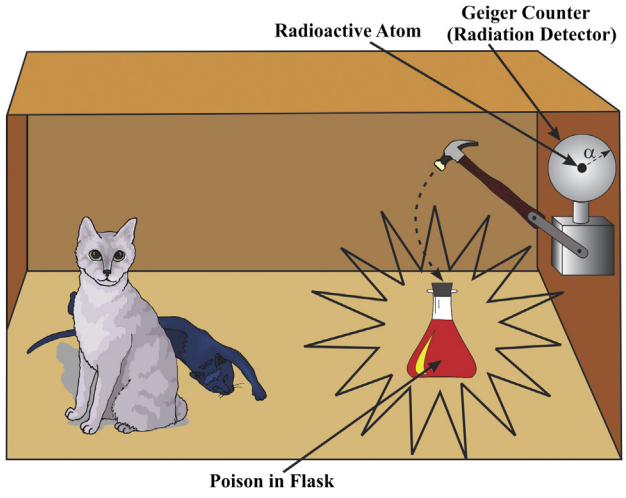

FIGURE V.7 Schrödinger's Cat, that is, his imaginary thought experiment. At a given half-life, a radioactive atom may or may not decay with the emission of radiation (illustrated with an alpha particle). The atom is surrounded by a spherical Geiger counter as the radiation detector. If the atom decayed, it would be detected by the Geiger counter, which would relay a signal that would release a hammer onto a glass flask containing poison; and the cat would be dead; however, with equal probability, the radioactive atom does not decay; and the cat thus remains alive. Without opening the box, it remains unknown if the atom had not decayed and the cat is alive, or the atom had decayed and the cat is dead. Thus, at the time of the half-life of the radioactive particle, the system remains a superposition of two different quantum states, that of the radioactive and decayed particle and that of the cat alive and dead. The two states of the cat alive and dead are illustrated. The reader should keep in mind that Schrödinger devised this thought experiment with the knowledge that the half-life of a radioactive atom is a statistical period of time, which is derived or determined when dealing with a large number of atoms. When dealing with a single radioactive atom or a small number of them, it cannot be known when the atom or a small number of them will decay.

the counter tube discharges and through a relay releases a hammer which shatters a small flask of hydrocyanic acid. If one has left the entire system to itself for an hour, one would say that the cat still lives if meanwhile no atom has decayed. The first atomic decay would have poisoned it. The Ψ-function of the entire system would express this by having in it the living and the dead cat (pardon the expression) mixed or smeared out in equal parts.

It is typical of these cases that an indeterminacy originally restricted to the atomic domain becomes transformed into macroscopic indeterminacy, which can then be resolved *by direct observation. That prevents us from so naively accepting as valid a "blurred model" for representing reality. In itself it would not embody anything unclear or contradictory. There is a difference between a shaky and out-of-focus photograph and a snapshot of clouds and fog banks.*

Reprinted with permission © 1980 American Philosophical Society.

The conclusions taken from Schrödinger's thought experiment was underscored by the Nobel Committee when it announced the Nobel Prize in physics for the year 2012 to David J. Wineland and Serge Haroche for "their ground-breaking experimental methods that enable measuring and manipulation of individual quantum systems" (see Hall of Fame, Part X). The announcement of the Nobel Committee included the following:

When it comes to the smallest components of our universe, our usual understanding of how the world works ceases to apply. We have entered the often paradoxical and difficult-to-comprehend realm of quantum physics. In this world, the same object can exist in different states simultaneously.

http://www.nobelprize.org/nobel_prizes/physics/laureates/2012/.

As pointed out by the statement of the Nobel Committee and in the thought experiment, known as Schrödinger's Cat, we should conclude that the easily seen and easy-to-comprehend physics of the macroscopic world that we live in cannot necessarily be applied to the subatomic world of particle physics. This was elaborated further by David Wineland (2012) in his Nobel lecture given on December 8, 2012, when he stated the following:

…Erwin Schrödinger (Schrödinger, 1935) realized that in principle, quantum mechanics should apply to a macroscopic system in a more complex way, which could then lead to bizarre consequences. In his specific example, the system is composed of a single radioactive particle and a cat placed together with a mechanism such that if the particle decays, poison is released, which kills the cat. Quantum mechanically we represent the quantum states of the radioactive particle as undecayed $= |\uparrow\rangle$ *or decayed* $= |\downarrow\rangle$*, and live and dead states of the cat as* $|\mathrm{L}\rangle$ *and* $|\mathrm{D}\rangle$*. If the system is initialized in the state represented by the wave function* $|\uparrow\rangle|\mathrm{L}\rangle$*, then after a duration equal to the half-life of the particle, quantum mechanics says the system evolves to a superposition state where the cat is alive and dead simultaneously, expressed by the superposition wave function:*

$$\psi = \frac{1}{\sqrt{2}}[|\uparrow\rangle|L\rangle + |\downarrow\rangle|D\rangle]\cdot\psi = \frac{1}{\sqrt{2}}[|\uparrow\rangle|L\rangle + |\downarrow\rangle|D\rangle] \qquad [V.18]$$

Schrödinger dubbed this an entangled state because the state of the particle is correlated with the state of the cat. That is, upon measurement, if the particle is observed to be undecayed, one can say with certainty that the cat is alive, and vice versa. But before measurement, the particle and cat exist in both states. The extrapolation of quantum mechanics from individual quantum systems to the macroscopic world bothered Schrödinger (and a lot of other people).

It was Max Born (1882−1970) who accurately interpreted Schrödinger's wave function ψ to provide the probability density ψ^2 of the atomic electron. No longer is the atomic electron envisioned to occupy a fixed orbit, but rather to have a probability of occupying given coordinates. The regions that the electrons occupy in space are defined according to orbitals. An orbital is a region in space where an electron is likely to be found with high probability (eg, >90%). Orbitals should not be confused with orbits, as the electron's position in the atom cannot be fixed to specific distances from the nucleus. Because we are dealing with probabilities in defining the locations of the electrons, the orbitals are represented as electron clouds of specific shape representing high densities of the atomic electrons. An electron could be found statistically anywhere from a distance very close to a nucleus (<0.53 Å) to a distance further away from the nucleus; however, high probabilities (>90%) will define the likelihood of finding an atomic electron at certain coordinates and therefore also define its orbital and the shape of the orbital.

The assignment of atomic electrons in three-dimensional space, which define atomic orbitals, depends on the following three variables:

1. *The principle quantum number* (n), which may have values of $n = 1, 2, 3,\ldots$, correspond to the energy level of the electron and the size or magnitude of the orbital. An orbital with a higher value of n will be larger in size or volume and its electrons of higher energy than an orbital with a lower value of n.
2. *The orbital quantum number* (ℓ), which is assigned values of $\ell = 0, 1, 2, 3,\ldots\ n - 1$, defines the shape of the orbital and identifies the orbital according to the following orbital types: *s, p, d,* and *f*. For example, spherical orbitals have the quantum number $\ell = 0$ and are identified as *s* orbital types; dumbbell-shaped orbitals have the quantum number $\ell = 1$ and are identified as *p* orbitals; and orbitals of clover-leaf shape have the quantum number $\ell = 2$ and are identified as *d* orbitals. The *f* orbitals with quantum number $\ell = 3$ are more complex in shape. The *s*, *p*, and *d* orbitals are illustrated in Figs. V.8–V.10

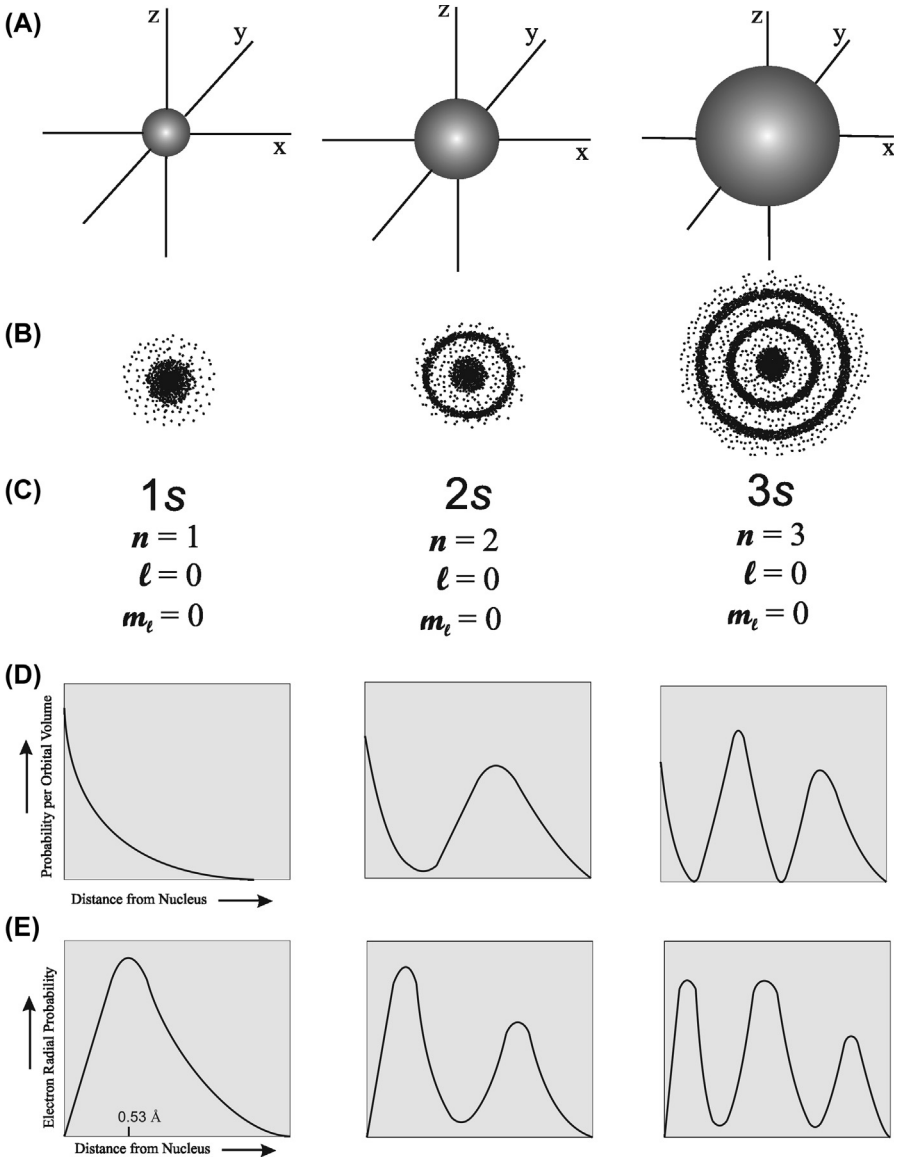

FIGURE V.8 Characteristics of the 1*s*, 2*s*, and 3*s* orbitals from left to right according to (A) spherical shape of increasing size and electron energy, (B) sketches of the electron density distributions along the cross-sections (radial) of the orbitals, (C) orbital identification with underlying quantum numbers, (D) electron probability positions per orbital volume as a function of distance from the nucleus, and (E) electron radial probability positions as a function of distance from the nucleus.

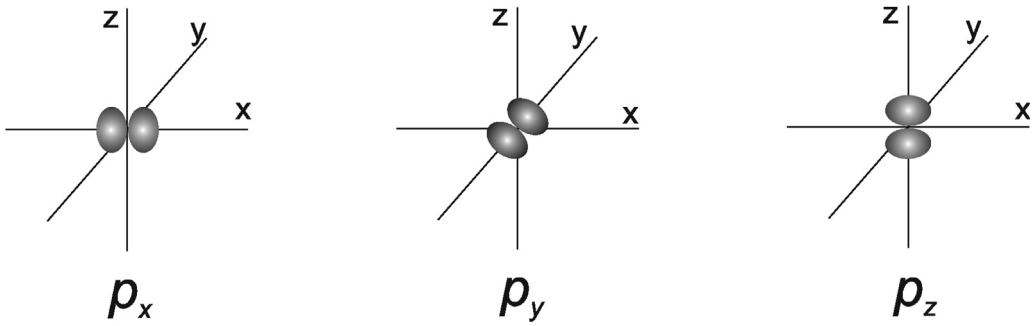

FIGURE V.9 Shape and orientations of the *p* electron orbitals identified according to their axis of orientation. The quantum numbers that define the *p* orbitals are $\ell = 1$, and m_ℓ will have values of -1, 0, or $+1$ yielding three possible orientations in space. The principle quantum number $n = 1, 2, 3\ldots$ are also associated with the *p* orbital to identify energy level. The principle quantum number, that may be assigned to the *p* orbital (eg, 1*p*, 2*p*, 3*p*…, not illustrated), will signify the energy level and size of the orbital.

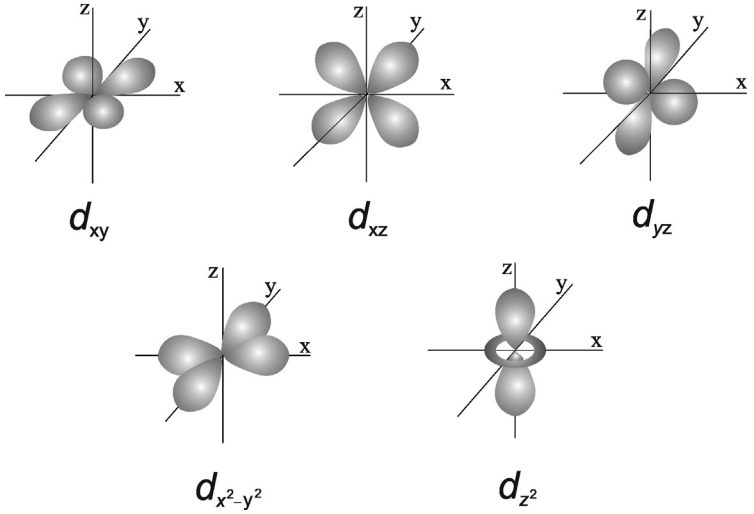

FIGURE V.10 Shapes and orientations of the *d* orbitals identified according to their axes of orientation. The quantum numbers that define the *d* orbitals are $\ell = 2$, and m_ℓ will have values of -2, -1, 0, $+1$, or $+2$, yielding five possible orientations in space. The d_{xy}, d_{xz}, and d_{yz} orbitals lie in the xy, xz, and yz planes, respectively. The $d_{x^2-y^2}$ orbital lies along the x and y axes, and the d_{z^2} orbital is oriented along the z axis. The principle quantum number that may be assigned to the *d* orbital (eg, 1*d*, 2*d*, 3*d*…, not illustrated), will signify the energy level and size of the orbital.

3. *The magnetic quantum number* (m_ℓ) can have values over the range of $m_\ell = -\ell$ to $+\ell$, and it will define the orientation in space of the orbital. For example, when $\ell = 2$, the magnetic quantum number, m_ℓ, will have values of -2, -1, 0, $+1$, $+2$, yielding five different spatial orientations of the *d* orbital, as illustrated in Fig. V.10. When $\ell = 1$, m_ℓ will have values of -1, 0, $+1$, yielding three different spatial orientations of the *p* orbitals, as illustrated in Fig. V.9. When $\ell = 0$, $m_\ell = 0$ and there will be no differing spatial orientations of the *s* orbital, as illustrated in Fig. V.8. The *s* orbital is a sphere, which cannot differ in shape and differs only in size and energy of the electrons according to the principle quantum number *n*.

The postage stamp illustrated here was issued by Sweden in 1982 to commemorate Schrödinger's discovery of his wave equation and the awarding of his Nobel Prize. It illustrates two electron orbital types, namely the *d* and *s* orbitals. The rules applied to the filling of atomic electrons into the various orbitals that constitute the buildup of elements in the periodic table are provided in the biographical sketch of Wolfgang Pauli. The simplest of all atoms is, of course, the hydrogen atom of atomic number 1, which possesses only one atomic electron. The next atom, of atomic number 2, is helium, with two electrons. The atomic number of each atom corresponds, of course, to the number of protons in the nucleus, which is also equal to the number of electrons that the neutral atom may possess in its ground state. The buildup of the neutral atoms of some selected elements according to the placement of the atomic electrons into specific orbitals is provided in Table V.2A.

Electron Orbitals *d* (left) and *s* (right)

The 1*s* orbital is found in all atoms of the elements in the periodic table, including the hydrogen atom. It is the orbital with electrons of the lowest energy. The hydrogen atom (H) has an atomic number of 1 and only one electron. That electron occupies the 1*s* orbital (see Table V.2A). Its electron configuration is noted as $1s^1$ and it reads as "one s one." The exponent one means "one electron in the *s* orbital". The number 1 before the *s* is the principle quantum number or energy level of the orbital.

TABLE V.2A Electron Configurations of Neutral Atoms in the Ground State

		K[a]	L		M			N			
		$n^b = 1$	$n = 2$		$n = 3$			$n = 4$			
Atomic No.	Element	*s*[c]	*s*	*p*	*s*	*p*	*d*	*s*	*p*	*d*	*f*
1	H	1									
2	He	2									
3	Li	2	1								
4	Be	2	2								
5	B	2	2	1							
6	C	2	2	2							
7	N	2	2	3							
8	O	2	2	4							
9	F	2	2	5							
10	Ne	2	2	6							
11	Na	2	2	6	1						
12	Mg	2	2	6	2						
13	Al	2	2	6	2	1					
⋮	⋮										
18	Ar	2	2	6	2	6					
⋮	⋮										
29	Cu	2	2	6	2	6	10	1			
⋮	⋮										
46	Pd	2	2	6	2	6	10	2	6	10	

[a] *Main quantum level. The electron energy level K is the closest to the nucleus. Other energy levels, namely, L, M, N, and O, are of increasing energy and distance from the nucleus.*
[b] *Principle quantum number.*
[c] *Orbital type.*
Data taken from Lide, D.R., 1997. CRC Handbook of Chemistry and Physics, 77th ed. CRC Press, Boca Raton.

The next most complex atom is that of helium (He), of atomic number 2, with two electrons (see Tables V.2A and B), and its electron configuration is written as $1s^2$, which reads "one s two," meaning two electrons in the *s* orbital of lowest energy (principle quantum number or level of 1). The next element in the period table is lithium (Li) of atomic number 3; and thus the atom of lithium has three electrons. Its electron configuration is noted as $1s^2 2s^1$, which reads as "two electrons in the 1*s* orbital and one electron in the 2*s* orbital." Notice here that only two electrons can fill the 1*s* orbital. The third electron in lithium must occupy another orbital, that of the next highest level or the 2*s* orbital. The reason for the exclusion of additional electrons to the orbital is explained by Pauli's Exclusion Principle, which permits not more than two electrons of opposite spin to occupy the same quantum or energy state, described in the biographical sketch of Wolfgang Pauli (see Hall of Fame, Part II).

The electrons of the 1*s* orbital are of the lowest energy and closest to the nucleus, as illustrated in Fig. V.8. According to Schrödinger's wave mechanics, the electrons in the 1*s* orbital can be anywhere from a distance closest to the nucleus to an infinite distance away from the nucleus; however, the electrons in this orbital will be found with highest probability at a distance of 0.53 Å, which is the distance calculated by Niels Bohr of closest approach of the atomic electron to the nucleus. The probability curves for the locations of the electrons in the 1*s*, 2*s*, and 3*s* orbitals are illustrated in Fig. V.8. Two types of probability curves are shown, namely, probability per orbital volume (Fig. V.8D) and radial probability (Fig. V.8E). The probability per unit volume of the 1*s* orbital shows the electron probability to be highest closest to the nucleus, because the orbital volume can be relatively large. The radial probability curve provides an electron density probability along the cross-section of the orbital and a clearer picture of the electron density distribution. Notice in Fig. V.8E that the electron density or cloud of the 1*s* orbital will be thickest at 0.53 Å distance from the nucleus. Electrons in the 2*s* orbital are found to overlap the 1*s* and extend with highest probability to a distance further away from the nucleus, forming a larger sphere with electrons of higher energy then the 1*s* electrons. The electrons in the 3*s* orbital are yet of higher energy and found with highest probability further away from the nucleus.

Another atom we may take as an example is that of sodium (Na), which is more complex, with 11 electrons. Its electron configuration provided in Table V.2B is $1s^2 2s^2 2p^6 3s^1$, which reads "two electrons in the 1*s* orbital, two electrons in the 2*s* orbital, 6 electrons in the 2*p* orbital, and one electron in the 3*s* orbital." Notice here that there can be as many as six electrons assigned to the *p* orbitals, because there are three types of *p* orbitals as illustrated in Fig. V.9, and only two electrons per orbital of opposite spin are possible. As the *p* orbitals are filled, the additional electron in the sodium atom is found in the next highest 3*s* orbital. The *d* orbitals are not formed until the higher quantum level ($n = 3$) is reached, as illustrated in Table V.2A. These orbitals can occupy as many as 10 electrons, because there are five different *d*-orbital types, which can be filled with two electrons of opposite spin. The copper (Cu) atom with 29 electrons has all of its *d* orbitals filled. It has the electron configuration $1s^2 2s^2 2p^6 3s^2 3p^6 3d^{10} 4s^1$, as given in Table V.2B. The *d* orbitals are of five types as illustrated in Fig. V.10. These can be filled by two electrons of opposite spin. Electrons will begin to fill the more complex *f* orbitals (not illustrated) in larger atoms of atomic number 58 (cerium) and higher.

Schrödinger's wave mechanics was the second formulation of quantum mechanics, the first being the mathematical matrix mechanics of Heisenberg. Schrödinger's wave mechanics provided scientists with a visual picture of the space coordinates occupied by the electron, which Heisenberg's mathematical matrix equations could not provide. The initial reaction of Heisenberg was disagreement with Schrödinger's new wave mechanics; however, Schrödinger demonstrated the equivalence of the matrix and wave versions of quantum mechanics.

In 1927 Schrödinger moved to Berlin to succeed Max Planck, who had retired the previous year, at the University of Berlin. He decided to leave Germany in 1933 with Hitler's coming to power that very year, as he witnessed the persecution of Jews. In late 1933 he left Berlin under a fellowship at Oxford University, the very year that he was awarded the Nobel Prize. Schrödinger was invited to lecture at Princeton in 1934 and offered a permanent position there, which he did not accept. Instead, after returning to Oxford, he accepted a position at the University of Graz in 1936, only to encounter again problems with Hitler's regime after Hitler annexed Austria in 1938. As a Nobel Laureate preferring to live outside the German state was taken as an affront, he fled Austria via Italy and returned to Oxford. While at Oxford, Schrödinger proceeded to the University of Ghent for a one-year term as visiting professor. In 1939 he took on the position of Director of the newly created School for Theoretical Physics at Dublin, where he remained until his retirement in 1955 (Nobel Lectures, Physics, 1922−1941). After his retirement he returned to Vienna, his birthplace, until his death on January 4, 1961. For decades Schrödinger was honored by Austria with his portrait on the coveted Austrian 1000 Schilling monetary bill issued in 1983, which remained legal tender in Austria until the Euro exchange in 2002.

Max Born (1882−1970) was awarded the Nobel Prize in physics in 1954 "especially for his statistical interpretation of the wave function." He was born December 11, 1882 in Breslau, Germany, which is now Wroclaw, a capital city of Lower Silesia in Southwestern Poland. He attended the Konig Wilhem Gymnasium in Breslau and studied mathematics and physics at the University of Breslau, which is now the University of Wroclaw. Max Born transferred to the University of Göttingen, where he

TABLE V.2B Nomenclature for Electron Configurations of Table V.2A

Atomic No.	Element	Electron Configuration
1	H	$1s^1$
2	He	$1s^2$
3	Li	$1s^2 2s^1$
4	Be	$1s^2 2s^2$
5	B	$1s^2 2s^2 2p^1$
6	C	$1s^2 2s^2 2p^2$
7	N	$1s^2 2s^2 2p^3$
8	O	$1s^2 2s^2 2p^4$
9	F	$1s^2 2s^2 2p^5$
10	Ne	$1s^2 2s^2 2p^6$
11	Na	$1s^2 2s^2 2p^6 3s^1$
12	Mg	$1s^2 2s^2 2p^6 3s^2$
13	Al	$1s^2 2s^2 2p^6 3s^2 3p^1$
⋮	⋮	⋮
18	Ar	$1s^2 2s^2 2p^6 3s^2 3p^6$
⋮	⋮	⋮
29	Cu	$1s^2 2s^2 2p^6 3s^2 3p^6 3d^{10} 4s^1$
⋮		⋮
46	Pd	$1s^2 2s^2 2p^6 3s^2 3p^6 3d^{10} 4s^2 4p^6 4d^{10}$

studied mathematics, physics, and astronomy, graduating in 1907. After a short period of work under J.J. Thomson at Cambridge, Born returned to Breslau in 1908. He accepted an appointment in 1912 to lecture at the University of Chicago in the Department of Physics headed by Albert A. Michelson. In 1915, Born was compelled to join the German armed forces and declined an offer to work under Max Planck at the University of Berlin. After the war he was appointed professor at the University of Frankfurt am Main, where his assistant Otto Stern began his research that led him to the Nobel Prize. In 1921 Max Born was appointed Professor of Physics at the University of Göttingen, where he remained until 1933 to carry out his historic statistical interpretations of quantum mechanics, collaborating with many great physicists of the time including Heisenberg, Pauli, his student Pascual Jordan, Enrico Fermi, J. Robert Oppenheimer, and Maria Goeppert-Mayer.

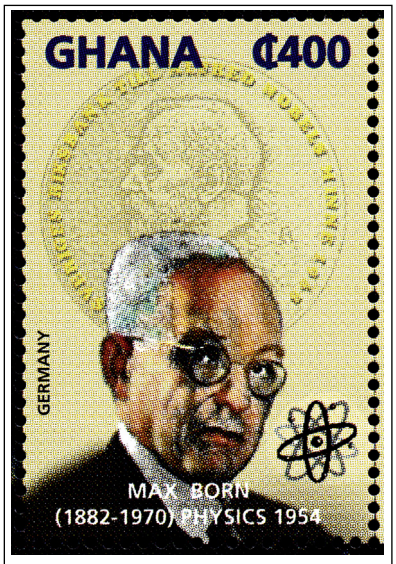

Max Born (1882–1970)

Schrödinger had interpreted his wave function ψ as the electron's matter-wave density distribution, that is, he wanted to dispense with the particulate properties of the electron and consider them to possess a continuous density distribution $|\psi|^2$, meaning that the electron as a wave could have a high density in some regions of space and lower in density in other regions. Max Born, however, interpreted the wave function ψ as providing a picture of the electron with its coordinates in space, and $|\psi|^2$ as the probability density of the electron (Born, 1926a,b,c,d; Born et al., 1926; Born and Oppenheimer, 1927; Born and Fock, 1928). Born's probability density interpretation is widely accepted today as that which gives the probability of finding the electron particle at particular coordinates in space. Born commented on this interpretation in his Nobel lecture (Born, 1954) as follows:

> *The work, for which I have had the honour to be awarded the Nobel Prize for 1954, contains no discovery of fresh natural phenomenon, but rather the basis for a new mode of thought in regard to natural phenomenon…For a brief period at the beginning of 1926, it looked as though there were, suddenly, two self-contained but quite distinct systems of explanation extant: (Heisenberg's) matrix mechanics and (Schrödinger's) wave mechanics. But Schrödinger himself soon demonstrated their complete equivalence…there came the* dramatic surprise*, the appearance of Schrödinger's famous papers (1926a,b,c,d,e). He took up quite a different line of thought which had originated from Louis de Broglie (1924, 1925). A few years previously the latter had made the bold assertion, supported by brilliant theoretical considerations, that wave-corpuscle duality, familiar to physicists in the case of light, must also be valid for electrons. To each electron moving free of force belongs a plane wave of a definite wavelength, which is determined by Planck's constant and the mass…Wave mechanics enjoyed a very great deal more popularity than the Göttingen or Cambridge version of quantum mechanics. It operates with a wave function ψ, which in the case of* one *particle at least, can be pictured in space, and it used the mathematical methods of partial differential equations which are in current use by physicists…He (Schrödinger) proposed to dispense with the particle representation entirely, and instead of speaking of electrons as particles, to consider them as a continuous density distribution $|\psi|^2$ or electric density $e|\psi|^2$. To us in Göttingen this interpretation seemed unacceptable in face of well established experimental facts. At that time it was already possible to count particles by means of scintillations or with a Geiger counter, and to photograph their tracks with the aid of a Wilson cloud chamber…an idea of Einstein's gave me the lead. He had tried to make the duality of particles − light quanta or photons − and waves comprehensible by interpreting the square of the optical wave amplitudes as probability density for the occurrence of photons. This concept could at once be carried over to the ψ-function: $|\psi|^2$ ought to represent the probability density for electrons (or other particles).*

Like many German scientists of Jewish descent, Max Born lost his professorship and was forced to leave Germany in 1933. He lectured at Cambridge from 1933 to 1936, and during the winter of 1935 to 1936 he spent 6 months working with C.V. Raman and his students at the Indian Institute of Science at Bangalore. In 1938 Born was appointed Professor of Natural Philosophy at the University of Edinburgh, where he remained until his retirement in 1953 [Nobel Lectures, Physics, 1942−1962 (1964)]. He died on January 5, 1970 in Göttingen, Germany. For additional reading see his autobiography (Born, 1978).

Paul A.M. Dirac (1902−1984) shared the Nobel Prize in Physics in 1933 with Schrödinger "for the discovery of new productive forms of atomic theory." Dirac was born in Bristol, England on August 8, 1902. He started his higher education in the field of electrical engineering at Bristol University. After receiving his bachelor of science degree in 1921, Dirac continued his studies at Bristol University until 1923. He then proceeded to St John's College at Cambridge, where he received his PhD degree in mathematics in 1926. He did not like the field of electrical engineering per se; however, his early studies in this field were useful to his future work, as reflected in a quotation provided in Sir Michael Berry's (1998) biographical sketch of Dirac:

Paul Dirac (1902–1984)

I owe a lot to my engineering training because it [taught] me to tolerate approximations. Previously to that I thought…one should just concentrate on exact equations all the time. Then I got the idea that in the actual world all our equations are only approximate. We must just tend to greater and greater accuracy. In spite of the equations being approximate, they can be beautiful.

The year following receipt of his doctorate degree, Dirac became a Fellow at St. John's College at Cambridge and carried out research in theoretical physics at the Cavendish Laboratory. At the Cavendish Laboratory, Dirac was introduced to Heisenberg's recent papers on quantum mechanics, and the following year, Dirac (1928a,b) published the quantum theory of the electron, which included new quantum wave mechanics incorporating the theory of relativity for relativistic electrons approaching the speed of light into Schrödinger's equation. Dirac's new quantum theory included a wave equation for the electron, the Dirac Equation, which could provide the dynamics of electron waves yielding physical predictions while satisfying the requirements of relativity (Berry, 1998). A result of Dirac's quantum theory of the electron was the prediction of the electron spin and the occurrence of a new electron, one of positive charge, known as the positron, the antiparticle of the negatron or negative electron. In his Nobel lecture, Dirac (1933) described how he came to the conclusion of the existence of the positron as follows:

There is [a] feature of these equations which I should like to discuss, a feature which led to the prediction of the positron….one sees that [the equation] allows the kinetic energy to be either a positive quantity greater than mc^2 *or negative quantity less than* $-mc^2$*…Now, in practice, the kinetic energy of a particle is always positive. We thus see that our equations allow for two kinds of motion for an electron, only one of which corresponds to what we are familiar with. The other corresponds to electrons with a very peculiar motion such that the faster they move, the less energy they have, and one must put energy into them to put them to rest…Thus, in allowing negative energy states, the theory gives something which appears not to correspond to anything known experimentally, but which we cannot simply reject by a new assumption. We must find some meaning for these states…We make use of the exclusion principle of Pauli, according to which there can be only one electron in any state of motion. We now make the assumptions that in the world as we know it, nearly all the states of negative energy for the electrons are occupied, with just one electron in each state, and that a uniform filling of all the negative-energy states is completely unobservable to us. Further,* any unoccupied negative-energy state, being a departure from uniformity, is observable and is just a positron. *An unoccupied negative-energy state, or* hole*, as we may call it for brevity, will have a positive energy, since it is a place where there is a shortage of negative energy. A hole is, in fact, just like an ordinary particle, and its identification with the positron seems the most reasonable way of getting over the difficulty of the appearance of negative energies in our equations. On this view the positron is just a mirror image of the electron, having exactly the same mass and opposite charge. This has already been confirmed by experiment.*

Dirac also predicted the phenomenon of annihilation, when a particle and its antiparticle (eg, negatron and positron) meet and are annihilated by the conversion of their electron masses into electromagnetic radiation. In his Nobel Lecture, Dirac explained:

From our theoretical picture, we should expect an ordinary electron, with positive energy, to be able to drop into a hole and fill up this hole, the energy being liberated in the form of electromagnetic radiation. This would mean a process in which an electron and a positron annihilate one another. The converse process, namely the creation of an electron and a positron from electromagnetic radiation, should also be able to take place. Such processes appear to have been found experimentally, and are at present being more closely investigated by experimenters.

The existence of the positron was experimentally discovered in 1932 by Carl D. Anderson while carrying out research on cosmic rays for which he was awarded the Nobel Prize in physics in 1936. Anderson also demonstrated together with his graduate student, Seth Neddermeyer, that gamma rays from "ThC" [^{212}Bi] would generate positrons, by pair production, after passing through substances such as lead. Pair production as predicted by Dirac is the creation of an electron and positron pair by the conversion of the energy of electromagnetic gamma radiation into the masses of two electrons of opposite charge, as illustrated in Fig. 8.20 of the chapter entitled "Electromagnetic Radiation: Photons." The electron and positron pair is produced when a gamma ray in excess of 1.02 MeV energy passes through the coulomb field of a nucleus. The minimum gamma-ray energy of 1.02 MeV is calculated in the chapter entitled "Electromagnetic Radiation: Photons" as the energy equivalent to twice the electron mass expressed in energy units of electron volts, or twice 0.511 MeV. The conversion is written as:

$$E_{\text{pair}} = m_{e^-}c^2 + m_{e^+}c^2 = 2mc^2 = 2(0.511\ \text{MeV}) = 1.022\ \text{MeV} \qquad \text{[V.19]}$$

Energy in excess of 1.02 MeV appears as the kinetic energy of the electron and positron produced, and is written as:

$$h\nu = 2mc^2 + E_{e^-} + E_{e^+} \qquad \text{[V.20]}$$

The postage stamp illustrated here was issued by Sweden in 1982 to commemorate Dirac's prediction of the positron, the antiparticle of the electron, which was subsequently discovered by Carl D. Anderson. The stamp shows a copy of an actual picture of the negative and positive electron tracks produced in a bubble chamber following pair production. The tracks are spiral in shape because of a magnetic field running perpendicular to the electron tracks forcing the charged particle paths to bend according to their charge and velocity.

Spiral Tracks of an Electron-Positron Pair

Dirac (1933) also postulated the existence of the antiparticle of the proton, that is, the antiproton or negatively charged proton. In his Nobel Lecture he explained:

> *One might perhaps think that the same theory could be applied to protons. This would require the possibility of existence of negatively charged protons forming a mirror-image of the usual positively charged ones…I think it is probable that negative protons can exist, since as far as the theory is yet definite, there is a complete and perfect symmetry between positive and negative electric charge, and if this symmetry is really fundamental in nature, it must be possible to reverse the charge on any kind of particle.*

The antiproton was indeed, in due time, discovered in 1955 by Emilio Segrè and Owen Chamberlain, for which they were awarded the Nobel Prize in physics in 1955. Dirac even went further to postulate the possibility of the existence of entire solar systems many light years away that would be built of antiparticles or antimatter, a theory which today still appears plausible. Dirac (1933) explained:

> *If we accept the view of complete symmetry positive and negative electric charge so far as concerns the fundamental laws of Nature, we must regard it rather as an accident that the Earth (and presumably the whole solar system), contains a preponderance of negative electrons and positive protons. It is quite possible that for some of the stars it is the other way about, these stars being built up mainly of positrons and negative protons. In fact, there may be half the stars of each kind. The two kinds of stars would both show exactly the same spectra, and there would be no way of distinguishing them by present astronomical methods.*

Dirac's accomplishments could have provided him with the worldwide fame of Einstein during his lifetime, but he shunned notoriety and remains to this day a figure hardly known outside the scientific community. Chaundy (2002) explains that this is due to the fact that Dirac was an introvert; he was shy and avoided publicity to the extreme. He liked to work alone and had very few graduate students. It is reported that a graduate student once asked Dirac if he could be his thesis advisor; and Dirac replied "Thank you, but I do not need any help at this time." To avoid publicity, Dirac contemplated refusing to accept the Nobel Prize. Chaundy (2002) reports that Dirac accepted the Nobel Prize because he was advised that, by refusing the prize, he would be given even greater publicity. Sir Michael Berry (1998) provides the following evaluation of Dirac's accomplishments by quoting the following words of the mathematician Mark Kac, who divided geniuses into two classes:

> *There are the ordinary geniuses, whose achievements one imagines other people might emulate, with enormous hard work and a bit of luck. Then there are the magicians, whose inventions are so astounding, so counter to all the institutions of their colleagues, that it is hard to see how any human could have imagined them. Dirac was a magician.*

In 1932 Dirac was appointed Lucian Professor of Mathematics at Cambridge, which is the same post once held by Sir Isaac Newton. Dirac was only 31 years of age when he was awarded the Nobel Prize in physics in 1933. He married Margit

Wigner, the sister of the Hungarian Nobel Laureate Eugene Wigner. In 1969 Dirac retired from Cambridge and joined Florida State University at Tallahassee. He died in Tallahassee on October 20, 1984. For further reading one is invited to peruse a biography by Kragh (1990) and his collected works provided by Dalitz (1995).

CLINTON DAVISSON (1881–1958) AND GEORGE PAGET THOMSON (1892–1975)

Clinton Davisson shared the Nobel Prize in physics in 1937 with George Paget Thomson "for their experimental discovery of the diffraction of electrons by crystals." Davisson was born in Bloomington, Illinois, USA on October 22, 1881. He was the son of Joseph Davission, a veteran of the Union Army in the Civil War and of Mary Calvert, a school teacher from Pennsylvania. In 1902 Clinton Davisson graduated from public high school in Bloomington with a mathematics and physics scholarship to the University of Chicago, where he found himself suddenly under the influence of Prof. Robert A. Millikan, who would eventually receive the Nobel Prize in physics in 1923 for his discovery of the elementary charge on the electron. Unable to finance his continued education after his first year at the university, Davisson took up employment at a Bloomington telephone company. Upon the recommendation of Prof. Millikan he was appointed assistant in physics at Purdue University in 1904. The same year he returned to the University of Chicago until 1905. Again under the recommendation of Prof. Millikan, Davisson took up an appointment as instructor in physics at Princeton University, where he remained until 1910, carrying out his duties as instructor as well as student of physics. During his tenure at Princeton he would study at the University of Chicago during the summer semesters, and eventually graduate with a BS degree from the University of Chicago in 1908. Davisson was awarded a fellowship in physics for 1910 to 1911 at Princeton, during which time he completed his PhD degree under Prof. and later Nobel Laureate Owen W. Richardson.

C. Davisson (1881–1958)

Having completed his doctorate degree, Clinton Davisson took on a position of instructor in the Department of Physics, Carnegie Institute of Technology, Pittsburg in 1911 and remained in that position until 1917. During his stint at Carnegie, Davisson spent a summer of leave in 1913 working in the Cavendish Laboratory under J. J. Thomson, who was awarded the Nobel Prize in physics in 1906 for the discovery of the electron. Little did Davisson know, during his stint at the Cavendish Laboratory with J.J. Thomson, that he would share the Nobel Prize in physics 24 years later with the son of J.J. Thomson.

Davisson was refused conscription into the army corps in 1917 and, in lieu of military service he accepted wartime employment in the Engineering Department of the Western Electric Company, which would later become Bell Telephone Laboratories, New York while on leave of absence from Carnegie Tech. After the end of the war, Davisson remained at the Bell Telephone Laboratories and resigned his position of Assistant Professor of Carnegie Tech.

At the Bell Telephone Laboratories, Davission carried out a series of experiments, which began in 1919, on thermionic electron emission and the emission and scattering of electrons upon positive ion and electron bombardment (Davisson and Pidgeon, 1920; Davisson and Germer, 1920; Davisson and Kunsman, 1922a,b, 1923). These experiments led to the discovery of electron diffraction by crystalline material in 1927.

Two occurrences led Davisson to the discovery of the diffraction of electrons by crystalline matter and thereby demonstrate the wave nature of the electron. The first was the hypothesis of de Broglie (1923a,b,c,d) from work on his doctoral thesis, that a particle of momentum, p, would display wave properties, and the wavelength of the matter-wave would be proportional to Planck's constant and inversely proportional to the mass and velocity of the particle, or:

$$\lambda = \frac{h}{p} = \frac{h}{mv} \qquad [V.21]$$

The other occurrence that led to the discovery of electron diffraction was provided by Davisson's previous work with coworkers. This work demonstrated the elastic scattering of electrons. In his Nobel lecture, Davission noted the following:

> *…the work was begun the day after copies of de Broglie's thesis reached America. The work actually began in 1919 with the accidental discovery that the energy spectrum of secondary electron emission has, as its upper limit, the energy of the primary electrons, even for primaries accelerated through hundreds of volts; that there is, in fact, an elastic scattering of electrons by metals…and then chance again intervened; it was discovered purely by accident, that the intensity of elastic scattering varies with the orientations of the scattering crystals. Out of this grew, quite naturally, an investigation of elastic scattering by a single crystal of predetermined orientation.*

The breakthrough in Davisson's work came in 1927 when Davisson and Germer were investigating the elastic collisions of electrons, as these were reflected off the surface of metallic nickel. A laboratory accident caused the glass housing of the electron gun and target apparatus to break, whereby the loss of vacuum formed an oxide layer on the surface of the nickel sample. To remove the oxide layer, they heated the nickel to a high temperature in a reducing atmosphere. This caused the surface of the nickel to crystallize. Repeating their experimentation with electron beams on the nickel sample produced different results. They noticed that the intensity of the reflected electron beam was confined to specific angles with respect to the energy and angle of the incident beam. This was characteristic of a diffraction of the electron beam similar to what Sir William and Sir Lawrence Bragg (Nobel Prize in physics, 1915) observed when X-rays are directed onto a crystalline substance. Their first report of the diffraction of electrons was made in April 1927 (Davisson and Germer, 1927a).

The apparatus used by Davisson and Germer (1927b) consisted of an electron gun that would direct the electron beam toward the nickel crystal. The intensity of the diffracted electron beam was measured with a Faraday cup rotated from 20 to 90° from the origin of the incident electron beam, as illustrated in Fig. V.11. The nickel crystal also could be rotated to permit the measurement of refracted electron beam intensities according to various azimuths of the crystal.

Davisson and Germer measured the most intense scattered electron beam at a 50° angle (ϕ) from the primary electron beam. This diffraction was caused by an electron beam created with an acceleration potential of 54 V, illustrated in Fig. V.12.

They tested the de Broglie relation, $\lambda = h/p$, on the scattered electrons to demonstrate the electron matter-wave. In Davisson's words (1937), the proof of the de Broglie matter wave for the electron was carried out as follows:

> *The de Broglie relation was tested by computing wavelengths from the angles of the diffraction beams and the known constant of the crystal [*d*], and comparing these with corresponding wavelengths computed from the formula* λ = h/p, *where* p, *the momentum of the electrons, was obtained from the potential used to accelerate the beam and the known value of* e/m *for electrons. If wavelengths computed from the formula agreed with those obtained from the diffraction data, the de Broglie relation would be verified.*

For example, the incident electron beam illustrated in Fig. V.12 was produced by acceleration across a potential difference of 54 V. The wavelength of this electron beam can be calculated according to the following relation derived by de Broglie according to Eqs. [III.6]−[III.9] (see Hall of Fame III):

$$\lambda = \frac{h}{p} = \frac{h}{m_0 v} = \frac{h}{\sqrt{2m_0 eV}} \qquad [V.22]$$

where h is Planck's constant, m_0 is the rest mass of the electron, e is the electron charge, and V is the applied voltage. A calculation of the wavelength of the 54 V electron beam according to the de Broglie relation (Eq. [V.22]) yields:

$$\lambda = \frac{h}{\sqrt{2m_0 eV}} = \frac{6.626 \times 10^{-34}\ \text{J s}}{\sqrt{2(9.11 \times 10^{-31}\ \text{kg})(1.6 \times 10^{-19}\ \text{C})(54\ \text{V})}} = 1.67 \times 10^{-10}\ \text{m} = 1.67\ \text{Å}$$

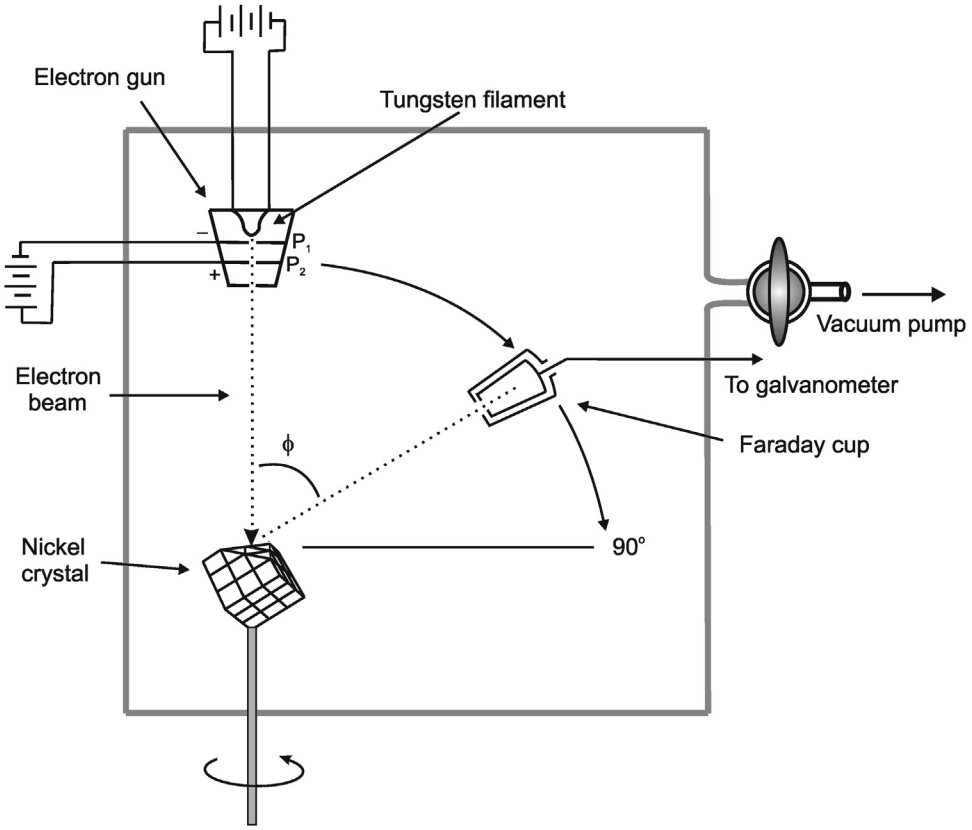

FIGURE V.11 A schematic diagram illustrating the disposition of the electron beam, nickel crystal, and collector (Faraday cup). The crystal could be rotated to bring a principal azimuth into a plane of observation. The Faraday cup could detect and measure the intensity of the electron matter-wave in varying directions from 20° (closest to the electron gun) to 90° (perpendicular to the plane of electron impact with the crystal. The electron emission from the tungsten filament was concentrated onto the opening of plate P_1 by giving the plate a potential more negative than that of the filament. The potential of P_2 was given a high positive value, and the difference between the potential of plate P_2 and that of the filament would determine the speed of the emergent electron beam. The distance from the end of the electron gun to the crystal target was only 7 mm, and the nickel crystal measured approx. $8 \times 5 \times 3$ mm. See Davisson and Germer (1927b) for detailed drawings of their apparatus.

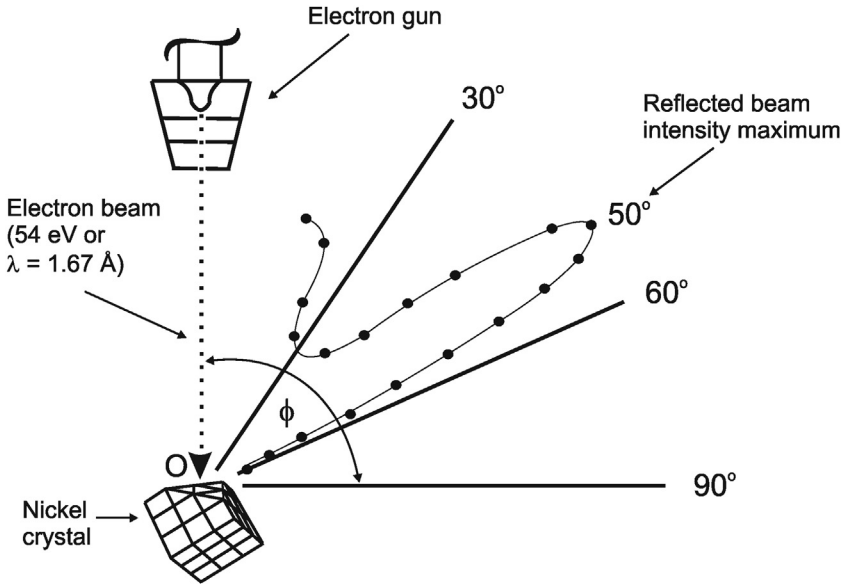

FIGURE V.12 A schematic diagram of the electron gun, the nickel crystal target, and Davisson and Germer's plot of the electron beam intensity as a function of the angle of reflection, ϕ. The relative intensities of the reflected beam are measured by the distance from the point O to any position on the reflected beam intensity plot. The maximum intensity of the reflected electron beam for an incident beam of 1.67 Å was measured at an angle $\phi = 50°$. A tungsten filament served as the electron source. See Davisson and Germer (1927b) for details.

Taking the electron beam angle of deflection $\phi = 50^\circ$ and the known spacing between the atomic nuclei of the nickel crystal ($d = 2.15$ Å), Davission and Germer (1927a) calculated the incident electron beam wavelength according to the diffraction equation as follows:

$$n\lambda = d\sin\varphi = 2.15\ \text{Å}\ \sin 50^\circ = 1.6469\ \text{Å} = 1.65\ \text{Å} \qquad [V.23]$$

which agrees very closely with the 1.67 Å for the wavelength calculated according to the de Broglie matter−wave relation.

Notice that Eq. [V.23] is slightly different than Bragg's Law for diffraction (ie, $n\lambda = 2d\sin\theta$) described by Eq. [III.52] in Hall of Fame III, because the electron beam in the above case did not penetrate the crystal lattice; rather the beam was diffracted off the surface layer atoms of the crystal lattice. Davisson and Germer (1927a) used low-energy electrons in their diffraction experiments. In such a case, the surface atoms of the crystal acted principally as the diffraction grating, because the electrons would not have sufficient energy to penetrate significantly to lattice layers below the outermost ordered layer of the crystal atoms. This was noted by Davission and Germer (1928) as follows:

> *…near grazing first-layer scattering is strongly predominant, and diffraction occurs as if waves were being scattered by a single layer of atoms only. Files of atoms serve as line gratings and ordinary line grating diffraction is observed.*

At about the same time as Davisson and Germer performed their diffraction experiments with low-energy electrons, George Paget Thomson in Aberdeen, UK independently demonstrated electron diffraction in thin metal foils with high-energy electrons, which could penetrate several layers of crystalline lattice and thereby obey Bragg's Law of diffraction, $n\lambda = 2d\sin\theta$, as described previously for X-ray diffraction (see Eq. [II.52] in Hall of Fame, Part III). A sketch of the life and work of George P. Thomson is provided in the following section.

The significance of the experimental demonstration of the electron matter-wave and consequently experimental verification of the de Broglie particle-wave theory was underscored by Davisson in his Nobel lecture on December 13, 1937 when he stated:

> *I will take time only to express my admiration of the beautiful experiments − differing from ours in every respect − by which Thomson in far-away Aberdeen demonstrated electron diffraction and verified de Broglie's formula at the same time as we in New York. And to mention, as closely related to the subject of this discourse, the difficult and beautifully executed experiments by which Stern and Estermann in 1929 (Estermann and Stern, 1930) showed that atomic hydrogen also is diffracted in accordance with the de Broglie-Schrödinger theory.*
>
> *Important and timely as was the discovery of electron diffraction in inspiring confidence in the physical reality of material waves, our confidence in this regard would hardly be less today, one imagines, were diffraction yet to be discovered, so great has been the success of the mechanics built upon the conception of such waves in clarifying the phenomena of atomic and subatomic particles.*

From 1930 to 1937 Davisson continued his research at the Bell Telephone Laboratories on electron optics and on the applications of electron diffraction in engineering. He subsequently studied the scattering of very slow electrons by metals, and during World War II he researched the development of various electronic devices and crystal physics problems (Nobel Lectures, Physics, 1922−1941 (1965)). Davisson retired from Bell Labs in 1946 and was visiting professor at the University of Virginia, Charlottesville, VA from 1947 to 1949. He died at the age of 76 on February 1, 1958 in Charlottesville.

George Paget Thomson shared the Nobel Prize in physics in 1937 with Clinton Davisson "for their experimental discovery of the diffraction of electrons by crystals."

G. Thomson (1892–1975)

Thomson was born at Cambridge in 1892 the son of J.J. Thomson, Nobel Laureate in physics in 1906. It has been stated in jest, "J.J. Thomson won the Nobel Prize in physics in 1906 for demonstrating that the electron was an elementary particle, whereas his son, G.P. Thomson, won the Nobel Prize in physics in 1937 for demonstrating that the electron was not a particle." The truth is, however, that G.P. Thomson, through his experimental discovery of electron diffraction, verified the de Broglie formula that describes the dual wave-matter property of the electron, that like other particles with kinetic energy exhibit the properties of a particle and of a wave. The postage stamp issued by the Guinean Republic commemorated G. P. Thomson's scientific discovery; although the reader will notice that his family name is misprinted on the postage stamp.

George Paget Thomson completed his undergraduate studies in mathematics and physics at Trinity College, Cambridge. He also completed a year of research work under his father at the Cavendish Laboratory, Trinity College, Cambridge. When the First World War broke out, Thomson served in the infantry for a short stint, and then was assigned to numerous scientific research positions with the Royal Flying Corps and several months in the United States as part of the British War Mission. After the war he spent 3 years as Fellow and Lecturer at Corpus Christi College, Cambridge.

In 1922 Thomson became Professor of Natural Philosophy at the University of Aberdeen and remained in that position until 1930. It was at the University of Aberdeen where J.P. Thomson carried out his historic research that led to the discovery of electron diffraction. The experimental demonstration of the diffraction of electrons was a significant step in physics, as it provided the evidence to verify the de Broglie equation, $\lambda = h/mv$, defining the wave nature of particles. Thomson arrived at his discovery in Aberdeen at about the same time as Davisson in New York. They announced their discoveries simultaneously in the same volume 119 of the journal *Nature* (Davisson and Germer, 1927a; Thomson and Reid, 1927); however, the experimental approach and the manner in which the diffraction was observed were completely different in the two camps. Davisson's discovery, described previously in this section, was accidental, whereas Thomson, inspired by the theory of de Broglie, set out from the start to prove the wave nature of the electron (Obituary, 1975 *Nature* **257**, 726). It is not unusual for scientific discoveries to be made by two groups totally independent of each other. When the time is right and the stage is set, the discoveries are made.

Quite opposite to the approach used by Davisson and Germer (1927a), who measured a beam of low-energy electrons (54 eV) as these deflected off the atomic plane of the crystal surface, Thomson and Reid (1927) used a beam of relatively high-energy electrons (20,000 to 60,000 eV), which would pass directly through the crystalline lattice of thin metal foils. The apparatus used by Thomson and Reid is illustrated in Fig. V.13.

Thomson et al. (1927, 1928, 1929) calculated the wavelength of the electron beam according to the de Broglie matter-wave theory defined previously in Eq. [V.22] corrected for the relativistic mass of the electron, or:

$$\lambda = \frac{h}{p} = \frac{h}{mv} \qquad [V.24]$$

where m, the relativistic mass of the electron, is defined as:

$$m = \frac{m_0}{\sqrt{1 - (v^2/c^2)}} \qquad [V.25]$$

where m_0 is the electron rest mass, v is the speed of the electron, and c is the speed of light in a vacuum. Eq. [V.24] can then be written as:

$$\lambda = \frac{h}{\left[m_0/\sqrt{1 - (v^2/c^2)}\right]v} \qquad [V.26]$$

and:

$$\lambda = \frac{h\sqrt{1 - (v^2/c^2)}}{m_0 v} \qquad [V.27]$$

Thomson (1928) used Eq. [V.27] from the de Broglie matter-wave theory to calculate the wavelength of the electron beam produced in their electron diffraction apparatus. He only needed to know the speed of the electron, v, which was calculated from the electron kinetic energy. The following expression for the electron kinetic energy permits the calculation of the speed of the relativistic electron:

$$K = mc^2 - m_0c^2 \qquad [V.28]$$

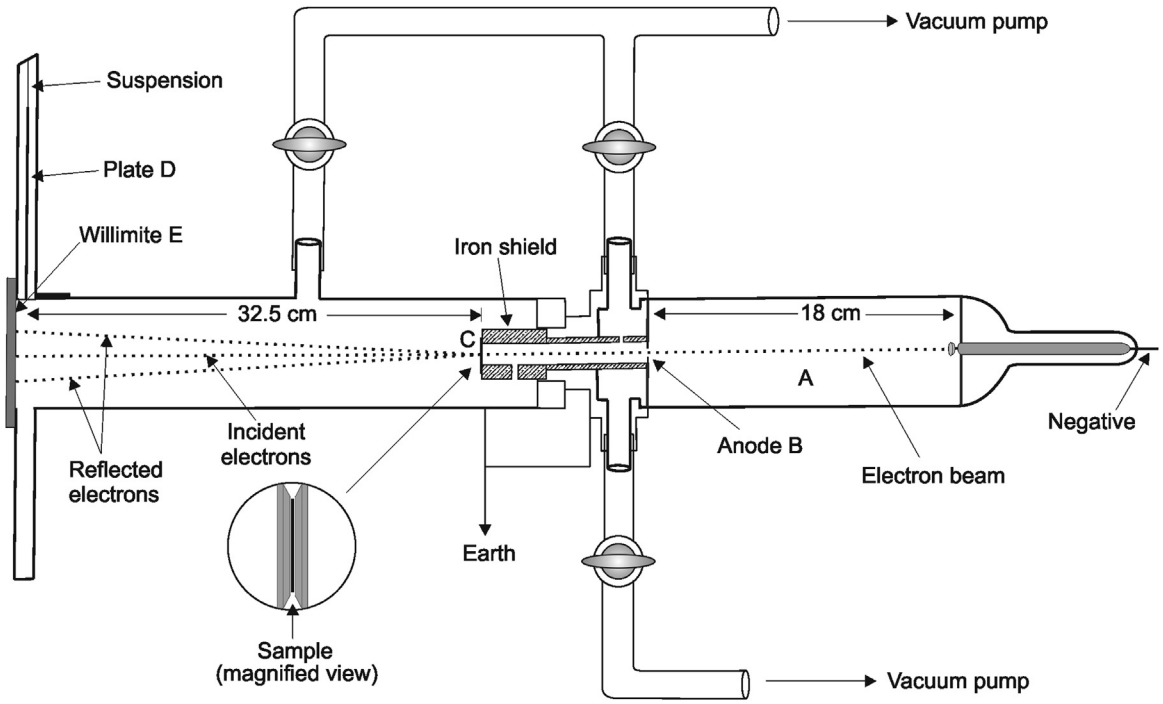

FIGURE V.13 Experimental arrangement used by Thomson and coworkers to demonstrate the diffraction of an electron beam by the crystalline lattices of thin metal and organic substances (see Thomson, 1928). The chambers of the apparatus were evacuated by a mercury vapor pump and the cathode rays were generated by an induction coil. The electron beam passed from right to left through tube A and through a fine tube of small bore (0.23 mm) and 6-cm length in the anode B. The electron beam exiting the anode would strike the thin foil (10^{-5} to 10^{-6} mm thick) of crystalline substance at C. The electron beam and its diffracted waves would travel on through the foil and onto a willimite screen at E on the far end of the apparatus. The willimite screen would glow green from fluorescence when bombarded by the electron beam. At the willimite screen, Thomson and coworkers could observe the image produced by the principal (unreflected) electron beam as a central spot, and the diffracted electron matter-waves as rings of diameter D, which surround the central electron beam. Permanent images of the electron beam and the surrounding rings of the diffracted waves were made by dropping a photographic plate from position D down into the path of the electron beam in front of the willimite screen. Thomson's original apparatus is on display at the Science Museum, Cavendish Laboratory, University of Cambridge.

where m is the relativistic mass of the electron and m_0 its rest mass. From the expression of m of Eq. [V.25], the particle kinetic energy can be written as:

$$K = \frac{m_0 c^2}{\sqrt{1-(v^2/c^2)}} - m_0 c^2 \qquad [V.29]$$

The electron rest energy in units of MeV is calculated as:

$$E = m_0 c^2 = \left(9.109 \times 10^{-31}\ \text{kg}\right)\left(2.9979 \times 10^{8}\ \text{m/s}\right)^2 = 8.186 \times 10^{-14}\ \text{J} \qquad [V.30]$$

The electron rest energy in joules is converted to units of MeV as:

$$8.186 \times 10^{-14}\ \text{J}/1.602 \times 10^{-19}\ \text{J/eV} = 0.511\ \text{MeV} \qquad [V.31]$$

The known constant value of the electron rest energy, 0.511 MeV, can be inserted into Eq. [V.29] to calculate the electron velocity, v, from the measured value of its kinetic energy, K, as:

$$K = \frac{0.511\ \text{MeV}}{\sqrt{1-(v^2/c^2)}} - 0.511\ \text{MeV} \qquad [V.32]$$

Thomson measured the kinetic energy of the electron beam produced in his apparatus in units of eV from an accurate measurement of the potential difference used to accelerate the electron toward the anode. From the measured value of K, he calculated the velocity of the electron according to Eq. [V.32].

Thomson used electron beams over the range of 20,000 to 60,000 V energy, which he reports to have wavelengths varying according to energy over the respective range of 0.8×10^{-9} cm to 0.5×10^{-9} cm (Thomson, 1938). For example,

in his early detailed report of electron diffraction, Thomson (1928) used an electron beam of 25,000 V energy and calculated the wavelength of the electron beam according to Eq. [V.27] to be about 0.75×10^{-9} cm. To arrive at the value of the electron wavelength, the velocity of the 25-keV electron is first calculated according to Eq. [V.29] as:

$$K = \frac{m_0 c^2}{\sqrt{1-(v^2/c^2)}} - m_0 c^2 \quad \text{or} \quad 0.025\ \text{MeV} = \frac{0.511\ \text{MeV}}{\sqrt{1-(v^2/c^2)}} - 0.511\ \text{MeV} \qquad [V.33]$$

which is transposed to solve for the electron velocity, v, as follows:

$$\sqrt{1-(v^2/c^2)} = 0.953 \qquad [V.34]$$

and:

$$1-\left(v^2/c^2\right) = (0.953)^2 \qquad [V.35]$$

and:

$$\frac{v^2}{c^2} = 1 - 0.90821 \qquad [V.36]$$

and:

$$v^2 = 0.09179c^2 \qquad [V.37]$$

or:

$$v = 0.3029c \qquad [V.38]$$

Thus, the value of $v = 0.3029c$ calculated here is the velocity of the electrons of 25,000 V energy, which is 0.3029 times the speed of light in a vacuum.

From the calculated value of v, the wavelength λ of the 25-keV electrons is calculated as:

$$\begin{aligned}\lambda &= \frac{h\sqrt{1-(v^2/c^2)}}{m_0 v} \\ &= \frac{6.626 \times 10^{-34}\ \text{J s}\sqrt{1-\dfrac{[(0.3029)(2.9979\times 10^8\ \text{m/s}]^2}{\left(2.9979\times 10^8\ \text{m/s}\right)^2}}}{(9.109\times 10^{-31}\ \text{kg})(0.3029)\left(2.9979\times 10^8\ \text{m/s}\right)} \\ &= 0.076 \times 10^{-10}\ \text{m} = 0.076\ \text{Å}\end{aligned} \qquad [V.39]$$

The above results agree closely with the calculated value of 0.75×10^{-9} cm reported by Thomson (1928).

Because the electrons used by Thomson were of relatively high energy, these would travel directly through the thin (10^{-5} to 10^{-6} mm) foil of crystalline substances such as platinum, aluminum, gold, nickel, and celluloid. By means of the apparatus illustrated in Fig. V.13 Thomson could observe that the electron beam would undergo diffraction by the atomic planes in the crystalline substances according to Bragg's Law:

$$n\lambda = 2d\sin\theta \qquad [V.40]$$

which was previously described for X-ray diffraction, where n is an integer 1,2,3…, d is the interatomic spacing or atomic planes in the crystal lattice, and θ is the glancing angle at which the electrons are reflected. Only electron beams with wavelengths of 1λ, 2λ, 3λ,… over the path length of travel ($2d\sin\theta$) between each successive crystal atomic plane will produce coherent reflected electron beams (see Fig. III.11 in Hall of Fame III). The incident electron beam would deflect off the atomic planes of the crystalline lattice in the same way as X-ray photons, as illustrated in Fig. V.14 and described by Thomson (1938) in his Nobel lecture as follows:

> *A narrow beam of cathode rays was transmitted through a thin film of matter. In the earliest experiment of the late Mr. Reid [Thomson's assistant, Alexander Reid] this film was of celluloid, in my own of metal. In both, the thickness was of the order of 10^{-6} cm. The scattered beam was received on a photographic plate normal to the beam, and when deployed showed a pattern of rings, recalling optical halos and the Debye-Scherrer rings well known in the corresponding experiment with X-rays.*

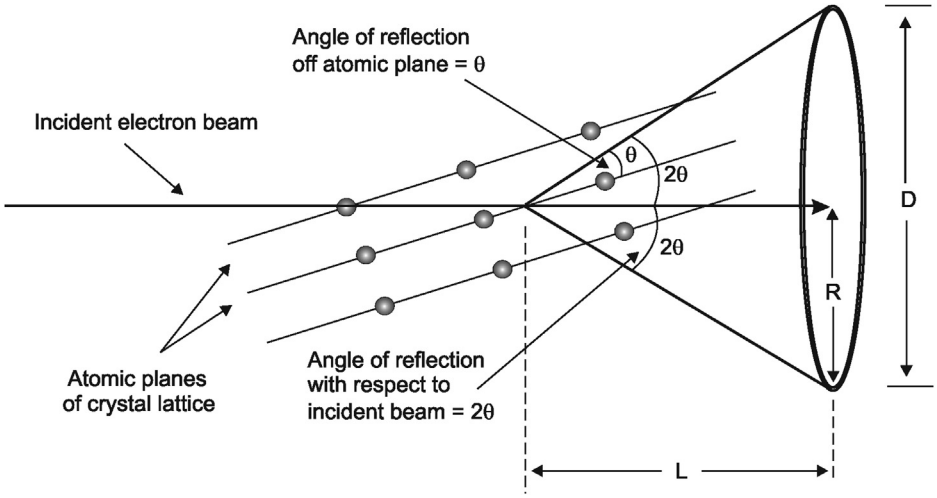

FIGURE V.14 The diffraction of an electron beam off an atomic plane of a crystal lattice as the beam passes through the lattice. The beam diffracts at an angle θ to the atomic plane and an angle 2θ with respect to the path of the incident electron beam. A ring of diffracted electrons is formed around the central electron beam, which was observed in real time by the willimite screen or by the image formed after exposure to a photographic plate placed normal to the electron beam, as illustrated in Fig. V.13. The diameter of the ring is a function of the angle of reflection (θ) and the distance or length (L) of travel of the diffracted beam.

An interference phenomenon is at once suggested. This would occur if each atom of the film scattered in phase a wavelet from an advancing wave associated with the electrons forming the cathode rays. Since the atoms of each small crystal of the metal are regularly spaced, the phases of the wavelets scattered in any fixed direction will have a definite relationship to one another. In some directions they will agree in phase and build up a strong scattered wave, in others they will destroy one another by interference. The strong waves are analogous to the beams of light diffracted by an optical grating.

Thomson took crystalline samples of known d spacing, that is, crystalline materials that had interatomic spacing predetermined by X-ray diffraction, and from the diameter of the ring produced by the reflection of an electron beam of known wavelength (λ) off a thin sample of a crystalline material, he could demonstrate that the electron beam satisfied Bragg's Law $n\lambda = 2d\sin\theta$.

Thomson could demonstrate that the electron beam behaved as a wave, as it would diffract along the atomic planes of a crystalline substance in accord with Bragg's Law in the same fashion as X-ray photons. For example, an electron beam of 25,000 V corresponding to a wavelength of 0.076 Å according to the de Broglie matter-wave theory (see calculations according to Eqs. [V.28]–[V.39]) was directed toward a thin foil sample of crystalline platinum. The d spacing of the platinum was previously measured by X-ray diffraction to be 3.92 Å (Thomson, 1927). If the distance of travel (L) of the diffracted beam from its origin in the platinum foil to the end of its path at the photographic plate was 32 cm (distance from the sample to the photographic plate, as illustrated in Fig. V.14), Thomson could calculate the first-order (1λ) angle of deflection that should correspond to Bragg's Law (Eq. [V.40]) as:

$$\sin\theta = \frac{\lambda}{2d} = \frac{0.076\ \text{Å}}{(2)\left(3.92\ \text{Å}\right)} = 0.00969 \qquad [V.41]$$

$$\theta = \sin^{-1} 0.00969 = 0.555^{\circ} \qquad [V.42]$$

If the diameter (D) of a first-order diffraction ring on the photographic plate measured 1.24 cm, the angle of deflection of the electron beam should agree with the following relationship derived by Ironside (1928), an assistant to G.P. Thomson:

$$\sin\theta = \frac{(1/4)(D)}{L} = \frac{D}{4L} \qquad [V.43]$$

$$\sin\theta = \frac{1.24\ \text{cm}}{(4)(32\ \text{cm})} = 0.009687 \qquad [V.44]$$

$$\theta = \sin^{-1} 0.009687 = 0.555^{\circ} \qquad [V.45]$$

Also, the angle of diffraction of the electron beam calculated above according to Bragg's Law (Eq. [V.40]) should satisfy the following geometric relation to the ring size:

$$\tan 2\theta = \frac{R}{L} \qquad [V.46]$$

where R is the radius of the ring as illustrated in Fig. V.14, and:

$$\tan 2(0.555^\circ) = \frac{R}{32\ \text{cm}} \qquad [V.47]$$

$$0.019375 = \frac{R}{32\ \text{cm}} \qquad [V.48]$$

$$R = 0.62\ \text{cm} \qquad [V.49]$$

Thomson thus demonstrated the de Broglie electron matter-wave. The materials tested by Thomson were polycrystalline meaning that the substance is built up of many crystals having different orientations, such as a powdered sample of single crystal grains. The effect of X-ray or electron diffraction of polycrystalline materials is the production of a diffraction pattern consisting of several concentric rings of various diameters about the central spot produced by the electron beam. An example of a typical electron ring diffraction pattern produced by Thomson (1935) on a photographic plate is shown in Fig. V.15.

During the winter of 1929 to 1930, Thomson was a nonresident lecturer at Cornell University, and afterward appointed professor at Imperial College, London. After completing his major work on electron diffraction, George Thomson became interested in neutron physics in the 1930s, and took up the study of nuclear energy once fission was discovered in 1939. When it became clear that fission had military possibilities during the Second World War, he became chairman of the confidential MAUD Committee, the British Committee set up in 1940 to study the possibilities of the utilization of nuclear fission for atomic weapons (Nobel Lectures, Physics, 1965; Anonymous, *Nature*, 1975). The MAUD Committee was established following a memorandum by Otto R. Frisch and Rudolf E. Peierls, both at Birmingham University, in which they predicted that a small mass of Uranium-235 could sustain a chain reaction that would serve as the basis for the making of an atomic weapon. MAUD was the code name for the secret British committee commissioned to research the military potential of nuclear fission. The origin of the code name MAUD is related in a historical account by Fakley (1983). When Denmark was occupied by the Germans, Niels Bohr sent a telegram to Otto Frisch, who had worked in Bohr's Copenhagen Laboratory, and at the end of the telegram asked Frisch to "Tell Cockcroft [Prof. J.D. Cockcroft] and Maud Ray Kent." Fakley (1983) explains that Maud Ray Kent was a cryptic reference to possibly uranium disintegration, and after the war the code name Maud Ray was identified to be a former governess to Bohr's children, who was living in the county of Kent.

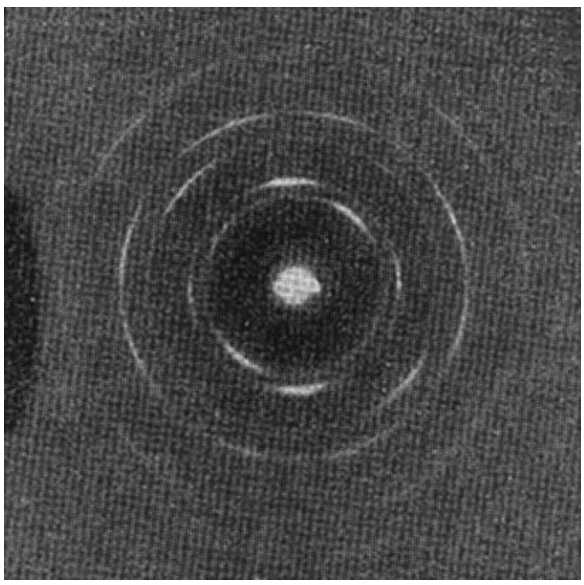

FIGURE V.15 Diffraction pattern of gold foil irradiated with an 85-keV electron beam. *From Thomson, G.P., 1935. Electron diffraction as a method of research. Nature 135, 492–495. Reprinted with permission from Macmillan Publishers Ltd., © 1935.*

From this cable the code name MAUD was chosen for the secret British Committee to study the feasibility of utilizing uranium fission for weapons development. The MAUD Committee concluded in 1941 that the development of a nuclear weapon was feasible, and George Thomson was authorized to hand over the conclusions of the Committee to American scientists Vaneveer Bush and James Conant (Nobel Lectures, Physics, 1965).

George Thomson held his post as Professor at Imperial College, London until 1952. That same year he became Master of Corpus Christi College, Cambridge where he had carried out his historic electron diffraction experiments and remained in that post until his retirement in 1962. As a hobby Thomson enjoyed building model ships. He died on September 17, 1975.

PIERRE VICTOR AUGER (1899–1993)

Pierre Auger (pronounced OH-ZHAY) was born in Paris, France on May 14, 1899. He did not win the Nobel Prize, but he made great contributions to the science of radioactivity including the discovery of the atomic Auger Effect, Auger electrons, and the showers of the cosmic radiation.

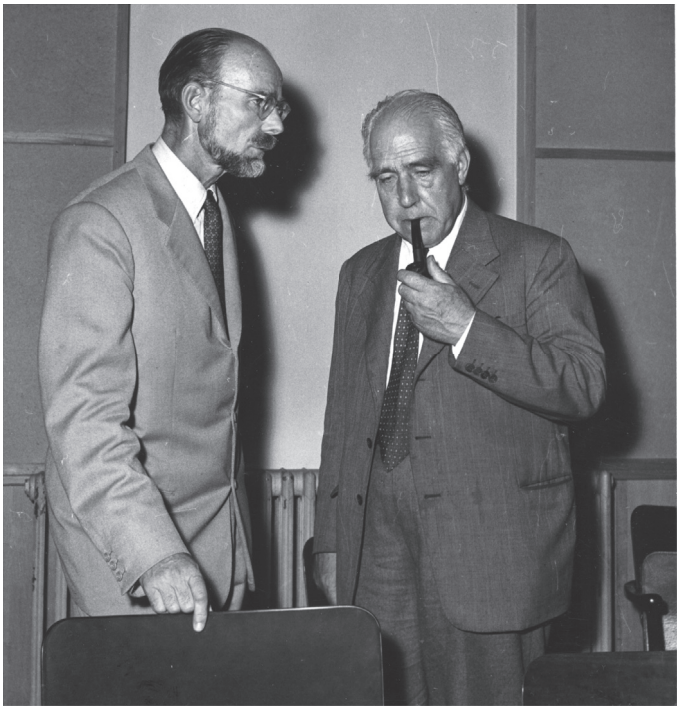

Pierre Auger (left) profile with Niels Bohr (right) with pipe
[UNESCO photograph, courtesy AIP Emilio Segre Visual Archives]

Pierre Auger studied at the Ecole Normale Supérieure de Paris from 1919 to 1922 and devoted his professional career to atomic and cosmic-ray physics. At the young age of 24 years, he discovered the emission of electrons from atoms excited by X-rays (Auger, 1923, 1925a,b). Pierre Auger irradiated krypton and argon gas with X-rays and discovered the emission of electrons. He reasoned that an X-ray photon causes the ejection of an atomic electron from a given shell or quantum level, leaving a vacancy behind. He further reasoned that an electron from the next outer shell could fill the vacancy, causing the emission of electromagnetic radiation that would correspond to the difference in the energy levels of the electrons in the outer and inner shells. For example, Auger noted that, if an electron in the K shell was ejected by an artificially produced X-ray photon, an electron from the next outer L shell could fill the vacancy resulting in the emission of energy, E, as electromagnetic radiation, which he described by the following equation:

$$E_{\text{X-ray}} = h\nu = E_{\text{L}} - E_{\text{K}} \qquad \text{[V.50]}$$

where E_{L} and E_{K} are the energy levels of the electrons in the L and K shells, respectively. The transition energy $h\nu$ may be emitted as an X-ray photon characteristic of the atom, or alternatively, the transition energy may be absorbed by an atomic electron resulting in its emission from the atom. The electron emitted in this fashion is identified as an Auger electron in the

name of Pierre Auger for his discovery and interpretation of this phenomenon. Lise Meitner (1923) also independently discovered Auger electrons the same year as Pierre Auger; however, the Auger electrons and the phenomenon that gives rise to these electrons, the Auger Effect, are named after Pierre Auger.

From this discovery of Meitner and Auger has developed the very important analytical technique of Auger electron spectroscopy (AES). The technique of AES involves irradiating the surface of a sample with an electron beam of energy sufficient to ionize the inner orbits of atoms, thereby inducing the concomitant emission of Auger electrons. The Auger-electron energy spectra drawn from the induced emissions serve as fingerprints of different atoms to enable their identification and quantitative analysis (Chourasia and Chopra, 1997; Mehlhorn, 1998). In 1978 Pierre Auger was recognized with the Gaede-Langmuir Award "for establishing the fundamental principle of Auger spectroscopy which has led to the most widely used surface analysis technique of importance to all aspects of vacuum science and technology."

Pierre Auger together with French physicist Roland Maze (Auger and Maze, 1938, 1939; Auger et al., 1938, 1939) discovered the extensive air showers of cosmic radiation, that is, the all-encompassing cascade of high-energy particles in the earth's atmosphere produced by the impact of relativistic galactic cosmic-ray particles with nuclei in the earth's atmosphere. In a comprehensive review on cosmic radiation, Cronin (1999) relates the work of Auger and Maze (1938), who demonstrated in Jean Perrin's laboratory in Paris that cosmic-ray particles separated by distances as large as 20 m arrived in time coincidence, which indicated that the particles were secondary particles, or part of a cascade of particles, from a primary or common source. Cronin (1999) relates that subsequent experiments by Auger et al. (1939) in the Alps demonstrated that particle coincidences were observed even at distances of 200 m apart. They observed cosmic-ray particles of very high energy up to 10^{15} eV. In their paper Auger et al. (1939) reported"

> *One of the consequences of the extension of the energy spectrum of cosmic rays up to 10^{15} eV is that it is actually impossible to imagine a single process able to give to a particle such an energy. It seems much more likely that the charged particles, which constitute the primary cosmic radiation, acquire their energy along electric fields of a very great extension.*

Yet cosmic-ray particles in excess of 10^{20} eV have been discovered since the first particle of about 10^{20} eV was discovered by Linsley (1962). Thus, in honor of Pierre Auger in an effort to study further properties of these ultra-high energy particles, the Pierre Auger Cosmic Ray Observatory has been established (Argirò, 2004). The observatory is an international effort designed to measure cosmic-ray particles of energy in excess of 10^{19} eV. These are rare, as the expected particle flux at these energies is approximately 1/km^2/year. Cosmic-ray particles of energy greater than 10^{20} eV are even more uncommon, as these strike the earth at about 1/km^2/century. The Pierre Auger Observatory constitutes the largest cosmic-ray detector ever built, encompassing an area of 3000 km^2 in western Mendoza Province, Argentina. As described by Argirò (2004), the observatory is designed with the installation of 1600 water Cherenkov detectors and four fluorescence detectors, each covering 3000 km^2. The large size of the detectors is required to achieve consistent statistics, and the combination of the two detection techniques are used to reconstruct the air showers to the greatest precision achievable. The overall objective is to measure the arrival direction, energy, and mass composition of 60 particle events per year with energies above 10^{20} eV and 6000 events per year above 10^{19} eV. The project is supported by UNESCO, the United Nations Educational, Scientific and Cultural Organization with headquarters in Paris. Currently more than 500 scientists and 100 institutions worldwide collaborate in the reading and interpretation of data. The construction of the Pierre Auger Observatory was completed in the year 2008 at a cost of approximately $50 million, which was shared among some 15 nations.

From 1948 to 1956, Pierre Auger was Director of the Department of Sciences for UNESCO, during which time he helped promote the creation of international research programs and the founding of CERN, the European Organization for Nuclear Research in 1954 with headquarters in Geneva. From 1967 until his retirement in 1970, Pierre Auger was Director of the Centre des Faibles Radioactivités (CFR), a joint laboratory of the Centre National de la Recherche Scientifique (CNRS) and the Commissiariat à l'Energie Atomique (CEA), France. Pierre Auger died in Paris on December 25, 1993.

Chapter 12

Atomic Electron Radiation

I believe that all young people think about how they would like their lives to develop. When I did so, I always arrived at the conclusion that life need not be easy; what is important is that it not be empty. And this wish I have been granted.

Lise Meitner, who Albert Einstein called "Our Madame Curie," a few years before her death. The life of Lise Meitner, like that of Marie Curie, could serve as an example for all on how hard work and dedication can overcome many obstacles no matter how insurmountable they may appear.

12.1 INTRODUCTION

Atomic electrons may be emitted from atoms as a result of a nuclear decay process referred to as internal conversion (IC). In such a process, an unstable nucleus decaying to a lower more stable state transmits its decay energy to an atomic electron, which is emitted from the atom with an energy corresponding to the nuclear decay energy less the binding energy of the electron to the atom. Another source of atomic electron radiation is the emission of Auger (pronounced OH-ZHAY) electrons. Auger electrons may be emitted by radioactive atoms, which have electron shell vacancies and undergo electron energy−level transitions. Radioactive atoms that decay by electron capture (EC) or IC decay processes leave vacancies in electron shells. External radiation impinging on atoms can also knock out electrons from inner orbitals of atoms (eg, photoelectron and Compton effects), leaving behind electron vacancies. When a vacancy occurs in an electron shell, an outer orbital electron will move to fill that vacancy. In such an electron energy−level transition, energy may be released in the form of x-radiation, or the energy of transition may be transferred to an atomic electron, causing the electron to be emitted from the atom as an Auger electron. The origins and properties of IC and Auger electrons are described in this chapter.

12.2 INTERNAL CONVERSION ELECTRONS

Decay by IC results in the emission of an atomic electron. This electron, called the internal conversion electron, is emitted from an atom after absorbing the excited energy of a nucleus. In this decay process an unstable nucleus decaying to a lower, more stable state transmits its decay energy to an atomic electron, which is emitted from the atom with an energy corresponding to the nuclear decay energy less the binding energy of the atomic electron. This mode of decay accompanies and even competes with gamma-ray emission as a deexcitation process of unstable nuclei.

The kinetic energy of the electron emitted is equivalent to the energy lost by the nucleus (energy of transition of the excited nucleus to its ground or lower energy state) less the binding energy of the electron. This is illustrated by the following equation:

$$E_e = (E_i - E_f) - E_b \quad [12.1]$$

where E_e is the kinetic energy of the IC electron; $(E_i - E_f)$ is the energy of transition between the initial, E_i, and the final, E_f, nuclear energies normally associated with gamma-ray emission; and E_b is the binding energy of the atomic electron. Lise Meitner and Otto Hahn in Germany (Meitner, 1924; Hahn and Mettner, 1924) were the first to interpret the origin of this monoenergetic electron energy as derived from the IC of the gamma-decay energy. Nobel Laureate Luis W. Alvarez at the University of California, Berkeley was the first to provide experimental evidence of IC of artificially produced radioactive atoms (Alvarez, 1938a).

Radioactivity: Introduction and History, From the Quantum to Quarks. http://dx.doi.org/10.1016/B978-0-444-63489-4.00012-5
Copyright © 2016 Elsevier B.V. All rights reserved.

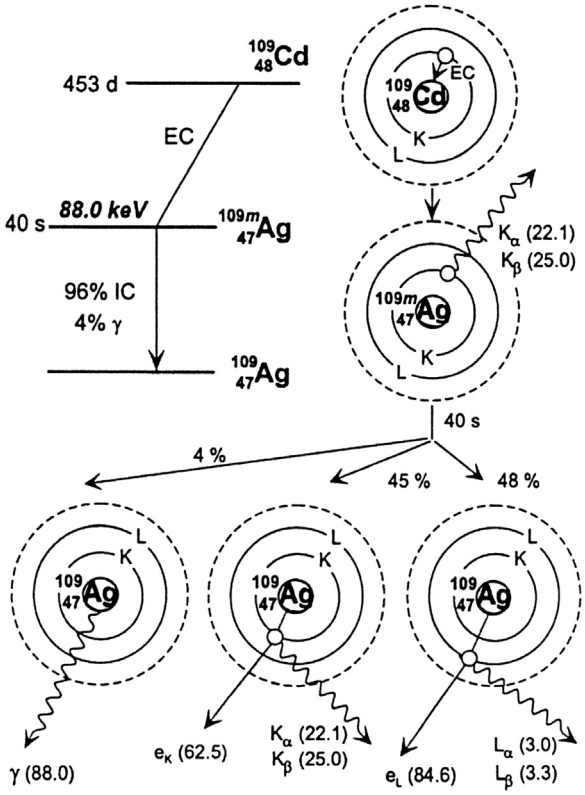

FIGURE 12.1 Decay scheme of ^{109}Cd(^{109m}Ag). The numbers in parenthesis indicate energy values in keV. The electron capture (EC) process occurs from *K*, *L*, and outer shells with probabilities of 79%, 17%, and 4%, respectively, but only *K*-capture is represented here. The ^{109m}Ag daughter decays by emission of 88.0-keV gamma rays with a 4% probability or by internal conversion (IC) with the probabilities of 45% and 48% for *K*- and *L*-shells. Internal conversion from shells higher than *L* contributes the remaining 3% (not illustrated). The *K* and *L* IC decays illustrated involve the ejection of a conversion electron with energy $e_K = 62.5$ keV or $e_L = 84.6$ keV, accompanied by the emission of an Ag *K*- or *L*-fluorescence X-ray photon ($K_\alpha = 22.1$, $K_\beta = 25.0$ keV, or $L_\alpha = 3.0$, $L_\beta = 3.3$ keV) or by the emission of Auger electrons (not represented) and X-ray photons following Auger electron emissions. *From Rachinhas, P.J.B.M., et al., 2000. Simulation and experimental results for the detection of conversion electrons with gas proportional scintillation counters. Nucl. Instrum. Methods Phys. Res., Sect. A 441, 468–478, reprinted with permission from Elsevier © 2000.*

An example of radionuclide decay by IC is found in Fig. 12.1, which illustrates the decay of the parent–daughter nuclides ^{109}Cd(^{109m}Ag). Note that the ^{109m}Ag daughter decays by IC with a 96% probability (ie, 45% for IC from the *K*-shell + 48% from the *L*-shell + 3% from higher electron shells—the latter 3% is not illustrated in Fig. 12.1), and decay occurs also via gamma emission with the remaining 4% probability (Rachinhas et al., 2000).

Because the emission of IC electrons competes with gamma-ray emission as an alternative mode of nuclear deexcitation, many radioactive nuclei that emit gamma radiation will also emit IC electrons. The degree to which this competition occurs is expressed as the total IC coefficient (α), which is the ratio of the rate of emission of IC electrons (e) to the rate of emission of gamma rays (γ) of equivalent energy, or:

$$\alpha = e/\gamma = N_e/N_\gamma \qquad [12.2]$$

where N_e and N_γ are the number of electrons and number of gamma-ray photons, respectively, emitted by a radionuclide sample in a given time interval for a given decay energy transition.

In other words, the IC coefficient is a quantitative measure of the number of IC electrons divided by the number of gamma rays emitted from a radionuclide sample for a given radionuclide energy transition.

Internal conversion electrons may be emitted from specific electron shells of atoms and may be expressed in terms of IC electrons and gamma rays of the same energy less the energy difference resulting from the binding energy of the electron as described by Eq. [12.1]. When expressed in terms of electrons emitted from specific shells, the shell-conversion coefficients are written with a subscript denoting the electron shell of origin, for example, α_K or e_K/γ, α_L or e_L/γ, and α_i or

e_i/γ, where $i = K$, L, M, and so on through the electron shells; and the total IC coefficient would be the sum of the shell-conversion coefficients, or:

$$\alpha = \alpha_K + \alpha_L + \alpha_M + \ldots \alpha_i \quad [12.3]$$

where α_K, α_L, α_M, and α_i are the shell-conversion coefficients for the L, K, M electrons, etc.

Values of IC coefficients are provided in reference tables on isotope decay, such as those found in Lederer and Shirley (1978). In general, IC coefficients are smaller in magnitude for gamma-ray-emitting nuclides of low Z and high-energy transitions, and larger for nuclides of high Z and low-energy transitions. This relationship is illustrated in Table 12.1, which lists a few radionuclides selected at random as examples in order of increasing Z number. As can be seen, larger IC coefficients occur when IC electrons are emitted with low-energy nuclear transitions as indicated by the large values of α associated with low gamma-ray energies and high Z. Also, It should be pointed out that the IC electron (e^-) energies listed are slightly lower than the gamma-ray energies. This is because the energy of the IC electron is equal to the energy absorbed from the decaying nucleus (transition energy) less the binding energy of the atomic electron described previously in Eq. [12.1]. On the other hand, gamma-ray energies serve as a measure of the exact quanta of energies lost by a nucleus.

The loss of atomic electrons through the emission of IC electrons leaves vacancies in atomic electron shells. The vacancies are filled by electrons from outer higher-energy shells, whereby there is a concomitant loss of energy as x-radiation. Emission of x-radiation resulting from electron filling of vacancies in electron shells (K, L, M…) is also listed in Table 12.1. This is a process that occurs in the daughter atoms; the X-rays are a characteristic of the daughter rather than of the parent.

Internal conversion electrons are identical in their properties to beta particles. They differ, however, in their origin. A beta particle is an electron created as a product of the decay of an atomic nucleus (beta decay); whereas an IC electron originates from an atomic electron shell. A characteristic difference between these two types of electrons is their energy spectra. A beta particle, as discussed in the chapter entitled "Beta Radiation and Beta Decay," is created as a result of the

TABLE 12.1 Relationship Between Gamma Radiation and Internal Conversion Electron Radiation, e^-, Associated With Several Nuclides Listed in Order of Increasing Z

Nuclide ^A_ZX	Gamma radiation (MeV)[a]	e^- (MeV)	$\alpha = e/\gamma$	X-rays[a]
$^{7}_{4}$Be	0.477 (10%)		7.0×10^{-7}	
$^{22}_{11}$Na	1.275 (100%)		6.7×10^{-6}	
$^{44}_{22}$Ti	0.068 (90%)	0.065	0.12	Sc K
	0.078 (98%)	0.073	0.03	
$^{57}_{27}$Co	0.014 (9%)	0.013	8.2	Fe K (55%)
	0.122 (87%)	0.115	0.02	
	0.136 (11%)	0.129	0.15	
$^{64}_{29}$Cu	1.34 (0.6%)	1.33	1.3×10^{-4}	Ni K (14%)
$^{87m}_{38}$Sr[b]	0.388 (80%)	0.386	0.21	Sr K (9.4%)
$^{119m}_{50}$Sn[b]	0.024 (16%)	0.020	5.13	Sn K (28%)
$^{125}_{53}$I	0.035 (7%)	0.030	13.6	Te K (138%)
$^{129}_{53}$I	0.040 (9%)	0.034	22	Xe K (69%)
$^{169}_{68}$Er	0.008 (0.3%)	0.006	220	Tm M
$^{181}_{74}$W	0.006 (1%)	0.004	46	Ta K (65%)
$^{203}_{80}$Hg	0.279 (82%)	0.275	0.23	Tl K (13%)
$^{239}_{94}$Pu	0.039 (0.01%)	0.033	461	U K (0.012%)
	0.052 (0.02%)	0.047	269	

[a] *Values in percent are radiation intensities or abundances.*
[b] *m denotes a metastable state.*

decay of an atomic nucleus; and beta particles are emitted with a broad spectrum or smear of energies ranging from near zero to E_{max}. However, an IC electron is emitted from an electron shell of a decaying atomic nucleus with a discrete line of energy of a magnitude equivalent to that of the energy lost by the nucleus less the electron binding energy. The energy of an IC electron can be used to estimate the energy lost by a nucleus.

Like beta particles, IC electrons dissipate their energy by ionization they cause in matter. The abundance of IC electrons emitted from some nuclide samples can be significant and should not be ignored. In certain cases, IC can play a significant role in radionuclide detection and measurement. Internal conversion electron energies are slightly lower than the true gamma-decay energy, because of the energy consumed in the ejection of the bound atomic electron (E_b in Eq. [12.1]).

An IC coefficient of large magnitude does not, however, necessarily signify the emission of a high abundance of IC electrons. For example, ^{239}Pu with a high IC coefficient ($\alpha = 461$) corresponding to a 0.039-MeV gamma-decay process emits only a trace of IC electrons, because of the low abundance of gamma decay (0.01%, see Table 12.1).

12.3 AUGER ELECTRONS

An Auger (pronounced OH-ZHAY) electron can be considered as the atomic analogue of the IC electron. In the EC decay processes, vacancies are left in electron shells (K, L, M…) that can be filled by atomic electrons from higher-energy levels. In the process of falling to a lower-energy shell to fill a vacancy, electron energy may be lost as a photon of x-radiation (see the chapter: "Electromagnetic Radiation − Photons"). Alternatively the energy liberated in the shift of an electron from its higher-energy state to a lower one can be transferred to an electron in an outer shell, resulting in the emission of the electron as an Auger electron.

At the young age of 24 years, Pierre Victor Auger at the Ecole Normale Supérieure de Paris discovered the emission of electrons from atoms excited by X-rays (Auger, 1923, 1925a,b). Pierre Auger irradiated krypton and argon gas with X-rays and discovered the emission of electrons. He reasoned that an X-ray photon causes the ejection of an atomic electron from a given shell or quantum level leaving a vacancy behind. He further reasoned that an electron from the next outer shell could fill the vacancy, causing the emission of electromagnetic radiation that would correspond to the difference in the energy levels of the electrons in the outer and inner shells. For example, Auger noted that if an electron in the K-shell was ejected by an artificially produced X-ray photon, an electron from the next outer L-shell could fill the vacancy, resulting in the emission of energy, E, as electromagnetic radiation, which he described by the following equation:

$$E_{\text{x-ray}} = h\nu = E_L - E_K \qquad [12.4]$$

where h is Planck's constant ($h = 6.62 \times 10^{-27}$ erg s $= 4.14 \times 10^{-15}$ eV s $= 6.62 \times 10^{-24}$ J s), ν is the photon frequency in units of s^{-1}, and E_L and E_K are the energy levels of the electrons in the L- and K-shells, respectively. The transition energy $h\nu$ may be emitted as an X-ray photon characteristic of the atom or, alternatively, the transition energy may be absorbed by an atomic electron resulting in its emission from the atom. The electron emitted in this fashion is identified as an Auger electron in the name of Pierre Auger for his discovery and interpretation of this phenomenon. Lise Meitner (1923) also independently discovered Auger electrons the same year as Pierre Auger; however, the Auger electrons and the phenomenon that gives rise to these electrons, the Auger effect, are named after Pierre Auger.

Auger electrons are defined as atomic electrons that are emitted from atoms after acquiring energy from an atomic electron transition within the atom. Electron transitions will occur when an atom becomes ionized by the loss of an electron from an inner shell. For example, an atom may become ionized by the ejection of an electron from an inner shell by one of several mechanisms, such as (1) irradiation with artificial external X-rays or irradiation with external electron beams, (2) the emission of an IC electron such as K-shell IC, or (3) by EC, also known as K-capture. The term K-capture refers to the capture of an electron from the K-shell by a nucleus. Electron capture from shells farther away from the nucleus (eg, L- and M-shells) are possible to a lesser degree. Capture from the K-shell predominates in the EC decay process. The vacancy left in the K-shell can be filled by an electron from an outer L-shell. In turn, the vacancy left in the L-shell could be filled by another electron from the outer M-shell, etc. The process of nonradiative rearrangement of atomic electrons as a result of the ionization of the atom in one of its inner shells is defined as the Auger effect (Borisenko and Ossicini, 2004). In the process of falling to a lower-energy shell to fill a vacancy, electron energy may be lost as a photon of x-radiation. The energy of the photon radiation is equivalent to the differences in the energy levels of the electrons in the outer and inner shells as described by the above Eq. [12.4]. The X-ray photon may be emitted from the atom, or alternatively the energy released in the electron transition can be transferred to an electron of an outer shell and cause its emission from the atom as an Auger electron. The energy of the Auger electron would be that defined by Eq. [12.4] less the binding energy, E_b, of the electron, or:

$$E_{\text{Auger}} = (E_L - E_K) - E_b \qquad [12.5]$$

The energy of the Auger electron is thus equivalent to the energy of the X-ray photon less the binding energy of the electron, or:

$$E_{\text{Auger}} = E_{\text{x-ray}} - E_b \qquad [12.6]$$

Values of the binding energies of electrons in various shells (K, L, M,…) are found in reference texts such as Lide (2010). Either of two processes, the emission of an X-ray photon or the emission of an Auger electron, can occur as a result of electron energy−level transitions from higher to lower energies. Auger electron emission competes with X-ray emission. An example of the Auger effect and the resultant emission of an Auger electron as compared to X-ray emission are illustrated in Fig. 12.2. The emission of an Auger electron from an atom will occur as a consequence of the following transitions: (1) an atom losses an atomic electron from an inner shell, leaving a hole or vacancy in that shell; (2) an electron from a higher-energy level fills the vacancy; and (3) the energy emitted in the transition of the electron from the higher to lower energy levels is transferred to an outer atomic electron, causing the electron to be emitted from the atom.

Whenever an X-ray photon causes the ejection of an atomic electron, another electron falls from an outer shell to a lower one to fill the vacancy, and there is a cascading effect of electrons falling from yet more distant shells to fill vacancies left behind until the atom reaches the ground or stable state. The downward transitions of electrons in this fashion produce additional X-ray photons of lower energy than the initial X-ray photon. The production of X-ray photons in this fashion is referred to as X-ray fluorescence.

Auger electron emission competes with X-ray emission, and it can accompany any nuclear decay process that results in the production of X-rays, such as a consequence of EC decay or nuclides that have IC in their decay. Like IC electron emission described previously, the EC decay process also results in the emission of appreciable quantities of x-radiation. Auger electron emission can reduce appreciably the abundance of X-ray emission normally expected to accompany radionuclide decay processes. The two competing processes of Auger electron emission and X-ray emission are important to consider in the detection and measurement of nuclides that decay by EC. This is measured by both the fluorescence yield and Auger yield. The fluorescence yield is the fraction of vacancies in a given electron shell that is filled with accompanying X-ray emission, and Auger yield is the fraction of vacancies that is filled resulting in the emission of Auger

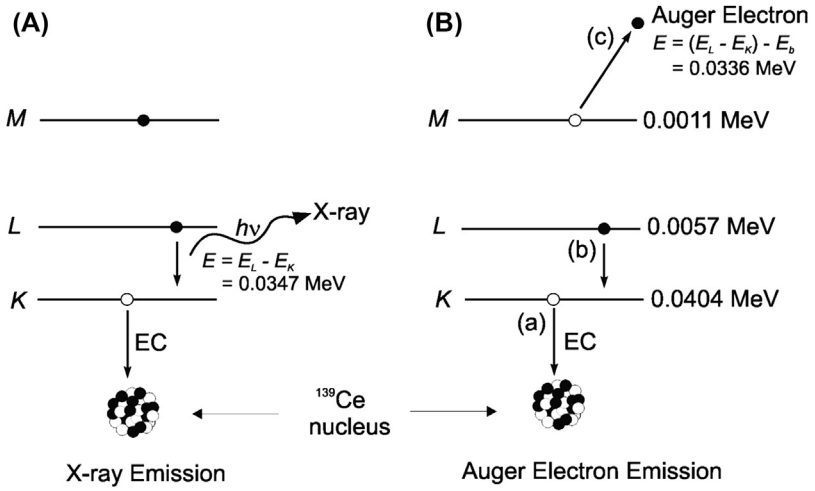

FIGURE 12.2 Decay of the radionuclide ^{139}Ce by electron capture (EC) resulting in (A) X-ray emission or (B) Auger electron emission. An electron vacancy in a shell is illustrated as an empty circle and an electron as a filled circle. Specific binding energies for cerium atomic electrons in K-, L-, and M-shells were obtained from Lide (2010) and are provided along the right-hand side of lines illustrating the various electron energy levels. The Auger effect or process by which an Auger electron is emitted from an atom occurs according to the following sequence, as noted in the figure: (1) an atom loses an atomic electron from an inner shell, leaving a hole or vacancy; (2) an electron from a higher-energy level fills the vacancy; and (3) the energy emitted in the electron transition in step (2) is transferred to an outer atomic electron, causing the electron to be emitted from the atom. The energy of the K X-ray illustrated above is equal to the electron transition ($E_{\text{x-ray}} = h\nu = E_L - E_K = -0.0057 - (-0.0404) = 0.0347$ MeV). The energy of the Auger electron is equal to the electron transition energy ($E_L - E_K$) less the binding energy of the electron (E_b) or, in other words, the X-ray energy less the binding energy of the electron ($E_{\text{Auger}} = 0.0347 - 0.0011 = 0.0336$ MeV). The daughter nucleus of the ^{139}Ce remains in an excited state after EC and emits a gamma ray (not illustrated). Also the loss of an Auger electron will leave an electron vacancy, which can be filled by an electron of an outer shell. This will produce another X-ray, which is not illustrated here. The electron filling the vacancy will, in itself leave another vacancy, which could be filled by yet another electron in an outer shell. The production of X-rays by this cascading effect of electron transitions from outer to inner shells is known as X-ray fluorescence.

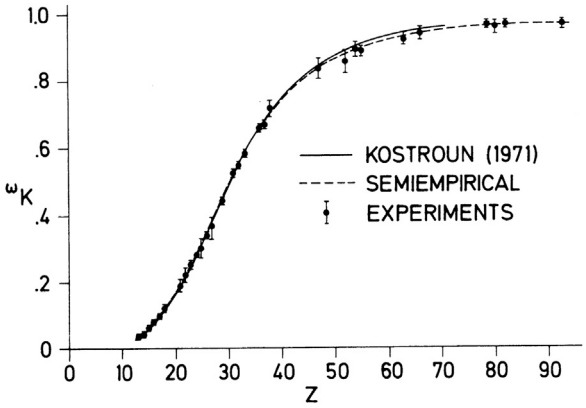

FIGURE 12.3 Fluorescence *K*-shell yields, ω_K, as a function of atomic number, *Z*: (—) according to Kostroun et al. (1971); (–) a best fit to selected experimental data; and (Ⓘ) critically evaluated experimental results. *From Bambynek, W., et al., 1972. X-ray fluorescence yields, Auger, and Coster-Kronig transition probabilities. Rev. Mod. Phys. 44, 716–813. http://dx.doi.org/10.1103/RevModPhys.44.716, reprinted with permission ©1972 by The American Physical Society.*[1]

electrons (Friedlander et al., 1964). For example, as described by Burhop and Asaad (1972), an initial vacancy in the *K*-shell may be filled either by the emission of *K* series x-radiation (fluorescence yield ω_K) or *K*-Auger electrons (Auger yield a_K), where:

$$\omega_K + a_K = 1 \qquad [12.7]$$

Fig. 12.3 illustrates the *K*-shell fluorescence yield as a function of nuclide atomic number. The *L*-shell, which consists of subshells, such as L_1, L_2, and L_3, can exhibit fluoresce yields characteristic of the subshells. The *L*-shell fluorescence yield also varies similarly with atomic number as the *K*-shell fluorescence yield, but it is several times lower in magnitude (Friedlander et al., 1964). When an Auger electron is emitted as a result of an electron transition from a higher subshell to a lower subshell of the same shell, it is referred to as a Coster–Kronig transition, which is a special type of Auger effect named in honor of Dirk Coster and Ralph Kronig from the Netherlands (Coster and Kronig, 1935). The ejected electrons in Coster–Kronig transitions are of very low energy ($\leq$1 keV), and in X-ray spectroscopy, they cause the broadening and lowering of intensities of corresponding X-ray lines.

Auger electron emission energies and intensities, including those arising from Coster–Kronig transitions, are measured and accounted for in radionuclide standardization by liquid scintillation counting (Grau Carles and Grau Malonda, 2006; Grau Malonda et al., 2006; Bé et al., 2006; Kossert and Grau Carles, 2008, 2010; Grau Carles and Kossert, 2009). As described previously both Auger and IC electron emissions possess discrete energies, and these energy lines can be envisaged by the electron emission spectra illustrated in Fig. 12.4. The emission spectrum illustrated in Fig. 12.4 provides an excellent picture of the energy magnitudes and monoenergetic character of Auger and IC electrons.

Certain radionuclides, such as ^{123}I, ^{125}I, ^{111}In, and ^{119}Sb, which decay by EC with significant intensities of Auger electron emissions, are receiving much attention for their applications in cancer therapy (Behr et al., 2000; Gao et al., 2013; Bodei et al., 2003; Capello et al., 2003; Chen et al., 2006; Constantini et al., 2007; Janson et al., 2000; Kassis, 2003; Michel et al., 2003; Thisgaard and Jensen, 2009; Zhang et al., 2014). The low energies of the Auger electrons emitted by these radionuclides, and consequently their short range in the human body, can increase the highly localized radiation-induced kill of cancer cells. The short range of travel of Auger electrons in human tissue assures maximal damage to malignant tumor cells while producing minimal harm to healthy tissue surrounding the tumor. An example can be taken from the work of Gao et al. (2013), who studied the use of ^{125}I brachytherapy to treat esophageal cancer. Brachytherapy is described in detail in chapter "Radioactivity and Our Well Being" of this book. In brief, it involves the insertion of seeds of a radionuclide into the tumor of a patient. The radioactive seeds generally measure approximately 3–4 mm in length and 1 mm in diameter. Seeds containing radioisotopes such as ^{111}In ($t_{½}$ = 2.8 days), ^{119}Sb ($t_{½}$ = 38.2 h), ^{123}I ($t_{½}$ = 13.0 h), and ^{125}I ($t_{½}$ = 60.2 days) emit Auger electrons and Coster–Kronig electrons that can kill tumor cells when sufficient doses

1. Readers may view, browse, and/or download material for temporary copying purposes only, provided these uses are for noncommercial personal purposes. Except as provided by law, this material may not be further reproduced, distributed, transmitted, modified, adapted, performed, displayed, published, or sold in whole or part, without prior written permission from the American Physical Society.

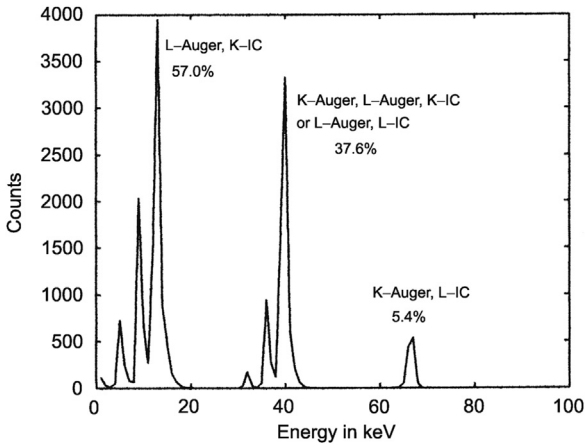

FIGURE 12.4 Simulation of the emission spectrum of Auger and internal conversion (IC) electrons of ^{125}I. The 36-keV γ-transition of ^{125}I is highly converted with a probability of 93.3%. As described by Grau Carles and Kossert (2009), three regions characterize the spectrum. The first region below 20 keV comprises about 57% of the spectral events. The peaks are created by the emission of *K*-IC electrons with about 3.7 keV, which may occur in coincidence with one or two *L*-Auger electrons stemming from the subsequent rearrangement processes of the preceding EC decay. Thus, the region shows three sharp peaks. The second region at about 40 keV contains about 37.6% of the counts. It corresponds to the coincident interaction of *K*-IC and *K*-Auger electrons or the interaction of *L*-IC electrons. *K*-Auger electrons may have energies between ∼21.8 and 31.8 keV. The energy of *L*-IC electrons is about 31 keV. Again, the emissions can be in coincidence, with one or two *L*-Auger electrons yielding the subdivision into three peaks. The third region above 60 keV contains coincidences of *L*-IC and *K*-Auger electron emissions and encompasses ∼5.4% of the total spectral events. *From Grau Carles, A., Kossert, K., 2009. Monte Carlo simulation of Auger electron spectra. Appl. Radiat. Isot. 67, 192–196, reprinted with permission from Elsevier © 2009.*

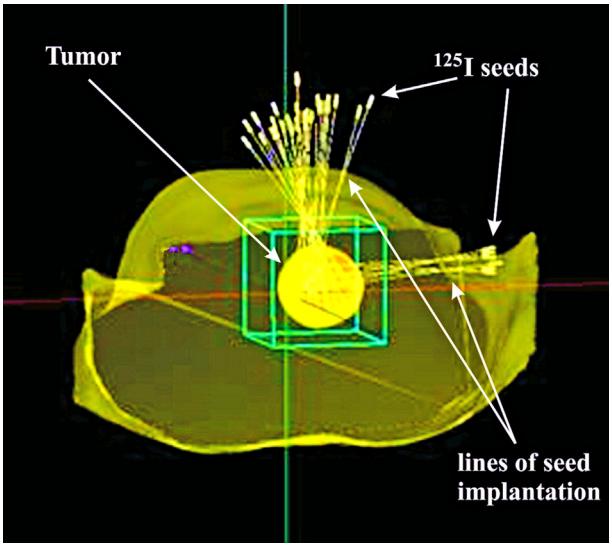

FIGURE 12.5 Preplanning of ^{125}I brachytherapy. The figure illustrates a three-dimensional image of the tumor with a computerized radioactive treatment planning system (TPS). The computerized TPS helps the physician plan the directions of insertion (illustrated as lines of seed implantation) of the radioactive seeds into the tumor of the patient. Lettering in the figure was added by the author. *From Gao, F., et al., 2013. CT-guided 125I brachytherapy for mediastinal metastatic lymph nodes recurrence from esophageal carcinoma: effectiveness and safety in 16 patients. Eur. J. Radiol. 82, e70–e75, reprinted with permission of Elsevier © 2013.*

of radiation are applied; and these electron emissions do not have sufficient energy to travel beyond the tumor, thereby protecting healthy tissue from the damaging effects of the radiation. The radioisotopes have relatively short half-lives; and the seeds can remain, without harm, in the body of the patient. Figs. 12.5 and 12.6 illustrate the implantation of seeds of ^{125}I into a tumor of a patient with esophageal cancer; and the disappearance of the tumor four months after the implantation of the ^{125}I seeds.

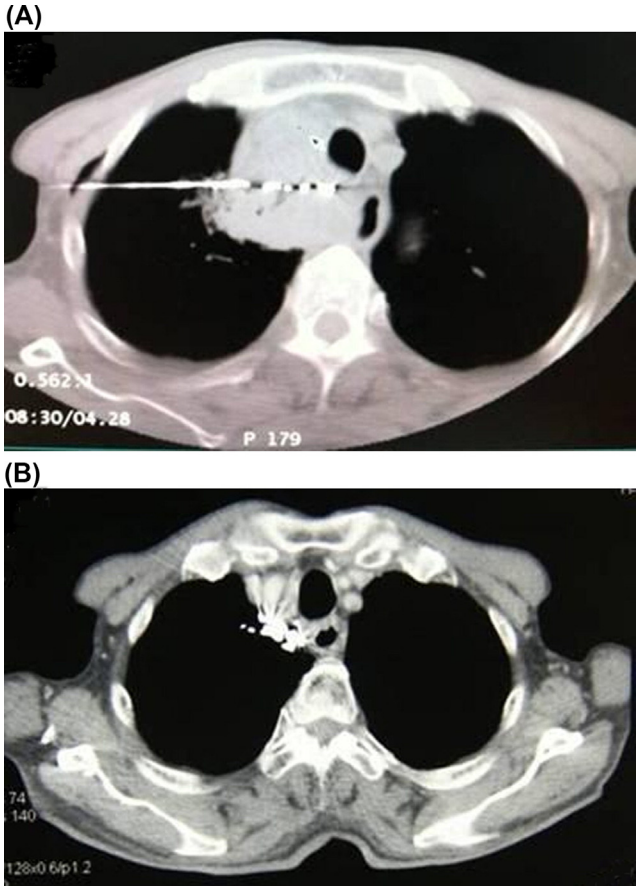

FIGURE 12.6 (A) During brachytherapy, a computed tomography scan (image slice) of the patient illustrates an applicator accurately inserted (horizontal line) into the tumor to implant ^{125}I seeds. (B) Four months after brachytherapy, a computed tomography scan shows that the tumor had disappeared, with radioactive seeds (white dots in location where round tumor had existed) remaining only. *From Gao, F., et al., 2013. CT-guided ^{125}I brachytherapy for mediastinal metastatic lymph nodes recurrence from esophageal carcinoma: effectiveness and safety in 16 patients. Eur. J. Radiol. 82, e70–e75, reprinted with permission of Elsevier © 2013.*

Another auspicious outcome of the discovery of the Auger effect is the development of Auger electron spectroscopy (AES). The technique of AES involves irradiating the surface of a sample with an electron beam of energy sufficient to ionize the inner orbitals of atoms, thereby inducing the concomitant emission of Auger electrons. The Auger electron energy spectra drawn from the induced emissions serve as fingerprints of different atoms to enable their identification and quantitative analysis (Chourasia and Chopra, 1997; Melhorn, 1998; Vandendael, 2010; and Unger and Hodoraba, 2013).

Chapter 13

Hall of Fame: Part VI

Victor F. Hess (1883−1964), Carl D. Anderson (1905−1991), Patrick M.S. Blackett (1897−1974), Hideki Yukawa (1907−1981), Cecil F. Powell (1903−1969), Emilio G. Segrè (1905−1989) and Owen Chamberlain (1920−2006), Donald A. Glaser (1926−2013), and Manuel Sandoval Vallarta (1899−1977)

In order to obtain exchange forces, we must assume that these mesons have the electric charge, and that a positive (negative) meson is emitted (absorbed) when the nucleon jumps from the proton state to the neutron state, whereas a negative (positive) meson is emitted (absorbed) when the nucleon jumps from the neutron to the proton. Thus a neutron and a proton can interact with each other by exchanging mesons just as two charged particles interact by exchanging photons.

Hideki Yukawa in his Nobel Lecture, December 12, 1949.

VICTOR F. HESS (1883−1964)

Victor Franz Hess was born on June 14, 1883 in Waldstein Castle near Peggau, approximately 75 km northwest of the city of Graz, Steiermark, Austria. He received the Nobel Prize in Physics in 1936 "for his discovery of cosmic radiation."

Victor Hess was entirely educated in Graz, attending Graz Gymnasium in 1893−1901 followed by higher education at the University of Graz, where he received a doctorate in 1910. Hess then went to the Physics Institute of the University of Vienna, located on the Turkenstrasse, where he briefly studied the science of radioactivity under the prominent physicist Professor Egon von Schweidler, who was among the first to discover late in 1899 that radiation emissions from radium and polonium could be deflected by a magnetic field. Others who made this observation independently about the same time were Friedrich Giesel of Braunschweig, Germany and Stefan Meyer of Vienna (Becquerel, 1903). Also in 1899−1900 Egon von Schweidler, Friedrich Giesel, Stefan Meyer, Henri Becquerel, and Pierre and Marie Curie had determined that beta rays from radioactive sources were fast electrons.

Victor F. Hess (1883–1964)

Radioactivity: Introduction and History, From the Quantum to Quarks. http://dx.doi.org/10.1016/B978-0-444-63489-4.00013-7
Copyright © 2016 Elsevier B.V. All rights reserved.

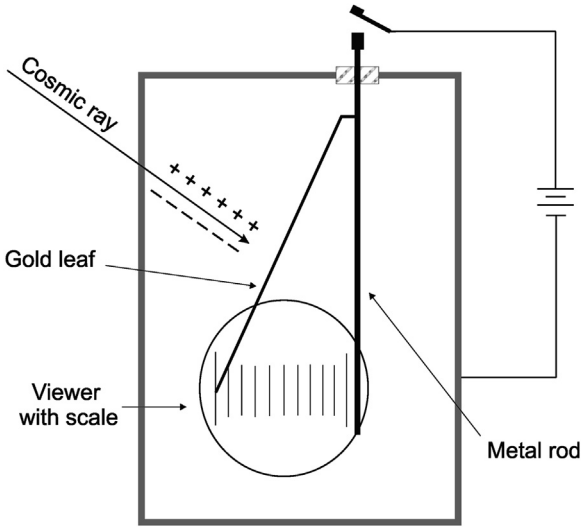

FIGURE VI.1 Schematic diagram of a gold-leaf electroscope. After charging with a battery the gold leaf moves to the left away from the metal support rod due to charge repulsion with the metal rod. When cosmic radiation enters the chamber, ion pairs are formed; and ions will discharge the gold leaf and rod so the flexible gold leaf returns toward the rod at a rate dependent on the rate of discharge. The rate of fall of the gold leaf toward the rod provides a measure of the radiation intensity.

From 1910 to 1920 Victor Hess was an assistant under Stefan Meyer at the Institute of Radium Research, during which time Hess made the pioneering observations that led to his discovery of cosmic radiation. The original building of the Institute of Radium Research, located at the intersection of Währinger Strasse and Boltzmanngasse in the ninth district of Vienna, can be visited today. It is now occupied by the Institute of Physical Chemistry, but the sign Radium Institut set in concrete can be seen above the door of the Boltzmanngasse entrance.

Around 1910 radioactivity was commonly measured with electroscopes. A schematic illustration of the basic components of a gold-leaf electroscope of the period is illustrated in Fig. VI.1. Electroscopes contained a metal rod, to one end of which was attached a thin metal foil, such as gold leaf. The metal rod and gold leaf were enclosed in an airtight chamber made of metal or glass through which one could observe the position of the gold leaf against a transparent scale placed in front of or behind the foil in the line of sight of the viewer. The metal rod, insulated from the chamber walls, was first charged with a few 100 volts from a battery, and the charged rod and gold leaf caused the foil to be repelled away from the rod, since like charges repel each other. When radiation enters the chamber, such as high-energy beta and gamma radiation or showers of cosmic rays, ionization of the air within the electroscope occurs and the ion pairs produced collect on the gold leaf and rod, causing their charge to become reduced so the gold leaf moves back toward the direction of the metal rod. The rate of fall of the gold leaf back toward the rod provides a measure of the radiation intensity. The instrument could not count the number of rays entering the chamber, but it was a very sensitive and could be calibrated with known sources to provide a measure of the number of ions collected in the chamber per unit of time. Hess (1912) calibrated his electrometers to measure the number of ions per cubic centimeter per second.

During the early 1900s high-penetrating radioactivity was detected with the electroscope in all parts of the globe, on the ground in valleys and on mountain tops, in buildings, in the air, in lake bottoms, on top of the Eiffel Tower, and even when protected with lead to shield the electroscope from known mineral sources of radioactivity. It was thought by some that the radioactivity was emanating from minerals on the Earth's surface, but it persisted at altitudes of tall buildings and structures such as the Eiffel Tower. Some thought that the radioactivity originated from sources in the air. Some scientists made balloon ascents during 1909–1911 to measure the ionization caused by this mysterious radioactivity, but their instrumentation developed defects and could not provide irrefutable evidence as to its source (Moritz, 1963).

During 1911–1913 Victor Hess made seven balloon ascents into the atmosphere up to heights of 5300 m. He carefully calibrated his instruments and took along with him three electroscopes to measure the ionization caused by the external radiation. To eliminate doubt and reduce error he thought it best to make simultaneous measurements of ionization at various heights with more than one instrument, to guard against failure or erratic readings. If the data from three instruments coincided, the results would provide the confidence needed for an interpretation. He found that at an altitude of 500 m the ionization dropped to about half that obtained on the soil surface. However, the readings increased proportionally with altitude as he ascended further. He found at 1000 m and upwards that the ionization produced by the

radioactivity noticeably increased, and further ascents to altitudes of 5000 m gave ionization readings at several times that at ground level (Hess, 1912, 1936, 1940). It was obvious to Hess that gamma rays from radium in air could not cause any increase in ionization with altitude, and he interpreted his results in the following words:

> *The only possible way to interpret my experimental findings was to conclude to the existence of a hitherto unknown and very penetrating radiation, coming mainly from above and being most probably of extra-terrestrial origin…*

This discovery by Hess opened the door to a new field of science, as underscored by Professor H. Pleijel, chair of the Nobel Committee for Physics, in his presentation speech on December 10, 1936:

> *The mystery of the origin of this radiation remained unsolved until Prof. Hess made it his problem… With superb experimental skill Hess perfected the instrumental equipment used and eliminated its sources of error. With these preparations completed, Hess made a number of balloon ascents to heights up to 5300 m, in 1911 and 1912. His systematic measurements showed that a decrease in ionization did occur up to 1000 m, but that it increased considerably thereafter… Later ascents and investigations made by successors of Hess in free balloons equipped with recording instruments showed that, at a height of 9300 m, radiation is about 40 times as intensive as on the earth's surface… From these investigations Hess drew the conclusion that there exists an extremely penetrating radiation coming from space, which enters the earth's atmosphere. This radiation, which has been found to come from all sides in space, has been called cosmic radiation… The new rays surpass in intensity and penetrating power everything previously known. They are capable of penetrating lead plates one meter thick and they have been detected on the floor of lakes with a depth of 500 m.*

In the autumn of 1931 Victor Hess set up an observatory on a 2300 m high mountain, the Hafelekar at Innsbruck, Austria, for continuous recording of fluctuations in intensity of cosmic rays. Higher mountains were available, but not accessible at all seasons of the year. Hess chose the Hafelekar, as the summit could be reached by suspended cable car from Innsbruck in 40 min all year round (Hess, 1932). He recorded a great number of results in continuous studies through all seasons, including the measurement of small, regular, daily fluctuations of radiation attributed to atmospheric influences, particularly electrical and magnetic effects in the highest layers of the atmosphere (Hess, 1939; Hess and Demmelmair, 1937; Hess et al., 1938a,b).

Following the historic discovery of cosmic radiation by Victor Hess in 1912, other researchers studied the physical properties of this penetrating radiation. One of the methods used was to observe and study the tracks of the cosmic rays by means of the Wilson cloud chamber. This led to the discovery of antimatter by Carl D. Anderson, the first observation of the positron, the positive electron, and the antiparticle of the negatively charged electron. Carl Anderson shared in the Nobel Prize Physics in 1936, and his biographical sketch and a brief description of his work are provided in the next section.

In 1919 Victor Hess was awarded the Ignaz L. Lieben Prize by the Austrian Academy of Sciences— the "Nobel Prize equivalent" established by the former Danube monarchy of old Austria, but discontinued by the National Socialists in 1938. The prize was revived in 2004 with a foundation from a US patron, Alfred Bader, chemist and founder of the chemical company Sigma-Aldrich, who had to escape the Nazi regime in Vienna in 1939 in a children's transport to England. First granted in 1862, this award was one of the most important science prizes in the history of old Austria. The new Lieben Prize is granted to young scientists from Bosnia-Herzegovina, Croatia, Slovakia, Slovenia, the Czech Republic, Hungary, and Austria for "outstanding work in the fields of molecular biology, chemistry and physics."

In 1919 Hess was named Extraordinary Professor of Experimental Physics at Graz University. In 1921−1923 he took leave of absence from his post in Austria to work in the United States as director of research at the US Radium Corporation and consultant to the US Bureau of Mines. He returned to the University of Graz in 1923, and in 1931 was appointed professor at Innsbruck University and director of its new Institute of Radiology. In 1931 Hess also established his cosmic ray observatory at the summit of Hafelekar mountain near Innsbruck.

In 1937 Hess returned to the University of Graz as professor of physics and director of the Physics Institute. However, two months after the "Anschlus," on March 13, 1938, Victor Hess was dismissed from his post because he had a Jewish wife and also was a representative of the sciences in the government of Chancellor Kurt von Schuschnigg (Moritz, 1963), who had opposed the German absorption of Austria. Schuschnigg's opposition to Hitler's occupation was successful until he lost the support of Benito Mussolini, and he was a Nazi prisoner until 1945. Fortunately a sympathetic Gestapo officer warned the Hess family that they would be taken to a concentration camp if they remained in Austria. Even a Nobel Laureate could not escape such a fate (see the biographical sketch of James Franck and his story of the pact with Niels Bohr and Max Planck to hide their gold Nobel medals from the Nazi regime in a solution of aqua regia). The Hess family escaped to Switzerland four weeks before the order came for their arrest (Moritz, 1963).

Victor Hess was appointed to a full professorship in 1938 at Fordham University in New York, and became an American citizen in 1944. At Fordham he carried out research on the measurement of environmental radioactivity, including measuring radium, artificial radioactivity in the atmosphere from nuclear testing, and the effects of radioactivity on human health. He retired from Fordham University in 1958, and died on December 17, 1964. The Victor F. Hess Prize was established in 1987 in Austria in his honor: it is awarded to PhD graduates who have produced an outstanding PhD dissertation at an Austrian university in the field of nuclear and particle physics. An excellent summary of the work and life of Victor Hess can be found in a thesis by Federmann (2003).

CARL D. ANDERSON (1905–1991)

Carl David Anderson was born in New York City on September 3, 1905. He shared the Nobel Prize in Physics in 1936 with Victor Hess. Anderson's share of the prize was awarded "for his discovery of the positron," the first experimental evidence of antimatter. He was only 31 years old at the time of the award and then the youngest person to have received the Nobel Prize. A yet younger Nobel Laureate would emerge, Tsung-Dao Lee from China, who was awarded the Nobel Prize in Physics in 1957.

Anderson's parents moved to Los Angeles from New York when he was seven, and he was educated in California. After high school in Los Angeles, he completed his undergraduate and graduate degrees at the California Institute of Technology (CalTech) in Pasadena; indeed, his entire professional career and scientific accomplishments were fulfilled at CalTech. He received his BSc degree in physics and engineering in 1927. Nobel Laureate Robert Millikan became his graduate advisor for his doctoral degree, and Anderson received a PhD in 1930 after research on photoelectrons produced by X-rays (Anderson, 1930). In his autobiography Anderson wrote concerning his PhD thesis and Millikan's involvement:

Carl D. Anderson (1905–1991)

> *"For this I thanked him, but not once during the three years of my graduate thesis work did he visit my laboratory or discuss the work with me." Then came postdoctoral work [that led to Anderson's improvement of the Wilson cloud chamber and discovery of the positron from cosmic-ray showers, and the Nobel Prize] again loosely supervised by Millikan, during which Anderson built and ran the Caltech Magnet Cloud Chamber (Weiss, 1999; Brown, 2000).*

Although such statements might seem unusual and cruel toward one's graduate advisor and a person as famous as Millikan, graduate students who are self-driven and gifted have had similar experiences at other institutions. Concerning this, William H. Pickering (1999), a former colleague of Anderson, wrote:

> *Millikan became Carl's graduate advisor. In those days graduate students had a great deal of freedom in their research. Consequently, Carl received very little direction from Millikan… In retrospect Anderson's achievement was due in part to*

R.A. Millikan's intuition that the study of cosmic rays was important and that Anderson had the experimental ability to build a superior cloud chamber. The intellectual climate at Caltech encouraged the young physicist. This was still the period when physics was being done with "love and string and sealing wax". Brilliant scientists with very little money or other support were pushing back the frontiers of physics and in the process giving us new concepts of the world. Anderson's "anti-matter" was the first step that led to the understanding of the nucleus.

After Anderson received his doctorate at the age of 25, Millikan suggested that he get a National Research Council fellowship and work at another institution to broaden his experience. He agreed and was accepted to work with A.H. Compton at Chicago, but Millikan changed his mind and convinced Anderson to stay at CalTech to work on cosmic radiation. Thus Anderson remained at CalTech as a research fellow in 1930–1933, during which time he made his historic discovery of antimatter.

To observe cosmic-ray interactions with matter, Anderson firstly made improvements on the Wilson cloud chamber detector (see C.T.R. Wilson in Hall of Fame, Part II) to provide clearer images of the tracks of elementary particles that would be produced when high-energy cosmic radiation interacted with the supersaturated vapor of the cloud chamber, and with various metals such as lead and aluminum inserted into the path of the particles. For his cloud chamber Anderson developed a vacuum-controlled piston that rapidly expanded a mixture of water and alcohol. The supersaturation produced in the cloud chamber by the water–alcohol mixture gave clearer images of the particle tracks than the pure water vapor originally used by Wilson. When a charged particle passes through the supersaturated vapor, very minute water droplets condense and become visible along the path of the ionizing particle, producing tracks like those of a jet traveling at high speed in the upper atmosphere. With proper illumination and timing, the tracks can be photographed with a conventional camera.

Anderson added a magnetic field around his cloud chamber. The magnetic field perpendicular to the path of the charged particle caused the particle path of travel to bend, and the degree of bend in the particle track produced by the magnetic field provided information as to the charge, mass, and energy of the particle. For example, when an applied magnetic field was directed normal to the path of a charged particle, the positively charged particle traveled in an upward direction and a negatively charged particle in the downward direction. The lower the mass of the particle and the lower its energy, the greater the bend or sharper the curvature of the particle path under a given magnetic field. With sufficient magnetic field strength the charged particles travel in circular paths across the magnetic field. By counting the number of droplets per unit length along the particle tracks Anderson could make measurements of the specific ionization of both positive and negative particles. The specific ionization and number of droplets formed are proportional to the particle mass and charge. Anderson was also able to determine the direction of travel of the charged particles by photographing their tracks in a cloud chamber containing lead or aluminum plates. Particles that traveled through the plates lost energy, and thus the track left by the particle after passing through the metal plate had a sharper bend under the effect of an applied magnetic field. In his Nobel lecture Anderson explained his technique:

…In the spring of 1932, a preliminary paper, on the energies of cosmic-ray particles was published [Anderson, 1932, 1933a] in which energies over 1 billion electron-volts were reported. It was here shown that particles of positive charge occurred about as abundantly as did those of negative charge, and in many cases several positive and negative particles were found to be projected simultaneously from a single center. The presence of positively charged particles and the occurrence of "showers" of several particles showed clearly that the absorption of cosmic rays in material substances is due primarily to a nuclear phenomenon of a new type.

Measurements of the specific ionization of both the positive and negative particles, by counting the number of droplets per unit length along the tracks, showed the great majority of both the positive and negative particles to possess unit electric charge. The particles of negative charge were readily interpreted as electrons, and those of positive charge were at first tentatively interpreted as protons, at that time the only known particle of unit positive charge.

If the particles of positive charge were to be ascribed to protons than those of low energy and sharp curvature in the magnetic field… should be expected to exhibit an appreciably greater ionization than the negatively charged electrons. In general, however, the positive particles seemed to differ in specific ionization only inappreciably from the negative ones… it seemed inadequate to account for the large number of particle tracks which showed a specific ionization anomalously small if they were to be ascribed to protons.

To differentiate with certainty between the particles of positive and negative charge it was necessary only to determine without ambiguity their direction of motion. To accomplish this purpose a plate of lead was inserted across a horizontal diameter of the chamber. The direction of motion of the particle could then be readily ascertained due to the lower energy and therefore the smaller radius of curvature of the particles in the magnetic field after they have traversed the plate and suffered a loss of energy.

Results were then obtained which could logically be interpreted only in terms of particles of a positive charge and a mass of the same order of magnitude as that normally possessed by the free negative electron. In particular, one photograph (see Fig. VI.2) shows a particle of positive charge traversing a 6 mm plate of lead. If electronic mass is assigned to this particle, its energy before it traverses the plate is 63 MeV and after it emerges its energy is 23 MeV. The possibility that this particle of positive charge could represent a proton is ruled out on the basis of range and curvature. A proton of the curvature shown after it emerges from the plate would have an energy of 200 keV, and according to previously well-established experimental data would have a range of only 5 mm whereas the observed range was greater than 50 mm. The only possible conclusion seemed to be that this track, was the track of a positively charge electron.

Anderson found many examples of positron tracks similar to that described above, and published his findings (Anderson 1932, 1933b). In addition, he determined the relative specific ionizations of the positive and negative electrons by counting the droplets of water vapor photographed in the particle tracks. He demonstrated that the mass and charge of the positive electron did not differ significantly from the magnitude of the mass and charge of the negative electron.

Another interesting finding first reported by Anderson and his first graduate student, Seth Neddermeyer, was that gamma rays from thorium C (ThC or ^{212}Bi) would give rise to positrons (Anderson, 1933c; Anderson and Neddermeyer, 1933). Such an observation was made independently by Irène Joliot-Curie and her husband Frédéric Joliot (1933) and Lise Meitner and K. Philipp (1933). An interesting example is that illustrated in Fig. VI.3, which shows the track of a positron emerging from a lead plate bombarded by ThC gamma rays and the passage of the positron through an aluminum plate. The charge and mass of the particle were determined by its direction of travel in a magnetic field and its specific ionization. The positron would travel in the opposite direction to that of the electron in a magnetic field normal to the path of travel, and its specific ionization would not differ greatly from that of the electron.

Occasionally Anderson and Neddermeyer observed the simultaneous appearance of two particles, both a positron and a negatron, either upon bombarding lead with ThC gamma rays or from the absorption of cosmic gamma radiation. Their photographs of the cloud chamber tracks were the first evidence of the conversion of energy into mass by the process now known as "pair production." Fig. VI.4 illustrates two examples of their cloud chamber photographs of the tracks produced by positron and negatron pairs after the absorption of cosmic gamma rays in a lead barrier.

A biographical sketch by William Pickering (1991), a colleague and coworker of Anderson in cloud chamber measurements of cosmic-ray showers (Anderson et al., 1934), noted that following his observation of the positive electron tracks in the cloud chamber photographs, Anderson consulted Robert Oppenheimer and Richard B. Feynman for their view on the phenomena of the origin and fate of the positive electron. Pickering relates:

Anderson said that he discussed the problem of the formation and disappearance of the positron with J. Robert Oppenheimer and, in retrospect, was surprised that Oppenheimer did not come up with this pair-production mechanism. He also commented that it was very difficult to understand Oppenheimer's answers to his questions. Later, when he talked with Richard P. Feynman, just the opposite was true. Feynman was clear and precise. Anderson's positron and J. Chadwick's neutron, discovered and reported in the Proceedings of the Royal Society *in 1932, were the first new fundamental particles.*

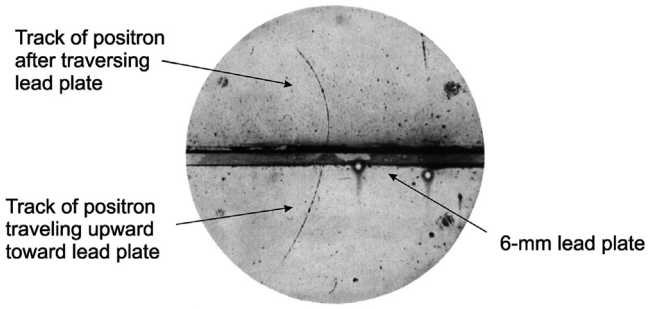

FIGURE VI.2 Historic cloud chamber photograph taken by Anderson of a track made by a 63 MeV positron that had traveled in the upward direction under the influence of a 15,000 G magnetic field in a cloud chamber. The positron emerges after traversing a lead plate with a lower energy of 23 MeV. Notice the sharper curvature of the particle track after it had lost energy in the lead plate. From the length of travel of the positively charged particle and its curvature, Anderson could conclude that the particle was not a proton, but a positively charged electron. *From Anderson, C.D., 1933b. The positive electron. Phys. Rev. 43, 491–498, http://dx.doi.org/10.1103/PhysRev.43.491, 1936, reprinted with permission by the American Physical Society © 1933 (Readers may view, browse, and/or download material for temporary copying purposes only, provided these uses are for noncommercial personal purposes. Except as provided by law, this material may not be further reproduced, distributed, transmitted, modified, adapted, performed, displayed, published, or sold in whole or part, without prior written permission from the American Physical Society.).*

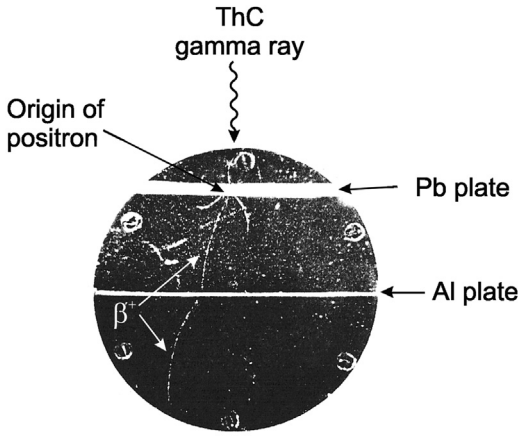

FIGURE VI.3 The cloud chamber track of a positron (β^+) originating from a 2 mm lead plate bombarded with ThC gamma rays from above. The track illustrates the path of the positron as it traveled toward a 0.5 mm aluminum plate and passed through the aluminum. Notice the slight curvature of the positron track before entering the aluminum and the sharper curvature after passing through it. The sharper curvature of the positron path in the magnetic field was due to its reduction in energy from 0.8 MeV before entering to 0.5 MeV after passing through the aluminum. *From Anderson, C.D., Neddermeyer, S.H., 1933. Positrons from gamma rays. Phys. Rev. 43, 1034–1035, http://dx.doi.org/10.1103/PhysRev.43.1034, reprinted with permission by the American Physical Society © 1933.*

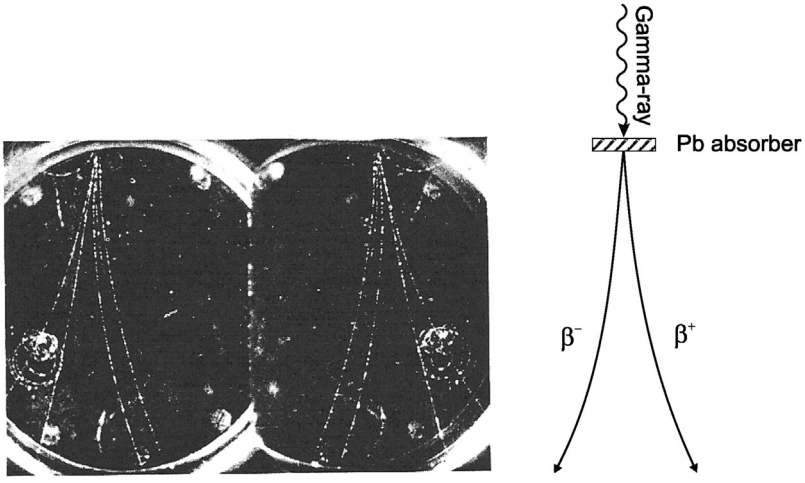

FIGURE VI.4 Photograph of cloud chamber tracks of positrons (curved tracks on the right) and negatrons (curved tracks on the left) from a common point of origin where gamma-ray photons of cosmic origin were absorbed by a lead barrier. The magnetic field was applied in the direction of the page of this book. The photograph was presented as a stereoscopic pair, and the direct image is on the left. A drawing to the right illustrates pair production; that is, the production of a negatron–positron pair from the energy of a gamma-ray photon in the region of the nucleus of an absorber material such as lead. The curved tracks illustrate the deflection of the negatron–positron pair by the magnetic field. *From Anderson, C.D., Neddermeyer, S.H., 1936. Cloud chamber observations of cosmic rays at 4300 meters elevation and near sea-level. Phys. Rev. 50, 263–271, http://dx.doi.org/10.1103/PhysRev.50.263, reprinted with permission by the American Physical Society © 1936.*

In the report of their findings, Anderson and Neddermeyer (1933) stated their observation:

> *One of the most striking phenomena, which have been observed in this experiment is the occasional simultaneous appearance of paired tracks consisting of one positive particle and one negative with a common point of origin… The process, which gives rise to the positrons is at present not known, but so far as these data go they are in accord with the view expressed by Blackett and Occhialini (1933) that the two particles may be formed by a process in which the energy of approximately 1 MeV required for the formation of a positive and negative electron is supplied by the impinging radiation.*

It was Nobel Laureate Patrick Blackett and his coworker Giuseppe P.S. Occhialini (1933) who recognized that the two particles, positron and negatron, are formed by the process known as "pair production," whereby the energy of 1.02 MeV

required for the production of the two particles is provided by the gamma radiation. In his Nobel Lecture Anderson (1936) explained the pair-production phenomenon:

> *…that the appearance of pairs of positive and negative electrons could be understood in terms of this theory [Dirac's theory] as the "creation" of a positive-negative electron pair in the neighborhood of an atomic nucleus. The energy corresponding to the proper mass of both of the particles, as well as to their kinetic energies is supplied, according to this view, by the incident radiation. Since the energy corresponding to the proper mass of a pair of electrons is approximately 1 MeV, one should expect gamma rays of energy greater than this amount to produce positrons in their passage through matter, and further that the sum of the kinetic energies of the positive and negative electrons should be equal to the energy of the radiation producing them diminished by approximately 1 MeV.*

In this statement Anderson described the process of pair production first theorized by Dirac (1928a,b), observed through cloud chamber track photographs by Anderson and Neddermeyer (1933), and interpreted by Blackett and Occhialini (1933). The gamma-ray photon energy required for pair production is, as noted by Anderson, equivalent to the sum of the masses of the electron and positron, described by the equation

$$E_{pair} = m_{e^-}c^2 + m_{e^+}c^2 = 2mc^2 = 2(0.511\ \text{MeV}) = 1.022\ \text{MeV} \qquad \text{[VI.1]}$$

The gamma-ray photon energy in excess of 1.022 MeV appears as the kinetic energy of the electron and positron created, and the overall pair-production phenomenon can be expressed as

$$h\nu = 2mc^2 + E_{e^-} + E_{e^+} \qquad \text{[VI.2]}$$

where $h\nu$ is the gamma-ray photon energy, $2mc^2$ is the equivalent energy of the mass of two electrons (ie, 1.022 MeV), and E_{e^-} and E_{e^+} are the kinetic energies of the electron and positron, respectively. By the time of Anderson's Nobel lecture in 1936, three sources of positrons were known, and he took the opportunity of his lecture to describe these: cosmic-ray showers of electron–positron pairs via pair production from cosmic gamma radiation; pair production via the absorption of gamma radiation in excess of 1 MeV from radionuclide sources; and positron emission via beta decay from radioactive elements, such as ^{30}P, ^{13}N, and ^{27}Si artificially produced by Joliot-Curie and Joliot (1934a–c), which decay by positron emission.

Subsequent studies reported in joint papers (Anderson and Neddermeyer, 1936; Neddermeyer and Anderson, 1937, 1938) provided evidence for the muon in cosmic-ray showers, a particle of "intermediate" mass; that is, of mass greater than the electron but less than the proton or neutron. They used a cloud chamber with a Geiger counter placed within it and coupled by means of a coincidence circuit to another Geiger counter placed above the cloud chamber. With such an arrangement the counters could trigger lighting and cameras, thereby increasing the probability of photographing cosmic-ray particle tracks, including images of tracks as the particles neared the end of their ranges, up to the location where they came to rest. Such images gave Anderson and Neddermeyer the mass and stability properties of the particle. The historic cloud chamber photograph illustrated in Fig. VI.5 is the first demonstrating the existence of the muon in cosmic-ray showers.

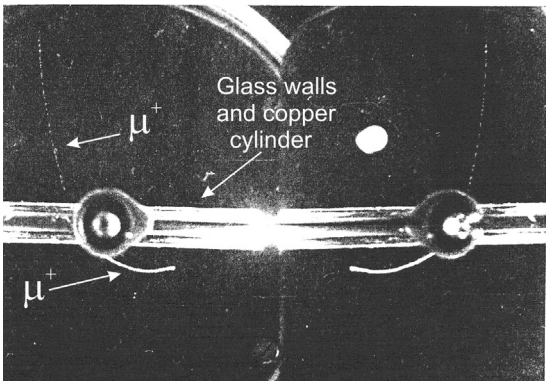

FIGURE VI.5 A track of a positive muon (μ^+) of about 10 MeV energy that had entered from above the cloud chamber and passed through the glass walls and copper cylinder of a Geiger counter in the center of the chamber. The muon track curved toward the right under the effect of a magnetic field of 7900 G. Notice the high droplet density (thickness) of the muon track after the muon emerged from the glass and copper barrier with an energy of only 0.21 MeV. The reduction in the muon's energy increased its specific ionization in the chamber. Its residual range after emerging from the barrier was 2.9 cm in the gas of the cloud chamber containing 2/3 He, 1/3 Ar, and alcohol vapor at a pressure of 1 atm, equivalent to 1.5 cm in air. The photograph was presented as a stereoscopic pair: the direct image is on the left. *From Neddermeyer, S.H., Anderson, C.D., 1938. Cosmic-ray particles of intermediate mass. Phys. Rev. 53, 88–89, http://dx.doi.org/10.1103/PhysRev.54.88.2, reprinted with permission by the American Physical Society © 1938.*

Neddermeyer and Anderson (1938) were able to calculate that the specific ionization of the particle before it traversed the glass and copper barrier was greater than that of a fast electron, and the very high specific ionization after traversing the barrier provided evidence of its intermediate mass. Data on the specific ionization and that provided on the curvature of the track before and after traversing the glass and copper barrier provided them with sufficient information to report an initial estimate of the particle mass at 240 electron masses. Their findings were subsequently confirmed by Street and Stevenson (1937). Later studies by Leighton et al. (1949) determined the muon mass to be 217 ± 4 electron masses. The muon is now classified to have a mass of 106 MeV/c^2, which is equivalent to 207 electron masses, and a lifetime of 2.2×10^{-6} s. Neddermeyer and Anderson (1938) were also able to provide initial information concerning the decay scheme of the muon from its track, illustrated in Fig. VI.5. In their paper they noted:

> *An interesting feature of the photograph is the fact that the particle is actually observed to come to rest in the gas of the chamber. No completely certain evidence of a subsequent disintegration can be found on the photograph. There are, however, three droplets which appear on the left-hand image, which is the direct view, and also on the right-hand mirror image. Stereoscopic observation shows that these droplets line up so as to indicate a short segment of an electron track emanating from the point in the gas at which the particle came to rest and directed toward the counter… These droplets may therefore indicate that the particle, after coming to rest, disintegrated by the emission of a positive electron.*

Their deductions from the early observations made in this historic photograph have proven to be true. The positive muon (μ^+) is known to decay to a positive electron (e^+) and a muon neutrino (ν_μ), and the negative muon (μ^-) decays to a negative electron (e^-) and anti-muon neutrino ($\overline{\nu}_\mu$), illustrated by the following equation:

$$\mu^{+/-} \rightarrow e^{+/-} + \nu_\mu + \overline{\nu}_\mu \qquad \text{[VI.3]}$$

Anderson became assistant professor at CalTech in 1933, the very year he made the discovery of antimatter that brought him the Nobel Prize three years later at the young age of 31. He did not become full professor until 1939. It is difficult to understand why CalTech denied Anderson the title of professor of physics until three years after his award of the Nobel Prize. Possibly he was simply too young, with insufficient experience as assistant professor. To have made a major discovery from work carried out during 1930–1933 as a research fellow when he was only 25–28 years of age, with the Nobel Prize awarded only a couple of months after his 31st birthday, was astounding. One can only surmise that the administration at CalTech did not award him the professorship until 1936 because of his youth.

In his autobiography, edited by Weiss (1999), Anderson revealed that in May 1942 Arthur H. Compton had asked him "to head a project to design and build an atomic bomb," but Anderson turned down the offer simply "on economic grounds." General Leslie R. Groves offered the job to J. Robert Oppenheimer five months later on October 15, 1942. In his autobiography Anderson wrote:

> *I believe my greatest contribution to the World War II effort was my inability to take part in the development of the atomic bomb. Thinking so brings me peace of mind.*

However, Anderson did contribute significantly to the war effort. During World War II he took part in the research at CalTech on the development of rocket launchers. Anderson's main responsibility was to help develop rocket launchers from aircraft that could be used against submarines detected by magnetic sensors. Rockets and launchers were also developed to be used from ships to facilitate Pacific island landings. Pickering (1991) noted that Anderson traveled to the Normandy beachhead in 1944 to observe the CalTech rockets under battlefield conditions. His student Seth Neddermeyer received his PhD at CalTech in 1935, then joined the staff at the University of Washington. Neddermeyer was later recruited into the Manhattan Project at Los Alamos and was one of the originators of the implosion technology for the atomic bomb. Rhodes (1986) wrote of Neddermeyer's involvement in the bomb development: "His idea of using explosives to squeeze a nuclear core to criticality saved the plutonium bomb when impurities threatened its design."

High-energy cosmic-ray nucleons collide with nuclei of the atmosphere, smashing the nuclei into subatomic particles and creating the cosmic-ray showers described in the chapter entitled "Cosmic Radiation." After the war Anderson continued his research on cosmic-ray showers at CalTech. He flew in B-29 bomber airplanes equipped with cloud chambers to study the cosmic-ray showers with support of the Office of Naval Research. On one of these flights, at 9300 m altitude, he obtained a cloud chamber photograph of a muon and its disintegration (Anderson et al., 1947). He and coworkers reported the decay of the positive muon to a positron. The muon neutrino obviously could not be detected in the cloud chamber.

$$\mu^+ \rightarrow e^+ + \nu_\mu \qquad \text{[VI.4]}$$

The muon came to rest in the cloud chamber, and the positron made a track at a 90 degree angle with respect to the disintegrating muon. The mass of the muon can be determined from the track left by the particle in the cloud chamber image based on the parameters of particle range, specific ionization, and track curvature in the magnetic field. On the basis

of the data obtained, they measured the muon mass at 200 electron masses, which is very close to the currently known mass of the muon at 207 electron masses. A subsequent study carried out by Anderson and coworkers (Leighton et al., 1949) at CalTech involved the analysis of 75 cloud chamber tracks of decaying cosmic-ray muons at sea level. Again the cloud chamber was subjected to a magnetic field (7250 G) to permit the charge determination of the particles and measurements of the track curvatures. From the numerous tracks analyzed, they observed a cosmic-ray muon spectrum over the range of 9–55 MeV, with a continuous distribution of intermediate energy values and a mean energy of 34 MeV.

Further studies by Anderson and coworkers focused on cloud chamber measurements of *V* particle decay in cosmic-ray showers (Leighton et al., 1953). *V* particles got their name from the V-shaped tracks they formed from a given point in cloud chambers. These were produced by the decay of neutral kaons (K^0) or charged kaons ($K^{\pm}$), also called *K* mesons. The neutral kaon exists in a short-lived $\left(K_S^0\right)$ or long-lived $\left(K_L^0\right)$ state with relative lifetimes of 0.9×10^{-10} s and 5×10^{-8} s, and the mass of the neutral kaon is 498 MeV/c^2. The charged kaons ($K^{\pm}$) have a lifetime of 1.2×10^{-8} s and mass of 494 MeV/c^2. The predominant decay modes of the charged kaons are the following (Sundareson, 2001):

$$K^{\pm} \rightarrow \mu^{\pm} + \nu_{\mu}\ (63\%) \qquad \text{[VI.5]}$$

$$K^{\pm} \rightarrow \pi^{\pm} + \pi^0\ (21\%) \qquad \text{[VI.6]}$$

$$K^{\pm} \rightarrow \pi^{\pm} + \pi^{+} + \pi^{-}\ (5.5\%) \qquad \text{[VI.7]}$$

$$K^{\pm} \rightarrow \pi^0 + e^{\pm} + \nu_e\ (5\%) \qquad \text{[VI.8]}$$

$$K^{\pm} \rightarrow \pi^0 + \mu^{\pm} + \nu_{\mu}\ (3\%) \qquad \text{[VI.9]}$$

$$K^{\pm} \rightarrow \pi^{\pm} + \pi^0 + \pi^0\ (2\%) \qquad \text{[VI.10]}$$

Other modes of decay of the charged kaon exist with abundances of less that 1%. The first-order neutral kaon modes of decay are

$$K^0 \rightarrow \pi^{+} + \pi^{-}\ (88\%) \qquad \text{[VI.11]}$$

and

$$K^0 \rightarrow \pi^0 + \pi^0\ (12\%) \qquad \text{[VI.12]}$$

The *V* particles, or particles that yield V-shaped tracks, were discovered by George D. Rochester and Clifford Charles Butler (Rochester and Butler, 1947) at the University of Manchester, England. They result from the decay of the neutral kaon, which has a mass of about 490 MeV/c^2. The neutral kaon cannot produce a track in the cloud chamber due to its lack of charge; however, its decay into positive and negative pi-mesons (pions) according to Eq. [VI.11] yields two tracks in a cloud chamber subjected to a magnetic field. The two tracks take the shape of a V due to the opposing pion paths and lack of track from an incoming neutral kaon. Fig. VI.6 illustrates a cloud chamber photograph of the tracks left by a neutral *V* particle (ie, neutral kaon, K^0). Notice that the V-shaped tracks appear in the left-center of the lower chamber of the

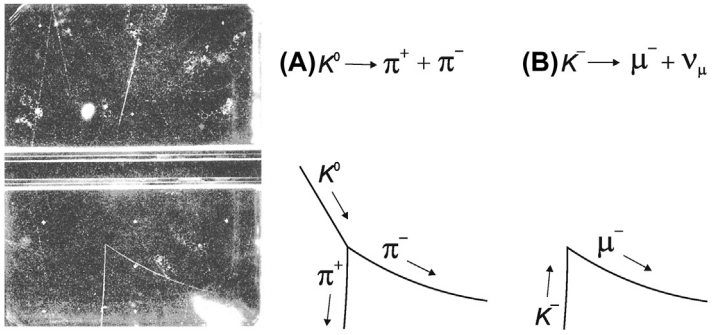

FIGURE VI.6 A cloud chamber photograph of the tracks of a probable *V* particle in a magnetic field of 5000 G. The cloud chamber consists of upper and lower chambers separated by the glass walls and copper tubing of a central Geiger counter. The V-shaped track appears left-center in the lower chamber. The V-shaped track was the result of one of two possible modes of kaon decay, namely a neutral kaon (K^0) decaying into positive and negative pions where the neutral kaon does not leave a track because of its lack of charge, or a negative kaon (K^-) entering the cloud chamber from below and decaying into a negative muon and neutrino. The neutrino obviously does not leave a track. *Cloud chamber photograph from Anderson and coworkers (Leighton, R.B., et al., 1953. The decay of* V^0 *particles. Phys. Rev. 89, 148–177, http://dx.doi.org/10.1103/PhysRev.89.148), reprinted with permission by the American Physical Society © 1953.*

apparatus. No track is left by the incoming particle, because it has no charge. Alternatively Anderson and coworkers (Leighton et al., 1953) proposed that the V-shaped track illustrated in Fig. VI.6 could also be due to a negative kaon decaying to a negative muon according to Eq. [VI.5].

Carl Anderson spent his entire professional career at CalTech. He served as professor there until 1976 at the age of 71, and died on January 11, 1991.

PATRICK M.S. BLACKETT (1897–1974)

Patrick Maynard Stuart Blackett was born in London, England on November 18, 1897. He was awarded the Nobel Prize in Physics in 1948 "for his development of the Wilson cloud chamber method, and his discoveries therewith in the fields of nuclear physics and cosmic radiation."

Patrick Blackett (1897–1974)

Blackett started his career as a naval cadet in 1914, taking part in the World War I naval battles of the Falkland Islands in December 1914 and Jutland in May 1916. He graduated from Osborne Naval College in 1917. After the war he studied physics at Cambridge University, England, and after graduation in 1921 began research on cloud chambers under Lord Rutherford at his Cambridge laboratory. Blackett first improved the Wilson cloud chamber by making it fully automatic, in the sense that a photograph of the illuminated tracks left by the elementary particles would be taken every 15 s (Blackett, 1922, 1927, 1929). His first challenge under Rutherford was to use the cloud chamber to photograph the process of transmutation of nitrogen into oxygen following the collision of an alpha particle with nitrogen. In 1919 Rutherford had made the discovery that nuclei of certain light elements, such as nitrogen, could be changed to another element by the impact of very fast alpha particles from radioactive sources, and in the process fast protons were emitted. Rutherford could not provide experimental evidence for the process of transmutation at the time of his discovery, and it was the next step to use the Wilson cloud chamber to see and measure, through photographic images of the particle tracks, what nuclear processes were occurring.

Patrick Blackett was meticulous in his approach to the use of the cloud chamber to observe and study nuclear transmutation. He first used the chamber to photograph and measure the collisions of alpha particles with nuclei of oxygen, hydrogen, and helium atoms to verify that normal collisions, where transmutations did not occur, were truly elastic collisions—that is, collisions where no energy was lost in the process. From the photographs of the nuclear tracks, Blackett measured the angles between the track of the α particle before collision and the tracks of both the deflected α particle and recoil atom after the collision, denoted as ϕ and θ, respectively, in Fig. VI.7. Notice that in Fig. VI.7B the α particle undergoes only a slight deflection (small ϕ), and continues to travel in almost a straight path after collision with hydrogen atoms because of the large difference in mass between the He and H nuclei.

Blackett (1923, 1948a) and coworkers (Blackett and Champion, 1931; Blackett and Hudson, 1927; Blackett and Lees, 1932b,c) based their study on the fact that, for truly elastic collisions, energy and momentum are conserved, and the angles

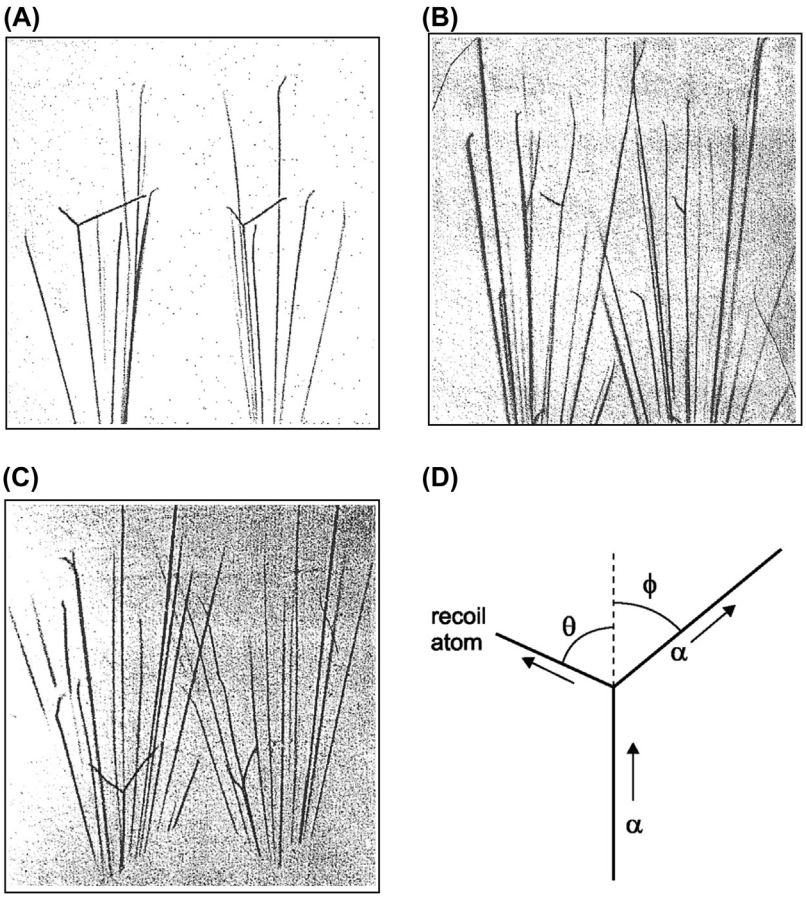

FIGURE VI.7 Cloud chamber tracks illustrating elastic collisions of alpha particle with (A) oxygen nucleus, (B) hydrogen nucleus, and (C) helium nucleus; and (D) a drawing of the geometry of the collisions. Only a few collisions are observed in the photographic images. *From Blackett, P.M.S., 1923. The study of forked α-ray tracks. Proc. Roy. Soc. London 103A, 62–80; Blackett, P.M.S., 1948a. Cloud chamber researches in nuclear physics and cosmic radiation. Nobel Lecture on December 13, 1948. In: Nobel Foundation Staff, (Eds.), Nobel Lectures, Physics, 1942–62, (1964). Elsevier Publishing, Amsterdam, reproduced with permission of the Royal Society.*

of atom recoil and α particle deflection would be a function of the mass of the α particle (M) and the mass of the recoil atom (m), according to the following equation:

$$\frac{M}{m} = \frac{\sin(2\theta + \phi)}{\sin \phi} \qquad \text{[VI.13]}$$

By measuring the angles of α particle deflection and atomic recoil, Blackett calculated the mass (m) of the recoil atom for each of the three types of collisions illustrated in Fig. VI.7, and compared the calculated values with the known atomic masses. Table VI.1 gives the measured angles of α particle deflection and atomic recoil, and calculated and known values of atomic mass. The very close agreement between the calculated and known masses of the recoil atoms demonstrated to Blackett that the collisions were not nuclear transmutations and were truly elastic collisions. This study on the forked tracks was one of the first quantitative measurements ever conducted on the dynamics of single collisions of subatomic particles.

As the next step in his quest to identify and measure nuclear transmutation via α particle collision Blackett (1922, 1923, 1925) and Blackett and Lees (1932a,b) conducted detailed studies of the relationship between the range of a recoil nucleus and its velocity. He determined the velocities of the recoil nuclei from the angles of the collision and the initial and final velocity of the α particle on the basis that the collisions were elastic. Studies on the bombardment of hydrogen, helium, nitrogen, and argon with α particles provided Blackett with the following formula for the range in air of a nucleus of mass m and atomic number Z:

$$R \approx mz^{-1/2} f(u) \qquad \text{[VI.14]}$$

TABLE VI.1 Measurements of Collisions of α Particles With Nuclei of Oxygen, Hydrogen, and Helium, and the Calculated Atomic Mass (m) of the Recoil Atoms

Recoil Atom	α Particle Deflection (ϕ)	Angle of Recoil (θ)	m (Calculated)	m (Known)
Oxygen	76°6′	45°12′	16.72	16.00
Hydrogen	9°21′	65°39′	1.024	1.008
Helium	45°49′	43°56′	4.032	4.00

From Blackett, P.M.S., 1923. The study of forked α-ray tracks. Proc. Roy. Soc. London 103A, 62–80; Blackett, P.M.S., 1948a. Cloud chamber researches in nuclear physics and cosmic radiation. Nobel Lecture on December 13, 1948. In: Nobel Foundation Staff, (Eds.), Nobel Lectures, Physics, 1942–62, (1964). Elsevier Publishing, Amsterdam, reprinted with permission from the Royal Society.

where $f(u)$ was roughly proportional to $v^{3/2}$. He needed the range measurements to facilitate identification of the recoil particles emerging from collision that were "abnormal" or inelastic.

In 1924 Blackett took 23,000 photographs of α particle collisions with nitrogen over a period of a few months. Each photograph had an average of 18 tracks, yielding in total over 400,000 tracks that had to be scrutinized for anomalous behavior which might show a nuclear transmutation. He found eight forked tracks which were different than the usual tracks of normal elastic collisions. These photographs were of the interaction of the α particle with the nitrogen nucleus, resulting in the transmutation of the nucleus to that of oxygen after the emission of a proton from the nucleus. One of these photographs is seen in Fig. VI.8. Blackett (1925) and Blackett and Lees (1932a) provided evidence that the transmutation

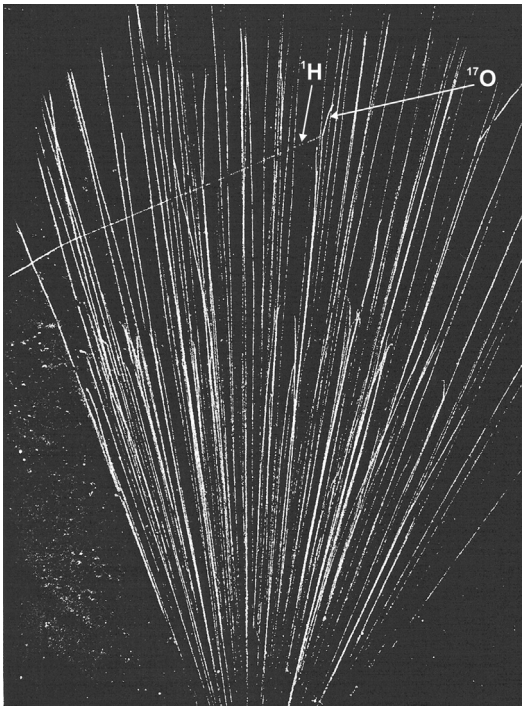

FIGURE VI.8 Alpha particle tracks, including one alpha particle collision with a nucleus of nitrogen resulting in the transmutation of the nucleus of a nitrogen atom into a nucleus of an oxygen atom. The photograph illustrates the capture of an alpha particle by a nitrogen nucleus with the emission of a proton (^{1}H). The thin beaded track toward the left and slightly backward is that of the ejected proton. The oxygen nucleus (^{17}O) created from a nucleus of nitrogen (^{14}N) made a short, thick track upward and slightly to the right of the alpha particle trajectory. Blackett (1925) noted that the beaded appearance of the proton tracks was evidence of the small ionization along them, since the ionization due to any particle is proportional to the square of its charge and the reciprocal of its velocity. The source of alpha particles was a mixture of thorium B + C, more commonly referred to as ^{212}Pb(^{212}Bi). The alpha particle tracks ending in the middle of the photograph were from the lower-energy alpha particles of the ^{212}Bi source. Notations and arrows are inserted into the original figure to facilitate identification of the tracks produced by the products of the nuclear transmutation. *From Blackett, P.M.S., Lees, D.S., 1932a. Investigations with a Wilson Chamber. I. On the photography of artificial disintegration collisions. Proc. Roy. Soc. London 136A, 325–338; Blackett, P.M.S., 1948a. Cloud chamber researches in nuclear physics and cosmic radiation. Nobel Lecture on December 13, 1948. In: Nobel Foundation Staff, (Eds.), Nobel Lectures, Physics, 1942–62, (1964), Elsevier Publishing, Amsterdam, reproduced with permission from the Royal Society.*

included the capture of the α particle by a nucleus of nitrogen with the concomitant emission of a proton from the new and larger nucleus. In his Nobel lecture Blackett (1948a) described the evidence from the photographs of the particle tracks and his reasoning:

Rutherford's original experiments, using the scintillation technique, were only capable of proving that when an alpha particle struck a nitrogen nucleus a fast proton occasionally was ejected, but they were not able to reveal what happened to the alpha particle after the collision. There were two possibilities. The alpha particle might leave the nucleus again as a free particle, or it might be captured, so forming a heavier nucleus. In the former case, one would expect to find a forked track showing the track of the incident alpha particle, with three emergent tracks due to the alpha particle, the ejected proton, and the recoil nucleus. The eight anomalous tracks all showed only two emergent particles, so proving that the assumed "disintegration" of nitrogen by alpha particles was in reality an "integration" process. Applying the principle of conservation of charge and mass, it was immediately deduced that the new nucleus formed must be a heavy isotope of oxygen $^{17}_{8}O$*; the nuclear reaction being*

$$^{4}_{2}\mathrm{He} + {}^{14}_{7}\mathrm{N} \rightarrow {}^{1}_{1}\mathrm{H} + {}^{17}_{8}\mathrm{O} \qquad \text{[VI.15]}$$

…These experiments gave for the first time detailed knowledge of what is now known to be a typical nuclear transformation process. Owing to the laborious nature of the task of photographing the collisions of natural alpha particles with nuclei, not very much subsequent work has been carried out with this method.

During 1924−1925 Patrick Blackett worked at the University of Göttingen with Nobel Laureate James Franck, and then returned to Cambridge. In autumn 1931 he began a collaboration with Giuseppe Occhialini to study the high-energy particles in cosmic radiation with the cloud chamber as the tool for the identification and measurement of the cosmic-ray particle interactions with atomic nuclei. Guiseppe "Beppo" Occhialini was a renowned physicist, born in Pesaro, Italy in 1907. He collaborated successfully with Patrick Blackett from 1931 to 1934 and with Nobel Laureate Cecil Powell from 1944 to 1947. Italian physicist Bruno Pontecorvo (1913−1993) once praised Occhialini when he toasted:

I drink not to Beppo, but to us all: may we collaborate with him, it is a practically sure way of winning a Nobel Prize.

Giuseppe "Beppo" Occhialini (left) and Patrick Blackett (right) From Amaldi Archives, Departimento di Fisica, Universita 'la Sapienza', Rome Courtesy of the AIP Emilio Segre Visual Archives

Early work with the use of the cloud chamber to photograph tracks of cosmic-ray particles was very tedious, as at the instant of expanding the chamber and taking the photograph it was not known whether or not one or more cosmic-ray particles or interactions would be occurring in the chamber. Hundreds, sometimes thousands, of photographs had to be

taken in the hope of photographing tracks of cosmic-ray particles and the cosmic-ray showers—that is, the particles resulting from the collision of high-energy cosmic-ray particles with atomic nuclei in the atmosphere.

Blackett and Occhialini (1932, 1933) made a great leap in the study of cosmic radiation by developing the counter-controlled cloud chamber. The apparatus utilized the coincidence circuitry developed by Nobel Laureate Walther Bothe in collaboration with Hans Geiger and Bruno Rossi at the Physikalisch-Technische Reichsanstalt in Berlin-Charlottenburg, Germany (Bothe, 1926, 1954). A coincidence circuit is an electronic device that analyzes the outputs of two or more radiation detectors, and when the electronic signals from the detectors are received by the coincidence circuit within a specified period of time (generally within a few microseconds), known as the coincidence time or coincidence window, the signal is accepted. If, for example, a cosmic-ray particle passes through two detectors, for example two Geiger–Müller counters, each of the detectors will produce an output signal simultaneously. The signal from each detector will pass the coincidence circuit, and the output signal from the coincidence circuit can be used to trigger any device, such as a radiation counter or a cloud chamber and its camera. Any signal received from only one of the detectors generally would be rejected by the coincidence circuit, because two signals from the two detectors would need to occur in coincidence within the very short time window of a few microseconds. A coincidence circuit was employed to trigger the detection of a cosmic-ray particle and the simultaneous expansion and photography of its track. An example of a coincidence circuit linked to a cloud chamber and camera is illustrated in Fig. VI.9.

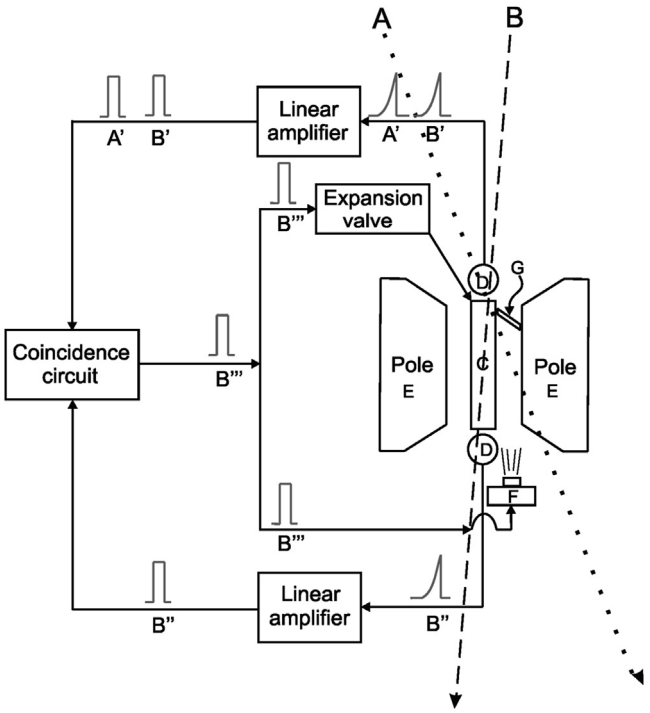

FIGURE VI.9 A schematic illustration of a counter-controlled cloud chamber apparatus. Two cosmic rays (A and B) are traveling through the apparatus from top to bottom. The heart of the apparatus is the cloud chamber (C), which is in the vertical position. A typical cloud chamber would measure approximately 17 cm in diameter and 3 cm in depth fully expanded. Above and below the chamber are Geiger–Müller counters (D), illustrated as circular tubes. The poles of an electromagnet (E) are facing the cloud chamber. Cosmic ray A is illustrated as passing through the Geiger–Müller counter above the cloud chamber and through the right-hand corner of the chamber. Cosmic ray A produces ionization in the Geiger–Müller counter resulting in an electric pulse A′, shown as a tail pulse traveling in the direction of the linear amplifier. Cosmic ray B travels through both Geiger–Müller counters and directly through the cloud chamber. The cosmic ray is detected by both Geiger–Müller counters producing electric tail pulses B′ and B″, illustrated traveling simultaneously toward the two linear amplifiers. The pulses are shaped after passing the linear amplifier. Pulse A′ is rejected by the coincidence circuit, because it was not received as two pulses arriving simultaneously at the circuit with a preset resolving time (window) of generally a few microseconds. Pulses B′ and B″, which arrive simultaneously at the coincidence circuit, are accepted; and the output of the coincidence circuit is a single pulse B‴. This pulse, resulting from cosmic ray B, travels simultaneously to an expansion valve to trigger the cloud chamber expansion and to a camera (F) to trigger its shutter and the illumination needed to photograph the tracks in the chamber. A mirror (G) located between the horizontal face of the cloud chamber and a pole of the magnet reflects the image of the cosmic-ray tracks in the direction of the camera lens.

The significance of the development of the counter-controlled cloud chamber was underscored by Blackett in his Nobel lecture (1948):

The method used, that of making an expansion of a cloud chamber at a random time and taking the chance that one of the rare cosmic rays would cross the chamber during the time of sensitivity—generally less than ¼ second—was much consuming of time and photographic film, since in a small chamber only some 2–5% of photographs showed cosmic-ray tracks.

Occhialini and I set about, therefore, the devising of a method of making cosmic rays take their own photographs, using the recently developed "Geiger-Müller counters" as detectors of the rays. [Walter] Bothe and [Bruno] Rossi had shown that two Geiger counters placed near each other gave a considerable number of simultaneous discharges, called coincidences, which indicated in general the passage of a single cosmic ray through both counters. Rossi devised a neat valve circuit by which such coincidences could easily be recorded.

Occhialini and I decided to place Geiger counters above and below a vertical cloud chamber, so that any ray passing through the two counters would also pass through the chamber. By a relay mechanism, the electric impulse from the coincident discharge of the counter was made to actuate the expansion of the cloud chamber, which was made so rapid that the ions produced by the ray had no time to diffuse much before the expansion was complete. Having made the apparatus ready, one waited for a cosmic ray to arrive and take its own photograph. Instead of a small fraction of photographs showing a cosmic ray track, as when using the method of random expansion, the counter-controlled chamber yielded a cosmic-ray track on 80% of the photographs.

A detailed description of the design and technique of the counter-controlled cloud chamber is given by Blackett (1934). The expansion of the cloud chamber would take only approximately 0.005 s to travel its full movement of 1 cm. Expansion was required to get the supersaturation of the water or alcohol in air to yield visible tracks by the collection of droplets along the paths left by the cosmic-ray particles. About 1/100 s after the cloud chamber expansion, the camera and illumination flash would be triggered. The flash would last 1/30 s. Initial magnetic field strengths of 3000 G were used, but high-energy cosmic rays would maintain straight paths. The magnetic field strengths were increased to 14,000 G to produce a curvature and direction to the paths of the charged particles, facilitating the identification of their mass, charge, and energy (Blackett, 1936; Blackett and Brode, 1936).

With the newly developed counter-controlled cloud chamber, Blackett confirmed Anderson's discovery of the positive electron, and demonstrated the existence of the cascading effect of the collisions of cosmic rays with atomic nuclei of the atmosphere producing a multitude of charged particles, which were named "cosmic-ray showers." In his Nobel lecture, Blackett explained:

During the late autumn of 1932, Occhialini and I, using our new counter-controlled cloud method, accumulated some 700 photographs of cosmic rays, among which grouped or associated rays were so striking a feature as to constitute a new phenomenon and to deserve a name. From their appearance they came to be known as "showers" of cosmic-ray particles.

Often half the rays in the cosmic-ray showers were positively charged and the other half negatively charged, particularly when the cosmic radiation passed through a high atomic number absorber such as a barrier of lead placed in the outer perimeter of the cloud chamber. Blackett also observed that the mass of the positively charged particles was close to the mass of the electron as determined by their range and specific ionization in the cloud chamber. Patrick Blackett was the first to conclude that these positive and negative electrons were due to the phenomenon of "pair production" theorized by Dirac. In his Nobel lecture Blackett (1948a) reflected on his finding:

So not only was Anderson's discovery of the positive electron further confirmed by a wealth of evidence, but it was proved that the newly discovered particles occurred mainly in showers along with approximately an equal number of negative electrons. This fact of the rough equality of numbers of positive and negative electrons, and the certainty that the former do not exist as a normal constituent of matter on earth, led us inevitably to conclude that the positive electrons were born together in collision processes initiated by high-energy cosmic rays. The energy required to produce such a pair is found from Einstein's famous equation to be $2mc^2 \cong 1$ *MeV. So was demonstrated experimentally for the first time the transformation of radiation into matter.*

Blackett explained that the abundant cosmic gamma radiation is converted in large part to positron–electron pairs in the cosmic-ray showers of our atmosphere via pair production, and thus finally the positron or antimatter of the electron, which was only previously theorized by Dirac to exist, was now a known entity. The equations describing pair production and the derivation of the energy required for it to occur (a minimum gamma-ray energy of 1.02 MeV) are given in Eqs. [VI.1] and [VI.2] of the previous biographical sketch on Carl Anderson and in Eqs. [8.40]–[8.42] of the chapter

entitled "Electromagnetic Radiation: Photons." In his Nobel lecture Blackett went further by explaining for the first time his observation of the phenomenon called "annihilation," where matter is changed into electromagnetic gamma radiation. He explained his historic observations:

> *Dirac's theory predicted that a positive electron would disappear by uniting with a negative electron to form one or more quanta. Occhialini and I suggested that the anomalous absorption of hard gamma rays by nuclei might be the result of the process of pair production, and that the observed re-emission of softer radiation might represent the emission of two 0.5 MeV quanta resulting from the annihilation of a positive and negative electron. Subsequent work has confirmed this suggestion.*

From Einstein's equation $E = mc^2$, Blackett knew that the energy equivalent of the mass of an electron was 0.51 MeV (see Eqs. [8.40]–[8.42] and subsequent calculations in the chapter entitled "Electromagnetic Radiation: Photons" for computation of the conversion of the electron rest mass of 9.109×10^{-31} kg to its energy equivalent of 0.51 MeV). Since the positron and electron are of the same mass, but opposite in charge, they each possess the energy equivalence of 0.51 MeV, and when the positive electron comes to rest, it encounters an electron and becomes annihilated, with the liberation of two quanta of 0.51 MeV gamma radiation or

$$e^+ + e^- = 2h\nu = 2(0.51\ \text{MeV}) \qquad \text{[VI.17]}$$

The two 0.51 MeV gamma rays from positron–electron annihilation are emitted in opposite directions.

By 1933 Blackett had made these major discoveries, for which he was awarded the Nobel Prize. He became professor at Birkbeck College, London in 1933, where he continued his research on cosmic radiation. In 1937 he succeeded Sir Lawrence Bragg at Manchester University in the post previously held by Ernest Rutherford, and here Blackett established his school of cosmic-ray research.

During World War II Blackett helped establish a research effort to combat U-boats, and became Director of Naval Operational Research at the Admiralty. He also worked on antiaircraft defense of England during the blitz. Mary Jo Nye (2004) writes in a biography on Blackett:

> *Outside physics, Blackett was well known for his role in developing the scientific field of operational research, and he is regarded as the "father" of operational research following his critical role on its diffusion throughout the British military command structure in World War II (Kirby, 2003). Although he had been a youthful naval officer in the First World War, he became a hero in the Second World War, credited with determining operational strategies for the antisubmarine campaign that turned the tide of the European war by late 1943.*

After the war, in 1945 Blackett resumed his research on cosmic radiation at the University of Manchester. In his Manchester laboratory George Rochester and Clifford Butler (1947) discovered the neutral kaon in the cosmic-ray showers. The particle has a mass of about 490 MeV/c^2, and is a product of collision of a high-energy cosmic-ray particle with an atomic nucleus in the atmosphere. Cosmic radiation was the natural atom-smasher and creator of subatomic particles in the cosmic-ray showers. The kaon is discussed in more detail in the previous biographical sketch of Carl Anderson.

It is not unusual in scientific research for discoveries to be made independently and almost simultaneously, within weeks of each other, by two research groups at opposite sides of the globe. When the time is right in science and the stage is set with previous discoveries, new findings will be made. Such was the case of Clinton Davission in the United States and George Paget Thomson in England; both had discovered experimentally the diffraction of electrons; both published their findings in the same volume of the journal *Nature* in 1927; and both shared in the Nobel Prize for their discovery. Fate is not always so rewarding. In the case of the positron, Carl Anderson was first to report the discovery in late 1932 and was thus rewarded the Nobel Prize for revealing this elementary particle. Some controversy arose in the British press over this, as Patrick Blackett and Guiseppe Occhialini waited until February 1933 to publish the discovery. In an essay McLean (2002) writes about Blackett:

> *In late 1932, Carl D. Anderson at Caltech published an observation of a positively charged particle, with mass smaller than a proton, in cosmic radiation… he initially characterized its production as a rare event. By February 1933, Blackett and Occhialini had completed a paper summarizing their analysis of some 500 tracks of cosmic-ray particles, of which 14 tracks were evidence of the anti-electron or positive electron, which they explicitly linked to Dirac's relativistic electron theory. Some physicists thought it unfortunate that Blackett and Occhialini appeared to have delayed publication, in order to get firmer data on the positive electron within the framework of Dirac's theory, so that it was Anderson who received the Nobel Prize in Physics for the "discovery of the positron" in 1936.*

Concerning the credit for the discovery of the positron, Mary Jo Nye (2004) writes in her authoritative biography of Blackett:

> *One of the great controversies over the awarding the Nobel Prize in Physics entered on Blackett's work, not in 1948, when he received the Prize, but in 1936 when he did not. The issue was that Carl Anderson alone received recognition in 1936 for discovery of the positron or positively charged electron, and British physicists continued to discuss the failure to recognize Blackett even after Blackett singly received the 1948 Prize… Blackett emphasized that Anderson at Pasadena had previously found tracks that seemed to indicate the existence of a positive electron. Only in one interview did Blackett add that his and Occhialini's work had been in progress for some months before they published their results from the Cavendish Laboratory in early 1933… What everyone acknowledged and admired in this matter was that Blackett behaved impeccably and did not himself engage in disputes about recognition for the positron.*

Blackett was very outspoken in science and politics. Nye (2004) writes that during the 1940 and 1950s Blackett was increasingly committed to the development of science and technology in India and the third world, which proved controversial. He also pleaded for setting up a special foreign aid fund for former colonies in the third world, which evoked anger and ridicule from many of his former colleagues. Nye explains, however, that "by 1964 the British political climate changed, and Blackett, who had been meeting with a scientific group advising the Labour Party's leadership, became scientific advisor in Harold Wilson's Ministry of Technology." Blackett had foresight in foreign affairs and the necessary ingredients for world peace, as shown by his push for massive foreign aid to third world countries. The following quotation, attributed to Blackett (Lovell, 1975), reflects current bilateral and international foreign aid programs:

> *The uneven division of power and wealth, the wide differences of health and comfort among the nations of mankind, are the sources of discord in the modern world, its major challenge and, unrelieved, its moral doom.*

Patrick Blackett became head of the Department of Physics at the Imperial College of Science and Technology, London in 1953. During the last decade of his scientific career he and a group under his direction studied magnetism in rocks, with the objective of determining the history of the Earth's magnetic field. The work at Imperial College under his direction and in other laboratories may provide evidence for the continental drift that has occurred over the course of geological history (Nobel Lectures, 1964).

Patrick Blackett was the author of several books, including *Military and Political Consequences of Atomic Energy* (1948b), *Lectures on Rock Magnetism* (1954), *Studies of War* (1962), and *Science, Technology and Aid in Developing Countries* (1971). He retired in 1963, and died in London on July 13, 1974.

HIDEKI YUKAWA (1907–1981)

Hideki Yukawa was born in Tokyo, Japan on January 23, 1907. He was awarded the Nobel Prize in Physics in 1949 "for his prediction of the existence of mesons on the basis of theoretical work on nuclear forces." The mesons were first theorized in 1935 by Yukawa as a particle which could account for the strong interactions that hold protons and neutrons together in the atomic nucleus. The mesons were discovered in 1947 in the cosmic radiation showers by Cecil F. Powell and Guiseppe P.S. Occhialini.

Hideki Yukawa (1907–1981)

Hideki Yukawa grew up in Kyoto and graduated from Kyoto University in 1929. After graduation he continued his studies and research in theoretical physics with an emphasis on elementary particles. From 1932 to 1939 he was an assistant professor and lecturer at Osaka University and a lecturer at Kyoto University.

At the very young age of 27, at Osaka University he took a bold step to publish (Yukawa, 1935) a revolutionary theory of nuclear forces that predicted the existence of the meson, an elementary particle that serves as an exchange particle of the strong interaction holding protons and neutrons together within the nucleus. The underlying question was what type of force strongly binds the protons and neutrons together in the atomic nucleus? The major forces, with which physicists were already well familiar, were gravity and electromagnetism. The reasoning used by Yukawa in his conception of the meson was given in his Nobel lecture of December 12, 1949 when he stated:

> *The meson theory started from the extension of the concept of the field of force so as to include the nuclear forces in addition to the gravitational and electromagnetic forces. The necessity of introduction of specific nuclear forces, which could not be introduced to electromagnetic interactions between charged particles, was realized soon after the discovery of the neutron, which was to be bound strongly to the protons and other neutrons. As pointed out by Wigner in 1933 [Eugene Wigner, Nobel Laureate in Physics 1963], specific nuclear forces between two nucleons, each of which can be either in the neutron state or the proton state, must have a very short range of the order of 10^{-15} m, in order to account for the rapid increase of the binding energy from the deuteron [nucleus of one proton and one neutron] to the alpha-particle [nucleus of two protons and two neutrons]. The binding energies of nuclei heavier than the alpha-particle do not increase as rapidly as if they were proportional to the square of the mass number A, i.e., the number of nucleons in each nucleus, but they are in fact approximately proportional to A [see Fig. 20.4 of the chapter entitled "The Atomic Nucleus"]. This indicates that nuclear forces are saturated for some reason.*

In his Nobel Lecture, Yukawa (1949) explained further that certain concepts of Werner Heisenberg and Enrico Fermi led him to the meson theory. Heisenberg (1932a,b, 1933c) had suggested that a force could be assumed between a neutron and proton due to an exchange of an electron, or more generally an electric charge, as in the case of a chemical bond between a hydrogen atom and a proton, eg, $H{\bullet}H^{+}$, the chemical bond depicted by the one dot between the hydrogen atom and proton, consists of a sharing of the electron between two hydrogen atoms or, in the words of Dunne (2002), "in this molecule the binding forces are associated with the continuous migration of the single electron from one atom to the other." Yukawa added that shortly after Heisenberg's theory was published, Fermi (1934a) developed a theory of beta decay based on the hypothesis of Pauli: that a neutron, as an example, could decay into a proton, an electron, and a neutrino, a neutral particle of near-zero mass. Yukawa explained that he searched for the particle that would represent the charge and binding force shared between the proton and neutron in the atomic nucleus.

In his Nobel lecture Yukawa explained that these concepts of Heisenberg, Pauli, and Fermi:

> *…gave rise, in turn, to the expectation that nuclear forces could be reduced to the exchange of a pair of an electron and a neutrino between two nucleons, just as electromagnetic forces were regarded as due to the exchange of photons between charged particles. It turned out, however, that the nuclear forces thus obtained were much too small (Tamm and Ivanenko, 1934), because the beta decay was a very slow process compared with the supposed rapid exchange of the electric charge responsible for the actual nuclear forces. The idea of the meson field was introduced in 1935 in order to make up this gap.*

Hideki Yukawa proposed his concept of the strong force holding protons and neutrons together as a particle (the name meson for this particle came later) with positive or negative charge that would be continuously emitted and absorbed by the proton and neutron, respectively. In other words, the meson would be an exchange particle that would hold the protons and neutrons as a unit in the atomic nucleus. Yukawa explained:

> *In order to obtain exchange forces, we must assume that these mesons have the electric charge, and that a positive (negative) meson is emitted (absorbed) when the nucleon jumps from the proton state to the neutron state, whereas a negative (positive) meson is emitted (absorbed) when the nucleon jumps from the neutron to the proton. Thus a neutron and a proton can interact with each other by exchanging mesons just as two charged particles interact by exchanging photons.*

Yukawa calculated the mass of the meson to be equivalent to approximately 200 electron masses. He knew that the nuclear forces between the proton and neutron states were of short range and of the order of 10^{-15} m, which would be the distance the meson would travel from proton to neutron or in the reverse direction. In harmony with the Heisenberg uncertainty principle, the creation and disappearance of an exchange particle such as the meson would be possible. The Heisenberg uncertainty principle in terms of energy and time, according to Eq. [V.16] of Hall of Fame, Part V, can be expressed as

$$\Delta E \Delta t \geq \frac{\hbar}{2} \qquad \text{[VI.18]}$$

The existence of the meson as an exchange particle, because of its additional mass, would break the laws of energy conservation ($E = mc^2$) if the meson existed for a time that exceeded

$$\Delta t \approx \frac{\hbar}{2\Delta E} \qquad \text{[VI.19]}$$

The meson could travel from a proton to another proton or as an exchange particle between proton and neutron if its lifetime (Δt) during that exchange was short enough to satisfy Heisenberg's uncertainty principle. Since the meson would travel at a speed less than that of light, its distance of travel would be defined by the term $c\Delta t$. Also the energy of the meson would be defined by Einstein's $\Delta E = mc^2$. Then Eq. [VI.19] can be written as

$$d \approx c\Delta t = \frac{\hbar c}{2\Delta E} = \frac{\hbar c}{2mc^2} \qquad \text{[VI.20]}$$

and

$$mc^2 \approx \frac{\hbar c}{2d} \approx \frac{(1.054 \times 10^{-34}\ \text{J s})(2.99 \times 10^{8}\ \text{m/sec})}{(2)(1 \times 10^{-15}\ \text{m})} \approx 1.57 \times 10^{-11}\ \text{J} \qquad \text{[VI.21]}$$

or

$$mc^2 \approx \frac{1.57 \times 10^{-11}\ \text{J}}{1.60 \times 10^{-19}\ \text{J/eV}} \approx 98.5 \times 10^{6}\ \text{eV} \qquad \text{[VI.22]}$$

and

$$m \approx 100\ \text{MeV}/c^2 \qquad \text{[VI.23]}$$

which is the estimated mass of the meson in energy units. Since the mass of the electron $m_e = 0.51\ \text{MeV}/c^2$, the mass of the meson, compared to the electron mass, would be

$$\frac{m}{m_e} = \frac{100\ \text{MeV}/c^2}{0.51\ \text{MeV}/c^2} \approx 200 \times \text{electron mass} \qquad \text{[VI.24]}$$

Yukawa estimated the mass of his theorized meson to be approximately 200 times that of the electron. His revolutionary theoretical work on the origin of the strong nuclear forces is commemorated in a postage stamp illustrated on page 460 issued in Japan in 1985. Yukawa's meson was finally discovered in cosmic radiation showers in 1947 by Cecil Powell, Guiseppe Occhialini, and Césare Lattes (Occhialini and Powell, 1947; Lattes et al., 1947) at the University of Bristol, England. Much interest in Yukawa's discovery ensued after World War II, which opened up an entire new field in the study of nuclear forces. Professor I. Waller, member of the Nobel Committee on Physics, underscored the importance of Yukawa's work in the Nobel award presentation speech on December 10, 1949:

> *…according to Yukawa's theory, the nuclear forces can be traced back to the exchange of mesons between the nucleons. These are continually emitting and absorbing mesons. Yukawa also studied the important question of whether the mesons can appear outside the nuclei. He found that the mesons can be created during the interaction of nucleons if these can deliver a sufficient amount of energy. Therefore, mesons cannot be created in ordinary nuclear reactions. Yukawa emphasized, however, that they can be expected to appear in the cosmic radiation, in which particles of great energy are found… Prof. Hideki Yukawa, in 1934, when you were only 27 years old, you boldly predicted the existence of new particles, now called "mesons" which you anticipated to be of fundamental importance for the understanding of the forces acting in the atomic nucleus. Recent experiments have provided brilliant support for your essential ideas. These ideas have been exceedingly fruitful and are a guiding star in present day theoretical and experimental work on atomic nuclei and on cosmic rays.*

The name meson attributed to Yukawa's particle is derived from the Greek word for "middle," as the meson acts as a mediator or go-between permitting one particle to change into another, thereby acting as a strong force holding the particles together in the nucleus. The meson predicted by Yukawa and discovered in cosmic radiation showers is called the π-meson or pion. Yukawa predicted that the π-meson would come in two charged forms, as noted earlier. The positive and negative forms (ie, the π^+ and π^-) were discovered in cosmic radiation showers, which are products of high-energy collision of cosmic-ray particles with nuclei of the Earth's atmosphere. The mass of the charged pions is 139.6 MeV/c^2, and they have a short lifetime of 2.6×10^{-6} s. More information on the abundance and properties of the pions is given in the chapter

entitled "Cosmic Radiation" on cosmic radiation. First evidence for the neutral pion (π^0) was provided by Bjorklund et al. (1950) at the Lawrence Berkeley Laboratory from gamma-ray photon emissions following the bombardment of various targets with protons accelerated to energies of 180 MeV. The neutral pion decays to two gamma-ray photons; it has a mass of 135 MeV/c^2 and a lifetime of 8.3×10^{-17} s (see the chapter: "Cosmic Radiation"). Confirmation of the neutral pion was provided by Carlson et al. (1950) by observing the tracks in photographic emulsions of scattered pairs of fast electrons produced by interactions with gamma-ray photon pairs, which are products of π^0 decay. These observations were made at an altitude of 70,000 ft, which provided evidence that the π^0 was produced in cosmic radiation showers. Additional evidence for the π^0 was supplied the following year by Panofsky et al. (1951) at the Lawrence Berkeley Laboratory by measuring the gamma-ray photon emission following the bombardment of targets with protons accelerated to energies of 330 MeV.

Prior to receiving the Nobel Prize and only about three years after the surrender of Japan in World War II, Yukawa was visiting professor at the Institute of Advanced Study at Princeton University during 1948–1949. In July 1949 he became visiting professor at Columbia University in New York until 1950. The importance of Yukawa's work and his international collaboration with the United States shortly after the war was a great example for peace and international cooperation. This was underscored by Carl Skottsberg, President of the Royal Academy of Sciences, on December 10, 1949 in the banquet speech following the awarding of the Nobel Prize to Hideki Yukawa:

> *Your fellow-workers in atomic research recognize the high intrinsic value of what you have done, and that's the reason why you are here today, the first Japanese to receive a Nobel Prize. You have told us already what this means, not only to you personally, but also to scientific life in Japan, an enlivening stimulation in these days of great distress. We can understand this. And are you not the very best example of the importance of science in bringing nations and races together? Not many years ago Japan and the United States stood against each other, armed to the teeth, bent upon destruction. Today you work happily in the midst of American colleagues.*

From Left to Right: Hideki Yukawa, Ernest Lawrence, Mrs. Yukawa, and Robert Serber standing outdoors at the Radiation Laboratory Berkeley in 1948 Courtesy of the AIP Emilio Segre Visual Archives, Yukawa Collection

In 1932 Yukawa became the first chair of the Yukawa Institute for Theoretical Physics at Kyoto University. He was among the 10 leading scientists and intellectuals who signed the Russell-Einstein Manifesto in 1955, discussed in Hall of Fame, Part IV of this book. Hideki Yukawa died on September 8, 1981 in Kyoto, Japan.

CECIL F. POWELL (1903–1969)

Cecil Frank Powell was born in Tonbridge, Kent, southeast of Greater London on December 5, 1903. He was awarded the Nobel Prize in Physics in 1950 "for his development of the photographic method of studying nuclear processes and his discoveries regarding mesons made with this method."

Cecil Powell grew up in humble surroundings. His grandfather was a successful and skilled gunsmith, and his father had inherited the company and craft. However, the business went bankrupt after his grandfather spent considerable

funds fighting a lawsuit over a hunting accident, in addition to falling demand due to the advent of industrial manufacture of guns making handicraft production less economic. His father had to work as a clerk in his brother's electrical business, and the family had to take up lodging in their residence to make ends meet. In his autobiography Powell (1987) relates:

> *My parents' life was hard and my mother was very anxious that her children should escape from the drudgery, which had been her lot. Her brother… had succeeded in getting into Trinity College, Cambridge, and had become an electrical engineer. My mother determined that I should secure a similar emancipation.*

Cecil Powell (1903–1969)

We can never overestimate the important role of our primary and secondary school teachers. Often it is a teacher in our formative youth who will impress us to the extent that he or she helps us find the vocation where we have the greatest potential to make a contribution to society. This is clear in the following statement from Powell's autobiography:

> *I was fortunate that at Judd School I came under the influence of a physics master who was devoted to his profession and an able teacher… the experiments in his class were well designed and gave scope for originality and skill. I used to be allowed to spend a lot of time there on my own. And he was a man of some taste and originality.*

Powell did well in secondary school and, after two attempts, won a scholarship in 1921 to Sidney Sussex College, Cambridge. C.T.R. Wilson, who would become Nobel Laureate in Physics in 1927, was a fellow at the college when Powell began his studies there. It was difficult for Powell to adjust to the transition from a small town to a big university, but he graduated with honors. He thought of becoming a teacher and was accepted to a post at Uppingham School; however, after serious thought about his future calling and ambitions, he approached Ernest Rutherford in 1925 about the possibility of becoming a research student at the Cavendish Laboratory. Rutherford agreed and arranged for C.T.R. Wilson to be his supervisor. The Cavendish was bustling with new scientific developments at the time Powell entered as a research student. Charles Eryl Wynn-Williams (1931, 1932) was developing automatic electronic scalers for the counting of radiation emissions, Patrick Blackett (1934) was building his automatic counter-controlled cloud chamber described previously, and John Cockroft and Ernest Walton (1932a,b), who would share the Nobel Prize in Physics in 1951, were developing methods for the acceleration of protons to high energies for experimentation on proton collisions with atomic nuclei. The environment at the Cavendish was perfect for any young budding scientist like Powell. His initial research under Wilson was to develop an improved all-glass cloud chamber for the study of the nature of condensation by different degrees of expansion of dust-free air. In his autobiography Powell relates how impressed he was that 20 years earlier

Wilson would ever have attempted to make a successful cloud chamber that would be capable of observing the paths of charged subatomic particles. Such work taught Powell the importance of perseverance, as he relates in his autobiography:

> *I always found it remarkable that Wilson should ever have attempted to make such a device [cloud chamber] but he succeeded 20 years before: Rutherford used to tell a story that on one occasion just before he went on a long vacation, he had left Wilson in the attempt, sitting glass-blowing at the blow-pipe and pedaling the foot-bellows. When he returned Wilson was in the same position and seemed to be engaged in exactly the same task.*

Powell's work on the cloud chamber led him to the discovery of the nature of steam discharge through nozzles, which had some impact on the design of steam turbines. He received his doctorate in 1927, and in 1928 moved to the University of Bristol as research assistant to A.M. Tyndall to study the mobility and nature of ions in gases. In 1935 he joined an expedition to Montserrat in the West Indies to study seismic activity on the island. That same year he became very interested in nuclear physics and decided to return to the Cavendish, which was bustling with new discoveries. It was an opportune time at the Cavendish, as in 1932 Blackett and Occhialini had discovered pair production, Chadwick had discovered the neutron, and Cockroft and Walton had successfully caused the disintegration of lithium by accelerated protons. Powell wanted to study particle scattering in a Wilson cloud chamber following the bombardment of light elements, such as lithium, beryllium, boron, carbon, and oxygen, by protons and deuterons with a Cockroft and Walton accelerator. However, research by Marietta Blau (1894−1970) and her assistant Hertha Wambacher (1903−1950) at the Radium Institute in Vienna had demonstrated that photographic emulsions could be used to detect subatomic particles, and could be more versatile than the cloud chamber. Powell relates in his autobiography:

> *The original intention was to study the scattering of fast neutrons by protons using a Wilson Chamber filled with hydrogen… But about this time W. Heitler, who had been in Bristol for some years, pointed out that Blau and Wambacher had successfully used "halftone" photographic emulsion to detect particles in the cosmic radiation and, since the method had the advantage of extreme simplicity, he thought we might begin by sending similar plates on to a mountain to see if we could simulate the Viennese results.*

The writer would like to divert from the work of Powell to touch briefly on the life and contributions of Marietta Blau, whose work on photographic emulsions helped pave the way for some of Powell's discoveries. She was born in Vienna in 1894 to a Jewish family and, after Lise Meitner, was among the first women to study physics at the University of Vienna, where she was awarded the doctorate in 1919. She did research without pay at the Radium Institute, University of Vienna from 1923 to 1938. She was forced to flee Austria in 1938 after the annexation of Austria by Germany. Blau supervised the doctoral studies of Hertha Wambacher at the University of Vienna. After completion of her doctorate Wambacher joined Blau in research, and they had a fruitful collaboration for about six years, mostly in the development of the emulsion technique for detection and measurement of subatomic particles originating from cosmic-ray collisions with atomic nuclei in the Earth's atmosphere (Blau and Wambacher, 1935, 1937; Blau, 1938). The work by Blau and Wambacher in 1937 yielded the detection of numerous images on photographic emulsions called "stars," as these images showed the track of a high-energy cosmic ray particle colliding with an atomic nucleus in the emulsion resulting in numerous tracks leading from the point of impact. As many as 12 tracks would be observed as straight lines stretching out in many directions from the point of impact of the cosmic-ray particle with the atomic nucleus. These tracks illustrated the shattering of an atomic nucleus into as many as 12 particles. Nobel Laureate Max Born (1969) credited Blau and Wambacher with the discovery of the photographic emulsion technique for the detection and measurement of tracks left by subatomic particles:

> *Another great advance was made by two Viennese ladies. Misses Blau and Wambacher (1937), who discovered a photographic method of recording tracks of particles. The grains of emulsion [ie, silver bromide grains suspended in an emulsion of gelatin] are sensitive not only to light but also to fast particles; if a plate exposed to a beam of particles is developed and fixed, the tracks are seen under the microscope as chains of black spots.*

Erwin Schrödinger twice nominated Blau for the Nobel Prize (Moore, 1989; Perlmutter, 2000). Blau escaped from Austria with the assistance of Albert Einstein and went to Mexico, where she worked as professor at the National Polytechnic University in Mexico City from 1939 to 1944. A copy of her Mexico City identity card, which she used during her escape to Mexico, is illustrated. After five years in Mexico, Marietta Blau held positions in industry in 1944−1948 in New York and was a research physicist at Columbia University from 1948 to 1950. Her career continued as associate physicist at the Brookhaven National Laboratory from 1950 to 1955 and finally associate professor at the University of Miami from 1955 to 1960 (Byers, 2000). While at Columbia and Brookhaven, Blau did pioneering work on the study of high-energy particle interactions with atomic nuclei (Blau and De Felice, 1948; Blau et al., 1953; Blau and Caulton, 1954; Blau, 1956; Blau and Oliver, 1956). Like Lise Meitner, she was born in an era which required great fortitude and perseverance for a woman to

overcome many obstacles in scientific research. Her Jewish heritage added to the hurdles and tortuous obstacles she had to overcome during her productive years, which kept her from achieving her maximum potential. Blau returned to her native Austria in 1960 at the age of 66 and died of cancer in Vienna in 1970. For additional reading on the life and scientific accomplishments of Marietta Blau the reader is invited to peruse a biography by Rosner and Strohmaier (2003), an extensive treatise by Perlmutter (2000), a book chapter by Halpern (1993), and a book chapter and article by Galison (1997a,b).

Marietta Blau (1894–1970)
Mexico City Identity Card dated 1941
Courtesy of the AIP Emilio Segre Visual Archives,
Gift of Prof. Robert Rosner

Cecil Powell grasped the photographic emulsion (or nuclear emulsion) technique pioneered by Blau and Wambacher, and improved its application to study nuclear disintegrations produced by artificially accelerated beams of protons and deuterons, and later to nuclear disintegrations produced by collisions of cosmic-ray particles. The purpose of the technique is to detect and measure atomic particles (ie, their mass, charge, and energy) by the tracks they leave behind in nuclear emulsions. The emulsion was a suspension of silver bromide crystals in gelatin supported on a transparent glass plate; currently transparent plastic plates are used. Charged particles produce ionization in the emulsion as the particle travels through the emulsion or until it comes to a stop within the emulsion. The ionization occuring within the silver bromide crystals yields electrons that are free to travel from one ion to another in the silver bromide until they are trapped at sites of defects within the silver bromide crystal structure. At a structural defect a silver ion absorbs the electron to become a silver atom. The crystals affected in this way by nuclear radiation become visible only after the application of a chemical "developer" which reduces all the silver ions of the affected crystals to metallic silver (observed as black grains or spots). The crystals, which do not contain reduced silver, are dissolved out of the emulsion by the chemical "fixer" leaving a black image produced by the nuclear radiation. A series of dark grains in the film emulsion denotes the track left by the nuclear particle. The intensity of the dark grains or the thickness of the track is a function of the specific ionization caused by the particle. Thus the thickness of a particle track in a nuclear emulsion is proportional to the mass and charge of the particle, as particles of higher mass and charge produce higher ionization in matter. However, the thickness of a particle track will be inversely proportional to the particle velocity, because a particle produces more ion pairs as it slows down before it comes to rest (see Fig. 4.6 of the chapter: "Alpha Radiation"). To observe the particle tracks in nuclear emulsions the photographic film must be wrapped in opaque paper to protect it from light, which would expose and darken the film. After exposure to nuclear radiation the protective wrapping is removed in a darkroom, and the film treated with chemical developer and fixer to yield dark particle tracks on a clear background. For additional reading on the theory and practice of nuclear emulsions see Gurney and Mott (1938), Barkas (1963), Rogers (1979), Mundy et al. (1983), and L'Annunziata (1987).

In his autobiography Powell (1987) explained clearly the advantages of nuclear emulsions over the cloud chamber to detect and measure atomic particles: nuclear emulsions are continuously sensitive, so as a detector the emulsion is sensitive throughout the duration of its exposure to the nuclear particles until the time of chemical development of the emulsion, unlike the cloud chamber, which is sensitive for only a few milliseconds at the instant of expansion of the chamber; nuclear emulsions can record with precision the point of entry of a particle and its direction of motion; and the nature of the particle (eg, mass and charge) and its range and energy can be determined by observations on the character of the tracks (eg, some nuclear particles come to a full stop in the emulsion and their range can be measured, and the thickness and shape of the track can characterize the speed, mass, and charge of the particle). The versatility of nuclear emulsion was demonstrated by Powell and his coworkers, and underscored by Professor A.E. Lindh, member of the Nobel Committee, in his Nobel presentation speech on December 11, 1950:

The photographic method used by Prof. Powell is based on the fact that after an electrically charged particle has passed through a photographic emulsion, the silver bromide grains of the emulsion can be developed, making the path of the particle appear as a

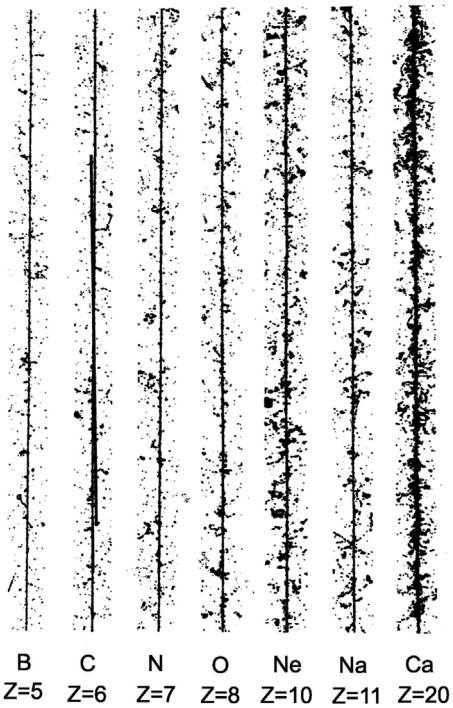

FIGURE VI.10 Examples of tracks in photographic emulsions of primary nuclei of cosmic radiation moving at relativistic velocities. The tracks produced by particles of higher mass and charge have a higher density of black grains. *From Powell, C.F., 1950. The cosmic radiation. Nobel Lecture at Stockholm, Sweden on December 11, 1950. In: Nobel Foundation Staff, (Eds.), Nobel Lectures, Physics, 1942–62, (1964). Elsevier Publishing, Amsterdam., with permission from the Nobel Foundation © 1950.*

> *dark line which is, actually, a series of blackened grains with longer or shorter intervals between. The distance between the grains is proportional to the speed of the particle; the greater the speed of the particle, the greater the distance, which circumstance is connected with the fact that a swift particle has less power of ionizing than a slow one.*

To demonstrate how clearly the ionizing power of a particle, governed by its speed, mass and charge, can be distinguished by the nuclear emulsion technique, in his Nobel lecture on December 11, 1950 Powell showed seven particle tracks, illustrated in Fig. VI.10, of primary cosmic ray particles recorded in various emulsions carried by high-flying balloons at altitudes of approximately 95,000 ft. In Fig. VI.10 it can be seen that if the particle speeds are similar, the thickness of the particle track in the emulsion is a function of the particle mass. Powell (1950) noted that experimental data, including data of Freier et al. (1948) and Bradt and Peters (1948), taken on the frequency of the nuclear tracks made by primary cosmic-ray particles at high altitudes provided much information on the relative abundances and speed of the nuclei of different chemical elements in primary cosmic radiation. He noted:

> *By observations at great altitudes we now know that the primary cosmic radiation is made up of atomic nuclei moving at speeds closely approaching that of light. It is possible to record the tracks of the incoming particles and to determine their charge; and thence the relative abundance of the different chemical elements. Recent experiments prove that hydrogen and helium occur most frequently, and the distribution in mass of the heavier nuclei appears to be similar to that of the matter of the universe. Thus elements more massive than iron or nickel occur, if at all, very infrequently.*

After World War II, Cecil Powell joined forces with Italian physicist Giuseppe Occhialini, who had previously worked with Nobel Laureate Patrick Blackett at the Cavendish Laboratory on cosmic radiation using the Wilson cloud chamber, leading to the interpretation of "pair production" and the discovery of the nuclear process of "annihilation" in cosmic-ray showers. Occhialini left the Cavendish in 1938 to return to Florence, Italy, and a few years later went to the University of São Paulo in Brazil to conduct research on cosmic radiation. During the war he took refuge in the Itatiaya mountains between São Paulo and Rio de Janeiro. Occhialini joined forces with Powell at the University of Bristol in 1945. Together with other researchers, including Brazilian physicist Césare Lattes, they employed nuclear emulsions to study the collisions of cosmic-ray particles with atomic nuclei.

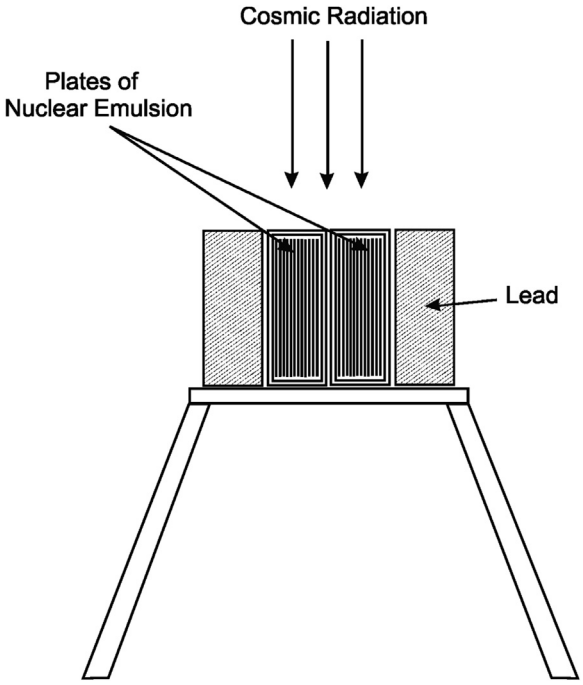

FIGURE VI.11 Stacks of 24 Ilford plates of nuclear emulsion supported in a vertical position between two blocks of lead shielding. (The Ilford plates came from Ilford Imaging, which is now a worldwide company. It was founded by Alfred Harmon, who made gelatine dry photographic plates in the basement of his house on Cranbook Road in Ilford, Essex, UK in 1879.) The plates each measured approximately 2 × 1 cm in area and contained a layer of silver bromide emulsion approximately 100−250 μm thick. The plates were kept in their original light-tight packing. Stacks of about 12 Ilford plates were housed in 0.5 mm tinned iron layered together in a vertical sandwich position between two lead shields. The lead shielding reduces background radiation from scattered cosmic-ray showers that could enter the plates at angles other than from directly above the plates. *From Camerini, U., et al., 1948. Observations on slow mesons of the cosmic radiation. Nature 162 (4116), 433−438, http://doi:10.1038/162433a0, reprinted with permission from Macmillan Publishers Ltd © 1948.*

The experimental setup involved stacking several nuclear emulsions supported on glass plates in a vertical position to improve chances that an incident cosmic radiation would enter one emulsion only and travel through it, or even come to a stop in that single emulsion. Only a cosmic ray incident to the vertical orientation of a plate of nuclear emulsion would have the opportunity to travel through the one emulsion and produce a track in it. Cosmic radiation that entered the plates at an acute angle, such as scattered cosmic radiation showers, would not produce a track. The experimental arrangement is illustrated in Fig. VI.11.

Powell and coworkers took two approaches to the study of cosmic radiation with nuclear emulsions, namely exposing the emulsions at very high altitudes of up to 95,000 ft (about 29 km) by placing the plates in a gondola aboard a large (37 m) hydrogen-filled balloon, or placing the plates of nuclear emulsion on mountains of various altitudes, such as 5500 m in the Bolivian Andes (Lattes et al., 1947), atop the Jungfraujoch in Switzerland at 3000 m, and on Kilimanjaro in Tanzania and Chacaltaya in Bolivia, both at 5500 m (Occhialini and Powell, 1948). Powell's objective in exposing nuclear emulsions at very high altitudes was to measure the abundances of the atomic nuclei in the primary cosmic radiation, which cannot be observed at lower altitudes because they undergo collisions and disintegrate with atomic nuclei of the atmosphere. Also, the primary cosmic ray nuclei arriving from intergalactic space would interact with atomic nuclei of the nuclear emulsions to produce "stars," which are tracks produced by the disintegrations of the colliding nuclei and the elementary nuclear particles (eg, alpha particles, neutrons, protons, electrons, and mesons) emitted in many directions from the point of impact (see Fig. VI.12). The tracks of these particles could then be studied for the determination of their mass, charge, and energy. On the other hand, at lower altitudes of mountain peaks the atmosphere would be free of the primary cosmic nuclei of high mass, and the nuclear emulsion exposures would therefore show the interactions of the nuclear particles of low mass and secondary cosmic radiation (ie, the products of the nuclear collisions of primary cosmic rays with nuclei of the atmosphere) with nuclei of the emulsion. In his Nobel lecture, Powell (1950) elucidated on his experimental approach based on the differences of cosmic radiation as a function of altitude:

> *The detailed study of the "mass spectrum" of the incoming nuclei [examples of the tracks of such incoming nuclei are shown in Fig. VI.10] has an important bearing on the problem of the origin of the primary particles; but it is complicated by the fact that,*

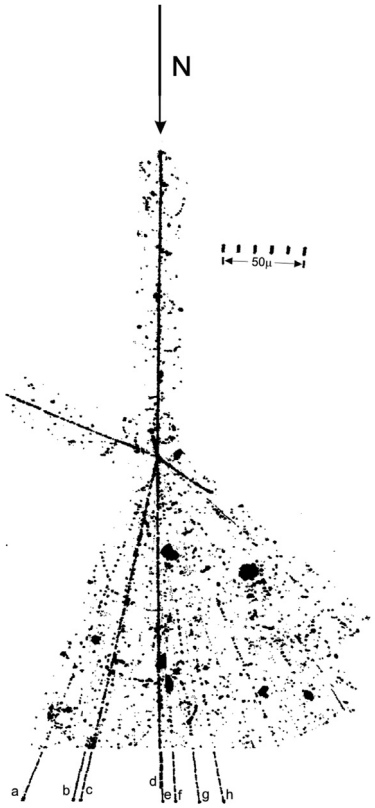

FIGURE VI.12 A cosmic radiation "star" produced in nuclear emulsion. The name "star" was attributed to the patterns of tracks produced when a high-energy particle collided with an atomic nucleus and the nuclei disintegrated in nuclear emulsions, yielding a star-like pattern of particle tracks in many directions. Here an incoming nitrogen nucleus of the primary cosmic radiation collides with a nucleus of the nuclear emulsion, and splits up into a lithium nucleus, an alpha particle, a deuteron, and a number of protons. Some π-mesons are created in the collision. The event was reported by Powell (1950) to be very exceptional, because by chance the tracks of many of the particles in the emulsion are long, so they can be identified and their energy determined. Powell (1950) identified the particles that produced the tracks and their energies. At the top of the "star": N, 28,000 MeV. At the bottom: (a) α particle, 220 MeV; (b) π-meson, 800 MeV; (c) proton, ie, ${}_1^1$H, 81 MeV; (d) Li, ∼10,000 eV; (e) ${}_1^1$H, 2000 MeV; (f) deuteron, ie, ${}_1^2$H, 3800 MeV; (g) π-meson, 1000 MeV; and (h) π-meson, 1200 MeV. *From Camerini, U., et al., 1948. Observations on slow mesons of the cosmic radiation. Nature 162 (4116), 433–438, http://doi:10.1038/162433a0, reprinted with permission from Macmillan Publishers Ltd © 1948.*

because of their large charge, the particles rapidly lose energy in the atmosphere by making atomic and nuclear collisions. They therefore rarely penetrate to altitudes less than 70,000 ft (∼21 km). It is for this reason that exposures at high altitudes are of particular interest.

A second reason for making experiments at extreme altitudes is that the primary nuclei commonly suffer fragmentation in making nuclear collisions. A primary nucleus of magnesium, aluminum [or nitrogen, see Fig. VI.12], for example, may decompose into lighter nuclei such as lithium, α-particles and protons. The mass spectrum at a given depth is therefore different from that of the primary radiation, and such effects are appreciable at 90,000 ft [27 km, where the air density is low, ∼0.05 kg/m^3]. They would be much reduced at 12,000 ft [3.6 km, where the air density is higher, ∼0.9 kg/m^3].

The primary protons and α-particles, because of their smaller charge, penetrate to much lower altitudes. In collisions they disintegrate the nuclei which they strike [see Fig. VI.12] and, in the process, lead to the creation of new forms of matter, the π-mesons of mass 274 m_e (Lattes et al., 1947; Piccioni, 1950; Fowler, 1950). These particles are usually ejected with great speed and proceed downward towards the earth.

In February 1947 Giuseppi Occhialini and Cecil Powell reported the existence of the π-meson (Occhialini and Powell, 1947). They observed six "star" formations in nuclear emulsions exposed to cosmic radiation, which demonstrated the existence of a previously unknown particle of small mass, but of mass greater than the electron mass. In each of the six star-like nuclear disintegrations out of 800 "stars" studied they observed that the disintegrations appeared to be caused by the entry of a slow charged particle, the meson, into the nucleus. They provided evidence by grain density

measurements that the meson slowed down and entered a nucleus causing the nucleus to disintegrate. Occhialini and Powell (1947) reported:

> *"The conclusion receives additional support from the observation that the number of grains per unit length of the [meson] track, which can be taken as a measure of the ionization produced by the particle, is greatest in the immediate neighborhood of the disintegrating nucleus and becomes less as we recede from it…" [It is a known fact that the ionization per unit length of travel by a charged particle is greatest when the particle is approaching the end of its range, as illustrated in Fig. 4.6 of the chapter entitled "Alpha Radiation."] We have now observed six of these events among a total of eight hundred stars. The probability, in any one case, that a charged particle, unrelated to the star, has, by chance, come to the end of its range within 1 μm of the disintegrating nucleus, is less than 1 in 10^5. We must therefore conclude that the particle entered the nucleus and produced a disintegration with the emission of heavy particles.*

About the same time that Powell's group reported tracks produced by this new particle, Don Perkins (1947) of Imperial College in London reported in the same volume of the journal *Nature* the observation of one track of the meson in nuclear emulsion. This track was obtained by exposing the emulsion to cosmic radiation for several hours aboard an aircraft at an altitude of 30,000 ft (9100 m). From the meson track he observed that the meson was absorbed by a nucleus, causing the nucleus to explode, as a star-like image was produced by numerous tracks of subatomic particles emitted in various directions from the point of impact. In his Nobel lecture, Powell (1950) stated:

> *The observation of two "events" [Powell's and Perkin's research] of a similar nature seemed to exclude completely the possibility of a juxtaposition of unrelated tracks and it appeared certain that we were observing the consequences of the capture of a negative meson by a nucleus of an atom in the emulsion and its resulting disintegration.*

Shortly after noting the observation of the π-meson tracks César Lattes, Occhialini, and Powell reported in October 1947 (Lattes et al., 1947) the observation of pion decay to a muon after examining plates of nuclear emulsion exposed in the Bolivian Andes at an altitude of 5500 m. They found 40 examples of nuclear disintegrations leading to the production of the muon. In their paper they noted:

> *that many of the observed mesons are locally generated in the "explosive" disintegration of nuclei.*

In his Nobel Lecture, Powell (1950) described the origins and fate of the pi-meson and muon in cosmic radiation showers, as derived from the tracks of these nuclear particles in nuclear emulsions exposed at high altitudes to cosmic radiation. Exposure times on mountain tops were often in the order of 35 days, after which the nuclear emulsions were treated with chemical "developer" and chemical fixer, and the tracks studied under the microscope. The origins of the π-mesons were the collisions of primary cosmic-ray nuclei with atomic nuclei of the upper atmosphere (above 22,000 m) resulting in nuclear disintegrations into smaller nuclear particles, as illustrated in Fig. VI.12; the absorption of a negatively charged π-meson by an atomic nucleus in the atmosphere, which also results in the explosion of the nucleus into smaller particles; and other sources of mesons, including high-energy protons and α particles that collide with atomic nuclei in the Earth's atmosphere to break up or "smash" the nuclei into numerous particles, including protons, neutrons, α particles, and mesons. Thus the forces in intergalactic space accelerate primary high-energy cosmic particles to relativistic speeds, and these collide with atomic nuclei in the Earth's atmosphere to smash atoms and produce high-energy secondary particles (eg, high-energy protons and α particles). These secondary particles, in turn, also serve as natural "atom smashers," producing a cascade or shower of protons, neutrons, electrons, pions, muons, and neutrinos in the Earth's atmosphere (see Fig. 14.3 of the chapter entitled "Cosmic Radiation").

The pions and muons were the new particles observed by Powell and his coworkers from their tracks in nuclear emulsions. In his Nobel lecture Powell (1950) discussed the origin and fate of the pions and muons:

> *When brought to rest in a photographic emulsion, the positive π-particles decay with the emission of a muon of mass 212* m_e *[see Fig. VI.13]. This particle commonly emerges with a constant velocity, so that its range varies only within the narrow limits due to straggling [notice in Fig. VI.13 that the muon tracks are of relatively constant length, which indicates a relatively constant velocity among the particles]. It follows that in the transmutation of the π-meson, the muon is accompanied by the emission of a single neutral particle. It has been shown that this neutral particle is of small rest-mass and that it is not a photon. It is therefore reasonable to assume, tentatively, that it is a neutrino, the particle emitted in the process of nuclear β-decay [see Eqs. [14.19] and [14.20] of the chapter entitled "Cosmic Radiation" for charged pion decay to muon and neutrino].*
>
> *When a negative π-meson is arrested in a solid material, it is captured by an atom, interacts with a nucleus and disintegrates it (Perkins, 1947, Occhialini and Powell, 1947). It follows that the particle has a strong interaction with nucleons,*

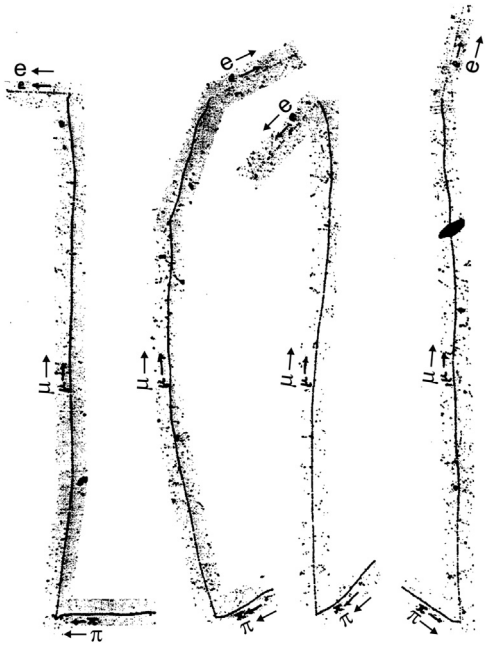

FIGURE VI.13 Photo-micrographs of four examples of the successive decay π-μ-e as recorded in photographic emulsions. *From Powell, C.F., 1950. The cosmic radiation. Nobel Lecture at Stockholm, Sweden on December 11, 1950. In: Nobel Foundation Staff, (Eds.), Nobel Lectures, Physics, 1942–62, (1964). Elsevier Publishing, Amsterdam, with permission from the Nobel Foundation © 1950.*

and in this respect its properties are similar to those predicted for the "heavy quanta" of Yukawa. [Powell here points out that they have discovered the π-meson as the transitory particle of very short lifetime predicted by Yukawa in 1935. Thus the π-meson was identified by Powell as the particle within the nucleus that acts as a go-between, permitting one particle to change into another, such as a proton into a neutron and vice versa, participating in the strong force holding the particles in the nucleus together.]

When π-mesons are created in nuclear collisions occurring in the atmosphere, they commonly transform, whilst in flight, into μ-mesons [i.e., muons] and neutrinos. It is these μ-particles, which form the "hard" or "penetrating" component of the cosmic radiation and they are responsible for most of the residual ionization in air at sea level [see Fig. 14.3 of the chapter entitled "Cosmic Radiation"]. The μ-mesons [i.e., muons] are penetrating because, unlike the π-mesons, they are able to traverse the nuclei with which they collide without interacting with them, and some of them reach great depths underground…

In addition to producing the charged π-mesons, the primary protons in making nuclear collisions also produce neutral π-particles (Bjorklund et al., 1950). The neutral π-mesons are very short-lived and each transforms spontaneously into two quanta of radiation [see Eq. [14.15] of the chapter entitled "Cosmic Radiation"]. Such a quantum, when it happens to pass near an atomic nucleus, can in turn transform into a pair of electrons, one positive and one negative; and the electrons can generate new photons in further collisions. A succession of such processes results in the production of the well-known cascades of electrons and photons which form the "soft" or easily absorbed component of the cosmic radiation (Carlson et al., 1950).

See Fig. 14.3 of the chapter entitled "Cosmic Radiation" for an illustration of the cascade of particles in cosmic radiation showers described by Powell.

One of Powell's assistants, H. Muirhead (see Occhialini and Powell, 1947), made a quantitative study of the grain densities along the tracks of the mesons (later identified as π-mesons) observed in six "star" formations to get an initial estimate of the particle mass. He counted the black grains in the nuclear emulsion to quantify the variation of the grain density along the tracks of protons so he could extrapolate or predict the distribution of grain density expected for particles of the same charge as the proton but of different mass. His initial estimate of the mass of the new particle was in the range of 100–230 m_e, where m_e is the mass of the electron. This was relatively close to the current figure for the mass of the charged pion, which is 139.6 MeV/c^2 or 274 m_e, since the ratio of the masses of the pion and electron in energy units is 139.6 MeV/c^2/0.51 MeV/c^2.

Powell and coworkers (Lattes et al., 1947) were able to deduce the masses of the pi-meson and muon by determining their ranges in the nuclear emulsions and comparing them to the ranges of the proton at various energies. Under the

magnification of a strong optical microscope they could count the grain densities in a particle track—that is, the number of grains per unit length of particle track. The method is described by Lattes et al. (1947):

> *In determining the grain density in a track, we count the number of individual grains in successive intervals of length 50 μm along the trajectory, the observation being made with optical equipment giving large magnification (2000×), and the highest available resolving power. Typical results for protons and mesons are shown in [Fig. VI.14],… and it will be seen that there is satisfactory resolution between the curves for particles of different types… We can therefore conclude that there is a significant difference in the grain-density in the tracks of the primary and secondary mesons [ie, pi-mesons and muons], and therefore a difference in the mass of the particles. The conclusion depends, of course, on the assumption that the π- and μ-particles carry equal charges.*

Lattes et al. (1947) concluded that the charges on the pi-mesons and muons were equal and unitarily equivalent to the magnitude of the electric charge (e). Their conclusion was based on the observation that the grain densities at the ends of the tracks for both particle types were consistent with particles of unitary electronic charge. For particles of double charge the grain densities would increase at the end of the particle track, that is, at the end of the particle range. See Fig. 4.6 of the chapter entitled "Alpha Radiation," illustrating how the α particle, which is of double charge, causes more ionization as it slows down and the highest ionization just before it reaches the end of its range. This is due to the fact that as the α particle slows down and comes close to a stop, the coulombic attractive forces between the particle and atomic electrons have more time to act, forcing the atomic electrons to latch on to the alpha particle so increased ionization occurs. Lattes et al. (1947) made a more precise comparison of the masses of the pi-mesons and muons from the track lengths. The π-meson had a track length of about 600 μm, whereas the length of the tracks of the muons in the nuclear emulsion exceeded 1000 μm. They estimated the ratio of the masses of the pi-mesons and muons $\left(m_\pi/m_\mu\right)$ to be about 1.5. This is quite close to the currently known value of 1.3, as the masses of the pi-mesons and muons are 139.6 MeV/c^2 and 106 MeV/c^2, respectively.

Nuclear emulsions served as excellent media for the recording and measurement of particle tracks. As mentioned previously, they were considered an improved method over the Wilson cloud chamber and had many advantages. The disadvantage of nuclear emulsions was the practical impossibility of causing magnetic deflections of the charged particles as they passed through the emulsions. Very high magnetic fields of the order of 10^6 G would be required, and the angle of

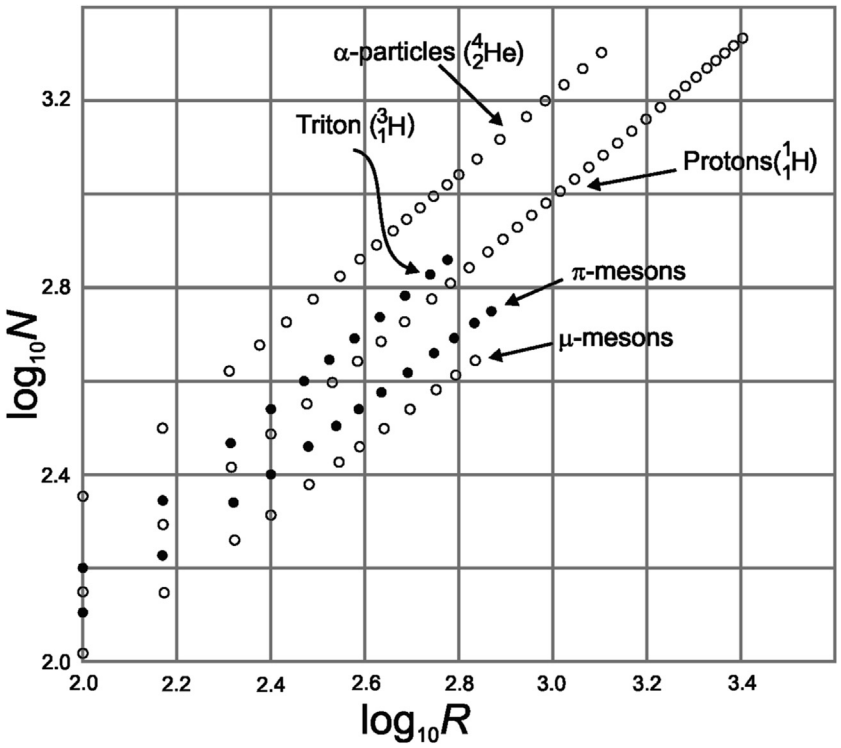

FIGURE VI.14 An approximate depiction of plots by Lattes et al. (1947) of the total number N of grains in a particle track of residual range R (scale divisions), where one scale division = 0.85 μm of nuclear emulsion. Notice that the greater the mass and charge of the cosmic-ray particle, the greater the developed grain densities of the particle track. The particles labelled mu-mesons in the figure above are now known to be muons, which are leptons rather than mesons.

coulomb scattering would be very small in the denser nuclear emulsion, complicating the interpretations of deflections. This disadvantage was clearly underscored by Powell and Rosenblum (1948):

> *It is well known that it is not possible, to make magnetic deflection experiments with photographic emulsions—analogous to those which have been so successful with the Wilson expansion chamber in experiments on cosmic radiation—by observations on the curvature, due to the magnetic field, of the trajectory of a particle in an emulsion.*

To circumvent this shortcoming, Powell and Rosenblum (1948) designed the experimental arrangement illustrated in Fig. VI.15 to permit the use of two face-to-face nuclear emulsions for the measurement of particle deflections in a magnetic field as the particle passes through a vacuum or gas. They arranged two photographic plates with their emulsions face to face in a suitable plate holder, which would keep the emulsions separated by a distance of 3 mm. The assembly was placed between the poles of an electromagnet providing a field of 8600 G and the planes of the emulsions arranged normal to the magnetic field. After traveling through emulsion 1 and while traversing the space between the two emulsions, positive particles are deflected upwards and negative particles downwards toward emulsion 2. The points of exit from emulsion 1 and point of entry into emulsion 2 of a particle permitted Powell and Rosenblum to calculate ρ, the radius of the curvature of the particle path, which is a function of the magnetic field strength (H) and the particle's mass and velocity or its momentum. In the words of Powell and Rosenblum (1948):

> *…in the space between the plates, it [the particle] will have moved in a spiral path. If we can identify the track of the same particle in the two emulsions, then the observed change in the direction of motion in traversing the air gap, and the distance between the points of exit and entry of the particle in the emulsions, allows us to calculate $H\rho$ for the particle; the magnitude of its momentum in the plane perpendicular to the field is thus determined. Further, if the particle comes to rest in the emulsion, its observed range gives a measure of its velocity as a function of its mass. The two observations taken together define the mass of the particle.*

Blackett and Brode (1936) demonstrated that the relation between the energy of an electron in (eV) and the magnetic field strength (H) and the radius of curvature of the particle path (ρ) was defined as

$$E = 300\,H\rho$$

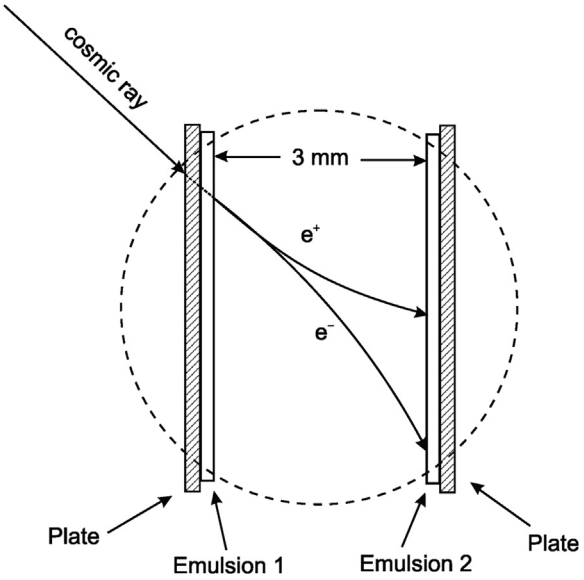

FIGURE VI.15 Experimental arrangement of Powell and Rosenblum (1948) designed to use nuclear emulsions in conjunction with applied magnetic fields to measure the deflections of cosmic-ray particles and calculate their charge and mass. Two photographic plates are placed 3 mm apart, and their nuclear emulsions are oriented face to face. The distance between the emulsions is exaggerated in the figure to illustrate the deflections produced by the magnetic field. The dashed circle represents the positions of the poles of a magnet in the front and rear of the photographic plates. The poles of the magnet provide an 8600 G magnetic field normal to the nuclear emulsions. Positive and negative particles (eg, electrons) originating from a cosmic-ray interaction in emulsion 1 on the left-hand side of the apparatus exit from emulsion 1 and are deflected in the magnetic field while traveling in the 3 mm space between the two emulsions. The positive electron path curves upward and the negative electron path bends downward into emulsion 2. The electrons may travel through the second emulsion or come to a full stop within the emulsion. The position of exit of a particle from emulsion 1 and its point of entry into emulsion 2 will define the arc or curvature of deflection.

For example, they calculated that the radius of curvature of the track of an electron of 10^{10} eV energy in a field of 14,000 G would be 24 m, or

$$\rho = \frac{1 \times 10^{10}\ \text{eV}}{(300)(14,000\ \text{G})} = 0.24 \times 10^{4}\ \text{cm} = 24\ \text{m} \qquad \text{[VI.25]}$$

The nuclear emulsion technique developed by Powell and his coworkers was a vital tool used by many researchers to determine the properties of high-energy cosmic radiation and the physics of elementary particles in general. Among these, a very important example can be taken from the work of Emilio Segrè, Owen Chamberlain, and coworkers, who used Powell's nuclear emulsion technique to study antinucleon annihilation and measure the resulting particle energies. This is described in detail in the subsequent biographical sketches on Emilio Segrè and Owen Chamberlain.

Cecil Powell staunchly opposed nuclear weapons and was one of the original proponents for total nuclear disarmament. He was cosignatory of the Russell-Einstein Manifesto of 1955 (Bone, 2005) calling for nuclear disarmament and world peace (see the biographical sketch on Leo Szilard in Hall of Fame, Part IV). Powell also chaired the first Pugwash Conference in 1957, which focused on the then most difficult and vital challenge facing mankind, nuclear disarmament and world peace. Cecil Powell died on August 9, 1969 in Milan, Italy.

EMILIO SEGRÈ (1905–1989) AND OWEN CHAMBERLAIN (1920–2006)

Emilio Segré and Owen Chamberlain were jointly awarded the Nobel Prize in Physics in 1959, in the words of the Nobel Committee "for their discovery of the antiproton."

The antielectron or positron had been discovered by Carl D. Anderson in 1932 in cosmic radiation showers, as described previously. This antiparticle of the electron was postulated by Dirac, who predicted antiparticles of all matter, including protons and neutrons. To confirm Dirac's theory, there was a need to provide evidence for the existence of the antiparticles of the nucleons—that is, the antiparticles of the proton and neutron. Emilio Segrè, Owen Chamberlain, and coworkers at the Lawrence Berkeley National Laboratory discovered the antiproton in 1955, and the antineutron was discovered by coworkers the following year.

Emilio Segrè, April 28, 1954
Photo courtesy of Berkeley Lab, © 2012
The Regents of the University of California,
Lawrence Berkeley National Laboratory

Due to the large mass of the proton or neutron, a large amount of energy would be required to produce a proton–antiproton pair or a neutron–antineutron pair. With sufficient energy a particle and its antiparticle would be produced as a

pair of particles, similar to the positron−electron pair production described earlier. The energy required for pair production of a proton−antiproton or neutron−antineutron would be equivalent to an excess of the mass equivalent energy of the two particles. The energy equivalence of the mass of the electron is only 0.51 MeV/c^2. Thus the production of the electron−positron pair requires energy in excess of the mass of two electrons or 1.02 MeV, as described in the chapter entitled "Electromagnetic Radiation: Photons." This low-energy threshold made possible the relatively facile observation of positron−electron pair production by Carl D. Anderson with gamma-ray sources in excess of 1.02 MeV. However, due to the relatively high mass of the proton (938.27 MeV/c^2), the scientific staff at the Lawrence Berkeley National Laboratory knew that a relatively large amount of energy in excess of two proton masses (>1876 MeV or 1.876 billion eV) would be required to produce a proton−antiproton pair. High-energy particles in the cosmic radiation showers can provide energies in excess of that required for nucleon pair production; however, the particle showers are random; and a steady source of high-energy particles would be needed to provide sufficient data to prove the existence of the antinucleon. The Lawrence Berkeley National Laboratory thus set out to construct a high-energy proton synchrotron capable of accelerating protons in the energy range of several billion electron volts or BeV—hence it was called a Bevatron, a name commensurate with the energy range of the protons it would produce (the current usage for this magnitude of energy is gigaelectron volts or GeV). The Bevatron began operation in 1954, and was utilized by Emilio Segrè, Owen Chamberlain, and coworkers to establish the existence of the antiproton unequivocally.

Owen Chamberlain (1920−2006)

The significance of the discovery of the antiproton by Segrè, Chamberlain, and coworkers at the Lawrence Berkeley National Laboratory was put into perspective in the Nobel Prize award ceremony speech given by Professor E. Hulthén, chair of the Nobel Committee for Physics, on December 11, 1959 [with author's comments in brackets]:

> *…Dirac's theory of particles and antiparticles, which may be designated, almost, as each other's mirror images. Both kinds of particles are conceived as arising through the formation of pairs and as reciprocally annihilating each other. The world in which we find ourselves belongs, by chance, to the one kind of particles, among which sporadically occurring antiparticles are very quickly destroyed. On account of the mirror symmetry it would be very difficult to decide whether a remote star or galaxy belonged to the one or the other kind of matter.*
>
> *There were probably very few physicists who at first ascribed to this side of Dirac's otherwise very valuable theory any real import until, quite suddenly and unexpectedly, the first antiparticle, the positive electron, was discovered by Anderson in cosmic radiation in the year 1931. Continued investigations showed that the new particle behaved in all respects according to Dirac's theory: that it was manifested, namely, in connection with some energetic process, always together with an ordinary electron, and that it disappeared in the same way and with equal suddenness. Today nothing is better known and clearly elucidated than this process of pair formation and annihilation.*

Nonetheless it now seemed desirable to test the validity of this remarkable theory upon the antiparticle to the proton, the nucleus of the hydrogen atom - a process which required, however, about 2000 times as great an amount of energy. Such quantas of energy do, certainly, occur in cosmic radiation, but in such a random way that it was finally realized that the only systematic way of investigating the process was through the controlled production of the antiproton by means of an accelerator with a sufficiently high capacity.

It has been said of the Bevatron, the great proton accelerator at Berkeley University in California, that it was constructed chiefly with a view to the production of antiprotons. This is perhaps an exaggeration, but in so far correct as its peak achievement, 6 milliard electron volts [ie, 6 billion eV or 6 GeV $= 6 \times 10^9$ *eV], was set with a view to the energy required for the pair formation of protons - antiprotons. That it was constructed in Berkeley was due to the tradition established there ever since Lawrence built the first cyclotron and McMillan developed the principle for the synchronization of relativistic particles.*

But even if antiproton research was thus first made possible through this technologically very impressive machine, the actual discovery and investigation of the antiproton was chiefly the merit of Chamberlain and Segrè. With similar methods an antiparticle to the neutron has subsequently been discovered, a discovery whose importance lies in the fact that the concept of the antiparticle was thereby extended to include also the neutral elementary particles.

As noted above, the energy equivalent to two proton masses (ie, 2×938.27 MeV $= 1876.5$ MeV ≈ 2 billion eV) would be the minimum or threshold energy required to convert energy into a proton−antiproton pair. However, Segrè, Chamberlain, and coworkers planned to accelerate protons with the Bevatron, and then have the protons collide against a stationary target to liberate sufficient energy to create the proton−antiproton pair. Due to transfer loss of energy to the stationary target, energy in excess of 2 billion eV would be required, as described by Chamberlain (1959) in his Nobel Lecture:

… the energy necessary to produce a proton-antiproton pair would be twice the proton rest energy, or about 2 billion electron volts. It was also known that high-energy collisions were necessary, such as those between high-energy particles and particles at rest. A likely process might be one in which a very fast proton struck a stationary neutron. The proton would have to have about 6 billion electron volts of energy in order that 2 billion electron volts might be available to make new particles… this fact was taken into consideration when the Bevatron energy, just 6 billion electron volts, was decided upon. Professor Edwin McMillan and the late Professor Ernest Lawrence were among the men who selected the energy of the Bevatron and were responsible for initiating its construction.

Following the collision of high-energy protons against a stationary target, both positive and negative particles would be created. The antiproton would be negatively charged; and the charge of the particles could easily be discriminated by their deflection in a magnetic field, as described by Chamberlain (1959) [with the author comments in brackets]:

To make this demonstration [the existence of the antiproton], it was necessary to show that after the Bevatron beam struck a piece of material, there were present among the particles issuing from nuclear collisions some particles of the same mass as that of the proton, but electrically negative, ie, with an electric charge opposite to that of the proton. It is not difficult to sort out particles that are electrically negative, for in a magnetic field the negative particles are deflected in one direction, while positive particles are deflected in the opposite direction.

In addition to identifying the charge of the particle, it was necessary for Segrè and Chamberlain to measure two independent properties of the same particle, such as its mass, momentum, energy, velocity, or range of travel in a given absorber. This latter property is a function of the mass and energy of a particle of given charge. To confirm the antiproton, Chamberlain (1959) explained that they decided to determine the momentum and velocity of the particle, from which its mass can be readily calculated. Particles originating from collisions of Bevatron-accelerated high-energy protons with atoms of target material would possess relativistic speeds (ie, travel at velocities close to the speed of light); and thus the momentum of the antiprotons would not be defined by the conventional relationship of $p = mv$, because the mass of a particle traveling at relativistic speeds would increase with its velocity according to Einstein's definition of relativistic mass shown by Eq. [III.46] in Hall of Fame, Part III, or

$$m = \frac{m_0}{\sqrt{1 - (v^2/c^2)}} \qquad \text{[VI.26]}$$

where m is the relativistic mass of the particle, m_0 is the particle rest mass, v is the particle velocity, and c is the velocity of light in a vacuum. In his Nobel lecture, Chamberlain (1959) explained how the Berkeley lab team measured particle momentum, velocity, and mass [with the author comments in brackets]:

Perhaps I may remind you of the nonrelativistic relationship between momentum and velocity, namely

$$p = mv \qquad \text{[VI.27]}$$

where p = *momentum,* m = *mass,* v = *velocity. Clearly, we may obtain the mass of a particle by measuring momentum and velocity, obtaining the mass as* m = p/v. *For particles travelling at nearly the speed of light, the expressions are not as simple as these; but it is still true that if momentum and velocity are simultaneously measured, then the mass of the particle may be determined. The relationships are*

$$p = \frac{mv}{\sqrt{1-(v^2/c^2)}} \quad \text{and} \quad m = \frac{p\sqrt{1-(v^2/c^2)}}{v} \qquad \text{[VI.28]}$$

The well-established method of measuring the momentum of atomic particles is to measure their deflection in a known magnetic field. In fact, one may set up a system of magnets through which only particles of a certain momentum interval pass [see Fig. VI.16]… The high-energy proton beam strikes a target, which might be a piece of copper. Fragments of nuclear collisions emerge from the target in all directions, some of which enter the region of the magnetic field, the rest being wasted. For certain values of momentum, negative particles are deflected by the correct amount and pass through the aperture in the collimator. Other particles are stopped by the walls of the collimator…The use of magnetic lenses was suggested to us by Dr. Oreste Piccioni, who pointed out that a greater number of useful particles would pass through the system if lenses were employed. I will not describe the lenses in detail, except to say that each lens is composed of three quadrupole magnets. The lens action is very similar to the action of a simple optical lens for light…

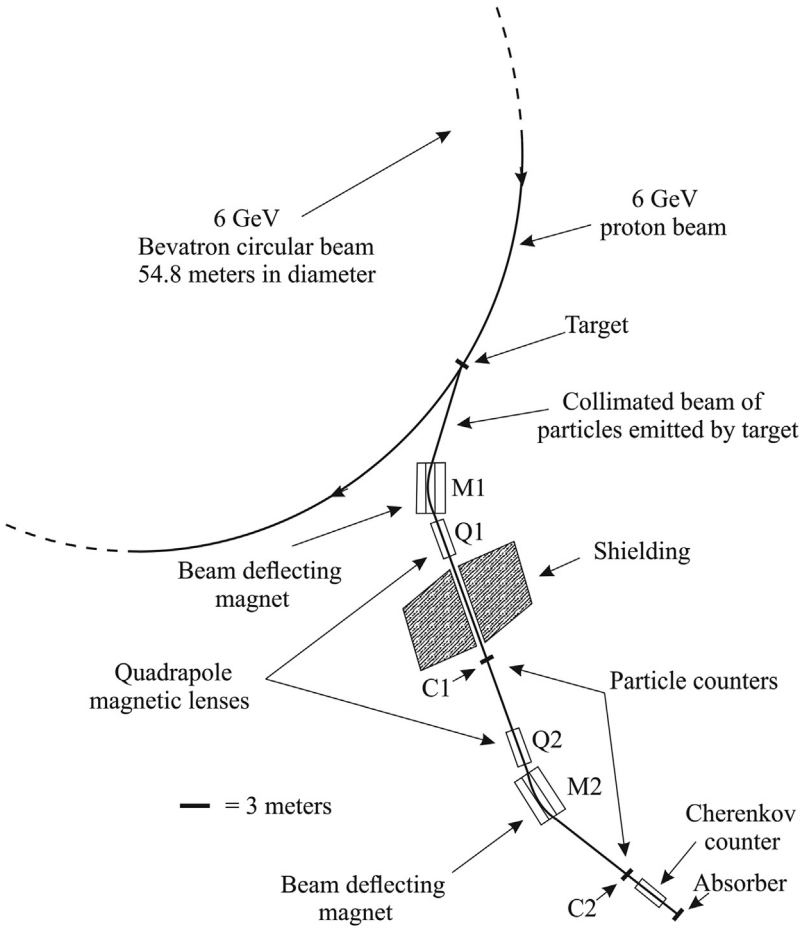

FIGURE VI.16 Plan view of the Lawrence Berkeley National Laboratory Bevatron and its associated particle spectrograph. *Adapted from Chamberlain, O., 1959. The Early Antiproton Work. Nobel Lecture, December 11, 1959. In: Nobel Foundation Staff, (Eds.), Nobel Lectures, Physics, 1942–62, (1964). Elsevier Publishing, Amsterdam, pp. 489–505.*

I have said that only negative particles would be present in the beam formed by the magnetic spectrograph, since positive particles would be deflected in the opposite direction and would not pass through the collimator. By reversing the magnetic field, however, we may use the same spectrograph to select positive particles, if these are desired. The final arrangement of magnets that we have used consists of two such spectrographs, one following the other [see Fig. VI.16].

The first spectrograph extends from the target to the first focus point. The second spectrograph extends from the first to the second focus point. The first spectrograph acted as a preliminary sorting device to provide a relatively pure beam of particles for the second spectrograph, where the experiment itself was performed. Now let us discuss the velocity of the antiprotons that may be found. The most copious production of antiprotons was expected to be at a velocity of 87 percent of the velocity of light, while the other background particles, such as mesons, would be travelling at approximately 99 percent of the velocity of light. To make the experiment somewhat easier, slightly slower antiprotons were chosen, with u, *= 0.78*c, *or 78 percent of the velocity of light [the variable* u *is the same as the variable* v *in Eq. [VI.28]]. The letters* u *and* v *are used often to represent the same variable, that of the particle velocity.]*

One of the simplest means of determining velocity is to measure the time of flight between two counters, and this was the method used. A counter was placed at the first focus point, and another counter at the second focus point. The spacing of these counters was 12 m. Mesons, which travel near the speed of light, would take 40 millimicroseconds (40 billionths of a second) to pass over this distance, but antiprotons of the same momentum would take 51 millimicroseconds. The difference of 11 millimicroseconds is not great, but it is within the capability of modern electronic circuits to distinguish with certainty between the two time intervals [see Fig. VI.16, where counters C1 and C2 are separated by a distance of 12 m along the beam of negatively charge particles].

The operation of the particle spectrograph associated with the Bevatron illustrated in Fig. VI.16 is explained in detail by Chamberlain (1959); a brief description is given here. The spectrograph, which is the instrumentation associated with the particle beam leading away from the circular Bevatron 9 GeV proton beam, was designed to determine the antiproton momentum and velocity and, from these two variables, permit the calculation of the particle mass from Eq. [VI.28] above. As described by Chamberlain (1959), the particle momentum is measured by its degree of deflection in a known magnetic field, and a system of magnets was selected so that only particles of a certain momentum could pass.

A stationary target of copper is placed in the path of the 6 GeV proton beam. When the high-energy protons collide with atoms of the stationary target, nuclear particles are emitted in all directions. A collimated beam of the emitted particles is led into a deflecting magnetic field (M1 in Fig. VI.16), whereby only particles of negative charge are deflected in a given direction. Particles of a momentum that does not allow their passage through this magnetic field are lost intentionally and do not continue along the beam. The beam now contains only negatively charged particles of a certain momentum. Quadrupole magnetic lenses Q1 and Q2 further condense the particle beam in a similar manner to optical lenses condensing a beam of photons of light. The shielding along the beam further collimates it by absorbing any particles that undergo scattering. Two particle counters C1 and C2 (eg, ionization detectors) are located along the beam of negatively charged particles at a distance of 12 m apart to permit time-of-flight measurements of the particle velocity. A second deflecting magnet, M2, further deflects only negatively charged particles into a Cherenkov counter.

The Cherenkov counter permits a second measurement of the particle velocity to confirm the accuracy of the first measurement and avoid any erroneous measurements of velocity that could occur when negatively charged mesons are detected simultaneously by counters C1 and C2 and wrongly interpreted as antiproton particles. The Cherenkov counter is described in detail in the chapter entitled "Cherenkov Radiation," but in brief it is based on the principle that a high-energy charged particle can travel at a velocity faster than the speed of light in transparent media such as air, glass, plastic, etc., although they cannot travel faster than the speed of light in a vacuum. When a high-energy charged particle travels at a speed in excess of the speed of light in a transparent medium, it creates a conical wave front, resulting in the emission of visible light at an angle θ relative to the direction of particle travel, as illustrated in Fig. VI.17.

The emitted radiation, known as Cherenkov radiation, was discovered by Nobel Laureate P.A. Cherenkov and is described in detail in Hall of Fame, Part VII. The angle of emission θ is a function of the particle velocity and the index of refraction of the transparent medium, according to the equation

$$\cos\theta = \frac{1}{\beta n} = \frac{1}{(v/c)n} \qquad [VI.29]$$

where θ is the angle of radiation emission relative to the path of particle travel, β is the relative phase velocity of the particle, ie, the velocity of the particle in the medium relative to the velocity of light in a vacuum or $\beta = v/c$, and n is the index

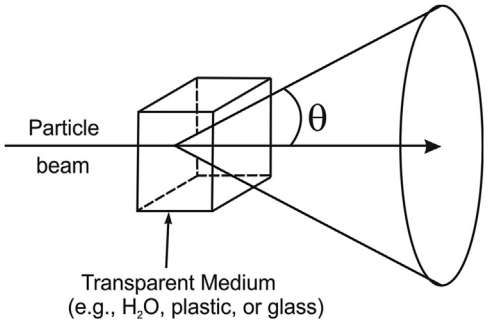

FIGURE VI.17 Cherenkov conical radiation wave front produced by a high-energy charged particle traveling in a transparent medium in a Cherenkov counter. The conical wave front is emitted at an angle θ relative to the path of travel of the charged particle.

of refraction of the medium within which the particle is traveling. In his Nobel lecture Chamberlain (1959) explained the need for the Cherenkov counter:

> *Unfortunately, when many mesons are passing through the system in close succession, it will sometimes happen that two mesons have exactly the right spacing between them to imitate an antiproton, ie, just 11 millimicroseconds. We will call this the accidental coincidence of two mesons. To avoid having the electronic circuits "fooled" by two mesons in close succession, it was considered important to have another method of determining velocity in use at the same time. For this purpose, a Cherenkov counter was constructed. In fact, the study of the Cherenkov counter was one of the first steps taken in the preparation of the experiment. I would like to describe it here. The basic principles of the Cherenkov radiation are familiar, since Professor Cherenkov must have been speaking from this rostrum just one year ago, but those principles especially relevant to the Cherenkov counter used in the antiproton experiment should be reviewed here. In an optical medium such as glass, light moves more slowly than in a vacuum. Although no particle may move faster than the speed of light in vacuum, a particle may move faster than the speed of light in glass. When this happens with an electrically charged particle, Cherenkov light is emitted, at different angles for particles of different velocity.*

Further confirmation of the antiproton was provided by evidence of the energy emitted in antiproton–proton annihilation. Segrè, Chamberlain, and coworkers, including Clyde Wiegand and Thomas Ypsilantis, identified particle tracks and measured the energy released by the explosive effect of antiproton interactions with atomic nuclei, which yielded conclusive evidence of proton and antiproton annihilation (Chamberlain et al., 1956). An example is the annihilation star illustrated in Fig. VI.18. Antiproton annihilation gives rise to mostly π mesons, on average about 4.8 pions per annihilation, plus other nucleons that result from the disintegration of a nucleus.

In the case of nucleon–antinucleon (eg, proton–antiproton or neutron–antineutron) interactions, the resulting annihilation is more complex than electron–positron annihilation. The electron–positron annihilation yields the practically immediate conversion of the two electron masses to electromagnetic energy (see Eq. [8.12] of the chapter entitled "Electromagnetic Radiation: Photons"). However, in the nucleus of the atom there is also the meson, predicted by Yukawa, which is an exchange particle between the nucleons, embodying the strong nuclear forces binding the nucleons. Thus the nucleon–antinucleon annihilation process involves the emission of π mesons, which in a matter of microseconds decay to photons or particles of zero rest mass. Segrè (1959), in his Nobel lecture on December 11, 1959, explained nucleon–antinucleon annihilation [with the author's comment's in brackets]:

> *By now we know a great deal about [nucleon] annihilation. It gives rise prevalently to π mesons. These, in a time of the order of 10^{-8} seconds, decay into μ mesons [now known to be muons, which are leptons rather than mesons] and neutrinos. The μ mesons [i.e., muons], in a time of the order of microseconds decay into electrons or positrons and neutrinos, and the electrons and positrons finally recombine to give gamma rays. In a few microseconds the total rest mass of the nucleon-antinucleon pair degrades to particles with rest mass zero, traveling away from the spot of the annihilation with the velocity of light. Direct annihilation into photons may occur, but is expected to be rare and thus far has never been observed with certainty. The reason for this difference between the behavior of electron-positron and nucleon-antinucleon pairs is, of course, that the latter can annihilate not only through the electromagnetic interaction giving rise to light quanta, but also through the specific nuclear interaction whose quanta are the pions [ie, π mesons]. This last interaction is much stronger than the electromagnetic one and when both are simultaneously present its effects overwhelm those of the electromagnetic interaction, which is the only [type of interaction] available to the electron-positron pair. The most significant result of the [nucleon–antinucleon] annihilation is that the annihilation process gives rise to an average of 4.8 pions per annihilation, about equally divided among positive, negative, and neutral pions [see Fig. VI.18]. These pions escape with a continuous energy distribution, the average kinetic energy being*

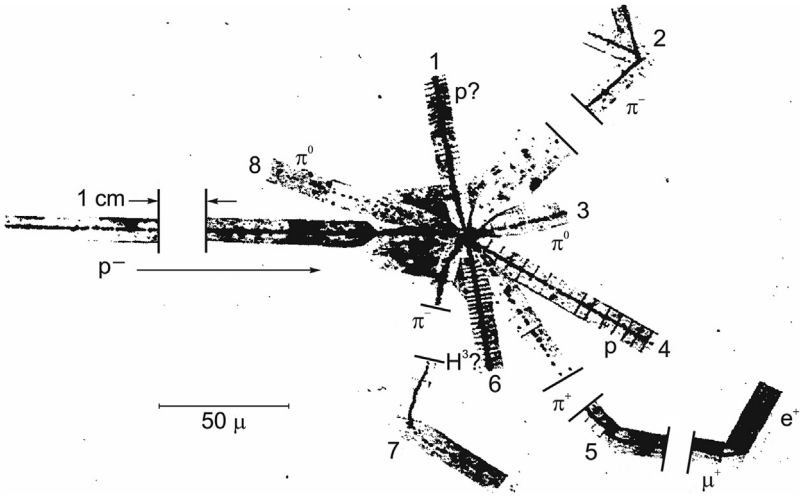

FIGURE VI.18 An annihilation "star" in nuclear emulsion resulting from an antiproton−proton interaction. The track of the antiproton indicates where it traveled from left to right. It comes to rest in the vicinity of a proton of a nucleus in the photographic emulsion, resulting in antiproton−proton annihilation and destruction of the nucleus. Tracks of particles resulting from the interaction show their various directions of travel away from the spot where the annihilation occurred. The particles are identified as (1) proton?, (2) π^--meson, (3) π^0-meson, (4) proton, (5) π^+-meson, (6) H^3?, (7) π^--meson, and (8) π^0-meson. The total visible energy released = 1300 MeV. *From Segré, E., 1959. Properties of Nucleons, Nobel Lecture, December 11, 1959. In: Nobel Foundation Staff, (Eds.,) Nobel Lectures, Physics, 1942-62, (1964). Elsevier Publishing, Amsterdam, taken from the work of Gösta Ekspong at Berkeley with permission from the Nobel Foundation © 1959.*

about 200 MeV. In about 4 percent of the annihilation cases at rest strange particles, K *mesons, are emitted. The escaping pions give rise in complex nuclei to secondary processes and thus a number of nucleons or light nuclei are also found among the particles emitted on annihilation. Sometimes the relatively rare* K *mesons interact producing a* Λ *hyperon and even more complicated hyperfragments have been observed.*

The Λ hyperon is a particle that interacts with the nuclear proton and neutron through the strong force. It is an electrically neutral and unstable particle with a mass higher than the neutron (1115.6 MeV/c^2) and a short lifetime (2.63×10^{-10} s). The Λ hyperon has the following two principal modes of decay (Sundareson, 2001):

$$\Lambda^0 \rightarrow p^+ + \pi^- \ (63.9\%) \qquad \text{[VI.30]}$$

$$\Lambda^0 \rightarrow n + \pi^0 \ (35.8\%) \qquad \text{[VI.31]}$$

The predominant mode of decay depicted by Eq. [VI.30] above was observed in cloud chamber images as V-shaped tracks, such as the track illustrated previously in Fig. VI.6.

As previously mentioned, Powell's nuclear emulsion technique permitted measurement of particle energies from the ranges and grain densities of their tracks. Thus Segrè, Chamberlain, and their coworkers were able to measure the energy liberated from the nucleon−antinucleon annihilation. To demonstrate proton−antiproton annihilation unequivocally, they needed to provide evidence that the energy released in the initial encounter of the proton and antiproton, according to Einstein's equation, would be greater than mc^2 (ie, the energy equivalent to the mass of the proton or antiproton) and possibly near the order of magnitude of $2mc^2$ (ie, the energy equivalent to the combined masses of the proton and antiproton). Thus the energy, E, released in the annihilation would be in the range

$$mc^2 < E \leq 2mc^2 \qquad \text{[VI.32]}$$

where m is the mass of the proton or antiproton and c is the velocity of light in a vacuum. The term $2mc^2$ is derived from the following equation, from which the maximum energy released in the proton−antiproton annihilation is calculated as

$$\begin{aligned} E &= m_p c^2 + m_{\bar{p}} c^2 = 2mc^2 \\ &= 2(1.672 \times 10^{-27}\ \text{kg})(2.9979 \times 10^8\ \text{m/s})^2 \\ &= 30.016 \times 10^{-11}\ \text{J} \end{aligned} \qquad \text{[VI.33]}$$

where $2mc^2$ represents the energy equivalent to the combined masses of the proton and antiproton.

Converting the energy in Joules to electron volts gives

$$E = \frac{30.053 \times 10^{-11}\ \text{J}}{1.602 \times 10^{-19}\ \text{J/eV}} = 18.76 \times 10^{8}\ \text{eV} = 1876\ \text{MeV} \quad \text{[VI.34]}$$

The 1876 MeV would be the maximum energy released in the annihilation, as it represents the conversion of the two proton masses to energy. However, the energy measured with a nuclear emulsion can be expected to fall short of the maximum energy released, because of the various neutrino and gamma-ray energies following pion and muon decays, the tracks of which would not be visible in the emulsion. In his Nobel lecture Emilio Segrè (1959) commented on the energy released from the annihilation:

> *Initially the effort was mainly directed toward establishing the fact that the energy released was* $2mc^2$ *(where* m *is the mass of the proton,* c *the velocity of light), thus furnishing a final proof of the annihilation. In the early investigations with photographic emulsions carried out in my group by Gerson Goldhaber and by a group in Rome led by [Edoardo] Amaldi, we soon found stars showing a visible energy larger than* mc^2*, giving conclusive evidence of the annihilation in pairs of proton and antiproton.*
>
> (Chamberlain et al., 1956).

This discovery of the antiproton facilitated the discovery of the antineutron via proton−proton collisions in the Bevatron at the University of California, Lawrence Berkeley National Laboratory the following year by Bruce Cork, Glen R. Lambertson, Oreste Piccioni, and William A. Wenzel (Cork et al., 1956). The antineutron possesses a neutral charge similar to the neutron. Its antiparticle, the antineutron, is composed of one antiup $(\overline{u})$ quark and two antidown $(\overline{d})$ quarks, and the neutron is composed of an up (u) quark and two down (d) quarks. Also, the antineutron possesses a magnetic moment opposite to that of the neutron. The importance of the discoveries of the antiproton and antineutron was underscored by Professor E. Hulthén, chair of the Nobel Committee for Physics, in the Nobel award ceremony on December 11, 1959:

> *The actual discovery and investigation of the antiproton was chiefly the merit of Chamberlain and Segrè. With similar methods an antiparticle of the neutron has subsequently been discovered, a discovery whose importance lies in the fact that the concept of the antiparticle was thereby extended to include also the neutral elementary particles.*

Brief biographical sketches of Emilio Segrè and Owen Chamberlain are provided in the following paragraphs.

Emilio Segrè was born into a Jewish family in Tivoli, some 25 km from Rome, Italy, on February 1, 1905. He entered the University of Rome to study engineering, but changed his field to study physics under Enrico Fermi, graduating in 1928 with a doctorate in physics.

After a stint in the Italian army from 1928 to 1929, Segrè worked at the University of Rome in 1929−1932 as assistant to Professor Orso Mario Corbino, who was director of the Institute of Physics and had a long history as supervisor to many famous physicists, including Fermi, Edoardo Amaldi, Oscar D'Agostino, Ettore Majorana, Bruno Pontecorvo, and Franco Rasetti. In 1930 Segrè obtained a traveling Rockefeller Foundation fellowship, which allowed him to study atomic spectroscopy under Nobel Laureates Otto Stern in Hamburg, Germany and Peter Zeeman in the Netherlands. In 1932 to 1935, with the status of assistant professor, Segrè carried out joint research under Enrico Fermi on Fermi's pioneering studies of slow neutrons and the creation of artificial radioisotopes with neutron bombardment. This work was carried out with Amaldi, D'Agostino, and Rasetti under Fermi's leadership (see Fermi et al., 1934). A detailed description of the work is given in the biographical sketch of Fermi in Hall of Fame, Part II. During this period, Rome was the leading center of nuclear research on neutron-induced nuclear transformations.

In 1936 Emilio Segrè made a visit to the Berkeley Radiation Laboratory established by Ernest O. Lawrence, and became interested in the radioactive isotopes residing in the scrap metal that was part of Lawrence's cyclotron. Lawrence sent him a molybdenum foil strip which was part of the deflector from the cyclotron. The foil contained unknown radionuclides after bombardment with deuterons in the cyclotron. In Segrè's biographical memoir, Jackson (2002) relates that Segrè understood that two possibilities of nuclear reactions of molybdenum with deuterons could occur. One was a (d,n) reaction, whereby the molybdenum nucleus captures the deuteron (consisting of a proton + neutron) and emits a neutron, resulting in an increase in the atomic number of the nucleus from $Z = 42$ to that of the then unknown element of $Z = 43$. An example of the (d,n) reaction is the following reaction of deuterium with stable ^{94}Mo:

$$^{94}_{42}\text{Mo} + {}^{2}_{1}\text{H} \xrightarrow{(\text{d,n})} {}^{95}_{43}\text{Tc}(\text{radioactive}) + {}^{1}_{0}\text{n} \quad \text{[VI.35]}$$

The other possible nuclear reaction with deuterium is a (d,p) reaction, whereby a molybdenum nucleus captures a deuteron followed by the emission of a proton, which is the following using ^{94}Mo as an example:

$$^{94}_{42}\mathrm{Mo} + ^{2}_{1}\mathrm{H} \xrightarrow{(\mathrm{d,p})} ^{95}_{42}\mathrm{Mo(stable)} + ^{1}_{1}\mathrm{H} \qquad \text{[VI.36]}$$

Segrè collaborated with chemist Carlo Perrier to analyze radionuclides in the strip; and they discovered a new element of atomic number 43, which would result from a (d,n) reaction such as that illustrated above. Eventually they named the new element "technetium," as it was the first artificially produced element (Perrier and Segrè, 1947), and the name is derived from the Greek for "artificial." Segrè became dissatisfied with his academic standing in the University of Palermo, as noted by Jackson (2002):

> *Rightly proud of having filled a gap in the periodic table by their discovery of technetium, Segrè apparently was disturbed by lack of recognition in Italy and by perceived hindrances to his career caused by academic and national politics in Rome… he began seriously in 1937 to look elsewhere for a position, at least in part because of the hints, and more, of trouble for Jews.*

Segrè remained as professor of physics and director of the Physics Laboratory of the University of Palermo in 1936−1938; but in 1938 Bennito Mussolini's facist government prohibited Jews from university positions. Thus Segrè sought asylum in America in 1938, together with his wife Elfriede and their one-year-old child Claudio. Emilio Segrè's mother was captured by the Nazis in 1943 and died at their hands; his father escaped capture but died of natural causes in 1944, shortly after his wife was taken (Jackson, 2002).

Segrè started work on radioisotopes at Ernest O. Lawrence's Radiation Laboratory; and later Lawrence gave Segrè a post as research associate. At the Berkeley Radiation Laboratory Segrè collaborated with Glenn T. Seaborg, resulting in the first isolation of the radioisotope technetium-99m, which is currently one of the most utilized isotopes in nuclear medicine (Segrè and Seaborg, 1938). In 1940 Segrè collaborated with Dale R. Corson and Kenneth R. MacKenzie to create yet another missing element of the periodic table, that of atomic number $Z = 85$. They used Lawrence's 60 in. cyclotron to bombard bismuth ($Z = 83$) with high-energy alpha particles (helium nuclei) and discovered the artificially produced radioactive element of atomic number $Z = 85$, namely astatine (Corson et al., 1940). They created astatine by the following reaction:

$$^{209}_{83}\mathrm{Bi(stable)} + ^{4}_{2}\mathrm{He} \rightarrow ^{211}_{85}\mathrm{At(radioactive)} + 2^{1}_{0}\mathrm{n} \qquad \text{[VI.37]}$$

The word astatine comes from the Greek *astatos*, meaning "unstable." Astatine-211 has a half-life of 7.2 h.

Segrè then collaborated with Seaborg, Joseph W. Kennedy, and Arthur C. Wahl in January 1941, using the cyclotron at Berkeley to synthesize plutonium-239 (element 93) by slow neutron bombardment of uranium. This work was kept secret until 1946, because Pu-239 turned out to be a fissile isotope eventually used in the implosion design for the atomic bomb (http://americanhistory.si.edu/). Segrè's involvement in this work remained secret until after the war in 1946, due probably to the fact that he was an alien, as related by Jackson (2002):

> *Segrè's position in the collaboration was rather bizarre because of government restrictions on aliens concerning topics viewed as sensitive. Matters became even more complex with the entry of the United States into the war.*

In 1943 Segrè joined the Manhattan Project in Los Alamos to conduct research on the development of the atomic bomb during World War II. Two of his former students from the Berkeley Radiation Laboratory, Clyde Wiegand and Owen Chamberlain, joined Segrè at Los Alamos. Segrè's group made critical studies on the spontaneous fission rate of plutonium. The fission rate proved to be too high to use enriched plutonium-239 in the bullet design of the atomic bomb, so uranium-235 was employed instead. The high spontaneous fission rate came mostly from the contaminant plutonium-240 isotope and not from the plutonium-239 (Jackson, 2002). Enriched plutonium-239 was reserved for the implosion design (see Hall of Fame, Part IV). In 1944 Segrè and his wife Elfriede became US citizens while they were in Los Alamos (Jackson, 2002).

After World War II Emilio Segrè returned to the University of California as professor of physics and group leader at the Berkeley Radiation Laboratory. Chamberlain and Clyde Wiegand joined Segrè's research group at the Radiation Laboratory, Chamberlain as a faculty member and Wiegand as laboratory staff assistant (Jackson, 2002). Segrè's group carried out research on nuclear isomerism, the effects of chemical bonding on the rates of electron capture decay, and high-energy proton bombardment of nuclei using a 184-in. synchrocyclotron (Jackson, 2002). As noted in the chapter entitled "Beta Radiation and Beta Decay," Segrè (1947) at the Berkeley Radiation Laboratory, University of California and R. Daudel (1947) at the Curie Laboratories of the Radium Institute in Paris were the first to suggest independently that the rate of decay of nuclei which undergo electron capture decay would be governed by extranuclear environments, such as chemical

bonding and pressure. Segrè and coworkers (Segrè and Wiegand, 1949, 1951; Leininger et al., 1949) demonstrated that chemical effects (ie, chemical bonding affecting orbital electrons) can alter the electron capture decay of beryllium-7.

After the 1954 completion of the Bevatron, capable of accelerating protons to 6 GeV, Segrè, Chamberlain, Clyde Wiegand, and Thomas Ypsilantis searched for the antiproton via the high energies liberated when 6 GeV protons were made to collide with stationary targets, as described in detail earlier. Their discovery of the antiproton in 1955 culminated in the awarding of the Nobel Prize in Physics in 1959 to Emilio Segrè and Owen Chamberlain. The Nobel Prize can be shared by no more than three people, and only Segrè and Chamberlain were selected by the Nobel Committee. There was some controversy over this award of the Nobel Prize to only two of the four authors of the paper announcing the discovery of the antiproton. Jackson (2002) provides some insight into this in his biography of Emilio Segrè:

> *The circumstances surrounding the discovery of the antiproton were not without controversy. Claims were raised that key ideas for the experiment had been stolen. Even within the group, feelings of injustice prevailed. The discovery paper has four authors (Chamberlain, Segrè, Wiegand, and Ypsilantis). The process of nomination and selection for Nobel Prizes is arcane, to say the least, but the practice of no more than three persons to share any one prize seems inviolate. There are those who feel that Wiegand was as deserving as any one to share the prize. Why he was not included is not publicly known. Wiegand's own recount of the initiation, construction, and operation of the 1955 experiment at a symposium in Berkeley in 1985 on the thirtieth anniversary of the discovery gives a glimpse of his own views. For his own part Segrè undoubtedly felt that as group leader responsible for marshaling the resources and fighting successfully to get the experiment scheduled, he deserved a significant share of the glory, regardless of who had actually taken the data. He now had the accolade that had eluded him 20 years earlier… Segrè was also disappointed not to share in the 1951 Nobel Prize in chemistry awarded to McMillan and Seaborg for his contributions to the work on plutonium.*

Emilio Segrè served as chair of the Department of Physics of the University of California, Berkeley during 1965–1966, and published a biography of Enrico Fermi in 1972. In 1974 he returned to the University of Rome, where he served for a year as professor before reaching the mandatory retirement age; and he was awarded an honorary chair at the University of Rome by the Italian parliament (Jackson, 2002). His autobiography (Segrè, 1993) was published posthumously. He was an avid photographer, and took many photos of scientists and scientific events. Many of these were donated to the American Institute of Physics, which has compiled an archive of the history of physics named after Segrè in his honor. The Emilio Segrè Visual Archives currently contains more than 30,000 photos of scientists and their work, available to the public via the internet in digital format (https://photos.aip.org/). Segrè died at the age of 84 of a heart attack while walking near his home in Lafayette, California.

Owen Chamberlain was born in San Francisco, California on July 10, 1920. He graduated from Dartmouth College with a bachelor's degree in physics in 1941, and continued studies in physics as a graduate student at the University of California, Berkeley. Here he took a course in optics given by Emilio Segrè. In a biographical memoir on Chamberlain, Steiner (2010) quotes from Segrè's autobiography (Segrè, 1993), commenting on Chamberlain's participation in his class:

> *In one of my optics courses there was a student who amused himself in finding flaws in the lectures. His objections, always polite, were often well taken and showed a critical and alert mind. I appreciated the young man, who obviously was interested in the course, and used his head, and I made friends with him. He was Owen Chamberlain.*

Chamberlain's studies at Berkeley were interrupted when the United States entered World War II on December 8, 1941 after the Japanese attack on Pearl Harbor. In early 1942 Ernest Lawrence, director of the Berkeley Radiation Laboratory, recruited faculty and students to work on the Manhattan Project, which was the concerted American research project to develop the atomic bomb. Chamberlain joined the Manhattan Project by first assisting Emilio Segrè in the measurement of spontaneous fission rates at Berkeley; and in 1943 he moved to Los Alamos with his wife to continue work on the project. At Los Alamos, Chamberlain worked under Segrè in research on nuclear cross-sections for intermediate-energy neutrons and rates of spontaneous fission of the heavy elements (see Nobel Lectures in Physics, 1942–1962 and the above biographical sketch of Segrè).

During his work in the Manhattan Project, Chamberlain believed firmly in the importance of developing the atomic bomb, because other countries would be doing the same. In a biography on Owen Chamberlain, Steiner (2010) explains that after the war Chamberlain saw how quickly and effectively the bomb ended the war, and the effect it had on the military. Steiner noted:

> *He [Chamberlain] soon became concerned that people who read the newspapers and realized that the atomic bomb had been instrumental in stopping the war would not comprehend what a revolution had occurred in the military. Within a few months he was taking an active part in the newly established organization called the Federation of Atomic Scientists, whose main goal was to prevent future nuclear wars.*

Chamberlain continued his graduate studies in 1946 at the University of Chicago under the guidance of Enrico Fermi. He completed his doctoral research on the diffraction of slow neutrons in liquids in 1948, and was awarded his doctorate in 1949. Fermi considered Chamberlain as his top student, who he encouraged to pursue his profession in experimental physics and teaching at the University of California at Berkeley, where he continued for the next 41 years. On return to Berkeley, Chamberlain started as instructor and was promoted to assistant professor in 1950. At this time Chamberlain joined forces with Segrè to colead "the Segrè-Chamberlain group at the Berkeley Radiation Laboratory" (Steiner, 2010). During 1953–1954 the Segrè–Chamberlain group carried out studies of nucleon–nucleon interactions using the 184 inch synchrocyclotron, and then advanced to use the Bevatron, capable of accelerating protons to energies in excess of 6 GeV, sufficient to produce antiprotons following collisions of 6 GeV protons with stationary targets, as described earlier. This work led to the discovery of the antiproton in 1956, reported in a paper coauthored by Chamberlain, Segrè, Clyde Wiegand, and Thomas Ypsilantis; the work also included several graduate students. Only the two group leaders, Chamberlain and Segrè, were awarded the Nobel Prize in 1959 for this work. However, Herbert Steiner (2010), who started his graduate studies under Segrè in 1953, provides insight into the lesser-known Wiegand and Ypsilantis:

> *We were all rather intimidated by Segrè, who didn't suffer fools lightly, but who also taught us a lot from his extensive experience, and his ability to focus on the essence of a problem. Owen was the person we would go to when we didn't understand something or when we wanted to learn more. The other senior member of the group was Clyde Wiegand, the superb experimental physicist who turned our naïve ideas into reality and taught us by example how physics should be done. Clyde was also the one to whom we would go to ask the questions we were too embarrassed to ask even Owen. One student, in particular, deserves special mention. He was Tom Ypsilantis, who was always full of ideas, and he played an increasingly important role in the activities of the group as time went on.*

Left to right: Clyde Wiegand (1915–1996), Owen Chamberlain, Emilio Segre, and Thomas Ypsilantis (1928–2000) converse in a laboratory Courtesy of the AIP Emilio Segre Visual Archives, Segre Collection

During the following years Chamberlain studied antiproton–nucleon interactions and the production of antineutrons from antiprotons. In the 1960s he pioneered the development and use of polarized (spin-aligned) proton targets to study spin dependence on high-energy processes, including the scattering of pi-mesons and protons on polarized proton targets; and in the 1970s and 1980s he participated in studies on the interactions of high-energy light nuclei with nuclear targets at the Berkeley Bevalac accelerator (Nobel Lectures, Physics, 1942–1962). The Bevalac was an accelerator consisting of the Bevatron linked to a linear accelerator, known as the super-HILAC. The linear accelerator would first accelerate nuclei, which were then fed into the Bevatron. The Bevalac at the Lawrence Berkeley Laboratory could accelerate all nuclei of the periodic table to relativistic speeds (ie, close to the speed of light). During his final years at Berkeley, Chamberlain worked with David R. Nygren (1938–) on the construction and development of the time projection chamber, which was subsequently utilized for studies of positron–electron interactions at the Stanford Linear Accelerator Center (Nobel Lectures, Physics, 1942–1962). The time projection chamber, invented by Nygren at the Berkeley Laboratory, was a particle detector that gave a three-dimensional picture of particle collisions occurring within the detector. This would allow the tracking of ionizing particles following a collision, thereby permitting the determination of the particle type and momentum and the position of the collision.

Owen Chamberlain died on February 28, 2006 as a result of complications of Parkinson's disease at his home in Berkeley, California at the age of 85.

DONALD A. GLASER (1926–2013)

Donald Arthur Glaser was born in Cleveland, Ohio on September 21, 1926. He was awarded the Nobel Prize in Physics in 1960 "for the invention of the bubble chamber."

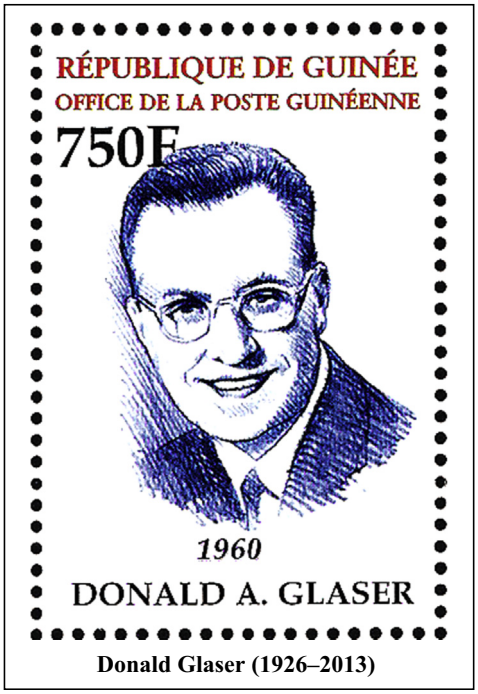

Donald Glaser (1926–2013)

Donald Glaser completed his primary and secondary education in the public schools of Cleveland Heights, Ohio. He received a BSc in physics and mathematics in 1946 at the Case Institute of Technology, now the Case Western Reserve University. (The new university was formed in 1967 by the federation of the Case Institute of Technology, founded in 1880 by philanthropist Leonard Case, Jr, and the Western Reserve University, founded in 1826.) He taught mathematics during the 1946 spring semester at the Case Institute of Technology, and the following autumn began his graduate studies at CalTech. Glaser completed his PhD work under the supervision of Nobel Laureate Carl Anderson in the autumn of 1949 and was awarded the degree the following year. His doctoral research was a study on the momentum spectra of high-energy cosmic radiation and mesons of cosmic-ray showers at sea level.

After completing his doctoral work, in 1949 Glaser began a teaching and research position in the Physics Department of the University of Michigan, and was promoted to the rank of professor in 1957. At Michigan he carried out the pioneering research that led to his invention of the bubble chamber for the identification and measurement of elementary atomic particles by the tracks of bubbles they leave behind in various liquids. He was aware of the need for a detector that could record many particle tracks on a real-time basis to permit the collection of mass data to improve our knowledge of the lifetimes, energies, and interactions of elementary nuclear particles. Particularly there was a need for a detector of large volume (several liters) to speed the collection of rare events in cosmic-ray interactions, unlike the thin photographic emulsions. With the development of a large-volume detector, sufficient data could be collected on rare events to improve the accuracy of the information that could be acquired from the particle tracks. One example of a rare event was the occurrence of "*V* particles" or "pothooks," so called because of the unusual V shape that appeared in some rare tracks in nuclear emulsion (see Fig. VI.6), such as those produced by kaons of cosmic radiation showers. Tracks of this type were observed only infrequently—about one a day with nuclear emulsions or cloud chambers placed on mountain tops. A large-volume detector, as noted by Glaser (1960), could provide more experimental information concerning the production, decay, and interactions of the new and yet rarely observed particles.

Glaser based his invention of the bubble chamber on the basis that nucleation of bubble formation could result from the passage of an ionizing (charged) particle through a superheated liquid. In other words, the ionization that would

occur along the path of travel of a charged particle would create microscopic bubbles or a vapor trail of the liquid, analogous to a vapor trail produced by a high-speed aircraft traveling in the upper atmosphere. The microscopic bubbles would be very small (10^{-6} cm) 1−2 ms after they were created and would grow larger with each millisecond of time. Such an effect occurs when a high-flying aircraft produces a vapor trail. The trail starts very fine, and then grows thicker with time. If the liquid selected was transparent, the particle path through the liquid could be photographed only a few milliseconds after a charged particle traversed the liquid. Glaser selected diethyl ether as the liquid medium for his initial experiment, because it had a relatively low boiling point (34.5°C), critical temperature (192.6°C), and critical pressure (35.6 atm.), and it was relatively inexpensive. Also, he chanced upon a relatively old publication by Kenrick et al. (1924) reporting that diethyl ether could be maintained quiescent at 130°C and 1 atm pressure for hours under very clean conditions; but the authors complained that at 140°C the liquid would erupt at erratic time intervals after being brought rapidly to 140°C. In disgust over this unexpected occurrence and prior to abandoning their experiment, Kenrick et al. (1924) reported a typical series of 30 consecutive times that this random boiling would erupt. Glaser (1960, 1994) relates that he made a histogram of the time intervals and got a Poisson distribution that corresponded to a random event with a mean time interval of 60 s. Glaser estimated that the combination of cosmic radiation and terrestrial background radiation would produce an ionizing event, on average, approximately once every 60 s in the hot diethyl ether of Kenrick et al. (1924). He proceeded to demonstrate that ionizing radiation could trigger boiling in the superheated diethyl ether; his experiment is illustrated in Fig. VI.19.

His first report on the formation of bubbles in liquids by ionizing radiation was the result of initial tests with diethyl ether in a glass tube kept at 140°C under a pressure of 20 atm (Glaser, 1952). He showed that the diethyl ether would erupt to a boil as soon as the pressure was released if exposed to a 12.6 mCi ^{60}Co source. When the diethyl ether was not exposed to the radiation source, eruptive boiling would not occur until about 68 s after release of the pressure, keeping in mind that hard cosmic-ray particles could traverse the liquid at an average of one every 34 s. His initial tests clearly showed that external radiation could cause bubble formation in superheated liquids, and the potential that the tracks of the very first minuscule bubbles formed by ionizing radiation might be observed if photographed almost immediately (a few milliseconds) after the particle traversed the liquid. Fig. VI.19 illustrates Glaser's initial experiment, the results of which were first reported in 1952 and subsequently in more detail in his Nobel lecture (Glaser, 1960) and recollections later in life (Glaser, 1994).

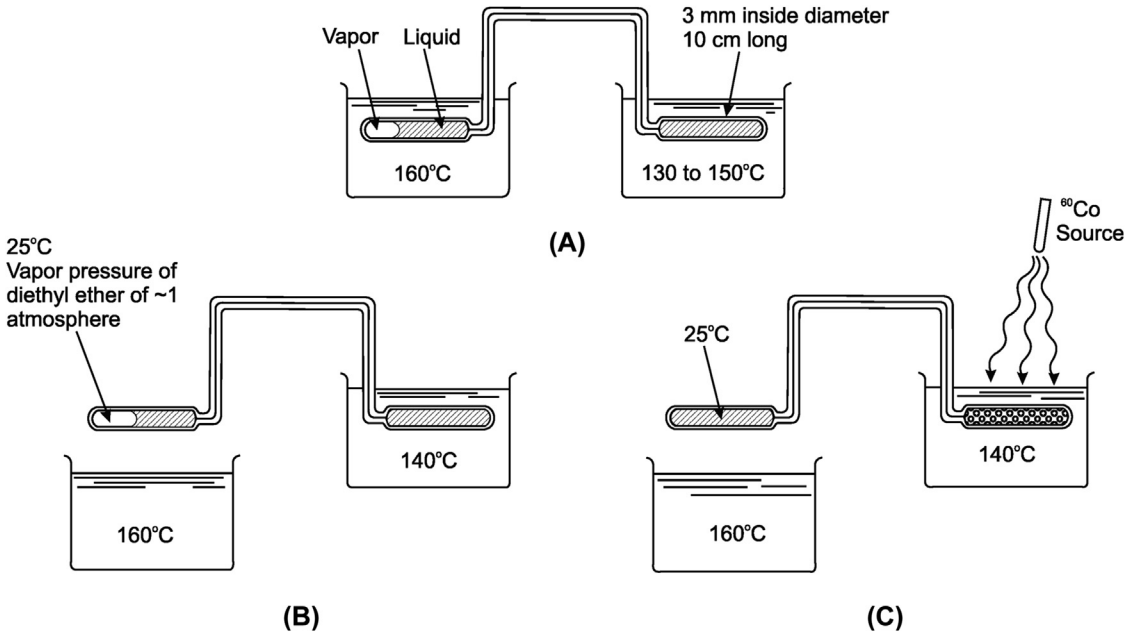

FIGURE VI.19 Glaser's experiment demonstrating that superheated diethyl ether could be made to boil by ionizing radiation. The experimental apparatus consisted of two glass bulbs containing diethyl ether connected with narrow-bore glass tubing. The diethyl ether in the bulbs was maintained at different temperatures to control the pressure on the enclosed liquid. The experiment proceeded as follows. (A) The pressure on the enclosed diethyl ether was initially high (~20 atm) due to the vapor pressure of the liquid at 160°C. The temperatures were maintained by oil baths. (B) The oil bath at 160°C was removed quickly, whereby the temperature in the bulb on the left dropped to 25°C, and the pressure on the overall system dropped to ~1 atm. The diethyl ether in the right-hand bulb at 140°C then became highly superheated. (C) Boiling is triggered in the superheated diethyl ether by radiation from the ^{60}Co source. *Adapted from Glaser, D.A., 1960. Elementary Particles and Bubble Chambers, Nobel Lecture, December 12, 1960. In: Nobel Foundation Staff, (Eds.), Nobel Lectures, Physics, 1942–62, (1964). Elsevier Publishing, Amsterdam; Glaser, D.A., 1994. Invention of the bubble chamber and subsequent events. Nucl. Phys. B (Proc. Suppl.) 36, 3–18, with permission from the Nobel Foundation © 1960.*

After demonstrating that ionizing radiation from ^{60}Co could initiate boiling in a superheated liquid, Glaser needed to determine whether or not a minimum ionizing particle could initiate boiling, and if such a particle would form very minute bubbles along its path of travel in the superheated liquid in the few milliseconds prior to the eventual growth of the bubbles into a more eruptive effect such as boiling. If minute bubbles along the particle path of a minimum ionizing particle were not observable, the device would have no application in cosmic-ray or high-energy particle physics. By "minimum ionizing particle" is meant any charged particle of low mass and high (relativistic) speed, such as cosmic-ray mesons.

To demonstrate the effect of the passage of a minimum ionizing particle in the superheated liquid, Glaser constructed numerous Pyrex glass bubble chambers of various shapes (round, oval, etc.) and a small volume (a few cm^3). He used a hot oil bath to keep the diethyl ether at the appropriate temperature, and a mechanical piston operated by a hand crank controlled the pressure above the diethyl ether. With the liquid at its appropriate temperature, Glaser reduced the pressure with a quick turn of the hand crank to achieve the superheated state. A few seconds later, when the diethyl ether was in its quiescent superheated state, a high-speed movie camera recorded the formation of bubbles and the onset of boiling. Glaser (1994) reported his recollections of the historic findings:

> *From these movies taken at 3000 pictures/second, one sees that the bubbles grow to more than a millimeter in diameter in 300 microseconds. Finer tracks were obtained by constructing an automatic device for expanding and recompressing the chamber every 10 seconds. Photographs of the chamber were taken with a xenon flashlamp whenever a vertical Geiger counter telescope indicated the passage of a penetrating cosmic ray particle during the few seconds of sensitive time following each expansion. These photographs [one is illustrated in Fig. VI.20] proved that bubble chambers could yield precision measurements of events involving minimum ionizing tracks.*

FIGURE VI.20 One of the first penetrating cosmic-ray tracks photographed by Glaser in a 3 cm^3 diethyl ether bubble chamber at 140°C with random expansion and counter-controlled flashlamp. The photograph was taken with a 10 μs flash delay and 20 μs flash duration. *From Glaser, D.A., 1953. Bubble chamber tracks of penetrating cosmic-ray particles. Phys. Rev. 91, 762–765, http://dx.doi.org/10.1103/PhysRev.91.762, reprinted with permission by the American Physics Society © 1953.*

Diethyl ether was the first liquid tested by Glaser, because it was conveniently available in his laboratory. After his initial demonstration of the first particle tracks by penetrating cosmic radiation in superheated diethyl ether, Glaser theorized that bubble nucleation in superheated propane and other liquids would also occur, and proceeded to research these liquids. He thought that liquid hydrogen would be a good candidate, particularly since physicists would be able to observe cosmic-ray or other high-energy particle interactions with protons. He did not have a cryogenics laboratory at his University of Michigan, Ann Arbor facilities, so in 1953 he joined Roger Hildebrand and Darragh Nagle at the University of Chicago to work on liquid hydrogen bubble chambers. Glaser (1994) related the momentum of work on the development of his invention at the time:

I was pleased to learn that Roger Hildebrand and Darragh Nagle at the University of Chicago wanted to make a liquid-hydrogen chamber and invited me to join them. Liquid hydrogen was soon shown to be radiation sensitive under the predicted conditions [Hildebrand and Nagle, 1953] and the race was on to make a track-forming chamber. John Wood at Berkeley was the first to succeed using liquid hydrogen with a chamber fabricated of glass and metal (Wood, 1954), a so-called dirty chamber, because boiling always began at the metal walls. The same technique works for other liquids but shortens the sensitive time making the chamber very inefficient for cosmic-ray experiments, but not interfering with pulse-beam accelerator experiments at all. Construction of large hydrogen bubble chambers became feasible because of this critical development.

Subsequent research by Glaser and coworkers demonstrated that other liquids such as isopentane (Glaser and Rahm, 1955), liquid xenon (Brown et al., 1956) and propane (Meyer et al., 1957) in addition to diethyl ether and hydrogen were suitable for track formation in bubble chambers. As noted by Glaser in his Nobel lecture on December 12, 1960:

Many other liquids were tested in our laboratory and in other places. No liquid that has been tested seriously has failed to work as a bubble chamber liquid. The choice of liquids depends only on the physical objectives of the experiment and on engineering and economic considerations… Water, of course, turns out to be the wrong substance to use in a bubble chamber, because it has a large surface tension and a high critical pressure.

Glaser et al. (1956) demonstrated that the particle velocities could be determined by the measurement of the relative ionization produced by the charged particles as they traveled through the bubble chamber. The relative ionization was measured by a determination of the bubble density along the particle track, ie, the number of bubbles formed per particle path length. The bubble densities produced by particles of known velocity and mass would be used as standards to determine the velocities and mass of the unknown particles. They could count bubble densities up to approximately 150 bubbles per centimeter on a photograph negative without error, due to fusion of neighboring bubble images along the particle track. Thus particle velocity and mass measurements were possible with the new bubble chamber.

Following the demonstration by Wood (1954) that bubble chambers could be constructed with metal walls, larger chambers were made of metal frames and glass windows. One of the first was a circular bubble chamber with 5 cm diameter glass windows and aluminum frame, followed by the construction of a 30 cm, 21 L propane chamber and Luis Alvarez's (1911–1988) 180 cm, 500 L liquid hydrogen chamber at Berkeley (Glaser, 1960). Magnetic fields could be applied to the new bubble chambers by external magnets to facilitate measurement of charge, momentum, and mass of a particle from its direction of deflection and radius of curvature, as described previously. As charged particles slowed they would take on a very small radius of curvature in the magnetic field, and even display a winding circular path. The new bubble chambers thus provided much information on the masses, lifetimes, decay schemes, branching ratios, etc. of the elementary particles. Some illustrative examples are provided in Figs. VI.21–VI.23 .

The K^+ meson has several modes of decay, as described by Eqs. [VI.5]–[VI.12]. Some of the decay schemes yield one or more π^o mesons. The neutral pion will not produce a track in any bubble chamber, but its conversion to positron–negatron (e^+e^-) pairs, which are formed in the proximity of the vertex of the K^+-meson decay, provides evidence of the π^o mesons, such as in the example illustrated in Fig. VI.24. Kalmus and Kernan (1967) took 240,000 photographs of 3×10^6 tracks of stopped K^+ mesons in a 76 cm bubble chamber filled with Freon. They were able to identify the K^+-meson decay schemes according to the characteristic patterns of particle tracks formed by π^o-meson conversion to e^+e^- pairs, as illustrated in Fig. VI.24.

In the Nobel Prize presentation speech on December 12, 1960, Professor Kai Siegbahn, member of the Swedish Academy of Sciences and later a recipient of the Nobel Prize in Physics in 1981 for his work on the development of high-resolution electron microscopy, spoke about the significance of Glaser's invention of the bubble chamber:

The Wilson [cloud] chamber has certainly played a tremendously important role, especially during the 1930's, which is referred to as "the golden age of nuclear physics", and there is no doubt that it was the Wilson chamber which made possible the greatest nuclear physical discoveries during that decade… This situation is completely different in the nuclear physics of today, where one now has at one's disposal particle accelerators with energies as high as 25 billion volts, for example the accelerator which has

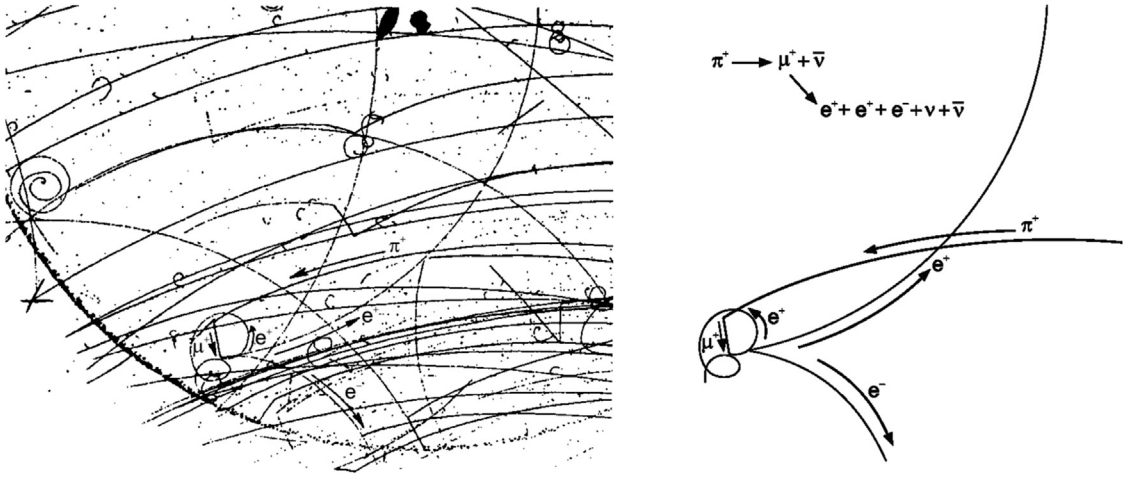

FIGURE VI.21 Bubble chamber tracks of the decay of a pion and a μ^+ (positive muon). On the left is the bubble chamber image with its many tracks, and on the right is a drawing of the tracks produced by the muon decay and the identified decay scheme. The slow muon track was stopped in a liquid hydrogen bubble chamber 30.5 cm in diameter and 15.25 cm in depth placed in a magnetic field of 8800 G. Out of 22,000 positive muons observed by Lee and Samios (1959), they found three events of μ^+ decay with three charged prongs (two positrons and one electron), such as the event illustrated here. The authors concluded that a positron and electron pair arise from the internal conversion of a gamma ray (internal pair production) arising from the decay scheme $\mu^+ \rightarrow e^+ + \nu + \overline{\nu} + \gamma$. *From Lee, J., Samios, N.P., 1959. Search for rare decay modes of the μ^+ meson. Phys. Rev. Lett. 3, 55–56, http://dx.doi.org/10.1103/PhysRevLett.3.55, reprinted with permission by the American Physical Society © 1959.*

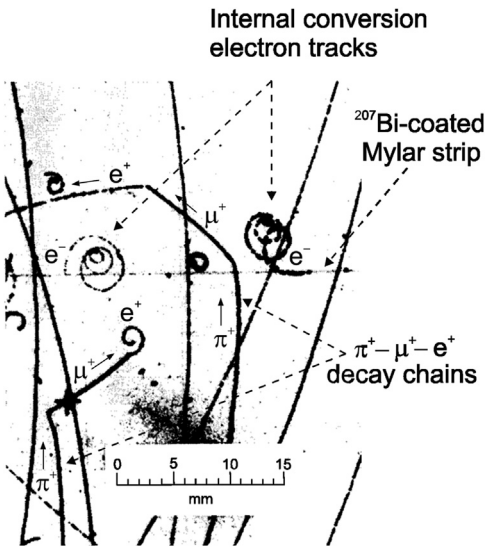

FIGURE VI.22 Particle tracks formed in a 10 L hydrogen bubble chamber exposed to a beam of π^+. Curvatures to particle paths were produced by a magnetic field of 20.85 kG, whereby positive and negative charged particles bend in opposite directions and the radius of curvature is a function of the particle momentum. The picture illustrates two 1.4 MeV/*c* internal conversion electron tracks. The internal conversion electrons originated from a ^{207}Bi source coated on the surface of a Mylar® (DuPont trademark) strip stretched across the bubble chamber. The tracks of the conversion electrons were used to calibrate the μ^+ momentum measurements. The tracks of two $\pi^+ - \mu^+ - e^+$ decay chains are seen here. *From Derenzo, S.E., 1969. Measurement of the low-energy end of the μ^+ decay spectrum. Phys. Rev. 181, 1854–1866, http://dx.doi.org/10.1103/PhysRev.181.1854, reprinted with permission by the American Physical Society © 1969.*

recently been built in the European Nuclear Research Center in Geneva. In other words, [particle] energies which are more than 1000 times larger than those which were earlier obtainable… It is obviously necessary to use a medium other than gas in order to be able to bring such particles to rest. Donald Glaser has succeeded in solving this problem, and his so-called "bubble chamber" is the high-energy nuclear physics counterpart to the low-energy nuclear physics Wilson chamber… One could say that Glaser's bubble chamber is an anti-Wilson chamber. Particle tracks in Glaser's chamber are composed of small gas bubbles in a liquid… The largest bubble chamber is surrounded by a powerful electromagnet which is capable of bending the paths of the particles so

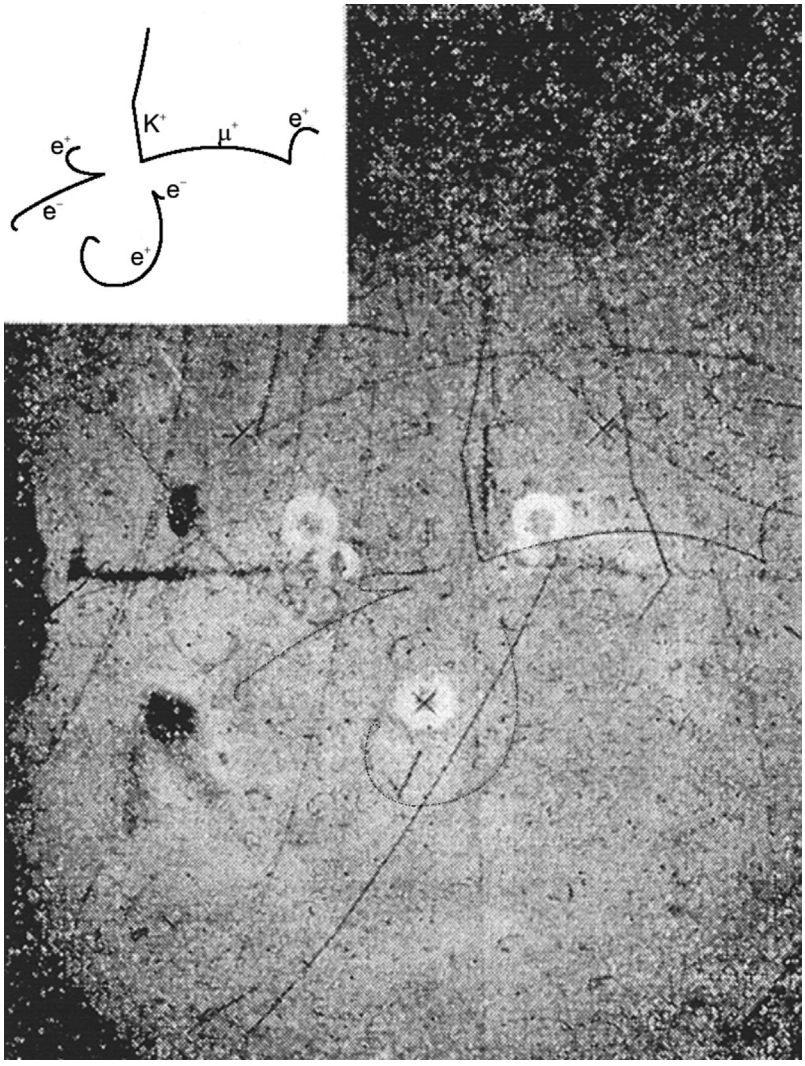

FIGURE VI.23 An enhanced photograph of the tracks produced by a K^+ meson that was stopped in a 76 cm Freon (C_3F_8) bubble chamber. A drawing of the relevant tracks is inset in the upper left-hand corner of the photograph. The positive kaon decayed according to the path $K^+ \rightarrow \pi^o + \mu^+ + \nu$. The μ^+ decays to a positron and neutrino. The neutrinos, of course, do not form tracks because of their lack of charge and near-zero mass. The π^o decays according to the pathway $\pi^o \rightarrow 2\gamma$, so the two gamma-ray photons convert to positron−negatron (e^+e^-) pairs. Notice the gap between the end of the K^+-meson track and the start of the two tracks formed by the (e^+e^-) pairs. The absence of tracks is due to the neutral charge of the π^o meson. *From Callahan, A.C., et al., 1966. Measurement of the $K^+_{\mu 3}$ decay parameters. Phys. Rev. 150, 1153−1164, http://dx.doi.org/10.1103/PhysRev.150.1153, reprinted with permission by the American Physical Society © 1966.*

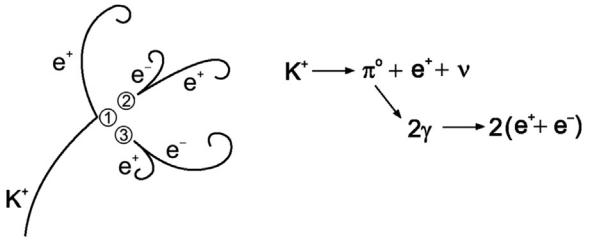

FIGURE VI.24 Schematic diagram of the bubble chamber particle tracks produced by the decay sequence $K^+ \rightarrow \pi^o + e^+ + \nu$ at vertex (1), followed by $\gamma \rightarrow e^+ + e^-$ at vertices (2) and (3). *From Kalmus, G.E., Kernan, A., 1967. Experimental study of $K^+ \rightarrow \pi^o + e^+ + \nu$ decay. Phys. Rev. 159, 1187−1194, http://dx.doi.org/10.1103/PhysRev.159.1187, reprinted with permission by the American Physical Society © 1967.*

that the faint bubble tracks become slightly curved. In this way one is able to identify the unknown atomic particles when they, traveling very close to the speed of light, pass through the chamber… Already a great amount of information has been obtained in this way and many important discoveries will no doubt follow in the near future by means of your method. It is unusual for a development in modern nuclear physics to be due to such a large extent to one single man [person].

Among the prominent findings facilitated by Donald Glaser's bubble chamber was evidence of the mechanisms of antiproton and antineutron annihilation. In 1955 Segrè, Chamberlain, and coworkers discovered the antiproton (Chamberlain et al., 1955); and the following year Cork et al. (1956) discovered the antineutron. For their discovery Segrè and Chamberlain were awarded the Nobel Prize in Physics in 1959. The discovery of the antinucleons was long awaited, since Dirac had predicted the positron or antiparticle of the electron in 1928, and the positron was discovered by Anderson in 1933. Dirac (1933) went further to predict the antiparticles of the nucleons. It is now known that the antiproton is a component of cosmic radiation, but its numbers are very small compared to the cosmic-ray protons (see Table 6.1). Not until the Bevatron high-energy accelerator capable of accelerating particles to energies of several billion electron volts was constructed at the Lawrence Berkeley Laboratory in California were the necessarily high proton accelerations and collisions possible to liberate sufficient energy for the creation of an adequate number of antiprotons to demonstrate their existence (Segrè, 1959; Chamberlain, 1959). It was expected that the newly discovered antiproton would undergo immediate annihilation upon direct contact with a proton (see Fig. VI.18). Another interaction of the antiproton ($\overline{\mathrm{p}}$) would be a charge−exchange reaction with a proton (p), as described by Eq. [VI.38], resulting in the production of a neutron (n) and antineutron ($\overline{\mathrm{n}}$), which on annihilation would produce an explosive star of particles consisting mostly of π mesons (Segrè, 1959).

$$\mathrm{p} + \overline{\mathrm{p}} \rightarrow \mathrm{n} + \overline{\mathrm{n}} \qquad \text{[VI.38]}$$

The charge−exchange process and subsequent antineutron annihilation, photographed in Glaser's bubble chamber, is illustrated in Fig. VI.25.

Donald Glaser continued his work as professor of physics at the University of California at Berkeley from 1959 to 1964. In 1962 he decided to change course in scientific research and entered the field of molecular biology. At Berkeley he and his students carried out significant research in the identification of human genes with defects that lead to a form of human skin cancer (Nobel Lectures, 1964). In 1970 he and two associates founded the first biotechnology company, which started an industry applying the findings of research in molecular biology to advances in the fields of agriculture and medicine. During the 1990s Glaser was professor of the Graduate School, Department of Molecular and Cell Biology, at the University of California, Berkeley. He and his students conducted research in the field of neurobiology and the human visual system, which is the best-known part of the brain. Their work included the construction of computational models of the human visual system that explain its performance in terms of its physiology and anatomy (Glaser and Barch, 1999;

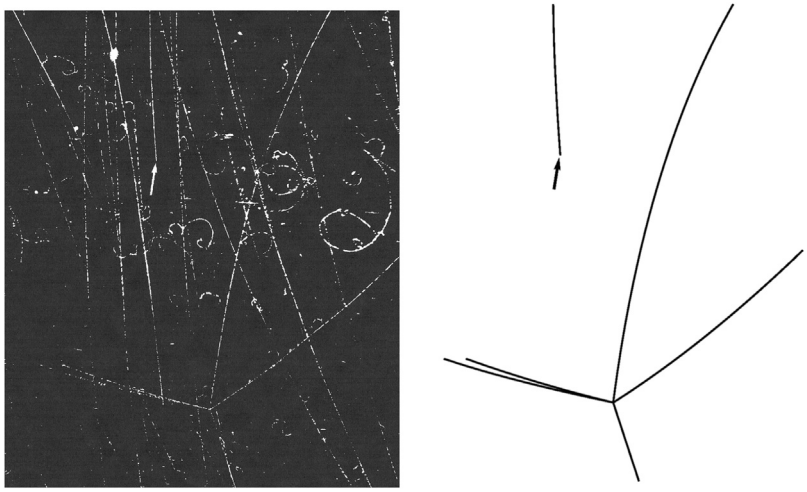

FIGURE VI.25 The photograph on the left shows tracks in a propane bubble chamber. The track of an antiproton is seen ending at the point marked by the arrow, where it underwent charge exchange with a proton to produce a neutron and antineutron, neither of which leaves tracks due to their lack of charge. However, the antineutron undergoes annihilation by causing the explosive star directly below. The distance between the charge exchange and star was 0.95 cm. *From Agnew, L.E., et al., 1958. p^-−p Elastic and charge exchange scattering at about 120 Mev. Phys. Rev. 110, 994−995, http://dx.doi.org/10.1103/PhysRev.110.994, reprinted with permission by the American Physical Society © 1958, and Segrè (1959).*

Kumar and Glaser, 1993, 1995; Chaudhuri and Glaser, 1991). Donald Glaser died at his home in Berkeley, California on February 28, 2013 at the age of 86.

MANUEL SANDOVAL VALLARTA (1899–1977)

Manuel Sandoval Vallarta was born on February 11, 1899 in Mexico City. During his career he made key contributions to our understanding of cosmic radiation, for which he was nominated for the Nobel Prize, and collaborated with the most notable physicists in the world as professor of physics at the Massachusetts Institute of Technology (MIT) and the Institute of Physics at the National Autonomous University of Mexico (UNAM). Much of the information given here about the life of Vallarta is obtained from the comprehensive biography by Alfonso Mondragón of the Institute of Physics, UNAM (Mondragón, 1999).

Manuel Sandoval Vallarta (1899–1977)

In 1912 Vallarta entered the National Preparatory School (Escuela Nacional Preparatoría) in Mexico City. A preparatory school in Mexico is academically similar to a junior college. During our early years of schooling, often one or two exceptional teachers may spark in us an interest or even a passion for a particular field of study. In the case of Vallarta there was Juan Mancilla y Rios, an outstanding professor of physics, José de Las Fuentes, professor of cosmology, and Sotero Prieto, professor of mathematics and theoretical physics, who awakened in Manuel Sandoval Vallarta a keen interest in physics.

At the age of 18 Vallarta entered MIT, and graduated there with a degree in electrical engineering in 1921. He continued his studies at MIT, gaining a doctorate in physics and mathematics in 1924. His doctoral dissertation, a mathematical interpretation of the Bohr atom, was entitled "Bohr's Atomic Model from the Standpoint of the General Theory of Relativity and the Calculus of Perturbations," and was published by MIT in 1924, No. 0125483. The year prior to receiving his doctorate, Vallarta became an assistant to the notable Vannevar Bush, who was professor of electrical engineering at MIT and would later become director of the US Office of Scientific Research and Development during World War II, directing almost all wartime military research and development, including initiation and early administration of the Manhattan Project. His research with others at MIT gave birth to digital circuit design theory. Bush gave Vallarta the task of investigating the mathematical techniques and operational calculus of Oliver Heavyside, who was a mathematical genius of the 19th century and predicted theoretically the origins of Cherenkov radiation (see the chapter: "Cherenkov Radiation"). Vallarta explained and demonstrated Heavyside's expansion theorem, which was scattered among several of Heavyside's "Electrical Papers," and published the mathematical proof in *Transactions of the American Institute of Electrical Engineers* (Vallarta, 1926a). At the same time he published papers in theoretical physics from MIT, including works on Sommerfeld's theory of fine structure and general relativity and a theory on the continuous X-ray spectrum (Vallarta, 1926b).

In 1927, at only 28 years of age, Manuel Sandoval Vallarta was awarded a Guggenheim fellowship to visit the University of Berlin, which was at the time one of the most advanced centers of theoretical physics in the world. Vallarta thus had the opportunity to study relativity with Albert Einstein, quantum physics with Max Planck, X-ray diffraction with Max von Laue, and quantum mechanics with Werner Heisenberg. He also traveled to Leipzig to study under Heisenberg, who

had established the uncertainty principle of quantum mechanics. During his fellowship in Germany, Vallarta remained affiliated with MIT and continued to publish research papers as sole author or jointly with Norbert Wiener in quantum physics and relativity in the journals *Nature*, the *Proceedings of the National Academy of Sciences USA*, and the *Zeitschrift für Physik* (Vallarta, 1927, 1929a,b; Wiener and Vallarta, 1929a–c). Norbert Wiener (1894–1964) was a famous child prodigy and professor of mathematics at MIT. He was awarded a BA in mathematics from Tufts College at the age of 14, and a PhD at Harvard in mathematics when he was merely 17 years old.

On his return to MIT after his fellowship and numerous publications, Manuel Sandoval Vallarta was given membership in the faculty of physics as assistant professor in 1929. He had a long and very successful career at MIT, being made professor of physics in 1939 and holding the chair for theoretical physics until 1946. During his tenure at MIT Vallarta was academic advisor to numerous students of physics and electrical engineering, including Julius Stratton, who became president of MIT, and Richard Feynman, who was awarded the Nobel Prize in Physics in 1965 for his contributions to the field of quantum electrodynamics. Feynman's first scientific publication was a paper coauthored with Vallarta in the journal *Physical Review* (Vallarta and Feynman, 1939) concerning the scattering of cosmic rays.

From Left to Right: Donald William Kerst (back to camera), Manuel Sandoval Vallarta, Niels Bohr, and Edward Gerjuoy (back to camera) cerca 1959 in discussion during lunch at the John Jay Hopkins Laboratory (General Atomic, formerly a division of General Dynamics Corporation, Courtesy of the AIP Emilio Segrè Visual Archives

The "Big Bang" theory on the origin of the universe was proposed originally by Georges Lemaître (1927, 1931a,b), as discussed in the chapter entitled "Cosmic Radiation." Manuel Sandoval Vallarta considered the possibility that cosmic radiation could provide evidence for Lemaitre's "Big Bang." He developed a quantitative theory of the effect of the Earth's magnetic field on the movement of the high-energy cosmic-ray particles, and thus the variable intensities of cosmic radiation as a function of the Earth's latitude. Vallarta began a collaboration with Georges Lemaitre, and discovered the effects of the Earth's magnetic field on the variable intensities of cosmic radiation with latitude. Vallarta, Lemaitre, and coworkers also developed theories on the origins of primary cosmic radiation and the effects of the magnetic field of the sun and rotation of the galaxy on cosmic-ray energies and intensities (Lemaître and Vallarta, 1933, 1936a,b; Vallarta and Godart, 1939; Vallarta, 1933, 1935, 1937a,b, 1939a,b, 1948, 1949, 1950, 1961; Vallarta et al., 1939, 1947). Similar studies were carried out at the same time by Nobel Laureate Arthur Compton and coworkers.

At MIT, Vallarta served as doctoral advisor to two younger Mexican nationals who were outstanding students of physics and had earned admission to the prestigious MIT Department of Physics: Alfredo Baños and Carlos Graef Fernández, who graduated with doctorates in physics from MIT in 1938 and 1940, respectively. During World War II much research in physics and electrical engineering was diverted to the war effort. This hindered Vallarta's research

programs somewhat, as he did not work on the Manhattan Project. For example, as explained by Mondragón (1999), Vannevar Bush's laboratory at MIT with a differential integrator, the most advanced computer of its time, was dedicated exclusively to military projects. This interrupted the programs calculating the periodic orbits of cosmic-ray particles used by Vallarta and his students. Thus in 1943−1946 Vallarta began looking more toward Mexico, and divided his time between the physics programs at MIT and UNAM.

In 1946 Manuel Sandoval Vallarta left his position of chair of theoretical physics at MIT to devote his time as teacher and administrator to strengthening the physics programs at the national institutions of learning and research in Mexico. During his career in Mexico, Vallarta served as undersecretary of the Ministry of Education, director of the National Polytechnic Institute, founder of the National Institute for Scientific Research, representative of Mexico to UNESCO and the International Atomic Energy Agency, and director of the National Institute of Nuclear Energy up to his death (Gall, 1977). As a former researcher and graduate thesis advisor at the Nuclear Center of the National Institute of Nuclear Energy in Mexico during 1975−1977, the writer can recall numerous conversations among the research staff reflecting esteem for Vallarta, which instilled pride and motivation in their work. Manuel Sandoval Vallarta died in Mexico City on April 18, 1977.

For additional reading on the life and work of Manuel Sandoval Vallarta, the reader can peruse Mondragón (1999) and Olvera and Silva (2009).

Chapter 14

Cosmic Radiation

It became clear that they [Arno Penzias and Robert Wilson] had found a background radiation, equally strong in all directions, independent of the time of the day and the year, so it could not come from the sun of our Galaxy…Continued investigations have confirmed that this background radiation varies with wavelength in a way prescribed by well-known laws for a space, kept at the temperature [of] 3K.

From the Nobel presentation speech on December 8, 1978 on the occasion of the presentation of the Nobel Prize in Physics to Arno Penzias and Robert Wilson for their discovery of cosmic microwave background radiation (CMBR) with a spectrum corresponding to a temperature arising from the original Big Bang.

14.1 INTRODUCTION

Two terms often referred to in this chapter are cosmic radiation and air showers of the cosmic radiation. Stable charged particles and nuclei with lifetimes of 10^6 years or longer originating from space, which strike the top of the atmosphere (TOA) from all directions, constitute what is known as **cosmic radiation**. On the other hand, **air showers of cosmic radiation**, or more simply showers of cosmic radiation, consist of cascades of subatomic particles and electromagnetic radiation resulting from nucleon—nucleon collisions of high-energy cosmic-ray particles from space with atomic nuclei of the earth's atmosphere. Cosmic rays are classified according to their origin in space, and air showers of cosmic radiation are characterized according to the products of collisions of high-energy cosmic-ray particles and nuclei with atoms of the earth's atmosphere.

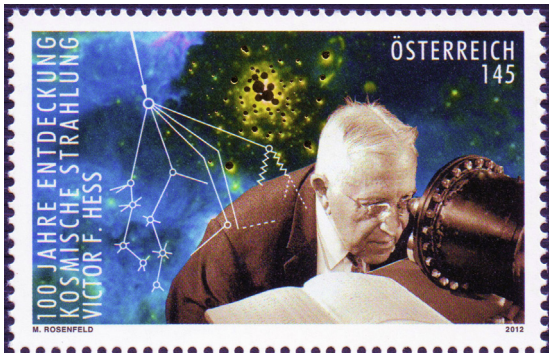

Victor F. Hess (1883–1964) and illustration of a cosmic ray particle (arrow) colliding with an atomic nucleus (circle) at the top of the atmosphere creating cosmic ray showers resulting from a cascade of particle collisions and reactions

The discovery of cosmic radiation is attributed to Victor Hess, who made seven balloon ascents from 1911 to 1913 into the atmosphere during the daytime, during the evening darkness, and even during a solar eclipse. On these ascents he took along three electroscopes that would measure the ionization caused by external radiation. He thought it best to make simultaneous measurements of ionization with more than one instrument to eliminate doubt in the event one instrument

Radioactivity: Introduction and History, From the Quantum to Quarks. http://dx.doi.org/10.1016/B978-0-444-63489-4.00014-9
Copyright © 2016 Elsevier B.V. All rights reserved.

might give erroneous readings. Hess found, that at an altitude of 500 m, the ionization dropped to about half of that obtained from the soil surface. However, the readings would increase proportionally with altitude as he would ascend beyond 1000 m. He found the ionization at 1500 m would increase to be approximately equal to that at the soil surface, and further ascents to altitudes of 5000 m would provide ionization readings of several times of that at the ground level (Hess, 1912, 1936, 1940). It was obvious to Hess that gamma rays, from radium in air, could not cause any increase in ionization with altitude where air got thinner, and he interpreted his results in the following words:

> *The only possible way to interpret my experimental findings was to conclude to the existence of a hitherto unknown and very penetrating radiation, coming mainly from above and being most probably of extra-terrestrial (cosmic) origin….*

Victor Hess was awarded the Nobel Prize in 1936 for his discovery of cosmic radiation.

The dose to the human body from cosmic radiation is of concern to astronauts, airline pilots, and persons living at high altitudes, as our atmosphere attenuates considerably cosmic radiation; and the dose to the human body consequently increases with altitude. Cosmic radiation is also of much concern as background interference in the measurement of low levels of radioactivity. The accurate measurement of radionuclides in our environment requires the suppression and accurate measurement of the background interference from cosmic rays.

14.2 CLASSIFICATION AND PROPERTIES

Cosmic radiation incident on the earth's atmosphere is classified into primary or secondary cosmic rays. As defined by Gaisser and Stanev (2002), primary cosmic rays are stable charged particles and nuclei accelerated at astrophysical sources, and secondary rays are particles produced via the interaction of the primaries with interstellar gas. The nuclear interactions of the accelerated primary cosmic-ray particles with interstellar medium produce stable nuclei of the light elements (eg, Li, Be, and B), as well as many fundamental particles including pions or π mesons of zero charge (π^0), which decay into gamma rays (see Eqs. [14.15] and [14.16]). Galactic gamma radiation has been mapped by the Compton Gamma Ray Observatory satellite. The satellite has provided an image of the galaxy produced by gamma rays of approximately 100 MeV (Simpson, 2001). The gamma-ray image compares closely to the visible-light image of the galaxy with which we are most familiar. Galactic gamma rays can cover the full energy range from <100 MeV to >10 TeV.

Primary cosmic-ray particles include protons, helium nuclei, electrons, and nuclei of most elements of the periodic table (eg, carbon, iron, oxygen, etc.) of stellar origin. Nuclei of the light elements lithium, beryllium, and boron ($Z = 3-5$) are classified as secondary radiation. The abundance of these light elements in cosmic radiation is highly enriched compared to the abundance of these elements in the universe, which is evidence that these are secondary nuclei created via collision (nuclear spallation interactions) with heavier primary particles during the interstellar propagation of primary nuclei. The radionuclide ^{10}Be ($t_{½} = 1.6 \times 10^6$ year) is found among other isotopes of the light elements in cosmic rays. From the measured abundance analysis of ^{7}Be, ^{9}Be, and the radioactive ^{10}Be in cosmic radiation, it is found that cosmic-ray particles remain contained in galactic magnetic fields for approximately 10^7 years before escaping into our atmosphere or intergalactic space. The mean interstellar density for propagation of the cosmic radiation is $\sim$0.2 atom/cm^3 (Simpson, 2001).

Nucleons of practically all elements of the periodic table will be found in cosmic radiation. Free protons account for about 80% of the primary nucleons; and approximately 15% are nucleons bound in helium nuclei (equivalent to alpha particles). Electrons constitute about 2% of the primaries. Nuclei of the elements of the periodic table, other than the previously mentioned H and He, make up the remaining components of cosmic radiation. Nuclei of the light elements (Li, Be, and B), which constitute secondary cosmic-ray particles, account for a small fraction ($\sim$0.3%) of cosmic-ray nuclei (see Table 14.1).

The composition of cosmic radiation will vary according to the 11-year solar cycle and the earth's magnetic latitude (Potgieter, 2008a). The earth's magnetic field, which extends well into space, affects the composition of the charged particles of cosmic radiation. The geomagnetic latitude effect was first reported by Clay (1928) and confirmed by Compton (1932, 1933), who measured cosmic-ray showers with ionization detectors while traversing latitudes onboard ocean vessels. Cosmic-ray particles will concentrate in the earth's Van Allen radiation belts, which extend from about 1000 to 60,000 km from the earth. The sea-level latitude effect of the electromagnetic and meson components of cosmic-ray interactions in the earth's atmosphere measured by Compton corresponded to an approximately 12 to 15 percent increase between the geometric equator and high latitudes. However, no information was obtained then on the latitude effect on the nucleonic component of cosmic radiation at sea level. Subsequent studies (Simpson, 1948, 1951, 2001) demonstrated a dramatic increase of 300 to 400 percent in the nucleonic component compared with a 10 to 15 percent increase in the meson component of cosmic radiation at sea level as one traveled from 0 to 70 degree latitude. This is particularly relevant to international airline pilots who are concerned about the cosmic radiation dose they accumulate when they travel frequently at high altitudes (12 km) and high latitudes (40–60 degree), where the radiation intensities are higher.

TABLE 14.1 Approximate Composition of Cosmic Radiation of Galactic Origin Incident on the Top of the Atmosphere (TOP)[a]

Radiation Type	Approximate Fraction (%)
H nuclei or protons (p^+ and p^-)[b]	80
He nuclei (equivalent to α particles)	15
Electrons (e^- and e^+)[c]	2
Heavier nuclei (eg, C, O, Mg, Fe, Si, etc.)[d]	1
Lighter nuclei ($Z = 3-5$, ie, Li, Be, and B)[e]	0.2

[a]*Cosmic radiation incident at the top of the terrestrial atmosphere includes all stable charged particles and nuclei with lifetimes on the order of 10^6 years or longer (Gaisser and Stanev, 2002).*
[b]*The ratio of antiprotons to protons ($\bar{p}/p$) is about 2×10^{-4} in the particle energy range of 10–20 GeV.*
[c]*The ratio of positrons to negatrons (e^+/e^-) varies from ~0.2 below 1 GeV to ~0.1 around 2 GeV and to ~0.05 at higher electron energies of 5–20 GeV.*
[d]*Nucleons of all of the elements of the periodic table stripped of their atomic electrons with the exception of the lighter nucleons listed above.*
[e]*The nuclei of Li, Be, and B are classified as secondary cosmic radiation, that is, particles produced by the interaction of the primaries with interstellar gas.*

Positrons and antiprotons are components of secondary cosmic radiation. Positrons are much lower in abundance than electrons (see Table 14.1). They are produced mainly via proton and nuclei interactions in the interstellar medium (Grimani, 2009). The differential flux of negatrons and positrons incident at the top of the atmosphere from galactic space is a function of particle energy. The positron fraction, measured as $e^+/(e^+ + e^-)$, decreases from ~0.2 below 1 GeV, to ~0.1 around 2 GeV and to ~0.05 at higher energies of 5 to 20 GeV (Grimani, 2009, 2005; Clem and Evenson, 2002; Gaisser and Stanev, 2002; Sundaresan, 2001). Antiprotons in the cosmic radiation were discovered by Golden et al. (1979, 1984). These are classified as secondaries, as antiprotons as well as positrons are produced by the interactions of primary cosmic radiation, principally protons with the interstellar matter, such as cosmic-ray nuclei (Adriani et al., 2010; Gaisser and Schaefer, 1992; Webber and Potgieter, 1989; Gaisser and Maurer, 1973). The proportions of antiprotons to protons ($\bar{p}/p$) is a function of energy, with ratios varying from $\sim 0.3 \times 10^{-5}$ to 1×10^{-5} in the energy range of ~0.2–1 GeV, from $\sim 2 \times 10^{-5}$ to 1×10^{-4} in the energy range of ~1–10 GeV, and from $\sim 2 \times 10^{-3}$ to 3×10^{-3} in the energy range of 10–180 GeV (Adriani et al., 2010; Beach et al., 2001; Basini et al., 1999; Mitchell et al., 1996; Hof et al., 1996). In summary, the approximate composition of galactic cosmic-ray particles is provided in Table 14.1.

Most galactic cosmic-ray particles possess energies from about 50 MeV to 10 GeV, as illustrated in Fig. 14.1, which provides the energy distributions of some of the major components of primary cosmic radiation for a particular period of the solar cycle. A series of very precise measurements of primary protons and helium nucleon intensities have been made by the AMS Collaboration (2000), Menn et al. (2000), Sanuki et al. (2000), Bellotti et al. (1999), and Boezio et al. (1999). Particle energies up to 10^{15} eV were first observed by Auger and Maze (1938, 1939), and a cosmic-ray particle of about 10^{20} eV energy was observed by Linsley (1963).

Protons in the kinetic energy range of 100 MeV to 10 GeV would have relativistic speeds ranging from 42.8 to 99.6 percent of the speed of light (ie, $0.428c$ to $0.996c$) calculated according to Eq. [10.12] of the chapter entitled "Neutron Radiation." For example, the relativistic speed of a proton with 10 GeV kinetic energy would be calculated according to the following equation:

$$u = c\sqrt{1 - \left(\frac{K}{mc^2} + 1\right)^{-2}} \qquad [14.1]$$

The rest energy of the proton (mc^2) is calculated as:

$$mc^2 = \left(1.6726 \times 10^{-27}\ \text{kg}\right)\left(2.9979 \times 10^{8}\ \text{m/s}\right)^2 = 1.503 \times 10^{-10}\ \text{J} \qquad [14.2]$$

which can be expressed in units of eV as follows:

$$\frac{1.503 \times 10^{-10}\ \text{J}}{1.602 \times 10^{-19}\ \text{J/eV}} = 938.2 \times 10^{6}\ \text{eV} = 938.2\ \text{MeV} \qquad [14.3]$$

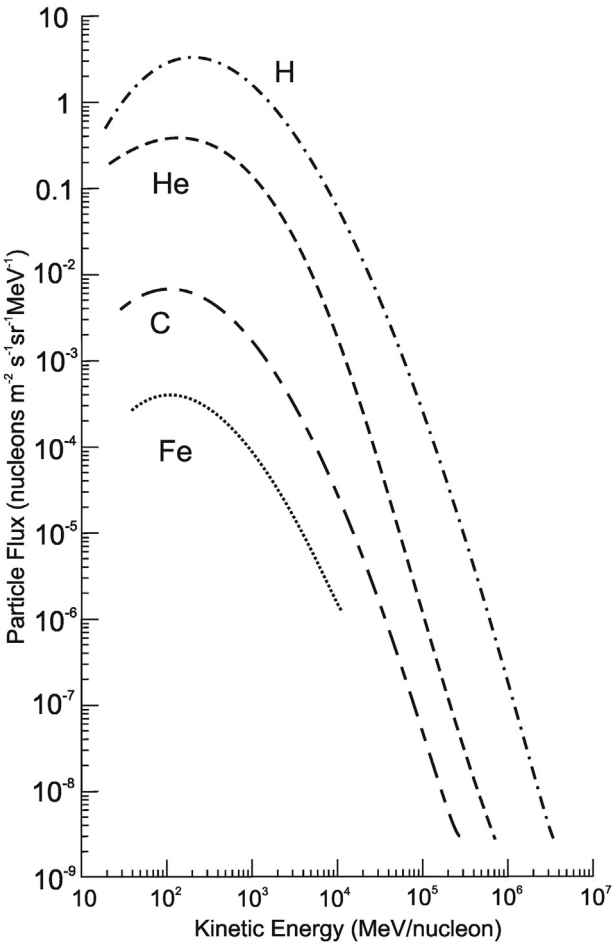

FIGURE 14.1 Approximate flux distributions of major components of primary cosmic radiation. *See Simpson, J.A., 1983. Elemental and isotopic composition of the galactic cosmic rays. Ann. Rev. Nucl. Part. Sci. 33, 323–381 and Gaisser, T.K., Stanev, T., 2002. Cosmic rays. In: Hagiwara et al. (Eds.), The Review of Particle Physics, Physical Review D66, University of California, Lawrence Berkeley Laboratories, pp. 23.1–23.19 for more precise data on nucleon flux as a function of particle energy.*

The relativistic speed of the 10-GeV proton can then be calculated as:

$$u = c\sqrt{1 - \frac{1}{(10^4\ \text{MeV}/938.2\ \text{MeV} + 1)^2}} = 0.996c \qquad [14.4]$$

A higher kinetic energy 100-GeV (10^5 MeV) cosmic-ray proton would have a relativistic speed of:

$$u = c\sqrt{1 - \frac{1}{(10^5\ \text{MeV}/938.2\ \text{MeV} + 1)^2}} = 0.999956c \qquad [14.5]$$

The speed of the 100-GeV proton, calculated according to Eq. [14.5], may also be calculated on the basis of the definition of the kinetic energy of the particle being the difference between the *total energy* of the particle and its rest energy (see Eq. [10.4] of the chapter: "Neutron Radiation")

or:

$$K = \gamma mc^2 - mc^2 = (\gamma m - m)c^2 \qquad [14.6]$$

or:

$$10^5\ \text{MeV} = (\gamma m - m)c^2$$

Converting the units of electron volts in the above equation to joules, and imputing the speed of light, provides:

$$\left(10^{11}\ \text{eV}\right)\left(1.602 \times 10^{-19}\ \text{J/eV}\right) = (\gamma m - m)\left(2.9979 \times 10^{8}\ \text{m/s}\right)^2 \quad [14.7]$$

from which the differences of the relativistic and rest masses of the proton can be calculated as:

$$\gamma m - m = \frac{1.602 \times 10^{-8}\ \text{J}}{8.9874 \times 10^{16}\ \text{m}^2/\text{s}^2} = 0.1782495 \times 10^{-24}\ \text{kg} \quad [14.8]$$

Inputting the known rest mass m of the proton (1.6726×10^{-27} kg) permits the calculation of the relativistic mass of the 100 GeV proton as:

$$\gamma m = 178.2495 \times 10^{-27}\ \text{kg} + 1.6726 \times 10^{-27}\ \text{kg} = 179.9221 \times 10^{-27}\ \text{kg} \quad [14.9]$$

Since by definition, $\gamma m = m/\sqrt{1 - (u^2/c^2)}$ (see Eq. [10.5] of the chapter: "Neutron Radiation"), we can write:

$$\frac{\gamma m}{m} = \frac{1}{\sqrt{1 - (u^2/c^2)}} \quad [14.10]$$

which transforms to read:

$$\left(\frac{m}{\gamma m}\right)^2 = 1 - \frac{u^2}{c^2} \quad [14.11]$$

or:

$$\frac{u^2}{c^2} = 1 - \left(\frac{m}{\gamma m}\right)^2 \quad [14.12]$$

Inputting the values for the relativistic and rest masses of the proton yields:

$$\frac{u^2}{c^2} = 1 - \left(\frac{1.6726 \times 10^{-27}\ \text{kg}}{179.9221 \times 10^{-27}\ \text{kg}}\right)^2 \quad [14.13]$$

$$\frac{u^2}{c^2} = 1 - (0.00929624)^2$$

$$\frac{u^2}{c^2} = 1 - 8.64200 \times 10^{-5}$$

$$u^2 = (0.9999135)c^2$$

and:

$$u = 0.999956c$$

where u is the relativistic speed of the 100-GeV proton exactly as calculated previously by Eq. [14.5].

High-energy cosmic-ray protons, as demonstrated above, approach the speed of light. Primary cosmic-ray nucleon intensity drops rapidly according to energy beyond several GeV, as illustrated in Fig. 14.1. The primary nucleon intensity from a few GeV to 100 TeV is described according to the power law:

$$I_{\text{N}}(E) = 1.8\, E^{-\alpha}\ \text{nucleons/cm}^2\ \text{s sr GeV} \quad [14.14]$$

where E is the energy per nucleon (including rest mass energy) and α is approximately 2.7.

As illustrated in Fig. 14.1, primary nucleon energies in excess of 1 TeV (ie, 10^{12} eV or 10^{6} MeV) are relatively few in number, and primary cosmic-ray particles with energies in excess of 10^{20} eV or 10^{14} MeV are very rare, but have been reported (Hörandel, 2010; Pierre Auger Collaboration, 2010; Scherini, 2010; Zavrtanik, 2010; Nagano and Watson, 2000; Bird et al., 1995; Hayashida et al., 1994; Linsley, 1963). The rarity of such extremely high-energy primary cosmic-ray particles can be visualized with the graph of primary cosmic-ray flux as a function of nucleon energy shown in Fig. 14.2.

The cosmic-ray scientific community is studying the knee and ankle regions of the cosmic-ray spectrum illustrated in Fig. 14.2. The knee region at particle energies of 10^{15}–10^{16} eV shows a decline in the particle flux, while the ankle region of the spectrum occurring between 10^{18} to 10^{19} eV shows a rise in particle flux. The origins of the knee and ankle regions of the

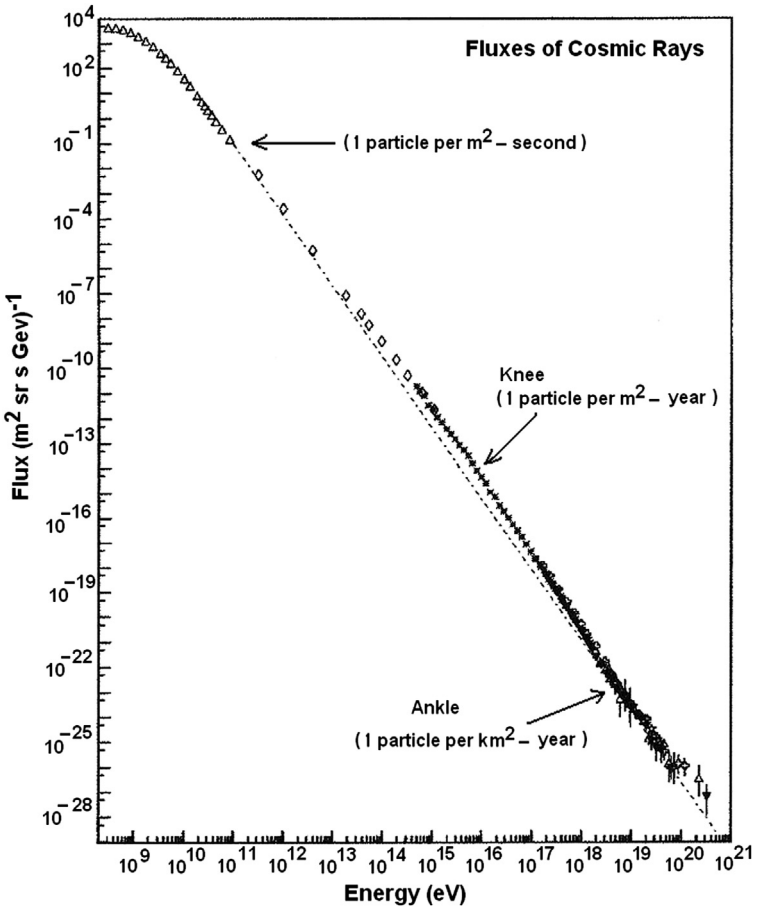

FIGURE 14.2 Spectrum of cosmic rays greater than 100 MeV. The cosmic rays consist predominantly of nucleons ranging in species from protons to iron nuclei with traces of nuclei of the heavier elements. Not included in the figure are notations for estimated cosmic-ray fluxes of about one particle/cm^2/s at the low energy end of 10^8 eV, and only on the order of one particle/km^2/century at the high-energy end of 10^{20} eV of the spectrum. *This figure was produced by Swordy, S., University of Chicago from published results of the LEAP, Proton, Akeno, AGASA. Fly's Eye, Haverah Park, and Yakutsk experiments. See Marcelli, L., 2011. Identification of the light nuclei component of cosmic rays with the PAMELA experiment. Nucl. Instrum. Methods Phys. Res., Sect. A, (630(1), 58–62.), and Bhattacharjee and Sigl, 2000. Reprinted with permission from Elsevier © 2000.*

energy spectrum is not fully understood, and these are now under intense research as described by Chiavassa (2010), Marcelli (2010), Blümer et al. (2009), Giller (2008), and Hörandel (2008a). The knee portion of the energy spectrum at about 4 PeV (~4 petaelectron volts, ie, $\sim 4 \times 10^{15}$ eV), as described by Hörandel (2008a), is caused by a break in the energy spectra of the light elements. The mean mass of the cosmic rays is found to increase as a function of energy in the knee region. The knee in the energy spectrum is most likely caused by a combination of the maximum energy reached during acceleration and leakage from the galaxy during propagation (Hörandel, 2008a). Theory for the production of the ankle region of the spectrum is summarized by Sundaresan (2001). It appears that the ankle is caused by a higher energy cosmic-ray population mixed in with a lower energy population at energies a couple of orders of magnitude below the ankle. The spectrum below 10^{18} eV is considered to be of galactic origin, and the higher energy population in excess of 5×10^{18} eV is considered to be of extragalactic origin (Marcelli, 2010; Allard et al., 2007; Cronin, 1999; Sundaresan, 2001).

Much attention in the cosmic-ray community is focused also on the mechanisms by which the cosmic-ray nucleons are accelerated in space to energies in excess of 10^{20} eV. Enrico Fermi (1949) proposed and calculated the acceleration of cosmic rays resulting from a series of collisions with magnetic fields or magnetic clouds traversing the universe whereby the cosmic-ray particles gain energy each time they bounce off the magnetic fields. This is now referred to as Fermi acceleration; and Cronin (1999) explains that subsequent work has shown that multiple "bounces" off turbulent magnetic fields associated with supernova shock waves is the more efficient acceleration process (Drury, 1983). The energy spectrum of cosmic rays supports the "standard picture," as described by Hörandel (2008a), that the bulk of galactic cosmic rays is accelerated in shocks of supernova remnants.

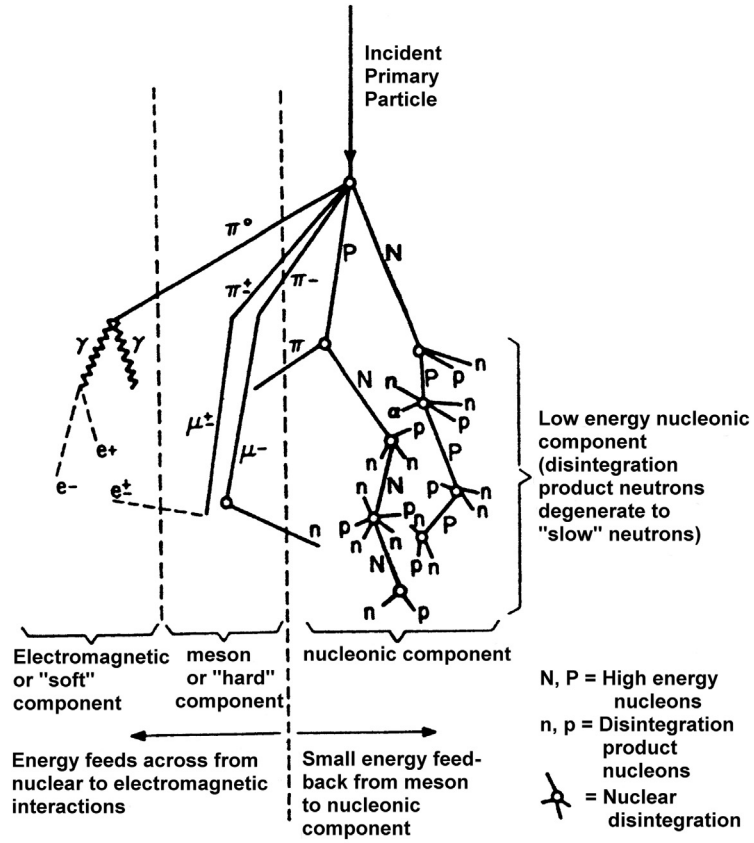

FIGURE 14.3 Schematic representation of the typical development of the secondary cosmic radiations within the atmosphere arising from an incident primary particle. *From Simpson, J.A., et al., 1953. Cosmic ray intensity-time variations and their origin: neutron intensity variation method and meteorological factors. Phys. Rev. 90, 934–950. http://dx.doi.org/10.1103/PhysRev.90.934; reprinted with permission © 1953 by the American Physical Society.*[1]

14.3 SHOWERS OF COSMIC RADIATION

Cosmic radiation consisting of high-energy nucleons striking the top of the atmosphere (TOA) collide with atoms of the air to produce a cascade of secondary subatomic particles and electromagnetic radiation referred to as showers of cosmic radiation. During the years that preceded the development of manmade high-energy particle accelerators, cosmic rays provided much information to the field of high-energy particle physics. The collisions of high-energy nucleons with atoms of the atmosphere provided natural "atom-smashers" that led to the early discovery of subatomic particles.

When a cosmic-ray particle strikes an atomic nucleus of a gaseous molecule of the atmosphere (eg, N_2, O_2, etc.), a nuclear disintegration follows producing high-energy secondary nucleons and charged and neutral π mesons (pions). These secondary nucleons collide with additional atomic nuclei of the atmosphere, producing a cascade of particles including mesons, nucleons of various masses, neutrons, and products of meson–nuclear interactions and meson decay, namely, photons (eg, gamma rays), positrons, negatrons, and neutrinos. Fig. 14.3 provides a good schematic of the various possible nucleon interactions that produce the cascade of secondary cosmic radiation in the atmosphere.

Mesons are strongly interacting particles of mass intermediate between that of the electron (0.511 MeV/c^2) and the proton (938 MeV/c^2). Among the mesons produced are (1) kaons (K-mesons), which have a mass of about 490 MeV/c^2, lifetimes of approximately 10^{-10} and 10^{-8} s for the neutral (K^0) and charged ($K^{\pm}$) kaon, respectively, decaying to pions and/or muons (see Eqs. [VI.5] to [VI.12] and Fig. VI.6 in the Hall of Fame, Part VI); and (2) the charged pions ($\pi^{\pm}$-mesons) that can decay into muons, such as described by Eqs. [14.19] and [14.20]. A neutral pion has a mass of 135 MeV/c^2 and a

1. Readers may view, browse, and/or download material for temporary copying purposes only, provided these uses are for noncommercial personal purposes. Except as provided by law, this material may not be further reproduced, distributed, transmitted, modified, adapted, performed, displayed, published, or sold in whole or part, without prior written permission from the American Physical Society.

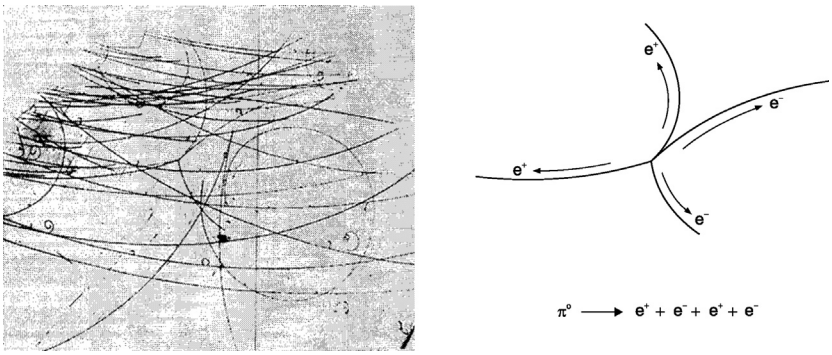

FIGURE 14.4 Photograph of a typical double internal conversion following π^0 decay on the left with a drawing of the specific tracks provided on the right. The tracks were produced in a hydrogen bubble chamber 30.5 cm in diameter and 15.25 cm in depth. A magnetic field of 5.5 G produced the curved deflection of the oppositely charged electrons. *From Samios, N.P., et al., 1962. Parity of the neutral pion and the decay $\pi^0 \rightarrow 2e^+ + 2e^-$. Phys. Rev. 126, 1844–1849, http://dx.doi.org/10.1103/PhysRev.126.1844; reprinted with permission © 1962 by the American Physical Society.*

lifetime of 8.3×10^{-17} s. It decays into two gamma-ray photons, as illustrated in Fig. 14.3, or into a positron–negatron pair and gamma ray with branching ratios of approximately 98.8% and 1.2%, respectively, for the two decay modes (Sundareson, 2001; Glasser et al., 1961) as follows:

$$\pi^0 \rightarrow \gamma + \gamma \,(98.798 \pm 0.032\%) \qquad [14.15]$$

$$\pi^0 \rightarrow e^+ + e^- + \gamma \,(1.198 \pm 0.032\%) \qquad [14.16]$$

The positron and negatron pair (e^+e^-), as products of the neutral pion decay, illustrated by Eq. [14.16], is a result of internal conversion of a gamma-ray photon (ie, internal pair production). The neutral pion decay may also manifest itself in a yet more rare form of dual internal conversion whereby two gamma-ray photons are converted to two positron–negatron pairs. The decay scheme is described by Eq. [14.17]; and the tracks from such a decay scheme produced in a bubble chamber are illustrated in Fig. 14.4.

$$\pi^0 \rightarrow e^+ + e^- + e^+ + e^- \qquad [14.17]$$

Out of eight million π^0 decays in 836,000 bubble chamber pictures, Samios et al. (1962) were able to find only 206 neutral pion decays with double internal conversion. The numerous neutral pions were produced by Samios et al. (1962) by the interactions of π^- mesons from a cyclotron with protons of the bubble chamber liquid according to the reaction:

$$\pi^- + p^+ \rightarrow n + \pi^0 \qquad [14.18]$$

The π^- mesons were slowed down with a polyethylene absorber and then allowed to stop in the hydrogen bubble chamber. The numerous bubble chamber photographs could be analyzed for the identification of specific tracks by a digitized scanning machine.

Any of the gamma rays can, in turn, produce positron–negatron pairs via pair production, and the positron can undergo annihilation to gamma radiation. The positive and negative pions are antiparticles. Charged pions have a mass of 139.6 MeV/c^2 and a lifetime of 2.6×10^{-6} s, much longer than that of the neutral pion. The positive pion decays to a positive muon and muon neutrino, whereas the negative pion decays into a negative muon and muon antineutrino, as illustrated by the following:

$$\pi^+ \rightarrow \mu^+ + \nu_\mu \qquad [14.19]$$

$$\pi^- \rightarrow \mu^- + \overline{\nu}_\mu \qquad [14.20]$$

The muon has a mass of 106 MeV/c^2 and lifetime of 2.2×10^{-6} s. The positive muon decays to a positron and muon neutrino, and the negative muon to a negatron and anti-muon neutrino, as illustrated in Fig. 14.3 and by the following equation:

$$\mu^{+/-} \rightarrow e^{+/-} + \nu_\mu + \overline{\nu}_\mu \qquad [14.21]$$

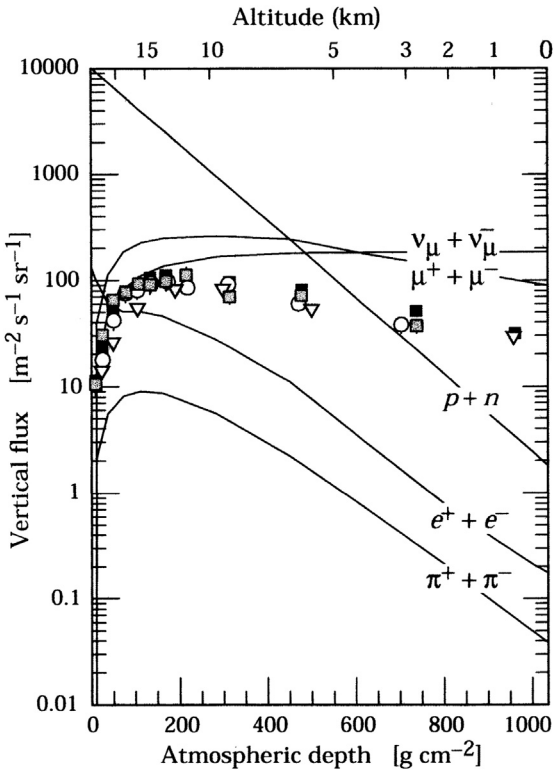

FIGURE 14.5 Vertical fluxes of cosmic rays in the atmosphere with $E > 1$ GeV estimated from the nucleon flux of Eq. [14.14]. The points show measurements of negative muons with $E_\mu > 1$ GeV. *From Olive, K.A., 2014. Particle Data Group. Chin. Phys. C38, 090001, http://pdg.lbl.gov, reprinted with permission, Lawrence Berkeley National Laboratory, © 2014 Regents of the University of California. The latest edition of the figure is available at the Particle Data Group website http://pdg.lbl.gov/http://pdg.lbl.gov.*

Slow negative muons undergo nuclear absorption by nucleons with sufficient high atomic number ($Z \approx 10$ or greater); however, for low Z nuclides such as carbon ($Z = 6$), slow negative muon decay occurs rather than absorption by the nucleus (Sundareson, 2001).

At sea level, muons are the most numerous of the charged particles resulting from cosmic ray interactions with atomic nuclei of the atmosphere. These have been measured with an intensity of 100 m^{-2} s^{-1} at sea level. The relative abundances of the cosmic radiation shower components in the atmosphere at different altitudes with energies in excess of 1 GeV are illustrated in Fig. 14.5. As illustrated in the figure, most muons are produced high in the atmosphere at an altitude of ~15 km where high-energy cosmic-ray nucleons undergo collision with nuclei of the atmospheric gases. Pions likewise are produced high in the atmosphere; however, their number at sea level is highly diminished due to the prompt decay of the neutral pion to gamma radiation and the decay of the charged pions to muons. The muon produced high in the atmosphere loses about 2 GeV of energy to ionization before reaching the ground; and the mean energy of the muon at the ground is ≈4 GeV (Gaisser and Stanev, 2002), and these travel at speeds close to the speed of light (>0.99c).

One might ask at this point the following question: If muons of the cosmic radiation showers are produced high in the earth's atmosphere (at altitudes of ~15,000 m or higher), travel at speeds close to the speed of light, and have an average lifetime of only 2.2×10^{-6} s, how could such muons be detected at sea level on the earth's surface? The question is an obvious one, as it would appear with classical mathematics that, with such a short lifetime, muons would never be expected to reach the earth. Let's say, for example, a muon is produced at the altitude of 15,000 m and it travels at the speed v of 0.99985c, which would correspond to a speed in units of m/s as:

$$0.99985c = (0.99985)(2.9979 \times 10^8 \text{ m/s}) = 2.99745 \times 10^8 \text{ m/s} \quad [14.22]$$

The classical calculation of its average distance d of travel during its lifetime would be:

$$d = (v)(t) = (2.99745 \times 10^8 \text{ m/s})(2.2 \times 10^{-6} \text{ s}) = 659.4 \text{ m} \quad [14.23]$$

Thus the muon would be expected to decay, according to classical transformations, after traveling 659 m on average, and therefore would never be detected on earth. However, for such a muon viewed by an observer on earth, he or she would view the two events: (A) the creation of the muon and (B) the decay of the muon, to occur in two locations in space-time coordinates. The Lorentz time transformations demonstrate that the two events, A and B, separated by the time interval Δt, will be dilated to the time interval Δt_{earth}, when viewed by an observer on earth. The time dilation is calculated according to the following Lorentz transformation derived by Einstein (see Eq. [C.38] in Appendix C, which provides his derivation of time dilation in relativity):

$$\Delta t_{\text{earth}} = \frac{\Delta t}{\sqrt{1 - (v^2/c^2)}} \qquad [14.24]$$

where v is the velocity of the particle and c is the invariable speed of light in a vacuum. For the muon traveling at $0.99985c$, we can calculate Δt_{earth} or the dilated lifetime of the muon as follows:

$$\Delta t_{\text{earth}} = \frac{\Delta t}{\sqrt{1 - (v^2/c^2)}} = \frac{2.2 \times 10^{-6}\ \text{s}}{\sqrt{1 - (0.99985)^2}} = \frac{2.2 \times 10^{-6}\ \text{s}}{0.01732} = 127.0 \times 10^{-6}\ \text{s} \qquad [14.25]$$

According to the dilated time of 127.0×10^{-6} s, the observer on earth will determine that the muon would travel, before it decays, a distance of:

$$d = (v)(\Delta t_{\text{earth}}) = \left(2.99745 \times 10^{8}\ \text{m/s}\right)\left(127.0 \times 10^{-6}\ \text{s}\right) = 38{,}067.6\ \text{m} \qquad [14.26]$$

which is well beyond the distance of 15,000 m elevation when it was created, permitting its detection on earth. The distance is only an average figure, because the muon lifetime of 2.2×10^{-6} s is an average lifetime. Notice that a similar calculation made in Hall of Fame, Part III (see Eqs. [III.24] to [III.28]) for the dilated lifetime of a muon traveling at a slower speed of $0.9993c$ was only 58.8×10^{-6} s compared to the above calculation of the dilated lifetime of 127.0×10^{-6} s for a muon traveling at a faster speed of $0.99985c$. Thus, the faster the relativistic speed of the muon, the longer will be its relativistic calculated lifetime.

The example provided above is a realistic one. The relativistic time dilation has been demonstrated by Bailey et al. (1977, 1979) based on the historical tests by Rossi and Hall (1941) on muons traveling close to the speed of light in cosmic radiation showers.

The historical work of Rossi and Hall entailed the measurement of the muon flux on Mt. Washington in New Hampshire at the altitude of 2000 m and at the mountain base. They found that the muon flux at both altitudes did not differ greatly, only by the ratio of 1.4, that is, the muon flux was only 1.4 times as high at the altitude of 2000 m compared to the ground level. Calculations based on a muon half-life of 1.5×10^{-6} s, the muon flux ratio for the two altitudes, should have been approximately 22 even when attributing the highest unrealistic speed of light to the muons. The actual low ratio of 1.4 could only be explained by applying the time dilation calculations for muons traveling at the speed of $0.994c$.

More recent experiments at CERN by Bailey et al. (1977, 1979) involved accelerating muons in a storage ring to speeds of up to $0.9994c$. The rates of decay of the accelerated muons were measured by detecting their electron decay-product emissions. The accelerated muons were found to have a lifetime 29.3 times longer than a muon at rest. This agrees perfectly with the calculated dilated lifetime of the muon according to the Lorentz transformation:

$$\Delta t = \frac{\Delta t_0}{\sqrt{1 - (v^2/c^2)}} \qquad [14.27]$$

where Δt_0 is the lifetime of the muon at rest, v the speed of the muon, and c the speed of light. The dilated lifetime of the muon at $0.9994c$ is calculated to be:

$$\Delta t = \frac{2.2 \times 10^{-6}\ \text{s}}{\sqrt{1 - (0.9994)^2}} = 63.52 \times 10^{-6}\ \text{s} \qquad [14.28]$$

The increase in the observed lifetime of the accelerated muons over the muons at rest is:

$$\frac{\Delta t}{\Delta t_0} = \frac{63.52 \times 10^{-6}\ \text{s}}{2.2 \times 10^{-6}\ \text{s}} = 28.9 \qquad [14.29]$$

This test of time dilation, provided by the muon lifetime measurements, is discussed in papers by Drumm et al. (1977), Thompson (2004), and Tomaschitz (2004).

14.4 COSMIC RAYS UNDERGROUND

The only significant cosmic radiation with energy sufficient to penetrate considerable depths of earth are charged muons and muon neutrinos. Thus, Tueros and Sciutto (2010) describe muons as the "penetrating component" of the cosmic-ray-induced showers, capable of reaching deep underground without interacting in the atmosphere. High-energy muons will traverse rock and lose energy via either direct ionization or radiative processes. The radiative processes include Bremsstrahlung production with concomitant positron−electron pair production and photonuclear interactions. Muon-induced spallation is another mechanism of energy loss. The muon cosmic-ray intensities diminish with depth as expected. This is a subject of concern in the measurement of very low levels of radiation. Consequently underground laboratories have been built to achieve the lowest possible background radiation interference in the counting of very low levels of natural radioactivity. Muon ranges in rock are measured in units of km-water-equivalent (km.w.e.) where 1 km.w.e. $= 10^5$ g/cm^2 of standard rock. Average ranges in standard rock ($Z = 11$, $A = 22$, $Z/A = 0.5000$, $\rho = 2.650$ g/cm^3) for muons of 10, 100, 1000, and 10,000 GeV are 0.05, 0.41, 2.45, and 6.09 km.w.e. The vertical muon intensity versus underground depth of standard rock has been determined. The muon vertical intensity drops from 10^{-6} cm^{-2}sr^{-1}s^{-1} to 10^{-12} cm^{-2}sr^{-1}s^{-1} over the range of rock depths from 1 to 10 km.w.e., respectively (Gaisser and Stanev, 2002).

Radiation from muons of cosmic-ray showers are significant underground. The mechanisms of muon energy loss are dependent on the muon energy. Tueros and Sciotto (2010) report a Monte Carlo program that simulates high-energy cosmic-ray showers underground. From nuclear data tables of Groom et al. (2001), they calculated the muon energy losses in standard rock by plotting the stopping power versus muon energy illustrated in Fig. 14.6. (Stopping power calculations are discussed in the chapter: "Beta Radiation and Beta Decay.") Muons traveling through matter will lose energy by several mechanisms including ionization, Bremsstrahlung production, pair production, and photonuclear reactions including spallation caused by muon collisions with nuclei. Tueros and Sciotto (2010) demonstrate from Fig. 14.6 that ionization losses are dominate at low muon energies (<100 MeV) and ionization losses predominate among the other mechanisms of energy loss and remain fairly constant at 1.5 to 2.2 MeV cm^2/g below 10 GeV (10^4 MeV) muon energy in standard rock. At muon energies >10 GeV, radiative energy losses steadily increase and reach the critical energy at ~0.7 TeV (693 GeV; see Fig. 14.6), which is the energy at which the ionization loss is equal to the radiative loss. The critical energy for muons in air is much higher, 3.6 TeV, as reported by Grieder (2001). Thus Tueros and Sciotto (2010) point out that Bremsstrahlung and pair production energy losses for muons in air is negligible with the exception of very high muon energies; whereas it is increasingly important underground for muon energies >50 GeV.

Another source of underground background interference from muons of the cosmic radiation showers is the production of gamma ray photons from radiative neutron capture reactions in hydrogen and elements encountered in rock and other

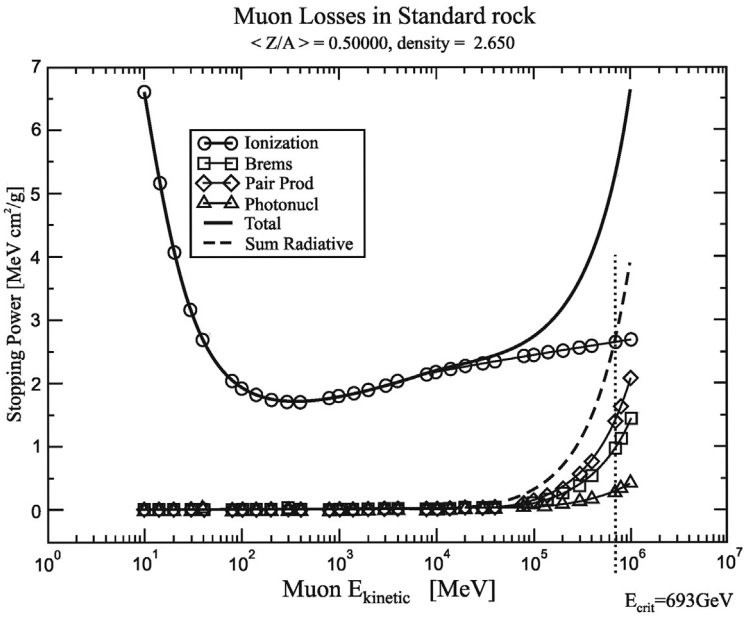

FIGURE 14.6 Muon energy loss versus muon energy in standard rock. The mechanisms of energy loss are identified as ionization, Bremsstrahlung production, pair production, and photonuclear reactions. *From Tueros, M., Sciutto, S., 2010. TIERRAS: A package to simulate high energy cosmic ray showers underground, underwater and under-ice. Comp. Phys. Commun. 181, 380−392, reprinted with permission from Elsevier © 2010.*

soil materials. Neutrons are produced by muon spallation reactions as well as photonuclear reactions arising from Bremsstrahlung radiative energy loss. Araújo et al. (2008) and Lindote et al. (2009) report a Monte Carlo simulation that provides a very good estimate of the absolute neutron yield in lead as $(1.31 \pm 0.06) \times 10^{-3}$ neutrons/muon/g/cm^2 for a mean muon energy of 260 GeV.

14.5 ORIGINS OF COSMIC RADIATION

The origins of galactic and extragalactic cosmic rays remains an unsolved problem, and reviews on this subject matter are provided by Potgieter (2010), Blasi (2008), Hörandel (2008b), and Gaisser (2001).

In brief, cosmic rays can originate from (1) energetic particles associated with mass ejections from solar flares and similar energetic solar events; (2) anomalous cosmic rays, which are particles of interstellar origin accelerated at the edge of the heliopause and accelerated at the termination shock in the solar wind; (3) high-energy particles of galactic origin far outside the heliosphere or our solar system; and (4) extragalactic sources, which give rise to particles of the highest energies of $\sim 10^{18}$ eV or higher.

The sun has been identified as one of the sources of high-energy cosmic-ray particles that hit the top of the atmosphere, and these particles can be accelerated during solar flares. The mass ejections associated with solar flares drive shocks into the interplanetary medium, where particles undergo acceleration via shocks in the heliosphere. Linked to these are the anomalous cosmic rays, which are classified as a subset of particles accelerated in the heliosphere; these are particles of interstellar origin accelerated at the termination shock in the solar wind (Gaisser, 2000). Neutron monitors are used to detect the secondary neutrons produced by the cosmic-ray nucleon collisions with nuclides of the earth's atmospheric molecules. The gamma-ray images of the galaxy taken in space provide evidence for the gamma radiation produced by interactions of the accelerated particles in the solar atmosphere in addition to gamma radiation originating from neutral meson decay described previously.

Galactic cosmic rays can arise from a supernova, which is the final stage in a star's evolution. During the death of a star, it explodes as a supernova, producing heavy particles and accelerating them in a shock wave into interstellar gas. Supernovae are sources of galactic cosmic rays, with particles undergoing acceleration to $\sim 10^{15}$ eV or higher. The interactions of these accelerating particles also serve as sources of gamma radiation that we detect throughout the galaxy.

Accelerated particles in excess of approximately 10^{18} eV or higher are considered to be possibly of extragalactic origin. Most galactic cosmic rays are confined by the magnetic field lines of the galaxy. Extragalactic cosmic-ray particles with sufficient energy to invade our galaxy (10^{18} to beyond 10^{20} eV) are relatively few in number, as discussed previously. Several theories and models exist for the origins of extragalactic cosmic rays and these are reviewed by Gaisser (2000).

14.6 COSMIC MICROWAVE BACKGROUND RADIATION AND THE BIG-BANG THEORY

The hot Big-Bang or "explosive" nucleosynthesis theory of the origin of the universe predicts the existence of a relic cosmic microwave background radiation (CMBR) left over by the Big-Bang. The first to describe a very hot and explosive beginning of the universe on a scientific basis was Georges Lemaître, a Belgian mathematician and Catholic Priest. Georges-Henri Lemaître obtained a doctorate in mathematics at the University of Leuran in 1920 and was ordained a Catholic Priest in 1923. That same year he studied at the University of Cambridge under astronomer Arthur Eddington and went on to study the following year at Harvard College Observatory in Cambridge, Massachusetts and also registered that year at the Massachusetts Institute of Technology (MIT) for a doctoral degree in the sciences. By 1927 he obtained his PhD degree at MIT and returned to Belgium as Professor at the University of Leuven. The very year he received his doctorate, Lemaître (1927) published his conclusions that the universe was expanding based on Einstein's general theory of relativity and the red-shift surrounding extragalactal bodies. In a biographical account, Midbon (2000) relates that following Edwin Hubble's systematic observations confirming the red shift, Lemaître sent a copy of his 1927 paper to British astronomer Arthur Eddington, who then realized that Lemaître had bridged the gap between observation and theory. Eddington therefore requested that an English translation of Lemaitre's paper be published in the March 1931 Monthly Notices of the Royal Astronomical Society (Lemaître, 1931a). Georges Lemaitre went further, to propose in a letter published in the journal *Nature* (Lemaître, 1931b) his interpretations that would lead to the Big-Bang theory. In a book, Mather and Boslough (1996) summarized Lemaître's theory as follows:

> *A letter Lemaître wrote to* Nature *magazine in 1931 was effectively the charter of what was to become the Big Bang theory. He theorized that this primordial explosion, occurring on "a day without yesterday," had burst forth from an extremely dense point of space and time. He began calling this the "primeval atom." By now Lemaître had become a celebrity in his own right for his revolutionary ideas. At an immense gathering of the British Association for the Advancement of Science in London the same year, he speculated before an audience of several thousand scientists that the cosmic rays may have originated in the primordial explosion. Eventually, he thought, they might prove to be material evidence of the universe's natural beginning.*

Georges Lemaître
(1894–1966)

In January of 1933, Georges Lemaître traveled with Albert Einstein for a series of seminars in California including a lecture at the California Institute of Technology (Caltech) in Pasadena. At one of these seminars after Lemaître detailed his theory on the explosive beginning of the universe, Einstein stood up, applauded, and acclaimed "This is the most beautiful and satisfactory explanation of creation to which I have ever listened" (Midbon, 2000). A photograph of Georges Lemaitre with Albert Einstein and Robert Millikan at Caltech during the seminars is provided below. There was, of course, some opposition to Lemaître's theory on the creation of the universe, as explained by Midbon (2000), particularly at Cambridge University, and it was Fred Hoyle, an astronomer at Cambridge, who had coined the term "Big Bang" in sarcasm to Lemaître's theory. Nevertheless, before Lemaître's death he was able to get satisfaction from the discovery by Nobel Laureates Arno Penzias and Robert Wilson in 1965 of the cosmic microwave radiation, the primordial radiation, that would be key evidence for the Big-Bang theory. These finding are subsequently discussed.

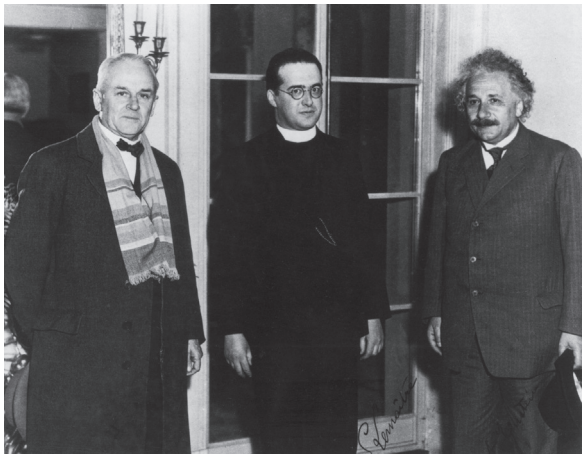

Left to right: Robert Millikan, Georges Lemaitre and Albert Einstein at Caltech on January 10, 1933
Courtesy of the Archives, California Institute of Technology and with clearance from the Albert Einstein Archives, Hebrew University of Jerusalem

A primordial relic radiation from a hot early beginning of the universe was first predicted by George Gamow in 1948 and by his students Ralph Alpher and Robert Herman in 1949 (see Alpher and Herman, 1988). Gamow (1948) made calculations of the conditions in the early stage of the universe and understood that the universe had to have a very hot beginning to prevent the coalescence of all hydrogen nuclei into heavier elements. In a story related by Stephen Hawking (1988), the often humorous Gamow convinced Hans Bethe to coauthor a paper in 1948 with Gamow's student Ralph Alpher whereby the authors would be cited as Alpher, Bethe, and Gamow so that the first letters of each author would coincide with the familiar names of the "alpha, beta, and gamma" radiations, which would be most appropriate for a paper on the beginnings of the universe. In their theory, they predicted a very hot and dense beginning of the universe, which today with the expanding universe would exhibit a residual photon radiation corresponding to a temperature that would have reduced to only a few degrees above absolute zero of the thermodynamic temperature Kelvin (ie, a few degrees >0 K). Alpher and Herman (1949) followed the temperature evolution of the early beginning of the universe and predicted a cooling down to a current temperature of 5 K. Alpher et al. (1953) went even further to carry out what was considered by Nobel Laureate Robert W. Wilson (1978) as the first thorough analysis of the early history of the universe, but failed to calculate or even mention their earlier prediction of 1949 that the universe would have cooled down to about 5 K.

It was not until 1965 did Arno Penzias and Robert Wilson at Bell Telephone Laboratories in New Jersey accidentally discovered a cosmic microwave background radiation. They were building and testing a new sensitive radio receiver, when they observed an excess noise that was of equal intensity regardless of the direction that the detector or antenna was pointing in the atmosphere. They concluded that the microwave radiation had originated from deep space even beyond our solar system and even our galaxy, because as the earth orbited the sun and rotated on its axis the antenna would be pointing to a different direction in space. At the same time a team of physicists led by Robert Dicke at Princeton University were studying microwaves to devise a system that would demonstrate the cosmic microwave background predicted by Gamow and Alpher. When Penzias and Wilson learned about this research work in search of the cosmic microwave background, they realized that they had discovered it. Penzias and Wilson (1965) reported their discovery in the *Astrophysics Journal* and Dicke et al. (1965) at Princeton reported the interpretation of the discovery in the same journal as back-to-back papers in the same issue. Penzias and Wilson shared the Nobel Prize in Physics 1978 for this discovery.

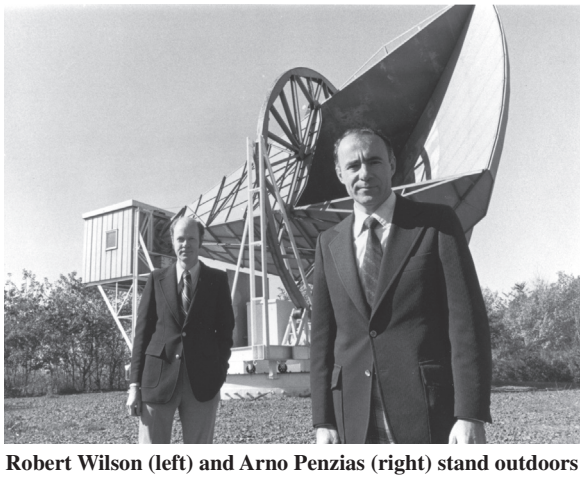

Robert Wilson (left) and Arno Penzias (right) stand outdoors by Bell Laboratories horn radio antenna in Crawford Hill, New Jersey
Courtesy of the AIP Emilio Segrè Visual Archives, Physics Today Collection

In the Nobel presentation speech, Proffessor Lamek Hulthén of the Royal Academy of Sciences on December 8, 1978 in Stockholm, Sweden, underscored the importance of the work and discovery of Penzias and Wilson. An excerpt of his speech is the following:

> *In the early 1960's a station was set up in Holmdel [Bell Laboratories, Holmdel, New Jersey] to communicate with the satellites Echo and Telstar. The equipment, including a steerable horn antenna, made it a very sensitive receiver for microwaves, ie, radio waves of a few cm wave length. Later radio astronomers Arno Penzias and Robert Wilson got the chance to adapt the instrument for observing radio noise, eg, from the Milky Way…The task of eliminating various sources of errors and noise turned out to be*

very difficult and time-consuming, but by and by it became clear that they had found a background radiation, equally strong in all directions, independent of the time of the day and the year, so it could not come from the sun or our Galaxy…Continued investigations have confirmed that this background radiation varies with wavelength in the way prescribed by well known laws for a space, kept at the temperature [of] 3 K. Our Italian colleagues call it "la luce fredda"—the cold light…But where does the cold light come from? A possible explanation was given by Princeton physicists Dicke, Peebles, Roll and Wilkinson (1965) and published together with the report of Penzias and Wilson (1965). It leans on a cosmology theory, developed about 30 years ago by the Russian born physicist George Gamow and his collaborators [Ralph] Alpher and [Robert] Herman. Starting from the fact that the universe is now expanding uniformly, they concluded that it must have been very compact about 15 billion years ago and ventured to assume that the universe was born in a huge explosion, the "Big Bang." The temperature must then have been fabulous: 10 billion degrees [K], perhaps more. At such temperatures, lighter chemical elements can be formed from existing elementary particles, and a tremendous amount of radiation of all wavelengths is released. In the ensuing expansion of the universe, the temperature of the radiation rapidly goes down. Alpher and Herman estimated that this radiation would still be left with a temperature around 5 K…Have Penzias and Wilson discovered 'the cold light from the birth of the universe'? It is possible—this much is certain that their exceptional perseverance and skill in the experiments led them to a discovery, after which cosmology is a science, open to verification by experiment and observation.

The significance of the discovery of the cosmic microwave background radiation corresponding to a temperature of approximately 3 K by Arno Penzias and Robert Wilson was commemorated in a postage stamp issued in Sweden. The stamp illustrated here shows a temperature of 3 K. A more precise figure has been determined to be a cosmic microwave background radiation corresponding to a 2.73-K blackbody radiation spectrum. This is discussed in more detail subsequently.

The precise spectrum of the cosmic microwave background radiation (CMBR) has been determined over three decades of frequency via many satellite, rocket, balloon, and ground measurements, and the cumulated data of radiant flux intensity as a function of radiation frequency is plotted in Fig. 14.7. The CMBR spectrum fits exactly to that predicted by a 2.73-K blackbody radiation spectrum whereby the brightness (B_ν) or intensity (I_ν) per unit of radiation frequency or wavelength is a function of the absolute temperature of the black body. The term "brightness" is used when measuring the radiant flux from a projected area of the surface of a blackbody, while the term "intensity" is used when reception of the radiant flux is measured (Woan, 2000). The Planck functions for the brightness or intensity are given by the following:

$$I_\nu(T) = B_\nu(T) = \frac{2h\nu^2}{c^2}\left[\exp\left(\frac{h\nu}{kT}\right) - 1\right]^{-1} \quad [14.30]$$

and:

$$I_\lambda(T) = B_\lambda(T) = B_\nu(T)\frac{d\nu}{d\lambda} = \frac{2hc^2}{\lambda^5}\left[\left(\frac{hc}{\lambda kT}\right) - 1\right]^{-1} \quad [14.31]$$

where I_ν and B_ν are the intensity or brightness, respectively, of blackbody radiation per unit frequency (W/m^2 Hz sr) and I_λ and B_λ are the intensity and brightness, respectively, of blackbody radiation per unit wavelength (W/m^2 m sr), h is Planck's constant (6.626×10^{-34} J s), c is the speed of light (2.99×10^8 m/s), k is the Boltzmann constant (1.38×10^{-23} J/K), and T is the temperature Kelvin (Woan, 2000).

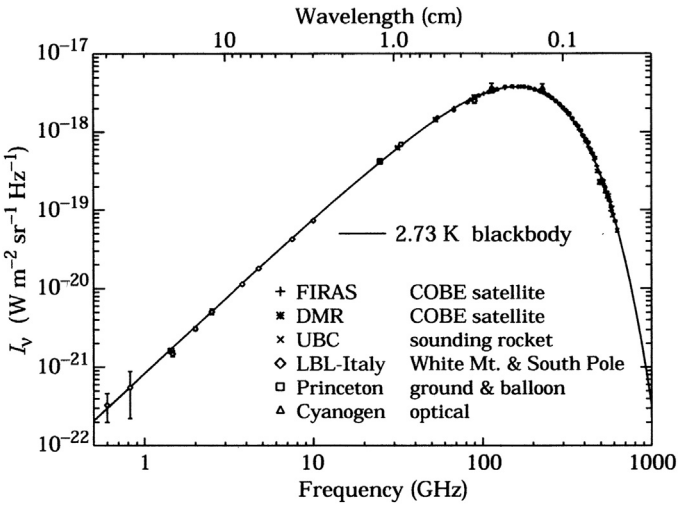

FIGURE 14.7 Precise measurement of the cosmic microwave background radiation (CMBR) spectrum. The line represents a 2.73-K blackbody, which describes the spectrum very well, especially around the peak of intensity. The spectrum is less well constrained at 10 cm and longer wavelengths. FIRAS, DMR, UBC, LBL-Italy, Princeton, and Cyanogen are sources of the experimental data points. *From Smoot, G.F., Scott, D., 2002. Cosmic background radiation. In: Hagiwara et al. (Eds.), Particle Data Group. Phys. Rev. D66, 010001-1, pp. 22.1–22.14; reprinted with permission, Lawrence Berkeley National Laboratory, © 2014 Regents of the University of California. The most up-to-date data is available on the Particle Data Group website http://pdg.lbl.gov.*

The precise determination of the cosmic microwave background radiation spectrum involved large teams of researchers and decades of work; and the significance of this work was underscored by the Nobel Committee with the award of the Nobel Prize in Physics 2006 to John C. Mather (NASA Goddard Space Flight Center, USA) and George F. Smoot (University of California, Berkeley, USA) "for their discovery of the blackbody form and anisotropy of the cosmic microwave background radiation." The award ceremony speech was given by Professor Per Carlson, Chairman of the Nobel Committee in Physics, on December 10, 2006, who highlighted the meaning of the precise measurement of the CMBR spectrum. An excerpt of his speech is the following, with the author's insertions in brackets:

This year's Nobel Prize in Physics is for another kind of astronomy, in which the instruments on the COBE [COsmic Background Explorer] satellite were used to observe radiation that was sent to us about 13 billion years ago, from another, much earlier era in the development of the universe.

At that time the character of the Universe had just altered. Previously it had been a dense, hot and impenetrable soup of electrons, protons and radiation. The temperature was so high and the Universe so dense that the radiation was swallowed up by the soup, just as light is veiled by fog. But the Universe is expanding, which means that its density and the temperature is sinking, and at the same time the energy of the radiation is lessening—which is the same as saying its wavelength is rising. The radiation that had previously been swallowed up by the soup was released—like when the fog lifts. The temperature had then sunk to 3000 degrees and it is estimated that the Universe was about 380,000 years old. The released radiation could continue its long, unimpeded journey through the Universe.

During the radiation's 13-billion-year journey the Universe has expanded mightily and its wavelength has extended one-thousand-fold, at the same time the temperature has dropped from 3000 to about three degrees above absolute zero. This cold background radiation fills the Universe and is a relic from its earliest stages, but it is invisible to the eye. The extended waves can be observed in the microwave area, with wavelengths of a few millimeters. It is this original radiation that the COBE satellite observed.

John Mather was responsible for the instruments on board COBE that were able to determine with great precision the temperature of the background radiation and also confirm that this spectrum had the characteristic blackbody form, characterizing the hot uniform state of the early Universe.

George Smoot was in charge of the instruments that were searching for very small variations—about one per 100,000—in the temperature of the background radiation in various directions. These variations would provide the seeds of the structures, in the shape of stars and galaxies, that evolved from the original hot, uniform soup. After collecting data for several years, it was possible to show that the small variations sought for really existed…Dr. Mather, Professor Smoot: Cosmology has become a precision science and your ground-breaking research laid the foundation for that. With your carefully calibrated instruments you have shown the cosmic microwave background radiation (CMBR) to follow very precisely a blackbody form.

In Prof. Per Carlson's speech, he describes the current form of the CMBR spectrum having the form of blackbody radiation spectrum resulting from the hot Big-Bang origin of the universe, which with the expansion of the universe over a period of 13 billion years, has cooled down to representing a current temperature of 2.75 K. Further expansion of the universe into the millions and billions of years to come would result in a further cooling of the universe with the blackbody radiation spectrum shifting to wavelengths of lower frequency and longer wavelengths of the cosmic microwave background radiation.

In his Nobel address, John C. Mather explained the impact of the determination of the precise cosmic microwave background radiation spectrum in his Nobel lecture as follows:

> *In the beginning was the Big Bang, so we now say with great certainty. The COsmic Background Explorer (COBE) satellite, proposed to NASA in 1974 and launched in 1989, provided very strong evidence for it: the spectrum of the cosmic microwave background radiation (CMBR) has the spectrum of an almost-perfect blackbody emitter at 2.725 ± 0.001 K, and the radiation is isotropic (the same in all directions) within 10 parts per million (rms) on angular scales of 7 degree and larger. This radiation is interpreted as the relic of an incredibly hot and dense early phase of the universe. In such a hot and dense phase, the creation, destruction, and energy equilibration of photons with one another and with all other forms of matter and energy would occur very rapidly compared with the expansion time scale of the universe. Such a state would immediately produce a blackbody radiation field. The expanding universe should preserve this blackbody spectrum, so measurement of any significant deviation from a perfect blackbody spectrum would either invalidate the whole idea of the Big Bang, or show that energy (eg, from decay of primordial particles) was added to the CMBR after the rapid equilibration ended…*
>
> *The fact that the radiation is isotropic to such a high degree is key evidence for its origin in the Big Bang…When I presented this spectrum at the January 1990 meeting of the American Astronomical Society in Crystal City (a suburb of Washington, D.C.), the audience of over 1000 people rose in a standing ovation. None of us on the COBE team anticipated this response, since the spectrum was not a surprise to us. In retrospect we now appreciate the reason for the enthusiasm. Not only was the spectrum beautiful to look at, but at one stroke it banished the doubts of almost everyone about the Big Bang theory. For so many decades, the intense combat between the Big Bang and Steady State advocates had continued, and for so many years, a series of small discrepancies between theory and measurement had been explained by ingenious people. Now it was over…The Big Bang theory was safe, and the universe was simple, simple enough for theorists to go on to the next problem.*

The blackbody radiation spectra plotted according to Eq. [14.30] over a broad range of radiation frequencies for three temperature levels, namely, 5.46, 2.73, and 1.36 K, are illustrated in Fig. 14.8. Compare the measured spectrum of the cosmic microwave background of Fig. 14.7 of radiation intensity per unit frequency with the calculated spectrum for a 2.73 K-blackbody of Fig. 14.8 (curve b). The measured cosmic microwave background spectrum of Fig. 14.7 is identical to

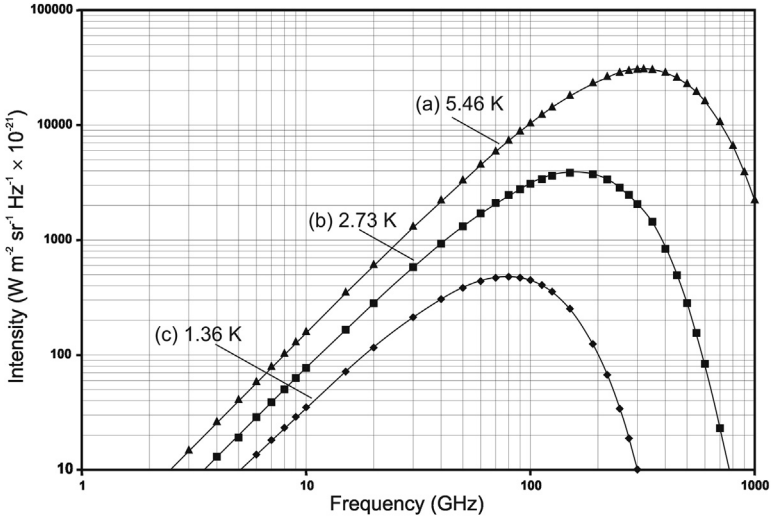

FIGURE 14.8 Logarithmic plots of the spectra of blackbody radiation depicting the intensity (I_ν) of the cosmic microwave background radiation (CMBR) as a function of radiation frequency (Hz) when the expanding universe was (a) hotter at 5.46 K and one-half its current size, (b) its current temperature of 2.73 K at its current size, and (c) its predicted one-half the current temperature when the universe expands to twice its size and cools to 1.36 K in approximately 100 million years.

the calculated radiation spectrum for a 2.73-K blackbody. The current precise calculated temperature corresponding to the measured cosmic radiation background is 2.73 K (Smoot and Scott, 2002).

A quick calculation of the temperature that corresponds to the cosmic microwave background spectrum can be made directly from Fig. 14.7 and Wien's displacement law that describes the inverse proportionality between the wavelength of maximum intensity of emission, λ_{max}, and temperature of a black body, that is, as the temperature of the black body decreases, the wavelength of maximum brightness (emission intensity) increases. This inverse proportionality was defined by the German Nobel Laureate Wilhelm Wien in 1893 as:

$$\lambda_{max} T = 2.9 \times 10^{-3}\ \text{mK} \qquad [14.32]$$

or:

$$\lambda_{max} = \frac{2.9 \times 10^{-3}\ \text{mK}}{T} \qquad [14.33]$$

Wilhelm Wien
(1864–1928)

Thus Wien's displacement law simply states that the maximum intensity of the blackbody radiation spectrum will occur at shorter wavelengths or higher radiation frequencies as the temperature of the blackbody increases. The following provide compelling evidence for the hot Big-Bang hypothesis for the origin or creation of the universe: (1) the residual temperature of only a few degrees (2.73 K), (2) the measured cosmic microwave background radiation (CMBR) spectrum that precisely corresponds to the blackbody radiation spectrum for 2.73 K (Fig. 14.7), and (3) the isotropy (uniformity in all directions) of the radiation among other data (see Smoot and Scott, 2002).

Wilhelm Wien (1864−1928) received the Nobel Prize in Physics in 1911 for his discoveries concerning the laws of thermal radiation and, in particular for his displacement law described above. The importance of Wien's work, reflected in the most recent findings on cosmic radiation, was underscored by E.W. Dahlgren, President of the Royal Swedish Academy of Sciences, on December 10, 1911 in the following excerpt of his Presentation Speech of the Nobel Prize to Wilhelm Wien:

> *The importance of Wien's displacement law extends in various directions…it provides one of the conditions which are required for the determination of the relationships between energy radiation, wavelength and temperature for black bodies, and thus represents one of the most important laws in the theory of heat radiation…Thus it became possible to determine the temperature of bodies, within fairly narrow limits, simply by seeking the wavelength at which radiation is greatest. The method has successfully been applied to the determination of the temperature of our light sources, of the sun, and of some of the fixed stars….*

What could not be foreseen at the time of Wilhelm Wien was that his law would be instrumental in determining the temperature of the universe from the wavelength of maximum brightness or intensity of the cosmic microwave background radiation.

The hot Big-Bang hypothesis describes the universe as having a very hot ($\sim 10^{10}$ K a second after the Big-Bang) and small, dense beginning with an expansion and cooling of the universe ever since the Big-Bang. The measured cosmic microwave background radiation illustrated in Fig. 14.7 provides evidence for the prediction of the Big-Bang creation and the ever-expanding and cooling of the universe. When the universe expands to twice its size, its temperature falls by half (Hawking, 1988). Consequently, when the universe was one-half its present size, its temperature would have been twice as hot (5.4 K) and the CMB radiation would have had a brightness peaking at a higher photon frequency, as illustrated in Fig. 14.8. Likewise, if we go further back in time when the universe was 1/100th its current size, the universe would have been a hundred-fold hotter than now, or 273 K, equivalent to 0°C. The CMB radiation would have had a spectrum shifted to yet higher frequencies and shorter wavelengths.

As we go further and further back in time to the Big-Bang, the universe was proportionally hotter, smaller, and more dense. The postage stamp and souvenir sheet issued in Macao, China illustrates the changes in the temperature of the universe from about 10^{32} K some 10^{-42} s after the Big-Bang to the current temperature of about 3 K some 15 billion years after the Big-Bang. The temperature at about a second after the Big Bang is estimated to have been about 10 billion degrees or 10^{10} K, and about 1 million years later the universe consisting then of only neutral hydrogen and smaller amounts of light elements would have expanded and cooled to about a few 1000 degrees or 10^3 to 10^4 K (Hawking, 1988). Because the microwave background photons interact very weakly with neutral hydrogen, the constitution of the universe at that time could be considered as the "surface of last scattering," that is, when the CMB radiation was scattered and continued to travel in all directions through the expanding universe with time. The CMB radiation shifts to longer wavelengths as the universe expands and cools. The universe is presently expanding by 5−10% every 10^9 years as determined by the Doppler effect of the velocity of travel of galaxies away from earth (Hawking, 1988). We could extrapolate, therefore, that the universe would expand to twice its current size and cool to one-half its current temperature to 1.36 K in approximately 10^{10} years. The cosmic microwave background radiation at that time in the future would be expected to be that corresponding to the spectrum of blackbody radiation at about 1.36 K, as illustrated in Fig. 14.8(c).

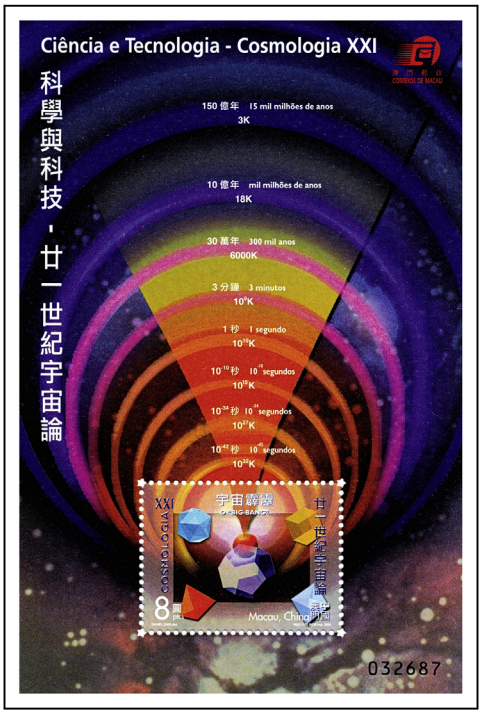

The differences between the current microwave background radiation intensity of the universe compared to that predicted for the universe when it expands to twice its current size are most easily recognized when plotting the blackbody radiation spectra at the current temperature of $T = 2.73$ K and the predicted temperature of 1.36 K on linear scales, as illustrated in Fig. 14.9.

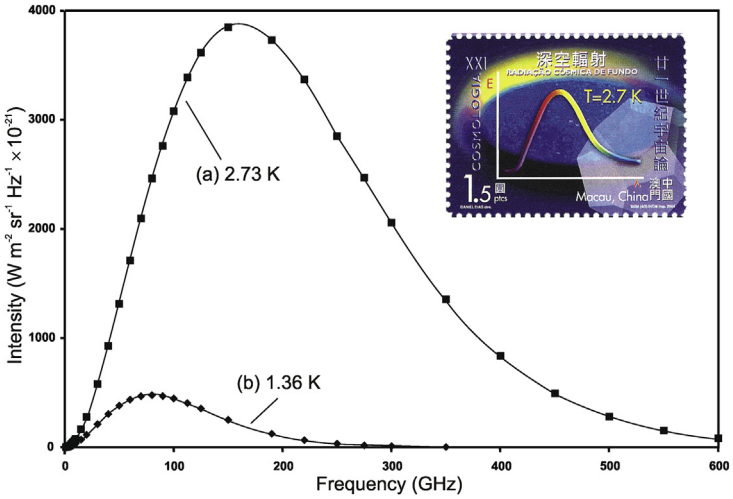

FIGURE 14.9 Linear plots of the spectra of blackbody radiation depicting the intensity of the cosmic microwave background radiation as a function of radiation frequency on a linear scale at (a) the current temperature ($T = 2.7$ K) and size of the universe and (b) the predicted temperature ($T = 1.3$ K) when the universe expands to twice its current size. The insert in the upper right corner of the graph is a picture of a postage stamp issued in Macao, China in 2004 commemorating the finding of the current cosmic microwave background radiation spectra corresponding to the linear spectra of blackbody radiation at $T = 2.7$ K.

14.7 RADIATION DOSE FROM COSMIC RADIATION AND OTHER SOURCES

Radiation dose, also referred to as absorbed radiation dose, is the amount of energy deposited in a given mass of a medium by ionizing radiation. The basic units used in the measurement of radiation dose and the recommended limits of radiation exposure and dose will be mentioned briefly here, as the monitoring of radiation for the dose received by the human body is essential not only for those working with radiation sources but also for the public in general.

Radiation exposure was historically measured by the roentgen (R), which is a measure of the quantity of radiation deposited in air from the amount of charge or ionization produced by the radiation in air. By definition $1\ R = 2.58 \times 10^{-4}$ C/kg of air at STP, that is, 1 R will produce 2.58×10^{-4} coulombs of ion pairs in 1 kg of air. The roentgen is a unit of exposure that is mostly historical and seldom used; it still occasionally appears on some dosimeter readings. Of more significance is the measure of absorbed dose, that is, the energy of radiation absorbed per unit mass of absorber. The original unit of absorbed dose is the rad, which is derived from the term "radiation absorbed dose." The rad has been replaced with the gray (Gy), which is the SI unit of absorbed dose. The use of SI units is recommended by the International Commission on Radiation Units and Measurements (ICRU). The rad and gray have the following equivalents:

$$100\ \text{rad} = 10^4\ \text{erg/g} = 1\ \text{Gy} = 1\ \text{J/kg} \quad [14.34]$$

$$1\ \text{rad} = 10\ \text{mGy} = 100\ \text{erg/g} \quad [14.35]$$

$$1\ \text{mrad} = 10\ \mu\text{Gy} \quad [14.36]$$

As $1\ \text{eV} = 1.602 \times 10^{-19}$ J we can convert the gray to units of electron-volt energy deposited in a kg of absorber or:

$$1\ \text{Gy} = 1\ \text{J/kg} = \frac{1\ \text{J/kg}}{1.602 \times 10^{-19}\ \text{J/eV}} = 6.24 \times 10^{18}\ \text{eV/kg} = 6.24 \times 10^{12}\ \text{MeV/kg} \quad [14.37]$$

Let us use the following example to illustrate the calculation of radiation dose:

A 1.5 cm^2 beam of gamma radiation consisting of 1-MeV photons with an emission rate of 5×10^8 photons/s is irradiated onto human tissue of density 1.1 g/cm^3. If 6.25% of the gamma radiation is absorbed by 1.25 cm thickness of the tissue (ie, 93.75% transmitted through the tissue), the rate of radiation dose administered to the tissue per second may be calculated as:

$$\text{dose} = \frac{\text{energy}}{\text{mass}} \quad [14.38]$$

and:

$$\text{dose/s} = \frac{\text{energy/s}}{\text{mass}}$$

$$= \frac{(5 \times 10^8 \text{ photons/s})(0.0625)(1 \text{ MeV/photon})}{(1.1 \text{ g/cm}^3)(1.5 \text{ cm}^2)(1.25 \text{ cm})} \quad [14.39]$$

$$= \frac{3.12 \times 10^7 \text{ MeV/s}}{2.0625 \text{ g}} = 1.51 \times 10^{10} \text{ MeV/s/kg}$$

If 1 Gray (Gy) is equivalent to 6.24×10^{12} MeV/kg (Eq. [14.37]), the dose rate in MeV/s/kg is converted to units of the Gray (Gy) as:

$$\text{dose (Gy/s)} = \frac{1.51 \times 10^{10} \text{ MeV/s/kg}}{6.24 \times 10^{12} \text{ MeV/kg/Gy}} = 0.00242 \text{ Gy/s} = 2.42 \text{ mGy/s}$$

Another formerly very common and historical unit of radiation dose is the rem. The rem is a measure of absorbed dose in biological tissue. This unit of measure is derived from the term "**r**oentgen **e**quivalent for **m**an" or "**r**oentgen **e**quivalent **m**ammal." The rem was created as a measure of dose of ionizing radiation to body tissue in terms of its estimated biological effect; its SI unit is the sievert (Sv) and:

$$100 \text{ rem} = 1 \text{ Sv} \quad \text{and} \quad 1 \text{ rem} = 10 \text{ mSv} \quad [14.40]$$

The rem or Sv (sievert) are referred to as units of equivalent dose, because the dose is measured on the basis of a weighting factor (w_R), which defines the relative hazard of radiation on the basis of the types and energies of the radiations by placing all radiation classes on the same dose level or equivalent (L'Annunziata, 1987). The weighting factor, formerly known as the quality factor (QF), is defined as the ratio of the gamma-ray or X-ray dose to the dose required to produce the same biological effect by the radiation in question. Table 14.2 lists the radiation weighting factors according to radiation type and energy, specified by the International Commission on Radiological Protection (ICRP). The weighting factor of a given radiation is a function of the radiation linear energy transfer (LET), that is, the radiation energy loss per path length of travel. As discussed in the chapter entitled "Beta Radiation and Beta Decay," radiations of high mass and charge, such as alpha particles or fission products, will have a higher LET than electrons or beta particles, muons, or X-ray or gamma-ray photons. Because photons will produce electrons as secondary particles, X- or gamma-ray photons are classified to have the same radiation weighting factor as electrons. According to the weighting factors provided in Table 14.2, alpha particles are considered to be 20 times more damaging to cells of the human body than beta particles (ie, electrons), muons, and X- or gamma radiation. However, alpha particles and other heavy nuclei have short ranges in matter compared to other

TABLE 14.2 Radiation Weighting Factors

Radiation	w_R
X- and gamma-rays, all energies	1
Electrons and muons, all energies	1
Neutrons <10 keV	5
10–100 keV	10
>100 keV to 2 MeV	20
2–20 MeV	10
>20 MeV	5
Protons (other than recoils) >2 MeV	5
Alphas, fission fragments, and heavy nuclei	20

Source: ICRP, 1991. Summary of recommendations. Ann. ICRP 21, 67–77. Pub. 103, Elsevier, Amsterdam, and Donahue, R.J., Fassó, A., 2002. Radioactivity and radiation protection. In: Hagiwara et al. (Eds.), Phys. Rev. D66, 01001-1, also ICRP, 2007. Pub. 103, Chapter 3. Biological aspects of radiological protection. Ann. ICRP 37 (2–4), 49–79, Elsevier, Amsterdam, reprinted with permission from Elsevier © 1991.

radiation types. Thus distance provides the best protection from alpha particles and other heavy nuclei. Also, the weighting factors for neutrons in Table 14.2 classify the neutrally charged neutrons as more hazardous to biological tissue than the charged electrons or muons. This is because neutrons will produce recoil protons and ions of higher mass via neutron collisions in body tissue.

The equivalent dose in Sv can be calculated from the weighting factors as:

$$\text{Sv} = \text{absorbed dose in grays} \times w_R \quad [14.41]$$

where the weighting factor expresses potential damage to cells, and long-term risk (primarily cancer and leukemia) from low-level chronic exposure, which is dependent on radiation type and other factors (ICRP, 1991; Donahue and Fassò, 2002). Using the notation of Lilley (2001) for average absorbed dose in tissue, Eq. [14.41] can be written as:

$$\text{Sv} = D_{T,R} \times w_R \quad [14.42]$$

where Sv is the equivalent dose in sieverts and $D_{T,R}$ is the average absorbed dose in tissue T from a given type of radiation R. For example, from the weighting factors of Table 14.2 and Eq. [14.41]. We can calculate that an average absorbed dose of 0.01 Gy from alpha particles ($w_R = 20$) will produce the same biological effect as a 0.2-Gy dose from X- or gamma radiation ($w_R = 1$). Likewise, a 0.1-Gy dose from 50-keV neutrons ($w_R = 10$) will produce the same biological effect as a 1 Gy-dose of electrons or beta-particles ($w_R = 1$). When more than one radiation type contributes to the absorbed dose, the equivalent dose is calculated according to the weighted sum of the contributions from each radiation type.

The ICRP (1991) recommendation for limits of exposure for radiation workers for whole-body dose is 20 mSv/year (2 rem/year) averaged over 5 years, with the dose in any 1 year $\leq$ 50 mSv (5 rem/year). It is estimated by the United States National Safety Council that the average person in the United States receives only 3.6 mSv (0.36 rem or 360 mrem) of accumulated radiation dose per year from all sources including cosmic radiation, medical X-rays, and natural radioactivity, etc. In most areas of the world, the whole-body equivalent dose rate is $\approx$0.4 to 4 mSv/year or 40–400 mrem/year, although in certain areas of the world the dose rate can range up to 50 mSv/year or 5 rem/year (Donahue and Fassó, 2002).

The radiation sources and their approximate average relative contribution to the dose received by the human body are radon ($\sim$55%), medical X-rays ($\sim$11%), internal radiation, ie, radiation from radionuclides within the human body ($\sim$11%), terrestrial radiation ($\sim$8%), cosmic radiation ($\sim$8%), nuclear medicine ($\sim$4%), consumer products ($\sim$3%), and other sources ($\sim$1%). Cosmic radiation contributes only a relatively small ($\sim$8% or $\sim$30 mrem) portion of the total annual radiation dose that the average person may receive from both manmade and natural radioactivity. Cosmic radiation, therefore, contributes only a small part to the total radiation that the human body receives by the average person during his or her lifetime. Natural radon is the largest source of radioactivity that may affect our health. This is followed with X-rays that we may receive from medical and dental diagnostic procedures, and internal radiation arising from radionuclides within our own bodies. Radiation used in nuclear medicine, such as in cancer diagnosis and treatment, and radioactivity from consumer products such as smoke detectors, lawn fertilizer, cigarettes, stone or brick masonry, and television sets, etc., contribute yet smaller amounts of radiation to the overall dose our bodies receive during our lifetimes. Finally, the vague term of "other sources" ($\sim$1%) cited earlier in this paragraph refers to radioactivity that might reach our bodies from radioactive waste associated with manmade radionuclides from nuclear power plants, nuclear weapons production and testing, and peaceful applications of radionuclides used in scientific research.

As we travel above sea level to higher altitudes in the earth's atmosphere, the dose rate from cosmic radiation will obviously increase, since the atmosphere serves as a shield to cosmic radiation. Persons who live several 1000 ft above sea level should expect to accumulate a higher dose from cosmic radiation over a period of a year than another person living at sea level in the same general region of the country. For example, Fig. 14.10 illustrates approximate cosmic radiation dose rates for persons in the State of Idaho. A person living in the city of Idaho Falls, Idaho (altitude = 4740 ft or 1445 m) could expect to receive more than twice the cosmic radiation dose over the period of a year than a person living in Sandpoint, Idaho (altitude = 2150 ft or 655 m). A person living in Leadville, Colorado, which is the highest city (10,150 ft or 3094 m) in the United States, should expect to receive several times the annual dose rate than a person at or near sea level in the same State. Nevertheless, the accumulated dose, received by the human body, at inhabitable altitudes of the world are very low and contribute only a small percentage ($\sim$8%) to the total body dose received from all sources.

If we travel to altitudes accessible only by aircraft (7–12 km above the earth), the dose from cosmic radiation increases, and the amount of increase will be a function of latitude, as illustrated in Fig. 14.11. At these high altitudes, the cosmic radiation of most concern is neutrons, charged particles including muons and protons (see Fig. 14.5), and gamma radiation. Although cosmic radiation is incident from above the earth's atmosphere, exposure to cosmic radiation showers in the atmosphere aboard airplanes is considered isotropic, that is, it should be incident from all directions. This is the result of scattering of radiation in all directions as a result of nucleon collisions in the atmosphere.

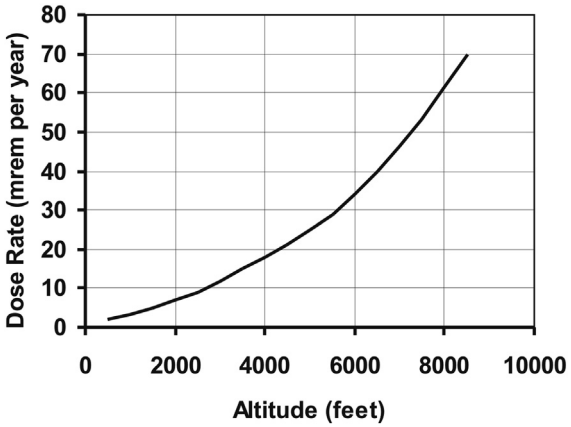

FIGURE 14.10 Approximate cosmic radiation dose rates as a function of inhabitable altitudes above sea level. *Data obtained from State of Idaho, Idaho National Engineering and Environmental Laboratory, Idaho Falls, http://www.oversight.state.id.us.*

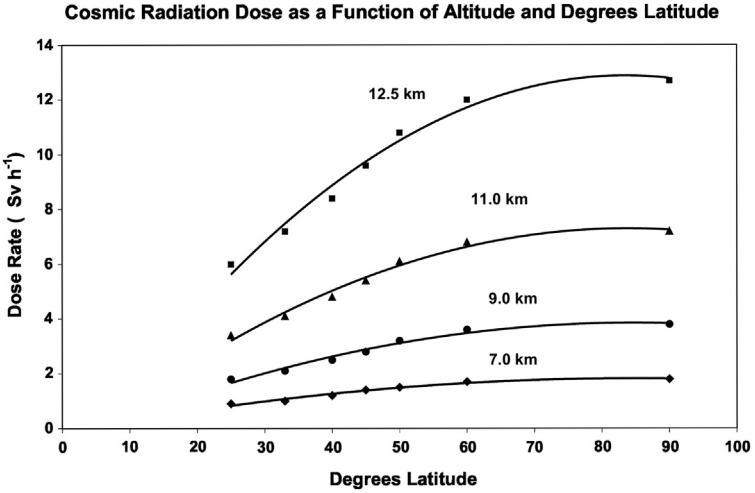

FIGURE 14.11 Cosmic radiation dose rate as a function of altitude above sea level and degrees latitude. The latitudes plotted are not precise; instead, the seven data points are plotted at the upper ends of the general latitude ranges of 0–25, 25–33, 33–40, 40–45, 45–50, 50–60, and 60–90 degrees, respectively. *Data from NRL, February 1998. The exposure of New Zealand aircrew to cosmic radiation. National Radiation Laboratory, Information Sheet 19, Christchurch, New Zealand, p. 6.*

Exposure to cosmic radiation is a concern to intercontinental airline pilots, who fly at high altitudes and high degrees of latitude and who compile large numbers of flight hours per year over long careers. Hammer et al. (2000) report a mean cosmic radiation dose estimate of 35 mSv for 509 pilots, who averaged 26.6 years of employment at an average of 481 flight hours per year. The accumulated cosmic radiation dose of 35 mSv over 26.6 years will yield an average dose rate of 1.3 mSv/year. The dose to aircrew is a function of altitude, latitude, and flight time (flight hours) at various altitudes and latitudes of flight, among other factors. The National Radiation Laboratory in New Zealand (NRL, 1998) provides statistics for national aircrew. They separated aircrew into four categories according to their altitudes, latitude, and yearly flying hours as provided in Table 14.3. Their conclusions are that flight crew exposure is of limited health significance. The dose rates are well within the ICRP (1991) recommendations for limits of exposure for radiation workers for whole-body dose set at 20 mSv/year. For pregnant women, however, the ICRP limit of dose is 2 mSv for the duration of pregnancy. Consequently, the study by NRL (1998) concludes that airline companies may apply a limit of 2 mSv for a pregnant member of the aircrew from the time of conception.

Astronauts, who circle the earth in orbit for extended periods of time, those who have traveled and plan to travel to the moon and back, and those who may travel to Mars have reason for concern of exposure to cosmic radiation where there is no protection by the earth's partially protective atmospheric shield. Fujitaka (2005) reports that a 1-week mission on the space schuttle will result in a radiation dose of 3.5 mSv; while astronauts would accumulate a dose of 43 mSv during a trip

TABLE 14.3 Cosmic Radiation Dose to Aircrew

Flight Altitudes (km)	Flight Latitudes (degrees)	Flight Hours (h/year)	Dose Rate (mSv/year)
7.0	—	500	<0.2
9.3–8.2	—	500–700	<0.5
11 (70%)[a]	Middle latitudes	1000	>3.5
12 (90%)[b]	0–40 (50%)[c] 40–60 (50%)[c]	1000	>6.5

[a] *Percent of flight time at 11 km altitude.*
[b] *Percent of flight time at 12 km altitude.*
[c] *Flight time equally divided (50%) between low (0–40) and high (40–60) latitudes.*
Source: Taken from data provided by NRL, February 1998. The exposure of New Zealand aircrew to cosmic radiation. National Radiation Laboratory, Information Sheet 19, Christchurch, New Zealand, p. 6.

to the moon. Travel from Earth to Mars would take 280 days and the return trip 256 days, during which time astronauts would accumulate 1850 mSv, and a stay on Mars for 439 days would expose astronauts to an additional 410 mSv, whereby each astronaut would accumulate a grand total of 2.26×10^3 mSv (Paschoa and Steinhäusler, 2010). A very interesting and stimulating note for thought is reported by Fujitaka (2005), that space travel to Pluto, which is at the boundaries of our solar system, would expose astronauts to a cosmic radiation dose of 70 Sv or 70,000 mSv, which is enough radiation to kill every cell in the human body. This may be so at current speeds of space travel, as NASA's New Horizons Mission spacecraft to Pluto was launched in June 2006, and it reached Pluto after nine years, in July of 2015. However, with the proper thrust systems, high speeds of space travel in a manned spacecraft, referred to as relativistic rocketry, would be possible (Westmoreland, 2010; Walter, 2006), which would minimize space travel time well out of our solar system and thus keep cosmic radiation dose to acceptable limits.

For further information on radiation dosimetry, the reader is invited to peruse books dedicated to this subject matter such as those by Bevelacqua (2010), Stabin (2009), and Cember and Johnson (2008).

Chapter 15

Hall of Fame: Part VII

Sergei Ivanovich Vavilov (1891–1951), Pavel Alekseyevich Cherenkov (1904–1990), Il'ja Mikhailovich Frank (1908–1990) and Igor Yevgenyevich Tamm (1895–1971)

Pavel Cherenkov, Il'ja Frank, and Igor Tamm shared the Nobel Prize in Physics in 1958 "for the discovery and interpretation of the Cherenkov Effect." Sergei Vavilov would have been nominated for the prize had he not passed away several years before.

The Editor of "NATURE" presents his compliments to Mr. P. A. Cherenkov and regrets he is unable to make use of the communication, returned herewith, entitled "VISIBLE RADIATION PRODUCED BY ELECTRONS MOVING IN A MEDIUM WITH VELOCITIES EXCEEDING THAT OF LIGHT".

The entire content of a letter of rejection from the journal *Nature* dated June 29, 1937 addressed to P.A. Cherenkov, who tried to publish his Nobel-winning discovery of Cherenkov radiation.

If you have chosen to become a scientist, realize that your whole life will be restless and devoted to a perpetual quest for something new in your field. Each scientist must have a gene for concern and must be an obsessed person.

A quote attributed to N.I. Vavilov (1887–1943) from Vavilov, Yu. N., Levshin, L., 2002. Opt. Spectrosc. 92 (6), 956–961.

SERGEI IVANOVICH VAVILOV (1891–1951)

Sergei Vavilov was born in Moscow in 1891. Sergei and his elder brother Nikolai both became prominent scientists. Their father was a successful merchant, who educated his sons with hope that they would inherit his business. However, Sergei studied physics and mathematics at Moscow University and Nikolai studied biology and became a prominent plant breeder. Biodata on Sergei Vavilov presented here was taken in part from comprehensive and authoritative reviews of Vavilov's life, contributions, and biography by Bolotovski et al. (1998, 2004) of the Lebedev Physics Institute, Moscow, and information provided in Moscow News (2006). Bolotovski et al. (1998) provide the most thorough and authoritative historical review of Sergei Vavilov's contribution to the development of Russian physics in the face of inconceivable political repression and persecution during the leadership of Joseph Stalin from the mid-1920s until Stalin's death in 1953 and the unyielding power of Stalin's henchman, Lavrenty Beria, from 1935 to 1953. Vavilov's biography by those who knew him (Bolotovski et al., 1998) provides insight into life during the Great Purge of the Soviet Union and the personal sacrifices made by Sergei Vavilov to assure the development of physics in the Soviet Union during those repressive years. The postage stamp illustrated here was issued in the former USSR in 1961 to commemorate 10 years following the death of Sergei Vavilov.

During his second year at Moscow University, Sergei Vavilov started research work in the laboratory of Pyotr Nikolaevich Lebedev (1866–1912), who was the first physicist to demonstrate the pressure exerted by light photons on solids and gases, which confirmed James Clerk Maxwell's theory that light has momentum and could thus exert pressure on solids. Vavilov graduated with honors from Moscow University in 1914 and shortly thereafter began service in the military during the First World War. He was taken prisoner by the German forces in 1917. Bolotovski et al. (2004) related the following account of his capture and escape:

He was interrogated by a German officer who happened to be a physicist, and they spent all night discussing physics, especially Max Planck's new theory of light. By morning the officer had helped Vavilov escape, and in February 1918 he appeared in Moscow.

From CERN Courier, November 12, 2004, http://cern.courier.com/cws/article/cern/29202, reprinted with permission © CERN 2004.

Radioactivity: Introduction and History, From the Quantum to Quarks. http://dx.doi.org/10.1016/B978-0-444-63489-4.00015-0
Copyright © 2016 Elsevier B.V. All rights reserved.

Sergei I. Vavilov (1891–1951)

Pyotr N. Lebedev (1866–1912)

Vavilov's father had lost all of his property and emigrated from Russia following the Russian Revolution of 1917 culminating in the defeat of the counterrevolutionaries of the civil war of 1918 to 1922. Sergei and his brother Nikolai, as budding scientists, remained to work in their homeland. Bolotovski et al. (2004) explains:

> *…they realized that they had to coexist with the Soviet government as many other Russian scientists did. The government had decided that use should be made of scientific and technical specialists "in spite of the fact that they have been nourished upon capitalist ideology." The 1920s were thus a period of great liberty for Russian scientists, despite civil war, widespread famine and economic collapse.*

From CERN Courier, November 12, 2004, http://cern.courier.com/cws/article/cern/29202, reprinted with permission © CERN 2004.

Sergei Vavilov began his career in 1918 working in the Physics and Biophysics Institute, Moscow, headed by Pyotr Petrovich Lazarev, a disciple of Lebedev. Here Vavilov started a research career in physical optics and specifically research in the field of photoluminescence, of which little was known at the time. Vavilov also lectured at Moscow University. He and his coworkers defined the laws of luminescence and mechanisms of luminescence quenching. They were the first to introduce the term "luminescent yield" as the ratio of luminescent energy to the energy of light creating the luminescence. In 1926, Vavilov and Vadim Levshin discovered a violation of Bouguer's Law in uranium glass. The law defines light attenuation by optically homogeneous or transparent media, variations of which are also known as Beer's Law or the Beer–Lambert Law. They found a reduction in the light absorption by the glass as the intensity of the incident light was increased. Bolotovski et al. (2004) explain that this is known as the photorefractive effect, which is described as resulting from the depopulation of the ground state by the incident beam. Vavilov thus introduced the term "nonlinear optics," which is now a branch of physics.

Sergei Vavilov's entire scientific career was in Russia, with the exception of a 6-month research stint at the Physikalisches Institut der Universität Berlin with Peter Pringsheim, the then-authoritative figure in the science of fluorescence (Pringsheim, 1949). Bolotovski et al. (2004) report (with the writer's insertions in brackets):

> *At the beginning of the 1930s the political climate in the USSR changed abruptly for the worse as Stalin consolidated his power. Numerous scientists were persecuted in Moscow, Leningrad and other cities. In March 1931 [Pyotr] Lazarev was suddenly arrested and later exiled in the Urals. Colleagues lost their jobs at the institute, including [Sergei]Vavilov, although he kept his position as university professor. Academicians trying to preserve the Lebedev-Lazarev scientific school recommended Vavilov as a full member of the USSR Academy of Sciences, and he was elected in 1932.*

From CERN Courier, November 12, 2004, http://cern.courier.com/cws/article/cern/29202, reprinted with permission © CERN 2004.

Around the time of his election to the Academy of Sciences, Vavilov was invited by the director of the Optical Institute of Leningrad (now Saint Petersburg) to bolster the activities of the institute and save its programs from being stopped by the government, which wanted to make way for the production of optical equipment, particularly for the military. Vavilov then became head of research of the State Optical Institute in 1932 and also head of the Academy of Science's Physics Department in Leningrad. Here Vavilov organized teams of young scientists to carry out research in neutron physics and luminescence.

In 1933, Sergei Vavilov had a doctoral student whose name was Pavel Alekseyevich Cherenkov. For his doctoral research, Vavilov proposed that Pavel Cherenkov work on the topic of "The luminescence of uranyl salt solutions under the influence of hard gamma radiation." High-energy gamma radiation would induce the production of a weak blue light from solutions of uranium salts, and it was thought at the time that this might be due to the occurrence of luminescence. The mysterious weak blue light was historically documented as seen by Marie Curie in 1910 with bottles of concentrated radium solutions aglow with a pale blue light, as related in a biography by her daughter Eve Curie (1941). Lucien Mallet (1926, 1928, 1929) also had studied the properties of the light and found that it would be emitted by a variety of transparent bodies when exposed to radioactive sources. However, Mallet did not determine the origin of the blue light. Vavilov put Cherenkov onto investigating the origins and properties of the mysterious light, which he thought to be fluorescence. Vavilov and Cherenkov apparently were not aware of the earlier observations of Curie or the previous studies by Mallet, and in any case they started the research to investigate what they thought was fluorescence. Sophisticated photomultiplier detectors were not available in 1933; however, Vavilov had developed a visual method of measuring low light intensities very close to the thresholds of human vision. To observe and measure the intensities of this weak light, Cherenkov had to adapt his eyes by remaining in a dark room for an hour or more before taking any measurements.

Cherenkov found that the weak light was emitted not only from the uranium salt in sulfuric acid solution when irradiated with strong gamma rays, but that there was a background glow from the solvent itself, that is, when sulfuric acid solution without the uranium solute was irradiated with the hard gamma. Bolotovski et al. (2004) give an account that Vavilov asked Cherenkov to check other solvents that were highly purified to see if these also emitted light when irradiated. Cherenkov investigated 16 different pure solvents and observed about the same intensity of blue light in all solvents when these were irradiated with the hard gamma radiation. Various attempts to quench the effect were unsuccessful, which provided evidence that the phenomenon was not fluorescence. What was occurring was obvious to them at this point. This was not fluorescence, but that the light emission was a new phenomenon of origin yet unknown to mankind. They had discovered a new radiation, which they reported in two papers back-to-back in the 1934 Proceedings of the USSR Academy of Sciences (Cherenkov, 1934a,b; Vavilov, 1934). In his paper, Vavilov provided a preliminary theory on the origin of the radiation. He proposed that Compton electrons produced by the hard gamma radiation would yield a type of bremsstrahlung radiation. He was correct in the conclusion that the mysterious light was being produced by the Compton electrons; however, the mysterious light was not the result of bremsstrahlung but was yet of unknown origin. It would not be until a few years later (1935–1938), with more research by Cherenkov (1936, 1937a,b,c,d, 1938a,b,c) under the directorship of Vavilov and theoretical calculations by Il'ja M. Frank and Igor Y. Tamm (1937), that it would be understood finally that the new radiation was produced by the Compton electrons when these electrons had sufficient energy to travel at a speed in excess of the speed of light in the transparent medium. The new radiation soon became known as "Vavilov–Cherenkov radiation" or "Cherenkov radiation."

Vavilov–Cherenkov radiation eventually became a very important tool in studies of high-energy physics (see the chapter: "Cherenkov Radiation"). Cherenkov counting, ie, the instrumental technique of detecting and counting the individual Cherenkov radiation wave fronts or emissions, has become a common means of analyzing the levels of activity or disintegration rates (disintegrations per minute) of radionuclides that emit high-energy β-particles (L'Annunziata, 1987, 2012e). As a consequence of the practical importance of the Vavilov–Cherenkov Effect, the Nobel Prize in Physics in 1958 for the discovery and interpretation of the Cherenkov Effect was awarded to Pavel Cherenkov, Il'ja Frank, and Igor Tamm. Sergei Vavilov would also have been nominated for the award had he not passed away in 1951, as the Nobel Prize is not awarded posthumously. Those who have had the opportunity to view the core of an operating nuclear reactor at the bottom of a pool of water may have witnessed the weak blue Cherenkov light surrounding the core. This Cherenkov radiation in the water surrounding the reactor core is produced mostly from Compton electrons produced as a result of high-energy γ-ray interactions with atomic electrons of the water or high-energy β-particles emitted as a result of fission-product decay. A photograph of the blue visible radiation of Cherenkov light in a reactor core is provided in Fig. VII.1.

In addition to his elected membership to the USSR Academy of Sciences in 1932, Sergei Vavilov was appointed Head of the State Optics Institute (currently the Vavilov State Optical Institute, or Gosudarstvennyy Opticheskiy Institute or GOI), and Head of the Physics Department of the Institute of Physics and Mathematics of the USSR Academy of Sciences in Leningrad. From this time on for the rest of his life, Sergei Vavilov devoted his professional career to helping and supervising young scientists and performing administrative duties required to build up research groups that would put Russian physics research at the forefront and at a par with the leading scientific physics research groups of the world. In 1934, the USSR Academy of Sciences moved from Leningrad to Moscow, and Sergei Vavilov and his Physics Department

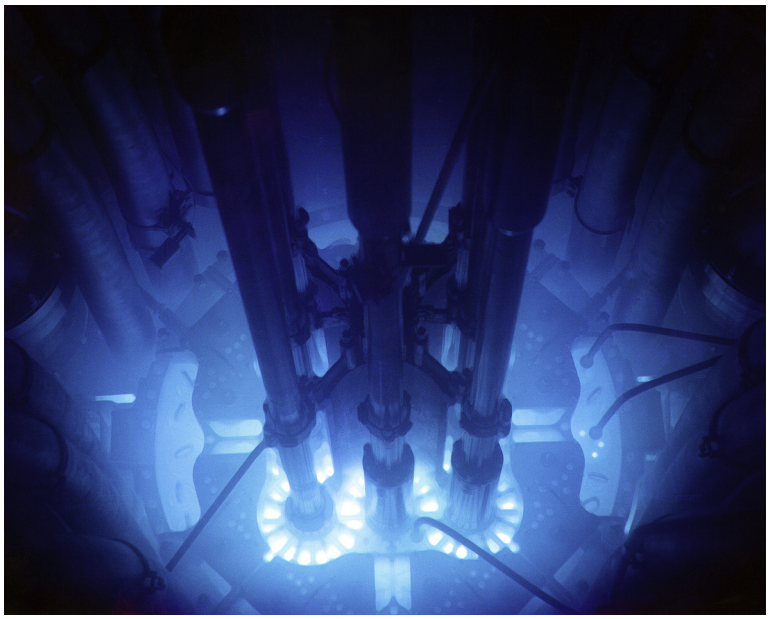

FIGURE VII.1 The Advanced Test Reactor (ATR) of the Idaho National Laboratory illuminating blue visible light by Cherenkov radiation. *Printed with permission, Digital Photo Archive, Department of Energy (DOE), courtesy of the AIP Emilio Segre Visual Archives.*

moved as well to Moscow, where they occupied the same building formerly used by the exiled Pyotr Lazarev. After the move to Moscow, Sergei Vavilov's Physics Department was transformed into the Physics Institute of the USSR Academy of Sciences (Fizicheskii Institut Akademya Nauk USSR, or FIAN), and Sergei Vavilov was appointed its director. Following Vavilov's proposal, the new institute was named the P.N. Lebedev Physics Institute after Pyotr Nikolaevich Lebedev (1866−1912), the pioneering physicist in whose laboratory Vavilov had the opportunity to work when he was a young student at Moscow University. Vavilov remained Director of FIAN his entire life. FIAN developed under Vavilov's direction from no more than about a couple dozen staff members and graduate students in 1932 to one of the largest and leading physics research institutes of the world. This was not easy for Sergei Vavilov to accomplish, as related by Bolotovski et al. (1998), due to the 1930s being a difficult time of political hysteria in Russia.

To survive and to be able to build FIAN as its director into an institute packed with the most qualified physicists who could work in relative tranquility at the forefront of science and as President of the USSR Academy of Sciences (1945−1951), Vavilov had to bow to the Communist Party and make ceremonial statements during symposia and conferences on many occasions, described by Bolotovski et al. (1998).

V. I. Veksler (1907–1966) and Phase Stability Principle

Sergei Vavilov would attract the best scientists to FIAN. As an example, in 1936 Vavilov had invited the young physicist Vladomir Iosifovich Veksler to join FIAN. Veksler would later be the first to develop the principle of phase stability (Veksler, 1944), which would permit the acceleration of particles to relativistic speeds in modern particle accelerators. This was independently discovered by E.M. McMillan (1945) at the University of California, Berkeley.

For their discovery, Veksler and McMillan shared the Atoms for Peace Award in 1963. The postage stamp illustrated here commemorates V.I. Veksler and his discovery of the principle of phase stability. The stamp illustrates a "star" consisting of numerous particle tracks emitted in various directions following the collision of a charged particle at relativistic speeds with an atomic nucleus in a synchrotron, developed as a consequence of Veksler's phase stability principle. Bolotovski et al. (2004) relate the development of particle accelerators under Vavilov's direction. They detail the account of how Vavilov believed that experiments in nuclear physics required particle accelerators that were larger than the 10-MeV cyclotron already available at the Radium Institute. Vavilov consequently called together a "cyclotron group" in the Lebedev Physics Institute to evaluate the possibility of constructing a larger, more powerful cyclotron. The general feeling of the group was that it would be impossible to jump over the relativistic barrier. However, after Veksler wrote two papers in 1944 on his new principle of phase stability (Veksler, 1944, 1945), Vavilov immediately recommended the papers for publication in the national journals and initiation of construction of a 30-MeV synchrotron at the Lebedev Institute. Veksler's new concept of phase stability was subsequently published in the international journal *Phys. Rev.* the following year. Veksler spoke the following of Vavilov (Bolotovski et al., 2004):

> *I was lucky in that as a young scientist I was invited in 1936 to join the staff of the Lebedev Institute [FIAN]. An exciting atmosphere of complete commitment to science prevailed in the institute. My first impression of Vavilov was that his attitude was extremely affable and straightforward.*

From CERN Courier, November 12, 2004, http://cern.courier.com/cws/article/cern/29202, reprinted with permission © CERN 2004.

It was in the 1940s that Sergei Vavilov was struck with one of the hardest blows of his lifetime, the arrest and death of his brother Nikolai Ivanovich Vavilov (1887−1943). Bolotovski et al. (1998, 2004), Yuori N. Vavilov (2002), and The Moscow News (2006) provide detailed accounts of the tragic history of Nikolai's arrest and demise at the peak of his career. Nikolai Vavilov was the elder brother of Sergei and a famous plant breeder and geneticist. By 1920, Nikolai had already made many scientific advances in the field of plant breeding and genetics. He had discovered the law of biological variability essential to plant breeding for crop improvement, and from 1922 to 1933 he organized numerous expeditions to 60 countries of the world and collected about a quarter million specimens of grain. This study of the world's plant resources enabled Nikolai to work out foundations for the selection and breeding of improved varieties in Russia. By 1929, Nikolai was elected President of the Agricultural Academy and elected member of the Academy of Sciences. Nikolai was head of the research institutes of plant breeding in Leningrad and genetics in Moscow. He set up many experimental stations in various parts of the USSR and directed their research programes. Nikolai's pioneering work was recognized worldwide, and the field of plant genetics and breeding, which Nikolai helped establish, would eventually become universally recognized as a vital field for agricultural production. The importance of plant breeding in the improvement of crop production and the reduction of famine in the world was underscored by the Nobel Committee when it awarded the Nobel Prize for Peace in 1970 to Norman Borlaug for his work in plant breeding and the green revolution. Unfortunately, in early 1935 a campaign was launched in the Soviet Union against genetics, which was branded the "handmaiden of the bourgeoisie" (Moscow News, 2006), and Nikolai Vavilov, as a world leader of genetics, had to defend his field of work, particularly against the sinister figure of Trofim Lysenko, his arch enemy. Lysenko promised quick crop improvements, against Nikolai Vavilov's slow process of systematic hybridization and selection, and Nikolai had to bear constant accusations of holding "idealist" Mendelian theories (Bolotovski et al., 2004). Stalin was particularly receptive to Lysenko's claims. Bolotovski et al. (2004) related the following:

> *…[Sergei] Vavilov was struck with the blow of the arrest, and later death, of his older brother Nikolai (1887−1943), an outstanding plant breeder and geneticist. The two brothers loved and influenced each other all their lives. Both were men of encyclopaedic knowledge, retentive memory, prodigious energy and personal charm, with a deep devotion to science. In the 1920s Nikolai had carved out a brilliant carrier in Russia. He was elected president of the Agricultural Academy and was at the head of research institutes of plant breeding in Leningrad and genetics in Moscow. He organized many expeditions throughout the world and created a huge seed collection. He also preserved and set up many experimental stations in different regions of the USSR and directed their programmes. However, Nikolai gained enemies driven by agronomist Trophim Lysenko and Marxist philosopher Isaak Present. Lysenko promised quick crop improvements, compared with Nikolai's slow process of systematic hybridization and selection, and from 1935 Nikolai had to bear constant accusations of holding "idealist" Mendelian theories. Thousands of his colleagues and followers were removed from their teaching and research positions; many were arrested and some were shot. Nikolai's agricultural programme was devastated and in 1940 he was arrested, tortured, tried and sentenced to be shot "for sabotaging Soviet agriculture and spying for England." (He had worked on genetics in the UK in 1913−1914.) A year later the sentence was commuted to 20 years of forced labour, and in 1943 he died of starvation in Saratov prison. After Nikolai's death, Sergei actively helped the family of his brother, and two of Nikolai's sons became cosmic-ray physicists at the Lebedev Institute.*
>
> *Not all of the sciences suffered as badly as biology, but Marxist philosophers assailed the "idealism" inherent in quantum mechanics and relativity theory. In 1937−1938 many physicists were arrested, and some were persecuted in the Lebedev Institute.*

Vavilov shielded the head of the Optics Division, Grigori Landsberg, the head of the Theory Division, [Igor] Tamm (whose brother, the chief engineer of the chemical factory, was arrested), and others; he [Sergei Vavilov] wrote directly to the chief prosecutor when Sergei Rytov, head of the Radiophysics Division, was arrested in 1937 (he was released in 1939).

From CERN Courier, November 12, 2004, http://cern.courier.com/cws/article/cern/29202, reprinted with permission © CERN 2004.

The postage stamp illustrated here was issued in the Russian Federation in the year 2000 to commemorate the pioneering work of Nikolai Vavilov and his discovery of the law of biological variability in 1920.

Nikolai I. Vavilov (1887–1943)

Bolotovski et al. (1998) analyze in detail the historical data including quotations from those who knew Sergei Vavilov to ascertain how Sergei could manage to continue to work diligently toward the creation of a national physics research institute of world renown for a government that, in the short period of only three years, had unjustly imprisoned and taken the life of his dear brother.

Sergei Vavilov was concerned with saving Soviet physics and the lives and welfare of those he could help. The state of affairs in physics was a shambles after the Second World War, and Stalin ordered assessments of army officers, executives of the defense ministries, and others, who might be helpful to the state and were imprisoned as enemies of the people, so that they might be released and offered positions. Bolotovski et al. (1998) elucidate that Stalin instructed his secret police chief [Lavrenty Pavolich] Beria to process the assessments. They noted that the fact that Sergei Vavilov's brother Nikolei had been purged was not an impediment to his appointment as President of the Academy of Sciences. Bolotovski et al. (1998) noted also that Stalin "approved" of the arrangement under which close relatives of top government and public figures were purged.

Pyotr L. Kapitsa (1894–1984)

The case of Pyotr Kapitsa (1894–1984) is an interesting example. Kapitsa was awarded the Nobel Prize in Physics in 1978 in the words of the Nobel Committee "for his basic inventions and discoveries in low-temperature physics." The postage stamp illustrated here was issued in 1994 by the Russian Federation to commemorate the 10th anniversary of the death of Pyotr Kapitsa. He was born in Kronstadt near Leningrad, USSR in 1894, and graduated in 1918 from the Petrograd Polytechnical Institute. His wife and two small children perished of illness during the chaos of the civil war that followed the Russian Revolution. After their deaths, Kapitsa left the USSR in 1921 to study at Cambridge University and eventually worked at the Cavendish Laboratory at Cambridge, England with Ernest Rutherford. He became a renowned physicist in England, starting as a Clerk Maxwell Student at Cambridge University from 1923 to 1926, Fellow of Trinity College in 1925, Assistant Director of Magnetic Research at the Cavendish Laboratory from 1924 to 1932, Fellow of the Royal Society in 1929, Messel Research Professor of the Royal Society from 1930 to 1934, and Director of the Royal Society Mond Laboratory from 1930 to 1934. In 1934 Kapitsa went to a scientific meeting in the USSR. His passport was seized and he was detained on Stalin's orders and not permitted to leave the country. He was required to form the new Institute for Physical Problems of the USSR Academy of Sciences in Moscow, and he thus arranged, through the help of Rutherford, to have his equipment at the Mond Laboratory shipped to Moscow. As head of the new institute, Kapitsa made many discoveries in the field of low-temperature physics and discovered superfluidity in helium. He was of great assistance to the success of the USSR in the Second World War, assisting particularly in the production of large quantities of liquid oxygen for the steel industry, and after the USSR victory was awarded the title of Hero of Socalist Labor in 1945, the highest award granted then to a civil servant. In 1946 he refused to work on the development of the hydrogen bomb, and thus fell out of favor with Stalin. He was punished and removed of his post as Head of the Institute of Physical Problems in August of 1946 by a decree of the USSR Council of Ministers, signed by Stalin, and exiled to his dacha near Moscow. He was forced to remain in exile until Stalin's death in 1953. Sergei Vavilov secretly helped Kapitsa at this time of need. Bolotovski et al. (1998) quoted A.A. Kapitsa, the widow of Pyoty Kapitsa, whereby she underscored that Sergei Vavilov had assisted Kapitsa in many ways without making his assistance known, which illustrates one of many examples of how Vavilov helped his colleagues whenever possible.

Yuri N. Vavilov, the son of Nikolai Vavilov, recalled his father's imprisonment and death in prison and the extent to which his uncle Sergei Vavilov helped his family in a letter in *Physics Today* (Bolotowsky and Vavilov, 1995). They noted the following (reprinted with permission from © 1995 AIP Publishing LLC):

> *[Sergei] Vavilov was a kind, responsive person. In his conduct he was motivated by the principles of Christian morality. He was the brother of Nikolai Ivanovich Vavilov (1887–1943), a distinguished biologist who perished in Stalin's prison and who was the father of one of the writers of this letter. The writer remembers with deep gratitude the loving care rendered to his family by his uncle Sergei after his father's arrest and death. He helped the writer to get an education and became a physicist. He also helped the writer's older brother, Oleg—a talented physicist who died under unclear circumstances.*

In 1945, Sergei Vavilov was elected President of the USSR Academy of Sciences. Some question how he could be appointed to such a position and how he could accept such a position in light of his brother's imprisonment and death. On this point, Bolotowski et al. (2004) comment with the following:

> *Vavilov was elected president of the USSR Academy of Sciences in July 1945. Many academicians thought there was not another scientist of so high a cultural level and such a provident, skillful administrator as Vavilov, and some recommended him for presidency. However, this could only have taken place if he were Stalin's choice, so it was very hard for him to accept, as his brother Nikolai had been murdered by Stalin's regime. The opinion of people close to Vavilov is that he accepted the post because he considered it his duty to serve science and the nation, rather than Stalin. During the time he was president he accomplished much to foster science in the USSR–the laboratories were better supplied with equipment and instruments, and the salaries of the researchers were increased.*

From CERN Courier, November 12, 2004, http://cern.courier.com/cws/article/cern/29202, reprinted with permission © CERN 2004.

Sergei Vavilov used his position as President of the USSR Academy of Sciences to try to attain exoneration for his brother Nikolai. Bolotovski et al. (1998) note that in 1955, four years after Sergei died, V.F. Sennikov, a staff member of FIAN, examined documents in the archives of the Ministry of State Security with the purpose of rehabilitating the innocent victims of Stalin's purges. They note that Sennikov was "particularly impressed [by Sergei] Vavilov's letter of 1949 addressed personally to Stalin in which he appealed for the exoneration of his brother. The letter included a detailed account of the life and work of N. Vavilov, described his openness and honest and straightforward manner of speaking. Vavilov firmly rejected all subversive actions attributed to his brother, claiming that the accusations against him were

slanderous. Vavilov ended his letter saying "if my brother N. Vavilov is not exonerated, I cannot remain President of the USSR Academy of Sciences." They note that the letter bears an inscription by Beria "Not authorized," and that there were no marks indicating that the letter was shown to Stalin.

As Director of the P.N. Lebedev Physics Institute and President of the USSR Academy of Sciences, Sergei Vavilov did all he could to help and protect staff and colleagues from Stalin's purges. There are numerous examples and the reader is invited to peruse the detailed accounts given by Bolotovski et al. (1998). The degree to which Vavilov played in the establishment of physics in the USSR is evidenced by the relatively numerous Nobel Laureates who emerged from the P.N. Lebedev Physics Institute, which he established from 1934 to the time of his death in 1951, and from the USSR Academy of Sciences over which Vavilov presided. Among these Noble Laureates are Pavel A. Cherenkov (1904−1990), Il'ja M. Frank (1908−1990), Igor Y. Tamm (1895−1971), Lev D. Landau (1908−1968), Aleksandr M. Prokhorov (1916−2002), Nikolai G. Basov (1922−2001), Andrei D. Sakharov (1921−1989, awarded the Nobel Prize for Peace), Pyotr L. Kapitsa (1894−1984), and Vitaly L. Ginzburg (1916−2009).

A final example of the numerous cases where Sergei Ivanovich Vavilov tried to help fellow scientists within the stressful atmosphere of Stalin's oppression within which they had to live and work is taken from the life of Vitaly Ginzburg, who shared the Nobel Prize in Physics in 2003 "for pioneering contributions to the theory of superconductors and superfluids." Vitaly Ginzburg did pioneering work on the interpretation of the Vavilov−Cherenkov Effect in collaboration with Il'ja Frank from 1939 to 1947. His contributions to the interpretation of the Vavilov−Cherenkov radiation did not begin to appear in print until 1940 in the *Journal of Physics* of the former USSR and in the *Proceedings of the USSR Academy of Sciences* some three years after the famous paper of Il'ja Frank and Igor Tamm (1937), which explained the radiation discovered by Vavilov and Cherenkov. Consequently Ginzburg did not share in the Nobel Prize for Physics in 1958 with Cherenkov, Frank, and Tamm. However, he was awarded the Nobel Prize for Physics 45 years later, as noted above, for a totally different contribution. Vitaly Ginzburg provides the following account [with the author's insertions in brackets] of Sergei Ivanovich Vavilov in his book *The Physics of a Lifetime* (Ginzburg, 2001, pages 395−396) with kind permission of Springer Science+Business Media © 2001 Springer-Verlag Berlin Heidelberg):

I have been working at FIAN since 1940 and, hence, for ten years I was at the Institute with S. I. Vavilov as its director…The point is that my wife Nina Ivanova Ginzburg (born Ermakova) was arrested in 1944, and after nine months in prison was 'sentenced' by the notorious KGB Special Consultation to a three-year confinement in a camp…Nina was freed in September 1945, but with a limited number of cities in which she was allowed to reside (Moscow was certainly excluded)…I began writing applications to the NKVD (I believe that this was the name of the VChK-OGPU-KGB at that time) with a request to register my wife in Moscow. But someone made me listen to reason and not write directly to the 'organs', but to do it through the Institute instead, because millions of people were imprisoned and exiled…I must say at once that I never received a positive answer and my wife could only return to Moscow in 1953 after a new amnesty which followed the death of the 'coryphaeus of all sciences' [ie, Josef Stalin]…When I went to Sergei Ivanovich [Vavilov] in this connection for the first time (it was at the end of 1947, or rather at the beginning of 1948), he agreed to 'back up' my application. The same was repeated the next year. When I went [to him] for the third time, he said approximately the following: 'I shall of course support you, but you know, my 'belle soeur' − a sister not only of my wife, but also of the wife of Vensin, the President of the Academy of Architecture − is also exiled. And we − two presidents of Academies…are applying for the registration of our belle soeur in Moscow, but they refuse.'

Sergei Ivanovich [Vavilov] died in 1951 when he was not yet sixty. He had an infarction and looked bad; I met him in the hall of the Institute not long before his death. He was very sad, and that is how I remember him. Dimitrii Vladimirovich Skobeltsyn became director of FIAN [after the death of Vavilov], and the last two times I asked for my application to be seconded I addressed him. When I went to him (for the second time, I believe), he said to me, 'My brother is in exile in Tsarevo-Kokshaisk (before 1919 this was the name of the present Yoshkar-Ola), and my application to register him at my place in Moscow has been declined.'

This is, properly speaking, the story of two directors. Of course, in light of what we know today about life in Stalin's times, nobody will be surprised at such information…D. V. Skobeltsyn was not only an academician, but also the chief expert or even the Head of the Soviet Delegation at UN negotiations on banning nuclear weapons, and, from 1950, Chairman of the Committee for the International Lenin Prize "for Consolidation of Peace Among Nations". And even such [important] people were refused permission to lodge their ostensibly guilty relatives in the places where they lived. In truth, nowhere could a man breathe freely.

For additional information, the reader should peruse an interesting paper by Yu N. Vavilov, a son of Nikolai Vavilov and nephew of Sergei Vavilov, coauthored by L. V. Leshin, the last undergraduate student of Sergei Vavilov (Vavilov and Levshin, 2002). Also, a paper by Kojevnikov (1996) entitled "President of Stalin's Academy: The Mask and Responsibility of Sergei Vavilov" is recommended.

PAVEL ALEKSEYEVICH CHERENKOV (1904–1990)

Pavel Alekseyevich Cherenkov was born on July 28, 1904 in the village of Novaya Chigla in the fertile agricultural region of Voronezh, USSR. He shared the Nobel Prize in Physics in 1958 "for the discovery and interpretation of the Cherenkov Effect." The unique radiation that is produced as a result of the Cherenkov Effect would subsequently become referred to as Cherenkov radiation or Vavilov–Cherenkov radiation in honor of Sergei Vavilov and Pavel Cherenkov, who were the first to discover the origin of the radiation.

Detailed information on the personal aspects of Cherenkov's life in the English language is limited. The biography provided by Pavel Cherenkov at the time of his Nobel Prize award in Stockholm in 1958 is one of the briefest biographies among all of the Nobel Laureates (see *Nobel Lectures, Physics, 1942–1962*), a sign of his modesty. A paper by his daughter Elena Cherenkova (2005) recently filled the gap with information on his life and experiences as a person and physicist. Also, the same year, one of his former colleagues, Boris Borisovich Govorkov (2005), published a paper on Cherenkov's equipment and work in fundamental physics. Personal information on Cherenkov's life and work is taken from these limited sources.

Pavel Cherenkov had a simple and humble upbringing as a young boy. He skated in winter on homemade ice skates. Pavel was a passionate reader, and would prefer reading at the village library in lieu of dancing or other amusements of young boys at the time. Pavel's father was a skilled farmer and shop owner. His mother died when Pavel was only two years of age. In 1928 Pavel Cherenkov graduated from Voronezh State University with major studies in physics and mathematics. After graduation from the university, Pavel Cherenkov worked as a school teacher in the Michurinsk county center. It was in Michutinsk in 1930 where he met his wife, Maria Alekseevna Putintseva, a graduate also of Voronezh State University in the field of philology. Maria's parents were well educated. Her father, Aleksey Mihaylovich Putinsev, was a professor of philology at Voronezh University, and her mother, Maria Mihaylovna, taught foreign languages at the same university. This was a time of great turmoil for both Pavel and Maria and for many in the USSR, as related by the following taken from Elena Cherenkova (2005):

> *My parents – beautiful, intellectual, industrious, well-educated, believed in bright horizons opened for the country and its young people. But the event took a very unexpected turn. In the late 1920s, the communist government launched an expropriation of farmers' property and forced collective farms. Aleksey Egorovich, Pavel's father, was exiled to the northern regions. In autumn of 1930, Maria's father Aleksey Mihaylovich Putsinsev was arrested in connection with the so-called "case of regions specialists." More than 90 people were persecuted in this high-scale trial. Similar processes were launched against both all independently-minded groups and all not independently-minded groups all over the country. Aleksey Mihaylovich was sentenced to five years of concentration camps. Pavel's and Maria's freedom was hanging in the balance too; they could be convicted by association.*

From Cherenkova (2005), reprinted with permission from Elsevier © 2005.

Pavel A. Cherenkov (1904–1990)

In 1930, Pavel Cherenkov went to Leningrad to carry out postgraduate studies in the School of the USSR Academy of Sciences. He and Maria were married in 1931, and Pavel was able to get a single room in a student dormitory where they had to accommodate five persons. The hardship and personal anguish with which Pavel and Maria had to cope is related by Elena Cherenkova (2005) as follows:

> *They [Pavel and Maria] settled in the postgraduate student's dormitory. Pavel managed to get a separate room! They had to house five people there – including Tatiana, Pavel's youngest sister (the life in the country was very hard in those years). Also Maria's mother joined them after her husband was imprisoned. In 1932, their son Aleksey was born. During the first years of his life, he was a sickly child. Food rationing was enforced in the country at that time. Maria was often unemployed. Her friends routinely shared their bread-cards. This bread was dried and sent to grandfather to the concentration camp. Pavel's only winter coat was also sent to her father. In 1932, Maria's father was released from the camp. He lost his strength and health. In spring of 1937 he died. At the end of 1937 Aleksey Egorovich, Pavel's father, was arrested again. By the sentence of 'the tribunal of three', without the investigation or trial, he was executed. Such was the family environment in which the young physicist Pavel Cherenkov had to live while undertaking his graduate studies and research.*
>
> From Cherenkova, 2005, reprinted with permission from Elsevier © 2005.

One can only imagine the determination and discipline that Pavel Cherenkov had to have to remain focused on his studies and research. It was in 1932 that Sergei Ivanovich Vavilov became Pavel Cherenkov's research adviser. Sergei Vavilov was renowned for his research studies on luminescence and fluorescence, which are processes that result in the emission of light by certain compounds as a consequence of atomic electron energy state transitions. Certain organic or inorganic compounds may absorb energy and become elevated to excited energy states via electron transitions, whereby the compounds may emit the excitation energy as light photons as the electrons fall back to lower energy states. For his PhD studies, Vavilov assigned Cherenkov the task of studying what was thought to be luminescence of uranyl salt solutions under the effect of hard gamma radiation. In his recollections published when he was approximately 81 years of age, Cherenkov (1986) explained:

> *The main purpose of these investigations was to make clear the mechanisms for the light emission and to compare it with the properties of ordinary photoluminescence radiation. Therefore, all measurements were carried out in parallel: exciting the luminescence by both radioactive sources and by visible light. As the luminescent materials, liquids and in particular solutions of uranium salts were, for reason of methodology chosen…at the same time, control experiments with solutions of other lumifors such as esculinium or fluorescein were carried out. But the uranium salts had become the main object of the investigations. It was planned to determine the laws of their light emission under radioactive rays, and to ascertain whether, in this case, there was something in common with photoexcitation luminescence…Making use of liquid lumifors gave one the possibility of choosing, over wide limits, the characteristics such as concentration, viscosity, temperature, which affect one of the general signs of luminescence: the finite lifetime of the excited states. This was approximately the theme of my dissertation work. One can see that there was no task to discover a new effect here.*
>
> From Cherenkov (1986), reprinted with permission from Elsevier © 1986.

Thus, Cherenkov clearly explained that his initial task was to study luminescence by the uranium salts, and that the outcome of the work, the discovery of a new phenomenon (Cherenkov Effect) and new radiation (Cherenkov radiation), was a fortuitous outcome of the work. Although it was not Cherenkov's intention to find a new type of radiation, his discovery, like most in science, was not accidental. In the words of Cherenkov (1986) in his recollections of the work:

> *…it would be perhaps incorrect to consider the discovery as an accidental one, since the conditions for it were, in fact, prepared by preceding successes in different spheres of physics.*
>
> From Cherenkov (1986), reprinted with permission from Elsevier © 1986.

Cherenkov did not have a spectrophotometer at his disposal, nor were photomultiplier detectors available in the early 20th century to measure light intensities; however, Vavilov had developed a technique of dark-adapting the human eye and a graded wedge to enable a visual measurement of relative intensities of light. Cherenkov used an experimental arrangement somewhat like that illustrated in Fig. VII.2.

Light emitted by luminescence or the Cherenkov radiation, which he would discover, was extremely weak and therefore difficult to measure with the apparatus illustrated in Fig. VII.2. Each day before beginning work, he had to remain

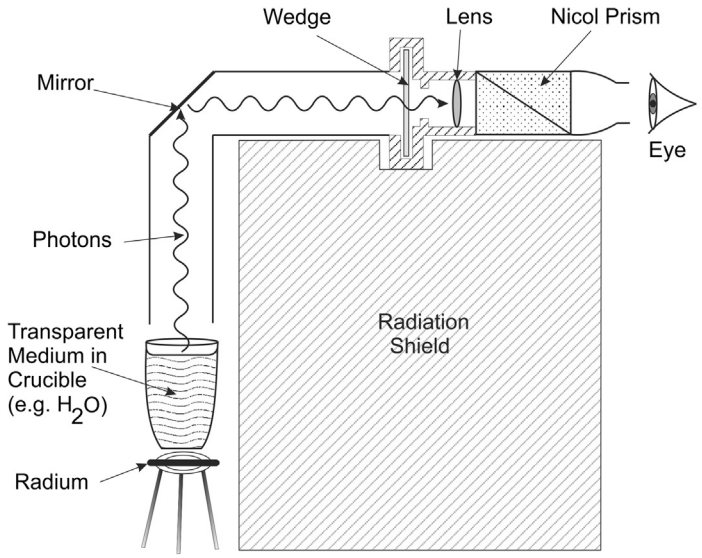

FIGURE VII.2 Writer's depiction of the basic elements of the experimental arrangement used by Cherenkov that resulted in his discovery of Cherenkov radiation. More detailed schematics of his apparatus are described by Cherenkov (1934a) and Govorkov (2005). The setup was made to observe and measure the intensity of luminescence in liquids in a dark room with the naked eye, and resulted in the discovery of Cherenkov radiation. A periscope type of arrangement was used by Cherenkov whereby he could measure the Cherenkov photon intensity from the other side of a suitable shield against harmful gamma radiation from the radium source. A crucible containing a pure liquid, such as water, is located behind the shield above the radium. Light emitted from the open top of the crucible would pass through the periscope arrangement reflecting off a mirror toward a wedge and collimating lens. A transparent graded wedge controlled by the observer was used to measure the intensities of the Cherenkov radiation. The Nicol prism provided information on the polarization of the radiation.

in a dark room for an hour to dark-adapt his eyes before starting any observations. Cherenkov's (1986) recollection on the crude apparatus, which he used in 1933, is the following:

> *The main difficulty of the work was in the necessity to detect this extremely weak light with a new method (using the threshold of vision), which had a distinctly subjective character. The accuracy of the method depended upon the conditions of the observer and was determined by many factors (tiredness, lack of sleep, and even mood) and to take strict account of these was, of course, complicated…as the detector the eye was used. This has a rather high sensitivity after adaptation to total darkness.*
>
> From Cherenkov (1986), reprinted with permission from Elsevier © 1986.

In his Nobel lecture in 1958, Cherenkov commented:

> *This method makes use of the human eye instead of the use of a light-measuring device. Since the sensitivity of an eye adapted to darkness is some tens of thousands of times greater than its sensitivity by daylight, this method was superior to others by virtue of its high sensitivity. Notwithstanding its subjectivity and the comparatively large errors in the measurements, this method was at the time the only one that could be used which permitted a quantitative determination of those extremely low light intensities.*

Pavel Cherenkov (1934a) measured the intensity of light emitted from the crucible when various substances were irradiated with the gamma rays from the radium source. He used 140 mg of radium, which yields high doses of radiation. High levels of gamma rays were needed because of the weak nature of the light emitted. He measured light intensity while irradiating various substances dissolved in solvents, and he would also irradiate the pure solvents to serve as blanks, as no luminescence would be expected from pure solvents such as water, sulfuric acid, propyl alcohol, acetone, carbon tetrachloride, etc. However, Cherenkov noticed a very weak light from the solvents when irradiated with the high-intensity gamma rays of the radium. The light emitted by the solvents was weaker in intensity than that emitted by the luminescent solutes. He could have simply subtracted this weak light from the blank solvents, as the objective of his research was to study luminescence. Fortunately he did not ignore this anomaly. Cherenkov discussed his observation with Sergei Vavilov, and they agreed Cherenkov should investigate this weak light from the solvents by further purifying the solvents to ascertain whether the light was a result of luminescent impurities or a property of the solvent when irradiated by the gamma radiation. To his amazement, Cherenkov observed no change in light intensity from the solvents even for the purest samples. Cherenkov (1934a) tested as many as 16 pure solvents and would observe the same light intensity when irradiated

with the radium source. Yet he had to make one more test to ascertain whether he was dealing with luminescence in these solvents or a totally new phenomenon. This test was that based on the property of quenching of luminescent substances by the addition of chemical additives, ie, chemical quenchers, or by heating. Thus, when luminescence occurs, the addition of chemical quenchers or heat will reduce the light intensity. Also, Cherenkov (1958) noted in his Nobel lecture that heating would also alter the polarization of the luminescence photons, as this would alter the mobility of the particles. He made the following comments in his Nobel lecture concerning the results of his test for quenching:

> *…the intensity of the light of fluids [pure solvents] cannot be influenced either by heating or by dissolving in them such active fluorescence quenchers as potassium iodide, silver nitrate, and many others. It has also been shown that the perceptible polarization which appears in this light cannot be altered either…Confirmation [of the discovery a new phenomenon] was forthcoming also in the unusual character of the polarization of this light. The main direction of the vector of the electric vibrations did not run perpendicularly to the excited beam, as is the case with polarized fluorescence, but parallel to it. Taken altogether, the results collected even during the first stage consequently gave rise to the statement that the light produced in fluids by the action of gamma rays is not a trivial phenomenon.*

Pavel Cherenkov (1934a,b) published his initial findings (ie, discovery paper) in the *Proceedings of the USSR Academy of Sciences*, and his supervisor Sergei Vavilov (1934) offered an interpretation for the origin of this unusual light in a short paper back-to-back with Cherenkov's. Vavilov thought the light might be due to Compton electrons. A subsequent interpretation by Frank and Tamm (1937) would show that Vavilov was correct concerning the Compton electrons as the origin of this new light; and that it would be Compton electrons traveling at relativistic speeds.

Only following Cherenkov's subsequent discovery in 1936 of the asymmetric properties of this light would it be confirmed that he was dealing with a phenomenon and type of radiation so far unknown. Cherenkov (1936) was able to demonstrate the space asymmetry of the light by providing experimental data to confirm that when solvents where irradiated with the gamma rays the light would be emitted forward in one direction with respect to the gamma-ray beam. Also Cherenkov demonstrated that an applied magnetic field would affect the direction of the light emitted, thus providing evidence that the Compton electrons deflected in the magnetic field were involved in the production of the light. To provide experimental evidence of this asymmetric property of the radiation and the effect of a magnetic field on the direction of photon emissions, Cherenkov devised an experimental arrangement that involved irradiating a transparent medium in a magnetic field with high-energy gamma rays; and a part of his experiment is illustrated in Fig. VII.3.

In the absence of a magnetic field, Cherenkov would set the measured intensity (I) of the light produced by the γ-rays as unity ($I = 1.0$), and any deviation of the measured light intensity as a result of the applied magnetic field as relative to

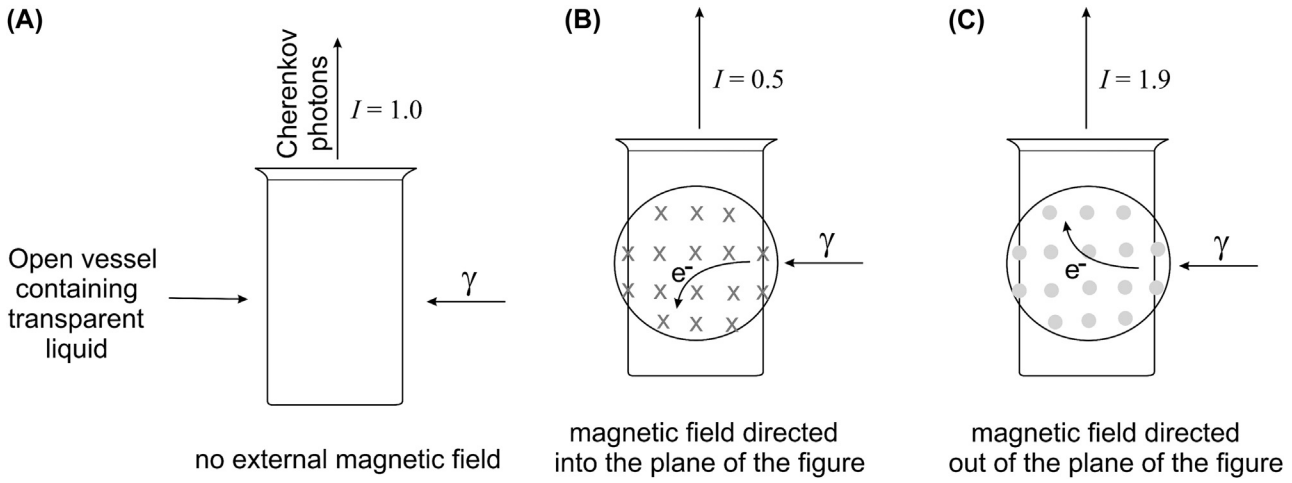

FIGURE VII.3 Cherenkov's experimental arrangement that provided evidence of the asymmetric property of the mysterious light and the involvement of Compton electrons in the production of the light (Cherenkov, 1936). The vessel located in the figure was made of platinum or glass and contained either water or pentane. The inside walls of the vessel were coated with a black layer to reduce reflection of the photons off the surfaces. A magnetic field of 9000 Gauss was applied perpendicular to the plane of the figure, and Cherenkov could reverse the field to be directed into or out of the plane of the figure. Three experimental conditions are illustrated whereby the Cherenkov photon intensities (I) out of the vessel openings are given in (A) the absence of an external magnetic field, (B) a magnetic field directed into the plane of the figure, and (C) a magnetic field directed out of the plane of the figure. Within a circle are illustrated the magnetic field lines directed into and out of the plane of the figure with $\times$ and ● symbols, respectively. The bent paths within the magnetic fields are those of Compton electrons. The source of γ-rays, equivalent to 0.5−1.0 g of radium, was placed to one side of the vessel with the gamma radiation collimated in the direction of the vessel. The radium source was shielded with 1 mm of lead to absorb β-particles. The photon intensities (I) were measured by Cherenkov using the visual periscope illustrated in Fig. VII.2.

unity. When the γ-ray source was placed at the side of a transparent liquid medium, as illustrated in Fig. VII.3, the observed light intensity would either double or be reduced to one-half depending on the direction of the magnetic field. Charged particles are deflected either upwards or downwards depending on their charge and the direction of the magnetic field. For example, if the magnetic field is directed into the plane of the page of this book (illustrated by × signs in Fig. VII.3), particles of positive charge are directed upward and those of negative charge (eg, Compton electrons) are directed downward. In the reverse, if the magnetic field is directed out of the plane of the page (illustrated by ● in Fig. VII.3), negative electrons are deflected upward and positively charged particles deflected downward. The Cherenkov light intensities measured were a function of the direction of the magnetic field indicating that electrons deflected upward in the direction of the vessel opening (Fig. VII.3) produced a measured light intensity approximately twice that produced in the absence of the magnetic field. Electrons deflected downward in the magnetic field produced a measured Cherenkov light intensity of about one-half of that measured in the absence of a magnetic field (see Fig. VII.3). Cherenkov now had firm evidence that electrons were the particles producing the mysterious light and that the light was asymmetric, that is, the photons were emitted in a direction similar to that of the Compton electrons. More details of this experiment are available from his original paper (Cherenkov, 1936) in the *Proceedings of the USSR National Academy of Sciences*. Cherenkov (1937a) subsequently demonstrated that high-energy β-particles produced the same light, thus confirming that high-energy electrons in transparent media were the origin of the light.

With the firm evidence at hand of the space asymmetry of the mysterious light, Cherenkov and his supervisor Sergei Vavilov knew they had discovered a new phenomenon. Thus, in 1936, two other physicists at the same institute as Cherenkov took interest in this new radiation. Il'ja Frank and Igor Tamm of the Theoretical Division of the P.N. Lebedev Institute of Physics of the USSR Academy of Sciences began their theoretical study on the origin and properties of the radiation. The theory established by Frank and Tamm (1937), following the initial discovery of the radiation and its properties by Vavilov and Cherenkov, states that Cherenkov radiation is produced when an electron travels in a transparent medium of refractive index n with a velocity exceeding the velocity of light in that medium, that is, the following threshold condition must be met for the production of Cherenkov radiation:

$$\beta n > 1 \qquad \text{[VII.1]}$$

where β is the relative phase velocity of the particle, that is, the velocity of the particle in a transparent medium divided by the speed of light in a vacuum, and the index of refraction n, is the ratio of the velocity of light in a vacuum to its velocity in the medium. The above condition is met when the particle travels in a transparent medium with a velocity exceeding that of light in the same medium. Under such circumstances, the particle will produce an electromagnetic "shock" wave analogous to the acoustical shock wave or sonic boom produced by supersonic aircraft. Light will be propagated in the direction of the electron, forming an angle θ with the path of the electron as a cone of light. The angle of emission of the photons would be defined by the equation:

$$\cos\theta = \frac{1}{\beta n} \qquad \text{[VII.2]}$$

As the electron energy increases, the value of β approaches a maximum value of 1.0. If water ($n = 1.332$ measured at 20°C at the wavelength of 589.0 nm) is the medium within which the electron travels, and we assign β its maximum value of unity, the value of θ would be calculated according to Eq. [VII.2] to be 41.3 degrees.

As described in the previous paragraph, the angle of emission of the photons relative to the direction of travel of the electron in water will vary according to the energy of the electron, and it will not exceed 41.3 degrees. For other substances with different indexes of refraction (n), the maximum angle of emission will therefore differ. Cherenkov (1937b) calculated the values of θ for three substances having distinctly different indexes of refraction and for electrons of different energies traveling in water, that is, different values of β. When the electron energy was selected to provide values of the electron relative phase velocity β to vary from 0.8 to 1.0, the angle of emission of the Cherenkov photons relative to the direction of electron travel were calculated to vary from 21°0′ to 41°40′ in water, from 34°20′ to 48°40′ in benzene, and from 41°0′ to 52°50′ in CS_2.

From Cherenkov's calculations it could be seen that, from a determination of the angle of emission in a given transparent medium of known index of refraction (n), it would be possible to determine the energy or velocity of the electron from a measured value of θ. This concept forms the basis of measuring particle velocity with modern ring-imaging Cherenkov (RICH) counters described in the chapter entitled "Cherenkov Radiation." Cherenkov (1937b) made an approximate measurement of the angles of emission (θ) for Cherenkov photons produced by the Compton electrons in water when bombarded with gamma rays from a radium source employing the experimental arrangement illustrated in Fig. VII.4.

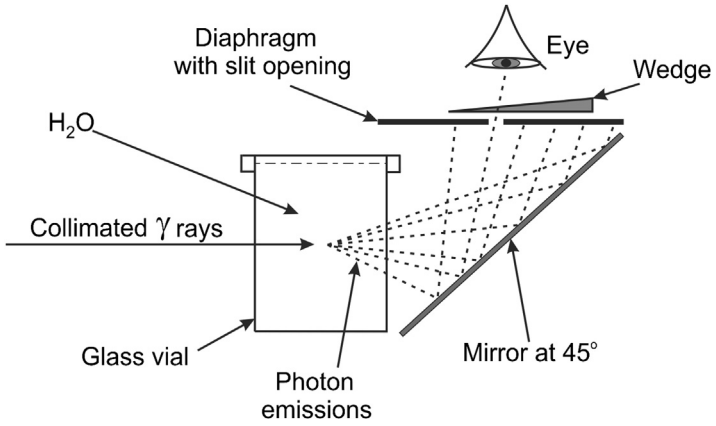

FIGURE VII.4 Writer's depiction of the experimental arrangement used by Cherenkov to measure angles of emission (θ) of light produced by the Compton electrons in water following the bombardment of the water with collimated gamma rays from a radium source. The angles were measured relative to the line of travel of the gamma rays. A more detailed illustration of the experimental setup is provided by Cherenkov (1937b).

The radium source used by Cherenkov had a very high activity (200−350 mCi) to provide sufficient light intensity to be measurable with the ocular system periscope arrangement illustrated in Fig. VII.2. A 2-mm lead plate at the orifice of the lead housing of the radium source (not illustrated in Fig. VII.4) was used to absorb any hard β-particles providing a pure γ-ray source. Horizontal movement of the diaphragm permitted readings of the light intensity at various angles of reflection relative to the direction of the γ-rays. The wedge, which is moved horizontally along the diaphragm slit, was calibrated to provide an approximate measure of the light intensity. The direction of the Compton electrons are themselves scattered at various angles relative to the direction of travel of the gamma rays. Thus, readings of the light intensities at various angles of reflection provided only an approximation of the angles of emission of the Cherenkov radiation relative to the direction of travel of the incident γ-rays.

Cherenkov (1937b) measured the angles of emission with respect to the direction of the incident γ-rays, and found the highest intensities of light between 0 degree and 30 degrees, which would obey the relationship $\cos\theta = 1/\beta n$. He used the very simple and imprecise visual apparatus illustrated in Fig. VII.4. As previously discussed, Cherenkov had calculated, when β is assigned the value of 1.0 for the highest-energy electrons possible, the value of θ should be 41°40′ with water as the medium. Thus, according to the relation $\cos\theta = 1/\beta n$, the angles of emission of Cherenkov photons in water could range anywhere between 0° and 41°40′ and cannot exceed 41°40′ in water. However, his data (Cherenkov, 1937b) indicated emissions of photons beyond 41°40′ of diminishing intensity to 90 degrees and beyond. This can be explained by the fact that Compton electrons produced by the incident γ-rays can be emitted at a large angle relative to the incident γ-ray. When only high-energy β-particles or electrons, in lieu of γ-rays, are incident on water, the angle of emission of Cherenkov photons does not exceed 41°40′, and the angle of emission will vary according to the energy or phase velocity β of the electrons.

The experimental data obtained by Cherenkov (1937b) provided the first experimental evidence of the relationship $\cos\theta = 1/\beta n$. In the case of water, which was assigned an index of refraction $n = 1.3371$, and taking the value of $\theta = 30°$, that is, the angle of highest intensity of light emission, Cherenkov calculated the phase velocity of the Compton electrons to be $\beta = 0.86$. This was the first estimate of the use of the Cherenkov Effect to measure the velocity of an elementary particle.

Cherenkov continued his experimentation and obtained recorded evidence of the unique asymmetric nature of the mysterious light using photographic plates. He was now able to demonstrate, by means of photographs, the direction of emission of the light photons with respect to the direction of the incident γ-rays on a sample of water. In June of 1937, Cherenkov submitted his historic findings concerning the evidence for the space symmetry of the radiation to the journal *Nature* for publication. However, Cherenkov's paper was rejected, and the letter of rejection is reproduced in Fig. VII.5.

In an article on his recollections of his historic work, Cherenkov (1986) related his reaction to the rejection to publish his work by the editors of *Nature* and the reactions of the scientific community. An excerpt of his comments [with the author's notations in brackets] is the following:

> *…I can only say it was not particularly a pleasure for me to be aware that my experiments were now and again classified as "spiritualism" and often paralleled with an erroneous effect, the notorious N-rays of Blondlot, which were finally settled by Wood. [Cherenkov refers here to the history of René R. Blondlot (1849−1930), who in 1903 claimed to have discovered N-rays, and many*

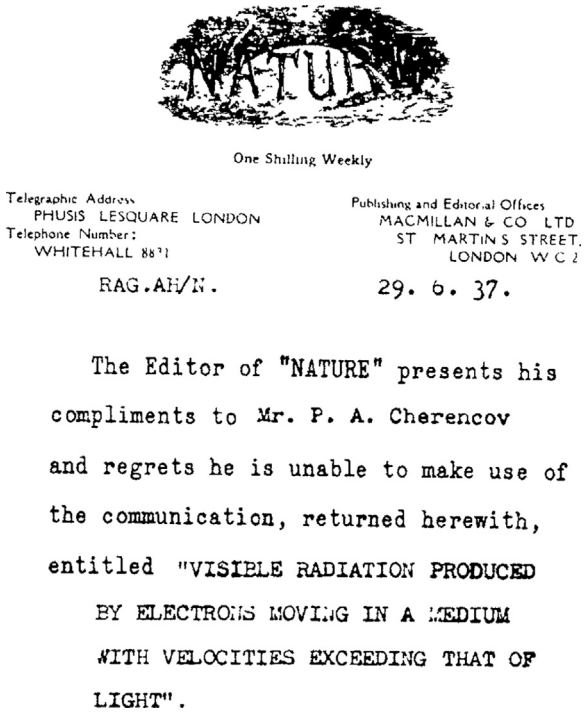

NATURE

One Shilling Weekly

Telegraphic Address
PHUSIS LESQUARE LONDON
Telephone Number:
WHITEHALL 8871

Publishing and Editorial Offices
MACMILLAN & CO LTD
ST MARTIN'S STREET,
LONDON W C 2

RAG.AH/N. 29. 6. 37.

The Editor of "NATURE" presents his compliments to Mr. P. A. Cherencov and regrets he is unable to make use of the communication, returned herewith, entitled "VISIBLE RADIATION PRODUCED BY ELECTRONS MOVING IN A MEDIUM WITH VELOCITIES EXCEEDING THAT OF LIGHT".

FIGURE VII.5 Letter to Pavel Cherenkov from the editors of the journal *Nature* rejecting his historic findings for publication. *From Cherenkov, P.A., 1986. At the threshold of discovery. Nucl. Instrum. Methods Phys. Res. A248, 1–4; reprinted with permission from Elsevier © 1986.*

scientists subsequently published articles on the origins and characteristics of the N-radiation. R.W. Wood of John Hopkins University later exposed the experimental results of Blondlot to be erroneous, misconceived, and the N-rays to be imaginary. The reader is invited to read an interesting historical account of the Blondlot N-rays by Lagemann (1977)]…Of course, sometimes there were pleasant exceptions. I still recall with great pleasure the exclamation by the greatest scientist of that epoch, Niels Bohr — "Wunderbar, Wunderschön", repeated several times after I demonstrated to him one of the most essential properties of the radiation, namely its space symmetry. Nevertheless, the atmosphere of distrust of the new effect from scientific opinion remained. The most open and sharp manifestation of this distrust was the refusal by the journal Nature *to publish a short paper submitted to me, summarizing the essence of the phenomena and its main properties. Evidently, it was a mistake of the editorial staff of* Nature *who did not take the article sufficiently seriously. Receiving a negative answer from them and, fortunately, also the text of the article, I consulted S.I. Vavilov and right then transferred it, to another envelope and sent it to the editors of the American journal* Physical Review. *They were more attentive to it and, rather soon, published it in the next issue of the journal. This was the beginning of an overall recognition of the experimental discovery of a hitherto unknown effect: the radiation of charged particles moving faster than light in a material medium.*

Reprinted with permission from Elsevier © 1986.

In only six weeks after *Nature* had rejected Cherenkov's article did Cherenkov's paper appear in the August 15, 1937 issue of *Physical Review* (see Cherenkov, 1937c). In his paper, Cherenkov described the experimental arrangement, illustrated in Fig. VII.6, that he used to demonstrate unequivocally the asymmetric character of the light. A liquid contained in a thin-walled glass vessel would be bombarded with γ-rays from one direction only, and light emitted from the liquid would be reflected off the cylindrical mirror completely surrounding the vessel. The light intensity would be recorded onto a photographic plate.

With the experimental setup illustrated in Fig. VII.6, Cherenkov used a high-intensity γ-ray source with an activity equivalent to 794 mg of radium and a long exposure time of 72 h to produce a suitable photographic image of the light emitted by the transparent medium in the glass vessel. He demonstrated that water and benzene would emit photons only in the onward direction, that parallel to the γ-ray beam. The photographic prints are reproduced in Fig. VII.7A and B. To illustrate the asymmetric character of the newly discovered radiation, Cherenkov compared the images of the radiation produced by the water and benzene with that produced by the luminescent compound esculin.

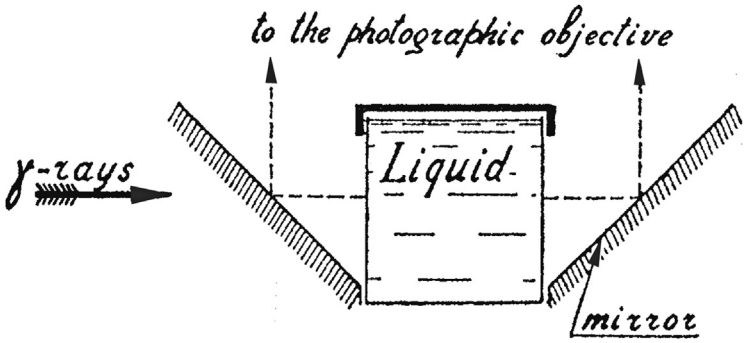

FIGURE VII.6 Experimental arrangement of Cherenkov used to demonstrate the unique direction of emission of the Cherenkov light photons with respect to the direction of the incident γ-rays on a sample of water. A glass vessel covered at the top was used to contain a pure liquid. The vessel was surrounded with a cylindrical mirror. Above the vessel was located a photographic lens and photographic plate. Gamma rays from thorium C (ThC) or radium (Ra) were incident on the sample from one side only, and the light emitted from the liquid reflected off the cylindrical mirror up toward the photographic lens and onto the photographic plate. *From Cherenkov, P.A., 1937c. Visible radiation produced by electrons moving in a medium with velocities exceeding that of light. Phys. Rev. 52, 378–379, https://journals.aps.org/pr/abstract/10.1103/PhysRev.52.378; reprinted with permission © 1937 by the American Physical Society. (Readers may view, browse, and/or download material for temporary copying purposes only, provided these uses are for noncommercial personal purposes. Except as provided by law, this material may not be further reproduced, distributed, transmitted, modified, adapted, performed, displayed, published, or sold in whole or part, without prior written permission from the American Physical Society.)*

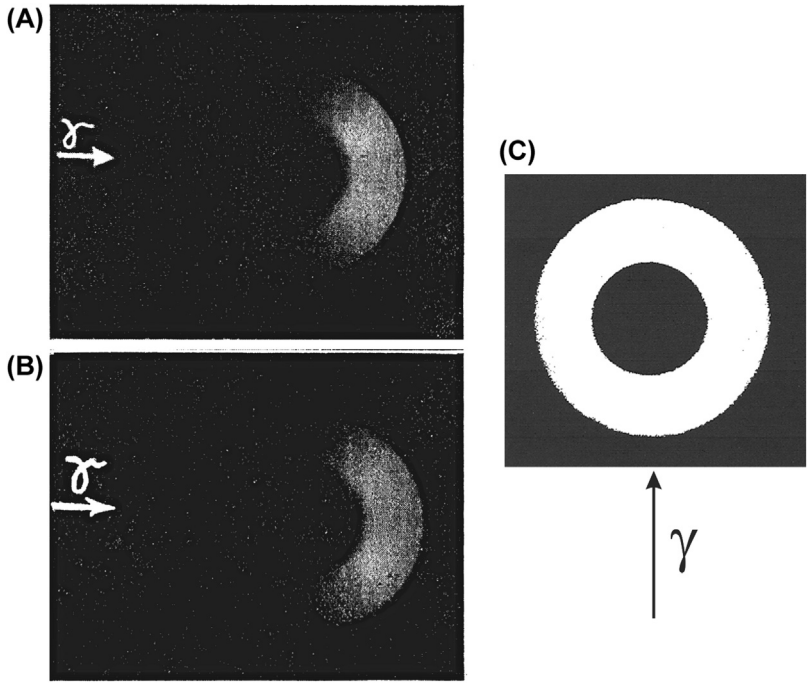

FIGURE VII.7 Photographs showing asymmetry of the radiation emitted by (A) water, $n = 1.337$, and (B) benzene, $n = 1.513$ (Cherenkov, 1937c), and the symmetric light emission in all directions by (C) a solution of the luminescent compound esculin (Cherenkov, 1958). The light produced a black image on the photographic negative after chemical development of the plate. The black image on the photographic negative is seen as a white image above on the positive photographic prints. The arrows show the direction of the incident γ-rays. In the case of (C), the luminescence in the center vessel resulted in the symmetrical emission of light from the vessel in all directions. Thus, the white circle from the more intense and symmetrical luminescence light reflected off the circular mirror that surrounded the vessel illustrated in the previous Fig. VII.6. *A and B are from Cherenkov, P.A., 1937c. Visible radiation produced by electrons moving in a medium with velocities exceeding that of light. Phys. Rev. 52, 378–379, https://journals.aps.org/pr/abstract/10.1103/PhysRev.52.378; reprinted with permission © 1937 by the American Physical Society; and C is from Cherenkov, P.A., 1958. Nobel lecture: radiation of particles moving at a velocity exceeding that of light, and some of the possibilities for their use in experimental physics, Stockholm, December 11, 1958. In: Nobel Foundation Staff (Eds.), Nobel Lectures, Physics, 1942–62. (1964). Elsevier Publishing, Amsterdam; reprinted with permission © The Nobel Foundation 1958.*

The luminescence produced by a solution of esculin emits visible radiation in all directions, distinct from Cherenkov radiation, which is illustrated by the photograph in Fig. VII.7C.

Any doubts about the validity of the mysterious radiation discovered by Cherenkov was finally put to rest after Cherenkov's radiation and its properties were investigated in detail and confirmed by George Collins and Victor Reiling (1938) at the University of Notre Dame. They published their experimental results in the journal *Physical Review*, the same journal that accepted Cherenkov's paper the year before. They carried out a detailed study confirming Cherenkov's findings on the direction of emission, spectroscopic properties, and intensity of unique radiation and reported the following:

> *Electrons of two million volts energy from an electrostatic generator were used to investigate the properties of the asymmetric radiation discovered by Cherenkov. This radiation is produced when electrons traverse a material medium with a velocity greater than the velocity of light in that medium. It was found for several solids and liquids [water, mica, glass, cellophane, etc.] that the direction of the emission of the radiation is accurately expressed by the relation, cos θ = 1/βn, and that the intensity maximum is quite sharp. The nature of the radiation from all solids and liquids investigated was found to be continuous and identical in appearance. The radiation apparently extends with increasing intensity from the infra-red to the ultraviolet absorption limit of the medium in which it is produced. Rough quantitative measurements of its intensity indicate that one 1.9 million volt electron in being brought to rest in water produces 40 quanta in a wavelength range 4000Å to 6700Å. These results are in good agreement with the classical explanation of the phenomenon given by Frank and Tamm (1937).*
>
> From Collins and Reining (1938), https://journals.aps.org/pr/abstract/10.1103/PhysRev.54.499, reprinted with permission © 1939 by the American Physical Society.

Subsequent work by Cherenkov (1938a,b,c) included a series of thorough experiments to demonstrate the theory presented by Frank and Tamm (1937) on his newly discovered radiation. Cherenkov made more meticulous measurements of the spatial distributions of Cherenkov photons which, according to the theory of Frank and Tamm (1937), obeyed the relationship $\cos\theta = 1/\beta n$. He measured the spatial distributions of the photons induced by high-energy electrons traveling in four liquids having different indexes of refraction (Cherenkov, 1938a, 1958). These are in order of increasing index of refraction n, water ($n = 1.3371$), cyclohexane (C_6H_{12}, $n = 1.4367$), benzene (C_6H_6, $n = 1.5133$), and ethyl cinnamate ($C_{11}H_{12}O_2$, $n = 1.58043$). At the same time, he tested two sources of γ-rays with differing energies, which would produce photo- and Compton electrons of different energies when a liquid was irradiated. The two γ-ray sources were (1) radium, which would produce electrons with a phase velocity $\beta = 0.847$; and (2) thorium C″ or ThC″ (ie, ^{208}Tl), which emits a high-energy 2.16 MeV γ-ray, yielding electrons with a phase velocity $\beta = 0.896$. To guarantee only the hardest components of the γ-ray emissions from the two sources, Cherenkov filtered the lower-energy γ-rays of radium with 2 mm of lead shielding and those of the higher-energy γ-rays of ThC″ with 12-mm lead shielding. He accurately measured the angles of emissions (θ) of the Cherenkov photons in the four liquids when irradiated with the γ-ray sources Ra or ThC″. By measuring (θ) in liquids of differing index of refraction (n) and sources of two electron energies (β), Cherenkov set out to demonstrate that the angle θ, which is the direction of emission of the Cherenkov photons relative to the line of flight by the electrons traveling in a medium at a velocity exceeding that of light in the same medium, satisfies the relation $\cos\theta = 1/\beta n$. The graphical representation of his measurements of θ in the four liquids when irradiated by either Ra or ThC″ is illustrated in Fig. VII.8.

From the experimental data provided in Fig. VII.8 Cherenkov was able to demonstrate that the angle θ, the light intensity maxima in the four liquids, would increase as with increasing index of refraction n as well as with increasing electron velocity of energy β. The index of refraction increases with each liquid tested from top to bottom of Fig. VII.8, and the electrons produced by the ThC″ are faster than those produced by the Ra source. In the four liquids, the light intensity maxima, measured as θ with respect to the direction of electron travel, enlarged with increasing n and increasing β. The experimentally observed values of θ measured by Cherenkov (1938a) and those calculated according to the theoretical relation $\cos\theta = 1/\beta n$ of Frank and Tamm (1938) were in very close agreement, demonstrating that the theory holds with experiment.

Pavel Cherenkov continued his thorough investigation into the properties of the newly discovered radiation. In another work published the same year as that previously described, Cherenkov (1938b) investigated the spectrum of the visible radiation produced by charged particles that traveled in a transparent medium at speeds faster than the speed of light in the medium. To measure the light intensity as a function of the wavelength of the visible light, Cherenkov suspended a source of up to 280 mCi of Ra(B+C) or ^{214}Pb(^{214}Bi) in a 2-mm glass tube in benzene by means of a thin wire in the center of a thin-walled (0.1-mm) glass vessel measuring 3 cm in diameter and 4.5 cm in height. The outside of the inner glass tube containing the radium was coated with silver to eliminate any Cherenkov photons that might be produced in the glass walls of the tube. The source provided high-energy β-particles to create the Cherenkov photons in benzene.

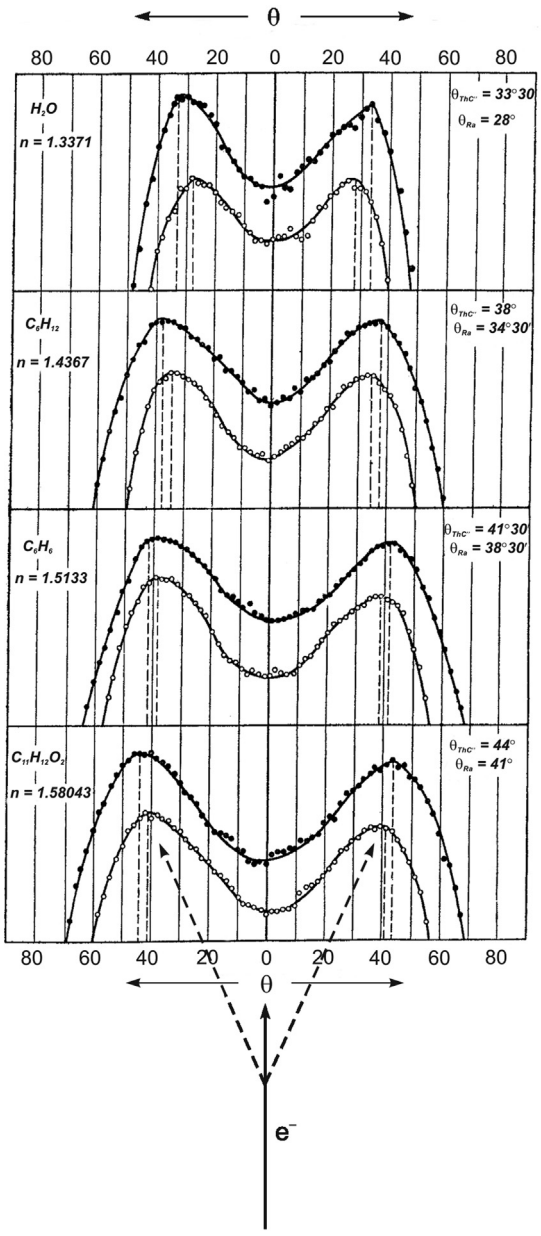

FIGURE VII.8 Spatial distribution of visible Cherenkov photon radiation produced by fast electrons in four liquid media and two sources of fast electrons. The liquid media tested were from top to bottom, water, cyclohexane, benzene, and ethyl cinnamate. The sources of fast electrons used were ThC″-producing electrons in the liquid media with a phase velocity $\beta = 0.896$ and radium-producing electrons with $\beta = 0.847$. In the lower part of the figure, the writer has inserted an arrow with a solid line to indicate the direction of travel of electrons at $\theta = 0$ and two arrows with dashed lines toward the light intensity maxima indicating the direction of travel of the majority of Cherenkov photons at an angle θ with respect to direction of the electrons. Large values of θ were measured by Cherenkov from 0 degree to 70 degrees, as illustrated, which are due to Compton scattering. Compton scattering results in the gamma-ray scattering of electrons at angles $\theta > 0$. *From Cherenkov, P.A., 1958. Nobel lecture: radiation of particles moving at a velocity exceeding that of light, and some of the possibilities for their use in experimental physics, Stockholm, December 11, 1958. In: Nobel Foundation Staff (Eds.), Nobel Lectures, Physics, 1942–62. (1964). Elsevier Publishing, Amsterdam; with permission © The Nobel Foundation 1958.*

Cherenkov (1938b) placed the radiation source at the entrance slit of a dual monochromator and lens arrangement to observe and measure the intensities of light at various wavelengths of the visible part of the spectrum. He would have to accustom his eyes to the dark for about an hour before making the measurements. The light intensity at various wavelengths of the visible spectrum of the Cherenkov photons was measured by Cherenkov to range between 4000 and 6000 Å, with the maximum intensity occurring at a wavelength of approximately 5100 Å.

Later in life, approximately 20 years after his historic research on the visible spectrum of the newly discovered radiation, Cherenkov commented on the spatial distribution and the visible spectrum of the radiation in his Nobel lecture given on December 11, 1958 as follows:

> *If we consider the picture [of the radiation] not in the [two-dimensional] plane but spatially, then the radiation must spread out along the surface of a cone whose axis forms the path of an electrically charged particle while the surface line forms with this axis the angle [θ].*
>
> *If we place [a] photographic plate perpendicular to the beam of high-speed particles [see Fig. VII.9], we shall obtain, in addition to an image of the track of the beam, also a photograph of the radiation in the form of a ring. This photograph [see Fig. VII.10] was obtained with the aid of a fine beam of protons in the accelerator of the United Institute for Nuclear Research at Dubna…we have in our considerations assumed some fixed frequency. In reality, however, the radiation spectrum is continuous. Since the medium exhibits dispersion,* i.e., *the refractive index is dependent on the frequency, this means that the light of different wavelengths is propagated at angles which, even with strictly constant velocity of the particles, differ somewhat from one another.*
>
> *Thus the radiation is broken up as in spectral analysis. The radiation cone will consequently show a definite intensity, and in the case of a medium with normal dispersion, the spectral red will lie in the inner part of the cone while the violet is on the outside. That this is actually so was shown by a photograph showing part of the ring with a colour plate.*

In a review of Cherenkov's work, Govorkov (2005) described three possible sources of radiation that can be produced with an electron traveling at relativistic speed through a transparent scintillating crystal. These would be (1) scintillation radiation, which is isotropic, that is, emitted in all directions; (2) Cherenkov radiation, which is conical, that is emitted as a cone at an angle θ with respect to the line of travel of the electron; and (3) bremsstrahlung radiation, which is emitted at angles close to 0° with respect to the line of travel of the electron. These were illustrated by Govorkov (2005) according to Fig. VII.11.

Finally, Cherenkov (1938c) measured the energy output of the radiation produced by electrons traveling in a medium at super-light velocity. This study was important to determine what portion of the total energy of the electron is dissipated in the generation of the Cherenkov radiation. According to the theory of Frank and Tamm (1937), the energy W emitted by an electron traveling in a medium at super-light velocity is calculated according to the equation:

$$W = \frac{e^2 l}{c^2} \int \omega d\omega \left(1 - \frac{1}{\beta^2 n^2}\right) \qquad \text{[VII.3]}$$

where l is the length of the electron path, c is the speed of light in a vacuum, ω is the cyclic frequency of the radiation, β is the electron phase velocity, ie, v/c as previously defined, and n is the refractive index of the medium. Cherenkov (1938c) explained that the velocity of the electron must exceed the phase velocity of light in the medium, where $\beta n > 1$. Also Cherenkov added that the motion of the electron in the medium involves a considerable change in velocity, and accordingly the magnitude of its phase velocity β will vary greatly for different sections of the electron path. Therefore, he

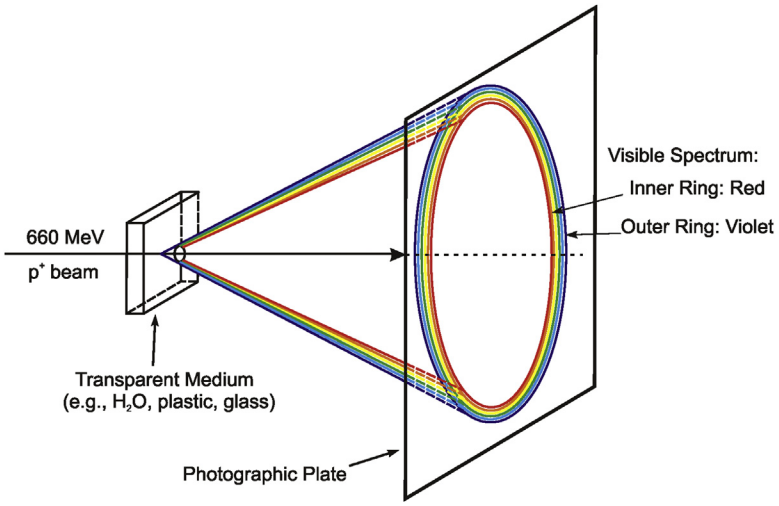

FIGURE VII.9 Diagram of an experimental arrangement for obtaining photographs of the cone section in the plane of a photographic plate placed perpendicular to the path of high-speed (660 MeV) protons in an accelerator beam. The color lines and their identification of the visible spectrum were added by the writer. *From Cherenkov's Nobel lecture given on December 11, 1958 with permission © The Nobel Foundation 1958.*

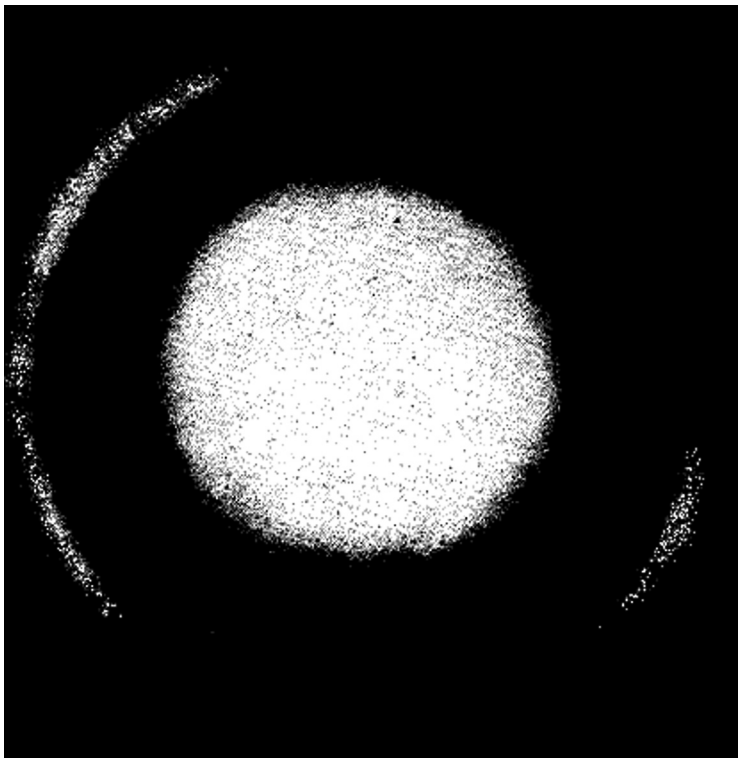

FIGURE VII.10 Photograph of a section of the Cherenkov radiation cone (outer circle) obtained by the experimental arrangement illustrated in Fig. VII.9. The central patch is that produced by the high-energy proton beam. *From Cherenkov, P.A., 1958. Nobel lecture: radiation of particles moving at a velocity exceeding that of light, and some of the possibilities for their use in experimental physics, Stockholm, December 11, 1958. In: Nobel Foundation Staff (Eds.), Nobel Lectures, Physics, 1942-62. (1964). Elsevier Publishing, Amsterdam; with permission © The Nobel Foundation 1958.*

concluded that, on the assumption that a relatively small region of the radiation spectrum is examined, within which n may be considered a constant, Eq. [VII.3] with reference to the true motion of the electron would be written as follows:

$$W = \frac{e^2}{c^2} \int \omega d\omega \int_{\beta n > 1} \left(1 - \frac{1}{\beta^2 n^2}\right) dl \qquad \text{[VII.4]}$$

where β depends on l. To facilitate the integration along l, Cherenkov substituted β and dl with V and dV, where V is the kinetic energy of the electron in keV and dV is the energy lost by the electron in the section of path dl.

Cherenkov next expressed the kinetic energy of the particle as the difference between its total energy and rest energy. As described in Eqs. [10.3]–[10.5] of the chapter entitled "Neutron Radiation," the total energy (E) of a particle is the sum of its kinetic (V) and rest energies (mc^2), or:

$$E = V + mc^2 = \gamma mc^2 \qquad \text{[VII.5]}$$

The kinetic energy V of the particle is then expressed as:

$$V = \gamma mc^2 - mc^2 \qquad \text{[VII.6]}$$

The term γmc^2 is dependent on the particle speed, as described previously by Eq. [10.5] of the chapter entitled "Neutron Radiation," where:

$$\gamma = \frac{1}{\sqrt{1 - (v^2/c^2)}} = \frac{1}{\sqrt{1 - \beta^2}} \qquad \text{[VII.7]}$$

Thus, the kinetic energy (V) of the electron can be expressed as:

$$V = \frac{mc^2}{\sqrt{1 - \beta^2}} - mc^2 \qquad \text{[VII.8]}$$

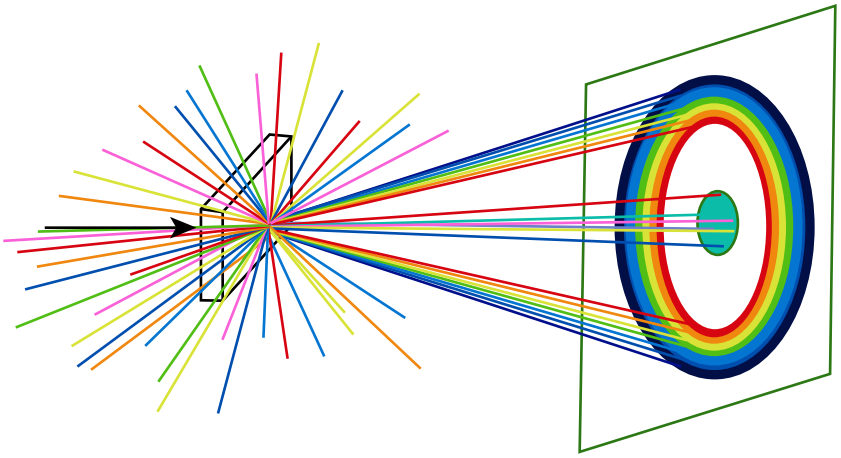

FIGURE VII.11 Three types of radiation that may be emitted when a relativistic electron travels through a transparent scintillating crystal, namely, (1) scintillation radiation, which is isotropic, that is, emitted in all directions illustrated in the left-hand portion of the figure; (2) Cherenkov radiation, which is conical, that is emitted as a cone at an angle θ with respect to the line of travel of the electron illustrated with the outer ring displaying the spectral lines of visible radiation at the right-hand portion of the figure; and (3) bremsstrahlung radiation, which is emitted at angles close to 0° with respect to the line of travel of the electron illustrated by the small gray circle at the center of the ring at the right-hand portion of the figure. The path of the electron is illustrated with the arrow at the far left of the figure. *From Govorkov, B.B., 2005. Cherenkov detectors in Cherenkov's laboratory. Nucl. Instrum. Methods Phys. Res. A553, 9–17; reprinted with permission from Elsevier © 2005.*

Cherenkov considered the rate of electron energy lost per path length in a given medium to be constant or $-dV/dl = k$, and that the value of k would differ for each medium and be proportional to the density of the medium. From Eq. [VII.8], Cherenkov expressed β^2 as:

$$\beta^2 = 1 - \frac{1}{[(V/mc^2)+1]^2} \quad \text{or} \quad \beta^2 = 1 - \left[\frac{1}{(V/mc^2)+1}\right]^2 \qquad \text{[VII.9]}$$

Substituting the value of β^2 from Eq. [VII.9] and the value $-dV/k$ for dl into Eq. [VII.4], Cherenkov (1938c) expressed the energy emitted by an electron at relativistic speed in a medium as:

$$W = \frac{e^2}{c^2}\int \omega d\omega \frac{1}{k}\int \frac{dV}{n^2\left[1-\left(1/[(V/mc^2)+1]^2\right)\right]} \qquad \text{[VII.10]}$$

He carried out the integration for W, the total energy emitted by the electron in water, within a range of frequencies from 536 to 556 mμ (5360–5560 Å) and electron energy range from 260 to 3000 keV. The electron energy spectrum would be that corresponding to a source of Ra(B + C), as Cherenkov would subsequently use this source of β-particles to determine experimentally the energy output of the Cherenkov photons. The value of k, a constant for each medium, was given the value of 1710 keV/cm for water. Beta particle energies below 260 keV were ignored, because only electron energies above 260 keV satisfy the threshold condition of $\beta > 1/n$ for the production of Cherenkov photons in water medium where $n = 1.334$ (see the chapter entitled "Cherenkov Radiation" for the calculation of the threshold electron energy for the production of Cherenkov photons in water). Cherenkov thus calculated W, the theoretical output of the radiation energy, to be 3.5×10^{-4} erg/s.

To compare the above theoretically calculated value of the energy output W with an experimentally determined value, Cherenkov (1938c) would measure the energy output for the same Cherenkov photon spectral region of 5360 to 5560 Å. He used an experimental arrangement whereby the Cherenkov photons were produced in a liquid medium within a 13-cm-diameter spherical glass cavity coated with reflecting magnesium oxide, an Ulbricht sphere, placed in a lead block. The liquid medium under investigation (H_2O was the first liquid to be used, and other liquids were tested subsequently) was placed inside the cavity in a round thin-walled glass vessel, 3.5 cm in diameter. The Cherenkov photons were produced by β-particles from a high-activity (135–193 mCi) source of Ra(B + C) located in an 8-mm-diameter spherical thin-walled (0.12-mm) glass ampule inside the liquid in the center of the spherical vessel. The ampule was coated with silver on its outer surface to reflect and eliminate Cherenkov photons produced in the ampule glass. A lead block protected the experimenter from the high levels of gamma radiation.

The Ulbricht sphere provided homogeneous Cherenkov photons in all directions even though the emission of a β-particle and consequent Cherenkov photons were asymmetrical. The size of the spherical vessel was carefully selected to provide a thickness layer of liquid sufficient to completely absorb the β-particles emitted by the Ra source, while at the same time insufficient to absorb to an appreciable extent the hard γ-rays from the source. In this way Cherenkov assured that any contribution by γ-rays to the production of Cherenkov photons would be insignificant.

The visible radiation would exit the cavity and pass through a 0.2-mm entrance slit of a monochromator. The observer would select the region of the spectrum ranging from 5360 to 5560 Å, with the mean wavelength at 5460 Å corresponding to the green line of the mercury arc. A wedge was controlled by the observer to determine radiation intensities using the criterion of the threshold of the eye conditioned to the dark.

Cherenkov carried out three series of experiments with Ra(B + C) sources of 193, 162, and 135 mCi activity. The results of the work yielded an experimental mean value of 4.1×10^{-4} erg/s per mCi of activity, which was very close to the theoretically calculated value of 3.5×10^{-4} erg/s per mCi.

Cherenkov (1938c) repeated the above experiment of theoretically calculated and experimentally measured energy outputs in five additional liquid media, namely benzene, cyclohexane, carbon disulfide, isobutyl alcohol, and carbon tetrachloride. The theoretical values were calculated according to Eq. [VII.10], varying only n and k for each medium. The absolute outputs differed for each medium because of the differences in index of refraction (n) and density (thus different k) of each medium; however, the experimental and calculated values for each medium were in close agreement.

One of the major outcomes of this work was Cherenkov's finding that the energy expended by the beta particles in the production of Cherenkov photons was small, on the order of 0.1% of the total energy of the beta particles.

In his Nobel lecture given on December 11, 1958, Cherenkov summarized the outcome of his discovery in 1934, his experimental research on the newly discovered radiation from 1934 to 1938, and the theory presented by Frank and Tamm in 1937 as follows:

> *The development of this theory [Frank and Tamm, 1937] completes a great cycle of research work which covers discovery, all-round experimental investigation, and the development of the theoretical basis of this phenomenon which established a new branch of physics – the optics of rays moving faster than light.*

Although, as noted above, the production of Cherenkov radiation is not a principal means by which charged particles may dissipate their energy in matter, the production of Cherenkov photons and their detection in matter later developed to be a vital tool in the biological, environmental, and physical sciences. In the biological sciences, the counting of Cherenkov photons is used commonly to analyze quantitatively the activity in disintegrations per minute (DPM) of the beta particle–emitting nuclide ^{32}P, an important radioisotope used as a tracer for phosphorus. This technique is discussed in detail in previous books by the writer (L'Annunziata, 1987, 2012e). In the environmental sciences, Cherenkov counting of the nuclide ^{90}Y, which emits high-energy beta particles, is utilized in the analysis of its parent nuclide ^{90}Sr (L'Annunziata, 1971, 2012e; L'Annunziata and Passo, 2002). In the physical sciences, the Cherenkov Effect has become a useful tool for the identification of elementary particles and information on their mass and velocity particularly following the development of ring-imaging Cherenkov (RICH) detectors reviewed by Sequinot and Ypsilantis (1994), Ypsilantis and Sequinot (1994), and L'Annunziata (2012e) and discussed in detail in the chapter entitled "Cherenkov Radiation" of this book. In his Nobel lecture, Cherenkov (1958) summarized the unique properties of Cherenkov radiation that would open a new field of physics proving to be of immense value in the detection and measurement of radionuclides and the identification of elementary particles and their mass and velocity. An excerpt of his comments [with the author's notations in brackets] listed according to application, is the following:

1. The presence of an energy threshold makes this type of counter [Cherenkov counter or detector] insensitive to the slow particles whose energy lies below the threshold. [In this statement, Cherenkov clearly points out that radionuclides that emit low-energy β-particles, for example, ^{3}H or ^{14}C, will cause no interference in the detection and counting of Cherenkov photons produced by β-particle emissions of ^{32}P in a liquid medium such as water. This is so because the threshold energy for the production of Cherenkov photons in water is 260 keV and the energy maxima of the β-particles emitted by ^{3}H and ^{14}C are 18.6 and 155 keV, respectively, well under the threshold energy of 260 keV.]
2. …The asymmetry of the radiation facilitates with this counter the measurement of those particles which are moving in the radiator in the direction of the cathode of the photomultiplier. Particles moving in the opposite direction are not measured by the counter. In other words, this type of counter has the distinction of focusing on a definite directional effect.
3. …one of the most important parameters of a particle – its mass – can be determined on the basis of measurements of its momentum and speed…It is evident without more ado that where the speed of a particle is within a certain range where β

[particle phase velocity], that fulfills the condition $\beta n > 1$, is still sufficiently different from 1, the speed of the particle, on the basis of the equation $\cos\theta = 1/\beta n$ and starting from the measured quantity θ and the known refractive index, can easily be calculated. When the type of the particle is known, speed measurements enable us to determine their energy also.

4. We have already noted the fact of the [Cherenkov] radiation having an energy threshold [that is, the particle must possess an energy in excess of the threshold to produce Cherenkov radiation], which renders the counter insensitive to low-energy particles. We thus have the possibility of altering the threshold energy E_0 when we choose a radiator with a suitable quantity n. It is clear that two counters set at degrees of threshold energy E_0' and E_0'', and switched on in the proper sequence according to the scheme of anticoincidence, will only measure those particles whose velocity is in the region of E_0' and E_0''. A procedure of this kind was successfully employed by [Emilio] Segrè and his collaborators in their outstanding work which led to the discovery of the antiproton.

An interesting paper on Cherenkov's professional work and his equipment is provided by one of his former colleagues Boris Borisovich Govorkov (2005) of the Lebedev Physical Institute (LPI), Moscow, from which some of the following notes on Cherenkov's professional career are provided here. In 1949, Pavel Cherenkov collaborated with Vladimir Iosifovich Veksler in the startup of the first European electron synchrotron, which accelerated electrons to energies of up to 250 MeV. Cherenkov became chief investigator in particle physics after the accelerator was put into operation. In 1959 he became the leader of the Photomesonic Laboratory in the LPI of the Russian Academy of Sciences, which he managed until 1986. Pavel Cherenkov then was appointed director of the High Energy Physics Department of the LPI, which staffed approximately 150 physicists, engineers, and technicians carrying out research in photonuclear processes and accelerator physics.

Pavel Alekseyevich Cherenkov died on January 6, 1990. In August of the following year, John Hubbell (1991) wrote a short article entitled "Faster than a Speeding Photon" commemorating Cherenkov's paper published in 1934 announcing his discovery of the light created by charged particles that traveled at speeds faster than light in a transparent medium. In his article, Hubbell underscored the significance of Cherenkov's work by the following statement: Pavel Alekseyevich Cherenkov casts a long shadow (or light actually) across both the history and future of radiation physics.

IL'JA MIKHAILOVICH FRANK (1908–1990) AND IGOR YEVGENYEVICH TAMM (1895–1971)

Il'ja Mikhailovich Frank and Igor Yevgenyevich Tamm shared the 1958 Nobel Prize in Physics with Pavel Alekseyevich Cherenkov "for the discovery and interpretation of the Cherenkov Effect." It was Pavel Cherenkov who discovered the effect in 1934 and measured the physical properties of Cherenkov radiation; however, it was Il'ja Frank and Igor Tamm, who in a joint publication in 1937, provided the interpretation of the origin and properties of the radiation. Their biographical sketches and work are presented jointly here since they worked together in providing the theoretical concepts needed to interpret the Cherenkov effect.

Il'ja M. Frank (1908–1990)

Il'ja Frank was born in Leningrad (now Saint Petersburg), Russia on October 23, 1908. He was a pupil of Sergei I. Vavilov at Moscow State University, graduating in 1930. The following year he was appointed scientific officer of the State Optical Institute, where S. I. Vavilov would become Head of Research the following year. In 1934 Frank joined the P.N. Lebedev Institute of Physics in Moscow, which was newly created under the directorship of S. I. Vavilov. It was that same year that Cherenkov (1934a,b) reported his discovery of a new radiation produced by high-energy electrons in a transparent media, and Vavilov (1934) presented his initial understanding of the origin of this unique radiation, which is currently referred to as Cherenkov radiation or Vavilov–Cherenkov radiation. Frank was awarded the doctorate in physical and mathematical sciences in 1935.

Igor Y. Tamm (1895–1971)

Igor Tamm was born in Vladivostok, Russian Empire on July 8, 1895. When he was five years of age, he moved with his family to Elizavetgrad (now Kiroovograd, Ukraine). He graduated from the Elizavetgrad Gymnasium in 1913 and then studied at the University of Edinburgh from 1913 to 1914. Like his future colleague Il'ja Frank, Igor Tamm studied physics and math at Moscow State University, graduating from the university in 1918. Upon graduation he continued his studies and teaching of physics and mathematics in several institutions including the Crimean and Moscow State Universities, the Polytechnical and Engineering Physical Institutes, and the J.M. Sverdiov Communist University (Nobel Lectures, Physics, 1942–62). He eventually achieved the rank of full professor and was awarded the doctorate in physics and mathematical sciences. Again like Il'ja Frank, in 1934 Igor Tamm joined the newly created P.N. Lebedev Institute of Physics in Moscow, which was established under the directorship of Sergei I. Vavilov.

Once Cherenkov had discovered a unique visible radiation produced by high-energy Compton electrons or high-energy (fast) β-particles; and once Cherenkov found that this light was polarized and that the light emission was asymmetric, that is, it was emitted only in the direction of the fast electrons (Cherenkov, 1934a,b, 1936), Cherenkov and his doctoral dissertation advisor and director of the P.N. Lebedev Institute, Sergei I. Vavilov, knew that they were dealing with a yet-unknown phenomenon. Il'ja Frank and Igor Tamm of the Theoretical Physics Division of the same institute took notice and went to work on the interpretation of this new phenomenon. Their findings were published in a joint paper entitled "Coherent Visible Radiation of Fast Electrons Passing through Matter" (Frank and Tamm, 1937). They explained the phenomenon as caused by a charged particle traveling in a medium at a speed in excess of the speed of light in that medium. It was known from Einstein's theory of relativity that matter could not travel in excess of the speed of light in a vacuum ($c = 2.99 \times 10^8$ m/s); however, in other gaseous, liquid, or solid transparent media the velocity of light will be less than its velocity in a vacuum, and an elementary charged particle with sufficient energy could travel in such media at speeds exceeded that of light. The charged particle in passing through the electron clouds of a medium would create an electromagnetic shock wave analogous to that of a "sonic boom" created by a jet airplane or projectile traveling in the atmosphere at a speed exceeding that of sound. Frank and Tamm (1937) described the Cherenkov Effect as follows, with the author's comments in brackets:

> *We shall consider an electron moving with constant velocity* v *along [an] axis through a medium characterized by its index of refraction* n *[The index of refraction,* n*, is by definition the ratio of the speed of light in a vacuum to its speed in a particular medium, and the value of* n *will vary from one medium to another]. The field of the electron may be considered as the result of*

superposition of spherical waves of retarded potential, which are being continually emitted by the moving electron and are propagated with the velocity (c/n). *[See Fig. VII.12] It is easy to see that all these consecutive waves emitted will be in phase along the directions making the angle* θ *with the axis of motion [of the particle], if only* v, n, *and* θ *do satisfy the condition:*

$$\cos\theta = \frac{1}{\beta n} \qquad \text{[VII.11]}$$

where $\beta = v/c$. *Thus, there will be a radiation emitted in the direction* θ, *whereas the interference of waves will prevent radiation in any other direction. Now the condition [of Eq. [VII.11]] can be fulfilled only if:*

$$\beta n > 1, \qquad \text{[VII.12]}$$

that is, only in the case of fast electrons in a medium, whose index of refraction n *for frequencies in question is markedly larger than 1.*

The term "fast electrons" used by Frank and Tamm (1937) above refers to electrons of such energy that they travel at a speed in excess of the speed of light in a particular medium. Also the term β is called the relative phase velocity of the particle ($\beta = v/c$) or the velocity of the particle in a medium divided by the speed of light in a vacuum.

Eq. [VII.11] derived by Frank and Tamm can be found from the distance of travel of the spherical wave front relative to the distance traveled by the electron, as seen in Fig. VII.12. In the words of Frank (1958) in his Nobel lecture:

…We have to consider each point of the particle trajectory as a source of waves. In this case the wave phase is determined by the instant of passage of the particle through a given point. Let us assume that at moment $t = -t_3$ *the emitter was at point* A_3, *at moment* $t = -t_2$ *at point* A_2, *at moment* $t = -t_1$ *at* A_1, *and, finally, at the moment of observation* $t = 0$ *at* A_0.

…the velocity of the waves is equal to the phase velocity of light c/n*…*

The surfaces of the rays are simply spheres whose radii for points A_3, A_2, A_1, *and* A_0 *are* $(c/n)t_3$, $(c/n)t_2$, $(c/n)t_1$, *and 0, respectively [see Fig. VII.12A]. The envelope of these spheres evidently represents a cone of circular cross section with the apex at* A_0. *Its generatrices in the plane of the drawing are* A_0B *and* A_0B'.

According to the Huygens' principle, the directions of the rays are defined by the radius vectors drawn from some centre of the waves to the point of tangency with the envelope. For example, in Fig. VII.12 it is A_3B *and* A_3B' *coinciding with the generatrices of the wave normal cone…*

From Fig. VII.12 it is not difficult to determine the magnitude of the threshold velocity. When the velocity diminishes, the distances between points A decrease. The threshold case arises when point A, occupies the position A_0' *on the surface of the sphere. [This case is depicted separately in Fig. VII.12B.] At lower velocities, one of the spheres lies completely within the other and they do not have a common envelope. In the threshold case [*$\beta n = 1$*], they have only a common point of tangency,* A_0'. *Thus evidently* $(c/n)t_3 = v_0 t_3$, i.e. $v_0 = c/n$. *The cone of wave normals is compressed in the direction of velocity v, and the wave cone transforms into a plane perpendicular to the axis of motion at point* A_0' *[Fig. VII.12B].*

From Fig, VII.12A, the equation defining the angle θ as a function of the particle phase velocity β and index of refraction n, ie, $\cos\theta = 1/\beta n$, is derived from the distances of travel of the wave front with respect to that traveled by the

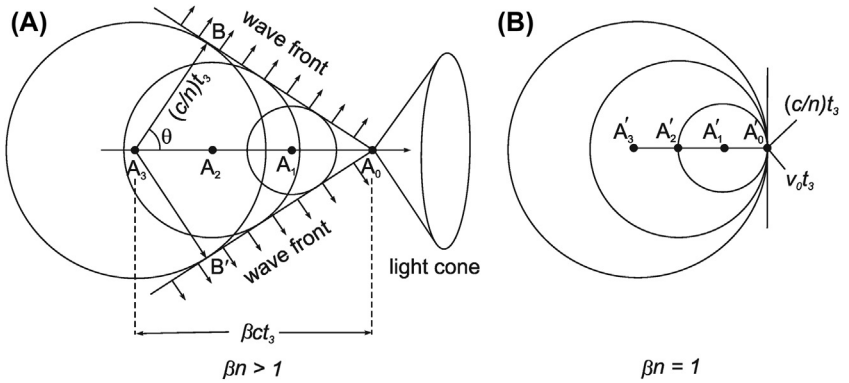

FIGURE VII.12 A Huygens construction of the spherical waves of retarded potential produced by a charged particle traveling along an axis in a refractive medium from points A_3 to A_0 at two velocities, namely (A) $\beta n > 1$ and (B) $\beta n = 1$. *Adapted from Nobel Lecture of Frank, I.M., 1958. Optics of light sources in refractive media. Nobel Lecture, December 11, 1958. In: Nobel Foundation Staff (Eds.), Nobel Lectures, Physics, 1942–62. (1964) Elsevier Publishing, Amsterdam; with permission © The Nobel Foundation 1958.*

charged particle. The velocity v of travel of the wave front in a particular medium is a function of the index of refraction n of the medium, since by definition $n = c/v$. The distance traveled by the wave front from A_3 to B of Fig. VII.12A is the product of velocity and time t or $A_3B = vt_3$, and the distance traveled by the charged particle in the same time span from A_3 to A_0 is the product of the particle velocity in the medium v_p and time t_3 or $A_3A_0 = v_pt_3$, which may be written as $A_3A_0 = (v_p/c)ct_3$. Since the particle phase velocity β is defined as v_p/c, the distance A_3A_0 traveled by the charged particle becomes $A_3A_0 = \beta ct_3$. The angle of emission θ of the Cherenkov radiation with respect to the direction of travel of the charged particle is defined as:

$$\cos\theta = \frac{AB}{A_3A_0} = \frac{(c/n)t_3}{\beta ct_3} = \frac{1}{\beta n} \qquad \text{[VII.13]}$$

Frank and Tamm (1937) calculated the total energy, W, radiated by an electron via the Cherenkov Effect through a cylindrical region of medium of length, l, where the axis of the cylinder coincided with the line of motion of the electron. Under the assumption that β is constant over a short length, dl, of the electron track, they derived the equation:

$$W = \frac{e^2 l}{c^2} \int\limits_{\beta n>1} \omega d\omega \left(1 - \frac{1}{\beta^2 n^2}\right) \qquad \text{[VII.14]}$$

where ω is the frequency of the Cherenkov radiation. The lower limit of the integral, $\beta n > 1$, is the threshold condition for the production of Cherenkov photons in any medium. Frank and Tamm (1937) established the equation to be valid provided that l should be large in comparison with the wavelength λ of the Cherenkov radiation emitted. Cherenkov (1938c) took Eq. [VII.14] of Frank and Tamm and evaluated the energy, W, radiated by an electron taking under consideration that the magnitude of β will vary greatly over the entire path length of the electron. Cherenkov (1938c) noted that the velocity of the electron will vary in various sections of its path of travel as it loses energy and thus the magnitude of β varies according to the sections of electron's path of travel in the medium. Thus, assuming that if a small region of the spectrum is examined whereby n may be considered a constant, Cherenkov (1938c) expressed Eq. [VII.14] with respect to the true motion of the electron as follows:

$$W = \frac{e^2}{c^2} \int \omega d\omega \int\limits_{\beta n>1} \left(1 - \frac{1}{\beta^2 n^2}\right) dl \qquad \text{[VII.15]}$$

where β is a function of l.

Frank and Tamm (1937) thus calculated the rate of radiated energy to be only 4.1 erg/s output per1 mCi of beta particle radioactivity. Thus, the electron energy loss via the emission of Cherenkov radiation would be a negligible quantity of energy in comparison to the energy lost by the electron or beta particle by other mechanisms such as ionization. Cherenkov (1938c) confirmed this through calculations and experimentation and concluded that the radiation expended by β-particles from Ra(B + C) via the emission of Cherenkov radiation amounts to a value of the order of only 0.1% of the total energy of the particles.

From Eq. [VII.14], Frank and Tamm (1937) deduced the following equation for the number of photons, N, emitted by an electron within the limits of a given spectral region confined by the wavelengths λ_1 and λ_2 for a constant β, that is, for a short length of the electron track where the phase velocity of the electron remains relatively constant, to be:

$$N = 2\pi\alpha \left(\frac{1}{\lambda_2} - \frac{1}{\lambda_1}\right)\left(1 - \frac{1}{\beta^2 n^2}\right) \qquad \text{[VII.16]}$$

where α is the fine structure constant ($\alpha \approx 1/137$). From Eq. [VII.16], Frank and Tamm (1937) calculated that a 500-keV electron, which would correspond to $\beta^2 = 0.75$, traveling in water, where $n = 1.33$, would produce approximately 10 photons per 0.1 cm within the visible region between $\lambda_1 = 4000$ Å and $\lambda_2 = 6000$ Å as follows:

$$N = 2(3.14)(1/137)\left(\frac{1}{4\times10^{-5}\text{ cm}} - \frac{1}{6\times10^{-5}\text{ cm}}\right)\left(1 - \frac{1}{(0.75)(1.33^2)}\right) = 94.1 \text{ photons/cm} \approx 10 \text{ photons/0.1 cm}$$

The above approximation by Frank and Tamm was confirmed with more precise calculations by Belcher (1953), who calculated the integral number of Cherenkov photons produced by an electron as a function of its varying phase velocity over the entire effective range of travel of the electron in water ($n = 1.33$) and Perspex plastic medium ($n = 1.50$). The effective range of travel of the electron is that of its highest energy or highest phase velocity ($\beta = \beta_{max}$) to a lower energy as a result of reduced velocity in the medium corresponding to the threshold phase velocity or $\beta = 1/n$, at which point

Cherenkov photons are not produced. The calculations of Belcher are treated in more detail in the chapter entitled "Cherenkov Radiation."

Following the publication of their joint work on the Cherenkov Effect in 1937 described above, for which they shared with Cherenkov the Nobel Prize in Physics in 1958, Frank and Tamm concluded their collaboration. However, Il'ja Frank continued to study the Cherenkov Effect, publishing a work on the possibility of interference phenomena in Cherenkov radiation emission (Frank, 1944).

Il'ja Frank continued to study Cherenkov radiation, undertaking numerous theoretical works with Vitaly Ginzburg on various extensions of the Cherenkov Effect as produced by dipoles, multipoles, and oscillators. These studies are reviewed in a comprehensive treatise on Cherenkov radiation and its applications by Jelley (1958). Frank became head of the Physics Department of Moscow State University in 1944 and was appointed head of the Neutron Laboratory of the Joint Institute of Nuclear Research in 1957. He composed an authoritative text entitled "Vavilov-Cherenkov Radiation, Theoretical Aspects," which was published in 1988 in the Russian language two years before his death. Vitaly Ginzburg (2001), also a Nobel Laureate and former collaborator of Frank, commented on Frank's theoretical treatise as follows:

> *…I naturally looked through Frank's book once again. What hard work was done, how many results were obtained! This [the book] is a memorial…This memorial and the name of Il'ja Mikhailovich will remain in the history of physics forever.*

With kind permission from Springer Science+Business Media © 2001 Springer-Verlag Berlin Heidelberg.

In a historical account, Bolotovski et al. (2004) wrote about Il'ja Frank's final work as follows:

> *Frank preserved his respect and affection for his beloved teacher [Sergei I. Vavilov] until the end of his days. He compiled and edited a collection of reminiscences about Vavilov, which was published in three volumes [See Frank, 1979, 1981, 1991]. Frank was very ill when he was working on the third volume in 1990 and afraid he would die without finishing the work. When he completed the manuscript he emerged from his study at home and joyfully informed his family that the book had been finished, adding: "Now at last I can die," He died a few days later.*

Il'ja Mikhailovich Frank died on June 22, 1990.

Igor Tamm, after his collaboration on the theoretical interpretation of the Cherenkov Effect with Il'ja Frank, continued to work on other concepts of theoretical nuclear physics and turned his attention to plasma physics. From 1934 and for the remainder of his life, Igor Tamm was head of the Department of Theoretical Physics of the P.N. Lebedev Physical Institute in Moscow. In 1948, Igor Tamm was commissioned by Igor Kurchatov, head of the Soviet atomic bomb project, to work on the development of the hydrogen (fusion) bomb. Tamm and some of his students, including 1975 Nobel Laureate for Peace Andrei Sakharov, became part of a specialized group at FIAN that worked on the fusion bomb. FIAN was the Physics Institute of the Academy of Sciences, the acronym for the Russian **F**izicheskii **I**nstitut **A**kademya **N**auk SSSR. It was later named the P.N. Lebedev Physics Institute. As an outcome of their collaboration, Tamm and Sakharov in 1952 proposed a Tokamak system as a means of achieving a controlled thermonuclear fusion (CTF) as a peaceful source of energy. The Tokamak is a word of Russian origin that is an acronym for a Russian phrase meaning "toroidal-chamber-magnetic coils," and the first Tokamak was successfully developed in the USSR around 1960. The Tokamak utilizes current-carrying coils that create a toroidal magnetic field confinement of heated plasma within a donut-shaped reactor, which is designed to achieve and maintain the high temperatures needed for the fusion of hydrogen nuclei. A current transmitted through the plasma creates magnetic field lines around the current to improve plasma confinement by preventing ion migration toward the walls of the torus. The Tokamak design remains the most promising for the future utilization of nuclear fusion as a peaceful source of energy. Fusion energy production by means of a commercial-scale reactor is assumed to be developed around the year 2050 (Sheffield, 2001). The Tokamak and nuclear fusion in general, as a future source of energy, is discussed in detail in the chapter entitled "Radioactivity and Our Well-Being" of this book.

In a recent book, Nobel Laureate Vitaly Ginzburg (2001) provided his personal reminiscences of Igor Tamm, from which a small excerpt is quoted as follows:

> *The theoretical Department of FIAN, established by Tamm in 1934, now bears his name. Originally it had five or six staff members and now it is one of the largest departments of its kind in the world. It has 60 researchers on its staff and hundreds of former postgraduate students and other researchers from the department now work successfully in laboratories all over the world. In more than 50 years there was not a single instance of serious interpersonal friction, let alone conflict. This is a rare situation, indeed, and it was, of course, Tamm who made it happen. It was unthinkable for him to disregard junior staff, to allow senior personnel or supervisors to add their names as authors to papers written by their subordinates, or to take precipitate or coercive administrative steps. On the contrary, he was ready to provide to his subordinates support, freedom of action, sympathy, and*

friendly comments…That was a very simple 'secret' of Tamm as a leader and mentor. Mature people in a team require sympathy and lack of any hindrance from the leader, while young people need freedom and guidance, when indicated, and that is all that is needed for the team to be successful. Its sounds simple but, unfortunately, it is not always practiced by administrators in science…He was typically fascinated with genuine mysteries, the problems of a fundamental character. Problems of this kind are especially hard to work on because years may pass without one getting any significant results. Such concerns, though, never worried Tamm; he never was guided by such desires as publishing a paper or, in general, 'to maximize the production rate.'…A person is called ambitious not only when he strives to attain a high position and control other people, but also when he strives to fulfill himself by producing good results and hoping to see them acclaimed. The latter kind of ambition is typically a necessary condition for successful research. So many gifted people…have failed to fulfill themselves because of their indifference and laziness, that is, essentially, lack of ambition. Tamm was ambitious in that sense of the term.

With kind permission from Springer Science+Business Media © 2001 Springer-Verlag Berlin Heidelberg.

Ginzburg (2001) described the last three years of Tamm's life, which were tragic. In 1967, he was struck with lateral amyotrophic sclerosis, and in February 1968 he became partially paralyzed by the illness and could survive only with a breathing machine; other machines were provided to enable him to sit and work at his desk. In his book, Ginzburg (2001) wrote the following recollections of Tamm's final years:

With a bitter smile, he used to say, "I am like a beetle on a pin." The first two years of his illness he managed to work a lot, he played chess, and was glad to see visitors. The fatal illness did not make him angry; indeed, he became gentler. When healthy he tended to conceal his warm feelings, apparently thinking they were unseemly, and illness freed him of that inhibition.

With kind permission from Springer Science+Business Media © 2001 Springer-Verlag Berlin Heidelberg

Igor Tamm died on April 12, 1971.

Chapter 16

Cherenkov Radiation

I still recall with great pleasure the exclamation of the greatest scientist of that epoch, Niels Bohr—"Wunderbar, Wunderschön", repeated several times after I demonstrated to him one of the most essential properties of the radiation, namely its space symmetry. Nevertheless, the atmosphere of distrust of the new effect [Cherenkov Effect] from scientific opinion remained. The most open and sharp manifestation of this distrust was the refusal by the journal Nature *to publish a short paper, summarizing the essence of the phenomena and its main properties.*

Pavel A. Cherenkov (1986), relating his reaction to the rejection of his work by the editors of *Nature* and the reactions of the scientific community. (From Cherenkov, P.A., 1986. At the threshold of discovery. Nucl. Instrum. Methods Phys. Res. Sect A 248, 1–4.)

16.1 INTRODUCTION

Photons of visible radiation are produced when a charged particle travels through a transparent medium at a speed greater than the speed of light in that medium. The medium may be any liquid or solid provided it is transparent. These photons are referred to as Cherenkov radiation, in honor of the Russian physicist Pavel A. Čerenkov for his basic research and discovery of the properties of this unique radiation (see Cherenkov, 1934a, 1937d). The process that gives rise to Cherenkov photons is referred to as the Cherenkov effect. In the scientific literature, four variations of the contemporary spelling or naming of Čerenkov radiation can be found, namely, (1) *Čerenkov radiation*, after the Russian, which is the spelling used by Pavel Čerenkov in his original papers (Cherenkov, 1934a,b, 1936, 1937a–d, 1938a–c); (2) *Vavilov–Čerenkov radiation*, in honor also of Sergei Ivanovich Vavilov (1891–1951), who was the doctoral research advisor to Pavel Čerenkov during the pioneering discoveries; (3) *Cherenkov radiation*, which provides the English pronunciation for the Russian Č; this is also the spelling used by Pavel Cherenkov (1986) in his last publication, and it is the spelling adopted by the Nobel Foundation (http://nobelprize.org/index.html); and (4) *Cerenkov radiation*, which is the anglicized version. All four versions of the spelling are found in the current scientific literature. Throughout this chapter, the writer will adopt the spelling *Cherenkov*, for the following reasons: (1) it conforms with that used by Pavel Cherenkov in his last paper (Cherenkov, 1986), entitled "At the Threshold of Discovery," which appeared in the journal *Nuclear Instruments and Methods in Physics Research*; (2) it is the spelling adopted by *Chemical Abstracts*; (3) it is the spelling adopted by the Nobel Foundation; and (4) it is the spelling adopted most often by authors of papers in the journal *Nuclear Instruments and Methods in Physics Research*.

The Cherenkov effect and the resulting radiation produced by a charged particle traveling in a transparent medium at a velocity exceeding the speed of light in that medium were predicted theoretically as early as 1888 by Oliver Heaviside (1888, 1889, 1892, 1899, 1912a,b), but long forgotten until the radiation was discovered finally by Cherenkov (see Cherenkov, 1934a,b) and interpreted by Frank and Tamm (1937). Heaviside's early prediction was based on a traveling point charge, as the electron was not discovered by J.J. Thompson until 1897. Govorkov (2005) reviewed the historical significance of Heaviside's prediction, namely, that Heaviside first predicted theoretically that a point charge (eg, electron) would produce a conical wave front whenever it were to travel at a speed greater than the speed of light in a medium. Heaviside's prediction was before Einstein's theory of relativity, which holds that matter cannot travel faster than light in a vacuum; however, matter can travel faster than light in a medium. In the time of Heaviside, even outer space was not considered to be a vacuum but to consist of an "ether," and therefore, according to Heaviside, the conical wave front would be produced in the ether as well as any other medium provided the point charge travels at a speed exceeding that of light. In the words of Govorkov (2005):

A genius, Heaviside was half a century in advance of his time in his calculations and predictions, but unfortunately he was not understood by his contemporaries. His works were forgotten, and scientists had to start from the beginning, this time from experiment [i.e., the experiments and discovery by Cherenkov (see Cherenkov 1934a,b, 1936, 1937a–d, 1938a–c)].

Radioactivity: Introduction and History, From the Quantum to Quarks. http://dx.doi.org/10.1016/B978-0-444-63489-4.00016-2
Copyright © 2016 Elsevier B.V. All rights reserved.

Oliver Heaviside (1850–1925)
Photo courtesy of AIP Emilio Segre Visual Archives, Brittle Books Collection

The German physicist, Arnold Sommerfeld (1904), also predicted a radiation wave front, that would be produced by an electron traveling at a speed exceeding the speed of light in a medium. Sommerfeld's prediction was with no apparent knowledge of the previous theories of Heaviside. Electrons, as well as other charged particles, with sufficient energy can indeed travel faster than light in media where light travels at speeds less than its speed in a vacuum. The speed of light in a transparent medium is defined by the index of refraction, n, of the medium, where $n = c/v$ and c is the velocity of light in a vacuum and v is the velocity of light in the medium. Heaviside (1912a) had even calculated the geometry and angle of emission of the electromagnetic wave front relative to the axis of travel of the charged particle. Also, Afanasiev et al. (1999) explains that the early theoretical predictions of Heaviside, namely, that a conical radiation wave front would arise when the point charge velocity exceeds the light velocity in a medium, had been forgotten by the scientific community until 1974 when, they were revived by Tyapkin (1974) and Kaiser (1974).

Cherenkov radiation was first observed by Marie Curie in 1910. She observed, in a dark room, a pale blue light from concentrated radium solutions, as related in a biography by her daughter Eve Curie (1937). The radiation was researched by Lucien Mallet (1926−1929). He found that the light would be emitted by a variety of transparent bodies when exposed to radioactive sources; however, the unique origin and anisotropic properties of the radiation were yet to be discovered. It was not until the extensive work of Cherenkov and Vavilov (see Cherenkov, 1934−1938) and the theoretical interpretations of Frank and Tamm (1937), who shared the 1958 Nobel Prize in Physics with Cherenkov, that the origin and properties of Cherenkov radiation was finally understood. Comprehensive treatments on the theory, properties, applications, and history of Cherenkov radiation are available from Frank (1960), Jelley (1958, 1962), Ritson (1961), and in a book by the writer (L'Annunziata, 2012d,e). A concise overview will be provided in this chapter.

Cherenkov radiation consists of a continuous spectrum of wavelengths extending from the ultraviolet region into the visible part of the spectrum peaking at about 420 nm (see Kulcsar et al., 1982; Claus et al., 1987). Only a negligible amount of photon emission is found in the infrared or microwave regions.

Cherenkov photon emission is the result of local polarization along the path of travel of the charged particle with the emission of electromagnetic radiation when the polarized molecules return to their original states (Gruhn and Ogle, 1980). This has been described by Marshall (1952), Siegbahn (1958), and others as the electromagnetic "shock" wave that is analogous to the acoustical shock wave or sonic boom created by supersonic aircraft. In the presentation speech of the Nobel Prize in Physics for 1958 awarded to Pavel Cherenkov, Il'ja Frank, and Igor Tamm for "the discovery and interpretation of the Cherenkov effect" on December 11, 1958, Prof. K. Siegbahn described Cherenkov radiation in the following words (with the author's notations in brackets):

> *The phenomenon can be compared to the bow wave of a vessel that moves through the water with a velocity exceeding that of the waves. In air, an analogous phenomenon occurs when a jet plane penetrates the so-called sound barrier at about 1000 km/hr,*

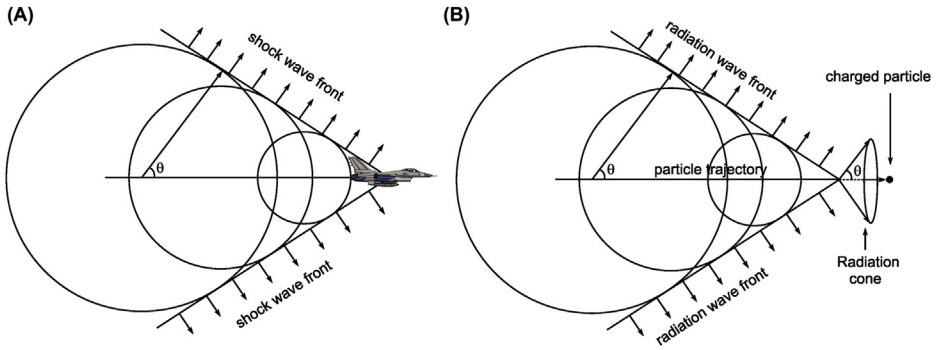

FIGURE 16.1 Conical wave fronts produced by (A) a jet traveling at supersonic speed and (B) a charged particle traveling at super-light speed in a transparent medium, ie, a speed exceeding the speed of light in the medium. The supersonic jet produces a conical shock wave front while the charged particle produces a conical wave front of Cherenkov radiation. The Cherenkov photons are emitted at an angle θ to the particle trajectory.

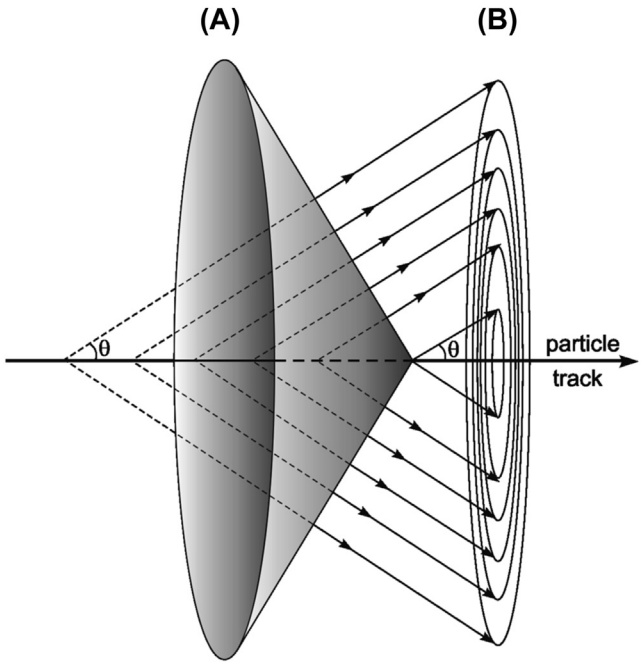

FIGURE 16.2 Cherenkov conical wave front in (A) three dimensions and (B) photon trajectories at angle θ (indicated by *arrows*) in two dimensions illustrating Cherenkov cones and the rings of Cherenkov photons produced along the particle track. The shaded region (A) is not the Cherenkov cone but rather its complementary wave front.

> *i.e., when the jet velocity exceeds the propagation velocity of the sound waves [See Fig. 16.1A]…The condition that is required to form the corresponding Cherenkov bow wave of ordinary light when a charged particle, e.g. an electron, traverses a medium is, analogously, that the particle moves with a velocity greater than that of light in the medium [Fig. 16.1B].*

The production of Cherenkov photons by a charged particle traveling in a transparent medium at a speed exceeding that of light in the medium is depicted as a conical wave front in a two-dimensional diagram in Fig. 16.1B. The photons are asymmetric and emitted in the direction of the particle trajectory at an angle θ relative to the particle track. The emission angle θ is a function of the particle phase velocity and the index of refraction of the medium, as described previously in the biographical sketches of Pavel Cherenkov, Il'ja Frank, and Igor Tamm. The conical Cherenkov radiation wave front is illustrated in three dimensions in Fig. 16.2. A cross section of the wave front yields rings of photon emissions in the direction of the particle trajectory. The diameter of a Cherenkov radiation ring, as illustrated in Fig. 16.2, is a function of the distance of the origin of the conical wave front (Fig. 16.2A) to the position of measurement of the Cherenkov radiation ring (Fig. 16.2B). As will be discussed further on in this chapter, the photon ring can be imaged and its radius measured. The ring radius may be used to calculate the phase velocity of the charged particle when the index of refraction of the medium is known.

16.2 THEORY AND PROPERTIES

The theory explaining the production of Cherenkov radiation in various types of transparent media was provided by Frank and Tamm (1937), and many of the properties of Cherenkov radiation, upon which the theory was based, were demonstrated experimentally by Cherenkov (1934a,b, 1936, 1937a–d, 1938a–c). These studies are described in detail in the biographical sketches on Cherenkov, Frank, and Tamm in the Hall of Fame Section, Part VII in this book. A brief summary of the theory will be provided here.

16.2.1 Threshold Condition

The threshold condition for the production of Cherenkov radiation in a transparent medium is given by:

$$\beta n = 1 \qquad [16.1]$$

where β is the relative phase velocity of the particle (v/c), that is, the velocity of the particle (v) divided by the speed of light in a vacuum (c), and n is the refractive index of the medium (ie, the ratio of the velocity of light in a vacuum to its velocity in the medium). Only charged particles that possess:

$$\beta > 1/n \qquad [16.2]$$

produce Cherenkov photons in transparent media (Frank and Tamm, 1937). The value of β of the charged particle is dependent on its kinetic energy, as reported by Jelley (1962):

$$E = m_0c^2\left[\frac{1}{\left(1-\beta^2\right)^{1/2}} - 1\right] \qquad [16.3]$$

where m_0 is the particle rest mass in grams, c is the velocity of light in a vacuum (equal to 2.99×10^{10} cm/s), and E is the kinetic energy in ergs (where 1.602×10^{-12} erg = 1 eV). Eq. [16.3] can be solved for β to give the expression for the phase velocity of the particle as a function of its energy, or:

$$\beta = \left[1 - \left(\frac{1}{(E/m_0c^2)+1}\right)^2\right]^{1/2} \qquad [16.4]$$

The value of the rest energy for an electron is $m_0c^2 = (9.11 \times 10^{-28}\ \text{g})\ (2.99 \times 10^{10}\ \text{cm/s})^2 = 8.14 \times 10^{-7}$ erg. The energy in ergs may be converted to electron volts as follows: $(8.14 \times 10^{-7}\ \text{erg})/(1.602 \times 10^{-12}\ \text{erg/eV}) = 511$ keV. Substituting the value of 511 keV for m_0c^2 in Eq. [16.4] and solving for β gives:

$$\beta = \left[1 - \left(\frac{1}{(E/511\ \text{keV})+1}\right)^2\right]^{1/2}. \qquad [16.5]$$

Thus the value of β, where electrons or beta particles are concerned, is dependent upon the electron energy, E, in keV according to Eq. [16.5].

16.2.2 Threshold Energies

As noted above, the particle phase velocity, β, is a critical factor in the production of Cherenkov photons in a medium of given index of refraction, n, that is, Cherenkov radiation will occur only when $\beta > 1/n$. Consequently the particle energy, upon which the particle phase velocity is dependent, is a critical factor. Thus a minimum or threshold energy of the particle must be reached when traveling in a medium of given index of refraction before Cherenkov photons will be produced. If we apply the threshold value of β for the production of Cherenkov photons from Eq. [16.1], that is, $\beta = 1/n$, to Eq. [16.5], we will obtain the threshold energy that electrons or beta particles must possess for the production of Cherenkov radiation as a function of the index of refraction of the medium as:

$$E_{\text{th}} = 511\ \text{keV}\left[\left(1 - \frac{1}{n^2}\right)^{-1/2} - 1\right] \qquad [16.6]$$

When water is the transparent medium, where $n = 1.333$ (at 20°C at the sodium line, ie, 589.0 nm), the threshold energy for the production of Cherenkov photons by electrons or beta particles is calculated according to Eq. [16.6] to be 262 keV (or 0.262 MeV) as follows:

$$\begin{aligned} E_{\text{th}} &= 511 \text{ keV}\left[\left(1-\frac{1}{n^2}\right)^{-1/2}-1\right] \\ &= 511 \text{ keV}\left[\frac{1}{\sqrt{1-\frac{1}{(1.333)^2}}}-1\right] \\ &= 262 \text{ keV} \end{aligned}$$

Thus, only electrons or beta particles that possess energy in excess of 262 keV or 0.262 MeV produce Cherenkov photons in water. The value of refractive index n is wavelength and temperature specific, that is, the index of refraction will vary slightly according to the temperature and wavelength of measurement; however, the value of $n = 1.333$ is often used for water as measured at 20°C and with a wavelength of 589.0 nm.

We can write Eq. [16.6] in general terms for the calculation of the threshold energy of charged particles of any mass as follows:

$$E_{\text{th}} = m_0c^2\left[\left(1-\frac{1}{n^2}\right)^{-1/2}-1\right] \qquad [16.7]$$

where m_0 is the particle rest mass and c is the velocity of light in a vacuum (2.99×10^{10} cm/s).

As described in Eq. [16.7], the threshold energy for the Cherenkov effect (ie, Cherenkov photon production) will vary according to the particle rest mass and index of refraction of the medium. The energy required for the production of Cherenkov photons, E_{th}, increases with particle mass, and it will be lower for media of higher index of refraction. For example, according to Eq. [16.7], electrons or beta particles traveling through polyethylene plastic of refractive index $n = 1.52$ will have the following calculated threshold energy of 167 keV or 0.167 MeV, which is considerably lower than the threshold energy of 262 keV or 0.262 MeV for the production of Cherenkov photons in water:

$$\begin{aligned} E_{\text{th}} &= m_0c^2\left[\left(1-\frac{1}{n^2}\right)^{-1/2}-1\right] \\ &= \left(9.10938 \times 10^{-28} \text{ g}\right)\left(2.99792 \times 10^{10} \text{ cm/s}\right)^2\left[\frac{1}{\sqrt{1-\frac{1}{(1.52)^2}}}-1\right] \\ &= 8.18707 \times 10^{-7} \text{ ergs}\left[\frac{1}{\sqrt{0.5671745}}-1\right] \\ &= \left(\frac{8.18707 \times 10^{-7} \text{ ergs}}{1.602 \times 10^{-12} \text{ ergs/eV}}\right)\left[\frac{1}{0.753109}-1\right] \\ &= (0.5110 \times 10^6 \text{ eV})(0.3278) = 0.167 \text{ MeV or } 167 \text{ keV} \end{aligned} \qquad [16.8]$$

Thus the use of plastic, which has a higher index of refraction than water, as a counting medium through which beta particles must travel, will reduce the threshold energy for the production of Cherenkov photons and increase the detection efficiency of radionuclides measured by Cherenkov counting (L'Annunziata and Passo, 2002).

TABLE 16.1 Particle Threshold Energies in MeV for the Production of Cherenkov Photons in Media (Cherenkov Radiators) of Different Index of Refraction

Medium	Index of Refraction (n)	Particle Threshold Energy (MeV)[a]		
		Electron[b]	Muon[c]	Proton[d]
Air	1.00027712[e]	21.2	4380.9	38,925.9
Silica aerogel[f]	1.05	1.16	240.7	2139.0
Water	1.333	0.262	54.3	482.1
Glass[g]	1.47	0.186	38.5	341.9
Plastic[h]	1.52	0.167	34.6	307.6
Ceramic[i]	2.1	0.070	14.5	128.7
Diamond	2.4	0.051	10.6	93.9

[a] *Calculated according to Eq. [16.7].*
[b] *Energy equivalent mass of electron* (m_0c^2) = 0.511 *MeV.*
[c] *Energy equivalent mass of muon* (m_0c^2) = 105.6 *MeV.*
[d] *Energy equivalent mass of proton* (m_0c^2) = 938.3 *MeV.*
[e] *Index of refraction of air measured at the sodium D line at STP (Lide, 2010).*
[f] *Silica aerogel index of refraction* (n) *will vary according to mode of manufacture. The value of 1.05 is taken from experiments by Brajnik et al. (1994, 1995) and Pestotnik et al. (2002).*
[g] *Borosilicate glass tested for electrons or beta particles by L'Annunziata and Passo (2002).*
[h] *Polyethylene plastic tested for electrons or beta particles by L'Annunziata and Passo (2002).*
[i] *Commercial ceramic tested for electrons or beta particles by Takiue et al. (2004).*

Table 16.1 lists the calculated threshold energies of particles of differing mass in media of differing index of refraction calculated according to Eq. [16.7]. A medium within which Cherenkov photons are produced is referred to as a *Cherenkov radiator*.

Data in Table 16.1 illustrate that the threshold energy for a particular particle decreases in media of increasing index of refraction. Also, the threshold energy required for the production of Cherenkov photons in any particular medium increases proportionally with the mass of the particle. Thus, by the selection of a medium of given index of refraction, it is possible to discriminate between particles of different energies or mass.

16.2.3 Photon Spatial Asymmetry

An important property of Cherenkov radiation is its asymmetry, that is, the directional emission of the Cherenkov photons. Cherenkov radiation is not emitted in all directions. When Cherenkov (1936) discovered the asymmetric properties of this radiation, he knew he had discovered a type of radiation yet unknown. Frank and Tamm (1937) explained the spatial asymmetry of the radiation as a result of the charged particle traveling in a medium at a velocity exceeding the velocity of light in the medium. Frank and Tamm (1937) theorized that when the phase velocity of the charged particle, β, exceeded the reciprocal of the index of refraction, n, of the medium, that is, $\beta > 1/n$, Cherenkov photons are emitted as a cone at an angle, θ, to the direction of the charged particle, as depicted in Fig. VII.12A in the biographical sketches of Il'ja Frank and Igor Tamm and in Fig. 16.1B and 16.2 in this chapter. According to the theory of Frank and Tamm (1937) the angle, θ, of photon emission would be defined by the relationship:

$$\cos\theta = \frac{1}{\beta n} \qquad [16.9]$$

Cherenkov (1937b) tested the theory of Frank and Tamm (1937) using gamma rays directed at a vessel of water to create high-energy electrons in the water via the Compton effect (see Fig. VII.4). He then measured the angles of emission of the photons relative to the direction of the incident gamma radiation. Cherenkov found a broad range of photon emission angles in water with a maximum around 30°. The maximum angle of emission would depend on the phase velocity of the Compton electron, β, and thus on the energy of the electron. Although Cherenkov definitely was able to demonstrate the spatial asymmetry of the newly discovered photons, the Compton electrons unfortunately are not unidirectional and can display wide angles of deflection relative to the direction of the gamma rays that created them. Consequently Cherenkov's results were not precise enough to demonstrate irrefutably Frank and Tamm's theory that $\cos\theta = 1/\beta n$. It was not until

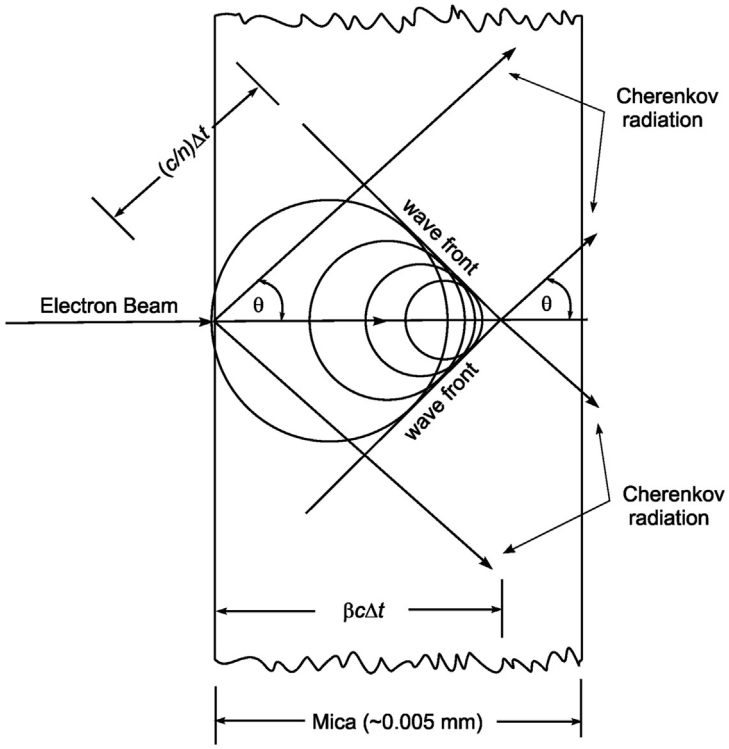

FIGURE 16.3 A thin section of mica used by Collins and Reiling (1938) and Wyckoff and Henderson (1943) as the transparent medium for the production of Cherenkov photons by a beam of high-energy electrons of uniform energy. The thin section of Cherenkov radiator would assure minimal loss of electron energy in traversing the mica.

mono-energetic electrons were used by researchers such as Collins and Reiling (1938) and Wyckoff and Henderson (1943) that the angle of photon emission, θ, could be accurately measured. They directed electrons of uniform energy into thin sections of transparent media such as mica, glass, cellophane, and water (see Fig. 16.3). A thin section of Cherenkov radiator assured insignificant loss of electron energy in traversing the medium.

According to the theory of Frank and Tamm (1937), the angle, θ, illustrated in Fig. 16.3, is defined by the equation:

$$\cos\theta = \frac{\text{distance of travel of radiation front in the medium}}{\text{distance of travel of charged particle in the medium}} \quad [16.10]$$

or:

$$\cos\theta = \frac{(\text{speed of light in the medium})(\Delta t)}{(\text{speed of particle in the medium})(\Delta t)} \quad [16.11]$$

where Δt is a time interval. Using the notation provided in Fig. 16.3, we can then write:

$$\cos\theta = \frac{(c/n)t}{\beta ct} \quad [16.12]$$

The term $(c/n)t$ represents the distance of travel of the radiation wave front measured by the product of the velocity of the light in the medium (c/n) and time (t), while the term βct measures the distance of particle travel according to $\beta ct = (v/c)ct = vt$, where v is the velocity of the particle in the medium, c the speed of light in a vacuum, and t is time. From Eq. [16.12] we obtain the expression:

$$\cos\theta = \frac{1}{\beta n}. \quad [16.13]$$

When $\beta = 1/n$, which is the threshold condition for the production of Cherenkov photons (Eq. [16.1]), the charged particle possesses a threshold energy where Cherenkov radiation is yet to be produced, that is, $\cos\theta = 1$ and $\theta = 0$.

When $\beta > 1/n$, the charged particle possesses sufficient energy and velocity to produce Cherenkov photons, which are emitted in the exact forward direction of the charged particle at an angle θ, as defined according to Eq. [16.13].

As the particle energy, E, of Eq. [16.4] increases to relativistic speeds, the value of β approaches unity and cos θ approaches $1/n$ of Eq. [16.13]. Thus, the maximum angle of emission of a Cherenkov photon produced by a charged particle in any transparent medium would occur when the charged particle possesses a high energy to the point where the value of β of Eq. [16.4] approaches unity, or:

$$\cos\theta = \frac{1}{n}, \text{ when } \beta \text{ approaches } 1, \qquad [16.14]$$

If we consider the case of mica as the transparent medium with index of refraction $n = 1.59$, such as that tested by Collins and Reiling (1938) and Wyckoff and Henderson (1943), the maximum possible angle of emission of Cherenkov photons in the mica are calculated to be:

$$\cos\theta = \frac{1}{1.59} = 0.6289$$

and:

$$\theta = 51.0^\circ$$

According to the theory of Frank and Tamm (1937), Cherenkov photons are emitted at more acute angles for charged particles just above their threshold energy and cannot exceed an emission angle of 51.0° in mica, even for the most energetic particles.

Collins and Reiling (1938) and Wyckoff and Henderson (1943) tested the theory of Frank and Tamm by shooting electrons of various energies at mica, and they measured accurately the angles of emission of the Cherenkov photons as a function of electron energy. They could then compare the experimentally obtained emission angles, θ, with those calculated according to the relation $\cos\theta = 1/\beta n$. The key component of their experimental arrangement illustrated in Fig. 16.4 included a conical mirror to reflect the Cherenkov photons such as that designed by Cherenkov (1937b) in his initial experiments with Compton electrons.

The theoretical angles of emission (θ) of Cherenkov photons produced by electrons in mica with an index of refraction, $n = 1.59$, are plotted in Fig. 16.5. According to the Frank and Tamm theory (1937), where $\cos\theta = 1/\beta n$, the theoretical angles of emission will vary from zero at the threshold electron energy to the highest emission angle for the relativistic electrons of highest energy where β approaches 1, its highest possible value. Collins and Reiling (1938) and Wycoff and Henderson (1943) found the experimentally measured angles of emission to agree very closely to the theoretical values over the electron energy range of 240 to 1900 keV within about 1 degree. In addition to mica, thin films of other transparent media of different index of refraction, including thin films of glass and cellophane, were tested by Wyckoff and Henderson (1943), and the measured and theoretically calculated values of θ agreed to within 1 degree. The slight

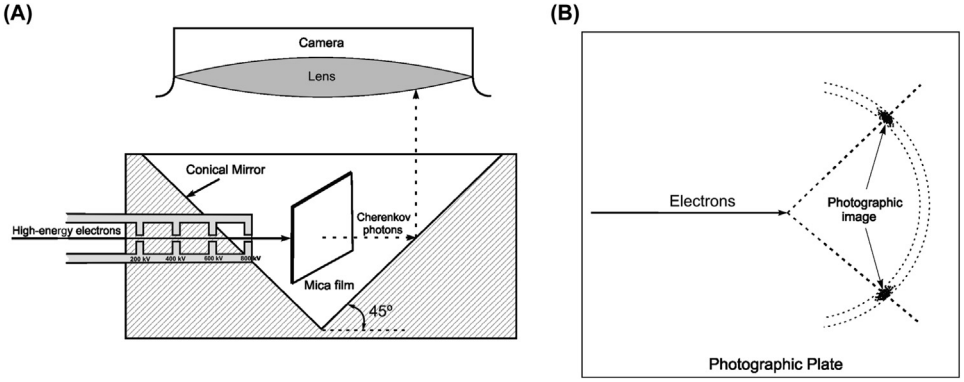

FIGURE 16.4 Basic experimental arrangement used by Collins and Reiling (1938) and Wyckoff and Henderson (1943) to demonstrate the relation $\cos\theta = 1/\beta n$. In (A) an electron gun provides electrons of uniform energy by accelerating electrons across potentials varying from 200 to 800 kV. Wyckoff and Henderson (1943) produced electrons with energies over the range of 240–815 keV and Collins and Reiling (1938) accelerated electrons up to 2000 keV. The electrons in (A) traverse the mica film and produce cones of Cherenkov radiation. The Cherenkov photons are produced only in the direction of the electrons, and the photons are reflected off the conical mirror toward the camera. The photographic plate in (B) provides two spots produced by the Cherenkov radiation cone reflected in two dimensions from which the angle θ can be calculated.

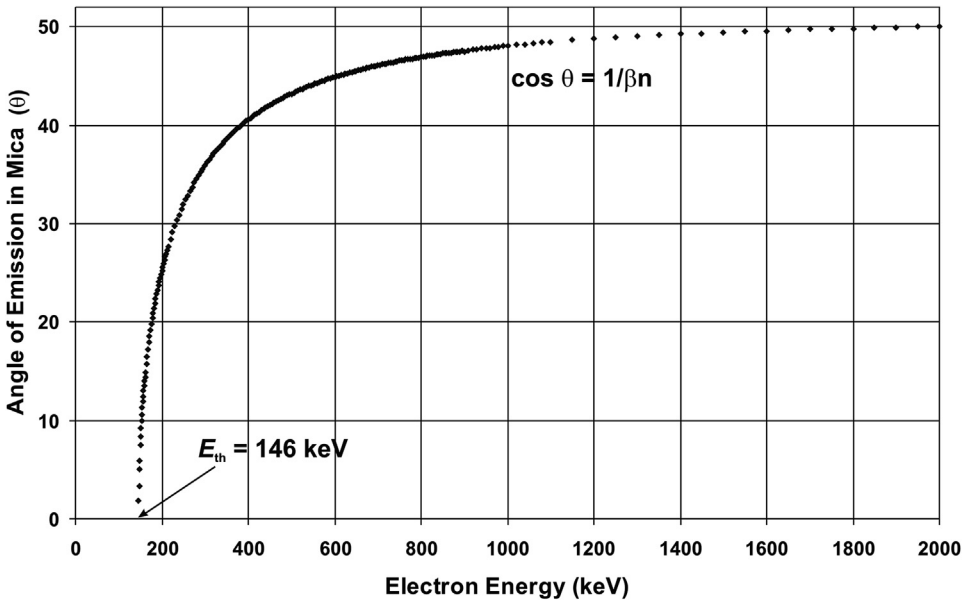

FIGURE 16.5 Cherenkov photon emission angles (θ) in mica of index of refraction, $n = 1.59$, as a function of electron energy calculated according to $\cos\theta = 1/\beta n$. The threshold energy E_{th} of electrons (146 keV) for the production of Cherenkov photons in the mica was calculated according to Eq. [16.7].

discrepancy between the measured and calculated values was considered due to slight unavoidable bending or imperfections of the thin films used.

We can conclude from the above that, for a particle of given mass and charge, the angle of emission of the Cherenkov photons will depend on the particle relative phase velocity (β), which is a function of its energy as well as the index of refraction of the medium. The maximum angle of emission of Cherenkov photons will, of course, differ for media of different index of refraction. In the fields of particle and nuclear physics, the Cherenkov effect has been exploited over the last decade for the identification of particles based on their velocity, which in any given medium of known index of refraction, will govern the angle of emission of the Cherenkov photons. The concepts of particle identification (PID) by measurement of Cherenkov emissions is discussed briefly later in this chapter and reviewed in detail by Va'vra (2000), Križan (2001), Joram (2002), and L'Annunziata (2012e).

16.2.4 Photon Spectrum and Radiation Intensity

Cherenkov radiation consists of a continuous spectrum of wavelengths extending from the near-ultraviolet region into the visible part of the spectrum, peaking at about 420 nm (Kulcsar et al., 1982; Claus et al., 1987). Only a negligible amount of photon emission is found in the infrared or microwave regions. In Cherenkov's early work (see Fig. VII.10 in Hall of Fame VII), he found the Cherenkov cone of radiation to comprise the visible spectrum. He observed specifically that the outer ring of the radiation cone was violet and its inner ring was red. Jelley (1958) explains that a medium is always dispersive, and consequently the radiation is restricted to those frequency bands for which $n(\omega) > 1/\beta$, where $n(\omega)$ is the index of refraction at a particular frequency band. Jelley adds that the absorption bands in media, which are transparent at visible wavelengths, limit the radiation to the near-ultraviolet and longer wavelengths.

In their classic interpretation of the Cherenkov effect, Frank and Tamm (1937) calculated the total energy, W, radiated by an electron via the Cherenkov effect through a cylindrical region of medium of length, l, where the axis of the cylinder coincided with the line of motion of the electron. Under the assumption that β is constant over a short length, dl, of the electron track, they derived the equation:

$$W = \frac{e^2 l}{c^2} \int_{\beta n > 1} \omega d\omega \left(1 - \frac{1}{\beta^2 n^2}\right) \qquad [16.15]$$

where ω is the frequency of the Cherenkov radiation. The lower limit of the integral, $\beta n > 1$, is the threshold condition for the production of Cherenkov photons in any medium. Frank and Tamm (1937) established the equation to be valid provided that l should be large in comparison with the wavelength λ of the Cherenkov radiation emitted. Cherenkov (1938c)

took Eq. [16.15] of Frank and Tamm and evaluated the energy, W, radiated by an electron taking under consideration that the magnitude of the electron velocity, ie, the magnitude of β, will vary greatly over the entire path length of travel of the electron. Cherenkov (1938c) thus expressed Eq. [16.15] with β as a variable depending on its length of travel l or:

$$W = \frac{e^2}{c^2}\int \omega d\omega \int_{\beta n>1}\left(1-\frac{1}{\beta^2 n^2}\right)dl \qquad [16.16]$$

Frank and Tamm (1937) thus calculated the rate of radiated energy per path length of travel, dW/dl, to be of the order of only several kilovolts per centimeter. Thus it was found that the electron or beta-particle energy loss via the emission of Cherenkov radiation would be a negligible quantity of energy in comparison to the energy lost by the electron by other mechanisms such as ionization. Cherenkov (1938c) confirmed this through calculations and experimentation and concluded that the radiation expended by β-particles from Ra(B + C) via the emission of Cherenkov radiation amounts to only a value of the order of only 0.1% of the total energy of the particles.

From Eq. [16.15] Frank and Tamm (1937) deduced the equation for the Cherenkov photon radiation intensity, ie, the number of photons emitted by an electron per path length of travel, as follows:

$$dN = 2\pi\alpha\left(\frac{1}{\lambda_2}-\frac{1}{\lambda_1}\right)\left(1-\frac{1}{\beta^2 n^2}\right)dl \qquad [16.17]$$

where dN is the number of photons emitted in path length dl within the spectral region defined by the wavelengths λ_1 and λ_2, α is the fine structure constant $\sim 1/137$, and β and n are the particle-phase velocity and the index of refraction of the medium, respectively. From Eq. [16.17], Belcher (1953) assumed the index of refraction to be constant over the spectral range studied and expressed the total number, N_E, of photons radiated along the track of a particle of initial energy E and brought to rest within the medium as:

$$N_E = 2\pi\alpha\left(\frac{1}{\lambda_2}-\frac{1}{\lambda_1}\right)\int_{\beta=\beta_{\max}}^{\beta=1/n}\left(1-\frac{1}{\beta^2 n^2}\right)dl \qquad [16.18]$$

where $\beta_{\max}$ is the maximum phase velocity, ie, the initial velocity of the particle, and $1/n$ is the limiting phase velocity of the particle, ie, the velocity at which Cherenkov photons cease to be produced. Belcher (1953) reduced Eq. [16.18] to read:

$$N_E = A\int_{\beta=\beta_{\max}}^{\beta=1/n}\left(1-\frac{1}{\beta^2 n^2}\right)dl \qquad [16.19]$$

where $A = 2\pi\alpha(1/\lambda_2 - 1/\lambda_1)$. For the spectral range of $\lambda_2 = 3000$ to $\lambda_1 = 7000$ Å, the value of A is calculated to be:

$$A = 2\pi\alpha\left(\frac{1}{\lambda_2}-\frac{1}{\lambda_1}\right) = 2(3.14)(0.007297)\left(\frac{1}{3\times10^{-5}\text{ cm}}-\frac{1}{7\times10^{-5}\text{ cm}}\right) = 874\text{ cm}^{-1} \qquad [16.20]$$

Over the defined spectral range, Eq. [16.19] is reduced to:

$$N_E = 874\int_{\beta=\beta_{\max}}^{\beta=1/n}\left(1-\frac{1}{\beta^2 n^2}\right)dl \qquad [16.21]$$

Belcher (1953) evaluated the integral defined by Eq. [16.21] by firstly determining the range-energy function for an electron in water ($n = 1.33$ and $\rho = 1.00$ g/cm^3) and Perspex plastic ($n = 1.50$ and $\rho = 1.18$ g/cm^3). He plotted the values of $(1 - 1/\beta^2 n^2)$ against the range of electrons in water and Perspex plastic. He then evaluated Eq. [16.21] by graphical integration to obtain the expected values of N_E as a function of electron energy in water or Perspex plastic, which is illustrated in Fig. 16.6. As can be seen in Fig. 16.6, photons are not produced by electrons below 0.175 MeV in the Perspex plastic or 0.260 MeV in water, which are the respective threshold energies for the Cherenkov effect in these two materials.

Frank and Tamm (1937) made an approximate calculation that a 500-keV electron, which would correspond to $\beta^2 = 0.75$, traveling in water, where $n = 1.33$, would produce approximately 10 photons per 0.1 cm within the visible region between $\lambda_1 = 4000$ Å and $\lambda_2 = 6000$ Å (see Eqs. [VII.16] in the previous section, Hall of Fame VII). Their approximation came very close to the above calculations of Belcher (1953), which indicate that a 0.500-MeV electron would produce approximately 20 photons in water (Fig. 16.6). With a range of 0.2 cm in water, the rate of photons production by a 0.5-MeV electron would be 10 photons per 0.1 cm.

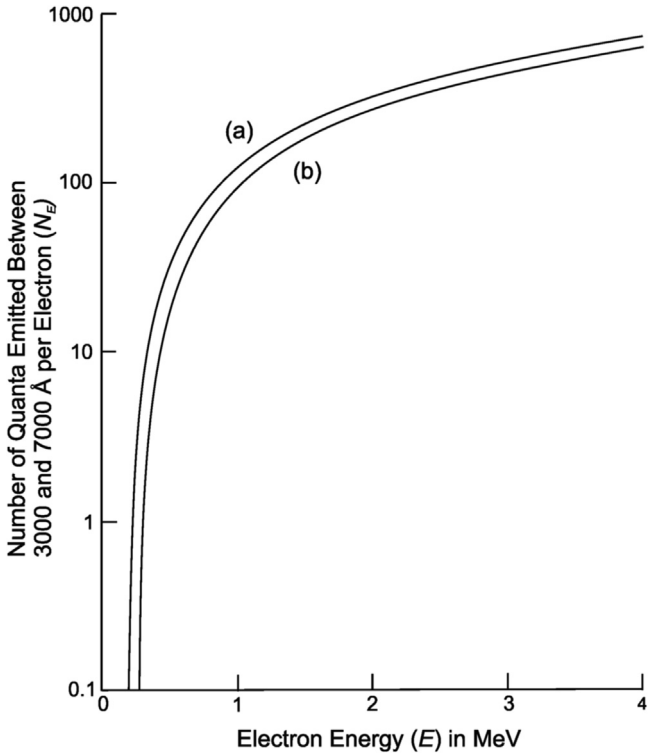

FIGURE 16.6 A plot of the number of Cherenkov photons in the spectral range of 3000−7000 Å produced by an electron in (a) Perspex plastic ($n = 1.50$) and (b) water ($n = 1.33$) over its entire range of travel as a function of electron energy. *From Belcher, E.H., 1953. The luminescence of irradiated transparent media and the Cerenkov effect. I. The luminescence of aqueous solutions of radioactive isotopes. Proc. Royal Soc. London Ser. A 216 (1124), 90−102 by Permission of the Royal Society.*

The above calculations for the number of photons emitted as a function of a single electron of known energy in a transparent medium are more complex when dealing with β-particles. This is so because β-particles are emitted from radioactive isotopes with a broad spectrum of energies between 0 and E_{max}, as depicted graphically in Fig. 6.1 of the chapter entitled "Beta Radiation and Beta Decay." In such a case, Belcher (1953) noted that it is necessary to combine the function N_E of Eq. [16.18] or [16.19] with the energy distribution function of the electrons released within the medium. He therefore elaborated that, if p_E is the probability of release of an electron possessing energy between the limits E and $(E + dE)$, then the average total intensity I of Cherenkov photon emission per electron is given by the following:

$$I = \int_0^{E_{max}} p_E N_E dE. \qquad [16.22]$$

The property of photon intensity is of particular relevance in studies on the measurement of Cherenkov radiation for Particle identification (PID) and radionuclide analysis, a subject to be dealt with later in this chapter. The photon intensity is also expressed in terms of the number of Cherenkov photons created per unit photon energy. As noted by Križan (2001) for particles above the threshold $\beta = 1/n$, that is $\beta > 1/n$, the number of Cherenkov photons emitted per unit photon energy in a medium of particle path length L is:

$$\frac{dN}{dE} = L\frac{\alpha}{\hbar c}\sin^2\theta \qquad [16.23]$$

where α is the fine structure constant (1/137), $\hbar$ is Planck's constant divided by 2π (ie, $h/2\pi = 6.582 \times 10^{-16}$ eV s), c is the speed of light in a vacuum or 2.998×10^{10} cm/s, and θ is, as previously defined, the angle of emission of the Cherenkov photons relative to the direction of travel of the charged particle. Taking the values of the aforementioned constants, the term $\alpha/\hbar c$ of Eq. [16.23] becomes 370 eV^{-1} cm^{-1}. From Eq. [16.23], Križan (2001) calculated that in 1 cm of water, a particle track where $\beta = 1$ (ultra-relativistic or most energetic particle possible) emits $N = 320$ photons in the

spectral range of visible light ($\Delta E \approx 2$ eV). Since the high-energy electron (eg, 1000 GeV) does not lose significant energy in 1 cm of water, otherwise the angle of emission would diminish as the electron loses energy and its velocity reduces, the above number of 320 photons is calculated as follows:

Since the angle of emission θ of the Cherenkov photons for a particle of given energy and velocity is defined by:

$$\cos\theta = \frac{1}{\beta n} \qquad [16.24]$$

and, because the charged particle at ultra-relativistic speeds approaches the speed of light in a vacuum or β approaches 1, we can write:

$$\cos\theta = \frac{1}{n} \qquad [16.25]$$

If water is the medium:

$$\cos\theta = \frac{1}{1.33} = 0.7518 \qquad [16.26]$$

and then:

$$\cos^{-1} 0.7518 = 41.3^\circ \qquad [16.27]$$

Thus the number of photons emitted (ΔN) over the energy range of the visible spectrum ($\Delta E \approx 2$ eV) in the particle path length of 1 cm in water is calculated according to Eq. [16.23] as:

$$\begin{aligned} \Delta N &= L\frac{\alpha}{\hbar c}\sin^2\theta\,\Delta E \\ &= (1\text{ cm})\left(370\text{ eV}^{-1}\text{cm}^{-1}\right)\left(\sin^2 41.3^\circ\right)(2\text{ eV}) \\ &= 320\text{ photons} \end{aligned} \qquad [16.28]$$

In the instrumental detection of individual Cherenkov photons there is an efficiency factor, which defines the efficiency of an instrument to detect the photons. With an average instrumental detection efficiency of $\varepsilon = 0.1$ over the spectral interval in the example given above, only $N = 32$ photons would be measured. The detection efficiency for Cherenkov photons should not be confused with the term counting efficiency of each particle that interacts with the medium, which is employed in radionuclide analysis, as it will be seen in this chapter that Cherenkov counting efficiencies can be >70% or >0.70.

The number of photons emitted per path length of electron travel in the wavelength interval between λ_1 and λ_2 is calculated by Sowerby (1971) according to:

$$\frac{dN}{dl} = 2\pi\alpha Z^2\left(\frac{1}{\lambda_2} - \frac{1}{\lambda_1}\right)\sin^2\theta \qquad [16.29]$$

where α is the fine structure constant ($e^2/\hbar\, c = 1/137$), z is the particle charge ($z = 1$ for electrons or beta particles), and the refractive index of the medium and particle velocity appear in the $\sin^2\theta$ term. Over the visible range of wavelengths from $\lambda_2 = 400$ to $\lambda_1 = 700$ nm, Eq. [16.29] becomes:

$$\begin{aligned} \frac{dN}{dl} &= 2(3.14)(0.007297)(1)^2\left(\frac{1}{4\times10^{-5}\text{ cm}} - \frac{1}{7\times10^{-5}\text{ cm}}\right)\sin^2\theta \\ &= 490\sin^2\theta\text{ cm}^{-1} \end{aligned} \qquad [16.30]$$

Sundaresan (2001) estimated the number of photons N per path length L to be:

$$N/L = 490\sin^2\theta\text{ cm}^{-1}, \qquad [16.31]$$

The emission angle θ would diminish as the particle loses energy and velocity. It can be considered constant over particle path lengths where the particle does not undergo significant energy loss.

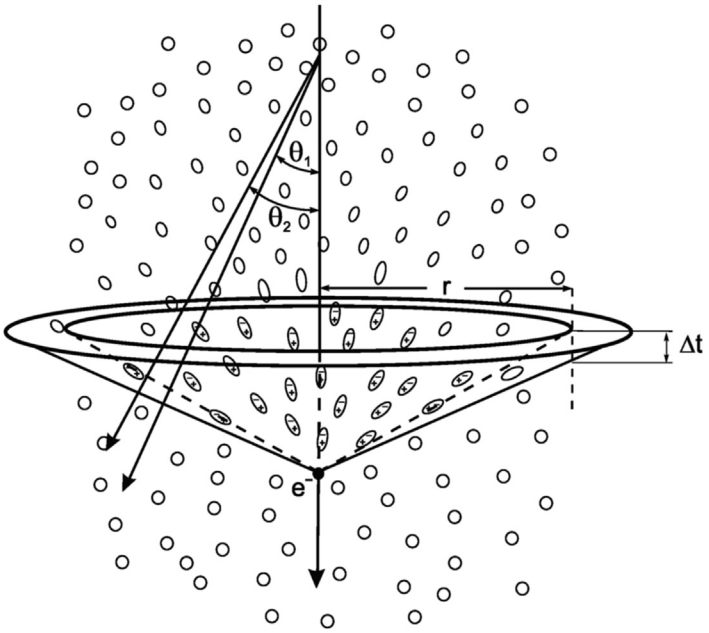

FIGURE 16.7 Depiction of the production of Cherenkov radiation in a dispersive medium and the resulting wave front expansion. The wave front spreading lengthens the excitation pulse on a time scale that is small in comparison to fluorescence decay. Δt is the duration of the light pulse along a line parallel to the axis of the particle at a distance r from the axis. *From Burden, D.L., Hieftje, G.M., 1998. Cerenkov radiation as a UV and visible light source for time-resolved fluorescence. Anal. Chem. 70 (16), 3426–3433, reprinted with permission © 1998 American Chemical Society.*

16.2.5 Duration of Cherenkov Light Flash

The Cherenkov effect is the result of a physical disturbance caused by a high-energy charged particle along its path of travel resulting in a directional anisotropic emission of light. Therefore, there is no chemical fluorescence nor the relatively long excitation decay times associated with fluorescence. Jelley (1958) and Burden and Hieftje (1998) calculated the width of a typical Cherenkov-generated pulse, or in other words, the duration of the photon flash, Δt, depicted in Fig. 16.7, which is a function of the spread of the Cherenkov wave front and the position of observation with respect to the particle trajectory. They approximated the duration of a the light pulse, Δt, over the range of Cherenkov photon wavelengths λ_2 and λ_1 observed at a distance r parallel to the particle path, as illustrated in Fig. 16.7, according to the following:

$$\Delta t = \frac{r}{\beta c}\left(\sqrt{\beta^2 n^2(\lambda_2) - 1} - \sqrt{\beta^2 n^2(\lambda_1) - 1}\right) \quad [16.32]$$

and:

$$= \frac{r}{\beta c}(\tan\theta_2 - \tan\theta_1) \quad [16.33]$$

Cherenkov radiation would encompass the entire spectrum of visible radiation as noted by Cherenkov (1958) whereby the inner ring of the Cherenkov cone would be red (longer wavelength) and the outer limit of the cone would be violet (shorter wavelength). Jelley (1958) calculated a flash duration $\Delta t = 5 \times 10^{-12}$ s for a light flash observed between the wavelength limits of 4000 Å (violet) and 6000 Å (orange) at a distance $r = 10$ cm to the side of the track of a fast electron traversing water where $\beta = 1$, average value of index of refraction $\overline{n} = 1.33$, the angle of emission at its maximum value of 41 degree. Burden and Hieftje (1998) calculated a light pulse duration $\Delta t = 326$ fs or 0.326×10^{-12} s for a 1-MeV electron traversing water where the light pulse is detected at a distance $r = 1$ cm parallel to the particle path of travel between the wavelengths of 300 and 350 nm or 3000 and 3500 Å.

16.3 CHERENKOV PHOTONS FROM GAMMA-RAY INTERACTIONS

Cherenkov (1934) discovered the radiation named after him by directing γ-rays from a radium source into pure transparent media such as water and other pure solvents. Gamma radiation produces Cherenkov photons indirectly through mostly Compton interactions, as the gamma radiation travels through the transparent medium. Compton electrons produce the Cherenkov photons provided they possess the threshold energy for Cherenkov photon production in the transparent medium (see Table 16.1).

A practical application is the measurement of Cherenkov photons in gamma-ray detection by the Cherenkov verification technique used in nuclear safeguards to verify the authenticity of irradiated nuclear fuel, which is one of the important tasks performed by the International Atomic Energy Agency (IAEA). The IAEA nuclear safeguards program audits the national declarations of nuclear fuel inventories to insure that no illicit diversion of nuclear material has occurred. High levels of gamma radiation are emitted by fission products in irradiated nuclear fuel. The irradiated fuel stored under water will produce Cherenkov light as a result of Compton scattering in the water surrounding the fuel. A Cherenkov Viewing Device containing a UV-transmitting lens coupled to a UV-sensitive charge-coupled device and image monitor enables the real-time imaging of the UV light portion of the Cherenkov radiation in the presence of normal room lighting (Attas et al., 1990, 1992; Attas and Abushady, 1997; Kuribara, 1994; Kuribara and Nemeto, 1994; Lindsey et al., 1999; IAEA, 2003; Chen et al., 2007; Håkansson and Jonter, 2007; Molander, 2008; Zendel, 2008; Grape et al., 2010). The presence of fission products and the nature of their distribution, as indicated by the Cherenkov glow, are used as evidence of fuel verification.

16.4 PARTICLE IDENTIFICATION

Cherenkov counters are applied in particle physics research for the determination of particle mass (m) and velocity (β) for particle identification (PID). Cherenkov detectors of various designs are applied to the discrimination and identification of high-energy particles, among which are (1) threshold and differential Cherenkov counters, (2) ring-imaging Cherenkov (RICH) detectors, and (3) Cherenkov counters that utilize time-of-propagation (TOP) and time-of-flight (TOF) measurements. Extensive reviews of the applications of Cherenkov detectors to PID are available in the journal literature, including Ullaland (2003), Va'vra (2003), Križan (2007, 2009), Websdale (2008), Iijima (2010), Engelfried (2011), Lippmann (2011), and Nappi (2011). A concise overview of the principles and techniques applied to the application of the Cherenkov effect to PID will be given here. For more comprehensive coverage of the instrumentation and techniques, the reader may peruse the extensive review articles cited above.

16.4.1 Threshold Cherenkov Counters

Threshold Cherenkov counters consist of Cherenkov detectors of differing refractive index, which may be utilized to discriminate particles of different mass based on the differing Cherenkov threshold energies that the detectors possess for the particles. For example, if we consider a beam of two types of particles of different mass (m), such as pions ($\pi^{\pm}$, $m = 139.6\ \text{MeV}/c^2$) and kaons ($K^{\pm}$, $m = 493.7\ \text{MeV}/c^2$), a Cherenkov detector may be selected of a given refractive index (n) such that the particle of higher mass does not produce Cherenkov radiation. This would be the case, if the threshold condition for the production of Cherenkov radiation is not met by the particle of higher mass, that is, $\beta < 1/n$. Sundareson (2001) describes another example of the application of two Cherenkov detectors of different refractive index, namely silica aerogel ($n = 1.01-1.03$) and pentane ($n = 1.357$), whereby particles of lower mass, such as 10-GeV kaons ($m = 493.7\ \text{MeV}/c^2$), produce Cherenkov photons in the two Cherenkov detector media, whereas particles of higher mass such as protons ($m = 939.3\ \text{MeV}/c^2$) produce Cherenkov photons only in the silica aerogel. Siudak et al. (2008) describe the use of a threshold Cherenkov detector of silica aerogel with refractive index $n = 1.05$, which exhibits a very high detection efficiency for pions with momenta $\geq$900 MeV/c. Thus, to detect K^{+} particles, a huge background of scattered pions could be suppressed using the aerogel Cherenkov detectors. Only the pions would produce Cherenkov photons; the kaons were below the threshold velocity. Adachi et al. (1995) describe a threshold Cherenkov counter for the identification of $\pi^{\pm}$ and $K^{\pm}$ in a particle beam. Silica aerogel with refractive index of 1.0127 with 14 cm thickness was used as the detector and photomultiplier tubes (PMTs) for the measurement of Cherenkov photons. The threshold momentum for the detection of $\pi^{\pm}$ and $K^{\pm}$ was determined to be 0.863 GeV/c and 3.05 GeV/c, respectively.

Two threshold Cherenkov detectors operated in tandem are described by Asaturyan et al. (2005) for the identification of $\pi/K/p$ particles. Two different aerogel materials were used with index of refraction $n = 1.030$ and 1.015, respectively.

TABLE 16.2 Threshold Momenta (P_{th} in GeV/c) for Particles in Two Aerogel Threshold Detectors of Refractive Index n

Type of Particle	P_{th} in $n = 1.030$	P_{th} in $n = 1.015$
μ	0.428	0.608
π	0.565	0.803
K	2.000	2.840
P	3.802	5.379

Reprinted from Asaturyan, R., et al., 2005. The aerogel threshold Cherenkov detector for the high momentum spectrometer in hall C at Jefferson Lab. Nucl. Instrum. Methods Phys. Res. Sect. A 548, 364–374, with permission from Elsevier © 2005.

The threshold momenta P_{th} in units of Gev/c for muons, pions, kaons, and protons in the two types of aeorogel detector materials are provided in Table 16.2.

The minimum momentum (ie, threshold momentum) at which a particle of mass, m, will exceed the phase velocity of light in the medium and produce Cherenkov photons, is a function of the particle mass and refractive index of the medium, n, as described by Asaturyan et al. (2005) according to the expression:

$$P_{\min}c = \frac{mc^2}{\sqrt{n^2-1}} \qquad [16.34]$$

where c is the speed of light in a vacuum. For example, the minimum momentum, $P_{\min}$, of the muon for the production of Cherenkov photons in aerogel of refractive index, $n = 1.030$, would be calculated as follows:

The energy equivalence of the muon mass, $m_\mu c^2 = 105.658$ MeV, is obtained from tables of physical constants (NIST, 2011) or calculated according to Eqs. [B.7]–[B.10] described in the chapter entitled "Basic Concepts and Definitions" of this book; and the minimum (threshold) muon momentum in the aerogel detector with index of refraction $n = 1.030$ is calculated as:

$$\begin{aligned} P_{\min}c &= \frac{m_\mu c^2}{\sqrt{n^2-1}} \\ &= \frac{105.658\ \text{MeV}}{\sqrt{(1.030)^2-1}} \\ &= 428.14\ \text{MeV} \\ P_{\min} &= 0.428\ \text{GeV}/c \end{aligned} \qquad [16.35]$$

which is equivalent to the value quoted in Table 16.2. An aerogel detector with refractive index $n = 1.015$ will yield a minimum muon momentum for the Cherenkov effect of 0.608 GeV calculated according to Eq. [16.34].

The difference in count rates from Cherenkov photons produced in the two detectors yields the relative numbers of the heavier and lighter particles. This is illustrated by Fig. 16.8, which is a plot of the number of photoelectrons (N_{pe}) collected by PMT photon detectors as a function of particle momentum (P) in GeV/c. From the figure it can be seen that the $n = 1.030$ aerogel will permit good pion/proton discrimination up to 4 GeV/c, while the $n = 1.015$ aerogel material can be used for pion/kaon discrimination in the momentum range of 1–3 GeV/c, and for pion/proton discrimination up to 6 GeV/c (Asaturyan et al., 2005).

As described previously in this chapter by Eq. [16.17], the number of Cherenkov photons emitted per path length of travel in the wavelength range of λ_1 and λ_2 is a function of the particle velocity β and the refractive index n of the medium or Cherenkov radiator, that is:

$$\frac{dN}{dl} = 2\pi\alpha Z^2\left(\frac{1}{\lambda_1}-\frac{1}{\lambda_2}\right)\left(1-\frac{1}{\beta^2 n^2}\right) \qquad [16.36]$$

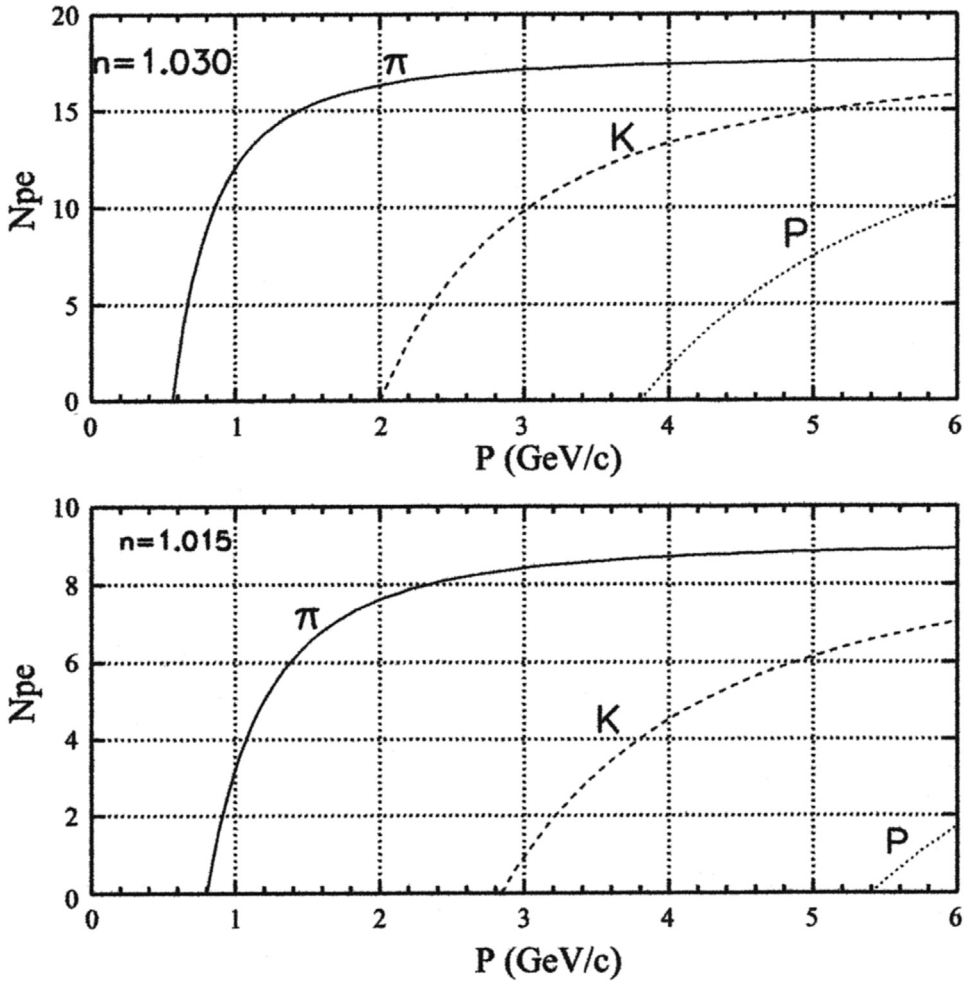

FIGURE 16.8 Particle separation using aerogel Cherenkov detectors with an index of refraction $n = 1.030$ (top) and $n = 1.015$ (bottom). Electrons (positrons) are above threshold over essentially the full momentum range. *Reprinted from Asaturyan, R., et al., 2005. The aerogel threshold Cherenkov detector for the high momentum spectrometer in hall C at Jefferson Lab. Nucl. Instrum. Methods Phys. Res. Sect. A 548, 364–374, with permission from Elsevier © 2005.*

where α is the fine structure constant (1/137) and Z is the charge on the particle. In most cases, $Z = 1$; and this term is often omitted from the equation; and the dependence of n on wavelength is ignored. As described by Asaturyan et al. (2005) and Denisov and Stoyanova (2006), Eq. [16.36] reduces to the expression for the number of Cherenkov photons produced by a particle of charge ($Z = 1$) per particle path length (L) of travel in the wavelength region between λ_1 and λ_2 to the following:

$$N = 2\pi\alpha L\left(\frac{1}{\lambda_1} - \frac{1}{\lambda_2}\right)\sin^2\theta \qquad [16.37]$$

where θ is given by the well-known expression $\cos\theta = 1/\beta n$.

All Cherenkov photons are not detected by the photodetectors; and thus the reflectivity M of a diffuse light box and the aerial fraction ε of coverage by the photodetectors must be included, as described by Carlson (1986), Poelz (1986), and Asaturyan et al. (2005), to give the expression for the average number of photons hitting the photomultuplier tubes, N_e, as:

$$N_e = 2\pi\alpha L\left(\frac{1}{\lambda_1} - \frac{1}{\lambda_2}\right)\left(1 - \frac{1}{\beta^2 n^2}\right)\frac{\varepsilon}{1 - M(1-\varepsilon)} \qquad [16.38]$$

From Eqs. [16.37] and [16.38], the number of Cherenkov photons detected is usually expressed as:

$$N_e = N_0 L \sin^2 \theta \qquad [16.39]$$

where N_e is similar to N_{pe} in Fig. 16.8, and N_0 is the "figure-of-merit" or "quality factor," characterized by Engelfried (2011) and Lippmann (2011) as the figure that describes the quality and wavelength interval of the photon detection system including the efficiency of light transmission, collection, and detection. Typical values of N_0 are between 30 and 180 cm^{-1} (Lippmann, 2011).

A gaseous carbon dioxide Cherenkov threshold detector has been designed for the measurement of 16.75-MeV gamma rays that accompany deuterium−tritium fusion (Mack et al., 2003, 2006; Caldwell et al., 2003; Kim et al., 2009b). The deuterium−tritium fusion reaction is discussed in detail in the chapter entitled "Radioactivity and Our Well-Being." The fusion reaction generally results in the release of 17.58-MeV energy with the emission of a 14-MeV neutron and 3.5-MeV alpha particle. Alternatively, 16.75-MeV gamma rays may accompany the deuterium−tritium fusion with a branching ratio on the order of $10^{-5}\gamma$/14 MeV neutron (Herrmann et al., 2010). Although the gamma-ray emission is less abundant, the observed high-energy gamma-ray signal in the Cherenkov detector is proportional to the observed 14-MeV fusion neutron yield and independent of neutron-induced gamma rays (Mack et al., 2003, 2006). The Cherenkov detection energy threshold is set by the pressure of the CO_2 gas, which detects the high-energy Compton electrons.

A Cherenkov detector arrangement reported by Perrino et al. (2001) provides an example of two Cherenkov detectors operated in tandem together with time-of-flight (TOF) measurements to discriminate between pions (π^+), positrons (e^+), and protons (p^+). The experimental setup consisted of a CO_2 gas detector ($n = 1.00041$) providing excellent detection for positrons, and a silica aerogel detector with a refractive index $n = 1.025$ providing (π, p) discrimination in the 1−4 GeV/c range with Cherenkov thresholds of 0.62 and 4.2 GeV/c for pions and protons, respectively. Pions and protons at 1 and 2 GeV/c are below the Cherenkov threshold in the CO_2 gas. Complementary data provided by TOF measurements between two BC408 scintillation detectors separated at a 23 m distance along the particle beam enabled the tagging of protons. TOF measurements are determined by signals between detectors permitting the determination of the speed of a particle, and with its total energy signal, the mass of the ion can be identified (Lilley, 2001).

Dual Cherenkov threshold detectors with aerogel radiators having two different refractive indices, $n = 1.015$ and 1.008, were designed by Allkofer et al. (2007, 2008) to operate in tandem to discriminate between kaons and protons in the momentum range of 4 to 8 GeV. Diffuse reflector foils coated with wavelength shifter increased the Cherenkov light yield by 50%. To discriminate between pions and kaons in the same 4 to 8 GeV momentum range, Horikawa et al. (2008) designed a threshold Cherenkov detector using perfluorobutane (C_4F_{10}) gas radiator, which has a refractive index $n = 1.00137$ at the 300-nm wavelength. In the C_4F_{10} gas, kaons are well below the threshold for the Cherenkov effect in the entire 4 to 8 GeV momentum range.

16.4.2 Ring Imaging Cherenkov Counters

The ring imaging Cherenkov (RICH) detector is designed principally for PID, as it can provide information on the velocity, β, and the charge of the particle, z; and complementary information provided by rigidity measurements using a magnetic tracker can provide the identity of the particle according to its mass (Pinto da Cunha, 2000). The accurate measurement of Cherenkov ring images for the determination of particle velocities was a major advancement in particle physics, as the particle velocity together with other particle properties mentioned above would lead to the identification of particles. The possibility of precisely measuring the dimensions of a Cherenkov ring image together with instrumental design proposals and calculations for the determination of particle velocities of electrons, muons, pions, kaons, and protons may be attributed to Arthur Roberts (1960 a,b). In one of his very detailed papers, Roberts (1960b) states the following:

> *A new type of Čerenkov radiation detector is proposed, in which the light emitted by a single particle traversing a radiator is imaged, by means of a lens or mirror focused at infinity, on the cathode of an image intensifier tube. The image is a ring, whose diameter measures accurately the Čerenkov cone angle, and thus the particle velocity. In addition the coordinates of the center of the circular image accurately indicate the orientation of the particle trajectory…*

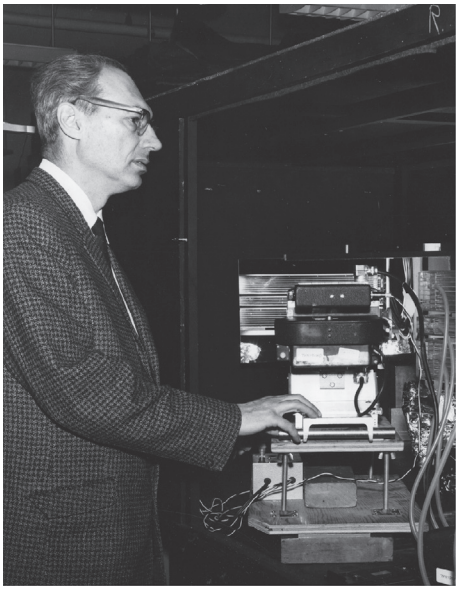

Arthur Roberts (1912–2004), circa 1963 at the High Energy Physics Division, Argonne National Laboratory. Arthur Roberts adjusting a spark-chamber test setup of the High Energy Physics Division of the Argonne National Laboratory. Printed with permission of Argonne National Laboratory, courtesy of AIP Emilio Segre Visual Archives

Some early designs of RICH detectors included the use of optical lenses to focus the Cherenkov photons as a ring image onto a photon-imaging plane, as described by Giese et al. (1970). Much of the pioneering work on RICH detectors was carried out by Thomas Ypsilantis and Jaques Sequinot (see Sequinot and Ypsilantis, 1977), and thorough treatments on the theory of RICH counters are available from Sequinot and Ypsilantis (1994) and Ypsilantis and Sequinot (1994). Several detector geometries and designs are reviewed by Glässel (1999), Ullaland (2003), Križan (2007), Iijima (2010), Kerzel (2010), and Engelfried (2011).

The classic spherical-mirrored RICH detector, reviewed by Sequinot and Ypsilantis (1977), was designed to accept particles that originate from any 4π direction; and this classical RICH geometry is illustrated in Fig. 16.9. The illustration shows a particle trajectory passing through a Cherenkov radiator of refractive index n enclosed in a spherical mirror. The Cherenkov photon detector has a concentric spherical surface of smaller radius. The space between the outer surface of the photon detector and inner spherical mirror is filled with a transparent medium of a given refractive index (eg, gas, C_4F_{10} ($n = 1.0015$), liquid, C_6F_{14} ($n = 1.276$), crystalline NaF ($n = 1.33$), or silica aerogel ($n = 1.01-1.02$)) to serve as the Cherenkov radiator (Pinto da Cunha et al., 2000). The Cherenkov radiator is chosen according to the mass and momenta of the particles to be identified, as the emission of Cherenkov radiation at an angle θ (or θ_c of Fig. 16.10) must satisfy the threshold condition $\beta > 1/n$. At the moment the particle penetrates the Cherenkov radiator, the Cherenkov radiation is emitted at an angle θ_c according to the particle velocity, β, and the refractive index (n) of the Cherenkov radiator as defined by Eq. [16.9] previously in this chapter, that is, $\cos\theta_c = 1/\beta n$. The radiator dimensions used by Pinto da Cunha et al. (2000) were 2 cm thickness and 50 cm radius. The Cherenkov photons are reflected off the inner surface of the outer spherical mirror as a ring of light onto the conical detector surface. The ring has a radius, r, which is measured to determine the particle velocity or particle mass, if its momentum is measured. An imaging detector is used to provide an image of the ring of Cherenkov light and its coordinates relative to the vertex.

As described by Engelfried (2011), the Cherenkov photons emitted under the angle θ_c are focused (in a small-angle approximation) by the spherical mirror of radius R onto a focal sphere of radius $R/2$, whereby the focal length $f = R/2$, upon which the photons form a ring of radius r (see Fig. 16.9) defined by the equation:

$$r = f\tan\theta_c = \frac{R}{2}\tan\theta_c \qquad [16.40]$$

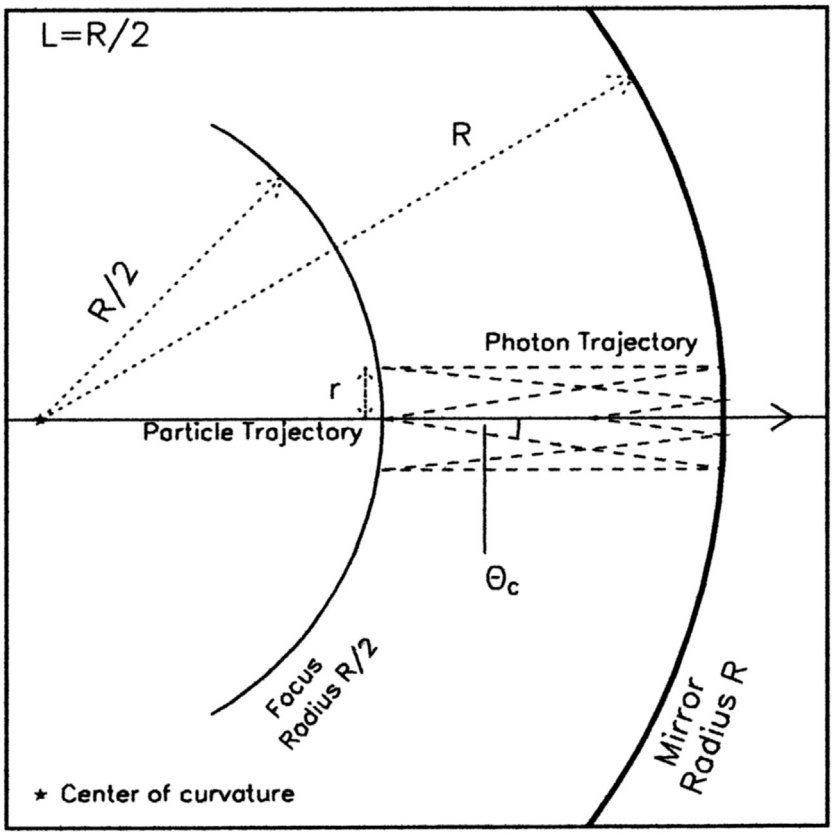

FIGURE 16.9 Working principle of a classical RICH detector. A spherical mirror surrounds a spherical photon detector. Cherenkov photon trajectories are drawn (*dashed lines*) in the small angle approximation surrounding the particle trajectory, which depict the emitted conical Cherenkov light and cone image (ring) reflected onto the detector surface. The radius of the light cone image is labeled *r*. *Reprinted from Engelfried, J., 2011. Cherenkov light imaging Fundamentals and recent developments. Nucl. Instrum. Methods Phys. Res. Sect. A, in press, with permission from Elsevier © 2011.*

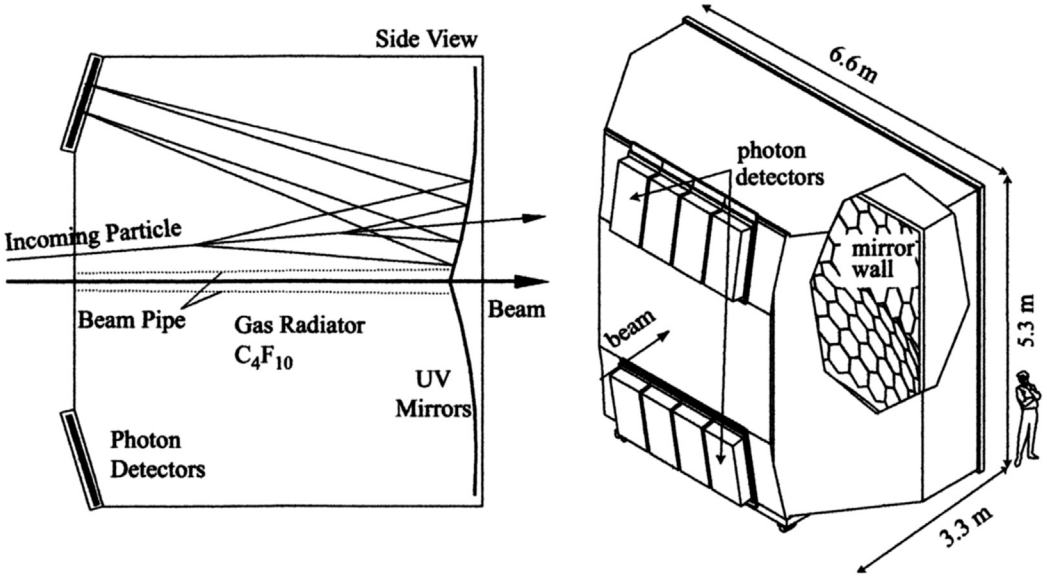

FIGURE 16.10 A scheme of the principle and an artist's view of the COMPASS RICH-1 detector. The side view (left) illustrates Cherenkov photons produced by an incoming particle inside the C_4F_{10} gas-filled detector and the focusing of the photons by mirrors onto the photon detectors for ring imaging. An exterior view (right) shows the locations of the photon detectors in the upper and lower halves of the detector and an inside view of a multifaceted photon focusing mirror wall. A sketch of a human figure is illustrated to the right to provide an idea of the magnitude of the detector. *Reprinted from Abbon, P., et al., 2011. Particle identification with COMPASS RICH-1. Nucl Instrum. Methods Phys. Res. Sect. A 631, 26–39, with permission from Elsevier © 2011.*

The number of photons detected is defined by Eq. [16.39] described previously.

Numerous RICH detectors have been designed with mirrors to reflect and focus the Cherenkov photons onto a suitable plane of photon detectors as well as lenses to enhance images of Cherenkov rings with the objective of measuring the radius r. An example of one of several RICH detectors now in use is the COMPASS RICH-1 detector described by Abbon et al. (2010, 2011) and illustrated in Fig. 16.10. (COMPASS is the acronym for Community Pentascale Project for Accelerator Science and Simulation, of which the lead institution is the Fermi National Accelerator Laboratory, Batavia, IL, USA). As illustrated in the figure (upper side view), an incoming nuclear particle enters the COMPASS RICH-1 detector, which is filled with gaseous C_4F_{10} radiator ($n = 1.00140$ at 150 nm). Cherenkov photons are produced along the particle path; and the ring image is condensed and reflected off a 21-m^2 wall of 116 spherical mirror elements toward a photon detector. Photon detectors are illustrated in both the upper and lower halves of the RICH detector to accommodate incoming particles either above or below a hadron beam. Ring imaging is provided by multianode PMT with pixel size of $\sim 4.2 \times 4.2$ mm^2 coupled to individual telescopes of fused silica lenses and a concentrator lens to enlarge the effective active area of the photon detectors. Examples of ring images provided by multianode photomultiplier detectors are illustrated in Figs. 16.11 and 16.14. Other RICH detector designs are used worldwide, such as the DIRC (Detector of Internally Reflected Cherenkov light) reviewed by Coyle et al. (1994), Aubert et al. (2002), Ratcliff (2003), and Križan (2007, 2009); the HERA-B RICH detector (particle detector of the Hadron-Elektron-Ringanlage, Hamburg, Germany) reviewed by Korpar (2003), Starič (2005), Gorišek (2004), and Ariño (2004); and the LHCb RICH detector (Large Hadron Collider beauty experiment at CERN) reviewed by Forty (2010), Kerzel (2010), Kim (2011b), and Mulheim (2011).

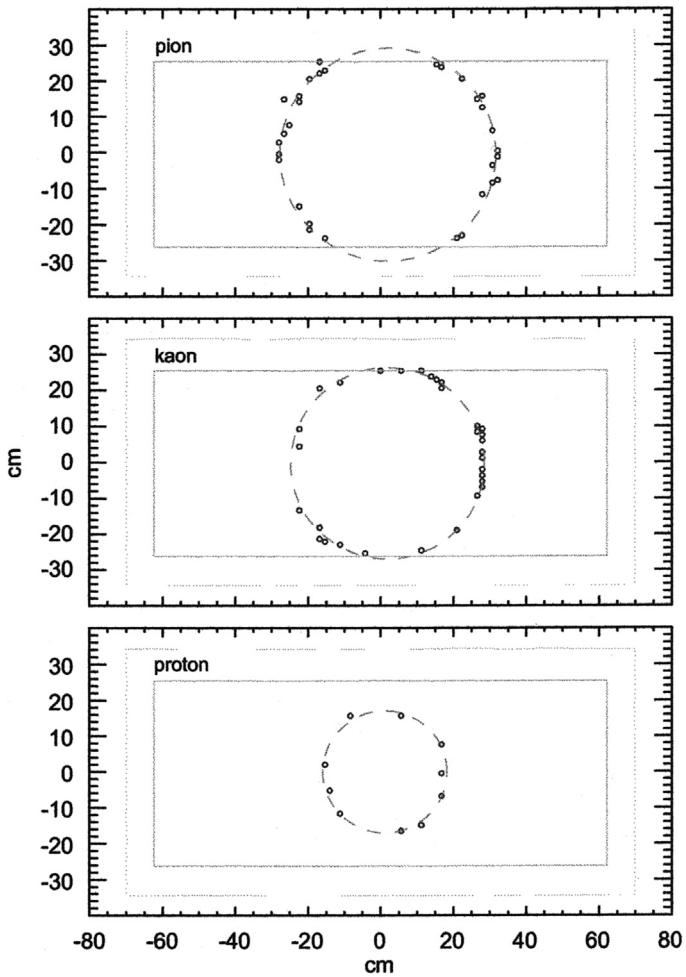

FIGURE 16.11 Sample event displays at 40-GeV/c pion (top), kaon (middle), and proton (bottom) rings in the RICH counter. Small circles indicate hit PMTs. The dashed circles show the rings reconstructed from the PMT hits. *Reprinted from Graf, N., et al., 2010. Charged kaon mass measurement using the Cherenkov effect. Nucl. Instrum. Methods Phys. Res. Sect. A 615, 27–32, with permission from Elsevier © 2010.*

For a Cherenkov radiator of given refractive index n, the radius r in the small angle approximation is a function of the particle mass m and momentum p according to the following (Engelfried, 2011):

$$r = f\sqrt{2 - \frac{2}{n}\sqrt{1 + \frac{m^2c^2}{p^2}}} \qquad [16.41]$$

Thus, if the particle momentum p is known or measured (eg, in a magnetic spectrometer, Engelfried, 2011), the particle mass m can be calculated from the radius r of the Cherenkov cone or ring; and conversely, if the particle mass is known, the particle velocity β or momentum p can be calculated. Also, as described by Lippmann (2011), with the knowledge of the Cherenkov angle θ and particle momentum p, the determination of the particle mass m is possible according to the following derivation:

Since the angle of Cherenkov photon emission θ is a function of the particle velocity and radiator refractive index n, or:

$$\cos\theta = \frac{1}{\beta n} \qquad [16.42]$$

and the particle phase velocity β is a function of its mass and momentum according to:

$$\beta = \frac{1}{\sqrt{\left(\frac{mc}{p}\right)^2 + 1}}, \qquad [16.43]$$

then the two Eqs. [16.42] and [16.43] can be combined to give an equation for the particle mass m as a function of its momentum and the angle of emission of the Cherenkov photons, that is:

$$m = \frac{p}{c}\sqrt{n^2\cos^2\theta - 1} \qquad [16.44]$$

For a given particle momentum p and given refractive index n of the Cherenkov radiator, it can be stated that, the smaller the mass of the particle, the greater will be the Cherenkov angle θ and the greater will be the radius r of the Cherenkov ring. This is illustrated by the Cherenkov ring images for pion, kaon, and proton particles at 40-GeV/c momentum in Fig. 16.11, which was obtained by Graf et al. (2010) with a RICH counter filled with CO_2 gas just above atmospheric pressure as the Cherenkov radiator. The CO_2 gas has a refractive index $n = 1.00045$ at the 300-nm wavelength, which gave threshold momenta of $p = 4.5$ GeV/c for pions, 17 GeV/c for kaons, and 31 GeV/c for protons.

Various radiator materials of differing index of refraction (n) are selected for RICH detectors in order to discriminate between particles of differing mass and momentum. For example, Kerzel (2010) and Lippmann (2011) describe the use of three radiator substances of differing refractive index to discriminate between particles in various ranges of momentum as illustrated in Fig. 16.12. These are silica aerogel ($n = 1.03$), which is used to detect and discriminate particles in the momentum range up to $\sim$10 GeV/c; C_4F_{10} ($n = 1.0014$) for the momentum range of $10 \le p \le 40$ GeV/c; and CF_4 ($n = 1.0005$) for particles in the range of $16 \le p \le 100$ GeV/c.

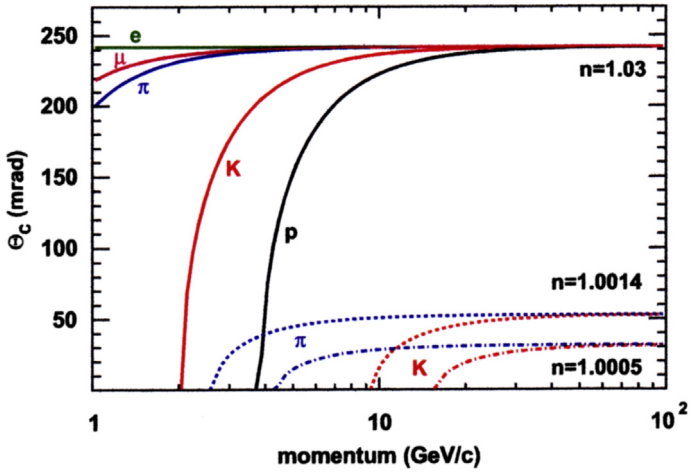

FIGURE 16.12 Cherenkov angles as a function of momentum for different particle species and for three different values of refractive index n corresponding to three radiator materials used in the LHCb RICH setup. *Reprinted from Kerzel, U., 2010. The LHCb RICH detectors. Nucl. Instrum. Methods Phys. Res. Sect. A 617, 283–286; Lippmann, C. (2011). Particle identification. Nucl. Instrum. Mehtods Phys. Res. Sect. A, in press, with permission from Elsevier © 2011.*

16.4.3 Proximity-Focusing RICH Counters

The proximity-focusing RICH detectors do not utilize mirrors or lenses to focus the Cherenkov ring image; rather the image is focused by proximity. As noted by Websdale (2008), proximity focusing effectively means no focusing. An example of a proximity-focusing RICH detector, used to discriminate kaons from pions with particle momentum up to 2.4 GeV/c, is that described by Mammoliti et al. (2011). The detector utilizes 1.5-cm-thick liquid Freon (C_6F_{14}) as the radiator and a CsI photoconverter separated by a distance of only 10 cm for Cherenkov ring imaging, illustrated in Fig. 16.13. A charged particle that exceeds its Cherenkov threshold energy in the liquid Freon ($n = 1.28$ at 180-nm wavelength) emits Cherenkov photons in the Freon in the form of a cone at an angle θ to the particle trajectory. The Cherenkov photons pass through a proximity gap filled with CH_4 at STP; and the photons are then converted into photoelectrons by a 300-nm-thick CsI film deposited onto electrode pad planes of a multiwire proportional chamber (MWPC) providing a two-dimensional localization of the Cherenkov photon hits (Garibaldi et al., 2003; Cusanno et al., 2004; Iodice et al., 2005; Lippmann, 2011). An average of 12.4 photoelectrons per ring are collected with a gain of $\sim 5 \times 10^4$, which provides the signal location for construction of the ring image (Mammoliti et al., 2011).

Cherenkov ring images are recorded commonly by a flat panel of numerous multianode PMTs. An example may be taken from the work of Artuso et al. (2006), which is illustrated in Fig. 16.14. Cherenkov photon hits onto individual PMTs produce the two-dimension signal localization of the Cherenkov photons, which are reconstructed into the ring image.

A schematic diagram of a typical proximity-focusing RICH counter is that described by Pestotnik et al. (2004), Matsumoto et al. (2004), Korpar et al. (2005), and Križan et al. (2005), which is illustrated in Fig. 16.15. The RICH detector employs two 5×5 cm^2 multiwire proportional chambers (MWPCs) to provide precise measurement of the particle track. MWPCs are gas ionization detectors, developed by Nobel Laureate Georges Charpak and coworkers (Charpak et al., 1968, 1970; Charpak, 1969, 1970; Charpak and Sauli, 1978, 1979), which contain an array or grid of uniformly spaced anode wires sandwiched between two outer grids of uniformly spaced cathode wires. The two outer cathode planes are oriented at right angles to one another, and the sandwich of these grids is contained in a chamber of proportional counting gas such as an $Ar + CH_4$ gas mixture. Output signals provide the x- and y-coordinates of the ionizing particles entering the grid.

As illustrated in Fig. 16.15, after passing through the first MWPC, the high-energy particles continue on to penetrate a silica aerogel Cherenkov radiator (10−25 mm thick). The refractive index ($n = 1.05$) of the aerogel provides discrimination of pions and kaons in the momentum range of 0.5−4 GeV/c. The Cherenkov photons produced in the aerogel are detected by an array of flat-panel multianode PMTs. The multichannel PMTs are connected to an analog memory board providing a read-out of the PMT signals. The position sensitivity of the readout yields a Cherenkov angle resolution per photon of 10 mrad (Matsumoto et al., 2004).

Križan et al. (2001) provide another excellent example of the use of position-sensitive PMTs to provide high-resolution images of Cherenkov rings (Fig. 16.16A). They used 2300 position-sensitive PMTs with a 2.8-m-long C_4F_{10} gas radiator

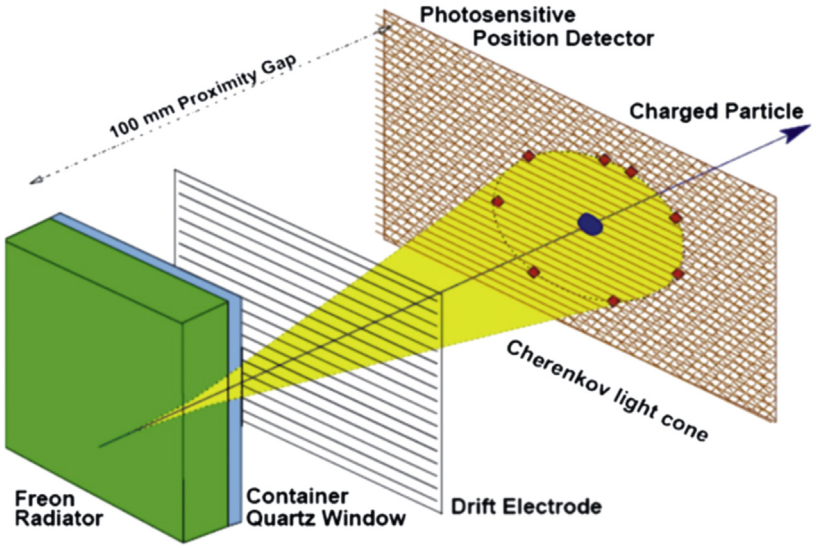

FIGURE 16.13 Artist's view of a proximity-focusing RICH counter. *Reprinted from Mammoliti, F., et al., 2011. A RICH detector for hadron identification at JLab. Appl. Radiat. Isot., in press, with permission from Elsevier © 2011.*

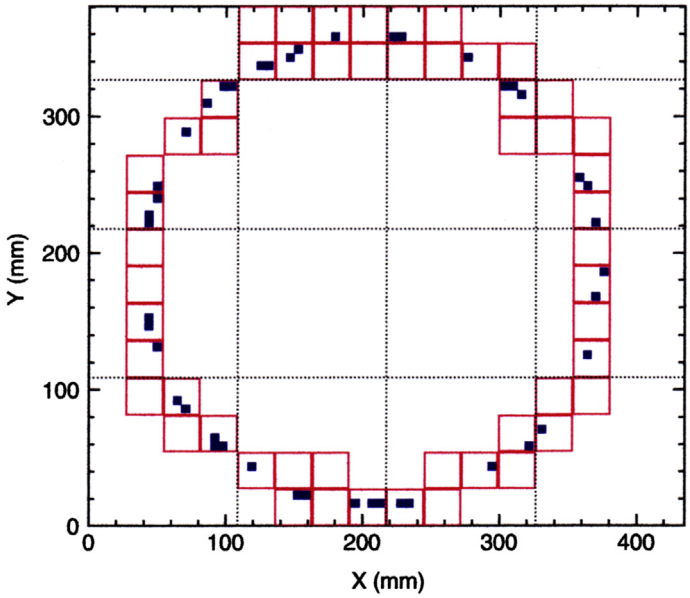

FIGURE 16.14 Cherenkov ring image. Each darkened square represents a hit. Each solid hollowed box corresponds to a multianode photomultiplier tube. *From Artuso, M., et al., 2006. Performance of a C_4F_8O gas radiator ring imaging Cherenkov detector using multi-anode photomultiplier tubes. Nucl. Instrum. Methods Phys. Res. Sect. A 558, 373–387. Reprinted with permission from Elsevier © 2006.*

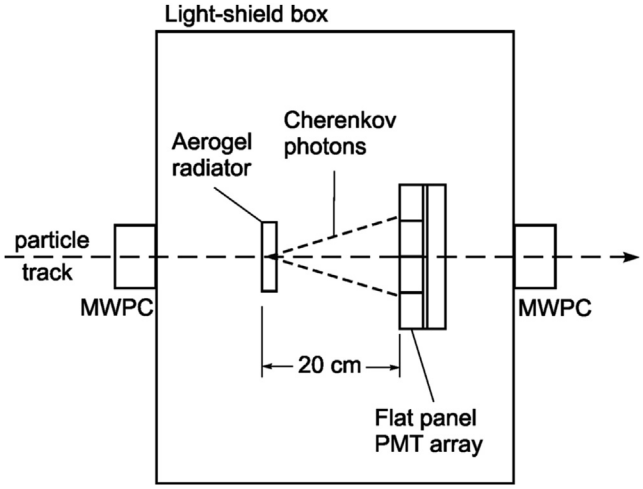

FIGURE 16.15 Experimental arrangement of a proximity-focusing RICH detector with an array of flat-panel position-sensitive PMTs. *Reprinted from Matsumoto, T., et al., 2004. Studies of proximity focusing RICH with an aerogel radiator using flat-panel multi-anode PMTs (Hamamatsu H8500). Nucl. Instrum. Methods Phys. Res. Sect. A 521, 367–377, with permission from Elsevier © 2004.*

($n = 1.00135$), yielding an average number of 32 Cherenkov photons per ring produced by 50-GeV/c kaons or pions and about twice that number of photons per ring when produced by overlapping e^+e^- pairs. Cherenkov photon resolutions of approximately 1 mrad provide discrimination of kaons and pions of momentum as high as 50 Gev/c. Examples of Cherenkov rings imaged by the signal outputs of position-sensitive PMTs are illustrated in Fig. 16.16.

A linear relation between Cherenkov angle θ_c and particle momentum is described by Križan et al. (2001) to be:

$$\theta_c^2 = \frac{\theta_0^2 - m^2}{p^2} \qquad [16.45]$$

where $\theta_0^2 = 2(n-1)$, m is the particle mass, and p is the particle momentum. The relation between the variables θ_c^2 and $1/p^2$, as defined by Eq. [16.45], is linear, and thus the plot of θ_c^2 against $1/p^2$ for a particle of given mass would be a straight line. Fig. 16.17 illustrates the linear relationship between θ_c^2 and $1/p^2$ for particles of different mass, namely, protons

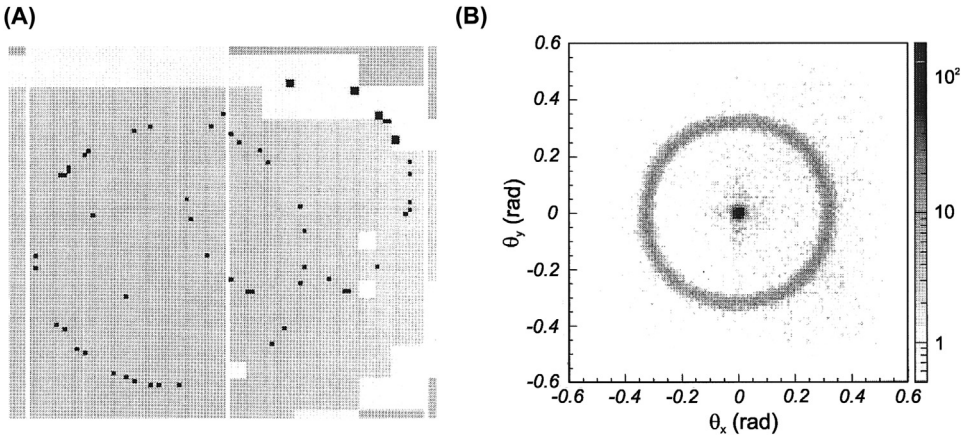

FIGURE 16.16 Cherenkov rings imaged by multichannel position-sensitive PMTs. (A) An event with two Cherenkov rings with single-photon resolutions of 0.7 mrad produced by two different particle trajectories in a 2.8-m perfluorobutane gaseous medium. *(From Križan, P., et al., 2001. The performance of the HERA-B RICH at high track densities. Nucl. Instrum. Methods Phys. Res. Sect. A 471, 30–34; printed with permission ©2001 IEEE.)* (B) A broader Cherenkov ring produced by a distribution of numerous PMT hits in the Cherenkov x,y space by 3 Gev/*c* pions traveling through a 2-cm-thick silica aerogel Cherenkov radiator. The central dark spot was produced by the particle beam. Background spots outside of the ring are produced by Cherenkov photons that are Rayleigh scattered in the radiator. *(Reprinted from Matsumoto, T., et al., 2004. Studies of proximity focusing RICH with an aerogel radiator using flat-panel multi-anode PMTs (Hamamatsu H8500). Nucl. Instrum. Methods Phys. Res. Sect. A 521, 367–377, with permission from Elsevier © 2004.)*

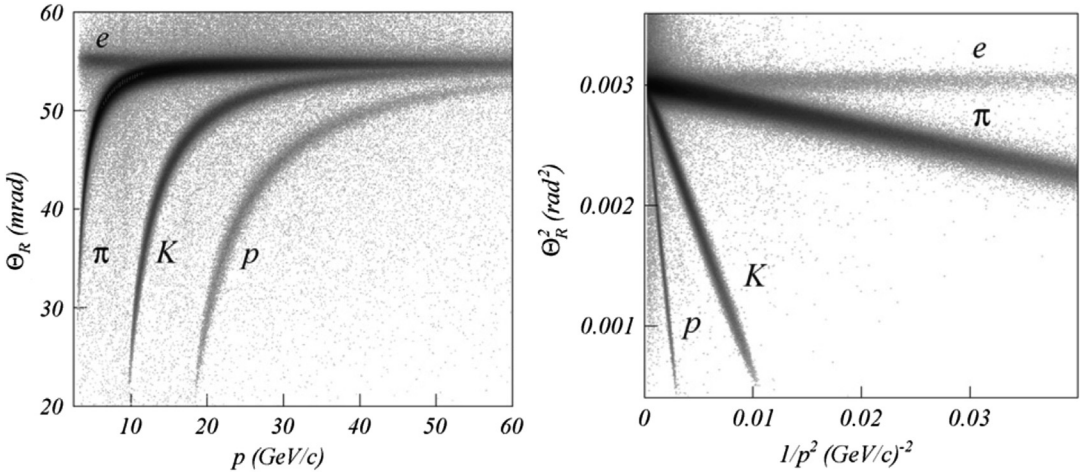

FIGURE 16.17 The measured-ring Cherenkov angle θ_R versus the particle momentum p (left) with Cherenkov thresholds at ~2.5, 9, and 17 GeV/*c* for pions, kaons, and protons, respectively, and θ_R^2 versus $1/p^2$ (right) in a C_4F_{10} gaseous radiator. *Reprinted from Abbon, P., et al., 2011. Particle identification with COMPASS RICH-1. Nucl Instrum. Methods Phys. Res. Sect. A 631, 26–39, with permission from Elsevier © 2011.*

($m = 938.27$ MeV/c^2), kaons ($m = 493.67$ MeV/c^2), pions ($m = 139.57$ MeV/c^2), and electrons ($m = 0.511$ MeV/c^2). In Fig. 16.17, the measured-ring Cherenkov angle is plotted as a function of the particle momentum, where the Cherenkov thresholds in gaseous C_4F_{10} radiator for electrons, pions, kaons, and protons are given. Abbon et al. (2011) points out with Fig. 16.17, that in the small-angle approximation, the relationship between the two variables θ^2 and $1/p^2$ is linear with a slope proportional to the squared mass of the corresponding particle; and the bands start at the Cherenkov threshold and have a common intercept corresponding to the maximum Cherenkov angle. Thus measurement of the Cherenkov angle of emission in radians (rad) can be used to determine the velocity of a particle from its momentum or identify the particle from its known momentum.

16.4.4 Time-of-Propagation Cherenkov Counters

A more recent concept in the application of Cherenkov detectors for PID is via the measurement of the time-of-propagation (TOP) of Cherenkov photons in a narrow (2 cm thick) quartz bar described by Akatsu et al. (2000), Ohshima (2000), Inami

(2008, 2011), Nishimura et al. (2010), Nishimura (2011), and Starič (2011). The basic structure of the TOP Cherenkov counter is illustrated in Fig. 16.18. The TOP detector consists of a quartz Cherenkov radiator bar (20 mm thick, 60 mm wide, 3150 mm long). The TOP counter utilizes the principle of total internal reflection of Cherenkov photons produced in the quartz radiator, and measures the position and precise arrival time of propagated photons at the radiator ends (Inami, 2011). Two mirrors are located at both ends for focusing the Cherenkov photons. The mirror is flat at the backward end to reflect the Cherenkov light toward the forward end, where butterfly-shaped mirrors and photon detectors are located. The Cherenkov photons are focused horizontally onto the photon detector plane; and the TOP is measured by position-sensitive multichannel phototubes. The method is based on the following principles: (1) the Cherenkov photon emission angle (θ_c) illustrated in Fig. 16.19 is a function of the particle velocity (β) according to the relation $\cos\theta_c = 1/\beta n$, where n is the refractive index of the Cherenkov radiator; (2) the TOP of photons in a light guide with internal-total-reflection characteristics can be calculated as a function of the photon emission angle; and (3) a correlation between TOP and photon emission angle would provide information on PID. Notice from the example provided in Fig. 16.19 that the Cherenkov photon emission angle created by the pion (π) is less acute than that created by the kaon (K) of the same momentum, and the TOP of the Cherenkov photons derived from the pion is shorter than derived by the kaon. As noted by Inami (2011), TOP differences of 200 ps or more are found for normal incident 2 GeV/c K^+ and π^+; the time resolution for single-photon detection needs about 40 ps. An additional property, that is utilized, is the TOF from the interaction point (see IP., illustrated in Fig. 16.18 at a 1-m distance) to the counter, which affects the difference in the Cherenkov photons' arrival time additively in most cases (Inami, 2011).

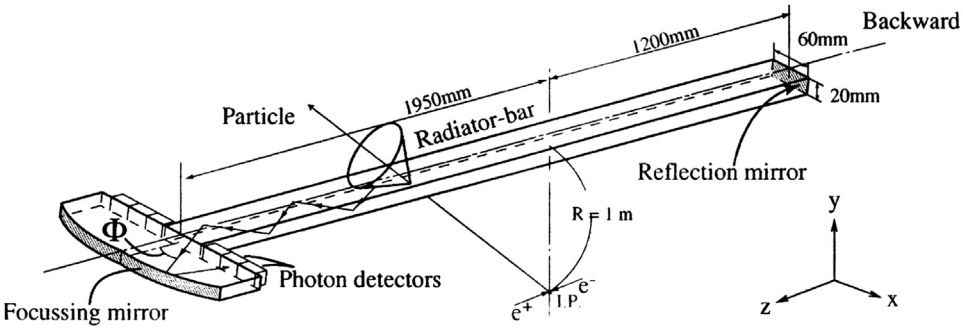

FIGURE 16.18 Structure of a TOP Cherenkov counter. Basic parameters are indicated in the figure. The bar (Cherenkov radiator) and mirrors are made of synthetic optical quartz ($n = 1.47$ at $\lambda = 390$ nm) and configured z-asymmetric to the interaction point (IP) of an asymmetric collider. The counters are placed 1 m radially distant from the interaction point to form a cylindrical structure. *Reprinted from Akatsu, M., et al., 2000. Time-of-propagation Cherenkov counter for particle identification. Nucl. Instrum. Methods Phys. Res. Sect. A 440, 124–135; Ohshima, T., 2000. Test result of time-of-propagation Cherenkov counter. Nucl. Instrum. Methods Phys. Res. Sect. A 453, 331–335; Enari et al., 2002, with permission from Elsevier ©2002.)*

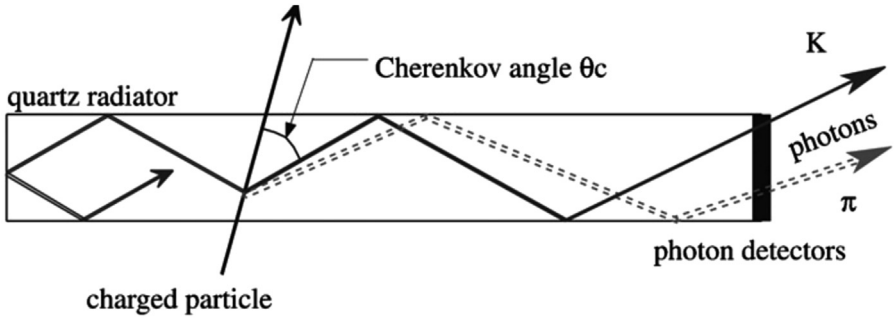

FIGURE 16.19 A side view schematic of the TOP concept. The path length difference of Cherenkov photons emitted from a pion and a kaon within the radiator bar results in a difference in arrival time at the photodetector. *Reprinted from Iijima, T., 2010. Recent topics of particle identification and photodetection. Nucl. Instrum. Methods Phys. Res. Sect. A 632 (1), 48–56; Nishimura, K., et al., 2010. An imaging time-of-propagation system for charged particle identification at a super B factory. Nucl. Instrum. Methods Phys. Res. Sect. A 623, 297–299; Nishimura, K., 2011. The time of propagation counter for Belle II. Nucl. Instrum. Methods Phys. Res. Sect. A, in press), with permission from Elsevier © 2010.*

16.4.5 Time-of-Flight Cherenkov Counters

For a beam of particles of known momentum, a measurement of the time-of-flight (TOF) between a start and stop counter (eg, Cherenkov detectors) separated by several meters yields the mass of the particle (Va'vra et al., 2009; Ronzhin et al., 2010), a property key to PID. The following principles and methodology discussed in this section pertain to TOF measurements employed in conjunction with proximity-focusing RICH detectors to supplement data for PID:

The relativistic momentum of the particle is expressed as:

$$p = \gamma m v \qquad [16.46]$$

where:

$$\gamma = \frac{1}{\sqrt{1-\beta^2}} \qquad [16.47]$$

is the relativistic Lorentz transformation factor (Airapetian et al., 2005; Lippmann, 2011), as described previously by Eq. [10.5] of the chapter entitled "Neutron Radiation" and Eq. [C.32] of Appendix C of this book, m is the particle mass, v is the particle velocity, and β is the relativistic phase velocity of the particle, that is, the velocity of the particle divided by the speed of light in a vacuum (v/c). From Eq. [16.46], Lippmann (2011) expresses the mass of the particle in terms of its momentum and phase velocity as:

$$m = \frac{p}{c\beta\gamma} \qquad [16.48]$$

where $\beta = v/c$; where the particle momentum may be determined by its curvature in a magnetic field and the particle velocity may be determined by TOF and Cherenkov radiation measurements. From Eqs. [16.47] and [16.48], we can write the expression:

$$\frac{mc}{p} = \frac{\sqrt{1-\beta^2}}{\beta} \qquad [16.49]$$

which can be transformed to express the particle velocity β in terms of its mass m and momentum p as:

$$\beta = \frac{1}{\sqrt{\left(\frac{mc}{p}\right)^2 + 1}} \qquad [16.50]$$

The particle phase velocity β, as described by Lippmann (2011), is determined by TOF measurements of the particle flight time t over a given distance L along the particle trajectory; and β would then be expressed as:

$$\beta = \frac{v}{c} = \frac{L}{tc} \qquad [16.51]$$

Eqs. [16.50] and [16.51] may be used to write an equation for the particle mass m from measurements of L, t, and p, as described by Lippmann (2011) as:

$$m = \frac{p}{c}\sqrt{\frac{c^2t^2}{L^2} - 1} \qquad [16.52]$$

Thus, for particles of known momentum, Cherenkov detectors separated by the distance L, which can register the start and stop signals for the measurement of t, can provide the data necessary to calculate the particle mass. In turn, Eq. [16.52] may be transposed to express the time t for a particle of mass m and momentum p to travel the distance L as:

$$t = \frac{L}{c}\sqrt{1 + \left(\frac{mc}{p}\right)^2} \qquad [16.53]$$

Lippmann (2011) points out that, if two particles with masses m_A and m_B carry the same momentum, their flight time difference can be calculated as:

$$|t_A - t_B| = \frac{L}{c}\left|\sqrt{1 + \left(\frac{m_A c}{p}\right)^2} - \sqrt{1 + \left(\frac{m_B c}{p}\right)^2}\right| \qquad [16.54]$$

Accurate measurements of the start and stop signals are provided by two radiation detectors. One detector is located upstream from the particle beam or trajectory and the second detector to provide the stop signal or end of the measured particle trajectory. Cherenkov photons, produced in the window of a PMT of a proximity-focusing RICH counter, have been used conveniently to provide the stop signal for TOF measurements (Adachi et al., 2007; Korpar et al., 2007; Križan, 2007, 2009; Križan et al., 2007; Iijima et al., 2008; Iijima, 2010). As illustrated in Fig. 16.20, Cherenkov photons, produced by a nuclear particle in the window of a microchannel plate photomultiplier tube (MCP-PMT), are used to provide a stop signal for the measurement of TOF, while the Cherenkov photons produced by the particle in passing through the aerogel detector yield ring imaging data. Thus, TOF measurements supplement other PID methods, such as RICH counting.

An example of an arrangement where the concept of proximity-focusing RICH and TOF measurements are combined in the same detector is taken from the work of Iijima et al. (2008). The concept is illustrated in Fig. 16.21. The start signal for the measurement of TOF of kaons and pions, illustrated in Fig. 16.21, is the interaction point (IP) and the stop signal is the signal registered by Cherenkov photons produced in the window of the PMT (referred to as a "Window Hit" in Fig. 16.21). The distance of particle travel L for the calculation of TOF t and particle mass according to Eqs. [16.52]–[16.54] is measured in the experimental arrangement illustrated in Fig. 16.21 as $L = 1.8\text{ m} + 0.2\text{ m}$. Cherenkov photons produced by the particle passing through the aerogel detector are detected by the PMTs to yield ring image data; and the detection of a Cherenkov ring photon is referred to as a "Ring Hit" in Fig. 16.21. In addition to ring image, additional TOF information on the particle is obtained by measuring TOF from the IP point to the aerogel detector (ΔTOF1 of Fig. 16.21) plus the TOP of the Cherenkov photon from the aerogel radiator to the PMT (ΔTOP of Fig. 16.21). Iijima et al. (2008) measured TOF differences for 2- and 4-GeV/c kaons and pions to be 147 and 37 ps, respectively, for the Ring Hits and 184 and 47 ps for the Window Hits. Such TOF measurements permit the identification of particles having momenta below the Cherenkov threshold (ie, when no Cherenkov photons are produced) in

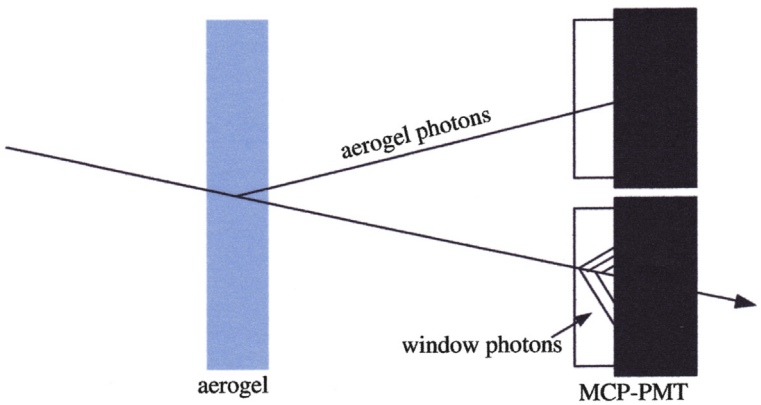

FIGURE 16.20 Schematic view of a combined proximity-focusing RICH and TOF counter. Cherenkov photons produced by the charged particle in passing through the window of the microchannel plate photomultiplier tube (MCP-PMT) provide the stop signal for TOF measurements. Cherenkov photons produced by the particle as it passes through the aerogel detector are detected by another MCP-PMT for ring imaging data. *Reprinted from Križan, P., 2009. Recent progress in particle identification methods. Nucl. Instrum. Methods Phys. Res. Sect. A 598, 130–137, with permission from Elsevier © 2009.*

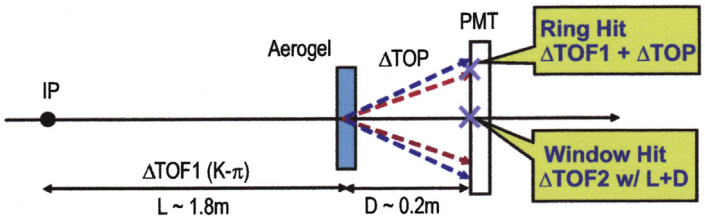

FIGURE 16.21 Concept of a RICH counter with TOF capability. *From Iijima, T., et al., 2008. Studies of a proximity focusing RICH with aerogel radiator for future Belle upgrade. Nucl. Instrum. Methods Phys. Res. Sect. A 595, 92–95; reprinted with permission of Elsevier © 2008.*

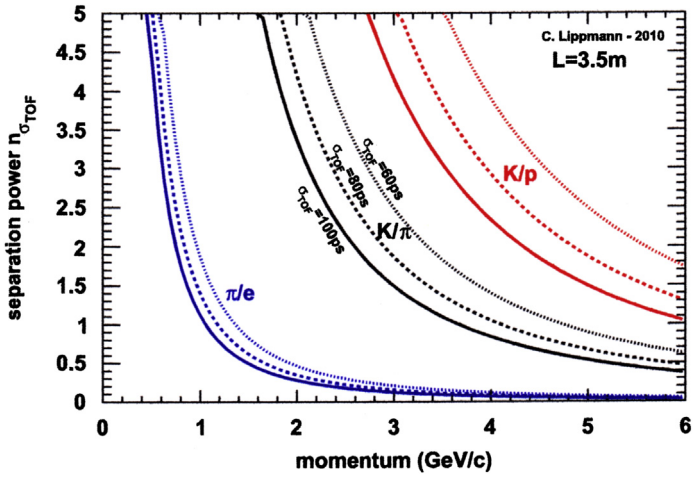

FIGURE 16.22 Particle separation with TOF measurements in three different system time resolutions ($\sigma_{TOF} = 60$, 80, and 100 ps) and for a track length $L = 3.5$ m. Infinitely good precisions on momentum and track length are assumed. *Reprinted from Lippmann, C., 2011. Particle identification. Nucl. Instrum. Mehtods Phys. Res. Sect. A, in press), with permission from Elsevier © 2011.*

the aerogel radiator of refractive index $n = 1.03-1.05$, which is ≈ 1.5 GeV/c for kaons and ≈ 3 GeV/c for protons (Iijima et al., 2008).

The MCP-PMT photodetector is a very fast device with a reported time resolution per single photons to be ~ 50 ps (Iijima et al., 2008). The power of TOF measurements to separate particles ($n_{\sigma_{TOF}}$) is a function of the TOF difference between the two particles ($t_A - t_B$) and the resolution of the TOF measurement (σ_{TOF}), or:

$$n_{\sigma_{TOF}} = \frac{|t_A - t_B|}{\sigma_{TOF}} \qquad [16.55]$$

With particle momentum $p >> mc$, Lippmann (2011) points out that the approximation:

$$\sqrt{1 + (mc/p)^2} \approx 1 + (mc)^2/2p^2 \qquad [16.56]$$

and from Eqs. [16.54]–[16.56], the separation power becomes:

$$n_{\sigma_{TOF}} = \frac{|t_A - t_B|}{\sigma_{TOF}} = \frac{Lc}{2p^2\sigma_{TOF}}\left|m_A^2 - m_B^2\right| \qquad [16.57]$$

For a given length (L) of measured particle trajectory of 3.5 m, the separation power of particles as a function of particle momentum and time resolution is illustrated in Fig. 16.22. Lippmann (2011) demonstrates from the separation power curves of Fig. 16.22 that assuming a time resolution in the range of 100 to 60 ps and requiring a separation power of $n_{\sigma_{TOF}} = 3$, the upper limits for the momentum are in the range of 2.1 to 2.7 GeV/c for K/π separation and 3.5 to 4.5 GeV/c for K/p separation.

Charles and Forty (2011) designed a Cherenkov detector consisting of a plate of quartz equipped with microchannel plate photomultipliers placed 12 m downstream of the interaction point. The detector has a specific design, which provides the Cherenkov angle (θ_C) and TOF measurements for the identification of particles of momentum up to 10 GeV/c.

16.5 NEUTRINO DETECTION AND MEASUREMENT

Because neutrinos do not carry charge, they do not produce the Cherenkov effect. However, neutrino interactions within very large bodies of transparent material can produce high-energy charged particles, which in turn produce Cherenkov photons. Photon detectors, namely PMT, are used to measure the Cherenkov photon intensity produced by the charged particles, which provides a measure of the neutrino flux.

The very large volumes of transparent material currently used for the detection of Cherenkov photons from neutrino interactions contain water or ice; and these have been designed to detect neutrinos from various sources such as solar neutrinos, atmospheric neutrinos of the cosmic ray showers, geo-neutrinos, artificially produced neutrinos arising from

nuclear reactors and accelerators, and ultra-high-energy (UHE) astrophysical neutrinos. The following large bodies of water or ice are utilized:

1. Heavy water (D_2O) weighing >1 kiloton in an underground vessel, such as that utilized by the Sudbury Neutrino Observatory (SNO) near Sudbury, Canada (Boudjemline et al., 2010) or light water (H_2O) weighing >50 kilotons contained in a large vessel underground, such as that utilized by the Super-Kamiokande Cherenkov detector under Mt. Ikenoyama, Japan (Fukuda et al., 2003; Nishino et al., 2009). Both vessels are surrounded by photomultiplier detectors for the detection of the Cherenkov photons.
2. Lake or ocean waters with Cherenkov photon detectors (PMTs) located deep within lake or ocean waters. In ocean waters, photon detectors have been placed at depths of up to 2.5 km. There are currently two large-scale neutrino telescopes in operation in lake or ocean waters, namely, the NT200 in Lake Baikal in Siberia (Aynutdinov et al., 2006, 2011) and the ANTARES (Astronomy with a Neutrino Telescope and Abyss Environmental RESearch) in the Mediterranean Sea (Carr, 2008; Aguilar et al., 2011; Brunner, 2011; Costantini, 2011).
3. Polar ice with Cherenkov photon detectors placed deep within holes drilled into the polar ice cap. The current large-scale neutrino telescope of this type is the IceCube/AMANDA (Antartic Muon and Neutrino Detector Array) at the South Pole (Achterberg et al., 2006; Berghaus, 2009; Montaruli, 2009b; Abbasi et al., 2010, 2011; Hultqvist, 2011).

The very large bodies of water or ice are required to detect the neutrino interactions, because of the high penetrating power of neutrinos due to their lack of charge and very low mass.

The Cherenkov photons that are detected, are those produced by charged particles resulting from neutrino interactions such as (1) elastic scattering (ES) of electrons by neutrinos in the detector medium, (2) neutrino charged current (CC) interactions with deuterium nuclei in heavy water, and (3) neutral current (NC) interactions of neutrinos with atomic nuclei of water or ice.

Electron Scattering. The ES of electrons by neutrinos, described by the following:

$$\nu_x + e^- \rightarrow \nu_x + e^- \qquad [16.58]$$

is sensitive to all neutrino flavors (where $x = e$, μ, or τ), but with a reduced sensitivity to the muon neutrino (ν_μ) and the tau neutrino (ν_τ). In the ES interaction described by Eq. [16.58], neutrino energy is transferred to an atomic electron; and the electron will, in turn, travel as a scattered electron in light water, heavy water, or ice at relativistic speeds and produce Cherenkov photons, as illustrated in Fig. 16.23. From this interaction and the anisotropic property of the Cherenkov radiation, the directional information of the neutrino can be determined.

Charged Current (CC) Interactions. The CC interaction with a deuterium nucleus or deuteron (d) is described as follows:

$$\nu_e + d \rightarrow p + p + e^- \qquad [16.59]$$

where the resultant energy of the electron (e^-) is well correlated with the energy of the electron neutrino (ν_e). The high-energy scattered electron produced from interactions 16.58 and the high-energy negatron from reaction 16.59 produce Cherenkov photons in transparent media. The electron neutrino ν_e is the only neutrino flavor that is able to convert the deuterium nucleus (ie, deuteron) into two protons and a negatron. The interaction of a neutrino with the deuteron described by Eq. [16.59], can be illustrated further whereby a neutron of the deuterium nucleus is transformed into a proton, as illustrated in Fig. 16.24.

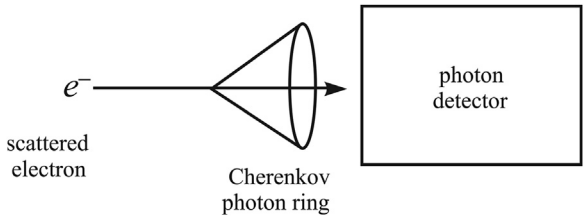

FIGURE 16.23 An electron with energy in excess of 262 keV traveling in H_2O, D_2O, or ice producing a Cherenkov photon ring; the direction of travel of the Cherenkov photons are determined by the photon detectors (eg, photomultiplier tubes). The anisotropic property of Cherenkov photons permits the design and orientation of photon detectors to register only Cherenkov photons traveling in a certain direction. Thus, the directional information of the neutrino can be determined.

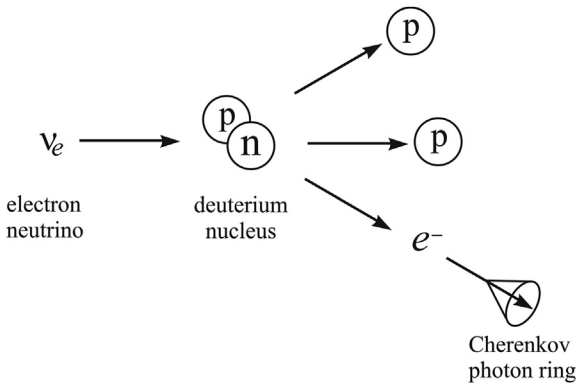

FIGURE 16.24 Charged current interaction of an electron neutrino with a deuterium nucleus, resulting in the transformation of a neutron (n) into a proton (p) and negatron (e^-). The negatron or negative electron travels in the heavy water to produce Cherenkov photons illustrated with a Cherenkov photon ring.

The interaction described by Eq. [16.59] and Fig. 16.24 is called a CC interaction because a charged W boson, which can carry either a positive or negative charge ($W^{\pm}$), acts as an intermediate vector in the transformation process of a neutron in the nucleus of deuterium (*d*) into a proton (*p*). The charged W^+ bosons act as exchange particles involved in the transformation of quark flavor, which in this interaction, involves the transformation of a down quark (d) of the neutron into an up quark (u) transforming the neutron into a proton. This is illustrated by the Feynman diagram of Fig. 16.25.

Another CC interaction that is currently employed to detect atmospheric neutrinos involves the creation of secondary muons by atmospheric neutrinos in large bodies of water, such as lakes, ocean floors, and Arctic ice. As described by Formaggio (2009), Katz (2009) and Abbasi et al. (2010), the following CC reaction results in the creation of high-energy muons, which travel at relativistic speeds (0.8*c*) and produce Cherenkov photons detected by photon detectors located deep within lakes, ocean floors, or Arctic ice:

$$\nu_\mu(\overline{\nu}_\mu) + N \rightarrow \mu^-(\mu^+) + X \qquad [16.60]$$

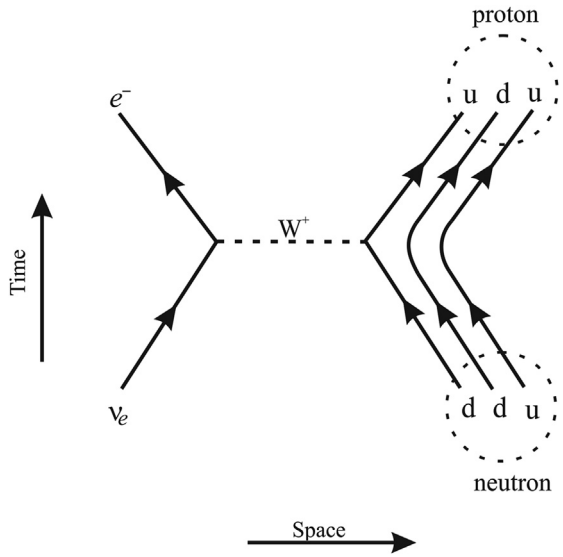

FIGURE 16.25 Feynman diagram illustrating the charged current (CC) interaction of an electron neutrino (ν_e) with a neutron of a deuterium nucleus via the mediation of a W^+ boson, resulting in the transformation of a down quark (d) of the neutron into an up quark (u), resulting in the transformation of the neutron into a proton. The diagram illustrates, on the lower left, an incoming electron neutrino (ν_e) interacting with a down quark (d) of a neutron (lower right) via a W^+ boson (dashed line). The down quark (d) of the neutron is transformed into an up quark (u) (upper right), thereby changing the neutron into a proton (upper right) with the creation of a negatron (e^-), illustrated with the arrow upward on the upper left of the diagram.

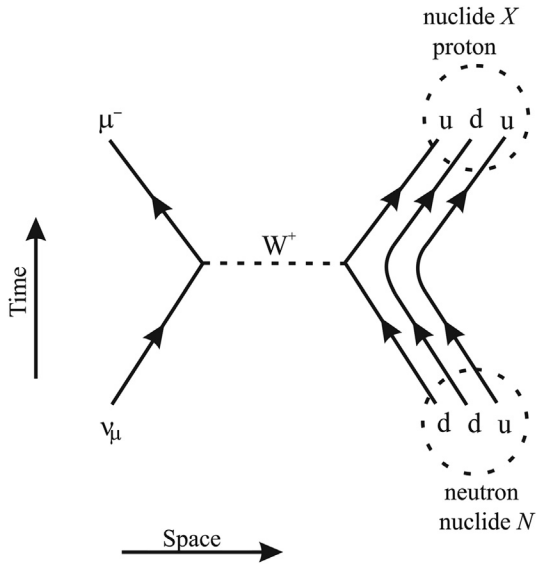

FIGURE 16.26 Feynman diagram describing the charge current interaction of a muon neutrino and a down quark of a nucleon in element *N*, mediated by a W^+ boson, converting the quark flavor from a down (d) quark to an up (u) quark with the production of a negative muon (μ^-). The conversion of the quark flavor from d to u results in the conversion of a neutron to a proton and consequently conversion of nuclide *N* to nuclide *X*.

where an atmospheric muon neutrinos (ν_μ) or muon antineutrinos ($\overline{\nu}_\mu$) interact with nuclei *N* of elements that surround the Cherenkov photon detector to produce charge muons (μ^- or μ^+) and nuclei of element *X*. The nuclei change from *N* to *X*, because in the charge current reaction mediated by a W^+ boson, the quark flavor within a nucleon is changed as illustrated by the Feynman diagram of Fig. 16.26.

Neutral Current (NC) Interactions. The Cherenkov photon detection and measurement of neutrinos via NC interactions of neutrinos with deuterium nuclei in heavy water is described by the following:

$$\nu_x + d \rightarrow p + n + \nu_x \qquad [16.61]$$

where ν_x is a neutrino of any flavor, that is $x = e$, μ, or τ, to represent the electron, muon, or tau neutrino, *d* is the deuteron or nucleus of deuterium, and *p* and *n* are the proton and neutron, respectively, liberated when the deuterium nucleus breaks apart. The reaction is called a NC interaction, because a neutral Z boson (Z^0) acts as the intermediate exchange particle in this interaction of a neutrino with the deuterium nucleus. The Z^0 boson does not change the flavor of quarks in a nucleon; however, the energy transferred causes the nucleus to break up into its proton and neutron component nucleons. An illustration of the NC interaction of a neutrino with a deuterium nucleus, by means of a Feynman diagram, is provided in Fig. 16.27.

All neutrino flavors react equally with deuterium in this NC reaction, which can provide a measure of the total neutrino flux for neutrino energies in excess of 2.2 MeV (Prior, 2009). The neutron produced in reaction 16.61 becomes quickly thermalized in the water; and the thermal neutron is subsequently captured by a deuterium (^{2}H) nucleus or by a nucleus of ^{35}Cl when the water is doped with a high concentration of NaCl. Neutron capture by ^{2}H or by ^{35}Cl results in the emission of gamma radiation. The gamma rays will interact with atomic electrons of the water to produce Compton electrons. All Compton electrons with energy in excess of the 262-keV threshold energy will produce Cherenkov photons in the water. The detection and measurement of the Cherenkov photons provide a measurement of the neutrino flux. The NC interaction in heavy water doped with NaCl is illustrated in Fig. 16.28.

An illustration of the layout of a NC detector, namely the SNO Cherenkov detector, which utilizes heavy water (D_2O), described previously for the detection and measurement of neutrinos, is found in Fig. 16.29. The SNO (Sudbury Neutrino Observatory) is located 2100 m underground in Sudbury, Ontario, Canada. Fig. 16.29 illustrates a person standing above the detector, which provides a perspective of the magnitude of the heavy water detector.

Ultra-high energy (UHE) astrophysical neutrino interactions with atomic nuclei can produce particles yielding Cherenkov radio waves, which are detected with antennas. For additional reading on the detection of neutrinos by the Cherenkov effect, the reader may peruse a detailed review by the writer in a previous book (L'Annunziata, 2012e).

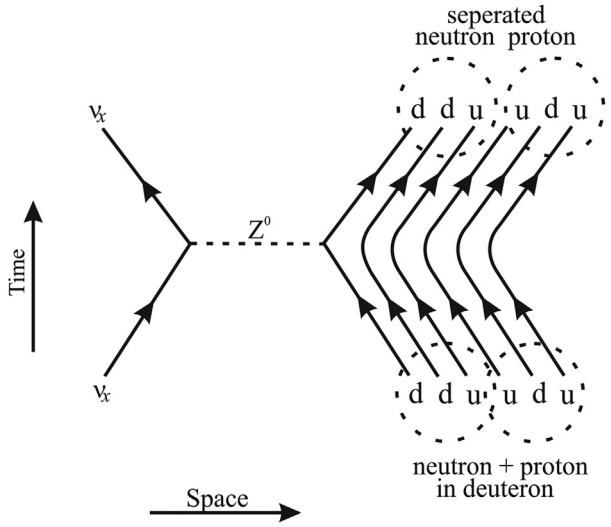

FIGURE 16.27 Feynman diagram describing a neutral current interaction of an electron, muon, or tau neutrino (where $x = e$, μ, or τ) with a down quark (d) of a neutron in a nucleus of deuterium (deuteron) via the neutral Z boson (Z^0) as an intermediate exchange particle. The flavor of the quark does not change, that is, the down quark (d) of the neutron remains a down quark; and thus the neutron does not change into a proton. However, energy of the neutrino is transferred; and the neutron and proton of the deuterium nucleus (lower right, dashed circles overlapping) break apart (upper right, dashed circles separated).

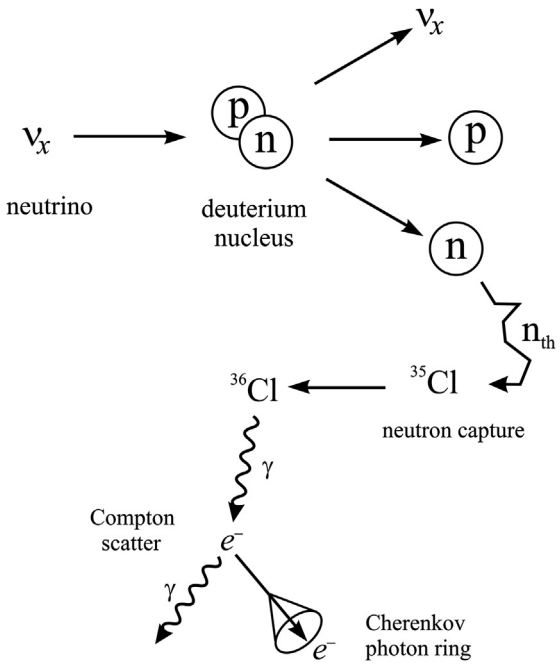

FIGURE 16.28 A neutral current interaction of a neutrino utilized for the detection of neutrinos of any flavor (electron, muon, or tau) where $x = e$, μ, or τ, in heavy water (D_2O) doped with a high concentration of NaCl. The neutrino interacts with a deuterium nucleus, causing the nucleus to break apart into its constituent proton and neutron. The neutron rapidly undergoes thermalization after several collisions (jagged path of arrow) with atomic nuclei; and the thermalized neutron (n_{th}) is captured by a ^{35}Cl nucleus. Gamma-ray emission from ^{36}Cl following neutron capture undergoes Compton scatter; and the Compton electrons, in excess of 262 keV energy, produce Cherenkov photons in the water. The Cherenkov photons are measured with suitable photon detectors (eg, photomultiplier tubes).

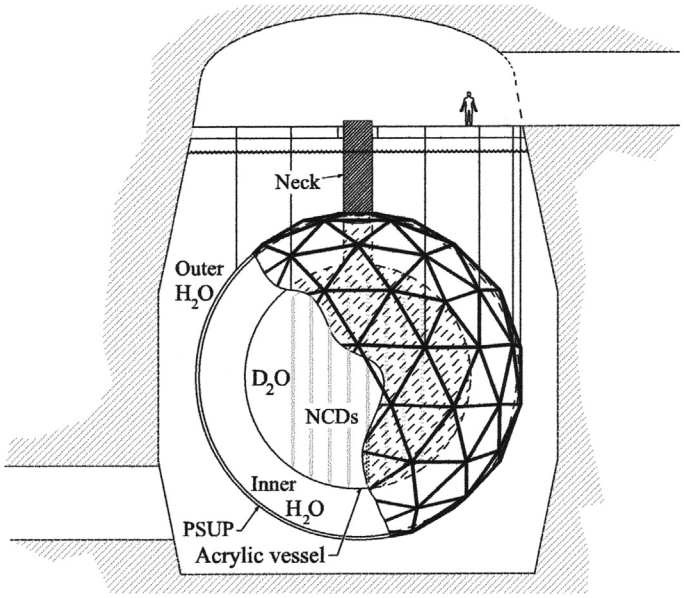

FIGURE 16.29 Layout of the SNO Cherenkov detector. The D_2O (1000 tons) is contained within an acrylic vessel. This volume could be accessed via the neck. The Neutral Current Detectors (NCDs), illustrated as vertical lines in the acrylic vessel housing the D_2O, were employed in the third phase of the experiment. The acrylic vessel was surrounded by water for shielding the radioactivity from the rock (outer H_2O) and photomultiplier tubes (inner H_2O). The photomultiplier support structure (PSUP) holds the photomultiplier tubes and light concentrators. A figure of a person is illustrated in the upper right to provide a perspective of the magnitude of the underground Cherenkov detector. *Reprinted from Boudjemline, K., et al., 2010. The calibration of the Sudbury Neutrino Observatory using uniformly distributed radioactive sources. Nucl. Instrum. Methods Phys. Res. Sect A 620, 171–181, with permission from Elsevier © 2010.*

16.6 APPLICATIONS IN RADIONUCLIDE ANALYSIS

Cherenkov radiation, when produced at significant levels, can be employed for the efficient measurement of radioactivity. This was first demonstrated by Belcher (1953), who used a liquid-nitrogen cooled single photomultiplier to measure Cherenkov radiation intensity in terms of count rates per millicurie (mCi) of various radionuclides in aqueous solution. However, it was not until coincidence counting with dual photomultiplier liquid scintillation analyzers became available commercially and in widespread use in the early 1960s, namely the Packard Tri-Carb 314 liquid scintillation analyzer, did practical research into Cherenkov counting for the measurement of radioactivity begin. (Modern Tri-Carb liquid scintillation counters are now produced by PerkinElmer Inc., Boston among other manufacturers.) Although the production of Cherenkov radiation does not involve the scintillation phenomenon, a conventional liquid scintillation counter can detect and count Cherenkov photons emitted from a given sample in a standard counting vial. The beta-particle emissions of certain radionuclides may be counted in water or in other suitable transparent medium without the use of scintillation fluor or any other chemical reagents. The radionuclide beta-particle emissions may even be counted in the dry state, albeit at a diminished counting efficiency, where the glass or plastic vial wall containing the sample serves as the transparent medium as the Cherenkov radiator. The percent counting efficiencies are calculated according to the equation:

$$\%E = \frac{\text{cpm}}{\text{dpm}} \times 100 \qquad [16.62]$$

where E is the counting efficiency defined by the ratio of the radioactive sample count rate in counts per minute to the sample disintegration rate or radioactivity in units of disintegrations per minute. When the sample radioactivity (dpm) is unknown and the sample radiation count rate is determined experimentally, the radioactivity is calculated from the detection efficiency according to the equation:

$$\text{dpm} = \frac{\text{cpm}}{E} \qquad [16.63]$$

The application of Cherenkov counting to the activity analysis of radionuclides is popular in those cases where the Cherenkov counting efficiency of the radionuclide of interest is adequate to meet particular detection limits required. Table 16.3 provides approximate Cherenkov counting efficiencies of a few radionuclides measured and listed according to

the E_{max} of the β particles emitted by each radionuclide. A more comprehensive table can be found in a reference book on the subject matter (L'Annunziata, 2012e). The E_{max} is listed, because the Cherenkov detection efficiency of radionuclides is a function of the threshold energy (E_{th}) and the refractive index (n) of the medium calculated according to Eq. [16.6]. For example, if water is the medium ($n = 1.333$), the Cherenkov counting efficiency would be a function of the number of β particles of $E > 262$ keV detected relative to the total number of β particles emitted by the radionuclide. Cherenkov counting is popular when counting efficiencies are adequate, because of the ease of sample preparation and low expense incurred in the preparation and disposal of samples. Because water is generally the medium of counting, samples are often left in a state suitable for subsequent tests such as chemical analysis, spectrometric analysis, chromatographic tests, or even chemical compound extraction and isolation. The application of Cherenkov counting to the analysis of specific radionuclides is reviewed in a previous book (L'Annunziata, 2012e).

TABLE 16.3 Experimentally Determined Cherenkov Counting Efficiencies

Nuclide	E_{max} (keV)[a]	Counting Efficiency[b] (%)	References
^{14}C	155 (100%)	1.5[c]	Takiue et al. (2004)
^{45}Ca	258 (100%)	2.3[c]	Takiue et al. (2004)
^{99}Tc	292 (100%)	1.0[d]	Scapita and Fisenne (1996)
^{59}Fe	273 (48.5%)	5.8[d]	Scapita and Fisenne (1996)
	475 (51.2%)		
^{90}Sr	546 (100%)	1.0	Rucker (1991) and Chang et al. (1996)
^{60}Co	Compton electrons[e]	5.6	Grau Carles and Grau Malonda (1995)
^{36}Cl	710 (98%)	6.6	Grau Carles and Grau Malonda (1995)
^{204}Tl	763 (98%)	4.0	Grau Carles and Grau Malonda (1995)
^{137}Cs	510 (92%)	4.8	Grau Carles and Grau Malonda (1995)
	1170 (8%)		
^{198}Au	960 (99%)	5.4	Parker and Elrich (1970)
^{47}Ca	660 (83%)	7.5	Parker and Elrich (1970)
	1940 (17%)		
^{228}Ac	2180 (10.1%)	10.0	L'Annunziata and coworkers (see Aleissa et al., 2008)
	1850 (9.6%)		
	1700 (6.7%)		
	1110 (53%)		
	640 (7.6%)		
	450 (13%)		
^{210}Pb(^{210}Bi)	1160 (from ^{210}Bi >99%)	18	Blais and Marshall (1988)
^{115m}Cd	680 (3%)	35	Bem et al. (1978) and Ramesh and Subramanian (1997)
	1620 (97%)		
^{89}Sr	1490 (100%)	42	Rucker (1991) and Chang et al. (1996)
^{228}Th	580 (from ^{212}Pb)[f]	53	Al-Masri and Blackburn (1994)
	1790 (from ^{208}Tl)[f]		
	2250 (from ^{212}Bi)[f]		
^{86}Rb	680 (8.5%)	53	L'Annunziata and coworkers (see Noor et al., 1996)
	1770 (91.5%)		

TABLE 16.3 Experimentally Determined Cherenkov Counting Efficiencies—cont'd

Nuclide	E_{max} (keV)[a]	Counting Efficiency[b] (%)	References
^{40}K	1310 (89%)	55	Pullen (1986)
^{32}P	1710 (100%)	57	Takiue et al. (1993)
^{234}Th	(from ^{234m}Pa)[f]	60	Navarro et al. (1997); Nour et al. (2002)
	2290 (99.8%)		
^{238}U	(from ^{234m}Pa)[f]	62	Blackburn and Al-Masri (1994)
^{90}Y	2280 (100%)	72	L'Annunziata and Passo (2002)
^{118}Re	2120 (79%)	53	Kushita and Du (1998)
	1970 (20%)		
	<1900 (1%)		
^{106}Ru(^{106}Rh)	2000 (from ^{106}Rh, 3%)	62	Carmon and Dyer (1987)
	2440 (from ^{106}Rh, 12%)		
	3100 (from ^{106}Rh, 11%)		
	3530 (from ^{106}Rh, 68%)		
^{234m}Pa	2290 (99.8%)	54	Grau Malonda and Grau Carles (1998a,b, 2000)
^{42}K	1970 (18.4%)	75	Buchtela and Tschurlovits (1975)
	3560 (81.3%)		
^{226}Ra/^{222}Rn	1505 (from ^{214}Bi, 16%)[f]	77	Blackburn and Al-Masri (1993) Al-Masri and Blackburn (1995a,b, 1999)
	1540 (from ^{214}Bi, 16%)[f]		
	3270 (from ^{214}Bi, 24%)[f]		
	650 (from ^{214}Pb)[f]		
^{34m}Cl	Several β-decay branches up to an energy maximum of 4500	57	Wiebe et al. (1980)
^{38}Cl	4913 (57.6%)	66	Wiebe et al. (1980)
	2770 (11.1%)		
	1111 (31.3%)		
^{18}F	635 (97%)	50%[g]	Wiebe et al. (1978)
^{214}Bi(^{214}Pb)	(See ^{226}Ra, this table)		

[a] *Where more than one beta-decay modes occur for a given radionuclide, the % abundance or relative intensities of each decay process is provided in parentheses.*
[b] *Counting efficiencies will vary from instrument to instrument and vial type (eg, glass or plastic). Also, measurements made with older, less efficient photomultiplier tubes provided lower counting efficiencies than can be expected from contemporary, more efficient phototubes. No attempt is made in this table to categorize the counting efficiencies according to the aforementioned governing factors that will affect the counting efficiency values reported. However, the counting efficiencies listed are intended to provide a general idea of their orders of magnitude relative to the energies of the beta-particle emissions. The counting efficiencies are values reported of nuclides in water without wavelength shifter unless otherwise noted.*
[c] *Measured in the dry state deposited onto the surface of high refractive index ceramic* ($n = 2.1$).
[d] *Measured in 10 mL aqueous 25 mM 7-amino-1,3-naphthalene disulfonic acid (ANSA) wavelength shifter.*
[e] *The Cherenkov photons from ^{60}C are due to Compton electrons produced by its 1.33 and 1.17 MeV gamma-ray emissions.*
[f] *Daughter nuclide.*
[g] *A combination of Cherenkov and scintillation counting in high refractive index methyl salicylate* ($n = 1.5369$).

Chapter 17

Hall of Fame: Part VIII

Ernest O. Lawrence (1901–1958), John Douglas Cockcroft (1897–1967) and Ernest Thomas Sinton Walton (1903–1995), Hans A. Bethe (1906–2005), Willard F. Libby (1908–1980), Edwin M. McMillan (1907–1991), and Glenn T. Seaborg (1912–1999).

Dr. Lawrence envisioned a radically different course—one which did not have those difficulties attendant upon the use of potential differences of millions of volts. At the start, however, it presented other difficulties and many uncertainties, and it is interesting to speculate on whether an older man, having had the same vision, would have ever attained its actual embodiment and successful conclusion. It called for boldness and faith and persistence to a degree rarely matched.

Statement by Dr. W.D. Coolidge in 1947 on presenting the Comstock Prize of the National Academy of Sciences to Nobel Laureate Ernest Lawrence for his achievement in the invention and development of the cyclotron. Lawrence displayed stubborn determination and perseverance in finding solutions that would make his idea of the cyclotron become a reality. The cyclotron remains to this day a vital source of radioisotopes on site in medical clinics and hospitals for use in medical diagnosis.

ERNEST LAWRENCE (1901–1958)

Ernest Orlando Lawrence was born in Canton, South Dakota on August 8, 1901. He was awarded the Nobel Prize in Physics in 1939 "for the invention and development of the cyclotron and for results obtained with regard to artificial radioactive elements." Lawrence received the Nobel Prize at a ceremony on the campus of the University of California, Berkeley on February 29, 1940. He was unable to travel to Stockholm for the traditional award presentation and ceremony due to the precarious travel conditions in the early stages of World War II. At the ceremony Professor R.T. Birge (1940), chair of the Department of Physics at Berkeley, delivered a detailed account of Lawrence's life and work, which was published in "Nobel Lectures, Physics 1922–1941." Some details of Lawrence's biography are taken from this speech.

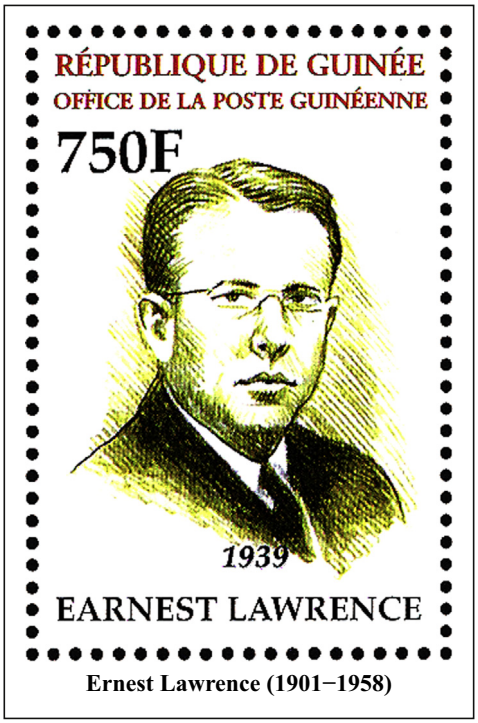

Ernest Lawrence (1901–1958)

Radioactivity: Introduction and History, From the Quantum to Quarks. http://dx.doi.org/10.1016/B978-0-444-63489-4.00017-4
Copyright © 2016 Elsevier B.V. All rights reserved.

Lawrence attended elementary and secondary schools in Canton and Pierre, South Dakota, and studied as an undergraduate at St. Olaf College and the University of South Dakota, where he received a BA degree in chemistry in 1922. He shunned the college fraternities to devote his time to study. Initially he planned to enter medicine, but it became evident to him and his teachers that his interest was physics. He carried out graduate studies at the University of Minnesota, where he received his MSc degree, and spent a year at the University of Chicago before going on to Yale University, where he was awarded a PhD in physics in 1925. Often a secondary school teacher or college professor has a tremendous influence on a successful student, and in Lawrence's case it was Professor W.F.G. Swann, his teacher for advanced study in physics at Minnesota. Lawrence followed Swann, his thesis advisor, to Chicago and Yale, where he completed his doctoral research in physics on the photoelectric effect. Lawrence became a very practical and relentlessly hard-working physicist, and was able to put theory into practice in the development of the cyclotron, an instrument that became vital for the study of the nucleus and the production of new radioactive isotopes useful in medicine, biology, and other fields. Lawrence learned from Swann, who is quoted as saying "Cut-and-try sometimes is more important than too prolonged theorizing." This proved to be the philosophy of Ernest Lawrence throughout his career: he would grasp the theory and put it into practice. The development of the cyclotron appeared possible only in theory.

Upon graduation at Yale, Lawrence remained there as a national research fellow and then assistant professor of physics. Swann left Yale, and the University of California saw the opportunity to attract Lawrence to the Berkeley campus, where he was appointed associate professor of physics in 1928 and then professor in 1930.

As a new member of the faculty at the University of California, Berkeley, Lawrence decided to research the atomic nucleus. As a young scientist he recalled the pioneering work of Ernest Rutherford, who bombarded the nucleus of atoms with alpha particles emitted by radium and discovered that almost the entire mass and energy of the atom is in the nucleus. In 1919, 10 years earlier, Rutherford had discovered that bombarding atoms of nitrogen with alpha particles resulted in the capture of the alpha particles by the nitrogen nucleus with the emission of a proton, thus converting the nitrogen into an isotope of oxygen as follows:

$$ {}_{2}^{4}\mathrm{He} + {}_{7}^{14}\mathrm{N} \rightarrow {}_{8}^{17}\mathrm{O} + {}_{1}^{1}\mathrm{H} \qquad \text{[VIII.1]} $$

Lawrence related in his Nobel lecture on December 11, 1951 in Stockholm, 12 years after receiving the Nobel Prize, how he clearly saw, following the work of Rutherford and his school, that "the next great frontier for the experimental physicist was surely the atomic nucleus." Unfortunately, alpha particles emitted by radionuclides were limited in their energies to approximately 4–8 MeV, and their intensities were very much limited to the amount or activity of the radioactive alpha particle source. Also, protons were much lighter particles and would have a better chance of penetrating the atomic electron coulombic barrier to collide with the nucleus. Lawrence thus contemplated the need to accelerate protons and other charged particles to energies sufficient to collide with atomic nuclei, so he could explore the energy of the nucleus.

One evening in 1929 Lawrence was reviewing the literature in the Berkeley Library when he came across a paper published in German by a Norwegian engineer, Rolf Wideröe (1928), concerning the multiple acceleration of positive ions. Lawrence could not read German easily, but was able to understand the principal approach to the problem from the various drawings in the article. Wideröe had described a glass linear acceleration apparatus where he used a 25,000 V potential to impart to positive potassium ions a 50,000 V potential. He achieved 50,000 V potassium ions with only 25,000 V, a twofold voltage amplification. Wideröe's demonstration of positive ion acceleration was based on the original concept of Swedish Professor Gustaf Ising (1924) for a linear accelerator of positive ions. Ising's principle for the multiple acceleration of positive ions involved the application of radiofrequency oscillating voltages to a series of cylindrical electrodes positioned in a linear fashion, as illustrated in Fig. VIII.1. The idea involved lining up hollow cylinders on the same axis through which the positive ions would be accelerated by a series of successive pushes across the same voltage potential. The accelerating electrodes, through which the ions pass, are successively longer in length due to the increasing velocity of the ions. Three such accelerating electrodes were illustrated in Ising's drawing of his original concept. On the basis of this idea, Ising is considered the father of the development of multiple acceleration.

Upon seeing Wideröe's paper employing the concept of multiple linear acceleration, Lawrence made some calculations. He concluded that to penetrate the coulomb barrier of atoms effectively, he would have to accelerate positive ions to energies in excess of 1 MeV, which would require an accelerator too long for practical laboratory purposes. Lawrence then began to visualize an accelerator consisting not of a large number of cylindrical electrodes in line, but of only two electrodes, which would be used over and over again by sending the positive ions back and forth through the electrodes in a circular fashion in a magnetic field. In relating his reaction after seeing Wideröe's paper, Lawrence (1951) stated:

> *…a little analysis of the problem showed that a uniform magnetic field had just the right properties – that the angular velocity of the ions circulating in the field would be independent of their energy so that they would circulate back and forth between suitable hollow electrodes in resonance with an oscillating electrical field of a certain frequency…*

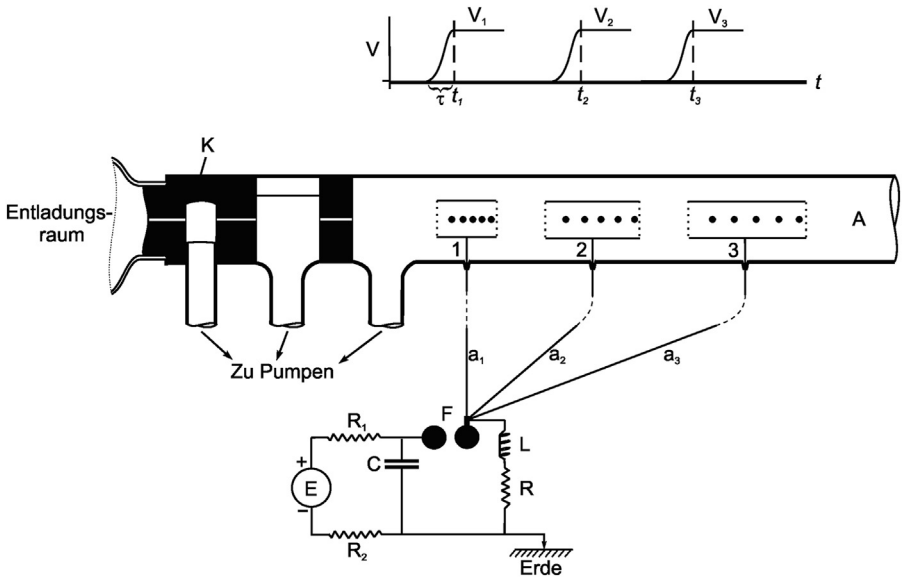

FIGURE VIII.1 The pioneering diagram of Gustaf Ising illustrating his concept of the multiple acceleration of ions. Positive potassium ions produced at K are accelerated from left to right through hollow cylindrical electrodes 1, 2, and 3. The voltage difference applied to each electrode is identical and illustrated graphically above the apparatus. *Adapted from Ising, G., 1924. Prinzip einer Methode zur Herstellung von Kanalstrahlen hoher Voltzahl. Ark. Mat. Astr. Fys. 18 (30), 1–4, as illustrated by Ernest Lawrence in the text of his Nobel lecture, reprinted with permission © The Nobel Foundation 1939.*

Thus Lawrence concluded that two hollow electrodes would be needed, with a relatively low voltage (eg, 4000 V) and oscillating positive and negative potential so that each instant the ions exit one electrode and enter the other, the charges on the electrodes would change in accord with the proper frequency, providing a "push" to the ions as they exit an electrode and thereby increasing their energy and velocity. In the Nobel award ceremony at Berkeley, Professor R.T. Birge (1940) described Lawrence's idea eloquently:

> *Wideröe had used two hollow cylinders, lined up on the same axis. Lawrence sketched a series of such cylinders, but in the case of atoms of small mass, which are most effective in nuclear disintegration, the necessary length of the apparatus would be too great. He next thought of the possibility of using a curved path. Now an electrically charged particle, entering into a magnetic field directed at right angles to the motion of the particle, proceeds to move in a circle constant speed. Moreover, the time to move through a half circle depends only on the charge and mass of the particle and on the strength of the magnetic field. It does not depend on the speed of the particle. The greater the speed, the greater the radius of the circle in which the particle moves [see Fig. VIII.2]. This important fact, which Lawrence immediately noted by writing down a very simple mathematical relation, gave him the idea of the present essential features of the cyclotron. All this happened within a few minutes of the time he had seen Wideröe's paper.*

On that day in 1929, after reading Wideröe's paper, Lawrence invented the principle of the cyclotron. Conceiving the principle of a new concept is one matter, but making it happen may be altogether a seemingly impossible hurdle. Birge (1940) related:

> *The next morning Dr. Lawrence told his friends that he had found a method for obtaining particles of very high energy, without the use of any high voltage. The idea was surprisingly simple and in principle quite correct—everyone admitted that. Yet everyone said, in effect, "Don't forget that having an idea and making it work are two very different things."*

This statement is a lesson to us in all fields of work and whatever the pursuit. Many good ideas that conform with known laws of nature may come to us, but to make these ideas or inventions a reality can be an insurmountable burden to most. The almost endless hours of toil, frustration, and sometimes borderline despair that one encounters necessitate stubborn determination to find solutions and turn an idea into a reality. We can be sure that Lawrence and many others who have achieved greatness have faced these tremendous hurdles. Birge (1940) quoted the remarks of Dr. W.D. Coolidge, then director of the Research Laboratory of the General Electric Company, in 1947 when he presented the Comstock Prize of

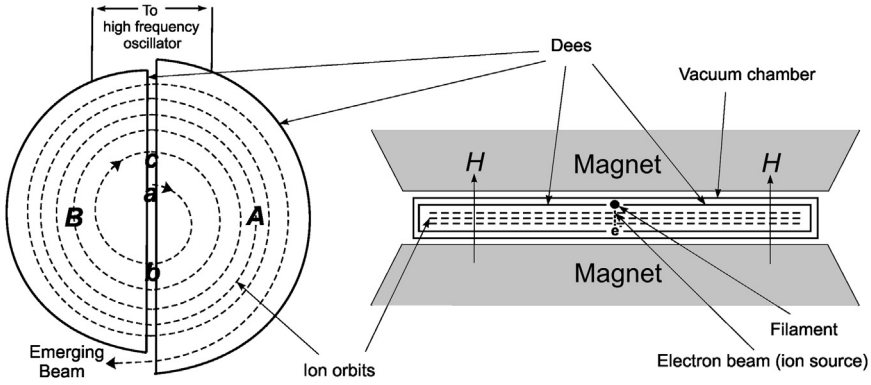

FIGURE VIII.2 Diagrams illustrating the cyclotron method of multiple acceleration of ions. On the left is a drawing of the top or bottom of the cyclotron electrodes, and on the right is a drawing of a side view with the electrodes between magnet poles. Two electrodes *A* and *B* in the form of semicircular hollow plates (called "dees" because they have the shape of the letter D) are mounted in a vacuum chamber with their diametral edges adjacent. The electrodes of the early cyclotron of Lawrence and Livingston measured only 24 cm in diameter; and the hollow semicircular chambers, through which the ions traveled, had a width of only 1 cm. The system is placed between the poles of a magnet whereby the magnetic field *H* is introduced normal to the plane of the plates. High-frequency electric oscillations are applied to the plates to give an oscillating electric field in the diametral region between them. A filament placed above the diametral region creates a stream of electrons that produces the needed positive ions, which are pulled out sideways by the oscillating electric field. The electrons are not drawn out into the cyclotron electrodes because of their very small radii of curvature in the magnetic field. The positive ions (eg, protons, deuterons, or helium nuclei) are accelerated by the oscillating electric field and travel with increasing speed and energy in a circular fashion of increasing radius in the magnetic field. The beam of positive ions emerges from the cyclotron to collide with specific targets, creating new elements, stable isotopes, radioisotopes, etc. *Adapted from Lawrence, E.O., Livingston, M.S., 1932. The production of high-speed light ions without the use of high voltages. Phys. Rev. 40, 19–35.*

the National Academy of Sciences to Lawrence. The prize is awarded only once in 5 years, and is considered one of the greatest honors bestowed by the Academy. Coolidge stated:

> *Dr. Lawrence envisioned a radically different course – one which did not have those difficulties attendant upon the use of potential differences of millions of volts. At the start, however, it presented other difficulties and many uncertainties, and it is interesting to speculate on whether an older man, having had the same vision, would have ever attained its actual embodiment and successful conclusion. It called for boldness and faith and persistence to a degree rarely matched.*

Experimental work on the development of the cyclotron began in 1930, and in the spring of that year Lawrence's first graduate student at Berkeley, Nels Edlefsen, constructed a crude model which gave evidence of working. In September 1930 they gave a preliminary report to a meeting of the National Academy of Sciences (Lawrence and Edlefsen, 1930). In autumn 1930 another graduate student, M. Stanley Livingston, improved on the model, which was only 4.5 in. (11.43 cm) in diameter. The diameter of the accelerator refers to the size of the chamber in which the ions move in a circular path of increasing radius. The first working cyclotron produced 80,000 V protons with less than 1000 V applied to the semicircular accelerating electrode. This was reported to the American Physical Society (Lawrence and Livingston, 1931a) as a demonstration of the cyclotron as a practical apparatus and principle for the acceleration of ions. The same year Lawrence and Livingston (1931b) reported the acceleration of protons to 0.5 MeV with only 5000 V potential applied to the electrodes.

Lawrence and Livingston (1932) described the basic design and principle of the cyclotron with a simple diagram, such as that illustrated in Fig. VIII.2. The cyclotron uses the principle of repeated acceleration of ions by means of resonance with an oscillating field. The ions circulate from the interior of one electrode to the interior of another, back and forth with increasing speed in a circular fashion. The hollow electrodes *A* and *B* in Fig. VIII.2 are placed between the poles of a magnet, and the magnetic field normal to the plane of the hollow plates causes the ions to deflect in a circular fashion with a radius of curvature dependent on the mass, charge, and velocity of the ions.

The oscillating electric field between the electrodes is vital to the operation of the cyclotron. As Lawrence and Livingston (1932) explained, if at one instant there is an ion in the region between the electrodes, and if electrode *A* is negative with respect to electrode *B*, the ion will be "pushed" and accelerated to the interior of electrode *A*. Within the hollow electrode the ion will travel along a circular path under the effect of the magnetic field. After completing a semicircular path in electrode *A*, as illustrated by the arc *a*…*b* in Fig. VIII.2, the ion emerges again between the electrodes. If the time consumed in the travel of this path (from point *a* to point *b* in Fig. VIII.2) is equal to the half-period of the electric oscillations, the electric field will have reversed and the ion will receive a second "push" and be accelerated into the interior of electrode *B* with higher velocity. The ion continues to travel in a circular path in electrode *B* and completes

another semicircular path with greater velocity and greater radius of curvature. Upon completion of this path in electrode *B* at point *c*, the ion again emerges between the electrodes and is again accelerated by the oscillating electric field to travel at greater speed into the interior of the opposing electrode with a path of greater radius of curvature. The process of acceleration repeats itself over and over until the ion achieves a radius of curvature such that it emerges from the cyclotron.

A vital characteristic of the cyclotron principle is that the time taken for an ion to complete a semicircular path is independent of the ion's velocity, and thus independent of the radius of the ion path. This is demonstrated by the calculations below and the elucidation given by Lawrence and Livingston (1932) following their demonstration of an 11 in. (28 cm) diameter cyclotron:

> *…the radius of the path is proportional to the velocity, so that the time required for the travel of a semi-circular path is independent of the ion's velocity. Therefore, if the ion travels its first half-circle in a half-cycle of the oscillations, it will do likewise on all succeeding paths. Hence it will circulate around on ever widening semi-circles from the interior of one electrode to the interior of the other, gaining an increment of energy on each crossing of the diametral region that corresponds to the momentary potential difference between the electrodes. Thus, if, as was done in the present experiments, high frequency oscillations having peak values of 4000 V are applied to the electrodes, and protons are caused to spiral around in this way 150 times, they will receive 300 increments of energy, acquiring thereby a speed corresponding to 1,200,000 V.*

The independence of the time of travel t of an ion along a semicircular path and its radius r and velocity v was demonstrated quantitatively by Lawrence and Livingston (1932). They equated the centrifugal force of an ion traveling along a circular path within an electrode with the magnetic force on the ion, as follows:

$$\frac{mv^2}{r} = \frac{Hev}{c} \qquad \text{[VIII.2]}$$

where m is the mass of the particle, H is the magnetic field, e is the ion charge, and c is the velocity of light in a vacuum. Eq. [VIII.2] may be inverted to read

$$\frac{r}{mv^2} = \frac{c}{Hev} \qquad \text{[VIII.3]}$$

or

$$\frac{r}{v} = \frac{mc}{He} \qquad \text{[VIII.4]}$$

Since the circumference of a circle is defined as $2\pi r$, the distance d of a semicircle would be πr. The time of travel of the ion along the semicircular path of an electrode is defined as

$$t = \frac{d}{v} = \frac{\pi r}{v} = \frac{\pi mc}{He} \qquad \text{[VIII.5]}$$

Thus the time of ion travel along a semicircular path is independent of the radius r and the velocity v. The particle of mass m and charge e was made to travel in phase with the oscillating electric field in the radiofrequency range by adjustment of the magnetic field H of the order of magnitude of 10,000 G.

The 1.2 million volt hydrogen ions produced by Lawrence and Livingston in their early 11 in. (28 cm) diameter accelerator were of sufficient energy to disintegrate the light lithium nucleus; but much higher energies would be needed to penetrate larger atomic coulombic barriers and disintegrate the heavier elements. Larger diameter cyclotrons would require larger magnets, because the spiraling path taken by the ions in the cyclotron are produced by a uniform magnetic field normal to their plane of travel. Thus the pole faces of the magnets had to be at least as large as the diameter of the cyclotron vacuum chamber.

The largest magnets to be found in any scientific laboratory in 1932 were 11 in. (28 cm). Fortunately, however, Lawrence obtained a larger magnet with the assistance of Professor L.F. Fuller at Berkeley, who was previously vice-president of the Federal Telegraph Company. The magnet was once intended for shipment to China, but considered obsolete for its intended purpose and never sent. Consequently, it was of no use to the telegraph company and a godsend for Lawrence. The diameter of the pole faces of the magnet measured 37 in. (94 cm). In addition, deuterium or heavy hydrogen ($^2_1$H) was discovered by Harold C. Urey, which opened the door to the acceleration of deuterons, a particle with twice the mass of the proton. Such particles could have twice the disintegrating power of protons of the same energy. With the larger magnet at hand, Lawrence proceeded to build a 27 in. (69 cm) diameter cyclotron, with the electrodes (dees) measuring 20 in. (51 cm) and having a width of 1.12 in. (2.8 cm). Using the new and larger cyclotron Lawrence and Livingston (1934) were able to accelerate protons ($^1_1$H) to 5 MeV energy. With yet further modification,

essentially increasing the size of the electrodes dees to a diameter of 24.5 in. (62 cm) and width of 1.75 in. (4.4 cm), Lawrence and Cooksey (1936) produced deuterons (heavy hydrogen, $^{2}_{1}$H) and helium ions (alpha particles, $^{4}_{2}$He) of 5 and 10 MeV energy, respectively. The helium ions would be accelerated to twice the energy of the deuterons, as explained by Lawrence and Cooksey (1936):

…The helium ions having twice the charge and mass relative to deuterons, receive twice the increments in energy each time they pass between the dees and arrive at the periphery with twice as much energy. Thus, apart from difficulties of producing doubly charged helium ions at the center, the cyclotron produces 10 MeV alpha particles as readily as 5 MeV deuterons.

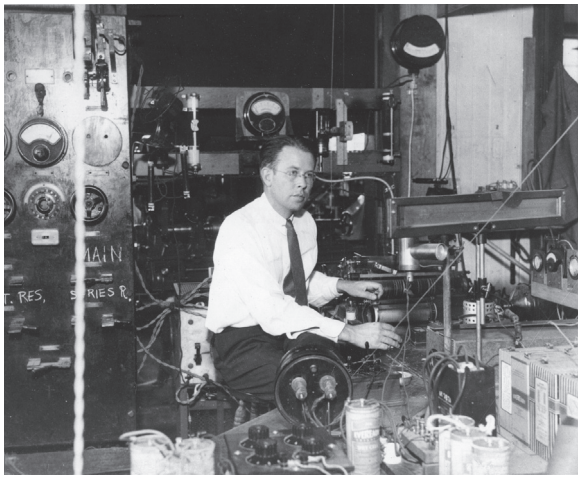

Ernest Lawrence at the control table of the 27-in. (69-cm) cyclotron
Reprinted with permission of the AIP Emilio Segre Visual Archives

The most significant outcome of the new and improved cyclotron demonstrated by Lawrence and Cooksey (1936) was the production of neutrons and artificial radioactive isotopes. Neutron fluxes higher than ever achieved were reported. For example, the neutron flux by the deuteron bombardment of various elements including beryllium was 10^5 times greater than that produced by a mixture of 1 Ci of radon and beryllium. Lawrence began to produce many new radioisotopes, as noted by Lawrence and Cooksey (1936):

With 5 MeV deuterons, it has been found possible (Lawrence, 1935) to produce radioactive isotopes of many of the elements throughout the periodic table. In many cases, the yields of the radioactive substances are quite large; as for example, a day's bombardment of sodium metal with 20 (microamperes) of 5 MeV deuterons produces more than 200 mg equivalent of radio sodium.

In 1939, the year Lawrence received the Nobel Prize, he and coworkers (Lawrence et al., 1939) at the Berkeley lab completed a larger 60-in. (1.5 m) cyclotron that produced 16 MeV deuterons. It had a magnet weighing 200 tons. In his Nobel lecture in Stockholm, Lawrence commented about the larger cyclotron:

…the cyclotron for the first time began to look like a well-engineered machine. It was with this machine that the discoveries of the transuranium elements were made, which have been rewarded this year by the award of the Nobel Prize in Chemistry [1951] to Edwin M. McMillan and Glenn T. Seaborg.

Lawrence and his coworkers wanted to engineer even bigger and more powerful cyclotrons that could produce protons and deuterons at yet higher energies. In his Nobel lecture Lawrence (1951) explained that Hans Bethe predicted they would encounter difficulties at this point, because of the relativistic increase in mass of the particles as they increase in energy in the course of acceleration. This would cause the ions to get out of resonance with the oscillating electric field. Lawrence (1951) added:

…the war prevented the building of this new machine and immediately afterwards Edwin McMillan (1945) and Vladomir Veksler (1944, 1945) independently came forward with the principle of phase stability, which transformed the conventional cyclotron to a much more powerful instrument for higher energies − the synchrocyclotron.

During World War II Lawrence collaborated in the Manhattan Project. He successfully developed the Calutron, which was an electromagnetic method of separating U-235 from other isotopes of uranium required for the enrichment of fissile U-235. In a biographical memoir, Luis Alvarez (1970) noted:

> *Lawrence spent several of the war wears perfecting the Calutron, or mass spectrometer method of separating ^{235}U from ordinary uranium. It is probably true that no one but Ernest Lawrence could have made a success of the Calutron process…The Calutron process was complicated and expensive relative to the gaseous diffusion process [an alternative method for enrichment of U-235], but once a single unit had worked, there was no doubt that the application of a large amount of money could produce enough material for a bomb.*

At the height of the Cold War, Lawrence and Edward Teller successfully argued for the creation in 1952 of a second laboratory to augment the efforts of the Los Alamos National Laboratory. Established at Livermore, California, it had a commitment to the team science approach to multidisciplinary research used by Lawrence (www.llnl.gov/about/history). In honor of Ernest Lawrence, it is named the Lawrence Livermore National Laboratory.

Particle accelerators of various types have been developed over the years from the 1930s to the present. Modern particle accelerators now produce ion beams with energies beyond 10,000 TeV, where 1 TeV = 10^{12} eV. For modern reviews of the history and state of the art of accelerators the reader may peruse works by Bryant (1992), Kullander (2005), and Steere (2005), and a book by Wilson (2001), as well as the chapter entitled "Electromagnetic Radiation: Photons" and Hall of Fame, Part X in this book.

Lawrence received the Nobel Prize not only for the invention and development of the cyclotron but equally, if not more so, for the results obtained therein in the production of new radioactive isotopes. Many of these new isotopes became, soon after their creation from the cyclotron, very useful tools for peaceful applications in nuclear medicine, radiation biology, and agricultural research among other fields of science that in a short term improved our lives and well-being. The significance of this development was underscored by Birge (1940) only 10 years after Lawrence and Edlefsen (1930) first reported the feasibility of the cyclotron:

> *With the cyclotron one can, as stated, transform every stable element into other forms. Some of the final products are themselves stable, but most of them are radioactive. The cyclotron is by far the best device for producing new radioactive substances. …there are about 335 artificially produced radioactive substances, of which 223 have been discovered by means of the cyclotron… Many of the artificially produced radioactive substances are proving of extraordinary value in medicine and biology.*

Marie Curie was one of the first to treat cancer patients with radium radiation. The cyclotron production of many new radioactive sources, differing in their modes of decay and consequently in the radiation types and energies emitted as well as differing half-lives, opened the door to a new frontier of nuclear medicine. Birge (1940) emphasized the importance of this by highlighting developments in medicine:

> *The great importance of radioactive elements in medicine and biology results chiefly from their use as so-called "tracer atoms" …They are now being used also in the direct treatment of various diseases…and shown very promising in the treatment of cancer, and other medical uses are constantly being found.*

Dr. Ernest Lawrence recognized the future applications of the newly created isotopes shortly after they were discovered with his cyclotron. At the Berkeley Radiation Laboratory he collaborated closely with his brother and medical scientist Dr. John Lawrence in research for medical applications of radioactive isotopes. His brother became director of the University of California's Medical Physics Laboratory and Ernest Lawrence became consultant to the Institute of Cancer Research at Columbia. The development of nuclear medicine continues to this day, such as in diagnosis and treatment of cancer with the use of isotopes and radiation in techniques as radiotherapy, computerized tomography, single photon emission computerized tomography, and positron emission tomography. These applications of radioactive isotopes in modern medicine are discussed in the chapter entitled "Radioactivity and Our Well-Being" to this book.

Ernest Lawrence died on August 27, 1958 at Palo Alto, California. After his death his radiation laboratory was officially named the Ernest O. Lawrence Berkeley Laboratory, or in brief the Lawrence Berkeley Laboratory. It is located in the Berkeley hills overlooking San Francisco Bay, and 13 Nobel Laureates have worked there since the radiation laboratory was established in 1928. Here Lawrence's tradition of a multidisciplinary team scientific approach continues to solve global problems in human health, technology, energy, and the environment (http://history.lbl.gov).

JOHN D. COCKCROFT (1897–1967) AND ERNEST T.S. WALTON (1903–1995)

John Douglas Cockcroft and Ernest Thomas Sinton Walton shared the Nobel Prize in Physics in 1951 "for their pioneer work on the transmutation of atomic nuclei by artificially accelerated atomic particles." They joined forces in 1928 at the

Cavendish Laboratory of Cambridge University under the directorship of Ernest Rutherford to work on high-voltage acceleration of protons. In 1932, by means of their newly developed accelerator, Cockcroft and Walton became the first to split the atom artificially and produce a nuclear disintegration by artificial means. They were thus able to demonstrate Einstein's equation of equivalence of mass and energy ($E = mc^2$) by measuring the total energy of the alpha particles liberated from a nucleus of Li-7 upon impact with a proton, and the differences in mass of the interacting proton and Li-7 nucleus and masses of the alpha particles. Some of the biographical data provided here is obtained from the autobiographies of Cockcroft and Walton written at the time of their Nobel award and available in "Nobel Lectures, Physics 1942–1962." Details concerning their collaborative research are taken from their scientific research papers published in *Nature* and the *Proceedings of the Royal Society of London*.

John Cockcroft (1897–1967)
Reprinted with permission from the Nobel Foundation © 1951

Ernest Walton (1903–1995)

John Cockcroft was born on May 27, 1897 at Todmorden, England, where he acquired his secondary education. During 1914–1915 he studied mathematics at Manchester University. Cockcroft served during World War I in the Royal Field Artillery, returning afterward to study electrical engineering at the College of Technology. He served 2 years' apprenticeship with the Metropolitan Vickers Electrical Company. His education and experience in electrical engineering would serve him well in the collaborative work with Ernest Walton on the development of a high-voltage proton accelerator. Following his apprenticeship he entered St. John's College and sat the mathematical tripos in 1924, then went on to work under Lord Rutherford at the Cavendish Laboratory. At first he collaborated on the production of intense magnetic fields and low temperatures with Piotr Kapitsa, who was later awarded the Nobel Prize for studies in low-temperature physics. In 1928 he joined with Walton at the Cavendish to work on the development of a high-voltage accelerator.

Ernest Walton was born at Dungarvan, County Waterford, on the south coast of Ireland, on October 6, 1903. He became a boarder at the Methodist College, Belfast in 1915, where he pursued studies in mathematics and science. In 1922 he entered Trinity College, Dublin on a scholarship, and completed honors courses in mathematics and experimental science with a major in physics. Walton graduated in 1926 with top honors in mathematics and physics, and was awarded an MSc degree in 1927. The same year he received a research scholarship and went to Cambridge University to work under Lord Rutherford at the Cavendish Laboratory, where he soon teamed up with John Cockcroft to develop the high-voltage accelerator with which the pair would become the first to produce nuclear disintegration by artificial means.

Left to Right: Sir John Cockcroft, Ernest Rutherford and Ernest Walton outside the Cavendish Laboratory, 1932 Reprinted with Permission, UK Atomic Energy Authority, courtesy AIP Emilio Segre Visual Archives

In 1919 Rutherford was the first to demonstrate the disintegration of light elements by bombarding them with alpha particles from radioactive sources. In particular, the most celebrated reaction was that whereby he demonstrated the transmutation of nitrogen into oxygen accompanied by the emission of a proton after bombarding the nitrogen with alpha particles from a radium source, illustrated by the following:

$$^{14}_{7}\mathrm{N} + ^{4}_{2}\mathrm{He} \rightarrow ^{17}_{8}\mathrm{O} + ^{1}_{1}\mathrm{H} \qquad \text{[VIII.6]}$$

Alpha particles from radioactive sources were limited in energy. Rutherford was aware that particles like protons, the newly discovered deuteron, and even higher-energy alpha particles were needed, at intensities and energies much higher than any particles that could be provided from any natural sources, to split large atoms, which possess greater binding energies than nitrogen. Steere (2005), in his review of particle accelerators, noted:

> *In a speech before the Royal Society of London in 1927, Rutherford expressed publicly the desire of the scientific community to accelerate charged particles to energies greater than those of natural α-decay in order to disintegrate nuclei with higher binding energies than nitrogen.*
>
> Rutherford (1929).

The energies and intensities of these particles had to be controlled in the laboratory for thorough studies of the constitution of the atomic nucleus and possible nuclear transmutations into various elements. At the Cavendish in 1927 Rutherford was aware that there was a race on to be the first and at the cutting edge in this field. The Swede Gustaf Ising (1924) had set the stage with his concept for particle acceleration, and Norwegian Rolf Wideröe (1928) was soon to demonstrate the feasibility of Ising's principle of particle acceleration. Ernest Lawrence at Berkeley and Robert Van de Graaff at Princeton would in a few years produce high-energy protons with the newly developed cyclotron and electrostatic generator, respectively. Rutherford wanted the Cavendish to be first to penetrate the atomic nucleus with accelerated particles, and an excellent historical account on "how a group of Cambridge scientists won the international race to split the atom" can be read in Cathcart's (2004) book *The Fly in the Cathedral*.

John Cockcroft began his research on the atomic nucleus under the directorship of Lord Rutherford in 1928. That same year George Gamow, a Ukrainian-born physicist, was visiting the Cavendish and discussed the theory of tunneling, where a relatively low-energy proton of only 100 keV, with its de Broglie wave property, had a high probability of penetrating the nucleus of boron and an even greater probability of penetrating the smaller lithium nucleus (Gamow and Houtermans, 1929). Cockcroft discussed the theory with Rutherford in 1928, who agreed he begin work on the problem. Cockcroft was soon joined by Ernest Walton, who had already done some previous work on the development of particle accelerators.

They started work by accelerating protons in a canal ray tube with voltages up to 280 kV and bombarded lithium, beryllium and other targets, searching for gamma radiation from the targets using a gold-leaf electroscope detector (Cockcroft and Walton, 1930). They did not detect any gamma rays from their targets, so decided to develop an apparatus that would accelerate protons to higher energies and search for alpha particles from the disintegration of lithium. With this

objective in mind they needed a system that could provide a steady high-voltage potential, so they devised a system of rectifiers which could provide a steady potential of 800 kV. Such high-voltage sources were not available for general laboratory use, but they devised a voltage multiplier circuit that would produce the needed high voltage by charging capacitors in parallel and releasing the charge in series (Cockcroft and Walton, 1932c; Walton, 1951).

With the capacity of achieving a voltage potential of 800 kV, Cockcroft and Walton successfully constructed an accelerator following tedious experimentation. The basic components of the accelerator are illustrated in Fig. VIII.3. Details in the design and description of the apparatus can be found in Cockcroft and Walton (1932c). In his Nobel lecture Cockcroft (1951) commented:

> *…the new apparatus was completed in early 1932. We were soon able to bring a narrow beam of 500 kV protons out through a thin mica window in the base of the experimental tube, and to measure their range as a function of energy.*

The first working accelerator built by Cockcroft and Walton, illustrated in Fig. VIII.3, was constructed of two glass tubes, A, which measured 3 ft (91 cm) in height and 14 in. (35.5 cm) in diameter. Between the glass tubes was a steel plate, B, to support the electrodes, C. To the steel plate, B, was attached externally a 3 ft^2 (8 m^2) piece of sheet metal, D, which acted as a stress distributor and was maintained at one-half of the potential applied to the electrodes. The electrodes were made of thin-walled steel tubes with the ends fitted with thick rings made from ¾ in. (2 cm) diameter steel to prevent automatic electronic emission. Protons (H^+) were produced by electron-impact ionization of hydrogen in the hydrogen discharge tube at the top of the accelerator, and accelerated at two gaps between electrodes, C, held at increasing potential difference descending to the bottom of the accelerator. The protons traveled from the top through the center of the

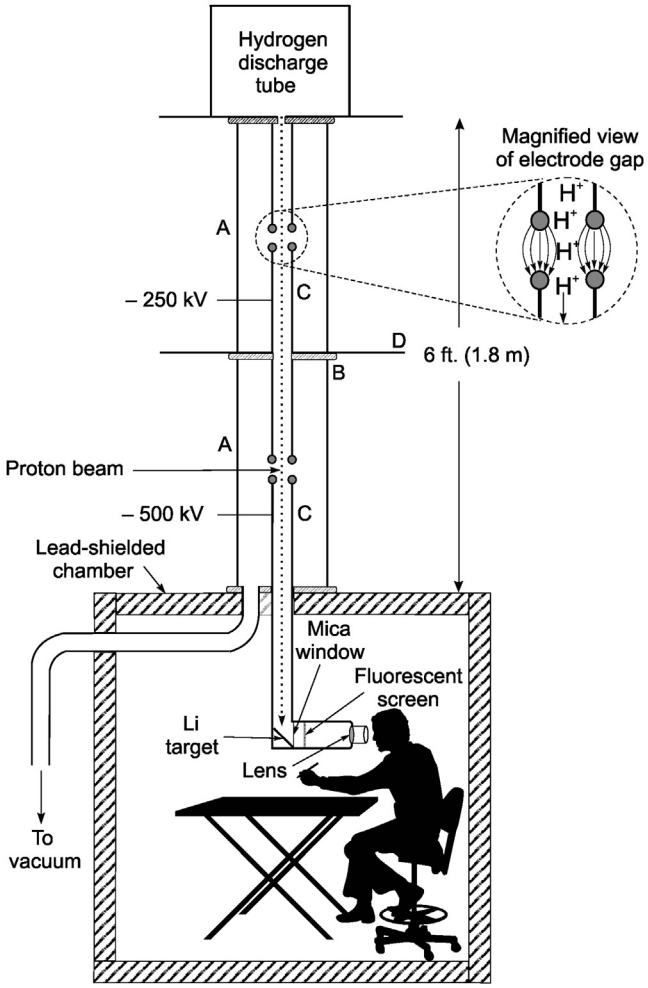

FIGURE VIII.3 Basic design (cross-section) of the Cockcroft and Walton accelerator of 1932. In a magnified view of a gap between electrodes, electric field lines are drawn to illustrate the acceleration of protons across the gap.

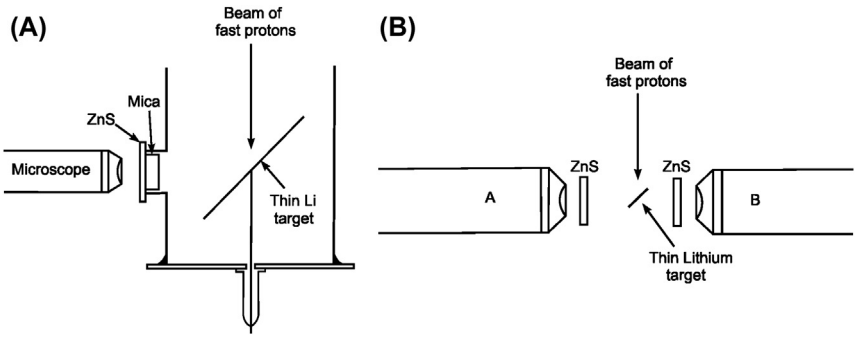

FIGURE VIII.4 Experimental arrangements of Cockcroft and Walton for (A) the detection of α particles by a single observer, and (B) recording the emissions of α particles in coincidence by two observers. The α particles were observed and counted during the bombardment of lithium with a beam of protons in the proton energy range of 125−500 kV. *From Cockcroft (1951), with permission from The Nobel Foundation © 1951.*

electrodes to the bottom to hit specific targets, such as lithium, illustrated in Fig. VIII.3. A thin mica window was placed close below the target to absorb any scattered protons of 600 kV energy; at the same time, it was thin enough to enable α particles from the target to escape and interact with a zinc sulfide fluorescent screen to produce scintillations and emission of visible light. An observer in a shielded chamber below the accelerator tower could count the scintillations of light produced by the α particles by observing these through the magnifying lens of a microscope.

Cockcroft and Walton resumed their experiments by bombarding the accelerated protons against a round 5 cm diameter lithium target and searching for α particles, as illustrated in Fig. VIII.4A. In his Nobel lecture, Cockcroft (1951) describes their experience:

> *Almost at once, at an energy of 125 kV, Dr. Walton saw the bright scintillations characteristic of α-particles, and a first primitive absorption experiment showed that they had a range of 8.4 cm. We then confirmed by a primitive coincidence experiment, carried out with two zinc sulfide (ZnS) screens and two observers tapping keys [Fig. VIII.4B], that the α-particles were emitted in pairs…More refined experiments showed that the energy of the α-particles was 8.6 million volts [MeV]. It was obvious then that lithium was being disintegrated into two α-particles with a total energy release of 17.2 million volts [MeV].*

Their finding was reported in *Nature* (Cockcroft and Walton, 1932b) and the *Proceedings of the Royal Society of London* (Cockcroft and Walton, 1932d). They achieved the first nuclear disintegration by purely artificial means.

The detection of two α particles of measured energy of 8.6 MeV each emitted in coincidence was sufficient evidence for Cockcroft and Walton (1932d) that a proton ($^{1}_{1}\mathrm{H}$) penetrated the nucleus of lithium ($^{7}_{3}\mathrm{Li}$), and the resulting nucleus would split into two α particles ($^{4}_{2}\mathrm{He}$) according to the reaction

$$^{7}_{3}\mathrm{Li} + {}^{1}_{1}\mathrm{H} \rightarrow {}^{4}_{2}\mathrm{He} + {}^{4}_{2}\mathrm{He} + 17.3\ \mathrm{MeV} \qquad \text{[VIII.7]}$$

In his Nobel lecture, Cockcroft (1951) related that Kenneth Bainbridge (1904−1996), with whom he had established a friendship during Bainbridge's Guggenheim fellowship at Rutherford's Cavendish Laboratory in 1933, had measured the mass of $^{7}_{3}\mathrm{Li}$ by mass spectrometry to be 7.0130 atomic mass units (u). This was the most precise measurement at the time for the mass of $^{7}\mathrm{Li}$. Cockcroft and Walton used the mass of the lithium nucleus, the known masses of the proton and α particle, and the measured energies of the α particles to confirm Einstein's equation of mass−energy equivalence ($E = mc^2$). Walton (1951) calculated the mass balance for reaction [VIII.7] as follows.

Sum of masses of $^{7}\mathrm{Li}$ and $^{1}\mathrm{H}$ less the sum of masses of the two α particles gives a mass decrease of

$$\begin{array}{rr} ^{7}\mathrm{Li} & 7.0130\ \mathrm{u} \\ ^{1}\mathrm{H} & \underline{1.0072\ \mathrm{u}} \\ & 8.0202\ \mathrm{u} \\ \text{Less } 2\ ^{4}\mathrm{He} & \underline{8.0022\ \mathrm{u}} \\ \text{Mass decrease} & 0.0180\ \mathrm{u} \end{array} \qquad \text{[VIII.8]}$$

The mass decrease or difference in mass of the combined lithium and proton and the two α particles should be manifested in the reaction as energy, ie, the combined energies of the two α particles, measured to be 17.3 MeV. The mass difference of 0.0180 u converted to energy according to $E = mc^2$ gives

$$\begin{aligned} E &= mc^2 \\ &= (0.0180\ \text{u})(931.494\ \text{MeV}/c^2)\ c^2 \\ &= 16.8\ \text{MeV}, \end{aligned} \qquad \text{[VIII.9]}$$

since by definition 1 u = 931.494 MeV/c^2. The 16.8 MeV calculated above by Walton represents their calculation of the Q value of reaction [VIII.7], which is the interaction of a proton with ^{7}Li yielding two alpha particles as reaction products. For this reaction they used protons accelerated to 600 keV energy. The total kinetic energy shared by the two alpha particles is calculated according to Eqs. [2.11] and [2.12] described in the chapter entitled "Basic Concepts and Definitions" of this book, namely

$$Q = K_{\text{Products}} - K_{\text{Reactants}} \qquad \text{[VIII.10]}$$

and

$$\begin{aligned} K_{\text{Products}} &= Q + K_{\text{Reactants}} \\ &= 16.8\ \text{MeV} + 0.6\ \text{MeV} \\ &= 17.4\ \text{MeV} \end{aligned} \qquad \text{[VIII.11]}$$

Their Q value calculation, based on the then less accurately known masses of the reactants and products, is quite close to the current online QCalc computer-calculated value of 17.3 MeV provided by the National Nuclear Data Center (www.nndc.bnl.gov/qcalc). The calculated energy released is shared by the two alpha particles as kinetic energy.

In addition to splitting the lithium atom with protons, Cockcroft and Walton (1932d) measured the minimum proton energy required to penetrate the lithium nucleus. They varied the energy of the proton beam by controlling the potential difference between the accelerator electrodes, and determined the rates by which the α particles were emitted by a lithium target as a function of proton energy. This was accomplished by counting the number of alpha particles emitted for a given time period of proton bombardment and converting the count/time to the unit counts/minute, ie, α particle counts per minute. The first sign of α particles appeared at the proton-beam energy of approximately 100 kV. The α particle count rate increased exponentially as the beam energy was increased to 500 kV. Their experiment demonstrated clearly that Gamow's prediction of tunnelling was correct: that the proton, being of relatively low mass, would penetrate the small atomic nucleus of lithium at the low energy of approximately 100 kV.

Cockcroft and Walton (1933) proceeded to study the disintegration of other light elements by the accelerated protons. Their next target was boron. They observed that in most interactions the proton would enter the boron nucleus in the proton−energy range of 115 kV and higher, followed by its disintegration into three α particles, ie,

$$^{11}_{5}\text{B} + {}^{1}_{1}\text{H} \rightarrow 3\ {}^{4}_{2}\text{He} \qquad \text{[VIII.12]}$$

Support for reactions [VIII.7] and [VIII.12] and the disintegration of lithium and boron was provided by photographs of particle tracks produced in a Wilson cloud chamber. A Stokes student, P.I. Dee, was at the Cavendish Laboratory working under C.T.R. Wilson on research with Wilson's cloud chamber. Rutherford diverted Dee to work with Cockcroft and Walton. A second accelerator was constructed by Dee and Walton, with a Wilson cloud chamber positioned directly below the proton beam. A shutter was constructed to absorb the beam when in the closed position and to open as appropriate when the cloud chamber expanded, also synchronized with the camera shutter and illuminating lamp. Dee and Walton (1933) took photographs of the tracks produced by two α particles when lithium was the target, and three α particle tracks were photographed when boron was the target.

In 1931 Harold Urey had discovered heavy hydrogen (ie, deuterium or $^{2}_{1}$H), an isotope of hydrogen with twice the mass of hydrogen. A small sample was made available to Cockcroft and Walton in 1933. They were then able to accelerate the deuterons, and study the effect of collisions with various targets. They observed the following reactions of accelerated deuterons with lithium and boron:

$$^{6}_{3}\text{Li} + {}^{2}_{1}\text{H} \rightarrow {}^{4}_{2}\text{He} + {}^{4}_{2}\text{He} \qquad \text{[VIII.13]}$$

$$^{6}_{3}\text{Li} + {}^{2}_{1}\text{H} \rightarrow {}^{7}_{3}\text{Li} + {}^{1}_{1}\text{H} \qquad \text{[VIII.14]}$$

$$^{10}_{5}\text{B} + {}^{2}_{1}\text{H} \rightarrow {}^{11}_{5}\text{B} + {}^{1}_{1}\text{H} \qquad \text{[VIII.15]}$$

Reactions [VIII.14] and [VIII.15] demonstrate the transmutation of one isotope into another. Cloud chamber photographs of particle tracks provided additional evidence of their findings.

Proceeding on to targets of greater mass, Cockcroft, Gilbert, and Walton irradiated carbon ($^{12}_{6}C$) in the form of graphite with accelerated protons or deuterons. They looked for α particles as products of a nuclear reaction, but could not find any after bombarding a graphite target with either protons or deuterons. In early 1934 they heard of the discoveries of Joliot-Curie and Joliot (1934a,b,c), who had produced radioactive positron-emitting elements by bombarding targets of aluminum, boron, and magnesium with α particles from polonium. They borrowed a Geiger counter from Kenneth Bainbridge, and discovered that delayed positrons were emitted after graphite was bombarded with a beam of 400−500 kV protons. The same effect occurred when the graphite was irradiated with a beam of deuterons. The radioisotope produced had a measured half-life of 10 min, corresponding to that of the radioisotope $^{13}_{7}N$ (Cockcroft et al., 1934a,b), and the radiation emissions were demonstrated to be positrons by their direction of deflection in a magnetic field and their absorption properties, characteristic of electrons. The reactions were therefore described to occur as follows:

$$^{12}_{6}C + {}^{1}_{1}H \rightarrow {}^{13}_{7}N \qquad \text{[VIII.16]}$$

$$^{12}_{6}C + {}^{2}_{1}H \rightarrow {}^{13}_{7}N + {}^{1}_{0}n \qquad \text{[VIII.17]}$$

The product ^{13}N decays by positron emission with a half-life ($t_{1/2}$) of 10 min, as follows:

$$^{13}_{7}N \xrightarrow{t_{1/2}=10\ \text{min}} {}^{13}_{6}C + \beta^{+} \qquad \text{[VIII.18]}$$

Cockcroft and Walton had now demonstrated the transmutation of carbon into the radioactive isotope ^{13}N. The same year Joliot-Curie and Joliot (1934a,b,c) had produced positron-emitting radionuclides from stable elements using α particles from polonium. These transmutations were not performed by totally artificial means, because the α particles were emitted naturally by polonium and consequently their energies were not controlled by humans. The production of ^{13}N by Cockcroft et al. (1934a,b) was carried out using artificially produced protons or deuterons of controlled energies. All variables were entirely under human control. This fact was emphasized by Professor I. Waller, member of the Nobel Committee for Physics, in Stockholm, Sweden on the occasion of the presentation of the Nobel Prize to Cockcroft and Walton on December 11, 1951:

> *The work of Cockcroft and Walton was a bold thrust forward into a new domain of research. Great difficulties had to be overcome before they were able to achieve their first successful experiments at the beginning of 1932. By then they had constructed an apparatus which, by multiplication and rectification of the voltage from a transformer, could produce a nearly constant voltage of about six hundred thousand volts. They had also constructed a discharge tube in which hydrogen nuclei were accelerated. Causing these particles to strike a lithium layer, Cockcroft and Walton observed that helium nuclei were emitted from the lithium. Their interpretation of this phenomenon was that a lithium nucleus into which a hydrogen nucleus has penetrated breaks up into two helium nuclei, which are emitted with high energy, in nearly opposite directions. This interpretation was fully confirmed. Thus, for the first time, a nuclear transmutation was produced by means entirely under human control.*

Professor Waller further underscored the significance of their work:

> *The analysis made by Cockcroft and Walton of the energy relations in a transmutation is of particular interest, because a verification was provided by this analysis for Einstein's law concerning the equivalence of mass and energy [$E = mc^2$]. Energy is liberated in the transmutation of lithium, because the total energy of the helium nuclei produced is greater than that of the original nuclei. According to Einstein's law, this gain in energy must be paid for by a corresponding loss in the mass of the atomic nuclei…In subsequent work, Cockcroft and Walton investigated the transmutations of many other atomic nuclei. Their techniques and results remain a model for nuclear research.*

Cockcroft and Walton (1934) and Cockcroft and Lewis (1936a,b) studied other reactions resulting from the bombardment of the light elements, including Li, Be, B, C, N, and O, with protons and deuterons. The Cockcroft and Walton accelerator is still used today, often as an ion injector for more sophisticated and powerful accelerators. For a review of the history and state of the art of particle accelerators the reader may peruse works by Murray and Holbert (2015), Iwata and Noda (2014), Choppin et al. (2013b), Amaldi and Hall (2015), and Sessler and Wilson (2014).

After concluding his collaboration with Walton in 1934, Cockcroft became head of the Royal Society Mond Laboratory in Cambridge. In 1939 he took up a wartime assignment as assistant director of scientific research in the Ministry of Supply, working on the application of radar to coastal and air defense. In 1944 he headed the Canadian Atomic Energy Program and was director of the Montreal and Chalk River Laboratories. In 1946 he returned to England to become

director of the Atomic Energy Research Establishment at Harwell. During 1954–1959 Cockcroft was a member of the scientific research staff of the UK Atomic Energy Authority. He was elected master of Churchill College, Cambridge in 1959, and was also chancellor of the Australian National University, Canberra. In 1960–1962 he was president of the Institute of Physics of the Physical Society, and in 1961–1963 president of the British Association for the Advancement of Science. John Cockcroft died on September 18, 1967.

When Ernest Walton began his collaboration with Cockcroft on a research scholarship at the Cavendish in 1928 he was only 25 years old. He received his PhD 3 years later, after completing their first joint publication on the preliminary development of their accelerator (Cockcroft and Walton, 1930). Before he reached his 29th birthday he and Cockcroft had developed a working accelerator (Cockcroft and Walton, 1932a; *Nature*, February, 13 1932) and split the atom of lithium with protons accelerated to energies of 125–400 keV (Cockcroft and Walton, 1932b; *Nature*, April 30, 1932). He was a Clerk Maxwell scholar at the Cavendish Laboratory during his collaboration with John Cockcroft from 1932 to 1934.

Ernest Walton returned as a fellow to Trinity College, Dublin. In 1946 he was appointed Erasmus Smith professor of natural and experimental philosophy at Trinity, and elected senior fellow there in 1960. Walton served on numerous scientific, governmental, and church committees in his home country of Ireland. Ernest Walton died in Belfast on June 25, 1995.

HANS A. BETHE (1906–2005)

Hans Albrecht Bethe was born on July 2, 1906 in Strasbourg, Alsace-Lorraine, which was then a part of Imperial Germany. He was awarded the Nobel Prize in Physics in 1967 "for his contributions to the theory of nuclear reactions, especially the discoveries concerning the energy production of stars." Bethe wrote a brief autobiography at the time of his Nobel Prize award, which was published in "Nobel Lectures, Physics 1963–1970." Specific dates and places of his study and work were obtained from this source.

Hans Bethe (1906–2005)

After studying at the Gymnasium in Frankfurt, in 1924 Hans Bethe went to the University of Frankfurt for 2 years, and completed his PhD degree in theoretical physics at the University of Munich in July 1928 under the guidance of Professor Arnold Sommerfeld. After completing his doctorate Bethe taught at the Universities of Frankfurt and Stuttgart for a semester at each institution. In autumn 1929 he transferred to the University of Munich and became Privatdozent in 1930; he remained there until autumn 1932. In the winter semester of 1932–1933 Hans Bethe was appointed to the faculty of the University of Tübingen. However, not long after Hitler came to power in 1933 a law was passed forbidding appointments in the civil service to anyone with Jewish ancestry. Bethe lost his faculty position because his mother was Jewish, although he personally did not consider himself Jewish. His mother had converted to the Lutheran Church and his father was also

Christian. At the time, Hans Bethe's expectations to pursue physics were low. He emigrated to England in October 1933 and was appointed to a temporary position of lecturer at the University of Manchester in 1933−1934. A fellowship at the University of Bristol followed in autumn 1934.

In February 1935 Bethe was offered an assistant professorship at Cornell University in Ithaca, New York. He emigrated to America, and after a little more than 2 years was promoted to full professor at Cornell in 1937. He remained a member of the physics faculty at Cornell for the rest of his life, and was absent only temporarily for sabbatical leaves and work in the Manhattan Project during World War II.

During the 1930s Hans Bethe made many of his major contributions to nuclear physics. The first was a series of three lengthy papers in the journal *Reviews of Modern Physics* in 1936 and 1937, comprising almost 500 pages of a comprehensive review of experimental and theoretical nuclear physics; he wrote alone and also with Robert F. Bacher and M. Stanley Livingston, who had collaborated previously with Ernest Lawrence in the development of the cyclotron in 1931−1934. The three papers (Bethe and Bacher, 1936; Bethe, 1937; Livingston and Bethe, 1937) were so comprehensive that together they became known as the Bethe Bible, and 50 years later were republished as a book by the American Institute of Physics (Bethe et al., 1986). The significance of his work in theoretical physics was underscored by Professor O. Klein, member of the Swedish Academy of Sciences, at the presentation of the Nobel Prize to Hans Bethe on December 11, 1967:

> *Bethe belonged to the small group of young theoretical physicists who, through skill and knowledge, were particularly qualified for tackling the many theoretical problems turning up in close connection with the rapidly appearing experimental discoveries. The centre of these problems was to find the properties of the force that keeps the protons and neutrons together in the nucleus, the counterpart of the electric force that binds the atomic electrons to the nucleus. Bethe's contributions to the solution to these problems have been numerous and are still continuing… Moreover, about the middle of the thirties he wrote, partly alone, partly together with some colleagues, what nuclear physicists at the time used to call the Bethe Bible, a penetrating review of about all that was known of atomic nuclei, experimental as well as theoretical.*

In April 1938 George Gamow convened a small conference of physicists and astrophysicists in Washington, DC, sponsored by the Carnegie Institution's Department of Terrestrial Magnetism. This gave the astrophysicists the opportunity to discuss with the nuclear physicists all that they know about the internal elemental constitution and properties of the stars. The conference highlighted a key problem that the astrophysicists needed to solve: the origin of the energy of the Sun. How could the Sun continue for thousands of millennia, before and during the evolution of the human race, to emit light and heat without exhausting its source of energy? At one time it was thought that radioactivity might be the answer, or even gravity forcing particles to reach high velocities and kinetic energies, but the energy yield from such sources would not be sufficient or long lasting, and the lack of sufficient amount of radioactive substances in the Sun's matter obviated radioactivity. Only months after the conference, taking into account the properties of the Sun, including the temperature, pressure, and elemental constitution of Sun matter, Hans Bethe found evidence for nuclear fusion and nuclear reactions as the key processes that provide the long-lasting energy of the Sun. This work was summarized in a lengthy paper on "Energy Production in Stars" submitted to the journal *Physical Review* in September 1938 and published there in March 1939 (Bethe, 1939). Bethe grasped the facts from the astrophysicists present at the conference, and in only three or four months provided the answers. The facts and reasoning Bethe used were eloquently described in Professor Klein's Nobel presentation speech:

> *During that conference and afterwards he [Bethe] seems also to have acquired the necessary astrophysical knowledge. This knowledge depended mainly on a pioneer work by [Arthur S.] Eddington from the year 1926, according to which the innermost part of the sun is a hot gas mainly consisting of hydrogen and helium. Owing to the high temperature, about 20 million degrees, − these atoms being dissolved into electrons and nuclei − the mixture, despite the high density − about 80 times that of water − really behaves like a gas. The amount of energy generation necessary to maintain this state was known from measurements of the radiation falling on the earth. Taken as a whole it is enormous, but very slow as compared to the size of the sun…This very slow burning together with the very high energy release from a given weight of fuel gives this source the high durability required by geology and the long existence of life on the earth.*

Bethe explained that all nuclei in a normal star are positively charged, and to react the nuclei would need to penetrate the coulomb potential barrier of others. He demonstrated that for a given temperature and equal conditions for all nuclei, the reactions that could occur most easily would be those between nuclei of the smallest value of W, defined by the following:

$$W = AZ_0^2 Z_1^2 \qquad \text{[VIII.19]}$$

where

$$A = A_0 A_1/(A_0 + A_1) \qquad \text{[VIII.20]}$$

and A_0 and A_1 are the atomic weights of the two colliding nuclei and Z_0 and Z_1 are their atomic numbers or the charges on the nuclei. Thus, as explained by Bethe, the simplest of all possible reactions would be that between two proton nuclei, or

$$^{1}_{1}\mathrm{H} + {}^{1}_{1}\mathrm{H} \rightarrow {}^{2}_{1}\mathrm{H} + \beta^{+} + \nu \qquad \text{[VIII.21]}$$

In this reaction one of the protons is converted into a neutron, forming deuterium with the emission of a positron and neutrino. The reaction was first suggested by von Weizsäcker (1937) and calculated by Bethe and Critchfield (1938), who demonstrated that the reaction is relatively very slow, because it involves the beta disintegration, and there would be no chance to observe such a slow reaction on Earth. However, Bethe explained that the unlimited time and very large supply of protons of very high energy in the stars would yield a rate of energy production that corresponded to the observed energy production in the Sun. The deuterons formed by this reaction quickly react with protons to yield ^{3}He, according to the reaction

$$^{2}_{1}\mathrm{H} + {}^{1}_{1}\mathrm{H} \rightarrow {}^{3}_{2}\mathrm{He} + \gamma \qquad \text{[VIII.22]}$$

which in turn, with the buildup on ^{3}He and a temperature of 15 million degrees, coalesce to form ^{4}He according to the following.

$$^{3}_{2}\mathrm{He} + {}^{3}_{2}\mathrm{He} \rightarrow {}^{4}_{2}\mathrm{He} + {}^{1}_{1}\mathrm{H} + {}^{1}_{1}\mathrm{H} \qquad \text{[VIII.23]}$$

Bethe demonstrated that at higher temperatures the following reaction would compete with the above reaction [VIII.23]:

$$^{4}_{2}\mathrm{He} + {}^{3}_{2}\mathrm{He} \rightarrow {}^{7}_{4}\mathrm{Be} + \gamma \qquad \text{[VIII.24]}$$

Bethe (1938, 1968) showed that the ^{7}Be formed above could further react with a proton to form ^{8}B

$$^{7}_{4}\mathrm{Be} + {}^{1}_{1}\mathrm{H} \rightarrow {}^{8}_{5}\mathrm{B} + \gamma \qquad \text{[VIII.25]}$$

which would yield two helium nuclei according to the reaction

$$^{8}_{5}\mathrm{B} \rightarrow {}^{4}_{2}\mathrm{He} + {}^{4}_{2}\mathrm{He} + \beta^{+} + \nu \qquad \text{[VIII.26]}$$

yielding neutrinos of very high energy. Ahmad et al. (2002) have detected solar neutrinos and found that the total number of neutrinos coming from the Sun do match predictions of nuclear fusion in the Sun.

In his Nobel lecture given in Stockholm on December 11, 1967, Hans Bethe provided arguments in favor of certain reactions:

> *I examined (Bethe, 1939) the reactions between protons and other nuclei, going up in the periodic system. Reactions between ^{1}H and ^{4}He lead nowhere, there being no stable nucleus of mass 5. Reactions of ^{1}H with Li, Be, and B, as well as with deuterons, are all very fast at the central temperatures of the sun, but just this speed of the reaction rules them out…In fact, and just because of this reason, all of the elements mentioned from deuterium to boron, are extremely rare on earth and in the stars, and can therefore not be important sources of energy.*

However, Bethe found that the next element in the periodic table, carbon, reacts very differently. Firstly, it is a relatively abundant element in the Sun, and, in the gaseous plasma of stellar temperature, the nucleus of ^{12}C would undergo the following cycle of reactions, referred to as the carbon−nitrogen (CN) cycle:

$$^{12}_{6}\mathrm{C} + {}^{1}_{1}\mathrm{H} \rightarrow {}^{13}_{7}\mathrm{N} + \gamma \qquad \text{[VIII.27]}$$

$$^{13}_{7}\mathrm{N} \rightarrow {}^{13}_{6}\mathrm{C} + \beta^{+} + \nu \qquad \text{[VIII.28]}$$

$$^{13}_{6}\mathrm{C} + {}^{1}_{1}\mathrm{H} \rightarrow {}^{14}_{7}\mathrm{N} + \gamma \qquad \text{[VIII.29]}$$

$$^{14}_{7}\mathrm{N} + {}^{1}_{1}\mathrm{H} \rightarrow {}^{15}_{8}\mathrm{O} + \gamma \qquad \text{[VIII.30]}$$

$$^{15}_{8}\mathrm{O} \rightarrow {}^{15}_{7}\mathrm{N} + \beta^{+} + \nu \qquad \text{[VIII.31]}$$

$$^{15}_{7}\mathrm{N} + {}^{1}_{1}\mathrm{H} \rightarrow {}^{12}_{6}\mathrm{C} + {}^{4}_{2}\mathrm{He} \qquad \text{[VIII.32]}$$

Bethe (1967) explained that reactions [VIII.27], [VIII.29], and [VIII.30] are radiative captures whereby the proton is captured by the nucleus and the energy of the reaction is emitted in the form of gamma radiation, which is converted into thermal radiation of the Sun. The remaining reactions [VIII.28] and [VIII.31] are spontaneous beta decays with lifetimes of only 10 min and 3 min, respectively, which are negligible in comparison to stellar lifetimes. The last reaction [VIII.32] is a nuclear reaction resulting in two nuclei as products of the collision. It is the most interesting, because the reaction closes the CN cycle, as the ^{12}C nucleus is reproduced from the same nucleus from which the reaction started. Thus Bethe (1967) classified the ^{12}C as a catalyst of a reaction resulting in the production of one ^{4}He nucleus, in which process two neutrinos are emitted that take away approximately 2 MeV energy together. The remaining energy, approximately 25 MeV per cycle, is released to keep the Sun warm. Bethe demonstrated that at higher stellar temperatures, when the CN cycle prevails there is a high probability for the reaction chain

$$^{16}_{8}O + {}^{1}_{1}H \rightarrow {}^{17}_{9}F + \gamma \qquad \text{[VIII.33]}$$

$$^{17}_{9}F \rightarrow {}^{17}_{8}O + \beta^{+} + \nu \qquad \text{[VIII.34]}$$

$$^{17}_{8}O + {}^{1}_{1}H \rightarrow {}^{14}_{7}N + {}^{4}_{2}He \qquad \text{[VIII.35]}$$

This reaction chain is not cyclic, but Bethe indicated that it feeds into the CN cycle, whereby the entire set of reactions is referred to as the CNO bi-cycle.

Bethe (1942) summarized his findings and the rationale that he used to investigate nuclear transmutations as the source of stellar energy. He pointed out:

> *We know, however, from radioactive measurements [radioisotope dating of rocks] that the age of the earth is at least 1500 million years. The sun is likely to be at least as old, and there is no reason to assume that its radiation 1500 million years ago was much less than it is now. In fact, it is certain that the radiation did not change appreciably during the last 500 million years, because during all this time life existed on earth [because life can tolerate only a narrow range of temperatures].*

Bethe explained that the solution to the problem of energy production in the Sun was unlocked when Rutherford discovered in 1919 the transmutation of atomic nuclei. He noted that Atkinson and Houtermans (1929) first suggested the possibility of nuclear transmutations as the source of stellar energy. Bethe proceeded to demonstrate that nuclear reactions, and specifically which nuclear reactions, would give sufficient energy and reaction rates to provide the energy supplied by the Sun over hundreds of millions of years. By using Einstein's equation of equivalence of energy and mass, $E = mc^2$, Bethe (1942) gave an illustrative example of the energy released when a nucleus of oxygen, namely ^{16}O, was created by the fusion of its constituent nucleons—that is, the fusion of eight protons and eight neutrons. Bethe showed that the mass of the ^{16}O nucleus was smaller than the sum of the masses of its eight protons and eight neutrons. He gave the following explanation to the mass difference:

> *Where did the remaining mass go to? Here the special relativity theory gives the answer: The smaller mass of ^{16}O indicates that this nucleus contains less energy than the 16 separate protons and neutrons. Energy is set free when the protons and neutrons combine to form a nucleus; in fact, that is the reason why a nucleus stays together at all. The amount of energy set free, the binding energy, can be calculated from the decrease in mass by* m *corresponds to a decrease of energy by* mc^2 *where* c *is the velocity of light.*

Bethe (1942) calculated firstly the sum of the masses of the constituent protons and neutrons of ^{16}O. He then took the difference of the sum of the masses of the constituent nucleons and the mass of the lighter ^{16}O nucleus. From the mass difference he calculated the energy released (readers should note that the proton and neutron masses used by Bethe in his calculations were based on the most accurately measured values at the time; these differ slightly from current more accurately measured values):

	Mass of 8 neutrons	8.0714 u (atomic mass units)
	Mass of 8 hydrogen atoms	8.0650
	Total	16.1364
Minus	Mass of ^{16}O atom	16.0000
	Mass change	0.1364 u

Corresponding energy change = 0.000205 ergs = 205 μergs, based on the conversion factor of 0.0015 ergs of energy per atomic mass unit (u).

On this calculation, Bethe (1942) commented:

> *This energy may seem very small, but it must be remembered that it is for a single oxygen nucleus! If we could produce a* gram *of oxygen nuclei by bringing half a gram of protons and half a gram of neutrons together, the energy set free would be* 7.7×10^{18} *ergs, or 210,000 kW-hours. The ordinary combustion of a gram of coal gives about 1/100 of a kilowatt-hour. Thus it is seen what tremendous energies are liberated when nuclei are formed from protons and neutrons: a very promising result when we are trying to explain the energy production in stars.*

In this calculation, for reasons of brevity Bethe did not show details of how he arrived at the energy equivalence of 210,000 kW-hours. The following calculations give all the details.

We can convert the mass difference of 0.1364 u calculated by Bethe to energy using Einstein's equation of equivalence of mass and energy, as follows:

$$\begin{aligned} E &= mc^2 \\ &= (0.1364\ \text{u})(1.66 \times 10^{-27}\ \text{kg/u})\left(3 \times 10^{8}\ \text{m/s}\right)^2 \\ &= 2.04 \times 10^{-11}\ \text{J} \end{aligned} \qquad \text{[VIII.36]}$$

The energy in joules (J) converted to energy in ergs becomes

$$\frac{2.04 \times 10^{-11}\ \text{J}}{1 \times 10^{-7}\ \text{J/erg}} = 2.04 \times 10^{-4}\ \text{ergs} = 204\ \mu\text{ergs}$$

These calculations give the energy released in the fusion of only eight protons and eight neutrons to form one nucleus of oxygen-16. To calculate the energy released by combining 0.5 g of protons and 0.5 g of neutrons to form 1.0 g of oxygen, we may first calculate the number of protons and neutrons contained in 0.5 g of each, as follows:

$$1\ \text{proton} = 1.6726 \times 10^{-24}\ \text{g} \quad \text{or} \quad \frac{1\ \text{proton}}{1.6726 \times 10^{-24}\ \text{g}} = 5.9787 \times 10^{23}\ \text{protons/g}$$

$$1\ \text{neutron} = 1.6749 \times 10^{-24}\ \text{g} \quad \text{or} \quad \frac{1\ \text{neutron}}{1.6749 \times 10^{-24}\ \text{g}} = 5.9705 \times 10^{23}\ \text{neutrons/g}$$

The number of protons or neutrons per gram of each nucleon $\approx 6 \times 10^{23}$ and 0.5 g of either nucleon number $\sim 3 \times 10^{23}$. Since $8\text{p} + 8\text{n} = 1\ ^{16}\text{O} = 1$ fusion reaction, we divide the number of protons (p) or number of neutrons (n) contained in 0.5 g of either by a factor of eight to arrive at the number of fusion reactions achieved with 0.5 g of p + 0.5 g of n, as follows:

$$\frac{3 \times 10^{23}\ \text{protons}/0.5\ \text{g}}{8\ \text{protons/fusion reaction}} = 3.75 \times 10^{22}\ \text{fusion reactions}/0.5\ \text{g}\ \ \text{p} + \text{n}$$

If one fusion reaction as calculated above yields 204 μergs of energy, then 3.75×10^{22} fusion reactions yield

$$\left(\frac{204 \times 10^{-6}\ \text{ergs}}{\text{fusion reaction}}\right)\left(3.75 \times 10^{22}\ \text{fusion reactions}\right) = 7.7 \times 10^{18}\ \text{ergs}$$

The energy liberated in ergs is converted to energy units in joules (J) and kilowatt-hours (kWh) as follows:

$$\left(7.7 \times 10^{18}\ \text{ergs}\right)\left(1 \times 10^{-7}\ \text{J/erg}\right) = 7.7 \times 10^{11}\ \text{J}$$

and

$$\frac{7.7 \times 10^{11}\ \text{J}}{3.6 \times 10^{3}\ \text{J/Wh}} = 2.1 \times 10^{8}\ \text{Wh} = 2.1 \times 10^{5}\ \text{kWh} = 210{,}000\ \text{kWh}$$

Bethe (1942) thus demonstrated that fusion and other nuclear reactions are immense sources of energy generated by the Sun. He also proceeded to demonstrate the reaction rates would correspond to the long life of the Sun based on laboratory data for nuclear reaction probabilities and values for the temperature of the Sun as calculated by astrophysicists on the basis

of calculations by Eddington (1926). Taking the nuclear reactions of the CN cycle described by Eqs. [VIII.27]–[VIII.32] as examples, Bethe calculated how long any nucleus at the center of the Sun will live, on average, before it is attacked by a proton and undergoes a nuclear transmutation. Thus at a temperature of 20,000,000°C, Bethe found the average lifetime for the following nuclei to be

^{12}C	2,500,000 years
^{13}N	10 min (spontaneous decay)
^{13}C	50,000 years
^{14}N	4,000,000 years
^{15}O	2 min (spontaneous decay)
^{15}N	20 years

Thus a complete CN cycle of the six reactions, with ^{12}C in the first reaction, acts as a catalyst for the formation of one ^{4}He nucleus consuming four protons (see reactions [VIII.27]–[VIII.32]), takes about 6,000,000 years. Bethe (1942) provided the following conclusions based on the reaction rates and nuclear fuel converted in the Sun:

> *We have found that about 40 microergs are set free for each helium nucleus produced in the sun, or 10 for each proton destroyed. One gram of the sun's material has been calculated to contain about 2×10^{23} protons. Therefore if all the protons can be converted into helium, the available energy supply is 2×10^{18} ergs per gram. At present the sun radiates about 2 ergs per gram of its mass. At this rate the energy supply will last for about 30 billion years. It is evident that our nuclear reactions represent a sufficiently plentiful source of energy.*

Hans Bethe was recruited by Oppenheimer to head the theoretical division of the secret nuclear weapons laboratory at Los Alamos during World War II to work on the fission bomb. After the success of the Manhattan Project he returned to Cornell University. Bethe told his biographer (Hall, 1995) why he decided to work on the bomb: "Rose [his wife] asked me to consider carefully whether I really wanted to continue to work on this. Finally, I decided to do it. The fission bomb had to be done, because the Germans were presumably doing it… The main reason was, I felt in this way I could make the greatest contribution to the war effort. After all, nuclear physics was my field." Edward Teller later tried to convince Bethe to work on the hydrogen fusion bomb, but Bethe declined. He became deeply involved with disarmament in the 1950s. He was a member of the US president's Science Advisory Committee in the 1950s, and remained involved in an advisory capacity nationally and internationally for decades.

Hans Bethe was an active member of Albert Einstein's Emergency Committee of Atomic Scientists, which drew public attention to the dangers of nuclear war and the peaceful applications of nuclear energy (see "Einstein the Pacifist" in Hall of Fame, Part III of this book). Although not active in the Pugwash movement focused on dialogue, disarmament, and the prevention of war, Bethe participated in the Pugwash meeting that took place at Stowe, Vermont, USA in 1961; and he also shared the Albert Einstein Peace Award with Nobel Peace Laureate Joseph Rotblat in 1992 (Tucker, 2005).

Hans Bethe died at the age of 98 on March 8, 2005.

WILLARD F. LIBBY (1908–1980)

Willard Frank Libby was born in Grand Valley, Colorado on December 17, 1908. He was awarded the Nobel Prize in Chemistry 1960 in "for his method to use carbon-14 for age determination in archeology, geology, geophysics, and other branches of science." Libby got his primary and secondary education at schools near Sebastopol, California during 1913–1926. He entered the University of California at Berkeley in 1927, and was awarded a PhD there in 1933. The same year Libby was appointed instructor in the Department of Chemistry at Berkeley, and by 1943 he had risen in the ranks at Berkeley to become associate professor of chemistry. In 1941 he was awarded a Guggenheim fellowship and chose to work at Princeton University. His fellowship was interrupted in December that year to work on America's war effort at Columbia University in the Manhattan District Project until 1945. (The Manhattan District Project is the abbreviated form of referring to the original codename of the Manhattan Engineering District for the military component of the project to produce the world's first nuclear weapons. The general codename of Manhattan Project was used subsequently.) All this time Libby remained on leave from his post at the Department of Chemistry at Berkeley.

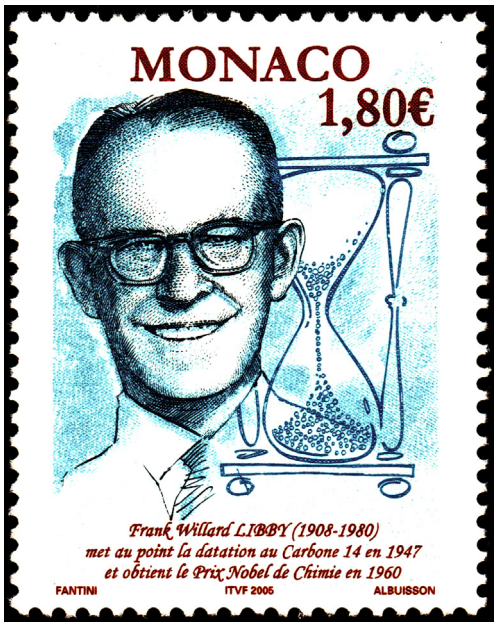

Willard Libby (1908–1980)

After the war, Libby was appointed in 1945 to the post of professor of chemistry at the Institute of Nuclear Studies at the University of Chicago. In 1954 President Eisenhower appointed him a member of the US Atomic Energy Commission, in which capacity he headed Eisenhower's international Atoms for Peace program to help promote peaceful applications of nuclear energy in various fields, including agriculture, medicine, hydrology, and industry. He resigned from this position in 1959 to take up a new post as professor of chemistry at the University of California, Los Angeles (UCLA), and was subsequently appointed as director of the Institute of Geophysics and Planetary Physics in 1962 (Nobel Lectures, Chemistry, 1964).

In his Nobel lecture given in Stockholm on December 12, 1960 and at an International Atomic Energy Agency (IAEA) international symposium on radioactive dating, Libby (1967) related the history of the carbon-14 dating technique. The sequence of events given here is taken in part from his historical account.

The origins of natural atoms of carbon-14, upon which Libby's dating technique is based, are neutrons produced in the Earth's atmosphere. In 1939 Korff and Danforth developed a boron−trifluoride counter for the detection of neutrons. Serge A. Korff and coworkers flew the counter on a balloon, and discovered that neutrons were produced in the atmosphere by the collision of cosmic rays at the top of the atmosphere (Korff, 1940). The intensity of the neutrons was found to be two neutrons per square centimeter of the Earth's surface per second. Korff (1940) indicated that the absorption of neutrons by nitrogen in the atmosphere would likely make carbon-14 according to the (n,p) reaction demonstrated artificially in a Wilson cloud chamber by Kurie (1934), Bonner and Brubaker (1936a,b), and Burcham and Goldhaber (1936):

$$^{14}_{7}\mathrm{N} + {}^{1}_{0}\mathrm{n} \rightarrow {}^{14}_{6}\mathrm{C} + {}^{1}_{1}\mathrm{H} \qquad \text{[VIII.37]}$$

The likely production of ^{14}C in the Earth's atmosphere was vital to the conception of the radiocarbon dating technique, as stated by Libby (1960) in his Nobel lecture:

> *Professor Korff noted in one of his papers announcing the discovery of neutrons [in the upper atmosphere] that the principal way in which the neutrons would disappear would be to form radiocarbon…knowing that there are about 2 neutrons formed per square centimeter per second, each of which forms a carbon-14 atom, and assuming that the cosmic rays have been bombarding the atmosphere for a very long time in terms of the lifetime of carbon-14 [half-life is 5730 years]…we can see that a steady-state condition should have been established, in which the rate of formation of carbon-14 would be equal to the rate at which it disappears to reform nitrogen-14 [radiocarbon decays by the emission of a beta particle to form stable nitrogen-14 according to Eq. [VIII.38]]. This allows us to calculate quantitatively how much carbon-14 would exist on earth [see Fig. VIII.5].*

$$^{14}_{6}\mathrm{C} \rightarrow {}^{14}_{7}\mathrm{N}\ (\text{stable}) + \beta^{-} + \overline{\nu} \qquad \text{[VIII.38]}$$

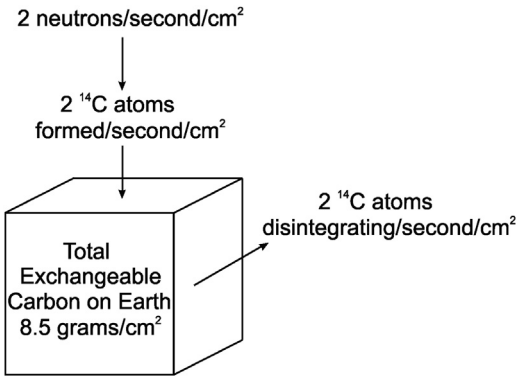

FIGURE VIII.5 Radiocarbon genesis and mixing. *Adapted from Libby, W.F., 1960. Radiocarbon dating. Nobel Lecture given in Stockholm on December 12, 1960. In: Nobel Foundation Staff (Eds.), Nobel Lectures, Chemistry, 1942–62. (1964). Elsevier Publishing, Amsterdam; reprinted with permission of Elsevier Science, Amsterdam.*

Anderson and Libby estimated the expected level of natural radiocarbon activity on the Earth from its expected rate of disintegration and the estimated amounts of carbon on Earth. Their estimation of carbon on Earth was obtained from a summation of the carbon content of the various carbon reservoirs on Earth reported by Libby (1960) in his Nobel lecture listed in Table VIII.1.

TABLE VIII.1 Carbon Reservoir Makeup (Libby, 1960)

Reservoir	Grams (C/cm^2)
Ocean, "carbonate"	7.25
Ocean, dissolved organic	0.59
Biosphere	0.33
Humus	0.20
Atmosphere	0.12
Total	8.5

As illustrated in Fig. VIII.5, neutrons are formed in the upper atmosphere at the rate of two neutrons per second per square centimeter, forming 2 ^{14}C atoms at the same rate. The newly formed ^{14}C exchanges with carbon on the Earth, constituting 8.5 g/cm^2. A steady-state condition is reached over a period of many thousands of years, with the disintegration rate of the $^{14}C = 2$ disintegrations per second (2 dps/cm^2) equaling its rate of formation. Converting the units of disintegrations per second to disintegrations per minute (DPM) and dividing by the amount of exchangeable carbon on Earth yields the estimated level of activity of ^{14}C on Earth, calculated by Libby and coworkers as follows:

$$^{14}\text{C Activity on Earth} \approx \frac{2\ \text{dps}}{8.5\ \text{g C}} \approx \frac{(2\ \text{dps})(60\ \text{s/m})}{8.5\ \text{g C}} \approx 14\ \text{DPM/g C} \qquad \text{[VIII.39]}$$

The production of carbon-14 in the atmosphere leading to the continuous labeling of all forms of carbon on Earth, as illustrated in Fig. VIII.5, was the basis for the conception of the carbon-14 dating technique, as Libby (1967) explained:

> *The real beginning of the history of radiocarbon dating as such was in the realization that the cosmic-ray production of radiocarbon in the high atmosphere leads to a continuous labeling of the biosphere and living matter, which is terminated at death. It is difficult to know when this idea was born, but it was very soon after the author's plan was fixed to detect the effects of cosmic rays on the Earth's atmosphere. It was necessary to know how a test could be made for the radiocarbon that must be present on Earth, according to Korff's measurements [natural radiocarbon was yet undiscovered]; in considering where to look for this natural radiocarbon, and how to detect it, it was realized that the supply of radiocarbon from the well-mixed system, consisting of the carbon dioxide in the air, and the dissolved salts in the ocean and in the biosphere would be cut off to any living being at the instant of death. For this, of course, the principle of radiocarbon dating was obvious – namely, that the decay of the radiocarbon normally present during life would measure the time elapsed since death – half of it being lost every 5730 years.*

In his Nobel lecture Libby (1960) elaborated further the historical account of the conception of carbon-14 dating:

…the agreement between the predicted and observed assays is encouraging evidence that the cosmic rays have indeed remained [relatively] constant in intensity over many thousands of years and that the mixing time, volume, and composition of the oceans have not changed either. We are in the radiocarbon dating business as soon as this has been said, for it is clear from the set of assumptions that have been given that organic matter, while it is alive, is in equilibrium with the cosmic radiation; that is, all the radiocarbon atoms which disintegrate in our bodies are replaced by the carbon-14 contained in the food we eat, so that while we are alive we are part of a great pool which contains the cosmic-ray produced radiocarbon [see Fig. VIII.6]. The specific activity is maintained at the level of about 14 disintegrations per minute per gram by the mixing action of the biosphere and hydrosphere. We assimilate cosmic-ray produced carbon-14 atoms at just the rate that the carbon-14 atoms in our bodies disappear to form nitrogen-14. At the time of death, however, the assimilation process stops abruptly. There is no longer any process by which the carbon-14 from the atmosphere can enter our bodies. Therefore, at the time of death the radioactive disintegration process takes over in an uncompensated manner and, according to the law of radioactive decay, after 5600 years [the most precise figure now is 5730 years] the carbon that is in our bodies while we are alive will show half the specific carbon-14 radioactivity that it shows now. Since we have evidence that this has been true for tens of thousands of years, we should expect to find that a body 5600 [now known to be 5730] years old would be one-half as radioactive as a present-day living organism.

The production of ^{14}C by cosmic radiation in the Earth's atmosphere, its thorough mixing in the carbon pool on Earth, and the decay of ^{14}C after the death of living systems is illustrated in Fig. VIII.6.

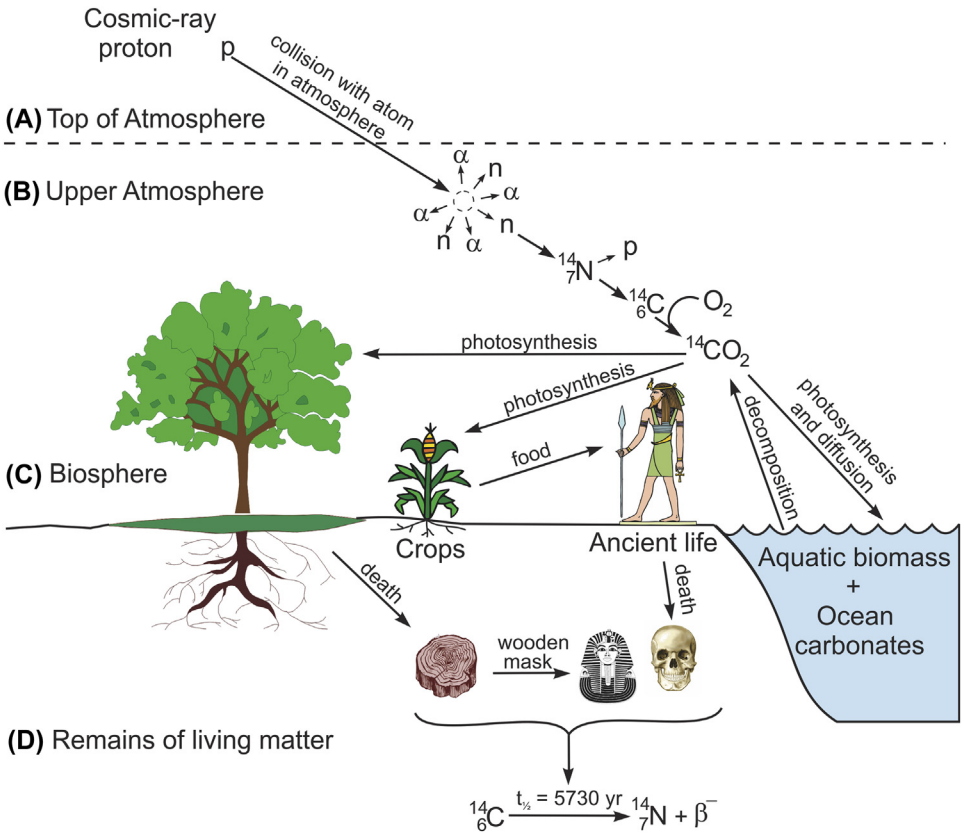

FIGURE VIII.6 The cycle of radiocarbon on Earth. Cosmic-ray protons enter (A) the top of the atmosphere and collide with atoms in the Earth's upper atmosphere (B). The collisions smash the atoms into their various nuclear components, including alpha particles, protons, and neutrons. The neutrons collide with nuclei of nitrogen and convert it to nuclei of radioactive carbon-14. The newly created carbon-14 is immediately oxidized to radioactive $^{14}CO_2$, which is absorbed with stable carbon dioxide into the Earth's reservoirs of organic and inorganic carbon, including all forms of living matter in its biosphere (C). At the moment of death, the remains of living matter (D) are no longer able to assimilate new radioactive ^{14}C, so the level of the radiocarbon in the remains begins to decay to lower levels of radioactivity, losing one-half of its activity after 5730 years from the time of death. This occurs in all forms of former living matter: human and animal remains, wood, artifacts made from wood, such as the mask of the mummy illustrated in (D), and pottery containing embedded charcoal.

Using the value of 14 DPM/g C as the estimated uniform specific activity of radiocarbon in the Earth's carbon reservoirs, Libby (1960) explained that the specific activity of the ^{14}C would diminish according to the radioactivity decay law given by Eq. [VIII.40]

$$N = N_0 e^{-\lambda t} \qquad \text{[VIII.40]}$$

where N is the number of ^{14}C atoms remaining after time t, N_0 is the number of atoms of ^{14}C at the time of initiating observations or time $t = 0$, e is the base to the natural logarithm, and λ is the decay constant defined as $\ln 2/t_{1/2}$ where $t_{1/2}$ is the half-life of the radioactive isotope. A derivation of Eq. [VIII.40] and some of its practical applications are provided in the chapter entitled "Radionuclide Decay, Radioactivity Units, and Radionuclide Mass." The terms N and N_0 may be replaced by A and A_0, as given in Eq. [VIII.41] for the activity or specific activity of the radioactive isotope at times t and t_0, respectively, because the number of atoms of a radioactive isotope in a given sample of material and the radioactivity of the isotope in the sample expressed in units of rate of disintegration (eg, DPM) are proportional.

$$A = A_0 e^{-\lambda t} \qquad \text{[VIII.41]}$$

Thus Libby and his coworkers based their conception of the ^{14}C-dating technique on the unalterable half-life of ^{14}C being 5730 years and the fact that assimilation of ^{14}C by a living organism would cease upon death. Libby reasoned that the level of ^{14}C in the sample would diminish with time after death according to the half-life of ^{14}C and defined by the decay Eq. [VIII.40] or [VIII.41]. The decay of ^{14}C and the consequent reduction in its activity over time in the carbon remains of an organism from its time of death is illustrated in Fig. VIII.7.

The graph in Fig. VIII.7 was constructed using Eq. [VIII.41], substituting the value of 1 or unity for A_0 and then calculating for A the fraction of ^{14}C activity remaining as a function of time t. For example, the fraction of the ^{14}C activity in the remains of a mummy 3000 years after the pharaoh's death would be calculated according to Eq. [VIII.41] as

$$\begin{aligned} A &= A_0 e^{-\lambda t} \\ &= (1)\left(e^{-(\ln 2/5730 \text{ years})(3000 \text{ years})}\right) \\ &= 0.696 \text{ or } 69.6\% \end{aligned} \qquad \text{[VIII.42]}$$

In turn, Libby reasoned that the radioactivity decay law would permit the calculation of t, the time in years from death or the age of a mummy, if the specific activity of ^{14}C in the reservoirs of carbon on earth (A_0) could be determined

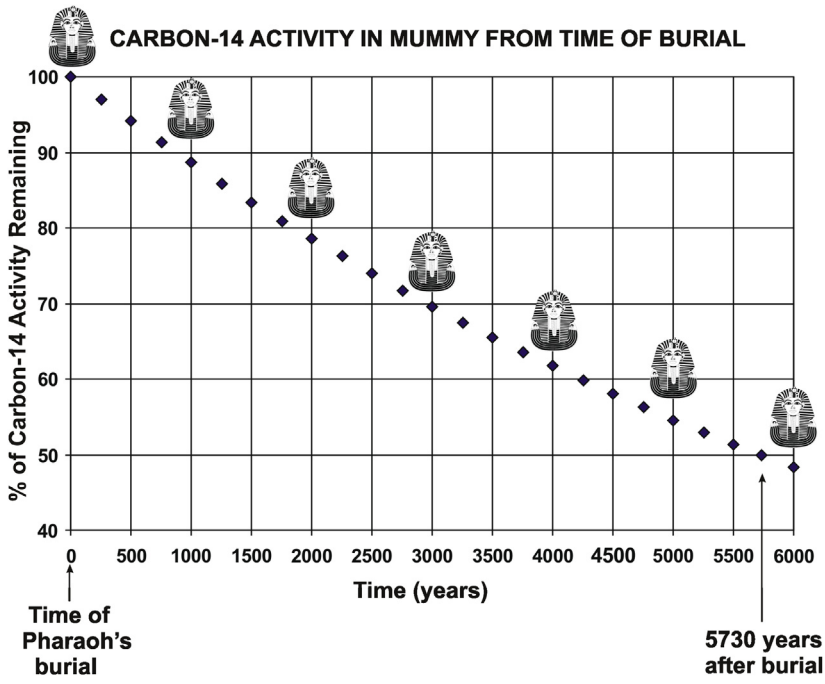

FIGURE VIII.7 Expected rate of ^{14}C decay in the remains of a mummy and its wooden burial mask from time of the pharaoh's death.

accurately, and if the ^{14}C specific activity, A, in the carbon remains of the mummy could be experimentally determined. Thus the time that had transpired from the time of death of the remains could be calculated from the following Eq. [VIII.43], which is derived from Eq. [VIII.41]:

$$t = \frac{1}{\lambda} \ln \frac{A_0}{A} \qquad \text{[VIII.43]}$$

As it was confirmed that radiocarbon was produced in the Earth's atmosphere, it was expected to exist in living material; but Willard Libby and his collaborator Ernest Carl Anderson had to demonstrate that it did indeed exist. The chart of the nuclides at that time had a vacant space where the isotope ^{14}C would be located. Radioactive measurement devices, such as gas ionization counters, were not very sensitive at that time, so they proceeded to concentrate the carbon-14 isotope in methane gas obtained from the sewage of the City of Baltimore with the assistance of A.V. Grosse of Temple University, who was developing thermal diffusion columns for the concentration of the carbon-13 isotope for medical applications (Anderson et al., 1947). Methane from the city sewage was used because it contained carbon from living organic matter but the radioactive carbon-14 would not have had time to decay to any appreciable level. In contrast, petroleum methane would have no ^{14}C, because it would have all decayed in the oil deposits of the Earth. Anderson et al. (1947a,b) did indeed find carbon-14 in the methane of living organic matter at about the specific activity predicted.

The next step in the process was to develop an instrument which could measure very low levels of radioactivity in a sample of carbon. Libby and coworkers could not use the isotope enrichment technique to analyze samples routinely for ^{14}C, because such methods were expensive and time-consuming. An isotope dating technique would not be useful if it cost several thousands dollars to analyze only one sample. It was necessary to find a routine method of measuring the radioactivity of carbon-14, and from as small a sample as possible, which would permit the analysis of numerous antiquities without sacrificing a large sample of the antiquity for the analysis.

Gas ionization detectors, such as proportional counters or Geiger–Müller counters, were popular instruments during the 1940s and 1950s, and remain reliable instruments for the detection and measurement of radioactivity today. In his Nobel lecture (1960) Libby related that such detectors then yielded an unshielded background count rate of about 500 counts per minute (cpm). The background radioactivity was due to high-energy radiation from natural radionuclides of terrestrial origins such as uranium, thorium, and potassium in cement used in the building foundation and other structural materials, as well as cosmic radiation. Shielding the detector with 8 in. of iron would absorb terrestrial sources of radioactivity and reduce the background count rate to about 100 cpm, principally from cosmic-ray muons. The cosmic-ray muons could penetrate metal shielding readily, so this background could not be eliminated by brute passive shielding. The background was still too high to detect carbon-14 in antiquities that contained less than 15 DPM per gram of carbon. Libby and his coworkers needed to achieve a 50–100-fold reduction in background to provide a high signal-to-noise ratio of sample-to-background radioactivity, particularly if old artifacts produced carbon-14 count rates of only 1–2 cpm. They devised a counter assembly, illustrated in Fig. VIII.8, known as the anticoincidence counter. This was described by Libby:

> *The 100 remaining counts due in main part to μ mesons [These particles are now known to be muons, which are leptons rather than mesons.] had to be removed. In order to do this we surrounded the counter with the carbon-dating sample in it with a complete layer of Geiger counters in tangential contact with one another and wire them so that when any one of these counters counts, the central counter with the dating sample is turned off for about 1/1000th of a second. In this way the μ mesons [i.e., muons] are eliminated from the record, so the background comes down to something between 1 and 6 counts per minute, depending on detailed counter and shield design. This is for a counter of about 1 liter volume capable of holding up to 5 g of carbon with counting rates of 75 counts per minute for living carbon, 37.5 counts for 5600 year-old carbon, 18.7 counts for 11,200 years, and 0.07 counts for 56,000 years.*

Libby's statement refers to the decay of radiocarbon in dead matter based on a half-life of 5600 years. The half-life of carbon-14 is now more accurately measured to be 5730 years. Samples were initially counted as carbon black deposited on the inner detector wall, with the detector filled with a suitable counting gas such as argon. Also, Libby converted samples to CO_2 or acetylene, which served as the counting gas, thereby providing higher sample count rates. The β particles emitted by the decaying carbon-14 atoms in the sample detector and cosmic-ray muons that penetrated the guard and sample detectors produced ion pairs in the gaseous media of the detectors. The ion pairs become separated by an applied potential and collected at a central anode and outer cathode wall of the detector, producing an output pulse which is registered by the scaler and counted or rejected by the anticoincidence circuit illustrated in Fig. VIII.8.

With a counter providing low background count rates, Libby and his graduate student Ernest Carl Anderson proceeded to analyze carbon-14 in living matter from various parts of the globe. Variable cosmic-ray intensity with latitude, discussed in detail in the chapter entitled "Cosmic Radiation," was a concern. It was estimated that it would take about 8000 years for the

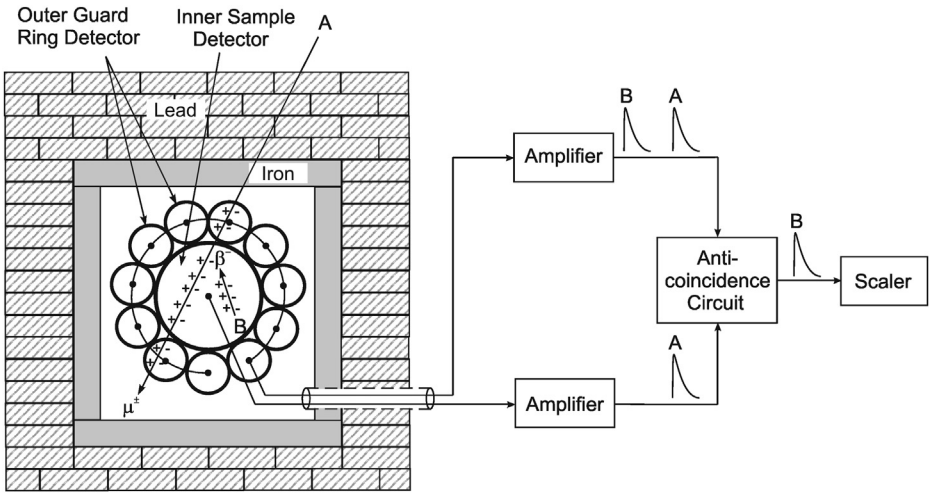

FIGURE VIII.8 Low-background anticoincidence counter and passive shielding. The counter assembled by Libby and coworkers consisted of 11 gas proportional or Geiger–Müller tubes surrounding a larger 1 L gas ionization sample detector located in the center. The outer tubes are coupled electronically so that any ionizing radiation that might penetrate one or more tubes within a time window of 0.001 s would produce an output pulse. A cosmic-ray muon (A) is illustrated passing through the guard ring detector and central sample detector, producing ionization in these detectors and coincident output pulses from each detector. An atom of carbon-14 (B) inside the sample detector emits a β particle which cannot penetrate outside the central detector wall, producing only one output pulse B. The coincident pulses produced by the cosmic-ray muon are rejected by the anticoincidence circuit, and only the pulse produced by the carbon-14 passes on to be counted by the scaler. The counts collected over a preset period of time (as long as 48 h) are summed by the scaler.

carbon-14 to be mixed in the atmosphere and ocean bodies, and thereby provide a relatively uniform carbon-14 specific activity around the globe. They needed to confirm that the known variation of cosmic-ray intensity with latitude and expected long time of mixing would not produce a wide variation in carbon-14 deposits in the carbon reservoirs around the globe. With a counting method at hand, E.C. Anderson devoted much of his PhD thesis to this problem (Anderson, 1949). He analyzed the ^{14}C specific activity (DPM/g C) in 18 samples from almost as many countries, from geomagnetic latitudes starting from 60° north to the equator, and as far south as 65° south. The carbon-14 specific activities of the samples were relatively uniform, varying only from 14.5 to 16.3 and providing an average value of 15.3 ± 0.1 DPM ^{14}C/g C. Libby (1960) commented on the ^{14}C specific activities found in the Earth's reservoirs:

> *They [data on natural abundance or specific activity of radiocarbon in the earth] show no appreciable differences even though they come from places varying in latitude from near the South Pole to near the North Pole. At the present time, ten years later, no evidence for variation has been found except in areas of extensive carbonate deposits where the surface waters may carry a considerable amount of old carbon dissolved, and thus reduce the carbon-14 level below the world-wide average for the biosphere-atmosphere-ocean pool as a whole. Fortunately, such conditions are relatively rare and generally easily recognized.*

Now equipped with the knowledge that living matter had a relatively uniform carbon-14 specific activity, Willard Libby and his coworkers were able to plot a curve, similar to that illustrated in Fig. VIII.9, which would predict the content of carbon-14 in ancient organic matter. Their dating curve was plotted using the universal radioisotope decay Eq. [VIII.40] and the relatively uniform content of carbon-14 in living matter of 15.3 DPM/g C. Libby (1955) expressed his dating equation as follows:

$$I = I_0 e^{-\lambda t} \qquad \text{[VIII.44]}$$

$$= 15.3 e^{-(\ln 2/5568 \text{ years})(t)} \qquad \text{[VIII.45]}$$

where I is the content of carbon-14 in units of DPM/g C in any dead matter after time t in years, I_0 is the carbon-14 content in living matter, and λ is the decay constant for carbon-14 or the ln 2/half-life. In 1955 the half-life of carbon-14 was measured to be 5568 years; the more precise figure accepted today is 5730 years. Libby reasoned that if the content of carbon-14 in ancient dead organic matter is determined experimentally in units of DPM/g C, then the age of the organic matter or time t that had transpired from the time of death could be calculated from Eqs. [VIII.44] and [VIII.45] as

$$t = \frac{1}{\lambda} \ln \frac{I_0}{I} \qquad \text{[VIII.46]}$$

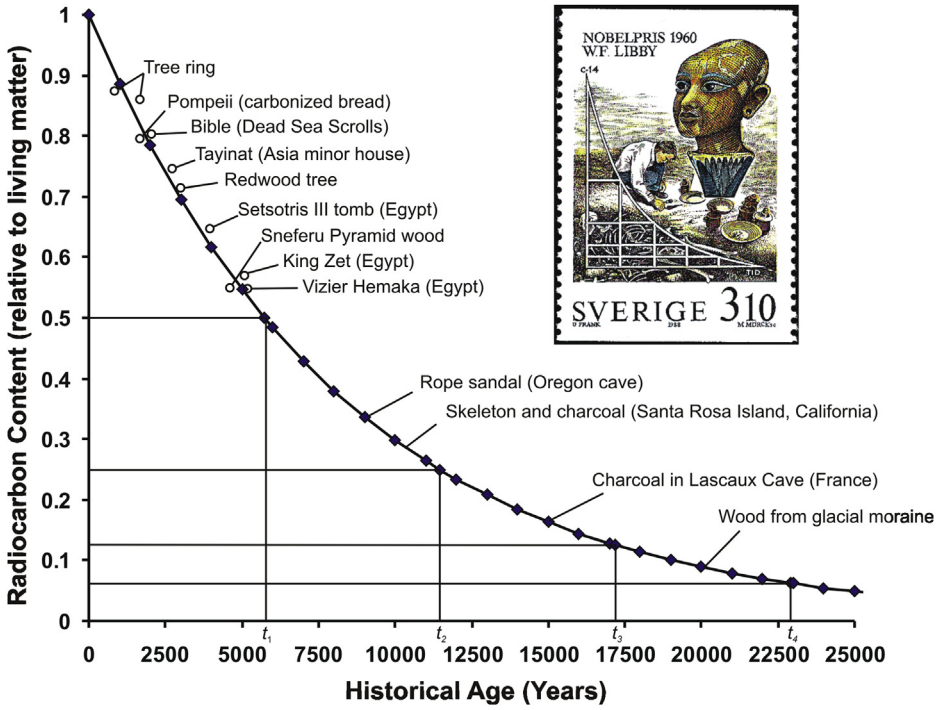

FIGURE VIII.9 The level of carbon-14 in dead organic matter relative to living matter as a function of the age of the organic matter from time of death. The curve is plotted according to the 5730 year half-life of carbon-14. The hollow circles along the curve from 1000 to 5000 years represent carbon samples of known age and measured carbon-14 content reported by Arnold and Libby (1949) on the basis of the then measured ^{14}C half-life of 5568 years. Samples identified on the curve from 9000 to 20,000 years have historical ages determined only by their carbon-14 content. Four carbon-14 half-lives are identified, namely t_1, t_2, t_3, and t_4 at 5730, 11,460, 17,190, and 22,920 years, respectively. The insert shows a postage stamp issued by Sweden in 1988 to commemorate the discovery of the carbon-14 dating technique, illustrating an archeologist with mummy, pottery, and carbon-14 decay curve.

$$t = \frac{1}{\ln 2/5568 \text{ years}} \ln \frac{15.3 \text{ DPM/g C}}{I}$$

For example, if the ^{14}C activity in a sample of a mummy was determined to be 8.2 DPM/g C, and using Libby's initial estimate of the specific activity of the Earth's carbon reservoirs as 15.3 DPM/g C, the age of the mummy would be calculated as

$$t = \frac{1}{\ln 2/5568 \text{ years}} \ln \frac{15.3 \text{ DPM/g C}}{8.2 \text{ DPM/g C}}$$

$$= \frac{1}{1.245 \times 10^{-4} \text{ years}^{-1}} \ln 1.86$$

$$= 4985 \text{ years}$$

With the accepted level of carbon-14 in living matter expressed as unity or given the value of 1, Libby (1955) calculated the fraction of carbon-14 that would be remaining in ancient dead matter after t years according to the equation

$$I = 1\, e^{-(0.693/5568 \text{ years})(t)} \qquad \text{[VIII.47]}$$

In this equation Libby used the value of 5568 years for the half-life of carbon-14, which is 2.8% lower than the current more precisely determined value of 5730 years. Eq. [VIII.47] was used by the writer to plot the carbon-14 decay with time in years with the value of 5730 years, where the carbon-14 radioactivity content in a given sample would relate to the age in years of that sample from its time of death. An example of such a curve is plotted in Fig. VIII.9.

With a decay curve such as that illustrated in Fig. VIII.9, Libby and coworkers had only to prove that antiquities of dead matter could be dated accurately. They needed to analyze antiquities of historically known age and compare the age determined by the carbon-14 dating method. Remains and artifacts of known age could be found only as far

back as 5000 years. The youngest would be tree rings, remains from Pompeii, Dead Sea Scrolls, remains from identified Egyptian tombs, etc. Their known ages correlated quite closely with ages determined by the carbon-14 dating method (see Fig. VIII.9). Thus Libby and coworkers had developed a technique which could be used to determine the ages of remains containing dead carbon as far back as approximately nine half-lives of carbon-14 or around 50,000 years. Beyond 50,000 years of age the level of carbon-14 would be too low and too close to background to determine accurately. Fig. VIII.9 illustrates the ages of remains determined by their carbon-14 content up to 20,000 years reported by Libby (1960). In his Nobel lecture given on December 12, 1960, Libby summarized the state of the art:

> *The dating technique itself is one which requires care, but which can be carried out by adequately trained personnel who are sufficiently serious-minded about it. It is something like, the discipline of surgery − cleanliness, care, seriousness, and practice. With these things it is possible to obtain radiocarbon dates which are consistent and which may indeed help roll back the pages of history and reveal to mankind something more about his ancestors, and in this way perhaps about his future.*

An important finding which affects the carbon-14 dating technique is the Suess effect, named after its discoverer (Suess, 1955). During the late 19th and early 20th centuries the use of fossil fuels for industry and domestic heating injected relatively large amounts of CO_2 free of carbon-14 into the atmosphere. Fossil fuels do not contain any carbon-14, as coal, oil, etc. are much older than the lifetime of the radioisotope. The infusion of ^{14}C-depleted CO_2 into the atmosphere lowered the overall specific activity of radiocarbon in the atmosphere by about 2%—the Suess effect. In the 1950s the Suess effect was abated by atmospheric tests of nuclear weapons, which infused carbon-14 into the atmosphere from nuclear weapon neutron reactions with atoms of nitrogen. Thus artificial carbon-14 was infused into the atmosphere by neutrons from nuclear weapons testing according to the same reaction that occurs naturally when neutrons from cosmic-ray collisions in the upper atmosphere collide with nitrogen (Eq. [VIII.37] and Fig. VIII.6). This produced the opposite effect of increasing the carbon-14 level in the atmosphere. Thus for carbon-14 dating a reference standard had to be made, uncontaminated by fossil-fuel CO_2 or the Suess effect. The primary modern reference standard for radiocarbon measurements, as described by Cook et al. (2003) and Salonen et al. (2012), is wood from an AD 1890 tree ring formed before the Suess effect and consequently uncontaminated by fossil-fuel CO_2. The carbon-14 activity of the AD 1890 wood was measured in the 1950s and corrected for ^{14}C decay to the year of growth to yield the absolute carbon-14 activity, found to be 226 Bq/kg C equivalent to 13.56 DPM/g C. Thus radiocarbon ages are expressed in years BP (before present), where present is the year 1950. For example, AD 0 is expressed as 1950 BP, and BC 3000 is expressed as 4950 BP.

Laboratories involved in radiocarbon dating use a secondary modern reference standard, namely Oxalic Acid SRM 4990C provided by National Institute of Standards and Technology (NIST), against which their sample activities are measured. The following equation described by Cook et al. (2003) and Salonen et al. (2012) is used in the calculation of radiocarbon age:

$$t = \frac{1}{\lambda} \ln \frac{A_{ON}}{A_{SN}} \qquad \text{[VIII.48]}$$

where t is time or age, λ is the decay constant = ln 2/5568 years or ln 2/Libby half-life of ^{14}C, A_{ON} is 74.59% of the measured net Oxalic Acid Secondary Standard SRM 4990C activity normalized for ^{13}C fractionation, and A_{SN} is the sample activity normalized for sample fractionation to $-25‰$. Notice the similarity of this equation and that used by Libby, Eq. [VIII.46]. The activities are normalized for ^{13}C fractionation, because the isotopes of carbon (^{12}C, ^{13}C, and ^{14}C) undergo fractionation or fluctuation in their ratios as a result of isotope effects in natural biochemical processes due to their mass differences. For in-depth treatments of carbon-14 aging measurements readers may peruse articles by Stuiver and Polach (1977), Mook and van der Plicht (1999), Taylor (2000), and Currie (2004). State-of-the-art techniques for measuring ^{14}C are reviewed by Buchtela (2003), Huber et al. (2003), Cook et al. (2003), Becker (2012), Salonen et al. (2012), and Steinhauser and Buchtela (2012).

Willard Libby married Leona Woods Marshall in 1966. Leona Marshall was a physicist in the team collaborating with Enrico Fermi in the construction of the first nuclear reactor under the stands of the University of Chicago's Stagg Field. She was the only woman present when the reactor went critical in a carefully controlled and sustained nuclear chain reaction lasting 4.5 min on December 2, 1942. She is shown in a photograph in Fig. II.12 of Hall of Fame, Part II with Fermi and his team commemorating the design, construction, and operation of the world's first nuclear reactor. She was the only woman and the youngest in Fermi's team at the onset of the Manhattan Project. She died in 1986 at the age of 67 (Folkart, 1986).

Libby remained professor of chemistry at UCLA until his retirement in 1976. He died in Los Angeles on September 8, 1980.

EDWIN M. McMILLAN (1907–1991)

Of Scottish descent, Edwin M. McMillan was born on September 18, 1907 at Redondo Beach, California. He was the first person to produce a transuranium element, in collaboration with Philip Abelson. He shared the Nobel Prize in Chemistry with Glenn T. Seaborg in 1951 for, in the words of the Nobel Committee, "their discoveries in the chemistry of the transuranium elements." Professor A. Westgren, chair of the Nobel Committee for Chemistry of the Royal Swedish Academy of Sciences, underscored McMillan's contribution during the Nobel award ceremony speech on December 10, 1951:

> *The first transuranium element of which there was definite proof was produced by McMillan and Abelson [Philip H. Abelson] in May 1940 at the University of California, by irradiating uranium with neutrons with the aid of the cyclotron built by Lawrence [Ernest O. Lawrence]. It was obtained as a disintegration product of a beta-radiating uranium isotope, which has a half-life of 23 minutes. Hahn [Otto Hahn] and Meitner [Lise Meitner] had also discovered this body, but their preparation was too weak for its daughter-product to be demonstrated. The Americans were able to investigate this thoroughly, and showed that it forms an isotope of element 93, that is to say, a transuranium element. They called it neptunium after the planet Neptune, whose orbit lies next outwards after Uranus in the solar system. By irradiating uranium with rapid neutrons or with heavy-hydrogen nuclei, deuterons, other neptunium isotopes were soon produced in Berkeley.*

McMillan wrote a brief autobiography at the time of his Nobel Prize award, which was published in "Nobel Lectures, Physics 1942–1962." Specific dates and places of his study and work were obtained from this source.

McMillan grew up in Pasadena, California, and as a high school student he attended public lectures at CalTech in Pasadena. After high school graduation in 1924 he entered CalTech, where he obtained his BSc degree in 1928 and MSc in 1929. McMillan then transferred to Princeton University and received his doctorate there in 1932.

Edwin M. McMillan (1907–1991)

Upon graduation from Princeton Edwin McMillan entered the University of California at Berkeley as a national research fellow. After two years at Berkeley he joined the staff at the Radiation Laboratory under Professor Ernest O. Lawrence, studying nuclear reactions and the design and construction of cyclotrons; and at the same time he became a faculty member of the Department of Physics at Berkeley. His appointment in the department began as instructor in 1935, with a promotion to assistant professor in 1936.

In 1939 the work of Otto Hahn and Fritz Strassmann in Germany demonstrating the discovery of nuclear fission in uranium was published; and McMillan, among others at Berkeley, worked quickly to confirm and expand on this momentous discovery. In his approach to investigate the capture of neutrons by uranium and fission, McMillan

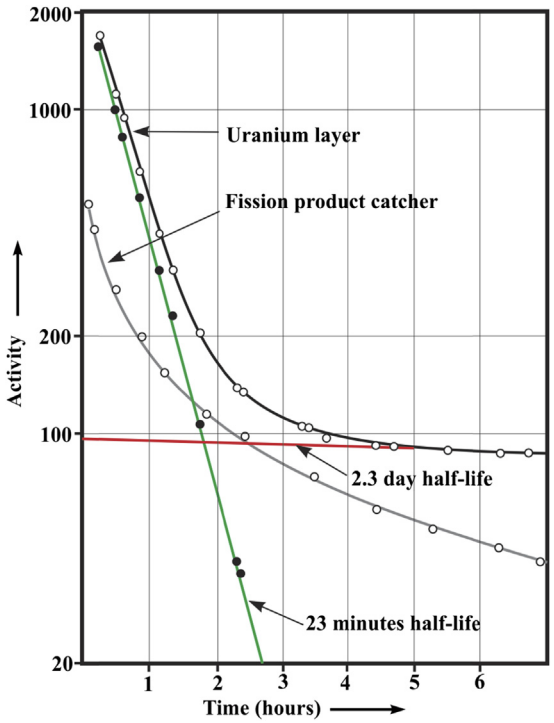

FIGURE VIII.10 Radioactivity decay curves of the uranium layer consisting of a mixture of $^{239}U + {}^{239}Np$ following neutron capture by ^{238}U of high-energy (fast) neutrons, depicted by the uppermost solid black curve with white circular data points; the almost horizontal straight red line, which is a 2.3 day half-life curve due to the decay of ^{239}Np; the steep straight green line with solid black data points, which is a 23 min half-life curve due to the decay of ^{239}U; and the fission product catcher, which contains numerous fission products each possessing differing half-life decay times. *Graph from McMillan, E.M., 1951. The transuranium elements: early history. In: Nobel Lecture, December 12, 1951. The Nobel Foundation, with permission of The Nobel Foundation © 1951.*

bombarded neutrons on to a thin layer of uranium in the form of ammonium urinate deposited as a thin suspension on a sheet of Bakelite. The sheet of uranium deposit was sandwiched with cellophane, designed to catch the numerous fission products away from the uranium layer. Because fission products are of lower mass than uranium (about half the mass), they would recoil with high energy away from the uranium layer and be absorbed into the surrounding cellophane. The cellophane was referred to by McMillan as a "fission product catcher." By catching the fission products away from the layer of uranium he was able to observe the radioactivity decay resulting from heavy radioactive atoms, which were too heavy to recoil out of the thin uranium layer, thus leaving the heavy radioactive atoms free from interfering background radiation from the fission products. The radioactive decay curves of the heavy atoms produced after neutron bombardment of uranium could then reveal the presence of any unknown heavy atoms that might be produced by the neutron capture of uranium. McMillan irradiated the thin uranium target material with neutrons produced by the bombardment of a beryllium target with 8 MeV deuterons in a 37 in. (94 cm) cyclotron according to the reaction $^{9}Be(d,n)^{10}B$. After neutron bombardment of the uranium, McMillan was able to resolve the decay curve of the neutron-bombarded "uranium layer" into two radioactivity decay curves yielding 23 min and 2.3 day half-lives, illustrated in Fig. VIII.10.

The uranium layer following neutron irradiation consisted of a mixture of two radioisotopes of differing decay rates. McMillan was able to resolve the separate decay curves of the two isotopes by drawing a straight line along the almost flat region of the decay curve of the uranium layer (almost horizontal red line for the 2.3 day half-life in Fig. VIII.10). He then subtracted the activity values of the 2.3 day half-life curve from the uranium layer decay curve, yielding the steep straight decay curve depicting an isotope with a 23 min half-life (steep green line in Fig. VIII.10). A similar procedure to resolve the individual decay curves of a mixture of two isotopes is described in the chapter entitled "Radionuclide Decay, Radioactivity Units, and Radionuclide Mass" and illustrated by Fig. 18.3. The reactions resulting from the bombardment of uranium with fast neutrons produced in the 37 in. (94 cm) cyclotron are illustrated in Fig. VIII.11.

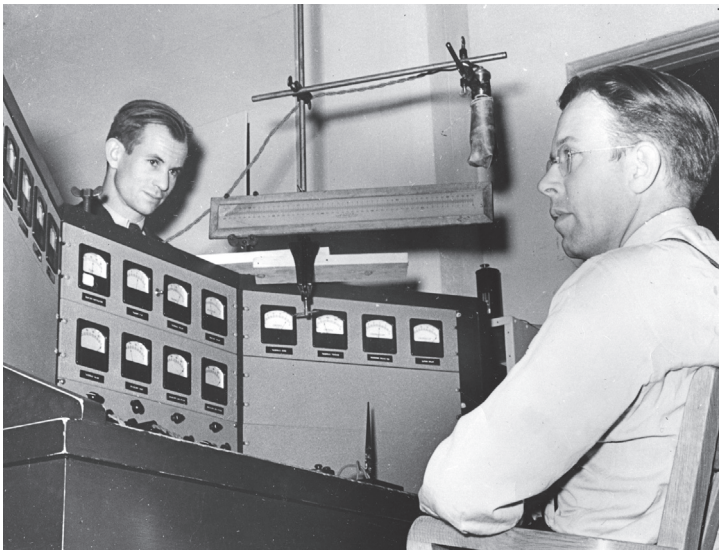

E. M. McMillan (left) and E. O. Lawrence (right) at the control panel of the 60-inch cyclotron at the University of California's Berkeley Radiation Laboratory, Berkeley, California
Printed with permission from Lawrence Berkeley National Laboratory, courtesy AIP Emilio Segre Visual Archives, Fermi Film Collection

Chemical studies of oxidation states of the isotope with the 2.3 day half-life demonstrated that it had a chemistry similar to uranium and was element 93—a new element with atomic number $Z = 93$ (McMillan and Abelson, 1940; McMillan, 1951). Element 93 was given the name neptunium. Beta decay of ^{239}Np with a half-life of 2.3 days leads to an isotope of yet another new element 94, namely the isotope ^{239}Pu, illustrated in Fig. VIII.11. McMillan had yet to identify element 94.

Subsequent to the production of ^{239}Np by the top two processes illustrated in Fig. VIII.11, McMillan proceeded to irradiate uranium with deuterons to explore the possibility of producing additional isotopes of elements 93 and 94. He explained this in his Nobel lecture (McMillan, 1951):

> *I then tried bombarding uranium directly with the 16-MeV deuterons from the cyclotron, in the hope that this might produce a different isotope of element 94 with a shorter life, giving a greater rate of alpha particle emission. This hope proved to be well founded, and a considerably stronger alpha-activity was found in the decay products of the element 93 separated from the deuteron-bombarded sample. The next slide [Fig. VIII.11] shows the nuclear reactions involved in the formation of the two isotopes of element 94.*

Full confirmation of the production of element 94 (plutonium) was not completed by McMillan, because in 1940 he was persuaded to discontinue his work and move to work on the development of radar for national defense at the Massachusetts Institute of Technology (MIT) Radiation Laboratory. In his Nobel lecture (McMillan, 1951) commented:

> *…I did not participate in the final proof of this [production of element 94], since I left Berkeley in November 1940, to take part in the development of radar for national defense. The rest of the story belongs to Seaborg [Glenn T. Seaborg], who took up the work after my departure…*

$$^{238}\mathrm{U} + \mathrm{n} \longrightarrow \gamma + {}^{239}\mathrm{U}\ (\text{instantaneous})$$
$$^{239}\mathrm{U} \longrightarrow \beta^- + {}^{239}\mathrm{Np}\ (23\ \text{minutes})$$
$$^{239}\mathrm{Np} \longrightarrow \beta^- + {}^{239}\mathrm{Pu}\ (2.3\ \text{days})$$
$$^{239}\mathrm{Pu} \longrightarrow \alpha + {}^{235}\mathrm{U}\ (24{,}000\ \text{years})$$
$$^{238}\mathrm{U} + \mathrm{d} \longrightarrow 2\mathrm{n} + {}^{238}\mathrm{Np}\ (\text{instantaneous})$$
$$^{238}\mathrm{Np} \longrightarrow \beta^- + {}^{238}\mathrm{Pu}\ (2.1\ \text{days})$$
$$^{238}\mathrm{Pu} \longrightarrow \alpha + {}^{234}\mathrm{U}\ (92\ \text{years})$$

FIGURE VIII.11 Nuclear reactions of cyclotron-produced fast neutrons (uppermost reaction) and 18 MeV deuterons (fifth reaction from the top) with ^{238}U and subsequent beta and alpha decay resulting in the formation of two isotopes of element 93, namely neptunium (^{239}Np and ^{238}Np), and two isotopes of element 94, namely plutonium (^{239}Pu and ^{238}Pu). The times in parenthesis on the right are the half-lives of the processes indicated. *From McMillan, E.M., 1951. The transuranium elements: early history. In: Nobel Lecture, December 12, 1951. The Nobel Foundation, with permission from The Nobel Foundation © 1951.*

Glenn T. Seaborg took over this work at the Berkeley Radiation Laboratory; and the final proof of the discovery of the artificially produced isotope of ^{238}Pu of the element 94 was made in late February 1941 by Seaborg, chemistry instructor Joseph W. Kennedy, and Seaborg's first graduate student, Arthur C. Wahl. The results were voluntarily withheld from publication until after World War II in 1946 (Jackson and Panofsky, 1996), because plutonium-239 was found to be highly fissionable with potential as a nuclear weapon (Hoffman, 2007). For his work on the discovery of element 94, McMillan was included as a coauthor of a 1946 paper in *Physical Review* reporting the production of element 94 from deuterons on uranium (Seaborg et al., 1946).

During World War II McMillan carried out research in national defense, including radar research at the MIT Radiation Laboratory (1940–1941), research at the US Navy Radio and Sound Laboratory in San Diego, California (1941–1942), and in the Manhattan Project on the development of the atomic bomb at Los Alamos (1942–1945). After J. Robert Oppenheimer was appointed director of the Los Alamos weapons laboratory, he made McMillan his principal advisor on technical issues starting in autumn 1942. His work in the Manhattan Project included the on-site selection of Los Alamos, the development of the gun-type or bullet-type device which was utilized to reach a critical mass in ^{235}U, and the development of diagnostics for the plutonium bomb, which involved an implosion assembly (Jackson and Panofsky, 1996). The basic design and principles behind the gun design and implosion assemblies of the atomic bombs developed at Los Alamos are described in Hall of Fame, Part IV of this book.

After World War II Edwin McMillan returned to pursue his research interests in particle acceleration and nuclear reactions. He had participated in planning the construction of a larger cyclotron at the Berkeley Radiation Laboratory with E.O. Lawrence. The problem with utilizing brute force to increase the energy of accelerated particles was keeping them in phase with an accelerating rf voltage, because as the particles traveled at yet higher energies and relativistic speeds, their masses would increase. In a biographical memoir Jackson and Panofsky (1996) describe how McMillan mulled over the problem in June 1945:

> *envisioned the idea of phase stability, which in a single stroke of invention made this brute force approach obsolete. McMillan recognized that when particles are accelerated in a radiofrequency field not at the crest of the radiofrequency amplitude but on the side of the waveform, the particles would be locked stable at a certain phase.*

McMillan published his idea in *Physical Review* in 1945 (McMillan, 1945), unaware that the Russian physicist Vladomir I. Veksler had published the idea earlier (Veksler, 1944) in a Russian journal. The paper did not reach the United States during the wartime. Jackson and Panofsky (1996) describe how McMillan later corresponded with Veksler on the matter; both understood that their ideas occurred independently, and they became close friends. It is common in science that when the stage is set with previous research on a subject matter, the same idea can come independently and almost simultaneously to research groups at opposite ends of the Earth. For their independent discoveries on phase stability Vladimir Veksler and Edwin McMillan were awarded jointly the Atoms for Peace Award in 1963. The principle of phase stability remains an important aspect in accelerating particles to speeds close to the speed of light in modern accelerators.

Edwin McMillan returned to work on particle acceleration at the Berkeley Radiation Laboratory in 1945. He was promoted to professor of physics at Berkeley in 1946, and in 1954 was appointed associate director of the Berkeley Radiation Laboratory. After the untimely death of Ernest O. Lawrence on August 27, 1958, the laboratory was renamed the Lawrence Radiation Laboratory and McMillan was appointed its director, a post which he held until 1973. He retired from the Berkeley faculty in 1974, but continued to participate in the work of the Lawrence Berkeley Laboratory until he suffered debilitating strokes in 1984.

Edwin McMillan died at the age of 83 at El Cerrito, California on September 7, 1991.

GLENN T. SEABORG (1912–1999)

Glenn T. Seaborg shared the Nobel Prize in Chemistry in 1951 with Edwin M. McMillan, in the words of the Nobel Committee "for their discoveries in the chemistry of the transuranium elements." He was codiscoverer of plutonium (element 94) with McMillan and coworkers, and is best known as codiscoverer of the transuranium elements 94–103 and element 106, which is named seaborgium in his honor. In the Nobel award ceremony speech on December 12, 1951, Professor A. Westgren, chair of the Nobel Committee for Chemistry, noted:

> *Seaborg, as leader of a comprehensive group of able colleagues, completed the studies of the transuranium elements. In doing this, he has written one of the most brilliant pages in the history of the discovery of chemical elements…By irradiating different sorts of heavy atoms with neutrons, protons, deuterons, helium nuclei, or, most recently, carbon nuclei, a great number of isotopes have been produced from the six transuranium elements. The study of these isotopes' formation and properties has yielded a wealth of scientific material.*

Seaborg was born in Ishpeming, Michigan on April 19, 1912 to parents who had immigrated in their youth from Sweden. The Swedish language was spoken at home, and was the first language that Glenn Seaborg spoke. He moved with

his family to California in 1912, and graduated as class valedictorian from the David Starr Jordan High School in the Los Angeles suburb of Watts in 1929. In high school Glenn Seaborg developed a keen interest in chemistry and physics, which he attributed to his high school teacher, Dwight Logan Reid (Hoffman, 2000). Many of us can recall our early high school days and identify one teacher who impressed or inspired us into finding our calling in life.

Glenn Seaborg's life during his youth was not easy. His mother wanted to move from the small town of Ishpeming to Los Angeles to provide more opportunities for her children. This meant his father had to give up permanent employment as a machinist, and he could not find any permanent or suitable employment after their move to Los Angeles. Glenn Seaborg had to work at several odd jobs to finance his college expenses, as Hoffman (2000) notes in the biographical memoirs of the Academy of Sciences:

> *He first obtained work in a warehouse as a stevedore and then found summer employment as a night laboratory assistant in the Firestone Tire and Rubber Company to earn money for his freshman year at the University of California, Los Angeles (UCLA). This made it just barely possible for him to enter UCLA in the depression year of 1929, since it was a tuition free public university and he could live at home and commute with friends some 20 miles to UCLA.*

On graduating from high school in 1929, Seaborg entered UCLA and graduated in 1939 with a doctorate in chemistry from the University of California at Berkeley; he then became an instructor at Berkeley. While at Berkeley he collaborated in the search for new isotopes with the use of Ernest Lawrence's 37 in. cyclotron (Livingood and Seaborg, 1938; Seaborg and Kennedy, 1939). Among the new isotopes discovered was iodine-131, which is to this day very useful in nuclear medicine for diagnostic and therapeutic treatment of the thyroid. This work gave Seaborg a good taste of the potential of nuclear reactions for finding new elements and isotopes.

The departure of Edwin McMillan from Berkeley in November 1940 gave Glenn Seaborg the opportunity to continue McMillan's work on the use of the cyclotron to search for new elements. This was right in the wake of McMillan's discovery of the first transuranium element 93 (neptunium) and potential discovery of element 94 (plutonium). Seaborg asked McMillan for permission to continue this work, and it was so agreed. With the collaboration of instructor Joseph W. Kennedy, Seaborg's first graduate student Arthur C. Wahl, and Emilio Segrè, Seaborg produced and identified the properties of plutonium as the isotope ^{238}Pu, which was prepared by the bombardment of uranium with deuterons. This was described by Seaborg in his Nobel lecture with the reactions illustrated in Fig. VIII.12.

Glenn T. Seaborg (1912–1999)

Simultaneous to the work on the production of ^{238}Pu described in Fig. VIII.12, Emilio Segrè collaborated with Seaborg and coworkers in the production and identification of ^{239}Pu. The isotope was produced by the fast-neutron capture in uranium-238 illustrated in Fig. VIII.11. Plutonium-239 was found to have a very long half-life (24,000 years) and to be

$$^{238}_{92}\mathrm{U} + {}^{2}_{1}\mathrm{H} \longrightarrow {}^{238}_{93}\mathrm{Np} + 2\mathrm{n}$$

$$^{238}_{93}\mathrm{Np} \xrightarrow[2.1\ \text{days}]{\beta^-} {}^{238}_{94}\mathrm{Pu}\ (90\ \text{years}, \alpha)$$

FIGURE VIII.12 The preparation of plutonium-238 by the bombardment of uranium oxide with 16-MeV deuterons from the 60 in. cyclotron in 1940. The isotope affected in the uranium oxide was uranium-238, yielding neptunium-238, which decays by beta emission with a 2.1 day half-life to yield plutonium-238. In parentheses is the mode of decay of the plutonium-238 (α emission) and the value (known at the time) of the half-life of 90 years. The half-life of plutonium is more accurately known today to have a value of 86.4 years. *From Seaborg (1951), printed with permission of The Nobel Foundation © 1951.*

fissionable. These findings were submitted to *Physical Review* in 1941, but voluntarily suppressed from publication until 1946 after World War II (Seaborg et al., 1946; Kennedy et al., 1946) because of the fissionable properties and potential weapons application of plutonium-239. In light of the proposal by McMillan to name element 93 neptunium after the planet Neptune, the planet beyond Uranus, from which uranium (element 92) was named, Seaborg explained that it was considered proper to name element 94 plutonium after the next planet, Pluto.

Glenn Seaborg was appointed assistant professor of chemistry in 1941 at the University of California, Berkeley. After the United States entered World War II, Seaborg was granted leave of absence from Berkeley to join the Manhattan Project in 1942. His main duty was to head a group working on the chemical purification of plutonium-239 to yield kilogram quantities of the fissionable isotope. In his Nobel lecture Seaborg explained that the principal problem was firstly to find a way to produce the plutonium on a large scale and then isolate it after production. The production of ^{239}Pu on a large scale would require an immense flux of neutrons from chain-reacting units of a nuclear reactor. The large source of neutrons in a nuclear reactor utilizing the neutron-induced fission chain reaction within uranium-235 was employed, as illustrated by Seaborg in Fig. VIII.13. The high flux of fast neutrons from the fission of ^{235}U was captured by ^{238}U in a uranium target to produce ^{239}U, which would decay by beta emission to ^{239}Np, which would undergo beta decay with a very short half-life to ^{239}Pu.

By 1944 the process for large-scale production and purification of ^{239}Pu was solved in the Manhattan Project, which gave Glenn Seaborg time to contemplate and plan his search for the synthesis and identification of elements beyond plutonium (element 94), namely elements 95 and 96. He solicited the assistance of collaborators in this endeavor, including Albert Ghiorso, an electric engineer who played an important role in the development of electronic instrumentation required for the radioactivity measurements, as Seaborg noted in his Nobel lecture. Seaborg's other collaborators included R.A. James and L.O. Morgan, who were young chemists with expertise in research on the chemistry of the transuranium elements. The identification of elements 95 and 96 caused great difficulty, as explained by Seaborg in his Nobel lecture:

> *There followed quite a period during which the attempts to synthesize and identify elements 95 and 96 bore no fruit. These unsuccessful experiments were based on the premise that these elements should be much like plutonium in that it should be possible to oxidize them to the (VI) oxidation state and utilize this in the chemical isolation procedures. It was not until the middle of the summer of 1944, upon the first recognition that these elements were part of an actinide transition series…As soon as it was recognized that these elements should be oxidized above the (III) state only with extreme difficulty, if at all, the identification of an isotope of element 96 followed immediately. Thus the isotope ^{242}Cm was identified [Seaborg et al., 1949a] in the summer of 1944 as a result of the bombardment of ^{239}Pu with 32 MeV helium ions in the Berkeley 60-in. cyclotron.*

The actinide transition series mentioned by Seaborg was elaborated in a biographical memoir by Hoffman (2000):

> *They were unsuccessful until Seaborg came up with the actinide concept of heavy-element electronic structure in which the 14 elements heavier than actinium (atomic number 89) are placed in the periodic table of elements as a* 5f *transition series under the lanthanide* 4f *transition series. A new periodic table incorporating this concept was published in* Chemical & Engineering News *in 1945.*

$$^{235}\mathrm{U} + \mathrm{n} \longrightarrow \text{fission products} + \text{energy} + \text{neutrons}$$

$$^{238}\mathrm{U} + \mathrm{n} \longrightarrow {}^{239}_{92}\mathrm{U} \xrightarrow[23.5\ \text{min.}]{\beta^-} {}^{239}_{93}\mathrm{Np} \xrightarrow[2.33\ \text{days}]{} {}^{239}_{94}\mathrm{Pu}$$

FIGURE VIII.13 The production of plutonium-239 with neutrons produced in the chain reaction resulting from neutron capture in ^{235}U. Neutrons captured by ^{238}U produced ^{239}U, which decays to ^{239}Pu following two beta decay processes. *From Seaborg (1951), printed with permission of The Nobel Foundation © 1951.*

Seaborg's concept of the actinide series of elements was a great breakthrough, but met with some opposition from the scientific community, as described by Ghiorso (1999); reprinted by permission from AIP Publishing LLC © 1999:

> *…although the chemistry of plutonium was well-known by then, that of the new elements was completely unknown. These factors meant that little progress had been made after many months of effort. Finally, Glenn made a big breakthrough when he formulated his theory that the transuranic elements were part of an actinide series, and, because they were trivalent in aqueous solution, they could be chemically separated from the plutonium target material. His theory of a rare earth-like series required a major realignment of the periodic table, and for many years the Seaborg hypothesis was fought by other chemists. In the end, his actinide theory was vindicated, especially after his insight made possible the chemical identification of elements up through element 103, which was later dubbed lawrencium.*

The identification of element 95 followed in late autumn 1944 (Seaborg et al., 1949b). In his Nobel lecture, Seaborg explained that element 95 (americium) was produced by the bombardment of ^{239}Pu with pile neutrons, namely neutrons from a nuclear reactor, as described in Fig. VIII.14; and, at the same time an isotope of element 96 (curium-242) results from the neutron capture by ^{241}Am to ^{242}Am, followed by beta decay to ^{242}Cm, as described by Fig. VIII.15.

Element 95 was given the name americium after America, in line with the earlier naming of its lanthanide homologue europium, named after Europe. Element 96 was named curium in honor of Pierre and Marie Curie, which is analogous to the earlier naming of its lanthanide homologue gadolinium after Johan Gadolin, the Finnish discoverer of the element yttrium.

Glenn Seaborg collaborated in the discovery of these numerous new elements of the actinide series; he did not claim credit. In his Nobel lecture on December 12, 1951 he tried to name as many as possible of the people who had contributed greatly to this work. In the case of americium (element 95), he named B.B. Cunningham as the first to isolate americium in 1945 at the wartime Metalurgical Laboratory (Cunningham, 1949); and he named L.B. Werner and I. Perlman as the first to isolate ^{242}Cm (element 96) at the Berkeley Department of Chemistry and Radiation Laboratory in 1947 (Werner and Perlman, 1951).

In December 1949 and January 1950 elements 97 (berkelium) and 98 (californium) were discovered, respectively. As described by Seaborg (1951), these elements were discovered by the cyclotron irradiation of ^{241}Am and ^{242}Cm with 35 MeV helium ions by S.G. Thompson, A. Ghiorso, and a young scientist, K. Street, Jr, with Seaborg's collaboration (Thompson et al., 1950a,b,c,d). The reactions of the 25 MeV helium ions with elements 95 and 96 to produce elements 97 and 98 were illustrated by Seaborg (1951) with the processes shown in Fig VIII.16.

The reactions illustrated in Fig. VIII.16 were not efficient, and produced only a few thousand atoms of this new element. Seaborg (1951) reported that the pioneering work of Miller et al. (1950) made carbon-ion bombardment of target atoms possible with the 60 in. cyclotron. Thus Ghiorso et al. (1951) were able to produce californium isotopes by the reactions illustrated in Fig. VIII.17.

Many isotopes of the numerous new elements were discovered; only a few were cited by Seaborg in his Nobel lecture. As noted by Ghiorso (1999a,b), Seaborg's insight enabled the chemical identification of elements up to atomic

$$^{239}\text{Pu} + \text{n} \longrightarrow {}^{240}\text{Pu} + \gamma$$

$$^{240}\text{Pu} + \text{n} \longrightarrow {}^{241}\text{Pu} + \gamma$$

$$^{241}_{94}\text{Pu}\ (14\ \text{years}) \xrightarrow{\beta^-} {}^{241}_{95}\text{Am}\ (475\ \text{years}, \alpha)$$

FIGURE VIII.14 The production of element 95 (americium) by the bombardment of plutonium by neutrons from a nuclear pile (reactor) followed by the beta decay of ^{241}Pu to ^{241}Am. The values in parentheses are the measured half-lives of the isotopes. *From Seaborg (1951), printed with permission of The Nobel Foundation © 1951.*

$$^{241}\text{Am} + \text{n} \longrightarrow {}^{242}\text{Am} + \gamma$$

$$^{242}_{95}\text{Am}\begin{pmatrix}16\ \text{hours upper state}\\ 100\ \text{years lower state}\end{pmatrix} \xrightarrow{\beta^-} {}^{242}_{96}\text{Cm}\ (162\ \text{days}, \alpha)$$

FIGURE VIII.15 The production of element 96 (curium) by the neutron capture by element 95 (^{241}Am) to yield ^{242}Am, followed by the beta decay of ^{242}Am to yield ^{242}Cm. The values in parentheses are the measured half-lives of the isotopes; and the two half-lives of ^{242}Am represent the measured half-lives of two metastable states of that isotope. *From Seaborg (1951), printed with permission of the Nobel Foundation © 1951.*

$$^{241}_{95}\mathrm{Am} + {}^{4}_{2}\mathrm{He} \longrightarrow {}^{243}_{97}\mathrm{Bk} + 2\mathrm{n} \quad (4.6\ \text{hours, K}/\alpha \cong 10^{3})$$

$$^{242}_{96}\mathrm{Cm} + {}^{4}_{2}\mathrm{He} \longrightarrow {}^{244}_{98}\mathrm{Cf} + 2\mathrm{n} \quad (45\ \text{min.}, \alpha)$$

FIGURE VIII.16 The cyclotron production of isotopes of elements 97 (berkelium) and 98 (californium) by the bombardment of 35 MeV helium ions with elements 95 (americium) and 96 (curium) respectively. The data in parentheses is the measured half-lives of the berkelium and californium isotopes, respectively. The term K/α represents two modes of decay of the berkelium isotope, namely K-capture or alpha emission, with K-capture predominating by approximately a thousand-fold. *From Seaborg (1951), printed with permission of The Nobel Foundation © 1951.*

$$^{238}_{92}\mathrm{U} + {}^{12}_{6}\mathrm{C} \longrightarrow {}^{244}_{98}\mathrm{Cf} + 6\mathrm{n} \quad (45\ \text{min.}, \alpha)$$

$$^{238}_{92}\mathrm{U} + {}^{12}_{6}\mathrm{C} \longrightarrow {}^{246}_{98}\mathrm{Cf} + 4\mathrm{n} \quad (36\ \text{hours}, \alpha)$$

FIGURE VIII.17 The cyclotron production of isotopes of element 98 (californium) by the cyclotron bombardment of carbon ions against a uranium target. *From Seaborg (1951), printed with permission of The Nobel Foundation © 1951.*

number 103. Again, the writer notes that Seaborg emphasized the collaboration and work of many people in this enormous task of producing the new elements of the actinide series. In his Nobel lecture Seaborg (1951) commented:

> *It should be emphasized that these nuclides are the product of the investigations of a number of laboratory groups besides our own. I should like to mention especially the work of W.M. Manning, M.H. Studier and coworkers of the Argonne National Laboratory in Chicago, Illinois, as well as the work of the United States Atomic Energy Commission's Los Alamos Laboratory, and the Chalk River Laboratory of the Canadian National Research Council. I feel that I should especially single out the contributions of my colleague Albert Ghiorso whose name, as you may have noticed, has come up time after time as I have gone through my description here of the work on the transuranium elements. Ghiorso has been a key man throughout and is one of those individuals without whom a laboratory such as ours simply could not run.*

Ion exchange was a technique pioneered and utilized by Glenn Seaborg and collaborators in the separation and purification of the new radioactive elements after their production; and it remains today a key method for the purification and subsequent quantitative analysis of radioisotopes (Vajda et al., 2012; Becker, 2012; Engelbrecht, 2012; L'Annunziata, 2012d; Salonen et al., 2012; Grate et al., 2012). The technique involves the elution of a mixture of various radioactive elements on a column of ion exchange resin. If the ionic forms of the elements are positively charged, they will adhere to the negative charge of a cation exchange resin. The elements are eluted from the column with particular solvents possessing certain pH and chemical properties that govern the rates of elution of elements from the column due to the varying degrees of retention that different cations have on ion exchange resins. A mixture of the elements in a small volume of solution is firstly added to the top of the column of ion exchange resin, followed by the slow addition of solvent. The solvent flows down the column by gravity or pressure, and is subsequently collected in fractions as it leaves the other end of the column. The solvent is often collected in tubes at a particular rate determined by the counting of drops that leave the column. Each fraction of solvent collected from the column is measured by a predetermined number of drops or volume collected per fraction. A photocell can count the drops of solvent as it leaves the column; and the collecting tubes can be changed automatically after a preset number of drops has been collected. The process is referred to as fraction collecting, and is now commonly used by chemists. When the correct solvent is found, the elements in ionic state can be eluted from the ion exchange column at different rates. In his Nobel lecture, Seaborg (1951) illustrated how the actinides were separated on a column of cation exchange resin (see Fig. VIII.18).

A photograph of Glenn Seaborg shows the ion exchange apparatus and fraction collector which he and his collaborators used. The apparatus contains, at the very top, a glass separatory funnel containing solvent supported on a ring stand. The separatory funnel has a stopcock with which the rate of flow of solvent can be controlled. The solvent flows down a transparent vinyl tube to a glass apparatus housing a column of ion exchange resin. A small volume of solution containing a mixture of elements is injected into the top of the ion exchange resin, and the solvent is allowed to flow down the column. Under the column can be seen a circular tray containing numerous holes to accommodate test tubes that will collect fractions of solvent as it exits the column. The rate of collection is determined by the experimenter, and the fraction collector can be set to rotate after a predetermined number of drops are counted by a photocell located directly under the column.

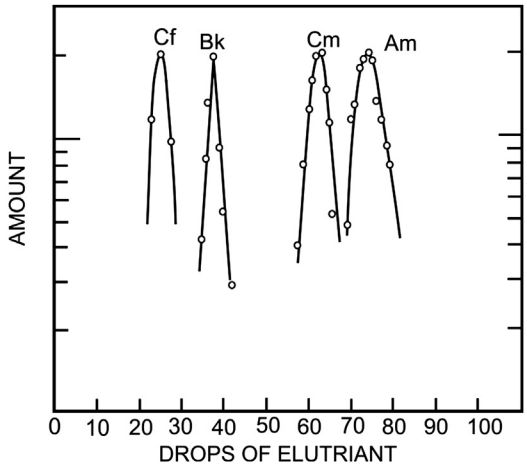

FIGURE VIII.18 Rates of elution of actinides on a column of cation exchange resin. The data for the actinides shown here is that of K. Street, Jr., S. G. Thompson, and G. T. Seaborg (1950) in which the cation exchange resin Dowex-50 was used and the elution performed at 87°C with ammonium citrate buffered with citric acid to a pH of 3.5 (total citrate concentration 0.2 M). *Reprinted with permission of the American Chemical Society © 1950.*

Seaborg is shown in the photograph writing the names of various actinides that were produced from elements 94–98; and alongside these are written the chemical homologues of these new elements, which belong to the lanthanide series, namely elements 63–66.

For the history of the production of heavier elements up to element 110, the reader may peruse a paper by Seaborg (1990) entitled "Transuranium Elements: A Half Century," available on the internet (www.osti.gov/accomplishments/documents/fullText/ACC0052.pdf).

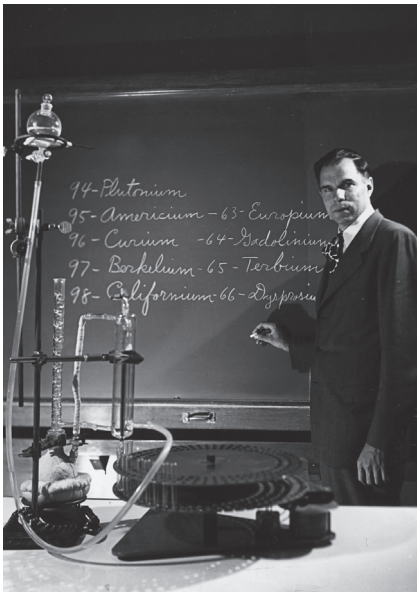

Glenn T. Seaborg writing on blackboard with ion exchange apparatus and fraction collector in foreground
Courtesy of The University of California, AIP Emilio Segre Visual Archives, Segre Collection

From 1946 to 1958 Seaborg was director of the Nuclear Chemistry Division, and in 1954 became associate director of the Berkeley Radiation Laboratory. In 1961 the president-elect asked Glenn Seaborg to chair the US Atomic Energy Commission (AEC), in which capacity he served from 1961 to 1971. During his tenure as AEC chair, Seaborg participated

in the negotiations that resulted in the Limited Test Ban Treaty prohibiting the atmospheric testing of nuclear weapons or testing under the sea (Ghiorso, 1999; Hoffman, 2000). Also during Seaborg's tenure, the AEC played a key role in the negotiation of the Non-proliferation Treaty (NPT) and the institution of national and international safeguards to ensure that nuclear materials are not diverted from peaceful applications to weapons manufacturing (Hoffman, 2000). The Treaty on the Non-Proliferation of Nuclear Weapons, with its international nuclear safeguards, remains an important international agreement that is monitored by the IAEA in signatory countries.

In 1971 Seaborg returned to his post as professor of chemistry at the University of California, Berkeley, where he taught classes and supervised the research work of more than 65 PhD students. He also served as associate director at large of the Lawrence Berkeley National Laboratory until his death in 1999 (Hoffman, 2000).

It is noted by biographers that Glenn Seaborg was listed in the Guinness Book of World Records as having the longest biographical sketch in *Who's Who in America*.

Element 106 was named seaborgium in his honor in 1997, 2 years before his death. He was the only living person to have had an element named in their honor.

Chapter 18

Radionuclide Decay, Radioactivity Units, and Radionuclide Mass

…the character of thorium radioactivity is unaltered by chemical treatment… It is well established that this property [radioactivity] is the function of the atom and not of the molecule. Uranium and thorium, to take the most definite cases, possess the property [radioactivity] in whatever molecular condition they occur... So far as the radioactivity of different compounds of different density and states of division can be compared together, the intensity of the radiation appears to depend only on the quantity of active element present. It is not at all dependent on the source from which the element is derived, or the process of purification to which it has been subjected, provided sufficient time is allowed for the equilibrium point to be reached…radioactivity is at once an atomic phenomenon and accompanied by…changes in which new types of matter are produced, these changes must be occurring within the atom, and the radioactive elements must be undergoing spontaneous transformation…Radioactivity may therefore be considered as a manifestation of subatomic…change.

Ernest Rutherford and Frederick Soddy (1902) relating their research conclusions on the phenomenon of radionuclide decay. In their statements cited above, which are taken from their classic research paper, which appeared in the *Philosophical Magazine*, they concluded (1) that the rates of decay of radionuclides, ie, radioactivity, cannot be altered by chemical treatment; (2) the intensity of the radiation emitted is a function of the mass or amount of radionuclide present; (3) the intensity of the radiation measured may require a period of time for equilibrium to be reached—this is the first historical account of the existence of decay equilibria that can exist; and (4) radionuclide decay results from changes within the atom or "subatomic change," where a radioactive element is transformed into another.

18.1 INTRODUCTION

The activity of a radioactive source or radionuclide sample is, by definition, its strength or intensity, or in other words the number of nuclei decaying per unit time (eg, disintegrations per minute or disintegrations per second). The activity of a given radionuclide in a sample is proportional to the number of radioactive atoms present in that sample. Consequently the activity of a radionuclide is also a measure of its mass. The activity decreases with time as a result of radionuclide decay. A unit of time in which there is an observable change in the activity of a given quantity of radionuclide may be very short, on the order of seconds, or very long, on the order of many years. The rate of decay of some nuclides is so slow that it is impossible to measure any change in radioactivity during our lifetime.

18.2 HALF-LIFE

Rates of radionuclide decay are usually expressed in terms of half-life. This is the time, t, required for a given amount of radionuclide to lose 50% of its activity. In other words, it is the time required for one-half of a certain number of nuclei to decay. The decay curve of ^{32}P (Fig. 18.1) illustrates the concept of half-life. In Fig. 18.1, the activity of the ^{32}P is plotted against time in days. It can be seen that, after every interval of 14.3 days, the radioactivity of the ^{32}P is reduced by half. Thus, the half-life, $t_{1/2}$, of ^{32}P is 14.3 days. It is not possible to predict when one particular atom of ^{32}P will decay; however, it is possible to predict statistically for a large number of ^{32}P radionuclides that one-half of the atoms would decay in 14.3 days.

The phenomenon of radioactivity decay and its measurement in terms of half-life was first observed by Ernest Rutherford (1900). He published his observations on the rate of decay of a certain isotope of thorium in the *Philosophical Magazine* in January 1900, less than four years after Henri Becquerel first reported the existence of radioactivity to the

Radioactivity: Introduction and History, From the Quantum to Quarks. http://dx.doi.org/10.1016/B978-0-444-63489-4.00018-6
Copyright © 2016 Elsevier B.V. All rights reserved.

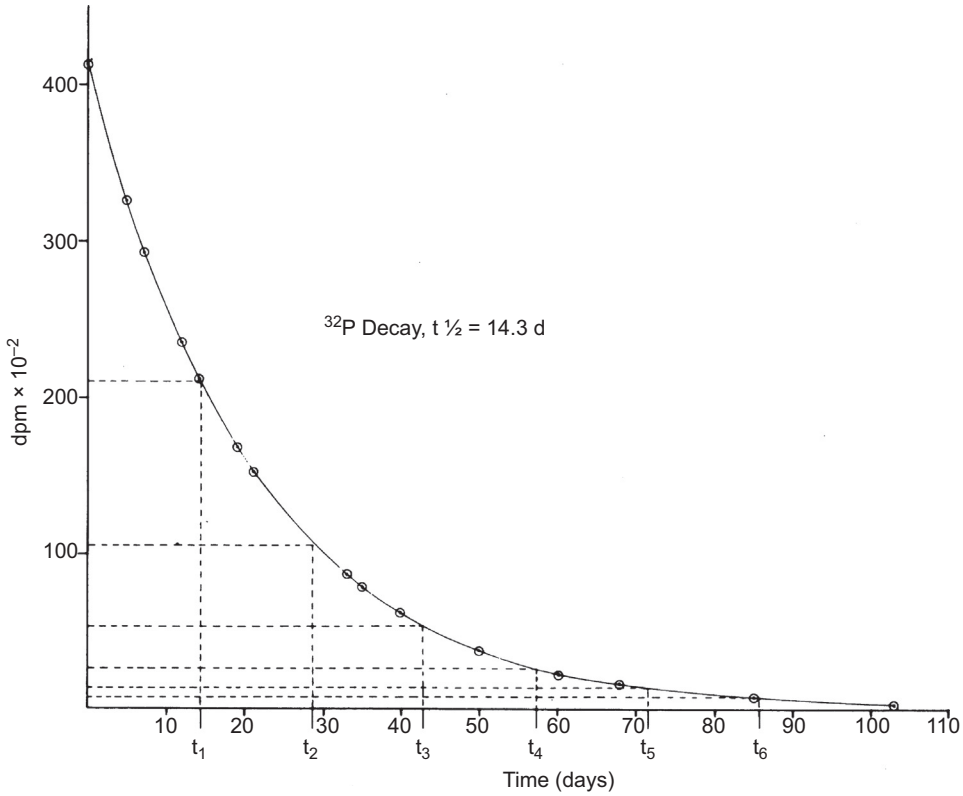

FIGURE 18.1 Decay of ^{32}P represented as a linear plot of activity in disintegrations per minute (dpm) against time in days. Horizontal and vertical lines between the ordinate and abscissa delineate ^{32}P activities (dpm) after six half-lives identified by the symbols t_1, t_2, t_3,…t_6. *From L'Annunziata, M.F., 1965, unpublished work of the writer.*

French Academy of Sciences in February and March 1996. Rutherford (1900) measured the rate of decay by the level of ionization the radiation would produce in air as a function of time, and he noted the following when he measured the half-life of a radionuclide sample to be 60 s [writer's comments are in brackets]:

> *…the intensity of the radiation has fallen to one-half its value after an interval of about one minute. The rate of leak [meaning rate of decay, or rate of ionization caused by the radiation] due to the emanation was too small for measurement after an interval of 10 minutes [i.e., 10 half-lives]… The current [produced by the ionization] reaches half its value in about one minute − a result which agrees with the equation given, for* $e^{-\lambda t} = 1/2$ *when* $t = 60$ *seconds.*

In his original paper, Rutherford (1900) did not use the term "half-life"; but he defined mathematically the concept of half-life. As we shall see subsequently in Eq. [18.6], the ratio of the number of radionuclides, N, in a sample at a given time, t, to the original number of nuclides, N_0, in that sample at time $t = 0$, is equal to $e^{-\lambda t}$, where e is the base to the natural logarithm, λ is a decay constant of that radionuclide, and t is the interval of time.

When radionuclide decay can be recorded within a reasonable period of time, the half-life of a nuclide can be determined by means of a semi-logarithmic plot of activity versus time, as shown in Fig. 18.2. Radionuclide decay is a logarithmic relation, and the straight line obtained on the semi-logarithmic plot permits a more accurate determination of the half-life.

Ernest Rutherford and Frederick Soddy (1902), in the *Philosophical Magazine*, summarized their findings on radioactivity and radionuclide decay as follows [the writer's insertions are in brackets]:

> *Turning from the experimental results to their theoretical interpretation, it is necessary to first consider the generally accepted view of the nature of radioactivity. It is well established that this property is the function of the atom and not of the molecule. Uranium and thorium, to take the most definite cases [examples], possess the property in whatever molecular condition they occur… So far as the radioactivity of different compounds of different density and states of division can be compared together, the intensity of the radiation appears to depend only on the quantity of active element [radioisotope] present.*

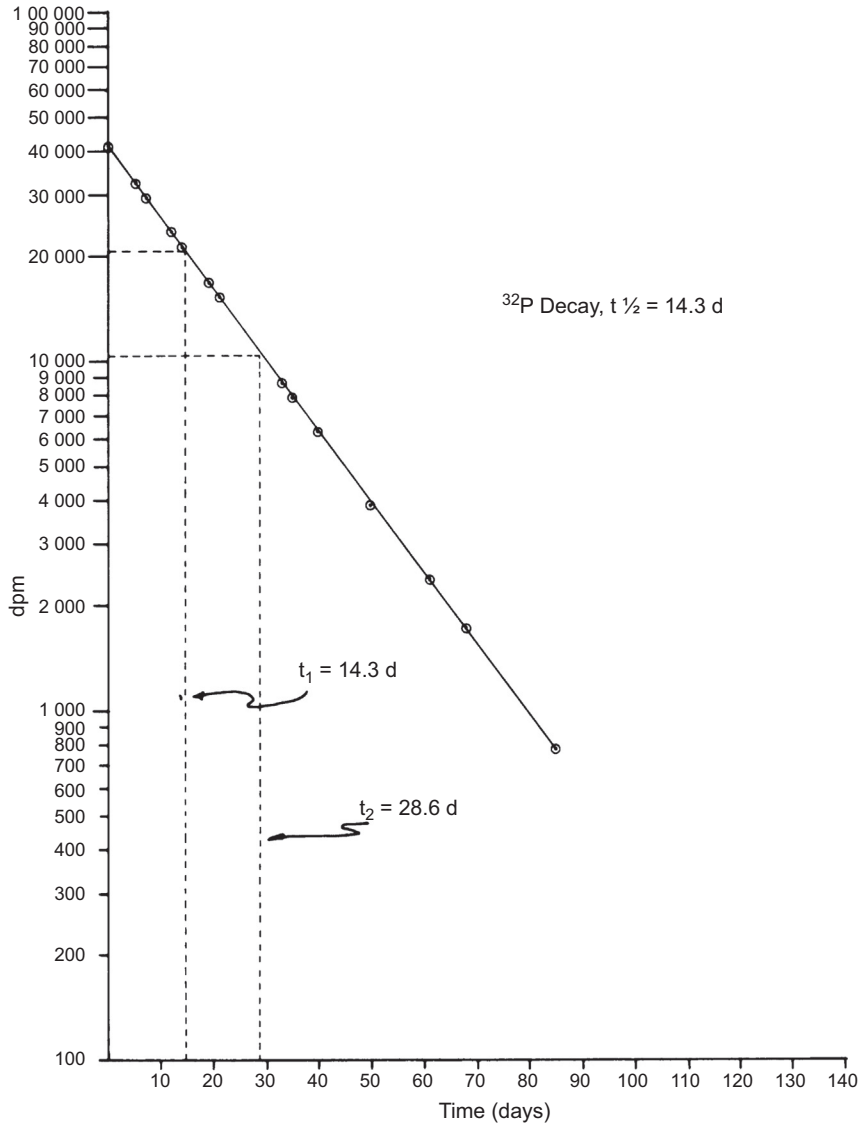

FIGURE 18.2 Semi-logarithmic plot of the decay of ^{32}P. One and two half-lives (t_1 and t_2) are delineated by horizontal and vertical lines between the ordinate and abscissa. *From L'Annunziata, M.F., 1965, unpublished work of the writer.*

The above statement by Rutherford and Soddy in 1902 that "the intensity of the radiation appears to depend only on the quantity of active element present" is defined subsequently in mathematical terms.

The number, ΔN, of atoms disintegrating in a given time, Δt, is proportional to the number, N, of radioactive atoms present. This relationship may be written as:

$$\Delta N/\Delta t = \lambda N \qquad [18.1]$$

or:

$$dN/dt = -\lambda N \qquad [18.2]$$

where λ is a proportionality constant, commonly referred to as the decay constant, and the negative sign signifies a decreasing number of radionuclides with time.

One condition must be fulfilled for Eq. [18.1] to be rigorously applicable: the total number of radioactive atoms being considered must be large enough to make statistical methods valid. For example, in the case of a single isolated atom of ^{32}P, there is no way to predict when the atom will decay. In fact, the atom might decay in the first second after $t = 0$

(the moment observations are initiated) or it might decay days or weeks later. The concept of half-life is a statistical one, which when applied to a large number of atoms, as is usually the case, allows an accurate calculation of the activity of radionuclides after a given time interval.

For radionuclide decay calculations, Eq. [18.2] must be transformed into a more suitable form and may be expressed as:

$$dN/N = -\lambda\, dt, \qquad [18.3]$$

which can be integrated between the limits N_0 and N and between t_0 and t, where t_0 is 0 (the moment observations are initiated), N_0 is the number of atoms originally present at time t_0, and N is the number of atoms remaining after time t:

$$\int_{N_0}^{N} dN/N = -\lambda \int_{t_0}^{t} dt \qquad [18.4]$$

to give:

$$\ln \frac{N_0}{N} = -\lambda t \qquad [18.5]$$

Eq. [18.5] may be written in exponential form as:

$$N = N_0 e^{-\lambda t} \qquad [18.6]$$

where e is the base of the natural logarithm, λ is the decay constant, and t is the interval of time. Eq. [18.6] is the form used to determine the decay of a radionuclide sample after a given time interval. To use Eq. [18.6], the value of the decay constant λ must be known, and this is different for each radionuclide. To determine λ for a particular radionuclide, a relationship between the decay constant and the half-life may be derived from the decay equation (Eq. [18.5]), which may be transposed to:

$$\ln \frac{N_0}{N} = \lambda t \qquad [18.7]$$

By definition, we know that after an interval of time corresponding to the half-life, half of the original activity remains. Therefore we may assign the original activity N_0 as unity, whereby after one-half life the remaining activity N would be one-half of unity, and Eq. [18.7] would become:

$$\ln \frac{1}{1/2} = \lambda t \qquad [18.8]$$

or:

$$\ln 2 = \lambda t_{1/2} \qquad [18.9]$$

where $t_{½}$ is the half-life of the radionuclide in units of time, namely, seconds, minutes, hours, days, or years, and:

$$0.693 = \lambda t_{1/2} \qquad [18.10]$$

The decay constant can then be defined as:

$$\lambda = \frac{0.693}{t_{1/2}} \qquad [18.11]$$

The value of λ can be calculated easily from the half-life of an isotope with Eq. [18.11]. The units used for λ are expressed in reciprocal time, s^{-1}, min^{-1}, h^{-1}, $days^{-1}$, or $years^{-1}$, depending on the half-life of the radionuclide and also on the time interval t used in Eq. [18.6]. For example, if ^{32}P, which has a half-life of 14.3 days, is used in an experiment, λ may be expressed in $days^{-1}$. The unit of the decay constant must agree with the time interval t of Eq. [18.6].

The following example illustrates the use of Eq. [18.6] to calculate the decay of a radionuclide sample within any time interval.

If a sample contained 3.7 MBq (megabecquerels, where by definition 1Bq = 1 disintegration per second or 1 dps; and 1 MBq = 10^6 dps) of ^{32}P on a given date and an investigator wished to determine the amount remaining after a 30-day period, he or she would first determine the decay constant for ^{32}P according to Eq. [18.11] and then calculate the

activity after the specified time period using the decay Eq. [18.6] as follows. The decay constant in units of days^{-1} is determined by:

$$\lambda = \frac{0.693}{t_{1/2}} = \frac{0.693}{14.3 \text{ days}} = 4.85 \times 10^{-2} \text{ days}^{-1}$$

With the calculated value of λ and the time interval t equal to 30 days, the activity of the remaining ^{32}P is determined by Eq. [18.6] expressed in terms of activity, or:

$$A = A_0 e^{-\lambda t} \quad [18.12]$$

and

$$\begin{aligned} A &= 3.7 \times 10^6 \text{ dps} \cdot e^{-\left[\left(4.85 \times 10^{-2} \text{ days}^{-1}\right)(30 \text{ days})\right]} \\ &= 3.7 \times 10^6 \text{dps} \cdot e^{-1.455} \\ &= 3.7 \times 10^6 \text{dps} \cdot 0.2334 \\ &= 8.64 \times 10^5 \text{dps} = 0.864 \text{ MBq} \end{aligned}$$

where A is the activity of the radionuclide in units of decay rate (eg, dps) after time t, and A_0 is the initial activity at time t_0 or $A_0 = 3.7$ MBq $= 3.7 \times 10^6$ dps, since by definition 1 MBq $= 1 \times 10^6$ dps. Thus after the 30-day period, the activity of ^{32}P decayed from an initial activity of 3.7 MBq to an activity of 0.864 MBq.

The decay equation has many practical applications, as it can be used as well to calculate the time required for a given radionuclide sample to decay to a certain level of activity. Let us consider the following example.

A patient was administered intravenously 600 MBq of [^{99m}Tc]-methylene diphosphate, which is a radiopharmaceutical administered for the purposes of carrying out a diagnostic bone scan. The doctor then wanted to know how much time would be required for the ^{99m}Tc radioactivity in the patient's body to be reduced to 0.6 MBq (0.1% of the original activity) from radionuclide decay alone ignoring any losses by bodily excretion. The half-life $t_{1/2}$ of ^{99m}Tc is 6.00 h. To calculate the time required, we can transpose Eq. [18.12] to:

$$\ln \frac{A_0}{A} = \lambda t \quad [18.13]$$

or:

$$t = \frac{1}{\lambda} \ln \frac{A_0}{A} \quad [18.14]$$

By definition (Eq. [18.11]), the decay constant λ of ^{99m}Tc is $0.693/t_{1/2}$ or 0.693/6.00 h. Solving Eq. [18.14] after inserting the value of λ and the relevant activities of ^{99m}Tc gives:

$$t = \left(\frac{6.00 \text{ h}}{0.693}\right) \ln \left(\frac{600 \text{ MBq}}{0.6 \text{ MBq}}\right) = 59.8 \text{ h} = 2.5 \text{ days}$$

In the case of a mixture of independently decaying radionuclides, the rate of decay of each nuclide species is independent of the other. However, the rate of decay of the overall sample is equal to the sum of the decay rates of the individual nuclide species. The cumulative decay of a mixture of independently decaying nuclides from the most simple case of a mixture of two nuclides to a more complex case of n number of radionuclides is described by:

$$N = N_1^0 e^{-\lambda_1 t} + N_2^0 e^{-\lambda_2 t} + \ldots N_n^0 e^{-\lambda_n t} \quad [18.15]$$

where N is the number of atoms remaining after time t, and N_1^0, N_2^0, and N_n^0 are the numbers of atoms originally present at time t_0 of 1, 2, and n number of nuclide species, and λ_1, λ_2, and λ_n are the decay constants of 1, 2, and n number of radionuclide species, respectively.

The semi-logarithmic decay plot of a mixture of two independently decaying radionuclides is not a straight line, contrary to pure radionuclide samples, but is a composite plot, as in the case of a mixture of ^{32}P and ^{45}Ca (see Fig. 18.3). If the half-lives of the two nuclides are significantly different, the composite curve may be analyzed so that the half-lives of

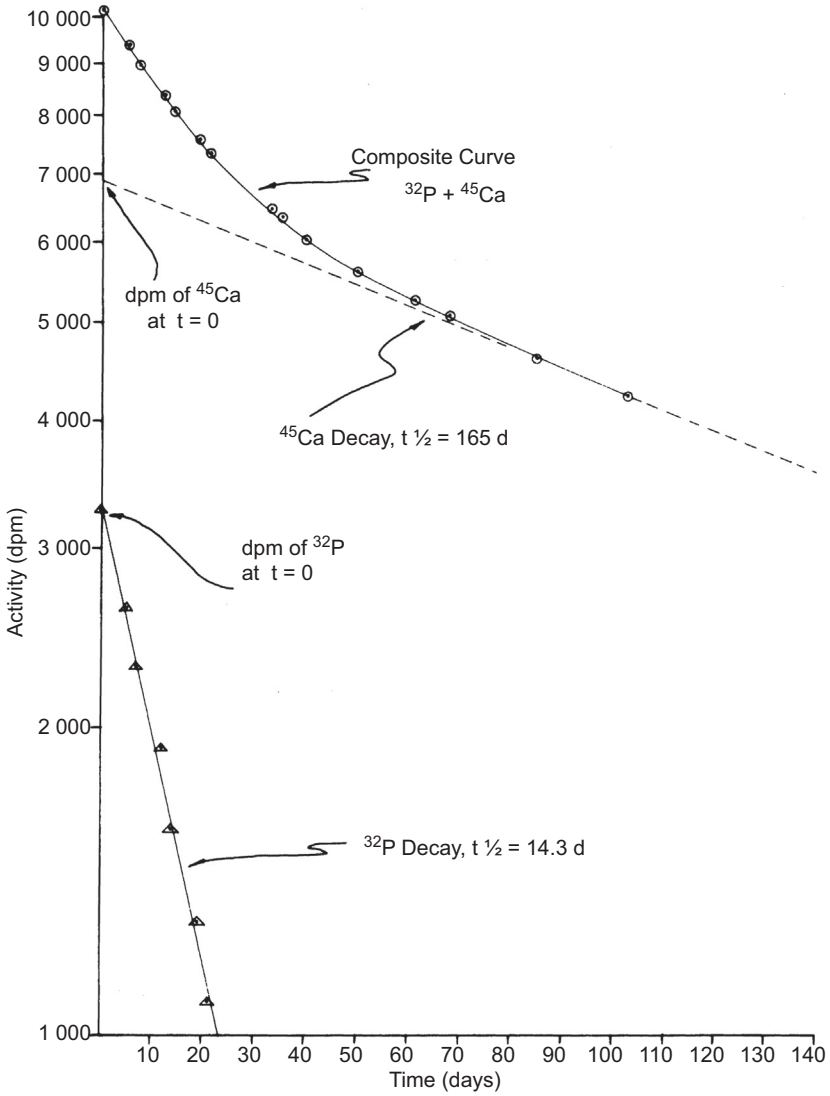

FIGURE 18.3 Semi-logarithmic decay curves of ^{32}P and ^{45}Ca isolated from a composite decay curve of a mixture of $^{32}P + {}^{45}Ca$. *From L'Annunziata, M.F., 1965, unpublished work of the writer.*

each radionuclide may be determined. If the decay of the composite mixture can be observed over a reasonable period of time, the composite curve will eventually yield a straight line representing the decay of the longer-lived nuclide after the disappearance of the shorter-lived nuclide (depicted in Fig. 18.3). This straight line may be extrapolated to time $t = 0$ so that the activity (dpm) of this nuclide at $t = 0$ can be found. The difference between the activity at $t = 0$ of the longer-lived nuclide and the total activity of the sample at $t = 0$ gives the activity at $t = 0$ of the shorter-lived nuclide. Likewise, further subtraction of points of the extrapolated decay curve from the composite curve yields the decay curve of the shorter-lived nuclide.

The half-lives of the two radionuclides are determined from the slopes of the two decay curves isolated from the composite curve. Eq. [18.7], which is expressed in natural logarithms, may be transformed to logarithms to the base 10 by:

$$2.30 \log(N_1/N_2) = \lambda(t_2 - t_1) \qquad [18.16]$$

or:

$$\log(N_1/N_2) = \frac{\lambda}{2.30}(t_2 - t_1) \qquad [18.17]$$

where N_1 and N_2 are the numbers of atoms or activity of the sample at times t_1 and t_2, respectively. As $\lambda/2.30$ of Eq. [18.17] is equal to the slope of the straight-line decay curve, the decay constant, λ, may be calculated from a graphical determination of the slope. With a calculated value of λ, the half-life of the nuclide is then calculated from Eq. [18.7].

Many radionuclides have very long half-lives, which make the graphic representation of their decay impossible. Some examples are ^{3}H ($t_{1/2} = 12.3$ years), ^{14}C ($t_{1/2} = 5.73 \times 10^{3}$ years), ^{40}K ($t_{1/2} = 1.3 \times 10^{9}$ years), and ^{174}Hf ($t_{1/2} = 2 \times 10^{15}$ years). In such cases, the half-lives can be calculated from Eqs. [18.2] and [18.11]. The decay rate or activity, A, in disintegrations per year (DPY) of a given radionuclide sample, defined by dN/dt of Eq. [18.2], is measured experimentally by counting the radiation emission per unit time, eg, counts per minute (CPM). The number of atoms of the radioassayed sample, defined by N of Eq. [18.2], must be known or determined by quantitative chemical analysis. This is simple for pure samples. For example, the number of atoms of ^{40}K in a pure sample of KCI is easily calculated from Avogadro's number (6.022×10^{23} molecules/mol) and the percentage natural abundance of ^{40}K (0.012%). Samples of unknown purity and isotopic abundance require a quantitative analysis of the element such as that provided by a mass spectral analysis of the isotopic abundance. The value of λ in years^{-1} is calculated as:

$$\lambda = \frac{dN/dt}{N} = \frac{A}{N} = \frac{\text{CPM}/E}{N}\left(5.25 \times 10^{5}\ \text{min/year}\right) \qquad [18.18]$$

where A is the sample nuclide activity in DPY, N is the number of atoms of the nuclide in the sample, CPM is the sample count rate (counts per minute) provided by the instrument radioactivity detector, E is the instrument counting efficiency, and 5.25×10^{5} min/year is the factor used to convert counts per minute (CPM) to counts per year (CPY). The half-life can then be calculated according to Eqs. [18.11] and [18.18], both of which define the value of λ.

Let us look at a practical example of the use of the above equations to determine the half-life of ^{40}K taken from the work of Grau Malonda and Grau Carles (2002). The accurate determination of the half-life of ^{40}K has very practical implications, as it is currently used by geologists to date a rock's formation based on the measurement of the quantity of the stable daughter nuclide ^{40}Ar. Grau Malonda and Grau Carles (2002) reported the accurate determination of the half-life of ^{40}K as follows:

They measured accurately the activity of ^{40}K in a sample of pure KNO_3 and applying the relationships of half-life to λ according to Eqs. [18.11] and [18.18]. They measured the ^{40}K specific activity in KNO_3 to be 12.24 ± 0.014 Bq/g by a very accurate CIEMAT/NIST efficiency-tracing liquid scintillation standardization method first conceived by Agustin Grau Malonda in 1978 and developed by him in collaboration with Bert M. Coursey as described in detail by Grau Malonda (1999) and L'Annunziata (2012b). Also, applying the known isotopic concentration of ^{40}K in KNO_3 of 0.01167% and the value of Avogadro's number 6.022×10^{23} atoms per mole, they could calculate the number of atoms of ^{40}K in 1 g of KNO_3 as follows:

$$\left(\frac{6.022 \times 10^{23}\ \text{atoms K/mole KNO}_3}{101.103\ \text{g KNO}_3\text{/mole KNO}_3}\right)\left(\frac{0.01167\ \text{atoms }^{40}\text{K}}{100\ \text{atoms K}}\right)$$

$$= 6.951 \times 10^{17}\ \text{atoms }^{40}\text{K/g KNO}_3$$

From Eqs. [18.11] and [18.18] we can write:

$$\frac{1}{\lambda} = \frac{t_{1/2}}{0.693} = \frac{N}{A} \qquad [18.19]$$

or:

$$t_{1/2} = 0.693\left(\frac{N}{A}\right) \qquad [18.20]$$

From the determined specific radioactivity of ^{40}K in KNO_3 and the number of atoms of ^{40}K per gram of KNO_3, Grau Malonda and Grau Carles (2002) calculated the half-life of ^{40}K as:

$$t_{1/2} = 0.693\left(\frac{6.951 \times 10^{17}\ \text{atoms }^{40}\text{K/g KNO}_3}{(12.24\ \text{dps }^{40}\text{K/g KNO}_3)(60\ \text{s/min})(5.25 \times 10^{5}\ \text{min/year})}\right)$$

and:

$$t_{1/2} = 1.248 \times 10^{9}\ \text{years}$$

From the mean of nine determinations, Grau Malonda and Grau Carles (2002) were able to assign the value of the half-life of ^{40}K to be $(1.248 \pm 0.004) \times 10^9$ years at a 95% confidence level.

Other radionuclides have very short half-lives, such as ^{209}Ra ($t_{½} = 4.6$ s), ^{215}At ($t_{½} = 1.0 \times 10^{-4}$ s), and ^{212}Po ($t_{½} = 2.98 \times 10^{-7}$ s). Half-lives of such short duration can be determined by delayed-coincidence radiation counting methods (Jakubek et al., 2010; Kurtukian-Nieto et al. 2008; Morozov et al., 2006, 2002, 1998; Schwarzschild, 1963; Oms, 2004; Petkov et al., 2003; Ohm et al., 1990), which involve the use of scintillation and semiconductor radiation detectors with detector response times as short as 10^{-11} s. The technique has also been applied to the measurement of the half-lives of excited nuclear states, such as the 8.7- and 98.1-ns half-lives of the 14.4- and 136.5-keV excited states of ^{57}Fe daughter nuclides, which emit gamma radiation, following the decay of ^{57}Co (Morozov et al., 2006, 2002). Radiation detectors with resolving times of fractions of a microsecond are set electronically so that a delay circuit will detect a radiation-induced pulse from the parent in coincidence with a radiation pulse produced from the daughter. Varying the delay time of the coincidence circuit results in a delay of the coincidence pulse rate, from which a decay curve of the very short-lived daughter nuclide can be plotted and the half-life determined.

The half-life of a radionuclide, as well as its decay mode(s), radiation emissions, energies, and intensities, is available from reference tables (L'Annunziata, 2012f; Lide, 2010).

18.3 GENERAL DECAY EQUATIONS

The simplest decay relationship between parent and daughter nuclides that can be considered is that of a parent nuclide that decays to form a stable daughter nuclide.

The decay of the radionuclide ^{33}P serves as an example. The parent nuclide ^{33}P decays with a half-life of 25.3 days with the production of the stable daughter ^{33}S, as indicated by:

$$^{33}_{15}\mathrm{P} \rightarrow ^{33}_{16}\mathrm{S}(\text{stable}) + \beta^- + \overline{\nu} \qquad [18.21]$$

Numerous radionuclides, such as ^{3}H, ^{14}C, ^{32}P, ^{35}S, ^{36}Cl, ^{45}Ca, and ^{131}I, decay by this simple parent–daughter relationship.

However, numerous other radionuclides produce unstable daughter nuclides. The simplest case would be that in which the parent nuclide A decays to a daughter nuclide B, which in turn decays to a stable nuclide C:

$$\mathrm{A} \rightarrow \mathrm{B} \rightarrow \mathrm{C}\ (\text{Stable}) \qquad [18.22]$$

In such decay chains, the rate of decay and production of the daughter must be considered as well as the rate of decay of the parent. The decay of the parent is described by the simple rate equation:

$$-\frac{dN_\mathrm{A}}{dt} = \lambda_\mathrm{A} N_\mathrm{A} \qquad [18.23]$$

which is integrated to the form:

$$N_\mathrm{A} = N_\mathrm{A}^0 e^{-\lambda_\mathrm{A} t} \qquad [18.24]$$

where N_A^0 is the number of atoms of the parent at the time $t = 0$ and N_A is the number of atoms after a given period of time $t = t_1$.

The decay rate of the daughter is dependent on its own decay rate as well as the rate at which it is formed by the parent. It is written as:

$$-\frac{dN_\mathrm{B}}{dt} = \lambda_\mathrm{B} N_\mathrm{B} - \lambda_\mathrm{A} N_\mathrm{A} \qquad [18.25]$$

where $\lambda_\mathrm{B} N_\mathrm{B}$ is the rate of decay of the daughter alone and $\lambda_\mathrm{A} N_\mathrm{A}$ is the rate of decay of the parent or rate of formation of the daughter. Eqs. [18.24] and [18.25] may be transposed into the linear differential equation:

$$\frac{dN_\mathrm{B}}{dt} + \lambda_\mathrm{B} N_\mathrm{B} - \lambda_\mathrm{A} N_\mathrm{A}^0 e^{-\lambda_\mathrm{A} t} = 0 \qquad [18.26]$$

which is solved for the number of atoms of daughter, N_B, as a function of time, to give:

$$N_\mathrm{B} = \frac{\lambda_\mathrm{A}}{\lambda_\mathrm{B} - \lambda_\mathrm{A}} N_\mathrm{A}^0 \left(e^{-\lambda_\mathrm{A} t} - e^{-\lambda_\mathrm{B} t}\right) + N_\mathrm{B}^0 e^{-\lambda_\mathrm{B} t} \qquad [18.27]$$

Although unnecessary in this treatment, the solution to Eq. [18.26] is given by Friedlander et al. (1964).

In decay schemes of this type, the following three conditions may predominate: (1) secular equilibrium, (2) transient equilibrium, and (3) the state of no equilibrium. Each of these cases will now be considered in detail.

18.4 SECULAR EQUILIBRIUM

The phenomenon of radioisotope decay equilibrium was first observed by Ernest Rutherford and Frederick Soddy in 1902, which they reported in their classic paper on "The Cause and Nature of Radioactivity." They reported their observations as follows:

> *Radioactivity is shown to be accompanied by chemical changes in which new types of matter are being continuously produced. These reaction products are at first radioactive, the activity diminishing regularly from the moment of formation. Their continuous production maintains the radioactivity of the matter producing them at a definite equilibrium value.*

Secular equilibrium is a steady-state condition of equal activities between a long-lived parent radionuclide and its short-lived daughter. The important criterion upon which secular equilibrium depends is the following: The parent must be long-lived compared to the life of the daughter nuclide; that is, negligible decay of the parent occurs during numerous half-lives of the daughter. In other words, the daughter must have a relatively short half-life compared to that of the parent. The relative differences in half-lives of the parent and daughter nuclides may be expressed as:

$$\lambda_A/\lambda_B \leq \sim 10^{-4} \qquad [18.28]$$

that is:

$$\lambda_A \ll \lambda_B \qquad [18.29]$$

where λ_A and λ_B are the respective decay constants of the parent and daughter nuclides. The importance of these two requirements can be clearly seen if the $^{90}Sr(^{90}Y)$ equilibrium is taken as an example.

The nuclide ^{90}Sr is the parent in the decay scheme:

$$^{90}_{38}\mathrm{Sr} \xrightarrow{t_{1/2}\,=\,28.8\ \text{years}} {}^{90}_{39}\mathrm{Y} \xrightarrow{t_{1/2}\,=\,2.7\ \text{days}} {}^{90}_{40}\mathrm{Zr}\ (\text{stable}) \qquad [18.30]$$

The long half-life of ^{90}Sr compared to the very short half-life of the ^{90}Y daughter satisfies the requirement for secular equilibrium. Over a quarter of a century is needed for it to lose 50% of its original activity. As will be seen, less than 3 weeks are required for secular equilibrium to be attained and, in this interim period, negligible decay of ^{90}Sr occurs. The relative differences of the half-lives of the ^{90}Sr parent and its ^{90}Y daughter can be measured by comparing their decay constants.

The decay constants for ^{90}Sr and ^{90}Y are easily calculated from their half-lives and Eq. [18.11], and the values are 6.60×10^{-5} days^{-1} and 2.57×10^{-1} days^{-1}, respectively. Consequently, in the comparison, $\lambda_A/\lambda_B = 2.57 \times 10^{-4}$, and this is in agreement with the order of magnitude required for secular equilibrium.

An equation for the growth of daughter atoms from the parent can be obtained from Eq. [18.27] by consideration of the limiting requirements for secular equilibrium. Since $\lambda_A \approx 0$ and $\lambda_A << \lambda_B$, $e^{-\lambda_A t} = 1$ and λ_A falls out of the denominator in the first term of Eq. [18.27]. If the daughter nuclide is separated physically from the parent (L'Annunziata, 1971), $N_B^0 = 0$ at time $t = 0$ (time of parent–daughter separation) and the last term would fall out of Eq. [18.27]. Thus, in the case of secular equilibrium, the expression of the ingrowth of daughter atoms with parent can be written as:

$$N_B = \frac{\lambda_A N_A^0}{\lambda_B}\left(1 - e^{-\lambda_B t}\right) \qquad [18.31]$$

If the observation of the ingrowth of the daughter is made over many half-lives of the daughter, it is seen that the number of atoms of the daughter approaches a maximum value $\lambda_A N_A^0/\lambda_B$, which is the rate of production of the daughter divided by its decay constant. The final form of Eq. [18.31] to be used for the calculation of the ingrowth of the daughter can be expressed as:

$$N_B = (N_B)_{max}\left(1 - e^{-\lambda_B t}\right) \qquad [18.32]$$

Since the activity of the daughter atoms, A_B, is proportional to the number of daughter atoms, or $A_B = k\lambda_B N_B$, where k is the coefficient of detection of the daughter atoms, Eq. [18.32] may also be written as:

$$A_B = (A_B)_{max}\left(1 - e^{-\lambda_B t}\right) \qquad [18.33]$$

Rutherford and Soddy (1902) were the first to write and interpret Eqs. [18.32] and [18.33] when they studied the equilibrium existing between radioactive thorium and a daughter radionuclide. They noted the following [the writer's comments in brackets]:

> *The radioactivity of thorium at any time is the resultant of two opposing processes: 1. The production of fresh radioactive material at a constant rate by the thorium compound, and 2. The decay of the radiating power of the active material with time. The normal or constant radioactivity possessed by thorium is an equilibrium value, where the rate of increase of radioactivity due to the production of fresh active material [daughter nuclide] is balanced by the rate of decay of radioactivity of that already formed…The experimental curve obtained with the hydroxide [this was the chemical form they used to separate the parent nuclide from the daughter] for the rate of rise of its activity from a minimum to a maximum value will therefore be approximately expressed by the equation* $I_t/I_0 = 1 - e^{-\lambda t}$, *where* I_0 *represents the amount of activity recovered when the maximum is reached, and* I_t *the activity recovered after time* t, λ *being the same constant as before. [Notice the similarity of Rutherford and Soddy's equation, which may be transposed to read* $I_t = (I_0)(1 - e^{-\lambda t})$, *and Eqs. [18.32] and [18.33].]*

Let us take an arbitrary example of equal activities of 100 dpm of parent ^{90}Sr and 100 dpm of daughter ^{90}Y in secular equilibrium and calculate and graphically represent the ingrowth of ^{90}Y with its parent and also the decay of ^{90}Y subsequent to the separation of parent and daughter nuclides (L'Annunziata, 1971). Identical activities of ^{90}Sr and ^{90}Y are arbitrarily chosen, because their activities are equal while in secular equilibrium prior to their separation. Fig. 18.4 illustrates the calculated growth of ^{90}Y (curve B) as produced by ^{90}Sr using Eq. [18.33] with $(A_B)_{max} = 100$. The decay of separated ^{90}Y (curve A) is plotted by simple half-life decay ($t_{1/2} = 2.7$ days). The dashed line (line C) represents the decay of ^{90}Sr, which is negligible during the period of observation ($t_{1/2} = 28.8$ years). The total activity (curve D) is the result of both ^{90}Sr decay and the ingrowth of ^{90}Y after the separation of the latter and is obtained by the addition of curve B to line C. It may be noted from Fig. 18.4, that after approximately six half-lives of ^{90}Y (~18 days), the growth of ^{90}Y has reached the activity of ^{90}Sr, after which both nuclides decay with the same half-life, that of the parent ^{90}Sr (28.8 years).

Ernest Rutherford and Frederick Soddy, in their classic paper on "The Cause and Nature of Radioactivity" in 1902 in the *Philosophical Magazine*, made the first published observation of what is now known as secular equilibrium. They were studying the radioactivity of an isotope of thorium and a daughter isotope, which they called ThX. The term "daughter isotope" for an isotope decay product was not then established, because knowledge of radioactivity was only then at its infancy. They summarized their findings with the following [the writer's comments are in brackets]:

> *The foregoing experimental results may be briefly summarized. The major part of the radioactivity of thorium—ordinarily about 54 percent—is due to a non-thorium type of matter, ThX, possessing distinct chemical properties, which is temporarily radioactive, its activity falling to half value in about four days. The constant radioactivity of thorium is maintained by the production of this material at a constant rate. Both the rate of production of the new material and the rate of decay of its activity appear to be independent of the physical and chemical condition of the system. [We now know that the activity of parent and daughter nuclides are equal in secular equilibrium and the value of "about 54 percent" reported by Rutherford and Soddy was precisely 50 percent.]*

As an example of the practical utility of this phenomenon, the application of secular equilibrium theory to the analysis of ^{90}Sr in biological systems is presented here.

One method reported by the Los Alamos National Laboratory (see Gautier, 1995) entails the initial chelation (complex formation) of strontium with the sodium salt of ethylenediaminetetraacetic acid (EDTA). The chelated strontium is then isolated by elution on an ion-exchange column. The eluted strontium is then precipitated as a carbonate. The activity of radioactive strontium, which will include ^{89}Sr + ^{90}Sr in the sample, is determined by low-background counting. Low-background liquid scintillation counting is most often used for the total ^{89}Sr + ^{90}Sr analysis, as described by Passo and Cook (1994) and Salonen et al. (2012). The isolated radiostrontium is then allowed to remain in the sample without further treatment for a period of about 2 weeks to allow for the ingrowth of ^{90}Y. About 2 weeks are needed to ensure the parent and daughter radionuclides are in secular equilibrium before the chemical separation of yttrium from strontium. From Eq. [18.33], it is calculated that after 2 weeks the activity of ^{90}Y grows to 97.4% of its original level. Carrier yttrium is then added to the dissolved radiostrontium, and the yttrium is precipitated as the hydroxide, redissolved, and reprecipitated as an oxalate. The step involving the precipitation of yttrium from the sample results in the separation of ^{90}Y from the radiostrontium. The separated ^{90}Y can then be assayed by suitable low-background radiation counting using liquid scintillation or Cherenkov counting (Passo and Cook, 1994 and L'Annunziata and Passo, 2002). The ^{90}Sr activity in the sample is determined from the activity of ^{90}Y by calculating the ^{90}Y decay from the time of separation (precipitation) of

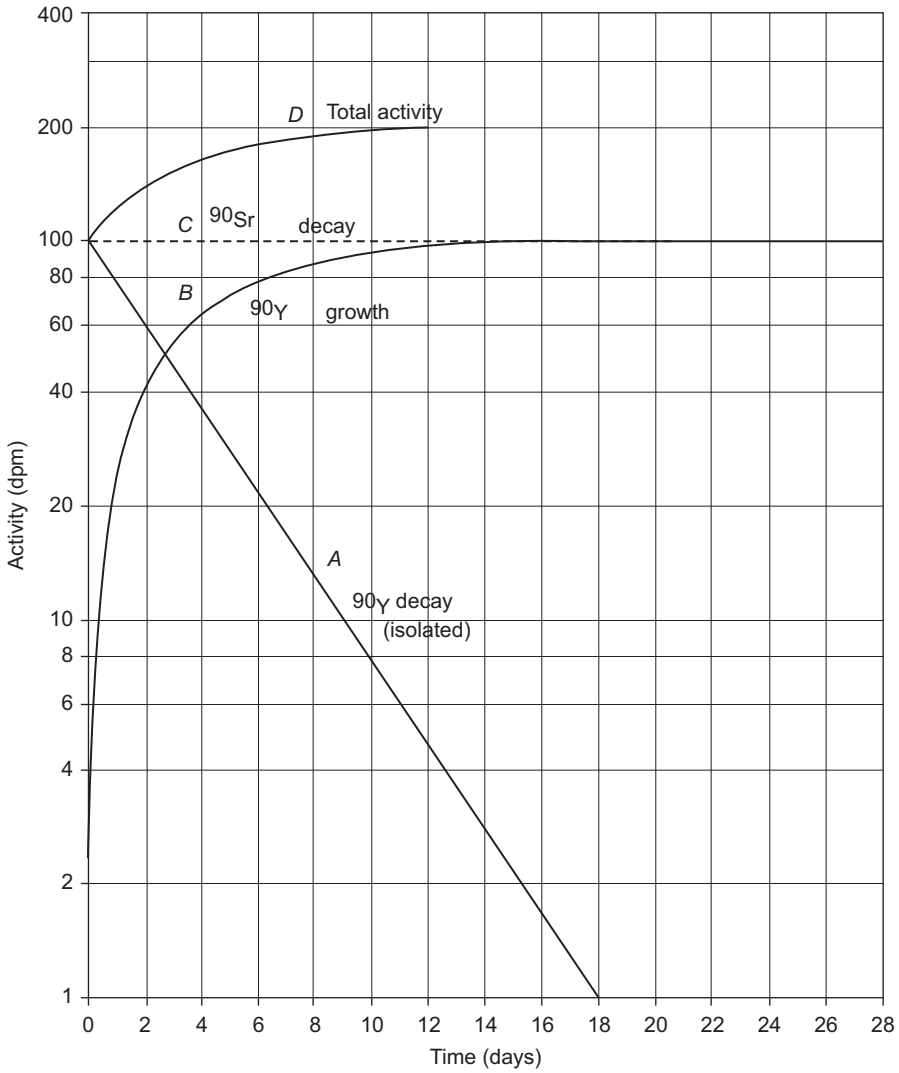

FIGURE 18.4 Growth and decay curves following the separation of ^{90}Sr(^{90}Y) in secular equilibrium. (A) Decay of isolated ^{90}Y. (B) Ingrowth of ^{90}Y with ^{90}Sr. (C) Decay of isolated ^{90}Sr. (D) Total activity from isolated ^{90}Sr, representing both ^{90}Sr decay and ^{90}Y growth until secular equilibrium is attained. *From L'Annunziata, M.F., 1971. Birth of a unique parent-daughter relation: secular equilibrium. J. Chem. Educ. 48,700–703, reprinted with permission © 1971 American Chemical Society.*

yttrium from strontium. This is possible because the parent and daughter radionuclides were at secular equilibrium (ie, ^{90}Sr dpm = ^{90}Y dpm) at time $t = t_0$ when the precipitation and separation of yttrium from strontium were carried out. The ^{89}Sr activity in the sample is determined from the difference between the total radiostrontium activity (^{89}Sr + ^{90}Sr) and the measured activity of ^{90}Sr.

Certain chemical processes in natural and biological systems can preferentially select either the parent or daughter nuclide and, in this manner, separate the two. For example, a research investigator could administer nuclides in secular equilibrium to a soil and plant system. At the time of administration, the nuclides are in secular equilibrium; that is, both the parent and daughter activities are equal. However, if in the course of the experiment the investigator obtains a plant sample for radioassay, which had preferably absorbed either the parent or daughter, problems ensue if the equilibrium phenomenon is not considered. Radioassay of plant tissue that had selectively concentrated the parent could show an initial progressive rise in radioactivity due to ingrowth of the daughter, whereas a selective concentration of the daughter would result in a sample showing an initial decrease in radioactivity. In cases such as these, it is necessary to isolate the parent radionuclide chemically and wait for a period of time sufficient to permit secular equilibrium to be reached ($\sim$2 weeks for the ^{90}Sr(^{90}Y) example) before analyzing the sample.

18.5 TRANSIENT EQUILIBRIUM

Like secular equilibrium, transient equilibrium is a steady-state condition between the parent and daughter nuclides. However, in transient equilibrium the parent–daughter nuclides do not possess the same activities but rather they decay at the same half-life, that of the parent nuclide.

The criterion upon which transient equilibrium rests is that the parent nuclide must be longer lived than its daughter, but not of the order of magnitude described by Eq. [18.28]; that is, it is necessary that $\lambda_A < \lambda_B$. However, the ratio λ_A/λ_B should fall within the limits $10^{-4} < \lambda_A/\lambda_B < 1$.

The decay chain of ^{100}Pd serves as an example of parent–daughter nuclides that may attain transient equilibrium. ^{100}Pd decays by electron capture to ^{100}Rh with a half-life of 96 h. The daughter nuclide ^{100}Rh decays by electron capture and positron emission to the stable nuclide ^{100}Ru. The half-life of the daughter nuclide is 21 h. The decay scheme may be represented as:

$$^{100}_{46}\text{Pd} \xrightarrow{t_{1/2} = 96\text{ h}} {}^{100}_{45}\text{Rh} \xrightarrow{t_{1/2} = 21\text{ h}} {}^{100}_{44}\text{Ru (stable)} \qquad [18.34]$$

The first criterion for transient equilibrium is satisfied in this case; the half-life of the parent nuclide is greater than that of the daughter. If the decay constants λ_A and λ_B are now calculated, we can determine whether or not the second criterion ($10^{-4} < \lambda_A/\lambda_B < 1$) is satisfied.

The value of λ_A, given by 0.693/96 h, is $7.2 \times 10^{-3}\ \text{h}^{-1}$, and that of λ_B, given by 0.693/21 h, is $3.3 \times 10^{-2}\ \text{h}^{-1}$. Consequently, the ratio $\lambda_A/\lambda_B = 2.2 \times 10^{-1}$ and lies within the limits of the second criterion.

If the general decay, Eq. [18.27], of the daughter nuclide is considered, the term $e^{-\lambda_B t}$ is negligible compared with $e^{-\lambda_A t}$ for sufficiently large values of t. Thus the terms $e^{-\lambda_B t}$ and $N_B^0 e^{-\lambda_B t}$ may be dropped from Eq. [18.27] to give:

$$N_B = \frac{\lambda_A}{\lambda_B - \lambda_A}\left(N_A^0 e^{-\lambda_A t}\right) \qquad [18.35]$$

for the ingrowth of the daughter nuclide as a function of time. Because $N_A = N_A^0 e^{-\lambda_A t}$, Eq. [18.35] may be written as:

$$\frac{N_B}{N_A} = \frac{\lambda_A}{\lambda_B - \lambda_A} \qquad [18.36]$$

From Eq. [18.36], it can be seen that the ratio of the number of atoms or the ratio of the activities of the parent and daughter nuclides is a constant in the case of transient equilibrium.

Since $A_A = k_A \lambda_A N_A$ and $A_B = k_B \lambda_B N_B$, where A_A and A_B are the activities of the parent and daughter nuclides, respectively, and k_A and k_B are the detection coefficients of these nuclides, Eq. [18.36] may be written in terms of activities as:

$$\frac{A_B}{k_B \lambda_B}(\lambda_B - \lambda_A) = \frac{A_A}{k_A \lambda_A}\lambda_A \qquad [18.37]$$

or:

$$\frac{A_B}{A_A} = \frac{k_B \lambda_B}{k_A(\lambda_B - \lambda_A)} \qquad [18.38]$$

If equal detection coefficients are assumed for the parent and daughter nuclides, Eq. [18.38] may be written as:

$$\frac{A_B}{A_A} = \frac{\lambda_B}{(\lambda_B - \lambda_A)} \qquad [18.39]$$

Thus, for transient equilibrium, Eq. [18.39] indicates that the activity of the daughter is always greater than that of the parent by the factor $\lambda_B/(\lambda_B - \lambda_A)$. Eq. [18.39] may likewise be written as:

$$\frac{A_A}{A_B} = 1 - \frac{\lambda_A}{\lambda_B} \qquad [18.40]$$

whereby the ratio A_A/A_B falls within the limits $0 < A_A/A_B < 1$ in transient equilibrium.

If an activity of 100 dpm is arbitrarily chosen for the daughter nuclide ^{100}Rh in transient equilibrium with its parent ^{100}Pd, the activity of ^{100}Pd can be found using either Eq. [18.39] or [18.40]. Eq. [18.39] gives:

$$\frac{100\text{ dpm}}{A_A} = \frac{3.3 \times 10^{-2}\ \text{h}^{-1}}{3.3 \times 10^{-2}\ \text{h}^{-1} - 7.2 \times 10^{-3}\ \text{h}^{-1}}$$

or:

$$A_A = 78 \text{ dpm}$$

With the use of Eq. [18.39] or [18.40], the decay of the daughter nuclide may be calculated as a function of parent decay in transient equilibrium. The ^{100}Pd–^{100}Rh parent–daughter decay in transient equilibrium is illustrated by curves A and B, respectively, of Fig. 18.5. The parent and daughter nuclides are shown to have respective activities of 78 and 100 dpm at time $t = 0$. As curves A and B show, the parent and daughter nuclides in transient equilibrium decay with the same half-life, that corresponding to the half-life of the parent.

If the parent and daughter nuclides were to be separated, the daughter nuclide would decay according to its half-life, as indicated by curve C. The isolated parent nuclide would, however, show an increase in activity with time owing to the ingrowth of daughter until transient equilibrium is attained. Curve D of Fig. 18.5 shows the ingrowth of daughter nuclide from a freshly isolated parent. Because $N_B^0 = 0$ at time $t = 0$ (time of separation of parent and daughter), the last term of Eq. [18.27] falls out, to give:

$$N_B = \frac{\lambda_A N_A^0}{\lambda_B - \lambda_A}\left(e^{-\lambda_A t} - e^{-\lambda_B t}\right) \quad [18.41]$$

The term $\lambda_A N_A^0/(\lambda_B - \lambda_A)$ describes the rate of production of the daughter divided by the difference between the daughter and parent decay constants, which will approach a maximum value that may be written as:

$$N_B = (N_B)_{max}\left(e^{-\lambda_A t} - e^{-\lambda_B t}\right) \quad [18.42]$$

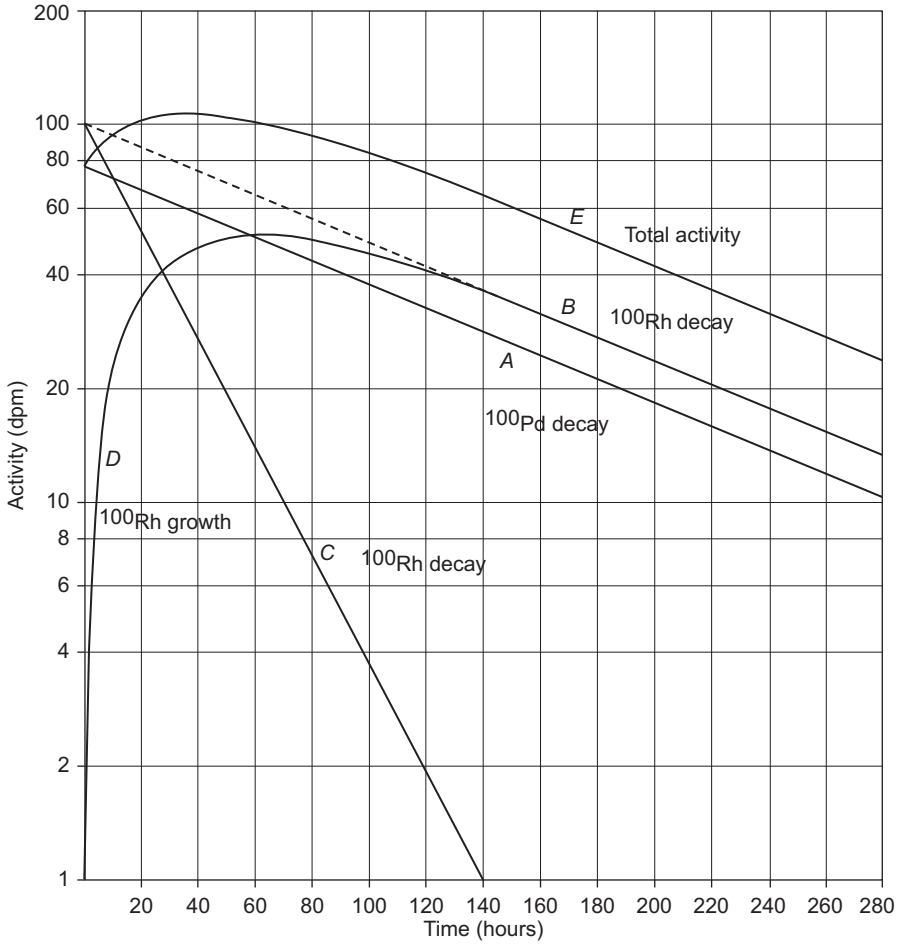

FIGURE 18.5 Growth and decay curves following the separation of ^{100}Pd(^{100}Rh) in transient equilibrium. (A) Decay of isolated parent nuclide ^{100}Pd. (B) Decay of ^{100}Rh daughter nuclide in transient equilibrium. The dashed portion of this curve represents ^{100}Rh decay if parent and daughter nuclides were not separated. (C) Decay of ^{100}Rh after separation from its parent. (D) The ingrowth of ^{100}Rh with the isolated parent ^{100}Pd. (E) Total activity from the isolated ^{100}Pd representing both ^{100}Pd decay and ^{100}Rh growth until transient equilibrium is attained. *From L'Annunziata, M.F., 1987. Radionuclide Tracers, Their Detection and Measurement. Academic Press, London, pp. 505, reprinted with permission from Elsevier © 1987.*

comparable to the case of Eq. [18.32]. Since the activity, A_B, of the daughter atoms is proportional to the number of daughter atoms, or $A_B = k_B\lambda_B N_B$, where k is as defined previously, Eq. [18.42] may also be written as:

$$A_B = (A_B)_{max}\left(e^{-\lambda_A t} - e^{-\lambda_B t}\right) \quad [18.43]$$

Because the maximum daughter activity in this sample is 100 dpm, Eq. [18.43] may be used to calculate the ingrowth of daughter nuclide with $(A_B)_{max} = 100$.

Curve E of Fig. 18.5 illustrates the total activity, that is, the activity of the isolated parent nuclide plus the ingrowth of daughter nuclide. It is found by summing curves A and D and consequently accounts for the simultaneous decay of the parent nuclide and the ingrowth of the daughter. Notice that the slopes of curves A, B, and E are identical when transient equilibrium is attained, that is, the rates of decay of both the parent and daughter are identical.

18.6 NO EQUILIBRIUM

The cases of secular equilibrium and transient equilibrium, which involve decay schemes whereby the parent nuclide is longer lived than its daughter, were just considered. In other cases in which the daughter nuclide is longer lived than its parent, $\lambda_A > \lambda_B$, no equilibrium is attained. Instead, the parent nuclide of shorter half-life eventually decays to a negligible extent, leaving only the daughter nuclide, which decays by its own half-life. The following decay scheme of ^{56}Ni serves as an example:

$$^{56}_{28}\text{Ni} \xrightarrow{t_{1/2} = 6.4 \text{ days}} {}^{56}_{27}\text{Co} \xrightarrow{t_{1/2} = 77.3 \text{ days}} {}^{56}_{26}\text{Fe (stable)} \quad [18.44]$$

The parent nuclide ^{56}Ni decays by electron capture with a half-life of 6.4 days, whereas its daughter ^{56}Co decays with the longer half-life of 77.3 days by electron capture and β^+ emission. Curve A of Fig. 18.6 illustrates the decay of the ^{56}Ni parent nuclide. The decay of ^{56}Ni is followed by the ingrowth (production) of the ^{56}Co daughter nuclide, shown by curve B. The ingrowth of the daughter is calculated from Eq. [18.27], of which the last term, $N_B^0 e^{-\lambda_B t}$, falls out because $N_B^0 = 0$ at time $t = 0$. The number of daughter atoms N_B of Eq. [18.27] may be converted to activity, A_B, by the term $A_B = k_B\lambda_B N_B$ as discussed previously. The total activity illustrated by curve C of Fig. 18.6 depicts both the simultaneous decay of parent nuclide and the growth and decay of the daughter determined by summing curves A and B. Notice from Fig. 18.6 that the parent nuclide activity in this example becomes negligible after around 55 days, after which the total activity, curve C, has a slope corresponding to the decay rate of the daughter nuclide.

18.7 MORE COMPLEX DECAY SCHEMES

Other decay schemes exist that involve a chain of numerous nuclides, such as:

$$A \rightarrow B \rightarrow C \rightarrow \ldots N \quad [18.45]$$

where nuclides A, B, and C are followed by a chain of a number N of decaying nuclides. A long decay chain of this type may be observed in the complex decay schemes of high-atomic-number natural radionuclides such as ^{232}Th, ^{238}U, and ^{235}U in Figs. 2.1 to 2.4 of chapter "Basic Concepts and Definitions" of this book. The complex decay scheme of ^{232}Th is illustrated in Fig. 18.7. The decay sequence of $^{232}_{90}$Th to $^{212}_{83}$Bi is described by the general Eq. [18.45]. However, the continuation of this decay scheme with $^{212}_{83}$Bi involves a branching decay of the type:

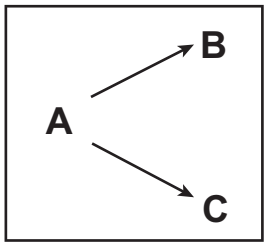

[18.46]

In this example, $^{212}_{83}$Bi is the parent of the two daughter nuclides $^{212}_{84}$Po and $^{208}_{81}$Tl. The half-life of ^{212}Bi is written under the nuclide symbol rather than along the arrows of Fig. 18.7, because the ^{212}Bi half-life is a function of the two decay processes and may be written as:

$$t_{1/2} = \frac{0.693}{(\lambda_A + \lambda_B)} \quad [18.47]$$

where λ_A and λ_B are the decay constants of the two separate decay processes.

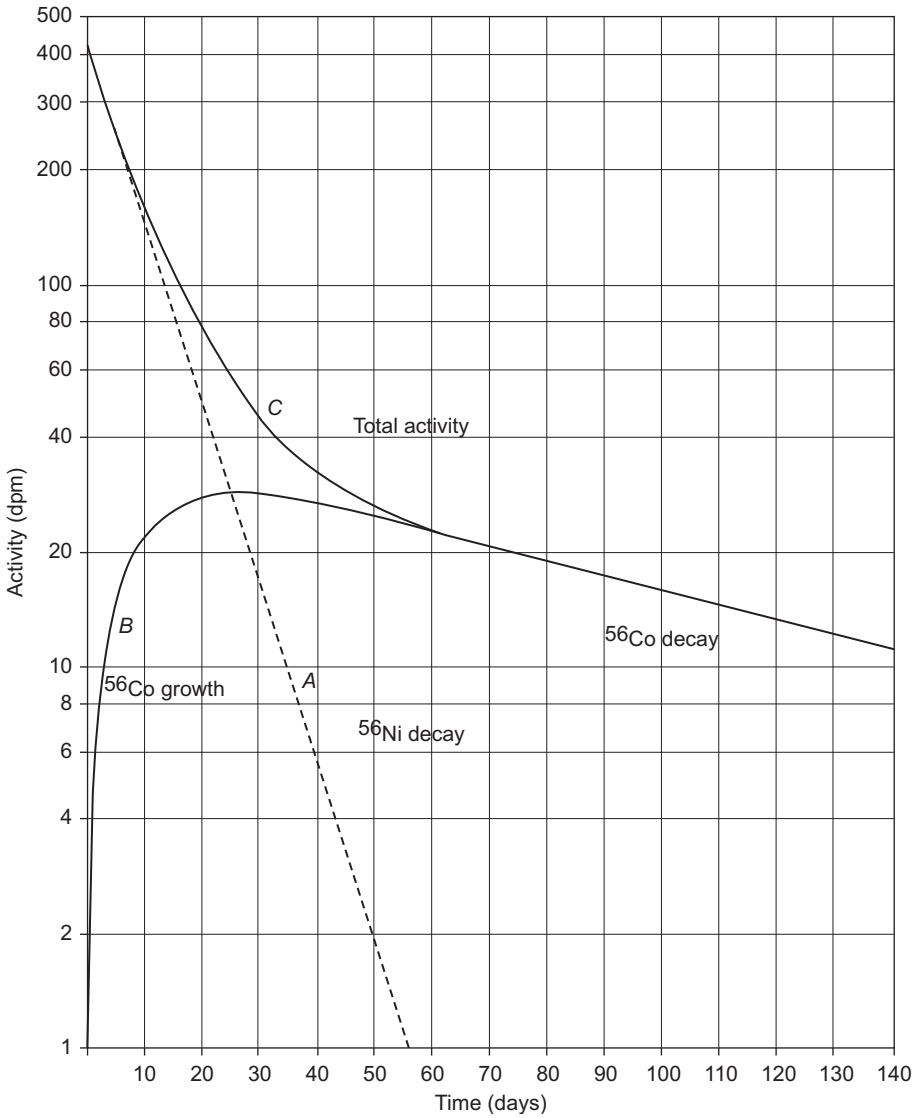

FIGURE 18.6 Growth and decay curves of the ^{56}Ni(^{56}Co) parent–daughter nuclides following the isolation or fresh preparation of the parent nuclide ^{56}Ni. (A) Decay of pure parent nuclide ^{56}Ni. (B) Ingrowth of daughter nuclide ^{56}Co. (C) Total activity representing both ^{56}Ni decay and the simultaneous growth and decay of ^{56}Co daughter. *From L'Annunziata, M.F., 1987. Radionuclide Tracers, Their Detection and Measurement. Academic Press, London, pp. 505, reprinted with permission from Elsevier © 1987.*

18.8 RADIOACTIVITY UNITS AND RADIONUCLIDE MASS

18.8.1 Units of Radioactivity

The units used to define radioactivity or, in other words, the activity of a radioactive source are written in terms of the number of atoms, N, disintegrating per unit of time, t. We can use Eq. [18.1] previously discussed in this chapter to calculate the activity of any given mass of radionuclide. The equation, namely $\Delta N/\Delta t = \lambda N$, defines the proportionality between the rate of decay of a radionuclide and the number of atoms of the radionuclide in a sample. As an example, we may use Eq. [18.1] to calculate the activity of 1 g of ^{226}Ra as follows:

$$\frac{\Delta N}{\Delta t} = \lambda N \qquad [18.48]$$

and:

$$\frac{\Delta N}{\Delta t} = \left(\frac{0.693}{t_{1/2}}\right)(N) \qquad [18.49]$$

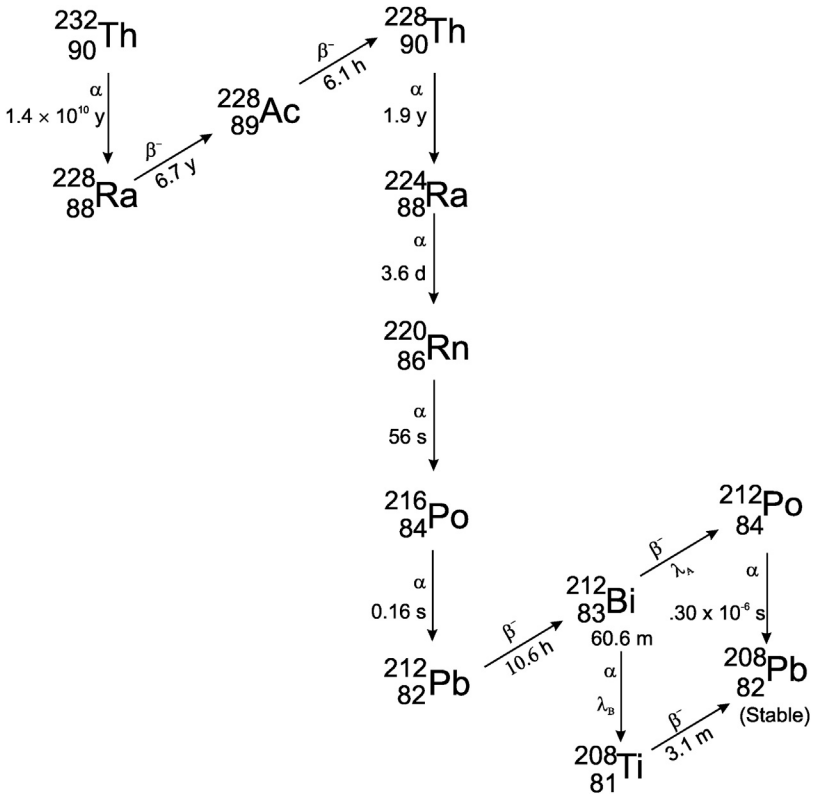

FIGURE 18.7 Decay scheme of natural ^{232}Th. The modes of decay (α or β^- emission) and half-lives of the radioisotopes are provided along each arrow of the decay scheme. Half-lives in years, days, hours, minutes, and seconds are abbreviated as y, d, h, m, and s, respectively.

where $\lambda = 0.693/t_{½}$ as derived previously (Eq. [18.11]). If we take the half-life, $t_{1/2}$, of ^{226}Ra to be 1599 years and substitute for N, in the preceding equation, the number of atoms per mol of ^{226}Ra, we can write:

$$\frac{\Delta N}{\Delta t} = \left(\frac{0.693}{1599 \text{ years}}\right)\left(\frac{6.022 \times 10^{23} \text{ atoms}}{226 \text{ g}}\right) \quad [18.50]$$

where, according to Avogadro's number, there are 6.022×10^{23} atoms per gram mole of substance. If we now convert the half-life of ^{226}Ra from units of years to minutes, we can calculate the number of ^{226}Ra atom disintegrations per minute (dpm) per gram according to:

$$\frac{\Delta N}{\Delta t} = \left[\frac{0.693}{(1599 \text{ years})(365 \text{ days/year})(24 \text{ hours/day})(60 \text{ min/hour})}\right]\left(\frac{6.022 \times 10^{23} \text{ atoms}}{226 \text{ g}}\right)$$

$$\frac{\Delta N}{\Delta t} = \left(\frac{0.693}{8.404 \times 10^{8} \text{ min}}\right)(2.665 \times 10^{21} \text{ atoms/g})$$

$$= 2.198 \times 10^{12} \text{ atoms/min/g}$$

The activity of 1 g of ^{226}Ra is the basis of the unit of radioactivity known as the curie (Ci). One curie is almost equal to the activity of 1 g of ^{226}Ra or, by definition:

$$1 \text{ Ci} = 2.22 \times 10^{12} \text{ dpm} = 3.7 \times 10^{10} \text{ dps} \quad [18.51]$$

Therefore, 1 Ci of activity or any multiple of the curie of any radionuclide defines the number of atoms disintegrating per unit of time in minutes or seconds.

The rate of decay in terms of time in seconds gives rise to a more internationally adopted Système International d'Unités (SI) unit of activity, which is the becquerel (Bq), where by definition:

$$1 \text{ Bq} = 1 \text{ dps} \quad [18.52]$$

Therefore, we can interrelate the curie and becquerel as follows:

$$1\ \text{Ci} = 2.22 \times 10^{12}\ \text{dpm} = 3.7 \times 10^{10}\ \text{dps} = 37\ \text{GBq} \quad [18.53]$$

Likewise, smaller units of the curie, namely the millicurie (mCi) and microcurie (μCi), may be interrelated with the becquerel as follows:

$$1\ \text{mCi} = 2.22 \times 10^{9}\ \text{dpm} = 3.7 \times 10^{7}\ \text{dps} = 37\ \text{MBq} \quad [18.54]$$

and:

$$1\ \mu\text{Ci} = 2.22 \times 10^{6}\ \text{dpm} = 3.7 \times 10^{4}\ \text{dps} = 37\ \text{kBq} \quad [18.55]$$

Another unit of activity recommended in the early 1960s by the International Union of Pure and Applied Physics, but less frequently used, is the rutherford, where 1 rutherford = 10^6 dps and 1 microrutherford would be equivalent to 1 dps or 1 Bq (Buttlar, 1968; Das and Ferbel, 1994).

18.8.2 Correlation of Radioactivity and Radionuclide Mass

From Eq. [18.48] and calculations made in the previous Section 18.8.1, we can see that, for radioactivity sources of a given level of activity, radionuclides of shorter half-life will contain a smaller number of radioactive atoms than radionuclides of longer half-life.

We can use Eq. [18.48] again to compare two radionuclides of relatively short and long half-lives to see the magnitude of the differences in radionuclide masses we would encounter for any given level of radioactivity. For example, we may take the radionuclide ^{32}P of 14.3-day half-life and the radionuclide ^{14}C of 5730-year half-life and calculate the activity per gram (eg, dpm/g) and grams per activity (eg, g/Ci) of each radionuclide for comparative purposes. These calculations are as follows.

1. **^{32}P, half-life = 14.3 days:**

$$\frac{\Delta N}{\Delta t} = \left(\frac{0.693}{t_{1/2}}\right)(N) \quad [18.56]$$

$$\frac{\Delta N}{\Delta t} = \left[\frac{0.693}{(14.3\ \text{days})(24\ \text{h/day})(60\ \text{min/h})}\right]\left(\frac{6.022 \times 10^{23}}{32\ \text{g}}\right)$$

$$= 6.32 \times 10^{17}\ \text{dpm per gram}\ ^{32}\text{P}$$

If, by definition, 1 Ci = 2.22×10^{12} dpm, we can convert the above activity per gram of ^{32}P to grams ^{32}P per curie as follows:

$$\frac{2.22 \times 10^{12}\ \text{dpm/Ci}}{6.32 \times 10^{17}\ \text{dpm/g}\ ^{32}\text{P}} = 3.51 \times 10^{-6}\ \text{g}\ ^{32}\text{P per Ci} \quad [18.57]$$

$$= 3.51 \times 10^{-6}\ \text{mg}\ ^{32}\text{P per mCi}$$

2. **^{14}C, half-life = 5730 years:**

$$\frac{\Delta N}{\Delta t} = \left[\frac{0.693}{(5730\ \text{years})(365\ \text{days/year})(24\ \text{h/day})(60\ \text{min/h})}\right]\left(\frac{6.022 \times 10^{23}}{14\ \text{g}}\right)$$

$$= 9.90 \times 10^{12}\ \text{dpm per gram}\ ^{14}\text{C}$$

This activity per gram of ^{14}C is converted to grams ^{14}C per curie as follows:

$$\frac{2.22 \times 10^{12}\ \text{dpm/Ci}}{9.90 \times 10^{12}\ \text{dpm/g}\ ^{14}\text{C}} = 0.224\ \text{g}\ ^{14}\text{C per Ci} = 0.224\ \text{mg}\ ^{14}\text{C per mCi} \qquad [18.58]$$

The calculated mass of ^{32}P in 1 Ci of activity is almost a million-fold less than the calculated mass of ^{14}C in 1 Ci of activity. In general, research with radionuclides involves the handling and analysis of lower levels of radioactivity in millicuries, microcuries, and picocuries, and so on. The masses of radioactive atoms in the milli-, micro-, and picocurie levels of radioactivity are obviously much smaller than encountered at the curie level.

Chapter 19

Hall of Fame: Part IX

Maria Goeppert-Mayer (1906–1972) and J. Hans D. Jensen (1907–1973), Eugene P. Wigner (1902–1995), Chen-Ning Yang (1922–), Tsung-Dao Lee (1926–), and Chien-Shiung Wu (1912–1997), Isidor Isaac Rabi (1898–1988), and Richard P. Feynman (1918–1988).

In concluding this discussion it may be appropriate to return to the theme introduced earlier in the paper and raise the question once again of the deeper, and possibly philosophical, meaning of the term "elementary" particle. As we have seen, the proton and neutron, which were once thought to be elementary particles are now seen to be highly complex bodies. It is almost certain that physicists will subsequently investigate the constituent parts of the proton and neutron…

This is an excerpt from the Nobel lecture on December 11, 1961 of Robert Hofstadter (1915–1990), who was awarded the Nobel Prize in Physics in 1961 for his work on the scattering of high-energy electrons on nucleons. By bombarding the atomic nuclei with high-energy electrons, he provided evidence that the proton and neutron are not elementary particles, but that they contain an inner structure that exhibit strong electric and magnetic forces.

The inestimable value of possessing a good idea, of indefatigably testing and perfecting it, is best illustrated by your precision-measurements of the magnetic moment of the neutron, one of the most difficult and at the same time most important tasks in nuclear physics.

This second quote is taken from the Nobel award ceremony speech of Professor E. Hulthén, member of the Nobel Committee for Physics, on the occasion of the awarding of the Nobel Prize in Physics in 1952 to Felix Bloch (1905–1983). The precise determination of the magnetic moment of the neutron provided additional confirmation that the neutrally charged neutron was not an elementary particle; rather it possessed an underlying structure of smaller charged particles.

MARIA GOEPPERT-MAYER (1906–1972) AND J. HANS D. JENSEN (1907–1973)

Our knowledge of the shell structure of the atomic nucleus has its beginnings with the independent work of Maria Goeppert-Mayer while at the Argonne National Laboratory in the United States (Goeppert-Mayer, 1948a,b, 1949) and J. Hans D. Jensen from the University of Heidelberg, Germany (Haxel et al., 1949). Their biographical sketches are included together, because they discovered independently and concurrently the nuclear shell structure while living in almost opposite sides of the globe and without any prior collaboration or correspondence. When the stage is set with numerous findings by previous scientific works of others, discoveries will be made. Such is the case with the discovery of the shell structure of the atomic nucleus by Maria Goeppert-Mayer and Hans D. Jensen. They later became close colleagues, and subsequently collaborated on a book on the nuclear shell structure (Goeppert-Mayer and Jensen, 1955). For this work they were awarded the 1963 Nobel Prize in Physics "for their discoveries concerning nuclear shell structure," which they shared with Eugene Paul Wigner. This award made Maria Goeppert-Mayer the second woman to receive the Nobel Prize in Physics since Marie Curie. The shell structure of the atomic nucleus is based on the finding that there is a certain number of protons or neutrons in the nucleus that attribute to a nucleus an unusual stability regardless of the number of other nucleons in the nucleus. This number of neutrons or protons is referred to as a "magic number." The significance of this discovery was underscored by the words of Professor I. Waller, member of the Nobel Committee for Physics, in his award ceremony speech given on December 12, 1963 (with the writer's insertion in brackets):

A paper published by Goeppert-Mayer in 1948 marked the beginning of a new era in the appreciation of the shell model. For the first time convincing evidence was there given for the existence of the higher magic numbers and it was stressed that the experiments support the existence of closed shells very strongly. Somewhat later Goeppert Mayer and independently Haxel, Jensen and Suess published the new idea, which was needed for the explanation of the higher magic numbers. The idea was that a nucleon should have different energies when it "spins" in the same or opposite sense…[in] the nucleus.

Radioactivity: Introduction and History, From the Quantum to Quarks. http://dx.doi.org/10.1016/B978-0-444-63489-4.00019-8
Copyright © 2016 Elsevier B.V. All rights reserved.

Maria Goeppert-Mayer was born on 28 June 1906 in Kattowitz, Upper Silesia, which was then a part of Germany. The city is now Kattowice in Upper Silesia in southern Poland. At only 4 years of age Maria moved with her family to Göttingen, Germany, where her father, Friedrich Goeppert, was appointed professor of pediatrics. Her father was the sixth generation of university professors in the family, and thus it was understood that Maria would study for and earn a university degree. In her autobiography, written at the time of receiving the Nobel Prize, she noted that it was taken for granted by herself and her parents that she would attend a university (Nobel Lectures, Physics, 1963–1970). Maria Goeppert's father had a great influence on her life. As noted by Joan Dash (1973): "He was after all a scientist." She was said to have been told by her father that she should not grow up to be a woman, meaning a housewife, and therefore decided, "I wasn't going to be *just* a woman."

Maria Goeppert-Mayer (1906–1972)

As in the life of Lise Meitner, it was very difficult for a woman to attend a university in the early part of the 20th century. Maria Goeppert had first to study in a privately endowed school that prepared girls for the entrance examination to university. She successfully passed her entrance examination and entered the University of Göttingen in 1924 to study mathematics, but slowly her interests drifted to physics. Goeppert passed her doctoral examination in 1930 with three current and future Nobel Laureates on her examination committee, namely Max Born, James Franck, and Adolf Windaus.

At the University of Göttingen, Maria Goeppert met Joseph Edward Mayer, who was working with James Franck as a fellow of the Rockefeller Foundation. After receiving her doctorate in 1930, she married Joseph Mayer and became Maria Goeppert-Mayer. That year she joined her husband at Johns Hopkins University, where he had a professorship in physical chemistry. She would not be able to join the faculty; and it would be 30 years before she was finally awarded a professorship. As noted in a biographical memoir by Robert Sachs (1979), "Opportunities for her to obtain a normal professional appointment at that time, which was at the height of the Depression, were extremely limited. Nepotism rules were particularly stringent then and prevented her from being considered for a regular appointment at Hopkins; nevertheless, members of the Physics Department were able to arrange for a very modest assistantship…" Using this, she carried out research in physical organic chemistry with her husband, and with Karl Herzfeld, and others.

Maria Goeppert-Mayer returned to the University of Göttingen to work in the field of physics with Max Born. With Born, she coauthored a chapter in the prestigious *Handbuch der Physik* (Born and Goeppert-Mayer, 1933). Her next paper in the journal *Physical Review* represents pioneering work on beta decay of atomic nuclei, in which she calculated the probability of double-beta ($\beta\beta$) disintegration of an atomic nucleus that involves the simultaneous emission of two beta particles and two neutrinos from the nucleus (Goeppert-Mayer, 1935), with a predicted very long half-life exceeding 10^{17} years for a nucleus undergoing double-beta decay. Her prediction set forth in this paper was demonstrated over 52 years later with the discovery in 1987 by Steven R. Elliott, Alan A. Hahn, and Michael K. Moe at the University of California, Irvine of double-beta decay of the isotope ^{82}Se with a half-life of greater than 10^{19} years (Elliott et al., 1986, 1987; Moe, 1986; Moe and Rosen, 1989). This is described in detail in the chapter entitled "Beta Radiation and Beta Decay." Maria Goeppert-Mayer's prediction was accurate. It took over a half-century to observe the phenomenon, because of the long half-life for this decay and the modern highly sensitive and accurate radiation

detection instrumentation required to observe double-beta decay. Currently research teams are investigating the phenomenon, as described in the chapter entitled "Beta Radiation and Beta Decay."

Left to right: Edward Teller, Maria Goeppert-Mayer, Joseph Edward Mayer, and James Franck
Photograph by Francis Simon, with permission courtesy AIP Emilio Segre Visual Archives

In 1939 Maria Goeppert-Mayer joined her husband in a move to Columbia University in New York, where he was appointed to a professorship in chemistry. However, she was given no more than an office without appointment by the chairman of the Physics Department (Sachs, 1979). Her first real position was at Sarah Lawrence College for Women, where she contributed to a science curriculum on a part-time basis during 1941−1945. The writer finds it of interest that it would take a women's college to provide a definite position for Maria Goeppert-Mayer. The Sarah Lawrence College did not start to admit male students until 1949. Goeppert-Mayer only taught at the women's college on an occasional basis, because she was offered another job by Harold Urey, who was heading a program for the separation of uranium-235 from natural uranium as part of the wartime effort to construct a nuclear weapon under what would eventually become known as Columbia University's Substitute Alloy Materials (SAM) Project (Sachs, 1979). In the spring of 1945 she worked with Edward Teller at Los Alamos on the properties of matter and radiation at extremely high temperatures, which had a bearing on Edward Teller's ambitious efforts toward the development of a thermonuclear weapon (Sachs, 1979).

In 1946 Maria's husband, Joseph Mayer, was appointed to a professorship in the Department of Chemistry and the Institute for Nuclear Studies of the University of Chicago. In a biographical memoir Sachs (1979) points out that nepotism rules did not permit the hiring of husband and wife in faculty positions; however, Maria took on a voluntary associate professor of physics position at the Institute for Nuclear Studies. Here she was hired again to work with Edward Teller within the original objectives of the Metallurgical Laboratory on the Manhattan Project, which ceased to exist on July 1, 1946. Nuclear energy research was then transferred to the newly established Argonne National Laboratory under the auspices of the Atomic Energy Commission (Sachs, 1979). At the Argonne National Laboratory Maria Goeppert-Mayer was able to research peaceful applications of nuclear energy, particularly reactor physics, serve as advisor to graduate research students of the University of Chicago, and research on her greatest contribution to science, the shell model of the atomic nucleus.

Maria Goeppert-Mayer's opportunity for discovery came while voluntarily collaborating at the University of Chicago's Institute for Nuclear Studies (now known as the Enrico Fermi Institute) with Edward Teller in a search for the cosmological model of the origin of the universe. While compiling data she studied the abundance of the elements and found that there were certain elements that were highly abundant; and she found a correlation between the abundance of these elements and specific numbers of neutrons and protons in their nuclei. While compiling data and formulating her thoughts on the relationship between nuclear stability and the numbers of neutron and protons in the nucleus, Maria Goeppert-Mayer had many discussions on the matter with Enrico Fermi. Robert G. Sachs, her first graduate student, relates the following story in a biographical memoir (Sachs, 1979): Enrico Fermi asked Maria "Is there any indication of spin−orbit coupling?" Maria then knew immediately that the nucleon spin states and the Pauli Exclusion Principle would be involved, and would restrict

the neutrons and protons in the nucleus to specific energy shells; and thus, certain numbers of filled or closed shells of neutrons and protons would predict nuclear stability. Sachs (1979) relates the story told by Joseph Mayer whereby Enrico Fermi had to leave his office after posing the question on spin−orbit coupling to Maria Goeppert-Mayer, but returned in less than 10 min. Maria was so excited over her finding that she began delivering to Fermi a rapid explanation of the phenomenon. He then left the office, commenting "Tomorrow, when you are less excited, you can explain it to me."

Maria published her findings in the records of the Argonne National Laboratory (Goeppert-Mayer, 1948a) and in the journal *Physical Review* (Goeppert-Mayer, 1948b, 1949). She discovered that J. Hans D. Jensen at the Institute of Theoretical Physics in Heidelberg, together with his collaborators Otto Haxel at the Max Planck Institute in Göttingen and Hans E. Suess of the Institute of Physical Chemistry at Hamburg, came to a similar conclusion that certain elements with particular numbers of neutrons and protons were particularly stable. Their paper was also published in the journal *Physical Review* (Haxel et al., 1949). It is interesting to note that the discoveries were made simultaneously and independently on both sides of the globe. When the stage is set, the discoveries will be made. Maria Goeppert-Mayer and J. Hans D. Jensen did not know each other at the time: they met when Maria traveled to Germany in 1950. They became close friends and collaborated in 1955 by coauthoring a book entitled *Elementary Theory of Nuclear Shell Structure* (Goeppert-Mayer and Jensen, 1955). The following year, Maria Goeppert-Mayer was elected to the National Academy of Sciences. The theory of the shell structure of the atomic nucleus received widespread acceptance, and the pair were jointly awarded the Nobel Prize in Physics in 1963 for this work.

Maria Goeppert-Mayer left Chicago with her husband Joseph in 1960 to take up a position as professor of physics at the University of California, San Diego, thus she was finally appointed to a professorship 3 years before receiving the Nobel Prize in Physics with J. Hans D. Jensen. She became the seventh generation of university professors on her father's side of the family, which was most fulfilling in light of the numerous obstacles to a professorship that she encountered early in life. J. Hans D. Jensen collaborated again with Maria as a visiting professor to the University of California, San Diego in 1961; and again by writing jointly a chapter on the shell model of the nucleus in Kai Siegbahn's well-known book on alpha-, beta-, and gamma-ray spectroscopy in 1965 (Goeppert-Mayer and Jensen, 1965).

Maria Goeppert-Mayer received honorary doctor of science degrees from Russell Sage College, Mount Holyoke College, and Smith College. These were all colleges for women; were it not for her untimely death in 1972, the writer believes that other institutions of higher learning which are not exclusively for women would also have awarded her honorary degrees.

J. Hans D. Jensen (1907–1973)

J. Hans D. Jensen was born the son of a gardener, Karl Jensen, on June 25, 1907 in Hamburg, Germany. In 1926 he completed his undergraduate studies at the Universities of Hamburg and Freiburg; and he was awarded the doctorate

degree in 1932 and Dr. habil. degree in 1936 at the University of Hamburg. In 1941 J. Hans D. Jensen became professor of theoretical physics at the Technische Hochschule in Hannover. He became professor of physics at the University of Heidelberg in 1949, which was the year he published with Otto Haxel and Hans E. Suess (Haxel et al., 1949) their findings on the shell structure of the atomic nucleus. In 1964 J. Hans D. Jensen was awarded a honorary doctorate degree at the Technische Universitat Hannover, and the University of Heidelberg appointed him as emeritus professor in 1969. He died in Heidelberg, Germany, on February 11, 1973. The above dates and places are taken from an autobiography prepared at the time of the presentation of the Nobel Prize (Nobel Lectures, Physics, 1963−1970).

In his Nobel lecture J. Hans D. Jensen described his reaction to finding the paper by Maria Goeppert-Mayer (1948a,b) on the concept of closed shells in nuclei, which he immediately compared to his work with Otto Haxel and Hans E. Suess as follows:

> *There in a recent issue of the* Physical Review*, I found a paper by Maria Goeppert-Mayer, "On closed shells in nuclei", where she too had collected the empirical evidence pointing out the significance of the magic numbers. That gave me courage to talk about her work, along with our results, in a theoretical seminar… The seminar turned into a long and lively discussion. I was very much impressed by the intensity with which Niels Bohr received, weighed, and compared these empirical facts, facts that did not at all fit into his own picture of nuclear structure… I remember our being elated when we found some hints in the still meagre data that was available at that time. Nevertheless, I did not feel very happy about the whole picture, and I was not really surprised when a serious journal refused to publish our first letter, stating "it is not really physics but rather playing with numbers". Only when I thought of the lively interest in the magic numbers which Niels Bohr had shown did I dare send the same letter to [Victor] Weisskopf who forwarded it to the* Physical Review*. Yet it was not until later, after I had presented our ideas in a Copenhagen seminar and been able to discuss them with Niels Bohr, that I finally gained some confidence.*

The numbers of protons and neutrons, correlated to particularly stable nuclei, were called the "magic numbers." In the words of Goeppert-Mayer in her Nobel lecture:

> *What makes a number magic is that a configuration of a magic number of neutrons, or of protons, is unusually stable whatever the associated number of the other nucleons. The magic numbers, as we know them today, are:*
>
> *2, 8, 20, 28, 50, 82, 126.*
>
> *And most importantly, they are the same for neutrons and protons.*

Nuclides containing a magic number of neutrons and/or protons are listed in Table IX.1. Goeppert-Mayer (1963) pointed out that Sn ($Z = 50$) is the element with the largest number of stable isotopes among all the elements in the periodic table. There are 6 stable nuclides with 50 neutrons and 7 stable nuclides with 82 neutrons, whereas normally one will find only 2 or 3 stable nuclei in the Chart of the Nuclides having identical numbers of neutrons.

Some nuclides are called "doubly magic," because they have equal numbers of protons and neutrons that are magic numbers. The nuclide ${}^{4}_{2}\mathrm{He}$ has a high binding energy, ie, it is very tightly bound (see Fig. 20.4 of the chapter: "The Atomic Nucleus"), and an extra proton or neutron cannot be attached to its nucleus, as evidenced by the fact that ${}^{4}_{3}\mathrm{Li}$ and ${}^{5}_{2}\mathrm{He}$ do not exist. In addition ${}^{16}_{8}\mathrm{O}_{8}$, which is also "doubly magic", is very stable. A large amount of energy would be required to remove a neutron from its nucleus; whereas the addition of an extra neutron to its nucleus to form ${}^{17}_{8}\mathrm{O}_{9}$ would result in a weakly bound neutron, which is evidenced by the low natural abundance of ${}^{17}\mathrm{O}$ (0.04%) compared to ${}^{16}\mathrm{O}$(99.76%).

The breakthrough in the development of the nuclear shell model came with the conclusion that the protons and neutrons in the nucleus exhibit nuclear spin-coupling effects, which result in shifts in their energy levels within the nucleus, similar to what occurs with electrons in their orbitals about the atom. Pauli's Exclusion Principle, which was applied to atomic electrons, is also applied to the nucleons in the nucleus. The exclusion principle states that no two protons or two neutrons in a nucleus could exist in the same quantum or energy state. The proton or neutron can exist in two spin quantum states, namely $+1/2$ (ie, spin-up) or $-1/2$ (ie, spin-down). Goeppert-Mayer explained in her Nobel lecture that there is a strong interaction between spin and orbital angular momentum, whereby spin-up and spin-down refer to the spin being parallel or antiparallel to the orbital angular momentum. She provided evidence that this spin interaction raised considerably the energy levels of nuclei that contained 9, 21, 29, 51, or 83 protons or neutrons, or 127 or 128 neutrons, thereby attributing a high degree of stability to nuclei that contain 2, 8, 20, 28, 50, 82 protons or neutrons, or 126 neutrons. The numbers 2, 8, 20, 28, 50, 82, and 126 refer to closed shells of protons or neutrons attributing a high degree of stability to nuclei with these nucleon numbers. The closed shells of nucleons in the highly stable nuclei are analogous to the closed electron shells of the noble gases, which attribute to these gases a high degree of

TABLE IX.1 Magic Number Nuclides

Number of Protons	2	8	20	28	50	82	126
	^{4}He	^{16}O	^{40}Ca	^{58}Ni	^{112}Sn	^{204}Pb	
		^{17}O	^{42}Ca	^{60}Ni	^{114}Sn	^{206}Pb	
		^{18}O	^{43}Ca	^{61}Ni	^{115}Sn	^{207}Pb	
			^{44}Ca	^{62}Ni	^{116}Sn	^{208}Pb	
			^{46}Ca	^{64}Ni	^{117}Sn		
			^{48}Ca		^{118}Sn		
					^{119}Sn		
					^{120}Sn		
					^{122}Sn		
					^{124}Sn		
Number of Neutrons	**2**	**8**	**20**	**28**	**50**	**82**	**126**
	^{4}He	^{15}N	^{36}S	^{48}Ca	^{86}Kr	^{136}Xe	^{208}Pb
		^{16}O	^{37}Cl	^{50}Ti	^{87}Rb	^{138}Ba	^{209}Bi
			^{38}Ar	^{51}V	^{88}Sr	^{139}La	
			^{39}K	^{52}Cr	^{89}Y	^{140}Ce	
			^{40}Ca	^{54}Fe	^{90}Zr	^{141}Pr	
					^{92}Mo	^{142}Nd	
						^{144}Sm	

From Goeppert-Mayer, M., December 12, 1963. The Shell Model. Nobel Lecture. http://www.nobelprize.org/nobel_prizes/physics/laureates/1963/mayer-lecture.pdf; reprinted with permission from the Nobel Foundation ©1963.

chemical inertness. Thus protons and neutrons exist in the nucleus in different energy states in structured orbitals similar to the external electron orbitals of the atom.

In her Nobel lecture Maria Goeppert-Mayer provided evidence for the increased instability of nuclei when additional neutrons are added to nuclei above the magic numbers, which represent closed shells at 2, 8, 20, 28, 50, 82, and 126 nucleons. Fig. IX.1 illustrates the decay energies of various nuclides with $N - Z = 3$ to $N - Z = 2$. Maria Goeppert-Mayer explained the curve as follows:

> *One would expect to find a smooth curve, sloping downward. Except for one point it is indeed so, This point is ^{39}Ar with 21 neutrons and 18 protons. A smooth interpolation of the curve would predict ^{39}Ar to be stable … However, ^{39}Ar is unstable against β^- emission by about 0.5 MeV. The explanation of this anomaly is the low binding energy of the 21st neutron, while the 19th proton into which it is transformed has the higher binding energy of the proton shell which closes at 20. That the energies drop again sharply is due to the fact that now $Z = 20$ is involved. These types of discontinuity occur at all magic numbers.*

A similar discontinuity of the β^- decay energies in the neighborhood of $N = 50$ is illustrated in Fig. IX.2. The addition of a single neutron to the nucleus of $N = 50$ increases the energy state of that nucleus, illustrated by the higher decay energy of the nucleus of ^{89}Sr with $N = 51$ compared to ^{85}Kr with $N = 49$. This is only one of several examples given by Goeppert-Mayer (1963) of nuclear stability attributed to the closing of a neutron shell at $N = 50$.

The highest magic number of 126 occurs only for the closing of a neutron shell. Thus it would be expected that the 127th and 128th neutrons would be less tightly bound; and that these nuclides would be at higher and less stable energy states compared to nuclides with 126 neutrons. This is just the case, as illustrated in Fig. IX.3. In the case of α-decay there is the emission of two neutrons together with two protons. As illustrated in Fig. IX.3, the α-particle decay energy is the highest for nuclides with 128 neutrons, and this drops sharply when the 128th and 127th neutrons are removed from the nucleus.

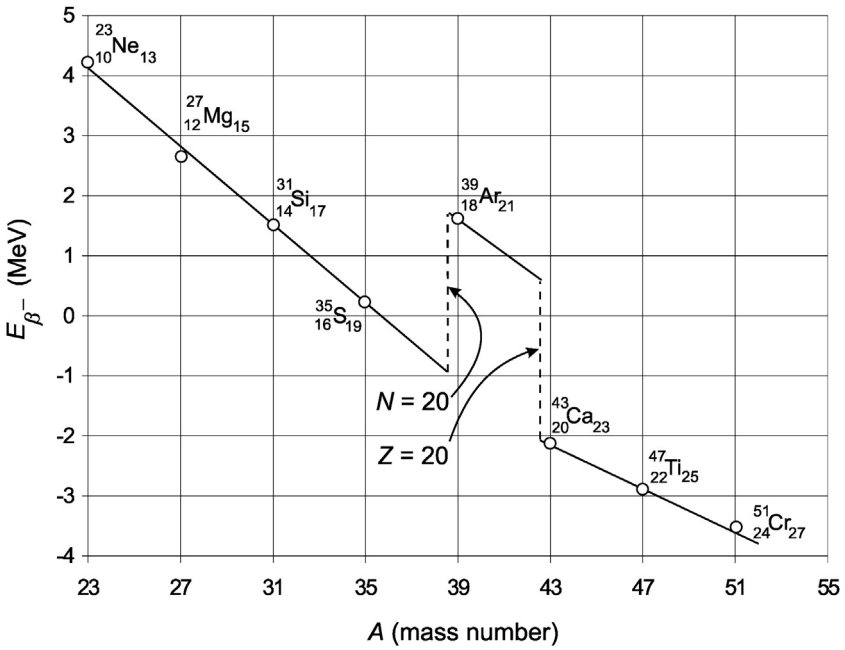

FIGURE IX.1 Beta decay energies in the neighborhood of $N = 20$. *From Goeppert-Mayer, M., December 12, 1963. The Shell Model. Nobel Lecture. http://www.nobelprize.org/nobel_prizes/physics/laureates/1963/mayer-lecture.pdf; reprinted with permission from the Nobel Foundation © 1963.*

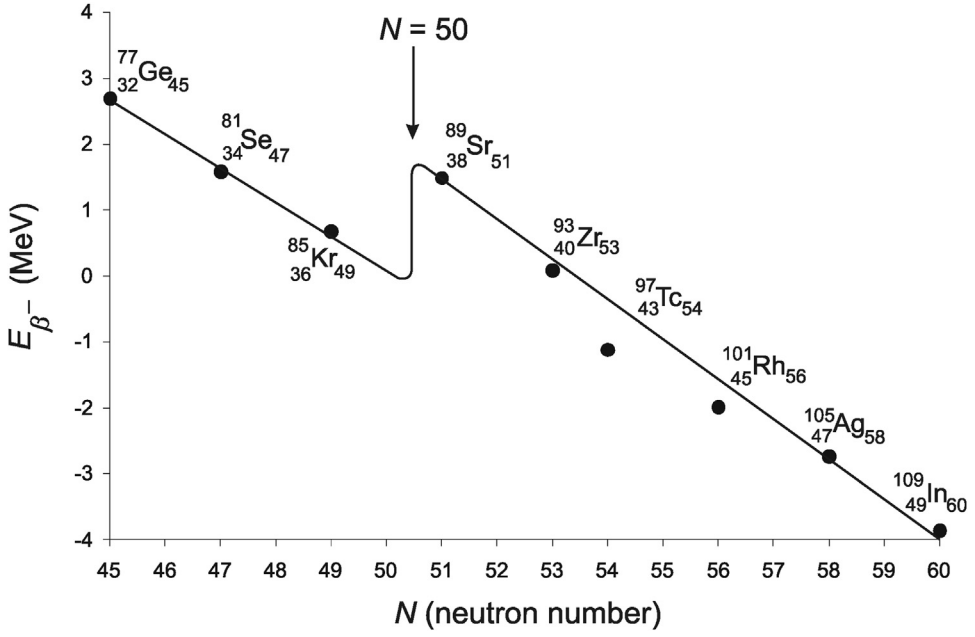

FIGURE IX.2 Beta decay energies in the neighborhood of $N = 50$. *From Goeppert-Mayer, M., December 12, 1963. The Shell Model. Nobel Lecture. http://www.nobelprize.org/nobel_prizes/physics/laureates/1963/mayer-lecture.pdf; reprinted with permission from the Nobel Foundation © 1963.*

For further information on this subject the reader is invited to peruse works by Goeppert-Mayer and Jensen (1955, 1965), Goeppert-Mayer (1964), Choppin et al. (2002), and Rowe and Wood (2010).

EUGENE P. WIGNER (1902–1995)

Eugene Paul Wigner was born on November 17, 1902 into a Jewish family in Budapest, Hungary, and was given the name Jenö Pál Wigner. He shared one-half of the Nobel Prize in Physics in 1963 for, in the words of the Nobel Committee, "his

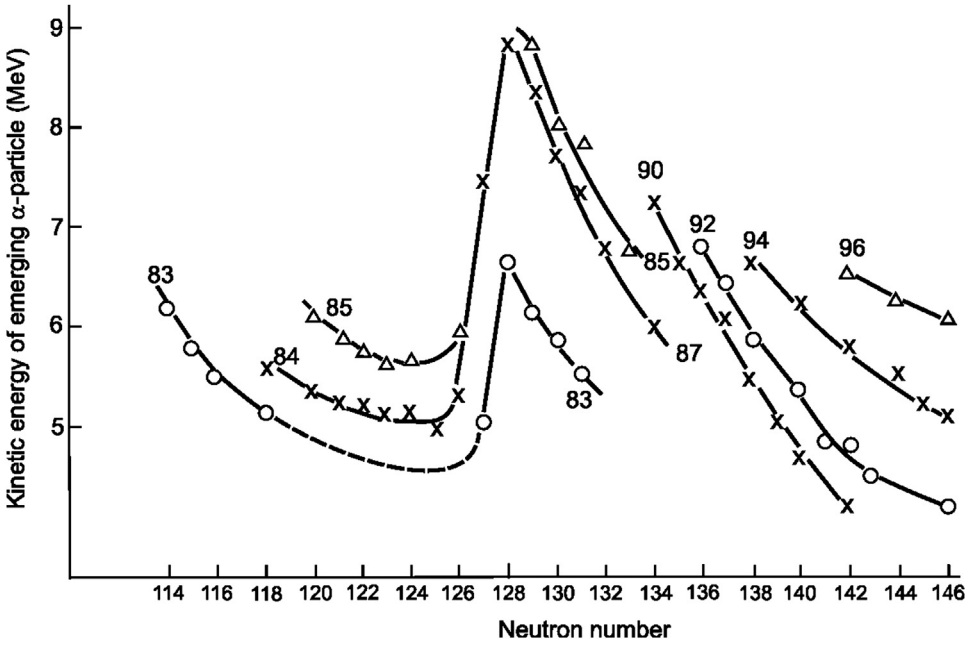

FIGURE IX.3 Energy release in alpha decays. *From Goeppert-Mayer, M., December 12, 1963. The Shell Model. Nobel Lecture. http://www.nobelprize.org/nobel_prizes/physics/laureates/1963/mayer-lecture.pdf; reprinted with permission from the Nobel Foundation © 1963.*

contributions to the theory of the atomic nucleus and the elementary particles, particularly through the discovery and application of fundamental symmetry principles." The other half of the prize was awarded to Maria Goeppert-Mayer and J. Hans D. Jensen, as described previously. The significance of Eugene Wigner's work was underscored in a statement by Professor I. Waller, member of the Nobel Committee for Physics of the Royal Swedish Academy of Sciences, on December 12, 1963:

> *In order to be able to calculate the motion of the nucleons it was, however, necessary to know also the forces which act between them. A very important step in the investigation of these forces was taken by Wigner in 1933 when he found, deducing from some experiments, that the force between two nucleons is very weak except when their distance apart is very small but that the force is then a million times stronger than the electric forces between the electrons in the outer part of the atoms. Wigner discovered later other important properties of the nuclear forces… Wigner could show that most essential properties of the nuclei follow from generally valid symmetries of the laws of motion. Earlier Wigner had performed pioneering work by studying such symmetries in the laws of motion for the electrons and had made important discoveries by investigating* e.g. *those symmetries which express the fact that the laws mentioned make no difference between left and right and that backward in time according to them is equivalent to forward in time. These investigations were extended by Wigner to the atomic nuclei at the end of the 1930s [sic] and he explored then also the newly discovered symmetry property of the force between two nucleons to be the same whether either of the nucleons is a proton or a neutron… Wigner has made many other important contributions to nuclear physics. He has given a general theory of nuclear reactions and has made decisive contributions to the practical use of nuclear energy.*

Eugene Wigner obtained his secondary education at the Lutheran Gimnazium in Budapest, where he had an excellent teacher whom he acknowledged all his life for motivating him to become an outstanding mathematician and scientist. If we are fortunate enough, we have all had one or more high school or college teachers who we remember to have had a great influence on our academic development and career. In the case of Eugene Wigner, one such was Laslo Ratz, his high school mathematics teacher, and another was Professor Michael Polanyi, his doctoral advisor at the Technische Hochschule in Berlin, which is today the Technische Universität Berlin or Technical University of Berlin. Wigner paid tribute to these teachers in his banquet speech given on the day of receiving the Nobel Prize:

> *I wish to say at this occasion a few words on a subject about which we think little when young but which we appreciate increasingly when we reflect on our intellectual development. I mean our indebtedness to our teachers… What I wish to draw*

attention to is how much of our interest in science, and how much of our attitude toward science, we owe to our teachers. My own history begins in the high-school in Hungary where my mathematics teacher, [Laslo] Ratz, gave me books to read and evoked in me a sense for the beauty of his subject. I cannot mention all to whom I am indebted but I do wish to mention the inspiration received from Polanyi.

Eugene P. Wigner (1902–1995)

At the University of Berlin, Eugene Wigner studied chemical engineering at the behest of his father, rather than the subjects of his real passion—mathematics and theoretical physics. His father was concerned that Eugene should pursue a field of study where he could easily find work to make a living. After obtaining a degree in chemical engineering at the Technische Hochschule in Berlin in 1925, Wigner pursued mathematics and physics, but his deep understanding of chemical engineering, acquired in Berlin, would come in handy years later in his work on peaceful applications of nuclear energy and the early development of nuclear reactors.

After completing his degree Wigner returned to Budapest to help his father manage a leather factory; but after a year or more in Budapest he returned to the University of Berlin to undertake a research assistantship. While in Berlin Wigner established friendships with pioneering physicists, including James Franck, Victor F. Weisskopf, Edward Teller, Dennis Gabor, and Leo Szilard, among others. In a biographical memoir, Seitz et al. (1998) note that, following the advice of Leo Szilard that Wigner should use his mathematical skills to write a book on group theory and its applications which would be understandable to physicists, Eugene Wigner wrote his classic book *Group Theory and Its Application to the Quantum Mechanics of Atomic Spectra* (Wigner, 1931).

In 1930 Eugene Wigner and his friend, countryman, and notable mathematician John von Neumann jointly accepted a shared (half-time) appointment at Princeton University, which lasted until 1936. Wigner then joined the faculty at the University of Wisconsin at Madison from 1936 to 1938, before returning to Princeton. He had hopes to return to his previous appointments and contacts at the University of Berlin. However, Adolph Hitler was appointed Chancellor in 1933; and Eugene Wigner knew that, with his Jewish background, he would be barred from research and teaching at the university. He thus decided to apply for American citizenship, and this was granted in 1937. Following the signing of the Munich Agreement in 1938 between the major powers of Europe permitting Nazi Germany to annex part of Czechoslovakia, Eugene Wigner was aware of the threat of the rising power of Hitler and convinced his parents to move to the United States (Seitz et al., 1998). Under similar threatening circumstances, Wigner's friend Leo Szilard escaped from Berlin to Vienna before moving to London, where Szilard filed his famous patent on an atomic bomb in 1934 well before nuclear fission was discovered by Otto Hahn and Fritz Strassmann in Germany

in 1939. It was Eugene Wigner who drove by car with Leo Szilard on July 16, 1939 to Albert Einstein's summer house at Peconic, Long Island, to convince Einstein to sign a letter (later to be drafted by Szilard) addressed to President Franklin Delano Roosevelt informing him of the possibility of nuclear weapons from nuclear chain reactions from fission, and the fear of the possibility that Germany could be working toward this end (see Hall of Fame, Part IV).

The secret American project, ie, the Manhattan Project, on the development of atomic weapons was initiated by President Roosevelt on October 9, 1941. Within the project Eugene Wigner was placed in charge of a theoretical group; and he put his knowledge of chemical engineering into the development of large reactors for the production of plutonium, together with nuclear physicists Alvin M. Weinberg and Edward Creutz, among others, at the secret Metallurgical Laboratory of the University of Chicago. Seitz et al. (1998) note that Wigner and his team designed large water-cooled, graphite, natural uranium 500 MW reactors that could produce optimally up to 500 g of plutonium per day. The first reactor for plutonium production was Hanford B, which was built in 13 months and began operation in September 1944. Eugene Wigner personally reviewed all blueprints for the first Hanford reactor, which was constructed by the Dupont Company (Seitz et al., 1998). Reactor B is now a national historic landmark, located in the southeast of the state of Washington off the Columbia River. When it began operation in 1944, the B reactor contained 64,000 rods of uranium, which were inserted into the reactor core; after about 6 weeks of neutron irradiation, the rods were removed, cooled in a pool of water, and then taken by train to another site for processing and separation of plutonium (www.hanford.gov/page.cfm/BReactor).

In a biographical memoir Seitz et al. (1998) noted that Eugene Wigner became aware after the testing of the first atomic bomb at Alamagordo in July 1945 that the United States would manufacture an arsenal; and although he was proud of his work toward the release of nuclear energy, Wigner did not want to contribute to the death of thousands of Japanese civilians. He thus joined 70 other personnel of the secret Metallurical Laboratory in signing the "Petition to the President of the United States" drafted by Leo Szilard on July 17, 1945, weeks before the bomb was dropped on Hiroshima (see Hall of Fame, Part IV for the text of the petition), in an attempt to avert the use of the bomb against Japan. The thought that many thousands of lives were saved on both sides by the use of the atomic bomb brought some solace to Eugene Wigner (Seitz et al., 1998).

Left to Right: Eugene P. Wigner, Walter H. Zinn, D. Bronk (President of NAS), Leo Szilard, J. Killian (Chairman of Atoms for Peace Committee), and Alvin M. Weinberg Presentation of the Atoms for Peace Award at the National Academy of Science, 1960. Printed with permission courtesy of the AIP Emilio Segre Visual Archives, Physics Today Collection

After World War II, Wigner turned his efforts toward the design of power reactors for peaceful production of electricity; and as director of research at the Clinton Laboratory, Oak Ridge (now known as the Oak Ridge National Laboratory), during 1946–47, he collaborated with Alvin Weinberg in writing their classic book entitled *The Physical Theory of Neutron Chain Reactors* (Weinberg and Wigner, 1958). As director of the Clinton Laboratory, Eugene Wigner initiated a program to train young scientists and engineers to become future leaders in the development of safe

and reliable reactors for peaceful applications of nuclear energy. The Atomic Energy Commission (U.S. AEC) was established on 1 January 1947 after much politicized debate; and, as noted by Seitz et al. (1998), Wigner did not want to continue as head of a laboratory in a complex and politicized environment. He returned to the faculty at Princeton University in 1947, where he remained to teach and advise numerous graduate students, including as many as 40 PhD students. Wigner was a member of the General Advisory Committee of the US AEC in 1952−1957 and 1959−1964. He retired from Princeton University in 1971 and died at Princeton on January 1, 1995.

CHEN-NING YANG (1922−), TSUNG-DAO LEE (1926−), AND CHIEN-SHIUNG WU (1912−1997)

Chen-Ning Yang and Tsung-Dao Lee were jointly awarded the Nobel Prize in Physics in 1957, in the words of the Nobel Committee "for their penetrating investigation of the so-called parity laws which has led to important discoveries regarding the elementary particles." After a thorough examination of scientific evidence (Lee and Yang, 1956), they confirmed that parity was conserved in many physical processes involving strong and electromagnetic interactions; and that there was no evidence of the conservation of parity in weak interactions, such as in beta decay of atomic nuclei and the decay processes of other elementary particles. In addition, Lee and Yang (1956) postulated some decay processes that might be investigated, including the beta decay of cobalt-60, which could provide evidence for the violation of parity in the weak interactions.

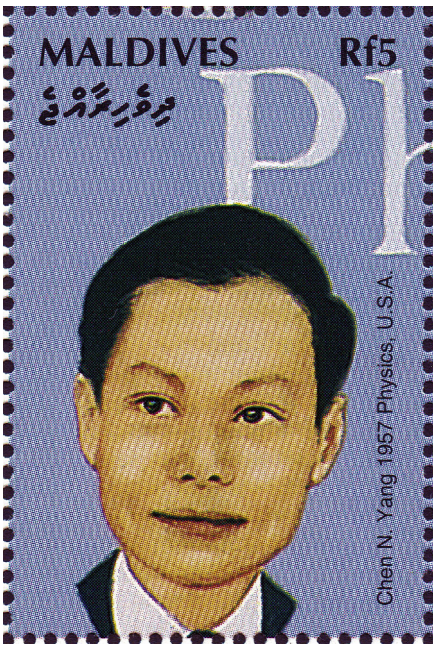

Chen-Ning Yang (1922–)

Tsung-Dao Lee (1926–)

Chien-Shiung Wu, together with collaborators (Wu et al., 1957), undertook the very difficult task of experimentally demonstrating that parity is not conserved in beta decay. The writer does not know why the Nobel Committee did not include Mrs. Chien-Shiung Wu with a share in the Nobel Prize awarded to Chen-Ning Yang and Tsung-Dao Lee, when it is known that up to three persons can share the Nobel Prize and in light of the fact that the work of Chien-Shiung Wu and her collaborators was vital to arrive at the conclusion that parity is not conserved in beta decay. There was thus good reason for including her in the award.

Chien-Shiung Wu (1912–1997) sitting at equipment
Printed with permission, courtesy of the AIP Emilio Segre Visual Archives, Physics Today Collection

Chen-Ning Yang was born in Hefei, Anhui Province, China, on October 1, 1922. He attended primary and high schools in Beijing, growing up in the academic environment of the prestigious Tsinghua University where his father was professor of mathematics. In 1937, at the age of 15, his family returned to Hefei after the Japanese invasion. In 1938 they moved to Kunming, Yunnan Province, China, where Chen-Ning Yang attended the National Southwest Associated University, graduating with a BSc degree in 1942. The National Southwest Associated University was established by merging celebrated universities including Peking University, Tsinghua University, and Nankai University when war broke out between China and Japan in 1937. Yang obtained his MSc degree in 1944 from Tsinghua University in Kunming, the temporary residence of the university during the Sino-Japanese War of 1937−1945. With a fellowship from Tsinghua University, Chen-Ning Yang gained admission to the University of Chicago, where he studied under Enrico Fermi and Edward Teller, receiving a PhD degree in 1948 at the age of 26. He remained at the University of Chicago an additional year as an instructor. The following year Yang joined the faculty of the Institute for Advanced Study at Princeton, New Jersey, and became a professor there in 1955 (Nobel Lectures, Physics, 1942−1962). At the Institute for Advanced Study Chen-Ning Yang collaborated fruitfully with Tsung-Dao Lee, with whom he shared the Nobel Prize in 1957. Chen-Ning Yang became a US citizen in 1964. He was appointed Albert Einstein professor of physics at the State University of New York (SUNY) at Stony Brook in 1965, and retired as emeritus professor from SUNY at Stony Brook in 1999. The C. N. Yang Institute for Theoretical Physics of SUNY at Stony Brook was named in his honor, and he served as its first director. Chen-Ning Yang has permanent residency in China and is honorary director of Tsinghua University in Beijing.

Tsung-Dao Lee was born on November 24, 1926 in Shanghai, China, where he completed most of his secondary (high school) education. He attended the National Chekiang University in Kweichow Province, China, during 1943−1944; and then studied at the National Southwest Associated University in Kunming, Yunnan, in 1945−1946. Lee had a gifted aptitude for physics. In his autobiography, presented at the time of the Nobel Prize award, Lee acknowledged the encouragement he received from Professor Ta-You Wu, who recognized Lee's early talents in the field of physics. After completing only his sophomore year at university, Tsung-Dao Lee was awarded a Chinese government fellowship for graduate studies in the United States. Lee studied at the University of Chicago under Enrico Fermi during 1946−1950 and was awarded a PhD degree with Fermi as his advisor. During 1950−1953 Lee worked as a lecturer and research associate at Yerkes Astronomical Observatory, Wisconsin, the University of California at Berkeley, and the Institute for Advanced

Study at Princeton. He joined the faculty of Columbia University in 1953 as an assistant professor; and by 1956, at the age of 29, he became the youngest full professor in Columbia University's faculty history (Nobel Lectures, Physics, 1942−1962). Lee became a naturalized US citizen in 1962, and retired from Columbia University as emeritus professor in 2012. Tsung-Dao Lee and Chen-Ning Yang both shared the Nobel Prize in Physics in 1957, becoming the first Chinese Nobel Laureates.

Chien-Shiung Wu was born in the town of Liuhe about 35 km north of Shanghai, China, on May 31, 1912. Much of the biographical data presented here is taken from Chien-Shiung Wu's memoirs, published by the National Academy of Sciences (Benczer-Koller, 2009). Her father was an academic and headmaster of Ming De School, which was one of the first schools admitting girls in China. He encouraged his daughter to study, and she was a pupil at his school up to 1923. At 11 or 12 years of age, in 1923, Wu left home to attend Soochow School for Girls, which was a boarding school. This school taught mainly the humanities, so Wu was thus unable to get formal learning in the sciences at the school. Nevertheless, she studied physics, chemistry, and mathematics at night from books borrowed from friends who attended normal high schools. Following graduation from Soochow School for Girls, Wu attended the Shanghai Gong Xue public school in 1929. After only 1 year at the school, Chien-Shiung Wu enrolled at 18 years of age at what would be become known as the National Central University in Nanjing. Wu enrolled to study mathematics as a major; and then changed her major to physics after her first year. She graduated with a BSc degree in 1934 with top honors in her class, and taught for a year at Chekiang University (Zhejiang University) in Hangzhou Province; simultaneously she carried out research in X-ray crystallography at the Academica Sinica under the guidance of female professor Jing-Wei Gu, who had studied in America.

With the encouragement of Professor Gu, Chien-Shiung Wu traveled by ship to the United States to attend the University of Michigan. In the biographical memoir of the National Academy of Sciences, Benczer-Koller (2009) relates the following account of when Wu arrived in California from China.

> *…upon her arrival she first visited the University of California at Berkeley, where she met another Chinese physics student, Luke Chia Yuan, who escorted her around campus. Luke introduced her to Professor Ernest Lawrence, who immediately, recognizing Miss Wu's intelligence and dedication, encouraged her to stay at Berkeley and pursue a Ph.D. In addition, she had also heard that the University of Michigan at that time did not accept women in the student union; the decision to stay at Berkeley was made easily.*
>
> From Benczer-Koller (2009); reprinted with permission by the National Academy of Sciences, courtesy of National Academies Press, Washington, DC.

Although Professor Lawrence was her official advisor for her doctoratal degree, she worked mainly under Emilio Segré and utilized her skills in the development of nuclear instrumentation to study fission products of uranium. She completed her doctorate in 1940 at the University of California at Berkeley. She made an important discovery concerning uranium fission products, which was vital to the successful operation of a nuclear reactor, namely the xenon effect or xenon poisoning. An account of this discovery is provided by Benczer-Koller (2009). In brief, xenon poisoning was the production and accumulation of two isotopes of xenon, ^{135m}Xe and ^{135}Xe, which have relatively short half-lives of 15.3 min and 19.1 h, respectively. The isotopes are uranium fission products that can accumulate in a nuclear reactor. They have a high neutron capture cross section. The accumulation of the xenon isotopes in a reactor results in the capture of neutrons vital to the neutron chain reaction and thus halts or hampers the continuation of the fission chain reaction. After a period of reactor downtime, the xenon isotopes will decay to a low level, permitting the optimum resumption of reactor operation. Methods were devised to compensate for the xenon effect. The very first patent for the nuclear reactor, which was filed by Enrico Fermi and Leo Szilard on December 10, 1944, included a control rod in the reactor design to compensate for this xenon effect. This compensatory control rod can be seen in Fermi and Szilard's original drawing from the patent, which is illustrated in Fig. IV.17 in Hall of Fame, Part IV.

After completion of her PhD at Berkeley, Chien-Shiung Wu wanted to continue her research work at Berkeley or another institution; however, this would be practically impossible for a woman, as Benczer-Koller (2009) relates:

> *She wanted to stay at Berkeley after completion of her Ph.D., but at that time major research-oriented U.S. universities were reluctant to hire women, Jews, Asians, or people of color in a tenure-track professorial position. But in 1942 the nation was at war, most physicists were engaged in the war effort, and young men were at the front. Chien-Shiung Wu accepted an offer of a teaching position at Smith College, a women's institution on the East Coast… Although Smith College was very*

supportive, it did not have a research infrastructure, which Chien-Shiung missed thoroughly… she left Smith in 1943 and accepted an offer from Princeton University as the first female instructor ever hired on the faculty. But she really needed to work in a laboratory. She was invited to join the Manhattan District Project at Columbia University in March 1944 as a senior scientist.

From Benczer-Koller (2009); reprinted with permission by the National Academy of Sciences, courtesy of National Academies Press, Washington, DC.

Wu married Luke Yuan, the countryman who introduced her to Ernest Lawrence at Berkeley, after he received his PhD at the California Institute of Technology in 1937. Within the Manhattan Project at Columbia University, Chien-Shiung Wu assisted in the development of the gaseous diffusion method for the separation and enrichment of ^{235}U and ^{238}U isotopes. Her husband Luke took an appointment with the Radio Corporation of America (RCA) at Princeton to work on the development of radar within the war effort.

After the war, Chien-Shiung Wu worked as a research associate in the Physics Department at Columbia University during 1946–1952. She finally obtained a tenure-track faculty position at Columbia as associate professor of physics in 1952. Benczer-Koller (2009) noted:

Chien-Shiung Wu was frequently honored and received many awards. She was promoted to an associate professorship at Columbia in 1952, the first woman to hold a tenured faculty position in the physics department…

Chien-Shiung Wu was promoted to professor of physics in 1958, the year following her pioneering work demonstrating parity violation in beta decay. Following this demonstration, Chen-Ning Yang and Tsung-Dao Lee were awarded the Nobel Prize in Physics in 1957. Although overlooked for a share in that Nobel Prize, Chien-Shiung Wu gained world fame as a leading nuclear physicist, and was awarded the professorship at Columbia a year later. Such was the plight of women in the physical sciences. Another female nuclear physicist at this time, who also encountered tremendous obstacles in getting a faculty appointment, was Maria Goeppert-Mayer, who was awarded a faculty position at the University of California, San Diego in 1960 three years before receiving the Nobel Prize in Physics in 1963 for her findings on the shell model of the atomic nucleus many years earlier.

In addition to her ground-breaking discovery of parity violation in beta decay, Chien-Shiung Wu was well known for her pioneering work in beta spectroscopy and beta decay theory, double-beta decay, and the development of very sensitive nuclear radiation detectors, among other fields. Garwin and Lee (1997) and Benczer-Koller (2009) provide detailed accounts of her work.

Chien-Shiung Wu was elected to the National Academy of Sciences in 1958, the same year she was awarded the professorship at Columbia. She received many honorary degrees, but the one she valued most was that from Princeton University, as underscored by Benczer-Koller (2009):

She was awarded many honorary degrees, but the first one that she truly appreciated was a Sc.D. from Princeton University (1958), awarded for the first time to a woman… She was the first woman to serve as president of the American Physical Society (1975)… Wu became a trailblazer for women and joined Marie Curie and Lise Meitner as the role model for future generations of aspiring female physicists.

Chien-Shiung Wu has been referred to as "the Chinese Marie Curie." She died in New York on February 16, 1997 after suffering a stroke. Her ashes were placed at a memorial site designed by Nobel Laureate Tsung-Dao Lee at the Ming De School in Changsha, Hunan Province, China.

Parity Violation in Beta Decay

Spatial parity involves the behavior of a physical system under the inversion of spatial coordinates (Sundaresan, 2001). This is equivalent to changing or transforming the coordinates (eg, x to $-x$ and vice versa) of a physical system, as illustrated in Fig. IX.4. As described by Sundaresan (2001), the parity operation is equivalent to going from a right-handed system of coordinates to one that is left-handed; and parity is conserved if the system has "left–right symmetry." In Fig. IX.4 the clock and its mirror image represent a change in the sign of coordinates. Both clocks function equally and tell the same time. They are identical and display symmetry, and parity is conserved. In natural systems we can find molecules in biological systems which are mirror images of each other. Both molecules display the same physical and chemical properties, and thus left–right symmetry.

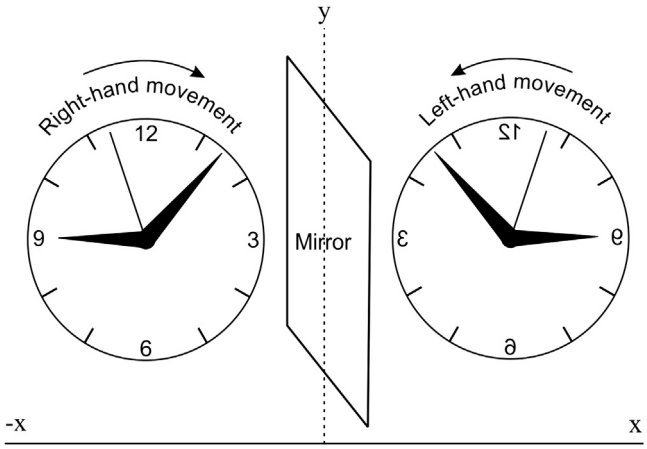

FIGURE IX.4 The inversion of the coordinates along the x axis ($-x$ to $+x$ and vice versa) resulting in spatial parity transformation of a clock yielding the mirror image of each. Both clocks run identically and display symmetry, and parity is conserved.

Elementary particles possess the quantum number, parity (P), which may be either $+1$ or -1, and are referred to as even parity or odd parity, respectively. Particles with even parity ($+1$) have states which possess an even angular momentum (ℓ); and those with odd parity (-1) have states possessing an odd value for angular momentum. The parity quantum number (P) is determined according to $P = (-1)^{\ell}$ where the angular momentum (ℓ) is an exponent. Parity is one of many quantum numbers that a particle may possess. A particle may have several quantum numbers, which will define the quantum state of the particle. An example was provided earlier for the atomic electron in Hall of Fame, Part II of this book, where the principal number n, orbital quantum number ℓ, magnetic quantum number m_ℓ, and the spin quantum number m_s all together will define the energy state and orbital of an atomic electron.

The principle of symmetry in nature was examined by Chen-Ning Yang in his Nobel lecture given on December 11, 1957. He used the example of a person whose heart is on the left side looking into a mirror; and the image in the mirror is that of a person with a heart on the right side. (Although the base of the human heart is really located along the midline of the body, the heart points to the left and about two-thirds of the mass of the heart are found on the left side of the body and the other one-third on the right side of the body. Thus it is common to refer to the heart being on the left side of the body.) Chen-Ning Yang (1957) provided the following example in his Nobel lecture:

> *One of the symmetry principles, the symmetry between the left and the right, is as old as human civilization… Of course, in daily life, left and right are quite distinct from each other. Our hearts, for example, are on our left sides… the laws of physics have always shown complete symmetry between the left and the right… To illustrate the point, we mention that if there existed a mirror image man [from another world] with his heart on his right side, his internal organs reversed compared to ours, and in fact his body molecules, for example sugar molecules, the mirror image of ours, and if he ate the mirror image of the food that we eat, then according to the laws of physics, he should function as well as we do… The law of right-left symmetry then leads also to a conservation law: the conservation of parity.*

Prior to the work of Nobel Laureates Lee and Yang (1956), and Chien-Shiung Wu and her collaborators (Wu et al., 1957), it was always assumed that right−left symmetry was conserved throughout all physical processes involving elementary particles and their reactions. This was explained clearly by Professor O. B. Klein, member of the Nobel Committee for Physics, during his award ceremony speech on the presentation of the Nobel Prize in Physics on December 11, 1957:

> *But what has the question of right and left to do with elementary particle physics?… it was assumed almost tacitly, that elementary particle reactions are symmetric with respect to right and left… That this assumption was made was very natural… it looked as if the electrons, the best known elementary particles, possessed no feature which would permit a distinction between right and left… In fact, most of us were inclined to regard the symmetry of elementary particles with respect to right and left as a necessary consequence of the general principle of right-left symmetry of Nature. Thanks to Lee and Yang and the experimental discoveries inspired by them we now know that this was a mistake. The starting-point of Lee and Yang in their revision of the whole question of right-left symmetry in elementary particle reactions were certain strange observations concerning a kind of new particles called K mesons, which looked as if they were in contrast with the assumption mentioned.*

After a thorough study of the various forces in nature, Lee and Yang (1956) began to question if right−left symmetry is conserved in all interactions. They researched for evidence of the symmetry and the conservation of parity among the forces that act between subatomic particles, namely the nuclear forces, electromagnetic forces, and weak forces. They found that there was considerable evidence that parity was conserved in the strong nuclear and the electromagnetic forces between particles; however, it was only assumed by the scientific community that right−left symmetry and parity conservation were consistent in the weak forces that govern decay interactions, such as beta decay and the decay of subatomic particles. In his Nobel lecture Chen-Ning Yang (1957) explained these forces as follows:

We list the four classes of interactions below. The [relative] strength of these interactions is indicated in the column on the right.

1. Nuclear Forces	1
2. Electromagnetic Forces	10^{-2}
3. Weak Forces (Decay Interactions)[1]	10^{-13}
4. Gravitational Forces	10^{-38}

The strongest interactions are the nuclear interactions which include the forces that bind nuclei together and the interaction between the nuclei and the π mesons… The second class of interactions are the electromagnetic interactions of which physicists know a great deal. In fact, the crowning achievement of the physicists of the 19th century was a detailed understanding of the electromagnetic forces. [The electromagnetic forces hold electrons in orbitals about the nucleus of an atom; and these are the forces involved in the collision and scattering between charged particles via the exchange of photons between them.]… The third class of forces, the weak interactions, was first discovered around the beginning of this century in the β-radioactivity of nuclei,… With the discovery of π−μ, μ−e decays and μ capture, it was noticed independently by Klein (1948), by Tiomno and Wheeler (1949), and by Lee, Rosenbluth and me (Lee et al., 1949), that these interactions have roughly the same strengths as β-interactions… About the last class of forces, the gravitational forces, we need only mention that in atomic and nuclear interactions they are so weak as to be completely negligible in all the observations with existing techniques.

The fact that parity conservation was assumed by the scientific community and never demonstrated was emphasized by Lee and Yang (1956), who proposed some experiments that might demonstrate right−left symmetry in the weak interactions, including beta decay. The basic principles of these experiments, as described by Yang (1957), are the following:

One constructs two sets of experimental arrangements which are mirror images of each other, and which contain weak interactions. One then examines whether the two arrangements always give the same results in terms of the readings of their meters (or counters).

When applying such an experiment to β decay, the readings of the meters or counters described above refer to the counting of β-particles emitted by the decaying nuclei. If the results of two readings are the same for nuclei arranged as mirror images, then one can demonstrate right−left symmetry in the beta decay and the conservation of parity. Chen-Ning Yang (1957) illustrated such as experiment in which cobalt-60, which decays by the emission of β-particles, is polarized in a magnetic field so that the radioactive ^{60}Co nuclei spin in a given direction. The magnetic field can then be reversed so that the ^{60}Co nuclei spin in the opposite direction (the nuclei become a mirror image of the first case). If the radioactivity counters that detect and count the emitted β-particles yield the same count rate when the nuclei are spinning in either direction, than right−left symmetry and parity would be demonstrated. This is illustrated in Fig. IX.5.

Chien-Shiung Wu became the physicist who demonstrated whether or not there is conservation of parity in the weak interactions, such as β decay. As related in her biographical memoir by Benczer-Koller (2009), Nobel Laureate Tsung-Dao Lee consulted with Chien-Shiung Wu because she was the leading experimentalist in β decay. They confirmed that there was no evidence in the scientific literature for parity conservation or nonconservation in the weak interaction, and that an experiment would be necessary to find an answer. Benczer-Koller (2009) notes that Chien-Shiung Wu knew that ^{60}Co,

1. The current relative strength of the weak forces has been revised to 10^{-6}.

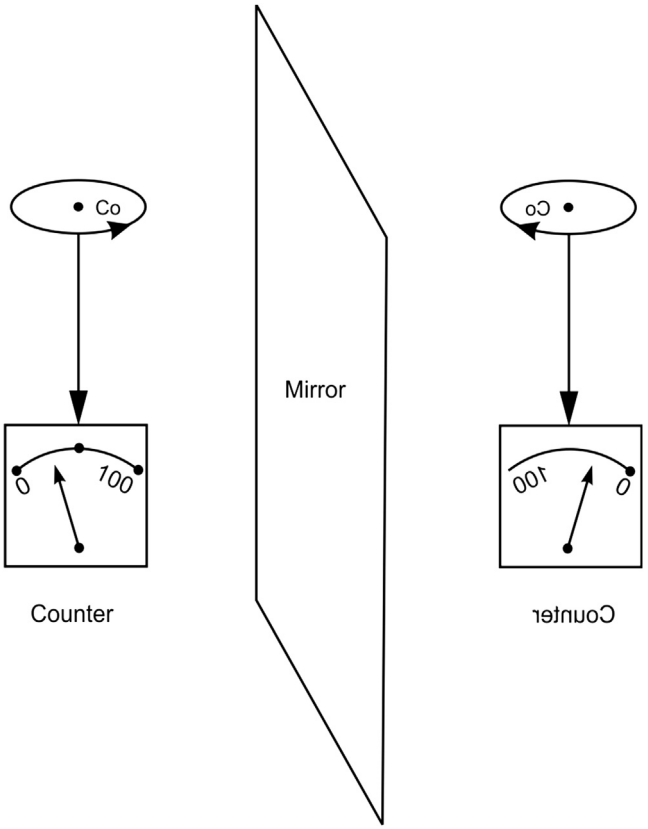

FIGURE IX.5 Experimental arrangement to test right–left symmetry and parity in β decay of ^{60}Co. In the first experiment (on the left), nuclei of ^{60}Co are aligned in a magnetic field so that the nuclei spin in a fixed direction. The number of β-particles emitted by the nuclei is counted over a fixed period of time (count rate) by a radiation detector fixed at a given location relative to the ^{60}Co source. In the second experiment (on the right) the magnetic field is reversed so that the radioactive ^{60}Co nuclei spin in the opposite direction, thereby creating the mirror image of the ^{60}Co nuclei in the first experiment. If the radiation detector yields the same count rate as in the first experiment then the β decay will exhibit right–left symmetry and conservation of parity. If the count rates are significantly different in the two cases, the β decay of ^{60}Co would demonstrate that parity is not conserved in the decay process. *From Yang, C.N., December 11, 1957. The law of parity conservation and other symmetry laws of physics. Nobel Lecture. In: Nobel Foundation Staff (Eds.), Nobel Lectures, Physics, 1942–1962 (1964), Elsevier Publishing, Amsterdam; printed with permission, © The Nobel Foundation 1957.*

which undergoes β decay, would be the isotope of choice for the experiment,because the spin of the ^{60}Co nucleus could be polarized in a certain direction with respect to emission of β-particles.

The design of the ultimate experiment to test parity symmetry in the weak interaction (ie, β decay) was left to Chien-Shiung Wu (Benczer-Koller, 2009). She designed an arrangement whereby an external magnetic field could polarize ^{60}Co nuclei so that their nuclear spins would be directed uniformly in a direction according to the external magnetic field. This required embedding the radioactive ^{60}Co in a cerium magnesium (cobalt) nitrate crystal at the extremely low temperature of about 0.003 K (Wu et al., 1957), which is very close to absolute zero. The very low temperature essentially eliminates thermal agitation and movement of the atomic nuclei; and thereby essentially freezes the polarized ^{60}Co nuclei in the orientation controlled by the external magnetic field. Such an experiment required expertise that was available at the low-temperature laboratory of the National Bureau of Standards (NBS) in Washington, DC, which is now the National Institute of Science and Technology (NIST). The NBS low-temperature laboratory had previous experience in the low-temperature alignment of atomic nuclei. Thus the experiment to demonstrate parity conservation would be a collaboration between Chien-Shiung Wu of Columbia University and Ernest Ambler, Raymond W. Hayward, Dale D. Hoppes, and Ralph P. Hudson of the NBS low-temperature laboratory (Forman, 1982, http://physics.nist.gov/GenInt/Parity/parity.html). The specific experimental arrangement that they designed is illustrated in Fig. IX.6.

The apparatus used by Chien-Shiung Wu and collaborators to test parity symmetry in β decay in ^{60}Co, illustrated in Fig. IX.6, consists of a cryostat housing the radioactive ^{60}Co (labeled as "specimen" in the figure) as a thin source (0.005 cm thick) embedded in CeMg nitrate to facilitate the polarization of the ^{60}Co nuclei, with the cryostat housing in a

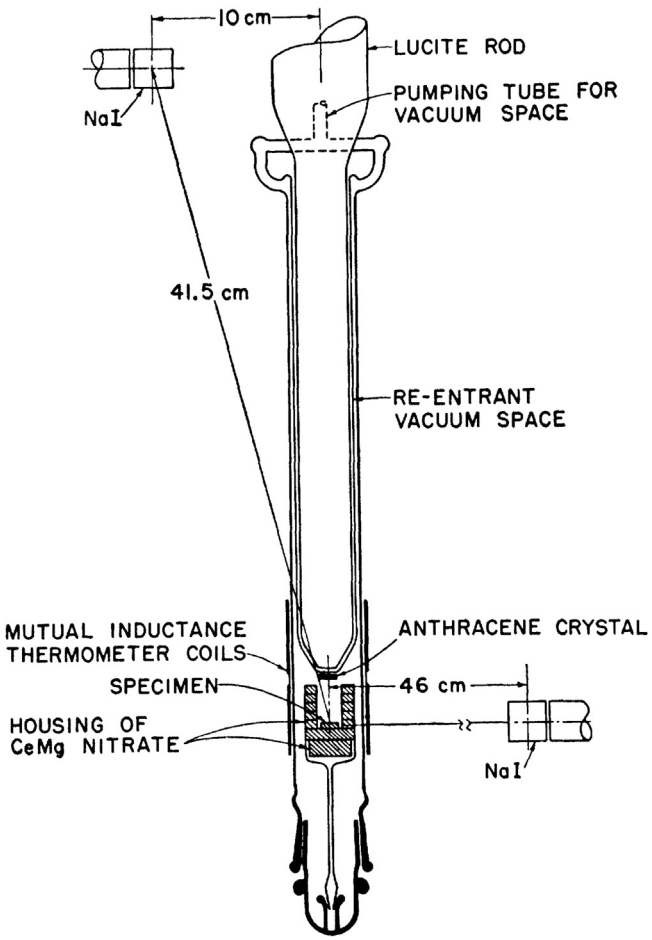

FIGURE IX.6 Schematic drawing of the ^{60}Co source, detector, and lower part of the cryostat used by Chien-Shiung Wu and collaborators at NIST to test parity conservation in beta decay. *From Wu, C.S., Ambler, E., Hayward, R.W., Hoppes, D.D., Hudson, R.P., 1957, Experimental test of parity conservation in beta decay. Phys. Rev. 105, 1413–1414 © 1957 American Physical Society, http://dx.doi.org/10.1103/PhysRev.105.1413.*

magnetic field at near absolute zero temperature. The anthracene crystal located about 1 cm above the ^{60}Co source is a scintillation detector sensitive to the β-particles emitted by the ^{60}Co. The anthracene scintillator emits a flash of light following the interaction of each β-particle with the crystal. The individual flashes of light are transmitted by the lucite rod to an external photomultiplier tube (PMT), which will convert the light to voltage pulses. Each voltage pulse is then counted over a fixed period of time, providing a count rate (eg, counts per minute) of the β-particles emitted by the ^{60}Co. Beta decay of ^{60}Co yields ^{60}Ni according to the following:

$$^{60}_{27}\mathrm{Co} \rightarrow {}^{60}_{28}\mathrm{Ni} + \beta^{-} + \overline{\nu} + \gamma \qquad \text{[IX.1]}$$

The antineutrino emitted in the β decay escapes without detection. The gamma radiation is emitted by the ^{60}Ni product nuclide, which is produced at an excited energy state resulting in the immediate emission of γ-rays before reaching a stable state. The γ-rays are detected by NaI solid scintillation detectors located over 40 cm away from the apparatus at the equatorial and near the polar position of the ^{60}Co (see Fig. IX.6). The NaI detectors were used by Wu and collaborators to measure the γ-ray anisotropy to provide a measure of the ^{60}Co nuclear polarization.

Before cooling and the application of an external magnetic field, the ^{60}Co nuclei exhibit thermal agitation and are not polarized. Thus the β-particles they emit under these conditions would be isotropic—that is, they would be emitted in all directions. Under these warm (ie, room temperature) conditions, Wu and her collaborators determined the count rate of the β-particles and labeled this as "$<\text{COUNTING RATE}>_{\text{warm}}$" (see Fig. IX.7). When the ^{60}Co specimen is cooled and the magnetic field applied, the ^{60}Co nuclei become polarized and remain rigid in their polarized state. The number of β-particles detected by the anthracene crystal over a fixed period of time under these conditions was determined and

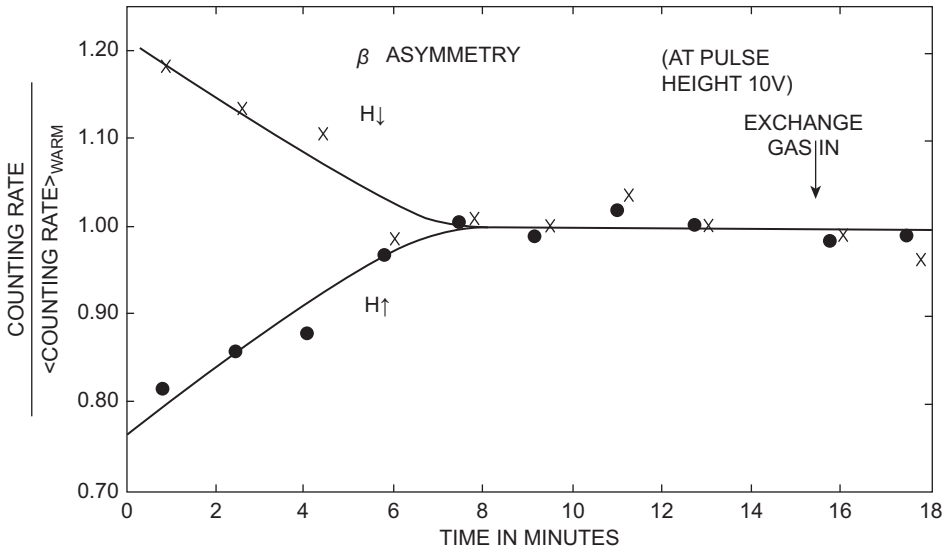

FIGURE IX.7 Beta particle asymmetry for polarizing fields pointing up and down. *From Wu, C.S., Ambler, E., Hayward, R.W., Hoppes, D.D., Hudson, R.P., 1957, Experimental test of parity conservation in beta decay. Phys. Rev. 105, 1413–1414 © 1957 American Physical Society, http://dx.doi.org/10.1103/PhysRev.105.1413.*

labeled as COUNTING RATE (see Fig. IX.7). The ratio of COUNTING RATE/<COUNTING RATE>$_{warm}$ was then used by Wu and coworkers to determine if the counting rate of the β-particles emitted by the ^{60}Co was higher or lower than the counting rate under warm conditions and in the absence of a magnetic field.

They discovered that when the magnetic field is applied in one direction (H↓ in Fig. IX.7) with the ^{60}Co nuclei at near absolute zero temperature and polarized in one direction, the β-particle counting rate was at its highest—higher than when the sample is at room temperature and in the absence of a magnetic field. Reversing the direction of the magnetic field (H↑ in Fig. IX.7) and thereby reversing the direction of polarization of the ^{60}Co nuclei resulted in a reduction of the β-particle counting rate to magnitudes below that determined when the sample was at room temperature and in the absence of a magnetic field. When the ^{60}Co is warmed slowly to room temperature, the ^{60}Co nuclei return to normal thermal agitation and lose their polarization after about 7 min of warming, as illustrated in Fig. IX.7.

As described above, the findings of Wu and her collaborators demonstrated that the β-particle emissions were not the same for the two spin directions of the ^{60}Co nuclei; that is, the β-particle emissions differed for the two mirror images of the ^{60}Co nuclei. Thus the β decay process in ^{60}Co nuclei does not exhibit right–left symmetry; in other words, this β decay violates parity. This is illustrated in Fig. IX.8.

The experiment of Wu and her collaborators at the NBS (NIST) demonstrated that β-particle emission from decaying ^{60}Co nuclei is greatest in the direction of the south pole of the nucleus, which is the pole that would point toward the north pole of an external magnetic field (Forman, 1982). This is labeled "our world" in Fig. IX.8. Once the significance of Chien-Shiung Wu's work was ascertained, other researchers, including Richard Garwin, Leon Lederman, and Marcel Weinrich at the Nevis Cyclotron Laboratories at Columbia University, detected asymmetry in muon decay, which broadened the acceptance of parity violation in weak interactions other than β decay (Garwin et al., 1957).

ISIDOR ISAAC RABI (1898–1988)

Isidor Isaac Rabi was born in 1898 into an orthodox Jewish family in Rymanów, Poland, which was part of the Austro-Hungarian Empire and under the control of Austrian-ruled Galicia at the time of his birth. His given name was Israel Isaac Rabi; but this name changed in an interesting course of events, as related by Ramsey (1993) in a biographical memoir. Shortly after his birth his father emigrated to New York City, and after a few months he had earned enough money so that infant Rabi and his mother could join him. At home in New York they gave young Israel Isaac the name "Izzy" for short. When it was time to register the boy in a public school, his mother gave his name as Izzy, and the school administration registered him as Isidor Isaac Rabi, thinking that Izzy was a short for Isidor. His family never corrected the

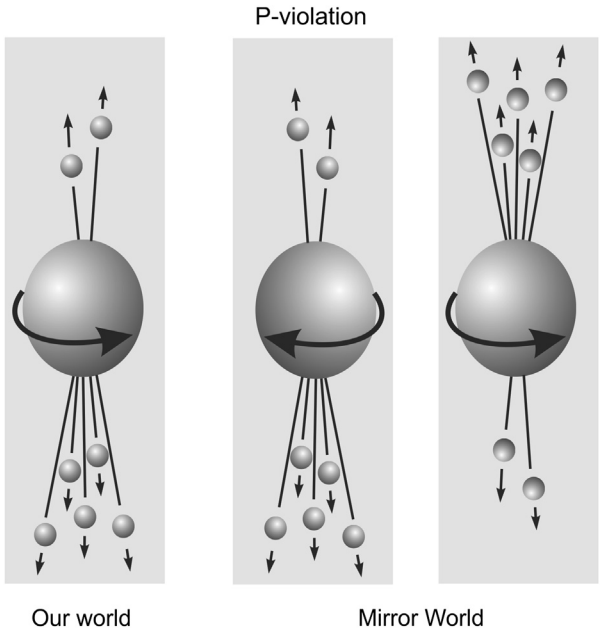

FIGURE IX.8 Parity violation in the decay of cobalt-60. The large spheres in the center represent groups of ^{60}Co nuclei. The β-particle emissions from the ^{60}Co nuclei are illustrated as smaller spheres, which are emitted predominantly in the direction opposed to that of the nuclear spin (*curving arrow*). The two orientations of the ^{60}Co nuclei in the "mirror world" were created in the laboratory by Wu and coworkers by polarization of the ^{60}Co nuclei in a magnetic field at near absolute zero temperature to fix the nuclei in one orientation, and then flipping the nuclei by polarization in an opposite direction. The beta emissions of the two ^{60}Co nuclei are not identical in their mirror images, and thus parity conservation is violated in the beta decay of ^{60}Co. *From Atkinson, D., 2006. Does quantum electrodynamics have an arrow of time? Studies Hist. Phil. Mod. Phys. 37, 528–541; reprinted with permission of Elsevier © 2006.*

error, and he continued through life with the name Isidor. He was awarded the Nobel Prize in Physics in 1944, in the words of the Nobel Committee "for his resonance method for recording the magnetic properties of atomic nuclei."

Isidor Isaac Rabi (1898–1988)

Life was not easy for young Rabi. He lived with his family in a Jewish ghetto in the Manhattan slums of New York, where his father worked in a sweatshop making clothing by day and at night in an unsuccessful grocery store, which was operated by his mother during the day (Ramsey, 1993). Isidor attended public schools in Brooklyn and Manhattan, during which time he acquired an interest in science through reading a book from the public library. Upon graduation from high school he entered Cornell University, and graduated with a BS in chemistry in 1919. He was unable to find suitable work in chemistry; and after 3 years of work in nonscientific employment, Rabi entered graduate school at Cornell and later transferred to Columbia University, graduating with the aid of fellowships with a PhD in physics in 1927 for his dissertation work on the magnetic properties of crystals.

With the aid of a fellowship Rabi was able to travel to study in Europe, where he had the opportunity to meet and work with such leading physicists as Niels Bohr, Wolfgang Pauli, Otto Stern, and Werner Heisenberg, among others. While working in the laboratory with Stern, Rabi became very interested in studying the magnetic properties of atomic nuclei; and he was able to develop further Stern's atomic beam method to make measurements with greater precision (Nobel Lectures, Physics, 1942–1962). In 1929 Rabi returned to Columbia University as lecturer in theoretical physics, and set up his own laboratory for the study of the magnetic properties of atomic nuclei with his own improvements on Stern's atomic beam method. In 1937 he was promoted to full professor at Columbia. During 1936–1940 Rabi and his coworkers, including P. Kusch, J. M. B. Kellogg, and S. Millman at Columbia University and J. R. Zacharias of Hunter College, established the magnetic resonance method of measuring nuclear magnetic moments and determined the magnetic resonance properties of atomic nuclei. Polykarp Kusch was awarded the Nobel Prize in Physics in 1955 for his accurate determination of the magnetic moment of the electron.

From 1940 and throughout World War II, Isidor I. Rabi took leave from Columbia to collaborate in the development of radar at Massachusetts Institute of Technology (MIT); and he served as consultant to J. Robert Oppenheimer, director of the Los Alamos nuclear research laboratory (Ramsey, 1993). After the war Rabi returned to Columbia to reestablish his molecular beam research, and became an effective chair of the Physics Department. As a member of the General Advisory Committee of the US AEC, he joined Enrico Fermi as strong opponents to the vigorous efforts toward the development of a hydrogen bomb. He and Norman F. Ramsey initiated the first proposals for the establishment of the Brookhaven National Laboratory; and he pioneered in advocating European collaboration for the establishment of CERN, the renowned European Organization for Nuclear Research (Ramsey, 1993). In 1959 Rabi was appointed a member of the board of governors of the Weizmann Institute of Science at Rehovoth, Israel; and he served as a member of the Science Advisory Committee of the International Atomic Energy Agency in Vienna (Nobel Lectures, Physics, 1942–1962).

Rabi was awarded the Nobel Prize in Physics specifically for his work on the magnetic resonance properties of atomic nuclei, which he had developed for the accurate measurements of nuclear magnetic moments. He and his coworkers (Rabi et al., 1938, 1939; Kellogg et al., 1939) demonstrated that atomic nuclei aligned in a magnetic field would precess in a similar fashion that a spinning top will precess under the force of gravity; and that the frequency of precession (ν), referred to as the Larmor frequency of precession (after Joseph Larmor), is a function of the magnitude of the magnetic field (H). A beam of nuclei precessing in a homogeneous magnetic field at a certain frequency will be exposed to radio waves. The atomic nuclei absorb energy from the radio waves when their frequency of precession coincides with the radio wave frequency; and, in so doing, the atomic nuclei change their spin direction against the magnetic field, as illustrated in Fig. IX.9. Rabi and coworkers (Kellogg et al., 1939) described the energy absorption of the nuclei according to the Bohr quantum relation

$$h\nu = \Delta E = E_{\max} - E_{\min} \qquad [IX.2]$$

where h is Planck's constant, ν is the frequency of precession, and $E_{\max}$ and $E_{\min}$ are the energy states of the nuclei after and before the absorption of the radio wave energy.

One of the molecular beam arrangements used by Rabi and his coworkers is illustrated in Fig. IX.10. A molecular beam is initiated at the far left of the evacuated chamber labeled O, which is the oven that produces the molecular or atomic vapor. The oven contains a slit opening only 0.03 mm wide to enable the atomic vapor to escape as a thin beam and travel through the chamber. The beam travels in a straight line from left to right through the center of the deflecting magnet A, followed by magnet C, which produces a homogeneous field, and then a refocusing magnet B before traveling on through a slit opening to a tungsten filament detector D at the far right of the chamber. At the center of the chamber a collimating slit S leads the beam on to an RF oscillating field R, which consists of two 0.32 cm copper tubes, 4 cm long, that carry current in opposite directions. The space between the pole faces of magnet C and the copper tubes for the oscillating field is only 1 mm for the passage of the atomic beam.

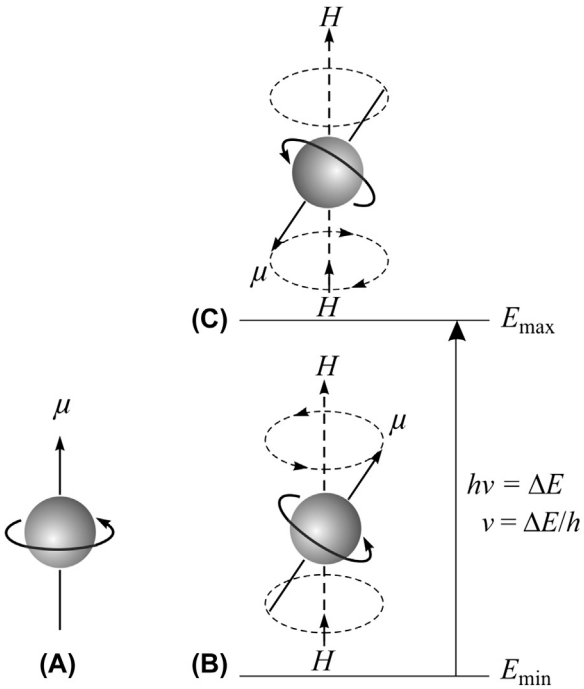

FIGURE IX.9 An atomic nucleus of spin quantum number ½ with magnetic moment μ in (A) the absence of an external magnetic field and (B) the presence of an external magnetic field (H). At E_{min} the nucleus maintains a spin aligned with the external magnetic field and precesses with frequency (ν) in accordance with the strength of the external magnetic field. At (C) the nucleus makes a quantum jump ($h\nu$) to a higher energy state E_{max}, aligning its spin against the magnetic field after exposure to radio frequency (RF, ie, radio waves of varying frequency) (ν), coinciding with the frequency of precession. Atomic nuclei of spin ½ have only two possible quantum spin states, one aligned to and the other against the external magnetic field. Examples are nuclei of odd mass, such as ^{1}H, ^{7}Li, ^{13}C, ^{15}N, ^{19}F, ^{29}Si, ^{31}P, ^{35}Cl, and ^{37}Cl or even mass and odd charge.

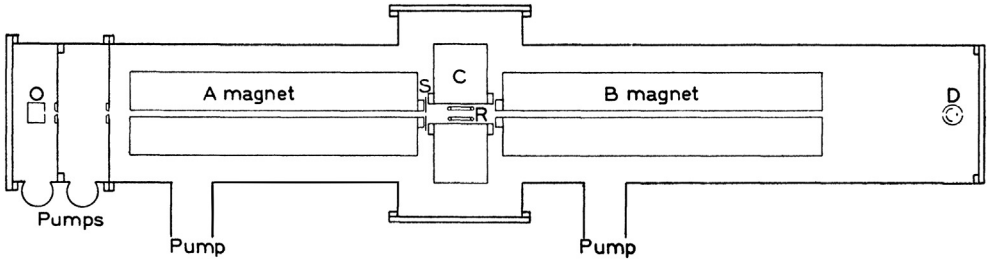

FIGURE IX.10 Schematic diagram of the experimental arrangement used by Rabi and coworkers for their molecular beam resonance method for measuring nuclear magnetic moments. *Reprinted with permission from Rabi, I.I., et al., 1939. The molecular beam resonance method for measuring nuclear magnetic moments. Phys. Rev. 55, 526–535 © 1939 American Physical Society, http://dx.doi.org/10.1103/PhysRev.55.526.*

In the very first report of nuclear magnetic resonance (NMR), Rabi et al. (1938) described the phenomenon that occurs when the atomic nuclei in the beam are exposed to an RF equal to their frequency of precession. They described how the nuclei undergo a reorientation of their nuclear spin and magnetic moment when the appropriate RF (ν) is found, as illustrated in Fig. IX.9. They noted that the quantum leap of reorientation of the atomic nuclei prevents their refocusing in the B magnetic field and blocks their arrival at the detector D. Rabi et al. (1938) noted the following [with the writer's notes in brackets]:

> *Consider a beam of molecules, such as LiCl, traversing a magnetic field which is sufficiently strong to decouple completely the nuclear spins from one another and from the molecular rotation. If a small oscillating magnetic field [radio frequency region R in Fig. IX.10] is applied at right angles to a much larger constant field [from magnetic poles at C in Fig. IX.10], a re-orientation of the nuclear spin and magnetic moment with respect to the constant field will occur when the frequency of the oscillating field is close to the Larmor frequency of precession of the particular angular momentum vector in question… the re-orienting field is*

placed in the region between the two magnets [region R in Fig. IX.10]. The homogeneous field is produced by an electromagnet [magnet C in Fig. IX.10] capable of supplying uniform fields up to 6000 G in a gap 6 mm wide and 5 cm long. In the gap is placed a loop of wire in the form of a hairpin (with its axis parallel to the direction of the beam) which is connected to a source of current at radiofrequency to produce the oscillating field at right angles to the steady field. If a re-orientation of a spin occurs in this field, the subsequent conditions in the second deflecting field [magnet C in Fig. IX.10] are no longer correct for refocusing, and the intensity at the detector goes down. The experimental procedure is to vary the homogeneous field for some given value of the frequency of the oscillating field until the resonance is observed by a drop in intensity at the detector and a subsequent recovery when the resonance value is passed.

Reprinted with permission from Rabi et al. (1938) © 1938 American Physical Society, http://dx.doi.org/10.1103/PhysRev.53.318.

An example of the detector response to ^{19}F nuclei in a molecular beam of NaF is provided in Fig. IX.11. The figure illustrates how the detector indicates a diminished response to the molecular beam, because when the atomic nuclei absorb an energy quantum from the RF, they undergo a reorientation of their nuclear spin and magnetic moment and cannot be detected in the beam reaching the detector. This discovery led to the development of NMR spectroscopy, which is currently one of the most popular methods of determining the structure of organic compounds in the chemical, biological, and medical sciences. Also, magnetic resonance imaging (MRI), an important imaging technique applied in the field of nuclear medicine, is another beneficial outcome of Rabi's findings in NMR. NMR spectroscopy and MRI are discussed later in this section.

In his Nobel Prize award ceremony speech Professor E. Hulthén described the magnetic resonance method of Rabi as follows:

Let us now for a moment touch upon Rabi's achievements… How does the atom react to the magnetic field?… this influence may be ascribed to a relatively slow precession movement on the part of the electron and the atomic nucleus around the field direction—a gyromagnetic effect most closely recalling the gyroscopic movement performed by a top when it spins around the vertical line. If the strength of the magnetic field is known, the magnetic factor of the electron and of the atomic nucleus can also be estimated by this means, provided that we can observe and measure these precessional frequencies. Rabi solved the problem in a manner as simple as it was brilliant. Within the magnetic field was inserted a loop of wire, attached to an oscillating circuit the frequency of which could be varied in the same manner as we tune in our radio receiving set to a given wavelength. Now, when the atomic beam passes through the magnetic field, the atoms are only influenced on condition that they precess in time with the electric current in the oscillating circuit. This influence might perhaps be described graphically: the nucleus performs a vault (salto)—the technical term for which is a "quantum jump"—thereby landing in another positional

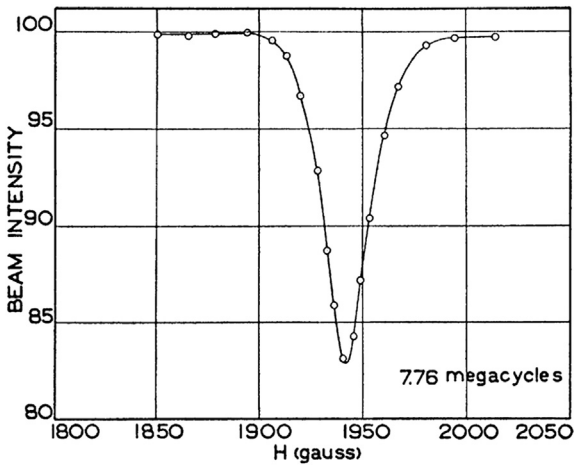

FIGURE IX.11 Resonance curve of the ^{19}F nucleus observed in NaF. The RF (ν) of 7.76 megacycles was measured for the quantum energy ($h\nu$) absorption by the ^{19}F nuclei at a magnetic field strength of approximately 1940 G. *Reprinted with permission from Rabi, I.I., et al., 1939. The molecular beam resonance method for measuring nuclear magnetic moments. Phys. Rev. 55, 526–535 © 1939 American Physical Society, http://dx.doi.org/10.1103/PhysRev.55.526.*

direction to the field. But this means that the atom has lost all chance of reaching the detector and of being registered by it… By this method Rabi has literally established radio relations with the most subtle particles of matter, with the world of the electron and of the atomic nucleus.

Nobel Lectures, Physics, 1942–62.

Isidor I. Rabi died in Manhattan on January 11, 1988. For a comprehensive review of Rabi's work and life, the reader may peruse his biographical memoir by Ramsey (1993) and a biography by John S. Rigden (1987).

Important Developments from Rabi's Work on Nuclear Magnetic Resonance

Magnetic Properties of Nucleons

Isidor Rabi's pioneering work on the magnetic resonance properties of the atomic nucleus inspired others to research deeper within the nucleus to investigate the properties of individual nucleons, particularly the neutron. Because the neutron is a neutral particle and a spinning charge would be needed to create a magnetic field, it was not expected to possess magnetic properties.

Luis Alvarez of the Radiation Laboratory at the University of California at Berkeley and Felix Bloch at Stanford University modified Isidor Rabi's molecular beam method to determine the magnetic moment of the neutron (Alvarez and Bloch, 1940). They were able to measure the magnetic moment of the neutron by passing a beam of thermal neutrons through a polarizing and analyzing plate of magnetized iron, as described by Bloch et al.:

The initial use of this magnetic resonance method has been made by Rabi and his collaborators (Rabi et al., 1939) in their famous experiments on molecular and atomic beams. Alvarez and Bloch (1940) have succeeded in applying the method to the neutron. In their experimental arrangement a beam of thermal neutrons passes through a polarizing and analyzing plate of magnetized iron. Between these two plates the neutrons are exposed to a magnetic field which has a constant component H_0 and at right angles to it an oscillating component with circular frequency ω and amplitude H_1. Under resonance conditions, there occurs in this field a reorientation of the neutron moments and thus a partial depolarization of the beam. Consequently, the total transmission through the analyzer is lowered so that resonance depolarization manifests itself by a drop in the transmitted intensity detected as one passes through resonance. From the measured value H_0 of the constant field at which resonance is observed and the frequency ω of the oscillating field, one obtains

$$\frac{\mu_N}{\hbar I_N} = \gamma_N = \frac{\omega}{H_0} \qquad \text{[IX.3]}$$

for the gyromagnetic ratio γ_N, defined as the magnetic moment of the neutron μ_N, divided by its angular momentum $\hbar I_N$. Assuming the spin of the neutron to be $I_N = ½$, the absolute value of the neutron moment was determined to be

$$|\mu_N| = (1.93 \pm 0.02)\mu_n \qquad \text{[IX.4]}$$

[where μ_n is the nuclear magneton $= 5.050 \times 10^{-27}$ JT^{-1}]. The fact that the sign of the neutron moment is actually negative has been shown in an earlier experiment of Powers (1938).

Bloch et al. (1948), reprinted with permission, © 1948 American Physical Society, http://dx.doi.org/10.1103/PhysRev.74.1025.

Felix Bloch and coworkers at Stanford University (Bloch et al., 1948) refined the measurement of the magnetic moment of the neutron and determined it to be $(-1.91307 \pm 0.0006)\mu_n$, which calculates to be $(-1.91307)(5.050 \times 10^{-27}\ \text{JT}^{-1}) = -0.966 \times 10^{-26}\ \text{JT}^{-1}$. This magnitude of the magnetic moment agrees with the current value included in the listing of fundamental physical constants reported by NIST (http://physics.nist.gov/cuu/index.html). See also Table 2.1 of chapter "Basic Concepts and Definitions".

Further studies were undertaken into the charge and magnetic properties of the nucleons by Robert Hofstadter (1915–1990) and his coworkers at Stanford University, who utilized an electron accelerator to bombard the atomic nucleus with high-energy electrons ranging in energies from a low end of 190 MeV to as high as 1 BeV (Hofstadter et al., 1953a,b;

Hofstadter and McAllister, 1955; McAllister and Hofstadter, 1956; Chambers and Hofstadter, 1956). His electron-scattering experiments against numerous atoms of the periodic table demonstrated that the radius of the atomic nucleus is a function of its mass number, according to the equation

$$R = r_0 A^{1/3} \qquad \text{[IX.5]}$$

where r_0 is a constant (currently with the value of 1.22×10^{-15} m) and A is the mass number or number of protons + neutrons in the nucleus (Hahn et al., 1956). Hofstadter was also able to determine that all atomic nuclei had a uniform charge density of $\sim 1.1 \times 10^{19}$ C/cm^3, with the exception of the nuclei of hydrogen and helium atoms, which contained a higher charge density of ~ 10 times and ~ 2 times that of the other atomic nuclei, respectively. The very high charge density of the hydrogen nucleus is understandable, because the nucleus of hydrogen contains nothing more than one proton.

Accelerated high-energy electrons could penetrate the nuclear Coulombic barrier and enter into a nucleus, such as that of the hydrogen atom, which contains only one proton, and the deuterium atom, which contains only one proton and one neutron. The high-energy electrons were bombarded against the hydrogen and deuterium atoms as liquid targets (ie, liquid hydrogen or liquid deuterium). The hydrogen atom (ie, liquid hydrogen) served as a source of protons for Hofstadter's electron-scattering experiments; however, neutrons in significant numbers are not available in confined spaces for bombardment experimentation. Thus he used liquid deuterium, which contains a proton and a neutron; the difference in scattering properties with hydrogen would provide information on neutron scattering. As described by Robert Hofstadter in his Nobel speech:

> *The difficulty is compounded by the experimental fact that neutron targets are obtained only by using the deuteron as a neutron carrier, for free neutrons in large numbers are unobtainable in confined spaces… Many of these difficulties were overcome in the work of Yearian and the author [Yearian and Hofstadter, 1958a,b] who used a difference method to compare the scattering from the deuteron and the proton. These investigators first showed that the neutron could not be represented as a point nucleon and that its magnetic moment was distributed in a manner similar to that of the proton.*

The magnetic and charge forces of an individual proton or neutron would scatter the high-energy electrons of varying energies in different directions, which Hofstadter and his coworkers carefully measured with magnetic spectrometers. From this work he was able to determine the distribution of electric charge in the nuclei, and provide evidence that the individual nucleons possessed internal charge and magnetic properties. The proton and neutron would no longer be considered as elementary particles; rather, these scattering experiments indicated that the nucleons contain some internal charge distribution. Thus the neutron, like the proton, possessed an internal structure with charge that attributed a magnetic property to the nucleons.

Concerning his findings on the internal charge distribution and magnetic properties of the proton and neutron, Hofstadter noted that the proton and neutron should no longer be considered as elementary particles; and that physicists would eventually determine their constituent parts. He stated in his Nobel lecture given on December 11, 1961:

> *If we now attempt to summarize the recent progress in nucleon structure determinations and in their interpretation, we may say that the proton and neutron are two different aspects of a single entity—the nucleon… A phenomenological and qualitative interpretation of the nucleon form factors then shows that the same charged mesonic clouds appear in both the neutron and proton… As we have seen, the proton and neutron, which were once thought to be elementary particles are now seen to be highly complex bodies. It is almost certain that physicists will subsequently investigate the constituent parts of the proton and neutron—the mesons of one sort or another… The history of physics shows that whenever experimental techniques advance to an extent that matter, as then known, can be analyzed by reliable and proved methods into its "elemental" parts, newer and more powerful studies subsequently show that the "elementary particles" have a structure themselves. Indeed this structure may be quite complex, so that the elegant idea of elementarity must be abandoned.*

In the years to come, physicists would determine the internal structure of protons and neutrons to consist of quarks that carry charge and gluons that bind the quarks together within the proton or neutron. Also, physicists would eventually determine that within the nucleus there is a constant transformation of a proton into a neutron and vice versa, a neutron into a proton. Thus Robert Hofstadter's prediction cited in the preceding quote, that the proton and neutron act as a "single entity—the nucleon," would eventually be demonstrated.

Robert Hofstadter (left) and President Ronald Reagan (right)
President Ronald Reagan presenting a Medal of Science Award to Robert Hofstadter in 1986. Photo: Mary Anne Fackelman-Miner, The White House, courtesy AIP Emilio Segre Visual Archives, Physics Today Collection with permission

Nuclear Magnetic Resonance Spectroscopy

As described above, Isidor Isaac Rabi carried out the pioneering research demonstrating that atomic nuclei behave like small spinning magnets, and in a magnetic field they will precess like spinning tops with a certain frequency depending on the strength of the external magnetic field. He then demonstrated that by exposing these gyrating nuclei to an RF, he could find the exact RF that would correspond to the frequency of the precessing nuclei. This would cause the nuclei to absorb the RF energy ($h\nu$) and consequently make a quantum leap to a higher energy while flipping to an alternate state of orientation against the magnetic field. This groundbreaking work on NMR was all done by Rabi and his coworkers with molecular beams of atomic nuclei in an apparatus under vacuum. Rabi's pioneering research set the stage for subsequent work by Felix Bloch (1905−1983) and Edward Purcell (1912−1997), who were able to develop NMR with the nucleus of the hydrogen atom to permit the application of the technique to liquids and solids outside of any vacuum chamber. This would enable a researcher in any laboratory to place a sample of an organic compound as a liquid or in solution in a suitable solvent within a magnetic field while subjecting the sample to an RF, and then record the energies of RF absorption by the protons on various atoms of the organic molecule, such as protons on carbon and nitrogen. Any researcher in any laboratory could then determine the molecular structure of an organic compound without destroying the sample with the very popular analytical technique that is now called NMR spectroscopy. Felix Bloch and Edward Purcell jointly received the Nobel Prize in Physics in 1952 for this work. The significance of this development in NMR was eloquently noted by Joachim Pietzsch (2014):

> *Rabi's findings were in the artificial environment of atomic beams in a vacuum, but working independently on hydrogen atoms, Bloch and Purcell developed the technique so that it could be applied to liquids and solids. Their breakthrough provided researchers with the potential to place any solid or liquid in an electromagnetic field, expose it to radio waves, and identify the specific atoms that make up the chemical, without affecting it in any perceptible way. Such a degree of chemical analysis had been unattainable until then—a statement based on substance rather than spin.*
>
> From Pietzsch (2014) for Nobelprize.org, www.nobelprize.org/nobel_prizes/physics/laureates/1952/speedread.html.

Felix Bloch (1905–1983)

Edward M. Purcell (1912–1997)
AIP Emilio Segre Visual Archives, Physics Today Collection with permission

NMR spectroscopy is one of the most powerful methods of identifying organic compounds or determining their molecular structure. Since the first commercial NMR spectrometer appeared in 1960, it has become an indispensable tool for the determination of the molecular structure of organic compounds from the magnetic properties of their atomic nuclei (eg, ^{1}H, ^{13}C, ^{19}F and ^{31}P) and the surrounding molecular electrons. Nuclei of certain atoms of odd mass, such as ^{1}H and ^{13}C, or even mass and odd charge have a net charge and a spin. The spinning charge of the nucleus creates a magnetic dipole (μ). If one places spinning proton nuclei, which are a component of most organic compounds, in a magnetic field (H), the axis of the magnetic dipoles of these nuclei will precess at an angle with respect to the magnetic field axis, as illustrated in Fig. IX.9. The precession of the nuclei with respect to the applied magnetic field axis occurs somewhat like the way a spinning top precesses under the force of the Earth's gravitational field. The angular velocity of this precession is a function of the strength of the applied magnetic field (H) and the effects of shielding caused by spinning electrons in the molecular environment of the proton nuclei.

Spherical nuclei of odd mass, such as ^{1}H, ^{13}C, ^{15}N, ^{19}F, and ^{31}P, possess a spin of ½, and when subjected to the external magnetic field the nuclei can possess two orientations, namely an orientation in the direction of the magnetic field (+½), as illustrated in Fig. IX.9, or an orientation against the magnet field (−½). While under the forces of a stable magnetic field (H) of an NMR spectrometer, the proton nuclei are irradiated with an RF energy tunable over a narrow range. When the variable RF is attuned to the precessional angular velocity of a given proton nucleus of a molecule, the two frequencies are in resonance. The applied energy at this resonance frequency (hv) is absorbed by the proton nucleus, the nucleus is caused to make a quantum leap in energy, and it flips or becomes aligned against the applied magnetic field (H), as illustrated in Fig. IX.9. The energy absorbed by the proton nucleus that causes it to reach the higher-energy spin state (ie, flipped or −½) is the energy measured by the NMR spectrometer. The NMR spectrometer measures the RF absorption energy by collecting the RF signal free-induction decay (FID) as the excited nuclei emit the excitation energy as they decay back to equilibrium (Rankin et al., 2014). The basic components and function of the NMR spectrometer are illustrated in Fig. IX.12.

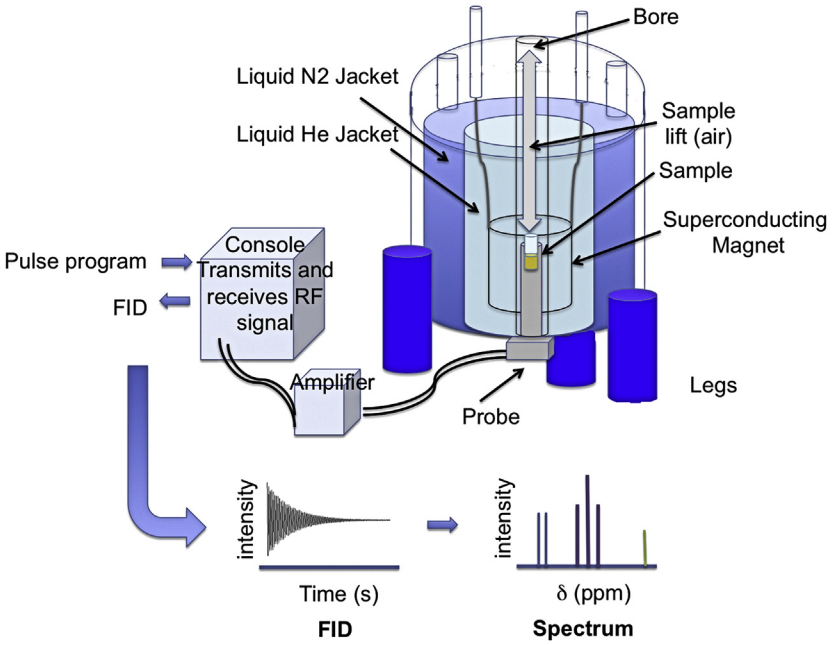

FIGURE IX.12 Simplified diagram of an NMR spectrometer. At the heart of the ^{1}H NMR spectrometer is a superconducting magnet. This must be kept at 4 K, so it needs to be immersed in liquid helium which is prevented from evaporating by vacuum and nitrogen jackets. The probe containing the RF coil sits in the bottom of the magnet within its bore. The sample is always contained within the ^{1}H NMR tube; it is gently dropped into the probe on a cushion of air. Here the superconducting magnet causes the protons to spin, and the RF coil sends RF pulses to excite them and collects the FID as they relax back to equilibrium. The pulse programs are created using a computer and sent to the console, which acts as both an RF transmitter and a receiver. The signals are amplified on transmission and receipt. The FIDs are Fourier transformed (mathematically deconvoluted) to produce ^{1}H NMR spectra of intensity versus chemical shift (δ) using a computer. *From Rankin, N.J. et al., 2014. The emergence of proton nuclear magnetic resonance metabolomics in the cardiovascular arena as viewed from a clinical perspective. Atherosclerosis 237, 287–300.*

Fortunately, in NMR spectroscopy the resonance absorption by proton nuclei is complicated by the shielding effect of electron clouds of varying densities in the environment of organic molecules. The electron cloud surrounding a nucleus also has charge and spin, and therefore produces its own characteristic magnetic field, which opposes or shields the externally applied field. The degree of shielding is a function of the electron cloud density, which will differ from nucleus to nucleus in the organic molecule because of the differing electronegativities of neighboring atoms. Therefore, protons in a molecule will absorb different resonance frequencies depending on their location in the molecule. This effect is referred to as the chemical shift. A proton which is highly shielded absorbs at a lower resonance frequency than a proton with reduced shielding. The presence of atoms of differing degrees of electronegativity (electron-withdrawing ability) in molecules as well as the differing three-dimensional orientation of atoms within molecules will cause a wide spectrum of shielding effects on neighboring protons. This gives rise to a wide spectrum of resonance absorption frequencies for protons, depending on the structural group to which the protons are attached, their neighboring atoms, and their spatial orientation in the molecule. Thus the differing resonance absorption frequencies or chemical shifts of protons in NMR spectroscopy provide an absorption spectrum, which serves as a means for identifying chemical groups and their spatial positions in organic molecules.

The chemical shift of a particular proton nucleus in a molecule is recorded with respect to the chemical shift of the protons on a reference molecule, eg, tetramethylsilane or $(CH_3)_4Si$, most often referred to as TMS. The difference in chemical shifts of a proton or group of protons in a molecule with respect to that of TMS is recorded and calculated in units of Hz, whereas the magnitude of the applied frequency is in the order of magnitude of MHz, a millionfold greater. The difference in chemical shift of a proton nucleus with respect to that of the reference molecule (eg, TMS) in Hz is divided by the applied frequency in MHz to record chemical shifts in convenient units of parts per million (ppm) expressed as δ (ppm) or τ (ppm), where $\tau = 10.0 - \delta$. Nuclei of even mass and even charge (eg, ^{12}C and ^{16}O) in a molecular structure do not possess a magnetic moment, and these nuclei are inert to the previously described effects of an external magnetic field. Deuterated solvents, such as $CDCl_3$ or D_2O which have no resonances in the region of ^{1}H, are used generally in the measurement of ^{1}H-NMR spectra.

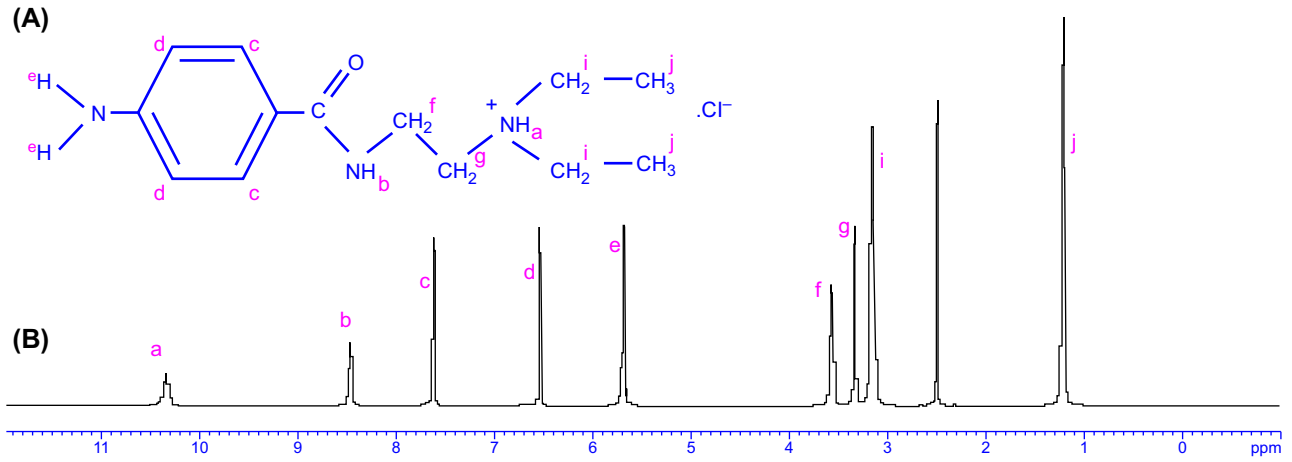

FIGURE IX.13 Proton NMR (^{1}H-NMR) spectrum of PCA dissolved in deuterated dimethyl sulfoxide $(CD_3)_2SO$ solvent. The proton absorption resonance peaks (chemical shifts measured in ppm) for each proton on the molecular structure of PCA are identified by letters a–j. *From Siva, S., et al., 2015. Fabrication of cyclodextrins-procainamide supramolecular self-assembly: shape-shifting of nanosheet into microtubular structure. Carbohydr. Polym. 122, 123–134; reprinted with permission from Elsevier © 2015.*

Examples of the power of ^{1}H-NMR are provided in Figs. IX.13 and IX.14. The protons and their chemical groups throughout the molecule of procainamide hydrochloride (PCA) are identified by the ^{1}H resonance absorption peaks. Reference tables help the analytical chemist identify the peaks. For example, electron-donating atoms or groups (eg, CH_3– and $-CH_2-$) generally yield a resonance peak further upfield (lower δ (ppm), such as peaks f, g, i, and j of Fig. IX.13) than electronegative atoms or groups (eg, NH_2–, –NH–, $-NH^+$, and aromatic –CH═) which yield a resonance peak further downfield (higher δ (ppm), such as peaks a–e in Fig. IX.13).

A yet more powerful advantage of NMR spectroscopy is that it can be used to determine the structures of organic compounds which are stereoisomers—that is, compounds that may differ only in the orientation in space of one or more atoms. This is illustrated by the proton NMR spectra of L-chiro-inositol and myo-inositol in Fig. IX.14. The two molecules differ only by the orientation in space of one proton and hydroxyl group on a single carbon atom of the cyclohexane ring. The two isomers can clearly be identified by their proton NMR spectra. The spectra illustrated in Fig. IX.14 were recorded by the writer in 1968, when NMR spectrometers utilized much weaker magnetic fields compared to modern instruments. The reader can compare the much higher resolution, ie, higher signal-to-noise ratios, attainable with modern NMR spectrometers, as illustrated by the highly resolved resonance peaks in Fig. IX.13.

For additional reading on the principles of NMR as well as mass spectrometry see works by Lambert et al. (2010), Jacobsen (2007), and Pavia et al. (2014).

Magnetic Resonance Imaging

Another remarkable outcome of the early pioneering NMR discoveries of Isidor Isaac Rabi in the 1930s is the invention of magnetic resonance imaging (MRI), which is now a common and invaluable technique worldwide in diagnostic and clinical medicine. Breakthroughs in research during the 1970s that brought the possibility of imaging from the NMR phenomenon are attributed to the work of Paul C. Lauterbur when he was professor of chemistry and radiology at SUNY at Stony Brook and Sir Peter Mansfield, professor of physics at the University of Nottingham. They were awarded the Nobel Prize in Physiology and Medicine in 2003, when MRI became a developed and advantageous technique utilized in many clinics and hospitals throughout the world. The significance of the development of MRI was underscored by Professor Hans Ringertz in delivering the presentation speech for the 2003 Nobel Prize in Physiology and Medicine on December 10, 2003:

> *To be able to visualize the inner organs of humans without invasive techniques is of paramount importance to modern medicine… Magnetic Resonance Imaging, MRI, represents a new modality for obtaining diagnostic medical images… MRI is important to monitor many diseases of most organs in the human body. Imaging with magnetic resonance is an invaluable aid in the whole healthcare chain from screening and detection, diagnosis and treatment, to follow up of diseases… Magnetic resonance occurs in magnetic fields between atomic nuclei and electromagnetic waves of radio frequencies. Atomic nuclei have a magnetic moment and in the magnetic field, their spin depends on the strength of the field. The direction of magnetization resulting from the*

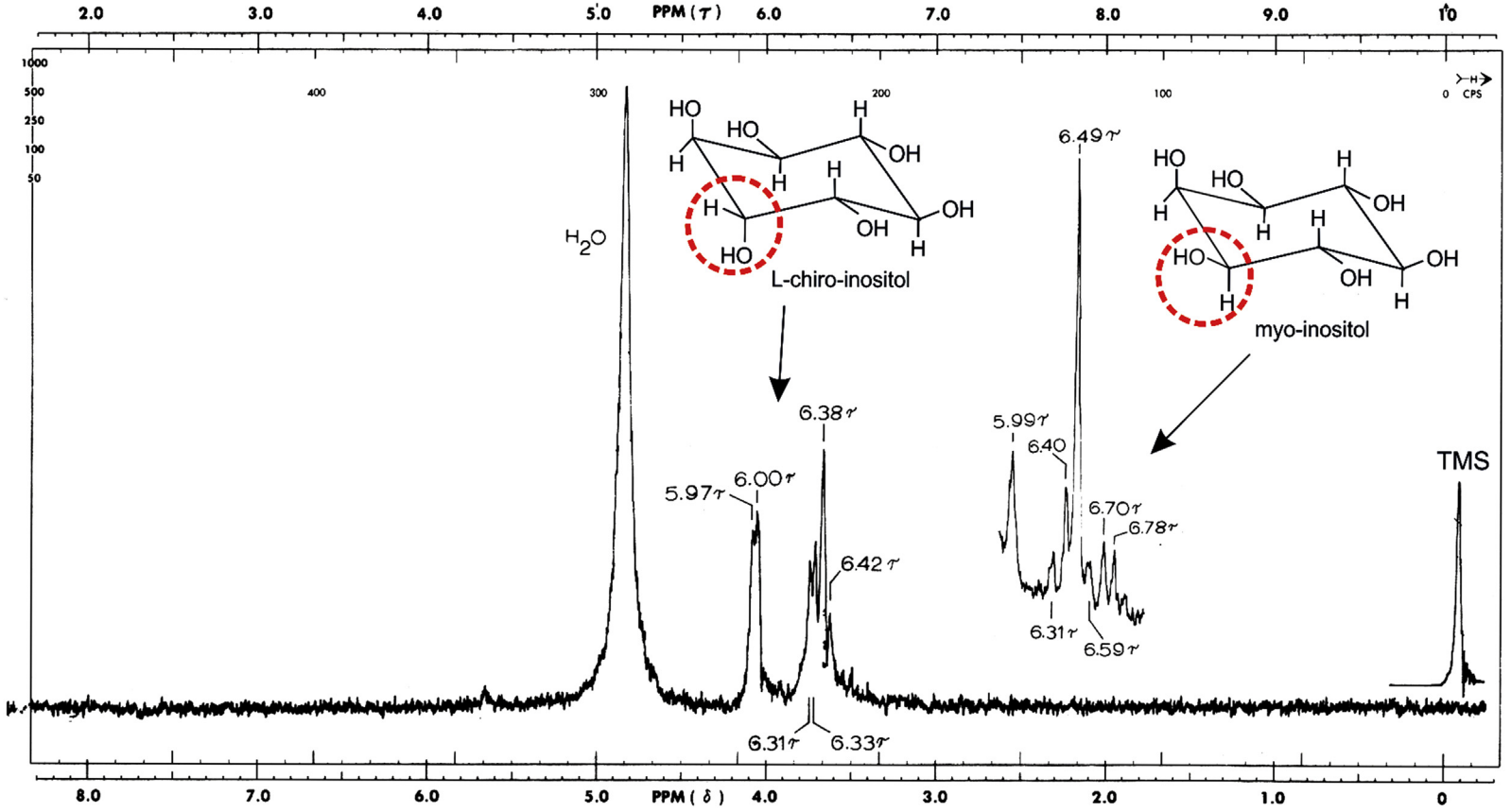

FIGURE IX.14 Proton NMR spectrum of L-chiro-inositol, and (inset to the right) the proton resonance spectrum corresponding to myo-inositol for comparison, in D_2O solvent. The only protons yielding a resonance absorption signal are those attached to the cyclohexane ring. The protons attached to the hydroxyl groups do not display a resonance absorption signal, because they exchange with deuterium from the D_2O solvent. The two stereoisomers differ in structure only at one carbon atom marked by the circle drawn over the two structures. The chemical shifts are measured here in δ (ppm) or τ (ppm), where $\tau = 10.0 - \delta$. *From L'Annunziata, M.F., 1970 (Ph.D. dissertation). The University of Arizona, Tucson. University Microfilms International (UMI), AAT 7104237. http://dissexpress.umi.com/dxweb/results.html?QryTxt=&By=L%27Annunziata&Title=&pubnum.*

magnetic moments can change. This happens when the nuclei are in resonance with radio waves of the same frequency as the frequency of their own rotation. In the same way the nuclei can send back radio waves, when there is a change in the direction of the magnetic moment… In the early 1970s Paul Lauterbur discovered the possibility to create a two-dimensional image by introducing gradients in the magnetic field. By analysis of the characteristics of the emitted radio waves, he was able to determine their origin. This made it possible to build up images of structures that could not be visualized with other methods. Peter Mansfield discovered further possibilities to utilize gradients in the magnetic field. He showed how the radio signals could be mathematically analysed, which made it possible to develop a useful imaging technique. Mansfield also showed how images could be achievable extremely fast using magnetic resonance. This became technically possible in clinical medicine about a decade later.

From www.nobelprize.org/nobel_prizes/medicine/laureates/2003/presentation-speech.html, © The Nobel Foundation 2003.

The MRI scanner is illustrated diagrammatically with its basic components in Fig. IX.15. As described by Cleary and Guimarães (2014) and illustrated in Fig. IX.15, the scanner consists of four main components: a magnet surrounding the patient; gradient coils in the *x*, *y*, and *z* planes of the magnet; an RF coil, which transmits the RF pulses needed to produce the MRI signal (known as the body transmit coil); and an RF receiver coil that picks up the resonance signal created in the patient. The patient is exposed to RF pulses, which are absorbed by the protons in the body. When the frequency of precession of the protons is equal to that of a transmitted RF, the protons will absorb a quantum of energy (*hv*) and orient themselves against the magnetic field. Upon deexcitation, the protons return to their lower-energy state, emitting an RF signal. The RF receiver coils are illustrated in Fig. IX.15 close to the body of the patient to optimize the RF signals received from the protons at various depths and organs within the patient's body.

A patient lying on the table is moved into the central magnet bore of the MRI scanner. The magnet contains superconducting coils cooled by liquid helium. A current flowing through the coils generates a magnetic field, B_o. Cooling with liquid helium maintains the temperature near absolute zero and gives near-zero resistance to electric current in the coils. The patient, within the magnet bore of the MRI scanner, is exposed to a spatially varying magnetic field (ie, magnetic field gradient) created by the *x*, *y*, and *z* gradient coils. Deexcitation times for proton nuclei (also referred to as relaxation times)

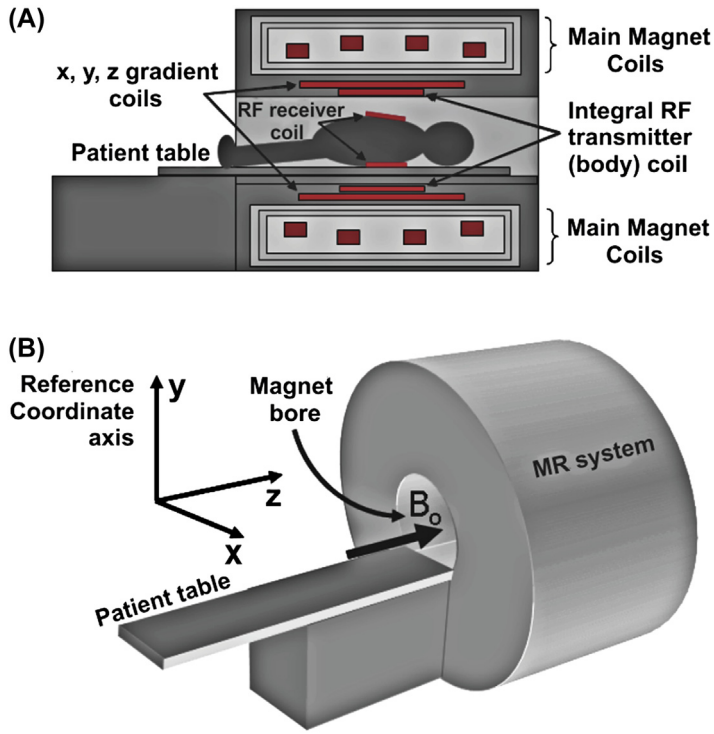

FIGURE IX.15 MRI system components: (A) cross-sectional diagram illustrating the relative locations of the main magnet coils, *x*, *y*, and *z* gradient coils, integral RF transmitter body coil, and RF receiver coils, with patient lying stretched out on a table within the central bore of the MRI system; (B) diagram of the outer view of the typical arrangement of a cylindrical-bore MRI system showing the magnet bore and the reference coordinate axis with the static B_o field direction along the z axis, and a table on which the patient lies and is moved into the magnet bore of the MRI system. *From Ridgway, J.P., 2010. Cardiovascular magnetic resonance physics for clinicians, part 1. J. Cardiovasc. Magn. Reson. 12, 71.*

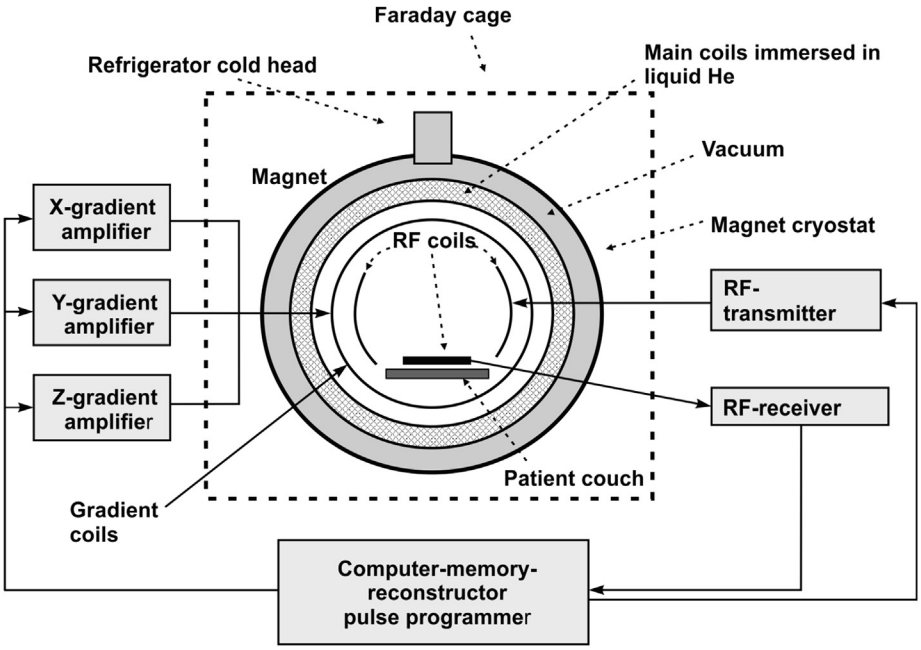

FIGURE IX.16 Schematic of the major components of the MRI scanner. *From McRobbie, D.W., 2014. Fundamentals of MR imaging, In: Anders Brahme (Ed.-in-Chief), Comprehensive Biomedical Physics, Magnetic Resonance Imaging and Spectroscopy, vol. 3. Elsevier, pp. 1–19; reprinted with permission © Elsevier 2014.*

differ among the protons within the body of the patient, because of the spatially variant magnetic field that the protons experience as a function of their location within an organ of the human body. Thus the RF receiver picks up varying RFs according to proton locations in the patient's body. The interconnections of the various components required for the operation of an MRI scanner are illustrated schematically in Fig. IX.16.

Because the organs of the patient have volume and are located at various depths in the body, the numerous spinning and precessing protons of water molecules within the organs will precess at various frequencies depending on the strength of the magnetic field where the protons are located within the body organs. Thus the variable RFs that the protons absorb depend on their depth or position within the organs of the patient, and the RFs they emit upon deexcitation permit the construction of an image by computer from the positional information.

MRI scanners are used in the tens of thousands worldwide in clinics and hospitals for medical diagnosis, cancer and other disease staging, and the evaluation of conditions following treatment. Images are generated as two-dimensional slices or even in three dimensions. An example of three-dimensional images is provided in Fig. IX.17. In the figure, a possible cardiovascular obstruction is identified (see blue arrow in Fig. IX.17B). Also the time-resolved images illustrate how the arteries and veins leading to and from the heart, as well as the heart itself, change in volume. These images were constructed with the aid of an MRI contrast agent containing gadolinium. Contrast agents are provided when needed to patients orally or intravenously prior to MRI scanning. A contrast agent shortens the relaxation times of protons in tissues where they are present; and the water protons in different tissues react differently to contrast agents and exhibit varying relaxation times, enhancing imaging contrast. Gadolinium-based contrast agents are applied to patients in chelated form, which allows the gadolinium to interact with neighboring proton nuclei of water molecules while preventing their absorption into the body, and ensures they are excreted rapidly from the body (Krishnamurthy, 2011).

A significant advantage of MRI over X-ray imaging is that the relatively low frequencies and long wavelengths of RFs possess low photon energies (10^{-6}–10^{-7} eV). Ionization of organic molecules requires energy in the range of 1–10 eV. Thus MRI of the human body causes minimal cellular damage. On the other hand, X-rays have a much shorter wavelength with higher photon energies in the range of 10^{4}–10^{5} eV. As noted by McRobbie (2014), ionization does not occur during MRI scanning.

RICHARD P. FEYNMAN (1918–1988)

Richard Phillips Feynman was born in New York City on 11 May 1918 in a Jewish family; although neither he nor his parents were in any way religious. His father, Melville Arthur Feynman, arrived in the United States in 1895 from Minsk,

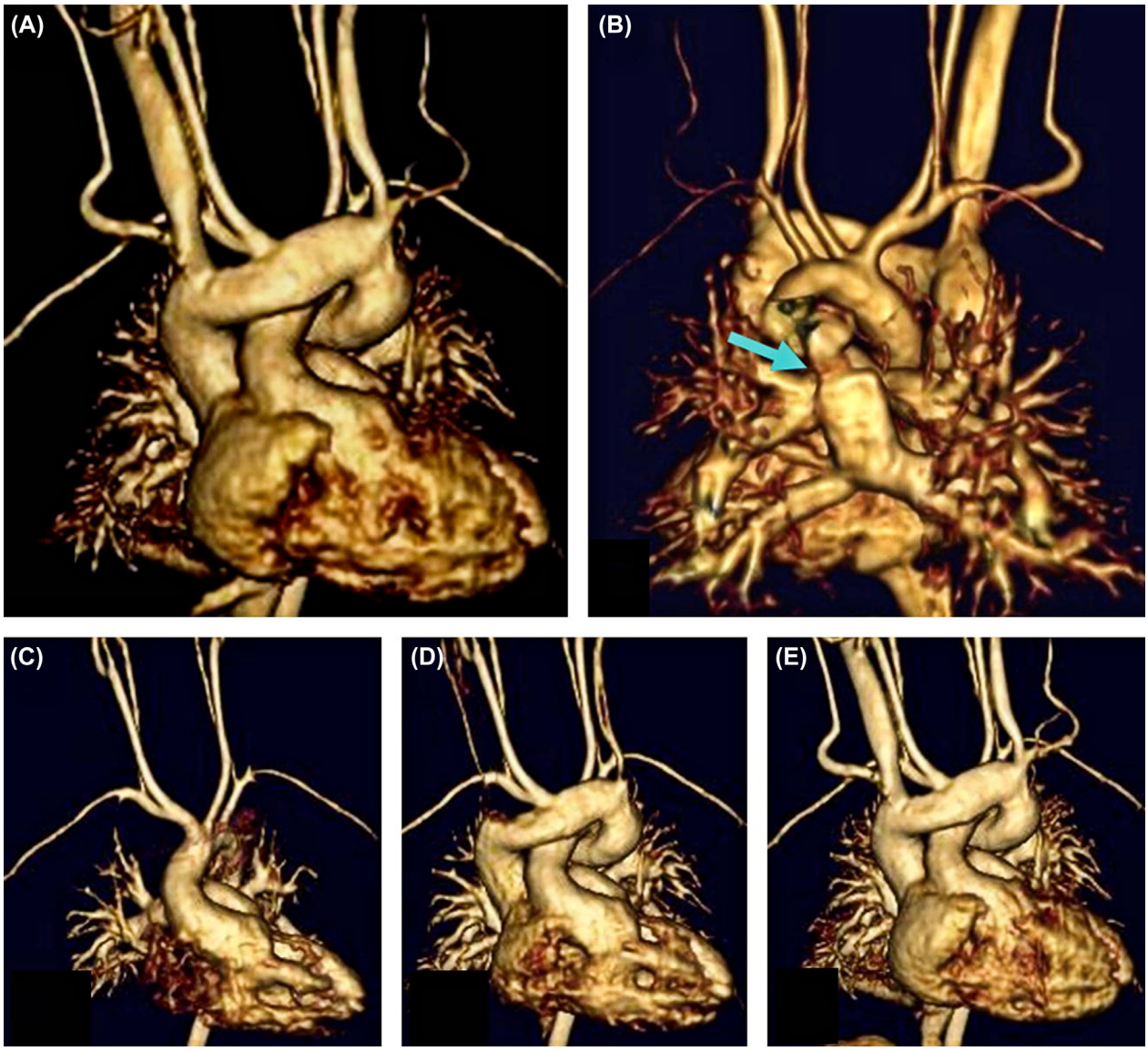

FIGURE IX.17 Time-resolved cardiovascular MRI angiography in a neonate. (A, B): anterior and posterior views of a three-dimensional volume-rendered MRI angiography showing the anomalous vertical vein draining into the left innominate vein, with associated obstruction caused by mass effect from the left mainstem bronchus (*arrow* in B); (C–E): anterior projections from successive dynamics of the time-resolved MRI angiography showing successive filling of the aorta and pulmonary artery, pulmonary veins, and the systemic veins on C, D, and E, respectively, following a lower-extremity intravenous injection of contrast. *From Krishnamurthy, R., Lee, E., 2011. Congenital cardiovascular malformations: noninvasive imaging by MRI in neonates. Magnetic Reson. Imag. Clin. North Amer. 19 (4), 813–822, reprinted with permission from Elsevier © 2011.*

Byelorussia, as a child with his parents; and his mother, Lucille Phillips, was born to German parents who had immigrated to America at a young age.

Richard Feynman's autobiography, which he submitted at the time of receiving the Nobel Prize in Physics in 1965, was one of the shortest biographies ever provided by a Nobel Laureate, which may reflect the fact that he shunned the publicity. Much of the information provided on his biography is taken from *Feynman's Biographical Memoirs of Fellows of the Royal Society*, written by Jagdish Mehra (2002).

Richard Feynman shared the Nobel Prize in Physics in 1965 with Sin-Itiro Tomonaga and Julian Schwinger for, in the words of the Nobel Committee, "their fundamental work in quantum electrodynamics, with deep-plowing consequences for the physics of elementary particles."

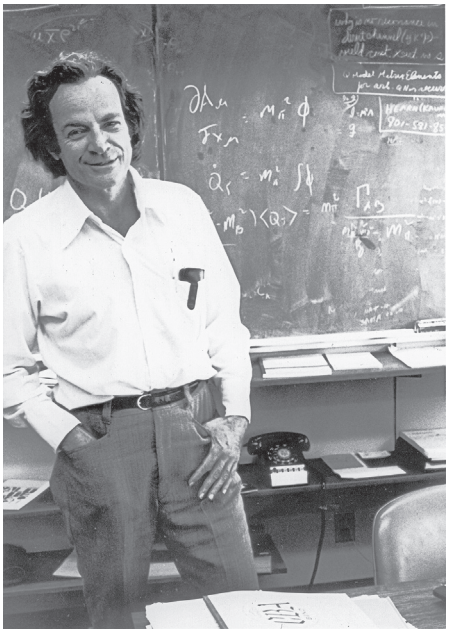

Richard P. Feynman standing in a classroom by a blackboard
With permission; courtesy of AIP Emilio Segre Visual Archives, Physics Today Collection

Richard Feynman was a gifted scientist and mathematician: at the age of 13 he taught himself calculus through reading. In his senior year at Far Rockaway High School in New York City he had an excellent physics teacher, Abram Bader, who recognized Feynman's talents. Jagdish Mehra (2002) relates that he received a letter from Bader in 1988, the year that Feynman died, describing his experiences with Feynman. Abram Bader was informed in advance by Feynman's chemistry teacher that Feynman was a gifted student, and Bader found this to be true on the first day of physics honors class. Bader explained that Feynman would become restless and sometime noisy and disruptive, because he was already very knowledgeable on the material presented in class. Thus Bader gave Feynman a book on advanced calculus (Woods, 1932). Young Feynman found the book very interesting, with mathematics that he learned to enjoy and even used to create games. He appreciated learning advanced mathematics on his own in high school, and was grateful to his teacher for giving him this attention. Mehra (2002) relates that Richard Feynman went through the entire book in a month, although it took a whole year for his teacher to master the subject.

Upon graduation from high school, Feynman entered the Massachusetts Institute of Technology, graduating with a BSc in physics in 1939. He had applied for admission to other universities, including the City College of New York and Columbia University; but Columbia had denied him admission—as related by Feynman, it had something to do with the filling of the Jewish quota for the freshman class (Mehra, 2002). At MIT he published his first paper in *Physical Review* with Professor Manuel Sandoval Vallarta (Vallarta and Feynman, 1939) on the scattering of cosmic rays by stars of a galaxy (described in Hall of Fame, Part VI of this book). After graduation from MIT, Feynman entered graduate school with a research assistantship under Professor John Archibald Wheeler. As described by Mehra (2002), Wheeler gave Feynman problems, and Feynman would solve them. However, when Wheeler gave him a problem that he could not solve, Feynman would begin to think about quantum electrodynamics (QED), which he had studied at MIT. QED is defined as a quantum field theory of the interactions of charged particles with electromagnetic fields, mainly the interactions of electrons and photons (Sundaresan, 2001). It describes mathematically how charged particles interact via the exchange of photons as virtual particles—that is, particles that are not actually detected. Thus a charged particle is scattered when it encounters the field of another similarly charged particle, and the scattering is in response to their fields via the exchange of photons. The photons are considered virtual because they are not detected; however, the electromagnetic field of a charged particle is detected by the reaction or response of another charged particle. Likewise, photons are the carriers of the electromagnetic force that maintains the electron orbitals at a distance from the atomic nucleus. The relatively large distance between the atomic nucleus and the orbital electrons of an atom is not "empty space"; rather the

space is filled with photons as the electromagnetic force carriers maintain the atomic nucleus and its electrons together. Feynman's first seminar as a graduate student at Princeton was attended by some of the most distinguished physicists and mathematicians of the time, including Albert Einstein, John von Neumann, Wolfgang Pauli, and Eugene Wigner, who chaired the seminar.

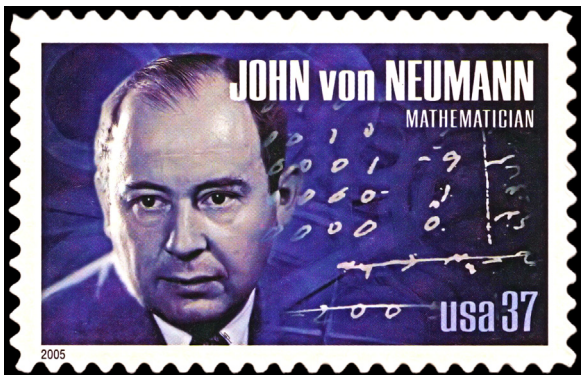

John von Neumann (1903–1957)
John von Neumann was a Hungarian and naturalized American mathematician, physicist and polymath. He was a key member of the Manhattan Project and of the Institute for Advanced Study at Princeton. He made significant contributions to development of game theory and quantum mechanics. Also, von Neumann was honored with the Enrico Fermi Award in 1956 for his scientific contribution to the theory and design of the digital computer; and his foresight into the role of computers in the control of atomic energy and in the advancement of the arts and sciences

Before Feynman could complete his PhD studies at Princeton, he was recruited in 1941 by Robert R. Wilson to work on the atomic bomb project (Mehra, 2002) at the Office of Scientific Research and Development. This body was created on 28 June 1941 to oversee all scientific research for the war effort under the direction of Vannevar Bush, who reported directly to President Franklin Delano Roosevelt. Feynman's doctoral dissertation advisor, John Archibald Wheeler, went to work on the bomb project at the Metallurgical Laboratory in Chicago with Eugene Wigner (Mehra, 2002). While working on the project, Feynman took a few weeks off to complete his degree and was awarded a PhD at Princeton in 1942.

Upon his return to the bomb project, all the recruited staff from Princeton moved to Los Alamos for full-time work on the development of the atomic bomb as a part of the Manhattan Project. Like many of his colleagues at Los Alamos, Feynman agreed to work toward the development of the A-bomb out of fear that Nazi Germany, where nuclear fission was discovered, could develop the bomb first. Richard Feynman was assigned to Hans Bethe's theoretical division. Bethe highly respected Feynman as a physicist and mathematician, and a person who was direct, straightforward, and trustworthy, so made him group leader. Feynman and Bethe developed the Bethe-Feynman formula for calculating the yield of a fission bomb, based on prior information provided by Robert Serber. The director of the Manhattan Project, J. Robert Oppenheimer, instructed his protégé Serber to give a series of lectures to the arriving scientific staff at Los Alamos, covering all that was then known about nuclear fission and the technology for the development of an atomic bomb, including mathematical formulas, graphs, and drawings. The lectures were carefully planned at a secret summer seminar at Berkeley attended by Oppenheimer, Serber, Hans Bethe, and Edward Teller. Robert Serber's lectures gave all newly recruited staff the information they needed to know: the purpose of the project, the basic background from which to proceed, and a clear meaning as to why they would be enclosed in a secret and fenced community with restricted travel. Edward Condon, associate director of the laboratory at Los Alamos, took notes during the lectures, and he and Serber prepared mimeographed copies for distribution as secret preparatory material for newcomers to the laboratory. These lectures remained classified material under the official Los Alamos Technical Report (LA-1) until their complete declassification and release in 1965. They are available as a book entitled *The Los Alamos Primer*, published by University of California Press in 1992 (Serber, 1992).

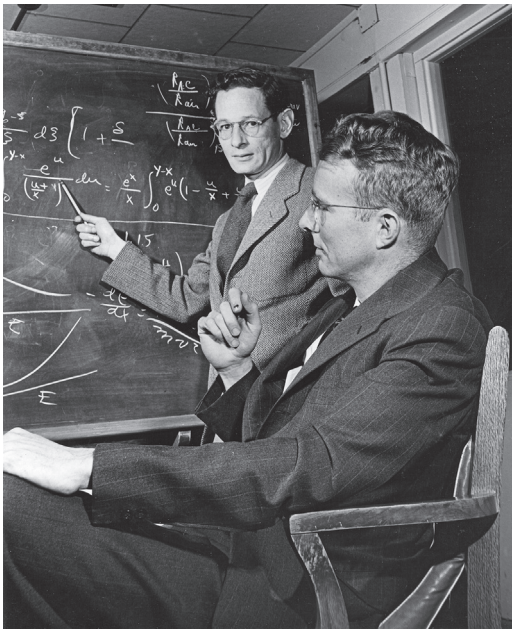

Robert Serber (standing at blackboard) and Luis W. Alvarez (seated) discussing calculations
Printed with permission, courtesy of the AIP Emilio Segre Visual Archives

At Los Alamos Feynman was successful; but bored in the isolated environment of the secret labs. He was alone. His wife, Arline Greenbaum, was suffering in a clinic in Albuquerque with tuberculosis, and could not join him. He and others at Los Alamos visited her. Mehra (2002) relates that for enjoyment Feynman would put his mathematical skills to work to decipher the combinations to locks where the various groups stored their papers. He used combinations of numbers corresponding to various mathematical constants or variations of these, such as $\pi = 3.14159$ or the base to the natural logarithm $e = 2.71828$. He was very successful in opening many locked papers and left intriguing notes for staff informing them of a breach in their security. Some were alarmed, at first suspecting a spy in their midst.

Feynman's wife Arline succumbed to her illness and died in the summer of 1945. In his biographical memoir, Mehra (2002) recounts that Feynman had to go to Albuquerque hastily to take care of Arline's burial, and borrowed Klaus Fuchs's car. It was discovered years later that Fuchs, a German-born British physicist, was a spy, and passed secret information to the Soviet Union from 1942 to 1949 (Rhodes, 1986). He confessed in 1950 to passing nuclear secrets to the Soviet Union on the Manhattan Project's atomic and fusion bomb work up to 1946, which was the year he returned to the UK. He served nine years in a UK prison, was stripped of his British citizenship, and emigrated to the communist German Democratic Republic.

After the war, Richard Feynman rejected an offer by Princeton University and followed Hans Bethe to Cornell University, where Feynman was appointed assistant professor after recommendations by Bethe and Robert F. Bacher to R. C. Gibbs, chair of the Department of Physics. Robert Bacher was professor of physics at Cornell, and worked closely with Oppenheimer throughout the Manhattan Project at Los Alamos. Feynman taught theoretical physics at Cornell in 1945−1950. During his time at Cornell he received offers from the Institute for Advanced Study at Princeton, which he rejected using the pretext that there were no teaching opportunities and he enjoyed lecturing when not occupied with research (Mehra, 2002). They then offered him a joint teaching and research position with Princeton University. He did not accept this or other offers from the University of California at Los Angeles and Berkeley, but the offers spurred increases in his salary and stature at Cornell with a promotion to associate professor. He eventually accepted a position at the California Institute of Technology (Caltech) in 1950, and remained there for the rest of his career.

In 1947 two important developments were reported at the Shelter Island Conference on Problems of Quantum Mechanics and the Electron: the finding of the "Lamb shift," named after Willis E. Lamb, who reported the finding with Robert C. Retherford at Columbia University (Lamb and Retherford, 1947); and the accurate measurement of the

anomalous magnetic moment of the electron by Polykarp Kusch and Henry M. Foley (Kusch and Foley, 1948), also at Columbia University. The Lamb shift is a small difference in two energy levels that the atomic electron orbitals of the hydrogen atom may possess; and the anomalous magnetic moment of the electron was the result of an accurate measurement of the electron magnetic moment, leading to the finding that its magnetic moment was higher than expected. This was explained by Ramsey (2008) in his biographical memoir of Kusch: "in 1947, when many theorists believed that the electron magnetic moment was exactly one Bohr magneton, Kusch and Henry M. Foley, by magnetic resonance experiments on different atomic states of gallium, indium and sodium, showed that the magnetic moment of the electron was 1.00119 ± 0.00005 Bohr magnetons…" Willis E. Lamb and Polykarp Kusch jointly shared the Nobel Prize in Physics in 1955 for their findings. The discoveries of Lamb and Kusch and their coworkers sparked much research in the field of QED, culminating in the joint award of the Nobel Prize in Physics in 1965 to Richard Feynman of Caltech, Julian Schwinger of Harvard University, and Sin-Itiro Tomonaga of Tokyo University of Education (now Tsukuba University). As explained by Professor Ivar Waller of the Nobel Committee for Physics in the Nobel presentation speech on December 11, 1965:

> *For the hydrogen atom, which has only one electron and consequently is the simplest atom to investigate theoretically, the calculation of the motion of the electron in the electric field of the nucleus led to results of such accuracy that 20 years elapsed until any error of the theory could be found experimentally. This occurred, however, in 1947 when Lamb and his collaborator Retherford discovered that some energy levels of hydrogen which should coincide theoretically were in fact somewhat shifted relative to each other.*
>
> *One important result of the work of this year's Nobel Prize winners Sin-Itiro Tomonaga, Julian Schwinger and Richard Feynman was the explanation of the Lamb-shift. Their work is, however, much more general and of deep general significance to physics. It has explained and also predicted several important phenomena. It is the continuation of some investigations performed in the late 1920's in order to find the general quantum mechanical laws according to which the atoms and in particular the electrons give rise to electromagnetic fields,* e.g. *emit light, and are influenced by such fields…*
>
> *Almost simultaneously with the discovery of the Lamb-shift another peculiarity was found by Kusch and his collaborator Foley, which made it clear that the magnetic moment of the electron is somewhat larger than had been assumed before…*
>
> *Schwinger had developed the formalism of the new quantum electrodynamics in several fundamental papers using partially methods similar to those of Tomonaga. He has also made this formalism more useful for practical calculations.*
>
> *Feynman used more radical methods for solving the problems of quantum electrodynamics. He created a new formalism which he made very useful for practical calculations by introducing a graphical interpretation called Feynman diagrams, which have become an important feature of modern physics. In the description used by Feynman the electromagnetic field did not any more appear explicitly. His description has been very valuable in elementary particle physics where it is necessary to consider besides the electromagnetic also other interactions.*
>
> *When considering the truth of quantum electrodynamics in its new form one has first of all to realize the extraordinary success of this theory in giving results in agreement with the experiments. For the Lamb-shift and for the anomalous part of the magnetic moment of the electron the agreement is within some parts in one hundred thousand respectively in a million and no disagreement has yet been found. Quantum electrodynamics is indeed one of the most accurate of all the theories of physics.*
>
> From Nobel Prize in Physics 1965—Presentation Speech; printed with permission © The Nobel Foundation 1965.

The famous Feynman diagrams described in Professor Waller's Nobel presentation speech were explained in detail by Feynman in one of his classic papers on calculations in QED (Feynman, 1949). The diagram he used to describe his calculations on the fundamental interaction between charges (ie, two electrons) in QED is illustrated in Fig. IX.18. Richard Feynman introduced these diagrams as a means of depicting, through sketches, the interactions among nuclear particles as shorthand for the equations that are used to put the interactions into more complex mathematical terms. In Fig. IX.18, Feynman (1949) used numbers 1, 5, and 3 to identify the coordinates of one electron, which he called particle a, and numbers 2, 6, and 4 to identify the coordinates of the second electron, particle b. He defined the Schrödinger wave function at a given time to be $\psi(x_a, x_b, t)$ of the coordinates x_a and x_b of particles a and b at time t. He then defined the term $K(x_a, x_b, t; x'_a, x'_b, t')$, written as $K(3,4; 1,2)$ according to Fig. IX.18, as the amplitude that particle a at x'_a at time t' will get to x_a at time t, while particle b at x'_b at time t' gets to x_b at time t. Feynman (1949) used this notation in his calculations on the interactions of electrons at short distances. The notations γ_μ at coordinates 5 and 6 of particles a and b of Fig. IX.18 are referred to by Feynman as Dirac matrices, where a virtual quantum (photon) is emitted by one particle and absorbed by the other.

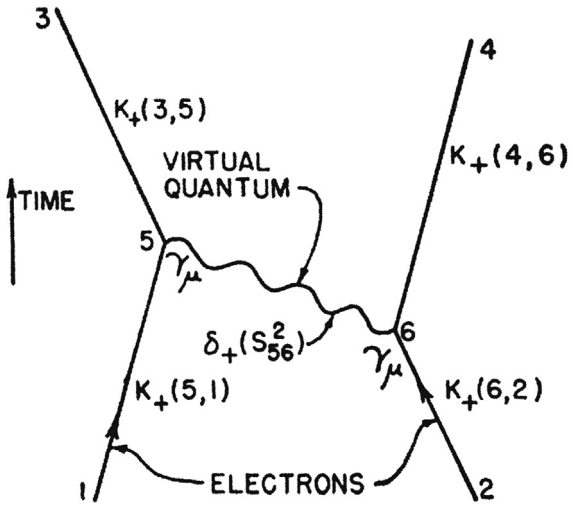

FIGURE IX.18 The fundamental interaction: the exchange of one quantum between two electrons. *From: Reprinted with permission from Feynman, R.P., 1949. Space-time approach to quantum electrodynamics. Phys. Rev. 76 (6), 769–789 © American Physical Society, http://dx.doi.org/10.1103/PhysRev.76.769.*

The electromagnetic force exists between charged particles, and will become manifest when the particles collide. For example, two electrons when they come into close proximity or collide will repel each other. The force exerted on the electron by another to cause its repulsion is carried by a virtual photon that is exchanged from one electron to the other. This electromagnetic interaction results in the absorption of the photon by an electron, providing it with momentum to be repelled. The electron emitting the photon undergoes recoil. Such an electromagnetic interaction of two electrons is illustrated by the Feynman diagrams in Figs. IX.18 and IX.19A. Feynman diagrams show particle interactions in coordinates of space and time. The axes are not quantitative—that is, the lengths of the lines or spacing between particles are not measures of relative time or distance. Particles are illustrated by solid lines, with arrows giving the particle direction. An arrow in the opposite direction indicates an antiparticle, and not a particle moving in the opposite direction. Virtual particles, ie, particles that do not appear outside the region of exchange, are illustrated as waves (for photons) or dashed lines for particles with a rest mass. Arrows are not used generally with the virtual particles. The Feynman diagrams of the electron collision illustrated in Figs. IX.18 and IX.19A show the transfer of a photon from one electron to another, and both electrons continue on in time. The interaction illustrated is simply a transfer of energy from one electron to another. The Feynman diagrams in Fig. IX.19B and C illustrate other electromagnetic interactions—electron annihilation and pair

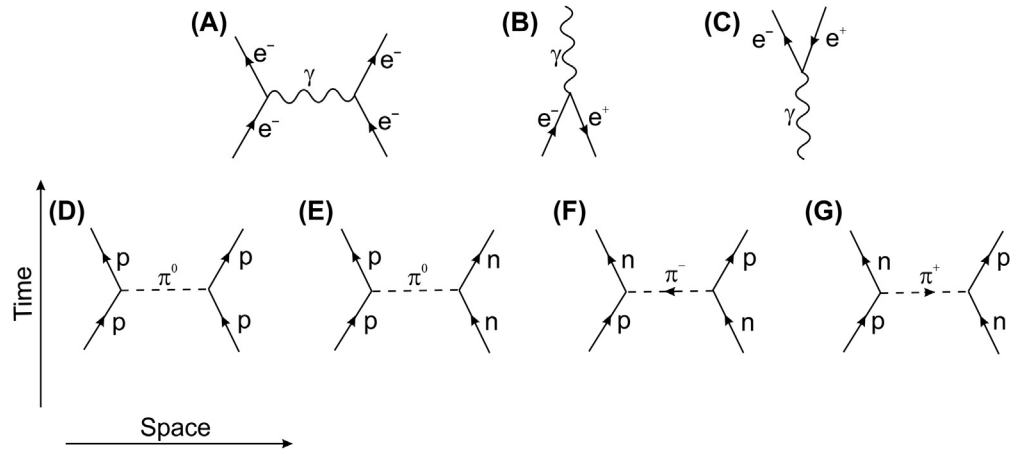

FIGURE IX.19 Feynman diagrams for some electromagnetic interactions: (A) Electron collision, (B) Electron annihilation, (C) Electron pair production. Feynman diagrams for Yukawa's postulated strong interactions involving π-mesons in the atomic nucleus: (D) π^0 exchange between protons, (E) π^0 exchange between a proton and neutron, (F) a negative meson, π^-, is absorbed when a proton jumps to the neutron state, and (G) a positive meson, π^+, is emitted when the proton changes into a neutron.

production, respectively. In the electron annihilation, an electron and its antiparticle (positron) combine and emit a quantum of electromagnetic radiation; while in pair production a quantum of electromagnetic radiation creates an electron and its antiparticle. Notice that the arrows pointing downward in Fig. IX.19B and C represent the antiparticle. A postage stamp issued in 2005 commemorates the life and accomplishments of Richard Feynman, with illustrations of some of his diagrams.

In Feynman's biographical memoir Mehra (2002) relates that after the Nobel award ceremony, Feynman was invited by Victor Weisskopf, then director general of CERN, to give a lecture. Among those attending was Ernst C. G. Stückelberg of the University of Geneva and University of Lausanne, who had made significant contributions to QED which both preceded and overlapped Feynman's work. Mehra (2002) notes that Feynman felt regret that "he himself was covered with glory and Stückelberg walked quietly alone." As a matter of fact most books list Feynman, Stückelberg, Tomonaga, and Schwinger as the four who had made major contributions to QED; however, Nobel Committee rules allow no more than three persons to share a Nobel Prize.

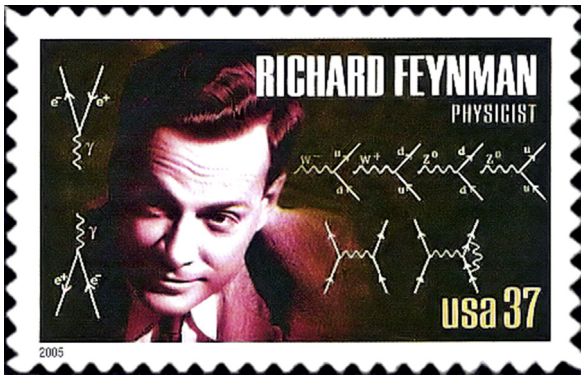

Richard Feynman (1918–1988)

Feynman diagrams illustrating the strong forces mediated by Yukawa's π-meson are illustrated in Fig. IX.19D–G. Fig. IX.19D illustrates protons exchanging a neutral pion, whereby one proton changes into another proton and vice versa. Also a neutron changes into a proton and a proton into a neutron with the exchange of a neutral pion, illustrated in Fig. IX.19E. Negative and positive pions can exchange with protons and neutrons, as illustrated in Fig. IX.19F and G, to change into their counterpart neutron and proton nucleons, respectively.

The postage stamp of Richard Feynman illustrates, in addition to the previously mentioned electron pair production, electron annihilation, and QED, other interesting phenomenon, including the role of the W^- and W^+ bosons as force carriers of the weak interaction in beta decay, and neutral current interactions involving the Z^0 boson. The use of such diagrams by Feynman was met at first with skepticism, but their applications were eventually recognized and currently the diagrams have widespread use. For interesting historical accounts of Feynman's diagrams see Kaiser (2005a) and Weiss (2005). For additional reading on the drawing rules and applications of Feynman diagrams see books by Mattuck (1992), Veltman et al. (1994), and Kaiser (2005b).

Among other significant contributions of Richard Feynman are the atomic theory of superfluid helium and his lectures on physics. Feynman enjoyed lecturing, and was known as "the Great Explainer." He made major contributions to physics education by means of his three-volume book, *The Feynman Lectures on Physics*, which is a compilation of lectures given to undergraduate students at Caltech in 1961–1963 authored by Richard P. Feynman, Robert B. Leighton, and Mathew Sands, originally published by Addison-Wesley in 1964 (see Feynman et al., 2011). This is considered one of the most popular physics texts ever written, having sold over a million copies in English and being translated into several languages. In 2013 Caltech made the book freely accessible to all via the Caltech website, http://feynmanlectures.caltech.edu/.

For further reading on the life and works of Richard Feynman, the reader may peruse comprehensive biographies by Gleick (1992) and Mehra (1994). Also, almost an entire issue of *Physics Today* (see Lubkin, 1989) was devoted to articles on Richard Feynman by persons who knew and worked with him.

Chapter 20

The Atomic Nucleus

Tomorrow, when you are less excited, you can explain it to me.

Sachs (1979)

So said Enrico Fermi to Maria Goeppert-Mayer when she tried with much excitement to explain to Fermi her discovery of a configuration of "magic numbers" of protons or neutrons in the nucleus, which attributed unusual stability to the nucleus regardless of the associated number of other nucleons.

20.1 INTRODUCTION

Ernest Rutherford (1911, 1919, 1920a,b) was the first to discover the atomic nucleus and measure the size of the nucleus of an atom. A detailed account of this work is given Hall of Fame, Part I of this book. In brief, Rutherford bombarded very thin gold foil (4×10^{-5} cm thick) with alpha particles. Most of the alpha particles traversed the gold foil almost as if the foil was not in their path; however, one alpha particle for every 20,000 particles would bounce back from the foil by more than 90 degrees from the direction of travel. Rutherford concluded that within much empty space of the atom there exists a massive central nucleus capable of knocking back the alpha particle to the direction from which it came. Rutherford expressed his reaction to the observed alpha particle back-scattering with the following statement, related by Feather (1940) in a biographical essay a few years following Rutherford's death:

It was quite the most incredible event that ever happened to me in my life. It was almost as incredible as if you fired a 15-inch shell at a piece of tissue paper and it came back and hit you. On consideration, I realized that the scattering backwards must be the result of a single collision, and when I made calculations I saw that it was impossible to get anything of that order of magnitude unless you took a system in which the greater part of the mass of the atom was concentrated in a minute nucleus.

20.2 NUCLEAR RADIUS AND DENSITY

Rutherford utilized his discovery of the scattering of alpha particles by the atomic nucleus to determine the nuclear radius of aluminum. By selecting a metal foil of low Z (aluminum, $Z = 13$) and thus low coulomb barrier to alpha penetration, and applying alpha particles of relatively high energy (7.7 MeV) from a natural source whereby defined alpha particle scattering at an acute angle due to coulombic repulsion would begin to fail, Rutherford (1919, 1920a,b) was able to demonstrate that the distance of closest approach of these alpha particles to the atom center according to Coulomb's law was equivalent to the nuclear radius of aluminum, $\sim 5 \times 10^{-15}$ m or 5 fm (5 fermi).

Since Rutherford's pioneering alpha particle scattering experiment, numerous nuclear scattering experiments have been carried out to measure the size of atomic nuclei, including electron scattering (Jansen et al., 1971; Sick, 1982), electron–proton scattering (Klarsfeld et al., 1986), electron–deuteron scattering (Sick and Trautmann, 1998), and high-energy beam interactions (Tanihata et al., 1985; Suzuki et al., 1999). The radius of an atomic nucleus obeys the general empirical formula

$$R = r_0 A^{1/3} \qquad [20.1]$$

where r_0 is a constant, referred to as the radius parameter, and A is the mass number of the nucleus (Tolhoek and Brussaard, 1954; Elton, 1958; Angeli and Csatlós, 1977). A detailed derivation of Eq. [20.1] is provided by Elton (1958). The value of the radius parameter r_0, was confirmed by Royer (2008) to be 1.22 fm. Obviously the radius of the nucleus will increase with mass number. For a small nucleus, such as the nucleus of ${}^{4}_{2}\mathrm{He}$ (equivalent to an alpha particle), the radius is calculated

Radioactivity: Introduction and History, From the Quantum to Quarks. http://dx.doi.org/10.1016/B978-0-444-63489-4.00020-4
Copyright © 2016 Elsevier B.V. All rights reserved.

to be 1.9×10^{-15} m or 1.9 fm. For larger nuclei, such as $^{27}_{13}$Al, $^{197}_{79}$Au, and $^{235}_{92}$U, the nuclear radii calculate to be 3.6, 6.9, and 7.4 fm, respectively.

Treating the nucleus as a sphere permits the calculation of the nuclear volume, and from the mass of the nucleus we can calculate the nuclear density ρ_N as

$$\rho_N = \text{mass/volume} = m_n A \Big/ \frac{4}{3}\pi R^3 \qquad [20.2]$$

where m_n is the mass of a nucleon (proton or neutron), A is the mass number, and R is the nuclear radius. The mass of either nucleon (the proton or neutron) may be used, as the two nucleons are very similar in mass and may be considered here as equal in mass, when only three significant figures are needed, namely 1.67×10^{-27} kg. Substituting $r_0 A^{1/3}$ for R in Eq. [20.2] gives

$$\rho_N = m_n \Big/ \frac{4}{3}\pi r_0^3 \qquad [20.3]$$

The value of the nuclear density calculated according to Eq. [20.2] or [20.3] gives the value of $\rho_N = 2.3 \times 10^{17}$ kg/m^3. Treating the nucleus as a sphere facilitates the density calculation as a good estimate, as available in current textbooks; however, most nuclei are not spherical and some may exhibit oscillations such as depicted by the liquid drop model of the nuclei. Some nuclei described by Gould et al. (2004) exhibit football-shaped quadrupole deformations and even pear-shaped octupole deformations (Krappe and Wahsweiler, 1967; Vogel, 1967, 1968; Aponik Jr. et al., 1970; Cline, 1993). Gould et al. (2004) describe the interior of a large nucleus as uniform (0.17 nucleons/fm^3), but the density falls off smoothly at the surface of the nucleus, dropping from 90% to 10% of the interior density over a distance of ~2.5 fm.

The density of the nucleus is extraordinarily high when compared with elements and materials consisting of atoms. For example, the atomic nucleus is 2.0×10^{13} times the density of lead (11.3×10^3 kg/m^3) or 1.2×10^{13} times the density of depleted uranium (19.1×10^3 kg/m^3). While the density of the nucleus is amazingly high, the nucleus consists of closely packed nucleons, and thus the nucleons themselves and even subnuclear particles, particularly leptons, would even have higher densities.

Subnuclear particles are classified into two groups, leptons and hadrons. The word leptons comes from the Greek *lepto*, meaning "refined" or "thin." **Leptons** are particles with no apparent substructure and are thus considered to be truly elementary or point particles; examples are electrons, muons, and their respective neutrinos and quarks. Leptons, with the exception of quarks, participate in electromagnetic and weak interactions. **Hadrons**, on the other hand, are more complex in subnuclear structure and participate in the strong nuclear force. Hadrons are classified into two groups, namely the **mesons** containing two quarks (eg, pion and kaon), and the **baryons** (from the Greek *barys*, meaning "heavy"), which are of higher mass and contain three quarks (eg, proton and neutron). The role of mesons as particles that mediate the strong nuclear force between the nucleons is discussed in the next section.

The high density of the nucleus and its constant value from nuclide to nuclide underscores the importance of a strong short-range nuclear force that exists between the nucleons (ie, protons and neutrons), keeping them closely packed regardless of the repulsive forces of the positively charged protons or the Z/N ratios of the nucleus among the thousands of nuclides that exist.

20.3 NUCLEAR FORCES

In the 1930s question arose concerning the force that was capable of holding the protons and neutrons together in the nucleus. It was unusual to find that the like positive charge of the protons, together with neutrally charged neutrons, did not repel each other, but rather were held tightly together into a very dense nucleus. It was expected that the force holding the nucleons together would be strong. Nobel Laureate Hideki Yukawa (1935, 1949) first postulated the strong force between nucleons. Before doing this, Yukawa understood that charged particles would interact through the exchange of photon particles. He noted that such a force, known as the electromagnetic force, would become manifest when the particles collide. For example, electrons would interact via the exchange of virtual photons, as illustrated by the Feynman diagram of Fig. 20.1 (A convenient way to illustrate the interactions and exchange forces between the elementary particles is with Feynman diagrams, which were devised by Nobel Laureate Richard Feynman (1918–1988). When he was a young scientist, he introduced the diagrams as a means of depicting, through sketches, the interactions among nuclear particles as shorthand for the equations that are used to put the interactions into more complex mathematical terms. Feynman diagrams show particle interactions in coordinates of space and time. The axes are not quantitative—that is, the length of the lines and spacing between particles are not measures of relative time or distance. Particles are illustrated by solid lines with

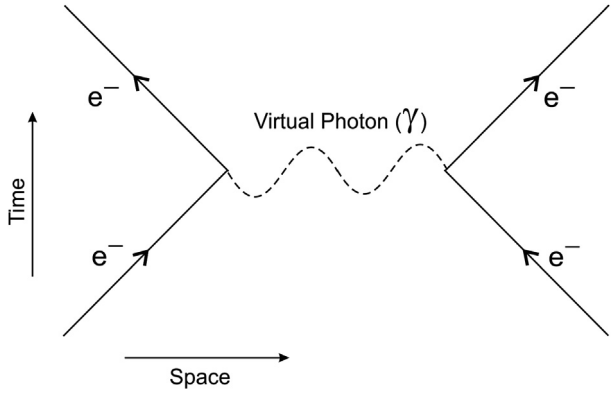

FIGURE 20.1 Feynman diagram illustrating the photon as a particle that mediates the electromagnetic force between two electrons. The electromagnetic interaction results in the absorption of the photon particle by an electron, providing it with momentum to be repelled. The electron emitting the photon undergoes recoil. The photon is illustrated as a dashed wave. It is referred to as virtual photon, because it is emitted and absorbed without being detected.

arrows giving the particle direction, whereas the arrows for antiparticles are drawn to point in the opposite direction. Virtual particles are illustrated as dashed waves for particles with zero rest mass (ie, photons or gluons) and dashed straight lines for particles with a rest mass.) in Fig. 20.1. Yukawa explained the strong force between nucleons by proposing a new particle, which would mediate the strong force between the nucleons. He predicted that the new particle would have a mass inversely proportional to the force between the nucleons; and that the mass of the particle would be intermediate of the proton and electron masses ($\sim 200 \times$ the electron mass). The new particle was named the meson, taken from the Greek *meso*, meaning "middle." The prediction of Yukawa was verified by the discovery of the π meson or pion by Giuseppe Occhialini and Cecil F. Powell (Occhialini and Powell, 1947, 1948). The strong force keeping the nucleons together is mediated by the exchange of π mesons between the nucleons. The pion is the carrier of Yukawa's nuclear force. It is found in three charge states, π^+, π^-, and π^0. They have the mass predicted by Yukawa and are unstable, eg, the π^+ has a mass of 139.5 MeV/c^2 and a mean lifetime of 2.6×10^{-8} s (Sundareson, 2001). The mediation of the strong force between a neutron and a proton in the nucleus is illustrated by the Feynman diagram in Fig. 20.2. The diagram illustrates a proton converting into a neutron and a neutron converting into a proton, and in the process a π^+ is exchanged between the two nucleons.

Pion exchange between nucleons, as the particle mediating the strong force, is explained on the basis of the subnuclear structure of the proton, neutron, and meson. The 1969 Nobel Laureate in Physics, Murray Gel-Mann (1964) and George Zweig (1964a,b) independently proposed the idea of a substructure to mesons and baryons, now universally referred to as quarks, which would possess quantum numbers and fractional charge. The mesons (eg, pion and kaon), which are of intermediate mass between that of the electron and proton, contain two quarks; whereas the baryons (eg, proton, neutron,

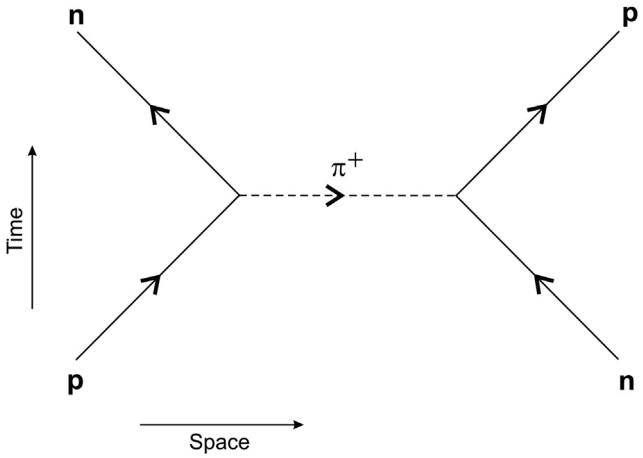

FIGURE 20.2 A Feynman diagram illustrating the mediation of the strong nuclear force between nucleons in the nucleus. A neutron (lower left) is transformed into a proton (upper left), and a proton (lower right) is transformed into a neutron (upper right) via the intermediary pi meson.

TABLE 20.1 Quark Compositions and Properties of Quark Components of Pi Mesons and Nucleons

Particle	Quark Composition	Properties of Quarks			
		Name[a]	Symbol	Charge	Mass
Mesons					
π^+	$u\bar{d}$	Up	u	$+\frac{2}{3}e$	2.3 MeV/c^2
π^-	$d\bar{u}$	Down	d	$-\frac{1}{3}e$	4.8 MeV/c^2
π^0	$u\bar{u}$, $d\bar{d}$	Antiup	$\bar{u}$	$-\frac{2}{3}e$	$m_{\bar{u}} = m_u$
		Antidown	$\bar{d}$	$+\frac{1}{3}e$	$m_{\bar{d}} = m_d$
Nucleons/Baryons					
P	uud				
n	udd				

[a]*Other quarks exist, such as the strange (s), charmed (c), bottom (b), and top (t) quarks, which are component quarks of other mesons and baryons.*

lambda, etc.), which are of higher mass, contain three quarks. The quark compositions of pi mesons (pions) and nucleons (proton and neutron), and the properties of the quarks are provided in Table 20.1. In the table it is seen that the π^+ contains an up quark (u) with charge of $+\frac{2}{3}e$ and an antidown $(\bar{d})$ quark with charge of $+\frac{1}{3}e$, yielding a total charge on the π^+ of $+1$. The π^- consists of a down quark (d) of charge $-\frac{1}{3}e$ and antiup quark $(\bar{u})$ of charge $-\frac{2}{3}e$, yielding an overall particle charge of -1. The π^0 is a mixture or superposition of $u\bar{u}$, $d\bar{d}$ quark pairs, referred to as mixing of quark pairs with overall neutral charge.

The proton, neutron, and all of the baryons, which are particles of higher mass than the mesons, contain three quarks. The quark content of the proton, as listed in Table 20.1, is two up quarks and one down quark (uud), with respective charges of $+\frac{2}{3}e$, $+\frac{2}{3}e$, and $-\frac{1}{3}$ e or a total charge of $+1$; whereas the neutron contains two down quarks and one up quark (udd), with a total charge of zero.

Quarks possess another property called color or color charge. The property of color or color charge has no relation to visible radiation as we see color; rather, color charge is a quantum number and source of force that quarks and antiquarks possess. Color charge was proposed by Oscar Wallace Greenberg (1964) at the University of Maryland as a quantum number; and proposed as a source of force between quarks by Mo-Young Han at Duke University and Yoichiro Nambu at the University of Chicago (Han and Nambu, 1965). To satisfy the Pauli exclusion principle stating that no two particles can exist in the same energy or quantum state, the concept of color charge was introduced as a quantum state and force between quarks. Three color-charge quantum states carried by quarks are red, blue, and green; and those carried by antiquarks are antired, antiblue, and antigreen. In the baryons, all of which possess three quarks such as the proton (uud) and the neutron (udd), there are three quarks with color charge, red, blue, and green. Quarks of different color charge possess an attractive force between each other, whereas quarks of like color repel each other. Mesons, which possess only two quarks, a quark and antiquark (see Table 20.1), display red and antired, blue and antiblue, or green and antigreen quantum states. There is an attractive force between a quark of a given color and its anticolor quantum state in mesons.

There are yet other particles in addition to quarks, called gluons, which exist in mesons and baryons. A gluon is a field particle like the electromagnetic photon, which has zero rest mass. Gluons differ from photons in that they interact directly with quarks and with each other; and, similar to quarks, they carry a color-charge quantum state. Quarks emit and absorb gluons. When a quark either emits or absorbs a gluon, the quantum state of the quark changes and thus the color charge of the quark also changes. The process of emission and absorption of gluons by quarks, which is discussed subsequently, is part of the mechanism by which the strong nuclear forces keep the protons and neutrons closely packed in the atomic nucleus. The force that exists between quarks of different quantum color states is called color force; and the theory that these forces play in the strong interactions is called quantum chromodynamics.

In summary, mesons mediate the strong forces between the protons and neutrons in the nucleus, and it is the energy exchange or quantum state changes between quarks and gluons of the mesons and nucleons that enable the strong nuclear forces to hold the protons and neutrons together in the nucleus. An example of a process whereby the strong nuclear forces between the nucleons come into play is illustrated by the Feynman diagram in Fig. 20.3. The figure illustrates the involvement of quarks and gluons in the transformation of a proton into a neutron and a neutron into a proton via the

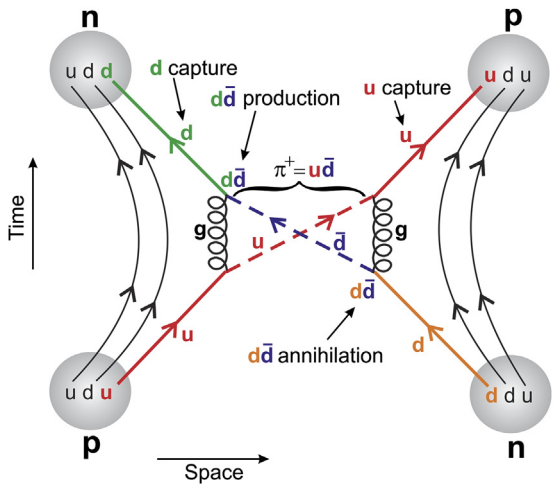

FIGURE 20.3 A Feynman diagram illustrating the mediation of a π^+ meson in the strong nuclear force between a proton and a neutron in the nucleus with the interaction of quarks and gluons. An up quark (u, *colored red*) in the proton on the lower left of the figure emits a gluon (g), illustrated by a helice in the left center of the figure, resulting in pair production of a $d\bar{d}$ pair. The down quark (d, *colored green*) is captured (*green line*), changing the proton on the lower left to a neutron (upper left). The antidown quark ($\bar{d}$, *colored purple*) created in the pair production is annihilated by a down quark (d, *colored brown*) of the neutron at the lower right of the figure. The *purple arrow* of the antidown quark points in the opposite direction, because it is an antiparticle; and, according to Feynman rules, antiparticles are identified by arrows in the opposite direction. The $d\bar{d}$ annihilation results in the destruction of the down quark of the neutron on the lower right with the emission of a gluon (g, *helice*) in the right center of the figure; and the up quark (u, *red colored*) is captured by the neutron on the lower right, converting it into a proton on the upper right of the figure.

mediation of a pi meson (π^+). Fig. 20.3 is an expanded diagram of that in Fig. 20.2 illustrating the involvement of the π^+ meson in the strong interaction between protons and neutrons in the atomic nucleus.

The mass of the nucleons as well as that of the mesons arises from the interaction of their quarks with the gluon field particles. Because gluons have a zero rest mass, the creation and absorption of gluons are a constant process in the nucleons attributing mass to the nucleons. As described by Gould et al. (2004), the mass of the nucleons comes from the interaction of the quarks with the nucleon field; and the nucleon is described as consisting of a core of three quarks confined within a sphere of radius $\sim$0.5−1.0 fm. Surrounding the core is a cloud of pions (pi mesons), which are themselves composed of quark−antiquark pairs.

The range of the strong nuclear force is very close to that of the radius of the nucleon core. We can use the uncertainty principle to calculate the range of interaction of the strong nuclear force mediated by the pi meson or pion. Nobel Laureate Werner Heisenberg published the uncertainty principle (Heisenberg, 1927), which is a basic concept of quantum physics. In terms of energy and time variables, Heisenberg's uncertainty principle can be expressed as

$$\Delta E \Delta t \geq \frac{h}{4\pi} \geq \frac{\hbar}{2} \qquad [20.4]$$

which states that the precision with which we measure the energy of an atomic particle (ΔE) is limited by the time available (Δt) to measure the particle energy, where h is Planck's constant ($h = 6.626 \times 10^{-34}$ J s) and $\hbar$ is a reduced form of Planck's constant ($\hbar = h/2\pi = 1.055 \times 10^{-34}$ J s $= 6.582 \times 10^{-22}$ MeV s). We can accurately calculate the energy of the pion from its mass; and from the Heisenberg uncertainty principle expressed by Eq. [20.4] we can state that the pion would violate the conservation of energy if it lasted for a period of time exceeding

$$\Delta t \approx \frac{\hbar}{2\Delta E} \qquad [20.5]$$

where ΔE is the energy needed to create a pion of mass m_π, defined by Einstein's equation of mass and energy as

$$\Delta E = m_\pi c^2 \qquad [20.6]$$

and Δt is the time it would take for the pi meson to travel from one nucleon to the other (eg, from a proton to a neutron or vice versa). The mass m_π of the π^+ or π^- = 139.5 MeV/c^2. Since the pi meson cannot travel faster than the speed of light, c, its distance (d) of travel is defined as

$$d = c\Delta t \qquad [20.7]$$

Thus the maximum distance that the pi meson could travel is calculated as

$$\begin{aligned} d &= c\Delta t = c\left(\frac{\hbar}{2m_\pi c^2}\right) \\ &= 2.99 \times 10^8 \text{ m/s}\left(\frac{6.582 \times 10^{-22} \text{ MeV s}}{2(139.5 \text{ MeV}/c^2)c^2}\right) \\ &= 7.0 \times 10^{-16} \text{ m} \approx 1 \times 10^{-15} \text{ m} \approx 1 \text{ fm} \end{aligned} \quad [20.8]$$

The range of the strong nuclear force mediated by the pion is thus ~1 fm, similar to that of the radius of the proton or neutron.

For more in-depth reading on subnuclear structure and its role in the strong nuclear force, see Sundaresan (2001), Heyde (2004), Martin and Shaw (2004), and Serway et al. (2005).

20.4 BINDING ENERGY

The total energy of the nucleus with its bound nucleons is always less than the total energy of the separate protons and neutrons, and this difference in energy is the binding energy (E_b) of the nucleus. The binding energy is equivalent to the energy required to pull apart a bound system, such as a bound nucleus, leaving its component protons and neutrons free of attractive forces. The binding energy is described by the equation

$$E_b = \sum_{i=1}^{n} m_i c^2 - Mc^2 \quad [20.9]$$

where m_i are the free component particles (protons and neutrons) of the nucleus numbered $i = 1$ to n, and M is the mass of the bound nucleus. We may use atomic mass units (u) to calculate the nuclear binding energies according to Eq. [20.9] for any nuclide, ${}^{A}_{Z}\text{X}$, of Z number of protons, A number of protons + neutrons, and $N = A - Z$ number of neutrons, as follows:

$$E_b = \left[(Zm_{{}^{1}_{1}\text{H}} + Nm_n - M_{{}^{A}_{Z}\text{X}})931.494 \text{ MeV}/c^2\right]c^2 \quad [20.10]$$

where $m_{{}^{1}_{1}\text{H}}$ is the atomic mass of hydrogen, m_n is the neutron mass, and $M_{{}^{A}_{Z}\text{X}}$ is the atomic mass of the nuclide of atomic number Z and mass number A, ie, ${}^{A}_{Z}\text{X}$ in atomic mass units; and by definition 1 u = 931.494 MeV/c^2. Atomic mass units are used in Eq. [20.10], because the number of electrons of the Z hydrogen atoms is the same as the electrons included in the atomic mass of the nuclide ${}^{A}_{Z}\text{X}$. The differences in electron binding energies of the hydrogen atoms and that of the nuclide are negligible and ignored. Let us take an example and use atomic mass units to calculate the binding energy for the helium nucleus, ie, ${}^{4}_{2}\text{He}$, which is equivalent to an alpha particle, as follows:

$$\begin{aligned} E_b &= \left[(2m_{{}^{1}_{1}\text{H}} + 2m_n - M_{{}^{4}_{2}\text{He}})931.494 \text{ MeV}/c^2\right]c^2 \\ &= \left[((2)(1.007825 \text{ u}) + (2)(1.008665 \text{ u}) - 4.002603 \text{ u})931.494 \text{ MeV}/c^2\right]c^2 \\ &= 28.296 \text{ MeV} \end{aligned} \quad [20.11]$$

Because nuclei vary in their number of nucleons or mass number (A), it is common to express the nuclear binding energy in terms of the number of nucleons in the nucleus—that is, the binding energy per nucleon or E_b/A. In the case of the nuclide ${}^{4}_{2}\text{He}$, the binding energy per nucleon is

$$E_b/A = 28.296 \text{ MeV}/4 = 7.07 \text{ MeV} \quad [20.12]$$

The values of the binding energies per nucleon for all of the nuclides provide a measure of how tightly bound the nucleons are within a particular nucleus. Fig. 20.4 illustrates graphically the difference in the values of the binding energy per nucleon (E_b/A) as a function of the mass number (A) of the nucleus for nuclides over the entire range of mass numbers.

From Fig. 20.4 it is seen that the highest nuclear stability is found in the region of mass number $A = 50$–70; and the most stable nuclei (those nuclei that are most tightly bound) belong to the "iron group," including ${}^{62}\text{Ni}$, ${}^{58}\text{Fe}$, and ${}^{56}\text{Fe}$, with binding energies per nucleon at a maximum of approximately 8.8 MeV. On either side of this maximum, illustrated in Fig. 20.4, are the smaller nuclei in the range of $A = 2$–20 with lower binding energies per nucleon, which could fuse to yield larger and more stable nuclei with the release of energy, and the very large nuclei in the range of about $A \geq 120$,

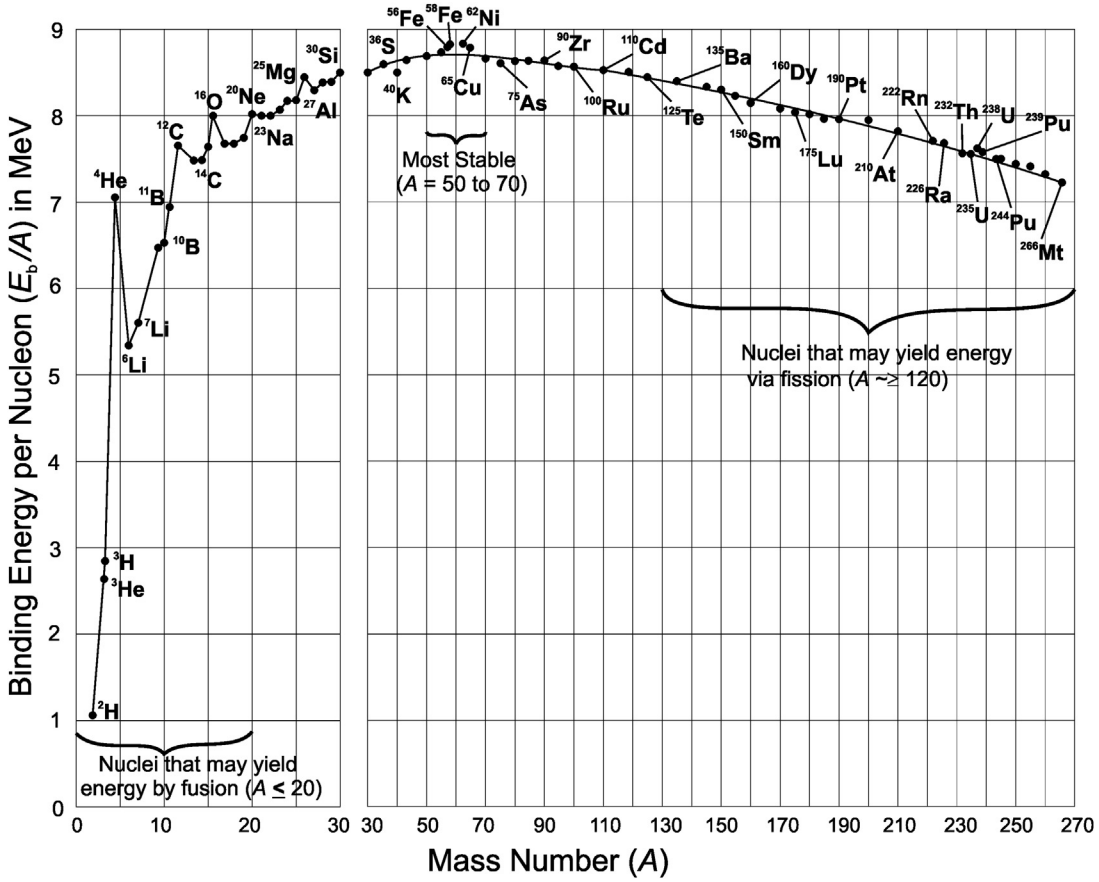

FIGURE 20.4 Binding energy per nucleon as a function of mass number. The scale between mass numbers 0 and 30 is broader than that illustrated for mass numbers 30–270. Several nuclides are identified along the curve. The most stable nuclei are ^{62}Ni, ^{58}Fe, and ^{56}Fe, with E_b/A values of 8.794, 8.792, and 8.790 MeV, respectively. Notice the small peak of highest stability at the top of the curve.

which could break apart into approximately equal mass number by fission to form smaller and more stable nuclei with the release of energy. Consequently, the size of the nucleus and its binding energy per nucleon will govern whether nuclear fusion or fission would be feasible; and the energy released in both cases can be estimated directly from Fig. 20.4 or by calculation. Let us take examples of both cases, fission and fusion.

20.4.1 Nuclear Fission

The nuclide ^{236}U, which results from the capture of a slow neutron by ^{235}U, is unstable. It takes on the characteristic of an unstable oscillating droplet. The nuclear droplet, which oscillates with the opposing forces of two positively charged nuclides, splits into two fragments with the liberation of an average energy of 193.6 MeV (Koch, 1995). The mass numbers of the fission fragments vary between 70 and 160; and the following is just one example illustrating the fission of ^{236}U into the nuclide fragments ^{90}Sr and ^{143}Xe with the emission of three neutrons:

$$^{236}_{92}\mathrm{U} \rightarrow {}^{90}_{38}\mathrm{Sr} + {}^{143}_{54}\mathrm{Xe} + 3^{1}_{0}\mathrm{n} \qquad [20.13]$$

The binding energy (E_b) of the ^{236}U nucleus, ie, the difference in mass of the ^{236}U nucleus and the combined mass of its free component nucleons, is calculated as follows:

$$E_b = (M_{92^1\mathrm{H}} + M_{144\mathrm{n}}) - M_{236_\mathrm{U}} \qquad [20.14]$$

where $M_{92^1\mathrm{H}}$ is the mass of 92 hydrogen atoms, $M_{144\mathrm{n}}$ is the mass of 144 neutrons, and M_{236_U} is the mass of the bound nucleus of the ^{236}U atom. As noted in the previous section, the mass of the hydrogen atom is used instead of the mass of the proton, because the mass of 92 electrons of the hydrogen atoms is the same as the 92 electrons in the atomic mass of $^{236}_{92}$U.

Using atomic mass units for the masses of the ^{236}U nucleus and its constituent nucleons, we calculate the binding energy (E_b) in atomic mass units (u) as

$$\begin{aligned} E_b &= [92(1.007825\ \text{u}) + 144(1.008665\ \text{u})] - 236.045561\ \text{u} \\ &= 237.96766\ \text{u} - 236.045561\ \text{u} = 1.922099\ \text{u} \end{aligned} \quad [20.15]$$

Although the masses of the electrons are included in the atomic masses, the electron masses can be ignored since these are the same for the ^{236}U and the 92 hydrogen atoms. Using Einstein's equation for the equivalence of mass and energy we can convert the binding energy to MeV or

$$\begin{aligned} E = mc^2 &= \left[(1.922099\ \text{u})\left(931.494\ \text{MeV}/c^2\right)\right]c^2 \\ &= 1790.42\ \text{MeV} \end{aligned} \quad [20.16]$$

Dividing the binding energy by the number of nucleons in the nucleus (mass number $A = 236$) will provide the binding energy per nucleon for ^{236}U or

$$(E_b/A)_{^{236}\text{U}} = 1790.42\ \text{MeV}/236 = 7.58\ \text{MeV/nucleon} \quad [20.17]$$

Similar calculations for the binding energies of the fission fragments ^{90}Sr and ^{143}Xe yield $E_b/A = 8.69$ MeV/nucleon for ^{90}Sr and 8.19 MeV/nucleon for ^{143}Xe. Estimated values of the binding energies per nucleon (E_b/A) as a function of mass number (A) can be obtained from Fig. 20.4. Because the binding energies per nucleon for the two fission products are slightly different, we could average the two values simply to get an estimated figure for the amount of energy released. We can now estimate the energy released from ^{236}U fission, or the Q value, using as an example the fission reaction of Eq. [20.13] as follows:

$$^{236}_{92}\text{U} \rightarrow {}^{90}_{38}\text{Sr} + {}^{143}_{54}\text{Xe} + 3{}^{1}_{0}\text{n}$$

$$Q = \left[(E_b/A)_{\text{fission products}} - (E_b/A)_{^{236}\text{U}}\right] \times 236\ \text{nucleons} \quad [20.18]$$

$$Q = \left[\left(\frac{(E_b/A)_{^{90}\text{Sr}} + (E_b/A)_{^{143}\text{Xe}}}{2}\right) - (E_b/A)_{^{236}\text{U}}\right] \times 236\ \text{nucleons}$$

$$Q = \left[\left(\frac{8.69\ \text{MeV/nucleon} + 8.19\ \text{MeV/nucleon}}{2}\right) - 7.58\ \text{MeV/nucleon}\right] \times 236\ \text{nucleons}$$

$$Q = 202\ \text{MeV}$$

Thus approximately 200 MeV is the amount of energy released from ^{236}U fission, ie, neutron-induced fission of ^{235}U. The magnitude of the energy released from neutron-induced fission of ^{235}U would be an average figure, because the actual amount of energy released would depend on the fission reaction, and there are many possible ways that the ^{236}U could break into two nuclides.

There are about 100 radionuclides of high mass number $A \geq 230$ that decay by spontaneous fission (SF), which involves the spontaneous noninduced splitting of the nucleus into two nuclides or fission fragments. A rough estimate of the energy released by fission reactions can be obtained quickly from Fig. 20.4. For example, ^{252}Cf undergoes spontaneous fission in 3% of the decay events as an alternative to alpha decay. An estimate of the energy released in the spontaneous fission is found by reading from Fig. 20.4 the binding energy per nucleon for a nuclide of mass number $A \approx 250$, which is about 7.5 MeV, and the binding energy per nucleon for fission fragments that have a mass number (A) in the range of 80−150, which varies between 8.5 and 8.3 or an average of ~8.4 MeV. The following calculation, in accordance with Eq. [20.18], gives the approximate energy released as

$$Q \approx [(8.4\ \text{MeV/nucleon}) - (7.5\ \text{MeV/nucleon})] \times 252\ \text{nucleons} \approx 230\ \text{MeV} \quad [20.19]$$

Nuclear fission as a source of neutrons is discussed in the chapter entitled "Neutron Radiation."

20.4.2 Nuclear Fusion

Nuclides of very low mass number ($A < 20$) have nuclei with relatively low binding energies per nucleon (see Fig. 20.4), and if these nuclei could coalesce, a larger, more tightly bound nucleus would form, and the overall process would release

energy as described by Eq. [20.9]. For example, if two nuclei of deuterium ($^{2}_{1}\mathrm{H}$) were to fuse into a nucleus of helium ($^{4}_{2}\mathrm{He}$), equivalent to an alpha particle, the energy released by the nuclear fusion can be estimated from Fig. 20.4. Taking the values of binding energy per nucleon (E_b/A) from Fig. 20.4 for $^{2}_{1}\mathrm{H}$ to be $\sim$1 MeV and that for $^{4}_{2}\mathrm{He}$ to be $\sim$7 MeV, the energy released is estimated from the following as

$$Q = \left[(E_b/A)_{^4\mathrm{He}} - (E_b/A)_{^2\mathrm{H}}\right] \times 4 \text{ nucleons} \qquad [20.20]$$

$$Q \approx [(\sim 7 \text{ MeV/nucleon}) - (\sim 1 \text{ MeV/nucleon})] \times 4 \text{ nucleons} \approx 24 \text{ MeV}$$

The energy released is more precisely determined by calculating the binding energy, E_b, for the $^{4}_{2}\mathrm{He}$ nucleus and the $^{2}_{1}\mathrm{H}$ nucleus according to Eq. [20.10]. The nuclear binding energy for $^{4}_{2}\mathrm{He}$ was previously calculated (see Eq. [20.11]) to be 28.296 MeV, and the binding energy per nucleon is $(E_b/A)_{^4\mathrm{He}} = 28.296 \text{ MeV}/4 = 7.074 \text{ MeV}$. The nuclear binding energy for $^{2}_{1}\mathrm{H}$ according to Eq. [20.10] is calculated as

$$\begin{aligned} E_b &= \left[(m_{^1\mathrm{H}} + m_n - M_{^2_1\mathrm{H}})931.494 \text{ MeV}/c^2\right]c^2 \\ &= \left[(1.007825032 \text{ u} + 1.00866492 \text{ u} - 2.014101778 \text{ u})931.494 \text{ MeV}/c^2\right]c^2 \\ &= 2.225 \text{ MeV} \end{aligned} \qquad [20.21]$$

The binding energy per nucleon for $^{2}_{1}\mathrm{H}$ is $(E_b/A)_{^2\mathrm{H}} = 2.225 \text{ MeV}/2 = 1.112 \text{ MeV}$. The energy released in the fusion of two nuclei of deuterium to a nucleus of helium is calculated according to Eq. [20.10] as

$$\begin{aligned} Q &= [7.074 \text{ MeV} - 1.112 \text{ MeV}] \times 4 \text{ nucleons} \\ &= 23.85 \text{ MeV} \end{aligned} \qquad [20.22]$$

The deuterium fusion reaction is written as

$$^{2}_{1}\mathrm{H} + {}^{2}_{1}\mathrm{H} \rightarrow {}^{4}_{2}\mathrm{He} + \gamma + 23.85 \text{ MeV} \qquad [20.23]$$

This calculated energy of 23.85 MeV for deuterium fusion agrees with the online computer-calculated value of 23.846 MeV provided by the Brookhaven National Laboratory of the National Nuclear Data Center (NNDC): www.nndc.bnl.gov/qcalc. The energy released in the deuterium fusion may also be calculated according to Eq. [2.11] of chapter "Basic Concepts and Definitions," namely,

$$Q = (m_R - m_P)c^2 \qquad [20.24]$$

where m_R and m_P are the rest masses of the reactants and products, respectively. For the fusion of two deuterium nuclei described in Eq. [20.23], the energy released is calculated using atomic mass units (u) as

$$\begin{aligned} Q &= \left([2(2.014101778 \text{ u}) - 4.00260325 \text{ u}]931.494 \text{ MeV}/c^2\right)c^2 \\ &= 23.85 \text{ MeV} \end{aligned}$$

where, by definition, 1 u = 931.494 MeV or 931.494 MeV/c^2.

The nuclear fusion reaction described by Eq. [20.23] is one that releases a relatively large amount of energy; but it has a low reaction cross-section or low probability of occurrence, and the energy not easily captured because most of it would be carried off by the gamma radiation. A more practical source of energy by nuclear fusion is the fusion of deuterium and tritium nuclei according to the reaction:

$$^{2}_{1}\mathrm{H} + {}^{3}_{1}\mathrm{H} \rightarrow {}^{4}_{2}\mathrm{He} + {}^{1}_{0}\mathrm{n} + 17.58 \text{ MeV} \qquad [20.25]$$

When comparing the energy released from neutron-induced fission of $^{235}\mathrm{U}$ ($\sim$200 MeV, see Eq. [20.18]) and that produced by the fusion of deuterium and tritium nuclei (17.6 MeV, see Eq. [20.25]), we can immediately see that there is more than a 10-fold greater magnitude of energy released by the neutron-induced fission reaction. However, if we evaluate the reactions in terms of fuel mass, we find that the deuterium–tritium fusion reaction is the most efficient for energy production. For example, let us now calculate and compare the energy yields per kilogram of fuel for both nuclear fission and nuclear fusion.

Neutron-induced ^{235}U fission energy yield:

$$\begin{aligned} E\ \text{yield}_{^{235}\text{U fission}} &= \frac{\text{Reaction energy release}}{\text{Fuel mass}} \\ &= \frac{200\ \text{MeV}}{(M_{^{235}\text{U}} + M_{\text{neutron}})\left(1.660 \times 10^{-27}\ \text{kg/u}\right)} \\ &= \frac{200\ \text{MeV}}{(235.04392\ \text{u} + 1.00866\ \text{u})(1.660 \times 10^{-27}\ \text{kg/u})} \\ &= 0.5104 \times 10^{27}\ \text{MeV/kg} \end{aligned} \quad [20.26]$$

Deuterium-tritium (D-T) fusion:

$$\begin{aligned} E\ \text{yield}_{\text{D-T fusion}} &= \frac{\text{Reaction energy release}}{\text{Fuel mass}} \\ &= \frac{17.6\ \text{MeV}}{(M_{^2\text{H}} + M_{^3\text{H}})\left(1.660 \times 10^{-27}\ \text{kg/u}\right)} \\ &= \frac{17.6\ \text{MeV}}{(2.01410\ \text{u} + 3.016049\ \text{u})(1.660 \times 10^{-27}\ \text{kg/u})} \\ &= 2.1077 \times 10^{27}\ \text{MeV/kg} \end{aligned} \quad [20.27]$$

In the above Eqs. [20.26] and [20.27], the notations $M_{^{235}\text{U}}$, M_{neutron}, $M_{^2\text{H}}$, and $M_{^3\text{H}}$ refer to the masses of ^{235}U, the neutron, deuterium, and tritium in atomic mass units (u). Taking the ratio of energy yields of nuclear fusion over fission yields

$$\frac{E\ \text{yield}_{\text{D-T fusion}}}{E\ \text{yield}_{^{235}\text{U fission}}} = \frac{2.1077 \times 10^{27}\ \text{MeV/kg}}{0.5104 \times 10^{27}\ \text{MeV/kg}} = 4.13 \quad [20.28]$$

Thus D-T nuclear fusion is more than four times as efficient as neutron-induced nuclear fission in terms of energy yield per mass of fuel consumption.

D-T fusion offers great promise as a future energy source, and would be more efficient and more environmentally friendly than neutron-induced fission. There are 437 nuclear power plants in 31 countries of the world operating on the basis of nuclear fission, which provide 16% of the world energy needs (IAEA, 2013a,b). However, nuclear fusion is still in the developmental stage. The fusion of light nuclei is not possible under normal temperature and pressure, because the repulsive coulombic forces between atomic electrons and between positive charges of atomic nuclei prevent the nuclei from mingling into the required close proximity for them to coalesce into one nucleus. However, at temperatures of about 100×10^6 °C the nuclei of atoms become plasmas in which nuclei and electrons move freely with high kinetic energy, sufficient for the nuclei to overcome their repulsive forces and combine. Because of the high temperatures required, the process is referred to as thermonuclear fusion.

In summary, the fusion of light nuclei, such as those of deuterium (^{2}H) and tritium (^{3}H), release an energy per nucleon (MeV/u) or energy per unit of material considerably greater than can be achieved by nuclear fission, as calculated above. Thermonuclear fusion requires a large energy input to achieve high temperatures and maintain nuclear plasma; but once achieved, the energy output is greater than the input. An additional advantage of the nuclear fusion of deuterium and tritium is that no hazardous radioactive wastes are direct products of the reaction. The products of the thermonuclear fusion of deuterium and tritium nuclei are alpha particles and neutrons. The neutrons can produce some radioactive isotopes in the surrounding reactor shielding material, but most would be short-lived and there would be no need to store radioactive waste in geological deposits for long periods of time, as is the custom with nuclear fission.

The advantages and future development of nuclear fusion are described in detail in the chapter entitled "Radioactivity and Our Wellbeing" of this book.

20.5 NUCLEAR MODELS

Since Ernest Rutherford's alpha-scattering experiment that led to the discovery of the atomic nucleus (Rutherford, 1911), physicists have used experimental and empirical data to establish nuclear models to describe the nucleus. The nuclear models that have been created provide insight into the stability of the atomic nucleus and an understanding of the processes of nuclear decay.

20.5.1 Liquid Drop Model

During a meeting of the Royal Society in London on February 7, 1929, the Russian-born physicist George Gamow (1904−1968) presented his thoughts on the properties of the nucleus and that the nucleus would possess forces similar to those of a liquid drop (Gamow, 1930). A very complete and detailed account of Gamow's conception of the liquid drop model of the nucleus is given by Stuewer (1997). The writer will give a small portion of this historical account, which provides the reasoning used by Gamow. At the time Gamow first presented his ideas on the liquid drop characteristics of the nucleus, the neutron had not been discovered and the alpha particle was thought to be the building block of the nucleus. In the discussion, Gamow (1929) commented:

> *Such an assembly of alpha particles with attractive forces between them, which vary rapidly with the distance may be treated somewhat as a small drop of water in which the particles are held together by surface tension.*

Gamow (1930) continued his development of the liquid drop model, still before the neutron was discovered by James Chadwick (1932a,b) to be a component particle of the nucleus. After the discovery of the neutron, Werner Heisenberg (1934) presented his analysis of exchange forces and general theory of nuclear structure at the seventh Solvay Conference in Brussels in October 1933. At the meeting, Heisenberg reported theory on nuclear structure, which could be "considered as corresponding to a form of Gamow's drop model made precise by the neutron hypothesis" (Stuewer, 1997). Only a year later, Heisenberg's student Carl Friedrich von Weizsäcker (1937) derived an empirical equation that would yield the binding energy of the nucleus as a function of its mass number (A), incorporating into the equation the various properties of the nucleus characteristic of a liquid drop. Von Weizsäcker's equation for the liquid drop model of the nucleus gained notoriety when Hans Bethe and Robert Bacher (Bethe and Bacher, 1936; Bethe, 1937) from Cornell University reworked Weizsäcker's equation to include a pairing energy, which was referred to subsequently as the Bethe-Weizsäcker mass formula.

George Gamow
Portrait of George Gamow (1904–1968) at middle age, Courtesy of American Institute of Physics, AIP Emilio Segre Visual Archives

Carl F. von Weizsäcker and Homi J. Bhabha
Left: Carl Friedrich Freiherr von Weizsäcker (1912–2007) and Right: Homi Jehangir Bhabha (1909–1966) dining during the 1936 Denmark Conference at the Niels Bohr Institute in Copenhagen. Photograph by Paul Ehrenfest, courtesy of the American Institute of Physics, AIP Emilio Segre Visual Archives

Gamow's original conception of the nucleus with the physical properties of a liquid drop soon became useful in the interpretation of nuclear fission. In December 1938 Otto Hahn and Fritz Strassman (Hahn and Strassman, 1939a,b) confirmed that barium ($Z = 56$) was a product of neutron bombardment of uranium ($Z = 92$). Hahn could not arrive at an explanation of how a nuclide of lower atomic number would result from the reaction of a neutron with a nucleus of much higher atomic number, and asked his former colleague and collaborator, Lise Meitner, for an explanation. Lise Meitner and Otto Frisch (1939) considered the recently developed concept of the nucleus having the properties of a liquid drop. They arrived at the conclusion that the capture of a neutron by the uranium nucleus attributed to the nucleus a degree of instability, whereby it would oscillate like a liquid drop forming a dumbbell shape (see Fig. 20.5), that the opposing coulomb forces of the fat

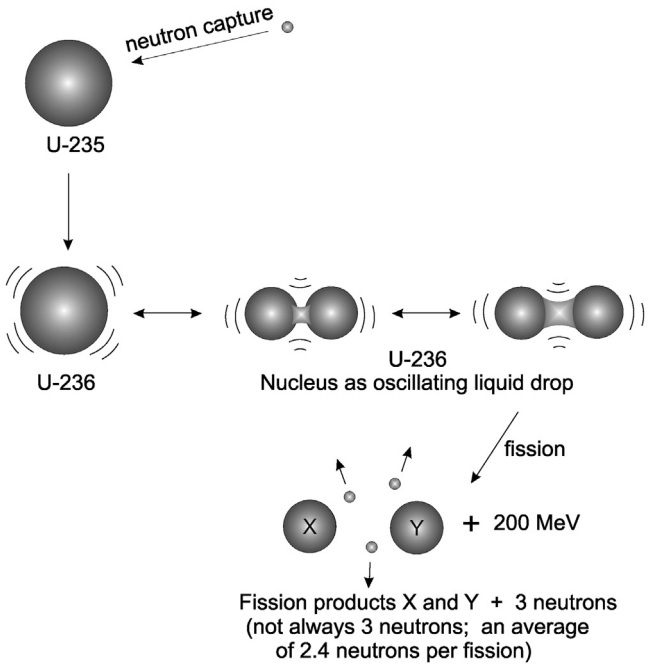

FIGURE 20.5 Neutron capture by uranium-235 and subsequent fission of unstable uranium-236. The capture of a slow neutron by uranium-235 yields the nuclide uranium-236, which is unstable, capable of oscillating like a liquid drop and breaking into two smaller nuclides, X and Y, generally of different masses and of atomic numbers that add up to $Z = 92$ (the atomic number of the parent uranium) plus the emission of an average of 2.4 neutrons and energy (approximately 200 MeV). The emission of three neutrons is illustrated. The uranium-236 nuclides break into two fission fragments in as many as 30 different possible ways, thus producing 60 different nuclide fission fragments.

sections of the dumbbell would cause the nucleus to split apart into two nuclides (fission fragments) of smaller atomic number, and that the sum of the atomic numbers of the two fission fragments would equal that of the original uranium ($Z = 92$). Meitner and Frisch concluded that if barium ($Z = 56$) was a product (fission fragment) of neutron bombardment of uranium ($Z = 92$), the other fission fragment would be krypton ($Z = 36$), as described by the following reaction:

$$^{235}_{92}\mathrm{U} + {}^{1}_{0}\mathrm{n} \xrightarrow{\text{fission}} {}_{56}\mathrm{Ba} + {}_{36}\mathrm{Kr} + x\,{}^{1}_{0}\mathrm{n} \qquad [20.29]$$

They coined the term "fission" by borrowing from biology a word used to describe the splitting of bacteria cells. The liquid drop model remains to this day an excellent means of describing nuclear fission, and the model formula has been used to predict spontaneous fission half-lives (Ronen, 2004).

Lise Meitner
Lise Meitner (1878–1968); courtesy of the American Institute of Physics, AIP Emilio Segre Visual Archives

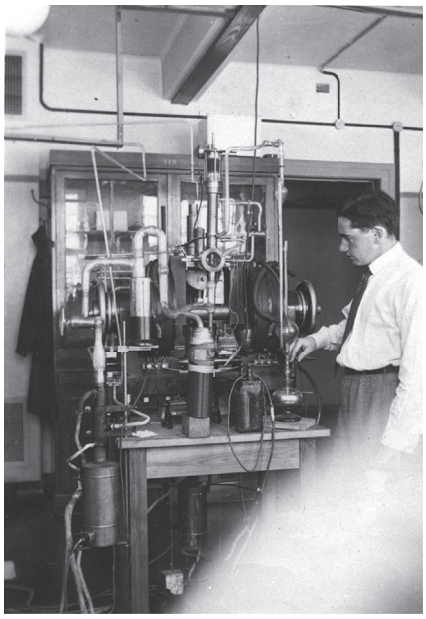

Otto Frisch
Otto R. Frisch (1904–1979) at yourng age working with laboratory equipment in Hamburg, Germany; courtesy of the American Institute of Physics, AIP Emilio Segre Visual Archives

Today the mathematical formula for this model is often referred to as the Weizsäcker liquid drop model formula or the semiempirical mass formula. It has been refined by many researchers to include theory with empirical measurements, including those described by Evans (1972), Friedlander et al. (1964), Ronen (2004), Serway et al. (2005), Mahboub (2008), and Royer (2008), and the formulas vary slightly among research reports; however, all have the basic mathematical structure of the equation first reported by von Weizsäcker. The liquid drop formula described by Evans (1972), Friedlander et al. (1964), Choppin et al. (2002), Gould et al. (2004), and Serway et al. (2005) is basically the following:

$$E_b = a_v A - a_s A^{2/3} - a_c \frac{Z(Z-1)}{A^{1/3}} - a_{sy} \frac{(N-Z)^2}{A} \pm \delta_p(Z, N) \qquad [20.30]$$

where E_b is the nuclear binding energy in MeV, A is the mass number, N is the neutron number, Z is the atomic number, a_v, a_s, a_c, and a_{sy} are coefficients for the volume energy, surface energy, coulomb energy, and symmetry energy, respectively, and $\delta_p(Z, N)$ is a pairing energy term (described subsequently). The values of the coefficients a_v, a_s, a_c, and a_{sy} reported by Woan (2000) are $a_v \approx 15.8$ MeV, $a_s \approx 18.0$ MeV, $a_c \approx 0.72$ MeV, and $a_{sy} \approx 23.5$ MeV. The coefficients vary slightly among research reports depending on the data used to obtain the mathematical best fit of the equation to measured values of nuclear binding energy, and the equation generally agrees with measured values to within a few percent for nuclides of $A > 40$. The various terms of the liquid drop equation (Eq. [20.30]) are described as follows.

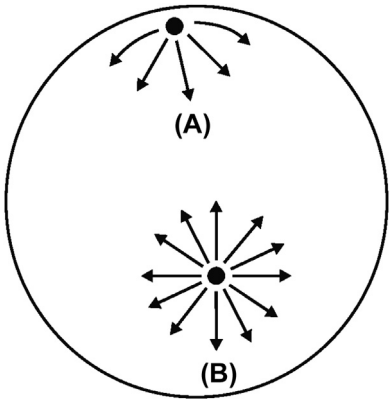

FIGURE 20.6 Nuclear forces (*arrows*) binding a nucleon at the nuclear surface (A) and a nucleon within the nucleus (B). The binding forces of the nucleon at the surface are unsaturated, as there are fewer neighboring nucleons with which to bind compared to nucleons within the nucleus. The phenomenon is similar to that which occurs in the binding of molecules of a liquid drop, resulting in surface tension.

20.5.1.1 Volume Energy a_vA

The volume energy term assigns a direct proportionality of the nuclear volume to the total binding energy of the nucleus, ie, the nuclear volume increases in proportion to the number of nucleons. The extension of the binding energy throughout the entire volume of the nucleus is a consequence of the short-range and saturation characteristics of the nuclear forces. The strong nuclear forces binding neutrons and protons in the nucleus extend throughout the nuclear volume.

20.5.1.2 Surface Energy $a_sA^{2/3}$

The surface energy term is negative, as the nuclear forces binding the nucleons are unsaturated at the surface, similar to the surface tension effect that occurs with a liquid drop (see Fig. 20.6), and there is thus a reduction of binding at the surface. The nucleons at the surface have fewer neighboring nucleons with which to bind, resulting in a reduction in binding energy as a function of surface area. The surface effect will increase with surface area, and the surface area of a sphere is defined as πr^2. Since the radius of the nucleus is proportional to the mass number ($r \propto A^{1/3}$), as defined by Eq. [20.1], the surface area term can be written as being proportional to $A^{2/3}$.

20.5.1.3 Coulomb Energy $a_c(Z(Z-1)/A^{1/3})$

The coulomb energy term takes into account the repulsive coulomb forces of the protons in the nucleus. The nucleus contains Z protons, and their long-range coulomb forces interact with the remaining $Z-1$ protons. The coulomb force therefore extends throughout the nucleus with radius proportional to $A^{1/3}$ (see Eq. [20.1]), which is included in this coulomb energy term of the liquid drop model.

The strong nuclear binding forces between neutrons and protons in the nucleus, which are of short range, counteract the coulomb repulsive forces. Thus in the Chart of the Nuclides among the stable nuclei with $Z > 20$ we find that their nuclei contain more neutrons than protons. If we look through the Chart of the Nuclides we notice that the stable nuclides of low atomic number ($Z \leq 20$) will have an *N/Z* ratio of ~ 1. However, as the atomic number increases ($Z > 20$), the *N/Z* ratio of the stable nuclides increases gradually, reaching as high as ~ 1.5 (eg, $^{209}_{83}\text{Bi}$, $Z = 83$, $N/Z = 1.518$). Furthermore, there are no stable nuclides of an atomic number greater than 83.

In brief, the importance of the *N/Z* ratio to nuclear stability is explained on the basis of the existence of strong short-range nuclear binding forces, which are charge independent, and the long-range repelling coulomb forces between protons. The short-range strong nuclear forces extend to a distance of ≈ 2 fm (2 fermi or 2×10^{-15} m), which is close to the radius of a small nucleus, such as that of ^4_2He (see Section 20.2 of this chapter). These attractive strong nuclear forces are binding exchange forces that have charge independence (see Section 20.3). The binding exchange forces therefore exist, regardless of charge on the particles, between two protons, two neutrons, and a proton and a neutron. Thus at short distances within 2 fm, the strong forces between n–n, n–p, and p–p are equal and charge independent. However, at distances beyond 2 fm there are repelling coulombic forces between the positively charged protons that act to force them apart. For nuclides of low Z, the attractive nuclear forces exceed the repelling coulombic forces when $N \approx Z$. However, increasing the number of protons (eg, $Z > 20$) further increases the strength of the repelling coulombic forces over a larger nucleus, which will tend to force

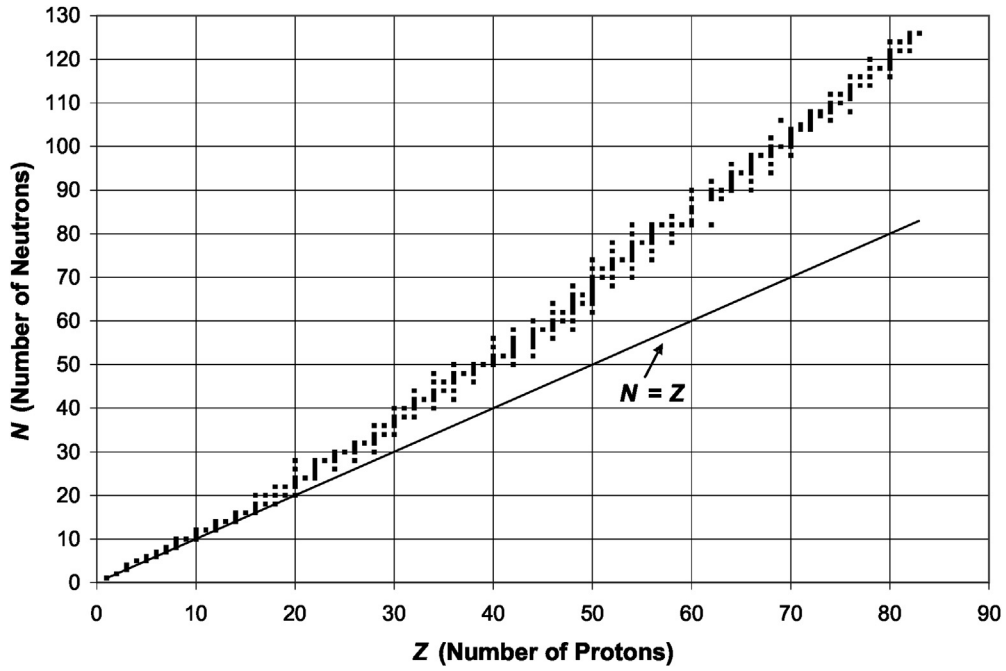

FIGURE 20.7 Plot of stable nuclides. The number of neutrons (N) is plotted against the number of protons (Z) in the nuclei of the stable atoms. The straight line represents $N = Z$. Only 13 nuclides in the region $Z \leq 20$ with an equal number of neutrons and protons ($N = Z$) are stable.

the nucleus apart. Therefore additional neutrons, $N > Z$, provide additional strong attractive nuclear forces needed to overcome the repelling forces of the larger proton population. Fig. 20.7 illustrates a plot of the stable nuclides as a function of their N and Z numbers. The N/Z ratio of the stable nuclides, as illustrated in Fig. 20.7, increases significantly as a function of Z for nuclides of $Z > 20$. As the atomic number increases further, $Z > 83$, all nuclides are unstable. Even though N/Z ratios reach 1.5, nuclear stability is not achieved when the number of protons in the nucleus exceeds 83.

20.5.1.4 Volume Symmetry $a_{sy}((N - Z)^2/A)$

The volume symmetry term quantifies the contribution of nuclear symmetry to the binding energy. Among the light nuclei, the unstable nuclei reside on either side of the symmetrical term $N = Z$. Thus a negative sign is assigned to this symmetry term, which increases according to $(N - Z)$. Nuclear stability among the larger nuclei is achieved by an increase in the N/Z ratio (see Fig. 20.7), as the strong short-range binding nuclear forces between neutrons and protons (see Section 20.3) are needed to hold the nucleus together over its entire volume. As these short-range n−p binding forces do not reach throughout the volume of the nucleus, the probability of occurrence of n−p binding within a nucleus would be inversely proportional to the nuclear volume or A^{-1}.

20.5.1.5 Pairing Energy $\pm\delta_p(Z,N)$

The pairing energy term may have a positive sign whereby the term adds to the nuclear binding energy, or a negative sign diminishing the nuclear binding energy. Nuclei that have an even number of protons and even number of neutrons (even Z, even N) are known to be the most stable of all nuclei due to proton−proton spin coupling and neutron−neutron spin coupling (see Section 20.5.2 below). The pairing energy term for the binding energy of these nuclei is assigned a value of $+34/A^{3/4}$ MeV. Nuclides with even Z−odd N or odd Z−even N are generally less stable than even−even nuclides, and thus the even−odd and odd−even (ie, odd A) nuclides are assigned a value of zero to the pairing energy term. The least stable of the nuclides are those with odd Z and odd N (odd−odd nuclides), and these are assigned a pairing energy term of $-34/A^{3/4}$ MeV. The negative value of this term diminishes the total binding energy of Eq. [20.30] for the liquid drop model. Thus the pairing energy term has the following values, as summarized by Woan (2000) and Gould et al. (2004):

$$\pm\delta_p(Z,\ N) \approx \frac{34}{A^{3/4}} \begin{Bmatrix} +1 & \text{for even-even} \\ 0 & \text{for } A \text{ odd} \\ -1 & \text{for odd-odd} \end{Bmatrix} \qquad [20.31]$$

The liquid drop model is useful in describing certain properties that may attribute stability or instability to atomic nuclei; and it has proven successful in explaining nuclear fission in large nuclei. However, the model does not provide insight into the fine organized structure and spin coupling of protons and neutrons in the nucleus that attribute stability to certain nuclei, as provided by the shell model described next.

20.5.2 Shell Model

Our knowledge of the shell structure of the atomic nucleus has its beginnings with the independent work of Maria Goeppert-Mayer while at the Argonne National Laboratory in the USA (Goeppert-Mayer, 1948a,b, 1949) and J. Hans D. Jensen from the University of Heidelberg, Germany (Haxel et al., 1949). They subsequently collaborated with a book on nuclear shell structure (Goeppert-Mayer and Jensen, 1955). For this work they were awarded the 1963 Nobel Prize in Physics. This award made Maria Goeppert-Mayer only the second woman to receive the Nobel Prize in Physics after Marie Curie.

Maria Goeppert-Mayer's opportunity for discovery came while voluntarily collaborating at the University of Chicago's Institute for Nuclear Studies (now known as the Enrico Fermi Institute). At the institute she collaborated with Edward Teller in a search for the cosmological model of the origin of the universe. While compiling data she studied the abundance of the elements, and found that there were certain elements that were highly abundant; she found a correlation between the abundance of these elements and specific numbers of neutron and protons in their nuclei. J. Hans D. Jensen at the Institute of Theoretical Physics in Heidelberg, together with his collaborators Otto Haxel at the Max Planck Institute in Göttingen and Hans E. Suess of the Institute of Physical Chemistry at Hamburg, came to a similar conclusion that certain elements with particular numbers of neutrons and protons were particularly stable. It is interesting to note that on both sides of the globe, the discoveries were made simultaneously and independently. When the stage is set, the discoveries will be made.

The numbers of protons and neutrons correlated to particularly stable nuclei were called the "magic numbers." In the words of Goeppert-Mayer in her Nobel lecture:

> *What makes a number magic is that a configuration of a magic number of neutrons, or of protons, is unusually stable whatever the associated number of the other nucleons. The magic numbers, as we know them today, are:*
>
> *2, 8, 20, 28, 50, 82, 126*
>
> *and most importantly, they are the same for neutrons and protons.*

Nuclides containing a magic number of neutrons and/or protons are listed in Table IX.1 of Hall of Fame, Part IX. Goeppert-Mayer (1963) pointed out that Sn ($Z = 50$) is the element with the largest number of stable isotopes among all of the elements in the periodic table. There are six stable nuclides with 50 neutrons and seven stable nuclides with 82 neutrons, whereas normally one will find only two or three stable nuclei in the Chart of the Nuclides having identical numbers of neutrons.

Some nuclides are called "doubly magic," because they have equal numbers of protons and neutrons that are magic numbers. The nuclide ${}^{4}_{2}\mathrm{He}$ has a high binding energy, ie, it is very tightly bound; and an extra proton or neutron cannot be attached to its nucleus, as evidenced by the fact that ${}^{4}_{3}\mathrm{Li}$ and ${}^{5}_{2}\mathrm{He}$ do not exist. In addition ${}^{16}_{8}\mathrm{O}_{8}$, which is also "doubly magic," is very stable. A large amount of energy is required to remove a neutron from the ${}^{16}_{8}\mathrm{O}_{8}$ nucleus; whereas the addition of an extra neutron to its nucleus to form ${}^{17}_{8}\mathrm{O}_{9}$ results in a weakly bound neutron, which is evidenced by the low natural abundance of ${}^{17}\mathrm{O}$ (0.04%) compared to ${}^{16}\mathrm{O}$ (99.76%).

The breakthrough in the development of the nuclear shell model came with the conclusion that the protons and neutrons in the nucleus exhibit nuclear spin coupling effects, which result in shifts in their energy levels within the nucleus, similar to what occurs with electrons in their orbitals about the atom. Pauli's exclusion principle, which was applied to atomic electrons, is also applied to the nucleons in the nucleus. The exclusion principle states that no two protons or two neutrons in a nucleus could exist in the same quantum or energy state. The proton or neutron can exist in two spin quantum states, namely $+1/2$ (ie, spin-up) or $-1/2$ (ie, spin-down). Goeppert-Mayer explained in her Nobel lecture that there is a strong interaction between spin and orbital angular momentum, whereby spin-up and spin-down refer to the spin being parallel or antiparallel to the orbital angular momentum. She provided evidence that this spin interaction raised considerably the energy levels of nuclei that contained 9, 21, 29, 51, or 83 protons or neutrons, or 127 or 128 neutrons, thereby attributing a high degree of stability to nuclei that contain 2, 8, 20, 28, 50, or 82 protons or neutrons, or 126 neutrons. The numbers 2, 8, 20, 28, 50, 82, and 126 refer to closed shells of protons or neutrons, attributing a high degree of stability to nuclei with these nucleon numbers. The closed shells of nucleons in the highly stable nulei are analagous to the closed electron shells

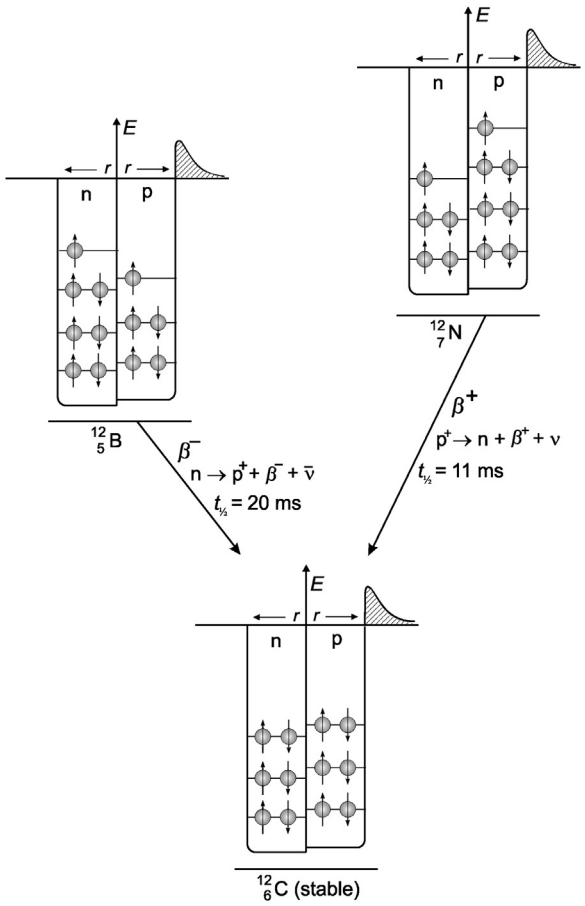

FIGURE 20.8 Nuclear potential energy-well illustrations of the pairing of nucleons in the isobars ^{12}N, ^{12}B, and ^{12}C. The neutrons and protons are illustrated with arrows to represent opposite spin states, spin-up (↑) and spin-down (↓). Only two nucleons of opposite spin state are allowed per energy level (E) in accord with the Pauli exclusion principle. The protons are illustrated at a higher energy level than the neutrons, because of the added positive coulomb potential of the protons. The ridge, at energy levels above those occupied by the protons, represents the coulomb potential barrier to charged particles from entering or escaping the nucleus. The nuclear radius is represented by r.

of the noble gases, which attribute to these gases a high degree of chemical inertness. Thus protons and neutrons exist in the nucleus in different energy states in structured orbitals, similar to the external electron orbitals of the atom. It was discussed previously how stability is achieved in the light nuclei ($Z < 20$) when $Z = N$, and this was illustrated in Fig. 20.7. In accordance with the exclusion principle, the nucleons are packed in the nucleus according to energy levels, with two protons of opposite spin and two neutrons of opposite spin per energy level. As a proton or neutron is added to the nucleus, it will occupy the next highest energy state; and the increase in energy state of the nucleus can decrease its stability. Fig. 20.8 illustrates how the additional proton in ^{12}N compared to ^{12}C attributes a higher energy state to the ^{12}N nucleus, whereby it decays to the stable ^{12}C by the conversion of a proton to a neutron via positive beta decay. Also, an extra neutron in the nucleus of ^{12}B places that nucleus in a higher energy state compared to ^{12}C. The ^{12}B achieves stability by conversion of the excess neutron to a proton to form stable ^{12}C via negative beta decay.

In her Nobel lecture Maria Goeppert-Mayer provided evidence for the increased instability of nuclei when additional neutrons are added to nuclei above the magic numbers, which represent closed shells at 2, 8, 20, 28, 50, 82, and 126 nucleons.

The highest magic number of 126 occurs only for the closing of a neutron shell. Thus it can be expected that the 127th and 128th neutrons would be less tightly bound; and that these nuclides would be at higher and less stable energy states compared to nuclides with 126 neutrons.

Additional material on the "shell model" of the nucleus and "magic numbers" of protons and neutrons in the nucleus is provided in Hall of Fame, Part IX. Also, further information on this subject matter is available in works by Goeppert-Mayer and Jensen (1955, 1965), Goeppert-Mayer (1965), Choppin et al. (2002), and Rowe and Wood (2010).

20.5.3 Collective Model

The collective model of the nucleus combines aspects of the liquid drop and shell models, and provides a description of the collective properties of the nucleus. The oldest model was the liquid drop described previously. This model was very useful in describing certain nuclear reactions, such as nuclear fission. After the liquid drop model came the shell model, which gave an organized picture of the nucleons in different energy states in structured orbitals. This provided an explanation for the stability of nuclei with certain "magic numbers." However, neither model could provide an explanation for excited states of the nucleus, which is the result or consequence of the collective action of the nucleus. The collective model, for which Aage Bohr (son of Niels Bohr) from the Niels Bohr Institute in Copenhagen, Ben Mottelson of the Nordic Institute for Theoretical Physics in Copenhagen, and James Rainwater of Colombia University in New York received the 1975 Nobel Prize in Physics, depicts the nucleus with both the properties of a liquid drop and the ordered structure of the nucleons, providing an explanation of excited states of the nucleus as a consequence of its rotations and vibrations.

Auge Bohr (1922–2009)

Ben R. Mottelson (1926–)

Certain nuclei, particularly heavy nuclei ($A > 150$), exhibit large electric quadrupole moments. This property is a charge distribution that deviates from what one would encounter with a symmetrical spherical nucleus. The property clearly indicates that certain nuclei are not spherical in shape, but are deformed or ellipsoidal in shape. Rainwater (1950) provided a solution by considering that there was an interaction between an inner core and outer surface of valence nucleons whereby the valence nucleons could influence the shape of the nucleus. The movement of the valence nucleons with respect to the core would cause a polarizing effect, resulting in a deformed nucleus as would be expected in the liquid drop model. Aage Bohr (1951) published ideas similar to those of Rainwater in a paper that was submitted prior to the publication of Rainwater's paper, demonstrating their independent discoveries. Bohr linked the movement of nucleons on the nuclear surface to oscillations of the nuclear shape, which would account for the large nuclear quadrupole moments. Bohr predicted collective excitations of the nucleus, namely vibrational excitations resulting in the periodic change in the shape of the nucleus, and rotational excitations which entail the rotation of the entire nucleus, not as a single body, but in a motion consisting of a surface wave of nucleons that propagates. In his Nobel address Aage Bohr stated: "The rotational motion resembles a wave traveling across the nuclear surface and the moment of inertia is much smaller than for a rigid rotation." The moment of inertia of the nucleus will change as its shape changes. This is analagous to the actions of a figure skater, who with outstretched arms will pull in his or her arms, thereby reducing the moment of inertia and resulting in a faster spin. In his Nobel lecture Aage Bohr illustrated the differences between the rotation of a rigid nucleus and one which has a nonrigid surface, as depicted in Fig. 20.9.

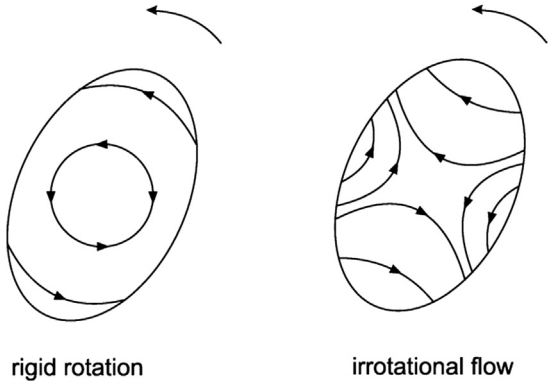

FIGURE 20.9 Velocity fields for rotational motion. For the rotation generated by irrotational flow, the velocity is proportional to the nuclear deformation (amplitude of the traveling wave). Thus for a spheroidal shape the moment of inertia is $\vartheta = \Im_{rig}(\Delta R/R)^2$, where $\Im_{rig}$ is the moment for rigid rotation, while R is the mean radius and ΔR (assumed small compared to R) is the difference between major and minor semiaxes. *From Bohr, A., 1975. Rotational motion in nuclei. Nobel Lecture, December 11, 1975. http://www.nobelprize.org/nobel_prizes/physics/laureates/1975/bohr-lecture.pdf; Bohr, A., 1992. Rotational motion in nuclei. In: Lundqvist, S. (Ed.) Nobel Lectures, Physics 1971–1980. World Scientific Publishing, Singapore, reprinted with permission © The Nobel Foundation 1975.*

Thus nuclear excitations would be expected from the nucleus rotating not as rigid body, but resulting from the movement of a surface wave of nucleons propagating about and around the surface of the nucleus. The nuclear deformations (elipsoidal shapes) would result from numerous nucleons acting in a collective manner as a wave on the surface of a more rigid inner nuclear core. The differing ellipsoidal shapes or rotational states of the nucleus are manifested as rotational bands in gamma-ray emission spectra, as subsequently discussed.

James Rainwater (1917–1986)
Photo from AIP Emilio Segre Visual Archives, Physics Today Collection with permission

Bohr and Mottelson (1953a,b) were able to correlate the energy of rotational states with gamma-ray emission spectra. The energy (E) of the rotational states for even–even nuclei would be defined by the equation

$$E = \hbar^2 \frac{I(I+1)}{2\vartheta} \qquad [20.32]$$

where I is the nuclear spin and ϑ is the moment of inertia. Some of the first examples of energy spectra proportional to $I(I+1)$ are illustrated in Fig. 20.10. For example, the ratio of spin state 4 to spin state 2 is $4(4+1)/2(2+1) = 3.33$, and the product of this ratio and the observed energy at spin state 2 yields $(3.33)(93\ \text{keV}) = 310\ \text{keV}$, as given in parenthesis for the calculated energy at spin state 4 of the radionuclide ^{180}Hf in Fig. 20.10.

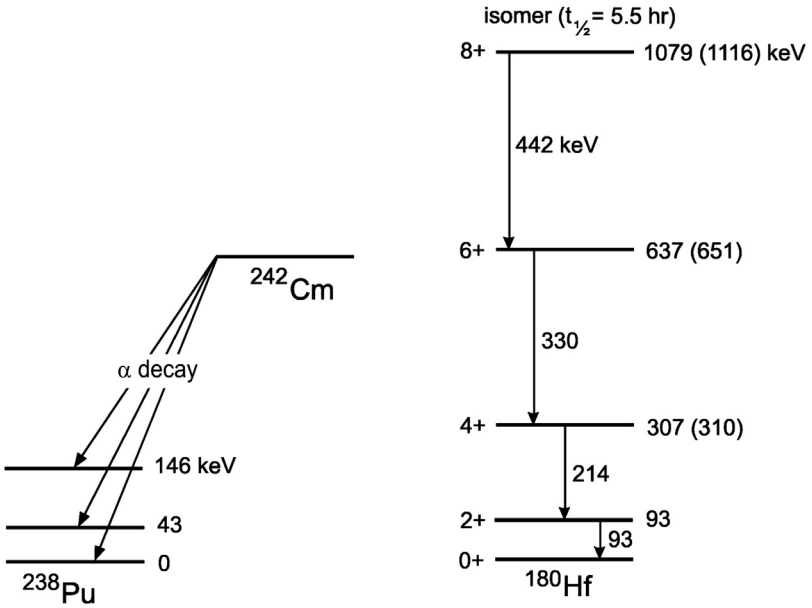

FIGURE 20.10 Rotational spectra for ^{238}Pu and ^{180}Hf. The spectrum of ^{180}Hf was deduced from the observed γ lines associated with the decay of the isomeric state. The nuclear spin states (0, 2, 4…) and parity (+) are given at the left of each energy plateau of ^{180}Hf, and the energies in keV are given to the right of each energy plateau. The *vertical arrows* pointing downward in the decay of ^{180}Hf represent the energy differences between the plateau and the magnitudes of the gamma-ray photon energies. The numbers in parenthesis are calculated from the energy of the first excited state, assuming the energies to be proportional to $I(I+1)$. *From Bohr, A., 1975. Rotational motion in nuclei. Nobel Lecture, December 11, 1975. http://www.nobelprize.org/nobel_prizes/physics/laureates/1975/bohr-lecture.pdf; Bohr, A., 1992. Rotational motion in nuclei. In: Lundqvist, S. (Ed.) Nobel Lectures, Physics 1971–1980. World Scientific Publishing, Singapore, reprinted with permission © The Nobel Foundation 1975.*

Similar calculations can be made to arrive at the calculated energy levels of 651 and 1116 keV of ^{180}Hf illustrated in Fig. 20.10. In his Nobel lecture, Bohr stated:

> *The spectrum of ^{238}Pu was established by Asaro and Perlman (1953) from measurements of the fine structure in the α-decay of ^{242}Cm. Subsequent evidence showed the spin-parity sequence to be 0+, 2+, 4+, and the energies are seen to be closely proportional to* I(I + 1).

These findings were the first to demonstrate that certain nuclear energy states can be explained on the basis that they constitute a nuclear rotational spectrum, thus providing convincing evidence for the collective model of the nucleus.

20.6 SUPERHEAVY NUCLEI

The superheavy elements (SHEs), also referred to as "superheavies," are those that contain nuclei with atomic number $Z > 104$. These do not occur naturally, and SHEs of atomic number $Z = 105$ to $Z = 118$ have been produced artificially. The quest to produce SHEs reached a seeming scientific and political impasse during the period 1965–1974, which is described in an interesting historical account by Dunn (2013) in the *National Geographic*. In this period the Lawrence Berkeley National Laboratory in California and Flerov Laboratory of Nuclear Reactions of the Joint Institute for Nuclear Research in Dubna, Russia both laid claim to the production of elements 102, 103, 104, 105, and 106. As Dunn (2013) describes, a dispute arose over which laboratory (Berkeley or Dubna) was the first to produce these elements. This dispute got ugly, as it was during the Cold War between the USA and Soviet Union. Dunn (2013) relates that compromise prevailed and "nuclear war" was averted by naming element 105 as dubnium, after the city of Dubna, and element 106 seaborgium after Glenn T. Seaborg, who was codiscoverer of the transuranium elements 94–103 and element 106.

The isotopes of the SHEs ($Z > 104$) which have been produced so far are unstable, with increasingly diminishing half-lives from elements 105 to 118. For example, the half-lives of these elements are measured in units of hours for element 105, minutes for elements 106 and 107, seconds for elements 108–114 and milliseconds for elements 115–118. While the SHEs produced so far (up to element 118) have very unstable nuclei, the current theory of shell structure of the atomic nucleus predicts certain "magic numbers" of protons and neutrons that would attribute a relatively high stability to yet much heavier elements.

The shell structure of the atomic nucleus with its magic numbers of protons and neutrons in the nucleus, first discovered by Maria Goeppert Meyer and Hans Jensen in 1948–1949, was described earlier in this chapter and in the Hall of Fame, Part IX. The shell structure describes the stable atomic nuclei as having magic numbers of 2, 8, 20, 26, 28, 50, and 82 protons or neutrons or 126 neutrons, which comprise closed shells of protons or neutrons in the nucleus of an atom that attribute to the atom exceptional stability. Atomic nuclei that are "doubly magic"—that is, those nuclei that contain magic numbers of closed shells for both protons and neutrons (eg, ^{4}He with $Z = 2$ and $N = 2$, ^{16}O with $Z = 8$ and $N = 8$, ^{40}Ca with $Z = 20$ and $N = 20$, ^{48}Ca with $Z = 20$ and $N = 28$, and ^{208}Pb with $Z = 82$ and $N = 126$)—are shown to be most stable.

The concept of the shell structure and magic numbers of protons and neutrons in the nucleus has been extended to the theory and synthesis of the SHEs. New magic numbers are predicted that would constitute closed shells of protons and neutrons in an atomic nucleus that would attribute stability to superheavy nuclei with $Z = 114$ and $N = 184$, or $Z = 120$ (Bender et al., 2001), or $Z = 126$ (Ćwiok et al., 1996). These magic numbers of closed shells of protons and neutrons are predicted to yield one or more elements with unusual stability, which could be measured with half-lives in thousands of years. These superheavy nuclides would have decayed, if they were produced at the time of the formation of the Earth, 4.5 billion years ago. Their predicted numbers of closed shells of protons and neutrons place them in the Chart of the Nuclides in a separate region referred to as the "Island of Stability," surrounded by a "Sea of Instability" composed of known and unstable radionuclides of very short half-life. Fig. 20.11 illustrates where the predicted Island of Stability would be found in the Chart of the Nuclides. The dark blue area and dark blue blocks in the region of $Z = 114–126$ and $N = 177–186$ identify the Island of Stability, surrounded by light blue, yellow, and green blocks representing the locations of very short-lived nuclides comprising the Sea of Instability.

Currently, element 114, namely flerovium, has been produced as isotopes with mass numbers in the range $A = 285$ to 289. Thus its heaviest known isotope (Fl-289) contains $A - Z = 289 - 114 = 175$ neutrons, which is below the predicted magic number of $N = 184$. Its measured half-life is reported to be 2.6 s. The difficulty lies in finding the mechanism of producing an isotope with the magic number of 184 neutrons, which would require adding an additional nine neutrons to flerovium-289, an isotope of element 114.

The predicted magic number of $Z = 120$, which would be element 120 with its predicted filled shell of protons, is yet to be produced. In a review on the shell structure of superheavy nuclei, Greiner (2008) notes that research utilizing meson field theory and other approaches indicates that the proton number $Z = 120$ should prove to be as much a magic number as $Z = 114$ (Rutz et al., 1997; Papazoglou et al., 1998, 1999; Beckmann et al., 2002). The corresponding magic number of neutrons for element 120 is predicted to be $N = 172$, and to a lesser degree $N = 184$ (Greiner, 2008). Work by R. A. Gherghescu, Greiner, and coworkers (Poenaru et al., 1987, 1989) calculated the potential energy surface of the $Z = 120$ nucleus; and the charge distribution of the $Z = 120$, $N = 184$ nucleus points to a hollow interior of that nucleus. This work

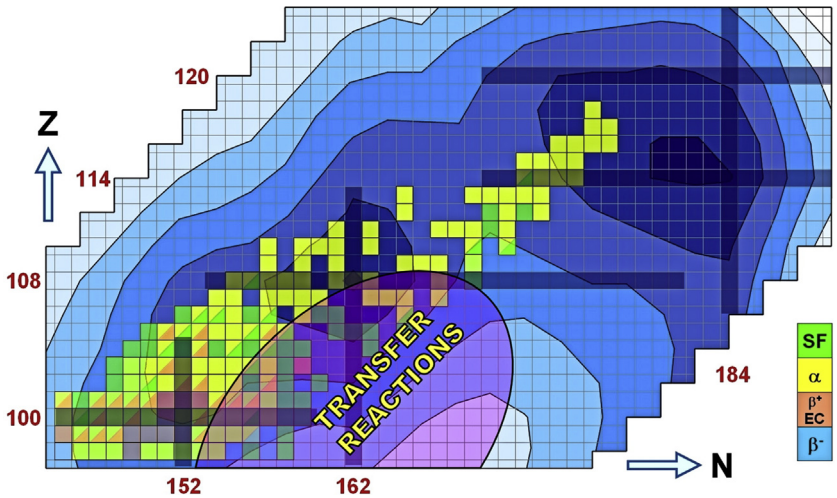

FIGURE 20.11 Section from the Chart of the Nuclides in the region of the heaviest known elements. The underlying contour plot shows the magnitude of shell stabilization according to microscopic–macroscopic calculations (Patyk et al., 1997). The predicted Island of Stability is clearly visible as a dark area close to $N = 184$ and $Z = 114$. Note that other calculations favor a closed proton shell at $Z = 120$ (Bender et al., 2001), or $Z = 126$ (Ćwiok et al., 1996) instead. Known nuclei are indicated with color-coded boxes according to their decay properties. The region of neutron-rich isotopes accessible via multinucleon transfer reactions is highlighted. *From Dvorak, J., et al., 2011. IRiS—Exploring new frontiers in neutron-rich isotopes of the heaviest elements with a new inelastic reaction isotope separator. Nucl. Instrum. Meth. Phys. Res. Sect. A 652, 687–691, reprinted with permission from Elsevier © 2011.*

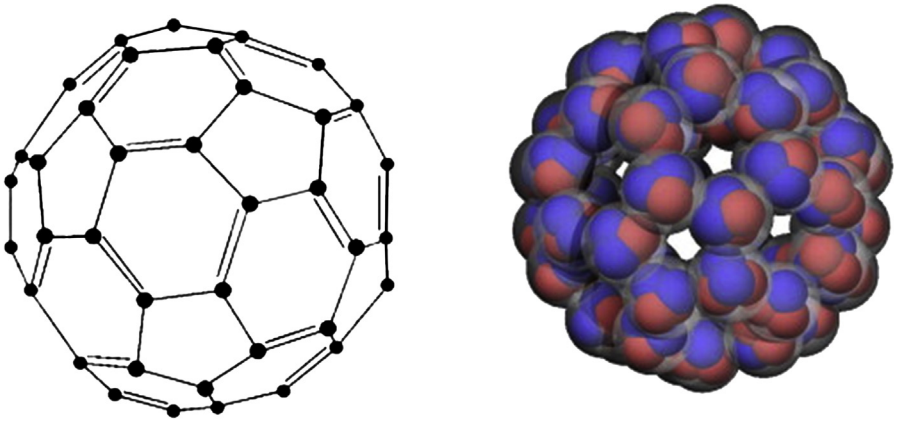

FIGURE 20.12 On the left is the typical molecular structure of the C_{60} carbon molecule fullerene. On the right is the nuclear case where the carbon atoms are replaced by α particles and the double bondings by additional neutrons. Such a structure would immediately explain the semihollowness of that superheavy nucleus, which is revealed in the mean-field calculations within meson field theories. *From Greiner, W., 2008. Structure of vacuum and elementary matter: from superheavies via hypermatter to antimatter—the vacuum decay in supercritical fields. In: Salomonson, S., Lindroty, E. (Eds.), Advances in Quantum Chemistry, vol. 53. Elsevier, pp. 99–150, reprinted with permission from Elsevier © 2008.*

indicates that such a nucleus would have a structure similar to the fullerene "buckyball" molecule that consists of 60 carbon atoms (C_{60}) in a spherical structure with hollow interior, as illustrated in Fig. 20.12. Greiner (2008) notes that these studies suggest that the nucleus with predicted doubly magic numbers $Z = 120$, $N = 184$ would consist of 60 α particles ($^4_2$He nuclei) with one additional binding neutron per α particle, as illustrated in Fig. 20.12. These studies point to a new frontier where elements beyond $Z = 118$ will be produced; and some of an exceptional stability with long half-lives measured to have magnitudes in the thousands of years. When the writer was a university student in the early 1960s, the shell structure of the atomic nucleus and the existence of magic numbers of protons and neutrons in the nucleus were an altogether new field. The buckyball structure of carbon molecules was unknown then. In years to come, amazing discoveries are expected with the production of new SHEs beyond element 118.

The current goal is to find the ways and means of producing neutron-rich SHEs within the Island of Stability. Dean and Hamilton (2011) describe the methods used by Yuri Oganessian and his team at the Flerov Laboratory of Nuclear Reactions at the Joint Institute for Nuclear Research in Dubna, Russia, and methods utilized at the Lawrence Livermore National Laboratory in California. Hofmann (2009) describes the fusion reactions based on lead and bismuth targets which were used by the Gesellschaft für Schwerionenforschung mbH in Darmstadt, Germany and/or at RIKEN in Wako, Japan for the synthesis of neutron-deficient isotopes of the elements 107–113; and the fusion reactions of ^{48}Ca projectiles with actinide targets whereby more neutron-rich isotopes of the elements 112–116 and even 118 were produced at the Flerov Laboratory of Nuclear Reactions. Also, the Lawrence Livermore National Laboratory produced elements 113–118 in a joint collaboration with the Flerov Laboratory. Elements 114 and 116 were named flerovium and livermorium in honor of the two laboratories.

The production of the SHEs 113–118 involved fusion reactions of "doubly magic" neutron-rich ^{48}Ca with massive actinide target elements. The ^{48}Ca stripped of its electrons is a highly stable nucleus containing magic numbers of both protons and neutrons ($Z = 20$ and $N = 28$). These nuclei are accelerated in a cyclotron against an actinide target, resulting in the fusion of the ^{48}Ca projectile and actinide according to the following examples:

$$^{243}_{95}\mathrm{Am} + ^{48}_{20}\mathrm{Ca} \rightarrow ^{288}_{115}\mathrm{Uup} + 3^1_0\mathrm{n} \rightarrow ^{284}_{113}\mathrm{Uut} + ^4_2\mathrm{He} \quad [20.33]$$

$$^{244}_{94}\mathrm{Pu} + ^{48}_{20}\mathrm{Ca} \rightarrow ^{292}_{114}\mathrm{Fl}^* \rightarrow ^{289}_{114}\mathrm{Fl} + 3^1_0\mathrm{n} \quad [20.34]$$

$$^{243}_{95}\mathrm{Am} + ^{48}_{20}\mathrm{Ca} \rightarrow ^{288}_{115}\mathrm{Uup} + 3^1_0\mathrm{n} \quad [20.35]$$

$$^{248}_{96}\mathrm{Cm} + ^{48}_{20}\mathrm{Ca} \rightarrow ^{296}_{116}\mathrm{Lv}^* \rightarrow ^{293}_{116}\mathrm{Lv} + 3^1_0\mathrm{n} \quad [20.36]$$

$$^{249}_{97}\mathrm{Bk} + ^{48}_{20}\mathrm{Ca} \rightarrow ^{297}_{117}\mathrm{Uus}^* \rightarrow ^{293}_{117}\mathrm{Uus} + 4^1_0\mathrm{n} \quad [20.37]$$

$$^{249}_{98}\mathrm{Cf} + ^{48}_{20}\mathrm{Ca} \rightarrow ^{294}_{118}\mathrm{Uuo} + 3^1_0\mathrm{n} \quad [20.38]$$

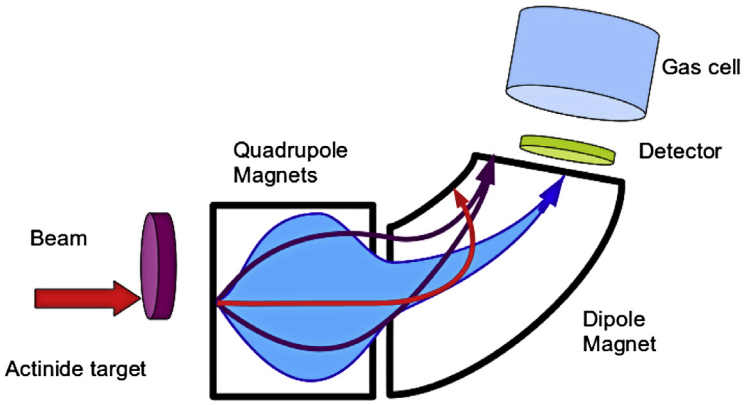

FIGURE 20.13 Schematic drawing of a separator based on a quadrupole design. Ions are focused in a pair of quadrupole magnets before they enter the dipole magnet, where they are separated according to their magnetic rigidity. The beam, which leaves the target without a nuclear interaction, has a low magnetic rigidity and is deflected to the inner wall of the dipole magnet. The intensity of the dipole field is tuned to guide the neutron-rich heavy transfer products into the focal plane detector (spectrometer mode) or the gas cell (product collection mode). *From From Dvorak, J., et al., 2011. IRiS—Exploring new frontiers in neutron-rich isotopes of the heaviest elements with a new inelastic reaction isotope separator. Nucl. Instrum. Meth. Phys. Res. Sect. A 652, 687–691, reprinted with permission from Elsevier © 2011.*

A new approach to the production of neutron-rich elements that reside in the Island of Stability is the application of multinucleon transfer reactions, reviewed by Dvorak et al. (2011) and Corradi et al. (2013). These reactions are usually carried out at lower projectile energies whereby one or more nucleons are transferred between the projectile and target nuclei. As described by Dvorak et al. (2011), these are deeply inelastic reactions in which the projectile and target nuclei come into contact and exchange a large number of nucleons before they separate. Dvorak et al. (2011) note that these reactions can yield a broad spectrum of products, including the neutron-rich isotopes of the heaviest elements. This technique requires lower and more gentle projectile energies than those used in fusion reactions, which can tend to "break up" target nuclei. A large source of neutron-rich isotopes that may be used in future multinucleon transfer reactions is highlighted in Fig. 20.11 in the region of the Chart of the Nuclides labeled "transfer reactions."

The acceleration of a beam of charged nuclei on to an actinide target for the production of SHEs can give numerous nuclear reaction products in addition to the SHEs. In addition, the SHEs produced to date all have short half-lives. The separation, detection, and measurement of newly produced SHEs require beam irradiation of target nuclei, then the separation of the beam nuclei and the scattered product ions which emerge from the target, followed by their detection and measurement. An instrument used to separate, detect, and measure reaction products of this type, referred to as a quadrupole separator/spectrometer, is designed to contain a combination of magnetic quadrupoles (multipoles) and a magnetic dipole, as described by Dvorak et al. (2011) and illustrated in Fig. 20.13.

When the beam of projectile nuclei strike the actinide target, reaction products (eg, transfer products) are scattered in many directions from the target material. These ions enter the separator, where quadrupole or multipole magnets will focus the product nuclei toward a central area in the first stage of the separator. The transfer products and nuclei of the original nuclear beam, which has not undergone any nuclear reaction, enter into the field of the dipole magnet, which will separate the ions according to their momentum rigidity (ie, their momentum-to-charge ratios). Ions of the nuclear beam, which had passed through the target material without reaction, are of low mass compared to the heavy transfer products. These ions thus have a lower magnetic rigidity and are deflected easily in the dipole magnetic field away from the detector and land on the inner wall of the dipole magnet. These ions are, in a sense, discarded. The dipole magnetic field is tuned to focus the superheavy transfer products on to a detector, which serves as a spectrometer for the determination of the particle mass and proton number for particle identification (Dvorak et al., 2011). An alternative mode of the separator is to remove the detector and replace it with a gas cell, as illustrated in Fig. 20.13, for the collection of the neutron-rich isotopes of the heaviest elements. The heavy elements are stopped in the gas cell—that is, the gas medium serves as a collector of the neutron-rich transfer products. The neutron-rich heavy elements in the collection gas can then be transferred to another experimental arrangement for measurement of their physical and chemical properties. Single- or double-charged ions are extracted from the gas via radiofrequency (RF) and direct current (DC) electrical fields through a nozzle with extraction times as short as 0.1 s (Dvorak et al., 2011). Another type of ion separator/spectrometer used to collect, detect, and measure the heavy ions is a solenoid-based design,

which utilizes a solenoid magnet to focus the transfer product ions according to momentum and charge on to a detector and/or gas cell collector. This design is described by Dvorak et al. (2011).

The future offers great promise for discoveries in the ways and means of producing neutron-rich SHEs with very long half-lives. P. Roy Chowdhury of the Saha Institute of Nuclear Physics in Kolkata, India and coworkers (Chowdhury et al., 2008) have modeled the decay modes of numerous isotopes of the SHEs, which indicate that a few isotopes could have half-lives which would measure from a few hundred years to as long as 100 million years. If these elements existed at the time of the creation of the Earth, they would not be found, as such isotope lifetimes would be too short compared to the age of the earth (4.5 billion years). If such elements are produced eventually, Dvorak et al. (2011) note that our knowledge of the isotopes in this region would open new fields in nuclear chemistry, nuclear and atomic physics, and nuclear astrophysics, of which the latter includes particularly nuclear processes that occur in supernovae.

For additional information the reader may peruse short and interesting articles by Dean (2008), Shiga (2011), and Dunn (2013).

20.7 CLUSTER RADIOACTIVITY

Cluster radioactivity is nuclear decay with the spontaneous emission of a particle heavier than an alpha particle with $Z \geq 6$. It is included in this part of the chapter because cluster radioactivity is an important phenomenon in the study of the properties of the nucleus, in particular nuclear stability and magic numbers.

Cluster radioactivity was first predicted by Sandulescu and Greiner (1977) and discovered by Rose and Jones (1984), who were the first to observe the emission of ^{14}C from the nucleus of ^{223}Ra. Since the discovery in 1984, intense experimental research at numerous institutions (see reviews by Price, 1989, 1994; Ronen, 1997; Bonetti and Guglielmetti, 1999; Santhosh et al., 2010) has uncovered numerous radionuclides of high mass number ($A \geq 221$) that emit clusters, including ^{14}C, ^{20}O, ^{23}F, ^{24}Ne, ^{28}Mg, and ^{32}Si. Radionuclides that exhibit cluster radioactivity are listed in Table 20.2 with their cluster decay modes and decay properties.

Cluster decay is a rare event that competes with alpha particle emission, ie, alpha decay. The probabilities of cluster decay for observed decay modes (ie, branching ratios) range from 10^{-9} to 10^{-17} of the alpha decay probability. All the decay modes listed in Table 20.2 yield product nuclei that possess magic numbers of protons ($Z = 82$) and/or neutrons ($N = 126$) with the exception of ^{211}Bi ($Z = 83$, $N = 128$), which is accompanied by the ^{14}C cluster in the decay of ^{225}Ac. However, in this exceptional case the ^{14}C cluster has the highest binding energy (BE) per cluster. Ronen (1997) compared the magic numbers, BEs per cluster, and Q values of the cluster decays listed in Table 20.2. From these comparisons, Ronen (1997) concluded the following.

1. The most likely mode of cluster radioactivity is when the light cluster has the highest BE per cluster and the daughter product is the doubly magic nucleus ^{208}Pb. We can see from Table 20.2 that, among the isotopes of Ra which yield the ^{14}C cluster, the decay mode yielding the doubly magic ^{208}Pb has the highest Q value. Also, among the isotopes of U and Pu, the decay modes that yield the doubly magic ^{208}Pb also have the highest Q values.
2. Nuclei that decay by cluster radioactivity have either a daughter that is magic ($N = 126$ or $Z = 82$) or a light emitted cluster with the highest BE per cluster. Nuclei that obey both conditions (magic number and highest BE per cluster for the emitted cluster) have shorter half-lives.

Because of the rarity of cluster radioactivity in comparison to alpha decay, the detection of emitted clusters must be done with a relatively high alpha activity. Certain solid-state nuclear track detectors insensitive to alpha particles (Durrani and Bull, 1987; Ilić and Durrani, 2003) serve as good means of detecting cluster radioactivity. However, Bonetti et al. (2001) point out that track detectors may not have enough A resolution to offer unambiguous identification. Thus to decide in favor of one of the most probable Ne clusters, Bonetti et al. (2001) resorted to theoretical calculations.

Several of the cluster decays listed in Table 20.2 are illustrated in Fig. 20.14, together with sections of the Chart of the Nuclides (Z versus N). This illustrates how cluster radioactivity competes with alpha particle emission, and results in large leaps in the Chart of the Nuclides from parent to daughter nuclides.

An important outcome of the discovery of cluster radioactivity was the reconfirmation of the magic numbers of closed shells of protons and neutrons in the nucleus that yield exceptional stability to atomic nuclei, discussed previously. Numerous works have been devoted to explaining the cluster decay process; these are summarized by Santhosh et al. (2010). There are two approaches to explaining the cluster decay process, namely that it is fission-like or alpha-like. In the fission model (Sandulescu et al., 1985; Greiner et al., 1985; Poenaru et al., 1985, 1986; Shi and Swiatecki, 1985; Shanmugam and Kamalaharan, 1988), the nucleus deforms continuously as the cluster penetrates the nuclear barrier. This would be somewhat similar to the nuclear fission process discussed previously. In the alpha-like or cluster model of decay

TABLE 20.2 Cluster Decay Modes and Properties[a]

Decay Mode[b]	Magic Number(s)[c]	*E* or *Q* Value (MeV)	Half-life (log $T_{½}$ (s))
$^{221}Fr \rightarrow {}^{207}Tl + {}^{14}C$	$N = 126$	29.28	14.5 ± 0.12
$^{221}Ra \rightarrow {}^{207}Pb + {}^{14}C$	$Z = 82$	30.34	13.0 ± 0.2
$^{222}Ra \rightarrow {}^{208}Pb + {}^{14}C$	$Z = 82$, $N = 126$	30.97	11.0 ± 0.06
$^{223}Ra \rightarrow {}^{209}Pb + {}^{14}C$	$Z = 82$	29.85	15.2 ± 0.05
$^{224}Ra \rightarrow {}^{210}Pb + {}^{14}C$	$Z = 82$	28.63	15.8 ± 0.12
$^{225}Ac \rightarrow {}^{211}Bi + {}^{14}C$	None	28.57	17.16 ± 0.06
$^{226}Ra \rightarrow {}^{212}Pb + {}^{14}C$	$Z = 82$	26.46	21.3 ± 0.2
$^{228}Th \rightarrow {}^{208}Pb + {}^{20}O$	$Z = 82$, $N = 126$	44.72	20.7 ± 0.08
$^{231}Pa \rightarrow {}^{208}Pb + {}^{23}F$	$Z = 82$, $N = 126$	46.68	26.0
$^{230}Th \rightarrow {}^{206}Hg + {}^{24}Ne$	$N = 126$	51.75	24.6 ± 0.07
$^{231}Pa \rightarrow {}^{207}Tl + {}^{24}Ne$	$N = 126$	54.14	22.9 ± 0.05
$^{232}U \rightarrow {}^{208}Pb + {}^{24}Ne$	$Z = 82$, $N = 126$	55.86	20.5 ± 0.03
$^{234}U \rightarrow {}^{210}Pb + {}^{24}Ne$	$Z = 82$	52.81	25.9 ± 0.2
$^{234}U \rightarrow {}^{206}Hg + {}^{28}Mg$	$N = 126$	65.26	25.7 ± 0.2
$^{236}Pu \rightarrow {}^{208}Pb + {}^{28}Mg$	$Z = 82$, $N = 126$	70.22	21.7 ± 0.3
$^{238}Pu \rightarrow {}^{208}Pb + {}^{30}Mg$	$Z = 82$, $N = 126$	67.00	25.7 ± 0.25
$^{238}Pu \rightarrow {}^{206}Hg + {}^{32}Si$	$N = 126$	78.95	25.3 ± 0.16

[a] *Decay mode, energy (E), and half-life data are from Price (1994) and Ronen (1997). The table is from L'Annunziata (2012g), reprinted with permission from Elsevier © 2012.*
[b] *Other cluster decays, not listed in the table, are $^{236}U \rightarrow {}^{206}Hg$ (N = 126) + ^{30}Mg, $^{236}Pu \rightarrow {}^{212}Pb$ (Z = 82) + ^{24}Mg, and $^{242}Cm \rightarrow {}^{208}Pb$ (Z = 82, N = 126) + ^{34}Si, reported by Tretyakova (1995), and $^{230}U \rightarrow {}^{208}Pb$ (Z = 82, N = 126) + ^{22}Ne and $^{226}Th \rightarrow {}^{208}Pb$ (Z = 82, N = 126) + ^{18}O, reported by Bonetti et al. (2001). The magic numbers of the product nuclei are in parenthesis, where the nucleus of ^{208}Pb is "doubly magic."*
[c] *The magic numbers are those of the cluster decay product nuclei.*

(Blendowske et al., 1987; Landowne and Dasso, 1986; Buck and Merchant, 1989; Malik and Gupta, 1989), the cluster is assembled in the nucleus in a similar fashion as the alpha particle is assembled before the cluster penetrates the nuclear potential barrier.

20.8 PROTON AND NEUTRON RADIOACTIVITY

In the previous chapters of this book various radionuclide decay modes are described as mechanisms whereby unstable nuclei emit particles and energy in their transitions from an elevated energy state to a lower or stable state (ground state). Some of these transitions to lower energy states involve the transformation of a proton to a neutron or a neutron to a proton in the nucleus, as in beta decay, whereby a nucleus arrives at a more stable ratio of protons/neutrons in the nucleus. Some artificially produced radionuclides—that is, radionuclides that are not encountered naturally, but those produced through nuclear reactions such as reactions facilitated with an accelerator—may possess an excess number of protons or neutrons. Such nuclei that are unstable due to an excess number of protons or neutrons are said to have exceeded their nucleon "drip line." The nucleon drip line, be it a proton drip line or neutron drip line, refers to the ratio of protons-to-neutrons in a nucleus (ie, the numbers of protons or neutrons in a nucleus) of a given element beyond which the isotopes of that element are unstable. Many isotopes produced by nuclear reactions via the bombardment of target nuclei with accelerated nuclei possess proton or neutron numbers beyond their drip lines and are unstable, with very short half-lives; and these are referred to as exotic isotopes. Such isotopes may undergo nuclear decay to a more stable state by emitting a proton or a neutron directly from the unstable nucleus. The nucleus literally "spits out" a proton or a neutron to achieve a more stable or optimum proton/neutron ratio. The direct emission of a proton or neutron from the nucleus is a decay process referred to as "proton radioactivity" or "neutron radioactivity," respectively. The process is also known as "proton emission" or "neutron emission," because of the very short half-lives of this decay process, measured most often in fractional seconds.

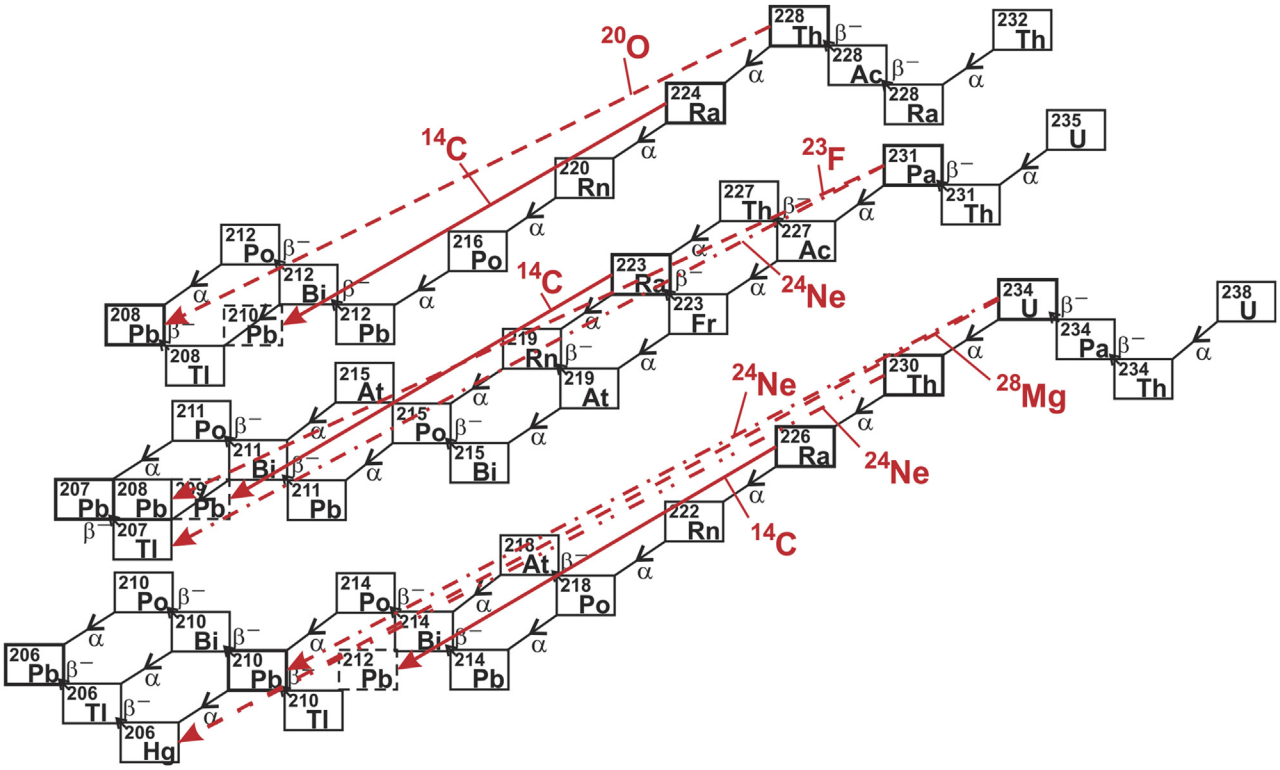

FIGURE 20.14 Cluster radioactivity of actinide nuclei. By emission of ^{14}C, ^{20}O,… "big leaps" in the periodic system can occur, just contrary to the known α-, β-, γ-radioactivities, which are also partly shown in the figure. *Caption and figure are from Greiner, W., 2008. Structure of vacuum and elementary matter: from superheavies via hypermatter to antimatter—the vacuum decay in supercritical fields. In: Salomonson, S., Lindroty, E. (Eds.), Advances in Quantum Chemistry, vol. 53. Elsevier, pp. 99–150, with red color added by the writer; reprinted with permission from Elsevier © 2008.*

As these radionuclides are produced artificially with very short half-lives, they are often referred to as "exotic nuclei." The decay process of direct "proton or neutron emission" may also be considered as exotic; however, much research is under way currently in this field, because it helps us understand the shell structure of the nucleus and its magic numbers of protons and neutrons in the stable nucleus.

20.8.1 Proton Radioactivity

The phenomenon of proton radioactivity is eloquently introduced by Blank et al. (2003), as quoted below, and this introduction applies also to the phenomenon of neutron radioactivity.

> *The atomic nucleus is made up of positively-charged protons and neutral neutrons, the nucleons. To form a stable atomic species, a balance between the number of neutrons and of protons has to be respected. For light nuclei, this requires an equal number of both nucleons. Beyond mass or nucleon number $A = 40$, stable atomic nuclei accommodate more neutrons than protons to outbalance the repulsion of the charged protons. The number of neutrons with respect to the number of protons increases until reaching a neutron number of $N = 126$ and a proton number $Z = 82$ for lead.*
>
> *Nuclei which do not respect this balance are unstable and decay by radioactive processes. For a minor disequilibrium, β decay occurs: an excess neutron is transformed into a proton and vice versa by emitting an electron/positron and an anti-neutrino/neutrino. If the imbalance between proton and neutron numbers is too large, the nuclear forces can no longer bind all nucleons and the atomic nucleus becomes particle-unstable. Thus the limits of nuclear stability are reached and the unstable nucleus will emit single excess nucleons or clusters of nucleons. The emission of clusters of two protons and two neutrons, a ^4He nucleus, was the first radioactivity observed and was called α radioactivity. It occurs mainly for very heavy nuclei in the lead to uranium region ($Z = 82$–92), but also for very proton-rich lighter nuclei. For the heaviest nuclear species, fission may occur, where the heavy nucleus splits into two medium-heavy pieces.*

Theoretical investigations [Goldansky, 1960, 1961] in the 1960s predicted that for medium-mass (A = 50−100) nuclei, other new radioactive decays might occur. For very proton-rich odd-Z nuclei, one-proton radioactivity, i.e., the emission of one single excess proton, should be observable, whereas for even-Z nuclei with a large proton excess, two-proton radioactivity, the emission of a pair of protons, should occur. Although these one-proton or two-proton emitting nuclei are particle-unbound, they may exhibit a measurable half-life due to the Coulomb barrier the protons have to tunnel through.

Reproduced from Blank et al. (2003), with permission © 2003 Elsevier Masson SAS. All rights reserved.

20.8.1.1 Beta-Delayed Proton Emission

The first observation of proton radioactivity was a proton emission from an excited state (elevated energy state) of a nucleus following beta decay (Barton et al., 1963), which is referred to as "beta-delayed proton emission." This process is abbreviated as β^+(p) or β^+(2p), to signify the emission of one proton or two protons from a nucleus that was the product of positron emission. Silicon-25 was the radionuclide from which beta-delayed proton emission was observed for the first time by Barton et al. (1963). The radionuclide was produced by bombarding aluminum with 97 MeV protons. The researchers also produced other radionuclides, namely ^{21}Mg, ^{17}Ne, and ^{13}O, that decayed by the same process after bombarding various elements with accelerated protons. They observed that all of the beta-delayed proton emissions, where a parent nuclide with a proton and neutron number (Z, N) is of the form $(2k + 2,\ 2k - 1)$, exhibited the following decay sequence:

$$(2k+2,\ 2k-1) \xrightarrow{\beta^+} (2k+1,\ 2k)^* \xrightarrow{p} (2k,\ 2k) \qquad [20.39]$$

In this reaction sequence, the notation above each arrow signifies the decay process (ie, β^+ for beta decay with positron emission and p for proton emission). The asterisk in Eq. [20.39] signifies an excited or elevated energy state of the daughter nuclide of the beta decay.

The beta-delayed proton emissions observed by Barton et al. (1963) in the decay of ^{25}Si, ^{21}Mg, ^{17}Ne, and ^{13}O exhibited decay sequences in accord with Eq. [20.39], which are written as

$$^{25}_{14}\mathrm{Si}_{11} \xrightarrow[t_{1/2}=220\ \mathrm{ms}]{\beta^+} {}^{25}_{13}\mathrm{Al}_{12} + \beta^+ + \nu \xrightarrow{p} {}^{24}_{12}\mathrm{Mg}_{12} + p \qquad [20.40]$$

$$^{21}_{12}\mathrm{Mg}_{9} \xrightarrow[t_{1/2}=122\ \mathrm{ms}]{\beta^+} {}^{21}_{11}\mathrm{Na}_{10} + \beta^+ + \nu \xrightarrow{p} {}^{20}_{10}\mathrm{Ne}_{10} + p \qquad [20.41]$$

$$^{17}_{10}\mathrm{Ne}_{7} \xrightarrow[t_{1/2}=109.2\ \mathrm{ms}]{\beta^+} {}^{17}_{9}\mathrm{F}_{8} + \beta^+ + \nu \xrightarrow{p} {}^{16}_{8}\mathrm{Ne}_{8} + p \qquad [20.42]$$

$$^{13}_{8}\mathrm{O}_{5} \xrightarrow[t_{1/2}=8.6\ \mathrm{ms}]{\beta^+} {}^{13}_{7}\mathrm{F}_{6} + \beta^+ + \nu \xrightarrow{p} {}^{12}_{6}\mathrm{C}_{6} + p \qquad [20.43]$$

The decay process, beta decay with positron emission (β^+), is written above each arrow and the half-life of the radionuclide below an arrow.

A typical decay scheme of beta-delayed proton emission, as an example, is illustrated in Fig. 20.15. The decay scheme illustrates ^{48}Fe, which decays with a half-life of 43.3 ms by beta decay with positron emission to a daughter nuclide ^{48}Mn. At an elevated energy state, 14.6% of the ^{48}Mn daughter nuclides decay by proton emission to the granddaughter nuclide ^{47}Cr. Gamma-ray emission accompanies daughter nuclide deexcitation. The decay equation is written as follows:

$$^{48}_{26}\mathrm{Fe}_{22} \xrightarrow[t_{1/2}=43.3\ \mathrm{ms}]{\beta^+} {}^{48}_{25}\mathrm{Mn}_{23} + \beta^+ + \nu \xrightarrow{p} {}^{47}_{24}\mathrm{Cr}_{23} + p \qquad [20.44]$$

Beta-delayed proton emission may involve the sequential emission of two protons following beta decay, as in the decay of ^{26}P, described by Honkanen et al. (1983). The decay of ^{26}P occurs according to the following sequence:

$$^{26}_{15}\mathrm{P}_{11} \xrightarrow{\beta^+} {}^{26}_{14}\mathrm{Si}_{12} + \beta^+ + \nu \xrightarrow{p} {}^{25}_{13}\mathrm{Al}_{12} + p \xrightarrow{p} {}^{24}_{12}\mathrm{Mg}_{12} + p \qquad [20.45]$$

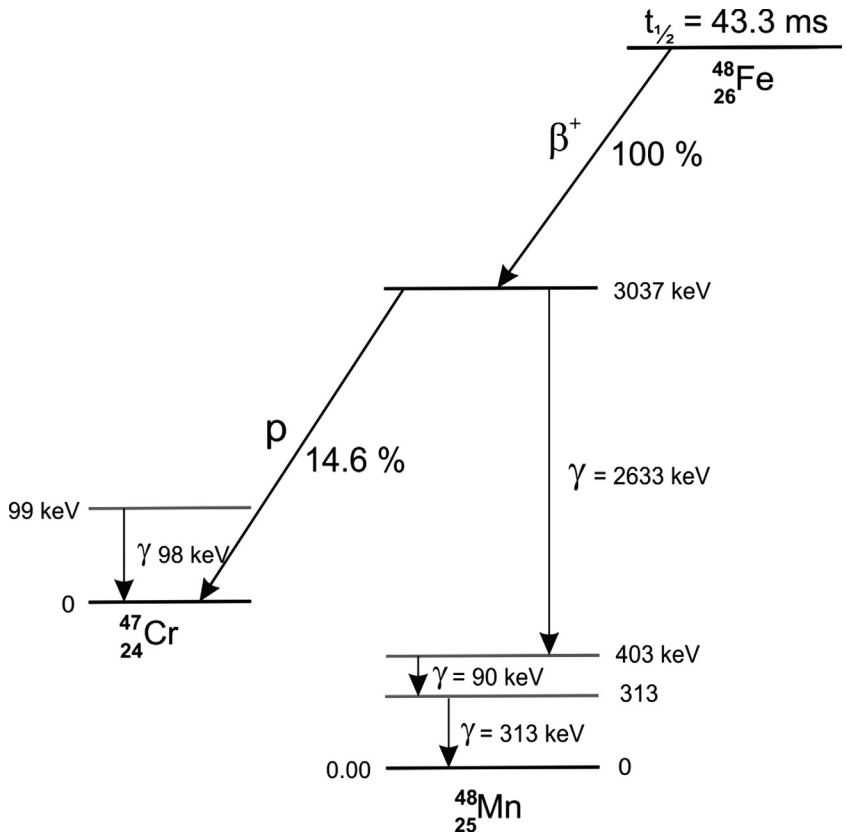

FIGURE 20.15 The scheme for beta-delayed proton emission in the decay of ^{48}Fe. The positron (β^+) and proton (p) emission intensities are from Audi et al. (2003). As illustrated, 14.6% of the elevated ^{48}Mn daughter nuclides undergo proton emission to ^{47}Cr. The remaining 85.4% decay by gamma-ray emission to the ground state of ^{48}Mn. *From Dossat, C., et al., 2007. The decay of proton-rich nuclei in the mass A = 36–56 region. Nucl. Phys. A 792, 18–86, reprinted with permission from Elsevier © 2007.*

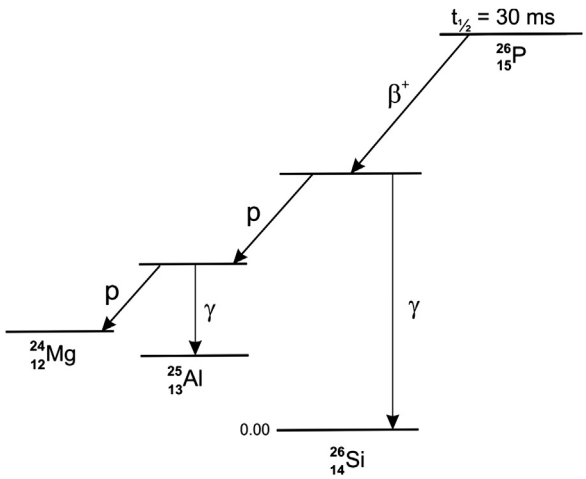

FIGURE 20.16 The scheme for the beta-delayed two-proton emission decay of ^{26}P according to the reaction sequence described by Eq. [20.45]. *Adapted from Honkanen, J., et al., 1983. Beta-delayed two-proton decay of ^{26}P. Phys. Lett. B 133B, 146–148, with permission from Elsevier © 1983.*

Such a decay scheme is abbreviated as β^+(2p), and its simplified decay scheme is illustrated in Fig. 20.16. As described by Honkanen et al. (1983), the two protons are not emitted simultaneously but in a sequential two-step process. As they explain and as illustrated in the decay scheme of Fig. 20.16, one proton is emitted to an energy level of an intermediate nucleus, which then becomes unbound to a subsequent emission of a second proton.

20.8.1.2 Direct Proton Emission

Proton emission from exotic nuclei may also occur directly from an unstable nucleus that possesses an excess number of protons, without the initial beta decay. Direct proton radioactivity occurs by the following sequence:

$$ {}^{A}_{Z}\mathrm{X}_{N} \rightarrow {}^{A-1}_{Z-1}\mathrm{Y}_{N} + p \qquad [20.46] $$

where a radionuclide X of atomic number Z, mass number A, and neutron number N emits a proton p to transform into an isotope of element Y of atomic number $Z - 1$, mass number $A - 1$, and neutron number N.

The first direct proton emission as a radioactive decay process was observed by Jackson et al. (1970) and Cerny et al. (1970) in the decay of ^{53m}Co, following the production of this exotic isotope of cobalt by the cyclotron bombardment of ^{40}Ca target with 81 MeV ^{16}O ions or the bombardment of an ^{54}Fe target with 32 MeV protons according to the reactions ^{40}Ca(^{16}O,2np)^{53m}Co and ^{54}Fe(p,2n)^{53m}Co, respectively. These abbreviated reaction notations with parentheses are described later in this chapter, and read as follows: "target nucleus (projectile, emitted particle) product nucleus." The ^{53m}Co was observed by Jackson et al. (1970) to decay with the direct emission of a 1.53 MeV proton, and the decay scheme is illustrated in Fig. 20.17.

The direct emission of a proton as a disintegration mode of a nuclear ground-state was first observed by Hofmann et al. (1982) in the direct proton decay of ^{151}Lu, and by Klepper et al. (1982) in the proton decay of ^{147}Tm. As noted by Klepper et al. (1982), this work demonstrated for the first time that direct proton decay is a possible disintegration mode of nuclear ground states similar to disintegration processes that occur with alpha and beta decay, as well as nuclear fission. The decay sequence, half-lives, and proton emission energies of the direct proton emission decay modes of the two radionuclides are the following:

$$ {}^{151}_{71}\mathrm{Lu} \xrightarrow{t_{1/2} = 80.6\ \mathrm{ms}} {}^{150}_{70}\mathrm{Yb} + \mathrm{p}\ (1.23\ \ \mathrm{MeV}) \qquad [20.47] $$

$$ {}^{147}_{69}\mathrm{Tm} \xrightarrow{t_{1/2} = 580\ \mathrm{ms}} {}^{146}_{68}\mathrm{Er} + \mathrm{p}\ (1.06\ \ \mathrm{MeV}) \qquad [20.48] $$

Two-proton radioactivity—that is, the direct emission of two protons from an atomic nucleus that has an excess number of protons, ie, beyond the proton drip line—is also possible. The two-proton emission from such a nucleus could occur in a sequential process, described by Blank et al. (2003) as follows:

> … *one-proton emission populates a well-defined quantal state in the one-proton daughter, before a second one-proton emission occurs to a two-proton daughter state.*

This sequential emission of two protons in nuclear decay is illustrated in the left-hand portion of Fig. 20.18. The term "mass excess" in the figure is a measure of the energy levels of each nuclear state, which is determined by the energy equivalence to mass of the nuclides. The mass excess, as defined by Audi et al. (2003a.b), is the difference between the atomic mass (in mass units) and the mass number for each nuclear state. Thus the mass excess is a measure of the energy levels, and is expressed usually in units of keV or MeV. The simultaneous emission of two protons from the nucleus

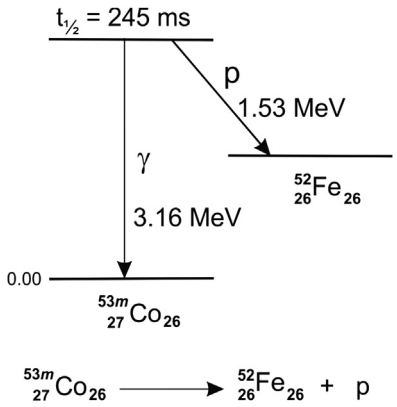

FIGURE 20.17 Direct proton emission decay scheme and decay equation of ^{53m}Co. *Adapted from Jackson, K. P., et al., 1970. ^{53m}Co: A proton-unstable isomer. Phys. Lett. B 33(4), 281–283., with permission from Elsevier © 1970.*

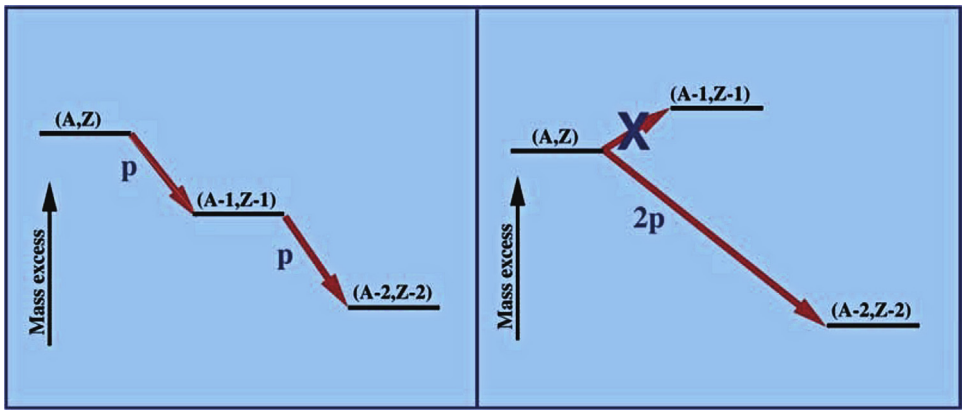

FIGURE 20.18 Schematic representation of sequential (left) and simultaneous (right) two-proton emission. If the one-proton daughter state is energetically not accessible, the emission has to be simultaneous. *Reproduced from Blank, B., et al., 2003. First observation of two-proton radioactivity from an atomic nucleus. C. R. Physique 4, 521–527 with permission © 2003 Elsevier Masson SAS. All rights reserved.*

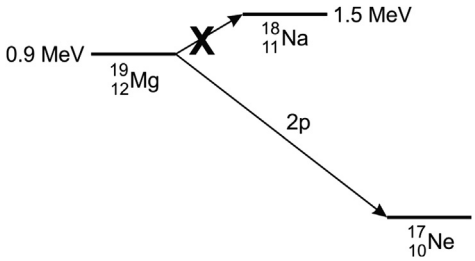

FIGURE 20.19 The predicted decay scheme by the simultaneous emission of two protons. *Adapted from Mukha, I., Schrieder, G., 2001. Two-proton radioactivity as a genuine three-body decay: the ^{19}Mg probe. Nucl. Phys. A 690, 280–283, with permission from Elsevier © 2001.*

could occur when the one-proton daughter state is energetically not possible (ie, a forbidden transition), as illustrated in the right-hand portion of Fig. 20.18. The simultaneous emission of two protons is explained by Blank et al. (2003) as follows:

> *…the nuclear pairing force, which couples two nucleons of the same type to gain energy, is responsible for the fact that the masses of even-Z nuclei (in our case those of the two-proton emitter and the two-proton daughter) are smaller than the one of the one-proton daughter, thus rendering one-proton emission impossible [see Fig. 20.18]. In such a case, the two protons have to be emitted simultaneously for energy conservation.*

Blank et al. (2003), reproduced with permission © 2003 Elsevier Masson SAS. All rights reserved.

An example of the simultaneous emission of two protons in a direct two-proton emission according to the sequence illustrated in the right-hand part of Fig. 20.18 is taken from the work of Mukha and Schneider (2001). They predicted the decay of ^{19}Mg to proceed by a simultaneous two-proton emission to ^{17}Ne due to the higher energy state of the one-proton emission daughter, as illustrated in Fig. 20.19. The predicted two-proton emission daughter nuclide ^{17}Ne was found to decay by simultaneous two-proton emission by Chromik et al. (1998). It is interesting to note here that the decay sequence from ^{17}Ne would stop at the production of stable ^{15}N, which contains the magic number of eight neutrons according to the following:

$$^{17}_{10}\mathrm{Ne} \xrightarrow[t_{1/2}=109\ \mathrm{ms}]{2p} {}^{15}_{8}\mathrm{O} + 2p \xrightarrow[122\ \mathrm{s}]{\beta^+} {}^{15}_{7}\mathrm{N}\ (\mathrm{stable}) + \beta^+ + \nu \qquad [20.49]$$

20.8.1.3 Detection and Measurement of Simultaneous Proton Radioactivity

The detection and measurement of protons emitted simultaneously during radionuclide decay are accomplished with position-sensitive detectors, such as the Si semiconductor microstrip detector arrangement illustrated in Fig. 20.20. Energy detectors can use solid scintillation or semiconductors. The principles behind these Si semiconductor and scintillation detection devices are provided in reviews by Verplancke et al. (2012) and L'Annunziata (2012c).

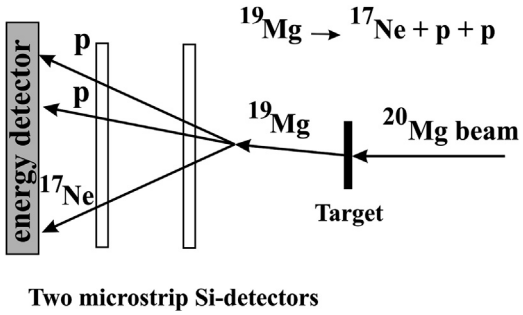

FIGURE 20.20 Experimental arrangement for simultaneous detection of the emission of protons and the ^{17}Ne daughter nuclide from ^{19}Mg disintegration. A beam of ^{20}Mg ions is accelerated to bombard against a target, resulting in a nuclear reaction causing a neutron "knock out" from the ^{20}Mg nucleus, yielding ^{19}Mg. The ^{19}Mg disintegrates in flight by the emission of two protons, producing the daughter nuclide ^{17}Ne. The directions of flight are determined by alignments of signals from the microstrip detectors; and the particle energies can be measured by scintillation detectors. *From Mukha, I., Schrieder, G., 2001. Two-proton radioactivity as a genuine three-body decay: the ^{19}Mg probe. Nucl. Phys. A 690, 280–283, reprinted with permission from Elsevier © 2001.*

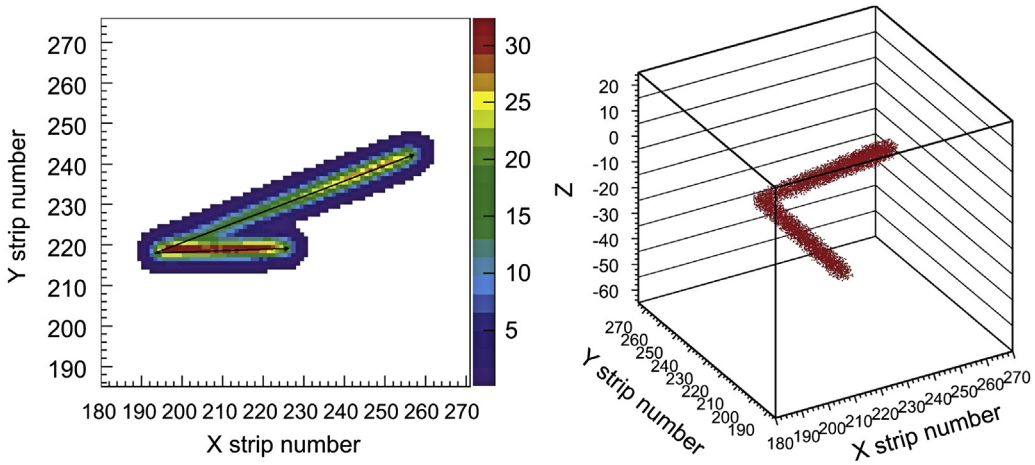

FIGURE 20.21 Two-dimensional (left) and three-dimensional (right) views of ^{45}Fe events as reconstructed from the strip information in X and Y. The color/gray code is indicative of the energy loss detected by the strips. *Reproduced from Blank, B., et al., 2010. A time projection chamber for the three-dimensional reconstruction of two-proton radioactivity events. Nucl. Instrum. Methods Phys. Res. Sect. A 613, 65–78, reprinted with permission from Elsevier © 2010.*

A gas electron multiplier detector is often used to detect and measure particles in nuclear reactions and decay. This is an advanced ionization detector which can provide images of particle tracks with X- and Y-direction readout strips. Gas electron multiplier detectors were introduced by Sauli (1997); and the current state of the art in the operation and applications of these detectors in particle physics is provided by Sauli (2014). An example of two- and three-dimensional images of a two-proton radioactivity event is illustrated in Fig. 20.21. This figure provides an image and the intensities of the two protons emitted simultaneously in the radioactive decay of ^{45}Fe. The radionuclide ^{45}Fe decays by beta-delayed proton emission; that is, the ^{45}Fe decays by positron emission to an elevated energy state of ^{45}Mn, which then emits simultaneously two protons to ^{43}V as described by the following decay sequence:

$$^{45}_{26}\mathrm{Fe} \xrightarrow[t_{1/2}=3.2\ \mathrm{ms}]{\beta^+} {}^{45}_{25}\mathrm{Mn} + \beta^+ + \nu \xrightarrow{2p} {}^{43}_{23}\mathrm{V} + 2p\ (1.1\ \ \mathrm{MeV}) \qquad [20.50]$$

The two protons that are emitted simultaneously share 1.1 MeV (Pfützner et al., 2002; Giovinazzo et al., 2002), which is written into the decay sequence of Eq. [20.50]. The relatively equal sharing of the 1.1 MeV energy by the two protons is evidenced in Fig. 20.21 by the relatively equal length of travel of the two protons in the gas ionization detector.

Another experimental arrangement used for the measurement of proton radioactivity is the optical time projection chamber (OTPC), developed by Miernik et al. (2007a,b) and utilized by Pomorski et al. (2011) for the beta-delayed emission of one, two, and three protons in the nuclear decay of ^{43}Cr. The OTPC, described by Pomorski et al. (2011),

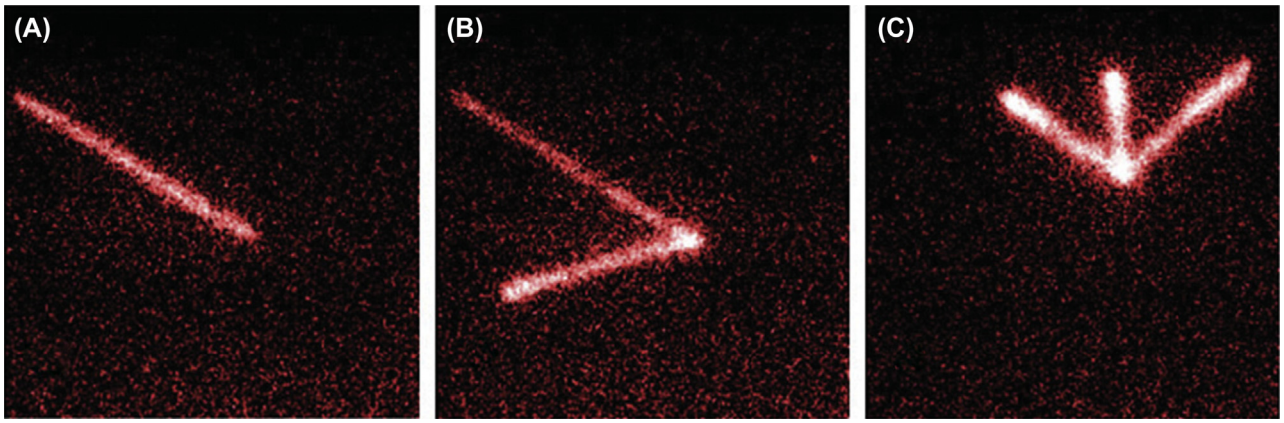

FIGURE 20.22 Example CCD images of ^{43}Cr decays by β-delayed proton(s) emissions, recorded in the synchronous mode of an OTPC detector in which the track of an incoming ion is not seen. The cases of emission of (A) a single proton, (B) two protons, and (C) three protons are shown. The ionizing power of the positron is too small to see its trace. In the synchronous mode of the OPTC detector the CCD camera image is started by a trigger, which avoids the image of the incoming heavy ions. *From Pomorski, M., et al., 2011. β-delayed proton emission branches in ^{43}Cr. Phys. Rev. C 83, 014306, reprinted with permission by the American Physical Society © 2011, http://dx.doi.org/10.1103/PhysRevC.83.014306.*

consists of an ionization counting chamber measuring $20 \times 20 \times 42$ cm^3 filled with a mixture of He, Ar, N_2, and methane gas. Charged particles (eg, protons) produce ionization (ie, ion pairs) in the gas; and the primary electrons drift in a uniform electric field toward a double-stage amplification structure formed by parallel-mesh flat electrodes. In this multiplication stage UV (ultraviolet) photons are emitted and the UV wavelengths are converted to the visual range by a thin luminescent foil providing an image of particle tracks, which are recorded by a charge-coupled device (CCD) camera and photomultiplier tube. CCD camera images of the simultaneous emission of one, two, and three protons from the beta-delayed proton emission decay of ^{43}Cr are illustrated in Fig. 20.22. The decay schemes are as follows:

$$^{43}_{24}\mathrm{Cr} \xrightarrow[t_{1/2}=21.6\ \mathrm{ms}]{\beta^+} {}^{43}_{23}\mathrm{V} + \beta^+ + \nu \xrightarrow{p} {}^{42}_{22}\mathrm{Ti} + p \qquad [20.51]$$

$$^{43}_{24}\mathrm{Cr} \xrightarrow[t_{1/2}=21.6\ \mathrm{ms}]{\beta^+} {}^{43}_{23}\mathrm{V} + \beta^+ + \nu \xrightarrow{2p} {}^{41}_{21}\mathrm{Sc} + 2p \qquad [20.52]$$

$$^{43}_{24}\mathrm{Cr} \xrightarrow[t_{1/2}=21.6\ \mathrm{ms}]{\beta^+} {}^{43}_{23}\mathrm{V} + \beta^+ + \nu \xrightarrow{3p} {}^{40}_{20}\mathrm{Ca} + 3p \qquad [20.53]$$

The branching ratios for the emission of one, two, and three protons were determined by Pomorski et al. (2011) to be 81, 7.1, and 0.1%, respectively.

Over 40 exotic nuclei have been identified that exhibit proton radioactivity. These are artificially produced via nuclear reactions; and they have short half-lives of the order of seconds or milliseconds. Their study has provided much insight into nuclear structure in terms of proton and neutron shells, nuclear stability, and proton and neutron drip lines. For further reading, extensive reviews on proton radioactivity are available in Pfützner et al. (2012), Pfützner (2013), and Roeckl and Mukha (2013).

20.8.2 Neutron Radioactivity

The term "neutron radioactivity" should not be confused with the emission of neutrons from heavy nuclei following nuclear fission reactions, or neutron emission as the result of the decay of nuclei by spontaneous fission. Somewhat analogous to proton radioactivity, described previously, neutron radioactivity refers to the direct emission of neutrons from light nuclei that possess an excess number of neutrons—that is, a number of neutrons beyond their neutron drip line.

20.8.2.1 Beta-Delayed Neutron Emission

Neutron radioactivity most commonly occurs as a beta-delayed process; that is, neutron emission from the atomic nucleus occurs following beta (β^-) decay. Beta-delayed neutron emission by fission products is an important source of

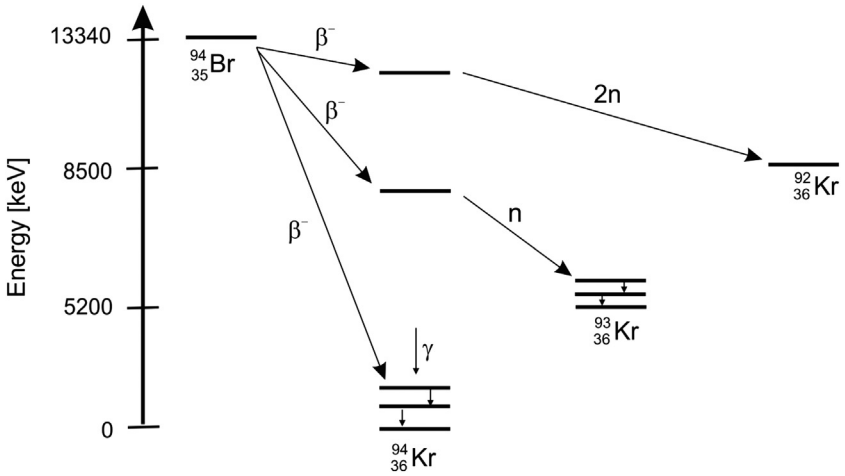

FIGURE 20.23 Beta-delayed neutron emission ($\beta^- n$ and $\beta^- 2n$) from neutron-rich ^{94}Br. *Adapted from Rykaczewski (2008), Holifield Radioactive Ion Beam Facility for the US Department of Energy: https://www.phy.ornl.gov/hribf/app/decay/neutrons.shtml.*

neutrons that contributes to the total number of neutrons responsible for the continuity of nuclear fission chain reactions in nuclear power reactors.

Beta-delayed neutron emission involves the emission of one or more neutrons from a neutron-rich nucleus when the neutrons exist in neutron-unbound states in a daughter nucleus at an elevated energy following beta decay (Birch et al., 2014). This decay process is abbreviated as $\beta^- n$, $\beta^- 2n$, or $\beta^- 3n$, for the emission of one, two, or three neutrons following beta decay. The emission of four neutrons from a beta-decay daughter nucleus at an excited state is possible, but not yet confirmed. The half-lives of nuclei that exhibit neutron radioactivity are considerably shorter than those that undergo proton radioactivity, because a neutron, due to its lack of charge, does not encounter any coulomb barrier to hinder its emission from a nucleus. When half-lives are very short ($<10^{-12}$ s), the process may be termed neutron emission rather than neutron radioactivity, as described by Thoennessen et al. (2013).

An example of beta-delayed neutron emission, namely $\beta^- n$ and $\beta^- 2n$, in the decay of ^{94}Br is illustrated in Fig. 20.23. The element bromine has an atomic number $Z = 35$, whereby the isotope ^{94}Br with a neutron number of 59 ($N = 94 - 35 = 59$) is very rich in neutrons. The beta decay of ^{94}Br leaves neutrons of the daughter nuclei ^{94}Kr at elevated unbound energy states, permitting their emission from the ^{94}Kr nucleus to form ^{93}Kr or ^{92}Kr, respectively. Either one or two neutrons are emitted simultaneously from the ^{94}Kr nucleus, and the neutron-emission decay sequences may be written as follows:

$$^{94}_{35}\mathrm{Br} \xrightarrow[t_{1/2}=70\ \mathrm{ms}]{\beta^-} {}^{94}_{36}\mathrm{Kr} + \beta^- + \overline{\nu} \xrightarrow{n} {}^{93}_{36}\mathrm{Kr} + n \qquad [20.54]$$

$$^{94}_{35}\mathrm{Br} \xrightarrow[t_{1/2}=70\ \mathrm{ms}]{\beta^-} {}^{94}_{36}\mathrm{Kr} + \beta^- + \overline{\nu} \xrightarrow{2n} {}^{92}_{36}\mathrm{Kr} + 2n \qquad [20.55]$$

Among the light nuclei ($Z \leq 28$), there are numerous isotopes for which the beta-delayed neutron emission probabilities have been measured. By the year 2014 a total of 203 nuclei had been identified as potential precursors to beta-delayed neutron emission; among these, the probabilities of $\beta^- n$ emission have been measured experimentally for 109 nuclei, whereas probabilities of $\beta^- 2n$ emission have been measured experimentally for only 19, and the probabilities of $\beta^- 3n$ emission measured in four nuclei (Birch et al., 2014). The beta-delayed emission of four neutrons (ie, $\beta^- 4n$), is yet to be measured. The nuclides that exhibit neutron radioactivity are found in the neutron-rich region of the Chart of the Nuclides, which is a Z versus N plot of the nuclides. These are illustrated in Fig. 20.24 for nuclides in the region of $Z \leq 28$. The radionuclides that decay by beta-delayed $1n$ emission ($\beta^- n$) are marked in red. Nuclides decaying by $\beta^- 2n$ and $\beta^- 3n$ are fewer in number, as mentioned previously. Also, as noted by Birch et al. (2014), all nuclides that decay by $\beta^- 2n$ also decay by $\beta^- 1n$ precursors; and all $\beta^- 3n$ precursors are also $\beta^- 2n$ and $\beta^- 1n$. Nuclides that exhibit negatron emission and neutron radioactivity reside in the neutron-rich side of the Chart of the Nuclides, ie, the region to the right of the black stable line of nuclides; whereas nuclides that decay by positron emission and exhibit proton radioactivity are found in the region to the left of the black line. Nuclides that decay by proton emission are not identified in Fig. 20.24; however, they reside among the yellow boxes of proton-rich nuclides to the left of the black boxes of stable nuclides.

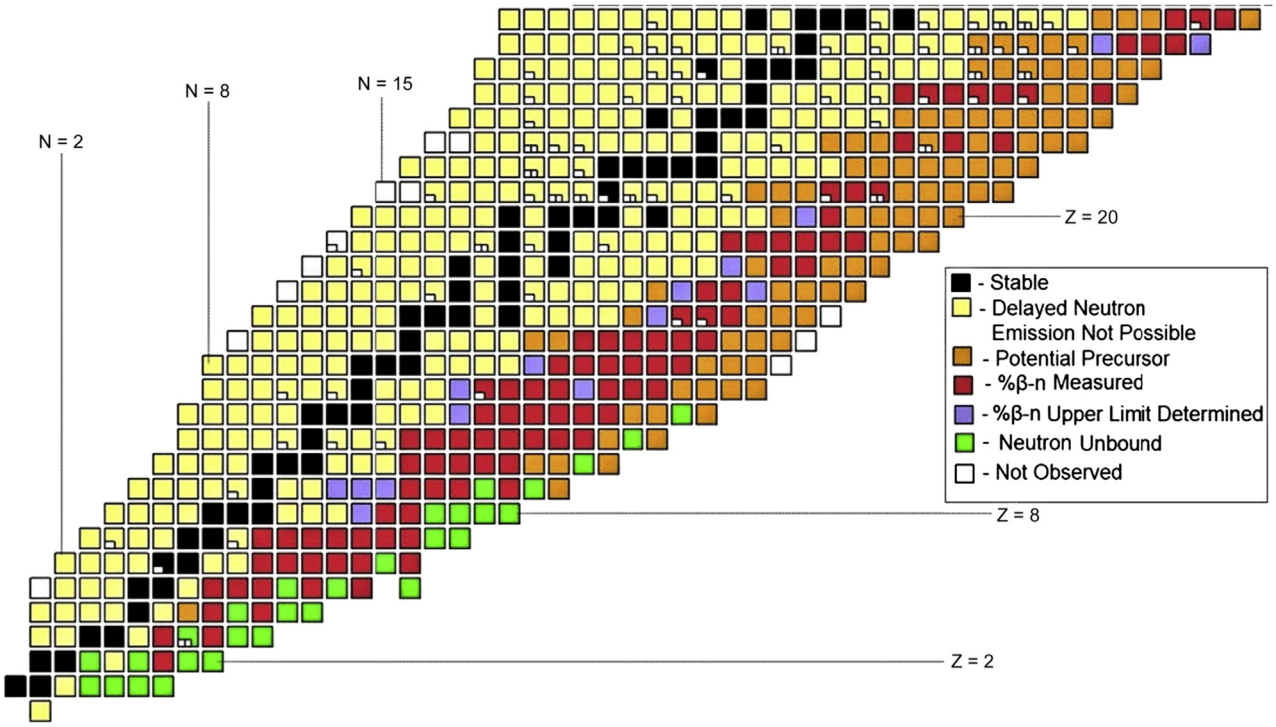

FIGURE 20.24 Chart of nuclides for $Z \leq 28$ nuclei. The coloring of the boxes indicates the measurement status of single-neutron decay emission probability, P_{1n}. *Small white boxes* indicate the existence of an isomer for that isotope. *Adapted from the NUCLEUS display software of the Atomic Mass Data Center: http://amdc.in2p3.fr/web/nubdisp_en.html.*

20.8.2.2 Direct Neutron Emission

The direct emission of neutrons from neutron-rich nuclei can occur; and in such cases the half-life is generally much shorter than proton emission, because neutrons will not encounter any coulomb barrier to their escape from the atomic nucleus. An example is the dineutron decay of neutron-rich ^{16}Be measured by Spyrou et al. (2012), which decays with a 200 ns half-life according to the following decay sequence:

$$^{16}_{4}\mathrm{Be} \xrightarrow{t_{1/2}\ =200\ \mathrm{ns}} {}^{14}_{4}\mathrm{Be} + 2n \qquad [20.56]$$

The emission of only one neutron or the sequential emission of two neutrons from ^{16}Be is not possible energetically, because the ground state of ^{15}Be is at a significantly higher energy than the parent ^{16}Be nuclide (Spyrou et al., 2012).

20.8.2.3 Detection and Measurement of Neutron Radioactivity

The detection and measurement of neutron radioactivity require instrumental techniques that are different to the gas ionization detection and measurement techniques described previously for proton radioactivity. The neutral charge on the neutron will not permit its detection by gas ionization. However, certain inorganic and organic plastic scintillators are sensitive to neutron interactions such as proton recoil following elastic scattering in organic and plastic scintillators. A review of methods for the detection and measurement of neutrons is provided by the writer in an earlier book (L'Annunziata, 2012c).

A method proposed by Caesar et al. (2013) for the detection and measurement of neutron radioactivity and the very short half-lives involved is described in detail by Thoennessen et al. (2013). A diagram of the instrumental arrangement is illustrated in Fig. 20.25, with the decay scheme of ^{16}B as an example. The neutron-rich nucleus of ^{16}B emits a neutron with a half-life of $<$190 ps according to the decay sequence

$$^{16}_{5}\mathrm{B} \xrightarrow{t_{1/2}\ <190\ \mathrm{ps}} {}^{15}_{5}\mathrm{B} + n \qquad [20.57]$$

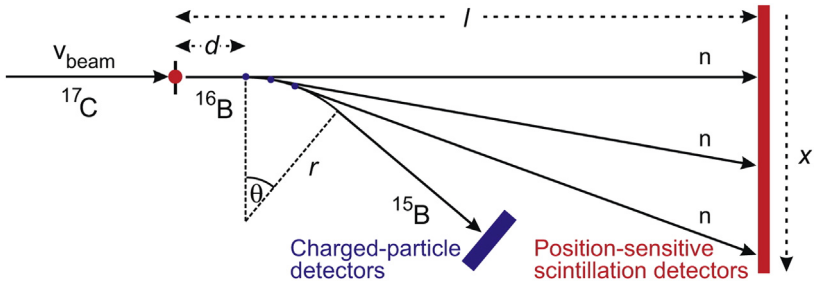

FIGURE 20.25 Schematics of the decay in a magnetic field technique. The incoming ^{17}C beam produces ^{16}B in the target (*red dot*), which enters a magnet field (bend radius r and deflection angle θ) after a drift distance d. The ^{16}B can then decay at different positions along the flight path (*blue dots*) into ^{15}B and a neutron. The ^{15}B fragments and neutrons are detected and identified in a set of charged-particle detectors and position-sensitive scintillation detectors (at a distance l of 1500 cm from the target), respectively. *Thoennessen, M., et al., 2013. Novel techniques to search for neutron radioactivity. Nuc. Instrum. Methods Phys. Res. Sect. A 729, 207–211, reprinted with permission from Elsevier © 2013.*

The very short half-life requires the measurement of the neutron emissions from the onset of the production of the ^{16}B. A method of half-life measurement illustrated in Fig. 20.25 is the measurement of the neutron distribution along position-sensitive scintillation detectors, known as the decay in a magnetic field method. As described by Thoennessen et al. (2013), the ^{16}B is produced by accelerating a beam of ^{17}C against a target material that knocks out a proton from the ^{17}C, producing ^{16}B. The reaction ^{17}C(-p)^{16}B occurs at the location identified by a red dot in Fig. 20.25. The decay sequence $^{16}\text{B} \rightarrow {}^{15}\text{B} + n$ at various times in flight is illustrated by three blue dots along the flight path of the ^{16}B, bent by a deflecting magnetic field with a bend radius r and a deflecting angle θ after a possible drift distance d. The deflecting magnetic field will bend the path of the charged particles away from the paths of the emitted neutrons, permitting the detection and counting of ^{15}B. The distribution of the neutrons measured along the distance x of the position-sensitive scintillation detectors (see Fig. 20.25) will provide a measure of the half-life of the nuclear decay. Decay times as short as 10 ps will show a concentration of neutrons detected near the zero-degree line (little deflection) at a distance l from the target. A longer half-life of the order of 500 ps to 1 ns will exhibit a distribution of neutrons further away from the zero-degree line along the distance x. Longer decay times of up to 100 μs will exhibit a spread further away from the zero-degree line.

For additional reading on neutron radioactivity the reader may peruse papers by Spyrou et al. (2012), Thoennessen et al. (2013), and Birch et al. (2014).

20.9 NUCLEAR DECAY MODES

Throughout this book numerous decay modes of atomic nuclei are described. These decay modes are manifested in general through the emission of nuclear radiation, such as α particles, β particles, γ-ray photons, protons, neutrons, and heavy cluster emissions. We also refer to the modes of nuclear decay as radioactive decay modes. The modes of nuclear decay are given specific nomenclature for reason of identification, such as alpha decay (α); beta decay, including negatron emission (β^-), positron emission (β^+), and electron capture (ε or EC); isomeric transition (IT, resulting in γ emission); proton emission (p); neutron emission (n); spontaneous fission (SF); and heavy cluster emission (^{14}C, ^{20}O, ^{23}F…). Most nuclear decay modes result in a transformation (ie, transmutation) of an atom of one element into another, as illustrated in Fig. 20.26. This figure depicts nuclear decay transitions that occur between blocks occupied by the various radionuclides in the Chart of the Nuclides, which is the periodic table of the nuclides (both stable and radioactive) separated in blocks according to their atomic number (Z) and neutron number (N). The nuclear decays generally lead to a change in the atomic number (Z), and consequently a change from one element to another. The emission of a neutron (n) from the nucleus, also illustrated in Fig. 20.26, results in no change in atomic number and thus no change of element between parent and daughter nuclides; rather, the emission of one or more neutrons from the nucleus results in a change in the mass number of the same element and in an isotope of the same element. Another mode of nuclear decay which does not result in a change in chemical elements between parent and daughter atoms is the IT mode, not illustrated in Fig. 20.26. The IT decay results in a change from one energy state of an atomic nucleus to a lower energy state with the emission of gamma (γ) radiation. Heavy cluster emission is the emission of nuclei larger than the helium nucleus (eg, ^{14}C, ^{20}O, etc.) from a heavy nucleus, which for reasons of space is not illustrated in Fig. 20.26.

Table 20.3 provides a list of nuclear decay modes, together with their description and examples of each.

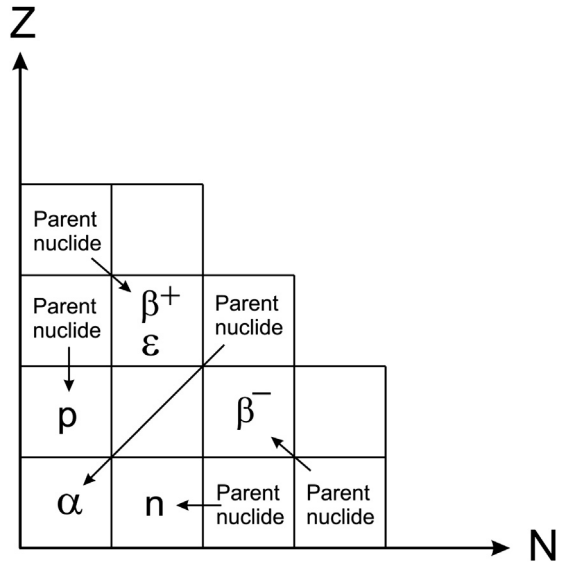

FIGURE 20.26 Nuclear decay mode transitions according to blocks occupied by the various nuclides in the Chart of the Nuclides, plotted according to their number of protons (Z) and number of neutrons (N) in the nucleus. Various nuclear decay modes are illustrated that result in changes in the number of protons (atomic number, Z) or neutrons (neutron number, N) between parent and daughter nuclides. The radiation emitted or the decay modes are written in the blocks occupied by the daughter nuclides. For example, positron (β^+) emission or EC (ε) decay results in a reduction in proton number ($Z-1$) and increase in neutron number ($N+1$); whereas negatron emission results in the opposite—an increase in the number of protons in the nucleus ($Z+1$) and a reduction in the number of neutron ($N-1$). Alpha (α) decay results in twofold reductions in the proton and neutron numbers in the nucleus ($Z-2$ and $N-2$). Proton (p) and neutron (n) radioactivity result in loss of one or more protons or neutrons, respectively.

20.10 NUCLEAR REACTIONS

A nuclear reaction is an interaction between two nuclear particles or two nuclei that yields products which are different from the reactants, that is, new nuclei are formed. If the interacting particles or nuclei only collide and separate without change, the process is referred to as **elastic scattering**. When a nuclear particle collides with a nucleus but only the nucleus undergoes excitation to a higher energy state, the process is referred to as an **inelastic collision**.

20.10.1 Reaction Types

The term "nuclear reaction" generally refers to the interaction of a projectile particle and a target nucleus that results in the production of a residual (product) nucleus and an ejected particle.

An example of a nuclear reaction is the following:

$$ {}^{1}_{0}\mathrm{n} + {}^{10}_{5}\mathrm{B} \rightarrow ({}^{11}_{5}\mathrm{CN})^{*} \rightarrow {}^{7}_{3}\mathrm{Li} + {}^{4}_{2}\mathrm{He} + 2.79\ \mathrm{MeV} \qquad [20.58] $$

In the example in Eq. [20.58] a neutron, ${}^{1}_{0}\mathrm{n}$, collides with the target nucleus, ${}^{10}_{5}\mathrm{B}$, and they coalesce to form an excited and unstable compound nucleus (abbreviated as CN*). The compound nucleus generally is not written, as it is very short-lived ($\sim 10^{-16}$ s). In this example the compound nucleus decays to yield the product nucleus ${}^{7}_{3}\mathrm{Li}$ and an ejected alpha particle, ${}^{4}_{2}\mathrm{He}$. The sum of the proton numbers and mass numbers must be equal on both sides of the reaction. For example, in Eq. [20.58] the proton numbers $0+5=3+2$ and mass numbers $1+10$ and $7+4$ are equal on both sides of the reaction. As illustrated in Eq. [20.58], there is kinetic energy released in this reaction to the amount of 2.8 MeV. This nuclear reaction is a very practical one, because it is used for the detection of thermal neutrons. The nuclide ^{10}B has a high natural abundance of 20%, and when incorporated into the crystalline structure of a solid scintillation detector, the crystal becomes a sensitive detector for thermal neutrons. The alpha particles ejected as a product of the reaction have a very short range of travel in the crystalline detector. The kinetic energy of the alpha particles is in the MeV range, and they dissipate their energy close to the point of neutron interaction. Solid scintillators of this type serve as good thermal neutron detectors.

Nuclear reactions between a specific projectile and target nucleus may result in more than one set of reaction products. For example, in his Nobel lecture Enrico Fermi noted:

> *Neutron bombardment of aluminum, that has a single isotope ^{27}Al, gives rise to three radioactive products: ^{24}Na, with a half-life of 15 h…; ^{27}Mg, with a half-life of 10 min…; and ^{28}Al with a half-life of 2 to 3 min…*

TABLE 20.3 Nuclear Decay Modes

Mode	Designation and Description	Example
α	**α emission**. A nucleus of helium ($^4_2$He) is emitted from the nucleus of the decaying atom.	$^{241}_{95}\text{Am} \rightarrow {}^{137}_{93}\text{Np} + {}^4_2\text{He}$
β^-	**β^- or negatron emission**. A neutron is converted to a proton, with the emission of a negative electron and an antineutrino. There is no change in mass number.	$^3_1\text{H} \rightarrow {}^3_2\text{He} + \beta^- + \bar{\nu}$
β^+	**β^+ or positron emission**. A proton is converted to a neutron, with the emission of a positive electron and a neutrino. There is no change in mass number.	$^{11}_6\text{C} \rightarrow {}^{11}_5\text{B} + \beta^+ + \nu$
ε or EC	**Electron capture**. An atomic electron (eg, K shell) is captured by a nuclear proton; and the proton is converted to a neutron with the emission of a neutrino. This is another form of beta decay, and there is no change in mass number. EC decay competes with positron emission.	$^{65}_{30}\text{Zn} \rightarrow {}^{65}_{29}\text{Cu} + \nu$
IT	**Isomeric transition**. The transition of a nucleus from an excited elevated energy state to that of a lower energy state, with the emission of gamma (γ)-ray photons. There is no change in atomic number or mass number. The mass number of the parent nuclide is designated with the letter *m* to signify a metastable state when the gamma-ray emission is not immediate or a "prompt gamma."	$^{119m}_{50}\text{Sn} \rightarrow {}^{119}_{50}\text{Sn} + \gamma$
SF	**Spontaneous fission**. The spontaneous splitting of a nucleus into two nuclear fragments with the emission of neutrons. The possible nuclear fission fragments vary; and there are numerous fragment combinations possible.	$^{252}_{98}\text{Cf} \rightarrow {}^{101}_{40}\text{Zr} + {}^{148}_{58}\text{Ce} + 3^1_0\text{n}$
p	**Proton emission**. The consecutive or simultaneous emission of one, two, or three protons from a proton-rich atomic nucleus. When two or three protons are emitted, the decay mode is identified as 2p or 3p, respectively.	$^{147}_{69}\text{Tm} \rightarrow {}^{146}_{68}\text{Er} + \text{p}$
n	**Neutron emission**. The emission of one or two neutrons from a neutron-rich nucleus. The simultaneous emission of two neutrons is identified as a 2n decay mode.	$^{16}_4\text{Be} \rightarrow {}^{14}_4\text{Be} + 2\text{n}$
β^+p	**Beta-delayed proton emission**. The emission of a proton from a populated elevated energy state of a proton-rich atomic nucleus following β^+ decay. The emission of two protons is designated as β^+2p.	$^{13}_8\text{O} \rightarrow {}^{13}_7\text{F} + \beta^+ + \nu \rightarrow {}^{12}_6\text{C} + \text{p}$
β^-n	**Beta-delayed neutron emission**. The emission of a neutron from a populated elevated energy state of a neutron-rich atomic nucleus following β^- decay. The emission of two neutrons is designated as β^-2n.	$^{94}_{35}\text{Br} \rightarrow {}^{94}_{36}\text{Kr} + \beta^- + \bar{\nu} \rightarrow {}^{93}_{36}\text{Kr} + \text{n}$
$2\beta^-$ or $\beta^-\beta^-$	**Double-β^- decay**. Two neutrons decay to two protons in an atomic nucleus, with the emission of two β^- particles and two antineutrinos.	$^{82}_{34}\text{Se} \rightarrow {}^{82}_{36}\text{Kr} + 2\beta^- + 2\bar{\nu}$
^{14}C,^{20}O…	**Cluster radioactivity**. The spontaneous emission of a particle heavier than an α particle with $Z \geq 6$, such as the emission of ^{14}C, ^{20}O, ^{23}F, ^{24}Ne, ^{28}Mg, ^{30}Mg, or ^{32}Si.	$^{221}_{87}\text{Fr} \rightarrow {}^{207}_{81}\text{Tl} + {}^{14}_6\text{C}$

The three reactions described by Fermi may be written as follows:

$$^1_0\text{n} + {}^{27}_{13}\text{Al} \rightarrow ({}^{28}_{13}\text{CN})^* \rightarrow \begin{cases} {}^{24}_{11}\text{Na} + {}^4_2\text{He} & Q = -3.13 \text{ MeV} \\ {}^{27}_{12}\text{Mg} + {}^1_1\text{H} & Q = -1.83 \text{ MeV} \\ {}^{28}_{13}\text{Al} + \gamma & Q = 7.72 \text{ MeV} \end{cases} \quad [20.59]$$

An intermediary compound nucleus is illustrated as decaying into three possible decay products. The above reactions that leave behind the residual nuclei of ^{24}Na and ^{27}Mg have negative Q values. These reactions are endoergic or endothermic. In these two cases, the neutron projectile must possess additional kinetic energy for the reaction to proceed. The reaction that produces the ^{28}Al residual nucleus has a positive Q value. This reaction is exoergic or exothermic, resulting in a release of energy. Low-energy neutrons, classified as slow or thermal neutrons, are sufficient for this reaction to proceed. The capture of slow neutrons by nuclei is accompanied generally by the immediate emission of one or more gamma-ray photons. The nuclei are left in a state of excitation after the neutron capture, and their ground state is reached after the emission of the gamma-ray quanta. The Q value, as a measure of reaction energy, is discussed in more detail further on in this section.

TABLE 20.4 Examples of Pickup and Stripping Reactions

Reaction	Condensed Notation[a]	Projectile Energy	References
Pickup Reactions			
${}^{13}_{6}C + {}^{1}_{1}H \rightarrow {}^{12}_{6}C + {}^{2}_{1}H$	${}^{13}_{6}C(p,d){}^{12}_{6}C$	12 MeV	Glover and Jones (1966)
${}^{12}_{6}C + {}^{3}_{1}H \rightarrow {}^{11}_{5}B + {}^{4}_{2}He$	${}^{12}_{6}C(t,\alpha){}^{11}_{5}B$	10 MeV	Honda et al. (1965)
${}^{20}_{10}Ne + {}^{2}_{1}H \rightarrow {}^{19}_{9}F + {}^{3}_{2}He$	${}^{20}_{10}Ne(d,h){}^{19}_{9}F$	52 MeV	Kaschl et al. (1970)
${}^{89}_{39}Y + {}^{2}_{1}H \rightarrow {}^{87}_{38}Sr + {}^{4}_{2}He$	${}^{89}_{39}Y(d,\alpha){}^{87}_{38}Sr$	12 MeV	Brien et al. (1972)
Stripping Reactions			
${}^{12}_{6}C + {}^{2}_{1}H \rightarrow {}^{13}_{6}C + {}^{1}_{1}H$	${}^{12}_{6}C(d,p){}^{13}_{6}C$	12 MeV	Glover and Jones (1966)
${}^{12}_{6}C + {}^{3}_{1}H \rightarrow {}^{13}_{6}C + {}^{2}_{1}H$	${}^{12}_{6}C(t,d){}^{13}_{6}C$	12 MeV	Glover and Jones (1966)
${}^{27}_{13}Al + {}^{3}_{2}He \rightarrow {}^{28}_{14}Si + {}^{2}_{1}H$	${}^{27}_{13}Al(h,d){}^{28}_{14}Si$	41 MeV	Munger and Peterson (1978)
${}^{194}_{78}Pt + {}^{3}_{2}He \rightarrow {}^{195}_{79}Au + {}^{2}_{1}H$	${}^{194}_{78}Pt(h,d){}^{195}_{79}Au$	41 MeV	Munger and Peterson (1978)

[a]*The condensed form of writing nuclear reactions is read as follows: target nucleus (projectile, ejected particle) product nucleus.*

The above reactions are described as possessing a compound nucleus, and those reactions may be referred to as **compound nuclear reactions**. Two other types of nuclear reactions are classified as **pickup** and **stripping reactions**. When high-energy nuclear projectiles are used to bombard a target nucleus, the interaction can be more direct: the projectile does not interact with all the nucleons of the target and thus does not reside in a compound nucleus; rather, the projectile may interact only with a few nucleons in specific nuclear shell-model orbits of the target. In such cases, the projectile may pick up or gain nucleons from the target nucleus in pickup reactions; or it may lose nucleons to the target in stripping reactions. Some early studies of pickup and stripping reactions that may occur in specific nuclear shell-model orbits are the works of Kaschl et al. (1970) and Brien et al. (1972). Examples of pickup and stripping reactions and the projectile energies at which these reactions were observed are listed in Table 20.4.

Spallation reactions are another class of nuclear reaction. Spallation occurs when a high-energy (>100 MeV) charged particle, such as a proton, strikes a nucleus and initially "knocks out" several nucleons from the target nucleus within a period of about 10^{-22} s, leaving the residual nucleus in an excited state. The excited residual nucleus may then immediately break up into numerous smaller components of smaller nucleons, such as helium and lithium nuclei, deuterons, mesons, and individual protons and neutrons, etc. In general, numerous neutrons are emitted from each spallation reaction, making this reaction a good neutron source. Nobel Laureate Glenn T. Seaborg is credited with coining the term "nuclear spallation" in his doctoral dissertation in 1937, deriving the word from the verb "spall," meaning to chip or crumble.

Nuclear spallation is a common occurrence in our atmosphere when high-energy cosmic ray particles (eg, cosmic ray protons) of energies ranging from 10^8 to $>10^{20}$ eV strike nuclei in the atmosphere, resulting in the fragmentation of nuclei into smaller nucleons constituting cosmic ray showers. Spallation reactions resulting from the interaction of high-energy particles in the cosmic ray showers colliding with nuclei in mineral deposits on the Earth's surface are attributed to the cosmogenic production of nuclides, such as ^{36}Cl (Stone et al., 1996; Licciardi et al., 2008).

There is current worldwide interest in the artificial production of spallation reactions as neutron sources, referred to as spallation neutron sources. Spallation neutron sources are accelerator-driven systems whereby protons are accelerated to high energies (1 GeV and above), which then collide with heavy metal targets resulting in nuclear spallation with the emission of neutrons useful in research (Slowiński, 2003; Mason et al., 2006; Thomsen, 2007; Zamani et al., 2008).

Two other nuclear reactions that are very important sources of energy are nuclear fission and nuclear fusion. These are discussed in greater detail in other parts of this book.

20.10.2 Reaction Notation

The nuclear reaction illustrated previously in Eq. [20.58] may be abbreviated as follows:

$$^{10}_{5}B(n,\alpha)^{7}_{3}Li \qquad [20.60]$$

which is written in the sequence

$$\text{target nucleus}(\text{projectile}, \text{ejected particle})\text{product nucleus}. \qquad [20.61]$$

This condensed form of writing the nuclear reaction, as written above in Eq. [20.60], reads as follows: a ^{10}B target nucleus bombarded by neutrons ejects an alpha particle, leaving the residual ^{7}Li nucleus. Particles, which are often either a projectile or an ejected particle (ejectile), in nuclear reactions are the following, with the abbreviation in parenthesis: proton ($^{1}_{1}$H or p), neutron (n), deuteron ($^{2}_{1}$H or d), triton ($^{3}_{1}$H or t), helium-3 ($^{3}_{2}$He or h), and helium-4, ie, the alpha particle ($^{4}_{2}$He or α). Neutrons as projectiles for nuclear reactions with target nuclei are easily available from nuclear reactions induced by alpha particles, such as the alpha particle bombardment of beryllium (ie, $^{9}_{4}\mathrm{Be}(\alpha, n)^{12}_{6}\mathrm{C}$), which provide neutrons with average energies of 5.7 MeV. The nuclear fission reactor is another excellent source of neutrons available as projectile particles to induce nuclear reactions. Accelerators are also good sources of neutrons via spallation reactions induced by high-energy particle collisions with target nuclei. Various sources of neutrons are described in the chapter entitled "Neutron Radiation." The cyclotron is an excellent source of high-energy positively charged particles and nuclei, such as protons, deuterons, triton ions, and helium-3 and helium-4 ions. In the cyclotron, target material is placed in the path of the accelerating ion, and numerous radionuclides are made via the nuclear reactions initiated by the bombardment of the positively charged projectiles with the target nuclei.

20.10.3 Energy of Reactions (Q Value)

The Q value of a nuclear reaction is a measure of the reaction energy. It is the difference between the kinetic energy of the reaction products and the kinetic energy of the original particles of the nuclear reaction (reactants). The Q value for the reaction illustrated in Eq. [20.58] is reported in the literature to be 2.79 MeV. The computer-calculated Q values for all nuclear reactions are readily available online from the NNDC: www.nndc.bnl.gov/qcalc/qcalcr.jsp (NNDC, 2016). At this website it is only necessary to identify the projectile, target nucleus, and ejected particle. There is no need to input or identify the residual nucleus, because the calculator can easily deduce the proton number and mass number of the residual nucleus by difference. The calculations made at this website are based on the data maintained by the Atomic Mass Data Center and on atomic mass evaluations reported by Audi et al. (2003b), Wapstra et al. (2003), and Möller et al. (1995). Q values for nuclear reactions are easy to calculate, and these calculations are discussed later in this section. The Q value is an important property of a nuclear reaction, because it tells us whether a reaction will release kinetic energy ($Q > 0$) or lose kinetic energy ($Q < 0$). When $Q = 0$, the reaction is referred to as *elastic scattering* whereby the projectile and target nucleus collide and exchange energy, but do not undergo any change. When the projectile and target nucleus collide and part of the kinetic energy of the projectile is transferred to the target nucleus, leaving the target at an excited energy state, the reaction is referred to as *inelastic scattering*. There is only energy transfer, but no change in atomic or mass number of the projectile or target nucleus, in inelastic scattering reactions.

To arrive at the equation for the calculation of reaction Q values let us abbreviate the nuclear reaction of Eq. [20.58] in the form

$$A + B \rightarrow C + D \qquad [20.62]$$

where projectile A bombards nucleus B, which leaves behind a residual nucleus C and ejected particle D. If the total energy of the reactants and products is conserved, we can write

$$E_A + E_B = E_C + E_D \qquad [20.63]$$

Also, the total energy (E) of a particle or nucleus is the sum of its kinetic energy (K) and its rest energy (m_0c^2), which is

$$E = K + m_0c^2 = K + E_0 \qquad [20.64]$$

where m_0 is the particle or nuclear rest mass, c is the speed of light in a vacuum, and E_0 is the rest energy. Furthermore, if we assume that the target nucleus is at rest, ie, it has zero kinetic energy, we can transform Eq. [20.63] to

$$K_A + m_Ac^2 + m_Bc^2 = K_C + m_Cc^2 + K_D + m_Dc^2 \qquad [20.65]$$

The total kinetic energy released or absorbed in the reaction, Q, is the difference of the kinetic energies of the products and the reactants. In other words, it is the differences in the kinetic energies gotten out of the reaction versus what was put into the reaction, or

$$Q = K_{\text{out}} - K_{\text{in}} \qquad [20.66]$$

Then from Eq. [20.65] we can write

$$Q = (K_C + K_D) - K_A = (m_A + m_B)c^2 - (m_C + m_D)c^2 \quad [20.67]$$

In accord with $E = mc^2$, Eq. [20.67] simply states

$$Q = E_{0,\ \text{reactants}} - E_{0,\ \text{products}} \quad [20.68]$$

where $E_{0,\ \text{reactants}}$ and $E_{0,\ \text{products}}$ are the rest energies of the nuclear reactants and products, respectively. Eqs. [20.67] and [20.68] may be simplified to read

$$Q = (m_{\text{reactants}})c^2 - (m_{\text{products}})c^2 \quad [20.69]$$

where $m_{\text{reactants}}$ and m_{products} are the combined masses of the nuclear reactants and products, respectively.

For example, in accordance with Eqs. [20.67] and [20.69], the Q value for the nuclear reaction described previously in Eq. [20.58] and rewritten here in condensed form,

$${}^{1}_{0}\text{n} + {}^{10}_{5}\text{B} \rightarrow {}^{7}_{3}\text{Li} + {}^{4}_{2}\text{He} \quad [20.70]$$

would be calculated as follows:

$$Q = (M_{^1\text{n}} + M_{^{10}\text{B}})c^2 - (M_{^7\text{Li}} + M_{^4\text{He}})c^2 \quad [20.71]$$

where $M_{^1\text{n}}$, $M_{^{10}\text{B}}$, $M_{^7\text{Li}}$, and $M_{^4\text{He}}$ are the masses of the neutron, ^{10}B reactants, and ^{7}Li and ^{4}He product nuclei, respectively, and c is the speed of light in a vacuum. We may use atomic mass units (u) taken from standard reference tables, since the five atomic electron masses of the reactants and the product nuclides are included on both sides of the equation. Thus using atomic mass units in Eq. [20.71] gives

$$Q = \left\{ \begin{matrix} (1.00866492\ \text{u} + 10.012937\ \text{u})(931.494\ \text{MeV/u}) \\ -(7.016004\ \text{u} + 4.00260325\ \text{u})(931.494\ \text{MeV/u}) \end{matrix} \right\}$$

$$Q = 2.79\ \text{MeV}$$

The Q value is positive, and is exactly the Q value calculated by the online computer program of the NNDC (www.nndc.bnl.gov/qcalc/). Thus energy is released in the nuclear reaction. In such a case, the reaction releases kinetic energy by conversion of some of the rest mass to kinetic energy according to

$$E_{\text{Total}} = E_K + m_0c^2 \quad [20.72]$$

Reactions with a positive Q value ($Q > 0$) are called **exoergic** or **exothermic**, since kinetic energy is released. When the Q value is negative ($Q < 0$) the reaction is called **endoergic** or **endothermic**, as kinetic energy is absorbed in the reaction. In such a case, the reaction could not take place unless energy is added to the reactant particle or projectile. For example, let us calculate the Q value of the nuclear reaction used by Ernest Rutherford (1919) whereby he discovered the proton:

$${}^{4}_{2}\text{He} + {}^{14}_{7}\text{N} \rightarrow {}^{17}_{8}\text{O} + {}^{1}_{1}\text{H} \quad [20.73]$$

$$Q = (M_{^4\text{He}} + M_{^{14}\text{N}})c^2 - (M_{^{17}\text{O}} + M_{^1\text{H}})c^2 \quad [20.74]$$

$$Q = \left\{ \begin{matrix} (4.00260325\ \text{u} + 14.00307401\ \text{u})(931.494\ \text{MeV/u}) \\ -(16.9991315\ \text{u} + 1.007825031\ \text{u})(931.494\ \text{MeV/u}) \end{matrix} \right\}$$

$$Q = -1.192\ \text{MeV}$$

This is exactly the Q value calculated by the NNDC online computer program (www.nndc.bnl.gov/qcalc/). The reaction is endoergic ($Q < 0$) or endothermic, as energy is absorbed in the reaction. The reaction would require more than 1.192 MeV of energy input for the reaction to occur. Since the target nucleus is at rest, it is the projectile particle or projectile nucleus that carries the kinetic energy needed for the reaction to take place. Furthermore, there is a threshold energy (E_{th}), which is by definition the minimum bombarding energy that the projectile particle must possess when Q is negative ($Q < 0$) for the reaction to take place. The threshold energy is calculated by the following equation, derived by Evans (1972):

$$E_{\text{th}} = -Q\left(\frac{M_1 + M_2}{M_2}\right) \quad [20.75]$$

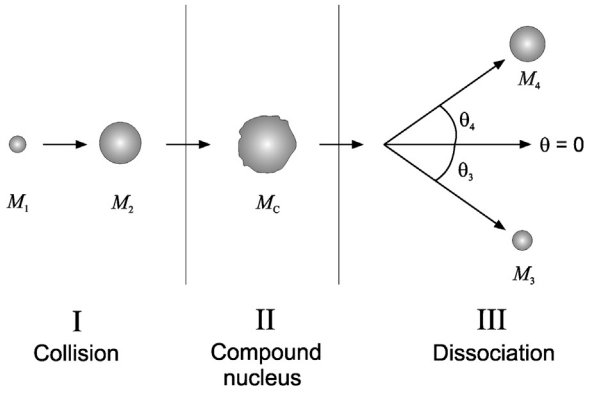

FIGURE 20.27 Three stages of a nuclear reaction, namely (I) collision where a projectile particle of mass M_1 collides with a target nucleus of mass M_2, forming a (II) compound or intermediate nucleus M_C of mass equivalent to the combined masses of the projectile and target nucleus, and (III) dissociation of the compound nucleus resulting in an ejected particle of mass M_3 and residual nucleus of mass M_4 expelled at angles θ_3 and θ_4, respectively.

where M_1 and M_2 are the masses of the projectile particle and target nucleus, respectively, as illustrated in Fig. 20.27. Using the Q value of -1.192 MeV, we can calculate the threshold energy of the alpha particle projectile for the reaction in Eq. [20.73] to take place as follows:

$$E_{\text{th}} = -(-1.192\ \text{MeV})\left[\frac{(4.00260325\ \text{u} + 14.00307401\ \text{u})(931.494\ \text{MeV/u})}{(14.00307401\ \text{u})(931.494\ \text{MeV/u})}\right] \quad [20.76]$$

$$= 1.533\ \text{MeV}$$

The calculated threshold alpha particle projectile energy of 1.533 MeV would be required for the reaction to take place. Rutherford (1919) used alpha particles from radium C′, which is today known as ^{214}Po. The alpha particles from ^{214}Po have energies of 7.8 MeV, well above the threshold energy for the reaction in Eq. [20.73] to take place. The NNDC online computer program (www.nndc.bnl.gov/qcalc/) provides a calculation of the reaction threshold energy in addition to the Q value of the reaction; and this online calculation of the reaction threshold energy agrees exactly with the above calculation of 1.533 MeV.

The projectile particle M_1 of Eq. [20.75] is illustrated in Fig. 20.27 traveling in the direction of the target nucleus M_2, which forms an intermediate compound nucleus M_C with a mass equivalent to the combined masses of the projectile particle and target nucleus. The compound nucleus then dissociates into an ejected particle M_3 and a residual nucleus M_4. Due to the very short lifetime of the combined nucleus ($\sim 10^{-22}$ s) or of an intermediate system that does not consist of the formation of a compound nucleus, Evans (1972) reports that M_C loses no appreciable energy due to ionization prior to dissociation into M_3 and M_4. When particle M_3 is ejected at an angle $\theta_3 = 0$, the energy of the projectile particle is at the minimum or threshold energy E_{th}. As the projectile particle energy is raised over the threshold energy, the ejected particles M_3 begin to appear at $\theta_3 > 0$.

20.10.4 Reaction Cross-Section

The reaction cross-section is, by definition, the measure of the probability that a nuclear reaction or process will occur. The cross-section has units of area (cm^2), and the term reaction cross-section is used because it depicts the effective area of the target nucleus. It is not a measure of the true cross-section of a target nucleus; rather, it is a measure of the effectiveness of the target nucleus to increase or reduce the probability of a nuclear reaction with a projectile particle. The larger the measured effective area or cross-section of the target nucleus, the greater will be the probability that a projectile particle will hit or interact with that nucleus. The probability that a projectile particle collides with a target nucleus will depend on the rate at which the projectile particles are bombarding the target material: the particle beam intensity (I = projectile particles/second), the number of target nuclei in the target material or the target nuclei density (n = # of nuclei/cm^3), the effective area of the target nucleus—that is, the cross-section (σ) of the target nucleus (cm^2)—and the thickness of the target material (cm). The variables affecting the probability of a nuclear reaction and consequently the rate of the reaction are illustrated in Fig. 20.28.

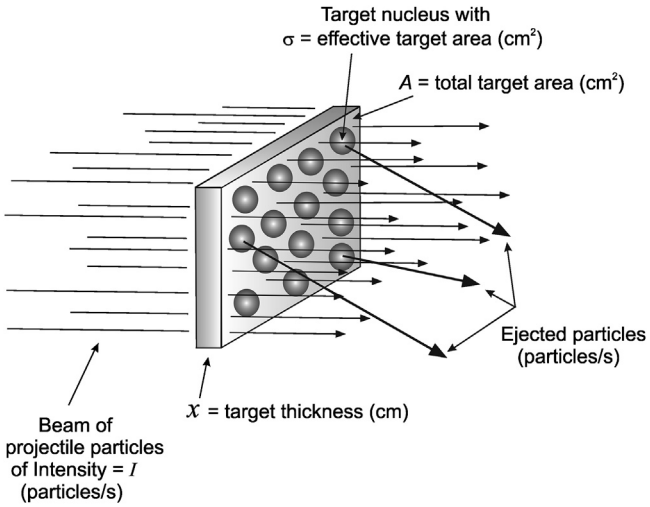

FIGURE 20.28 Reaction target area. A beam of projectile particles bombards a material containing target nuclei of cross-section (σ). Some of the projectile particles react with the target nuclei, resulting in the ejection of particles as products of the nuclear reaction. The reaction rate is measured by a detector sensitive to the ejected particles.

The rate of a nuclear reaction is a function of the effective target area exposed to the projectile particle beam. The effective target area is a product of the total number of target nuclei in the target material and the reaction cross-section (σ) of the target nuclei. The number (#) of target nuclei in the target material is dependent on the density of the target nuclei and the target volume, which is

$$\#\text{ of target nuclei} = n(Ax) \tag{20.77}$$

where n in the target nuclei density (# of nuclei/cm^3), A is the target area (cm^2), and x is the target thickness (cm). The effective target area is then calculated as

$$\text{Effective target area} = (\#\text{ of target nuclei})(\sigma) \tag{20.78}$$

$$= n(Ax)\sigma \tag{20.79}$$

We can reason that the rate of the reaction is related to the particle bean intensity as the effective target area is to the total target area, or

$$\frac{\text{Rate of reaction (particles/s)}}{\text{Beam intensity (particles/s)}} = \frac{\text{Effective target area (cm}^2\text{)}}{\text{Total target area (cm}^2\text{)}} \tag{20.80}$$

or

$$\frac{R}{I} = \frac{n(Ax)\sigma}{A} \tag{20.81}$$

and

$$R = In\sigma x \tag{20.82}$$

where R in the rate of the reaction (ejected particles/s), I is the projectile beam intensity (projectile particles/s), n is the density of target nuclei (# of target nuclei/cm^3), σ is the reaction cross-section (cm^2), and x is the target thickness (cm). The cross-section may be determined experimentally from the reaction rate, projectile beam intensity, target nuclei density, and target thickness. As described in the previous section on reaction Q value, the rate of a nuclear reaction will also depend on the energy of the projectile particles bombarding the target nuclei. Thus reaction cross-sections are reported together with the projectile particle energy (Kelley et al., 2005; He et al., 2006; Janczyszyn et al., 2006; Zhou et al., 2010; Madani et al., 2010). Thorough treatments of reaction cross-section are given by Evans (1972), Friedlander et al. (1964), and Serway et al. (2005).

The common unit of measure for the reaction cross-section is the barn, where 1 b $= 1 \times 10^{-24}$ cm^2. This measure of cross-section was first used by Baker et al. (1943), and proposed by Marshall P. Holloway and Charles P. Baker (1944) as

the unit of measure for the cross-section in secret technical reports of the Los Alamos National Libraries during the Manhattan Project. Holloway and Baker (1944, 1972) reported that, while measuring reaction cross-sections at Purdue University, they tried to come up with a suitable unit of measure. They thought of the word "Oppenheimer," but discarded the idea because of the word's length. They also considered the "Bethe," but discarded that because of possible confusion with the widespread use of "beta." They also considered using the name "John" after John Manley, who headed the Purdue Project, but discarded that because the word had widespread use for purposes other than the name of a person. One of the authors had a rural background, and on farms in the countryside the barn was always the largest building and could be seen at a distance. There was a very common colloquial term, "big as a barn," which is still used today. It was common to say of sportsmen with a poor aim, such as poor marksmen, archers, or golfers, that "they couldn't hit the side of a barn." Barns were built generally longer than they were wide, and thus the side or length was the largest part of a barn. They thus reported that the unit "barn" was appropriate, because a cross-section of 10^{-24} cm^2 for nuclear processes was very large and really "as big as a barn." Submultiples and multiples of the barn are also used, such as the millibarn (mb $= 10^{-3}$ b) and the kilobarn (kb $= 10^{3}$ b).

20.11 RADIOACTIVE NUCLEAR RECOIL

When a decaying nucleus discharges or emits a particle, such as an alpha particle, beta particle, gamma-ray or X-ray photon, or neutrino, the nucleus will recoil in a fashion somewhat like a cannon recoils when it shoots a cannon ball from its barrel. The energy of recoil is a function of the mass and energy of the particle that is emitted as well as the mass of the nucleus. This may appear intuitively obvious if we relate the process to that of a cannon: the heavier the cannon for a given mass and velocity of cannon ball, the less will be the recoil energy. Even radionuclides that emit electrons or photons from their atomic shell, such as Auger electrons and X-rays, respectively, will experience some recoil effect, albeit much less than would occur when a heavy particle, such as the alpha particle, is emitted from a nucleus. In accordance with the principles of conservation of momentum, nuclear recoil will occur in all nuclear decay processes with the conservation of momentum between the emitted particle and the product nucleus, as illustrated in Fig. 20.29.

Various textbooks give reference to equations for calculating nuclear recoil energies for some particular particle emissions. However, van Rooyen et al. (2008) and Szucs et al. (2009) provide relativistic and nonrelativistic expressions for all particle emissions, including alpha particles, beta particles, Auger electrons, neutrinos, and gamma-ray and X-ray photons. Detailed derivations of the equations are not included by these authors, so the derivations are provided here.

20.11.1 Relativistic Expressions

When a particle is emitted by a decaying nucleus, it possesses a kinetic energy (K_p), which is the difference of the total particle energy (E_p) and its rest energy (m_pc^2) or

$$K_p = E_p - m_pc^2 \qquad [20.83]$$

And if the expression of energy, momentum, and particle mass is written as previously described in this book (see Eq. [8.4] of the chapter entitled "Electromagnetic Radiation: Photons")

$$E_p^2 = p_p^2c^2 + \left(m_pc^2\right)^2 \qquad [20.84]$$

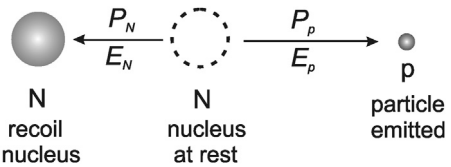

FIGURE 20.29 Nuclear recoil resulting from the energy imparted to a nucleus (N) at rest (*dashed circle*) by the emission of a particle (p) by the nucleus. Conservation of energy and momentum requires that the energy of the nucleus at rest be equal to the energy of the recoil nucleus + the energy of the emitted particle, ie, E_N (at rest) $= E_N$ (recoil) $+ E_p$; and the momentum of the recoil nucleus P_N is equal the momentum of the emitted particle P_p, ie, $P_N = P_p$.

where p_p is the particle momentum and c is the speed of light in a vacuum. From Eqs. [20.83] and [20.84] we can write

$$\left(K_p + m_p c^2\right)^2 = p_p^2 c^2 + \left(m_p c^2\right)^2 \quad [20.85]$$

which becomes

$$K_p^2 + 2m_p c^2 K_p + \left(m_p c^2\right)^2 = p_p^2 c^2 + \left(m_p c^2\right)^2 \quad [20.86]$$

and reduces to

$$K_p^2 + 2m_p c^2 K_p = p_p^2 c^2 \quad [20.87]$$

Solving Eq. [20.87] for the particle momentum gives

$$p_p = \frac{\sqrt{K_p^2 + 2m_p c^2 K_p}}{c} \quad [20.88]$$

According to the laws of conservation of momentum, we can write

$$p_N = p_p \quad [20.89]$$

where p_N is the momentum of the nucleus as a result of the emission of the particle. From Eqs. [20.88] and [20.89] we can equate the expressions for the nuclear and particle momentum as

$$\frac{\sqrt{K_N^2 + 2m_N c^2 K_N}}{c} = \frac{\sqrt{K_p^2 + 2m_p c^2 K_p}}{c} \quad [20.90]$$

where K_N and m_N are the kinetic energy and mass, respectively, of the recoil nucleus. If the total energy of the nucleus (E_N), in terms of its momentum and mass, is written according to Eq. [20.84],

$$E_N^2 = p_N^2 c^2 + \left(m_N c^2\right)^2 \quad [20.91]$$

and with $p_N = p_p$ we can express the total energy of the nucleus as

$$E_N^2 = \left(\frac{\sqrt{K_p^2 + 2m_p c^2 K_p}}{c}\right)^2 c^2 + \left(m_N c^2\right)^2 \quad [20.92]$$

which becomes

$$E_N^2 = K_p^2 + 2m_p c^2 K_p + m^2 c^4 \quad [20.93]$$

Eq. [20.93] is reduced to the simple expression of the total energy of the nucleus as

$$E_N = \sqrt{K_p^2 + 2m_p c^2 K_p + m_N^2 c^4} \quad [20.94]$$

If by definition the kinetic energy of the nucleus K_N—that is, its recoil energy—is the difference of its total energy, E_N, and its rest energy, $m_N c^2$, then

$$K_N = E_N - m_N c^2 \quad [20.95]$$

From Eqs. [20.94] and [20.95] we can arrive at the final expression for the kinetic energy of the recoil nucleus in terms of the particle kinetic energy (K_p), particle mass (m_p), and mass of the recoil nucleus (m_N)

$$K_N = \sqrt{K_p^2 + 2m_p c^2 K_p + m_N^2 c^4} - m_N c^2 \quad [20.96]$$

Eq. [20.96] is the fully relativistic expression for the calculation of the nuclear recoil energy for particle emissions that possess nonzero rest mass, such as alpha particles, beta particles, and Auger electrons. For particle emissions consisting of gamma-ray and X-ray photons, which have a zero rest mass, the term $2m_p c^2 K_p$ will fall out of Eq. [20.96]; and in the case of the neutrino, which has a near-zero rest mass, the term $2m_p c^2 K_p$ becomes negligible and can be dropped out of Eq. [20.96] so that it simplifies to

$$K_N = \sqrt{K_p^2 + m_N^2 c^4} - m_N c^2 \quad [20.97]$$

Eq. [20.97] is thus used to calculate the nuclear recoil energies for gamma-ray and X-ray photons or neutrino emissions. We should keep in mind that the recoil nucleus is that of the daughter nucleus, because it is the daughter nucleus that recoils after the nucleus discharges or expels a particle.

20.11.2 Nonrelativistic Expressions

20.11.2.1 Nuclear Recoil Energy From Alpha Particle Emissions

For relatively very heavy particles, such as the alpha particle, a more simple nonrelativistic calculation of the nuclear recoil energy may also be used. The nonrelativistic expression of the nuclear recoil energy for alpha particle emissions is derived subsequently. The nonrelativistic expression of the kinetic energy of the alpha particle is defined as

$$K_\alpha = \frac{1}{2} m_\alpha v^2 \qquad [20.98]$$

where m_α and v are the mass and velocity of the particle, respectively. Its nonrelativistic momentum would be simply

$$p_\alpha = m_\alpha v \qquad [20.99]$$

Multiplying Eq. [20.98] by $2m_\alpha$ gives

$$2m_\alpha K_\alpha = (m_\alpha v)^2 = p_\alpha^2 \qquad [20.100]$$

Eq. [20.100] relates the alpha particle mass, energy, and momentum. Conservation of momentum of the alpha particle (p_α) and recoil nucleus (p_N) dictates

$$p_\alpha = p_N \qquad [20.101]$$

and then from Eqs. [20.100] and [20.101] we can write

$$\sqrt{2m_\alpha K_\alpha} = \sqrt{2m_N K_N} \qquad [20.102]$$

where m_N and K_N are the mass and kinetic energy of the recoil nucleus. Squaring both sides of Eq. [20.102] and solving for K_N gives

$$K_N = \left(\frac{m_\alpha}{m_N}\right) K_\alpha \qquad [20.103]$$

Eq. [20.103] was used in Section 4.2 of the chapter entitled "Alpha Radiation" (see Eq. [4.8]) for calculation of the recoil energy resulting from the 5.545 MeV alpha particle emitted from ^{241}Am. The relativistic expression, provided in Eq. [20.96], yields the same result.

20.11.2.2 Nuclear Recoil Energy From Gamma-Ray, X-Ray, and Neutrino Emissions

For gamma-ray photons and X-ray photons, which have zero rest mass, and neutrinos, which have near-zero rest mass, we can express their momentum (see Eqs. [8.5] and [8.6] of the chapter entitled "Electromagnetic Radiation: Photons") as

$$p_p = \frac{E_p}{c} \qquad [20.104]$$

where p_p is the momentum of the gamma-ray photon, X-ray photon, or neutrino, E_p is the particle energy (ie, photon or neutrino energy), and c is the speed of light in a vacuum. If the nonrelativistic expression of the kinetic energy of the recoil nucleus is

$$K_N = \frac{1}{2} m_N v^2 \qquad [20.105]$$

where K_N is the kinetic energy of the recoil nucleus, m_N is the mass of the recoil nucleus, and v is its velocity, then multiplying both sides of Eq. [20.105] by $2m_N$ gives

$$2m_N K_N = (m_N v)^2 = p_N^2 \qquad [20.106]$$

where p_N is the momentum of the recoil nucleus. As momentum is conserved, we can write

$$p_N^2 = p_p^2 = 2m_N K_N = \frac{E_p^2}{c^2} \qquad [20.107]$$

Solving Eq. [20.107] for the kinetic energy of the recoil nucleus gives

$$K_N = \frac{1}{2}\left(\frac{E_p^2}{m_N c^2}\right) \qquad [20.108]$$

where E_p^2 is the energy of the gamma-ray photon, X-ray photon, or neutrino, and m_N is the mass of the recoil nucleus.

20.11.3 Sample Calculations

20.11.3.1 Nuclear Recoil from Alpha Emissions

In the chapter entitled "Alpha Radiation" of this book (see Eq. [4.8]), the nonrelativistic expression for recoil energy was used to determine the recoil energy imparted to a nucleus as a result of alpha particle emission of 5.545 MeV that occurs in the following decay of ^{241}Am:

$$^{241}_{95}\mathrm{Am} \rightarrow {}^{237}_{93}\mathrm{Np} + {}^{4}_{2}\mathrm{He} \qquad [20.109]$$

The relativistic expression provided by Eq. [20.96] will be used. Since nuclear recoil occurs after the nucleus emits a particle, it is the daughter nuclide that recoils. We will use atomic mass units (u) and the conversion factor of 931.494013 MeV/u to convert mass to energy units. Relevant data from nuclear tables (eg, Lide, 2010) is the mass of the alpha particle and that of ^{237}Np, which are 4.00150617 u and 237.048166 u, respectively. Thus from Eq. [20.96] the nuclear recoil energy is calculated as

$$\begin{aligned} K_N &= \sqrt{K_p^2 + 2m_p c^2 K_p + m_N^2 c^4} - m_N c^2 \\ &= \left\{ \sqrt{\begin{array}{l}(5.545\ \text{MeV})^2 + 2(4.00150617\ \text{u}) \\ (931.494013\ \text{MeV/u})(5.545\ \text{MeV}) \\ +[(237.048166\ \text{u})(931.494013\ \text{MeV/u})]^2\end{array}} \right\} - (237.048166\ \text{u})(931.494013\ \text{MeV/u}) \\ &= 0.0936\ \text{MeV} \end{aligned} \qquad [20.110]$$

The recoil energy of 0.0936 MeV agrees with the nonrelativistic calculation made in the chapter entitled "Alpha Radiation", Section 4.2 (see Eq. [4.8] and the subsequent calculation). The nuclear recoil energy is 1.68% of the alpha particle energy. In general, the nuclear recoil energy resulting from alpha particle emissions is about 2% of the alpha particle energy. This is relatively high for recoil energies and is characteristic of alpha particle emissions, because the alpha particle is massive. We see much smaller nuclear recoil energies resulting from beta particle emissions of similar energies to the alpha particle, because the alpha particle is massive compared to the electron or beta particle. The mass of the alpha particle is 7294 times that of the electron (ie, $\alpha/e = 4.00150617$ u/0.000548579 u). An analogy can be made by comparing the recoil imparted to a cannon upon firing a cannon ball compared to the kick imparted to a pistol upon firing a 0.45 caliber bullet.

20.11.3.2 Nuclear Recoil from Beta Emissions

Let us calculate the recoil energy imparted to a nucleus by the emission of a beta particle. The following decay of ^{109}Pd by beta particle emission may serve as an example:

$$^{109}_{46}\mathrm{Pd} \rightarrow {}^{109\mathrm{m}}_{47}\mathrm{Ag} + \beta^-(E_{\max} = 1.03\ \text{MeV}) + \overline{\nu} + \gamma \qquad [20.111]$$

Beta particles are emitted with a broad spectrum of energies, from zero to $E_{\max}$, because the decay energies are shared with a neutrino. We will select the maximum energy (1.03 MeV) that the negative beta particle may possess when the antineutrino energy is at its minimum (near zero) to calculate the maximum recoil energy that the particle may impart to the nucleus. We will not calculate here any nuclear recoil energy that the gamma ray may impart to the nucleus. Again, as in the previous example, the nucleus that undergoes the recoil is that of the daughter nuclide, because it is the daughter that is produced when the beta particle is emitted from the nucleus. Also, we will use the relativistic expression of the recoil energy (Eq. [20.96]) for the calculation. Relevant data from nuclear reference tables for the calculation is the mass of the

beta particle (ie, electron mass) and that of ^{109m}Ag, which are 0.000548579 u and 108.904756 u, respectively. The nuclear recoil energy is calculated as

$$K_N = \sqrt{K_p^2 + 2m_pc^2K_p + m_N^2c^4} - m_Nc^2$$

$$= \left\{ \sqrt{\begin{array}{l}(1.03 \times 10^6 \text{ eV})^2 + 2(5.48579 \times 10^{-4} \text{ u}) \\ (931494013 \text{ eV/u})(1.03 \times 10^6 \text{ eV}) \\ +[(108.904756 \text{ u})(931494013 \text{ eV/u})]^2\end{array}} \right\} - (108.904756 \text{ u})(931494013 \text{ eV/u}) \quad [20.112]$$

$$= 10.41 \text{ eV}$$

As we see from this example, the previous example, and Table 20.5, the energies imparted by the massive alpha particles to recoil nuclei are measured in tens of thousands of electron volts, whereas energies imparted by the relatively miniscule beta particle range mostly from a few to several hundred electron volts, and energies imparted to nuclei by gamma-ray and X-ray photons and neutrino emissions are yet smaller.

20.11.3.3 Nuclear Recoil From Gamma-Ray Photon, X-Ray Photon, or Neutrino Emissions

Let us consider an example of a nuclide that decays exclusively by electron capture, with the emission of neutrinos and gamma radiation. The nuclide ^{7}Be decays to ^{7}Li, with the emission of neutrinos of 0.862 MeV at 89.6% relative intensity and 0.384 MeV at the remaining 10.4% intensity. The ^{7}Li daughter nuclides resulting from the lower 0.384 MeV neutrino emissions decay to the ground state, with the emission of gamma radiation of 0.478 MeV. The decay scheme of ^{7}Be is illustrated in Fig. 6.9 of the chapter entitled "Beta Radiation and Beta Decay," and the decay equation is the following:

$$^7_4\text{Be} \xrightarrow{\text{EC}} {}^7_3\text{Li} + \nu + \gamma \quad [20.113]$$

We can use Eq. [20.97] to calculate the nuclear recoil energy resulting from the emission of a neutrino or gamma-ray photon. Let us calculate the recoil energy imparted to the ^{7}Li nucleus resulting from the emission of a 0.862 MeV neutrino. The mass of ^{7}Li obtained from physical data tables is 7.016004 u, and the constant for conversion of atomic mass units to energy is 931.494013 MeV/u.

$$K_N = \sqrt{K_p^2 + m_N^2c^4} - m_Nc^2 \quad [20.114]$$

$$K_N = \left\{ \sqrt{\begin{array}{l}(8.62 \times 10^5 \text{ eV})^2 + \\ [(7.016004 \text{ u})(931494013 \text{ eV/u})]^2\end{array}} \right\} - (7.016004 \text{ u})(931494013 \text{ eV/u})$$

$$= 56.84 \text{ eV}$$

This calculated value is in agreement with the experimental measurement of the ^{7}Li recoil energy of 56 ± 1 eV by 2002 Physics Nobel Laureate Raymond Davis Jr (Davis, 1952). The recoil energy is higher than that calculated above for the recoil energy imparted by the beta particle emission to a ^{109m}Ag nucleus (Eq. [20.112] and subsequent calculation), because of the relatively small mass of the ^{7}Li nucleus. We can see from Table 20.5 that, when comparing particle emissions of the same mass and energy, higher recoil energies will result from nuclei of smaller mass.

20.11.4 Radioactive Recoil Effects

The implications of nuclear recoil are numerous, including applications of hot-atom chemistry where chemical bonds are broken by recoiling nuclei, facilitating the preparation of radionuclides with high specific activity by means of the Szilard-Chalmers effect. Also, nuclear recoil during radioactive decay of naturally occurring radionuclides can create disequilibrium when the recoil liberates the nuclide from its mineral lattice. These recoil effects will be discussed subsequently.

TABLE 20.5 Recoil Energies in Electron Volts (eV) Imparted to Nuclei of Various Masses by Emitted Particles of Various Energies

	Alpha Particles[a]				
Nuclear Mass	E_α = 1.5 MeV	E_α = 2 MeV	E_α = 4 MeV	E_α = 6 MeV	E_α = 8 MeV
150 u	4.0E4 eV	5.3E4 eV	10.7E4 eV	16.0E4 eV	21.3E4 eV
175	3.4E4	4.6E4	9.1E4	13.7E4	18.3E4
200	3.0E4	4.0E4	8.0E4	12.0E4	16.0E4
225	2.7E4	3.6E4	7.1E4	10.7E4	14.2E4
250	2.4E4	3.2E4	6.4E4	9.6E4	12.8E4
	Beta Particles[b]				
Nuclear Mass	E_β = 0.5 MeV	E_β = 1 MeV	E_β = 2 MeV	E_β = 4 MeV	E_β = 6 MeV
10 u	40.84 eV	108.35 eV	324.42 eV	1078.27 eV	2261.53 eV
20	20.42	54.27	162.21	539.13	1130.76
50	8.17	21.71	64.88	215.65	452.30
100	4.08	10.85	32.44	107.82	226.15
150	2.72	7.23	21.63	71.88	150.77
200	2.04	5.43	16.22	53.91	113.08
250	1.63	4.34	12.98	43.13	90.46
	Gamma-Ray Photons, X-Ray Photons, or Neutrinos[c]				
Nuclear Mass	E_γ = 0.5 MeV	E_γ = 1 MeV	E_γ = 2 MeV	E_γ = 4 MeV	E_γ = 6 MeV
10 u	13.42 eV	53.68 eV	214.71 eV	858.83 eV	1932.38 eV
20	6.71	26.84	107.35	429.42	966.19
50	2.68	10.74	42.94	171.77	386.47
100	1.34	5.37	21.47	85.88	193.24
150	0.89	3.58	14.32	57.25	128.82
200	0.67	2.68	10.74	42.94	96.62
250	0.54	2.15	8.59	34.35	77.29

[a]*Nuclear recoil energies resulting from alpha particle emission are expressed in exponential form. For example, the nuclear recoil energy imparted to a nucleus of mass 150 u by an alpha particle emitted with energy of 1.5 MeV is 4.0E4 or 4.0 × 10^4 eV. Also, nuclear recoil energies for nuclear masses of <150 u are not listed for alpha particle emissions, because only nuclei of relatively high mass (A > 140 u) are unstable to alpha particle emission. The recoil energies resulting from alpha particle emissions are calculated by Eq. [20.103], ie,* $K_N = (m_\alpha/m_N)K_\alpha$.

[b]*The recoil energies resulting from beta particle emissions are calculated according to Eq. [20.96], ie,* $K_N = \sqrt{K_p^2 + 2m_pc^2K_p + m_N^2c^4} - m_Nc^2$.

[c]*Recoil energies resulting from gamma-ray photon, X-ray photon, or neutrino emissions were calculated according to Eq. [20.97],*

ie, $K_N = \sqrt{K_p^2 + m_N^2c^4} - m_Nc^2$.

20.11.4.1 Szilard-Chalmers Process

Szilard-Chalmers is an important process which is key to the preparation of radionuclides with high specific activity. The historical background that led to the discovery of the Szilard-Chalmers process is relevant, and is presented briefly in the biographical sketch on Leo Szilard in Hall of Fame, Part IV of this book. Leo Szilard started a search for an element that would undergo a chain reaction with neutrons years before neutron-induced nuclear fission was discovered. With this in mind, Szilard began a collaboration of nuclear research with T.H. Chalmers at the Physics Department of the Medical College of St. Bartholomew's Hospital, London. This research did not result in the discovery of the neutron-induced chain reaction, but led to other important work, including the discovery of a photoneutron (γ,n) source—that is, the induction of neutron emission by gamma- or X-radiation—and the Szilard-Chalmers effect, which is

the rupture of a chemical bond between an atom and a molecule of which the atom is a constituent, as a result of nuclear recoil during radioactive decay of that atom.

Szilard and Chalmers (1934b) used iodine as the indicator for neutrons produced by a $^{9}Be(\gamma,n)^{8}Be$ photoneutron (γ,n) source, as the neutrons would induce radioactivity in iodine by creating radioiodine via neutron capture. An important outcome of this work was the discovery of the Szilard-Chalmers process, whereby radionuclides may be easily separated and isolated from their parent atoms and consequently high specific activities of radionuclides may be obtained which otherwise would be difficult when both the target and product atoms are isotopes. For example, Szilard and Chalmers (1934a,b) surrounded 150 mg of radium (gamma-ray source) with 25 g of beryllium in a sealed container of 1 mm thick platinum. The Ra-Be neutron source was immersed in 100 mL of ethyl iodide. The neutrons produced radioactive ^{128}I from stable ^{127}I by neutron capture. The ^{128}I would precipitate as radioactive silver iodide ($Ag^{128}I$) after the addition of water containing silver ions (Ag^{+}). However, a control experiment without the neutron source produced no radioactivity over background in the silver iodide precipitate. This experiment indicated that the chemical bond between the carbon atom of the ethyl group and the ^{128}I was broken after ^{127}I neutron capture, because free unbound ionic $^{128}I^{-}$ would precipitate with the Ag^{+} to produce radioactive $Ag^{128}I$ precipitate in the aqueous phase (see Fig. IV.9 of Hall of Fame, Part IV for an illustration of this process).

Leo Szilard (1898–1964)
Leo Szilard holding newspaper declaring that President Harry S. Truman announces on September 23, 1949 that the Soviet Union had tested the atomic bomb. This was 15 years after Szilard searched for the nuclear chain reaction while discovering the Szilard-Chalmers Effect and 10 years after nuclear fission was discovered in Germany. Although Szilard fought hard to pervent the use of the atom bomb against Japan and to prevent a weapons race, he holds the newspaper showing that the weapons race had begun. Argonne National Laboratory photo, courtesy of the American Institute of Physics, AIP Emilio Segre Visual Archives

The energy of bonding between the carbon and iodine atoms is about 2 eV, which is higher than the neutron recoil energy. Consequently, the rupture of this bond is due to the gamma recoil when the ^{128}I undergoes gamma emission upon deexcitation after neutron capture. Some atoms of ^{128}I could recombine with the free ethyl group and even exchange with some stable atoms of ^{127}I, but if these processes are slow and are further reduced by the addition of water or even alcohol to dilute the organic phase, the precipitate of radioactive inorganic iodide proceeds, yielding a highly enriched radioactive ^{128}I with minimal ^{127}I.

The Szilard-Chalmers process remains to this day a very practical application to isolate high-specific-activity radioactive sources from the medium in which the radionuclide sources were synthesized. A few examples taken from the literature are editorial reviews by Eckelman et al. (2008) and Koster et al. (2012), the isolation of high-specific-activity

radioisotopes after cyclotron production (Bonardi et al., 2004; Birattari et al., 2001), the preparation of high-specific-activity ^{64}Cu (Van Elteren et al., 1999; Gielow, 1990; Barnes et al., 1986; Hetherington et al., 1986; Sekine, 1986), the production of high-specific-activity ^{166}Ho (Zeisler and Weber, 1998), the preparation of high-specific-activity ^{117m}Sn for medical applications (Mausner et al., 1992), high-specific-activity ^{186}Re (Jia and Ehrhardt, 1997), the optimized production of ^{18}F (Alfassi et al., 1986), high-specific-activity radiohalfnium complexes (Abbe and Marques-Netto, 1975; Marques-Netto and Abbe, 1975), high-specific-activity ^{51}Cr (Vimalnath et al., 2014; Harbottle, 1954; Green and Maddock, 1949), high-specific-activity ^{56}Mn (Zahn, 1967a,b), high-specific-activity radioisotopes of tin (Spano and Kahn, 1952), the concentration of high specific activities of the radioisotopes of Groups IV and V elements (Murin and Nefedov, 1955), and the production of high-specific-activity ^{99}Mo and ^{90}Y (Tomar et al., 2010).

20.11.4.2 Radioactive Disequilibrium

When chemical bonds are broken after radioactive nuclear recoil, the recoiling nucleus may be displaced from the chemical structure (eg, mineral lattice) within which it resided. The liberated nuclide, which may be part of a natural decay chain, may then be leached from mineral deposits into ground water, creating disequilibrium among the natural radionuclides. For example, Labidi et al. (2010) measured the isotopic levels of ^{234}U/^{238}U and ^{226}Ra/^{234}U in waters of Tunisia and found a disequilibrium between the two members of the ^{238}U decay series, which may be due to the direct action of nuclear recoil during radioactive decay and preferential leaching. The U-238 natural decay series was discussed and illustrated previously in Fig. 2.2 of the chapter entitled "Basic Concepts and Definitions" of this book. The researchers estimated the annual effective radiation doses due to the ingestion of the mineral waters to be well below the 0.1 mSv/year reference dose level. Fernandes et al. (2006) studied the radioecological characteristics of a uranium mining site in Brazil and point out that, as suggested by Ivanovich (1994) and Ivanovich and Harmon (1992), disequilibrium between Ra and U isotopes may be due to precipitation/dissolution reactions, alpha recoil, diffusion, and the Szilard-Chalmers effect. Almayahi et al. (2012) found elevated ^{226}Ra/^{238}U ratios in soil and sand systems, which may be the result of the Szilard-Chalmers effect causing disequilibrium in the decay series and elevated radon concentrations.

The activity ratios of ^{234}U/^{238}U were studied by Paces et al. (2002) for evidence of ground-water flow patterns in the USA. They found that ^{234}U enters solution preferentially from rocks as a result of mechanisms related to its origin by radioactive decay of ^{238}U, including alpha recoil damage of crystal-lattice sites containing ^{234}U and the Szilard-Chalmers effect, as well as radiation-induced oxidation of ^{234}U. Similar disequilibrium effects of natural radioactivity, which may be due to nuclear recoil following alpha decay in the ^{238}U decay series, were observed by Dowdall and O'Dea (2002) and Davis and Krogh (2000). Disequilibrium among radionuclides in the natural decay series was underscored by Adloff (1989) to occur by "natural Szilard-Chalmers reactions" all along the radioactive decay series, triggered mostly by nuclear recoil effects after alpha decay. Adloff summarizes that these effects have found a wide range of applications in environmental studies such as geochronology, weathering, sedimental processes, and oceanic chemistry.

Chapter 21

Hall of Fame: Part X

Luis W. Alvarez (1911−1988), Murray Gell-Mann (1929−), George Zweig (1937−), Oscar Wallace Greenberg (1932−), Moo-Young Han (1934−), and Harald Fritzsch (1943−), Jerome I. Friedman (1930−), Henry W. Kendall (1926−1999), and Richard E. Taylor (1929−), Sheldon L. Glashow (1932−), Abdus Salam (1926−1996), and Steven Weinberg (1933−), Gerardus 't Hooft (1946−) and Martinus J.G. Veltman (1931−), Carlo Rubbia (1934−) and Simon van der Meer (1925−2011), Yoichiro Nambu (1921−), Makoto Kobayashi (1944−) and Toshihide Maskawa (1940−), François Englert (1932−) and Peter W. Higgs (1929−), and Serge Haroche (1944−) and David J. Wineland (1944−).

Who ordered that?

This comment was made by Nobel Laureate I. I. Rabi after the discovery of the muon, a "heavy electron" (lepton) with no known role in nuclear interactions. Muons were discovered in cosmic ray showers by Carl D. Anderson and Seth Neddermeyer at the California Institute of Technology (CalTech) in 1936.

When the Nobel Prizes were first awarded in 1901, physicists knew something of just two objects which are now called "elementary particles": the electron and the proton. A deluge of other "elementary" particles appeared after 1930; neutron, neutrino, μ meson [muon], π meson, heavier mesons, and various hyperons. I have heard it said that "the finder of a new elementary particle used to be rewarded by a Nobel Prize, but such a discovery now ought to be punished by a $10,000 fine".

This quote is from the Nobel lecture of Willis E. Lamb, Jr on December 12, 1955. In an interview with George Zweig at CERN (European Organization for Nuclear Research) Physics Department on December 13, 2013, Zweig claims that these words by Willis Lamb were the "older generation talking" (Charitos, 2013, http://ph-news.web.cern.ch/content/interview-george-zweig). According to Zweig's response to Lamb's humorous statement, the young pioneering physicists were anxiously awaiting the discovery of new particles which would provide new answers to the structure of matter. Also, at the time that Willis Lamb made the comment (1955), the general thought was that the proton, neutron, mesons, and hyperons were elementary particles. We now know, as discussed in this chapter, that the hadrons (proton, neutron, mesons and hyperons) are not elementary particles; rather, they are composed of yet smaller particles, namely quarks and gluons.

LUIS W. ALVAREZ (1911−1988)

Luis Walter Alvarez was born in San Francisco, California on June 13, 1911, the son and grandson of physicians Walter C. Alvarez and Luis F. Alvarez. Luis W. Alvarez was awarded the Nobel Prize in Physics in 1968 "for his decisive contributions to elementary particle physics, in particular the discovery of a large number of resonance states, made possible through his development of the technique of using a hydrogen bubble chamber and data analysis." He also discovered the radioactive decay process known as electron capture (EC) or K-capture, which competes with positron emission in beta decay; and was the first to measure experimentally the complete beta particle and neutron emissions in a nuclear decay process known as beta-delayed neutron emission.

Radioactivity: Introduction and History, From the Quantum to Quarks. http://dx.doi.org/10.1016/B978-0-444-63489-4.00021-6
Copyright © 2016 Elsevier B.V. All rights reserved.

Luis W. Alvarez (1911–1988)

After his high school education Luis Alvarez entered the University of Chicago, where he completed his entire college education; he gained a bachelor of science degree in 1932, a master of science in 1934, and a doctorate in 1936. Nobel Laureate Arthur H. Compton was his doctoral dissertation advisor. Alvarez had the talent and knowledge to construct excellent Geiger counters for radiation detection, and thus Compton invited him to use specially designed Geiger counters to study the direction of incoming cosmic ray particles. By means of specifically orienting Geiger counter tubes and coincidence counting methods of positively charged particles (ie, protons) at the favorable geomagnetic latitude (29°N) and elevation (2310 m) provided by Mexico City, Luis Alvarez and Arthur Compton (1933) were able to obtain evidence to support the theory of Georges Lemaître and Manuel Sandoval-Vallarta, Manuel (1933) that charged particles of the cosmic radiation are deflected by the Earth's magnetic field. This was Alvarez's first major publication; and Compton, as Alvarez's supervisor, included himself as a coauthor but gave major credit to Luis Alvarez. As related by Trower (2009), Alvarez took this noble act by Compton as an example in later life to encourage his staff to take major credit as principal authors of papers in work to which they had contributed heavily.

In a biographical memoir, Trower (2009) points out that Luis Alvarez was not an exceptional student. He noted the following:

> *An accomplished but unexceptional student, Luie along with Bill Shockley was interviewed by Stanford psychologist Lewis Terman for his famous longitudinal study of the gifted. Neither was selected, nor would either have qualified for Mensa membership, but both received Nobel Prizes (which none of the 1528 "Termites" did).*

This is an important observation by Trower. The writer has also in his career witnessed gifted students who did not become great achievers. A passion for one's field of work, imagination, and a drive to achieve are generally more powerful ingredients in success than a gifted intellect.

After completing his graduate studies at the University of California in 1936, Luis Alvarez joined Ernest O. Lawrence's group at the Radiation Laboratory of the University of California at Berkeley. At the Radiation Lab, Alvarez (1937, 1938a,b) was able to demonstrate for the first time radioactive decay by EC, also known as K-capture, which had only been proposed previously by beta decay theory. EC is described in detail in the chapter entitled "Beta Radiation and Beta Decay," and this decay process often competes with positron emission as a means of nuclear decay. Alvarez (1938a,b) first

demonstrated K-capture in the decay of gallium-67, where the nucleus captures an atomic electron from the K-orbital, and the electron combines with a nuclear proton to form a neutron within the nucleus. He was able to confirm this decay process by measuring the characteristic K X-ray quantum from the daughter nuclide ^{67}Zn. The decay process, demonstrated by Alvarez (1938a), was the following:

$$^{67}_{31}\mathrm{Ga} \xrightarrow{\mathrm{EC}} {}^{67}_{30}\mathrm{Zn} + \nu + K \text{ x-rays} + \gamma \qquad [X.1]$$

Gamma radiation, included in Eq. [X.1], often accompanies such a decay process; and Alvarez measured this to be emitted from the ^{67}Zn daughter nuclide. He was also able to measure the emission of internal conversion electrons as a mode of decay, which often competes with gamma emission, as described in the chapter entitled "Atomic Electron Radiation" of this book.

While at the Radiation Laboratory, Luis Alvarez collaborated with Felix Bloch (Alvarez and Bloch, 1940) in the measurement of the magnetic moment of the neutron by passing a beam of thermal neutrons through polarizing and analyzing plates of magnetized iron, as described in Hall of Fame, Part IX of this book. Thus in only four years after graduating with a doctoral degree from the University of Chicago (1936−1940), Luis Alvarez was able to accomplish two major pioneering achievements: demonstrating the capture of a K-shell electron by an atomic nucleus, and determining the magnetic moment of the neutron. Trower (2009) best characterized the significance of Alverez's achievements as follows:

> *Bethe [Hans Bethe] noted that nuclei could cannibalize their innermost atomic electrons but was discouraged about the prospects that the effect would ever be seen. Luie [Luis Alvarez] experimentally demonstrated nuclear K-capture. Bethe despaired that the magnetic moment of the neutron, a fundamental constant, would prove to be beyond measuring. Luie measured it, and Felix Bloch calculated its value.*

In 1940 Luis Alvarez joined the Radiation Laboratory at the Massachusetts Institute of Technology (MIT), where he was responsible for the development of three major radar systems vital to the war effort: the microwave early warning system; the Eagle high-altitude bombing system; and a blind-landing system, which was of great value for civilian as well as military aircraft, known as GCA or ground-controlled approach (Nobel Lectures, Physics, 1963−1970). In 1943 Alvarez was invited by J. Robert Oppenheimer to join the Manhattan Project. After a short stint with Enrico Fermi at the University of Chicago, Alvarez joined the research effort at Los Alamos, where he was responsible for the development of detonators for the plutonium bomb.

After the war, Luis Alvarez returned to the University of California at Berkeley to devote his time to the development and application of particle accelerators. Alvarez (1949) carefully studied the decay of ^{17}N, which had a measured half-life of 4.2 s produced with the 184-inch (467.4 cm) cyclotron, and found that it decayed by beta-delayed neutron emission, abbreviated $\beta(n)$. The theory behind $\beta(n)$ decay was developed by Niels Bohr and John Archibald Wheeler (Bohr and Wheeler, 1939), but Alvarez was the first to measure precisely a complete decay scheme with beta particle and neutron emission energies. Beta-delayed neutron emission involves the emission of neutrons from excited elevated states of a neutron-rich nucleus following beta decay, as illustrated in Fig. X.1. Alvarez was able to determine the maximum beta particle energy of ^{17}N decay by means of Feather analysis, which involves the measurement of the maximum energy of beta particle emissions according to their range in an absorber previously calibrated with reference standards for beta emissions of known energy maxima. The technique was named after Norman Feather (1904−1978), who developed the method (Feather, 1938). Alvarez determined the neutron energies originating from the beta-delayed neutron emission of ^{17}N decay from the energies of the ^{16}O nuclear recoils measured by gas proportional counters. Beta-delayed neutron emission is discussed in detail in the chapter entitled "The Atomic Nucleus."

The beta-delayed neutron emission in the decay of neutron-rich ^{17}N, illustrated by the decay schemes in Fig. X.1, may be written as follows:

$$^{17}_{7}\mathrm{N} \xrightarrow{\beta^-} {}^{17}_{8}\mathrm{O} + \beta^- + \overline{\nu} \xrightarrow{n} {}^{16}_{8}\mathrm{O} + \mathrm{n} \qquad [X.2]$$

As illustrated in Fig. X.1A, Alvarez identified three beta transitions, which leads to three elevated energy states of ^{17}O with a concomitant emission of a neutron from each of these excited or elevated energy states. In his drawing illustrated in Fig. X.1A, Alvarez provides three lines for beta particle transitions identified with the β symbol and a neutron emission (arrows pointing downward, identified by the letter n) from each of three energy levels of the decay scheme. The lengths of the three arrows pointing downward differ according to their energy, which he symbolized with a bell curve oriented in a

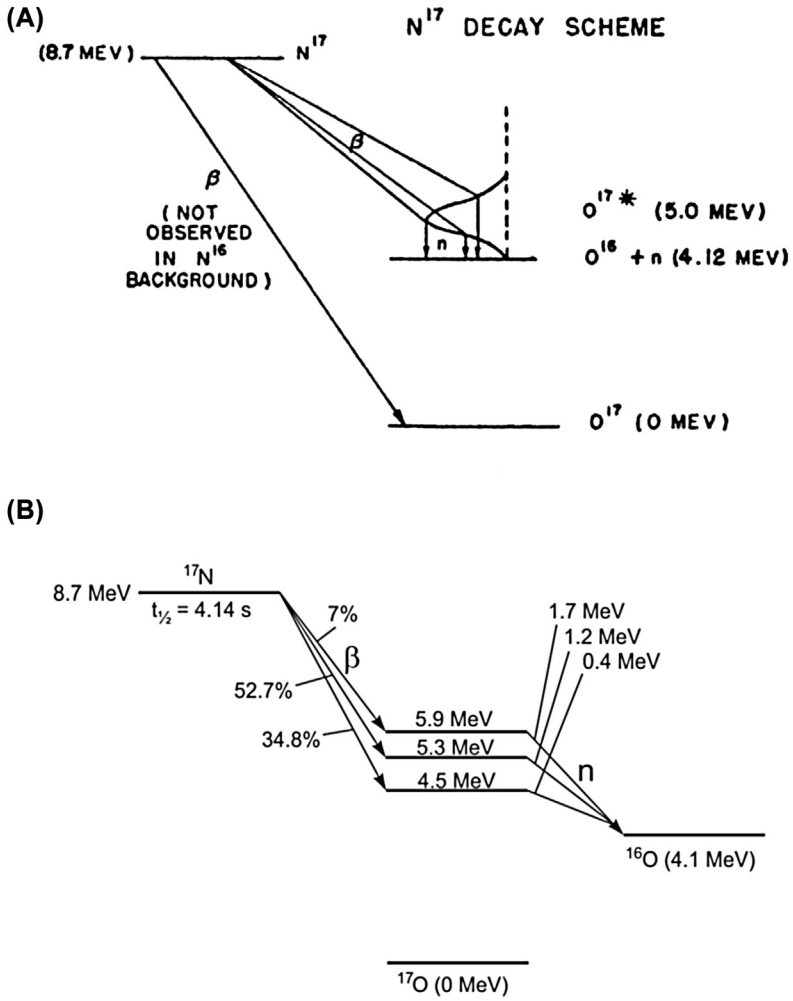

FIGURE X.1 The radioactive decay of nitrogen-17 by beta-delayed neutron emission, abbreviated $\beta(n)$. The decay scheme is illustrated according to (A) the original decay scheme from the work of Luis Alvarez (1949), http://dx.doi.org/10.1103/PhysRev.75.1127, reprinted with permission by the American Physical Society © 1949; and (B) a more modern depiction of the decay scheme with data on neutron energies from Ohm et al. (1976) and current nuclear decay data. A relatively very weak beta transition with a 0.6% intensity, resulting in the emission of a 0.8 MeV neutron, is not illustrated. It should be noted that during the early and mid-part of the 20th century it was the practice to write the mass number of a nuclide in superscript to the right of the symbol for the element, such as N^{17} in the drawing by Alvarez (1949). It is now the practice to write the mass number in superscript to the left of the symbol for the element, eg, ^{17}N.

horizontal position. His measurements of the three neutron energies were approximately 0.5, 1.0, and 1.8 MeV (Alvarez, 1949), which are very close to the current values provided in Fig. X.1B. Alvarez's work is amazing when considering that he had to manufacture his own radiation measurement instrumentation, which cannot compare with modern instrumentation currently available to researchers.

In 1954 the Bevatron proton linear accelerator came into operation at the Lawrence Berkeley National Laboratory. The Bevatron was a proton synchrotron capable of accelerating protons to impart energies in billions of electron volts, from which the name Bevatron (**b**illions of **eV** synchro**tron**) was derived. Thus Alvarez turned his attention to research on proton collisions using the Bevatron. Particles from such high-energy collisions would have very short lifetimes, of the order of 10^{-10} s or less. In April 1953 Alvarez met Donald Glaser at the annual meeting of the American Physical Society. Glaser, who was at the time a postdoctoral research student at the University of Michigan, had invented a bubble chamber filled with liquid diethyl ether, which proved very useful for the production and imaging of tracks produced by the

collisions of high-energy particles in cosmic radiation showers. Alvarez decided to develop a bubble chamber filled with liquid hydrogen, as he would be researching the collisions of high-energy protons. Hydrogen would be the ideal medium for a bubble chamber, because it would be advantageous to study the collisions of high-energy protons against the nuclei of hydrogen atoms, which are protons.

Alvarez and his coworkers successfully developed the hydrogen bubble chamber, which yielded tracks of numerous newly discovered particles following the collisions of high-energy protons within the bubble chamber (Alvarez, 1972). Although the newly discovered particles had very short lifetimes (10^{-10} s or less), he could measure their lifetimes by the lengths of their tracks, which could be as long as several centimeters taking into account that the particles travel at close to the speed of light. The newly discovered particles were known as *strange particles* because of their unusual properties, including short lifetimes and high mass compared to the proton and neutron. The importance of the hydrogen bubble chamber and newly discovered particles was underscored by Professor S. von Friesen, member of the Swedish Academy of Sciences, in his award ceremony speech on the occasion of the awarding of the Nobel Prize to Luis Alvarez on December 11, 1968:

> *One could, however, suspect the existence of particles with considerably shorter life-spans and with such small track-lengths that they are impossible to measure. In this case one is obliged, instead, to study the tracks of their disintegration products and the tracks of the reactions they produce in collision with other particles. The pattern of tracks thus becomes very complicated; the correct interpretation of what actually occurs requires acute powers of discernment and a particularly advanced experimental technique. It is in this field that Professor Luis Alvarez has made the contributions for which he is today being rewarded.*
>
> *He has with insight and determination developed the bubble-chamber, invented by the Nobel Prize winner in Physics, Donald Glaser, into an invaluable instrument for this type of investigation. Alvarez' bubble-chamber contains many hundreds of litres of hydrogen, reduced to a temperature of minus 250°C, which thus becomes fluid. When the particle passes through the liquid, it is warmed to boiling point along the track it leaves. In the wake are a trail of bubbles that can be photographed whilst still very small. The photographs are able, in this way, to reproduce accurately the path of the particle. Because the chamber contains only hydrogen, it is evident that all reactions must occur with hydrogen nuclei, protons. This considerably simplifies the interpretation of the phenomenon. The cost of this instrument, capable of producing about a million photographs annually, was two million dollars.*
>
> *The photographs must be studied and measured with great accuracy. In order to carry out this enormous task, Alvarez and his assistants have constructed a series of more and more delicate automatic scanning and measuring instruments capable of transferring the information from the photographic film into a state suitable for treatment by computer. In this field, too, Alvarez has made contributions of a pioneering nature.*
>
> *With the establishment of the hydrogen bubble-chamber, entirely new possibilities for research into high-energy physics present themselves. Results have already been apparent in the form of newly-discovered elementary particles. The first, very short-lived, so called "resonance particle" was found in 1960. Since then there have been a whole series of discoveries made by Alvarez' group in Berkeley, California and in other laboratories where Alvarez' material is being used or where his methods and programs are adopted. Practically all the discoveries that have been made in this important field of high-energy physics have been possible only through the use of methods originated by Professor Alvarez.*

From Nobel Lectures, Physics, 1963–1970, Elsevier, Amsterdam, 1972, © The Nobel Foundation 1968, Nobelprize.org. Nobel Media AB 2014. Web. 9 Apr 2015. www.nobelprize.org/nobel_prizes/physics/laureates/1968/press.html, reprinted with permission.

An example of numerous tracks produced in the hydrogen bubble chamber by a cascade of strange particles is provided by one of Alvarez's photographs, illustrated in Fig. X.2. An entire zoo of strange particles and resonance states was discovered with the hydrogen bubble chamber, including the lambda (Λ^0), sigma (Σ^+, Σ^-, and Σ^0), xi (Ξ^- and Ξ^0), and delta (Δ^{++}, Δ^+, Δ^0, and Δ^-) particles. The resonance particles, referred to above, are the very short-lived particles such as the delta (Δ) particles with lifetimes of the order of 10^{-24} s, which is too short a lifetime to produce any measurable track length in the hydrogen bubble chamber. The limit of the bubble chamber was a measurable track length of 1 μm or 10^{-6} m. A particle that would produce a track length of only 10^{-6} m in the bubble chamber before decaying would have a measurable lifetime. The lifetime measured according to the length of the particle track would be a dilated lifetime according to Einstein's theory of relativity and the Lorentz transformation, as described by Eq. [III.21] in Hall of Fame, Part III of this book. The particles measured in the bubble chamber travel close to the speed of light; and the measurement of time taken in the reference frame of the laboratory of a particle traveling at relativistic speed in its proper frame of

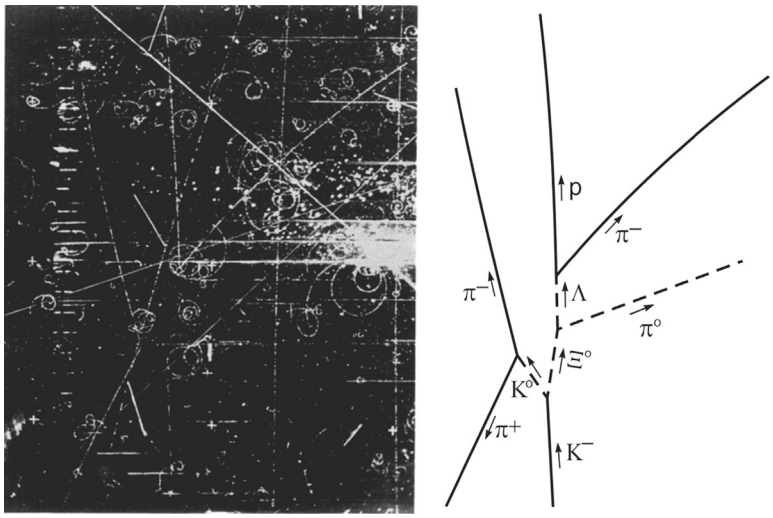

FIGURE X.2 Photograph and sketch of Ξ^0 event. *(From Alvarez (1959), http://dx.doi.org/10.1103/PhysRevLett.2.215, reprinted with permission by the American Physical Society © 1959.)* On the left is a photograph with the particle tracks.

reference will be a dilated measurement. Serway et al. (2005) describe this dilated lifetime measurement in the laboratory as t_{lab}; and they calculate this dilated lifetime of a particle traveling at $0.99c$ (0.99 times the speed of light) for a distance of only 10^{-6} m according to the following:

$$t_{lab} = \frac{d}{v} = \frac{10^{-6}\text{ m}}{(0.99)(2.99 \times 10^{8}\text{ m/s})} = 0.33 \times 10^{-14}\text{ s} \qquad [X.3]$$

where t_{lab} is the particle lifetime as measured by an observer in the reference frame of the laboratory, d is the distance of travel of the particle, ie, the particle track length in the bubble chamber, and v is the particle velocity in meters/second. Serway et al. (2005) point out that the proper lifetime of the particle (ie, the lifetime of the particle in the reference frame of the particle), identified as t_{proper}, would be shorter, as calculated according to relativity (see Eq. [III.21] in Hall of Fame, Part III of this book), as follows:

$$t_{proper} = (t_{lab})\sqrt{1 - \frac{v^2}{c^2}} = \left(0.33 \times 10^{-14}\text{ s}\right)\sqrt{1 - \frac{(0.99c)^2}{c^2}} = 4.6 \times 10^{-16}\text{ s} \qquad [X.4]$$

If we consider a particle traveling at yet a faster speed of $0.9995c$ and apply the same calculations, we will arrive at the proper lifetime of the particle t_{proper} to be 1.0×10^{-16} s. Thus particles with lifetimes shorter than 10^{-16} s could not be measured by Alvarez from a bubble chamber track. Serway et al. (2005) note that particles of very short lifetimes, such as the resonance particles with lifetimes of the order of 10^{-23} s, are deduced from resonance peaks produced by plots of cross-section versus energy of decay products.

The zoo of strange particles and resonance states revealed by the hydrogen bubble chamber and the techniques developed by Luis Alvarez remained unorganized in terms of any systematic interrelationship between the particles until the independent work of Murray Gell-Mann and Yuval Ne'eman established the Eightfold Way, which is a sort of periodic table of these strange particles. This is reviewed later in this chapter.

Luis Alvarez died on September 1, 1988 in Berkeley. For a very complete review of his life and work, the reader is encouraged to peruse the biographical memoir by Trower (2009).

MURRAY GELL-MANN (1929–)

Murray Gell-Mann was born in the Manhattan district of New York City in 1929. He was valedictorian at Columbia Grammar and Preparatory School in New York, having skipped three years of classes, so he entered Yale University at the young age of 15. At Yale Gell-Mann graduated with a bachelor of science degree in physics in 1948; and in 1951 at the age of 21 he received his doctoral degree at MIT under the supervision of Victor Weisskopf. He was awarded the Nobel Prize in Physics in 1969 "for his contributions and discoveries concerning the classification of elementary particles and their interactions."

Murray Gell-Mann (1929–)

In 1951–1952 Murray Gell-Mann was an instructor at the University of Chicago. He was promoted to assistant professor in 1953, associate professor in 1954, and professor in 1956. To establish some order to the chaos of the menagerie or zoo of strange and resonance particles discovered by Luis Alvarez and others with high-energy proton collisions, the theory of strangeness was established in 1954 by Gell-Mann (Gell-Mann and Pais, 1954) at the University of Chicago and independently by Kazuhiko Nishijima (Nakano and Nishijima, 1953; Nishijima, 1954, 1956), who was professor of physics at Osaka City University, the University of Tokyo, and Kyoto University. Professor Nishijima was born in Tsuchiura, Japan on October 4, 1926 and died on February 15, 2009 in Tokyo. In an original paper Tadao Nakano and Kazuhiko Nishijima wrote

> *After the completion of this work, the authors knew in a private letter from Prof. Nambu to Prof. Hayakawa that Dr. Gell-Mann has also developed a similar theory.*

This statement reflects the almost simultaneous and independent discoveries by persons at opposite ends of the earth, which sometimes occurs in scientific research. When the stage is set with findings from the research of others, discoveries or breakthroughs will be made.

Strangeness

Strangeness (S) is a quantum number assigned to particles. The term strangeness was established before the discovery of quarks to explain differing rates of reaction when strange particles were produced and when they decayed. A *law of conservation of strangeness* states that the sum of the strangeness quantum numbers between reacting particles or the quantum number of a decaying particle should be equal to the sum of strangeness numbers of the reaction products or decay products. A violation of the law might explain differing decay rates of the products compared to their rates of production. When the theory of quarks was established in the 1960s (described subsequently in this section), the strangeness quantum number (S) was defined by the number of strange quarks (s) that constitute a part of the internal structure of the particle. The quark structures of baryons and mesons are provided in Tables X.1 and X.2 and discussed later in this chapter. The strange (s) quark is attributed a strangeness value of −1. For example, the proton and neutron contain no strange quarks, and thus have a strangeness of 0. Sigma (Σ^+, Σ^0, or Σ^-) particles each contain one strange quark, and thus have a strangeness value of −1. Particles with two strange quarks, such as the xi (Ξ^- and Ξ^0), are

TABLE X.1 Quark Structure and Properties of Baryons[a]

Particle	Symbol	Quark Structure[b]	Charge[c]	Rest Mass (MeV/c^2)	Lifetime (s)
Proton	p^+	uud	$+\frac{2}{3}+\frac{2}{3}-\frac{1}{3}=+1e$	938.3	Stable
Neutron	n	udd	$+\frac{2}{3}-\frac{1}{3}-\frac{1}{3}=0$	939.5	886[d]
Lambda	Λ^0	uds	$+\frac{2}{3}-\frac{1}{3}-\frac{1}{3}=0$	1115.7	2.6×10^{-10}
Sigma	Σ^+	uus	$+\frac{2}{3}+\frac{2}{3}-\frac{1}{3}=+1$	1189.4	0.8×10^{-10}
	Σ^0	uds	$+\frac{2}{3}-\frac{1}{3}-\frac{1}{3}=0$	1192.6	7.4×10^{-20}
	Σ^-	dds	$-\frac{1}{3}-\frac{1}{3}-\frac{1}{3}=-1$	1197.4	1.5×10^{-10}
xi	Ξ^0	uss	$+\frac{2}{3}-\frac{1}{3}-\frac{1}{3}=0$	1314.9	2.9×10^{-10}
	Ξ^-	dss	$-\frac{1}{3}-\frac{1}{3}-\frac{1}{3}=-1$	1321.7	1.6×10^{-10}
Delta	Δ^{++}	uuu	$+\frac{2}{3}+\frac{2}{3}+\frac{2}{3}=+2$	1232	6.0×10^{-24}
	Δ^+	uud	$+\frac{2}{3}+\frac{2}{3}-\frac{1}{3}=+1$	1232	6.0×10^{-24}
	Δ^0	udd	$+\frac{2}{3}-\frac{1}{3}-\frac{1}{3}=0$	1232	6.0×10^{-24}
	Δ^-	ddd	$-\frac{1}{3}-\frac{1}{3}-\frac{1}{3}=-1$	1232	6.0×10^{-24}
Omega	Ω^-	sss	$-\frac{1}{3}-\frac{1}{3}-\frac{1}{3}=-1$	1672.4	8.2×10^{-11}
Lambda[e]	Λ_c^+	udc	$+\frac{2}{3}-\frac{1}{3}+\frac{2}{3}=+1$	2286	2.0×10^{-13}
	Λ_b^0	udb	$+\frac{2}{3}-\frac{1}{3}-\frac{1}{3}=0$	5619	1.4×10^{-12}

[a] *Data is from the Berkeley National Laboratory Particle Data Group, 2013. Beringer, J., et al. (Particle Data Group), Phys. Rev. D86, 010001 (2012) and 2013 partial update, http://pdg.lbl.gov/2013/listings/contents_listings.html.*
[b] *The quark structure listed is that of the particle and not of the antiparticle. All baryon antiparticles contain the antiquarks with resulting opposite charge. For example, the antiproton would contain the quark structure $\overline{uud}$ with an overall opposite charge of the proton, ie, $-\frac{2}{3}-\frac{2}{3}+\frac{1}{3}=-1e$. All baryons listed have spin quantum number ½ with the exception of the delta particles and the omega minus particle, which have the spin quantum number 3/2.*
[c] *The total charge on the particle is provided as the sum of the individual quark charges. The particle charge is a multiple of the electron charge* e.
[d] *The neutron is stable in the confines of the nucleus.*
[e] *Baryons containing a subscript "c" or "b" are baryons containing a charm (c) quark or a bottom (b) quark, respectively. These are referred to as charmed or bottom baryons. The b quark is also called a beauty quark; and a baryon containing a b quark may also be referred to as a beauty baryon.*

attributed a strangeness value of -2. The omega (Ω^-) particle contains three strange quarks, and it is thus assigned a strangeness value of -3. Particles containing a strange antiquark ($\bar{s}$), such as the kaon K^+ particle, would have a strangeness quantum number of $+1$, opposite to that of a particle with a strange quark (s). The assignment of the strangeness quantum number (S) to a particle, as described above, obeys the following formula:

$$S = -\left(n_S - n_{\bar{S}}\right) \qquad [X.5]$$

where n_S is the number of strange quarks (s) that the particle holds, and $n_{\bar{S}}$ is the number strange antiquarks ($\bar{s}$) comprised by a particle.

The strangeness quantum number facilities the interpretation of differing reaction or decay rates among the particles. As noted by Serway et al. (2005), the slow decay rates of some strange particles can be explained by inferring that while the strong and electromagnetic interactions obey the law of conservation of strangeness, the weak interaction does not obey the law; and decay reactions which violate strangeness conservation exhibit relatively slow decay rates via the weak interaction, ie, a mechanism of decay involving the weak nuclear force. The following examples of reactions and decay of strange particles illustrate conservation of strangeness. The strangeness quantum numbers (S) are included under each particle in parentheses. The reactions are taken from Luis Alvarez's Nobel lecture (Alvarez, 1972).

1. The interaction of a K^- meson with a proton,

$$\begin{gathered} K^- + p \rightarrow \Xi^0 + K^0 \\ (-1) + (0) \rightarrow (-2) + (+1)^0 \end{gathered} \qquad [X.6]$$

TABLE X.2 Quark Structure and Properties of Mesons[a]

Particle	Symbol	Antiparticle	Quark Structure[b]	Charge[c]	Rest Mass (MeV/c^2)	Lifetime (s)
Pion[d]	π^+	π^-	$u\bar{d}$	$+\frac{2}{3}+\frac{1}{3}=+1e$	139.6	2.6×10^{-8}
	π^0	self[e]	$--^{e}$	0[e]	135.0	8.5×10^{-17}
Kaon[f]	K^+	K^-	$u\bar{s}$	$+\frac{2}{3}+\frac{1}{3}=+1$	493.7	1.2×10^{-8}
	K_S^0	$\overline{K_S^0}$	$d\bar{s}, \bar{d}s$	0[c]	497.6	8.9×10^{-11}
	K_L^0	$\overline{K_L^0}$	$d\bar{s}, \bar{d}s$	0[c]	497.6	5.1×10^{-8}
Eta	η^0	self[i]	$--^{g}$	0[g]	547.9	$<10^{-18}$
Eta prime	$\eta^{0\prime}$	self[i]	$--^{g}$	0[g]	957.8	2.2×10^{-21}
Rho	ρ^+	ρ^-	$u\bar{d}$	$+\frac{2}{3}+\frac{1}{3}=+1$	775.3	0.4×10^{-23}
Omega	ω^0	self[i]	$u\bar{u}, d\bar{d}$	0[c]	782.6	0.8×10^{-22}
Kaon[h]	K^{*+}	K^{*-}	$u\bar{s}$	$+\frac{2}{3}+\frac{1}{3}=+1$	891.6	3.3×10^{-23}
	K^{*0}	$\overline{K}^{*0}$	$d\bar{s}$	$-\frac{1}{3}+\frac{1}{3}=0$	895.8	1.4×10^{-23}
Phi	φ	self[i]	$s\bar{s}$	$-\frac{1}{3}+\frac{1}{3}=0$	1019.4	1.5×10^{-22}
D meson	D^+	D^-	$c\bar{d}$	$+\frac{2}{3}+\frac{1}{3}=+1$	1869.6	1.0×10^{-12}
	D^0	$\overline{D^0}$	$c\bar{u}$	$+\frac{2}{3}-\frac{2}{3}=0$	1864.9	4.1×10^{-13}
J/Psi	J/ψ	self[i]	$c\bar{c}$	$+\frac{2}{3}-\frac{2}{3}=0$	3096.9	0.8×10^{-20}
B meson	B^+	B^-	$u\bar{b}$	$+\frac{2}{3}+\frac{1}{3}=+1$	5279.3	1.6×10^{-12}
	B^0	$\overline{B^0}$	$d\bar{b}$	$-\frac{1}{3}+\frac{1}{3}=0$	5279.6	1.5×10^{-12}
Upsilon	Υ	self[i]	$b\bar{b}$	$-\frac{1}{3}+\frac{1}{3}=0$	9460.3	1.3×10^{-20}

[a] *Data is from the Berkeley National Laboratory, Particle Data Group, 2013. Beringer, J., et al. (Particle Data Group), Phys. Rev. D86, 010001 (2012) and 2013 partial update, http://pdg.lbl.gov/2013/listings/contents_listings.html.*
[b] *The quark structure listed is that of the particle and not of the antiparticle.*
[c] *The total charge on the particle is provided as the sum of the individual quark charges. The particle charge is a multiple of the electron charge* e.
[d] *The oppositely charged meson is the antiparticle of the other. They differ in their quark structure. Antiparticles have an opposed quark structure to their respective particle. For example, the positive pion (π^+) has the $u\bar{d}$ quark structure; whereas its antiparticle, the negative pion, has the opposed quark structure $d\bar{u}$ with the sum of its quark charges amounting to $-\frac{1}{3}-\frac{2}{3}=-1$. Another example, the neutral kaon (K^0), has the $d\bar{s}$ quark structure, while the antiparticle of the neutral kaon $\left(\overline{K^0}\right)$ has the opposed $\bar{d}s$ quark structure and a charge of $-\frac{1}{3}+\frac{1}{3}=0$.*
[e] *The particle is its own antiparticle, and its quark structure is a composite of the up–antiup and down–antidown quarks: $u\bar{u}-d\bar{d}\big/\sqrt{2}$.*
[f] *The K_S^0 and K_L^0 are relatively short- and long-lived states of the neutral kaon.*
[g] *The quark structure is a composite of quark–antiquark pairs.*
[h] *Resonance state.*
[i] *The particle is its own antiparticle.*

2. The reaction of a negative pion with a proton,

$$\pi^- + p \rightarrow \Lambda^0 + K^0$$
$$(0) + (0) \rightarrow (-1) + (+1) \qquad \text{[X.7]}$$

The following illustrate differing lifetimes for particle decays that obey strangeness conservation and proceed by the strong nuclear force, and others that violate strangeness conservation and exhibit relatively slower decay rates by the weak nuclear force.

1. The decay of a neutral sigma particle,

$$\Sigma^0 \rightarrow \Lambda^0 + \gamma \quad \left(\Sigma^0 \text{ lifetime } = 6\times10^{-20}\text{ s}\right)$$
$$(-1) \rightarrow (-1) + (0) \quad \text{(strangeness is conserved)} \qquad \text{[X.8]}$$

2. The decay of the delta particle,

$$\Delta^+ \rightarrow p + \pi^0 \quad \left(\Delta^+ \text{ lifetime } = 6 \times 10^{-23} \text{ s}\right)$$
$$(0) \rightarrow (0) + (0) \quad \text{(strangeness is conserved)} \qquad \text{[X.9]}$$

3. The decay of the positive kaon,

$$K^+ \rightarrow \pi^+ + \pi^0 \quad \left(K^+ \text{ lifetime } = 1.24 \times 10^{-8}\text{s}\right)$$
$$(+1) \rightarrow (0) + (0) \quad \text{(strangeness is not conserved)} \qquad \text{[X.10]}$$

4. The decay of the neutral xi,

$$\Xi^0 \rightarrow \Lambda^0 + \pi^0 \quad \left(\Xi^0 \text{ lifetime } = 2.9 \times 10^{-10} \text{ s}\right)$$
$$(-2) \rightarrow (-1) + (0) \quad \text{(strangeness is not conserved)} \qquad \text{[X.11]}$$

Yuval Ne'eman (1925–2006)
University of Hawaii High Energy Physics Group, courtesy of AIP Emilio Segre Visual Archives

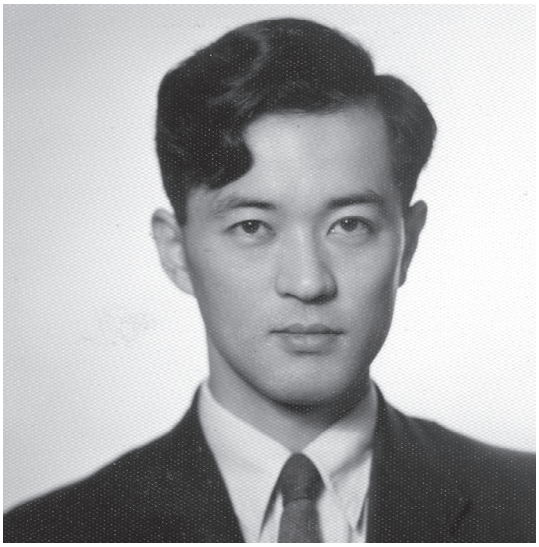

Kazuhiko Nishijima (1926–2009)
With permission of AIP Emilio Segre Visual Archives

The Eightfold Way

Physicists needed to find a further degree of order for the numerous strange particles discovered with the hydrogen bubble chamber. We will recall the work of Dmitri Ivanovich Mendeleev (1834−1907), the Russian chemist who discovered an order among the chemical elements according to their atomic weight and valence (Mendeleev, 1864, 1869), which is now referred to as the periodic table of the elements. Mendeleev's placement of the elements in a periodic table permitted an organized arrangement of the known elements not only according to their atomic weights and valence, but also according to their properties; and the prediction of elements to be discovered where vacancies or gaps occurred in the table. In an attempt to find a practical organization of the newly discovered and numerous strange particles, physicists strove to find where certain properties of the particles could be organized into a table analogous to the periodic table of the elements.

Murray Gell-Mann at the Synchrotron Laboratory at CalTech and Yuval Ne'eman, an Israeli theoretical physicist, independently arrived at a systematic organization of numerous particles, which is known as the Eightfold Way (Gell-Mann, 1961; Ne'eman, 1961). The Eightfold Way was subsequently described in a book jointly coauthored and edited by Gell-Mann and Ne'eman (1964). The particles are organized according to their spin (s) and plots of their

strangeness (S) and charge (Q) quantum numbers. Firstly the particles are grouped according to spin ½ baryons, spin 0 mesons, and spin 1 mesons; and then each group of particles is arranged by plotting their strangeness (S) against their charge (Q). The results formed octets of the subatomic particles interlinked by triangles and hexagons, as illustrated in Figs. X.3–X.5. Murray Gell-Mann coined the organization of these octets of strange particles as the Eightfold Way, referring to "the Noble Eightfold Path," one of the principal teachings of Buddha. The Eightfold Path of Buddha is a teaching that leads to tranquility and insight.

The octets illustrated in Figs. X.4 and X.5 are interesting, because the antiparticle of each meson is found at opposite ends of the hexagons. While the original number of particles in each hexagon was only eight (thus the name octet and Eightfold Way), the original arrangement in Fig. X.4 contained only seven particles; and Gell-Mann predicted the missing η^0 particle of this octet (Gell-Mann, 1961). The missing η^0 was discovered subsequently by Pevsner et al. (1961) and identified by Bastien et al. (1962). This is similar to the history of the periodic table of the elements, when gaps in the table were filled by subsequently discovered elements. An additional meson, the η'^0, was discovered by Dauber et al. (1964). This particle fitted appropriately in the center of the hexagon.

The original number of particles in the hexagon of Fig. X.5 was eight. However, the phi (ϕ) meson was subsequently discovered (see Amsler et al., 2008). The phi meson fits conveniently in the center of the hexagon of Fig. X.5.

When the Eightfold Way of plotting particles was applied to the high-mass spin $^3/_2$ baryons, a different pattern was found. The pattern resulted in an array of 10 particles, referred to as a decuplet, which is illustrated in Fig. X.6. However, at the time the Eightfold Way was proposed independently by Gell-Mann and Ne'eman in 1961, the sigma minus (Ω^-) baryon had not been discovered. This particle was predicted by the Eightfold Way plot (yellow circle at the bottom of Fig. X.6) and later discovered by a team of physicists at the Brookhaven National Laboratory (Barnes et al., 1964). They identified and measured the Ω^- track and its decay products in a hydrogen bubble chamber when a high-energy (5.0 BeV/c) K^- meson interacted with a proton in the chamber, which is illustrated in Fig. X.7.

When the Eightfold Way was first proposed by Gell-Mann and Ne'eman, it was received with some skepticism until the missing particles predicted by the Eightfold Way plots were discovered. The Eightfold Way then received widespread acceptance with an underlying question: "What is the reason behind the interrelationship of the baryons and mesons to cause them to be associated in such a manner depicted by the Eightfold Way plots?" Physicists arrived at a conclusion that

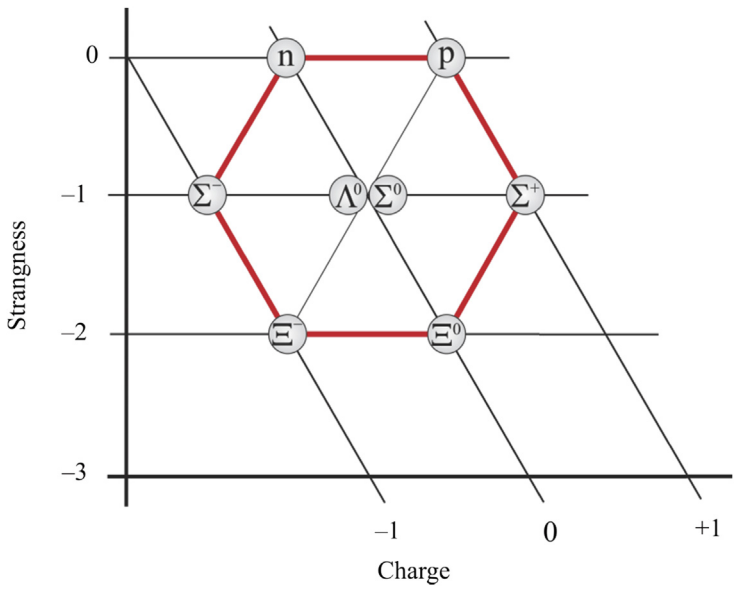

FIGURE X.3 Octet of spin ½ baryons. A baryon contains three quarks, and a quark has a spin equal to ½. The neutron and proton along with the other baryons in this figure contain three quarks, two of which have parallel spins (eg, ↑↑) and the other is opposite (eg, ↓). Two opposite spins cancel one another, resulting in a total spin of ½.

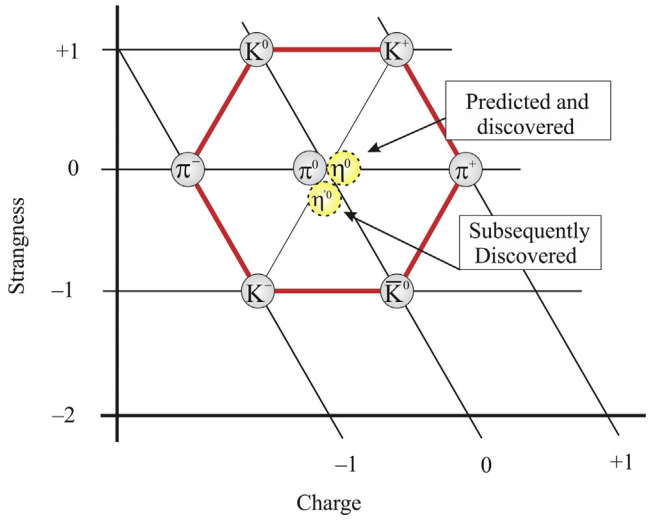

FIGURE X.4 Octet of zero-spin (or spin 0) mesons. All mesons contain only two quarks, each of which has a spin of ½; and the quarks in the above mesons possess opposite spin (ie, ↑↓) which cancel each other, yielding zero spin. The eta (η) particles at the center of the octet in broken circles colored yellow were not included at the time of the original formulation of the Eightfold Way; however, Gell-Mann (1961) predicted the neutral eta particle (η^0). Both the η^0 and η'^0 were subsequently discovered.

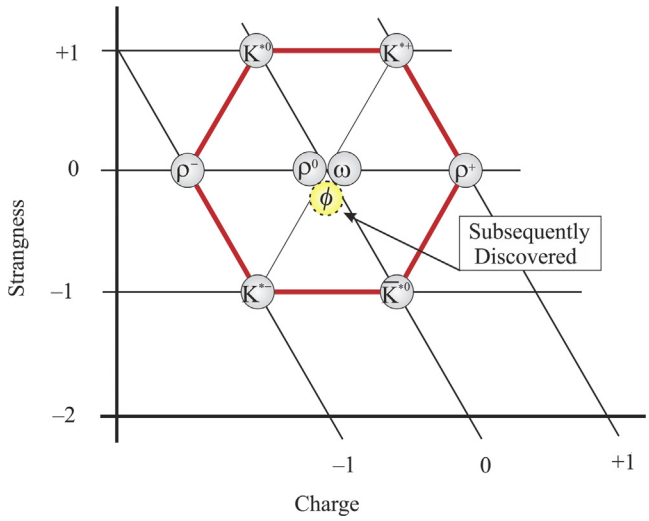

FIGURE X.5 Octet of spin 1 (double-spin) mesons. All mesons contain only two quarks, each of which is a spin ½ particle. The quarks in the mesons illustrated above would have parallel spins (eg, ↑↑); thus their total spin is the sum of the two (ie, ½ + ½) or a spin equal to 1.

the baryons and mesons were not elementary particles like the electron and neutrino, which have no underlying structure. They began to consider what might be the underlying structure of the proton, neutron, and other baryons as well as the mesons, which led to the proposal by Murray Gell-Mann and George Zweig that the baryons and mesons contained other particles, now known as quarks, as well as forces that hold the quarks together within these subatomic particles.

Quarks

Murray Gell-Mann and George Zweig independently put forward a model in 1964 that the baryons and mesons contained what Gell-Mann called "quarks" (Gell-Mann, 1964) and Zwieg called "aces" (Zweig, 1964a,b). The word "quarks" was adopted by the scientific community, probably due to the fact that Gell-Mann's proposal of the existence of quarks was

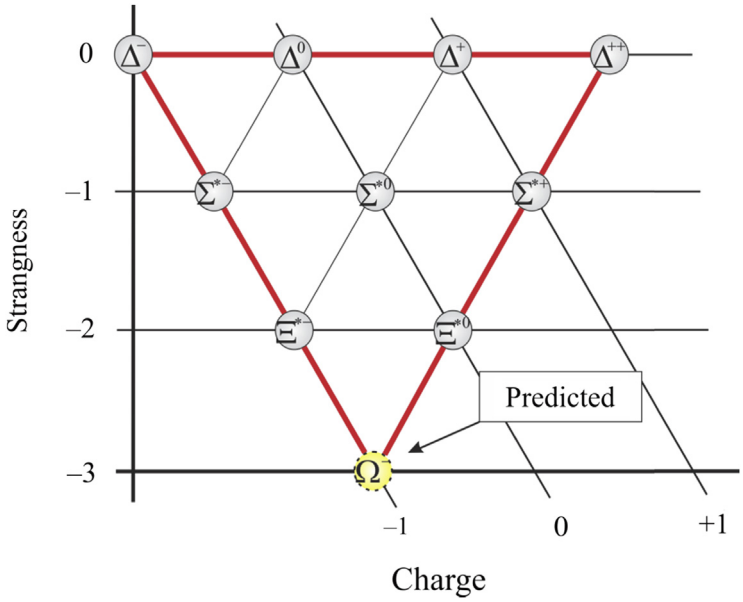

FIGURE X.6 Plot of strangeness versus charge of high mass and spin 3/2 baryons (also referred to as triple-spin baryons, because they possess three times the spin of a proton or neutron). The plot yields a pattern of 10 particles (decuplet): a quartet of delta (Δ) particles, a triplet of sigma (Σ) particles, a doublet of xi (Ξ) particles, and a missing but predicted omega (Ω^-) particle, which was discovered three years later at the Brookhaven National Laboratory to fit exactly in the predicted location.

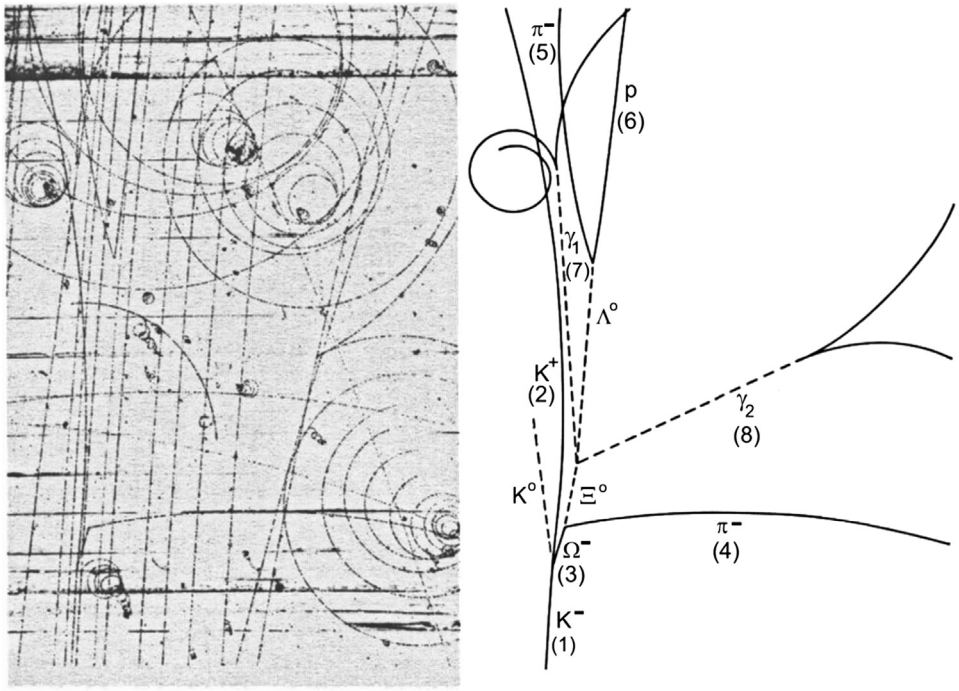

FIGURE X.7 Left: A hydrogen bubble chamber photograph of particle tracks. Right: A line diagram extracted from the numerous tracks of the photograph, which shows the sequence of events. The track of the incoming K^- meson appears entering the bubble chamber from the bottom, interacting with a proton of the liquid hydrogen in the bubble chamber and producing a Ω^- hyperon (track 3), and K^+ (track 2) and K^0 mesons (a *dashed or broken line*, because neutral particles do not form tracks). The Ω^- hyperon then decays into a neutral xi (Ξ^0) baryon and a π^- (track 4). The Ξ^0 decays into neutral lambda (Λ^0) and π^0. There is no visible track for the π^0 at the end of the Ξ^0 track, because the π^0 has a very short lifetime (8.5×10^{-17} s). The π^0 decays into two gamma-ray photons (γ_1 and γ_2, tracks 7 and 8). Both γ_1 and γ_2 undergo pair production into a positron (e^+ and e^-), which are seen as tracks diverting in opposite directions and bending in a magnetic field applied to the bubble chamber. The Λ^0 decays into a π^- (track 5) and a proton (track 6). *The figure is from Barnes, V.E., et al., 1964. Observation of a hyperon with strangeness minus three. Phys. Rev. Lett. 12 (8), 204–207, http://dx.doi.org/10.1103/PhysRevLett.12.204, reprinted with permission by the American Physical Society © 1964.*

published in the international journal *Physics Letters*, to which all had access, while George Zweig's work remained for years unpublished as a CERN internal report, for unfortunate reasons which are discussed in the biographical sketch of Zweig later in this chapter.

In his original paper Gell-Mann (1964) acknowledges that he named the particles "quarks," pronounced "kwôrks" to rhyme with "forks," from the phrase "Three quarks for Muster Mark!" in James Joyce's *Finnigan's Wake* (1939, Viking Press, New York, p. 383). The phrase "Three quarks for Muster Mark!" was appropriate for selecting the designation "quark," because Gell-Mann proposed three quarks as constituent particles of the known baryons and mesons of the time. Gell-Mann represented the three quarks with the abbreviations u, d, and s, which currently are named the *up*, *down*, and *strange* quarks.

Gell-Mann (1964) expressed the need to find an explanation for the link between the baryons and mesons of the Eightfold Way, and presented a mathematical model for quarks. An excerpt from his original paper (Gell-Mann, 1964) describes the properties of the proposed quarks:

> *If we assume that the strong interactions of baryons and mesons are correctly described in terms of the broken "eightfold way", we are tempted to look for some fundamental explanation of the situation… A simpler and more elegant scheme can be constructed if we allow non-integral values for the charges… We then refer to the members* $u^{\frac{2}{3}}$, $d^{-\frac{1}{3}}$, *and* $s^{-\frac{1}{3}}$ *of the triplet as "quarks" q and the members of the anti-triplet as anti-quarks* $\bar{q}$. *Baryons can now be constructed from quarks by using the combinations (qqq)… while mesons are made out of* $(q\bar{q})$…
>
> From Gell-Mann, M., 1964, reprinted with permission from Elsevier © 1964.

Gell-Mann's statement proposes that each quark possesses a charge that is a fractional charge of the electron; namely the up quark (u) would have a charge of $+\frac{2}{3}e$, the down quark (d) would possess a charge of $-\frac{1}{3}e$, and the strange quark (s) would have a charge of $-\frac{1}{3}e$, where e is the charge of the positive electron (ie, positron). The antiquarks referred to in Gell-Mann's statement would possess a charge of opposite sign to the quarks, so the antiup $(\bar{u})$, antidown $(\bar{d})$, and antistrange $(\bar{s})$ quarks would possess charges of $-\frac{2}{3}e$, $+\frac{1}{3}e$, and $+\frac{1}{3}e$, respectively. This was the first time that the scientific community envisaged a charge smaller than that of the electron. It had always been considered that the electron, as an elementary particle, possessed the elementary charge (ie, -1 for the negatron and $+1$ for the positron), and that this charge could not be subdivided into smaller entities. In his paper, Murray Gell-Mann proposed that the baryons (eg, proton and neutron) would possess three quarks, which he abbreviated as (qqq); while the mesons would possess two quarks, specifically a quark and an antiquark, which he abbreviated as $(q\bar{q})$. The sum of the fractional charges of the quarks in the baryons or mesons would add up to the total charge of the baryon or meson.

It should be noted here that George Zweig, while at CERN, also proposed independently the existence of quarks in more detail and length (Zweig, 1964a,b). George Zweig called the quarks "aces"; and the name adopted for these elementary constituents of baryons and mesons is "quarks" for reasons discussed further on in this chapter in the biographical sketch of George Zweig.

Tables X.1 and X.2 provide the currently known quark structure of baryons and mesons, illustrating how quarks with their fractional charges constitute baryons and mesons, and the sum of their fractional charges equal the total charge of the baryon or meson. For example, from Table X.1, the proton contains two up quarks and a down quark (ie, uud), and the sum of the fractional quark charges $+\frac{2}{3}+\frac{2}{3}-\frac{1}{3}$ equals $+1$; whereas the neutron possesses one up quark and two down quarks (ie, udd) and the sum of the fractional quark charges of the neutron $+\frac{2}{3}-\frac{1}{3}-\frac{1}{3}$ equals 0. Mesons contain a quark and an antiquark. Examples of mesons, their quark and antiquark constituents, fractional quark charges, and total charge are provided in Table X.2. For example, the π^+ listed in Table X.2 possesses an up quark (u) and an antidown $(\bar{d})$ quark; and the sum of the fractional quark and antiquark charges for the $u\bar{d}$ combination $+\frac{2}{3}+\frac{1}{3}$ equals $+1$. The antiparticle of the π^+ is the π^-, also listed in Table X.2. The π^- possesses the antiquarks of the π^+. Antiquarks possess an opposite charge to the quarks. Thus, as listed in Table X.2, the π^- contains the antiup $(\bar{u})$ and down (d) quarks; and the sum of the fractional antiquark and quark $(\bar{u}d)$ combination $-\frac{2}{3}-\frac{1}{3}$ equals -1.

Murray Gell-Mann (1964), in his original paper proposing quarks, elaborated further:

> *Since charge and baryon number are exactly conserved, one of the quarks* $\left(\text{presumably } u^{\frac{2}{3}} \text{ or } d^{-\frac{1}{3}}\right)$ *would be absolutely stable, while the other member of the doublet would go into the first member very slowly by β-decay or K-capture.*
>
> From Gell-Mann (1964), reprinted with permission from Elsevier © 1964.

In this statement Gell-Mann refers firstly to the laws of conservation of charge and conservation of baryon number whenever a reaction or decay occurs that would involve a change in one of the quarks within a baryon or meson. The *laws*

of conservation of charge and *conservation of baryon number* state that the sum of the charges or sum of the baryon numbers before a decay or reaction takes place must equal (ie, balance) the sum of the charges or sum of the baryon numbers after the decay or reaction occurs. The baryon number (B) is a quantum number. Quarks possess a baryon number of ⅓ and antiquarks −⅓; and the baryon number of all particles, including baryons, mesons, and leptons, are calculated according to

$$\mathrm{B} = \frac{1}{3}\left(n_{\mathrm{q}} - n_{\overline{\mathrm{q}}}\right) \qquad [\mathrm{X.12}]$$

where B is the baryon number, n_{q} is the number of quarks that the particle contains, and $n_{\overline{\mathrm{q}}}$ is the number of antiquarks. Baryons, which contain three quarks, have a baryon number of +1; antibaryons, which contain three antiquarks, have a baryon number of −1; mesons contain a quark and an antiquark and thus have a baryon number of 0; and leptons, which are elementary particles, also have a baryon number of 0.

Another proposal concerning quarks made by Gell-Mann (1964) was the transformation of one quark into another, which would be expected to occur in the β decay or EC decay processes. This is clear in the following statement from Gell-Mann (1964):

> *one of the quarks* $\left(\text{presumably } u^{\frac{2}{3}} \text{ or } d^{-\frac{1}{3}}\right)$ *would be absolutely stable, while the other member of the doublet would go into the first member very slowly by β-decay or K-capture.*

As described in the chapter entitled "Beta Radiation and Beta Decay," the beta decay process could involve the creation of a negatron (β^-), when a neutron is converted to a proton during nuclear decay; the creation of a positron (β^+), when a proton is converted to a neutron during nuclear decay; and K-capture (ie, EC), when a nuclear proton is converted to a neutron following the capture of a K-orbital atomic electron by the proton.

George Zweig independently described the same processes of quark transformation in β decay in his original papers (Zweig, 1964a,b), but he used the term "aces" for "quarks." It is interesting how two persons at opposite ends of the globe (Gell-Mann at CalTech in Pasadena, California and Zweig at CERN in Europe) arrived independently and almost simultaneously at the same theory. Several years later Richard Feynman (1969) introduced a similar model of elementary particles as constituents of hadrons, which he called "partons." The partons were proposed as point-like components within hadrons as a model to explain highly inelastic electron−nucleon scattering at high energies. Bjorken and Paschos (1969) at the Stanford Linear Accelerator Center (SLAC) proposed that the parton model be tested, comparing it to the models of quarks or aces proposed earlier by Gell-Mann and Zweig. When evidence for the existence of quarks was finally provided by Nobel Laureates Jerome I. Friedman, Henry W. Kendall, and Richard E. Taylor (Nobel Prize in Physics in 1990) by inelastic scattering of electrons on protons and bound neutrons, the partons proved to be the same point-like particles proposed by Gell-Mann and Zweig (namely quarks or aces). The term "partons" is used at times to mean "quarks and gluons."

Years later Harald Fritsch worked with Murray Gell-Mann and Heinrich Leutwyler (Fritzsch and Gell-Mann, 1972; Fritsch et al., 1973) to make major contributions to the establishment of quantum chromodynamics (QCD), a theory first introduced by Moo Young Han and Yoichiro Nambu (Han and Nambu, 1965; Nambu, 1966). QCD is the current theory describing the strong force that binds or holds the quarks together within the baryons and mesons, and is described later in this chapter.

From 1972 to 2002 Gell-Mann was director of the John D. and Catherine T. MacArthur Foundation, which supports creative people and effective institutions committed to building a more just, verdant, and peaceful world. He also played a major role in the founding of the Santa Fe Institute in 1984. The Santa Fe Institute is a transdisciplinary research community that expands the boundaries of scientific understanding. Its aim is to discover, comprehend, and communicate common fundamental principles in complex physical, computational, biological, and social systems that underlie many of the most profound problems facing science and society today (www.santafe.edu). Professor Murray Gell-Mann remains affiliated today with the Santa Fe Institute as a distinguished fellow and life trustee.

GEORGE ZWEIG (1937−)

George Zweig was born in 1937 into a Jewish family in Moscow, USSR, where his parents had moved from Germany in 1933 after Adolf Hitler's inauguration as chancellor of Germany. His father was a structural engineer, and obtained a contract with the government of the Soviet Union (Russia) to assist in the preparation for a war with Germany, which his father foresaw as inevitable. After the termination of the contract, George Zweig moved with his parents to Vienna, Austria, where they tried to convince his father's parents to leave Europe for America. When Nazi Germany annexed

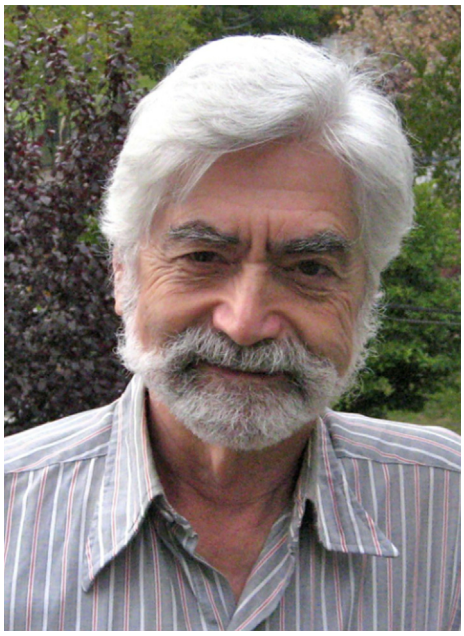

George Zweig (1937–)
Reproduced with permission © Erica Jen

Austria in March 1938, George Zweig emigrated to America with his parents. They settled in Detroit, Michigan, and their immigration was possible after the personal intervention of two Michigan senators, Arthur H. Vandenberg and Prentiss M. Brown. As related by George Zweig (see Charitos, 2013), their efforts failed to get US Department of State approval for admission of his father's parents into the United States; and they sadly were shipped as prisoners numbered 869 and 870 on January 26, 1942 to Riga, Latvia, where they were executed by the Nazis. Zweig also related that, as a structural engineer, his father designed factories for the war effort, including a factory for B-24 bombers with an assembly line over a mile long, which produced one B-24 bomber per hour.

For his undergraduate studies, George Zweig majored in mathematics at the University of Michigan, and also took numerous courses in physics. After completing his undergraduate studies in 1959, Zweig pursued a PhD in theoretical physics at CalTech, Pasadena under the supervision of Richard P. Feynman. He completed his doctoral degree in physics at CalTech in 1963.

While at CalTech in 1963, Zweig began to be concerned over the decay of the phi meson (φ), which was not decaying into the expected mode of $\rho + \pi$; rather, the φ meson was decaying into the energetically less favored $K^+ + K^-$ mode. Zweig presented his concerns to Feynman during the spring of 1963, including the possibility of φ meson decay involving aces (now known as quarks), whereby the aces would be constituent particles of mesons (see Charitos, 2013). Feynman shrugged off Zweig's idea of aces as a bizarre solution to a problem that did not exist, because Feynman thought the φ meson decay experiment was wrong. Although rebuffed by Feynman, Zweig remained engrossed on the problem and continued to explore the matter further during 1963; and he prepared a paper describing mathematically his complete theory of aces that he would try to publish.

In 1964 Zweig was a visiting theoretical physicist at CERN with financial support from the US Air Force Office of Scientific Research and the National Academy of Science/National Research Council. He prepared his model of aces in a paper entitled "An SU(3) Model for Strong Interaction Symmetry and Its Breaking," with the intention of submitting it to the journal *Physical Review*; however, the head of the Theory Division, Leon Van Hove, refused to let Zweig publish the paper, and it remained unpublished as an internal CERN document in its initial unrevised form (see Zweig, 1964a, CERN preprint 8182/TH.401, January 17, 1964) and in a revised form (Zweig 1964b, CERN Report 8419/TH.412, February 21, 1964). As related by Zweig in an interview published by the Department of Physics at CERN (see Charitos, 2013), Leon Van Hove would not allow Zweig to submit the paper to *Physical Review* because the journal is published by the American Physical Society. Van Hove claimed that all reports from CERN could be published only in European journals, regardless of the fact that Zweig's salary, overheads, and publication costs were financed by American institutions. Also, Zweig tried

to get the theory secretary Madame Fabergé to retype his paper for publication, but she refused, informing Zweig that Van Hove had instructed her not to type any of Zweig's papers. In an interview (Charitos, 2013), George Zweig elaborated further on the obstacles he had encountered with Van Hove concerning his theory on aces (ie, quarks):

> *I was scheduled to give a theory seminar at CERN titled "Dealer's Choice: Aces are Wild." Van Hove cancelled the seminar, and I was not allowed to reschedule it. When Van Hove and Kokedee published a book four years later reprinting articles on the quark model they did not include either of the CERN reports. Van Hove deliberately and systematically tried to keep my work from public view.*
>
> From Charitos (2013), CERN "Interview with George Zweig," http://ph-news.web.cern.ch/content/interview-george-zweig.

One can only try to surmise why Leon Van Hove would oppose the publication in 1964 of George Zweig's original theory of the existence of aces as constituent particles of baryons and mesons, particularly if the paper was mathematically sound. We can image that in 1964 Zweig's theory was a very bold step, even revolutionary. Zweig was then a young man, only 27 years of age; and an older supervisor in a leading position might find it difficult to accept a most unusual theory from a youngster who had just graduated. Also, Zweig's theory was possibly hard to fathom by Van Hove and others, because at the time the universal thinking was that the proton and neutron were elementary particles (ie, it was widely believed that the proton and neutron could not be broken down into any smaller constituent particles), and any proposal to the contrary would be considered very ground-breaking. In addition, it was also thought that there could be no fractional charge on a particle; that is, it was generally believed there was no charge smaller than the charge on the electron, namely the basic charge of -1 or $+1$. The proposal of Zweig (1964a,b) could be considered by his supervisors to be too extraordinary and unacceptable coming from a young budding scientist. However, a less specific theory where aces were hypothetical and were called quarks, coming from an already renowned physicist such as Murray Gell-Mann, could be given consideration by the scientific community. In any case, in light of the short (two-page) paper published on February 1, 1964 of Murray Gell-Mann's theory of quarks in the journal *Physics Letters* (Gell-Mann, 1964), some sort of declaration could have been made immediately by CERN that it possessed an earlier very detailed paper, dated January 17, 1964, by George Zweig describing a related theory. Zweig's detailed theory of aces (ie, quarks) registered as a 1964 CERN report (CERN-TH-412) can be accessed online via the CERN document server of the CERN Accelerator Science website (http://cdsweb.cern.ch/record/570209?ln=en). Many were skeptical in the 1960s of the theory of quarks until evidence for their existence was provided years later, as discussed further on in this chapter. Zweig's original paper (Zweig, 1964a,b) was finally published 16 years later in a book edited by Lichtenberg and Rosen (Zweig, 1980).

In George Zweig's initial report on aces (Zweig, 1964a,b), he assigned the baryon number ⅓ to each of three aces, identified as p_o, n_o, and Λ_o. He assigned nonintegral electron charges to each ace, namely p_o and n_o contained charges of $+⅔$ and $-⅓$, respectively, and Λ_o contained the charge of $-⅓$. The aces p_o, n_o, and Λ_o were equivalent to what we now identify as the u, d, and s quarks—the up, down, and strange quarks. Zweig (1964a,b) described the three aces as "fundamental units from which all mesons and baryons are to be constructed."

Zweig (1964a,b) elaborated further on how one ace, namely ace n_o, would be heavier than ace p_o, which would render ace p_o stable, thereby allowing the transformation of n_o into p_o:

> *we are able to conjecture that n_o is heavier than p_o, making p_o completely stable (like p) but allowing the decay*

$$n_o^{-1/3} \rightarrow p_o^{+2/3} + e^- + \nu \qquad [X.13]$$

just as

$$n \rightarrow p + e^- + \nu" \qquad [X.14]$$

In this statement, Zweig (1964a,b) considers ace n_o to have a mass greater than ace p_o allowing the transformation of ace n_o to ace p_o in beta decay where e^- is the β particle, which is always accompanied by neutrino (ν) emission (Eq. [X.13]). We now refer to ace n_o as the d quark and ace p_o as the u quark; and, as postulated by Zweig (1964a,b), the d quark does possess a mass greater than that of the u quark (see Table X.3). In addition, we now know Zweig's prediction to be correct; that is, the d quark (ace n_o) changes to a u quark (ace p_o), resulting in a transformation of a neutron (n) to a proton (p) in beta decay (Eq. [X.14]), as illustrated in Fig. X.8.

TABLE X.3 Quarks and Their Properties[a]

Quark	Symbol	Charge[b]	Mass[c]
Up	u	$+\frac{2}{3}e$	2.3 ± 0.6 MeV/c^2
Down	d	$-\frac{1}{3}$	4.8 ± 0.4
Strange	s	$-\frac{1}{3}$	95 ± 5
Charm	c	$+\frac{2}{3}$	1275 ± 25
Bottom	b	$-\frac{1}{3}$	4.18 ± 0.03 GeV/c^2
Top	t	$+\frac{2}{3}$	173.0 ± 0.5

[a] *All quarks are spin ½ particles. Data is from the Berkeley National Laboratory, Particle Data Group, 2013. J. Beringer et al. (Particle Data Group), Phys. Rev. D86, 010001 (2012) and 2013 partial update, http://pdg.lbl.gov/2013/listings/contents_listings.html.*
[b] *The charge is a fraction multiple of the electron charge e. The antiquarks, ie, $\overline{u}$, $\overline{d}$, $\overline{s}$, $\overline{c}$, $\overline{b}$ and $\overline{t}$, have opposite charge to values listed.*
[c] *The masses of the u, d, s, and c quarks are in units of MeV/c^2, while the much heavier b and t quarks are in units of GeV/c^2. Masses are measured from scattering experiments.*

Gell-Mann (1964) came to the same conclusion as Zweig (1964a,b). Gell-Mann referred to the subnucleon constituents as quarks rather than aces, and pointed out that for β decay to occur, one of the quarks would have to be transformed into another. This is exactly the current mode of describing β decay in terms of quarks. In negatron (β^-) emission from a decaying nucleus, a neutron is converted to a proton; and for this to occur, a down quark (d) of a neutron is converted to an up quark (u) whereby the neutron which contains the three quarks "udd" becomes a proton containing the three quarks "udu," as illustrated in the Feynman diagram in Fig. X.8. Quark transformation in β decay remains today the current understanding of this nuclear decay process.

Thus both Murray Gell-Mann and George Zweig postulated the existence of quarks in 1964; however, they did not know at the time that these subatomic particles would ever be discovered or evidence for their existence ever found. It even

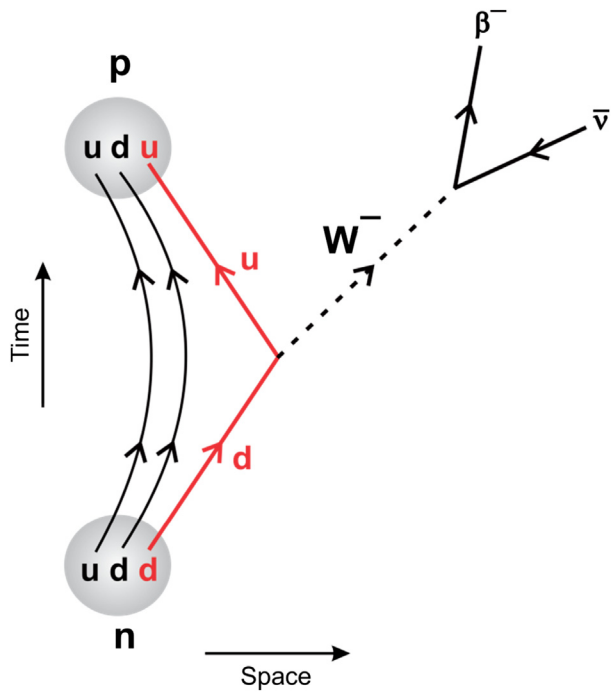

FIGURE X.8 Feynman diagram illustrating negatron (β^-) emission in beta decay. A down quark (d) of a neutron (lower left of figure) is transformed into an up quark (u) whereby the neutron changes into a proton (upper left of figure) with the emission of a W^- boson, which transforms into a negative electron (β^-) and antineutrino ($\overline{\nu}$). The W^- boson serves as a carrier of the weak interaction of elementary particles that occurs in beta decay. The quark transformation is depicted in red, and the quarks that undergo no change are in black.

can be conjectured that Gell-Mann thought that possibly quarks did not really exist but were purely hypothetical mathematical entities when he wrote the following in his original proposal of quarks:

> *It is fun to speculate about the way quarks would behave if they were physical particles of finite mass (instead of purely mathematical entities…)… A search for stable quarks… at the highest energy accelerators would help to reassure us of the non-existence of real quarks.*

On the other hand, George Zweig proposed quarks as real entities. He concluded in his original CERN report (Zweig 1964a,b), after listing all of the logical possibilities in interpreting the results of his paper:

> *…there is also the outside chance that the model is a closer approximation to nature than we may think, and that fractionally charged aces abound within us.*

This statement was as close as Zweig could come to saying that aces (ie, quarks) were real.

An important question was presented by George Zweig (1964a,b) in his original paper on aces:

> *What is the particle (or particles) that is responsible for binding the aces?*

This question would be answered years later with the theory of QCD, which defines the constant emission and absorption of gluons responsible for the strong force that binds the aces (ie, quarks) into baryons and mesons. QCD is described later in this chapter.

The first evidence for the existence of quarks was found by inelastic scattering of electrons on protons and bound neutrons during 1967−1973 at SLAC, with collaboration of physicists of MIT. For this work Jerome I. Friedman and Henry W. Kendall of MIT and Richard E. Taylor of SLAC were awarded the Nobel Prize in Physics in 1990. This work is described later in this chapter.

In an interview given by the Department of Physics at CERN (see Charitos, 2013) George Zweig explained why he referred to quarks as aces. He replied that he considered aces to be fundamental point particles (ie, elementary particles) like the leptons; and that similar to the leptons (see Table X.4), the aces had fields that entered into the electromagnetic and weak currents. Because there were four leptons known at the time, Zweig conjectured that there might be four aces (as in a deck of cards), which could equal the number of leptons. In that sense, Zweig was again correct: the number of quarks does equal the number of leptons. There are six quarks known to exist as well as six leptons. The balance between leptons and quarks in nature is commemorated with a postage stamp from Macau, China, which lists the six leptons on the left and six quarks on the right.

TABLE X.4 Leptons and Their Properties[a]

Particle	Symbol	Antiparticle	Rest Mass (MeV/c^2)	Lifetime (s)
Electron	e^-	e^+	0.511	Stable
Electron neutrino	ν_e	$\overline{\nu_e}$	$<2 \times 10^{-6}$	Stable
Muon	μ^-	μ^+	105.7	2.20×10^{-6}
Muon neutrino	ν_μ	$\overline{\nu_\mu}$	<0.19	Stable
Tau	τ^-	τ^+	1776.8	2.9×10^{-13}
Tau neutrino	ν_τ	$\overline{\nu_\tau}$	<18.2	Stable

[a]*Data is from the Berkeley National Laboratory, Particle Data Group, 2013. J. Beringer et al. (Particle Data Group), Phys. Rev. D86, 010001 (2012) and 2013 partial update, http://pdg.lbl.gov/2013/listings/contents_listings.html. All leptons are spin ½ particles and all are classified as elementary particles; that is, they are considered to be point-like with no internal structure.*

In addition to the **up (u), down (d), and strange (s)** quarks proposed by Murray Gell-Mann and George Zweig, three other quark flavors (the various types of quarks are referred to as flavors) were discovered. Evidence for the fourth quark flavor, namely the **charm (c) quark**, was provided by the discovery of the J/Ψ meson following the work of Burton Richter at SLAC and Samuel Ting at the Brookhaven National Laboratory, for which they were awarded the Nobel Prize in Physics in 1976.

A fifth flavor, the **bottom (b) or beauty quark** was discovered as the constituent quark of the upsilon meson at the Fermi National Laboratory (Fermilab) in 1977 by the E288 Collaboration under the leadership of Leon M. Lederman (Nobel Laureate in Physics 1988). The upsilon meson contains the bottom (b) and antibottom $(\overline{b})$ quarks. The sixth quark is the **top (t) or truth quark**, which was discovered in 1995 by the CDF and DØ experiments at Fermilab. Makato Kobayashi and Toshihide Maskawa were awarded the Nobel Prize in Physics in 2008 for their prediction of the top and bottom quark flavors.

Discoveries of the various quark flavors are discussed further on in this chapter, and their properties are provided in Table X.3.

In 1977 Richard Feynman nominated Murray Gell-Mann and George Zweig for the Nobel Prize in Physics for the work that led to their independent proposals in 1964 of the theory of quarks as constituent particles of the baryons and mesons and the basic building blocks of matter. The mathematically sound theories for the existence of quarks presented by Murray Gell-Mann and George Zweig in 1964 sparked the search and eventual discovery of quarks by means of high-energy inelastic scattering experiments. Feynman's nomination was made after irrefutable evidence for the existence of quarks was provided by deep inelastic scattering of electrons on protons and bound neutrons at SLAC, as well as other experimental evidence provided by neutrino-nucleon scattering, high-energy electron−positron annihilation, and proton−proton collision experiments.

A copy of the Nobel Prize nomination acknowledgment letter from the Nobel Committee addressed to Richard Feynman is illustrated in Fig. X.9. This Nobel Prize nomination is significant, because the proposals made by Gell-Mann and Zweig sparked the search for and discovery of quarks that has advanced immeasurably our understanding of the structure of matter and the natural changes that matter can undergo. We can compare the theory of quarks presented by Gell-Mann and George Zweig to the discovery of the proton by Ernest Rutherford (Nobel Prize, 1908), the discovery of the electron by J.J. Thomson (Nobel Prize, 1906), the discovery of the neutron by James Chadwick (Nobel Prize, 1935), and the discovery of the neutrino by Frederick Reines and Clyde Cowan, Jr (Nobel Prize, 1995). All of these particles constitute the basic building blocks of matter. Quarks are the basic particles upon which the proton and neutron can be formed; and the theory of Gell-Mann and Zweig that proposed quarks represents one of the greatest advances in the history of physics.

Feynman's nomination of Murray Gell-Mann and George Zweig for the Nobel Prize presented a conundrum for the Nobel Committee, because Murray Gell-Mann had already been awarded a Nobel Prize "for his contributions and discoveries concerning the classification of elementary particles and their interactions." If the Nobel Committee were to award the prize to George Zweig, they could not avoid including Gell-Mann, whose theory in 1964 also sparked the search and discovery of quarks. The Nobel Committee had already mentioned Gell-Mann's work on quarks in the presentation speech at the time of awarding his first Nobel Prize, without mention of George Zweig's work (presumably they had no knowledge

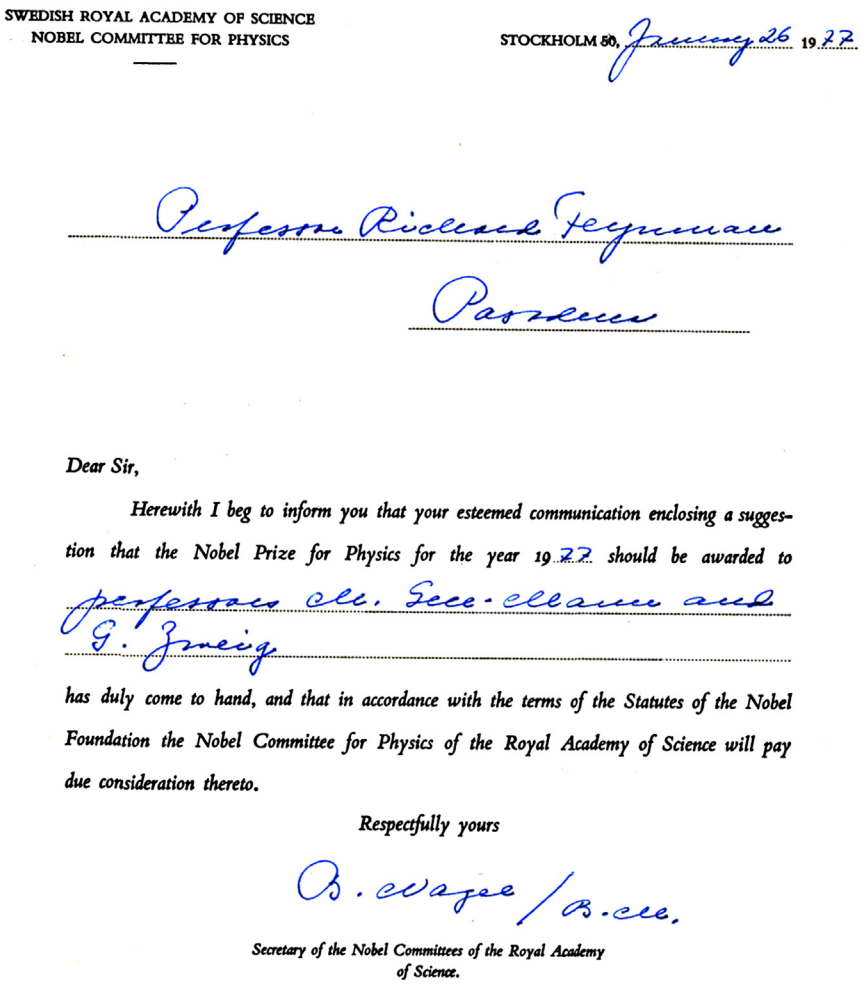

SWEDISH ROYAL ACADEMY OF SCIENCE
NOBEL COMMITTEE FOR PHYSICS

STOCKHOLM 50, January 26 1977

Professor Richard Feynman

Pasadena

Dear Sir,

Herewith I beg to inform you that your esteemed communication enclosing a suggestion that the Nobel Prize for Physics for the year 1977 should be awarded to

professors M. Gell-Mann and G. Zweig

has duly come to hand, and that in accordance with the terms of the Statutes of the Nobel Foundation the Nobel Committee for Physics of the Royal Academy of Science will pay due consideration thereto.

Respectfully yours

S. Wagse / S.cc.

Secretary of the Nobel Committees of the Royal Academy of Science.

FIGURE X.9 Letter of January 1977 from the Nobel Committee for Physics acknowledging the nomination by Professor Richard Feynman of Professors M. Gell-Mann and G. Zweig for the Nobel Prize in Physics. *From Zweig, G., 2010. Memories of Murray and the quark model. Int. J. Mod. Phys. 25 (20), 3863–3877, reproduced with permission © George Zweig.*

of his paper, as it remained an internal CERN document), when on December 11, 1969 Professor Ivan Waller, member of the Nobel Committee for Physics, stated:

> *Gell-Mann has also found that "The Eightfold Way" can be described very simply by assuming that all particles which interact strongly with each other are composed of only three kinds of particles which he called quarks and of the corresponding anti-particles. The quarks are peculiar in particular because their charges are fractions of the proton charge which according to all experience up to now is the indivisible elementary charge.*
>
> From Nobel Lectures, Physics, 1965–1970, "Nobel Prize in Physics 1969—Presentation Speech," Nobelprize.org, Nobel Media AB 2014.

George Zweig's biographical data is available from the website of the MacArthur Foundation (http://www.macfound.org/fellows/113/), from which the following information was obtained. Zweig remained on the faculty of CalTech as professor of physics (1964–1998) and a member of the Jason Division of the Institute for Defense Analysis (1965–1972). In 1970 he turned his research interests toward neurobiology. Zweig's research is concerned with the effects of sound waves that enter the ear, and the mapping of sound on to the spatial dimensions of the cerebral cortex. He is founder and president of Signition, a laboratory focused on applications of wavelets to characterization of speech, nonstationary spectral estimation, and the multiresolution characterization of shapes. He has been a fellow at the Los Alamos National Laboratory since 1985 and a visiting scientist at the MIT Research Laboratory of Electronics since 1999.

George Zweig was awarded a MacArthur fellowship in 1981. The MacArthur Fellows Program awards unrestricted fellowships to talented individuals who have shown extraordinary originality and dedication in their creative pursuits and a marked capacity for self-direction (http://www.macfound.org).

In 2015 George Zweig was awarded the J. J. Sakurai Prize by the American Physical Society for "his independent proposal that hadrons are composed of fractionally charged fundamental constituents, called quarks or aces, and for developing its revolutionary implications for hadron masses and properties."

For additional reading on the history of quarks, the reader is invited to peruse papers by Zweig (2010, 2014). The latter paper, entitled "Concrete Quarks," provides a thorough history of events leading to the discovery and acceptance of concrete quarks, and describes the very different proposals concerning quarks made by Zweig and Gell-Mann. The reader should also find the interview with George Zweig at CERN Department of Physics published by Charitos (2013) to be very informative.

OSCAR WALLACE GREENBERG (1932–), MOO-YOUNG HAN (1934–), AND HARALD FRITZSCH (1943–)

When the existence of quarks in baryons and mesons was proposed by George Zweig (1964a,b), he asked an important question in his pioneering papers: "What is the particle (or particles) that is responsible for binding the aces?" We may interpret this question as meaning: "What are the particles and forces that bind the aces (ie, quarks) within the baryons and mesons?"

Shortly after quarks were proposed by Gell-Mann (1964) and Zweig (1964a,b), physicists observed that certain baryons, such as the Δ^{++} with three constituent up quarks (uuu), the Δ^{-} with its three down quarks (ddd), and the Ω^{-} with its three strange quarks (sss), all contain three identical quarks with parallel or aligned spins. All quarks are fermions with spin ½; and physicists noted that the quarks must satisfy the Pauli exclusion principle, which is attributed to Wolfgang Pauli (1900–1958) and described in Hall of Fame, Part II. The exclusion principle states that no two identical fermions can exist in the same quantum or energy state. The three identical quarks in the Δ^{++}, Δ^{-}, and Ω^{-} particles with aligned spins would violate this principle. Physicists noted that a new quantum number had to be identified for all quarks.

In the very year that Gell-Mann and Zweig proposed the existence of quarks, Oscar Wallace Greenberg (Oscar Wallace Greenberg is an American physicist born in 1932. He is professor of physics at the University of Maryland at College Park.) introduced a three-valued charge degree of freedom to quarks (Greenberg, 1964), which means that this new charge quantum number would be different for each of the three quarks. It would be different than the electric charge, but analogous to it, and eventually would become known as color charge. Color charge is analogous to electric charge only in terms of the attraction between opposite charge and repulsion that occurs between like charge. About the same time Moo-Young Han (Moo-Young Han was born in Seoul, Korea in 1934. He is a naturalized American physicist, and has been professor of physics at Duke University since 1967.) at the Department of Physics at Syracuse University in New York and Yoichiro Nambu of the Enrico Fermi Institute for Nuclear Studies at the University of Chicago introduced what would later become known as color charge as a gauge symmetry (Han and Nambu, 1965; Nambu, 1966), which is a mathematical means of describing how physical fields interact with matter. This pioneering work of Oscar W. Greenberg, Moo-Young Han, and Yoichiro Nambu set the stage for what would become quantum chromodynamics (QCD), which is the theory describing the strong force that holds the quarks within baryons and mesons.

In 1971 and 1972 the German theoretical physicist Harald Fritzsch (Harald Fritzsch was born in 1943 in Zwickau, Germany. He studied physics in Leipzig from 1963 to 1968; and in 1968 he escaped from the German Democratic Republic with a friend via Bulgaria and in a folding canoe across the Black Sea into Turkey. His daring escape is described in the book *Escape from Leipzig* (Fritzsch, 2008). He studied at the Technical University of Munich, where he received his doctorate under Heinrich Mitter, and worked with Werner Heisenberg in 1971. He is known for his contributions to the development of QCD and the Standard Model of elementary particles. He has collaborated with Murray Gell-Mann at SLAC at Stanford University and at CERN in Geneva. He is currently professor emeritus at the Ludwig-Maximilian University, Munich.), while on leave from the Max-Planck-Institut für Physik und Astrophysik at Munich, collaborated with Murray Gell-Mann at CalTech (Fritzsch and Gell-Mann, 1971, 1972); and the following year Fritzsch collaborated further with Gell-Mann and a Swiss theoretical physicist, Heinrich Leutwyler, on leave from the Institute for Theoretical Physics, Bern (Fritzsch et al., 1973). This collaboration established the term "color" for the quantum states of quarks and also gluons, which are particles that mediate the strong interaction between quarks. They described how quarks and gluons would form the building blocks of baryons and mesons in the theory of what we now refer to QCD.

Quantum Chromodynamics

QCD is the theory describing the strong force between the quarks and gluons that constitute baryons and mesons. Gluons are bosons that mediate the strong interaction between quarks; they act as the "glue" that binds quarks within the baryons and mesons. Baryons, as described previously, are made of three quarks, such as the proton with the **uud** combination of quarks and the neutron with the **udd** combination. The quarks are held together strongly by the emission and absorption of gluons. A postage stamp from Macau, China commemorates the initial proposal of the quark theory by Gell-Mann and Zweig in 1964 and the subsequent development of QCD. The three color charges of quarks in a baryon are illustrated on the postage stamp with interlinking gluons, which mediate the strong force between the quarks. Also shown on the stamp is a blue quark of a meson and its antiblue antiquark depicted in yellow, utilizing the complementary color of blue for the anticolor charge of blue.

The color charge of quarks should not be confused with color as we perceive the various wavelengths of visible light, nor with electrical charge; rather, color charge represents different quantum states of quarks existing within baryons and mesons. To facilitate the visualization of the concept of color charge as a quantum state, the three colors of red, green, and blue were selected for the three quarks in a baryon, as illustrated in Fig. X.10. Quarks of different color experience an attractive force between them; whereas quarks of a like color repel each other. The three quarks of a baryon always occupy different quantum states; each of the three quarks possesses a red, green, or blue color charge; and the overall or combined color of the three quarks is white or neutral, which is analogous to white light of the visible spectrum. However, the color charge quantum state of quarks has absolutely no relation to color as we know it in our visible world. Mesons, on the other hand, consist of only two quarks, namely a quark and an antiquark. The quark contains a color charge (red, green, or blue); and the antiquark contains an anticolor charge (antired, antigreen, or antiblue). Thus a meson could contain a red quark and an antired antiquark, a blue quark and an antiblue antiquark, or a green quark and an antigreen antiquark. The quantum states of a quark color charge and the anticolor charge of the antiquark are attracted to each other within a meson (see Fig. X.10). The combination of a colored quark and its anticolored quark (eg, red quark and antired antiquark, green quark and antigreen antiquark, or blue quark and antiblue antiquark) is also overall neutral.

Illustrative examples of quark color charge are provided by the quark structures of a proton and negative pion in Fig. X.10. On the left of the figure is a proton, which contains two up (u) quarks and one down (d) quark. Mesons contain a quark and an antiquark. The meson illustrated in this figure is that of the negative pion. It contains a down (d) quark and an antiup ($\overline{u}$) quark. The quarks in the mesons are also attracted to each other via the color charge, and the strong force mediated by the emission and absorption of gluons. The color charge of mesons differs from that of baryons. The color charge of a quark can be red, green, or blue; however, an antiquark of the meson must possess the anticolor of red, green, or blue. The meson illustrated in Fig. X.10 is shown with a blue and antiblue antiquark. If we use colors to

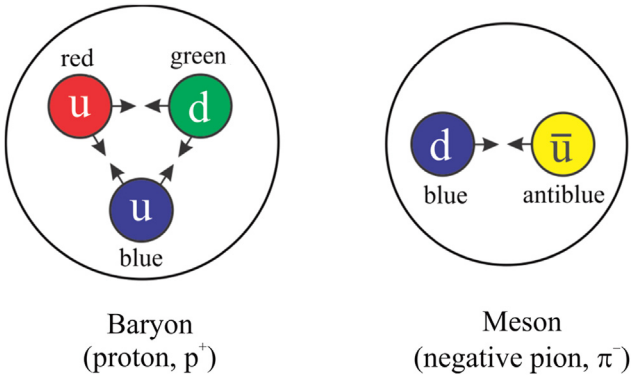

FIGURE X.10 Color charge of quarks in baryons and mesons. Baryons consist of three quarks (*red, green, and blue*), which are attracted to each other by means of the strong force mediated through the emission and absorption of gluons (illustrated by *arrows*). Mesons contain only two quarks, namely a quark and an antiquark, attracted to each other by means of the strong gluon force (see Fig. X.11).

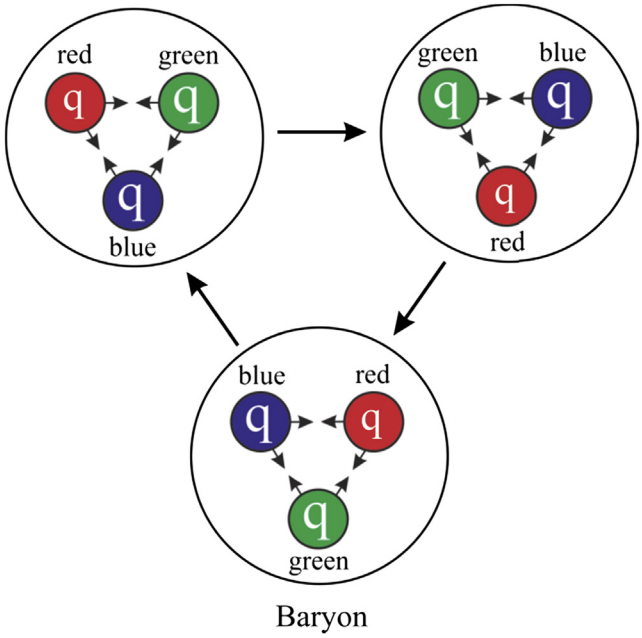

FIGURE X.11 A baryon contains three quarks (q); and the color charges of the quarks are denoted as *red, green, or blue*. The quarks will constantly emit and absorb gluons, resulting in a continuous change of quark color charge.

depict color charge in mesons, the antiblue, antigreen, and antired would be represented with the complementary colors of red, green, and blue, which are cyan, magenta, and yellow, respectively. The combination of a color charge of a quark and anticolor charge of the antiquark is neutral, just as the combination of a color and its complementary color would be white.

Quarks constantly emit and absorb gluon particles, which is the process responsible for the strong force between quarks. When quarks emit or absorb gluon particles, the quarks will change color charge. Thus there is a constant change of color charge among the quarks, as illustrated in Fig. X.11. There are eight gluon particles, which are carriers of this strong force, and these carry two color charges, a color and an anticolor, such as a red−antigreen gluon $\left(g_{r\bar{g}}\right)$, a green−antired gluon $\left(g_{g\bar{r}}\right)$, a red−antiblue gluon $\left(g_{r\bar{b}}\right)$, a blue−antired gluon $\left(g_{b\bar{r}}\right)$, a blue−antigreen gluon $\left(g_{b\bar{g}}\right)$, a green−antiblue gluon $\left(g_{g\bar{b}}\right)$, etc. For example, when a red quark emits a red−antigreen gluon, it becomes a green quark; and a green quark which absorbs this gluon converts into a red quark. The constant change of quark color charge via the emission and absorption of gluons is illustrated in Fig. X.11; and a Feynman diagram depicting change of quark color charge mediated by the emission and absorption of gluons between quarks is illustrated in Fig. X.12.

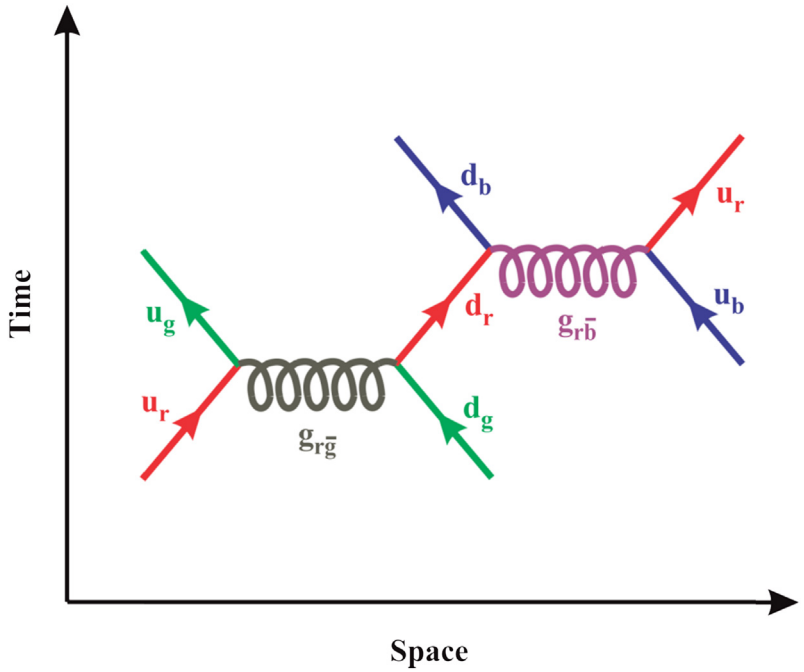

FIGURE X.12 Feynman diagram of QCD depicting the change in color charge of quarks due to the emission and absorption of gluons. The diagram illustrates the following changes of color charge among quarks. Starting at the lower left of the diagram, a red up quark (u_r) emits a red–antigreen gluon $\left(g_{r\bar{g}}\right)$ and changes to a green up quark (u_g). A green down quark (d_g) absorbs the red–antigreen gluon and changes to a red down quark (d_r). The down red quark (d_r) emits a red–antiblue gluon $\left(g_{r\bar{b}}\right)$ and changes to a blue down quark (d_b). A blue up quark (u_b) then absorbs the red–antiblue gluon $\left(g_{r\bar{b}}\right)$ and changes to a red up quark (u_r).

The constant emission and absorption of gluons between quarks in baryons and quarks and antiquarks in mesons results in a superposition of red, green, and blue color charges in baryons and mesons and antired, antigreen, and antiblue color charges in mesons. The superposition of color charges as well as the combination of a quark color charge and its anticolor charge of the antiquarks in a meson results in an overall white or neutral color charge in baryons and mesons.

For additional information on QCD the reader may peruse books by Fritzsch (1983, 2012), Fritzsch and Gell-Mann (2015), Nambu (1985), and Han (1999).

JEROME I. FRIEDMAN (1930–), HENRY W. KENDALL (1926–1999), AND RICHARD E. TAYLOR (1929–)

As discussed previously, the theory of quarks was proposed independently by Murray Gell-Mann and George Zweig in 1964, after which came the theory of quark color charge by Oscar W. Greenberg, Moo-Young Han, and Yoichiro Nambu in 1964 and 1965. The next development was the theory of QCD, which described the strong force between quarks in baryons and mesons mediated by the emission and absorption of gluons by quarks developed by Harald Fritzsch and coworkers during 1971 to 1973. The question remaining among physicists was "Will the existence of quarks and gluons ever be demonstrated?"

Evidence for the existence of quarks and gluons within the nucleons (protons and neutrons) was finally demonstrated by Jerome I. Friedman and Henry W. Kendall of MIT and Richard E. Taylor of SLAC and their coworkers. For this work the Nobel Prize in Physics in 1990 was awarded to Friedman, Kendall, and Taylor for, in the words of the Nobel Committee, "their pioneering investigations concerning deep inelastic scattering of electrons on protons and bound neutrons, which have been of essential importance for the development of the quark model in particle physics."

Jerome I. Friedman was born in Chicago, Illinois on March 28, 1930. His parents, Selig and Lillian Friedman, née Warsaw, immigrated to the USA from Russia with little formal education but a love for books, learning, and the arts. His parents placed the highest priority on the education of their children. Jerome Friedman received his primary and high school education in Chicago. He became interested in physics during his high school years after reading a book by Albert Einstein on relativity. Friedman did not have to go far for his higher education: he applied to the University of Chicago, because of its outstanding reputation in physics; and he wanted to study under Enrico Fermi, who was among the most notable physicists of the time. Friedman was admitted into the Physics Department of the University of Chicago in 1950

with a full scholarship, which was fortunate, because his family had no means to support his higher education. After receiving the MSc degree in 1953, Friedman studied for his PhD with Enrico Fermi as advisor. Fermi died unfortunately after a sudden illness in 1954 (see Hall of Fame, Part II); and Friedman continued his doctoral studies, which he completed in 1956, under the supervision of John Marshall.

In 1957 Friedman joined the research group of Robert Hofstadter at the High Energy Physics Laboratory of Stanford University. Hofstadter received the Nobel Prize in Physics in 1961 for, in the words of the Nobel Committee, "his pioneering studies of electron scattering in atomic nuclei and for his thereby achieved discoveries concerning the structure of the nucleons." With Hofstadter's group at SLAC, Jerome Friedman acquired much expertise in studying electron elastic and inelastic scattering by proton and deuteron nuclei. At SLAC Friedman began to collaborate with Henry Kendall, a member of the group, and become acquainted with Richard Taylor, who was also at SLAC completing his doctoral thesis.

In 1960 Friedman was appointed to the faculty of the Department of Physics at MIT. As professor at MIT, Jerome Friedman and Henry Kendall initiated a collaboration with W.K.H. Panofsky, director of SLAC, and Richard Taylor among other physicists at SLAC to carry out research on nuclear electron scattering utilizing the new 20 GeV Stanford Linear Accelerator. This collaboration between MIT and SLAC from 1979 to 1955 on inelastic scattering by the protons and neutrons in hydrogen and deuterium provided the first experimental evidence for the existence of quarks and gluons within the inner structure of the nucleons.

Jerome Friedman was appointed director of the Laboratory for Nuclear Science at MIT in 1980, and was head of the Physics Department at MIT from 1983 to 1988. He is currently emeritus professor of physics at MIT.

Left to right: Richard Taylor, Henry Kendall, and Jerome Friedman
Taylor, Kendall, and Friedman celebrating the award of the 1990 Nobel Prize in Physics. Standing; clasped hands. Printed with permission of the American Institute of Physics, AIP Emilio Segre Visual Archives, Physics Today Collection

Henry W. Kendall was born in Boston, Massachusetts on December 9, 1926. In primary school he had a reading disability which held him back, but he later overcame this. Most of his teenage years were spent at Deerfield Academy, an outstanding college preparatory high school in Deerfield, Massachusetts. In his autobiography written at the time of receiving the Nobel Prize, Henry Kendall claims to have been a poor student due to his fascination with outside interests and his personal exploration of science and engineering. His father encouraged him in his personal projects until they became hazardous, such as the cultivation of pathogenic bacteria. After graduation from high school he joined the US Merchant Marine Academy in 1945, resigned after a year, and then entered Amherst College with a major in mathematics and an interest in physics. During his college years he became experienced as a diver, and wrote two successful books on shallow-water diving and underwater photography.

Karl T. Compton, a prominent physicist, president of MIT, and brother of Nobel Laureate Arthur H. Compton, was a family friend. He encouraged Kendall to apply to MIT, and Kendall was accepted by the MIT School of Physics in 1950. He received his PhD degree there in 1955 under the supervision of Martin Deutsch, an Austrian-American physicist who was well known for his discovery of positronium.

After receiving the doctoral degree, Henry Kendall was awarded a National Science Foundation research fellowship for two years, which provided him with research opportunities at MIT and the Brookhaven National Laboratory and a chance to join Robert Hofstadter's group at Stanford University. Here Hofstadter was utilizing a 300-foot (92 m) linear electron accelerator to study electron inelastic scattering by the nuclear proton and neutron. At Stanford, Henry Kendall met and

worked with Jerome Friedman and become acquainted with Richard Taylor, who was then a graduate student. Kendall also had the opportunity to get to know W.K.H. Panofsky, who would become responsible for the new two-mile (3.2 km) linear electron accelerator yet to be built at SLAC.

In 1957, after five years at Stanford, Kendall moved back to MIT as a member of the faculty; Jerome Friedman had also returned. Kendall and Friedman's prior collaboration at Stanford University and their work with Richard Taylor at Stanford set the stage for a collaborative effort where the three would join forces in 1964 with other coworkers at SLAC to explore, through the early 1970s, the substructure of the proton and neutron via inelastic scattering of electrons. This collaboration led to their joint award of the Nobel Prize in Physics in 1990.

Henry Kendall was a founding member of the Union of Concerned Scientists, and became chair of the organization in 1974. He suffered a mishap while diving in the waters of Wakulla Springs State Park, Florida, and drowned on February 15, 1999 at the age of 72.

Richard E. Taylor was born on November 2, 1929 in Medicine Hat, a small town in Alberta, Canada. His father had Northern Irish and Scottish parents who homesteaded in the prairies of Canada, and his mother was an American born to Norwegian immigrants. In high school Taylor did well in mathematics and developed an interest in physics, which he attributes to his talented high school teachers. He studied mathematics and physics at the University of Alberta, and completed his MSc degree there in 1952 with a thesis on an attempt to detect double-beta decay with a Wilson cloud chamber.

On graduation from the University of Alberta, Richard Taylor was admitted to the doctoral program at Stanford University. After a year of study and hard work he joined the research group at the High Energy Physics Laboratory to work on the new linear accelerator. In 1958 he joined a research group at the École Normale Supérieure in Paris for experiments with a linear accelerator in Orsay, France. Taylor returned to the USA in 1961 for a short stint at the Lawrence Berkeley Laboratory; and the following year returned to Stanford University, where the new two-mile linear accelerator was under construction at SLAC. After two years at Stanford he was able to join the research group and faculty at SLAC and work closely with its director, Wolfgang K. H. Panofsky, and collaborators at CalTech and MIT, including Jerome Friedman and Henry Kendall at MIT, with whom he shared the Nobel Prize in Physics in 1990 for their work on the scattering of high-energy electrons that provided the very first evidence for point-like charged quarks and the neutral gluons in protons and neutrons.

The significance of the discovery of quarks and gluons was underscored in the Nobel Prize award ceremony speech given by Professor Cecilia Jarlskog of the Royal Swedish Academy of Sciences on December 8, 1990:

> *One of the most important tasks of physics is to provide us with a clearer picture of the world we live in. We know that the observable universe is much larger than any of us could imagine and is even, perhaps, no more than just an island in an ocean of universes. But the creation also has another unfathomable frontier—that towards smaller and smaller constituents: molecules, atoms and elementary particles… The special roles of the proton and the neutron are evident [;] among other things they are responsible for more than 99 percent of our weight. But what roles did the other particles play? Where had nature's elegance and beauty gone? Was there a hidden order not yet discovered by man? There could be order but only at the price of postulating an additional, deeper level in nature—perhaps the ultimate level—consisting of only a few building blocks. Such an idea had been advanced and the new building blocks were called 'quarks'… This year's Laureates lit a torch in this darkness. They and their coworkers examined the proton (and later on also the neutron) under a microscope—not an ordinary one, but a 2 mile-long electron accelerator built by Wolfgang K.H. Panofsky at Stanford, California… They looked for the electron undergoing a large deflection… The electrons ricocheted off hard point-like objects inside the proton. These were soon shown to be identical with the quarks, thus simplifying the physicist's picture of the world; but the results could not be entirely explained by quarks alone. The Nobel Prize-winning experiment indicated that the proton also contained electrically neutral constituents. These were soon found to be 'gluons', particles gluing the quarks together in protons and other particles. A new rung on the ladder of creation had revealed itself and a new epoch in the history of physics had begun.*
>
> From nobelprize.org, Nobel Media AB 2014, www.nobelprize.org/nobel_prizes/physics/laureates/1990/presentation-speech.html, reprinted with permission.

The work of Jerome I. Friedman, Henry W. Kendall, Richard E. Taylor, and their collaborators at MIT and SLAC in the search for quarks and gluons within the nucleons began with the construction of a two-mile (3.2 km) electron accelerator buried 25 feet (7.6 m) underground at SLAC on the campus of Stanford University, and continued during 1967–1973. The experimental results have been described in great technical detail by each of the Nobel Laureates (Friedman, 1991; Kendall, 1991; Taylor, 1991), and in an account by Michael Riordan (1992).

The newly constructed accelerator at SLAC could accelerate electrons to the energy of 20 GeV (ie, 20 billion electron volts). The researchers carried out numerous experiments, which involved the bombardment of liquid hydrogen or deuterium targets with high-energy electrons. The objective was to search for inelastic scattering that would provide evidence for constituents within the protons or neutrons of the target material. The nuclei of the hydrogen atoms in the accelerator target provided pure protons as target material for the bombarding electrons; while the deuterium nuclei contain both a proton and a neutron. The experimental difference in deflections produced by the two targets would provide evidence for the effect of neutrons on the bombarding electrons.

We can recall the historic experiments carried out by Ernest Rutherford, Hans Geiger, and Ernest Marsden over a century ago (see Hall of Fame, Part I), where they bombarded a very thin gold foil (5×10^{-5} cm thick) with alpha particles. Most of the alpha particles passed through the gold foil as if it were not even present in the path of the bombarding particles; but they observed the occasional deflection of alpha particles at acute angles and even back in the direction from which they came. Rutherford concluded that the deflections of the alpha particles were caused by a nucleus within the atoms of gold, and thereby discovered the atomic nucleus. In a somewhat similar approach, Jerome Friedman, Henry Kendall, Richard Taylor, and their collaborators at MIT and SLAC bombarded the proton and neutron within the atomic nucleus with high-energy electrons to measure and analyze any deflections that could occur. The theory that quarks could exist within the proton and neutron as point-like objects that carry fractional electric charge had been presented by Murray Gell-Mann (1964) and George Zweig (1964a,b); and that neutral gluons would mediate the strong force between the quarks within the nucleons was described by the theory of QCD, discussed earlier in this chapter. The question to be answered was the following: would measurements of inelastic scattering of high-energy electrons bombarding the proton or neutron within the atomic nucleus show the nucleons to be relatively homogeneous with respect to their internal structure, or would the inelastic deflections of electrons provide evidence for an internal structure within the nucleons?

As described by Riordan (1992), the first promising results were observed in 1968 when corrections were made for radiative effects of observed electron scattering; and it was determined that deep inelastic scattering of electrons by the nucleons did occur and was not due to radiative effects. In other words, something dense within the proton and neutron was causing the electron scattering. Additional more accurate measurements demonstrated that the electron scattering could be correlated with the fractional charges of the differing quark compositions of the proton (uud) and the neutron (udd); however, certain calculations indicated that the electrons were deflected by about half the mass of the nucleon. This would occur if about half the mass of the nucleon contained, in addition to quarks, neutral gluons, which would not interact with the bombarding charged electrons. This was described by Jerome Friedman (1990) in his Nobel lecture:

> *A sum rule generally relates an integral of a cross section (or of a quantity derived from it) and the properties of the interaction hypothesized to produce that reaction… Sum rule evaluations within the framework of the parton [ie, quark–gluon] model provided an important element in identifying the constituents of the nucleon… The experimental value was about one-half the value predicted on the basis of the simple three-quark model of the proton, and it was also too small for a proton having three valence quarks in a sea of quark-antiquark pairs. The Kuti-Weisskopf model (1971) which included neutral gluons, in addition to the valence quarks and the sea of quark-antiquark pairs, predicted a value… that was compatible with this experimental result.*

Thus the experimental evidence produced by the deep inelastic electron scattering experiments provided evidence that the proton and neutron contain three charged quarks, namely the uud quark combination in the proton and the udd quark grouping in the neutron; and that the quarks within the nucleons are found within a sea of neutral gluons. Further experiments during 1969–1979 provided yet more evidence for the existence of quarks and gluons within the nucleons. As outlined by Riordan (1992), these include the neutrino–nucleon scattering experiments (Budagov et al., 1969; Perkins, 1972) at CERN also known as the European Organization for Nuclear Research. Due to their neutral charge and near-zero mass, neutrinos do not commonly interact with matter; however, neutrinos can interact via the weak force, as in the reverse beta decay described previously in this book. At CERN, intense beams of high-energy neutrinos directed against massive target material provided evidence for point-like structures within the nucleons, characteristic of three charged quarks. Sum rules described by Friedman provided additional evidence that half of the momentum carried by a proton or neutron in the neutrino–nucleon interactions was carried by the quarks, which left behind by difference the neutral gluons to carry off the remaining half of the momentum.

Most convincing to the scientific community of the existence of quarks and qluons was visible evidence provided by high-energy positron–electron collisions (Hanson et al., 1975; Brandelik et al., 1979; Barber et al., 1979; Berger et al., 1979; Biebel, 2001). An example is the large electron–positron (LEP) collider built by CERN, which had a circumference of 27 km and was constructed in a tunnel 100 m underground near Geneva, Switzerland. The tunnel passed through the border of France and Switzerland. The accelerator was dismantled in 2001 to allow the large hadron collider (LHC) to take its place. The LEP collider was operated as a synchrotron to accelerate positrons and electrons to travel close to the speed

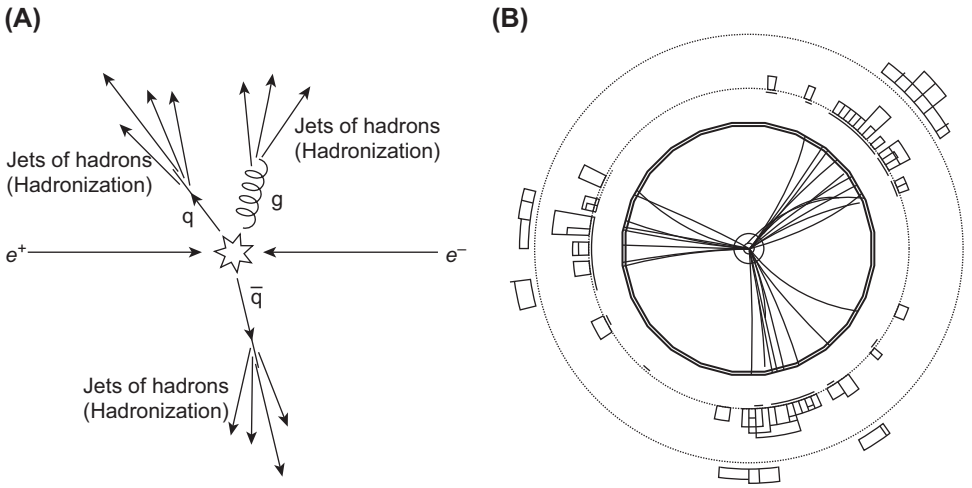

FIGURE X.13 Hadron jets formed as a result of a high-energy collision and annihilation of a positron and electron produced in an electron−positron collider. (A) On the left is a collision of a high-energy positron and electron in a positron−electron collider producing a quark (q) and antiquark ($\overline{q}$) traveling apart in opposite directions and a gluon (g), resulting in the production of three jets of hadrons traveling away from the point of collision. *(From Driga, O., 2012. Soft hadron production at the LHC. Prog. Part. Nucl. Phys. 67, 434−439, reprinted with permission from Elsevier © 2012.)* (B) On the right is an example of recordings of three hadron jets from an e^+e^- annihilation recorded in the jet chamber of a particle detector. The three jets include two jets produced by a quark−antiquark pair and the emission of a gluon by the separated quark−antiquark pair. The jets of hadrons are shown in the plane perpendicular to the direction of the e^+ and e^-, which annihilated in the center of the detector. Charged particles produce curved jets, bent by a solenoidal magnetic field; and uncharged particles produce straight lines. The boxes outside the circular region represent recordings of the energy deposited by the neutral and charged particles in the outer components of the particle detector. *(From Biebel, O., 2001. Experimental tests of the strong interaction and its energy dependence in electron-positron annihilation. Phys. Reports 340, 165−289, reprinted with permission from Elsevier © 2001.)*

of light, with energies as high as 209 GeV. Positrons and electrons traveled in opposite directions, and the positron and electron beams were made to collide at certain stations along the 27 km circular part of the accelerator. At the points of interaction of the positrons and electron were very large detectors that would surround the positron and electron beams and record the particles and energy emitted following a positron and electron collision.

A high-energy positron and electron collision results in the annihilation of both the positron and the electron, which can generate the emission of a quark (q) and antiquark ($\overline{q}$) pair together with the radiation of a gluon, as illustrated in Fig. X.13A. As the quark and antiquark travel further apart, more energy is released, resulting in the production of additional quark−antiquark pairs and gluons. After all the energy is released from the quark−antiquark separation, the quarks, antiquarks, and gluons created then associate according to color charge and combine to form colorless hadrons, namely baryons consisting of red, green, and blue quarks and mesons composed of quark and antiquark combinations. The hadrons appear as streams or jets emitted from the point of collision of the positron and electron in the direction of emission of the original quark, antiquark, and gluon created in the e^+e^- annihilation. This process by which jets of hadrons are produced from quarks, antiquarks, and gluons is referred to as hadronization, and serves as the signature for quarks and gluons. Hadron jets were first reported to arise from high-energy positron−electron collisions studied by the Lawrence Berkeley National Laboratory and SLAC (Hanson et al., 1975); and the visible evidence of gluons was first reported as a third hadron jet from a gluon emission in addition to the two hadron jets arising from the production of a quark−antiquark pair in a high-energy e^+e^- annihilation recorded by the Deutsches Elektronen-Synchrotron at Hamburg, Germany (Barber et al., 1979; Berger et al., 1979; Brandelik et al., 1979).

Fig. X.14 illustrates the process of hadronization as it occurs in the electron−positron collider by a mechanism referred to as cluster fragmentation. As described by Biebel (2001) and illustrated in Fig. X.14, hadronization may occur in the following sequence. A high-energy positron and electron collide and annihilate, possibly involving initial-state photon radiation (γ), and an intermediate boson (Z^0) turns into a quark and antiquark—an up (u) quark and antiup ($\overline{u}$) quark are illustrated in Fig. X.14 as an example. Gluons radiate, illustrated as curly lines, and split into quark−antiquark pairs (branching lines originating from the gluons), which produces a shower of partons (referring to a grouping of quark, antiquark, and gluon). The quarks, antiquarks, and gluons transition into hadrons (ie, baryons and mesons). Finally, the hadrons undergo decay (branching arrows leading from hadrons).

The energy liberated by the separation of quark and antiquark, resulting in a parton shower and hadronization, is a result of a property of quarks known as asymptotic freedom, which describes the strong force between quarks. The

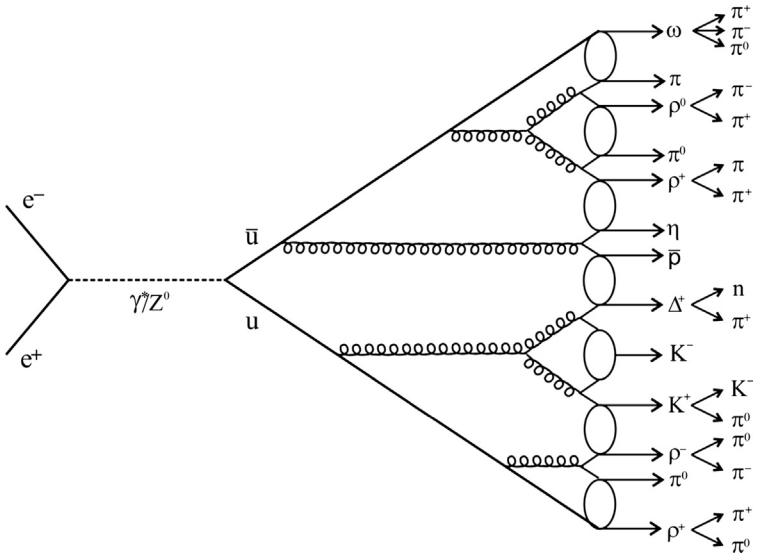

FIGURE X.14 Feynman diagram of hadronization *From Biebel, O., 2001. Experimental tests of the strong interaction and its energy dependence in electron-positron annihilation. Phys. Reports 340, 165–289 and adapted from Sjöstrand, T., 1988. Status of fragmentation models. Int. J. Mod. Phys. A 3, 751–804; reprinted with permission from Elsevier © 2001.*

property of asymptotic freedom between quarks was developed by David Gross of the University of California, Santa Barbara, Frank Wilczek of MIT, and David Politzer of CalTech, for which they were awarded the Nobel Prize in Physics in 2004. Asymptotic freedom is a property of QCD whereby the bond between quarks is weakest at the shortest distance between quarks and the strength of the bond between quarks increases with distance, which extends to the diameter of a nucleon. Thus within the nucleon quarks are kept in close proximity, loosely bound, and free to move about. As quarks are separated, such as in the production of a quark and antiquark pair after an e^+e^- annihilation, the strength of their bond increases as the distance between them increases. It is therefore considered that quarks, as elementary particles, cannot be isolated. The effects of their separation, the production of hadron jets in an electron–positron collider, can serve as the signature for their existence.

The postage stamp illustrated here commemorates the Beijing electron–positron collider (BEPC) and the measurement of hadron jets following the collision of a high-energy positron and electron. The positron and electron beams are illustrated as different colored beams which approach each other from opposite directions (left- and right-hand parts of the figure). The beams interact at the center of the figure, resulting in an e^+e^- annihilation within the very center of a detector (surrounding red object). The hadron jets (dotted lines and curves) originating from the point of e^+e^- collision are detected and measured by the surrounding detector.

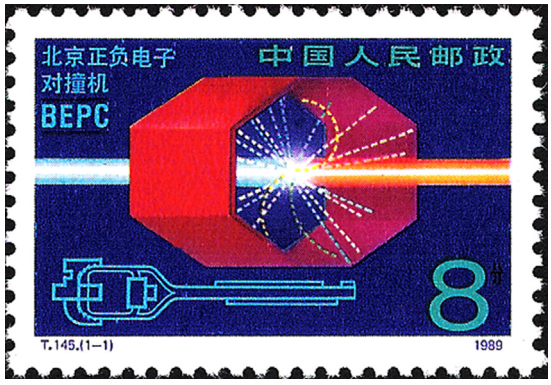

Hadron jets in the Beijing electron-positron collider (BEPC)

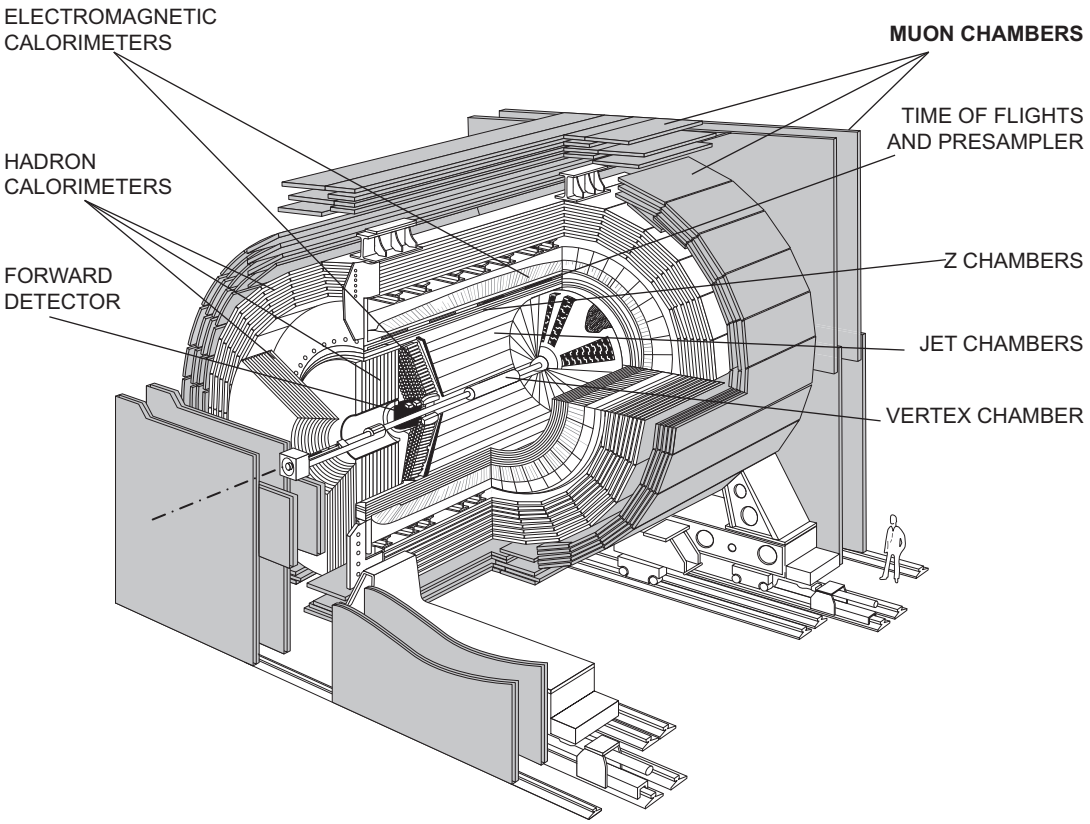

FIGURE X.15 The OPAL (**O**mni-**P**urpose **A**pparatus for **L**EP) detector for the LEP at CERN. The detector surrounds the beams of electrons and positrons that approach the detector from opposite directions through a beam pipe at the very center of the detector. The dashed line on the left front of the detector indicates the line of flight of one of the electron beams. The antiparticle electron beam approached the detector from the other end, which is not visible. *From Korytov, A., 2009. Muon detectors for colliders. Nucl. Instrum. Methods Phys. Res. Sect. A 598, 175–182, reprinted with permission from Elsevier © 2009.*

The actual detector that surrounds the location where the beams of accelerated high-energy electrons and positrons are made to collide is massive. The OPAL detector used for the LEP collider at CERN is illustrated in Fig. X.15. A very small human figure is illustrated standing in the lower right-hand corner to indicate the immense size of detectors utilized around points of interaction of accelerator beams. The OPAL detector was 12 m in length, 12 m high, and 12 m wide, and was designed to measure the interactions of high-energy electrons and positrons. The jet chamber, where hadron jets were recorded, measured 4 m in diameter.

A detector is immense to permit the measurement of particle momenta and energy. The large size of the jet chamber permits the measurement of particle momentum from the curvature of charged particles in the magnetic field; and because of the high energy of these particles, a jet chamber radius of 2 m is required to provide a measurable curvature (see examples of jets with curvatures illustrated in Fig. X.13B, and the postage stamp commemorating the Beijing electron–positron collider). The matter surrounding the jet chamber consists of layers of massive detectors (calorimeters) where particle energy is completely absorbed to determine their energy. The electromagnetic calorimeters are constructed of lead glass to measure gamma photon and electron energies. Particles exiting the electromagnetic calorimeters are detected by hadron calorimeters, which consist of layers of iron sandwiched with planes of particle detectors. The vertex chamber, illustrated in Fig. X.15, facilitates a precise measurement of the z coordinate of the charged particles close to the e^+e^- point of interaction. A time-of-flight system provides information on the time of transit of a particle from the point of e^+e^- interaction, which can assist in particle identification. Forward detectors are located at both ends of the detector to measure particle energies that are emitted at small angles relative to the electron and positron beam line. The muon chambers are the outermost detectors, covering the outer barrel and endcap regions of the detector to facilitate the detection of muons that are highly penetrating and pass through both the electromagnetic and the hadron calorimeters.

As described previously, the theory of quarks, first proposed independently by Murray Gell-Mann and George Zweig in 1964, followed by the discovery of quarks and gluons during the following decade and half represent one of the greatest

breakthroughs in the history of science. This was eloquently stated by Riordan (1992) with the following statement, which underscores are current understanding of the building blocks of matter:

> *The existence of quarks is recognized today as a cornerstone of the standard model, currently the dominant theory of particle physics. In this theory, all matter is composed of elementary quarks and leptons, and the forces between these particles are carried by gauge bosons such as the photon and gluons.*

SHELDON L. GLASHOW (1932–), ABDUS SALAM (1926–1996), AND STEVEN WEINBERG (1933–), GERARDUS 'T HOOFT (1946–) AND MARTINUS J.G. VELTMAN (1931–), AND CARLO RUBBIA (1934–) AND SIMON VAN DER MEER (1925–2011)

The Nobel Prize in Physics in 1979 was awarded to Sheldon L. Glashow of Harvard University, Abdus Salam of the International Center for Theoretical Physics, Trieste, Italy and Imperial College, London, United Kingdom, and Steven Weinberg of Harvard University for, in the words of the Nobel Committee, "their contributions to the theory of the unified weak and electromagnetic interaction between elementary particles, including, inter alia, the prediction of the weak neutral current."

Sheldon L. Glashow was born in New York City in 1932 to Jewish parents who had immigrated from czarist Russia. Glashow graduated from the Bronx High School of Science in 1950. He received a BA degree at Cornell University in 1950 and a doctoral degree in 1959 at Harvard University, under Nobel Laureate Julian Schwinger. Glashow became professor of physics at Harvard in 1966. He is currently Higgins professor of physics emeritus at Harvard and Metcalf professor of mathematics and physics at Boston University.

Abdus Salam was born in Jhang, Pakistan on January 29, 1926. He completed his MA degree in 1946 as an award-winning scholarship student at Punjab University and gained an honors degrees in mathematics and physics at St. John's College, Cambridge, United Kingdom. Salam completed his doctoral degree in theoretical physics at Cambridge in 1951, then returned to Pakistan and headed the Mathematics Department at Punjab University in 1952. He was chief scientific advisor to the president of Pakistan during 1961–1974; and he spearheaded the establishment of the International Center of Theoretical Physics in Trieste, Italy in 1964, becoming its first director from then until 1993. Abdus Salam died at the age of 70 in Oxford, England on November 21, 1996.

Steven Weinberg was born in 1933 in New York City to Jewish immigrant parents. He graduated from the Bronx High School of Science in 1950 alongside Sheldon Glashow. After a year of study at the Niels Bohr Institute in Copenhagen, Weinberg received his PhD at Princeton University in 1957. From 1959 to 1966 he carried out research at Columbia University and the University of California at Berkeley. In 1966–1969 Weinberg was Loeb lecturer at Harvard University and visiting professor at MIT. In 1969 he accepted a professorship at MIT, and in 1973 Weinberg was given the chair at Harvard previously occupied by Julian Schwinger. In 1982 he moved to the University of Texas at Austin, where he holds the Josey Regental chair in science. At the University of Texas at Austin Weinberg is a member of the Physics and Astronomy Departments, where he remains active in research on elementary particle physics and cosmology.

The **weak force** in nature was explained by Enrico Fermi as the force involved in beta decay, which is the decay of radionuclides resulting in beta particle emission (β^+ or β^-) or EC; and the **electromagnetic force** is the force exchanged between charged particles mediated by the photon, described previously in quantum electrodynamics (QED). The theory of the unified weak and electromagnetic interaction between elementary particles first described by the above Nobel Laureates (Glashow, 1961; Salam and Ward, 1964; Weinberg, 1967) proposed a merging of the weak and electromagnetic forces into a unified electroweak interaction. John Clive Ward (1924–2000) did not share the Nobel Prize with Glashow, Salam, and Weinberg, presumably because only three persons can share a Nobel Prize. The unification implied that the weak force could involve two types of interaction, namely an interaction involving a **charged current**, where particles change in identity, such as a neutron changing into a proton, or an interaction involving a **neutral current**, where particles do not change in identity. The very short range of interaction of the weak forces predicted the existence of very large particles of high mass that would mediate this weak force. These were named the W^+ and W^- particles that would mediate the charged current interactions and a neutrally charged particle Z^0 that would mediate the neutral current interactions.

Fig. X.16A illustrates a charged current reaction where an electron neutrino reacts with a deuterium nucleus, resulting in the transformation of a neutron into a proton. Other examples of charged current reactions are those that occur in beta decay, illustrated in Fig. X.8 earlier in this chapter and Fig. X.17. A neutral current reaction is shown in Fig. X.16B. In this

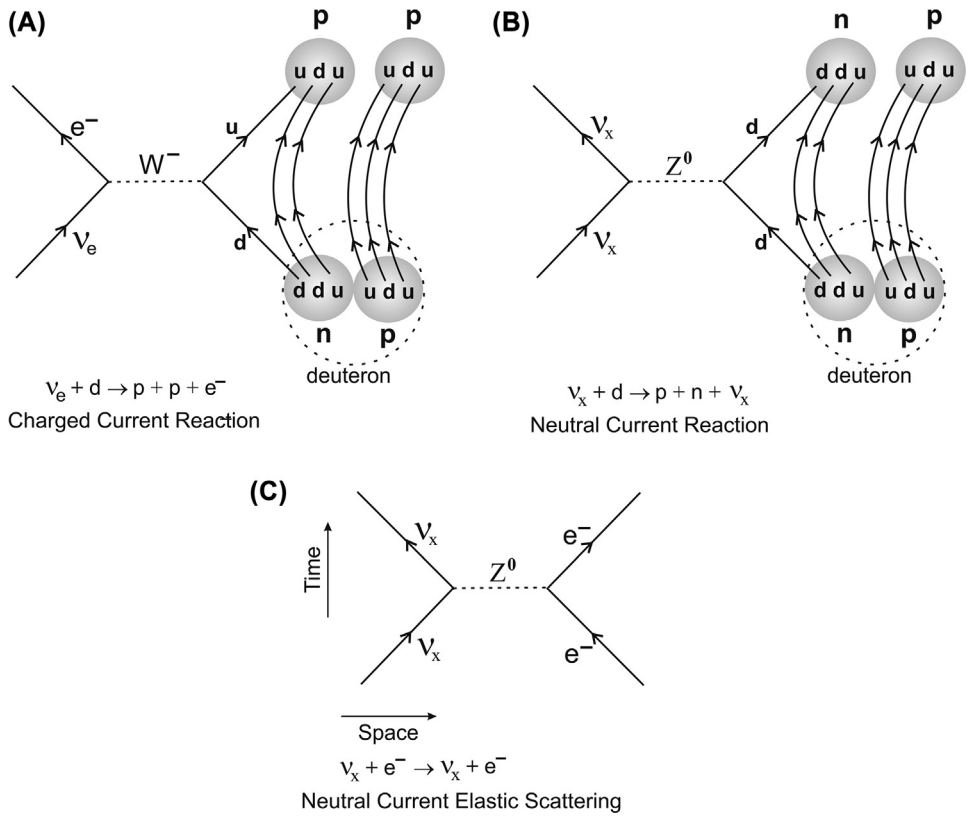

FIGURE X.16 Feynman diagrams describing charged current and neutral current reactions that are key reactions used to detect solar neutrinos at the Sudbury Neutrino Observatory at Sudbury, Canada reviewed in a previous book by the writer (L'Annunziata, 2012e). (A) A charged current reaction of an electron neutrino with a deuterium nucleus. (B) A neutral current reaction of a neutrino of any flavor with a nucleus of deuterium, where x = e, μ, or τ. (C) An elastic scattering of an electron by a neutrino of any flavor.

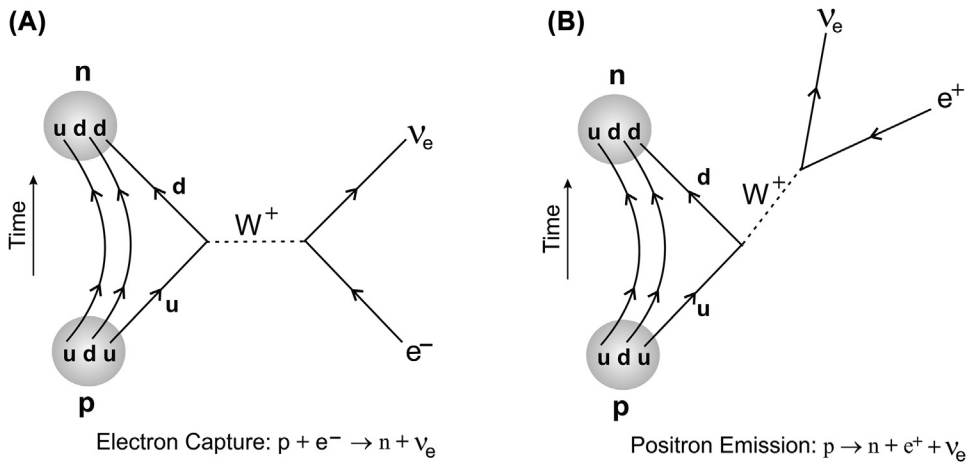

FIGURE X.17 Feynman diagrams describing nuclear beta decays mediated by the W particle: (A) EC decay, and (B) positron (e^+) emission. A Feynman diagram describing negatron (e^-) emission in beta decay is illustrated in Fig. X.8 earlier in this chapter.

case, a neutrino of any flavor reacts with a deuterium nucleus. Neither the neutron nor the proton of the deuterium nucleus changes identity; and the nucleons of the deuterium nucleus separate into individual neutron and proton. Another neutral current interaction is illustrated in Fig. X.16C. In this example, a neutrino, which carries no charge, interacts with an electron, causing the electron to scatter. The elastic scattering is mediated by a Z^0 particle. This reaction was first observed

by Hasert et al. (1973) in a very large 6.3 m^3 bubble chamber Gargamelle filled with Freon CF_3Br and exposed to neutrino and antineutrino beams at the CERN proton synchrotron.

The unified weak and electromagnetic interaction between elementary particles proposed by Sheldon Glashow, Abdus Salam, Steven Weinberg, and their coworkers was eloquently described by Professor Bengt Nagel of the Royal Academy of Sciences in the Nobel award ceremony speech given on December 8, 1979:

> *When one began to study the atomic nucleus in the first decades of our century, two new forces were discovered: the strong and the weak nuclear forces. Unlike gravitation and electromagnetism these forces act only over distances of the order of nuclear diameters or less. The strong force keeps the nucleus together, whereas the weak force is responsible for the so called beta decays of the nucleus… The theory which is awarded this year's prize, and which was developed in separate works by the prizewinners in the 60's, has extended and deepened our understanding of the weak force by displaying a close relationship to the electromagnetic force: these two forces emerge as different aspects of a unified electroweak interaction. This means e.g., that the electron and the neutrino belong to the same family of particles; the neutrino is the electron's little brother. Another consequence of the unified theory is that there should exist a new kind of weak interaction. It was formerly assumed that weak processes could occur only in connection with a change of identity of the electron to neutrino (or vice versa); such a process is said to proceed by a charged current, since the particle changes its charge. The theory implies that there should also be processes connected with a neutral current in which the neutrino—or else the electron—acts without changing identity.*
>
> From http://www.nobelprize.org/, with permission © The Nobel Foundation.

The interactions between charged particles (eg, electron scattering) mediated by the photon (γ) in an electromagnetic interaction, illustrated in Fig. X.18A, exhibit a similarity to the weak interaction between a particle without charge (eg, neutrino) and an electron mediated by a Z^0 particle, illustrated in Fig. X.18B. The photon, which possesses no mass, has an infinite range; but the Z^0 particle was predicted to have a very large mass (91.2 GeV/c^2) and thus a very short range of interaction. The $W^{\pm}$ particles also possess a very large mass, which was determined to be 80.4 GeV/c^2. This is greater than the mass of an atom of iron-56, which is 52.1 GeV/c^2. The range of interaction of $W^{\pm}$ and Z^0 particles is of the order of 10^{-18} m, which is less than the diameter of a nucleon (proton or neutron); and they have a very short lifetime of $\sim 10^{-25}$ s. The short lifetime may be expressed as a tenth of a millionth of a millionth of a millionth of a millionth of a second.

In the electromagnetic interaction illustrated in Fig. X.18, an electron with a given kinetic energy approaches another electron, and the two electrons are scattered via a force mediated by the photon (γ). The photon may be considered as a virtual particle (ie, a particle that is not detected), as the photon is emitted by one electron and absorbed by the other. Likewise, the electron that has absorbed a photon from the other can also emit a photon to be absorbed by the other electron. The exchange of photons can be visualized as two persons playing catch with a ball; however, the photon energy (ie, electromagnetic force) transferred between the two electrons triggers the scattering of the two electrons in different directions. In a similar fashion, a neutrino of any flavor (ie, ν_e, ν_μ, or ν_τ) with a given kinetic energy can

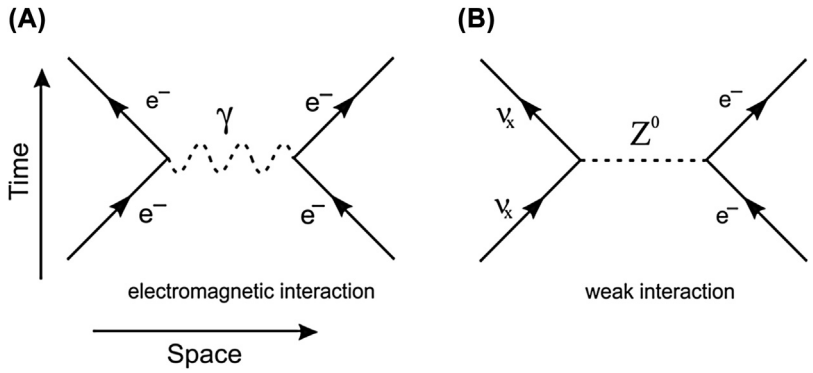

FIGURE X.18 Feynman diagrams illustrating the differences between (A) an electromagnetic interaction between two electrons and (B) a weak interaction between a neutrino and an electron.

pass through matter and encounter an electron, whereby the neutrino and electron are scattered in different directions. The force producing the scatter is mediated by the emission of a Z^0 boson, which is a carrier of the force between the neutrino and electron. The Z^0 bosons, which are very short-lived, act as exchange particles between the neutral (ie, uncharged) neutrino and the charged electron in a fashion similar to the photon particle, which serves as the exchange particle of the force between two charged particles, such as the two charged electrons in Fig. X.18A.

Postage stamps were issued in commemoration of the formulation of the electroweak theory proposed by Glashow, Salam, and Weinberg; and the eventual discovery of the Z^0 particle by Carlo Rubbia and coworkers at CERN in 1983. In the stamp commemorating the electroweak theory, notice the correlation between the γ photon and the positive and negative electrons to both sides of the photon; and the Z boson with neutrinos to both sides. Likewise, the W^- and W^+ bosons are illustrated as the exchange particles in beta decay. The negatron (e^-) and antineutrino ($\bar{\nu}$) particles emitted in negative beta decay (ie, β^- emission) are situated above and below the W^- boson (the exchange particle in negatron emission). Also, the positron (e^+) and neutrino (ν) particles emitted in positive beta decay (ie, β^+ emission) are located above and below the W^+ boson (the exchange particle in positron emission).

In his Nobel lecture, Carlo Rubbia (1984) gave credit to Oskar Klein, who in 1938 had the premonitory vision to classify the bosons that we now call the $W^{\pm}$ and Z^0 particles as very similar to photons in their role as exchange particles in the weak interactions:

> *It was Oskar Klein who, in 1938, first suggested that the weak interactions could be mediated by massive, charged fields. Although he made use of Yukawa's idea of constructing a short-range force with the help of massive field quanta, Klein's theory established also a close connection between electromagnetism and weak interactions. We now know that his pre-monitory vision is embodied in the electroweak theory of Glashow, Weinberg and Salam… It is worth quoting Klein's view directly:*
>
> *The role of these particles, and their properties, being similar to those of the photons, we may perhaps call them "electro-photons" (namely electrically charged photons).*

The mass of the Z^0 boson, equivalent to 91.197 GeV/c^2, is compared to that of the photon (γ) shown on the postage stamp commemorating the discovery of the Z^0 boson by Carlo Rubbia and coworkers at CERN in 1983. The discoveries of the $W^{\pm}$ and Z^0 bosons are described later in this chapter.

Electroweak Unification

Discovery of Z Boson

The theory of electroweak unification described above, which predicted the $W^{\pm}$ and Z^0 bosons, was a significant advancement to our understanding of the electromagnetic and weak interactions. However, the $W^{\pm}$ and Z^0 particles were yet to be discovered, and physicists encountered numerous problems in using the theory to make calculations to determine particle properties and related physical quantities. Thus many were reluctant to accept the theory. Not until the work of Professor Martinus J.G. Veltman at the University of Utrecht and his doctoral graduate student Gerardus 't Hooft were the complicated mathematical expressions worked out to make quantitative calculations permitting widespread acceptance of the electroweak unification (Veltman, 1970; 't Hooft, 1971a,b; 't Hooft and Veltman, 1972). For this work, 't Hooft and Veltman were awarded the Nobel Prize in Physics in 1999, as described in the Nobel Committee press release announcing the award:

> *While the theory of electro-weak interaction developed in the 1960s was a great step forward, the research community at first found it difficult to accept. When they tried to use the theory for calculating in more detail the properties of the new W and Z particles (and many other physical quantities) it gave unreasonable results… Martinus J.G. Veltman had developed the* Schoonschip *computer program which, using symbols, performed algebraic simplifications of the complicated expressions that all quantum field theories result in when quantitative calculations are performed… In spring 1969, Veltman was joined by a 22-year-old pupil, Gerardus 't Hooft…With the help of Veltman's computer program, 't Hooft's partial results were now verified and together they worked out a calculation method in detail. The non-abelian gauge theory of electro-weak interaction had become a functioning theoretic machinery and it was possible, just as it had become for quantum electrodynamics 20 years previously, to start performing precise calculations… As described above, the theory of the electro-weak force predicted the existence of the new W and Z particles right from the start. But it was only through 't Hooft's and Veltman's work that more precise prediction of physical quantities involving properties of W and Z could start.*
>
> From Press release "The 1999 Nobel Prize in Physics," www.nobelprize.org/nobel_prizes/physics/laureates/1999/press.html.

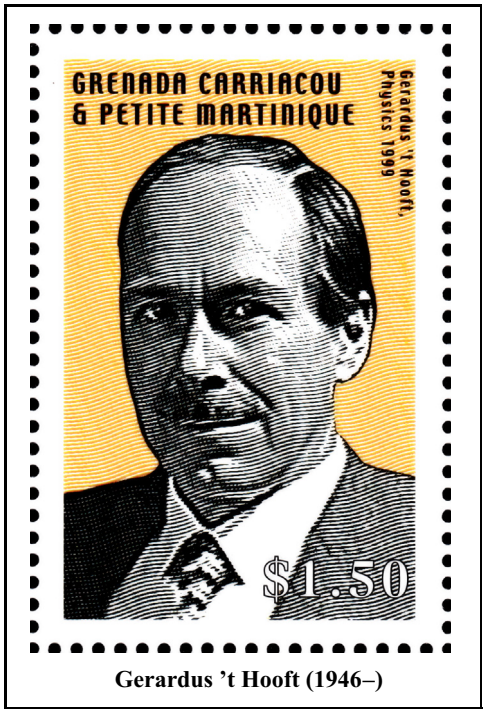

Gerardus 't Hooft (1946–)

Martinus J. G. Veltman (1931–)

Martinus J.G. Veltman was born in 1931 in the town of Waalwijk, in the southern part of the Netherlands. At the age of nine he saw the German army march into the Netherlands, and at the age of 13 his town was liberated by the Allied forces. In his autobiography, Veltman (1999) relates how his family escaped the famine winter of 1944−1945, when many

Dutch died of hunger, because the northern part of the country remained occupied. He studied physics at the University of Utrecht in 1948, for which he thanked his high school teacher: Veltman was uncertain as to the direction to take after high school, and his teacher took the time to visit Veltman's home and advise his parents to send him to Utrecht. Many can relate to a high school teacher being influential in helping them make an important decision for their future. Martinus Veltman (1999) underscores this fact in his autobiography:

> *…my physics high school teacher came to my home and suggested to my parents to send me to the University… I am still grateful to this high school teacher, Mr. Beunes, as he did the extra thing, going to my parent's house. Since then I have found out that many physicists owe their career to a good high school teacher.*

In 1955 Veltman got a job as assistant to Professor Michels at the Van Der Waals Laboratory in Amsterdam, and later the same year he moved to Utrecht to study for his master's degree under Professor Leon Van Hove. After a two-year stint in military service, Van Hove accepted Martinus Veltman as a doctoral student in theoretical physics at Utrecht University. He received his PhD degree in 1963, and in 1966 was awarded a professorship at Utrecht University as successor to Van Hove, who had moved in 1960 to become director of the Theory Division at CERN in Geneva, Switzerland. Veltman also went to CERN in 1961 to follow Van Hove, before eventually returning to Utrecht. In 1963−1964 Veltman worked at SLAC, during which time he constructed his Schoonschip computer program, which enabled the symbolic manipulation of the complex mathematics needed to solve equations that would lead to the determination of the properties of the $W^{\pm}$ and Z^0 bosons predicted by the unified electroweak theory. In 1972 Gerardus 't Hooft became Veltman's doctoral student at Utrecht University, where they collaborated in the work that lead to their joint award of the Nobel Prize in Physics in 1999. Martinus J.G. Veltman was awarded the John D. and Catherine T. MacArthur chair in the physics faculty at the University of Michigan at Ann Arbor in 1981. Veltman had many graduate students in particle and theoretical physics, some of whom moved on to other very different and successful fields of endeavor. Even his daughter Hélène completed a thesis in particle physics at Berkeley before going on to a successful career in the banking world in London. In this respect, Martinus J.G. Veltman (1999) made an interesting observation concerning studies in the field of theoretical physics:

> *…theoretical physics is a good science to be educated in, it prepares for no job in particular but the scientific methods learned are of use in many positions in modern society. So never worry too much what kind of job you will get after finishing a theoretical physics education. For example, the first Prize in Economic Sciences in Memory of Alfred Nobel went to Tinbergen, a former theoretical physicist. And nowadays the banking world is full of particle theorists.*

Martinus J.G. Veltman is now a retired emeritus professor in the town of Bilthoven in the Netherlands.

Geradus 't Hooft was born in 1946 in Dan Helder in the Netherlands and grew up in The Hague. In primary and high school, 't Hooft excelled in science and mathematics as well as languages. At the age of 16 he won second place in the Dutch Math Olympiad—he might have won first place if it were not a simple mistake made out of nervousness, as explained in his autobiography ('t Hooft, 1999). In 1964 he entered Utrecht University to study particle physics. Here he joined forces with Professor Martinus J.G. Veltman, with whom he shared the Nobel Prize in Physics in 1999. After obtaining his PhD in 1972, 't Hooft went to work at CERN in Geneva. Here he made calculations concerning the strong interaction, whereby he predicted asymptotic freedom among quarks, which was evidenced at CERN by deep inelastic scattering experiments of protons on nucleons, as discussed previously. Asymptotic freedom among quarks in the nucleon describes how quarks move freely within the nucleons, because the energy binding the quarks within the nucleons is weakest when the quarks are at their closest proximity, and the strength of the bond between the quarks increases as the distance between the quarks increases. This is a key factor preventing the isolation of quarks, as described previously. Gerardus 't Hooft mentioned his findings at a small conference at Marseille in 1972; as he notes ('t Hooft, 1999), the only person who listened or understood what he had said was Kurt Symanzik, who urged 't Hooft to publish the idea, stating that if he did not publish it, someone else would do so. 't Hooft had even made a remark about the finding in a previous paper ('t Hooft, 1971b), but not one person picked up on his observation. Also, 't Hooft (1999) related that Veltman told him his theory would be worthless if he could not explain why quarks could not be isolated. 't Hooft did not publish or pursue the theory further; and eventually the Nobel Prize in Physics in 2004 was awarded to David J. Gross, H. David Politzer, and Frank Wilczek "for the discovery of asymptotic freedom in the theory of the strong interaction." In 1974 Gerardus 't Hooft was appointed assistant professor at Utrecht University; in 1976 he was guest professor at Stanford and Harvard University. In 1978 't Hooft was named full professor at Utrecht, and in 2011 distinguished professor.

The Nobel Prize in Physics in 1999 was awarded to Martinus J.G. Veltman and Geradus 't Hooft years after the $W^{\pm}$ and Z^0 particles were discovered by Carlo Rubbia, Simon van der Meer, and coworkers at CERN in 1983. It was the earlier work of Veltman and 't Hooft that enabled the precise calculations of the masses $W^{\pm}$ and Z^0 particles and their consequent discoveries with the aid of the superproton synchrotron (SPS) at CERN, described later in this section. The importance of

our knowledge of this work was underscored by Professor Cecilia Jarlskog of the Royal Swedish Academy of Sciences in her Nobel Prize award ceremony speech on December 10, 1999:

> *In order to describe the building blocks of nature we must have language, a theory. This year's Laureates in Physics, Gerardus 't Hooft and Martinus Veltman, have made a decisive contribution to this language. Their contributions concern electromagnetic and weak interactions of the building blocks of matter. Electromagnetism is the interaction which is responsible, for instance, for the existence of atoms. The principal actor here is the photon—light—because without light there would be no electromagnetism. Weak interactions also have their own agents: three particles that unfortunately have not been honored by beautiful and dignified names but are simply called W-plus, W-minus and Z. In spite of their dull names, these particles are of paramount importance. Consider, for example, W-plus. We know that the sun is like an oven. But who makes the fire there? The particle W-plus, of course! Without weak interactions the sun would not shine!*

The role of the W-plus particle (ie, W^+ boson) referred to in this statement are heat-producing reactions of the sun that involve the emission of positrons (β^+), a form of beta decay. There are nuclear decays and nuclear reactions in the heat-producing reaction cycle of the sun, as described by Hans Bethe in his Nobel lecture of 1967 (see Hall of Fame VIII). These reactions involve the transformation of a proton to a neutron with the emission of positrons and a neutrino mediated by a W^+ boson, as illustrated previously in Fig. X.17.

Following the work of 't Hooft and Veltman, the properties of the $W^{\pm}$ and Z^0 bosons could be predicted; however, there was still the need to demonstrate the existence of these particles, as they were yet to be discovered. The $W^{\pm}$ and Z^0 bosons would possess a high mass, as noted previously, greater than that of an atom of iron. The $W^{\pm}$ and Z^0 particles could be produced by quark–antiquark annihilation or fusion, as illustrated in the Feynman diagrams of Fig. X.19. Quarks and antiquarks cannot be isolated. Thus the quarks and antiquarks for the annihilation reactions would be provided by high-energy collisions between proton (p) and antiproton ($\overline{p}$) beams accelerated in opposite directions in the SPS at CERN in Geneva, Switzerland. It took the determination and drive of Carlo Rubbia from Italy to spearhead the work of the largest project in physics at the time, which required hundreds of research scientists at CERN over a period of several years to undertake the design of the SPS and its particle detectors, and the ingenuity of Simon van der Meer from the Netherlands, who made it possible to accumulate large numbers of antiprotons in a synchrotron accelerator and storage ring, without which the production and detection of the $W^{\pm}$ and Z^0 particles would not have been possible.

The Feynman diagrams in Fig. X.19 also include products of the decay of the $W^{\pm}$ and Z^0 particles. The detection and measurement of these decay particles would serve as the signature for the production of the W^+, W^-, or Z^0 particles following a high-energy proton–antiproton ($p\overline{p}$) collision. For example, the following are possible production and decay reactions for the W^+, W^-, or Z^0 particles following a high-energy $p\overline{p}$ collision:

$$p + \overline{p}(ie, \overline{u}d) \rightarrow W^- + X, \quad \text{and} \quad W^- \rightarrow e^- + \overline{\nu} \qquad [X.15]$$

$$p + \overline{p}\left(ie, u\overline{d}\right) \rightarrow W^+ + X, \quad \text{and} \quad W^+ \rightarrow e^+ + \nu \qquad [X.16]$$

$$p + \overline{p}\left(ie, \overline{u}u \text{ or } d\overline{d}\right) \rightarrow Z^0 + X, \quad \text{and} \quad Z^0 \rightarrow e^+ + e^- \text{ or } \mu^+ + \mu^- \qquad [X.17]$$

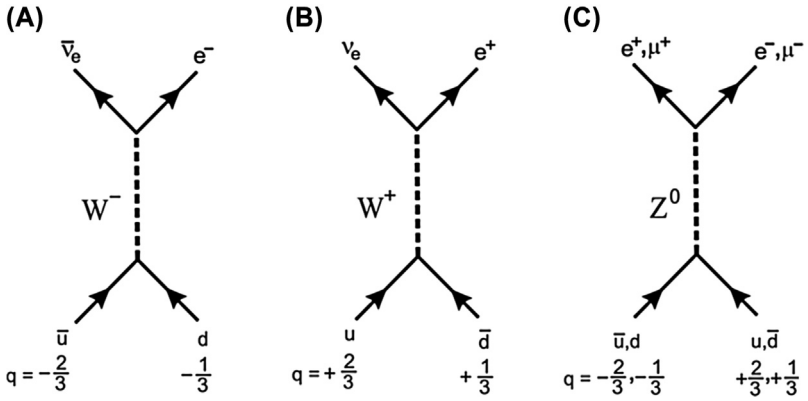

FIGURE X.19 Feynman diagrams for the direct production of the W^+, W^-, and Z^0 particles in high-energy proton–antiproton collisions via quark–antiquark annihilation: (A) the fusion and annihilation of an antiup quark and a down quark to produce a W^-, which decays to an antielectron neutrino and an electron; (B) an up quark and an antidown quark fuse to form a W^+, which decays to an electron neutrino and a positron; (C) either an antiup and up quark ($\overline{u}u$) or a down and antidown quark $\left(d\overline{d}\right)$ fuse to form a Z^0, which may decay to either a positon–electron pair (e^+, e^-) or muons of opposite charge (μ^+, μ^-). The quark charges (q) are provided below each quark. *Adapted from Rubbia, C., 1984. Experimental Observation of the Intermediate Vector Bosons W^+, W^- and Z^0. Nobelprize.org. Nobel Media AB 2014. http://www.nobelprize.org/nobel_prizes/physics/laureates/1984/rubbia-lecture.html.*

These reactions describe the fusion of a quark and antiquark from a proton−antiproton collision to yield a W^+, W^-, or Z^0 particle and X. As described by Rubbia (1984), the X in the reactions refers to the fragmentation of spectator partons, or, in other words, the sum of particle debris (numerous other particles) from interactions of other protons that do not produce the W^+, W^-, or Z^0 particle.

Carlo Rubbia (1934–)
At Boston University Commencement, 3 March 1988, recipient of honorary degree. Courtesy of the American Institute of Physics, AIP Emilio Segre Visual Archives

Simon van der Meer (1925–2011)

Carlo Rubbia was born in 1934 in Gorizia, a small town in northern Italy on the border with Yugoslavia, about 80 km from the Austrian border. After high school Rubbia studied physics at the Scuola Normale in Pisa, and completed his studies there with a thesis on cosmic radiation in 1958. He then proceeded to the United States to continue his studies and undertake research with particle accelerators at Columbia University. At Columbia, Carlo Rubbia carried out work on parity violation in the weak interactions, and received a doctorate in 1959. After a year and half at Columbia, Rubbia returned to Europe in 1960 to join the research group using the proton synchrotron at CERN in Geneva; here he carried out research in weak interactions, including measurements of parity violation in lambda hyperon decay. In 1971 CERN completed the first hadron collider with intersecting storage rings (ISRs), consisting of two storage rings for proton and antiproton circulation in opposite directions. The rings intersected in eight locations (see Fig. X.20), which permitted proton−antiproton collision. The ISRs gave Rubbia much accelerator experience which would be vital to the successful collisions of high-energy protons and antiprotons that led to the discovery of the $W^{\pm}$ and Z^0 bosons over a decade later. In 1976 Carlo Rubbia, David Cline, and Peter McIntyre (Rubbia et al., 1977) proposed the construction of an SPS, which would accelerate protons and antiprotons in counter-rotating beams to energies of up to 270 GeV. The new SPS would provide center-of-mass proton−antiproton collision energies of 540 GeV, sufficient to produce the $W^{\pm}$ and Z^0 bosons; this was successfully accomplished in 1983 by Carlo Rubbia, Simon van der Meer, and numerous coworkers at CERN (discussed in more detail later in this chapter). In addition to his work at CERN, Rubbia was appointed Higgins professor of physics at Harvard University, where he would spend one semester per year until 1989. He was then appointed to the post of director general of the CERN Laboratory for a five-year term from 1989 to 1994, and directed attention to research on renewable energy resources. From 1999 to 2005 Carlo Rubbia was president of ENEA, the Italian National Agency for New Technologies, Energy, and Sustainable Economic Development; and from 2005 to 2009 he was principal scientific advisor to CIEMAT, which is Spain's scientific research organization for energy, the environment, and technology. In 2009 Carlo Rubbia was appointed as special advisor to the secretary-general of the UN Economic Commission for Latin

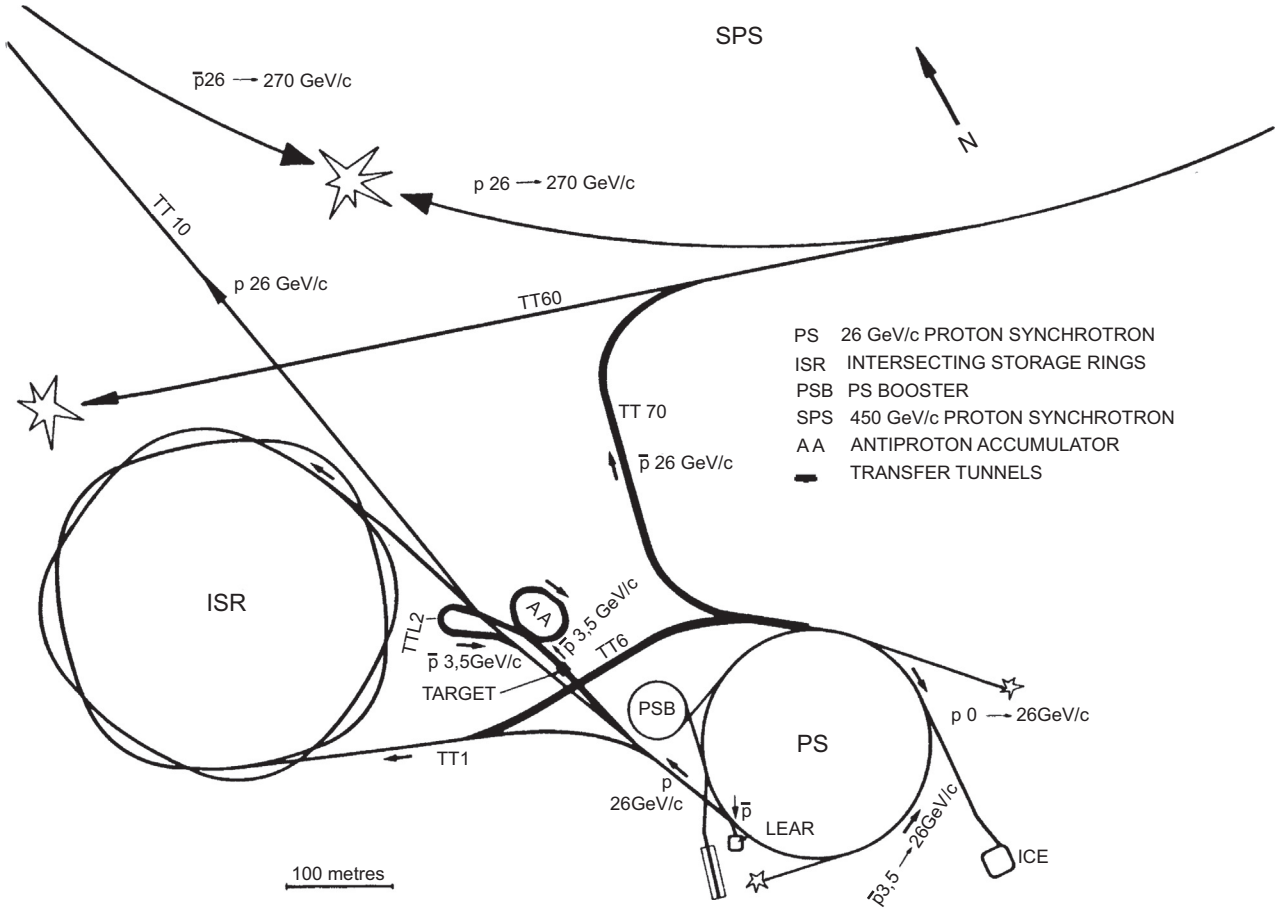

FIGURE X.20 The CERN proton−antiproton collider complex. TTs (transfer tunnels) for antiprotons are illustrated in heavier lines. *Denegri, D., 2004. The discovery of the W and Z. Phys. Reports 403−404, 107−145, reprinted with permission from Elsevier © 2004.*

America and the Caribbean. Since 2010 he has been scientific director of the Institute for Advanced Sustainability Studies in Potsdam, Germany.

Simon van der Meer was born in 1925 in The Hague in the Netherlands, where he grew up. His father was a teacher and his mother was from a family of teachers; thus learning and a good education were of primary importance, and van der Meer relates in his autobiography ("Simon van der Meer—Biographical," Nobelprize.org, Nobel Media AB 2014, www.nobelprize.org/nobel_prizes/physics/laureates/1984/meer-bio.html) that his parents made many sacrifices to assure a good education for their children. In 1943 he went to the Gymnasium in The Hague, where he passed his final exam in the sciences; but during the German occupation the universities were closed. Simon van der Meer was obliged to attend the humanities section of the Gymnasium for the next two years; but he gives a lot of credit and thanks to a very inspiring physics teacher who during that time let van der Meer assist him in the preparation of numerous demonstrations. After the war, from 1945 he studied technical physics at the University of Technology in Delft. This was a newly created curriculum of a high standard, but not the intense theoretical nuclear physics education that some of his colleagues enjoyed at the time. However, van der Meer reflected that this may have turned out to be an asset, because his highly practical and technical experience and education gave him the ability to make major contributions to the accelerator field. The stochastic cooling technique that he first proposed was vital to the success of CERN's discovery of the $W^{\pm}$ and Z^0 bosons in 1983, and gained him the Nobel Prize, as discussed later. After completing an engineering degree in 1952, van der Meer worked at the Philips Research Laboratory in Eindhoven; and in 1956 he moved to join the newly established CERN in Geneva. He remained at CERN for the rest of his professional career. During the late 1970s Simon van der Meer was made joint project leader with R. Billinge in the development of the antiproton accumulator and stochastic cooling technique utilized in the low-energy antiproton ring (LEAR). Without the stochastic cooling, discussed later, the discovery of the $W^{\pm}$ and Z^0 bosons in 1983 would not have been possible. Simon van der Meer retired from CERN in 1990, six years after receiving the Nobel Prize. He died on March 4, 2011 in Geneva, Switzerland.

The Nobel Prize in Physics in 1984 was awarded to Carlo Rubbia and Simon van der Meer, in the words of the Nobel Committee "for their decisive contributions to the large project, which led to the discovery of the field particles W and Z, communicators of the weak interaction." Recognition for the discovery of the $W^{\pm}$ and Z^0 particles was given to CERN as well as the Nobel Laureates, as Professor Gösta Ekspong of the Swedish Royal Academy of Sciences stated in the Nobel award ceremony speech on December 8, 1984 [with comments by the writer in brackets]:

The large project mentioned in the citation is the antiproton project at CERN, the international centre for research devoted to the study of elementary particles, which has 13 European states as members [CERN currently has 20 member states]. CERN straddles, in a unique way, the border between two countries, Switzerland and France, and has grown progressively in importance over the 30 years of its life. The international character is underlined by the fact that Carlo Rubbia is Italian, Simon van der Meer is Dutch and the collaborators in the various phases of the project are scientists, engineers, and technicians of many nationalities, either employed by CERN or in one of the many universities or research institutes involved in the experiments. The project has been made possible by collaboration, by the pooling of financial resources and of scientific and technical skill… two conditions had to be fulfilled in order to produce the W and Z in particle collisions: The first is that the particles must collide at sufficiently high energy so that the conversion of energy into mass could create the heavy W and Z particles. The second is that the number of collisions must be large enough to give a chance of seeing the rare creation process taking place. The name of Rubbia is connected with the first condition, that of van der Meer with the second. Rubbia's proposal was to use the largest accelerator at CERN, the SPS, as a storage ring for circulating antiprotons as well as for protons, circulating in the opposite direction. The particles in the two beams would cross the French-Swiss border about 100,000 times every second for a whole day or more, to be repeated with new beams during months of operation. Antiprotons cannot be found in nature, in any case not on Earth. But they can be created at CERN where sufficient energy is available at the other accelerator, the PS [proton synchrotron]. The antiprotons are accumulated in a special storage ring, built by a team led by van der Meer… his ingenious method, called stochastic cooling, enables an intense antiproton beam to be built up. The signals from produced particles are recorded in huge detector systems set up around two collision points along the periphery of the SPS storage ring. The largest of these detectors [UA1 detector] was designed, built and operated by a team led by Rubbia. A second large detector [UA2 detector] was built by another team, operating it in parallel with the first one, nicely confirming the extremely important results… the discoveries of the W and Z were made at CERN—the dream of better understanding the weak interaction, which turns out to be weak just because the W and Z are so very heavy. The weak interaction is unique in that it can change the nature of a particle, for example transforming a neutron into a proton or vice versa. Such transformations are crucial for the sun and it is the weakness of the interaction which leads to the very slow burning of the nuclear fuel of the sun and thus creates the conditions on earth which can support life. At first radioactive decays were the only weak interaction phenomena available for study. Nowadays thanks to accelerators and storage rings this field of research is quite large… The modern electroweak theory contains not only the electromagnetic photons as communicators of force but also the communicators W and Z which act as a kind of shock-absorber, especially noticeable in hard collisions—such as those which must have occurred frequently during the Big Bang era at the early stage of the evolution of our universe. The collisions in the CERN collider may be hard enough to break loose the communicators, the shock-absorbers, for a short moment. The resulting fireworks of newly produced particles have been observed in the detectors, and the signs showing the presence of the W and Z have been seen and a start has been made on measuring their properties… The discovery of the W and Z particles will go down in the history of physics like the discovery of radio waves and the photons of light, the communicators of electromagnetism.

From "The 1984 Nobel Prize in Physics—Presentation Speech," Nobelprize.org, Nobel Media AB 2014, www.nobelprize.org/nobel_prizes/physics/laureates/1984/presentation-speech.html, with permission.

The CERN proton−antiproton collider complex consisted of a large SPS, measuring 7 km in circumference, which utilized beams of protons and antiprotons fed to it by a smaller proton synchrotron (PS) and proton and antiproton storage rings. The complex, which straddles the borders of Switzerland and France, is illustrated in Fig. X.20. A complete history of the establishment and operation of the CERN proton−antiproton collider and its application to the discovery of the $W^{\pm}$ and Z^0 particles is provided by Denegri (2004). In brief, a proton beam of 26 GeV is established by the PS, depicted by the synchrotron ring at the lower right of Fig. X.20, to direct against a fixed target which produces low-energy antiprotons of 3.5 GeV at a rate of 1 antiproton ($\overline{p}$) per 10^6 incident protons. The LEAR is the small ring in the lower right of Fig. X.20. The low-energy 3.5 GeV antiprotons are stochastically cooled and accumulated in the antiproton accumulator (labeled AA). The small ring labeled ICE at the very lower right-hand portion of Fig. X.20 was used for the initial cooling experiment where stochastic cooling of the particle beams was tested in 1977 (Carron et al., 1978). Stochastic cooling, described later, is a method used to compress the particles into a narrow and dense beam. Protons and antiprotons of up to 26 GeV from the PS can be transferred along separate transfer tunnels (TTs) to the ISRs illustrated at the lower left of

Fig. X.20. The ISRs consist of two storage rings for 26 GeV protons and antiprotons traveling in opposite directions, and have eight intersecting points which provide areas where experimentation with relatively low-energy proton–antiproton collision can be undertaken. Other TTs, identified as TT 10 and TT 70 in Fig. X.20, are used to transfer the 26 GeV protons and antiprotons, respectively, to the large 8 km SPS. The entire ring of the SPS is not illustrated, because of its large diameter relative to the much smaller PS. The SPS accelerates separate beams of protons and antiprotons traveling in opposite directions to 270 GeV. The proton and antiproton beams are made to collide head on to yield a center of mass energy of 540 GeV, which is sufficient energy to produce the $W^{\pm}$ and Z^0 particles (Rubbia, 1984).

The general idea for the production of the high-energy proton–antiproton beams was first presented by Rubbia, McIntyre, and Cline (1977). The major problem with the idea was how to get sufficient antiprotons, because they can only be produced in small numbers. As mentioned, the collision of 26 GeV protons against a fixed target can produce antiprotons of 3.5 GeV at a rate of 1 antiproton ($\overline{p}$) per 10^6 incident protons. In other words, it takes a beam of 1 million protons to produce 1 antiproton. Because of the low interaction cross-section for the production of a detectable number of $W^{\pm}$ and Z^0 particles, antiprotons have to be produced and accumulated in very intense and dense beams or bunches, with antiproton luminosities in the order of 10^{28}–$10^{29}/cm^2/s$. The accumulation of beams with such large numbers of antiprotons could only be achieved by a method called stochastic cooling, first proposed by van der Meer (1972) and developed through his efforts and leadership.

Stochastic cooling reduces the energy spread and divergence of the charged particles in the synchrotron storage rings so that the particles are concentrated and compressed into a narrow and dense beam. The method involves firstly a detector, known as a particle pick-up, which detects individual charged particles that are diverging away from the center of gravity of the particles in the beam. The detector sends a signal to another device called a kicker, which applies an electric field to push the divergent particle back toward the center of the particle beam. The method is repeated with all particles that deviate from the center of mass of the beam. Because the beam of charged particles circulates a storage ring over 100,000 times a second and stochastic cooling is repeated in every cycle, the particle beam can be compressed into a narrow and dense bunch in minutes. The term "cooling" is used because the method is analogous to the reduction of the random nature of motion of the molecules of a gas when the gas is cooled. Stochastic cooling reduces the tendency of the charged particles to divert away from the very center of the beam. By compressing the beams into narrow, dense bunches of particles, the probability of proton–antiproton collisions is increased, providing larger numbers of $W^{\pm}$ and Z^0 events needed to confirm their production. An illustration of the effect of stochastic cooling on reducing the spread of a particle beam is shown in Fig. X.21. An overview of stochastic cooling is given by Marriner (2004).

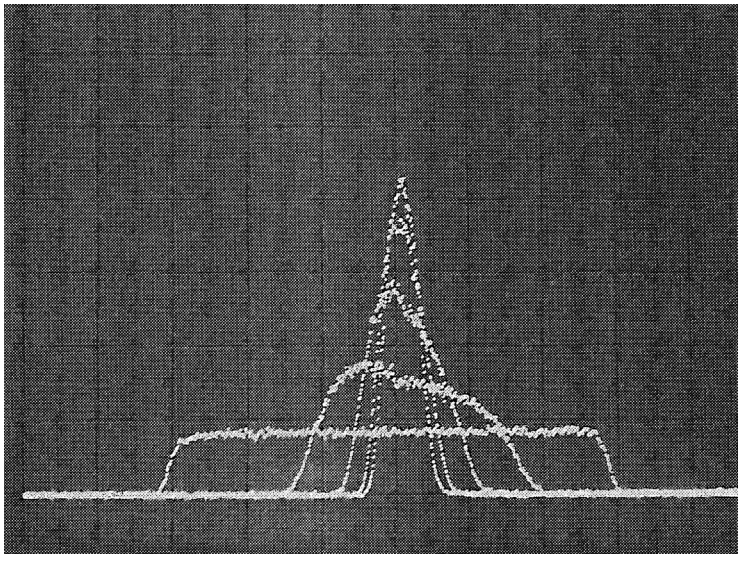

FIGURE X.21 Demonstration of stochastic momentum cooling in the initial cooling experiment (ICE). The momentum distribution of 5×10^7 circulating protons was first spread out; then cooling was turned on. Scans after 1, 2, and 4 min show the concentration of the protons into a narrow momentum bite. The signal height is proportional to the square root of particle density, and the width of the trace is proportional to $\Delta p/p$ where p is the particle momentum. *From Koziol, H., Möhl, D., 2004. The CERN antiproton collider programme: accelerators and accumulation rings. Phys. Reports 403–404, 91–106 reprinted with permission from Elsevier © 2004.*

The development of stochastic cooling was vital to the production of sufficient numbers of $W^{\pm}$ and Z^0 production and decay events to provide irrefutable evidence for their existence. This was underscored be Denegri (2004):

The conversion of the SPS into a $p\overline{p}$ collider of sufficient luminosity was the key ingredient culminating in the discoveries of the W and Z in 1982/83. There is no doubt that C. Rubbia with his understanding of accelerator physics, his enthusiasm and power of conviction played a central role in this phase of the project. It allowed to bring to fruition the idea of "stochastic cooling" (phase-space compactification of the antiproton beam in this case) proposed [by van der Meer 1972] and tested in the mid-1970s by Simon van der Meer, and which was the key to attain the required antiproton intensities.

Two very large particle detectors, identified as UA1 and UA2, were placed along the SPS storage ring at locations where the proton and antiproton beams are made to collide. The detectors were massive, and constructed in a cylindrical shape similar to the detector illustrated in Fig. X.15, shown earlier in this chapter. The UA1 and UA2 detectors measured 5.8 m in length and 2.3 m in diameter. The two detectors were interchangeable, and could be rolled and positioned in place to surround the proton and antiproton particle beams of the SPS according to which detector was preferred. The detector would surround the particle beams precisely where the two beams were made to collide. The numerous particles emitted in all directions following a proton−antiproton collision could be detected by UA1 or UA2, their particle tracks imaged, and the particle energies measured.

The UA1 detector was the largest imaging drift chamber at the time of its construction, and began operation in 1981. Charged particles emitted after a proton−antiproton collision produced ionization in an argon−methane gas mixture within the drift chamber. The electrons produced as a result of the ionization would drift in an electric field created by 170,000 field wires, and the electrons were collected by over 6000 sensing wires. The sensing wires were arranged geometrically to give physicists a three-dimensional image of the particle tracks. An 800-ton electromagnet was used to create a magnetic field sufficient to curve the tracks of the charged particles, which can be identified by the particle momentum and track curvatures. Electromagnetic and hadronic calorimeters were layered outside the electromagnet to measure electron and photon energies and hadron energies, respectively. Muon chambers constituted the outermost part of the detector, to absorb and measure muon energies (see Fig. X.15 for a general picture of a typical detector). The UA2 detector was more limited in scope. It was used to measure precisely the energies of the particles as they passed through its various absorbing materials. As described by CERN and Sauli (2004), the UA2 was used to measure the masses of the W and Z particles more accurately, as it could more accurately measure the jets of hadrons and their energies for particle mass determinations (http://home.web.cern.ch/about/experiments/ua2). Detailed information on the various detectors used with high-energy colliders to capture and measure the energies of the particles and their momentum and mass can be obtained from Fabjan (2003).

Examples of images of particle tracks resulting from $W^{\pm}$ and Z^0 production and decay are shown in Figs. X.22−X.24.

The term "gondola" in the caption of Fig. X.22 refers to one of the many electromagnetic detectors made of lead located around the central detector. The name "gondola" was given to these detectors because of their boat shape. Fig. X.22 illustrates the measurement of the electron energy from the decay of a W particle; however, the neutrino from the same decay is not detected. The neutrino is the only particle that the detector is unable to detect, due to its very low mass and neutral charge, as described in Hall of Fame II. Thus the detection of the W^+ or W^- according to its decay reaction $W^{\pm} \rightarrow e^{\pm} + \nu_e$ must be accomplished by the determination of the energies of all the particles resulting from the $p\overline{p}$ collision and annihilation, and deducing the energy of the electron neutrino by difference from the expected overall energy deposits from a W^+ or W^- decay in the detector. This was described by Carlo Rubbia (1984) in his Nobel lecture, when he stated:

The process we want to observe is

$$p + \overline{p} \rightarrow W^{\pm} + X, \quad W^{\pm} \rightarrow e^{\pm} + \nu_e \qquad [X.18]$$

where X represents the sum of the debris from the interactions of the other protons (spectators). Although the detection of high-energy electrons is relatively straight forward, the observation of neutrino emission is uncommon in colliding-beam experiments. The probability of secondary interactions of the neutrino in any conceivable apparatus is infinitesimal. We must therefore rely on kinematics in order to signal its emission indirectly. This is achieved with an appropriately designed detector [Astbury et al., 1978] which is uniformly sensitive, over the whole solid angle, to all the charged or neutral interacting debris produced by the collision. Since collisions are observed in the center of mass, a significant momentum imbalance may signal the presence of one or more non-interacting particles, presumably neutrinos.

Fig. X.22 is an image of the particle track.

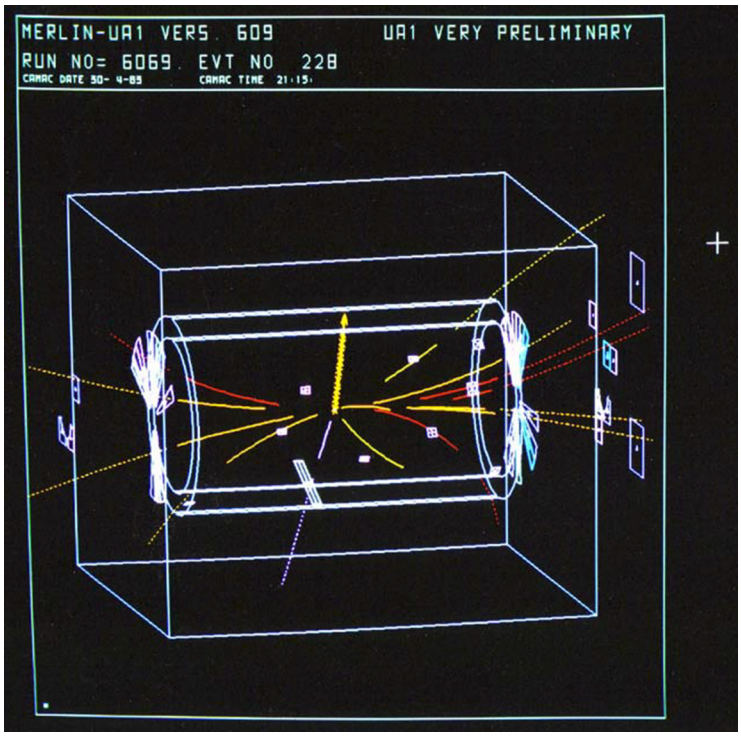

FIGURE X.22 One of the very first W → electron + neutrino events seen in the UA1 detector, as visible on the interactive graphic display (Megatek). Color coding is used for tracks and energy deposits in calorimetric cells. The high-momentum electron track is pointing almost downwards toward a large energy deposit in a "gondola" (oblong white rectangle). The missing transverse energy vector is the thick yellow arrow pointing upwards. *From Denegri, D., 2004. The discovery of the W and Z. Phys. Reports 403–404, 107–145, reprinted with permission from Elsevier © 2004.*

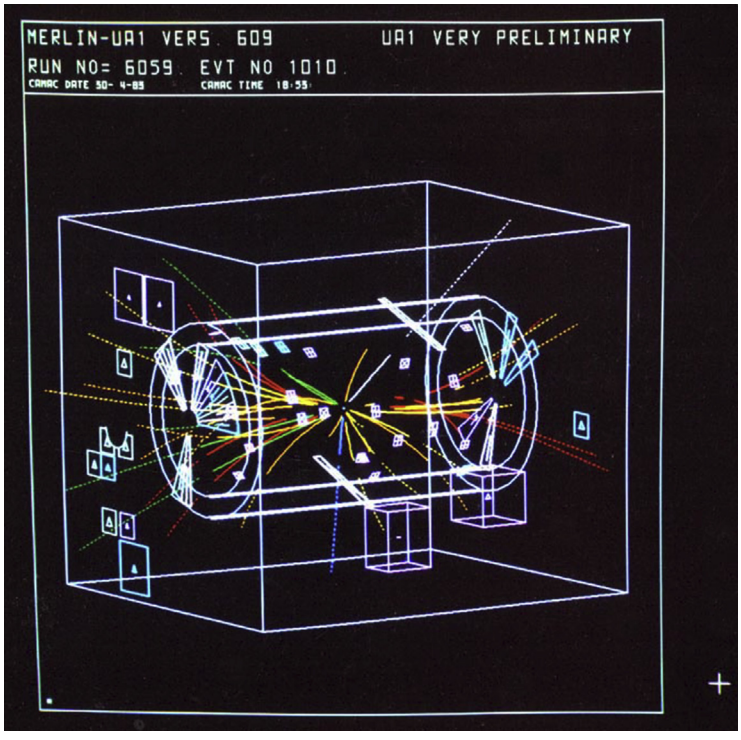

FIGURE X.23 One of the first $Z^0 \rightarrow e^+ + e^-$ events seen in the UA1 detector, as visible on the Megatek. The high-momentum e^+ and e^- tracks are straight, and point to large energy deposits in two "gondolas" in white. Smaller momentum tracks and energy deposits are color coded. *From Denegri, D., 2004. The discovery of the W and Z. Phys. Reports 403–404, 107–145, reprinted with permission from Elsevier © 2004.*

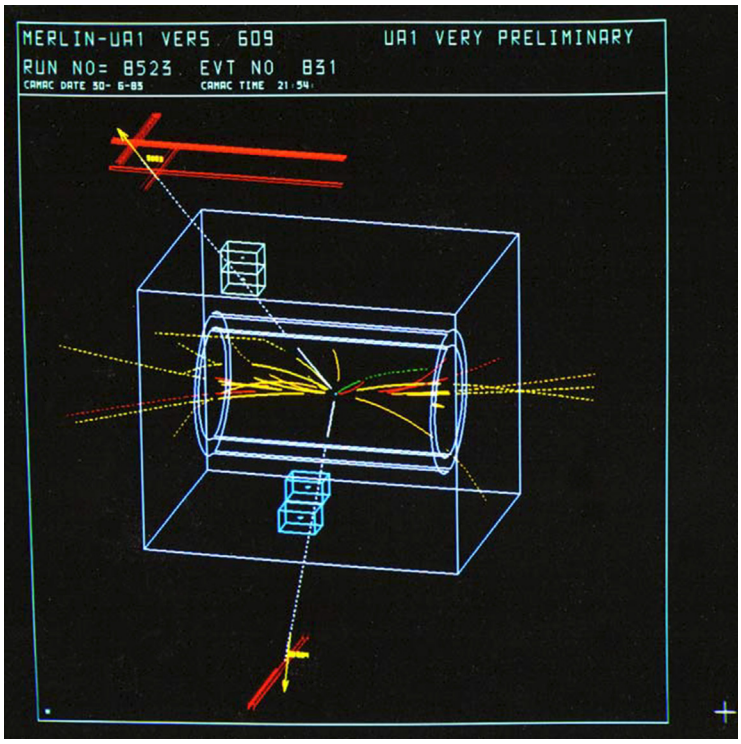

FIGURE X.24 One of the $Z^0 \rightarrow \mu^+ + \mu^-$ events in the UA1 detector. Muon tracks are visible in the tracker (straight hard tracks) and their intercept with muon chambers (yellow arrows in chambers coded in red), as well as their minimum ionizing particle deposits in the hadron calorimeter cells (illustrated as boxes). *From Denegri, D., 2004. The discovery of the W and Z. Phys. Reports 403–404, 107–145, reprinted with permission from Elsevier © 2004.*

YOICHIRO NAMBU (1921–), MAKOTO KOBAYASHI (1944–), AND TOSHIHIDE MASKAWA (1940–)

Yoichiro Nambu (1921–)
Courtesy of the American Institute of Physics, AIP Emilio Segre Visual Archives, Physics Today Collection

Makoto Kobayashi (1944–)
KEK, courtesy of the American Institute of Physics, AIP Emilio Segre Visual Archives, W.F. Meggers Gallery of Nobel Laureates

Toshihide Maskawa (1940–)
Kyoto Sangyo University, courtesy of the American Institute of Physics, AIP EmilioSegreVisual Archives, W.F. Meggers Gallery of Nobel Laureates

Half of the Nobel Prize in Physics in 2008 was awarded to **Yoichiro Nambu** of the Enrico Fermi Institute, University of Chicago, for, in the words of the Nobel Committee, "the discovery of the mechanism of spontaneous broken symmetry in subatomic physics." The other half of the prize was awarded equally to **Makoto Kobayashi** of the High Energy Accelerator Research Organization (KEK), Tsukuba, Japan and **Toshihide Maskawa** of the Yukawa Institute of Theoretical Physics, Kyoto University and Kyoto Sangyo University, Japan "for the discovery of the origin of the broken symmetry which predicts the existence of at least three families of quarks in nature."

The following biographical information was obtained from the autobiographical sketches made by the Nobel Laureates at the time of the Nobel Prize award in 2008 and subsequent updated information available at http://www.nobelprize.org/nobel_prizes/physics/laureates/2008.

Yoichiro Nambu was born in Tokyo, Japan in 1921 and grew up in the provincial city of Fukui. From 1940 to 1942 he studied physics at the Imperial University of Tokyo, graduating with an MS degree. During World War II Nambu was drafted into the army to work on radar research. After the war he returned to the University of Tokyo as a research associate, and was awarded his doctoral degree there in 1952. From 1952 to 1956 Yoichiro Nambu was a professor at the newly created Osaka City University. While still holding a post at Osaka, he became a visiting professor of the Institute for Advanced Study at Princeton and a research associate at the University of Chicago. In 1956 Nambu was appointed to the position of associate professor at Chicago, and promoted to full professor in 1958 and distinguished service professor in 1971. He served as chair of the Department of Physics at the University of Chicago in 1973−1976, and was again promoted to become the Henry Judson distinguished professor in 1976 until his retirement in 1991 as emeritus professor. Nambu became a naturalized citizen of the USA in 1970. He received many awards, including Japan's Order of Culture in 1978, the US National Medal of Science in 1982, the J. J. Sakurai Prize of the American Physical Society in 1994, and Israel's Wolf Prize in Physics in 1994. His share of the Nobel Prize in Physics in 2008 was for his work, begun in 1959, that led to his discovery of the mechanism of spontaneous broken symmetry in subatomic physics.

Makoto Kobayashi was born in Nagoya, Japan in 1944 during World War II. He and his parents were evacuated from the city; and shortly after the war ended in 1945, his father passed away. At only two years of age, Makoto Kobayashi returned to Nagoya with his mother to find their home destroyed by the bombings. They were forced to move into the home of his mother's parents, where the family of his cousin Toshiki Kaifu was also living—Kaifu would grow up to become Japan's prime minister. Makoto Kobayashi obtained his elementary, middle school, and high school education in Nagoya. While a high school student, he read a book entitled *The Evolution of Physics* by Albert Einstein and Leopold Infeld, first published in 1942. This sparked his interest in physics, and he chose physics for his studies at

Nagoya University, where the internationally famous Shoichi Sakata worked in the Faculty of Physics. Sakata (1911−1970) is known for his theoretical work in particle physics, and in particular for the Sakata model, which was an early foundation to the quark model of the structure of matter. Makoto Kobayashi carried out his graduate studies under the supervision of Shoichi Sakata, earning a PhD at Nagoya University in 1972. At Nagoya Makoto Kobayashi met and began to collaborate with Toshihide Maskawa, with whom he would eventually share the Nobel Prize. Upon graduation from Nagoya, Kobayashi joined the Physics Department of Kyoto University, where he again joined forces with Maskawa, who had also moved from Nagoya to Kyoto. This collaboration resulted in their sharing of the Nobel Prize in Physics in 2008 for the discovery of the origin of the broken symmetry, which predicts the existence of at least three families of quarks in nature. In 1979 Kobayashi was appointed assistant professor at the National Laboratory for High Energy Physics (KEK), now known as the High Energy Accelerator Research Organization. In 1982 he was a visiting scientist at CERN at the time the W boson was discovered, described earlier in this chapter. In 1989 Kobayashi was appointed head of KEK's Physics Division II, which participated in the planning and construction of the B factory accelerator. The B factory began operation in 1999, with the purpose of demonstrating CP (charge parity) violation in the B meson system. As described by Makoto Kobayashi (2008) in his Nobel lecture, the B factory is an accelerator capable of producing B mesons in large quantities (up to 1 million B meson pairs per day). Electron−positron colliders, ie, $e^+ + e^- \rightarrow B^+ + B^-$, were built for this purpose. There were two electron−positron colliders built almost simultaneously at B factories, namely the KEKB at KEK in Tsukuba, Ibaraki Prefecture, Japan and the PEPII at SLAC in the USA. These were called the Belle (KEKB) and BaBar (PEPII), and consisted of large international teams. The B factory demonstrated CP violation in the B meson system resulting from quark mixing of the six-quark model (Kobayashi, 2008). In 2003 Makoto Kobayashi was appointed director of KEK's Institute of Particle and Nuclear Studies, and in 2006 he retired from this post to become emeritus professor of KEK. In 2007 he was appointed executive director of the Japan Society for the Promotion of Science. Makoto Kobayashi has received many awards, including the Nishina Memorial Prize in 1979, the J.J. Sakurai Prize in 1985 awarded by the American Physical Society, the High Energy Particle Physics Prize in 2007 awarded by the European Physical Society, and the Order of Culture in 2008 from the government of Japan.

Toshihide Maskawa was born in Nagoya, Japan in 1940. He was not an outstanding student in high school; but after graduating from Nagoya City Kouyou High School in 1958 and a hard year of study, he entered Nagoya University to pursue a career in the field of theoretical physics. Like his future collaborator Makoto Kobayashi, with whom he would eventually share in the Nobel Prize, Toshihide Maskawa studied under the famous theoretical physicist and teacher Shoichi Sakata. He graduated with a PhD in physics from Nagoya in 1967. He then joined Kyoto University as a research associate in 1967, where he began a collaboration with Makoto Kobayashi that led to their sharing the Nobel Prize in Physics in 2008, described later. In 1976 Maskawa was promoted to the rank of professor at Yukawa Institute of Theoretical Physics, Kyoto University; and in 1990 he became a councilor of Kyoto University. Toshihide Maskawa returned to his position of professor at the Yukawa Institute of Theoretical Physics from 1995 until his retirement as professor emeritus at Kyoto University in 1997. He then became distinguished professor at Nagoya University in 2003, and in 2009 was appointed to the position of director at Kobayashi-Maskawa Institute for the Origin of Particles and the Universe at Nagoya University. He has received numerous awards jointly with Makoto Kobayashi in addition to the Nobel Prize; among these are the J.J. Sakurai Prize in 1985, the Asahi Prize in 1994, and Japan's Order of Culture.

The contributions made by the Nobel Laureates in Physics 2008 were introduced to the audience at the award ceremony by Professor Lars Brink, member of the Royal Swedish Academy of Sciences and of the Nobel Committee for Physics, on December 10, 2008 when he stated the following:

> *The Earth is round. This simple sentence contains so much. It shows how we human beings see the objects around us in symmetric shapes… The sentence also shows the importance of symmetries in determining the laws of physics. These laws do not allow the Earth to be flat or square. They have a built-in symmetry. But the Earth is not exactly round. Its radius at the equator is slightly bigger than at its poles. There are mountains and valleys. So physicists would say that symmetry is "weakly broken."*

In our daily lives we encounter symmetries and how these symmetries can be spontaneously broken. For example, Fig. X.25 illustrates a top spinning in the center of a circle. If we stand at any position on the circle and observe the spinning top, it will appear the same regardless of the position from which we make the observation. However, when the spinning top comes to rest or reaches its "ground state" it falls into a position where its symmetry is spontaneously broken. The top resting in the circle will appear different to an observer from any location on the circle.

Professor Lars Brink, in the Nobel award ceremony speech, underscored the importance of Yoichiro Nambu's discovery of the mechanism of spontaneous broken symmetries in subatomic particle physics and radioactivity decay; and the consequences

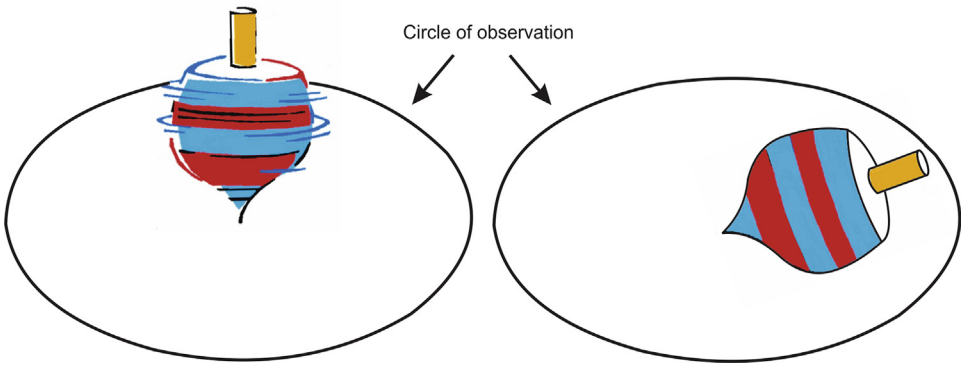

FIGURE X.25 Symmetry breaking in everyday life. On the left is a spinning top at the very center of a circle. If we stand on the line defining the circle at any location of the 360 degree surrounding the spinning top, we will observe no change in the shape of the top: the spinning top will be symmetrical in all respects. On the right is the same top after it lost its kinetic energy and fell to a stable ground state. Now if we observe the fallen top from any location around the circle, we see that the top is different in shape at each location from which we make the observation. The symmetry of the spinning top was spontaneously broken.

of the findings of Makato Kobayashi and Toshihide Maskawa in their mathematical explanation of the origin of broken symmetry, which led to the prediction of six quarks in nature and the predominance of matter over antimatter in our universe:

> *The decisive idea came from Yoichiro Nambu, who in 1960 showed that the fundamental laws of nature can exhibit spontaneous broken symmetries… There can be strong restrictions from large symmetries that are not seen directly in physical experiments, at least at the energies that can be produced in today's large particle accelerators. The symmetries are there as a consequence of the fundamental laws of physics, but for a system in its ground state there are no direct signs of the restrictions that symmetry should impose… Mirror symmetry is important for fundamental laws, too. It caused a major sensation when Lee and Yang [Tsung-Dao Lee and Chen-Ning Yang, described in Hall of Fame, Part IX] pointed out in 1956 that this is not necessarily true in radioactive decays [symmetry breaking in the weak interaction], a fact that was very quickly confirmed [see the experiment of Chien-Shiung Wu in Hall of Fame, Part IX]. Nevertheless, it was thought that mirror symmetry [i.e., parity symmetry or P symmetry] would indeed apply to all particle reactions if it were combined with the operation of changing a particle to its antiparticle [charge conjugation symmetry or C symmetry]. However, in 1964 Cronin and Fitch [James W. Cronin and Val L. Fitch] discovered, very surprisingly, that this combined symmetry [CP symmetry] could also be very weakly broken in certain special processes. During the late 1960 and 1970s the Standard Model that is now used to describe elementary particle physics was developed, partly based on Nambu's ideas. However, it could not explain this weak symmetry breaking, so the question arose of how one could extend the model without destroying the results that had so successfully been compared to experiments. In 1972 Makoto Kobayashi and Toshihide Maskawa examined the possibility of introducing more fundamental particles – quarks – and found that if there are six different quarks, the theory can indeed break the symmetry. It was a daring assumption, since at that time the everyday world seemingly needed only two different kinds of quarks [an up quark and a down quark, the two constituent quarks of the proton and neutron], whereas three had already been discovered [the up (u), down (d) and strange (s) quarks]. Kobayashi and Maskawa suggested that there should be three more [charm (c), bottom (b), and top (t) quarks]. These were eventually discovered, the last one in 1994. During the past decade, elementary particle physicists have measured Kobayashi and Maskawa's theory with great precision and found that it really does fit the data. Nature is endowed with six different quarks, at least at the energies that have so far been accessible. This also leads to an imbalance [broken symmetry] between matter and antimatter, a fact that Andrei Sacharov pointed out early on. Thanks to this imbalance, we are here today. Symmetry breaking allows for a world of matter.*
>
> From "The Nobel Prize in Physics 2008—Presentation Speech," Nobelprize.org, Nobel Media AB 2014. www.nobelprize.org/nobel_prizes/physics/laureates/2008/presentation-speech.html, with permission).

This speech by Brink refers to two types of symmetry, namely mirror symmetry or parity (abbreviated P), which refers to a mirror image of a physical system, and charge conjugation symmetry (abbreviated C), which refers to the changing of the sign (ie, electric charge and quantum numbers of particles, such as the changing of a particle into its antiparticle).

The first indication of the possibility of symmetry breaking in nuclear physics was the result of scientific evidence studied by Tsung-Dao Lee and Chen-Ning Yang (Lee and Yang, 1956), which confirmed that parity was conserved in many physical processes involving the strong and electromagnetic interactions; but that there was no evidence to the conservation of parity in the weak interactions, such as beta decay. Thus Lee and Yang (1956) postulated that some beta

decay processes, such as the beta particle emission from cobalt-60, should be investigated for the possibility of violation of parity in the weak interactions. In light of this, the following year Chien-Shiung Wu and coworkers (Wu et al., 1957) demonstrated violation of parity in the emissions of beta particles from cobalt-60 nuclei: the breaking of mirror symmetry in the beta decay of cobalt-60, as discussed in detail in Hall of Fame, Part IX. Thus in the weak interactions mirror symmetry or parity can be broken.

It had always been thought that matter and antimatter obeyed equally the same laws of physics (charge conjugation or C symmetry), although there was always a predominance of matter over antimatter. After the demonstration of the breaking of mirror symmetry, ie, parity violation, in beta decay by Wu et al. (1957), it was thought by physicists that the two symmetries, charge and mirror symmetry, referred to as CP symmetry, could not be broken simultaneously. However, in 1964 James Cronin, Val Fitch, and coworkers at the Brookhaven National Laboratory (see Christenson et al., 1964) demonstrated that the neutral kaon particle, albeit a small fraction of the kaon particle, can undergo decay which violates both mirror and charge symmetry. In other words, they display CP asymmetry. James Cronin and Val Fitch received the Nobel Prize in Physics in 1980 for this discovery.

The demonstration of CP asymmetry by Cronin and Fitch involved the decay of the neutral kaon, which has two different decay modes and two very different lifetimes, one being much shorter than the other. The neutral kaon with a short lifetime ($\tau = 8.9 \times 10^{-11}$ s) is denoted as K_S^0, and the neutral kaon with the longer lifetime ($\tau = 5.1 \times 10^{-8}$ s) is designated K_L^0. The short- and longer-lived neutral kaons have different modes of decay, which are the following:

$$K_S^0 \rightarrow \pi^0 + \pi^0 \left(\tau = 8.9 \times 10^{-11}\ \text{s}\right)$$
$$K_L^0 \rightarrow \pi^0 + \pi^0 + \pi^0 \left(\tau = 5.1 \times 10^{-8}\ \text{s}\right) \qquad [X.19]$$

Cronin, Fitch, and coworkers produced kaons at the Alternating Gradient Synchrotron at the Brookhaven National Laboratory in New York. After traveling several meters, the short-lived neutral kaons decayed completely to nonexistence, leaving behind the long-lived neutral kaons. The kaon particle is a meson consisting of equal amounts of matter and antimatter, namely a quark and an antiquark. Cronin, Fitch, and coworkers observed that a small number (approximately two in every 1000 decays) of the longer-lived kaons did not decay into three neutral pions; but rather into two neutral pions. This provided evidence of an imbalance of matter and antimatter, and a violation of CP symmetry. The imbalance between matter and antimatter, or broken CP symmetry, was the first evidence of why matter prevailed over antimatter during the creation of the universe at the time of the Big Bang. After the Big Bang (see the chapter: "Cosmic Radiation"), possibly fractions of a second afterward, there were likely equal amounts of matter and antimatter; however, CP asymmetry could have favored matter over antimatter, so the world we now live in is created of matter. There is only a very small amount of antimatter in our universe. If there remained equal proportions of matter and antimatter after the Big Bang, we would not exist, because matter and antimatter annihilate each other whenever they come into contact. Matter prevailed over antimatter. This was underscored by the Nobel Committee press release after the announcement of the award of the Nobel Prize in Physics 2008 to Yoichiro Nambu, Makoto Kobayashi, and Toshihide Maskawa:

> *A hitherto unexplained broken symmetry of the same kind lies behind the very origin of the cosmos in the Big Bang some 14 billion years ago. If equal amounts of matter and antimatter were created, they ought to have annihilated each other. But this did not happen, there was a tiny deviation of one extra particle of matter for every 10 billion antimatter particles. It is this broken symmetry that seems to have caused our cosmos to survive. The question of how this exactly happened still remains unanswered.*

In 1960 Yoichiro Nambu introduced the concept of spontaneous broken symmetry into particle physics for the first time (Nambu, 1960a,b; Nambu and Jona-Lasinio, 1960a,b). Nambu had expertise in the principles and theoretical calculations of spontaneous broken symmetry in superconductivity; and in the above papers he and Giovanni Jona-Lasinio translated these principles into a model for elementary particles. He explained that the symmetry of a physical system can be broken simultaneously when it falls to a lower energy state. Just like the spinning top observed from a circle (Fig. X.25) eventually falls to a lower energy state, resulting in a spontaneous broken symmetry, Nambu (2008) in his Nobel lecture (presented by Giovanni Jona-Lasinio of the Sapienza University of Rome on December 8, 2008) described a similar analogy of an elastic rod:

> *Spontaneous symmetry breaking (SSB), which is the main subject of my talk, is a phenomenon where a symmetry in the basic laws of physics appears to be broken. In fact, it is a very familiar one in our daily life, although the name SSB is not [The name is due to Baker and Glashow (1962).]. For example, consider an elastic straight rod standing vertically. It has a rotational symmetry; it looks the same from any horizontal direction. But if one applies increasing pressure to squeeze it, it will bend in some direction, and the symmetry is lost. The bending can occur in principle in any direction since all directions are equivalent. But you do not see it unless you repeat the experiment many times. This is SSB.*

As eloquently described by the Royal Swedish Academy of Sciences ("The Nobel Prize in Physics 2008—Illustrated Presentation," Nobelprize.org, Nobel Media AB 2014. www.nobelprize.org/nobel_prizes/physics/laureates/2008/illpres.html), Yoichiro Nambu explained the low mass of the pi meson compared to the proton and neutron. As described in the chapter entitled "The Atomic Nucleus," the pi meson mediates the strong interaction binding the protons and neutrons together in the atomic nucleus. Its mass (139.6 MeV/c^2) is only a small fraction ($\sim$15%) of the masses of the proton (938.3 MeV/c^2) or neutron (939.5 MeV/c^2). Currently it is understood that the original symmetry that was present at the Big Bang was spontaneously broken symmetry; and the destruction of this symmetry only a fraction of a second after the Big Bang creation of the universe resulted in the assignment of varying masses to particles.

After Nambu and Jona-Lasinio introduced broken symmetry into particle physics, Makoto Kobayashi and Toshihide Maskawa mathematically studied the origin of this broken symmetry, which led to their prediction that there should be a total of six quarks. Only three quarks were known to exist at that time, namely the up, down, and strange quarks. The remaining three quarks were eventually discovered, confirming their prediction. These six quarks together with six leptons now form the basis for what is called the Standard Model of elementary particles.

In his Nobel lecture, Maskawa (2008) described how he and Kobayashi came up with the mathematical matrix that predicted a total of six quarks. They first tried to solve the gauge theory mathematics with a four-quark model—that is, one additional quark over the three known quarks. When the CP violation could not be explained with four quarks, they found a solution with the use of six quarks. This led to their prediction (Kobayashi and Maskawa, 1973) that there existed six quarks. An excerpt of his Nobel lecture is the following:

> *We started to study CP violation based on the quartet quark model in the electro-weak unified gauge theory… attempting to explain how CP violation could be understood as a four-quark model. We fought a tough struggle for a month or so. And one day, while taking a bath, I thought: No good model exists which can explain CP violation in the four-quark model if we stick to the renormalizable theory of weak interaction. So I made up my mind to write a negative paper, which proved that CP violation cannot be explained in the four-quark model in a framework of renormalizable electro-weak theory. Deciding to finish this work by writing a poor paper and thinking up an excuse, I got out of the bath tub. Probably this may have freed me from sticking to the four-quark model. Suddenly, I recognized that it must work well in the six-quark model. It was already clear from our many trials and calculations up until then that a complex phase could remain there. In the framework of unified electro-weak gauge theory, there is a scalar field called the Higgs field. When it develops a non-vanishing vacuum expectation value, the quark fields acquire their masses. If we rewrite the quark fields into those, which have definite masses, then the charged current operators in the weak interaction develop a unitary matrix* U. *If a complex phase appears in the matrix elements of* U, *CP violation occurs… It, however, took a long time: more than 30 years and vast efforts of many experimenters to really verify this theory.*

Makoto Kobayashi also explained in his Nobel lecture (Kobayashi, 2008) how he and Maskawa (Kobayashi and Maskawa, 1973) arrived at the conclusion that there should be six quarks in nature, which would mean three unknown quarks in addition to the three known quarks:

> *We found that even if we relax the conditions… we cannot make any realistic model of CP violation with four quarks. This implies that there must be some unknown particles besides the fourth quark. I thought that this was quite strong and an important conclusion of our argument.*
>
> *Then we considered a few possible mechanisms of CP violation by introducing new particles. We proposed the six-quark model as one such possible mechanism… We thought that this mechanism of CP violation is very interesting and elegant, but we had no further reason to single out the six-quark model from the other possibilities. The model was not so special, because if the system has sufficiently many particles, it is not difficult to violate CP symmetry. However, the subsequent experimental development pushed up the six-quark model to a special position.*
>
> *In 1974, the J/ψ particle was discovered [Aubert et al., 1974; Augustin et al., 1974], and soon it turned out that it is the bound state of the fourth quark c and its anti-particle…*
>
> *In 1975, the τ-lepton was discovered [Perl et al., 1975]. This discovery had a significant effect on our model. The τ-lepton is the fifth member of leptons. Although it is a lepton, it suggested the existence of a third family in the quark sector, too. That was when people began to pay attention to our model…*
>
> *In 1977, the Upsilon particle was discovered [Herb et al., 1977], and it turned out that it is a bound state of the fifth quark b and anti-b. The discovery of the last quark, t, occurred as recently as in 1995 [Abe et al., 1995; Abachi et al., 1995], but before that time the six-quark model became a standard one.*

Once the three quarks predicted by Kobayashi and Maskawa were finally discovered, which confirmed a total of six quarks to be among the fundamental particles that make up matter, the Standard Model of particle physics was confirmed. The Standard Model explains the fundamental or elementary particles (ie, particles that are not broken down further into

other particles, or at least not known to be made of any other particles), and how these fundamental particles interact according to three of the four fundamental forces (also referred to as fundamental interactions) in nature. The confirmation of the Standard Model was emphasized by Makoto Kobayashi (2008) in his Nobel lecture, when he illustrated the model (see Fig. X.26) and stated:

> *We know that ordinary matter is made of atoms. An atom consists of the atomic nucleus and electrons. The atomic nucleus is made of a number of protons and neutrons. A proton and a neutron are further made of two kinds of quarks, u and d. Therefore the fundamental building blocks of ordinary matter are the electron and two kinds of quarks, u and d.*
>
> *The standard model, which gives a comprehensive description of current understanding of the elementary particle phenomena, however, tells us that the number of species of quarks is six. The additional quarks are called s, c, b and t. The reason why we do not find them in ordinary matter is that they are unstable in the usual environment. Similarly, the electron belongs to a family of six members called leptons. Three types of neutrinos are included among these six.*
>
> *Another important ingredient of the standard model is fundamental interactions. Three kinds of interactions act on the quarks and leptons. The strong interaction is described by Quantum Chromodynamics (QCD) and the electro-magnetic and weak interactions by the Weinberg-Salam-Glashow theory in a unified manner.*

The Standard Model of particle physics, illustrated in Fig. X.26, consists of 12 fundmental particles which are the basic building blocks of matter. These particles are considered elementary (ie, they cannot be broken down to smaller particles, or are not known to contain smaller constituents). All matter is made up of these particles, six quarks and six leptons. The six quarks are illustrated in Fig. X.26 as a superposition of three particles colored red, green, and blue. The three colors represent a property of quarks known as color charge, which constantly changes when the quarks interact by the strong force known as QCD. The fundamental particles are organized into three columns, from left to right, which are referred to as three generations. The first generation consists of the up (u) and down (d) quarks and the electron (e) and electron neutrino (ν_e); the second generations contains the charm (c) and strange (s) quarks and the muon (μ) and muon neutrino (ν_μ); and the third generation comprises the top (t) and bottom (b) quarks and the tau (τ) lepton and tau neutrino (ν_τ). The first generation of elementary particles are all stable, and constitute the building blocks of ordinary matter of our world and that of the universe, including the matter that makes up our body, food, and the things we may see and feel in our day-to-day lives. The fundamental particles of the second and third generations are higher in mass than their previous generation. The particles of the second generation are higher in mass than the first; and those of the third generation are higher in mass than the second. The second and third generations of charged particles are building blocks of particles that are very unstable, encountered or produced in high-energy accelerator environments or cosmic ray collisions in the atmosphere, and they decay to particles of the first generation.

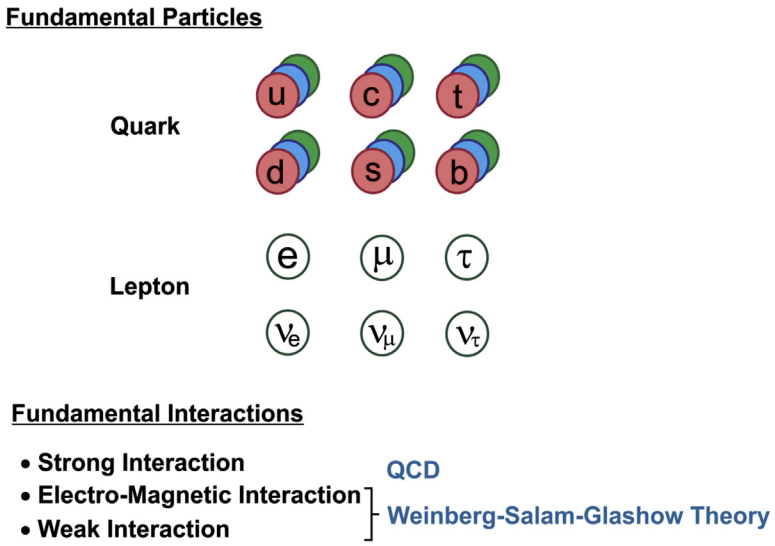

FIGURE X.26 The Standard Model. *From Kobayashi, M., 2008. CP Violation and Flavor Mixing. Nobel Lecture, December 8, 2008, Nobelprize.org. Nobel Media AB 2014. http://www.nobelprize.org/nobel_prizes/physics/laureates/2008/kobayashi-lecture.html, printed with permission from the Nobel Foundation © 2008.*

Illustrated in Fig. X.26 are three fundamental interactions or forces that act upon the fundamental particles to govern how they interact with each other and the relative strengths of their interaction. The form of their interaction and the strength of the interaction will govern the structure of matter. For example, the strong interaction is the force that holds the up and down quarks together to form the proton and neutron, and it holds the protons and neutrons together in the atomic nucleus. Not included, but implied, in Fig. X.26 presented by Makato Kobayashi in his Nobel lecture are the gauge bosons, which are the particles that act as the carriers of the fundamental forces or interactions between the fundamental particles. These bosons are the gluon (g), the photon (γ), and the W^+, W^-, and Z^0 particles, which are included in the illustration of the Standard Model in Fig. X.27. The carriers of the strong force are the gluons. The exchange of gluons between the quarks constitutes the strong interaction, which is defined by QCD, described previously. It is the strongest interaction or force in nature. The electromagnetic interaction is weaker in strength; and the carrier of this force is the photon (γ), which carries the force of attraction or repulsion between charged particles. It is the force that maintains the orbital electrons of an atom further away from the nucleus, which is at the very center of the atom. The weak interaction is yet weaker than the electromagnetic interaction. The W^+ and W^- bosons are the carriers of the weak force in radioactive beta decay; and the Z^0 particle is the carrier of neutral-current weak interactions, such as the neutrino–electron scattering described previously in this chapter.

Not included in Figs. X.26 or X.27 is a fourth interaction or force known as gravity, which is the weakest of all forces. It is not included in the Standard Model because gravity is a force that acts on macroscopic particles or particles of large mass, such as the planets and the physical entities that surround the planets. The Standard Model only defines the fundamental subatomic particles that are the building blocks of matter. Gravity, which would involve the graviton (not yet discovered) as the boson or carrier of gravitational force, cannot yet be included in the Standard Model. This is why the

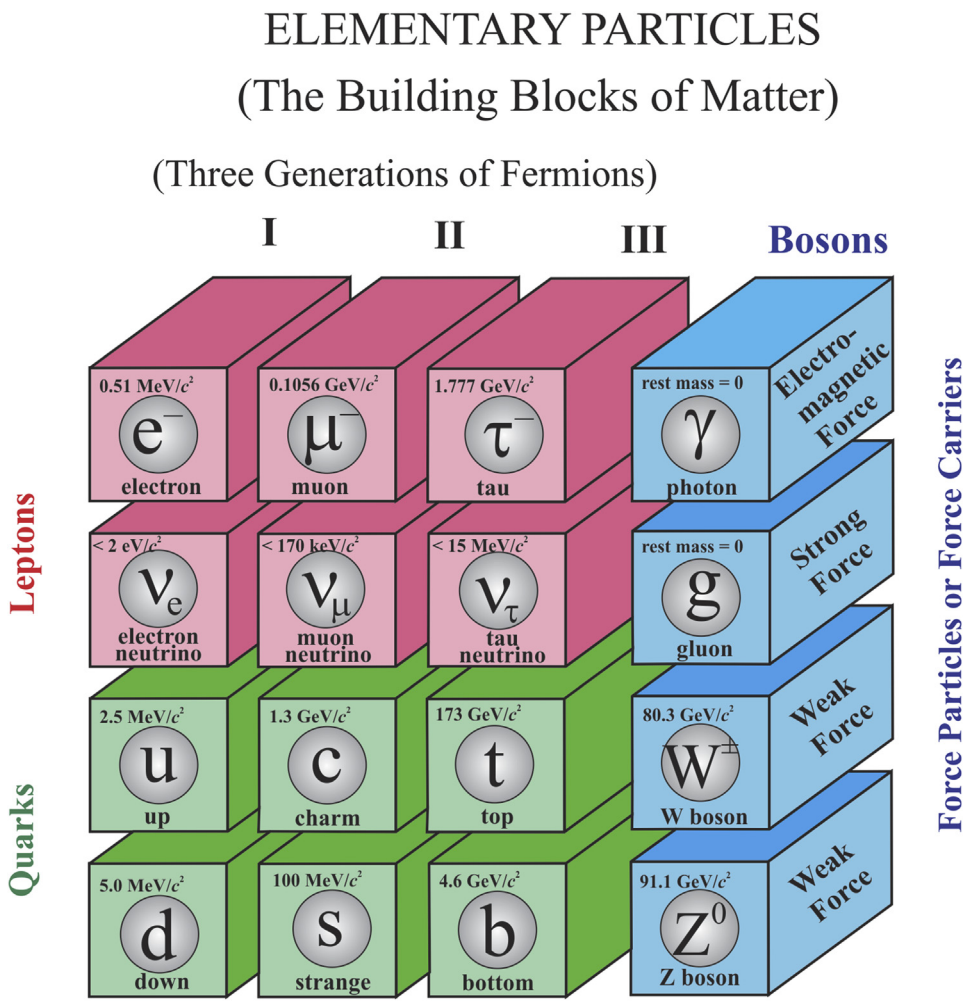

FIGURE X.27 The Standard Model of elementary particles (ie, building blocks of matter) up to the year 2012, prior to the discovery of the Higgs boson.

model is called "the theory of almost everything." When physicists are able to include the fourth force in nature, namely gravity, in the Standard Model, it may then possibly be called "the theory of everything."

FRANÇOIS ENGLERT (1932–) AND PETER W. HIGGS (1929–)

François Englert of the Université Libre de Bruxelles, Brussels, Belgium and Peter W. Higgs of the University of Edinburgh, Edinburgh, Scotland were awarded the Nobel Prize in Physics in 2013, in the words of the Nobel Committee, "for the theoretical discovery of a mechanism that contributes to our understanding of the origin of mass of subatomic particles, and which recently was confirmed through the discovery of the predicted fundamental particle [ie, the Higgs boson] by the ATLAS and CMS experiments at CERN's Large Hadron Collider."

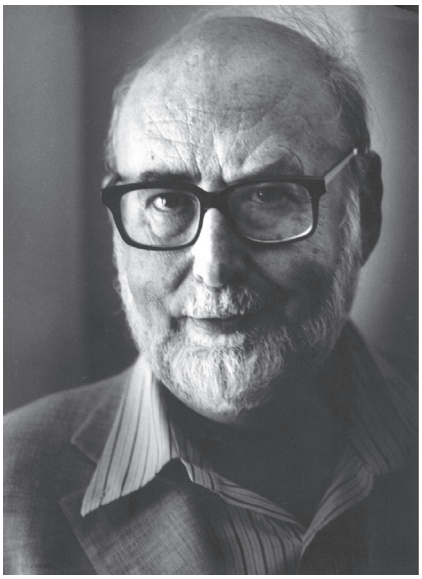

François Englert (1932–)
Portrait of François Englert, Wolf Foundation Prize in Physics, courtesy of the American Institute of Physics, AIP Emilio Segre Visual Archives

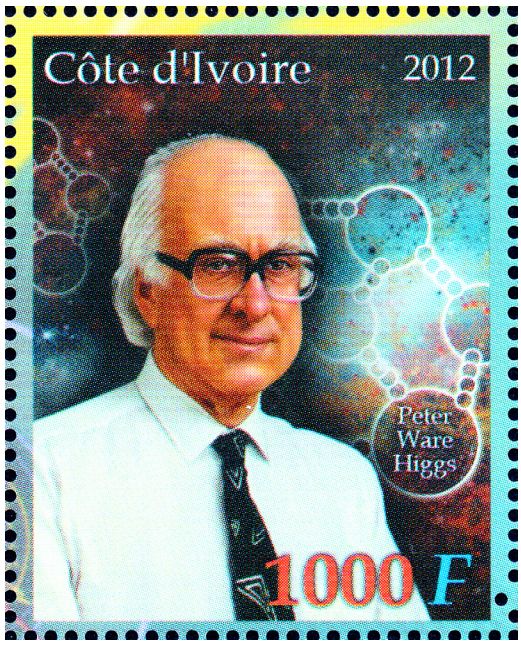

Peter W. Higgs (1929–)

Autobiographical sketches by François Englert and Peter Higgs were supplied to the Nobel Committee at the time of the award of the Nobel Prize in Physics in 2013, from which the following information was obtained (www.nobelprize.org/nobel_prizes/physics/laureates/2013/).

François Englert was born in Belgium in 1932. His parents and brother, a family of Polish Jews, emigrated to Belgium from Poland in 1924, looking for a better life and needing to escape from the antisemitic environment in Poland at the time. Less than a year after the German invasion of Poland, Nazi Germany invaded Belgium. François Englert was only seven years of age at the time; but old enough to be well aware of the situation. Two years after the invasion, all Jews was forced by the Nazis to wear the Star of David to identify their Jewish ethnicity; and only months thereafter the Nazis began to deport Jews to the concentration and extermination camps. Fortunately François Englert, his parents, and his brother survived, thanks to Belgians who took great risks and showed much generosity in hiding them from the Nazis. He, his brother, and his parents were separated and hidden in locations unknown to each other to facilitate secrecy. François Englert was looked after at first by Camille and Louise Jourdan, the owners of a cafe-restaurant in Lustin, a village in the Ardennes. As related by Englert, his protectors had a daughter, Yvonne, who taught him music and piano, which offered him a glimmer of hope in a time of despair and desperation. Englert eventually had to flee Lustin after a denunciation. However, he was fortunate again to be protected by a priest, Warnon of Annevoie, in a small town in the Ardennes, where he was reunited with his family. The priest presented the Englert family to the villagers as Christians, and they remained protected until the end of the war. François Englert was baptized and attended a Catholic college, Notre-Dame de Bellevue, in Dinant, Namur; and his brother was enrolled in a seminary school, dressed in soutane to

disguise him as a student for the priesthood. François Englert maintains a loving memory of his parents, who always put the lives of their children above their own preservation, and had the astuteness to make the right moves at the right times to achieve their escape from Nazi persecution. Englert related, however, that all his family who remained in Poland were murdered by the Nazis. After the war François Englert completed high school in Belgium, and developed an interest in mathematics. In 1955 he completed his undergraduate degree in electromechanical engineering at the Free University of Brussels (Université Libre de Bruxelles—ULB). Englert continued his studies at the university with an assistantship to finance his living, and was awarded a master's degree in physics in 1958 and his PhD in 1959. After receiving his doctorate, Englert was offered a two-year position at Cornell University, Ithaca, New York as a research associate under a young Professor Robert Brout. Together, Englert and Brout created a lifelong friendship and a long-lasting collaboration. When François Englert was scheduled to leave Cornell University in 1961 and return to his home country and university, he was offered a position as professor at Cornell. Englert preferred to return to Belgium. In turn, Robert Brout received a Guggenheim fellowship to ULB; and after a few months there, he decided to settle in Brussels with his family with a position at ULB. Robert Brout acquired Belgian nationality, and jointly directed with François Englert the theoretical physics group at ULB. Their collaboration resulted in their historic paper (Englert and Brout, 1964) that led to the Nobel Prize in Physics in 2013 for François Englert and Peter W. Higgs for the Brout-Englert-Higgs (BEH) mechanism, described later. Brout was not included in the Nobel Prize because he died in Brussels on May 3, 2011, and the award is not granted posthumously. In his autobiographical sketch provided at the time of the Nobel Prize award in 2013 (www.nobelprize.org/nobel_prizes/physics/laureates/2013/englert-bio.html), François Englert highlighted the work accomplished in collaboration with Robert Brout:

> *In Brussels, we resumed our analysis on spontaneous symmetry breaking, both in the statistical theory of phase transition and, inspired mainly by Nambu's work, in field theory. This is how we discovered the mass generating mechanism that may now indeed be viewed as a phase transition from a high temperature phase in the early Universe, where elementary particles were massless, to the present low temperature phase where their mass arises from a generalisation of spontaneous symmetry breaking to Yang-Mills fields, namely the BEH mechanism.*

Englert was awarded the Wolf Foundation Prize in Physics 2004 for pioneering work that led to the insight of mass generation whenever a local gauge symmetry is realized asymmetrically in the world of subatomic particles. He is emeritus professor at ULB and professor of the Faculty of Exact Sciences, Sackler School of Physics and Astronomy at Tel Aviv University, Israel.

Peter W. Higgs was born in 1929 in the Elswick district of Newcastle-upon-Tyne, UK. He received his BSc degree in physics in 1950 with first-class honors, an MSc degree a year later, and a PhD in 1954 at King's College, University of London. He then moved in 1954 to the University of Edinburgh, Scotland, UK, where he remained for two years. In 1956 Higgs returned to London under an ICI research fellowship for a year at University College and a little more than a year at Imperial College. He then returned to University College to occupy a post as temporary lecturer in mathematics. In 1960 Peter Higgs was awarded a lectureship in mathematical physics at the Tait Institute, School of Physics and Astronomy, University of Edinburgh. At the University of Edinburgh, Higgs was promoted to reader in 1970. He was made a fellow of the Royal Society of Edinburgh in 1974, the Peter Higgs Chair of Theoretical Physics in 1980, fellow of the Royal Society in 1983, and fellow of the Institute of Physics in 1991. He retired from the University of Edinburgh as professor emeritus in 1996. The awards and honorary degrees bestowed on Peter Higgs are too numerous to include here, but the reader may review them on the www.nobelprize.org website.

At the time of the Nobel lecture of Makoto Kobayashi in 2008, an intense search for the Higgs boson was well under way, and would change the Standard Model of particle physics which Kobayashi presented in his Nobel lecture (Fig. X.26). It all started in 1964, when three groups of physicists published three papers in the journal *Physical Review Letters* providing the foundations of a theory on how the mass of particles could arise by a mechanism of spontaneous symmetry breaking, now referred to as the Higgs mechanism. The mechanism would require a field that would permeate throughout the universe, and the existence of a boson. The three groups consisted of Robert Brout and François Englert of ULB (Englert and Brout, 1964), Peter Higgs of the University of Edinburgh (Higgs, 1964), and Gerald Guralnik and Tom Kibble of Imperial College, London, together with Carl Richard Hagen, who was at Imperial College on leave from the University of Rochester, New York (Guralnik et al., 1964). Peter Higgs subsequently wrote a paper (Higgs, 1966) which described the boson as massive, stating that its transverse states were the quanta of the gauge field. The boson eventually became known as the Higgs boson; and the field that is constant throughout space is now called the Higgs field. For their theoretical papers, which would initiate the largest research project the world has known in the search for the Higgs boson, the six theoretical physicists were honored with the J. J. Sakurai Prize in 2010 by the American Physical Society. It was

then known that the discovery of the Higgs boson would eventually bring a Nobel Prize; but that no more than three persons could share a Nobel award.

Some of the best explanations of the Higgs mechanism and the discovery of the Higgs boson are provided by the Nobel Foundation in both advanced and general formats, and were published at the time of the award of the Nobel Prize in Physics in 2013 ("The Nobel Prize in Physics 2013—Popular Information," Nobelprize.org. Nobel Media AB 2014. http://www.nobelprize.org/nobel_prizes/physics/laureates/2013/popular.html). Only a very brief narrative is provided here.

The Higgs mechanism is based on the existence of a constant invisible field that exists throughout the universe, known as the Higgs field. The Higgs particle is a quantum vibration of the Higgs field. The Standard Model, which describes the elementary particles and the forces by which they interact, is based on an established symmetry (described previously), such as mirror symmetry or parity. The photon that mediates the electromagnetic force is massless, and the massless photon obeyed symmetry in all respects; however, the massive $W^{\pm}$ and Z^0 bosons mediating the weak forces encountered in radioactive beta decay violated symmetry, as described previously. However, Englert and Brout (1964), Guralnik et al. (1964), and Higgs (1964) came to the rescue of the Standard Model with the establishment of a mechanism by which particles can acquire mass and yet break the intrinsic symmetry of nature. Particles would acquire mass only to the degree to which they interact with the Higgs field that permeates throughout space. Thus a particle that interacts strongly with the Higgs field would acquire a high mass (eg, $W^{\pm}$ boson, mass $= 80.3\ \text{GeV}/c^2$), a light particle (eg, electron, mass $= 0.51\ \text{MeV}/c^2$) would interact weakly with the field, and a particle with zero mass (eg, photon) would not interact with the Higgs field.

The Higgs mechanism is explained on the basis of the mathematical equations of the Standard Model that involve the three interactions among the elementary particles, namely the strong, electromagnetic, and weak interactions. These equations require symmetry, such as mirror symmetry. At the instant of the Big Bang creation of the universe, the temperature and consequently the energy state were at their highest, when all particles were massless and only symmetry abounded. However, about one billionth of a second (10^{-11} s) after the Big Bang, the energy state dropped to a lower level and symmetry was broken. The Higgs mechanism affords a means for the symmetry and its breaking to exist simultaneously, whereby the symmetry remains hidden. An analogy used by many in describing this mechanism is that of a bowl which contains a ball at its very bottom, as illustrated in Fig. X.28 (left). The bowl and the ball in its most stable position at the very bottom of the bowl are perfectly symmetrical, such as would be the case for the symmetry of the elementary particles at the instant of the Big Bang. Now, if the bottom of the bowl was pushed upwards to produce a hump in the center of the bowl to take the form of a Mexican hat or that of the bottom of a champagne bottle, the ball would be at the top of the hump and perfectly symmetrical, but unstable, as illustrated in Fig. X.28 (right). The ball can roll down from the hump in any direction. In such a situation, the Mexican hat retains it symmetry; however, after the ball rolls down from the hump, the symmetry becomes hidden. This latter picture of the ball having rolled down from the hump is analagous to the spontaneous symmetry breaking that occurred among the elementary particles a billionth of a second after the Big Bang. This spontaneous symmetry breaking in the Higgs field at a point away from the symmetrical Big Bang position is

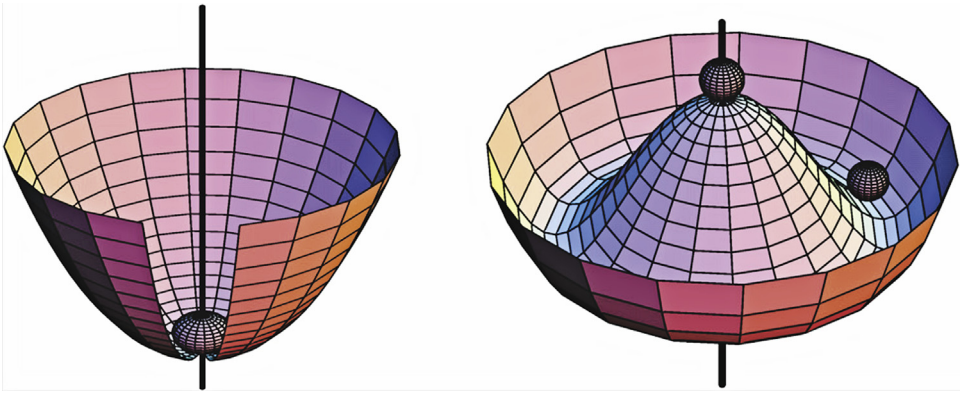

FIGURE X.28 Two-dimensional visualization of scalar potentials. The left plot shows a symmetric potential, under rotation around the vertical axis, with a stable minimum where the ball is resting. This resembles a bowl with a ball at the very bottom. A slit is cut out of the wall to allow the reader to see the ball at the bottom. The right figure, resembling a Mexican hat (or bottom of a champagne bottle), illustrates spontaneous symmetry breaking. The symmetric configuration at the top of the hat is unstable. The system will pick up any stable configuration along the brim. *From Davier, M., 2007. The Higgs boson of the standard model. Compt. Rend. Phys. 8 (9), 986–998, reprinted with permission from Elsevier Masson SAS © 2007. All rights reserved.*

called the phase transition of the Higgs field. The Nobel Foundation provides an excellent explanation of how the phase transition resulted in the production of the Higgs boson and the three remaining bosons that possess mass, namely the W^+, W^-, and Z^0 bosons:

> *In order for the phase transition to occur, four particles were required but only one, the Higgs particle, survived. The other three were consumed by the weak force mediators, two electrically charged W particles and one Z particle, which thereby got their mass. In that way the symmetry of the electroweak force in the Standard Model was saved—the symmetry between the three heavy particles of the weak force and the massless photon of the electromagnetic force remains, only hidden from view.*

Evidence to support the theory of the Higgs mechanism proposed in 1964 required the discovery of the Higgs boson, which would not be confirmed until almost 50 years later. The only effective means of producing the Higgs boson, which was predicted to have a high mass greater than 114 GeV/c^2, is by taking two beams of high-energy particles produced by an accelerator and directing the beams to collide head on. The Higgs boson has a short lifetime of $\sim 10^{-22}$ s, and thus cannot be detected directly. If the particle is produced in an accelerator, the detectors will register particles of the Higgs boson decay and their energies. The mass of the Higgs boson can be determined from the energies of the decay particles.

From the 1990s physicists made use of accelerators at two laboratories to search for the Higgs boson, namely the Tevatron accelerator at Fermilab (Fermi National Accelerator Laboratory) in Batavia outside Chicago, Illinois, USA and the accelerators at CERN, which straddle the border of Switzerland and France. Fermilab made significant contributions to the search for the Higgs boson. The Tevatron was used to collide 8 GeV protons against antiprotons in an accelerator ring with a 4 mile (6.4 km) circumference. On July 2, 2012 Fermilab reported (CDF Collaboration et al., 2012) that they had closed in on the mass range of the Higgs boson to be 115−140 GeV/c^2. However, Fermilab's Tevatron shut down on September 29, 2011, as it could not compete with CERN's Large Hadron Collider (LHC).

CERN's LHC is the world's largest accelerator, and the largest machine ever constructed. It consists of a 27 km ring which is connected to the smaller 7 km SPS, constructed 100 m below the Earth's surface. A map of the LHC above ground and its arrangement below the Earth's surface is shown in Fig. X.29; and a picture of the beam tunnel is provided in Fig. X.30. To underscore the enormousness of the LHC, compare its size to the much smaller SPS illustrated in Fig. X.20 earlier in this chapter and in Fig. X.29 below. The LHC first started up on September 10, 2008; and by 2012 it could accelerate narrow beams of up to 10^{15} protons up to an energy of 4 TeV traveling near the speed of light in opposite

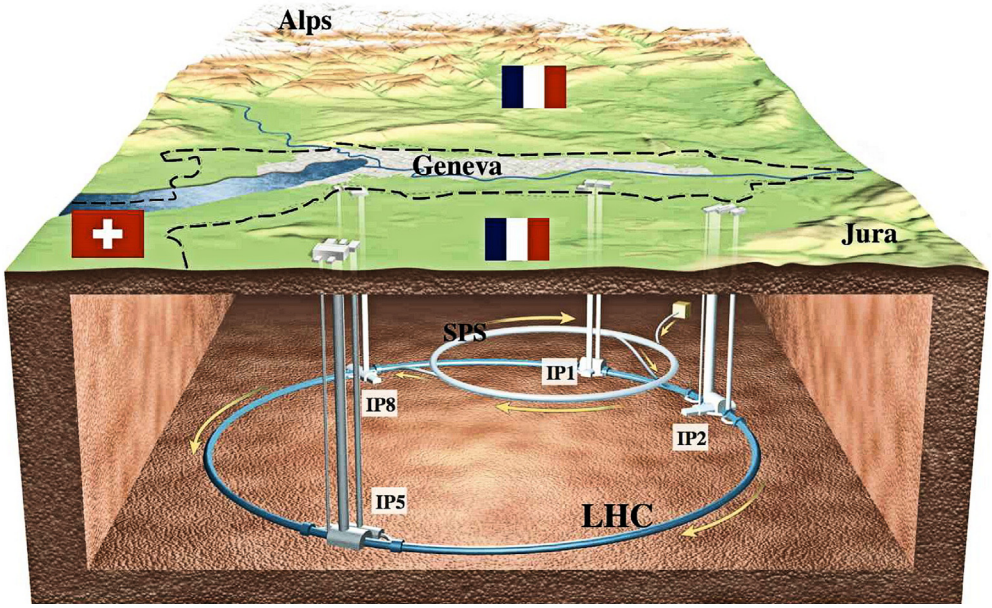

FIGURE X.29 Schematic diagram of the underground beam lines of CERN's LHC with the SPS as proton injector and four interaction regions (labeled IP). Particle detectors surround the interaction regions where protons traveling in opposite directions (yellow arrows) are made to collide head on. The topographical map illustrates the border between Switzerland and France (dashed line), which straddles the LHC and SPS. Above are the city of Geneva and Lake Geneva; and in the distance are the Alps and the department of Jura, France. *From Brüning, O., et al., 2012. The large hadron collider. Prog. Part. Nucl. Phys. 67, 705−734, reprinted with permission from Elsevier © 2012.*

FIGURE X.30 Beam tunnel and beam pipe of CERN's LHC. To one side of the beam line is a mobile robot (iMORO) on wheels; this was developed at the Intelligent Hydraulics and Automation Department of Tampere University of Technology, Finland as part of the PURESAFE (Preventing Human Intervention for Increased Safety in Infrastructures Emitting Ionizing Radiation) project. *From Khan, D.I., et al., 2014. Functional failure modes cause-consequence logic suited for mobile robots used at scientific facilities. Reliabil. Eng. Sys. Safety 129, 10-18, reprinted with permission from Elsevier © 2014.*

directions (see yellow arrows in Fig. X.29), yielding a combined energy of 8 TeV when made to collide at interaction points along the beam line (see interaction points identified in Fig. X.29).

Among the 20 member countries of CERN and 100 cooperating nations, as many as 6000 persons altogether worked at CERN and affiliated laboratories needed for the discovery of the Higgs boson, including the analysis of data collected by the detectors and other activities required for the proper operation and maintenance of the LHC.

Two massive detectors, namely the ATLAS detector and the CMS detector, were utilized at interaction points IP1 and IP5 noted on Fig. X.29, respectively. Staff analyzing data from each detector worked independently, so the staff at one detector could not influence the other; and when sufficient data was collected the results of the two groups were compared to confirm findings, such as the calculated mass of the Higgs boson. The mass of the Higgs boson can be determined from the energies of its decay particles. Each detector is designed to surround completely the proton−proton interaction point to identify the elementary particles that are emitted and determine their energies.

A cut-away drawing of the ATLAS detector is shown in Fig. X.31. The enormous size of the detector is indicated by the small human figures illustrated at its base. The electromagnetic calorimeters (colored green) measure gamma-ray photon and electron energies; and the hadron calorimeters (orange) detect and measure particles that exit the electromagnetic calorimeters. The end-cap and barrel toroids (gray) constitute the magnet system. The magnetic field generated can bend the paths of travel of charged particles to facilitate the determination of their charge and momentum. An inner solenoid, located close the proton−proton interaction point, creates a high magnetic field of 2 T surrounding the inner detector to bend the path of charged particles, permitting the determination of their charge and momentum. The CMS detector, which is not illustrated here for brevity, is yet more massive than the ATLAS, weighing over 14,000 tons and equipped with a higher magnetic field of 4 T, although it is about half its length and height. For detailed descriptions of the ATLAS and CMS detectors used to find and measure the mass of the Higgs boson, readers can peruse papers by Maiani, (1999), Mirabito (2010), Jakobs (2011), Sharma (2012), Spieler (2012), and Ventura (2013).

The production of the Higgs boson by means of high-energy proton−proton collisions in the LHC requires the transfer of energy into the mass of the Higgs boson. Several mechanisms are possible for Higgs boson production; however, the two principal mechanisms used in the LHC are **gluon fusion**, the predominant mechanism, which involves the fusion of

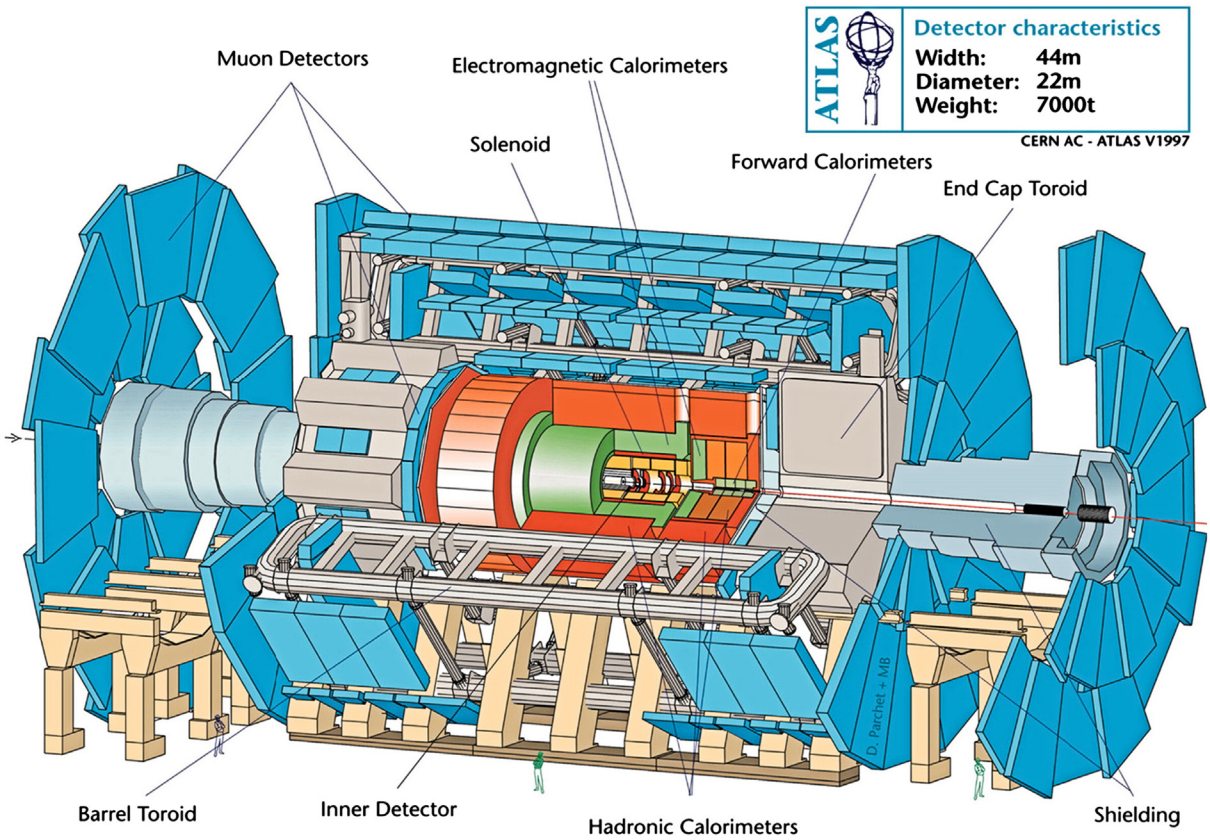

FIGURE X.31 The ATLAS muon spectrometer. The spectrometer is the outer layer (in blue) of the detector (~22 m height, 44 m in length and 7000 tons in weight); 5500 m^2 covered by muon detectors or 400,000 single drift tube detectors, grouped in 1200 chambers. *From Sharma, A., 2012. Muon tracking and triggering with gaseous detectors and some applications. Nucl. Instrum. Meth. Phys. Res. Sect. A 666, 98–129, reprinted with permission from Elsevier © 2012.*

two gluons following the collision of two high-energy protons, and **vector boson fusion**, which is a secondary mechanism involving the collision of two quarks from two colliding protons, whereby the two quarks exchange a W boson which then emits a Higgs boson. The gluon fusion and vector boson fusion mechanisms are illustrated in Fig. X.32.

The production of a Higgs boson in the LHC is a rare event (about one event in 10 billion other decay events). Detecting the occurrence of a rare Higgs boson production and decay event against a background of hundreds of other particle decays occurring at an interaction point within the ATLAS or CMS detectors is a gargantuan task, and can only be accomplished with the work of thousands of staff at CERN and collaborating institutions. Thus the detection of the Higgs boson required computer data analysis of hundreds of millions of proton–proton collisions collected over a period of several years, involving the analysis of ~30 million gigabytes annually with the cooperation of 42 countries linked to the Worldwide LHC Computing Grid (http://wlcg.web.cern.ch/). The work required the identification and analysis of signature decay modes of the Higgs boson.

Two principal decay modes of the Higgs boson are decays to four leptons (muons or electrons) or two photons, which are shown in Feynman diagrams in Figs. X.33 and X.34. The decay of the Higgs boson to two photons represents a complete conversion of mass into energy; and a determination of the energy of the photons with the aid of the surrounding spectrometers of the ATLAS and CMS detectors can give a direct measure of the mass of the boson. The decay of the Higgs boson to four leptons (muons or electrons) or two photons is considered a signature for the identification and mass measurement of this boson, but the signature pathways have to be identified against a background of hundreds of other particles created during high-energy proton–proton collisions. An example of the particle emissions that occur simultaneously to the signature decay schemes is shown in Fig. X.35, which simulates four muon emissions following the decay of the Higgs boson as measured by the ATLAS and CMS detectors. The numerous electromagnetic calorimeters, muon detectors, and imaging detectors surrounding the central interaction point of the two detectors aid in the discrimination of signature Higgs boson decay schemes over the multiple background particle emissions.

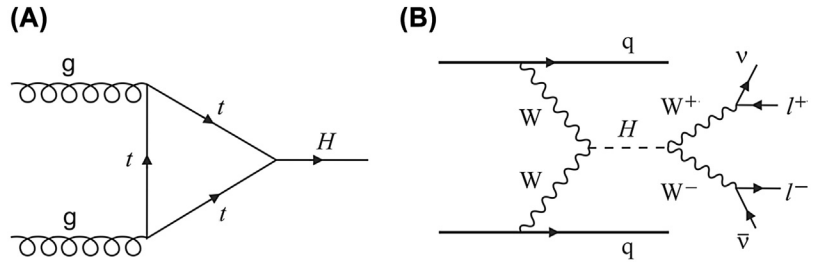

gluon fusion vector boson fusion

FIGURE X.32 Two principal mechanisms of Higgs boson production via proton−proton collision in CERN's LHC are illustrated by Feynman diagrams. (A) Gluon fusion, which involves the fusion of two gluons from two colliding protons followed by a *t*-quark fermion loop *(Adapted from Gastmans, R., et al., 2011. Higgs production at the large hadron collider: Phenomenological model and theoretical predictions. Nucl. Phys. B 850, 53−95; Dudas, E., et al., 2013. Low scale supersymmetry breaking and its LHC signatures. Nucl. Phys. B 870, 353−358; Ghosh, D., et al., 2013. Looking for an invisible Higgs signal at the LHC. Phys. Lett. B 725, 344−351; Nicolaidou, R., Sirois, Y., 2015. The Higgs boson discovery and measurements. C. R. Physique 16, 379−393.)* (B) vector boson fusion, whereby two quarks from colliding protons exchange a W boson, which produces a Higgs boson. One of several decay mechanisms of the Higgs boson is also illustrated, where the Higgs boson decays to W^+ and W^- bosons which decay respectively to a positively charged lepton and neutrino and a negatively charged lepton and antineutrino. *(From Cranmer, K., Bowman, R.S., 2005. Physics GP: A Genetic Programming approach to event selection. Comp. Phys. Comm. 167, 165−176, reprinted with permission from Elsevier © 2005.)* The lepton (*l*) may be either an electron (e), or muon (μ).

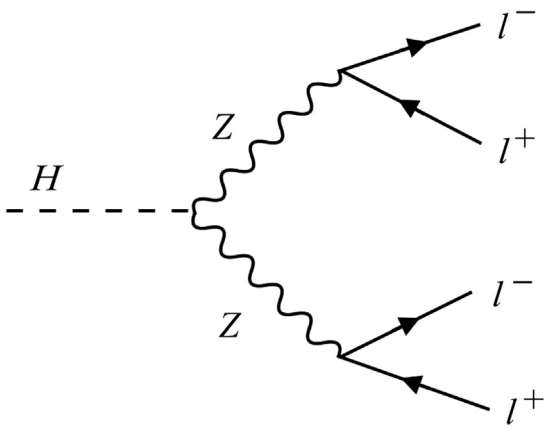

FIGURE X.33 Feynman diagrams illustrating Higgs boson decay to four leptons. The Feynman diagram illustrates a Higgs boson decaying to two Z bosons that decay into two lepton (*l*) pairs, where *l* represents a muon, μ, or an electron, e. *Adapted from Dittmaier, S., Schumacher, M., 2013. The Higgs boson in the standard model—from LEP to LHC: expectations, searches, and discovery of a candidate. Prog. Part. Nucl. Phys. 70, 1−54.*

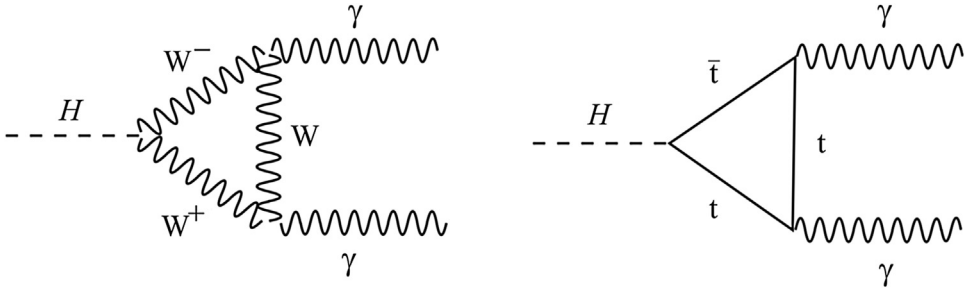

FIGURE X.34 Feynman diagrams illustrating the decay of the Higgs boson to two photons. The Higgs boson decays to a loop of W bosons or top quarks, which decay to two photons. *From Nicolaidou, R., Sirois, Y., 2015. The Higgs boson discovery and measurements. C. R. Physique 16, 379−393, reprinted with permission from Elsevier Masson SAS © 2015. All rights reserved.*

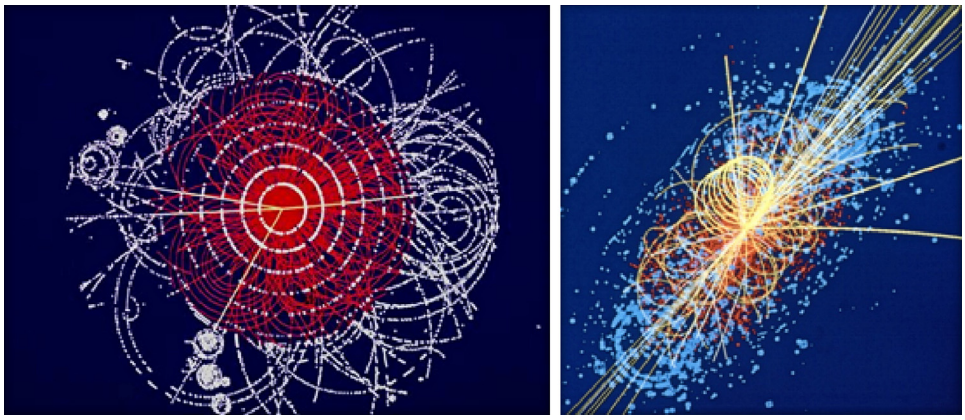

FIGURE X.35 Simulation of Higgs decaying into four muons in ATLAS (left) and CMS (right). This is the "goldplated" discovery decay mode: the guiding principle of the ATLAS and CMS muon systems. *From Sharma, A., 2012. Muon tracking and triggering with gaseous detectors and some applications. Nucl. Instrum. Meth. Phys. Res. Sect. A 666, 98–129, reprinted with permission from Elsevier © 2012.*

At CERN's LHC the ATLAS and CMS Collaborations, which are the two groups of physicists that collected and analyzed the data from the ATLAS and CMS detectors, announced on July 4, 2012 that they had irrefutable evidence of a new particle with a mass in the neighborhood of 126 GeV/c^2. After a long search of over two decades of work involving thousands of collaborators from many countries, this new particle was found to possess the properties of the Higgs boson predicted by the BEH mechanism described previously. Only three months later the Nobel Committee for Physics announced on October 8, 2013 the award of the Nobel Prize in Physics in 2013 to François Englert and Peter Higgs. Three persons or a combination of persons and organizations can share in a Nobel Prize; and it is assumed that Robert Brout did not have a share because he had died in 2011. CERN could have shared one-third of the prize; but the writer believes CERN was not given the award because another institution, Fermilab in the USA, had also made earlier significant contributions toward the discovery of the Higgs boson before Fermilab shut down its Tevatron in September 2011.

On March 17, 2015, CERN announced the most accurate measurement of the Higgs boson mass to be 125.09 ± 0.24 GeV, with a precision of better than 0.2%. In this statement CERN underscored the importance of finding the Higgs boson, and described the main decay signatures used in the detection of the boson:

> *The Higgs boson is an essential ingredient of the Standard Model of particle physics, the theory that describes all known elementary particles and their interactions… The Higgs boson decays into various different particles. For this measurement, results on the two decay channels that best reveal the mass of the Higgs boson have been combined. These two decay channels are: the Higgs boson decaying to two photons; and the Higgs boson decaying to four leptons—where the leptons are an electron or muon.*
>
> http://home.web.cern.ch/about/updates/2015/03/lhc-experiments-join-forces-zoom-higgs-boson.

The two decay schemes cited in this statement, namely Higgs decay to two photons or four leptons (electrons or muons) were discussed previously and illustrated by Feynman diagrams in Figs. X.33 and X.34. The CERN statement underscored the Higgs boson as a new essential ingredient of the Standard Model. The form of illustrating the Standard Model customarily showed 16 building blocks of matter representing the leptons, quarks, and gauge bosons, as illustrated in Fig. X.27. Now, with the discovery of the Higgs boson, the Standard Model has acquired a circular design to illustrate the 12 elementary particles that make up matter, together with the four gauge bosons that mediate the three forces in nature, namely the electromagnetic force mediated by the photon (γ); the weak nuclear force, including radioactive beta decay mediated by the W^+ and W^- bosons and weak interactions mediated by the Z^0 boson; and the strong nuclear force mediated by the gluon (g), which includes the force holding the quarks together within the baryons and the force holding the protons and neutrons together within the atomic nucleus. An example of the circular design is shown in Fig. X.36 with the Higgs boson in the very center, as it is the degree of interaction of the elementary particles with the Higgs field that determines whether a particle will possess mass or none at all.

For further reading on the Higgs boson and its discovery, the reader may peruse books by Baggott (2012) and Butterworth (2015).

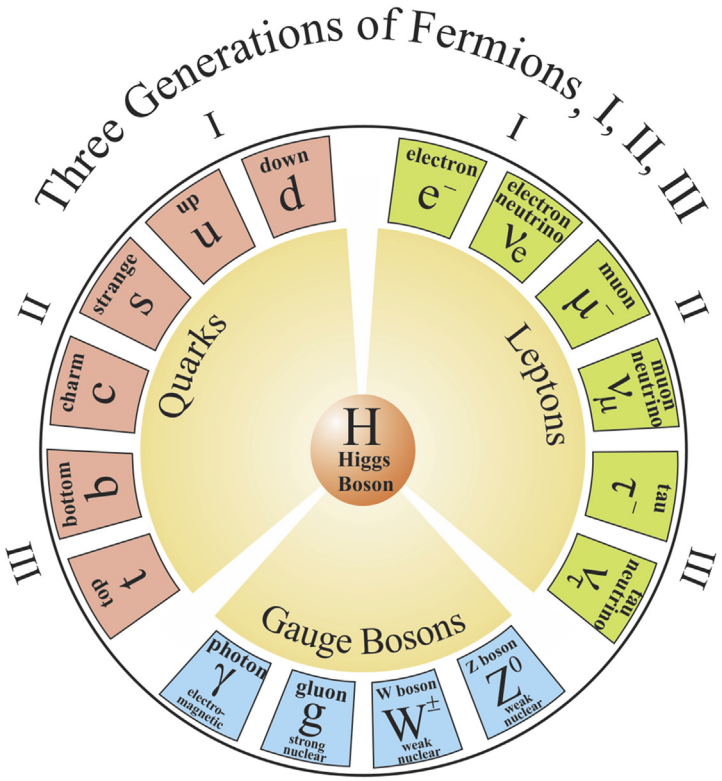

FIGURE X.36 The Standard Model of elementary particles. The quarks and leptons are the fundamental particles upon which all other particles and matter are built; and the gauge bosons are the force carrier particles which govern the interaction of the elementary particles. The Higgs boson at the very center governs the mass of the various quarks and leptons according to their individual degree of interaction in the Higgs field. *Circular design adapted from Butterworth, J., September 7, 2013. What's Next? New Scientist, 219 (2933), vi–vii.*

SERGE HAROCHE (1944–) AND DAVID J. WINELAND (1944–)

Serge Haroche of the Collège de France and Ecole Normale Supérieure, Paris, France and David J. Wineland of the National Institute of Standards and Technology (NIST) and the University of Colorado, Boulder, Colorado, USA shared the Nobel Prize in Physics in 2012 for, in the words of the Nobel Committee, "ground-breaking experimental methods that enable measuring and manipulation of individual quantum systems."

Serge Haroche (1944–)

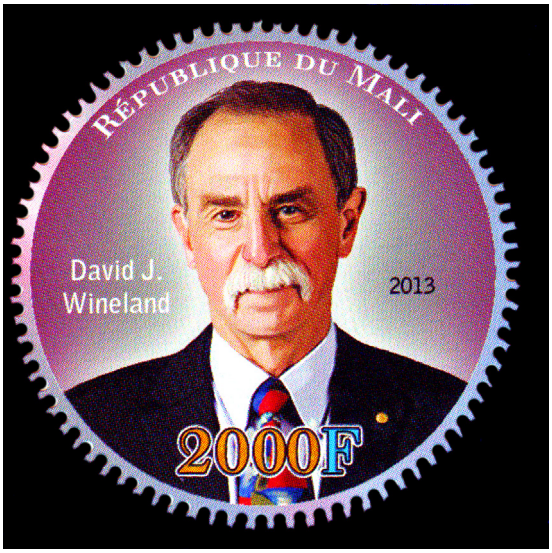

David J. Wineland (1944–)

Serge Haroche and David J. Wineland provided very extensive autobiographies to the Nobel Committee at the time of the Nobel award; these can be found on the website of the Nobel Foundation (www.nobelprize.org/nobel_prizes/physics/laureates/2012/). Brief biographical sketches are provided here from data obtained from their autobiographies.

Serge Haroche was born into a Jewish family in 1944 in Casablanca, Morocco. His father was a lawyer who practiced in Rabat. His mother was raised in Casablanca after her family emigrated to Morocco from Russia following the Bolshevik revolution in the 1920s. Serge Haroche grew up in Morocco, where he witnessed the events leading to the independence of Morocco from France; and in 1956, when independence came, he accompanied his parents and siblings to settle in France.

In Paris, Haroche studied at the Lycée Carnot, where he quickly went to the head of his class. Here he earned his baccalauréat, which is the French high school degree. Haroche was interested in several academic fields of study, and became fascinated with science and its associated mathematics. He embarked on two years of strenuous study and preparation in math and classical physics for examinations that earned him admission into the Ecole Normale Supérieure (ENS) in 1963, after ranking first in the national examination. At the ENS, Serge Haroche was immediately immersed in modern physics and the field of quantum physics. Among his teachers were Alfred Kastler (1903−1984), Nobel Laureate in Physics in 1966 "for the discovery and development of optical methods for studying Hertzian resonances in atoms," and Claude Cohen-Tannoudji (1933−), who shared the Nobel Prize in Physics in 1997 with Steven Chu and William D. Phillips "for development of methods to cool and trap atoms with laser light." In 1967 Haroche began his thesis under the supervision of Claude Cohen-Tannoudji at the ENS.

During his PhD studies Serge Haroche became interested in the interaction of atoms with microwave photons, which would eventually lead him to earning the Nobel Prize. After gaining his PhD, Haroche became a postdoctoral fellow at Stanford University in the laboratory of Arthur L. Schawlow (1921−1999), who would later share the Nobel Prize in Physics in 1981 with Nicolaas Bloembergen "for their contribution to the development of laser spectroscopy." During his postdoctoral year, Serge Haroche became interested in studying Rydberg states of atoms, which possessed very excited atomic levels with energies close to the atom's ionization limit, and the use of lasers to prepare and manipulate atomic matter in the excited Rydberg states. Haroche later used these techniques in his pioneering work with others that earned him the Nobel Prize. He proposed his research ideas to the director of the ENS Physics Department, and was awarded a research position at the ENS in 1973. Haroche was interested in teaching in addition to research, and in 1975 he was appointed to the position of professor at the Paris VI University. In 1981 he received an offer from Harvard University for a full-time professorship, but he was not willing to leave Paris and his research group. However, Yale University in New Haven offered him a one-term yearly position that allowed him to carry out research on both sides of the Atlantic, which he accepted and continued for a few years.

In the early 1990s Serge Haroche decided it was best to devote his full time to his group in Paris to carry out research ideas on the nondestructive manipulation and observation of photons, which would lead eventually to the Nobel Prize. These ideas originated with Haroche's collaboration with Brazilian physicists in Rio de Janeiro, where he participated in a French−Brazilian workshop in quantum optics in 1983. Haroche particularly noted that Luiz Davidovich and Nicim Zagury, two quantum optics theorists from Rio, were familiar with the Paris experimental work on cavity QED; and they worked on the theoretical aspects of the Paris experiments, described later in this chapter. Serge underscored the collaboration of Jean-Michel Raimond and Michel Brune. In particular, he noted that the first ideas of the nondestructive counting of photons emerged in contacts with Jean-Michel Raimond during communication between New Haven, Rio de Janeiro, and Paris. Haroche also noted that Brune was an exceptionally gifted student who stayed on to collaborate after completing his PhD thesis on the two-photon Rydberg atom maser. Both Raimond and Brune remained to collaborate with Haroche in research that led to the trapping and quantum nondemolition (QND) measurement of photons and eventually to the Nobel Prize. With Haroche's Brazilian colleagues, the two groups in Paris and Rio de Janeiro wrote a lengthy paper in the journal *Physical Review* (Brune et al., 1992) describing in detail the experiments planned for the preparation and manipulation of circular Rydberg states and reflective cavities able to trap photons for a very long time. Haroche noted that it took 15 years to get an experimental setup that would allow them to observe the alterations in Rydberg states and the nondestructive counting of photons that they had predicted in the early 1990s, described later. Haroche and his research group recognized that their work involving the trapping of photons was complementary to the work of David Wineland's group in Boulder, Colorado, where they were trapping atoms.

In June 2000 Serge Haroche was elected professor of the prestigious Collège de France; and in 2006 he and Jean-Michel Raimond authored a comprehensive book on the physics of atoms in cavities entitled *Exploring the Quantum: Atoms, Cavities and Photons*. In 2012 Haroche was elected to the position of administrator of the Collège de France, which gave him the opportunity to contribute to the expansion of the college with new labs in physics, biology, and chemistry.

David J. Wineland was born in 1944 in Wauwatosa, Wisconsin, just outside Milwaukee. He grew up in Sacramento, California, and graduated from Encina High School, now Encina Preparatory High School, in Sacramento in 1961. His

father graduated in engineering from CalTech in 1931; his mother was also a professional, but left her career to remain at home with David and his sister Judy. David Wineland's parents experienced the Great Depression in the United States, and emphasized the importance of frugality and a good education to improve one's chances of good employment. Thus Wineland was determined to attend college, and always strived to maintain high grades in school. He liked mathematics, and in his senior year he took his first physics class, enjoying the application of math to physics. Here he realized how mathematics helped answer how many things function in our day-to-day world.

After graduation from high school, David Wineland entered the prestigious University of California, Davis, close to Sacramento, with a major in mathematics. With hard work, he was among the top of his class. Wineland's interest was in physics and mathematics, and he knew that the University of California at Berkeley was among the most reputable schools in the country in this field. Thus in his junior year at Davis he transferred to the Berkeley campus, where he graduated with a BSc degree in 1965. Like many serious students, Wineland had one teacher who had a great influence on him: he noted in his autobiography that Frederick Byron was a great teacher of classical physics who taught the most difficult class while at the same time stimulating his students to enjoy the work. It was Byron who advised Wineland to apply for admission to Harvard University for graduate studies in physics. Wineland applied to Harvard, with an application the University of California at Berkeley as backup, as he considered Berkeley to be among the top graduate schools in the field.

David Wineland started his graduate studies at Harvard in 1965 in a class of 26 students. He was concerned about entering Harvard, thinking that there would be 25 geniuses and himself. Instead, he discovered that there were only two geniuses among the 26; and the remaining students were ordinary like himself, but highly motivated and working hard to do well. At Harvard, Wineland joined Norman Ramsey's research group. He was awarded a PhD in 1970 with a dissertation on the atomic deuterium maser. Wineland felt the need to immerse himself more in physics, and thus joined Hans Dehmelt's research group at the University of Washington in Seattle with a postdoctoral position to work on Dehmelt's electron magnetic moment experiment. During this work Wineland recognized that systematic shifts would be smallest for a single trapped electron, and he focused on obtaining that goal as his primary project while at Seattle. Thus Wineland researched the trapping of ions, which gave him much experience in the future work that would lead eventually to the Nobel Prize.

After the postdoctoral work, David Wineland searched for an academic position, but the university posts available did not provide the possibility of carrying out a large, viable research project. However, in 1975 he took on a research position with the Time and Frequency Division of the National Bureau of Standards (now the National Institute of Standards and Technology—NIST) in Boulder, where he could easily form a research group. In his autobiography (www.nobelprize.org/nobel_prizes/physics/laureates/2012/wineland-bio.html), Wineland praised those with whom he collaborated at NIST, including Wayne Itano, Jim Bergquist, Bob Drullinger, Chris Monroe, Ignacio Cirac, Peter Zoller, Till Rosenband, and Didi Leibfried, among others. In 1985 Wineland's group demonstrated the first atomic clock that employed laser cooling, which was based on a hyperfine transition in $^{9}Be^{+}$ ions. The laser cooling was important to suppress relativistic time dilation. The group was also able to demonstrate a two-qubit (quantum bit) logic gate, which was a project in quantum processing first proposed by Ignacio Cirac and Peter Zoller in 1995. Wineland applauded the work of Till Rosenband, who became a permanent staff member in 2006, for his development of an atomic clock based on $^{27}Al^{+}$ ions, which is the clock with the lowest systematic error of approximately one in 10^{17}. David Wineland is currently working at NIST with Didi Leibfried to research the use of atomic ions in quantum information processing.

At the time of receiving the Nobel Prize in 2012, David Wineland had completed 38 years of research at the National Bureau of Standards and NIST. He praised the laboratory director, Katharine Gebbie, for her support and encouragement; and noted in his autobiography that a measure of her success is that he was the fourth NIST person, after Bill Phillips, Eric Cornell, and Jan Hall, to receive a Nobel Prize during her tenure as lab director.

Joining NIST was fortuitous, because it gave Wineland the opportunity to focus on research that led to the Nobel Prize; and to teach and serve as doctoral research advisor at the University of Colorado in Boulder, where he joined the faculty in the year 2000 and remains as adjoint professor of physics. David Wineland notes in his autobiography that many of his young students ask his advice. His comments in this respect are the following:

> *I've often been asked for advice to give to young students. Of course there's no one answer that fits all, but for me, because of my upbringing, it's been pretty simple. I would suggest finding something interesting (even if you change your mind) and give it your best possible effort. That means hard work, and although not everybody above you will appreciate it, most of them will recognize it and support you. And, as nice as it is to be recognized for accomplishments, I think the biggest reward for me has been just to have the opportunity to explore new ideas. The physics has never been a job; it's more like a hobby—and just the process of doing research is extremely interesting and rewarding.*

"David J. Wineland—Biographical," Nobelprize.org, Nobel Media AB 2014, August 4, 2015, www.nobelprize.org/nobel_prizes/physics/laureates/2012/wineland-bio.html.

In addition to the Nobel Prize in Physics in 2012, which he shared with Serge Haroche, David Wineland is the recipient of several other prestigious awards, including the 1990 Davission-Germer Prize "for his outstanding contributions to research on trapped ions, including leading one of the two groups to first demonstrate laser cooling of an atomic species, and developing the most accurate atomic clock based on atomic ions." In 2010 Wineland was awarded the Benjamin Franklin Medal, with J. Ignacio Cirac and Peter Zoller, "for their theoretical proposal and experimental realization of the first device that performs elementary computer-logic operations using the quantum properties of individual atoms." For additional information on quantum computing, the reader may peruse a paper by Christopher R. Monroe and David J. Wineland (2008) entitled "Quantum Computing with Ions."

In Hall of Fame, Part III of this book, we saw the discovery by Max Planck in the year 1900 that electromagnetic radiation is emitted in discrete energies corresponding to different energy states of a body. Planck named the discrete radiation energy as "the quantum." The magnitude of this energy will be the product of Planck's constant (h) times the frequency of the electromagnetic radiation (v). In that chapter, the writer referred to the relationship $E = hv$ as the Planck−Einstein equation, because it was Albert Einstein who in 1905 described the photoelectric effect by explaining that a photon of light was a particle with energy sufficient to knock out an orbital electron of an atom. In the same chapter, the writer noted the work of the French scientist Louis de Broglie in 1923, who extended further the quantum theory of matter by demonstrating that all particles of matter possess a wave nature, just as all waves of electromagnetic radiation have a particle nature. Thus the field of quantum physics was established, whereby particulate matter can be described to have a dual nature—that of a particle and that of a wave. The particle−wave duality in nature led to a field of study known as quantum mechanics or quantum physics, which takes into account the particle−wave duality of matter.

Since the discovery of quantum physics in the early 1900s, scientists have demonstrated many times over the dual particle−wave nature of matter. In an early example, Clinton Davisson and George Paget Thomson demonstrated in 1927 that electrons, which are particles of known rest mass, could be diffracted by the atomic lattice of crystalline material, similar to the manner by which visible light is diffracted by a crystal into a rainbow of wavelengths. In another example, gamma or x-radiation of given wavelength was demonstrated by Arthur H. Compton in 1923 to act as a particle by knocking out an orbital electron from an atom; and the electromagnetic radiation scattered at an angle away from the liberated electron in a manner similar to two billiard ball collisions. Thus, the wave nature of the gamma or x-radiation displayed its particle nature in the collision.

From the discovery of the energy quantum by Max Planck in 1900 up to the work of Serge Haroche and David Wineland, it had not been possible to measure simultaneously various quantum states of matter. For example, it was possible to detect a photon and measure its energy with a photomultiplier tube, which can measure the energy of the photon via the photoelectric effect. However, the process of measuring the energy of the photon resulted in the destruction of that photon. The conundrum of measuring the quantum states of matter without altering or destroying the quantum properties before the pioneering independent work of Haroche and Wineland was eloquently described in the Nobel award ceremony speech of Professor Björn Jonson, member of the Royal Swedish Academy of Sciences and chair of the Nobel Committee for Physics, on December 10, 2012:

> *In the quantum world, light, atoms, nuclei and elementary particles are all described as being both particles and waves. Quantum physics has been extremely successful in modern physics. But to really observe matter at the quantum level one encounters major problems since almost any attempt to make a measurement causes the quantum properties to simply disappear. It has therefore been a dream since the dawn of quantum physics to be able to study individual quantum systems. This dream has now become a reality.*
>
> *This year's Nobel Laureates, together with their research groups, have used cleverly designed experiments to successfully perform the trick of controlling and measuring single isolated quantum systems without destroying their quantum properties. Serge Haroche and David Wineland have opened the door to the observation of the most fundamental quantum world… They have shown how to study and control and count quantum systems. One may call this mastering without touching—since the enchantment of the micro-world would otherwise disappear. Their experimental methods have many things in common. David Wineland captures individual electrically charged atoms, ions, in an electrostatic trap, and cools, measures and controls them with photons of light. If the temperature is close to absolute zero, both the energy and the frequency of oscillation of the ion can only obtain certain distinct values; they are what we call quantised. By shining laser light on the ion it can then be put in a state called superposition, a state simultaneously occupying two different energy levels! The superposition of energy can then be transferred into a corresponding superposition of vibrational states, also with laser light. A superposition has been transferred without destroying it.*
>
> *Serge Haroche takes the opposite approach—he captures single photons between two perfectly reflecting mirrors and keeps them there long enough to be able to measure and control them. This is done with the aid of very highly excited atoms, which pass*

the trap and tickle the photons just a bit. These atoms act like antennas that gather information about the number of photons in the trap and about their condition. This is simply spying at the quantum level. It is also remarkable to note that Haroche can study single photons, given that a regular 9 W bulb emits more photons in a billionth of a second than there are people on earth.

Both Laureates represent a research field called quantum optics, a field where the interaction between light and matter is studied at a fundamental level… Their research has given us new tools for future experiments and is therefore of the highest scientific interest. Their research also provides hope for the construction of future super-fast computers based on quantum physics… Their experiments have also led to the development of extremely accurate optical clocks that will eventually become the new time standard. Today they have already achieved an accuracy of about a hundred times more than today's clocks based on caesium. This accuracy is so unimaginable that if you could let such a clock run for a period of time corresponding to the age of the universe, it would only lag by a few seconds.

(With permission from "The Nobel Prize in Physics 2012—Presentation Speech," Nobelprize.org, Nobel Media AB 2014, August 13, 2015, www.nobelprize.org/nobel_prizes/physics/laureates/2012/presentation-speech.html.

David Wineland and Serge Haroche took independently two different and similar approaches to study fundamental interactions between light and matter. Wineland at the NIST Laboratory in Boulder trapped electrically charged atoms and measured their quantum states with photons of light. Haroche at the ENS in Paris took the opposite approach: he trapped photons and then measured their properties by sending atoms through a cavity containing the trapped photons. The two experimental arrangements used by Wineland and Haroche to study quantum optics are illustrated in Fig. X.37.

David J. Wineland's technique, on the left in Fig. X.37, involved trapping ions within an electric field created by electrodes, illustrated as four columns surrounding the trapped ions. The ions are trapped in an environment free of external environmental interactions by isolating them in a vacuum state at extremely low temperature. A laser pulse, illustrated in Fig. X.37, is used to reduce the thermal motion of the ions in the trap to their lowest energy state by using radiative forces of the laser to reduce the random thermal velocities of the ions, referred to as laser cooling of atoms (Hänsch and Schawlow, 1975; Wineland and Dehmelt, 1975; Wineland and Itano, 1979). The development of methods to cool and trap atoms with laser light was the basis for awarding the Nobel Prize in Physics in 1997 to Steven Chu of Stanford University, Claude Cohen-Tannoudji of the Collège de France, ENS, Paris, and William D. Phillips of NIST at Gaithersburg, Maryland, USA. As described by Phillips (1989), the temperature of the trapped atoms is reduced to the microkelvin range. An image of three trapped beryllium ions is shown in Fig. X.38.

With the ions trapped in their lowest state of thermal motion, David Wineland could then study the changes in quantum states of the trapped ions by directing a laser pulse at them, placing the ions into a superposition state, which is the simultaneous existence of two distinct energy states. Serge Haroche (2012) described Wineland's technique as follows:

In the Boulder experiments [carried out by Wineland's team at NIST], the ions' internal degrees of freedom (making up the "spin") are coupled to the external motion of the particles in the trap undergoing a mechanical oscillation, whose quanta are phonons [collective vibrational motions of atoms that may oscillate at a definite frequency within a lattice of atoms or molecules]. The coupling is achieved by irradiating the ions with properly tuned laser beams producing transitions between the ion internal energy levels accompanied by the absorption or emission of phonons.

With the use of properly tuned lasers, Wineland's research group could irradiate the trapped ions at their lowest energy state into a higher, albeit intermediate, energy level between two energy states, so that the ions are made to exist as a superposition of two energy states. In such an intermediate superposition energy state, the ions can be considered to have an equal probability to exist in either the lower or the higher energy state.

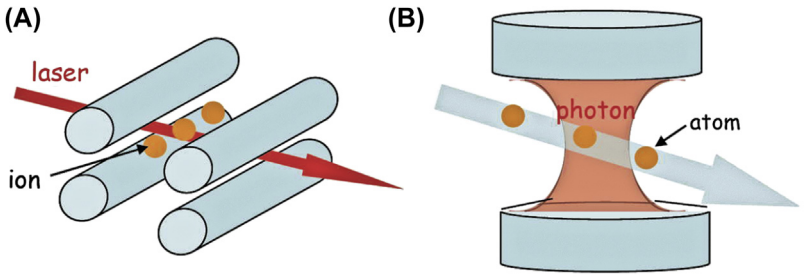

FIGURE X.37 Scheme of the NIST ion trap (A) and of the ENS photon box (B). *From the Nobel lecture of Serge Haroche given on December 8, 2012, reprinted with permission © The Nobel Foundation 2012, www.nobelprize.org/nobel_prizes/physics/laureates/2012/haroche-lecture.pdf.*

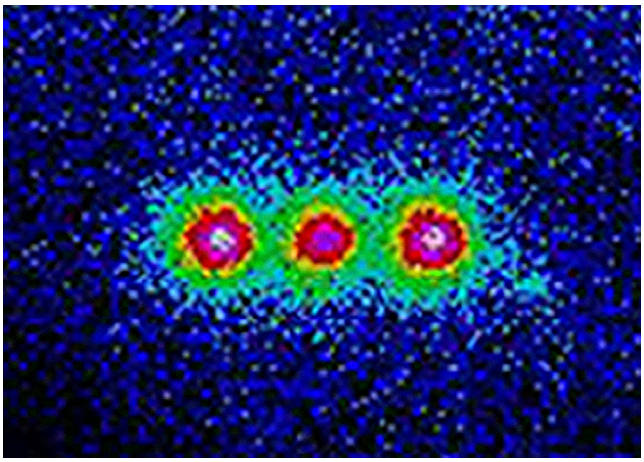

FIGURE X.38 This image shows the fluorescence from three trapped beryllium ions illuminated with an ultraviolet laser beam. Black and blue areas indicate lower intensity, and red and white higher intensity. NIST physicists used three beryllium ions to demonstrate a crucial step in a procedure that could enable future quantum computers to break today's most commonly used encryption codes. *Courtesy NIST.*

The creation of a superposition of two energy states in trapped ions opens the door to the construction of powerful quantum computers that use individual atoms to carry out complex calculations much faster than conventional modern computers. As described by Monroe and Wineland (2008), the potential power of a quantum computer would be derived from the superposition states of the trapped ions. A conventional computer utilizes a digital bit, which can have the value of 0 or 1; but a quantum computer would utilize the simultaneous superposition states and have a value of both 0 and 1 at the same time, known as a qubit. Monroe and Wineland (2008) point out that a system with two cubits would contain simultaneously the four values of 00, 01, 10, and 11. Thus a quantum computer with N number of trapped ions, each of which can be elevated to two superposition states, could simultaneous manipulate 2^N numbers. A quantum computer with 300 trapped ions, each of which stores a quantum bit, could hold 2^{300} values. This would amount to more values than the number of particles in the universe (Monroe and Wineland, 2008).

Serge Haroche and his coworkers measured changes in the quantum state of atoms by directing a beam of atoms at photons, and in so doing were able to measure the birth and death of photons without destroying them. This work represents the very first successful method of measuring photon intensities (ie, photon numbers) without destroying the photon. Historically, prior to this work a photon could only be detected by its interaction (eg, via the photoelectric effect), or with our eyes, where photon energy is absorbed and then transmitted to our brain, or via an instrumental detector, such as a photomultiplier tube whereby photon energy is transmitted to an electric pulse via the photoelectric effect. In his Nobel lecture, Serge Haroche described eloquently the significance of the nondestructive detection and measurement of photons, also referred to as the QND measurement of photons:

> *When you see light, the photons, which strike your eye, your camera, or your photodetector, are converted by the photoelectric effect into an electron, or some kind of electric current and the photon is destroyed in the process. The situation is not essentially different from the brute force collisions occurring in a cloud chamber or a particle accelerator. Seeing light amounts to collecting the debris of the photons colliding with a photosensitive surface. If you detect a click in your photon counter, the photon is no longer there and has been replaced by the vacuum, zero photons instead of one! What we were looking for instead was a process by which a click in our nondestructive detector would leave the photon intact afterwards, allowing the measurement to be repeated again and again, on the same photon… For this purpose, a special kind of atomic detector was required, which was transparent to radiation but still sensitive enough to register an imprint of a single photon. And we needed also a very good photon box, an open structure keeping the photons for a very long time, enabling us to repeat the measurement again and again with successive atoms crossing the box one by one.*

A photograph of the photon box is shown in Fig. X.39. The box contains two reflective cavities which act as two mirrors, separated by 2.7 cm distance. The reflective surfaces are made of superconducting niobium, and are cooled to a very low temperature slightly above absolute zero. These are the most reflective mirrors ever manufactured. Microwave photons are made to bounce back and forth within the two cavities long enough for a single photon to travel a distance of 40,000 km before the photon becomes lost or absorbed. The photon box provides a means of housing or trapping photons for a relatively long period of time, sufficient to direct a beam of Rydberg atoms into and through the open cavity so that

FIGURE X.39 The ENS photon box (photograph by Michel Brune). The mirrors have a diameter of 5 cm and are 2.7 cm apart (for a clear view, they are further apart in this picture than in the actual experimental setup). *From the Nobel Lecture of Serge Haroche (2012); reprinted with permission from the Nobel Foundation © 2012.*

the atoms can interact and measure the trapped photons. Rydberg atoms, named after the Swedish physicist Janne Rydberg (1854−1919), are excited atoms with an atomic diameter much larger than normal atoms, so an outer single orbital electron is very distant and shielded from the core of atomic electrons, to the extent that the outer atomic electron displays an electric potential identical to that of a single electron of the hydrogen atom.

A schematic of the ENS arrangement whereby a beam of atoms is directed through the open reflective cavity to interact with trapped photons in the photon box is illustrated in Fig. X.37B. Essentially the method involves directing a beam of Rydberg atoms (4200 atoms per second) through the photon box with its reflective cavities. The Rydberg atoms directed toward the trapped photons possess an orbital electron similar to that of a neutral hydrogen atom. The de Broglie electron waves of the Rydberg atoms have a uniform amplitude around a circular orbit, resulting in a zero electric dipole, illustrated in Fig. X.40A. The beam of Rydberg atoms traverses an opening between the reflective cavities of the photon box, interacts with a photon, and exits the box cavity, leaving the reflecting photon behind in the box. The beam intensity of the Rydberg atoms is carefully controlled to monitor the photon interactions within the box. The interaction of a Rydberg atom with a microwave photon in the reflective cavities of the photon box will alter the de Broglie wave phase of the Rydberg orbital electron, as illustrated in Fig. X.40B. The phase shift of the Rydberg atoms that exit the photon box will indicate the presence or absence of a photon in the reflective cavity of the box. Thus Haroche and his coworkers at the ENS can measure a single photon and determine its lifetime.

The technique was described by Haroche in his Nobel lecture given on December 8, 2012:

> *In order to probe the photons, we send across the cavity [photon box] a special kind of Rydberg atoms, called "circular," in which the outer electron orbits on a circle of large diameter, about a thousand times bigger than an ordinary ground state atom [see Fig. X.40]. These excited Rubidium atoms are prepared with lasers and radiofrequency excitation, using a modified version [Nussenzveig et al., 1993] of a procedure invented by Daniel Kleppner and Randy Hulet at MIT in 1983 [Hulet and Kleppner, 1983]. According to quantum theory, the orbiting Rydberg electron is also a wave, which has a de Broglie wavelength, and the*

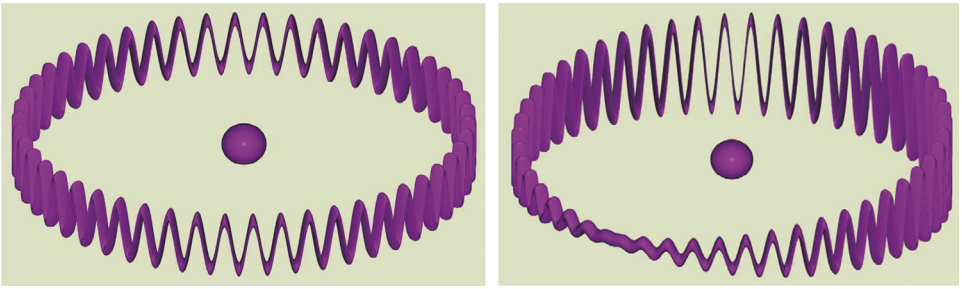

FIGURE X.40 Sketch of circular Rydberg atom electron waves. (A-left image) In an energy eigenstate, the de Broglie electron wave has a uniform amplitude around the circular orbit, resulting in a zero electric dipole; (B-right image) in a superposition of adjacent circular Rydberg states, the de Broglie waves interfere positively on one side of the orbit and destructively on the other side, yielding a net electric dipole which rotates in the orbital plane. *From the Nobel lecture of Serge Haroche (2012), reprinted with permission of the Nobel Foundation © 2012.*

condition of a stable orbit is that there is an integer number of these wavelengths along the circumference [see Fig. X.40A]. This number, called the principal quantum number of the Rydberg atom, is equal to 51 or 50 in our experiments (these Rydberg states are called e *and* g *respectively in the following)…*

In the e *and* g *Rydberg states, the circulating de Broglie wave has a uniform amplitude, resulting in an electron charge density centered at the atomic nucleus, yielding a zero electric atomic dipole [see Fig. X.40A]. In order to prepare an electric dipole, a pulse of resonant microwave can be applied to the atom, bringing it in a superposition of the two adjacent* e *and* g *states, with respectively 51 and 50 nodes in their wave function. This superposition of states can be referred to as a "Schrödinger cat" because it implies an atom at the same time in two levels, reminding us of the famous cat that Schrödinger imagined suspended between life and death. [see biographical sketch of Erwin Schrödinger in Hall of Fame, Part V]. A better name should be a "Schrödinger kitten," because it is made of a single atom and thus very small. The two de Broglie waves making up this "kitten" interfere constructively at one end of the orbit and destructively at the other end, resulting in a net electric dipole, rotating in the orbital plane at 51 GHz [see Fig. X.40B]. This dipole behaves as a rotating antenna extremely sensitive to microwave radiation [the microwave photons reflecting in the photon box]. It can also be described as the rotating hand of a clock, ticking at 51 GHz.*

When microwave radiation, non-resonant with the transition between the two states e *and* g*, impinges on the atom [ie, the Rydberg atom], it cannot absorb it and hence the photons remain intact, ensuring the non-demolition character essential to our experiments. However, the effect of this non-resonant light is to shift the atomic energy levels [of the Rydberg atom] slightly and hence alter the rotating frequency of the atomic dipole, our clock hand. This light shift effect had been discovered in 1961 by Claude Cohen-Tannoudji in his seminal optical pumping studies [Cohen-Tannoudji, 1983]. Light shifts are proportional to the field energy, i.e., to the photon number… In the case of Rydberg atoms, the effect is then very large, resulting in a phase shift of the atomic dipole after the atom leaves the cavity which can reach the value of 180°, the dipole jumping in two opposite directions when the photon number changes by one unit. Measuring this phase shift amounts to counting the photon number without destroying the light quanta.*

The first evidence for the QND measurement of photons (that is, the detection of a photon without destroying it) was reported in the journal *Nature* by Serge Haroche and coworkers (Nogues et al., 1999); and the absolute recording of the birth and death of a photon trapped within a cavity (photon reflective box) was also reported in the journal *Nature* eight years later by Haroche and coworkers (Gleyzes et al., 2007). In this more recent paper providing a measurement of the photon lifetime, Haroche and coworkers reported that the Rydberg atoms were prepared in a superposition of *e* and *g* states, and the microwave photons trapped in the reflective cavity (photon box) interact with the superposition states to enable the detection of a microwave photon in the cavity and measurement of its lifetime. The experimental setup, illustrated in Fig. X.41, is described in detail in papers by Gleyzes et al. (2007) and Haroche et al. (2013).

In the experimental arrangement illustrated in Fig. X.41, as described by Gieyzes et al. (2007), a beam of rubidium atoms in the Rydberg state *g* originates at O. The beam passes through a microwave pulse in R_1, which generates a superposition of states *e* and *g* of the Rydberg atoms. The superposition of the *e* and *g* states in the beam then enters the reflective cavity C (the photon box), where trapped microwave photons reflect back and forth from the concave and reflective cavity walls. In C the superpositioned states *e* and *g* of the Rydberg atoms interact with a reflecting photon, but do not destroy the photon. If a photon is present in the cavity, it undergoes a nonresonant interaction with the Rydberg atom, shifting the phase of its atomic dipole, but the photon is not destroyed. The atomic beam exiting C is probed by a second microwave resonant field at R_2 before entering a state-selective ionization detector D, which will determine the *e* or *g* state of an atom. The relative phase of the fields in R_1 and R_2 will determine the probability of finding the atom in the *g* state when the cavity C is empty (ie, when no photon is present or $n = 0$), or the *e* state when the cavity contains one

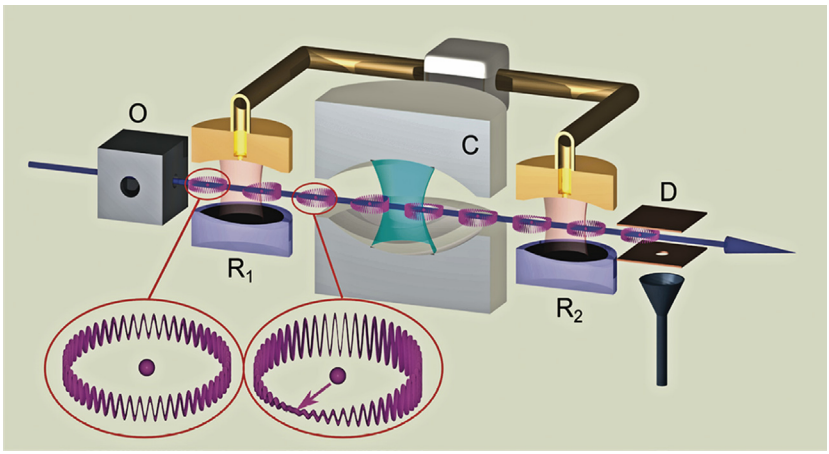

FIGURE X.41 Detecting single photons with a Rydberg clock. Rubidium atoms are prepared in a circular Rydberg state ("g"), with the excited valence electron depicted as a circular de Broglie wave having constant amplitude (left inset). The first microwave pulse, in R_1, is resonant with the transition frequency between the initial state and a neighboring Rydberg state ("e"), and generates a dipole (right inset) that evolves at the atomic transition frequency. The atoms, at a rate of about 4200 per second, then traverse a cavity at C made of two highly reflective mirrors. If a photon is present, the atoms' nonresonant interactions with the field shift the phase of their atomic dipoles but do not absorb the photon. The atoms then undergo a second microwave pulse in R_2 before their final state is detected by ionization at D. *From Haroche, Brune, M., and Raimond, J.-M. (2013), reprinted with permission, American Institute of Physics © 2013.*

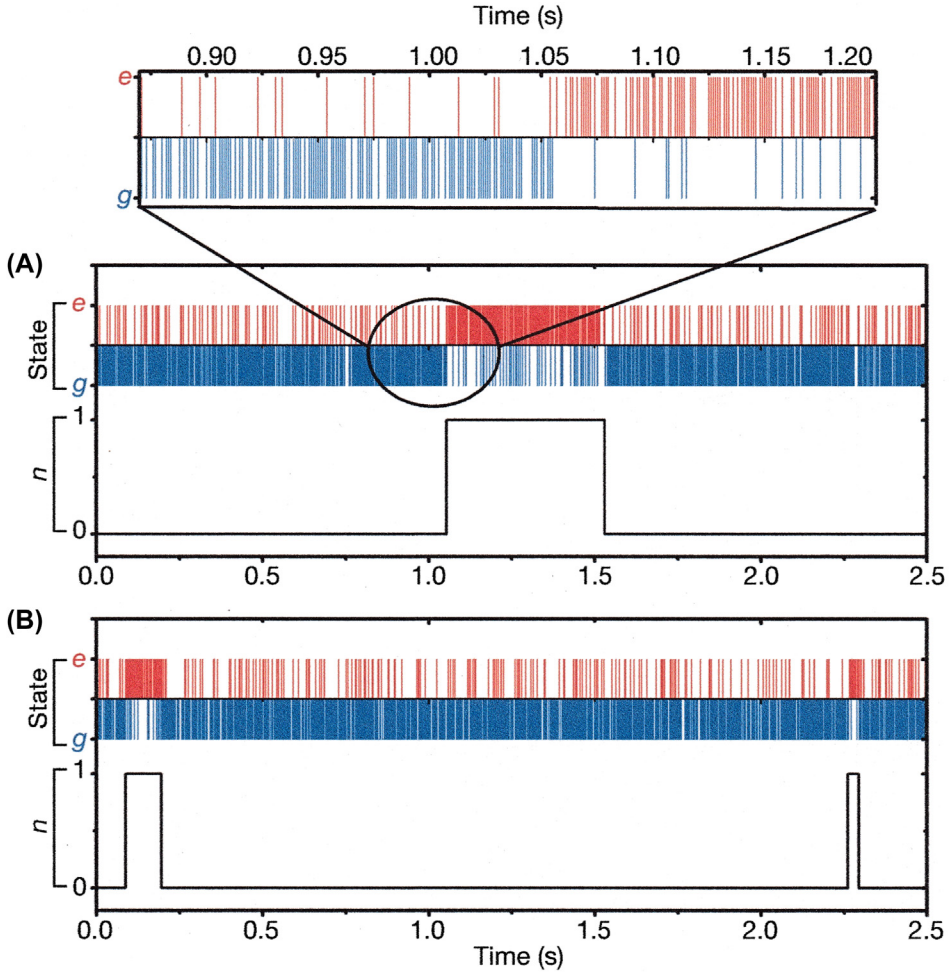

FIGURE X.42 (A) QND detection of a single photon. Red and blue bars show the raw signal, a sequence of atoms detected in *e* or *g*, respectively (upper trace). The inset zooms into the region where the individual detection events can be more clearly visualized and where the statistics of the detection events suddenly change, revealing the quantum jump from $|0\rangle$ to $|1\rangle$. The photon number (n) inferred by a majority vote over eight consecutive atoms is shown in the lower trace, revealing the birth, life, and death of an exceptionally long-lived photon. (B) Similar signals showing two successive single photons, separated by a long time interval with the cavity in vacuum. *From Gleyzes, S., Kuhr, S., Guerlin, C., Bernu, J., Deléglise, S., Hoff, U.B., Brune, M., Raimond, J.-M., Haroche, S., 2007. Quantum jumps of light recording the birth and death of a photon in a cavity. Nat. Lett. 446, 297–300, reprinted by permission from Macmillan Publishers Ltd © 2007.*

photon ($n = 1$). They report that a probability of finding two photons in a thermal field where the cavity temperature $T = 0.8K$ is only 0.3%.

A measured sudden change in the g to e state in the atom beam exiting the photon cavity would signify the creation or birth of a photon in the cavity; and the reverse change of state would signal the death of the photon. Haroche and coworkers (Gleyzes et al., 2007) provide interesting examples of the signals detecting the birth, life, and death of photons with this experimental setup. They provide the plots illustrated in Fig. X.42, which show detector outputs that monitor the photon changes in the reflective photon box (cavity C). In Fig. X.42A, Gleyzes et al. (2007) explain that this plot represents a 2.5 s sequence of 2241 detection events recording the birth, life, and death of a single photon. The plot illustrates first a predominance of the g state (blue bars), indicating an absence of a photon in C. Then a sudden change from the g to e states of the Rydberg atoms in the detection sequence at time $t = 1.054$ s indicates the creation of a photon in cavity C, which disappears after time $t' = 1.530$ s. In this plot, Gleyzes et al. (2007) demonstrate an exceptionally long-lived photon, which reflected back and forth within the photon box for 0.476 s (ie, $t' - t = 1.530 - 1.054$ s). During the 0.476 s of its lifetime, this particular photon traveling at the speed of light (299,792.458 m/s) had traveled back and forth between the cavity mirrors for close to 143,000 km.

This pioneering work demonstrated for the first time the detection of photon particles during the entire lifetime of the photon without the destruction of the photon. For additional research on this topic, the reader may peruse papers by Haroche and coworkers with stunning titles, such as "Seeing a Single Photon without Destroying It" (Nogues et al., 1999), "Quantum Jumps of Light Recording the Birth and Death of a Photon in a Cavity" (Gleyzes et al., 2007), and "Atomic Clocks for Controlling Light Fields" (Haroche et al., 2013).

Chapter 22

The Atom as We Know and Use It

I want to address the scientific community as a whole. You are doing fundamental work, pushing forward the frontiers of knowledge, but often you do it without giving much thought to the impact of your work on society. Precepts such as 'science is neutral' or 'science has nothing to do with politics', still prevail. They are remnants of the ivory tower mentality, although the ivory tower was finally demolished by the Hiroshima bomb… We need to convey the message that safeguarding our common property, humankind, will require developing in each of us a new loyalty: a loyalty to mankind. It calls for the nurturing of a feeling of belonging to the human race. We have to become world citizens… I believe that the prospects for the acceptance of this new loyalty are now better than at the time of the Russell-Einstein Manifesto. This is so largely because of the enormous progress made by science and technology during these 40 years. The fantastic advances in communication and transportation have shrunk our globe. All nations of the world have become close neighbors. Modern information techniques enable us to learn instantly about every event in every part of the globe. We can talk to each other via the various networks. This facility will improve enormously with time, because the achievements so far have only scratched the surface. Technology is driving us together. In many ways we are becoming like one family… What we are advocating in Pugwash, a war-free world, will be seen by many as a Utopian dream. It is not Utopian. There already exist in the world large regions, for example, the European Union, within which war is inconceivable. What is needed is to extend these to cover the world's major powers. In any case, we have no choice. The alternative is unacceptable. Let me quote the last passage of the Russell-Einstein Manifesto: We appeal, as human beings, to human beings: Remember your humanity and forget the rest. If you can do so, the way lies open for a new paradise; if you cannot, there lies before you the risk of universal death.

Excerpt from the Nobel Lecture of nuclear physicist Joseph Rotblat, recipient of the Nobel Prize for Peace in 1995, which he shared with the Pugwash Conferences on Science and World Affairs "for their efforts to diminish the part played by nuclear arms in international politics and, in the longer run, to eliminate such arms" (www.nobelprize.org/nobel_prizes/peace/laureates/1995/rotblat-lecture.html).

22.1 INTRODUCTION

This final chapter is intended by the writer to summarize briefly some of the material covered in this book with respect to our knowledge of the structure of the atom, the forces that hold the atom together, how we have pictured the atom, and how we may use the energy of the atom for the betterment of mankind. All the historical accounts of the scientific achievements related in the previous chapters have given us a good picture of the atom and the energy that it holds. Using this energy exclusively for peace and the betterment of mankind is our obligation.

22.2 FROM DEMOCRITUS' "ATOMOS" TO QUARKS AND GLUONS

Over 2000 years ago the Greek philosopher Democritus taught the theory of atomism, which held that all matter was made up of minute, indivisible, and indestructible components called atoms. It would take physicists over 20 centuries to demonstrate the existence of atoms as basic components of the elements that constitute matter. Contrary to what was thought before the 20th century, scientists revealed that atoms were not indivisible but made up of yet much smaller constituents.

Research into the structure of the atom all began with the discoveries of X-radiation by Wilhelm C. Röntgen in 1895 and radioactivity from salts of the element uranium by Henri Becquerel in 1896. After these initial discoveries by Röntgen and Becquerel, advances into the structure of the atom progressed very fast. Relative to the findings from previous centuries, the advances made by physicists into atomic structure occurred exponentially. In the 20th century alone, the world

Radioactivity: Introduction and History, From the Quantum to Quarks. http://dx.doi.org/10.1016/B978-0-444-63489-4.00022-8
Copyright © 2016 Elsevier B.V. All rights reserved.

acquired almost all we know of the atom and its structure. Only 1 year after the discovery of radioactivity, J. J. Thomson discovered the electron, identified it as a particle, and determined the charge-to-mass (e/m) ratio of the electron. The following year, 1898, Marie and Pierre Curie demonstrated that the mysterious radiation discovered by Becquerel originated from the element of uranium; and that the same type of radiation was also emitted from the element of thorium. A few years thereafter, Marie Curie isolated the radioactive elements of radium and polonium.

The knowledge that radiation was emitted by atoms sparked research by Ernest Rutherford, Frederick Soddy, J. J. Thomson, and Paul Villard to characterize this radiation into alpha particles, beta particles, and gamma rays. Gamma rays would later be characterized by Albert Einstein to consist of photon particles similar to those of visible light but of shorter wavelength. Such a characterization by Einstein was a great step forward following the discovery by Max Planck of the quantum theory. Planck developed his quantum theory after determining that the energy levels (ΔE) of radiation emitted over a wide spectrum of wavelengths and frequencies corresponded to discrete multiples of a constant (Planck's constant h) times the frequency of the radiation (ν). Thus Planck's quantum dictated that energy was emitted from atoms in discrete energies ($\Delta E = h\nu$), which may be pictured as packets of energy referred to as energy quanta. The word quantum was most fitting for the phenomenon, as it is derived from the Latin *quantus*, meaning "how much."

With a basic knowledge of the properties of radiation emitted by radioactive atoms, Ernest Rutherford discovered the atomic nucleus in 1911. To do this, Rutherford and his assistants bombarded a thin foil of gold metal with alpha particles emitted by radioactive atoms. Almost all the alpha particles passed through the gold foil, as if the atom was empty space. However, a very small number of the alpha particles (one in 8000) would ricochet back toward the direction from which it came. From this Rutherford concluded that there exists a relatively small and massive body in the atom which would cause the alpha particle to bounce back from the atoms of gold metal. He called this small massive body the atomic nucleus. By measuring angles of deflection of the alpha particles, Rutherford could mathematically calculate the radius of the atomic nucleus to be approximately 10^{-15} m.

The next great discovery on the structure of the atom came in 1919, when Ernest Rutherford bombarded molecules of air with alpha particles of energy sufficient to knock out protons from the nucleus of nitrogen atoms of the air. The location of the electron in the atomic structure was described by Niels Bohr in a series of papers published during 1913−1921. Niels Bohr presented to the world calculations demonstrating that atomic electrons would exist in orbitals at distances away from the atomic nucleus. The orbitals would represent specific quantized energies. The number of orbital electrons with their negative unit charge would equal the positive charge of the protons in the nucleus of the neutral atom.

Thus by 1919 much had been discovered concerning the atom, the electron, its relative location in the atom and its charge, the atomic nucleus and its size, and the proton as a constituent of the nucleus and its charge. The existence of the neutron was not yet known. The neutron remained elusive because of its neutral charge, which made it difficult to detect at the time. However, in only 20 years (1898−1919) more had been discovered on the atom and its nucleus than was known the previous 20 centuries since Democritus' teaching of *atomos*.

Ironically, G. P. Thomson, the son of J. J. Thomson, and Clinton Davisson demonstrated independently in 1927 that the electron particle discovered by J. J. Thomson in 1897 would act as a wave, thus demonstrating the dual particle-wave nature of matter. This discovery came on the heels of Louis Victor de Broglie's theory in 1923 of the dual nature of matter and light: that matter could be interpreted as having the properties of light with wavelength and frequency or the properties of a particle with mass. A common joke among physicists at the time was that "The father, J. J. Thomson, received the Nobel Prize for proving that the electron was a particle; and his son, G. P. Thomson, won the Nobel Prize for demonstrating that the electron was not a particle, but a wave." This was all in jest, because it was demonstrated that the electron as well as other particles exhibit a dual nature: that of a particle and that of a wave.

A more complete picture of the atomic nucleus remained unknown until James Chadwick discovered the neutron in 1932. It was known by 1930 that a highly penetrating radiation was emitted when beryllium metal was bombarded with alpha particles. However, the characterization of this radiation as neutrons was elusive, because of the particle's neutral charge, which gave it a high power of penetration in matter and also made it difficult to detect: the neutron's neutral charge would not cause ionization and would enable the neutron to pass through lead and other metals easily with little or negligible interaction. However, James Chadwick used ingenuity to demonstrate that the neutron could interact with a barrier made up of a proton-rich substance such as paraffin. The neutrons would collide with the protons of the paraffin, knocking them out of the waxy substance as free protons. Due to their positive charge, protons are easy to detect and have a short range of travel in matter. By determining the energy of the protons emitted from the paraffin, James Chadwick could demonstrate that the neutrally charged neutrons had a mass similar to the protons.

Following this discovery of the neutron in 1932, the basic structure of the atom was complete: protons and neutrons are held together in the nucleus by a yet unknown strong nuclear force, and the atomic electrons are located in discrete quantized energy orbitals at a relatively great distance from the atomic nucleus. The nucleons—the protons and neutrons

that make up the atomic nucleus—were thought to be fundamental or elementary particles that were indivisible. This belief remained for over 30 years until 1964, when George Zweig and Murray Gell-Mann independently proposed the existence of quarks as constituents of the nucleons; the quarks were later discovered by others.

With a complete picture of the nucleus as consisting of proton and neutrons, the origin of alpha particles and gamma radiation in nuclear decay could be better understood. Both of these radiation types were emitted with discrete energy lines. The alpha particles, which consisted of a combination of two protons and two neutrons, would be emitted or "spit out" of the nucleus of unstable radioactive atoms with discrete energies. Such a phenomenon would occur only in large atoms that had a heavy nucleus—that is, a nucleus with an atomic number (proton number) greater than 83. The nucleus would have to be large to allow a portion of the nucleus to be "spit out" as an alpha particle. The emission of gamma radiation from a decaying atomic nucleus was well understood to be discrete energy quanta emitted from the nucleus as it decayed to a lower or stable energy state. A conundrum existed for the scientific community in understanding what was happening when beta particles were emitted by unstable decaying atomic nuclei. Firstly, beta particles were equivalent to electrons, and electrons could not exist in the nucleus. Thus the beta particle must be created by the atomic nucleus during its decay. However, when considering a sample containing many atoms of a given unstable radioactive isotope, the beta particles emitted would all possess a different energy. If the decay energy of a nucleus was a given value and the emission of the beta particle brought the nucleus to a stable energy state, several questions arose. Why would the beta particle possess an energy lower than the decay energy? Where did the remaining energy go? Why would the beta particle energies be emitted over a wide spectrum, from close to zero energy up to the maximum decay energy of the nucleus? The conundrum was solved in theory by Wolfgang Pauli in an open letter he wrote in 1930 to the participants at a meeting on radioactivity in Tübingen, Germany. In this letter he proposed the existence of another particle, namely the neutrino, which would be created along with the beta particle as a product of beta decay and would share the energy of beta decay with the beta particle. The neutrino would be very difficult to detect because of its near-zero mass and neutral charge. The particle can travel through the center of the Earth without interacting with anything. So difficult was this particle to detect that its existence would not be demonstrated until 25 years later, by Frederick Reines and Clyde Cowan, Jr.

Neutron radiation proved to be an excellent means of producing numerous radioactive artificial isotopes of the elements. Enrico Fermi headed a team of scientists during 1939−1940 that produced over 65 artificial radioisotopes by the irradiation of elements with neutrons. He observed that neutrons with their neutral charge could penetrate the coulombic barrier of the atom without difficulty and intimately approach the atomic nucleus to be captured by the nucleus, creating an atomic nucleus of higher mass or of different atomic number and mass number, when the capture of the neutron resulted in the emission of a proton or alpha particle. Many new radioisotopes which were created artificially in this manner and by other means, such as the cyclotron invented by Ernest Lawrence in 1931, proved to be very useful for the betterment of humankind in the fields of biological research and the diagnosis and treatment of cancer.

Neutron capture by an atomic nucleus also resulted in the discovery in 1939 of nuclear fission of uranium-235 by Otto Hahn and Fritz Strassman; and shortly thereafter Lise Meitner and Otto Frisch interpreted fission as the splitting of a large nucleus into two parts, with the emission of a relatively large amount of energy. In addition, nuclear fission resulted in the emission of neutrons; and Walter Zinn and Leo Szilard in 1939 determined accurately that the fission reaction resulted in the emission of generally two or three neutrons per reaction, with an average figure of about 2.5 neutrons per fission. The determination that more than one neutron is emitted for each neutron captured by the uranium nucleus in the fission reaction led to the conclusion that nuclear chain reactions were possible. The scientific community then knew that the production of a nuclear fission chain reaction, when sufficient atoms of uranium-235 (or plutonium-239) were present, would produce an atomic bomb. Scientists realized that nuclear fission was a double-edged sword. Nuclear fission in the form of an uncontrolled chain-reacting bomb would threaten the continued survival of humankind; but on the other hand, a controlled chain reaction would provide an immense source of energy in the form of electric power for our development and well-being.

In 1939, the same year that nuclear fission was discovered, energy production in stars was described in detail by Hans Bethe. It entailed the fusion of two atomic nuclei, resulting in the production of a large amount of energy. Knowledge can be used to pursue adverse objectives; and in this case nuclear fusion was used by Edward Teller and Stanislaw Ulam to design hydrogen bombs in 1951, which are much more powerful and devastating than the fission-based atomic bomb. The development of large stockpiles of these devastating bombs, as a result of an arms race between nations, holds the potential of destroying all humans on Earth. On the other hand, the fusion of two atomic nuclei to produce energy for electric power is now considered the energy of the future, whereby fusion reactors will eventually replace nuclear power reactors to produce a relatively safe source of electrical power with an endless source of fuel, as described in detail in this book.

When the writer was a doctoral student in the 1960s, it was taught in class that the proton and neutron in the atomic nucleus were elementary or fundamental particles; that is, it was believed these particles could not be broken down

further into smaller constituents. However, in 1964 George Zweig and Murray Gell-Mann proposed independently that the proton and neutron contained yet smaller particles, referred to as quarks. The proton and neutron in the atomic nucleus would contain different combinations of two quarks, now known as the up (u) quark and the down (d) quark. The proton would contain two up quarks and a down quark (uud); and the neutron would contain one up quark and two down quarks (udd). These quarks would possess a fractional charge whereby the u quark has a fractional positive charge of the electron charge or $+\frac{2}{3}e$; and the down quark has a fractional negative charge of the electron charge or $-\frac{1}{3}e$. This would leave the overall charge on the proton with 2 u quarks and 1 d quark as $(+\frac{2}{3}e) + (+\frac{2}{3}e) + (-\frac{1}{3}e) = +1e$. The overall charge on the neutron with 1 u quark and 2 d quarks would be $(+\frac{2}{3}e) + (-\frac{1}{3}e) + (-\frac{1}{3}e) = 0$. George Zweig also postulated in 1964 that a force would have to exist to maintain the quarks confined in the proton and neutron. Three quarks within a proton and their relative size to that of the proton are illustrated in Fig. 22.1. The existence of

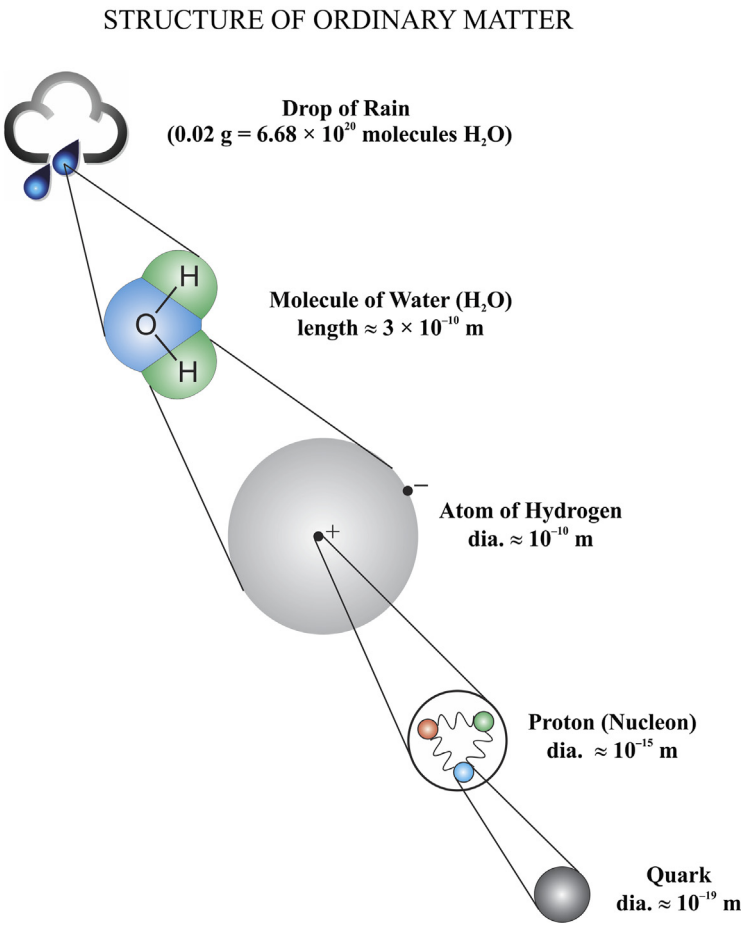

FIGURE 22.1 The hydrogen atom. The term "ordinary matter" is used here to mean matter which we observe in day-to-day life; and not matter that is produced via the collision of atomic particles. We can start with a drop of rain, visible to the naked eye. A conventional drop weighing 0.02 g would contain as many as 6.7×10^{20} molecules of water (H_2O). A single molecule of water, measured with radiation of much shorter wavelength than visible light, such as X-ray diffraction, is only $\sim 3 \times 10^{-10}$ m in length. An atom of hydrogen from that molecule would have a diameter defined by its nucleus (small dot at the center) and its surrounding electron orbital (represented by the surrounding shaded area). The hydrogen atom has a diameter of approximately 10^{-10} m. Bombardment of the atom with particles of very short wavelength permits the measurement of the dimensions of all atom components. The atomic nucleus is very small compared to the whole atom, being approximately 1/10,000 the size of the atom. Thus there is a relatively large distance between the nucleus and its surrounding orbital electron. We can compare this distance to that of a baseball, which has a diameter of 7.5 cm, in the center of a circular field with a diameter of 0.75 km. The distance between the nucleus and an electron orbital, although relatively large, is not considered empty space, because it contains an electromagnetic force mediated by the emission and absorption of photons between the positively charged proton and negatively charged orbital electron. This force holds the nucleus and outer electrons of atoms together. A single nucleon (proton or neutron) of the nucleus measures approximately 10^{-15} m in diameter and contains three quarks of red, green, or blue color charge and gluons (illustrated as waves between the quarks). The quarks in the nucleon are held together by the strong force mediated by the continuous emission and absorption of gluons between the quarks. A component quark is yet 1/10,000 times smaller than the proton or neutron, or 10^{-19} m.

quarks and the force that holds them together in a nucleon (proton or neutron) remained a theory and was not demonstrated until the early 1970s.

Prior to the discovery of quarks another theory was created that would explain the forces that hold the quarks within a nucleon. During 1964 and 1965 Oscar W. Greenberg, Moo-Young Han, and Yoichiro Nambu presented the theory that the quarks would possess another property called color charge, denoted as red, green, and blue color charge. This property had no relation whatsoever to color; but the term "color" was convenient to describe this new charge because the combination of red, green, and blue results in an overall colorless or neutral charge. Then came the development, by Harald Fritzsch and coworkers in 1971 and 1973, of the theory of quantum chromodynamics to describe the strong force between the quarks in the proton and neutron, which would be mediated by the constant emission and absorption of gluons by the quarks. The constant emission and absorption of gluons by quarks result in the continuous change of quark color charge—that is, the quarks will change constantly to red, green, or blue charge, as described in this book. The gluons are depicted by waves interconnecting the colored quarks in Fig. 22.1. Evidence for the existence of quarks and gluons was provided by Jerome Friedman, Henry Kendall, Richard Taylor, and coworkers, for which they were awarded the Nobel Prize in Physics in 1990. The experimental evidence for the existence of quarks and gluons in the nucleons is described in this book.

An interesting point to consider is the fact that gluons are exchange bosons that mediate the force between the quarks in the protons and neutrons of the atomic nucleus. The gluons act as the "glue" that binds the quarks within the nucleons. Gluons also mediate the strong force that holds the protons and neutrons together to form the atomic nucleus. Although gluons are themselves massless, their energy, ie, binding energy, contributes to 99% of the total mass of an atom. As originally described by Albert Einstein, energy is equivalent to mass ($E = mc^2$). The contribution of the gluon binding energy to the total mass of an atom is an astonishing 99%! In other words, almost all the mass of an atom is derived essentially from the gluon binding energy. To illustrate this amazing fact, the writer has calculated the masses of the various constituents of atoms of low, intermediate, and high atomic numbers (Z). These are listed in Table 22.1 to provide a picture of the contribution of the mass equivalent of the gluon binding energy to the total mass of small, medium, and large atoms. The gluon binding energies are calculated by summing the masses of the electrons and the up and down quarks, and subtracting the sum from the total known mass of each atom.

Although astonishing, it is now understood that the gluon, which is massless, is responsible for 99% of the mass of an atom. This mass is derived from the energy of the massless gluons, which is an energy that binds the quarks together in the atomic nucleus. Thus, in essence, 99% of the mass of our bodies and all matter that we observe on Earth and beyond are derived from energy. This amazing fact was underscored by Jim Baggott (2012) is his popular book where he described how 99% of the mass of all forms of matter that we see and feel each day is derived from the energy of gluons, which are massless. A short quote from his book is the following:

> *…the masses of the quarks are quite small, accounting for just one per cent of the mass of a proton or neutron. The other 99 per cent is derived from the energy carried by the massless gluons which flit between the quarks and bind them together. In the Standard Model the concept of mass, as an intrinsic property of measure of an amount of substance, has gone. Mass is instead constructed entirely from the energy of the interactions that occur between elementary quantum fields and their particles.*

From Baggott, J., 2012. Higgs, The Invention and Discovery of the God Particle, Oxford University Press, p. 221, www.oup.com.

22.3 THE PARTICLE ZOO

Subatomic particles are numerous, and with that in mind they are often referred to as "the particle zoo." Some are known constituents of matter; others are particles of yet unknown function that are produced naturally via high-energy collisions of cosmic radiation with atoms of air at the top of the atmosphere or artificially in high-energy particle colliders. The numerous subatomic particles are described in the previous chapters of this book, and their organization or classification can be confusing. A brief description and classification of the various groups of these particles is provided here.

The classification of subatomic particles is based upon their spin quantum numbers and whether or not the particles are elementary or composite (see Figs. 22.2–22.4). Elementary particles have no internal structure, ie, they are not composed of other particles or not known to be composed of other particles; whereas the composite particles can be broken down further into other particles.

Subatomic particles are classified into two types, namely **fermions** and **bosons**, as illustrated in Fig. 22.2. The fermions (named after Enrico Fermi) are particles with half-integral spin (1/2, 3/2…). Fermions obey the Pauli exclusion principle, which states that no two identical particles in an atom can possess the same quantum state.

TABLE 22.1 Mass Contributions of the Various Components of Atoms to the Total Mass of the Atom for Atoms of Low, Intermediate, and High Atomic Numbers (Z)

Atomic Component	Quantity	Mass (MeV/c^2)	Mass (kg)[a]	% of Atomic Mass[b]
Hydrogen-1 ($Z = 1$)				
Electrons	1	0.510[c]	9.1×10^{-31}	0.05
Photons (extranuclear)[d]	—	0.000136	Negligible	Negligible
Proton up (u) quarks[e]	2	4.6	82.0×10^{-31}	0.49
Proton down (d) quarks[f]	1	4.8	85.6×10^{-31}	0.51
Sum[g]	—	9.9	177.0×10^{-31}	1.05
Gluon binding energy[h]	—	928.9	1.656×10^{-27}	98.95
Carbon-12 ($Z = 6$)				
Electrons	6	3.06[c]	54.5×10^{-31}	0.03
Photons (extranuclear)[d]	—	0.000624	Negligible	Negligible
Proton up (u) quarks[e]	12	27.6	492.0×10^{-31}	0.25
Proton down (d) quarks[f]	6	28.8	513.4×10^{-31}	0.26
Neutron up (u) quarks[e]	6	13.8	246.0×10^{-31}	0.12
Neutron down (d) quarks[f]	12	57.6	1026.8×10^{-31}	0.52
Sum[g]	—	132.03	2353.5×10^{-31}	1.18
Gluon binding energy[h]	—	11,045.9	19.690×10^{-27}	98.82
Iron-56 ($Z = 26$)				
Electrons	26	13.26[c]	236.4×10^{-31}	0.03
Photons (extranuclear)[d]	—	0.0208	0.37×10^{-31}	Negligible
Proton up (u) quarks[e]	52	119.6	2132.1×10^{-31}	0.23
Proton down (d) quarks[f]	26	124.8	2224.8×10^{-31}	0.24
Neutron up (u) quarks[e]	30[i]	69.0	1230.0×10^{-31}	0.13
Neutron down (d) quarks[f]	60[i]	288.0	5134.1×10^{-31}	0.55
Sum[g]	—	614.7	$10{,}957.8 \times 10^{-31}$	1.18
Gluon binding energy[h]	—	51,488.4	91.786×10^{-27}	98.82
Barium-138 ($Z = 56$)				
Electrons	56	28.56[c]	509.1×10^{-31}	0.02
Photons (extranuclear)[d]	—	0.137	2.4×10^{-31}	Negligible
Proton up (u) quarks[e]	112	257.6	4592.1×10^{-31}	0.20
Proton down (d) quarks[f]	56	268.8	4791.8×10^{-31}	0.21
Neutron up (u) quarks[e]	82[i]	188.6	3362.1×10^{-31}	0.15
Neutron down (d) quarks[f]	164[i]	787.2	$14{,}033.1 \times 10^{-31}$	0.61
Sum[g]	—	1530.9	$27{,}290.6 \times 10^{-31}$	1.19
Gluon binding energy[h]	—	126,927.0	226.268×10^{-27}	98.81
Bismuth-209 ($Z = 83$)				
Electrons	83	42.33[c]	754.6×10^{-31}	0.02
Photons (extranuclear)[d]	—	0.372	6.6×10^{-31}	Negligible
Proton up (u) quarks[e]	166	381.8	6806.2×10^{-31}	0.20

Continued

TABLE 22.1 Mass Contributions of the Various Components of Atoms to the Total Mass of the Atom for Atoms of Low, Intermediate, and High Atomic Numbers (*Z*)—cont'd

Atomic Component	Quantity	Mass (MeV/c^2)	Mass (kg)[a]	% of Atomic Mass[b]
Proton down (d) quarks[f]	83	398.4	7102.1×10^{-31}	0.20
Neutron up (u) quarks[e]	126[i]	289.8	5166.2×10^{-31}	0.15
Neutron down (d) quarks[f]	252[i]	1209.6	$21{,}563.1 \times 10^{-31}$	0.62
Sum[g]	—	2322.3	$41{,}398.8 \times 10^{-31}$	1.19
Gluon binding energy[h]	—	192,341.7	342.880×10^{-27}	98.81

[a] *From conversion factor:* $1\ MeV/c^2 = 1.782661 \times 10^{-30}\ kg$.

[b] *The atomic mass of hydrogen-1* $= 1.007825\ u$

$$= (1.007825\ u)(931.494013\ MeV/u) = 938.783\ MeV$$
$$= (1.007825\ u)(1.66053873 \times 10^{-27}\ kg/u) = 1.6735 \times 10^{-27}\ kg$$

The atomic mass of carbon-12 $= 12\ u$

$$= (12\ u)(931.494013\ MeV/u) = 11,177.93\ MeV$$
$$= (12\ u)(1.66053873 \times 10^{-27}\ kg/u) = 19.926 \times 10^{-27}\ kg$$

The atomic mass of iron-56 $= 55.934939\ u$

$$= (55.934939\ u)(931.494013\ MeV/u) = 52,103.06\ MeV$$
$$= (55.934939\ u)(1.66053873 \times 10^{-27}\ kg/u) = 92.882 \times 10^{-27}\ kg$$

The atomic mass of barium-138 $= 137.905232\ u$

$$= (137.905232\ u)(931.494013\ MeV/u) = 128,457.898\ MeV$$
$$= (137.905232\ u)(1.66053873 \times 10^{-27}\ kg/u)$$
$$= 228.997 \times 10^{-27}\ kg$$

The atomic mass of bismuth-209 $= 208.980374\ u$

$$= (208.980374\ u)(931.494013\ MeV/u) = 194,663.967\ MeV$$
$$= (208.980374\ u)(1.66053873 \times 10^{-27}\ kg/u)$$
$$= 347.020 \times 10^{-27}\ kg$$

[c] *The energy equivalent mass of the electron is* $0.510\ MeV/c^2$.

[d] *Photons are the carriers of the weak electromagnetic force, which provides the binding energy between the nucleus and the orbital electron. There is only one orbital electron in* ***hydrogen-1****, which has a binding energy of* $13.6\ eV/c^2$. *There are six orbital electrons in the* ***carbon-12*** *atom in three orbital subshells, with combined binding energies amounting to* $624.2\ eV/c^2$. *There are 26 orbital electrons in the* ***iron-56*** *atom, with combined binding energies of* $20.8\ keV/c^2$. *There are 56 orbital electrons in the* ***barium-138*** *atom, with combined binding energies of* $137.8\ keV/c^2$. *There are 83 orbital electrons in the* ***bismuth-209*** *atom, with combined binding energies of* $372.0\ keV/c^2$.

[e] *The mass of the up (u) quark is* $\sim 2.3\ MeV/c^2$.

[f] *The mass of the down (d) quark is* $\sim 4.8\ MeV/c^2$.

[g] *The sum is the total of all masses of the atomic constituents, with the exception of the energy of the massless gluons that bind the quarks within the protons and neutrons of the nucleus.*

[h] *The gluon binding energy constitutes the remaining mass of the atom, which is found by the difference of the atomic mass less the sum of the masses of all other components of the atom.*

[i] ***Iron-56*** *contains 26 protons and 30 neutrons in the nucleus.* ***Barium-138*** *contains 56 protons and 82 neutrons in the nucleus.* ***Bismuth-209*** *contains 83 protons and 126 neutrons in the nucleus.*

For each of the fermions there exists a distinct antiparticle. Among the fermions are the quarks and **leptons**, which are elementary particles (see Fig. 22.3). The word lepton is derived from the Greek *leptós*, meaning small. Also among fermions are the baryons, which are composite particles containing three quarks. The word **baryon** is derived from the Greek word *barus*, meaning heavy. The other class of nuclear particle is the boson, named after the Indian physicist Satyendra Nath Bose (1894−1974). Bosons have integral spins (0, 1, 2…), and do not obey Pauli's exclusion principle, ie, two bosons may possess the same quantum state. Bosons may be elementary particles such as photons and gluons, or may be composite particles referred to as **mesons**, which contain a quark and an antiquark. The elementary particles constitute the Standard Model as the building blocks of all matter, as described in the previous chapter of this book.

Particles are also classified according to whether they are elementary or composite, as illustrated in Figs. 22.2−22.4. The elementary particles do not have any known substructure; that is, they have no known underlying structure. Among these are the elementary bosons, namely the photon (γ), gluon (g), $W^{\pm}$ boson, Z^0 boson, and the Higgs boson;

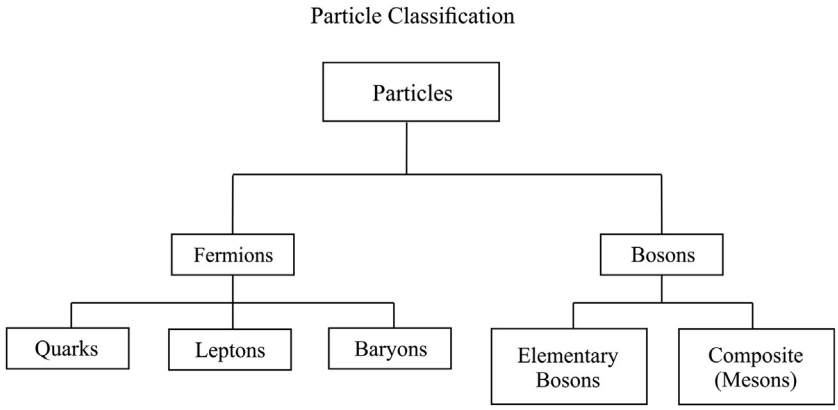

FIGURE 22.2 The classification of subatomic particles. The fermions obey the Pauli exclusion principle, and possess odd half-integer spin (ie, 1/2, 3/2… ie, half an odd integer). The bosons do not obey the Pauli exclusion principle, and possess integer spins (ie, 0, 1…). Bosons may be elementary bosons, which cannot be broken down into smaller particles. Examples are the photon (γ), gluon (g), $W^{\pm}$, and Z^0 particles, and the Higgs (H^0) boson. Composite bosons can be broken down into smaller particles, such as the mesons, which contain a quark and an antiquark.

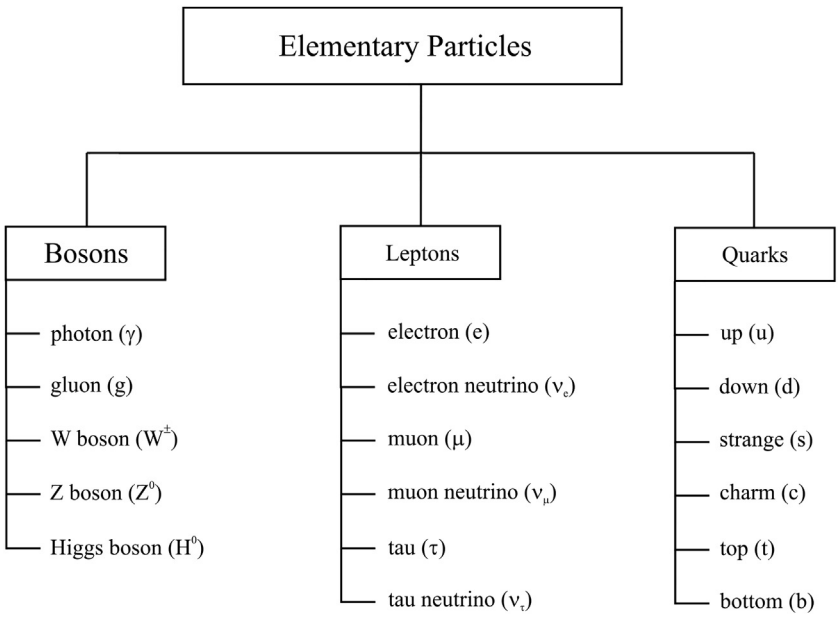

FIGURE 22.3 The elementary particles are particles that cannot broken down into smaller constituents or that are not known to contain smaller particles. The elementary particles (all the particles listed above) constitute the Standard Model of the building blocks of matter.

the leptons, including the electron (e), muon (μ), and tau (τ) particles and their respective neutrinos; and the quarks, of which there are six types or flavors, namely the up (u), down (d), strange (s), charm (c), top (t), and bottom or beauty (b) quark.

Hadrons are composite particles which have an underlying structure of quarks held together by the strong force mediated by the energy of gluons. The word hadron is derived from the Greek word *hadrós*, meaning thick. The hadrons are classified as either **baryons**, which contain three quarks, such as the proton, neutron, and hyperons, or **mesons**, which contain only two quarks (a quark and an antiquark), such as the pion, kaon, etc. The hadrons are categorized in Table 22.4.

Among the elementary bosons listed in Fig. 22.3, the photon, gluon, and the $W^{\pm}$ and Z^0 particles act as exchange particles in one of three fundamental forces or interactions in nature. Table 22.2 lists the **fundamental forces** in nature and their properties.

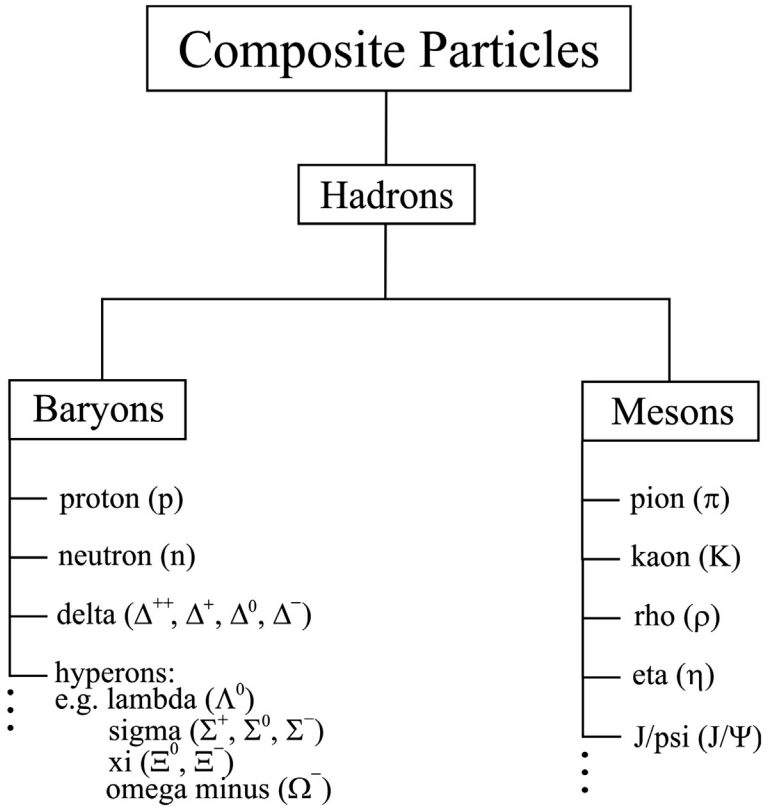

FIGURE 22.4 The composite particles are called hadrons, which comes from the Greek *hadrós*, meaning thick, because the hadrons contain quarks held together by gluons. The baryons contain three quarks; and the mesons are composed of two quarks, specifically a quark and an antiquark. Both baryons and mesons also contain gluons that represent the strong force holding the quarks within each particle. The hyperons are called strange baryons, because they contain at least one strange (s) quark and do not contain either a charm (c), bottom (b), or top (t) quark.

TABLE 22.2 Fundamental Forces in Nature

Force	Relative Strength[a]	Range	Field Particle(s)[b]	Particles Affected[c]
Electromagnetic	$\approx 1/137$	Infinite	Photon (γ)	Charged particles
Weak	$\approx 10^{-6}$	$\approx 10^{-18}$ m	$W^{\pm}$ and Z^{0}	Leptons and quarks
Strong	≈ 1	$\approx 10^{-15}$ m	Gluon (g)	Hadrons and quarks
Gravity	$\approx 10^{-40}$	Infinite	Graviton?[d]	All particles

[a] *The strength of the force or interaction relative to the strong force arbitrarily given the value of 1.*
[b] *A force carrier particle that mediates the electromagnetic, weak, and strong interactions, and gravity.*
[c] *The electromagnetic, weak, and strong interactions will affect only certain particles.*
[d] *The graviton is hypothetical, and has not yet been demonstrated.*

22.3.1 The Electromagnetic Force

The electromagnetic force is exhibited when particles of like charge repel one another or when particles of opposite charge attract each other. Such a force is exchanged between the two particles by means of a virtual photon, ie, electromagnetic quantum, as illustrated in Fig. 22.5. The distance or range of the electromagnetic force is considered infinite, because it is effective at very short distances, such as when an electron (eg, β particle) travels to close proximity of another electron within an atom and the two electrons are scattered due to their like charge, and is also exhibited at great distances within the vast electromagnetic fields of the galaxies. The electromagnetic force is weaker than the strong nuclear force by a factor of 1/137, which is known as the fine structure constant ($\alpha = 1/137.035 = 7.297 \times 10^{-3}$).

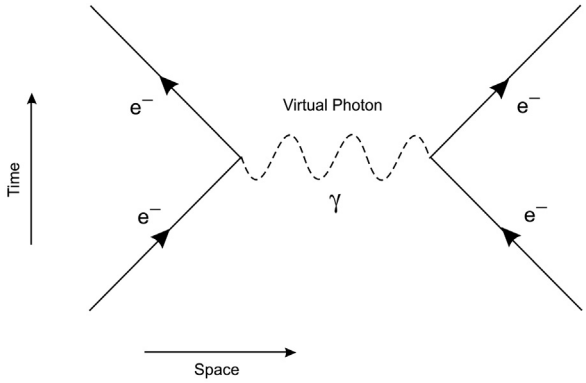

FIGURE 22.5 A Feynman diagram depicting the photon as the exchange particle of the electromagnetic force between two electrons, resulting in electron scattering. The photon mediates the electromagnetic force between the two electrons. The electromagnetic interaction results in the absorption of the photon particle by an electron, providing it with momentum to be repelled. The electron emitting the photon undergoes recoil. The photon is illustrated as a dashed wave. It is referred to as a virtual photon, because it is emitted and absorbed without being detected.

22.3.2 The Weak Force

The weak force, also referred to as the weak nuclear force or weak interaction, is the controlling force involved in charged current and neutral current interactions, including beta decay, as described in detail in Hall of Fame, Part IX of this book. Beta decay involves the conversion of a neutron and proton in the atomic nucleus. Therefore, the distance or range of the weak force is short (10^{-18} m), ie, not exceeding the diameter of a proton or neutron. Because of the very short distance of interaction, it is called the weak force or weak interaction, although it is stronger than gravity (see Table 22.2). With a strength of 10^{-6} relative to the strong nuclear force, the weak force is weaker than the electromagnetic force.

The $W^{\pm}$ and Z^0 bosons are the mediating particles of the weak force. An example is where the $W^{\pm}$ boson mediates the weak force in beta decay, which results in either negatron or positron emission. Beta decay with negatron (e^-) emission involves the conversion of a neutron into a proton, as described in the chapter entitled "Beta Radiation and Beta Decay." In this beta decay process, a neutron converts into a proton when a down quark (d) of the neutron transforms into an up quark (u), as illustrated in the Feynman diagram in Fig. 22.6. The conversion of the down quark to an up quark involves the emission of the W^- boson as the exchange particle, which decays into a negative electron (ie, negatron, symbolized as e^- or β^-) and antineutrino $(\overline{\nu_e})$. The Feynman diagram in Fig. 22.6 illustrates a neutron which contains three quarks, ie, one up quark and two down quarks (udd), transforming into a proton which also contains three quarks, ie, two up quarks and a down quark (uud). In the process, a W^- boson is emitted, which decays into a negative electron (e^-), also known as a negatron or negative beta particle (β^-), and an electron antineutrino $(\overline{\nu_e})$. A negatively charged boson (W^-) mediates the negatron (β^-) emission, to balance the creation of the positively charged proton from the neutral charge of the original neutron. Thus a negatively charged electron is emitted.

In the case of beta decay resulting in positron (e^+ or β^+) emission, the antiparticle of the W^-, which is denoted as W^+, is the mediating particle or, in other words, the field particle, ie, the force-carrying particle. This is the particle that carries the energy and momentum from one particle to another, as illustrated in Fig. 22.7. This beta decay process is the opposite of that described in the previous paragraph, and proceeds as follows. A proton, which has a quark composition of one down quark and two up quarks (duu), converts into a neutron, which has a quark composition of two down quarks and one up quark (dud), when an up quark (u) changes into a down quark (d), as illustrated in Fig. 22.7. In the process, a positively charged W^+ boson is emitted as the carrier of this weak force, which balances the positive charge lost in the conversion of the proton to the neutron; and a positive electron (e^+), ie, positron (β^+), is emitted.

The lifetimes of the $W^{\pm}$ bosons are very short ($\sim 10^{-25}$ s), as they are massive particles (80.3 GeV/c^2) with a mass much greater than that of the proton or neutron. The short lifetime of these particles render them undetectable in beta decay measurements. Taking into account the very large mass of the $W^{\pm}$ bosons, their maximum range can be estimated on the basis of the Heisenberg uncertainty principle to be only 10^{-18} m (according to Eq. [VI.20] of Hall of Fame, Part VI of this book). The equation and calculation of the estimated range are as follows.

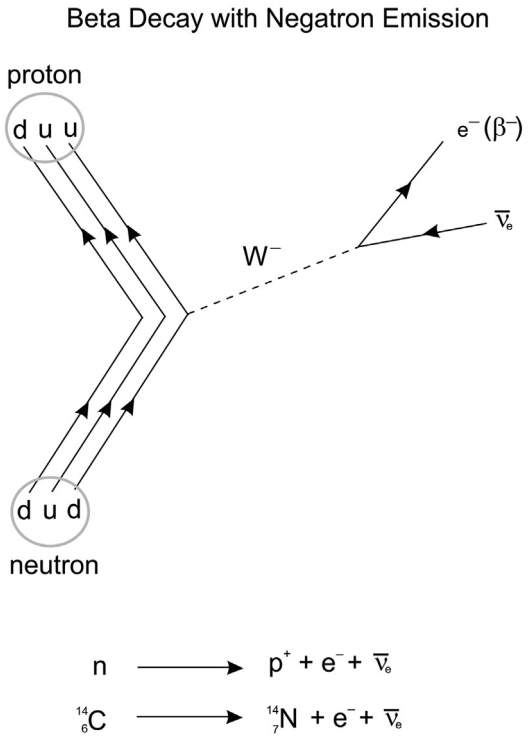

FIGURE 22.6 Feynman diagram illustrating beta decay with negatron emission where a neutron converts to a proton with the emission of a negative electron (beta particle) and an antineutrino. An example is provided by the beta decay of ^{14}C to ^{14}N. The diagram is read from left to right in the direction of the arrows as follows: a d quark of a neutron transforms into a u quark, whereby the neutron then becomes a proton with the emission of a W^- boson which acts as a field exchange particle for the creation and emission of a negative electron, also referred to as a negative β particle or negatron, and the emission of an antineutrino. Antiparticles are illustrated with an *arrow* in the opposite direction.

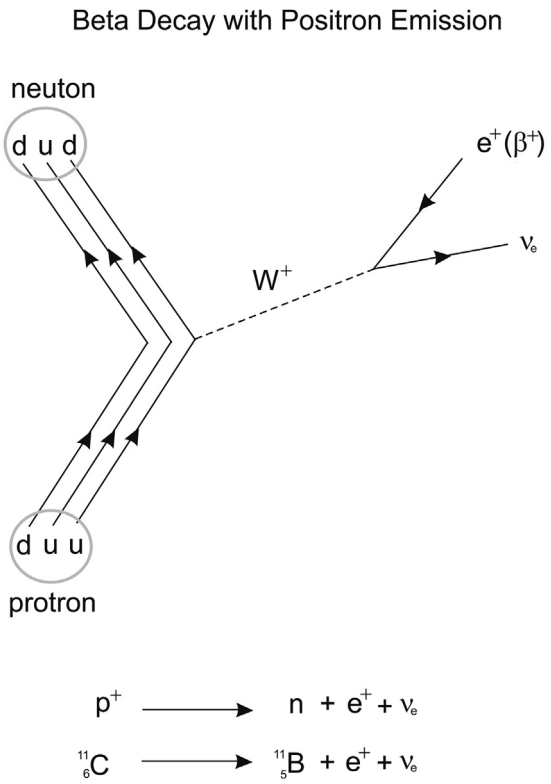

FIGURE 22.7 Feynman diagram illustrating beta decay with positron emission, where a proton converts to a neutron with the emission of a positive electron (ie, positive β particle or positron) and a neutrino. An example is provided by the beta decay of ^{11}C to ^{11}B.

For the $W^{\pm}$ bosons with a mass of 80 GeV/c^2, the maximum range of travel would be calculated as

$$d = c\Delta t = c\left(\frac{\hbar}{2m_W c^2}\right)$$

$$= 2.99 \times 10^8 \text{ m/s}\left(\frac{6.582 \times 10^{-22} \text{ MeVs}}{2(80 \times 10^3 \text{ MeV}/c^2)c^2}\right)$$

$$= 0.12 \times 10^{-17} \text{ m} \approx 1 \times 10^{-18} \text{ m}$$

Inverse beta decay, which involves the interaction of a neutrino with a neutron or antineutrino with a proton, is described in the chapter entitled "Beta Radiation and Beta Decay." This phenomenon is commonly used in the detection of neutrinos. The reactions of inverse beta decay (see reactions II.19 and II.20 of Hall of Fame, Part II of this book) involve the conversion of quark flavor with the transformation of a proton to a neutron, or vice versa, a neutron to a proton, and the $W^{\pm}$ bosons as field particles.

All forms of beta decay, including the rare double-beta (ββ) decay, are also mediated by W^- bosons, as illustrated in Fig. 6.13 of Chapter "Beta Radiation and Beta Decay."

The Z^0 boson possesses a neutral charge and a mass of approximately 92 GeV/c^2. Because of its neutral charge, the Z^0 boson is a field particle that mediates or transfers neither charge nor mass in particle interactions. Such interactions are referred to as **neutral current** (NC) weak interactions, such as the neutrino-electron scattering reaction illustrated in Fig. 22.8, which is an interaction used to detect solar neutrinos in liquid scintillation detectors. Another neutral current reaction involving the Z^0 boson, used to detect solar neutrinos, is that which occurs when a neutrino reacts with a deuterium nucleus, whereby neither a proton nor neutron of the deuterium nucleus changes identity. Rather, the combined neutron and proton of the deuterium nucleus separate, as described by the following:

$$\nu + \text{d} \xrightarrow{Z^0} \text{p} + \text{n} + \nu$$

Contrary to neutral current interactions, the $W^{\pm}$ bosons are field particles that mediate **charged current** (CC), where either the W^+ or W^- carries and transfer charge, as illustrated in Figs. 22.6 and 22.7.

$W^{\pm}$ and Z^0 bosons are virtual particles of high mass of approximately 80 and 92 GeV/c^2, respectively. They are very short-lived (approximately 10^{-25} s) and may be considered as photons, which acquire mass as exchange particles via the Higgs mechanism. The same concept holds for the origin of mass of protons and neutrons. The mass of protons (938 MeV/c^2) and neutrons (939 MeV/c^2) represents the principal source of the mass of all matter, as these nucleons constitute the heart of matter. The surrounding electrons of the atom are of relatively very low and almost negligible mass (0.51 MeV/c^2) compared to the mass of the proton and neutron. The protons contain three quarks (duu) with a total mass of only ~9 MeV/c^2, and neutrons contain three quarks (ddu) with a total mass of ~10 MeV/c^2. Thus quarks contribute ~9 MeV/938MeV ≈ 1% of the total mass of protons and ~10 MeV/939MeV ≈ 1% of the total mass of neutrons. The remaining 99% of the mass of the protons and neutrons is attributed to energy ($E = mc^2$) of the massless gluons, which are emitted and absorbed constantly by the quarks within the protons and neutrons. This binding energy of the massless gluons is the source of ~99% of the mass of all matter in the universe acquired through the Higgs mechanism.

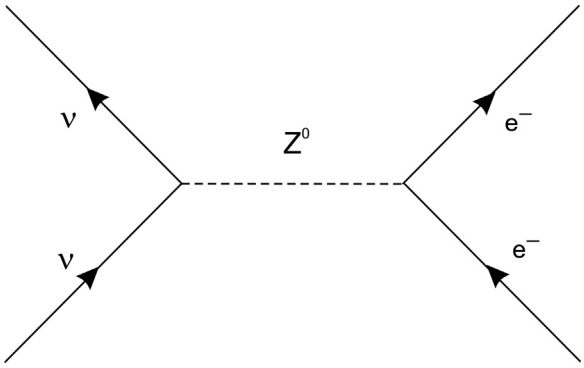

FIGURE 22.8 A Feynman diagram illustrating the mechanism by which a Z^0 boson acts as the field particle or force exchange particle in the interaction of a neutrino with an electron, resulting in an elastic scattering reaction. The interacting neutrino imparts kinetic energy to the electron, resulting in neutrino-electron scattering.

22.3.3 The Strong Force

The strong force is the short-range (10^{-15} m) force that holds the protons and neutrons together in the atomic nucleus. It is also the force that binds the quarks together within the protons and neutrons. Hideki Yukawa explained the strong force between nucleons in the atomic nucleus by proposing a new particle that would have a mass inversely proportional to the force between the nucleons; the mass of the particle would be intermediate of the proton and electron masses ($\sim 200 \times$ the electron mass). The new particle was named the meson, taken from the Greek *meso*, meaning middle. The prediction of Yukawa was verified by the discovery of the π meson or pion by Ochialini and Powell (1947, 1948). The strong force keeping the nucleons together is mediated by the exchange of π mesons between the nucleons. A detailed description of the role of the pion in the strong nuclear force that binds the protons and neutrons together in the atomic nucleus and the role of gluons in the strong nuclear force holding the quarks within the proton or neutron is provided in the chapter entitled "The Atomic Nucleus." The function of gluons in binding the quarks within the protons and neutrons is described in Hall of Fame, Part X.

22.3.4 Gravity

The force of gravity is the weakest among the four fundamental forces of nature listed in Table 22.2. It is the attractive force between two bodies that is directly proportional to the product of their masses and inversely proportional to their distance. The gravitational force is about 10^{-38} times weaker than the electromagnetic force and 10^{-34} times weaker than the weak nuclear force. Thus gravity has no significant influence on the interactions between subatomic particles. As there is a field particle in the other three forces in nature, it is predicted that the graviton would be the particle that mediates the gravitational force. This particle remains hypothetical. Currently only three of the four forces in nature are included in the Standard Model of elementary particles, namely the electromagnetic, weak, and strong interactions. The force of gravity is not yet a part of the Standard Model. The unification of the four fundamental forces in nature, which would include gravity, with general relativity and quantum theory to form the "theory of everything" is yet to be achieved. This goal is commemorated in a postage stamp from Macao, China illustrated here. The postage stamp illustrates a graph of the four fundamental forces of nature, with the "intensity of interaction" on the ordinate (y axis), "energy" on the abscissa (x axis), and an image of Albert Einstein. Four curves are labeled and colored as gravity (yellow curve), electromagnetic (purple), weak or fraca (orange), and strong or forte (red). The relative strengths of the four forces are illustrated along with the four curves as a dream or visualization whereby some day the four curves would conjoin, in the hope that in the future a theory will be available to explain their unification.

Unification of Forces

22.4 IMAGES OF THE ATOM

We have come a long way in the past century. The atom is no longer hypothetical. We know the structure of the atom as well as we know the structure of the cell of a living organism. We can obtain images of individual atoms in the structure of matter and see how the arrangements of these atoms make up the structures of matter in our world.

In our day-to-day lives we take photographs of anything we can see with our naked eye. Photons of visible light reflect off the surface of matter, and the reflected light enters the lenses of our eyes. The various intensities and shades of light and the various wavelengths that reach the eye together produce images of whatever we see, similar to a photographic camera. The wavelengths of visible light are too long (380−760 nm) to penetrate into atomic lattice structures and diffract from them to produce images; and images of atoms organized in matter would be too small for us to see with the naked eye. On the other hand, X-rays have short wavelengths (10−100 pm) equivalent to the lengths of the bonds between atoms. These X-rays can penetrate matter and be diffracted within the organized crystalline lattices of atoms. Measurement of the intensities of the diffracted X-rays can provide an image of the atoms as they are arranged within the crystalline structure of matter. The technique was first developed by the father-and-son team Sir William and Sir Lawrence Bragg in 1914, which earned them the Nobel Prize in Physics in 1915. The technique has been refined in modern science to produce many thousands of images of the arrangement of atoms in crystalline structures, which are referred to as electron density contour maps. An example of a picture of the electron density contour map of the atoms of carbon and hydrogen organized in the structure of benzene is illustrated in Fig. 22.9A. As described by Garcia-Granda and Mantejo-Bernardo (2013) in their comprehensive review of X-ray diffraction techniques, an electron density function reveals the molecular structure (arrangement of atoms) from which a crystal is made. They note that the electron density is concentrated in the vicinity of the atomic nucleus of the atoms in the crystal, which show peaks of the electron density maxima (positions of the atoms) as illustrated in Fig. 22.9A. Images of the arrangement of atoms in very complex and large molecules are determined by this technique. An excellent example is provided by the three-dimensional arrangement of the atoms in the enzyme fumarase, which is composed of 510 amino acids with a total molecular weight of 54,637 Da (illustrated in Fig. 1.43 in the chapter "Radioactivity and Our Well Being" of this book).

The hydrogen atom, which is the smallest of all atoms, consisting of only one proton for the atomic nucleus and one orbital electron, has been magnified by Stodolna et al. (2013) by a method called photoionization microscopy to provide an image of the nodal structure of the electron orbital. The instrumentation used by Stodolna et al. (2013) is illustrated in Fig. 22.10; and an image of the hydrogen atom with its nodal structure of the electron orbital is illustrated in Fig. 22.11. As described by Stodolna et al. (2013), the photoionization microscope provides a direct macroscopic projection of the electronic quantum state of the hydrogen atom. A very brief description of the operation of the microscope is as follows.

A beam of hydrogen atoms is formed by photoionization of H_2S gas in a vacuum chamber. A photon beam of 213 nm breaking an H−S bond and liberating a hydrogen atom (red ball) is illustrated at the far left of Fig. 22.10. The hydrogen atoms pass through a 3 mm aperture at collimator (a); and between regions (b) and (c) of Fig. 22.10.

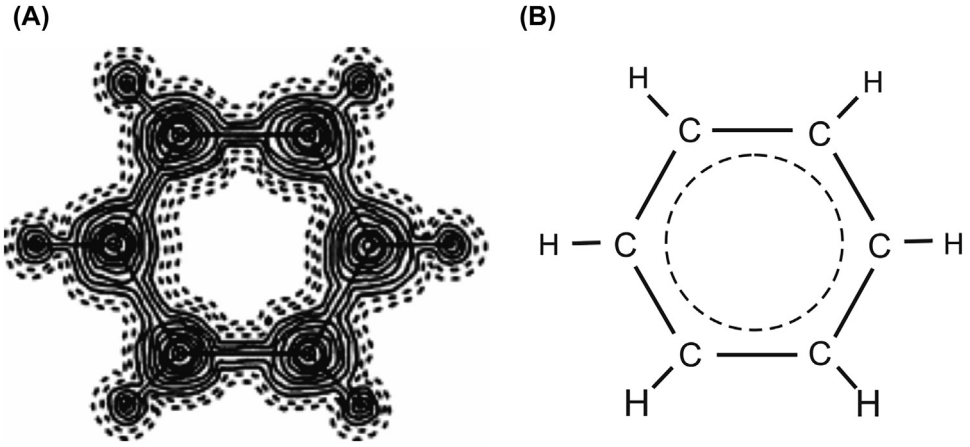

FIGURE 22.9 The orientation of carbon and hydrogen atoms in the benzene molecule, pictured as (A) a projection of the electron density contour map for benzene on the plane of the molecule *(from Garcia-Granda, S., Montejo-Bernardo, J.M., 2013. X-Ray Absorption and Diffraction|X-Ray Diffraction − Single Crystal. In: Jan Reedijk (Ed.-in-Chief), Reference Module in Chemistry, Molecular sciences and Chemical Engineering, Elsevier, Amsterdam, pp 1−15, reprinted with permission from Elsevier © 2013)*, and (B) the written chemical structure of benzene with its six carbon atoms bonded into a hexagonal ring with a single atom of hydrogen bonded to each atom of carbon.

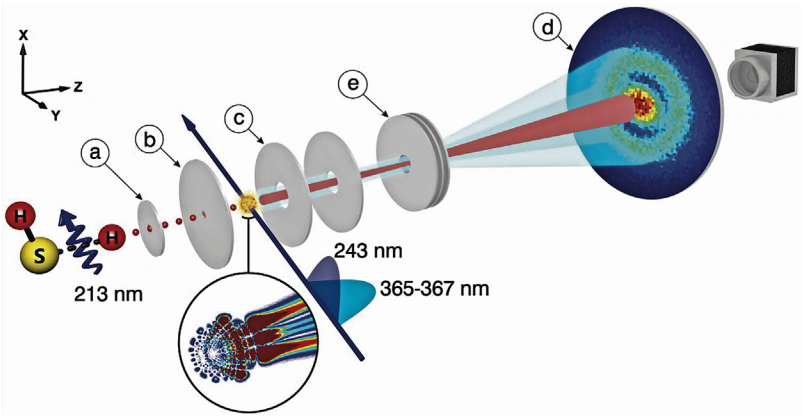

FIGURE 22.10 Basic components of the photoionization microscope, which provides a magnified image of the hydrogen atoms' electron orbital. *From Stodolna, A.S., et al., 2013, Hydrogen atoms under magnification: direct observation of the nodal structure of stark states. Phys. Rev. Lett. 110, 213001−213005, reprinted with permission from Elsevier © 2013.*

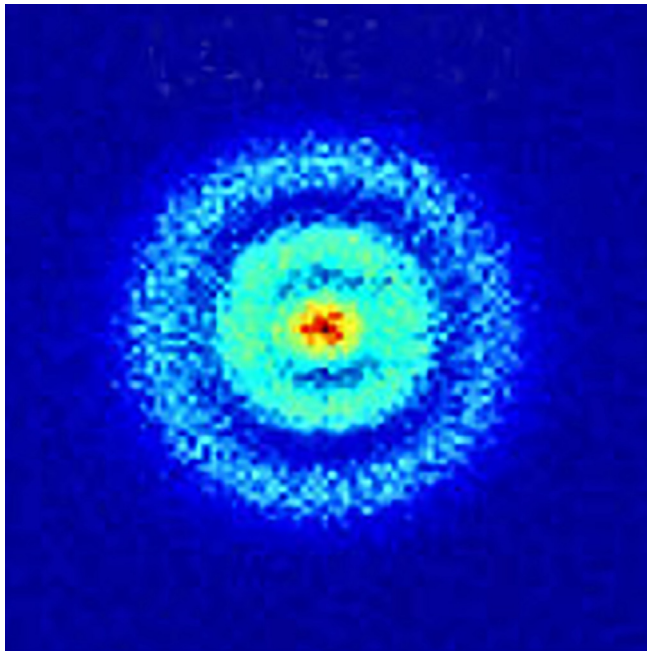

FIGURE 22.11 Hydrogen atom under magnification. At the very center the red-yellow region is that occupied by the nucleus, and the light cloudy regions away from the center are images created by an interference pattern of photoelectrons excited to the 2*s* and 2*p* orbital quantum states. *From Stodolna, A.S., et al., 2013, Hydrogen atoms under magnification: direct observation of the nodal structure of stark states. Phys. Rev. Lett. 110, 213001−213005, reprinted with permission from Elsevier © 2013.*

The hydrogen atoms at their ground state are excited to higher energy orbital quantum states, namely the 2*s* and 2*p* orbitals, by means of a two-photon transition with a pulse 243 nm laser followed by a tunable 365−367 nm UV laser. The photoelectrons are then accelerated by means of a voltage difference across the repeller (b) and extractor (c) electrodes to travel on through an Einzel lens (e), and collide with a two-dimensional microchannel plate detector and phosphor screen at (d). A camera consisting of a charged-coupled device, illustrated at the far right of Fig. 22.10, then captures the image of the hydrogen atom.

As described by Smeenk (2013) in a technical review of the newly developed microscope, there are two portions of the electron waves produced during the photoionization process. One portion of the wave is initially directed toward the two-dimensional phosphor screen and detector, and another portion is directed initially away from the detector. The repeller electrode (b) and extractor electrode (c) force all photoelectrons toward the two-dimensional detector;

however, an interference pattern is created, because of the two initially different directories of the photoelectrons. This interference pattern provides an image of the nodal structure of the electron orbital populated by an excitation pulse from the laser. The microscope is also known as a "quantum microscope," as it provides an image of an electron orbital quantum state.

22.5 THE ATOM IN OUR FUTURE

At the very beginning of this chapter is an excerpt from the Nobel lecture of Joseph Rotblat given in 1995. He underscored the fact that scientists and leaders of the world powers have an obligation to work toward the advancement and survival of humankind. We have learned more of the atom in the 20th century than we knew in the previous 20 centuries. Technology is advancing exponentially. When the writer went to elementary school, there were no ball-point pens. All students had to carry to school a bottle of writing ink and a pen. There were no transistor radios; a telephone call from a land-line required speaking first to an operator; and international calls were not possible. Throughout the writer's high school and undergraduate university education, there were no electronic calculators or computers. We used slide rules for mathematical calculations. Very large computers for mathematical calculations became available during the writer's years in graduate school in the 1960s. Electronic hand-held calculators with all the mathematical functions only became available in the 1970s.

The internet arrived in the 1990s, and the world started to become smaller. Now students of all ages access the internet on a hand-held device. We can communicate both visually and verbally with almost anyone in the world with the push of a button on our personal computer or hand-held device. Over the past 10 years we have become accustomed to expect new technological advances almost every day. With the world getting smaller and smaller in terms of international communication, travel, trade, and collaboration, what occurs in one nation can have an effect on all nations. Large scientific projects and very significant technological advances are no longer carried out by a single person or nation; rather, they are the result of international collaborations.

In the comprehensive introductory part of the book (chapter "Radioactivity and Our Well Being"), the writer described numerous advances made in the application of nuclear science and radioactivity to the betterment of humankind, including very important fields such as the use of nuclear radiation and radioactivity in the diagnosis and treatment of cancer and the development of nuclear fusion to provide a very safe form of energy for electric power with an endless source of fuel (deuterium) from our ocean waters. Nuclear fusion is the most promising energy source for future electric power. Space travel will also be powered by nuclear fusion. There is great promise that scientists from many countries now working together will harness the energy of the atom with nuclear fusion in the not too distant future, as described in detail in the chapter "Radioactivity and Our Well Being." This would mean limitless fuel for electric power free of radioactive fuel elements and free of radioactive waste now generated by fission nuclear reactors.

With the exponential growth of scientific development, it is impossible for us to predict what the next generation will bring. Out future, however, hangs in a delicate balance. Described in this book is the dark history of the development of the atomic fission bomb, and the even worse and more powerful and devastating hydrogen fusion bombs, which number in the tens of thousands (close to 16,000 nuclear weapons) in worldwide arsenals today. Added to this is the past development of other types of weapons of mass destruction, including chemical and biological. The world has at its disposal the power to destroy humankind several times over. From the Nobel lecture of Joseph Rotblat, a portion of which is given at the start this chapter and in Hall of Fame, Part IV, we must keep in mind that the very promising future, that scientific and technological advances can bring to all humankind, rests on our elimination of all nuclear weapons and other weapons of mass destruction. This has priority over any other achievement we may want to accomplish.

Appendix A

Particle Range–Energy Correlations

Figs. A.1–A.4

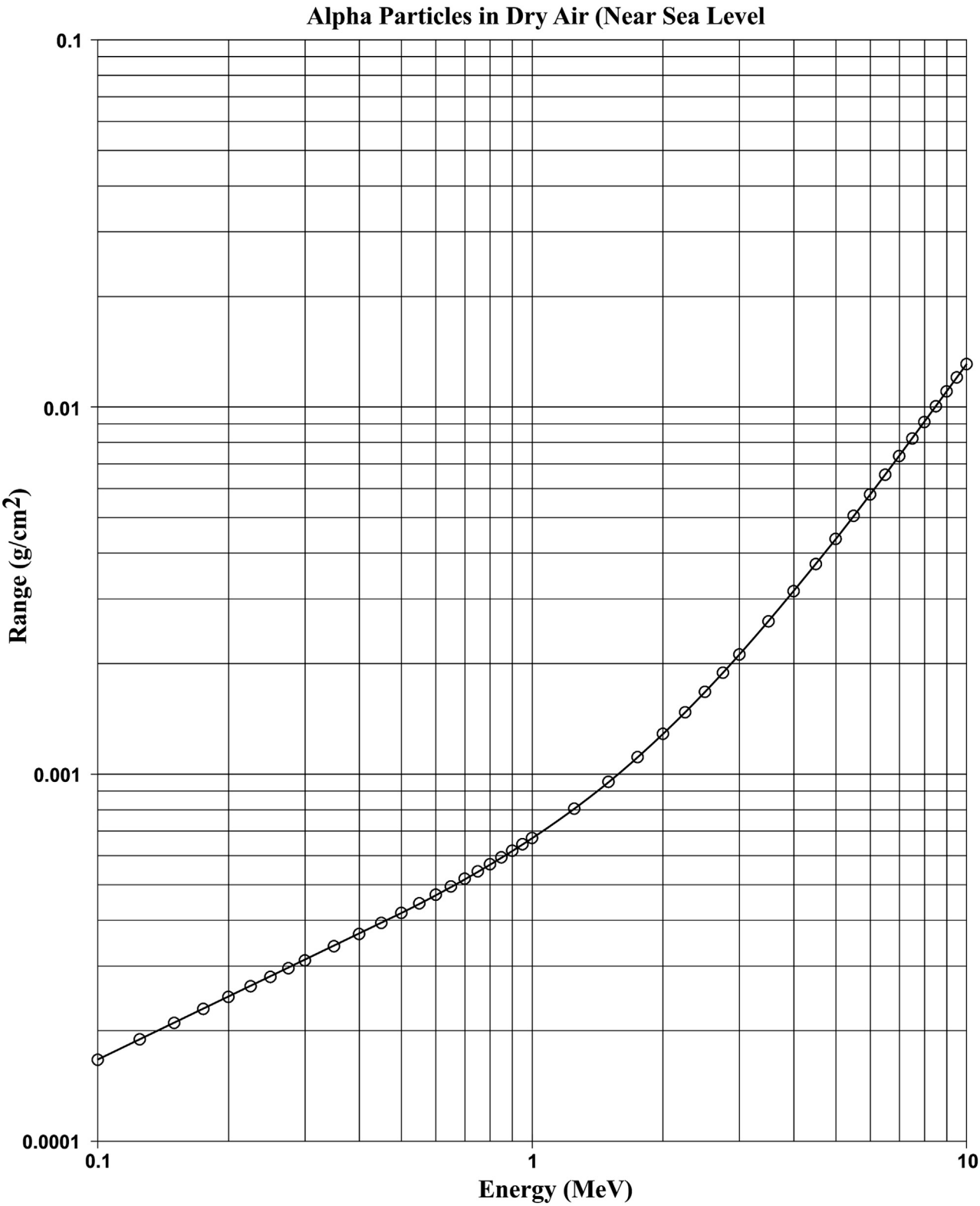

FIGURE A.1 Range−energy relationship for alpha particles in air. The range in cm can be obtained by dividing the above range by the density of air ($\rho = 0.001226$ g/cm^3 at standard temperature and pressure (STP)). For example, the range of a 5.5 MeV alpha particle from the graph is read as 0.005 g/cm^2, and dividing by the density of air yields a calculated linear range of 4 cm. The range−energy relationship is plotted from data provided by the National Institute of Standards and Technology database ASTAR (2016) for continuous slowing down approximation ranges, from which very precise calculated values of range may be found: http://www.nist.gov/pml/data/star/index.cfm.

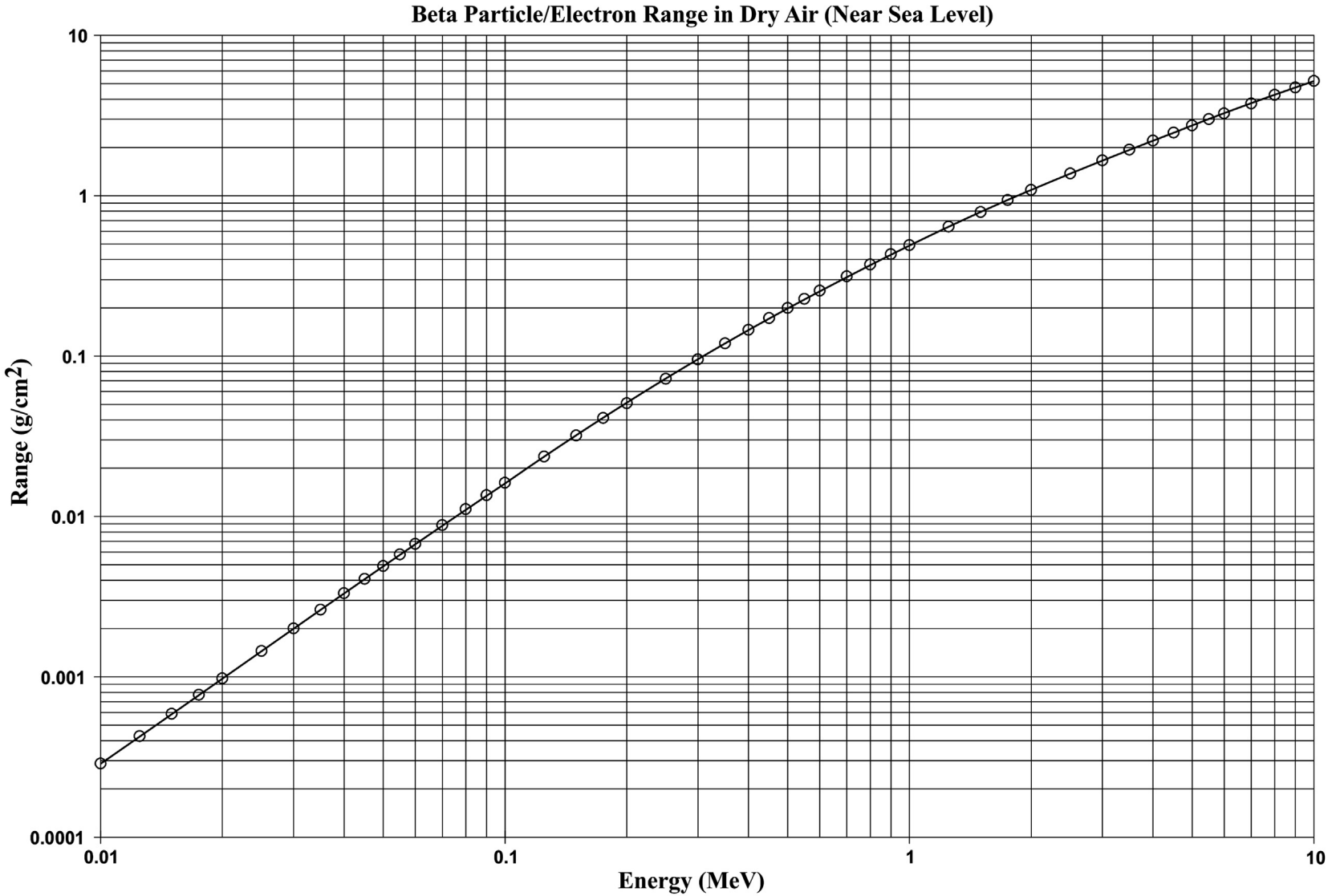

FIGURE A.2 Range–energy relationship for beta particles or electrons in air. The range in cm can be obtained by dividing the above range by the density of air ($\rho = 0.001226$ g/cm^3 at STP). For example, the range of a 1.0 MeV beta particle from the graph is read as 0.48 g/cm^2, and dividing by the density of air yields a calculated linear range of 390 cm. The range–energy relationship is plotted from data provided by the National Institute of Standards and Technology database ESTAR (2016) for continuous slowing down approximation ranges, from which very precise calculated values of range may be found: www.nist.gov/pml/data/star/index.cfm.

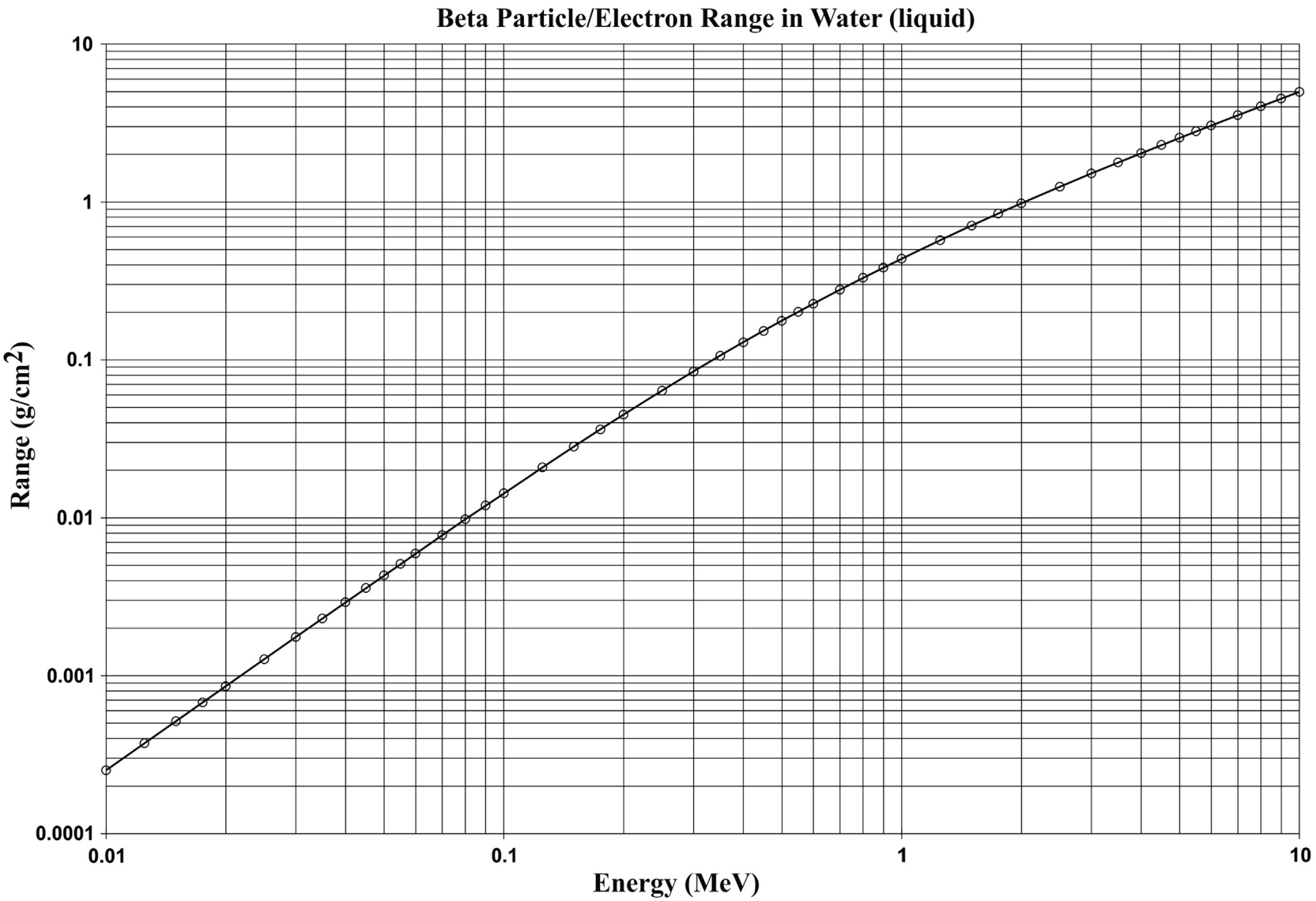

FIGURE A.3 Range–energy relationship for beta particles or electrons in water (liquid). The range in cm can be obtained by dividing the above range by the density of water ($\rho = 1.00$ g/cm^3 at STP). For example, the range of a 1.0 MeV beta particle from the graph is read as 0.43 g/cm^2, and dividing by the density of water yields a calculated linear range of 0.43 cm. The range–energy relationship is plotted from data provided by the National Institute of Standards and Technology database ESTAR (2016) for continuous slowing down approximation ranges, from which very precise calculated values of range may be found: www.nist.gov/pml/data/star/index.cfm.

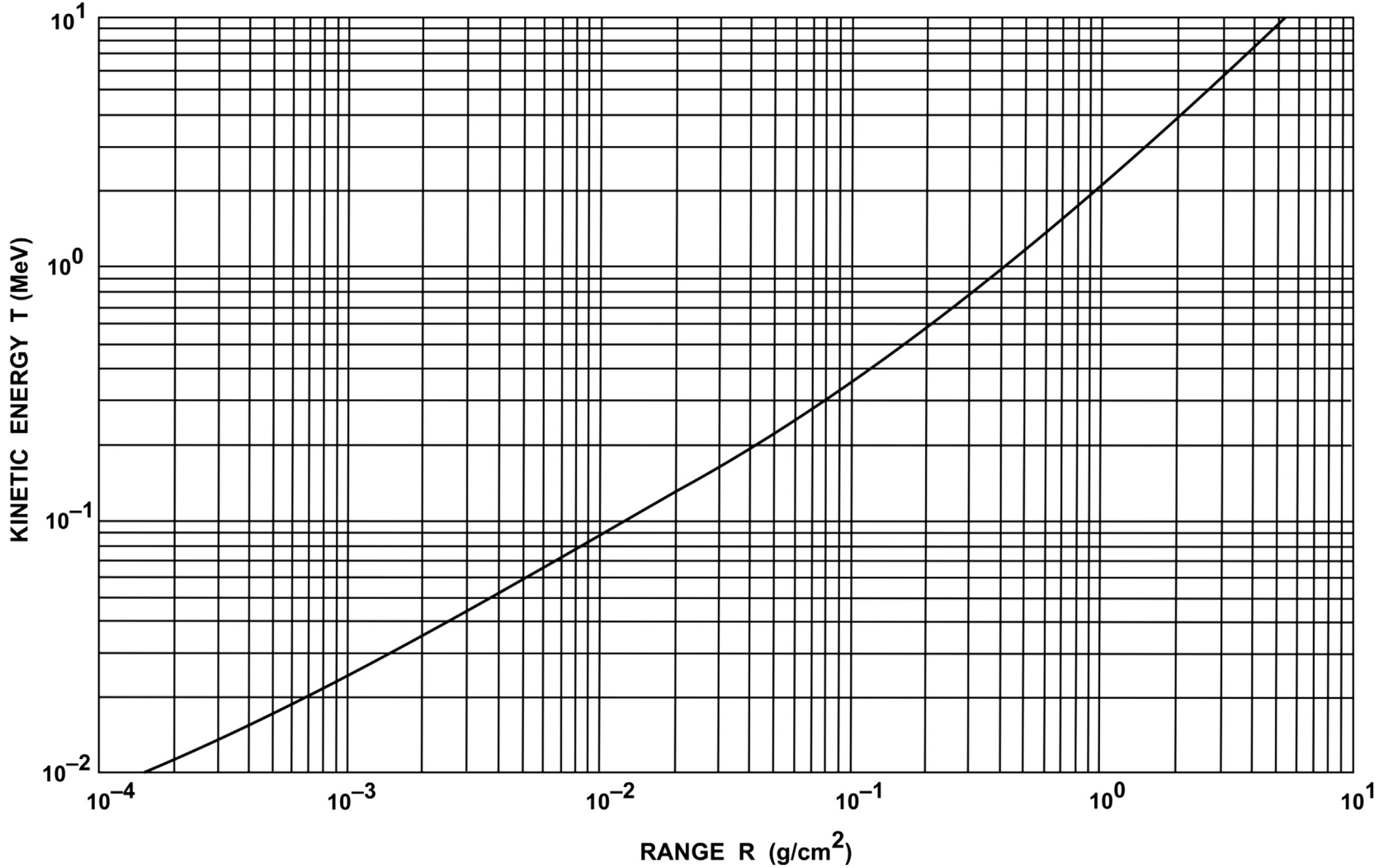

FIGURE A.4 Beta particle range–energy curve for absorbers of low atomic number. The curve is described by the formulas $R = 0.412T^{1.27-0.0954 \ln T}$ for $0.01 \leq T \leq 2.5$ MeV and $R = 0.530T - 0.106$ for $T > 2.5$ MeV, where T is the beta particle energy in MeV. *From US Public Health Service, 1970, Radiological Health Handbook, Publ. No. 2016. Bureau of Radiological Health, Rockville, MD.*

Periodic Table of the Elements

	IA	IIA	IIIB	IVB	VB	VIB	VIIB	VIIIB			IB	IIB	IIIA	IVA	VA	VIA	VIIA	VIIIA
1	1 H 1.00794 Hydrogen																	2 He 4.0021 Helium
2	3 Li 6.941 Lithium	4 Be 9.0122 Beryllium											5 B 10.811 Boron	6 C 12.011 Carbon	7 N 14.007 Nitrogen	8 O 15.999 Oxygen	9 F 18.998 Fluorine	10 Ne 20.180 Neon
3	11 Na 22.990 Sodium	12 Mg 24.305 Magnesium											13 Al 26.918 Aluminum	14 Si 28.085 Silicon	15 P 30.974 Phosphorus	16 S 32.066 Sulfur	17 Cl 35.453 Chlorine	18 Ar 39.948 Argon
4	19 K 39.098 Potassium	20 Ca 40.078 Calcium	21 Sc 44.956 Scandium	22 Ti 47.867 Titanium	23 V 50.941 Vanadium	24 Cr 51.996 Chromium	25 Mn 54.938 Manganese	26 Fe 55.845 Iron	27 Co 58.933 Cobalt	28 Ni 58.693 Nickel	29 Cu 63.546 Copper	30 Zn 65.39 Zinc	31 Ga 69.723 Gallium	32 Ge 72.61 Germanium	33 As 74.921 Arsenic	34 Se 78.96 Selenium	35 Br 79.904 Bromine	36 Kr 83.80 Krypton
5	37 Rb 85.468 Rubidium	38 Sr 87.62 Strontium	39 Y 88.906 Yttrium	40 Zr 91.224 Zirconium	41 Nb 92.906 Niobium	42 Mo 95.94 Molybdenum	43 Tc (98)[a] Technetium	44 Ru 101.07 Ruthenium	45 Rh 102.90 Rhodium	46 Pd 106.42 Palladium	47 Ag 107.87 Silver	48 Cd 112.41 Cadmium	49 In 114.82 Indium	50 Sn 118.71 Tin	51 Sb 121.76 Antimony	52 Te 127.60 Tellurium	53 I 126.90 Iodine	54 Xe 131.29 Xenon
6	55 Cs 132.90 Cesium	56 Ba 137.33 Barium	57-71*	72 Hf 178.49 Hafnium	73 Ta 180.95 Tantalum	74 W 183.84 Tungsten	75 Re 186.21 Rhenium	76 Os 190.23 Osmium	77 Ir 192.22 Iridium	78 Pt 195.08 Platinum	79 Au 196.97 Gold	80 Hg 200.59 Mercury	81 Tl 204.38 Thallium	82 Pb 207.2 Lead	83 Bi 208.98 Bismuth	84 Po (209)[a] Polonium	85 At (210)[a] Astatine	86 Rn (222)[a] Radon
7	87 Fr (223)[a] Francium	88 Ra 226.02[b] Radium	89-103**	104 Rf (261)[a] Rutherfordium	105 Db (262)[a] Dubnium	106 Sg (263)[a] Seaborgium	107 Bh (264)[a] Bohrium	108 Hs (265)[a] Hassium	109 Mt (266)[a] Meitnerium	110 Ds (271)[a] Darmstadtium	111 Rg (272) Roentgenium	112 Cn (277) Copernicium	113 Uut (284) Ununtrium[c]	114 Fl (285) Flerovium[d]	115 Uup Ununpentium[c]	116 Lv Livermorium[d]	117 Uus Ununseptium[c]	118 Uuo Ununoctium[c]

Key to Chart

Atomic Number — 79 — Au — 196.97 — Gold — Name

Symbol — Atomic Weight — Electron configuration from top to bottom in K, L, M, N, O, P, to Q energy levels

*Lanthanides	57 La 138.90 Lanthanum	58 Ce 140.11 Cerium	59 Pr 140.91 Praseodymium	60 Nd 144.24 Neodymium	61 Pm (145)[a] Promethium	62 Sm 150.36 Samarium	63 Eu 151.96 Europium	64 Gd 157.25 Gadolinium	65 Tb 158.92 Terbium	66 Dy 162.50 Dysprosium	67 Ho 164.93 Holmium	68 Er 167.26 Erbium	69 Tm 168.93 Thulium	70 Yb 173.04 Ytterbium	71 Lu 174.97 Lutetium
**Actinides	89 Ac (227)[a] Actinium	90 Th 232.04[b] Thorium	91 Pa 231.04[b] Protactinium	92 U 238.03 Uranium	93 Np 237.05[b] Neptunium	94 Pu (244)[a] Plutonium	95 Am (243)[a] Americium	96 Cm (247)[a] Curium	97 Bk (247)[a] Brekelium	98 Cf (251)[a] Californium	99 Es (252)[a] Einsteinium	100 Fm (257)[a] Fermium	101 Md (258)[a] Mendelevium	102 No (259)[a] Nobelium	103 Lr (260)[a] Lawrencium

[a]A value in parenthesis denotes the mass number of the longest lived isotope of the element.
[b]Atomic weight of the most commonly available long-lived isotope of the element.
[c]The names of elements 113, 115, 117, and 118 are the Latin equivalents of the atomic numbers. Element 112 was created in 1996 at the GSI, Darmstadt, Germany. The discovery of element 113 was attributed to RIKEN in Japan by the IUPAC in 2016. The discovery of elements 115 and 118 were attributed to the JINR, Dubna, Russia and LLNL in the USA in 2015. The discovery of Element 117 was credited to the JINR, LLNL and ORNL in 2015.
[d]Element 114, Flerovium, is named after Georgy Flyorov, the founder of the JINR, Dubna, Russia; and element 116 is named after the LLNL in the USA.

Appendix C

Derivation of the Lorentz Transformations

The Lorentz transformations are used in many books to calculate length contraction, time dilation, and changes in mass in relativity. However, the origin of the Lorentz transformations—that is, the derivation of the equations—is seldom provided in books. The derivation of the Lorentz transformations, on the basis of that described by Einstein (1916a,b), is given here for the convenience of the reader.

The calculations of relativity, provided by Einstein (1916a,b) as examples, are found in Hall of Fame, Part III in this book. In that section the reader will find that Einstein applies a system of equations known as the "Lorentz transformations," as follows:

$$x' = \frac{x - vt}{\sqrt{1 - (v^2/c^2)}}, \quad y' = y \quad \text{and} \quad z' = z \qquad [C.1]$$

and

$$t' = \frac{t - \frac{v}{c^2}x}{\sqrt{1 - (v^2/c^2)}} \qquad [C.2]$$

where x', y', z', and t' are the space–time coordinates in a reference frame O' traveling at a velocity v relative to reference frame O, defined by coordinates x, y, z, and t; and c is the invariable velocity of light in a vacuum. The two reference frames are illustrated in Fig. C.1.

The Lorentz transformations were derived by Einstein (1916a, pp. 131–135 as translated by Robert W. Lawson). In Einstein's derivation he explained the various mathematical procedures that lead to the Lorentz transformations, but he did

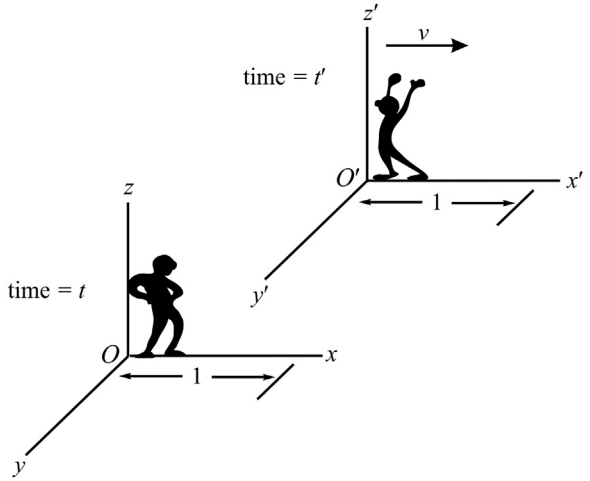

FIGURE C.1 Two frames of reference in space and time. An event in space and time in reference frame O' is defined by space–time coordinates x', y', z', and t', traveling at a velocity v relative to reference frame O, defined by coordinates x, y, z, and t. Two observers are illustrated, one with hands on hip in reference frame O and the other with waving hands in reference frame O'. A unit of measurement is illustrated along the x-axis of each reference frame. This is a basic unit of length, such as 1 m.

not write out each step in the derivation. For the convenience of the reader, the detailed derivation of the Lorentz transformations (ie, Eqs. [C.1] and [C.2]) from the explanation given by Einstein (1916a,b) is provided here.

Einstein (1916a,b) considered firstly only events that are measured along the x-axis (see Fig. C.1). He explained that events in coordinate system O are described according to the axis x and time t; and in coordinate system O' they are described according to the axis x' and time t'. The derivation is based on finding x' and t' (Eqs. [C.1] and [C.2]) when x and t are known. Einstein pointed out that light along the x-axis of coordinate system O travels at the velocity

$$x = ct \quad \text{or} \quad x - ct = 0 \tag{C.3}$$

and likewise, for coordinate system O' light will travel at the same speed or

$$x' - ct' = 0 \tag{C.4}$$

As the speed of light c is constant for both coordinates, Einstein (1916a,b) concluded that there must be a proportionality of the space−time events in one coordinate system with those in the other coordinate system. Thus he established the proportionality constants λ and μ between the two coordinate systems for events along the positive x-axis and negative x-axis, namely

$$\text{events along positive } x\text{-axis}: x' - ct' = \lambda(x - ct) \tag{C.5}$$

$$\text{events along negative } x\text{-axis}: x' + ct' = \mu(x + ct) \tag{C.6}$$

Adding Eqs. [C.5] and [C.6] gives

$$2x' = \lambda x + \mu x - \lambda ct + \mu ct \tag{C.7}$$

Transposing variables within Eq. [C.7] gives

$$2x' + \lambda ct - \mu ct = \lambda x + \mu x \tag{C.8}$$

or

$$2x' + (\lambda - \mu)ct = (\lambda + \mu)x$$

and

$$x' = \left(\frac{\lambda + \mu}{2}\right)x - \left(\frac{\lambda - \mu}{2}\right)ct \tag{C.9}$$

Einstein (1916a,b) assigned the letters a and b to the constants $(\lambda + \mu)/2$ and $(\lambda - \mu)/2$, respectively, so that Eq. [C.9] would read as follows:

$$x' = ax - bct \tag{C.10}$$

Eq. [C.10] is an important step to the derivation of the Lorentz transformation which defines the value of x' (ie, Eq. [C.1]) in reference frame O' for known values of x and t in reference frame O. Eq. [C.10] was obtained by adding Eqs. [C.5] and [C.6]. To continue with the derivation, the equation defining t' (ie, Eq. [C.2]) is needed. Einstein (1916a,b) noted that he also subtracted Eqs. [C.5] and [C.6], although he did not illustrate the steps—probably for reasons of brevity. These steps are included here to give the detailed derivation. Subtracting Eq. [C.6] from Eq. [C.5] gives

$$-2ct' = \lambda x - \mu x - \lambda ct - \mu ct \tag{C.11}$$

or

$$2ct' = -\lambda x + \mu x + \lambda ct + \mu ct \tag{C.12}$$

and transposing Eq. [C.12] gives

$$(\lambda - \mu)x + 2ct' = (\lambda + \mu)ct \tag{C.13}$$

or

$$ct' = \left(\frac{\lambda + \mu}{2}\right)ct - \left(\frac{\lambda - \mu}{2}\right)x \tag{C.14}$$

Substituting the letters a and b for the constants $(\lambda + \mu)/2$ and $(\lambda - \mu)/2$, respectively, gives

$$ct' = act - bx \qquad [C.15]$$

Eqs. [C.10] and [C.15] were established by Einstein (1916a,b) as the key to the solution to the derivation of the Lorentz transformations, namely Eqs. [C.1] and [C.2]. It only remains to determine the values of a and b.

Einstein (1916a,b) sets the origin of the reference frame O' at $x' = 0$, whereby Eq. [C.10] becomes

$$0 = ax - bct \qquad [C.16]$$

and

$$x = \frac{bc}{a}t \qquad [C.17]$$

Since x/t or distance/time is the velocity v, Eq. [C.17] may be written as

$$\frac{x}{t} = v = \frac{bc}{a} \qquad [C.18]$$

where v is the velocity of observer O' situated at $x' = 0$, moving relative to observer O at the origin $x = 0$. Thus v is the relative velocity of one reference frame to the other, or the velocity of the observer in frame O' relative to the observer in frame O. If a rod measuring 1 m is placed at the origin of each reference frame, as illustrated in Fig. C.1, the observers would find that the rod measured 1 m when they take the measurement in their own reference frame; but if an observer in reference frame O takes a measurement of the rod in frame O' traveling at a velocity v relative to O, the observer in reference frame O measures the rod to be of a different length, according to the Lorentz transformation (Eq. [C.1]). This will also be the case for an observer in reference frame O' who measures the rod in frame O when traveling at a velocity v relative to O. To arrive at this Lorentz transformation (Eq. [C.1]), Einstein (1916a,b) proposed that the observer at O take a picture or "snapshot" of O' at a given time $t = 0$ for the start of the observation. When $t = 0$, Eq. [C.10] can be written as

$$x' = ax \qquad [C.19]$$

Einstein (1916a,b) points out that the 1 m rod is separated by the distance $\Delta x'$ when measured by the observer in O', so Eq. [C.19] becomes

$$\Delta x' = a\Delta x \quad \text{or} \quad \Delta x = \frac{1}{a} \qquad [C.20]$$

Einstein (1916a,b) then proposed that the picture ("snapshot") be taken from O' at $t' = 0$, and that t be eliminated from the previously derived Eqs. [C.10] and [C.15]. For brevity, Einstein (1916a,b) did not illustrate how this was performed, but the writer proceeds through all the steps here for clarity. We firstly rewrite Eqs. [C.10] and [C.15], and then eliminate t from these equations as follows:

$$\text{Eq. [C.10]}: x' = ax - bct$$

$$\text{Eq. [C.15]}: ct' = act - bx$$

If by definition $t = x/v$ and, as previously defined, $b = va/c$, we can rewrite Eq. [C.10] as

$$x' = ax - \frac{av}{c}c\frac{x}{v} \quad \text{or} \quad x' = ax - ax = 0 \qquad [C.21]$$

Also Eq. [C.15] can be written at $t' = 0$ to become

$$act = bx \qquad [C.22]$$

We can eliminate t from Eq. [C.22], with the previously defined $t = x/v$ and $b = va/c$ as follows

$$ac\frac{x}{v} = \frac{va}{c}x \quad \text{or} \quad ax\left(\frac{c}{v}\right) = a\left(\frac{v}{c}\right)x \qquad [C.23]$$

or

$$ax = a\left(v^2/c^2\right)x \qquad [C.24]$$

Subtracting Eq. [C.24] from Eq. [C.21] gives

$$x' - ax = -a\left(v^2/c^2\right)x \quad [C.25]$$

which transforms to

$$x' = ax - a\left(v^2/c^2\right)x \quad [C.26]$$

or

$$x' = a\left(1 - v^2/c^2\right)x \quad [C.27]$$

Einstein (1916a,b) points out that from Eq. [C.27] we can conclude that two points on the x-axis which measure 1 unit relative to O will be seen on the photo or "snapshot" taken from O' as the distance

$$\Delta x' = a\left(1 - v^2/c^2\right) \quad [C.28]$$

The two photographs or "snapshots" taken from each reference frame would be identical, thus Einstein (1916a,b) equates Eqs. [C.20] and [C.28], or

$$\Delta x = \Delta x' \quad [C.29]$$

that is

$$\frac{1}{a} = a\left(1 - v^2/c^2\right) \quad [C.30]$$

or

$$a^2 = \frac{1}{1 - \left(v^2/c^2\right)} \quad [C.31]$$

and

$$a = \frac{1}{\sqrt{1 - \left(v^2/c^2\right)}} \quad [C.32]$$

With the constant a now fully defined by Eq. [C.32] and the constant b defined by Eq. [C.18], namely $b = va/c$, Einstein (1916a,b) inserted the expressions for a and b into Eqs. [C.10] and [C.15] to yield the Lorentz transformations as follows.

From Eq. [C.10] we have

$$x' = ax - bct$$

Inserting the expression of a from Eq. [C.32] and that for $b = va/c$ into the above equation gives

$$x' = \frac{1}{\sqrt{1 - \left(v^2/c^2\right)}}x - v\frac{1}{\sqrt{1 - \left(v^2/c^2\right)}}t \quad [C.33]$$

and

$$x' = \frac{x - vt}{\sqrt{1 - \left(v^2/c^2\right)}} \quad [C.34]$$

From Eq. [C.15] we have

$$ct' = act - bx$$

or

$$t' = at - \frac{bx}{c} \quad [C.35]$$

Inserting the expression of a from Eq. [C.32] and that for $b = va/c$ into Eq. [C.35] gives

$$t' = \frac{1}{\sqrt{1 - \left(v^2/c^2\right)}}t - \frac{(va/c)x}{c} \quad [C.36]$$

or

$$t' = \frac{1}{\sqrt{1-(v^2/c^2)}}t - \frac{1}{\sqrt{1-(v^2/c^2)}}(v/c^2)x \qquad [C.37]$$

or

$$t' = \frac{t - \frac{v}{c^2}x}{\sqrt{1-(v^2/c^2)}} \qquad [C.38]$$

Eqs. [C.34] and [C.38] are the Lorentz transformations used to determine the values of x' and t' in reference frame O', which travels at the velocity v relative to reference frame O when the values of x and t of reference frame O are known. Einstein (1916a,b) pointed out that the Lorentz transformations along the x-axis described by Eqs. [C.34] and [C.38] can be extended to include events in other axes by appending these equations with $y' = y$ and $z' = z$.

The Lorentz transformations have proven to be very useful in making calculations of the time dilation that cosmic shower radiations are observed to undergo when traveling at very fast (relativistic) speeds toward the Earth. A practical example of the use of the Lorentz transformations is provided in the biographical sketch of Albert Einstein in Hall of Fame, Part III in the case of muons of very short lifetime (2×10^{-6} s) created in the upper atmosphere and traveling at close to the speed of light toward Earth. The lifetime of the muons as measured from Earth is dilated, or in other words the measured lifetime of the muons is increased, which permits an observer on Earth to detect their arrival on the Earth's surface. An example of length contraction is provided in the same Hall of Fame, Part III with respect to muons in cosmic radiation showers traveling at near the speed of light in the atmosphere from the height of a mountain top to the mountain base.

References

Aaserud, F., August 2003. Hilde Levi: 1909–2003, Obituary. Niels Bohr Institute Archive, Copenhagen.

Abachi, et al., D0 Collaboration, 1995. Observation of the top quark. Phys. Rev. Lett. 74 (14), 2632–2638. arXiv:hep-ex/9503003.

Abbasi, R., et al., 2010. The energy spectrum of atmospheric neutrinos between 2 and 200 TeV with the AMANDA-II detector. Astropart. Phys. 34, 48–58.

Abbasi, R., et al., 2011. Search for neutrino-induced cascades with five years of AMANDA data. Astropart. Phys. 34, 420–430.

Abbe, J.C., Marques-Netto, A., 1975. Szilard-Charlmers effects in halfnium complexes. J. Inorg. Nucl. Chem. 37, 2239–2242.

Abbon, P., et al., 2010. Design and construction of the fast photon detection system for COMPASS RICH-1. Nucl. Instrum. Methods Phys. Res. Sect. A 616, 21–37.

Abbon, P., et al., 2011. Particle identification with COMPASS RICH-1. Nucl. Instrum. Methods Phys. Res. Sect. A 631, 26–39.

Abe, et al., CDF Collaboration, 1995. Observation of top quark production in pp collisions. Phys. Rev. Lett. 74 (14), 2626–2632. arXiv:hep-ex/9503002.

Abela, R., et al., 2010. Analytical applications of synchrotron radiation. TrAC Trends Anal. Chem. 29 (6), 447–576.

Abele, H., 2000. The standard model and the neutron β-decay. Nucl. Instrum. Methods Phys. Res. Sect. A 440, 499–510.

Achterberg, A., et al., 2006. First year performance of the IceCube neutrino telescope. Astropart. Phys. 26, 155–173.

Adachi, I., et al., 1995. Study of a threshold Cherenkov counter based on silica aerogels with low refractive indices. Nucl. Instrum. Methods Phys. Res. Sect. A 355, 390–398.

Adachi, I., et al., 2007. A study of proximity focusing RICH with aerogel radiator. Nucl. Instrum. Methods Phys. Res. Sect. A 580, 1042–1045.

Adkisson, P., Tumlinson, J., 2003. Edward F. Knipling 1909–2000, a biographical memoir. Biograph. Mem. 83, 3–15.

Adloff, J.P., 1989. Radioactive disequilibrium in nature: origin, facts and applications. Int. J. Radiat. Appl. Instrum. Part C 33 (3), 257.

Adriani, O., et al., PAMELA Collaboration, 2010. PAMELA results on the cosmic-ray antiproton flux from 60 MeV to 180 GeV in kinetic energy. Phys. Rev. Letts. 105, 121101, arXiv:1007.0821v [astro-ph.HE].

Afanasiev, G.N., et al., 1999. On Tamm's problem in the Vavilov-Cherenkov radiation theory. J. Phys. D: Appl. Phys. 32, 2029–2043.

Aggarwaal, P., et al., 2012. Isotope hydrology. Int. Assoc. Hydrol. Sci. 484.

Agirò, S., 2004. Status and perspectives of the Pierre Auger Cosmic Ray Observatory. Eur. J. Phys. C 33, s947–s949.

Agnew, L.E., et al., 1958. p^-–p elastic and charge exchange scattering at about 120 Mev. Phys. Rev. 110, 994–995.

Aguilar, M., et al., AMS Collaboration, 2002. The Alpha Magnetic Spectrometer (AMS) on the International Space Station: part I – results from the test flight on the space shuttle. Phys. Rep. 366 (6), 331–405.

Aguilar, J.A., et al., 2011. Time calibration of the ANTARES neutrino telescope. Astropart. Phys. 34, 539–549.

Ahmad, Q.R., et al., SNO Collaboration, 2002. Direct evidence for neutrino flavor transformation from neutral-current interactions in the Sudbury Neutrino Observatory. Phys. Rev. Lett. 89 (011301), 1–6.

Airapetian, A., et al., 2005. The time-of-flight technique for the HERMES experiment. Nucl. Instrum. Methods Phys. Res. Sect. A 540, 305–310.

Akatsu, M., et al., 2000. Time-of-propagation Cherenkov counter for particle identification. Nucl. Instrum. Methods Phys. Res. Sect. A 440, 124–135.

Alcaraz, J., et al., 2000. Leptons in near earth orbit. Phys. Lett. B484, 10–22.

Aleissa, K.A., Almasoud, F.I., Islam, M.S., L'Annunziata, M.F., 2008. Radium-228 analysis of natural waters by Cherenkov counting of actinium-228. Appl. Radiat. Isot. 66, 1954–1963.

Alfassi, Z.B., et al., 1986. Optimation of the production of $Na^{18}F$ by use of the Szilard–Chalmers reaction following irradiation of fluorine compounds with 14 MeV neutrons. J. Radioanal. Nucl. Chem. 100 (2), 263–268.

Allard, D., et al., 2007. On the transition from galactic to extragalactic cosmic-rays: spectral and composition features from two opposite scenarios. Astropart. Phys. 27 (1), 61–75.

Allaveisi, F., et al., 2013. Effect of gamma sterilization on microhardness of the cortical bone tissue of bovine femur in presence of N-Acetyl-L-Cysteine free radical scavenger. Phys. Med. 30 (3), 314–319.

Allen, A.D., February 2001. Szilard endorsed nuclear medicine by example. Phys. Today Lett. Online 1.

Allkofer, Y., et al., 2007. A novel aerogel Cherenkov detector for DIRAC-II. Nucl. Insrtrum. Methods Phys. Res. Sect. A 582, 497–508.

Allkofer, Y., et al., 2008. A new aerogel Cherenkov detector for DIRAC-II. Nucl. Insrtrum. Methods Phys. Res. Sect. A 595, 84–87.

Almayahi, B.A., et al., 2012. Effect of the natural radioactivity concentrations and $^{226}Ra/^{238}U$ disequilibrium on cancer diseases in Penang, Malaysia. Rad. Phys. Chem. 81, 1547–1558.

Al-Masri, M.S., Blackburn, R., 1994. Simultaneous determination of ^{234}Th and ^{228}Th in environmental samples using Cerenkov counting. Radiochim. Acta 65, 133–136.

Al-Masri, M.S., 1996. Cerenkov counting technique. J. Radioanal. Nucl. Chem. Articles 207, 205–213.

Al-Masri, M.S., Blackburn, R., 1995a. Application of Cerenkov radiation for the assay of ^{226}Ra in natural water. Sci. Total Environ. 173/174, 53–59.
Al-Masri, M.S., Blackburn, R., 1995b. Radiochemical determination of ^{226}Ra using Cerenkov counting. J. Radioanal. Nucl. Chem. Articles 195, 339–344.
Al-Masri, M.S., Blackburn, R., 1999. Radon-222 and related activities in surface waters of the English Lake District. Appl. Radiat. Isot. 50, 1137–1143.
Almeida, A.P., et al., 2014. Phase contrast X-ray microtomography of the *Rhodnius prolixus* head: comparison of direct reconstruction and phase retrieval approach. Rad. Phys. Chem. 95, 243–246.
Alpher, R.A., Herman, R.C., 1949. Remarks on the evolution of an expanding universe. Phys. Rev. 75 (7), 1089–1095.
Alvarez, L.W., et al., 1959. Neutral cascade hyperon event. Phys. Rev. Lett. 2 (5), 215–219.
Alpher, R.A., Herman, R.C., 1988. Reflections on early 'big bang' cosmology. Phys. Today (August) 41 (8), 24–34.
Alpher, R.A., et al., 1953. Physical conditions in the initial stages of the expanding universe. Phys. Rev. 92, 1347–1361.
Alvarez, L.W., 1937. Nuclear K electron capture. Phys. Rev. 52 (2), 134–135.
Alvarez, L.W., 1938a. Electron capture and internal conversion in Gallium-67. Phys. Rev. 53 (7), 606.
Alvarez, L.W., 1938b. The capture of orbital electrons by nuclei. Phys. Rev. 54 (7), 486–497.
Alvarez, L.W., 1949. N^{17}, a delayed neutron emitter. Phys. Rev. 75 (8), 1127–1132.
Alvarez, L.W., 1970. Ernest Orlando Lawrence 1901–1958, a Biographical Memoir. National Academy of Sciences, Washington, DC, pp. 251–294.
Alvarez, L.W., 1972. Recent development in particle physics. Nobel lecture. December 11, 1968. In: Nobel Lectures, Physics 1963–1970, Elsevier Publishing Company, Amsterdam, pp. 241–290.
Alvarez, L.W., Bloch, F., 1940. A quantitative determination of the neutron moment in absolute nuclear magnetons. Phys. Rev. 57, 111–122.
Alvarez, L.W., Compton, A.H., 1933. A positively charged component of cosmic rays. Phys. Rev. 43 (10), 835–836.
Amaldi, E., Fermi, E., 1935. Absorption of slow neutrons. Ricerca Sci. 6, 344–347.
Amaldi, E., Fermi, E., 1936a. Groups of slow neutrons. Ricerca Sci. 7 (1), 310–313.
Amaldi, E., Fermi, E., 1936b. Diffusion of slow neutrons. Ricerca Sci. 7 (1), 393–395.
Amaldi, E., et al., 1935. Artificial radioactivity produced by neutron bombardment. II. Proc. R. Soc. London A149 (868), 522–558.
Amaldi, E., et al., 1937. Artificial generator of neutrons. Ricerca Sci. 8 (2), 40–43.
Amaldi, U., Hall, G., 2015. Particle Accelerators: From Big Bang Physics to Hadron Therapy. Springer, p. 284.
AMS Collaboration, 2000. Cosmic protons. Phys. Lett. B490, 27–35.
Amsler, C., et al., 2008. Particle Date Group. Review of particle physics. Phys. Lett. B 667, 1–1340.
Anderson, C.D., 1930. Space distribution of X-ray photoelectrons ejected from the K and L atomic energy levels. Phys. Rev. 35, 1139–1145.
Anderson, C.D., 1932. The apparent existence of easily detectable positives. Science 76, 238.
Anderson, C.D., 1933a. Energy loss and scattering of cosmic-ray particles. Phys. Rev. 43, 381.
Anderson, C.D., 1933b. The positive electron. Phys. Rev. 43, 491–498.
Anderson, C.D., 1933c. Free positive electrons resulting from the impacts upon atomic nuclei of the photons from ThC. Science 77, 432.
Anderson, C.D., 1936. The production and properties of positrons. Nobel Lecture, December 13, 1939. In: Nobel Lectures, Physics, 1922–1941 (1965). Elsevier Publishing, Amsterdam.
Anderson, C.D., Neddermeyer, S.H., 1933. Positrons from gamma rays. Phys. Rev. 43, 1034–1035.
Anderson, C.D., Neddermeyer, S.H., 1936. Cloud chamber observations of cosmic rays at 4300 meters elevation and near sea-level. Phys. Rev. 50, 263–271.
Anderson, C.D., et al., 1934. The mechanism of cosmic-ray counter action. Phys. Rev. 45, 352–363.
Anderson, E.C., 1949. Natural Radiocarbon (Ph.D. thesis). University of Chicago, Chicago.
Anderson, E.C., et al., 1947a. Radiocarbon from cosmic radiation. Science 105, 576–577.
Anderson, E.C., et al., 1947b. Natural radiocarbon from cosmic radiation. Phys. Rev. 72, 931–936.
Anderson, C.D., et al., 1947c. On the mass and the disintegration products of the mesotron. Phys. Rev. 72, 724–727.
Anderson, H.H., et al., 1969. Excitation potentials and shell corrections for the elements $Z_2 = 20$ to $Z_2 = 30$. Phys. Rev. 180, 373–380.
Anderson, H.L., et al., 1939a. Production of neutrons in uranium bombarded by neutrons. Phys. Rev. 55, 797–798.
Anderson, H.L., et al., 1939b. Neutron production and absorption in uranium. Phys. Rev. 56, 284–286.
Anderson, I.S., et al., 2010. Neutron Imaging and Applications: A Reference for the Imaging Community (Neutron Scattering Applications and Techniques). Springer, p. 400.
Andreo, P., et al., 2005. Calibration of photon and electron beams. In: Podgorsak, E.B. (Ed.), Review of Radiation Oncology Physics: A Handbook for Teachers and Students. International Atomic Energy Agency (IAEA), Vienna, pp. 301–355.
Angeli, I., Csatlós, M., 1977. Fine structure in the mass number dependence of rms charge radii. Nucl. Phys. A 288 (3), 480–492.
Anonymous, 1975. Obituary. Sir George Thomson. Nature 257, 726.
Ansell, G., Rotblat, J., 1948. Radioactive iodine as a diagnostic aid for intrathoractic goitre. Br. J. Radiol. 21, 552–558.
Aoyama, M., et al., 2013. Inter and intra basin scale transport of ^{137}Cs in the Pacific Ocean. In: Isotopes in Hydrology, Marine Ecosystems and Climate Change Studies. Proceedings of an International Symposium, Monaco, 27 March–1 April 2011, vol. 2. International Atomic Energy Agency, Vienna, pp. 571–578.
Aoyama, S., et al., 1927. Die Abhängigkeit der Röntgenabsorptionsspektren von der chemischen Bindung. Z. Phys. 44 (11–12), 810–833.
Aponick Jr., A.A., et al., 1970. Quadrupole and hexadecapole deformations in rare earth nuclei. Nucl. Phys. A 159 (2), 367–384.
APS, June 2012. This month in German history, June 1911: invention of the Geiger counter. Am. Phys. Soc. News 21 (6), 2.

Araújo, H.M., et al., 2008. Measurements of neutrons produced by high-energy muons at the Boulby Underground Laboratory. Astropart. Phys. 29, 471–481.

Argo, C., et al., 2012. Weight loss resistance: a further consideration for the nutritional management of obese Equidae. Vet. J. 194, 179–188.

Argonne National Laboratory, 1963. Reactor Physics Constants. ANL-5800, second ed. United States Atomic Energy Commission, Washington, DC.

Ariño, I., et al., 2004. The HERA-B ring imaging Cherenkov counter. Nucl. Instrum. Methods Phys. Res. Sect. A 516, 445–461.

Arnison, G., et al., UA1 Collaboration, 1983a. Experimental observation of isolated large transverse energy electrons with associated missing energy at $\sqrt{s} = 540$ GeV. Phys. Lett. 122B, 103–116.

Arnison, G., et al., UA1 Collaboration, 1983b. Experimental observation of lepton pairs of invariant mass around 95 GeV/c^2 at the CERN SPS collider. Phys. Lett. 126B, 398–410.

Arnold, J.R., Libby, W.F., 1949. Age determinations by radiocarbon content: checks with samples of known age. Science 110, 678–680.

Arrhenius, S., 1922. Presentation speech for the Nobel Prize in Physics 1921 awarded to Albert Einstein. December 10, 1922. In: Nobel lectures, Physics 1901–1921 (1967). Elsevier Publishing, Amsterdam.

Artuso, M., et al., 2006. Performance of a C_4F_8O gas radiator ring imaging Cherenkov detector using multi-anode photomultiplier tubes. Nucl. Instrum. Methods Phys. Res. Sect. A 558, 373–387.

Arvanitoyannis, I.S., 2010. Carbohydrates, pp. 561–600. In: Irradiation of Food Commodities. Elsevier, Amsterdam, p. 710.

Arzumanov, S., et al., 2000a. Neutron lifetime measured by monitored storing of untra-cold neutrons. Nucl. Instrum. Methods Phys. Res. Sect. A 440, 511–516.

Arzumanov, S., et al., 2000b. Neutron lifetime measured by monitored storing of ultra-cold neutrons with detection of inelastically scattered neutrons. Phys. Lett. B 483, 15–22.

Arzumanov, S., et al., 2009. A new project to measure the neutron lifetime using storage of ultracold neutrons and detection of inelastically scattered neutrons. Nucl. Instrum. Methods Phys. Res. Sect. A 611, 186–188.

Asaro, F., Perlman, I., 1953. Patterns in alpha spectra of even-even nuclei. Phys. Rev. 91, 763–764.

Asaturyan, R., et al., 2005. The aerogel threshold Cherenkov detector for the High Momentum Spectrometer in Hall C at Jefferson Lab. Nucl. Instrum. Methods Phys. Res. Sect. A 548, 364–374.

Ashley, R.P., et al., 2000. Steady-state D–^{3}He proton production in an IEC fusion device. UWFDM-1144. Fusion Technology Institute, University of Wisconsin, Madision, p. 6.

Astbury, A., et al., 1978. A 4x solid-angle detector for the SPS used as a proton-antiproton collider at a centre-of-mass energy of 540 GeV, Proposal. CERN-SPSC 78-6/P92.

Atekwana, E.A., Krishnamurthy, R.V., 1998. Seasonal variations of dissolved inorganic carbon and $\delta^{13}C$ of surface waters: application of a modified gas evolution technique. J. Hydrol. 205, 265–278.

Atkinson, D., 2006. Does quantum electrodynamics have an arrow of time? Studies Hist. Phil. Mod. Phys. 37, 528–541.

Atkinson, R. d'E., Houtermans, F.G., 1929. Aufbaumöglichkeit in Sterren. Z. Phys. 54, 656–665.

Attas, M., Abushady, I., 1997. Cerenkov Viewing Device for Spent Fuel Verification at Light Water Reactors. IAEA Inspector Training Manual. © IAEA, Vienna. Atomic Energy of Canada, Ltd, Pinawa, Manitoba.

Attas, M., et al., 1990. A Cherenkov viewing device for used-fuel verification. Nucl. Instrum. Methods Phys. Res. Sect. A 299, 88–93.

Attas, M., et al., 1992. An ultraviolet imager for nuclear safeguards inspectors. In: Proceedings of the International Meeting on Electron Tubes and Image Intensifiers. San Hose, CA, February 10–12, 1992. Proc. SPIE, vol. 1655, pp. 50–57.

Aubert, J.J., et al., E598 Collaboration, 1974. Experimental observation of a heavy particle. Phys. Rev. Lett. 33 (23), 1404–1406.

Aubert, B., et al., 2002. The BABAR detector. Nucl. Instrum. Methods Phys. Res. Sect. A 479, 1–116.

Audi, G., et al., 2003a. The NUBASE evaluation of nuclear and decay properties. Nucl. Phys. A 729, 3–128.

Audi, G., et al., 2003b. The AME2003 atomic mass evalustion (II). Tables, graphs, and references. Nucl. Phys. A 729, 337–676.

Auditore, L., et al., 2005. Study of a 5 MeV electron linac based neutron source. Nucl. Instrum. Methods Phys. Res. Sect. B 229, 137–143.

Auger, P., 1923. Secondary β rays produced in a gas by X-rays. Compt. Rend. 177, 169–171.

Auger, P., 1925a. Sur les rayons β secondaires produits dans un gaz par des rayons-X. Compt. Rend. 180, 65–68.

Auger, P., 1925b. Sur l'effect photoélectrque compose. J. Phys. Radium 6, 205–208.

Auger, P., Maze, R., 1938. Les grandes gerbes cosmiques de l'atmosphere. C. R. Acad. Sci. Ser. B 207, 228–230.

Auger, P., Maze, R., 1939. Extension et Pouvoir Pénétrant des Grandes Grebes de Rayons Cosmiques. Compt. Rend. 208, 1641–1643.

Auger, P., et al., 1938. Heavy electrons in cosmic ray showers originating in the atmosphere. Compt. Rend. 206, 1721–1723.

Auger, P., et al., 1939. Extensive cosmic-ray showers. Rev. Mod. Phys. 11, 288–291.

Augustin, J.E., et al., SLAC-SP-017 Collaboration, 1974. Discovery of a narrow resonance in e^+e- annihilation. Phys. Rev. Lett. 33 (23), 1406–1408.

Auslender, V.L., et al., 2004. Bremsstrahlung converters for powerful industrial electron accelerators. Radiat. Phys. Chem. 71, 295–297.

Avignone III, F.T., 2010. The Majorana ^{76}Ge double-beta decay project. Prog. Part. Nucl. Phys. 64 (2), 258–260.

Aydin, E.G., et al., 2008. Equilibrium and pre-equilibrium calculations of neutron production in medium–heavy targets irradiated by protons up to 100 MeV. Ann. Nucl. Energy 35, 2306–2312.

Aynutdinov, V., et al., 2006. Search for a diffuse flux of high-energy extraterrestrial neutrinos with the NT200 neutrino telescope. Astropart. Phys. 25 (2), 140–150.

Aynutdinov, V., et al., 2011. The Baikal Neutrino Project: present and perspective. Nucl. Instrum. Methods Phys. Res. Sect. A 628, 115–119.

ASTAR, 2016. Stopping Power and Ranges for Protons and Helium Ions (Alpha Particles). NISTIR 4999. Physical Measurement Laboratory, National Institute of Standards and Technology. http://www.nist.gov/pml/data/star/index.cfm.

Baas, H.W., 2004. Neutron Activation Analysis of Inhomogeneous Samples. Delft University Press, p. 174.

Bacon, G.E., 1969. Neutron Physics. Wykeham Publications, London.

Baggott, J., 2012. Higgs: The Invention and Discovery of the God Particle. Oxford University Press, p. 221. http://www.oup.com.

Bagnaia, P., et al., UA2 Collaboration, 1983. Evidence for $Z^0 \rightarrow e^+e^-$ at the CERN $\bar{p}p$ collider. Phys. Lett. 129B, 130–140.

Bailey, J., et al., 1977. On muon lifetimes and time dilation. Nature 268, 301–305.

Bailey, J., et al., 1979. Final report of the CERN muon storage ring including the anomalous magnetic moment and the electric dipole moment of the muon, and the direct test of relativistic time dilation. Nucl. Phys. B 150, 1–75.

Bainbridge, K.T., 1952. Effect of chemical combination of radioactivity confirmed. Chem. Eng. News 30, 654.

Baker, C.P., et al., 1943. Cross Section for the Reaction 20(230,240)10. Los Alamos Technical Report, LAMS-2, p. 63.

Baker, M., Glashow, S.L., 1962. Spontaneous breakdown of elementary particle symmetries. Phys. Rev. 128 (5), 2462–2471.

Balasubramanian, P.S., 1997. Anodically oxidized aluminum layer as a useful substrate for the fabrication of ^{147}Pm sources for beta-ray thickness gauges. J. Radioanal. Nucl. Chem. 223 (1–2), 79–81.

Balasubramanian, P.S., 1998. A simple procedure for the fabrication of high activity beta-radiation sources of ^{147}Pm for use in beta-ray thickness gauges. J. Radioanal. Nucl. Chem. 229 (1–2), 157–160.

Baldassini, W.A., et al., 2015. Bioanalytical methods for the metalloproteomics study of bovine longissimus thoracis muscle tissue with different grades of meat tenderness in the Nellore breed (*Bos indicus*). Food Chem. 169, 65–72.

Bambynek, W., et al., 1972. X-ray fluorescence yields, Auger, and Coster-Kronig transition probabilities. Rev. Mod. Phys. 44, 716–813.

Bangham, D.H., Franklin, R.E., 1946. Thermal expansion of coals and carbonised coals. Trans. Faraday Soc. 42, B289–B294.

Banner, M., et al., UA2 Collaboration, 1983. Observation of single isolated electrons of high transverse momentum in events with missing transverse energy at the CERN $\bar{p}p$ collider. Phys. Lett. 122B, 476–485.

Bao, Q., et al., 2014. Degradation of 2-mercaptobenzothiazole in aqueous solution by gamma irradiation. Rad. Phys. Chem. 103, 198–202.

Barabash, A.S., et al., 2007. Search for β^+ EC and ECEC processes in ^{74}Se. Nucl. Phys. A 785 (3–4), 371–380.

Barabash, A.S., et al., 2008. Search for β^+ EC and ECEC processes in ^{112}Sn and $\beta^-\beta^-$ decay of ^{124}Sn to the excited states of ^{124}Te. Nucl. Phys. A 807 (3–4), 269–281.

Barany, A. (Ed.), 1999. The Nobel Prizes 1999 Les Prix Nobel: Nobel Prizes, Presentations, Biographies, and Lectures. Almquiest & Wiksell International, Stockholm.

Barber, D.P., et al., 1979. Discovery of three-jet events and a test of quantum chromodynamics at PETRA. Phys. Rev. Lett. 43 (12), 830–833.

Barkas, W.H. (Ed.), 1963. Nuclear Research Emulsions: Pure and Applied Physics. Academic Press, London, p. 518.

Barnes, V.E., et al., 1964. Observation of a hyperon with strangeness minus three. Phys. Rev. Lett. 12 (8), 204–207.

Barnes, R.K., et al., 1986. Polarographic quantification of the specific activity of copper-64 produced by Szilard–Chalmers reactions. Appl. Radiat. Isot. 37, 1241.

Barthakur, N.N., 1983. The β-ray gauge as a leaf surface wetness detector. Int. J. Appl. Radiat. Isot. 34 (11), 1549–1552.

Barthe, N., et al., 2012. High-resolution beta imaging. In: L'Annunziata, M.F. (Ed.), Handbook of Radioactivity Analysis, third ed. Elsevier, Amsterdam, pp. 1209–1242.

Bartke, W., 1997. Who was Who in the People's Republic of China (Part of Reed Elsevier). K.G. Saur Verlag & Co. KG, Munich, p. 517.

Barton, R., et al., 1963. Observation of delayed proton radioactivity. Can. J. Phys. 41, 2007–2025.

Bartusiak, M., Sunday, March 17, 1996. The Woman Behind the Bomb. Washington Post.

Basini, G., et al., 1999. The flux of cosmic-ray antiprotons from 3.7 to 24 GeV. In: Proc. 26th Int. Cosmic Ray Conf., Salt Lake City, vol. 3, p. 101.

Basnayaka, U., et al., 2014. Diffraction-enhanced synchrotron imaging of bovine ovaries ex vivo. J. Med. Imaging Rad. Sci. 45 (3), 307–315.

Bassham, J.A., et al., 1950. The path of carbon in photosynthesis. J. Biol. Chem. 185, 781–787.

Bastien, P.L., et al., 1962. Decay modes and width of the η meson. Phys. Rev. Lett. 8 (3), 114–117.

Basu, S.K., 2003. Hand Book of Oceanograohy. Global Vision Publishing, Delhi.

Battista, J., van Dyk, J., 2002. London celebrates fifty years of cobalt-60 radiotherapy. Can. Med Phys. Newsl. 48 (1), 15.

Bayanov, B., et al., 2009a. A neutron producing target for BINP accelerator-based neutron source. Appl. Radiat. Isot. 67, S282–S284.

Bayanov, B., et al., 2009b. First neutron generation in the BINP accelerator based neutron source. Appl. Radiat. Isot. 67, S285–S287.

Bayanov, B., et al., 2010. Dosimetry and spectrometry at accelerator based neutron source for boron neutron capture. Radiat. Meas. 46 (10), 1462–1464.

Bé, M.-M., et al., 2006. Detailed calculation of *K*- and *L*-Auger electron emission intensities following radioactive disintegration. Appl. Radiat. Isot. 64, 1435–1439.

Beach, A.S., et al., 2001. Measurement of the cosmic-ray antiproton-to-proton abundance ratio between 4 and 50 GeV. Phys. Rev. Lett. 87, 271101.

Beatty, J.J., et al., 2004. New measurement of the cosmic-ray positron fraction from 5 to 15 GeV. Phys. Rev. Lett. 93, 241102.

Beck, L., 2014. Recent trends in IBA for cultural heritage studies. Nucl. Instrum. Methods Phys. Res. Sect. B 332, 439–440.

Beck, L., et al., 2011. IBA techniques: examples of useful combinations for the characterization of cultural heritage materials. Nucl. Instrum. Methods Phys. Res. Sect. B 269, 2999–3005.

Beck, M., 2010. The KATRIN experiment. J. Phys. Conf. Ser. 203 (1), 012097.

Becker, J.S., 2012. Inorganic mass spectrometry of radionuclides. In: L'Annunziata, M.F. (Ed.), Handbook of Radioactivity Analysis, third ed. Elsevier, Amsterdam, pp. 833–870.
Beckerly, J.G., 1945. What is the "Geiger-Nuttall law"? Am. J. Phys. 13 (3), 158–159.
Beckmann, Ch., et al., 2002. Nuclei, superheavy nuclei, and hypermatter in a chiral SU(3) model. Phys. Rev. C 65 (2), 024301.
Becquerel, A.H., 1896. On the rays emitted by phosphorescence. C. R. Acad. Sci. Paris 122, 420.
Becquerel, A.H., 1996. On the invisible rays emitted by phosphorescent bodies. C. R. Acad. Sci. Paris 122, 501.
Becquerel, A.H., 1901. The radio-activity of matter. Nature 63, 396–398.
Becquerel, A.H., 1903. On radioactivity, a new property of matter. Nobel Lecture, December 11, 1903. In: Science Incorporated Elsevier (Ed.), Nobel Lectures in Physics, 1901–1970, Nobel Lectures, Physics, 1901–1921 (1967), vol. 1. Elsevier Publishing, Amsterdam.
Behnken, H., 1927. Die Absolutbestimmung der Dosisinheit "1 Röntgen" inder Physicalisch-Technischen Reichsanstalt. Strahlentherapie 26, 79–100.
Behr, T., et al., 2000. Therapeutic advantages of Auger electron-over beta emitting radiometals or radioiodine when conjugated to internalizing antibodies. Eur. J. Nucl. Med. 27 (7), 753–765.
Belcher, E.H., 1953. The luminescence of irradiated transparent media and the Cerenkov effect. I. The luminescence of aqueous solutions of radioactive isotopes. Proc. R. Soc. London Ser. A 216 (1124), 90–102.
Bellotti, R., et al., 1996. Measurement of the negative muon spectrum between 0.3 and 40 GeV/*c* in the atmosphere. Phys. Rev. D53, 35.
Bellotti, R., et al., 1999. Balloon measurements of cosmic-ray muon spectra in the atmosphere along with those of primary protons and helium nuclei over midlatitude. Phys. Rev. D60, 052002.
Bem, E.M., et al., 1978. The use of Cherenkov radiation in the measurement of cadmium-115m in blood and other tissues. Bull. Environ. Contam. Toxicol. 19, 677–683.
Benczer-Koller, N., 2009. Chien-Shiung Wu 1912–1997. National Academy of Sciences, Washington, DC, pp. 1–17.
Bender, M., et al., 2001. Shell stabilization of super- and hyperheavy nuclei without magic gaps. Phys. Lett. B 515 (1–2), 42–48.
Benson, A.A., et al., 1952. The path of carbon in photosynthesis. XVI. Kinetic relationships of the intermediates in steady state photosynthesis. J. Am. Chem. Soc. 74, 4477–4482.
Benny, P.G., et al., 2011. Evaluation of the efficiency and throughput of a gamma irradiator treating municipal sewage sludge. Appl. Radiat. Isot. 69 (3), 604–606.
Berger, Ch., et al., 1979. Evidence for gluon bremsstrahlung in e^+e^- annihilations at high energies. Phys. Lett. 86B (3–4), 418–425.
Berger, M.J., Hubbell, J.H., 1997. Photon attenuation coefficients. In: Lide, D.R., Frederikse, H.P.R. (Eds.), Handbook of Chemictry and Physics, 77th ed. CRC Press, Boca Raton, pp. 10-250–10-254.
Berger, M.J., Seltzer, S.M., 1982. Stopping Powers and Ranges of Electrons and Positrons. NBSIR 82-2550. Nat. Bureau Standards Publ, p. 168.
Berger, M.J., et al., 2010. XCOM: Photon Cross Sections Database 8 (XGAM). The National Institute of Standards and Technology (NIST). http://www.nist.gov/pml/data/xcom/index.cfm.
Berghaus, P., for the IceCube Collaboration, 2009. Muons in IceCube. Nucl. Phys. B (Proc. Suppl.) 196, 261–266.
Berry, M., February 1998. Paul Dirac: the Purist Soul in Physics. Physics World, p. 36.
Bethe, H.A., 1933. Quantenmechanik der Ein- und Zwei-Electronen-Probleme. In: Geiger, H., Scheel, K. (Eds.), Handbuch der Physik, second ed., vol. 24, Part I. Springer, Berlin.
Bethe, H.A., 1937. Nuclear physics II. Nuclear dynamics, theoretical. Rev. Mod. Phys. 9, 69–244.
Bethe, H.A., 1939. Energy production in stars. Phys. Rev. 55, 434–456.
Bethe, H.A., 1942. Energy production in stars. Am. Sci. 30 (4), 243–264.
Bethe, H.A., 1967. Energy production in stars. Nobel Lecture on December 11, 1967, Stockholm. In: Nobel Foundation Staff (Ed.), Nobel Lectures, Physics, 1942–1962 (1964). Elsevier Publishing, Amsterdam.
Bethe, H.A., 2000. The German uranium project. Phys. Today 53 (7), 34–36.
Bethe, H.A., Ashkin, J., 1953. Passage of radiations through matter. In: Segré, E. (Ed.), Experimental Nuclear Physics, vol. 1. J. Wiley, New York.
Bethe, H.A., Bacher, R.F., 1936. Nuclear physics I. Stationary states of nuclei. Rev. Mod. Phys. 8, 82–229.
Bethe, H.A., Critchfield, C.L., 1938. The formation of deuterons by proton combination. Phys. Rev. 54, 248–254.
Bethe, H.A., Peierls, R.E., 1934. The neutrino. Nature 133, 532.
Bethe, H.A., Placzec, G., 1937. Resonance effects in nuclear processes. Phys. Rev. 51, 450–484.
Bethe, H.A., et al., 1986. Basic Bethe: Seminal Articles on Nuclear Physics, 1936–1937. American Institute of Physics, New York.
Bevelacqua, J.J., 2010. Basic Health Physics: Problems and Solutions. Wiley-VCH, Hoboken, p. 768.
Bevilacqua, R., et al., 2007. PhoNeS: a novel approach to BNCT with conventional radiotherapy accelerators. Nucl. Instrum. Methods Phys. Res. Sect. A 572, 231–232.
Bhabha, H.J., 1933. For the absorption of cosmic radiation. Z. Phys. A Hadrons Nucl. 86 (1–2), 120–130.
Bhabha, H.J., 1936. The scattering of positrons by rlectrons with exchange on Dirac's theory of the positron. Proc. R. Soc. A 154, 195–206. http://dx.doi.org/10.1098/rspa.1936.0046.
Bhabha, H.J., Heitler, W., 1937. The passage of fast electrons and the theory of cosmic showers. Proc. R. Soc. London A 159, 432–458.
Bhabha, H.J., 1938a. On the penetrating component of cosmic radiation. Proc. R. Soc. London A 164 (917), 257–294.
Bhabha, H.J., 1938b. Nuclear forces, heavy electrons and β-decay. Nature 141 (3559), 117–118.
Bhabha, H.J., 1939. The fundamental length introduced by the theory of the mesotrpn (meson). Nature 143 (3616), 276–277.
Bhabha, H.J., 1937. Negative protons in cosmic radiations. Nature 139 (3514), 415–416.

Bhattacharjee, P., Sigl, G., 2000. Origin and propagation of extremely high-energy cosmic rays. Phys. Rep. 327, 109–247.
Biebel, O., 2001. Experimental tests of the strong interaction and its energy dependence in electron-positron annihilation. Phys. Rep. 340, 165–289.
Biersack, H.-J., Freeman, L.M., 2007. Nuclear Medicine Concise. Springer Verlag, p. 380.
Bijma, J., et al., 2013. Climate change and the oceans – what does the future hold? Mar. Poll. Bull. 74, 495–505.
Billington, D., 1992. Radioisotopes (introduction to biotechniques). BIOS Sci. 168.
Birattari, C., et al., 2001. Review of cyclotron production and quality control of "high specific activity" radionuclides for biomedical, biological, industrial, and environmental applications at INFN-LASA. In: Marti, F. (Ed.), "Cyclotrons and Their Applications 2001". Proceedings of Sixteenth International Conference. American Institute of Physics, Melville, New York.
Birch, M., et al., 2014. First compilation and evaluation of beta-delayed neutron emission probabilities and associated half-lives for $A \leq 72$ nuclei. Nucl. Data Sheets 120, 66–69.
Bird, D.J., et al., 1995. Detection of a cosmic ray with measured energy well beyond the expected spectral cutoff due to cosmic microwave radiation. Astrophys. J. 441, 144–150.
Birge, R.T., 1940. Account of Professor Lawrence's Work. Speech given at Presentaion Ceremony of Nobel Prize, Physics to Ernest O. Lawrence on February 29, 1940 at The University of California, Berkeley. In: Nobel Lectures, Physics, 1922–1941 (1965). Elsevier Publishing, Amsterdam.
Bjorken, J.D., Paschos, E.A., 1969. Inelastic electron-proton and γ-proton scattering and the structure of the nucleon. Phys. Rev. 185 (5), 1975–1982.
Bjorklund, R., et al., 1950. High energy photons from proton-nucleon collisions. Phys. Rev. 77, 213–218.
Blackburn, R., Al-Masri, M.S., 1993. Determination of radon-222 and radium-226 in water samples by Cerenkov counting. Analyst 118, 873–876.
Blackburn, R., Al-Masri, M.S., 1994. Determination of uranium by liquid scintillation and Cerenkov counting. Analyst 119, 465–468.
Blackett, P.M.S., 1922. On the analysis of alpha-ray photographs. Proc. R. Soc. London 102A, 294–318.
Blackett, P.M.S., 1923. The study of forked α-ray tracks. Proc. R. Soc. London 103A, 62–80.
Blackett, P.M.S., 1925. The ejection of protons from nitrogen nuclei, photographed by the Wilson method. Proc. R. Soc. London 107, 349–360.
Blackett, P.M.S., 1927. An automatic cloud chamber for the rapid production of alpha ray photographs. J. Sci. Instrum. 4 (14), 433–439.
Blackett, P.M.S., 1929. On the design and use of a double camera for photographing artificial disintegrations. Proc. R. Soc. London 123A, 613–629.
Blackett, P.M.S., 1934. On the technique of the counter controlled cloud chamber. Proc. R. Soc. London 146A, 281–289.
Blackett, P.M.S., 1936. The measurement of the energy of cosmic rays. I. The electro-magnet and cloud chamber. Proc. R. Soc. London 154A, 564–573.
Blackett, P.M.S., 1948a. Cloud chamber researches in nuclear physics and cosmic radiation. Nobel Lecture on December 13, 1948. In: Nobel Foundation Staff (Ed.), Nobel Lectures, Physics, 1942–62 (1964). Elsevier Publishing, Amsterdam.
Blackett, P.M.S., 1948b. Military and Political Consequences of Atomic Energy. Turnstile Press, London.
Blackett, P.M.S., 1954. Lectures on Rock Magnetism. The Weizmann Press, Tel Aviv.
Blackett, P.M.S., 1962. Studies of War. Oliver and Boyd, London.
Blackett, P.M.S., 1971. Science, Technology and Aid in Developing Countries. Edinburgh University Press, Edinburgh.
Blackett, P.M.S., Brode, R.B., 1936. The measurement of the energy of cosmic rays. II. The curvature measurements and the energy spectrum. Proc. R. Soc. London 154A, 573–587.
Blackett, P.M.S., Champion, F.C., 1931. The scattering of slow alpha particles by helium. Proc. R. Soc. London 130A, 380–388.
Blackett, P.M.S., Hudson, E.P., 1927. The elasticity of the collisions of alpha particles with hydrogen nuclei. Proc. R. Soc. London 117A, 124–130.
Blackett, P.M.S., Lees, D.S., 1932a. Investigations with a Wilson Chamber. I. On the photography of artificial disintegration collisions. Proc. R. Soc. London 136A, 325–338.
Blackett, P.M.S., Lees, D.S., 1932b. Further investigations with a Wilson Chamber. II. The range and velocity of recoil atoms. Proc. R. Soc. London 134A, 658–671.
Blackett, P.M.S., Lees, D.S., 1932c. Further investigations with a Wilson Chamber. III. The accuracy of the angle determination. Proc. R. Soc. London 136A, 338–348.
Blackett, P.M.S., Occhialini, G.P.S., 1932. Photography of penetrating corpuscular radiation. Nature 130, 363.
Blackett, P.M.S., Occhialini, G.P.S., 1933. Some photographs of the tracks of penetrating radiation. Proc. R. Soc. London 139A, 699–726.
Blais, J.S., Marshall, W.D., 1988. Determination of lead-210 in admixture with bismuth-210 and polonium-210 in quenched samples by liquid scintillation counting. Anal. Chem. 60, 1851–1855.
Blank, B., et al., 2003. First observation of two-proton radioactivity from an atomic nucleus. C. R. Phys. 4, 521–527.
Blank, B., et al., 2010. A time projection chamber for the three-dimensional reconstruction of two-proton radioactivity events. Nucl. Instrum. Methods Phys. Res. Sect. A 613, 65–78.
Blasi, P., 2008. Origin of high energy cosmic rays: a short review. Nucl. Instrum. Methods Phys. Res. Sect A 588, 166–170.
Blasko, J.C., et al., 1998. In: Ernstoff, M.S., Heaney, J.A., Peschel, R.E. (Eds.), Prostate Cancer. Blackwell Science, Cambridge, MA, p. 137.
Blau, M., 1938. Photographic tracks from cosmic rays. Nature 142, 613.
Blau, M., 1956. Hyperfragments and slow K-mesons in stars produced by 3 BeV protons. Phys. Rev. 102, 495–501.
Blau, M., Coulton, M., 1954. Inelastic scattering of 500-MeV negative pions in emulsion nuclei. Phys. Rev. 96, 150–160.
Blau, M., et al., 1953. Meson production by 500 MeV negative pions. Phys. Rev. 92, 516.
Blau, M., De Felice, J.A., 1948. Development of thick emulsions by a two-bath method. Phys. Rev. 74, 1198.
Blau, M., Oliver, A.R., 1956. Interaction of 750 MeV pi-mesons with emulsion nuclei. Phys. Rev. 102, 489–494.
Blau, M., Wambacher, H., 1935. Über die Empfindlichkeit desensibilisierter photographischer Schichten in Abhängigkeit vom Luftsauerstoff und von derKonzentration der Desensibilatoren. Mitteilungen des Institutes für Radiumforschung Nr, 367. Akad. Der Wissenschaften Wien, Mathematisch-naturwissenschaftliche Klasse, Sitzungsberichte, Abteilung IIa, Band 144, Heft 1-10, S. 403.

Blau, M., Wambacher, H., October 2, 1937. Dsintegration processes by cosmic rays with the simultaneous emission of several heavy particles. Nature 140, 585.

Blendowske, R., et al., 1987. Microscopic calculation of the ^{14}C decay of Ra nuclei. Nucl. Phys. A 464, 75–89.

Blewett, J.P., 1988. Synchrotron radiation – 1873 to 1947. Nucl. Instrum Methods Phys. Res. Sect. A 266, 1–9.

Bloch, F., et al., 1948. A quantitative determination of the magnetic moment of the neutron in units of the proton moment. Phys. Rev. 74 (9), 1025–1045.

Blümer, J., et al., 2009. Cosmic rays from the knee to the highest energies. Prog. Part. Nucl. Phys. 63, 293–338.

Bodei, L., et al., 2003. Radionuclide therapy with iodine-125 and other Auger-emitting radionuclides: experimental models and clinical applications. Cancer Radiother. Radiopharm. 18, 861–877.

Boehm, F., Wu, C.S., 1954. Internal bremsstrahlung and ionization accompanying beta decay. Phys. Rev. 93, 518–523.

Boezio, M., et al., 1999. The cosmic-ray proton and helium spectra between 0.2 and 200 GeV. Astrophys. J. 518, 457.

Boezio, M., et al., 2000a. The cosmic-ray electron and positron spectra measured at 1 AU during solar minimum activity. Astrophys. J. 532, 653.

Boezio, M., et al., 2000b. Measurements of the flux of atmospheric muons with the CAPRICE94 apparatus. Phys. Rev. D62, 032007.

Bohr, A., 1951. On the quantization of angular momenta in heavy nuclei. Phys. Rev. 81, 134–138.

Bohr, A., December 11, 1975. Rotational Motion in Nuclei. Nobel Lecture. http://www.nobelprize.org/nobel_prizes/physics/laureates/1975/bohr-lecture.pdf.

Bohr, A., 1992. Rotational motion in nuclei. In: Lundqvist, S. (Ed.), Nobel Lectures, Physics 1971–1980. World Scientific Publishing, Singapore.

Bohr, A., Mottelson, B.R., 1953a. Interpretation of isomeric transitions of electric quadrupole type. Phys. Rev. 89, 316–317.

Bohr, A., Mottelson, B.R., 1953b. Rotational states in even-even nuclei. Phys. Rev. 90, 717–719.

Bohr, N., 1913. On the constitution of atoms and molecules. Philos. Mag. 26 (6), 1–25.

Bohr, N., 1914. On the spectrum of hydrogen. Address to the Physical Society of Copenhagen, December 20, 1913. Physik Tidsskrift 12, 97, translated by A.D. Udden "The Theory of Spectra and Atomic Constitution – Three Essays 1922.". In: Moulton, F.R., Schifferes, J.J. (Eds.), Autobiography of Science. Doubleday, New York, 1950.

Bohr, N., 1921a. Atomic structure. Nature 107, 104–107.

Bohr, N., 1921b. Atomic structure. Nature 108, 208–209.

Bohr, N., December 11, 1922. The structure of the atom. Nobel Lecture. In: Nobel Lectures, Physics 1922–1941 (1965). Elsevier Publishers, Amsterdam.

Bohr, N., 1928. The quantum postulate and the recent development of atomic theory. Nature 121, 580–591.

Bohr, N., 1936. Neutron capture and nuclear constitution. Nature 137, 344–348.

Bohr, N., 1939. Disintegration of heavy nuclei. Nature 143, 330.

Bohr, N., 1950. Open letter to the United Nations. Science 112 (2897), 1–6.

Bohr, N., Lindhard, J., 1954. Electron capture and loss by heavy ions penetrating through matter. K. Dan. Vidensk. Selsk. Mat. Fys. Medd. 28 (7), 1–30.

Bohr, N., Wheeler, J.A., 1939. The mechanism of nuclear fission. Phys. Rev. 56 (5), 426–449.

Bohr, N., et al., 1926. Quantum mechanics II. Z. Phys. 35 (8/9), 557–615.

Bolotovski, B.M., Vavilov, Y.N., Kirkin, A.N., 1998. Sergei Ivanovich Vavilov, the man and the scientist: a view from the threshold of the 21st century. Phys. Usp. 41 (5), 487–504.

Bolotovski, B.M., Vavilov, Y.N., Schmeleva, A.P., November 12, 2004. Sergei Vavilov: Luminary of Russian Physics. CERN Courier. Institute of Physics, London.

Bolotowski, B.M., Vavilov, Yu, N., 1995. Sergei Vavilov, honored in Russia, still little known in the west. Phys. Today 48 (12), 11–13.

Boltz, C.L., 1970. Ernest Rutherford. Heron Books, Norwich, p. 371.

Bonardi, M.L., et al., 2004. Cyclotron production and quality control of "high specific activity" radionuclides in "no-carrier added" form for radioanalytical applications in the life sciences. J. Radioanal. Nucl. Chem. 250 (3), 415–419.

Bonbardieri, E., et al., 2007. Advances in Nuclear Oncology. Informa Healthcare, p. 600.

Bone, A., October 1, 2005. The Russell-Einstein Manifest and the Origins of Pugwash. Eric Fawcett Memorial Lecture to Canadian Pugwash and Science for Peace. Joint Forum of the Canadian Pugwash Group and Science for Peace, p. 11.

Bonetti, R., Guglielmetti, A., 1999. Measurements of cluster radioactivity. In: Greiner, W., Gupta, R.K. (Eds.), Heavy Elements and Related New Phenomena, vol. II. World Scientific, Singapore, p. 1168.

Bonetti, R., et al., 2001. Cluster decay of ^{230}U via Ne emission. Nucl. Phys. A 686, 64–70.

Bonn, J., et al., 2000. The Mainz neutrino mass experiment. In: Proceedings of the XIX International Conference on Neutrino Physics and Astrophysics (Neutrino-2000), Sudbury, Canada, June 16–21, 2000.

Bonn, J., et al., 2001. The Mainz neutrino mass experiment. Nucl. Phys. B – Proc. Suppl. 91 (1–3), 273–279.

Bonner, T.W., Brubaker, W.M., 1936a. The disintegration of nitrogen by neutrons. Phys. Rev. 49, 223–229.

Bonner, T.W., Brubaker, W.M., 1936b. The disintegration of nitrogen by slow neutrons. Phys. Rev. 49, 778.

Boone, M.N., et al., 2014. High spectral and spatial resolution X-ray transmission radiography and tomography using a color X-ray camera. Nucl. Instrum. Methods phys. Res. Sect. A 735, 644–648.

Borisenko, V.E., Ossicini, S., 2004. What Is What in the Nanoworld: a Handbook on Nanoscience and Nanotechnology. Wiley-VCH Verlag GmbH & Co. KgaA, Weinheim.

Born, M., 1926a. The quantum mechanics of the impact process. Z. Phys. 37 (12), 863–867.

Born, M., 1926b. Quantum mechanics in impact process. Z. Phys. 38 (11/12), 803–840.

Born, M., 1926c. Zur Wellenmechanik der Stossvorgänge. Göttingen Nachr. Math. Phys. Kl. 146–160.

Born, M., 1926d. The adiabaten principle in the quantum mechanics. Z. Phys. 40 (3/4), 167–192.
Born, M., 1954. The statistical interpretation of quantum mechanics. In: Nobel Foundation Staff (Ed.), Nobel Lectures, Physics, 1942–62 (1964). Elsevier Publishing Co., Amsterdam.
Born, M., 1969. Atomic Physics. Blackie and Son, Ltd., Glasgow, pp. 36–37.
Born, M., 1978. My Life: Recollections of a Nobel Laureate (1978), first U.S. ed. Schribner, p. 308.
Born, M., Fock, V., 1928. Bewas des Adiabatensatzes. Z. Phys. 51, 165–180.
Born, M., Oppenheimer, R., 1927. Quantum theory of molecules. Ann. Phys. 84 (20), 457–484.
Born, M., Goeppert-Mayer, M., 1933. Dynamische Gittertheorie der Kristalle. In: Handbuch der Physik, Band 24/2. Verlag Julius Springer, Berlin, pp. 623–794.
Bornemann, A., et al., 2003. The impact of calcerous nannofossils on the pelagic carbonate accumulation across the Jurassic-Cretaceous boundary interval. Palaeogeogr. Palaeoclimatol. Palaeoecol. 199, 187–228.
Bothe, W., 1926. The interconnection between elementary radiation activities. Z. Phys. 37, 547–567.
Bothe, W., 1954. The coincidence method. Nobel Lecture. In: Nobel Foundation Staff (Ed.), Nobel Lectures, Physics, 1942–62 (1964). Elsevier Publishing, Amsterdam.
Bothe, W., Becker, H., 1930. Künstliche Erregung von Kern-Strahlen. Z. Phys. 66, 289.
Bothe, W., Geiger, H., 1924. Über das Wesen des Compton effecks. Z. Phys. 26, 44.
Boudjemline, K., et al., 2010. The calibration of the Sudbury Neutrino Observatory using uniformly distributed radioactive sources. Nucl. Instrum. Methods Phys. Res. Sect. A 620, 171–181.
Bouyer, J., Lefrançois, T., 2014. Boosting the sterile insect technique to control mosquitoes. Trends Parasitol. 30 (6), 271–273.
Bowen, I.S., et al., 1934. A very high altitude survey of the effect of latitude upon cosmic ray intensities and an attempt at a general interpretation of cosmic ray phenomena. Phys. Rev. 46, 641–652.
Bowen, I.S., et al., 1936. The latitude effect in cosmic rays at altitudes of up to 29,000 feet. Phys. Rev. 50, 579–581.
Bowen, I.S., et al., 1937. The influence of the earth's magnetic field on cosmic-ray intensities up to the top of the atmosphere. Phys. Rev. 52, 80–88.
Bradley, R.S., 2015. Marine sediments. In: Paleoclimatology, third ed. Elsevier, Amsterdam, pp. 196–277.
Bradt, H.L., Peters, B., 1948. Investigation of the primary cosmic radiation with nuclear photographic emulsions. Phys. Rev. 74, 1828–1837.
Bragg, W.L., 1913. The diffraction of short electromagnetic waves by a crystal. Proc. Cambridge Phil. Soc. 17, 43–57.
Bragg, W.L., 1914a. The analysis of crystals by the X-ray spectrometer. Proc. R. Soc. London Ser. A 89, 468–489.
Bragg, W.L., 1914b. X-rays and Crystaline Structure. Morse King Publishers, p. 802.
Bragg, W.L., 1922. The diffraction of X-rays by crystals. Nobel Lecture, September 6, 1922. In: Nobel Lectures, Physics, 1901–1921 (1967). Elsevier Publishing, Amsterdam.
Brajnik, D., et al., 1994. Measurement of ^{90}Sr activity with Cherenkov radiation in a silica aerogel. Nucl. Instrum. Methods Phys. Res. Sect. A 353, 217–221.
Brajnik, D., et al., 1995. Determination of high energy β-emitters with a Ge spectrometer or Cherenkov radiation in a silica aerogel. Sci. Total Environ. 173/174, 225–230.
Brandelik, et al., 1979. Evidence for planar events in e^+e^- annihilation at high energies. Phys. Lett. 86B (2), 243–249.
Brasch, A., Lange, F., Waly, A., Banks, T.E., Charlmers, T.A., Szilard, L., Hopwood, F.L., 1934. Liberation of neutrons from beryllium by X-rays: Radioactivity induced by means of electron tubes. Nature 134, 880.
Braun, R., et al., 2007. Joseph Rotblat: Visionary for Peace. Wiley-VCH, p. 371.
Brien, M., et al., 1972. States of ^{87}Sr populated by deuteron pick-up from ^{89}Y. Nucl. Phys. A 185, 289–302.
Bridge, E.S., et al., 2014. Bird migration and avian influenza: a comparison of hydrogen stable isotopes and satellite tracking methods. Ecol. Indic. 45, 266–273.
Brower, H., 1985. An addendum to "Some misunderstandings about Millikan's oil drop experiment". J. Chem. Educ. 62 (5), 455.
Brown, A., 2012. Keeper of the Nuclear Conscience: The Life and Work of Joseph Rotblat. Oxfor University Press, p. 288.
Brown, J.L., Glaser, D.A., Perl, M.L., 1956. Liquid xenon bubble chambers. Phys. Rev. 102, 586–589.
Brown, L.M., 2000. Book review: the discovery of Antimatter: the autobiography of Carl David Anderson, the youngest man to win the Nobel Prize. Phys. Today 53 (10), 81.
Browne, E., et al., 1986. Table of Radioactive Isotopes. John Wiley & Sons, New York.
Brune, M., Haroche, S., Raimond, J.M., Davidovich, L., Zagury, N., 1992. Manipulation of photons in a cavity by dispersive atom-field coupling: quantum-nondemolition measurements and generation of "Schrödinger cat" states. Phys. Rev. A 45, 5193–5214.
Brüning, O., et al., 2012. The large hadron collider. Prog. Part. Nucl. Phys. 67, 705–734.
Brunner, J., for the ANTARES Collaboration, 2011. The ANTARES neutrino telescope—status and first results. Nucl. Instrum. Methods Phys. Res. Sect. A 626–627, S19–S24.
Bryant, P.J., 1992. A brief history and review of accelerators. In: Proceedings, General Accelerator Physics, vol. I. CERN, Geneva, pp. 1–16.
Bryne, J., 1994. Neutrons, Nuclei and Matter, an Exploration of the Physics of Slow Neutrons. Institute of Physics, London.
Buchtela, K., 2003. Gas ionization detectors, pp. 123–178. In: L'Annunziata, M.F. (Ed.), Handbook of Radioactivity Analysis, second ed. Elsevier Science Publishers, Amsterdam, p. 1273.
Buchtela, K., Tschurlovits, M., 1975. A new method for determination of ^{89}Sr, ^{90}Sr, and ^{90}Y in aqueous solution with the aid of liquid scintillation counting. Int. J. Appl. Radiat. Isot. 26, 333–338.

Buck, B., Merchant, A.C., 1989. Cluster model calculations of exotic decays from heavy nuclei. Phys. Rev. C 39, 2097–2100.
Budagov, I., et al., 1969. Measurement of structure factors in inelastic neutrino scattering. Phys. Lett. 30B (5), 364–368.
Bullen, T.D., Kendall, C., 1998. Tracing of weathering reactions and water flowpaths: a multi-isotope approach, pp. 611–646. In: Kendall, C., McDonnell, J.J. (Eds.), Isotope Tracers in Catchment Hydrology. Elsevier, Amsterdam, p. 839.
Burcham, W.E., Goldhaber, M., 1936. The disintegration of nitrogen by slow neutrons. Proc. Cambridge Phil. Soc. 32, 632–636.
Burcham, W.E., Jobes, M., 1994. Nuclear and Particle Physics. Longman Scientific & Technical, Essex.
Burden, D.L., Hieftje, G.M., 1998. Cerenkov radiation as a UV and visible light source for time-resolved fluorescence. Anal. Chem. 70 (16), 3426–3433.
Burhop, E.H.S., Asaad, W.N., 1972. The Auger effect. In: Bates, D.R., Esterman, I. (Eds.), Advances in Atomic and Molecular Physics, vol. 8. Academic Press, New York, pp. 163–184, p. 299.
Butcher, S.I., 2005. The origins of the Russell-Einstein Manifesto. In: Boutwell, Jeffrey (Ed.), Pugwash History Series, Number One. Pugwash Conferences on Science and World Affairs, pp. 1–35.
Butterworth, J., September 7, 2013. What's Next? New Sci. 219 (2933), vi–vii.
Butterworth, J., 2015. Most wanted particle: the inside story of the hunt for the Higgs, the heart of the future of physics. Experiment 304.
Buttlar, H.V., 1968. Nuclear Physics, an Introduction. Academic Press, New York.
Byers, N., 2000. Marietta Blau. University of California, Los Angeles. Website. http://cwp.library.ucla.edu.
Caesar, C., et al., 2013. Beyond the neutron drip line: the unbound oxygen isotopes ^{25}O and ^{26}O. Phys. Rev. C 88, 034313.
Caffee, M.W., et al., 1992. Isotopic composition of chlorine in groundwater from the Wawona basin, Yosmite National Park. Eos Trans. Am. Geophys. Union 73, 173.
Caldwell, S.E., et al., 2003. Observation of d–t gamma rays. Rev. Sci. Instrum. 74 (3), 1837–1841.
Calinescu, I., et al., 2013. E-Beam SO_2 and NO_x removal from flue gases in the presence of fine water droplets. Rad. Phys. Chem. 85, 130–138.
Callahan, A.C., et al., 1966. Measurement of the $K^+_{\mu 3}$ decay parameters. Phys. Rev. 150, 1153–1164.
Calvin, M., 1949. The path of carbon in photosynthesis VI. J. Chem. Educ. 26, 623–657.
Calvin, M., 1953. The path of carbon in photosynthesis. Chem. Eng. News 31, 1622–1625.
Calvin, M., Benson, A.A., 1948. The path of carbon in photosynthesis. Science 107, 476–480.
Calvin, M., Bassham, J.A., Benson, A.A., 1950. Chemical transformations of carbon in photosynthesis. Fed. Proc. 9 (2), 524–534.
Camerini, U., et al., 1948. Observations on slow mesons of the cosmic radiation. Nature 162 (4116), 433–438.
Campbell, D.B., et al., 2008. Evaluation of radioactive background rejection in ^{76}Ge neutrino-less double-beta decay experiments using a highly segmented HPGe detector. Nucl. Instrum. Methods Phys. Res. Sect. A 587, 60–67.
Canberra Nuclear, 1996. Neutron detection and counting. In: Canberra Nuclear Instruments Catalog, ninth ed. Canberra Industries, Meriden, CT, pp. 37–39.
Capello, A., et al., 2003. Peptide receptor radionuclide therapy in vitro using [In-111-DTPA(0)]octreotide. J. Nucl. Med. 44 (1), 98–104.
Carlson, A.G., et al., 1950. Nuclear transmutations produced by cosmic-ray partcles of great energy – Part V. The neutral meson. Phil. Mag. 41, 701.
Carlson, P., 1986. Aerogel Cherenkov counters: construction principles and applications. Nucl. Instrum. Methods Phys. Res. Sect. A 248, 110–117.
Carmon, B., Dyer, A., 1987. Čerenkov spectoscopic assay of fission isotopes II. Čerenkov counting of ^{106}Ru on UV-colour-quenched solutions containing other β-emitters. J. Radioanal. Nucl. Chem. Articles 109, 229–236.
Caroll, J., Lerche, I., 2003. Sedimentary Processes: Quantification Using Radionuclides (Radioactivity in the Environment). Elsevier Science, Amsterdam, p. 282.
Carr, J., 2008. Data from the ANTARES neutrino telescope. Nucl. Instrum. Methods Phys. Res. Sect. A 588, 80–85.
Carron, G., et al., 1978. Stochastic cooling tests in ICE. Phys. Lett. B 77, 353–354.
Casnati, E., et al., 1998. The effect of delta rays on the ionometric dosimetry of proton beams. Phys. Med. Biol. 43, 547–558.
Caso, C., et al. Particle Physics Group, 1998. Review of particle physics. Eur. Phys. J. C 3 (1–4), X1–12.
Cathcart, B., 2004. The Fly in the Cathedral: How a Group of Cambridge Scientists Won the International Race to Split the Atom. Farrar, Straus and Giroux, New York, p. 320.
CDF Collaboration, et al., 2012. Updated Combination of CDF and D0 Searches for Standard Model Higgs Boson Production with up to 10.0 fb-1 of Data. FERMILAB-CONF-12-318-E; CDF Note 10884; D0 Note 6348. http://arxiv.org/abs/1207.0449.
Celiktas, C., 2011. A method to determine the gamma-ray linear attenuation coefficient. Ann. Nucl. Energy 38 (9), 2096–2100.
Cember, H., Johnson, T., 2008. Introduction to Health Physics, fourth ed. McGraw-Hill Medical, New York, p. 864.
Cengiz, A., Almaz, E., 2004. Internal bremsstrahlung spectra of β^- particle emitters using the Monte Carlo method. Radiat. Phys. Chem. 70, 661–668.
CERN Courier, 2004. Bookshelf: Marietta Blau – Sterne der Zertrümmerung. January/February 2004, vol. 44 (No. 1).
Cerny, J., et al., 1970. Confirmed proton radioactivity of ^{53m}Co. Phys. Lett. B 33 (4), 284–286.
Chadwick, J., 1932a. Possible existence of a neutron (Received February 27, 1932). Nature 129, 312.
Chadwick, J., 1932b. The existence of a neutron (Received May 10, 1932). Proc. R. Soc. A 136, 692–708.
Chadwick, J., 1935. The neutron and its properties. Nobel Lecture, December 12, 1935. In: Nobel Lectures, Physics 1922–1941 (1965). Elsevier Publishers, Amsterdam.
Chadwick, J., Goldhaber, M., 1934. A 'nuclear photo-effect': disintegration of the diplon by γ-rays. Nature 134, 237–238.
Chamberlain, O., 1959. The early antiproton Work. Nobel Lecture, December 11, 1959. In: Nobel Foundation Staff (Eds.), Nobel Lectures, Physics, 1942–62 (1964). Elsevier Publishing, Amsterdam, pp. 489–505.

Chamberlain, O., Segrè, E., Wiegand, C., Ypsilantis, T., 1955. Observation of antiprotons. Phys. Rev. 100, 947–951.

Chamberlain, O., Chupp, W.W., Ekspong, A.G., Goldhaber, G., Goldhaber, S., Lofgren, E.J., Segrè, E., Wiegand, C., Amaldi, E., Baroni, G., Castagnoli, C., Franzinetti, C., Manfredini, A., 1956. Phys. Rev. 102, 921.

Chambers, E.E., Hofstadter, R., 1956. Structure of the proton. Phys. Rev. 103 (5), 1454–1463.

Chandra, S., Lorey II, D.R., 2007. SIMS ion microscopy imaging of boronophenylalanine (BPA) and $^{13}C^{15}N$-labeled phenylalanine in human glioblastoma cells: relevance of subcellular scale observations to BPA-mediated boron neutron capture therapy of cancer. Int. J. Mass Spec. 260, 90–101.

Chang, T.-M., et al., 1996. Rapid and accurate determination of $^{89/90}Sr$ in radioactive samples by Cerenkov counting. J. Radioanal. Nucl. Chem. Articles 204, 339–347.

Chard, T., 1995. An Introduction to Radioimmunoassay and Related Techniques, fifth ed. Elsevier, p. 328.

Charitos, P., December 13, 2013. Interview with Grorge Zweig. Newsletter of the PH Department. CERN. http://ph-news.web.cern.ch/content/interview-george-zweig.

Charpak, G., 1969. Particle detection by gas discharges. J. Phys. (Paris) Colloq. 2, 86–96.

Charpak, G., 1970. Evolution of the automatic spark chambers. Ann. Rev. Nucl. Sci. 20, 195–254.

Charpak, G., Sauli, F., 1978. The multistep avalanche chamber: a new high-rate, high-accuracy gaseous detector. Phys. Lett. 78B, 523–528.

Charpak, G., Sauli, F., 1979. Multiwire proportional chambers and drift chambers. Nucl. Instrum. Methods 162, 405–428.

Charpak, G., et al., 1968. The use of multiwire proportional counters to select and localize charged particles. Nucl. Instrum. Methods 62, 262–268.

Charpak, G., et al., 1970. Some developments in the operation of multiwire proportional chambers. Nucl. Instrrum. Methods 80, 14–34.

Chase, G.D., Rabinowitz, J.L., 1968. Principles of Radioisotope Methodology, third ed. Burgess Publishing Company, Minneapolis, pp. 140–143.

Chaudhuri, A., Glaser, D.A., 1991. Metastable motion anisotropy. Vis. Neurosci. 7 (4), 397–407.

Chen, P., et al., 2006. Nuclear localizing sequences promote nuclear translocation and enhance the radiotoxicity of the anti-CD33 monoclonal antibody HuM195 labeled with In-111 in human myeloid leukemia cells. J. Nucl. Med. 47 (5), 827–836.

Chen, J.D., et al., 2007. Long-Cooled Spent Fuel Verification Using a Digital Cherenkov Viewing Device. International Atomic Energy Report IAEA-SM-367/14/07.

Chengzhi, L., 2011. Agronomy in space – China's crop breeding program. Space Policy 27, 157–164.

Cherenkov, E., 2005. Pavel Cheerenkov – a person and a physicist – through the eyes of his daughter. Nucl. Instrum. Methods Phys. Res. A553, 1–8.

Cherenkov, P.A., 1934a. Visible light from clear liquids under the action of gamma radiation. C. R. Dokl. Akad. Nauk SSSR 2 (8), 451–454.

Cherenkov, P.A., 1934b. Sichtbares Leichten von Reinen Flüssigkeiten unter der Einwirkung von γ-Strahlen. C. R. Dokl. Akad. Nauk SSSR 2 (8), 455–457.

Cherenkov, P.A., 1936. Die Wirkung eines Magnetfeldes auf das durch Gamma-Strahlen Hervorgerfene sichtbare Leuchten der Flüssigkeiten. Dokl. Akad. Nauk SSSR 3 (9), 413–416.

Cherenkov, P.A., 1937a. Sichtbares Leuchten der Reinen Flüssigkeiten unter der Einwirkung von Harten β-Strahlen. Dokl. Akad. Nauk SSSR 14 (3), 101–105.

Cherenkov, P.A., 1937b. Winkelverteilung der Intensität des Leuchtens, das durch γ-Strahlen in Reinen Flüssigkeiten Hervorgerufen wird. Dokl. Akad. Nauk SSSR 14 (3), 105–107.

Cherenkov, P.A., 1937c. Visible radiation produced by electrons moving in a medium with velocities exceeding that of light. Phys. Rev. 52, 378–379.

Cherenkov, P.A., 1937d. Visible radiation of pure liquids under the action of fast electrons. Byull. Akad. Nauk SSSR 4-5, 455–492.

Cherenkov, P.A., 1938a. Spatial distribution of visible radiation produced by fast electrons. Dokl. Akad. Nauk SSSR 21 (7), 319–321.

Cherenkov, P.A., 1938b. The spectrum of visible radiation produced by fast electrons. Dokl. Akad. Nauk SSSR 20 (9), 651–655.

Cherenkov, P.A., 1938c. Absolute output of radiation caused by electrons moving within a medium with super-light velocity. Dokl. Akad. Nauk SSSR 21 (8), 116–121.

Cherenkov, P.A., 1958. Nobel Lecture: radiation of particles moving at a velocity exceeding that of light, and some of the possibilities for their use in experimental physics. Stockholm, December 11, 1958. In: Nobel Foundation Staff (Ed.), Nobel Lectures, Physics, 1942–62 (1964). Elsevier Publishing, Amsterdam.

Cherenkov, P.A., 1986. At the threshold of discovery. Nucl. Instrum. Methods Phys. Res. A248, 1–4.

Cheryl, K., et al., 2012. Transfusion-associated graft-versus-host disease: a case report and review of literature. J. Am. Acad. Dermatol. 66 (4), e141–e143.

Chiavassa, A., 2011. Studies of the knee of the cosmic rays primary spectrum through measurements in the 10^{16}–10^{18} eV energy range. Nucl. Instrum. Methods Phys. Res. Sect. A 630 (1), 183–188.

Chikamoto, M.O., et al., 2012. Variability in North Pacific intermediate and deep water ventilation during Heinrich events in two coupled climate models. Deep Sea Res. II 61–64, 114–126.

Chmielewski, A.G., Haji-Saeid, M., 2004. Radiation technologies: past, present and future. Radiat. Phys. Chem. 71, 17–21.

Chmielewski, A.G., et al., 2012. Treatment of off-gases containing NO_x by electron beam. Catal. Today 191, 159–164.

Choppin, G.R., et al., 2002. Radiochemistry and Nuclear Chemistry, third ed. Elsevier, Amsterdam, p. 720.

Choppin, G., et al., 2013a. Radiation biology and radiation protection. In: Radiochemistry and Nuclear Chemistry, fourth ed. Elsevier, Amsterdam, pp. 445–491.

Choppin, G., et al., 2013b. Particle accelerators. In: Radiochemistry and Nuclear Chemistry, fourth ed. Elsevier, Amsterdam, pp. 493–512.

Chourasia, A.R., Chopra, D.R., 1997. Auger electron spectroscopy. In: Settle, Frank A. (Ed.), Handbook of Instrumental Techniques for Analytical Chemistry. Prentice Hall, Upper Saddle River, New Jersey, pp. 791–808.

Chowdhury, P. Roy, et al., 2008. Search for long lived heaviest nuclei beyond the valley of stability. Phys. Rev. C 77, 044603.
Christenson, J.H., Cronin, J.W., Fitch, V.L., Turlay, R., 1964. Evidence for the 2π decay of the K^0 meson. Phys. Rev. Lett. 13 (4), 138–141.
Christian, P.E., Waterstram, K., 2007. Nuclear Medicine and PET/CT Technology and Techniques. Mosby, p. 688.
Chromik, M.J., et al., 1998. Two-proton decay of the first excited state of ^{17}Ne. AIP. Conf. Proc. 481, 187. http://dx.doi.org/10.1063/1.59548. Conf. August 10–15, 1998, Gatlinburg, Tennessee.
Chu, L., et al., 2011. Effect of gamma irradiation on activities and physicochemical characteristics of sewage sludge. Biochem. Eng. J. 54 (1), 34–39.
Cipiti, B.B., Kulcinski, G.L., 2005. The production of ^{13}N using beam-target D–^{3}He fusion reaction. Fusion Sci. Technol. 47, 1245–1249.
Clapp, T.G., et al., 1995. The On-line Inspection of Sewn Seams. National Textile Center Annual Report (August), pp. 221–230.
Clark, R.W., 1970. Einstein: The Life and Times. Avon Books, New York, p. 681.
Clarke, R., 2005. Incoherent source/synchrotrons. In: Guenther, E.D. (Ed.-in-Chief), Encyclopedia of Modern Optics. Elsevier, Amsterdam, pp. 217–224.
Claus, R., et al., 1987. A waveshifter light collector for a water Cherenkov detector. Nucl. Instrum. Methods Phys. Res. Sect. A 261, 540–542.
Clay, J., 1928. Penetrating radiation. Proc. R. Acad. Amsterdam 31, 1091.
Clay, J., 1934. Dutch cosmic ray expedition, 1933. Physics I 363–382.
Cleary, J., Guimarães, A.R., 2014. Magnetic resonance imaging. In: Pathobiology of Human Disease, A Dynamic Encyclopedia of Disease Mechanisms. Elsevier, pp. 3987–4000.
Cleland, M.R., Stichelbaut, F., 2013. Radiation processing with high-energy X-rays. Rad. Phys. 84, 91–99.
Cleland, M.R., et al., 1991. Evaluation of a new X-ray processing facility. Nucl. Instrum. Methods Phys. Res. Sect. B 56-57 (2), 1242–1245.
Clem, J.M., Evenson, P.A., 2002. Positron abundance in galactic cosmic rays. Astrophys. J. 568, 216–219.
Cline, D., 1993. Quadrupole and octupole shapes in nuclei. Nucl. Phys. A 557, 615–634.
Coakley, K.J., 2001. Neutron lifetime experiments using magnetically trapped neutrons: optimal background correction strategies. Nucl. Instrum. Methods Phys. Res. Sect. A 469, 354–363.
Coakley, K.J., 2007. Optimal proton trapping strategy for a neutron lifetime experiment. Nucl. Instrum. Methods Phys. Res. Sect. A 577, 702–707.
Cobelli, C., Gianna, D.F., 2001. Tracer Kinetics in Biomedical Research: From Data to Model. Springer, p. 468.
Cockcroft, J.D., 1951. Experiments on the interaction of high-speed nucleons with atomic nuclei. Nobel Lecture, December 11, 1951, Stockholm, Sweden. In: Nobel Foundation Staff (Ed.), Nobel Lectures, Physics, 1942–62 (1964). Elsevier Publishing, Amsterdam.
Cockcroft, J.D., Lewis, W.B., 1936a. Experiments with high velocity positive ions. V. Further experiments on the disintegration of boron. Proc. R. Soc. London 154A (881), 246–261.
Cockcroft, J.D., Lewis, W.B., 1936b. Experiments with high velocity positive ions. VI. The disintegration of carbon, nitrogen, and oxygen by deuterons. Proc. R. Soc. London 154A (881), 261–279.
Cockcroft, J.D., Walton, E.T.S., 1930. Experiments with high velocity positive ions. Proc. R. Soc. London 129A (811), 477–489.
Cockcroft, J.D., Walton, E.T.S., 1932a. Artificial production of fast protons. Nature 129, 242.
Cockcroft, J.D., Walton, E.T.S., 1932b. Disintegration of lithium by swift protons. Nature 129, 649.
Cockcroft, J.D., Walton, E.T.S., 1932c. Experiments with high velocity positive ions. (I) Further developments in the method of obtaining high velocity positive ions. Proc. R. Soc. London 136A (830), 619–630.
Cockcroft, J.D., Walton, E.T.S., 1932d. Experiments with high velocity positive ions. (II) The disintegration of elements by high velocity protons. Proc. R. Soc. London 137A (831), 229–242.
Cockcroft, J.D., Walton, E.T.S., 1933. Disintegration of light elements by fast protons. Nature 131, 23.
Cockcroft, J.D., Walton, E.T.S., 1934. Experiments with high velocity positive ions. III. The disintegration of lithium, boron, and carbon by heavy hydrogen ions. Proc. R. Soc. London 144A (853), 704–720.
Cockcroft, J.D., et al., 1934a. Production of induced radioactivity by high velocity protons. Nature 133, 328.
Cockcroft, J.D., et al., 1934b. Experiments with high velocity positive ions. IV. The production if induced radioactivity by high velocity protons and diplons. Proc. R. Soc. London 148A (863), 225–240.
Cohen, D.D., et al., 2008. Experimental bremsstrahlung yields for MeV proton bombardment of beryllium and carbon. Nucl. Instrum. Methods Phys. Res. Sect. B 266, 1149–1153.
Cohen-Tannoudji, C., 1962 (thesis). Annales de Physique (Paris), vol. 7, 423 and 469.
Cole, L.A., 2010. Quantitative hCG assays, pp. 223–228. In: Cole, L.A., Butler, S.A. (Eds.), Human Chorionic Gonadotropin. Elsevier, p. 378.
Collins, G.B., Reiling, V.G., 1938. Čerenkov radiation. Phys. Rev. 54, 499–503.
Constantini, D.L., et al., 2007. ^{111}In-labeled Trastuzumab (Herceptin) modified with nuclear localization sequences (NLS): an Auger electron-emitting radiotherapeutic agent for HER2/neu-amplified breast cancer. J. Nucl. Med. 48 (8), 1357–1368.
Cook, G.J.R., et al., 2007. In: Clinical Nuclear Medicine, fourth ed. A Hoddar Arnold Publication, p. 896.
Cook, G.T., et al., 2003. Environmental liquid scintillation counting. In: L'Annunziata, M.F. (Ed.), Handbook of Radioactivity Analysis, second ed. Elsevier Science, Amsterdam, pp. 537–607.
Cook, I., et al., 2003. Fusion reactor safety. Report on the 7th IAEA Technical Committee Meeting held at Cannes, France, June 13–16, 2000 Nucl. Fusion vol. 40 (11), 1535–1750.
Compton, A.H., 1923a. A quantum theory of the scattering of X-rays by light elements. Phys. Rev. 21 (5), 483–502.
Compton, A.H., 1923b. The spectrum of scattered X-rays. Phys. Rev. 22 (5), 409–413.
Compton, A.H., 1927. X-rays as a branch of optics. Nobel Lecture, December 12, 1927. In: Nobel Lectures, Physics, 1922–1941 (1965). Elsevier Publishing, Amsterdam.

Compton, A.H., 1932. Variation of the cosmic rays with latitude. Phys. Rev. 41, 111–113.
Compton, A.H., 1933. A geographic study of cosmic rays. Phys. Rev. 43, 387–404.
Compton, A.H., Simon, A.W., 1925a. Measurements of β-rays associated with scattered X-rays. Phys. Rev. 25, 306–314.
Compton, A.H., Simon, A.W., 1925b. Directed quanta of scattered X-rays. Phys. Rev. 26, 289–299.
Compton, A.H., Woo, Y.H., 1924. The wavelength of molybdenum K_α rays when scattered by light elements. Proc. Natl. Acad. Sci. 10 (6), 271–273.
Cork, B., et al., 1956. Antineutrons produced from antiprotons in charge-exchange collisions. Phys. Rev. 104, 1193–1197.
Corradi, L., et al., 2013. Multinucleon transfer reactions: present status and perspectives. Nucl. Instrum. Methods Phys. Res. Sect. B 317, 743–751.
Corson, D.R., MacKensie, K.R., Segrè, E., 1940. Artificially radioactive element 85. Phys. Rev. 58 (8), 672–678.
Cosmic abundances of matter. In: Waddington, C.J. (Ed.), 1988. A.I.P. Conf. Proceedings No. 183, p. 111.
Costantini, H., 2011. The ANTARES deep-sea neutrino telescope: operation and calibration. Nucl. Instrum. Methods Phys. Res. Sect. A 639 (1), 26–29.
Coster, D., Nishina, Y., Werner, S., 1923. Röntgenspektroskopie. Über die Absorptionsspektren in derL-Serie der Elemente La(57) bis Hf(72). Z. Phys. 18 (1), 207–211.
Coster, D., Kronig, R.D.L., 1935. A new type of Auger effect and its influence on the X-ray spectrum. Physica 2 (1–12), 13–24.
Coursey, B.M., 2014. Opportunities for scientists to influence policy: when does radiation metrology matter in development of national policy? Appl. Radiat. Isot. 87, 142–147.
Coursey, B.M., Nath, R., 2000. Radionuclide Therapy. Physics Today, p. 9. Online, April 2000.
Coursey, B.M., et al., 1993. Radioassays of yttrium-90 used in nuclear medicine. Nucl. Med. Biol. 20 (5), 693–700.
Coutu, S., et al., 2000. Energy spectra, altitude profiles and charge ratios of atmospheric muons. Phys. Rev. D62, 032001.
Cowan Jr., C.L., 1964. Anatomy of an Experiment: An account of the Discovery of the Neutrino. Annual Report. Smithsonion Institution, p. 409.
Cowan Jr., C.L., et al., 1953. Large liquid scintillation detectors. Phys. Rev. 90 (3), 493–494.
Cowan Jr., C.L., et al., 1956. Detection of the free neutrino: a confirmation. Science 124, 103–104.
Coyle, P., et al., 1994. The DIRC counter: a new type of particle identification device for B factories. Nucl. Instrum. Methods Phys. Res. Sect. A 343, 292–299.
Cranmer, K., Bowman, R.S., 2005. PhysicsGP: a genetic programming approach to event selection. Comp. Phys. Commun. 167, 165–176.
Cronin, J.W., 1999. Cosmic rays: the most energetic particles in the universe. Rev. Mod. Phys. 71 (2), S165–S172.
Crookes, W., 1878. V. The Bakarian Lecture – One the illumination of lines of molecular pressure, and the trajectory of molecules. Phil. Trans. R. Soc. London 170, 135–164.
Crookes, W., 1903a. The emanation of radium. Proc. R. Soc. (London) A71, 405–408.
Crookes, W., 1903b. Certain properties of the emanation of radium. Chem. News 87, 241.
Crow, J.F., 2004. Addendum: Leo Szilard 1898–1964. Addendum to Maas, W. (2004). Leo Szilard. A personal remembrance. Genetics 167, 555–558.
Csikai, J., 1987. In: CRC Hand Book of Fast Neutron Generators, vol. 1. John Wiley and Sons, New York, p. 256.
Cucinotta, F.A., et al., 1998. The effects of delta rays on the number of particle-track traversals per cell in laboratory and space exposures. Rad. Res. 150, 115–119.
Cunningham, B.B., 1949. The Transuranium Elements: Research Papers, Paper No. 19.2. In: The first isolation of americium in the form of pure compounds; microgram-scale observations on the chemistry of americium, NNES PPR, vol. 14B. McGraw-Hill Book Co., Inc., New York.
Curie, E., 1937. Madame Curie: A Biography. Country Life Press, p. 448.
Curie, M., 1911. Radium and the new concepts in chemistry. Nobel Lecture on December 11, 1911. In: Nobel Foundation Staff (Ed.), Nobel Prize Lectures in Chemistry, 1901–1970 (1967). Elsevier Science, Amsterdam vol. 1, 1901–1921, vol. 2, 1922–1941, vol. 3, 1942–1962.
Curie, P., 1905. Radioactive substances, especially radium. Nobel Lecture on June 6, 1905. In: Science Incorporated Elsevier (Ed.), Nobel Lectures in Physics, 1901–1970, Nobel Lectures, Physics, 1901–1921 (1967), vol. 1. Elsevier Publishing, Amsterdam.
Currie, L.A., 2004. The remarkable metrological history of radiocarbon dating. J. Res. Natl. Inst. Stand. Technol. 109, 185–217.
Cusanno, F., et al., 2004. A RICH detector for strangeness physics in Hall A at Jefferson Lab. Nucl. Instrum. Methods Phys. Res. Sect. A 525, 163–167.
Ćwiok, S., et al., 1996. Shell structure of the superheavy elements. Nucl. Phys. A 611 (2–3), 211–246.
Calloway, E.H., et al., 2011. Three-dimensional computed tomography for evaluation and management of children with complex chest wall anomalies: useful information or just pretty pictures? J. Pediatr. Surg. 46 (4), 640–647.
Chaundy, R., 2002. Paul Dirac: the unsung genius. In: Depth News, BBC Newsmakers, Friday, July 5, 2002. http://news.bbc.co.uk.
Dahlgren, E.W., 1911. Presentation speech of Nobel Prize Physics to Wilhelm Wien. In: Science Incorporated Elsevier (Ed.), Nobel Lectures in Physics, 1901–1970, Nobel Lectures, Physics, 1901–1921 (1967), vol. 1. Elsevier Publishing, Amsterdam.
Dalitz, R.H. (Ed.), 1995. The Collected Works of P. A. M. Dirac: Volume I: 1924–1948. Cambridge University Press, p. 1334.
Dannen, G., January 1997. The Einstein-Szilard Refrigerators. Sci. Am. 90–95.
Dannen, G., 1998. Leo Szilard the Inventor. In: Marx, George (Ed.), Leo Szilard Centenary Volume, Proccedings of the Leo Szilard Centenary, Budapest, February 9–11, 1998. Eötvös University, Eötvös Physical Society, Budapest.
Dannen, G., March 2001. Szilard's inventions patently halted. Phys. Today 54 (3), 102–104. http://dx.doi.org/10.1063/1.1366083.
Daraktchieva, Z., the NEMO Collaboration, 2009. Search for neutrinoless double beta decay with NEMO 3 experiment. Nucl. Phys. A 827, 495c–497c.
Das, A., Ferbel, T., 1994. Introduction to Nuclear and Particle Physics. John Wiley & Sons, New York.
Dash, J., 1973. A Life of One's Own: Three Gifted Women and the Men They Married, first ed. Harper & Row, p. 231.
Dauber, P.M., et al., 1964. Properties of the 960-MeV boson. Phys. Rev. Lett. 13 (14), 449–454.
Daudel, R., 1947. Alteration of radioactive periods of the elements with the aid of chemical methods. Rev. Sci. 85, 162.

Davier, M., 2007. The Higgs boson of the Standard Model. C. R. Phys. 8 (9), 986–998.
Davis Jr., R., 1952. Nuclear recoil following neutrino emission from beryllium 7. Phys. Rev. 86 (6), 976–985.
Davis, D.W., Krogh, T.E., 2000. Preferential dissolution of ^{234}U and radiogenic Pb from α-recoil-damaged lattice sites in zircon: implication for thermal histories and Pb isotopic fractionation in the near surface environment. Chem. Geol. 172, 41–58.
Davisson, C., 1937. The discovery of electron waves. Nobel Lecture, December 13, 1937. In: Nobel Lectures 1922–1941. Elsevier Publishing Co., Amsterdam.
Davisson, C., Germer, L.H., 1920. The emission of electrons from oxide-coated filaments under positive bombardment. Phys. Rev. 15, 330–332.
Davisson, C., Germer, L.H., 1927a. The scattering of electrons by a single crystal of nickel. Nature 119, 558–560.
Davisson, C., Germer, L.H., 1927b. Diffraction of electrons by a crystal of nickel. Phys. Rev. 30, 705–741.
Davisson, C., Germer, L.H., 1928. Diffraction of electrons by a single layer of atoms. Phys. Rev. 31, 135.
Davisson, C., Kunsman, C.H., 1922a. The secondary electron emission from nickel. Phys. Rev. 20, 110.
Davisson, C., Kunsman, C.H., 1922b. The scattering of electrons by aluminum. Phys. Rev. 19, 534–535.
Davisson, C., Kunsman, C.H., 1923. The scattering of low speed electrons by platinum and magnesium. Phys. Rev. 22, 242–258.
Davisson, C., Pidgeon, H.A., 1920. The emission of electrons from oxide-coated filaments. Phys. Rev. 15, 553–555.
Dean, J.A., 1995. Analytical Chemistry Handbook. McGraw-Hill, New York.
Dean, T., July 26, 2008. Higher, Higher! New Scientist, pp. 32–35.
de Broglie, L., 1923a. Waves and quanta. Nature 112, 540.
de Broglie, L., 1923b. Ondes et quanta. Compt. Rend. 177, 507–510.
de Broglie, L., 1923c. Quanta de lumière, diffraction et interférence. Compt. Rend. 177, 548–550.
de Broglie, L., 1923d. Les quanta, la théorie cinétique des gas et la principe de Fermat. Compt. Rend. 177, 630–632.
de Broglie, L., 1924. Rescherches sur la théorie des quantas (thesis). Paris.
de Broglie, L., 1925. Rescherches sur la théorie des quantas. Ann. Phys. (Paris) 3 (10), 22–128.
Dee, P.I., Walton, E.T.S., 1933. A photographic investigation of the transmutation of lithium and boron by protons and of lithium by ions of the heavy isotope of hydrogen. Proc. R. Soc. (London) 141A (845), 733–742.
de Hevesy, G., 1944. Some applications of isotopic indicators. Nobel Lecture, December 12, 1944. In: Nobel Lectures, Chemistry 1942–1962 (1964). Elsevier Science, Amsterdam.
de Hevesy, G., Levi, H., 1936a. Action of slow neutrons on rare-earth elements. Nature (London) 137, 185.
de Hevesy, G., Levi, H., 1936b. The action of neutrons on rare-earth elements. K. Dan. Vidensk. Selsk. Mat. Fys. Medd. 14 (5), 1–3.
de Hevesy, G., Paneth, F., 1913a. Die Löslichkeit des Bleisulfids und Bleichromats. (RaD). Z. Anorg. Chem. 82, 223.
de Hevesy, G., Paneth, F., 1913b. RaD als 'Indikator' des Bleis. Z. Anorg. Chem. 82, 322.
Demanes, D.J., et al., 2011. High-dose-rate monotherapy: safe and effective brachytherapy for patients with localized prostate cancer. Int. J. Radiat. Oncol. Biol. Phys. 81 (5), 1286–1292.
Denegri, D., 2004. The discovery of the W and Z. Phys. Rep. 403–404, 107–145.
Denisov, S.P., Stoyanova, D.A., 2006. Cherenkov counters in experiments at IHEP accelerator. Radiat. Phys. Chem. 75, 856–861.
Derenzo, S.E., 1969. Measurement of the low-energy end of the μ^+ decay spectrum. Phys. Rev. 181, 1854–1866.
Desilets, D.M., et al., 2010. Nature's neutron probe: land surface hydrology at an elusive scale with cosmic rays. Water Resour. Res. 46, W11505. http://dx.doi.org/10.1029/2009WR008726.
Desilets, D.M., Zreda, M., 2013. Footprint diameter for a cosmic-ray soil moisture probe: theory and Monte Carlo simulations. Water Resour. Res. 49, 3566–3575. http://dx.doi.org/10.1002/wrcr.20187.
Desrosiers, M.F., et al., 2005. Irradiation decontamination of postal mail and high-risk luggage. In: Gazsó, L.G., Ponta, C.C. (Eds.), Radiation Inactivation of Bioterrorism Agents, NATO Science Series I: Life and Behavioural Sciences, vol. 365. IOS Press, The Netherlands, pp. 115–126.
de Viguerie, L., et al., 2010. Revealing the *sfumato* Technique of Leonardo da Vinci by X-ray fluorescence spectroscopy. Angew. Chem. Int. Ed. 49 (35), 6125–6128.
Devincenzi, T., et al., 2014. Dose-dependent response of nitrogen stable isotope ratio to proportion of legumes in diet to authenticate lamb meat produced from legume-rich diets. Food Chem. 152, 456–461.
Dewey, M., et al., 2009. Prospects for a new cold neutron beam measurement of the neutron lifetime. Nucl. Instrum. Methods Phys. Res. Sect. A 611, 189–192.
Dicke, R.H., et al., 1965. Cosmic black-body radiation. Astrophys. J. 142, 414–419.
Dirac, P.A.M., 1928a. The quantum theory of the electron. Proc. R. Soc. (London) A 117, 610–612.
Dirac, P.A.M., 1928b. The quantum theory of the electron, Part II. Proc. R. Soc. (London) A 118, 351–361.
Dirac, P.A.M., 1933. Theory of electrons and positrons. Nobel Lecture, December 12, 1933. In: Nobel Lectures, Physics, 1922–1941 (1965). Elsevier Publishing, Amsterdam.
Dittmaier, S., Schumacher, M., 2013. The Higgs boson in the Standard Model—From LEP to LHC: Expectations, searches, and discovery of a candidate. Prog. Part. Nucl. Phys. 70, 1–54.
Dolan, T.J., 1982. Fusion Research: Principles, Experience and Technology. Pergamon Press, New York.
Domanus, J.C., 2004. Practical Neutron Radiography. Springer, p. 292.
Donahue, R.J., Fassó, A., 2002. Radioactivity and radiation protection. In: Hagiwara, et al. (Eds.), Phys. Rev., vol. D66, 01001-1.

Dong, J., et al., 2014. Calibration and validation of the COSMOS rover for surface soil moisture measurement. Vadose Zone J. http://dx.doi.org/10.2136/vzj2013.08.0148.
Dossat, C., et al., 2007. The decay of proton-rich nuclei in the mass A = 36−56 region. Nucl. Phys. A 792, 18−86.
Dowdall, M., O'Dea, J., 2002. $^{226}Ra/^{238}U$ disequilibrium in an upland organic soil exhibiting elevated natural radioactivity. J. Environ. Radioact. 59 (1), 91−104.
Downing, R.G., Arif, M., 2008. Neutron Radiography: Proceedings of the Eighth World Conference: Wcnr-8. Destech Pubns Inc., p. 800
Dracos, M., 2009. Possibility of detecting neutrinoless double beta decays using nuclear emulsions. Rad. Meas. 44, 729−732.
Driga, O., 2012. Soft hadron production at the LHC. Prog. Part. Nucl. Phys. 67, 434−439.
Drobny, J.G., 2012a. Equipment used for radiation processing of polymers, pp. 27−81. In: Ionizing Radiation and Polymers. Elsevier, p. 298.
Drobny, J.G., 2012b. Electron beam processing of commercial polymers, monomers, and oligomers, pp. 101−147. In: Ionizing Radiation and Polymers. Elsevier, p. 298.
Drobny, J.G., 2012c. Industrial applications of ionizing radiation, pp. 149−212. In: Ionizing Radiation and Polymers. Elsevier, p. 298.
Drumm, H., et al., 1977. On muon lifetimes and time dilation. Nature 268 (5618), 301−305.
Drury, L.O.'C., 1983. An introduction to the theory of diffuse shock acceleration of energetic particles in tenuous plasmas. Rep. Prog. Phys. 46, 973−1027.
Dudas, E., et al., 2013. Low scale supersymmetry breaking and its LHC signatures. Nucl. Phys. B 870, 353−358.
Dugdale, A.H.A., et al., 2011. Effects of season and body condition on appetite, body mass and body composition in ad libitum fed pony mares. Vet. J. 190, 329−337.
Dugdale, A.H.A., et al., 2012. Body condition scoring as a predictor of body fat in horses and ponies. Vet. J. 194, 173−178.
Düllman, Ch. E., et al., 2010. Production and decay of element 114: high cross sections and the new nucleus ^{277}Hs. Phys. Rev. Lett. 104, 252701.
Dunn, R., May 2013. Elements. Nat. Geogr. 2013, 112−121.
Dunne, P., 2002. A reappraisal of the mechanism of pion exchange and its implications for the teaching of particle physics. Phys. Educ. 37 (3), 211−222.
Dunoyer, L., 1911. Sur la realisation d'un rayonnement materiel d'origine purement thermique. Cinetique experimentale. Le Radium 8, 142−146.
Durrani, S.A., Bull, R.K., 1987. Solid State Nuclear Track Detection: Principles, Methods, and Applications. Pergamon Press, Oxford, p. 304.
DuVernois, M.A., et al., 2000. Cosmic-ray electrons and positrons from 1 to 100 GeV: measurement with HEAT and their interpretation. Astrophys. J. 559, 296−303.
Dvorak, J., et al., 2011. IRiS—Exploring new frontiers in neutron-rich isotopes of the heaviest elements with a new inelastic reaction isotope separator. Nucl. Instrum. Methods Phys. Res. Sect. A 652, 687−691.
Dyck, V.A., et al. (Eds.), 2005. Sterile Insect Technique: Principles and Practice in Area-Wide Integrated Pest Management. Springer, p. 787.
Dyson, F.J., 2007. Edward Teller, 1908 2003. Biographical Memoir. National Academy of Sciences, Washington, DC, p. 21.
Di Carli, M.F., Murthy, V.L., 2011. Cardiac PET/CT for the evaluation of known or suspected coronary artery disease. Radiographics 31 (5), 1239−1254.
Dalrymple, G.B., January 1, 2001. The Age of the Earth in the Twentieth Century: a Problem (Mostly) Solved, vol. 190. Geological Society, London, pp. 205−221. Special Publications.
Dean, D.J., Hamilton, J.H., 2011. Resource letter NSM-1: new insights into the nuclear shell model. Am. J. Phys. 79 (1), 5−16.
ESTAR, 2016. Stopping Power and Ranges for Electrons. NISTIR 4999. Physical Measurement Laboratory, National Institute of Standards and Technology. http://www.nist.gov/pml/data/star/index.cfm.
Enari, Y., et al., 2002. Progress report on Time-of-Propagation counter − a new type of ring imaging Cherenkov detector. Nucl. Instrum. Methods Phys. Res. Sect. A 494, 430−435.
Eary, J.F., Brenner, W., 2007. Nuclear Medicine Therapy. Informa Healthcare, p. 500.
Eckelman, W.C., et al., 2008. True radiotracers: are we approaching theoretical specific activity with Tc-99m and I-123? Nucl. Med. Biol. 35, 523−527.
Eddington, A.S., 1926. Bakerian Lecture − Diffuse matter in interstellar space. Proc. R. Soc. London A111, 424−456.
Editorial, 2013. Due credit. Nature 496 (7445), 270.
Egan, C.K., et al., 2014. Material specific X-ray imaging using an energy-dispersive pixel detector. Nucl. Instrum. Methods Phys. Res. Sect. B 324, 25−28.
Ehman, W.D., Vance, D.E., 1991. Radiochemistry and Nuclear Methods of Analysis. John Wiley & Sons, New York.
Einstein, A., 1905a. Über einen die Erzeugung und Verwandlung des Lichtes betreffenden heuristischen Gesichtspunkt. Ann. Phys. Leipzig 17, 132−148.
Einstein, A., 1905b. Zur Elektrodynamik bewegter Körper. Ann. Phys. (Ser. 4) 17, 891−921.
Einstein, A., 1905c. Ist die Träheit eines Körpers von seinem Energieinhalt abhängig? Ann. Phys. (Ser. 4) 18, 639−641.
Einstein, A., 1905d. Über die von der molekularkinetischen Theorie der Wärme geforderte Bewegung von in ruhenden Flüssigkeiten suspendierten Teilchen. Ann. Phys. 17 (8), 549−560.
Einstein, A., 1911. Über den Einfluß der Schwerkraft auf die Ausbreitung des Lichtes. Ann. Phys. Leipzig 35, 898−908.
Einstein, A., 1915. Erklärung der Perihelbewegung des Merkur aus der allgemeinem Relativitätstheorie. SPAW 1915, 831−839.
Einstein, A., 1916a. Relativity, The Special and the General Theory. Translation by Robert W. Lawson, 1961. Three Rivers Press, New York, p. 188.
Einstein, A., 1916b. Die Grundlage der allgemeinen Relativitätstheorie. Ann. Phys. Leipzig 49, 769−822.
Einstein, A., July 11, 1923. Fundamental ideas and problems of the theory of relativity. [Nobel] Lecture delivered to the Nordic Assembly of Naturalists at Gothenburg. In: Nobel Lectures, Physics, 1901−1921 (1967). Elsevier Publishing, Amsterdam.
Einstein, A., 1931. The world as I see it. In: Living Philosophies. Simon and Schuster, New York, pp. 3−7.
ElBaradei, M., 2004. Nuclear power, an evolving scenario. IAEA Bull. 46 (No. 1), 4−8.

Elder, F.R., et al., 1947. Radiation from electrons in a cyclotron. Phys. Rev. 71, 829.
Elder, F.R., et al., 1948. Radiation from electrons accelerated in a cyclotron. Phys. Rev. 74, 52.
El-Dessouky, H.T., Ettouney, H.M., 2002. Fundamentals of Salt Water Desalination. Elsevier Science, Amsterdam, p. 690.
Elliott, S.R., Vogel, P., 2002. Double beta decay. Ann. Rev. Nucl. Part. Phys. 52, 115–151.
Elliott, S.R., Hahn, A.A., Moe, M.K., 1986. Experimental investigation of double-beta decay in ^{82}Se. Phys. Rev. Lett. 56, 2582–2585.
Elliott, S.R., Hahn, A.A., Moe, M.K., 1987. Direct evidence for two-neutrino double-beta decay in ^{82}Se. Phys. Rev. Lett. 59, 2020–2023.
Elliott, S.R., et al., 2006. Pulse shape analysis in segmented detectors as a technique for background reduction in Ge double-beta decay experiments. Nucl. Instrum. Methods Phys, Res. Sect. A 558, 504–510.
Elkin, L.O., March 2003. Rosalind Franklin and the double helix. Phys. Today 61.
El Naschie, M.S., 2000. On Nishina's estimate of the critical mass for fission and early nuclear research in Japan. Chaos, Solitons Fractals 11, 1809–1818.
El-Nemr, K.F., 2011. Effect of different curing systems on the mechanical and physico-chemical properties of acrylonitrile butadiene rubber vulcanizates. Mater. Des. 32 (6), 3361–3369.
Elster, J., Geitel, H., 1903. Über die durch radioactive Emanation erregte scintillierende Phosphoreszenz der Sidot-Blende. Phys. Z. 4, 439–440.
Elton, L.R.B., 1958. A semi-empirical formula for the nuclear radius. Nucl. Phys. 5, 173–178.
Emery, P., Buch, M.H., May 5, 2012. Towards an optimum strategy in rheumatoid arthritis. Lancet 379, 1682–1683.
Engelbrecht, R., 2012. Environmental radioactivity monitoring. In: L'Annunziata, M.F. (Ed.), Handbook of Radioactivity Analysis, third ed. Elsevier, Amsterdam, pp. 695–726.
Engelfried, J., 2011. Cherenkov light imaging—Fundamentals and recent developments. Nucl. Instrum. Methods Phys. Res. Sect. A 639 (1), 1–6.
Engelmann, J.J., et al., 1990. Charge composition and energy spectra of cosmic-ray nuclei for elements from Be to Ni – Results from HEAO-3-C2. Astron. Astrophys. 233, 96–111.
Englert, F., Brout, R., 1964. Broken symmetry and the mass of gauge vector mesons. Phys. Rev. Lett. 13 (9), 321–323.
Escobar, I.C., Schäfer, A.I. (Eds.), 2010. Sustainable Water for the Future: Water Recycling versus Desalination, vol. 2. Elsevier, p. 416.
Eshwarappa, K.M., et al., 2007. Comparison of photoneutron yield from beryllium irradiated with bremsstrahlung radiation of different peak energy. Ann. Nucl. Energy 34, 896–901.
Eskandari, M.R., Kashian, S., 2009. Design of moderator and multiplier systems for D-T neutron source in BNCT. Ann. Nucl. Energy 36, 1100–1102.
Estermann, I., Stern, O., 1930. Beugung von Molekularstrahlen. Z. Phys. 61, 95–125.
Estermann, I., Stern, O., 1933. Ueber die magnetische Ablenkung von Wasserstroffmolekuelen und das magnetische Moment des Protons II. Z. Phys. 85, 17–24.
Estermann, I., et al., 1933. Magnetic moment of the proton. Nature 132 (3326), 169.
Evangelisti, L., et al., 2013. Boron neutron capture therapy and ^{18}F-labelled borophenylalanine positron emission tomography: a critical and clinical overview of the literature. Appl. Radiat. Isot. 74, 91–101.
Evans, R.D., 1972. The Atomic Nucleus. McGraw-Hill, New York.
Ezhov, V.F., et al., 2009. Magnetic storage of UCN for a measurement of the neutron lifetime. Nucl. Instrum. Methods Phys. Res. Sect. A 611, 167–170.
Fabjan, C.W., 2003. Collider detectors for multi-TeV particles. In: Robert A. Meyers (Ed.-in-Chief), Encyclopedia of Physical Science and Technology, third ed., Elsevier Science, Amsterdam, pp. 253–268.
Fajans, K., Göring, O.H., 1913. Über das Uran X_2-das neue Element der Uranreihe. Phys. Z. 14, 877–884.
Fakley, D.C., 1983. The British Mission. Los Alamos Science, Winter/Spring, pp. 186–189.
Fantidis, J.G., et al., 2009. A transportable neutron radiography system based on a SbBe neutron source. Nucl. Instrum. Methods Phys. Res. Sect. A 606, 806–810.
Farhataziz, Rodgers, M.A.J., 1987. Radiation Chemistry, Principles and Applications. VCH Publishers, Inc, New York.
Farkas, J., 2004. Food irradiation. In: Mozumder, A., Hatano, Y. (Eds.), Charged Particle and Photon Interactions with Matter. Marcel Dekkar, New York, pp. 785–812.
Farkas, J., 2006. Irradiation for better foods. Trends Food Sci. Technol. 17, 148–152.
Farkas, J., Mohácsi-Farkas, C., 2011. History and future of food irradiation. Trends Food Sci. Techn. 22 (2–3), 121–126.
Faw, R.E., Shultis, J.K., 2004. Radiation sources. In: Meyers, R.A. (Ed.), Encyclopedia of Physical Science and Technology. Academic Press, pp. 613–631.
Feather, N., 1932. The collisions of neutrons with nitrogen nuclei. Proc. R. Soc. A 137, 229–242.
Feather, N., 1938. Further possibilities for the absorption method of investigating the primary β-particles from radioactive substances. Proc. Cambridge Phil. Soc. 34, 599–611.
Feather, N., 1940. Lord Rutherford. Blackie & Son, Ltd.
Fedak, G., 2002. Origin of Marquis Wheat. Eastern Cereal and Oilseed Research Centre, Agriculture and Agri-Food Canada, Ottawa. http://sci.agr.ca/ecorc/au/marquis_e.htm.
Feher, J.J., 2012. Quantitative Human Physiology, An Introduction. Elsevier, p. 904.
Feinberg, G., et al., 2009. LiLiT – a liquid lithium target as an intense neutron source for nuclear astrophysics at the Soreq Applied Research Accelerator Facility. Nucl. Phys. A 827, 590c–592c.
Feld, B.T., Weiss Szilard, G. (Eds.), 1972. The Collected Works of Leo Szilard: Scientific Papers. MIT Press, Cambridge, p. 642.
Federmann, G., 2003. Viktor Hess und die Entdeckung der Kosmischen Strahlung. In: Dimplomarbeit zur Erlangung des akademischen Grades Magister der Naturwissenschaften. Institut für Radiumforschung und Kernphysik, Vienna.

Fernandes, H.M., et al., 2006. Radioecological characterization of a uranium mining site located in a semi-arid region in Brazil. J. Environ. Radioact. 88, 140–157.

Feshbach, H., 1952. The coulomb scattering of relativistic electrons and positrons by nuclei. Phys. Rev. 88 (2), 295–297.

Fenyves, E., Haiman, O., 1969. The Physical Principles of Nuclear Radiation Measurements. Academic Press, New York.

Fermi, E., 1934a. Versuch einer theorie der β-Strahlen. Z. Phys. 88, 161–177.

Fermi, E., 1934b. Attempt at a theory of beta rays. Nuovo Cimento 11, 1–21.

Fermi, E., 1934c. Radioactivity induced by neutron bombardment. Nature 133, 757.

Fermi, E., 1934d. Possible production of elements of atomic number higher than 92. Nature 133, 898–899.

Fermi, E., 1938. Artificial radioactivity produced by neutron bombardment. Nobel lecture, December 12, 1938. In: Nobel Lectures, Physics, 1922–1941 (1965). Elsevier Publishing, Amsterdam.

Fermi, E., 1940a. Reactions produced by neutrons in heavy elements. Science 92, 269–271.

Fermi, E., 1940b. Reactions produced by neutrons in heavy elements. Nature 146, 640–642.

Fermi, E., 1949. On the origin of the cosmic radiation. Phys. Rev. 75 (8), 1169–1174.

Fermi, E., Amaldi, E., 1936. On the absorption and the diffusion of slow neutrons. Phys. Rev. 50, 899–928.

Fermi, E., Amaldi, E., D'Agostino, O., Rasetti, F., Segre, E., 1934. Artificial radioactivity produced by neutron bombardment. Proc. R. Soc. London A146 (857), 483–500.

Fermi, E., Amaldi, E., Wick, G.C., 1938. On the albedo of slow neutrons. Phys. Rev. 53, 493.

Ferronsky, V.I., Polyakov, V.A., 2012. Isotopes of the Earth's Hydrosphere. Springer, p. 630.

Feynman, R.P., 1949. Space-time approach to quantum electrodynamics. Phys. Rev. 76 (6), 769–789.

Feynman, R.P., 1969. The behavior of hadron collisions at extreme energies. In: High Energy Collisions: Third International Conference at Stony Brook. Gordon & Breach, NY, p. 237.

Feynman, R.P., 1974. Cargo Cult Science. Caltech's 1974 Commencement Address.

Feynman, R.P., et al., 2011. The Feynman Lectures on Physics, The New Millennium Edition. Basic Books, p. 1552.

Filby, R.H., 1995. Isotopic and nuclear analytical techniques in biological systems: a critical study. Part IX. Neutron activation analysis. Pure Appl. Chem. 67 (11), 1929–1941.

Finger, P.T., 2009. Radiation therapy for orbital tumors: concepts, current use, and ophthalmic radiation side effects. Surv. Ophthalmol. 54 (5), 545–568.

Fiorini, E., 2007. Neutrinoless double beta decay. Nucl. Phys. B – Proc. Suppl. 168, 11–16.

Fiorini, E., 2008. Double beta decay. Nucl. Phys. A 805, 313c–319c.

Firestone, R.B., et al., 1996. Table of Isotopes, eighth ed., vols. I and II. John Wiley & Sons, New York.

Flammersfeld, A., 1946. Eine Beziehung zwischer Energie und Reichweite fürBeta-Strahlen kleiner und mittlerer Energie. Naturwissenschaften 33, 280–281.

Fletcher, H., 1982. My work with Millikan on the oil-drop experiment. Physics Today 35 (6), 43–47.

Fletcher, S.H., 1992. Harvey Fletcher (1884–1981) A Biographical Memoir. National Academy of Sciences, Washington, DC, pp. 165–193.

Folkart, B.A., November 13, 1986. Leona Marshall Libby Dies; Sole Woman to Work on Fermi's 1st Nuclear Reactor. Los Angeles Times.

Formaggio, J.A., for the SNO Collaboration, 2009. Measurement of atmospheric neutrinos at the Sudbury Neutrino Observatory. Nucl. Phys. A 827, 498c–500c.

Forman, P., 1982. The Fall of Parity. NIST, Washington, DC. http://physics.nist.gov/GenInt/Parity/parity.html.

Forty, R., 2010. The RICH system of LHCb. Nucl. Instrum. Methods Phys. Res. Sect. A 623, 294–296.

Fowler, P.H., 1950. Nuclear transmutations produced by cosmic-ray particles of great energy. III. Nature of the slower particles. Phil. Mag. 41, 169–184.

Fowler, W.A., Oppenheimer, J., 1938. Scattering and loss of energy of fast electrons and positrons in lead. Phys. Rev. 54 (5), 320–324.

Fox, M.S., 1998. Some recollections and reflections on mutation rates. Genetics 148, 1415–1418.

Frame, P.W., April 1997. Tales from the atomic age. Fermi strikes gold and Hevesy invents Neutron activation analysis. Health Physics Newsletter.

Franck, J., December 11, 1926. Transformations of kinetic energy of free electrons into excited energy of atoms by impacts. Nobel Lecture. In: Nobel Lectures. Physics 1922–1941. Elsevier Publishing Co., Amsterdam.

Franck, J., 1935. Remarks on photosynthesis. Chem. Rev. 17, 433–438.

Franck, J., Hertz, G., 1914a. Über Zusammenstösse zwischen Elektronen und den Molekülen des Quecksilberdampfes und die Ionisierungsspannung desselben. Verh. Phys. Ges. Berlin 15, 457–467.

Franck, J., Hertz, G., 1914b. Über die Erregung der Quecksilberresonanzlinie 253.6p.p. durch Elektronentösse. Verh. Phys. Ges. Berlin 15, 512–517.

Franck, J., Rosenberg, J.L., 1964. A theory of light utilization in plant photosynthesis. J. Theor. Biol. 7, 276–301.

Franck, J., Hughes, D.J., Nickson, J.J., Rabinowitch, E., Seaborg, G.T., Stearns, J.C., Szilard, L., June 11, 1945. The Franck Report. Report of the Committee on Political and Social Problems, Manhattan Project. U.S. National Archives, Record Group 77, Manhattan Engineer District Records, Harrison-Bundy File, Folder #76. Metallurgical Laboratory, University of Chicago, Washington, DC.

Frank, I.M., 1944. Interference phenomena in the case of Cherenkov radiation. C. R. Dokl. Akad. Nauk SSSR 42 (8), 341–344.

Frank, I.M., 1958. Optics of light sources in refractive media. Nobel Lecture, December 11, 1958. In: Nobel Foundation Staff (Ed.), Nobel Lectures, Physics, 1942–62 (1964). Elsevier Publishing, Amsterdam.

Frank, I.M., 1960. Optics of light sources moving in refractive media. Science 131, 702–712.

Frank, I.M., 1979. Sergei Ivanovich Vavilov: Ocherki I Vospominaniia, vol. 1. Nauka, Moscow, p. 296.

Frank, I.M., 1981. Sergei Ivanovich Vavilov: Ocherki I Vospominaniia, vol. 2. Nauka, Moscow, p. 350.

Frank, I.M., 1988. Izluchenie Vavilova-Cherenkova: Voprosy Teorii (Vavilov-Cherenkov Radiation: Theoretical Aspects). Nauka, Moscow, p. 285.
Frank, I.M., 1991. Sergei Ivanovich Vavilov: Ocherki I Vospominaniia, vol. 3. Nauka, Moscow, p. 374.
Frank, I., Tamm, Ig, 1937. Coherent visible radiation of fast electrons passing through matter. Dokl. Akad. Nauk SSSR 14 (3), 109–114.
Franklin, R.E., Gosling, R.G., 1953a. The structure of sodium thymonucleate fibers. I. The influence of water content. Acta Crystallogr. 6, 673.
Franklin, R.E., Gosling, R.G., 1953b. The structure of sodium thymonucleate fibers. II. The cylindrically symmetrical Patterson function. Acta Crystallogr. 6, 678.
Franklin, R.E., Gosling, R.G., 1953c. Molecular configuration in sodium thymonucleate. Nature 171 (4356), 740–741.
Franklin, R.E., Gosling, R.G., 1953d. Evidence for 2-chain helix in crystalline structure of sodium deoxyribonucleate. Nature 172, 156.
Franklin, R.E., Gosling, R.G., 1955. The structure of sodium thymonucleate fibers. III. The three-dimensional Patterson function. Acta Crystallogr. 8, 151.
Freitas, E.D.C., et al., 2010. Secondary scintillation yield in high-pressure xenon gas for neutrinoless double beta decay ($0\nu\beta\beta$) search. Phys. Lett. B 684, 205–210.
Friedrich, W., et al., 1912. Interferenz-Erscheinungen bei Röntgenstrahlen. Sitzunsber. Königl. Bayerisch. Akad. Wiss. 303–322.
Friedlander, G., Kennedy, J.W., Miller, J.M., 1964. Nuclear and Radiochemistry, second ed. John Wiley & Sons, New York, p. 585.
Friedman, J.I., December 8, 1990. Nobel Lecture. http://www.nobelprize.org/nobel_prizes/physics/laureates/1990/friedman-lecture.html.
Friedman, J.I., 1991. Deep inelastic scattering: comparisons with the quark model. Rev. Mod. Phys. 63 (3), 615–628.
Frisch, O., 1978. Lise Meitner, nuclear pioneer. New Sci. 80 (1128), 426–428.
Frisch, R., Stern, O., 1933. Ueber die magnetische Ablenkung von Wasserstoffmolekuelen und das magnetische Moment des Protons I. Z. Phys. 85, 4–16.
Fritzsch, H., 1983. Quarks: The Stuff of Matter. Basic Books, p. 297.
Fritzsch, H., 2008. Escaoe from Leipzig. World Scientific, p. 140.
Fritzsch, H., September 2012. The History of QCD. CERN Courier.
Fritzsch, H., Gell-Mann, M., 1972. Current algebra: quarks and what else? In: Proceedings of the XVI Int. Conf. on High Energy Phys, vol. 2, p. 135.
Fritzsch, H., Gell-Mann, M., 2015. 50 Years of Quarks. World Scientific, p. 500.
Fritsch, H., Gell-Mann, M., Leutwyler, H., 1973. Advantages of the color octet gluon picture. Phys. Lett. 27B, 365–368.
Fritz, P., et al., 2006. Stereotactic, single-dose irradiation of stage I non-small cell lung cancer and lung metastases. Rad. Oncol. 1, 30.
Frost, E.B., 1896. Further experiments with X-rays. Sci. New Ser. 3 (65), 465–467.
Frost, E.B., April 1930. The first X-ray Experiment in America? Dartmouth Alumni Magazine, pp. 383–384.
Fujitaka, K., 2005. High-level doses brought by cosmic rays. Int. Congr. Ser. 1276, 124–128.
Fukuda, S., et al., 2003. The Super-Kamiokande detector. Nucl. Instrum. Methods Phys. Res. Sect. A 501, 418–462.
Fukuda, Y., et al., 2010. InP solid state detector for measurement of low energy solar neutrinos. Nucl. Instrum. Methods Phys. Res. Sect. A 623 (1), 460–462.
Fuller, W., 2003. Who said 'helix'? Right and worng in the story of how the structure of DNA was discovered. Nature 424 (6951), 876–878.
Freier, P., et al., 1948. Evidence for heavy nuclei in the primary cosmic radiation. Phys. Rev. 74, 213–217.
Franck, J., Herzfeld, K., 1941. Contribution to a theory of photosynthesis. J. Phys. Chem. 45, 978–1025.
Grau Malonda, A., 1999. Free Parameter Models in Liquid Scintillation Counting. Editorial CIEMAT, Madrid, ISBN 84-7834-350-4, p. 416.
Gillon, S.M., 2006. 10 Days That Unexpectedly Changed America (History Channel Presents). Crown/Archtype Publishers, p. 272.
Gaisser, T.K., 2000. Origin of cosmic radiation. Astron. AIP Conf. Proc 558 (2001), 27–42.
Gaisser, T.K., 2001. Origin of cosmic radiation. Astron. AIP Conf. Proc. 558, 27–42.
Gaisser, T.K., Maurer, R.H., 1973. Cosmic $\overline{p}$ production in interstellar pp collisions. Phys. Rev. Lett. 30, 1264–1267.
Gaisser, T.K., Schaefer, R.K., 1992. Cosmic-ray secondary antiprotons: a closer look. Astrophys. J. 394, 174–184.
Gaisser, T.K., Stanev, T., 2002. Cosmic rays. In: Hagiwara, et al. (Eds.), The Review of Particle Physics, Physical Review, vol. D66. University of California, Lawrence Berkeley Laboratories, pp. 23.1–23.19.
Galison, P.L., 1997a. Marietta Blau: Between Nazis and nuclei, pp. 146–159. In: Image and Logic: A Material Culture of Microphysics. University of Chicago Press, p. 982.
Galison, P.L., November 1997b. Marietta Blau: between Nazis and nuclei. Phys. Today 42–48.
Gall, R., 1977. Manuel Sandoval Vallarta. Phys. Today 30 (12), 70.
Gambarini, G., et al., 2014. Online in vivo dosimetry in high dose rate prostate brachytherapy with MOSkin detectors: in phantom feasibility study. Appl. Radiat. Isot. 83, 222–226.
Gamow, G., 1928. Zur Quantentheorie des Atomkernes. Z. Phys. 51, 204–212.
Gamow, G., 1930. Mass defect and nuclear constitution. Proc. R. Soc. London A 126, 632–644.
Gamow, G., 1948. Evolution of the universe. Nature 162, 680–682.
Gamow, G., Houtermans, F., 1929. Quantenmechik der radioactive Kerns. Z. Phys. 57 (7–8), 496–509.
Gamow, G., Teller, E., 1936. Selectrion rules for the β-disintegration. Phys. Rev. 49, 895–899.
Gamow, G., Teller, E., 1937. Some generalizations of the β transformation theory. Phys. Rev. 51, 289.
Garcia-Granda, S., Montejo-Bernardo, J.M., 2013. X-ray absorption and diffraction | X-ray diffraction – single crystal. In: Jan Reedijk (Ed.-in-Chief), Reference Module in Chemistry, Molecular sciences and Chemical Engineering , Elsevier, Amsterdam, pp. 1–15.
Gardner, M.B., 1981. Harvey Fletcher. Phys. Today 34 (10), 116.

Gardner, R.P., et al., 2004. A semi-empirical model for a ^{90}Sr beta-particle transmission thickness gauge for aluminum alloys. Nucl. Instrum. Methods Phys. Res. B 213, 357–363.

Garibaldi, F., et al., 2003. A proximity focusing RICH detector for kaon physics at Jefferson lab Hall A. Nucl. Instrum. Methods Phys. Res. Sect. A 502, 117–122.

Garinoa, C., et al., 2014. Determination of the electronic and structural configuration ofcoordination compounds by synchrotron-radiation techniques. Coord. Chem. Rev. 277–278, 130–186.

Garwin, R.L., Lederman, L.M., Wein rich, M., 1957. Observations of the failure of conservation of parity and charge conjugation in meson decays: the magnetic moment of the free muon. Phys. Rev. 105, 1413–1414.

Garwin, R.L., Lee, T.-D., 1997. Chien-Shiung Wu. Phys. Today 50 (10), 120–122.

Gastmans, R., et al., 2011. Higgs production at the large hadron collider: phenomenological model and theoretical predictions. Nucl. Phys. B 850, 53–95.

Gao, F., et al., 2013. CT-guided ^{125}I brachytherapy for mediastinal metastatic lymph nodes recurrence from esophageal carcinoma: effectiveness and safety in 16 patients. Eur. J. Radiol. 82, e70–e75.

Gat, J.R., 2005. Isotope Hydrology. World Scientific, p. 200.

Gautier, M.A. (Ed.), 1995. Health and Environmental Chemistry: Analytical Techniques, Data Management, and Quality Assurance. Los Alamos National Laboratory, Los Alamos, NM. Manual LA-10300-M, vol. III, UC-907, pp. WR190-1–WR190-16.

Gautreau, R., Savin, W., 1999. Theory and Problems in Modern Physics, second ed. McGraw-Hill, New York.

Gaye, O., et al., 2013. Robust stabilization of the current profile in tokamak plasmas using sliding mode approach in infinite dimension. Control Eng. Pract. 21 (10), 1350–1358.

Gearheart, D.M., et al., 2007. An improved approach to external beam radiation therapy for intra-abdominal cavity lesions for rural cancer centers. Med. Dosim. 32 (4), 271–277.

Gehman, V.M., et al., 2010. Systematic effects in pulse shape analysis of HPGe detector signals for $0\nu\beta\beta$. Nucl. Instrum. Methods Phys. Res. Sect. A 615, 83–92.

Geiger, H., 1908. The scattering of the alpha particles by matter. R. Soc. Proc. A 81, 174–177.

Geiger, H., Marsden, E., 1909. On a diffuse reflection of the α-particles. Proc. R. Soc. A 82, 495–500.

Geiger, H., Müller, W., 1928a. Elektronenzählohr zur Messung schwächster Aktivitäten. Naturwissenschaften 16 (31), 617–618.

Geiger, H., Müller, W., 1928b. Die Elektronenzählohr. Phys. Z. 29, 839–841.

Geiger, H., Müller, W., 1929a. Technische Bemerkungen zum Elektronenzählohr. Phys. Z. 30, 489–493.

Geiger, H., Müller, W., 1929b. Demonstration des Elektronenzählohrs. Phys. Z. 30, 523.

Geiger, H., Nuttall, J.M., 1911. LVII. The ranges of the α particles from various radioactive substances and a relation between range and period of transformation. Phil. Mag. Series 6 22 (130), 613–621.

Gell-Mann, M., March 15, 1961. The Eightfold Way: A Theory of Strong Interaction Symmetry. Report CTSL-20, TID-12608. Synchrotron Laboratory, California Institute of Technology, Pasadena.

Gell-Mann, M., 1964. A schematic model of baryons and mesons. Phys. Lett. 8 (3), 214–215.

Gell-Mann, M., Ne'eman, Y., 1964. The Eightfold Way. W. A. Benjamin, Inc., New York, Amsterdam, p. 302.

Gell-Mann, M., Pais, A., 1954. Theoretical views on the new particles. In: Bellamy, E.H., Moorhouse, R.G. (Eds.), Proceedings of the 1954 Glasgow Conference on Nuclear and Meson Physics, 1955. Pergamon Press, London, New York.

Gerlach, W., Stern, O., 1922a. Der experimentelle Nachweis des magnetischen Moments des Silberatoms. Z. Phys. 8, 110–111.

Gerlach, W., Stern, O., 1922b. Das magnetische Moment des Silberatoms. Z. Phys. 9, 353–355.

Gerward, L., 1999. Paul Villard and his discovery of gamma rays. Phys. Perspect. 1, 367–383.

Gerward, L., Rassat, A., 2000. Paul Villard's discovery of gamma rays – a centenary. C. R. Acad. Sci. Paris t. 1 Ser. IV 965–973.

Ghassoun, J., et al., 2010. Detailed dose distribution prediction of Cf-252 brachytherapy source with boron loading dose enhancement. Appl. Radiat. Isot. 68 (2), 265–270.

Ghiorso, A., Thompson, S.G., Street Jr., K., Seaborg, G.T., 1951. Californium isotopes from bombardment of uranium with carbon ions. Phys. Rev. 81, 154.

Ghiorso, A., 1999a. Glenn Theodore Seaborg. Phys. Today 52 (8), 77–78.

Ghiorso, A., 1999b. Obituary: Glenn T. Seaborg (1912–99). Nature 398, 472.

Ghosh, D., et al., 2013. Looking for an invisible Higgs signal at the LHC. Phys. Lett. B 725, 344–351.

Gibbs, W.W., 1998. A massive discovery. Sci. Am. 279 (2), 18–20.

Gibson, J.A.B., Piesch, E., 1985. Neutron Monitoring for Radiological Protection. Technical Report Series No. 252. International Atomic Energy Agency, Vienna.

Gielow, P., 1990. Preparation of ^{64}Cu-labelled diethyl-HIDA. Appl. Radiat. Isot. 41 (2), 237–238.

Giese, R., et al., 1970. A high resolution Cherenkov chamber. Nucl. Instrum. Methods 88, 83–92.

Giller, M., 2008. Cosmic rays between the knee and the ankle. J. Phys. G 35 (2), 023201.

Ginzburg, V.L., 2001. About Igor Evgenevich Tamm. In: The Physics of a Lifetime: Reflections on the Problems and Personalities of 20th Century Physics. Springer, Berlin, pp. 351–359.

Ginzburg, V.L., 2001. In commemoration of Sergei Ivanovich Vavilov. In: The Physics of a Lifetime: Reflections on the Problems and Personalities of 20th Century Physics. Springer, Berlin, pp. 395–396.

Ginzburg, V.L., 2001. In the memory of Ilya Mikhailovich Frank. In: The Physics of a Lifetime: Reflections on the Problems and Personalities of 20th Century Physics. Springer, Berlin, pp. 403–410.
Giovinazzo, J., et al., 2002. Two-proton radioactivity of ^{45}Fe. Phys. Rev. Lett. 89 (10), 102501.
Glaser, D.A., 1952. Some effects of ionizing radiation on the formation of bubbles in liquids. Phys. Rev. 87, 665.
Glaser, D.A., 1953. Bubble chamber tracks of penetrating cosmic-ray particles. Phys. Rev. 91, 762–765.
Glaser, D.A., 1960. Elementary particles and bubble chambers, Nobel Lecture, December 12, 1960. In: Nobel Foundation Staff (Eds.), Nobel Lectures, Physics, 1942–62 (1964). Elsevier Publishing, Amsterdam.
Glaser, D.A., 1994. Invention of the bubble chamber and subsequent events. Nucl. Phys. B (Proc. Suppl.) 36, 3–18.
Glaser, D.A., Barch, D., 1999. Motion detection and characterization by an excitable membrane: The bow wave model. Neurocomputing 26–27, 137–146.
Glaser, D.A., Rahm, D.C., 1955. Characteristics of bubble chambers. Phys. Rev. 97, 474–479.
Glaser, D.A., et al., 1956. Bubble counting for the determination of the velocities of charged particles in bubble chambers. Phys. Rev. 102, 1653–1658.
Glaser, G., 1880. The fourth state of matter. Science 1 (5), 58–59.
Glashow, S.L., 1961. Partial-symmetries of weak interactions. Nucl. Phys. 22 (4), 579–588.
Glässel, P., 1999. The limits of the ring image Cherenkov technique. Nucl. Instrum Methods Phys. Res. Sect. A 433, 17–23.
Glasser, R.G., et al., 1961. Mean lifetime of the neutral pion. Phys. Rev. 123, 1014–1020.
Gleick, J., 1992. Genius: The Life and Science of Richard Feynman. Pantheon Books.
Glendenin, L.E., 1948. Determination of the energy of beta particles and photons by absorption. Nucleonics 2, 12–32.
Gleyzes, S., Kuhr, S., Guerlin, C., Bernu, J., Deléglise, S., Hoff, U.B., Brune, M., Raimond, J.-M., Haroche, S., 2007. Quantum jumps of light recording the birth and death of a photon in a cavity. Nat. Lett. 446, 297–300.
Glover, R.N., Jones, A.D.W., 1966. Stripping and pick-up reactions on the carbon isotopes. Nucl. Phys. 84, 673–682.
Goeppert-Mayer, M., 1935. Double beta-disintegration. Phys. Rev. 48, 512–516.
Goeppert-Mayer, M., 1948a. On Closed Shells in Nuclei. United States Atomic Energy Commission, AECD – 1818. Argonne National Laboratory, p. 5.
Goeppert-Mayer, M., 1948b. On closed shells in nuclei. Phys. Rev. 74, 235–239.
Goeppert-Mayer, M., 1949. On closed shells in nuclei, II. Phys. Rev. 75, 1969–1970.
Goeppert-Mayer, M., December 12, 1963. The Shell Model. Nobel Lecture. http://www.nobelprize.org/nobel_prizes/physics/laureates/1963/mayer-lecture.pdf.
Goeppert-Mayer, M., 1964. The shell model. Science 145, 999–1006.
Goeppert-Mayer, M., Jensen, J.H.D., 1955. Elementary Theory of Nuclear Shell Structure. Wiley, New York, p. 284.
Goeppert-Mayer, M., Jensen, J.H.D., 1965. Shell Closure and *jj* Coupling. In: Siegbahn, Kai (Ed.), Alpha-, Beta- and Gamma-Ray Spectroscopy. North Holland Publishers, Amsterdam, pp. 557–581.
Gogulancea, V., Lavric, V., 2014. Flue gas cleaning by high energy electron beam – modeling and sensitivity analysis. Appl. Thermal Eng. 70 (2), 1253–1261.
Goldansky, V.I., 1960. On neutron-deficient isotopes of light nuclei and the phenomena of proton and two-proton radioactivity. Nucl. Phys. 19, 482–495.
Goldansky, V.I., 1961. Two-proton radioactivity. Nucl. Phys. 27 (4), 648–664.
Golden, R.L., et al., 1979. Evidence for the existence of cosmic-ray antiprotons. Phys. Rev. Lett. 43, 1196–1199.
Golden, R.L., et al., 1984. Energy dependence of the $\overline{p}/p$ ratio in cosmic rays. Astrophys. Lett. 24, 75–83.
Goldsmith, B., 2004. Obsessive Genius: The Inner World of Marie Curie (Great Discoveries). W.W. Norton & Co., p. 320
Goldstein, D., 2001. In defense of Robert Andrews Millikan. Am. Sci. 89 (1), 54. January/February.
Goldstein, G.R., 2001. A review essay on "Lise Meitner and the Dawn of the Nuclear Age" by Patricia Rife. Peace Change 26 (1), 95–105.
Gómez, H., et al., 2007. Background reduction and sensitivity for germanium double beta decay experiments. Astropart. Phys. 28, 435–447.
Gonfiantini, R., et al., 1998. Isotopes in groundwater hydrology, pp. 203–245. In: Kendall, C., McDonnell, J.J. (Eds.), Isotope Tracers in Catchment Hydrology. Elsevier Science, Amsterdam, p. 839.
Goodman, B., Maggio, J., Scott, C., 2006. Einstein's letter: July 16, 1939. In: 10 Days that Unexpectedly Changed America. History Channel, A&E Television Networks, New York.
Goodstein, J.R., 1991. Millikan's School, A History of the California Institute of Technology. W. W. Norton & Co., New York.
Goodstein, D., 2001. In defense of Robert Andrews Millikan. Am. Sci. 89 (1), 54–60.
Gorelink, G.E., 1995. Moscow Physics, 1937. In: Tragicheskie Sud'by (Tragis Destinies). Nauka, Moscow, pp. 54–75.
Gorišek, A., 2004. Particle identification performance of the HERA-B RICH. Nucl. Instrum. Methods Phys. Res. Sect A 518, 590–592.
Gould, C.R., et al., 2004. Nuclear physics. In: Meyers, R.A. (Ed.), Encyclopedia of Physical Science and Technology. Academic Press, Orlando, pp. 721–738.
Govorkov, B.B., 2005. Cherenkov detectors in Cherenkov's laboratory. Nucl. Instrum. Methods Phys. Res. A553, 9–17.
Grado-Caffaro, M.A., Grado-Caffaro, M., 2010. An ultrarelativistic approach to derive the photon rest-mass as a function of wavelength. Optik 121, 214–215.
Grado-Caffaro, M.A., Grado-Caffaro, M., 2013. Photon rest-mass and velocity versus wavelength. Optik 124, 2549–2550.
Grado-Caffaro, M.A., Grado-Caffaro, M., 2014. On the wavelength dependence of the photon rest-mass. Optik 125, 212–213.
Graf, N., et al., 2010. Charged kaon mass measurement using the Cherenkov effect. Nucl. Instrum. Methods Phys. Res. Sect. A 615, 27–32.

Granqvist, G., 1915. Presentation Speech for the Nobel Prize in physics 1914. In: Nobel Lectures, Physics 1901–1921 (1967). Elsevier Publishing, Amsterdam.

Grape, S., et al., 2010. Modeling Cherenkov light from irradiated nuclear fuel assemblies using GEANT. In: IAEA Symposium on International Safeguards "Preparing for Future Verification Challenges", November 1–5, 2010, Vienna.

Grassi, N., 2009. Differential and scanning-mode external PIXE for the analysis of the painting. "Ritratto Trivulzio" by Antonello da Messina. Nucl. Instrum. Methods Phys. Res. Sect. B 267, 825–831.

Grate, J.W., O'Hara, J., Egorov, O.B., 2012. Automated radiochemical separation, analysis, and sensing. In: L'Annunziata, M.F. (Ed.), Handbook of Radioactivity Analysis, third ed. Elsevier, Amsterdam, pp. 1179–1207.

Gratta, G., Wang, Y.F., 1999. Towards two-threshold, real-time solar neutrino detectors. Nucl. Instrum. Methods Phys. Res. Sect. A 438, 317–321.

Grau Carles, A., Grau Malonda, A., 1995. Radionuclide standardization by Cherenkov counting. Appl. Radiat. Isot. 46, 799–803.

Grau Carles, A., Grau Malonda, A., 1996. Applicación de al Radiación Cherenkov a la Metrología de Radionucleidos, vol. 22, 28040. Editorial CIEMAT, Avda. Complutense, Madrid, p. 140.

Grau Carles, A., Grau Malonda, A., 2006. Computational aspects in modeling the interaction of low-energy X-rays with liquid scintillators. Appl. Radiat. Isot. 64, 1515–1519.

Grau Carles, A., Kossert, K., 2009. Monte Carlo simulation of Auger electron spectra. Appl. Radiat. Isot. 67, 192–196.

Grau Malonda, A., Grau Carles, A., 1998a. The anisotropy coefficient in Cerenkov counting. In: Proc. ICRM 1997. National Institute of Standards and Technology, Gaithersburg, MD.

Grau Malonda, A., Grau Carles, A., 1998b. The anisotropy coefficient in Cerenkov counting. Appl. Radiat. Isot. 49 (9–11), 1049–1053.

Grau Malonda, A., Grau Carles, A., 2000. Standardization of electron-capture radionuclides by liquid scintillation counting. Appl. Radiat. Isot. 52, 657–662.

Grau Malonda, A., Grau Carles, A., 2002. Half-life determination of ^{40}K by LSC. Appl. Radiat. Isot. 56, 153–156.

Grau Malonda, A., et al., 2006. Mean values of LMM Auger transition in a KLM model. Appl. Radiat. Isot. 64, 1485–1491.

Green, J.H., Maddock, A.G., 1949. (n, γ) recoil effects in potassium chromate and dichromate. Nature 164, 788–789.

Greenberg, O.W., 1964. Spin and uinitary spin independence in a paraquark model of baryons and mesons. Phys. Rev. Lett. 13, 598–602.

Greiner, W., et al., 1985. An exotic nuclear decay of ^{223}Ra by emission of ^{14}C nuclei. Z. Phys. A 320, 347–348.

Greiner, W., 2008. Structure of vacuum and elementary matter: from superheavies via hypermatter to antimatter—the vacuum decay in supercritical fields. In: Salomonson, S., Lindroty, E. (Eds.), Advances in Quantum Chemistry, vol. 53. Elsevier, pp. 99–150.

Grieder, P.K.F., 2001. Cosmic Rays at Earth: Researcher's Reference Manual and Data Book. Elsevier, Amsterdam, p. 1093.

Grimani, C., 2005. Upper limit to the cosmic-ray positron flux generated at the pulsar polar cap. In: Proc. of the 29th Int. Cosmic Ray Conf. (Pune, India, August 3–10, 2005), vol. 3, pp. 9–12.

Grimani, C., 2009. Origin of cosmic-ray positrons. In: Proc. of the 31st Int. Cosmic Ray Conf. Lódź, Poland, July 7–15, 2009.

Groom, D.E., et al., 2001. Muon stopping power and range tables 10 MeV to 100 TeV. At. Data Nucl. Data Tables 78, 183–356.

Gruhn, C.R., Ogle, W., 1980. In: Peng, C.-T., Horrocks, D.L., Alpen, E.L. (Eds.), Liquid Scintillation Counting, Recent Applications and Developments, vol. 1. Academic Press, New York, London, pp. 357–374.

Grünewald, M.W., 1999. Experimental tests of the electroweak standard model at high energies. Phys. Rep. 322 (3–4), 125–346.

Grünewald, Th, 1984. Food preservation, pp. 271–301. In: L'Annunziata, M.F., Legg, J.O. (Eds.), Isotopes and Radiation in Agricultural Sciences, Animals, Plants, Food and the Environment, vol. 2. Academic Press, London, p. 356.

Gullstrand, A., 1923. Presentation speech, The Nobel Prize in physics 1923. In: Nobel Lectures, Physics 1922–1941 (1965). Elsevier Publishing, Amsterdam.

Gullstrand, A., 1925. Presentation speech, The Nobel Prize in physics 1924. In: Nobel Lectures, Physics 1922–1941 (1965). Elsevier Publishing, Amsterdam.

Gupta, B., Agarwal, R., 2011. Hydrogels for wound healing applications, pp. 184–227. In: Rimmer, S. (Ed.), Biomedical Hydrogels. Elsevier, p. 269.

Guralnik, G.S., Hagen, C.R., Kibble, T.W.B., 1964. Global conservation laws and massless particles. Phys. Rev. Lett. 13 (20), 585–587.

Gurney, R.W., Condon, E.U., 1928. Wave mechanics and radioactive disintegration. Nature 122, 439.

Gurney, R.W., Mott, N.F., 1938. The theory of the photolysis of silver bromide and the photographic latent image. Proc. R. Soc. London 164A, 151–167.

Gutiérrez-Fernández, J., et al., 2014. Crystal structures of *Ophiostoma piceae* sterol esterase: structural insights into activation mechanism and product release. J. Struct. Biol. 187, 215–222.

Hahn, B., et al., 1956. High-energy electron scattering and the charge distributions of selected nuclei. Phys. Rev. 101 (3), 1131–1142.

Hacker, B., et al., July/August 1998. Celebrating Edward Teller at 90. Sci. Technol. Rev. 29.

Hahn, O., Meitner, L., 1918. Die Muttersubstanz des Actiniums, eines neues radioactives Element von langer Lebendauer. Phys. Z. 19, 208–218.

Hahn, O., Meitner, L., 1924. Das β-strahlenspektrum von Radium und seine Deutung. Z. Phys. 26, 161–168.

Hahn, O., Strassmann, F., 1939a. Über den Nachweis und das Verhalten der bei Bestrahlung des Urans mittels Neutronen entstehenden Erdalkalimetalle. Naturwissenschaften 27, 11–15.

Hahn, O., Strassmann, F., 1939b. Nachweis der Entstehung activer bariumisotope aus Uran und Thorium durch Neutronenbestrahlung; nachweis weiterer aktiver Bruchtucke bei der Uranspaltung. Naturwissenschaften 27, 89–95.

Håkansson, A., Jonter, T., 2007. An Introduction to Nuclear Non-Proliferation and Safeguards. SKI Report 2004:44, ISSN:1104-1374. Swedish Nuclear Power Inspectorate, p. 140.

Halevi, P., 1982. Fletcher and the oil drop. Phys. Today 35, 104.

Hall, B., 1995. A tribute to Hans Albrecht Bethe. Cornell Magazine. August–September Issue.
Halpern, A., 1988. Schaum's 3000 Solved Problems in Physics. McGraw-Hill, New York.
Halpern, L., 1993. Marietta Blau (1894–1970). In: Grinsten, L.S., Rose, R.K., Rafailovich, M.H. (Eds.), Women in Chemistry and Physics: A Bibliographic Sourcebook. Greenwood Press, Westport, Connecticut, p. 736.
Hammer, G.P., et al., 2000. Comparing different methods of estimating cosmic radiation exposure of airline personnel. Radiat. Environ. Biophys. 39, 227–231.
Han, M.Y., 1999. Quarks and Gluons: A Century of Particle Charges. World Scientific, p. 158.
Han, M.Y., Nambu, Y., 1965. Three-triplet model with double SU(3) symmetry. Phys. Rev. 139, B1006–B1010.
Han, L., et al., 2011. A male- and female-sterile mutant of Kentucky bluegrass (*Poa pratensis* L.) induced by space radiation. Sci. Horticult. 131, 67–73.
Hänsch, T., Schawlow, A., 1975. Cooling of gases by laser radiation. Opt. Commun. 13, 68.
Hanson, G., et al., 1975. Evidence for jet structure in hadron production by e^+e^- annihilation. Phys. Rev. Lett. 35 (24), 1609–1612.
Harbottle, G., 1954. Szilard-Charlmers reaction in crystalline compounds of chromium, radiochemical analysis. J. Chem. Phys. 22, 1083.
Harms, A.A., Wyman, D.R., 2005. Mathematics and Physics of Neutron Radiography. Springer, p. 184.
Haroche, S., December 8, 2012. Controlling Photons in a Box and Exploring the Quantum to Classical Boundary. Nobel Lecture. http://www.nobelprize.org/nobel_prizes/physics/laureates/2012/haroche-lecture.pdf.
Haroche, S., Brune, M., Raimond, J.-M., 2013. Atomic clocks for controlling light fields. Phys. Today 66 (1), 27–32.
Hasert, F.J., et al., 1973. Search for elastic muon-neutrino electron scattering. Phys. Lett. B 46, 121–124.
Hatch, M.D., Slack, C.R., 1966. Photosynthesis by sugarcane leaves. A new carboxylation reaction and the pathway of sugar formation. Biochem. J. 101, 103–111.
Hawking, S.W., 1988. A Brief History of Time. Bantam Press, London.
Hawryluk, R.J., et al., 1994. Confinement and heating of a deuterium-tritium plasma. Phys. Rev. Lett. 72, 3530–3533.
Haxel, O., Jensen, J.H.D., Suess, H.E., 1949. On the "Magic Numbers" in nuclear structure. Phys. Rev. 75, 1766.
Hayashida, N., et al., 1994. Observation of a very energetic cosmic ray well beyond the predicted 2.7 K cutoff of the primary energy spectrum. Phys. Rev. Lett. 73, 3491–3494.
Haynes, W.M. (Ed.), 2013. CRC Handbook of Chemistry and Physics, 94th ed. CRC Press.
He, G., et al., 2006. Cross-section measurements for (n, 2n), (n,p) and (n, α) reactions on strontium isotopes at the neutron energy about 14 MeV. Annals Nucl. Energy 33 (1), 37–42.
Heaviside, O., 1888. The electromagnetic effects of a moving charge. The Electrician 22, 147–148.
Heaviside, O., 1889. On the electromagnetic effects due to the motion of electricity through a dielectric. Phil. Mag. 27, 324–339.
Heaviside, O., 1892. Electrical Papers, vol. II. Macmillan & Co., London, pp. 494–497.
Heaviside, O., 1899. Note on the motion of a charged body at a speed equal to or greater than that of light, pp. 533–536. In: Electromagnetic Theory, Volume 2, 1899, published by The Electrician Printing and Publishing Co., London, Reprinted in 2001 by Elibron Classics. Adamant Media Corp., Boston, p. 592.
Heaviside, O., 1912a. Theory of the steady rectilinear motion of a point-charge or 'electron' through the ether when $u < v$ and when $u >$ v, pp. 25–28. In: Electromagnetic Theory, Volume 3, 1912, published by The Electrician Printing and Publishing Co., London, Reprinted in 2001 by Elibron Classics. Adamant Media Corp., Boston, p. 556.
Heaviside, O., 1912b. The steady rectilinear motion in its own line of a terminated electrified line when $u > v$, and interpretation of the impure conical wave following an electron, pp. 30–33. In: Electromagnetic Theory, Volume 3, 1912, published by The Electrician Printing and Publishing Co., London, Reprinted in 2001 by Elibron Classics. Adamant Media Corp., Boston, p. 556.
Heding, L., 2012. Radioimmunoassays for Insulin, C-Peptide and Proinsulin. Springer, p. 88.
Heilbron, J.L., 2003. Ernest Rutherford and the Explosion of Atoms. Oxford University Press, New York, p. 139.
Heisenberg, W., 1926a. Quantum mechanics. Naturwissenschaften 14, 989–994.
Heisenberg, W., 1926b. Multi-boby problem and resonance in the quantum mechanics. Z. Phys. 38 (6/7), 411–426.
Heisenberg, W., 1926c. Fluctuation appearances and quantum mechanics. Z. Phys. 40 (7), 501–506.
Heisenberg, W., 1927. Über den anschaulichen Inhalt der quantentheoretischen Kinematik und Mechanik. Z. Phys. 43, 172–198.
Heisenberg, W., 1929. The development of the quantum theory 1918–1928. Naturwissenschaften 17, 490–496.
Heisenberg, W., 1932a. Über den Bau der Atomkerne. I. Z. Phys. 77, 1–11.
Heisenberg, W., 1932b. Über den Bau der Atomkerne. II. Z. Phys. 78, 156–168.
Heisenberg, W., 1933a. Development of quantum mechanics. Nobel Lecture, December 11, 1933. In: Nobel Lectures, Physics 1922–1941 (1965). Elsevier Publishing Co., Amsterdam.
Heisenberg, W., 1933b. Werner Heisenberg – biography. In: Nobel Lectures. Physics 1922–1941 (1965). Elsevier Publishing Co., Amsterdam.
Heisenberg, W., 1933c. Über den Bau der Atomkerne. III. Z. Phys. 80, 587–596.
Heisenberg, W., 1946. Über die Arbeiten zur technischen Ausnutzung der Atomkernenergie in Deutschland. Naturwissenschaften 33 (11), 325–329.
Herb, S.W., et al., 1977. Observation of a dimuon resonance at 9.5-GeV in 400-GeV proton-nucleus collisions. Phys. Rev. Lett. 39 (5), 252–256.
Herrmann, H.W., et al., 2010. Diagnosing inertial confinement fusion gamma ray physics. Rev. Sci. Instrum. 81 (10), 10D333.
Hertz, G., 1926. The results of the electron-impact tests in the light of Bohr's theory of atoms. Nobel Lecture, December 11, 1926. In: Nobel Lectures. Physics 1922–1941. Elsevier Publishing Co., Amsterdam.
Hertz, G., 1933. Manufacture of pure heavy hydrogen isotope by diffusion. Naturwissenschaften 21, 884–885.

Hertz, H.R., 1887a. Über sehr schnelle slectrische Schwingungen. Ann. Phys. 267 (7), 421–448.
Hertz, H.R., 1887b. Über einen Einfluss des ultravioletten Lichtes auf die electrische Entladung. Ann. Phys. 267 (8), 983–1000.
Hertz, H.R., 1888a. Über die Einwirkung einer geradlinigen electrischen Schwingung auf eine benachbarte Strombahn. Ann. Phys. 270 (5), 155–170.
Hertz, H.R., 1888b. Über die Ausbreitungsgeschwindigkeit der electrodynamischen Wirkungen. Ann. Phys. 270 (7), 551–569.
Hertz, H., 1892. Über den Durchgang von Kathodenstrahlen durch dünne Metallschichten. (The passage of cathode rays through thin metal layers). Wied. Ann. Phys. 45, 88.
Hertz, K.L., Hilton, N.R., Lund, J.C., Van Scyoc, J.M., 2003. Alpha-emitting radioisotopes for switchable neutron generators. Nucl. Instrum. Methods Phys. Res. A 505, 41–45.
Herzberg, G., Teller, E., 1933. Schwingungsstruktur der Elektronenübergänge bei mehratomigen Molekülen. Z. Phys. Chem. 21, 410–446.
Hess, V.F., 1912. Über Beobachtungen der durchdringenden Strahlung bei sieben Freiballonfahrten. Phys. Z. 13, 1084–1091.
Hess, V.F., September 1932. The cosmic ray observatory at the Hafelekar. Terr. Mag. Atmos. Elect. 399.
Hess, V.F., 1936. Unsolved problems in physics: tasks for the immediate future in cosmic rays studies. Nobel Lecture, December 12, 1939. In: Nobel Lectures, Physics, 1922–1941 (1965). Elsevier Publishing, Amsterdam.
Hess, V.F., 1939. The significance of variations in cosmic ray intensity and their relation to solar, earthmagnetic and atmospheric phenomena. Rev. Mod. Phys. 11, 153–157.
Hess, V.F., 1940. The discovery of cosmic radiation. Thought (Fordham Q.) 15, 225–236.
Hess, V.F., Demmelmair, A., 1937. World-wide effect in cosmic ray intensity, as observed during a recent magnetic storm. Nature 140, 316–317.
Hess, V.F., et al., March 1938a. Relations between terrestrial magnetism and cosmic ray intensity. Terr. Mag. Atmos. Elect.
Hess, V.F., et al., 1938b. Cosmic rays and the Aurora of January 25–26. Nature 141, 686–687.
Hetherington, E.L., et al., 1986. The preparation of high specific activity copper-64 for medical diagnosis. Int. J. Rad. Appl. Instrum. 37 (12), 1242–1243.
Heyde, K.L.G., 2004. Basic Ideas and Concepts in Nuclear Physics, An Introductory Approach, third ed. Institute of Physics Publishing, Bristol, p. 360.
Higashi, T., et al., 2003. Preliminary results of low pressure discharge experiments of a cylindrical inertial electrostatic confinement fusion device aimed for a small neutron source. Fusion Sci. Technol. 44, 544–548.
Higgs, P.W., 1964. Broken symmetries and the masses of gauge bosons. Phys. Rev. Lett. 13 (16), 508–509.
Higgs, P.W., 1966. Spontaneous symmetry breakdown without massless bosons. Phys. Rev. 145 (4), 1156–1164.
Hildebrand, R.H., Nagle, D.E., 1953. Operation of a Glaser bubble chamber with liquid hydrogen. Phys. Rev. 92, 517–518.
Hirose, K., et al., 2013. Plutonium in southern hemisphere ocean waters. In: Isotopes in Hydrology, Marine Ecosystems and Climate Change Studies. Proceedings of an International Symposium, Monaco, 27 March–1 April 2011, vol. 1. International Atomic Energy Agency, Vienna, pp. 493–500.
Hirsch, R.L., 1967. Inertial-electrostatic confinement of ionized fusion gases. J. Appl. Phys. 38 (11), 4522–4535.
Hobson, K.A., 2007. An isotopic exploration of the potential of avian tissues to track changes in terrestrial and marine ecosystems. Terr. Ecol. 1, 129–144.
Hobson, K.A., 2008. Applying isotopic methods to tracking animal movements. Terr. Ecol. 2, 45–78.
Hof, M., et al., 1996. Measurement of cosmic-ray antiprotons from 3.7 to 19 GeV. Astrophys. J. Lett. 467, L33.
Hofmann, S., 2009. Superheavy elements. Lect. Notes Phys. 764, 203–252.
Hofmann, S., et al., 1982. Proton radioactivity of ^{151}Lu. Z. Phys. A – At. Nucl. 305, 111–123.
Hoffman, D.C., 2000. Glenn Theodore Seaborg, 1912–1999. In: Biographical Memoirs, vol. 78. The National Academy Press, Washington, DC, pp. 235–256.
Hoffman, D.C., 2007. Glenn Theodore Seaborg, 19 April 1912–25 February 1999. Biogr. Mems. Fell. R. Soc. 53, 327–338.
Hofstadter, E., McAllister, R.W., 1955. Electron scattering from the proton. Phys. Rev 98 (1), 217.
Hofstadter, E., et al., 1953a. Scattering of high-energy electrons and the method of nuclear recoil. Phys. Rev 91 (2), 422.
Hofstadter, E., et al., 1953b. High-energy electron scattering and nuclear structure determinations. Phys. Rev. 92 (4), 978–987.
Holbert, K.E., Murray, R.L., 2015. Information from isotopes, pp. 198–219. In: Nuclear Energy, seventh ed. Elsevier, p. 550.
Holden, N.E., 1997a. Table of isotopes. In: Lide, D.R. (Ed.), CRC Handbook of Chemistry and Physics, 77th ed. CRC Press, Boca Raton, FL, pp. 11-38–11-143.
Holden, N.E., 1997b. Neutron scattering and absorption properties. In: Lide, D.R. (Ed.), CRC Handbook of Chemistry and Physics, 77th ed. CRC Press, Boca Raton, FL, pp. 11-144–11-158.
Holdren, J.P., 2005. Joseph Rotblat (1908–2005). Science 310, 633.
Holland, H., Turekian, K. (Eds.), 2014. Treatise on Geochemistry Surface and Groundwater, Weathering and Soils, second ed., vol. 7. Elsevier, Amsterdam.
Holloway, M.G., Baker, C.P., 1944. Note on the Origin of the Term "barn". Technical Report LAMS-523. Los Alamos, p. 4.
Holloway, M.G., Baker, C.P., 1972. How the barn was born. Phys. Today 25 (7), 9.
Holstein, B.R., 2009. The mysterious disappearance of Ettore Majorana. Carolina International Symposium on Neutrino Physics. J. Phys. Conf. Ser. 173 (1–6), 012019. http://dx.doi.org/10.1088/1742-6596/173/1/012019.
Honda, T., et al., 1965. Nuclear direct interaction in the ^{12}C(t,α)^{11}B reaction. Nucl. Phys. 62, 561–574.
Hönisch, B., et al., 2012. The geological record of ocean acidification. Science 335 (6072), 1058–1063.
Hönisch, B., Allen, K.A., 2013. Paleoceanography, Physical and Chemical Proxies | Carbon Cycle Proxies (δ11B, δ13Ccalcite, δ13Corganic, Shell Weights, B/Ca, U/Ca, Zn/Ca, Ba/Ca). In: Scott A. Elias (Ed.-in-Chief), Encyclopedia of Quaternary Science, second ed., Elsevier, Amsterdam, pp. 849–858.

Honkanen, J., et al., 1983. Beta-delayed two-proton decay of ^{26}P. Phys. Lett. 133B, 146–148.
Hopper, V.D., Biswas, S., 1950. Evidence concerning the existence of the new unstable elementary neutral particle. Phys. Rev. 80, 1099–1100.
Hörandel, J.R., 2008a. Cosmic-ray composition and its relation to shock acceleration by supernova remnants. Adv. Space Res. 41, 442–463.
Hörandel, J.R., 2008b. The origin of galactic cosmic rays. Nucl. Instrum. Methods Phys. Res. Sect. A 588, 181–188.
Hörandel, J.R., 2010. Cosmic rays at the highest energies. Prog. Part. Nucl. Phys. 64, 351–359.
Horikawa, S., et al., 2008. The C_4F_{10} Cherenkov detector for DIRAC-II. Nucl. Instrum. Methods Phys. Res. Sect. A 595, 212–215.
Huang, N.M., et al., 2009. γ-Ray assisted synthesis of Ni_3Se_2 nanoparticles stabilized by natural polymer. Chem. Eng. J. 147, 399–404.
Hubbell, J.H., 1969. Photon Cross Sections, Attenuation Coefficients, and Energy Absorption Coefficients from 10 keV to 100 GeV. NSRDS-NBS 29, Natl. Stand. Ref. Data Ser. National Bureau of Standards (U.S.), p. 80.
Hubbell, J.H., August 26, 1991. Faster than a speeding photon. Curr. Contents 34, 10.
Huber, G., et al., 2003. Radioisotope mass spectrometers, pp. 799–843. In: L'Annunziata, M.F. (Ed.), Handbook of Radioactivity Analysis, second ed. Elsevier Science Publishers, Amsterdam, p. 1273.
Huh, C.-A., 1999. Dependence of the decay rate of ^{7}Be on chemical forms. Earth Planet. Sci. Lett. 171, 325–328.
Huisman, H., et al., 2000. Dynamical effects in proton–proton bremsstrahlung for non-coplanar geometrics. Phys. Lett. B 476, 9–14.
Hulet, R.G., Kleppner, D., 1983. Rydberg atoms in "circular" states. Phys. Rev. Lett. 51 (16), 1430–1433.
Hulthén, L., December 8, 1978. Presentation speech for the Nobel Prize in physics 1978. Stockholm. In: Lundqvist, S. (Ed.), Nobel Lectures, Physics 1971–1980. World Scientific Publishing Co., Singapore.
Hulthén, E., December 11, 1959. Award Ceremony Speech. Stockholm, The Nobel Prize in Physics 1959. http://www.nobelprize.org.
Hultqvist, K., 2011. IceCube: physics, status, and future. Nucl. Instrum. Methods Phys. Res. Sect. A 626–627, S6–S12.
IAEA, 2007. Nuclear Technology Review 2007. International Atomic Energy Agency, Vienna.
IAEA, 2000a. Nuclear Techniques in Integrated Plant Nutrient, Water and Soil Management. IAEA, Vienna, p. 479.
IAEA, 2000b. Environmental Isotopes in the Hydrological Cycle, Principles and Applications, vols. 1–6. International Atomic Energy Agency, Vienna.
IAEA, 2001. Introduction of Nuclear Desalination: A Guidebook. IAEA, Vienna, p. 281.
IAEA, 2002. Assessment of Soil Phosphorus Status and Management of Phosphatic Fertilizers to Optimize Crop Production. IAEA, Vienna, p. 473.
IAEA, 2003. Safeguards techniques and equipment. In: International Nuclear Verification Series. International Atomic Energy Agency, Vienna, ISBN 92-0-109403-5, p. 82.
IAEA, 2004a. Isotope Hydrology and Integrated Water Resources Management. IAEA-CSP-23. IAEA, Vienna, p. 487.
IAEA, 2004b. Radiation Processing of Polysaccharides for Health Care Applications. International Cooperative Agreement. IAEA, Vienna, p. 39.
IAEA, 2004c. Nuclear Technology Review 2004. International Atomic Energy Agency, Vienna.
IAEA, 2005a. World Survey of Activities in Controlled Fusion Research, 10th ed. International Atomic Energy Agency, Vienna.
IAEA, 2005b. Nuclear Technology Review 2005. International Atomic Energy Agency, Vienna.
IAEA, 2005c. Gamma Irradiators for Radiation Processing. IAEA, Vienna, p. 40.
IAEA, 2005d. Optimization of the Coupling of Nuclear Reactors and Desalination Systems. IAEA, Vienna.
IAEA, 2005e. Nutrient and Water Management Practices for Increasing Crop Production in Rainfed Arid/Semi-arid Areas. IAEA, Vienna, p. 221.
IAEA, 2006. Nuclear Technology Review 2006. International Atomic Energy Agency, Vienna.
IAEA, 2008. Field Estimation of Soil Water Content: A Practical Guide to Methods, Instrumentation and Sensor Technology. Training Course CD Series (No. 30, 2008). International Atomic Energy Agency, Vienna, p. 129.
IAEA, 2009. Nuclear Technology Review 2009. International Atomic Energy Agency, Vienna, Austria.
IAEA, 2010. Nuclear Technology Review 2010. International Atomic Energy Agency, Vienna, Austria.
IAEA, 2011. Nuclear Technology Review 2011. International Atomic Energy Agency, Vienna, Austria.
IAEA, 2012. Nuclear Technology Review 2012. International Atomic Energy Agency, Vienna, Austria, p. 170.
IAEA, 2013a. Nuclear Technology Review 2013. International Atomic Energy Agency, Vienna, Austria, p. 109.
IAEA, 2013b. Isotopes in Hydrology, Marine Ecosystems and Climate Change Studies. In: Proceedings of an International Symposium, Monaco, 27 March–1 April 2011, vols. 1 & 2. International Atomic Energy Agency, Vienna.
Ianni, A., et al., 2005. How to observe ^{8}B solar neutrinos in liquid scintillator detectors. Phys. Lett. B 627, 38–48.
ICRP, 1991. Summary of Recommendations. Annals of the ICRP 21(Pub. 103). Elsevier, Amsterdam, pp. 67–77.
ICRP, 2007. Pub. 103, Chapter 3. Biological Aspects of Radiological Protection. Ann. ICRP 37 (2–4), 49–79. Elsevier, Amsterdam.
Iijima, T., 2010. Recent topics of particle identification and photodetection. Nucl. Instrum. Methods Phys. Res. Sect. A 632 (1), 48–56.
Iijima, T., et al., 2008. Studies of a proximity focusing RICH with aerogel radiator for future Belle upgrade. Nucl. Instrum. Methods Phys. Res. Sect. A 595, 92–95.
Ilić, R., Durrani, S.A., 2003. Solid state nuclear track detectors, pp. 179–237. In: L'Annunziata, M.F. (Ed.), Handbook of Radioactivity Analysis, second ed. Elsevier, Amsterdam, p. 1273.
Inami, K., 2008. Development of a TOP counter for the super B factory. Nucl. Instrum. Methods Phys. Res. Sect. A 595, 96–99.
Inami, K., On behalf of the Belle II - PID Group, 2011. TOP counter prototype R&D. Nucl. Instrum. Methods Phys. Res. Sect. A 639 (1), 298–301.
Iodice, M., et al., 2005. Performance and results of the RICH detector for kaon physics in Hall A at Jefferson Lab. Nucl. Instrum. Methods Phys. Res. Sect. A 553, 231–236.
IPCC, 2007. Climate Change 2007: Impacts, Adaptation and Vulnerability. Contribution of Working Group II to the Fourth Assessment Report of the Intergovernmental Panel on Climate Change. Cambridge University Press, Cambridge, UK.

Ironside, R., 1928. The diffraction of cathode rays by thin films of copper, silver and tin. Proc. R. Soc. London A119, 668–673.
Ising, G., 1924. Prinzip einer Methode zur Herstellung von Kanalstrahlen hoher Voltzahl. Ark. Mat. Astr. Fys. 18 (30), 1–4.
Isotope Products Laboratories, 1995. Californium-252 fission foils and neutron sources. In: Radiation Sources for Research, Industry and Environmental Applications. Isotope Products Laboratories, Burbank, CA, p. 55.
Issa, F., et al., 2013. Boron and gadolinium neutron capture therapy. In: Reedijk, Jan, Poeppelmeier, Kenneth (Eds.), Comprehensive Inorganic Chemistry II, from Elements to Applications, second ed., vol. 3. Elsevier, Amsterdam, pp. 877–900.
Ito, K., 2002. Values of "pure science": Nishina Yoshio's wartime discourse between nationalism and physics, 1940–1945. Historical Studies in the Physical and Biological Sciences 33 (1), 61–86. University of California Press. http://www.jstor.org/stable/10.1525/hsps.2002.33.1.61.
Ivanovich, M., 1994. Uranium series disequilibrium: concepts and applications. Radiochim. Acta 64, 81–94.
Ivanovich, M., Harmon, R.S., 1992. Uranium Series Disequilibrium: Applications to Earth, Marine and Environmental Sciences. Clarendon Press, Oxford, p. 910.
Iwanenko, D.D., Pomeranchuk, I.Y., 1944a. On the maximal energy attainable in a betatron. Dokl. Akad. Nauk SSSR 44, 364.
Iwanenko, D.D., Pomeranchuk, I.Y., 1944b. On the maximal energy attainable in a betatron. Phys. Rev. 65 (11–12), 343.
Iwashita, Y., et al., 2011. Satellite pulsed tiny neutron source at Kyoto University, Sakyo. Nucl. Instrum. Methods Phys. Res. Sect. A 634 (1, Suppl. 1), S97–S99.
Iwata, Y., Noda, K., 2014. Chapter 8.10 Ion Linac and synchrotron. In: Reference Module in Biomedical Sciences, from Comprehensive Biomedical Physics. Elsevier, Amsterdam, pp. 153–168.
Jackson, J.D., Panofsky, W.K.H., 1996. Edwin Mattison McMillan, 1907–1991. In: Biographical Memoirs. National Academy Press, Washington, DC, pp. 213–241.
Jackson, K.P., et al., 1970. ^{53m}Co: a proton-unstable isomer. Phys. Lett. B 33 (4), 281–283.
Jackson, J.D., 2002. Emilio GinoSegrè 1905–1989. In: Biographical Memoirs, vol. 81. National Academy Press, Washington, DC, pp. 1–25.
Jacobsen, N.E., 2007. NMR Spectroscopy Explained: Simplified Theory, Applications and Examples for Organic Chemistry and Structural Biology. Wiley-Interscience, p. 688.
Jahn, H.A., Teller, E., 1937. Stability of polyatomic molecules in degenerate electronic states. I. Orbital degeneracy. Proc. R. Soc. A 161, 220–235.
Jaklevic, J.M., Madden, N.W., Wiegand, C.E., 1983. A precision beta gauge using a plastic scintillator and photomultiplier detector. Nucl. Instrum. Methods Phys. Res. 214 (2–3), 517–518.
Jakobs, K., 2011. Physics at the LHC and sLHC. Nucl. Instrum. Methods Phys. Res. Sect. A 636, 51–57.
Jakubek, J., et al., 2011. Direct observation of decay of radioactive nuclei with spatial and time coincidence technique. Nucl. Instrum. Methods Phys. Res. Sect. A 633 (Suppl. 1), S203–S205.
Janczyszyn, J., et al., 2006. Measurement and calculation of cross section for (p,x) reactions on natural Fe for 650 MeV protons. Ann. Nucl. Energy 33 (7), 633–639.
Janni, J.F., 1982. Proton range-energy tables, 1 keV – 10 GeV. At. Data Nucl. Date Tables 27, 147–339.
Jansen, J.A., et al., 1971. Nuclear charge radii of ^{12}C and ^{9}Be. Nucl. Phys. A 188 (2), 337–352.
Janson, E., et al., 2000. Nuclear localization of In-111 after intravenous injection of [In-111-DTPA-D-Phe(1)]-octreotide in patients with neuroendocrine tumors. J. Nucl. Med. 41 (9), 1514–1518.
Jebri, S., et al., 2013. Effect of gamma irradiation on bacteriophages used as viral indicators. Water Res. 47 (11), 3673–3678.
Jelley, J.V., 1958. Čerenkov Radiation and Its Applications. Pergamon Press, New York, p. 296.
Jelley, J.V., 1962. Čerenkov radiation: its origin, properties and applications. Contemp. Phys. 3, 45–47.
JET Team, 1992. Fusion energy production from a deuterium-tritium plasma in the JET tokamak. Nucl. Fusion 32, 187–201.
Jeynes, C., et al., 2012. "Total IBA" – where are we? Nucl. Instrum. Methods Phys. Res. Sect. B 271, 107–118.
Jia, W., Ehrhardt, G.J., 1997. Enhancing the specific activity of ^{186}Re using an inorganic Szilard-Charlmers process. Radiochim. Acta 79 (1–4), 131–136.
Johansson, A., Wilkin, C., 2009. Hard bremsstrahlung in the $pp \rightarrow pp\gamma$ reaction. Phys. Lett. B 673, 5–8.
Johansen, G.A., Jackson, P., 2004. Isotope Gauges for Industrial Process Measurements. John Wiley & Sons Ltd, Chichester, UK. http://dx.doi.org/10.1002/0470021098.fmatter.
Joliot-Curie, I., 1931. Sur l'excitation des rayons gamma nucléaires du bore par les particules alpha. Énergie quantique du rayonnement gamma du polonium. C. R. Acad. Sci. (Paris) 193S, 1415–1417.
Joliot-Curie, I., Joliot, F., 1932. Èmission de protons de grande vitesse par les substances hydrogénées sous l'influence des rayons γ trés pénétrants. Comptes Rendus (Paris) 194S, 273–275.
Joliot-Curie, I., Joliot, F., 1933. Contribution à l'étude des électrons positifs. Comptes Rendus (Paris) 196S, 1105–1107.
Joliot-Curie, I., Joliot, F., 1934a. Artificial production of a new kind of radioelement. Nature 133, 201.
Joliot-Curie, I., Joliot, F., 1934b. Un nouveau type de radioactivité. Comptes Rendus 198S, 254–256.
Joliot-Curie, I., Joliot, F., 1934c. Séparation chimique des nouveaux radioéléments émetteurs d'électrons positifs. Comptes Rendus 198S, 559–561.
Joliot-Curie, I., Savitch, P., 1938a. Sur les radioelement de période 3,5 heures formé dans l'uranium irradié par les neutrons. Comptes Rendus 206S, 906–908.
Joliot-Curie, I., Savitch, P., 1938b. Sur la nature du radioélements de période 3,5 heures formé dans l'uranium irradié par les neutrons. Comptes Rendus 206S, 1643–1644.
Joliot-Curie, I., Savitch, P., 1939. Sur les radioélements formés dans l'uranium et le thorium irradiés par les neutrons. Comptes Rendus 208S, 343–346.

Joliot, F., Joliot-Curie, I., 1935. Chemical evidence of the transmutation of elements. Nobel Lecture on December 12, 1935. In: Nobel Foundation Staff (Ed.), Nobel Prize Lectures in Chemistry, 1901–1970 (1967). Elsevier Science, Amsterdam vol. 1, 1901–1921, vol. 2, 1922–1941, vol. 3, 1942–1962.

Jones, H.G., 1973. Estimation of plant water status with the beta-gauge. Agric. Meteorol. 11, 345–355.

Joram, C., 2002. The evolution of the Cherenkov imaging technique in high energy physics. Nucl. Phys. B (Proc. Suppl.) 109B, 153–161.

Jungk, R., 1956. Heller als tausend Sonnen. Scherz & Goverts, p. 368.

Jungk, R., 1957. Staekere end Tusind Sole: Atomforskernes Skaebne. Jespersen og Die, p. 309.

Jungk, R., 1958. Hotter than a Thousand Suns: A Personal History of the Atomic Scientists. Harcourt Brace, New York, p. 369.

Kaiser, D., 2005a. Physics and Feynman's diagrams. Am. Sci. 93 (March–April), 156.

Kaiser, D., 2005b. Drawing Theories Apart: The Dispersion of Feynman Diagrams in Postwar Physics. University of Chicago Press, Chicago, p. 376.

Kaiser, T.R., February 8, 1974. Heaviside radiation. Nature 274, 400–401.

Kakuee, O., et al., 2012. External PIXE analysis of an Iranian 15th century poetry book. Nucl. Instrum. Methods Phys. Res. Sect. B 273, 178–181.

Kallman, H., 1950. Scintillation counting with solutions. Phys. Rev. 78 (5), 621–622.

Kalmus, G.E., Kernan, A., 1967. Experimental study of $K^+ \rightarrow \pi^o + e^+ + \nu$ decay. Phys. Rev. 159, 1187–1194.

Kantarelou, V., et al., 2011. X-ray fluorescence analytical criteria to assess the fineness of ancient silver coins: application on Ptolemaic coinage. Spectrochim. Acta B 66, 681–690.

Karelin, Y.A., et al., 1997. Californium-252 neutron sources. Appl. Radiat. Isot. 48 (10–12), 1563–1566.

Kaschl, G.Th., et al., 1970. Proton pick-up from ^{19}F, ^{20}Ne and ^{22}Ne. Nucl. Phys. A 155, 417–442.

Kassis, A.I., 2003. Cancer therapy with Auger electrons: are we almost there? J. Nucl. Med. 44 (9), 1479–1481.

Katz, L., Penfold, A.S., 1952. Range-energy relations for electrons and the determination of beta-ray end-point energies by absorption. Rev. Mod. Phys. 24 (1), 28–44.

Katz, U.F., 2009. Underwater neutrino telescopes. Nucl. Phys. B. (Proc. Suppl.) 188, 245–251.

Kaufman, R.M., 2010. Transfusion reactions, pp. 256–257. In: Mushin, S.B., Greene II, H.L. (Eds.), Decision Making in Medicine, third ed. Elsevier, p. 726.

Kawauchi, S., Benson, A.A., Hayes, P., Calvin, M., 1952. The path of carbon in photosynthesis. J. Am. Chem. Soc. 74, 4477–4482.

Kazkaz, K., The Majorana Collaboration, 2005. The Majorana search for neutrinoless double-beta decay. Nucl. Phys. B – Proc. Suppl. 143, 550.

Kearns, E., et al., 1999. Detecting massive neutrinos. Sci. Am. 281 (2), 64–71.

Keisch, B., 2003. The Atomic Fingerprint: Neutron Activation Analysis. University Press of the Pacific, p. 64.

Kellogg, et al., 1939. The magnetic moments of the proton and the deuteron. Phys. Rev. 56, 728–743.

Kelley, K.C., et al., 2005. ^{148}Gd production cross section measurements for 600- and 800-MeV protons on tantalum, tungsten, and gold. Nucl. Phys. A 760 (3–4), 225–233.

Kendall, C., McDonnell, J.J. (Eds.), 1998. Isotope Tracers in Catchment Hydrology. Elsevier Science, Amsterdam, p. 839.

Kendall, C., et al., 2014. Environmental isotope applications in hydrologic studies. In: Holland, H., Turekian, K. (Eds.), Treatise on Geochemistry, Surface and Groundwater, Weathering and Soils, second ed., vol. 7. Elsevier, Amsterdam, pp. 274–327.

Kendall, H.W., 1991. Deep inelastic scattering: experiments on the proton and the observation of scaling. Rev. Mod. Phys. 63 (3), 597–614.

Kennedy, J.W., Seaborg, G.T., Segrè, E., Wahl, A.C., 1946. Properties of $^{239}94$. Phys. Rev. 70, 555.

Kenrick, F.B., et al., 1924. The superheating of liquids. J. Phys. Chem. 28, 1297–1307.

Kerzel, U., 2010. The LHCb RICH detectors. Nucl. Instrum. Methods Phys. Res. Sect. A 617, 283–286.

Kesler, S.E., et al., 2012. Global lithium resources: relative importance of pegmatite, brine and other deposits. Ore Geol. Rev. 48, 55–69.

Kesterbaum, D., 1998. Neutrinos throw their weight around. Science 281 (5383), 1594–1595.

Khachan, J., Samarian, A., 2007. Dust diagnostics on an inertial electrostatic confinement device. Phys. Lett. A 363, 297–301.

Khan, D.I., et al., 2014. Functional failure modes cause-consequence logic suited for mobile robots used at scientific facilities. Reliab. Eng. Sys. Saf. 129, 10–18.

Khaton, M.M., Shaik, M.M., 2011. Sterile Insect Technique to Control Destructive Insect Pest Melon Fly: Optimize the Ratio of Irradiated Males to Be Released for the Suppression of Melon Fly (*Bactrocera Cucurbitae*). Lap Lambert Academic Publishing.

Kim, D.-W., 2006. Yoshio Nishina and two cyclotrons. Hist. Stud. Phys. Biol. Sci. 36 (2), 243–273.

Kim, I.J., Jung, N.S., Jung, H.D., Hwang, Y.S., Choi, H.D., 2008. A D–D neutron generator using a titanium drive-in target. Nucl. Instrum. Methods Phys. Res. Sect. B 266, 829–833.

Kim, H.S., et al., 2009a. Development of a beta gauge system for a fabric density measurement. Appl. Radiat. Isot. 67, 1213–1215.

Kim, Y., et al., 2009b. In: Anstracts ICOPS 2009. IEEE International Conference on Plasma Science, June 1–5, 2009. Plasma Sciece, ISBN 978-1-4244-2617-1.

Kim, T.-H., et al., 2011. Gamma ray irradiation for sludge solubilization and biological nitrogen removal. Rad. Phys. Chem. 80 (12), 1386–1390.

Kim, G.Y., On behalf of the LHCb RICH Collaboration, 2011. The RICH detectors for the upgraded LHCb experiment. Nucl. Instrum. Methods Phys. Res. Sect. A 639 (1), 278–281.

Kim, H.H., et al., 2013a. Reduction of toxicity of antimicrobial compounds by degradation processes using activated sludge, gamma radiation, and UV. Chemosphere 93 (10), 2480–2487.

Kim, I.J., et al., 2013b. Accurate measurement of bromine contents in plastic samples by instrumental neutron activation analysis. Anal. Chim. Acta 769, 22–29.

Kimura, K., 1951. Dr. Yoshiro Nishina. Nature 168 (4272), 453.

Kirby, M., 2003. IFORS' operational research hall of fame, Patrick Maynard Stuart Blackett. Int. Trans. Op. Res. 10, 405–407.

Kirkham, D., 1982. Fletcher and the oil drop. Phys. Today 35 (11), 15.

Klarsfeld, S., et al., 1986. Determination of the deuteron mean square radius. Nucl. Phys. A 456 (3), 373–396.

Klassen, W., 2003. Edward F. Knipling: titan and driving force in ecologically selective area-wide pest management. J. Am. Mosq. Control Assoc. 19 (1), 94–103.

Klein, O., Nishina, Y., 1928. The scattering of light by free electrons according to Dirac's new relativistic dynamics. Nature 122 (3072), 398–399.

Klein, O., Nishina, Y., 1929. Über die Streuung von Strahlung durch freie Elektronen nach der neuen relativistischen Quantendynamik von Dirac. Z. Phys. 52 (11–12), 853–868.

Klein, O., 1938. In: Proc. Symp. on Les Nouvelles Theories de la Physique, Warsaw, 1938 (Institut International de Coopération Intellectuelle, Paris, 1939), p. 6.

Klein, O., 1948. Mesons and nucleons. Nature 161 (4101), 897–899.

Klepper, O., et al., 1982. Direct and beta-delayed proton decay of very neutron-deficient rare-earth isotopes produced in the reaction ^{58}Ni + ^{92}Mo. Z. Phys. A At. Nucl. 305, 125–130.

Kloft, W.J., 1984. Entomology. In: L'Annunziata, M.F., Legg, J.O. (Eds.), Isotopes and Radiation in Agricultural Sciences, Animals, Plants, Food and the Environment, vol. 2. Academic Press, London, pp. 51–103.

Klug, A., 1968. Rosalind Franklin and the discovery of the structure of DNA. Nature 219 (5156), 808–810, 843–844.

Knapp, A.K., et al., 1985. An evaluation of beta attenuation for estimating aboveground biomass in a tallgrass praire. J. Range Manage. 38 (6), 556–558.

Knipp, J.K., Uhlenbeck, G.E., 1936. Emission of gamma radiation during the beta decay of nuclei. Physica III (6), 425–439.

Knipling, E.F., 1955. Possibilities of insect control or eradication through the use of sexually sterile males. J. Econ. Entomol. 48 (4), 459–462.

Knipling, E.F., 1957. Controlled eradication of screw-worm fly by atomic radiation. Sci. Mon. 85 (4), 195–202.

Knipling, E.F., 1959. Sterile-male method of population control. Science 130 (3380), 902–904.

Knipling, E.F., 1960a. Use of insects for their own destruction. J. Econ. Entomol. 53 (3), 415–420.

Knipling, E.F., 1960b. The eradication of the screwworm fly. Sci. Am. 203 (4), 54–61.

Kobayashi, M., Maskawa, T., 1973. CP violation in the renormalizable theory of weak interactions. Prog. Theor. Phys. 49 (2), 652–657.

Kobayashi, M., 2008. CP violation and flavour mixing. Nobel Lecture, December 8, 2008. Nobelprize.org. Nobel Media AB 2014. http://www.nobelprize.org/nobel_prizes/physics/laureates/2008/kobayashi-lecture.html.

Koch, L., 1995. Radioactivity and fission energy. Radiochim. Acta 70/71, 397–402.

Kojevnikov, A., 1996. President of Stalin's Academy. The mask and responsibility of Sergei Vavilov. Isis 87 (1), 18–50.

Kolhinen, V.S., et al., 2010. Accurate Q value for the ^{74}Se double-electron-capture decay. Phys. Lett. B 684 (1), 17–21.

Konoki, K., et al., 2010. Binding of diarrheic shellfish poisoning toxins to okadaic acid binding proteins purified from the sponge *Halichondria okadai*. Bioorg. Med. Chem. 18, 7607–7610.

Koppers, A.A.P., et al., 2000. Dating crystalline groundmass separates of altered Cretaceous seamount basalts by the Ar-40/Sr-39 incremental heating technique. Chem. Geol. 166 (1–2), 139–158.

Koppers, A.A.P., et al., 2003. High-resolution Ar-40/Ar-30 dating of the oldest oceanic basement basalts in the western Pacific basin. Geochem. Geophys. 4 (11), 8914.

Korff, S.A., June 1940. On the contribution to the ionization at sea level produced by the neutrons in the cosmic radiation. Terrestial Magn. Atmos. Electr. 45, 133–134.

Korff, S.A., Danforth, W.E., 1939. Neutron measurements with boron-trifluoride counters. Phys. Rev. 55, 980.

Korpar, S., 2003. HERA-B RICH. Nucl. Instrum. Methods Phys. Res. Sect. A 503, 41–45.

Korpar, S., et al., 2005. RICH with multiple aerogel layers of different refractive index. Nucl. Instrum. Methods Phys. Res. Sect. A 553, 64–69.

Korpar, S., et al., 2007. Proximity focusing RICH with TOF capabilities. Nucl. Instrum. Methods Phys. Res. Sect. A 572, 432–433.

Kortschak, H.P., Hartt, C.E., 1966. Effects of varied conditions on carbon dioxide fixation in sugarcane leaves. Naturwissenschaften 53, 253.

Kortschak, H.P., et al., 1965. Carbon dioxide fixation in sugarcane leaves. Plant Physiol. 40, 209–213.

Korytov, A., 2009. Muon detectors for colliders. Nucl. Instrum. Methods Phys. Res. Sect. A 598, 175–182.

Kossert, K., Grau Carles, A., 2008. Study of a Monte Carlo rearrangement model for the activity determination of electron-capture nuclides by means of liquid scintillation counting. Appl. Radiat. Isot. 66, 998–1005.

Kossert, K., Grau Carles, A., 2010. Improved method for the calculation of the counting efficiency of electron-capture nuclides in liquid scintillation samples. Appl. Radiat. Isot. 68, 1482–1488.

Köster, U., et al., 2012. Production of radioisotopes with high specific activity by photonuclear reactions: from a "wild idea" to reality. Radiother. Oncol. 102 (Suppl. 1), S102–S103.

Kostroun, V.O., et al., 1971. Atomic radiation transition probabilities to the 1s state and theoretical K-shell fluorescence yields. Phys. Rev. A3, 533–545.

Koziol, H., Möhl, D., 2004. The CERN antiproton collider programme: accelerators and accumulation rings. Phys. Rep. 403–404, 91–106.

Kragh, H., 1990. Dirac: A Scientific Biography. Cambridge University Press, p. 399.

Krane, K.S., 1988. Introductory Nuclear Physics. John Wiley & Sons, New York.

Krappe, H.J., Wahsweiler, H.G., 1967. Stability of nuclei against pear-shaped deformations. Nucl. Phys. A 104 (3), 633–641.

Krása, A., et al., 2010. Neutron production in a Pb/U-setup irradiated with 0.7−2.5 GeV protons and deuterons. Nucl. Instrum. Methods Phys. Res. Sect. A 615, 70−77.
Krasaechai, A., et al., 2009. Low-energy ion beam modification of horticultural plants for induction of mutation. Surf. Coatings Technol. 203, 2525−2530.
Kraus, Ch, et al., 2005. Final results from phase II of the Mainz neutrino mass search in tritium decay. Eur. Phys. J. C 40 (4), 447−468.
Kreiner, A.J., et al. (Eds.), 2011. 14th International Conference on Neutron Capture Therapy. Appl. Radiat. Isot., vol. 69(12), p. 1631.
Krishnamurthy, R., Lee, E., 2011. Congenital cardiovascular malformations: noninvasive imaging by MRI in neonates. Magn. Reson. Imag. Clin. North Am. 19 (4), 813−822.
Kristensen, H.M., Norris, R.S., September 9, 2014. Worldwide deployments of nuclear weapons, 2014. Bull. At. Sci. 70 (5). Nuclear Notebook.
Kristiansen, J.R., et al., 2010. Coupling between cold dark matter and dark energy from neutrino mass experiments. New Astron. 15, 609−613.
Križan, P., 2001. Recent progress in Čerenkov counters. IEEE Trans. Nucl. Sci. 48 (4), 941−949.
Križan, P., 2007. Detectors for particle identification. Nucl. Instrum. Methods Phys. Res. Sect. A 581, 57−64.
Križan, P., 2009. Recent progress in particle identification methods. Nucl. Instrum. Methods Phys. Res. Sect. A 598, 130−137.
Križan, P., et al., 2001. The performance of the HERA-B RICH at high track densities. Nucl. Instrum. Methods Phys. Res. Sect. A 471, 30−34.
Križan, P., et al., 2005. Proximity focusing RICH with flat panel PMT as photon detector and aerogel as radiator. Nucl. Instrum. Methods Phys. Res. Sect. A 553, 58−63.
Križan, P., et al., 2007. Proximity focusing RICH with TOF capabilities. Nucl. Phys. B (Proc. Suppl.) 172, 227−230.
Krönig, B., Friedrich, W., 1918. Physikalische und Biologische Grundlagen der Strahlentherapie. Urban & Scharzenberg, Berlin.
Kubo, R., 1990. Yoshio Nishina, the Pioneer of modern physics in Japan. In: Address at the Nishina Centennial Symposium, December 5,1990. Japan Medical Association, Tokyo.
Kubo, R., 2008. Yoshio nishina, the Pioneer of modern physics in Japan. Lect. Notes Phys. 746, 17−26. http://dx.doi.org/10.1007/978-4-431-77056-5_2. Springer, Japan.
Kudo, H., 1995. Radioactivity and fusion energy. Radiochim. Acta 70/71, 403−412.
Kulcsar, F., Teherani, D., Altmann, H., 1982. Study of the spectrum of Cherenkov light. J. Radioanal. Chem. 68, 161−168.
Kullander, S., 2005. Accelerators and Nobel Laureates, p. 30. http://nobelprize.org/physics/articles/kullander/index.html.
Kumamoto, Y., et al., 2011. Temporal and spatial variations in bomb-produced radiocarbon along BEAGLE2003 lines—Revisits of WHP P06, A10, and I03/I04 in the Southern Hemisphere Oceans. Prog. Ocean. 89, 49−60.
Kumar, T., Glaser, D.A., 1993. Initial performance, learning, and observer variability for hyperacuity tasks. Vis. Res. 33, 2287−2300.
Kumar, T., Glaser, D.A., 1995. Depth discrimination of a crowded line is better when it is more luminant than the lines crowding it. Vis. Res. 35, 657−666.
Kuribara, M., 1994. Spent fuel burnup estimation by Cerenkov glow intensity measurement. IEEE Trans. Nucl. Sci. 41 (5), 1736−1739.
Kuribara, M., Nemoto, K., 1994. Development of new U.V. − I.I. Cerenkov viewing device. IEEE Trans. Nucl. Sci. 41 (1), 331−335.
Kurie, F.N.D., 1934. A new mode of disintegration produced by neutrons. Phys. Rev. 45, 904−905.
Kurtukian-Nieto, T., et al., 2008. A new analysis method to determine β-decay half-lives in experiments with complex background. Nucl. Instrum. Methods Phys. Res. Sect. A 589, 472−483.
Kusch, P., Foley, H.M., 1948. The magnetic moment of the electron. Phys. Rev. 74, 250−263.
Kushita, K.N., Du, J., 1998. Radioactivity measurements of ^{188}Re by Cherenkov counting. Appl. Radiat. Isot. 49 (9−11), 1069−1072.
Kyle, R.A., Shampo, M.A., 2002. Rosalyn Yalow − pioneer in nuclear medicine. Mayo Clin. Proc. 77, 4.
Kusnir, M.M., et al., 2004. Simultaneous quantitative analysis of isobars by tandem mass spectrometry from unresolved chromatographic peaks. J. Mass Spectrom. 39 (5), 532−540.
Kamohara, K., et al., 2011. Staged resternotomy for a retrosternal giant aneurysm of the thoracic aorta using an inferior T-shaped ministernotomy. Ann. Thorac. Surg. 92 (5), 1911−1913.
Lal, D., 2009. Cosmogenic isotopes. In: Steel, et al. (Eds.), Encyclopedia of Ocean Sciences. Academic Press/Elsevier Science, Amsterdam, pp. 678−687.
Lal, D., Peters, B., 1967. Cosmic ray produced radioactivity on the earth. Handb. Phys. 46 (2), 551−612.
Lawrence, E.O., et al., 1939. Initial performance of the 60-inch cyclotron of the William H. Crocker Laboratory, University of California. Phys. Rev. 56, 124−125.
Labidi, S., et al., 2010. Natural radioactivity levels in mineral, therapeutic and spring waters in Tunisia. Radiat. Phys. Chem. 79, 1196−1202.
Lacoste, V., 2010. Review of radiation sources, calibration facilities and simulated workplace fields. Radiat. Meas. 45 (10), 1083−1089.
Lagemann, R.T., 1977. New light on old rays: N rays. Am. J. Phys. 45 (3), 281−284.
Lakosi, L., Nguyen, C.T., 2008. Neutron interrogation of high-enriched uranium by a 4 MeV linac. Nucl. Instrum. Methods Phys. Res. Sect. B 266, 3295−3301.
Lamb, W.E., Retherford, R.C., 1947. Fine structure of the hydrogen atom by a microwave method. Phys. Rev. 72, 241−242.
Lambert, B., Martin, J., 2013. Sterilization of implants and devices, pp. 1339−1353. In: Ratner, B.D., Hoffman, A.S., Schoen, F.J., Lemons, J.E. (Eds.), Biomaterials Science, third ed. Elsevier, p. 1555.
Lambert, J.B., et al., 2010. Organic Structural Spectroscopy, second ed. Prentice Hall, p. 552.
Landowne, S., Dasso, C.H., 1986. Novel aspects of the carbon decay mode of radium. Phys. Rev. C 33, 387−389.
L'Annunziata, M.F., 1970. The University of Arizona (Ph.D. dissertation). University Microfilms International (UMI), Tucson. AAT 7104237. http://dissexpress.umi.com/dxweb/results.html?QryTxt=&By=L%27Annunziata&Title=&pubnum=.

L'Annunziata, M.F., 1971. Birth of a unique parent-daughter relation: secular equilibrium. J. Chem. Educ. 48, 700–703.

L'Annunziata, M.F., 1984. Agricultural biochemistry: reaction mechanisms and pathways in biosynthesis. In: L'Annunziata, M.F., Legg, J.O. (Eds.), Isotopes and Radiation in Agricultural Sciences, vol. 2. Academic Press, London, pp. 105–182.

L'Annunziata, M.F., 1987. Radionuclide Tracers, Their Detection and Measurement. Academic Press, London, p. 505.

L'Annunziata, M.F. (Ed.), 2012a. Handbook of Radioactivity Analysis, third ed. Elsevier Science, Amsterdam, p. 1379.

L'Annunziata, M.F., 2012b. Liquid scintillation analysis, principles and practice. In: L'Annunziata, M.F. (Ed.), Handbook of Radioactivity Analysis, third ed. Elsevier, Amsterdam, pp. 423–573.

L'Annunziata, M.F., 2012c. Solid scintillation analysis. In: L'Annunziata, M.F. (Ed.), Handbook of Radioactivity Analysis, third ed. Elsevier, Amsterdam, pp. 1021–1115.

L'Annunziata, M.F., 2012d. Flow-cell analysis. In: L'Annunziata, M.F. (Ed.), Handbook of Radioactivity Analysis, third ed. Elsevier, Amsterdam, pp. 1117–1178.

L'Annunziata, M.F., 2012e. Cherenkov counting. In: L'Annunziata, M.F. (Ed.), Handbook of Radioactivity Analysis, third ed. Elsevier, Amsterdam, pp. 935–1019.

L'Annunziata, M.F., 2012f. Table of radioactive isotopes. Appendix A. In: Handbook of Radioactivity Analysis, third ed. Elsevier Science, Amsterdam, p. 1379.

L'Annunziata, M.F., 2012g. Radiation physics and radionuclide decay. In: L'Annunziata, M.F. (Ed.), Handbook of Radioactivity Analysis, third ed. Elsevier, Amsterdam, pp. 1–162.

L'Annunziata, M.F., Legg, J.O. (Eds.), 1984a. Isotopes and Radiation in Agricultural Sciences, vol. 1. Soil-Plant-Water Relationships. Academic Press, London, p. 292.

L'Annunziata, M.F., Legg, J.O. (Eds.), 1984b. Isotopes and Radiation in Agricultural Sciences, vol. 2. Animals, Plants, Food and the Environment. Academic Press, London, p. 356.

L'Annunziata, M.F., Passo Jr., C.J., 2002. Cherenkov counting of yttrium-90 in the dry state; correlations with phosphorus-32 Cherenkov counting data. Appl. Radiat. Isot. 56, 907–916.

L'Annunziata, M.F., Gonzalez, I.J., 1977. Soil metabolic transformations of carbon-14-*myo*-inositol, carbon-14-phytic acid, and carbon-14-iron(III) phytate. In: Soil Organic Matter Studies, vol. I. International Atomic Eneregy Agency, Publication No. IAEA-SM-211/66, Vienna, Austria, pp. 239–253.

L'Annunziata, M.F., et al., 1977. Microbial epimerization of *myo*-inositol to *chiro*-inositol in soil. Soil Sci. Soc. Amer. J. 41, 733–736.

Lanouette, W., with Silard, B., 2013. Genius in the Shadows, A Biography of Leo Szilard, the Man Behind the Bomb. Skyhorse Publishing, New York, p. 613.

Lappin, G., Temple, S., 2006. Radiotracers in Drug Development. CRC Press, Boca Raton, p. 320.

Larijani, B., et al. (Eds.), 2006. Chemical Biology: Applications and Techniques. John Wiley & Sons, p. 272.

Lattes, C.M.G., Occhialini, G.P.S., Powell, C.F., 1947. Observation on the tracks of slow mesons in photographic emulsions. Nature 160, 453–456.

Lauer, W.C. (Ed.), 2006. Desalination of Seawater and Brackish Water. American Waterworks Association, p. 780.

Lavrenkov, K., et al., 2007. A potential to reduce pulmonary toxicity: the use of perfusion SPECT with IMRT for functional lung avoidance in radiotherapy of non-small cell lung cancer. Radiother. Oncol. 83 (2), 156–162.

Lawrence, E.O., 1935. Transmutation of sodium by deuterons. Phys. Rev. 47, 17–27.

Lawrence, E.O., 1951. The evolution of the cyclotron, Nobel Lecture given on December 11, 1951 in Stockholm, Sweden. In: Nobel Lectures, Physics, 1922–1941 (1965). Elsevier Publishing, Amsterdam.

Lawrence, E.O., Edlefsen, N.E., 1930. The production of high-speed protons without the use of high voltages. Science 72, 376–377.

Lawrence, E.O., Livingston, M.S., 1931a. The production of high-speed protons without the use of high voltages. Phys. Rev. 37, 1707.

Lawrence, E.O., Livingston, M.S., 1931b. The production of high-speed protons without the use of high voltages. Phys. Rev. 38, 834.

Lawrence, E.O., Livingston, M.S., 1932. The production of high-speed light ions without the use of high voltages. Phys. Rev. 40, 19–35.

Lawrence, E.O., Livingston, M.S., 1934. The multiple acceleration of ions to very high speeds. Phys. Rev. 45, 608–612.

Lawrence, E.O., Cooksey, D., 1936. On the apparatus for the multiple acceleration of light ions to high speeds. Phys. Rev. 50, 1131–1140.

Lawson, C.G., Krause, C., November 2004. Documenting history: minutes of the New Piles Committee meetings. Nucl. News 36–38.

Lederer, M.C., Shirley, V.S., 1978. In: Brown, E., et al. (Eds.), Table of Isotopes, seventh ed. John Wiley & Sons, New York.

Lee, J., Samios, N.P., 1959. Search for rare decay modes of the μ^+ meson. Phys. Rev. Lett. 3, 55–56.

Lee, K.K.M., Steinle-Neumann, G., 2008. Ab-initio study of the effects of pressure and chemistry on the electron-capture radioactive decay constants of ^{7}Be, ^{22}Na and ^{40}K. Earth Planet. Sci. Lett. 267, 628–636.

Lee, S.-H., et al., 2013. The transport of close-in fallout plutonium in the northwest Pacific Ocean: tracing the water mass movement using ^{240}Pu/^{239}Pu atom ratio. In: Isotopes in Hydrology, Marine Ecosystems and Climate Change Studies. Proceedings of an International Symposium, Monaco, 27 March–1 April 2011, vol. 1. International Atomic Energy Agency, Vienna, pp. 513–521.

Lee, T.D., Yang, C.N., 1956. Question of parity conservation in weak interactions. Phys. Rev. 104, 254–258.

Lee, T.D., et al., 1949. Interaction of mesons with nucleons and light particles. Phys. Rev. 75, 905.

Lee, Z., et al., 2005. Multimodal and three-dimensional imaging of prostate cancer. Comput. Med. Imaging Graph. 29, 477–486.

Leighton, R.B., et al., 1949. The energy spectrum of the decay particles and the mass and spin of the mesotron. Phys. Rev. 75, 1432–1437.

Leighton, R.B., et al., 1953. The decay of V^0 particles. Phys. Rev. 89, 148–177.

Leininger, R.F., Segrè, E., Wiegand, C., 1949. Experiments on the effect of atomic electrons on the decay constant of ^{7}Be. II. Phys. Rev. 76, 897.

Lemaître, G., 1927. Un universe homogène de masse constante et de rayon croissant relevant compte de la vitresse radiale des nébuleuses extragalactiques. Ann. Soc. Sci. Brux. A47, 41–49.
Lemaître, G., 1931a. A homogeneous universe of constant mass and increasing radius accounting for the radial velocity of extragalactic nebulae. Mon. Not. R. Astron. Soc. 91 (1), 483–490.
Lemaître, G., 1931b. The evolution of the universe. Nature 128 (3234), 704–706 (Suppl., October 24, 1931.
Lemaître, G., Vallarta, M.S., 1933. On Compton's latitude effect of cosmic radiation. Phys. Rev. 43, 87.
Lemaître, G., Vallarta, M.S., 1936a. On the geomagnetic analysis of cosmic radiation. Phys. Rev. 49, 719.
Lemaître, G., Vallarta, M.S., 1936b. On the allowed cone of cosmic radiation. Phys. Rev. 50, 493.
Lenard, P., 1894. Über Kathodenstrahlen in Gasen von atmosphärischem Druck und im äussersten Vakuum. (Cathode rays in gases at atmospheric pressure and in the highest vacuum. Wied. Ann. Phys. 51.
Lenard, P., 1899. Erzeugung von Kathodenstrahlen durch ultraviolettes Licht. (Production of cathode rays by ultraviolet light). Sitzber. Kaiserl. Akad. Wiss. Wien. 2, 19th October, also Ann. Phys.
Lenard, P., 1902. Über die lichtelektrische Wirkung. Ann. Phys. 8, 149–198.
Lerouge, S., 2010. Sterilisation and cleaning of metallic biomaterials. In: Niinomi, M. (Ed.), Metal for Biomedical Devices. Elsevier, pp. 303–326, p. 420.
Leung, K.K.H., Zimmer, O., 2009. Proposed neutron lifetime measurement using a hybrid magnetic trap for ultra-cold neutrons. Nucl. Instrum. Methods Phys. Res. Sect. A 611, 181–185.
Levi, H., 1985. George de Hevesy: life and Work. Hilger, p. 147.
Levine, I.N., 1999. Quantum Chemistry, fifth ed. Prentice Hall, p. 739.
Levinger, J.S., 1953. Effects of radioactive disintegrations on inner electrons of the atom. Phys. Rev. 90, 11–25.
Libby, W.F., 1955. Radiocarbon Dating, second ed. The University of Chicago press, Chicago, p. 175.
Libby, W.F., 1960. Radiocarbon dating, Nobel Lecture given in Stockholm on December 12, 1960. In: Nobel Foundation Staff (Ed.), Nobel Lectures, Chemistry, 1942–62 (1964). Elsevier Publishing, Amsterdam.
Libby, W.F., 1967. History of radiocarbon dating. In: Radioactive Dating and Methods of Low-level Counting. Proceedings of a Symposium, Monaco. International Atomic Energy Agency, Vienna, pp. 3–25.
Licciardi, J.M., et al., 2008. Cosmogenic ^{36}Cl production rates from Ca spallation in Iceland. Earth Planet. Sci. Lett. 267, 365–377.
Lide, D.R., 1997. CRC Handbook of Chemistry and Physics, 77th ed. CRC Press, Boca Raton.
Lide, D.R., 2010. CRC Handbook of Chemistry and Physics, 81st ed. CRC Press, Boca Raton, pp. 10–220.
Liedvogel, M., et al., 2011. The genetics of migration on the move. Trends Ecol. Evol. 26 (11), 561–569.
Lilley, J., 2001. Nuclear Physics, Principles and Applications. John Wiley & Sons, Ltd, West Sussex, p. 393.
Linden, R.A., et al., 2009. Technique of outpatient placement of intraprostatic fiducial markers before external beam radiotherapy. Urology 73 (4), 881–886.
Lindh, A.E., 1950. Presentation speech for the Nobel Prize in physics 1950. In: Nobel Foundation Staff (Ed.), Nobel Lectures, Physics, 1942–62 (1964). Elsevier Publishing, Amsterdam.
Lindhard, J., Scharff, M., 1960. Recent developments in the theory of stopping power. I. Principles of the statistical method. In: Penetration of Charged Particles in Matter. National Academy of Sciences-National Research Council, Publication 752, p. 49.
Lindhard, J., Scharff, M., 1961. Energy dissipation by ions in the keV region. Phys. Rev. 124, 128–130.
Lindsey, C.S., et al., 1999. Nuclear fuel assembly assessment project and image categorization. In: Proceedings of the Ninth Workshop on Virtual Intelligence, Dynamic Neural Networks. Royal Institute of Technology, KTH, Stockholm, Sweden, June 22–26, 1998. Proc. SPIE 3728, pp. 491–499.
Lindop, P.J., Rotblat, J., 1961. Shortening of life and causes of death in mice exposed to a single whole-body dose of radiation. Nature 189, 645–648.
Lindop, P.J., Rotblat, J., 1965. Life-shortening in mice exposed to radiation: effects of age and hypoxia. Nature 208, 1070–1072.
Lindote, A., et al., 2009. Simulation of neutrons produced by high-energy muons underground. Astropart. Phys. 31, 366–375.
Litherland, A.E., et al., 2007. Isobar separation at very low energy for AMS. Nucl. Instrum. Methods Phys. Res. Sect. A 259 (1), 230–235.
Linsley, J., 1963. Evidence for a primary cosmic-ray particle with energy 10^{20} eV. Phys. Rev. Lett. 10, 146–148.
Lionaes, A., 1970. Presentation speech, the Nobel Peace prize 1970. In: Heberman, F.W. (Ed.), Nobel Lectures, Peace 1951–1970. Elsevier Publishing Co., Amsterdam, 1972.
Lipkin, H.J., White, M.G., 1950. Scattering of positrons and electrons by nuclei. Phys. Rev. 79 (5), 892L–893L erratum 80(4), 770L.
Lippmann, C., 2012. Particle identification. Nucl. Instrum. Methods Phys. Res. Sect. A 666, 148–172.
Lis, G.J., et al., 2014. Distribution of selected elements in calcific human aortic valvesstudied by microscopy combined with SR-μXRF: Influence of lipids on progression of calcification. Micron 67, 141–148.
Liu, L., Huh, C.-A., 2000. Effect of pressure on the decay rate of ^{7}Be. Earth Planet. Sci. Lett. 180, 163–167.
Liu, Y., et al., 2009. Preparation of high-stable silver nanoparticle dispersion by using sodium alginate as a stabilizer under gamma radiation. Rad. Phys. Chem. 78, 251–255.
Livingood, J.J., Seaborg, G.T., 1938. Radioactive iodine isotopes. Phys. Rev. 53, 1015.
Livingston, M.S., Bethe, H.A., 1937. Nuclear physics III. Nuclear dynamics, experimental. Rev. Mod. Phys. 9, 245–390.
Lobashev, V.M., et al., 1999a. Direct search for mass of neutrino and anomaly in the tritium beta-spectrum. Phys. Lett. B 460, 227–235.
Lobashev, V.M., et al., 1999b. Neutrino rest mass and anomaly in the tritium β spectrum. Nucl. Phys. A654, 982c–987c.
Lobashev, V.M., et al., 1999c. Neutrino mass and anomaly in the tritium beta-spectrum. Results of the "Troitsk ν-mass" experiment. Nucl. Phys. B (Proc. Suppl.) 77, 327–332.

Lobashev, V.M., et al., 2000. Neutrino mass anomaly in the tritium beta-spectrum. In: Proceedings the XIX International Conference on Neutrino Physics and Astrophysics (Neutrino-2000), Sudbury, Canada, June 16–21, 2000.

Loeber, C.R., 2002. Building the Bombs: A History of the Nuclear Weapons Complex. Sandia National Laboratories, Albuquerque, p. 262.

Loeffler, J., et al., 2012. Application of current radiation deleivery systems and radiobiology. In: Ellenbogen, R., Abdulrauf, S., Sekhar, L. (Eds.), Principles of Neurological Surgery, third ed. Saunder, New York, pp. 697–706.

Lorentz, H.A., 1904. Electromagnetic phenomena in a system moving with any velocity smaller than that of light. Proc. R. Neth. Acad. Arts Sci. 6, 809–831.

Los Alamos Science, 1997. The Reines-Cowan Experiments, 1953–1956. Detecting the Poltergeist. Number 25.

Lovell, B., 1975. Blackett, Patrick Maynard Stuart, Baron Blackett of Chelsea. In: Biographical Memoirs of the Fellows of the Royal Society, vol. 21. Royal Society, London, pp. 1–115, p. 564.

Loveland, W., 2004. Nuclear chemistry. In: Myers, R.A. (Ed.), Encyclopedia of Physical Science and Technology, third ed. Elsevier, Amsterdam, pp. 597–615.

Lowenthal, G., Airey, P., 2001. Practical Applications of Radioactivity and Nuclear Radiations. Cambridge University Press, p. 366.

Luo, N., et al., 2010. Proton bremsstrahlung and its radiation effects in fusion reactors. Fusion Eng. Des. 85, 39–45.

Lubkin, G.B., 1989. Special issue. Richard Feynman. Phys. Today 42 (2), 22.

Luft, R., 1977. Presentation speech. The Nobel Prize in physiology or medicine 1977. In: Lindsten, J. (Ed.), Nobel Lectures, Physiology and Medicine 1971–1980. World Scientific Publishing, Singapore, 1992.

Maas, W., 2004. Leo Szilard. A personal remembrance. Genetics 167, 555–558.

Macfarlane, R.D., Kohman, D.P., 1967. Natural alpha radioactivity in medium-heavy elements. Phys. Rev. 121, 1758–1769.

Mack, J.M., et al., 2003. Observation of high-energy deuterium–tritium fusion gamma rays using gas Cherenkov detectors. Nucl. Instrum. Methods Phys. Res. Sect. A 513, 566–572.

Mack, J.M., et al., 2006. Remarks on detecting high-energy deuterium–tritium fusion gamma rays using a gas Cherenkov detector. Radiat. Phys. Chem. 75, 551–556.

Madani, J.H., et al., 2010. Microscopic study of deuteron–nucleus total reaction cross section at medium energies. Nucl. Phys. A 839 (1–4), 42–50.

Madias, J., 2014. Electric furnace steelmaking. In: Seetharaman, S. (Ed.), Treatise on Process Metallurgy, vol. 3 Industrial Processes. Elsevier, p. 1745.

Magaritz, M., et al., 1990. A new method to determine regional evapotranspiration. Water Resour. Res. 26, 1759–1762.

Magaud, P., et al., 2004. Nuclear fusion reactors. In: Cutler J. Cleveland (Ed.-in-Chief), Encyclopedia of Energy, Elsevier, pp. 365–381.

Mahatni, S., 2014. Homi Jehangir Bhabha. Vigyan Prasar Science Portal. http://www.vigyanprasar.gov.in/scientists/bhabha/BHABHANEW.HTM.

Mahboub, K., 2008. A simple theoretical approach to the liquid drop model. Ann. Nucl. Energy 35, 1381–1385.

Mahjour-Shafiei, et al., 2006. Proton–proton bremsstrahlung towards the elastic limit at 190 MeV incident beam energy. Phys. Lett. B 632, 480–484.

Maiani, L., 1999. The large hadron collider project. Fusion Eng. Des. 46, 433–447.

Majorovits, B., 2010. Segmented HPGe detectors for the search of neutrinoless double beta-decay. Prog. Part. Nucl. Phys. 64 (2), 264–266.

Malik, S.S., Gupta, R.K., 1989. Theory of cluster radioactive decay and of cluster formation in nuclei. Phys. Rev. C 39, 1992–2000.

Mallet, L., 1926. Luminescence of water and organic substances subjected to gamma radiation. C. R. Acad. Sci. (Paris) 183, 274–275.

Mallet, L., 1928. Spectral study of the luminescence of water and carbon disulfide under gamma radiation. C. R. Acad. Sci. (Paris) 187, 222–223.

Mallet, L., 1929. The ultra-violet radiation of substances subjected to γ-rays. C. R. Acad. Sci. (Paris) 188, 445–447.

Mammoliti, F., et al., 2011. A RICH detector for hadron identification at JLab. Appl. Radiat. Isot. 69 (8), 1118–1120.

Manjunatha, H.C., Rudraswamy, B., 2009. Exposure of bremsstrahlung from beta-emitting therapeutic radionuclides. Rad. Meas. 44, 206–210.

Manjunatha, H.C., Rudraswamy, B., 2010. Bremstrahlung exposure of tissues from beta-therapeutic nuclides. Nucl. Instrum. Methods Phys. Res. Sect. A 621, 581–589.

Mapleston, P., 1997. Film thickness gauges meet market needs for quality, cost. Mod. Plast. 74, 73–76.

Marburger III, J.H., 2001. Enrico Fermi's Impact on Science. Address given at the Italian Embassy, Washington, DC, Centennial Celebration of the Birth of Enrico Fermi, November 27, 2001.

Marcelli, L., On behalf of the PAMELA Collaboration, 2011. Identification of the light nuclei component of cosmic rays with the PAMELA experiment. Nucl. Instrum. Methods Phys. Res. Sect. A 630 (1), 58–62.

Marcelli, A., et al., 2012. Biological applications of synchrotron radiation infrared spectromicroscopy. Biotechnol. Adv. 30, 1390–1404.

Markowicz, A.A., VanGrikin, R.E., 1984. Composition dependence of bremsstrahlung background in electron-probe X-ray microanalysis. Anal. Chem. 56, 2049–2051.

Mameli, A., et al., 2008. CR-39 detector based thermal neutron flux measurements, in the photo neutron project. Nucl. Instrum. Methods Phys. Res. Sect. B 266, 3656–3660.

Mann, W.B., 1978. A Handbook of Radioactivity Measurements Procedures. National Council on Radiation Protection and Measurements. CCRP Report No. 58, Washington, DC.

Marques-Netto, A., Abbe, J.C., 1975. Szilard-Charlmers effects in halfnium chelates. J. Inorg. Nucl. Chem. 37, 2235–2238.

Marra, P.P., et al., 2010. Migratory connectivity. In: Encyclopedia of Animal Behavior. Academic Press, pp. 455–461.

Marriner, J., 2004. Stochastic cooling overview. Nucl. Instrum. Methods Phys. Res. Sect. A 532, 11–18.

Marshall, J., 1952. Particle counting by Cerenkov radiation. Phys. Rev. 86, 685–693.

Martin, A., et al., 2014. Radiation-curing of acrylate composites including carbon fibres: a customized surface modification for improving mechanical performances. Rad. Phys. Chem. 105, 63–68.
Martin, B., Shaw, G., 2004. Particle physics, elemenetary. In: Meyers, R.A. (Ed.), Encyclopedia of Physical Science and Technology. Academic Press, Orlando, pp. 617–648.
Martins, M.N., Silva, T.F., 2014. Electron accelerators: history, applications, and perspectives. Rad. Phys. Chem. 95, 78–85.
Martin, R.C., et al., 1997. Development of high-activity ^{252}Cf sources for neutron brachytherapy. Appl. Radiat. Isot. 48 (10–12), 1567–1570.
Martin, R.C., et al., 2000. Production, distribution and applications of californium-252 neutron sources. Appl. Radiat. Isot. 53, 785–792.
Martínez, S.A., et al., 2010. Evaluation of neutron production in new accelerators for radiotherapy. Radiat. Meas. XXX, 1–4.
Masefield, J., 2004. Reflections on the evolution and current status of the radiation industry. Radiat. Phys. Chem. 71, 8–15.
Maskawa, T., 2008. What Does CP Violation Tell Us? Nobel Lecture, December 8, 2008, Nobelprize.org. Nobel Media AB 2014. http://www.nobelprize.org/nobel_prizes/physics/laureates/2008/maskawa-lecture.html.
Mason, T.E., et al., 2006. The spallation neutron source in Oak Ridge: a powerful tool for materials research. Phys. B 385–386, 955–960.
Masuda, K., et al., 2006. Spatial distribution of D–D/D–^{3}He advanced fuels fusion reactions in an inertial electrostatic confinement device. In: Proceedings of the 21st IAEA Conference on Fusion Energy, Chengdu, October 16–21, 2006, IAEA-CN-149, pp. 1–8. IC/P7-9.
Mather, J.C., Boslough, J., 1996. The Very First Light: The True Story of the Scientific Journey Back to the Dawn of the Universe. Basic Books, New York, pp. 41–42, 328 p.
Materne, S., et al., 2009. PENeLOPE—on the way towards a new neutron lifetime experiment with magnetic storage of ultra-cold neutrons and proton extraction. Nucl. Instrum. Methods Phys. Res. Sect. A 611, 176–180.
Matsumoto, T., et al., 2004. Studies of proximity focusing RICH with an aerogel radiator using flat-panel multi-anode PMTs (Hamamatsu H8500). Nucl. Instrum. Methods Phys. Res. Sect. A 521, 367–377.
Mattuck, R.D., 1992. A Guide to Feynman Diagrams in the Many-Body Problem, second ed. Dover Publications, Mineola, New York, p. 429.
Mausner, L.F., et al., 1992. Improved specific activity of reactor produced ^{117m}Sn with the Szilard–Chalmers process. Appl. Radiat. Isot. 43 (9), 1117–1122.
Mavunda, R.D., et al., 2004. Bremsstrahlung spectra from diagnostic X-rays. Radiat. Phys. Chem. 71, 991–992.
Maxwell, J.C., 1859. On the stability of the motion of Saturn's rings. Astron. Soc. Mon. Not. XIX, 297–304.
Maxwell, J.C., 1861a. On physical lines of force, Part 1. The theory of molecular vortices applied to magnetic phenomena. Phil. Mag. XXI, 161–175.
Maxwell, J.C., 1861b. On physical lines of force, Part 2. The theory of molecular vortices applied to electric currents. Phil. Mag. XXI, 281–291 and 338–348.
Maxwell, J.C., 1862a. On theories of the constitution of Saturn's rings. Edinb. R. Soc. Proc. IV, 99–101.
Maxwell, J.C., 1862b. On physical lines of force, Part 3. The theory of molecular vortices applied to statical electricity. Phil. Mag. XXIII, 12–24.
Maxwell, J.C., 1862c. On physical lines of force, Part 4. The theory of molecular vortices applied to action of magnetism on polarized light. Phil. Mag. XXIII, 85–95.
Maxwell, J.C., 1865. A dynamical theory of the electromagnetic field. Phil. Trans. R. Soc. CLV, 459–512.
Maxwell, J.C., 1868. On a method of making a direct comparison of electrostatic and electromagnetic force; with a note on the electromagnetic theory of light. Phil. Trans. R. Soc. CLVIII, 643–658.
Maxwell, J.C., 1873. A Treatise on Electricity and Magnetism. Macmillan & Co, London, p. 425.
Mayba, I.I., 1997. Ukranian physicist contributes to the discovery of X-rays. Mayo Clin. Proc. 72, 658.
McAllister, R.W., Hofstadter, R., 1956. Elastic scattering of 188-Mev electrons from the proton and the alpha particle. Phys. Rev. 102 (3), 851–856.
McDougall, I., Harrison, T.M., 1999. Geochronology and Thermochronology by the ^{40}Ar/^{39}Ar Method. Oxford University Press, New York, p. 269.
McGrath, J., et al., 2010. Detecting multi-hit events in a CdZnTe coplanar grid detector using pulse shape analysis: a method for improving background rejection in the COBRA $0\nu\beta\beta$ experiment. Nucl. Instrum. Methods Phys. Res. Sect. A 615, 57–61.
McKellar, A.R.W., 2010. High-resolution infrared spectroscopy with synchrotron sources. J. Molec. Spectros. 262, 1–10.
McLane, V., et al., 1988. Neutron cross sections. In: Neutron Cross Section Curves for $Z = 1–100$, vol. 2. Academic Press, San Diego.
McLean, A., April 5, 2002. The most versatile physicist of his generation. Science 296 (5565), 49–50.
McLean, I.D., Martensen, J., 2014. Specialized imaging. In: Marchiori, D. (Ed.), Clinical Imaging, third ed. Elsevier Science, Amsterdam, pp. 44–78.
McMillan, E., Abelson, P.H., 1940. Radioactive element 93. Phys. Rev. 57, 1185–1186.
McMillan, E.M., 1945. The synchrotron – a proposed high energy accelerator. Phys. Rev. 68, 143–144.
McMillan, E.M., 1951. The Transuranium Elements: Early History. Nobel Lecture, December 12, 1951. The Nobel Foundation.
McQuarrie, D.A., 1983. Quantum Chemistry. University Science Books, Mill Valley, p. 517.
McRobbie, D.W., 2014. Fundamentals of MR imaging. pp. 1–19, In: Anders Brahme (Ed.-in-Chief), Comprehensive Biomedical Physics, Magnetic Resonance Imaging and Spectroscopy, vol. 3. Elsevier.
Mederski, H.J., 1961. Determination of internal water by beta gauging technique. Soil Sci. 92, 143–146.
Mederski, H.J., Alles, W., 1968. Beta gauging leaf water status: influence of changing leaf characteristics. Plant Physiol. 43, 470–472.
Mehra, J., 1994. The Beat of a Different Drum. The Life and Science of Richard Feynman. Clarendon Press, Oxford.
Mehra, J., 2002. Richard Phillips Feynman, 11 May 1918–15 February 1988. Biogr. Mem. Fell. R. Soc. 48, 97–128.
Mehta, K., et al., 2003. Applicability study on existing dosimetry systems in high-power bremsstrahlung irradiation. Radiat. Phys. Chem. 68, 959–962.
Meitner, L., 1923. Das beta-Strahlenspektrum von UX_1 und seine Deutung. Z. Phys. 17, 54–66.
Meitner, L., 1924. Uber die Rolle der γ-strahlen beim Atomzerfall. Z. Phys. 26, 169–177.

Meitner, L., Philipp, K., 1933. Die bei Neutronenenregung auftretenden Elektronenbahnen. Naturwissenschaften 21, 286–287.
Meitner, L., Frisch, O.R., February 11, 1939. Disintegration of uranium by neutrons: a new type of nuclear reaction. Nature 143 (3615), 239–240.
Meitner, L., Strassmann, F., Hahn, O., 1938. Künstliche Emwandlungsprozesse bei Bestrahlung des Thoriums mit Neutronen; Auftreten isomer Reihen durch Abspaltung von α-Strahlen. Z. Phys. 109, 538–552.
Melhorn, W., 1998. 70 years of Auger spectroscopy, a historical perspective. J. Electron Spect. Relat. Phenom. 93 (1), 1–15.
Melhus, C.S., Rivard, M.J., 2006. Towards HDR ^{252}Cf brachytherapy: shielding assessment of a linear accelerator vault. Brachytherapy 5 (2), 83–84.
Mendeleev, D.I., 1864. The dependence between the properties of the atomic weights of the elements. J. Russ. Chem. Soc.
Mendeleev, D.I., 1869. The dependence between the properties of the atomic weights of the elements. Z. Chem. 12, 405–406.
Meneses, A.A.M., et al., 2012. Segmentation of synchrotron radiation micro-computed tomography images using energy minimization via graph cuts. Appl. Radiat. Isot. 70, 1284–1287.
Menn, W., et al., 2000. The absolue flux of protons and helium at the top of the atmosphere using IMAX. Astrophys. J. 533, 281–297.
Menviel, L., et al., 2012. Simulating atmospheric CO_2, 13C and the marine carbon cycle during the Last GlacialeInterglacial cycle: possible role for a deepening of the mean remineralization depth and an increase in the oceanic nutrient inventory. Quat. Sci. Rev. 56, 46–68.
Menzel, R.G., Smith, S.J., 1984. Soil fertility and plant nutrition, pp. 1–34. In: L'Annunziata, M.F., Legg, J.O. (Eds.), Isotopes and Radiation in Agricultural Sciences, Soil-Plant-Water Relationships, vol. 1. Academic Press, London, p. 292.
Mercer, J.A., et al., 2007. A non-intrusive neutron device for in situ detection of petroleum contamination in soil. Nucl. Instrum. Methods Phys. Res. Sect. B 263, 217–220.
Messier, M.D., 2006. Review of neutrino oscillation experiments. In: Flavor Phys. and CP Violation Conf., Vancouver 2002. hep-ex/0606013v1 5 June 2002.
Mettler, F.A., Guiberteau, M.J., 2005. Essentials of Nuclear Medicine Imaging. Saunders, p. 592.
Meyer, D.I., Perl, M.L., Glaser, D.A., 1957. Scattering of K^+ mesons by protons. Phys. Rev. 107, 279–282.
Michael Lederer, C., Shirley, V.S. (Eds.), 1978. Table of Isotopes, seventh ed. John Wiley & Sons, New York.
Michaudon, A., 2000. From alchemy to atoms. The making of plutonium. Los Alamos Sci. 26, 62–73.
Michel, R., et al., 2003. A comparison of 4 radionuclides conjugated to antibodies for single-cell kill. J. Nucl. Med. 44 (4), 632–640.
Midbon, M., March 24, 2000. A day without yesterday: Georges Lemaître & the big bang. Commonweal 18–19.
Miernik, K., et al., 2007a. First observation of β-delayed three-proton emission in ^{45}Fe. Phys. Rev. C 76, 041304(R).
Miernik, K., et al., 2007b. Optical time projection chamber for imaging nuclear decays. Nucl. Instrum. Methods. Phys. Res. Sect. A 581 (1–2), 194–197.
Miethe, A., 1924. Zuschriften und vorläufige Mitteilungen. Naturwissenschaften 12 (29), 597–598.
Miley, G.H., Sved, J., 1997. The IEC – a plasma-target-based neutron source. Appl. Radiat. Isot. 48 (10–12), 1557–1561.
Miller, R.B., 2003. Food irradiation using bremsstrahlung X-rays. Radiat. Phys. Chem. 68, 963–974.
Miller, R.B., 2005. Food Irradiation. Springer, Berlin, New York, London, p. 246.
Miller, J.F., et al., 1950. Acceleration of stripped C^{12} and C^{13} nuclei in the cyclotron. Phys. Rev. 80, 486.
Millikan, R.A., 1910. The isolation of an ion, a precision measurement of its charge, and the correction of Stoke's law. Science 32 (822), 436–448.
Millikan, R.A., 1911. The isolation of an ion, a precision measurement of its charge, and the correction of Stoke's law. Phys. Rev. (Ser. I) 32, 349–397.
Millikan, R.A., 1913. On the elementary electrical charge and the Avogadro constant. Phys. Rev. 2 (Ser. 2) 109–143.
Millikan, R.A., 1914. A direct determination of "*h*". Phys. Rev. 4, 73–75.
Millikan, R.A., 1916a. Einstein's photoelectric equation and contact electromotive force. Phys. Rev. 7, 18–32.
Millikan, R.A., 1916b. A direct photoelectric determination of Planck's "*h*". Phys. Rev. 7, 355–388.
Millikan, R.A., 1921. The distinction between intrinsic and spurious contact E.M.F.S. and the question of the absorption of radiation by metals in quanta. Phys. Rev. 18, 236–244.
Millikan, R.A., 1924. The electron and the light-quant from the experimental point of view. Nobel Lecture, May 23, 1924. In: Nobel Lectures, Physics 1922–1941 (1965). Elsevier Publishing, Amsterdam.
Millikan, R.A., Begeman, L., 1908. On the charge carried by the negative ion of an ionized gas. Phys. Rev. 26, 197–198.
Millikan, R.A., Boweb, I.S., 1926. High frequency rays of cosmic origin I. Sounding ballon observations at extreme altitudes. Phys. Rev. 27, 353–361.
Millikan, R.A., Cameron, G.H., 1928. High altitude tests on the graphical, directional, and spectral distributions of cosmic rays. Phys. Rev. 31, 163–173.
Millikan, R.A., Neher, H.V., 1935. The equatorial latitude effect in cosmic rays. Phys. Rev. 47, 205–208.
Millikan, R.A., 1950. The Autobiography of Robert A. Millikan. Prentice Hall, New Jersey, 311 p.
Milne, S., Hinde, R., 2005. Joseph Rotblat 1908–2005. Nature 437, 634.
Mirabito, L., 2010. The Compact Muon Solenoid detector. Nucl. Instrum. Methods Phys. Res. Sect. A 623, 345–347.
Mitchell, J.W., et al., 1996. Measurement of 0.25–3.2 GeV antiprotons in the cosmic radiation. Phys. Rev. Lett. 76 (17), 3057–3060.
Mitchell, E., et al., 1999. Demystifying the synchrotron trip: a first time user's guide. Structure 7 (5), R111–R121.
Miura, N., et al., 2010. Intermolecular vibrational study in liquid water and ice by using far infrared spectroscopy with synchrotron radiation of MIRRORCLE 20. Spectrochim. Acta A 77, 1048–1053.
Mizota, C., 2009. Temporal variations in the concentration and isotopic signature of ammonium- and nitrate–nitrogen in soils under a breeding colony of Black-tailed Gulls (*Larus crassirostris*) on Kabushima Island, northeastern Japan. Appl. Geochem. 24 (2), 328–332.
Moe, M.K., 1986. Double-beta decay in ^{82}Se, ^{128}Te, and ^{130}Te. AIP Conf. Proc. 150, 1012–1016.
Moe, M.K., Rosen, S.P., November 1989. Double-beta decay. Sci. Am. 48–55.

Molander, M., 2008. Quantitative Image Analysis of Cherenkov Light from Nuclear Fuel Assemblies. ISSN: 1401-5757. Uppsala University, p. 41. UPTEC F08 047.
Molins, R.A. (Ed.), 2001. Food Irradiation: Principles and Applications. John Wiley & Sons, New York.
Möller, P., et al., 1995. Nuclear ground-state masses and deformations. At. Data Nucl. Data Tables 59, 185−381.
Molnar, G., 2004. Handbook of Prompt Gamma Activation Analysis: With Neutron Beams. Springer, p. 423.
Monahan, F.J., et al., 2012. Authentication of grass-fed beef using bovine muscle, hair or urine. Trends Food Sci. Technol. 28, 69−76.
Mondragón, A., 1999. Manuel Sandoval Vallarta y la física en México. Ciencias 53, 32−39 (Enero-Marzo).
Monroe, C.R., Wineland, D.J., August 2008. Quantum computing with ions. Sci. Am. 64−71.
Montaruli, T., 2009. Neutrino astronomy in the ice. Nucl. Phys. B (Proc. Suppl.) 188, 239−244.
Mook, W.G., van der Plicht, J., 1999. Reporting ^{14}C activities and concentrations. Radiocarbon 41, 227−239.
Moore, W., 1989. Schrödinger, Life and Thought. Cambridge University Press, pp. 479−480.
Victor Hess. In: Moritz, C. (Ed.), 1963. Current Biography Yearbook 1963. H.W. Wilson Company, New York, pp. 180−182.
Mora, G., 2003. Temperature and salinity changes in the Caribbean sea during glacial/interglacial intervals as inferred from elemental and isotopic data. In: Geol. Soc. Amer Annual Meeting, Seattle, November 2−5, 2003.
Morozov, V.A., et al., 1998. Nuclear experimental techniques − three-dimensional delayed coincidence single-crystal scintillation time spectrometer. Instrum. Exp. Tech. 41 (5), 609.
Morozov, V.A., et al., 2002. High-sensitivity delayed-coincidence spectrometer to search for short-lived nuclear states. Nucl. Instrum. Methods Phys. Res. Sect. A 484, 225−232.
Morozov, V.A., et al., 2006. Measurement of the half-life for two ^{57}Fe excited states by a single-crystal scintillation time spectrometer. Nucl. Instrum. Methods Phys. Res. Sect. A 566, 448−451.
Morrison, J.W., 1960. Marquis wheat − a triumph of scientific endeavor. Agric. Hist. 34 (4), 182−188.
Morrissey, R.F., Herring, C.M., 2002. Radiation sterilization: past, present and future. Radiat. Phys. Chem. 63, 217−221.
Moscow News, 2006. Father of Russian genetics and selection of plants. Mosc. News 15. Tuesday, May 2, 2006.
Moseley, H.G.J., 1913. The high frequency spectra of the elements. Phil. Mag. 26 (1), 1024−1034.
Moseley, H.G.J., 1914. The high frequency spectra of the elements. Phil. Mag. 27 (2), 703−713.
Moskowitz, C., July 21, 2014. Proton spin mystery gains a new clue. Sci. Am. (On-line). http://www.scientificamerican.com/article/proton-spin-mystery-gains-a-new-clue1/.
Moussavi-Zarandi, A., 2008. Determination of beryllium by use of photonuclear activation techniques. Appl. Radiat. Isot. 66, 158−161.
Mozumder, A., et al., 1968. Theory of radiation chemistry. IX. Mode and structure of heavy particle tracks in water. Am. Chem. Soc. Ser. Adv. Chem. 1, 27.
Muheim, F., On behalf of the LHCb RICH Collaboration, 2011. The ring imaging Cherenkov detectors of the LHCb experiment. Nucl. Instrum. Methods Phys. Res. Sect. A 639 (1), 11−14.
Mukha, I., Schrieder, G., 2001. Two-proton radioactivity as a genuine three-body decay: the ^{19}Mg probe. Nucl. Phys. A 690, 280−283.
Mukoyama, T., Shimizu, S., 1974. The effect of pressure on orbital electron capture. Phys. Lett. 50A (4), 258−260.
Müller, A.R., et al., 2009. A low-temperature proton detector for a neutron lifetime experiment. Nucl. Instrum. Methods Phys. Res. Sect. A 611, 289−292.
Mundy, J.N., et al. (Eds.), 1983. Methods in Experimental Physics, vol. 21. Academic Press, New York and London, p. 504.
Munger, M.L., Peterson, R.J., 1978. Proton stripping reactions on ^{194}Pt, ^{196}Pt and ^{198}Pt. Nucl. Phys. A 303, 199−216.
Munn, A.J., et al., 2012. Energy and water use by invasive goats (*Capra hircus*) in an Australian rangeland, and a caution against using broad-scale allometry to predict species-specific requirements. Comp. Biochem. Physiol. Part A 161, 216−229.
Murai, K., et al., 2013. A large-scale mutant panel in wheat developed using heavy-ion beam mutagenesis and its application to genetic research. Nucl. Instrum. Methods Phys. Res. Sect. B 314, 59−62.
Murin, A.N., Nefedov, V.D., 1955. Concentration of artificial radioactive isotopes of groups IV and V by method of recoil atoms. Primen. Mechenykh At. Anal. Khim. Akad. Nauk SSSR 75−78. UCRL Trans.
Murray, R.L., 1993. Nuclear Energy. An Introduction to the Concepts, Systems, and Applications of Nuclear Processes, fourth ed. Pergamon Press, Oxford, p. 437.
Murray, R.L., 2001. Nuclear Energy. An Introduction to the Concepts, Systems, and Applications of Nuclear Processes, fifth ed. Elsevier Butterworth-Heinemann, Amsterdam, p. 490.
Murray, R.L., 2009. Nuclear Energy. An Introduction to the Concepts, Systems, and Applications of Nuclear Processes, sixth ed. Elsevier Publishers, Amsterdam, p. 497.
Murray, R.L., Holbert, K.E., 2015. Nuclear Energy. An Introduction to the Concepts, Systems, and Applications of Nuclear Processes, fifth ed. Elsevier Butterworth-Heinemann, Amsterdam, p. 513.
Mutterlose, J., et al., 2005. Mesozoic calcareous nanofossils − state of the art. Palaeontologische Z. 79, 113−133.
National Academy of Sciences, 1992. Oceanography in the Next Decade: Building New Partnerships. National Academy Press, Washington, DC, p. 202.
Naeem, H.S., 2012. A Comparison Radiation Analyzing Methods Between NAA and XRF. Lap Lambert Academic Publishing, p. 200.
Nagano, M., Watson, A.A., 2000. Observations and implications of the untrahigh-energy cosmic rays. Rev. Mod. Phys. 72, 689−732.
Nagaoka, H., 1903. On two constants A_1 and A_2 in the kinetic theory of gases. Nature 69, 79−80.
Nagaoka, H., 1904a. On a dynamical system illustrating the spectrum lines and the phenomena of radio-activity. Nature 69 (1791), 392−393.

Nagaoka, H., 1904b. LV. Kinetics of a system of particles illustrating the line and the band spectrum and the phenomena of radioactivity. Phil. Mag. Ser. 6 7 (41), 445–455.
Nagaoka, H., 1904c. A dynamical system illustrating the spectrum lines. Nature 70, 124–125.
Nagaoka, H., 1907. The eruption Kraktoa and the pulsation of the earth. Nature 76, 89–90.
Nagaoka, H., 1908a. Satellites of yellow and green lines of mercury. Nature 77, 581–582.
Nagaoka, H., 1908b. Zeeman effect in weak magnetic fields. Nature 79, 221.
Nagaoka, H., 1909. Difference between longitudinal and transversal Zeeman effects in helium lines. Nature 81, 188.
Nagaoka, H., 1910. Zeeman effect of the yellow mercury line λ 5770. Nature 83 (2114), 276–277.
Nagaoka, H., 1924. Isotopes of mercury and bismuth and the satellites of their spectral lines. Nature 114, 245.
Nagaoka, H., 1925a. Preliminary note on the transmutation of mercury into gold. Nature 116 (2097), 95–96.
Nagaoka, H., 1925b. Die Umwandlung von Quecksilber in Gold. Naturwissenschaften 13 (31), 682–684.
Nagaoka, H., 1925c. Note préliminaire sur la transmutation du mercure en or. J. Phys. Radium Ser. VI 6 (7), 209–216.
Nagaoka, H., 1932. Variations of latitude and great earthquakes. Nature 130, 541.
Nagaoka, H., Sugiura, Y., 1923a. Easy method of observing the Stark effect. Nature 111, 431.
Nagaoka, H., Sugiura, Y., 1923b. On the regularities of the spectral lines of iron and the atomic magnetic field. Nature 112, 359.
Nagaoka, H., Sugiura, Y., 1924. Spectroscopic evidence of isotopic elements. Nature 113, 532–534.
Nagaoka, H., et al., 1924. Isotopes of mercury and bismuth revealed in the satelites of their spectral lines. Nature 113 (2839), 459–460.
Nagaoka, H., Takamine, T., 1913. Anomalous Zeeman effect in the satellites of mercury lines. Nature 91, 660–661.
Nakahata, M., 2000. Neutrinos underground. Science 289 (5482), 1155–1156.
Nakayama, F.S., Ehrler, W.L., 1964. Beta ray gauging technique for measuring leaf water content changes and moisture status of plants. Plant Physiol. 39, 95–98.
Nakano, T., Nishijima, K., 1953. Charge independence for *V*-particles. Prog. Theor. Phys. 10, 581–582.
Nambu, Y., 1960a. Quasi-particles and gauge invariance in the theory of superconductivity. Phys. Rev. 117 (3), 648–662.
Nambu, Y., 1960b. Axial vector current conservation in weak interactions. Phys. Rev. Lett. 4 (7), 380–381.
Nambu, Y., 1966. A systematics of hadrons in subnuclear physics. In: de Shalit, A., Feshbach, H., Van Hove, L. (Eds.), Preludes in Theoretical Physics. North Holland, Amsterdam.
Nambu, Y., 1985. Quarks: Frontiers in Elementary Particle Physics. Wspc, p. 240.
Nambu, Y., 2008. Spontaneous Symmetry Breaking in Particle Physics: A Case of Cross Fertilization. Nobel Lecture, December 8, 2008, Nobelprize.org. Nobel Media AB 2014. http://www.nobelprize.org/nobel_prizes/physics/laureates/2008/nambu-lecture.html.
Nambu, Y., Jona-Lasinio, G., 1961a. Dynamical model of elementary particles based on an analogy with superconductivity. Phys. Rev. 122 (1), 345.
Nambu, Y., Jona-Lasinio, G., 1961b. Dynamical model of elementary particles based on an analogy with superconductivity. II. Phys. Rev. 124 (1), 246.
Nappi, E., 2011. Advances in charged particle identification techniques. Nucl. Instrum. Methods Phys. Res. Sect. A 628, 1–8.
Nasser, A.F., 2009. Drug Metabolism Handbook: Concepts and Applications. Wiley, New York, p. 1064.
Navarro, N., et al., 1997. Standardization of ^{234}Th by Cerenkov counting. Appl. Radiat. Isot. 48 (7), 949–952.
Ne'eman, Y., 1961. Derivation of strong interactions from a gauge invariance. Nucl. Phys. 26, 222–229.
Neddermeyer, S.H., Anderson, C.D., 1937. Note on the nature of cosmic-ray particles. Phys. Rev. 51, 884–890.
Neddermeyer, S.H., Anderson, C.D., 1938. Cosmic-ray particles of intermediate mass. Phys. Rev. 53, 88–89.
Newburgh, R., Peidle, J., Rueckner, W., 2006. Einstein, Perrin, and the reality of atoms: 1905 revisited. Am. J. Phys. 74 (6), 478–481.
New England Journal of Medicine, 2011. First results of phase 3 trial of RTS, S/AS01 malaria vaccine in African children. NEJM 365 (20), 1863–1875. http://www.nejm.org/doi/full/10.1056/NEJMoa1102287.
New York Times, October 23, 2011. Two Cheers for the Malaria Vaccine. http://www.nytimes.com/2011/10/24/opinion/two-cheers-for-the-malaria-vaccine.html?_r=0.
New York Times, 2012. http://www.nytimes.com/2011/11/22/science/rare-krypton-81-isotope-helps-track-water-in-ancient-nubian-aquifer.html?src=dayp.
Nico, J.S., et al., 2005. Measurement of the neutron lifetime by counting trapped protons in a cold neutron beam. Phys. Rev. C 71 (5), 055502.
Nicolaidou, R., Sirois, Y., 2015. The Higgs boson discovery and measurements. C. R. Phys. 16, 379–393.
Nielsen, D.R., Cassel, D.K., 1984. Soil water management, pp. 35–65. In: L'Annunziata, M.F., Legg, J.O. (Eds.), Isotopes and Radiation in Agricultural Sciences, Soil-Plant-Water Relationships, vol. 1. Academic Press, London, p. 292.
Nimz, G.J., 1998. Lithogenic and cosmogenic tracers in catchment hydrology, pp. 247–289. In: Kendall, C., McDonnell, J.J. (Eds.), Isotope Tracers in Catchment Hydrology. Elsevier Science, Amsterdam, p. 839.
Nimz, G.J., et al., 1993. Extremely low 36Cl.Cl values in deep ground water at Wawona, Yosemite National Park, California: evidence for rapid upwelling of deep crustal waters? Eos Trans. Am. Geophys. Union 74, 582.
Nimz, G.J., et al., 1997. 36Cl.Cl ratios in geothermal systems: preliminary measurements from the Coso field. Geotherm. Resour. Council Trans. 21, 211–217.
Nishijima, K., 1954. Some remarks on the even-odd rule. Prog. Theor. Phys. 12, 107–108.
Nishijima, K., 1956. On the theory of hyperons and heavy mesons. Fortschr. Phys. 4, 519–559.
Nishimura, K., On behalf of the Belle II Particle Identification Group, 2011. The time of propagation counter for Belle II. Nucl. Instrum. Methods Phys. Res. Sect. A 639 (1), 177–180.

Nishimura, K., et al., 2010. An imaging time-of-propagation system for charged particle identification at a super B factory. Nucl. Instrum. Methods Phys. Res. Sect. A 623, 297–299.
Nishina, Y., 1925. LVIII. On the L-absorption spectra of the elements from Sn(50) to W(74) and their relation to the atomic constitution. Phil. Mag. 49 (291), 521–537. Series 6.
Nishina, Y., 1928. The polarisation of Compton scattering according to Dirac's new relativistic dynamics. Nature 122 (3083), 843.
Nishina, Y., Rabi, I.I., 1928. Verh. Dtsch. Phys. Ges. 3, 6. Reihe 9.
Nishina, Y., Ray, B.B., 1926. Relative intensity of X-ray lines. Nature 117 (2934), 120–121.
Nishina, Y., et al., 1937. On the nature of cosmic ray particles. Phys. Rev. 52, 1198–1199.
Nishina, Y., et al., 1939a. On the mass of the mesotron. Phys. Rev. 55, 585–586.
Nishina, Y., et al., 1939b. Fission of thorium by neutrons. Nature 144, 547–548.
Nishina, Y., et al., 1940a. Cosmic-ray intensities and air masses. Phys. Rev. 57, 663.
Nishina, Y., et al., 1940b. Air mass effect on cosmic ray intensity. Phys. Rev. 57, 1050.
Nishina, Y., et al., 1940c. Fission products of uranium by fast neutrons. Phys. Rev. 58, 660.
Nishina, Y., et al., 1940d. Fission products of uranium produced by fast neutrons. Nature 146, 24.
Nishina, Y., et al., 1941a. Cosmic rays at a depth equivalent to 1400 meters of water. Phys. Rev. 59, 401.
Nishina, Y., et al., 1941b. Fission products of uranium by fast neutrons. Phys. Rev. 59, 323.
Nishina, Y., et al., 1942. Einige Spaltprodukte aus der Bestrahlung des Urans mit schnellen Neutronen. Z. Phys. 119 (3–4), 195–200.
Nishino, H., et al., 2009. High-speed charge-to-time converter ASIC for the Super-Kamiokande detector. Nucl. Instrum. Methods Phys. Res. Sect. A 610, 710–717.
NIST, 2011. The NIST Reference on Constants, Units, and Uncertainty. National Institute of Standards and Technology, Physical Measurement Laboratory, Gaithersburg, MD, USA. http://physics.nist.gov/cuu/Constants/.
NNDC, 2016a. National Nuclear Data Center, Brookhaven National Laboratory, "Q-value Calculator (QCalc)". http://www.nndc.bnl.gov/qcalc/.
NNDC, 2016b. National Nuclear Data Center, Brookhaven National Laboratory, "Nuclear Decay Data (NuDat)". Decay Radiation Data, NuDat 2.5. http://www.nndc.bnl.gov/nudat2/.
Nobel Foundation Staff (Ed.), 1964. Nobel Lectures, Chemistry, 1942–62. Elsevier Publishing, Amsterdam.
Nobel Lectures, Physics, 1922–1941, 1965. Elsevier Publishing, Amsterdam.
Nobel Foundation Staff (Ed.), 1964. Nobel Lectures, Physics, 1942–1962. Elsevier Publishing, Amsterdam.
Nobel Foundation Staff (Ed.), 1972. Nobel Lectures, Physics 1963–1970. Elsevier Publishing, Amsterdam.
Nobel Prize in Physics 1965 – Presentation Speech, 1965. Nobel Prize.org. Nobel Media AB 2014. http://www.nobelprize.org/nobel_prizes/physics/laureates/1965/press.html.
Nobel Foundation Staff (Ed.), 1967. Nobel Prize Lectures in Chemistry, 1901–1970. Elsevier Science, Amsterdam vol. 1, 1901–1921, vol. 2, 1922–1941, vol. 3, 1942–1962.
Noborio, K., et al., 2006. Confinement of ions in an inertial electrostatic confinement fusion (IECF) device and its influence on neutron production rate. Fusion Eng. Des. 81, 1701–1705.
Nogues, G., Rauschenbeutel, A., Osnaghi, S., Brune, M., Raimond, J.M., Haroche, S., 1999. Seeing a single photon without destroying it. Nature 400, 239–242.
Noor, A., Zakir, M., Rasyid, B., Maming, L'Annunziata, M.F., 1996. Cerenkov and liquid scintillation analysis of the triple label ^{86}Rb-^{35}S-^{33}P. Appl. Radiat. Isot. 47, 659–668.
Nordling, C., 1994. Presentation speech, the Nobel Prize in physics 1994. In: Ekspong, G. (Ed.), Nobel Lectures, Physics 1991–1995 (1997). World Scientific, Singapore.
Norman, H.C., et al., 2009. Stable carbon isotopes accurately predict diet selection by sheep fed mixtures of C_3 annual pastures and saltbush or C_4 perennial grasses. Livest. Sci. 121, 162–172.
Northcliffe, L.C., 1963. Passage of heavy ions through matter. Ann. Rev. Nucl. Sci. 13, 67–102.
Nour, S., et al., 2002. ^{234}Th analysis of marine sediments via extraction chromatography and liquid scintillation counting. Appl. Radiat. Isot. 57, 235–241.
Novick, A., Szilard, L., 1950. Experiments with the chemostat on spontaneous mutations of bacteria. Proc. Natl. Acad. Sci. U. S. A. 36, 708–719.
Novick, A., Szilard, L., 1951. Genetic mechanisms in bacteria and bacterial viruses. I. Experiments on spontaneous and chemically induced mutations of bacteria growing in the chemostat. Cold Spring Harb. Symp. Quant. Biol. 16, 337–343.
Novick, A., Szilard, L., 1952. Anti-mutagens. Nature 170, 926–927.
NRL, 1998. The Exposure of New Zealand Aircrew to Cosmic Radiation. National Radiation Laboratory, Christchurch, New Zealand, p. 6. Information Sheet 19, February 1998.
Nuclear Technology Review Update, 2005. International Atomic Energy Agency, Vienna, p. 36.
Nuclear Technology Review, 2004. International Atomic Energy Agency, Vienna, p. 94.
Nuclear Technology Review, 2006. International Atomic Energy Agency, Vienna, p. 127.
Nussenzveig, P., et al., 1993. Preparation of high-principal-quantum-number "circular" states of rubidium. Phys. Rev. A 48 (5), 3991–3994.
Nye, M.J., 2004. Blackett, Physics, War, and Politics in the Twentieth Century. Harvard University Press, Cambridge, p. 249.
O'Shaughnessy, C.M., et al., 2009. Measuring the neutron lifetime using magnetically trapped neutrons. Nucl. Instrum. Methods Phys. Res. Sect. A 611, 171–175.
Obregewitsch, R.P., et al., 1975. Estimating relative leaf water content with a simple beta gauge calibration. Agron. J. 67, 729–732.

Occhialini, G.P.S., Powell, C.F., 1947. Nuclear disintegrations produced by slow charged particles of small mass. Nature 159, 186–190.
Occhialini, G.P.S., Powell, C.F., 1948. Observations on the production of mesons by cosmic radiation. Nature 162, 168–173.
Ochiai, K., et al., 2007. Thin slit streaming experiment for ITER by using D-T neutron source. Fusion Eng. Des. 82, 2794–2798.
Ochsner, T.E., et al., 2013. State of the art in large-scale soil moisture monitoring. Soil Sci. Soc. Am. J. 77 (6), 1888–1919.
O'Leary, G.J., Incerti, M., 1993. A field comparison of three neutron moisture meters. Aust. J. Exp. Agric. 33, 59–69.
Ogando, J., 1993. Nuclear web gauging keeps pace with processor needs. Plast. Technol. 39, 46–49.
Ohm, H., et al., 1976. Beta-delayed neutron emission following the decay of ^{17}N. Nucl. Phys. A274, 45–52.
Ohm, H., et al., 1990. Delayed-coincidence measurement of subnanosecond lifetimes in fission fragments. In: The Spectroscopy of Heavy Nuclei 1989 Proceedings of the International Conference on the Spectroscopy of Heavy Nuclei, Agia Pelagia, Crete, June 25–July 1, 1989. Institute Physics Conference Series. No. 105. Adam Hilger, Ltd., Bristol, pp. 323–328.
Ohnishi, M., et al., 2007. Development of convergent D–D fusion neutron generator with large pulse current. Fusion Sci. Technol. 52, 1101–1104.
Ohno, T., 2013. Particle radiotherapy with carbon ion beams. EPMA J. 4, 9.
Ohshima, T., 2000. Test result of time-of-propagation Cherenkov counter. Nucl. Instrum. Methods Phys. Res. Sect. A 453, 331–335.
Oliphant, M.L., 1943. Classified Memo Submitted to the British Directorate of Atomic Energy. University of Birmingham Archive, UK.
Olive, K.A., 2014. Particle data group. Chin. Phys. C38, 090001. http://pdg.lbl.gov.
Olvera, A.M., Silva, M.J.J., 2009. Dr. Manuel Sandoval Vallarta, su vida, su trabajo y si invaluable aportación para eo desarroll de la ciencia an México. Bol. UPIITA (19), 11. http://www.boletin.uipiita.ipn.mx.
Olzem, J., et al., 2007. Cosmic-ray positron identification through bremsstrahlung conversion. Nucl. Phys. B (Proc. Suppl.) 173, 51–55.
Oms, J., 2004. Lifetime extraction from delayed-coincidence experiments by a direct deconvolution method. Nucl. Instrum. Methods Phys. Res. Sect. A 527, 598–603.
Ongena, J., van Oost, G., 2004. Energy for future centuries. Will fusion be an inexhaustible, safe and clean energy source? Fusion Sci. Technol. 45, 3–14.
Oganessian, Y., 2007. Heaviest nuclei from ^{48}Ca-induced reactions. J. Phys. G. Nucl. Part. Phys. 34 (4), R165.
Oganessian, Y., et al., 2010. Synthesis of a new element with atomic number Z = 117. Phys. Rev. Lett. 104, 142502.
Oseen, C.W., 1926. Presentation speech for the Nobel Prize in physics 1925 on December 10, 1926. In: Nobel Lectures. Physics 1922–1941 (1965). Elsevier Publishing Co., Amsterdam.
Otten, E.W., Weinheiner, C., 2008. Neutrino mass limit from tritium β decay. Rep. Prog. Phys. 71 (8), 6201.
Owens, A., 2012. Synchrotron light sources and radiation detection metrology. Nucl. Instrum. Methods Phys. Res. Sect. A 695, 1–12.
Perlman, I., Ghiorso, A., Seaborg, G.T., 1950. Systematics of alpha radioactivity. Phys. Rev. 77 (1), 26–50.
Perrier, C., Segré, E., 1937. Some chemical properties of element 43. J. Chem. Phys. 5 (9), 712–716.
Plaß, W.R., et al., 2008. Isobar separation by time-of-flight mass spectrometry for low-energy radioactive ion beam facilities. Nucl. Instrum. Methods Phys. Res. Sect. B 266 (19–20), 4560–4564.
Price, P.B., 1989. Heavy particle radioactivity. Ann. Rev. Nucl. Part. Sci. 39, 19–42.
Pringsheim, P., 1949. Fluorescence and Phosphorescence. Interscience Publishers, Inc., New York, London, p. 792.
Paces, J.B., et al., 2002. ^{234}U/^{238}U evidence for local recharge and patters of ground-water flow in the vicinity of Yucca Mountain, Nevada, USA. Appl. Geochem. 17, 751–779.
Pachoa, A.S., Steinhäusler, F., 2010. Cosmic radiation, including its effects on airline crew, frequent flyers, and space travel. In: Radioactivity in the Environment, vol. 17. Elsevier, Amsterdam, pp. 87–121, p. 244.
Panofsky, W.K.H., et al., 1951. The gamma-ray spectrum resulting from capture of negative π^- mesons in hydrogen and deuterium. Phys. Rev. 81, 565–574.
Papazoglou, P., 1998. (Ph.D. thesis). University of Frankfurt.
Papazoglou, P., et al., 1999. Nuclei in a chiral SU(3) model. Phys. Rev. C 59, 411.
Papiz, M.Z., Winter, G., 2010. Biomolecular X-ray crystallography, structure determination methods. In: John Lindon (Ed.-in-Chief), Encyclopedia of Spectroscopy and Spectrometry, Elsevier, Amsterdam, pp. 185–193.
Park, Y.J., et al., 2009. Performance characteristics of a prompt gamma-ray activation analysis (PGAA) system equipped with a new compact D–D neutron generator. Nucl. Instrum. Methods Phys. Res. Sect. A 606, 243–247.
Park, M., et al., 2010. Data acquisition system implemented with various platforms for KSTAR diagnostic systems. Fusion Eng. Des. 85, 350–355.
Parker, R.P., Elrick, R.H., 1970. Cerenkov counting as a means of assaying β-emitting radionuclides. In: Bransome Jr., E.D. (Ed.), The Current Status of Liquid Scintillation Counting. Grune and Stratton, New York, London, pp. 110–122.
Pasachoff, N., 1996. Marie Curie and the Science of Radioactivity. Oxford University Press, New York, Oxford, p. 112.
Pasachoff, N., 2005. Ernest Rutherford: Father of Nuclear Science. Enslow Publishers, Berkeley Heights, NJ, p. 128.
Passo Jr., C.J., Cook, G.T., 1994. Handbook of Environmental Liquid Scintillation Spectrometry. A Compilation of Theory and Methods. Packard Instrument Company, Meriden, CT.
Patel, S.B., 1991. Nuclear Physics, an Introduction. John Wiley & Sons, New York, p. 346.
Patil, B.J., et al., 2010a. Measurement of angulare distribution of neutron flux for the 6 MeV race-track microtron based pulsed neutron source. Appl. Radiat. Isot. 68, 1743–1745.
Patil, B.J., et al., 2010b. Simulation of e–γ–n targets by FLUKA and measurement of neutron flux at various angles for accelerator based neutron source. An. Nucl. Energy 37, 1369–1377.
Patrono, C., et al., 2011. Radioimmunoassay in Basic and Clinical Pharmacology. Springer, p. 611.

Patyk, Z., et al., 1997. Masses and shapes of heaviest nuclei. Nucl. Phys. A 626 (1−2), 337−340.
Paul, W., Steinwedel, H., 1955. Interaction of electrons with matter. In: Siegbahn, K. (Ed.), Beta- and Gamma-ray Spectroscopy. North-Holland, Amsterdam.
Paul, M., et al., 1986. A new ^{36}Cl hydrologic model and ^{36}Cl systematics in the Jordan River/Dead Sea system. Nature 321, 511−515.
Paul, S., 2009. The puzzle of neutron lifetime. Nucl. Instrum. Methods Phys. Res. Sect. A 611, 157−166.
Pauli, W., 1924. Zur Frage der theoretischen Deutung der Satelliten eineger Spektrallinien und ihrer Beeinflussung durch magnetische Felder. Naturwissenschaften 12, 741−743.
Pauli, W., 1925. Über den Zusammenhang des Abschlusses der Electronengruppen in Atom der Komplexstruktur der Spectren. Z. Phys. 31, 765−783.
Pauli, W., 1946. Exclusion principle and quantum mechanics. Nobel Lecture, December 13, 1946. In: Nobel Foundation Staff (Ed.), Nobel Lectures, Physics, 1942−62 (1964). Elsevier Publishing, Amsterdam.
Pavia, D.L., et al., 2014. Introduction to Spectroscopy, fifth ed. Cengage Learning, p. 748.
Peeters, A., et al., 2010. How costly is particle therapy? Cost analysis of external beam radiotherapy with carbon-ions, protons and photons. Radiother. Oncol. 95 (1), 45−53.
Penney, L., 1967. Homo Jehangir Bhabha 1909−1966. Biogr. Mem. Fellows R. Soc. 13, 35−55.
Penzias, A.A., Wilson, R.W., 1965. A measurement of excess antenna temperature at 4080 Mc/s. Astrophys. J. 142, 419−421.
Perkins, D.H., 1947. Nuclear disintegrations by meson capture. Nature 159, 126.
Perkins, D.H., 1972. Review talk on experimental neutrino physics. In: Proc.16th Int. Conf. on High-Energy Phys. (Chicago 1972), vol. 4, p. 189.
Perl, M.L., et al., 1975. Evidence for anomalous lepton production in e^+e^- annihilation. Phys. Rev. Lett. 35 (22), 1489−1492.
Perlman, I., Ypsilantis, T.J., 1950a. Consistency of Nuclear Radii of Even-Even Nuclei from Alpha-Decay Theory. United States Atomic Energy Commission Report UCRL-613, February 27, 1950, p. 15.
Perlman, I., Ypsilantis, T.J., 1950b. Consistency of nuclear radii of even-even nuclei from alpha-decay theory. Phys. Rev. 79, 30−34. http://prola.aps.org/abstract/PR/v79/i1/p30_1.
Perlmutter, A., 2000. Marietta Blau's Work after World War II. Manuscript Biography No. MB 2001-251. American Institute of Physics, College Park, Maryland, p. 44.
Perrier, C., Segrè, E., 1947. Technitium: the element of atomic number 43. Nature 159 (4027), 24.
Perrin, J., December 30, 1895. New Experiments on the Kathode Rays. Paris Academy of Sciences.
Perrin, J., 1896. New experiments on the kathode rays. Nature 53 (1370), 298−299.
Perrin, J., 1909. Mouvement Brownian et réalité moléculaire. Ann. Chim. Phys. 18 (8), 5−114.
Perrin, J., 1910. Brownian Movement and Molecular Reality. Translated by F. Soddy. Taylor & Francis, London, p. 114.
Perrin, J., 2010. Brownian Movement and Molecular Reality. Translated by F. Soddy. Dover Publications, Mineola, New York, p. 114.
Perrin, J., 2014. Brownian Movement and Molecular Reality. Translated by F. Soddy. Nabu Press, p. 114.
Perrino, R., et al., 2001. Performances in the aerogel threshold Cherenkov counter for the Jefferson Lab Hall A spectrometers in the 1-4 GeV/*c* momentum range. Nucl. Instrum. Methods Phys. Res. Sect. A 457, 571−580.
Perry, M.F., 2007. Remembering the oil-drop experiment. Phys. Today 60 (5), 56−60.
Pestotnik, R., et al., 2002. Investigation of ^{90}Sr detection with Cherenkov radiation in silica aerogels. In: Proceedings of IEEE Symposium on Nuclear Science and Medical Imaging Including Nuclear Power Systems. November 4−9, 2001, San Diego. IEEE, Piscataway, NJ.
Pestotnik, R., et al., 2004. Proximity focusing RICH with flat panel PMT (Hamamatsu H8500) as photon detector and aerogel radiator. Nucl. Instrum. Methods Phys. Res. Sect. A 525, 158−162.
Petersen, A.L., et al., 2012. Liposome imaging agents in personalized medicine. Adv. Drug Deliv. Rev. 64, 1417−1435.
Petkov, P., et al., 2003. Lifetime determination in delayed-coincidence experiments using the differential decay-curve approach. Nucl. Instrum. Methods Phys. Res. Sect. A 500, 379−385.
Pevsner, A., et al., 1961. Evidence for a three-pion resonance near 550 Mev. Phys. Rev. Lett. 7 (11), 421−423.
Pfützner, M., 2013. Particle radioactivity of exotic nuclei. Phys. Scr. T152, 014014 (14 pp.).
Pfützner, M., et al., 2002. First evidence for the tw-proton decay of ^{45}Fe. Eur. Phys. J. A 14, 279−285.
Pfützner, M., et al., 2012. Radioactive decays at limits of nuclear stability. Rev. Mod. Phys. 84, 567−619.
Phanchaisri, B., et al., 2012. Expression of OsSPY and 14-3-3 genes involved in plant height variations of ion-beam-induced KDML 105 rice mutants. Mutat. Res. Fund. Mol. Mech. Mutat. 734, 56−61.
Phillips, W.D., 1989. Laser cooling and trapping of neutral atoms. Rev. Mod. Phys. 70 (3), 721−741.
Piccioni, O., 1950. On the secondary particles of local penetrating showers. Phys. Rev. 77, 6−10.
Pichler, G.P., et al., 2013. A critical analysis of whole body bioimpedance spectroscopy (BIS) for the estimation of body compartments in health and disease. Med. Eng. Phys. 35, 616−625.
Pichlmaier, A., et al., 2000. MAMBO II: neutron lifetime measurement with storage of ultra-cold neutrons. Nucl. Instrum. Methods Phys. Res. Sect. A 440, 517−521.
Pickering, W.H., 1991. Biography: Carl David Anderson, September 3, 1905−January 11, 1991. California Institute of Technology, Institute Archives, Pasadena, p. 16.
Piefer, G.R., et al., 2005. Design of an ion source for ^{3}He fusion in a low pressure IEC device. Fusion Sci. Technol. 47, 1255−1259.
Piel, A., 2009. Famous Scholars from Kiel: Hans Geiger. University of Kiel, Kiel, Germany. http://www.uni-kiel.de/ps/cgi-bin/fo-bio.php?nid=geiger&lang=e.

Pierre Auger Collaboration, 2010. A study of the effect of molecular and aerosol conditions in the atmosphere on air fluorescence measurements at the Pierre Auger Observatory. Astropart. Phys. 33, 108–129.

Pietzsch, J., 2014. The Attraction of Spin. The Nobel Prize in Physics 1952-Speed Read. Nobelprize.org. Nobel Media AB 2014. http://www.nobelprize.org/nobel_prizes/physics/laureates/1952/speedread.html.

Pinto da Cunha, J., et al., 2000. On the reconstruction of Cherenkov rings from aerogel radiators. Nucl. Instrum. Methods Phys. Res. Sect. A 452, 401–421.

Pleijel, H., 1933. Presentation speech, December 10, 1933. The Nobel Prize in physics 1932 and 1933. In: Nobel Lectures, Physics 1922–1941 (1965). Elsevier Publishing, Amsterdam.

Pleijel, H., 1935. Presentation speech, December 10, 1935. The Nobel Prize in physics 1935. In: Nobel Lectures, Physics 1922–1941 (1965). Elsevier Publishing, Amsterdam.

Pleijel, H., 1936. Presentation speech, December 10, 1936. The Nobel Prize in physics 1936. In: Nobel Lectures, Physics 1922–1941 (1965). Elsevier Publishing, Amsterdam.

Poelz, G., 1986. Aerogel Cherenkov counters at DESY. Nucl. Instrum. Methods Phys. Res. Sect. A 248, 118–129.

Poenaru, D.N., et al., 1985. Atomic nuclei decay modes by spontaneous emission of heavy ions. Phys. Rev. C 32, 572–581.

Poenaru, D.N., et al., 1986. Calculated half-lives and kinetic energies for spontaneous emission of heavy ions from nuclei. At. Data Nucl. Data Tables 34, 423–538.

Poenaru, D.N., et al., 1987. Cold fission as heavy ion emission. Z. Phys. A 328 (3), 309–314.

Poenaru, D.N., et al., 1989. Inertia and fission paths in a wide range of mass asymmetry. Z. Phys. A 333 (3), 291–298.

Poirier, R.K., et al., 2012. Central arctic paleoceanography for the last 50 kyr based on ostracode faunal assemblages. Mar. Micropaleontol. 88–89, 65–76.

Pollock, H.C., 1983. The discovery of synchrotron radiation. Am. J. Phys. 51 (3), 278–280. http://dx.doi.org/10.1119/1.13289.

Pomorski, M., et al., 2011. β-delayed proton emission branches in ^{43}Cr. Phys. Rev. C 83, 014306.

Potgieter, M.S., 2008. Solar cycle variations and cosmic rays. J. At. Solar Terr. Phys. 70, 207–218.

Potgieter, M.S., 2010. The dynamic heliosphere, solar activity, and cosmic rays. Adv. Space Res. 46, 402–412.

Potter, K.M., 1994. In: CAN-CERN Accelerator School: 5th General Accelerator Physics Course, Jyväskylä, Finland, September 7–18, 1992, pp. 117–129. http://dx.doi.org/10.5170/CERN-1994-001.117.

Povinec, P., Sanchez-Cabeza, J.A. (Eds.), 2006. International Conference on Isotopes and Environmental Studies. Aquatic Forum 2004, October 25–29, Monaca (Radioactivity in the Environment), vol. 8. Elsevier Science, Amsterdam, p. 660.

Povinec, P.P., et al., 2012. Marine radioactivity analysis, pp. 769–832. In: L'Annunziata, M.F. (Ed.), Handbook of Radioactivity Analysis, third ed. Elsevier, Amsterdam, p. 1379.

Povinec, P.P., et al., 2013. Distribution of tritium and ^{137}Cs in south Indian ocean waters – implications of water transport processes. In: Isotopes in Hydrology, Marine Ecosystems and Climate Change Studies. Proceedings of an International Symposium, Monaco, 27 March–1 April 2011, vol. 1. International Atomic Energy Agency, Vienna, pp. 89–95.

Powell, C.F., 1950. The cosmic radiation. Nobel lecture at Stockholm, Sweden on December 11, 1950. In: Nobel Foundation Staff (Ed.), Nobel Lectures, Physics, 1942–62 (1964). Elsevier Publishing, Amsterdam.

Powell, C.F., 1987. Cecil Powell, Fragments of Autobiography. University of Bristol, p. 28.

Powell, C.F., Rosenblum, S., 1948. A new method for the determination of the mass of mesons. Nature 161, 473–475.

Powers, P.N., 1938. The magnetic scattering of neutrons. Phys. Rev. 54 (10), 827–838.

Powsner, R.A., Powsner, E.R., 2006. Essentials of Nuclear Medicine Physics, second ed. Blackwell Publishing, p. 224.

Price, P.B., 1994. Recent advances in cluster radioactivities. In: Scheid, W., Sandulesco, A. (Eds.), Frontier Topics in Nuclear Physics. Plenum Press, New York, p. 510.

Pullen, B.P., 1986. Cerenkov counting of ^{40}K in KCl using a liquid scintillation spectrometer. J. Chem. Educ. 63, 971.

Puluj, J., 1883. Strahlende Elektroden-Materie und der sogenannte vierte Aggregatzustand. Druck und Verlag von Carl Gerold's Sohn, Vienna, p. 86.

Puluj, J., 1889. Radiant electrode matter and the so-called fourth state. In: Physical Memoirs Selectred and translater from Foreign Sources. Physical Society of London, vol. 1. Taylor and Francis, London, pp. 233–331. Part 2.

Puluj, J., 1896. On kathode rays. Proc. Phys. Soc. London 14, 178.

Puluj, J., 1915. Ukraina und ihre Internationale Politische Bedeutung. Druck von Adolf Holzhausen, Vienna, p. 41.

Quinn, S., 1996. Marie Curie: A Life. Addison Wesley, 509 pp.

Raghaven, R.S., 1976. Inverse β decay of ^{115}In $\rightarrow$ ^{115}Sn*: a new possibility for detecting solar neutrinos from the proton-proton reaction. Phys. Rev. Lett. 37, 259–262.

Rambalde, E., et al., 2013. SPECT/CT with ^{99m}Tc-MDP in a patient with monostotic fibrous dysplasia of the rib. Rev. Esp. Med. Nucl. Imagen Mol. 32 (2), 126–127.

Rykaczewski, 2008. Holifield Radioactive Ion Beam Facility for the US Department of Energy. https://www.phy.ornl.gov/hribf/app/decay/neutrons.shtml.

Rogers, A., 1979. Techniques of Autoradiography. Elsevier/North Holland Biomedical Press, Amsterdam.

Rabi, I.I., et al., 1938. A new method of measuring nuclear magnetic moment. Phys. Rev. 53, 318.

Rabi, I.I., et al., 1939. The molecular beam resonance method for measuring nuclear magnetic moments. Phys. Rev. 55, 526–535.

Rabinowitch, E., 1964. Editorial. Bell Atomic Scientists. October, 16–20.

Rachinhas, P.J.B.M., et al., 2000. Simulation and experimental results for the detection of conversion electrons with gas proportional scintillation counters. Nucl. Instrum. Methods Phys. Res. Sect. A 441, 468–478.

Radchenko, V.M., et al., 2000. Curium-248 standard neutron source. Appl. Radiat. Isot. 53, 833–835.

Radel, R.F., et al., 2007. Detection of highly enriched uranium using a pulsed D–D fusion source. Fusion Sci. Technol. 52, 1087–1091.

Rahaman, S., et al., 2008. Q values of the ^{76}Ge and ^{100}Mo double-beta decays. Phys. Lett. B 662, 111–116.

Rahmani, F., Shahriari, M., 2010. Hybrid photoneutron source optimization for electron accelerator-based BNCT. Nucl. Instrum. Methods Phys. Res. Sect. A 618, 48–53.

Rainwater, J., 1950. Nuclear energy level argument for a spheroidal nuclear model. Phys. Rev. 79, 432–434.

Ramesh, A., Subramanian, M.S., 1997. Trace determination of tellurium using liquid scintillation and Cerenkov counting. Analyst 122, 1605–1610.

Ramsay, W., Soddy, F., 1903. Experiments in radioactivity, and the production of helium from radium. Proc. R. Soc. 72, 204–207.

Ramsey, N.F., 1993. I. I. Rabi 1898–1988. A Biographical Memoir. National Academy of Sciences, Washington, DC.

Ramsey, N.F., 2008. Polykarp Kusch 1911–1993. A Niographical Memoir. National Academy of Sciences, Washington, DC.

Rankin, N.J., et al., 2014. The emergence of proton nuclear magnetic resonance metabolomics in the cardiovascular arena as viewed from a clinical perspective. Atherosclerosis 237, 287–300.

Rant, J., et al., 2006. Neutron radiography examination of objects belonging to the cultural heritage. Appl. Radiat. Isot. 64, 7–12.

Ratcliff, B.N., 2003. Imaging rings in ring imaging Cherenkov counters. Nucl. Instrum. Methods Phys. Res. Sect. A 502, 211–221.

Ray, A., et al., 1999. Observation of large change of ^{7}Be decay rate in Au and Al_2O_3 and its implications. Phys. Lett. B 455, 69–76.

Ray, A., et al., 2009. Observation of enhanced orbital electron-capture nuclear decay rate in a compact medium. Phys. Lett. B 679, 106–110.

Ražem, D., Katušin-Ražem, B., 2008. The effects of irradiation on controlled drug delivery/controlled drug release systems. Rad. Phys. Chem. 77, 288–344.

Reguera, B., et al., 2013. Toxic microalgal blooms: what can nuclear techniques provide for their management? In: Isotopes in Hydrology, Marine Ecosystems and Climate Change Studies. Proceedings of an International Symposium, Monaco, 27 March–1 April 2011, vol. 1. International Atomic Energy Agency, Vienna, pp. 483–491.

Reid, A., 1928. The diffraction of cathode rays by thin celluloid films. Proc. R. Soc. London A119, 663–668.

Reines, F., 1960. Neutrino interactions. Ann. Rev. Nucl. Sci. 10, 1–26.

Reines, F., 1963. Neutrinos, old and new. Science 141, 778–783.

Reines, F., 1979. The early days of experimental neutrino physics. Science 203, 11–16.

Reines, F., 1982. Neutrinos to 1960. Personal recollections. J. Phys. 43 (12), C8–C237.

Reines, F., 1994. 40 years of neutrino physics. Prog. Part. Nucl. Phys. 32, 1–12.

Reines, F., 1995. In: Barany, A. (Ed.), The Neutrino: From Poltergeist to Particle. Nobel Lecture, December 8, 1995. The Nobel Prizes 1999 Les Prix Nobel: Nobel Prizes, Presentations, Biographies, and Lectures. Almquiest & Wiksell International, Stockholm.

Reines, F., Cowen Jr., C.L., 1953. Detection of the free neutrino. Phys. Rev. Lett. 92, 330.

Reines, F., Cowen Jr., C.L., 1956. The neutrino. Nature 178, 446–449.

Reines, F., Cowen Jr., C.L., 1957. Neutrino physics. Phys. Today 10 (8), 12–18.

Reines, F., Cowen Jr., C.L., Harrison, F.B., McGuire, A.D., Kruse, H.W., 1960. Detection of the free antineutrino. Phys. Rev. 117 (1), 159–173.

Resnik, D.B., 2012. Editorial: Plagiarism: words and ideas. Account. Res. 19 (5), 269–272.

Reynolds, G.T., Harrison, F.B., Salvini, G., 1950. Liquid scintillation counters. Phys. Rev. 78 (4), 488.

Rhodes, R., 1986. The Making of the Atomic Bomb. Touchstone/Simon & Schuster, New York, p. 886.

Rhodes, R., March 28, 1999. Atomic Physicist, Enrico Fermi. Time.

Ridgway, J.P., 2010. Cardiovascular magnetic resonance physics for clinicians, part 1. J. Cardiovasc. Magn. Reson. 12, 71.

Rife, P., 1999. Lise Meitner and the Dawn of the Nuclear Age. Birkhäuser, Boston, p. 432.

Rigden, J.S., 1987. Rabi: Scientist & Citizen. Alfred P. Sloan Foundation series. Basic Books, p. 302.

Riordan, M., 1992. The discovery of quarks. Sci. New Ser. 256 (5061), 1287–1293.

Ritson, D.M., 1961. Techniques in High Energy Physics. Interscience, New York.

Rizzutto, M.A., et al., 2014. External-PIXE analysis for the study of pigments from a painting from the Museum of Contemporary Art. Nucl. Instrum. Methods Phys. Res. Sect. B 332, 411–414.

Roberts, A., 1960a. Čerenkov detector accurately measuring velocity and direction over a wide range. Rev. Sci. Instrum. 31, 579–580.

Roberts, A., 1960b. A new type of Čerenkov detector for the accurate measurement of particle velocity and direction. Nucl. Instrum. Methods 9, 55–60.

Robson, J.M., 1950a. Radioactive decay of the neutron. Phys. Rev. 77, 747A.

Robson, J.M., 1950b. Radioactive decay of the neutron. Phys. Rev. 78, 311–312.

Rochester, G.D., Butler, C.C., 1947. Evidence for the existence of new unstable elementary particles. Nature 160 (4077), 855–857.

Roeckl, E., Mukha, I., 2013. Q values of radioactive decay: examples from nuclear physics and related fields. Int. J. Mass Spectr. 349–350, 47–56.

Roentgen, W.C., 1895. Über eine neue Art von Strahlen. Sitzungsber. Würzbg. Phys. Med. Ges. 9, 132–141.

Roentgen, W.C., 1896. On a new kind of rays. Nature 53 (1369), 274–276.

Rohrlich, F., Carlson, B.C., 1954. Positron-electron differences in energy loss and multiple scattering. Phys. Rev. 93, 38–44.

Rollion-Bard, C., et al., 2011. Boron isotopes as pH proxy: a new look at boron speciation in deep-sea corals using 11B MAS NMR and EELS. Geochim. Cosmochim. Acta 75, 1003–1012.

Ronen, Y., 1997. Systematic behaviour in cluster radioactivity. Ann. Nucl. Energy 24 (2), 161–164.
Ronen, Y., 2004. Indications of the validity of the liquid drop model for spontaneous fission half-lives. Ann. Nucl. Energy 31, 323–329.
Ronzhin, A., et al., 2010. Development of a 10 ps level time of flight system in the Fermilab Test Beam Facility. Nucl. Instrum. Methods Phys. Res. Sect. A 623, 931–941.
Rose, H., Jones, G.A., 1984. A new kind of natural radioactivity. Nature 307, 245.
Rosenberg, J.L., 2004. The contributions of James Franck to photosynthesis research: a tribute. Photosynth. Res. 80, 71–76.
Rosner, R., Strohmaier, B., 2003. Marietta Blau – Sterne der Zertrümmerung. Biographie einer Wegbereiterin der modernen Teilchenphysik. Böhlau Verlag, Vienna, p. 192.
Rosolem, R., et al., 2013. The effect of atmospheric water vapor on neutron count in the cosmic-ray soil moisture observing system. J. Hydrometeorol. 14, 1659–1671. http://dx.doi.org/10.1175/JHM-D-12-0120.1.
Rossi, B., Hall, D.B., 1941. Variation of the rate of decay of mesotrons with momentum. Phys. Rev. 59, 223–228.
Rost, B., et al., 2008. Sensitivity of phytoplankton to future changes in ocean carbonate chemistry: current knowledge, contradictions and research directions. Mar. Ecol. Prog. Ser. 373, 227–237.
Rotblat, J., 1939. Emission of neutrons accompanying the fission of uranium nuclei. Nature 143 (3629), 852.
Rotblat, J., 1949. Some applications of radioactive tracers in medicine. Br. Sci. News 201–204.
Rotblat, J., 1955a. The 15 MeV linear acceleratorat St. Bartholomew's hospital. Nature 175, 745–747.
Rotblat, J., 1955b. The hydrogen-uranium bomb. Bull. At. Sci. 11 (May 1955), 171–172, 177.
Rotblat, J., 1962. Science and World Affairs: A History of the Pugwash Conferences. Dawsons of Pall Mall, p. 92.
Rotblat, J., 1997. Reminiscences on the 40th anniversary of the Rissell-Einstein Manifesto. In: Towards a Nuclear-weapoin-free World. Proceedings of the Forty-fifth Pugwash Conference on Science and World Affairs, Hiroshima, Japan, July 23–29, 1995, pp. 225–230.
Rotblat, J., Ikeda, D., 2006. A Quest for Global Peace: Rotblat and Ikeda on War, Ethics and the Nuclear Threat. I. B. Tauris, p. 180.
Rowe, D.J., Wood, J.L., 2010. Fundamentals of Nuclear Models. World Scientific, Hackensack, NJ, p. 676.
Roy, R.R., Reed, R.D., 1968. Interactions of Photons and Leptons with Matter. Academic Press, New York.
Royer, G., 2008. On the coefficients of the liquid drop model mass formulae and nuclear radii. Nucl. Phys. A 807 (3–4), 105–118.
Rubbia, C., McIntyre, P., Cline, D., 1977. In: Faissner, H., Reithler, H., Zerwas, P. (Eds.), Proceedings of the International Neutrino Conference, p. 683. Aachen, 1976, Viewweg, Braunschweig.
Rubbia, C., 1984. Experimental Observation of the Internediate Vector Bosons W^+, W^- and Z^0. Nobelprize.org. Nobel Media AB 2014. http://www.nobelprize.org/nobel_prizes/physics/laureates/1984/rubbia-lecture.html.
Rucker, T.L., 1991. Calculational method for the resolution of ^{90}Sr and ^{89}Sr counts from Cerenkov and liquid scintillation counting. In: Ross, H., Noakes, J.E., Spaulding, J.D. (Eds.), Liquid Scintillation Counting and Organic Scintillators. Lewis Publishers, Chelsea, MI, pp. 529–535.
Russell, A.S., 1925. Transformation of mercury into gold. Nature 116 (2913), 312.
Russell, B., 1956. The Autobiography of Bertrand Russell 1914–1944. Little, Brown Publishers.
Rutherford, E., 1899. Uranium radiation and the electrical conduction produced by it. Phil. Mag. Ser. 47 (5), 109–163.
Rutherford, E., 1900. A radioactive substance emitted from thorium compounds. Phil. Mag. Ser. 49 (5), 1–14.
Rutherford, E., 1903. The magnetic and electric deviation of the easily absorbed rays from radium. Phil. Mag. Ser. 6, 177–187.
Rutherford, E., 1905a. Charge carried by the α rays from radium. Nature 71 (1844), 413–414.
Rutherford, E., 1905b. Charge carried by the α and β rays of radium. Phil. Mag. Ser. 6 10 (56), 193–208.
Rutherford, E., 1906. Retardation of the alpha particle from radium in passing through matter. Phil. Mag. Ser. 12 (6), 134–146.
Rutherford, E., 1911. The scattering of α and β particles by matter and the structure of the atom. Phil. Mag. Ser. 21 (6), 669–688.
Rutherford, E., 1913. The structure of the atom. Nature 92 (2302), 423.
Rutherford, E., 1919. Collision of α-particles with light atoms. Nature (London) 103, 415–418.
Rutherford, E., 1920a. Bakerian Lecture: nuclear constitution of atoms. Proc. R. Soc. London 97A, 374–401.
Rutherford, E., 1920b. Nuclear constitution of atoms. Proc. R. Soc. London 97A, 374–401.
Rutherford, E., 1927. Structure of the radioactive atom and origin of the alpha rays. Phil. Mag. 4 (22), 580–605.
Rutherford, E., 1929. Annual address to the Royal Society. Proc. R. Soc. London 122A, 1–23.
Rutherford, E., 1936. The development of the theory of atomic structure. In: Needham, J., Pagel, W. (Eds.), Background to Modern Science. Macmillan Company, New York, pp. 61–74.
Rutherford, E., Geiger, H., 1908a. The charge and nature of the alpha particle. Proc. R. Soc. A 81, 162–173.
Rutherford, E., Geiger, H., 1908b. An electrical method of counting the number of α-particles from radioactive substances. Proc. R. Soc. A 81, 141–161.
Rutherford, E., Soddy, F., 1902. The cause and nature of radioactivity. Phil. Mag. 4, 370–396.
Rutz, K., et al., 1997. Superheavy nuclei in self-consistent nuclear calculations. Phy. Rev. C 56, 238.
Snow, W.M., et al., 2000. A measurement of the neutron lifetime by counting trapped protons. Nucl. Instrum. Methods Phys. Res. Sect. A 440 (3), 528–534.
Stromholm, D., Svedberg, T., 1909a. Untersuchungen uber die chemie der radioactiven grundstoffe. I. Z. Anorg. Chem. 61, 338–346.
Stromholm, D., Svedberg, T., 1909b. Untersuchungen uber die chemie der radioactiven grundstoffe. II. Z. Anorg. Chem. 61, 197–206.
Seaborg, G.T., December 12, 1951. The Transuranium Elements: Present Status. Nobel Lecture. http://www.nobelprize.org/nobel_organizations/nobelfoundation/publications/lectures/index.html.

Seaborg, G.T., 1990. Transuranium Elements: A Half Century. Lawrence Berkeley National Laboratory Report LBL-29445. http://www.osti.gov/accomplishments/documents/fullText/ACC0052.pdf.
Sachs, R.G., 1979. Maria Goeppert Mayer 1906–1972. National Academy of Sciences, Washington, DC, pp. 311–328.
Salam, A., Ward, J.C., 1964. Electromagnetic and weak interactions. Phys. Lett. 13 (2), 168–171.
Salonen, L., et al., 2012. Environmental liquid scintillation counting. In: L'Annunziata, M.F. (Ed.), Handbook of Radioactivity Analysis, third ed. Elsevier Science, Amsterdam, pp. 625–693.
Salvany, T., et al., 2012. Geomorphic evolution of the Piton des Neiges volcano (Réunion Island, Indian Ocean): Competition between volcanic construction and erosion since 1.4 Ma. Geomorphol. 136, 132–147.
Samec, K., et al., 2009. Design of a compact high-power neutron source—The EURISOL converter target. Nucl. Instrum. Methods Phys. Res. Sect. A 606, 281–290.
Samios, N.P., et al., 1962. Parity of the neutral pion and the decay $\pi^{o} \rightarrow 2e^{+} + 2e^{-}$. Phys. Rev. 126, 1844–1849.
Sandoval-Vallarta, M., 1924. Bohr's Atomic Model from the Standpoint of the General Theory of Relativity and the Calculus of Perturbations. Massachusetts Institute of Technology, Boston. No. 0125483.
Sandulescu, A., Greiner, W., 1977. Mass asymmetry in fission, fusion and mass transfer due to the fragmentation in valleys. J. Phys. G. 3 (8), L189.
Sandulescu, A., et al., 1985. Comment on "Exotic nuclear decay of ^{223}Ra by emission of ^{14}C nuclei". Phys. Rev. Lett. 54, 490.
Sanna, V., et al., 2013. Nanoformulation of natural products for prevention and therapy of prostate cancer. Cancer Lett. 334, 142–151.
Santhosh, K.P., et al., 2010. Cluster formation probability in the trans-tin and trans-lead nuclei. Nucl. Phys. A 838, 38–49.
Sanuki, T., et al., 2000. Precise measurement of cosmic-ray proton and helium spectra with the BESS spectrometer. Astrophys. J. 545, 1135–1142.
Sarkadi-Priboczki, E., 2013. Novel ^{11}C-radioisotope Method for Catalysis Study. Lap Lambert Academic Publishing, p. 72.
Sauli, F., 1997. GEM: a new concept for electron amplification in gas detectors. Nucl. Instrum. Methods Phys. Res. Sect. A 386, 531–534.
Sauli, F., 2014. Gas electron multiplier (GEM) detectors: principles of operation and applications. In: Brahme, A. (Ed.), Volume 8: Radiation Sources and Detectors in Comprehensive Biomedical Physics. Elsevier, pp. 368–406.
Savchuk, W., 2006. The naturalist I. P. Puluj and the discovery of X-rays. In: Kokowski, M. (Ed.), The Global and the Local: The History of Science and the Cultural Integration of Europe. Proceedings of the 2nd ICESHS, Cracow, Poland, September 6–9, 2006. European Society for the History of Science (ESHS), pp. 133–241.
Sayen, S., Guillon, E., 2014. Aging effect on Zn retention on a calcareous soil: column experiments and synchrotron X-ray micro-spectroscopic investigation. Sci. Total Environ. 487, 545–556.
Scagliusi, S.R., et al., 2012. Radiation-induced degradation of butyl rubber vulcanized by three different crosslinking systems. Rad. Phys. Chem. 81, 991–994.
Scapita, S.C., Fisenne, I.M., 1996. Cerenkov counting as a compliment to liquid scintillation counting. Appl. Radiat. Isot. 47, 795–800.
Scherini, V., For the Pierre Auger Collaboration, 2011. Search for ultra-high energy photons with the Pierre auger observatory. Nucl. Instrum. Methods Phys. Res. Sect. A 630 (1), 226–229.
Schoenberger, J., et al., 2004. Evaluation of the clinical value of bone metabolic parameters for the screening of osseous metastases compared to bone scintiigraphy. BMC Nucl. Med. 4, 3.
Schoenborn, B.P., 2006. How single hydrogen atoms came into view. Forty years devoted to neutron techniques for structural biology. Los Alamos Sci. 30, 196–203.
Schroeder, M.R., 1982. Fletcher and the oil drop. Phys. Today 35, 15–104.
Schroeder, S., et al., 2008. Cardiac computed tomography: indications, applications, limitations, and training requirements: report of a writing group deployed by the Working Group Nuclear Cardiology and Cardiac CT of the European Society of Cardiology and the European Council of Nuclear Cardiology. Eur. Heart J. 29 (4), 531–556.
Schrödinger, E., 1915a. Notice regarding capillary pressure in gas blasts. Ann. Phys. 46 (3), 413–418.
Schrödinger, E., 1915b. The theory of drop and rise tests on Brownian motion particles. Phys. Z. 16, 289–295.
Schrödinger, E., 1917a. The acoustics of the atmosphere. Phys. Z. 18, 445–453.
Schrödinger, E., 1917b. Addendum to my essay: on the acoustics of the atmosphere. Phys. Z. 18, 567–574.
Schrödinger, E., 1921. Isotopia and Gibbs paradox. Z. Phys. 5, 163–166.
Schrödinger, E., 1926a. Quantisierung als Eigenwertproblem I. Ann. Phys. 79 (4), 361–376.
Schrödinger, E., 1926b. Quantisierung als Eigenwertproblem II. Ann. Phys. 79 (6), 489–527.
Schrödinger, E., 1926c. Über das Verhaltnis der Heisenberg-Born-Jordan'schen Quantenmechanik zu der meinen. Ann. Phys. 79 (8), 734–756.
Schrödinger, E., 1926d. Quantisierung als Eigenwertproblem III. Ann. Phys. 80 (13), 437–490.
Schrödinger, E., 1926e. Quantisierung als Eigenwertproblem IV. Ann. Phys. 81 (18), 109–143.
Schrödinger, E., 1926f. The constant crossover of micro- to macro molecules. Natirwissenschaften 14, 664–666.
Schrödinger, E., 1926g. An undulatory theory of the mechanics of atoms and molecules. Phys. Rev. 28 (6), 1049–1070.
Schrödinger, E., 1927. Energieaustausch nach der Wellenmechanik. Ann. Phys. 83 (15), 956–968.
Schrödinger, E., 1935. Die gegenwärtige Situation in der Quantenmechanik. Naturwissenschaften 23 (48), 807–812.
Schultz, H., May 2005. Nobel efforts. Nat. Geogr. Mag. 1.
Schulz, H.D., Zabel, M., 2006. Marine Geochemistry. Springer, p. 574.
Schwarzschild, A., 1963. A survey of the latest developments in delayed coincidence measurements. Nucl. Instrum. Methods 21, 1–16.
Science Incorporated Elsevier (Ed.), 1967. Nobel Lectures, Physics, 1901–21. Elsevier Publishing, Amsterdam.

Science Incorporated Elsevier (Ed.), 1967. Nobel Lectures in Physics, 1901–1970. Nobel Lectures, Physics, 1901–1921, vol. 1. Elsevier Publishing, Amsterdam.

ScienceWeek, February 23, 2001. History of Physics: Millikan's Oil Drops, Electron Charge, and Cooked Data, vol. 5. No. 8.

Seaborg, G.T., Kennedy, J.W., 1939. Nuclear isomerism and chemical separation of isomers in tellurium. Phys. Rev. 55, 410.

Seaborg, G.T., et al., 1946. Radioactive element 94 from deuterons on uranium. Phys. Rev. 69, 366–367.

Seaborg, G.T., James, R.A., Ghiorso, A., 1949. The new element curium (atomic number 96), NNES PPR. In: The Transuranium Elements: Research Papers, Paper No. 22.2, vol. 14B. McGraw-Hill Book Co., Inc., New York.

Seaborg, G.T., James, R.A., Morgan, L.O., 1949. The New Element Americium (Atomic Number 95), NNES PPR. In: The Transuranium Elements: Research Papers, Paper No. 22.1, vol. 14B. McGraw-Hill Book Co., Inc., New York.

Seaborg, G.T., McMillan, E.M., Kennedy, J.W., Wahl, A.C., 1946a. Radioactive element 94 from deuterons on uranium. Phys. Rev. 69, 366–367 (Submitted January 28, 1941).

Seaborg, G.T., Wahl, A.C., Kennedy, J.W., 1946b. Radioactive element 94 from deuterons on uranium. Phys. Rev. 69, 367–368 (Submitted March 7, 1941).

Seelig, C., 1954. A. Einstein "Ideas and Opinions, Based on Mein Weltbild". Bonzana Books, New York, pp. 8–11.

Segré, E., 1947. Possibility of altering the decay rate of a radioactive substance. Phys. Rev. 71, 274–275.

Segré, E., 1959. Properties of nucleons, Nobel Lecture, December 11, 1959. In: Nobel Foundation Staff (Ed.), Nobel Lectures, Physics, 1942–62 (1964). Elsevier Publishing, Amsterdam.

Segré, E., 1968. Nuclei and Particles. W. A. Benjamin, New York.

Segré, E., 1972. Enrico Fermi, Physicist. University of Chicago Press, p. 276.

Segré, E., 1973. Otto Stern, 1888–1969. Biographical Memoir. National Academy of Sciences, Washington, DC.

Segré, E., 1993. A Mind Always in Motion: The Autobiography of Emilio Segrè. University of California Press, p. 332.

Segré, E., Seaborg, G.T., 1938. Nuclear isomerism in element 43. Phys. Rev. 54 (9), 772.

Segré, E., Wiegand, C.E., 1949. Experiments on the effect of atomic electrons on the decay constant of ^{7}Be. Phys. Rev. 75, 39.

Segré, E., Wiegand, C.E., 1951. Erratum: experiments on the effect of atomic electrons on the decay constant of ^{7}Be. Phys. Rev. 81, 284.

Sekine, T., et al., 1986. Application of nuclear recoil to radioisotope enrichment of copper-64. J. Nucl. Sci. Technol. 23 (12), 1064–1068.

Seitz, F., Vogt, E., Weinberg, A.M., 1998. Eugene Paul Wigner, 1902–1995. Biographical Memoir, National Academies Press, Washington, DC, pp. 1–26.

Seltzer, S.M., Berger, M.J., 1982a. Evaluation of the collision stopping power of elements and compounds for electrons and positrons. Int. J. Appl. Radiat. Isot. 33, 1189–1218.

Seltzer, S.M., Berger, M.J., 1982b. Procedure for calculating the radiation stopping power for electrons. Int. J. Appl. Radiat. Isot. 33, 1219–1226.

Seltzer, S.M., Berger, M.J., 1984. Improved procedure for calculating the collision stopping power of elements and compounds for electrons and positrons. Int. J. Appl. Radiat. Isot. 35 (7), 665–676.

Selwyn, R.G., et al., 2007. A new internal pair production ratio of ^{90}Y: the development of a non-destructive assay for ^{90}Y and ^{90}Sr. Appl. Radiat. Isot. 65, 318–327.

Sequinot, J., Ypsilantis, T., 1977. Photo-ionization and Cherenkov ring imaging. Nucl. Instrum. Methods 142, 377–391.

Sequinot, J., Ypsilantis, T., 1994. A historical survey of ring imaging Cherenkov counters. Nucl. Instrum. Methods Phys. Res. Sect. A 343, 1–29.

Serber, R., 1992. The Los Alamos Primer, the First Lectures on How to Build an Atomic Bomb. University of California Press.

Serebrov, A., et al., 2005. Measurement of the neutron lifetime using a gravitational trap and a low-temperature Fomblin coating. Phys. Lett. B 605, 72–78.

Serway, R.A., et al., 2005. Modern Physics, third ed. Brooks/Cole – Thomson, Belmont, CA, p. 600.

Sessler, A., Wilson, E., 2014. Engines of Discovery: A Century of Particle Accelerators. World Scientific Publishing, p. 280.

Shamoo, A.S., Resnik, D.B., 2009. Responsible Conduct of Research. Oxford University Press, New York, 2.

Shanmugam, G., Kamalaharan, B., 1988. Application of a cubic barrier in exotic-decay studies. Phys. Rev. C 38, 1377–1381.

Shapley, D., 1978. Nuclear weapons history: Japan's wartime bomb projects revealed. Science 199 (4325), 152–157.

Sharma, S.K., et al., 2010. Explosive detection system using pulsed 14 MeV neutron source. Fusion Eng. Des. 85 (7–9), 1562–1564.

Sharma, A., 2012. Muon tracking and triggering with gaseous detectors and some applications. Nucl. Instrum. Methods Phys. Res. Sect. A 666, 98–129.

Sharma, A., et al. (2014). Mycotoxins | Immunological techniques for detection and analysis, pp. 869–877. In: Carl A. Batt (Ed.-in-Chief), Encyclopedia of Food Microbiology, vol. 2, second ed. Elsevier, pp. 863.

Sheffield, J., 2001. The future of fusion. Nucl. Instrum. Methods Phys. Res. Sect. A 464, 33–37.

Shi, J., et al., 2014. Comparison of space flight and heavy ion radiation induced genomic/epigenomic mutations in rice (*Oryza sativa*). Life Sci. Space Res. 1, 74–79.

Shi, Y.J., Swiatecki, W.J., 1985. Estimate of radioactive decay by the emission of nuclei heavier than α-particles. Nucl. Phys. A 438, 450–460.

Shiga, D., June 11, 2011. Heaviest elements yet join the periodic table. New Sci. 11.

Shimizu, S., et al., 2014. Preliminary analysis for integration of spot-scanning proton beam therapy and real-time imaging and gating. Phys. Med. 30 (5), 555–558.

Shu, F., et al., 2000. Enhanced visibility of hydrogen atoms by neutron crystallography on fully deuterated myoglobin. Proc. Natl. Acad. Sci. 97 (8), 3872–3877.

Shu, W.M., et al., 2004. Characteristics of a promising tritium process monitor detecting bremsstrahlung X-rays. Nucl. Instrum. Methods Phys. Res. Sect. A 521, 423–429.

Shu, W.M., et al., 2006. Monitoring of tritium in diluted gases by detecting bremsstrahlung X-rays. Fusion Eng. Des. 81, 803–808.
Sick, I., 1982. Precise nuclear radii from electron scattering. Phys. Lett. B 116 (4), 212–214.
Sick, I., Trautmann, D., 1998. On the rms radius of the deuteron. Nucl. Phys. A 637 (4), 559–575.
Siegbahn, K., 1958. Presentation speech, Nobel Prize in physics, Stockholm, December 11, 1958. In: Nobel Foundation Staff (Ed.), Nobel Lectures, Physics, 1942–62 (1964). Elsevier Publishing, Amsterdam.
Siegbahn, K., 1960. Presentation speech, Nobel Prize in physics, Stockholm, December 12, 1960. In: Nobel Foundation Staff (Ed.), Nobel Lectures, Physics, 1942–62 (1964). Elsevier Publishing, Amsterdam.
Siegert, M.J., 2013. Glacial landforms, ice sheets | growth and decay. In: Scott A. Elias (Ed.-in-Chief), Encyclopedia of Quaternary Science, second ed. Elsevier, Amsterdam, pp. 877–883.
Sime, R.L., 1996. Lise Meitner: A Life in Physics. University of California Press, Berkeley, p. 526.
Šimkovic, F., 2010. Double beta decay: a problem of particle, nuclear and atomic physics. Prog. Part. Nucl. Phys. 64 (2), 219–227.
Simpson, J.A., 1948. The latitude dependence of neutron densities in the atmosphere as a function of altitude. Phys. Rev. 73, 1389–1391.
Simpson, J.A., 1951. Neutrons produced in the atmosphere by cosmic radiations. Phys. Rev. 83, 1175–1188.
Simpson, J.A., 1983. Elemental and isotopic composition of the galactic cosmic rays. Ann. Rev. Nucl. Part. Sci. 33, 323–381.
Simpson, J.A., 2001. The cosmic radiation. In: Bleeker, J.A.M., Geiss, J., Huber, M.C.E. (Eds.), The Century of Space Science, vol. 1. Kluwer Academic Publishers, Dordrecht, The Netherlands, pp. 117–151.
Simpson, J.A., et al., 1953. Cosmic ray intensity-time variations and their origin: neutron intensity variation method and meteorological factors. Phys. Rev. 90, 934–950.
Simpson, J.A., Garcia-Munoz, M., 1988. Cosmic-ray lifetime in the galaxy: experimental results and models. Space Sci. Rev. 46, 205–224.
Singh, B., Batra, R.K., 1987. A method for calculating mass attenuation coefficients of beta particles. Appl. Radiat. Isot. 38 (12), 1027–1031.
Singh, B.P., Kumar, B., 2005. Isotopes in hydrology, hydrogeology, and water resources. Alpha Sci. 250.
Sinha, V., et al., 2014. A novel method for NDT applications using NXCT system at the Missouri University of Science & Technology. Nucl. Instrum. Methods Phys. Res. Sect. A 750, 43–55.
Siudak, R., et al., 2008. A threshold Cherenkov detector for K+/π+ separation using silica aerogel. Nucl. Instrum. Methods Phys. Res. Sect. A 596, 311–316.
Siva, S., et al., 2015. Fabrication of cyclodextrins-procainamide supramolecular self-assembly: shape-shifting of nanosheet into microtubular structure. Carbohyd. Poly. 122, 123–134.
Sjöstrand, T., 1988. Status of fragmentation models. Int. J. Mod. Phys. A 3, 751–804.
Skidmore, M.S., et al., 2009. Neutron sources for in-situ planetary science applications. Nucl. Instrum. Methods Phys. Res. Sect. A 608, 403–409.
Skottsberg, C., December 10, 1949. Banquet speech, Nobel Banquest, Stockholm. In: Holmberg, A. (Ed.), Les Prix Nobel en 1949. Nobel Foundation, Stockholm.
Slater, R.J. (Ed.), 2002. Radioisotopes in Biology, second ed. Oxford University Press, p. 328.
Slowiński, B., 2003. Spallation reactions and accelerator-driven systems. Appl. Energy 75, 129–136.
Smeenk, C.T.L., 2013. A new look at the hydrogen wave function. Physics 6, 58.
Smoot, G.F., Scott, D., 2002. Cosmic background radiation. pp. 22.1–22.14. In: Hagiwara et al. (2002). Phys. Rev. D66, 010001-1.
Snell, A.H., Miller, L.C., 1948. On the radioactive decay of the neutron. Phys. Rev. 74, 1217–1218.
Snell, A.H., et al., 1950. Radioactive decay of the neutron. Phys. Rev. 78, 310–311.
Snow, W.M., et al., 1973. Stopping power of Al, Cu, Ag, Au, Pb, and U for 5–18 MeV protons and deuterons. Phys. Rev. 8B, 1854–1863.
Soddy, F., 1913a. Inter-atomic charge. Nature 92, 399–400.
Soddy, F., 1913b. Radioactivity. Chem. Soc. Annu. Rep. 10, 262–288.
Soddy, F., 1913c. The radio-elements and the periodic Law. Chem. News 107, 97–99.
Soddy, F., 1922. The origins of the conceptions of isotopes. Nobel Lecture, December 12, 1922. In: Nobel Lectures, Chemistry 1901–1921 (1966). Elsevier Publishing Co., Amsterdam.
Soddy, F., 1924. The reported transmutation of mercury into gold. Nature 114 (2859), 244–245.
Soddy, F., Cranston, J.A., 1918. The parent of actinium. Nature 100, 498–499.
Sokaras, D., et al., 2011. The new external ion beam analysis setup at the Demokritos Tandem accelerator and first applications in cultural heritage. Nucl. Instrum. Methods Phys. Res. Sect. B 269, 519–527.
Soliman, Y.S., et al., 2013. Dosimetric studies for gamma radiation validation of medical devices. Appl. Radiat. Isot. 71 (1), 21–28.
Sommerfeld, A., 1904. Zur electronentheorie, II. Grundlage für eine allgemeine dynamik des elektrons. Nachrichten von der Gesellschaft der Wissenschaften zu Göttingen. Math. Phys. Kl. 1904, 363–439.
Soo, R.A., et al., 2009. First-line systemic treatment of advanced stage non-small-cell lung cancer in Asia: consensus statement from the Asian Oncology Summit 2009. Lancet 10 (11), 1102–1110.
Sorensen, T.L.M., et al., 2006. New light for science: synchrotron radiation in structural medicine. Trends Biol. 24 (11), 500–508.
Souza, C.D., et al., 2011. Analysis of the necessary radioprotection procedures in manufacture of iodine-125 sources used in brachytherapy: a preliminary study. Prog. Nucl. Energy 53, 66–72.
Sowerby, B.D., 1971. Čerenkov detectors for kow-energy gamma-rays. Nucl. Instrum. Methods 97, 145–149.
Spano, H., Kahn, M., 1952. Enrichment of tin activity through the Szilard-Chalmers separation. J. Am. Chem. Soc. 74, 568–569.
Spieler, H., 2012. Electronics and data acquisition. Nucl. Instrum. Methods Phys. Res. Sect. A 666, 197–222.

Spinks, J.W.T., Woods, R.J., 1990. An Introduction to Radiation Chemistry, third ed. John Wiley & Sons, Inc., New York.
Spyrou, A., et al., 2012. First observation of ground state dineutron decay: ^{16}Be. Phys. Rev. Lett. 108, 102501.
Stabin, M.G., 2009. Radiation Protection and Dosimetry, an Introduction to Health Physics. Springer, New York, p. 396.
Starič, M., HERA-B RICH group, 2005. HERA-B RICH: performance and physics impact. Nucl. Instrum. Methods Phys. Res. Sect. A 553, 210–214.
Starič, M., 2011. Pattern recognition for the time-of-propagation counter. Nucl Instrum. Methods Phys. Res. Sect. A 639 (1), 252–255.
Steere, A.R., 2005. A Timeline of Major Particle Accelerators (Masters of Science in Physics thesis). Michigan State University, Dept. of Physics and Astronomy, East Lansing, MI.
Stefański, T., et al., 2013. Metabolism of soluble rapeseed meal (*Brassica rapa* L.) protein during incubations with buffered bovine rumen contents in vitro. J. Dairy Sci. 96, 440–450.
Steigman, G., 1977. Secondary antiprotons: a valuable cosmic-ray probe. Astrophys. J. 217, L131–L133.
Steinhauser, G., Buchtela, K., 2012. Gas ionization detectors. In: L'Annunziata, M.F. (Ed.), Handbook of Radioactivity Analysis, third ed. Elsevier, Amsterdam, pp. 191–231.
Steiner, H., 2010. Owen Chamberlain 1920–2006, a Biographical Memoir. National Academy of Sciences, Washington, DC, p. 22.
Stephen, A.D., et al., 2011. Exploring the bond topological and electrostatic properties of benzimidazole molecule via experimental and theoretical charge density study. J. Mol. Struct. 989, 122–130.
Stern, O., 1920. Eine direkte Messung der thermischen Molekulargeschwindigkeit. Z. Phys. 2, 49.
Stern, O., 1921. Ein Weg zur experimentellen Pruefung der Richtungsquantelung im Magnetfeld. Z. Phys. 7, 249.
Stodolna, et al., 2013. Hydrogen atoms under magnification: direct observation of the nodal structure of Stark states. Phys. Rev. Lett. 110, 213001–213005.
Stone, J.O., et al., 1996. Cosmogenic chlorine-36 from calcium spallation. Geochim. Cosmochim. Acta 60 (4), 679–692.
Strachan, J.D., et al., 1994. Fusion power production from TFTR plasmas fueled with deuterium and tritium. Phys. Rev. Lett. 72, 3526–3529.
Street, J.C., Stevenson, E.G., 1937. New evidence for the existence of a particle of mass intermediate between the proton and electron. Phys. Rev. 51, 1005.
Street Jr., K., et al., 1950. Chemical properties of californium. J. Am. Chem. Soc. 72 (10), 4382–4385.
Stuewer, R.H., 1997. Gamow, alpha decay, and the liquid-drop model of the nucleus. In: Harper, E., Parke, W.C., Anderson, D. (Eds.), George Gamow Symposium, ASP Conference Series, vol. 129. Astronomical Society of the Pacific, San Francisco, pp. 30–43.
Stuiver, M., Polach, H.A., 1977. Reporting ^{14}C data. Radiocarbon 19, 355–363.
Suess, H.E., 1955. Radiocarbon content in modern wood. Science 122, 415–417.
Sundaresan, M.K., 2001. Handbook of Particle Physics. CRC Press, Boca Raton, FL, p. 446.
Suortti, P., 2003. X-ray, synchrotron radiation, and neutron diffraction. In: Robert A. Meyers (Ed.-in-Chief), Encyclopedia of Physical Science and Technology, third ed. Elsevier, Amsterdam, pp. 989–1023.
Susha Lekshmi, S.U., et al., 2014. A critical review of soil moisture measurement. Measurement. http://dx.doi.org/10.1016/j.measurement.2014.04.007.
Sutton, S.R., Newville, M., 2014. Synchrotron X-ray spectroscopic analysis. In: Heinrich Holland, Karl Turekian (Eds.-in-Chief), Treatise on Geochemistry, second ed., vol. 15. In: Analytical Geochemistry/Inorganic INSTR Analysis, Elsevier, Amsterdam, pp. 213–230.
Suzuki, T., et al., 1999. Nuclear radii of ^{17,19}B and ^{14}Be. Nucl. Phys. A 658 (4), 313–326.
Swallow, T., Kirby, R.S., 2008. Cancer of the prostate gland. Surgery (Oxford) 26 (5), 213–217.
Swimbanks, D., 1995. Physicists reveal glimpses of Japan's atomic bomb effort. Nature 376 (6538), 281–366.
Szilard, L., 1925. Über die Ausdehnung der Phänomenologischen Thermodynamik auf die Schwankungserscheinungen. Z. Phys. 32, 753–788.
Szilard, L., 1929. Über die Entropieverminderung in einem thermodynamischen System bei Eingriffen intelligenter Wessen. Z. Phys. 53, 840–856.
Szilard, L., Chalmers, T.A., 1934a. Chemical separation of the radioactive element fromits bombarded isotope in the Fermi effect. Nature 134, 462.
Szilard, L., Chalmers, T.A., 1934b. Detection of neutrons liberated from beryllium by gamma rays: a new technique for inducing radioactivity. Nature 134, 494–495.
Szilard, L., Chalmers, T.A., 1935. Radioactivity induced by neutrons. Nature 135, 98.
Szucs, Z., et al., 2009. Recoil effect on β-decaying in vivo generators, interpreted for ^{103}Pd/^{103m}Rh. Appl. Radiat. Isot. 67, 1401–1404.
Tarter, B., July/August 1998. Happy birthday, Edward! Science & Technology Review. In: Celebrating Edward Teller at 90. Lawrence Livermore National Laboratory. UCRL-52000-98-7/8. https://str.llnl.gov/str/pdfs/07_98.pdf.
't Hooft, G., 1971a. Renormalization of massless Yang-Mills fields. Nucl. Phys. B 33 (1), 173–199.
't Hooft, G., 1971b. Renormalizable Lagrangians for massive Yang-Mills fields. Nucl. Phys. B 35 (1), 167–188.
't Hooft, G., 1999. Gerardus 't Hooft – Biographical. Nobelprize.org. Nobel Media AB 2014. http://www.nobelprize.org/nobel_prizes/physics/laureates/1999/thooft-bio.html.
't Hooft, G., Ventman, M., 1972. Regularization and renormalization of gauge fields. Nucl. Phys. B 44 (1), 189–213.
Tabata, T., Ito, R., Okabe, S., 1972. Generalized semiempirical equations for the extrapolated range of electrons. Nucl. Instrum. Methods 103, 85–91.
Tait, W.H., 1980. Radiation Detection. Butterworths, London.
Takahashi, Y., et al., 2010. Development of landmine detection system based on the measurement of radiation from landmines. Appl. Radiat. Isot. 68 (12), 2327–2334.
Takamatsu, T., et al., 2006. Inertial electrostatic fusion device with an ion source using a magnetron discharge. Nucl. Fusion 46, 142–148.

Takiue, M., et al., 1993. Reliability of activity determined by Cerenkov measurements in a liquid scintillation counter. In: Noakes, J.E., Schönhofer, F., Polach, H.A. (Eds.), Liquid Scintillation Spectrometry 1992, Radiocarbon, pp. 69–73.

Takiue, M., et al., 1996. Accuracy of Cerenkov measurements using a liquid scintillation spectrometer. Appl. Radiat. Isot. 47, 123–126.

Takiue, M., et al., 2004. Cerenkov counting of low-energy beta-emitters using a new ceramic with high refractive index. Appl. Radiat. Isot. 61, 1335–1337.

Tamburini, F., et al., 2010. A method for the analysis of the $\delta^{18}O$ of inorganic phosphate extracted from soils with HCl. Eur. J. Soil Sci. 61 (6), 1025–1032.

Tamm, I.E., 1958. General characteristics of radiations emitted by systems moving with super-light velocities with some applications to plasma physics. Nobel Lecture, December 11, 1958. In: Nobel Foundation Staff (Ed.), Nobel Lectures, Physics, 1942–62 (1964). Elsevier Publishing, Amsterdam.

Tamm, I., Ivanenko, D., 1934. Exchange forces between neutrons and protons and Fermi's theory. Nature 133, 981–982.

Tanaka, H., et al., 2009a. Charastics comparison between a cyclotron-based neutron source and KUR-HWNIF for boron neutron capture therapy. Nucl. Instrum. Methods Phys. Res. Sect. B 267, 1970–1977.

Tanaka, H., et al., 2009b. Improvement of dose distribution in phantom by using epithermal neutron source based on the Be(p, n) reaction using a 30 MeV proton cyclotron accelerator. Appl. Radiat. Isot. 67, S258–S261.

Taylor, C.C.W., 1999. The Atomists: Leucippus and Democritus. University of Toronto Press, Toronto.

Taylor, L.S., et al., 1970. Linear Energy Transfer. ICRU Report 16. International Commission on Radiation Units and Measurements, Washington, DC.

Taylor, R.E., 1991. Deep inelastic scattering: the early years. Rev. Mod. Phys. 63 (3), 573–596.

Taylor, R.E., 2000. Fifty years of radiocarbon dating. Am. Sci. 88, 60–67.

Tanihata, I., et al., 1985. Measurement of interaction cross sections and radii of He isotopes. Phys. Lett. B 160 (6), 380–384.

Telegdi, V.L., October 2000. Szilard as inventor: accelerators and more. Phys. Today 53 (10), 25.

Teller, E., 1930. Über das Wasserstoffmolekülion. Z. Phys. 61, 458–480.

Teller, E., 1931. Der Diamagnetismus bon freien Elektronen. Z. Phys. 67, 311–319.

Teresawa, M., Kihara, M., 1996. Basic characteristics of synchrotron radiation and its related facilities and instrumentation. In: Saisho, H., Gohshi, Y. (Eds.), Applications of Synchrotron Radiation to Materials Analysis. Elsevier, Amsterdam, pp. 1–78.

Tharwat, M., et al., 2014. Image enhancement using MCNP5 code and MATLAB in neutron radiography. Appl. Radiat. Isot. 89, 30–36.

Thisgaard, H., Jensen, M., 2009. Production of the Auger emitter ^{119}Sb for targeted radionuclide therapy using a small PET-cyclotron. Appl. Radiat. Isot. 67, 34–38.

Thoennessen, M., et al., 2013. Novel techniques to search for neutron radioactivity. Nucl. Instrum. Methods Phys. Res. Sect. A 729, 207–211.

Thompson, K.A., 2004. Relativity, special. In: Meyers, R.A. (Ed.), Encyclopedia of Physical Science and Technology, third ed. Elsevier, Amsterdam, pp. 117–141.

Thomsen, K., 2007. A compound target concept for pulsed spallation sources. Nucl. Instrum. Methods Phys. Res. Sect. A 580, 1597–1599.

Thomson, G.P., 1927. The diffraction of cathode rays by thin film of platinum. Nature 120, 802.

Thomson, G.P., 1928. Experiments in the diffraction of cathode rays. Proc. R. Soc. London A 119, 600–609.

Thomson, G.P., 1929. The crystal structure of nickel films. Nature 123, 912.

Thomson, G.P., 1935. Electron diffraction as a method of research. Nature 135, 492–495.

Thomson, G.P., 1938. Nobel lecture. "Electronic waves", June 7, 1938. In: Nobel Lectures, Physics 1922–1941 (1965). Elsevier Publishing Co., Amsterdam.

Thomson, G.P., Reid, A., 1927. Diffraction of cathode rays by a thin film. Nature 119, 890–895.

Thomson, J.J., 1897. Cathode rays. Phil. Mag. 44, 293–316.

Thomson, J.J., 1904. XXIV. On the structure of the atom: an investigation of the stability and periods of oscillation of a number of corpuscles arranged at equal intervals around the circumference of a circle; with application of the results to the theory of atomic structure. Phil. Mag. Ser. 6 7 (39), 237–265.

Thompson, S.G., Ghiorso, A., Seaborg, G.T., 1950a. Element 97. Phys. Rev. 77, 838.

Thompson, S.G., Ghiorso, A., Seaborg, G.T., 1950b. The new element berkelium (atomic number 97). Phys. Rev. 80, 781.

Thompson, S.G., Street Jr., K., Ghiorso, A., Seaborg, G.T., 1950c. Element 98. Phys. Rev. 78, 298.

Thompson, S.G., Street Jr., K., Ghiorso, A., Seaborg, G.T., 1950d. The new element californium (atomic number 98). Phys. Rev. 80, 790.

Tiomno, J., Wheeler, J.A., 1949. Energy spectrum of electrons from meson decay. Rev. Mod. Phys. 21, 144.

Titus, K.J., et al., 1997. A preliminary investigation of a beta-particle transmission gauge for seam quality determination. Text. Res. J. 67, 23–24.

Toennies, J.P., et al., 2011. Otto Stern (1888–1969): the founding father of experimental atomic physics. Ann. Phys. (Berlin) 523 (12), 1045–1070.

Tolhoek, H.A., Brussaard, P.J., 1954. On the theory of alpha disintegration and the determination of nuclear radii. Physica 21 (1–5), 449–470.

Tomar, B.S., et al., 2010. Studies on production of high specific activity ^{99}Mo and ^{90}Y by Szilard Chalmers reaction. Radiochim. Acta 98, 499–506.

Tomaschitz, R., 2004. Cosmic time dilation: the clock paradox revisted. Chaos Solut. Fract. 20, 713–717.

Tomiyasu, K., et al., 2010. Particle-in-cell simulation of magnetic-assisted electrostatic confinement device. Fusion Eng. Des. 85 (5), 728–733.

Tossell, J.A., 2002. Does the calculated decay constant for ^{7}Be vary significantly with chemical form and/or applied pressure? Earth Planet. Sci. Lett. 195, 131–139.

Townsend, J.S., 1901. XVII. The conductivity produced in gases by the motion of negatively charged ions. Phil. Mag. Ser. 6 1 (2), 198–227.

Townsend, J.S., 1902. LXVI. The conductivity produced in gases by the aid of ultra-violet light. Phil. Mag. Ser. 6 3 (18), 557–576.

Townsend, J.S., 1903a. XXXVIII. The conductivity produced in gases by the aid of ultra-violet light. Phil. Mag. Ser. 6 5 (28), 389–398.

Townsend, J.S., 1903b. LXXVI. The genesis of ions by the motion of positive ions in a gas, and a theory of the sparkling potential. Phil. Mag. Ser. 6 (35), 598–618.

Tracz, G., et al., 2009. Pulsed thermal neutron source at the fast neutron generator. Appl. Radiat. Isot. 67, 1148–1155.

Trček, B., Jojer, H., 2010. Recharge of springs, pp. 88–127. In: Kresic, N., Stevanovic, Z. (Eds.), Groundwater Hydrology of Springs. Elsevier, Amsterdam, p. 573.

Tremsin, A.S., et al., 2014. Bright flash neutron radiography capability of the research reactor at the McClellan Nuclear Research Center. Nucl. Instrum. Methods Phys. Res. Sect. A 748, 46–53.

Trenn, T.J., 1986. The Geiger-Müller counter of 1928. Ann. Sci. 43 (2), 111–135.

Tretyakova, S.P., 1995. Study of cluster decay of heavy nuclei. Radiat. Meas. 25 (1–4), 279–282.

Treves, S.T. (Ed.), 2006. Pediatric Nuclear Medicine/PET, third ed. Springer, p. 542.

Trimmer, J.D., 1980. The present situation in quantum mechanics: a translation of Schrödinger's "Cat Paradox" paper. Proc. Am. Phil. Soc. 124 (5), 323–338.

Trower, W.P., 2009. Luis Walter Alvarez 1911–1988. National Academy of Sciences, Washington, DC.

Tsoulfanidis, N., 1995. Measurement and Detection of Radiation, second ed. Taylor and Francis, Washington, DC.

Tsumune, D., et al., 2013. Global distributions of ^{137}Cs, ^{239,240}Pu and the ratio of ^{239,240}Pu/^{137}Cs in an ocean general circulation model. In: Isotopes in Hydrology, Marine Ecosystems and Climate Change Studies. Proceedings of an International Symposium, Monaco, 27 March–1 April 2011, vol. 2. International Atomic Energy Agency, Vienna, pp. 493–499.

Tsybin, A.S., 1997. New physical possibilities in compact neutron sources. Appl. Radiat. Isot. 48 (10–12), 1577–1583.

Tucker, A., March 8, 2005. Obituary – Hans bethe. Guardian.

Tueros, M., Sciutto, S., 2010. TIERRAS: a package to simulate high energy cosmic ray showers underground, underwater and under-ice. Comp. Phys. Commun. 181, 380–392.

Tumul'kan, A.D., 1991. Typical calibration curves for beta thickness gauges. Meas. Tech. 34 (1), 24.

Turner, J.E., 1995. Atoms, Radiation and Radiation Protection, second ed. John Wiley & Sons, New York.

Tyapkin, A.A., 1974. The first theoretical prediction of the radiation discovered by Vavilov and Čerenkov. Sov. Phys. Uspekhi 17, 288.

Unger, W.E.S., Hodoroaba, V.-D., 2013. Surface chemical analysis at the micro- and nanoscale. In: Czichos, H. (Ed.), Handbook of Technical Diagnostics. Springer-Verlag, Berlin.

Unno, Y., et al., 2011. High sensitive standard measurement to determine strength of an I-125 brachytherapy source. In: Nuclear Science Symposium and Medical Imaging Conference (NSS/MIC), 2011 IEEE, October 23–29, 2011, Valencia, pp. 377–381.

UCSD, 2005. The Register of Leo Szilard Papers 1898–1998, MSS 0032. Mandeville Special Collections Library. Geisel Library, University of California, San Diego.

Uhlenbeck, G.E., Goudsmit, S., 1925. Ersetzung der Hypothese vom unmechanischen Zwang durch eine Forderung bezfiglich desinneren Verhaltens jedes einzelnen Elektrons. Naturwissenschaften 13 (47), 953–954.

Uhlenbeck, G.E., Goudsmit, S., 1926. Spinning electrons and the structure of spectra. Nature 117 (2938), 264–265.

Uhlenbeck, G.E., 1976. Fifty years of spin, personal reminiscences. Phys. Today 29 (6), 43–48.

UIC, 2005. Nuclear Fusion Power. UIC Nuclear Issues Briefing Paper No. 69, June 2005. Uranium Information Centre, Ltd, Melbourne, Australia, p. 5.

Ullaland, O., 2003. Update in particle identification. Nucl. Phys. B (Proc. Suppl.) 125, 90–99.

Underwood, M., 2008. Joseph Rotblat: influences, scientific achievements and legacy. Phys. Educ. 43 (6), 604–612.

Underwood, M., 2009. Joseph Rotblat: A Man of Conscience in the Nuclear Age. Sussex Academic Press, p. 160.

Unger, W.E.S., 2005. Surface analysis | auger electron spectroscopy. In: Worsfold, P., Townshend, A., Poole, C. (Eds.), Encyclopedia of Analytical Science, second ed. Elsevier Science, Amsterdam, pp. 466–474.

Unno, Y., et al., 2012. Measurement of anisotropic angular distributions of photon energy spectra for I-125 brachytherapy sources. Appl. Radiat. Isot. 70, 2240–2242.

Upham, L.V., Englert, D.F., 2003. Radionuclide imaging. In: L'Annunziata, M.F. (Ed.), Handbook of Radioactivity Analysis, second ed. Elsevier Science, Amsterdam, pp. 1063–1127.

USDA-ARS, 2006. http://www.screwworm.ars.usda.gov/HISTORY1.htm.

U.S. EPA, 2013. Nondestructive Multielement Instrumental Neutron Activation Analysis. U.S. Environmental protection Agency, p. 28.

U.S. EPA, 2014. Mail Irradiation. http://www.epa.gov/rpdweb00/sources/mail_irrad.html.

U.S. News & World Report, August 15, 1960. Leo Szilard, Interview: President Truman Did Not Understand, pp. 68–71.

U.S. Public Health Service, 1970. Radiological Health Handbook. Publ. No. 2016. Bureau of Radiological Health, Rockville, MD.

Velikyan, I., 2014. Radionuclides for imaging and therapy in oncology, pp. 285–325. In: Chen, X., Wong, S. (Eds.), Cancer Theranostics. Academic Press/Elsevier Publishers, San Diego, p. 516.

Vajda, N., et al., 2012. Alpha spectrometry. In: L'Annunziata, M.F. (Ed.), Handbook of Radioactivity Analysis, third ed. Elsevier, Amsterdam, pp. 364–423.

Vallarta, M.S., 1925. Sommerfeld's theory of fine structure from the standpoint of general relativity. MIT Bull. 83.

Vallarta, M.S., 1926a. Heavyside's proof of his expansion theorem. Trans. Am. Inst. Elect. Eng. XLV, 429–434.

Vallarta, M.S., 1926b. Theory of the Continuous X-ray Spectrum (Contribution from the Rogers Laboratory of Physics). MIT, p. 7.

Vallarta, M.S., 1927. Bemerkungen zu der Arbeit von Herrn G. von Gleich: zur Massenveränderlichkeit im Zweikörperproblem. Z. Phys. A 40 (11–12), 893–894.

Vallarta, M.S., 1929a. On Einstein's unified field equations and the Schwarzchild solution. Proc. Natl. Acad. Sci. U.S.A. 15 (10), 784–788.
Vallarta, M.S., 1929b. Quantum theory and special relativity. Nature 124 (3122), 336.
Vallarta, M.S., 1933. The interpretation of the azimuthal effect of cosmic radiation. Phys. Rev. 44, 1.
Vallarta, M.S., 1935. On the longitude effect of cosmic radiation. Phys. Rev. 47, 647.
Vallarta, M.S., 1937a. Cosmic rays and the magnetic moment of the sun. Nature 139, 839.
Vallarta, M.S., 1937b. Longitude effect of cosmic radiation and the position of the earth's magnetic centre. Nature 139, 24–25.
Vallarta, M.S., 1939a. Present status of the theory of the effect of the earth's magnetic field on cosmic rays. J. Frankl. Inst. 227 (1), 1–29.
Vallarta, M.S., 1939b. The determination of the energy spectrum of primary cosmic rays. Rev. Mod. Phys. 11, 239.
Vallarta, M.S., 1948. Cosmic rays and the magnetic field of the moon. Nature 161 (4095), 646–647.
Vallarta, M.S., 1949. Galactic rotation effect and the origin of cosmic radiation. Rev. Mod. Phys. 21, 356.
Vallarta, M.S., 1950. On the energy spectrum of heavy nuclei in primary cosmic radiation. Phys. Rev. 77, 419.
Vallarta, M.S., 1961. Theory of the geomagnetic effects of cosmic radiation. In: Cosmic Rays, Enyclopedia of Physics, vol. 9/46/1. Springer, pp. 88–129.
Vallarta, M.S., Feynman, R.P., 1939. The scattering of cosmic rays by the stars of a galaxy. Phys. Rev. 55, 506.
Vallarta, M.S., Godart, O., 1939. A theory of world-wide periodic variations of the intensity of cosmic radiation. Rev. Mod. Phys. 11, 180.
Vallarta, M.S., et al., 1939. Galactic rotation and the intensity of cosmic radiation at the geomagnetic equator. Phys. Rev. 55, 1.
Vallarta, M.S., et al., 1947. The determination of the sign and the energy spectrum of primary cosmic radiation. Phys. Rev. 71, 393.
Van der Meer, S., 1972. Stochastic Damping of Betatron Oscillations in the ISR. Internal Report CERN ISR-PO/72-31.
van den Akker, J., et al., 2011a. Salinity effects from evaporation and transpiration under flood irrigation. J. Irrig. Drain. Eng. 137 (12), 754–764.
van den Akker, J., et al., 2011b. Use of stable isotopes deuterium and oxygen-18 to derive evaporation from flood irrigation on the basis of pan evaporation techniques. J. Irrig. Drain. Eng. 137 (12), 765–778.
Vandendael, I., 2010. Use of Auger Ekectron spectroscopy to study an industrial process. Lambert Acad. Publ. 228.
Van Elteren, J.T., et al., 1999. Voltammetry detection of copper in high specific activity ^{64}Cu. Appl. Radiat. Isot. 51, 15–19.
van Loon, R., van Tihhelen, R., 2004. Radiation dosimetry in medical exposure. A short historical overview. Ann. Assoc. Belge. Radioprot. 29 (2), 163–174.
Van Rooyen, J., et al., 2008. A possible in vivo generator ^{103}Pd/^{103m}Rh—Recoil considerations. Appl. Radiat. Isot. 66, 1346–1349.
Vavilov, S.I., Levshin, V.L., 1926. The relation between fluorescence and phosphorescence in solid and liquid media. Z. Phys. 35, 920–936.
Vavilov, S.I., 1934. О возможныч Цричинач синеҐо γ-свечения жидкостей. C. R. Dokl. Akad. Nauk SSSR 2, 457–459.
Vavilov, Yu. N., November 11, 2002. The Work and the Life of S. I. Vavilov. CERN Seminar 21 November 2002. CERN Weekly Bulletin. Issue 46.
Vavilov, Yu. N., Levshin, L.V., 2002. Sergei Ivanovich Vavilov: an outstanding scientist, an organizer of Soviet science, a statesman and a public figure. Opt. Spectrosc. 92 (6), 956–961.
Va'vra, J., 2000. Particle identification methods in high energy physics. Nucl. Instrum. Methods Phys. Res. Sect. A 453, 262–278.
Va'vra, J., 2003. Novel photon detectors for RICH applications. Nucl. Instrum. Methods Phys. Res. Sect. A 502, 172–182.
Va'vra, J., et al., 2009. Beam test of a time-of-flight detector prototype. Nucl. Instrum. Methods Phys. Res. Sect. A 606, 404–410.
Veksler, V.I., 1944. A new method of accelerating relativistic particles. C. R. Dokl. Akad. Nauk SSSR 43 (8), 329–331.
Veksler, V.I., 1945. A new method of accelerating relativistic particles. J. Phys. USSR 9, 153–158.
Veksler, V.I., 1946. Concerning some new methods of acceleration of relativistic particles. Phys. Rev. 69, 244.
Veltman, M., 1970. Generalized ward identities and Yang-Mills fields. Nucl. Phys. B 21 (2), 288–302.
Veltman, M., 1999. Martinus J.G. Veltman – Biographical. Nobelprize.org. Nobel Media AB 2014. http://www.nobelprize.org/nobel_prizes/physics/laureates/1999/veltman-bio.ht.
Veltman, M., Goddard, P., Yeomans, J. (Eds.), 1994. Diagrammatica: The Path to Feynman Diagrams. Cambridge University Press, Cambridge, p. 296.
Ventura, A., 2013. The ATLAS muon trigger: experience and performance in the first 3 years of LHC pp runs. Nucl. Instrum. Methods Phys. Res. Sect. A 732, 48–51.
Verplancke, et al., 2012. Semiconductor detectors, pp. 299–362. In: L'Annunziata, M.F. (Ed.), Handbook of Radioactivity Analysis, third ed. Elsevier Science, Amsterdam, p. 1379.
Vetter, R.J., 2010. Radiation exposure in the preoperative environment. Perioper. Nurs. Clin. 5, 125–135.
Villard, P., 1894a. On the carbonic hydrate and the composition of gas hydrates. C. R. Acad. Sci. Paris 119, 368–371.
Villard, P., 1894b. Experimental study of gas hydrates. Ann. Chim. Phys. 11 (7), 353–360.
Villard, P., 1896. Combinaison de l'argon avec l'eau. C. R. Hebd. Séances Acad. Sci. Paris 123, 377–379.
Villard, P., 1899. Sur l'action chimique des rayons X. C. R. Acad. Sci. Paris 129, 882–883.
Villard, P., 1900a. On the chemical action of the X-rays. Phil. Mag. 49, 244.
Villard, P., 1900b. Sur la réflexion et la refraction des rayons cathodiques et des rayons déviables du radium. C. R. Acad. Sci. Paris 130, 1010–1012.
Villard, P., 1900c. Sur le rayonnement du radium. C. R. Acad. Sci. Paris 130, 1178–1179.
Villard, P., 1900d. Rayonnement du radium. Séances Soc. Fr. Phys. 45–46.
Villard, P., 1908. Instruments de mesure á lecture directe pour les rayons x. Sunstitution de la méthode électrométrique aux autres methods de mesure en radiology. Scleromètre et quantimètre. Arch. Électr. Méd. 16, 692–699.
Vimalnath, K.V., et al., 2014. Large scale production of ^{51}Cr for medical application in a medium flux research reactor: a comparative investigation of Szilard–Chalmers process and direct (n,γ) route. Appl. Radiat. Isot. 91, 104–108.

Vogel, P., 1967. On the nuclear octupole deformation in the $218 \leq A \leq 232$ region. Phys. Lett. B 25 (2), 65–67.
Vogel, P., 1968. On nuclear octupole deformations. Nucl. Phys. A 112 (3), 583–593.
Volkman, J.K. (Ed.), 2006. Marine Organic Matter: Biomarkers, Isotopes and DNA. Springer, p. 374.
Volkerts, M., et al., 2001. Proton-deuteron bremsstrahlung at 190 MeV. Nucl. Phys. A 684, 510c–512c.
von der Hardt, P., Röttger, H., 2013. Neutron Radiography Handbook: Nuclear Science and Technology. Springer, p. 180.
von Laue, M., 1912. Eine quantitative Prüfung der Theorie für die Interferenzerscheinungen bei Röntgenstrahlen. Sitz. Königl. Bayerisch. Akad. Wiss. 363–373.
von Laue, M., 1913. Concerning the detection of X-ray interferences. Nobel lecture, November 12, 1915. In: Nobel Lectures, Physics 1901–1921 (1967). Elsevier Publishing, Amsterdam.
von Weizsäcker, C.F., 1937. Über Elementumwandlungen im Innern Sterne. Phys. Z. 38, 176.
Vreysen, M.J.B., et al., 2007. Area-Wide Control of Insect Pests: From Research to Field Implementation. Springer, p. 789.
Wilson, R.W., 1978. Nobel Lecture: The Cosmic Microwave Background Radiation. Nobelprize.org. Nobel Media AB 2914. Web. January 14, 2016. http://www.nobelprize.org/nobel_prizes/physics/laureates/1978/wilson-lecture.html.
Wagner Jr., J.R., et al., 2014. Extrusion, second ed. Elsevier, Amsterdam, p. 620.
Waller, I., 1949. Presentation speech, December 12, 1949. Nobel Prize in physics 1949. In: Nobel Foundation Staff (Eds.), Nobel Lectures, Physics, 1942–62 (1964). Elsevier Publishing, Amsterdam.
Walstrom, P.L., Bowman, J.D., Penttila, S.I., Morris, C., Saunders, A., 2009. A magneto-gravitational trap for absolute measurement of the ultra-cold neutron lifetime. Nucl. Instrum. Methods Phys. Res. Sect. A 599, 82–92.
Walter, U., 2006. Relativistic rocket and space flight. Acta Austronaut. 59, 453–461.
Walton, E.T.S., 1951. The artificial production of fast particles. Nobel lecture, December 11, 1951. In: Nobel Foundation Staff (Eds.), Nobel Lectures, Physics, 1942–62 (1964). Elsevier Publishing, Amsterdam.
Wan, B.N., et al., 2007. The first plasma of EAST. In: 21st IAEA Fusion Energy Conference, Chengdu, China, October 16–21, 2007.
Wang, Z., 2007. Science and the state in modern China. Isis 98, 558–570.
Wang, C., et al., 2008. Development of a new Cf-252 source for remote afterloading neutron brachytherapy: Implications and applications. Brachytherapy 7 (2), 161–162.
Wapstra, A.H., et al., 2003. The AME2003 atomic mass evaluation (I). Evaluation of input data, adjustment procedures. Nucl. Phys. A 729, 129–336.
Wasserman, S.R., et al., 2012. Rapid-access, high-throughput synchrotron crystallography for drug discovery. Trends Pharmacol. Sci. 33 (5), 261–267.
Watson, J.D., Crick, F.H.C., 1953. A structure for deoxyribose nucleic acid. Nature 171 (4356), 737–738.
Webber, W.R., Potgieter, M.S., 1989. The artificial production of nuclear gamma-radiation. Astrophys. J. 344, 779.
Websdale, D.M., 2008. Review of Cherenkov imaging devices in particle and nuclear physics experiments. Nucl. Instrum. Methods Phys. Res. Sect. A 595, 12–18.
Webster, H.C., 1932. The artificial production of nuclear γ-radiation. Proc. R. Soc. A 136, 428–453.
Wei, J., 2003. Synchrotrons and accumulators for high-intensity proton beams. Rev. Mod. Phys. 75 (4), 1383–1432.
Weinberg, A.M., Wigner, E.P., 1958. The Physical Theory of Neutron Chain Reactors. University of Chicago Press, p. 801.
Weinberg, S., 1967. A model of leptons. Phys. Rev. Lett. 19 (21), 1264–1266.
Weise, W.L., Martin, G.A., 1989. A Physicists Desk Reference. American Institute of Physics, New York, p. 94.
Weiss, P., 2005. Dr. Feynman's doodles. How one scientist's simple sketches transformed physics. Sci. News 168 (3, July 16), 40.
Weiss, R.J. (Ed.), 1999. The Discovery of Anti-matter: The Autobiography of Carl David Anderson, the Youngest Man to Win the Nobel Prize. World Scientific, River Edge, NJ, p. 144.
Werner, L.B., Perlman, I., 1951. First isolation of curium. J. Am. Chem. Soc. 73 (11), 5215–5217.
Westmoreland, S., 2010. A note on relativistic rocketry. Acta Astronaut. 67, 1248–1251.
Wideröe, R., 1928. Über ein neues Prinzip zur Herstellung hoher Spannungen. Arch. Elektrotech. 21, 387–406.
Wiebe, L.I., et al., 1978. Čerenkov counting and Čerenkov scintillation counting with high refractive index organic ligands using a liquid scintillation counter. Int. J. Appl. Radiat. Isot. 29, 391–394.
Wiebe, L.I., et al., 1980. Liquid scintillation counting of radionuclides emitting high-energy beta radiation. J. Radioanal. Chem. 60, 385–394.
Wietfeldt, F.E., 2000. A measurement of the neutron lifetime by counting trapped protons. Nucl. Instrum. Methods Phys. Res. Sect. A 440, 528–534.
Wien, W., 1893. Eine neue Beziehung der Strahlung schwarzer Korper zum zweiten Hauprsatz der Warmtheorie. Sitz. Akad. Wiss. 9, 55–62.
Wiener, N., Vallarta, M.S., 1929a. Unified field theory of electricity and gravitation. Nature 123 (3096), 317.
Wiener, N., Vallarta, M.S., 1929b. On the spherically symmetrical statistical field in Einstein's unified theory of electricity and gravitations. Proc. Nat. Acad. Sci. U.S.A. 15 (4), 353–356.
Wiener, N., Vallarta, M.S., 1929c. On the spherically symmetrical statical field in Einstein's unified theory: a correction. Proc. Nat. Acad. Sci. U.S.A. 15 (10), 802–804.
Wigner, E., 1931. Gruppentheorie und Ihre Anwendung auf die Quantenmechanik der Atomspektren. F. Vieweg und Sohn, Braunschweig.
Wigner, E., 1933. On the mass defect of helium. Phys. Rev. 43, 252–257.
Wilkins, M.H.F., et al., 1953. Molecular structure of deoxypentose nucleic acids. Nature 171 (4356), 738–740.
Wilkinson, D.H., 2007. Super-allowed Fermi beta-decay: the neutron lifetime; G_A/G_V. Nucl. Instrum. Methods Phys. Res. Sect. A 574, 1–2.
Williams, J.L., Dunn, T.S., 1979. Radiation sources-gamma. Radiat. Phys. Chem. 14, 185–201.
Williamson, L.M., 1998. Transfusion associated graft versus host disease and its prevention. Heart 80, 211–212.

Wilson, E.J.N., September 19, 1996. In: Fifty Years of Synchrtrons. CERN Accelerator Conference. https://accelconf.web.cern.ch/AccelConf/e96/PAPERS/ORALS/FRX04A.PDF.

Wilson, C.T.R., 1911. On the method of making visible the paths of ionizing particles through a gas. Proc. R. Soc. London A85, 285–288.

Wilson, C.T.R., 1912. On the expansion apparatus for making visible the tracks of ionizing particles in gases and some results obtained by its use. Proc. R. Soc. London A87, 277–291.

Wilson, C.T.R., 1923. Investigations on X-rays and β-rays by the cloud method I – X-rays. Proc. R. Soc. London A104, 1–24.

Wilson, C.T.R., 1927. On the cloud method of making visible ions and the tracks of ionizing particles. Nobel lecture, December 12, 1927. In: Nobel Lectures, Physics 1922–1941, Elsevier Science Publishers, Amsterdam.

Wilson, E.J.N., 2001. An Introduction to Particle Accelerators. Oxford University Press, p. 272.

Wineland, D.J., December 8, 2012. Superposition, Entanglement, and Raising Schrödinger's Cat. Nobel Lecture. http://www.nobelprize.org/nobel_prizes/physics/laureates/2012/wineland-lecture.html.

Wineland, D.J., Dehmelt, H., 1975. Proposed 10^{14} $\Delta v<v$ laser fluorescence spectroscopy on TI+ mono-ion oscillator III. Bull. Am. Phys. Soc. 20, 637.

Wineland, D.J., Itano, W.M., 1979. Laser cooling of atoms. Phys. Rev. A 20, 1521–1540.

Woan, G., 2000. The Cambridge Handbook of Physics Formulas. Cambridge University Press, Cambridge.

Wolfe, R.R., 1992. Radioactive and Stable Isotope Tracers in Biomedicine: Principles and Practice of Kinetic Analysis. Wiley-Liss, p. 480.

Wolfe, R.R., Chinkes, D.L., 2004. Isotope Tracers in Metabolic Research: Principles and Practice of Kinetic Analysis, second ed. Wiley-Liss, p. 488.

Wolfson, R., 2003. Simply Einstein, Relativity Demystified. W. W. Norton & Co. Ltd, New York, p. 261.

Woo, Y.H., 1924. Note on absorption measurements of the X-rays reflected from a calcite crystal. Proc. Nat. Acad. Sci. 10 (4), 145–148.

Woo, Y.H., 1925a. The Compton Effect (Ph.D. dissertation). T-08048. The University of Chicago.

Woo, Y.H., 1925b. The intensity of the scattering of X-rays by recoiling electrons. Phys. Rev. 25 (4), 444–451.

Woo, Y.H., 1925c. The compton effect and tertiary X-radiation. Proc. Nat. Acad. Sci. 11 (2), 123–125.

Woo, Y.H., 1926. The distribution of energy between the modified and the unmodified rays in the compton effect. Phys. Rev. 27 (2), 119–129.

Woo, Y.H., 1930a. On the intensity of total scattering of X-rays by monoatomic gases. Proc. Nat. Acad. Sci. 16 (12), 814–816.

Woo, Y.H., 1930b. Intensity of total scattering of X-rays by monoatomic gases. Nature 126 (3179), 501–502.

Woo, Y.H., 1931a. Temperature and diffuse scattering of X-rays from crystals. Phys. Rev. 38 (1), 6–14.

Woo, Y.H., 1931b. On the intensity of total scattering of X-rays by gases I. Proc. Nat. Acad. Sci. 17 (8), 467–470.

Woo, Y.H., 1931c. On the intensity of total scattering of X-rays by gases II. Proc. Nat. Acad. Sci. 17 (8), 470–475.

Woo, Y.H., 1932. The scattering of X-rays by polyatomic gases. Phys. Rev. 39 (4), 555–560.

Wood, J.G., 1954. Bubble tracks in a hydrogen-filled Glaser chamber. Phys. Rev. 94, 731.

Woods, F.S., 1932. Advanced Calculus. Ginn and Company, p. 397.

Wooldridge, D.E., 1936. The Separation of Gaseous Isotopes by Diffusion (Doctoral dissertation). California Institute of Technology, Pasadena, California.

Wooldridge, D.E., Smythe, W.R., 1936. The separation of gaseous isotopes by diffusion. Phys. Rev. 50, 233–237.

Wu, B., Becker, J.S., 2011. Imaging of elements and molecules in biological tissues and cells in the low-micrometer and nanometer range. Int. J. Mass Spectrom. 307, 112–122.

Wu, C.S., Ambler, F., Hayward, R.W., Hoppes, D.D., Hudson, R.P., 1957. Experimental test of parity conservation in beta decay. Phys. Rev. 105, 1413–1414.

Wu, D.L., et al., 2009. Flower color chimera and abnormal leaf mutants induced by $^{12}C^{6+}$ heavy ions in *Salvia splendens* Ker-Gawl. Scientia Horticulturae 121 (4), 462–467.

Wu, H., et al., 2010. Mutations in cauliflower and sprout broccoli grown from seeds flown in space. Adv. Space Res. 46, 1245–1248.

Wüstling, S., et al., 2006. A large, 64-pixel PIN-diode detector for low-energy beta-electrons. Nucl. Instrum. Methods Phys. Res. Sect. A 568, 382–387.

Wyckoff, H.O., Henderson, J.E., 1943. The spatial asymmetry of Cerenkov radiation as a function of electron energy. Phys. Rev. 64 (1 and 2), 1–6.

Wynn-Williams, C.E., 1931. The use of thyratrons for high-speed automatic counting of physical phenomena. Proc. R. Soc. London 132A, 295–310.

Wynn-Williams, C.E., 1932. A thyratron scale-of-two counter. Proc. R. Soc. London 136A, 312–324.

Xiao, B.J., et al., 2008. EAST plasma control system. Fusion Eng. Des. 83, 181–187.

Xie, S., et al., 2014. Effects of acid/alkaline pretreatment and gamma-ray irradiation on extracellular polymeric substances from sewage sludge. Rad. Phys. Chem. 97, 349–353.

Yagi, N., 2014. Synchrotron radiation, pp. 17–33. In: Anders Brahme (Ed.-in-Chief), Comprehensive Biomedical Physics. In: Radiation Sources and Detectors, vol. 8. Elsevier, Amsterdam, p. 418.

Yaksic, A., Tilton, J.E., 2009. Using the cumulative availability curve to assess the threat of mineral depletion: the case of lithium. Resour. Policy 34, 185–194.

Yalow, R.S., 1977. Radioimmunoassay: a probe for fine structure of biologic systems. Nobel lecture, December 8, 1977. In: Lindsten, J. (Ed.), Nobel Lectures, Physiology and Medicine 1971–1980 (1992). World Scientific Publishing, Singapore.

Yalow, R.S., Berson, S.A., 1959. Assay of plasma insulin in human subjects by immunological methods. Nature 184, 1648–1649.

Yamasaki, S., et al., 2011. Unspiked K–Ar dating of Koolau lavas, Hawaii: evaluation of the influence of weathering/alteration on age determinations. Chem. Geol. 287, 41–53.

Yamauchi, K., et al., 2006. Performance of neuton/proton source based on ion-source-assisted cylindrical radially convergent beam fusion. IEEJ Trans. Fund. Mat. 126, 1177–1182.

Yang, C.N., 1957. The law of parity conservation and other symmetry laws of physics. Nobel lecture, December 11, 1957. In: Nobel Foundation Staff (Ed.), Nobel Lectures, Physics, 1942–1962 (1964). Elsevier Publishing, Amsterdam.

Yang, Y., et al., 2007. Explosives detection using photoneutrons produced by X-rays. Nucl. Instrum. Methods Phys. Res. Sect. A 579, 400–403.

Yang, S., et al., 2013. Structural augmentation with biomaterial-loaded allograft threaded cage for the treatment of femoral head osteonecrosis. J. Arthroplasty 25 (8), 1223–1230.

Yanus, S.O., et al., 2010. Analytical Methods Using Instrumental Neutron Activation Analysis: Determining the Radionuclides, Concentrations and Differential Factors of Biological Samples. VOM Verlag Dr. Müller, p. 84.

Yearian, M.R., Hofstadter, R., 1958a. Magnetic form factor of the neutron. Phys. Rev. 110 (2), 552–564.

Yearian, M.R., Hofstadter, R., 1958b. Magnetic form factor of the neutron at 600 MeV. Phys. Rev. 111 (3), 934–939.

Yi, C.Y., et al., 1999. Mass attenuation coefficients of β^+-particles. Appl. Radiat. Isot. 51, 217–227.

Yoshikawa, K., et al., 2007a. Research and development of a compact discharge-driven D–D fusion neutron source for explosive detection. Nucl. Instrum. Methods Phys. Res. Sect. B 261, 299–302.

Yoshikawa, K., et al., 2007b. Research and development on humanitarian landmine detection system by use of a compact D–D fusion neutron source. Fusion Sci. Technol. 52, 1092–1095.

Yoshiyuki, S., Hiroshi, T., 1999. Development of a small-sized painting thickness gauge based on a beta-ray transmission technique. Radioisotopes 48 (3), 163–171.

Young, N.A., 2014. The application of synchrotron radiation and in particular X-ray absorption spectroscopy to matrix isolated species. Coord. Chem. Rev. 277–278, 224–274.

Ypsilantis, T., Sequinot, J., 1994. Theory of ring imaging Cherenkov counters. Nucl. Instrum. Methods Phys. Res. Sect. A 343, 30–51.

Yu, X., et al., 2007. Characteristics of phenotype and genetic mutations in rice after spaceflight. Adv. Space Res. 40, 528–534.

Yukawa, H., 1935. On the interaction of elementary particles I. Proc. Phys. Math. Soc. Jpn. 17, 48–57.

Yukawa, H., 1949. Meson theory in its developments. Nobel lecture, December 12, 1949. In: Nobel Foundation Staff (Ed.), Nobel Lectures, Physics, 1942–62 (1964). Elsevier Publishing, Amsterdam.

Yukawa, H., 1951. Prof. Hantaro Nagaoka. Nature 168 (4271), 409.

Zahn, U., 1967a. A study of the recoil behavior of ^{56}Mn atoms in dilute solutions of manganese carbonyl compounds. Radiochim. Acta 7, 170–175.

Zahn, U., 1967b. Recoil reactions in crystalline ^{56}Mn carbonyls. Radiochim. Acta 8, 177–178.

Zallen, D.T., 2003. Despite Franklin's work, Wilkins earned his Nobel. Nature 425 (6953), 15.

Zamani, M., et al., 2008. A spallation neutron source based on Pb target surrounded by U blancket. Radiat. Meas. 43, S151–S155.

Zavrtanik, D., 2011. Results from the Pierre Auger observatory. Nucl. Instrum. Methods Phys. Res. Sect. A 630 (7), 166–170.

Zeeman, P., 1897. The effect of magnetism on the nature of light emitted by a substance. Nature 55 (1424), 347.

Zeisler, S.K., Weber, K., 1998. Szilard-Charlmers effect in holmium complexes. J. Radioanal. Nucl. Chem. 227, 105–109.

Zendel, M., 2008. IAEA safeguards equipment. Int. J. Nucl. Energy Sci. Technol. 4 (1), 72–80.

Zhang, L., et al., 2014. CT-guided radioactive 125I seed implantation treatment of multiple pulmonary metastases of hepatocellular carcinoma. Clin. Radiol. 69, 624–629.

Zhou, L.B., et al., 2006. Effects of ion beam irradiation on adventitious shoot regeneration from in vitro leaf explants of *Saintpaulia ionahta*. Nucl. Instrum. Methods Phys. Res. Sect. B 244, 349–353.

Zhou, F., et al., 2010. Measurements of the ^{89}Y(n,γ)^{90m}Y cross-section in the neutron energy range of 13.5–14.6 MeV. Nucl. Instrum. Methods Phys. Res. Sect. B 268 (9), 1367–1369.

Zhu, Y., et al., 2014. Synchrotron-based X-ray microscopic studies for bioeffects of nanomaterials. Nanomed. Nanotechnol. Biol. Med. 10, 515–524.

Ziessman, H.A., et al., 2005. Nuclear Medicine: The Requisites, third ed. Mosby, p. 704.

Zinn, W.H., Szilard, L., 1939. Emission of neutrons by uranium. Phys. Rev. 56, 619–624.

Zito, R.R., Schiferl, D., 1987. Electron capture decay in Jovian planets. ICARUS 72, 647–649.

Zreda, M., et al., 2008. Measuring soil moisture content non-invasively at intermediate spatial scale using cosmic-ray neutrons. Geophys. Res. Lett. 35, L21402. http://dx.doi.org/10.1029/2008GL035655.

Zreda, M., et al., 2012. COSMOS: the cosmic-ray soil moisture observing system. Hydrol. Earth Sys. Sci. 16, 4079–4099.

Zuber, K., 2003. Spectroscopy of low energy solar neutrinos using CdTe detectors. Phys. Lett. B 571, 148–154.

Zucchiatti, A., Redondo-Cubero, A., 2014. Ion beam analysis: new trends and challenges. Nucl. Instrum. Methods Phys. Res. Sect. B 331, 48–54.

Zweig, G., 1964a. An SU_3 Model for Strong Interaction Symmetry and Its Breaking. CERN Report preprint 8182/TH.412, January 17, 1964. http://cdsweb.cern.ch/record/352337?ln=en.

Zweig, G., 1964b. An SU_3 Model for Strong Interaction Symmetry and Its Breaking II. CERN Report 8419/TH.412, 21 February 1964, p. 86. http://cdsweb.cern.ch/record/570209?ln=en.

Zweig, G., 1980. An SU_3 model for strong interaction symmetry and its breaking II. CERN Report 8419/TH.412, February 21, 1964. In: Lichtenberg, D.B., Rosen, S.P. (Eds.), Developments in the Quark Theory of Hadrons, A Reprint Collection, vol. I: 1964–1978, Hadronic Press, Inc., Nonantum, Mass, pp. 22–101.

Zweig, G., 2010. Memories of Murray and the quark model. Int. J. Mod. Phys. 25 (20), 3863–3877.

Zweig, G., 2014. Concrete quarks – the beginning of the end. In: EPJ Web of Conferences, vol. 71. http://dx.doi.org/10.1051/epjconf/20147100146, 00146. http://www.epj-conferences.org/articles/epjconf/pdf/2014/08/epjconf_icnfp2013_00146.pdf.

Index

'*Note*: Page numbers followed by "f" indicate figures, "t" indicate tables, and "b" indicate boxes.'

A

Abelson, Philip, 610
Abolition of war, 353
Accelerated electrons
  properties of, 286–287
Accelerated protons/deuterons, 595
Accelerators, 46
  Cockcroft and Walton and, 589–590
  first artificial transmutation with, 589–590
  Ising and, 584, 585f, 591
  Rutherford and, 589–590
  Wideröe and, 584–585, 591
Aces, 740–742
  as Zweig's term for quarks, 743–750
Actinide series, 616
Actinide transition series, 615
Actinium decay chain, 74, 75f
Advanced Photon Source, 287–288, 290f
Agricultural production
  isotopes and radiation in, 23–37
Air showers of cosmic radiation, 434, 501–504
Alamogordo, 152
Alchemists, 97
Alpha decay, 123–126
Alpha decay energy
  half-life and, 126–127, 127f
Alpha particle emissions, 124f
  energy lines of, 125f, 148
Alpha-particle energy
  half-life and, 126
Alpha-particle induced reactions, 366t, 367–368
  neutron activities from, 367
  neutron energies from, 367
Alpha particles, 97–98, 123, 124f, 126, 130, 132–134
  charge and nature of, 98
  charge of, 99–100, 99f
  deflection of, 97–98
  electronic counter of, 102
  energy of, 125–126
  interactions, 128–129
  linear range, 130–134, 191, 816f
  mass of, 100–101
  nuclear assembly of, 126
  nuclear back-scattering of, 103–104
  nuclear escape of, 127f
  origin and properties, 801
  ranges in dry air, 816f
  ranges of, 106–107, 130–134, 191–192
  wave nature of, 126–127
Alpha radiation, 95–97
Alpher, Ralph, 508–509
Alvarez, Luis W., 488, 729–734
  Bloch and, 731
  Compton and, 730
  discovery of beta(n) decay, 731–732
  discovery of internal conversion, 435
  discovery of K-capture, 730–731
  Glaser and, 732–733
  hydrogen bubble chamber and, 732–733
  latitude effect on cosmic radiation, 730
  in Manhattan Project, 731
  neutron magnetic moment and, 662, 731
Amaldi, Edoardo, 481
Americium (element 95)
  production of, 616
Anderson, Carl D., 74, 144, 293–294, 422–423, 445–453, 459–460
  antimatter discovery, 447–448
  Compton and, 451
  Feynman and, 448
  kaon studies by, 452
  Manhattan project and, 451
  Millikan and, 446–447
  muons in cosmic ray showers and, 450
  muon studies by, 451–452
  Neddermeyer and, 448–450
  observation of pair production by, 448, 449f
  Oppenheimer and, 448
  positron discovery, 448
  Wilson cloud chamber and, 447
Anderson, Herbert, 326
Anderson, Robert, 58
Angular momentum, 164–165, 392
Animal disease vectors
  isotopes in avian influenza studies, 33
Animal health and production
  isotope tracer techniques in, 33
  radioimmunoassay in, 30–31
Annihilation, 158–159, 475–476
  antineutron-neutron, 491
  antiproton-proton, 479–480
  Dirac and, 422
  Einstein's equation $E = mc^2$ and, 458–459
  energy released in, 274–275
  first observation of, 458–459
  mass-energy conversion in, 220–221
  positron-negatron, 274–275, 275f
  principle of, 422
  radiation, 274–275, 295
Anode, 82
ANTARES, 575
Anthracene scintillator, 655–656
Anticathode, 82–83
Anticoincidence circuit, 607f
Anticoincidence counter
  for ^{14}C dating, 606
  Libby and, 606, 607f
  principle of, 606, 607f
Antimatter
  discovery of, 293–294, 447, 448f, 451
  first demonstration of, 458–459
Antineutrino, 158–159
  in negatron emission, 168
  spin property of, 169
Antineutron
  annihilation of, 491
  antiquark composition of, 481
  discovery of, 474, 481
Antiparticle, 220–221, 294–295, 422
  Dirac and, 421–423
Antiproton
  Bevatron and, 474–475
  charge-exchange reaction of, 491
  in cosmic radiation, 491
  criteria for its identification, 476
  discovery of, 423, 474
  Segrè and Chamberlain and, 423
Antiproton–proton annihilation
  evidence for antiproton discovery, 479
  image of, 480f
  pi-mesons emitted from, 479
Antiquark, 735–736, 742, 751
  charges of, 742, 746t
  color charges of, 751–752
  quantum states of, 751
A number, 68–69, 123
Argon
  discovery of, 94
Argonne National Laboratory, 639, 641–642
Armaments race, 357–358, 403
Astatine
  discovery of, 482
Asymmetric photons, 548–549
Asymptotic freedom, 757–758
  definition, 757–758
  description of, 765
ATLAS Collaboration, 788
ATLAS detector
  description of, 785, 786f

Atom, hydrogen
image of, 812–813
Atomic bomb
against our use of, 343, 346–353
first detonation by Soviet Union, 355
first detonation by USA, 339
first realization of potential of, 801
Szilard and, 323f–324f
Atomic bomb designs
gun assembly with ^{235}U, 339–340, 339f
implosion assembly with ^{239}Pu, 339f, 340
Atomic bomb, Germany and
Germany's scuttled effort, 412–413
Heisenberg and, 412–413
Szilard patent for, 322f–324f
Uranium Project, 413
Atomic bomb project
in Japan, 233–234
Manhattan Project, 327, 330f, 339–340, 342, 344f, 346
Atomic components
masses of, 804t–805t
Atomic constituents
properties of, 67–68
Atomic electron configurations, 418t
nomenclature for, 420t
principal electron energy levels, 395, 396t
principal quantum numbers for, 395, 396t
quantum energy sublevels, 395, 396t
Atomic electron radiation
origin, 435
Atomic electrons
configurations of the elements, 154, 156f
energy levels of, 154
Atomic mass units, 370
definition, 67–68, 70
energy equivalence of, 70, 172, 687
Atomic number, 123, 133, 137, 175f, 391–392, 67
characterization by Moseley, 249–250
definition, 68
Atomic orbitals
magnetic quantum number and, 417f
orbital quantum number and, 416–417, 417f
principal quantum number and, 416–417, 417f
Atomic pile, 151, 334
Atomic Scientists Association, 346–347
Atomic structure
Rutherford's determination of, 101
Atomic weight, 133
Atomism, 79–80
Atoms, 79–80
blueberry muffin model of, 119
images of, 812–814
and our future, 814
plum pudding model of, 119
radius of, 128–129
Attractive nuclear forces, 176
Auger effect, 433
definition, 438
process of, 439f
X-ray and Auger electron emission in, 439
Auger electron emissions, 433–434, 436f, 439f
in cancer therapy, 440–441
Auger electrons, 433–435, 438–442
Auger Effect and, 433–434
definition, 438
discovery, 312, 433–434
energy of, 438–439, 439f
first particle track of, 141–143
following EC decay, 179
mechanism of emission, 438
origin of, 277, 433–434
Auger electron spectroscopy, 434, 442
Auger, Pierre V., 433–434
Auger Effect and, 433–434
Auger electrons and, 312
cosmic radiation showers and, 433–434
discovery of Auger electrons, 433–434, 438
Meitner and, 433–434
Roland Maze and, 433–434
Auger yield, 439–440
Avogadro, Amadeo, 116
Avogadro's number, 116, 635–636
Perrin's calculation of, 116

B

Bacher, Robert F., 597, 689–690
Bainbridge, Kenneth, 593
Ballistic Missile Defense Organization, 357
Balmer series, 392
Baños, Alfredo, 493–494
Barkla, Charles G., 248–249, 251–252
discovery of secondary X-rays, 252
discovery of wave property of X-rays, 252
origin of K- and L-series X-rays and, 252
X-ray fluorescence discovery by, 252
Barn
definition, 720–721
origin of barn unit, 721
Bartky, Walter, 342
Baryon number
formula for, 742–743
as quantum number, 742–743
Baryon number conservation
law of, 742–743
Baryons, 751
composition of, 807f
definition, 680
quark color charge in, 682, 752f
quark composition of, 752f, 803–805
quarks color charge changes in, 753
quark structure and properties of, 736t
quark structure of, 681–682, 742, 806
strange, 807f
three quarks of, 751
three quark structure of, 742
Beauty baryon, 736t
Beauty quark, 736t
Becquerel, Henri, 83, 89–90, 94, 443, 799–800
Beijing electron-positron collider (BEPC), 758
Beria, Lavrenty Pavolich, 519, 524–525
Berson, Solomon, 30–31
Beta decay, 761f, 808, 809f
competing positron and EC decay in, 178f, 182
definition, 167
electron capture, 179
maximum energy of, 176–177
modes of, 183–184
N/Z ratios and, 176
proton-neutron conversion in, 743
quark transformation in, 743, 746, 808
types of, 167
$W^{\pm}$ bosons in, 810
Beta decay, branching, 183–184
criteria for, 183–184
pathways of, 183–184
Beta decay, double, 184–190
beta energy spectrum of, 189–190
criteria for, 186–187
decay energy calculation of, 187
decay energy of, 186–190
description, 184
discovery of, 185–186
Elliott, Hahn and Moe and, 640–641
Goeppert-Mayer and, 185–186
half-lives of, 186–187
quark transitions in, 189f
via electron capture, 188
via positron emission, 188
Beta decay, double/neutrinoless, 188–190
beta energy spectrum of, 189–190
decay energy of, 189–190
search for, 188
theory of, 188, 189f
Beta decay, quarks in
Gell-Mann and Zweig and, 746
Zweig and, 745
Beta decay theory
Fermi and, 169
Beta-delayed neutron emission, 710–711, 729, 731
discovery of, 731, 732f
Beta-delayed proton emission, 705–706, 706f
Beta particle, absorption and transmission, 192–195
exponential character of, 192–193
industrial applications, 194–195
thickness measurements from, 194
Beta particle energy
maximum, 175f
Beta particle, interactions with matter, 190–192
absorber density and, 190
mechanisms of, 190
positrons *vs.* negatrons, 192
Beta-particle radiation
energy spectra of, 148
Beta particles, 94–97, 156b, 167
vs. atomic electron, 167
bremsstrahlung and ionization energy loss, 198
bremsstrahlung from, 190
electron orbital excitation by, 190
energy spectra of, 154
energy spectrum of, 168–169

ionization by, 190
maximum energy of, 167–169
origin and properties, 801
origin of, 118, 167
as product of nuclear decay, 411
proof of inexistence in nucleus, 411
ranges in absorbers of low Z, 819f
ranges in dry air, 817f
ranges in low Z absorbers, 819f
ranges in water, 818f
ranges of, 190–192
scattering of, 190
stopping power of, 190
Beta radiation, 95
Beta thickness gauge, 194
Beta transmission thickness gauges, 194–195
Bethe-Feynman formula, 673–674
Bethe, Hans, 355, 588, 596–601, 689–690
Bacher and Livingston and, 597
duration of solar CN cycle, 600–601
Einstein and, 600–601
energy from fusion and, 599
energy production in stars and, 597
fusion energy in stars discovered by, 801
lifetimes of solar nuclei and, 600–601
in Manhattan Project, 600–601
meeting with astrophysicists, 597
neutrino detection and, 159
nuclear fusion in the sun and, 598
Rotblat and, 600–601
solar CNO bi-cycle and, 599
solar (CN) cycle of, 598–599
solar energy and, 597–600
solar lifetime and, 600–601
solar neutrino production and, 598
stopping power formula and, 195–197
Teller and, 600–601
Bevalac accelerator, 484
Bevatron
Alvares and, 732–733
antineutron discovery with, 481
antiproton velocities from, 476–478
particle spectrographs of, 476–478, 477f
Bevatron particle spectrograph
antiproton velocities from, 478
operation of, 478
Bevatron proton synchrotron
antiproton discovery with, 474–476, 491
antiproton relativistic mass and momentum from, 476–478
GeV proton energy from, 474–476
LBNL and, 474–476
McMillan and Lawrence and, 476
B factory
CP violation and, 774–775
Bhabha Atomic Research Centre, 264–265, 268
Bhabha, Homi J., 264–268
Bhabha scattering and, 265
naming of meson by, 267
relativistic time dilation and, 266–267
Bhabha scattering, 264–265, 266f
in high-energy physics, 265–266
Big Bang, 495, 508–509, 777
creation and, 783–784
Big Bang theory, 506–513
cosmic microwave background radiation and, 507
evidence for, 512–513
Lemaître and, 506–507
Bikini Atoll, 357
Binding energy, 308
electron, 435
of gluons, 803
nuclear, 187
Binding energy, nuclear, 375
calculation of, 599, 684
definition, 684
deuterium, 307
Hans Bethe and, 599
of ^{236}U, 685–686
Binding energy per nucleon
calculation of, 684
fusion *vs.* fission and, 684–685, 685f
nuclear stability and, 684
of ^{236}U, 685–686
Biological research, isotopes in, 20–23
anabolic and catabolic reactions in, 21
biological pathways and, 21
Hevesy and, 20–21
inositol phosphate metabolism and, 23f
pathways in photosynthesis and, 21–23
tracer technique in, 23
Black-body radiation, 205
definition, 204–205
Blackett, Patrick M.S., 294, 449–450, 453–460, 464–465
annihilation observed by, 458–459
cosmic-ray showers and, 458
nuclear collision measurements by, 453–454
Occhialini and, 456–457
pair production identification by, 458
proof of nuclear transmutation by, 455–456
Wilson cloud chamber automation by, 453, 457
Blau, Marietta, 465–466
cosmic ray showers studies of, 465
Einstein and, 465–466
escape from Nazi regime, 465–466
Nobel Prize nomination of, 465–466
photographic emulsion techniques of, 465
Bloch, Felix, 639
magnetic moment of neutron and, 662
NMR spectroscopy and, 664
Bohr, Aage, 396–397, 696
Bohr atom
atomic electron spectroscopy and, 395
Balmer series of, 393
creation of modern physics from, 408
electrons in quantum orbits of, 391–393
energy quantum absorption by, 392–393
energy quantum emission from, 392–393
hydrogen electron energy levels in, 394–395
inert gases and, 395
Lyman series of, 393, 395
Paschen series of, 393
quantized electron angular momentum in, 392
shortcomings in theory of, 408
spectral emission lines from, 394–395
Bohr, Niels, 101, 155–156, 232, 391–400, 408, 419, 432–433, 532–533
beta(n) decay theory of, 731
the Bohr atom and, 391–393
complementarity argument of, 412
electron orbitals and, 800
escape from Nazi occupation, 396
heavy nuclei disintegration theory of, 396
liquid drop model of nucleus and, 396
Manhattan Project and, 396–397
nuclear fission and, 396
nuclear nonproliferation and, 396–399
Open Letter to the UN, 398
Oppenheimer and, 396–397
as pacifist, 396–397
quantum electron orbits in atoms, 396f
quantum theory of atomic structure, 391–395, 400
Roosevelt and, 396–397
Rutherford and, 391
Rydberg formula and, 392–393
Weisskopf and, 396–397
Bohr's magneton, 164
Bohr's quantum theory, 407
Boltzmann, Ludwig, 309
Booster synchrotron, 287–288
Borlaug, Norman, 523–524
Born, Max, 407–424, 465, 640–641
electron probability density and, 421
interpretations of quantum mechanics, 419–420
Schrödinger and, 421
Boron-neutron capture therapy (BNCT), 374
advantages of, 17–18
applications of, 17–18
with liposome nanoparticles, 20
mechanism of, 17, 18f
Bose, Satyendra Nath, 803–805
Bosons, 780, 805–806, 806f
description of, 803–805
Bothe, Walther, 457–458
Bottom baryons, 736t
Brachytherapy, 14, 440–441
definition, 14
principle of, 14
in prostate cancer treatment, 15f
Brackett series, 392
Bragg's Law, 240, 427, 430–431
equation for, 248–249
Bragg, William H. and William L., 47, 51, 238–243, 812
atomic arrangement of NaCl and, 241
atomic structures of crystalline matter and, 242
crystal interatomic distance analysis, 238
first images of atoms in matter, 242
X-ray crystal structure analysis, 238, 240
X-ray spectrometer and, 238–239

Bragg, William L., 46–47, 51, 238–243
  Bragg's law and, 239–240
  the writer and, 242
  X-ray diffraction crystal structure analysis, 239
Branching decay
  definition, 172
Breeder reactors, 372
  Szilard and Fermi and, 339
Bremsstrahlung, 82, 195, 278–279
  artificial production of, 280
  beta-particle production of, 280
  electron accelerator production of, 281
  energy loss by, 198
  external, 283
  factors affecting, 195
  inner/internal, 281, 283
  intensity of, 278–279
  origin of, 276, 278
  photon energies of, 280
  production by cosmic-ray positrons, 279
  production of, 373
  properties of, 278
Bremsstrahlung intensity, 278–279
Bremsstrahlung production
  absorber atomic number and, 280
Bremsstrahlung radiation, 197–198
Brockhouse, Bertram N., 46
Brout-Englert-Higgs (BEH) mechanism, 781–782
Brout, Robert, 781–783, 788
  Englert and, 781–782
Brownian motion, 114–115, 213
Brown, Prentiss M., 743–744
Brune, Michel, 790
Bubble chamber
  advantages of, 485, 488–491
  antineutron annihilation tracks in, 491
  antiproton track in, 491f
  development of, 485–488
  Glaser and, 485
  internal conversion electron tracks in, 489f
  invention of, 485
  kaon and decay product tracks in, 488
  particle charge and momentum with, 488
  particle lifetimes and decay schemes with, 488
  particle mass and velocity measurements with, 488
  positive kaon and muon tracks in, 490f
  positive muon and pion tracks in, 489f
  principle of, 485–486
Bulletin of Atomic Scientists, 343
Bush, Vannevar, 432–433, 492–494
Butler, Clifford Charles, 452–453, 459
Byrnes, Jimmy, 342

C

Cadmium-109
  electron capture decay of, 436
Calorimeters, 759
Calutron, 589
Calvin–Benson–Bassham cycle, 22–23
Calvin, Melvin, 21–22
Carbon-14
  steady state condition on earth of, 602
  synthesis in upper atmosphere, 602
Carbon-14 dating
  anticoincidence counter for, 605–606, 607f
  Libby and, 603, 605–606, 607f, 608–609
  principle of, 603, 605–606, 607f, 608–609
  Suess effect and, 608–609
Carbon–nitrogen (CN) cycle, 598, 601
Castle Bravo, 347–348, 356–357
Cathode, 82
Cathode rays, 80–84, 90, 94–95, 115, 117–118, 121, 276, 114
Cathode ray tubes, 80–82, 117, 121f, 276
Cerenkov radiation. *See* Cherenkov radiation
Cerium-144
  decay scheme of, 272–273
CERN, 219, 742–745, 747, 749–750, 756, 759, 762–763, 765–771, 775, 781, 784, 786, 787f, 788
Chadwick, James, 46, 144, 303–309, 689–690
  binding energy of deuterium, 308
  Geiger and, 304
  neutron discovery by, 304, 800
  "neutron hypothesis" of, 304–305
  neutron mass determination and, 304
  neutron mass determination by, 305–308
  nuclear binding energy and, 306–307
  Rutherford and, 304
Chalmers, T.H., 324–325, 726–727
  photoneutron sources and, 325
  Szilard and, 324–325
  Szilard-Chalmers effect and, 325, 326f
Chamberlain, Neville, 326
Chamberlain, Owen, 423, 482–483
  antiproton discovery and, 474–485
  Clyde Wiegand and, 479
  Fermi and, 484
  in Manhattan Project, 483
  Segrè and, 483–484
  Thomas Ypsilantis and, 479
Changes in quantum states, 793
Charge
  particle charge, 68
Charge conjugation symmetry, 776–777
Charge conservation
  law of, 742–743
Charged current, 808
  definition, 760
Charged current interactions, 576f–577f, 762, 810
  examples of, 761f
  W^+ and W^- bosons and, 761f
Charged current reactions
  description of, 760
Charged particle breakup reaction, 366t
Charged particle direct reaction, 366t
Charged particle interactions, 199–200
  mechanisms of, 195
Charge, particle
  nuclear charge, 68
Charpak, Georges, 568
Chart of the Nuclides
  precursor to, 137
Cherenkov cone or ring, 537–539, 543f, 549f, 565f–571f, 573f, 575f–576f, 578f
Cherenkov conical radiation wave front, 479f
Cherenkov counter, 478, 479f
Cherenkov counting, 521, 579–581
Cherenkov effect, 521, 527–528, 540–545, 547–548. *See also* Cherenkov radiation
Cherenkov, P.A., 478–479, 527–543
  acceptance by *Physical Review*, 532–533
  discovery of Cherenkov radiation, 527–541, 532f, 547
  discovery of unknown radiation, 521
  experimental techniques of, 528–529, 530f, 532f, 534f, 535, 537–540
  freedom in balance, 527–541
  Igor Tamm and, 530–531
  Il'ja Frank and, 530–531
  Joseph Stalin's purges and, 527–541
  particle velocity measurement by, 532
  radiation energy output, 537–540
  rejection by journal *Nature*, 532–533
  research findings, 521
  Sergei Vavilov and, 521, 528–531
  student years, 528
Cherenkov radiation, 275, 492, 527–528, 529f, 542, 545, 548
  advantages in applications of, 540–541
  angle of emission, 531, 532f, 535–536, 548–549, 552–554, 555f, 558, 564
  applications of, 540
  asymmetric property of, 530–531, 533–535, 534f, 540, 548–549
  beta-particle energy output as, 540
  Cherenkov radiator, 579
  Compton electrons and, 530–531, 552–555, 530f
  confirmation of discovery, 535
  conical wavefront of, 537–539, 543f, 549f, 565f–566f, 568f–571f, 573f, 575f–576f, 578f
  conversion of cpm to dpm in counting of, 579
  electron or beta-particle energy and, 535
  electrons and beta-particles and, 550–552, 552t, 557f
  energy radiated by, 537–538, 543–544, 555–558
  Frank and, 521
  gamma radiation and, 530, 532f, 534f
  gamma rays and, 535, 552–555, 559–560
  high-energy beta-particles and, 530–532, 535
  high-energy electrons and, 532, 535
  image from reactor pool, 522f
  index of refraction and, 531, 535, 550–551, 552t, 555f
  intensities of, 555–558, 557f
  interpretation by Frank and Tamm, 542–544

Lucien Mallet and, 521, 548
Marie Curie and, 521, 548
MCR-PMT photodetectors for, 574
muons and, 552t
neutrino CC interactions and, 575, 577
neutrino electron scattering and, 575
neutrino measurements with, 574
neutrino NC interactions and, 577, 578f
in nuclear safeguards, 560
number of photons emitted as, 544
origin of, 530–531, 547–549
particle energy and, 531, 550, 553–554, 555f
particle energy discrimination, 540–541, 552
particle identification from, 560
particle mass and velocity and, 560
particle mass discrimination by, 552
particle phase velocity and, 531, 550
particle rest mass and, 550–551, 552t
particle speed and momentum and, 540
particle threshold energy and, 550–553, 552t
particle velocity and, 531
percent counting efficiencies, 579–581
photon detection efficiency, 558
photon intensity of, 535
photon pulse duration, 559
photon ring from, 537–539, 543f, 549f, 565f–566f, 568f–571f, 573f, 575f–576f, 578f
properties of, 540–541
protons and, 552t
radionuclide activity analysis from, 579
radionuclide counting efficiencies, 579–581
ring and cone spatial distribution of, 537
ring imaging Cherenkov (RICH) counters of, 563–564
spatial asymmetry of, 552–555
spectrum of, 535–536, 548, 555–558
Tamm and, 521
theory of Frank and Tamm, 531
threshold Cherenkov counters, 560
threshold condition for, 531, 535, 542–544, 550
TOF Cherenkov counters, 572
TOP Cherenkov counters, 570–571
total neutrino flux measurements by, 577
Vavilov and, 521
Cherenkov radiator
definition, 552
Cherenkov radio waves, 577
Cherenkov ring images, 563–564, 568–569, 569f–570f
Cherenkov threshold detector, 563
CIEMAT, 767–768
Climate change, 41–42
Cline, David, 767–768
Clinton, Bill, 357
Cloud chamber
C.T.R. Wilson and, 464–465
Cloud chamber, counter controlled,
advantages of, 458
operation of, 457f
Cluster fragmentation, 757
Cluster radioactivity, 702–703
of actinide nuclei, 704f
vs. alpha-emission, 702
binding energy per cluster and, 702
definition, 702
discovery of, 702
known clusters, 702
magic numbers and, 702
models for, 702–703
Cm-242, 615
CMS Collaboration, 788
CMS detector
description of, 785
Cobalt-60
parity violation in decay of, 657
polarized, 654–655
Cockcroft, J. and Walton, E.
accelerated ^{2}H reactions and, 594
artificial transmutation of ^{12}C to ^{13}N, 595
confirmation of Einstein's $E = mc^2$, 593–595
demonstration of proton tunneling by, 594
disintegration of ^{11}B with ^{1}H beam, 594
equivalence of mass and energy and, 589–590
first artificial transmutation, 589–590, 593
Gamow's tunneling theory and, 594
principle of accelerator by, 592–593
proton accelerator development by, 589–593
Cockcroft, John D., 464–465, 589–596
Cohen, Samuel T., 356–357
Coincidence circuit, 457
Coincidence time, 457
Coincidence window, 457
Collective model, nuclear, 696–698
nuclear shape oscillations in, 696–697
quadrupole moments in, 696
Collins, George, 535
Color charge, 750, 779, 803
quantum chromodynamics and, 803
Color charge, quark
in baryons, 682
definition, 682
in mesons, 682
as quantum state, 682
Color force
definition, 682
Complementarity argument
Bohr and, 412
Heisenberg and, 412
Complex decay schemes, 634
Compound nucleus, 151, 381, 385–388
Compton, Arthur H., 226–230, 292, 451
Compton Effect and, 227
cosmic-ray latitude effect and, 230
Wu Youxun and, 228
Compton effect, 228f, 230, 292–293, 300
confirmation of the photon particle by, 230
discovery, 227
photon energy loss in, 293
quantum theory of light and, 227–228
recoil electron energy in, 227–228
scattered quantum energy in, 227–228
wavelength shift in, 292
Wilson cloud chamber images of, 228, 229f–230f
Wu Youxun and, 231
X-ray scattering intensities in, 228, 229f
Compton electrons, 229f, 530–531, 535, 552–553
first particle track of, 141–143
Compton scatter, 195, 292, 536f
photon energy in, 293
Compton-scatter photon, 292
Compton–Wu Effect, 231
Computed axial tomography (CAT). *See* X-ray computed tomography (CT)
Conant, James, 432–433
Conical wave fronts, 548–549, 549f
Conservation of strangeness
examples of, 736–738
Conservation of strangeness law, 735–736
violation of in weak interactions, 736–737
Controlled thermonuclear fusion (CTF), 60, 375–377, 545
Controlled thermonuclear reactors, 60–66, 375–377
Cork, Bruce, 481
Cormack, Allan M., 6
Corson, Dale R., 482
Cosmic microwave background radiation, 506–513, 495
Big-Bang theory and, 511
blackbody form and anisotropy of, 510
blackbody form of, 510–511
blackbody spectrum of, 514f
blackbody temperature of, 510f, 511–512
discovery of, 508–509
interpretation of, 508
isotropic character of, 511
Mather and Smoot and, 510
spectrum of, 509, 510f, 511–512
spectrum of expanding universe, 513
temperature of, 509
Cosmic radiation, 462, 495
anomalous, 506
classification and properties, 496–500, 497t
composition of, 496, 497t
discovery of, 445
energy spectrum of, 500f
extragalactic, 506
galactic, 497t, 506
hard and soft components of, 470–471
interstellar density of, 496
latitude effect of, 496
origins of, 506
particle kinetic energies of, 498
pion decay in, 471f
primary, 496–497, 498f, 499
proton relativistic masses of, 499
proton relativistic speeds of, 498–499
relativistic particle speeds of, 497
secondary, 496–497
showers, 462, 501–505
underground, 505–506

Cosmic radiation, air showers
abundances of particle components in, 503
charged pion decay in, 502
definition, 495, 501
discovery of, 458
energy loss of muons in rock, 505
measured dilated lifetime of muon in, 504
mechanisms of muon energy loss in, 505
muon decay in, 502
muon ranges of, 505
negative meson nuclear capture in, 470
negative muon nuclear absorption of, 503
neutral pion decay in, 502f
penetrating component of, 505
pion decay to muon in, 470
secondary nucleons of, 501
secondary radiation of, 501f
subatomic particles in, 501
vertical particle fluxes of, 503f
Cosmic-ray nucleons
Fermi acceleration of, 500
flux distributions of, 497–498
mechanisms of acceleration, 500
Cosmic-ray positrons
measurement of, 279
Cosmic ray soil moisture observing system, 29–30
Coster, Dirk, 232, 313, 440
Coster–Kronig electrons, 440–441
Coster–Kronig transition, 440
Counting efficiency, 579
Cowan, Clyde L. Jr., 156b, 157–163
discovery of neutrino by, 801
in Manhattan Project, 157–158
neutrino detection and, 157
Pauli and, 135
Reines and, 157–162
CP symmetry, 775–776
Cronin and Fitch and, 777
definition, 775–776
in neutral kaon decay, 777
violation of, 777
Creation of the “new physics”, 408
Creation of universe
CP asymmetry and, 777
matter over antimatter, 777
Critical mass, 323f–324f
Szilard and, 321–324
Cronin, James W., 775–777
Crooke’s tubes, 80–81, 84, 87–88, 114, 276
Crookes, William, 84–86, 114, 128
Crop fertilizer use efficiency
isotopes and, 26–30
Crop water use efficiency
isotope water signatures and, 30
neutron moisture probe and, 26–30
Cross section, reaction, 719–721
definition, 719
Cuban Missile Crisis, 358
Curie Institute, 92
Curie, Iréne
life before marriage with Frédéric Joliet, 144
Curie, Marie and Pierre, 90–93, 799–800
birth of nuclear medicine and, 2
coining of the word radioactive by, 91
discovery of polonium and radium, 94
leukemia and, 146
polonium and radium, 91
radiation sickness and, 91
radiation therapy and, 92
uranium and thorium and, 91
Cyclotron
applications in medicine and biology, 589
development of, 586–588
invention of, 583–585
Lawrence and, 585–588
McMillan and Seaborg and, 588
principle of, 585, 586f, 587
radioisotope production by, 583–584
radioisotope production with, 588–589

D

D’Agostino, Oscar, 481
Daladier, Édouard, 326
Daudel, Raymond
Electron capture decay and, 183
Davis, Raymond Jr., 182, 725
Davisson, Clinton, 407–408, 424–433, 459
de Broglie matter-wave and, 425
elastic scattering of electrons, 425
electron diffraction and, 425, 426f, 427
electron wavelength calculation of, 425
electron wave properties and, 800
Germer and, 425, 426f
proof of de-Broglie matter-wave, 425, 427
de Broglie electron matter-wave, 432
de Broglie, Louis Victor, 46–47, 207–210, 364–365, 395, 407–408, 414, 421, 425, 428
particle-wave duality and, 203, 207–210, 792, 800
wave-particle duality of electron and, 208, 425, 426f, 427–432
de Broglie matter wave, 425, 427
de Broglie wavelengths, 364–365
calculation of, 209
equation for, 208–209
Decay chains, natural
^{232}Th decay chain, 74
^{235}U/actinium decay chain, 74, 75f
^{238}U decay chain, 74, 75f
Decay constant, 624–625
calculation of, 624–625
definition, 624
Decay energy, 123–126
alpha, 123–124
double beta, 186–188
electron capture, 180–182
negatron, 171–174
positron, 176–179
Decay energy (Q_{β^-}), 167, 171–174
Decay energy (Q_{β^+}), 176–178
Decay equilibria, 629–634
Decay in a magnetic field
method, 713, 713f
technique, 713f
Decay modes, nuclear
description of, 713
transitions in, 714f
Decay of the Higgs boson, 787f
Decuplet
of spin 3/2 baryons, 741f
de Hevesy, George, 49–50, 313
Paneth and, 21
Rutherford and, 20–21
Delta baryon, 166, 736t, 738, 741f, 807f
Delta rays, 199–200
definition of, 143
description of, 200
Democritus, 79–80
atomism and, 799
DEMO fusion reactor, 61
Density, 679–680
Desalination of seawater, 58
Desalination plants
nuclear power and, 59
world numbers, 59
Detection efficiency, 558
Determination of energy or velocity, 531
Deuterium fusion, 687
Deutsch, Martin, 754
Deviable rays, 94
Diffraction, 46–47
Diffraction of an electron beam, 431f
Diffusion cascade, 401
Dirac, Paul A.M., 233, 407–424
antiparticle prediction, 422
as introvert and genius, 423
prediction of annihilation, 422
prediction of antiproton, 423
prediction of pair production, 422
prediction of the positron, 422
quantum theory of electron, 422
Direct neutron emission, 712
Direct proton emission, 707–708
Discrimination between particles, 552
Disequilibrium, radioactive
from nuclear recoil, 728
Szilard-Chalmers effect and, 728
Disintegration rate, 67
Displacement law of radioisotopes, 137
DNA structure
Franklin and, 243
d,n reactions, 374
Dose, absorbed radiation
to aircrew from cosmic radiation, 517, 518t
to astronauts from cosmic radiation, 517–518
by average person per year, 516
calculation of, 514–515
from cosmic radiation, 516, 517f
definition, 514
gray unit of, 514
latitude and altitude effects, 516, 517f
limits for radiation workers, 516
quality factor for, 515–516
rad unit of, 514
rem unit of, 515

Sievert unit of, 515
sources of, 516
weighting factor for, 515–516
Dose, radiation
definition, 514
units in measurement of, 514
Dose, radiation equivalent
calculation of, 516
Dosimeter
pocket, 90
Double-beta decay
decay energy of, 186–188
discovery of, 185–186, 640–641
Goeppert-Mayer and, 640–641
neutrinoless, 188–190
Double-spin mesons, 166
Doubly magic nuclides, 694
Down quark, 188–189, 576
charge and mass of, 681–682
fractional charge of, 801–803
mass of, 804t–805t
Dual beta decay. *See* Beta decay; branching
Dunoyer, Louis, 163–164

E

Earth
age of, 69, 72
Eaton, Cyrus, 351–352
EC decay
branching, 183–184
chemical and pressure effects in, 182–183
energies of, 180–182
principles of, 179–180
Eddington, Arthur, 223–224
Eddington, S., 597
Edlefsen, Nels, 586
Electromagnetic interaction, 780
Effective atomic numbers, 199
Eightfold Way, 734, 738–740
Gell-Mann and Ne'eman and, 739–740
organization of particles by, 738–739
prediction of eta particle and, 739
prediction of sigma particle from, 739
quarks and, 748–749
of spin 1/2 baryons, 738–739
of spin 3/2 baryons, 739
of spin 0 mesons, 738–739
of spin 1 mesons, 738–739
Einstein, Albert, 46, 70, 92–93, 102–103, 110, 115, 205–206, 210–226, 303, 312–313, 317, 326–327, 330f, 343, 351–353, 407–408, 421, 465–466, 811, 827
anti World War I manifesto and, 224
Brownian motion and, 114, 213
discovery of photon particle by, 46–47, 102, 121–122, 205–206, 211–213, 256, 259, 269–270, 407, 800
Eddington and, 223–224
Emergency Committee of Atomic Scientists and, 225f–226f, 226f, 601
emigration to United States, 224
interaction of gravitational mass and photons, 223–224
law of photoelectric effect, 210, 212–213, 259–260
Lemaître and, 507
letter to Franklin D. Roosevelt, 225, 326–327, 328f
Lorentz transformations and, 110, 207, 823–824
as mailbox for Szilard, 326–327
Manhattan Project and, 326–327
Marie Curie and, 92
Marietta Blau and, 465
Max Planck medal and, 204
Meitner, Lise and, 313, 317, 435
Millikan and, 213
Nobel prize and, 224–225
as pacifist, 225–226
Pauli and, 153
photoelectric effect and, 121–122, 269–270
photoelectric effect interpretation by, 211
photoelectric equation of, 291
Planck and, 212
quantum theory interpretation by, 211
relativistic length contraction and, 213–216, 215f, 218f, 219, 823–829
relativistic time dilation and, 213–214, 215f, 216–217, 823–827
relativity and, 213–224, 823–827. *See also* Relativity
Russell and, 226, 348–349
Russell–Einstein Manifesto and, 226, 303, 348–351
Sachs and, 225
Szilard and, 225, 319, 321, 324, 326–327, 341f
Einstein–Bohr formula, 256
Einstein–Planck relation, 292–293
Einstein's energy-mass equivalence $E = mc^2$, 70, 124, 220–222, 294, 306–308, 362, 375–376, 459, 462, 480, 589–590, 683, 686, 801, 803
calculation of fusion energy by, 600
confirmation by Cockcroft and Walton, 593, 595
demonstration of, 458, 590, 593, 595, 599–600
Einstein's letters to Roosevelt, 225, 326–327, 328f, 330f, 341f, 342
Szilard and, 225, 324, 330f, 340–342
White House reply, 330f
Einstein's light quanta
Millikan and, 259
Einstein's theory of relativity, 110, 213–223, 823–827
relativistic length contraction and, 213–216, 823–827
relativistic mass and, 221–222, 476
relativistic time dilation and, 213–214, 216–220, 266–267, 504, 733–734, 823–827
Stern and, 163–164
Elastic collisions, 195, 379–380, 453
Elastic scattering, 47, 379–380, 575
definition, 379, 714
Elastic scattering of electrons, 425
ElBaradei, Mohamed, 398–399
Electrical radiometers, 84, 85f
Electricity and magnetism
unification of, 111
Electrode matter, 84, 85f, 87
Electromagnetic force, 760, 807, 808f
atomic structure and, 802f
description and strength, 807
photons as carriers of, 672–673
in QED, 676–677
Electromagnetic interaction
Feynman diagram of, 762–763
in QED, 676–677
Electromagnetic interactions, 148
Electromagnetic quantum, 807
Electromagnetic radiation, 438
interactions with matter, 291–302
properties of, 291
spectrum of, 112f
Electron binding energy, 270, 437–438, 439f
Electron capture (EC), 167, 179–183, 276f, 436f, 438, 439f, 729
decay energy calculation, 181–182
description of, 276
discovery of, 730–731
Electron capture decay
basic principles of, 179–180
in Be-7, 180f
chemical and pressure effects in, 182–183
description of, 179
Na-22 and, 177–178
neutrino energy calculation in, 181
neutrino energy in, 182
positron emission and, 179–181
transition and neutrino energy of, 179
Electron charge, 259
Electron de Broglie wavelength
calculation of, 425, 428
Davisson and, 425
Thomson and, 428
Electron density contour map, 812
Electron density map, 51
Electron diffraction, 425, 427
predicted by de Broglie, 209
Electron diffraction and,
proof of de-Broglie matter-wave, 432
Electron energy, 395, 405f, 555f
Electron excitation, 128
Electron groupings in quantum orbits, 391–392
Electron gun, 287–288
Electron, high-energy
radiation sources in scintillating crystal, 537
Electron kinetic energy, 428–429
Electron matter-wave, 425, 426f, 427
Electron orbital, 812
definition, 415
Schrödinger's wave function and, 415
Electron orbital excitation, 195

Electron, probability density of atomic, 415, 416f, 419, 421
Electrons, 117–119, 121, 312, 532
antiparticle of, 274–275
Cherenkov threshold energies of, 552t
discovery of, 117
magnetic moment of, 164
naming of, 118
origin of, 118
ranges in dry air, 191t, 817f
ranges in low Z absorbers, 190–191
ranges in water, 818f
rest energy calculation of, 294, 550
Electrons, atomic
binding energies of, 439
Electrons, high energy
deep inelastic scattering in nucleons, 756
Electron transitions, 277
atomic, 438
Electron velocity, 429–430
Electron volt
definition of, 70
Electron wavelength, 429–430
Electroweak force, 148, 763
Electroweak theory, 763
Electroweak unification, 763
Elementary particles
definition of, 778–779
quarks and leptons, 803–805
Elliott, Steven R., 640–641
Elster, Julius, 128
Emergency Committee of Atomic Scientists, 225, 226f
Emission angle, Cherenkov, 548–549, 558
Emulsion, 466–467
Endoergic or endothermic reaction
definition, 71
Endoergic reaction, 715
Endothermic reaction, 715
Energy as quanta of radiation, 393
Energy-level transitions, electron
X-ray *vs.* Auger-electron emission in, 439
Energy quanta, 800
discovery of, 203
Planck's discovery of, 269–270
Energy, Cherenkov radiated, 555–556
Englert, François, 781–788
Brout and, 781–782
Eniwetok, 357
Enrichment of isotopes, 401
Epithermal neutrons, 17
Erg
definition of, 70
Estermann, Immanuel, 164
Eta particle, 166
Ether, 85–86, 114
European Organization for Nuclear Research. *See* CERN
Exclusion Principle, Pauli, 153, 422
atomic orbital electron and, 154
description of, 153–154
Exoergic or exothermic reaction
definition, 71
Exotic isotopes, 703–704
Exotic nuclei, 703–704, 710
Experimental Breeder Reactor-I, 58–59
Exposure, radiation
roentgen and, 514
External beam radiation therapy
cobalt therapy in, 10
3D conformal radiotherapy, 12, 13f
4D conformal radiotherapy in, 14
intensity modulated therapy in, 12, 13f
Leksell Gamma Knife in, 11–12, 12f
with protons and heavy ions, 15
in radiation oncology, 11
X-ray photons in, 10

F

Fajans, Kasimir, 312
Faraday cylinder, 115
Fast and intermediate neutrons, 381
Fast neutrons, 28, 369
Fat Man, 340
Feather analysis, 192–193
Feather, Norman, 128–129, 305–306, 731
Federation of Atomic Scientists, 483
Fermi beta decay, 148
negative beta decay, 149f
neutron-proton transformations in, 148–149
positive beta decay, 149f
Fermi, Enrico, 58, 120, 147–153, 156–157, 312–313, 321–322, 324, 326, 332–334, 336f–337f, 355, 461, 481, 500, 641–642, 714, 361, 679
atomic pile and, 151
beta decay theory of, 148, 150
escape from Mussolini's regime, 147–148
first self-sustaining nuclear chain reaction and, 151
Leona Marshall and, 609
letter to Szilard on reactor, 334
Manhattan Project and, 152
neutrino and, 148, 156b
neutron capture isotope production and, 801
neutron-induced nuclear reactions and, 150
radioisotope production and, 151
reactor patent with Szilard and, 334, 335f–337f, 338
Szilard and, 151
thermal neutron capture and, 150–151
transmutations with neutrons and, 146
Fermions
definition, 68, 154
description of, 803–805
Fermi–Szilard reactor patent, 334–335, 339
first page of, 335f
heavy water reactor in, 336f
sequence of reactor events and, 337f
Fernández, Carlos Graef, 493–494
Feynman diagrams
description of, 676–677
QED described by, 675
Feynman, Richard P., 448, 493, 670–677, 680–681, 743
Bethe and, 673–674
Bethe and, 673–674
Feynman diagrams and, 674–675
in Manhattan project, 673–674
Manuel Sandoval Vallarta and, 672–673
Reines and, 157
Fine structure constant, 807
First X-ray images, 88
Fissile materials, 372
breeding of, 372
Fissionable isotopes, 372
Fission fragments, 382–383
Fission, nuclear, 382–383
chain reaction from, 371–372
neutron-induced, 369–372
nuclear drop in, 369
in plutonium-239, 372
Q value of U-236 fission, 369
of Th-232, U-238 and Np-237, 372
in uranium-233, 372
in uranium-235, 369
Fission phenomena, 396
Fission *vs.* fusion
advantages of fusion, 688
energy yields per fuel mass, 687–688
Fitch, Val L., 775–777
Fletcher, Harvey, 255–264
charge on the electron and, 255–259
Millikan and, 255–264
posthumous memoir on oil-drop experiment, 260
role in oil-drop experiment, 260
Fluorescence, 98, 128
Fluorescence yield, 439–440
Fluorescent, 80–81
Food irradiation, 56, 281
Force binding quarks, 682–683, 747, 750–753
Zweig and, 747
Force, electromagnetic
virtual photons and, 680–681, 681f
Forces/interactions in Nature
classification of, 654, 654t, 807–811, 807t
Force, strong nuclear
pion and, 680–681, 811
quark-gluon interactions and, 683f
range of, 683, 807t, 811
Yukawa and, 680–681
Franck–Hertz apparatus, 405f
Franck–Hertz experiment, 406f
arrangement and principle of, 405–407
atomic quantum energy states and, 404–407
Bohr's quantum theory and, 404–407
James Franck and Gustav Hertz and, 404–407
quantized energy transfer to atom, 404–407
Franck, James, 400–402
efforts against nuclear weapon use, 402
Henry Stimson and, 402
in Manhattan Project, 402
Nazi Germany and, 402
proof of Bohr's quantum theory and, 400
Seaborg and, 402
Szilard and, 402

Franck Report
call for international agreement on prevention of nuclear warfare, 403–404
call for international nuclear weapons control, 404
call for international organization for peace, 403–404
nuclear nonproliferation and, 402–404
potential nuclear arms race and, 403–404
potential total mutual destruction, 403–404
proposal against use of atomic bomb, 403–404
Frank, Il'ja M., 521, 531
Cherenkov effect theory and, 541–546
Cherenkov radiation origins and properties, 541–546
Cherenkov radiation theory and Vitaly Ginzburg, 545
Sergei Vavilov and, 545
Frank, James, 58, 339
Franklin, Rosalind, 51, 243–248
Crick and, 247–248
Crick and Wilkins and, 246
crucial x-ray data on DNA structure, 248
discovery of helical DNA, 244–245
DNA structure analysis by, 243
DNA X-ray diffraction photo, 245–246
early death and loss of Nobel, 246–248
petition for publication of DNA work, 247
Raymond Gosling and, 244–245, 247
Watson and, 246
Watson and Crick and, 245–246
Wilkins and, 244–245
X-ray diffraction photos of DNA, 244–245
Friedman, Jerome I., 743, 747, 753–760
demonstration of quarks and gluons, 753
discovery of quarks and, 803
Hofstadter and, 754
Frisch, Otto R., 58, 233, 311, 326, 346, 396, 432–433, 690–691
interpretation of nuclear fission by, 801
nuclear fission and, 313–314
Fritzsch, Harald, 743, 750–753
color charge and, 750–751
Gell-Mann and Leutwyler and, 750–751
gluons and, 750–751
quantum chromodynamics and, 803
Fuchs, Klaus
as Manhattan Project spy, 674
Fumerase
atomic structure of, 812
Fundamental interactions, 778–779
Fundamental interactions/forces
in the Standard Model, 780
Fundamental particles. *See* Elementary particles
Fusion, nuclear, 375–377
D-D fusion, 376–377
definition, 375
D-T fusion, 375–377
between ^{2}H and ^{3}H, 687
between ^{2}H nuclei, 687
as future source of energy, 60–66, 801
inertial electrostatic confinement, 377–378
Fusion power reactor
energy output from, 62
major components of, 61–62
plasma magnetic confinement in, 62–63
principle of operation, 61–62
tritium breeding by, 62
Fusion reactions, 374
Fusion reactor. *See* Nuclear Fusion reactor

G

Gamma radiation, 94, 96–97, 124–126, 179, 271–273
absorption edges of, 300
attenuation of, 296, 298, 300
discovery of, 94
energy lines of, 148
energy of, 124–125
galactic, 496
from neutron capture, 381
origin and properties, 801
origin of, 271, 291
Gamma-ray emission, 167–168, 436
following beta decay, 173f, 177, 179f–180f, 182
Gamma-ray interactions, 560
Gamma-ray photon
pair production from, 220
Gamma rays, 95, 552–553, 563
discovery of, 93–96
energy of, 271–273
frequency calculation of, 271
internal conversion of, 502
momentum of, 271
origin of, 270, 275–276
wavelength calculation of, 271
Gamma-ray spectrometry
photoelectric effect and, 212
Gamma recoil, 325, 326f
Gamow, George, 126–127, 508–509
Big-Bang Theory and, 508
tunneling theory of, 591, 594
Gas electron multiplier, 709
Gaseous diffusion
diffusion cascade in, 401
Gustav Hertz and, 400–401
isotope enrichment by, 400–401
principle of, 400
technique of, 400–401
Gas ionization, 95
Gas ionization detector
development of, 107–108
invention of, 104–106
Geiger counters, 102, 108, 144–145
Geiger, Hans, 98–101, 103, 106–107, 126, 128–129, 457, 756
Geiger–Muller counter and, 108
proportional counter and, 106
radiation counter and, 107–108
radioactivity counter and, 102, 104–106
Rutherford and, 103–104
Geiger, Johannes "Hans", 103–108
Müller and, 108
Geiger–Müller counter, 126, 146
counting plateau of, 108
development of, 108
Geiger–Nuttall apparatus, 106f
Geiger–Nuttall Law, 107, 126
Geitel, Hans, 128
Gell-Mann, Murray, 734–743, 746–747, 750–751, 759–760
Eightfold Way and, 738–739
Fritsch and, 743
Leutwyler and, 743
proposal of quarks by, 681–682
quark theory and, 800–803
strangeness theory of, 735
Gerlach, Walter
work with Stern, 164
Germer, Lester, 407–408, 425
Ghiorso, Albert, 615
Giesel, Friedrich, 443
Ginzburg, Vitaly, 526, 545–546
Glaser, Donald A.
Anderson and, 485–492
bubble chamber development, 485–488
invention of bubble chamber, 485–492
Glashow, Sheldon H., 760, 762
Global warming
delta ^{13}C and greenhouse gases, 41–42
delta ^{18}O and ocean deoxygenation, 42
isotopes in studies of, 41
Gluon binding energy, 804t–805t
mass of matter and, 810
Gluons, 79–80, 166, 682, 750–752, 755, 780, 803, 805–806, 729
binding energy of, 803
color-charge quantum states of, 682
contribution to atomic mass, 803, 804t, 805t
contribution to mass of nucleon, 166, 803, 804t, 805t
definition, 751
description of, 682
discovery of, 753, 755–756
emission and absorption between quarks, 682
emission and absorption of, 752, 753f
as force carrier between quarks, 802f
as force exchange bosons, 803
as "glue" binding quarks, 803
as quark binding force, 747, 752f
role in strong nuclear force, 682
visible evidence for, 756–757
Goeppert-Mayer, Maria, 639–645, 652, 694, 679
Born and, 640–641
double-beta decay and, 640–641
Fermi and, 641–642
magic numbers and, 643
in Manhattan Project, 641
nuclear shell structure and, 642
Teller and, 641
Urey and, 641
Goldhaber, Gerson, 481
Gold-leaf electroscope, 311, 444, 444f

Gondola, 771
Göring, Otto H., 312
Goudsmit, Samuel, 164–165
Graaff, Robert Van de, 591
Graef Fernández, Carlos, 493–494
Gravitational force, 780–781
Gravitational mass
  photon interaction in, 223–224
Graviton, 780–781, 811
Gravity, 780–781, 811
Gray
  definition, 11, 35–36
Greenberg, Oscar Wallace, 682, 750–753
  quark color charge and, 803
Green revolution, 34–35
Gross, David J., 757–758, 765
Groves, Leslie R., 342, 346, 451
Gun assembly atomic bomb, 339f

H

Hadron calorimeters, 759
Hadronization
  Feynman diagram of, 758f
  process of, 757
  from quarks and gluons, 757
  sequence in LEP, 757
Hadron jets, 758–759
  in electron-positron collider, 757f
  quarks and gluons in, 757f
Hadrons, 680, 807f
  description of, 806
Hahn, Alan A., 640–641
Hahn, Otto, 58, 77–78, 233, 309–318, 326, 346, 355, 396, 435, 610–611, 690–691
  discovery of fission by, 801
  Fermi Prize and, 315, 317
  Fritz Strassmann and, 147, 151
  at the Kaiser Wilhelm Institute, 310
  Meitner and, 310, 316–317
  with Meitner and nuclear fission, 313
  nuclear fission and, 313–314
  Rutherford and, 310
Half-life, 621–628
  definition, 621
  graphical measurement of, 622
Half-life measurement
  of long-lived radionuclides, 627
  for mixture of two radionuclides, 626–627
  of short-lived radionuclides, 628
Half-value thickness, 297–298, 300, 384
Hallwachs, Wilhelm
  photoelectric effect and, 211
Han, Moo Young, 743, 750–753
  quark color charge and, 803
Harmful algal blooms, 43–45
  definition, 43–44
  poisoning from, 43–44
  receptor binding assay for toxins from, 43–44
Haroche, Serge, 415, 789–798
Hawking, Stephen, 508
Haxel, Otto, 642, 694
H-bombs, 350, 353–355, 356f, 357–358
Health sciences
  nuclear medicine in, 2–20
Heavy ion therapy, 15–17
  advantages over proton therapy, 15–16
  advantages over X-ray photon therapy, 16–17, 16f
  carbon ions in, 15–16
Heaviside, Oliver, 492, 548f
  prediction of Cherenkov effect, 547–548
Heisenberg uncertainty principle
  meson mass prediction by, 461–462
Heisenberg, Werner, 233, 407–424, 461, 683, 689–690
  quantum mechanics and, 408
  Uncertainty Principle and, 410–411
  Uncertainty Principle of, 409
Herman, Robert, 508–509
Hertz, Gustav, 27, 400–402
  gaseous diffusion for isotope enrichment and, 400–401
  ^{2}H enrichment by, 400
  proof of Bohr's quantum theory and, 400
  ^{235}U enrichment in Russia by, 401
Hertz, Heinrich, 112, 121, 269
  photoelectric effect discovery, 211
Hess, Victor F., 443–446
  cosmic radiation discovery by, 495–496
  cosmic ray fluctuations and, 445
  discovery of cosmic radiation and, 444–445
  escape from Nazi regime, 445
  Lieben Prize and, 445
Higgs boson, 805–806
Higgs mechanism, 810
  origin of mass and, 782–783
Higgs, Peter W., 781–788
Hildebrand, Roger, 488
Hiroshima, 339–340, 349–350, 353
Hiroshima bomb
  ivory tower mentality and, 799
Hitler, Adolf, 326, 340
  assassination attempt on, 206
Hodgkin, Dorothy, 52
Hofstadter, Robert, 754–755, 639
  electron scattering on nucleons, 662–663
  nuclear charge density and, 662–663
  nuclear radius and, 662–663
  nucleon internal structure and, 663
Hounsfield, Godfrey N., 6
Hove, Leon Van, 744–745, 765
Hydrogen bubble chamber, 729
  development of, 733
  dilated particle lifetimes and, 733–734
  discovery of sigma particle with, 739
  particle lifetime measurements by, 733
  particle track production in, 733
  particle tracks in, 734f
  resonance particle discoveries by, 733–734
  sigma particle track in, 741f
  strange particles and, 733
  tracks of strange particles in, 733–734
Hydrogen "Super" bomb, 355, 356f
  father of, 353–354
  as fission-fusion-fission device, 347–348, 356f
  function and reactions of, 356
  nuclear fallout from, 356
  Rotblat and, 347
  Teller–Ulam assembly, 355
  warning from Rotblat and, 356
Hyperons
  definition, 807

I

IAEA, 398–399
I-125 brachytherapy, 440–441
IC coefficient, 438
IceCube/AMANDA, 575
Ig Nobel Prize for Peace, 358
Implosion assembly atomic bomb, 339f
Index of refraction, 551, 552t, 555
  definition, 548
Inelastic collision
  definition, 714
Inelastic neutron reactions, 195
Inelastic scattering, 46–47, 379–381, 717
  definition, 380–381
Inert gases, 395
Inertial electrostatic confinement fusion, 377–379
  applications, 379f
Inner bremsstrahlung. *See* Internal bremsstrahlung
Insect pest control
  radiation sterilization for, 24–26
Institute for Nuclear Research, Moscow, 171
Internal bremsstrahlung, 179
  in beta decay, 281
  electron capture and, 281
Internal conversion, 435, 436f
  discovery of, 435
  gamma-ray emission and, 436
  IC coefficient, 436–437
  nuclear decay by, 436
Internal conversion coefficients
  dependency on Z and transition energy, 437
Internal conversion decay
  gamma-ray emission and, 435
Internal conversion electrons, 435–438, 489f
  electron shell origins of, 436–437
  energies of, 435, 437–438
  properties of, 437–438
  shell conversion coefficients of, 436–437
Internal conversion, gamma ray, 489f
Internal pair production, 295–296, 295t, 489f
International agreement on total prevention of nuclear warfare, 403–404
International Atomic Energy Agency (IAEA)
  nuclear nonproliferation and, 399
International control of nuclear armaments, 404
International organization for peace, 403
Intersecting storage rings
  proton-antiproton collisions with, 767–768
  of proton synchrotron, 767–768

Inverse beta decay, 169–170, 810
antineutrino and, 169
detection of solar neutrinos by, 170
discovery of neutrinos by, 158, 160f, 161
neutrino and, 169–170
neutrino energy in, 170
quark flavor conversion in, 810
Reines and Cowan, Jr., and, 158–161
Iodine-125
Auger and IC electron emissions in, 441f
Iodine-125 brachytherapy, 441f
Ionization, 128, 134, 195
by alpha particles, 129
energy loss by, 198
Ionization energy
calculation of, 394
Ion pair formation, 128
Ion trap, NIST, 793f
Irradiation
industrial applications of, 281
Irradiation of blood, 55
Irradiation of domestic sewage, 57
Irradiation of hospital waste, 56
Ising, Gustaf, 319, 584, 585f
Island of Stability, 701
Isobars
definition of, 69
Isomeric energy states, 273
Isomeric transition, 271, 273
Isomers, nuclear
definition, 69–70
Isotones
definition, 70
Isotope dilution, 27
Isotopes
definition of, 69
discovery of, 137
ITER project, 60–61
ITER Tokamak, 61
fusion reactor, 64f
size and energy output, 63
Iwanenko and Pomeranchuk radiation, 286

J

James, R.A., 615
Jensen, J. Hans D., 639–645, 694
Bohr and, 643
nuclear shell structure and, 642–643
Joint European Torus reactor, 60–61
Joliet-Curie, Iréne, 74–76, 143–147, 312–313, 361
artificial production of radioisotopes, 2
leukemia and, 147
Paul Savitch and, 147
Joliet-Curie, Iréne and Joliet, Frédéric
birth of radiochemistry and, 146
contribution to nuclear power, 147
early work leading to discovery of neutron, 144
element transmutation and, 145
first artifically produced positrons and, 144–146
first artificial transmutation by, 146
nuclear reactions and, 145
origin of the term "radioisotopes" and, 146
radioisotope synthesis and, 144–146
Joliet, Frédéric, 74, 143–147, 361
life before marriage with Iréne Curie, 143
Jona-Lasinio, Giovanni, 777

K

Kaiser Wilhelm Institute, 309–310
Kaon, neutral
discovery of, 459
Kaons, 166
in cosmic ray showers, 452
Kaons (K-mesons), 501–502
Kapitsa, Pyotr L., 525
KATRIN experiment, 171
K capture, 438, 729–731. *See also* Electron capture
description of, 276
Kendall, Henry W., 743, 747, 753–760
demonstration of quarks and gluons, 753
discovery of quarks and, 803
Hofstadter and, 754–755
Martin Deutsch and, 754
Kendrew, John, 52
Kennedy, Joseph W., 614
Kilotons TNT equivalent, 340, 356–357
Kinetic energy, 361–364, 550
Kirchhoff, Gustav
Planck and, 203–204
thermal radiation and, 204–205
Klein–Nishina formula, 232
Klein, Oskar, 763
Knipling, Edward F., 24–25
Kobayashi, Makoto, 748, 773–781
broken symmetry origin, 774
Maskawa and, 774–775
matter *vs.* antimatter, 775–776
prediction of six quarks, 775–776
quark families, 774
Standard Model and, 782–783
symmetry breaking, 775–776
Korea Superconducting Tokamak Advanced Research (KSTAR), 60–61
Kronig, Ralph, 440
K-series X-rays, 252
KSTAR fusion reactor, 63f
Kubo, Ryogo, 233
Kundt, August, 80, 83–84
Kurchatov, Igor, 545
Kusch, Polykarp, 659

L

Lambda hyperon
mass and decay modes of, 480
Lambertson, R., 481
Lamb shift, 674–675
Lamb, Willis E. Jr., 729
Landsberg, Grigori, 523–524
Large electron-positron (LEP) collider, 756–757, 759
hadron jets in, 757f
Large hadron collider (LHC), 756–757, 784, 784f, 785f, 786–788
Larmor frequency, 659
Lattes, Césare, 462, 467
Lauterbur, Paul C., 667–669
Law of the photoelectric effect, 212–213
Lawrence Berkeley National Laboratory, 474, 589
Lawrence, Ernest O., 46, 77, 233, 284–285, 358, 476, 481, 591, 614
Calutron and, 589
cyclotron production of radioisotopes, 2
Edlefsen and, 586
^{235}U enrichment and, 589
invention of cyclotron by, 583–589, 801
in Manhattan Project, 589
Rutherford and, 584
Lawrence Livermore National Laboratory, 357, 358b
Lawrence and Teller and, 589
Lazarev, Pyotr Petrovich, 520–522
Lebedev, Pyotr Nikolaevich, 80, 83–84, 519–522
Lederman, Leon M., 748
Lee, Tsung-Dao, 649–657, 775–777
Leksell, Lars, 11–12
Lemaître, Georges, 493, 506–507, 730
Big-Bang theory of, 506–507
Eddington and, 506–507
Einstein and, 507
Lenard, Philipp von, 120–122, 121f
Einstein and, 121–122
photoelectric effect and, 121, 211
Lenard window, 121
Leptons, 778–779, 803–805
definition, 680
properties of, 748t
Leucippus, 79
Leutwyler, Heinrich, 743, 750–751
Levi, Hilde, 49–50
Libby, Willard, 601–609
Anderson, 606–607
anticoincidence counter of, 606–607
carbon in earth's reservoirs and, 603
^{14}C dating equation of, 606–608
^{14}C dating technique of, 603–608
^{14}C steady-state activity on earth and, 603–604
Leona Marshall and, 609
Lifetime
half-life and, 388–389
Light photon, 407–408
Light quanta, 421
Linear absorption coefficient, 193–194, 296
Linear accelerator (LINAC), 287–288, 289f
bremsstrahlung and neutron production with, 373–374
Linear attenuation coefficient, 296–300
Linear energy transfer, 195–201
charged particle interactions in, 199–200
definition, 35–36, 199, 515–516
energy restricted form of, 199
as function of energy and range, 199–200
particle mass and charge and, 199–201
particle range and, 201t
types of energy loss in, 199f
values in water, 199–200

Linear ranges, 130, 132, 133t
Liquid drop model, nuclear
  Coulomb energy of, 692–693
  Gamow and, 689–694
  Heisenberg and, 689–690
  Meitner and Frisch and, 313
  nuclear fission and, 690–691
  pairing energy of, 693–694
  surface energy of, 692
  volume energy of, 692
  volume symmetry of, 693
  Weizsäcker formula for, 689–691
Liquid scintillation, 158–159
Little Boy, 339–340
Livingston, M. Stanley, 586, 597
Lord Rayleigh, 94
Lorentz, Hendrick A., 109–110
  Lorentz transformations and, 109–110, 214
Lorentz transformations, 109–110, 214, 286–287, 504, 733–734, 823–827
  applications of, 827
  Einstein's derivation of, 823
  relativity and, 214
Los Alamos National Laboratory, 355, 589
L-series X-rays, 252
Lucky Dragon, 347–348
Ludwig, Anna Berta, 81–82
Luminescence, 528
Luminosity
  in colliding beam facilities, 265–266
Luminosity detector
  Bhabha scattering and, 265–266
Lyman, Balmer, or Paschen series, 393f
Lyman series, 392, 395f
Lysenko, Trofim, 523–524

M

MacKenzie, Kenneth R., 482
Magic numbers
  definition, 643
  doubly magic, 643
  Fensen and, 639
  Goeppert-Mayer and, 639
  nuclear stability and, 694
Magnetic field
  origin of earth's, 111
Magnetic moment, 68, 164–165
Magnetic moment, electron
  discovery by Stern and Gerlach, 164
  molecular beam method and, 164
Magnetic moment, proton
  discovery by Stern, 164
  discovery by Stern and Gerlach, 164
Magnetic quantum number, electron, 154, 155t, 417
Magnetic resonance imaging (MRI)
  in diagnostic and clinical medicine, 667–669
  Rabi and, 661
Majorana, Ettore, 188, 481
Majorana neutrino, 188–189
Mallet, Lucien, 521, 548
Manhattan Project, 151–152, 157, 225, 324, 327–329, 330f, 339–340, 344f, 346, 347f, 351–352, 355, 358b, 396–398, 401–402, 483, 492, 615, 641, 648
Mansfield, Peter, 667–669
Marine acidification
  delta ^{11}B indicators of, 42
  effects measured with ^{45}Ca, 42
  isotopes in studies of, 41–42, 42f
Marine resources, 41–46
Marsden, Ernest, 98, 103–104, 128–129, 756
Marshall, Leona
  Fermi and, 609
  first nuclear reactor and, 609
Maskawa, Toshihide, 748, 773–781
  broken symmetry origin, 774
  Kobayashi and, 775
  matter over antimatter, 775–776
  prediction of six quarks, 775–776
  quark families, 774
  symmetry breaking, 775–776
Mass
  energy equivalence of, 67, 70–72, 803, 804t, 805t
Mass absorption coefficient, 193–194
Mass attenuation coefficients, 193–194, 297–298, 300, 301f–302f
  positrons *vs.* negatrons, 192–194
Mass defect
  definition, 307
Mass excess
  definition, 707–708
Mass number, 123, 137, 144, 175f, 68
  definition, 68
Mass of matter
  binding energy of gluons and, 803, 804t, 805t
Mass of the Higgs boson, 784
Mass spectrometry, 69
Mass-thickness, 130–133, 133t, 190, 193–194
Mather, John C., 510–511
Matter over antimatter, 775–776
  evidence for during creation, 777
  symmetry breaking and, 775–776
Matter-wave, 425–432
MAUD Committee
  Bohr, Frisch and Peierls and, 432–433
  origin of, 432–433
  Thomson, G.P. and, 432–433
Max Planck Medal, 204
Maxwell, James Clerk, 110–113
  electricity and magnetism unification and, 111
  electromagnetic theory of, 113
  electromagnetic wave theory of, 109
Mayer, Joseph Edward, 640
Maze, Roland, 434
McIntyre, Peter, 767–768
McMillan, Edwin M., 476, 522–523, 610–613
  Abelson and, 610
  first transuranium element, 610
  Lawrence and, 610
  Manhattan Project and, 613
  phase stability and, 286
  production of neptunium and, 610–611
Meitner, Lise, 58, 77–78, 156b, 232–233, 309–318, 326, 346, 396, 433–434, 465, 610, 690–691, 435
  Auger electrons and, 312
  Coster and, 312–313
  discovery of Auger electrons, 438
  escape from Nazi Germany, 312–313
  Fermi Prize and, 315, 317
  with Hahn and Strassmann, 312–313
  Hahn, Otto and, 309–313, 435
  interpretation of nuclear fission by, 801
  at the Kaiser Wilhelm Institute, 309–311
  Meitnerium and, 317
  nuclear fission and, 312–314
  Otto Frisch and, 147, 313, 315
  Planck and, 309–310
  protactinium and, 312
Mendeleev, Dimitri Ivanovich, 738
Menon, M.G.K., 268
Meson field, nuclear
  Yukawa theory of, 461
Meson, nuclear
  exchange particle between nucleons, 461
  positive or negative charge of, 461
  strong nuclear force and, 461
Mesons, 469–470, 501–502
  composition of, 807f
  definition, 680
  discovery of, 460
  nuclear forces and, 460
  prediction of, 460
  quark-antiquark structure of, 742
  quark color charge in, 752f
  quark color charges of, 682
  quark composition of, 751, 752f, 803–805, 806f
  quarks color charge changes in, 753
  quark structure and properties of, 737t
  quark structure of, 681–682, 742, 806
p-Mesons, 462–463, 468–469
Meson theory, 461
Metallurgical Laboratory (Met Lab), 151, 152f, 339, 355, 402, 641, 648
Metastable state, 273
Meyer, Stefan, 443–444
Millikan–Fletcher oil drop experiment, 261
Millikan, Robert A., 255–264
  at Caltech, 262
  charge on the electron and, 255–259
  cosmic ray latitude effect and, 260
  Einstein and, 256
  Fletcher and, 255–264
  photon particle and, 259
Minimum ionizing particle, 487
Mitterrand, François, 93
Moe, Michael K., 640–641
Molecular beams, 163–164
  discovery of, 163–164

Mole of substance, 116
Momentum
  relativistic expression of, 271
Morgan, L.O., 615
Moseley, Henry G.J., 248–251
  atomic number characterization by, 249–250
  prediction of missing elements by, 249–250
  Rutherford and, 250–251
  X-ray emission spectra of the elements by, 248–249
  X-ray spectrometry and, 248–249
Mottelson, Ben, 696
Mo-Young Han, 682
MRI scanner
  principle of, 669
MRI scanning
  advantage over X-rays, 670
  gadolinium contrast agents in, 670
Mrs. Eleanor Roosevelt, 342
Müller, Walter, 108
  Geiger and, 108
Multiwire proportional chamber
  definition, 568
Munich Agreement, 647–648
Munich Pact, 326
Muons, 450, 501–502
  in cosmic radiation showers, 217
  Cherenkov threshold energies of, 552t
  discovery in cosmic ray showers, 450
  mass and decay scheme, 451
  relativity and, 217
Mussolini, Benito, 326, 445, 482

N

Nagaoka, Hantaro, 118–120
  structure of the atom and, 119
  transmutation of mercury by, 119–120
Nagasaki, 340, 353
Nagle, Darragh, 488
Nambu, Yoichiro, 682, 743, 750, 773–781
  quark color charge and, 803
  spontaneous broken symmetry, 774
  symmetry breaking and, 777
Nanoparticles
  in cancer imaging and therapy, 18–20
  definition, 19
National Bureau of Standards (NBS), 655
National Institute of Science and Technology (NIST), 655
Natural abundance, isotope
  definition of, 37–39, 69
Natural abundances, 175f
Neddermeyer, Seth, 293–294, 422, 448, 729
  Manhattan Project and, 451
Ne'eman, Yuval, 734, 739–740
  Eightfold Way and, 738–739
Negatron
  fate of, 274
  mass of, 171
Negatron beta decay
  of C-14, 172f
  of Cs-137, 173f
  of I-131, 173f
Negatron decay energy
  calculation of, 171–174
Negatron emission
  B-12 and, 175
  basic principles of, 168–169
  description of, 167–168
  Feynman diagram of, 746f
Negatron (β^-) emission, 167–174
Nehru, Jawaharlal, 267
Neptunium (Z = 93)
  McMillan and, 611f
  McMillan and Abelson and, 610, 612
  production of, 610, 611f, 612
Neptunium decay chain, 77f, 78
Neutral atom
  definition, 68
Neutral current, 575
  definition, 760
Neutral current detectors, 579f
Neutral current interactions, 578f, 762, 808, 810
  examples of, 761f
  Z^0 bosons and, 761f
Neutral current neutrino detector, 577
Neutral current reactions
  description of, 760
Neutral-current weak interactions, 780
Neutral kaon decay
  CP symmetry violation in, 777
  matter over antimatter and, 777
Neutral pion, 462–463, 501–502
Neutrino, 153, 155–156, 158–159
  in beta decay, 801
  detection of, 170
  energy of in electron capture decay, 179
  Fermi and, 169
  flavor oscillation of, 170–171
  Majorana, 188
  mass of, 170–171
  Pauli and, 169
  in positron emission, 168
  properties of, 168
  Reines and Cowan and, 169
  spin property of, 169
Neutrino charged current, 575
Neutrino charged current interactions
  electron neutrino and deuterium, 575, 576f
  muon neutrino and nuclei, 575, 576f
  W^+ boson and, 576f
Neutrino detection and measurement
  charged current interactions, 574–577
  Cherenkov counters for, 574–577
  electron scattering interactions, 574–577
  neutral current interactions, 574–577
  neutrino interaction in, 574–577
Neutrino-electron interaction
  Feynman diagram of, 762f
Neutrino-electron scattering, 810
Neutrino electron scattering interactions, 575
Neutrino interactions, 575
Neutrino mass, 170–171
  vs. electron mass, 171
  measurement of, 171
Neutrino neutral current interactions
  with deuterium nucleus, 577, 578f
  Z^0 bozon and, 577
Neutrino oscillations
  discovery of, 170–171
Neutrinos, high energy
  interactions against nucleons, 756
Neutrino spectroscopy, 170
Neutrinos, solar
  Bethe and, 598
  (CN) cycle and, 598
  origin of, 598
Neutron
  magnetic moment determination of, 662
Neutron absorption cross-section, 381
Neutron activation analysis, 49–50
  advantages of, 49
  discovery of, 49–50
  Levi and de Hevesy and, 49–50
  principle of, 49
  prompt-gamma, 49, 49f
  sensitivity of, 49
Neutron-antineutron pair production
  energy requirement for, 474–475
Neutron attenuation, 383–388
Neutron bomb
  Cohen and, 356–357
  fast neutrons from, 356–357
Neutron capture, 381
  description, 381
  gamma-ray emission from, 159
Neutron capture reactions, 381
Neutron capture therapy
  with boron-10, 17–18
  with gadolinium-157, 18
Neutron cross-sections, 381, 383–388
  definition, 383
  thermal, 381
Neutron decay, 388–389
  Q value of, 389
Neutron diffraction
  discovery by Shull, 46–47
  mapping hydrogen atoms with, 46–47
Neutron drip line, 710
Neutron emission, 703–704
Neutron emission, beta delayed
  decay scheme of, 711f
  definition, 711
  1n, 2n, and 3n emissions, 711
Neutron-induced chain reactions, 324–325
Neutron-induced fission, 366t
Neutron interactions, energetic
  mechanisms of, 195
Neutron lifetime, 388
  measurement of, 388–389
Neutron moderator
  Szilard and, 321–322
Neutron number, 175f
Neutron radiation
  absorption coefficient of, 383
  from accelerated deuterons, 374–375
  accelerator sources of, 374–375
  beam intensity, 383–384

Neutron radiation (*Continued*)
cross-section, 384
from D-D and D-T fusion, 377–378
detection of, 381–382
discovery of, 304
half-value thickness, 384
from IECF device, 377
moderators of, 379–380
from nuclear spallation, 375
from photoneutron reactions, 372–374
from proton beams, 375
range of, 383
Neutron radioactivity, 703–713
definition, 703–704, 710
detection and measurement of, 712–713
theory of, 704–705
Neutron radioactivity, direct
half-lives *vs.* proton radioactivity, 712
Neutron radiography, 48
applications of, 48
principle of, 48
vs. X-ray radiography, 48
Neutrons, 144
classification of, 361–365
decay of, 150
elastic scattering of, 379
energy, velocity and wavelength of, 361–362, 363f
interactions with matter, 379–383
properties, 361, 379
quark composition of, 682, 808
quark structure of, 801–803
relativistic, 365
rest energy of, 364
stability of, 68
wavelength and velocity, 364–365
Neutron scattering, 379–380
elastic and inelastic, 46–47
molecular structure analysis with, 46–47
Neutron source, portable, 378
applications, 378
Neutron sources, 366–379
alpha-particle induced reactions, 367
monoenergetic, 366t
New Piles Committee, 58, 339
New radioactive isotopes, 584
Newton
as unit of force, 222–223
Nickel-56 decay scheme, 634
Nishijima, Kazuhiko, 738
Strangeness theory of, 735
Nishina, Yoshio, 232–235
aerial bombing loss of 27-inch cyclotron, 234
Bohr and, 232
cosmic-ray research by, 233
cyclotron construction by, 233
Dirac and, 233
Heisenberg and, 233
60-inch cyclotron and, 233
60-inch cyclotron destruction and, 235
Japan's atomic bomb sproject and, 233–234
Lawrence and, 233
muon discovery by, 233
Nagaoka and, 232
nuclear fission research of, 233
Pauli and, 232
Rabi and, 232
rebuilding of post-war RIKEN by, 235
Rutherford and, 232
Tomonaga and, 233
uranium critical mass calculations, 234
Yukawa and, 233
Nishiwaki, Yasushi, 347–348
NMR spectroscopy
chemical shift in, 666
chemical structural analysis with, 664–665
development by Bloch and Purcell, 664
electron cloud shielding effects in, 666
identification of atomic groups by, 667
principle of, 665
Rabi and, 661
stereoisomer identification by, 667
Nobel Committee, on quark theory
credit for Gell-Mann, 748–749
lack of credit for Zweig, 748–749
Noble gas hydrates
discovery of, 94
Nonelastic reactions, 379, 381–382
neutron capture in, 381–382
Nonlinear optics, 520
Nonrelativistic calculations
errors in, 365, 366f
NT200, 575
Nuclear arms nonproliferation, 398–399
Nuclear arms race
current stockpiles worldwide, 357
nuclear weapons sites worldwide, 357
nuclear weapons stockpiles in 1985, 357
Nuclear bremsstrahlung, 281–283
in nuclear fusion, 282
in proton-neutron capture, 282–283
Nuclear chain reactions, 321, 322f
discovery of potential applications, 801
Szilard and, 321–322
Nuclear decay modes, 713
Nuclear disarmament, 343, 346–347
Pugwash Conferences and, 303, 345, 347f, 349f, 351–353
Rotblat and, 303, 348–353
Russell-Einstein Manifesto and, 303
Szilard and, 342, 352f
Nuclear emulsion technique
advantages of, 466–467
applied magnetic fields and, 472–473, 473f
cosmic ray particle measurements by, 467
cosmic ray 'star' formation in, 469f
disadvantage of, 472–473
experimental setup for, 468
identification of pi-mesons by, 469f
mechanism of particle track production in, 466
pion and muon properties from, 470–471
'stars' in, 468
Nuclear fission, 58–59, 379, 685–686, 801
discovery of, 313–316
Hahn and, 313–317
Meitner and, 313–317
Strassmann and, 313–316
Nuclear forces, 461
Nuclear forces, strong
prediction of meson and, 461
short range of, 461
Yukawa's meson theory of, 462
Yukaya and, 461
Nuclear fusion, 58, 60–66, 686–688
in sun, 598
Nuclear fusion reactor
advantages *vs.* fission, 60, 63–66, 65f
past and future, 60–61
principles of, 60
Nuclear isomers, 271–273
energy states of, 271
Nuclear models, 689–698
Nuclear nonproliferation, 226, 397–399, 402
Szilard and, 340
Nuclear Nonproliferation Treaty, 353
Nuclear potential barrier, 126–127, 127f
Nuclear power, 322f
from fission reactors, 58–66
future prospects, 58–59
Szilard and Fermi patent for, 324
Nuclear power plants
Szilard and Fermi patent for, 322
world numbers, 58–59
Nuclear radius, 679–680
Nuclear reactions, 366, 714–721
cross sections of, 719–720
definition, 714
description of, 714
energy of (Q values), 717–719
first man-made, 101
notation for, 716–717
pickup and stripping, 716, 716t
Q values of, 715
rates of, 720
spallation reactions, 716
Nuclear reactor, 323f, 332, 371–372
co-invention by Fermi and Szilard, 151
description of, 334
Fermi-Szilard patent for, 334
invention of, 58
moderator for, 371–372
peaceful applications of, 151–152
plutonium production with, 151–152
Nuclear reactor, first
graphite moderator for, 334
at University of Chicago, 334
Nuclear reactor moderators, 379
Nuclear reactor, patent for
by Fermi and Szilard, 151
Nuclear recoil, 325
daughter nuclide, 124
energy of, 124–125
following EC decay, 182
Nuclear recoil energy, 177
Nuclear resonance, 385–388
Nuclear safeguards, 560
Nuclear spallation, 375
definition, 375

Nuclear stability
atomic number limit of, 176
doubly magic numbers and, 694, 699
magic numbers and, 694
N/Z ratio and, 692–693
Nuclear startstrahlung. *See* Nuclear bremsstrahlung
Nuclear transmutation
Cockcroft and Walton and, 593
first by artificial means, 593
first demonstration from natural sources, 591
first evidence of, 455–456
Rutherford and, 591
Nuclear-weapon-free world, 353
Nuclear weapons, 351
abolition of, 350
universal death from, 350
use of, 350
worldwide number of, 814
Nucleon annihilation, 479–480
Nucleon–antinucleon annihilation
pi-meson emission from, 479–480
Nucleon drip line, 703–704
Nucleon mass
from gluon emission and absorption, 683
Nucleons, 79–80
composition of, 683
definition, 70
internal charge distribution of, 663
magnetic property of, 663
origin of mass of, 810
quark structure of, 682t
size of, 802f
Nucleus, 101, 124f, 128–129
alpha-particle deflection by, 129
alpha-particle scattering by, 128–129
discovery of, 104, 119
radius of, 98, 128–129
Nucleus, atomic
charge density of, 662–663
density of, 680
discovery of, 679
quantum energy leap in NMR, 660f, 661–662, 665
radius of, 662–663, 679–680
shell structure of, 639, 642–644
size of, 802f
Nuclide nomenclature, 68–70
Nuclides
artificial and radioactive, 68
definition of, 68
isomeric states of, 69–70
natural, 68
symbol for, 68
Nuttall, John Mitchell, 106–107, 126
Nygren, David R., 484

O

Occhialini, Guiseppe P.S., 294, 449–450, 456, 459–460, 462, 467, 680–681
Ocean circulation and mixing
natural and anthropogenic radionuclides in, 43
Ocean warming
delta ^{18}O measurements and, 42
Octet
of spin 1/2 baryons, 739f
of spin 0 mesons, 740f
of spin 1 mesons, 740f
Oganessian, Yuri, 700
Oil-drop experiment
electron charge by, 256
Fletcher's memoir on, 260–262
of Millikan and Fletcher, 256–257, 256f
Oliphant, Marcus, 284–286
synchrotron concept and, 284–285
Omega particle, 166
One-proton radioactivity, 704–705
OPAL detector
description of, 759f
recording of Hadron jets by, 759
Open Letter to the United Nations, 398
Oppenheimer, J. Robert, 152, 355, 397, 451, 731
Optical time projection chamber, 709–710
Orbital quantum number, electron, 154, 155t, 416
Orbitals, electron, 155t
Ordinary matter
definition of, 779, 802f

P

Pair production, 167, 195, 220–221, 293–296, 300, 423, 448, 475–476
Anderson and Neddermeyer and, 422
Blackett and Occhialini and, 449–450
by bremsstrahlung photon, 279
definition, 293–294
demonstration of, 449f
Dirac and, 422
Dirac theory of, 450
discovery of, 422
electron-positron energy in, 294
energy-mass conversion in, 220
energy requirement, 294, 450
first identification of, 458
internal, 502
principle of, 422
Paladium-100
transient equilibrium in, 632
Paneth, Frederic, 20–21
Panofsky, W.K.H., 754–755
Parent-daughter decay
no equilibrium in, 634
Parity, 783
conservation of, 649, 653
definition, 652, 653f
mirror symmetry and, 776
as quantum number, 653
violation of, 649
Parity conservation
test for in beta decay, 655f–656f
Parity violation, 777
symmetry breaking in beta decay, 776–777
Wu and, 776–777
α-Particle, 101, 123–134, 129
β-Particle, 101, 167, 171, 173–174, 175f
Particle energy, 554
total, 286
Particle identification
ring imaging Cherenkov counters and, 563–564
threshold Cherenkov counters and, 560–574
Particle mass, 560, 567
Particle phase velocity, 550
Particle relativistic momentum, 572
Particle rest mass, 550–551
Particles, composite
baryons and mesons, 805–806, 807f
classification of, 807f
definition, 803
Particles, elementary
classification of, 806f
definition, 803
description of, 805–806
Particle spectrograph, 478
Particles, subatomic
classification of, 803, 805, 806f, 807f
Particle threshold, 552t
Particle velocities, 563–564
Particle-wave duality, 207–209, 407–408, 425–432
Particle wavelength
de Broglie equation for, 208
Particle zoo, 803–811
definition, 803
Partons, 743, 756–757
Feynman theory of, 743
Paschen series, 392
Pauli exclusion principle, 153–154, 418–419, 682, 695f, 750, 803–805
applied to nucleons, 694–695
description of, 68
nuclear shell model and, 643–644
Pauli, Wolfgang, 153–157, 417–418, 461, 750
Einstein and, 153
Exclusion Principle of, 153–154
neutrino hypothesis of, 154–157
neutrino theory of, 148
Reines and Cowan and, 134
theory of neutrino and, 801
Peierls, Rudolf E., 327–329, 432–433
neutrino detection and, 159
Penzias, Arno, 507, 495
Penzias, Arno and Wilson, Robert
cosmic microwave background radiation discovery by, 508–509
Periodic law of radioisotopes, 136–137, 138f
Perrier, Carlo, 482
Perrin, Jean B, 114–116
Avogadro's number and, 116
charge on cathode rays and, 114–115
molecules and, 114–115
Perutz, Max, 52
Petition to the President of the United States, 225
Szilard and, 343, 344f

Phase stability, 522–523, 588
discoveries on, 613
McMillan and Veksler and, 588, 613
synchrocyclotron and, 588
Phase transition, 783–784
Phase velocity, relative
applications of, 549–550, 552, 555–556, 567, 572
definition, 207
Phonons
definition, 793
Phosphorescence, 89
Phosphorescent lamp, 86
Phosphorus-32
decay scheme of, 274f
Photoelectric effect, 118, 121–122, 195, 222, 270, 291, 300–301
definition, 211
Einstein's equation for, 212
Einstein's quantum photon and, 259
electron shell in, 300–301
light quantum frequency and, 212
Photoelectric effect law
Einstein and, 211–212
Photoelectrons, 121
energy of, 269–270
Photographic emulsion technique. *See also* Nuclear emulsion technique
particle mass *vs.* track density, 467f
Photoionization microscopy, 812, 813f
Photon, 780
birth and death measurement of, 794
Einstein's discovery of, 46–47, 121–122, 205–206, 211–213, 269–270, 800
nondemolition measurement of, 794
nondestructive counting of, 790
nondestructive measurement of, 792–793
quantum nondemolition measurement, 790
range of interaction, 762
trapping of, 790
wave-particle duality of, 269–271
Photon box, ENS, 793f
description of, 794–795
trapping photons in, 794–795
Photoneutron assembly, 373f
Photoneutron converter, 373f
Photoneutron sources, 366t, 372–374
discovery of, 325
Photon interactions
mechanisms of, 195, 291–296
Photon, long-lived
birth, life and death of, 796
0.5 second lifetime of, 796
Photon particle
Einstein and, 46–47, 121–122, 205–206, 211–213, 259, 269–270, 800
Millikan and, 255–256, 259
Photon ring Cherenkov, 548–549, 563–571, 565f, 566f, 568f–571f
Photons, 200, 291–292, 421, 805–806
discovery by Einstein, 46–47, 121–122, 205–206, 211–213, 269–270, 800
effective mass of, 222
electric and magnetic fields of, 111
as electromagnetic field particle, 808f
energy of, 222
as energy quanta, 212
momentum of, 270
particle and wave nature of, 112f, 121–122
wavelength calculation of, 270
Photons, trapped in box
birth, life and death of, 798
143,000 km travel of, 798
measurement with Rydberg atoms, 794–795
photon lifetime measurement of, 795–796
Photon trapping
Haroche and, 790, 792–793
photon measurement and control, 792–793
Raimond and, 790
Photonuclear reactions, 372–373
on bertllium mining, 372–373
for neutron raioagraphy, 372–373
Piccioni, Oreste, 481
Pickup nuclear reactions, 716
Pierre Auger Cosmic Ray Observatory, 434
Pierre Curie, 90–93
Pi-meson, neutral
decay of, 470–471
Pi mesons, 166, 462–463, 501–502
in cosmic ray showers, 469–470
discovery of, 680–681
origins of, 470
quark structure of, 682t
in strong nuclear force, 680–681, 811
Pitchblende, 91
Planck–Einstein equation, 205–206, 208, 269–270, 270, 280, 292–293, 792
Planck, Max, 121–122, 203–206, 391, 407–408, 800, 167
energy quantum and, 203
Planck's constant and, 205
quantum theory of, 269
radiation quantum discovery, 792
Planck's constant, 205, 167
definition of, 269
conversion of units of, 270–271
in quantum physics, 205
Plant breeding
"green revolution" in, 34–35
Norman Borlaug and, 34–35
radiation induced mutations in, 33–37
Plant breeding, mutation
cosmic rays in space in, 36
heavy ion beams in, 35–36
radiation induced, 35
X-, gamma and neutron irradiation in, 35
Plasma, 60–65, 375, 378–379
Plutonium-239, 615f
discovery of, 613–615
Kennedy and Wahl and, 614–615
large-scale production of, 614–615
naming of, 614–615
preparation from U-238, 372
Seaborg and McMillan and, 612–613
Seaborg and Segrè and, 614–615
Plutonium production reactors, 355
PMT photon detectors, 561
Politzer, H. David, 757–758, 765
Polonium
discovery of, 91–92
Pomeranchuk, Isaak, 286
Pontecorvo, Bruno, 456, 481
Positon emission
basic principles of, 174–179
C-11 and, 174
EC decay and, 180–182
Positron decay energy, 176–179
calculation of, 176–179
Positron-electron collisions
quarks and gluons from, 756–757
Positron (β^+) emission, 167, 174–179, 175f, 177f–179f
description of, 174
energy spectra of, 174
minimum decay energy for, 174
Na-22 and, 177–178
N-12 and, 174–175
N-13 and, 177
Positron emission tomography (PET), 7–9
hybrid PET/CT, 9
mechanism of, 7, 8f
medical advantages of, 8–9
principle of, 8f
Positronium, 274–275
Positrons, 144, 422
Anderson and, 422
controversy over discovery of, 459–460
discovery of, 422, 447–448
fate of, 274–275
mass of, 176
sources of, 294, 450
Potential energy well, 127f
Powell, Cecil F., 102, 460, 462–474, 680–681
cosmic ray particle studies of, 467f
C.T.R. Wilson and, 464–465
discovery of pi-meson, 469–470
first Pugwash Conference and, 474
Lattes and, 467
muon discovery, 470–471
neutral pi-meson discovered by, 470–471
nuclear emulsion techniques of, 466
Occhialini and, 467
photographic emulsion techniques of, 467f
pion discovery, 470–471
primary cosmic ray nuclei and, 468–469
Rutherford and, 464–465
secondary cosmic radiation and, 468–469
Yukawa's meson discovered by, 470–471
Present, Isaak, 523–524
President Franklin Roosevelt, 327, 340, 397
Primary cosmic ray nuclei, 468–469
Primary ionization, 190
Principle quantum number, electron, 154, 155t, 395, 416, 418–419
Probability density for electrons, 415, 419, 421
Probability positions of atomic electrons, 415, 416f, 419, 421

Prompt gamma NAA
advantages of, 49
applications, 49
Prompt gamma-rays, 49f
Proportional counter
invention of, 106
Proton
Cherenkov threshold energies of, 552t
discovery of, 102
magnetic moment of, 164
quark composition of, 682, 808
quark structure of, 801–803
rest energy of, 497
Proton–antiproton, 474–476
Proton–antiproton annihilation
energy released from, 480–481
mass-energy conversion in, 480–481
Proton-antiproton collider, CERN, 768f
description of, 769–770
sequence in operation of, 769–770
Proton-antiproton collision
in superproton synchrotron, 766
W^+, W^- and Z^0 particles from, 766f, 767
Proton–antiproton pair production
Bevatron and, 476
energy requirement for, 474–476
Proton beam therapy, 15–17
mechanics of, 16f
principle and advantages of, 15
Proton emission, 703–704
Proton emission, beta delayed
decay scheme for, 705
definition, 705
principle of, 705
sequential emission of 2p in, 705
Proton-induced gamma-ray analysis
analysis of low *Z* elements by, 53
Proton-induced X-ray emission (PIXE), 50
applications, 54
elemental analysis with, 53
principle of, 53
Proton number, 68
Proton radiation
from D-D fusion, 377–378
from D-He fusion, 377–378
Proton radioactivity, 703–713
definition, 703–704
theory of, 704–705
Proton radioactivity, direct
decay scheme of, 707f
first observation of, 707
principle of, 707
sequential emission of 2p, 707
simultaneous emission of 2p, 707–708
Proton radioactivity, simultaneous
decay schemes of, 709–710
detection and measurement of, 708–710
imaging of, 710f
2p and 3p emission in, 708f, 709f, 709–710
proton track imaging of, 709f
Proton source, portable, 377–378
applications, 378
Proton spin crisis, 166
Proton synchrotron, CERN
proton-antiproton production in, 769
Proximity-focusing RICH counters
Cherenkov angle *vs.* particle momentum, 569f–570f
Cherenkov light cone in, 568f
Cherenkov ring imaging with, 568–570, 568f–569f
description of, 568f
particle identification with, 570f
particle velocity from, 570f
pion and kaon discrimination with, 568–570, 568f–569f
proton, kaon, pion and electron discrimination with, 569f–570f
Pugwash Conference, 345, 352, 303, 709
foundation of, 352–353
international scale of, 351–352
Joseph Rotblat and, 351–352
Nobel Peace Prize, 352–353
objective of, 343
Russell-Einstein Manifesto and, 343
Pugwash movement
involvement in peace treaties, 352
Nobel Foundation and, 352
nuclear disarmament and, 352
nuclear test ban and nonproliferation treaties and, 352
Puluj, Ivan Pavlovich, 80, 83–89, 85f, 114
electrode matter characterization by, 85–86, 86f
phosphorescent lamp of, 86, 87f, 88
Puluj, Johan. *See* Puluj, Ivan Pavlovich
Puluj's phosphorescent lamp, 86–88, 87f

Q

Q_α, 123–124
Q_{β^-}, 172–174, 172f, 173f
Q_{β^+}, 176–178, 177f, 178f
Q_{EC}, 178f–180f, 179–182
QCalc, 370–371
QND measurements
Haroche and, 794
of photons in a box, 794
Quadrupole separator/spectrometer, 701
Quantized energies, 392
Quantized energy levels, 407
Quantum
energy, 269
particle energy as, 121–122
Quantum chromodynamics (QCD), 682, 743, 750–751, 753f, 756
definition, 751
gluons in, 747
strong force between quarks and, 803
Quantum computers
potential of, 794
superposition states or qubits in, 794
trapped ions and, 794
Quantum electrodynamics (QED)
theory of, 672–673
Quantum, energy
Planck's discovery of, 205–206
Quantum energy sublevels, 395
Quantum, gamma-ray
emission of following neutron capture, 150–151
Quantum mechanics, 409–410, 415
ambiguity of Bohr atom in, 411–412
Bohr's complementarity argument, 412
Heisenberg and, 408
Heisenberg and electron wave-particle duality, 411–412
Quantum microscope, 813–814
Quantum nondemolition (QND) measurement of photon, 790
Quantum numbers
of the atomic electron, 154
definition, 653
of subatomic particles, 165
Quantum numbers, atomic electron, 155t
Quantum of energy, 392
transferred to atom, 404–405
Quantum optics, 792–793
Quantum, photon
Einstein and, 206, 211–213, 221–223, 259–260
Quantum physics
Haroche and Wineland and, 792–793
particle-wave duality in, 792–793
quantum systems in, 792–793
Quantum, radiation
definition, 205–206
Quantum states
nondestructive measurement of, 792–793
Quantum structure, 411
Quantum theory, 206
atomic structure, 391–393, 395
discovery, 205
Max Planck and, 167, 205–206, 205f, 800
Quark-antiquark annihilation
proton-antiproton beams and, 766
Quark color charge
constant changes in, 752f, 753
Quark flavors
definition, 748
discovery of, 748
Quark fractional charge
Gell-Mann and, 742
Zweig and, 745–746, 746t
Quarks, 79–80, 166, 735–736, 740–742, 755, 778–779, 800–801, 729
asymptotic freedom of, 757–758, 765
in baryons and mesons, 681–682, 742
charges of, 742, 746t
color charge, 682, 751, 779, 802f, 803
confirmation of six, 778–779
CP violation and, 778
discoveries of c, b, and t quarks, 778
discovery of, 753, 755–756
Eightfold Way and, 742
evidence for, 747
evidence found for, 743
Gell-Mann and, 743
Gell-Mann and Zweig theory of, 740–743
Gell-Mann's theory of, 742

Quarks (*Continued*)
prediction of six in nature, 778
properties of, 746t
quantum states of, 751
six flavors of, 805–806
size of, 802f
spin, 165
in strong force, 811
up, down, and strange, 742
visible evidence for, 756–757
Zweig and, 743, 745–746
Zweig and Gell-Mann and, 801–803
Quarks, particles, real
Zweig *vs.* Gell-Mann and, 747
Quark transformation
Gell-Mann and Zweig and, 743
Zweig and, 745
Q value, 71–72, 123–124, 295–296, 367, 369–370, 389, 594
calculation of, 71
Cockcroft and Walton calculations, 593–594
of D-D and D-T reactions, 374
definition of, 71
from fission reactions, 686
from fusion reactions, 686–687
of ^{1}H and ^{7}Li reaction, 593–594
from ^{2}H fusion, 687
kinetic energy of products and, 71–72
reaction energetics and, 71
of ^{236}U fission, 686
Q-value Calculator (QCalc), 367
Q value, negative, 718
Q value, positive, 715
Q value, reaction
calculation of, 717–718
definition, 717
positive or negative, 718
stages of, 719f
threshold energy of, 718–719

R

Rabi, Isador Isaac, 232, 657–670, 729
magnetic resonance method of, 659, 660f, 661–662
nuclear magnetic resonance and, 664
Oppenheimer and, 659
Stern and, 659
Race, nuclear armaments, 403
Radiation
alpha, 123–124
annihilation, 274–275
atomic electron, 435–438
beta, 167–176, 190–199
bremsstrahlung, 278–283
Cherenkov, 275, 547–560
cosmic, 495–506
electromagnetic properties of photon, 111, 112f, 269
gamma, 271–274
neutron, 361–379
particle-wave nature of, 269–271
synchrotron, 284–287
X-rays, 276–284
Radiation absorbed dose, 514
Radiation curing of materials, 56
Radiation curing of rubber, 56
Radiation dose, 514–518
Radiation dosimetry, 95
Radiation frequency, 111
Radiation intensity, 95, 299
definition, 296
Radiation, nuclear
relative ranges in matter, 191–192
Radiation oncology, 92
Marie Curie and, 10
Radiation processing, 54–58
applications, 54–57
benefits of, 58
definition, 54
technique involved, 57
Radiation processing of polymers, 57
Radiation production of vaccines, 57
Radiation purification of flue gas, 57
Radiation sickness, 91
Radiation sterilization
of blood, 55
of healthcare products, 55
of human donor tissue, 55
of hydrogels, 55
of insects, 56
of mail, 57
Radiation technology, 46–58
Radiation therapy, 92
external beam, 10–14
radiation oncology in, 10–18
Radioactive decay
definition, 67
modes, 713
Radioactive fallout, 356
Radioactive fission products, 356
Radioactive nanoparticles
active targeting in cancer therapy, 19
in cancer therapy, 18–20
in cancer therapy and imaging, 19
liposomes as, 19
mechanisms of in cancer therapy, 19
passive targeting in cancer therapy, 19
Radioactivity, 579
definition, 1, 67, 621
discovery of, 89
medical applications of, 2–20, 92
Radioactivity units
becquerel (Bq), 636
curie (Ci), 636
Radiochemistry, 76
beginning of, 97
birth of, 146
Radiography
colored X-ray images and, 2–3, 3f
X-ray diagnostic, 2–3
Radioimmunoassay
in animal health and production, 30–32
principle of, 30–31, 32f
sensitivity of, 31–32
technique in, 31–32
Yalow and Berson and, 30–31
Radioisotope decay equilibria,
Rutherford and Soddy and, 629–630
secular equilibrium in, 629–632
transient equilibrium, 632–634
Radioisotopes, 69
applications in biology and medicine, 2–23, 147
definition of, 69
Radionuclide
definition, 68
Radionuclide activity
half-life *vs.* mass of, 637
radionuclide mass and, 635–638
Radionuclide activity decay
calculation of, 624–625
equation for, 624
equilibria in, 629–634
mixture of radionuclides and, 625
mixture of two radionuclides and, 625–626
Radionuclide decay chains
decay and production of daughters in, 628
neptunium decay chain, 77f
Th-232 natural decay chain, 74, 74f, 636f
U-235 natural decay chain, 74–75, 75f
U-238 natural decay chain, 74–75, 75f
Radionuclide mass
radionuclide activity and, 635–638
Radionuclides, artifically produced, 74–78
by alpha-particle bombardment, 76
by cyclotron, 77–78
Fermi and, 76–77
Joliot-Curies and, 75–76
Lawrence and, 77
neptunium decay chain, 77f, 78
by neutron bombardment, 76–77
by thermal neutron capture, 77
Radionuclides, natural, 72–74
conditions for occurrence, 72
of cosmogenic origin, 72t, 73
decay chains of, 74
long-lived, 73–74
Radiosurgery, 11–12
Radium
discovery of, 91–92
Raimond, Jean-Michel, 790
Rainwater, James, 696–697
Ramsey, William, 94
discovery of inert gases by, 136
Ranges
of alpha particles in dry air, 130–134, 191t
of alpha-particles in various absorbers, 131–133
of beta particles in absorbers of low Z, 190–191, 191t, 819f
of beta particles or electrons in air, 191t, 817f
of beta particles or electrons in water, 191t, 818f
Rasetti, Franco, 481
Rate of decay, nuclear, 67, 621–634
radionuclide mass and, 635–638
Reaction cross-section, 720–721
Reactor moderator, 337–339

Reagan, Ronald, 357
Receptor binding assay
for harmful algal bloom toxins, 45
principle of, 44
Recoil energy, 167–168, 172, 721–725, 721f
Recoil energy, calculations of
from alpha emissions, 724, 726t
from beta emissions, 724–725, 726t
from gamma-, X-ray-, and neutrino emissions, 725, 726t
Recoil energy, radioactive nuclear
nonrelativistic expressions for, 723–724
relativistic expressions for, 721–723
Recoil nucleus, 181, 379–381
Recoil, radioactive nuclear, 721–728
description of, 721
effects of, 725–728
radioactive disequilibrium from, 728
in Szilard-Chalmers process, 727
Red tides. *See* Harmful algal blooms
Refractive index, 550, 560
Regaud, Claudius, 92
Reid, Alexander, 427
Reiling, Victor, 535
Reines, Frederick, 156b, 157–163
Cowan, Jr., and, 158–159, 161–163, 160f, 162f
discovery of neutrino by, 801
Fermi and, 158
in Manhattan Project, 157
neutrino detection and, 157
Pauli and, 159, 135
Reines, Frederick and Cowan, Jr., Clyde
detection of neutrino by, 158–161
neutrino detection scheme of, 160f
neutrino detector of, 160f–161f
Pauli and, 161
Relativistic calculations
particle speed and wavelength, 364–365
Relativistic Heavy-Ion Collider, 166
Relativistic mass, 221, 287, 362, 428
calculations of, 222–223, 410
Relativistic speed
definition, 221
Relativistic time dilation
of cosmic ray muons measured on earth, 504
in muon decay measurements, 266–267
observed with muons in synchrotron, 504
Relativity, 213
Einstein's theory of, 213–224, 823–827
energy and mass in, 220–223
equivalence of mass and energy, 220–221
evidence for, 217–220
frames of reference in, 213, 214f, 823
gravitational mass and photons in, 223–224
length contraction in, 213–216, 215f, 218f, 219
muon lifetime dilation and, 217–219
particle dilated lifetimes and, 733–734
particle proper lifetimes and, 733–734
space-time coordinates in, 213, 214f, 823–827
time dilation in, 213–214, 215f, 216–217, 823–827
Rem
definition, 515
Repelling coulombic forces, 176
Research reactors, 46
Resonance effect
in neutron capture, 151
Resonances, nuclear
definition, 381–382
Resonance states, 733–734
Rest energy, 286–287, 361–362, 550
Rest mass, 221, 287
definition, 67–68
Reverse beta decay, 158–159
RICH detectors, 563–569, 565f, 567f–569f
Richter, Burton, 748
RIKEN, 232
Ring imaging Cherenkov (RICH) counters
angles of emission *vs.* particle momentum in, 567
Arthur Roberts and, 563–567
Cherenkov cone angle and, 563–567, 565f
Cherenkov ring dimensions from, 563–567, 565f
dimension, 566f
index of refraction and, 567
particle discrimination with, 567
particle identification with, 563–567
particle mass and Cherenkov ring, 566f
particle mass from emission angle, 566f
particle momentum from, 566
particle velocity, charge and mass measurements with, 563–567
particle velocity or mass from, 565f, 566
photon ring dimensions and, 566
photon ring imaging with, 565f, 566–568, 569f
proximity focusing, 567
ring images from, 566f, 568f–570f
working principle of, 565f, 566
Roberts, Arthur, 563–564
Rochester, George D., 452–453, 459
Röntgen, 80–82, 87
definition, 514
Röntgenogram, 82
Röntgen photographs, 88
Röntgen rays, 80, 82, 88
Röntgen Unit, 95
Röntgen, Wilhelm C., 80–84, 82f, 86, 94, 276, 799–800
first x-ray images by, 81–82
Roosevelt, Franklin D., 326–329, 328f, 330f, 341f
Einstein's letter and, 329f
Rosalind Franklin Award, 248
Rosalind Franklin University, 248
Rossi, Bruno, 457–458
Rotblat, Joseph, 345–349, 352, 352f, 356, 601, 814, 303, 799
abolition of war and, 353
Atomic Scientists Association and, 346–347
biological effects of radiation and, 348
Chadwick and, 346
cyclotron research and, 346
Einstein and, 351
first hydrogen bomb detonation and, 347
Manhattan Project and, 346, 347f
Nobel Peace Prize, 352–353
nuclear disarmament and, 345–347
nuclear medicine and, 347
nuclear-weapon-free-world and, 353
prediction of neutron number from ^{235}U fission, 346
Pugwash Conferences and, 351–352
radioactive fallout and, 348
Russell and, 348
Russell-Einstein Manifesto and, 348–353
Ulam and, 347
Rubbia, Carlo, 763, 766–768, 771
discovery of W^+, W^- and Z^0 particles, 765–766, 769
Rubidium-86
decay scheme of, 272f
Russell, Bertrand, 226, 343, 348–349, 303
Russell–Einstein Manifesto, 226, 343, 348–353, 463, 799
Einstein and, 303
Powell and, 474
Pugwash Conferences and, 351–352
reading of proclamation of, 349f
Rotblat and, 349f
Russell and, 303
signatories of, 351–353
Rutherford, Ernest, 72, 79, 95–106, 108, 119, 126–129, 232, 391, 584, 679, 756, 800, 123
alpha-particle deflections and, 97–98
artificial production of stable isotope, 2
characterization of alpha particle by, 97
charge and mass of alpha particle and, 99–100
discovery of atomic nucleus by, 800
discovery of proton by, 102, 800
first measurement of half-life, 621–622
first nuclear reaction and, 101
Geiger and, 98–99
nature of radioactivity and, 622–623
radiation nomenclature and, 95–96, 191–192
radioactivity counter and, 105–106
radionuclide decay and, 621
secular equilibrium and, 630
Soddy and, 97
structure of atom and, 101
transmutation and, 101
Rydberg atoms
definition, 794–795
measurement of trapped photons with, 795–796
"Scrödinger cat" states of, 795–796
two Rydberg state superpositions of, 795–796

Rydberg electron
de Broglie wavelength of, 795–796
Rydberg formula, 393
Balmer series and, 392–393
the Bohr atom and, 392–393
Brackett series and, 392–393
electron orbital radiation emission lines and, 394
ionization energy from, 394
Lyman series and, 392–393
Paschen series and, 392–393
photon emissions from atoms and, 392–393
quantized atomic electron energy levels from, 394
Rydberg, Janne, 392–393
Rydberg state alterations
observation of, 790
Rydberg states
definition, 790

S

Sachs, Alexander
Einstein's letter to Roosevelt and, 225, 327
Sakata, Shoichi, 774–775
Sakharov, Andrei, 60–61, 357, 775–776
hydrogen (fusion) bomb and, 545
Nobel Prize 1975 for Peace, 545
Tokamak and, 545
Salam, Abdus, 760, 762
Sandoval Vallarta, Manuel, 492–494, 730
Alfredo Baños and, 493
Carlos Graef Fernández and, 493
Feynman and, 493
Julius Stratton and, 493
latitude effects on cosmic radiation, 493
Lemaître and, 493
magnetic field-cosmic ray effects, 493
MIT chair in theoretical physics, 493
Norbert Wiener and, 492–493
Vannevar Bush and, 492
Sarah Lawrence College, 641
Savitch, Paul, 312–313
Scattering neutron, 46–47
Schmidt, Gerhard, 91
Schrödinger, Erwin, 395, 407–424, 465–466
breakaway from Germany's Nazi regime, 419
escape from Austria after Hitler's annexation, 419
matter-wave duality and, 414
movements of atomic electron wave, 414
radioactive decay and, 413–414
Schrödinger's cat, 414
wave function of, 414
wave mechanics of, 414
Schrödinger's Cat, 414f, 795–796
superposition of quantum states and, 414–415
Wineland and, 415
Schrödinger's wave function
electron orbitals and, 415
Max Born and, 415
probability of electron coordinates in, 415
Schrödinger's wave mechanics
atomic electron configurations and, 419
space coordinates of atomic electrons, 419
Schwinger, Julian, 671–672, 674–675
Scintillation proximity assay, 44–46, 44f, 45f
Seaborg, Glenn T., 318, 402, 588, 613–619, 698, 716, 78
discovery of elements 94-103 and 106, 614–618, 615f–617f
discovery of iodine-131, 614
discovery of plutonium with McMillan, 613
Ghiorso, James and Morgan and, 615
Lawrence and, 614
in Manhattan Project, 615
McMillan and, 614
production of element 94, 614–615, 615f
production of element 95, 616, 616f
production of element 96, 616, 616f
production of elements 97 and 98, 617–618, 617f
production of ^{238}Pu and ^{239}Pu, 614
Segrè and, 614
transuranic and actinide series of, 616
Sea of Instability, 699
Secondary ionization, 190
Secular equilibrium, 629–631
application in radionuclide analysis, 630–631
criterion for, 629
definition, 629
discovery of, 630
graphical depiction of, 631f
interpretation by Rutherford and Soddy, 630
Segrè, Emilio, 423, 484, 614
antiproton discovery and, 482–483
antiproton discovery by, 474–485
chemical effects on EC decay rates, 482–483
Clyde Wiegand and, 479
discovery of astatine, 482
discovery of technetium, 482
electron capture decay and, 183
escape from Nazi regime, 482
Fermi and, 152, 481
isolation of ^{99m}Tc, 482
Lawrence and, 481–482
in Manhattan Project, 482
Seaborg and, 482
Thomas Ypsilantis and, 479
Sequinot, Jaques, 564
Serber, Robert, 673–674
Condon and, 673–674
as lecturer at Los Alamos, 673–674
Shell model, nuclear, 694–695
magic numbers and, 694
spin coupling in, 694–695
Showers of cosmic radiation, 433, 501–504
Shull, Clifford G., 46
Siegbahn, Manne, 230, 253–255
discovery of M- and N-series X-rays, 253
electron orbitals identification and, 254
X-ray spectroscopy and, 253
Silver-109m
internal conversion decay of, 436
Single photon emission computed tomography. *See* SPECT
Sklodowska, Maria, 90–91
Slow (thermal) neutrons, 28
Smoot, George F., 510
SNO Cherenkov detector, 577, 579f
Soddy, Frederick, 135–137, 800
discovery of isotopes and, 67
He gas and alpha particles, 136
isotope decay laws and, 135–136
isotope nomenclature by, 137
nature of radioactivity and, 622–623
Periodic Law of, 138f
radioisotope displacement law and, 137
radioisotope periodic law of, 136–137
radionuclide decay and, 621
Ramsey and, 136
Rutherford and, 135–136
secular equilibrium and, 630
Sodium-22
decay scheme of, 273
Soil moisture neutron gauge, 28
Sommerfeld, Arnold, 236
Pauli and, 153
prediction of Cherenkov effect, 548
Soviet Union hydrogen bomb
first test of, 357
Sakharov and, 357
Space-time continuum, 213
Spallation neutron sources, 716
Spallation, nuclear
definition, 716
Seaborg and, 716
Spallation reaction, 366t
Spatial distribution, 537
Specific activity, 27
Specific ionization, 134
definition, 15–16, 141–143
Specific quantum energy states, 404–405
SPECT
mechanism of, 6–7
in medical diagnosis, 7
Spectral line, 394–395
Spectroscopy, 394–395
Speed of light
definition of, 270
Speer, Albert, 413
Spin, 164
description of, 68
Spin 1/2 baryons, 165
Spin 3/2 baryons, 166
Spin 0 mesons, 166
Spin 1 mesons, 166
Spin quantum number, 155t
of the electron, 154, 164–165
of the neutron, 165
of the proton, 165
quark structure and, 165
Spontaneous breaking symmetries
discovery of, 775–776, 776f, 783f
Nambu and, 775–776

Spontaneous fission, 361, 366t, 368–369
  definition, 686
Spontaneous fission neutron sources
  properties and applications, 368
Spontaneous symmetry breaking
  origin of mass and, 782–783, 783f
Stable isotopes, 27, 69
Stalin, Josef, 519, 520, 524–526
Stalin's purges, 526
Standard Model
  bosons, leptons and quarks of, 806f
  building blocks of matter and, 759–760
  description of, 778–779
  of elementary particles, 778
  elementary particles in, 780
  fundamental forces in, 780
  fundamental particles in, 779
  hidden symmetry in, 783–784
  Kobayashi and, 778–779
  Kobayashi and Toshihide and, 778
  prediction of six quarks of, 778
  quarks, leptons and bosons of, 788, 789f
Star Wars, 357
Statistical nature of radioactive decay, 413–414
Steady-state condition, 603, 602
Steiner, Herbert, 484
Sterile insect technique
  boosted SIT and, 25, 26f
  gamma- and X-rays for, 24–25
  Knipling and, 25
  malaria mosquito control by, 25
  Medfly control with, 25
  principle of, 24–25
  screwworm eradication by, 25
  tsetse fly eradication by, 25
Sterilization of tissue from human donors, 55
Stern–Gerlach experiment, 164, 165f
Stern, Otto, 163–166
  Einstein and, 163
  Gerlach and, 163–164
  Immanuel Estermann and, 164
  molecular beam technique and, 163–164
Stimson, Henry L., 342, 402
Stochastic cooling
  concentration of antiproton beams by, 769
  definition, 769–770
  principle of, 770
  van der Meer and, 770
  in W^+, W^-, and Z^0 production, 771
Stokes, George, 257–258
Stokes' law, 257–258
Stoney, George Johnstone, 118
Stopping power, 195–201
  calculation of, 195–197
  collision and radial energy loss in, 197
  definition, 195–197
  positrons *vs.* negatrons, 192
Storage ring, 287–289
Strange antiquark
  strangeness number of, 735–736
Strange baryons, 807
Strangeness
  law of conservation of, 735–736
  as quantum number, 735–736
Strangeness quantum number, 736–737
  formula for assignment of, 735–736
  strange quarks and, 735–736
Strangeness theory
  Gell-Mann and Nishijima and, 735
Strange (s) quark
  strangeness number of, 735–736
Strassmann, Fritz, 58, 77–78, 233, 312–313, 326, 346, 355, 396, 610–611, 690–691
  discovery of fission with Otto Hahn by, 801
  Fermi Prize and, 315, 317
  nuclear fission and, 313–314
Strategic Defense Initiative, 357
Stratton, Julius, 493
Streicher, Julius, 321
Strong force, 811
  atomic nucleus and, 802f
  mediated by gluons, 803
  nucleon binding and, 811
Strong interaction, 148, 780
Strong nuclear force, 187
  stability of atomic nucleus and, 800–801
Strontium-90(yttrium-90)
  decay scheme of, 370
  secular equilibrium of, 629, 631f
Stückelberg, Ernst C. G., 677
Subnuclear particles
  density of, 680
Substitute Alloy Materials (SAM), 641
Sudbury Neutrino Observatory (SNO), 170–171, 575
Suess, Hans E., 642, 694
Sun
  nuclear fusion in, 598
"Super" bomb, 348
Supercritical mass, 339f, 340
Superheavy elements
  definition, 698
  detection and measurement of, 701, 701f
  Island of Stability and, 699, 699f
  new magic numbers and, 699
  predicted hollow interiors of, 699–700
  production of, 700
  Sea of Instability and, 699, 699f
Superheavy nuclei, 698–702
Super-Kamiokande Cherenkov detector, 170–171, 575
Super-Kamiokande Collaboration, 170–171
Superposition, 792–793
Superposition of two different quantum states, 414f
Superposition wave function, 415
Superproton synchrotron (SPS), CERN, 765–766, 768f, 784f
  detection of W^+ and W^- in, 771
  image of W decay event in, 772f
  image of Z^0 decay in, 772f–773f
  as proton-antiproton storage ring, 769
  UA1 and UA2 detectors for, 769, 771
  W^+, W^-, and Z^0 bosons from, 767–768
Surface density, 131, 133t, 190
Switchable neutron generators, 367–368
Switchable neutron sources, 367–368
Symanzik, Kurt, 765
Symmetry
  breaking of, 775
  parity violation in beta decay, 783
  particle masses and, 778
  spontaneous breaking of, 775, 778
Symmetry breaking, 783–784, 783f
  Kobayashi and Toshihide and, 778
  prediction of six quarks by, 778
Synchrotron
  beam line, 288f
  booster ring, 289f
  construction of, 284–285
  phase stability in, 286
  principle of, 286
  storage ring, 287–288, 288f
  undulators, 288
  wigglers, 288
Synchrotron concept
  Marcus Oliphant and, 286
Synchrotron radiation, 284–290
  applications, 287–290
  from astronomic bodies, 284, 285f
  beam lines, 287–288
  components of, 287–288
  definition, 284
  discovery of, 284–286
  production of, 285f
  properties of, 286–287
Szilard-Chalmers effect, 728
  definition, 324–325, 726–727
  discovery of, 727
  principle of, 727f
Szilard-Chalmers process, 726–728
  applications of, 727–728
  description of, 325, 326f
  discovery, 324–325
  high specific activity isotopes and, 325
  Szilard and Chalmers and, 726–727
Szilard–Einstein pump, 321
Szilard, Leo, 58, 318–346, 328f, 330f, 336f–337f, 339, 351, 352f, 355, 402, 726–727
  atomic bomb and, 324
  atomic bomb patent, 340
  campaign against use of nuclear weapon, 341f, 342–343
  Chalmers and, 324–325
  critical mass and, 323–324
  Einstein and, 225, 319
  Einstein's letters to FDR and, 326–327, 328f, 330f, 341f, 647–648
  Eleanor Roosevelt and, 342
  escape from Nazi Germany, 321
  Fermi and, 332
  first conception of atomic bomb, 321
  at first Pugwash Conference, 352
  The Franck Report and, 342
  Gabor and, 320
  letters to Fermi on reactor, 332–333
  Manhattan Project and, 324

Szilard, Leo (*Continued*)
nuclear arms control and, 340
nuclear chain reaction and, 321
nuclear disarmament and, 343
opposition to atomic bomb use, 340
patent for atomic bomb, 92–93, 321, 322f–324f, 323–324, 647–648
patent for nuclear reactor, 321–322, 323f
patent on electron microscope, 320
patents on accelerators, 319
patents with Einstein, 321
photoneutron sources and, 325
Pugwash Conferences and, 343
Szilard–Chalmers effect, 325
U-235 fission and, 326, 801
at University of Berlin, 319
von Laue and, 319
Zinn and, 326

T

Takaaki Kajita, 170–171
Tamm, Igor Y., 60–61, 521, 523–524, 531
Andrei Sakharov and, 545
Cherenkov effect theory and, 541–546
Cherenkov radiation origins and properties, 541–546
controlled thermonuclear fusion and, 545
Ginzburg and, 545–546
hydrogen (fusion) bomb and, 545
and Igor Kurchatov, 545
Tata Institute of Fundamental Research, 267
Taylor, Richard E., 743, 747, 753–760
demonstration of quarks and gluons, 753
discovery of quarks and, 803
Technetium
discovery of, 482
as first artificial element, 482
Perrier and Segrè and, 482
Technetium-99m
first isolation of, 482
Segrè and Seaborg and, 482
Teller, Edward, 326–327, 353–359, 589, 601
design of hydrogen bomb by, 801
establishment of the LLNL and, 357
Fermi and, 355
first nuclear reactor and, 355
Gamow and, 354–355
hydrogen "Super" bomb and, 355
Ig Nobel Prize for Peace and, 358
as leader in nuclear weapons race, 357
Manhattan project and, 355
reactor safety and, 358
studies in Germany, 354
Szilard and, 355
Ulam and, 355
Teller–Ulam assembly
components and function of, 355–356, 356f
Teller–Ulam hydrogen bomb
first testing of, 357
Tevatron accelerator
Higgs boson search and, 784
The Franck Report, 342
Theory of everything, 811
Thermal neutrons, 17
most probable energy, 381
Thermonuclear fusion, 375, 688. *See also* Nuclear fusion
Thermonuclear war, 348
Thick-target materials
definition of, 283
Thomson, George Paget, 424–433, 429f, 459
Bragg's law and, 427, 429–431
as Chairman of MAUD Committee, 432
electron diffraction and, 427, 429–432
electron velocity calculation of, 428–430
electron wavelength calculation of, 428–430
electron wave properties and, 800
proof of de-Broglie matter-wave, 428
Reid and, 428–430
Thomson, Joseph John, 84–86, 90, 102, 116–118
electron discovery by, 85–86, 117–118, 799–800
electron properties and, 117
't Hooft, Gerardus, 763, 765–766
Thorium, 91
Thorium-232
decay scheme of, 636f
^{232}Th or thorium decay chain, 74
Threshold Cherenkov counters
discrimination between pions, positrons, 562f
gamma-ray detection with, 562f
gamma-ray measurement with, 561
index of refraction and, 560–563
lighter particles and, 561
muon, pion, kaon and proton discrimination with, 560–563, 561t, 562f
particle identification with, 560–563
particle mass and, 560–563
PMT photon detectors for, 561
and protons, 562f
relative abundances of heavier and, 561
threshold condition, 550
threshold momenta, 561t
threshold momentum, 561
threshold particle energy, 550, 553–554, 555f
threshold particle momentum in, 560–563, 561t, 562f
Time-of-flight Cherenkov counters
kaon and pion discrimination with, 573–574
particle identification with, 573–574, 574f
particle mass determination with, 572
particle velocity measurements with, 572
principle of, 572–574
Time-of-propagation Cherenkov counters
particle identification with, 570–571
pion and kaon discrimination with, 570–571
principle of, 570–571
Time projection chamber, 484
Ting, Samuel, 748
Tin-119m
decay scheme of, 273, 274f
Tokamak, 60–61
function of, 545
Tamm and Sakharov and, 545
Tomonaga, Sin-Itiro, 671–672, 674–675
Total attenuation, gamma-ray, 301f–302f
coefficients, 300
Total linear attenuation coefficients, 297–298
Total mass attenuation coefficients, 299t
Total mutual destruction, 403
Total neutrino flux, 577
Townsend Discharge, 105
Townsend, John Sealy, 105
Transfer reactions, 701
Transient equilibrium, 632–634
criteria for, 632
definition, 632
graphical depiction of, 633
parent-daughter activities in, 632
Transition energy, 125, 438
alpha-particle, 125
Transition intensity, 271
Transition probability, 271
Transmutation, 119–120
first artificial, 101–102
Transmutations, 361
Trapped beryllium ions
image of, 794f
Trapped ions
laser cooling of, 793
manipulation into superposition state, 793
photon measurement and control of, 792–793
quantum state changes in, 793
superposition energy states of, 792–793
Wineland and, 792–793
Trapped ion superposition states
quantum computers and, 794
Winelend and, 794
Trapping photons, 794–795
Trinity test, 152
Triple-spin baryons, 166
Truman, Harry S., 355
Tunneling, proton
Gamow and, 591
theory of, 591
Two-proton radioactivity, 704–705

U

U-235 critical mass
energy released from, 329
Peierls and energy released from, 327–329
^{235}U decay chain, 74, 75f
Uhlenbeck, George, 164–165
Ulam, Stanislaw, 759–760
design of hydrogen bomb by, 801
hydrogen "Super" bomb and, 355
Teller and, 355

Uncertainty principle, 409f, 410, 414
applications of, 410
applied to proof of inexistence of electron in nucleus, 410–411
concept of, 409
Heisenberg and, 409–410
mathematical expression of, 410
particle energy and time and, 411
particle momentum and location and, 411
range of strong nuclear force and, 683
theory of, 410
wave-particle duality and, 411
Undulators, 288, 289f–290f
Unification of forces, 811
Unified electroweak interaction, 760
United Nations, 397
Universal death, 350
Universe
Big-Bang theory of, 510
cooling of, 511
cooling temperature of, 510
cosmic microwave background radiation of, 513
expansion of, 510–511, 513
predicted temperature of, 513, 514f
temperature of, 512
University of Heidelberg, 639
University of Mainz, 171
^{238}U or uranium decay chain, 74, 75f
Up quarks (u), 188–189, 576
charge and mass of, 681–682
fractional charge of, 801–803
mass of, 804t–805t
Uranium, 90–91
Uranium-233
preparation from Th-232, 372
Uranium-235
energy released from fission chain, 331t, 332f
fission energy, 370–371, 372t
neutron chain reaction in, 331f
thermal neutron cross section, 385–388
Uranium Club, 108
Uranium hexafluoride (UF_6), 401
Uranium project, 413
Uranverein, 108
Urey, Harold C., 21, 587–588, 594, 641
Manhattan Project and, 342
Einstein and, 225–226
Emergency Committee of Atomic Scientists and, 225, 226f
Szilard and, 342

V

Vallarta. *See* Sandoval Vallarta
Vandenberg, Arthur H., 743–744
van der Meer, Simon, 765–768, 771
discovery of W^+, W^- and Z^0 bosons, 769
Van Hove, Leon
opposition to Zweig's theory, 744–745
Zweig's theory of quarks and, 744–745
Vavilov–Cherenkov Effect. *See* Cherenkov Effect
Vavilov–Cherenkov radiation, 527, 542. *See also* Cherenkov radiation
Vavilov, Nikolai I., 521
arrest and death of, 523–524
Lysenko and, 523–524
as pioneer in plant breeding, 523–524
Vavilov, Sergei I., 519–526, 530–531, 542–543, 545
arrest and death of Nicolai Vavilov and, 522–523
Cherenkov and, 521
as defender of Russian physicists, 525–526
discovery of unknown radiation, 521
Joseph Stalin's purges and, 524–526
Laventry Beria and, 519–526
as leader of Russian physics, 521–524
nonlinear optics and, 520
as President of USSR Acad. Sciences, 525
research on luminescence, 520–521
Stalin's regime and, 519–526
Vitaly Ginzburg and, 526
Vector boson fusion, 785–786
Veksler, Vladomir I., 588, 613
atoms for peace award and, 522–523
phase stability and, 286, 522–523
Veltman, Martinus J. G., 763, 765–766
Villard, Paul, 93–96, 94f, 800
Becquerel and, 94–95
discovery of gamma radiation by, 94–96
discovery of gaseous hydrates by, 94
gamma radiation and, 191–192
radiation dosimetry and, 95
Villard unit, 95
Violation of strangeness
examples of, 738
von Helmholtz, Herman
Planck and, 203–204
von Laue, Max, 46–47, 51, 235–238
correlation of X-ray wavelength and lattice constants, 237
discovery of X-ray diffraction, 237
discovery of X-ray wave nature, 237–238
Einstein and, 238
lattice theory of crystals and, 237–238
Planck and, 236
von Lenard, Philipp, 120–122
von Neumann, John, 672–673
von Schuschnigg, Kurt, 445
von Schweidler, Egon, 443
von Weizsäcker, Carl Friedrich, 689–690
V particles, 452–453, 485

W

Wahl, Arthur C., 614
Walton, Ernest T.S., 464–465, 589–596
$W^{\pm}$ and Z^0 bosons
properties of, 810
Ward, John Clive, 760
Water resources, 37–41
Water resources management
^{36}Cl/Cl ratios in, 40–41
delta ^{13}C in, 40
delta ^{18}O and ^{2}H in, 39–40
delta ^{87}Sr in, 41
isotope delta values in, 39
lithogenic and cosmogenic nuclides in, 38f
noble gas isotopes in, 41
stable isotope techniques in, 37
Watson, Edwin M., 327, 329f–330f
Wave function, 414
Wave-matter property of the electron, 428–429
Wave mechanics, 414
Wave-particle duality, 207–209, 407–408, 411, 421, 425, 426f, 427–432, 800
de Broglie and, 364–365
$W^{\pm}$ boson, 576, 780, 805–806, 808
in beta decay, 810
calculation of range of, 810
discovery, 188–189
in CC interactions, 810
mass of, 762, 810
maximum range of, 808
range of interaction, 762
W^+ bosons
beta decay and, 766
as field particle in positron emission, 808, 809f
positron emission and, 763
in quark flavor transformations, 576–577, 576f
W^- bosons, 188–189
in beta decay, 746f
decay of, 808
as field particle in negatron emission, 808, 809f
negatron emission and, 763
Weak force, 760, 808–810
Weak interactions, 148, 188–189, 808
Weak nuclear force, 808
Weapons, nuclear, 225–226, 233–234, 303, 323–324, 327, 328f, 330f, 339–344, 339f, 341f, 344f, 346–359, 356f
Wedgewood, Thomas
thermal radiation and, 204–205
Weight fractions, 132–133
Weinberg, Alvin, 58, 339
Weinberg, Steven, 760, 762
Weisskopf, Victor, 396–397, 677
Wenzel, William A., 481
Wheeler, John Archibald
beta(n) decay theory of, 731
White House, 330f
White light, 113
Whole-body counter, 161
Wholesale destruction of civilian life, 403–404
Wideröe, Rolf, 319, 584
Wiegand, Clyde, 479, 482, 484
antiproton discovery and, 483–484
Nobel Prize Physics 1959 and, 483–484
Wiener, Norbert, 492–493
Wien's displacement law, 512
Wien, Wilhelm, 236, 512
exponential law of, 204–205
Wigglers, 288, 289f–290f

Wigner, Eugene P., 58, 326–327, 339, 461, 645–649
Einstein's letter to FDR and, 647–648
nuclear weapons and, 648
plutonium production and, 648
strong nuclear force and, 645–646
Szilard and, 647
von Neumann and, 647–648
Wilczek, Frank, 757–758, 765
Wilson Cloud Chamber, 488–491
Compton and Auger electron tracks in, 143f
Compton scattering and, 228
design of, 140f
development of, 139
first alpha-particle tracks in, 141–143
first beta-particle tracks in, 141–143
operation of, 139–141
particle track formation in, 140f, 141
primary and secondary electron tracks in, 141–143
Wilson, C.T.R., 137–143, 408
development of cloud chamber by, 139
Wilson, Robert W., 507–508, 495
Wineland, David J., 415, 789–798
at NIST, 791
Wood, John, 488
Wu, Chien-Shiung, 649–657, 775–777
Lawrence and Segre and, 651
Lawrence and Segre and, 651
in Manhattan Project, 652
parity violation and, 652
parity violation in beta decay, 649–657
parity violation in Co-60 decay, 657, 658f
as pioneering female physicist, 652
test for parity conservation, 655, 656f
Tsung-Dao Lee and, 654–655
xenon poisoning/xenon effect and, 651
Wu, Youxun, 230–231
collaboration with Compton, 231
Compton and, 228
Wu Youxun Prize, 231
W^+, W^- and Z^0 bosons
conditions for production of, 769
production of, 766
from quark-antiquark annihilation, 766
Wynn-Williams, Charles Eryl, 464–465

X

Xenon-143
decay scheme of, 370–372
Xenon effect, 651
definition, 336f
Xenon poisoning/xenon effect discovery, 651
X-radiation, 82–83, 438
artificial, 83
definition of, 275–276
energy lines of, 277
following EC decay, 179
following internal conversion, 437–438
origin of, 83, 277, 291
X-ray computed tomography (CT), 82–83, 436f
2D-CT cross sectional images, 5f
3D-CT images, 5f
hybrid SPECT/CT in, 7
imaging technique of, 4f
in medical diagnosis, 3–6
principle of, 4–5
SSD 3D-CT images, 5–6
synchrotron radiation for, 6
X-ray crystallography, 51
birth of, 242–243
X-ray crystallography/diffraction, 51–52
applications, 52
in molecular structure analysis, 51–52
principle of, 51–52
with synchrotron radiation, 52
X-ray diffraction, 50, 812
Bragg's Law and, 240
discovery, 237
Franklin and DNA structure, 244–245
X-ray diffraction crystal structure analysis
W.L. Bragg and, 239
X-ray emission, 439f
Auger electron emission and, 439–440
X-ray fluorescence analysis, 439f
applications, 54
Barkla and, 252
description of, 439
principle of, 54
X-ray fluorescence (XRF) spectrometry, 50
X-ray photons, 292, 433–434
X-rays, 80–82, 87–88, 242, 291. *See also* X-radiation
from beta-particle emission, 283
classification of, 275–276
discovery of, 80, 84
line spectra of, 283
medical imaging with, 87–88
origin of, 270, 275–276
spectral lines of, 276–277
transmission of, 81t
X-ray spectrometer
of W.H. and W.L. Bragg, 241f
X-ray spectrometry
Moseley and, 248
Siegbahn and, 254
X-ray tube, 82–83, 82f, 86
X-ray wavelengths
Wien and Sommerfield estimations of, 236–237

Y

Yalow, Rosalyn, 30–31
Yang, Chen-Ning, 649–657, 775–777
parity and, 653
Ypsilantis, Thomas, 479, 484, 564
antiproton discovery and, 483–484
Yttrium-90
decay scheme of, 295f
Yukawa, Hideki, 233, 680–681, 811
Fermi and, 461
Heisenberg and, 461
meson mass prediction of, 461–462
meson prediction by, 460–463
meson theory of, 461
Pauli and, 461
Russell-Einstein Manifesto and, 463
Yukawa's meson
in cosmic radiation showers, 462
discovery of, 462
pion or pi-meson, 462–463
properties of, 462–463

Z

Z^0 boson, 780, 805–806, 808
discovery of, 763
mass of, 763
in neutral current interactions, 577, 578f, 810
in neutrino-electron scattering, 810f
range of interaction of, 762
Zeeman effect, 113, 269
Zeeman, Pieter, 113, 269
Zeeman effect and, 113
Zero-spin mesons, 166
Zinn, Walter, 58, 326, 332, 339, 346, 355
Szilard and, 326
U-235 fission and, 326, 801
Z number, 123
Zweig, George, 740–751, 756, 759–760, 729
Feynman and, 744
force binding quarks and, 750
force confining quarks and, 801–803
name "aces" for quarks and, 742
proposal of quarks by, 681–682
quark baryon number and, 745
quark charges and, 745
quark theory and, 800–803
Sakurai Prize for quark theory, 750
theory of quarks and, 744–745
theory of quarks hidden from public, 740–742
Van Hove and, 744–745
Zweig's Nobel Prize nomination
Feynman's and, 748, 749f